AIC 2015 TOKYO

Color and Image

Midterm Meeting of the International Colour Association (AIC)

19-22 May 2015 Tokyo, Japan

Proceedings

日本色彩学会
THE COLOR SCIENCE ASSOCIATION OF JAPAN

AIC

MCS 2015

Time Table

Hour	5/19 Tue	5/20 Wed
8:00		8:00 - 9:00 **Registration** Reception Hall
9:00		9:00 - 9:30 **Opening ceremony** sola city Hall; 9:00 -17:00 **Exhibition** Terrace Room
10:00	10:00-17:30 **EC Meeting** Room A	9:30 -10:30 **Keynote** sola city Hall; 10:30-10:45 **Group Photo**
11:00		10:45-11:15 Coffee Break; 11:15-12:45 OS1 **Color Imaging** (15min x 6) sola city Hall; 11:15-12:45 OS2 **Color Environment Design** (15min x 6) Room C
12:00		12:45-14:15 Lunch
13:00	13:00-20:00 **Registration** Reception Hall	
14:00		14:15-15:45 PS1 **Poster 1** Lobby / Room B
15:00		15:45-16:00 Coffee Break
16:00		16:00-17:30 OS3 **Colorimetry** (15min x 6) sola city Hall; 16:00-17:30 OS4 **Color Vision, Psychophysics** (15min x 6) Room C
17:00		17:30-19:00 **Study Group1** Room A; 17:30-19:00 **Study Group2** Room C
18:00	18:00-20:00 **Welcome Reception** sola city Hall	
19:00		
20:00		
21:00		
22:00		

5/21 Thu

- 8:00 - 8:30 **Registration** — Reception Hall
- 8:30 - 9:15 **Invited Talk(MCS)** — sola city Hall
- 9:20 -10:40 MCS1 **Multispectral Imaging System** (20min x 4) — sola city Hall
- 9:20 -10:35 OS5 **Color Education & Culture** (15min x 5) — Room C
- 10:40-11:00 **Coffee Break** 10:35-11:00
- 11:00-12:20 MCS2 **Multispectral Color Science** (20min x 4) — sola city Hall
- 11:00-12:15 OS6 **Color and Culture** (15min x 5) — Room C
- 12:15-13:45 **Lunch**
- 13:45-15:15 PS2 **Poster 2** — Lobby / Room B
- 15:15-15:30 **Coffee Break**
- 15:30-16:30 **AIC General Assembly** — sola city Hall
- 16:30-17:45 **Judd Award Lecture** — sola city Hall
- 17:45-22:30 **Banquet**
- 9:00 -17:00 **Exhibition** — Terrace Room

5/22 Fri

- 8:00 - 8:30 **Registration** — Reception Hall
- 8:30 - 9:15 **Invited Talk** — sola city Hall
- 9:20 -10:35 OS7 **Appearance, Lighting**(15min x 5) — sola city Hall
- 9:20 -10:35 OS8 **Color Deficiency** (15min x 5) — Room C
- 10:35-10:50 **Coffee Break**
- 10:50-11:50 OS9 **Cosmetics, Material Perception**(15min x 4) — sola city Hall
- 10:50-11:50 OS10 **Color Psychology** (15min x 4) — Room C
- 11:50-12:35 **Closing ceremony** — sola city Hall
- 12:45-18:30 **Optional Tour**
- 9:00 -10:50 **Exhibition** — Terrace Room

Hour
8：00
9：00
10：00
11：00
12：00
13：00
14：00
15：00
16：00
17：00
18：00
19：00
20：00

Floor map (sola city Conference Center)

1F

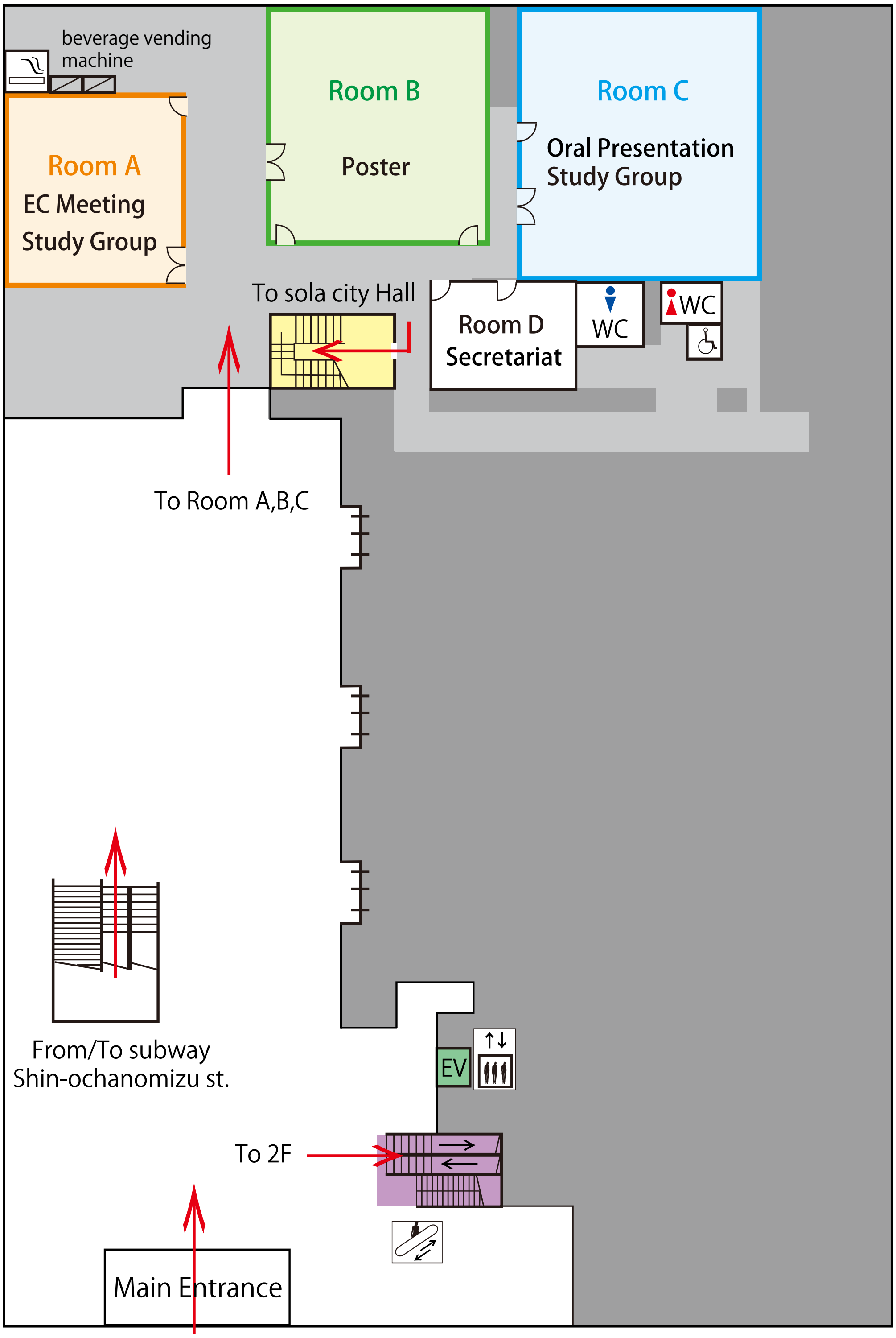

From/To JR ochanomizu st.

2F

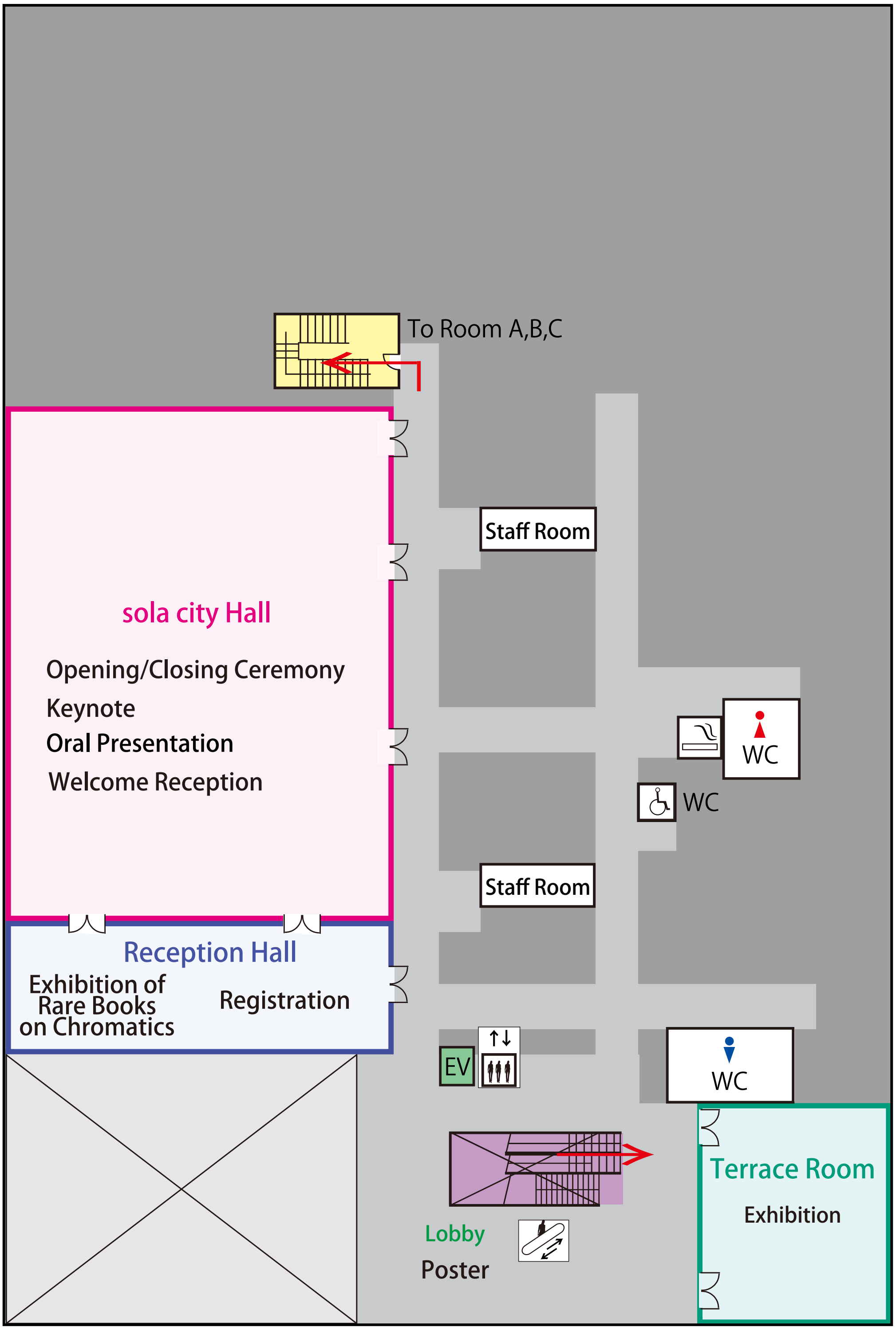
To Room A,B,C
sola city Hall
Opening/Closing Ceremony
Keynote
Oral Presentation
Welcome Reception
Staff Room
WC
WC
Staff Room
Reception Hall
Exhibition of Rare Books on Chromatics
Registration
EV
WC
Terrace Room
Exhibition
Lobby
Poster

MCS 2015

AIC2015 TOKYO
Color and Image

Midterm Meeting of the International Colour Association (AIC)

19-22 May 2015, Ochanomizu sola city Conference Center, Tokyo, Japan

Proceedings

Editors: Hirohisa Yaguchi
Katsunori Okajima
Taiichiro Ishida
Kikuko Araki
Motonori Doi
Yoshitsugu Manabe

日本色彩学会
THE COLOR SCIENCE ASSOCIATION OF JAPAN

AIC

Contents

AIC President's Message 5

AIC - International Colour Association 6

Color Science Association of Japan President's Preface 7

Welcome to AIC2015 TOKYO 8

Welcome to MCS2015 TOKYO 10

AIC 2015 Committees 11

MCS 2015 Committees 14

Cooperation & Support 14

Scientific Program 15

- Wednesday, May 20, 2015 15
- Thursday, May 21, 2015 19
- Friday, May 22, 2015 23

Keynote Lecture, Invited Talks, Judd Award Lecture 25

- Keynote Lecture 26
- Invited Talk (MCS) 27
- Invited Talk 33
- Judd Award Lecture 39

Oral Papers 61

MCS Oral Papers 360

Poster Papers 407

MCS Poster Papers 1265

Author Index 1356

AIC 2015 Sponsors 1363

Proceedings

Published May, 2015
by the Steering Committee of AIC2015 TOKYO
The Color Science Association of Japan
3-17-42, Shimo-ochiai, Shinjuku-ku, Tokyo 161-0033, Japan

Graphical design by Kikuko Araki
Printed by Tsujino Planning Office, Inc.

AIC President's Message

For a second time the AIC is to hold a conference in Japan, in Tokyo this time, thanks to the initiative of the Color Science Association of Japan. On the first occasion, the 8th AIC Congress was held in Kyoto, and everyone remembers it as a great event. This year it is to be mid-term meeting dedicated to "Image and Color". This is a very modern issue that encompasses many fields: from acquisition and reproduction of color images to processing the images and their use in computer vision. Many other interesting topics are also included, such as color in computer graphics, colorimetry, digital archiving of art, color vision, color psychology and emotion, environmental color, design, color culture and color education. All of them in their relationship to color images. The conference will also include the16th International Symposium on Multispectral Color Science, opening the science of color to the world of spectral imaging of large projections today.

We live in a world full of images. Communication between humans relies increasingly on the acquisition and use of images in any method of exchanging information. Optoelectronic audiovisual media of acquisition and reproduction of images and the internet have revolutionized the way we communicate and images are continuously used in color. As a result, new challenges arise: the reliability and quality of images, the development of new algorithms of image processing in order to find new applications, for example in computer vision or in medicine, etc.

Color is an added and differential value in images. We can say that it brings a great deal of transcendental information to those images that are part of our daily life. The visual images that form our eyes together with the retina and the brain processes involved, acquire a higher dimension when they are in color. We can say the same for the images obtained with a camera. I think the opportunity to discuss and exchange ideas in the field of color images at this conference will be extraordinary.

The Color Science Association of Japan is one of the most active regular members of the AIC. Proof of this is the high participation of Japanese scientists in all the AIC congresses and the participation of its members in the management of the AIC as members of the Executive Committee and as Chairs of Study Groups. From these lines I want to publicly thank these efforts that have supported the AIC since its founding and recognize the prestige of so many Japanese scientists in the field of color. I would also like to thank the great effort and work done by the organizing committee of AIC 2015 to enable this conference to be the success which I am sure it will be. The quality of the communications which are collected together in this book is sufficient proof of the magnificent meeting we are going enjoy together.

I wish all attendees a fruitful and enjoyable AIC 2015!

Javier Romero
President, International Colour Association

AIC - International Colour Association

AIC Executive Committee

President	Javier Romero
Past President	Berit Bergström
Vice President	Nick Harkness
Secretary/Treasurer	Tien-Rein Lee
Committee Members	Jin-Sook Lee
	Maria João Durão
	Nancy Kwallek
	Gabriela Nirino

AIC Regular Members

Argentina	GRUPO ARGENTINO DEL COLOR
Australia	COLOUR SOCIETY OF AUSTRALIA
Brazil	ASSOCIAÇÃO PRÓ-COR DO BRASIL
Bulgaria	COLOUR GROUP – BULGARIA
Canada	COLOUR RESEARCH SOCIETY OF CANADA
Chile	ASOCIACIÓN CHILENA DEL COLOR
China	COLOR ASSOCIATION OF CHINA
Finland	SUOMEN VÄRIYHDISTYS SVY RY
France	CENTRE FRANÇAIS DE LA COULEUR
Germany	DEUTSCHER VERBAND FARBE
Great Britain	THE COLOUR GROUP
Hungary	HUNGARIAN NATIONAL COLOUR COMMITTEE
Italy	GRUPPO DEL COLORE ASSOCIAZIONE ITALIANA COLORE
Japan	COLOR SCIENCE ASSOCIATION OF JAPAN
Korea	KOREAN SOCIETY OF COLOR STUDIES
Mexico	ASOCIACIÓN MEXICANA DE INVESTIGADORES DEL COLOR
Netherlands	NEDERLANDSE VERENIGING VOOR KLEURENSTUDIE
Norway	FORUM FARGE
Portugal	ASSOCIAÇÃO PORTUGUESA DA COR
Slovenia	SLOVENSKO ZDRUZENJE ZA BARVE
Spain	COMITÉ ESPAÑOL DEL COLOR
Sweden	STIFTELSEN SVENSKT FÄRGCENTRUM
Switzerland	PRO/COLORE
Taiwan	COLOR ASSOCIATION OF TAIWAN
Thailand	THE COLOR GROUP OF THAILAND
United States	INTER-SOCIETY COLOR COUNCIL

AIC Associate Members

INTERNATIONAL ASSOCIATION OF COLOR CONSULTANTS/DESIGNERS, North America
COLOUR MARKETING GROUP, USA

AIC Study Groups

Study Group on Color Education (CE)
Chair: Robert Hirschler (Hungary and Brazil)
Study Group on Environmental Color Design (ECD)
Chair: Verena M. Schindler (Switzerland)
Study Group on Color Vision and Psychophysics (CVP)
Chair: Katsunori Okajima (Japan)
Study Group on The Language of Color (LC)
Chair: Dimitris Mylonas (United Kingdom)

Color Science Association of Japan President's Preface

As the President of the Color Science Association of Japan I would like to welcome all of our participants to AIC2015, being held from May 19th to the 22nd in Tokyo.

Eighteen years ago in 1997 the Color Science Association of Japan held Asia's first international Congress in Japan's old capital of Kyoto, where participants from various countries had the chance to deepen friendships through lively discussions on their research, while simultaneously learning about Japan's traditions and colors. We are very happy that once again, eighteen years since then, the AIC's Midterm Meeting will once again be held in Japan.

The AIC is composed of members from more than 30 countries, and many people from various nations are gathering in Tokyo for AIC2015. We would like for this not only to be a place for research reports and scientific and technical discussions, but hope from the bottom of our hearts that it will be a chance for developing friendships which go beyond the boundaries of location or age. We, the members of the Color Science Association of Japan, have planned the program of AIC2015 Tokyo to be one that participants can enjoy. We hope you will feel happy that you participated in AIC2015 Tokyo. Additionally, to commemorate AIC2015 Tokyo, at the conference site on May 19th we will hold a symposium entitled "Considering Color and Japanese Culture from the Perspective of Food, Clothing, and Shelter" and, on the 20th, an exhibition of rare books by well-known authors such as Michel-Eugène Chevreul.

Now Tokyo is bustling with energy in preparation for the 2020 Olympic Games. We hope AIC2015 participants can observe Tokyo as it grows even more dynamically, and further develops the infrastructure to handle this major international event smoothly.

We, the members of the Color Science Association of Japan, are looking forward to meeting you in Tokyo.

Takayoshi Fuchida

President, The Color Science Association of Japan

Welcome to AIC2015 TOKYO

On behalf of the Steering Committee of AIC2015 TOKYO, I would like to welcome you all to the Midterm Meeting of the International Colour Association in the exciting and traditional city of Tokyo, from May 19-22, 2015.

The meeting is organized by the International Colour Association and the Color Science Association of Japan in cooperation with Ministry of Education, Culture, Sports, Science and Technology (MEXT), Ministry of Economy, Trade and Industry, National Institute of Advanced Industrial Science and Technology, Science Council of Japan, The Tokyo Chamber of Commerce and Industry.

This meeting will provide a unique forum, bringing together researchers, academics, students, artists, architects, industrialists, engineers, designers, computer scientists, lighting experts, media types, exhibitors and business leaders. This year the 16th International Symposium on Multispectral Color Science (MCS 2015) is organized as part of AIC2015. We have chosen "Color and Image" as a theme of AIC2015. The word "image" has a very wide meaning; not only visible presentation, such as imaging devices, displays, pictures, etc., but also a presentation of anything from people's minds. So, we have called for papers from a variety of fields as follows:

Color Imaging
Color Image Processing
Computational Color Image
Color in Computer Graphics
Color Reproduction
Color Image Quality
Multispectral Color Science
Multispectral Imaging
Multispectral Image Acquisition / Display
Spectral Image Applications
Colorimetry / Colorimetric Imaging / Lighting
Digital Archiving of Art
Color Vision / Psychophysics / Physiology
Color Psychology / Emotion
Perception of Material / Surface Quality
Color Image Design
Color Environmental Design
Cosmetics
Personal Color
Color Culture
Color Education

Although as many as 324 papers have been submitted from more than 20 countries, we have to accept a limited number of papers because of limitation of time and space. Finally, we selected 60 oral and 172 papers presentations covering a diverse range of color research and applications based on peer reviews by the International Program Committee.

We have invited three speakers who all are admirable leaders in their fields. Following the opening ceremony on Wednesday, May 20, Ms. Kazuyo Sejima, the recipient of the prestigious Prizker Architecture Prize with Ryue Mishizawa of SANNA, will deliver the Keynote Lecture on the title “The Gathering Space” focusing on her recent works. She will introduce the environment and architecture enhanced by color. During the morning session, invited papers are presented. On Thursday, May 21, Professor Jon Y. Hardeberg of the Gjøvik University College, Norway will give an invited lecture, “Multispectral colour imaging: time to move out of the lab?” He has beeen recommended by MCS and will talk about his main research interests which includes multispectral color imaging, print and image quality, colorimetric device characterization, color management, and cultural heritage imaging. On Friday, May 22, the final day, Professor Hidehiko Komatsu of National Institute for Physiological Sciences talks on “Neural representation of color in visual cortex.” He is currently project leader for a large research project “Brain and Information Science on shitsukan (material perception)” funded by MEXT and will talk on neural representation of color in higher visual cortex, neural mechanisms of gloss perception, texture processing, and multimodal integration in material recognition.

Following the General Assembly on Thursday, May 21, the AIC Judd Awards ceremony will be held. The 2015 Judd Award is to be received by Professor Françoise Viénot, Muséum National d’Histoire Naturelle, France. She will deliver the Judd Award Lecture on “On the dimensionality of the colour world.”

Finally, I would like to note acknowledgements as the Chair of the Steering Committee. The journey today would not have been possible without a dedicated and hard working Steering Committee all of whom have devoted a considerable amount of time to ensuring that AIC2015 TOKYO will be a great success. I would like to offer my personal and sincere thanks to all of you.

I would also like to thank our sponsors whose generosity and support is greatly appreciated. I would like to ask that you all reciprocate their support when you are seeking products or services offered by our sponsors.

I hope that you all leave the AIC2015 with warm feelings for the exciting city of Tokyo, will have renewed friendships and made new friends in the global color community, and, importantly, be refreshed and stimulated with new ideas to further develop your research in the world of color.

Hirohisa Yaguchi
Chair, Steering Committee of AIC2015 TOKYO

Welcome to MCS2015 TOKYO

As a MCS general chair, I would like to welcome all of you to AIC/MCS2014 TOKYO, which is held in Tokyo, Japan, during May 19–22, 2015. This year, the 16th International Symposium on Multispectral Color Science (MCS 2015) is organized as part of AIC2015 TOKYO.

Many aspects of the multi- and hyper- spectral image acquisition, analysis, and rendering have been extensively researched and studied along with the technological advances in hardware devices, software systems, and signal processing algorithms. Also, spectral imaging science and technology is more and more exploited in numerous applied technologies such as computer vision, computer graphics, biology, medicine, cosmetics, digital archiving, printing, display, and remote sensing. As a consequence, a variety of problems generally encountered have been reformulated, successfully solved, and sometimes cast into their new contexts rising new scientific challenges.

The first MCS symposium was launched at Chiba University, Japan in 1999. Since 2001 the multispectral symposium has been organized by a consortium of international researchers, mostly incorporated into larger international conferences and continues to grow. The 16th International Symposium (MCS2015 TOKYO) builds on the tradition to bring together researchers in the field of spectral color science and imaging.

We received about 40 paper submissions to the MCS group. The AIC/MCS Program Committee finally decided to accept 8 papers for MCS oral, about 20 papers for MCS poster, and some papers for AIC poster from the contributed papers, based on peer reviews by the International Program Committee. Paper presentations related on MCS are scheduled mostly on Thursday, May 21. The morning session starts with an invited lecture by Professor Jon Y. Hardeberg (Gjøvik University College, Norway), entitled “Multispectral colour imaging: time to move out of the lab,” which is then followed by the Oral session. The poster presentations are in the afternoon.

I wish that all participants will successfully exchange their knowledge, technologies, and ideas with old and new friends, and enjoy the conference and the most beautiful season in Japan.

Shoji Tominaga
General Chair of MCS2015 Tokyo

AIC 2015 Committees

Organizing committee

Asao Komachiya, Chair
Mitsuo Ikeda
Takuzo Inagaki
Naoyuki Osaka
Hiroshi Kansaku
Hitoshi Komatsubara
Tsuneo Suzuki
Shinya Takahashi
Goro Baba
Shoji Tominaga
Hideaki Hayashi
Takayoshi Fuchida
Masao Yamagishi

Steering committee

Chair	Hirohisa Yaguchi
Secretary	Yoshitsugu Manabe
Treasurer	Yoko Mizokami
	Kazuo Yamaba
Technical Program	
	Katsunori Okajima
	Shoji Tominaga (MCS)
	Taiichiro Ishida
	Takuzo Inagaki
	Shinya Takahashi
	Shinji Nakamura
	Norihiro Tanaka
Publicity	Motonori Doi
	Kohji Yoshimura
	Kikuko Araki
Local	Takahiko Horiuchi
	Ikuko Narita

Funding committee

Takayoshi Fuchida, Chair
Akira Kitabatake
Hitoshi Komatsubara
Tsuneo Suzuki
Takaaki Suzuki
Yoko Matsuda
Hiroyuki Shinoda
Katsunori Okajima
Shinya Takahashi
Hiroshi Shimazaki
Yoko Mizokami

Local arrangements committee

Takahiko Horiuchi, Chair
Ikuko Narita
Keita Hirai
Noriko Yata
Shoko Isawa
Tomoko Mitsutake
Yoshihiko Azuma
Wataru Iwai
Masako Yamada

Finance committee

Yoko Mizokami, Chair
Masayuki Osumi
Kazuo Yamaba

International Scientific Committee

Berit Bergstrom, Sweden
Monica Billger, Sweden
Valerie Bonnardel, United Kingdom
José Caivano, Argentina
Vien Cheung, United Kingdom
Osvaldo Da Pos, Italy
Motonori Doi, Japan
Mark Fairchild, United States
Karin Fridell Anter, Sweden
Brian Funt, Canada
Davide Gadia, Italy
Jeremie Gerhardt, Germany
Paul Green-Armytage, Australia
Helen Gurura, South Africa
Aran Hansuebsai, Thailand
Jon Hardeberg, Norway
Nick Harkness, Australia
Markku Hauta-Kasari, Finland
Javier Hernandez-Andres, Spain
Bernhard Hill, Germany
Keita Hirai, Japan
Robert Hirschler, Brazil
Takahiko Horiuchi, Japan
Po-Chieh Hung, United States
Mitsuo Ikeda, Thailand
Francisco Imai, United States
Taiichiro Ishida, Japan
Hyeon Jeongsuk, Korea
Maria Joaodurao, Portugal
Eric Kirchner, Netherlands
Michael Kriss, United States
Youngshin Kwak, Korea
Nancy Kwallek, United States
Derry Law, Hong Kong
Tien-Rein Lee, Taiwan
Wen-Yuan Lee, Taiwan
Reiner Lenz, Sweden
Lindsay Macdonald, United Kingdom
Yoshitsugu Manabe, Japan
Alamin Mansouri, France
Gabriel Marcu, United States
John Mccann, United States
Manuel Melgosa, Spain
Yoichi Miyake, Japan
Yoko Mizokami, Japan
Nathan Moroney, United States
Judith Mottram, United Kingdom
Dimitris Mylonas, United Kingdom
Shinji Nakamura, Japan
Shigeki Nakauchi, Japan
Sérgio Nascimento, Portugal
Juan Luis Nieves, Spain
Gabriela Nirino, Argentina
Peter Nussbaum, Norway
Tomoko Obama, Japan
Katsunori Okajima, Japan
Li-Chen Ou, Taiwan
Jussi Parkkinen, Malaysia
Carinna Parraman, United Kingdom
Marius Pedersen, Norway
Katia Ripamonti, United Kingdom
Alessandro Rizzi, Italy
Javier Romero, Spain
Maurizio Rossi, Italy

Tetsuya Sato, Japan

Verena M. Schindler, France

James Shyu, Taiwan

Cecilia Sik Lanyi, Hungary

Andrew Stockman, United Kingdom

Pei-Li Sun, Taiwan

Vincent C. Sun, Taiwan

Shoji Sunaga, Japan

Shin'ya Takahashi, Japan

Norihiko Tanaka, Japan

Elza Tantcheva, United Kingdom

Kulthida Teachavorasinskun, Thailand

Shoji Tominaga, Japan

Masaru Tsuchida, Japan

Seiichi Tsujimura, Japan

Norimichi Tsumura, Japan

Eva M. Valero, Spain

Francoise Viénot, France

Yuh-Chang Wei, Taiwan

Stephen Westland, United Kingdom

Haisong Xu, China

Hirohisa Yaguchi, Japan

Sari Yamamoto , Japan

Yasuki Yamauchi, Japan

Kohji Yoshimura, Japan

MCS 2015 Committees

General Chair

Shoji Tominaga, Japan

Program Committee of MCS 2015

Francisco Imai, United States
Jon Yngve Hardeberg, Norway
Markku Hauta-Kasari, Finland
Bernhard Hill, Germany
Alamin Mansouri, France
Yoichi Miyake, Japan
Jussi Parkkinen, Malaysia
Norimichi Tsumura, Japan
Philipp Urban, Germany

Local Committee of MCS 2015

Shoji Tominaga, Japan
Masaru Tsuchida, Japan
Keita Hirai, Japan

Cooperation & Support

In Cooperation With:

Ministry of Economy, Trade and Industry

Ministry of Education, Culture, Sports, Science and Technology

National Institute of Advanced Industrial Science and Technology

Science Council of Japan

The Tokyo Chamber of Commerce and Industry

With the Support of:

Architectural Institute of Japan

Color Universal Design Organization

Coating Equipment Manufacturers Association of Japan

The Illuminating Engineering Institute of Japan

The Imaging Society of Japan

Information Processing Society of Japan

The Institute of Electrical Engineers of Japan

The Institute of Electronics, Information and Communication Engineers

The Institute of Image Information and Television Engineers

Japan Ergonomics Society

Japanese Cosmetic Science Society

Japanese National Committee of CIE

Japanese Society for the Science of Design

The Japanese Psychological Association

The Japanese Psychonomic Society

The Japanese Society of Ophthaimological Optics

The Japanese Society of Printing Science and Technology

The Japan Paint Manufacturers Association

Japan Society of Colour Material

The Japan Society of Home Economics

Japan Society of Kansei Engineering

The Japan Society of Mechanical Engineers

The Optical Society of Japan

The Society of Cosmetic Chemists of Japan

The Society of Photography and Imaging of Japan

Vision Society of Japan

Suga Weathering Technology Foundation

Keynote Lecture

9:30 - 10:30 sola city Hall

Chair: Hirohisa Yaguchi

The Gathering Space

Kazuyo SEJIMA

Oral Papers

11:15-12:45 (sola city Hall)
OS1: Color Imaging

Chairs: Alessandro Rizzi & Takahiko Horiuchi

OS1-1 How Multi-Illuminant Scenes Affect Automatic Colour Balancing
Liwen Xu and Brian Funt

OS1-2 The Generalised Reproduction Error for Illuminant Estimation
Graham Finlayson and Roshanak Zakizadeh

OS1-3 Rank-Based Camera Spectral Sensitivity Estimation
Graham Finlayson and Maryam Mohammadzadeh Darrodi

OS1-4 Comparing Colour Camera Sensors Using Metamer Mismatch Indices
Ben Hull and Brian Funt

OS1-5 Advanced Measurement Technology for Image Clarity
Hideo Kita and Shigeo Suga

OS1-6 Painting by Numbers: Transforming Fields and Edges to Vectors
Carinna Parraman, Paul O'Dowd and Mikaela Harding

11:15-12:45 (Room C)
OS2: Color Environment Design

Chairs: Taiichiro Ishida & Jin-Sook Lee

OS2-1 Perception of Colours Illuminated by Coloured Light
Shabnam Arbab and Barbara Szybinska Matusiak

OS2-2 Effects of Furniture Colour on Apparent Volume of Interior Space
Keishi Yoshida and Masato Sato

OS2-3 Ideal GRID Model for Color Planning of Living Space
Tien-Rein Lee

OS2-4 Case Studies of Color Planning for Urban Renewal
Sari Yamamoto

OS2-5 Building Colours in Taipei – Taking Wanhua District as an Example
Chia-Chi Chang, Ting-Tsung Ho and Li-Chen Ou

OS2-6 Pritzker Prize Laureates' Colour Preferences
Malvina Arrarte-Grau

16:00-17:30 (sola city Hall)
OS3: Colorimetry

Chairs: Haisong Xu & Yoshitsugu Manabe

OS3-1 Computing Tristimulus Values: An Old Problem for a New Generation
Zhifeng Wang, Tianyi Li, M. Ronnier Luo, Manuel Melgosa, Michael Pointer and Changjun Li

OS3-2 Variability in Colour Matches between Displays
Phil Green, Srikrishna Nuduramati and Ivar Farup

OS3-3 A Comparison Study of Camera Colorimetric Characterization Models Considering Capture Settings Adjustment
Jingyu Fang, Haisong Xu and Wei Ye

OS3-4 Evaluation and Analysis of *YUTEKI-TENMOKU* Visual Effect on Traditional Ceramic Applied Gonio- Photometric Spectral Imaging and Confocal Type Laser Scanning Microscopy
Masayuki Osumi

OS3-5 Measuring Skin Colours Using Different Spectrophotometric Methods
YuZhao Wang, Ming Ronnier Luo, Xiao Yu Liu, Haiyan Liu and BinYu Wang

OS3-6 Assessing Light Appearance in Shopping Mall
Yuteng Zhu, Ming Ye, Wenjie Huang, Muhammad Farhan Mughal, Muhammad Safdar and Ming Ronnier Luo

16:00-17:30 (Room C)
OS4: Color Vision, Psychophysics

Chairs: Yoko Mizokami & Li-Chen Ou

OS4-1 Pupillary Light Reflex Associated with Melanopsin and Cone Photorecetors
Seiichi Tsujimura and Katsunori Okajima

OS4-2 Experimental Research on EEG Characteristics in Red, Green, Blue, and White Color Space Consequent on the Degree of Depression
Heewon Lee, Hanna Kim, Jiseon Ryu and Jinsook Lee

OS4-3 Hue-Tone Representation of the Nayatani-Theoretical Color Order System
Hideki Sakai

OS4-4 Colour Appearance in the Outdoor Environment
Ya-Chen Liang, Li-Chen Ou and Pei-Li Sun

OS4-5 Color Play: Gamification for Color Vision Study
Shida Beigpour and Marius Pedersen

OS4-6 Using Visual Illusions to Expand the Available Colors for Making Mosaics
I-Ping Chen and Wei-Jie Chiou

Study Group Meetings

17:30-19:00 (Room A)

Study Group on Environmental Color Design

Chair: Verena M. Schindler

17:30-19:00 (Room C)

Study Group on The Language of Color

Chair: Dimitris Mylonas

Poster Papers

14:15-15:45 Poster 1 (Room B/Lobby)

Chairs: Shoji Sunaga & Norihiro Tanaka

Room B : PS1-1~64
Lobby : PS1-65~87

PS1-1 Colour Image, Fashion Design and Identity
Larissa Noury

PS1-2 Contemporary Art and the Unfoldings of Colour
Laura Carvalho

PS1-3 Comparison of Slovene Colour Identities by Researchers A. Trstenjak and M. Tusak with Colors on Slovenian Municipality Flags
Vojko Pogacar

PS1-4 A Comparison of Color Schemes and Images in the Package Design of Sweets in the US and Japan
Kyoko Hidaka

PS1-5 Human Monochromatic Impressions on Multi-chromatic/Colorless Phenomena and Concepts
Ayana Deguchi, Akira Asano, Chie Muraki Asano and Katsunori Okajima

PS1-6 How to Create a Colour Education that Fosters Price-winning Design Students
Ivar Jung

PS1-7 Influence of Odors Function and Colors Symbolism in Odor-Color Associations: Comparative Study between Rural and Urban Regions in Lebanon
Léa Nehmé, Reine Barbar, Yelena Maric and Muriel Jacquot

PS1-8 Differences of Generation Dependences of Preferences between Colors and Styles in Women's Fashion
Chie Muraki Asano, Kanae Tsujimoto, Akira Asano and Katsunori Okajima

PS1-9 Effect of Color Appeared in Signage to Identify Gender of Thai
Chanida Saksirikosil, Kitirochna Rattanakasamsuk and Ploy Srisuro

PS1-10 Development of Three Primary-color Transparent Cubes for Learning Subtractive Color Mixing Visually
Keiichi Miyazaki

PS1-11 Multicolor LED Lighting Device with a Microprocessor for Demonstrating Effects of Lighting on Color Appearance
Takashi Nakagawa

PS1-12 The Effect of Environment Colour on Behavioural Inhibition
Nicholas Ciccone and Stephen Westland

PS1-13 Influence of Light Incident Angle and Illuminance Intensity on Visual Comfort and Clarity
Yinqiu Yuan, Li-Ching Chuo, Hsin-Pou Huang and Ming-Shan Jeng

PS1-14 Colour Terms in the Interior Design Process
Douha Y Attiah, Vien Cheung, Stephen Westland and David Bromilow

PS1-15 Effects of Classroom Wall Color on Students
Fazila Duyan and Rengin Ünver

PS1-16 A Study on the Evaluation Process of Facade Colour Parameters
Esra Küçükkılıç Özcan and Rengin Ünver

PS1-17 Correlation between Personal and Classroom color Preferences of Children
Rengin Ünver and Fazila Duyan

PS1-18 Research on the Coexistence of Color between Buildings and Exterior Advertising that Create a Cityscape ~ focusing on the Okamoto district of Kobe ~
Yoshifumi Takahashi and Ikuko Narita

PS1-19 Colour Management in the Colour Design Process
Per Jutterstrom

PS1-20 Exploring Combinations of Color Patterns in Nature
Akemi Yamashita and Naoko Takeda

PS1-21 Visual Impressions Induced by Colours of Facial Skin and Lips
Mei-Ting Liu, Hsing-Ju Hung, Wen-Ling Deng and Li-Chen Ou

PS1-22 International Comparison of Uses of Color for Pictograms
Yuki Akizuki, Michico Iwata and Hirotaka Suzuki

PS1-23 The Influence of Color on the Perception of Cartographic Visualisations
Zbyněk Štěrba and Jan D. Bláha

PS1-24 Evaluation of Colour Appearances Displaying on Smartphones
X. Gao, E. Khodamoradi, L. Guo, X. Yang, S. Tang, W. Guo, Y. Wang

PS1-25 Colour Management for High Dynamic Range Imaging
Keith D. M. Findlater

PS1-26 Development of a Wide-Gamut Digital Image Set
Stephen Westland, Qianqian Pan, Yuan Li and Soojin Lee

PS1-27 Construction of Display Profiles Using Simplicial Maps and Application to Color Reproduction of Displays
Masashi Yamamoto and Jinhui Chao

PS1-28 "Psycolorsynthesis": An Introduction of 10-Color Communication Method
Chiori Ohnaka

PS1-29 Perceptually Inspired Gamut Mapping between Any Gamuts with Any Intersection
Javier Vazquez-Corral and Marcelo Bertalmío

PS1-30 Color Correction Operation for 3D Scanning Models
Kai-Lin Chan, Lin Lu, Tzung-Han Lin, Hung-Shing Chen, Chia-Pin Cueh and Kang-Yu Liu

PS1-31 Correcting for Induction Phenomena on Displays of Different Size
Marcelo Bertalmío

PS1-32 KANSEI Evaluation of Color Images Presented in Different Blue Primary Displays
Toshiya Hamano, Takashi Fuseda, Tomonori Tashiro, Tomoharu Ishikawa, Hiroyuki Shinoda, Kazuhiko Ohnuma, Keisuke Araki and Miyoshi Ayama

PS1-33 New Proposal for Advanced Measurement Technology for Image Clarity
Hideo Kita, Shigeo Suga and Jack A. Ladson

PS1-34 Analysis of Color Appearance of Metallic Colors and Pearlescent Colors Using Multi-angle Spectrophotometer
Yu-Wen Chiu, Hung-Shing Chen, Chia-Pin Cueh and Kang-Yu Liu

PS1-35 HDR imaging - Automatic Exposure Time Estimation - A novel approach
Miguel Angel Martinez-Domingo, Eva M. Valero, Javier Hernández-Andrés and Javier Romero

PS1-36 Real-time Green Visibility Ratio Measurement
Motonori Doi, Akira Kimachi and Shogo Nishi

PS1-37 Evaluation of 20 p/d-safe Colors Used in Image Color Reduction Method for Color Deficient Observers
Takashi Sakamoto

PS1-38 Silkscreen Printing on Cotton Fabrics with Soil Colorant
Somporn Jenkunawat, Pratoomthong Trirat and Kulthanee Siriruk

PS1-39 Estimation of the Environment Illumination Color Using Distribution of Pixels
Noriko Yata, Yuki Arai and Yoshitsugu Manabe

PS1-40 A Spectral Reflectance Measurement System for Human Skin by Using Smartphone
Seungwan Hong, Norihiro Tanaka and Kosuke Mochizuki

PS1-41 Colour Management for High Quality Reproduction on Uncoated Papers
Maja Strgar Kurecic, Lidija Mandic, Ante Poljicak and Diana Milcic

PS1-42 A Real-Time Multi-spectral CG Rendering Method for Building with Scene Illumination
Chihiro Sakurai, Norihiro Tanaka and Kosuke Mochizuki

PS1-43 Color Mapping between a Pair of Similar Facial Images with and without Applying Cosmetics
Lin Lu, Hung-Shing Chen and Neng-Chung Hu

PS1-44 The Consistent Color Appearance Based on the Display-referred
Yasunari Kishimoto, Hitoshi Ogatsu and Hirokazu Kondo

PS1-45 The Study of Museum Lighting: The Optimum Lighting and Colour Environment - the Proposal for the Colour Quality Index -
Yuki Nakajima and Takayoshi Fuchida

PS1-46 Developing Test Targets for Color Management of Full Color Three-dimensional Printing
Yu-Ping Sie, Pei-Li Sun, Yun-Chien Su, Chia-Pin Cueh and Kang-Yu Liu

PS1-47 The Effect of Training Set on Camera Characterization
Semin Oh, Youngshin Kwak and Heebaek Oh

PS1-48 Reproducing the Old Masters: A Study in Replicating Dark Colours with Inkjet Printing
Melissa Olen and Joseph Padfield

PS1-49 A New Metric for Evaluating the Closeness of Two Colors
Yasuki Yamauchi, Yusuke Iida, Yuki Kawashima and Takehiro Nagai

PS1-50 Image and Color Space Clustering for Image Search
Akinobu Hatada

PS1-51 Restoration of Color Appearance by Combining Local Adaptations for HDR Images
Yuto Kubo, Takao Jinno and Shigeru Kuriyama

PS1-52 Image Quality Index for Perceiving Three-dimensional Effect in Mobile Displays
Chun-Kai Chang, Hirohisa Yaguchi and Yoko Mizokami

PS1-53 Imageries of Edible Souvenirs Evoked by Colours and Visual Textures of Packages
Shuo-Ting Wei

PS1-54 A Study of the Preference and Orientation of "The Sense-oriented"
Takashi Inaba

PS1-55 Color Peference Measured by Paper-Format Implicit Association Test
Shinji Nakamura and Aya Nodera

PS1-56 SSVEP Response Study for Low Semantic Images
Syntyche Gbèhounou, Enrico Calore, Francois Lecellier, Alessandro Rizzi and Christine Fernandez-Maloigne

PS1-57 My Own Colours
Kristiina Nyrhinen

PS1-58 Hue and Tone Effects on Color Attractiveness in Mono-Color Design
Uravis Tangkijviwat and Warawan Meksuwan

PS1-59 A Study on Silver Metallic Color Preference - A Comparison of Responses between Japanese and Thai People -
Mikiko Kawasumi, Kamron Yougsue, Chanprapha Phuangsuwan, Kanrawee Tawonpan and Ken Nishina

PS1-60 Colors' Relations to Other Things in My Works
Helena Lupari

PS1-61 Color Preference of Preschoolers : Compared to Adults' Surmise
Wei-Chun Hung, Pei-Li Sun and Li-Chen Ou

PS1-62 Influence of the Typical Color in Object Memory Task
Mikuko Sasaki and Yasuhiro Kawabata

PS1-63 Neural Basis of Color Harmony and Disharmony Based on Two-color combination
Takashi Ikeda and Naoyuki Osaka

PS1-64 Psychological Hue Circle of Blind People and Development of a Tactile Color Tag for Clothes
Saori Okudera, Ken Sagawa, Yuko Nakajima, Natsumi Ohba and Shoko Ashizawa

PS1-65 Examination of Method for Decreasing Unpleasantness Caused by Strong Brightness of Smart-phone Displays in Dark Adaptation
Itsuki Miyamae, Hyojin Jung, Saori Kitaguchi and Tetsuya Sato

PS1-66 A Spectral-based Color Vision Deficiency Model Compatible with Dichromat and Anomalous Trichromat
Hiroaki Kotera

PS1-67 Colour Information in Design
Seahwa Won, Stephen Westland, Kishore Budha and Bruce Carnie

PS1-68 Relationship between Perceived Whiteness and Color Vision Characteristics
Ichiro Katayama, Koichi Iga, Shoko Isawa and Tsuneo Suzuki

PS1-69 An Experiment of Color Rendering with 3D Objects
Laura Blaso, Cristian Bonanomi, Simonetta Fumagalli, Ornella Li Rosi and Alessandro Rizzi

PS1-70 Adapting and Adapted Colors under Colored Illumination
Mitsuo Ikeda, Chanprapha Phuangsuwan and Kanwara Chunvijitra

PS1-71 Color Constancy Depends on Initial Visual Information
Chanprapha Phuangsuwan, Mitsuo Ikeda and Kanwara Chunvijitra

PS1-72 Neighboring Color Effect on the Perception of Textile Colors
Youngjoo Chae, John H. Xin and Tao Hua

PS1-73 The Impact of Light at the Perception of Colours in Architecture, State of the Art Study and Suggestions for Further Research
Shabnam Arbab and Barbara Szybinska Matusiak

PS1-74 Evaluation of Cloth Roughness and Smoothness by Visual and Tactile Perceptions: Investigation of Cloth Photography Method for Online Shopping
Tomoharu Ishikawa, Yuya Akagawa, Kazuma Shinoda, Shigeru Inui, Kazuya Sasaki, Keiko Miyatake and Miyoshi Ayama

PS1-75 Study of Color Preferences of Gac Fruit Blended with Mixed Mushroom Juice
Wattana Wirivutthikorn and Somporn Jenkunawat

PS1-76 Luminance Contrast of Thai Letters Influencing Elderly Vision
Kitirochna Rattanakasamsuk

PS1-77 Color Rendering Analysis Based on Color Pair Evaluation under Different LED Lighting Conditions
Qing Wang, Haisong Xu, Jianqi Cai and Wei Ye

PS1-78 The Relationship between Whiteness Perception of Watercolor Illusions and Color Vision Characteristics
Shoko Isawa, Koichi Iga, Ichiro Katayama and Tsuneo Suzuki

PS1-79 Influence of Daylight Illumination in the Visual Saliency Map of Color Scenes
Juan Ojeda, Juan Luis Nieves and Javier Romero

PS1-80 Comparison between Multispectral Imaging Colors of Single Yarns and Spectrophotometric Colors of Corresponding Yarn Swatches
Lin Luo, Hui-Liang Shen, Si-Jie Shao and John H. Xin

PS1-81 New Color Rendering Index Based on Color Discriminability and Its Application to Evaluate Comfortability of Illuminants
Yasuhisa Nakano, Toshiki Nagasaki, Ryu Toyota, Jiro Kohda and Takuo Yano

PS1-82 Color Monitoring Method under High Temperature during Oven Cooking
Yuji Nakamori, Hiroyuki Iyota, Hideki Sakai, Taiki Matsumoto and Shuhei Nomura

PS1-83 Woodblock Printing as a Means for 2.5D and 3D Surface Evaluation
Teun Baar, Melissa Olen, Carinna Parraman and Maria Ortiz Segovia

PS1-84 The Relationships between Colors of Neck, Cheek, and Shaded Face Line Affects Beauty of Made-up Face
Youhei Ishiguro, Mamiko Nakato, Erika Tokuyama, Nao Matsushita and Minori Yamahara

PS1-85 Experimantal Method Suggested for Optical Observation of Anisotropic Scattering
Akio Kawaguchi and Hirofumi Ninomiya

PS1-86 Color Measurement of Meat in Cooking under LED Lightings with Different Spectral Distributions
Akari Kagimoto, Risa Shiomi, Shino Okuda, Mami Masuda, Katsunori Okajima, Hideki Sakai and Hiroyuki Iyota

PS1-87 Color Temperature and Illuminance of Main Streets with Day and Night Illumination in the Center of Osaka, Japan
Haruyo Ohnoh

Invited Talk (MCS)

8:30 - 9:15 sola city Hall

Chair: Shoji Tominaga

Multispectral colour imaging: Time to move out of the lab?

Jon Yngve HARDEBERG

Oral Papers

9:20-10:40 (sola city Hall)
MCS1: Multispectral Imaging System

Chairs: Lindsay MacDonald & Masaru Tsuchida

MCS1-1 Surface Spectral Reflectance Estimation with Structured Light Projection
Grzegorz Mączkowski, Krzysztof Lech and Robert Sitnik

MCS1-2 Multispectral Imaging System Based On Tuneable LEDs
Muhammad Safdar, Ming Ronnier Luo, Yuzhao Wang and Xiaoyu Liu

MCS1-3 Evaluation of Hyperspectral Imaging Systems for Cultural Heritage Applications Based on a Round Robin Test
Sony George, Irina Mihaela Ciortan and Jon Yngve Hardeberg

MCS1-4 Spectral Gigapixel Imaging System for Omnidirectional Outdoor Scene Measurement
Motoki Hori, Naoto Osawa, Keita Hirai, Takahiko Horiuchi and Shoji Tominaga

9:20-10:35 (Room C)
OS5: Color Education & Culture

Chairs: Verena M. Schindler & Kohji Yoshimura

OS5-1 Are There Ugly Colours?
Ilona Huolman

OS5-2 A Novel Experience in Color Teaching: Master in Color Design & Technology
Alessandro Rizzi, Maurizio Rossi, Cristian Bonanomi and Andrea Siniscalco

OS5-3 The Ambiguous Term of "Saturation"
Karin Fridell Anter, Harald Arnkil and Ulf Klarén

OS5-4 Colour Education and Real Life Colour
Ulf Klarén and Karin Fridell Anter

OS5-5 Color Universes for the Chilean Heritage
Elisa Cordero and Eréndira Martínez

11:00-12:20 (sola city Hall)
MCS2: Multispectral Color Science

Chairs: Jon Yngve Hardeberg & Keita Hirai

MCS2-1 Handheld Hyperspectral Imaging System for the Detection of Skin Cancer
Xana Delpueyo, Meritxell Vilaseca, Santiago Royo, Miguel Ares, Ferran Sanabria, Jorge Herrera, Francisco J. Burgos, Jaume Pujol, Susana Puig, Giovanni Pellacani, Jorge Vázquez, Giuseppe Solomita and Thierry Bosch

MCS2-2 Empirical Disadvantages for Color-Deficient People
Joschua Simon-Liedtke and Ivar Farup

MCS2-3 Spectral Reflectance Recovery Using Natural Neighbor Interpolation with Band-Divided Linear Correction
Tzren-Ru Chou and Tsung-Chieh Sun

MCS2-4 Evaluation of Gastrointestinal Tissue Oxygen Saturation Using LEDs and a Photo Detector
Yoshitaka Minami, Takashi Ohnishi, Koki Kato, Hiroyuki Wasaki, Hiroshi Kawahira and Hideaki Haneishi

11:00-12:15 (Room C)
OS6: Color and Culture

Chairs: Tien-Rein Lee & Shin'ya Takahashi

OS6-1 Forsius' Second Colour Order Diagram of 1611 from the Iconic Point of View
Verena M. Schindler

OS6-2 Five Colours - A Study of Chinese Traditional Colour
Jie Xu

OS6-3 Meeting New Challenges in Colour Tendencies in Norway
Kine Angelo and Alex Booker

OS6-4 The Image of the Color Red in Letters: A Study Based on the Historical Backgrounds of Russia and Japan
Sasha Krysanova

OS6-5 Japanese Color Names Reflecting Dyeing: With a Focus on Their Color Terms in Brown Regions Including More than 100 Browns
Kohji Yoshimura, Yuko Yamada and Stephen Shrader

Poster Papers

13:45-15:15 Poster 2 (Room B/Lobby)

Chairs: Yasuki Yamauchi & Takuzi Suzuki

Room B : PS2-1~64
Lobby : PS2-65~85

PS2-1 Changes of Color Names and Coloring Materials in Japan
Norifumi Kunimoto

PS2-2 Differences in the Drawings and the Color of the Violence in Children from Three Different Cultures
Georgina Ortiz Hernandez and Mabel López

PS2-3 Color and Image of the City in Environmental Design of Kazimir Malevich
Yulia Griber

PS2-4 Comparative Study about Preference Tendency to Spatial Color Based on Color Recognitions and Emotions among Nations : Focused on Korea and Malaysia
Ji-Young Oh, Heykyung Park, Mai Neo, Jian-Yuan Soh and Min Jae Lee

PS2-5 The Analysis of Door Color on the Traditional Palace of the Kingdom of Joseon
Lu Chen and Jin Sook Lee

PS2-6 Comparison among Three Methods for Thai Colour Naming
Pichayada Katemake, Dimitris Mylonas, Lindsay MacDonald and Amara Prasithrathsint

PS2-7 A Study on Elements Perceived as Traditional among Fabrics and Colors for Hanbok
Ji Hyun Sung and Yung Kyung Park

PS2-8 The Positive Impact of Image by Colour for Vulnerable People
Maria Elena Chagoya

PS2-9 Faith in the Power of Color : Spiritual Revival from the East Japan Earthquake Disaster
Yumi Awano

PS2-10 Types of Smart Cities | Cities Built from the Scratch and Old Cities Transformed into Smart Cities: What Kind of Colours can We Use?
Ana C. Oliveira

PS2-11 The Use of English Colour Terms in Big Data
Dimitris Mylonas, Matthew Purver, Mehrnoosh Sadrzadeh, Lindsay MacDonald and Lewis Griffin

PS2-12 A Proposal of Colour Universal Design Game for Learning Dichromats' Confusion Colours
Shigehito Katsura and Shoji Sunaga

PS2-13 Colour Management: Managing the Intuitive Issue, the Gamut Issue and the Engagement Issue
Philip Henry and Stephen Westland

PS2-14 Suggestion for Teaching Natural Colors through Investigation and Analysis of Current Color Education for Children in Korea
Shin Sangeun, Choi Sueran, Kim Saetbyul and Kim Yoosun

PS2-15 Color Mixture Learning using Personal Computer for Basic Design
Tomoko Mitsutake, Katsuyuki Aihara and Yosuke Yoshizawa

PS2-16 The Art of Colour Harmony: The Enigmatic Concept of Complementary Colours
Harald Arnkil

PS2-17 A Study on Influence of the Culture and Art Experience of Senior Citizens from Relationships between Culture and Art Education Space and Color Emotion Assessment
Hyeyun Son, Yunsun Park and Jinsook Lee

PS2-18 Impressions of Buildings Derived from the Combined Effects of Exterior Colour, Material, and Window Shape
Kazumi Nakayama and Masato Sato

PS2-19 Analysis of Current Colors of Native Plants Growing Naturally in Korea
Yoosun Kim, Sueran Choi, Saetbyul Kim and Sangeun Shin

PS2-20 Effects of Accent Colour on the Apparent Distance to a Wall and the Apparent Volume of an Interior Space: The Validation Experiment in an Actual Space
Wataru Kamijo, Keishi Yoshida and Masato Sato

PS2-21 Metamer Mismatching as a Measure of the Color Rendering of Lights
Hamidreza Mirzaei and Brian Funt

PS2-22 Visual Impression of a Real Room Affected by Lighting Conditions and by Colour and Texture of the Walls
Jau-Yi Wu, Henry Pan and Li-Chen Ou

PS2-23 Suggesting Appropriate Color Range for Indoor Space Based on EEG Measurement
Hanna Kim, Heewon Lee, Mijin Lee and Jinsook Lee

PS2-24 Development of the Interior Color Coordination Recommendation System of Living Space for University Student Living Alone Using Genetic Algorithm
Tatsunori Matsui, Keiichi Muramatsu, Kazuaki Kojima, Mai Kawashima and Miho Saito

PS2-25 Chromatic Integration of the Architectural Surfaces with the Environment: Analysis and Classification of Case Studies
Alessandro Premier and Katia Gasparini

PS2-26 Color Appearance of Red Printing Ink for Color Vision Deficiency
Terumi Kato, Yoko Mizokami, Masami Shishikura, Shinichiro Taniguchi, Tomomi Takeshita, Fumiko Goto and Hirohisa Yaguchi

PS2-27 A Study on the Utilization of Korean Saekdong Color in the Textile Arts
Kum-Hee Ryu

PS2-28 Color Adjustment for an Appealing Facial Photography
Kyeongah Jeong and Hyeon-Jeong Suk

PS2-29 Understanding Popular Relationships among Colors through the Network Analysis for Crowd Sourced Color Data
EunJin Kim and Hyeon-Jeong Suk

PS2-30 Eliciting the Color Bizarreness Effect Using Photographs
Aiko Morita and Saki Funakoshi

PS2-31 Texture in Color Emotions
Ivana Tomic, M Mar Lazaro, Ana Carrasco-Sanz, Ana Benjumea, Li-Chen Ou, Jose Antonio Garcia, Igor Karlovic and Rafael Huertas

PS2-32 Individual's Color Preference and Personality of Feeling Active and Passive Good Emotion, Pleasantness and Comfortableness
Shin'ya Takahashi and Takashi Hanari

PS2-33 Colour Emotions for Antioxidant-Enriched Virgin Olive Oils
Luis Gómez-Robledo, Piedad Limon, Ruperto Bermejo and Manuel Melgosa

PS2-34 A Study on Difference in Color Sensibility Judgment between Professionals & Non-professionals
Younjin Lee

PS2-35 Age Effects on Garments Color Harmony
Min Huang, Zeyang Li, Guihua Cui, Haoxue Liu and M. Ronnier Luo

PS2-36 Effects of Color and Aroma of Roasted Tea on the Predicted Taste and Palatability
Atsushi Haruta, Kosuke Asano, Akihisa Takemura, Shino Okuda and Katsunori Okajima

PS2-37 A Study of Relationship between Physical Value and Psychological Value in PCCS
Tadayuki Wakata and Miho Saito

PS2-38 Psychological Effects of Meal Tray Color on the Visual Palatability of Meals among Individuals with Low Vision - The Effects of Brightly Toned Colors
Keiko Tomita, Maya Inamura and Kimiko Ohtani

PS2-39 A Comparison between the Impact of Short and Long Wavelengths of Light on Sleepiness and Mood
Mengxi Yun, Sayaka Aritake, Sunao Uchida and Miho Saito

PS2-40 Experimental Study of Common Factors between Impressions of Wall-Paper Colors and Sounds in Living Environments
Miho Saito, Yuriko Oishi and Taiichiro Ishida

PS2-41 The Investigation of Factors Influencing the Impression of Color Harmony
Yuh-Chang Wei and Wen-Guey Kuo

PS2-42 The Hidden Image – A Strategy to Put an Unwanted Phenomenon in Its True Light
Salome Egger

PS2-43 Does Colour Really Affect Pulse Rate and Blood Pressure ?
Soojin Lee and Stephen Westland

PS2-44 Effects of Font Size on Visual Comfort for Reading on a Tablet Computer
Hsin-Pou Huang, Yi-Ho Bai and Li-Chen Ou

PS2-45 Influence of Spectral Component of White Light on the Discomfort Glare - Contribution of Image and Non-image Forming Pathways -
Toshihiro Toyota and Taka-Aki Suzuki

PS2-46 Low-chroma Colors Suppress Luminance-driven Brain Activation Measured by fMRI
Ippei Negishi and Keizo Shinomori

PS2-47 A New Evaluation Method Using the 100-hue Test and Age Trends in Color Distinction Ability
Masayuki Harada

PS2-48 Study on Image Statistics When Color Attracts Human Attention
Yasuhiro Hatori, Ichiro Kuriki, Kazumichi Matsumiya and Satoshi Shioiri

PS2-49 Prior Knowledge Modulates Peripheral Color Appearance
Bilge Sayim, Erik Myin and Tilde Van Uytven

PS2-50 Decision of Validness in Custom Color Name of JIS Z 8102
Yosuke Yoshizawa

PS2-51 Evaluation of Color Appearance under LED and OLED Lighting Based on the Data Obtained by a New Color Category Rating Method
Taiichiro Ishida, Yasuki Yamauchi, Takehiro Nagai, Hiroyuki Kurimoto, Yuhei Shoji and Tatsuya Tajima

PS2-52 Influence of Position of Colored Panels to Entire Pattern's Visibility
Ryouta Nakaya, Ippei Negishi and Keizo Shinomori

PS2-53 A Color Coordination Support System Based on Impression from Color and Readability of Text
Yoshihiko Azuma, Kazuhiro Yamamoto, Miyuki Kobayashi and Eri Komiyama

PS2-54 Study on Visual Recognition of Specula Reflection about Silk and Cotton Textile
Eun Jung Lee and Masayuki Osumi

PS2-55 An Experiment on Color Differences Using Automotive Gonioapparent Samples
Manuel Melgosa, Luis Gómez-Robledo, Esther Perales, Elisabet Chorro, Francisco Miguel Martínez-Verdú and Thomas Dauser

PS2-56 Legibility of Printed Thai Letters Comparison on Young and Elderly
Boonchai Waleetorncheepsawat

PS2-57 On the Perceived Brightness of Whites
Dragan Sekulovski, Kees Teunissen, Mart Peeters, Yue-Jun Sun and Remy Broersma

PS2-58 Smart Lighting Providing Different Optimal Visiual Illumination for Different Objects
Neng-Chung Hu, Horng-Ching Hsiao and Li-Chi Su

PS2-59 Prediction of Acceptable Lightness Difference in Painting on Automobile Surface with Different Materials Based on Multi-angle Measurement
Kohei Wakai

PS2-60 Visual Perception and Criteria for Good Lighting
Johanna Enger and Anahita Davoodi

PS2-61 Space Brightness Affected by a Scenic View through a Window
Shogo Yamada, Ryousuke Tanaka, Hiroyuki Shinoda and Yasuhiro Seya

PS2-62 Influence of Surface Properties on Material Appearance
Ming-Kang Lan, Tien-Rein Lee and Vincent C. Sun

PS2-63 Visual Evaluation of a Wooden-finish Room and the Colorimetry of Wood
Shigeko Kitamura, Jun Tsuchiya and Shoji Sunaga

PS2-64 Total Appearance of Metallic Coatings using a Stereo Capture System
Min-Ho Jung, Vien Cheung and Peter A. Rhodes

PS2-65 Statistical Image Analysis for Evaluating Face Shine: Cosmetic Research
Takanori Igarashi, Takahiro Naoki, Masataka Seo and Yen-Wei Chen

PS2-66 High Dynamic, Spectral and Polarized Natural Light Environment Acquisition
Philippe Porral, Patrick Callet and Philippe Fuchs

PS2-67 Development of Skin Reflectance Prediction Model Using a Skin Data
Kaida Xiao, Mengmeng Wang, Tushar Chauhan, Jingjing Yin, Changjun Li, Ronnier Luo and Sophie Wuerger

PS2-68 Comparing CSI and PCA in Amalgamation with JPEG for Spectral Image Compression
Muhammad Safdar, Ming Ronnier Luo and Xiaoyu Liu

PS2-69 A System for Analyzing Color Information with the Multi-spectral Image and Its Application
Junyan Luo, Yoko Mizokami, Hirohisa Yaguchi, Yohei Takara, Fuminori Ando, Takahiro Fujimori and Naoki Noro

MCS Poster Papers

PS2-70 Quality Comparison of Multispectral Imaging Systems Based on Real Experimental Data
Raju Shrestha and Jon Y. Hardeberg

PS2-71 LED-based Gonio-hyperspectral System for the Analysis of Automotive Paintings
Francisco J. Burgos, Meritxell Vilaseca, Esther Perales, Elísabet Chorro, Francisco M. Martínez-Verdú, José Fernández-Dorado, José L. Alvarez-Muñoz and Jaume Pujol

PS2-72 Multispectral Image Estimation from RGB Image Based on Digital Watermarking
Kazuma Shinoda, Aya Watanabe, Madoka Hasegawa and Shigeo Kato

PS2-73 Image Correction for a Multispectral Imaging System Using Interference Filters and Its Application
Shogo Nishi and Shoji Tominaga

PS2-74 Development of Multi-bands 3D Projector
Ryotaro Miwa, Yoshitsugu Manabe and Noriko Yata

PS2-75 Perceived Quality of Printed Images on Fluorescing Substrates under Various Illuminations
Steven Le Moan and Ludovic Gustafsson Coppel

PS2-76 To Predict Reality in Virtual Environments : Exploring the reliability of colour and light appearance in 3D-models
Beata Stahre Wästberg, Jacqueline Forzelius and Monica Billger

PS2-77 Altering Perceived Depth of Objects with Colored Lighting
Ruth Genevieve Ong and Nan-Ching Tai

PS2-78 A Model for Estimation of Overprinted Colors on *Nishiki-e* Printings
Sayoko Taya, Takuzi Suzuki, Noriko Yata and Yoshitsugu Manabe

PS2-79 Ethical Considerations on Gene Therapy for Color-Deficient People
Joschua Simon-Liedtke

PS2-80 Robust Cross-Domain Reflectance Estimation
Christoph Godau

PS2-81 Colorama: Extra Color Sensation for the Color-Deficient with Gene Therapy and Modal Augmentation
Joschua Simon-Liedtke

PS2-82 Benchmarking a Grating-based Spectral Imaging System
M. James Shyu and Ting-Yun Lin

PS2-83 Experimental Evaluation of Chromostereopsis with Varying Spectral Power Distribution of Same Color
Masaru Tsuchida, Minoru Mori, Kunio Kashino and Junji Yamato

PS2-84 Haze and Convergence Models: Experimental Comparison
Jessica El Khoury, Jean-Baptiste Thomas and Alamin Mansouri

PS2-85 Hyperspectral Reflectance Reconstruction Using a Filter-based Multispectral Camera
Wei-Chun Hung, Pei-Li Sun and Raymond Jiang

Judd Award Lecture

16:30 - 17:45 sola city Hall

Chair: Nick Harkness

On the dimensionality of the colour world
Françoise VIÉNOT

Invited Talk

8:30 - 9:15 sola city Hall

Chair: Katsunori Okajima

Neural Representation of Color in Visual Cortex

Hidehiko KOMATSU

Oral Presentation

9:20-10:35 (sola city Hall)

OS7: Appearance, Lighting

Chairs: Ronnier Luo & Hiroyuki Shinoda

OS7-1 Assessing Glare Using LED Sources Having Different Uniformity Patterns
ShiNing Ma, Yang Yang, Ming Ronnier Luo, XiaoYu Liu and BinYu Wang

OS7-2 Evaluation of the Performance of Different Colour Rendering Indices Employed in LEDs
Haiting Gu, Xiaoyu Liu, Ming Ronnier Luo, Binyu Wang and Haiyan Liu

OS7-3 A Study on the Lighting of Bathroom for the Elderly
Jiyoung Park, Chanung Jeong, Eunji Seo and Jinsook Lee

OS7-4 Sitting Posture Based Lighting System to Enhance the Desired Mood
Hyunjoo Bae, Haechan Kim and Hyeon-Jeong Suk

OS7-5 Colour Lighting Based on Chromatic Strength
Toru Kitano, Tetsuji Yamada and Kosuke Oshima

9:20-10:35 (Room C)

OS8: Color Deficiency

Chairs: Youngshin Kwak & Takashi Sakamoto

OS8-1 Influences to Color Constancy by Wearing the Optical Dichromatic Filter or the Aged Lens Filter under Static and Rapidly-Changed Colored Illuminations
Mio Hashida, Ippei Negishi and Keizo Shinomori

OS8-2 Spectral Functional Filters for Optical Simulation of Dichromats in Color Discrimination
Keizo Shinomori, Kanae Miyazawa and Shigeki Nakauchi

OS8-3 What Are Memory Colors for Color Deficient Persons?
Jia-Wun Jian, Hung-Shing Chen and Ronnier Luo

OS8-4 Establishment of a Model Colour Palette for Colour Universal Design
Kei Ito, Tomomi Takeshita, Fumiko Goto, Masafumi Nishigaki, Teruo Kobayashi, Mitsumasa Hashimoto, Yosuke Tanaka, Koichi Iga, Shunsuke Watanabe, Koki Okagawa and Mitsuyoshi Maekawa

OS8-5 Color Universal Design
Yasuyo G. Ichihara

10:50-11:50 (sola city Hall)

OS9: Cosmetics, Material Perception

Chairs: Takanori Igarashi & Motonori Doi

OS9-1 An Investigation of the Appearance Harmony Using Real Materials and Displayed Images
Midori Tanaka and Takahiko Horiuchi

OS9-2 The Colour of Gold
Lindsay MacDonald

OS9-3 Preferred LED Lighting for Wood Surfaces and Colored Surfaces
Markus Reisinger

OS9-4 Development of a Facial Imaging System and New Quantitative Evaluation Method for Pigmented Spots
Kumiko Kikuchi, Yuji Masuda, Tetsuji Hirao, Kiyoshi Sato, Yoko Mizokami and Hirohisa Yaguchi

10:50-11:50 (Room C)

OS10: Color Psychology

Chairs:Osvaldo Da Pos & Shinji Nakamura

OS10-1 Colour Preference and Harmony for Athletic Shoe Designs
Wei-Hsuan Chao, Ji-Yuan Huang, Chung-Chien Lan and Li-Chen Ou

OS10-2 A Study on Silver Metallic Color Preference - A Comparison of Responses by Age and Gender in Thailand -
Kamron Yongsue, Mikiko Kawasumi, Chanprapha Phuangsuwan and Kanrawee Tawonpan

OS10-3 Effects on Impression of Taste in Color Stimuli
Masato Sakurai, Yusuke Michinaka and Takahiro Yoshikawa

OS10-4 The Color Image of Dichromats and Anomalous Trichromats
Yuria Noguchi and Muneo Mitsuboshi

Keynote Lecture, Invited Talks, Judd Award Lecture

Keynote Lecture

Wednesday, May 20, 9:30-10:30 (sola city Hall)

The Gathering Space

Kazuyo SEJIMA
SANAA, Japan

Focusing on her recent works, Kazuyo Sejima will introduce the environment and architecture enhanced by color.
(In Japanese, with interpreting Japanese into English)

Kazuyo Sejima (Japan)

photo:Takashi Okamoto

Kazuyo Sejima studied architecture at the Japan Women's University before going to work for Toyo Ito. She launched her own practice in 1987. In 1995, she established SANAA with Ryue Nishizawa. Her own works include, House in a Plum Grove and Inujima Art House project. SANAA's main works include the 21st Century Museum of Contemporary Art in Kanazawa, Rolex Learning Center, EPFL, the Louvre Lens, and the New Museum of Contemporary Art. SANAA's current projects include the Grace Farms Project in Connecticut, USA, and the Bezalel Academy of Arts and Design in Jerusalem, Israel. In 2010 Kazuyo Sejima was appointed director of the Venice Biennale. And in the same year, Kazuyo Sejima and Ryue Nishizawa of SANAA were the recipients of the prestigious Pritzker Architecture Prize.

Invited Talk (MCS)

Thursday, May 21, 8:30-9:15 (sola city Hall)

Multispectral colour imaging: Time to move out of the lab?

Jon Yngve HARDEBERG and Raju SHRESTHA
The Norwegian Colour and Visual Computing Laboratory
Gjøvik University College, Gjøvik, Norway

Jon Y. Hardeberg (Norway)

He is currently Professor of Color Imaging at Faculty of Computer Science and Media Technology, Gjøvik University College, Norway and member of the Norwegian Color and Visual Computing Laboratory. His current main research interests include multispectral color imaging, print and image quality, colorimetric device characterization, color management, and cultural heritage imaging.His professional memberships include IS&T, SPIE, and ISCC. He is the Norwegian delegate to Division 8 of the CIE.

Multispectral colour imaging: Time to move out of the lab?

Jon Yngve HARDEBERG and Raju SHRESTHA
The Norwegian Colour and Visual Computing Laboratory
Gjøvik University College, Gjøvik, Norway

ABSTRACT

In this paper we present and discuss our recent research using three approaches for fast and cost-effective acquisition of multispectral colour images; using a stereoscopic camera with additional optical filters, using an extension of the traditional colour filter array beyond the conventional three channels, and using active LED illumination in conjunction with RGB or panchromatic area image sensors. An important goal for this work is to achieve faster and more practical solutions for multispectral colour imaging, paving the way for new application areas and more widespread use, beyond the scope of the resarch laboratories.

1. INTRODUCTION

In the past decades there has been a significant volume of research carried out in the field of multispectral colour imaging, that is, imaging systems and methodologies in which the spectral reflectance of the imaged scene is captured and processed, while one of the goals of the resulting imagery remains visual inspection; therefore precise colour information is of high importance in the imaging workflow.

The focus of much of this research has been to facilitate a type of systems that usually requires that the multispectral colour image is captured using multiple subsequent captures (e.g. systems based on filter wheels, liquid crystal tunable filters, or active lighting together with a panchromatic area imaging sensor), or a line-by-line scanning of the scene (e.g. systems based on prisms or gratings coupled with area imaging sensors). Both these approaches have serious shortcomings with regards to the usability of the systems, in particular when applied to real-world scenes with moving objects.

Multispectral colour imaging has shown its usefulness in many application domains such as cultural heritage, medical imaging, biometrics, remote sensing, food quality etc., and its scope continues to grow. Refer to Hardeberg (2001) and Shrestha (2014) for a comprehensive overview of the research field. However, the applications are so far mostly limited to research laboratories. Key obstacles to broader application include cost, user-friendliness, and speed.

Recently, new approaches for faster and more practical multispectral colour image acquisition have been proposed, including the three promising ideas of using multispectral colour filter arrays (MCFA), using two colour cameras with additional optical filters in a stereoscopic configuration, and using active LED illumination in conjunction with RGB or panchromatic area image sensors.

In this paper we present briefly our recent research using these three approaches, discuss their advantages and disadvantages, as well as directions for further research aiming for faster, cheaper, and more user friendly solutions for multispectral colour imaging.

2. THE MULTISPECTRAL COLOUR FILTER ARRAY APPROACH

The MCFA approach is based on an extension of the conventional colour filter array (CFA) to using more than three channels. Baone and Qi (2000) made a proposal of such an MCFA based imaging system, whose main purpose was classification, where they used four bands in the middle and low wave infrared region in addition to the conventional three in the visible spectrum. They also proposed a new demosaicking algorithm that aimed to better restore the image by maximizing a-posteriori probability. A recent work by Lu et al. (2009) also focused on constructing MCFAs to capture a NIR band along with the visible bands. The purpose of this work was the simultaneous capture of high quality visible and NIR image pair. Another work by Brauers and Aach (2006) proposes an MCFA with narrow band filters in the visible range. Here also, a demosaicking algorithm has been proposed, which attempts to make use of the inter-band correlation by low pass filtering of the channel differences.

A MCFA based multispectral camera introduces several design issues that need to be handled, even before considering possible issues related to the eventual real production of imaging sensors and systems (Lapray et al. 2014). Notable ones include the choice of the number of filters and their selection for the acquisition system, the spatial arrangement of the filters, and the demosaicking algorithm.

In (Shrestha et al. 2011a), we used the algorithm proposed by Miao and Qi (2004) to construct MCFAs of different sizes, based on the probability of appearance of the corresponding spectral bands. We simulated acquisitions of several spectral scenes using 6, 8, and 10-channel systems, and compared the results with those obtained by the conventional regular MCFA arrangement, evaluating the precision of the reconstructed scene spectral reflectances in terms of spectral RMS error, goodness-of-fit coefficient (GFC) and colorimetric CIEDE2000 colour differences. Using the proposed approach we significantly improved the precision, in particular for an eight-channel MCFA we reduced the average CIEDE2000 colour difference by up to 50%.

In (Wang et al. 2013a), we proposed to use a discrete wavelet transform (DWT) for MCFA demosaicking. In (Wang et al. 2013b), we proposed two vector based median filtering methods for MCFA demosaicking. One solved the demosaicking problems by means of vector median filters, and the other applied median filtering to the demosaicked image as a subsequent refinement process to reduce artefacts. To evaluate the performance of these algorithms, a simulation framework was constructed with the capability of simulating image acquisition, mosaicking, demosaicking and quality assessment. Through this work we have proved the feasibility of MCFA demosaicking.

3. THE STEREOSCOPIC CAMERA APPROACH

As the second approach towards fast and practical one-shot multispectral colour image acquisition we propose to use two colour cameras in a stereoscopic configuration, and equip them with appropriate optical filters. In a related previous work Hashimoto and Kishimoto (2008) proposed a two-shot 6-band multispectral system using a commercial digital camera and a custom colour filter. But, this still needed two subsequent shots, and custom filter needed to be constructed. Ohsawa et al. (2004) proposed a one-shot six band HDTV camera systems, and they have shown that the six band system achieved more accurate colour estimation. The system they proposed used a beam splitter and specially designed filters, and thus construction and operation of the system was still complex and costly.

In our work (Shrestha et al. 2010; 2011b; 2011c), we have extended this idea further with a more simplified approach using a stereo camera, and a pair of filters selected from among a set of readily available filters. The best pair of filters is selected from this set such that they modify the sensitivities of the two cameras in such a way that the resulting spectral sensitivities are optimal with regards to the precision of the resulting spectral reflectance data. Depending on application, optimal filters could be selected for more accurate colour reproduction. The stereoscopic configuration of the two cameras also provides a solution to the image alignment problem by means of stereo matching algorithms. An appropriate state of the art stereo matching algorithm can be used. Furthermore, the use of a stereo camera makes the system capable of capturing three dimensional images simultaneously along with the multispectral colour images. Thus the system can be used as a “two-in-one” multispectral-stereo system.

The proposed approach has been investigated with simulations as well as experimentally. Simulations have been performed with several pairs of real as well as imaginary cameras, and a set of two hundred and sixty five optical filters from Omega Optical, Inc. And, experimental studies have been conducted with arguably the world’s first modern digital 3D still camera from Fujifilm, the FinePix REAL 3D W1. The performance of the system has been evaluated both spectrally and colorimetrically based on spectral reconstruction of the scene reflectance and the scene colour reproduction respectively. Root mean square error (RMSE) and CIELAB ΔE*ab have been used as spectral and colorimetric evaluation metrics respectively for computing estimation errors. Both simulations and experiments have shown that the proposed system performed better than RGB system both spectrally and colorimetrically.

4. THE LED ACTIVE ILLUMINATION APPROACH

The third approach is based on multiplexed LED (Light Emitting Diode) illumination. In a typical LED illumination based multispectral imaging (LEDMSI) system, a number of narrow band LED illuminations in a certain wavelength range is used to capture images with a digital monochrome camera (Park et al. 2007, Christens-Barry et al. 2009). Since switching of LEDs can be done electronically, synchronized with the image capture by a camera through a programmable micro-controller or a computer, the imaging process is quite fast. Availability of many different colors and high intensity LEDs with peak wavelengths spanning the visible range and even infrared region has made the construction of a more effective multispectral colour imaging system possible.

We proposed a LEDMSI based multispectral film scanner for obtaining accurate digital color images from analog films (Shrestha et al. 2012). In one of our recent works, we proposed a LEDMSI system that uses an RGB camera in place of monochrome camera (RGB-LEDMSI), which increases the speed of acquisition by a factor of three (Shrestha & Hardeberg 2013a). An important step in a LEDMSI system design is the choice and number of LEDs to be used. We proposed a novel LED selection method for RGB-LEDMSI system in Shrestha et al. (2012). The method selects optimal combination of three different types of LEDs for each exposure, each type of LED lying in one of the three regions corresponding to the spectral sensitivities of the three camera channels. Simulation and experimental results have shown that the performance of the proposed RGB-LEDMSI systems are comparable to the corresponding monochrome camera based LEDMSI systems both in terms of spectral and colorimetric estimations, but at a significantly higher speed.

Another important aspect in LEDMSI is uniform illumination over the imaged scene. Moreover, we strive for all the LEDs have the same intensity profile. We proposed a LED matrix design method for equal intensity and uniform illumination in a LEDMSI (Shrestha & Hardeberg 2013b). Equal intensity LEDs can be achieved by using more LEDs whose intensity is low, and fewer LEDs whose intensity is high. For a given number of different types of LEDs, the proposed method generates an optimal or near-optimal arrangement of LEDs based on probability of appearances of the LEDs, which is calculated based on the intensity profiles of the LEDs and spectral sensitivity of the camera used. The method has shown to be effective in generating LED matrix design in terms of both spatial uniformity and consistency of LED distribution.

6. CONCLUSIONS AND PERSPECTIVES

In conclusion, our research so far has convinced us that the three proposed approaches can be viable alternatives for affordable acquisition of multispectral colour images. However there is obviously still much work to be done, e.g. concerning algorithms for interpolation in the filter array, as well as concerning the problem of occlusion in the stereo capture. Another promising research direction is addressing the problem of determining the illuminant in uncontrolled environments, so as to be able to recover the spectral reflectances of the scene without cumbersome calibration procedures (Shrestha & Hardeberg, 2014).

ACKNOWLEDGEMENTS

We would like to sincerely thank everyone at the Norwegian Colour and Visual Computing Laboratory and beyond, who have participated in our research on spectral imaging over the years; especially the current PhD students Xingbo Wang, Ferdinand Deger, Ruven Pillay, and Hilda Deborah, and postdoctoral researchers Sony George, Osamu Masuda, and Steven Le Moan.

REFERENCES

Baone, G.A., Qi, H. (2000) Demosaicking methods for multispectral cameras using mosaic focal plane array technology, in Spectral Imaging: Eighth International Symposium on Multispectral Color Science, SPIE Proceedings, 6062, 75–87

Brauers, J., Aach, T. (2006) A color filter array based multispectral camera, in Proc. 12. Workshop Farbbildverarbeitung, German Color Group, Ilmenau, Germany

Christens-Barry, W. A., et al. (2009) Camera system for multispectral imaging of documents, *in* Sensors, Cameras, and Systems for Industrial/Scientific Applications X, SPIE Proceedings, 7249, 724908

Hahshimoto, M., Kishimoto, J. (2008) Two-shot type 6-band still image capturing system using commercial digital camera and custom color filter, Fourth European Conference on Colour in Graphics, Imaging and Vision, IS&T

Hardeberg, J.Y. (2001) Acquisition and Reproduction of Color Images: Colorimetric and Multispectral approaches, Universal Publishers/dissertation.com, Parkland, FL, USA

Lapray, P.-J. et al. (2014) Multispectral Filter Arrays: Recent Advances and Practical Implementation. *Sensors*, 14(11): 21626-21659
Lu, Y.M., et al. (2009) Designing color filter arrays for the joint capture of visible and near-infrared images, in IEEE Proc. International Conference on Image Processing, pp. 3797-3800
Miao, L., Qi, H. (2004) A generic method for generating multi-spectral filter array, in IEEE Proc. International Conference on Image Processing,.
Ohsawa, K., et al. (2004) Six band HDTV camera system for spectrum-based color reproduction, *Journal of Imaging Science and Technology* 48; 85-92
Park, J. I., et al. (2007) Multispectral imaging using multiplexed illumination, *in* IEEE International Conference on Computer Vision (ICCV), pp. 1–8
Shrestha, R., Hardeberg, J.Y. (2010) Multispectral Image Capture using two RGB cameras. European Signal Processing Conference (EUSIPCO), Aalborg, Denmark
Shrestha, R., et al. (2011a) Spatial arrangement of Color Filter Array for Multispectral Image Acquisition. In Sensors, Cameras, and Systems for Industrial, Scientific, and Consumer Applications XII, SPIE Proceedings, 7875, 787502
Shrestha, R., et al. (2011b) One-Shot Multispectral Color Imaging with a Stereo Camera. Digital Photography VII, SPIE Proceedings, 7876, 787609
Shrestha, R., et al. (2011c) Multispectral imaging using a stereo camera: Concept, design and assessment, *EURASIP Journal on Advances in Signal Processing* **2011**(1), 57
Shrestha, R., et al. (2012) LED based multispectral film scanner for accurate color imaging. The 8th International Conference on Signal Image Technology and Internet based Systems (SITIS), IEEE, Pages 811-817, Sorrento, Naples, Italy
Shrestha, R., Hardeberg, J.Y. (2013a) Multispectral Imaging Using LED Illumination and an RGB Camera. The 21st Color and Imaging Conference, IS&T, pp. 8-13, Albuquerque, NM, USA
Shrestha, R. & Hardeberg, J.Y. (2013b) LED matrix design for multispectral imaging, *in* Proc. The 12th International AIC Congress, pp. 1317–1320
Shrestha, R. (2014) Multispectral imaging: Fast acquisition, capability extension, and quality evaluation, PhD dissertation, University of Oslo
Shrestha, R. & Hardeberg, J.Y. (2014) Spectrogenic imaging: A novel approach to multi-spectral imaging in an uncontrolled environment. *Optics Express*, 22(8): 9123-9133
Wang, X. et al. (2013a) Discrete wavelet transform based multispectral filter array demosaicking. Colour and Visual Computing Symposium, IEEE, Gjøvik, Norway, pp. 1-6
Wang, X.; et al. (2013b) Median filtering in multispectral filter array demosaicking. Digital Photography IX, SPIE Proceedings, 8660, 86600E

Address: Jon Y. Hardeberg, The Norwegian Colour and Visual Computing Laboratory
Faculty of Computer Science and Media Technology, Gjøvik University College
P.O. Box 191, N-2802 Gjøvik, Norway, http://www.colourlab.no
E-mail: jon.hardeberg@hig.no

Invited Talk

Friday, May 22, 8:30-9:15 (sola city Hall)

Neural Representation of Color in Visual Cortex

Hidehiko KOMATSU
Division of Sensory and Cognitive Information, National Institute for Physiological Sciences
School of Life Science, SOKENDAI (The Graduate University for Advanced Studies)

Hidehiko Komatsu (Japan)

He is currently Professor of Division of Sensory and Cognitive Information, National Institute for Physiological Sciences, Japan. His current main research interests include neural representation of color in higher visual cortex, neural mechanisms of gloss perception, texture processing, and multimodal integration in material recognition.
He is currently project leader for a large research project "Brain and Information Science on SHITSUKAN (material perception)" funded by the Ministry of Education of Japan.

Neural Representation of Color in Visual Cortex

Hidehiko KOMATSU,[1,2]
[1]Division of Sensory and Cognitive Information, National Institute for Physiological Sciences
[2] School of Life Science, SOKENDAI (The Graduate University for Advanced Studies)

ABSTRACT

To understand how the object color is represented in our visual system, we need to understand at least two things: how the wavelength composition of the light is transformed to the color signal and how the surface reflectance property of the object is represented in our visual system. Numerous attempts have been made to answer to the former question, and we now know that color signal is conveyed from the retina to the higher visual cortex along a specific visual pathway through several steps of signal transformation. Attempts to answer to the latter question have emerged only recently. These studies have shown that neurons selectively responsive to specific range of gloss exist in higher ventral visual area and that these neurons encode perceptual parameters of gloss. These two lines of studies in combination will shed light on how the object color is represented in our visual system.

1. 'COLOR OF LIGHT' VS 'COLOR OF OBJECT'

When one says "this apple is red", he is not talking about the wavelength composition of the light coming into his eye from the apple. Instead, he is talking about some property intrinsic to an apple which makes the apple red. Numerous attempts have been previously made to understand the neural mechanisms of color vision, but most of those studies have concerned on the question about how the different wavelength compositions of the light yield different color perception. As the results of the efforts by many scientists, we are now approaching to a stage where we can make a coherent explanation about the neural mechanisms of color vision from the responses of the retinal photoreceptors to the neuron activities in the higher visual cortex. However, to what extent are we able to talk about the mechanisms of color perception with regard to the intrinsic properties of objects? In relation to the surface color, some important studies have shown the involvement of area V4 in color constancy that is related to the estimation of surface color (Zeki, 1983). However, estimation of the surface albedo is not the whole story on the surface color of objects. Surface gloss generated by the surface reflections that depends on the directions of the illumination and view point significantly affects the appearance of the object surface. For example, a matte yellow object is perceived simply as an yellow object, but if the object has a strong gloss and becomes shiny, it comes to possess golden appearance (Okazawa et al., 2011). Therefore, in order to be able to more fully talk about the object color that is associated with intrinsic properties of objects, we need to understand how gloss is represented in our visual system as well as how the wavelength composition of the light is transformed to the color signal in the visual system.

2. NEURAL REPRESENTATION OF 'COLOR OF LIGHT'

Neural processes to extract color from the wavelength composition of the light have been extensively studied and the processing of such color information in the early stage of the visual pathway is well established. Color signals originate by comparing signals of cones with different wavelength sensitivities (L cone, M cone, S cone) in the retina. This process yields two types of color signals, namely (L - M) and (S - (L + M)) signals (two-axes representation of color)(Komatsu, 1998). These color signals are relayed at the parvo- and konio-cellular layers of the lateral geniculate nucleus (LGN) and sent to the primary visual cortex (V1) in the cerebral cortex. In V1, these two types of color signals are combined to generate neurons that are selectively responsive for particular hues and neurons tuned for various directions in the hue circle are formed (multi-axes representation of color)(Lennie et al., 1990; Hanazawa et al., 2000; Wachtler et al., 2003).

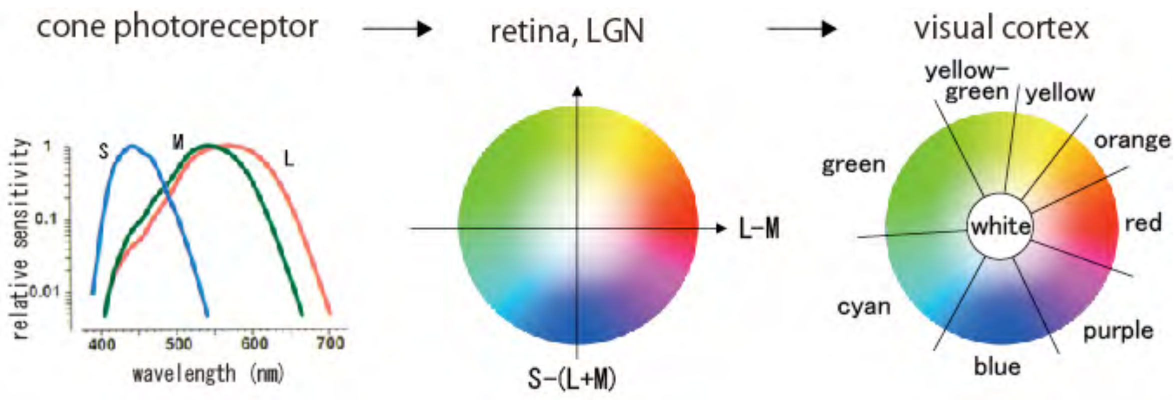

Figure 1: Color signal transformation in the visual system.

Color signal is transmitted from V1 through the ventral visual pathway including areas V2 and V4 to the higher ventral area (inferior temporal cortex = IT cortex in macaque monkey). IT cortex contains multiple subregions where color selective neurons are clustered. In these subregions, neurons have sharp color selectivity (Komatsu et al., 1992; Conway et al., 2007; Yasuda et al., 2010; Namima et al., 2014) and exhibit responses that are closely correlated with color perception or color related behaviors (Koida & Komatsu, 2007; Matsumora et al., 2008). In both humans and macaques, damage in the higher ventral area causes severe deficits in color perception, and it is thought that this area is responsible for color perception.

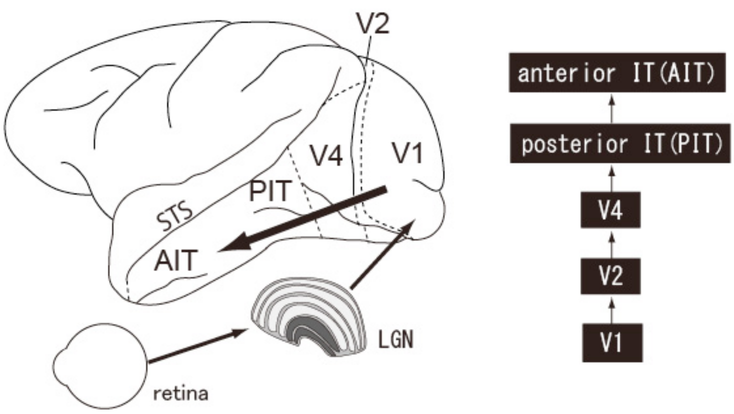

Figure 2: Ventral visual pathway in macaque visual cortex.

3. NEURAL REPRESENTATION OF GLOSS

In contrast to the accumulation of knowledge on the neural processing of 'color of light', far less is known about how 'color of object' is processed in the visual system. In the field of engineering and psychophysics, however, characterization of surface properties related to 'color of object' has made significant advancement in recent years. Especially, surface gloss has been extensively studied in terms of the directional specificity of surface reflection, and psychophysical studies have revealed the importance of the presence of the highlight and its spatial relationship with shadings (Beck & Prazdny, 1981; Kim & Anderson, 2010) as well as possible image features related to gloss perception (Nishida & Shinya, 1998; Motoyoshi et al., 2007). Based on these backgrounds, we have conducted a series of experiments to study neural representation of gloss in the visual cortex. We applied functional MRI (fMRI) to the macaque monkey, and recorded brain activities to object images with specular and matte surfaces. When we compared the responses to these images, it was found that stronger responses to the specular objects compared with the matte objects were observed in the visual areas along the ventral visual pathway (Okazawa et al., 2012). Especially, we found localized activities in restricted areas in the IT cortex including central part of the superior temporal sulcus (STS). Next, we conducted single neuron recordings from the region in the central STS, and examined the neural responses to object images with a variety of gloss. We found that neurons selectively responsive to specific range of gloss (gloss selective neurons) are accumulated in this region, and that as a population, these gloss selective neuron systematically represented a variety of gloss (Nishio et al., 2012). A previous study identified two sets of perceptual gloss parameters that form the dimensions of psychophysically uniform gloss space: contrast gloss (c) that corresponds to a non-linear combination of specular reflectance and diffuse reflectance and distinct-of-image gloss (d) that corresponds to the sharpness of highlight (Ferwerda et al., 2001). We found that responses of the gloss selective neurons are closely related to the perceptual gloss parameters (c and d), and that population activities of gloss selective neurons can precisely estimate the perceptual gloss parameters of the stimuli (Nishio et al., 2014). These results shed some light on how gloss is represented in the visual system.

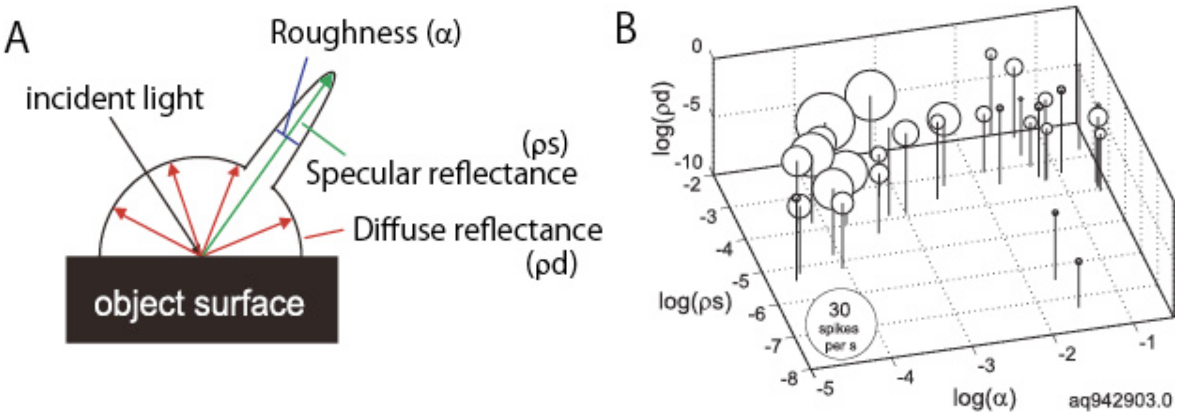

Figure 3: (A) Physical parameters related to gloss. (B) Responses of an example of gloss selective neuron (modified from Nishio et al. 2012).

4. CONCLUSIONS

Substantial knowledge has been accumulated on the neural representation of 'color of light'. Now, we are gradually learning about how gloss is represented in the visual system. We expect that by combining these knowledges, understanding on the representation of 'color of object' will be advanced. At the same time, we need to consider about new problems. For example, how are the information on the color of light and that on the surface reflection integrated when we perceive the color of object? Futhermore, there are many optical properties other than gloss such as transparency and translucency that affects the appearance of object. At this moment, we know nothing about the neural representation of those optical properties. To fully understand the mechanisms on how we perceive color of objects, development of the research in material perception or 'Shitsukan' should play a key role (Fleming et al. 2015).

ACKNOWLEDGEMENTS

This work was supported by a Grant-in-Aid for Scientific Research on Innovative Areas "Shitsukan" (22135007) from MEXT, Japan

REFERENCES

Beck, J., and Prazdny, S. (1981). Highlights and the perception of glossiness. *Percept Psychophys, 30*, 407-410.

Conway, B. R., Moeller, S., and Tsao, D. Y. (2007). Specialized color modules in macaque extrastriate cortex. *Neuron, 56* (3), 560-573.

Ferwerda, J. A., Pellacini, F., and Greenberg, D. P. (2001). A psychophysically-based model of surface gloss perception. *Proceedings of SPIE Human Vision and Electronic Imaging, 4299*, 291-301.

Fleming, R.W., Nishida, S., and Gegenfurtner, K. (2015) Visual perception of Materials: the Science of Stuff. *Vis Res, in press.*

Hanazawa, A., Komatsu, H., and Murakami, I. (2000). Neural selectivity for hue and saturation of colour in the primary visual cortex of the monkey. *Eur J Neurosci, 12* (5), 1753-1763.

Kim, J., and Anderson, B. L. (2010). Image statistics and the perception of surface gloss and lightness. *J Vis, 10* (9), 3.

Koida, K., and Komatsu, H. (2007). Effects of task demands on the responses of color-selective neurons in the inferior temporal cortex. *Nat Neurosci, 10* (1), 108-116.

Komatsu, H. (1998). Mechanisms of central color vision. *Curr Opin Neurobiol, 8* (4), 503-508.

Komatsu, H., Ideura, Y., Kaji, S., and Yamane, S. (1992). Color selectivity of neurons in the inferior temporal cortex of the awake macaque monkey. *J Neurosci, 12* (2), 408-424.

Lennie, P., Krauskopf, J., and Sclar, G. (1990). Chromatic mechanisms in striate cortex of macaque. *J Neurosci, 10* (2), 649-669.

Matsumora, T., Koida, K., and Komatsu, H. (2008). Relationship between color discrimination and neural responses in the inferior temporal cortex of the monkey. *J Neurophysiol, 100* (6), 3361-3374.

Motoyoshi, I., Nishida, S., Sharan, L., and Adelson, E. H. (2007). Image statistics and the perception of surface qualities. *Nature, 447* (7141), 206-209.

Namima, T., Yasuda, M., Banno, T., Okazawa, G., and Komatsu, H. (2014). Effects of luminance contrast on the color selectivity of neurons in the macaque area V4 and inferior temporal cortex. *J Neurosci, 34* (45), 14934-14947.

Nishida, S., and Shinya, M. (1998). Use of image-based information in judgments of surface-reflectance properties. *J Opt Soc Am A Opt Image Sci Vis, 15* (12), 2951-2965.

Nishio, A., Goda, N., and Komatsu, H. (2012). Neural selectivity and representation of gloss in the monkey inferior temporal cortex. *J Neurosci, 32* (31), 10780-10793.

Nishio, A., Shimokawa, T., Goda, N., and Komatsu, H. (2014). Perceptual gloss parameters are encoded by population responses in the monkey inferior temporal cortex. *J Neurosci, 34* (33), 11143-11151.

Okazawa, G., Goda, N., and Komatsu, H. (2012). Selective responses to specular surfaces in the macaque visual cortex revealed by fMRI. *Neuroimage, 63* (3), 1321-1333.

Okazawa, G., Koida, K., and Komatsu, H. (2011). Categorical properties of the color term "GOLD". *J Vis, 11* (8), 1-19.

Wachtler, T., Sejnowski, T. J., and Albright, T. D. (2003). Representation of color stimuli in awake macaque primary visual cortex. *Neuron, 37* (4), 681-691.

Yasuda, M., Banno, T., and Komatsu, H. (2010). Color selectivity of neurons in the posterior inferior temporal cortex of the macaque monkey. *Cereb Cortex, 20* (7), 1630-1646.

Zeki, S. (1983). Colour coding in the cerebral cortex: the reaction of cells in monkey visual cortex to wavelengths and colours. *Neuroscience, 9* (4), 741-765.

Address: Prof. Hidehiko KOMATSU, Division of Sensory and Cognitive Information, National Institute for Physiological Sciences, Nishigo-Naka 38, Myodaiji, Okazaki, Aichi, 444-8585, JAPAN
E-mails: komatsu@nips.ac.jp

Judd Award Lecture

Thursday, May 21, 16:30-17:45 (sola city Hall)

On the dimensionality of the colour world

Françoise VIÉNOT
Centre de recherche sur la conservation (CRC, USR 3224)
Muséum national d'Histoire naturelle

Françoise Viénot (France)

Emeritus professor, Muséum National d'Histoire Naturelle, Paris. Expert in color vision and appearance measurement, research on colorimetry, photometry, gloss metrics and LED illumination. French representative and former officer of CIE Division 1 (Vision), chair of CIE TC 1-36 "Chromaticity diagram with physiologically significant axes", vice-president of CIE-France. Newton medal (Colour Group of Great Britain) and Verriest medal (International Colour Vision Society).

On the dimensionality of the colour world

Françoise VIÉNOT

Centre de recherche sur la conservation (CRC, USR 3224)
Muséum national d'Histoire naturelle

ABSTRACT

Whereas, for colorimetric purpose, the three-dimensionality of colour cannot be circumvented and clearly refers to cone fundamentals, we examine situations where a reduced or expanded dimensionality could be experienced. Besides the case of individuals such as dichromats who suffer from a limited number of cone photopigments and enjoy two-dimensional colour vision, specific contexts or specific operations may require additional dimensions which could be supported by rod signals or melanopsin signals.

1. INTRODUCTION

Since the seminal hypothesis of Thomas Young and the studies from Maxwell and Helmholtz during the 19th century, it has been firmly established that colour is three-dimensional. Physiological, psychophysical and genetic studies have confirmed the 19th century statements so that standardization bodies, colour industry, image technology have developed tools and methods to improve numerous colour products.

It is often claimed that the three dimensions of colour originate from the presence of three families of cones in the retina. Yet, the cone signals are processed within the retina and in the brain structures so that colour construction aims at identifying objects and materials in our surrounding. Colour vision starts with the capture of photons by the long-wave sensitive (LWS) cones, the middle-wave sensitive (MWS) cones and the short-wave sensitive (SWS) cones. At the second stage, retinal ganglion cells combine the cone signals into three channels: one achromatic channel, supported by the “magno-cellular” pathway where cone signals are added, and two chromatic channels, supported by the “parvo-cellular” and the “konyo-cellular” pathways where cone signals are opposed. Retinal signals are processed in the brain in various contrasting combinations, ultimately delivering highly tuned colour responses.

Whereas the three-dimensionality of colour is consensually accepted it is of interest to examine situations where the colour dimensionality could be reduced or expanded.

2. THE THREE-DIMENSIONAL CIE COLOUR SPACE

2.1 The cone fundamentals

The three colour dimensions hypothesis has been validated by Psychophysics much earlier than Physiology and Genetics has isolated cone families and sequenced the genetic code of cone pigments (Nathans et al., 1986).

As early as 1886, König and Dieterici were able to determine accurate spectral sensitivity of the fundamental sensations. By asking colour normal observers and dichromatic observers to perform colour-matches, they were able to derive spectral sensitivity curves of the fundamental sensations that conform the most recent proposals (Stockman and Sharpe, 2000).

CIE technical committee 1-36 was established for proposing chromaticity diagrams based on the best set of colour-matching functions and cone fundamentals available nowadays. Cone fundamentals are based on Stiles and Burch (1959) experimental colour matches and validated by Physiology. A physiologically designed MacLeod-Boynton chromaticity diagram (MacLeod and Boynton, 1979) is proposed as well as a cone-fundamental-based (x_F, y_F) chromaticity diagram. All data are now fixed (CIE, 2006; CIE, in press; Viénot and Walraven, 2007). Specifying colour in the LMS space will offer novel opportunities to solve problems of colour measurement and colour perception in everyday life and industry.

In the future, refinements, such as colour vision variability due to photopigment polymorphism, would not weaken the three-dimensionality hypothesis. It would secure the hypothesis.

2.2 Metamerism

Comparison between the richness of the spectral information available in the Physics domain and the reduced number of signals generated at the entrance of the visual system has led colour scientists to investigate at length the metamerism phenomenon.

In colorimetry, the basic experiment is a colour match between two metameric stimuli. Practically, colorimetry reduces the stimulus to a unique three component object. Indeed, the visual system is unable to finely analyse the spectral content of the stimulus. In the three-dimensional colour space, metamerism is just concealed.

Nevertheless the volume of ignored parts of the stimulus is amazing as illustrated by Kelly and Wyszecki (See figure 2(3.8.4) in Wyszecki and Stiles, 1982). It leaves room to numerous spectral power distributions with some remarkable properties.

3. SMALL DIMENSIONALITY COLOUR WORLDS

3.1 One or two photoreceptors (individual dimensionality)

3.1.1 Achromatopsia

Cases of one-dimensional colour vision are rare. Achromatopsia is a very rare case of inherited total colour blindness, mainly including blue-cone monochromacy with a relative occurrence of 1:100,000 diagnosed cases (Sharpe et al., 1999).

Achromatopsia cases with total loss of all three cone opsin genes have been well documented by Nordby (he is an achromat) and Sharpe who examined the society from Guam, an island in Micronesia, known from Oliver Sacks' book entitled "The Island of the Colorblind" (1997), where about 10% of the population suffers from inherited achromatopsia.

3.1.2 Dichromatism

Conversely, two-dimensional colour vision is common among mammals, apart from primates. In humans, dichromacy is well characterized. About 2% of the male population is dichromatic. Dichromacy is of genetic origin. Dichromats lack one family of cone pigments. It has been verified since 1986 by Nathans and colleagues that dichromats lack the corresponding gene sequence.

During the 20th century, dichromatic colour vision has been well documented, showing dichromatic Rayleigh matches. Hue discrimination is impaired around 590 nm for protanopes and deuteranopes, or around 490 nm for tritanopes. Colour appearance is distorted. After a few reports from diagnosed unilateral dichromats, Judd (1948), Meyer and Greenberg (1988) and our group (Viénot et al., 1995; Brettel et al., 1997) have illustrated for the colour normal observer the colour appearance for dichromats.

The colour-blindness simulation is two-step.

In the LMS colour space, it is easy to find the colours that are confused by a dichromat. They lie on a line parallel to the axis corresponding to the missing fundamental. Our simulation was produced on a video-display, Cathode-Ray-Tube type, in which we could control the intensity of the three primaries. Yet, on a CRT, the definition of the stimulus is three-dimensional and linearly related to cone excitations.

Then we had to render a plausible appearance of the image. Reproducing how an image appears to dichromats was challenging. Given that a dichromat confuses a given red and a given green, how would these confused colours be perceived, and how should they be represented? Should the representation be red? Or green? Or yellow?

Appearance for a protanope→

Appearance for a deuteranope→

Figure 1. Simulation, for the normal eye, of the appearance of a flower bed for the dichromat (Viénot et al., 1995).

In his pioneer study, Judd had carefully reviewed the literature about unilateral colour defects which shows that for protanopic and deuteranopic observers, the colour perception of the spectrum is confined to two hues, yellow and blue. Judd's choice has been to represent, for a normal colour observer, all corresponding colours that are confused by dichromats by a unique sample of hue 5PB or hue 5Y of the Munsell Book of Colors. Precisely, Judd has given quantitative estimates of the colour perceptions typical of protanopic and deuteranopic observers for the whole range of Munsell colours. The same choice was retained by Meyer and Greenberg in a computer graphics simulation of dichromatic vision, prior to ours.

Our choice has been to maintain the normal colour appearance of white and greys and the same two hues of the stimuli at 475 nm and at 575 nm for protanopes, deuteranopes and normal trichromats. Finally, a photograph from a flower bed, at the Jardin des Plantes in Paris, has served to illustrate the simulation (Figure 1).

Now softwares have been written by many groups, some of them being available online. Figure 2 shows, for a trichromat, how the AIC 2015 logo (1st line) appears for a protanope (2nd line) and a deuteranope (3rd line).

Figure 2. Colour-blind simulation of the AIC 2015 logo.

3.2 Specificity of the luminance information (operational dimensionality)

The visual system network distinguishes between chromatic and achromatic pieces of information, the latter being prominent. Practically, the most efficient visual signals in nature which help the individual to localize targets and to move in the environment are based on luminance contrast.

Although the normal individual colour vision is trichromatic, behavioural responses to situations implicating resolution of high spatial and temporal frequencies depend principally on an achromatic mechanism with a spectral sensitivity much like $V(\lambda)$. Provided that the detection of high spatial frequencies or high temporal modulations depends on luminance contrast only, the chromaticity of the stimulus does not modify visual performance. Psychological evidence is obtained using the techniques of heterochromatic flicker photometry or minimally distinct border, among others. Thus, the high frequency spatial colour vision reduces to one dimension.

Lennie et al. (1993) recognize that the nature of underlying post-receptoral mechanisms is equivocal. Either LWS and MWS cone signals are directly summed into the magno-cellular pathway, or they are indistinctly processed so as issuing an additive signal.

3.3 The colour of illumination (contextual dimensionality)

Colour specification is well controlled by lighting engineers. With the emergence of solid-state technologies, much care is taken to correctly assess the colour of light. Indeed, for humans, the reference to qualify white light is natural daylight that needs only two variables to be qualified: the illuminance at earth level and the colour temperature.

Having measured the spectral power distribution (SPD) of real daylights, Judd and co-authors (1964) concluded, however, that distributions could be satisfactorily reconstituted by using only the first two principal components derived from principal component analysis (PCA). Later, Hernández-Andrés and colleagues (2001) concluded that more than two characteristic vectors were needed for good reconstruction. Even though they observed some departure of clear-sky colour from the CIE daylight locus, the chromaticities they measured are pretty much aligned along a unique curve.

Given the shape of the daylight locus and the dominance of the first two principal components in the analysis of daylight distribution, the question arises whether the three-dimensional colour specification that is used to specify the colour of material items is the one that should be used to scale illumination. We will see later in this paper that a specific visual channel is excited by light which might imply that the dimensions of the colour illumination world are only two.

4. EXPANDED DIMENSIONALITY COLOUR WORLDS

4.1 Additional photopigments (individual dimensionality)

Whereas the colour image domain exploits at best the three dimensions of colour, the questions arises whether the colour vision of the observer who looks at images could be more than three-dimensional.

4.1.1 Tetrachromatic mothers

Anomalous trichromats possess three cone pigment families. Nevertheless, one pigment family differs from the normal's cone pigment. Men inherit the LWS and the MWS pigment genes from their mother. The likelihood that behavioural tetrachromacy exists in carriers of anomalous trichromacy was addressed by Jordan (Jordan et al., 2010). Although most carriers of colour anomaly do not exhibit four-dimensional colour vision, Jordan and colleagues found 1 of 24 female carriers who exhibited tetrachromatic behavior on a colour matching test (Rayleigh matches). Genetic analysis showed that this mother had three well-separated cone photopigments in the longwave spectral region in addition to her short-wave cone which makes the sum of cone families equal to four. Nevertheless, it may be noted that this human observer has been just able to express trichromacy in a task where the canonical normal colour observer expresses dichromacy.

4.1.2 Fish and birds tetrachromatic vision

Fish and birds possess four families of cones. Although narrower tuning of the cone sensitivity might impair differential sensitivity, behavioural tests show that birds and fish enjoy tetrachromatic colour vision (Kelber and Osorio, 2010).

4.2 Additional receptors: rods and melanopsin (operational dimensionality)

Besides extra cone pigments, there are two photopigment families other than cone pigments, and with a different spectral sensitivity, which could be candidate to increase the dimensionality of colour vision.

4.2.1 Rod contribution

Rods, the spectral absorption of which, measured in the corneal plane, peaks at 507 nm, are active at mesopic levels.

Clarke (1973) and Trezona (1973) in early AIC conferences, demonstrated how to achieve a tetrachromatic colour match that holds at photopic and scotopic levels. To match every monochromatic radiation, they needed four primary matching stimuli of which they used one or another set of three. A unique match could be reached by iterative convergence. While the unique answer is recorded on the basis of the known colour sensations, this procedure ensures physiological identity of quantum absorption in four receptor responses.

4.2.2 Melanopsin interaction

During the past decade, it has been discovered that a few retinal ganglion cells contain a photopigment named melanopsin which can absorb photons before they reach the cone and rod layers. The melanopsin spectral sensitivity peaks at about 490 nm (estimated at the entrance of the eye), between SWS cones and rods' peak sensitivity. The so-called intrinsically photosensitive retinal ganglion cells (ipRGC) are stimulated at high mesopic and photopic illuminance levels (Dacey et al., 2005).

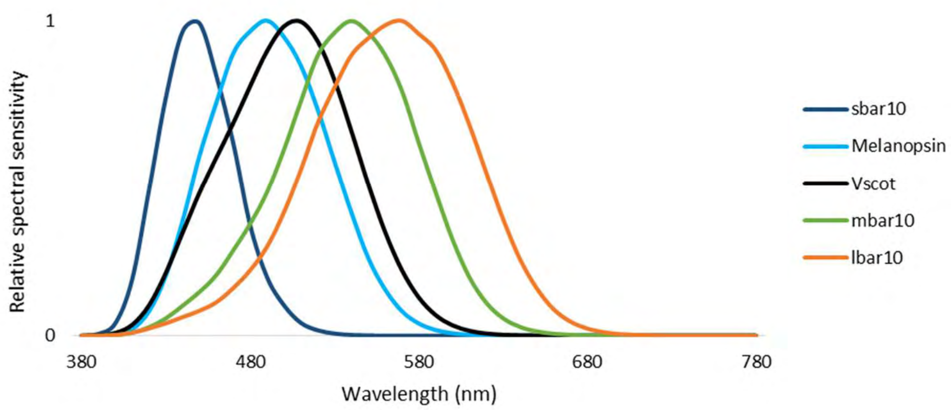

Figure 3. Cone, rod and ipRGC spectral sensitivities.

Using pharmacological tracers in the monkey brain, it has been shown that ipRGCs project to cortical and sub-cortical areas of the brain (Dacey et al., 2005; Hannibal et al., 2014). They convey information that is not principally devoted to image formation but mediate other visual functions such as the circadian rhythm and the pupillary reflex, and influence awareness and mood (Lucas et al. 2014).

The effect of the spectrum on non-image forming fonctions.

As pupil aperture is easy to record in real situations, we conducted experiments to test whether it was possible to drive the pupil response in accordance with the excitation of rods and ipRGCs (Viénot et al., 2012). Our experiments rest on the fact that metamers could differently address rods and ipRGCs. To investigate this question, at least 5 independent primaries are necessary. In a multi-LED light booth equipped with 7 types of colour LEDs, we could modulate the light spectrum, maintaining the white illumination at the same luminous level and the same CCT. Thus, the LEDs were driven so as to obtain metameric white lights that would excite rods and ipRGCs at most or at least (Figure 4). We continuously photographed the pupil of the observers under each 7 colour LED illumination to measure the pupil diameter.

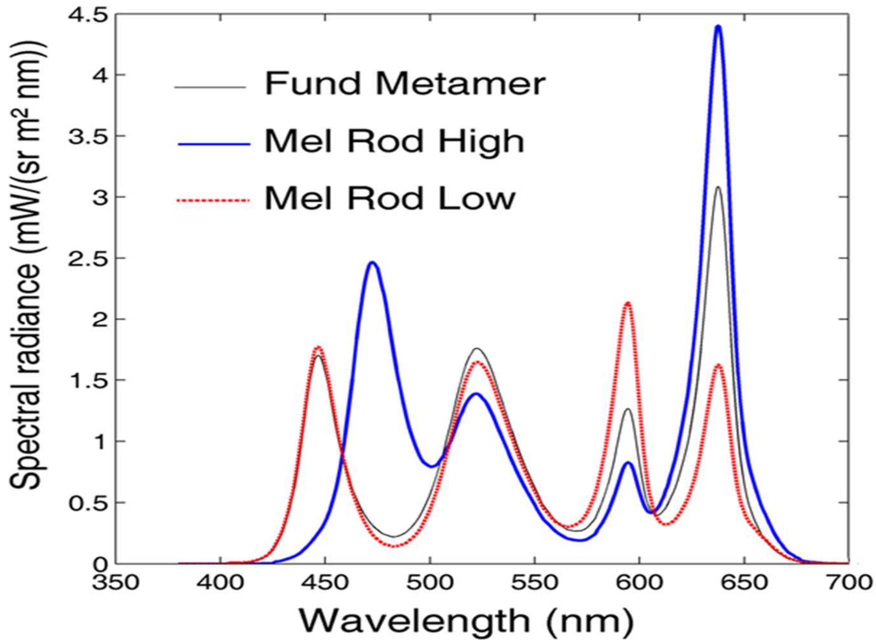

Figure 4. Two metameric white lights that would excite rods and ipRGCs at most or at least (Viénot et al., 2012).

Indeed, we verified that, with metameric white lights that generate identical signals in cones, the pupil diameter varies depending upon the spectral content of the light, which indicates that the light spectrum has an effect on visual functions, besides consciously seeing colours.

For domestic lighting, we draw attention to the possibility that driving the pupil reflex and possibly other non-image forming visual functions using unnatural spectrum would generate an uncomfortable behaviour.

Whether melanopsin interacts with cone colour vision is still unsolved. Brown et al. (2012) have hypothesized that ipRGCs may contribute to distinguishing brightness. Horiguchi et al. (2013) collected detection (difference) thresholds to many stimuli, using four-primary stimuli. Trichromatic theory explains foveal sensitivity, with no need to invoke a fourth photopigment. At high photopic levels where rods are not active, a fourth photopigment is required to explain peripheral sensitivity.

4.3 Four pigments and colour constancy (operational dimensionality)

Colour constancy is a visual phenomenon which we encounter every day. The perceived colours of reflecting surfaces remain satisfactorily stable despite changes in the spectrum of the illuminating light.

Where discounting for the illuminant change originates from is not understood yet. Simple models rely on the von Kries coefficient laws and state that the global change of illumination can be extracted from proportional changes of the cone excitations triggered by the reflecting surfaces in the scene. The gain change could operate within the retina.

However modern scientists question the complexity of colour constancy. They argue that the visual system makes a distinction between the estimation of the illuminant and the changes of surface reflectances.

Foster and colleagues (Craven and Foster, 1992; Foster, 2011) settle experiments where they introduced changes in illuminant colour and/or changes of material colour properties. They showed that subjects had been capable of correctly discriminating the two situations. They concluded that the visual system is provided with information about a changing world in "advance of the generation of a more elaborate and stable perceptual representation".

Hyperspectral images of natural scenes have revealed the occurrence of metamers in nature which indirectly means that the natural world is higher dimensional that the CIE colorimetry world (Foster et al., 2006). Of interest is the recent analysis of Barrionuevo and Cao (2014) who showed that the natural object spectra are not only discriminable by cones but that part of the spectral information can be decoded by melanopsin. Principal component analyses conducted on the excitations of rhodopsin, cone opsins, and melanopsin for natural hyperspectral images revealed that the sum of all responses ("L M S R I", with "I" for ipRGC) may contribute to the magno-cellular pathway and respond to irradiance levels. The PCA further suggests that rod and ipRGC signals also may contribute to post-receptoral pathway components that oppose LWS and MWS cone, with various combinations.

The putative role of a fourth photopigment to disambiguate the colour material factor from the colour illumination factor has been addressed in the context of colour constancy. In the future, investigation of the role of melanopsin signals might bring renewed knowledge about colour constancy as well as to the concept of colour temperature.

4.4 The generalized metameric approach. Metamers in the four- or five-dimensional framework

In the context of the three cones space, metameric colour stimuli have different spectral power distributions, but they excite the three families of cones similarly.

Investigation of the metamer domain has been facilitated using the concept of "metameric blacks" introduced by Gunter Wyszecki in 1953. (A simple example might be: given two real metameric stimuli, a metameric black is obtained by subtracting the SPD of one stimulus from the other.) Wyszecki presented the view that the spectral power distribution of metamers consists of two component spectral distributions: the fundamental distribution, named "fundamental metamer", that controls the three cone responses (and consequently the colour specification of the stimulus) and a secondary distribution that has no effect on cones, which he named a "metameric black". Cohen and Kappauf, in 1982, presented a procedure for accomplishing the decomposition of any visual stimulus into the fundamental metamer and the black component.

Adding a metameric black to a fundamental metamer has no effect on cone responses. However adding a metameric black to the fundamental metamer may well modify the responses of the rods and of the melanopsin cells. In order to investigate the domain of metamers in a space of higher dimensionality than the cone fundamentals', it is possible to extend Cohen and Kappauf's procedure for producing SPDs that excite or do not excite identified photoreceptors. Let us note that two metamers for a dichromat may not be metameric for the trichromat, two metamers for a trichromat may not be metameric for a four receptor visual system, two metamers for a four receptor system may not be metameric for a five receptor system, etc

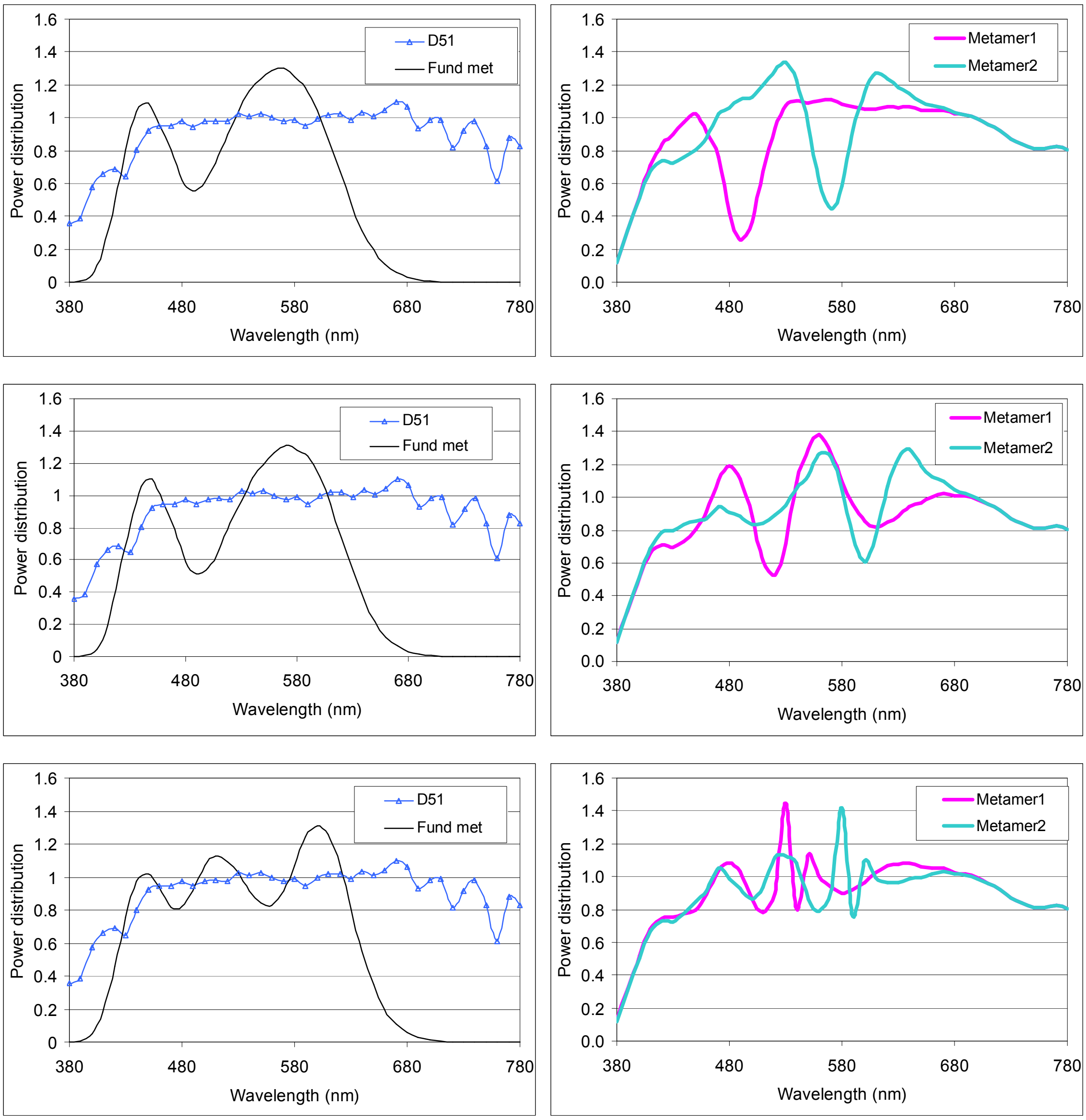

Figure 5. Metamers of daylight at 5100 K

Figure 5 shows examples of metamers of daylight at 5100 K for a variety of dimensionality of the visual receptor system. On the first line, the graphs show metamers for the deuteranope who lacks MWS photopigment. On the second line, the graphs show metamers for the normal trichromat. On the third line, the graphs show metamers that match for the three cone types as well as for rods and melanopsin cells. The left column presents the SPD of natural daylight at 5100 K and its fundamental metamer. In a previous paper, we already mentioned that, in the three-dimensional colour space, the fundamental metamer distribution resembles the SPD of modern light-emitting diodes. Thus while LED lighting mimics the colour of natural light it does not suit rod and melanopsin cells natural excitation. The right column presents two arbitrary chosen metamers with markedly different spectral power distribution. It can be seen that, as the dimensionality of the receptor system increases, the number of crossings of the two metameric stimulus functions increases. Note also that Metamer 1 and

Metamer 2 designed for the deuteranope would appear reddish and greenish to a colour normal observer.

4.5 The necessity of categorisation (contextual dimensionality)

Whereas receptor-level colour coding ensures continuous capture of the available information about the environment, we tend to group into categories the colour we perceive.

It is not clear whether categorization can be included in a dimensionality framework, for dividing the information into a small number of well-defined regions of the colour space tears the continuous dimensions of colour and introduces irregularities in the colour space (Jameson, 2005). Further, language, as a normative process of colour space segmentation, influences the way colour samples are grouped based on their perceptual similarities (Bonnardel, 2013).

What is accepted is that color categorization helps us to reliably and quickly identify objects and materials within a scene. It is an essential perceptual phenomenon.

CONCLUSION

On the one hand, stating that colour vision is three-dimensional strictly applies to the cone fundamental space. It has helped the CIE to found standard colorimetry and recently to revisit the cone fundamental space (CIE, 2006).

On the other hand, the dimensionality of colour vision may vary depending on the individual, the task and the context. It is a challenge for the future to establish relationships between one or another colour space and to find the best way to define the colour of the world.

ACKNOWLEDGMENTS

I am grateful to Hans Brettel for fruitful discussions and to the colleagues who nominated me for the Judd award.

REFERENCES

Barrionuevo, P. A. and Cao, D., 2014. Contributions of rhodopsin, cone opsins, and melanopsin to postreceptoral pathways inferred from natural image statistics. *Journal of the Optical Society of America* A, 31(4), A131.

Bonnardel, V., 2013. Color categories. In: *A Symposium on Colour Vision In Memory of Yves Le Grand*, CIE, MNHN, Paris, France.

Brettel H., Viénot F. and Mollon J. D., 1997. Computerized simulation of color appearance for dichromats. *Journal of the Optical Society of America* A 14: 2647–2655.

Brown T. M., Tsujimura S., Allen A. E., Wynne J., Bedford R., Vickery G., Vugler A., and R. J. Lucas, 2012. Melanopsin-based brightness discrimination in mice and humans, *Current Biology* 22: 1134-1141.

Clarke F. J. J., 1973. Needs and prospects for a tetrachromatic system of large field colorimetry. In: *Colour 73*, 2nd Congress of the International Colour Association, York, pp. 319-324.

Cohen J. B. and Kappauf W. E., 1982. Metameric color stimuli, fundamental metamers, and Wyszecki's metameric blacks, *American Journal of Psychology* 95: 537–564.

Commission Internationale de l'Eclairage: Fundamental Chromaticity Diagram with Physiological Axes - Part 1, CIE 170-1-2006

Craven, B. J. and Foster, D. H., 1992. An operational approach to colour constancy. *Vision Research* 32: 1359-1366.
Dacey, D. M., Liao, H.-W., Peterson, B. B., Robinson, F. R., Smith, V. C., Pokorny, J. and Gamlin, P. D., 2005. Melanopsin-expressing ganglion cells in primate retina signal colour and irradiance and project to the LGN. *Nature* 433(7027): 749–754.
Foster D. H., Amano K., Nascimento S. and Foster M. J., 2006. Frequency of metamerism in natural scenes. *Journal of the Optical Society of America* A 23: 2359–2372.
Foster, D. H., 2011. Color constancy. *Vision Research* 51(7): 674–700.
Hannibal, J., Kankipati, L., Strang, C. E., Peterson, B. B., Dacey, D., & Gamlin, P. D., 2014. Central projections of intrinsically photosensitive retinal ganglion cells in the macaque monkey: Central projections of intrinsically photosensitive RGCs in macaque. *Journal of Comparative Neurology* 522(10): 2231–2248.
Hernández-Andrés J., Romero J., Nieves J. L. and Lee Jr R. L., 2001. Color and spectral analysis of daylight in southern Europe. *Journal of the Optical Society of America* A 18(6): 1325-1335.
Horiguchi H., Winawer J., Dougherty R. F. and Wandell B. A., 2013. Human trichromacy revisited. *Proceedings of the National Academy of Science USA* 110: E260–E269.
Jameson, K., 2005. Culture and Cognition: What is Universal about the Representation of Color Experience? *Journal of Cognition and Culture*, 5(3): 293–348.
Jordan, G., Deeb, S. S., Bosten, J. M. and Mollon, J. D., 2010. The dimensionality of color vision in carriers of anomalous trichromacy. *Journal of Vision* 10(8):12, 1–19.
Judd D. B., 1948. Color perceptions of deuteranopic and protanopic observers. *J Res Nat Bur Stand (USA)* 41:247–271.
Judd D. B., MacAdam D. L. and Wyszecki G., 1964. Spectral distribution of typical daylight as a function of correlated color temperature, *Journal of the Optical Society of America* 54: 1031-1040.
Judd, D. B., Macadam, D. L., Wyszecki, G., Budde, H. W., Condit, H. R., Henderson, S. T. and Simonds, J. L., 1964. Spectral Distribution of Typical Daylight as a Function of Correlated Color Temperature. *Journal of the Optical Society of America* 54(8): 1031.
Kelber, A. and Osorio, D., 2010. From spectral information to animal colour vision: experiments and concepts. *Proceedings of the Royal Society B: Biological Sciences* 277(1688): 1617–1625.
König A. and Dieterici C., 1886. Die Grundempfindungen und ihre Intensita¨ts-Vertheilung im Spectrum. *Sitzungsberichte Akademie der Wissenschaften*, Berlin, 805–829.
Lennie, P, Pokorny, J and Smith, VC, 1993. Luminance. *Journal of the Optical Society of America* A 10: 1283-1293.
MacLeod D. I. A. and Boynton R. M., 1979. Chromaticity diagram showing cone excitation by stimuli of equal luminance. *Journal of the Optical Society of America* 69:1183-1186.
Meyer G. W. and Greenberg D. P., 1988. Color-defective vision and computer graphics displays. *IEEE Comp Graph Appl* 8: 28–40.
Nathans, J., Thomas, D. and Hogness, D., 1986. Molecular genetics of human color vision: the genes encoding blue, green, and red pigments. *Science* 232(4747): 193–202.
Report of U.S. Secretariat Committee on Colorimetry and Artificial Daylight, *CIE Proceedings*, Vol. 1, Part 7, Stockholm, 1951.
Sharpe L. TL, Stockman A., Jägle H. and Nathans J., 1999. Opsin genes, cone photopigments, color vision, and color blindness. In *Color Vision: From genes to perception*, eds : Gegenfurtner K R and Sharpe L T , Cambridge University Press, New York, pp. 3-52.

Stiles W. S. and Burch J. M., 1959. NPL colour-matching investigation: Final report (1958). *Optica Acta* 6: 1-26.

Stockman A. and Sharpe L. T., 2000. Cone spectral sensitivities and color matching. In *Color Vision: From genes to perception*, eds : Gegenfurtner K R and Sharpe L T , Cambridge University Press, New York, pp. 53-87.

Stockman A. and Sharpe L. T., 2000. Spectral sensitivities of the middle- and long-wavelength-sensitive cones derived from measurements in observers of known genotype. *Vision Research* 40: 1711–1737.

Trezona P. W., 1973. Tetrachromatic colour measurement. In: *Colour 73*, 2nd Congress oft he International Colour Association, York, pp.324-328..

Viénot F., Brettel H., Ott L., Ben M'Barek A. and Mollon J. D., 1995. What do colour-blind people see? *Nature* 376: 127-128.

Viénot, F., Brettel, H., Dang, T.-V. and Le Rohellec, J., 2012. Domain of metamers exciting intrinsically photosensitive retinal ganglion cells (ipRGCs) and rods. *Journal of the Optical Society of America* A 29(2): A366.

Viénot F., Walraven P., 2007, Colour-matching functions, physiological basis. In: Janos Schanda (Editor) *Colorimetry, Understanding the CIE system*, Wiley, pp. 219-243.

Wyszecki G. and Stiles W. S., 1982. Color science: Concepts and methods, Quantitative data and formulae, Wiley.

Wyszecki G., 1953. Valenzmetrische untersuchung des Zusammenhanges zwischen normaler und anomaler Trichromasie. *Farbe* 2:39–52.

Address: Prof. Françoise VIÉNOT
Centre de recherche sur la conservation (CRC, USR 3224)
Sorbonne Universités
Muséum national d'Histoire naturelle
Ministère de la Culture et de la Communication, CNRS
CP21, 36 rue Geoffroy-Saint-Hilaire, 75005 Paris, France.

BIBLIOGRAPHY
Françoise VIÉNOT

AWARDS

VIÉNOT F., 2014, *ISCC Macbeth Award*, Inter-Society Color Council News, Issue 468, Fall 2014

VIÉNOT F., *Verriest Medal, The International Colour Vision Society*, 22nd Biennial ICVS Symposium, Winchester UK, 15 July 2013.

VIÉNOT F., "Novelty of metameric LED white lights", *Newton medal, The Colour Group of Great Britain*, London, 13th April 2012.

VIÉNOT F., "From gloss scaling to gloss constancy". Presentation of "The David Palmer lecture", *The Colour Group* (Great Britain), London, 12th January 2006.

VIÉNOT F., Prix de la meilleure communication, *LE CLUB VISU - SID-FRANCE*, 18 juin 1997.

VIÉNOT F., Prix Alfred Monnier de *l'Association Française de l'Eclairage*, 20 mars 1997.

VIÉNOT F., Médaille de l'Universidad de Granada, 1996.

BOOKS

Commission Internationale de l'Eclairage, 2006, CIE 170-1:2006 "*Fundamental Chromaticity Diagram with Physiological Axes - Part 1*", report of CIE TC 1-36, 45 p.

ROQUE G., BODO B. & VIÉNOT F. (eds), 1997, *Michel-Eugène CHEVREUL. Un savant, des couleurs!* MNHN/EREC, Paris, 277 p.

KOWALISKI P., 2ème édition actualisée par VIÉNOT F. & SÈVE R., 1990, *Vision et mesure de la couleur*, Coll. Physique fondamentale et Appliquée, Masson, Paris.

BOOK CHAPTERS

VIÉNOT F., 2015, Peut-on mesurer l'apparence ? Actes de l'Université européenne « Observation et pensée », *Université Paris-Diderot* (in press).

VIÉNOT F., LE ROHELLEC J., 2012, Colorimetry and physiology: the LMS specification. In : FERNANDEZ-MALOIGNE C., ROBERT-INACIO F., MACAIRE L., *Digital color. Acquisition, Perception, Coding and Rendering* Digital Signal and Image Processing Series, ISTE, Wiley, pp. 1-27.

VIÉNOT F., LE ROHELLEC J., 2012, Colorimétrie et physiologie : la spécification LMS. In : FERNANDEZ-MALOIGNE C., ROBERT-INACIO F., MACAIRE L.(Eds.), *Couleur numérique : acquisition, perception, codage et rendu (Traité Signal et Image, IC2)*, Hermès, Lavoisier, pp.19-42, planche couleur page i.

VIÉNOT F., GENDRON F., 2009, L'attrait du brillant et de la couleur. L'éclat de la pierre polie. In : M-H. Moncel et F. Fröhlich (éditeurs), *L'homme et le précieux. Matières minérales précieuses*, BAR International Series 1934, pp. 111-118. http://precieux.mnhn.fr/?page_id=250

VIÉNOT F., 2008, L'éclairage à base de LEDs. In : P. Mottier (co-ordonnateur) *Les diodes électroluminescentes pour l'éclairage* (traité EGEM), Hermes. . pp. 207-239 et IV-VI. Traduction anglaise : Quality of white light from LEDs. In: P. Mottier (editor) *LEDs for Lighting Applications*, ISTE Wiley, 2009, pp 197-232. ISBN: 9781848211452

VIÉNOT F., WALRAVEN P., 2007, Colour-matching functions, physiological basis. In: Janos Schanda (Editor) *Colorimetry, Understanding the CIE system*, Wiley, pages 219-243.

VIÉNOT F., 2006, La vision en couleur des surfaces. In : *La couleur. Lumière, vision et matériaux*, sous la direction de Mady Elias et Jacques Lafait, Belin, collection Échelles, 27-78. www.lumilog.com

VIÉNOT F., 2001, L'usage de l'écran de visualisation dans le test de vision des couleurs. In: *Les dyschromatopsies*, rapport annuel des Sociétés d'Ophtalmologie de France, coordonnateur J. Leid, *Bull.Soc.Ophtal.Fr.* : 145-151.

RIGAUDIÈRE F.,VIÉNOT F., 2001, Quelques bases physiques, psychophysiques et neurophysiologiques de la sensation colorée. In: *Les dyschromatopsies*, rapport annuel des Sociétés d'Ophtalmologie de France, coordonnateur J. Leid, *Bull.Soc.Ophtal.Fr.* : 23-37.

VIÉNOT F., 1999, La couleur, une vue de l'esprit. In: *Mille cerveaux, mille mondes*, sous la direction de P. BUISSERET, Nathan/HER & MNHN, Paris, France, pp. 101-104.

BRETTEL H., VIÉNOT F., 1999, Web design for the colour-blind user. In: *Colour Imaging: Vision and Technology*, edited by L.W. MacDonald and M.R. Luo, John Wiley & Sons Ltd., pp.55-71.

VIÉNOT F., 1998, Perception de la couleur. In: M. BOUCART, M.-A. HÉNAFF & C. BELIN (eds.), *Vision : aspects perceptifs et cognitifs*, SOLAL, Marseille, pp. 149-168 (**Conférence invitée** à la *Société de Neuropsychologie de Langue Française*, Paris, décembre 1997)

VIÉNOT F., 1997, Parallèle entre certaines observations de Chevreul et les acquis récents sur les mécanismes visuels. In: G. ROQUE, B. BODO & F. VIÉNOT (eds.), *Michel-Eugène Chevreul. Un savant, des couleurs!* MNHN/EREC.1997. Paris, pp.147-158.

DENIEUL P., BRETTEL H., MONOT A., VIÉNOT F., 1992, Vision et visualisation. In: *Systèmes Optiques*, Les Editions de Physique, Les Ulis, France, pp.315-337. http://dx.doi.org/10.1051/bib-sfo:2002027

VIÉNOT F. & CHOUARD P., 1992, Définition des principales couleurs applicables aux végétaux. In: *Le Bon Jardinier*, 153° ed., Editions Pierre Anglade, Paris, pp.1079-1093, 2 planches couleur.

VIÉNOT F., 1991, Transition from photopic to scotopic light assessments and possible underlying processes. In: B.B.LEE & A. VALBERG (Eds.), *From Pigments to Perception,* Plenum Publishing Corporation, New York, pp.41-51. (**Conférence invitée** au colloque *Nato advanced workshop on Advances in understanding visual processes. Convergence of neurophysiological and psychophysical evidence*. Roros, Norway, 6-10 August 1990)

FLEURY P., DENIEUL P., VIÉNOT F., 1985, Vision. Dans: *Encyclopaedia Universalis,* 2° ed., pp.942-949.

VIÉNOT F., 1983, Can variation in macular pigment account for the variation of colour matches with retinal position? In: MOLLON J.D. and SHARPE L.T. (Eds), *Colour Vision: Physiology and Psychophysics,* Academic Press, London, pp.107-116. (**Conférence invitée** au colloque *Colour vision. A NATO conference*, Cambridge, August 23-27, 1982)

ARTICLES

VIENOT F., BRETTEL H., 2014, The Verriest lecture: Visual properties of metameric blacks beyond cone vision. J. Opt. Soc. Am. A / Vol. 31, No. 4 / April 2014. A38-A46. http://dx.doi.org/10.1364/JOSAA.31.000A38 On line December 19, 2013.

COMAR A., BARRET F., OBEIN G., SIMONOT L., MENEVEAUX D., VIENOT F., DE SOLAN B., 2014, A leaf BRDF model taking into account the azimuthal anisotropy of monocotyledonous leaf surface. *Remote Sensing of Environment*, 1: 112-121.

ARNAULT E, BARRAU C, NANTEAU C, GONDOUIN P, BIGOT K, VIÉNOT F. et al., 2013, Phototoxic Action Spectrum on a Retinal Pigment Epithelium Model of Age-Related Macular Degeneration Exposed to Sunlight Normalized Conditions. PLoS ONE 8(8): e71398. doi:10.1371/journal.pone.0071398

DELPORTE, C., SAUTROT, S., BEN CHOUIKHA, M., VIÉNOT, F., ALQUIÉ, G., 2013, Biological tissue identification using a multispectral imaging system. *Sensors, Cameras, and Systems for Industrial and Scientific Applications XIV. Proceedings of the SPIE*, Volume 8659, article id. 86590H, 9 pp. (2013).

COMAR, A., BARET, F., VIÉNOT, F., YAN, L. and DE SOLAN, B., 2012. Wheat leaf bidirectional reflectance measurements: Description and quantification of the volume, specular and hot-spot scattering features. *Remote Sensing of Environment*, 121: 26-35.

VIÉNOT F., BRETTEL H., DANG T.-V., LE ROHELLEC J., 2012, Domain of metamers exciting intrinsically photosensitive retinal ganglion cells (ipRGCs) and rods, *J. Opt. Soc. Am. A* 29, Issue 2, pp. A366-A376 (2012).

DELPORTE, C., BEN CHOUIKHA, M., SAUTROT, S., VIÉNOT, F., ALQUIÉ, G., 2012, Multispectral device for help in diagnosis. In: Widenhorn, R; Nguyen, V; Dupret, A. (Eds.), Sensors, Cameras, And Systems For Industrial And Scientific Applications XIII Book Series: Proceedings of SPIE Volume: 8298, Article Number: 82980P. [hal-00671010 - version 1]

SARKAR A., F. AUTRUSSEAU, F. VIÉNOT, P LE CALLET, and L. BLONDÉ, 2011, "From CIE 2006 physiological model to improved age-dependent and average colorimetric observers," *J. Opt. Soc. Am. A* 28, 2033-2048.

BEHAR-COHEN F., MARTINSONS C., VIÉNOT F., ZISSIS G., BARLIER-SALSI A., CESARINI J.-P., ENOUF 0., GARCIA M., PICAUD S., ATTIA D., 2011, Light-emitting diodes (LED) for domestic lighting: Any risks for the eye?, *Progress in Retinal and Eye Research*, 30/ 239-257.

VIÉNOT F., CORON G., LAVÉDRINE B., 2011, LEDs as a tool to enhance faded colours of museums artefacts, *J. Cultural heritage*, Volume 12, Issue 4, Pages 431-440. doi:10.1016/j.culher.2011.03.007. https://www.em-consulte.com/revue/culher/s200/2141.

GED G., OBEIN G., SILVESTRI Z., LE ROHELLEC J., VIÉNOT F., 2010, Recognizing Real Materials from their Glossy Appearance, *Journal of Vision,* 10(9):18, 1–17. http://www.journalofvision.org/content/10/9/18

LABORIE B., VIÉNOT F., LANGLOIS S., Methodology for constructing a colour-difference acceptability scale. *Ophthalmic and Physiological Optics*, 30: 568–577, 2010.

VIÉNOT F., DURAND M.-L., MAHLER E., 2009, Kruithof's rule revisited using LED illumination. *J. Mod. Optics*, 56 : 1433-1446.

MAHLER E., EZRATI J.-J., VIÉNOT F., 2009, Testing LED Lighting for Colour Discrimination and Colour Rendering. *Color Research & Application*, 34 : 8-17.

VIÉNOT F, MAHLER E., EZRATI J.-J., BOUST C., RAMBAUD A., BRICOUNE A., 2008, Color appearance under LED illumination: The visual judgment of observers. *Journal of Light and Visual Environment*, 32 :208-213.

VIÉNOT F, SERREAULT L., PARDO FERNANDEZ P., 2006, Convergence of experimental multiple Rayleigh matches to peak L- and M- photopigment sensitivity estimates, *Visual Neuroscience*, 23: 419-427.

BOUST C., BEN CHOUIKHA C., BRETTEL H., VIÉNOT F., BERCHE S. & ALQUIÉ G., 2006, Color Enhancement of Digital Images by Experts and Preference Judgments by Observers. *The Journal of Imaging Science and Technology*. 2006, **50**: 1-11.

RIGAUDIÈRE F., LEID J., VIÉNOT F, LE GARGASSON J.-F., 2006, Comprendre et tester les déficiences de la vision des couleurs de l'enfant, en pratique. *J Fr d'Ophtalmologie*, **29** :87-102.

HARRAR M., VIÉNOT F., 2005, Regulation of chromatic induction by neighboring images. *J. Opt. Soc. Am A.*, 22: 2197-2206.

OBEIN, G., KNOBLAUCH, K., & VIÉNOT, F., 2004. Difference scaling of gloss: Nonlinearity, binocularity, and constancy. *Journal of Vision*, *4*(9), 711-720, http://journalofvision.org/4/9/4/ , doi:10.1167/4.9.4.

HARRAR, M., & VIÉNOT, F. (2004). A study on chromatic contrast regulation [Abstract]. *Journal of Vision*, *4*(11), 11a, http://journalofvision.org/4/11/11/, doi:10.1167/4.11.11.

OBEIN, G., PICHEREAU, T., HARRAR, M., MONOT, A., KNOBLAUCH, K., & VIÉNOT, F. (2004). Does binocular vision contribute to gloss perception? [Abstract]. *Journal of Vision*, *4*(11), 73a, http://journalofvision.org/4/11/73/, doi:10.1167/4.11.73.

HARRAR M., VIÉNOT F., GIRAUDET G., BAILLET G., 2003, Is glare spectrally selective ? *Perception*, Vol. 32, Suppl., p. 149.

HARRAR M., GIRAUDET G., BAILLET G., VIÉNOT F., 2003, Effet d'un éblouissement coloré sur les fonctions visuelles, *LR'O°08*, pages 6-10.

OBEIN G., KNOBLAUCH K., CHRISMENT A., VIÉNOT F., 2002, Perceptual scaling of the gloss of a one-dimensional series of painted black samples. *Perception*, Vol. 31, Suppl., p. 65.

VIÉNOT F., 2002, Michel-Eugène Chevreul: From laws and principles to the production of colour plates. *Color Research and Application :* 27 : 4-14. (**Conférence invitée** à l'*Inter-Society Color Council 2nd Panchromatic Conference,* Color in its surround, February 19-21, 2000, Savannah, U.S.A.).

VIÉNOT F., CHIRON A., 2001, Michel-Eugène Chevreul and his colour classification system. *Color Research and Application*, 26 : S20-S24. (**Conférence invitée** à l'*International Colour Vision Society*, 1999).

VIÉNOT F., 2001, Retinal distribution of the macular pigment and the cone effective optical density from colour matches of real observers. *Color Research and Application*, 26: S264-S268.

REGAN B.C., JULLIOT C., SIMMEN B., VIÉNOT F., CHARLES-DOMINIQUE P., MOLLON J.D., 2001, Fruits, foliage and the evolution of primate colour vision. *Phil. Trans. Royal Soc.*, 356: 1-55.

LE ROHELLEC J., VIÉNOT F., 2001, Interaction of luminance and spectral adaptation upon Benham subjective colours. *Color Research and Application,* 24:S174-S179.

MELGOSA M., RIVAS M.J., HITA E., VIÉNOT, 2000, Are we able to distinguish color attributes?, *Color Research and Application*, 25, 356-367.

VIÉNOT F., 1999, Le rendu des couleurs dans son contexte. Antériorité du regard des peintres sur l'analyse des scientifiques. *Techne, Centre de recherche et de restauration des musées de France*, Nos 9-10, p. 74-91.

VIÉNOT F., BRETTEL H., MOLLON J., 1999, Digital video colourmaps for checking the legibility of displays by dichromats. *Color Research and Application,* 24 : 243-252.

DIAZ NAVAS J.A., CHIRON A., VIÉNOT F., 1998, Tracing a metameric match to individual variations of colour vision. *Color Research and Application*, 23: 379-389.

BEN CHOUIKHA M., VIÉNOT F., LU G.N., 1998, Colorimetric characterization of a buried triple p-n junction photo-detector. *Displays***,** vol.19, n°:30, pp. 105-110.

BÈCLE P., MONOT A., VIÉNOT F., EYQUEM D., 1998, Detecting gradient and discriminating shape from texture. *Perception*, vol.27, suppl., p.204.

LE ROHELLEC J., VIÉNOT F., 1998, The effect of luminance and spectral adaptation upon subjective colours. *Perception*, vol.27, suppl., p.174-175.

REGAN B.C., JULLIOT C., SIMMEN B., VIÉNOT F., CHARLES-DOMINIQUE P., MOLLON J.D., 1998, Frugivory and colour vision in *Alouatta seniculus*, a trichromatic platyrrhine monkey. *Vision Research*, 38: 3321-3329.

BRETTEL H., VIÉNOT F., MOLLON J., 1997, Computerized simulation of color appearance for dichromats. *J. Opt. Soc. Am.,* vol.14, 2647-2655.

PEFFERKORN S., CHIRON A., VIÉNOT F., 1996, Développement d'une méthode de photométrie visuelle mésopique. *Bull. du Bureau National de Métrologie*, vol.106, pp.19-35.

DIAZ NAVAS J.A., CHIRON A., VIÉNOT F., 1996, Tracing a metameric match to individual variations of colour vision. *Perception,* vol.25, suppl., p.15.

REGAN B.C., VIÉNOT F., CHARLES-DOMINIQUE P.C., PEFFERKORN S., SIMMEN B., JULLIOT C., MOLLON J.D., 1996, The colour signals that fruits present to primates. *Investigative Ophthalmology & Visual Science*, Vol.37, p.S648.

VIÉNOT F., BRETTEL H., OTT L., BEN M'BAREK A., MOLLON J. D., 1995, What do colour-blind people see?, *Nature*, vol. 376, pp.127-128.

LE ROHELLEC J., VIÉNOT F., 1994, Dependence of Fechner-Benham colours upon luminance adaptation, *Perception*, vol.23, suppl., p.91.

LE ROHELLEC J., VIÉNOT F., 1992, Change in the colours of Benham's top with exposure time. *Perception,* vol.21, suppl.2, p.76.

VIÉNOT F., CHIRON A., 1992, Heterochromatic flicker photometry is phase-dependent at mid-mesopic levels. *Perception,* vol.21, suppl.2, p.77.

VIÉNOT F. & LE ROHELLEC J., 1992, Reversal in the sequence of the Benham colours with a change in the wavelength of illumination. *Vision Res.*, Vol.32, pp.2369-2374.

VIÉNOT F. & CHIRON A., 1992, Brightness Matching and Flicker Photometric Data Obtained Over the Full Mesopic Range. *Vision Res.*, Vol.32, pp.533-540.

VIÉNOT F. & LE ROHELLEC J., 1990, Hue reversal in the colours of Benham's top with change in illumination wavelength. *Perception,* vol.19, pp.358-359.

VIÉNOT F., 1990, A portable apparatus for measuring wavelength discrimination in man. *J. Physiol. (Lond.),* vol.426, p.4P.

VIÉNOT F., 1987 (publié en 1989), What are observers doing when making color-matches? *Farbe,* vol.34, pp.221-228. (**Conférence invitée** au colloque *International Colour Association (AIC) interim meeting: Wyszecki and Stiles Memorial Symposium on Color Vision Models*, Florence, Italie, 10-13-juin 1987)

MORELAND J.D., VIÉNOT F., 1988, Macular pigment multiplicity. In: 11th European Conference on Visual Perception (ECVP), Bristol, G.B., *Perception,* vol.17, n°3, p.380.

CHIRON A., VIÉNOT F., 1988, Direct comparaison and flicker matches at high mesopic levels. In: 11th European Conference on Visual Perception (ECVP), Bristol, G.B., *Perception,* vol.17, n°3, p.371.

COOPER H.M., CHARLES-DOMINIQUE P., VIÉNOT F., 1986, Signification de la coloration des fruits en fonction de la vision des vertébrés consommateurs. *Mémoires du Muséum national d'Histoire naturelle ,* Série A, Zoologie, tome 132 (Entretiens du Muséum, Vertébrés et Forêts tropicales humides d'Afrique et d'Amérique), pp.131-143.

BOURDY C., VIÉNOT F., MONOT A., CHIRON A., 1985, Spatial contrast detection for colour patterns under selective chromatic adaptation. *Displays: Technology and applications,* vol.6, n°1, pp.43-51.

BOURDY C., VIÉNOT F., MONOT A., CHIRON A., 1983, Spatial sensitivity of the human visual system under selective chromatic adaptation: shape of the contrast sensitivity curves, foveal versus peripheral vision. *J. of Optics* (Paris), vol.14, n°5, pp.225-233.

VIÉNOT F., 1983, Color-match changes between the fovea and the perifovea. *Color Research and Application,* vol.8, n°4, pp.215-220.

BOURDY C., VIÉNOT F., MONOT A., CHIRON A., 1982, Forme des courbes de sensibilité au contraste des mécanismes colorés isolés en vision fovéale et en vision périphérique. *L'Année Psychologique,* vol.82, pp.19-27.

VIÉNOT F., 1980, Relations between inter-and intra-individual variability of color-matching functions. Experimental results. *J. Opt. Soc. Am.,* vol.70, n°12, pp.1476-1483.

VIÉNOT F., 1977, About the statistics of color-matching functions. *Farbe,* vol.26, n°3-6, pp.205-212.

VIÉNOT F., 1977, New equipment for the measurement of color-matching functions. *Color Research and Application,* vol.2, n°4, pp.165-170.

CONFERENCE PAPERS

VIÉNOT F., 2013, Light Emitting Diodes: quality assessment and visual comfort, Cultural heritage conservation science and sustainable development: experience, research, innovation International conference in the frame of the 50th anniversary of the Centre de recherche sur la conservation des collections – CRCC, Paris, 23, October 2013.

VIÉNOT F., 2013, Metamerism beyond colour vision. *22nd Symposium of the International Colour Vision Society*, Winchester, UK, 14-18 July 2013, p. 42. (**Verriest Medallist 2013**)

VIÉNOT F., 2013, Virtual Restoration of Faded Colours of %Museums Artefacts using LED Lighting. Proceedings of AIC2013, 12th International AIC Congress, Newcastle upon Tyne, 8 July 2013, page 101. (**Conférence invitée**)

BARRAU C., NADOLNY C., VILLETTE T., VIÉNOT F., 2013, Effects of selective blue-violet spectral subtractions on colour perception. *22nd Symposium of the International Colour Vision Society*, Winchester, UK, 14-18 July 2013, p. 123.

LE ROHELLEC J., VIÉNOT F., ANTON J.-L., NAZARIAN B., ATTIA D., MERCKEL O., ROSENFELD F., LAVÉDRINE B., 2013, A study of the sustained pupil response under a variety of LED illuminations. Proc. CIE Centenary, Paris, 15 April 2013.

VIÉNOT F., 2012, Gloss Characterization, a Cyclic Approach. In: *Predicting Perceptions: Proceedings of the 3rd International Conference on Appearance*. Lulu Press, Edinburgh UK, pp. 7-9. ISBN 978-1-4716-6869-2. (**Conférence invitée**)

DELPORTE C., BEN CHOUIKHA M., SAUTROT S., VIÉNOT F AND ALQUIÉ G, 2012, Multispectral device for help in diagnosis, *Proc. SPIE* 8298, 82980P (2012); http://dx.doi.org/10.1117/12.909107

FALKENSTERN K., BONNIER N., BRETTEL H., FELHI1 M., VIÉNOT F., 2011, Adaptively Selecting a Printer Color Workflow. *19th Color and Imaging Conference*, November 7 – 11, 2011, San Jose, CA, The Society for Imaging Science and Technology, 205-210, octobre 2011, Paris, France, 6 pages.

ROBERT-INACIO F., PERRIN M., FAVIER S., VIÉNOT F., DANG T.-V., LE ROHELLEC J. & KUSSENER E., Eye-tracking for pupil diameter extraction, ECEM 2011, 16th European Conference on Eye Movements, 21-25 August, 2011, Marseille, France.

FALKENSTERN K., BONNIER N., BRETTEL H., PEDERSEN M., VIÉNOT F., 2011, Weighing quality attributes. *21st Symposium of the International Colour Vision Society*, Kongsberg, Norway, 1-5 July 2011, p. 88.

VIÉNOT F., DANG T.-V., LE ROHELLEC J., BRETTEL H., 2011, Domain of metamers exciting melanopsin. *21st Symposium of the International Colour Vision Society*, Kongsberg, Norway, 1-5 July 2011, p. 84.

VIÉNOT F., BAILACQ S., ZOUAOUI L., LE ROHELLEC J., 2011, Variation of the pupillary reflex with the spectral power distribution of the light. Proceedings of the 27th session of the CIE, *CIE197:2011*, 940-944.

FALKENSTERN K., BONNIER N., BRETTEL H., PEDERSEN M., VIÉNOT F., 2011, Using Metrics to Assess the ICC Perceptual Rendering Intent, *Proc. SPIE*, Volume 7867 -- *Image Quality and System Performance VIII*, Burlingame, California, 2011.

ROUCHON V., ZERDOUN M., ESTÈVE J.-L., VIÉNOT F., LAVÉDRINE B., BARTHEZ J., 2010, Tonalité rouge des papiers anciens observés en lumière transmise : de l'observation à l'interprétation. In : Monique Zerdoun et Caroline Bourlet, actes du colloque "Matériaux du livre médiéval", collection Bibliologia de Brepols 30 :56-70. Turnhout, Belgique, Brepols, 55-70.

LABORIE B., LANGLOIS S., VIÉNOT F., 2010, Short-term colour discrimination: appearance and cognitive approach. *AVA CHRISTMAS MEETING 2010*, December17-18, 2010, Paris, France. *Perception*, 2011, volume 40, page 112, P2.

VIÉNOT F., LE ROHELLEC J., ZOUAOUI L., 2010, Case reports of the effect of the spectral power distribution of metamer lights on pupil aperture, *AVA CHRISTMAS MEETING 2010*, December17-18, 2010, Paris, France. *Perception*, 2011, volume 40, page 104, T1.

FALKENSTERN K., BONNIER N., BRETTEL H., PEDERSEN M., VIÉNOT F., 2010, Using Image Quality Metrics to Evaluate an ICC Printer Profile, *18th Color and Imaging Conference*, November 8 – 12, 2010, San Antonio, Texas, The Society for Imaging Science and Technology, 244-249.

LABORIE B., LANGLOIS S., VIÉNOT F., 2010, A PDP as a colorimetric tool to investigate colour vision. *15th International Workshop on Inorganic and Organic Electroluminescence & 2010 Int. Conference on the Science and Technology of Emissive Displays and Lighting & XVIII Advanced Display, Technologies* International Symposium, September 27-October 1, 2010, St. Petersburg, Russia, pp.300-301.

ATTIA D., BARLIER-SALSI A., BEHAR-COHEN F., CÉSARINI J. P., ENOUF O., GARCIA M., MARTINSONS C., MERCKEL O., PICAUD S., VIÉNOT F., ZISSIS G., 2010, Potential health impacts of LED lighting. *LS12-WhiteLED3, White LEDs and solid state lighting 3rd international conference*, July 11-16, Eindhoven, The Netherlands.

VIÉNOT F., DURAND M.-L., MAHLER E., 2009, The effect of LED lighting on performance, appearance and sensations, *Proceedings of the CIE Light and Lighting Conference,* Budapest, 27-29 May 2009. *CIE x034:2010*: 161:166.

LABORIE B., VIÉNOT F., LANGLOIS S., 2009, Construction d'un illustrateur de différence de couleur. In : ROBERT-IGNACIO F., *Cours et application industrielles de l'imagerie numérique couleur*, Toulon, France, Editions Fred Valou, 2009, p. 194-196. ISBN: 978-2-9532792-0-7. *Ecole d'Hiver sur l'Image Numérique Couleur*, Toulon, 13-16 janvier 2009, Prix du meilleur poster jeune chercheur,

VIÉNOT F., JUSTIN T., NETTER E., MILLEVILLE S., ECHARD J.-P., LAVÉDRINE B., An optical study of natural materials used in museum collections: wood and straw. *Materials & Sensations 2008*, Pau, Oct. 22–24, e-proceedings : p.117-120.

ECHARD, J.-P., VIÉNOT, F., BAK, A., EZRATI, J.-J., 2008, Apparence finale d'un érable ondé verni : rugosité des interfaces, in *De la peinture de chevalet à l'instrument de musique: vernis, liants et couleurs, actes du colloque, 6-7 Mars 2007. Paris Cité de la musique*, pp. 129-132.

VIÉNOT F, MAHLER E., EZRATI J.-J., BOUST C., BRICOUNE A., Color appearance under LED illumination: The visual judgment of observers. *First International Conference on White LEDs and Solid State Lighting*, Tokyo, Japan, 29 nov 2007. (**Conférence invitée**)

VIÉNOT F, LED lighting for museums, toward the highest quality of light. 3a Conferenza Nazionale del Gruppo del Colore. Torino, Italie, 25 oct 2007. (**Conférence invitée)**

VIÉNOT F, EZRATI JJ, BOUST C, MAHLER E, Grading LED illumination : from colour rendering indices to specific light quality indices. *CIE 26th session*, Beijing 2007, D1:22-25.

OBEIN G., VIÉNOT F., 2007, Modelling the BRDF of a series of matt to glossy black samples. *Proceedings of the CIE Expert Symposium on Visual Appearance, CIE publication x032:2007*, pp.67-74 (2007)

VIÉNOT F., BAK A., ECHARD J.-P., 2007, The peculiar BRDFs of flamed maple. *Proceedings of the CIE Expert Symposium on Visual Appearance, CIE publication x032:2007*, pp.230-234 (2007).

PLANTIER J., AUBRY J.P., VIÉNOT F., OSSARD G., ROUMES C., 2007, Chromatic Contrast Sensitivity Functions, *Perception*, Vol. 36, Suppl., 198.

HARRAR M., BRETTEL H., VIÉNOT, F., 2006, About the limited additive properties of colour appearance models. *Perception*, Vol. 35, Suppl., 191.

PLANTIER, J., AUBRY, J., VIÉNOT, F., OSSARD, G., & ROUMES, C., 2006, Luminance equilibrium of chromatic pairs at different eccentricities [Abstract]. *Journal of Vision*, *6*(6), 702a, http://journalofvision.org/6/6/702/, doi:10.1167/6.6.702.

VIÉNOT F., 2006, Origins and history of the Standard Observers, *CIE Expert Symposium on 75 Years of the CIE Standard Colorimetric Observer*, Ottawa, Canada, 16 May 2006, CIE x030:2006, 7p.. (**Conférence invitée)**

LAVÉDRINE B., GILLET M., VIÉNOT F., GARNIER C., MAHLER E., 2006, Évaluation de la photosensibilité et étude d'un dispositif d'éclairage à diodes électroluminescentes de photographies anciennes en couleurs. *Couleur et temps, La couleur en conservation et restauration*, Actes des 12es journées d'études de la Section française de l'institut international de conservation, 21-24 juin 2006, *SFIIC*, Champs sur Marne, pages 272-279. ISBN 2-905430-16-8.

BEN CHOUIKHA M., PLACAIS B., POULEAU G., SAUTOT S., VIÉNOT F., 2006, Benefits and Drawbacks of two Methods for Characterizing Digital Cameras, *CGIV 2006 Proceedings*, Society for Imaging science and Technology, 185-188.

VIÉNOT F., 2006, Introduction à la couleur : de l'expérience visuelle à la mesure. *Couleur et temps, La couleur en conservation et restauration*, Actes des 12es journées d'études de la Section française de l'institut international de conservation, 21-24 juin 2006, SFIIC, Champs sur Marne, pages 13-21. ISBN 2-905430-16-8. (**Conférence invitée)**

EZRATI J.-J., PÉRIGNON P., BRICOUNE A., SERREAULT L., HARRAR M., VIÉNOT F., MAHLER E., 2005, Light-emitting diodes: a future for museum lighting? *ICOM 14th Triennial Meeting 2005*, Vol. II, 26th September 2005.

VIÉNOT F., SERREAULT L., 2005, Is it possible to derive the maximum wavelength of M and L photo pigments using multiple-Rayleigh matches? *XVIIIth Symposium of the International Colour Vision Society*, Lyon, 8-12 July 2005, p. 22.

MAHLER E., EZRATI J.-J., VIÉNOT F., 2005, Designing a colour discrimination test to assess colour rendering of LED sources. *XVIIIth Symposium of the International Colour Vision Society*, Lyon, 8-12 July 2005, p. 53.

HARRAR M., BAILLET G., BOURDONCLE B., BRETTEL H., O'REGAN K., VIÉNOT F., 2005, Comparison of colour appearance changes assessed by observers versus predicted by CIECAM02, in *Proceedings of 10th Congress of the International Colour Association*, Granada (Granada, 8-13 May 2005), pp. 643-646.

VIÉNOT F., MAHLER E., SERREAULT L., HARRAR M., EZRATI J-J., PÉRIGNON P., BRICOUNE A., 2005, Discriminating colours under LED illumination, in *Proceedings of 10th Congress of the International Colour Association*, Granada (Granada, 2005), pp. 33-36.

BOUST C., CITTADINI F., BEN CHOUIKHA M., BRETTEL H., VIÉNOT F., BERCHE S., ALQUIÉ G., 2004, Does an expert use memory colors to adjust images? , *12th Color Imaging Conference IS&T*, Scottsdale, AZ, Nov. 9, 2004; p. 347-353.

VIÉNOT F., OBEIN G., 2004, Is Gloss recognized as a surface property? Proceedings of *MS 2004, 1st International Workshop on Materials and Sensations*, Pau, France, 27th to 29th October 2004, pages 77-82.

HARRAR, M., VIÉNOT F., 2004, What is controlling chromatic contrast in a complex scene? Proceedings of *CGIV 2004 - Second European Conference on Color in Graphics, Imaging and Vision*, Aachen, Germany, Volume 2, ISBN / ISSN: 0-89208-250-X, pp. 51-54.

OBEIN G., LEROUX T., KNOBLAUCH K., VIÉNOT F., 2003, Visually relevant gloss parameters. *Proceedings of 11th international Metrology congress*, Toulon, 20-23 octobre 2003, 6p.

DUMONT E., BRÉMOND R., BOUST C., DA COSTA E., VIÉNOT F., Assessment of the visual quality of tone-mapped images for visibility experiments. *CIE 152 :2003, Proc. of the 25th session of the CIE, San Diego 25 June - 2 July 2003* : D4-82-85.

BOUST C., CHAHINE H., VIÉNOT F., BRETTEL H., BEN CHOUIKHA M., ALQUIÉ G., 2003, Color correction judgements of digital images by experts and naive observers. *PICS 2003*: The PICS Conference, An International Technical Conference on The Science and Systems of Digital Photography, including the Fifth International Symposium on Multispectral Color Science, Rochester, NY; May 13, 2003; p. 4-9; ISBN / ISSN: 0-89208-245-3.

LE ROHELLEC J., BRETTEL H., VIÉNOT F., 2003, Contribution of achromatic and chromatic contrast signals to Fechner-Benham subjective colours. In : J.D. Mollon (ed.), *Normal and defective colour vision*. Oxford University Press, 2003, Proc. *International Colour Vision Society* Symposium, Cambridge, U.K. : 143-151.

VIÉNOT F., DAVID L., 2003, An algorithm to assess the detectability of spatio-temporal patterns at any illumination. Proceedings of the CIE Symposium'02 *Temporal and Spatial Aspects of Light and Colour Perception and Measurement*, 22-23 August 2002, Veszprém, Hungary, CIE x025:2003 : 73-80.

VIÉNOT F., 2002, Mesopic vision. In : *VISION (Vehicle and Infrastructure Safety Improvement in Adverse Conditions and Night Driving), Société des Ingénieurs de l'Automobile (ed.)*, Rouen, 24-25 septembre 2002, CD-ROM Proceedings : 8 p. (**Conférence invitée).**

VIÉNOT F., BOUST C., DA COSTA E., BRÉMOND R., DUMONT E., 2002, Évaluation psychométrique de la fidélité visuelle des images numériques / Psychometric assessment of the look and feel of digital images, In : *DSC 2002*, *Driving Simulation Conference, INRETS-RENAULT (ed.)* : 301-311.

VIÉNOT F., BOUST C., BRÉMOND R., DUMONT E., 2002, Rating tone-mapping algorithms for gradations. CGIV 2002 : In : *The First European Conference on Color in Graphics, Imaging and Vision* (CGIV), Poitiers, France, April 2002, IS&T, Springfield, USA, Volume 1 : p. 221-225.

VIÉNOT F., 2002, Report on a fundamental chromaticity diagram with physiologically significant axes, in *9th Congress of the International Colour Association,* Proceedings of SPIE Vol. 4421, 565-570 (**Conférence invitée).**

VIÉNOT F., BENHALIMA F., BRETTEL H., BOURDONCLE B., COLONNA DE LEGA A., 2002, Rating of tinted ophthalmic lenses, in *9th Congress of the International Colour Association*, Proceedings of SPIE Vol. 4421, 271-274.

VIÉNOT F., MONOT A., OBEIN G., 2001, Sensation visuelle : effets de moirés, de brillant, de lustre et de transparence. *Colloque " Jouer la lumière : le textile, la lumière et l'œil ",* Musée de la Mode et du Textile / Union centrale des arts décoratifs, 12 et 13 novembre 2001, Paris, 12 pages.

VIÉNOT F., BRETTEL H., 2001, Color display for dichromats. In: *Color imaging: Device-independent color, Color hardcopy, and Graphic arts VI,* R. Eschbach and G. G. Marcu, Eds., Proceedings of SPIE, Vol. 4300, 199-207.

OBEIN G., LEROUX T., VIÉNOT F., 2001, Bi-directional reflectance distribution factor and gloss scales. *Human vision and electronic imaging VI,* Bernice E. Rogowitz, Thrasyvoulos N. Papps, Editors, Proceedings of SPIE Vol. 4299 : 279-290.

OBEIN G., LEROUX T., VIÉNOT F., 2000, Variability of the 3d repartition of haze with the incident beam geometry. First international Conference on *Color Graphics and Image Processing*, October 1-4, 2000, Saint-Etienne, France. Pages 296-299.

OBEIN G., DOMONT S., BRETTEL H., VIÉNOT F., 2000, Contrast appearance under mesopic adaptation. A comparison between a simulation and the reality. *NPL Colour and Visual Scales 2000*, 3-5 April 2000, Egham, GB, 4 pages.

BEN CHOUIKHA M., VIÉNOT F. 1999, Colorimetric characterization of a color dedector implemented in a BiCMOS technology. *IS&T/SPIE's International Technical Group Newsletter, Vol.9, n°2, p.1&9.*

VIÉNOT F., BRETTEL H., DOMONT S., BORDENAVE E., 1999, Predictive simulation of mesopic vision. *CIE Publ.133, CIE 24rd session*, Warsaw, pp.107-111.

BÈCLE P., VIÉNOT F., MONOT A., EYQUEM D., 1998, Gradient and shape detection from texture. *1998 OSA Annual Meeting / ILS-XIV*, Baltimore, U.S.A., October 4-9, 1998, p.92.

BEN CHOUIKHA M., VIÉNOT F., LU G.N.: Temperature Effects on Colorimetric Accuracy of the BTJ Color Detector. In: *Advanced Focal Plane Arrays and Electronic Cameras II,* SPIE international sumposium on Electronic Image Capture and Publishing. Zurich 18-20 may 98. Vol: 3410. pp.204-214.

BEN CHOUIKHA M., VIÉNOT F., LU G.N., 1998, Characterization of a color sensitive photodedector implemented in a BiCMOS technology. in *Color and Document Imaging Conference, IS&T/SPIE's 10th Annual symposium: Electronic Imaging 98,* janvier 1998. Vol. 3300, pp 198-206.

BEN CHOUIKHA M., LU G.N., ALQUIÉ G., VIÉNOT F., 1997, Caractérisation d'un capteur de couleur réalisé par une technologie de circuits intégrés. In *VISU 97*, 10èmes Journées d'Etudes, Club VISU / SID-France, 3-4 avril 1997, Poitiers, France, pp.73-77.

BRUSQUE C., GANDON A., CARTA V., VIÉNOT F., 1997, Etalonnage d'une chaîne de production de diapositives par imageur numérique. In *VISU 97*, 10èmes Journées d'Etudes, Club VISU / SID-France, 3-4 avril 1997, Poitiers, France, pp.61-64.

VIÉNOT F., BRETTEL H., 1997, Palettes de couleur infographiques pour daltoniens. In *VISU 97*, 10èmes Journées d'Etudes, Club VISU / SID-France, 3-4 avril 1997, Poitiers, France, pp.65-68).

VIÉNOT F., PEFFERKORN S., CHIRON A., 1997, Photometry in the mesopic domain. *CIE x012-1997, Proc. of the NPL -CIE-UK Conference, Visual scales; photometric and colorimetric aspects*, 24-26 March 1997, Teddington, UK, pp. 52-55.

LE ROHELLEC J., VIÉNOT F., 1997, Distant colour induction on Fechner-Benham top. In: C.R.Cavonius (ed.), *Colour Vision Deficiencies XIII,* pp.459-464.

PEFFERKORN S., CHIRON A., VIÉNOT F., 1997, Effect of longitudinal chromatic aberration on photometric matches using an heterochromatic square-wave grating. In: C.R.Cavonius (ed.), *Colour Vision Deficiencies XIII,* pp.403-407.

VIÉNOT F., BEN M'BAREK A., OTT L., 1997, Screening colour vision with an LMS calibrated display. In: C.R.Cavonius (ed.), *Colour Vision Deficiencies XIII,* pp.339-349.

VIÉNOT F., 1996, Traitement de l'information chromatique dans les réseaux rétiniens. *Huitièmes Journées Neusosciences et Sciences de l'Ingénieur NSI 96*, Marly-le-Roi, 6-8 mai 1996, pp.153-160. (**Conférence invitée**)

VIÉNOT F., 1996, Fundamental chromaticity diagram with physiologically significant axes, report of the activity of CIE TC 1-36, *CIE x010-1996, Proc. of the CIE expert symposium '96 Colour standards for image technology*, 25-27 March 1996, Vienna, Austria, pp. 35-40. (**Conférence invitée**)

PEFFERKORN S., CHIRON A., VIÉNOT F.,1995, Mesopic photometry based on heterochromatic spatial contrast sensitivity measurements. *CIE 119-1995-23rd session*, New Dehli, pp.73-74.

VIÉNOT F., CHIRON A., PEFFERKORN S., 1995, Multiple approaches in heterochromatic photometry. Consequences for mesopic photometry. *CIE x009 - 1995, Proc. of the CIE Symposium on Advances in Photometry*, 1-3 December 1994, Vienna, Austria, pp.40-49. (**Conférence invitée**)

VIÉNOT F., CHIRON A., 1995, Rod and cone signal processing in mesopic heterochromatic photometry. In: B. DRUM (ed.), *Colour Vision Deficiencies XII,* Kluwer Academic Publishers, The Netherlands, pp.325-332.

LE ROHELLEC J. & VIÉNOT F., 1995, Contribution of two colour-opponent mechanisms to Fechner-Benham subjective colours. In: B. DRUM (ed), *Colour Vision Deficiencies XII*, Kluwer Academic Publishers, The Netherlands, pp. 251-258.

VIÉNOT F., OTT L., BEN M'BAREK A., 1994, LMS based colour vision test on CRT. *JERMOV, Montpellier,* p.216.

VIÉNOT F., 1994, Heterochromatic photometry. Visual capacities in the mesopic range. *IV Reunion Nacional de Optica*, Granada (Esp.), 15 Septiembre 1994, pp.XLV-L. (**Conférence invitée**)

VIÉNOT F., 1993, Fundamental chromaticity diagram with physiologically significant axes: report of the activities of CIE committee TC 1-36. *OSA Annual Meeting Technical Digest*, p.83.. (**Conférence invitée** au congrès annuel de l'Optical Society of America, Toronto, Canada, October 3-8, 1993)

PEFFERKORN S., VIÉNOT F., CHIRON A. & BRETTEL H., 1993, Problem of spectroradiometric calibration of polarized displays. In: *EURODISPLAYS '93*, proceedings of the 13th International Display Research Conference, Le Club Visu, SID - France, pp. 443-446.

VIÉNOT F. & FONTVIEILLE C., 1993, Evaluation of the "Différenciateur de Tonalité": an apparatus for measuring wavelength discrimination. In: DRUM B. and MORELAND J.D. (Eds), *Colour Vision Deficiencies XI*, Kluwer Academic Publishers, The Netherlands, pp.365-372.

BRETTEL H., CHIRON A., VIÉNOT F., GLASSER J., 1992, Etude du papillotement des écrans à cristaux liquides. In *VISU 92*, 8emes Journées d'Etudes organisées par le Club VISU / SID-France, 27-28 octobre 1992, Angers, France, pp.69-70.

VIÉNOT F., 1991, Poster session on Brightness and colour, chaired by Françoise Viénot, *CIE proceedings, 22nd session*, Vol.2, pp.105-106, Melbourne, 5 juillet 1991. (**Conférence invitée**)

VIÉNOT F. & CHIRON A., 1991, Comparison of heterochromatic flicker photometry and direct comparison brightness matching data over the spectrum. *CIE proceedings, 22nd session*, Melbourne, Vol.1, Part 1, Division 1, pp.41-42.

VIÉNOT F., CHIRON A., 1991, Mesopic luminous matches of protanopic and deuteranopic observers. In: DRUM B., MORELAND J.D. and SERRA A. (Eds), *Colour Vision Deficiencies X*, Kluwer Academic Publishers, Dordrecht, The Netherlands, pp.413-419.

VIÉNOT F., BRETTEL H., 1991, Vers une colorimétrie Physiologique. In: *VISU91*, 8emes Journées d'Etudes organisées par la SEE (Club VISU) 29-30 mai 91, Perros-Guirec, France, pp.54-55.

BRETTEL H., VIÉNOT F., MORELAND J.D., 1988, Adaptation de la méthode de photométrie par mouvement aux écrans de visualisation. In: *VISU 88,* 5èmes Journées Nationales d'Etudes organisées par le Club Visu, Gif-sur-Yvette, France, pp.53-54.

VIÉNOT F., BOUHARD F., SCHOEFFTER M., 1987, "Le différenciateur de tonalité": an apparatus for measuring wavelength discrimination. In: VERRIEST G. (ed), *Colour Vision Deficiencies VIII,* proc. of the 8th international IRGCVD symposium, Junk, the Hague, pp.253-258.

VIÉNOT F., BOUHARD F., SCHOEFFTER M., 1985, An equipment to measure wavelength discrimination. In: *Mondial Couleur 85*, actes du 5eme congrès de l'Association Internationale de la Couleur, réalisation Centre Français de la Couleur, Paris, France, p.62.

VIÉNOT F., 1985, Cone interrelations in color-matches. In: *Mondial Couleur 85*, actes du 5eme congrès de l'Association Internationale de la Couleur, réalisation Centre Français de la Couleur, Paris, France, pp.33-1,33-6.

BOURDY C., VIÉNOT F., MONOT A., CHIRON A., 1984, Spatial contrast detection for colour patterns under selective chromatic adaptation. In: GIPSON C.P. (ed), Proc. of a workshop on "*Colour coded vs monochrome electronic displays*", NATO, Farnsborough, G.B., pp.28.1-28.15.

VIÉNOT F., 1984, Color matches on large fields, changes with retinal area stimulated or with duration of presentation. in: VERRIEST G. (ed), *Colour Vision Deficiencies VII, Documenta Ophthalmologica Proc. Ser.*, Junk, The Hague, pp.121-125.

VIÉNOT F., 1981, Color match changes between the fovea end perifovea. In: *COLOR 81*, proc. of the 4th congress of the International Colour Association, Deutsche farbwissen schaftliche Gesellschaft e.V., Berlin, Deutschland, pp.B21-B23.

VIÉNOT F., 1978, Statistical study of the color-matching functions. In: *COLOR 77*, proc. 3rd congress of the International Color Association AIC, Adam Hilger, Bristol, pp.273-276.

Proceedings

Oral Papers

How Multi-Illuminant Scenes Affect Automatic Colour Balancing

Liwen XU, Brian FUNT
School of Computing Science, Simon Fraser University

ABSTRACT

Many illumination-estimation methods are based on the assumption that the imaged scene is lit by a single source of illumination; however, this assumption is often violated in practice. We investigate the effect this has on a suite of illumination-estimation methods by manually sorting the Gehler et al. ColorChecker set of 568 images into the 310 of them that are approximately single-illuminant and the 258 that are clearly multiple-illuminant and comparing the performance of the various methods on the two sets. The Grayworld, Spatio-Spectral-Statistics and Thin-Plate-Spline methods are relatively unaffected, but the other methods are all affected to varying degrees.

Keywords

Colour balancing, illumination estimation, digital photography.

INTRODUCTION

The usual first step in automatic colour balancing of digital imagery is to estimate the chromaticity of the illumination. Although there are some recent exceptions (Beigpour 2014; Gijsenij 2012; Joze 2013), most illumination-estimation methods assume that the relative spectral power distribution of the illumination is constant throughout the scene. However, many scenes contain multiple illuminants with differing SPDs, and we investigate the effect this has on automatic colour balancing.

Somewhat surprisingly, the Gehler et al. (Gehler 2008) "Colorchecker" data set of 568 images, which is widely used in evaluating competing illumination-estimation methods, contains many images of multiple-illuminant scenes. For example, Figure 1 depicts an indoor scene that also includes a window through which daylight is clearly falling on the counter. Is the scene illuminant the light from inside the room or outside the window? Figure 2 shows an outdoor scene with at least three illuminant types: the cloudy sky, the shadowed areas, and the traffic light.

Each image in the Colorchecker dataset contains an Xrite/Macbeth ColorChecker, which is used to provide a ground-truth measure of the illumination's 'colour'. However, since many of the scenes do contain multiple illuminants, a single such measurement cannot possibly represent the colour of all the illuminants correctly, but rather must represent some sort of compromise. Whether the illumination-estimation method assumes there is a single illuminant or multiple illuminants, a single colorchecker cannot correctly represent the ground-truth illumination in a multi-illuminant scene. In this paper, we investigate how much of an effect this has on a representative set of illumination-estimation methods; namely, MaxRGB (Funt 2012), Grayworld (Weijer 2007), Shades-of-Gray (Finlayson 2004), Edge-based (Weijer 2007), N-jet (Gijsenij 2010) , Thin-Plate-Spline (Shi 2011) and Spatio-Spectral Statistics (Chakrabarti 2012).

SCENE CLASSIFICATION

The Gehler et al. dataset (Gehler 2008) contains 568 images taken with two digital single lens reflex cameras, a Canon 5D and a Canon 1D. All images were saved in Canon RAW format. Each image contains an Xrite/Macbeth ColorChecker for reference. The image coordinates (measured by hand) of each Colorchecker square are provided with the dataset. In the tests below, we used the Shi et al. (Shi 2011) reprocessed version of the Gehler et al. data. The original dataset consists of non-linear TIFF images that were automatically generated from the RAW data. The reprocessed dataset contains PNG images that are linear and do not include any automatic white balancing or de-mosaicing.

We manually sorted the original 568 images into two groups according to whether the images were of single-illuminant or multiple-illuminant scenes. Sorting in this way is difficult because it can be hard to discern the nature of the scene illumination from the image. Figure 1 shows a typical case where the presence of multiple sources of illumination is very clear. Similarly, the traffic light in Figure 2 is an obvious additional illuminant. Figure 3 shows a situation in which it seems pretty clear that there is only a single illuminant. Figure 4 shows a somewhat ambiguous case, since there are areas in direct sun and others in shadow. The Colorchecker itself appears to be partly in sun and partly in shadow. There are also the clouds in the distance. However, this appears to be a typical outdoor scene basically dominated by sunlight/skylight and so we classified it as a single-illuminant scene. If we were to be any more strict in our interpretation of what constitutes a single-illuminant scene then almost the entire dataset would be classified as multiple-illuminant. Based on this type of analysis of each image, the 568 dataset is divided into 310 single-illuminant and 258 multiple-illuminant scenes. We denote the two images subsets as S (single) and M (multiple), and the full set of 568 images as F. The complete lists of image numbers for sets S and M are listed in the Appendix.

Figure 1 Example of a multiple-illuminant scene with light coming both from the room and window.

Figure 2 Example of a multiple-illuminant scene containing a visible light source.

Figure 3 Example of a clearly single-illuminant scene.

Figure 4 Example of a somewhat ambiguous scene with sunlight and shadow but classified as single-illuminant nonetheless.

COMPARATIVE PERFORMANCE ON SINGLE-VERSUS MULTIPLE-ILLUMIANT SCENES

We evaluate the illumination-estimation performance of all the methods separately on subset S, subset M, and the complete set F. The illumination-estimation methods are MaxRGB (Funt 2012), Gray-World (Weijer 2007), Shades of Gray (Finlayson 2004), Edge Based (Weijer 2007), N-jet (Gijsenij 2010), TPS (Shi 2011) and Spatio-Spectral Statistics (Chakrabarti 2012). The image pixels occupied by the Colorchecker in each image areas are replaced with zeros for the tests. These methods all estimate the rg-chromaticity of the illumination. The error in a given estimate is measured relative to the measured ground-truth illumination chromaticity. The error is evaluated in terms of the angular difference in degrees between the two chromaticities after each chromaticity is converted to a 3-vector as (r, g, 1-r-g). The overall accuracy across a given test set of images is reported in terms of the mean, median, RMS and maximum errors.

Table 1: Comparative illumination-estimation performance evaluated in terms of angular error. MaxP (MaxRGB w/o preprocessing), MaxM (MaxRGB after median filtering, GW (Grayworld), EB (Edge-Based, first and second order), 1-jet (Gamut mapping), 2-jet (Gamut mapping), SSS-ML (Spatio-Spectral Statistics with maximum likelihood, SSS-GP (Spatio-Spectral Statistics with general prior). Md (Median), Mn (Mean).

	Set S				Set M				Complete Dataset			
	Md	Mn	RMS	Max	Md	Mn	RMS	Max	Md	Mn	RMS	Max
MaxP	4.6	7.3	9.9	27	16	14	16	50	9.1	10	13	50
MaxM	3.1	5.3	7.8	26	8.8	10	13	42	4.7	7.7	11	42
GW	4.0	5.5	7.3	25	3.3	3.8	4.7	15	3.6	4.8	6.2	25
SoG (norm=6)	2.9	4.8	6.8	23	7.4	8.4	10	36	4.5	6.4	8.7	36
EB1 (norm=6)	2.6	4.6	6.8	26	7.2	9.0	12	38	3.8	6.6	9.4	38
EB1 (norm=1)	3.8	4.7	5.6	17	3.4	4.1	4.9	16	3.6	4.4	5.3	17
EB2	2.7	5.0	7.2	28	8.9	9.9	13	47	4.4	7.2	10	47
1-jet 3-fold	2.8	4.4	6.2	24	6.0	7.7	9.9	32	4.1	5.9	8.1	32
2-jet 3-fold	2.9	4.3	6.1	21	5.9	7.7	9.8	32	4.2	5.9	8.0	32
TPS 3-fold	2.6	3.5	4.5	17	3.0	3.6	4.5	15	2.7	3.5	4.5	17
SSS-ML	2.9	3.7	4.8	22	3.1	3.7	4.5	15	3.0	3.7	4.7	22
SSS-GP	2.9	3.6	4.7	22	3.0	3.6	4.4	15	3.0	3.6	4.6	22

The MaxRGB tests include MaxRGB without preprocessing and MaxRGB with median filtering MaxM (Funt 2012). The N-jet algorithms are tested using threefold cross-validation. Because the images are from two different cameras and the training is specific to each camera, we train and test on the images from each camera separately and then combine the results. TPS is also evaluated using threefold cross-validation.

DISCUSSION

The results in Table 1 show that the effect of multiple scene illuminants on illumination-estimation performance varies substantially across the various methods. MaxRGB is strongly influenced by the presence of multiple illuminants. Whether MaxRGB includes image preprocessing or not, the presence of multiple illuminants seriously influences the results. As Table 1 shows, the error is approximately tripled. For example, the median error for the MaxRGB variant MaxM rises from 3.1 to 8.8 degrees for the change from subset S to subset M. In other words, MaxRGB works very well when the single-illuminant assumption holds, but fails when it is violated. Since MaxRGB is based on estimating the maximum value in each of the R, G, B channels, it is particularly vulnerable to the presence of light sources such as the traffic light in Figure 2.

Interestingly, Grayworld's performance appears to be unaffected by the presence of multiple illuminants since the median angular error on sets S, M and F is 4.0, 3.3, and 3.6, respectively. Although its overall performance is poorer than several of the other methods, it has the advantage of being stable. The Shades of Gray approach is controlled by the choice of the Minkowski norm to vary between the extremes of Grayworld and MaxRGB. A norm of 6 has been reported to work well (Finlayson 2004). As a compromise between Grayworld and MaxRGB, however, its performance is then affected by the presence of multiple illuminants, with a median angular error of 2.9, 7.4 and 4.5, on sets S, M and F, respectively.

Just as Shades of Gray is more sensitive to the presence of multiple illuminants than Grayworld, the Edge-Based method using norm = 6 is more sensitive than the Edge-Based method using norm = 1. For the norm = 1 case, Edge-Based is simply averaging derivatives within each RGB channel instead of the RGB values themselves. With norm = 6, the Edge-Based method weights the large derivatives, which are likely to arise from illumination boundaries in multiple-illuminant scenes, more heavily thus leading to a concomitant increase in angular error. The performance of the 1-jet and 2-jet Gamut Mapping methods also degrades when the single-illuminant assumption is violated. For 1-jet, the median angular on S of 2.8 degrees increases to 6.0 degrees for M. Gamut mapping assumes that the gamut of RGBs and the gamuts of their derivatives are limited by the illuminant. In the presence of multiple illuminants these image gamuts expand such that the constraint used to estimate the illuminant is no longer as strong or accurate.

The learning-based methods appear to account for the presence of multiple illuminants quite well. The performance of the Spatio-Spectral Statistics methods tends to be very good and quite unaffected by multiple illuminants. With median angular errors of 2.6 (set S), 3.0 (set M) and 2.7 (set F), the Thin-Plate Spline method (TPS) is both the least affected by multiple illuminants and also attains the minimum error of all the methods on each of the three datasets.

ACKNOWLEDGMENT

Funding was provided by the Natural Sciences and Engineering Research Council of Canada

REFERENCES

Beigpour, S., C. Riess, J. van d Weijer, and E. Angelopoulou. 2014. Multi-illuminant estimation with conditional random fields. *IEEE Trans. on Image Processing* 23(1): 83-96.

Chakrabarti, A. K. Hirakawa, and T. Zickler. 2012. Color constancy with spatio-spectral statistics. *IEEE Transactions on Pattern Analysis and Machine Intelligence* 34(8): 1509-1519. Accompanying computer implementation downloaded from http://vision.seas.harvard.edu/colorconstancy/. Accessed February 23, 2015.

Finlayson, G. and E. Trezzi. 2004. Shades of gray and colour constancy. *In Proc. IS&T/SID 12th Color Imaging Conf.* Springfield, VA, 37-41.

Funt, B., and L. Shi. 2012. MaxRGB reconsidered. *Journal of Imaging Science and Technology* 56(2): 020501-1-020501-10.

Gehler, P., C. Rother, A. Blake, T. Minka, and T. Sharp. 2008. Bayesian color constancy revisited. In *Proc. IEEE Computer Society Conf. on Computer Vision and Patern Recognition.* Anchorage, Alaska, 1-8.

Gijsenij, A., T. Gevers, and J. van deWeijer. 2010. Generalized gamut mapping using image derivative structures for color constancy. *Int. J. Computer Vision.* 86, 127-139. Accompanying computer implementation downloaded from http://colorconstancy.com/. Accessed February 27, 2015.

Gijsenij, A., R. Lu, and T. Gevers. 2012. Color constancy for multiple light sources. *IEEE Trans. on Image Processing* 21(2): 697-707.

Joze, H.R.V. and Mark S. Drew. 2013. Exemplar-based colour constancy and multiple illumination. *IEEE Trans. on Pattern Analysis and Machine Intelligence* 36(5): 860-873.

Shi, L., W. Xiong, and B. Funt. 2011. Illumination estimation via thin-plate spline interpolation. *J. Opt. Soc. Am. A 28(5*): 940-948. Accompanying computer implementation downloaded from http://www.cs.sfu.ca/~colour/code/. Accessed February 25, 2015.

Shi, L. and B. Funt. Re-processed version of the Gehler color constancy dataset of 568 images. Downloaded from http://www.cs.sfu.ca/~colour/data/shi_gehler/. Accessed Sept. 2014.

Weijer, J. van de, T. Gevers, and A. Gijsenij. 2007. Edge-based color constancy. *IEEE Trans. Image Processing.* 16(9): 2207-2214.
Accompanying computer implementation downloaded from http://lear.inrialpes.fr/people/vandeweijer/software. Accessed February 25, 2015.

APPENDIX

Image numbers of single-illuminant scenes: 1 2 3 4 7 10 11 12 14 17 18 19 21 23 27 32 33 34 35 36 37 38 39 40 41 44 45 46 47 48 49 50 52 54 56 57 58 59 63 64 65 66 67 68 69 70 71 76 77 78 79 80 81 82 83 84 85 86 87 88 89 90 91 92 93 94 95 96 99 100 101 102 103 104 105 106 107 108 109 110 111 112 113 114 115 116 117 118 119 121 122 126 127 128 129 130 131 132 134 135 136 137 139 140 141 142 143 144 147 149 150 151 152 153 154 155 156 157 158 159 160 161 162 163 164 165 166 168 169 170 171 172 173 174 176 177 178 179 180 185 186 187 188 189 191 193 196 197 199 200 203 204 206 212 219 224 225 226 227 228 229 230 232 233 234 235 248 249 250 251 253 254 255 256 257 258 259 260 261 262 264 265 266 267 268 269 270 271 273 274 275 281 282 283 285 286 287 288 289 291 292 293 295 298 299 300 301 302 303 304 305 306 307 308 309 310 342 343 344 353 355 358 359 362 364 365 367 372 377 381 384 386 394 395 396 398 401 402 407 410 411 414 416 417 418 419 420 422 423 424 425 427 428 429 430 431 432 433 434 436 437 439 441 444 449 451 453 454 455 456 458 459 461 462 463 466 473 474 475 478 479 480 482 484 487 489 490 491 493 494 496 500 502 503 504 516 522 528 530 536 537 538 541 543 546 549 560 561 562 564

Image numbers of multiple-illuminant scenes: 5 6 8 9 13 15 16 20 22 24 25 26 28 29 30 31 42 43 51 53 55 60 61 62 72 73 74 75 97 98 120 123 124 125 133 138 145 146 148 167 175 181 182 183 184 190 192 194 195 198 201 202 205 207 208 209 210 211 213 214 215 216 217 218 220 221 222 223 231 236 237 238 239 240 241 242 243 244 245 246 247 252 263 272 276 277 278 279 280 284 290 294 296 297 311 312 313 314 315 316 317 318 319 320 321 322 323 324 325 326 327 328 329 330 331 332 333 334 335 336 337 338 339 340 341 345 346 347 348 349 350 351 352 354 356 357 360 361 363 366 368 369 370 371 373 374 375 376 378 379 380 382 383 385 387 388 389 390 391 392 393 397 399 400 403 404 405 406 408 409 412 413 415 421 426 435 438 440 442 443 445 446 447 448 450 452 457 460 464 465 467 468 469 470 471 472 476 477 481 483 485 486 488 492 495 497 498 499 501 505 506 507 508 509 510 511 512 513 514 515 517 518 519 520 521 523 524 525 526 527 529 531 532 533 534 535 539 540 542 544 545 547 548 550 551 552 553 554 555 556 557 558 559 563 565 566 567 568.

Address: Brian Funt, School of Computing Science, Simon Fraser University,
8888 University Drive, Burnaby, British Columbia V5A 1S6, Canada
E-mails: funt@sfu.ca, xuliwenx@gmail.com

The Generalised Reproduction Error for Illuminant Estimation

Graham FINLAYSON, Roshanak ZAKIZADEH
School of Computing Sciences, University of East Anglia, UK

ABSTRACT

In a recent publication "Reproduction Angular Error: An Improved Performance Metric for Illuminant Estimation", British Machine Vision Conference (2014), it was argued that the commonly used Recovery angular error – the angle between the RGBs of the actual and estimated lights- is flawed when it is viewed in concert with how the illuminant estimate is used. Almost always, we use the illuminant estimate to make an image reproduction where the colour bias due to illumination is removed or reduced. It was shown that, when a single algorithm was used to estimate the light for a fixed scene viewed under a range of illuminants and where similar reproductions were produced when the estimate was 'divided out', the recovery angular error would, counterintuitively, vary widely. The Reproduction angular error introduced in that paper remedies this flaw by measuring the angle between a true white patch and the white that is reproduced when an illuminant estimate is made. In this paper we generalize the reproduction error concept to consider how well a range of colours are reproduced. We show how an illuminant estimate can be used to map the colours in a Macbeth colour checker for the actual illumination to reference lighting conditions. Then we evaluate the error of reproduction using the mean CIE Delta E. This new Generalised Reproduction error metric is used to compare the performance of a variety of different algorithms. Significantly, the rank-order of the reproduction angular error is quite similar to that established with the generalized reproduction error. Based on our experiments we propose that the simpler reproduction angular error can be used as a proxy to our generalised metric to assess the performance of illuminant estimation algorithms.

1. INTORODUCTION

The colours in an image captured by a digital camera are affected by the illuminant under which the scene is captured. Unlike human visual system which is able to perceive the colours constant regardless of illumination, the sensors of a camera capture a colour signal which is confounded by the illumination. To make the colours pleasant and usable by many computer vision tasks, the illuminant of the scene is estimated by reasoning about the distribution of colours in the image. In a second step, the colour of the illuminant is divided out from the colours of the image thereby removing the colour bias due to the illumination.

Illuminant estimation algorithms range from simple statistics-based methods to algorithms that use more complex statistics to learning-based methods. The *recovery error* which is the angle between the estimated and the ground-truth illuminant is commonly used to evaluate the performance of an illuminant estimation algorithm. The average (mean or median) recovery error, for a set of training set of images, is used as an index to compare and rank different algorithms.

However, in recent work (Finlayson & Zakizadeh 2014), a problem with the recovery error was identified. It was shown that the same scene viewed under two different colours of light where the same algorithm is used to estimate the illuminant can result in two very different angular errors. This is a problem because when each of the estimated lights are divided out from their respective images almost the same image reproduction results. Finlayson and Zakizadeh argued that the performance of illuminant estimation algorithms should be tied to how illuminant estimates are used. They are used to discount the colour bias die to illumination in making an image reproduction. Their new metric, called Reproduction Angular Error, measures the angle between the colour (RGB vector) of a white surface corrected using the estimated illuminant and the one corrected using the ground-truth illuminant (resulting in a true white patch). Significantly, this reproduction error provides a stable error for the same scene viewed under different lights and this gels with the fact that the corresponding reproductions look similar. Moreover, the new metric while broadly ranking algorithms the same as recovery angular error introduced several local changes in algorithm rank.

In this paper, we seek to measure the difference between a range of colours (not just a white patch) which are reproduced by the estimated and ground-truth illuminants. This is not as easy as it first sounds as when image data sets are compiled we often have the image and the measured white point but not the appearance of the scene under a ground truth illuminant. In out approach we first show how to make a synthetic set of Macbeth colour checkers for different illuminants for a known camera. Second we show how to make reproductions of the Macbeth colour images when the illuminant colour is discounted using the illuminants estimated by different algorithms (for the algorithm estimates we use the data provided by Gijsenij et al. 2011). Then these reproductions are compared with the actual colours in a Macbeth checker for the reference lighting condition. The CIE Lab ΔE (Sharma et al. 2005) is used to measure the colour difference between the colours of the checker reproduced by the estimated lights and those under reference lighting condition. If the correct illuminant is estimated then a very small ΔE would result. Conversely, poor estimates result in large average ΔEs.

According to this new *generalised reproduction error* we can rank the performance of different algorithms. Crucially, we show that the ranking provided is almost the same as the recently introduced – and much simpler to calculate – reproduction angular error. This paper further validates the usefulness of the reproduction angular error metric.

2. BACKGROUND

The most commonly used metric for evaluating illuminant estimation algorithm is the recovery angular error:

$$err_{recovery} = \ cos^{-1}(\frac{\underline{E}_{est}\cdot \underline{E}_{act}}{|\underline{E}_{est}||\underline{E}_{act}|}) \qquad (1)$$

which is the angle between the estimated RGB of illuminant $\underline{E}_{act}$ and the ground-truth RGB illuminant $\underline{E}_{est}$. Recently, this recovery angular error was shown to have the problem of introducing a wide range of errors when a given algorithm estimates the illuminant for a given scene (Finlayson & Zakizadeh 2014) viewed under a wide range of illuminants. This behaviour is problematic because when the different illuminant estimates are 'divided out' similar reproductions result. It is these reproduced images that are respectively assessed in photography or used in computer vision. To solve this problem, the Reproduction Angular

Error was proposed The Reproduction angular error is defined to be the angle between the RGB of a white surface when the actual and the estimated illuminations are 'divided out'.

$$err_{recovery} = \; cos^{-1}\left(\frac{(\underline{E}_{act}/\underline{E}_{act}) * (\underline{E}_{act}/\underline{E}_{est})}{\sqrt{3}\left|\underline{E}_{act}/\underline{E}_{est}\right|}\right) \qquad (2)$$

3. GENERALISED REPRODUCTION ERROR

The Reproduction angular error assesses the performance of illuminant estimation algorithms according to how well white is reproduced when the colour bias due to illumination is removed. Here we wish to generalise this idea to consider how a range of colours are reproduced. Our idea is to provide a method for synthesising the RGB image of a Macbeth colour checker under an actual light and then use the RGB estimate of the illuminant – made by an algorithm – to correct the image colours (to remove the colour bias due to illumination). This corrected Macbeth checker is then compared with the actual reproduction (when the true illuminant is used).

In constructing our model, we use the set of spectra for 24 Macbeth colour checker patches and the 23 lights from the SFU dataset (Barnard et al. 2002). For camera sensitivity functions we use the Sony DXC-930 CCD (Barnard et al. 2002) but the sensitivities of any particular camera can be used in the problem formulation. Equation (3) teaches that the camera response (ρ^k) whose spectral sensitivities are denoted $R^k(\lambda)$ for the surface spectra ($S(\lambda)$) and the illuminant spectra ($E(\lambda)$) is calculated as:

$$\rho^k = \int_{380}^{700} R^k(\lambda)S(\lambda)E(\lambda)d\lambda \qquad (3)$$

For all numerical calculations, we assume the visible spectrum runs from 380 to 780 Nanometres and we use a 4 Nanometres sampling interval. For each of the 23 lights we, using (3), generate 24 RGBs. These 23 synthetic checker images encapsulate our understanding of how the checker appears under different lights. We wish to generalise this understanding so that we could, given the RGB of any target light, synthesise the appearance of the checker for any illuminant. Denoting the 24x3 RGBs for a Macbeth colour checker as *M*, we model *M* as a linear sum of three basis Macbeth colour checkers:

$$M \approx \sum_{i=1}^{3} M_i m_i \qquad (4)$$

In (4), m_i denotes a scalar weight and the optimal basis in a least-squares sense are found using Characteristic Vector Analysis (Maloney 1986) (in this case of the 23 synthetic Macbeth checker images). Crucially, we found the best basis models our data extremely well with the actual and 3-basis approximation being visually almost the same in appearance.

We chose a 3-dimensional linear model because illumination is defined by 3 numbers: the RGB of the light or the RGB of the estimated light. Let us place the RGB for the white reflectance in the Macbeth checker for each basis term M_i in the 3 columns of a calibration matrix Ω. Denoting an RGB of a light as $\underline{E}$, the linear combination of the columns of Ω defines the weights $\underline{m}$ used in Equation (4):

$$\underline{m} = \Omega^{-1}\underline{E} \qquad (5)$$

In (5), the illuminant vector E could be the actual light or the estimate made by an algorithm. Figure 1a shows one input image and four synthetic checkers. The image is from the SFU (Barnard et al. 2002) database. For this scene a white patch was also measured. Algorithms such as pixel-based gamut mapping will attempt to infer an estimate which ideally will be close to the measured light.

With the measured and actual RGBs of the light in hand, we generated from our linear model (4) and using (5) to find our model coefficient the appearance of the actual checker (Fig. 1b) and the one that pixel based gamut mapping infers (Fig. 1c). The third checker is the correct answer (Fig. 1d). The white patch is equal to [1,1,1]. All 3 images are scaled so that the brightest pixel value across all the colour channels is 1 and a gamma of .5 is applied.

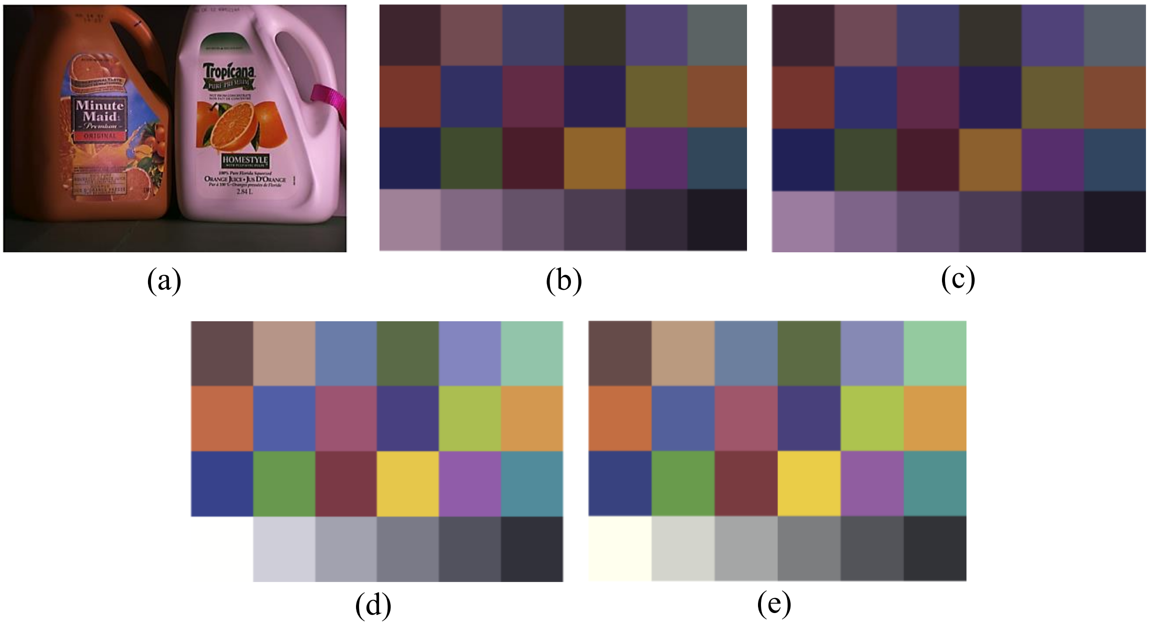

Figure 1: (a) Image from SFU dataset, (b) Synthetic colour checker under the ground truth light under which Fig. 1a was taken, (c) Synthetic colour checker under the estimation of the same ground truth light made by pixel-based gamut mapping algorithm, (d) Synthetic colour checker under the reference light and (e) Corrected colour checker by pixel-based gamut mapping algorithm.

So far, we have focussed on explaining how we synthesise the colours of the Macbeth colour checker for a target light. But, we ultimately seek to model the appearance of a checker under an actual light when it is corrected to the reference checker (fig. 1d) using the wrong illuminant estimate.

Denoting, respectively, the checker under the reference (white light), the actual coloured light and the estimated coloured light as M^{ref}, M^{act} and M^{est}, the estimated reproduction, $\widetilde{M}^{ref}$, is calculated as:

$$\widetilde{M}^{ref} = M^{act}T \quad , \quad T = [M^{est}]^{+}M^{ref} \qquad (6)$$

In (6), $[M^{est}]^{+}$ denotes the Moore-Penrose inverse. That is, T is the least-squares fit from the checker viewed under the estimated light to the reference lighting conditions. This 3x3 matrix T is then applied to the checker under the actual light.

The *Generalised Reproduction Error* for the i^{th} Macbeth colour checker patch is:

$$err_i = \| f(\widetilde{M}_i^{ref}) - f(M_i^{ref}) \| \quad (7)$$

where f maps an RGB to CIE LAB. Note the function f must map the camera values to corresponding XYZs and then the standard CIE Lab formulae can be used.

In Fig. 1e we show an actual checker under a coloured light corrected using the estimated light of pixel gamut mapping and the procedure described in (6). Note the reproduction is reasonable but there remains a slight yellowish cast.

4. RESULTS

Here we use the 321 images from the SFU dataset (Barnard et al. 2002). This data set has linear images and a variety of objects are imaged under 11 lights (ranging from quite yellowish to very blue). All images were captured with the SONY DXC-930. A variety of algorithms, including those listed in Table 1, were tested by Gijsenij et al. 2011 who makes all the estimated RGBs available to the community. We can thus calculate for all Macbeth colour checker images and the overall median generalised reproduction error. Then according to this global median we can rank the algorithms.

In Table 1 we list the algorithms and record the rank for the Recovery and Reproduction angular errors and the new Generalised Reproduction error.

Table 1. Comparison of ranking of algorithms based on reproduction angular errors and generalised reproduction errors.

	Recovery angular error		Reproduction angular error		Generalised Reproduction Error	
Method	Median error	Rank	Median error	Rank	Median error	Rank
Grey-world	7.0°	9	7.49°	9	7.02	9
MaxRGB	6.5°	8	7.44°	8	6.13	8
Shades-of-gray	3.7°	**7**	3.94°	6	3.26	6
1st grey-edge	3.2°	5	3.59°	5	3.12	5
2nd grey-edge	2.7°	4	3.04°	4	2.88	4
Pixel-based gamut	2.267°	**2**	2.83°	3	2.64	3
Edge-based gamut	2.278°	**3**	2.70°	2	2.59	2
Intersection-based gamut	2.09°	1	2.48°	1	2.46	1
Heavy tailed-based	3.45°	**6**	4.11°	7	3.74	7

While the rankings of all three metrics are almost similar it is clear recovery angular error ranks algorithms a little differently from reproduction angular error. Further in (Finlayson & Zakizadeh 2014) it was shown that the rankings are statistically different. And, this fact draws attention to the care the algorithm designer needs to take using the appropriate metric to assess their algorithm. The reproduction angular error assesses how well an algorithm reproduces white (i.e. when the estimated illuminant is divided out). Generalised reproduction error builds on this concept and accounts for the error for other surface colours. The ranks for the generalised reproduction error are almost identical to the reproduction angular error. Indeed – space prohibits us elucidating on this point here – the rankings are not statistically significantly different. We can conclude, for the data tested, that the simple reproduction error can be used as a proxy for the generalised reproduction error developed here.

5. CONCLUSION

Reproduction angular error measures the angle between a true white patch and the white patch that results when an algorithm's estimate is 'divided out' from the image. In this paper we generalised reproduction angular error to assess not only how white is reproduced but, instead, all the colours on a Macbeth colour checker. The generalised reproduction error is the CIE Lab colour difference of a reference checker and a reproduction that results when the same checker viewed under an actual coloured light is colour corrected using an estimate of that light supplied by an algorithm. Like the simple reproduction angular error the same algorithm/scene pair returns very similar error independent of the colour of the light to be estimated (because in all cases the resulting reproductions are similar). We observed that the ranking of a selection of algorithms based on the generalised reproduction error ΔEs are very similar to the ranks given by the simple reproduction angular metric. Thus, while the generalised reproduction error provides a finer grained summary of the 'goodness' of an illuminant estimation algorithm, the simpler reproduction angular error can be used to assess algorithm performance.

ACKNOWLEDGEMENTS

We thank EPSRC for supporting this research (grant: H022236).

REFERENCES

Barnard, K., L. Martin, B. Funt, and A. Coath. 2002. A data set for color research. *Color Research & Application, 27(3):147–151.*

Finlayson, D. G. and R. Zakizadeh. 2014. Reproduction angular error: an improved performance metric for illuminant estimation. In *Proc. British Machine Vision Confernece 2014, Nottingham, UK, September 1-5, 2014*.

Gijsenij, A., T. Gevers, and J. Van De Weijer. 2011. Computational color constancy: Survey and experiments. *IEEE Transactions on Image Processing, 20(9):2475-2489.*

Maloney, L. T. 1986. Evaluation of linear models of surface spectral reflectance with small numbers of parameters. *J. Opt. Soc. America A, 3(10), 1673-1683.*

Sharma, G., W. Wu, and E. N. Dalal. 2005. The ciede2000 color-difference formula: Implementation notes, supplementary test data, and mathematical observations. *Color Research & Application, 30(1):21-30.*

Address: School of Computing Sciences, University of East Anglia,
Norwich Research Park, Norwich, NR4 7TJ, UK
E-mails: r.zakizadeh@uea.ac.uk, g.finlayson@uea.ac.uk

Rank-Based Camera Spectral Sensitivity Estimation

Graham Finlayson, Maryam Mohammadzadeh Darrodi
School of Computing Sciences, University of East Anglia, UK

ABSTRACT

The spectral sensitivity function of a camera can be determined directly in the laboratory by detailed, and lengthy, measurements. Alternatively, and much more rapidly, the camera spectral sensitivities can be estimated through linear regression. However, compared with the lab based approach, the regression based estimates are not as accurate. In part, the poor performance is due some assumptions of the regression methods not holding exactly true. Indeed, prior art regression algorithms work with the assumption that a camera has a linear response. This is either not exactly the case or not the case at all. Here we develop a novel camera spectral sensitivity estimation technique that can recover the spectral sensor curves even when the camera has a non linear response. Our method assumes only that the rank-order of the final camera measurements is the same as the linear camera response. Experiments validate our method.

1. Introduction

The main contribution of this work is to present an estimation technique that is able to recover camera spectral sensitivity for both linear and non-linear camera responses. A camera has linear response, if when the physical signal entering the camera is scaled, the recorded RGBs scale by the same amount (e.g. double the light equals double the response). The images most people have access to (e.g. rendered jpegs from mobile phones) are the result of a long processing pipeline and are non-linear. One part of this process is the application of a color correction matrix which converts recorded sensor response to display RGBs (e.g. linear sRGB). In this scenario our method seeks to discover the linear transform of the sensor spectral sensitivities.

In this paper, we set forth an estimation technique that recovers spectral sensitivities assuming only that the recorded sensor values have the same rank order as those measured by the sensor (or of the sensor values post color correction). Importantly, almost all of the manipulations that an image undergoes preserves rank-order. For example, image gamma (approximately raising to the power of 0.5) is a monitonically increasing function. Contrast manipulation Ian S-shaped curve) also preserves rank-order. We show that the pairwise relationship between the responses of two spectral stimuli mathematically force the underlying spectral sensitivity to lie in one half of the space of all spectral sensitivity functions. Many pairs of responses induces many half-space constraints and the intersection of these is a surprisingly small set of candidate spectral sensitivity functions. One member of this intersection set is found using an appropriate optimization criteria.

We validate the results of rank-based spectral estimation for a Nikon camera using ground truth spectral data that were previously measured at National Physical Laboratory [1]. Good recovery is shown for linear raw and non-linear rendered images. We compare our recovery to that provided by a prior art linear regression method[2]. That method fails completely for the non-linear rendered image scenario.

2. METHODOLGY

In this paper we focus on cameras with three-channel response of red, green and blue. The typical camera response at jth pixel from ith sensor can be modelled as:

$$p_{ij} = \mathrm{f}(\int_{\omega} E(\lambda)\, S_j(\lambda) Q_i(\lambda) d\lambda + N_i), \qquad i = 1,2,3 \tag{1}$$

where p_{ij} is the camera response, $E(\lambda)$ is the spectral power distribution of the scene illuminant, $S_j(\lambda)$ is the surface reflectance imaged at pixel j and $Q_i(\lambda)$ is the spectral response of sensor i at wavelength λ. The integral is taken over the visible spectrum ω. Noise for each sensor is denoted as N_i and f() denotes a non-linear rendering function. Prior art estimation algorithms ignore N_i and f() to simplify Eq.1 for each channel as:

$$p_j = \int_{\omega} E(\lambda)\, S_j(\lambda) \mathrm{Q}(\lambda) d\lambda = \int_{\omega} C_j\,(\lambda) Q(\lambda) d\lambda \equiv \underline{c}_j \underline{q}. \tag{2}$$

Where $C(\lambda) = E(\lambda)S(\lambda)$. It is useful to translate (2) into the language of linear algebra. In (2), $\underline{c}_j$ denotes the 1×31 vector of sampled measurements (when we measure 31 wavelengths across the visible spectrum 400 to 700 Nanometres with 10Nm intervals) and $\underline{q}$ is the 31×1 single channel sensor spectral sensitivity. For N colors, we can attempt to estimate $\underline{q}$, when we have the $N \times 1$ vector of single channel responses $\underline{P}$ and the corresponding $N \times 31$ matrix C (with $\underline{c}_j$ being its jth row). Given the linear form of (2) sensor estimation can be written as a linear regression of the form below:

$$\min_{\underline{q}} \left\| C\underline{q} - \underline{P} \right\|^2 \tag{3}$$

Solving (3) by $\underline{q} = [C^t C]^{-1} C^t \underline{P}$ according to [4], does not provide a stable solution due to the limited dimensionality of matrix C [3]. Mathematically, the matrix $C^t C$ has a high condition number and, so, has a numerically unstable inverse.

Many spectral estimation algorithms begin with Equation (3) and attempt to solve for $\underline{q}$ in a more numerically robust way. Often, this is achieved by adding additional constraints into the problem formulation. For example in [2], sensors were assumed to belong to a low dimensional smooth basis and also that they should be unimodal. The resulting respective linear and linear inequality constraints led to sensor estimating being formulated as a quadratic programming problem [2]. Importantly, the constrained minimisation delivered much improved spectral sensitivity estimation. However, even this improved technique ignores the role of f() but, often, this cannot be ignored: camera responses are non linear (and when this is the case no existing method delivers good estimation performance).

Solving for $\underline{q}$ is much harder if the camera response is non-linear (i.e. when N_i and f() are not ignored). In this article we also take a constraint based approach for finding $\underline{q}$ [2]. The difference is in the linear constraints that improve upon the robustness of estimation technique for non-linear data. Our key observation is that is f() is assumed to be a monotonically increasing function then this means that the ranks of the non-linear RGB counts are the same as for their linear counterparts. Ranked single channel response for P_1 and P_2 implies:

$$f(P_1) > f(P_2) \Rightarrow P_1 > P_2 \rightarrow \left(\underline{c}_1 - \underline{c}_2\right).\underline{q} > 0 \tag{4}$$

The inequality in (4) expresses the general form of a linear constraint derived from ranking the order of the single channel camera response of two colors. For N color samples we can choose $\binom{N}{2}$ number of pairs to form the above linear constraint. The power of this linear constraint is in that it holds for both linear and non-linear data.
The intersection of all these 'half space' constraints results in a solution space that delimits a region of sensor space. As such, any sensor that satisfies all the ranking constraints is a possible solution to the sensor estimation problem. We choose the sensor that predicts the rank order of the response, integrates to unity, lies in a 7-dimensional Sine basis and is smoothest. This optimization is solved using Quadratic Programming.

3. EXPERIMENTS AND RESULTS

In this section we explain the experiments carried out for validation and evaluation of the estimated rank based spectral sensitivity functions of Nikon camera. An SG colour checker, was placed approximately in the centre of the floor of a VeriVide cabinet, facing upwards towards the D65 illuminant. The position of the camera relative to the color checker was chosen to be approximately at 45 degrees angle. For each patch in the checker, the camera signal was obtained by averaging the red, green and blue channel response over the central area of the patch resulting in matrix P for the 140 colors. We took both raw and rendered images of the same scene. The matrix C of colour signal measurement was obtained using a PR670 spectra radiometer.

We compare the estimated sensors $\hat{Q}$ using the ground truth spectral response functions measured (in a rigorous lab based experiment) at NPL [1]. We compare recovery for both the linear camera image and the nonlinear rendered image (the jpeg produced by the Nikon camera pipeline). In the latter case we seek to recover the camera sensitivities multiplied by the camera's 3x3 colour correction matrix T. Here, we use the work of [5] to recover the colour correction matrix T and we apply it to the measured spectral sensitivities to provide ground truth for spectral estimation using a rendered (jpeg) image. Figure 1 illustrates these estimated sensors (red dashed line) and ground truth data (blue solid lines).

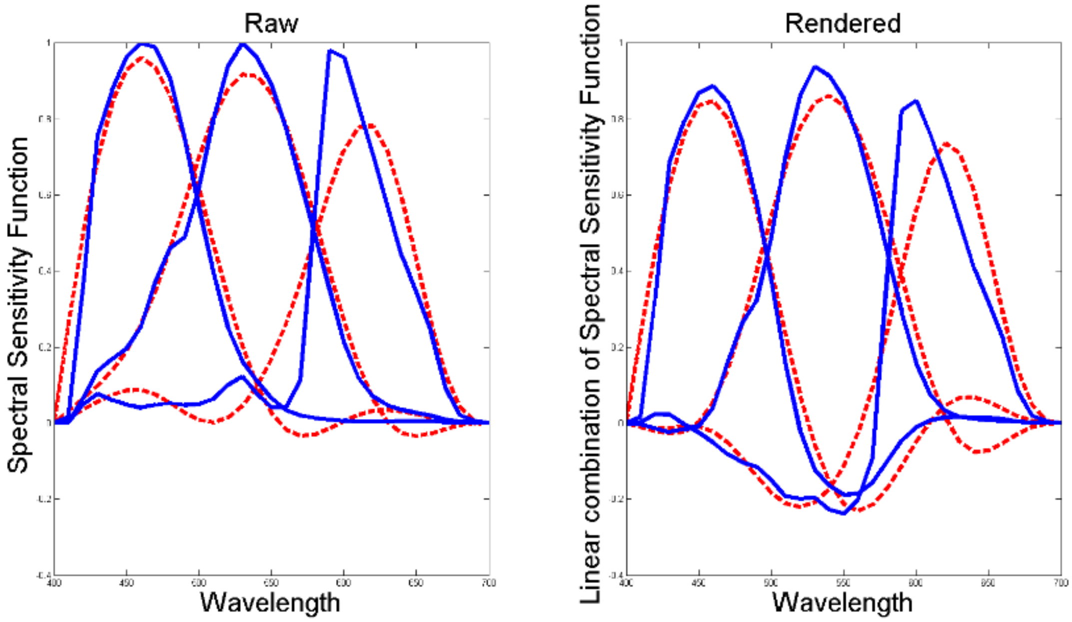

Figure 1: Nikon spectral sensitivity function estimated using rank based technique (red-dashed) and ground truth data (blue solid) on raw (Left) and rendered (right) data.

We also, numerically, evaluate the performance of our estimation technique by comparing it to a prior art quadratic programming estimation technique [2]. For this, we use Vora and Trusell's error [6] metric. Vora values close to 0 indicate the estimated sensors sample spectra – produce camera RGBs - close to those measured by the actual camera. The maximum Vora Value is 100. The Vora value is powerful as it teaches that two cameras with similar looking spectral profiles typically sample light in the same way. The Vora Value also capture the idea that the RGBs from a given camera can be linearly mapped to approximate measurements made by another (see [6] for a full discussion and derivation of the Vora Value).

Vora values for both raw and rendered data for the Rank-Based Spectral Estimation method (RBS) are shown in Table 1. That is, we calculate the Vora Value by comparing the estimated curves (plotted in red) in Figure 1 with the actual curves (plotted in blue). In both cases a very low Vora Value is found. That is the recovered sensors sample light very similarly to the actual sensors. The 'Rendered' results refer to the fact we are estimating the sensors multiplied by the colour correction matrix for the highly non-linear camera jpeg image.

In contrast the QP method [2] (based on assuming a camera has linear response) works well for the raw data but, as expected, terribly for the non-linear rendered data. A Vora Value of 65 teaches that the recovered sensitivities sample light nothing like the actual.

Estimation Technique	**Raw**	**Rendered**
RBS	5	6
QP	9	65

Table 1: Table of Vora values. RBS: Rank based spectral estimation. QP: Prior art quadratic programming estimation technique [2].

4. CONCLUSION

In this paper we have shown that the rank order of camera response is a powerful tool for solving the camera spectral sensitivity function (multiplied by colour correction in the case of rendered image). We have shown that this estimation technique is robust for both raw and rendered images. We validated our estimated sensors using measured spectral sensitivity functions from National Physical Laboratory. We show that prior art estimation technique fail to estimate spectral response function in the same consistent manner as our rank based technique. Experiments demonstrate that relatively good estimation is possible given a single image with known spectra.

REFERENCES

[1] Mohammadzadeh Darrodi M, Finlayson G.D., Goodman T., Mackiewicz M. 2014. A reference data set for camera spectral sensitivity estimation. *Journal of the Optical Society of America* (31): 381-391.

[2] Finlayson G.D., Hordley S., and Hubel P.M. 1998. Recovering device sensitivities with quadratic programming. In *The Sixth Color Imaging Conference*: Color Science, Systems, and Applications, 90-95.

[3] Maloney L.T. 1986. Evaluation of linear models of surface spectral reflectance with small numbers of parameters,. *Journal of the Optical Society of America* (3): 1673–1683.

[4] Moore E. 1920. On the reciprocal of the general algebraic matrix. *Bull Am Math Soc*, (26): 394-39.

[5] Kim S. J., Lin H. T., Lu Z., Susstrunk S., Lin S., and Brown M.S., 2012. A new in-camera imaging model for color computer vision and its application. *IEEE Transactions on Pattern Analysis and Machine Intelligence* 34(12): 2289-2302.

[6] Vora P.L., Fareel J.E., Tietz J.D., and Brainard D., (HP, 1997). Digital color cameras - 2 Spectral response, In HP Technical Report.

Address: Dr Maryam Mohammadzadeh Darrodi, School of Computing Sciences
University of East Anglia, Norwich Research Park, Norwich, NR4 7TJ, UK
E-mails: M.Darrodi@uea.ac.uk, G.Finlayson@ uea.ac.uk

Comparing Colour Camera Sensors Using Metamer Mismatch Indices

Ben HULL and Brian FUNT
School of Computing Science, Simon Fraser University

ABSTRACT

A new method of evaluating the colorimetric accuracy of a color camera is proposed that is based on the size (appropriately normalized) of the metamer mismatch volume induced by a change of 'observer' from camera to human eye and vice-versa. The degree of metamer mismatching indicates the range in the discrepancy of the colour signals that can arise and as such is a more well-founded measure of colorimetric accuracy than traditional spectral-based measures such as the root mean squared difference in fit between the camera and eye's sensitivity functions.

1. INTRODUCTION

It is well known that only a colour camera that satisfies the "Luther condition" (Luther 1927) can provide colorimetrically accurate colour images. Of course, colorimetric accuracy is only one issue of concern, and not necessarily the most important one, in terms of overall image quality. However, there are many situations—for example, dermatological imaging or paint and dye applications—in which it would be desirable to have a camera act as an imaging colorimeter. The Luther condition requires the camera sensitivity functions and the human eye's sensitivity functions to be within a linear transformation of one another. The problem with this condition is that it is all or none. If there is not an exact match then how is the discrepancy to be measured?

We address this question using the volume metamer mismatch index (VMMI) (Logvinenko 2014b) and compare the indices obtained for the sensitivity functions of the 28 digital cameras Jiang et al. (Jiang 2013) measured. The VMMI is a measure of the amount of metamer mismatching that can occur between two different observers for a given light. In this paper, one observer is fixed and defined by the human cone fundamentals; the other observer is defined by the spectral response functions of the colour camera being evaluated. Metamer mismatching for a pair of observers (sometimes called 'observer metamerism') refers to the fact two lights that induce an identical sensor response in one observer (i.e., match), may induce non-identical sensor responses in the second observer. The set of all possible such non-identical responses forms a convex volume in colour space referred to as the metamer mismatch volume.

The intuition behind using the degree of metamer mismatching in evaluating the colour fidelity of a digital camera is that if two lights match for the human observer, then it follows that ideally the camera should produce an identical RGB response to the two lights. If it does not, or if it produces identical RGB responses to lights that the human observer sees as distinct, then there cannot exist a one-to-one mapping between camera response and perceived colour. The greater the degree of metamer mismatching, the greater the ambiguity in the mapping between camera response and perceived colour, and hence, the less colorimetrically accurate the camera will be.

2. CAMERA VOLUME METAMER MISMATCH INDEX (CVMMI)

The Camera Volume Metamer Mismatch Index (CVMMI) is a measure of the amount of metamer mismatch between a particular camera sensor and the reference human observer. The CVMMI is a particular case of the VMMI in which: (*i*) the spectral response functions (Figure 1) of the reference human observer are those defined by the Govardovskii et al. model of photopigment responsivity (Govardovskii 2000) with peak photopigment optical density of 0.3 and peak absorbances of 430nm, 530nm, 560nm; and (*ii*) the metamer mismatch volumes are computed for lights that are for the first observer metameric to the equal-energy illuminant.

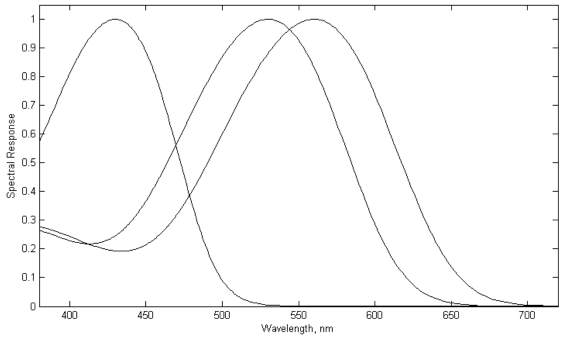

Figure 1: The relative spectral response functions for the reference human observer based on the Govardovskii et al. model of the cone sensitivities.

2.1 Calculating the Metamer Mismatch Volume

The metamer mismatch volume (MMV) for a given colour signal (i.e., XYZ, LMS or RGB, depending on the colour sensors used) recorded by the first observer in response to a given light is the set of all colour signals arising from lights that are metameric to the given colour signal that could possibly be recorded by the second observer. Logvinenko (Logvinenko 2014b) suggests that the size of the MMV can be measured in various ways, such as terms of its ‘diameter’, its area when projected into a 2D chromaticity space, or its three-dimensional volume. In this paper, we choose to use the cube root of its three-dimensional volume.

We calculate the MMV for the second observer given colour signal, Ψ_1, of the first observer using the new method Logvinenko describes (Logvinenko 2014b). This method is based on randomly choosing a set of 3 monochromatic lights and then finding a linear combination of the chosen lights that is metameric to Ψ_1. The response, Ψ_2, of the second observer to this linear combination provides a point in the MMV. Since this computation is fast, it can be repeated thousands of times with different sets of monochromatic lights thereby leading to lots of points on the boundary of the MMV. The convex hull of this set of these points provides a good approximation to the MMV.

2.2 Volume Metamer Mismatch index

While the volume of the MMV provides a measure of the amount of metamer mismatching, it varies in proportion to light intensity and to any linear transformation of the spectral sensitivity functions. To obtain a measure that is unaffected by these factors, Logvinenko (Logvinenko 2014b) introduces the Volume Metamer Mismatch Index (VMMI). The VMMI is defined as ratio of the volume of the MMV relative to the volume of the convex hull of the spectral curve for the second observer (see Eq. 8 of Logvinenko 2014b for the formal definition). Since light intensity affects both volumes equally, as does a linear transformation of the sensitivity functions, the ratio remains unaffected.

The VMMI for the case of the reference human observer to a camera as the second observer provides a measure of how well or poorly the given camera is at representing colours as seen by the human observer. A high VMMI means that lights that look the same to the human observer can end up with significantly different RGB outputs from the camera. For the reverse case, that of the VMMI for a change from camera as the first observer to human as the second observer, the VMMI gives a measure of how well the camera preserves differences seen by the human eye. A high camera-human VMMI indicates that two lights that look very different to the human eye may be indistinguishable to the camera.

The VMMI can be computed for any colour signal Ψ_1 of the first observer in response to a light. In terms of using the VMMI as a measure of the colour fidelity of cameras, however, we define Ψ_1 to be the colour signal of the first observer in response to the equal-energy spectrum. This single case is taken as being representative of the degree of metamer mismatching for all spectra since the color signal corresponding to the equal-energy case has the largest VMMI. At the other extreme, is the colour signal of monochromatic light, for which there are no metamers.

It is possible for a camera to have a low human-camera VMMI (for colour signal of equal-energy spectrum) while having a high camera-human VMMI, and vice versa. For a camera to be colorimetrically accurate, both must be low. Therefore, we define the Camera Sensor Metamer Mismatch Index (CSMMI) as the average of the two.

2.3 Restricting the lights

Lights leading to colour signals on the boundary of the MMV have spectra that are non-zero at only three wavelengths. Such lights are not very representative of lights that are actually encountered by cameras in practice, although imaging a laser-based display would be a clear exception. The problem with evaluating the CSMMI for monochromatic lights is that a small difference in the camera response at a particular wavelength can lead to a high degree of potential metamer mismatching. The volume of the MMV correctly represents the range of possible responses, but this may not be what is desired in practice where monochromatic lights rarely arise, and also where the camera's sensor sensitivity functions may not have been measured all that precisely at every wavelength.

To avoid the problem of small differences in the sensor response functions leading to large differences in the CSMMI, we replace the monochromatic lights with lights having a Gaussian-shaped spectrum. Metamers are then found using linear combinations of three such lights with peaks centered at three different wavelengths. Since the set of lights is being restricted, the resulting MMVs are smaller and strictly inside the theoretical MMVs based on linear combinations of 3 monochromatic lights.

Figure 2 shows examples of the light spectra formed as a linear combination of Gaussian spectra with standard deviations of either σ=25 or σ=50. At σ=25, the Gaussian spectra are more similar the peaks in LED spectra. The spectra formed as a linear combination of three Gaussian spectra with σ=50 are closer to typical broadband light sources. We denote the CSMMI indices computed using Gaussian spectra of σ=25 and σ=50 CSMMI25 and CSMMI50, respectively.

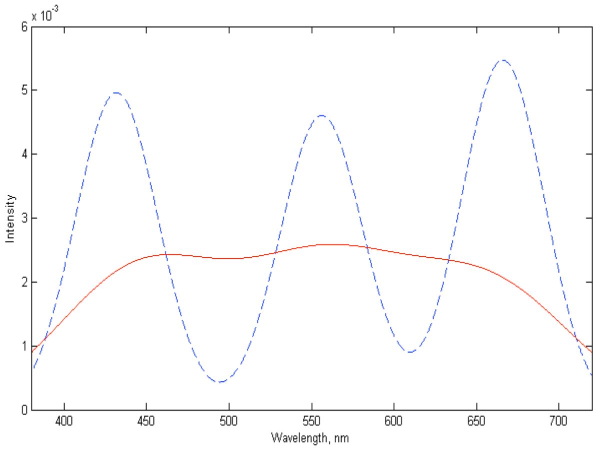

Figure 2: Two spectra that are metameric to the equal-energy spectrum formed as linear combinations of Gaussian lights of standard deviation σ=25 (dashed blue curve) and σ=50 (solid red curve).

3. RESULTS AND DISCUSSION

We computed the CSMMI25 and CSMMI50 measures for the sensor sensitivity functions of the 28 cameras measured by Jian et al. (Jiang 2013). The computation was based on finding 10,000 metameric lights as described above.

Jiang et al. rank the cameras in terms of two measures. The first is the departure from the Luther condition as measured in terms of the Root Mean Squared error in the best linear fit of the camera sensitivites to the CIE-1931 2-degree color matching functions. The second measure is the average CIEDE00 color difference taken over the 1269 Munsell reflectance spectra (Parkkinen 1989) illuminated by CIE D65 and measured between the transformed camera coordinates (i.e., best camera estimate of XYZ) and the true CIE XYZ. The RMS difference is a general measure, but using the average CIEDE00 over a set of reflectances is not. The problem is not only that the set of reflectances is limited, but that the reflectances are not lights. A general measure of camera colour fidelity must include the space of all lights, not just the space of lights reflected from surfaces under D65. In any case, Jiang et al. show that there is only a very limited correlation between the rankings that the two measures provide.

Figure 3 plots the RMS and CSMMI50 measures for the 28 cameras sorted in order of increasing CSMMI50. The two measures follow the same general trend, but there are significant disagreements between the two measures. The fact that the RMS measure can sometimes be small while the CSMMI is large is an indication of the problem with using the similarity of the camera and eye spectral sensitivity functions as a measure of colour fidelity since the CSMMI reveals that relative small differences as measured in terms of RMS can in fact lead to large colour differences between the camera and eye.

Of course, the CSMMI25 and CSMMI50 can be expected to be very correlated. Figure 4 shows that the two indices track one another closely with a few exceptions. Camera 6, for example, has a higher relative CSMMI25 than CSMMI50. This indicates that the colour fidelity of that camera will be poorer for lights with spectra having narrowband peaks than lights with strictly broadband spectra.

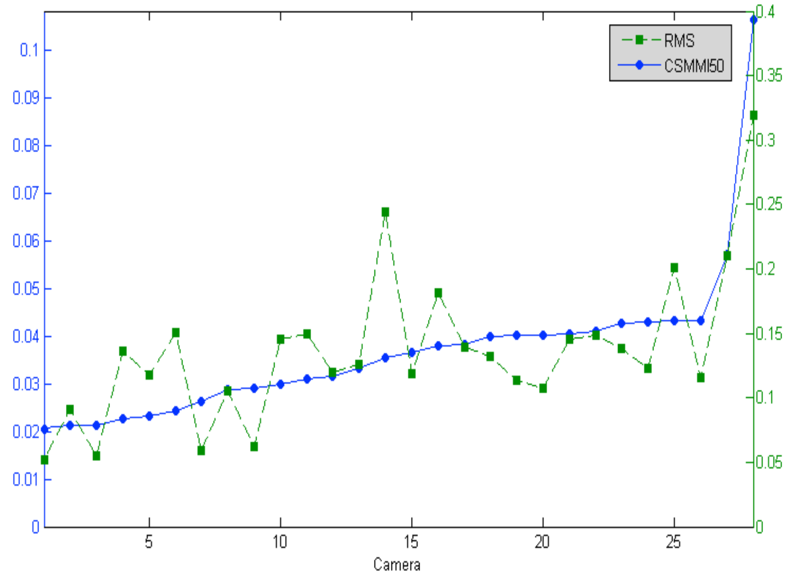

Figure 3: The RMS (dashed green) and CSMMI50 (solid blue) measures for each of the 28 cameras with the results sorted in left−to−right order in terms increasing CSMMI50. Left axis CSMMI50 index. Right axis RMS value.

Note that since the MMVs for the σ=50 lights are significantly smaller than the MMVs of the σ=25 lights the range of the CSMMI50 indices is always smaller than that of the CSMMI20 indices.

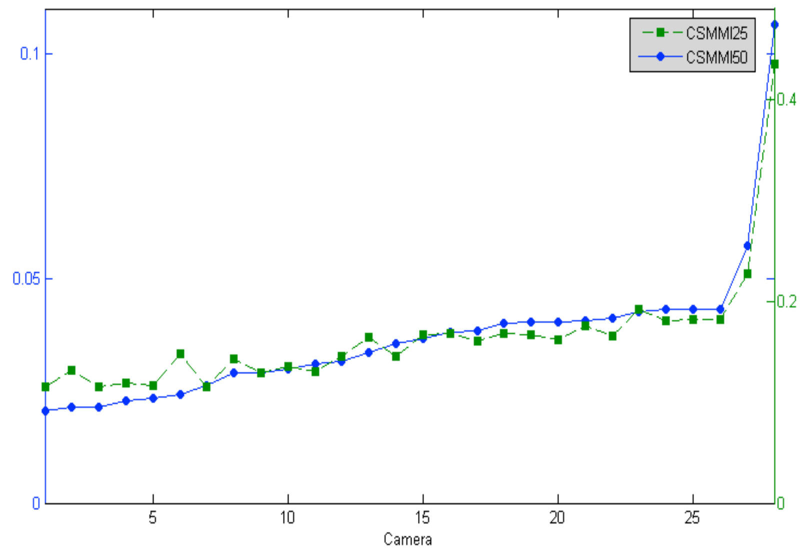

Figure 4: Comparison of the CSMMI50 and CSMMI25 indices. Cameras are ordered in terms of increasing CSMMI50. The relative scale of the two plots has been adjusted so that they overlap for comparison.

4. CONCLUSION

Digital colour cameras do not generally satisfy the Luther condition and therefore will not produce images that are entirely colorimetrically accurate. The Luther condition is all or none. To compare the colorimetric accuracy of cameras requires a different measure, for which the RMS error in the best linear fit of the camera sensitivity functions to the human cones is often used. As an alternative, we propose a new measure, the camera sensor metamer mismatch index (CSMMI), based on Logvinenko's (Logvinenko 2014b) volume metamer mismatch index, which in turn is based on the amount of metamer mismatching that is induced by a change from the eye's sensitivity functions to a camera's and vice-versa. As such, it provides a principled measure of the colorimetric accuracy of a camera.

ACKNOWLEDGEMENTS

Funding was provided by the Natural Sciences and Engineering Research Council of Canada.

REFERENCES

Govardovskii, V., N. Fyhrquist, T. Reuter, D. Kuzmin, and K. Donner. 2000. In search of the visual pigment template. *Visual Neuroscience*. 17, 509-528.

Jiang, J., D. Liu, J. Gu, and S. Susstrunk. 2013. What is the Space of Spectral Sensitivity Functions for Digital Color Cameras? In *IEEE Workshop on Applications of Computer Vision (WAVC)* 168-179.

Logvinenko A., B. Funt B. and C. Godau. 2014a. Metamer mismatching. *IEEE Trans. on Image Processing*, 23, 34-43.

Logvinenko, A. 2014b. Colour variations arising from observer-induced metamer mismatching, *www.researchgate.net*, Accessed Oct. 2014.

Luther, R., 1927. Aus dem Gebiet der Farbreizmetrik. Zeitschrift für technische *Physik* (8) 540-558.

Parkkinen, J., J. Hallikainen, and T. Jaaskelainen. 1989. Characteristic spectra of Munsell colors. *Journal of Optical Society of America A*, 6(2) 318–322.

Address: Brian Funt, School of Computing Science, Simon Fraser University, 8888 University Drive, Burnaby, British Columbia, Canada, V5A 1S6.
E-mails: bhull@sfu.ca, funt@sfu.ca

Advanced Measurement Technology for Image Clarity

Hideo Kita, Shigeo Suga
SUGA Test Instruments Co., Ltd.

ABSTRACT

Evaluation of object surface structure has traditionally involved the assessment of familiar optical properties known as Gloss and Haze. More recently, the optical property attributed to object surface structure or structural internal optical effects, have gained major importance because such property can vary, while the traditional properties of gloss and haze remain constant, and vice-versa. This optical property is known as Image Clarity. We designed a test apparatus to quantify this optical phenomenon, which exists in both reflection and in transmission mode. Image Clarity is then converted to a numerical index whose values are high when the specimen reflects, or transmits the image clearly and is low when the specimen blurs the image.

1. FORWARD

Many have experienced this sense of quality and luxury by noticing sharp images in the form of silhouettes of surrounding trees and buildings reflected on a body panel of a stylish car, which happened to catch your eye. The overall quality perception of an object is developed by examining various optical properties of a surface; such as image sharpness, color, gloss, and haze reflecting from its surface.

Among optical properties, the degree that an image of an object can be viewed clearly without distortion is called Image Clarity. This optical property occurs in images that are either reflected or transmitted.

Viewing the image of the optical mask in reflection from two anodized aluminum plates is shown in Figure 1. The left plate is clearly defined and sharp. This plate has high Image Clarity values. The right plate is blurred and the optical mask is barely recognizable. This plate has low Image Clarity values. Image Clarity is a measure of this observed phenomenon, expressed numerically. Image Clarity values are high when the image can be seen clearly and Image Clarity values are low when the image appears blurry.

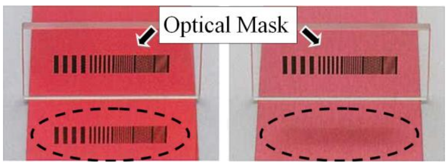

Figure 1: Reflected Image Clarity Illustrated

Recently, the phenomenon of Image Clarity is attracting much attention as a factor in the quantitative evaluation of how objects appear. This is occurring because the phenomenon is becoming recognized and understood. In addition to traditional measurements of Color, Gloss, and Haze, Image Clarity is being utilized in many diverse industrial fields. For example, external appearance has a significant influence on the perceived quality and value of products; such as the paint finish like piano black, orange peel or mirror finish on automobiles and other products, post cards[i], anodized aluminum, aluminum alloys and plastics whose surface is mirror finish and texturing. As a result of using Image Clarity values and controlling the manufacturing process, products are produced that have high Image Clarity values. This means that images reflecting off surfaces or transmitted through objects can be seen clearly and distinctly. Also, for glossy post cards, Image Clarity values are used for evaluation since it enables evaluation of differences in Image Clarity even when measured Gloss values are nearly equal.

Furthermore, materials; such as packaging for electronic components, films (glass) for liquid crystal displays and smart phones require high Image Clarity values to show text and screen images clearly. Image Clarity values are used because they provide differences in visual appearance and distinctness of image, while traditional methods of analysis do not. It is interesting to note that there are cases where low Image Clarity values are a requirement; for instance, in the case of liquid crystal displays. Not only is high transmittance a requirement but so are low Image Clarity values. Low values of reflection Image Clarity are required to reduce glare by minimizing the intensity of reflection.

2. MEASUREMENT PRINCIPLE OF IMAGE CLARITY

Assessment of Image Clarity may be obtained by reflectance and transmittance modalities. Examples of two modalities used for these measurements are shown below. Figure 2 illustrates the Geometry for Image Clarity by Reflection and Transmission.

In Figure 2, the optical path begins with illumination from a light source and after passing through the source aperture-slit, it is collimated by the collimating lens and directed onto a specimen. Then, the image of source aperture-slit, reflected from or transmitted through a specimen, is collected and focused by the de-collimating lens on the optical mask. The light receptor detects the fractional amount of transmitted radiation passing through the optical mask.

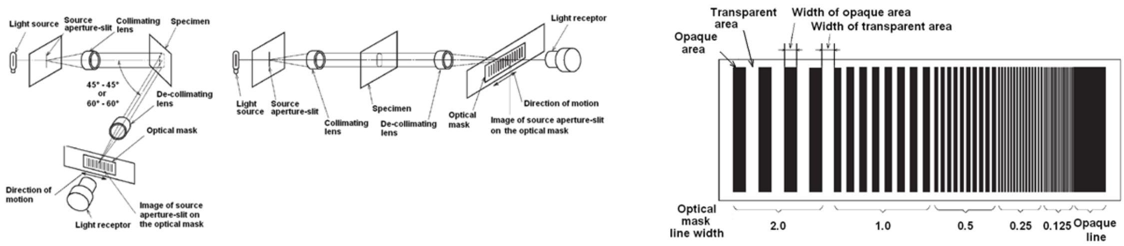

Figure 2: Illustrates the Geometry for Image Clarity and Optical Mask

The optical mask is illustrated in Figure 2. The geometric ratio of the opaque areas to the corresponding transparent areas is 1:1. There are 5 groups of comb patterns each having different segment widths; namely, 2.0, 1.0, 0.5, 0.25, and 0.125 mm. The data used for image analysis, which directly relates to Image Clarity, are acquired by scanning the intensity of radiation passing through the optical mask, shown as “Movement of optical mask” in Figures 3 and 4, Measurement of Image Clarity. Image Clarity, C(n)(%), is determined mathematically by the equation presented as equation (1). The largest amount of light received by the light receptor is the maximum light intensity, M_n. The least amount of light received by light receptor is the minimum light intensity, m_n. “n” is optical mask line width.

$$C_{(n)} = \frac{M_n - m_n}{M_n + m_n} \times 100 \qquad (1)$$

Referring to Figure 3, for a test specimen such as a perfect mirror, where the reflected image appears clear and distinct at the optical mask, the image of the source aperture-slit is replicated on the optical mask perfectly within the diffraction limits of the optical system. This means that the image of the slit is fully transmitted when the optical mask is in Position 1, and blocked completely when the light is in front of the opaque part when the optical mask is in Position 2. In this case, the amount of light received by image detector is as shown in right of Figure 3. The difference between the maximum and minimum light intensities is large; therefore, the Image Clarity value is high.

Conversely, a matt surface test specimen with a dull finish causes the image to blur and distort. That distortion of the image of aperture-slit on the optical mask will be large as shown in Figure 4, Measurement of Low Image Clarity. This means that the image of aperture-slit is not fully transmitted when the optical mask is in Position 3, nor is it blocked completely when the light is in front of the opaque part of the optical mask in Position 4. The representation of the light intensities for Image Clarity having low numerical values is shown in right of Figure 4. The difference between the maximum and minimum light intensities is small; therefore, the Image Clarity value is low.

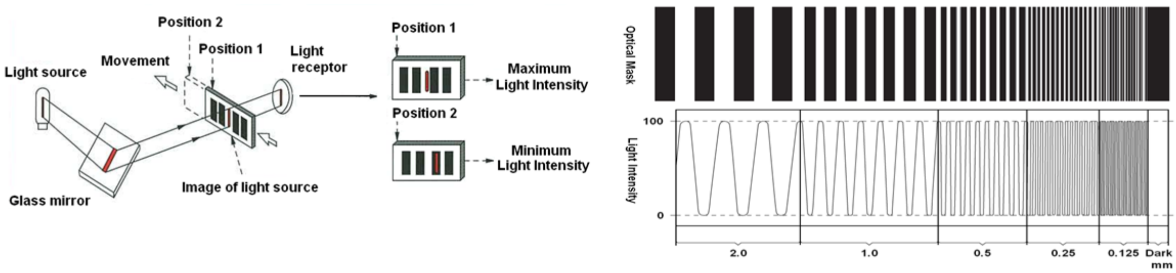

Figure 3: Measurement of High Image Clarity

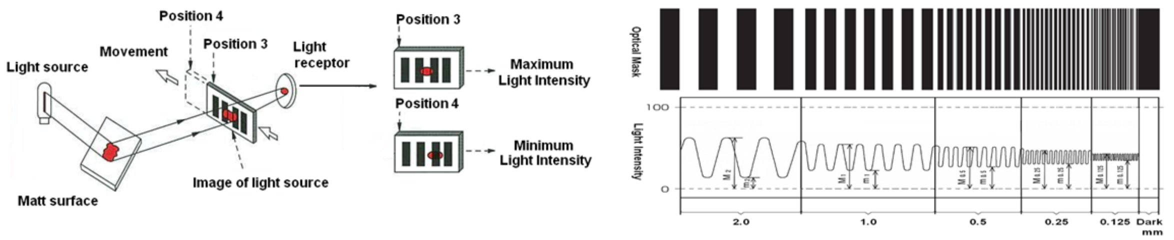

Figure 4: Measurement of Low Image Clarity

And also it is desirable to select optical mask line width depending on conformity to the visual assessment. Image Clarity values of five optical mask line widths are measured at the same time. For high Image Clarity specimens, use 0.125 mm and 0.25 mm in line width, for medium Image Clarity specimens, use 0.50 mm in line width and for low Image Clarity (matt) specimens, use 1.0 mm and 2.0 mm in line width.

3. A COMPARISON OF IMAGE CLARITY VERSUS GLOSS AND HAZE

3.1 Comparison of Measured Values for Gloss and Image Clarity

Four different tile specimens (Figure 5) that are similar in Gloss yet have different Image Clarity were selected for analysis. The tile designated A1 is a black glass, A2 is PVC, A3 is a painted plate, and A4 is a ceramic tile.

By the visual assesement, first, there is no discernable difference in Gloss among any of the specimens. Second, there are large differences in Image Clarity among all the specimens.

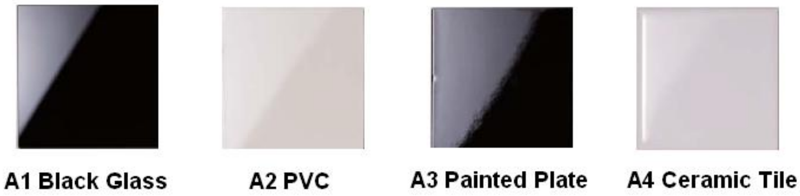

Figure 5: Reflective Test Specimens

The specimens were measured for Gloss at 60˚ and 20˚ in accordance with ISO 2813[ii] and Image Clarity in accordance with ISO 17221[iii] , using an Image Clarity Meter Model ICM-1T[1]. These data are presented in Table1.

One observes that the Gloss values at 60˚ are nearly the same, approximately 90 GU. Whereas the Gloss values at 20˚ and the Image Clarity values plot in descending order, A1 > A2 > A3 > A4. However the Gloss values at 20˚ do not show any obvious difference. Therefore, Gloss values at 20˚ and 60˚ do not conform to visual impressions. On the other hand, the Image Clarity C(0.25) values show large differences and those differences conform to visual impressions.

Table1 Measured Values for Reflective Test Specimens

Test Specimen	A1	A2	A3	A4
Gloss Value GU (60˚)	90.8	90.9	87.7	87.1
Gloss Value GU (20˚)	86.5	82.3	77.0	72.3
Image Clarity C(0.25)	99.5	32.0	18.9	1.6

3.2 A Comparison of Haze and Image Clarity

Four different transparent plastic specimens (Figure 6) that have different Haze values and Image Clarity values were selected for this analysis. The specimens B1 through B3 are plastic films. Specimen B4 is an anti-glare film.

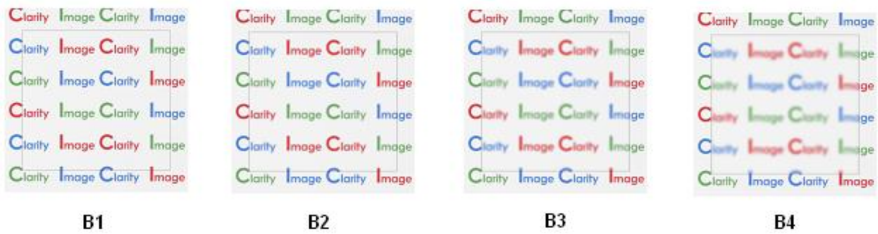

Figure 6: Transparent Test Specimens

By the visual assesment, specimens B1, B2 and B3 have the same high Image Clarity. The Image Clarity values of specimen B4 is distinctly lower than the grouping of the other three. The Haze of specimen B1 is barely discernable. Specimen B2 & B4 have low Haze values and specimen B3 has the highest Haze values.

The films were measured for Haze values on a Haze Meter, HZ-V3[2] in accordance with ISO 14782[iv] and Image Clarity in accordance with ISO 17221, using an Image Clarity Meter Model ICM-1T. These data are presented in Table 2.

---

[1] Manufactured by SUGA Test Instruments Co., Ltd., Shinjuku-ku, Tokyo, Japan

The Haze values increased (B1 < B2 < B3) and Image Clarity values decreased (B1 > B2 > B3), while cloudiness by visual impression increased. Therefore both sets of measured values conformed to visual impressions.

Table2 Measured Values for Transparent Test Specimens

Test Specimen	B1	B2	B3	B4
Haze Value (%)	1.6	14.1	33.2	14.7
Image Clarity C(2.0) (%)	97.1	90.4	88.5	38.4

However, in case of B4, the anti-glare film, the transmitted image is obviously hazier and appears indistinct when compared to plastic film B2. The evaluation of the Haze values gave similar values of about 14 for both specimens, but that result does not conform to visual impressions. On the other hand, the Image Clarity C(2.0) values were 90.4 for B2 and 38.4 for B4. This large difference in measured values conforms to visual impressions. From these observations and results, we conclude that the Image Clarity values are useful in the evaluation to determine the degree of glare. This is especially cogent for anti-glare films that have significant light diffusion properties.

4. CONSIDERATION OF DIFFERENCES IN RESULTS DUE TO DIFFERENCES IN METHODS OF EVALUATION

Differences between measured values of Gloss & Haze compared to Image Clarity are due to differences in Measurement Principles. Gloss values are determined by amount of reflected light within a small solid angle. In other words, Gloss largely depends on the amount of light reflected by an object. Haze is defined as percentage of light deviating by more than 2.5° from the incoming light transmitted through test specimen. These metrics do not access or measure image clarity.

Conversely, Image Clarity, either reflectance or transmittance measurement, is obtained by quantifying the amount of light transmitted through the optical mask at a particular spatial frequency. For example, in case of measuring Image Clarity for optical mask with 2 mm widths, the amount of light transmitted through optical mask is the greatest when image appears fully within the 2 mm transparent part of optical mask, and the detection is the smallest when image appears fully within 2 mm blocking part of optical mask. In such case, Image Clarity values will be the highest at 100 %. This phenomenon corresponds directly to the spatial frequency of the specimen texture. The degree of Image Clarity is influenced by the clearness, surface irregularities and haziness of surfaces. Gloss meters and Haze meters do not correctly access this phenomenon. Image Clarity is not the same as and should not be confused with Gloss or Haze.

5. PRECISION OF MEASUREMENT DATA

The confidence in a measurement system is directly related to its precision. The Image Clarity Meter was examined for its repeatability and reproducibility limit with 95% probability in accordance with ISO 5725-1[v] . The repeatability r and reproducibility R for Image Clarity by reflection measurements were performed at 6 different test laboratories for 6 different types of painted plates. For Image Clarity by transmission, measurements

---

[2] Manufactured by SUGA Test Instruments Co., Ltd., Shinjuku-ku, Tokyo, Japan

were performed at 6 different test laboratories using 4 kinds of transparent resins. The repeatability and reproducibility are presented in Table 3.

Table3 Repeatability and Reproducibility Data for Image Clarity

Measurement Conditions	C(0.5)		C(2.0)	
	r	***R***	***r***	***R***
Reflectance	**0.2～0.3**	**0.7～1.9**	**0.6～0.7**	**1.0～2.3**
Transmittance	**0.1～0.5**	**0.4～1.2**	**0.1～0.9**	**0.2～1.8**

6. CONCLUSIONS

We described the significance of Image Clarity evaluation by comparisons with traditional Gloss and Haze evaluations. Image Clarity is widely used as an evaluation and analysis tool in Sensory Evaluation, since it captures differences in visual properties. This is not possible with only traditional methods of evaluation.

A new paradigm of assessing the quality of finishes using Image Clarity delivers to manufacturers the information and data that they need to perfect their materials and processes to perfect high quality finishes. This technique offers significant, valuable information that is not available from conventional sources, such as Gloss and Haze.

ACKNOWLEDGEMENTS

The authors gratefully acknowledge Mr. Jack A Ladson, Color Science Consultancy, for his contributions for this paper.

REFERENCES

[i] *Research on Paper Quality of Glossy Postcards for Inkjet Printers,* Research Paper, Institute for Posts and Telecommunications Policy (IPTP) Monthly Report 2003.1 No.172, Toyoichi Hosokawa, Mitsuyasu Kitajima

[ii] ISO 2813 *Paints and varnishes, Determination of specular gloss of non-metallic paint films at 20 degrees, 60 degrees and 85 degrees*

[iii] ISO 17221 *Plastics — Determination of image clarity (degree of sharpness of reflected or transmitted image)*

[iv] ISO 14782 Plastics, *Determination of haze for transparent materials*

[v] ISO 5725-1 *Accuracy (trueness and precision) of measurement methods and results — Part 1: General principles and definitions*

Address: Hideo Kita, Calibration Dept, SUGA Test Instruments Co., Ltd.,
5-4-14, Shinjuku, Shinjuku-ku, Tokyo, 160-0022, JAPAN
E-mails: kita@sugatest.co.jp

Painting by Numbers: Transforming Fields and Edges to Vectors

Carinna Parraman, Paul O'Dowd, Mikaela Harding
The Centre for Fine Print Research, University of the West of England,
Bower Ashton Campus, Kennel Lodge Road, Bristol, BS3 2JT, UK

ABSTRACT

This paper considers alternative approaches to image making and printing that moves from the on-screen representation of images and painting applications, to the physical generation and methods for surface deposition or *2.5D printing*. The research investigates the application of new materials and print processes, as an alternative to four-colour separation and half-toning and departs from traditional halftone screening that uses a vector approach to image construction. The first aspect of the paper describes a non-photorealistic rendering image segmentation algorithm that is used to create a series of colour texture layers. The second part of the paper describes a preparatory UV curing additive that can be used to increase the textured qualities of the brush strokes.

1. INTRODUCTION

The theoretical and practical objective of this research is to gain a deeper understanding of how physical artworks can be created that incorporate both analogue (paint, ink, graphite) and digital (vector); and could be described as containing textural or 2.5D qualities.

Contemporary printing has evolved as a process that is capable of printing flat areas of colour, alongside text, blends of colour and photographic images. In the emerging 2.5D and 3D print market, there is now a requirement to develop methods that can reproduce textures that have the look and feel of, for example, brushstrokes of old master paintings, or as created in a painting software. Current colour painting software tends to mimic how layers of colour are applied as if one were painting. Research so far has considered the shape of brushes, edges, opacity, pressure but less so about the textural qualities of the brush mark or the over-layering of layers of colour, or how to simulate watercolour, ink, oil paints and acrylics.

Texture is a visual attribute that enables us to distinguish the differences between materials (substances or substance out of which a thing is or is made), identify the structure and shape of objects, and discriminate edges in a complex pictorial scene. In order to gain an understanding to create verisimilitude with materials, we can study lighting techniques, drawing and painting techniques used by artists (Bayer, 2004; Hollman, 2004; Jordan, 1995; Constable, 2007) along-side scientists working on human vision and texture perception. Three main characteristics identified as useful in determining the qualities of a surface texture are: value, repetition and edges. (Landy, 1996; Klatzky, 2010) In our search for an identification of what are the basic constituents to identify, classify and reproduce texture, (Marr, 1980) differentiates between image and representation, and the use of what he describes as *primitives* to describe a shape. There are two primary classes of shape primitive: surface based (2D) and volumetric (3D). Of special interest, volumetric primitives involve the spatial distribution of a shape and vectors to describe its dimensions, along with shading and texture gradients.

In previous research, the authors considered how by observing the brush strokes of painters, (Parraman, 2012; 2013) images can be generated through the use of lines, modulation of similar strokes and a repetitive over layering of paint. Inspired by the meticulous painting methods by artists such as Van Gogh and Seurat, the objective for the experiment was to create a vector-driven painting machine that applied a brush loaded with paint to paper in a methodical and mechanical way, yet remain human analogous.

Whilst a vector approach (digital format) is highly machine repeatable, the resulting individual painted brush strokes (analogue) are not. We study the creation of non-uniform but harmonious painting effects across paper substrates through the actuation and placement of the brush, and the flow of paint. We are developing a contemporary approach that is based on vector or .SVG (Scalable Vector Graphics), which provides a set of instructions to drive CNC paths. In software programmes, a vector path is a series of mathematical elements that describe a set of lines, curves, arcs, and a combination of all to form closed shapes. A path can be *stroked* to obtain different thickness or colours, or used as input for other elements such as pressure, gradients in height, and blends to include opacity and translucency. We consider a vector-based drawing philosophy as significant to gaining an understanding of alternative approaches, which break away from pixels (digital screen resolution) and halftones (analogue print resolution).

2. RELATED LITERATURE

Non-photorealistic rendering (NPR) is a body of research which interprets digital formats (captured visual scenes or original works) and renders them with an alternate artistic expression. Typical source formats are pixel based images, although NPR can also be derived from 3D models and determined algorithmically without a prior source.

The utility in NPR can be functional, for instance 'unrealistic' shading schemes aid in the visualisation of complex parts drawn in computer-aided design (Gooch et al, 1998). The utility of NPR can also be to provide a purely artistic interpretation from a source, or to provide interactive software tools to aid in the creation of stylised digital art works. Of particular interest, a subset of NPR is stroke based rendering (SBR) which interprets pixels to strokes. We consider strokes as analogous to vectors, representing a series of movements with magnitudes and directions.

Often SPR seeks to emulate famous painterly styles, such as impressionism (Kasao, 2006; Yang, 2008), oriental ink painting (Ning, 2011; Cheok, 2007), or pen-and-ink illustration (Winkenbach, 1994). In this way SPR is motivated to model characteristics of effectors (i.e. a horsehair brush), mediums (i.e. watercolour) and substrates (i.e. canvas) to synthesise a convincing screen based render (Curtis, 1997). Our motivation is not to render the illusion of painterly styles with pixels. Rather we explore the operation of print apparatus for the tangible production of texture, which originate in painterly styles. As such the characteristics of effector, medium and substrate are inherent to the apparatus we use; we are focused on deriving the appropriate effector movement from digital sources.

We draw on NBR literature for algorithms to determine image segmentation, stroke placement and stroke characteristics that are transferable to machine control, detailed in section [3]. We intend to send a printer a sequence of movements and gestures, rather than a field of pixels to raster to a screen or to scan on to a substrate.

There are many examples of prior works that utilise a machine to produce art in more human analogous ways. Lindemeier (2013) includes a review of early painting machines and related artists; 'eDavid' (Lindemeier, 2013), 'Paul' (Tresset, 2013) and a humanoid robot (Kudoh, 2009) are painting machines that closer approximate human movement. All three approaches utilise digital camera data to compare the working canvas against a digital source image. These three approaches therefore attempt to emulate the progressive development of paintings, stroke by stroke, by utilising predominantly 2D visual feedback during operation. In our approach we attempt to extract this chronological information from digital source images, by interpreting fields of pixels through segmentation and edges, to create a time-series composition of many-layered vectors. We develop this level of automation so that we may later experiment with controlling the generation of texture and expressive mark making.

3. IMAGE SEGMENTATION METHODOLOGY

We have developed a methodology inspired by the NPR algorithms for texture directionality described by Kasao et al through several papers (Kasao, 2006; Kasao 1998a; Kasao1998b). We use the convolution of a source image for texture directionality and edge detection. We implement a simpler K-Means clustering algorithm for image segmentation.

As an iterative algorithm, the K-means clustering progressively divides an image up into a predetermined number of segmentations, with a result analogous to a paint-by-numbers template. We experiment with low numbers of segmentations, such as 16 or 20, as we expect to run each segmentation as a paint layer. The segmentations do not necessarily map the spatial relationship of pixels, nor remain a fixed size of image partition. The segmentations group pixels by their similarity in calculated properties. Each segmentation is re-evaluated to generate the average characteristics of their assigned pixel grouping, thus altering the subsequent criteria for pixel assignment. The iterative algorithm ends when no more pixels are eligible to be reassigned, and therefore the segmentation averages have attained stable characteristics.

The segmentation minimises the Euclidean distance of six variables; x coordinate distance between a pixel and a possible segmentation centroid x coordinate (D_x), y coordinate distance between a pixel and possible segmentation y centroid coordinate (D_y), a pixel edge strength versus a possible segmentation average edge strength (D_e), a pixel texture directionality versus a possible segmentation average texture directionality (D_d); and the distance in colour space between a pixel hue, saturation brightness value, against the average hue, saturation brightness of a possible segmentation (D_h, D_s, and D_b respectively).

The variables D_x, D_y, D_e, D_d, D_h, D_s and D_b are given weighted influence by a fixed gain value, *Kx, Ky, Ke, Kd, Kh, Ks, Kb* respectively. In this way, an image can be segmented with little regard for pixel spatial relationship (K_x, K_y as small values, 0.01 works well), and high regard for texture directionality and edge strength (K_e and K_d as large values, such as 2.5). The Euclidean distance is thus calculated between each pixel and each segmentation (D_{ps}) as:

$$\Delta x = \sqrt{(D_x * K_x)^2}$$

$$\Delta y = \sqrt{(D_y * K_y)^2}$$

$$\Delta d = \sqrt{(D_d * K_d)^2}$$

$$\Delta e = \sqrt{(D_e * K_e)^2}$$

$$\Delta h = \sqrt{(D_h * K_h)^2}$$

$$\Delta s = \sqrt{(D_s * K_s)^2}$$

$$\Delta b = \sqrt{(D_b * K_b)^2}$$

$$D_{ps} = \sqrt{\Delta x + \Delta y + \Delta d + \Delta e + \Delta h + \Delta s + \Delta b}$$

The smallest D_{ps} value assigns the pixel to the related segment cluster. We have used values Kx = , Ky = , Ke = , Kd = , Kh = , Ks = , Kb = to good effect.

The completed segmentation combined with the pixel edge strength and texture directionality provides useful data for machine control. Each segmentation provides the average hue, saturation and brightness values for the assigned pixels, creating a finite palette of colours (equal to the number of segmentations) to paint. The segment average edge strength value provides the order in which to conduct the painting, where strong edges are likely to be outlines or highlights, and performed last in the painting order. The segment average edge strength also provides a means to select a brush size, where low edge strength indicates a uniform area of an image, and so a large brush and a low density of strokes per canvas size can be adopted. Importantly, the information relating to individual pixels is preserved, so the brush stroke length and direction can be mapped from a pixel texture directionality and edge strength, creating a non-uniform characterisation of strokes within a single segmentation of pixels.

4. DEVELOPMENT OF INKS

The second aspect of this project is the development of a water-based UV LED curable medium that can be added to artist's inks and pigments to create a UV curable paint. In normal UV resin bases for inks and paints, the viscosity of the individual components are as low as possible to ensure satisfactory production as well as good flow behaviour of the liquid formulation. However in this application, the resin needs to be viscous in order to hold the texture of the paintbrush mark when the ink/paint is deposited.

UV LED systems potentially offer a greener alternative to conventional mercury vapour lamps used to UV cure coatings for ink, wood/furniture, electronics and other industries. The main advantages of the LED lamps are that they are more energy efficient – using up to 60% less energy than mercury UV lamps, more cost efficient – lamp lifetimes of up to 10,000 hours, and more environmentally friendly – irradiation in the near visible region (380-410 nm), no formation of ozone when curing in air and no mercury lamps to dispose of at the end of their life.

In the current formulation, the medium contains a hydrophilic aliphatic urethane acrylate solution in water, containing 50% acrylated products. This has a 95% solids content and so is easily diluted with water. Tripropylene glycol diacrylate (TPGDA) acts as a reactive dilutant monomer that also promotes adhesion to substrate, hardness and scratch resistance of the cured layer (Mashouf, 2014). Other additives are used to further increase adhesion to substrate and flow of the medium.

Because of the long wavelength absorption characteristics, which are also better suited to commercially available LED's, acylphosphine oxides are particularly useful for the polymerization of pigmented formulations where irradiation at longer wavelength is desired. This family of photo initiators are used due to the high reactivity of the photo chemically formed phosphonyl radicals that arise from the high electron density at the phosphorus atom. Furthermore, the pyramidal structure of the radicals provide more favourable steric conditions for the unpaired radical site to react with monomers to initiate and propagate the polymerization reaction (Yagci, 2012).

A tertiary amine, N-vinyl pyrrolidinone (NVP), is used in the formulation to help in overcoming oxygen inhibition (Husar, 2014). Oxygen inhibition is due to the fact that molecular oxygen, at ambient conditions, exists as a diatomic molecule with a triplet diradical electronic ground state. Due to these triplet and radical characteristics, oxygen has high chemical reactivity towards the phosphonyl radicals created by the photo initiator, leading to the early termination of the polymerization reaction. (Miller, 2003) Therefore the free-radical photo polymerization reaction that occurs within the formulation can be inhibited significantly by oxygen in the atmosphere. The final ingredients in the UV LED formulation are mattefying silica to reduce the glossiness of the cured medium and the artist's pigment/materials to colour the formulation.

4. CONCLUSIONS

The paper describes methods for segmenting an image using NPR algorithms that can be exported as vector or .SVG documents that provides a set of instructions to drive CNC paths to a painting rig. Philosophically, we believe an image originally composed or acquired as vectors provides a richer description of an image, which would be especially suited to machine production. Through a process of segmentation and edges, fields of pixels are transcribed into many-layered vectors. The NPR algorithms are the starting point to transcribe the vectors into textured brushstrokes using paint and a highly experimental printer rig. The printer rig is capable of applying multilayers of artist's paints that include both traditional and UV curable inks (as described in section 4). The user is able to change the appearance of the layers ie. changes to translucency and viscosity by modifying the paints by hand, as well as change the direction of the brushstroke and the arc of the brush stroke by modifying the software, thus enabling the user to extend a greater control over the multi-layering process.

ACKNOWLEDGEMENTS

This work was supported by Arts and Humanities Research Council, Follow-on Funding, Impact and Engagement, Research Grant Ref: AH/L015277/1

REFERENCES

Bayer, A. 2004. *Painters of Reality*. New York: Yale University Press.

Cheok, A.D., Z.S. Lim and R.T.K. Tan 2007. *Humanistic oriental art created using automated computer processing and non-photorealistic rendering,* Computers Graphics 31(2), 280-291.

Constable, M. 2007. *The Painted Photograph: Technical Commonality between the Digital Composite and the Pre-Modern Painting*, World Conference on Educational Multimedia, Hypermedia and Telecommunications. Vancouver: Canada.

Curtis, C.J., S.E. Anderson, J.E. Seims, K.W. Fleischer, and D.H. Salesin 1997. Computer-generated watercolour, Proc. 24th Annual Conference on Computer Graphics and Interactive Techniques, SIGGRAPH '97, pp. 421-430. ACM Press/Addison-Wesley.

Gooch, A., B. Gooch, P. Shirley, and E. Cohen 1998. A non-photorealistic lighting model for automatic technical illustration, Proc. 25th Annual Conference on Computer Graphics and Interactive Techniques, SIGGRAPH '98, pp. 447-452. ACM, NY

Hollman, E. and J. Tesch 2004. *Trick of the Eye, Trompe L'oeil Masterpieces*. Prestel.

Husar, B. 2014 *Experimental Comparison Of Various Anti-Oxygen Inhibition Strategies In LED Curing*, RadTech, Vienna University of Technology.

Jordan, W.B. and P. Cherry 1995. *Spanish Still Life from Velázquez to Goya*. London: National Gallery.

Kasao, A. and K. Miyata 2006, *Algorithmic painter: a NPR method to generate various styles of painting*, The Visual Computer 22(1), 14-27.

Kasao, A. and M. Nakajima 1998a. *A resolution independent nonrealistic imaging system for artistic use*, Proc. IEEE International Conference on Multimedia Computing and Systems, pp. 358-367 (1998a)

Kasao, A. and M. Nakajima 1998b. *K-means algorithm using texture directionality for natural image segmentation*, IEICE tech. report. Image Engineering 97(467), 17-22.

Klatzky R.L. and S. J. Lederman 2010. *Multisensory Texture Perception*, Multisensory Object Perception in the Primate Brain. Naumer, M.J. and J. Kaiser (Eds.) Springer.

Kudoh, S., K. Ogawara, M. Ruchanurucks and K. Ikeuchi 2009. *Painting robot with multi-fingered hands and stereovision,* Robotics and Autonomous Systems 57(3), 279-288.

Landy, M. 1996. *Texture Perception*, Encyclopedia of Neuroscience. Adelman, G. (Ed.) Amsterdam: Elsevier

Lindemeier, T., S. Pirk, and O. Deussen 2013. *Image stylization with a painting machine using semantic hints*, Computers Graphics 37(5), 293-301.

Marr, D. and E. Hildreth 1980. *Theory of Edge Detection*, Proc. of the Royal Society of London. Series B, Biological Sciences, Vol. 207, No. 1167: 187-217.

Mashouf, G., M. Ebrahimi, and S. Bastani. 2014. *UV curable urethane acrylate coatings formulation: experimental design approach*, Pigment & Resin Tech., 43 (2) 61-68.

Miller, C.W., C. E. Hoyle, S. Jönsson, C. Nason, T. Y. Lee, W. F. Kuang and K. Viswanathan, 2003. *N-Vinylamides and Reduction of Oxygen Inhibition in Photo polymerization of Simple Acrylate Formulations,* Photo initiated Polymerization, *ACS Symposium Series*, 847, 2–14.

Ning, X., H. Laga, S. Saito, and M. Nakajima 2011. *Contour-driven Sumi-e rendering of real photos*, Computers Graphics. 35(1), 122 -134.

Parraman, C. 2013. *The development of vector based 2.5D print methods for a painting machine*, Proc. IS&T Elec. Imaging Sci. & Tech. 8652.

Parraman, C. 2012. *Dark Texture in Artworks*, IS&T Elec. Imaging Sci. & Tech. 8292.

Tresset, P. and F.F. Leymarie 2013. *Portrait drawing by Paul the robot*, Computer Graphics 37(5), 348-363.

Winkenbach, G. and D.H. Salesin 1994. *Computer-generated pen-and-ink illustration*, Proc. 21st Annual Conference on Computer Graphics and Interactive Techniques, SIGGRAPH '94, pp. 91-100. ACM, New York.

Yagci, Y. et al, 2012. *Photoinitiated Polymerization: Advances, Challenges, and Opportunities,* Macromolecules, 43, 6245–6260.

Yang, C.K. and H.L. Yang 2008. *Realization of Seurat's pointillism via non-photorealistic rendering*, The Visual Computer 24(5), 303-322.

E-mails: Carinna.Parraman@uwe.ac.uk, Paul3.O'Dowd@uwe.ac.uk, Mikaela.Harding@uwe.ac.uk

Perception of colours illuminated by coloured light

Shabnam ARBAB, Barbara Szybinska MATUSIAK
Faculty of Architecture and Fine Art, Norwegian University of Science and Technology (NTNU)

ABSTRACT

The present paper reports the findings from a scale model experiment dealing with the assessment of colour under different colour temperatures of light. The data presented in this paper is a part of the findings from a large experiment. The mixed methods approach, which associates both qualitative and quantitative evaluation of the visual environment have been used to answer the following question: *How is the perception of colour influenced by the colour temperature (CT) of light?* The light in this case is a mixture of direct light from a light panel and light reflected from a coloured facade. A questionnaire was used to assess nine alternatives; each of them was a combination of one of three different colours of façade and one of three CTs of light. Forty-seven participants evaluated two different stimuli: Colour of façade and colour of light. Visitors of the exhibition participated as subjects in the experiment.

The experiment was carried out during the exhibition entitled “Colour in the city” at Trondhjems Kunstforening and it was sponsored by the Norwegian Research Council as a part of the yearly so called “research day” activities in Norway.

The results show that both, the colour temperature of light and the colour of façade, have significant impact on the colour perception; CT has stronger effect. It was also found that the nuances shift toward the same direction with the same colour temperature of light for each façade. A similar tendency was observed for the hue. The statistical analysis resulted with trustworthy and precise results that we are happy to present at the AIC-2015.

1. INTRODUCTION

Colour is not the property of objects, spaces or surfaces; it is the sensation caused by certain qualities of light that the eye recognizes and the brain interprets. The colours of the environment influence our experiences of light and the need for lighting – and vice versa: the qualities of light are essential for our perception and experience of colour. Therefore, light and colour are inseparable. Recent studies put the spotlight on considering simultaneously both colour and light due to their importance for architecture and their effect on the quality of life of users as well as on the minimizing energy consumption in buildings.

As it was stated above, light and colour are, however, largely two separate fields of research and most of the research deals with completely other questions than their spatial interaction (Arbab and Matusiak 2015). Considering what was mentioned, the main research question is formulated as follows:

How is the perception of colour influenced by light?

In order to carry out comprehensive analysis about the impact of light on colour perception there is a need to merge qualitative and qualitative approaches since the strengths of both could provide the best understanding. A mixed methods approach, which associates both qualitative and quantitative evaluation of the visual environment, will be used to answer the research questions.

2. METHOD

In order to answer the question, a model with two rooms in the scale 1:10 was used; Each room 50cm x 50cm x 40cm represented a living room 5m x 5m x 4m in the 1:10 scale to be large enough to allow a comfortable observation of an outdoor facade as well as the interior. The walls, ceiling and floor were constructed using 3mm MDF boards. On the outside the models were painted in black colour and on the inside they were painted in grey NCS S 5500-N.

A sample with the reference colour NCS S 1500-N was placed in the first room having large window-like opening toward the street; 14 colour samples (Table 1) were placed in the adjacent room with no opening to the street but illuminated by the white light (6500K) from translucent ceiling. The visitors could deserve if and in which way the colour perception depends on the colour temperature of light. The experiment has been repeated with three different facades, yellow, dark red and light blue; see Figure 3, something that enabled testing of the impact of the colour of the façade. The visitors were asked to assess which of the 14 colour samples looks most similar to the reference colour.

Table 1. 14 selected colour samples

NCS Colour samples code		
NCS S 1505-Y40R	NCS S 1510-Y90R	NCS S 1515-R90B
NCS S 1505-Y70R	NCS S 1502-R	NCS S 1510-B
NCS S 1505-Y80R	NCS S 1502-R50B	NCS S 1502-B50G
NCS S 1505-Y90R	NCS S 1510-R60B	NCS S 1500-N
NCS S 1510-Y80R	NCS S 1510-R90B	

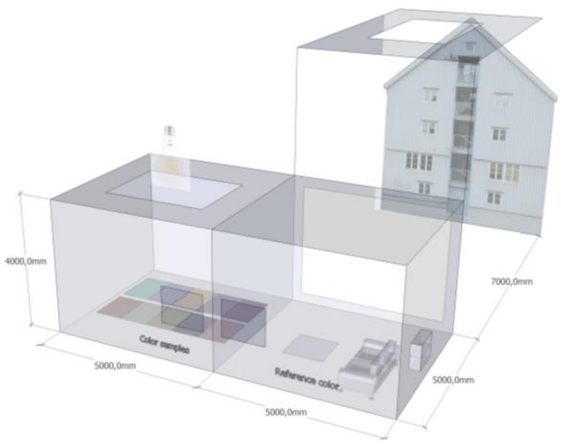

Figure 1: Illustration of the model.

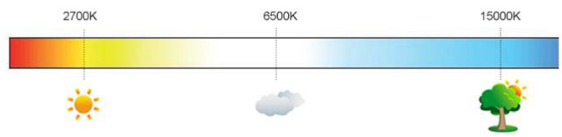

Figure 2: Stimuli 1: Three colour temperatures of light used in the experiment.

Figure 3: Stimuli 2: Three facade colouration to test. From left to right: NCS S 5030-Y80R / NCS S 2002-B / NCS S 4030-Y30R.

The experiment was carried out during the exhibition entitled “Colour in the city” at Trondhjems Kunstforening (Group 2014) and it was sponsored by the Norwegian Research Council as a part of the yearly so called “research day” activities in Norway, and the main objective was to examine the impact of the colour temperature (CT) of light (Figure 2) on visual perception of coloured surfaces in the scale model study.

The subjects were the visitors of the exhibition and participants of the research day, some of them were artists and researchers squinted with colour design or study. The aim was to have as many participants as possible. Since all the subjects received all stimuli, this experiment had within-subject design. It was full factorial approach and all possible combinations of independent variables were distributed in a completely randomized order.

The experiment was independent of weather condition and time of the day. The light was produced by two different light sources: LED based, full-spectrum light panel and LED based Philip hue bulbs. Pilot study was done to select the colour samples from wide spectrum of hues and nuances, to provide a final check of elements and instruments and to ensure a smooth conduct of the experiment. Then analysis of pilot study was done to find out whether further refinements were needed. During the pilot study the time required for running the experiment was also estimated.

Experimental design and planning, Subject selection, Sample selection, Configuration of experimental set-up, Pilot study, Main study, Analysis and reporting were just different stages of this project necessary to make the results more reliable:

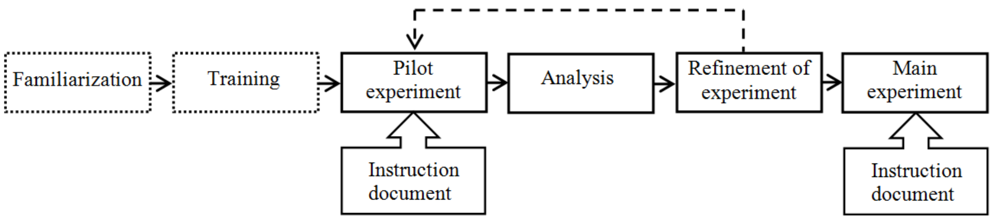

Figure 4: Flowchart of test administration stages (Bech and Zacharov 2007).

The colour samples were chosen from the NCS colour selection, and because of the time limitation of the experiment, it was necessary to narrow down from 71 to 14 samples. To make selection easier, the blackness of all samples was kept at the same level, namely 15%. The procedure for narrowing number of samples was the visual assessment by 5 people who were asked: which of a large number of comparison samples in the test room looked most similar to reference sample in the reference room.

To keep the same light level in both rooms, illuminance was measured in both rooms for each façade. Two Philip hue lamps and two layers of diffusing paper were used in the test room to adjust the light level and to create even light distribution.

3. RESULTS AND DISCUSSION

The overview of answer distribution is shown in Figure 5. The graph indicates the answer distribution on all 9 alternatives.

The effect of the CT of light and colour of façade on the responses was tested by a Stuart-Maxwell test (Stuart 1955, Trujillo-Ortiz 2005), where a computed SM value is evaluated using the chi-2 distribution. This test allows only pairwise comparisons and the results are summed up in Table 3. As is apparent from the low probability values, both the colour of the façade and the colour temperature of light, have significant effects on the answers, with a slightly stronger effect for CT.

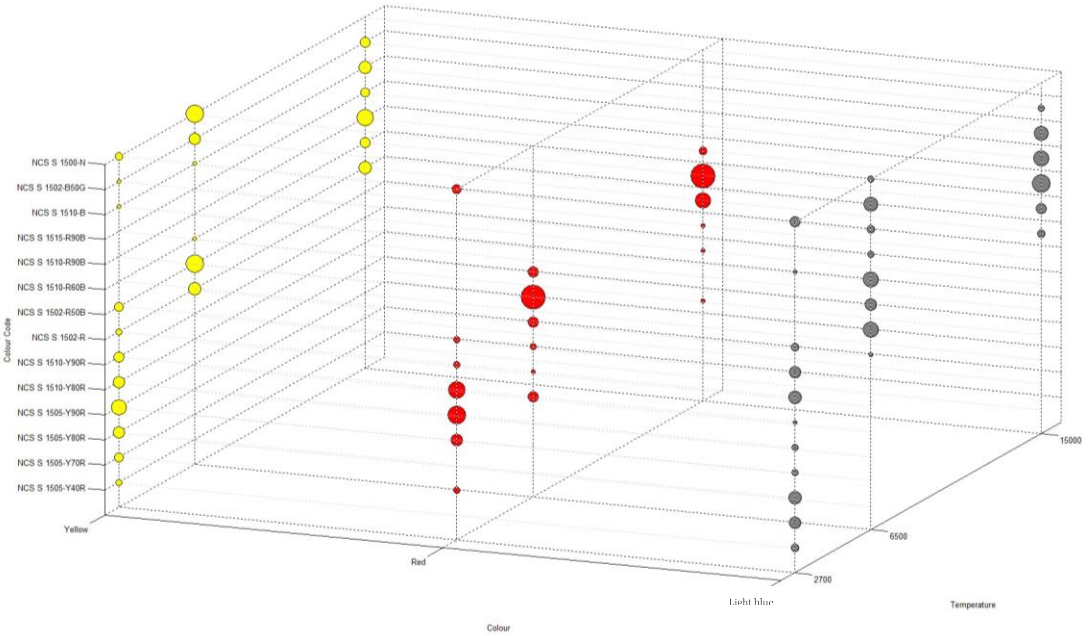

Figure 5: General overview about answer distributions.

In this experiment, all the colour samples had the same blackness on the nuance part but the chromaticity of colours was different. Figure 6 shows the average value of chromaticness. The differences in chromaticness of selected colour samples with different colours of façade are small and the yellow façade resulted with the lowest average of chromaticness. The differences due to different CT of light are bigger, higher temperature contributes to highest chromaticness.

Out of the three colours of façade, only yellow façade did not present in a way that we expect to have been affected by CT of light (Figure 7). See Table 4 for distribution of answers of nuances for each stimulus. Up to now, the effect of each stimulus was analysed but there is another way of analysing data, the interaction of both stimuli for 9 alternatives can be analysed separately. For example for Red façade with CT of 2700 K the tendency of answers is toward the yellowish colour with 90% red and the nuance toward the higher chromaticness. Full analysis of each alternative on NCS colour circle and triangle are available from authors upon request.

Table 3. Stuart-Maxwell analysis (probability values < 0.05 are considered as significant).

Statistical Analysis			
Comparison	SM value	d.f.	Prob
2700 K vs. 6500 K	101.9	13	3.3e-16
2700 K vs. 15000 K	120.1	13	0
6500 K vs. 15000 K	79.1	13	8.2e-12
Light-blue vs. red facade	99.8	13	8.9e-16
Light-blue vs. yellow facade	59.0	13	4.0e-8
Red vs. yellow facade	67.7	13	1.1e-9

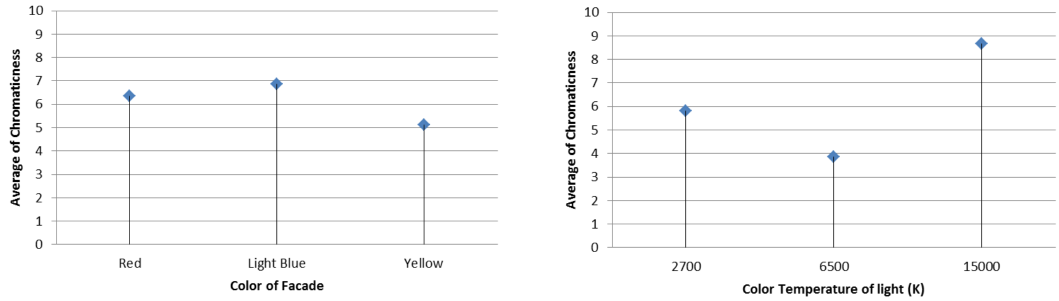

Figure 6: average of chromaticness under different stimuli.

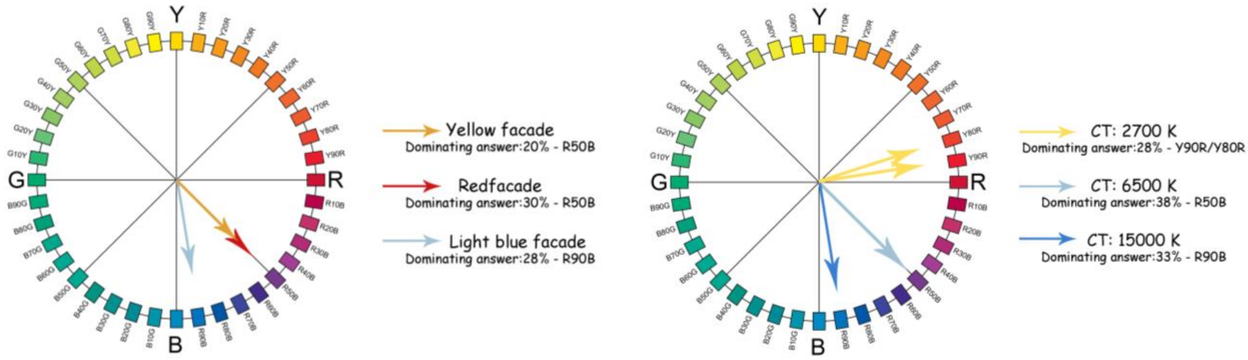

Figure 7: Effect of two stimuli on the hue: Colour of façade and CT.

Table 4. Dominating answers for nuances with different stimuli

Stimuli	Colour of facade			Colour temperature of light (K)		
	Yellow	Red	Light Blue	2700	6500	15000
Dominating answer (%) - Nuances	36% - 1502	51% - 1510	42% - 1510	37% - 1505	60% - 1502	66% - 1510

Another part of the experiment was to use spectral power distribution as a visual representative of light spectrum produced by a lamp. Figure 8 shows the relative intensities of a light source at each wavelength which was measured on the reference sample for three different colour temperatures of light in the same setting as evaluated in main experiment. The quality of light created by different light sources could be compared in this graph.

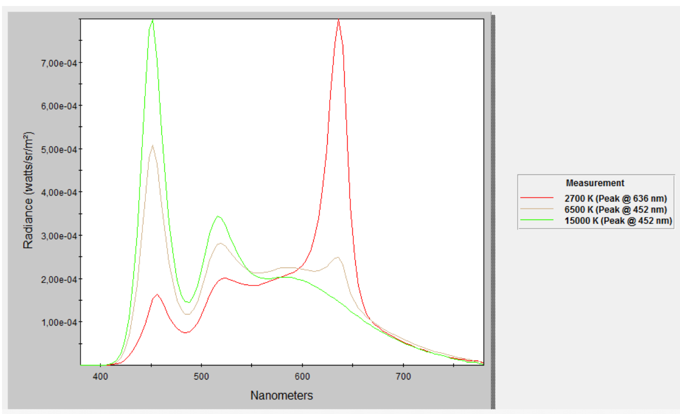

Figure 8: Spectral power distribution of light reflected from reference sample for three colour temperatures of light.

As expected, the results show that the effect of CT of light plays an important role in the perception rather than the façade; this coincides with the subject's answer.

Table 5. Comparison of CT (K) in 9 alt. as well as nutural facade with CT of light panel

CT of light panel	CT of light on reference colour With nutral grey	CT of light on ref. colour with red facade	CT of light on ref. colour with light blue facade	CT of light on ref. colour with yellow facade
2700	2589	2387	2743	2511
6500*	6007	5771	7006	6054
15000*	12425	12530	17879	12975

*After measuring spectral distribution on the light panel, it was found that the CT that was fixed on the light panel was not exactly equal with the measured by the PR-655 SpectralScan. The panel displayed 6500 and 15000 K and the measured values were respectively 6700 and 16200 K.

4. CONCLUSIONS

This paper discussed the interaction between light and colour on the perception of colour surfaces. Two predictors act as independent variables: Colour of façade and CT of light. In this experiment we attempted to make the model, the illumination and the outdoor environment as real as possible. The results of this study lead to the following conclusions:

If the effect of each stimulus was considered separately, the CT of light was found as most important predictor for the evaluations of all nine alternatives even though the colour of façade had effect as well.

But if the interaction of CT of light and colour of facade for each alternative were considered then the shifts from yellowish to bluish when the CT of light was increased was registered. The shift toward bluish stopped at the purple in the case of red façade, while the two other facades contributed to the shift closer to the bluish. So the effect of façade is weaker than CT of light, exactly like what we have experienced in with real overcast sky.

ACKNOWLEDGEMENTS

The authors gratefully acknowledge the contribution of Veronika Zaikina, members of the *Light & Colour Group* and Peter Svensson, professor at the Department of Electronics and Telecommunications of NTNU, for their assistance in conducting the experiment.

REFERENCES

Arbab, S. and Matusiak, B. S. The impact of light at the perception of colours in architecture, state of the art study and suggestions for further research. In AIC 2015, *Proceedings of Colour and image*. Tokyo.

Bech, S. and Zacharov, N. 2007. Perceptual audio evaluation-Theory, method and application, John Wiley & Sons.

Light and Colour Group. 2014. Colour in the City [Online]. Available: http://www.ntnu.no/trykk/publikasjoner/FargeiByen/

Stuart, A. 1955. A test for homogeneity of the marginal distributions in a two-way classification. Biometrika, 412-416.

Trujillo-Ortiz, A. 2005. StuMaxtest. Matlab Central.

Address: Shabnam Arbab, Dept. of Arch. Design, Form and Colour Studies, Norwegian University of Science and Technology (NTNU), Alfred Getz vei 3, 7491 Trondheim, Norway
E-mails: Shabnam.arbab@ntnu.no, barbara.matusiak@ntnu.no

Effects of Furniture Colour on Apparent Volume of Interior Space

Keishi YOSHIDA, Masato Sato
Division of Environmental Sciences, Kyoto Prefectural University

ABSTRACT

This study was conducted to evaluate the effects of furniture colour on the apparent volume of the interior space of a house. Psychological experiments were conducted using one-tenth scale models of a room. It was found that white solids were found to make the interior space appear more spacious compared with the other colours. As for the solids used to simulate beds, the taller the solid, the apparent volume of interior space becomes more cramped. As for the solids used to simulate cabinets, all solids except for the white solids made the interior space appear cramped, and increasingly so with increasing volume, whereas the white solids hardly made the interior space appear cramped, regardless of their volumes. In case of the solids having the same volume, interior space placed the solids used to simulate beds appeared more cramped than those placed the solids used to simulate cabinets.

1. INTRODUCTION

Since the concept of minimalism has become popular, the interior spaces of houses have become more compact than ever before. Therefore, it has become important issue how to make interior spaces appear spacious. Colours of interior components is one of the most successful methods for achieving this goal. There are many psychological effects of colour; advancing colour, receding colour, expanding colour, contracting colour and so on. It is evident that some of these effects play important roles in people's perceptions of interior spaces. The colours of the walls, floor, and ceiling of a room have a strong influence on the apparent volume of the room. Some studies have been conducted to evaluate the effects of the wall colour on the apparent volume of a room. One study found the effects of accent colour on the apparent distance to a front wall. Because interior spaces are usually furnished, it is clear that furniture colour must also influence the apparent volume of a room. However, only a few studies have been conducted on the effects of furniture colour on the apparent volume of a room.

The purpose of this study is to evaluate the effects of furniture colour on the apparent volume of the interior space of a house.

2. EXPERIMENTAL METHOD

A series of psychological experiments were conducted to evaluate the apparent volume of an interior space using a one-tenth scale model of a room measuring 2.4 m in ceiling height and 3.6 m in width and depth. The walls and floor were painted in the achromatic colour N8. A luminous ceiling comprising a milk white acrylic plate that transmitted light was included to maintain uniform interior illuminance. Fluorescent lamps of a high colour-rendering type were installed above the acrylic plate. The average interior illuminance level was approximately 250 lx. Seven types of rectangular solids were placed in the scale model of the room, one at a time, to simulate furniture pieces such as beds and cabinets. The six colours (Red, brown, blue, black, grey and white) used in the experiments were red, blue, brown, white, grey, and black. There were 42 experimental patterns made up of combinations of the six colours and seven solids. A standard model simulating the room without a solid and a comparison model with a solid inside were presented side by side. Figure 1 shows the experimental configuration, and figure 2 shows seven comparison models, each with a solid inside, and the dimension of the solids.

The subjects consisted of 17 females and 3 males from the 20–26 years age group. The subjects had no colour-vision deficiencies. The experimental patterns were randomly presented to each subject. The magnitude estimation method was applied to evaluate the apparent volume of the room. The 20 subjects were asked to look inside each model through a viewing aperture in the rear wall and to report what they perceived to be the volume of the comparison model relative to that of the standard model. The volume of the standard model was set to a reference value of 100.

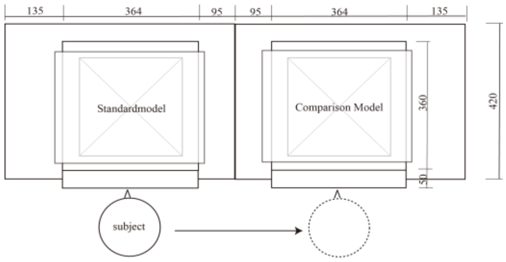

Figure 1: Experimental configuration.

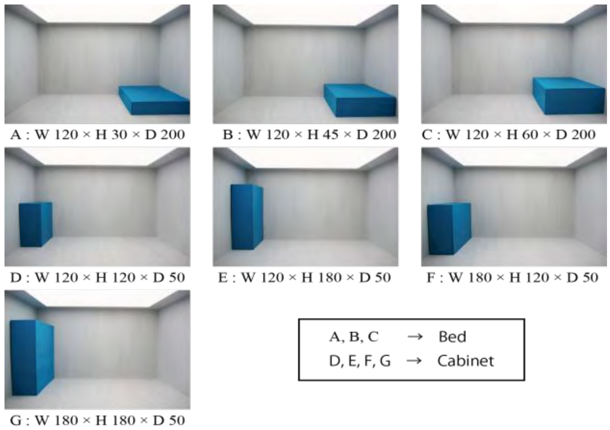

Figure 2: Comparison models with the solids inside the model and the dimension of the solids.

3. RESULTS AND DISCUSSION

3.1 Comparison of rectangular solids

Table 1 shows the "Magnitude average value" or "M value" for each colour and solid combination. Red coloured had the highest average value and blue coloured had the lowest average value for each solid. The white solids had the highest M values for all solids. The black, red, and brown solids had the lowest M values. The white solid brightness was N9.5, and the brightness of the scale model wall was N8. The white solid brightness was closer to the wall brightness than the brightness of any other colour, and therefore, the white solids emphasised the unity between the scaled model interior and the solid more than the other solids. This is believed to be the reason that the white solids had the highest M values. The advancing–receding phenomenon of the red and blue colours was also observed. However, some of the brown solids had M values that were not lower than the blue solids. The reason for this is that, although brown is an advancing colour like red, brown suggests the idea of wooden furniture. Thus, the brown solids rarely produced a feeling of strangeness and were less noticeable than the red solids.

Table 1. Magnitude average values by Solid colour and Comparison model.

		Comparison model						
		A	B	C	D	E	F	G
Solid colour	Red	91.57	86.08	75.68	91.93	88.6	87.52	80.98
	Brown	92.54	88.2	79.19	94.66	85.1	88.87	82.01
	Blue	96.05	87.85	78.61	93.19	92.1	93.19	83.52
	Black	94.28	84.3	78.11	91.13	88.45	87.27	80.05
	Grey	95.63	90.16	83.27	97.38	93.31	91.15	84.99
	White	101.73	95.04	83.78	99.66	95.95	97.3	93.76

	Maximum value		Minimum value

3.2 Differences in apparent volume with differences in height

As for the solids used to simulate beds, the taller solids of all colours, the apparent volume of interior space becomes more cramped. The differences in the M values of the different colours were not significant, however, the black solids made the interior space appear more cramped than the white solids, even though the solids were 45-cm high. The results suggest that it is important to pay attention to the balance of height and colour when choosing a bed.

As for the solids used to simulate cabinets, two comparisons of the differences in apparent volume were made to assess the effect of differences in cabinet height for the same width. The results are shown in Figure 3. T-tests were conducted to clarify the relationship between the apparent volume and the colour. In the case of solids D and E, the brown and grey colours had statistically significant effects (level of significance 0.05) on the apparent volume. In the case of solids F and G, all colours except white had statistically significant effects. The wider the width of the solid, the apparent volume of interior space becomes more cramped by a solid of greater height. This means that the interior space appeared more cramped with solids of greater volume, even for the same change in height. With the white solids, however, the apparent volume of the interior space was largely unaltered by changes in the solids' heights, regardless of their width and volume, and the differences were not statistically significant.

3.3 Differences in apparent volume with differences in width

As for the solids used to simulate cabinets, two comparisons of the differences in apparent volume were made to assess the effect of differences in cabinet width for the same height. The results are shown in Figure 4. The t-test results showed that, in the case of solids D and F, the red, brown, and grey colours had statistically significant effects on the apparent volume. In case of solids E and G, the red, blue, black, and grey colours had statistically significant effects. However, the white did not have a statistically significant effect in any case. As with the differences in apparent volume with differences in height, for all of the solids except the white solids, the taller the solid was, the apparent volume of interior space becomes more cramped by a solid of greater width. With the white solids, however, the apparent volume of the interior space was largely unaltered by changes in the solids' heights, regardless of their width and volume. These results indicate that the greater the volume of a solid, the apparent volume of interior space becomes more cramped by increases in solid height or width. On the other hand, the white solids hardly made the interior space appear cramped at all, regardless of differences in height or width.

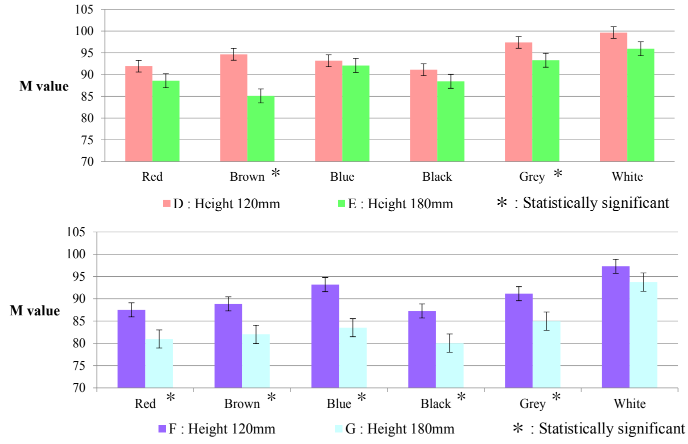

Figure 3: Differences in apparent volume with differences in height.

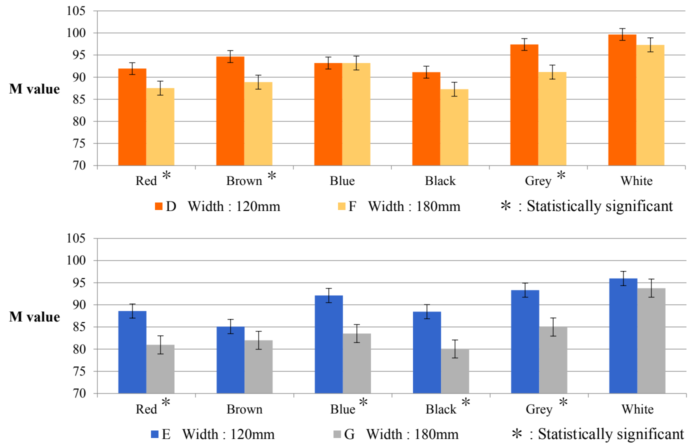

Figure 4: Differences in apparent volume with differences in width.

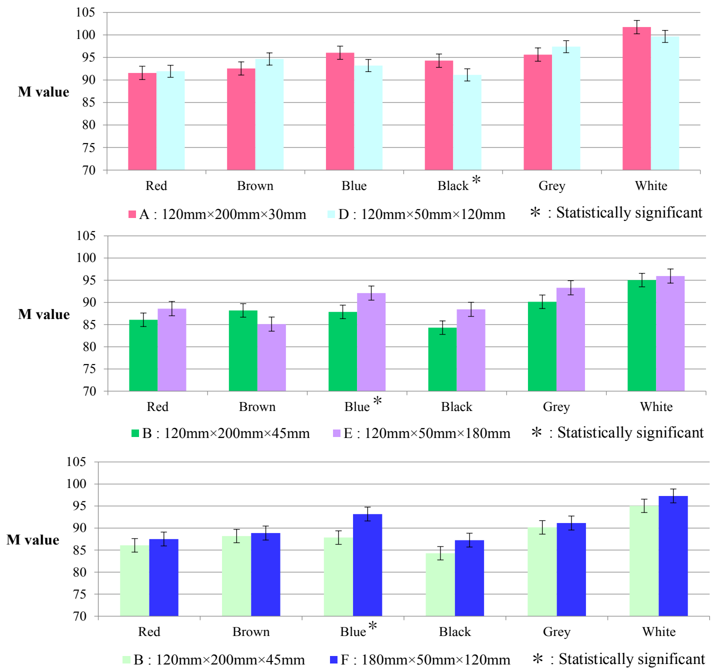

Figure 5: Differences in apparent volume for horizontal and vertical solids of the same volume.

3.4 Differences in apparent volume for each solid volume

T-tests were conducted to clarify the relationship between the apparent volume of the interior space and the position (horizontal or vertical) of a solid of given volume in the space. In this study, the solids used to simulate beds (A, B, and C) were placed horizontally and the solids used to simulate cabinets (D, E, F, and G) were placed vertically. The results are shown in Figure 5. In the case of solids A and D, although black was statistically significant, the differences in apparent volume were small on the whole. It can be concluded that there were no differences between the horizontal solid (A) and the vertical solid (D). In the cases of B and E, and B and F, although the blue was statistically significant, the vertical solids had a tendency to make the apparent volume of interior space becomes more spacious than the horizontal solids of all colours. These results indicate that greater volumes of vertical solids tended to make the apparent volume of interior space become more spacious than greater volumes of the horizontal solids.

4. CONCLUSIONS

This study was conducted to evaluate the effects of furniture colour on the apparent volume of the interior space of a house. The results can be summarized as follows.

1) It was found that the white solids make interior spaces appear more spacious than any other colors. Black, red and brown solids made the interior space appear cramped.

2) As for the solids used to simulate beds, the taller the solid was, the apparent volume of the interior space becomes more cramped.

3) As for the solids used to simulate cabinets, all solids except the white solids made the interior space appear cramped, and increasingly so with increasing volume, whereas the white solids hardly made interior space appear cramped, regardless of their volumes.

4) In case of the solids having the same volume, interior space placed the solids used to simulate beds appeared more cramped than those placed the solids used to simulate cabinets.

REFERENCES

Sato, M., 2013. *Effects of accent colour on apparent distance to a front wall and apparent volume of an interior space*, Proceedings of AIC Color' 13, Vol. 2, 555-558

Sawa, Y. 2000. *Color of various upholsteries and their desirable color coordination,* Bull. Mukogawa Women's Univ. Nat. Sci., 48, 9-17

Address: Prof. Masato SATO, Division of Environmental Sciences,
Kyoto Prefectural University, 1-5 Hangi-cho, Shimogamo,
Sakyo-ku, Kyoto 606-8522, JAPAN
E-mail: ma_sato@kpu.ac.jp

Ideal GRID Model for Color Planning of Living Space

Tien-Rein Lee
Department of Information Communications
Chinese Culture University

PREFACE

Color plays a key role in shaping human environments: the visual sense is an important part of human perception; it corresponds to the way people create, design and communicate their living spaces. In many cultures around the globe, different cultural traditions have made use of color for product applications of all parts of daily life, and matters of communication. Color has sometimes been described as a matter of individual perception and personal views, but this research claims to consequentially make use of color characteristics in the process of urban design and city planning. It suggests a layout for city color planning based on an overall Grid Model that uses hue, saturation and values to arrange spatial elements in a systematic way, while integrating historical and culture specific features. It also refers to three different modes of color arrangement: The Color Order System, the Chinese Five-Elements Theory, and the rainbow colors. It is assumed that color arrangements based on a grid model can be applied on micro, medium and macro levels; expanding from personal living sphere to public space, and towards a mega-level setting. While each level is marked by different characteristics, such as functional, aesthetic and symbolic meaning, a grid-based color order planning can be adjusted not just to the different levels of urban spaces, but contribute to communicating a city's color identity.

1. INTRODUCTION

Grid systems have been included in the methods of urban design and city planning for a long time: The old city of Chang'an (which has been called Xi'an since the Ming dynasty), in the south-western part of China (today's Sichuan province), allows insight into methods of urban design from its early beginnings. While its origins go back as far as to Neolithic times, during the Tang Dynasty (618—907), Chang'an was regarded as one of the largest cities in the world, much like Constantinople (Istanbul) and Baghdad. The structure of this early modern metropolis followed a grid pattern of 108 quarters and two large marketplaces in its eastern and western parts. This kind of model layout followed functionality regarding the placement of the Imperial Palace and its immediate administrative and urban environment; and it has served as a prototype in the city planning of several other Asian capitals, evident in the city structure of Kyoto (Japan). Looking at modern day's New York City, the island of Manhattan is called

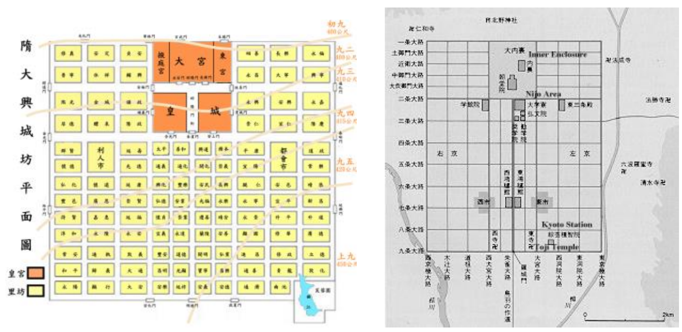

Figure 1: Grid city structures of Chang'an and Kyoto

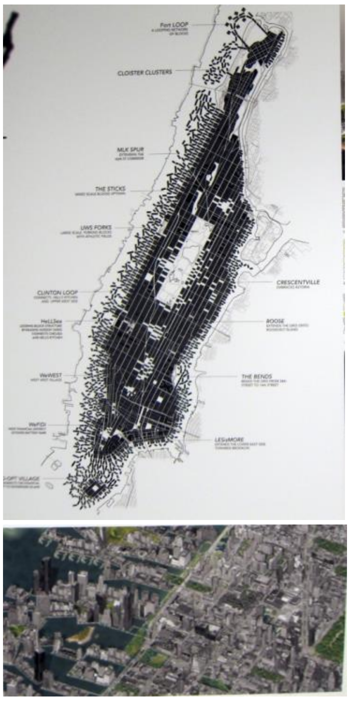

Figure 2: “Greatest Grid” – urban structure of Manhattan, New York City, U.S.A.

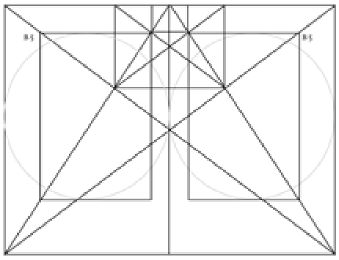

Figure 3: 9-parts shaped grid by Van de Graaf

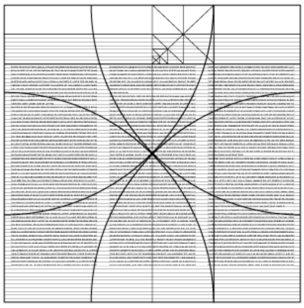

Figure 4: Grid system applied for ancient scrolls typography

the "Greatest Grid": Since its planning had started in 1811, these grid lines have resembled the social, architectural, financial and emotional veins of New York's urban life. In fact, grids have been applied in city planning throughout the United States (Knight, Nairn, 2013). Grid systems also play an important role in modern graphic design. A page can be divided into nine parts with the help of double diagonals and a guideline (Van de Graaf, 1946). The method results in margins with ratios of 2:3:4:6, where the original area has the ratio 2:3. In his works on typography, Tschichold appreciated this method and made it popular in his writings on the proportions and forms of books (Tschichold, 1955, 1975). Rosarivo shows how many of the classic books were designed via a module he calls MODULE 1.5. (Rosarivo, 1948). In fact, Christian monks made use of measurements divisible by three to create books that were holy according to the Christian faith, reminding of the holy trinity, while 2000 years old scrolls have been found using 8 mm line spacing: the method of dividing something in eight parts (triangulation) was known at that time, and the number eight is a holy number within Judaism (Gärde, 2007). Modern computer graphics allow to make use of grid systems for all kinds of layouts. Grid system functions include orientation, and in a neutral, mathematical sense, they are essential in building structures for human living spheres, regardless of culturally or geographically influential factors. The grid provides a useful, efficient tool that can be applied under a variety of different conditions, for achieving clearly defined purposes of city planning in all parts of the world. But can it be utilized for color planning? How to develop a standard model of color planning based on a grid system, applicable for small scale to large scale urban space?

2. GRID SYSTEMS AND COLOR ARRANGEMENT

City color planning is concerned with color selection for human living spheres. But how to find the most satisfying solution for a settlement? Color order systems have been developed after the natural color spectrum, or based on the measurements of human subjects’ visual responses to color. Different color order systems have been suggested by scientists throughout the centuries, with the color space of the Munsell color system specifying colors based on the three color dimensions hue, value (lightness), and chroma (color purity) being one of the most prevailing ones. Color order systems arrange color nuances based on different approaches: The Opponent Theory puts Red and Green as opposed at 180 degrees on two edges of its circle, and Blue and Yellow on the other;

while the rainbow colors follow a color order as it can be watched in the natural phenomenon. Color planning can make use of the directional functions of a grid, and add a color-coded order. Color order systems can be applied for city color planning and urban design projects by differentiating city center and districts, integrating neighborhoods and landmarks, and emphasizing directions and traffic guidance systems. A previous proposal of an urban color system for the City of Taipei, Taiwan, has included a district and neighborhood color analysis, and an overall city color layout. Three different modes of color arrangement have been proposed: The traditional Chinese Five Elements Theory, the Opponent Theory, and the rainbow colors. The Chinese Five Elements Theory is closely related to the theory of Wind and Water (Feng Shui), a traditional Chinese pattern of systematically understanding nature and natural events. The Chinese Five Elements Theory associates the natural phenomena Wood (Blue-Green/East), Fire (Red/South), Gold/Metal (White/West), Water (Black/North), and Earth (Yellow/Center) with colors and the cardinal directions of the compass dial. Each element and its color are also associated with a range of other characteristics like taste, smell, shape, and much more. Read in the clockwise direction, the Theory is applied following the seasonal changes of the year: Spring (Blue-Green), Summer (Red), Late Summer (Yellow), Fall (White), and Winter (Black): this order is understood as the natural "constructive cycle". A second cycle called the "destructive cycle" is defined as controlling and restricting the element considered as opposed to the prevailing one: Wood (Blue-Green/East), controls Earth (Yellow/Center); Fire (Red/South) controls Gold/Metal (White/West); Earth (Yellow/Center) controls Water (Black/North), Gold/Metal (White/West) and controls Wood (Blue-Green/East), and Water (Black/North) controls Fire (Red/South). The system is linked to a person's birthdate, so that recommendations can be given for color decisions contributing to a harmonically balanced life. This color order is very helpful for color decisions made on a personal level (regarding room colors, clothing or things of daily use), but it cannot be generalized and applied to public space. A color concept for a metropolis

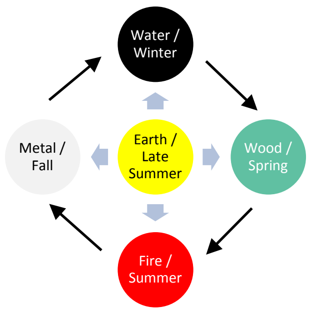

Fig. 5: The Five Elements in the seasons

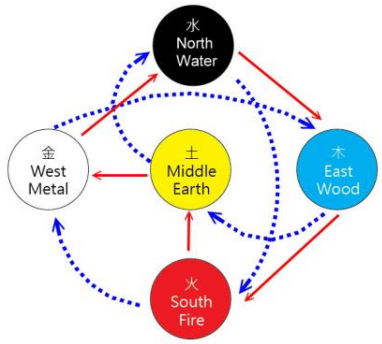

Fig. 6: The constructive and destructive cycles

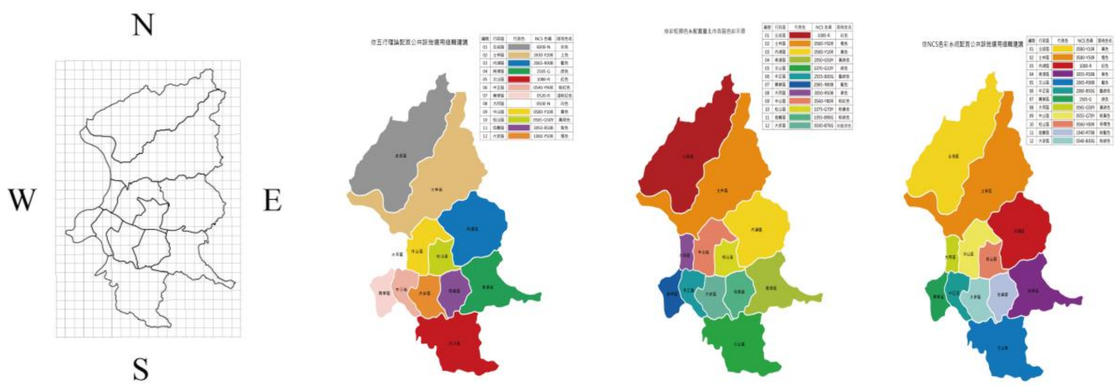

Figure 7: Used grid system and proposed color order systems in Taipei, Taiwan.

would have to use a more universally applicable system, adding an aesthetical dimension to function.

3. GRID SYSTEM COLOR PLANNING AND CITY IDENTITY

Color planning for public places includes functional, aesthetic and communicative goals: colors can represent city districts in the four cardinal directions, traffic systems may provide orientation by using these colors emphasizing bridges, highways, etc. Aesthetic value can be achieved by varying color shades for houses and landmarks, integrating a districts special highlights and harmonizing the general public appearance of places. The combination of grid systems and color order systems allows gradations and scaling of different sizes and ratios. It can also be adjusted to a city's layout, size, and specific proportional challenges of urban design.

Figure 8: Proposed colored Traffic Guidance System in Taipei, Taiwan.

Figure 9: Proposed colored traffic signs in Taipei, Taiwan.

It is suggested that Grid Color Systems can serve for urban design in different parts of the world, providing colorful layouts that help to identify an ideal color concept for different urban life-styles and traditions.

Cities are determining color identities related to the colors of traditional construction, or based on future-oriented tasks: geographical, climatic, and cultural influences all add individual features to the basic functions of an established common infrastructure, creating a unique appearance of the urban living sphere. These factors can constitute limitations for applying the Color Grid Model, but they can also be solved through it: The scalability and gradation of the Grid System make it a useful tool that can flexibly be adjusted to the local characteristics and circumstances. Furthermore, the flexibility of the Color Grid Model avoids creating indistinguishable neighborhoods and construction that would be leveling a city's special profile. On the contrary: The Color Grid Model can integrate a city's characteristic features and emphasize them as important parts of a city's specific identity. From small scale to medium to large scale dimensions, the Color Grid Model can serve for individual, public, and urban space color solutions.

4. CONCLUSION

The grid system is an ideal baseline (blue print) for rational arrangements, through thoughtful plans it matches the characteristics of color order and variations for any rational approach to utilize colors. It can create marginal effects for space planning with different needs. The proposed Grid Model for Color Planning of this research can integrate functions of communal infrastructure and suitable color components for the existing, unique local and traditional, or modern exterior design elements. It can help to develop a coherent color code that translates unique characteristics of a city into a comprehensive city color concept. The suggested Grid Model of Color Planning can be applied in all parts of urban life: starting from small scale color analysis of the neighborhood, regarding wall painting or garden architecture, street lamps and guidance systems; proceeding to medium size color recommendations of urban districts, applying color to district directions, landmarks, bridges, etc.; towards large scale color applications in the city's total urban space, such as colored subway lines and other transportation systems, public buildings, and so on. This prototype of Grid Model Color Planning can be universally applied but adjusted to the local needs of citizens in every part of the world, by integrating basic requirements of a community, while respecting local or regional peculiarities. As the responsibility for such an important, long-term project must not be left to isolated initiatives, it should involve all public authorities and private parties concerned with the creation and design of urban color spaces: like the government, residents, architects, and others.

REFERENCES

Gabriel, J. W. (September 1981). Color in Townscape, W. H. Freeman & Co.

Gärde, Marcus (2007) "The Way of Typography" http://www.bachgarde.com/html/works/gridsystem.html.

Glenwood (January 11, 2012). "Museum of the City of New York: the Greatest Grid & the Unfinished Grid." http://www.glenwoodnyc.com/manhattan-living/museum-city-new-york-greatest-grid-unfinished-grid/.

Knight, Paul; Nairn, Daniel(January 1, 2013). "Infographics. "http://www.thegreatamericangrid.com/infographics.

Linton, H. (January 1, 2003). Color in Architecture : Design Methods for Buildings, Interiors, and Urban Spaces, McGraw-Hill Professional Publishing.

Porter, J.-P. L. D. L. T. (2005). Doors Of The World, W. W. Norton & Co Inc.

Porter, J.-P. L. D. L. T. (2005). Windows Of The World, W. W. Norton & Co Inc.

Swirnoff, L. (February 1, 2003). The Color of Cities: An International Perspective, McGraw-Hill Professional Publishing.

Tschichold, Jan, (1955)"The Proportion of the Book (1975,)"The Form of the Book"

Van de Graaf, J. A. (1946): "Nieuwe berekening voor de vormgeving",

Tien-Rein LEE
Address: Dept. of Information Communications, Chinese Culture University
No. 55, Hwa-Kang Rd, Shilin, Yang-Ming-Shan, Taipei 11114, Taiwan
Email: trlee@faculty.pccu.edu.tw,

Case studies of Color Planning for Urban Renewal

Sari YAMAMOTO

Faculty of Art and Design, University of Tsukuba

ABSTRACT

Environmental color design in Japan, especially façade color, has long been considered a matter of individual choice. The Landscape Act was passed in 2004 by the Ministry of Land, Infrastructure and Transport, the purpose of which was to promote a more aesthetic approach to landscape and streetscapes, and also encourage the development of regional identity. We investigated each of these Landscape Plans, especially regarding the regulation of color, and determined that most towns use the Munsell Color System to manage façade color. 80 % of them use this system. As already mentioned, color regulation is mostly determined through restrictions regarding Chroma, however, this does not necessarily help in developing local features. We researched some unique cases in which color regulation was used in the development of streetscapes. The first case study is Girona in Spain. 30 years ago, old buildings were renovated, and street façades were renewed and colored. The second case study is the University of Tsukuba's color planning for its student accommodation facilities. The third case study is the public sign system in Tsukuba. The fourth case study is our bus color design for the town of Hitachi. Again, it is not façade color planning, but it helped to create a unique local feature for the city through the graphic design for buses and bus stops. With these case studies, I hope to have shown that color is not a minor issue and can be a useful tool in urban renewal and in creating a positive and life-affirming environment.

1. Background- the current status of local ordinance

Generally speaking, environmental color design in Japan, especially façade color, has long been considered a matter of individual choice. Consequently there has been little thought of coordinating façade color at a civic level. Because of this, the Landscape Act was passed in 2004 by the Ministry of Land, Infrastructure and Transport, the purpose of which was to promote a more aesthetic approach to landscape and streetscapes, and also encourage the development of regional identity. This legislation has only been partially successful.

As of January 2013 there were 568 landscape administrative organizations in Japan. "Landscape administrative organization" meaning a town or city council body tasked with managing the local landscape. Within these 568 organizations, only 384 towns have developed a "Landscape Plan" in accordance with national legislation.

We investigated each of these Landscape Plans, especially regarding the regulation of color, and determined that most towns use the Munsell Color System to manage façade color. 80 % of them use this system, with, for example, a directive like, "within Chroma 6 in case of Hue R". In other cases recommendations are based on color palette.

Restrictions regarding color only seem to be in effect for historical towns and cities, but not for unique landscape. It may be very useful for council administrators who are not confident making aesthetic decisions. However, the current legislation can be misinterpreted to allow any color to be used within the limitations, and to organize these limitations on the basis of Chroma may be detrimental to developing design sense, and spoil the overall color harmony of a particular area.

A survey was conducted using questionnaires in each of the 384 towns in 2013/2014. We asked whether local features were thought to be enhanced by the Landscape Plan. Less than 40% answered "Yes" and 60% answered "No" or "Undecided". People were also asked to rank which points they thought were effective in developing features of the local area in the Landscape Plan. Among these points were building color, height, shape and location. The responses are shown in Table 1. Color ranked highest, indicating that local government consider color to play a crucial role in making the most of their local features.

Table 1: Average Rank
(Which point is effective in developing features of the local area ?)

Point	Average Rank
Building Color	1.8
Building Height	3.3
Building Shape	3.6
Building Material	4.2
Outdoor advertisement	4.6
Building layout	4.8
Building greening	4.9
Others	7.8

As already mentioned, color regulation is mostly determined through restrictions regarding Chroma, however, this does not necessarily help in developing local features. We researched some unique cases in which color regulation was used in the development of streetscapes.

2. Case study 1

The first case study is Girona in Spain. 30 years ago, old buildings were renovated, and street façades were renewed and colored. The architect, Josep Fuses Comalada, planned the color scheme, which originated from the façade colors of the old city. In general, it was usual for local governments to use white, or off-white, when repainting or coloring buildings because it is cheap. However in this case they did not do so, and used a variety of colors which would have been found in the old city, such as 'almagro', traditionally considered the color of cow's blood, 'ochre' and 'sienna-red ochre'. Figure 2 is a diagram of the color design, showing the sophistication of the color production; although not so many colors are used, there is nevertheless an impression of great variety. Nowadays, there are many visitors to see the colorful streetscape of Girona. Thanks to this success, similar color planning is being applied to areas of redevelopment on the other side of the river. In Comalada's project, chemical paints were used due to cost restrictions, however, the new development uses natural paints. This is a very successful instance of urban renovation integrating streetscape color design.

Figure 1: Girona in Spain

Figure 2: Diagram of the color design

3. Case study 2

The second case study is the University of Tsukuba's color planning for its student accommodation facilities. The planning for this took several years. As with Girona, buildings were renovated, and at the same time, their façades were given a different color. Approximately 30 years have passed since the dormitories were built and the plumbing systems were out of date; renovation was needed. At first, it was planned that only the plumbing should be overhauled, however the university decided to recolor the façades at the same time to highlight to students the renovation of their accommodation. We have renovated approximately 5 buildings per year since 2009; there are a lot of student dormitories on our campus and it is impossible to renovate all the buildings at the same time.

Before renovation, the façades were beige or off-white. Although different colors were used to complement the concavo-convex shape of buildings or other façade features, the overall color harmony of each area was also considered. High Chroma colors were used, however these were carefully coordinated; for example, similar high Chroma colors are used for accents on adjacent buildings to give a sense of rhythm. In some cases these accent colors are designed to appear as gradation from certain angles. Mainly warm colors were used, to foster a positive and pleasant atmosphere.

The response from students is that the colored façades are cheerful and make the dormitories more appealing as habitats. This case study is a good indication of the importance of color and is informative for other renovation projects, as there are many buildings of this kind, that date back to 30 or 40 years ago.

Figure 3: Color design for Students Accomodation in the University of Tsukuba

4. Case study 3

The third case study is the public sign system in Tsukuba. This is not façade color planning as such, but sign design, which I think can also play an important role in creating unique character in an urban environment. We planned and designed a sign system for Tsukuba from 2005 to 2009, including the creation of sign guidelines, and 30 of these signs can be seen around the exits of the train station in the town center. We thought very deeply about the background color of the sign and decided on dark gray, after creating mock-ups for a field survey, so that the sign and its environment are harmonized. On the other hand, signs need to stand out, and we therefore included "art-posts" with the signs. These were made with natural materials such as stone and wood. These "art-posts" on the side of the signs, and monochrome photos on the reverse side of the signs have contributed positively to the town's environment and also give each sign a unique character. This sign system has been influential for other towns in Japan, and received an award from the Japanese Society for the Science of Design in 2009.

Figure 4: Sign Design for Tsukuba City

5. Case study 4

The fourth case study is our bus color design for the town of Hitachi. Again, it is not façade color planning, but it helped to create a unique local feature for the city through the graphic design for buses and bus stops.

Because of a decline in passenger numbers, many railway branch lines have fallen into disuse, and the routes have come to be served by bus lines. However, buses are often less punctual than trains and therefore have trouble retaining their customer base. For this reason, the government is promoting the BRT, or Bus Rapid Transit scheme, which repurposes unused railway lines as bus routes that cannot be used by other road vehicles.

In Hitachi, the railway branch line closed in 2005. Following this, the city council, in conjunction with residents who live near the old line, developed a BRT and solicited bids for the branding and graphic design. We revised the winning designs for practical application to the BRT, including the bus stops and other graphics. The concepts behind our design were:

1. To spread awareness of the BRT among Hitachi residents
2. To create a clear color scheme based on the winning design
3.To unify the graphics through the use of repeated design elements, such as color and shape
4. To respect local motifs in order to make citizens to have their attachments to our design and BRT.

The results were as follows:

1. A large BRT logo on the side and rear of the buses.
2. The use of a high chroma blue and simplified graphic design.
3. The creation of a Hitachi BRT logo, repeated on buses, bus stop signs and other PR merchandise.
4. The creation of different bus stop designs using elements that reference local culture in the immediate area.

The design has been well received by local residents, and the number of passengers has increased, making the business more profitable. This case shows that high quality design and color planning can strengthen a local population's relationship with their town and their environment, and can be a sound financial investment.

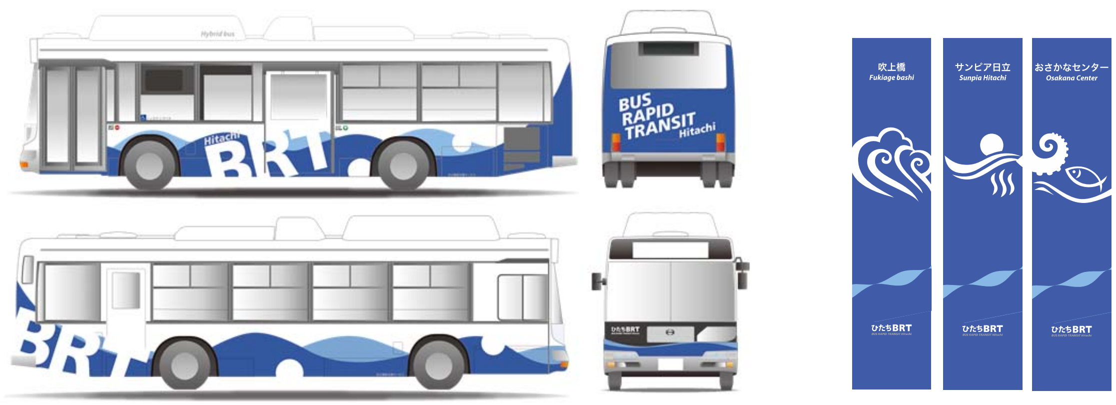

Figure 5: Color Design for Hitachi City Bus

6. Conclusion

The government has yet to devote serious attention to how color can be used in urban design, and there is a misapprehension that using more color is good, when in fact it leads to a lack of harmony. With these case studies, I hope to have shown that color is not a minor issue and can be a useful tool in urban renewal and in creating a positive and life-affirming environment. We hope that the power of the color will be used more in the process of making cities unique and beautiful.

References

Yamamoto Sari, Seo Minjung, Maki Kiwamu and Kumazawa Takayuki, *Local Government Policy of Landscape Planning for Local Features*, Summaries of technical papers of annual meeting, Architectural Institute of Japan, E-1, pp.517-520, 2014

Seo Minjung, Yamamoto Sari, *Relationship between Color Design Standard and Local Features in Local Government Policies and Environmental Planning,* Proceeding of the Annual Conference, Japanese Society for the Science of Design, 61(61), pp.266-277, 2014

Yamamoto Sari*, Environmental Color planning in Girona, Spain,* Summaries of technical papers of annual meeting, Architectural Institute of Japan, E-1, pp.513-514, 2013

Yamamoto Sari, *A Case study of Environmental Color and Sign for Sightseeing*, Journal of Tourism Sciences, 5, pp.31-34, 2013

Sari Yamamoto, Minjung Seo, Mao Kudo and Mitsuo Seki, *Design for the Bus Rapid Transit in Hitachi City,* Proceeding of the Annual Conference, Japanese Society for the Science of Design, 60(60), pp.186-187, 2013

Nishikawa Kiyoshi and Yamamoto Sari, *Public Sign for Tsukuba City,* Annual Design Review of Japanese Society for the Science of Design, *1*4(14), pp.26-31, 2009

Address: Dr. Sari YAMAMOTO, Faculty of Art and Design, University of Tsukuba,
1-1-1 Tennodai, Tsukuba, Ibaraki, 305-8574, Japan
E-mail: y-sari@geijutsu.tsukuba.ac.jp

Building Colours in Taipei – Taking Wanhua District as an Example

Chia-Chi CHANG[1], Ting-Tsung HO,[2] Li-Chen OU,[1]
[1] Graduate Institute of Applied Science and Technology, National Taiwan University of Science and Technology, Taiwan
[2] Graduate Institute of Color and Illumination Technology, National Taiwan University of Science and Technology, Taiwan

ABSTRACT

The study aims to investigate building colours in the Wanhau district of Taipei. Aims of this study include (a) to create a palette of building colours on 6 main roads in Wanhua district, (b) to analyse and improve the colour palette using CIELAB system, and (c) to develop guidelines of urban colour planing for this area. On the 6 main roads, all bulidings were measured colorimetrically, resulting in a total of 421 colours measured. According to the measurement results, most of the colours were warm colours, with high lightness and low chroma. Guidelines of building colours for this area are proposed on the basis of the colour survey results and the recent psychophysical findings of colour harmony. And a psychophysical experiment was carried out to study colours emotion and colour preference for building colours.

1. INTRODUCTION

Colours of urban buildings are an essential factor affecting the appearance of a landscape. Urban colours reflect a city's image and characteristics, and are related to the residents' feelings about their living environment. Due to the fast industrial development in cities of Taiwan, in addition to the lack of proper urban planning and the lack of regulations, landscapes in either urban or rural areas have become less and less attractive. As one of the most important visual factors in an architectural design, colour can easily change the impression of a landscape. Unfortunately, there has not been an urban colour system developed specifically for Taipei City using modern technologies of the CIE (International Commission of Illumination). To address the issue, this study investigated the building colour usage in Wanhua District. There are a number of historical, old buildings in Wanhua District, providing valuable cues or tendency in urban colour usage in this area.

2. METHODS

The present research adopted the colour matching methods developed by Lenclos (2004) for survey of building colours in Wanhua district. The NCS 1950 Index, a standard fandeck of the Natural Colour System, together with the NCS Colour Scan, a portable colour measuring device for collecting NCS values, were used during the colour survey.

Six main roads of the Wanhua District, including Zhonghua Road, Kangding Road, Wanda Road, Guilin Road, Bangka Boulevard and Xizang Road, were surveyed to cover a large range of Wanhua District. The main colour that covers 4/5 exterior surface of each building was measured using the NCS fandeck and the NCS Colour Scan. The NCS data collected during the colour survey were converted into CIELAB values for data analysis.

In addition, in order to study perceived colour emotion of building colours for Wanhua District, this study also conducted psychophysical experiments on three main roads of this area, including Guilin Road, Zhonghua Road and Kunming Road. A total of 62 buildings were evaluated. A total of 30 observers, including 15 males and 15 females, assessed 5 colour-emotion scales: warm-cool, heavy-light, active-passive, harmony-disharmony and like-dislike. The categorical judgment method was used for data collection and analysis.

3. RESULTS

A total of 421 buildings were measured in colorimetric terms. As a result, most of the colours were found to have hue angles between 30 and 120 degrees, with lightness ranging between 30 and 94 (see Figure 1a) and chroma lower than 50 (see Figure 1b). Only a few colours were found to have chroma values higher than 50 for colours in the hue region from 30 to 120 degrees. In addition, the buildings in the north part of Wanhua District were found to appear darker than those located in the south of the area, suggesting a tendency related to the historical background of the region

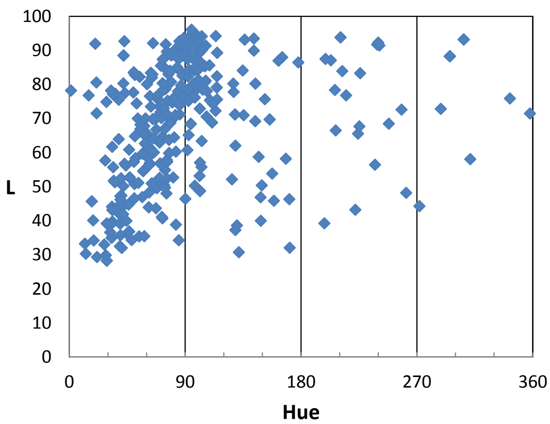

(a)

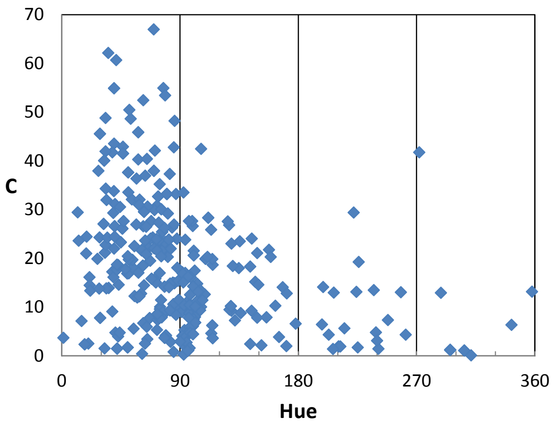

(b)

Figure 1. Distribution of measured colours for 421 bulidings in (a) the lightness-hue diagram and (b) the chroma-hue diagram

According to the results, most of the measured colours had a lightness ranging from 80 to 90, accounting for 24% of all colours measured, followed by the range 70 to 80 (19%), 90 to 100 (15%) and 60 to 70 (12%), as shown in Table 1 (a), suggesting that most of the building colours were light colours. In terms of chroma, most of the colours were in the range 0 to 10 (40%), followed by the range 10 to 20 (24%) and 20 to 30 (23%), as Table 1 (b) shows. This suggests that most of the colours were low-chroma colours. For hue, as Table 1 (c) demonstrates, it is clear that most of the colours were in the range 0 to 90 degrees, accounting for 56% of all colours measured, suggesting that most of the colours were warm colours.

Table 1. Distribution of measured colours in terms of (a) lightness, (b) chroma and (c) hue

(a)

Lightness range	20-30	30-40	40-50	50-60	60-70	70-80	80-90	90-100
Percentage	1%	8%	9%	12%	12%	19%	24%	15%

(b)

Chroma range	0-10	10-20	20-30	30-40	40-50	50-60	60-70
Percentage	40%	24%	23%	6%	5%	1%	1%

(c)

Hue range (in degree)	0-90	90-180	180-270	270-360
Percentage	56%	36%	6%	3%

One of the aims of this study was to improve the colour palette according to recent psychophysical findings of colour harmony (e.g. Ou and Luo, 2006; Szabó et al., 2010). Based on these findings, a number of common principles of colour harmony have been identified:

- Equal-hue and equal-chroma. Any two colours varying only in lightness tend to appear harmonious when combined together.
- High lightness. The higher the lightness score of each constituent colour in a colour pair, the more likely it is that they will appear harmonious.
- Unequal lightness scores. Small lightness variations (i.e., less than around 15 units of CIELAB colour difference) between the constituent colours in a colour pair may reduce the harmony of that pair.

According to these principles, it is more likely to create colour harmony if the lightness of each constituent colour is enhanced (i.e. the “high lightness” principle) and chroma being reduced (the “equal chroma” principle). As Table 1 indicates, 91% of the measured colours had lightness values higher than 40. Thus, the *recommended* building colours should have lightness values higher than 40, as illustrated by the green lines in Figure 2(a). The lightness range between 30 and 40 is regarded as *tolerable*, as shown by the orange lines in the graph. Those having lightness lower than 30 are *unacceptable*, as illustrated by the red lines.

Regarding the chroma, Table 2 shows that 87% of the colours had chroma values lower than 30. Note, as Table 3 indicates, 92% of the colours had a hue range from 0 to 180 degrees, most of which were in fact in the range from 30 to 120 degrees. Thus, the *recommended* building colours are those having chroma lower than 30 for hue angle ranging from 30 to 120 degrees, or those having chroma lower than 10 for the other hue region, as illustrated by the green lines in Figure 3(b). The chroma range between 30 and 50 for hue angle ranging from 30 to 120 degrees, and chroma range between 10 and 50 for hue angle ranging from 0 to 30 and from 120 to 180 degrees, are regarded as *tolerable*, as illustrated by the orange lines. The rest of the areas shown in the graph are *unacceptable*, as illustrated by the red lines.

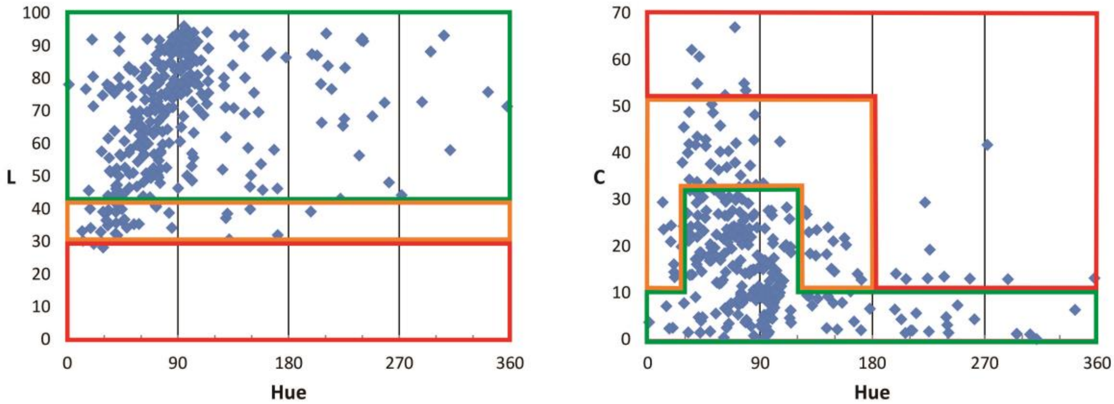

(a) (b)

Figure 2. Proposed guidelines in the form of (a) the lightness-hue diagram and (b) the chroma-hue diagram, where the areas divided by green, orange and red lines represent the recommended, tolerable and unacceptable building colours.

According to the guidelines of building colour planning as illustrated in Figures 2 (a) and (b), the original palette of building colours were revised. Figures 3 (a) and (b) show the distribution of the two colour palettes, the original in grey and the revised in blue, in the lightness-hue diagram and in the chroma-hue diagram, respectively.

To see how much the revised colour palette has improved compared with the original palette, Ou and Luo's colour harmony model (2006) was used to calculate the predicted colour harmony values, also called the CH values, for both colour palettes. The higher CH value being predicted, the more harmonious the colour combination appears. As Table 2 shows, the CH values are all higher for the revised colour palette than for the original palette, for all of the 6 main roads in Wanhua district. According to the table, for both the original and the revised colour palettes, the CH value is the highest for Xizang Road and the lowest for Kangding Road. This finding is perhaps due to the fact that there were more light colours for buildings on Xizang Road than for the other areas, and that there were more dark colours for buildings on Kangding Road than for the other areas.

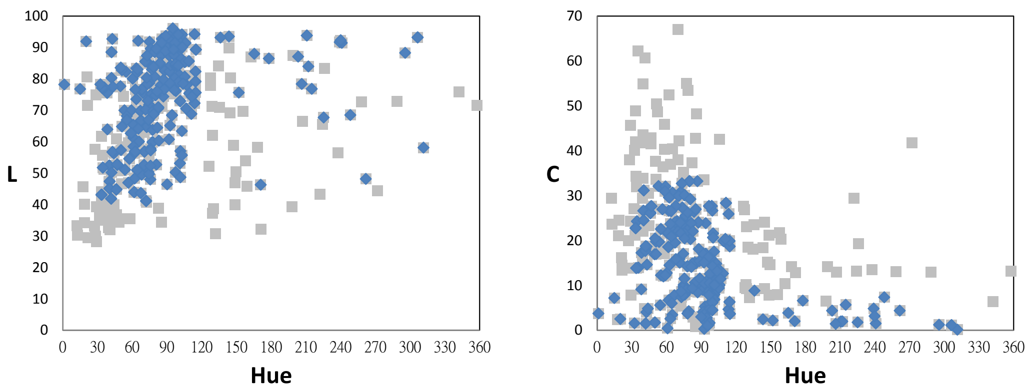

(a) (b)

Figure 3. Original colours (in grey) and of the enhanced colours (in blue) distributed in (a) the lightness-hue diagram and (b) the chroma-hue diagram

Table 2. CH values for the original and revised colour palettes for buildings on the 6 main roads in Wanhua District

	Zhonghua Road	Guilin Road	Xizang Road	Bangka Boulevard	Kangding Road	Wanda Road	All areas
Original	0.66	0.58	0.74	0.37	0.22	0.62	0.53
Revised	0.80	0.72	0.89	0.53	0.35	0.73	0.66

Moreover, 62 buildings of the Wanhua district were visually assessed by 30 observers. Most of the colours were found to have hue angles between 30 and 120 degrees, with lightness ranging between 20 and 95 (see Figure 4a) and chroma lower than 50 (see Figure 4b). The tendency of results is like Figure 1.

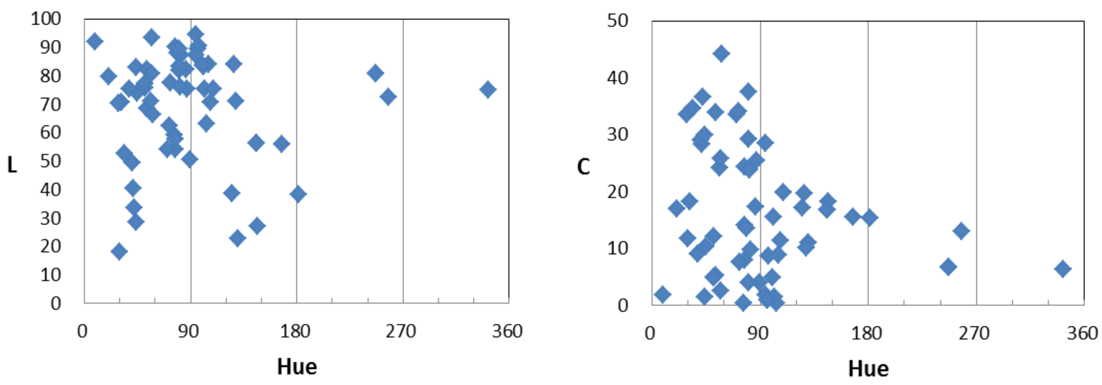

(a) (b)

Figure 4. Distribution of measured colours for the evaluated 62 buildings in (a) the lightness-hue diagram and (b) the chroma-hue diagram

As Table 3 shows, the average of Like score are all minus in the 3 roads. It indicates that observers didn't like building colours in Wanhua district especially in Guilin Road. Interestingly, Heavy score indicates that observers fell a little heavy. We think probably have relations with some of old and dirty buildings. According to the result of correlation with colour emotions scales in Figures 5. Active and Harmony have high correlation (R^2>0.7) with Like. It indicates that building colour are the more active and harmony, the more observers like. We follow the guidelines of building colour planning as illustrated in Figures 2 (a) and (b), to calculate the average of Like scores for "recommended" and "unacceptable" building colours, as shown in Table 4. As a result, the mean "recommended" score is higher than the mean "unacceptable" score.

Table 3. Average score of 5 colour-emotion scales for building colours on the 3 roads in Wanhua District.

	Like score	Harmony score	Active score	Heavy score	Warm score
Zhonghua Road	-0.10	0.38	0.08	0.38	0.00
Guilin Road	-0.25	0.45	-0.07	0.20	0.00
Kunming Road	-0.15	0.49	-0.02	0.23	0.16
All areas	-0.16	0.46	-0.01	0.26	0.09

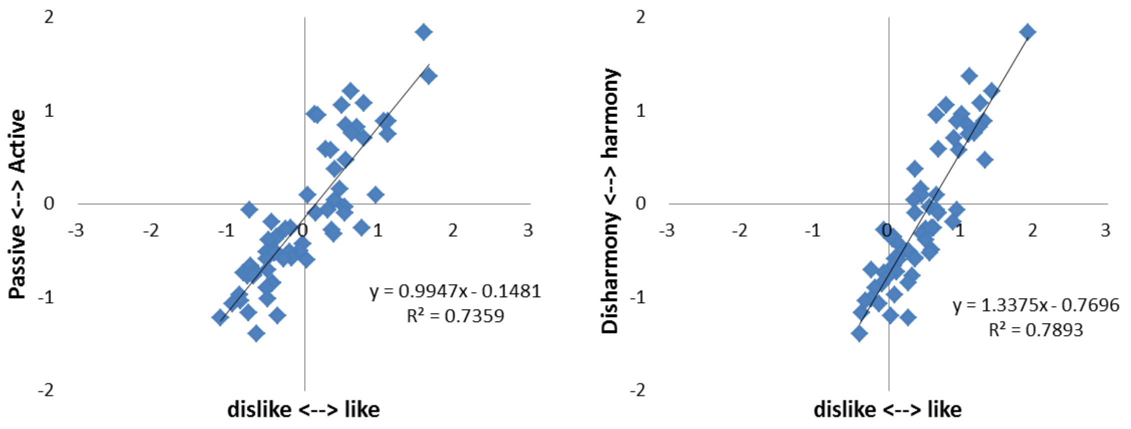

(a) (b)

Figure 5. Correlation between perceived colour preference and the other colour emotion scales: (a) active-passive and (b) harmony-disharmony.

Table 4. Average Like scores for "recommended" and "unacceptable" building colours

	All areas	recommended	unacceptable
Like score	-0.13	-0.04	-0.31

4. CONCLUSION

This study investigated building colours in Wanhua District. According to the measurement results, most of the colours were warm colours, with high lightness and low chroma. Based on these results, together with recent colour harmony findings (Ou and Luo, 2006; Szabó et al., 2010), guidelines of building colours for Wanhua district is proposed, as illustrated in Figures 2 (a) and (b). And the result of experiment shows better Like scores for buildings using the "recommended" than the "unacceptable" colours. Future studies will focus on how the findings can generalise to other areas.

AKNOWLEDGEMENTS

This work was supported in part by the Ministry of Science and Technology, Taiwan (MOST 103-2420-H-011-002-MY2).

REFERENCES

Ou, L. and Luo, M. R. 2006. A colour harmony model for two-colour combinations. *Color Research and Application* 31: 191-204.

Lenclos J. P. 2004. *Colors of the World – A Geography of Color*. W.W. Norton & Company.

Szabó, F., Bodrogi, P. and Schanda, J. 2010. Experimental modeling of colour harmony. *Color Research and Application* 35: 34-49.

Address: Chia-Chi Chang, Graduate Institute of Applied Science and Technology,
National Taiwan University of Science and Technology
43, Section 4, Keelung Road, Taipei, Taiwan
E-mails: jackie7089@gmail.com, lichenou@mail.ntust.edu.tw

Pritzker Prize Laureates' Colour Preferences

Malvina ARRARTE-GRAU
Architect, Landscape Architect, Colour Designer
ColorARQ Lima-Peru, SG ECD

ABSTRACT

It is unquestionable that architects dress in black, that their models are usually white and that they manifest an incomprehensible love for concrete. Consequently, in the website of the Pritzker Architecture Prize, the profession's highest honor since 1979, the work of the laureates stands out for its colourless appearance. The reason why colour is not noticed at first might be because it acts as neutral, blending in with the compositions.

For the purpose of this study it has been important to define *achromatic* and *neutral* in the context of architecture. According to colour theory pure achromatics contain no hue or colour, but near neutrals extend to nuances of low chromaticity, as brown and tans. Applied to buildings, neutrals and near neutrals allow other tones to stand out as chromatic in the composition. Under this principle, it is possible to catalogue neutrals according to the setting.

The object of the study is a sample of projects by the Pritzker Prize winners. The range of work which composes the portfolio of the elite is vast. The criterion for the selection is oriented towards the colour aspect of the projects. Initially the source was the '*selected works*' section and '*official website*' of the awardees (if applicable) in the Pritzker Prize website, being later complemented by other internet sources. A general impression led to catalogue the architects according to their preference for colour usage. Four tendencies were identified: *chromatic*; *near neutrals* for warm nuances of low chromaticity; *achromatics,* including black and gray; and *white*, as a sub-category of the achromatics. Common characteristics amongst the laureates have been pointed out, for a better understanding of their approach to colour.

1. INTRODUCTION

In order to find out if the preconception of non-coloured architecture amongst architects is certain, the Pritzker Prize, one of the most important international recognitions in architecture, has been used as an example of the use of colour by a select group of architects. The Prize was first given in 1979 to Philip Johnson, author of the Glass House. The next year it was granted to Luis Barragan, renowned for his coloured buildings and exterior spaces. The Pritzker Prize was established by Jay Pritzker and his wife Cindy to encourage and inspire creativity in the profession. One hundred thousand dollars and a bronze medallion are granted each year by the Pritzker Foundation to honour a living architect who demonstrates talent, vision and commitment, and who has contributed to the world and to humanity through the art of architecture. Until 2014, the laureates total thirty-seven architects from four continents.

Since ancient times stone, earth, wood and vegetable fibres have been the components of buildings and the point of departure of architectural colours. Nowadays processed construction materials and finishes come in a range of options, from those which resemble the natural to the most sterile and artificial ones. Both natural and processed materials may serve the purpose of complementing building exteriors, delicately echoing the surroundings, reflecting, blending in, weaving a texture or making contrast. The colours of buildings may be categorized as *chromatic*, *achromatic* or *near neutral*. In theory achromatics contain very little or no chroma. These are reduced to black, white and shades of grey, allowing slight variations in tone. Near neutrals are low in saturation. Within the architectural context these are often related to local materials, climate and geology. The spectrum of near neutral colours varies from very light to dark nuances, including those of soil, mud, brick and stone, wood and rust.

2. METHOD

Colour tendencies amongst Pritzker awardees have been analyzed by reviewing the works of each architect, mainly through internet sources: the Pritzker Prize official website, the architects' websites -if applicable-, and complementary information. After the revision, four possibilities have been proposed as tendencies of colour use and labeled with initials: C for chromatic; N for near neutral, which include natural materials of warm hues; A for achromatic, including shades of gray, black and materials such as glass, steel and concrete; and finally, W for white, settled apart as a sub-category of the achromatics.

This study is based on the external aspect of buildings. The range of size and character of the projects by Pritzker laureates implies a degree of complexity in the selection of images. These have been limited to photos which depict the building as an object, showing its shape and finishing materials. A priori the Pritzker website displays a dominance of achromatics and near neutrals. In order to demonstrate this, the criteria for defining the colour tendency of each architect will give priority to colour: the architect will be considered in favour of colour if he uses it recurrently, even if not in the majority of his/her projects.

After reviewing the portfolio and biography of each architect, and defining his/her colour tendency, the information gathered from the websites has been conveniently ordered in Table 1. This has served to visualize common denominators amongst the architects. Additionally, a timeline (Figure 1.) and a map (Figure 2.) in relation to the use of colour have been elaborated. The results are drawn from the graphics and the four tendencies are commented in the discussion.

3. RESULTS AND DISCUSSION

The revision of the projects in the '*Selected Works'* section of the Pritzker Prize annual book gives a first impression of the colour tendency of each architect. Though, for a better understanding of the colour preferences of Pritzker architects it has been necessary to complement the data with google searches. Table 1. summarizes biographical information gathered in this process: year and place of birth, education, work, influences, background details and additional abilities.

It is worth mentioning that since the beginning of World War II the United States became home to many European artists and intellectuals who imparted the principles of Modernism in universities. The influence of Le Corbusier, Aalto, Kahn and Mies van der Rohe are a common denominator amongst architects, and the laureates are no exception.

The particular abilities of the architects influence their design approach. For instance, Ando, Zumthor and Wang Shu trained in woodwork and crafts. Painting is a common interest to Johnson, Meier, Hollein, Hadid and Portzamparc. Soto de Moura started to study scupture. Jean Nouvel is inspired by cinema, as Aldo Rossi was, by theatre. Urban planning is the major of Tange, Maki, Foster, Mayne and Koolhaas. Barragan speaks of aesthetics and spirituality, as Shigueru Ban is moved by humanitarian concern. Others centered in innovative solutions, or in the context.

AWARD YEAR	AWARDEE	YEAR OF BIRTH	ORIGIN	ARCHITECTURAL EDUCATION	TRAINING AND WORK	INFLUENCES	PERSONAL	OTHER ABILITIES	COLOUR TENDENCY
1979	Philip JOHNSON	1906- 1905	Cleveland, Ohio, U.S.A.	Harvard, Architecture and Master of Architectural History	curator at MOMA, architect at 34	Le Corbusier, Mies van der Rohe, Minimalism and Pop-Art		critic, historian, collector of American art	A
1980	Luis BARRAGAN	1902- 1988	Guadalajara, MEXICO	Guadalajara School of Engineering	landscape architect	Corbusier, Morocco, Guadalajara School	spiritual values	landscape architect	C
1981	James STIRLING	1926- 1992	Glasgow, U.K.	Liverpool School of Architecture	James Gowan (London), Michael Wilford (partner)	late works of Le Corbusier			C
1982	Kevin ROCHE	1922	Dublin, Ireland/ U.S.A.	Dublin, IIT (Chicago)	Eero Saarinen (Michigan), Dinkeloo (partner)	Mies van der Rohe, Eero Saarinen			A
1983	Ieoh MING PEI	1917	Canton, CHINA / U.S.A.	Pennsylvania, MIT, Harvard	U.S. planning, international	Breuer, Gropius			A
1984	Richard MEIER	1935	New Jersey, U.S.A.	Cornell University	early practice, residential	Le Corbusier, FLW, Aalto, old european masters		expressionist painting	W
1985	Hans HOLLEIN	1934- 2014	Vienna, AUSTRIA	Academy of Fine Arts, School of Architecture (Vienna)	U.S., Sweden, Vienna	Mies, FLW, Neutra		artist, furniture and jewellry designer	N
1986	Gottfried BÖHM	1929	Offenbach-am-Main, GERMANY	Technische Hochschule and Academy of Fine Arts (Munich)	Dominicus Böhm, Rudolf Schawrtz (Cologne), Cajetan Baumann (N.Y.)	father and grandfather, Mies, Gropius	grandfather and father church designers, wife		N
1987	Kenzo TANGE	1913- 2005	Imabari, Shikoku Island, JAPAN	University of Tokyo	Tange Laboratory, reconstuction of Hiroshima, Bologna and Catania	Le Corbusier		urban planning	A
1998	Oscar NIEMEYER	1906- 2012	Rio de Janeiro, BRAZIL	School of Fine Arts of Brazil	Lucio Costa, was appointed to be architect of Brasilia	Lucio Costa, Le Corbubusier			W
1988	Gordon BUNSHAFT	1909- 1990	Buffalo, N.Y., U.S.A.	MIT	Worked with industrials designers, and for SOM until he became partner	Mies van der Rohe, Le Corbusier.			A
1989	Frank GEHRY	1929	Toronto, CANADA	Southern California, Harvard	André Remondet (Paris)	Corbusier, Balthasar Neumann, French Roman churches			C
1990	Aldo ROSSI	1931- 1997	Milan, ITALY	Milan Polytechnic	editor of Casabella	drama, theatre		writer, theatre	C
1991	Robert VENTURI	1947	Philadelphia, U.S.A.	Princeton, American Academy in Rome	Eero Saarinen, Louis Kahn, John Rauch (partner), DSB (partner)	Louis Kahn, Le Corbusier, Aalto, barroque, Palladio	Denise Scott Brown (wife and partner)		C
1992	Alvaro SIZA	1933	near Oporto, PORTUGAL	Escola de Belas Artes (U.of Porto)	early practice		father architect		N
1993	Fumihiko MAKI	1928	Tokyo, JAPAN	U. of Tokyo, Cranbrook Academy of Art, Harvard	SOM and Sert Jackson. Founder of Metabolists.	Kenzo Tange, Eliel Saarinen, Post-Bauhaus internationalism, early modern in Japan, FLW		urban design	A
1994	Christian DE PORTZAMPARC	1944	Casablanca, Morocco / Marseille, FRANCE	École de Beaux Arts (Paris)	New York, team of sociologists	Le Corbusier		painter	A
1995	Tadao ANDO	1941	Osaka, JAPAN	self-taught (from books, trips and tradition), trained with a joiner	fired from several offices	Corbusier, Mies, Aalto and FLW		amateur boxer, builder	A
1996	Rafael MONEO	1937	Tudela, SPAIN	Escuela Superior Técnica de Madrid, Spanish school in Rome	Saenz de Olsa, Utzon (Copenhague)	Nordic style, Dutch School			N
1997	Sverre FEHN	1924 –2009	Kongsberg, Buskerug, NORWAY	actual Oslo School of Architecture and Design	Jean Prouve (Paris), he met Le Corbusier.	architecture, Aalto, Korsmo, Prouve.			N
1998	Renzo PIANO	1937	Genoa, ITALY	Milan Polytechnic	Louis Kahn (Philadelphia), Makowski (London), Rice and Rogers (partners)	Le Corbusier, Prouve, Fuller, Nervi. Italian roots.	family of builders		C
1999	Norman FOSTER	1935	Manchester, U.K.	University of Manchester, Yale	Buckminster Fuller, Team 4 and Richard Rogers (partners)	Paul Rudolph, Vincent Scully, Serge Chermayev, Eames		urban planning	C
2000	Rem KOOLHAAS	1944	Indonesia / Rotterdam, NETHERLANDS	Architectural Association, London	founder of OMA (Madelon Vriesendorp, Elia and Zoe Zenghelis)		father writer, grandfather architect, wife	worked in journalism, writer, urbanist	A
2001	Jacques HERZOG & Pierre DE MEURON	1950	Basel, SWITZERLAND	Swiss Federal Institute of Technology (Zurich)	lectured, then opened their practice	Sharoun, Aalto, Rossi. No paradigms.			C
2002	Glenn MURCUTT	1936	London/ New Guinea/ Sidney, AUSTRALIA	University of South Wales, Sidney	Ancher, Mortlock, Murray and Wooley (Sidney). Now small practice	Mies van der Rohe, David Thoureau, Aalto, Barragan, FLW	father interested in architecture		N
2003	Jørn UTZON	1918- 2008	Copenhague, DENMARK	Royal Academy of Fine Arts (Copenhague)	Ahlberg (Sweden), Aalto (Finland)	Aalto, Asplund, Wright.	Cousin sculptor, father naval architect	sailor, training for naval officer	N
2004	Zaha HADID	1950	Bagdad, Iran / London, U.K.	American U. of Beirut (Maths), Architectural Association (London)	Oma with Elia Zhengelis and Rem Koolhaas (she became partner)	Eng. Peter Rice, Niemeyer, Russian Avant-garde		Artist; interior, furniture, clothing	A
2005	Thom MAYNE	1944	Connecticut, Indiana, California, U.S.A.	Pomona and Southern California, Harvard U.	Victor Gruen. Fired. Founded Morphosis (antini, Stafford, Brickler, Rotondi) and SCI-Arc			urban planner	A
2006	Paulo MENDEZ DA ROCHA	1928	Vitoria, Espirito Santo, BRASIL	Mackenzie Presbiterian University	early practice, masterpiece Athletic Club of Sao Paulo	Paulist Brutalist avant garde		urbanist	A
2007	Richard ROGERS	1933	Florence, Milan, London, U.K.	Architectural Association (London), Yale	Ernesto Nathan Rogers (Milan), Team 4 (partner), Renzo Piano (partner)	pupil of Rudolph and Stirling. Italy; Frank Lloyd Wright	ex-wife architect Wendy Rogers	cities	C
2008	Jean NOUVEL	1945	Fumel, SW FRANCE	Ecole de Beaux Arts (Paris) ÉÉ	Claude Virilio, Gilbert Lezenes, Jean-Francois Guyot and Pierre Soria	cinema, Virilio	ex-wife filmmaker; actual Swedish		C
2009	Peter ZUMTHOR	1943	Basel, SWITZERLAND	Pratt Institute (N.Y.), Kunstgewerbeschule	consultant at Canton of Graubürde (monument preservation)	not influenced by global tendencies		trained as a joiner	N
2010	Kazuyo SEJIMA & Ryue NISHIZAWA	1956 1966	North and South of Tokyo, JAPAN	Japan Women U. / Yokohama U.	Toyo Ito & Associates	Le Corbusier, Mies van der Rohe , Niemeyer, Koolhaas, Ghery, Siza			A
2011	Eduardo SOUTO DE MOURA	1950	Porto, PORTUGAL	School of Fine Arts (sculpture), School of Architecture, U. of Porto	Alvaro Siza	Donald Judd, Mies van der Rohe, Siza; collegues: Rossi, Herzog	wife architect	sculptor	N
2012	Wang SHU	1963	Urumqi, Xinjiang, CHINA	Nan Nanjing Institute of Technology	founded Amateur Architecture Studio (Hangzhou)		wife architect Lu Wenyu	crafts, literature	N
2013	Toyo ITO	1941	Seul / Tokyo, JAPAN	University of Tokyo	Kiyonori Kikutake, founded URBOT, Toyo Ito & Associates	Le Corbusier, Mies van der Rohe , Isozaki, Kikutake, Koolhaas	his father liked to draw plans		C
2014	Shigeru BAN	1957	Tokyo, JAPAN	Architecture Institute (S. California), Cooper Union	Arata Isozaki, NGO Voluntary Architects Network	Alvar Aalto		paper architecture	N

Table 1.

Figure 1. The timeline shows the sequence of Pritzker Laureates from 1979 until 2014 and their colour preferences.

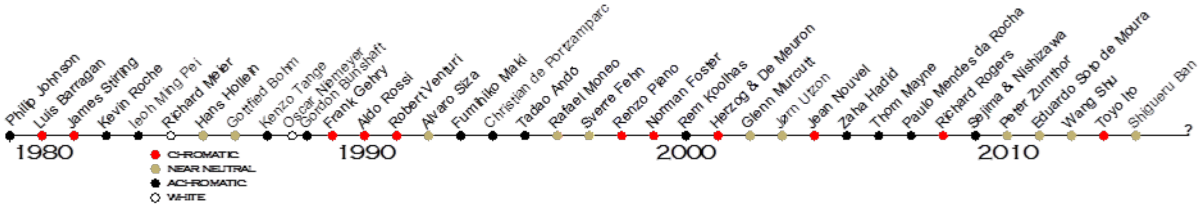

The timeline indicates the tendency of colour use by each architect, suggesting that colour has been in vogue around the 1980, 1990 and 2000. It is evidenced that during the last fifteen years, the architects who represent colour have been less frequent, giving way to more who use achromatics and near neutrals towards 2015. The immediate influence of Pritzker recipients on new generations is undeniable, but the moment of completion of each project determines available materials and technologies, and therefore, design possibilities, so there is an additional component to be considered in the former assumption.

Figure 2. Architects by zone or region

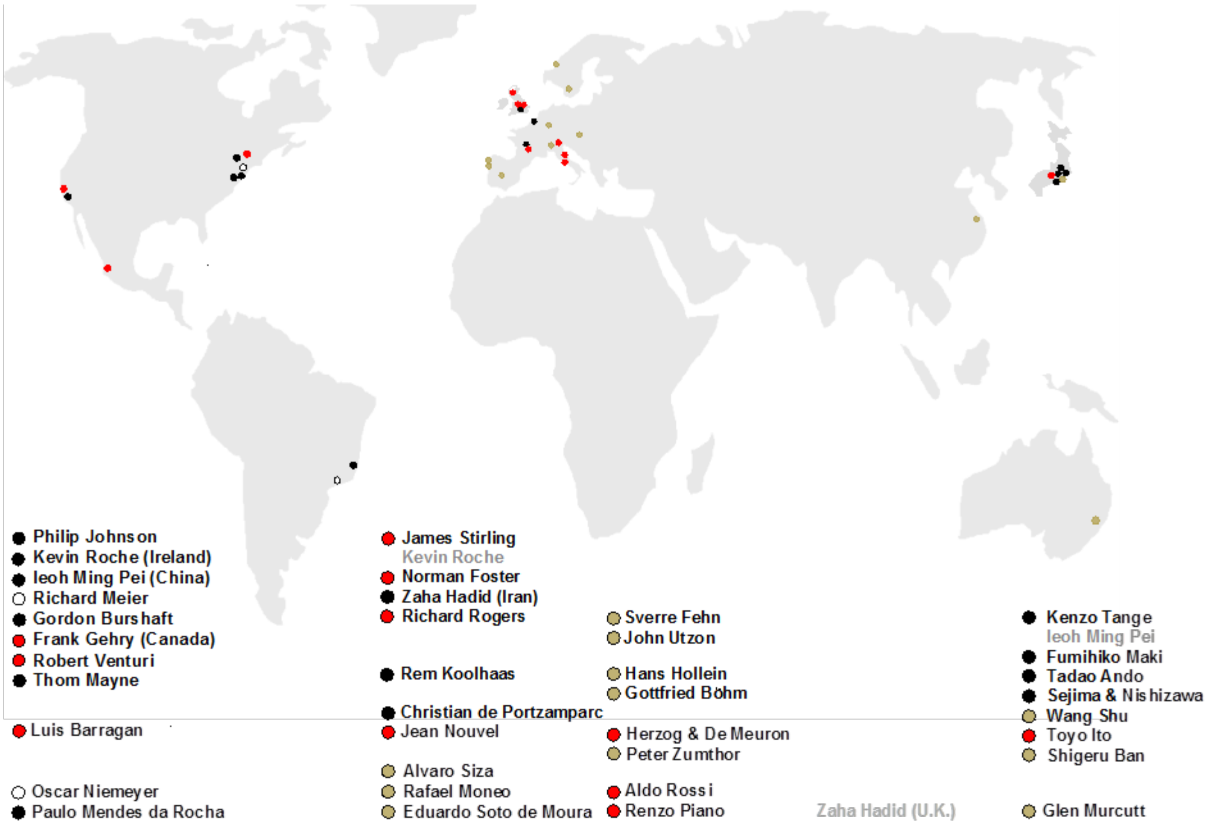

The second illustration (Figure 2.) shows the origin or main place of operation of the architects. It could be inferred that the location of each project directs, in principle, the colour possibilities of its exterior. In order to find common points as regards colour tendeny and location, the sequence of the comments follows the main country or continent from which they work.

The architects from the United States are Philip Johnson, Richard Meier, Gordon Bunshaft, Robert Venturi and Thom Mayne. Ieoh Ming Pei, Kevin Roche and Frank Gehry, who settled in the in the U.S. early in their careers, are also considered in this group. The genuine approaches of Richard Meier, who exclusively uses white, and Robert Venturi, who publicly rejected black and white in rebelling against radical ideas of modernism, demonstrate contundency as regards colour. Still, achromatics appear dominant in this region. Impressive titanium façades by Frank Ghery, have made it difficult to identify him for colour, as he shows versatility in this respect.

Even if colour is part of the Mexican tradition, Luis Barragan has no less merit for being a pioneer of colour in Modern architecture. He uses it artistically in outdoor spaces and interior views in combination with white, to emphasize volume and receding planes.

In Brazil large scale developments by Oscar Niemeyer and brutalist buildings by Edoardo Mendez da Rocha, show scarce colour. Though chromatics as used to point certain elements in Niemeyer's work, it is more of an exception. White plaster and exposed concrete are used in a neutralizing mode, rendering whole buildings, giving way to the overwhelming shapes that characterize the Brazilian urban landscape.

The architects from the Iberian Peninsula Alvaro Siza and Edoardo Soto de Moura, from Portugal, and Rafael Moneo, from Spain, exhibit the use of local stone and white plaster. Rafael Moneo showcases fine projects in brick. The predominant tendency for these architects is near neutrals.

Jean Nouvel and Christian de Portzamparc, work with avant-garde technology. Both of them employ a variety of surface materials, including plants and coloured lighting. In the projects by Nouvel, colour is applied in innovative techniques on expressly prepared materials. The buildings by Christian Portzamparc stand out for a sophisticated achromatic appearance, complemented by textures.

The buildings by Rem Koolhaas propose original solutions with unprecedented architectural form, contributing with ideas to the built environment, but he is not fond of colour in the simplistic way, as an element that will transform a building. So far, his work stands out as achromatic.

The British architects James Stirling, Richard Rogers and Norman Foster, have used colour to characterize building parts and enhance structures, making there more human. On the other hand, the inventive use of materials by Zaha Hadid is exclusively achromatic.

From Basel, Herzog & De Meuron and Peter Zumthor, stand out for their fine craft and use of materials. Zumthor employs the textures of natural stone and wood as essential elements in his compositions. Herzog & De Meuron apply colour in a refined manner accentuating volume and creating fabrics from structure and surface.

Aldo Rossi and Renzo Piano master colour in various ways. Rossi uses color to emphasize volume and to codify building elements, defining façade proportions. Piano uses diverse materials and technologies, exhibiting concepts with strong colour presence.

Several houses by Glen Murcutt present metal sheets on the façade. In the Australian landscape this follows horizontal patterns perceived in the surroundings and reflect the natural elements. He also uses wood, colour and white, for specific situations, blending in with nature. The proportion of materials sets him in the near neutral tendency.

The fact that in this world selection eight architects are from Eastern Asia (22% of the total, considering that Sejima & Nishizawa work together, and that I.M. Pei settled in the U.S.), and six from Japan, is quite significative. Four of these architects have been awarded the Prize in the last five years, corroborating the consequences of globalization and substantial development in the region. Tradition in the fine craft of materials and a taste for the subtle favours the preference for achromatics and near neutrals in this group.

A selection of architects serves to exemplify each the four colour tendencies. There is a small percentage amongst the thirty-seven Pritzker winners who have been notorious for chromatic designs in the way of Luis Barragan. These are: Aldo Rossi, Herzog&De Meuron, Renzo Piano, Jean Nouvel and Robert Venturi. Colour is also an important element in projects by Norman Foster, Richard Rogers and Toyo Ito. On the other hand Jørn Utzon, Sverre Fehn, Gottfried Böhm, Wang Shu and Shigeru Ban show a marked preference for natural materials. Concrete is a favourite of Tadao Ando, Paulo Mendes da Rocha and Kenzo Tange. The achromatics have inmortalized Philip Johnson and they are main ingredients in the work of insubordinate taste of Zaha Hadid, Thom Mayne and Rem Koolhaas. The architects who rely on white for their buildings are Richard Meier and Oscar Nyemeyer. Apart from them, Alvaro Siza, Fumihiko Maki, I.M. Pei, Sejima&Nishizawa, Toyo Ito, and probably most in this elite, are authors of iconic white buildings.

4. CONCLUSIONS

As regards the preference for colourless designs by Pritzker architects, it is confirmed that the scale tilts towards non-colours. Even if 35% of the laureates have used chromatic colour in several projects, their joint portfolios in a span of nearly 66 years show that achromatics and natural materials recurr in their work, while colour is the exception. Although the analysis of the timetable and the world map may have an arbitrary component, history and origin are a way to understanding colour use. Architects from diferent parts of the world show inclination to similar tendencies, and this depends on the moment in time, amongst other factors. Perhaps there is no urge to look for colour as such in coloured buildings. Instead, the subtleties of achromatics and material dimensions are there to be discovered and broaden the palette.

REFERENCES

Arrarte-Grau M. 2008. On the Bonding of Colour and Architecture: Colouring Modes. Stockholm, Sweden. In *Colour-Effects and Affects, AIC Color 2008, Proceedings*, ed. by I. Kortbawi. Stockholm: Scandinavian Colour Institute.

Koolhaas R. et al. 2001. *Colours: Rem Koolhaas/Oma, Norman Foster, Alessandro Mendini*. Basel, Berlin, Boston: Birkhäuser. 12-13

Office Profiles Architects. *Amateur Architecture Studio*. (Accessed February 27, 2015). http://www.chinese-architects.com/en/amateur.

Richard Meier & Partners Architects LLP. *Richard Meier Partners Architects Splash* Comments. (Accessed February 27, 2015). http://www.richardmeier.com/.

Home | The Pritzker Architecture Prize. *Home | The Pritzker Architecture Prize*. January 1, 2015. (Accessed February 27, 2015.). http://www.pritzkerprize.com/.

Toyo Ito & Associates, Architects. *Toyo Ito & Associates, Architects*. (Accessed February 27, 2015). http://www.toyo-ito.co.jp/.

Color Theory. *Wikipedia*. Wikimedia Foundation, n.d. Web. 27 Feb. 2015. http://en.wikipedia.org/wiki/Color_theory.

Address: Malvina ARRARTE-GRAU / Parque José de Acosta 226, Apt. 401, San Isidro, Lima 27, PERU
E-mail: colorarq@gmail.com

Computing Tristimulus Values: An Old Problem for a New Generation

Zhifeng Wang,[1] Tianyi Li,[1] M Ronnier Luo,[2] Manuel Melgosa,[3] Michael Pointer,[2] Changjun Li [1]
[1] School of Electronics and Information Engineering, University of Colour and Technology Liaoning, China
[2] School of Design, University of Leeds, UK
[3] Department of Optics, University of Granada, Spain

ABSTRACT

CIE tristimulus values (TSVs) are defined in terms of integrations and all the integrands involved have no analytical expressions: therefore accurate computation of the TSVs becomes a problem, a problem which has been noticed by scientific researchers possibly since the early 1930s. Various computational methods are available and disagreements between these methods can be large. This paper addresses this problem and shows that it becomes even worse with some current industrial applications. However, the problem is completely avoidable if a unified method is used to calculate the TSVs. The paper compares all available methods including the CIE recommended method and the ASTM weighting tables, the Oleari method and the LLR method, together with a newly developed LWL method, and it is found that this new LWL method gives the best results. It is therefore recommended for use for the computation of TSVs using data obtained at any measurement wavelength interval.

1. INTRODUCTION

Tristimulus values (TSVs) of object colours are defined by integrations:

$$V = \int_a^b W_V(\lambda)R(\lambda)d\lambda \text{, with } V = X \text{, } Y \text{ and } Z \tag{1}$$

where $W_X(\lambda) = \kappa S(\lambda)\bar{x}(\lambda)$, $W_Y(\lambda) = \kappa S(\lambda)\bar{y}(\lambda)$, $W_Z(\lambda) = \kappa S(\lambda)\bar{z}(\lambda)$. Here $S(\lambda)$ is the relative spectral power distribution (SPD) of an illuminant, $\bar{x}(\lambda)$, $\bar{y}(\lambda)$, $\bar{z}(\lambda)$ are the CIE 1931 (2°) or 1964 (10°) standard colorimetric observers or colour matching functions (CMFs), and $R(\lambda)$ is the reflectance (transmittance) function of a reflecting (transmitting) object colour. (a,b) is the visible range of wavelengths with a = 360 nm and b = 830 nm, and k is the normalizing factor defined for reflecting (transmitting) object colours and is given by $k = 100/\int_a^b S(\lambda)\bar{y}(\lambda)d\lambda$. However, the integrands involved in Eq. (1) have no equivalent analytical expressions, hence CIE[1] recommended that the integrations should be replaced by numerical summations:

$$V = \sum_{i=0}^{n} W_V(\lambda_i)R(\lambda_i)\Delta\lambda \text{, with } V = X \text{, } Y \text{ and } Z \tag{2}$$

at wavelength intervals $\Delta\lambda = 1\,\text{nm}$.

It seems that calculating TSVs using Eq. (2) should be straightforward provided that the reflectance values at 1 nm intervals are known over the full range of wavelengths. However, in practice these data are rarely available, since reflectance data are typically measured by a spectrophotometer at an interval much larger than 1 nm, for example 10, or even 20 nm, and often over a narrower wavelength range than 360 nm to 830 nm. Thus, for practical applications, there is still a problem of how to compute the TSVs. Since CIE makes has no precise recommendation on how to deal with this, there are many methods available for computing TSVs. Different methods lead to different results and the differences obtained can be large, which can cause problems in current industrial applications. Firstly, consider an example. Table 1 lists the differences in terms of CIELAB colour difference units using a number of different methods with the measured 1 nm, and then simulated 10 nm and 20 nm data, for a Munsell colour sample. In Table 1, S represents the CIE standard 1 nm summation method, which computes TSVs using the 1 nm data and 1 nm summation formula (Eq. 2) using the CIE F11 fluorescent illuminant and the CIE 1931 CMFs. This set of TSVs, denoted by XYZs, can be considered as the true TSVs of the sample. Also a number of other sets of TSVs, denoted by XYZb, were computed using the simulated 10 nm and 20 nm reflectance factors and some other available computation methods: these methods will be introduced in the next section. Ideally, XYZs and XYZb should be the same, but they are not. The values in bold and in the shaded area are the inconsistencies between different methods for 10 nm and 20 nm data respectively. Furthermore, the difference between XYZb1 obtained by method 1 and XYZb2 obtained by method 2 can be large. The values below/above the diagonal in Table 1 are for 20 nm/10 nm data and correspond to the CIELAB colour differences between the TSVs obtained using any two different methods, hence they represent the accuracies associated with the corresponding methods. It can be seen the values underlined are all greater than zero, which means no method replicates the accurate result XYZs: the smaller the value the better is the corresponding method. For the data having a 10 nm wavelength interval, the LWL, LLR and CIE-R methods are similar and are better than all the others. The worst method is the DS method which an error of 9.3 CIELAB colour difference units. For the data that has a 20 nm wavelength interval, the T6 and LLR methods are similar, and are better than all others, but they have error of 0.6 CIELAB colour difference units. The disagreements between methods can be as large as 11.1 CIELAB units for 10 nm data, and 31.8 CIELAB units for 20 nm data.

The CIE provides no recommendations for TSV computation from measured data at measurement intervals greater than 5 nm. Thus, in practice, various approaches have been used for computing TSVs, which can lead to a big discrepancy between two different methods from the same set of spectral data as shown by the above example which can cause problems. For example, a fashion designer asks a dyehouse to dye a fabric and provides spectral reflectance data at 10 nm intervals rather than a physical sample in order to save time and the cost. The requirement for the reproduction is, for example, less than 0.5 CIELAB units. If the dyehouse uses a different method for computing TSVs, it is highly possible that the dyed fabric might be rejected though the company thinks the requirement is satisfied. Another example occurs with cross media colour reproduction. In the colour reproduction chain, both the source (e.g. a camera) and destination (e.g. a printer) devices are characterized, so that the device dependent colour spaces are linked to the device independent CIE XYZ space. If the methods for computing the XYZ values are different between the characterization processes of the source and destination devices, it cannot be guaranteed that the reproduction will be accurate.

Table 1: The performance of different methods used to compute TSVs (underlined row for 20 nm interval data and underlined column for 10 nm data) for a Munsell sample under CIE illuminant F11 and the CIE 1931 standard colorimetric observer, measured as CIELAB colour differences. Values in the shaded area are for 20 nm interval data and values in bold for 10 nm interval data.

	S	T5	T6	LWL	LLR	CIER	OWT0	OWT2	DS	T5N	T6N
S	-	1.8	0.6	0.7	0.6	1.5	5.2	2.2	26.6	1.7	2.6
T5	0.3	-	1.3	1.2	1.2	0.4	6.4	2.1	25.5	0.1	0.8
T6	0.3	**0**	-	0.1	0.1	0.9	5.5	2	26.3	1.2	2
LWL	0.1	**0.1**	**0.2**	-	0	0.8	5.5	1.9	26.3	1.1	2
LLR	0.1	**0.2**	**0.2**	**0**	-	0.8	5.5	1.9	26.3	1.1	2
CIER	0.1	**0.1**	**0.2**	**0**	**0**	-	6.1	2	25.7	0.3	1.2
OWT0	1.8	**1.9**	**1.9**	**1.9**	**1.9**	**1.9**	-	4.6	31.8	6.3	7.1
OWT2	0.9	**0.9**	**0.9**	**0.9**	**0.9**	**0.9**	**1.1**	-	27.5	2.1	2.7
DS	9.3	**9.3**	**9.3**	**9.3**	**9.3**	**9.3**	**11.1**	**10.1**	-	25.5	24.9
T5N	-	-	-	-	-	-	-	-	-	-	0.9
T6N	-	-	-	-	-	-	-	-	-	-	-

2. AVAILABLE METHODS FOR COMPUTING TSV

The various computation methods are briefly introduced in chronological order of their development; further details can be found in reference 2.

2.1 Direct Selection Method

Direct selection (DS) is the simplest method and it has probably been used since 1932[3]. For measured reflectance at interval $\Delta\lambda>1$ nm, select one value from every $\Delta\lambda$ data from the spectral power distribution (SPD) and standard observer (CMF), and then carry out the corresponding summations as shown in Eq. (2).

2.2 ASTM E308-1985 and E308-1995 Weighting Tables

The American Society for Testing and Materials (ASTM) standardized a set of weighting tables in 1985 (E308-1985) and 1995 (E308-1995). Each set includes 36 weighting tables covering 9 illuminants (six continuous illuminants A, C, D50, D55, D65 and D75, plus the three fluorescent illuminants FL2, FL7 and FL11); each illuminant being combined with the two CIE standard colorimetric observers (1931 and 1964) and two different wavelength intervals (10 nm and 20 nm). All these tables cover a wavelength range from 360 nm to 780 nm. The ASTM E308-1985 weighting tables are denoted as Table 5 (T5) and must be used with bandpass corrected reflectance data. The E308-1995 weighting tables are denoted as Table 6 (T6) and must be used with the measured reflectance data directly.

Recently, ASTM[4] recommended that the 20 nm weighting data in both sets of tables should not be used. ASTM now recommends that, when the measured reflectance data for using T6 or the bandpass corrected reflectance for using T5, are at 20 nm intervals, they should be interpolated using the third-order Lagrange formulae to compute 10 nm reflectance data, and then the corresponding 10 nm weighting table should be used to compute TSVs. In this paper, this new recommendations are denoted T6N and T5N, respectively.

2.3 CIE Recommendations

For measured data with $\Delta\lambda \le 5$ nm, CIE recommends that the DS method can be used. For $\Delta\lambda = 10$ nm or $\Delta\lambda = 20$ nm, the measured data can be interpolated into 1 nm data and then the 1 nm summation can be used. This recommendation is named the CIE-R method in this paper. However, CIE[1] also suggested that for $\Delta\lambda = 10$ nm or $\Delta\lambda = 20$ nm, the ASTM T5 or T6 or the LLR method (which will be introduced later) may be used.

2.4 The Zero- and Second-Order Oleari Weighting Tables

In 2000, Oleari [5] proposed a method for the computation of TSVs based on a local power (zero or second-order) expansion for the product of the SPD of the illuminant/source and the CMFs. It was shown that the second-order method was better than ASTM T6. To avoid repeated computations, Li *et al.*[6] have derived zero- and second-order weighting tables based on Oleari's work. Henceforth, these zero- and second- order weighting tables will be termed the OWT0 and OWT2 methods, respectively.

2.5 LI-LUO-RIGG Method

IN 2004, Li, Luo and Rigg gave a method for computing weighting tables for calculating TSVs. The method (LLR) requires solutions to the following equations:

$$Au_V^{(\Delta\lambda)} = a_V^{(\Delta\lambda)}, \text{ with } V = X, Y \text{ and } Z \tag{5}$$

The unknown $\mathbf{u}_V^{(\Delta\lambda)}$ are the weights in the V directions. The matrix A and the right hand vector $a_V^{(\Delta\lambda)}$ can be found in the original paper [7].

2.6 LI-WANG-LUO Method

Similar to the LLR method, the least square method [8] (denoted as the LWL method) also requires solving three linear systems of equations:

$$\mathbf{B}\mathbf{u}_V^{(\Delta\lambda)} = \mathbf{a}_V^{(\Delta\lambda)}, \text{ with } V = X, Y \text{ and } Z \tag{6}$$

Here, the right hand side vectors are the same as those of the LLR method and coefficient matrix B is also tri-diagonal. It has been shown[2] that when $\Delta\lambda$ is large, the matrix B approaches the matrix A, and therefore in this situation the LWL and LLR methods have nearly the same performance. However, when $\Delta\lambda$ is small, these two methods will perform differently, which is confirmed by the experimental results presented in the next section.

3. COMPARISONS OF ALL METHODS

The comparison procedure used in this paper is the same as that used in references 2 and 7. Here, the 1 nm standard reflectance factors were measured from a set of 1096 Pantone samples between 360 nm and 780 nm. Thus, TSVs can be computed using the 1 nm summation methods and this set of TSVs are considered as standard. Then, the simulated 10 nm or 20 nm reflectance factors can be obtained and the TSVs, denoted as XYZb, can be obtained using a particular method under a particular illuminant and CMF combination. Finally, the CIELAB colour differences between XYZs and XYZb are computed. Since ASTM methods are also compared, the visible range considered here is from 360 nm to 780 nm. Six CIE illuminants and the CIE 1931 and 1964 CMFs were used. The illuminants were the three continuous illuminants D65, D50, and A, plus the three CIE fluorescent illuminants FL2, FL7 and FL11. In order to save space, the computed colour differences in Table II have been grouped into continuous and fluorescent illuminant groups (C-ILLs and F-ILLs) respectively. Then the median colour difference from each group is considered as the general performance for each method.

Table II: Median CIELAB colour differences for 10nm and 20nm using different methods under all continuous illuminants/two CMFs (C-ILLs) and Fluorescent illuminants/two CMFs (F-ILLs)

Method	10nm		20nm	
	C-ILLs	F-ILLs	C-ILLs	F-ILLs
T5	0.0111(6)	0.035(4)	0.1329(7)	0.2793(6)
T6	0.0033(2)	0.0408(5)	0.0287(3)	0.2199(4)
LWL	0.0013(1)	0.0095(1)	0.0243(2)	0.1263(2)
LLR	0.0038(3)	0.0107(2)	0.0216(1)	0.1238(1)
DS	0.0258(8)	7.3893(8)	0.3306(9)	4.6193(10)
CIE-R	0.0073(4)	0.0337(3)	0.0644(4)	0.1604(3)
OWT(0)	0.0094(5)	1.3594(7)	0.1173(5)	0.8284(7)
OWT(2)	0.0197(7)	0.5928(6)	0.2967(8)	0.9454(8)
T5N			0.1184(6)	0.2552(5)
T6N			0.7054(10)	0.9635(9)

Table II lists the median results for 10 nm and 20 nm measurement interval data. Values in brackets indicate the ranking of the corresponding methods. It can be seen that the LWL method ranks first for the 10 nm interval data and second for the 20 nm interval data. The LLR method ranks first for the 20 nm interval data and second for the 10nm interval data for F-ILLs. These two methods are better than all other methods. The worst method overall is the DS method. Comparing the four ASTM methods for the 20 nm interval data, T6 is the best, T5N is the second best and the T6N is the worst. In theory, the T5 and the CIE-R method are the same if the third order interpolation method is used for the CIE-R method. However, in this test, the Sprague method is used for the interpolation not the Lagrange method. This might be the reason that the CIE-R method performs better than the T5 method, as shown in Table II.

Further tests with $\Delta\lambda$ being equal to 2, 3, 4, 5, 6 and 7 nm, respectively were also conducted. It was found that in each case the LWL method performs the best. This result is very encouraging. It was also found that the LLR method performs much worse when the measuring wavelength interval is small.

4. CONCLUSIONS

We have reviewed the problem of accuracy in the computation of tristimulus values. Results from different methods can be quite different which can cause problems in current industrial applications. It is highly desirable that a single optimal method be adopted by CIE. To further this aim, a comprehensive comparison has been made using 1096 Pantone samples. The results show that the method of Li-Wang-Luo (LWL) performs the best for wavelength intervals not greater than 10 nm and performs the second best when the measuring interval is 20 nm. The LWL method is simple to implement and can be recommended for the computation of CIE XYZ tristimulus values from reflectance (transmittance) data measured at any wavelength interval.

ACKNOWLEDGEMENTS

This research has been supported by National Natural Science Foundation of China (Grant number 61178053) and Ministerio de Educación y Ciencia of Spain (Research project FIS2013-40661-P), with European Regional Development Fund (ERDF).

REFERENCES

1. CIE Publ. 15:2004. *Colorimetry*, 3rd Edition. CIE Central Bureau: Vienna; 2004.
2. Li CJ, Luo MR, Melgosa M and Pointer MR, *Testing the Accuracy of Methods for the Computation of CIE Tristimulus Values Using Weighting Tables*, Color Research and Application, 2015.
3. Hardy AC, Pineo OW. *The computation of trichromatic excitation values by the selected ordinate method*. J Opt Soc Am 1932;22:430.
4. ASTM E308-13. *Standard practice for computing the colors of objects by using the CIE system*. American Society for Testing and Materials (ASTM; 2013).
5. Oleari C. Spectral-reflectance-factor deconvolution and colorimetric calculations by local-power expansion. Color Res Appl 2000;25:176-185.5.
6. Li CJ, Oleari C, Melgosa M, Xu Y. *Methods for computing weighting tables based on local power expansion for tristimulus values computations*. J Opt Soc Am A 2011;28:2243-2252.
7. Li CJ, Luo MR, Rigg B. A new method for computing optimum weights for calculating CIE tristimulus values. Color Res Appl 2004;29:91-103.
8. Li CJ, Luo MR, Wang G. *Recent progress in computing weighting tables for calculating CIE tristimulus values*. Proc. SPIE 6033, 198-207 (2006).004;29:91-103.

Address: Prof. Changjun Li, School of Electronics and Information Engineering,
University of Science and Technology Liaoning, 185 Qianshan Road, Anshan, China
E-mail:cjliustl@sina.com

Variability in colour matches between displays

Phil GREEN,[1] Srikrishna NUDURUMATI,[2] Ivar FARUP[1]
[1] Colour and Visual Computing Laboratory, Gjøvik University College, Norway
[2] Global Graphics Software Ltd., Cambridge, UK

ABSTRACT

The variability between colour matches made by different observers on displays is a concern which has been addressed in several previous studies. Inter-observer variability in perceived colour matches was investigated in an experiment in which 21 observers matched a series of test colours, with the reference stimulus on a CRT and the test stimulus on an LCD display. Reference and test colour patches with a 2 degree angular subtense were presented on adjacent displays with a separation between reference and test stimuli of 7cm, and with an opaque black mask covering the remainder of the display screens. The first reference colour was a mid-tone neutral gray, followed by nine chromatic colours. Observers adjusted the test colour to produce a perceived match to the reference, and the resulting colours were measured with a Konica-Minolta CS-1000 telespectroradiometer. The results showed considerable variability in the matches in luminance. In *u'v'* chromaticity, observer variability was found to be less than in luminance, but much higher in blues than in greens and neutrals, suggesting a possible observer metamerism effect.

1. INTRODUCTION

The CIE 1931 Standard Colorimetric Observer was derived by pooling the colour matching functions of multiple observers. These original experiments, and subsequent ones in the following decades, recorded significant variability between matching functions of individual observers. While the typically smooth reflectance spectra of surface colours do not tend to give rise to significantly large inter-observer differences in colour matches, the nature of the spectral emission of self-luminous displays, often characterised by narrow peaks, is more likely to interact with differences in retinal spectral sensitivity to generate inter-observer variation in cross-media colour matches in cases where different colorant technologies are employed. Such inter-observer differences have been reported in previous studies (e.g. Oicherman 2007; Shaw, 2010; Sarkar 2010; Parab 2010; Sarkar 2011).

Modern displays use a variety of light-emitting technologies with very different spectral characteristics, and the goal of the present experiment was to provide experimental data on colour matches made by observers between two different types of displays.

2. EXPERIMENTAL

Following a small pilot study with 6 observers, 21 observers took part in the main phase of the experiment, in which 10 reference colours were matched between a CRT display (employing phosphors as the light-emitting technology) and an LCD display (with LED backlight).[1]

[1] The experiment was undertaken by the second author during his employment as an Early-stage Researcher in the Marie Curie Initial Training Networks (ITN) CP7.0 project.

2.1 Displays

The displays were a CRT (Lacie Softproofing Display) and an LED-backlit IPS-LCD (Dell U2412M). The R, G, B primaries of the two displays were measured with a Konica-Minolta CS1000 telespectroradiometer, and the spectral radiances are shown in Figure 1 below. The colour gamut of the two displays can be seen in CIE u',v' coordinates in Figure 2.

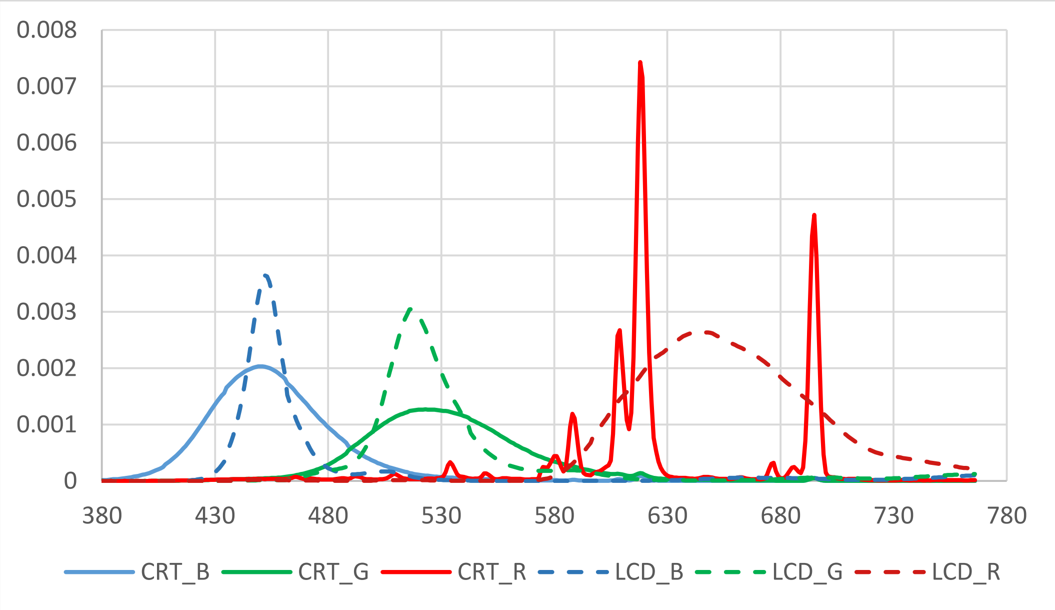

Figure 1: Spectral radiances of CRT and LCD display primaries in the experiment.

Since the dynamic range and colour gamut of the CRT was smaller than that of the LCD, the CRT was used to present the reference colours which observers then matched on the LCD. The neutral gray was presented first to provide an initial reference for brightness matching by observers. Display variability was evaluated by measuring a series of colours over a period of 12 hours after initial warm-up, using the K-M CS1000 TSR. The mean differences from the mean white point luminance over the period were 0.42 and 0.12 cd m^{-2} for the CRT and LCD respectively.

The observer visual matches and the instrumental measurement were performed at the same location on the displays, so the matches were unaffected by any spatial non-uniformity of the displays. There was a warm-up period of at least 15 minutes for the displays and the TSR prior to measurements and observations.

2.2 Observers

Following a pilot study with six observers, 21 observers aged 24-55 participated in the experiment. An Isihara test was conducted prior to the experiment for those observers had not previously performed such a test, and one was found to be colour deficient. Non-expert observers were given training in colour mixing. Observer repeatability was evaluated by observers performing matches between similar patches during each run of the experiment.

2.2 Reference Colours

10 colours were selected in RGB coordinates and displayed on the reference (CRT) display). The resulting colours were measured with the TSR and are shown in CIE u',v' coordinates

in Figures 2, where the reference colours are labelled 1-10. Some of the reference colours lie close to or on the boundary of the CRT gamut, but are within the gamut of the LCD display.

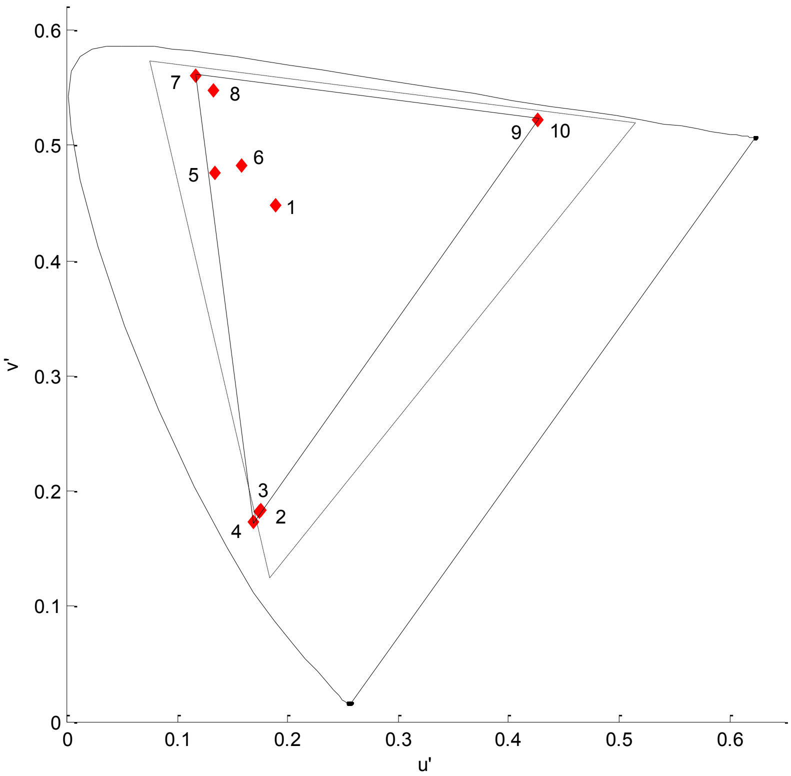

Figure 2: Reference colours in CIE u',v' with gamut of CRT (solid) and LCD (dashed) displays

2.3 Experimental Setup

The experiment was conducted in a completely dark room with the display colour patches being the only stimuli. Reference and test patches were circular and 3.5 cm in diameter. Observers were located one metre from the display faceplate, so that the colour stimulus gave an angular subtense of 2°. In order to exclude any effect due to the display backlight within the faceplate, the patches were observed through circular openings made within an opaque black sheet placed in front of the displays. The displays were placed adjacent to each other so that the reference and the test targets were located at approximately 7 cm apart. This is essentially an aperture mode rather than object mode viewing condition.

2.4 Experiment

In the experiment the reference colour was shown on the CRT display and the test colour shown simultaneously on the LCD display. Observers were asked to match the appearance of the test to the reference colour. To do this they were provided with three computer mice with two-way spherical scroll controlling the amounts of individual primaries (R, G & B) of the test colour, together with a keyboard control for adjustment of the brightness. Once the observer was satisfied with the match, the corresponding R, G, B values were recorded and subsequently measured with the TSR positioned at the observer location in the same viewing conditions.

3. RESULTS

CIE XYZ values for the reference colours and the observers matches were calculated from the measured radiances using the CIE 1931 Standard Colorimetric Observer, as shown in eqn. 1 below.

$$X = 683 \sum_{767}^{380} L(\lambda)\bar{x}(\lambda)$$

where $L(\lambda)$ is the measured spectral radiance (in W sr^{-1} m^{-2}) at 1nm intervals and $\bar{x}(\lambda)$ is the vector of matching function values for X; and Y and Z are computed analogously. The constant 683 results in Y tristimulus values in units of cd m^{-2}.

Since the experiment was conducted in a dark room with no adapting white and colours were judged in aperture mode, there is no reference white or illuminant and hence the data cannot be converted to a colour space such as CIELAB. For this reason the variability between the reference colour and the observer matches is shown in terms of luminance ΔY and chromaticity *Δu',v'* (CIE 2014). The results are shown in Table 1. [We note that if the data is converted to CIELAB, using the display peak white as the reference white as is commonly done in colour management, the average CIELAB 1976 ΔE^*_{ab} colour difference from the reference is 19.5 and the inter-observer variability (expressed as the mean colour difference from the mean, or MCDM) is 10.4, which gives a misleading impression of the accuracy of the matches.]

Table 1.Differences in luminance ΔY and chromaticity Δu',v' between reference colours and observer matches

	ΔY			*Δu'v'*		
Colour	Median	Max	95th percentile	Median	Max	95th percentile
1	6.57	9.6	9.51	0.0107	0.0244	0.0201
2	0.65	1.27	1.15	0.0207	0.0543	0.0537
3	0.91	2.91	2.32	0.0373	0.1023	0.0819
4	2.46	5.7	5.5	0.012	0.0526	0.0491
5	5.31	14.33	12.85	0.0128	0.0198	0.0197
6	4.01	14.9	13.62	0.0178	0.0256	0.0235
7	9.1	36.43	30.99	0.0134	0.0572	0.0391
8	3.54	32.98	23.94	0.0267	0.1424	0.1421
9	2.32	9.04	8.52	0.0253	0.047	0.0469
10	3.17	13.32	13.21	0.0238	0.0506	0.0492
Mean	3.8	14.05	12.16	0.0201	0.0576	0.0525

The variability in luminance matches is very high for some colours, shown by 95th percentile ΔY values of up to 30.99. The matches in u',v' chromaticity have smaller variability, as seen in Figures 3-5, where the reference colour is shown in red and the observer matches in black.

It should be noted that where the reference colours are close to the gamut boundary, the direction of possible matches in chromaticity space by observers was constrained.

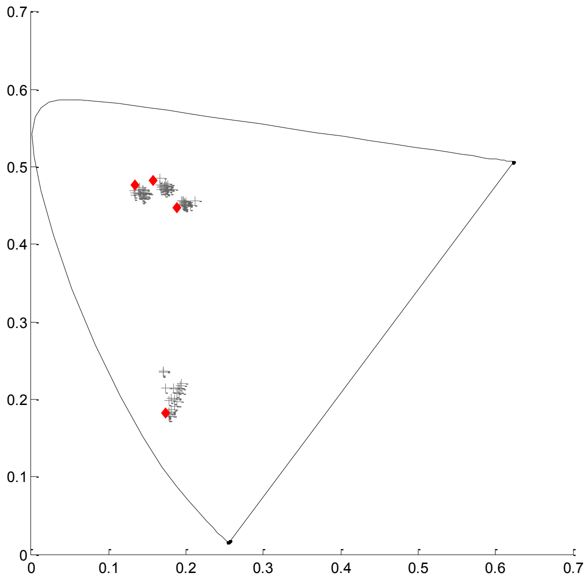

Figure 3. CIE u',v' coordinates of reference colours (red marker) and corresponding observer matches for colours 1, 2, 5 and 6

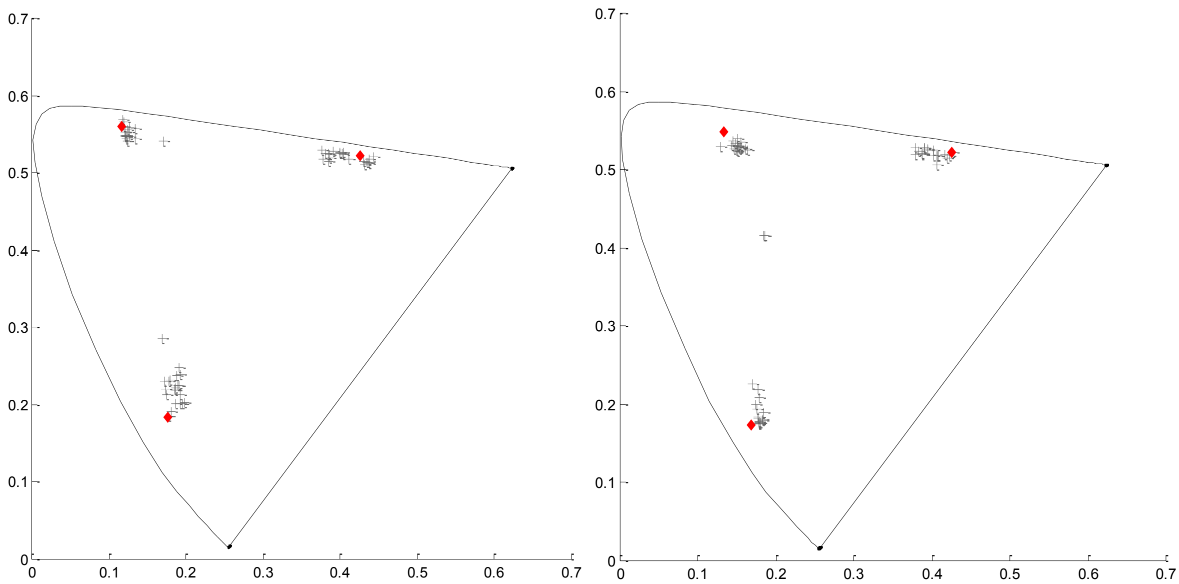

Figure 4-5. CIE u',v' coordinates of reference colours (red marker) and corresponding observer matches for colours 3, 7 & 10 and 4, 8 & 9 respectively

It can be seen from Figures 3-5 that observer variability in greenish and neutral colours is relatively small, while in red (colours 9-10) and blue (colours 2-4) regions it is considerably higher. The three blue reference colours are located at near-identical chromaticity coordinates, and the pattern of observer matches is very similar between the three, suggesting a possibly systematic difference in the way individual observers made the matches. A similar pattern can be seen in the two red colours, although less pronounced.

4. CONCLUSIONS

Observers matched a set of 10 reference colours presented on a CRT display, using an LED-backlit LCD display. Significant variability was seen in the luminance of the matches, suggesting that luminance is of less importance than chromaticity in an aperture-mode colour matching task. Variability in matching of chromaticity was small in some colours, but relatively high in certain colours, notably in blue. The similar trend seen in the matches for colours of similar chromaticity suggests there is a possible observer metamerism effect arising from different cone sensitivities of the observers. However, further analysis is needed to confirm this possibility. If present, it would be consistent with results obtained in other studies.

The results also indicate that aperture mode colour matches should be evaluated in luminance and chromaticity, with higher tolerances in luminance.

ACKNOWLEDGEMENTS

This work was supported by Marie Curie Initial Training Networks (ITN) CP7.0 N- 290154.

REFERENCES

Shaw, M. and Fairchild, M. (2002) *Evaluating the 1931 CIE Color Matching Functions,* Col. Res. Appl. 27(5) 316–329

Oicherman, B. (2007) *Effects of colorimetric additivity failure and of observer metamerism on cross-media colour matching*, (PhD thesis) University of Leeds, UK

Parab, N. and Green, P. (2011) *Soft proofing of printed colours on substrates with optical brightening agents*, Proc. SPIE 7866 doi:10.1117/12.872219

Sarkar, A., L. Blondé, P. Le Callet, F. Autrusseau, J. Stauder, P. Morvan, (2010) *Toward Reducing Observer Metamerism in Industrial Applications: Colorimetric Observer Categories and Observer Classification*, Proc IS&T 18th Color Imaging Conf. 307-313

Sarkar, A., F. Autrusseau, F. Viénot, P. Le Callet, L. Blondé, (2011) *From CIE 2006 Physiological Model to Improved Age-Dependent and Average Colorimetric Observers*, J. Opt. Soc. Am. (JOSA A), 28(10) 2033-48

CIE Technical Note 001:2014 *Chromaticity Difference Specification for Light Sources*, Vienna: CIE

Address: Prof. Phil GREEN, Colour and Visual Computing Laboratory,
Gjøvik University College, Teknologivn. 22, 2815 Gjøvik, Norway
E-mails: philip.green@hig.no, srisrikrishna9@gmail.com, ivar.farup@hig.no

A comparison study of camera colorimetric characterization models considering capture settings adjustment

Jingyu Fang,[1] Haisong Xu,[1,*] Wei Ye [2]
[1] State Key Laboratory of Modern Optical Instrumentation, Department of Optical Engineering, Zhejiang University, Hangzhou 310027, China
[2] State Key Laboratory of Industrial Control Technology, Zhejiang University, Hangzhou 310027, China

ABSTRACT

Capture settings must be fixed for colorimetric characterization models of digital camera, which greatly limits the application of the cameras. In order to overcome this disadvantage, a correction procedure for capture settings adjustment was proposed in this study. To investigate the performance of the correction comprehensively, four kinds of widely-used characterization models were employed in this correction procedure as the mapping technique, including look-up table (LUT), polynomial regression, artificial neural networks (ANN) and support vector machine (SVM). The results show that the correction procudure is applicable for all kinds of colorimetric characterizations.

1. INTRODUCTION

The colorimetric characterization of digital camera is of fundamental importance for its scientific applications such as image based colorimetric measurement and color communication. Color characterization of still digital camera can be divided into two methods, i.e. spectral sensitivity-based one and target-based one, in which the latter is more generally used for its low cost and convenience. Until now, there are mainly four kinds of widely-used target-based characterization models, namely LUT (Hung 1993), polynomial regression (Hong *et al*. 2001), ANN (Cheung *et al*. 2002), and SVM (Yang 2013). The mappings from device-dependent camera RGB signals to device-independent CIE XYZ values defined by the conventional characterization models can yield reasonable color accuracy. These models, however, which require camera capture settings to be fixed from sample training to practical measurement, do not make full use of the dynamic range and adaptability of the digital camera. Whenever the capture settings used in practical measurement are adjusted, the sample training process has to be performed again according to the changed settings. To overcome this inconvenience, a correction procedure was proposed in this study to compensate the error resulted from the changes of camera capture settings. Besides utilizing the mappings derived from conventional characterization models, this correction procedure introduces two processes, i.e. equivalent transformation step and scale factor step, based on the imaging system, of which the performance was validated through an experiment using the camera of Nikon D3x.

2. METHOD

The characterization model involves training part and testing part. The training procedure is conducted in the same way as the conventional one except that the capture settings are recorded, while for the testing part the correction procedure is carried out to compensate the prediction error resulted by different capture settings with comparison to those in training part.

2.1 Capture settings correction procedure

The correction procedure for capture settings adjustment should be performed in following four steps:

1) To transform the pixel values in the image of testing targets to equivalent ones corresponding to the training stage using the Eq. (1) below. This step builds the bridge between different capture settings including ISO sensitivity, f-number and exposure time, denoted as *S*, *N*, and *T* respectively in Eq. (1).

$$\frac{P_{ts}}{P_{eq}} = \frac{T_{ts}S_{ts} / N_{ts}}{T_{tr}S_{tr} / N_{tr}} \tag{1}$$

where the subscripts *ts* and *tr* stand for the testing and training ones respectively, and *eq* represents the equivalent ones.

2) To search among training samples to find the one that is the nearest to the testing sample in *rg* chromaticity coordinates of camera RGB color space. Then to scale the equivalent pixel values caculated by step 1 to match the values of the corresponding training sample. The scale factor, *K*, is calculated by Eq. (2)

$$K = \frac{R_{tr} + G_{tr} + B_{tr}}{R_{eq} + G_{eq} + B_{eq}} \tag{2}$$

where *R*, *G*, and *B* are the pixel values of red, green, and blue channels.

3) To apply the scaled RGB values to the conventional colorimetric characterization models, of which the parameters are determined through training procedure. For the four models employed in this study, LUT model was modified since a regular look-up table could not be obtained by the digital camera, so the weighted mean of the 8 neighbourhood points was chosen as the predicted values. Three order polynomial expansions were adopted for the polynomial regression, resulting in the size of transform matrix being 20×3. For the popular ANN and SVM algorithms in the field of machine learning, the MATLAB neural network toolbox and an open library of libsvm (Chang *et al*. 2011) were used by default parameters without optimization for direct and effective comparison. Through the colorimetric characterization, the scaled tristimulus values XYZ could be obtained.

4) To scale back the XYZ values from step 3 to the predicted ones. The scaling factor in this step is the reciprocal of *K* in Eq. (2).

The scale factor step is involved to reduce the error caused by the nonlinear relationship between RGB and XYZ. Following the above steps, the RGB signals of images with different capture settings can be transformed to the corresponding XYZ tristimulus values without any more training.

2.2 Experiments

In the experiment, a light booth of GretagMacbeth SpectraLight III was used to provide stable lighting environment, in which a GretagMacbeth DC color chart was placed as the color target. The odd and even numbered patches of DC color checker were adopted as the training and testing samples, respectively. A Nikon D3x DSLR camera was employed to obtain the different RGB values under various capture settings. And the measuring geometry is 45/0, while the exposure time and ISO sensitivity were changed in the experiment to investigate the impact of camera settings adjustment.

3. RESULTS AND DISCUSSION

For the first phase of the experiment, the exposure time was the only variable while ISO and f-number were fixed as 100 and 5.6, respectively. The training samples were captured with correct exposure of 1/15s, while the testing samples were imaged with the exposure time ranged from 1/2s to 1/1000s. As the result, the comparion of the prediciton performance, in terms of ΔE^*_{ab}, between different characterization models is illustrated in Figure 1.

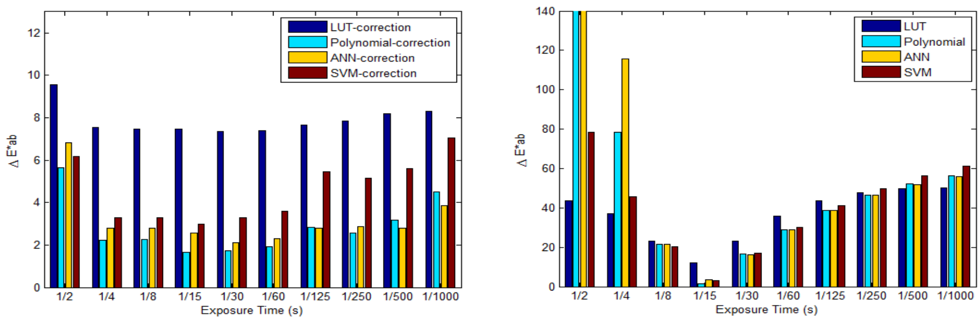

(a) models with correction procedure *(b) models without correction procedure*

Figure 1: Comparision of prediciton performance, in terms of ΔE^*_{ab}, between different characterization models

As can be seen from Figure 1, it is as expected that the prediction performance of all the four models achieve the best at the exposure time of 1/15s at which the training and testing settings are the same. The performance without correction procedure deteriorates with the camera settings being changed, while that with correction procedure remain at a stable level as the settings varies. As for the performance difference among the four models, the polynomial regression model is the best, while LUT is the worst due to the limited number and nonuniform color distribution of training samples for digital cameras. Since ANN and SVM were conducted using their default parameters, their prediction accuracies could be degraded accordingly. It could be concluded that either overexposure or underexposure should be avoided in applications as the prediction error with expsoure time at both end increases slightly.

For the second phase of the experiment, ISO sensitivity and expsoure time varied at the same time in order for right exposure, while the aperture was set as f/5.6. The training samples were captured with the ISO sensitivity of 100, while testing samples were photographed with ISO speed ranged from 100 to 6400. And the exposure time was halved when the ISO speed doubled according to the reciprocity law. The relationship between prediciton error and ISO sensitivity is shown in Figure 2, which shows that the correction procedure is applicable to ISO speed. There is a tendancy that the prediction error becomes bigger as the ISO speed increases, which results from the low signal to noise ratio for high ISO speed. Hence, it is recommanded that ISO 3200 or 6400 should be avoided to set unless the lighting is too weak.

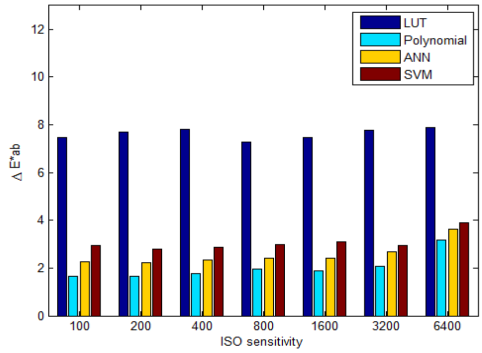

Figure 2: Prediction error of four characterization models with correciton procedure for different levels of ISO sensitivity

4. CONCLUSIONS

A correction procedure for camera colorimetric characterization was proposed in this study to compensate the prediciton error caused by capture settings adjustment. An experiment using Nikon D3x camera was conducted to validate the correction for four kinds of characterization models. It is indicated that the color prediction accuracy of all the four conventional models deteriorates badly as the gap between the image capture settings of training and testing becomes wider. On the contrary, the color differences achieved by the proposed correction based on the four models remain at a stable level with the capture settings being changed. Thereby, it can be concluded that this correction procedure for adjustable capture settings is applicable to different kinds of conventional colorimetric characterization models for camera imaging applications. In addition, the ISO sensitivity higher than the maximum of the standard ISO range (100-1600 for Nikon D3x) and the exposure value out of the dynamic range of the camera should be avoided.

REFERENCES

Chang, C-C. and C-J. Lin. 2011. LIBSVM: a library for support vector machines. ACM Transactions on Intelligent Systems and Technology 2(3): 27.

Cheung, V.T.L. and S. Westland. 2002. Color Camera Characterization Using Artificial Neural Networks. In 10th Color and Imaging Conference: Color Science and Engineering Systems, Technologies, and Applications, ed. by P. Hubel and I. Tastl. Scottsdale: Arizona, 117-120.

Hong, G.W., M.R. Luo, and P.A. Rhodes. 2001. A study of digital camera colorimetric characterization based on polynomial modelling. Color Research and Application 26(1), 76-84.

Hung, P-C. 1993. Colorimetric calibration in electronic imaging devices using a look-up-table model and interpolations. Journal of Electronic Imaging 2(1), 53-61.

Yang, B., H.Y. Chou and T.H. Yang. 2013. Color reproduction method by support vector regression for color computer vision. OPTIK 124(22), 5649-5656

Address: Zhejiang University, 38# Zheda Road, Hangzhou, 310027, CHINA
E-mails: chsxu@zju.edu.cn

Evaluation and Analysis of *YUTEKI-TENMOKU* Visual Effect on Traditional Ceramic Applied Gonio-Photometric Spectral Imaging and Confocal Type Laser Scanning Microscopy

Masayuki OSUMI
Office Color Science Co., Ltd.

ABSTRACT

The object of this study was developped obsevation and everuation way combined gonio-photometric spectral imaging and conforcal type laser scanning microscopy for traditional ceramics *YUTEKI-TENMOKU*. The flat shape ceramic plate was prepared with oxidation calcinating, and the glaze was composed feldspar, lime, silica stone, kaolinate, and red iron oxide. These were typical glaze components of *YUTKI-TEMOKU*. The spectral imaging illuminant direction was 15, 45 and 75 degree from normal direction. To get highly accurate spectrum, each wavelength images were compensated to small pixel shift by black/white lattice pattern measuring. As the result, regarding distribution in CIELAB color space, the image of 15 degree angle had wide distribution of L* by metal reflection. On the other hands, images of 45 and 75 degree angle were narrow distribution and disapeared metal reflection. *YUTEKI-TENMOKU* has various visual effects depend on optics dimension. And confocal type laser scanning microscopy observation was succeeded clearly getting three dimensional orientation of metal crystalline surface.

1. INTRODUCTION

TENMOKU ceramics were produced in Zhejiang Province of Chinese Southern Sung Dynasty, and it was considered to be brought to Japan by Zen priest around 800 years ago in Kamakura period. Especially, these were prized in japanese traditional tea ceremony and one of the sought-after item in *CHANO-YU*. *YUTEKI-TENOMOKU* is kind of these type ceramic, and many traditional tea bowls were designated a national tresure. The glaze was included a lot of iron ingredient, and the visual feature is oil droplet pattern on black ground of the cermic surface. These pattern was appearanced by precipitation of iron crystaline and one of the important optical manifestation, that is gonio-apparent and anisotropic color. It is nececsary analisys corelation between changing of color appearance with various optical dimension and orientation of iron crystaline in glazing layer to clarify chractarizing about these ceramics color appearance.

2. METHOD

2.1 Sample Preparation

The flat shape plate of *YUTEKI-TENOMOKU* ceramic was prepared with oxidation calcinating, and the applied glaze was composed feldspar $(Na,K,Ca,Ba)(Si,Al)_4O_8$, lime $Ca(OH)_2$, silica stone $Si(OH)_4$, kaolinate $Al_2Si_2O_5(OH)_4$, and red iron oxide Fe_2O_3 ingredient. Sample size was 10cm by 10cm of square. The thcikness of glaze layer was contrloed by dipping time and prepared 10 different thickness plates. The glaze layer thickness was related size of oil droplet pattern.

2.2 Colorimetric way

The detail measuring way of color was applied the gonio photometric spectral imaging system which was composed liquid crystaline tunable filter, white LED illuminant, and Peltier cooling monochrome CCD image sensor. Illuminant direction was 15, 45 and 75 degree from normal direction, and detect direction was normal against sample.

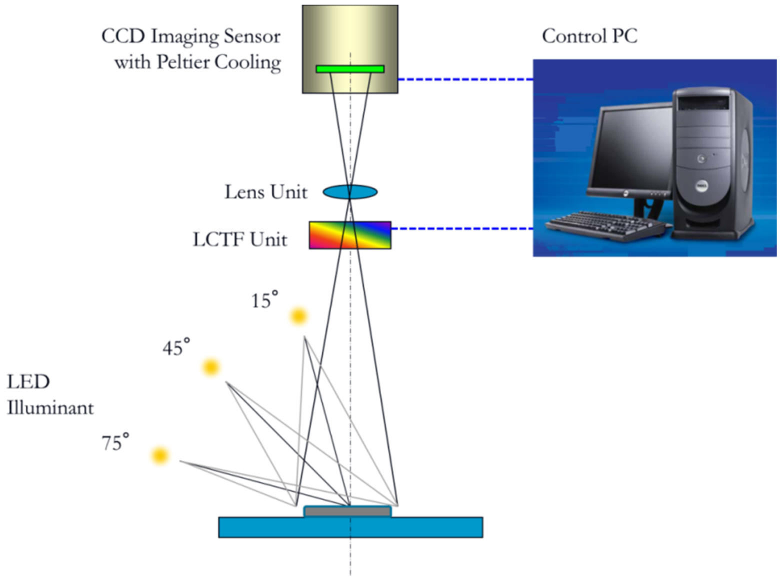

Figure 1: Gonio-photometric spectral imaging system.

To get highly accurate gonio-photometric reflectance spectrum and imaging information, each wavelength sample images were compensated by measuring of black/white lattice pattern to sence small shift amount of x and y direction before measuring ceramic sapmle. The lattice pattern image applied pixel shift compensation were shown in Fig. 2. Before compensation, measuring image was a lot of false color around black lattice line and reflectance profile was not horisontal. On the other hands, the image applied pixel shift compensation was disappeard false color.

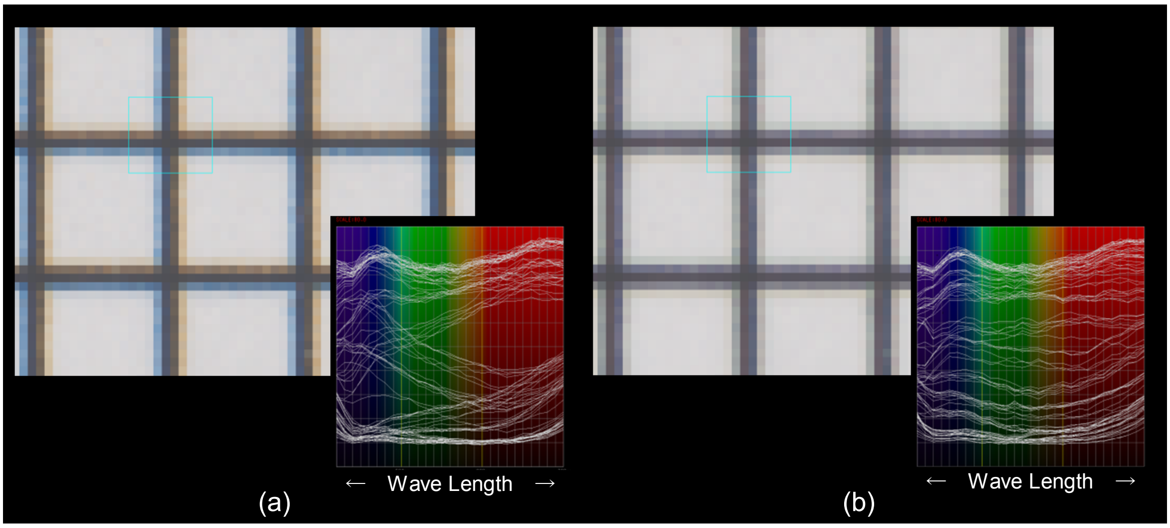

Figure 2: Pixel shift compensation by lattice pattern.
(a):before compensation. (b):after compensation.

The measuring results of sample plate by this way, three angle illuminant image were shown in Fig. 3.

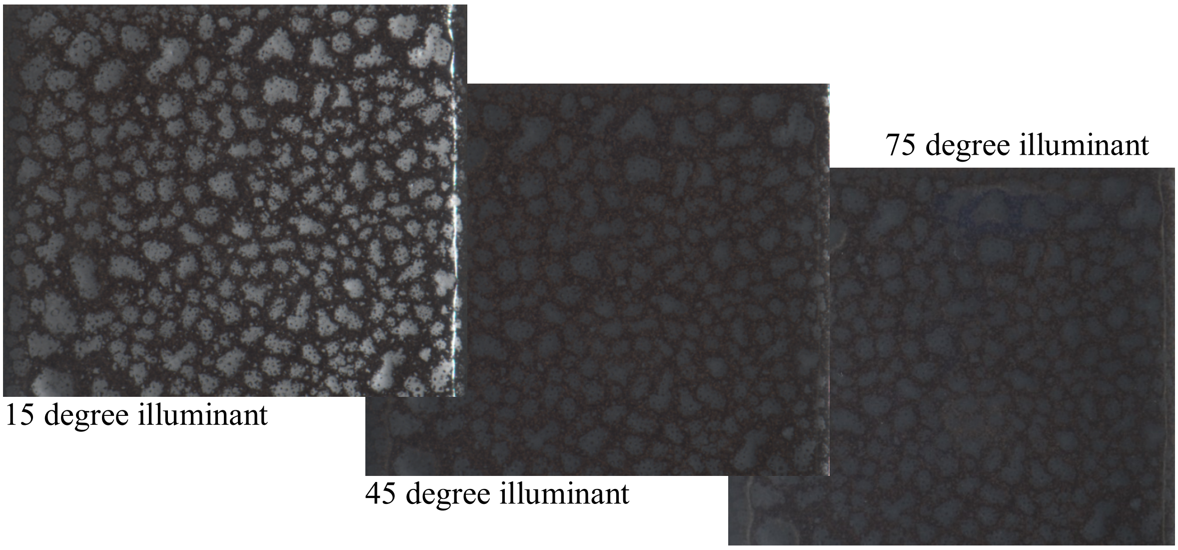

Figure 3: Measuring Image result of YUTEKITENMOKU ceramic plate by gonio-photometric spectral imaging.

2.3 Confocal type laser scanning microscopy observation

Also the three dimensional measuring way of iron crystaline distribution in glazing layer was applied confocal type laser scanning microscopy, and model VK-X100 made by KEYENCE was used. This microcopy was applied laser scanning technology, and allowing three dimensional reconstructions of topologically complex object by computer calculation, and can be sence interior structure with images of non-opaque specimen. In this experiment, observation magnification was 1000 times.

3. RESULTS AND DISCUSSION

3.1 Spectral Imaging observation

As the result, CIELAB coordinate value, number of color appearance and information entropy of each illuminant angle mesurements were shown in Table 1. Basically, *YUTEKI-TENMOKU* substrate color is black, and *a**, *b** value were almost zero, but color was slighty changed and angle dependent. The shade color, that is 75 degree illuminant angle image was bluish than the other angle. The distribution in CIELAB color space calculated from measured spectral image of each illminant angle was different. Especially, image of 15 degree angle had wide distribution of L* direction by metal reflection. On the other hands, images of 45 and 75 degree angle were narrow distribution profile and disapeared metal reflection. *YUTEKI-TENMOKU* has various visual effects depend on optics dimension. CIELAB color space distribution of each illuminant angle is shown in Fig. 4.

Table 1: Measuring Image result of YUTEKITENMOKU ceramic plate by gonio-photometric spectral imaging.

	L*	a*	b*	Number of color appearance	Information Entropy
15 degree	27.63	1.57	-0.52	785	5.72
45 degree	20.26	1.84	-0.48	120	4.07
75 degree	21.65	1.28	-1.75	233	4.41

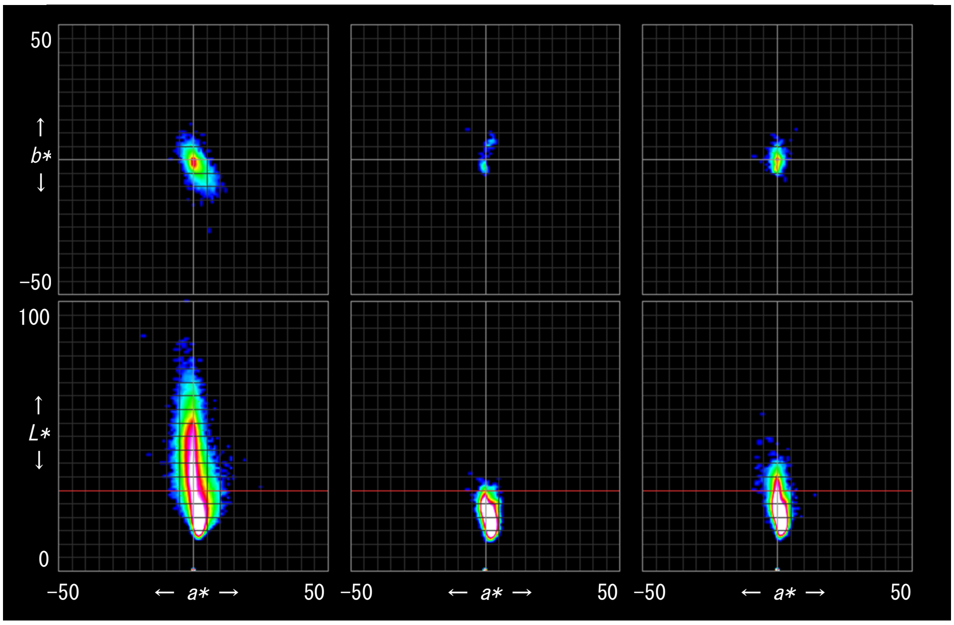

Figure 4: Measuring L distribution of YUTEKITENMOKU ceramic plate by gonio-photometric spectral imaging of 15, 45 and 75 degree illuminant.*

In this figure, upper three isometric graph are distribution of each angle at L^*=40. The L^* distribution of each illuminant angle were shown in Fig. 5. The horizontal axis was width direction of ceramic sample plate, and vertical axis is L^*. Figure 4 and 5 are related with number of color appearance and information entropy in Table 1. The distribution of 15 degree image is wider than the other angle distribution by metal crystalline reflection, especially, L^* distribution is quite large.

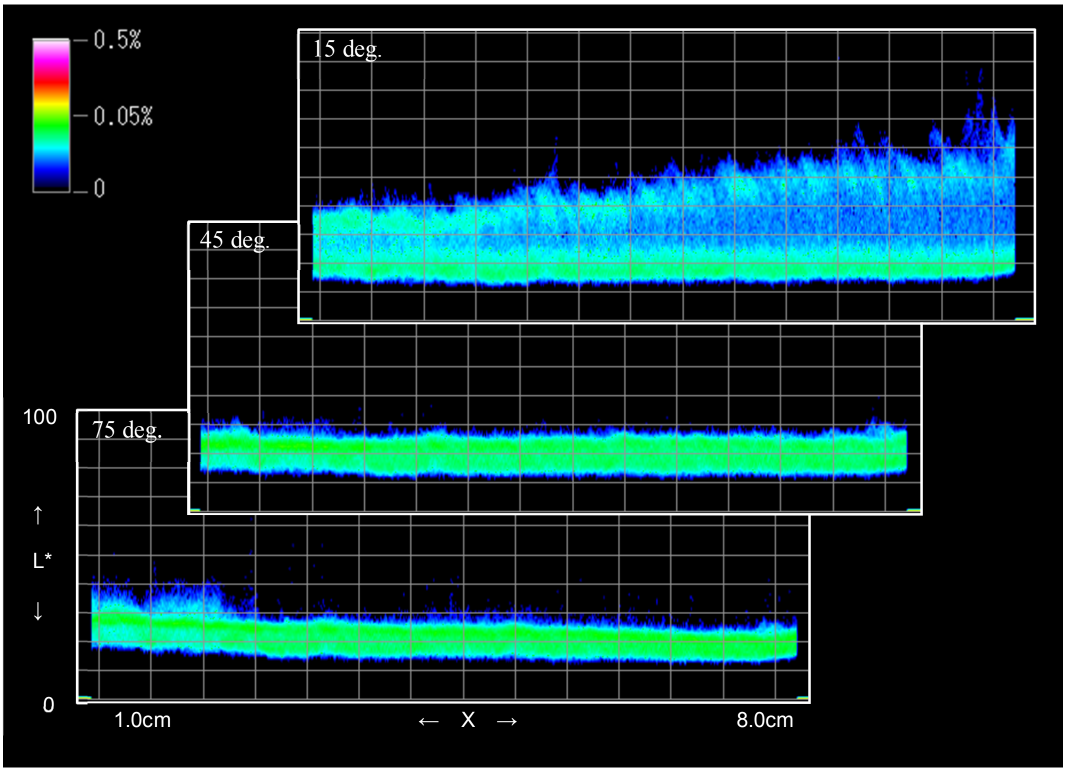

Figure 5: Measuring L distribution of YUTEKITENMOKU ceramic plate by gonio-photometric spectral imaging of 15, 45 and 75 degree illuminant.*

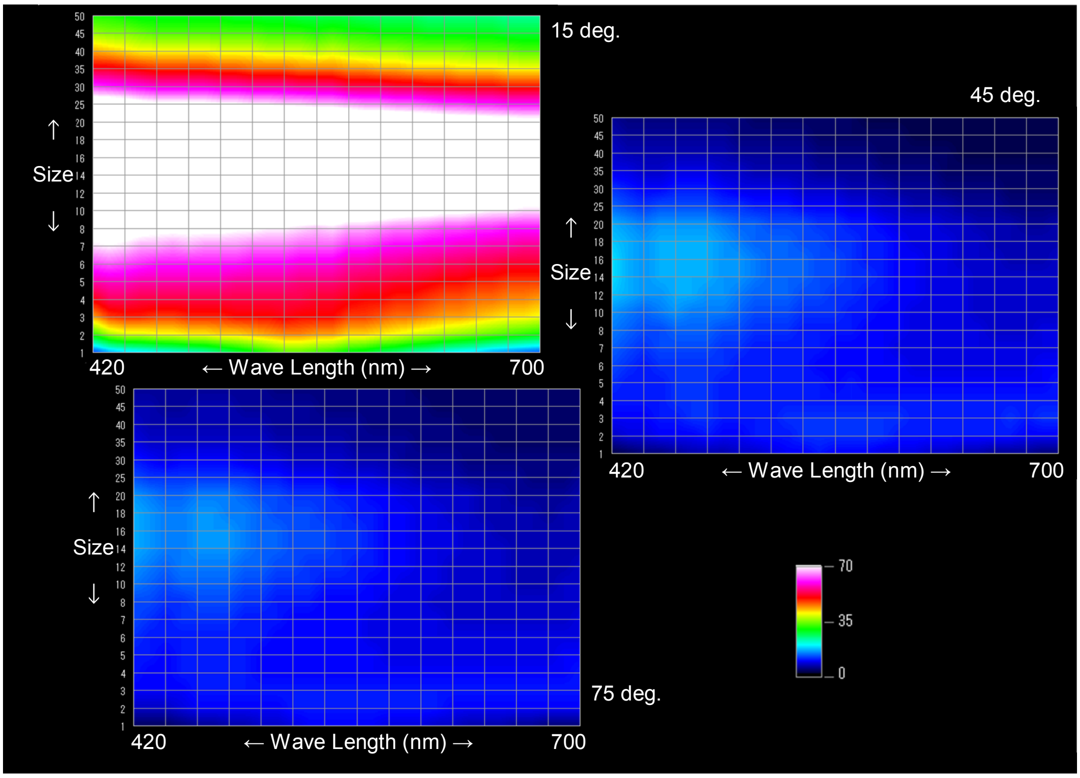

Figure 6: Measuring L distribution of YUTEKITENMOKU ceramic plate by gonio-photometric spectral imaging of 15, 45 and 75 degree illuminant.*

The Laplacian filter value calculation results of each angle are shown in Fig. 6. After measuring sample plate, the Laplacian filter value of each 10nm wavelength from 420 to 700nm measured spectral imaging data was calculated with various filter size by equation 1. This value is applied secondary deviation and one of the deformed contour intensifying filter. The size meaning is number of pixel and average area of filter calculation and related spatial frequency.

$$\nabla^2 f(x,y) = \frac{\partial^2 f(x,y)}{\partial x^2} + \frac{\partial^2 f(x,y)}{\partial y^2} = f_{xx}(x,y) + f_{yy}(x,y) \qquad (1)$$

The image of 15 degree illuminant, the Laplacian filter value was different and extremely huge compare with the other illuminant angle image. On the other hands, 45 and 75 illuminant image was similar and all image was not dependent on wavelength.

3.2 Confocal type laser scanning microscopy observation

The microscopy observation was succeeded clearly getting three dimensional orientation information of metal crystalline reflection surface. The measuring result was shown in Fig 7. The left image was laser and optics synthetic image, and recognized iron crystalline. And the glazing layer has sea island structure. The large particle crystalline was oriented almost horizontally. The non-iron crystalline area has various colors. The right image was three dimensional bird's-eye view drawing of the left side image. The iron crystalline was distributed around 2 or 3 micron of vertical direction, and glaze layer thick ness is around 5 to 10 micron. These orientation and distribution were correlated with various colors visual effects depend on optics dimension of *YUTEKI-TENMOKU*.

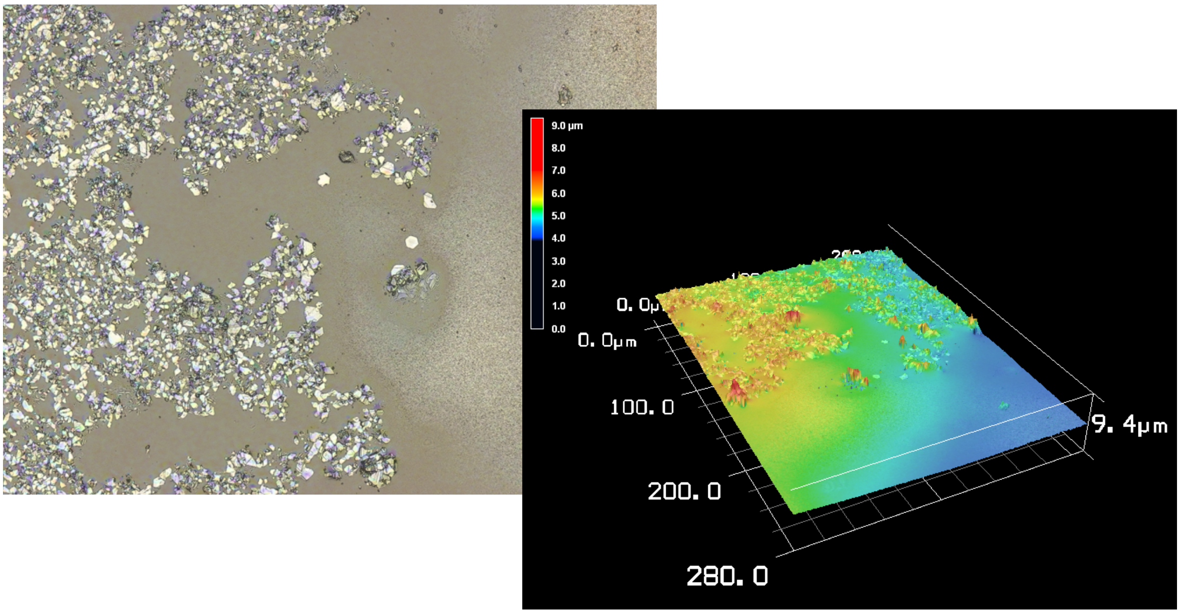

Figure 7: Example of Confocal type laser scanning microscopy.

4. CONCLUSIONS

YUTEKI-TENMOKU has various visual effects depend on optics dimension. And microscopy observation was succeeded clearly getting three dimensional orientation information of metal crystalline reflection surface. The benefit of combined with gonio-photometric spectral imaging and confocal type laser scanning microscopy analysis way was shown in this study. This imaging technology was quite useful for traditional ceramics characterizing.

ACKNOWLEDGEMENTS

The sample pleparation was supported and cooperated with Tokuemon Nishiyama of *YANBETAKOGAMA*.

REFERENCES

Takashima, H. 1994. *TOUJIKIYUU NO KAGAKU*, Uchida Rokakuho.

Seubert, C. 2013. *Measurement and Modeling of Aluminium Flake Coatings*, BYK Gardner User Meeting Presentation Document.

Taguchi, S. 2013. *Surface Structure and Color of Chogin- and Mameitagin-coins Used in the Edo Period*, AIC2013 Proceedings vol.4:1493-1496.

Robert, H. 1987. *Confocal scanning laser ophthalmoscope*. Applied Optics, vol.26, issue 6:1492-1499.

Brakenhoff, GJ. 1988. *3-dimensional imaging of biological structures by high resolution confocal scanning laser microscopy*, Scanning Microscopy, vol.2:33-40

Address: Masayuki OSUMI, Office Color Science Co., Ltd.,
Shinyokohama 3-20-12 Shinyokohama Bosei Bld. 402, Kuhoku-Ku
Yokohama City,222-0033, JAPAN
E-mails: masayuki-osumi@nifty.com

Measuring skin colours using different spectrophotometric methods

YuZhao WANG,[1] Ming Ronnier LUO,[1,2*] XiaoYu LIU,[1,3] HaiYan LIU,[4] and BinYu WANG[4]
[1] State Key Laboratory of Modern Optical Instrumentation, Zhejiang University, Hangzhou, China
[2] School of Design, University of Leeds, UK
[3] College of science, Harbin Engineering University, Harbin, China
[4] Thousand Lights Lighting (changzhou) Limited, Changzhou, China
*m.r.luo@leeds.ac.uk

ABSTRACT

This study investigates the skin colours. The goal is to understand the skin colour difference between different races, between genders, between different positions, and between different measuring methods. 47 observers from four skin groups were measured in terms of their spectral reflectance using 5 methods: two spectrophotometers, one tele-spectroradiometer, one camera and visual method. The data were analyzed and all the differences were successfully revealed. Also, the uncertainly of each method's uncertainty was established. Only the results of spectrophotometric data were reported. The results reveal the systematic trends between different body locations, between different genders, between skin groups and between spectrophotometers having different geometries.

1. INTRODUCTION

The topic of measuring skin color has long been extensively studied due to the strong interests from the photographic, digital imaging, cosmetic, medical applications. However the measuring methods and objectives of different applications are very different. For example, the contact method like spectrophotometer has been widely used for medical to detect skin related diseases and graphic applications for clour reproduction and communication. The non-contact method has been used for the appearance related application such as cosmetic, Chinese medicines, skin lighting. Also, with different illumination/viewing geometry, the measurement results could be quite different (Sun and Fairchild, 2001; Xiao, et al, 2012). However, in some of the databases such as SOCS (ISO, 1998) the measurement results were obtained using different methods. This would lead to quite different results for the same sample. In order to establish standard in this regard, basic study should be done to reveal the measuring difference between different methods. In this paper, we will discuss about the characteristics of human skin colour and the difference of different measurements.

2. METHOD

In the present study, four different measuring methods, five different measuring devices and tools were used. They include 3 non-contact methods (a digital camera, a skin colour chart for visual assessment, a spectroradiometer), and 2 contact methods including 2 spectrophotometers having different geometries: 45°:0° and di:8°. A D65 fluorescent simulator hand on the ceiling was used to illuminate the subject for visual assessment.

In total, 47 subjects from four skin groups participated in the experiment: 20 Chinese, 10 Pakistanis, 10 Caucasians, 5 Africans and 2 Sri Lankan. They were renamed as Chinese, Sub-Asian, Caucasian and Dark skin groups. Note the skin colours of Sri Lankan and African showed the darkest colours so that the name Dark was used. For each subject and each method except the visual match, eight locations of the body were measured: forehead, right cheek, left cheek, hand back, fist back, palm, inner forearm and outer forearm. For the visual match against a Pantone skin chart, three different observers measured only the forehead and the right cheek separately. In total, 408 data were obtained. It was found that some large difference between the contact and ono-contact methods, only the results based on the two spectrophotometers differed in illumination\viewing geometry (45°:0° and di:8°) were compared in this study. Methods from other methods will be reported elsewhere

3. RESULTS AND DISCUSSION

3.1 Colour Variation between Different body Locations

Figure 1 shows the results from the di:8° geometry. The results measured using the 45°:0° geometry were very similar. In Figure 1, the mean results from all the 20 Chinese subjects and plot them in CIELAB a^*-b^* and L^*-C_{ab}^*.

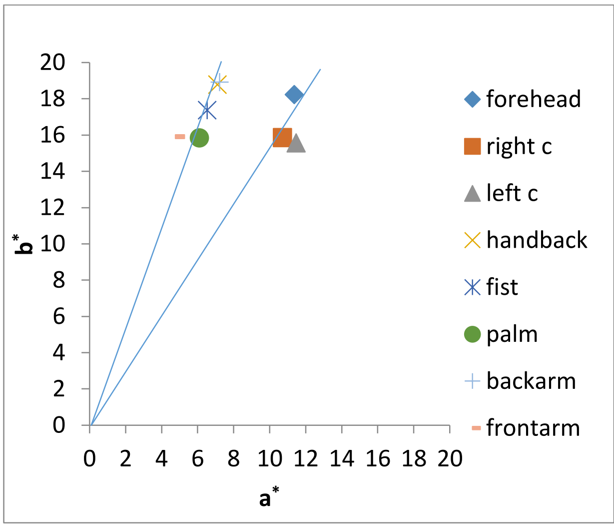

(a)

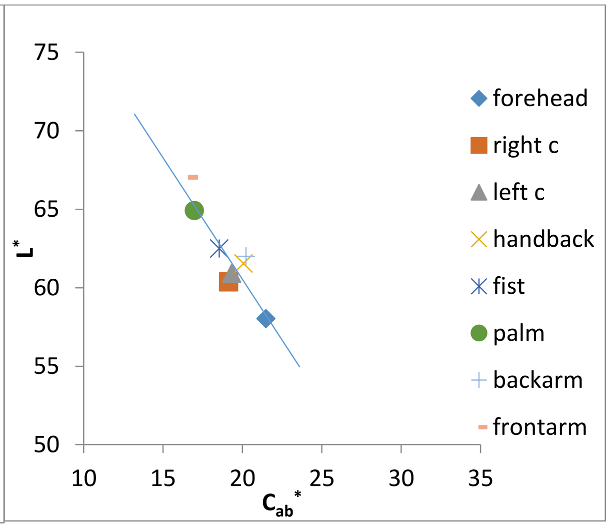

(b)

Figure 1: Chinese averaged data in a) in a^*-b^* plane, and b) L^*-C_{ab}^* plane

From Figure 1a, some systematic patterns can be seen. All the colours had hue angles red-yellow region. The data from eight locations are divided into two groups: one group contains all facial colours (forehead, right cheek and left cheek), while the other group contains all arm colours (hand back, fist, palm, outer forearm and inner forearm.) And within each group, the colours were very close in hue angle. It can be seen that arm colours are yellower than facial colours. This is expected due to the former colours are less exposed to the sun.

Figure 1b plots the same data in L^*-C_{ab}^* plane. It can be seen that all colours lie in a more or less straight line with an intercept to the L^* axis. This Line is close to the definition of

'Whiteness' as defined by NCS. Luo et al (2011) who developed whiteness and blackness model based on NCS colour atlas data. It was found that whiteness and blackness scales are visual sensations as the distance from the sample to the white and black point (L^* of 100 and of 0), respectively. The shorter the distance means a whiter or blacker colour, respectively. The results in Figure 1b clearly demonstrate that the arm colours are whiter than facial colours for Chinese subjects. A whiter colours also mean lower Chroma and higher lightness colours. This systematic patterns are similar to the Caucasian and Sub-Asian groups, but not to the Dark skin group.

Figure 2 shows the averaged data of the dark skin group also from di:8° geometry. As can be seen in Figure 2b, the trend is different from that in Figure 1b. Here, all colours are located on so call blackness scale. Figure 2a shows that all colours had similar hue with facial colours slightly redder than arm colours, similar to that in Figure 1a. However, the palm colour appears the most yellower and the brightest among all colours.

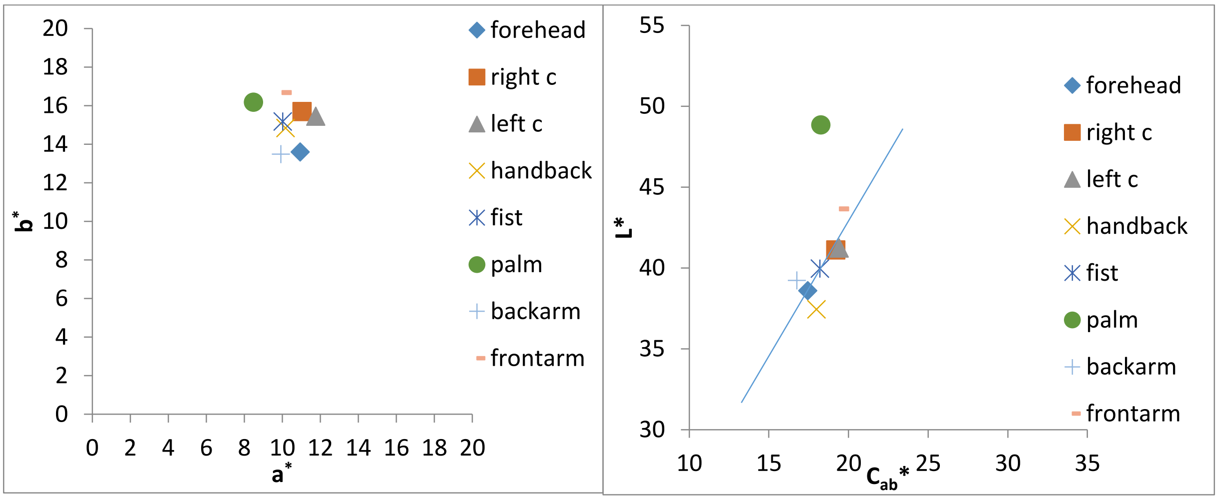

(a) *(b)*

Figure 2: Averaged data of the dark skin group in a) a^*-b^* and b) L^*-C_{ab}^* planes.

3.2 Colour Variation between Different Subject Groups

Figure 3 plots all the colours for all subject groups in L^*-C_{ab}^* for a) 45°:0° and b) di:8° spectrophotometers. Both figures showed the same trend, i.e. the colours following the whiteness and blackness scales. This indicates that both spectrophotometric methods gave similar results.

The most obvious trend is that Caucasian and Chinese colours have the largest lightness values, follow by Sub-Asian and the dark skin group the smallest. Also, as described earlier, the colours of the three subject groups except dark skin group, they all lie in whiteness scale. As for the dark skin group, they lie on blackness scale.

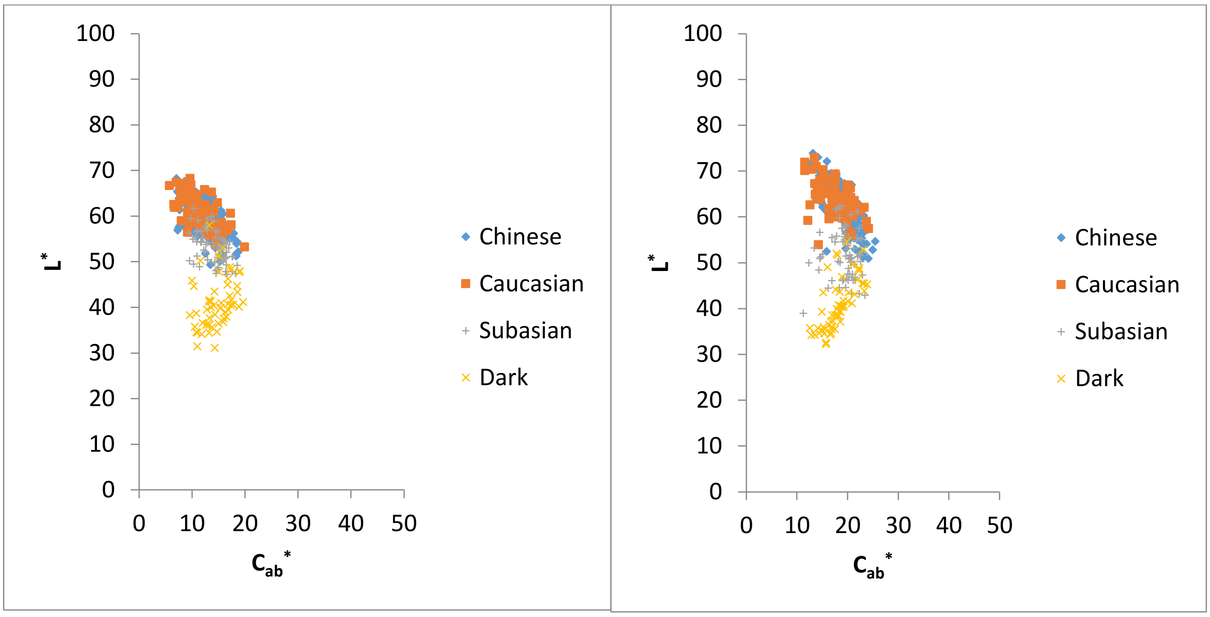

(a) *(b)*

Figure 3: All data plotted on L^*-C_{ab}^* plane a) for 45º:0º, and b) for di:0º instruments

3.3 Colour variation between Different Genders

The results also revealed that female and male's skin colours are different. Again, same clear trend was found between the two spectrophotometric methods. Figure 4 plots the data from the Chinese group to illustrate trend in a^*-b^* and L^*-C_{ab}^* planes respectively. The results clearly showed that the skin colours for both genders had very similar hue but female colours are less colourful (see Figure 4a), and all data fall in the same line representing whiteness scale, with female colours whiter than male colours.

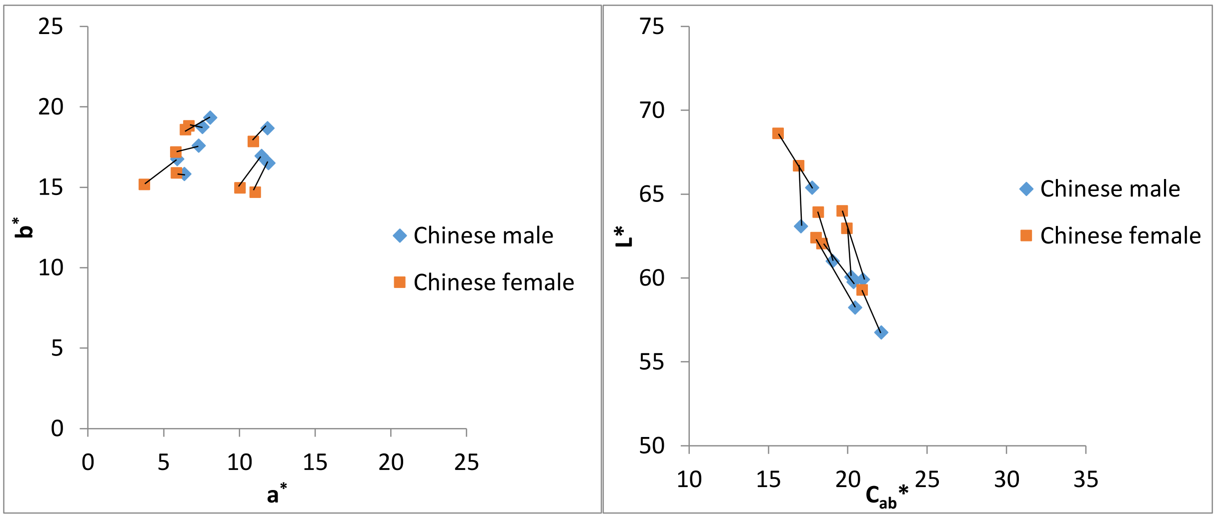

(a) *(b)*

Figure 4: Gender difference of Chinese skin colour in a) a^*-b^* and b) L^*-C_{ab}^* planes

3.4 Colour variation between Different Geometry of Spectrophotometric Methods

The last comparison was made between the results from two spectrophotometers having different geometry. Figure 5 shows the mean spectral reflectance functions of all Chinese skin colours between the two spectrophotometers studied. It can be seen that the two curves agree very well until reach 550nm, for which 45º:0º are higher than di:8º geometry. Figure 6 shows the Chinese data of two measuring geometries (45º:0º and di:8º) on a^*-b^* and L^*-C_{ab}^* planes. Figure 6b clearly showed that the 45º:0º results are less colourful and darker than those of di:8º. This indicates that a skin colour reflecting more light in long wavelength will result in an increase in Chroma and Lightness.

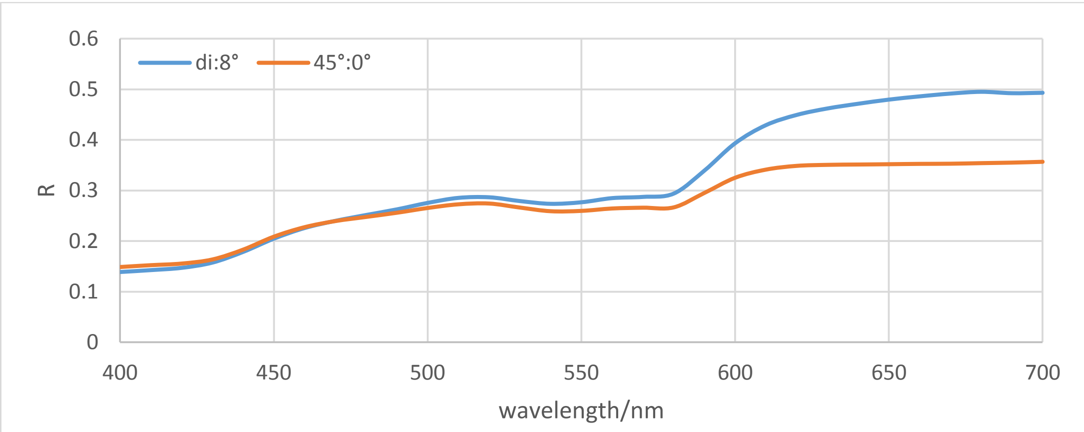

Figure 5: Difference of two measurement

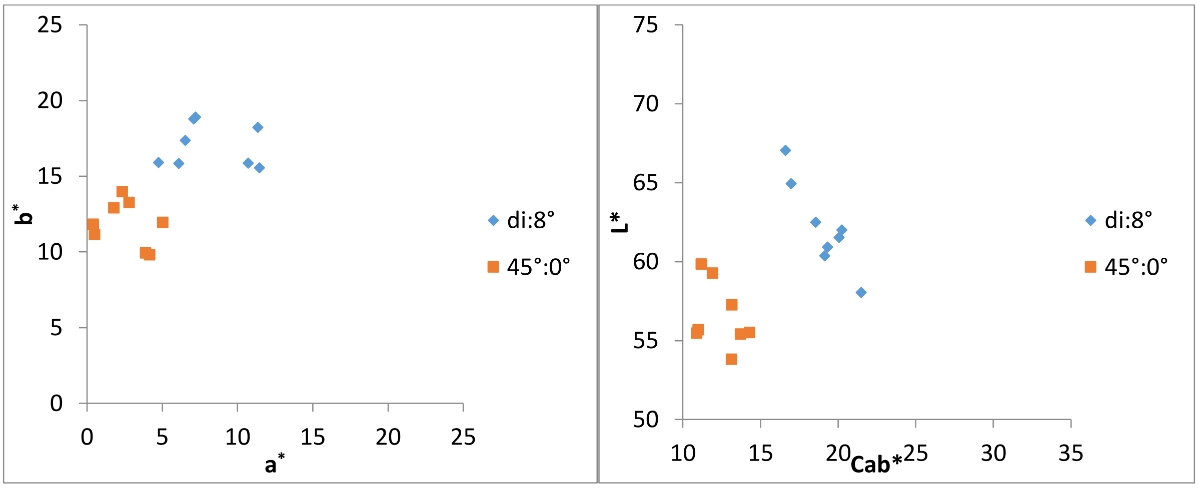

(a) *(b)*

Figure 6: Chinese averaged data of di:8º and 45º:0º in a) a^*-b^* plane, and b) L^*-C_{ab}^* plane

4. CONCLUSIONS

Five methods were employed to measure skin colours. It was found that the results are somewhat different. This paper is focused on the measurements based upon two spectrophotometers having geometries of 45°:0° and di:8°. The results reveal the following systematic trends:

- Comparing between different body locations, arm colours are yellower and whiter than facial colours for all skin groups except that of dark skin group, for which their colours lie in the blackness scale.
- Comparing different genders, female colours are yellower and whiter than male colours.
- Comparing different skin colours, the difference is mainly in lightness, Chinese and Caucasian gave the largest and dark group is the smallest.
- Finally, di:8° geometry data will have a higher spectral reflectance above 550nm, which results in lighter and more colourful appearance than those of 45°:0°.

ACKNOWLEDGEMENTS

The authors really appreciate the help from all the subjects participated in the experiment.

REFERENCES

Q. Sun, and M. D. Fairchild. 2001 *Statistical Characterization of Spectral Reflectances in Spectral Imaging of Human Portraiture*, IS&T/SID Ninth Color Imaging Conference, 73-79.

Q. Sun, and M. D. Fairchild. 2001. *A New Procedure for Capturing Spectral Images of Human Portraiture*, Proceedings, AIC color01, Rochester, USA

K. Xiao, N. Liao, F. Zardawi, H. Liu, R. V. Noort, Z. Yang, M. Huang, and J. M. Yates. 2012. *Investigation of Chinese skin colour and appearance for skin colour reproduction*, Chinese optics letters, COL 10(8), 083301

M. R. Luo, G. Cui, and Y. J. Cho. *The NCS-like colour scales based on CIECAM02*, The 21th Color and Imaging Conference, 6-8 November 2013, Albuquerque, NM, USA, 177-179.

Address: Prof. Ming Ronnier LUO, Key State Laboratory of Modern Optical Instrumentation, Zhejiang University, N.38, Zheda Road, Hangzhou, 310027, CHINA
E-mails: M.R.Luo@leeds.ac.uk

Assessing Light Appearance in Shopping Mall

Yuteng ZHU, [1] Ming YE, [1] Wenjie HUANG, [1] Muhammad Farhan Mughal, [1]
Muhammad Safdar [1] and Ming Ronnier LUO, [1, 2]
[1]Key State Laboratory of Modern Optical Instrumentation, Department of Optical Engineering, Zhejiang University, Hangzhou, China
[2]School of Design, University of Leeds, Leeds, UK

ABSTRACT

The current investigations of lighting appearance in rooms are mostly carried out in carefully controlled compartments or rooms. In order to verify the conclusions drawn from earlier studies, the lighting appearance of 21 different shops in two representative modern shopping malls in the city of Hangzhou, China, were investigated. The aim was to study the lighting appearance in real environment and eventually to establish an imaging-based method for quantifying the visual perception in real living environment, i.e. image processing software from image, via calibration, visual modelling and prediction. The CIECAM02 colour appearance model was used as a colorimetric metric to predict the room appearance. It was found that rooms with similar luminance, a light with higher CCT (Correlated Colour Temperature) appears brighter than that with lower CCT. However, as luminance levels varies from shop to shop in practical environment instead of being constant, higher CCT is perceived to be more yellowish but not occur to be brighter in our experiment. The comparison of room appearance between CIECAM02 prediction and visual assessment was shown. It was found that CIECAM02 predicts well for colorfulness and hue composition but not brightness in real rooms. An extension equation was used to adjust the brightness scale of CIECAM02 and the new model turned out to predict brightness well.

1. INTRODUCTION

Lighting appearance in rooms is of great importance for lighting research. Most of the previous works on lighting appearance were conducted in well-controlled environment, like Li et al. (2014) and Ohno and Fein (2014) in a room, and Rea and Freyssinier (2013) in a viewing cabinet. There is a need to investigate the earlier results in controlled environment to be agreed with those from the real environment, for which mixed lightings frequently take place. In this paper, the experimental data and analysis in scaling room appearance of modern shopping malls in city will be provided. The investigation of lighting appearance in shops can offer the basis for applying colour science in real environments.

2. METHOD

2.1 Overviews

In the current study, the experiment was conducted in 21 shops of two modern shopping malls to look into the lighting appearance. Both physical measurement and psychophysical assessment were carried out simultaneously.

2.2 Experimental shops

The categories of shops included costume, shoes, cosmetics, jewellery, watches and food products with different styles of decoration and ambiance. Figure 1 shows the experimental situation in a shop. A large size white cardboard (1.2×0.8 m^2) attached with an Xrite Macbeth ColorChecker Chart was used to be placed in front of a region representing typical illumination area.

Figure 1: An example of experimental situation in a shoes store.

A PhotoResearch PR670 tele-spectroradiometer (denoted as TSR hereafter) was used to measure luminance, CCT, SPD, u'v' coordinates. The cardboard had L*, a*, b* values of 80.8, -0.25 and 0.19 under D65 and CIE 1964 standard colorimetric observer. Figure 2 shows the percentages in ranges of CCT, luminance, CIE-Ra and lighting technologies investigated. It can be seen that the CCTs are in the range of 2500 to 4000K. This indicates that most shops apply a yellowish and warmer ambiance to create a 'comfort' environment as reported by Liu et al. (2014).The luminance range is mainly between 80 cd/m^2 and 200 cd/m^2. The colour rendering values in CIE-R$_a$ in shops are reasonably high, i.e. mostly above 80. Many shops apply different lighting technologies to produce special ambient effect to illuminant their products. Furthermore, the LED lightings have been well populated over 65%. The concept of energy conservation has been well received by the modern shopping mall.

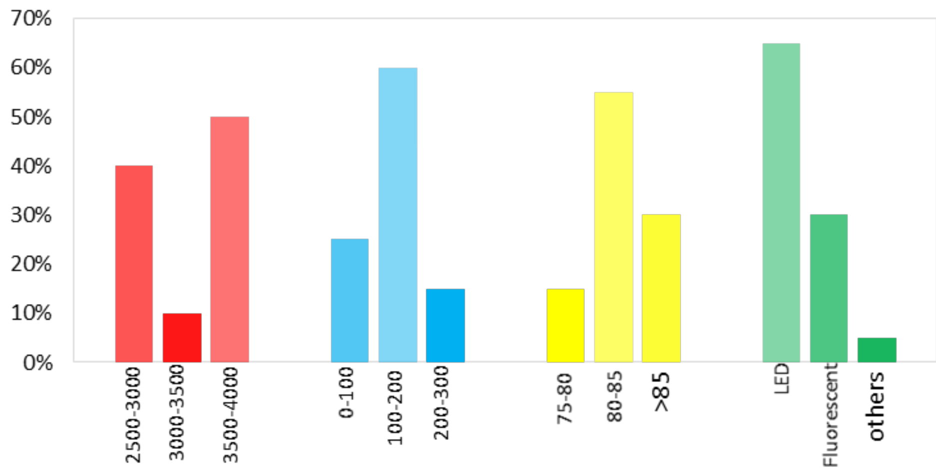

Figure 2: The distribution of CCT, luminance, CIE-Ra and the percentages of different illumination technologies.

2.3 Categorical judgement

The categorical judgement was used to describe light appearance in shops by three normal colour vision observers in the psychological experiment. The attributes of brightness and colourfulness were assessed using a 6-point categorical scale in terms of word-pairs (dark-brightness and not colourful - colourful describe for brightness and colourfulness, respectively). Taking brightness as an example, the scores are -3) 'very dark', -2) 'dark', -1) 'a little dark', 1) 'a little bright', 2) 'bright' and 3) 'very bright'.

Hue composition is an attribute for colour perception of the reflected lights from the white board (see Figure 1). A colour is described as a composition of two unique colours, red-yellow, yellow-green, green-blue or blue-red (see Figure 3). The observers were asked to give the percentage of two neighbouring unique colours to match their colour perception of light appearance in rooms.

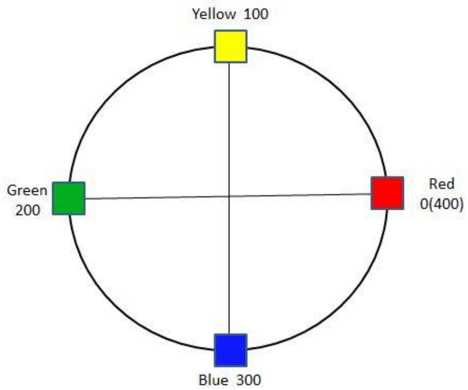

Figure 3: Hue circle with four unique colours.

2.4 Experimental Procedure

As mentioned earlier, a white cardboard having a size of 1.2×0.8 m^2 was used to measure the reflected lights, with a distance of 2 meters from the measuring devices or observers' position. Firstly, an image was captured by a Canon digital camera with an Xrite Macbeth ColorChecker Chart on the surface of the white cardboard. Then the lighting parameters, were measured by the TSR. In the visual assessment experiment, three normal colour vision observers scaled the brightness, colourfulness and hue composition of the light appearance after a 2 minutes' adaption.

3. RESULTS AND DISCUSSION

3.1 The effect of CCT on the attributes of appearance

Before data analysis, the scales were first transformed from -3 ~ 3 to 0 ~ 6 using an offset and the percentage of hue composition was transformed into 0 - 400 hue quadrature (see Figure 3). The relationship between CCT and appearance attributes, including brightness, colourfulness and hue composition was analysed. It can be seen that the perceived brightness is not proportional to luminance (see Figure 4a) as CCT and luminance have a combined influence on the attribute of perceived brightness. In order to study the CCT effect on perceptual brightness, data with similar luminance were selected and plotted in Figure 4b. The trend is obvious that a higher CCT makes the room appear brighter.

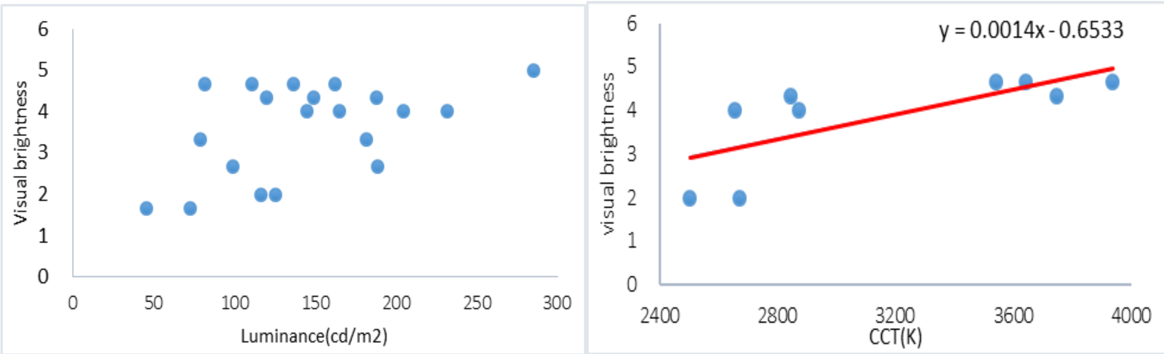

(a) (b)

Figure 4: a) The relation between luminance and visual brightness, b) CCT effect on visual brightness for similar luminance data.

The effect of CCT on colorfulness was also analyzed (see Figure 5). The results showed that a shop with a higher CCT would appear less colorful and more likely to be perceived as neutral white. The reason can be that for CCT below 3500K, lower CCT looks more yellowish while higher CCT is closer to white and appears less colorful. This agrees with that found by Li et al (2014).

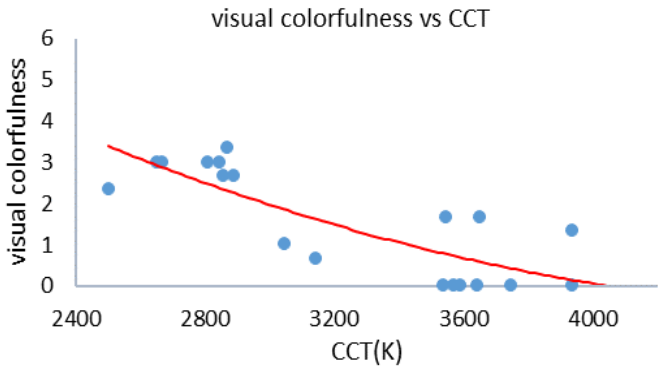

Figure 5: The relationship between CCT and visual colorfulness.

3.2 The comparison of visual perception and CIECAM02 prediction

The CIECAM02 model (CIE, 2004) was utilised to predict visual perceptions on brightness, colorfulness and hue composition as well. The comparison of the predictions and visual brightness, colorfulness and hue composition results are shown in Figures 6 and 7 respectively. It shows the CIECAM02 predicts well to the colorfulness and hue composition results but not to the brightness results.

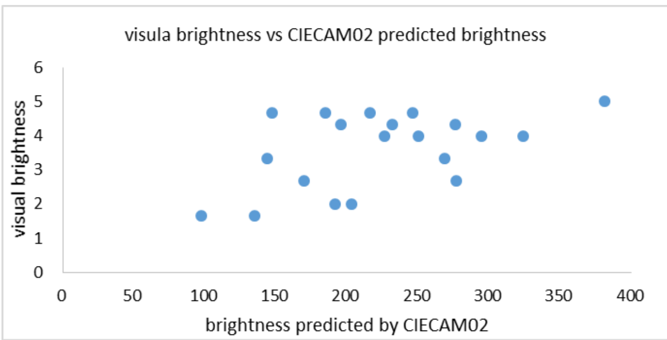

Figure 6: The relationship between CIECAM02 predicted and visual brightness.

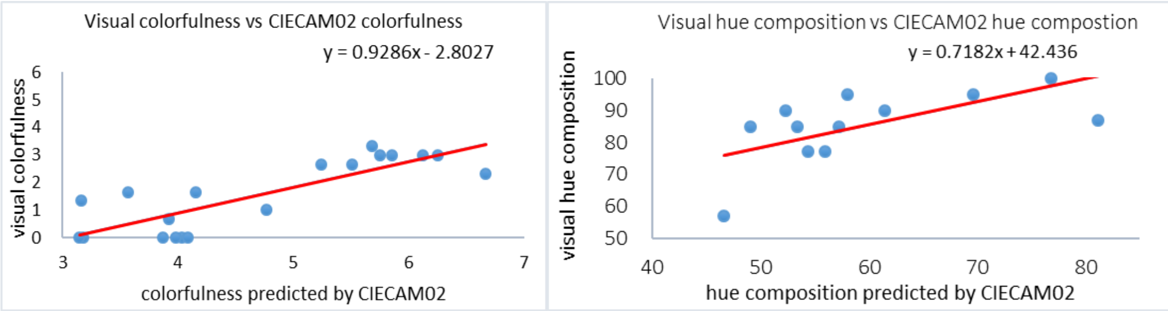

Figure 7: The relationship between CIECAM02 predicted and visual colorfulness (left) and hue composition (right).

3.3 The modified CIECAM02 in consideration of CCT effect on visual brightness

In the CIECAM02 model, CCT has no impact on brightness prediction. However, Figure 4b strongly reveals a trend that higher CCT leads to a brighter perception. So an extension, a linear function normalized at 2850K as given in equation (1) was applied.

$$Q' = Q \times (4.2 \times 10^{-4} \times T - 0.2) \qquad (1)$$

where T means CCT value, Q is the brightness computed by the original CIECAM02 and Q' is the brightness by the modified model. According to Eq. (1), CCT was then implemented as a variable for brightness prediction. The result demonstrates that the new model predicts the brightness well against experimental visual data comparing Figures 8a and 8b.

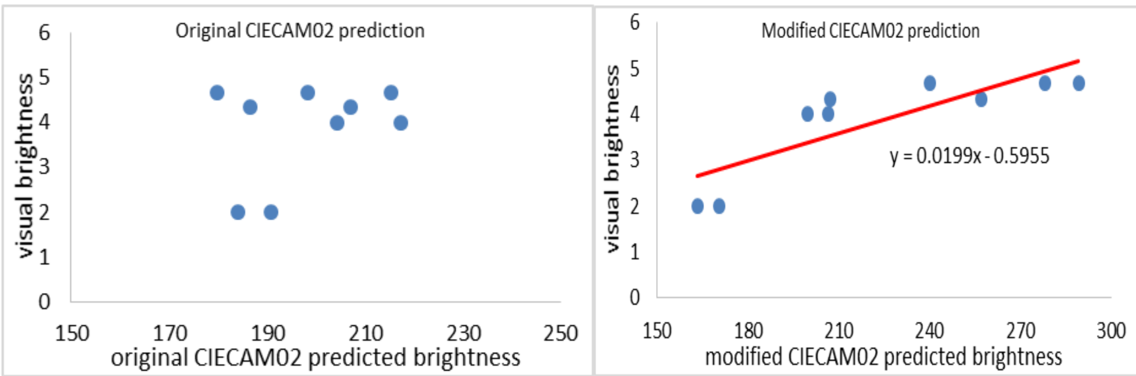

(a) (b)

Figure 8. a) The relation between original CIECAM02 brightness prediction and visual brightness, b) modified CIECAM02 brightness prediction against visual brightness.

4. CONCLUSIONS

In this paper, the appearance of lighting in shopping malls has been investigated via physical and psychophysical measurements. The CIECAM02 model was applied to predict the perceptual attributes and a comparison of visual data and prediction data was made. The results showed that CCT and luminance had a combined effect on the perception of brightness. With similar luminance level, a light with higher CCT made the room to be perceived brighter and less colorful. The CIECAM02 model predicts well on colorfulness and hue composition but not brightness. Hence, an extension of the model was applied considering the effect of CCT and it turned out to fit quite well with visual brightness perception.

ACKNOWLEDGEMENTS

The authors would like to give their sincere thanks to the managers of two shopping mall for providing different stylish shops to conduct the experiment in this research.

REFERENCES

Liu, X. Y., M. R. Luo and H. Li. 2014. *A study of atmosphere perceptions in a living room*, Light. Res and Tech., DOI: 1477153514528934, published on line in April, 2014.

Li, H., M.R. Luo, X.Y. Liu, B.Y. Wang and H.Y. Liu. 2014. *Assessing appearance in a lite room.* Private communication.

Rea, M.S. and J.P. Freyssinier. 2013. *White lighting*, Colour Research and Application, 38(2), 82-92.

Ohno, Y. and M. Fein. 2014. *Vision experiment of acceptable and preferred white light chromaticity for lighting.* Proc., CIE 2014 Lighting Quality and Energy Efficiency, 192 – 199.

CIE. 2004. CIE 159:2004. *A colour appearance model for colour management systems: CIECAM02*, Vienna.

Hunt, R.W.G. and M.R. Pointer. 2011. *Measuring Colour.* New York: John Wiley & Sons.

Hinks, D. and S. Renzo. (2011), *Review of retail store lighting: implications for colour control of products*. Coloration Technology, 127: 121–128. doi: 10.1111/j.1478-4408.2011.00286.x

Li, H., M.R. Luo and X.Y Liu. 2014. *Scaling appearance in a room illuminated by LED sources*. CIE 2014; x039:63-72.

Muhammad, S., M.R.Luo, H. Li, L.H. Xu and Y. Yang. 2014. *An imaging method for measuring room appearance*. 7th CJK Lighting Conference.

Address: Prof. Ming Ronnier LUO, Key State Laboratory of Modern Optical Instrumentation, Zhejiang University, N.38, Zheda Road, Hangzhou, 310027, CHINA
E-mails: M.R.Luo@leeds.ac.uk

Pupillary light reflex associated with melanopsin and cone photorecetors

Sei-ichi Tsujimura,[1] Katsunori Okajima,[2]
[1] Faculty of Sciences and Engineering, Kagoshima University, Japan
[2] Faculty of Environment and Information Sciences, Yokohama National University

ABSTRACT

Retinal ganglion cells containing the photopigment melanopsin are intrinsically photosensitive in primates. Several studies have shown that the intrinsically photoreceptive retinal ganglion cells project to the pupillary control center in the pretectum. Here, we independently stimulated human ipRGCs and cones, and investigated how signals driven by ipRGCs and cone-mediated signals contribute to the pupillary control mechanism. A four-primary illumination system that enables independent stimulation of each photoreceptor class was used to present the following three types of test stimuli. The transient pupil responses to these stimuli were measured. It was found that the transient pupil response to ipRGC stimuli had a longer latency than the responses to the LMS-cone and light flux stimuli. The longer latency suggests that signals from ipRGCs in the non-image forming pathway travel more slowly than that of the LMS achromatic mechanism in the image forming pathway.

1. INTRODUCTION

The intrinsically photoreceptive retinal ganglion cells (ipRGCs), which contains photopigment melanopsin, mediate signals to the pupillary control center in the pretectum. The ganglion cell is photosensitive and receives signals from classical photoreceptors. Although both cone- and ipRGC-mediated signals contribute to pupillary light reflex it is difficult to investigate how these signals are summed. Here, we independently stimulated human cones and ipRGCs, and investigated how cone- and ipRGC-mediated signals contribute to the pupillary control mechanism.

2. METHODS

2.1 Apparatus

An eight-channel, four-primary illumination system (Brown *et al.*, 2012) that enables independent stimulation of each photoreceptor class was used to present the following three types of test stimuli: one varying L-, M- and S-cone stimulation only without change in stimulation of ipRGCs (LMS-cone stimulus), another varying radiant flux of the stimuli without change in spectral composition which reduced/increased the radiant flux uniformly at all wavelengths (Light flux stimulus) and the other varying ipRGC stimulation without change in stimulation of L-, M- and S-cones (ipRGC stimulus). The intense test and adapting fields were used which minimized the involvement of rods. The test and adapting fields had a CIE coordinate of (0.57, 0.36) and a luminance of 1,221 cd m^{-2} for the test field and 355 cd m^{-2} for the adapting field, respectively. The transient pupil responses to these stimuli were measured.

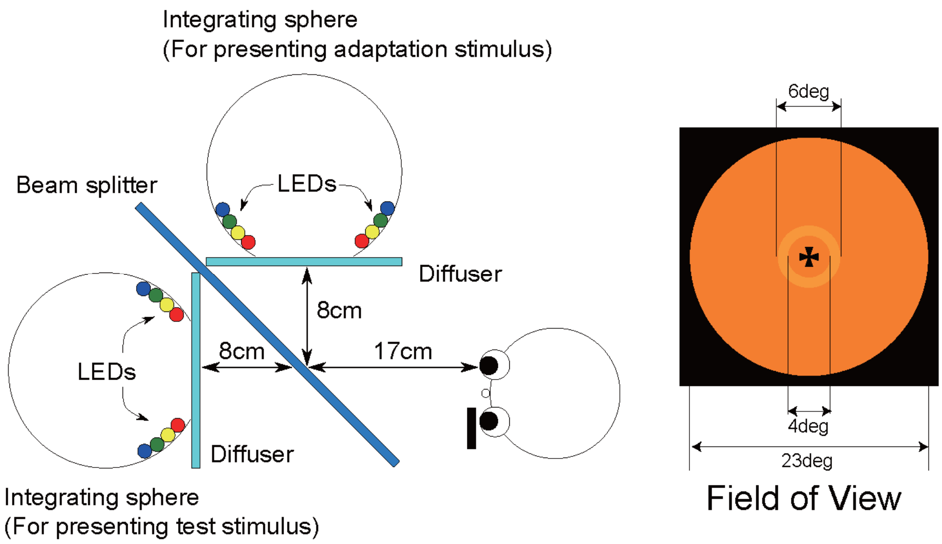

Figure 1 Eight channel, four-primary stimulation system

2.2 Spectral sensitivity curve for melanopsin ganglion cell

The test stimuli were generated based on the cone and ipRGC spectral sensitivities. The 10-deg cone fundamentals proposed by Stockman *et al.* (Stockman *et al.*, 1999, 2000) were used to calculate the stimulation of Long-wavelength sensitive cone (L cone), Middle-wavelength sensitive cone (M cone) and Short-wavelength sensitive cone (S cone). We estimated the spectral sensitivity curve of ipRGCs based on a pigment template nomogram with a peak wavelength, λ_{max}, of 480 nm and ocular optical properties. The lens and macular pigment density spectra were those of Stockman *et al*. The fraction of incident light absorbed by the receptor depends on peak axial optical density (D_{peak}). We tentatively chose 0.1 as the D_{peak} for ipRGC. We assumed that neither the S cones nor the ipRGC affect the photopic luminance efficiency function (*i.e.*, luminance), despite using photopic luminance units (cd m^{-2}). Similar to S-cone stimulation (Boynton and Kambe, 1980), one ipRGC stimulation was defined as the level of ipRGC stimulation produced by an equal energy spectrum of luminance 1 cd m^{-2}. The resultant spectral sensitivity function of ipRGC in a 10-deg field displayed a peak of 872 at a wavelength of 493 nm. The shape of spectral sensitivity curve we estimated is similar to that proposed by Lucas and his colleagues (Enezi *et al.*, 2011). We further considered the human macular pigment density at 10-deg for the estimation.

2.3 Procedure

Five visually corrected observers (age range 21–23 years) participated in the experiment. All observers had normal color vision according to the Ishihara color blindness test. All observers gave their written informed consent, and the study was approved by the local research ethics committee. The observers were seated 25 cm from the diffuser and monocularly fixated upon a black Maltese cross, which subtended 1.8° and was always present at the center of the diffuser. After an initial adaptation period of 5 min, we began a session of experimental trials. We used a ramp stimulus presented for 500 ms.

The pupil of the right eye was imaged using a video camera (Dragonfly, Point Grey Research, Canada) located 0.5 m from the observer and 28° nasal to the visual axis. The video image was fed into a personal computer and analyzed using LabVIEW and IMAQ Vision software (National Instruments) at a frequency of 60 Hz. The pupil was located using thresholding and edge detection techniques, allowing the pupil diameter to be analyzed.

3. RESULTS AND DISCUSSION

3.1 Influence of a modulation of ipRGC on amplitude of pupil response

Since both Light flux and LMS-cone stimuli modulated cones in the same way these stimuli were indistinguishable for cones. Therefore, the difference could be attributed to the difference in stimulation with or without ipRGC modulation. Pupil responses to the Light flux stimulus and to the LMS-cone stimulus were shown in Fig 2. It was found that the amplitude elicited by LMS-cone stimulus was significantly higher than that by the Light flux stimulus. The average pupil response was 0.24±0.06 mm for the LMS-cone stimulus, 0.20±0.07 mm for the Light flux stimulus and 010±0.04 mm for the ipRGC stimulus. In other words, the modulation of ipRGC in Light flux stimulus influenced amplitude of the pupil response, suggesting that the ipRGC stimulation suppresses pupillary amplitude response.

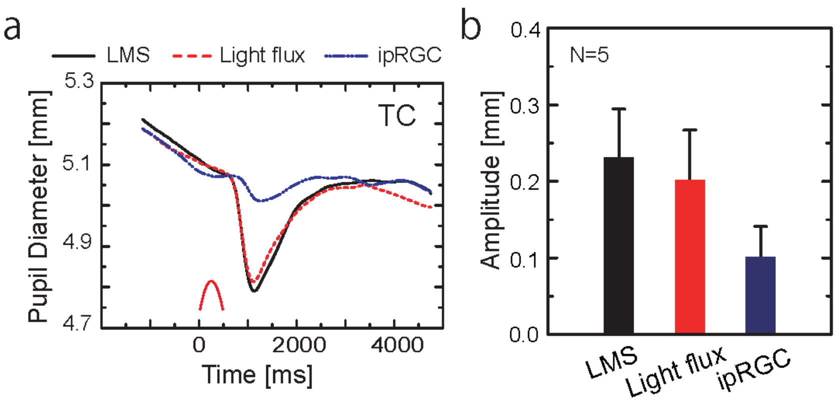

Figure 2 Pupillary responses and its amplitudes to the LMS-cone stimulus (black), to Light flux stimulus (red) and to the ipRGC stimulus (blue).

3.2 Sluggish pupillary response to the ipRGC stimulus

Typical normalized pupil responses are shown in Fig. 3. The horizontal axis represents a time and the vertical axis represents pupil diameters in mm to the test stimuli. The black curve represents curves for the LMS-cone stimulus, the red curve for the Light flux stimulus and the blue curve for the ipRGC stimulus. It was found that the transient pupil response to the ipRGC stimulus had a longer latency than those to the LMS-cone and to the Light flux stimuli. The average pupil latencies were 814±39 ms for the LMS-cone stimulus, 821±41 ms for the Light flux stimulus and 1,377±618 ms for the ipRGC stimulus. The longer latency to the ipRGC stimulus was consistent with those in the previous study (Lucas *et al*., 2001; Tsujimura *et al*., 2011), suggesting that the ipRGC-mediated signals in the non-image forming pathway travel more slowly than the LMS cone-mediated achromatic signals in the image forming pathway. These results suggested that the pupil responses to the LMS-cone stimulus and to the Light flux stimulus are mediated by cones and those to the ipRGC stimulus are mediated by ipRGCs.

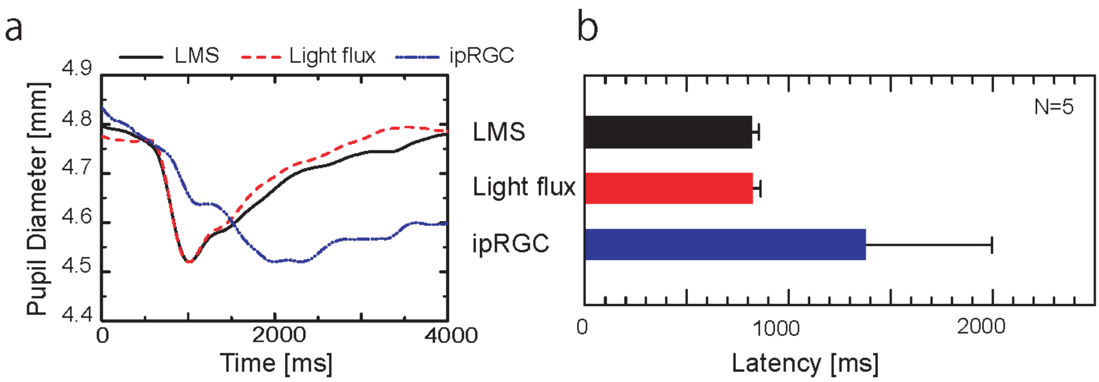

Figure 3 Normalised pupillary responses to the LMS-cone stimulus (black), to Light flux stimulus (red) and to the ipRGC stimulus (blue).

4. CONCLUSIONS

It was found that the transient pupil response to ipRGC stimuli had a longer latency than the responses to the LMS-cone stimulus and to the Light flux stimulus. The results indicate that we successfully demonstrated the pupillary response to ipRGCs under conditions where ipRGCs are isolated in humans. The longer latency suggests that signals from ipRGCs in the non-image forming pathway travel more slowly than that of the LMS-cone mediated signals in the image forming pathway.

ACKNOWLEDGEMENTS

This work was partly supported by grants by the Ministry of Education, Science, Sports, and Culture of Japan, KAKENHI (26280103 and 10381154 to S.T.).

REFERENCES

Boynton, R. M. and N. Karnbe 1980. *Chromatic Difference Steps of Moderate Size Measured along Theoretically Critical Axes*. Color Research & Application **5**(1): 13-23.

Brown, T.M.*, Tsujimura, S.*, Allen, A.E., Wynne, J., Bedford, R., Vickery, G., Vugler, A., and Lucas, R.J. 2012. *Melanopsin-Based Brightness Discrimination in Mice and Humans*. Current Biology 22, 1134-1141.*Equal contribution

Enezi, J., Revell, V., Brown, T., Wynne, J., Schlangen, L., and Lucas, R. (2011). *A "melanopic" spectral efficiency function predicts the sensitivity of melanopsin photoreceptors to polychromatic lights.* J Biol Rhythms 26, 314-323.

Lucas, R. J., R. H. Douglas, et al. 2001. *Characterization of an ocular photopigment capable of driving pupillary constriction in mice*. Nat Neurosci **4**(6): 621-626.

Stockman, A., L. T. Sharpe, et al. 1999. *The spectral sensitivity of the human short-wavelength sensitive cones derived from thresholds and color matches*. Vision Research **39**(17): 2901-2927.

Stockman, A. and L. T. Sharpe 2000. *The spectral sensitivities of the middle- and long-wavelength-sensitive cones derived from measurements in observers of known genotype*. Vision Res **40**(13): 1711-1737.

Tsujimura, S. and Tokuda, Y. 2011. *Delayed response of human melanopsin retinal ganglion cells on the pupillary light reflex*. Ophthalmic and Physiological Optics 31, 469-479.

Address: Dr. Sei-ichi Tsujimura, Department of Information Science and Bioengineering, Kagoshima University, 1-21-40, Koorimoto, Kagoshima 890-0065 JAPAN
E-mail: tsujimura@ibe.kagoshima-u.ac.jp

Experimental Research on EEG Characteristics in Red, Green, Blue, and White Color Space consequent on the Degree of Depression

Heewon LEE[1], Hanna KIM[2], Jiseon Ryu[1], Jinsook LEE[3]
[1] Doctor Course, Dept. of Architectural Engineering, CNU, Korea
[2] Noroo Paint & Coatings Co., Ltd, NPCI, Korea
[3] Professor, Dept. of Architectural Engineering, Chungnam National University, Korea

ABSTRACT

This study is intending to analyze the brain wave property in color space in red, green, blue and white according to the depression level. This study conducted the experiment on 6 female subjects in their 20s~30s, and the experiment result is as follows: First, after conducting self-diagnosis check of BDI-II depression, this study divided the subjects into non-depressive group and depressive group. Then, after measuring the brain wave in color space of red, green, blue and white, this study analyzed the occurrences of RB(Relative Beta Power Spectrum), and RAB(Ratio of Alpha to Beta)indicators in the frontal lobe which has rational thought and cognitive function.

As a result of the analysis, it was found that the green and white color used in this experiment had an effect on relaxation and stability of the depressive group, but in the case of the red and blue color also used in the experiment had an inhibition effect on the depressive group's relaxation and stability; through the result, this study was able to learn that when a person makes a design of indoor color environment, the person should be careful in the use of the red, blue color.

1. INTRODUCTION

1.1 Background and Purpose of the Study

Among the factors that affect our emotions, we are living in various colors that are embedded in the spaces and objects we encounter every day. Color controls emotions and inturn changes behaviors, in addition to influencing state of mind to maintain emotional stability and impacting bodily functions including circulatory system, heartbeat, blood pressure, and tensions in the nerve system and muscles. As explained, color may provide various energy to people through its inherent wavelengths, and may maintain body and mind to be stable and balanced. Color is proactively being used in psychology, medicine, as well as marketing, emotional engineering, architecture, and industrial design, and many research are being conducted, ushering in an era of color. Such trend is especially stimulating many scientific researches to prove that color is effective in healing the body and mind. Of course, we are referring to studies on color that link human emotions to physiological reactions and brain waves.

However, looking into the preceding research works, there have been researches on depression and color, but the analytical research on brain wave in a life-size Mock-up of color space consequent on depression inventory is actually insufficient. Hereupon, this study is intending to make a comparative analysis of brain wave property in color space of a life-size Mock-up using BDI-II(Beck Depression Inventory-II)which is the most widely used among self-report test papers developed to measure depressive symptoms.

1.2. Research Method & Scope

This study measured and researched the brain wave in color space consequent on the severity of depression targeting adults in their 20s~30s. This study conducted the research as shown in (Figure 1).

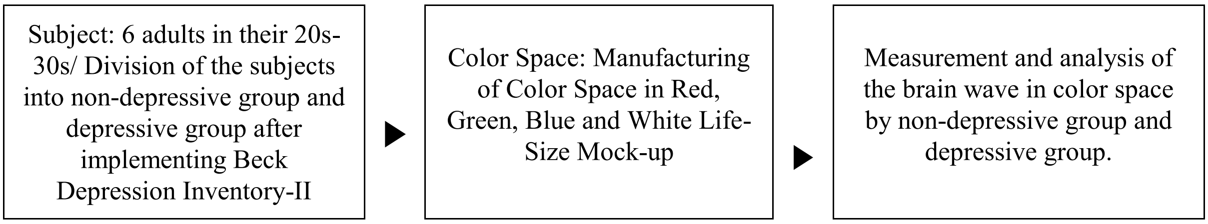

Figure 1. Method of the study implementation

2. SPECIFICS OF THE STUDY

2.1 Research method

2.1.1 Experiment environment

This study conducted the BDI-Ⅱ Depression Inventory at a laboratory of C School. This study used the laboratory located the innermost in order to minimize interrupting factors, such as external noise at a time of testing.

The space comprised of four rooms each with 1500㎜×1500㎜×2400㎜ dimesions. D65 standard light source lighting devices were 600 ㎜×600 ㎜, with the light intensity of 100㏓. In order to minimize visual error from texture and linkage that may arise when walls are covered with colored papers, the rooms were painted in red (5R 4/14, S2070-R), green (7.5G 5/8, S2555-G), blue (7.5BG 5/8, S2555-B30G), and white(N9.5, S0500-N). By minimizing sound and light that may be distracting to the experiment, a stable environment was established, and air circulation was provided in white room in order to prevent subjects from becoming drowsy, thereby achieving an environment with minimal measurement error.

2.1.2. Experiment Method

At the time of BDI-Ⅱ Depression Inventory progress, this study conducted the experiment by giving subjects enough time for reading and understanding instructions related to testing before proceeding with the test on subjects.

During brain wave measurement, the subjects were guided to sit comfortably in a chair in the middle of the white room, and electrodes were attached to them. In order to reduce anxiety in an unfamiliar space, the subjects stayed in the white room for five minutes before being sent to a colored room for one minute for measurement. In order to prevent after-image effect of the previous room, they were led to the white room again for five minutes, before being sent to another colored room to have their brain wave measured as shown in (Figure 2)

Figure 2. Brain wave measurement in each colored room

2.2. Measuring Tools

2.2.1. Beck Depression Inventory(Beck Depression Inventory-Ⅱ: BDI-Ⅱ)

BDI-Ⅱ was created through modifying & complementing the existing BDI(which is made on the basis of depression symptoms, measuring the type and severity level of depression)according to DSM-IV's depressive disorder diagnostic criteria by Beck et al.,; there is no change in its number of questions(21) and scoring method, but most questions except a few questions were partly modified or completely changed.

In case of BDI, it evaluates the symptoms occurring during the past 1 week, whereas BDI-II is designed to evaluate the symptoms during the past 2 weeks, and each question has a subtitle specifying what is evaluated. In addition, the most noticeable change in BDI-II is that it is designed to evaluate all the decrease & increase in sleep and appetite.

2.2.2. Brainwave measuring test

For the brainwave measurement in this study, I used PolyG-I (Laxtha, Inc., Korea), a computerized polygraph system that can simultaneously measure the brainwave, electrocardiogram (ECG), and electromyogram (EMG) that occur in the human body. The device includes as hardware wireless brainwave measuring equipment (WEEG-8) and as software the real-time data collection and time series analysis program (Telescan). In applying electrodes for the purpose of measuring brainwave, ten-twenty electrode system of the International Federation was used to install electrodes on the pre-frontal (Fp1, Fp2), the frontal (F3, F4), the parietal (P3, P4), the Occipital (O1, O2), and the left-right earlobes (A1, A2) as shown in Table 1. To measure heartbeat, I attached a snap electrode on the wrist. The subject’s brainwave signal was filtered with 0.5-50 ㎐ pass filter and converted with 16bit AD (Analog-Digital converter) before the date was saved to computer for collection purpose.

2.3. Subject Composition

The subjects of this research included people in their twenties and thirties without a history of psychological, cranial, or optical diseases. The methodology and the goal of this research was adequately explained to them, after which they agreed to volunteer with the explicit knowledge of cautions.

After implementing Beck Depression Inventory II, this study proceeded with the brain wave experiment by dividing the subjects into non-depressive group and depressive group.

3. EXPERIMENT RESULTS AND ANALYSIS

After implementing Beck Depression Inventory II, this study proceeded with the brain wave experiment by dividing the subjects into non-depressive group and depressive group. In the brainwave experiment, brainwave variance was measured by monitoring it with the data collection and analysis program called Telescan from LAXTHA, which is a computerized polygraph system. For respective channels, the measured values were put to relative power analysis.

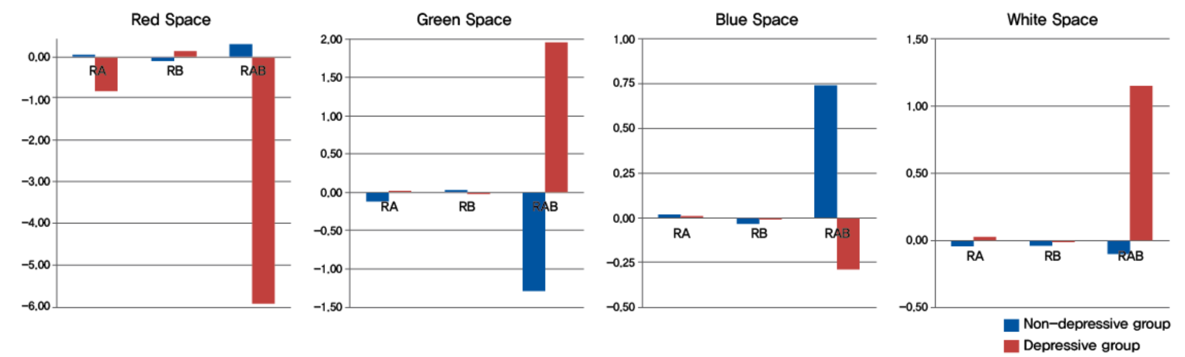

figure 3. Graph for indicator-specific brainwave variance in different color spaces

The analysis was performed on the brainwave indicators of RA (Relative Alpha Power Spectrum, 8-13/4-50 ㎐) that represents relaxation and stability, RB (Relative Beta Power Spectrum, 13-30/4-50 ㎐) that represents tension, alertness, and concentration, and RAB (Ratio of Alpha to Beta, 8-13/13-30 ㎐) that represents the alpha/beta ratio.

(Figure 3) shows in a graph the results of the brainwave measured in response to color spaces in the frontal that has rational thinking and cognitive ability for different indicators.

4. CONCLUSIONS

This study intended to look into the property of brain wave in color space in red, green, blue and white between the non-depressive group and depressive group consequent on Beck Depression Inventory-II results.

The research progress was conducted in three stages as follows:

1) In an effort to divide the subjects into non-depressive group and depressive group through Beck Depression Inventory-II, this study conducted the test on 6 adults in their 20s~30s, and measured their brain wave using PolyG-I.

2) This study conducted brain wave measurement in color space consisting of red(5R 4/14, S2070-R), green(7.5G 5/8, S2555-G), blue(7.5BG 5/8, S2555-B30G), white(N9.5, S0500-N).

The analysis result consequent on research progress is as follows:

The following is the result of the experiment, in which we measured brain wave in the frontal lobe of the subjects, which is responsible for rational thinking and cognitive abilities. In the red room, non-depression group showed increased RA and RAB indices and decreased RB index, while depression group displayed decreased RA and RAB, and increased RB index. In the green room, non-depression group had decreased RA and RAB and increased RB, while depression group had increased RA and RAB indices and decreased RB index. In the blue room, non-depression group had increased RA and RAB

indices, and decreased RB index, while depression group had increased RA index and decreased RB and RAB index. In the white room, all indices decreased for non-depression group, but depression group had increased RA and RAB indices and decreased RB index.
We learned that green and white used in the experiment had a relaxing and stabilizing effect for depression group, while red and blue used prevents such effects for depression group. We concluded that color environment designers must be wary of using red and blue for interior, and we learned that color stimulation affects brain waves depending on the degree of depression.
This study has a limit to generalization of the number of subjects. Accordingly, it is judged that there is a need for follow-up research on diverse subjects and experimental spaces in the light of the number of subjects, their age and gender, etc.

† This study was supported in 2014 by National Research Foundation of Korea (NRF) with funding from the Korean government (Ministry of Science, ICT and Future Planning) (No. 2008-0061908).

REFERENCES

Myung-sig KIM, Im-soon LEE, Chang-seon LEE. 2007. *The Validation Study Ⅰ of Korean BDI-Ⅱ: In Female University Students Sample.* The Koeran Journal of Clinical Psychology 26(4) 997-1014.

Hyung-mo Sung, Jung-bum KIM, Young-nam PARK, Dai-seok BAI, Sun-hee LEE, Hyun-nie AHN. 2008. *A Study on the Reliability and the Validity of Korean Version of the Beck Depression Inventory-Ⅱ(BDI-Ⅱ)*. Journal of the Korean Society of Biological Therapies in Psychiatry 14(2) 201-212.

Ji-A LEE. 2010. *Study on Color Preference and Color Sensibility of Depressed Patients. Master's Thesis*. Graduate School of Health Science&Welfare Management Pochon CHA University

Jin-sook LEE, Hee-won LEE, Hanna KIM, Ji-seon RYU. 2014. *A Basic Study on the Physiological Responses to the Color Stimulation in Red, Blue, Green, and White in Accordance with Youth's Concentration*. Collected Paper from Korea Society of Color Studies. 28(1) 177-86.

Heun-joo HONG, Soo-mi KIM, Beom-cheon LEE, Dong-hee LEE, and Seong-gwan AHN. 2009. *The Influence that Color Therapy Exercises on Stress and Brainwave Variation*. Journal of the Korean Society for Aesthetics and Cosmetology. 7(1) 51-59.

Beck TA, Streer RA, Brown GK. 1996. *Maunal for the BDI-Ⅱ*. The psychological corporation. San Antonio, TX

Address : Heewon LEE, Dept. of Architectural Engineering, College of Engineering, Chungnam National University, 99 Daehak-ro, Yuseong-gu, Daejeon 305-764. Korer
E-mails:bluesky4r@paran.com, hnkim@noroo.com,woman602@hanmail.net ,js_lee@cnu.ac.kr

Hue-Tone Representation of the Nayatani-Theoretical Color Order System

Hideki SAKAI
Graduate School of Human Life Science, Osaka City University

ABSTRACT

The Nayatani-Theoretical (NT) color order system is a new opponent-color-type system proposed by Nayatani based on his color-appearance and color-vision studies in 2003. The NT system has color attributes, whiteness, blackness, grayness, chroma and opponent-hue; the colors with the same attributes irrespective of hues have the same perceived whiteness or blackness (i.e., perceived lightness), the same degree of vividness, and also the same color tone. However, its tones are not explicitly stated in the NT system so far. Therefore, we introduced the categorical tone representation to the NT system. This makes the NT system more useful for various purposes. The tone concept has been widely used in the artistic fields of painting and color design from the old days. The NT tone categories introduced in this paper can be used for selecting the color combinations in those artistic fields. In the color science field, the color stimuli extracted based on the tone categories are frequently used in a wide variety of sensory testing of vision. The NT tones are also suitable for such scientific purposes, because its tones are derived based on the color-appearance studies and have well-defined colorimetric values. This colorimetric background will be of help when analyzing the sensory data.

1. INTRODUCTION

A lot of color order or color designation systems have been proposed from past to present (Fairchild 2013). We now have various types of color systems, and some of them are widely used. However, it seems that we have not yet found an ideal one. Even widely used systems have pros and cons. There is still more room for improvement. Thus, we expect many more new candidates will be proposed in the future.

In such a situation, the Nayatani-Theoretical (NT) color order system was proposed by Nayatani based on his color-appearance and color-vision studies in 2003 as a new candidate (Nayatani 2003, 2004). The NT system designates a color with the attributes, whiteness w, blackness bk, grayness gr, chroma C_{NT}, and opponent-hue H_{NT}. The colors with the same NT attributes [w, bk, gr, C_{NT}] irrespective of hues [H_{NT}] have the same perceived whiteness or blackness (i.e., perceived lightness), the same degree of vividness, and also the same color tone (Nayatani and Komatsubara 2005). This is the primary feature of the NT system, that is, the inclusion of the color tone concept in it. However, its tones are not explicitly stated in the NT system so far. Therefore, in this paper, we introduced the categorical tone representation to the NT system with hue divisions. We believe that this makes the NT system more useful for various purposes.

2. BRIEF SUMMARY OF NT SYSTEM

2.1 Structure of NT system

The color solid of the NT system is shown in the Figure 1. It consists of six primary colors, red (R), green (G), yellow (Y), blue (B), white (W), and black (Bk). It adopts three opponent-colors axes, not only red-green (R-G) and yellow-blue (Y-B), but also white-black (W-Bk). It has the reference gray (Gr) in the center.

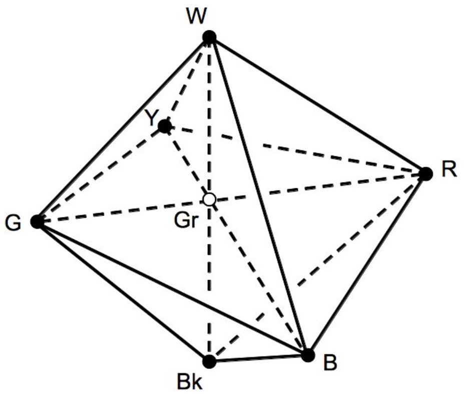

Figure 1: The color solid of the NT color order system.

The system has several unique features. It introduces an orthogonal coordinate using the city-block metric (Nayatani 2002) as shown in the Figure 2. It designates a color using whiteness *w*, blackness *bk*, grayness *gr*, chroma C_{NT} and hue H_{NT}. The color P in the Figure 2 (1), for example, has the attributes [*w*=0, *bk*=0, *gr*=0, C_{NT}=10, H_{NT}=Y100]. The maximum chroma, i.e., the chroma of pure color (PC), is different for different hue H_{NT} (Nayatani 2004). It clearly defines the grayness attribute, which is not defined explicitly in many other color order systems such as Munsell system and Natural Color System (Nayatani and Sakai 2014).

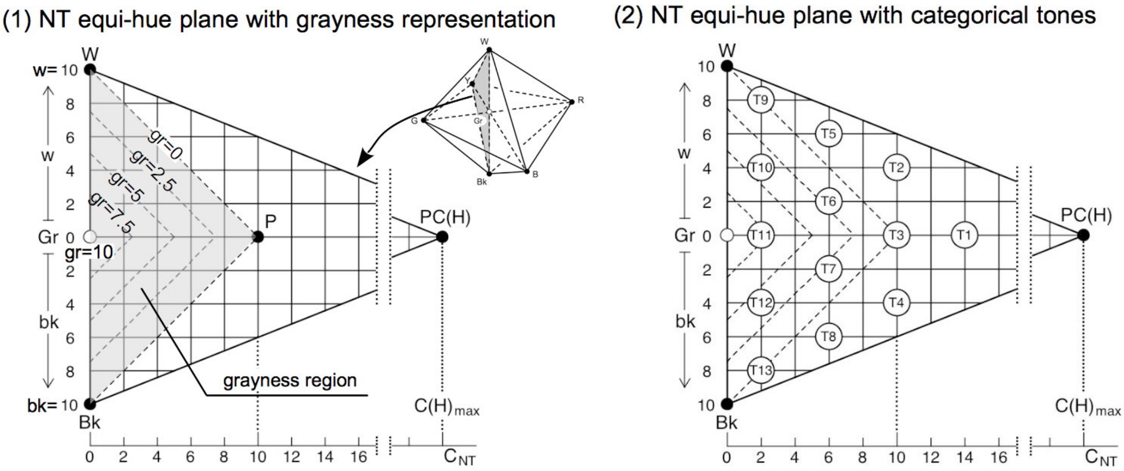

Figure 2: Equi-hue plane of NT system. (1) Grayness region, (2) categorical tones.

The NT system belongs to the category of Color Appearance Space (CAS) as discussed in the previous paper (Nayatani and Sakai 2007) and the name "Theoretical" comes from the fact that it can be theoretically derived from any Uniform Color Space (UCS) using the chromatic strength (CS) function and unique hue data. The concept of chromatic strength was originally proposed by Evans and Swenholt (1967) and it contains essential information on color appearance. Chromatic strength function and unique hue data are the necessary elements of NT system.

2.2 Derivation of NT color attributes

In this paper, CIELAB with D65 white point and 2-deg. observer is used as a base UCS. For the chromatic strength function, CS(k_1k_2; h_{ab}) is used (Nayatani 2004). For the primary opponent-color hues, the hue angles h_{ab} = 26, 91, 162, and 262 degrees are used as shown in the Table 1, which correspond approximately to the Munsell hues 5R, 5Y, 5G, and 2.5PB, respectively. Note that, in the preceding papers, the Munsell color attributes H V/C were mainly used to describe the NT system for simplicity (Nayatani et al. 2004, 2005, 2011, 2014). For example, Munsell chroma C was used as the NT chroma C_{NT}. We newly adopt CIELAB as the base UCS. However, no fundamental features of NT system discussed so far have changed at all. New C_{NT} derived from C^*_{ab} by Eq.(1) (see below) has the same meaning (Nayatani and Komatsubara 2005) and shows almost the same numerical values.

Table 1. Correspondence among NT opponent-color hues, CIELAB h_{ab}, and Munsell H.

NT Hue H_{NT}	CIELAB h_{ab} [deg.]	Munsell H (approx.)	proportional coefficient k_H
R100	26	5 R	2.3015 for $26 \le h_{ab} < 91$
Y100	91	5 Y	1.6748 for $91 \le h_{ab} < 162$
G100	162	5 G	2.2852 for $162 \le h_{ab} < 262$
B100	262	2.5 PB	2.4673 for $262 \le h_{ab} < 386$

Transform equations from the CIELAB color attributes [L^*, C^*_{ab}, h_{ab}] to NT color attributes [w, bk, gr, C_{NT}, H_{NT}] are as follows:

For chroma, the following equation is used.

$$C_{NT} = k_C \cdot \mathrm{CS}(h_{ab}) \cdot C^*_{ab} \,, \qquad (1)$$

where k_C = 0.14164 is the proportional coefficient, which is determined to make C_{NT} be the same scale as Munsell C on average.

For hues, first, identify in which opponent-hue section a color with h_{ab} is in, then, calculate the hue steps ΔH_{NT} between the two neighboring primary colors by the following equation.

$$\Delta H_{NT} = k_H \cdot \{1/\mathrm{CS}(h_{ab})\}^2 \cdot \Delta h_{ab} \,, \qquad (2)$$

where k_H is the proportional coefficient in the fourth column of Table 1.

For whiteness and blackness, first, correct the lightness scale that becomes L^*_{cr} = 50 when L^* = 55, then, obtain the perceived lightness $L^*_{cr,eq}$, finally transform it to w or bk.

$$L^*_{cr,eq} = k_L \cdot \mathrm{CS}(h_{ab}) \cdot L^*_{cr} \,, \qquad (3)$$

$$w \text{ or } bk = (1/5) \cdot (L^*_{cr,eq} - 50) \,, \qquad (4)$$

where k_L = 0.75029 for C_{NT} = 10. For other C_{NT} values, additional equations are used. See the previous paper (Nayatani and Sakai 2011) for details.

For grayness, the following equations are used (Nayatani and Sakai 2014).

$$gr = 10 - [(w \text{ or } bk) + C_{NT}] \,, \qquad \text{for } (w \text{ or } bk) + C_{NT} < 10 \qquad (5)$$

$$gr = 0 \,, \qquad \text{for } (w \text{ or } bk) + C_{NT} \ge 10 \qquad (6)$$

3. CATEGORICAL TONE DETERMINATION

In NT system, the colors with the same attributes [w, bk, gr, C_{NT}] irrespective of hues [H_{NT}] have the same tone attribute as already explained in the INTRODUCTION. Thus, It can be said that the NT system is the Hue-Tone system on its own. However, categorical tones are usually used in color design fields (Kobayashi 1981, Chung and Ou 2001, Nayatani and Komatsubara 2005). For example, Kobayashi (1981), the inventor of his Color Image Scale, defined the tone by "Colors belonging to the same tone have a common image in spite of their hue differences."

Considering these needs, we decided to introduce the categorical tone representation to the NT system. We placed the most vivid tones at [w=0, bk=0, gr=0, C_{NT}=14, H_{NT}=any] indicated as T1 and defined totally 13 tones from T1 to T13 as shown in the Figure 2 (2). Every tone has the definite NT attributes [w, bk, gr, C_{NT}, H_{NT}]. Therefore, by using the transform equations in Sec.2.2 inversely, they can be easily transformed to colorimetric values [L^*, C^*_{ab}, h_{ab}]. Figure 3 shows the colored image of 13 tones with eight hues, H_{NT}=R100, R50-Y50, Y100, Y50-G50, G100, G50-B50, B100, and B50-R50. The RGB values used in this colored image were obtained by transforming the CIELAB [L^*, C^*_{ab}, h_{ab}] values to the 24-bit sRGB color values (IEC 1999). Note that, however, several colors in tones T1, T2, T3, and T4 are out of sRGB range. Note also that this tone category is just an example. You can change the number of categorical tones or can adjust the interval between tones as you like by using NT system.

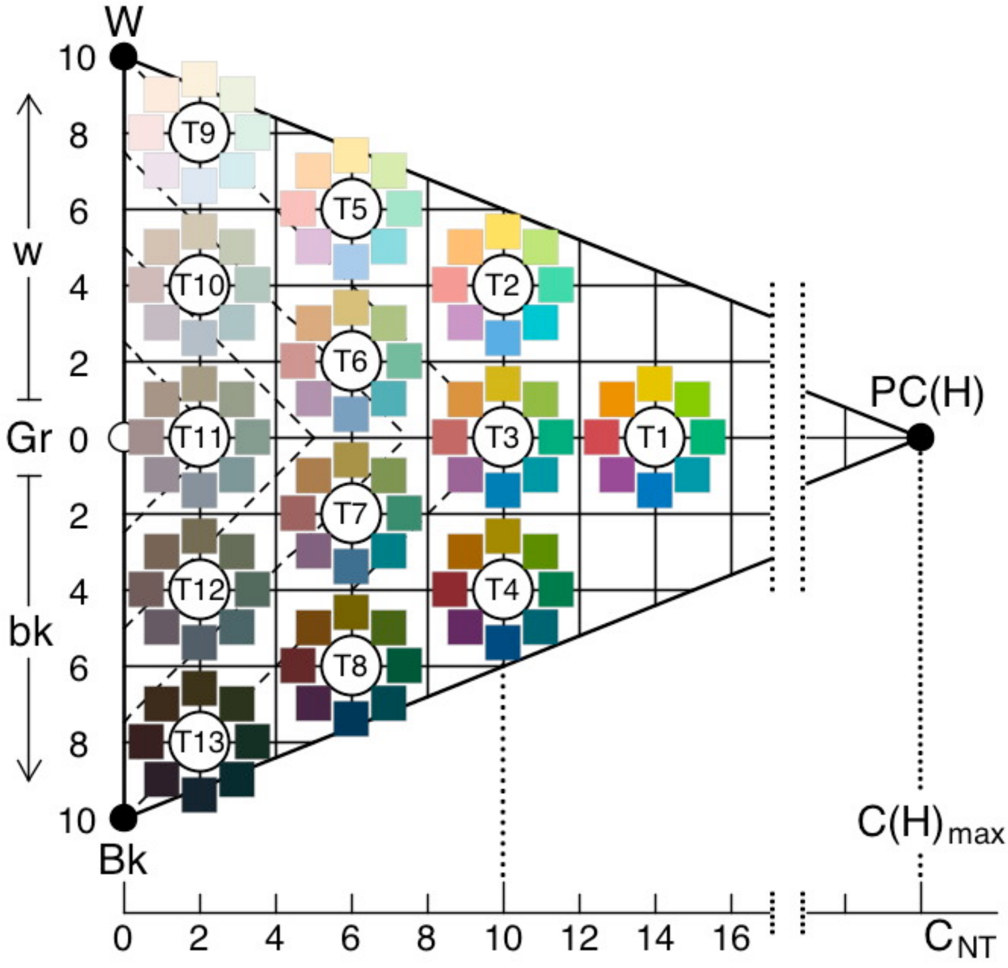

Figure 3: Categorical tone representation of NT system (Colored image).

4. CONCLUSIONS

The tone concept has been widely used in the artistic fields of painting and color design from the old days. The NT tone categories, for example, can be used for selecting the color combinations in those artistic fields (Sakai and Nayatani 2009).

In the color science field, the color stimuli extracted based on the tone categories are frequently used in a wide variety of sensory testing of vision. The NT tones are also suitable for such scientific purposes, because its tones are derived based on the color-appearance studies and have well-defined colorimetric values. This colorimetric background will be of help when analyzing the sensory data.

REFERENCES

Chung, M.C., L.C. Ou. 2001. Influence of Holistic Color Interval on Color Harmony. *Color Research and Application* 26 (1): 29-39.

Evans, R.M., B.K. Swenholt 1967. Chromatic Strength of Colors: Dominant Wavelength and Purity. *Journal of the Optical Society of America* 57 (11): 1319-1324.

Fairchild, M.D. 2013. *Color Appearance Models, Third Edition.* Chichester: John Wiley and Sons.

IEC 61966-2-1. 1999. *Multimedia systems and equipment- Colour measurement and management - Part 2-1*: Colour management- Default RGB colour space - sRGB. International Electrotechnical Commission.

Kobayashi, S. 1981. The Aim and Method of the Color Image Scale. *Color Research and Application* 6 (2): 93-107.

Nayatani, Y. 2002. A Hue Rectangle and Its Color Metrics in a Modified Opponent-Colors System. *Color Research and Application* 27 (3): 171-179.

Nayatani, Y. 2003. A Modified Opponent-Colors Theory Considering Chromatic Strengths of Various Hues, *Color Research and Application* 28 (4): 284-297.

Nayatani, Y. 2004. Proposal of an Opponent-Colors System Based on Color-Appearance and Color-Vision Studies, *Color Research and Application* 29 (2): 135-150.

Nayatani, Y., H. Komatsubara. 2005. Relationships among Chromatic Tone, Perceived Lightness, and Degree of Vividness. *Color Research and Application* 30 (3): 221-234.

Nayatani, Y., H. Sakai. 2007. Proposal of a New Concept for Color-Appearance Modeling. *Color Research and Application* 32 (2): 113-120.

Nayatani, Y., H. Sakai. 2011. Predictions of Munsell Values with the Same Perceived Lightness at Any Specified Chroma Irrespective of Hues - Determination of Any Tonal Colors. *Color Research and Application* 36 (2): 140-147.

Nayatani, Y., H. Sakai. 2014. Gray and Grayness - its Complexities in Color Appearance of Surface Colors. *Color Research and Application* 39 (1): 37-44.

Sakai, H., Y. Nayatani. 2009. Proposal for selecting two-color combinations with various affections. Part II: Demonstration of the System. *Color Research and Application* 34 (2): 135-140.

Address: Dr. Hideki SAKAI, Graduate School of Human Life Science,
Osaka City University, Sugimoto 3, Sumiyoshi-ku, Osaka, 558-8585, JAPAN
E-mail: hsakai@life.osaka-cu.ac.jp

Colour Appearance in the Outdoor Environment

Ya-Chen LIANG, Li-Chen OU, Pei-Li SUN
Graduate Institute of Color and Illumination Technology
National Taiwan University of Science and Technology, Taiwan

ABSTRACT

A psychophysical experiment of colour appearance, in terms of hue, lightness and colourfulness, was conducted outdoors to investigate colour appearance in the outdoor environment. The experiment was conducted outdoors on a sunny day by 14 observers at the same time, in the same place, where there was no glare in the observer's viewing field. The reference white, reference colourfulness and each test colour were all placed on a vertical panel covered with a medium grey cloth. The test colours included 42 colour patches selected randomly from the Practical Coordinate Color System to cover a wide range of hue, lightness and chroma. The 14 observers with normal colour vision were asked to estimate the lightness, colourfulness and hue for each test colour. The experimental results show high correlation between visual data and values predicted by CIECAM02 in terms of the three colour appearance scales. Although the perceived lightness also shows high correlation, experimental data suggests that the observers were more sensitive to variation in lightness for greyish colours than for highly saturated colours.

1. INTRODUCTION

Existing colour appearance models such as CIECAM02 (CIE Publication-159 2004) have typically been developed using displays, prints and other media. Nevertheless, these studies have been limited to indoor conditions. It has been unclear whether or not such colour appearance models also apply to the outdoor environment. CIECAM02 has defined three surround conditions, dark, dim and average. The average surround condition describing luminance level of around 1,000 cd/m^2 may not suffice to use in the outdoor environment, as the outdoor luminance can be easily beyond 10,000 cd/m^2. The luminance level of surround higher than 10,000 cd/m^2, also called the "bright surround condition", for which CIECAM02 did not seem to show satisfactory predictive performance (e.g. Park *et al.* 2015).

There is much greater variation in the luminance of light source outdoors (i.e. the day light) than indoor lights, due to unpredictable weather conditions. The human visual system has considerable ability to adapt to such variation. More importantly, the illumination level is way higher in the outdoor environment than indoor lighting. Colour applications for indoor conditions are quite different than those for the outdoor environment. The latter include outdoor colour measurement which is essential for architectural colour design and urban colour planning.

Several issues need to be addressed properly before a colour appearance experiment can be appropriately carried out outdoors. First, the selection of the experimental location is crucial. There should be no glare within visual range of the observer, so that the white tile serving as the reference white is the brightest in the viewing field. Moreover, outdoor luminance varies all the times due to the position of the sun and the weather conditions. To overcome these issues, all observers in the study must assess colour appearance of each colour sample at the same time, in the same place. And this was exactly how the present study was carried out.

2. METHODS

2.1 Experimental set-up

As described above, the experiment was conducted outdoors on a sunny day (afternoon) by all observers at the same time, in the same place, where there is no glare in the observer's viewing field. The reference white, the reference colourfulness and each test colour patch were all placed on a vertical panel covered with a medium grey cloth. During the experiment, the mean luminance value of the reference white was 13,050 cd/m^2 (SD = 2,639), as measured using a Konica Minolta CS-100A, a portable colour meter.

As shown in Figures 1 (a) and (b), the viewing distance for all observers was about 300 to 400cm, where the locations of each observer varied in terms of both viewing distance and viewing angle. To see whether this would result in significant colour difference for different observers, the CS-100A portable colour meter was used to measure the test colours from various locations of each observer. The measurement result shows a mean CIELAB colour difference of 1.38, which was thought acceptable in such an experimental condition.

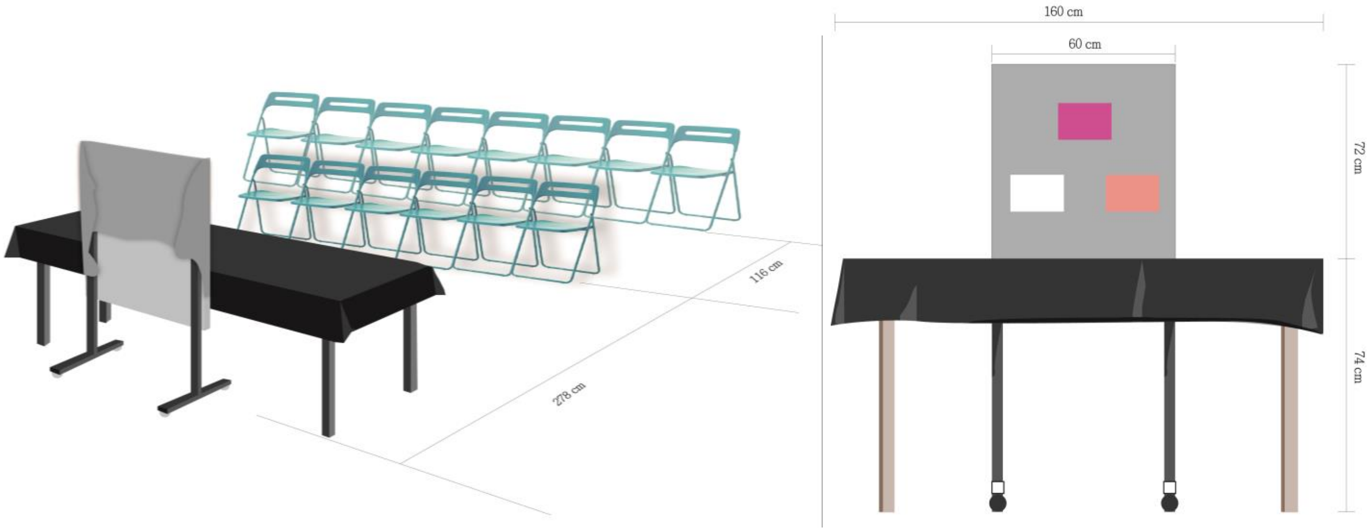

(a) (b)

Figure 1: Experimental set-up: (a) the 14 observers conducted the experiment simultaneously with a viewing distance of about 300-400cm, (b) each test colour, together with a reference white and a reference colourfulness, presented against a medium grey background on a black table

2.2 Colour samples

The test colours included 42 colour patches selected randomly from the Practical Coordinate Color System to cover a wide range of hue, lightness and chroma. The 42 colours included 6 achromatic colours for further data analysis.

During the experiment, for each test colour, the reference white, reference colourfulness and the test colour itself were measured in terms of the tristimulus values using the CS-100A portable colour meter. Figures 2 (a) and (b) show distribution of the 42 colour samples in CIELAB colour space according to the measurement results, illustrating a wide spread of colour samples in terms of hue, lightness and chroma.

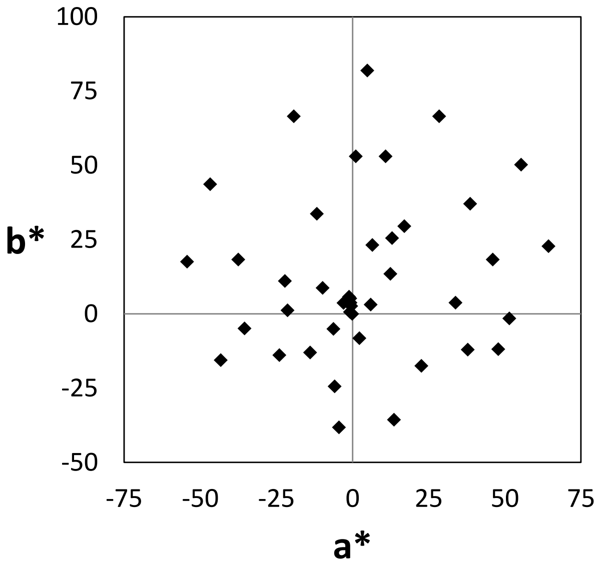

(a)

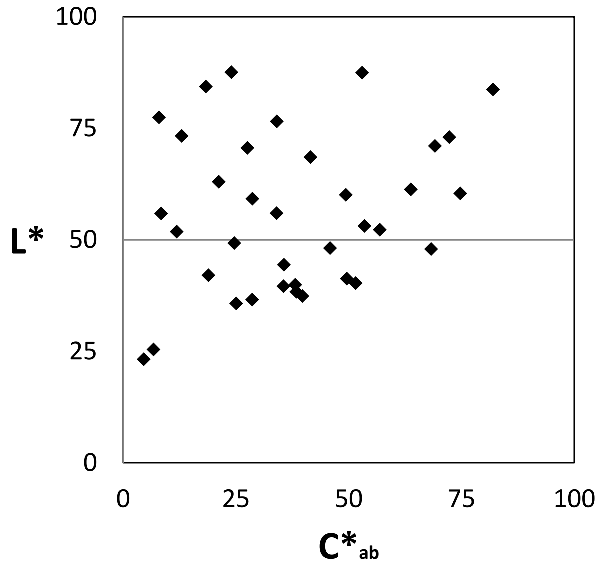

(b)

Figure 2: The 42 colour samples in (a) CIELAB a-b* and (b) L*-C*$_{ab}$ diagrams*

2.3 Observers

A total of 14 observers with normal colour vision were asked to estimate the lightness, colourfulness and hue for each test colour. The observers were all Taiwanese citizens, and were postgraduate students at the National Taiwan University of Science and Technology. Prior to the experiment, the observers received trainings of definitions of hue, lightness and chroma using the Munsell Color Book.

The 42 colour samples were presented individually in random order. To assess lightness of each test colour, the reference white was assigned to have a lightness value of 100. To assess colourfulness, the reference colourfulness was assigned to have a colourfulness value of 40. The hue quadrature was used to assess hue of each test colour in terms of proportion of red, yellow, green and blue in colour mixture that can match the test colour.

3. RESULTS

To see how well CIECAM02 performed in predicting hue, lightness and colourfulness for colour patches presented in the outdoor environment, the visual results were plotted against the predicted CIECAM02 values, as shown in Figures 3 (a)-(c) for hue, lightness and colourfulness, respectively. High correlation was found for all of the three scales, with a coefficient of determination (R^2) of 0.99 for hue, 0.82 for lightness and 0.89 for colourfulness. The results indicate good predictive performance of CIECAM02 for colour appearance in the outdoor environment, with the predicted values accounting for 99% of the total variance in the visual data of hue, 82% for lightness and 89% for colourfulness.

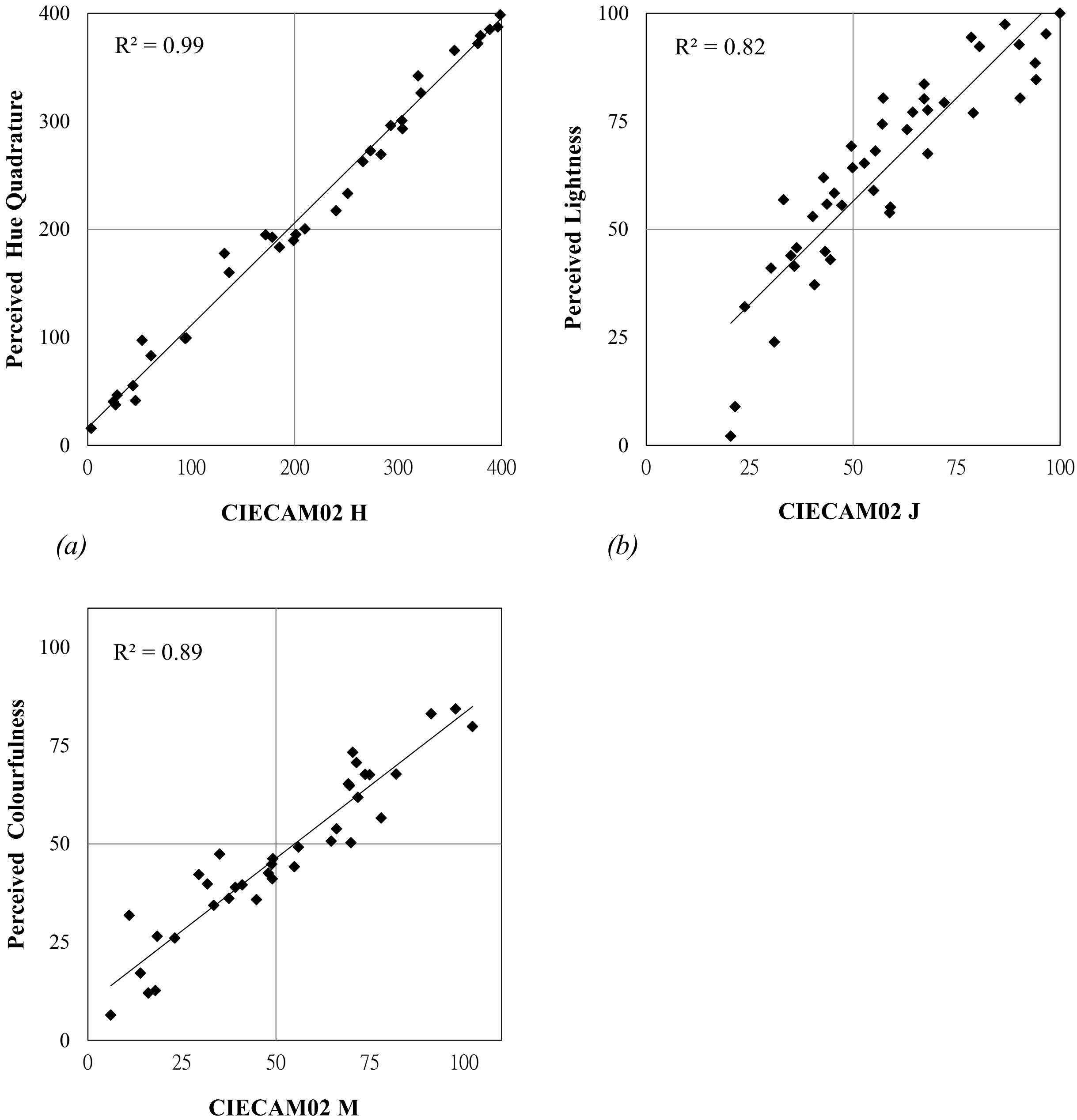

(a) *(b)*

(c)

Figure 3: Comparisons between visual results and predicted CIECAM02 values in terms of (a) hue, (b) lightness and (c) colourfulness

Note, however, that although experimental results show a coefficient of determination of 0.82 for lightness, as demonstrated in Figure 3 (b), which seems to suggest a close correlation between the visual results and the predicted value in lightness, the scatter graph illustrated in Figure 3 (b) shows a somewhat curvy trend line; colour samples having low CIECAM02 J values tended to be rated extremely low in lightness.

It is tempting to assume that the two data points located lowest in Figure 3 (a) being the outliers. To see whether this was the case, the experimental data were separated into five groups defined by CIECAM02 M (colourfulness): those with the M values lower than 5 (i.e. the achromatic colours), those with the M values greater than 5 and lower than 30, those with the M values greater than 30 and lower than 50, those with the M values greater than 50 and lower than 70, those with the M values greater than 70. As Figure 4 demonstrates, the five colourfulness groups seem to show different tendencies in terms of slope of trend line; the higher colourfulness, the lower slope of trend line. The achromatic colour group (i.e. M < 5) shows the highest slope, while the group with the highest colourfulness values (i.e. M > 70) shows the lowest slope. This seems to suggest that the observers were more sensitive to variation in lightness for greyish colours than for highly saturated colours.

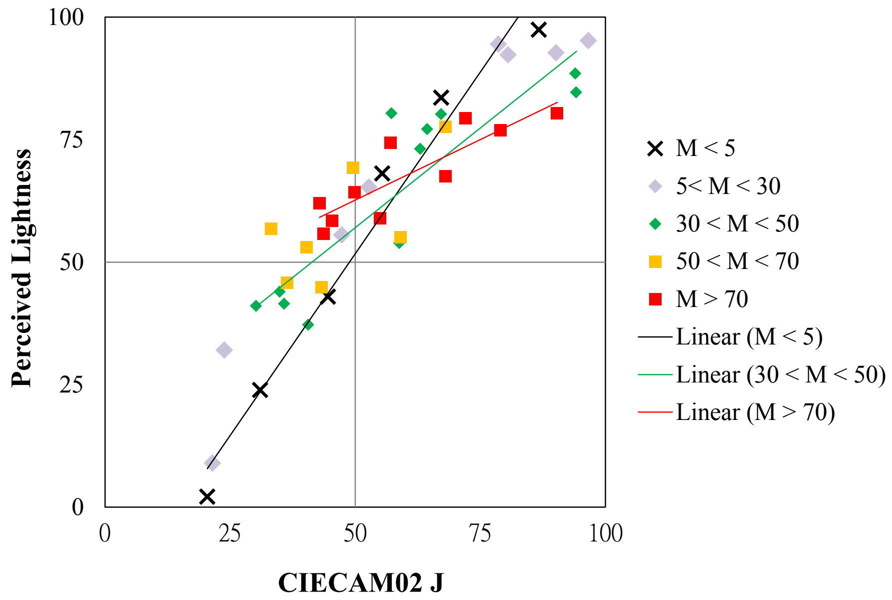

Figure 4: Perceived lightness plotted against CIECAM02 J for five colourfulness groups defined by CIECAM02 M

4. CONCLUSION

The experimental results show high correlation between the visual data and the predicted values by CIECAM02 in terms of the three colour appearance attributes: hue, lightness and colourfulness. While the perceived lightness also shows high coefficient of determination (0.82) as shown in Figure 3 (b), suggesting good predictive performance of CIECAM02 for outdoor environment, Figure 4 demonstrates different tendencies in terms of slope of trend line; the higher colourfulness, the lower slope of trend line. The result suggests that the observers were more sensitive to variation in lightness for greyish colours than for highly saturated colours. Whether the finding only applies in the outdoor environment or it may also occur in the average surround condition will require further study using more dark colour samples in the experiment.

ACKNOWLEDGEMENTS

This work was supported in part by the Ministry of Science and Technology, Taiwan (MOST 103-2420-H-011-002-MY2).

REFERENCES

CIE Publication-159. 2004. *A Colour Appearance Model for Colour Management Systems: CIECAM02*. Vienna: CIE Central Bureau.

Park, Y., Luo, M. R., Li, C. J., and Kwak, Y. 2015. *Refined CIECAM02 for bright surround conditions*, Color Research and Application 40 (2) 114-124.

Address: Li-Chen OU, Graduate Institute of Color and Illumination Technology, National Taiwan University of Science and Technology 43, Section 4, Keelung Road, Taipei, Taiwan
E-mails: lycperry@gmail.com, lichenou@mail.ntust.edu.tw, plsun@mail.ntust.edu.tw

Color Play: Gamification for Color Vision Study

Shida BEIGPOUR[1], Marius PEDERSEN
The Norwegian Colour and Visual Computing Laboratory, Gjøvik University College

ABSTRACT

The study of color perception in humans is an important ongoing research which currently mainly relies on psychophysical studies. Most psychophysical studies are prune to limitations which can highly reduce the scalability and repeatability of their experiments, cause over-fitting, and fail to fully engage subjects in performing the given tasks. Gamification is becoming a popular approach in obtaining large amount of data, and making the tasks more interesting for subjects. We design a game called Color Play which consists of a series of simple color mixing and matching tasks. This game engages both the children and adults in experimenting with different colors and color spaces. Through this game, the players would learn about different color spaces while at the same time becoming subjects of our color perception study. By analyzing the players' performance we investigate the differences between the RGB and HSV color spaces, and compare the importance of luminance versus chroma.

1. INTRODUCTION

While the human visual system can be studied in biology using sophisticated techniques like MRI, research on human color perception as a rather cognitive process, relies mainly on the study of the human behavior given visual stimuli. These studies analyze the results and performance of human subjects which take part and perform a set of tasks manually or semi-manually (e.g., segmenting objects in an image or rating images).

Performing such experiments is often time consuming, tedious, and can involve paid subjects. This all limit the number of subjects. Moreover, the tasks can be boring for the subjects and due to tiredness they might tend to pay less attention toward the end. Repeating the experiment (especially by other scientists) is not straightforward. Often these studies use participants from one location (e.g., their university), and mostly involve adults as collecting data from children requires much more effort. Lastly, the very controlled set up and lab environment results in a less natural behavior from the users, especially when they feel that their behavior is being controlled (Heppner et al. 2007).

In the current work, we investigate "gamification" as a method to tackle all the above challenges in psychophysical studies. The main goal of our study is to investigate the intuitiveness and ease of color matching and color mixing tasks in different color spaces, namely for the widely used RGB and HSV, and for different colors. The main purpose of our gameplay framework is to take a typical color mixing/matching scenario out of the laboratory environment and bring it to the context of everyday life. We study how people interact with colors and color spaces in work and leisure. Such study would help us analyze people's relation with color spaces based on the practical scenarios like finding the desired color mixture for a room, a graphic design, website, advertisement, video game, and so on.

We briefly list our main contributions: showing the advantage of gamification in psychophysical studies to improve the subjects' experience as well as the performance and

[1] S. Beigpour is now with the Chair for Computer Graphics at University of Siegen, Germany.

quality of the study; designing a portable and robust system to take advantage of public spaces as a platform to reach wide variety of subjects (e.g., age, gender, nationality); using a game environment we help subjects to present more natural behavior compared to a controlled lab environment; and finally as a result we study the intuitiveness of the RGB and HSV color spaces as well the importance and contribution of chroma and luminance for human observers in daily life. We provide quantitative data analysis.

2. RELATED WORK

Schwarz et al. (1987) designed a study on the effect of color spaces on color matching with a large number of naive subjects (96) in which 14 pages of instructions were handed out. Each subject matched five colors six times each for a total of 30 trials. They concluded that in their study: first, subjects were faster in matching using RGB and opponent color space; second, having a lightness axis helped with matching lightness more than having a hue or chroma axis helped with matching hue or chroma; third, significant learning occurred with respect to matching time and closeness; fourth, inexperienced subjects using the RGB color model matched rapidly but inaccurately in comparison with other color models; and fifth, the opponent, LAB, YIQ, and HSV color models require learning to use effectively.

Douglas and Kirkpatrick (1996) studied the effectiveness of color models with respect to interface feedback level. The experiment was performed for four groups of naive subjects (12 in each group). Each group was tested for a combination of the color model (RGB or HSV) and one of the two interfaces with different feedback. The subjects were required to perform a color matching task (30 target colors with the time limit of maximum three minutes per color). They concluded that the color model does not play a role in time or accuracy of the matching task, while higher level of feedback results in more accuracy.

Luo et al. (2005) designed an experiment to study the sources of uncertainty in color matching experiments. They have presented quantitative results comparing each source and concluded that the observers play the main role in such uncertainty. Furthermore, they have provided solutions for various types of uncertainty.

Flatla et al. (2011) proposed a framework that simplifies the design of *calibration games* as a way to improve both the performance and the user experience while performing a tedious task like calibration. They conclude that the gamification does significantly improve the enjoyment, and that even though there are some differences in the recorded data it does not reduce the utility of the data for calibration.

2. METHOD

In our gamification approach, the user is provided with a tangible environment consisting of four Philips Hue color light bulbs and the Playstation3 Move™ controller to interact with the game. The *feedback* element is provided by setting the bulbs to change color based on the user's action. We also provide scores to make the game more *competitive*.

2.1 Technical Specifications

We use a set of Philips Hue bulbs to represent the colors since they are capable of displaying a wide range of colors and their control interface is straight forward. Three bulbs are set to represent the three primaries in the color space to be studied and a fourth bulb displays the color produced by the subject. As the bulbs use colored LEDs, they are relatively robust and consistent over time. Furthermore, they don't heat up much. On the other hand, as they are mainly targeted for commercial use to provide household ambient lighting, their gamut is rather limited to the common indoor and outdoor illuminant colors (e.g., dark green and cyan are outside the gamut).

To overcome this limitation, we created a look-up table for the colors using a Konica Minolta CS1000 tele-spectro-radiometer mapping the values in the sRGB color gamut to their corresponding values for the bulbs. This look up table helps us find a set of colors which can be displayed by these bulbs as well as the exact values to be provided to the bulb in order to display the desired colors. Since the color reproduction function of the bulb turned out to be nonlinear and complex, using a look-up table to convert the values between the game's sRGB system and the bulb is a reasonable choice.

Furthermore, we use the open source code of Perl (2012) for tracking the PS3 Move™ controller with the help of a webcam. The tracking is quite robust to occlusions.

2.2 Game Setup

Figure 1 presents a schematic view of the game setup. We divide the space to equal horizontal portions, each of which is assigned to one of the three bulbs who stand for each of the primaries of a color space (i.e., Red, Green, and Blue for RGB). When the subject places the controller in each of these areas, the corresponding bulb is activated. The vertical dimension is divided to three areas, namely, *up*, *middle*, and *down*. Therefore for example placing the controller in the area assigned to the first bulb in the up or down areas will result in an increase or decrease (respectively) in the contribution of that bulb in the color mixed by users. The *middle* area is design to introduce a null state which helps users get better control of the changing bulbs, where no change occurs in the bulbs. The total number of steps in each color channel of each color space is kept constant to avoid giving more importance to chromatic and none chromatic characteristics of the color spaces.

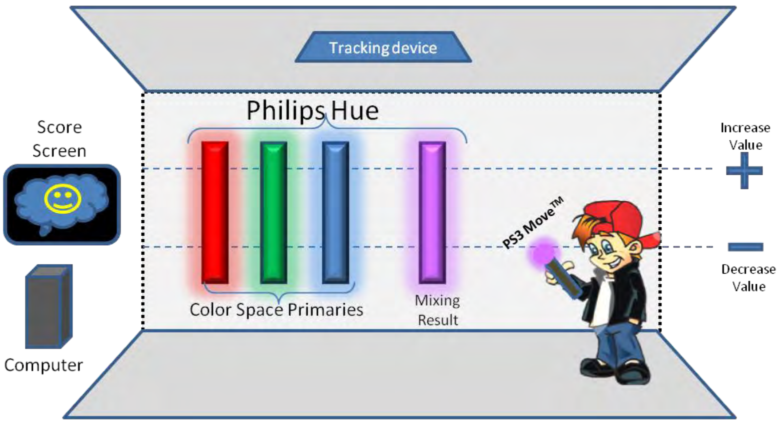

Figure 1: Schematic view of the game setup and its components.

The fourth bulb displays the color mixed by the player. The player needs to match this color to the color of the patch given on the screen. The screen also shows the player their score upon completing each round of the game.

At each instance of the game, one of the target colors is displayed in a large patch on the screen next to a few lines of instructions. The order of colors is random. The screen is placed in a way that the player can not see the target bulb and the patch on the monitor at the same time, so that they need to rely on their idea of that color. This way we can better study which characteristics of the color are more important for people. We setup the game inside a dark room to avoid the effect of ambient illumination and provide better contrast for the bulbs and the monitor.

Target Colors: We've chosen six colors, namely: Sand (RGB:206,188,96), Pimento (230,97,69), Sapphire (88,10,226), coral Pink (244,121,129), Lemon (225,238,24), pastel Purple (216,157,237).

3. EXPERIMENTS AND DISSCUSSION

In this section we provide details on our data analysis. First we define our metrics. Then we present the results for supervised and unsupervised experiments. Finally we compare the contribution of chroma versus luminance using the intra-observer data analysis.

2.1 Metrics

We use Median Observer Time (MOT) in seconds as a notion of how intuitive it is to mix and match colors in each space. The median is chosen since it is more robust to outliers. Luo et al. (2005) define *observer accuracy* as "the closeness of the agreement between the result of each individual observer and a true value of the measurement, i.e. the mean of all the observations for each color". Following Luo et al. (2005), we define Average Inter-Observer Inaccuracy $AIOI_{CS}$ for each color C and color space S in CIE ΔE^*_{ab} as:

$$AIOI_{cs} = (1/n) \sum_{i}^{n} \Delta E^*_{ab} \left(T_{CS}, P_{CS_i} \right),$$

where $T_{CS} = (1/n) \sum_{i}^{n} P_{CS_i}$, and P_{CS_i} is a player's result for each C and S. The number of observations is n. We have also calculated the difference between the T_{CS} and the actual match (from the look-up table explained before). We refer to this error as Average Observer Error (AOE) also in ΔE^*_{ab} units.

2.2 Supervised Experiment

For the first experiment, we asked 14 adult male and female subjects (8 expert and 6 naive subjects) with corrected to normal eye-sight to reproduce the six target colors in each of the two color spaces. They were also required to take a color deficiency test prior to the game to make sure they all have normal color vision. Two subjects repeated the experiment to provide data for the intra-observer study.

Questionnaires were provided to the participants to evaluate their experience. The subjects were asked to rate the game (on a scale of 1 to 5) based on how fun and how hard it is to play. Overall, the players rated the game as "fun" (4.1/5) and with "average difficulty" (2.98/5). On average, each color has been played about 35 times.

2.3 Unsupervised Experiment

In the second experiment we had the visitors voluntarily play as many colors as they like. These subjects were male and female between 22 and 27 years old and not included in the supervised experiment. The order of colors were random. On average, each color was played 5.2 times for RGB and 4.5 times for HSV.

2.3 Data Analysis

Figure 2 summarizes the analysis of the supervised and unsupervised experiments respectively. According to the top row, HSV is a more intuitive color space as the naive subjects were faster in mixing colors compared to RGB. On the other hand, the subjects performed similarly in both color spaces based on their unanimity (AIOI). In average, coral pink and pastel purple were the most and least accurately mixed colors respectively (AOE). Even though, the naive group took longer time in RGB, both groups performed similarly in average regarding their AIOI and AOE.

The AOE is more than twice the AIOI, and it is quite high for a perceptual difference. This shows that the subjects' perception of the bulb color was quite far from its actual color value measured accurately using the tele-spectro-radiometer. There are several possible reasons for that, including the surround effect, and that the players did not have the screen and the bulb next to each other. This is an indication of cognitive processes affecting our perception of colors.

Based on Figure 2 bottom row, when players’ task was to only play one color and space each, they were less unanimous among themselves maching in HSV (high AIOI). This indicates that as Schwarz et al. (1987) expressed, HSV requires learning to use effectively.

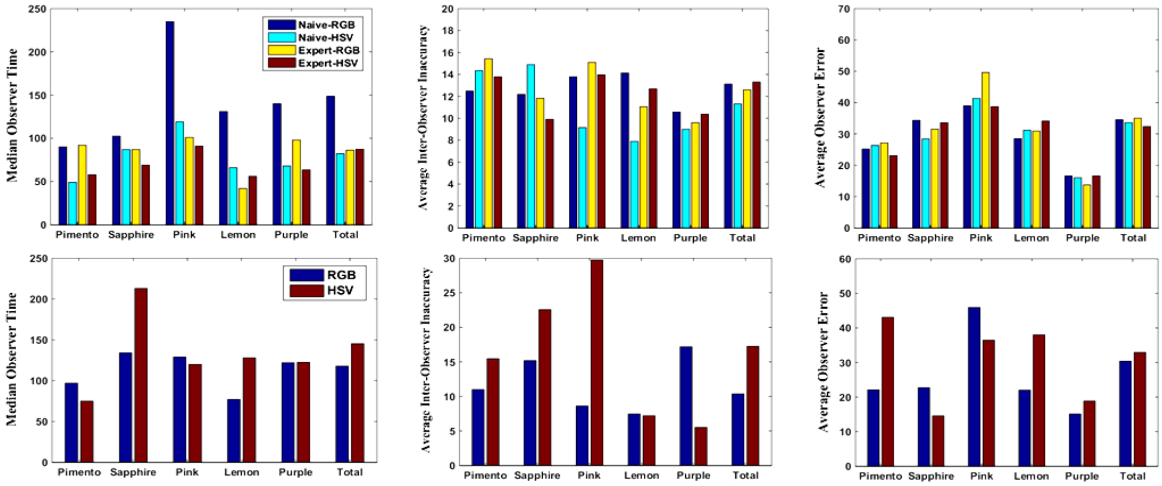

Figure 2: Top and bottom rows present supervised and unsupervised experiments respectively. From left to right: the MOT in seconds, AIOA and AOE in ΔE^*_{ab}.

To compare the contribution of chroma versus luminance we use the intra-observer data gathered from two expert subjects. Table 1 compares the Average Intra-Observer inaccuracy (AAO), as a measure of repeatability, and Average Matching Error (AE), absolute error, between the two color spaces in Chroma and Luminance. Based on the obtained values, subjects performed better in matching luminance than chroma in both color spaces.

Table 1. Intra-observer study:subjects matched better in Luminance than croma.

	Time	Number	AAO-Chroma	AAO-Luminance	AE-Chroma	AE-Luminance
RGB	73.5	32	8.6	5.5	41.8	21.3
HSV	75.1	33	7.0	5.3	41.5	24.8

2.3 Challenges

An inevitable challenge in a serious game is the *meta-gaming* (McCallum 2012). For example, a player might try to intentionally play bad. But it's difficult to ensure that there are no loopholes in the game rules, and restricting the game could limit the players' natural behaviour and bias the results. Having many subjects, reduces the effect of such outliers.

4. CONCLUSIONS

In this paper we took advantage of gamification in designing a study on human color perception. The designed game was used to gather information about the intuitiveness of mixing and matching colors in two different color spaces (i.e., RGB and HSV). The results of a supervised and controlled experiment indicate that HSV is a more intuitive colorspace as the subjects were faster in mixing colors compared to RGB. Results also indicate that subjects better matched in luminance compared to chroma. In an unsupervised experiment subjects were less unanimous matching in HSV.

Future work includes gathering data with more subjects. It can also include studies of the effect of gender, nationality, and age. The game can also be adapted for the observers to mix their favorite color, or for color memory experiments. It could also be interesting to see if one can detect color deficient players through the game.

ACKNOWLEDGEMENTS

This work has been funded by the Regional Research Funds of Norway Innlandet through the Colourplay project. We would like to thank Vitensenteret Innlandet and Simon McCallum for their valuable input to the project.

REFERENCESDouglas, S. and T. Kirkpatrick. Do color models really make a difference? *In Proceedings of the SIGCHI Conference on Human Factors in Computing Systems*, pages 399–ff. ACM, 1996.

Flatla, D.R, C. Gutwin, L.E. Nacke, S. Bateman, and R.L Mandryk. Calibration games: Making calibration tasks enjoyable by adding motivating game elements. *In Proceedings of the 24th Annual ACM Symposium on User Interface Software and Technology*, pages 403–412, New York, NY, USA, 2011. ACM.

Heppner,P., B. Wampold, and D. Kivlighan. *Research Design in Counseling*. Research, Statistics, and Program Evaluation Series. Cengage Learning, 2007.

Luo, W., MR. Luo, S. Westland, A. Tarrant, and A. Robertson. Measuring the uncertainty of colour matching. *AIC Colour 05 – 10th congress of the International Colour Association*. Pages 1087-1090. 2005 McCallum, S. Gamification and serious games for personalized health. *Studies in health technology and informatics*, 177:85–96, 2012

Perl T.. *Cross-platform tracking of a 6dof motion controller using computer vision and sensor fusion*. Master's thesis, Technischen Universität Wien, 2012.

Schwarz, M.W., W. B. Cowan, and J. C. Beatty. An experimental comparison of RGB, YIQ, LAB, HSV, and opponent color models. *ACM Transactions on Graphics*, 6(2):123–158, 1987.

Address: Shida Beigpour, PhD, Chair for Computer Graphics, Faculty IV
University of Siegen, Hölderlin Street 3, 57068 Siegen, Germany
E-mails: shida.beigpour@uni-siegen.de, marius.pedersen@hig.no

Using Visual Illusions to Expand the Available Colors for Making Mosaics

I-Ping CHEN, Wei-Jei CHIOU,
Institute of Applied Arts, National Chiao Tung University

ABSTRACT

Mosaic is an ancient art form of creating images by arranging pebbles, small pieces of ceramics, or other colored material called tesserae. One of the challenges in creating mosaics is the limited number of colors of the material. In order to create the desired colors that do not exist, mosaic artists have to make great efforts to learn principles of color mixture of tesserae which is not always intuitive. In this research, we attempt to look for other possible solutions for increasing available colors by applying two different visual illusions, Craik-O'brien-Cornsweet illusion and neon color spread illusion, to the mosaic design. To find out the optimal set of parameters to maximize the effect of illusion, we designed a series of computer-simulated experiments to examine how parameters such as the size of tesserae, the width and the color of grout, and the slope of luminance grading affect the magnitude of these two illusions. The results show that the magnitude of Craik-O'brien-Cornsweet illusion is remarkably stable across all manipulated values of parameters. The neon color spread illusion, by contrast, is sensitive to scale of tesserae, and width and color of the grout lines. Increasing the width of the grout lines will enhance the neon color spread illusion while increasing the size of tesserae would weaken the illusion. The magnitude of neon color spread varies with hues of grout. Green grout generates the strongest illusion, followed by red, blue and yellow grout in that order. We also create an Ehrenstein figure with ceramic tesserae according to the results of the experiment and the illusion effect of this physical version supports the conclusion of the experiment of neon color spread illusion.

1. INTRODUCTION

Mosaic is a discrete form of art. Unlike the case of painting, where the artist can produce a wide range of colors by mixing colors on his/her pallete, in mosaic making the artist has to work with a very small number of colors carried by the available tesserae. While not completely impossible, it is very difficult to achive color mixture effect by arranging colored tesserae in a specific way, the reason being that the grain size of mosaic elements is considerably larger than the color elements in a Pointillism painting. The top priority in the consideration of the arrangement of the tesserae should be given to conveying the spatial structure of the picture, not to the color mixture effect. It takes great talent and skill to make a mosaic work that excels both in form and color (Locktov & Clagett, 2002).

Given the color constraints faced by mosaic artists, we are highly motivated to seek for ways to expand the useful color range for the artists. In this study we try to make use of two color-related visual illusions, Craik-O'brien-Cornsweet illusion (Cornsweet, 1970) and the neon color spread illusion (Bressan et al., 1997), to increase the subjective number of colors in a mosaic.

In the original form of the Craik-O'brien-Cornsweet illusion, two panels of identical luminance are connected to each other by an 'amplified' luminance edge (aka. the Cornsweet edge) in the middle (Cornsweet, 1970, see Figure 2). The polarity suggested by this 'amplified edge' would bleed into these two side panels, making the panel by the dark side of the edge look darker (the right panel in Figure 1), the panel by the bright side brighter (the left panel in Figure 1).

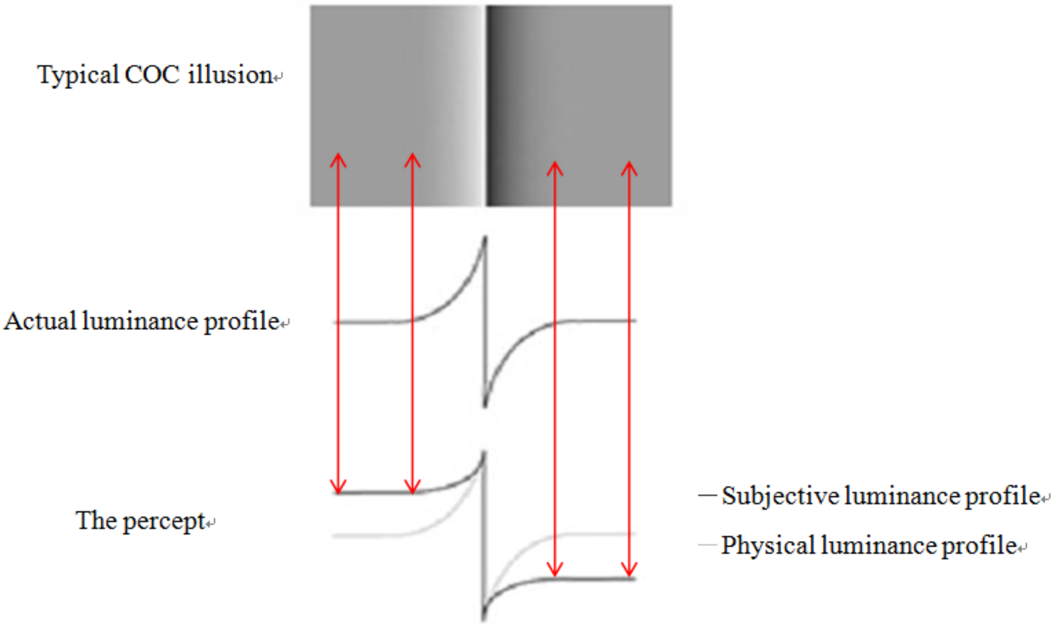

Figure 1: Illustration of the Craik-O'brien-Cornsweet illusion.

Several forms of the neon color spread illusion have been described in the literature (see Bressan et al., 1997 for a review). Two of them are shown in Figure 2.

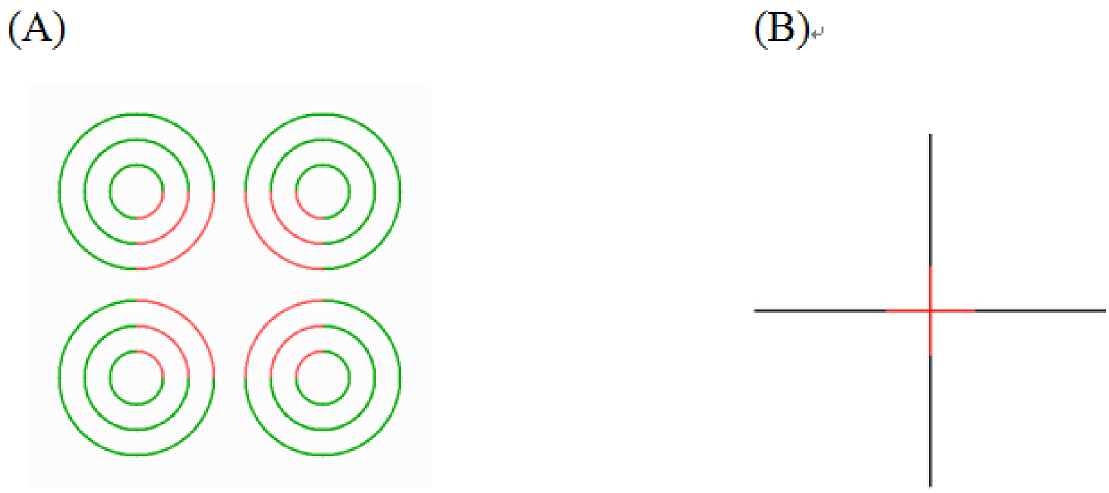

Figure 2: The neon color spread. (A) The version by Dario Varin; (B) The version by Tuijl (Bressan et al., 1997).

In all forms of the neon spread illusion, the color of some fine line pattern bleeds into the surrounding background, making a shaped area tinted with the color of the fine line.

We figured that the above two illusions have the potential of increasing available colors in a mosaic without having to increase the number of physical colors of the tesserae. Two sets of psychophysics experiments were carried out to determine the optimal parameters for creating the strongest color effect.

2. METHOD

The first set of psychophysics experiments manipulated (1) grain size of the tesserae, (2) the width of grout lines, (3) the slope of luminance grading, to map out the optimal range of these parameters. In the second of experiment, the effect of: (1) size of the tesserae, (2) the width of grout lines, (3) the color of grout lines, on the magnitude of neon color spread were measured with the method of adjustment

2.1 Materials for studying the discrete version of COC illusion

Figure 3 shows the discrete version of the COC illusion along with a blown up view the lluminance profile near the Cornsweet edge. To use the method of constant stimuli to gauge the magnitude of illusion, there are five levels of luminance difference spanning from significantly brighter to significantly darker between the left and the right half of the stimuli. The subjective eqality point was derived from the psychometric function as the index to the strength of the illusion.

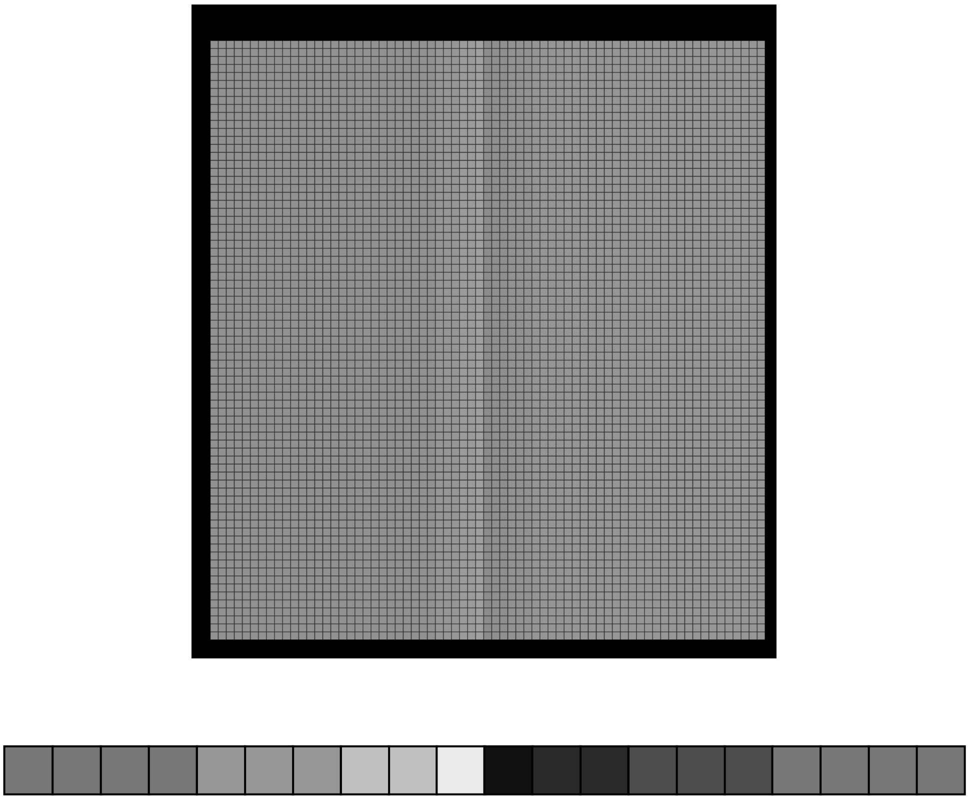

Figure 3: The discrete COC stimulus used in the first set of experiment. Notice that the grain size, line width, and the slope of the luminance gradient were manipulated in this experiment.

2.2 Experimental Procedure for studying the discrete version of the COC illusion

A typical method of constant stimuli procedure was adopted in this eperiment. The participant was asked to judge whether the left half of the stimulus looks brigher than the right half. There were 30 trials for each of the five luminance difference level, making the total number of trials 150 in a complete session.

2.3 Materials for measuring the magnitude of the neon color spread illusion

In the second set of experiment, we used method of adjustment to measure the effect of the neon color spread. The stimulus layout is illustrated in Figure 4.

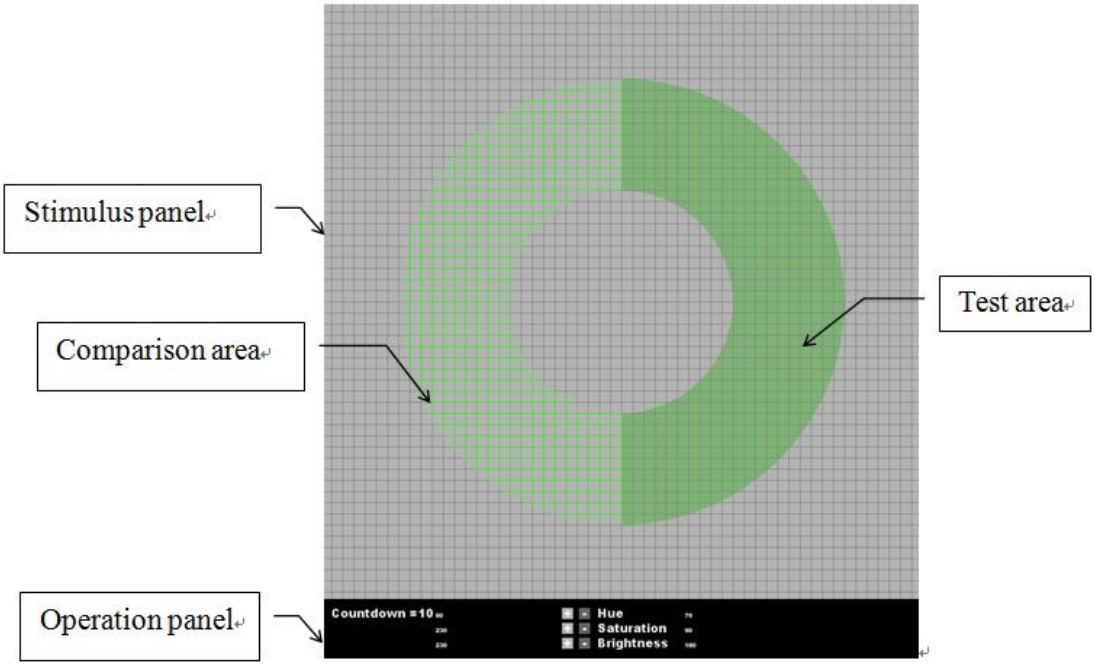

Figure 4: Stimulus layout and the operation panel in the neon color experiment. Notice that the between-line space in the comparison area is of the identical grey of the rest background. The color of the between-line space is subject to the participant's adjustment.

2.4 Experimental Procedure for neon color experiment

The participants needed to adjust the color appearance of the color of the between-line space in the test area utill it matches that of the comparison area by controlling the hue, saturation, and the brightness slide bars on the operation panel.

3. RESULTS

3.1 The COC eperiment

Effect of Grain Size Of the two levels of grain size used in this study (10 x 10 pixels vs. 20 x 20 pixels), we found a tendency of obtaining larger illusion effect with bigger grains. However, the difference is not statistically significant (p=0.27 > 0.05).

Effect of Line Width Of the two levels of line width used in this study (1 vs. 2 pixels), we found a clear pattern of larger line width produces stronger illusion effect (p=0.02).

Effect of Luminance Slope Of the two levels of luminance slope used in this study (on average, 15 units/step vs 22.5 units/step), we did not find significant difference in the illusion strength (p=0.88).

3.1 The neon spread eperiment

Effect of Grain Size The effect of grain size was very significant in the neon experiment (p<0.01), the bigger the grain, the stronger the sense of neon spread was iduced.

Effect of Line Width The effect of line width was also very significant in the neon experiment (p<0.01), the wider the line, the stronger the sense of neon spread was iduced.

Effect of Hue We tested four different hues, red, yellow, green, and blue, the results being that green was significantly more potent in inducing neon spread than all other hues, and there was no difference among red, yellow, and blue.

4. CONCLUSIONS

We found, in the computer simulation mode, great effect of both the COC and the neon color spread illusion in discrete forms. The magnitute of the COC illusion is relatively stable across all levels of parameters tested in this study, only significantly modulated by levels of line width.

In the case of the neon color spread, the effect is not only more dramatic but also much easier to apply to real art creation. The artist can apply chosen colors to grout lines, and the area circumscribed by the line would be tinted with the colors. The effect is somehow hue-dependent. Of the four basic colors tested in this study, green bleeds most aggressively. Both the size of tesserae and the line width affect the magnitude of the illusion.

To check whether our conclusion holds for reflective instead of illuminating surface (Bressan, 1995), we did an informal comparison with physical Ehrenstein figures (Ejima et al., 1984) as shown in Figure 5. The general patterns hold in the physical version. However, the size of illusion becomes smaller in the real version.

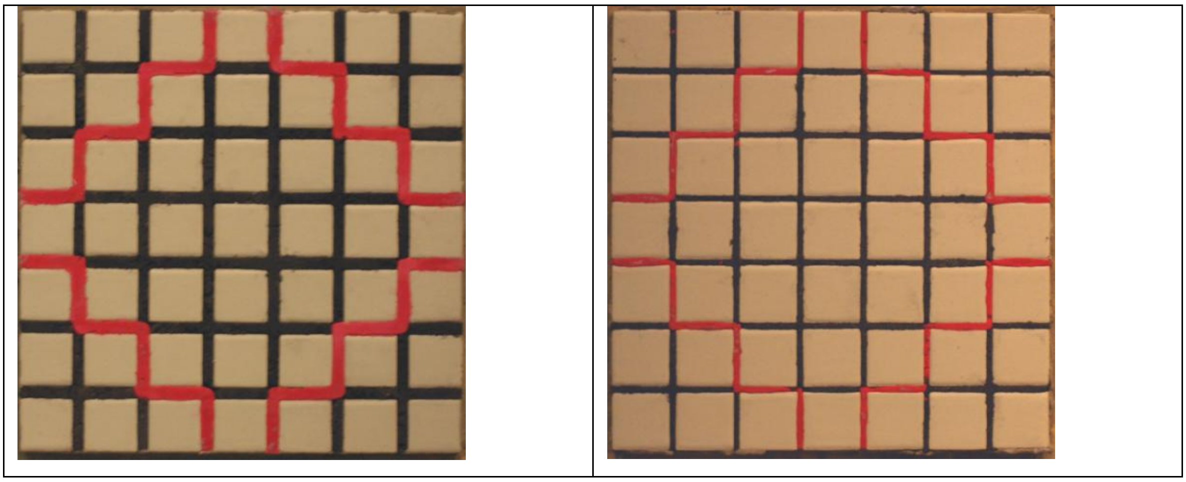

Figure 5: Two physical Ehrenstein figures of different line widths.

ACKNOWLEDGEMENTS

This research was supported by Taiwan's National Science Council (95-2411-H-009-019).

REFERENCES

Bressan, P. 1995. *A closer look at the dependence of neon color spreading on wavelength and illuminance*. Vision Research (35) 375-379.

Bressan, P., E. Mingolla L. Spillmann and T. Watanabe 1997. *Neon color spreading: a review*. Perception (26) 1353-1366.

Cornsweet, T. N. 1970. *Visual perception*. NY: Academic Press.

Ejima, Y., C. Redies S. Takahashi and M. Akita 1984. *The neon color effect in the Ehrenstein pattern: Dependence on wavelength and illuminance*. Vision Research (24) 1719-1726.

Locktov, J., & Clagett, L. P. (2002). *The art of mosaic design*. Rockport Publishers

Redies, C. and L. Spillmann 1981. *The neon color effect in the Ehrenstein illusion.* Perception (10) 667-681.

Address: Prof. I-Ping CHEN, Institute of Applied Arts,
National Chiao Tung University, 1001 University Road, Hsinchu, Taiwan 300, ROC
E-mails: iping@faculty.nctu.edu.tw,

Are There Ugly Colours?

Ilona Huolman
Helsinki Metropolia University of Applied Sciences
Degree Programme in Technology and Design

ABSTRACT

This paper presents a case study of my colour education classes, how students of Graphic-, Textile- and Industrial Design investigate and intentionally express their concepts of disharmony.

For centuries artists have asked what kinds of colour combinations are harmonic, affording aesthetic pleasure to the viewers. In the Finnish art education, teaching of colour relationships is still largely based on traditional notions of harmony. Many kinds of theories have been formed of colour harmonies. We have seen endlessly beautiful, harmonic paintings, all kinds of images in the different media. Colour harmony based on abstract and formal ordering, unity, balance or pleasantness has to a large extent ceased to motivate artists (Arnkil 2013).

What does the opposite, disharmony, mean? If harmony affords aesthetic pleasure and "tranquillity of mind", does disharmony afford aesthetic discomfort and "disturbance of mind"? How can we create aesthetic discomfort? It raises conflicting feelings when there is no visual hierarchy and equal "visual powers" are fighting with each other causing frustrations and aesthetic discomfort. If the main message is not clear nor do we even know what to look for first in the disharmonic picture that might cause the feeling there is something unknown and repulsive and something even scary to us.

The target of ugliness in the meaning of disharmony is, generally speaking, difficult for the students to achieve. Is it possible to achieve disharmony at all? It is also a kind of paradox that when students try to create chromatic harmony and beauty they fail, whereas when their primary task is to create disharmony they achieve something very interesting, fresh and good looking, something they would never have achieved, had they worked in the accustomed manner.

1. INTRODUCTION

In my colour education, it is most important that the students learn to develop efficiently their sensibility to make their own exact observations of colours. I use a number of exercises where students are learning by doing. This case study exercise is one of them. When they are painting and working with coloured papers (Josef Albers 2006) they have to make and analyse their own perceptions of different colour interactions in different colour comparisons. Become good visual professionals, e.g. designers, students should learn to open their eyes, understand what they see and how they react as individuals when they look at colours in any environment.

Colour harmony is the subject of endless texts offerings advice to the artists and designers and generally speaking disharmony is mentioned to be the opposite, something disturbing or unusual. If harmony is related to beauty, is disharmony related to ugliness? In the exercise, their tasks were to create an as disharmonic painting as they can and make observations of their own way to solve the question of disharmony. Officially disharmony was defined as the opposite visual term of harmony. In my opinion, disharmony is a visual term which means there is no visual hierarchy and the main message is not clear nor do we even know what to look for at first in the disharmonic picture. These kinds of aspects cause frustrations and aesthetic discomfort. Here is my "theoretical" example of disharmony. It represents at the same time visual chaos: the elements are distributed randomly, there is no rhythm and no visual cohesion (Figure 1).

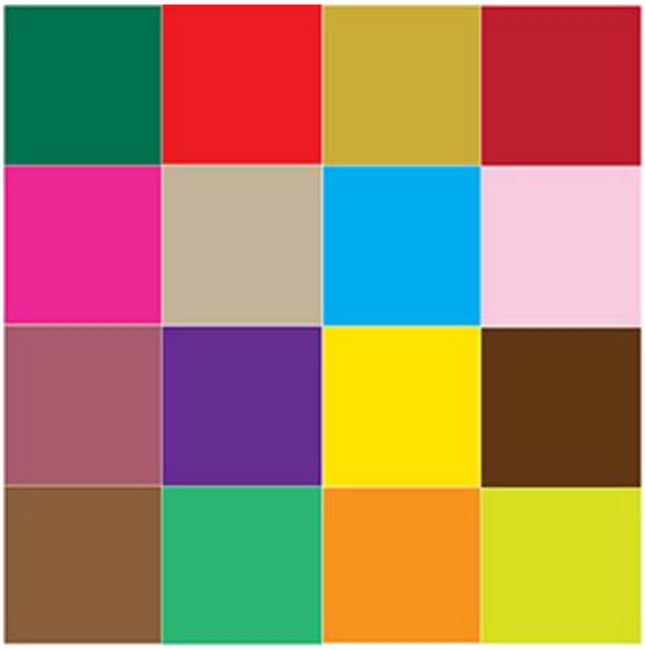

Figure 1: Example of disharmony.

2. METHOD

The exercise is simply called "Disharmonic painting". Instructions for the exercise were to discuss the visual terms "harmony" and its opposite, "disharmony". The students should think and ask themselves if harmony affords aesthetic pleasure and tranquillity of mind and what does disharmony afford? How can I create aesthetic discomfort? What does disharmony mean personally to me?

The students should not be shown examples of disharmony. Instead, they should think visually and make sketches about what kind of compositions and colours will establish disharmony in the best way in their own opinion. The topic could be approached freely. Finally, they should execute a disharmonic painting which is as disharmonic as possible in size A3 with gouache or acrylic colours.

The first reactions of the students after receiving instructions to the exercise "Disharmonic painting" are always disbelief and laughter. They think "disharmonic painting" is very easy and fast to do. It is usual that they have never tried to paint in a disharmonic way an "ugly" painting before.

In general, they begin to paint with the "ugly colours", with colours and compositions they hate. The painting processes are very interesting to follow as a teacher. When the processes approach the end, many students begin to express their amazed feelings and observations: their paintings are not so disharmonic although they tried to use "ugly colours" and imperfect compositions!

3. RESULTS AND DISCUSSION

The students tried in general to establish disharmony by establishing ugliness. There were two main approaches. The subject is narrative and there is something odd, disgusting and even scary about it. Another general topic is an abstract composition with a lot of colours. The students´ most common arguments for their disharmonious paintings were: disgusting topic, restless composition and ugly colours meaning for example colours with low saturation for example browns, greens with strong yellows, reds and blues. The second most common arguments had to do with "too many colours". They used more colours than what they usually do. They mixed new colours they never used before and what they had not liked at all.

It was interesting to share and discuss notions of what constitutes disharmony and ugliness after all. The students noticed that disharmony and ugliness are not always the same thing. Disharmony is a visual term and ugliness is quite a subjective and also a cultural learned matter. Disgusting topics include for example establishing instructively cultural and individual notions of ugliness. What ugliness means is more of a philosophical matter in our time and in our western culture now.

What constitutes disharmony in the picture? We drew a conclusion that all these anomalous colours, contrasts, details and compositions did not produce absolute disharmony in the meaning of totally aesthetic discomfort or chaos. Instead, disharmonic elements, anomalies created visual tension and fresh attractiveness. In that way their alleged disharmony turned into harmony in the meaning of affording aesthetic pleasure.

In the end, the students learned to understand that harmony and disharmony are equally important in art, graphic design and in all visual expression. With both harmony and disharmony highly interesting contrast can be created. The students also learn that there are no ugly colours in the absolute meaning: their ugly colours turned out to be the opposite in the way they used them.

I have had this exercise "Disharmonic painting" at my colour education now for many years. Always as the students failed in their task, finding it hard to achieve the set goal of disharmony, frustration set in. It feels paradoxical, even absurd, to fail when you have been allowed to do just that in the beginning, to create a disharmonious or as they think in general, "an ugly picture instead of a good looking one". At the same time this exercise has encouraged the students to create something different and new to themselves. I often heard:" I would have never done anything like this without the exercise!" That has been a way to exceed themselves and has given them a strong feeling of success after all. By giving up preference for harmony, they accepted dissonance to be as desirable as consonance (Albers 2006).

4. CONCLUSIONS

We achieved a kind of harmony through disharmony: A disharmoniously coloured painting can also afford aesthetic pleasure. We considered dynamic harmony in the way Josef Albers describes it: "Besides a balance through colour harmony, which is comparable to symmetry, there is equilibrium possible between colour tension, related to a more dynamic asymmetry" (Albers 2006).

Conclusions are in general that if there is no absolute colour harmony there is no absolute colour disharmony either. Also there are no absolutely ugly or beautiful colours but a very large and rich spectrum of different colour combinations. There are no absolutely failed compositions either. Everything depends on what we need in a certain actual context. Historical, cultural and individual qualities define how we understand the terms harmony and disharmony in a Western culture. These visual terms are not direct synonyms to the adjectives beauty and ugly.

Neuroscientist Beau Lotto expresses in his studies (Lotto 2013) that he learned to foresee what the next colour is people would choose when they can freely combine different colours at Lotto´s experiment. He said that we like to use side by side colours in the same way they occur in nature because we are used to that.

But we have seen in art history how new colour combinations could also be beautiful after we have become accustomed to them. Impressionism, Fauvism and Expressionism were at first badly received and their colours regarded as most disharmonious and ugly (Honour & Fleming 1992) but their works are highly valued today. These trends taught us to see a new kind of beauty and harmony. The students will be these agents of cultural evolution of colour images in the future.

ACKNOWLEDGEMENTS

I will acknowledge my mentor and colleague Harald Arnkil for wise comments and support to my study.

REFERENCES

Albers, Josef 2006. *Interaction of Color* 42-43.

Arnkil, Harald 2013. *"Colour harmony: from dualism to living perception". Proceedings of the AIC 2013: 12th International AIC Congress.* Lindsay MacDonald, Stephen Westland, Sophie Wuerger (eds.)The Colour Group (Great Britain).

Honour H. & Fleming J. 1992. *A World History of Art* 601, 652-653.

Lotto, Beau 2013. *Do you see the same than me?* Horizon, BBC/ Prisma Document, Yle Finland.

Address: MA Ilona Huolman, Degree programme in Technology and Design,
Helsinki Metropolia University of Applied Sciences, Lummetie 2,
FI-01300 Vantaa, FINLAND
E-mail: ilona.huolman@metropolia.fi

A novel experience in color teaching: Master in Color Design & Technology

Alessandro RIZZI,[1] Maurizio ROSSI,[2] Cristian BONANOMI,[1] Andrea SINISCALCO[2]
[1] Dept. of Computer Science, Università degli Studi di Milano
[2] Dept. of Design, Politecnico di Milano

ABSTRACT

Experiences in the teaching of color are central to the AIC community. The difficulties in this goal are due to the intrinsic multidisciplinary nature of color and to its many different possible applications and related technologies. Moreover, colors have emotional, cultural and symbolic valences and designing with color can sometimes look like a matter of personal preference. In order to be able to teach all aspects related to color and make the student experience them, Università degli Studi di Milano and Politecnico di Milano have organized in the 2014-2015 the first edition of the Master in Color Design & Technology with the aim of providing in-depth training in the complex field of color design and color technology. The master aims at forming professionals able to manage the technological and design complexities of using color in creative and industrial processes and in many application domains: from industrial product design to interior architecture, from communication to fashion and entertainment, and even in designing the urban environment. The master's program is organized in two separate learning phases. The first phase is theoretical, while the second part consists of project works to make students apply what they have learned in the fundamentals in scenarios of typical color design. At the end of all these modules, students are called for an internship in one of the companies or research centers related to the master.

Figure 1: Three moments involving the students, during the lessons: From left: practicing with a spectrophotometer, in the middle: using color atlases, at right: exercise for the Design Week about color trends.

1. INTRODUCTION

The Master, organized by Politecnico di Milano and Università degli Studi di Milano, aims to provide in-depth training in the complex field of color design and technologies, to form professionals able to use color in creative and industrial processes and in numerous application domains. Before being allocated in the internship the students completed the two learning phases that constitute the training part of the Master. The first phase, conducted at the Università degli Studi di Milano, is theoretical, and it is divided in four modules: perception and color history, colorimetry and color systems, digital color and color application. The second, held at Politecnico di Milano, part consists of five project works to make students apply what they have learned in the fundamentals in five scenarios of typical color design: color for communication, color for fashion design, color for interior design, color for industrial product design, color for urban space. In the following, details about the two phases are presented.

2. DIDACTIC OF THE MASTER

2.1 The theoretical fundamentals

Perception and color history

The aim of the first module was to present culture and color history, and the aspects of perception that are the basis of its complexity. The perceptual mechanisms that affect the color and vision in general have been examined in order to enable the students to recognize and design them.

Colorimetry and color systems

Although color is a subjective characteristic, colorimetry is needed to measure, standardize, communicate and represent in an accurate way the color of a surface or a light source. The theoretical basis of perception, colorimetry, photometric and radiometric measures have been presented in this second part as well as the color atlases, an alternative way to select, represent and communicate color. The module presented the essential technical skills that are the basis of the color designer, whatever the application areas on which it will choose to specialize in the future. The fundamentals have been presented both through frontal lessons, and practical or laboratory activities. Students have been encouraged not only to understand the laws that govern, i.e. a spectrophotometer, but also to learn how to use it correctly.

Digital color

With the diffusion of new technologies, more and more aspects of communication and color reproduction are becoming digital. In this module theoretical and practical fundamentals for manage, view and reproduce the digital color applied to different media have been provided, with particular attention to the limitations and problems associated with the use of different devices and color profiles.

Color applications

The success of a project that requires the conscious choice of colors depends on the experience, the preparation and the diligence of the designer. This module showed how the knowledge acquired in the previous modules can be applied in most professional fields and applications, through examples and case studies deriving from different contexts: marketing, visual communication, restoration of cultural heritage, photography, architecture, product and lighting design and more. A week later the beginning of the Master, in Milan started *the Design Week*, one of the most important world event related to the topic of design. Students were asked to actively participate to the event, looking for future trends in colors and finishing and reasoning about the change in the use of colors, in terms of decorations and schemes, from 1950s to now and more.

2.2 The project works

Color for communication

This module focused on the function and communicative dimension of color within the project of Communication Design. The idea focus on the fact that each communicative artifact arises from a series of choices that fit into a well-defined design process. The design and implementation of a brand start from the visual identity (name, brand, logo, lettering, packaging, integrated communication) that ensures the recognition and affirmation of the company. It is clear the importance of color in this strategy: the visual identity is built on the evocative and persuasive aspects of the chromatic language.

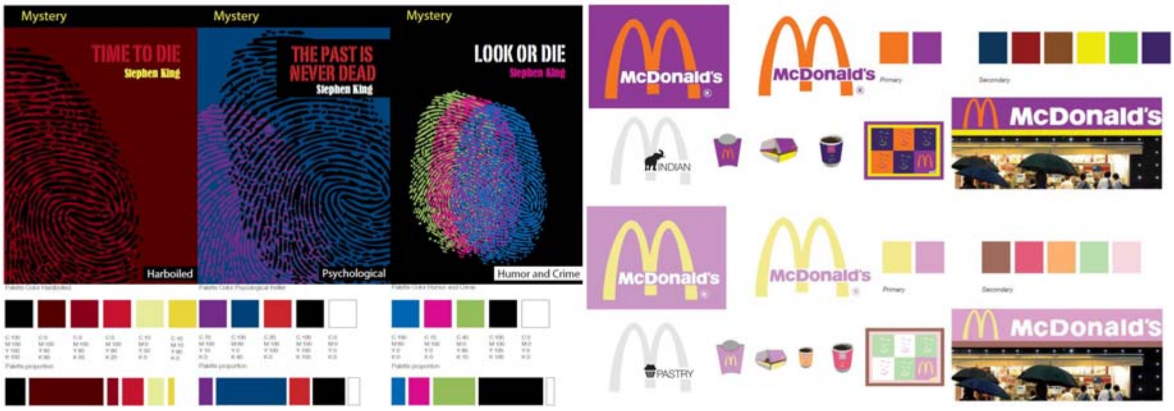

Figure 2: Project Work "Color for communication" teachers Elena Caratti and Elisabetta Del Zoppo, works of Sandra Niggl, Simona Troiano, and Sara Ubaldini.

Color for fashion design

This project work is dedicated to the study of the color texturing in fashion with the aim of being able to offer the same product with different color variation, in order to reach culturally different markets and to offer the sensation of a personal choice to individual consumers. The starting point is the construction of the color palette, composed by individual colors, for the fashion collection, combined in two or three main approaches in relation to the messages conveyed, their aesthetic and social characteristics. The basic concepts of pigments for dyeing and printing textiles as well as the quality standards for the marketing of fashion products have been presented: clothing, footwear and accessories.

Figure 3: Project Work "Color for fashion design" teachers Nello Marelli and Renata Pompas. On the left work of Francis Wild. On the right, students at work.

Color for interior design

The project work on interiors design is dedicated to the analysis of the application possibilities of a chromatic design, for the creation of innovative retail spaces, that can ensure a harmonious relationship, with the values from the image communicated by the brand and corporate identity. Starting from practical applications, examples of different approaches to retail design have been shown, proposing a new type of commercial space (permanent or temporary) where the color is integral part of the experience design.

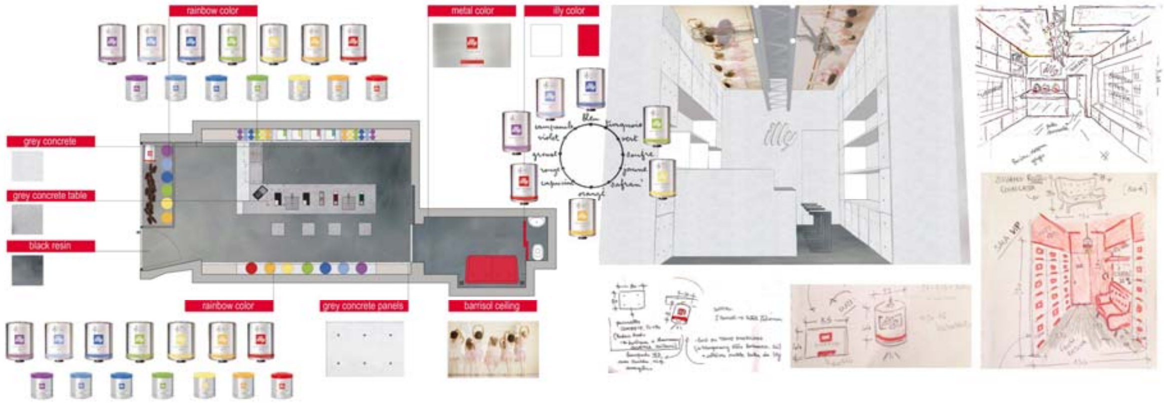

Figure 4: Project Work "Color for interior design" teachers Arturo Dell'Acqua Bellavitis and Lorenzo Morganti. Work of Costanza Fausone and Ilaria Sarà.

Color for industrial product design

The aim of this project work is to develop a methodology to design through the simulation of a CMF project (Color/Material/Finishes) of a real product (a branded coffee machine in the specific case). The students have gone through all of the methodical phases needed for the definition of the identity of the product: study of the market (position, competitors…), study and definition of the target, study of CMF trends in the sector and creation of CMF scenarios. The CMF responsible for the De Longhi group taught to the class about tendencies, brought samples of the colours used at present on the market and a new prototype ready for the commercial launch. After this first part students have gone through the proposal phase with the design of colours, materials and finishes to apply to the new product. The final output for the presentation have been shown also to the responsible from De Longhi that integrated the notes of the teachers with comments based on their experience on the real market.

Figure 5: Project Work "Color for product design" teachers Stefania Perenich and Francesca Valan. Work of Suheir Darhouth, Beatriz Travieso and Joni Kirk.

Color for urban space

This part of the master program dealt with the close relationship between architecture and urban space. The aspects related to the interaction between the human being and the natural environment has been analyzed. It will be highlighted the role of the "perceptual project" for the growth of civic and urban identities. The module analyzed the issues related to the phenomena of perception and color in the urban scale by providing theoretical and procedural tools with the support of pictures, cognitive maps and case studies.

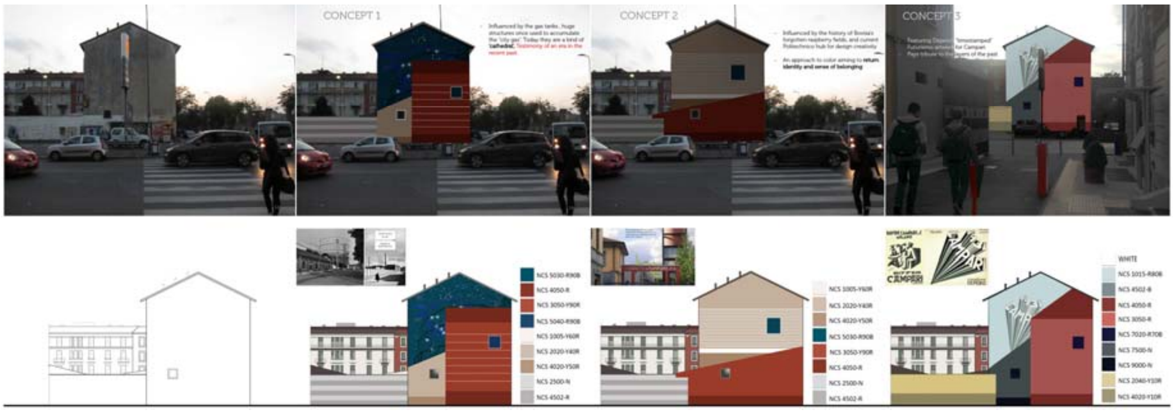

Figure 6: Project Work "Color in urban spaces" teachers Giulio Bertagna and Aldo Bottoli. Work of Salma Hussein and Tanja Polegubic.

Interim checks on students' learning progress are scheduled both for the theoretical part and the project works, where they have to work in group to present a final project for each module. After the internship they have to provide a final report considering goals achieved and skills developed during the experience that will be judge by the academic board during the final exam.

2.3 Empowerment

Some hours of the master program have been dedicated to the company empowerment: some of the companies (NCS, Barbieri, Mammafotogramma, Flukso, Barco, X-rite, Konica Minolta, Fontegrafica, Mantero, Missoni, Elementi Moda, F.lli Giovanardi, Oikos, De Longhi, Nankai Co Ltd, Merck, TIGER Coatings GmbH & Co. KG and Materis Paints) willing to host interns came in the classroom to tell their story and explain why there is the need of a color expert. They also brought devices and materials to show to the students. Moreover, were made two visits to companies that deal with color design: Clariant Color Work and Lechler, who opened us the doors of their laboratories. Empowerment supports the student's process of personal and professional growth by developing development the ability to form relationships and to work successfully in a variety of dynamics.

3. CONCLUSIONS

We are working to launch the second edition of the master. The teaching staff will receive useful information from the interviews that we are doing to the students, faculty, and the companies involved. Meanwhile we are writing this paper, the first edition of the Master in Color Design & Technology is ending. The students, coming from all around the world

(Italy, Australia, Germany, Egypt, Lebanon, Colombia), are engaged in the internship at one of the many companies related to the Master, in view of the final exam, in March. The hosting companies operate in various sectors: chemistry, fashion, product design, and measurement instrumentation as demonstration that color has a multidisciplinary nature and many different applications.

ACKNOWLEDGEMENTS

We would like to thanks: Associazione Italiana Colore, Konica Minolta and SIOF for the patronage and sponsorship; Lechler, Missoni, Barbieri, Materis Paint, Boero Group, Ceramica Vogue, Barco, Mamma Fotogramma Studio, Flukso, Federchimica AVISA, Digiworld, Elementi Moda s.r.l., Create, OIKOS, GMG-Color, X-Rite Pantone, Mantero, FlintGroup, Clariant, Fontegrafica, NCS, Coop la Meridiana, Chiron Sas, Eurojersey, Studio Valan, Progetto Iride and Unione Industriali di Como for the success of the Master. Finally, thanks to the teachers of the master for their dedication and professionalism.

BASIC REFERENCES OF THE MASTER

Ball, P. 2003. *Bright Earth: Art and the Invention of Color*, University of Chicago Press.

Berlin, B. and P. Kay 1969. *Basic Color Terms: Their Universality and Evolution.* University of California Press.

Braddock, S.E. M O'Mahony. 1999. *Techno Textiles: Revolutionary Fabrics for Fashion and Design*. Thames & Hudson.

Fletcher, A. 2004, *Beware wet paint*, Phaidon.

Hoffman, D. 2009. *The interface theory of perception: Natural selection drives true perception to swift extinction*. In Object categorization: Computer and human vision perspectives, S. Dickinson, M. Tarr, A. Leonardis, B. Schiele (Eds.) Cambridge, UK: Cambridge University Press, 148–165.

Hunt, R. W. G. 2004. *The Reproduction of Colour. 6th Edition*. Wiley.

Lefteri, C. 2001. *Plastic, materials for inspirational design*, Rotovision.

McCann, J.J. A. Rizzi. 2011. *The Art and Science of HDR Imaging*. Wiley.

Oleari, C.1998. *Misurare il colore*, Hoepli.

Ramanath R., W. E. Snyder, Y. Yoo, M. S. Drew , 2005. *Color image processing pipeline,* IEEE Signal Processing Magazine 22(1) 34-43.

Wyszecki, G. W.S. Stiles. 2000. *Color Science: Concepts and Methods, Quantitative Data and Formulae, 2nd ed.*, Wiley.

Address: Prof. Maurizio ROSSI, Department of Design, Politecnico di Milano,
Via Durando 38/A, 20158 Milano, ITALY
E-mails: alessandro.rizzi@unimi.it, maurizio.rossi@polimi.it,
cristian.bonanomi@unimi,it, andrea.siniscalco@polimi.it

The ambiguous term of "saturation"

Karin FRIDELL ANTER, Harald ARNKIL, Ulf KLARÉN
SYN-TES Nordic Interdisciplinary Network on Colour and Light

ABSTRACT

Ambiguous use of colour terms creates misunderstandings in the colour classroom, among professionals and in customer services. One obvious example is the term *saturation. Saturation* is not a common colour term in everyday language, but is widely used in the professional languages of art, design and science. There it has got several parallel definitions. In art and design parlance it most often refers to the "intensity" or "vividness" of a colour much in the same sense as NCS *chromaticness* and Munsell *chroma.* It can also be used as an equivalent of "depth", where "deep colours" and "strong colours" are not the same. NCS uses *saturation* for the relationship between chromaticness and whiteness, a variable that cannot be perceived, where the calculated values have no logical connection to perception and which gives a totally ambiguous value to the black elementary colour. We understand the concept of *NCS-saturation* as a deviation from the NCS's solid foundations in human perception and suggest that it is reconsidered and possibly excluded from the NCS's set of parameters. *NCS-saturation* is one of many attempts to categorise colours as deep or saturated in a meaning that does not coincide with their chroma/ chromaticness. Other similar attempts have been made by, among others, Tryggve Johansson, who created a previous version of the natural colour system, and also within the NCS as a "dual attribute" called deepness. We see the need for further investigations of the perceived colour quality of depth.

1. INTRODUCTION

Ambiguous use of colour terms creates misunderstandings in the colour classroom, among professionals and in customer services. One obvious example is the term *saturation* (German *Sättigung*, French *saturation*, Spanish *saturación*). *Saturation* is a generic word that one nevertheless seldom comes across in casual speech about colour. It is widely used in professional languages of art, design and science, though, and there it has got several parallel definitions. To add to the confusion, the words *chroma, chromaticness*, *chromaticity*, *purity* and *colourfulness* are also used, referring to more or less the same thing.[1]

2. *SATURATION* IN ART AND IN EVERYDAY LANGUAGE

The word *saturation* comes from the Latin word *saturare* (*satur* full). In everyday language*, saturation* is not a common colour term, but in art and design parlance, it is widely used, most often referring to the "intensity" or "vividness" of a colour much in the same sense as NCS *chromaticness* and Munsell *chroma.*

[1] Arnkil et al. 2015 includes discussions on several difficulties in colour terminology.

The term *saturation* features in digital colour management in the colour models HSL (Hue, Saturation, Lightness) and HSV or HSB (Hue, Saturation, Value/Brightness). Both HSL and HSV/HSB are cylindrical colour spaces, but with different mappings of the colour variables, resulting in two dramatically different interpretations of *Saturation*.[2] The term *saturation* is also used in chemistry, referring to the limit where a fluid cannot resolve more of another substance. In painting it can similarly refer to the concentration of the pigment or to the relative contents of chromatic pigment and white. These relative contents affect the chromatic properties of the painted surface differently depending on the pigment. Some pigments, such as yellow ochres, yield their most intense appearance unmixed. For those, *chemical saturation* and *chromaticness* coincide. Other pigments, notably blue ones, such as deep ultramarine, become more chromatic when mixed with a little white. For those, the visual property yielded by maximum chemical saturation could be called *depth*.

3. *SATURATION* IN COLORIMETRIC LANGUAGE

In the context of a colorimetric colour space the saturation of a colour can be understood as its proximity to its fully chromatic outer limit (Billmayer & Saltzmann 1981 p50) In Hermann von Helmholtz's words, saturation is the proportional mixture of "white" and pure monochromatic light of equal brightness. The same thing is said by Rolf Kuehni, who also clarifies how colorimetric language makes a distinction between *saturation* and *chromaticness*. Varying the brightness of a coloured lamp in total darkness is equivalent to varying its chromaticness. The brighter a red lamp shines, the higher its chromaticness. Kuehni concludes: "Chromaticness is an absolute measure of chromatic content of a colour regardless of its brightness, while saturation is a measure of the chromatic content of colours of equal brightness" (Kuehni 1983, p39f).

4. NCS *SATURATION*

In the NCS system, developed by the Judd award winning researchers Hård, Sivik and Tonnquist based on the findings of Ewald Hering (Hering 1964), saturation is used in a way that clearly differs from *chromaticness*. In the following text we refer to this as *NCS-saturation*. According to the definition given in the NCS atlas, colours that lie on a straight line from *NCS black* (S) possess equal saturation; thus *NCS-saturation* is defined as the relationship between *chromaticness* and *whiteness*. The illustration in the NCS atlas gives numeric values for each of the shown three lines (m=0,25, m= 0,50, m=0,75) where *m* refers to the Swedish word *mättnad*, which is used for the same concept as *NCS-saturation* (Svensk Standard 2004). (Fig. 1) The comprehensive scientific presentation of the NCS (Hård et al. 1996 p 188), gives the following equation for *NCS-saturation*:[3]

$m = c/(c+w)$ (m: NCS-saturation, c: chromaticness, w: whiteness)

Colours that possess equal *NCS-saturation* constitute what is called a "shadow series", a term that we find similarly used in the Ostwald system (Ostwald & Birren 1969). They

---

[2] Wikipedia. http://en.wikipedia.org/wiki/HSL_and_HSV. Accessed 15.2.2015.

[3] In the comprehensive Swedish presentation of NCS (Hård & Svedmyr 1995), the NCS research team instead defines *mättnad* as m=c/w. This means that *m* can vary between 0 and ∞, which would give other figures in our discussion about *NCS-saturation* but not alter the principal conclusions.

display the perceived variation of a single coloured surface (or object) in an idealised progression from fully lit to totally shaded, approximating the perceived gradient of colour in a depiction of a round or cylindrical object in directional light.[4] Thus the concept of *NCS-saturation* does not (and does not claim to) refer to "vividness", but instead denotes a colour property that could rather be interpreted as "depth".

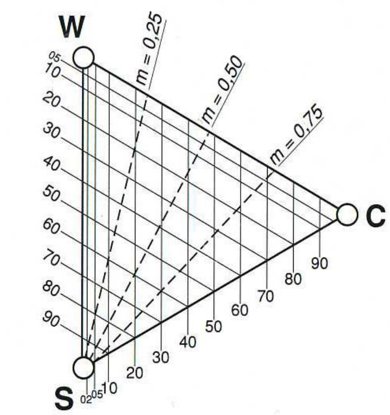

Figure 1: Lines of equal NCS-saturation, from NCS atlas 2004. The lines in the atlas are not precisely drawn – according to the definition the line for m=0,50 should go from S to the nuance 0050 and the line for m=0,75 from S to the nuance 0075.

Tryggve Johansson, who developed an earlier version of the natural colour system, also uses the concept of saturation (Swedish *mättnad*) in a similar way. He explicitly distinguishes between saturation and *colour strength* (Swedish *färgstyrka*), and uses *saturation* as a synonym for *depth.* He also presents the idea of *oversaturated* (övermättade) colours, by which he meant colours that are deeper than the colour that has maximum colour strength. Yellow colours cannot be oversaturated – there is no yellow colour deeper than the strongest one – whereas green, red and especially blue colours can increase in saturation beyond the most chromatic colour (Fig 2) (Johansson 1952 p4-6; Johansson 1965 p22-24)[5]. In pointing out this difference between colours of blue and yellow hue, Johansson implicitly acknowledges an observation that also influences everyday language. Colours with bluish hues are also called blue when they have a great amount of blackness, whereas yellowish colours with the same blackness are called brown or olive (Berlin & Kay 1991, Sivik & Hård 1984).

It is unfortunate that the same word – saturation – has been given these different and partly contradictory meanings. Further analysis of the concept of *NCS-saturation* also shows that it is not perceptually consistent, but rather a mathematical play with the numerical values of abstract parameters. For example, in the case of nearly black colours that can barely be distinguished visually, the *NCS-saturation* varies between the lowest (0) and highest (1) possible value (see table 1).

---

[4] It should, however, be noticed that the colour gradient of shading in real spatial contexts depends on the complex situation and cannot be simplified to a straight line in a theoretical model.

[5] Also discussed in Hård et al. 1996 p181-183.

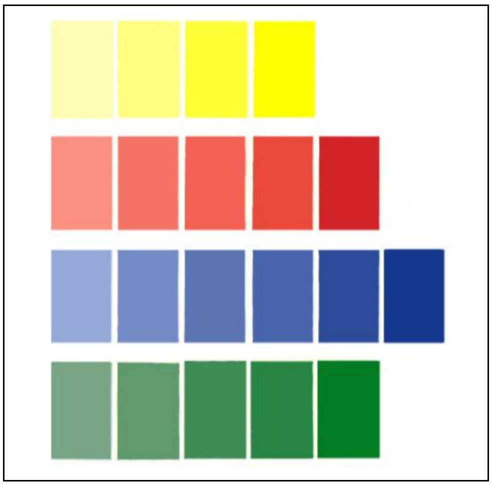

Figure 2: An illustration from Johansson 1965 p22, with Johansson's caption: "Note the difference between colour strength and saturation. The most saturated colours are placed furthest to the right. Those with the highest colour strength are placed as number four from the left." (Our translation and reconstruction of pixelated figure).

Table 1. Calculated NCS-saturation for nuances very close to elementary black.

Nuance	Blackness (s)	Chromaticness (c)	Whiteness (w)	m= c/(c+w)	
9900	99	0	1	0/1 = 0	On grey scale W-S
9800	98	0	2	0/2 = 0	On grey scale W-S
9700	97	0	3	0/3 = 0	On grey scale W-S
9901	99	1	0	1/1 = 1	On scale S-C
9802	98	2	0	2/2 = 1	On scale S-C
9703	97	3	0	3/3 = 1	On scale S-C
9801	98	1	1	1/2 = 0,5	
9701	97	1	2	1/3 = 0,33	
9702	97	2	1	2/3 = 0,67	

The table reveals that the grey scale between white and black has *NCS-saturation* = 0. Here *NCS-saturation* coincides with *chromaticness* in a way that creates no conflict with any of the generic meanings of *saturation*. The scale of deep colours, between black and the maximally chromatic colour C, offers much more problems. Here the calculated *NCS-saturation* is maximal. Thus absolute NCS-saturation is a quality of all chromatic elementary colours, whereas white has zero saturation. The NCS-saturation of elementary black cannot be mathematically calculated, and in the graphical NCS model, black is the end point of all lines showing NCS-saturation; this simply makes no sense. Thus, the concept of *NCS-saturation* is misleading in two ways. First, the term *saturation* is not a good choice, as it inevitably leads to thinking about other colour qualities than those referred to by *NCS-saturation*. More serious, however, is the fact that NCS, which is based on colour perception, introduces a variable that cannot be perceived, where the calculated values have no logical connection to perception and which gives a totally ambiguous value to the black elementary colour. This is not a matter of mere terminology - the concept of *NCS-saturation* would be as illogical and irrelevant to perception whatever it was called.

5. NCS DEEPNESS

In addition to *NCS-saturation*, the comprehensive scientific presentation of NCS includes a concept called *deepness* (Hård et al. 1996 p219). The term is tentatively suggested by the authors who point out that it may be ambiguous. Colours with deepness are characterized by a simultaneous resemblance to both black (S) and the maximal colour (C). Colours around the middle of the scale between S and C have the maximal deepness, according to this definition. Based on phenomenological analysis, the authors hypothesize that the deepness value (dv) can be calculated with the following equation:

$$dv = 40 \cdot s \cdot c/(w^2 + 1000)$$

This means that the nuance 5050 has maximal deepness = 100. Elementary black (S) and the maximal colour (C) both have deepness = 0, as does the white elementary colour. Lines of iso-deepness are shown red in Figure 3, which also shows lines connecting nuances with similar values of the analogically defined concepts greyness and clearness. The NCS authors call the three concepts "dual attributes". They mention that it is also possible to observe a corresponding category of colours that have simultaneous resemblance to two chromatic elementary colours. One example of such "dual attributes" is termed *orangeness*.

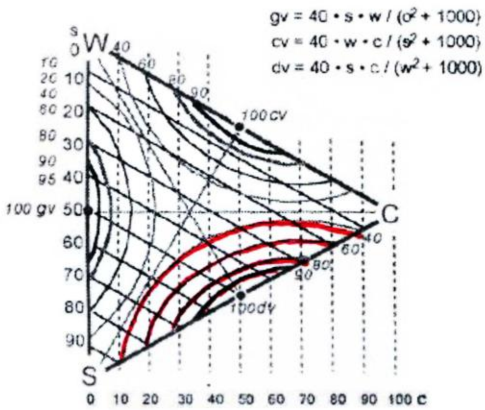

Figure 2: Lines of equal deepness, from Hård et al.1996 (Marked with red by us).

When looking at the colour triangle one can see some similarity between *NCS-deepness* and Tryggve Johansson's definition of *saturation*. For bluish hues, Johansson's maximally saturated (oversaturated) colour would approximately equal the nuance with *NCS-deepness* = 100. There is, however, an important difference: In Johansson's analysis, yellow colours cannot be oversaturated and the most saturated yellow nuance is the maximally chromatic one. In NCS, however, the concept of deepness is used irrespective of hue. Also Paul Green-Armytage (2002) indentifies a zone of “deep colours”. Starting from the nuance triangle of NCS, he treats all hues in the same way, but his zone of "deep colours" does not fully coincide with *NCS-deepness*.

6. CONCLUSIONS

Colours can be perceived as deep, in a meaning that does not coincide with their chroma/ chromaticness. There are a number of attempts to define this quality and arrange it into the order of a colour system, and here the term *saturation* is often used. We see the need for further investigations of the perceived colour quality of depth.

The colour changes caused by successive shading are an interesting field of study, and in this NCS is a useful tool for documentation and analysis of observed phenomena. It is then important to see the system as a tool, not as a model, and not force the dynamics and complexity of real life into symmetry and linearity.

The NCS has solid foundations in human perception of colours. We understand the concept of *NCS-saturation* as a deviation from this approach and suggest that it is reconsidered and possibly excluded from the NCS's set of parameters.

REFERENCES

Arnkil, H. (ed.) (2015). *Colour and Light - Concepts and confusions,* 2:nd edition. Aalto Univ. Art+Design+Architecture, https://shop.aalto.fi/p/208-colour-and-light/.

Berlin, B. & Kay, P. (1991). *Basic Color terms: Their Universality and Evolution.* Berkeley and Los Angeles.

Billmayer, F. W. Jr. & Saltzmann, M. (1981). *Principles of Color Technology*. Wiley.

Green-Armytage, Paul (2002). Colour Zones – Explanatory diagrams, colour names, and modifying adjectives. *9th Congress of the International Colour Association:* 861-864.

Hering, E. (1964). *Outlines of a Theory of the Light Sense* (Zur Lehre vom Lichtsinne. Wien 1878). Cambridge Mass.

Hård, A. & Svedmyr, Å.(1995). *Färgsystemet NCS. Tanke, tillkomst, tillämpning.* Färgantologi bok 1. Stockholm: Byggforskningsrådet

Hård, A, L. Sivik & G. Tonnquist (1996). "NCS Natural Color System - from Concepts to Research and Applications." *Color Research and Application* 21: 180-220.

Johansson, T. (1952). *Färg.* Stockholm

--- (1965). *Färgboken, färglära för praktiskt bruk*. Svenska Slöjdföreningen

Kuehni, R. (1983). *Color: Essence and Logic*. Van Nostrand Reinhold.

Ostwald, W. & F. Birren (Eds.) (1969). *The Color Primer*. Van Nostrand Reinhold.

Sivik, L. & A. Hård (1984). *Namn på färger*. Färginstitutet, Färgrapport F24.

Svensk Standard (2004). *NCS Färgatlas SS 19102:2004*. Stockholm: SIS.

Address: Prof. Karin Fridell Anter, Noreens väg 71, S-752 63 Uppsala SWEDEN
E-mails: karinfa@explicator.se, harald.arnkil@aalto.fi, ulf@klaren.se

Colour Education and Real Life Colour

Ulf KLARÉN, Karin FRIDELL ANTER
SYN-TES Nordic Interdisciplinary Network on Colour and Light

ABSTRACT

In this paper, we address three problems of traditional colour education: (1) The idea that colour education must base itself on simplified cases as it is seen as impossible to analyse complex perception. (2) The consequent formulation of a traditional "colour knowledge" that is too abstract to relate to our real life experiences. (3) The misunderstanding that subjective experiences are valid only for the experiencing individual.

We claim that colour (and light) education must take its starting point in complex situations based on real life experience, that theoretical and descriptive concepts must apply to such situations, and that it is to a great extent possible to describe complex human experiences intersubjectively.

Our conclusions are based on findings and approaches of the interdisciplinary research project 'SYN-TES' (2010-2011) treating colour and light as a coherent field of knowledge (Fridell Anter et al 2012). SYN-TES is summed up in a book on colour and light for humans, in a spatial context (Fridell Anter and Klarén 2014).

1. COLOUR EDUCATION

In most cases colour education focuses on colour phenomena as such, and without taking into account the visual spatial experience. Colour education has no coherent field of knowledge. The content has often been determined by causal needs from different interest groups. For example, the fact that colour education has set out from surface colours in even and uniform light is a pragmatic response to the needs of artists or designers who regarded colours as a tool for pictorial art and for pattern design.

The lack of a holistic approach is in part obscured by abstraction of colour from its natural function in the living context. Artists and educators have been preoccupied by the thought of reducing colour to systems. It has been professionally important to have the use of systems describing mutual relationships between colours. However, useful for particular purposes, systematizing means that colours are represented by notations and colour samples and thus abstracted from their normal context. The nominal colours described in colour systems often are regarded as the "true" and constant colours beyond the accidental colours experienced in the complex world around. Separated from the complexity, a variety of colour phenomena might be clearly demonstrated, but with no connection to a complex spatial world they do not contribute to knowledge related to our every day experiences.

The physical theory describing perceived colours as caused by spectral power distribution also contributes to the notion of colour as something detached from the living context of the world. The Japanese philosopher Januchi Murata remarks that Newton's dark chamber is a device in which a light phenomenon that is inseparable from spatiality is made up into a light phenomenon that is independent of spatial constitution (Murata 2007: 82).

With simplifications – or limitations – of a similar kind, education on light is often restricted to a technical approach using concepts based on a theory on the human visual systems' response to radiation, and to a large extent using physical measurements that cannot fully describe the complex dynamics of vision or the mutual nature of colour and light experiences.

To humans, the experiences of colour and light are mentally inseparable; colour and light together form our experience of space. Colours are an integral part of the human life-world; they are sensory qualities that are to be taken as “properties of the bodies which are actually perceived through these properties (Husserl 1970: 30). In this sense colours *are* the visual world and never appear isolated.

To conclude: The pedagogical problem of colour and light education is not too high a degree of complexity, but the opposite.

2. COLOUR AND LIGHT IN THE REAL WORLD

Colour and light education must take its starting-point from the human living and active relationship to the world around. Like all other living creatures, humans are naturally adapted to the surrounding world. We have our own specific perceptual ecological niche (Gibson 1979). Colour as such has no spatial extension, and colour separated from a spatial context is an abstraction; colour appearance without a connection to space is inconceivable. The human perceptual and cognitive systems – the mode of experience and the abilities to analyse and take stock of position in an ever-changing environment – are fundamental to human adaptation to the world around (Noë 2004: 1–3).

Perceptual adaptation is not limited to basic physiological reactions. It involves interplay between the individual and the world on many levels. These include the basic level of innate reactions (categorical perception), the level of perceptual understanding based on direct experience of the world, and the level of indirect cultural experience (Figure 1).

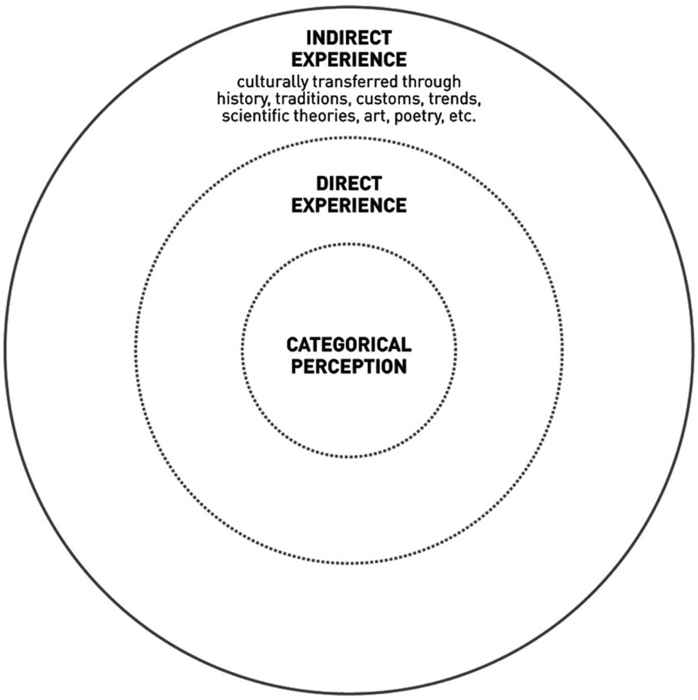

Figure 1: Experience levels (Klarén 2012: 25-28).

Colour and light experiences belong to the human perceptual niche and they have their distinctive features from this fact. They are properties of the world taken in relation to the perceiver or depend on both colour perceivers and their environment. (Thompson 1995: 177). Colour and light are natural, but non-physical (Noë 2004: 155). An absolute dichotomy between subjectivity and objectivity is thus hardly applicable to colour and light experiences.

The manifoldness of human colour and light experiences cannot be quantified or mapped in detail. But although our experiences are subjective by nature, our basic perceptual and mental conditions are functionally equal. Human experiences are largely intersubjective, and valid far beyond the individual. Each individual is a subject. However, by sharing and comparing experiences, individuals get a similar understanding of the world. When an external phenomenon is experienced and carefully described (in words and/or measurements) individuals can verify whether experiences of the phenomenon "fit" the description. This is the original core principle of empirical investigation. When it comes to colour and light experiences the only reality available to human senses is the human phenomenal world (Husserl 1936/1970:108-109).

3. A NEW PEDAGOGIC APPROACH

A pedagogy describing the coherent spatial interaction between colour and light calls for broad perspectives on aims and purpose of the human colour and light experience. Colour and light education should have its starting-point in phenomenology - in a wide sense of the word

It is possible to rationally describe and analyse colour and light within a complex context, but this requires other tools and concepts than those used in traditional colour and light education. People have a great tacit experience of colour and light in real life, and colour phenomena become clear and comprehensible only when they are discussed as part of a living everyday context, which is spatial by nature.

The interaction of colour and light in a living context may be successively analysed and understood by alternating systematic use of well-defined concepts and practice and reflection. There are as yet no widely applied concepts describing coherent spatial colour and light phenomena, and there is a great need for more research to develop useful methods and concepts. There are, however, a few approaches that have reached a certain spread. For example David Katz in the 1930s presented a number of concepts that names and defines appearance of colour in the spatial context, on surfaces, in transparency, in light sources, etc. (Katz 1935: 6f). *PERCIFAL - perceptual spatial analysis of colour and light* is a relatively late attempt to describe spatial colour/ light experiences (Klarén 2011).

Originally a method for visual evaluation of light presented by Anders Liljefors (Liljefors 2005), PERCIFAL is developed and pedagogically tested in the framework of the SYN-TES project (Klarén 2011). PERCIFAL aims at getting a firmer grasp of the total perceptual effect of colour and light through observation and concepts related to human experience, attention and reflection. Colour and light in the spatial context are described with eight well-defined concepts. The process resembles that of artists; working from the whole to the parts less essential details are sacrificed in favour of the overall impression. One can thereby describe important basic aesthetic and visually functional spatial qualities that are difficult to reveal by other means.

Colour and light education should aim at understanding colour and light phenomena as part of a greater whole, primarily developing the ability to focus attention towards important or relevant visual features in complex colour and light contexts, and – not least – acquiring relevant and well-defined concepts and put them in practice.

Colour and light pedagogy should be reflection, rather than reliance on isolated examples of elementary visual phenomena and abstract physical measurements.

REFERENCES

Fridell Anter, K., C. Häggström, U. Klarén, and B. Matusiak. 2012. A trans-disciplinary approach to the spatial interaction of colour and light. In the proceedings of *CIE 2012 - International Commission of Illumination - "Lighting Quality and Energy Efficiency"*, Hangzhou, China.

Fridell Anter K., and U. Klarén (Eds). 2014. *Färg & Ljus. För människan – i rummet* (Colour & Light. For humans – in a spatial context). Stockholm: Svensk Byggtjänst. Forthcoming in English.

Gibson J.J. 1979 *The Ecological Approach to Visual Perception.* Hillsdale, NJ: Laewrence Erlbaum

Husserl, E.1936/1970. *The Crisis of the European Science and Trancendental Phenomenology.* Trans. David Carr Everston. IL: Northwestern Univ. Press

Katz, D.1935. *The World of Colour.* London: Routhledge.

Klarén U. 2011. *PERCIFAL – Perceptual spatial analysis of colour and light.* Background and study guidelines. SYN-TES report 3E. Stockholm: Konstfack. www.konstfack.se/SYN-TES

Klarén, U. 2012. Natural experience and Physical Abstractions – On epistemology of colour and light. In Arnkil H.(Ed.), K. Fridell Anter, U. Klarén. *Colour and Light – Concepts and confusions.* Helsinki: Aalto University. http://books.aalto.fi/p/208-colour-and-light/

Liljefors, A. 2005. *Lighting – Visually and Physically. Revised edition*. Stockholm: KTH Lighting Laboratory

Murata, J. 2007. *Perception, Technology, and Life-Worlds (Collection UTCP 1)*. Tokyo: The University of Tokyo Center for Philosophy

Noë A. 2004. *Action in Perception.* Cambridge, MA: The MIT Press

Thompson, E. 1995. *Color Vision, A Study in Cognitive Science and the Philosophy of Perception*. London/New York: Routledge.

Address:Ass.Prof.em Ulf KLARÉN, Metkroken 4, 193 41 Sigtuna, SWEDEN
E-mails: ulf@klaren.se, karinfa@explicator.se

Color Universes for the Chilean Heritage

Elisa CORDERO,[1] Eréndira MARTÍNEZ,[2]
[1] Instituto de Arquitectura y Urbanismo, University Austral of Chile
[2] Independent Designer

ABSTRACT

The Government of the Libertador's Region in Chile, south of Santiago (the capital city), has decided to add value to its cultural heritage through the design of two new Interpretation Center buildings for the region. The first will shelter the 11,000 year old archaeological and paleontological site in a lagoon. The second project is related to the work of the famous "chamanto" poncho weavers, high-quality and beautiful woven pieces that received the Award for Excellence. A thorough color study was conducted in each place, including field visits, interviews, photographs, watercolor paintings, samplings and chromatic surveying. Theses colors should be used for the architecture, museography, and graphic art. Colors found were arranged into color universes specially created for each project. A color universe is a conceptual arrangement of colors related to its origin, ownership, culture, and space, among others. The full study, universes and their applications in the project's general image –from architecture to market products– are presented here.

1. INTRODUCTION

In 2013, the Government of the Libertador's Region in Chile, decided to design two new Interpretation Center buildings for the region, to add value to its cultural heritage. The O'Higgins Region is an exporter of mining products, in particular, copper and its derivatives. Its fertile soils have also favored the development of agriculture and agribusiness. The best wine that is produced in Chile, also comes from this region. But its touristic potential is not so much exploited, so the possible construction of these new centers are an excellent proposal to maximize its development.

These projects were designed by a team of architects, designers, anthropologists, engineers, and other professional most of them from the University Austral in Chile. They were delivered to the authorities of the Region in the hope they will get the means from the Chilean Government, to build them someday.

The architecture team entrusted each center with a study on color that includes the creation of color palettes to be used in the design of the architecture, museography, and graphic art. A thorough color study was conducted in each center, including field visits, interviews, photographs, watercolor paintings, samplings and chromatic surveying.Colors found were arranged into color universes specifically created for each project. A color universe is a conceptual arrangement of colors related to its origin, ownership, culture, and space, among others. These universes were then used to create the color palettes. The full study, universes and their applications in the project's general image –from architecture to market products– are presented here.

2. THE FIRST PROJECT: THE PALEONTOLOGICAL CENTER

The first project aims to shelter the 11,000 year old archaeological and paleontological site of the Tagua Tagua lagoon. In this place, bones of mastodons and other smaller mammals –including deer, horses, and rodents– have been found, as well as human remains belonging to an ancient extinct culture.

2.1 Methodology

The first project focused on the colors of the landscape, architecture, soil and museum pieces, mainly bones and arrow tips. Samples were taken of the land in different site locations and depths, where the bones were found, all with the NSC color palette. A study of the colors of the environment was also made, taking into account the landscape, architecture and objects.

Figure 1: Colour survey of an arrow tip ca 10.000 BP (Elisa Cordero, 2013).

2.2 Results

The colors found during field visits were arranged vertically, their place corresponding to the landscape in a geographical/spatial sense. At the top the colors of the sky and mountains; in the middle, architecture and objects; below, the land and the bones buried in it.This universe of colors was proposed to be used in the architectural, museographic and graphic design projects.

The architectural project offers a journey through the history of the place, starting with prehistory, in a showroom of bones found 13 meters deep and ending with recent history, in the ex-patrimonial house. The architects used the colors to create the atmospheres they needed in their showrooms. The graphic design team created their own color palettes from the color universe for brand design, paperwork and merchandising.

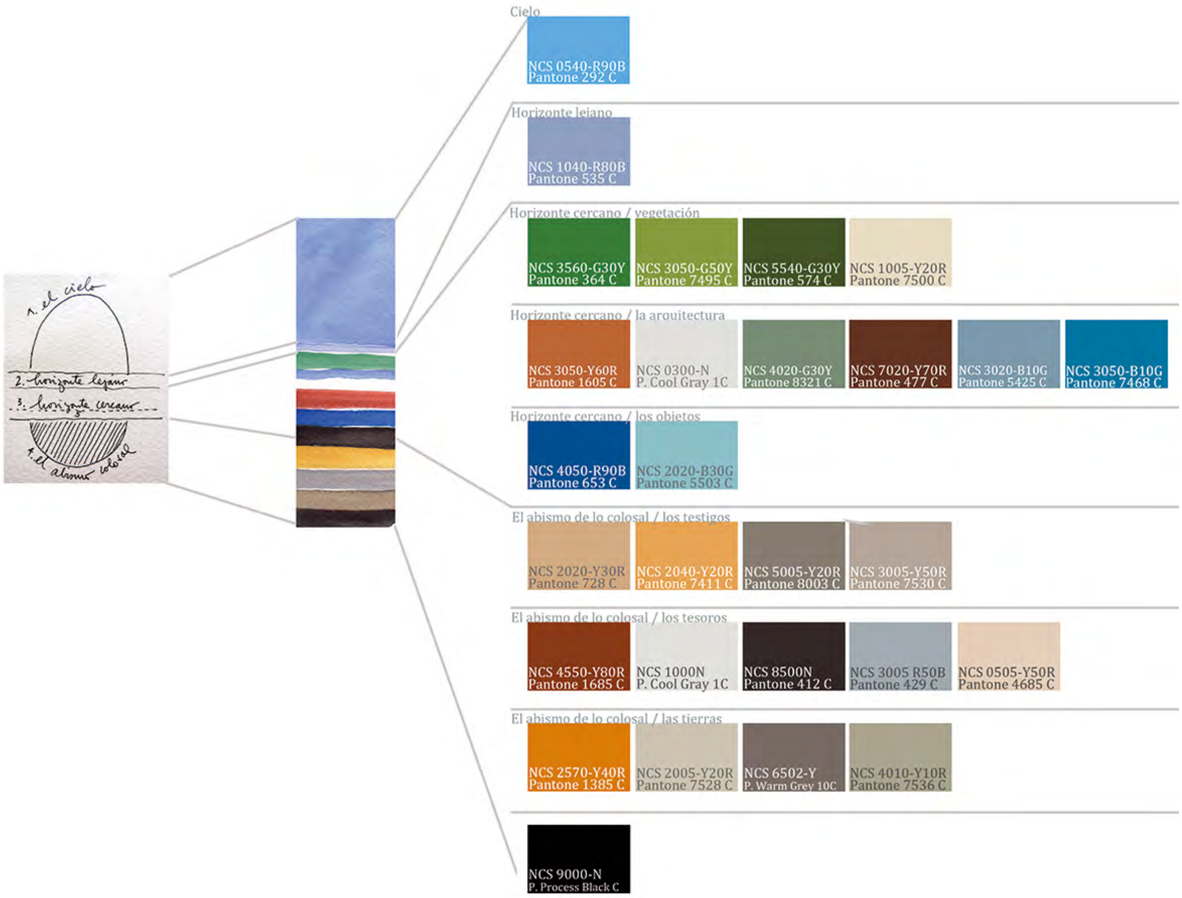

Figure 2: Color universe created from the colours from landscape, architecture, soil and museum pieces, ordered in a vertical way (Elisa Cordero, 2013).

Figure 3: The Graphic Design uses colors from the color universe. Here, the logo and its possibilities (Eréndira Martínez, 2013).

3. THE SECOND PROJECT: THE CHAMANTO CENTER

The second project is related to the work of the famous “chamanto” poncho weavers, beautiful high-quality woven pieces that received the Award for Excellence issued by Unesco in 2011. These master pieces are woven in the small village of Doñihue, of 15,000 people. Only women are authorized to do it, and the weaving technique is inherited from generation to generation in secret. The fabrication of one piece can take 6 months of lonely work, and they can be sold for around 5.000 dollars. The pieces are bought by country men who participate in a typical Chilean sport called "rodeo", where two men in horses must stop a young cow on a certain point inside a round corral. Many of these men are rich landowners, and the chamanto-poncho is an elegant and expensive dressing piece that displays their economic status and masculinity.

3.1 Methodology

This project focused on the colors of the threads used by weavers, and the colors of the landscape of Doñihue village. The colors of the ancient chamantos were studied in the "Museo del chamanto", some of which are up to 100 years old.

For current chamantos, the village weavers of Doñihue were sampled. The first step to approach the world of the weavers was to coordinate interviews to find out, for example, what meaning was given to the colors, which are the most common ones and how they decide the colors of each piece. Photos of the chamantos were taken as well as color samples and color surveys of the threads, parallel to the observation of the landscape, architecture and objects, studied through photos, sketches and color surveying.

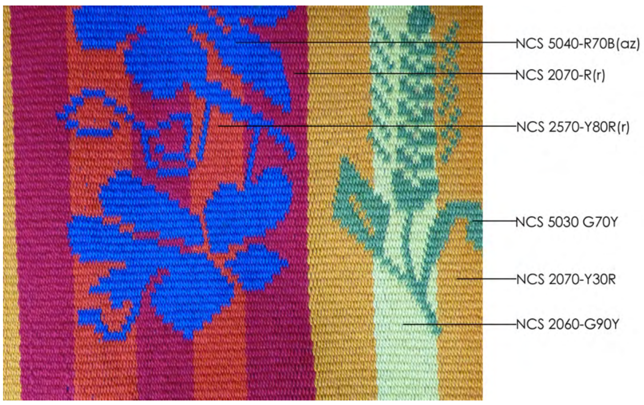

Figure 4: Color Survey with NCS of a Chamanto (Elisa Cordero, 2013).

3.2 Results

The investigation showed that the designs are closely linked to country life, for they mostly represent flowers, fruits and animals. These elements were the basis for sorting colors in a geographical way (with the 4 cardinal directions) in this way: North, warm light: Yellow. South, cool light: Blue. East, rising sun: White. West, night: Black. In the center, the central valley of Chile, with its green fields and lands, split by the bright crimson of wine. From this scheme, the colors of the exterior are arranged within the project. Outside, each of the four corners of the architectural project dons one of the colors of the cardinal directions. Each room in the interior will also take on the color of each direction depending on its orientation.

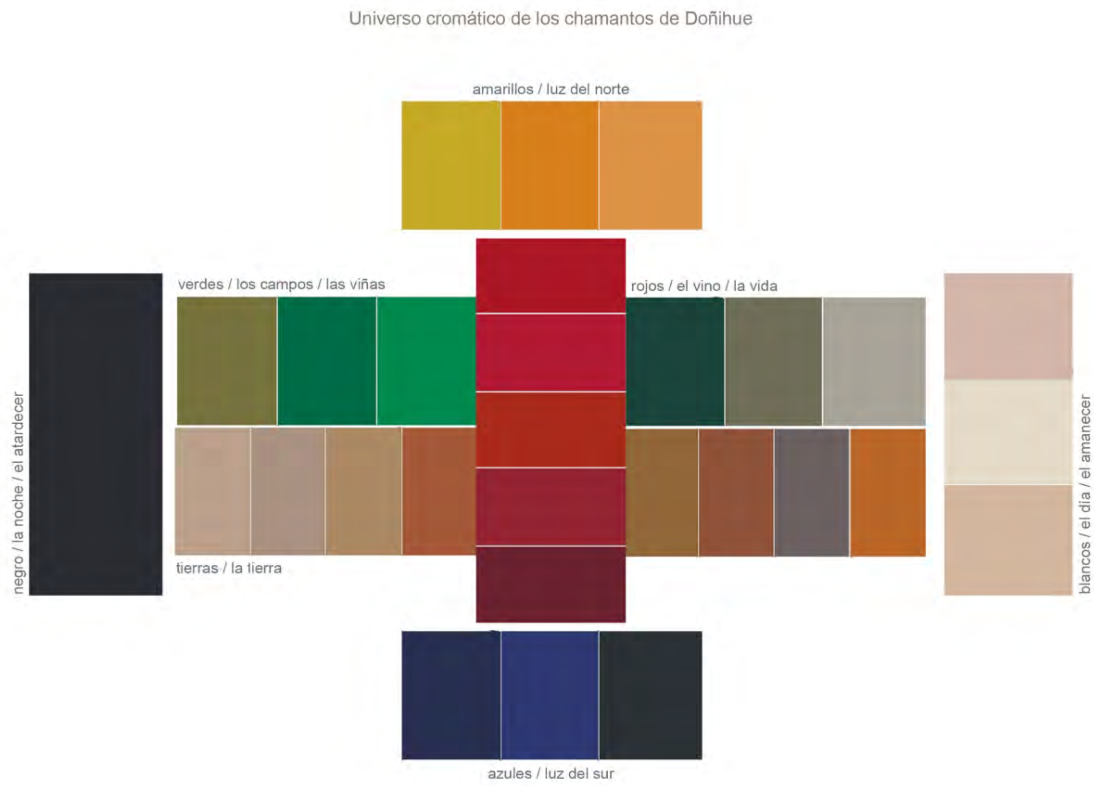

Figure 5: Color universe created on the colors of the threads and the landscape of Doñihue village, ordered in a geographical way *(Elisa Cordero, 2013).*

Figure 5: The architecture Project used the color universe for the fassade (Institute of Architecture Archiv, 2013).

The graphic design team created their own color palettes from the color universe for brand design, paperwork and merchandising.

Figure 6: Some examples of the use of the color universo on graphic pieces (Eréndira Martínez, 2013).

4. CONCLUSIONS

The assignment of the management team to create a color palette for the entire interpretation centers project was a challenge, because it was not only to create a useful palette, but to create an order that made sense to the project itself. This was achieved in both cases thanks to a deep study of the place where the project was to be deployed, which included space, landscape and social aspects (through interviews). The universe of colors is the temporal, spatial and social expression of a (current or past) historical moment, expressed through the language of colors. Because of these characteristics, is inextricably linked to the architectural project and other projects (graphic design, museology, landscaping) that make up the overall project.

Address: Prof. Elisa CORDERO, Institute of Architecture and Urbanism, University Austral of Chile, Faculty of Architecture and Arts,

Elena Haverbeck s/n, Isla Teja, Valdivia, CHILE.
E-mails: elisacordero@uach.cl, eremartinez@gmail.com,

FORSIUS' SECOND COLOUR ORDER DIAGRAM OF 1611 FROM THE ICONIC POINT OF VIEW

Verena M. SCHINDLER
Art and Architectural Historian, Zollikon
Atelier Cler Études Chromatiques, Paris
Chair of the Study Group on Environmental Colour Design (ECD) of the Association Internationale de la Couleur (AIC)

ABSTRACT

In her AIC 2009 paper the author demonstrated how important the cultural and historical context of colour order systems is for understanding them. This is especially the case for the colour order system of pastor, astronomer, mathematician, natural philosopher and astrologer Sigfrid(us) Aron(us) Forsius (ca. 1550–1624) that is illustrated by two diagrams in his *Physics, or a Description of the Qualities and Properties of Natural Things* of 1611. As the manuscript remained in the Archives of the Royal Library of Stockholm unpublished for more than 330 years until Johan Nordström published the transcription of the handwritten text in 1952, serious and critical debate of his work, and thus of his colour order diagrams, as well as its impact and acknowledgement previous to 1952 is non-existent. On the basis of printed evidence of his time, the author showed that Forsius' second diagram could perfectly be interpreted as a sphere, contradicting Kuehni and Schwarz's thesis (*Colour Ordered*, 2008) of a "linear" system. The present paper rejects Werner Spillmann's thesis (2001) that the colour order of Forsius' second diagram is incompatible with a sphere. The author bases her hypothesis on her own observations of the armillary sphere at the Globe Museum of the Austrian National Library in Vienna which show that Forsius' second scheme can be interpreted as a colour sphere. Hence, Forsius introduced a spherical colour system long before Otto Runge's Farben-Kugel (Colour Sphere) of 1810. These observations will be demonstrated with pictorial evidence. Further, Forsius' diagrams are considered in the context of contemporary colour theories such as those of François d'Aguilon (1566-1617), Athanasius Kircher (1602–1680) and Robert Fludd (1574–1637).

1. INTRODUCTION

1.1 Description of Forsius' colour diagram

First I'd like to describe Sigfrid(us) Aron(us) Forsius' second diagram in the possibly most neutral way. Figure 1 shows a geometrical form representing a circle. Within the circle, a straight vertical line is connecting two points of its cicumference as a diameter. Two curved lines either side of this vertical line connect the same two points on the top and the bottom. Small circles are set outside the circumference on the top and at the bottom. The one at the bottom is filled in with ink, and thus appears black. Five horizontal lines run across the circular form. The largest runs perpendicularly through the midpoint of the vertical line, thus through the center of the circle. Two horizontal lines further cut the upper semicircle in equidistant sections. Two other runs through the lower semicircle in the same way.

Handwritten colour names appear horizontally in the figure, with the exception of the four names (from left to right) ‘red’, ‘yellow’, ‘green’ and ‘blue’ that are midway between the top and the bottom, and going the length of both sides of the circumference and also the two curved lines. Further two colour names on the top left are written going along the interior side of the circumference.

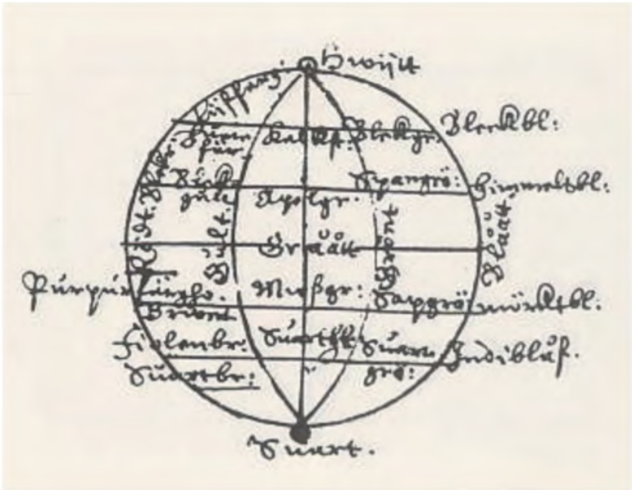

Figure 1: Sigfrid Aron Forsius: Second colour order diagram, manuscript folio 421v of 1611.

1.2 Forsius’ manuscript

Forsius’ drawing elucidates visually how colours organize in a geometrical form according to his philosophical ideas. It sounds amazing, but Forsius’ diagramme seems to be one of the earliest showing visual evidence of the relationship between colours. The drawing appears in Book 9, Chapter VII entitled ‘On vision’ (Kiiskinen 2007: 355) of his manuscript on *Physics, or a Description of the Qualities and Properties of Natural Things* completed in 1611. The nine books on physics deal with principles of nature and are written in the grand tradition of Aristotle. Colour is discussed in the last chapter, which deals with the senses and is specifically related to the sense of sight or vision.

Forsius himself mentioned his manuscript for the first time in a dedication to his 1610 astrological prediction, dated August 1, 1609, and completed it in Stockholm in 1611. It was the first text on the topic written in Old Swedish and included 485r folio pages. After his death two attempts to publish it in 1626 and 1652 failed. Forsius’ manuscript remained thus in the Archives of the Royal Library of Stockholm unpublished until Johan Nordström published the transcription of the handwritten text in 1952.

2. INTERPRETATION OF GEOMETRICAL FIGURE

2.1 On different interpretations since 1952

Concerning Forsius’ scheme there is no agreement among scholars, whether the scheme is meant to be a linear system, or rather a sphere. Some researchers adhere to a three-dimensional interpretation (Feller and Stenius 1970), seen as a “World of Colours” (Hesselgren 1984: 220), however, the latter points at “some difficulty in making the perspective drawing of the sphere.” This same argument will be taken up later (Kuehni

2003: 34–36) and Forsius' scheme will be put forward as a 'linear system' because of two reasons: "First, how to properly draw a transparent sphere was well known in the seventeenth century from several earlier books on perspective and geometry. Second, the text does not indicate that Forsius had a three-dimensional arrangement in mind." (Kuehni and Schwarz 2008: 45–46) More recently, Jones argues that "This model, if interpreted as three-dimensional, is surprisingly modern, (1) in its recognition of four primary hues and their complementarity, (2) in its use of the white-grey-black scale as a second parameter, and (3) in the introduction of a third dimension in which all the other colours fade to a central grey". Based on former articles (Spillmann 1993; Kuehni and Schwarz 2008), however, Jones concludes that "the weight of opinion now seems to favour a two-dimensional interpretation" (Jones 2013: 179).

2.2 Forsius' background

Forsius was a pastor, astronomer, mathematician, natural philosopher. When he began to write his 1611 manuscript, he was a professor of astronomy at the University of Uppsala (Sweden), where he lectured not only astronomy, but also geography and astrology (which also included meteorology and weather forecasts). It is important to note that in 1607 he was the first to publish an almanac calculating astronomical data of star positions at the local horizon for Stockholm and Åbo (Turku, in Finnish). In 1612, Forsius was appointed Royal Astronomer (Astronomus Regius) by King Gustav II Adolf, and in 1613 he was given the exclusive privilege of editing and printing almanacs. Forsius was a scientist of great knowledge, particularly in mathematics, and was called Sweden's first astronomer (Schindler 2009). This is especially significant contextually and historically for the interpretation of Forsius's scheme.

2.3 Armillary sphere

The author claims thus that such an armillary sphere was the basis of Forsius colour diagram. The armillary sphere is a device to determine celestial positions and demonstrate the motion of the stars around the Earth. Its name comes from the Latin *armilla*, since its skeleton is made of graduated metal circles linking the poles and representing the equator, the ecliptic, meridians and parallels. In Forsius' times, a ball representing the Earth (and later, the Sun) is placed in its center. Before the telescope was introduced in the 17th century, the armillary sphere was the prime instrument of all astronomers. In sum, a *sphera mundi* (armillary sphere) was the model and not a *mappa mundi* (globe) as in Philipp Otto Runge's *Farben-Kugel* of 1810 (Spillmann 2009: 40; Runge 1999).

2.4 A matter of perspective

Being an astronomer implies specific ways of drawing such an armillary sphere that can deffer from those of a painter. Circles can become straight lines depending of the point of view. Albrecht Dürer's *Nude Woman with Zodiac* is just one illustration of the fact that an armillary sphere could be composed of straight lines representing imaginary circles. As well, the symbol of the Portuguese Empire of the time gives much insight.

3. COLOUR ORDER

Some scholars base their arguments on the widely spread Aristotelian philosophy of the Middle Ages based on the four-colour theory (Parkhurst and Feller 1982: 226). The same authors also point at Alberti's six primary colours as the ancestor of Forsius' scheme. John Gage, however, notes a lack of coherence in the organization of colours, e.g., orange is located between yellow and black, and not between red and yellow (Gage 1997: 166). Another argument is put forward concerning the order of the four main colours. "A powerful argument against reading the Forsius diagram as a sphere has been put forward by Werner Spillmann. If the central horizontal line is to be read as a circle seen from the side, the colours are not in the right order." (Green-Armytage 2005: 349–351; Spillmann 2001)

The author bases her hypothesis on her own observations of the armillary sphere at the Globe Museum of the Austrian National Library in Vienna, which show that Forsius' scheme could be interpreted as a colour sphere. Looking from a specific angle, the colour order is changed in such a way that the order of the colours will constitute a hue circle corresponding to that of the NCS-System, flipped horizontally.

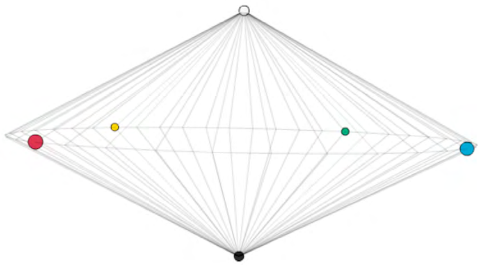

Figure 2: NCS double cone from the navigator, flipped horizontally.
© http://www.ncscolour.com/en/natural-colour-system/

ACKNOWLEDGEMENTS

Sandra Baer Heuer and Johannes Heuer, VorankerSpace for Temporary Artists Vienna.

REFERENCES

Caivano, J. L. 1995. *Sistemas de orden del color*, Serie Difusión 12, Buenos Aires: Secretaría de Investigaciones en Ciencia y Técnica, Facultad de Arquitectura, Diseño y Urbanismo.

Feller R. L. and A. S. Stenius 1970. On the Color Space of Sigfrid Forsius 1611, *Color Engineering* 8(3), 48–51.

Forsius, S.A. 1611. *Physica,* Universitatis Upsaliensis 2, ed. Nordström, J. editor, Uppsala: Lundequist.

Gage, J. 1997. *Kulturgeschichte der Farbe: Von der Antike bis zur Gegenwart*, Ravensburg: Ravensburger Buchverlag.

Green-Armytage, P. 2005. *Colour, language, and design*, PhD thesis, University of Western Australia, Faculty of Architecture, Landscape and Visual Arts.

Hård A. 1969. Quality Attributes of Colour Perception (10:1), *AIC Color 69*, *Book of Abstracts of the 1st Congress of the Association Internationale de la Couleur*, Stockholm.

Hesselgren, S. 1984. Why Colour Order Systems? *Color Research and Application*, 9(4), 220–228.

Jones, W. J. 2013. *German Colour Terms: A Study in their Historical Evolution from Earliest Times to the Present*, John Benjamins.

Kiiskinen, T. 2007. *Sigfrid Aronus Forsius. Astronomer and Philosopher of Nature*, Frankfurt am Main: Europäischer Verlag der Wissenschaften Peter Lang GmbH.

Kuehni, R. G, 2003. *Color Space and Its Divisions, Color Order from Antiquity to the Present*, New York: A John Wiley.

Kuehni, R. G. and A. Schwarz 2008. *Colored Ordered*, *A Survey of Color Order Systems from Antiquity to the Present*, Oxford: University Press.

Parkhurst C. and R. L. Feller 1982. Who Invented the Color Wheel? *Color Research and Application* 7(3), 217–230.

Runge, P. O. 1999. *Farbenkugel: Konstruktion der Verhältnisse aller Mischungen der Farben zueinander und ihrer vollständigen Affinität (1810); mit Notizen zur Farbe und deren Briefwechsel mit Goethe*, Köln: Tropen-Verlag; Stuttgart-Bad Cannstatt:frommann-holzboog.

Schindler, V. M. 2009. Forsius' Colour Order System (1611): Its Cultural and Historical Context and its Impact on Contemporary Colour Culture, *Proceedings of the 11th Congress of the Association Internationale de la Couleur*, ed. by Dianne Smith, Paul Green-Armytage, Margaret A. Pope and Nick Harkness. CD. Sydney: Colour Society of Australia.

Schindler. V. M. 2009a. Forsius e i suoi diagrammi di ordinamento dei colori (1611), *Luce & Immagini* 14(4), 13–15.

Spillmann, W. 1993. Philipp Otto Runge—ancestor of the 20th century colour order systems. *Proceedings of the 7th Congress of the Association Internationale de la Couleur,* ed. by Antal Nemcsics and János Schanda, Budapest: Hungarian National Colour Committee and Technical University of Budapest, Vol. C14, 6–14.

Spillmann, W. 2001. Farbskalen, Farbkreise, Farbsysteme, Wallisellen: *Applica*, Special Issue.

Spillmann, W. (Ed.) 2009. *Farb-Systeme 1611-2007*, with texts by V. M. Schindler, S. Wettstein, et al., and an introduction by Karl Gerstner, Schwabe Verlag: Basel.

Address: Verena M. SCHINDLER, Atelier Cler Etudes Chromatiques, 64 rue Vergniaud, 75013 Paris, FRANCE
E-mail: verenam.schindler@uzh.ch

Five Colours - A Study of Chinese Traditional Colour

Jie, XU
The School of Arts, Loughborough University

ABSTRACT

This research gives an overview of Chinese traditional colour, and intends to investigate the characteristics and the principles of the Five Colours in a Chinese cultural context. This study may inspire the designers in contemporary graphic design field.

The Five Colours are the earliest and basic colours that recorded in Chinese history. It first appeared in the book Shu Ki (before 221 A.D.). 'Fully displayed in the Five Colours, so as to form the ceremonial robes; - it is yours to see them clearly' (translated by Legge. 1879). These representative samples can reflect the common characteristics of traditional colour usage. Therefore, this research focuses on the Five Colours, which are Red, Cyan, Yellow, Black and White.

The research context unites three independent and related fields of study: ontology of the Five Colours, colour theory, and the Five Colours in relation to the Five Elements: Red-Fire; Cyan-Wood; Yellow-Earth; Black-Water; and White-Metal.

The methodology includes: a literature review, quantitative data collection, correlation analysis, visual research and a case study.

The research shows that the original meaning of Five Colours derives from certain natural scenes that specifically refer to some substances, for example, the original meaning of black is refer to mark on a man's face. However, the colour names can become abstract nouns when they develop as the metaphors that refer to the different ideas. For instance, the extensional meaning corresponds to the Five Elements. The symbolisation of the Five Colours also extends the contents to associate with other concepts and sensations.

In addition, from the comparison with different colour system, the colours are not primary colours in modern chromatics classification. Instead the Five colours are close to the natural colour hue and the colour combination reflects the tones, which profoundly influences the Chinese traditional aesthetics.

In conclusion, colour can be discussed as a concept rather than just a visual element in the Chinese traditional cultural context. The philosophical 'balanced' thinking of the Five Elements applies the premier principle to the colour applications. Consequently, the concept of 'harmony' develops as the fundamental theory of Chinese traditional aesthetics.

1. INTRODUCTION

When I reviewed the traditional Chinese colours, which gives more imagination and evocation just by the colour names. For example, one of the colour called Xiangsi Hui (Warm Grey), which direct translated meaning is the grey of lovesickness. And the subtleness of shades appears in traditional paintings and crafts are always appealing. Is there any principle of the colour application? To which extent graphic designer are using the five Chinese traditional colours and their meanings?

In the current graphic design research context, this subject has yet to be studied systematically. This research therefore complements the existent explorations of archaeology and social culture. Further, it may add or widen the horizon of historical and contemporary understandings of colour.

2. METHOD

The methods combine primary and secondary data collections. By using a systematic methodology, the original meanings and development of the Five Colours were examined from different aspects: etymology and chromatic. Attempt to restore and synthesise the concept of the Five Colours. The evidence potentially enables the answer of initial research question, which is there any principle of the colour application.

2.1 Sample Preparation

The study first focuses on the etymology of Five Colours from the Oracle (Xu Zhong Yu, 2006) (Fig. 1), which was the earliest hieroglyph, we see the description of the original story and the primary meanings attributed of the Five Colours. The diagram has been further extended with the definitions of the word class in linguistic.

Oracle	Chinese Name	English Name	Word Class	Original Meaning
	黄	Yellow	Abstract Noun, Adjective	The bulleye of target with mud
	赤	Red	Abstract Noun, Adjective	A man dancing on the fire
	青	Cyan	Abstract Noun, Adjective	The ore from coal mining
	黑	Black	Abstract Noun, Adjective	A mark or stain on man’s face
	白	White	Abstract Noun, Adjective	Air from the mouth

Figure 1: Naming of Five Colours

On the other hand, by using the principle of the Five Elements, which is the foundation of Chinese philosophy, to determine the Five Colours. The Five Elements: Metal, Wood, Water, Fire and Earth, are the summary of nature that known as a cyclical transforming system, which based on generating and overcoming, and reveal the law of the universe. According to the principle of association with the colours, it demonstrates a series of chromatography that incurs the relationship of harmony and contrast colour presentations (Fig. 2).

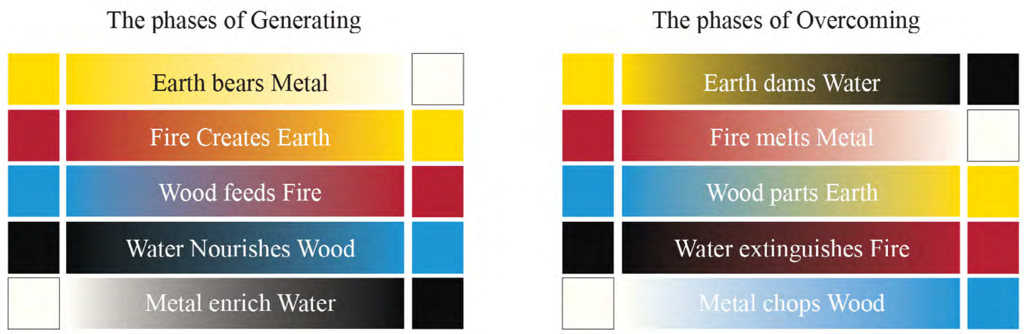

Figure 2: Phases of Five Colours

As there is a tight cultural connection between China and Japan since ancient times. A well-documented Japanese traditional colour profile is a good case study of establishing a modus of naming, the classifying and determining any unique characteristics, as well as the way of research. The case study has selected 372 colours from Japanese traditional colours as the research samples, whereby each refers to a Chinese traditional colour.

2.2 Experimental Procedure

There are four main types of colour systems: RYB, RGB, CMYK and NCS, which contain both additive and deductive methods of colour mixing. The comparison of the samples reveals that the difference between Chinese traditional colour and other colour system in hue, value, and chroma by using Munsell colour theory (Fig. 3). The precise analysis visually demonstrates and determines the constitution and attribute of the Five Colours in chromatics. The five colours are not the primary colour and the tone is close to the natural colour classification.

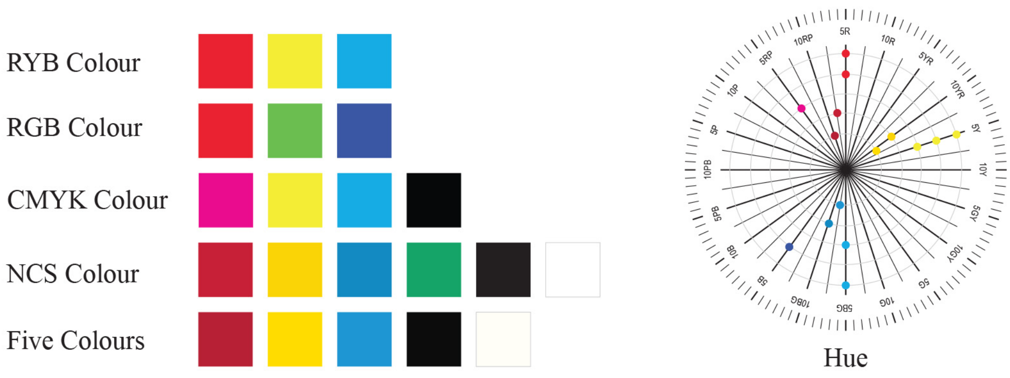

Figure 3: Colour Comparison Table

According to the book The Yellow Emperor's Inner Classic (478 B.C.) the Five Colours represent the Five Elements and many other concepts (Fig. 4). Based on principle, a quasi-experimental test is designed to see, whether people can associate the colours with the associated ideas according to ancient theory.

Five Colours	Five Elements	Five Directions	Five Seasons	Five Tastes	Five Senses	Five Emotions
Cyan	Wood	East	Spring	Sour	Sight	Anger
Red	Fire	South	Summer	Bitter	Touch	Happiness
White	Metal	West	Autumn	Spicy	Taste	Worry
Black	Water	North	Winter	Salt	Hearing	Fear
Yellow	Earth	Central	Seasons	Sweet	Smell	Sadness

Figure 4: Association of Five Colours

3. RESULTS AND DISCUSSION

Through the oracle description it shows that the Five Colours original meaning derives from the live scene (Fig.1), which reflects that colour is the most expressive feature of the memory from the image. In this sense, imagery colour is a narrative form of visualisation.

Moreover, the Five Colours correspond to the Five Elements and other concepts in Chinese cultural context. The colour symbolism is to visualise the abstract concepts and ideas. The balanced and harmony principle of the Five Elements influences the usage of the Five Colours.

From the comparison of other colour system, there is no explicit evidence state that the Five Colours are the primary colours in modern chromatics. NCS colour has the most similar hue to the Five Colours. These 'natural' tones were considered as the basic colours in ancient Chinese pigment.

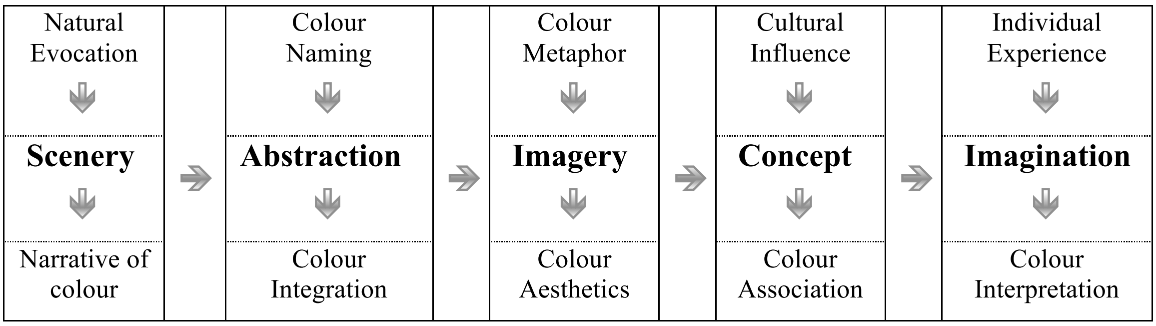

Figure 5: Chinese traditional colour mapping

The mapping (Fig.5) shows the variation of the colour status in different stages. The earliest recognition based on the impression of a particular scene. This feature of memory was combined with psychological factors and extends the connotation meanings. The colour abstraction developed as a metaphor to refer to many other concepts when associated with certain cultural contexts. Eventually the colour symbolism allows the evocation of the imagination by individual experiences.

Additionally, the quasi-experiment test was invited 36 audiences from different countries, the result shows that most of the audience failed in the test to associate the Five Colours with other concepts according to the ancient rules. There is no direct map to today's world in the colour matching. Once set free from a given cultural background, any interpretation will have a deviation according to the newly changed circumstances.

The limitations of the result, such as, language is inadequate in description of the colours, even it is a concrete noun, and the audience still has individual interpretation. One colour name may suggest a range of tones. I selected 327 samples to study the Japanese traditional colours, it shows that Japanese people uses more of the concrete nouns as colour names. In most of the cases, the colour naming denotes something in particular. Unlike Chinese tradition, the way that Japanese people divides colour into specific categories that avoid the distinction of colour as much as possible.

4. CONCLUSIONS

According to this paper, it shows that the cognitive bias of the colours derives from the process of abstract naming. There is no accurate term or parameter to quantify volume of colours. As colour can evoke different imaginings from different experiences, in this sense the way of interpreting colours is similar to that of interpreting images.

The ancient Chinese attributed a naturalistic manifestation to the colours. The Five Colours are therefore highly associated with the natural elements (Five Elements) and constituted an inner cyclical system, which generates and overcomes in the relationships of influencing each other. Furthermore, this belief that the nature law affected the moral, social and philosophical idea of Chinese traditional colour (Fig.6 , Fig.7).

Figure 6: Mogao Caves Painting

(Cave 285, Wei Dynasty)

Figure 7: China Five Coloured Flag

(1921-1928)

Central to the research question, in order to decode the colour, it is imperative to understand the significance of a particular cultural dimension. Traditional Chinese colour which is combined with other disciplines and cultural contents, negates the metaphor for the fixed cultural meanings. The 'balanced' thinking in philosophy of the Five Elements applies the premier principle to colour applications. Hence, the concept of 'harmony' was developed as the fundamental theory in Chinese traditional aesthetics.

Through the study of Chinese traditional colour, the enlightenment to the designers is that the colour has power of symbolism with its abstract form. The meaning of form refers to narratives, cultural contexts, and philosophical concept and so on. Therefore, colour is not only can be seen as a visual element but a symbolic image to visualise the abstract concepts or synesthesia other feelings. It implies that a good designer should be also a colourist who deeply understands the colour as a visual tool.

ACKNOWLEDGEMENTS

Thanks to many people who provided various help and encouragement along the way. I would like to express my appreciation and thanks to my advisor Professor Roberta Bernabei, for her constant support and consultation for this research.

A special thanks to my partner. Without her unstinting support this research would not have been possible. I am sincerely grateful to my mother and father for all of the sacrifices and supports. Every single step I have achieved is because of them.

REFERENCES

RILEY, C. 1995. *Color Codes: modern theories of color in philosophy, painting and architecture, literature, music and psychology.* Hanover; London: University Press of New England.

ALBERS, J. 2013. *Interaction of Color.* 4th Ed. New Haven and London: Yale University Press

ANONYMOUS. 1996. *The Book of Songs.* translated by WALEY, A. New York: Grove Press,

VOLLMER, J. 1980. *Five Colours of the Universe: Symbolism in Clothes and Fabrics of the Ch'ing Dynasty (1644-1911).* China: The Gallery.

BURCHHARDT, T. 2009. *Foundations of oriental art and symbolism*. Indiana: World Wisdom, Inc.

XU, Z. S. 2006. *Oracle Dictionary*. Sichuan: Sichuan Publishing.

NI, M.S. 1995. *The Yellow Emperor's Classic of Medicine.* Boston: Shambhala Publications, Inc.

2015. Traditional colors of Japan. [online]. [viewed 20/10/14]. Available from: <http://irocore.com>

2013. Chinese Traditional Colors. [online]. [viewed 5/11/14]. Available from: <http://archive.today/TlsGt>

Address: Johnny Xu Jie, The School of Arts, Loughborough University
Loughborough, LE11 3TU, United Kingdom
E-mails: j.xu4-14@student.lboro.ac.uk

Meeting New Challenges in Colour Tendencies in Norway

Kine ANGELO and Alex BOOKER,
Department of Architectural Design, Form and Colour, Faculty of Architecture and Fine Art, Norwegian University of Science and Technology (NTNU)

ABSTRACT

A recent debate in the Norwegian press, and in part raised by the authors through the exhibition Colour in the City in Trondheim 2014, points to a dramatic change in the colour pallet used both in the repainting of existing buildings and as a dominant tendency in recent architecture. This is exemplified in a substantial shift towards an achromatic pallet. Jotun, the major provider of paint in Norway, has noted that 80% of the exterior paint sold in recent years has been white, grey, brown or black. This is counter to a long tradition of chromatic variation in both vernacular and 19th and 20th century architecture. Colour and materiality play an essential role in shaping our place and identity. Colour is information, it tells us about history, about status, about territories and functions. Previously distinct chromatic neighborhoods are being eroded and new property developments build without any chromatic character or differentiation. Area character as distinct architectural styles and chromatic qualities is an important contribution to the identity and differentiation in the urban environment; it provides both a means of identification, navigation affordance and generator of aesthetic atmospheres in the architectural gestalt. Place is more than a street number, it is an ensemble of qualities and relationships that make meaning; materiality and colour are the key component in this process. The scope of this paper will be an analysis of the drivers of this process from developer to the architect to the consumer with the intention of developing a colour program methodology that meets the pressures of increasing urban densification.

Figure 1: The Waterfront Warehouses in Trondheim and neighboring area.

1. INTRODUCTION

The city of Trondheim dates back over a thousand years, and the contempory building mass contains all the varieties of architectural styles, sizes and materials. But the image of Trondheim and its main identity is foremost associated with the remaining clusters of older wooden and plaster rendered buildings painted with pictorial colours in easily apprehended relationships between hues and nuances. As of today, this is only a small element in the city's overall chromatic and material gestalt.

Colours in architectural context are the contextual result of the past and the present. Architectural colours are determined by variables of geography, such as culture, tradition, symbolic meaning and local resources. Other, time-related variables are preferences for a colour at a given period in history, the socio-political context and new technological advances. In short, the interactions of these variables have resulted in a present colour scheme of both governed regulations and ungoverned preferences and colour accessibility. However, none of these are perfectly or permanently consolidated, and all are susceptible to changes in patterns of use, of ownership and the tendencies of fashion; this last fifteen years exemplified by a drift from chromatic to a achromatic colour palette.

Figure 2: The traditional chromatic colour palette of Trondheim is drifting towards achromatic colours (right picture is manipulated to show all houses in grayscale).

A methodology is in general a guideline system used in a specific discipline for solving a task or a problem; i.e. methods, tools, techniques, rules and postulates. In proposing a methodology for the city of Trondheim it was therefor a priority to identify the main task or problem, in addition to finding out who may – and how to - implement them.

Buildings in Norway are regulated by two laws:
1. Cultural Heritage Act: The Act comprises buildings of conservation interest and buildings with conservation status, less than 10% of the buildings in the country.
2. Planning and Building Act: The Act mainly provides a framework for land use, transportation planning and the urban development, and comprises the buildings without conservation status or interest.

The responsibility and authority of building regulation in Norway is governed by elected councils in the Norwegian municipalities, and the methodology and the professional expertise involved varies a great deal within each municipality. Buildings with conservation status or interest have a well-founded methodology for dealing with architectural conservation, governed by people with an expertise within this field, but there is a lack of an overall colour methodology. The remaining 90% of the buildings are governed by regulations in the zoning plans and seldom includes any regulation of colour.

There is no existing archive showing if there has ever been a colour methodology for the city, and the material that does exist is fragmented and difficult to access. As the majority of the registered buildings in Trondheim are mostly in private ownership as residential houses or commercial buildings, and with a lack of a consistent colour methodology, the colours chosen for the urban realm of Trondheim are mostly determined by the competence or fancies of the owners and the property developers.

In 2014, in co-operation with the Municipality of Trondheim[1], we initiated a pilot project for colour registration of a selected area in the city, with the intention of finding the contemorary city's colour pallet to create a public archive and a reference for both historic colours and as a basis for analyses of current tendencies and future colour methodology.

2. METHOD

The colour registration was restricted to the registration of the nominal[2] colours of the façades visible to the public, including cladding, foundation and most significant building components such as doors, window frames and window sashes. However, our perception of a façade colour is affected by several other variables, for example surrounding colours and texture and we registered the most basic information about the materials and textures of the façade surfaces in addition to the colour notations, i.e. if the wooden cladding has vertical or horizontal boards, or if the finish of the plaster renderings is fine or rough. Other variables that affect how we perceive a colour are but generally described in the overall userguide in the finished report (light conditions, human visual conditions and other variables).

2.1 Colour Registration

The colour reference system chosen for the colour registration was NCS - Natural Color System and Norwegian Standard since 1984. Each building was photographed, and the façade colours were scanned with a NCS colour scanner and notes down For the roof colours and multicoloured façades with an inherent material colour, such as slate tiles, bricks or prefabricated façade panels, we noted down the perception of the overall colour impression as one colour notation together with information about the material properties. The method for finding nominal and perceived colours of façades is well researched and documented by the Swedish architect and researcher Karin Fridell Anter [2].

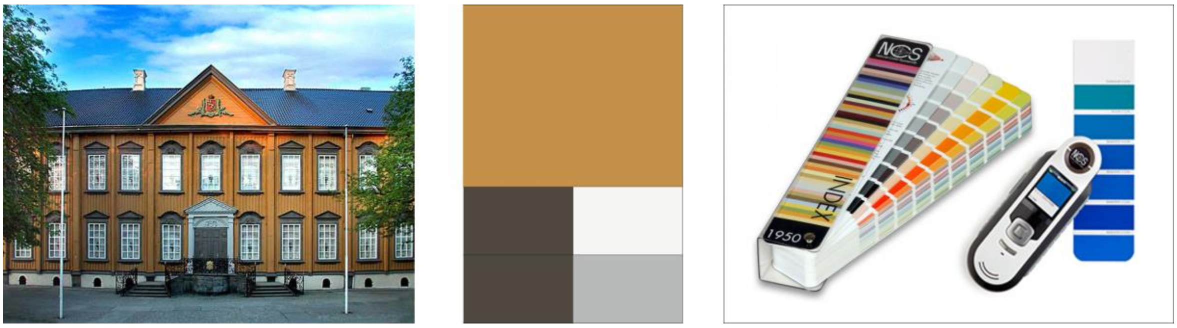

Figure 3: Example of picture and colour palette of registered building (Stiftsgården), where the NCS notations were found using NCS Index and NCS Color Scan 2.

---

[1] Office of Urban Planning in the Municipality of Trondheim.
[2] Karin Fridell Anter and Åke Svedmyr, *Färgen på huset*.
[3] Grete Smedal, *The Colours of Longyearbyen - An Ongoing Project*.

2.2 Public Archive

The material registered in the colour registration in this pilot project will be made publicly accessible through the Municipality of Trondheim in May 2015. The archive will provide an historical document of the colour palette of Trondheim as of today, and be a reference for both historical comparisons, present colour practice and tendencies, and used for future analyses. The archive can function both as inspiration and a guideline for the public in choosing colours for their buildings, provide information and knowledge about colours in an architectural context and give examples of traditional building articulation through the use of colour and its impact on perceived form and volume (for example, see figure 5).

3. RESULTS AND DISCUSSION

The NCS-system is commonly known and used as a colour reference system in Norway, but the system is not yet as commonly used as a tool for colour analyses and as a design tool. The method used in the pilot project was adopted from Norwegian interior architect Grete Smedals well established practice as a colour designer both nationally and internationally [3].

The system was also used as a tool for visual communication of the registered colours to show the colour palette of all registered colours in the pilot project. By plotting in the registered NCS notations in the NCS triangle (nuance) and NCS circle (hue), we can clearely identify the range of hues and nuances significant to the specific area or street, and communicate to the public what colours to choose from when repainting buildings or programming new buildings within the same area or street to stay within the contemporarely colour palette (see figure 4).

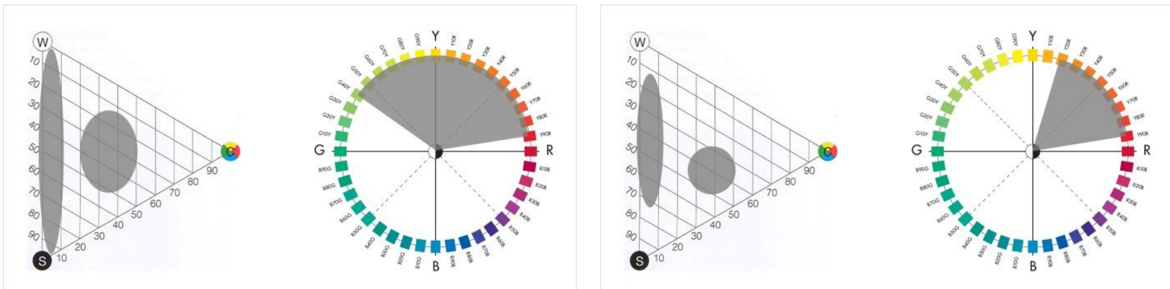

Figure 4: Left: Colour palette of all colours in the pilot project. Right: Colour palette in one street (Kjøpmannsgata).

However, we can speak of “area character” or “a coherent rhythm of buildings in a street” at micro and macro levels, but these characteristics are under pressure from the requirement for increased urban density, from radical shifts in architectural scale and proportion and not least from the often reflective surfaces of mass-production materials that in many cases offer very limited colour choice. These aspects are not discussed in this paper and will need further research before addressed and included in the current proposal for a colour methodology.

Another aspect of densification of the urban realm is that human colour vision was evolved to enable to distinguished object from background. The more complex the city becomes, there is an even stronger need for colour regulation to ensure a good hierarchy of colours and a good visual clarity.

4. CONCLUSIONS

Are colours in the urban realm of a private or public concern? The main design idea by using this methodology is that by identifying a colour palette for a city by colour registration of the facades, you can give the public the choice of choosing their own colours within the identified colour palette. In time, this data may be implemented in the city's Zoning Regulations and the Municipal Development Plan for a stronger effect to gain more control over visual clariry and the city's colour identity in a complex urban realm.

> The idea that colour should or could be controlled is anathema to many people, who regard it as one of their few remaining personal freedoms. Nevertheless, colour is already controlled in a significant number of ways that are taken for granted. Landowners still control large areas of town and country, and can dictate colour. Where individuals have relinquished control, government, institutions and public services have assumed control over civic design at many levels. Part of that control extends to colour, which is used in a variety of ways to express identity, impart information and in some cases to give warnings. But it is not clear who controls or coordinates these various uses. In principle many of the uses can be individually justified but the collective effect is often confused. There are two reasons for this: the sheer volume of uses, and the difficulties in achieving effective design and colour coordination between individuals and organizations. This is especially true where the former still believe that colour choice should be a personal matter. One solution is a design guide. (Michael Lancaster, *Colour in the Urban Context*)

By identifying the task of a proposed colour methodology to ensure a good visual clarity and the problem identified to losing the means to do so by a drift towards achromatic colours, we can propose a colour methodology to take back the city's image and identity. During the last year the discussion of colour in the media has fucused on whether to choose chromatic or achromatic colours, whereas the discussion should be directed to wich hue or nuance to choose, and how to use the colours in articulation of a building or the public realm.

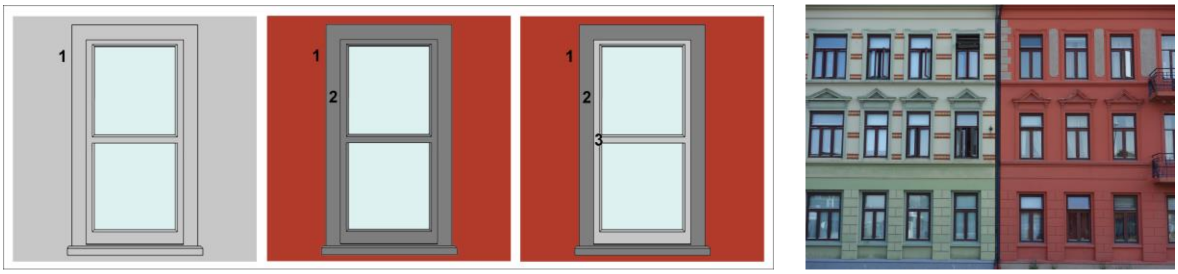

Figure 5: Traditional threefold division of cladding (1), window frame (2) and window sash (3). The colour registration showed tendencies for building elements being reduced to fewer contrasting colours than originally designed or becoming completely monochrome.

The limitations in the pilot project to a registration of colours only in parts of the city center of Trondheim does not give a full picture of the complexity of the city as a whole. The center has a stronger building regulation due to the fact that most of the buildings of concervations interest and regulation are situated in this area. The center also consists of more public buildings than the rest of the city and are therefore more easily regulated and controlled. But it has provided basis for a proposed colour methodology, by relatively simple means and possibility for a clear communication to the public.

The next, interesting possibility the colour registration gives a basis for will be to take the analyses further and include architectural styles, new cladding materials and building volume. For example, if a wooden building stands next to a modern construction made of concrete and glass, what would be a good hue and/or nuance combination to enrich both buildings?

ACKNOWLEDGEMENTS

Susanne Saue and Hilde Bøkestad from the Office of Urban Planning in the Municipality of Trondheim. Mette Bye from the Office of Conservation in the Municipality of Trondheim. Bjørg Helene Andorsen, master student of Aarchitecture at NTNU.

REFERENCES

Drange, T. Aanensen, H.O. Brænne, J. 1992. Gamle trehus. Universitetsforlaget.
Fridell Anter, K. Svedmyr, Å. 2001. *Färgen på huset*. Byggforskningsrådet.
Lancaster, M. 2002. *Colour in the Urban Context.* The Institute of Historic Building Conservation (IHBC).
URL: http://ihbc.org.uk/context_archive/75/urbancolour/colour.html
Smedal, G. 2009. *The Colours of Longyearbyen - An Ongoing Project*. Eget forlag.
Valberg, A. 2005 Light Vision Color, Chichester: John Wiley & Sons, Ltd.

Address: Assistant Prof. Kine ANGELO, Department of Architectural Design, Form and Colour, Faculty of Architecture and Fine Art, Norwegian University of Science and Technology, Anton Getz vei 3, 7491 Trondheim, NORWAY
E-mails: kine.angelo@ntnu.no, alex.booker@ntnu.no.

The Image of the Color Red in Letters: A Study Based on the Historical Backgrounds of Russia and Japan

Sasha KRYSANOVA
Graduate School of Letters, Kansai University

ABSTRACT

Color has been an important topic for thousands of years. In this research I will focus on the use of the color red in letters. The purpose of the survey is to discover the differences in point of view about color between Russia and Japan and to examine the traditional meanings of red in the two countries. The key points covered are the historical significance that people have attributed to this color. Use of the color red is prevalent all over the world. Red pigments were used for paintings on walls in caves, for graves, and in many other ways. It is obvious that people have a common perception of this color. But history also gives cultural meanings to colors. How they were symbolized in the past and some historical images of colors still influence the image of the color red today. For example, in Russia, red letters for celebrations are common. Red is associated with happy occasions, and is considered the color of strength and of life force. In contrast, in Japan this color can have positive meanings, but sometimes it is the color of *kegare,* a traditional concept of defilement. It is taboo to use the color red for letters in Japan. In this study, I will consider these different interpretations of the color red. This study is related not only to our lifestyles today, but to the cultural history of etiquette and manners in Russia and Japan.

1. INTRODUCTION

In Japan, writing letters or names in red is taboo. Using red letters is considered inauspicious. The following sentence about the appropriate color of ink was found in a book of manners.

> When you write letter of appreciation it is good manners to use black or blue ink (blue black which is almost black). A highlighter or pastel color ink is not suitable. Do not use red because it is the color of demand note or a letter of break off relations. Use dark black for celebration and light black for invitations or letter of appreciation (Tetsuo 2011: 22).

By searching on the internet with the keywords "write letter with red ink" in Japanese, we also can find many writings saying that it is good manners to not use red ink on letters or cards that you give to people. The reason, why people say to avoid this color were various. Mainly I could divide them into four categories.

1. On graves that are purchased while alive, the name of alive person is written in red.
2. Japanese warriors used red on a challenge.
3. Historically they would write the prisoner's name in red.
4. The rumor is that, if you write someone's name in red, his life will be shortened.

In all these reasons we can see inauspicious meanings of red letters. On the contrary, in Russia, those taboos are not seen. Moreover, red letters are frequently used in relation with celebrations. One example is red letters on celebration cards. In this survey, I compared frequency of using red letters on Russian and Japanese postcards related to celebrations. To measure the color red, I used the color cards "新配色カード199a". These cards are based on Practical Color Co-ordinate System which defines 2: R for red and 3: yR for yellowish red. The color numbers used are v2, v3 and dp2 for old cards (COLOR ENTERPRISE CO., LTD).

2. METHOD

At first, printed letters on birthday cards were compared. On Russian web site selling post cards (ЗАО"ПРАЗДНИК"), 63% of 48 cards had messages in red. On Japanese web site selling postcards (TOKYU HANDS INC), it was 12% of 221(9 % was in English). Secondly, I searched New Year cards. On Russian web site (ЗАО"ПРАЗДНИК"), 49% of 101 cards had messages in red. On Japanese web site (年賀.ORG.), it was 18% of 230 cards. Then, I observed the usage of red printed letters in the past(19^{th} and 20^{th} centuries). Here, 19% of 880 Russian New Year Cards (Retropost. Ru.), 6% of 401 Japanese New Year cards (Ideafactory Corporation), had red letters. It is observed that Russian post cards have more red letters than Japanese. Also, on Japanese post cards a tendency was found, to use very limited quantity of red for letters. For instance, one phrase representing celebration and red for seals (name seals are not included in this research). On the other hand, in Russia, especially on current cards, not only is the main phrase but also (on many cards) long messages and wishes were printed in red. In addition, all hand written postcard that seems to written only with red ink, could found on the Russian web site which collecting old post cards for Easter (Россия в красках). For these reasons, it is possible to say that Russian people have different point of view for using the color red for letters.

3. RESULTS AND DISCUSSION

As red and blood is one of the highest association in many different countries including Russia and Japan, discussion will be focused on the image of blood in the two countries. Religions are very important factor considering this matter. In Japan, a traditional concept of defilement, *kegare*, existed. Tadao Kobayashi states that Japanese red color had two sides, positive and negative. On one hand, it was a color which had magical power, it could chase bad spirits away. Also it was used in festivals as a color of celebration. But, on the negative side, it was a minor, taboo color especially when it associated with *kegare* of blood. Blood from woman's childbirth and menstruation was called "*akafujyo*" (赤不浄) which means "red uncleanliness" (Kobayashi 2002). The Japanese folk customs dictionary "*Nihon minzoku daijiten*" also has an explanation of blood and *akafujyo.* In addition, the dictionary shows examples of customs related to this thought like "*Nagare-kanjyo* " (流れ灌頂) and "*Ketsubonkyo*" (血盆経). The first one is a custom of purify the soul of woman who died while giving childbirth. The red material was put on the riverside, and passengers sprinkled water on it. When the red color dissapeared, it was thought that the dead woman could rest in peace. "*Ketsubonkyo*" is blood pool sutra. It is said that this beliefe came from China. It says that the blood that woman sheds on giving birth and menstruation could cause defilement for other people which gets her into blood pool after her death (Hayashi 1999). Noboru Miyata indicates the relations beteween *kegare* of blood and historical prohibition of eating meat. Also he clames that Buddhist “nonkilling” ethics is also an important factor. Furthermore, in Edo period, with growth of wet-rice farming, horses and cows became an indespensible labor saving device that discouraged people from eating them (Miyata 1996). From these reasons we can guess the gradual development of avoiding blood in Japan. In the Russian Orthodox religion, as in Western Europe, the color red associated with the Passion of Christ and His shed blood. On Easter, this color is used on Easter eggs and vestments. Perhaps it was the reason of using red letters on postcards related to Easter in Russia. Also, compare to Japan, Russia has a different history on relations with animals. People historically had various meats for eating and used the animals fur. Russia was known as one of the biggest fur trading countries since the medieval period. Fur was nesesarry to protect people from the cold climate, and it was an important property for country (Nishimura 2003). These historical backgrounds should have made the image of blood in Russia different from it in Japan.Of course, it does not mean that taboos related to blood do not existed in Russia. On this point, research will be continued.

4. CONCLUSIONS

In this study, it is observed that in Russian post cards related to celebrations, red letters were used more frequently than those in Japan. These differences are caused by various reasons including the ink problem and history of using color in writing. Here, I picked up the historical image of blood that is thought to be related to the color red in letters. As a conclusion, it seems that not only religion, but also the differences of life styles are involved. In future work, more data samples related to red letters will be collected.

REFERENCES

Hayashi Hideo. 1999. *Nihon minzoku daijiten(日本民俗大辞典)*. Tokyo: Yoshikawakobunkan.

Kobayashi Tadao. 2002. Nihon no Shikakubunka wo yomu(日本の視覚文化を読む). *Kunizukuri to kenshu* (98): 28-31.

Miyata Noboru. 1996. *Kegare no minzokushi: Sabetsu no bunkateki yoin(ケガレの民俗誌ー差別の文化的要因)*. Kyoto: Jinbun Shoin.

Nishimura Saburo. 2003. *Fur in Mankind History(毛皮と人間の歴史)*. Tokyo: KINOKUNIYA COMPANY LTD.

Tetsuo Shuichi (ed.), 2011. *Croissant Special Edition: Chanto shita tegami to hagaki ga kakeru hon(クロワッサン特別編集[新装版]ちゃんとした手紙とはがきが書ける本)*.Tokyo: Magazine House, Ltd.

COLOR ENTERPRISE CO., LTD. Available online, www.sikiken.co.jp. Accessed: July 27, 2015.

ЗАО“ПРАЗДНИК”. Available online, www.prazdnikcom.ru. Accessed: July 27, 2015.

Ideafactory Corporation. Available online, http://www.fuyuki-nenga.com/. Accessed: July 27, 2015.

Retropost. Ru. Available online. retropost.ru. Accessed: July 27, 2015.

TOKYU HANDS INC. Available online, http://hands.net/. Accessed: July 27, 2015.

年賀.ORG. Available online, http://www.nenga.org/. Accessed: July 27, 2015.

Россия в красках. Available online, http://ricolor.org/. Accessed: July 27, 2015.

Address: Kansai University, 3-3-35, Yamate-cho, Suita-shi, Osaka, 564-8680,JAPAN
E-mail: k298324@kansai-u.ac.jp

Japanese Color Names Reflecting Dyeing: With a Focus on Their Color Terms in Brown Regions Including More than 100 Browns

Kohji YOSHIMURA,[1] Yuko YAMADA,[2] Stephen SHRADER[3]
[1] Department of English, Kansai Gaidai College
[2] Color Instructor, Illustrator
[3] Department of Foreign Languages, Kansai Gaidai University

ABSTRACT

A variety of color terms such as *shijyu-hachi cha*, *hyaku nezu*, meaning "forty-eight browns, one hundred mouse colors," were used in the mid and late Edo period (A.D. 1651-1868) in Japan. At that time the most popular colors were browns, and the second most popular were mouse colors. Japanese color names for browns reflect Japan's *iki* aesthetic, and the defiant spirit of the Edo period people whose lives had become more affluent. The purpose of this paper is to show the main characteristics of Japanese color terms reflecting wood culture, i.e., dyeing, and 132 *cha*-named colors (despite the name 48). Color names based on the nomenclature of the forty-eight browns are used to refer to colors in Japanese fabrics, such as those for *kimono* in the 21st century. *Shijyu-hachi cha* (48 browns) embodies the *iki* aesthetic. For us, *iki* connotes the ability to live well with contradictory things by valuing how they complement and are a part of each other.

1. INTRODUCTION: "48 BROWNS" INCLUDING OVER 100 BROWNS

Among Japanese expressions for color terms, there is a famous phrase, *shijyu-hachi cha, hyaku nezu*, which means "forty-eight browns, one hundred mouse colors." As this expression suggests, from the mid to late Edo period (1651-1868) the most popular colors were browns, and the second most popular were mouse colors. Although not the focus of this article, the third most popular were indigos. Japanese color names for browns reflect Japan's *iki* aesthetic revealed in its color culture, and the defiant spirit of the Edo period people whose lives had become more affluent. Kunio Fukuda writes in his Dictionary of Strange Color Names (*Kimyo-na Siki-mei Jiten*, in Japanese, 1993: 13) that subdued, neutral colors matched the *iki* aesthetic, and that people favored color names with *cha* (tea) or *nezu* (mouse), hence the phrase *shijyu-hachi cha, hyaku nezu*. He argues that the number 48 was chosen because it sounded good, involved word play, and was lucky (p. 53). This paper will explain the existence through the years of 132 *cha*-named colors (despite the name 48), show that color names based on the nomenclature of the forty-eight browns are used in the 21st century in Japanese clothing as well as abroad, and additionally discuss the connotations of the number 48 in the phrase *shijyu-hachi cha* (48 browns).

2. A SUMMARY OF THE HISTORY OF BROWN DYE INGREDIENTS AND TEA PRIOR TO THE EDO PERIOD

Many Japanese color names reflect Japanese dyeing culture. The color name *cha-iro* (tea color) originated in the use of tea infusion as a dye during the Muromachi period (1336-1573). For example, *sencha-iro* (*sencha* is a type of green tea; *iro* means color) was a color produced by dyeing with the infusion of *sencha* from refined buds of the tea plant. *Sencha* came to be widely drunk by commoners in the Edo period (1603-1868), and the color names incorporating *cha* became common as revealed in the phrase *shijyu-hachi cha, hyaku nezu*. Many of these color terms used interesting contrasts revealing the hidden resistance among the common people to the control of the ruling class. It is thought that the first use of the Chinese character for tea (茶) was in the "*Cha Jing*" (*The Classic of Tea*, or "*Chakyo*" 『茶経』in Japanese), written around 760 by Lu Yu (Rikuu, 陸羽 in Japanese, 733-804) during the Tang Dynasty (618-907).

During the Nara period *tencha* (纏茶: half fermented tea) seems to have been brought to Japan from China by the Japanese envoy to Tang China. Actual tea production in Japan started in 805 when Saicho (最澄: 767-822) brought tea seeds from Tang China. Tea was presented to the Emperor. The courtiers of the Heian period (794-1185) began drinking tea in the form of tea-tasting competitions (*toucha*: 闘茶), and in the mid-Muromachi period (15th century) tea was a luxury item used in the tea ceremony. Among *samurai* and Buddhist priests tea was first drunk to ward off drowsiness. With the abandonment of the Japanese envoy to Tang China, tea declined in Japan; however, in 1191 Eisai (栄西:1141-1215) revitalized tea by bringing tea seeds and small tea plants from Southern Song China (1127-1279). From the late Heian to early Kamakura periods he had learned in China's Zen temples, which valued simplicity, the way of drinking tea that had developed from the Tang to Southern Song Dynasties.

The color names for browns before the Edo period did not use *cha* for their nomenclature. Heian period color names for browns included such terms as *kourozen* (黄櫨染), a yellowish brown dyed twice, but not using tea as a dye. It was a color forbidden to commoners. When the Edo period later came, some browns which had once been allowed only to the ruling class came to be permitted to the common people, which made them popular. The key point here is that it was the use of tea (*cha*) as a dye that caused this change, hence its wide popularity as a color name. Other browns of the Heian period, similar to *kourozen*, did not use tea as a dye. Another Heian color was *shira-tsurubami*, (白橡) a color produced from one of Japan's most ancient dyes, using the chestnut oak and acorns. Unlike *kourozen*, *shira-tsurubami* was actually prescribed for common people. *Aka-shira-tsurubami* (reddish *shira-tsurubami*), on the other hand, was reserved for high ranking officials only, and was produced with a dye based on madder (茜). *Ao-shira-tsurubami* (bluish *shira-tsurubami*) was used for everyday informal wear, but only by the Emperor. It was produced by cross-dyeing with *kariyasu* (*miscanthus tinctorius*) and lithospermum root. Unlike *shira-tsurubami*, *ao-shira-tsurubami* did not use chestnut oak, which was inexpensive and thought to be more appropriate for commoners. *Ki-tsurubami* was yet another brown color produced by dyeing with acorns and lye. Another color took its name from the Japanese word for cloves, *choji*. *Choji-zome* (丁子染) was produced in one of two ways. *Honzome* (本染) referred to *choji-zome* which was actually produced with expensive cloves, while *daiyou-zome* (代用染) referred to *choji-zome* which had been produced with red bayberry (楊梅) rather than cloves. *Choji-zome* was also called *kou-zome* (香染) or *koki-kou* (濃き香), and the *kou* in both of these color compounds refers to an aromatic wood. *Usu-kou*, also called *kou-iro*, was produced from lightly dyeing with cloves, and was light yellowish brown. The *kou* in its name comes from the use of incense as a dye. *Suou-kou* (蘇芳香) was similar to another color called *aka-kou* (a reddish variant of *kou-iro*, explained above). *Suo-kachi* was similar to *suou-kou*, but of an even deeper brown. These were some of the many browns prior to the Edo period, and demonstrate how people back to the early days of Japan's history were sensitive to slight differences in color. While later in the Edo period people began to use terms incorporating *cha* to refer to browns, before the Edo period there were many distinct names for these colors.

In the Edo period color names with *cha* came to be widely used, but tea was not the only ingredient used in the production of these colors. Dyeing materials used in the Edo period included red bayberry, sappan, *kariyasu*, peels of *ume*, madder, turmeric, indigo, small dried sardines, and other things. The Edo colors *usu-cha* and *shira-cha* were similar to the Heian colors *shira-tsurubami*, *kou-iro*, and *usu-kou*. They were a pale brown, sometimes with a yellowish or reddish tint, similar to a beige. Dye produced with the peel of red bayberry was most loved from the early to mid-Genroku period (1688-1704), and became popular again in the Bunka-Bunsei period (1787-1843). *Kyara* denotes a type of high quality aromatic resin, but from the mid-Edo period *kyara-cha* referred to a dark yellowish brown produced by dyeing with something other than (the very expensive and rare) *kyara*. The Edo period government established the "Sumptuary Regulation," preventing farmers from living a life of luxury. By decree of this law, all people regardless of status were prohibited from wearing luxurious kimono. In 1642 this law prohibited the use of silk in *kimono* belts and neckbands, and in 1643 it prohibited the use of purple and reddish-pink. In 1663 this law was expanded to include the *samurai* and commoners. Although the people of that time followed the law in practice, the *iki* spirit included resistance to it.

3. "48 BROWNS" ACTUALLY INCLUDES 132 BROWNS

The origins of *cha-iro* (tea/brown color) names have many origins, including plants (*azuki* beans, Japanese white birch, mulberry, kelp, mandarin orange, willow, fallen leaves, and fruits such as persimmons and loquats), plant-based dyes (indigo, Japanese horse chestnut, and tea, among others), dyeing methods (*momo-shio*—*momo* literally means one-hundred, suggesting the large number of times something is dyed, while *shio* usually would mean salt, but when used in the context of dyeing refers to insertion into dye, and taken together means a deep color produced from multiple rounds of dyeing, i.e. *youkan-iro*, a brown produced with this method and named after a kind of sweet jelly of *azuki* beans), birds (sparrows, bush warblers, Japanese crested ibises, black kites, Eurasian siskins, and others), animals (mice, sea-otters, and so on), personal names (Enshu, Kempo, Shikan, Shikou, Souden, Danjurou, Baikou, Rikan, Rikyu, Rokou, Roshun, among others), place-names (Edo, Kishu, Tang, Momo-yama, etc.), furniture (such as *kawarake*, or unglazed earthenware), architecture (like *nando*, a storeroom), tools (such as *toishi*, a whetstone), spices (such as *choji*, cloves), aromatic trees and woods (such as *kyara*, a high-quality agarwood product that was deep brown, and agarwood itself), things related to fortunes and omens (such as *chitose*, meaning one thousand years; *takara*, treasure; *kin*, gold; *fuku-jyu*, long life and happiness; and *yama-buki*, here meaning a gold coin), symbols (such as the tea *ikou-cha*, which referred to a tea that had been drunk by people who held high social status—the *ikou* refers to this status—and symbolized the power they commanded, making it popular when it later came to be drunk by commoners), colors (red, blue, yellow, white, green, gray, and tea-brown), physical features (such as *okina-cha*, a near-white brown that takes its name from the gray hair of an *okina*, an aged man). In addition, there are browns that take their names from word play (such as *kobicha* (媚茶), a color name derived from *kobu-cha*, or kelp brown, and also from the verb *kobiru*, meaning to butter someone up by fawning on them), from honorific expressions such as *omeshi-cha* (御召茶: a bluish, subdued brown named after a kind of high-quality *chirimen*, silk crepe-like fabric, loved by the 11th *shogun* Tokugawa Ienari, which subsequently came to be known as *omeshi*, itself is the honorific form of the verb "to wear"), and *bunjin-cha* (文人茶), which is an expression referring to fashionable and sophisticated people at that time (*bun* meaning literature, *jin* meaning people, and *cha* meaning tea, or people of tea and letters, such as the literati). Browns, unlike mouse colors, did not have color names that made reference to astronomical phenomena or river names. *Cha-iro* (茶色: tea color, brown) comes from the color of the drink tea, and includes 132 colors, which are typically divided into a three part classification system proposed by Nagasaki (1996), but which we have revised. Here we will explain his system and our modifications to it.

Nagasaki divided the browns into three categories, *aka-cha*, *ki-cha*, and *ao(midori)-cha*, which respectively mean red tea (brown), yellow tea, and blue (green) tea. He proposed this system based on different types of drinking tea, *ban-cha*, *sen-cha*, and *hiki-cha* (also known as *matcha*, thick green tea), and argued for this classification system noting that tea was used in the dyeing process. *Aka-cha* is a color category that he uses to describe colors similar to the drinking tea *ban-cha*, and they basically correspond to each other (but the first term represents the color category and the second term is the actual tea it is based on). Similarly, *ki-cha* is based on the tea type *sen-cha*, and *ao(midori)-cha* is based on *hiki-cha*. However, the fact is that while some of the browns are produced by dyeing with tea, some colors with the *cha* name use tea combined with other things, and some do not use tea at all. As part of our research we listed as many browns as we could find, and tried fitting them into Nagasaki's framework. We expanded the categories of his original proposed system by changing the names to better reflect a wider variety of browns, have added browns that were not in his original categories, and also added a fourth category of colors that include *cha* in the name, but are actually gray. Nagasaki himself did not attempt to fully list the *cha* colors in categories in this way.

Among the *ban-cha* colors, which Nagasaki called *aka-cha* (as do we; *aka-cha* means "red tea/brown"), are a total of 22 colors: *aka-cha*, *aka-koge-cha*, *azuki-cha*, *beni-ebi-cha* (紅海老), *danjyurou-cha*, *edo-cha*, *enshu-cha*, *kaba-cha* (which has three different Chinese characters with the same pronunciation, each counted as one color, 椛・蒲・樺), *kuri-ume-cha*, *kuri-kane-cha*, *kouetsu-cha*, *shikan-cha*, *shoujou-cha*, *suzume-cha*, *tangara-cha*, *tousei-cha* (当世), *toki-cha*, *momo-yama-cha*, *ume-cha*, and *usu-ume-cha*.

Nagasaki called the *sen-cha* category *ki-cha* when he referred to it as a color category name; however, we renamed it *ki-aka-kara-ki-cha*, which means "from yellow-red (tea brown) to yellow (tea brown)." It includes the following 30 colors: *bunjin-cha* (文人), *cha-iro*, *cha-kasshoku*, *choji-cha*, *hiwa-cha*, *kaki-cha*, *kawarake-cha*, *ki-cha* (黄茶), *ki-kara-cha* (黄唐), *ki-gara-cha* (黄雀・黄枯), *ki-kara (ki-gare) cha* (木枯), *kishu-cha*, *kara-cha*, *kin-cha*, *kenpou-kuro-cha*, *ki-miru-cha*, *koge-cha* (焦茶), *kobi-cha* (媚茶), *koi-uguisu-cha* (濃鶯), *konbu-cha*, *kuwa-cha*, *mikan-cha*, *ran-cha* (欄茶), *shibu-cha*/*shibucha-iro*, *sen-cha*/*senji-cha-iro*, *senjicha-zome*, *takara-cha*, *uguisu-cha*, and *yamabuki-cha*.

Finally, Nagasaki has the *hiki-cha* category, which he calls *ao(midori)-cha* when he refers to the colors in it rather than the tea; we call this category *midori-kara-ao-cha* ("from green to blue" tea brown). It includes these 21 colors: *ai-tono-cha* (藍砥・藍礪), *ao-cha*

(青茶), *icou-cha* (威光・威公), *fukujyu-cha*, *gin-onando-cha* (銀御納戸茶), *jinkou-cha/tono-cha* (沈香茶・殿茶), *kusayanagi-cha*, *maccha-iro*, *ryoku-cha*, *omeshi-cha*, *sensai-cha/senzai-cha* (千歳・千哉・千才・仙斎・千載・仙歳), *shinsai-cha*, and *yanagi-cha*.

We are also proposing a new category of colors with *cha* in their name, but which are more gray than brown – the following 56 colors would previously have been organized under the system above, but we will be recategorizing them. The 7 dark grays formerly in the *aka-cha* category are *ebi-cha* (海老・蝦・葡萄), *ebi-kawa-cha*, *kuri-kawa-cha*, and *momo-shio-cha* (百塩・百入). Three grays formerly under *aka-cha* are *kara-cha* (唐茶, the *kara* comes from a Japanese way to refer to Tang, which came to mean "new, beautiful"), *souden-kara-cha*, and *souden-cha*. Two light grays that would have originally fallen into the *aka-cha* category are *toki-gara-cha* and *toki-cha*. The 15 colors originally in the *ki-aka-kara-ki-cha* category, but now in the new category include the following dark grays: *ochiba-cha*, *kara-cha/kare-cha* (枯茶), *kanze-cha*, *kogarashi-cha/kogare-cha/kikara-cha* (木枯), *kurokobi-cha*, *kuro-cha/kurocha-iro*, *kogarashi-cha*, *goku-koge-cha*, *susu-take-cha*, *miru-cha*, *su-miru-cha/su-miru-cha-iro*, *mukashi-kara-cha* (昔枯・昔唐), *rakko-cha,* and *rokou-cha*, the following 8 grays: *tono-cha* (砺・砥・礪), *nezumi-cha/nezu-cha*, *hai-cha*, *biwa-cha* (枇杷・琵琶), and *furu-cha*, and these 7 light grays: *awa-cha*, *usu-cha*, *usu-sira-cha*, *kuwa-iro-sira-cha*, *shigaraki-cha* (信楽), *shira-cha/shiro-cha* (白茶), and *rikyu-sira-cha* (利休白茶). From the *midori-kara-ao-cha* category, we are moving the 10 dark grays: *ai-koi-cha* (藍濃), *ai-kobi-cha* (藍媚), *ai-sumi-cha* (藍墨・相済), *ai-miru-cha* (藍海松), *onando-cha/nando-cha*, *sikou-cha*, *yanagi-susutake-cha* (柳煤竹), and *rikan-cha*, the 2 grays: *iwai-cha* (岩井) and *rikyu-cha*, and these 2 light grays: *baikou-cha* and *mamegara-cha* (豆殻). The colors listed so far were formerly divided into three categories, but we put them into a new category we call *kurai-hai-kara-akarui-hai-no-cha* (meaning dark gray to light gray cha/tea/browns). There are also three colors that did not fit into the original system: *okina-cha* (the *cha* color closest to white), *kara-take-cha*, and *roshun-cha*.

4. COLOUR TERMS OF "48 BROWNS" IN MERCHANDISE

The *cha* colors listed above are one aspect of Japan's traditional culture, which lives on in the fact that many of the *cha* colors continue to be used in Japan today, especially among specialists and in industry. Japan's *geisha* and *maiko* (teenagers who are in training to become *geisha*) are highly-trained professional entertainers and performers of Japan's traditional arts, who wear *kimono* that reflect Japan's color culture. Many of the terms introduced above are used to refer to colors in Japanese fabrics, such as those for *kimono*. The clothing for *kabuki* also makes use of fabrics using these colors. Another example is pottery, where some of the *cha* color terms are still used. Additionally, some shops are named after the colors. There has also been one example of how one of the colors has been used overseas – in 2011, the American company Fender produced a guitar at the request of a Japanese musician using the color *omeshi-cha*, which they named "grayish olive green."

5. CONCLUSION: THE CONNOTATION OF 48 IN "48 BROWNS"

The number 48 is traditionally a significant number in Japanese culture, and can be seen in other phrases such as *shi-jyu-hachi-no-seigan* (a phrase referring to the forty-eight wishes of the Amida Buddha), and *kuchiba-shi-jyu-hachi-shoku* (forty-eight decayed-leaves colors). Although the phrase *shijyuhachicha, hyakunezu* (forty-eight browns, one-hundred mouse colors) states a clear number of colors, in fact the number of browns and mouse colors are both over one hundred. There are thus some questions about why these numbers were chosen in the first place, and why the number given for browns is smaller even though the actual list of color names is similar when we compare the browns and mouse colors. Kunio Fukuda (1993: 52-55) gives three reasons. First, he suggests that perhaps the number forty-eight is the same as the number of characters in a well-known poem which would have been even more widely known at that time, *Iroha*, which uses the Japanese syllabary and expresses Buddhist ideas. Second, he gives the possibility that forty-eight might have been chosen even though it was a bit different from the actual number because it involved some word play and sounded good, and this was seen as more important than accuracy. Third, he writes that the number might have been chosen for good luck, pointing out that the Chinese character for eight, 八, has a special additional meaning of good fortune and prosperity, and was often used to mean something similar to "a lot" regardless of the actual number of things being counted. Fukuda calls it the "magic number" of the Edo period, a part of Japanese culture carried on into modern society.

Interestingly, the number four traditionally has negative associations in Japan, since it sounds like the word for death; however, here it appears with the eight in forty-eight. The reason for this odd combination may be the interesting contrast it provides – one that would have been meaningful to people at that time, and today as well. It is the idea expressed in the yin and yang symbol (something that is good, for example, may contain the seeds or elements of its opposite). Aesthetically there is an enjoyment of putting opposites together which is revealed in the phrase, and is at the heart of the *iki* aesthetic. This can also be seen in the color terms themselves, which sometimes put opposites together (as in *ai-koi-cha*, in which the *ai* and *cha* are actually opposite colors). Earlier we mentioned the defiant spirit of the Edo people. The common people were resistant to the Sumptuary Regulation, and followed it outwardly but rejected it inwardly. This was revealed in the naming of the colors (i.e. the use of *cha* itself in naming the colors was a rejection of the Regulation). This reflects an aspect of Japanese culture referred to as *omote*/*ura*: outwardly saying one thing while internally thinking something else, and while this might be seen as being two-faced in English-speaking culture, it is not necessarily seen this way in Japan. Another interpretation of the 48 is that it embodies the *iki* aesthetic we have described – it was a kind of resilient and simultaneously restrained resistance to authority that took a sophisticated form in various aspects of life at that time. *Iki* connotes the ability to live well with contradictory things by valuing how they complement and are a part of each other, an outlook that is important to protect in the challenging world we live in today.

REFERENCES

Fukuda, Kunio 1993. *Kimyo-na Siki-mei Jiten*, Tokyo: Seiga-Shobou.

Nagasaki, Seiki 1996, 2006. *Nihon-no Dento-Syoku: Sono Shiki-mei to Shiki-cho* (*The Traditional Colors of Japan*) (written in Japanese), Kyoto: Kyoto-Shoin.

Uchida, Hiroyuki 2008. *Teihon Wa-no Iro Jiten*, Tokyo: Shikaku Design Kenkyu-Sho.

Address: Prof. emer. Kohji YOSHIMURA, Department of English, Kansai Gaidai College, 16-1, Nakamiya-Higashino-cho, Hirakata City, Osaka, 573-1001, JAPAN
E-mails: yoshim-k@kansaigaidai.ac.jp; yoshim-k@rk2.so-net.ne.jp

Assessing Glare Using LED Sources Having Different Uniformity Patterns

ShiNing MA[1], Yang YANG[1], Ming Ronnier LUO[1,2*], XiaoYu LIU[1,3], and BinYu WANG[4],
[1]State Key Laboratory of modern optical instrument, Zhejiang University, Hangzhou, China,
[2] Colour, Imaging and Design Research Centre, University of Leeds, UK
[3]College of science, Harbin Engineering University, Harbin, China
[4]Thousand Lights Lighting (Changzhou) Limited, Changzhou, China
*m.r.luo@leeds.ac.uk

ABSTRACT

Glare has been a problem in lighting design because it can cause safety accidents and visual impairment. For LED source, the existing standards may not be suitable because of its high luminance intensity, small size and non-uniform distribution. In this work, an experiment was conducted to investigate the indoor LED discomfort glare. The physical parameters studied included luminance intensity, the size of LED matrix, the pattern of LED luminance distribution, the background luminance, and the LED positioned angle above the sight line. The results showed that the five parameters all had statistic significant effect on human sensation of glare. Finally,the visual glare was used to test two different glare models. The results domenstrated that there are still some rooms to improve the accuracy of the model, especially for the non-uniform LED patterns.

Keyword: LED, discomfort glare, UGR

1. INTRODUCTION

LED (light-emitting diode) lighting source has become the most important clean source because of its special characters such as energy-saving and long service life. More importantly, LED source can be tuneable whose luminance, chromaticity, spectrum and pattern can be adjusted with different application requirements. These strengths make it possible to be developed as intelligent lighting source to provide functionalisation, personalisation and with internet.

However, glare is a serious problem in LED lighting design due to its small size. It can cause visual fatigue and excessive glare which could result in safety accidents and visual impairment. Here the research is concentrated on indoor discomfort glare. For traditional lighting sources such as incadescent or fluorescent, Cai (2013) reported different vision models to describe indoor discomfort glare such as UGR, VCP, and BGI , while they can only be used in some restricted conditons such as medium area and medium luminance. The problem is that these glare indices cannot be used to precisely predict glare caused by LED which has high luminance intensity, small size and non-uniform distribution. As the LED is rapidly replacing traditional lighting source, it is necessary to evaluate LED lighting quality especially the discomfort glare. With this in mind, CIE has established a Joint technical committee to investigate the prediction of glare for the non-uniform LED sources.

Over the past several years, several studies have been reported that many parameters exert strong impact on observer's perception of glare. Akashi et al. (2013) discovered that blue LED and cyan LED could have the lowest BCD luminance (borderline of comfort and discomfort) of discomfort glare compared with other colour's LED. By using fluorescent luminaires, Zhang et al. (2012) conducted a research on the effects of lighting source's color temperature on discomfort glare. Ayama et al. (2013) redefined the glare model UGR by calculating the luminance of LED glare source in HDR (high dynamic range) image and come up with the concept called 'effective glare luminance'.

Therefore, the purpose of the present research is to generate a glare viusal database and to analyse the relationship between lighting parameters and discomfort glare. Furthermore, it is still necessary to evaluate the existed indoor discomfort glare indices and improve them to some extent by analysing the collected data.

2. METHOD

2.1 Experimental Conditions

The experiment was carried out in an enclosed room without window. The apparatus is shown in Figure 1. LED elements were arranged in a four-by-four matrix, within an area of 16cm*16cm. These LEDs were Lambertian light source. The colour temperature of them was 4100K. The LED panel was placed on the background board covered with white cloth. The horizontal distance between observer's eyes and LED lighting source was 2.5 m. The distance between eye and computer display was 60 cm. The height of table was approximately 75 cm. For the display, the height was 32 cm and the width was 55 cm.

During the experiment, in order to simulate real working situation, the observers were asked to look horizontally at the computer display and enjoy the oil paintings presented randomly on the display. As for the subjective glare rating scale, Table 1 shows the detail.

Totally, there are twenty observers, eleven males and nine females in their twenties or thirties (the average age was 24 years) with normal colour vision, participated in the experiment.

2.2 Experimental Parameters

The experiment was divided into 2 parts. In Experiment 1, the effects of LED luminance intensity, the whole LED size, background luminance and LED positioned angle above the sight line were mainly investigated. Note that every bright LED has the same luminance in this experiment. LED luminance intensity corresponds to 5 levels (0.46, 1.65, 4.66, 9.57, and 16.79 cd) measured by PR670 (product of Photo Research). As the figure 2 shows, there were 3 matrices of LED sizes including 1*1, 2*2 and 4*4. There were two backgrounds (dark (0 lux) and bright (105 lux)). It had two LED positioned angles above the sight line, 10 degree and 20 degree.

Table 1. Subjective glare rating

category	name
1	imperceptible
2	just perceptible
3	noticeable
4	just uncomfortable
5	uncomfortable
6	just intolerable
7	intolerable

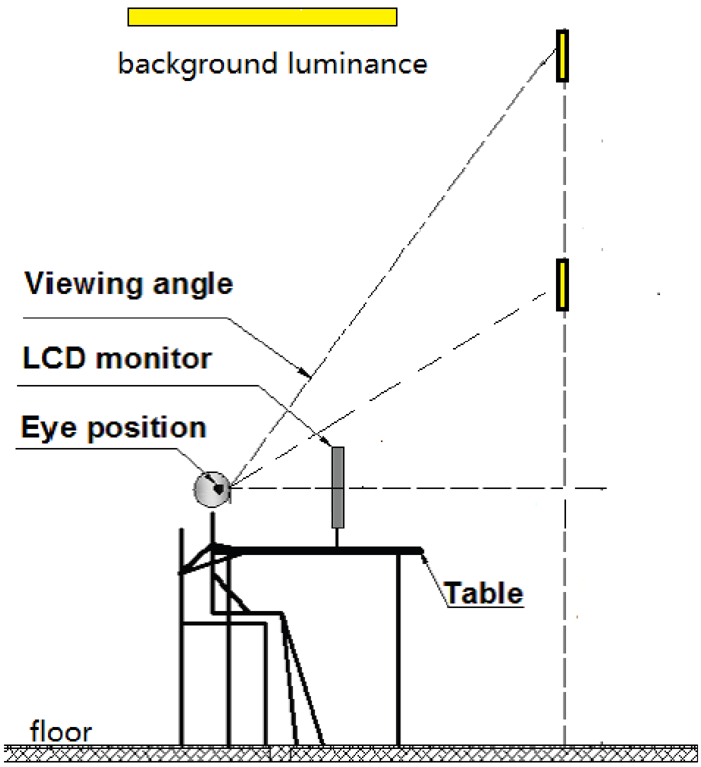

Figure 1: Experiment apparatus

In Experiment 2, the pattern of LED distribution was changed so that the uniformity of glare source was varied. There were 12 kinds of LED patterns with different luminance distribution of LED panel while the LED luminance intensity was set the same (20.79cd). Shown in figure 3, the luminance contrast between outside part and inside part had 10 different levels. Another two patterns included 1*1 LED matrix and 4*4 LED matrix. Also in Experiment 2, LED positioned angle above the sight line and background luminance were set the same as Experiment 1.

Overall, there are 108 different lighting conditions in this experiment assessed by 20 observers, each one did twice. In each lighting condition, 20 observers visually assessed the glare. In total, 2160 estimations were made.

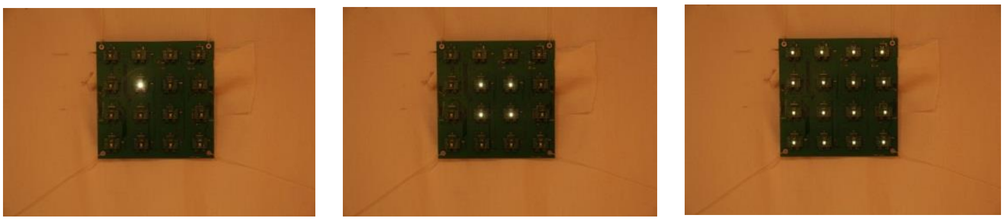

Figure 2: LED matrix in experiment 1

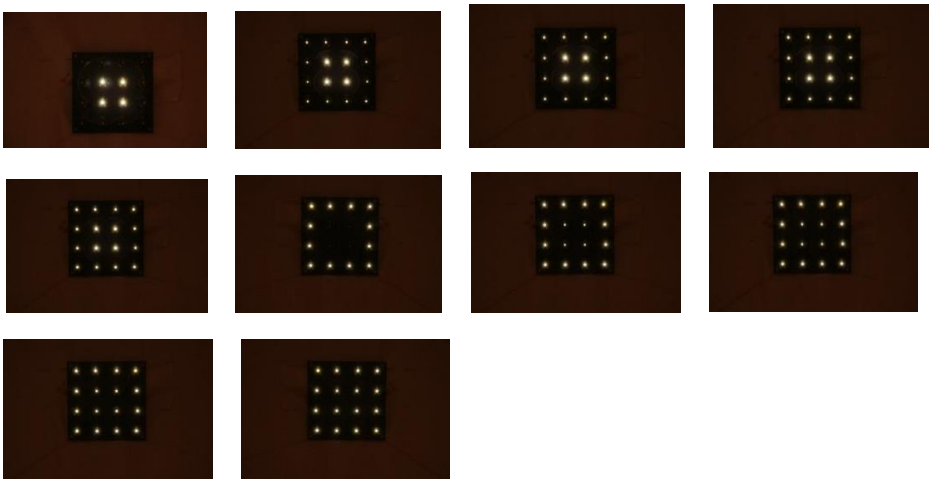

Figure 3: LED pattern with different contrast level between outside and inside

3. RESULTS AND DISCUSSION

3.1 Lighting Parameters on Perceived Glare

Statistical analyses were performed using SPSS version 16.0. For Experiment 1, the four parameters including LED luminance, matrix size, background luminance and LED positioned angle above the sight line. All had strong relationship with glare. After two-way factorial analysis of variance (ANOVA), it was found statistically significant interaction ($p=0$ and $p<0.05$) between glare rating score and all the parameters investigated in Experiment 1. For luminance, it is obvious that average glare rating score increases as the glare luminance increases. For the size of LED matrix, the glare rating score increases as the size increases. For background luminance, the sensation of glare in dark background is stronger than in bright background when other conditions are all the same. For the LED positioned angle above the sight line, the sensation of glare increases with the decrease of angle.

For Experiment 2, the most important parameter discussed here is the non-uniformity of LED lighting source. After two-way factorial analysis of variance (ANOVA), the results indicate statistically significant interaction ($p=0.002$ and $p<0.05$) between glare rating score and LED non-uniformity, or uniformity of LED pattern. Glare rating score increases with an increase of contrast between the inner and outer luminance. In other words, the discomfort glare increases as the increase of non-uniformity level.

3.2 Testing Models' Performances

Finally, the visual results were used to test UGR and BGI models. These were selected because the two models are known to have best performance in predicting the previous datasets (Cai, 2013). Parts 1 and 2 data represent the data from Experiments 1 and 2 respectively. Table 2 shows the predictive performance of the two models in terms of correlation coefficient (R value) for Part 1, Part 2 and combined data. Figure 4 plots the UGR predictions against the subjective ratings. It can be clearly seen that UGR model can predict Part 1 discomfort glare results better than those of Part 2. Figure 5 plots the BGI predictions against the subjective ratings. Similar to UGR model, BGI predicts Part 1 discomfort glare results better than those of Part 2. However, both models predict the combined data well, i.e. r values of 0.93 and 0.94 respectively. The results in Table 2 clearly indicate that both models gave good predictions to the combined data. They can predict better for Part 1 data than the Part 2 data. This implies that there is a room to improve the models in predicting the data having non-uniform LED patterns.

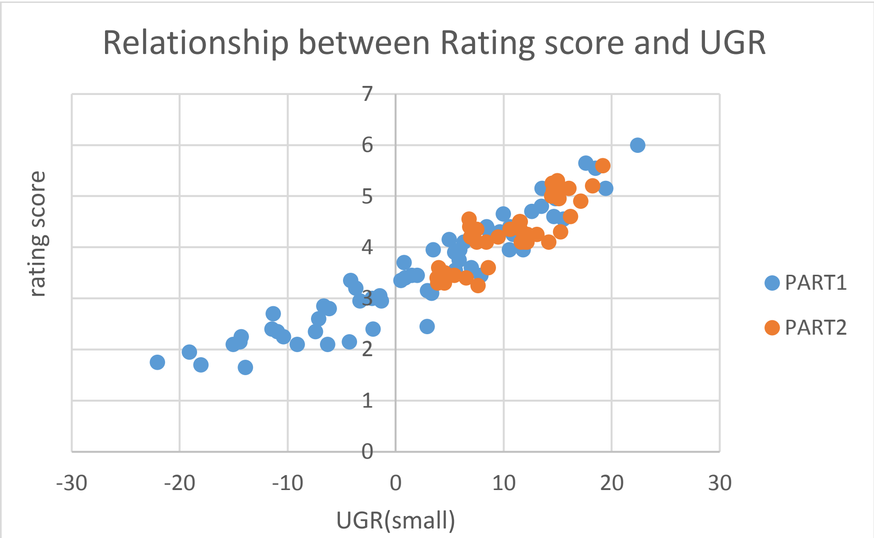

Figure 4: Relation between UGR and glare rating score

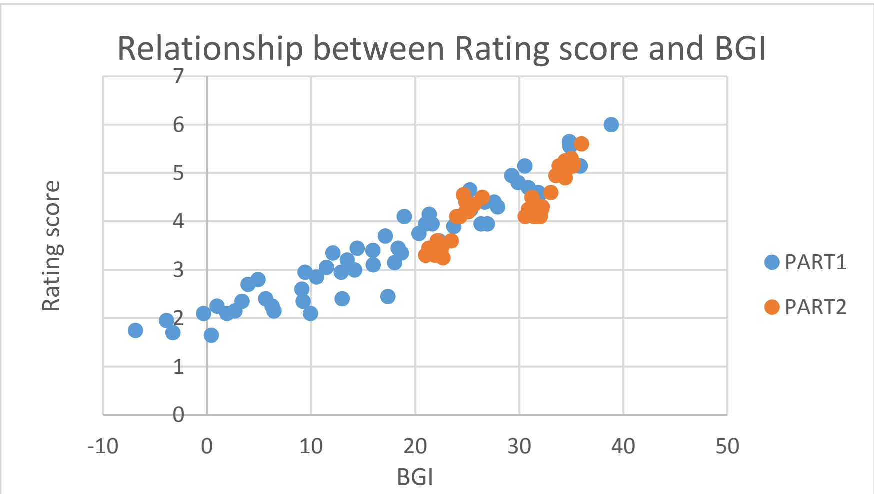

Figure 5: Relation between BGI and glare rating score

Table 2. R value in different conditions

	UGR	BGI
Part 1	0.94	0.95
Part 2	0.84	0.85
Combined	0.93	0.94

4. CONCLUSIONS

Two experiments investigating the relation between human sensation of glare and physical parameters of LED luminance, matrix size, background luminance, LED positioned angle above the sight line and non-uniformity were conducted. After data analysis, some important phenomena have been discovered. Firstly, all five parameters had significant impact on glare perception. Secondly, although UGR and BGI models can predict the combined glare data to some extent, there are still some rooms for improving in predicting non-uniform patterns. A new model is required by taking non-uniformity arrngments of LEDs into consideration.

ACKNOWLEDGEMENTS

The authors would like to thank the support from the National Natural Science Foundation of China. The project number is No. 61475142 and its title is 'Modelling the Indoor glare'.

REFERENCES

Akashi, Y., Asano, S., Kakuta, Y. (2013) Visual mechanisms of discomfort glare sensation caused by LEDs. In *Proceedings of CIE Centenary Conference: Toward a New Century of Light*: Paris, 327-330.

Ayama, M., Tashiroi, T., Kawanobe, S., Kimura-Minoda, T., Kohko, S., & Ishikawa, T. (2013) Discomfort glare of white LED sources of different spatial arrangements. In *Proceedings of CIE Centenary Conference: Toward a New Century of Light*: Paris, 119-122.

Cai, H., & Chung, T. (2013) Evaluating discomfort glare from non-uniform electric light sources. *Lighting Research and Technology*, 45(3), 267-294.

Zhang, J., Tu, Y., Liu, L., et al. (2012) The influence of correlated colour temperature of luminaire on overhead glare perception. In *Proceedings of CIE 2012: Lighting Quality and Energy Efficiency*: Hangzhou, 470-476.

Address: Prof. M. R. Luo, Department of Optical Engineering, Zhejiang University,
No.38 in Zheda Road, Xihu district, Hangzhou, China
E-mails: M.R.Luo@leeds.ac.uk

Evaluation of the Performance of Different Colour Rendering Indices Employed in LEDs

Haiting GU,[1] Xiaoyu LIU,[1,2] Ming Ronnier LUO,[1,3] Binyu WANG,[4] Haiyan LIU,[4]
[1] State Key Laboratory of Modern Optical Instrumentation, Zhejiang University
[2] College of science, Harbin Engineering University
[3] School of Design, University of Leeds
[4] Thousand Lights Lighting (changzhou) Limited

ABSTRACT

The goal of this study is to investigate the performance of various uniform colour spaces (UCSs) and colour rendering indices (CRIs) for evaluating colour rendering quality of light sources. An experiment was carried out to include colourful test samples and light sources of different types and correlated colour temperatures (CCTs). Ten observers participated to view identical samples placed in two cabinets under a pair of sources respectively, and judged their colour difference according to a grey scale. The results indicated that CAM02-UCS gave the best correlation with the visual results among all the UCSs tested. It was also concluded that all the colour fidelity indices gave similar performance and they outperformed colour preference indices in predicting the visual results.

1. INTRODUCTION

Colour Rendering Index (CRI) is one of the most important criterions. CIE-R_a is the only internationally accepted measurement for evaluating the colour rendering properties of a light source. It was proposed by the International Commission on Illumination (CIE) in 1974 and has been widely employed in the lighting industry. However, recent studies have shown that perceived colour qualities of newer LED light sources are not well described by CIE-R_a. The problem may arise due to some drawbacks associated with CIE-R_a, such as the use of low saturated test samples, the outdated colour space and chromatic adaptation transform. Hence, various new CRIs have been developed to update the present CIE-R_a.

In order to recommend one CRI as a new method for measuring and specifying colour rendering, many researchers have focused on investigating the performance of new CRIs. Li et al. (2011) conducted an experiment using 15 coloured textile samples placed in two cabinets under five light sources, while observers evaluated the change of colour appearance of samples according to a grey scale. They concluded that an index based on CAM02-UCS gave the best performance. A similar experiment done by Sándor and Schanda (2006) also showed that CIECAM02 colour appearance model provided best correlation with visual conditions. Boissard et al. (2014) also performed the experiment using a paired comparison method and observers to assess several aspects of colour quality. Their results indicated that perceived colour differences were better dealt by the CIECAM02 Uniform Colour Space (UCS), naturalness was well described by colour fidelity indices and colourfulness was well described by gamut based indices.

This paper describes an experiment conducted in a dark room with an aim to evaluate the performance of existing UCSs and CRIs.

2. EXPERIMENTAL

2.1 Apparatus

Three viewing cabinets placed side by side were used in the experiment. The walls and bottom of these cabinets were painted in medium grey matt paint, which had CIELAB values of 53, 1.0 and 1.0 for L*, a* and b* values respectively measured under D65 and CIE 1964 standard colorimetric observer. One cabinet was a VeriVide cabinet, providing traditional light sources including fluorescent lamps and a tungsten bulb. Another one was equipped with a 16-channel LEDs illuminator named Telelumen Light Replicator, which was supplied by Telelumen Limited Liability Company in US. The third one was illuminated by a self-built tunable LED cluster. This LED cluster included 10 monochromatic LEDs and one white LED. Figure 1 plots their SPDs. The desired CCT, luminance level and CIE-R_a value could be achieved by adjusting the intensity of each LED.

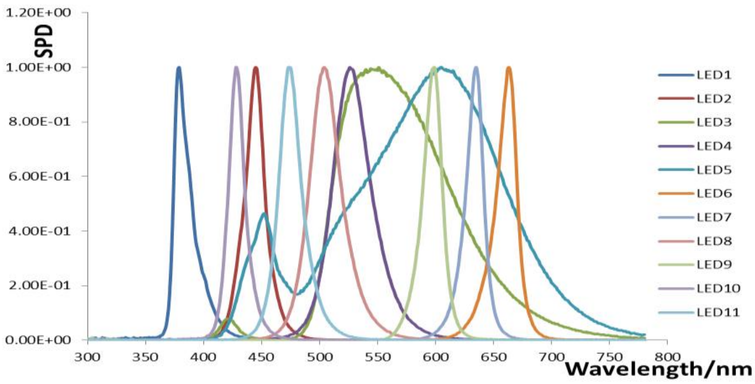

Figure 1: SPDs of 11 LEDs.

2.2 Pilot Experiment

The so-called 'test-sample method' adopted in this experiment requires observers to evaluate colour difference of identical samples illuminated by a reference and a test light source. Based on this, the grey backgrounds of two cabinets for adaptation should be visually alike. However, it was found that the bottom colour of two cabinets looked quite different while they had almost the same physical properties (CCT, luminance and chromaticity coordinates). The problem arises in part from the well-known shortcoming of V(λ) function, or 2° $\bar{y}$ colour matching function, i.e. it has insufficient energy in the blue end of spectrum.

A pilot experiment was therefore conducted to match the grey background in the cabinet illuminated by reference light sources and that illuminated by test sources. Five observers participated in this visual matching experiment. Telelumen was adjusted accroding to each observer's assessments to obtain a visually matched reference light source.

Nine visually matched reference light sources were obtained. Afterwards, the matched two grey backgrounds under a pair of light sources were measured by a JETI Specbos 1211uv spectroradiometer (called TSR hereafter). Spectral measurements were carried out under 0^o:45^o geometry. Figures 2a and 2b plot the individual results of a target of 2850K in u'v' diagram calculated in 2^o and 10^o observers respectively. It can be seen that the points are closer to the target in Figure 2b than in Figure 2a. This indicates that CIE 1964 or 10^o standard colorimetric observer performed better than that of 1931 or 2^o. In addition, the distance between 9 pairs of light sources in u'v' chromaticity diagram were calculated and the differences between the mean and each individual were averaged. This is known as MCDM (mean from colour difference of the mean) method. The MCDM values are 0.004 and 0.003 using 2° and 10° observers respectively. This is again confirmed that CIE 1964 standard colorimetric observer performed better than CIE 1931 standard one.

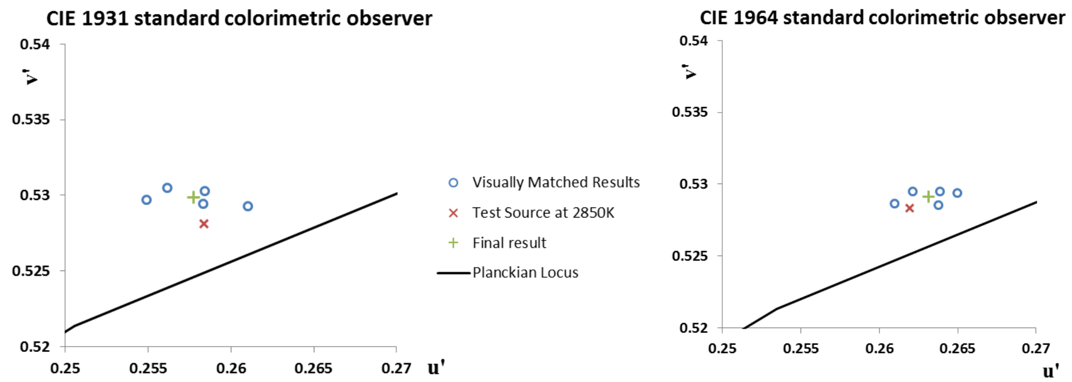

(a) *(b)*

Figure 2: u'v' chromaticity diagram of visually matched results (a: 2°observer; b: 10°observer).

2.3 Experimental Setup and Method

Nine pairs of light sources were investigated in this experiment. Their SPDs were reflected from a white tile positioned in the center of the bottom of the cabinet and also measured by TSR under the same illumination/viewing geometry. Table 1 lists the engineering data of the 18 light sources at 3 CCTs (2850K, 4000K and 6500K). Note that all the reference light sources were set about 60 cd/m^2 luminance higher than their corresponding test light sources, in order to have a visual matched brightness of the bottom surface under a pair of light sources as found in the pilot experiment. This is mainly caused due to the diffuse test source and spot reference source used in the experiment.

Table 1. Colorimetric properties of the 18 light sources.

Pair	Light sources	CCT(K)	Luminance (cd/m^2)	CIE-R_a
1	Test/Reference source	2814/2841	153/215	98/93
2	Test/Reference source	3955/3864	177/240	84/95
3	Test/Reference source	6280/6214	164/221	95/98
4	Test/Reference source	2812/2772	161/226	89/94
5	Test/Reference source	2829/2900	160/229	65/90
6	Test/Reference source	3960/3886	161/240	86/91
7	Test/Reference source	3953/3933	162/229	60/93
8	Test/Reference source	6308/6167	161/187	88/98
9	Test/Reference source	6322/5883	160/215	64/92

Thirty samples were chosen from various existing colour rendering sample sets, i.e. CIE-R_a, CQS and CRI2012. Figure 3 shows their distribution in CIELAB colour space, which reveals that they gave a satisfactory coverage. All the samples had a size of 7.5 cm by 5 cm to subtend about 5° at the observers' eyes with a viewing distance of 50cm.

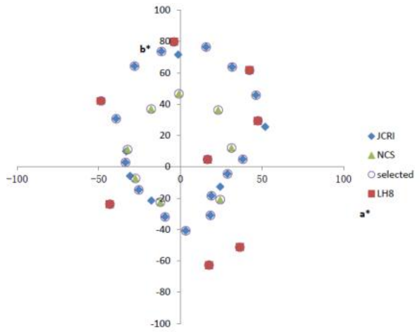

Figure 3: Sample distribution in CIELAB colour space.

Ten observers (5 male, 5 female) aged from 20 to 34 participated in the experiment. Before the experiment, they all passed the Ishihara colour vision test. Besides, they also took part in a small training session in order to be familiar with evaluation standards and to judge lightness, chroma and hue composition more accurately.

The whole experiment was carried out in a dark room without ambient light, as shown in Figure 4a. Before the start of experiment, observers were required to adapt to the dark condition for one minute. During this period, they were given an oral instruction of the experiment. Observers were then required to adapt to the grey backgrounds of two cabinets for one minute. In the experiment, according to a grey scale (see Figure 4b) placed in the cabinet of reference illuminant, observers reported colour difference in terms of grade values ranged from 1 (large difference) to 5 (no difference). Moreover, percentages of individual colour difference were also estimated, such as lightness difference, chroma difference and hue difference adding to 100. For each observer, the sequences of samples and light sources were all randomised.

In total, 12240 evaluations were accumulated, i.e. 4 questions × (30+4) samples × 9 pairs of sources × 10 observers.

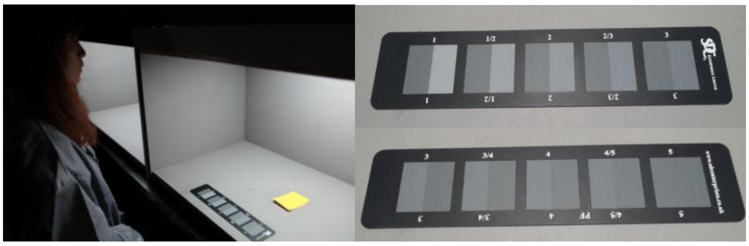

(a) *(b)*

Figure 4: (a) Photo of experimental situation (b) A grey scale.

3. RESULTS AND DISCUSSION

3.1 Observer Variability

Inter- and intra-observer variabilities were investigated in terms of the standardized residual sum of squares (STRESS) (García et al, 2007). A lower STRESS value indicates a smaller dispersion and better agreement. Inter-observer variability, which is also known as observer accuracy, was calculated between individual observer's results and mean observer's results. Meanwhile intra-observer variability, which is also known as observer repeatability, was calculated between each observer's first and second evaluations for the four repeated samples. The results showed that a mean value of 36 ranged from 31 to 46, and of 34 ranged from 21 to 49 for the inter- and intra- observer variabilities, respectively. This implies that intra- is slightly smaller than inter- observer variability as expected.

In addition, observers showed poor performance under pairs of sources 1, 3, and 8. This was mainly caused by the high CIE-R_a values for both the reference and test light sources. The higher the CIE-R_a value of test light source, the smaller the perceived colour difference will be. It is well known that observers perform less consistently for assessing colour difference of small magnitude, which leads to high STRESS values consequently.

3.2 UCSs' performance

The raw data reported by observers in terms of grade values (1-5) were converted into visual colour difference (ΔV) in CIELAB units via a fitted equation. Ideally, observers would find almost no lightness difference between two identical samples. However, it was found in the pilot experiment that observers required a higher luminance for the reference sources. Hence, the undesired visual lightness differences were calculated and removed from the total colour differences.

The visual chromatic differences obtained were employed to evaluate the performance of 4 different uniform colour spaces (UCSs), namely CIEU*V*W*, CIELAB, CIELUV and CAM02-UCS. Firstly, colour coordinates of 30 samples in different UCSs were calculated. Secondly, the colour differences between 30 sample pairs under each pair of light sources were calculated. These calculated colour differences (ΔE_i) were then compared with the corresponding averaged visual colour differences (ΔV_i) of ten observers. As mentioned earlier, 3 pairs of sources with high CIE-R_a values were removed to make results more reasonable. Pearson correlation coefficient (r) was used to indicate the agreement between the calculated and visual colour differences. It was found that CAM02-UCS provided the best correlation, followed by CIEU*V*W*, CIELUV and CIELAB the worst, with r values of 0.58, 0.53, 0.52 and 0.34, respectively. The results indicate that CAM02-UCS gave the overall best performance on evaluating colour fidelity of light sources. This also agrees with the previous work reported by other researchers (Li et al, 2011; Sándor and Schanda, 2006).

3.3 CRIs' performance

Observers' visual data were also used to test different CRIs, which can be divided into two categories. One category includes colour fidelity based CRIs, namely CIE-R_a, CQS, CRI-CAM02UCS and CRI2012 and the other includes colour preference CRIs, namely FSCI, FCI, GAI and MCRI. The mean visual colour difference of 30 samples under each pair of light sources was used to represent visual data for that pair of sources. Afterwards, the obtained visual results were compared with different CRIs of each test light source calculated from its SPD. Table 2 summarizes the performance of each CRI in terms of pearson correlation coefficient values.

From Table 2, it can be seen that all the four colour fidelity based CRIs gave similar good performance in terms of r values ranged from 0.79 to 0.91. All the fidelity indices agreed better with the perceived colour difference than those of colour preference indices, which gave quite poor correlations. Overall, CQS marginally outperformed the other colour fidelity indices. The results confirmed that colour preference based CRIs gave bad fit to the colour fidelity data.

Table 2. Performance of different CRIs in terms of r values

CRI	CIE-R_a	FSCI	FCI	GAI	MCRI	CRI-CA M02UCS	CQS	CRI2012
r values	-0.908	0.100	0.404	0.479	0.028	-0.862	-0.909	-0.792

4. CONCLUSIONS

A psychophysical experiment was carried out to investigate the performance of various UCSs and CRIs on evaluating colour fidelity of light sources. It is learned that a visual match of the grey backgrounds between the reference and test fields is strongly required. Also, the results obtained from the perception of colour difference reveal that test light sources with high CIE-R_a values are not recommended to use, since observers are unable to scale small colour differences accurately and consistently.

It was found that CAM02-UCS correlated with visual results best among all the 4 UCSs tested. CIEU*V*W*, which is used to calculate CIE-R_a, and CIELUV also showed good performance with slightly lower correlations. On the contrary, CIELAB worked worst in predicting visual results.

In considering CRIs' performances, all the colour fidelity indices gave similar accuracy and outperformed colour preference indices in terms of r values. On the whole, CQS performed marginally better than the other three fidelity indices while MCRI showed worst prediction of visual results.

REFERENCES

García, P. A., R. Huertas, M. Melgosa and G.H. Cui. 2007. Measurement of the relationship between perceived and computed color differences. *JOSA A*, 24(7): 1823-1829.

Jost-Boissard, S., P. Avouac, and M. Fontoynont. 2014. Assessing the colour quality of LED sources: Naturalness, attractiveness, colourfulness and colour difference. *Lighting Research and Technology*: 1477153514555882.

Li, C., M.R. Luo, G.H. Cui, and C.J. Li. 2011. Evaluation of the CIE colour rendering index. *Coloration Technology* 127(2): 129-135.

Sándor, N., and J. Schanda. 2006. Visual colour rendering based on colour difference evaluations. *Lighting Research and Technology* 38(3): 225-239.

Address: Prof. Ming Ronnier LUO, State Key Laboratory of Modern Optical Instrumentation, Zhejiang University, 38 Zheda Road, Hangzhou,310007, CHINA
E-mails: m.r.luo@leeds.ac.uk

A Study on the Lighting of Bathroom for the Elderly

Jiyoung PARK,[1] Chanung JEONG,[2] Eunji SEO,[2] Jinsook LEE[3]
[1] Ph.D, Dept. of Architectural Engineering, Chungnam National University, Korea
[2] Master Course, Dept. of Architectural Engineering, Chungnam National University, Korea
[3] Professor, Dept. of Architectural Engineering, Chungnam National University, Korea

ABSTRACT

In this study, I have come up with the luminance and color temperature that are appropriate for elderly people who are 65 or older, in the bathroom of houses that adopt direct LED light from the ceiling. To come up with a lighting environment in the bathroom space for the elderly, I combined the verified appropriate scope of luminance and color temperature with the analysis of the influence from the evaluation variables. As a result, the lighting environment in the bathroom space for elderly people who are 65 or older required the color temperature of 3000 K and the luminance of 400 lx.

1. INTRODUCTION

A bathroom is at once a space for satisfying the physiological needs of humans and a space for health care and rest. While its size is small compared to other units of a house, it accommodates a variety of behaviors. So, it requires sanitary and functional kind of lighting, and furthermore, since most bathrooms are closed without windows, the role of light looms even bigger. Moreover, as a bathroom registers the most accidents involving elderly people among all parts of a residential space and visual ageing follows health condition in influencing an elderly person's ability to perform activities of daily living, lighting should be applied while considering the visual characteristics of elderly people.

Also, the bathrooms for collective housing in Korea that is being sold or accommodating residents lately have direct light buried in the ceiling. And as LED has begun to be adopted for residential indoor lighting, studies should reflect such a trend for bathroom space.

Thus, in this study, I have come up with the luminance and color temperature that are appropriate for elderly people who are 65 or older, in the bathroom of houses that adopt direct LED light from the ceiling.

2. EXPERIMENTAL METHOD

The size of the bathroom space chosen for the experiment is 3000 (W) Ⅹ 2000 (L) Ⅹ 2000 (H) mm, and it includes a wash basin, a toilet, a bath tub, a mirror etc. The bathroom includes two pieces of direct light buried in the ceiling. The light chosen for the wash basin and the toilet is rectangular with the size of 1200 Ⅹ 150 mm, while the round-shaped ones used for the center above the bath tub and above the center of the bathroom have a diameter of 150 mm, all adopting LED.

Four different levels of color temperature presented for the experiment are 3000 K, 4000 K, 5000 K, and 6000 K, while six levels of luminance used for it are 100 lx, 200 lx, 300 lx, 400 lx, 500 lx, and 600 lx. The color temperature was measured using a chroma meter (CL-200, Minolta) directly under the experimental light source, while luminance was measured as an average luminance for the bathroom space, in KS 5-point method, using an illuminometer (T-10, Minolta), at the height of 85 cm above the floor.

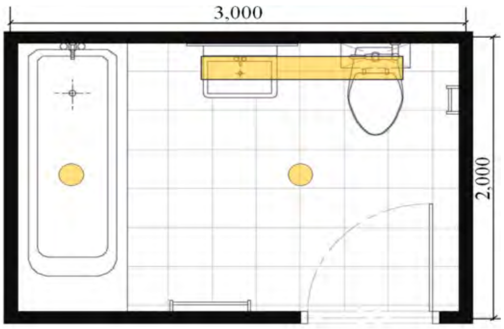

Fig 1. Overview of the experimental space

Fig. 2. Composition of the experimental space

Table 1. Physical properties of the rectangular ceiling light and spectral distribution

Color temperature	CRI [Ra]	Spectral distribution
3000 K	80	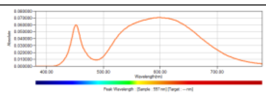
4000 K	79	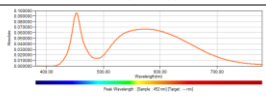
5000 K	77	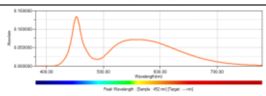
6000 K	75	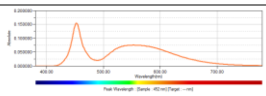

Table 2. Physical properties of the round shaped ones *ceiling light and spectral distribution*

Color temperature	CRI [Ra]	Spectral distribution
3000 K	78	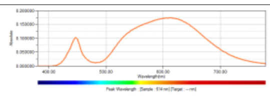
4000 K	81	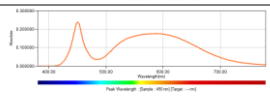
5000 K	81	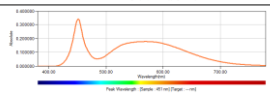
6000 K	80	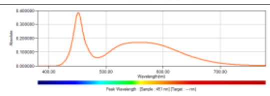

The 15 subjects who participated in the experiment were at least 65 years old and below 86 (average age 75). To rule out the influence of any artificial light sources around including the daylight, the experiment was conducted in a windowless space and in sequential comparison. The subjects were instructed to adjust for 1 minute to the provided lighting environment and then verbally express the appropriateness (how bright) and preference (how much preferred) of the brightness on the 5-point scale (5 points for Very much so, 3 points for So-so (appropriate for brightness), and 1 point for Never), while the researcher recorded their responses on the evaluation sheet.

3. EXPERIMENT RESULTS AND ANALYSIS

The analysis of the group average for the category of 'Bright' is as shown in Fig 3. For all color temperature levels, respondents found it the most appropriate at 300 to 400 lx, found 500 lx somewhat bright, and found 600 lx very bright. And they found 200 lx somewhat dark and 100 lx very dark. In her study, Jinsook LEE (2014) saw that those respondents in their 20s or 30s found 300 lx the most appropriate as the brightness for general lighting in the bathroom space. When compared with the study that surveyed elderly people who are 65 or older, one can see that the group of respondents who are 65 or older comes close to the group of those in their 20s or 30s, thus preferring similar levels of brightness, or demands 100 lx or so more.

The analysis of the group averages in the evaluative category of 'Preferred' is as shown in Fig 4. 3000 K is highly rated in all categories compared to the other color temperature levels, and notably, 3000 K is the most preferred at 300 to 400 lx, now found to be the appropriate brightness. The study by Jinsook LEE (2014) showed that as the appropriate color temperature for general lighting in the bathroom space, those in their 20s or 30s prefer 3000 K most. This agrees with the study involving the elderly who were 65 or older, and one sees that different age groups do not differentiate widely but share similar preference of color temperature.

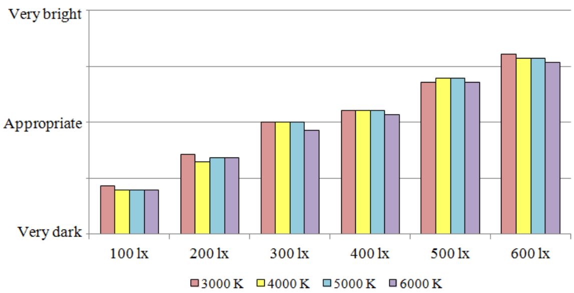

Fig. 3. Analysis of group averages in the evaluative category of 'Bright'

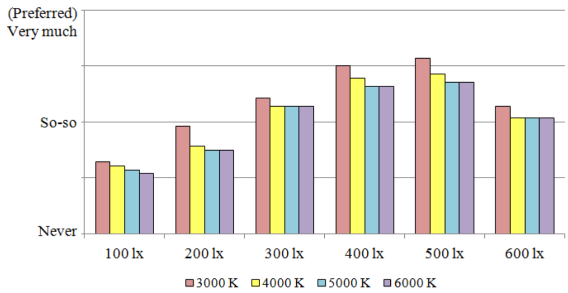

Fig. 4. Analysis of group averages in the evaluative category of 'Preferred'

I performed H-test by Kruskal-Wallis to see if there exist any significant differences among the results of the luminance evaluation at the same color temperature. As a result, all came up with a statistical significance (p-value) of less than 0.05 (with a significance level of 5%), thus showing that there a significant differentiation with levels of luminance. Therefore, I think scrupulous consideration should be given to brightness in designing lighting environment for a bathroom space (Table 3).

Table 3 . Test of statistical significance among levels of luminance at the same color temperature

Behavior	**Type of lighting**	**Color temperature**	**Statistical significance (P)**
			Bright
General	Direct light from ceiling	3000 K	0.000*
		4000 K	0.000*
		5000 K	0.000*
		6000 K	0.000*

* : Significance level below 0.05,

I performed H-test by Kruskal-Wallis to see if there exist any significant differences among the results of the color temperature at the appropriate luminance. As a result, all came up with a statistical significance (p-value) above 0.05 (with a significance level of 5%), thus showing that there is no significant differentiation with levels of color temperature (Table 4).

Table 4. Test of statistical significance among levels of color temperature at the appropriate luminance

Behavior	**Type of lighting**	**Color temperature**	**Statistical significance (P)**
			Preferred
General	Direct light from ceiling	300 lx	0.916
		400 lx	0.375

* : Significance level below 0.05

For a quantitative analysis of the visual effects of the experimental variables, I performed multiple regression analysis to analyze the influence of different evaluation variables. The multiple and partial correlation coefficients obtained from the analysis are as shown on Table 5. Overall, correlation coefficient was minimum 0.5 and luminance registered the greatest influence.

'Preference' with regard to the color temperature and luminance of 'direct light from ceiling' registered a high correlation coefficient of $R=0.9962$ ($R^2=0.9925$). As for the scope of factors, luminance was 84.83%, thus registering bigger influence than color temperature. To look at the quantity by category, respondents preferred 300 to 500 lx at the color temperature of 3000 K, with the greatest influence registered at 3000 K and 400 to 500 lx.

Table 5. Influence of evaluation variables

Evaluation criterion	**Multiple correlation coefficient (R^2)**	**Partial correlation coefficient (scope)**	
		Color temperature	**Luminance**
Preferred	0.9925	0.916(0.300)	0.996(1.678)

R^2=0.9925

Classification / Variable	Category	Number of samples	Standardized category quantity	Partial correlation coefficient	Variable scope	Variable scope quantity
Color temperature	3000 K	6	0.201	0.916	0.300	15.17%
	4000 K	6	-0.014			
	5000 K	6	-0.087			
	6000 K	6	-0.099			
Luminance	100 lx	4	-0.968	0.996	1.678	84.83%
	200 lx	4	-0.521			
	300 lx	4	0.179			
	400 lx	4	0.622			
	500 lx	4	0.709			
	600 lx	4	-0.021			

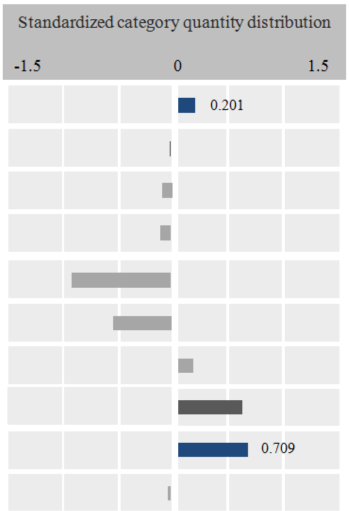

Fig. 5. Analysis of category-specific influence of different evaluation criteria

4. CONCLUSIONS

To come up with a lighting environment in the bathroom space for the elderly, I combined the verified appropriate scope of luminance and color temperature with the analysis of the influence from the evaluation variables. As a result, the lighting environment in the bathroom space for elderly people who are 65 or older required the color temperature of 3000 K and the luminance of 400 lx.

ACKNOWLEDGEMENTS

This work was supported by LED System Lighting R&D program of KEIT, [10042955, Integrated Optical, Emotion and Energy saving Assessment Techniques, and User Centered Guidelines Development for LED System Lighting.

REFERENCES

Jin-Sook, LEE. and Ji-Young, PARK. 2014. *Identifying the Appropriate Illuminance and Color Temperature of LED Lighting for Different Behaviors in Bathroom Space*, Journal of the Korea Society of Color Studies, 28(3), 179-188.

Address : Jiyoung Park, Dept. of Architectural Engineering, College of Engineering, Chungnam National University, 99 Daehak-ro, Yuseong-gu, Daejeon 305-764. Korea
E-mails: jiyoung1355@hanmail.net, chanwung2000@nate.com, sej4468@naver.com, js_lee@cnu.ac.kr

Sitting Posture Based Lighting System to Enhance the Desired Mood

Hyunjoo BAE,[1] Haechan KIM,[1] Hyeon-Jeong SUK[1]
[1] Department of Industrial Design, KAIST

ABSTRACT

As a cue of desired mood, we attempted to identify types of sitting posture when people are involved in various tasks during their working hours. After having attached six pressure sensors and one distance sonsor to an office chair, we first recorded participants' postures while they took part in four different tasks. From the seven sensors, we gathered five sets of data related to the head, lumbar, hip, thigh pressure and the distance between the backrest and the body and then classified them. We derived four types of sitting posture that were mapped into the different tasks. In addition, we requested subjects to take poses that might be suitable for the each of the four task types. In this way, we tried to compare the matches between postures and tasks in natural setting with those in controlled situation. The comparison yielded no statistical significance and consequently, we moved on to the development of a posture based lighting system that manipulates the quality of office lighting and is operated by changes in one's posture. Facilitated by this system, color temperature ranging between 3000 K and 7000 K and illumination ranging between 300 lx and 700 lx were modulated. This study demonstrates how human emotion can interact with lighting mediated through physical behavior.

1. INTRODUCTION

There have been demands for higher qualities of daily life by extending the role of lighting system. LED lighting system in particular, has benefits to easily control its illumination and color temperature, offering users wide possibilities of desirable lighting environment. Thus, efforts are currently underway to investigate the optimal lighting environment to enhance the task productivity and emotional satisfaction. For example, some studies has conducted a study to determine the proper lightings for educational situation(Lee et al. 2013, Wessolowski 2014). As a cue of desired mood, physical behavior reacted to the user contexts have been studied such as automated posture analysis for detecting subject's interest level(Mota and Picard 2003). Especially when it comes to office, it is determined that sitting postures have high feasibility and can be detected robustly with sensing chair(Mutlu et al. 2007). In this regard, we aim to examine the feasibilities of sitting postures as a cue of desired mood. Also, we attempt to propose a posture-based lighting system focusing on office environment that provides optimal quality of lighting for different user contexts.

2. EXPERIMENTAL PLAN

In order to obtain the quantitative data when people have different sitting postures during their working hours, we planned an empirical study by attaching sensors to an office chair. Differently from thoroughly carried out studies on human ergonomics, we tried to reduce the number of sensors as much as possible while minimizing the loss of meaningful data. Moreover, we also intended to find a synergetic match between types of posture and those of task. Finally we anticipated to map out appropriate lighting contents unconsciously modulated by one's sitting postures.

2.1 Participants

A total of 10 college students participated and their average age was 21.50 years (SD = 1.78 years) Their average height of 167.30 cm and weight of 59.20 kg, and both genders were evenly recruited. In order to prevent abnormal sitting posture caused by poor eyesight, we acquired higher than 0.7 score in eyesight. Also participants should not have experience of having treatment for pain of neck, shoulder, legs or arms.

2.2 Experimental Setup

The experimental room was set up to resemble an office environment. Sitting postures on the office chair were observed while participants were taking part in the given tasks presented on computer monitor(Figure.1). To identify the postures, we attached six pressure sensors and one distance sensor to an office chair. To find the relevant locations of sensors we referred to the related research(Park et al. 2012) and then covered the chair with cotton fabric(Figure 1). While a participant was sitting we received signals from their head, lumbar, hip, thigh pressure and the signal of backrest-body distance at every 5 Hz. We transformed the signals into manageable data utilizing Arduino Processing. In addition, to measure the body angle, markers were attached on their joint of shoulder, hip and knee and the side view were recorded. The monitor was set to be center of the participants, and the distance between the monitor and the eyes was 50 cm. The chair's height was adjusted depending on the participant's height to keep 90 degree of knee angle. To reduce influence by lighting, the experiment was conducted under a constant illuminant (5000 K, 600 lux).

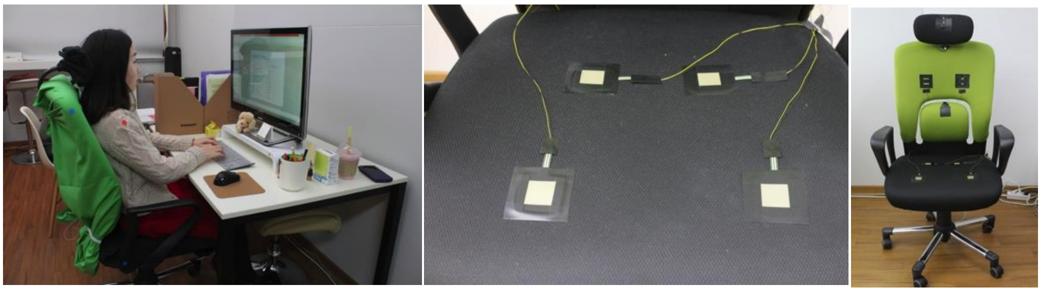

Figure 1: Experimental environment and Sensor equipped office chair.

2.3 Experimental Procedure

The empirical study involved two steps. In part 1, we observed participant's unconscious postures while they were working on the following four tasks: (1) memorizing words, (2) playing Tetris®, (3) reading magazine articles, and (4) relaxing. Memorizing words was for strong attention with high workload, while playing Tetris® game was considered as attentive but with low workload. Also, reading simple articles was associated with medium level of concentration as well as workload. As reading material we provided with six articles that were nor much informative. Finally, relaxing was expected to release participants from any types of tasks, and participants were listening to meditation music. In this way, the four tasks were carefully devised. Each task took seven minutes until completed and the tasks were given in random order(Figure 2). In part 1, participants were not informed that their posture was being recorded.

In part 2, on the other hand, the purpose of the experiment was revealed. Participants were asked to consciously take postures that best fit to the given task type. They sat in different positions approximately for 10 seconds and the request was repeated three times in random order(Figure 2).

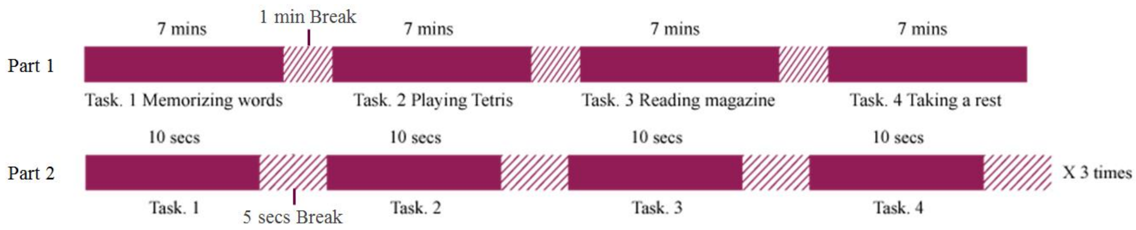

Figure 2: Experimental process of part2.

3. RESULTS AND ANALYSIS

3.1 Data Extraction

After having collected the data from both part 1 and 2, we focused on the replicated parts that appeared consistently. In part 1, when participants maintained certain posture for longer than 30 seconds, it was considered as one posture. We cropped out the 15 second-segment from the middle of the posture and then averaged them for each sensor value. Finally, a total of 45 segments (the number of observed postures which maintained longer than 30 secs) were collected from part 1, the unconscious sitting postures (Figure 3). In part 2, we applied the identical method but observed only 5 seconds. Since we requested to pose three times, we collected a total of 15 second-segment and then averaged them for each sensor value. Therefore, 40 segments (4 tasks × 10 participants) were collected from part 2, the conscious sitting postures (Figure 4).

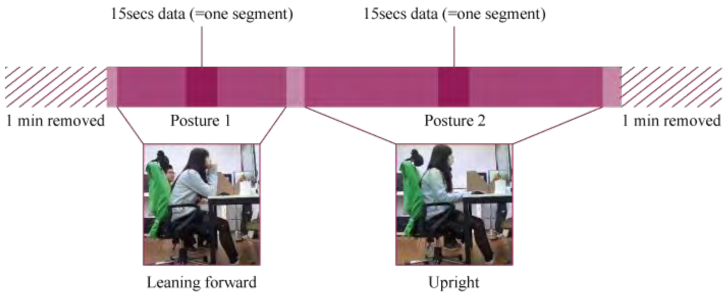

Figure 3: Process of extracting data from part1.

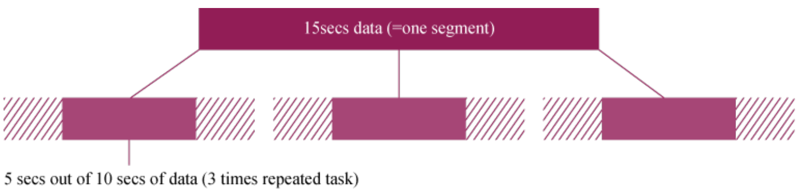

Figure 4: Process of extracting data from part2.

3.2 Classification of Sitting Postures based on the Sensor Values

Based on a total of 85 extracted posture segments, we classified them in following four kinds of postures: (P1) leaning forward (under 85 degree), (P2) upright (between 85 and 95 degree), (P3) upright with the lumbar supporting, (P4) leaning backward. We distinguished (P2) from (P3), because of different range of lumbar pressure. Furthermore, to confirm the statistical difference between posture types, we one-way independent ANOVA test based on the sensor values of each posture. The analysis yielded a statistical significance [$F(3,81) = 22.033$, $p<.05$] indicating that each posture can be profiled with a noticeable difference. For example, backrest-body distance was significantly bigger than other postures while participants leaning forward. During upright with the lumbar supporting and leaning backward, the lumbar pressure was significantly bigger than other postures. Subsequently, all 85 segments from observed postures could be classified in four posture types(Figure 5).

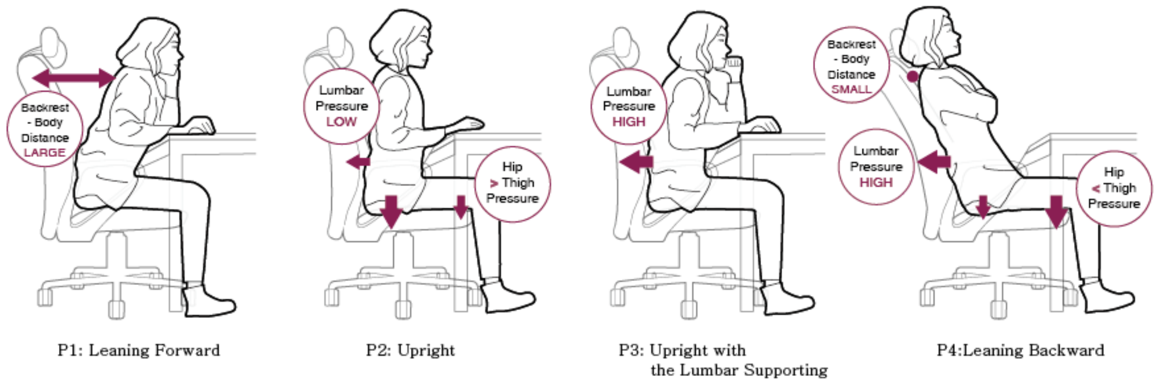

Figure 5: Posture classification process and criteria.

In addition, the Figure 6 illustrates the flow of signal processing to sort out the sensor signal into the corresponding postures.

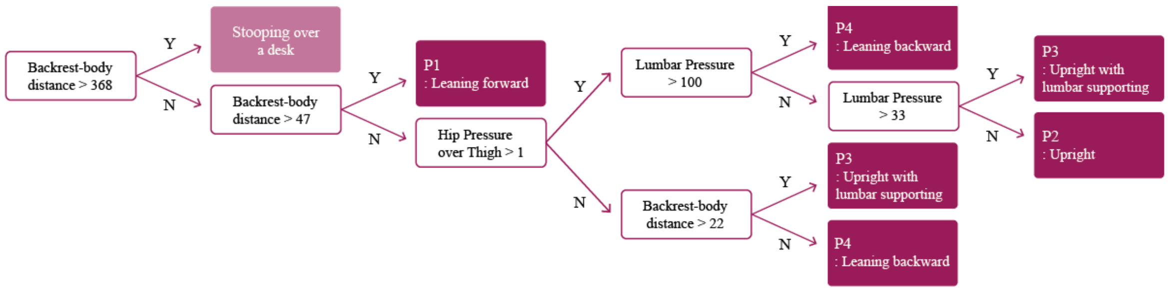

Figure 6: Process of signal to be corresponded to one of the four posture types.

3.3 The relationship between postures and tasks

Then we tried to explore whether the postures could be represent the user's task or not. Chi test was conducted to compare the frequency of observed posture types depending on unconscious and conscious tasks. Differently from anticipation, the difference between the unconscious postures in part 1 and conscious postures in part 2 did not show a statistical significance at an alpha level of 0.05 in each task. Therefore, the sum of posture frequency of both parts was used for statistical analysis (Table 1).

Table 1. Posture frequency depending on task types.

	P1	P2	P3	P4
(1) Memorizing Words	11	6	3	3
(2) Playing Tetris®	7	7	5	2
(3) Reading Articles	4	5	11	2
(4) Relaxing	0	0	2	20

The results indicate that postures are influenced by the task. There was a significant association between the task types and the posture types [χ^2 (9, N=85) = 62.087, p < .05]. While participants were memorizing words, leaning forward posture was most frequently observed. While playing game, leaning forward posture and upright posture were dominant identically. Whereas, during reading articles, upright with the lumbar supporting posture was quite frequent. In addition, while relaxing, frequency of leaning backward posture was definitely higher than other postures. That is, people are unconsciously and consciously leaning forward when working intensively, whereas leaning backward during relaxing.

4. DISCUSSION

4.1 General Discussion

The empirical study showed sitting postures could be classified in posture types based on signals. Also, sitting postures appeared differently related to the concentration level of works. Since the postures reflect user's states, it can be used as a novel lighting control interface. To some disappointment, there was weak similarity between unconscious and conscious postures in memorizing words out of four task types. It could be assumed that that intensive working caused some tiredness and it affected on inconsistent tendency of postures. As such, to make more reliable posture sorting algorithm, accurate and stable signals of sensor should be collected. Also, more in-depth studies would be worthwhile to investigate the relationship between sitting postures and task types.

4.2 Application of posture based lighting system

Finally we developed a posture based lighting system that manipulates the quality of office LED lighting and is operated by changes in one's posture. As previous studies have revealed there are optimal combinations of color temperature and correlated illumination that can enhance people's affective experience. They demonstrated that higher color temperature (7500 K versus 3000 K) is more activating in the point of mental level (Deguchi and Sato 1992) and low color temperature lighting creates a lowering of central nervous system activity(Noguchi and Sakaguchi 1999). In addition, the efficiency of learning increases under high color temperature and high illuminance lighting, whereas the lighting of low color temperature and low illuminance was proper for relaxing(Lee et al. 2013, Wessolowski 2014). Consequently, for the concentration required activities, high color temperature - high illuminance lighting condition is needed to users, on the other hand, low color temperature - low illuminance lighting is suggested for relaxation.

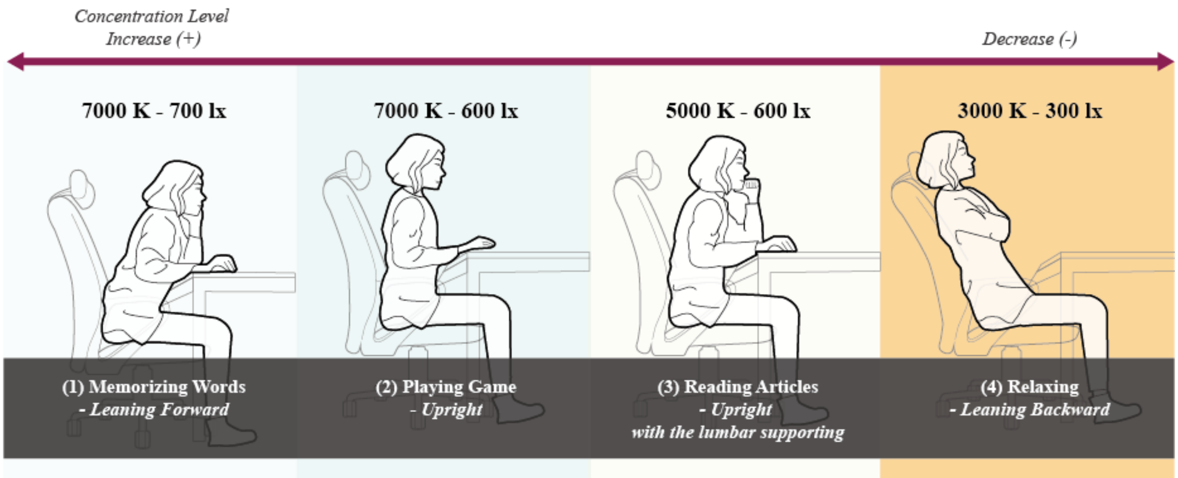

Figure 8: Four scenarios of posture-based lighting system.

Through the previous researches and the real demonstration under high rendering LED ambient lighting room, the modified illumination ranges between 300 lx and 700 lx, and correlated color temperatures range between 3000 K and 7000 K. After real-time posture classification by Arduino Processing, color temperature and illuminance of LED lighting can be adjusted to offer desired mood of users. Thus, optimal lighting presets for each task can be produced by one's posture. Four representative lighting scenarios were generated as follow: (1) for the strong attention with leaning forward posture, 7000 K - 700 lx lighting will apply, (2) for the attentive task such as playing game with upright posture, 7000K - 600 lx lighting will apply, (3) for the medium level of concentration in daily life like reading, 5000K - 600 lx will apply, and (4) for the relaxation, 3000K - 300 lx lighting will apply. Ultimately, this system might increase intuitiveness and unobtrusiveness of lighting control interface for office environment. Furthermore, with the larger number of participants, more accurate posture classification algorithm should be developed. Also the verification experiment will be conducted in these posture-based lighting scenarios.

5. CONCLUSION

This study investigates the feasibility of posture classification based on simple sensor equipped chair. Through the experiment, it was determined that postures of users are related to different concentration level of tasks. Also, there is no significant difference between unconscious and conscious sitting postures from identical task. Wide possibility of automated indoor lighting system to provide desired mood using sitting postures was explored. The empirical findings of this research can be utilized for interaction between human emotion and lighting mediated through physical behavior.

REFERENCES

Deguchi, Takatsugu, and Masahiko Sato. 1992. The effect of color temperature of lighting sources on mental activity level. *The Annals of physiological anthropology* 11 (1):37-43.

Lee, J, K Choi, N Na, and HJ Suk. 2013. LED Lighting for Educational Environment: Focusing on Math and Multimedia Based Tasks for 4th Grade Elementary School Students in South Korea. 12th Cogress of International Color Association AIC 2013, New Castle.

Mota, Selene, and Rosalind W Picard. 2003. Automated posture analysis for detecting learner's interest level. Computer Vision and Pattern Recognition Workshop, 2003. CVPRW'03, Villanova, 49-49.

Mutlu, Bilge, Andreas Krause, Jodi Forlizzi, Carlos Guestrin, and Jessica Hodgins. 2007. Robust, low-cost, non-intrusive sensing and recognition of seated postures. Proceedings of the 20th annual ACM symposium on User interface software and technology UIST 2007, Newport, 149-158.

Noguchi, Hiroki, and Toshihiko Sakaguchi. 1999. Effect of illuminance and color temperature on lowering of physiological activity. *Applied human science: journal of physiological anthropology* 18 (4):117-123.

Park, Jae Hee, Seung Hee Kim, Min Uk Kim, Hee Dong Han, Young Soo Shim, and Taeil Son. 2012. Measurement of Body Weight Distributions on a Seat Pan for Various Sitting Postures. *Journal of the Ergonomics Society of Korea* (Published online).

Wessolowski, Nino. 2014. Wirksamkeit von dynamischem Licht im Schulunterricht. Hamburg-Eppendorf: Universtitaet Hamburg.

Address: Prof. Hyeon-Jeong Suk, Department of Industrial Design, KAIST
Bldg. N25, 291 Daehak-ro, Yuseong-gu, Daejeon, 305-701, KOREA
E-mails: bhjoo@kaist.ac.kr,kimhaechan@kaist.ac.kr,h.j.suk@kaist.ac.kr

Colour Lighting Based on Chromatic Strength

Toru KITANO, Tetsuji YAMADA, Kosuke OSHIMA
Iwasaki Electric Co., Ltd.

ABSTRACT

In its technical report CIE 94: Guide for Floodlighting, the International Commission on Illumination (CIE) defines the recommended luminance for illuminating an object with white-colour light. However, it does not define recommended luminance for illuminating an object with coloured light. Accordingly, we conducted a matching experiment on the object illuminated with white-colour light and the object illuminated with coloured lights, for finding the luminance ratios when the both objects are perceived as having equal chromatic strength, and derived recommended luminance for colour lighting. As a result, we found that the recommended luminance for colour lighting can be expressed by a variable differing depending on the *u'v'* chromaticity of the illuminated object. In addition, we conducted a verification experiment to confirm whether derived recommended luminance is utilized for actual lighting design. In detail, we conducted an experiment to confirm whether the object is equally conspicuous when the object is illuminated with different coloured lights to the identical chromatic strength. We verified that the recommended luminance for colour lighting can be utilized for actual lighting design.

1. INTRODUCTION

Emergence of full-colour LED lighting has increased opportunities to illuminate towers, bridges, monuments, etc. with vivid coloured lights. In its technical report CIE 94: Guide for Floodlighting, the International Commission on Illumination (CIE) defines the recommended luminance for illuminating an object with white-colour light such as mercury lamp and high-pressure or low-pressure sodium lamp as 4 cd/m^2 (poorly lit zones), 6 cd/m^2 (average zones) and 12 cd/m^2 (brightly lit zones) according to the brightness of the surroundings. However, it does not define recommended illuminance and luminance for illuminating an object with coloured light. As a result, it is impossible to easily calculate the quantity of light required for giving the suitable appearance.

Accordingly, we conducted a matching experiment on the object illuminated with white-colour light and the object illuminated with coloured lights, for finding the luminance ratios when the both objects are perceived as having equal chromatic strength, and derived recommended luminance for colour lighting.

2. DERIVATION OF THE RECOMMENDED LUMINANCE

2.1 Matching Experiment

Figure 1 shows a schematic diagram of experimental equipment. The subjects included 10 males and females in their 30s to 40s with normal colour vision.

To begin with, the subject sits in the chair in a dark room and observes black paper of luminance L_B located in front for 5 minutes to adapt his/her eyes. As shown in Figure 1, the black paper is provided with two right and left circular holes opened symmetrically by the center of the visual field beforehand, which are covered with the same kind of black paper during adaptation. There is a white wall ahead of the black paper, and the left portion of the wall viewed from the subject is uniformly illuminated with white-colour light of correlated colour temperature 5,000 K, and the right portion of the wall is uniformly illuminated with coloured light. A partition is installed at the center of the white wall so that right and left light will not be mixed.

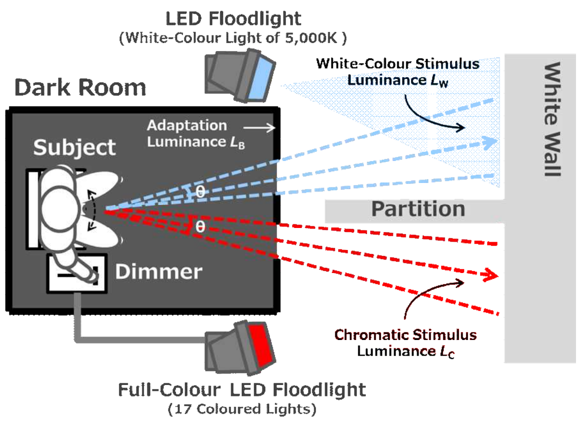

Figure 1: Schematic diagram of experimental equipment.

After the adaption, the black paper covering the holes is removed to present to the subject a stimulus by white-colour light (to be referred to as the white-colour stimulus) and that by coloured light (to be referred to as the chromatic stimulus) through the holes. When observing both stimuli, the subject was instructed to swing his/her face to the right and left to look at the center of the right and left stimuli. The subject was allowed to freely adjust the luminance L_C of the chromatic stimulus with a dimmer at hand until he or she perceives as the strength equal to the white-colour stimulus of luminance L_W. The subjects were taught that the strength was a “concept combining brightness and conspicuousness.” After matching was completed, the then luminance L_C of the chromatic stimulus was measured and a different chromatic stimulus was presented again to make matching.

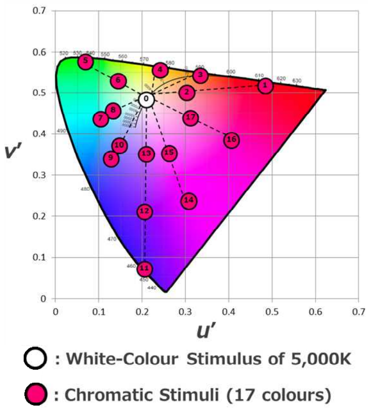

No.	u'	v'	No.	u'	v'
0	0.210	0.484	9	0.129	0.343
1	0.485	0.521	10	0.147	0.371
2	0.305	0.494	11	0.199	0.073
3	0.333	0.543	12	0.214	0.212
4	0.243	0.554	13	0.217	0.353
5	0.071	0.577	14	0.308	0.239
6	0.145	0.529	15	0.265	0.353
7	0.105	0.437	16	0.407	0.385
8	0.133	0.455	17	0.316	0.436

Figure 2: u’v’ chromaticity of the white-colour and chromatic stimuli.

Figure 2 shows the *u*’*v*’ chromaticity of the white-colour and chromatic stimuli. Totally 17 colours were used for the chromatic stimuli. Assuming the same 3 conditions as in the CIE94, 4, 6 and 12 cd/m^2, for the luminance L_W of the white-colour stimulus, the then adaptation luminance L_B was assumed to be 5% of L_W (0.2, 0.3 and 0.6 cd/m^2, respectively). The viewing angle θ of the presented stimuli assumed 3 sizes of 5°, 15° and

30°. This viewing angle was determined, assuming a situation to view an illuminated object from near, medium and far distances. The matching experiment was conducted in 3 times for each different luminance L_W of the white-colour stimulus, and matching was implemented 153 times in total (17 colours × 3 conditions × 3 sizes).

2.2 Experimental Results

Figure 3 shows the results of the $\log(L_W/L_C)$ values, that of the luminances L_C of the chromatic stimuli perceived as equal strength to the white-colour stimulus at $L_W = 4$ cd/m^2 and $\theta = 5°$, in the form of a box plot. Nos. 1 to 17 in Figure 4 are common with Figure 2.

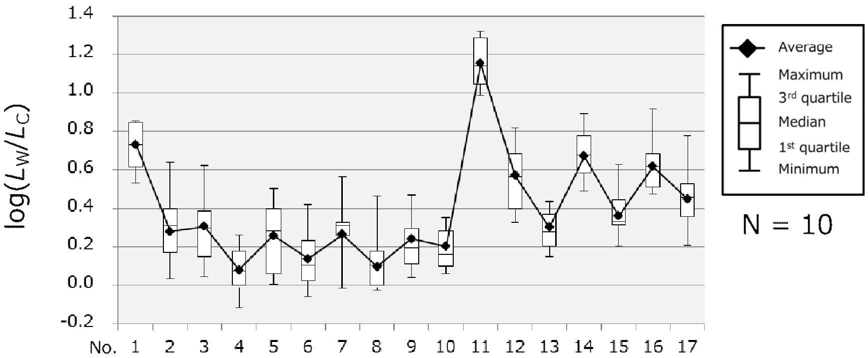

Figure 3: Results of the $\log(L_W/L_C)$ values.

The L_W/L_C ratios are proportional to the strength of that chromatic stimuli (to be referred to as the chromatic strength) and indicate that the chromatic stimuli are higher chromatic strength than the white-colour stimulus in case of $L_W/L_C > 1.0$, and they are lower chromatic strength than the white-colour stimulus in case of $L_W/L_C < 1.0$. According to Figure 3, the colour with the highest chromatic strength among Nos. 1 to 17 was No. 11, blue, and that with the lowest chromatic strength was No. 4, yellow. Also, among chromatic colours with the same dominant wavelength (for example, Nos. 11, 12 and 13), Figures 2 and 3 show that the one with higher excitation purity (No. 11 in this case) was the higher L_W/L_C ratios, and higher chromatic strength. This phenomenon was the same as the Helmholtz-Kohlrausch phenomenon in which the brightness of a perceived colour changes when the excitation purity is increased. These results showed a similar tendency in the experimental results with the different luminance L_W of the white-colour stimulus and different viewing angle θ of the presented stimulus.

As shown in Figure 3, the results of the L_C/L_W ratios varied greatly among the subjects depending on the chromatic colours. If the recommended luminance for colour lighting is derived, assuming the average value of the L_C/L_W ratios of the 10 subjects to be a representative value, the recommended luminance could be too low for about half of them. Accordingly, this study attempted to derive the recommended luminance for colour lighting, assuming the third quartile of the results to be the representative value of the L_C/L_W ratios.

2.3 Derivation of the Recommended Luminance

The CIE recommends the empirical formulas (1) and (2) which compare the brightness of the luminance L_1 and L_2 of different colours. Formula (1) represents the brightness by a correction coefficient f consisting of luminance and xy chromaticity. When Formula (1) holds, L_1 and L_2 are of the same brightness. When the *xy* chromaticity is D65 (0.313, 0.329), $f = 0$ holds.

$$\log (L_1) + f_1 = \log (L_2) + f_2 \tag{1}$$

$$f = 0.256 - 0.184y - 2.527xy + 4.656x^3y + 4.657xy^4 \tag{2}$$

Then, it is assumed that the luminance L_1 of Formula (1) is the luminance L_W of the 5,000 K white-colour stimulus, and that the luminance L_2 is the luminance L_C of the chromatic stimulus. Furthermore, if $f = 0$ holds in case of the 5,000 K white-colour stimulus, Formula (1) can be expressed as Formula (3), using the new correction coefficient f'. Since $f' = \log (L_W/L_C)$ is allowed by deforming Formula (3), a regression Formula (4) for calculating the correction coefficient f' was obtained by multiple regression analysis, assuming $\log (L_W/L_C)$ values obtained from the experimental results to be explained variables and variables consisting of the *u'v'* chromaticity of the chromatic stimuli to be explanatory variables.

$$\log (L_W) = \log (L_C) + f' \tag{3}$$

$$f' = 1.023 - 2.79v' + 46.1u'v'^3 + 141u'^3v'^2 - 196u'^2v'^3 \tag{4}$$

$$L_C = L_W / 10^{f'} \tag{5}$$

If Formula (3) is deformed, the recommended luminance L_C for colour lighting can be expressed by Formula (5). Now, suppose based on the CIE 94 that the recommended luminance L_W for illuminating an achromatic object with 5,000 K white-colour light has 3 levels 4 cd/m^2, 6 cd/m^2 and 12 cd/m^2, the recommended luminance L_C for colour lighting can be presented in Table 1. Figure 4 shows the relations between $10^{f'}$ values and *u'v'* chromaticity coordinates. It is seen that the recommended luminance L_C for colour lighting is a variable differing depending on the *u'v'* chromaticity of the illuminated object.

Table 1. Recommended luminance for colour lighting.

Brightness of the surroundings	Recommended luminance L_W (White-colour light)	Recommended luminance L_C (Coloured light)
Poorly lit zones	4 [cd/m^2]	$4/10^{f'}$ [cd/m^2]
Average zones	6 [cd/m^2]	$6/10^{f'}$ [cd/m^2]
Brightly lit zones	12 [cd/m^2]	$12/10^{f'}$ [cd/m^2]

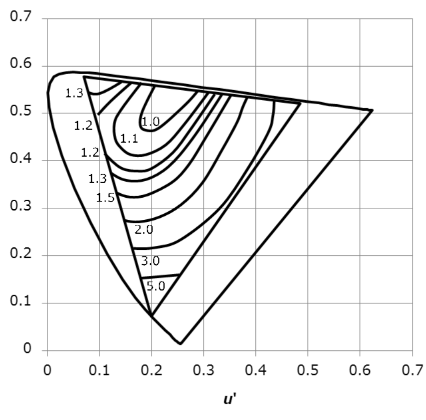

Figure 4: Relations between $10^{f'}$ values and u'v' chromaticity coordinates.

3. VERIFICATION OF THE RECOMMENDED LUMINANCE

3.1 Verification Experiment

A verification experiment was conducted to see whether derived recommended luminance based on chromatic strength for colour lighting is utilized for actual lighting design. In detail, an experiment was conducted to see whether the object is equally conspicuous regardless of light colour when the object is illuminated with different coloured lights to the identical chromatic strength. The subjects included 6 males and females in their 20s to 40s with normal colour vision.

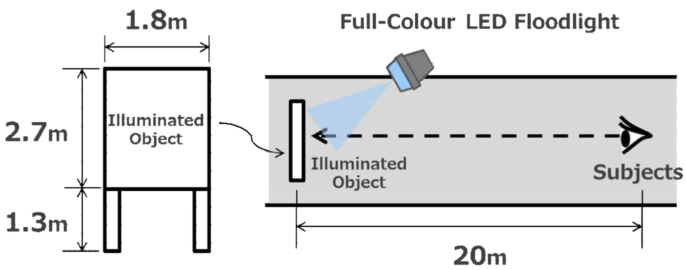

Figure 5: Schematic diagram of verification experiment.

The verification experiment was conducted on the factory campus passage at night. Firstly, a white wall sized to 2.7 m in length and 1.8 m in width was installed at the height of 1.3 m above the passage as an illuminated object as shown in Figure 5. And, the subjects were positioned 20 m away from the white wall. At this time, the viewing angle is 8° vertically × 5° horizontally. Next, using the full-colour LED floodlight used in the matching experiment, the white wall was alternately illuminated with white-colour light of correlated colour temperature 5,000 k (No. 0 in Figure 2) and coloured lights (Nos. 1, 3 to 5, 7 to 15, and 17 in Figure 2). The coloured lights used in the verification experiment were 14 colours optionally selected from all 17 kinds of coloured lights used in the matching experiment. When this is done, two patterns of lighting were performed; an equal-luminance lighting pattern to illuminate so that the overall luminance of the white wall will be 12 cd/m^2, and an equal-strength lighting pattern to illuminate so that the whole white wall will be $12/10^{f'}$ [cd/m^2] (the luminance of the white wall illuminated with white-colour light is same 12 cd/m^2). The subjects evaluated the impressions of all 14 colours in the two lighting patterns, respectively, using the 7-level evaluation scale (-3: Do not feel so strongly, -2: Do not feel so, -1: Do not rather feel so, 0: No opinion, 1: Rather feel so, 2: Feel so, 3: Feel so strongly), in response to the question, “Is the white wall illuminated with coloured light more conspicuous than when illuminated with white-colour light?”

3.2 Results and Discussion

Figure 6 shows the results of the verification experiment. The results are the average value of 6 subjects and shown in bar graphs with a standard error. In the equal-luminance lighting patterns in Figure 6, the evaluation results varied between -1 to 3 in all 14 colours. Particularly, the evaluation of No. 1 (red), No. 5 (green), No. 11 (blue) and No. 14 (purple) resulted in 2 or above. These results are generally consistent with those of the matching experiment. In the equal-strength lighting patterns on the other hand, the evaluation results concentrated between -1 to 1 in all colours except for No. 5 (green) in Figure 6. As mentioned above, it was confirmed that if the object was illuminated to the identical chromatic strength, the object illuminated with white-colour light and coloured light respectively could be controlled to the same extent of conspicuousness. Because the white wall illuminated with No. 5 (green) coloured light is significantly more conspicuous than when illuminated with white-colour light, however, improvement of Formula (4) has to be also examined in the future. From a viewpoint of the characteristics of arranged illumination, however, it is presumed that illumination resulting in sufficient conspicuousness will not be a practical problem. Based on the above-mentioned results, the recommended luminance for colour lighting can be utilized for actual illumination design.

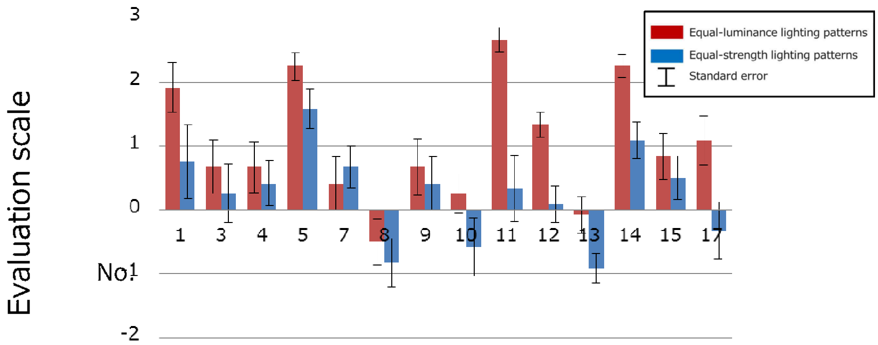

Figure 6: Results of the impression evaluation.

3. CONCLUSIONS

The matching experiment was conducted to obtain the luminance L_C of the chromatic stimulus perceived as equal strength to the luminance L_W of the white-color stimulus of the correlated colour temperature 5,000 K. Based on the obtained results of the L_W/L_C ratios, the 3-level recommended luminance for colour lighting was derived as shown in Table 1. Since every colour has different chromatic strength, the recommended luminance for colour lighting is a variable to be calculated from the $u'v'$ chromaticity of the illuminated object. As shown in Figure 4, the blue colour region has the highest chromatic strength and the yellow colour region has the lowest. For this reason, the blue colour region is the lowest recommended luminance and the yellow colour region is the highest. It was verified whether the derived recommended luminance based on chromatic strength for colour lighting can be utilized for actual illumination design. The white wall was illuminated with 14 different colour light to evaluate its conspicuousness. As a result, the white wall illuminated with white-colour light and coloured light respectively could be controlled to the same extent of conspicuousness.

REFERENCES

CIE 1993. *CIE 94 Guide for Floodlighting.*

Kaiser, P. K. 1986. Methods of heterochromatic brightness matching. *CIE J.* 5(2): 57-59.

Address: Toru KITANO, Iwasaki Electric Co., Ltd., Bakurocho-daiichi Bldg. 2F, 1-4-16, Nihonbashi-bakurocho, Chuo-ku, Tokyo, 103-0002, JAPAN

E-mails: kitano-tooru@eye.co.jp, yamada-tetsuji@eye.co.jp, ooshima-kousuke@eye.co.jp

Influences to color constancy by wearing the optical dichromatic filter or the aged lens filter under static and rapidly-changed colored illuminations.

Mio HASHIDA,[1] Ippei NEGISHI,[2] Keizo SHINOMORI,[2]
[1] Information Systems Engineering Course, Graduate School of Engineering, Kochi University of Technology
[2] School of Information, Kochi University of Technology

ABSTRACT

Human beings have an ability to estimate an original color of an object regardless of color of a illumination, that is called as color constancy. There are many arguments about mechanisms of color constancy and it has not been confirmed yet. The color constancy also exists on red-green color deficient observers. Thus, in the process of investigating the mechanism, we tried to evaluate effects to color constancy by innate adaptation and learning in color deficiency and by the long-term adaptation in aging. We especially tried to estimate whether this evaluation could be made by measurement of the color constancy on a color normal observer wearing the functional filters; the optical dichromatic filter and the aged lens filter. The color normal observer wearing one of these filters would have simulated perception of dichromats or elder person, but he or she could not have the innate or long-term adaptation and learning.

We additionally used the rapidly-changed colored illumination to minimize the short-term adaptation (von Kries type of adaptation) in possible mechanisms of color constancy, especially at retina. Experimental conditions of this research would be the extreme case distorting the color constancy effect. By these reasons, this study would have the other purpose that we would be able to estimate the maximum difference of color constancy between dichromats, elderly people and young color-normal observers.

In this study, we performed two experiments. In Experiment 1, we performed categorical color naming by 11 basic colors for OSA Uniform Color Scales (558 chips) under one of illuminations; white, red and blue (about 17.5 cd/m^2) lights. The categorical color naming was made four times on one chip by three states; wearing no filter, the dichromatic filter, or the aged lens filter. In Experiment 2, we used 134 chips (at L=0 and L=1) under the rapidly-changed colored illuminations at 5 seconds interval and other conditions were identical with Experiment 1.

In Experiment 1, under the condition of wearing the dichromatic filter, we observed typical changes in the result of the categorical color naming that can be predicted by effects of the dichromat filter under each illuminant's colors and it means that we could not find any distortion of color constancy. Additionally, we found that almost no change in color constancy by wearing the aged lens filter, in the measurement by the categorical color naming. In Experiment 2, the result was almost the same with the result of Experiment 1. The accuracy of color constancy became worse, but tendency of color naming was almost the same between static and rapidly-changed colored illuminations.

The results of this study indicate that color constancy, at least as long as measured by the categorical color naming, is robust against the change of spectral distribution of

reflected lights from objects by filters and rapid change of illumination. It supports that color constancy strongly reflects the higher-order brain processing like estimation of illumination, rather than the simple short-term adaptation effect at retina.

1. INTRODUCTION

Color constancy is the phenomenon that we can still discern original color of object's surface even when the color of illumination light has been changed. Possible contributing factors for the color constancy are;

1. Adaptation effect to cones and/or later processes (ex. von Kries type of adaptation)
2. Illumination estimation and/or estimation of spectral reflectance of the object using visual environment of background (surroundings)
3. Statistical estimation (Use of secondary statistics and/or Bayesian probability)

However, the mechanism of color constancy is still unclear though many researches have been conducted and many factors have been argued.

Previous study has been revealed that color constancy works on aged observers and color deficient observers, in limited conditions (Ma et al., AIC2012). We aimed to investigate color constancy of such observers, however, it was difficult to assemble sufficient number of them. Thus, we applied goggles with functional spectral filter simulating the color discrimination of dichromats or aged people to young people with normal color vision to measure color constancy. This method had the additional merit that the effect of long-term adaptation for congenital lack of one type of cones or age-related changes can be ignored. It would cause that the difference between normal and filter-simulated vision would reflect the worst and direct influences, meaning that the color constancy with these filters would help to reveal the mechanism of color constancy.

We additionally used the rapidly-changed colored illumination which changes illumination color in every 5 seconds in the order of Red-White-Blue-White- (or reversal order). Under this rapidly-changed colored illumination, we expected that the short-term adaptation (von Kries type of adaptation) in the possible mechanism of color constancy, especially at retina, would be minimized.

Overall, we expected that the experimental condition of this research would be the extreme case distorting the color constancy effect. By these reasons, this study would have the other purpose that we would be able to estimate the maximum difference of color constancy between dichromats, elderly people and young color-normal observers.

2. METHOD

2.1 Filters for experiments

One filter was the optical dichromatic filter, "Variantor (by Itoh Optical Industrial Co.)," which is the functional spectral filter simulating the color discrimination of dichromats for color normal observer. The other filter was the aged lens filter, "Simulation Filters of an Aged Human Lens (by Geomatec Co.)," simulating the age-related ocular lens density of 75 years old person for 32 years old observer. The color normal observer wearing one of these filters would have pseudo-perception of dichromats or elder person, but he or she could not have the innate or long-term adaptation and learning.

2.2 Stimulus

We used three kinds of illumination lights (white, red and dark) of which luminance was set to the equal value (about 17.5 cd/m2) measured on a white calibration plate (CS-A5, Konica Minolta Co.Ltd.) placed on the 45-degree-angled stand in the booth. We measured luminance and the chromaticity coordinates of the illumination lights on the white calibration plate placed on the stand by luminance and color meter (CS-200, Konica Minolta Co.Ltd.).

- White; L=17.59 cd/m2, (x,y)=(0.317, 0.350)
- Red; L=17.39 cd/m2, (x,y)=(0.635, 0.349)
- Bue; L=17.23 cd/m2, (x,y)=(0.144, 0.069)

2.3 Subjects and apparatus

Subjects were four university students (two males and two females) of color normal. Color vision was evaluated by Ishihara color vision test, Standard Pseudoisochromatic Plates (SPP) and D-15 test.

The experiment was carried out in a stimulus presentation booth created by neutral color (gray) in the darkroom. We installed a LCD projector above the booth to make an arbitrary-colored illumination light and put the stand that was angled 45 degrees to place color chips in the booth. An experimenter sat next to the stimulus presentation booth and controlled the projector to change illumination light and recorded response of the color naming.

2.4 Experimental procedure

We conducted two experiments of categorical color naming in this research. In experiment 1, we performed categorical color naming by 11 basic colors (white, black, red, green, yellow, blue, brown, orange, purple, peach and gray) for Optical Society of America Uniform Color Scales (558 chips) under one of illuminations; white, red and blue (about 17.5 cd/m^2) lights. The categorical color naming was made four times on one chip by three states; wearing no filter, the dichromatic filter, or the aged lens filter. The color name and the number of the same color-name in 4 sessions were plotted on the coordinates of the OSA uniform color system (j-g axes). We performed this experiment for all combinations on each subject ; 558 color chips X 3 observation condition (without the filer, with the optical dichromatic filter and with the aged lens filter) X 4 sessions.

At first, the subject conducted the dark adaptation for 5 minutes in the dark room. Depending on the experimental condition, the subject wore the optical dichromatic fiter or the aged lens fiter. The experimenter turned on one kind of the illumination light from the CD projector, and the subject was adapted to the illumination light and the filter in 5 minutes. Then, the subject was asked to pick up one color chip and to place it on the stand (with black gloves). The subject performed the categorical color naming by 11 basic color terms.

In Experiment 2, we used 134 chips (at L=0 and L=1) of OSA Uniform Color Scales under the rapidly-changed colored illuminations at 5 seconds interval and the color naming was performed only when the illumination color was red or blue. Other conditions were identical with Experiment 1.

3. RESULTS AND DISCUSSION

3.1 Experiment 1

Figure 1 shows the normalized number of color chips using each color name. With no filter, blue illumination reduced green, yellow and red naming significantly. With the dichromatic filter, it tended to change response as reduction of the naming in pink, orange and yellow caused by the decrease of retinal illuminance and the less long wavelength component. With the aged lens filter, there was the reduction of green and orange naming under blue and red illumination, respectively.

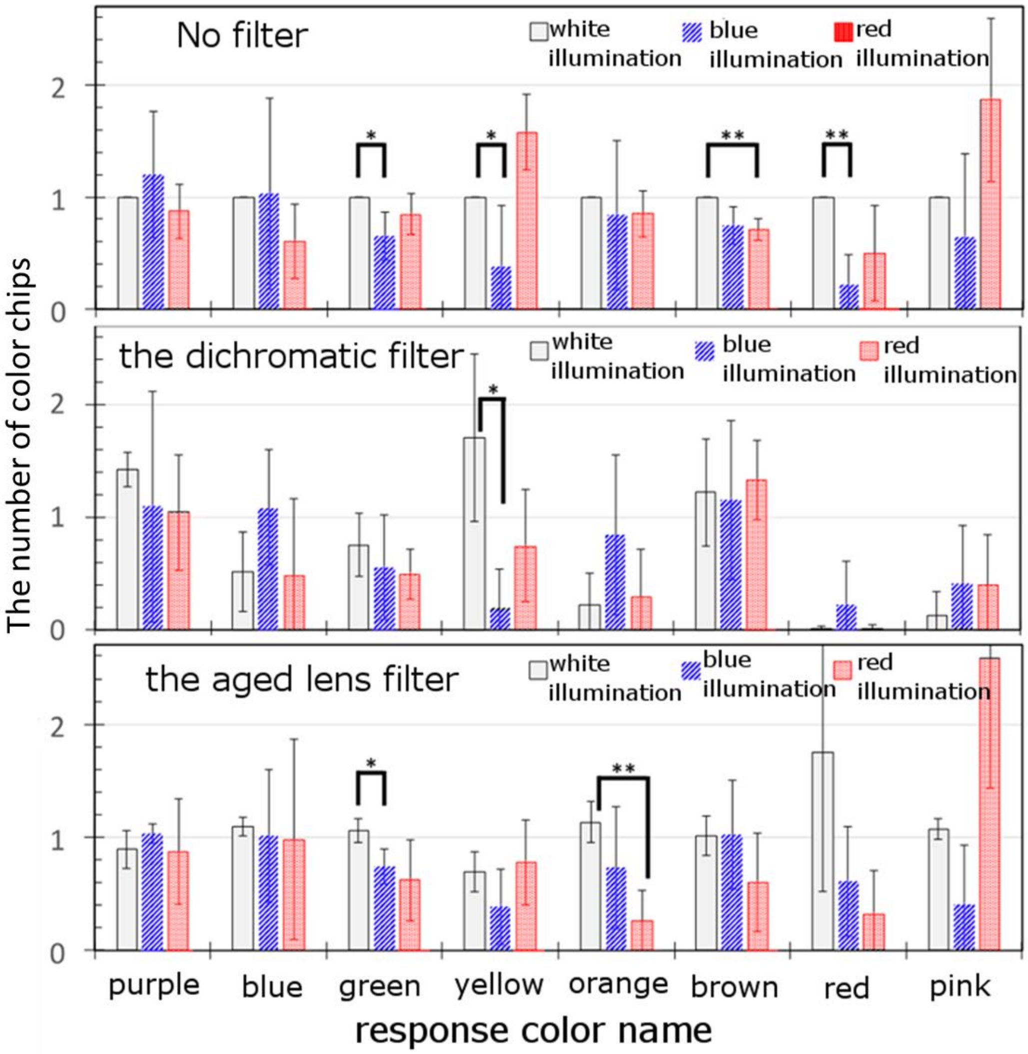

Figure 1: The normalized color chips for each color response.

In Experiment 1, under the condition of wearing the dichromatic filter, we observed typical changes in the result of the categorical color naming that could be predicted by effects of the dichromat filter under each illuminant's colors. No distortion of color constancy could be found. It means that the mechanism of color constancy should be composed by simple factors like color adaptation. Additionally, we found that almost no change in color constancy by wearing the aged lens filter, in the measurement by the categorical color naming.

3.2 Experiment 2

Figure 2 shows the number of color chips obtained the same (matched) response (using the same color name) between a certain illumination condition and white illumination.

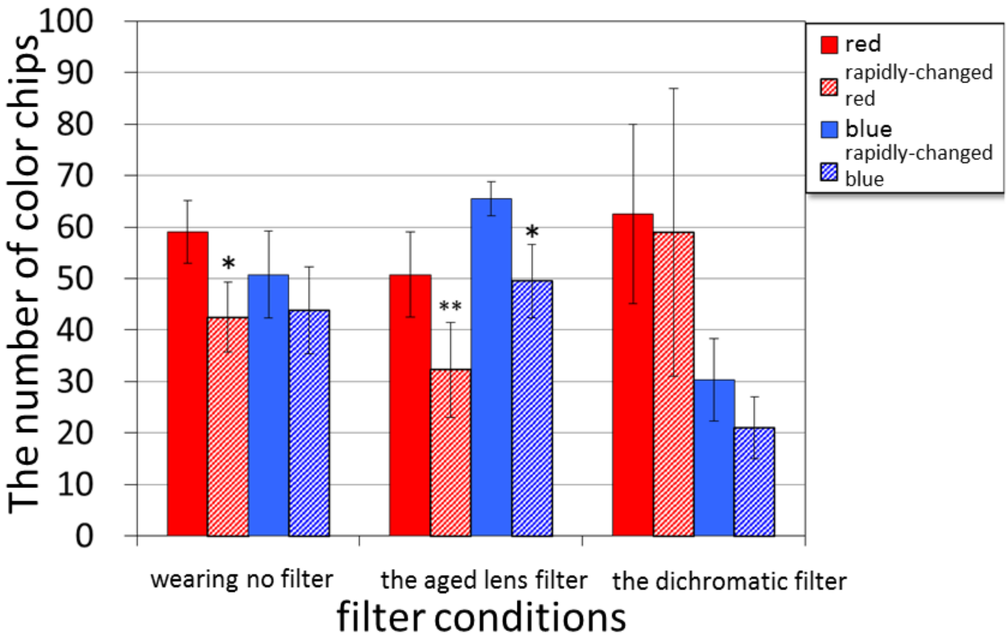

Figure 2: The number is response of color was coincident with steady white illumination.

In Experiment 2, the accuracy of color constancy became significantly worse with no filter and with aged lens filter conditions. The number of match response decreased when the rapidly-changed colored illuminations under red illumination in condition of wearing no filter and the aged lens filter. The effect of aged lens filter is minimum, observing the similar tendency in condition of wearing no filter and the aged lens filter. However, under the blue illumination, the result of the aged lens filter is more better than wearing no filter. Those reason is considered to the aged lens filter has property that decrease blue response a little.

On the other hand, this tendency was not much observed under the red illumination with the dichromatic filter. Although the number of match response was decreased overall when the illumination changes the rapidly-changed colored illuminations, but significant decrease was not observed. It is considered that the property of the dichromatic filter which makes the reduced response of red.

However, tendency of the naming was almost identical even under such the rapidly-changed illuminations in all conditions compared to the static illumination. It means that adaptation of cone photoreceptor has to take only around 1 second, suggesting that the rapid processing obtained by learning, like spectral reflectivity estimation or statistical estimation, also contributes color constancy mechanism.

From the results of the experiments, two factors contribute to color constancy mechanism. One is early stage of visual processing like adaptation of cone photoreceptor or gain control of signal. The other is higher processing like spectral reflectivity estimation or statistical estimation. The reason why these factors contribute is still unclear and further researches are needed.

4. CONCLUSIONS

In Experiment 1, under the condition of wearing the dichromatic filter, we observed typical changes in the result of the categorical color naming that can be predicted by effects of the dichromat filter under each illuminant's colors and it means that we could not find any distortion of color constancy. Additionally, we found that almost no change in color constancy by wearing the aged lens filter, in the measurement by the categorical color naming. In Experiment 2, the result was almost the same with the result of Experiment 1. The accuracy of color constancy became worse, but the tendency of color naming was almost the same between static and rapidly-changed colored illuminations. From the results of the experiments, two factors contribute to color constancy mechanism. One is early stage of visual processing like adaptation of cone photoreceptor or gain control of signal. The other is higher processing like spectral reflectivity estimation or statistical estimation.

ACKNOWLEDGEMENTS

This research was supported by JSPS KAKENHI Grant Number 24300085 to IN and KS.

REFERENCES

Ma, R., K. Kawamoto and K. Shinomori 2012. *Color constancy on red-green color deficient observers under illuminant change on confusion lines*, Conference Proceedings of AIC 2012 (T.R. Lee and J. Shyu eds.) 534-537.

Address: Prof. Keizo SHINOMORI, School of Information, Kochi University of Technology, 185 Tosayamada-miyanokuchi, Kami-city, Kochi 782-8502, JAPAN
E-mails: 175083b@gs.kochi-tech.ac.jp, negishi.ippei@kochi-tech.ac.jp, shinomori.keizo@kochi-tech.ac.jp

Spectral functional filters for optical simulation of dichromats in color discrimination

Keizo SHINOMORI,[1] Kanae MIYAZAWA,[2] Shigeki NAKAUCHI[3]
[1] School of Information, Kochi University of Technology
[2] Itoh Optical Industrial Co., Ltd.
[3] Department of Computer Science and Engineering, Toyohashi University of Technology

ABSTRACT

For dichromats, we should not use combinations of colors on such confusion lines for signs, indications, textbooks and other important notices. This concept was called as Color Universal Design. However, in many cases, it was not practical to measure all colors by a colorimeter, mostly because designers in color normal initially could not recognize problems in some color combinations. We though that if we would make the spectral functional filter to check the color combinations for dichromats, it would be more flexible, faster and easier to find initially-unexpected problems in color combinations.

Cone sensitivities of L- and M-cones, however, mostly overlap, and it was not possible to eliminate the stimulation of one type of cones by a spectral filter. Instead, we tried to simulate the ability of color discrimination defined by CIELAB color difference. We used 5745 modeled Munsell color chips under D65 illumination. The color difference was defined between each Munsell chip and the white starting point. In the next step, we assumed the spectrally band-pass filter which has two square-wave-shape peaks and three bottoms in its transmittance defined with 9 parameters. To simulate dichromat's color discrimination, from the spectral reflectance, we calculated LMS cone stimulations. We used the assumption that L- and M-cone stimulations always equal zero for protanope and deuteranope, respectively. Then, the tri-stimulus values were reversely calculated and we compared the CIELAB color differences between modeled protanope and deuteranope and each filter. The best filter was selected to minimize the "error" by changing 9 filter parameters under Genetic Algorithm. We successfully have made three kinds of the dichromatic filters even for commercial products ("Variantor" by Itoh Optical Industrial Co.); universal (U) type, protan (P) type and deutan (D) type. The U-type of the filter was designed to select worse case between P- and D-types in terms of color discrimination.

These filters were evaluated by Ishihara-plate, Standard Pseudoisochromatic Plates (SPP), D-15 and 100-hue test. As planned, results of SPP and 100-hue tests indicated that color normal observers wearing P- and D-type filters were evaluated as protanope and deuteranope, respectively, although the result of D-15 indicated that D-type filter were not significantly different with the result of no filter. The results with the universal filter indicated mixture and/or middle of protanope and deuteranope.

1. INTRODUCTION

Human has three types of photoreceptors called as cones. When we see objects in a bright environment, cones are used in visual dection processing. However, some people, classified as dichromats, do not congenitally have one type of cones and color discrimination using only that cone is theoretically impossible. Protanope and deuteranope do not have functioning L- and M-cones at retina, respectively, and additionally, it has been thought that they have no Red-Green opponency. Although there are some arguments of color perception of dichromats, especially about perception of red and green, it has been well accepted that dichromats cannot discriminate colors on confusion lines in chromatic coordinates, corresponding the lost type of cones.

For the Color Universal Design. However, in many cases, it was not practical to measure all colors by a colorimeter, mostly because designers in color normal initially could not recognize problems in some color combinations. It was more practical to take digital pictures of scenes and to present them in modified colors converted by special software like UDing Simulator (TOYO INK). We made the spectral functional filter to check the color combinations for dichromats and it would be more flexible, faster and easier to find initially-unexpected problems in color combinations.

2. METHOD

2.1 Plan for spectral functional filters

Cone sensitivities of L- and M-cones, however, mostly overlap, and it was not possible to eliminate the stimulation of one type of cones by a spectral filter. Cone sensitivities of L- and M-cones, however, mostly overlap, and it was not possible to eliminate the stimulation of one type of cones by a spectral filter.

Instead, we tried to simulate the ability of color discrimination defined by CIELAB color difference. For that purpose, firstly, we defined the color set for evaluation. We used 5745-modeled Munsell color chips under D65 illumination. The modeled reflectance of each Munsell chip consisted of the offset reflectance function (as the average of 1239 Munsell chips) and three fundamental reflectance functions (obtained by principle component analysis) multiplied by three independent parameters for each chip. Here, we set the luminance factor Y to make Y/Y_0 equaled 0.1, meaning that Munsell Value was approximately 3.8. The color difference was defined between each Munsell chip and the neutral chip (N/3.8).

In the next step, we assumed the spectrally band-pass filter which has two square-wave-shape peaks and three bottoms in its transmittance. This spectral band-pass filter was defined with 9 parameters; two parameters for the transmittance of two square-wave-shape peaks, three parameters for the transmittance of three buttoms and four parameters for the boarder wavelengths of two square-wave-shape peaks. Filter effects were simply obtained by using the filter transmittance. To simulate dichromat’s color discrimination, from the spectral reflectance, we calculated each Munsell chip's XYZ tri-stimulus values with CIE 1931 color matching function (Wyszecki and Stiles 1982) and obtained LMS cone stimulations by Smith-Pokony cone fundamentals (Smith and Pokorny 1975). We used the assumption that L- and M-cone stimulations always equal zero for protanope and deuteranope, respectively. Then, the tri-stimulus values were reversely calculated from LMS stimulations and used for color difference calculation. Finally, we compared the CIELAB color differences between modeled protanope and deuteranope. Figure 1 shows the CIELAB color difference of the 5745 modeled Munsell color chips under D65 illumination for color normal (Left panel), the modeled protanope (Center panel) and deuteranope (Right panel). Using these steps, the CIELAB color differences of each spectrally band-pass filter were also calculated. The best filters, defined as the best match to the color differences of thoretical protanope and deuteranope as shown in Figure 1, were selected to minimize the "error" by changing 9 filter parameters under Genetic Algorithm.

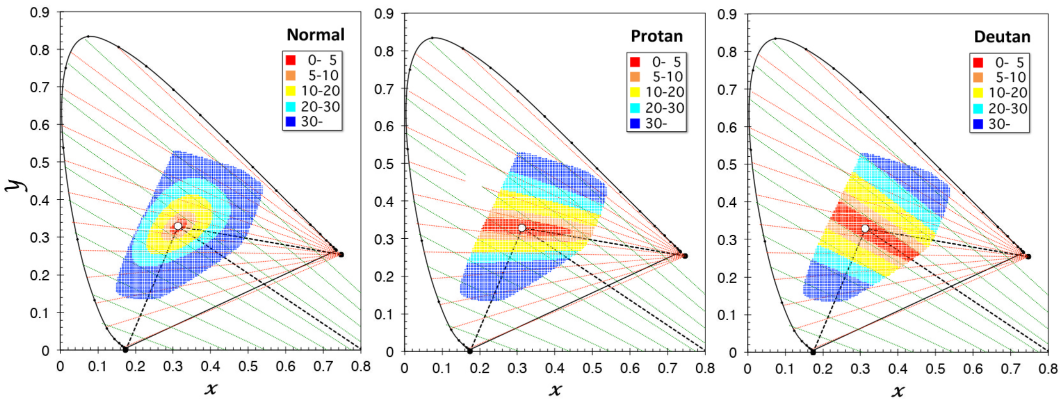

Figure 1: CIELAB color difference of modeled Munsell chips for color normal, modeled protanope and deuteranope.

For the purpose of the Color Universal Design. it can be more convenient to wear only one type of the spectral filter continuously. Thus, we defined "universal" type of dichromats as simulating worse color discrimination between protanope and deuteranope. In practical calculation, in the universal (U) type, color differences were defined as the worse value of theoretical protanopic and deuteranopic observers. Figure 2 shows the CIELAB color difference of the modeled Munsell color chips under D65 illumination with theoretically best protan (Left panel), deutan (Center panel) and universal filters (right panel). As expected, even the U-type of the filter was designed to select worse case between the P- and D-types in terms of color discrimination, the theoretical color differences was the about the middle of the P- and D-types because of the limitation of the filter transmittance with 9 parameters.

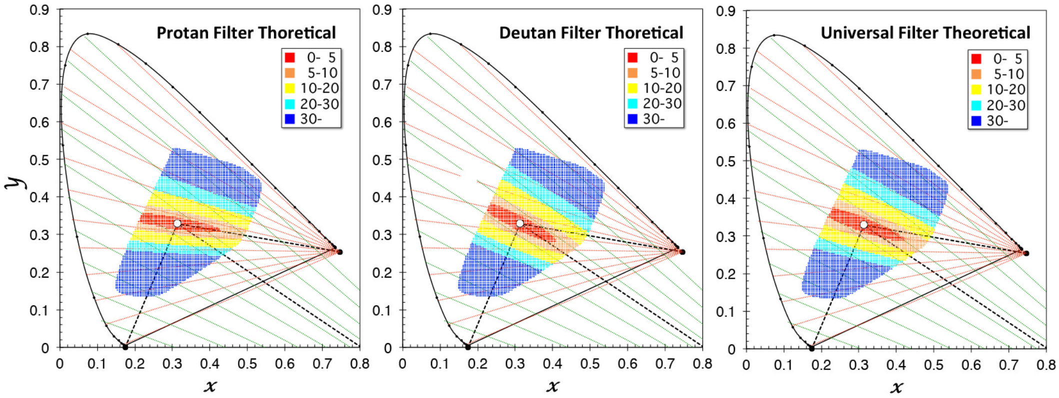

Figure 2: CIELAB color difference of modeled Munsell chips with theoretically best protan, deutan and universal filter.

We successfully have made three kinds of the dichromatic filters even for commercial products ("Variantor" by Itoh Optical Industrial Co.); universal (U) type, protan (P) type and deutan (D) type.

2.2 Evaluation of filters by traditional color tests

These filters were evaluated by traditional color vision tests; Ishihara-plate (38 plates edition), Standard Pseudoisochromatic Plates (SPP), D-15, Farnsworth-Munsell 100-hue test (FM 100-hue test) and 100 hue test (ND100) (Japan Color Enterprise Co.,Ltd.). ND100 is the new type of 100 hue test developed to measure more precise color discrimination with 100 color caps instead of 85 caps in FM 100 hue-test. In this sudy, only the result of FM100 would be presented. All color tests were performed in the light booth (Macbeth Jadge II, x-rite Co.,Ltd.) under one Day-light (6500K) fluorescent lamp. The illuminance of the buttom of the booth was about 660 lux.

Fifteen observers (11 male and 4 female) in age from 20 to 22 years participated in Ishihara, SPP and D-15 tests. Six observers (4 amle and 2 female) from them also participated in FM 100 hue test and additional nine observers (3 male and 6 female) in age from 22 to 51 years participated to FM100. Two of additional observers in FM 100 hue-test were authors. All tests were performed by one eye which was selected by the observer.

3. RESULTS AND DISCUSSION

3.1 Evaluation of filters in terms of classification as dichromats

Test error scores of each color vision test were used to evaluate the ability of simulating color discrimination on dichromats by filters. The observer's test error score wearing each filter was obtained and compared to criteria of color vision test to classify dichromats. Figure 3 shows test error scores as the average of 15 observers for each color test with each filter type including with no filter condition. Error bars denote doubled standard error of the mean (2S.E.M.). In Figure 3, only not-statistically-significant difference was denoted by lines and n.s. and all other differences were statistically-significant ($p < 0.01$).

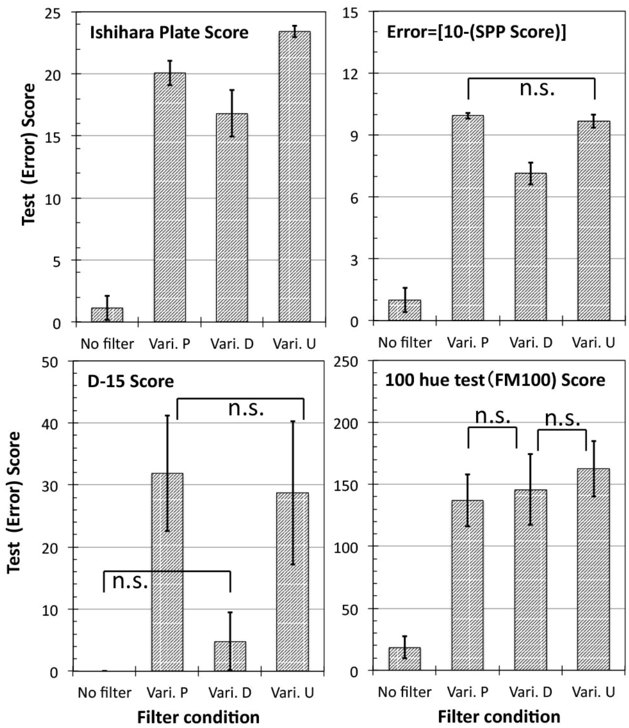

Figure 3: Test error scores in Ishihara-plate, SPP, D-15 and FM 100 hue test.

In the Ishihara plate test, one failed or unexpected recognition of a numeric number is counted as one error score and the worst score is 25. The criterion to doubt color deficiency on the observer is 4. All filters' error scores were enough high to judge as dichromats. In the SPP test, one correct answer is counted as one point and criterion of color vision normal is (more than) 8 points. For clarify of comparison with other tests, we calculated the test error score as [10 – SPP score], meaning that the error score more than 2 suggests dichromats. Again, all filters' error scores were enough high as dichromats. In both test, the score was significantly lower with the D-type filter compared to other filters.

In the D-15 test, test error score with D-type filter was not significantly different with the error score with no filter, meaning that D-type is simulating a weak dichromats or anomalous trichromats rather than strong dichromats. This result can be explained as the limitation of the spectral functional filter. As shown in Figure 1, assumption of the absence of M-cone response on deuteranope will make much less color difference compared to protanopes. However, the spectral functional filter can make almost the same color difference between P-, D- and U-types of filters, causing that D-type filter effect can be recognized as "weak deuteranopic" compared to a real deuteranope.

Contrary, in the FM 100-hue test, there was no significant difference between P- and D-type filters. The criterion of the FM 100-hue test estimated by Verriest et al. (1982) was 6.41±2.41(SD) as the average of left and right eyes in the age group of 20-29 years old. Error scores of all filters were significantly higher than the criterion.

3.2 Evaluation of filters in terms of protan/deutan classification

We also evaluated whether P- and D-type filters would be able to be classified as protanopic and deuteranopic observers, respectively, by the color tests. Ishihara-plate (38 plates edition) has 4 plates for protan/deutan classification (No.22-25). With P-type filter, correctly classification (one numeral seen) was 3.20 (80.0%) when the maximum is 4 and no classification (no numeral seen) was 0.47 (11.7%). With U-type filter, the result was close to the P-type filter. Correctly classification was 3.40 (85.0%) and no classification (no numeral seen) was 0.47 (11.7%).

Contrary, with D-type filter, correctly classification was 0.13 (3.3%) and no classification was 0.07 (1.7%). In other cases, observers could see both numbers correctly. The result of the previous literature (Birch 1997) indicating that the protan/deutan classification plates were more effective for deuteranope than for protanopes. However, it was obtained by Birch's method (1997) in which one number, which was more clearer or brighter than the other, was selected as one number. Thus, this study's result of seeing both numbers was not strange and NOT meaning the failure of the D-type filter classification. Because we did not take this method for Ishihara protan/deutan classification plates, alternative measurement should be performed for the further study.

Distributions of errors in FM 100-hue test has also been used for protan/deutan classification (Fransworth 1943). We refered protan (17 and 64), deutan(15 and 58) and tritan (5 and 46) axes used in FM 100-hue test scoring tool (v.3.0, Munsell Color Services Lab.). Figure 4 shows distribution of mean errors from 15 observers with filters. The P- and D-type filters were different and the U-type filter was mixture and/or middle of P- and D-type filters. One difference in the distribution between filters and dichromats should be mentioned that the distributions of filters were not showing high peak of errors at certain number of 100-hue test as frequently observed in dichromats (Fransworth 1943; Kinnear 1970). We expect that because the filters are not making confusion lines, which are caused by loosing signals from one type of cones, but making color discriminations more difficult, the errors distributed in many directions not a few directions.

4. CONCLUSIONS

By the idea of simulating the ability of color discrimination defined by CIELAB color difference, we successfully have made three kinds of the dichromatic filters even for commercial products ("Variantor" by Itoh Optical Industrial Co.); universal (U) type, protan (P) type and deutan (D) type. These filters were evaluated by Ishihara-plate, Standard Pseudoisochromatic Plates (SPP), D-15 and 100-hue test. As planned, results of SPP and 100-hue tests indicated that color normal observers wearing P- and D-types filters were evaluated as protanope and deuteranope, respectively, although the result of D-15 indicated that D-type filter were not significantly different with the result of no filter. The results with the universal filter indicated mixture and/or middle of protanope and deuteranope.

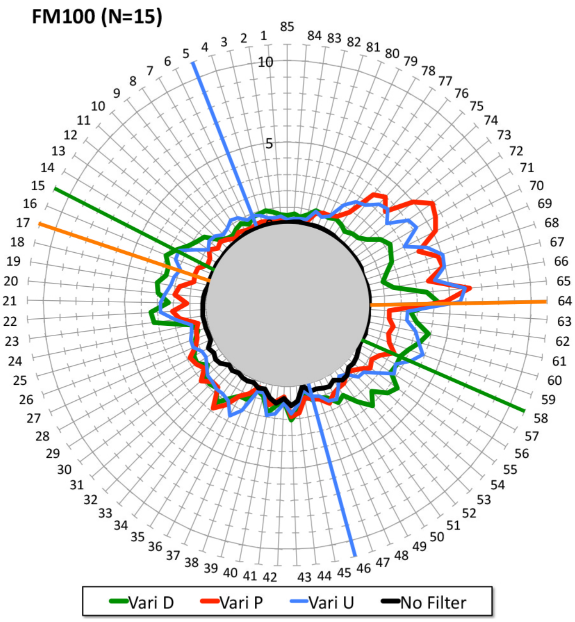

Figure 4: Distribution of mean errors from 15 observers with filters.

ACKNOWLEDGEMENTS

This research was supported by JSPS KAKENHI Grant Number 24300085 to KS and SN. We gratefully acknowledge Takuya HANAKAWA for subject testing.

REFERENCES

Birch, J. 1997. *Efficiency of the Ishihara test for identifying red-green colour deficiency*, Ophthalmic and Physiological Optics, 17(5), 403-408.

Fransworth, D. 1943. *The Farnsworth-Munsell 100-hue and dichotomous tests for color vision*, Journal of the Optical Society of America 33(10), 568-578.

Kinnear, P.R. 1970. *Proposals for scoring and assessing the 100-hue test*, Vision Research 10, 423-433.

Smith, V.C. and J. Pokorny 1975. *Spectral sensitivity of the foveal cone photopigments between 400 and 500 nm*, Vision Research 15(2), 161-171.

Smith, V. C., J. Pokorny and T. Yeh 1993. *The Farnsworth-Munsell 100-hue test in cone excitation space,* Colour Vision Deficiencies XI (pp. 281-291). Springer Netherlands.

Verriest, G., J. van Laethem and A. Uvijls 1982. *A new assessment of the normal ranges of the Fransworth-Munsell 100-hue test scores*, American Journal of Ophthalmology 93 635-642.

Wyszecki, G. and W.S. Stiles 1982. *Color Science: Concepts and Methods, Quantitative Data and Formulae*. Hoboken: John Wiley and Sons.

Address: Prof. Keizo SHINOMORI, School of Information, Kochi University of Technology, 185 Tosayamada-miyanokuchi, Kami-city, Kochi 782-8502, JAPAN
E-mails: shinomori.keizo@kochi-tech.ac.jp, k-miyazawa@itohopt.co.jp, nakauchi@tut.jp

What are Memory Colors for Color Deficient Persons ?

Jia-Wun Jian[1], Hung-Shing Chen[2] and Ronnier Luo[3]
[1]Graduate Institute of Color and Illumination Technology, National Taiwan University of Science and Technology, Taiwan
[2]Graduate Institute of Engineering, National Taiwan University of Science and Technology, Taiwan
[3]Department of Colour Science, University of Leeds, UK

ABSTRACT

Color-deficient persons are unable to discriminate some specific colors and hence have great difficulties in their lives. The mechanism of memory color for color vision defect is less clear until now. The aim of this study is to realize what are perceived colors on the familiar objects for people with color vision deficiency (CVD), and buildup the rating database of memory color for color-deficient persons. The rating data was analyzed by modified bivariate Gaussian function. the high memorized area of normal color vision forms a smaller rating ellipses on CIE $u'_{10}v'_{10}$ chromaticity diagram, however the results of CVD would form different degrees of memory-color rating ellipses. By analyzing the rating results of memory colors for the chosen familiar objects, it is possible to determine the severity of CVD for a subject according to the distribution of the memory-color rating ellipses.

1. INTRODUCTION

Color vision deficiency (CVD) is a common functional defect. There are around 8% male and 0.2% female suffering from color vision deficiency in the world [1]. People with abnormal color vision are unable to discriminate some specific colors and hence suffering in their lives. Because cone cells are absent or the peak of sensitivity is shifted, people with CVD cannot sense some specific colors as the people with normal color vision [2].

Memory color can be categorized into short-term or long-term, depending on the delay between adaptation and reproduction [3]. In order to investigated the memory color effect for color vision deficiency, total 13 kinds of test images used in the experiment include the following familiar objects: apple (two types of red and yellow), lemon (two types of yellow and green), banana (yellow), orange (orange), tomato (red), leaf (green), sky (blue), strawberry (red), Asian skin (Asian facial skin) and cauliflower (milk white). All of the test objects are arranged in Table 1.

Table 1. The test familiar objects

Name	(a) Banana	(b) Orange	(c) Yellow Lemon	(d) Cauliflower	(e) Asian Skin
Image					
Name	(f) Strawberry	(g) Sky	(h) Tomato	(i) Green Leaf	(j) Green Lemon
Image					
Name	(k) Blueberry	(l) Yellow Apple	(m) Red apple		
Image					

2. METHOD

In this study, two kind of experiments were designed: CVD's memory color rating distributions of 13 familar objects were investagted (Exp-1) and their rating results were compared with normal color vision obsevers (Exp-2). A well-calibrated monitor (sRGB) was used to display the test images of familiar objects, and the visual assessment experiment was conducted in a dark room to find the degrees of the CVDs' memroy color.

2.1 CVD subjects

Eight subjects with deutan color vison were invited to join the experiment. As listed in Table 2, two of them are deuteranomaly (mild deutan; Sub.3 and Sub.8), and the other eight subjects are deuteranopia (strong deutan). All of the subjects are male and Taiwan-Tech college students. Subjects were asked to conduct two color vision tests to verify their degrees and types of color vision deficiency with Anomaloskope and Ishihara plate. All of the color vision tests were carried out twice, where "1st" and "2nd" in the table represent the diagnosing result of the 1st and 2nd time respectively.

Table 2. Color vision diagnosing results of all subjects

Subject	Anormaloskope (1st / 2nd)	Ishihara plate (1st / 2nd)
Sub.1	Strong D / Strong D	Strong D / Strong D
Sub.2	Strong D / Strong D	Strong D / Strong D
***Sub.3**	Strong D / Strong D	Mild D / Mild D
Sub.4	Strong D / Strong D	Strong D / Strong D
Sub.5	Strong D / Strong D	Strong D / Strong D
Sub.6	Strong D / Strong D	Strong D / Strong D
Sub.7	Strong D / Strong D	Strong D / Strong D
***Sub.8**	Normal / Normal	Strong D / Strong D

Ps: Symbol * means mild degree; alphabet D means deutan color vision.

2.2 Experimental Procedure

Before memory color rating experiment, subjects were asked to stay in the dark room for 1 minute, then the staff would turn on the program and select one of test image, each image was rendered into a large numbers (150~200) of different color objects, while keeping the luminance near constant (Fig. 1). According to each subject's mental capacity, score with the range between +1 and -1 was given whether the image colors were matched the subject memory or not. After finishing all memory color rating tests, the experiment rating results were further modelled by modified bivariate Gaussian function *R* (Eq. (1)) [4, 5],

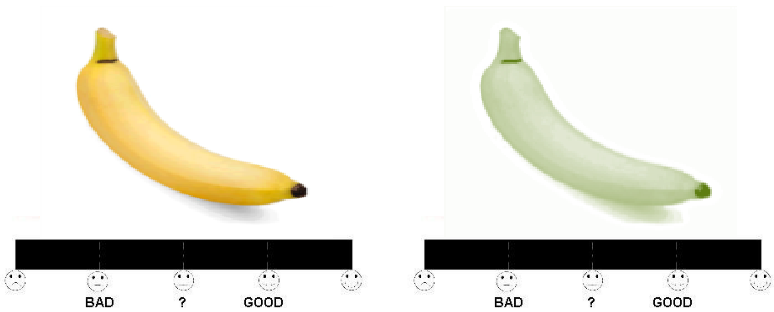

Figure 1: Two examples of rendered different object colors.

$$
\begin{aligned}
d\left(u'_{10}, v'_{10}\right) &= \left\{ \left[\begin{pmatrix} u'_{10} \\ v'_{10} \end{pmatrix} - \begin{pmatrix} a_3 \\ a_4 \end{pmatrix} \right]^T \begin{bmatrix} a_1 & a_5 \\ a_5 & a_2 \end{bmatrix} \left[\begin{pmatrix} u'_{10} \\ v'_{10} \end{pmatrix} - \begin{pmatrix} a_3 \\ a_4 \end{pmatrix} \right] \right\}^{1/2} \\
R\left(u'_{10}, v'_{10}\right) &= a_7 + a_6 \cdot e^{-\frac{1}{2} d\left(u'_{10}, v'_{10}\right)^2}
\end{aligned} \tag{1}
$$

where (u'_{10}, v'_{10}) means the use of CIE 1964 (10 degrees) Color Matching Functions in the calculation of u' v' chromaticity coordinate. The $d(u'_{10}, v'_{10})$ and $R(u'_{10}, v'_{10})$ are Mahalanobis distance and memory color rating at the (u'_{10}, v'_{10}) chromaticity coordinate respectively. Parameters a_1, a_2,.., and a_7 are the constants determined the observed data. The experiment flowchart is shown in Figure 2.

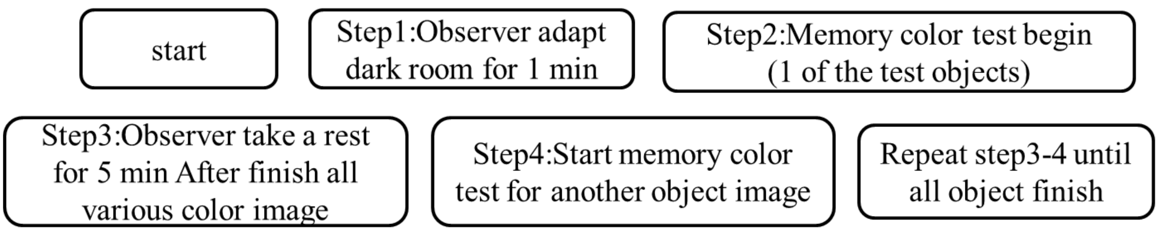

Figure 2: Flowchart illustrating the sample process.

3. RESULTS AND DISCUSSION

In Experiment 1, we collected the highest score data of all subjects, then draw the memory color rating distribution map of the mean values on CIE $u'_{10}v'_{10}$ chromaticity diagram. By plotting memory color rating distribution map, we could figure out what are memory colors of the people with deutan color vision perceived colors for the 13 familiar objects. Deutan memory color rating distribution map of mean values of all subjects are shown in Figure 2. In additions, Figure 3 shows the mean scores and all subject's highest scores plotted on $u'_{10}v'_{10}$ chromaticity diagram.

When analysing the experiment data, we used the Root Mean Square Deviation (RMSD) to calculate Inter- and Intra-observer variability. Intraobserver variability is each observer's first test and second test result data variation. And Interobserver variability is the difference between each test data and the average data, and the results of Inter- and Intra-observer variability are shown in Table 3. Besides, the color variations ($\Delta E^*_{u'10v'10}$) were calculated between individual $u'_{10}v'_{10}$ values and mean $u'_{10}v'_{10}$ values in Figure 3, and the result is shown in Table 4.

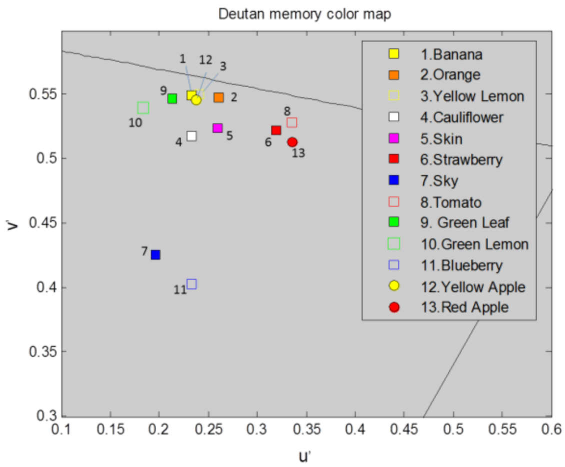

Figure 3. Deutan memory color rating map of the 13 familiar objects in terms of mean data of the highest scores.

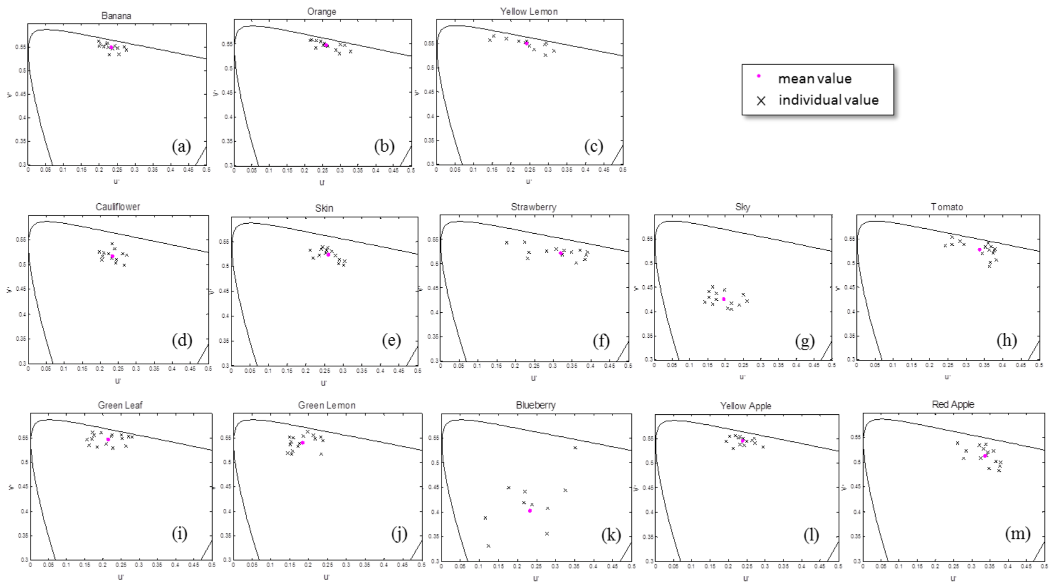

Figure 4. CIE $u'_{10}v'_{10}$ plots of the top memory color scores and the mean values of 8 Deutan color visions (for 13 familiar objects).

Table 3 Inter- and Intra-observer variability of the rating data (for 13 familiar objects).

No.	1	2	3	4	5	6	7
Object	banana	Orange	Yellow Lemon	Cauliflower	Asian Skin	Strawberry	Sky
Inter-observer	0.399	0.400	0.424	0.482	0.473	0.415	0.416
Intra-observer	0.456	0.448	0.476	0.435	0.476	0.353	0.415
No.	8	9	10	11	12	13	
Object	Tomato	Green Leaf	Green Lemon	Blueberry	Yellow Apple	Red Apple	
Inter-observer	0.425	0.531	0.576	0.485	0.462	0.496	
Intra-observer	0.475	0.561	0.662	0.453	0.526	0.473	

Table 4 Color varivations ΔE^*_{u10v10} between individual $u'_{10}v'_{10}$ data and mean $u'_{10}v'_{10}$ data (for 13 familiar objects).

No.	1	2	3	4	5	6	7
Object	banana	Orange	Yellow Lemon	Cauliflower	Asian Skin	Strawberry	Sky
Color variation	0.023	0.030	0.035	0.021	0.025	0.058	0.036
No.	8	9	10	11	12	13	
Object	Tomato	Green Leaf	Green Lemon	Blueberry	Yellow Apple	Red Apple	
Color variation	0.045	0.038	0.033	0.074	0.023	0.033	

In Experiment 2, we compare the memory color rating results between normal color visons and 2 degrees of deutan color visions (mild deutans and strong deutans). The test images for comparsion include 5 kinds of common familiar objects, which are strawbey, tomato, Asian skin, orange and banana. we anylized the rating scores of memory colors by modified bivariate Gaussian function, and draw the score distrubution ellepes on $u'_{10}v'_{10}$ chromaticity diagram, where the rating scores of normal color visons were retrieved from our earlier corrected memory color data (total 18 subjects; 12 males and 8 females; 2014), and their $u'_{10}v'_{10}$ rating ellipses based on score 0.0 and score 0.3 are shown in Figure 4.

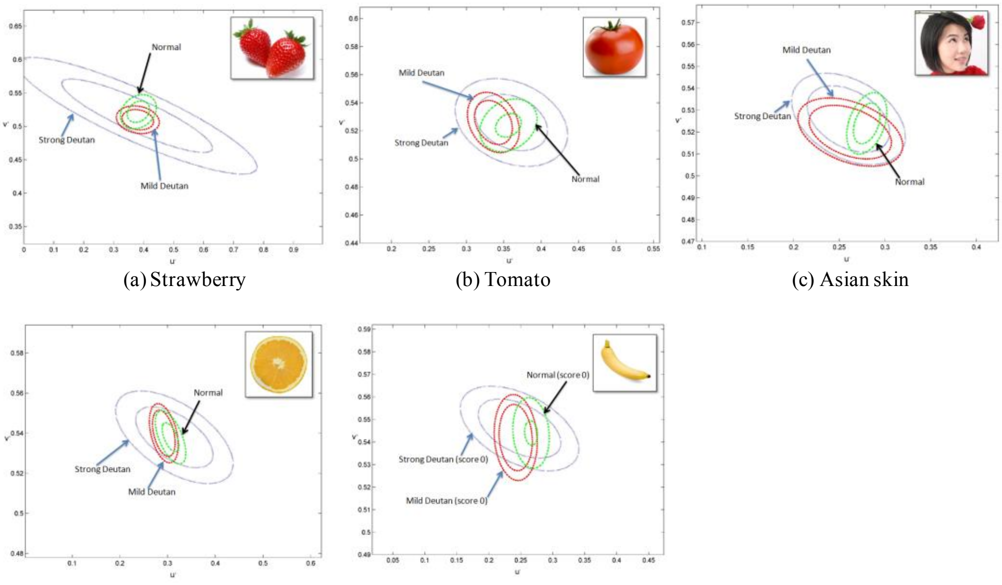

(a) Strawberry (b) Tomato (c) Asian skin

(d) Orange (e) Banana

Figure 4. Memory color rating comparisons between normal color vision and deutan color vision, where outer and inner green/ red/ blue ellipses represent the rating boundaries of normal/ mild/ strong color visions corresponding to score 0.0 and score 0.3 respectively.

4. CONCLUSIONS

In this study, memory color rating distribution map based on mild/ strong deutan color visions was investigated. The memory color rating results between normal color vison and deutan color visions (mild deutans and strong deutans) were compared. The modified bivariate Gaussian function was applied to form memory color rating ellipses of deutan color visions on $u'_{10}v'_{10}$ chromaticity diagram. The degrees of deutn color vision show stronger when the sizes of rating ellipses show bigger. This study could help us realize more about color vision mechanism between color vison deficieny and normal color vision. We hope this analysical results are beneficial to color vision deficiency's research. Our future works hope to add more subjects with different severities and color vision types to clarify memory color mechanism of abnormal color visions.

REFERENCES

[1] A. Stockman, D. I. A. MacLeod, and N. E. Johnson , "Spectral sensitivities of the human cones," Journal of the Optical Society of America A, vol.10 (1993).

[2] P. Bodrogi, T. Tarczali, "Colour memory for various sky, skin, and plant colours: effect of the image context," Color Research & Application 26.4: 278-289 (2001).

[3] Rigmor C. Baraas, "Color Constancy of Red-Green Dichromats and Anomalous Trichromats," Visual Psychophysics and Physiological Optics. Vol. 51, No.4, pp. 2286-2293 (2010).

[4] Smet KA, Ryckaert WR, Pointer MR, Deconinck G, Hanselaer P, "Memory colours and colour quality evaluation of conventional and solid-state lamps," Opt Express (25): 26229-44 (2010).

[5] Kevin A.G. Smet, Yandan Lin, Balázs V. Nagy, Zoltan Németh, Gloria L. Duque-Chica,

Jesús M. Quintero, Hung-Shing Chen, Ronnier M. Luo, Mahdi Safi, and Peter Hanselaer, "Cross-cultural variation of memory colors of familiar objects," Optics Express, Vol. 22, Issue 26, pp. 32308-32328 (2014).

Postal address: 43, Keelung Road, Section 4, Taipei, Taiwan
E-mails: m10325005@mail.ntust.edu.tw, bridge@mail.ntust.edu.tw, m.r.luo@Leeds.ac.uk

Establishment of a Model Colour Palette for Colour Universal Design

Kei ITO [1], TomomiTAKESHITA [2], Fumiko GOTO [2], Masafumi NISHIGAKI [2],
Teruo KOBAYASHI [3], MitsumasaHASHIMOTO [3], Yosuke TANAKA [4], Koichi IGA [4],
Shunsuke WATANABE [4], Koki OKAGAWA [4], Mitsuyoshi MAEKAWA [5]
[1] Institute of Molecular and Cellular Biosciences, University of Tokyo
[2] DIC Corporation (DIC Graphics Corporation, DICColour Design, Inc.)
[3] Japan Paint Manufacturers Association (JPMA)
[4] NPO Colour Universal Design Organization
[5] Industrial Research Institute of Ishikawa

ABSTRACT

Colour Universal Design (CUD) is a user-oriented design system to allow information to be conveyed accurately to people with diverse types of colour vision. Because of genetic variations or eye diseases, some people cannot easily distinguish certain combinations of colours. However, it is not practical to avoid all such combinations when painting graphic objects that require multiple colours, such as public signs, graphs and drawings, maps, and web pages. An alternative approach is to adjust the hue, saturation or brightness of each colour to maximise mutual separation. To achieve this, we organised a collaborative project to establish a palette of least confusing colours with precisely defined colour values. We first asked people with common-type (normal) colour vision to classify several thousands of colour chips into groups of colour categories. We then asked colour-blind people to examine these chips and discard those that appear confusing. We finally asked colour-blind and low-vision people to examine and adjust the remaining colours to establish a set of colours that are most distinguishable from each other, and obtained a palette of 20 colours: nine vivid colours suitable for small objects such as signs, graphs and characters, seven relatively pale colours for painting large objects such as maps and backgrounds, and four shades of achromatic colours that are least confusing with chromatic ones. Considering that colour-coded information in real life is presented in three ways–painting, process colour printing and display panels– we fine-tuned colours and made suggested colour definitions in Munsell values, CMYK values with industry-standard profiles, and RGB values in sRGB colour space. The palette is being used in a wide variety of products.

1. INTRODUCTION

About 8-10 % of Caucasoid males and 4% of Asian males, as well as one in several hundreds of females are so called red-green colour-blind, who cannot discriminate certain combination of colours even if they are clearly distinguishable by the people with common-type colour vision. Depending on the problematic cone cells in the retina, they are classified as protan (problem in L cones) and deutan (problem in M cones). In addition, some of the people who suffer from low-vision also have difficulty in distinguish colours, because S cone cells, which accounts for only a few percent of the retinal cells, tend to disappear first by retinal diseases, causing tritan-like color vision.

The fact that colour-blind and low-vision people cannot distinguish certain colours does not necessarily mean that they cannot distinguish all the tones of colours in that category. The colours that are hard to distinguish by these people tend to lie on straight lines called confusion lines on CIE xy charts (Pitt 1935, Figure 1). The colours appear much less confusing if they do not lie on the same confusion line. This is most exemplified by traffic lights. Even though colour-blind people have difficulty distinguishing red and green, few of them have problems with traffic lights, because red is deliberately shifted to yellowish and green to bluish colours, avoiding the combination that lie on a single confusion line.

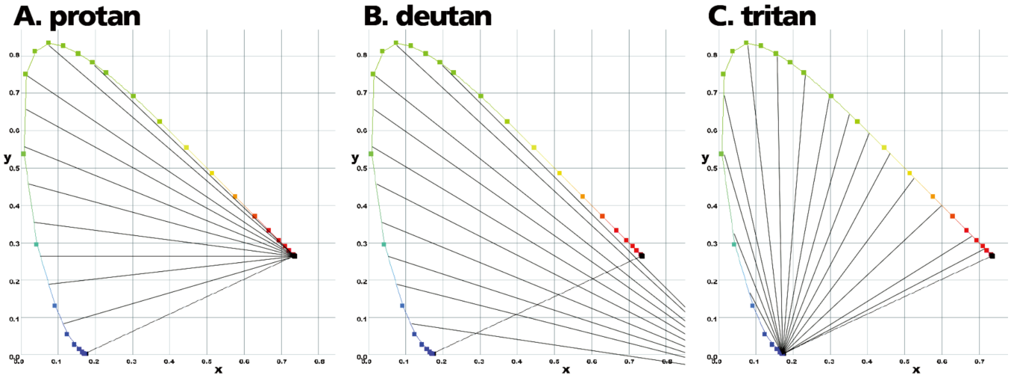

Figure 1: Confusion lines of the three major types of colour blindness.

Such fine-tuning of colours is a potentially promising way to provide information in many colours while keeping accessibility to diverse people. Although convenient algorithms for detecting potentially confusing colours have been established (Brettel et al. 1997) and are now implemented in popular graphic software such as Illustrator and Photoshop, fine-tuning of colours is not easy for designers who usually have only limited knowledge about the characteristics of various colour vision types.

For designers it should be most convenient, if they can have a palette of colours that are already fine-tuned for maximum distinction. To this aim we organised a collaborative project between research institutes (University of Tokyo and Industrial Research Institute of Ishikawa), leading company and industry association of the Japan's printing and painting industry (DIC Corporation and Japan Paint Manufacturers Association), and an NPO of colour-blind people that advises CUD (Colour Universal Design Organization).

2. METHOD

2.1 Sample Preparation

We used two types of colour sample chips that are *de facto* standards for ordering colours in Japan's printing and painting industry, respectively. The first is DIC Colour Guide library by DIC Corporation, which features 2,230 colours published in five volumes: Vol. 1 and 2 and Traditional Colours of Japan, France and China. The second set is the Standard Paint Colours by the Japan Paint Manufacturers Association (JPMA). The original set of JPMA samples feature 1,500 colours distributed evenly according to the Munsell colour system. Every two years, 600-700 colours are selected from this set and published as Standard Paint Colours. For fine-tuning colours for CMYK process printing, colour charts with various shades of cyan, magenta and yellow were specially made by DIC.

2.2 Experimental Procedure

Examination and selection of colours were performed in the form of "jamboree," where 10-15 people with various colour-vision types gather and examine colour samples together. This ensured quick comparison of conflicting colours by different types of people and fast screening of alternative colours for the best possible compromise. All sessions were performed under D65 lighting.

3. RESULTS AND DISCUSSION

3.1 Selection of colours than can easily be called with distinct colour names

Humankind use colour names to describe the colours they perceive and to communicate with other people about colours. Although there are millions of colours, the ranges of colours whose names are difficult to describe are not suitable for presenting colour-coded information. Therefore we first selected the range of colours that are easy to be named.

Based on the consulting experience of the designers at DIC Colour Design Inc., we first selected 27 colour names. These included three achromatic colours (black, grey and white), 12 high-saturation colours that are often used for painting small objects, and 12 low- or middle-saturation colours that are often used for painting large objects (Figure 2).

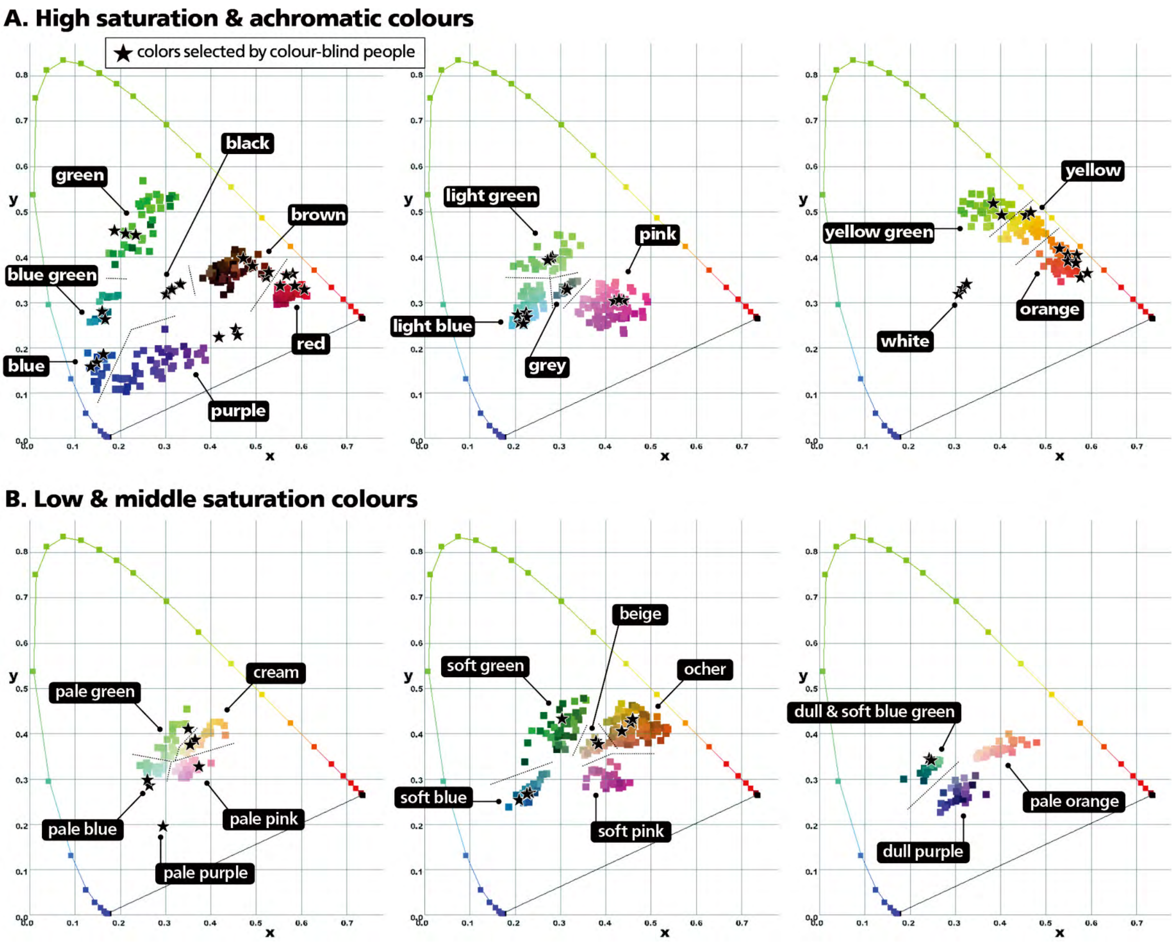

Figure 2: Distribution of the colours for specific colour names selected by common-type and colour-blind people

We then asked five designers with common-type colour vision to categorise the 2,230 DIC Colour Guide sample chips. Only the chips whose colour names seem apparent were grouped, and the chips whose colour names were difficult to describe were discarded. As expected, the resulted groups of colour chips formed uniquely distributed clusters in the CIE xy colour space (coloured squares in Figure 2).

Although colour-blind people can also recognise colours using colour names, the range of colours described by a particular colour name is not the same as those used by common-type people. For example, some shades of red appear green or brown to colour-blind people, but certain range of red colours can distinctly be felt as red. To identify such range of colours for each colour category, we then showed the above sets of colour chips to a jury of colour-blind people (protanope and deuteranope) and asked to select the chips that they can recognise with the same colour name (Star symbols in Figure 2).

The results were striking but understandable. The ranges of colour chips selected by the colour-blind people were distributed at either side of the confusion lines. For example, only yellowish red chips that were above the confusion line connecting red and green were selected as red, and only the bluish green chips that were below that confusion line were chosen as green. Likewise, only reddish purple chips above the confusion line connecting purple and blue (for protanope) and purple and green (for deuteranope) were selected as purple. Bluish purple, including violet, were not selected because they appear confusing with blue (for protanope) or green (for deuteranope). Similarly, only yellowish pink was selected, because other ranges of pink appear confusing with light blue (for protanope) or light green (for deuteranope). Among the 27 sets of colour chips, colour-blind people were not able to select any chip for soft pink, pale orange and dull purple, because all the chips selected by the common-type people for these colour names appeared confusing with the chips of other colours by colour-blind people. Thus, we obtained a set of 24 colours.

3.2 Adjustment of colours for paint colours

The DIC Colour Guide is designed for special-colour printing that uses pre-mixed ink for each colour. Because commercial printing with tens of special-colour inks is not practical, we first developed a practical version of the colour palette for the JPMA Standard Paint Colours for painting industry, in which special pre-mixed colours are used more commonly. Because JPMA Colours are based on Munsell colour space, we first converted above-mentioned 24 ranges of colours to Munsell values. Because of the fewer number of sample chips, the JPMA Standard Colours lacked some of the colours that were found useful for clear distinction of colours. Most notably, it lacked the yellowish red between Munsell values R7.5 and R10. JPMA therefore made new colour chips at R8.75 specially for this project. It also made several other colours for bluish green. Using these, we were able to select 24 chips of the JPMA standard colours (Figure 3A).

The selected colours had a few problems when it would be used for practical applications. First, It had only one shade of grey even though in many cases different shades of grey are useful. Second, the number of low- and middle-saturation colours did not match the number of high-saturation colours. We therefore tried to increase the number of achromatic and low/middle-saturation colours by selecting candidate colours (Figure 3B). After examination by colour-blind people, colours that were hard to distinguish were deleted (x symbols), and the hue, saturation and brightness of some colours were adjusted for better distinguishability (white arrows), resulting in a set of 31 colours (Figure 3C).

So far, colour combinations that are difficult to distinguish for low-vision people had not been considered. It is not easy to set a model case of low-vision, because many eye diseases are progressive. We therefore asked people who suffered from retinal detachment or retinopathy of prematurity, whose symptoms in the retinae remain rather stable. In addition, we asked another person whose colour vision of one eye showed complete tritan characteristics for unknown reasons. After another session with both colour-blind and low-vision people, many colours, especially those in the middle-saturation range, were determined confusing and had to be discarded (Figure 3D-1). In total 20 colours (nine high-saturation, seven low-saturation, and four achromatic colours) were selected eventually. Two remaining colours in the middle-saturation range (yellow and green) were designated as alternative colours that can be used instead of high-saturation colours.

3.3 Adjustment of CMYK values for process colour printing

Next, we made a similar colour palette for printing (Figure 3D-2). For practical multi-colour print, we made the set for CMYK process-colour printing. Paint and print have rather different gamut. To make the best use of CMYK gamut, we adjusted each colour by making charts with varying levels of cyan, magenta and yellow and selecting the colours that are most distinguishable. To ensure consistency of reproduction, CMYK values were determined with precisely controlled profile (DIC Standard SFC_AM2.0), which is essentially similar to the industry standard Japan Color 2001 Coated printing profile.

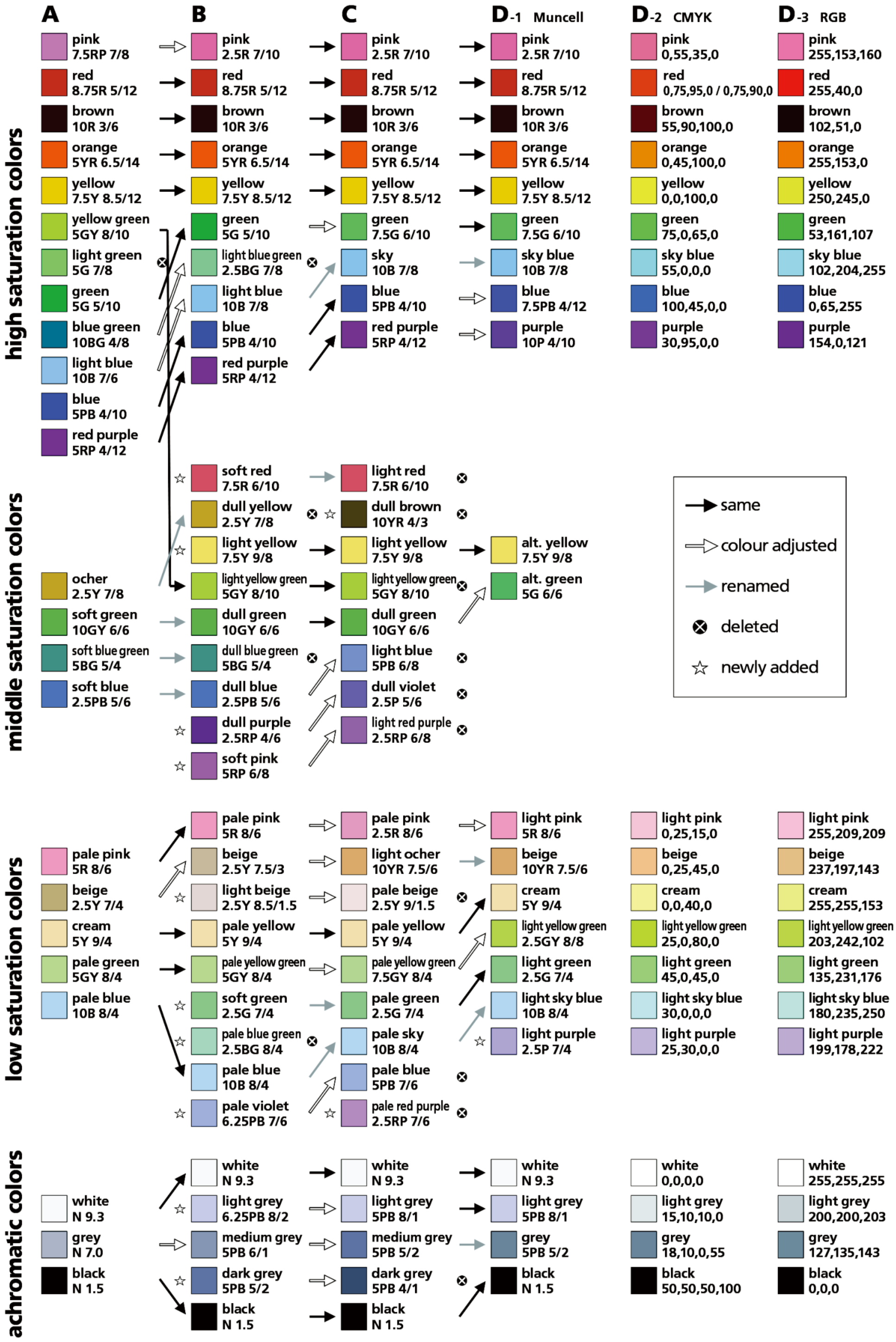

Figure 3. Colours for each version of the model colour palette

3.4 Adjustment of RGB values for display panels

The final set of colour palette is for the displays of computers, mobile devices, TV sets, and digital signage. Most of these use LCD displays, where colours are defined with RGB values. Among the two industry-standard colour space for such displays –sRGB and Adobe RGB– we chose sRGB because (1) it is also the standard for Internet web sites and PDF documents, and (2) the latter is used only for specific purposes such as photography printing. Using a precisely calibrated LCD monitor, we adjusted each colour to make the best use of the specific gamut of the sRGB colour space (Figure 3D-3).

3.5 Application of the model colour palette

The JPMA, CMYK and GRB versions of the palettes were released in mid 2009, late 2009, and late 2011, respectively. To help choosing the most distinguishable colours, we provided for each set the lists of colours that are especially easy or relatively difficult to discriminate. A handbook was released in 2014 to provide detailed information of each colour set as well as the lists of recommended and unrecommended colour combinations.

Since its release, the colour palette is used by a wide variety of products including train line maps, signs in public spaces, graphs and drawings in the textbooks of elementary and high schools, as well as graphic interface of electronic devices. The colours were also reproduced for plastic materials of colour-coded trash boxes and buttons of TV remote controllers. With slight modification, the colours were also used for public information services such as colour-coded maps and alert charts for the web sites of the national meteorological agency, as well as tsunami hazard alert systems of TV broadcast networks.

4. CONCLUSIONS

The model colour palette provides for the first time a systematic way for conveying colour coded information that is least confusing for people with diverse colour vision types. By defining colours not with Yxy or L*a*b* values, which are mostly used only by scientists, but with industry-standard paint colour chips and CMYK and RGB values, the palette has become instantly useful for designers who shape the colour environment of the real world.

ACKNOWLEDGEMENTS

We thank DIC, JPMA and Nihon Shikiken for preparing specially-made sample colour chips and colour charts, Akira Kitabatake for the discussion about colour names and definitions, and colour-blind and low-vision collaborators who provided constructive comments.

REFERENCES

Brettel, H., Viénot, F. and Mollon, J. D. 1997. *Computerized Simulation of Color Appearance for Dichromats*, Journal of the Optical Society of America 14 (10) 2647–2655.

Pitt, F.H.G. 1935. *Characteristics of dichromatic vision,* Medical Research Council, Report of the Committee on the Physiology of Vision, XIV; Special Report Series, 200.

Address: Prof. Kei Ito, Institute of Molecular and Cellular Biosciences,
The University of Tokyo, 1-1-1 Yayoi, Bunkyo-ku, Tokyo 113-0032, Japan
emails : itokei@iam.u-tokyo.ac.jp, ito@cudo.jp

Color Universal Design

Yasuyo G. Ichihara*1*2
[1] Faculty of Informatics, Kogakuin University
[2]NPO Color Universal Design Organization (CUDO)

ABSTRACT

The present study investigates the tendency of individuals to categorize colors. Humans recognize colors by categorizing them with specific color names such as red, blue, and yellow. When an individual having a certain type of color vision observes an object, they categorize its color using a particular color name and assume that other people will perceive the color in an identical manner. However, there are many variations in human color vision caused by photoreceptor differences in the eye, including red and green confusion. Thus, another person with a different type of color vision may categorize the color using another name. To address this issue, we attempt to determine the differences in the ranges of colors that people with different types of color vision categorize using particular color names. In the modern urban environment, most visual information, including warning signs and notice boards, is coded by color. Finding the common color categories among different types of color vision is an important step towards achieving Color Universal Design, a visual communication method that is viewer-friendly irrespective of color vision type. Herein we report on a systematic comparison between people with common (C-type) and deutan (D-type) color vision. Analysis of protan (P-type) color vision will follow in a subsequent report.

1. INTRODUCTION

In Japan, about 5% of men and 0.2% of women see color differently (so-called red-green confusion) than the general population, due to genetic differences. The percentage is higher in Europe and the United States; up to 10% of men in some countries. Visual information presented using various colors is generally easy to understand, but because of these differences in color vision, the use of colors can actually cause confusion. Modern society is filled with visual information comprising multiple colors, but the appearance of this information is often designed only with regard to people with the most common form of color vision. Designs employing certain ranges of colors can sometimes lead to ineffective communication or even accidents for the people who perceive colors differently. To avoid such misperceptions, the concept of “barrier-free color” or “color universal design” (CUD) has been advocated, with the goal of creating designs that are understandable regardless of the type of color vision.

Recently, computer software and glasses that provide a virtual experience of colors perceived by individuals with red-green confusion have become available, such as VisCheck, the CUD-proof function of Adobe Photoshop and Illustrator, and the Variantor glasses. However, these tools fail to indicate how individuals with different types of color vision recognize color categories.[1] In the present study, we compared the ranges of colors that people with common and red-green confusion color vision perceive when a particular color name is presented.

There are three major types of color vision: common (C-type), protan (P-type), and deutan (D-type). Individuals with P- or D-type color vision are often regarded negatively as being “colorblind”, color “anomalous” or having color vision “deficiency” compared to those with the “normal” C-type color vision. In order to avoid misleading impressions and promote more positive attitudes towards individuals with P- or D-type color vision, just two of the many types of genetic polymorphisms, we believe it is important to stem the use of words that are imbued with a negative connotation. We therefore refrain from using terms such as “normal”, “anomalous”, or “blind”.

2. METHOD

2.1 Study Overview

Using a light source to fully render color properties, subjects were asked to classify color chips of 1,050 different colors into 20 color categories. Subjects were also asked to choose one color chip for each category that they felt was the most representative of the given color name. The 20 color category names included the 11 basic color names (white, black, red, green, yellow, blue, brown, orange, purple, pink, and gray) proposed by Berlin and Kay[1)]. In order to analyze not only categories of high saturation colors but also low saturation colors, 9 additional color category names were used (beige, cream, yellowish-green, light green, blue-green, light blue, bluish-purple, purple, and reddish-purple. Considering that the ranges of colors covered by these names would occupy only discrete areas of the color space, we also made the “Color name unknown” category to avoid the risk of subjects feeling compelled to classify a color chip they had difficulty judging as belonging to a specific color category.

2.2 Subjects

Four subjects with C-type (trichromatic) color vision (Ishihara Test 38 plates – pass) and 4 subjects with complete deuteranope vision (strong D-type, Panel D15 test – fail). Color vision types were diagnosed at the Department of Ophthalmology, Jikei University School of Medicine.

Table 1. Subjects’ characteristics

Subject No.	Age (years)	Gender
C-type color vision No. 1	46	Female
C-type color vision No. 2	21	Female
C-type color vision No. 3	22	Male
C-type color vision No. 8	21	Male
D-type color vision No. 1	41	Male
D-type color vision No. 2	66	Male

D-type color vision No. 3	25	Male
D-type color vision No. 4	62	Male

2.3 Test Equipment/Light Source

Standard lighting equipment: RW standard color viewer; color appraisal AAA fluorescent lamp ($x=0.3425$, $y=0.3520$, luminance=7,500 cd/m^2); measured with a luminance and colorimeter (CS-1000; Konica Minolta, Tokyo Japan).

2.4 Background Color

White ($x=0.3370$, $y=0.3483$, $Y=62.18$)

We first compared color perception with white and black backgrounds and observed a significant difference between the two. Considering that many colors used in public signs and printed materials, like magazines, are presented on bright rather than dark backgrounds, we chose the white background for subsequent tests.

2.5 Color Samples

We used the Toyo Color Finder (CF) with 1,050 color chips (size: 3.2 × 1.2 cm^2, colored area: 2.4 × 1.2 cm^2), a color sample book published by Toyo Ink Manufacturing Co., as the color samples for color category classification. The reasons for using the Toyo Ink chips include the following.

(1) They evenly cover a range of colors used in commercial printing. (2) A large quantity of precisely colored chips is readily available. (3) Considering the burden attributed to classifying colors and resolution over the entire color range, a quantity of about 1,000 colors was deemed appropriate. It typically took 2.5 hours for one subject to complete the entire task.

3. RESULTS

3.1 Color Perception Influenced by Background Color

We first asked the 4 subjects with C-type color vision to categorize colors on the black background (standard tabletop of the RW standard color viewer) and on the white background (a white sheet of paper placed on the color viewer tabletop). Some color chips were selected as a particular color when presented on the white background but not when presented on the black background, and vice versa. Selected color chips with significant differences between the different backgrounds are shown in Table 2.

Table 2. Selected color chip data using different background colors

CF No.	XYZ-Y	Yxy-x	Yxy-y	Color category names	Number selected according to background
10114	21.1	0.4702	0.357 2	brown	White – Black = 1 – 4
10845	12.35	0.4058	0.392 2	brown	White – Black = 0 – 3
10594	55.72	0.3763	0.388 3	beige	White – Black = 1 – 4
10220	78.62	0.3725	0.404 3	yellowish-green	White – Black = 3 – 0
10239	59.44	0.3713	0.463	yellowish-green	White – Black = 4 – 0
10243	60.02	0.3588	0.447 6	yellowish-green	White – Black = 3 – 0
10645	36.76	0.2969	0.387 1	light green	White – Black = 3 – 0
10404	16.31	0.184	0.234 8	blue	White – Black = 3 – 0
10408	10.16	0.2116	0.244 4	blue	White – Black = 3 – 0
82 Purple	6.29	0.2414	0.148 5	bluish-purple	White – Black = 1 – 4
10946	6.86	0.3223	0.331 5	black	White – Black = 1 – 4

3.2 Results of C-type Color Vision (Ishihara Test 38 plates – pass)

The color chips selected by all 4 subjects with C-type color vision presented for each color name are shown in Figs. 3-1 and 3-2. For white and blue-green, none of the color chips were unanimously selected by the 4 subjects. For white, this was most likely because the Toyo color chips contain essentially no ink that appears white; because it is made for printing on white printing paper, white ink is not required. For blue-green, midway between blue and green, this was most likely because blue-green may not be established as a definite color category even among individuals with C-type color vision, at least in Japan; thus reflecting large differences based on the subjective experiences of individuals.

3.3 Results of D-type Color Vision (Panel D15 test – fail)

The color chips selected by all 4 subjects with D-type color vision are presented in Figs. 4-1 and 4-2. In addition, because of the wider variation among subjects with D-type color vision, colors selected by 3 of the 4 subjects are also shown in Figs. 5-1 and 5-2. For white, gray, green, purple, cream, yellowish-green, light green, blue-green, bluish-purple, and reddish-purple, there were no instances where all 4 subjects selected the same color chip. Of these, for white, light green, bluish-purple, and reddish-purple, even 3 of the 4 subjects did not select the same color chip. In addition, the color categories for brown and pink were broader than those for subjects with C-type color vision. Characteristically, the former (brown) extended to a dark yellow range, whereas the latter (pink) extended to a reddish-purple range.

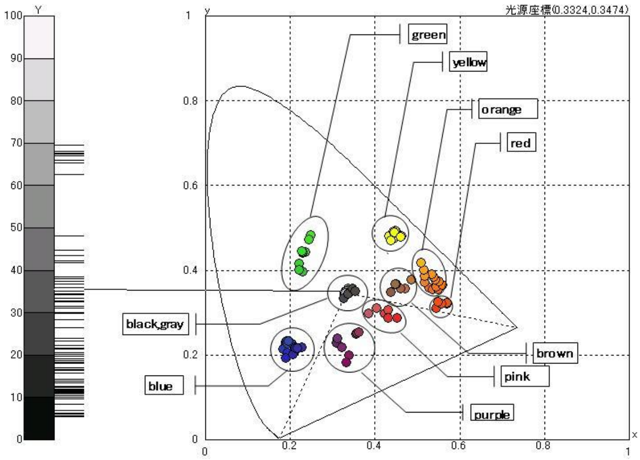

Fig. 3-1 Color chips selected by all 4 subjects with C-type color vision (basic colors)

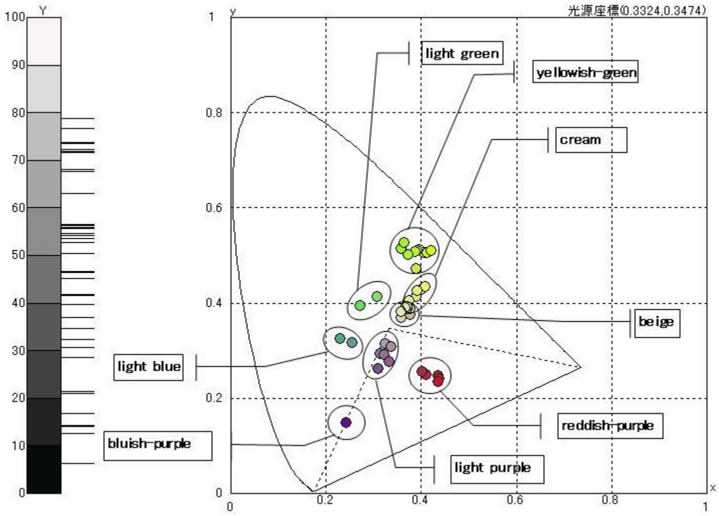

Fig. 3-2 Color chips selected by all 4 subjects with C-type color vision (non-basic colors)

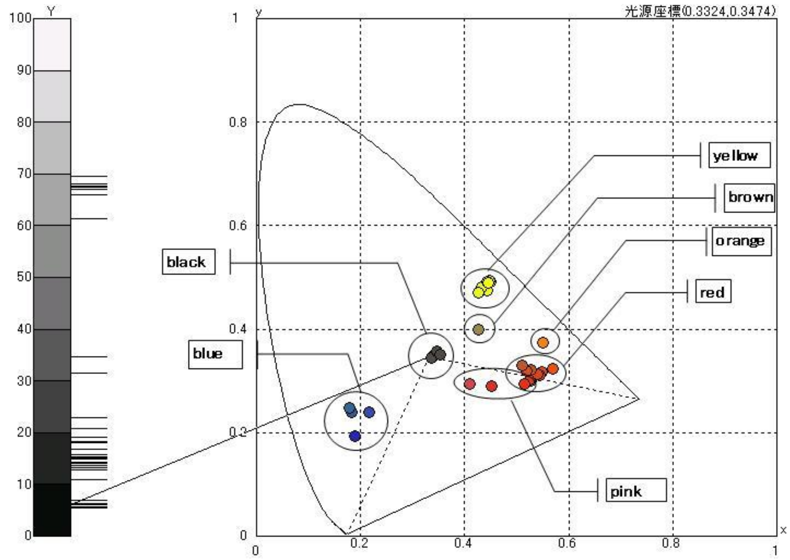

Fig. 4-1 Color chips selected by all 4 subjects with D-type color vision (basic colors)

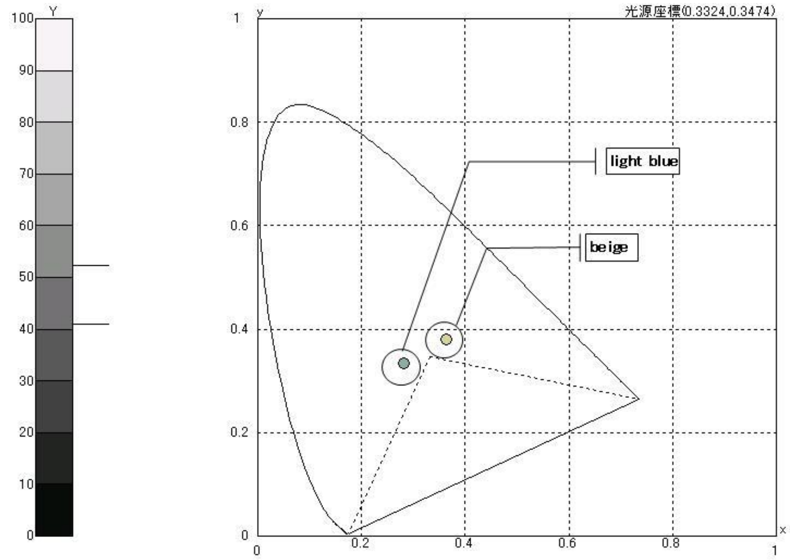

Fig. 4-2 Color chips selected by all 4 subjects with D-type color vision (non-basic colors)

Color categories for D-type subjects included beige and light blue.

3.4 Comparison of Color Name Recognition between Color Vision Types

Finally, we compared the color chips selected by subjects with C- or D-type color vision (color chips selected by at least 3 of the 4 subjects in each group, Fig. 6); those selected by subjects with C-type but not by those with D-type color vision (number of C-type subjects who selected the color vs number of D-type subjects who chose the chip differ by ≥3 [4:0, 4:1, 3:0], Fig. 7); and conversely, color chips selected by D-type subjects but not by C-type subjects (Fig. 8).

As shown in Fig. 6, there were no color chips that were commonly selected for white, gray, blue-green, bluish-purple, light purple, and reddish-purple. For purple, only one color chip was selected in common. In particular, for light purple, purple, and reddish-purple, there were color chips commonly selected by most subjects with C-type color vision, but they were not commonly recognized as the corresponding color name by subjects with D-type color vision (Fig. 7).

Colors represented by these color chips must be used with caution when designing visual information, because they would not be perceived as the same color by individuals with different types of color vision. Colors selected commonly by D-type but not by C-type subjects included red in brown regions, brown in dark yellow regions, yellowish-green in yellow regions, yellow in yellowish-green regions, and pink in warm-color gray regions (Fig. 8). Usage of color tones in these regions may also impair effective color-based communication.

Moreover, some colors recognized unanimously by the C-type subjects were not recognized as the corresponding colors by subjects with D-type color vision. These include color chips of high saturation yellowish-green, high saturation brown, low saturation orange, bluish-purple, and green on the confusion line with gray (Fig. 7).

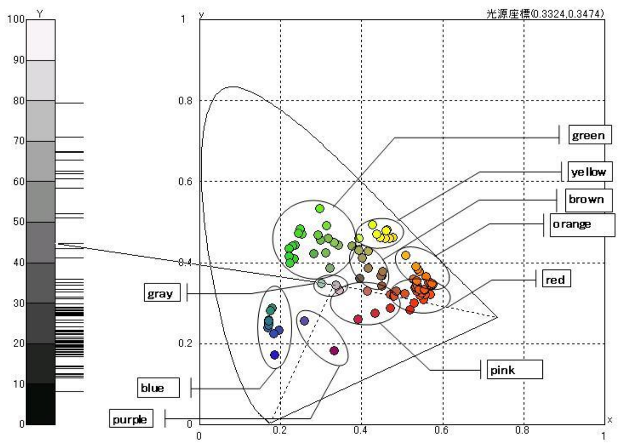

Fig. 5-1 Color chips selected by 3 of the 4 subjects with D-type color vision (basic colors)

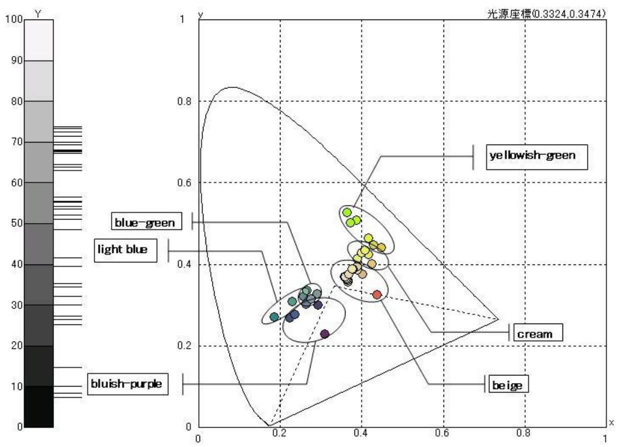

Fig. 5-2 Color chips selected by 3 of the 4 subjects with D -type color vision (non-basic colors)

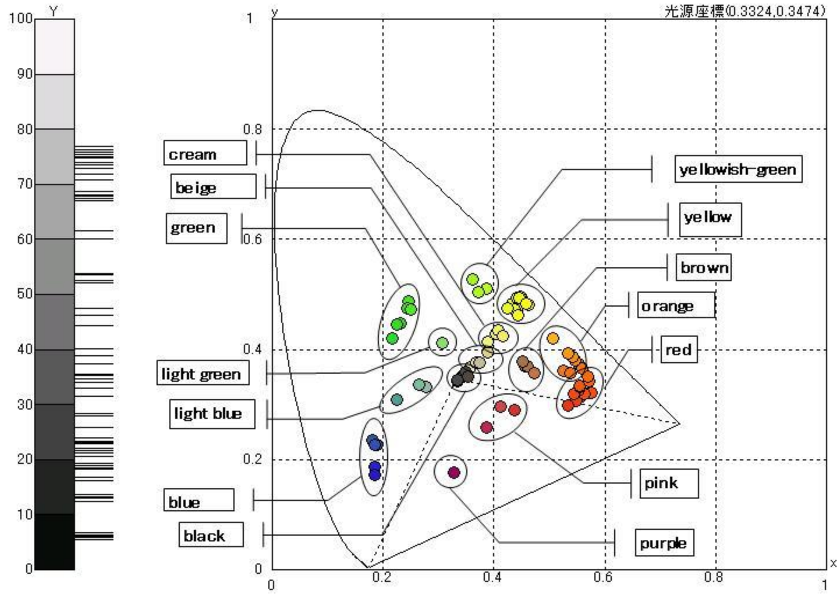

Fig. 6 Color chips selected by 3 or more subjects with C- or D-type color vision
(Colors that may possibly be used for color universal design)

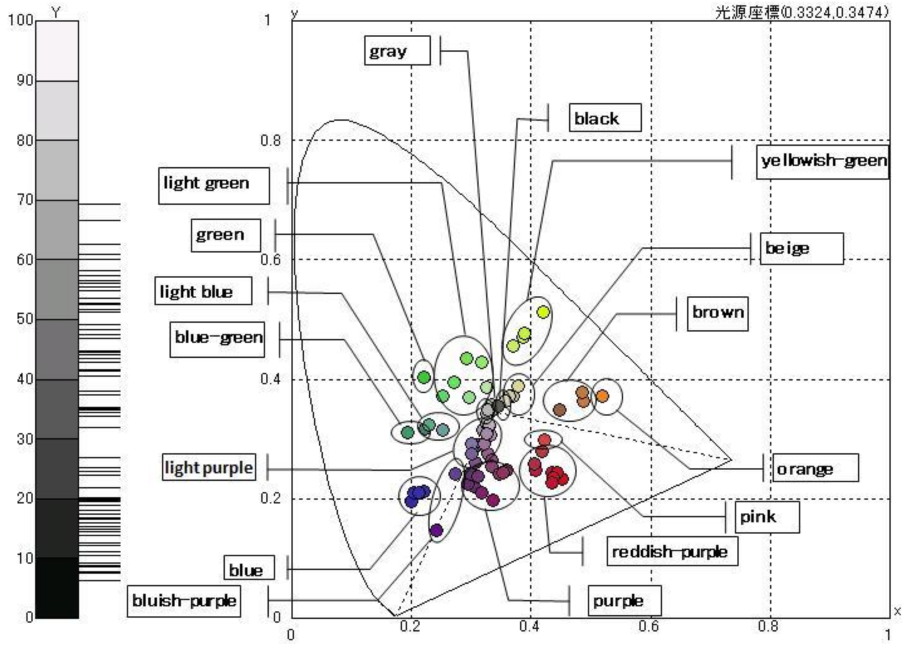

Fig. 7 Color chips selected by subjects with C-type color vision but not by subjects with D-type color vision

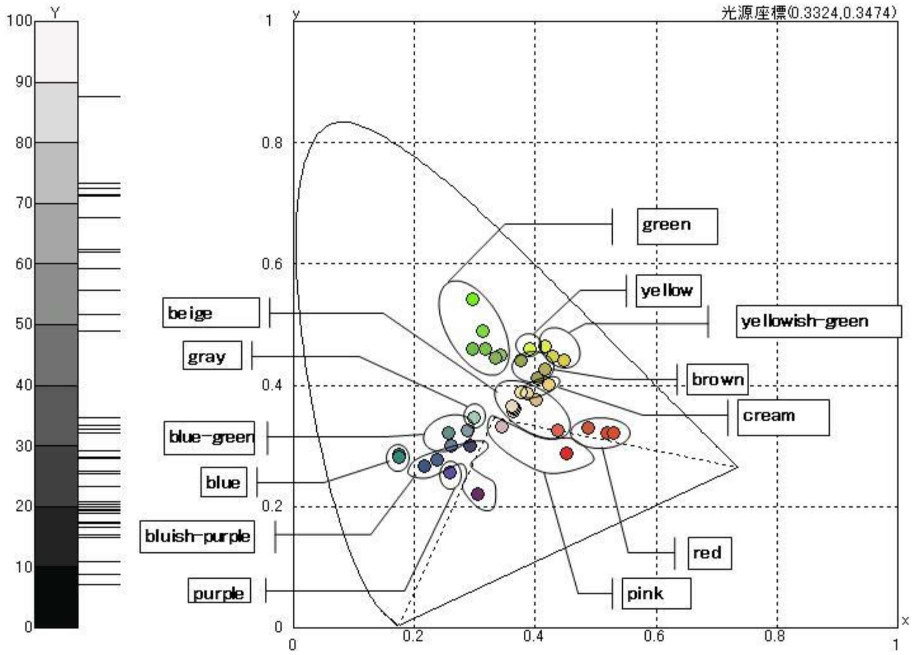

Fig. 8 Color chips selected by subjects with D-type color vision but not selected by subjects with C-type color vision

4. CONCLUSION AND FUTURE OUTLOOK

Our present study shows that color chips commonly selected by subjects with C- or D-type color vision exist for many color names. However, even for these colors, slight deviations in color tones may lead to color recognition using different color names. In future studies, data presented herein, combined with luminance information (reflectance Y or Munsell value) in the Yxy color space, will be compared three-dimensionally. In addition, the extent of individual differences and differences in the distribution of color tones felt to be most representative of a color name will be analyzed to further explore the differences in color category perception. An identical set of tests have already been conducted by 4 subjects with P-type color vision. Common and different features among C-, P- and D-type color vision will be analyzed in future studies.

Colors that are unanimously recognized as the same color name regardless of color vision type are good candidates for color universal design to facilitate color-name-based communication among individuals with different types of color-vision. Our study identified ranges of colors that are perceived differently depending on color vision type. Most notably, we identified ranges of colors that are perceived by individuals with C-type color vision with a certain color name but not by those with D-type color vision using the same color name. Such colors should be avoided when designing materials to be used in public places.

By replacing such colors with adjacent color tones that eliminate differences in color name recognition, color-coded designs that are difficult for those with different types of color vision to distinguish can be avoided.

ACKNOWLEDGEMENTS

This study was supported by a Grant-in-Aid for Challenging Exploratory Research (No. 21650071). We are grateful to Tomoyuki Takada and Ikutaka Kawada of Toyo Ink Manufacturing Co. for supplying information on the study materials. We also express our gratitude to Yosuke Tanaka of the NPO Color Universal Design Organization (CUDO) for help in recruiting subjects. We also thank all of the subjects for their participation in this study.

REFERENCES

[1] Brent Berlin, Paul Kay [Basic Color Terms], Their Universality and Evolution (The David Hume Series))(1969, 1991)

[2] Ichihara YG. Okabe M. Iga K.. Tanaka Y. Musha K. Ito K..,“Color Universal Design -The Selection of Four Easily Distinguishable Colors for all Color Vision Types- “EI2008 Color Imaging XIII:Processing, Hardcopy, and Application, SPIE Vol.6807 pp.6807O1~8 (2008)

[3] Ichihara Y.G., “Color constancy in Japanese Animation, EI2006 Internet Imaging”, Color Imaging XI:Processing, Hardcopy, and Application SPIE Vol.6058 pp.60580c1~8 (2006)

[4] Ichihara Y.G. Nakadomari S,Takeuchi H,Satoru Miyauchi S,Kitahara K., “A fMRI Study of Color Related Visual Cortex V4- Retinex processing from the fMRI study on V4 -Artistic Research of coloured Picture Using Functional MRI”, SPIE The International Society for Optical Engineering EI2002 Internet Imaging, Retinex40 SPIE Vol.4662 , 428 (2002)

[5] Ichihara YG,Nakadomari S,Takeuchi H,Satoru Miyauchi S,Kitahara K., “The difference between seeing a random colour dot picture and reading shapes from the same colour dot picture in the Ishihara pseudoisochromatic plates -Artistic research of coloured picture using functional MRI- “, AIC2001 Rochester Proceeding 2001 SPIE Vol.4421, 327-330, (2001)

[6] Ichihara YG., “What do you see in a digital color dot picture such as the Ishihara pseudoisochromatic plates? “, SPIE The International Society for Optical Engineering EI2001 Internet Imaging, vol. 4311, 419-426,(2001)

[7] Ichihara YG., “Suitable digital color palette (DPC) for individual human color vision sensitivity”, SPIE The International Society for Optical Engineering EI2000 Internet Imaging, vol. 3964, 168-174,(2000)

[8] K. Wakita and K shimamura, “SmartColor: disambiguation framework for the colorblind”, In Assets ’05:Proc. of the 7th international ACM SIGACCESS conference on Computers and accessibility, 158-165,(2

An Investigation of the Appearance Harmony using Real Materials and Displayed Images

Midori TANAKA and Takahiko HORIUCHI
Graduate School of Advanced Integration Science, Chiba University, Chiba, Japan

ABSTRACT

Color harmony has long been of interest to researchers in different fields who design the colors of various objects. When sensing harmony among actual objects, not only the harmony among the colors but also the appearance of harmony of the materials is an important consideration. In the previous study (Tanaka et. al., AIC2014), we investigated the appearance of harmony of various materials by conducting psychophysical experiments to collect quantitative data. In this study, we further investigated the appearance harmony using actual objects and rendered images and conducted the psychophysical experiments. Our results indicated that the sample pairs with similar reflection and texture patterns were viewed as harmonious, even though their materials were different. Furthermore, the appearance harmony of the materials was significantly affected by the subjects' reactions to the visual information of the displayed samples with/without monitor.

1. INTRODUCTION

Color harmony has interested researchers involved in color design based on various objects for a long time (e.g., Judd & Wyszecki, 1975; Hård, & Sivik, 2001; Burchett, 2002). By contrast, other traits related to harmony have not been investigated deeply in previous studies. The relationship between product identity and shape has been discussed (e.g., Bar & Neta, 2006; Nasser & Marjan, 2010; Ye, et al., 2014), but these studies investigated the preference for a single shape such as a kettle (Nasser & Marjan, 2010) or a chair (Ye, et al., 2014), whereas they did not consider two-shape combinations. Chen et al. investigated the relationship between preferences for color-pairs and shapes, but they did not discuss two-shape combinations. In the field of texture analysis, a single texture has been used in preference analyses. In 2014, Qiao et al. began the study of texture harmony (Qiao et al., 2014).

Recently, the analysis of material appearance has been studied actively. Most of these studies have focused on visual estimates of the specific properties of materials, such as glossiness, translucency, or roughness. According to experimental studies of material harmony, most of our empirical knowledge of harmony is based on specific material clusters in the actual field of industrial design, such as combinations of wood or stone used in architecture, or combinations of metals used in the car production. However, to the best of our knowledge, there have been no previous studies of the appearance harmony of materials.

Thus, in the present study, we investigated the appearance harmony of materials based on psychophysical experiments. Although numerous materials are mixed in the real world, the harmony among different materials has received little attention. In this study, we investigated the harmony across material categories.

2. EXPERIMENTAL STIMULI

2.1 Materials dataset

To investigate the perception of materials without being influenced by shape, we produced a dataset of 30 exemplars (size = 50 × 50 mm). The individual exemplars were selected from 10 material categories, i.e., stone, metal, glass, plastic, leather, fabric, paper, wood, ceramic, and rubber, thereby covering a wide range of material appearances. The materials are shown in Fig. 1. As noted by Albertazzi and Hurlbert (2013), color has a strong influence on perceptual qualities. However, it is difficult to collect uniform material exemplars of various hues, so we only collected exemplars with low saturation. In Fig. 2, the symbol "×" represents the location of each exemplar on the CIE xy chromaticity diagram. The number of exemplars in each material category was unequal because they were collected according to the differences in their surface properties. The material samples were used to generate 435 round-robin pairs, which were coupled arbitrarily and presented to the subjects, i.e., two samples each time.

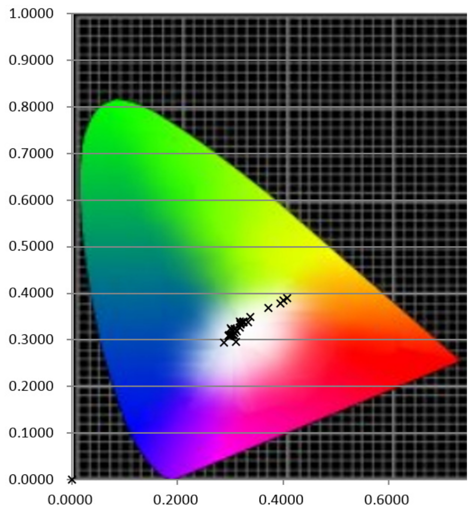

Fig. 1. Material dataset of 30 exemplars. *Fig. 2. Chrominance of the material samples.*

2.2 Image dataset

We hypothesized that when materials are reproduced on a monitor, the following factors might strongly affect the perceptual harmony: intensity, color reproduction, and resolution. Thus, we constructed an imaging system to facilitate the accurate reproduction of the real-world display materials, where the camera system comprised an RGB camera and a standard lens. The camera used to obtain a linear camera output was a Canon EOS 5D Mark II, with a *sRAW2* image size of 2784 × 1856 pixels and a quantization level of 14 bits. We then prepared a color image dataset by capturing the materials which placed in a viewing booth. The output monitor was an Apple 15.4" MacBook Pro with Retina display, where the widescreen, LED-backlit IPS screen had a glossy finish, with a native resolution of 2880 × 1880 pixels and 220 pixels per inch. Using a calibration process, we verified that the intensity and chromaticity of the real materials and their images reproduced on the display were almost equivalent.

3. EXPERIMENTAL METHODS

We conducted two different experiments, as follows.

(1) Experiment A:

Sample pairs were placed such that their surfaces and viewing directions were perpendicular to the subject. In this experiment, subjects assessed the harmony or disharmony of each sample pair based on their two-dimensional surface appearance.

(2) Experiment B:

The static sample pairs used in Experiment B were photographed using a digital camera. Subjects assessed the appearance harmony or disharmony of each sample pair appeared on the images displayed on a calibrated monitor.

After dark adaptation for two 2 min, the subjects evaluated the pairs according to each experimental method. A forced-choice, 10-point scale was used to rate harmony-disharmony. The subjects determined the appropriate rating for each combination from 1 (disharmony) to 10 (harmony) and recorded them on answer sheets. In each experiment, 435 pairs were evaluated and over 30 pairs were then selected from the 435 pairs to confirm the reproducibility of the experimental results. The subjects were asked to wear gloves in order to avoid the possibility of tactile effects confounding their assessments. In each experiment, the subjects conducted the evaluation in a specified order and they changed the evaluation samples themselves. Five subjects participated in this experiment. All of the subjects were native Japanese with normal color vision.

4. EXPERIMENTAL RESULTS

4.1 Intra- and inter-participant variances

The intra-participant variance was calculated as the average variances in the ratings between the two sessions. The inter-participant variance was calculated as the average ratings for each of 435 pairs by five participants.

Table 1 summarizes the intra- and inter-participant variances in the ratings. The intra-subject variance was based on 30 samples, which were shown twice. The inter-subject variance in the right row of Table 1 shows the average variance of the ratings among 435 pairs. As shown in Table 1, we confirmed that the variance in the intra-subject ratings was less than the variance in the inter-subject ratings.

Table 1. Variances in the Inter- and intra-participant ratings.

Experiment	Inter-var.	Intra-var.
A	0.52	3.73
B	0.32	2.77

The observed variance had one notable feature, as shown in Table 1, i.e., the ratings in Experiment A varied among subjects, whereas the ratings in Experiment B were stable among subjects. This suggests that the richness of the real-world information was sensitive to the perceptual harmony ratings. These results show that the evaluations of appearance harmony using actual material samples differed from the surface appearance assessments obtained based on captured images.

4.2 Perceptual harmony ratings within and across the categories of materials

Table 2 summarizes the averaged perceptual harmony ratings for all subjects within the same material category and across different material categories in each experiment. As shown in Table 2, the ratings for sample pairs within the same material category were higher than the ratings across material categories. In all the experiments, the "Metal-Metal" pair had the highest harmony ratings. By contrast, the harmony ratings for "Leather-Leather" and "Paper-Paper" were categorized as perceptual disharmony. These results suggest that the perceptual harmony ratings depended on the materials, where two samples within the same material category could be perceived as having appearance disharmony. Interestingly, the harmony rating for "Paper-Metal" was higher than for "Paper-Paper". This indicates that the perceptual harmony of the pairs in different material categories could be higher than that of pairs within the same material category. Metal, plastic, ceramic and rubber shared the most harmony with each other across material categories. "Glass-Plastic" also had a high perceptual harmony rating. These results indicate that materials can be harmonized across material categories.

Table 2. Averaged harmony ratings for the categories of materials.

Experiment	Within material	Across materials
A	6.68	4.02
B	6.43	4.14

4.3 Changes in harmony between experiments

As shown in Table 2, the average ratings in Experiments A and B did not differ significantly. However, there were some notable differences between the experiments. For the pair of plastic and rubber, the average rating indicated harmony in Experiments A (7.60) and B (7.30). For the pair of glass and rubber, the average rating changed from disharmony in Experiments A (4.80) to harmony in Experiment B (6.80). In this case, the appearance of the material may have differed between the real objects and the displayed images.

Some of the ratings for each pair differed in the experiments. Table 3 shows the ratings and pairs that changed greatly between experiments. In Experiment B, the average ratings across all subjects changed by a maximum +4.8 (pair 6 and 13) from Experiment A to B. Pair 6 (chrome, metal) and 13 (gray calfskin, leather), as shown in Fig. 3(a), had low ratings in Experiment A because their surface properties differed greatly in appearance. However, this difference could not be perceived when this pair was displayed on the monitor in Experiment B. By contrast, the average rating across all subjects changed by a minimum of –5.2 (pair 12 and 14) from Experiment A to B. Pair 12 (pig suede, leather) and 14 (cotton, fabric) had a high rating in Experiment A because their surface textures and colors were similar. However, in Experiment B, a low rating was obtained due to the low resolution of the monitor, as shown in Fig. 3(b). In these cases, the material appearance may have differed between the real objects and the displayed images.

Table 3. Harmony changes between experiments.

Experiment	Up (pair)	Down (pair)
A→B	+4.8 (6-13)	-5.2 (12-14)

(a) (b)

(a) Pair 6 (metal) and 13 (leather) , (b) Pair 14 (fabric) and 12 (leather)

Fig. 3. Pairs that changed significantly between experiments.

4.4 Distributions of samples in the appearance harmony space

We performed a principal component analysis (PCA) of all the ratings across materials to facilitate the visualization of the distributions of material classes in the appearance harmony feature space. We created a 30 × 30 diagonal matrix where the lines and columns represented the 30 material samples. Each element in the matrix showed the average rating for a pair, where we assumed symmetry among the rating. The diagonal components were considered to be the maximum ratings because a diagonal showed the ratings for pairs of materials. We derived 30 dimensions and 30 PCs from the matrix. Therefore, materials with the same harmony properties had the same PC coefficients. In all of the experiments, the first three PCs accounted for almost 92% of the variance. It should be noted that the remaining 8% of the variance in the distribution was accounted for by the other 27 dimensions. Thus, regardless of the methods used to determine the appearance harmony among materials, we can obtain an approximation of the overall distribution simply by using the first three PCs.

Figure 4 shows the ratings for each sample projected onto the first two PCs where each image is color coded by its true class membership. The open circles indicate the average for each material class and the same color corresponds to the same material category. The observed distribution in the PC space has several key features. As shown in Figure 4(a), with the exceptions of wood and fabric, the material categories overlapped with each other in Experiment A. This indicates that the degree of harmony did not depend on the material clusters in a stationary state, unlike the objects that could be moved. Furthermore, most of the material categories overlapped with each other in Experiment B, as shown in Figure 4(b). This suggests that the degree of harmony did not depend on the material clusters in the displayed images.

5. CONCLUSIONS

We investigated the appearance harmony among various materials by conducting three psychophysical experiments using the following real materials and their displayed images. In Experiment A, the samples were placed such that their surfaces and viewing directions were perpendicular to the subject. In Experiment B, static sample images were displayed on a monitor. Based on the intra- and inter-participant variances, we found that the perceptual harmony ratings were sensitive to the richness of the information available in the real world. In addition, the ratings were sensitive to the reflectance properties obtained by tilting objects. However, the perceptual harmony ratings were insensitive to the poor information obtained from rendered images.

Based on subjective assessments, we confirmed that sample pairs with similar surface properties were viewed as harmonious, although the materials were different. Indeed, the appearance harmony of the materials differed between static real samples and static images. The results of the PCA indicated that the degree of harmony did not depend on the material clusters in a stationary state and the displayed images.

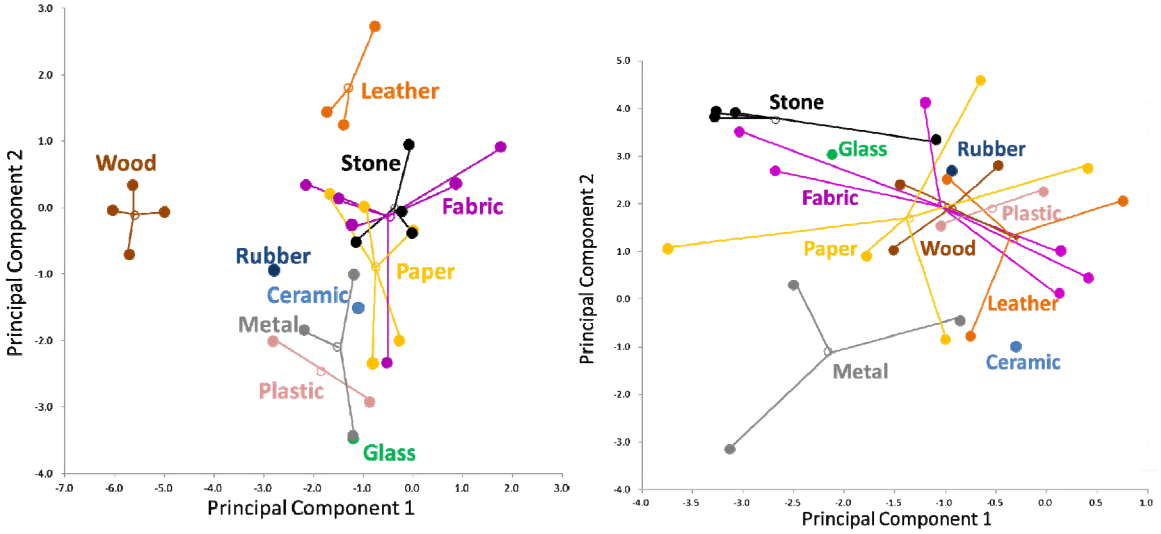

(a) Experiment A. *(b) Experiment B.*

Fig. 4. Distribution of samples in the first two PCs.

ACKNOWLEDGEMENTS

This work was supported by Grant-in-Aid for Scientific Research on Innovative Areas "Shitsukan" (No. 25135706) from MEXT, Japan.

REFERENCES

Bar, M. and M. Neta 2006. *Humans prefer curved visual objects*, Psychological Science 17 645–648.

Burchett, K.E. 2002. *Color harmony*. Color Res Appl. 27 28–31.

Chen, N., Tanaka, K., Matsuyoshi, D. and Watanabe, K. 2013. *Cross preference for color combination and shape*, Proc. Asia Color Association Conference, 98–101.

Hård, A. & Sivik, L. 2001. *A theory of colors in combination: A descriptive model related to the NCS color-order system*. Color Res Appl. 26 4–28.

Judd, D.B. & Wyszecki, G. 1975. *Color in Business*, Science and Industry, 3rd edition. New York: Wiley 390–396.

Nasser, K.M. & Marjan, T. 2010. *Design with emotional approach by implementing Kansei engineering—Case study: Design of kettle*, Proc. International Conference on Kansei Engineering and Emotion Research 625–632.

Qiao, X., Wang, P., Li, Y. and Hu. Z. 2014. *Study on a correlation model between the Kansei image and the texture harmony*, International Journal of Signal Processing, Image Processing and Pattern Recognition 7 73–84

Tanaka, M. and T. Horiuchi, 2014. *An Investigation of the Appearance Harmony of Materials*, Proc. AIC2014 Interim Meeting.

Ye, Y., Zhang Z. & He, R. 2014. *Study on design of chair shaping based on Kansei engineering,* International Journal of Scientific & Engineering Research 5 273–276.

Address: Ms. Midori Tanaka, Graduate School of Advanced Integration Science,
Chiba University, Yayoi-cho 1-33, Inage-ku, Chiba, 263-8522 JAPAN
E-mails:midori_t@graduate.chiba-u.jp, horiuchi@faculty.chiba-u.jp

The Colour of Gold

Lindsay W. MacDonald
3DImpact Research Group, Faculty of Engineering, University College London

ABSTRACT

The reflection from the surface of gold consists of both a body colour (dark and diffuse) and specular highlights (bright and metallic). Surface normals and albedo are calculated by regression over a subset of the intensity values from a set of images taken in an illumination dome. The specular component of reflectance is modelled as a Lorentzian function of radial angle from the specular peak direction. Rendering the surface by a model that adds diffuse and specular components at each pixel for any direction of incident illumination gives a good simulation of the appearance of the original object. It is shown how for gold this conforms to the Shafer dichromatic model of reflectance.

1. INTRODUCTION

There is nothing absolute about the colour of an object surface: it changes continually with illumination and orientation. So how can we define the colour of a surface? Given many images of the same object, even under the same light from many angles, what is the 'true' surface colour? Colorimetry specifies the colour of an object as the product of the illuminating power by the reflectance factor of the surface by the sensitivity of the observer, integrated over all wavelengths of the visible spectrum. This is the basis of the ubiquitous CIE system, but it relies on the assumption that the surface is perfectly matte so every point reflects the incident light equally in all directions, i.e. that it is perfectly Lambertian. In fact almost all real materials exhibit some angular dependence in the way they reflect light, and this behaviour must be taken into account when modelling the appearance of the object, by adding a gloss component to the underlying diffuse colour. The added light may appear as a sheen over the surface or as localised specular highlights, but its effect is to modulate the lightness and thereby change the colour stimulus.

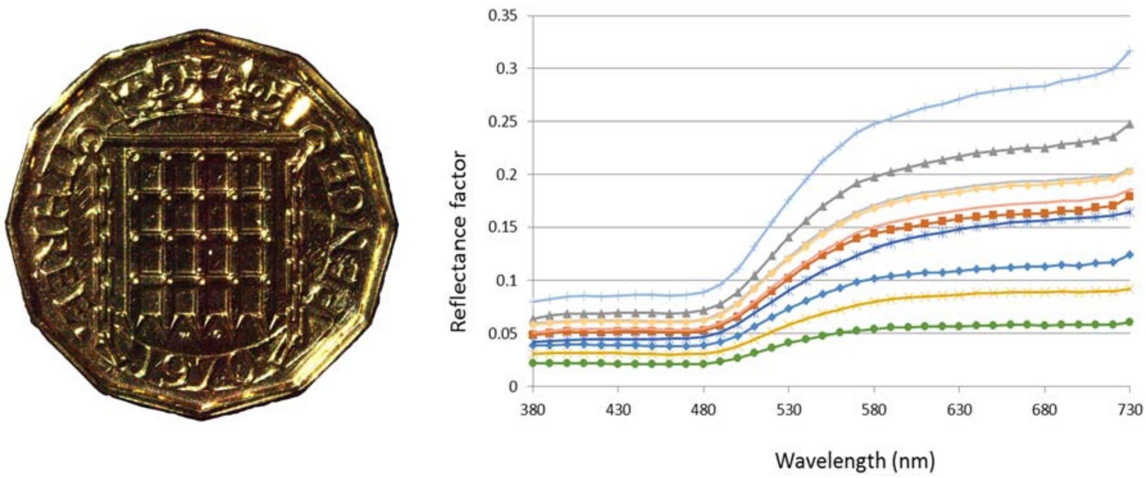

Figure 1. (left) Reverse of gold-plated threepence; (right) Reflectance spectra of 10 measurements.

This is especially true of gold, which combines glitter, specularity and sheen over a wide range of angles to give it a uniquely lustrous quality that sets it apart from ordinary materials.

To specify the colour of gold only by a single colorimetric triplet, or even by a single reflectance spectrum, would be dull indeed. As an example, a freshly gold-plated silver English threepence was selected as a test object and measured with an Xrite i1Pro spectrophotometer. The spectral reflectance distributions from 10 successive measure-ments are shown in Fig. 1. The characteristic rise in reflectance at 540nm corresponds to an energy band at 2.3 eV in pure gold where free electrons in the d-band can make the transition to unoccupied states in the conduction band (Saeger & Rodies, 1977). It is evident in the set of measurements that, although the shape of the curve remains the same, the magnitude of the reflectance varies by a factor of 5. This can be explained by the measurement geometry of the instrument, which is designed for measurement of flat surfaces, such as prints on paper, which may or may not be glossy. The 45° angle of incident light and 0° angle of view for the sensor ensures that the specular component of reflection is avoided. But when the instrument is removed and then brought back each time with the aperture in a different position over the relief surface of the coin, a different distribution of scattered light reaches the sensor and the reading changes. The majority of the variation in the measured colorimetric values is in the luminance, not the colour: in CIE 1931 chromaticity the range in x,y,Y is [0.3988±0.0023, 0.4000±0.0013, 19.75±4.38] and in $L^*a^*b^*$ the corresponding range is [51.18±5.04, 44.79±0.04, 26.40±2.13].

2. DOME IMAGE PROCESSING

The dome imaging system at UCL enables sets of images of an object to be taken with illumination from different directions. A hemisphere of 104 cm diameter is fitted with 64 flash lights, calibrated so that the geometric centroid coordinates of every light source are known to within 3mm (MacDonald *et al*, 2015). A Nikon D200 digital camera at the 'north pole' captures a series of 64 colour images, each illuminated from a different direction and all in pixel register. This enables the object to be visualised from a fixed viewing angle, i.e. vertically from above, for many different angles of incident light. Image sets captured by the system can be visualised by the polynomial texture mapping (PTM) technique, which has numerous applications in archaeology and cultural heritage (Earl *et al*, 2010).

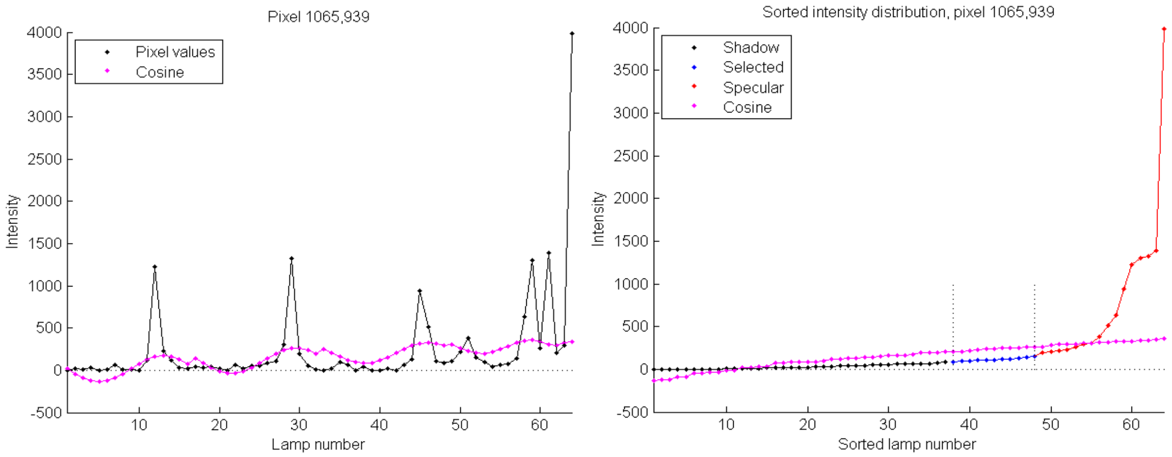

Figure 2. Intensity distributions for a single pixel: (left) in lamp order; (right) sorted.

The difficulty with gold, and indeed with all shiny and glossy materials, is that they reflect strongly in the specular direction. So in the vector of 64 intensity values for any pixel, there are a few values much larger than the others, corresponding to positions where the surface normal is close to the bisector of the angle between the illumination vector (toward the light) and the view vector (toward the camera). This results in images with high dynamic range where a few pixels may be 100 times greater in value than the majority. In the dome, images are captured and processed as linear 16-bit per channel (range 0–65535), setting the lens aperture to *f*/11 to avoid over-exposure. Fig. 2 shows the intensity distribution for a single pixel on the rim at the upper left edge of the coin. One value is ~4000 and five are in the range 1000–1500 but most others are less than 200. The magenta curve shows what the intensities would be for a perfectly matte (Lambertian) surface with the same albedo and normal angle. It is clear that the specular peaks are much greater in intensity than the cosine, but all other values are lower. Thus the metallic gold surface is generally darker than the diffuse equivalent, except for a few bright highlights.

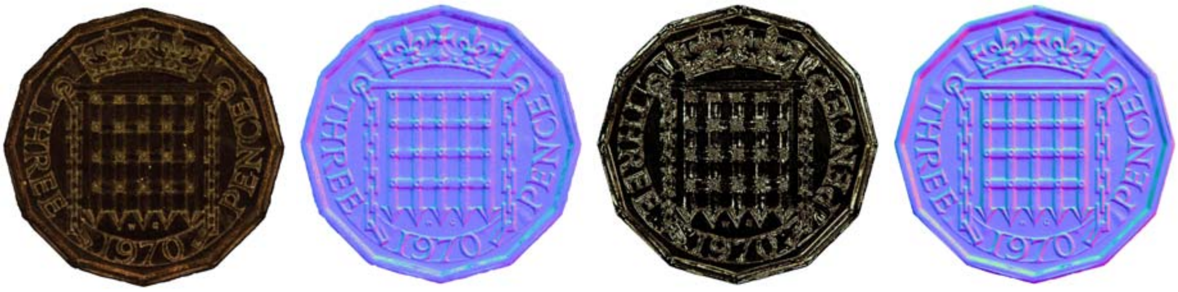

Figure 3: Image components derived from processing the original set of 64 images: (left to right) albedo, normals, specular colour, specular normals.

The processing method is to identify from the intensity distribution of a 3x3 pixel neighbourhood (9x64=576 values in total) a range of 100 values between the shadow and specular regions, which are taken to be representative of the non-specular 'body colour' of the object (the blue dots in Fig. 2 right). Then using the principle of 'shape from shading', a regression is performed on the corresponding lamp vectors to estimate the most probable direction of the surface normal at that pixel (MacDonald, 2014). The albedo is the magnitude of the normal vector, and its appearance is surprisingly dark (Fig. 3 left). The surface normals are represented in Fig. 3 by the standard false-colour coding with X values in red, Y in green and Z in blue. Note that the image set was taken with a Nikkor 200mm macro lens plus a 40mm extension ring, so the coin diameter of 21.0 mm spans 2060 pixels in the image. This means that the spatial resolution is 98 pixels/mm, i.e. 1 pixel represents 10.2 microns on the surface of the coin.

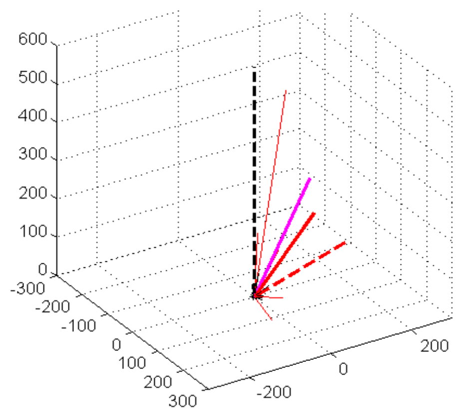

Figure 4. Vectors for a single pixel, showing view vector (black), normal (magenta), ideal specular (red dashed) and computed specular (thick red).

The second stage of processing is to determine the specular vector at each pixel, i.e. the direction of maximum specular reflectance. First the ratio, or specular quotient, is calculated between the actual intensity value and the diffuse component for each lamp. (This would be the black value divided by the magenta value for each of the 64 points in Fig. 2.) For semi-matte surfaces the quotient values are typically in the range 0.5 to 2.5, but for high gloss and shiny metallic surfaces they may be very large. In this case the maximum value over the image of the coin is 3,878 which is indicative of the high dynamic range of the imagery. To facilitate the computation, a compression function is applied to the quotient by a power function with fractional exponent. In this case an exponent of 0.5 (i.e. square root) has been used, giving a maximum quotient value of 62.3. A weighted sum is made of all the normalised lamp vectors above a threshold of 0.2 and within 60° of the normal vector, using the magnitude of the quotient as the weighting factor. For the pixel in Fig. 2 there are five specular vectors, shown by the thin red lines in Fig. 4, with the result shown by the thick red line. One might suppose that the specular angle should be exactly double that of the normal, as it would be for a perfect mirror surface, but in fact there is a great deal of variation. This is caused not only by noise, but also by the fixed sampling positions on the dome. Moreover granularity and surface imperfections, such as scratches and dust, cause perturbations in the direction of the strongest reflectance. The scatter is clear when the specular angle wrt the Z axis is plotted against the normal angle for 10,000 points randomly selected throughout the image (Fig. 5). Instead of lying along the line of slope 2 they are spread over a wide range of angles, both greater than and less than the normal angle. The horizontal lines of red dots in the figure are computational artefacts, where the specular vector lies exactly toward the lamp, so they indicate the incident angles of the five lamp tiers in the dome at 10°, 27°, 45°, 63° and 80°.

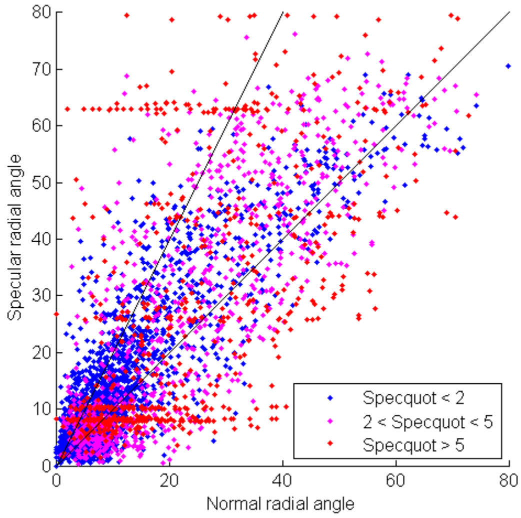

Figure 5. Specular vs normal angles for 10,000 random points in image.

The specular colour at each pixel is computed from the colours of the selected specular values, using the same weighting factors derived from the specular quotients. The resulting colour for the whole coin is shown in Fig. 2 (centre right) and it is apparent that the colour balance is slightly greenish, certainly less red than the albedo. The relationship can be explored by plotting corresponding values for a random selection of 10,000 points throughout the image area. In Fig. 6 albedo colours are shown as black dots and the specular colours as red dots in a normalised R,G,B cube. Also shown are lines representing the first principal component of each cluster of points, which tend in different directions. The albedo (body colour) is darker and on the red side of the neutral axis, whereas the specular colour is lighter and on the green side of the neutral axis. Both are below neutral on the blue axis, meaning that both are yellowish. (Note that all images were taken with the Nikon camera white balance set to 'flash', not auto-white, and that the images were corrected to ensure that equal values of R,G,B would correspond to neutral grey, before the image processing was undertaken.) The two vectors in RGB colour space (denoted by the red and black lines in Fig. 6) may be considered as equivalent to the interface and body colours identified by Shafer (1985) in his proposal for a dichromatic model of reflection from a material surface.

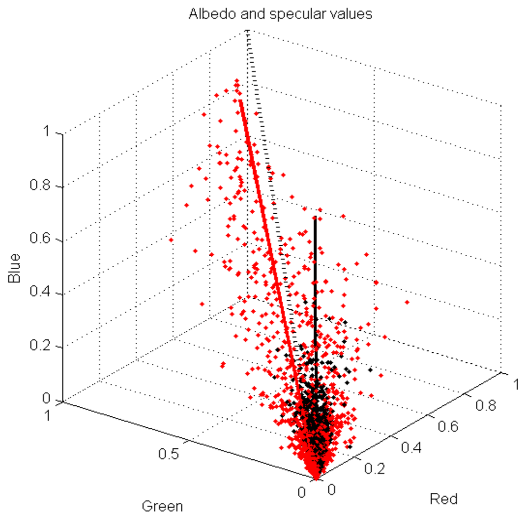

Figure 6. Specular vs albedo colours for 10,000 random points in image.

3. IMAGE RENDERING

The distribution of the specular quotient around the specular peak angle has been found for a variety of materials to be modelled well by a modified Lorentzian function (MacDonald, 2014), which takes the form of a curved peak plus a linear flank:

$$f(\omega) = \frac{p_a}{1+(\omega/p_s)^{p_e}} + \left(1 - \frac{\omega}{180}\right) \tag{1}$$

where $\omega = \mathrm{acosd}(\mathbf{L} \cdot \mathbf{S})$ is the specular radial angle in degrees between the lamp vector and specular vector. Thus the distribution is characterised at each pixel in terms of three parameters: p_a is the amplitude, p_s is the scale and p_e is an exponent. The flank is not fitted to the distribution of quotient values, but is assumed to be an invariant cone of value 1 at the apex and 0.5 at 90° from the specular vector. In this model the exponent p_e of the peak term is not constant = 2, as for a standard Lorentzian, but can vary over the range 1-10. The parameters of the curve are determined for each pixel from the distribution of specular quotient values in the polar plane. The angle of the specular vector is translated to the centre of the plane, and the angles of all incident lamp vectors are translated by an equal amount. Delaunay triangulation is applied to the distribution of points on the polar plane; when plotted as a mesh in 3D, with quotient value on the Z axis, the distribution forms a polyhedral central peak surrounded by an irregular flank (Fig. 7).

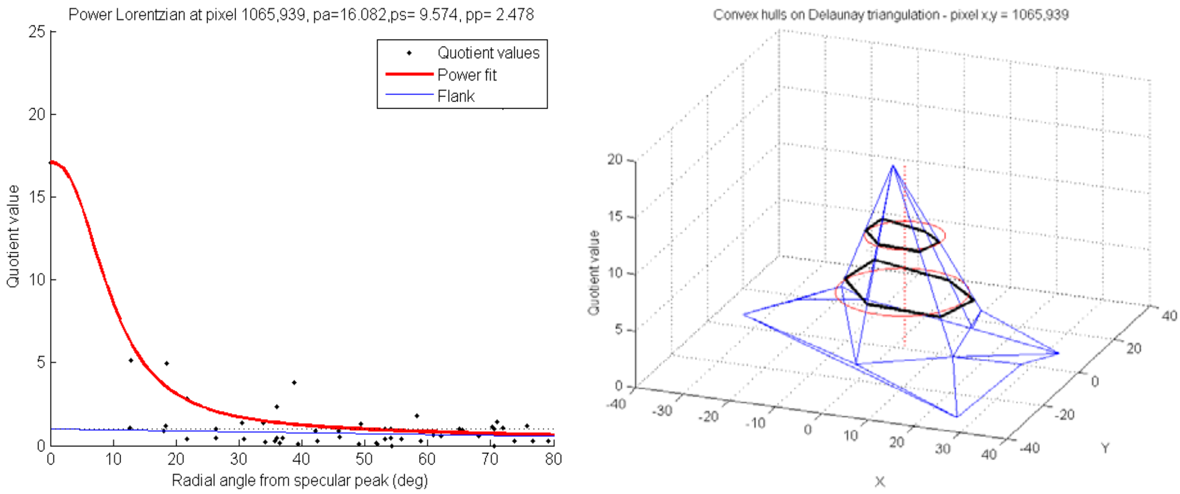

Figure 7. (left) Lorentzian distribution of intensity as a function of radial angle; (right) Profile modelled on the polar angle plane, fitting to Delaunay triangulation.

The complete model for rendering images under a single light source adds the diffuse and specular terms:

$$A_m I = \mathbf{L} \cdot \mathbf{N} A_{rgb} + (f(\omega) - 1) S_{rgb} A_m / S_m \tag{2}$$

where A_{rgb} is the albedo colour, S_{rgb} is the specular colour, A_m is the monochrome albedo (weighted sum of the R,G,B channels of A_{rgb}), and S_m is monochrome specular intensity. This gives images that are realistic in appearance and a good match to actual photographs (Fig. 8). It is important to recognise that the specular reflection is not isolated at the specular peak angle, but extends over a wide range of angles. Without this broad flank in the specular reflectance distribution the rendering would be darker with scattered pinpoint highlights and would not be realistic.

Figure 8 juxtaposes the actual photographic image taken in the dome illuminated by lamp 60 with the image rendered by Eq. 2. Although not identical, the two are similar in terms of the overall tonality and distribution of highlights. Because the model is based on a continuous function of angle, images can be rendered for a virtual light source at any position in the hemisphere.

Figure 8. (left) Photographic image for dome lamp 60; (right) image rendered with light from same direction.

Thus the colour of gold can be represented as a sum of two components: a dark reddish-yellow 'body colour', the albedo corresponding to the diffuse reflectance from the material, plus a bright greenish-yellow highlight with a broad angular distribution around the specular peak. A more complete model would need to take into account the Fresnel effect, which causes the spectrum of the reflected light to flatten at angles of incidence greater than 70° (Cook & Torrance, 1982). This is confirmed by observations of gold materials in which the perceived colour changes from yellowish, when the incident light is normal to the surface, to whitish as the angle of incidence is increased (Okawaza & Komatsu, 2013). Conversely, multiple reflections from facets on the surface cause the spectrum of the reflected light to be multiplied and hence to appear darker and more saturated. When the object is diffusely illuminated, with incident light from many directions, the characteristic golden radiance suffuses the whole surface and brings it to life.

REFERENCES

Cook, R.L. and Torrance, K.E. (1982). *A reflectance model for computer graphics*. ACM Transactions on Graphics, 1(1):7-24.

Earl G., K. Martinez and T. Malzbender (2010). *Archaeological applications of polynomial texture mapping: analysis, conservation and representation*, J. Archaeological Science, 37(8):2040-2050.

MacDonald, L.W. (2014) *Colour and Directionality in Surface Reflectance*, Proc. Conf. on Artificial Intelligence and the Simulation of Behaviour (AISB), April 2014.

MacDonald, L.W., A.H. Ahmadabadian and S. Robson (2015). *Determining the Coordinates of Lamps in an Illumination Dome*. Proc. SPIE Conf. on Optical Metrology, Videometrics, Range Imaging and Applications, Munich, June 2015.

Okazawa, G. and Komatsu, H. (2013). *Image statistics for golden appearance of a painting by a Japanese Edo-era artist Jakuchu Ito*. Proc. Computational Color Imaging Workshop (pp. 68-79). Springer.

Saeger, K.E. and J. Rodies (1977). *The colour of gold and its alloys*. Gold Bulletin, 10(1):10-14.

Shafer, S.A. (1985). *Using Color to Separate Reflection Components*, Color Research & Application, 10(4):210-218.

Address: Dr Lindsay MACDONALD, 3DIMPact Research Centre,
Department of Civil, Environmental and Geomatic Engineering,
University College London, Gower Street, London, UK
E-mail: lindsay.macdonald@ucl.ac.uk

Preferred LED lighting for wood surfaces and colored surfaces

Markus REISINGER[1]
[1] Lucerne School of Engineering and Architecture

ABSTRACT

The usage of Light Emitting Diodes (LEDs) as light sources in architectural lighting applications is quickly increasing. The present research addressed questions of material appearance by comparing effects of different LED-spectra. Preferred visual appearance is accessed for a set of 12 colors taken from the Natural Color System (NCS) catalog and a set of 8 types of wood surfaces. The results of this study demonstrates that certain hues fit better to lighting with higher correlated color temperature (cooler light) and other hues fit better to lighting with lower CCT (warmer light). Concerning the appearance of the wood surfaces the results are not fully conclusive. The observed reactions lead to the assumption that mainly hue determines the correlated light temperature of the LED light source that is preferred.

1. INTRODUCTION

The perceived atmosphere of an interior space is a whole of all consisting elements. Lighting as part of this constructed environment influences the visual appearance of objects and materials. A previous study (Lasauskaite Schüpbach, Reisinger and Schrader, 2015) evaluating lighting preferences for surfaces demonstrated that choice of the optimal lighting depends on the material and its typical characteristics. Light sources with a CCT of 3000K are preferred for red carpet and synthetic turf materials. For light blue flagstone and blue MDF materials light sources with 4000K CCT are preferred. Conversations with design experts, interior architects and architects are supporting the assumption to use warmer light for warm hues and cooler light for cooler hues. The first hypothesis tested is that people have clear preferences for warm or cold lighting, depending on the hue of the surface. Among lighting specialists it is well accepted that human skin and natural materials as wood surfaces suit better than others to judge lighting quality. The second part of the study is of explorative character and concerned with the appearance of different types of natural wood surfaces.

2. METHOD

In this study appearance of 12 color samples from the Natural Color System (NCS) catalog and 8 different types of wood are examined. Comparison is done side by side using two cabinets illuminated by LED light sources of different color temperature.

2.1 Materials

Two sets of materials are used to evaluate light preferences. The first set consists of 12 samples of NCS colors (NCS, Sweden). This are 4 highly saturated colors in yellow, red, blue, green and 4 saturated colors in hues exactly positioned in between. In the NCS hue circle this 8 samples show equal distances and include the two major axes with the so called unique hues. The latter mentioned hues were additionally presented in pastel versions.

Figure 1: Set of 12 NCS color samples.

Precise technical characteristics of the used color samples are found in table 1.

Table 1. Characteristics of the 12 color samples.

NCS-color tone	NCS lightness	CIE Yxy			CIE La*b*		
		Y	*x*	*y*	*L*	*a**	*b**
S0580-Y	0.86	65.1	0.48	0.48	84.5	6.1	99.5
S0580-Y50R	0.62	34.5	0.55	0.40	65.4	46.6	69.0
S1080-R	0.32	11.7	0.57	0.32	40.8	58.3	28.9
S3055-R50B	0.3	10.6	0.30	0.21	38.8	33.6	-27.9
S1565-B	0.45	21.6	0.18	0.24	53.6	-24.7	-36.3
S2060-B50G	0.48	24.0	0.20	0.34	56.1	-45.6	-9.6
S1565-G	0.52	26.9	0.25	0.45	58.9	-53.4	19.5
S0565-G50Y	0.78	54.0	0.40	0.49	78.4	-22.6	66.4
S0520-Y50R	0.86	67.8	0.38	0.36	85.9	13.6	22.8
S0520-R50B	0.85	67.7	0.31	0.31	85.8	7.6	-8.6
S0520-B50G	0.88	73.3	0.29	0.33	88.6	-14.2	-2.9
S0520-G50Y	0.93	82.3	0.34	0.38	92.7	-9.9	23.7

Note. CIE Yxy for 10° observer. La*b* reference light D65.

The second set consists of 8 types of wood surfaces: Fir, Staghorn sumac wood, Maple wood, Poplar, Red oak, Robinia, Beech wood and Plum wood. Color properties of these samples are described by their typical spectral reflection characteristics (see Fig. 2).

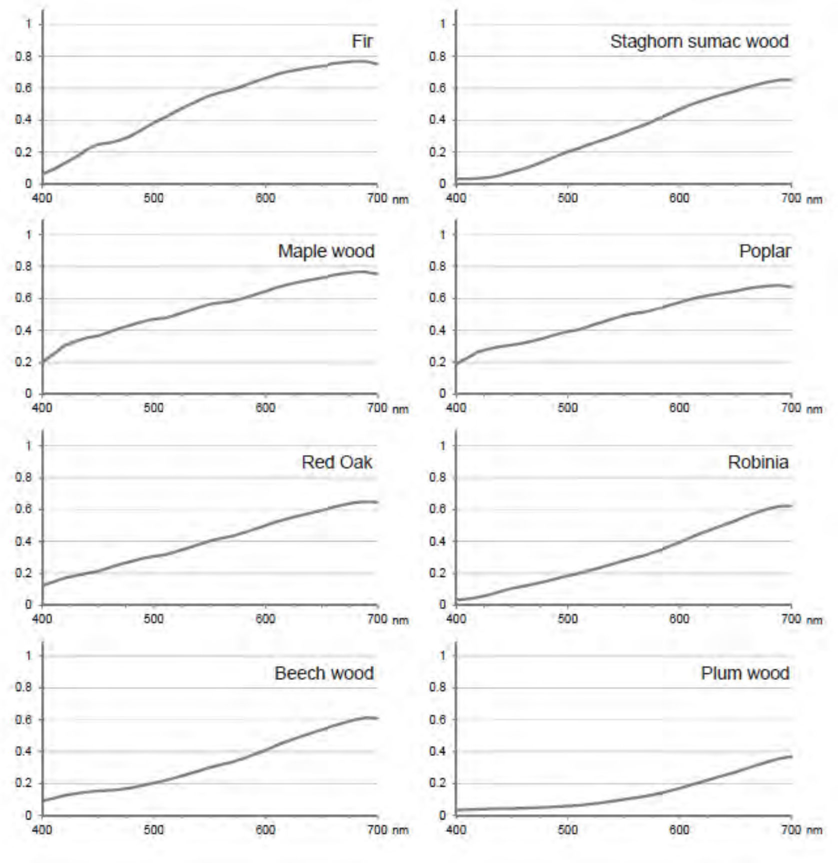

Figure 2: Spectral reflectance curves for the 8 wood samples

Visual preference is accessed by comparing visual appearance under two light conditions. Both scenes are illuminated with LED light sources: warm light with a CCT of approx. 3000K and cold light with a CCT of approx. 4000K. The Color Rendering Index (CRI) is for all used light sources (Xicato, USA) above 95. The average illumination level in both cabinets is 1400 lx. Measurements are done using a Illuminance Meter T-10 (Konica Minolta Sensing, Japan).

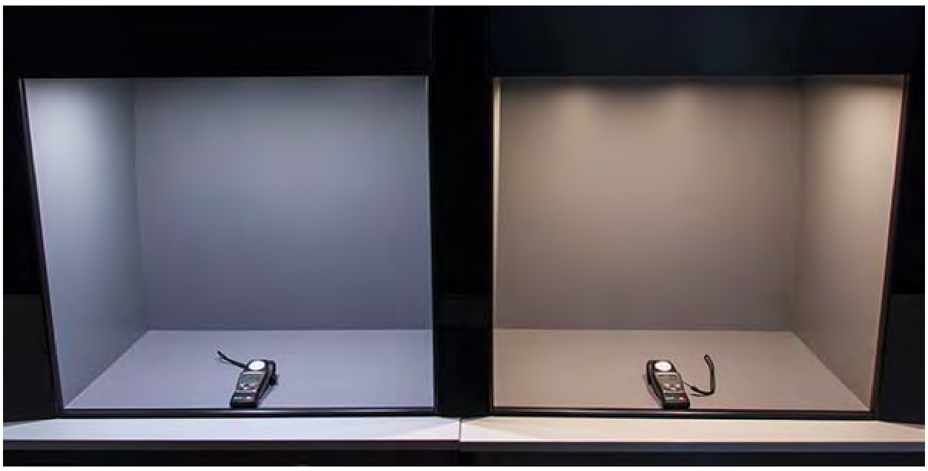

Figure 3: Two lighting cabinets illuminated by LED light sources of different CCT.

All participants assessed visual appearance by viewing the samples in front of a grey neutral background.

2.2 Procedure

27 interior architecture students (25 women: mean age 25 years) are participating in the experiment. None of the participants had color deficiency which is assessed with the Ishihara, 1999 color deficiency test. By performing a forced choice task participants expresses their preference for one out of two light conditions. The study design is within-persons (all participants are confronted with all experimental conditions).

3. RESULTS AND DISCUSSION

The light preferences for each of the 12 NCS samples are shown in Fig. 4. To address the question if materials are preferred under cold or warm light in a statistical manner, nonparametric two-tailed binomial tests are executed. Tests for light preferences on each of the materials are done with significance at 0.05 level using the IBM SPSS 22 statistical software package. The proportion of students' preferences is compared to 50% (chance level). The tests reveal, that participants have significant preference seeing red (NCS S1080-R) under the warm light condition, P = 0.002. The warm light is also preferred for purple color (NCS S3055-R50B), for the blue (NCS S1565-B) the cold light condition is preferred. However in both cases the difference from chance level only approached significance (P = .052). The proportion of preferences for other 9 materials does not significantly differ from the chance (P > .12).

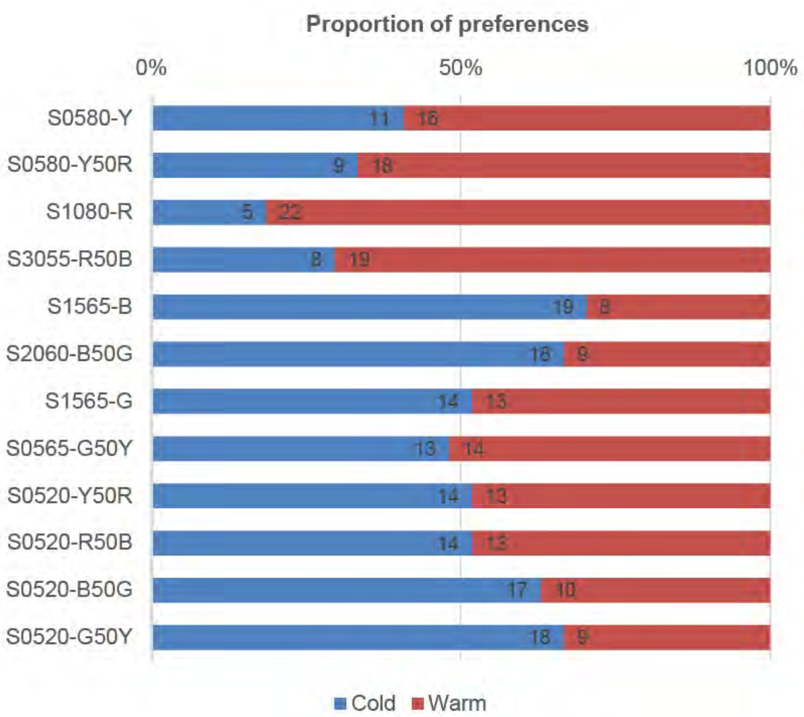

Figure 4: Preferences for appearance of 12 NCS color samples in coolish or warmish light.

The results for the 8 wood surfaces are summarized in Fig. 5. The descriptive percentage of light preference reveals that staghorn sumac wood is rather preferred in warm light condition, whereas appearance of robinia is preferred in cold light condition. Statistically are this differences not significant, but they point out that choice of wood type may ask for specific light considerations.

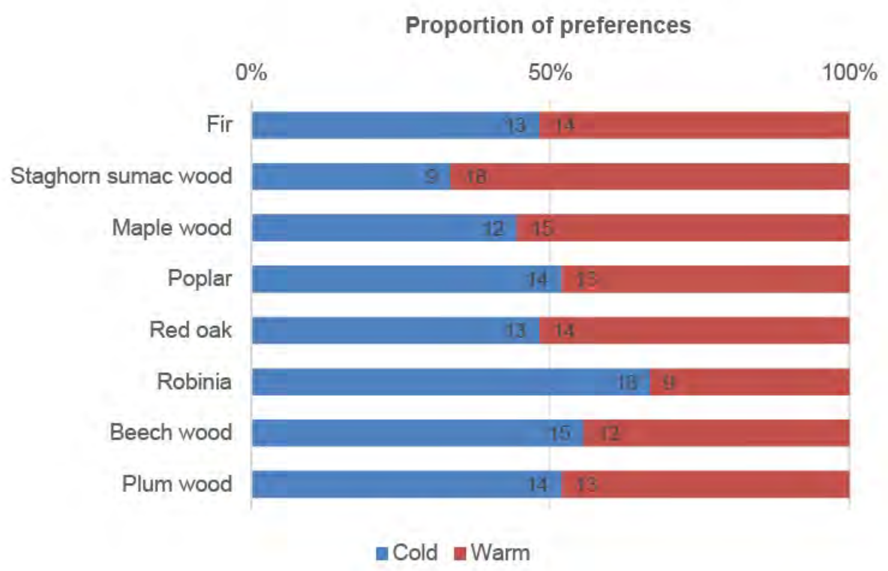

Figure 5: Preferences for appearance of 8 wood samples in coolish or warmish light.

.

4. CONCLUSIONS

The study confirmed that LED lighting with a CCT of 3000K is generally preferred for reddish hues. Light that fosters a cooler visual impression (CCT of 4000K) is generally preferred for bluish hues. Preferences for other hues and the pastel samples did not differ significantly from chance level. The explorative study about appearance of different wood types is not fully conclusive. Although it has shown that cooler light suit certain wood surfaces as robinia better, it cannot be explained by the measured spectral reflection characteristics. It can be assumed that for wood surfaces besides the reflection characteristics, respectively the hue, also grain, texture pattern and gloss might influence light preference.

In this study light sources with excellent color rendering characteristics are used, hence visual appearance for all samples is very close to the appearance under a CIE reference source. Although it is known from literature that visual preference of colors relates specifically to vividness and naturalness of its appearance (Bodrogi et. al., 2013), the use of LED types that emphasize vibrancy of colors is not considered for the reported experiment. All observed effects on preference thus can be attributed to the difference in correlated color temperature of the chosen LED light sources.

REFERENCES

Bodrogi, P., S. Brückner, T.Q. Khanh, and H. Winkler. 2013. *Visual Assessment of Light Source Color Quality*. Color Research & Application 38(1) 4-13.

Ishihara, S. 1999. *Ishihara's Tests for Colour Deficiency*. Tokyo: Kanehara & Co.

Lasauskaite Schüpbach, R., M. Reisinger, and B. Schrader 2015. *Influence of Lighting Conditions on the Appearance of Typical Interior Materials*, Color Research & Application 40(1) 50-61.

Address: Markus REISINGER, Department of Interior Architecture, Lucerne School of Engineering and Architecture,
Technikumstrasse 21, 6048 Horw, SWITZERLAND
E-mail: m.reisinger@lightingresearch.eu

Development of a facial imaging system and new quantitative evaluation method for pigmented spots

Kumiko KIKUCHI,[1,2] Yuji MASUDA,[1] Tetsuji HIRAO,[1] Kiyoshi SATO,[1] Yoko MIZOKAMI,[2] Hirohisa YAGUCHI[2]
[1] Shiseido Research Center
[2] Graduate School of Advanced Integration Science, Chiba University

ABSTRACT

The quantitative evaluation of skin color and skin chromophore distribution is important in dermatology, physiology, pharmacology, and cosmetic science. Various methods that evaluate facial pigmentation using image analysis have been proposed. These models provide visual information about the melanin distribution; however, the current methods cannot provide quantitative information on individual pigmented spots such as variation in size, shade of color, and distribution pattern. In this study, we describe our facial imaging system and pigment-specific image-processing techniques, and we also propose an image evaluation method that focuses on the analysis of individual pigmented spots on a wide area of the face. First, a facial imaging system that is equipped with an illumination unit and a high-resolution digital camera was developed. Facial images were captured and converted to *XYZ tristimulus values* from RGB values based on calibration using skin color chips. Next, to determine the melanin and hemoglobin concentration, we established pigment-specific image processing techniques based on relational expressions between *XYZ tristimulus values* and skin chromophore concentration. Finally, to obtain the features of individual pigmented spots in a cheek image, we established a simple object-counting algorithm that calculates spot size, colorimetric value, melanin concentration, and other features. Experimental results confirm that our system provides a reliable measurement with high precision and repeatability for skin color distribution on a wide area of the face. Applying the new methodology for individual pigmented spots to cheek skin images, the age-related changes of pigmented spots were clearly demonstrated. In conclusion, our techniques for skin color and individual pigmented spots allow us not only to determine the visual information about the melanin distribution, but also to understand the characteristics of individual pigmented spots on the face.

1. INTRODUCTION

The quantitative evaluation of skin color and skin chromophore distribution is important in dermatology, physiology, color science, and cosmetic science. Various studies have been conducted on the development of methods to evaluate facial pigmentation using image analysis (Tsumura, Haneishi, and Miyake, 1999; Masuda et al., 2001). These methods are based on the optical properties of light interaction with the components of the skin and provide visual information about the melanin distribution. However, such methods have not addressed in detail the quantitative information of individual pigmented spots, such as variation in size and colorimetric values or distribution patterns. In this study, we describe a facial imaging system that provides a reliable measurement for skin color distribution and pigment-specific image-processing techniques, and we also propose an image evaluation method that focuses on the analysis of individual pigmented spot on a wide area of the face.

2. METHOD

This paper is organized as follows: Section 2 of the paper discusses the facial imaging system and algorithm that provide colorimetric values for skin, having high accuracy, simplicity, and reproducibility. It also proposes a pigment-specific image processing technique based on a relational expression between *XYZ tristimulus values* and skin chromophore concentration. Furthermore, it describes an object-counting algorithm that evaluates the individual pigmented spots. In Section 3, we performed validation tests of the imaging system and investigated the age-related changes of pigmented spots and skin color by applying the new methodology, and Section 4 concludes the paper.

2.1 Facial Imaging System and Quantification of Color Values

We developed a facial imaging system that consists of an illumination unit and a high-resolution digital camera (Figure 1). The illumination unit employs fluorescent lamps (FPL30EX-D; Toshiba, Tokyo, Japan) with a correlated color temperature of 6,700 K. The lamps were designed to provide diffuse illumination over a wide field of the subject's face to eliminate shadows and artifacts from specular reflections. Figure 2 shows the lightness distribution on a mannequin model, which indicates that the illumination unit is sufficiently accurate for analyzing facial skin color. A Canon CMOS digital photo-camera (EOS Kiss X3; Canon, Tokyo, Japan) containing of 4,500 (horizontal) × 3,000 (vertical) effective picture elements was used. It was equipped with a Canon lens (EF 35 mm F2; Canon, Tokyo, Japan). Facial images were captured with a neutral gray color chip (Murakami Color Research Laboratory, Tokyo, Japan) as the standard for color and brightness and stored as uncompressed tagged image file format (TIFF) images at a resolution of 1,500 × 1,500 pixels and 72 dots per inch (dpi).

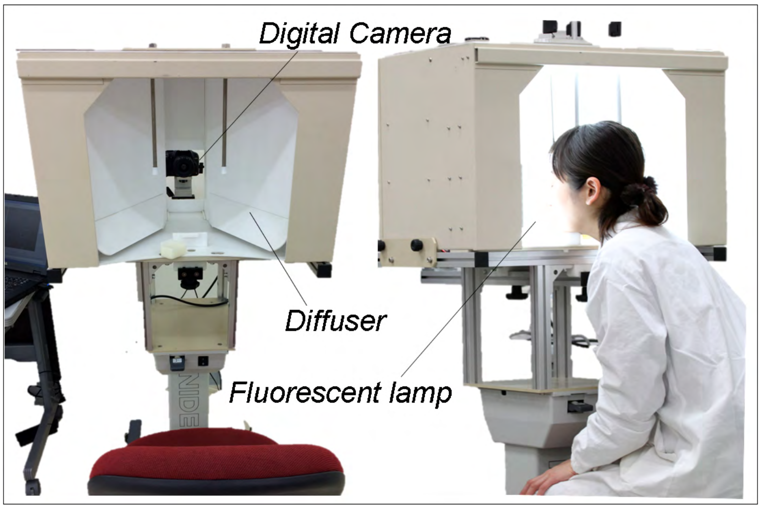

Figure 1: Facial imaging system.

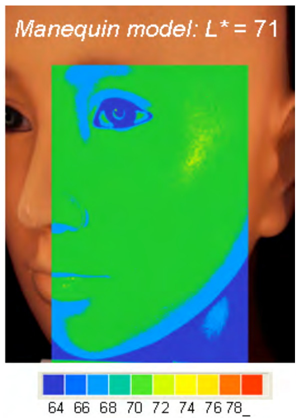

Figure 2: Lightness distribution of a mannequin model.

To ensure highly accurate conversion from linear RGB to *XYZ tristimulus values*, particularly in the skin color range, 100 color chips were selected based on experimentally acquired skin color data. Each color chip was captured by the imaging system to obtain all RGB color signals outputted from the camera and were measured with a contact-type spectrophotometer (CM-700d; Konica Minolta Sensing, Tokyo, Japan) to obtain the *XYZ* *tristimulus values*. The RGB image information was converted into XYZ data using values obtained by multiple regression analysis. The conversion expressions are written as follows:

$$X = 0.001645R + 0.001116G + 0.000314B + 2.585143$$

$$Y = 0.001110R + 0.002080G + 0.000065B + 2.359088$$

$$Z = 0.000439R + 0.000610G + 0.002439B + 2.757769$$

Figure 3 shows the relationship between the *XYZ tristimulus values* measured using a spectrophotometer and the estimated values obtained from the digital camera data. In addition, values in the L*a*b* color space (1976 CIELAB) were calculated from the *XYZ tristimulus values* using this system.

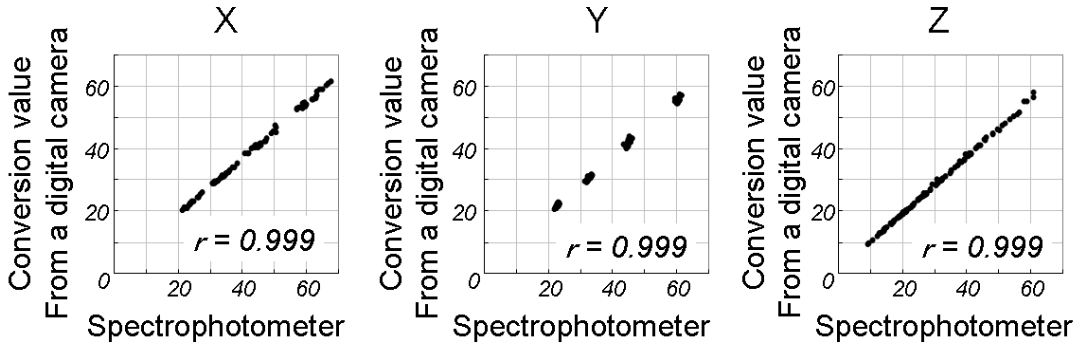

Figure 3: Comparison of XYZ values from a spectrophotometer and those converted from digital camera data.

2.2 Conversion from XYZ Values to Skin Chromophore Concentration

To determine melanin and hemoglobin concentrations, we established pigment-specific image processing techniques based on relational expressions between *XYZ tristimulus values* and skin chromophore concentration. In previous studies, skin chromophore concentration (i.e., melanin and hemoglobin) was calculated from skin spectral reflectance (Shimada et al., 2000; Masuda et al., 2009). These studies suggested that the skin chromophore concentration could be calculated by a multiple regression analysis, assuming that the absorbance spectrum is a linear sum of the absorbance spectra of melanin, oxygenated hemoglobin, and deoxygenated hemoglobin. Here, we suggest that the concentration of melanin and total hemoglobin can be estimated from *XYZ tristimulus values* obtained from a color image. Spectral reflectance data from the cheeks of 60 women were obtained using a colorimeter. The *XYZ tristimulus values* were calculated from the spectral reflectance of the skin for an illuminant D65 and 2° visual field. In addition, the concentrations of melanin and total hemoglobin were calculated according to methods in the previous studies. A linear regression equation to predict the concentration of melanin was then determined using multiple regression analysis with the logarithm (base 10) of the inverse *XYZ tristimulus values* as independent variables and melanin concentration as a dependent variable. Similarly, we used regression to predict the hemoglobin concentration. The melanin and hemoglobin concentration were calculated according to the following equations.

$$\text{Melanin index} = -4.861\log_{10}(1/X) + 1.268\log_{10}(1/Y) + 4.669\log_{10}(1/Z) + 0.063$$

$$\text{Hemoglobin index} = -32.218\log_{10}(1/X) + 37.499\log_{10}(1/Y) - 4.495\log_{10}(1/Z) + 0.444$$

By fitting this equation to the XYZ images, we obtained the melanin and hemoglobin distribution images.

2.3 Detection and Quantification of Pigmented Spots

To quantify individual pigmented spots within a cheek image, we adopted an object-counting algorithm that enables us to calculate their size and colorimetric value. The melanin distribution images were used, and the regions of interest were manually selected. The algorithm for pigmented spot extraction consists of smoothing, binarization, region labeling, and candidate cropping. Various stages of this analysis are shown in Figure 4. In the smoothing step, images are processed using a Gaussian filter with a half-value width of 4.0 mm to correct the rough undulations of the surface (Figure 4(a)), and processed three times using a median filter of 5 × 5 pixels to remove spike noise (Figure 4(b)). After noise reduction, the melanin images are converted to binary images (Figure 4(c)) using a threshold optimized for the detection of pigmented spots. Furthermore, the connected-component labeling algorithm that gives each separate connected group of pixels a unique label is applied (Figure 4(d)) to calculate the number, sizes, and colorimetric values of the individual spots. Finally, spots are then identified as areas greater than 2 mm^2 to remove pores (Figure 4(e)).

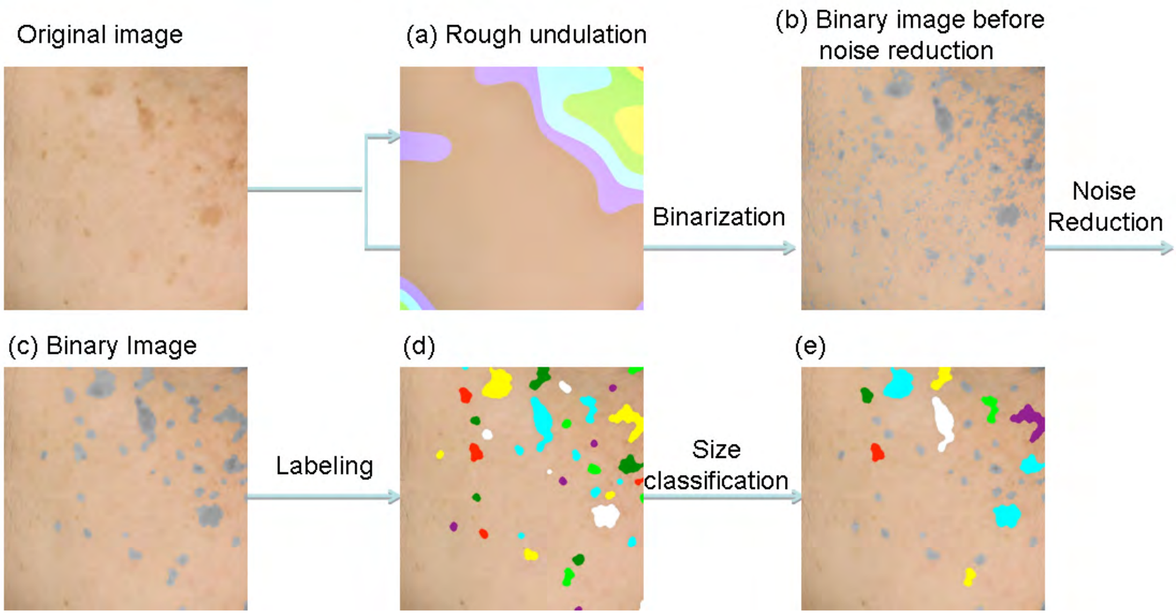

Figure 4: Schematic flow of the image processing for pigmentation analysis.

2.4 Method validation

To validate the accuracy of quantitative image analysis, the spectral reflectance of the cheek and lower eyelid of 32 Japanese women (age range 34–59 years; mean age 44.3 years) was measured using the contact-type spectrophotometer (CM-700d) with a probe head aperture of approximately 7 mm. At the same time, facial images of the same 32 subjects were obtained using the imaging system. In all facial images, regions of interest were selected in the same areas as those measured using the spectrophotometer. Melanin concentration and L*a*b* values were calculated from the spectral reflectance, and the correlation between the two types of measurement system was determined.

2.5 Color Variation of Pigmented Spots Due to Aging

Applying the new methodology for skin chromophore and individual pigmented spot analysis to cheek skin images, we investigated the relationship between the characteristics of spot occurrence and age. Six-hundred and forty-three healthy Japanese women aged 20–80 years were enrolled in the study. They were classified into nine groups: 22 subjects in group A (20–24 years old), 76 in group B (25–29 years old), 76 in group C (30–34 years old), 76 in group D (35–39 years old), 76 in group E (40–45 years old), 76 in group F (45–49 years old), 76 in group G (50–54 years old), 76 in group H (55–59 years old), and 89 in group I (60–80 years old). Informed consent was obtained from all participants. Subjects washed their face and rested for 40 min under conditions of 23° C and 45% relative humidity.

3. RESULTS AND DISCUSSION

Figures 5(a)–(d) compare the values of the facial images of our system with those of the spectrophotometer for $L*$, $a*$, $b*$, and melanin concentration in the cheek, respectively. The correlation coefficients between the spectrophotometer and facial images were higher than 0.900 for all parameters for the cheek. In addition, similar results were confirmed for the lower eyelids (data not shown). These results confirm that our system for facial imaging is sensitive enough to analyze not only colorimetric values but also melanin concentration with a good spatial distribution.

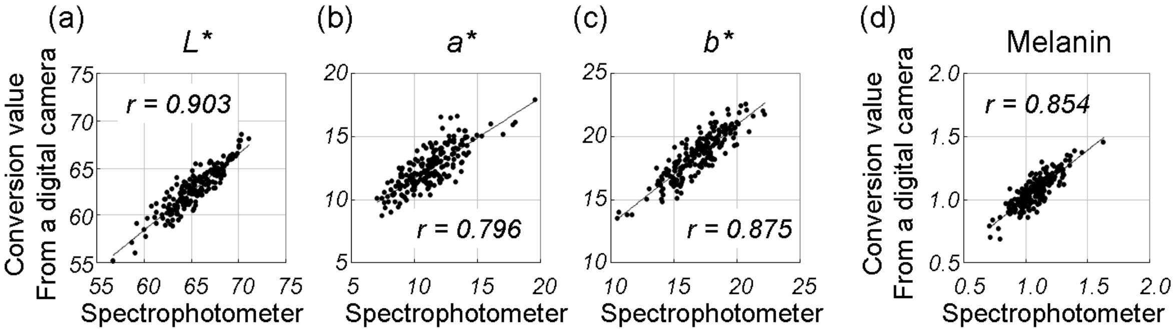

Figure 5: Comparison between the facial imaging system and spectrophotometer results.

The results of the cheek image analysis of 643 Asian women show that the proposed method is sufficiently sensitive to permit the measurement of colorimetric value, number, and size of individual pigmented spots. The differences of the parameters for each group were analyzed using one-way repeated analysis of variance. In this analysis, p-values less than 0.05 were assessed as statistically significant. Figure 6(a) shows that the number of spots per cheek on one side increased with age in a statistically significant manner (correlation coefficient of 0.613). The parameters of size and colorimetric values for spots on the cheek were plotted independently. The number of pigmented spots detected in the 643 women totaled 8,372. The size results indicate that there is a high probability of pigmented spots greater than 10 mm^2 in those older than 40 years (data not shown). Figure 6(b) shows that the colorimetric value $L*$ of spots significantly decreased with age (correlation coefficient of −0.211). Figure 6(c) shows that the $C*_{ab}$ of individual spots significantly increased with age (correlation coefficient of 0.339). For the colorimetric value h_{ab}, no significant changes were observed (Figure 6(d)).

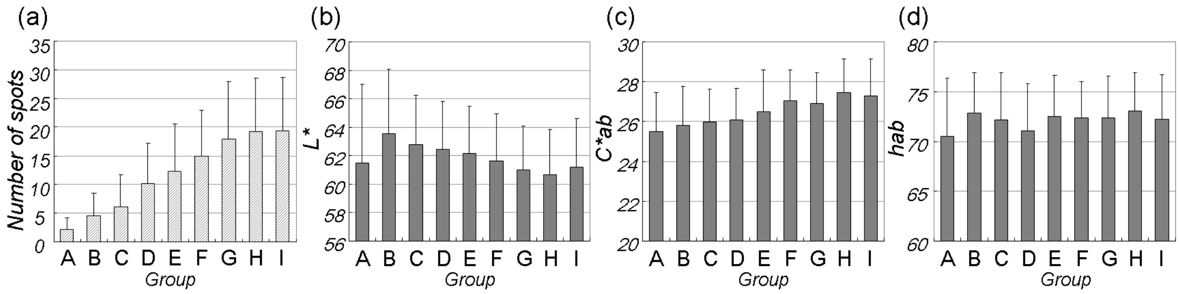

Figure 6: Age-dependent spot changes: (a) number of spots per cheek on one side, values for (b) L^*,(c) C^*_{ab}, and (d) h_{ab}.

4. CONCLUSIONS

Our techniques to determine skin chromophores and individual pigmented spots allow us not only to provide the visual information about the melanin distribution but also to understand the characteristics of various pigmented spots in a face. The results from our validation indicate that our system provides colorimetric data for skin that is highly accurate, simple to acquire, and reproducible. The data obtained in this study will be very useful for improving our knowledge about the aging of skin.

ACKNOWLEDGMENTS

The authors thank Dr. Mariko Egawa for her helpful discussion and suggestions.

REFERENCES

Tsumura, N., H. Haneishi, and Y. Miyake. 1999. Independent-component analysis of skin color image. *Journal of the Optical Society of America A* 16 (9): 2169-2176.

Masuda, Y., M. Takahashi, T. Sakamoto, M. Shimada, M. Itoh, and T. Yatagai. 2001. An innovative method to measure skin pigmentation. *Journal of the Society of Cosmetic Chemists of Japan.* 35: 325-332 (in Japanese).

Shimada, M., Y. Masuda, Y. Yamada, M. Itoh, M. Takahashi, and T. Yatagai. 2000. Explanation of human skin color by multiple linear regression analysis based on the modified Lambert-Beer law. *Optical Review* 7 (4): 348-352.

Masuda, Y., T. Yamashita, T. Hirao, and M. Takahashi. 2009. An innovative method to measure skin pigmentation. *Skin Research and Technology* 15 (2): 224-229.

Address: Kumiko KIKUCHI, Shiseido Research Center, 2-2-1 Hayabuchi, Tsuzuki-ku, Yokohama 224-8558, JAPAN

E-mail: kumiko.kikuchi1@to.shiseido.co.jp

mizokami@faculty.chiba-u.jp

yaguchi@faculty.chiba-u.jp

Colour Preference and Harmony for Athletic Shoe Designs

Wei-Hsuan CHAO, Ji-Yuan HUNG, Chung-Chien LAN, Li-Chen OU
Graduate Institute of Color and Illumination Technology, National Taiwan University of Science and Technology, Taiwan

ABSTRACT

A psychophysical experiment was conducted using athletic shoes, a product commonly seen and used in our everyday activities, as an example to study colour preference and harmony. A total of 404 test images were generated from two original shoe images, one from Nike and the other from Adidas, each manipulated by varying the two-colour combinations of the shoe design, including the main colour of the shoe and the logo colour (i.e. the Nike tick and the Adidas stripes). Twenty observers with normal colour vision, including 10 males and 10 females, participated in the visual assessment. Each observer was asked to rate each shoe images using two 6-step semantic scales, like/dislike and harmonious/disharmonious. The experimental results show that the color preference rating relied strongly on the main colour of the shoe regardless of the logo colour, while the color harmony rating was affected not only by hue similarity but also lightness difference between the main colour and the logo colour.

1. INTRODUCTION

Colour preference and harmony have both been concidered the most essential factors in the design of colour combinations. The relationship between these two attributes of colour has been extensively studied. For example, Schloss and Pamer (2011) recently found that colour preference and harmony both tended to increase as hue similarity increases, while preference relies more strongly on component color preference and lightness contrast. Nevertheless, most existing studies of colour preference and harmony, including Schloss and Palmer's research as mentioned above, have used abstract, contextless colour patches as the stimuli in the experiments. It is still unclear whether the results can also apply to real-world product designs. To address this issue, athletic shoes, a product commonly seen and used in our everyday activities, were taken as an example in our study of colour preference and harmony.

Basic shoes of two brands, Nike and Adidas, were selected to generate the experimental images. Aims of the study included (1) using recoloured images in two athletic shoes as the stimuli, (2) using colours from real athletic shoes on the market to generate test images as the stimuli, and (3) the results would be analysed for the effects of hue and lightness difference on colour preference and harmony.

2. METHODS

For each shoe image, two areas were recoloured according to the following definitions: (1) the "logo colour" means the logo shown on the shoe (i.e. the Nike tick and the Adidas stripes); (2) the "main colour" means the main body of the shoe. Colour preference was defined as how much the observer liked the combination of the logo colour and the main colour. Colour harmony was defined as how well the logo colour and the main colour went together as shown in the shoe images.

For logo colours, we selected four tones, saturated (S), light (L), muted (M) and dark (D), each consisting five hues, red (R), yellow (Y), green (G), blue (B) and purple (P). For main colours, we only selected eight colours, containing four hues, each having two lightness levels, including saturated red (SR), light red (LR), saturated yellow (SY), dark yellow (DY), light blue (LB), dark blue (DB), light purple (LP) and dark purple (DP). All colour samples were shown in Figure 1.

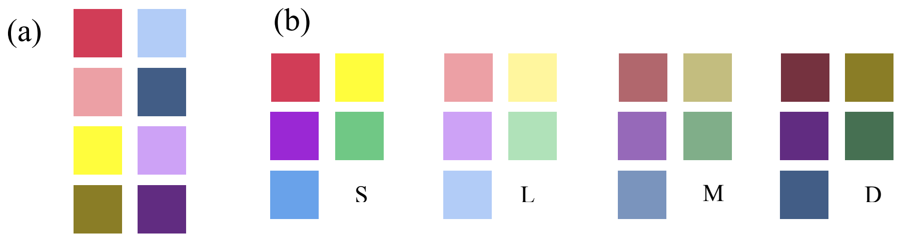

Figure 1: Colour samples used in the experiment: (a) the main colours and (b) the logo colours.

In the psychophysical experiment, we used 404 recoloured images of athletic shoes as the stimuli, presented on a calibrated computer display situated in a darkened room. The 404 images were generated from two original shoe images, one from Nike and the other from Adidas, each manipulated by varying the two-colour combinations of the shoe design, including the main colour of the shoe and the logo colour (i.e. the Nike tick and the Adidas stripes), as shown in Figure 2. Each of the two original shoe images were recoloured using 202 colour combinations, consisting of 152 pairs selected from CIELAB space to cover a wide variety of hue, lightness and chroma, and 50 colour pairs selected from real athletic shoes currently available on the market.

Figure 2: schematic diagrams of Nike and Adidas.

Twenty Taiwanese observers with normal colour vision, including 10 males and 10 females, participated in the visual assessment. Each observer was asked to rate each shoe images using two 6-step semantic scales, like/dislike and harmonious/disharmonious, as measures of colour preference and colour harmony, respectively.

3. RESULTS

3.1 colour preference for athletic shoes

Mean hues of main colur and main colour for preference ratings with Nike and Adidas athletic shoes in Figure 3, there were similar show that preference ratings is higher when dark blue (DB) as main colour with blue (B) as logo colour. When dark blue (DB) as main colour with some logo colour, it bring higher preference ratings. It was worth noting that dark blue (DB) with purple (P), the preference ratings was drop, the result was agree with original research. However, the dark yellow (DY) as main colour with any logo colour had lower preference ratings that everyone didn’t like it. We surmise that dark yellow (DY) make disgusting that it look like excrement.

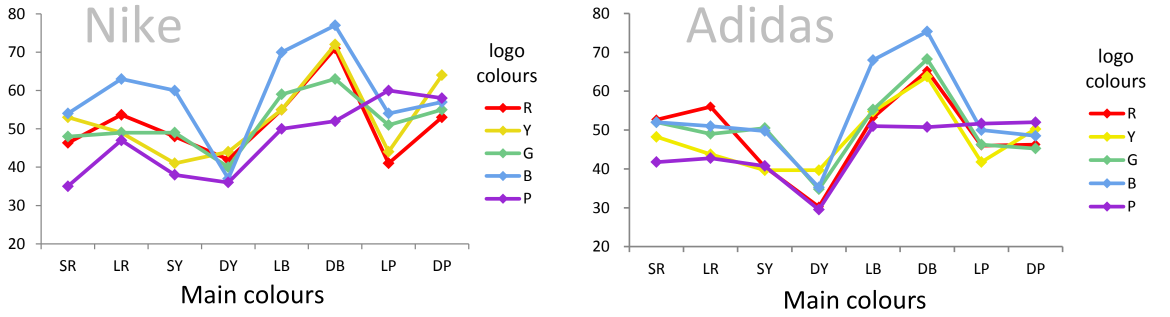

Figure 3: Preference ratings for the hue of logo colours against each main colour.

Preference ratings of Main colour in different hue difference in Figure 4. We can found that preference ratings of dark blue (DB) and light blue (LB) as main colour were higher than others, but the dark yellow (DY) as main colour had lower preference ratings. Again, proving that observers like blue colour much, instead yellow colour wasn't, especially dark yellow (DY).

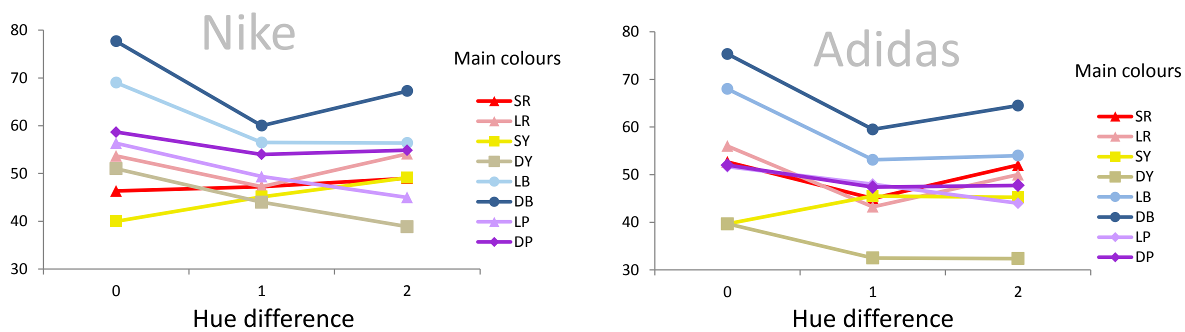

Figure 4: Preference ratings plotted against hue difference.

Mean lightness of logo colour and different main colour for preference ratings in Figure 5. We can see that dark blue (DB) as main colour with different lightness as saturated (S), light (L), muted (M), that higher preference; instead, the dark yellow (DY) as main colour with different lightness as saturated (S) and light (L) had lower preference. Above all, dark blue (DB) and dark yellow (DY) in colour preference experiment, former was most like colour combination, another wasn't.

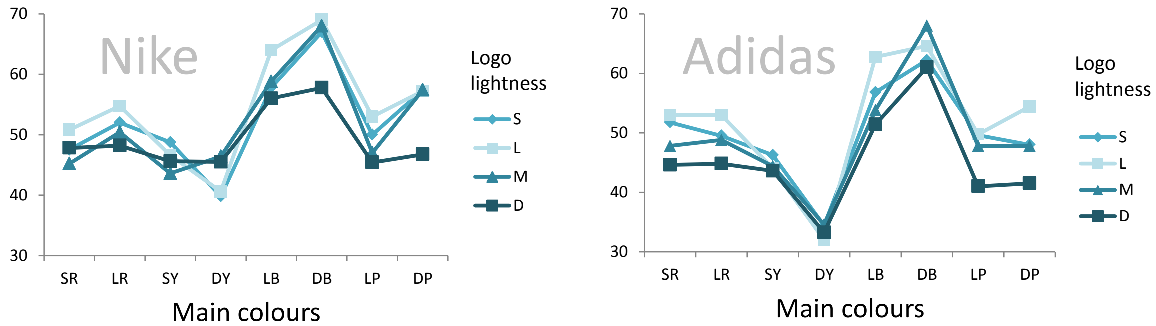

Figure 5: Preference ratings for each lightness level of logo colours against each main colour.

3.2 colour harmony for athletic shoes

Mean hues of logo colour and main colour for harmony ratings with Nike and Adidas athletic shoes in Figure 6. We can found harmony ratings is higher when light blue (LB) and dark blue (DB) as main colour with blue (B) as logo colour and dark yellow (DY) with yellow (Y). When dark yellow (DY) as main colour with purple (P) as logo colour, bring lower harmony ratings. In harmony ratings, we can found that the logo colour were similar with main colour, harmony ratings were higher, no matter the colour everyone like or not.

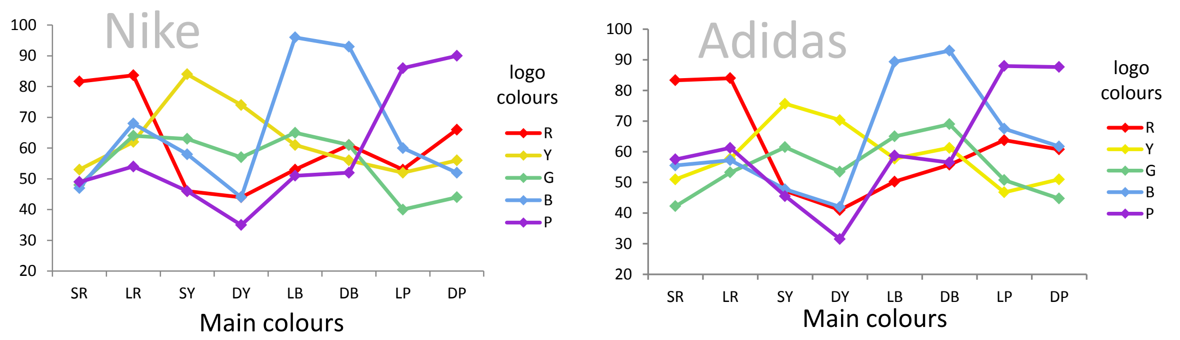

Figure 6: Harmony ratings for the hue of logo colours against each main colour.

Harmony ratings of main colour in different hue difference in Figure 7. Those pictures proved the hues difference less, the harmony ratings better. In other words, when main colour was similar to logo colour, the harmony was stronger.

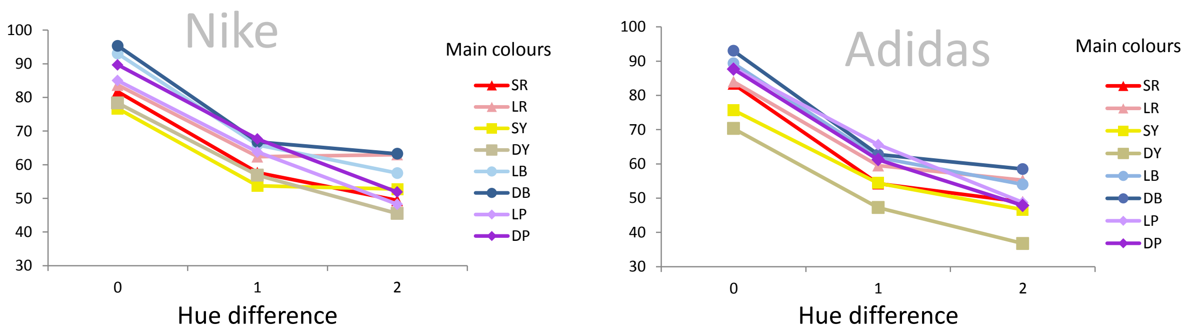

Figure 7: Harmony ratings plotted against hue difference.

Mean lightness of logo colour and different main colour for harmony ratings in Figure 8. We can find that there were many peak values in those pictures, most in light (L), muted (M) as lightness of logo colour. That is, main colour with light (L), muted (M) as lightness as logo colour, the harmony ratings was better. However, when the dark yellow (DY) as main colour with light (L) as lightness as logo colour, the harmony ratings was lower. We surmised observers might influenced by preference.

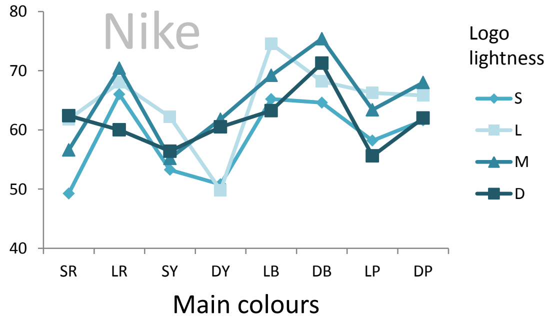

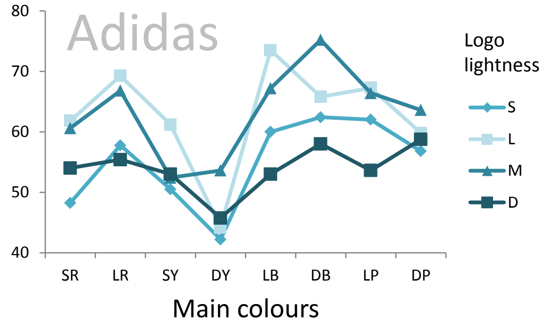

Figure 8: Harmony ratings for each lightness level of logo colours against each main colour.

4. CONCLUSION

Although all athletic shoes were comprised of main colours and logo colours (i.e. the logo colours in this study) in the experiment, the perceived color preference was affected mainly by the main colour of the shoe, while the perceived color harmony was affected not only by hue similarity but also by lightness difference between the main colour and the logo colour.

For colour preference, the blue tone was highly rated, while the yellow tone felt dull and dark and was thus not preferred. For colour harmony, the experimental results show that the smaller hue difference, the more harmonious. In addition, when the main colour with light (L), muted (M) as lightness as logo colour, the harmony ratings was better.

The results also show that shoe colors preferred by female observers tended to be liked by male observers, while shoe colors preferred by male observers were not necessarily liked by female observers. For colour preference, the two gender groups had a correlation coefficient of 0.63, however, high correlation between male and female data in terms of colour harmony, with a correlation coefficient of 0.83.

These results can help refine and clarify existing theories of colour preference and harmony based on contextless colour patches.

AKNOWLEDGEMENTS

This work was supported in part by the Ministry of Science and Technology, Taiwan (MOST 103-2221-E-011-138).

REFERENCES

Schloss, K.B. and S.E. Palmer 2011. *Aesthetic response to color combinations:preference, harmony, and similarity*, Atten Percept Psychophys 73(2) 551-571.

Address: Master. Wei-Hsuan CHAO, Graduate Institute of Color and Illumination Technology, National Taiwan University of Science and Technology, 43, Section 4, Keelung Road, Taipei, 10607, TAIWAN
E-mails: m10225009@mail.ntust.edu.tw

A study on silver metallic color preference - A comparison of responses by age and gender in Thailand –

Kamron YONGSUE[1], Mikiko KAWASUMI[2], Chanprapha PHUANGSUWAN[1], and Kanrawee TAWONPAN[1]
[1]Faculty of Mass Communication Technology, Rajamangala University of Technology Thanyaburi, Thailand
[2]Faculty of Science and Technology, Meijo University, Japan

ABSTRACT

This paper describes the outcome of the research about the designing conditions for more attractive surface color of the silver metallic productos. It is significant for us to understand the customer's visual preference for each product in each nation. In this paper, we will show you the relationship between the surface colors of silver metallic products and the customer's desired feelings such as the feeling of "high-quality". Especially we will report the comparative results of observation by age and gender in Thailand.

1. INTRODUCTION

Thailand is one of the countries that have many factories of Japanese manufacturer such as cars, home appliances and textiles, and those products are popular for Thai people. We also can see many metallic colors here such as fridges and cameras. We are currently researching the relationship between the surface colors of silver metallic products and the desired feelings of the customer.

The visual appearance of a product is very important for the customers and the desired impression and color preference may be different by age and gender. In this research we would like to find out the attractive silver metallic color for Thai customers and compare these effects among age and gender.

2. METHOD

A questionnaire on the Web was used for our investigation and written both in Thai and in English. In previous survey, we investigated in English. But we translated it into Thai language this time in order to add the respondents who live in local region including elderly people. Figure 1 shows a part of our questionnaire. Computer graphics were used to represent the surface colors of metallic products. Their surfaces have slightly different silver metallic colors: reddish, yellowish, bluish, and so on, and each color was controlled in ten hues of the Munsell color system: **P**, **RP**, **R**, **YR**, **Y**, **GY**, **G**, **BG**, **B**, and **PB** as shown in figure 2. We set five target feelings: "clean / pure", "relaxing / comforting", "high-quality", "stylish / chic", and "favorite", which were chosen as the most important desired feelings by Japanese customers in previous study. The respondents answered with color that they felt was the most "high-quality", for example, for seven target products: a fridge, a television, a DVD player, a laptop computer, a digital camera, a smartphone, and a music player as shown in figure 3.

Figure 1: A part of questionnaire.

Figure 2: Ten colored products.

Table 1: Target feelings.

In English	In Thai
Clean / pure	สะอาด / บริสุทธิ์
Stylish / chic	มีรสนิยม / แฟชั่น
High – quality	คุณภาพสูง
Relaxing / comforting	ผ่อนคลาย / สะดวกสบาย
Favorite	ชื่นชอบ

Figure 3: Target products.

Figure 4: A scene of answering questionnaire.

Table 2: Respondents.

Gender / Age group	Male	Female	Total
Teens ~ twenties	62	75	137
Thirties ~ forties	40	59	99
Over fifties	34	51	85
Total	136	185	321

We requested that the screen size of a computer should be not less than twelve inches, because it may be hard to distinguish the differences among ten hues on a small display. The required time was about twenty minutes on average. However the elderly people took a lot of time over forty minutes. We instructed every question in Thai in the next seat and helped them to fill the answer sheets. Finally, more than three hundred persons have cooperated with us in Thailand, as shown in Table 2. We've compared the results among gender and three age groups: teen – twenties, thirties – forties, and over fifties.

3. COMPARATIVE RESULTS BY AGE AND GENDER

Our results are shown in Figures 5 by line graphs. The horizontal axis shows the Munsell hue: **P**, **RP**, **R**, **YR**, **Y**, **GY**, **G**, **BG**, **B**, and **PB**, and the vertical the percentage of choice for the hue. Different line types indicate the products: a fridge, a television, a DVD player, a laptop computer, a digital camera, a smartphone, and a music player. It shows the comparative results by five feelings for all Thai people.

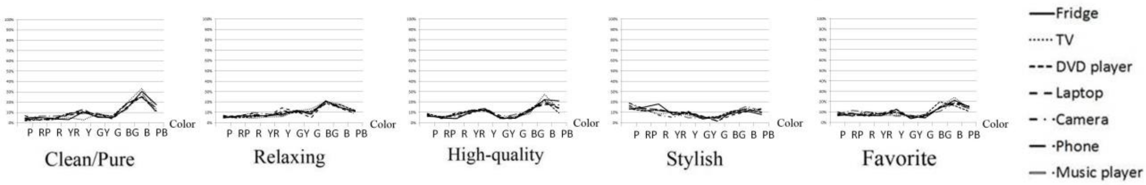

***Figure 5**: Comparative results by feeling.*

We can see that most Thai selected Munsell **B** for the feeling of "clean/pure" and **BG** for the "relaxing". Also, they selected **B** and **YR** for "high – quality" and purplish silver for "stylish". In addition, we could confirm that "clean / pure" has the highest correlation with "favorite" (r = 0.75 ~ 0.92) for all product except a music player. "High-quality" also has high correlation with "favorite" for a fridge, a laptop, a computer, and a camera (r = 0.81 ~ 0.90).

Figure 6 shows the comparative results among three age groups. It became clear that most people under forties preferred bluish silver for the feeling of "clean / pure" in every product, , many elderly people preferred yellowish silver also, especially in the personal mobile product: a laptop computer, a camera, a smart phone, and a music player. As everyone knows, color appearance of an elderly person is difference from a young person by aging process of the lens. However we could not find out any difference clearly in a statistical analysis (p > 0.05) and also couldn't confirm a big difference between male and female, as shown in Figure 7.

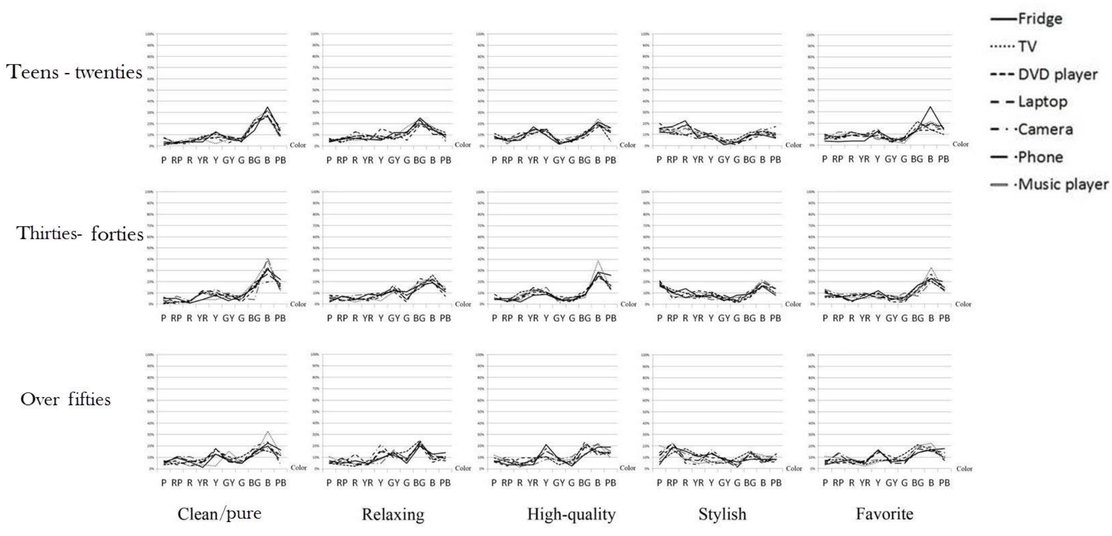

***Figure 6**: Comparative results by three age group.*

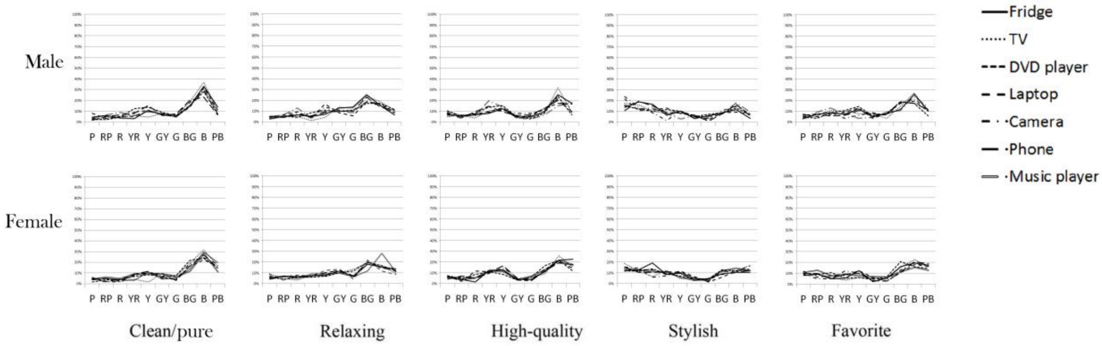

***Figure** 7: Comparative results by gender*.

4. SUMMARY AND FUTURE PLANS

We've examined the silver metallic preference in Thailand and compared the results by three groups of age and gender. As the results, we could grasp the characteristic of Thai people's preference. For example, Thai selected **B** for the feeling of "clean/pure" and **BG** for "relaxing". The former is the same result as other countries, but the latter is difference from others.

Our next issue is to investigate by using other adjectives such as "modern", "creative / innovative", and "advanced", because Thai people chosen these adjectives as an important desired feeling for a metallic product. We plan to examine the relationship between these new adjectives and the surface colors.

ACKNOWLEDGEMENTS

We appreciate the help received from official staffs and elderly people from Department of Social Welfare Development Center for Older Person, Bureau of Social Welfare Service, Department of Social Development and Welfare, Ministry of Social Development and Human Security in Pathumthani in Thailand, lecturers, staffs and students from Rajamangala University of Technology Thanyaburi in Thailand, and other many Thai people.

REFERENCES

Saito, M., 1994. *A cross-cultural study on color preference in three Asian cities: Comparison between Tokyo, Taipei and Tianjin*. Japanese psychological Research 36(4): 219-232.

Xin, J.H., Cheng, K.M., Taylor, G., Sato, T., Hansuebsai, A., 2004a. *Cross-Regional Comparison of Colour Emotions Part I:Quantitative Analysis*. Color Research and Application 29(6): 451-457.

Xin, J.H., Cheng, K.M., Taylor, G., Sato, T., Hansuebsai, A., 2004b. *Cross-Regional Comparison of Colour Emotions Part II:Qualitative Analysis*. Color Research and Application 29(6): 458-466.

Kawasumi, M., 2013. *A Comparative Study in Asian Countries on Color Preference for Factory Products*. In Proceedings of the 1st Conference of Asian Color Association, ed. by Vichai Payackso. Thanyaburi: Rajamangala University of Technology Tanyaburi, 26-27.

Kawasumi, M., 2014. *A Comparative Study in Asian Countries on Color Preference of industrial products*. *In 2nd* conference of Asian Color Association, ed. by Tien-Rein LEE. Taipei: Chinese Culture University, 268-271.

Address: Kamron Yongsue,
Faculty of Mass Communication Technology,
Rajamangala *University* of Technology Thanyaburi
39 Moo1, Rangsit-Nakhonnayok Rd. Klong 6, Thanyaburi Pathum Thani 12110
Thailand
E-mails: ykamron@gmail.com, future@meijo-u.ac.jp
karamenn@gmail.com, ktawonpan@gmail.com

Effects on Impression of Taste in Color Stimuli

Masato SAKURAI, Yusuke MICHINAKA, Takahiro YOSHIKAWA
Department of Media Informatics, College of Informatics and Human Communication,
Kanazawa Institute of Technology

ABSTRACT

To examine the effect on the impression of taste by color stimuli from the aspect of the three attributes of color (hue, lightness, and chroma) the impression of five basic tastes (sweetness, sourness, bitterness, saltiness, and umami) for the color stimuli were measured using the subjective evaluation. The color stimuli were uniformly selected from Munsell color system. In the results, the evaluation values increases with the regions between 5RP and 5YR on Munsell hue circle for the impression of sweetness and the regions between 5YR and 5GY on the hue circle for the impression of sourness. And in those hues, the evaluation value increases with the value of chroma. Therefore, the colors of reddish purple, red, and orange obtain the impression of sweetness and those of orange, yellow, and yellowish green give the impression of sourness with an increasing of the value of chroma. Dark achromatic colors obtain the high evaluation value in the impression of bitterness and its value increases with a decreasing of the value of lightness. Thus, the value of lightness affects the impression of bitterness.

1. INTRODUCTION

It is well-known that colors affect the impression of teste to humans. Previous studies have already reported that reddish purple, red, and orange colors highly obtain the impression of sweetness, yellow and green colors affect the impression of sourness, and grayish color highly obtains the impression of bitterness (Moga 1974, Kinoshita et al. 2010). And it is reported to associate the impression of sweetness with pink, orange, and red colors and to do that of sourness with yellow color as similar to the results of the above studies (Okuda et al. 2002). However, it is not clear how the three attributes of color – hue, lightness and chroma have an effect on the impression of the five basic tastes – sweetness, bitterness, sourness, saltiness and umami, from the point of view in the quantitative measurement. Also there are some literatures suggesting a connection, that colors for use in the food package enhance the willingness to buy a product when they are the impression close to actual food taste, then pass along information to become the criteria of judgment for buying (Kinoshita et al. 2010). So it seems to be the importance of investigating to the three attributes of color quantitatively. The purpose of this study is to examine the effect on the impression of taste by color stimuli from the aspect of the three attributes of color.

2. METHOD

2.1 Stimuli

Ten hues of the chromatic color (5R, 5YR, 5Y, 5GY, 5G, 5BG, 5B, 5PB, 5P, 5RP) and five of the achromatic color (N1, N3, N5, N7, N9) on the hue circle of Munsell color system were selected as the color stimuli in this experiment. In each hue of chromatic color, twenty-five stimuli were regularly chosen with the values of Munsell Value and Chroma in Munsell notation. Thus, there were around 257 stimuli in total. Table 1 shows the stimuli used in this experiment. The stimuli were presented by 24-inch display (Dell, UP2414Q) placed in front of the observer and the viewing distance was 500 mm. They were displayed into the square at a visual angle of 15 deg in the center of the screen, and set N5 as the background color. Referring to the values of tristimuls values (*XYZ*) of Munsell color with D_{65} light source in JIS Z 8721 (JIS 1993.), those colors were made. The mean value of ΔE_{ab}^* in all the stimuli is 4.94 as shown in Table 1.

Table 1. Stimuli in this experiment.

H	V	C	No. of colors	Ave. ΔEab^*
5R	2 - 9	1 - 20	25	4.88
5YR	2 - 9	1 - 16	25	5.36
5Y	3 - 9	1 - 14	25	5.64
5GY	3 - 9	1 - 14	26	5.35
5G	2 - 9	1 - 20	25	4.93
5BG	2 - 9	1 - 16	25	4.50
5B	1 - 9	1 - 12	25	4.68
5PB	2 - 8	1 - 16	25	4.42
5P	2 - 7	1 - 28	25	5.04
5RP	2 - 8	1 - 22	26	5.27
N	1 - 9		5	1.23
Total			257	4.94

2.2 Procedure

After three minutes light adaption by the D_{65} fluorescent lamps in experimental booth, the observers were asked to evaluate the impression of basic tastes (i.e. sweetness, sourness, bitterness, saltiness and umami) in stimuli presented, to each taste on a five-point scale (1: feel hardly, 2: feel slightly, 3: feel somewhat, 4: feel, 5: feel very much). The stimuli were presented randomly and the duration time was left to observer's discretion. The gray image of N5 was displayed as the inter-stimulus stimulus to remove the effect of the previous stimulus. In one session, the observer performed the evaluation of 257 times and three sessions were carried out for one observer. It was 771 times in total. Prior to the expriment, the observers had an enough time to practice for the evaluation.

2.3 Apparatus

The experimental booth was covered with a black curtain. It was illuminmated by the D_{65} fluorescent lamps and the illumination of screen in the display was around 350 lx. The display was placed in front of the observer and the viewing distance was 500 mm. The observers were asked to respond with the ten key when they evaluate the stimulus.

2.4 Observers

Twenty observers participated in this experiment. They were ten female and ten male students. They have the normal color vision.

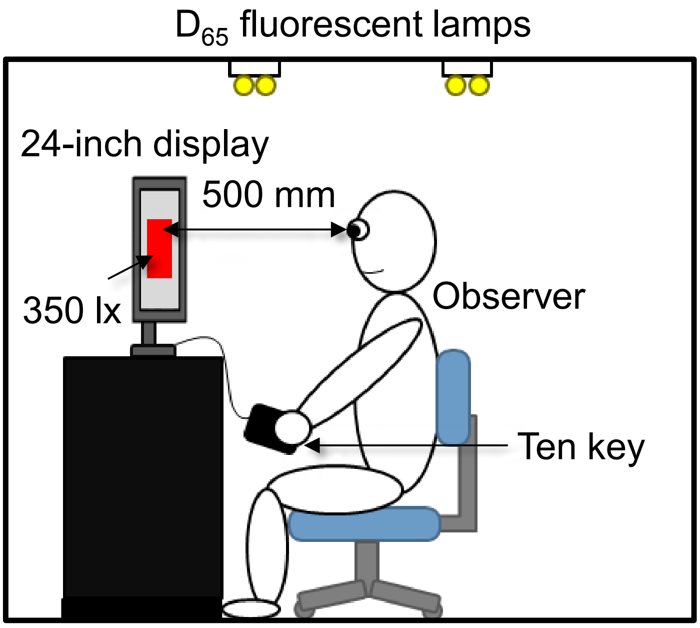

Figure 1: Apparatus.

3. RESULTS AND DISCUSSION

3.1 Effect of Hue

Figure 2 shows the results of the impression of five basic tastes (sweetness, sourness, bitterness, saltiness, and umami) on hue circle based on all the observers' responses. Figure 2 (a) – (e) indicate sweetness, sourness, bitterness, saltiness, and umami, respectively. The circumference in each panel represents the hue circle and each hue corresponds to the focal color in the hue used in this experiment (i.e. color of the highest chroma value in the hue). The radius indicates the subjective evaluation value in the experiment. In this figure the average values from all the observers' responses are connected.

As shown in this figure, particularly, the evaluation values increases with the regions between 5RP and 5YR in sweetness and the regions between 5YR and 5GY in sourness in Figure 2 (a) and (b), respectively. The colors of reddish purple, red, and orange obtain the impression of sweetness while those of orange, yellow, and yellowish green give the impression of sourness. For bitterness, saltiness, and umami in Figure 2 (c) – (e), the effects of hue are relatively small. On the other hand, N1 and N3 of achromatic colors obtain the high evaluation value in the impression of bitterness, and lightness affects the impression of bitterness as the mentioned in the next paragraph. The tendency of the results in hue effect corresponds to the results of previous studies (Kinoshita et al. 2010, Moga 1974, Okuda et al. 2002).

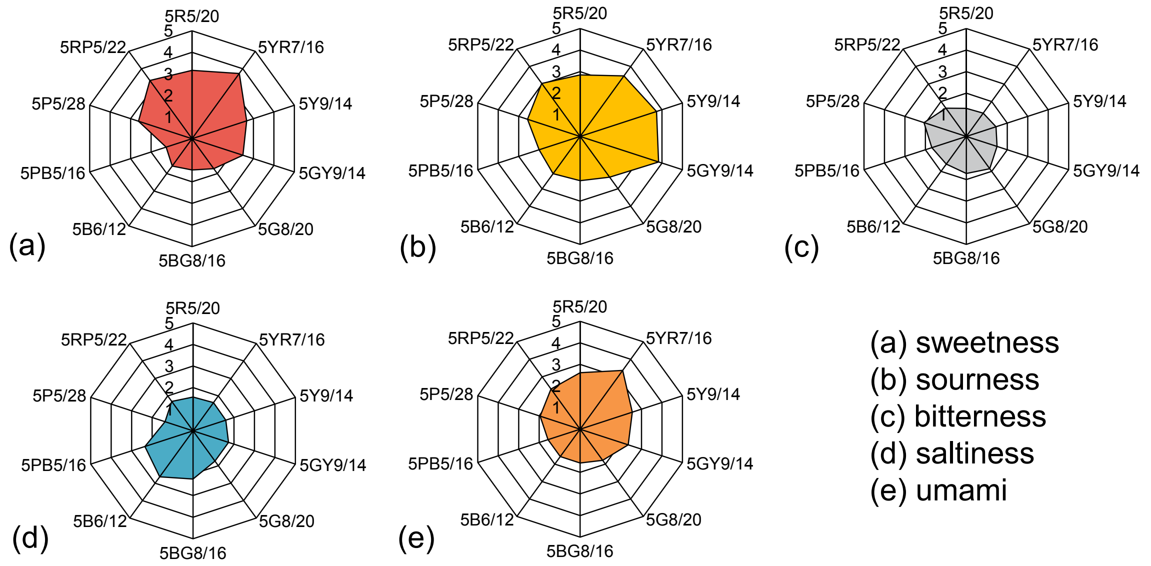

Figure 2: Effect of hue in the average results of the impression of five basic tastes for ten focal colors (i.e. color of the highest chroma value in the hue) . (a): sweetness, (b): sourness, (c): bitterness, (d): saltiness, and (e): umami. The circumference and radius represent the hue circle and the subjective evaluation value, respectively.

3.2 Effect of Lightness

Figure 3 shows the results of the impression of bitterness as a function with the value of lightness based on all the observers' responses. The horizontal and vertical axes indicate the value of lightness and the subjective evaluation value of bitterness, respectively. As the typical results, the average values of N, 5GY-/6, and 5G-/8 are plotted. In this figure, the evaluation value increases with a decreasing of the value of lightness in each color. It means that the value of lightness affects the impression of bitterness and it associates the impression of bitter with dark colors. This result corresponds to that of previous study (Kinoshita et al. 2010).

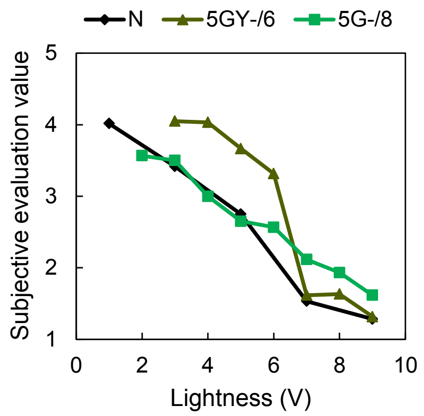

Figure 3: Average results of the impression of bitterness as a function with the value of lightness for N, 5GY-/6, and 5G-/8.

3.3 Effect of Chroma

Figure 4 (a) – (b) show the results of the impression of sweetness and sourness as a function with the value of chroma based on all the observers' responses, respectively. The horizontal and vertical axes indicate the value of chroma and the subjective evaluation value of sweetness and sourness, respectively. As the typical results, the average values of 5RP5/-, 5R5/-, and 5YR7/- are plotted in sweetness of Figure 4 (a) and those of 5GY9/-, 5Y9/-, and 5YR7/- are represented in sourness of Figure 4 (b).

In Figure 4 (a), the evaluation value increases with the value of chroma and then is saturated over 10 in the value of chroma in all the colors. It means that the value of chroma affects the impression of sweetness in reddish purple, red, and orange colors and it associates the impression of sweetness with high chroma value of those colors. In Figure 4 (b), the evaluation value increases with the value of chroma and then has a tendency saturated over 12 in the value of chroma in all the colors as well as the results of sweetness. It means that the value of chroma affects the impression of sourness in yellowish green, yellow, and orange colors and it associates the impression of sourness with the high chroma value in those colors. These results correspond to that of previous study (Kinoshita et al. 2010, Moga 1974, Okuda et al. 2002).

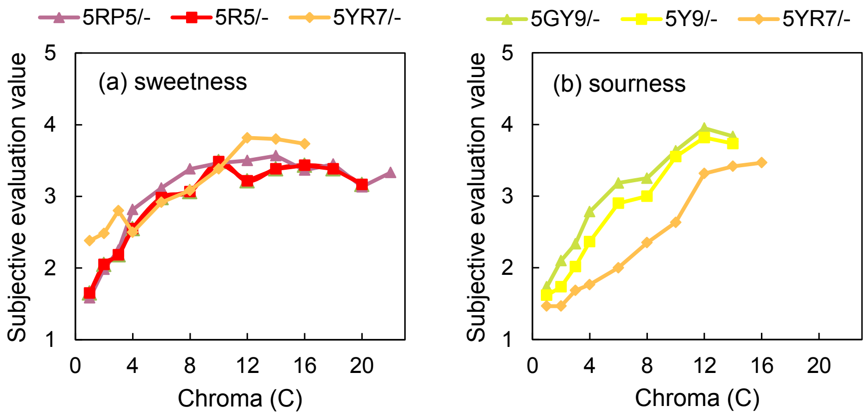

Figure 4: Average results of the impression of sweetness and sourness as a function with the value of chroma. (a): sweetness for 5RP5, 5R5, and 5YR7 (b): sourness for 5GY9, 5Y9, and 5YR7.

4. CONCLUSIONS

To examine the effect on the impression of taste by color stimuli from the aspect of the three attributes of color (hue, lightness, and chroma) the impression of five basic tastes for the color stimuli were measured using the subjective evaluation of five-point scale. The color stimuli were uniformly selected from Munsell color system. They included ten hues of chromatic colors and N of achromatic color. The value of lightness and chroma ranged from 1 to 9 and from 1 to 28, so that about 25 colors from each chromatic hues and 5 achromatic colors were selected and the total was 275 stimuli. The observers were asked to subjectively evaluate the impression of five basic tastes (sweetness, sourness, bitterness, saltiness, and umami) for the stimulus presented by the display using the five-point scale. In the results, the evaluation values increases with the regions between 5RP and 5YR on Munsell hue circle for the impression of sweetness and the regions between 5YR and 5GY on the hue circle for the impression of sourness. And in those hues, the evaluation value increases with the value of chroma and then is saturated over 10 - 12 in the value of chroma. It means that the colors of reddish purple, red, and orange obtain the impression of sweetness while those of orange, yellow, and yellowish green give the impression of sourness with an increasing of the value of chroma. N1 and N3 of achromatic colors obtain the high evaluation value in the impression of bitterness. And the evaluation value increases with a decreasing of the value of lightness including 5G and 5GY stimuli. It means that the value of lightness affects the impression of bitterness and it associates the impression of bitter with dark colors.

ACKNOWLEDGEMENTS

This work was supported by JSPS KAKENHI (Grant-in-Aid for Young Scientists (B)) Grant Numbers 26750007.

REFERENCES

Japanese Industrial Standards (JIS) 1993. Colour specification−Specification according to their three attributes, JIS Z 8721 (in Japanese).

Kinoshita, T., K. Matsuda, and K. Ayabe 2010. Effects of taste image by three attributes of color, *Journal of Design Research Association* 54, 107-112 (in Japanese).

Moga, J.A. 1974. Influence of color on taste thresholds, *Chem. Senses Flavor* 1 (1), 115-119.

Okuda, H., M. Tasaka, A. Yui, and S. Kawazoe 2002. Correlation between the image of food colors and the taste sense –The case of Japanese twenties-, *Journal of Cookery Science of Japan* 35(1), 2-9 (in Japanese).

Address: Masato SAKURAI (Dr. Eng.),
Department of Media Informatics,
College of Informatics and Human Communication,
Kanazawa Institute of Technology,
3-1 Yatsukaho, Hakusan, Ishikawa, 924-0838, JAPAN
E-mails: masato@neptune.kanazawa-it.ac.jp

The color image of dichromats and anomalous trichromats

Yuria NOGUCHI,[1] Muneo MITSUBOSHI,[2]
[1] Graduate School of Human Sciences, Kanagawa University
[2] Department of Human Sciences, Kanagawa University

ABSTRACT

We measured color image of color vision deficients using SD scales, and compared the results with those of color vision normals. Eleven colors chips, 8 vivid color (red , orange , greenish-yellow , yellow green , bluish-green , greenish-blue , blue , purple) , and achromatic colors (white , gray, black) were selected from the New Color Collections (199a) of the Japan Color Research Institute, and displayed on a black sheet .The size of stimulus was 3×3cm. Those colors were observed one by one by the participant through a square opening of black mask of the same size as stimulus to avoid mutual influence between adjacent colors. All the stimuli were observed under natural fluorescent lights with chromaticities of (.364 , .379) and the average illumination was 842 lx . Four color vision deficients (one protan, one deutan , and two deuteranomats) and 13 color vision normals participarted.

General tendency was that the point on each SD scale shifted towards right hand, i. e. negative image or affection, in color vision deficients. For red, orange, and white colors, there existed several substantially different color images (SD scales) between color vision deficients and color vision nomals. Image of blue, purple, gray, and black showed little difference between them. Images to greenish-yellow and yellow green were slightly different.

In terms of individual images (SD scales), images clustered in "activity ", e.g. "crowded-lonely", "powerful-non powerful", or " showy-quite" were much different for color vision deficients and color vision normals.

1. INTRODUCTION

There have been much data concerning how color vision deficinets recognize color and how differently they perceive colors from color vision normals (Graham & Hsia, 1958; Fletcher & Voke, 1985; Mitsuboshi & Hasegawa, 1987; CUDO, 2009; Noguchi, 2013). But little investigation has been made into how color vision deficients feel for colors, in other words, what kind of images they have to colors.

Many studies by SD method in the past show that there are generally three factors covering images to colors; i.e. "evaluation", "activity", and "potency" (Oyama et al. 1965). Such estimation is, however, for color vision normals.

What image they have to color and how different their images are from those of color vision normals are the scheme of the present report.

Color vision deficient may give same color name as color vision normals to a particular color, with different image (Kawamoto et al, 2008). Images clustered in potency were largely different in their participants. Saito et al , 2010), on the other hand, reported that there was little difference in their images between color vision dificients and normals.

2. METHOD

2.1 Color Stimuli

Eleven color chips, eight vivid red , orange , greenish-yellow , yellow green , bluish-green , greenish-blue , blue , purple , white , gray (Gy-5,0), and black which were selected from the New Color Collections (199a) of the Japan Color Research Institute. Their size was of 3×3cm. They were attached on the black background paper.

All the stimuli were observed under natural fluorescent lights with chromaticities of (.364 , .379) and the average illumination was 842 lx .

2.2 SD Scale

Figure 1 shows the SD scales used. These scales were evaluated with seven points.

1. light—dark	11. beautiful—ugly
2. elegant—vulgar	12. calm—frivolous
3. like—dislike	13. monotonous—changeful
4. get annoyed—mind	14. plain—heavy
5. natural—unnatural	15. romantic—realistic
6. amiable—not amiable	16. modern—ancient
7. warm—cool	17. young—old
8. crowded—lonely	18. smart—rustic
9. powerful—not powerful	19. open—closed
10. showy—quiet	20. profound—light
	21. clean—dirty

Figure 1: SD scales used.

2.3 Participants

Paid experienced 2 male dichromats (1 protan and 1 deutan) and 2 male anomalous trichromats (deuteranomats) , ranging from 27 to 73 years old, participated in this study. They were all recruited from CUDO organization. They had been tested their type of color vision at ophthalmological clinics

13 male and female color vision normals, who were all naive to this kind of color experiment and not paid, were also recruited so that their results can be compared. They had been tested their color vision by Ishihara Pseudoisochromatic Plates. They were all students of Kanagawa University at the age of around 20.

2.4 Experimental Procedure

11 colors of chips were observed one by one by the participant through a square opening of black mask of the size same as stimuli to avoid mutual influence between adjacent colors. The participants evaluated each 11 colors of images using 21 SD scales with 7 points.

3. RESULTS AND DISCUSSION

Figures 2 and 3 show SD average profile of the color vision deficients and color vision nomals for red and blue colors. Red is one of colors which showed remarkable difference between color vision deficients and normals. Blue is, on the other hand, one of colors which showed small differences. Dotted and solid lines indicate average results for color vision deficients and color vision normals respectively.

Table 1 shows the summary of individual images (SD scales) showing large difference , more than 2.0 points on each scale, between color vision deficients and normals in each color. Tha data for red and blue colors are excluded, which can be referred to Figures 2 and 3.

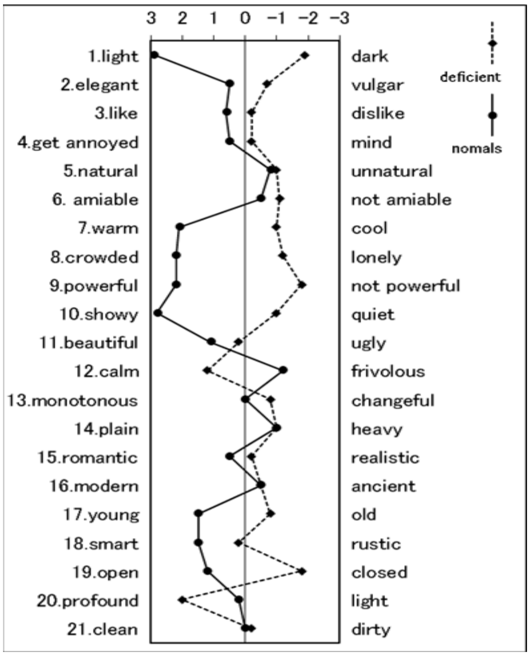

Figure 2: Average image to red.

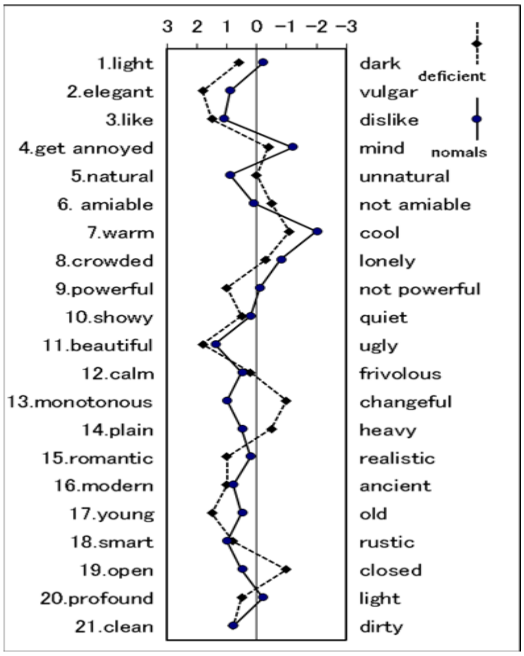

Figure 3: Average image to blue.

Points on individual images (SD scales) shifted generally towards right hand in each scale, i.e. towards negative image or emotion in color vision deficients .

For red color, images of warm-cold, crowded-lonely, powerful-not powerful , and showy-quiet, all of which may be clustered into "activity", shifted towards right hand in the color vision deficients. Images of romantic-realistic, modern-ancient, which may be clustered into "modernness", were similar between them .

For blue color, images of monotonous-changeful and open-closed shifted towards right in color vision deficients. But, images of other scales are generally analogous between them

Table1 shows that orange color also give different image, more than red, to color vision deficients and nomals. That is predictable because orange and red are quite similar in their image for color vision normals (Oyama et al., 1965). Many of images showing large difference were also from "activity ". Both red and orange colors are not perceived "red" nor "orange" as color vision normals do, but maybe look yellowish for them. It seems natural to postulate that images to such colors differ for color vision deficients.

It is, however, interesting that images for "narural-unnatural", "plain-heavy", or "modern-ancient" were little different between them despites of difference of appearance of color. This result suggest that such images are created not by color, but other factors like brightness or shape.

It is predictably that images of blue or bluish colors did not show great difference between color vision deficients and normals, for color vision deficients perceive blue color as "blue" (Graham & Hsia, 1958 ; Mitsuboshi and Hasegawa, 1987) .

Table 1: Scales showing large difference between color vision deficients and color vision nomals in each color except red and blue.

Color	SD scale
Orange	amiable—not amiable
	warm—cool
	crowded—lonely
	powerful—not powerful
	showy—quiet
	plain—heavy
	young—old
	smart—rustic
	open—closed
yellow green	like—dislike
	beautiful-ugly
	plain—heavy
White	like—dislike
	amiable—not amiable
	calm—frivolous
	romantic—realistic
	smart—rustic
greenish-yellow	amiable—not amiable
	powerful—not powerful
	plain—heavy
	young—old
	smart—rustic
bluish-green	not greatly different
greenish-blue	not greatly different
Purple	not greatly different
gray	not greatly different
black	not greatly different

The results that images to yellowish colors were rather different between color vision deficients and normals seem difficult to compromise with the hypothesis of their recognition of color, since they both see the same "yellow" color. This may partly be explained by the fact that yellowish colors used in the present study included some green, like yellow green and greenish yellow, which is assumed to look different from color vision normals.

Images by white were unpredictably different between color vision deficients and normals with those to gray and black little different. It is possible that image by gray or black is essentially weak for both color vision deficients and normals. Image by white is, on the other hand, strong forming somehow difference between them.

4. CONCLUSIONS

Images to colors by color vision deficients are different from color vision normals depending color. General tendency was that the point on each SD scale shifted towards right hand, i. e. negative image or affection, in color vision deficients. For red, orange, and white colors, there existed several substantially different color images (SD scales) between color vision deficients and color vision nomals. But Image of blue, purple, gray, and black showed little difference between them. Images to greenish-yellow and yellow green were slightly different.

In terms of individual images (SD scales), images clustered in "activity ", e.g. "crowded-lonely", "powerful-non powerful", or " showy-quite" were much different for color vision deficients and color vision normals. Images of "narural-unnatural", "plain-heavy", or "modern-ancient" were, on the other hand, showed little difference between them. The latter suggest that such images are not created by color, but some other factors.

Thus we have to pay attention to difference in image between color vision deficients and normals when we construct color universal design.

ACKNOWLEDGEMENTS

We greatly appreciate Yuka Asano for conducting experiments with color vision normals with the authors' advice, which was a partial fulfillment of graduation thesis submitted to Department of Human Sciences, Kanagawa University in 2012 academic year.

REFERENCES

Color Universal Design Organization(CUDO). 2009. *CUD* . Tokyo: Heart Publishing Co Ltd. (in Japanese).

Fletcher R. and J. Voke. 1985. *Defective Colour Vision fundamentals, diagnosis and management.* Bristol: Adam Hilger Ltd.

Graham, C. H. and Y. Hsia. 1958 The spectral luminosity curve for a dichromatic eye and a normal eye in the same person. *Proc. Natl. Acad. Sci.* 44, 46-49.

Kawamoto K. , Wake T. , and T. Yasuma. 2008. Identified color and impression of color deficiencies on color categorization, *The collection of papers of the Color Science Association of Japan, Supplement* 32:124-125. (in Japanese).

Mitsuboshi M and Hasegawa H. 1987. *Color vision, In Encyclopedia of Color, pp.170-247.* Tokyo: Asakura Publishing Co Ltd. (in Japanese).

Noguchi, Y. 2013. The effect of hatching on the word recognition of the color vision deficients using reaction time. *Bulletin of Human Sciences, Kanagawa University* 7: 5-17. (in Japanese).

Oyama, T., Soma, I., Tomiie, T., and H. Chijiiwa. 1965. A factor analytical study on affective responses to color. *Acta Chromatica* 1 (4):164-173.

Saito H. , Asano Y. , and M. Watanabe . 2010. The impression differences in color vision characteristics, *The collection of papers of the Color Science Association of Japan, Supplement* 34: 56-57. (in Japanese)

Address: Yuria Noguchi, Graduate School of Human Sciences,
Kanagawa University, 3-27-1 Rokkakubashi, Kanagawa-ku, Yokohama, 221-8686, JAPAN
E-mails: r201370189ih@kanagawa-u.ac.jp
Address: Prof. Muneo Mitsuboshi, Department of Human Sciences,
Kanagawa University , 3-27-1 Rokkakubashi, Kanagawa-ku, Yokohama, 221-8686,
JAPAN
E-mails: mitsum01@kanagawa-u.ac.jp

Proceedings

MCS Oral Papers

Surface spectral reflectance estimation with structured light projection

Grzegorz MĄCZKOWSKI,[1] Krzysztof LECH,[1] Robert SITNIK,[1]
[1] Institute of Micromechanics and Photonics, Warsaw University of Technology

ABSTRACT

Several solutions were developed to reconstruct reflectance spectra of surfaces. Most of them focus on 2D acquisition of more than three spectral channels. The bands are separated by filtering the illumination spectrum or the light falling on the camera sensor. Recently more complex solutions have emerged, which combine the multispectral information with shape in 3D. We present a robust method of spectral reflectance estimation for points sampled on a 3D surface in a structured light projection system. The proposed solution does not need any additional hardware apart from the devices used in the classic structured light projection setup. It utilizes a calibrated color CCD camera and a DLP projector, which projects sine fringes in order to provide precise 3D point coordinates. Additionally, the projector is used as a light source for multispectral image capture by displaying uniform color fields. Simultaneous acquisition of the 3D shape information, as well as the multispectral data is possible in a single sequence of images. They are corrected for illumination non uniformity, ambient light and camera noise.

Two approaches are verified for the design of optimal projected hues. In the first one the saturated CMY fields are displayed. In the second approach three hues are found by an optimization algorithm which uses emission spectrum of the projector and quantum efficiency of the camera in order to minimize intensity variations between channels.

The presented method reconstructs a point cloud representing the surface with spectral reflectance estimated for each point. It uses the Wiener inverse method for the spectrum reconstruction. We provide evaluation of accuracy of the proposed method and show results of scanning painting samples created with different techniques, as an example application of cultural heritage digitization.

1. INTRODUCTION

Some very recent developments focus on spectrum reconstruction from minimal input data and no a priori information. They need two images of a scene, captured with different illuminants (Jiang and Gu 2012) or with and without a filter (Shrestha at. al. 2011). These methods provide robust solutions to multispectral imaging problem.

Recently also the 3D acquisition systems emerge, which combine shape information, encoded as a point cloud, with spectral or colorimetric data (Tonsho at. al. 2001, Mansouri at. al. 2007, Simon-Chane at. al. 2013). These achievements are innovative and promising in cultural heritage digitization, but they are also complex and expensive. On the other hand, they address the problem of angular reflectance properties of the 3D surface, which is important, but difficult to solve. In this work we take a different approach and propose a simple and low-cost solution, which enhances an ordinary 3D scanner with structured light projection (SLP) in order to equip it with spectral reflectance estimation capability at each registered point. Being aware of the hardware limitations and simplified acquisition model, which does not take into account illumination and observation directions with respect to the surface orientation, we propose the illumination optimization procedure. It improves the reflectance reconstruction results, providing a robust measurement method.

2. CONCEPT OF THE SETUP

The setup joins the concept of the structured light projection system, with additional acquisition step, which provides data for the spectral reflectance reconstruction.

2.1 3D scanner

The SLP system is built with a digital camera and a DLP projector, which provides active illumination. In our case the sine fringe projection technique is used. During the acquisition a set of images with shifted pattern, along with binary codes for the phase unwrapping, is captured. After automatic processing it yields a point cloud corresponding to the digitized surface. Normally each point in the cloud has assigned a color value, coming from one of the registered images, which was acquired with the projector displaying uniform white background. Such color information has relatively low quality, which is only slightly improved by adjusting the camera white balance. In the following study we propose to swap this data with the calibrated color map, derived from the estimated reflectance spectrum. Because in the image acquisition path just a single camera is used, there is one-to-one correspondence between the calibrated color value and the point in cloud and no additional texture mapping is necessary.

The tested setup features 2.8Mpix color, CCD camera and off-the-shelf FullHD DLP projector. It is calibrated with the method described in (Sitnik 2002), so that it has working volume of size 150x150x80mm and achieves resolution of 0.1mm, measured as the average distance between points in the captured cloud.

2.2 Spectrum reconstruction method

The multispectral methods for reflectance reconstruction need to operate on more than three, linearly independent spectral channels. Different methods and applications use diverse number of bands, either narrow or wide (Fischer and Kakoulli, 2006). Most of them use between six and ten channels, which is sufficient, when the appropriate algorithm for the reconstruction is chosen. The most widely used approaches include the Wiener inverse method and/or PCA-based one (Kang, 2006: 203). The former one uses signal and noise covariance in order to balance the inverse problem of increasing the dimensionality of the response from a few channels to the full spectrum sampled with a predefined resolution. The PCA-based methods use statistical information gathered from a large number of spectral samples in order to derive basis vectors, describing the set of samples.

In this work the Wiener inverse approach is used. The spectral filtering is realized by taking three images with a trichromatic camera, illuminated with different projected hues. This way nine channels can be captured with three acquisitions. Additionally each captured image is corrected for the camera noise and uneven illumination with the method described in (Mączkowski at. al. 2012).

3. DLP PROJECTOR MODEL

The available DLP projectors use mainly two kinds of light sources: tungsten lamps and LEDs. Both of these solutions are not ideal for faithful color reproduction and spectral reconstruction. Measurements of spectral response of sample off-the-shelf devices show, that their emission spectral power distribution (SPD) is very non-uniform, with high peak around blue region and much smaller power in the red region of the spectrum (Figure 1a). Especially LED-based projectors are a poor choice for the proposed application, because they often exhibit wide ranges with no, or very small emission, which gives no sensitivity in these parts of the spectrum. Therefore in the further analysis the classic DLP projector, with tungsten lamp and filter wheel is used.

In order to take the advantage of the DLP projector in spectral measurements its characterization must be performed in order to find a relation between R, G and B values, which drive the output and produce the resulting SPD. For this purpose the spectral response $s_i(\lambda)$ in every channel of the projector was measured separately with a spectrophotometer. Additionally the total response, summed over the whole spectrum was measured at a range of supplied intensity levels between 100 and 250, with 10 levels interval. Based on this data a response model was found by least squares fitting of the power function to the intensity response. Based on the gamma coefficient found this way the final relation between input RGB values and the output SPD is derived as in Eq. 1.

$$S(\lambda)=s_R(\lambda)\left(\frac{R}{255}\right)^{\gamma}+s_G(\lambda)\left(\frac{G}{255}\right)^{\gamma}+s_B(\lambda)\left(\frac{B}{255}\right)^{\gamma} \quad (1)$$

The model was verified in two ways. In the first approach the hardware gamma correction was manually adjusted in the projector, so that two sets of responses for gamma 2.0 and 2.2 were collected. The model was found in both cases and the response was linearized. The resulting relations were identical, as is shown in Figure 1b, which proves that the model works for different gamma parameters.

In the second verification stage the reconstructed response was compared with the measured one for arbitrarily chosen RGB coefficients. The procedure was repeated for five different set of coefficients and in all cases the root mean square diffrence between the responses did not exceed 1%. Example pair of characteristics is depicted in Figure 1c. In the whole reasoning the assumption is made, that the γ coefficient is the same for all channels and does not change with wavelength. Furthermore, the emission spectrum is considered constant for the whole illuminated area, so that differences between pixels are neglected.

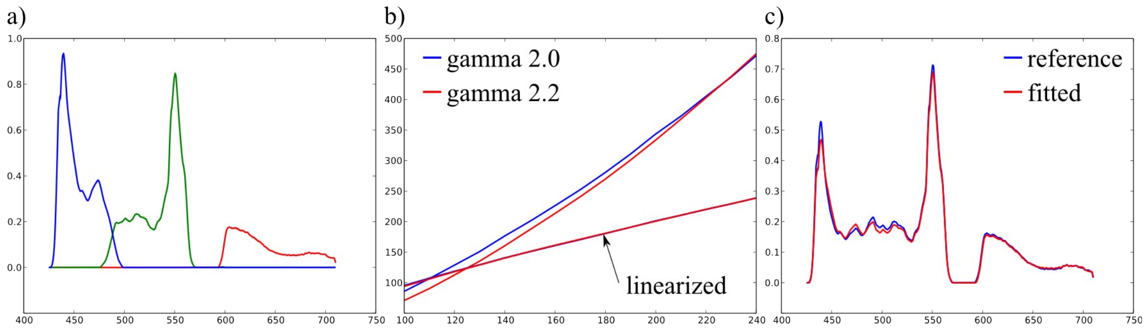

Figure 1: Spectral analysis of the DLP projector: a) response in channels R, G and B; b) results of response linearization; c) reconstruction of the SPD for R239, G228, B176.

4. OPTIMIZATION OF THE ACQUISITION PARAMETERS

Optimization of the acquisition parameters requires an image registration model, which describe how the spectral channels' intensity is captured. It equals the total irradiance $S_l(\lambda)$, emitted by a light source in the band l, filtered by the surface spectral reflectance $r(\lambda)$ and the detector sensitivity $D_k(\lambda)$ in the channel k, integrated over the visible spectrum (Eq. 2).

$$I_{kl}=\int D_k(\lambda)S_l(\lambda)r(\lambda)d\lambda \quad (2)$$

Input multispectral signal comprises of all combinations of light source spectral bands and camera channels. In this study the camera channels are equivalent to R, G and B spectral sensitivity of a CCD matrix with the Bayer color filter. For simplification the attenuation of the optical system is not considered separately, however the 8bit quantization of the intensity, resembling the actual camera behavior is taken into account.

The light source bands are chosen from three different hues, displayed by the DLP projector. It can be observed, that the pairs with projected red hue and captured blue channel and vice versa will likely produce low imaged intensity and low signal to noise ratio. To avoid this the cyan, magenta and yellow hues are displayed as the primary colors, so that relatively even exposure in all channels and high signal level is achieved.

The method of DLP bands selection is based on a simulation, which finds the solution minimizing the root mean square error between the reference and reconstructed spectral reflectance for different projected colors. The displayed hues are changed by manipulating the proportions between the nominal cyan, magenta and yellow channels. The procedure uses the model from Eq. 2 to calculate the camera response in each band. Spectral characteristics of the ColorChecker target patches are used as a set of reference reflectances *r(λ)*. Light source emission spectrum in channel *l* is calculated from the displayed $C_lM_lY_l$ with the projector model from Eq. 1, and the detector sensitivity corresponds to the camera color channel *k*. Once the camera response in each band is found for the reference color patches, the Wiener inverse spectrum reconstruction model is established. Afterwards it is used to recover reflectance spectra of another set of representative samples, which come from spectrophotometric measurements of painted surfaces.

In the initial attempt a non-linear solver was employed to find the optimal sets of CMY coordinates of the projected hues, which give the best results of the spectral reconstruction of the chosen samples. Unfortunately, the model proved to be not sensitive enough for the channels parametrization. To overcome this problem another approach was proposed. Because the parameter space is only three-dimensional and in practice can be sampled in only 256 levels, corresponding to the possible color values displayed by the DLP in each channel, it was possible to calculate the objective function for different parameters combinations. The error function was defined as the total RMS error of spectrum reconstruction for 24 representative samples, drawn from measured reflectances.

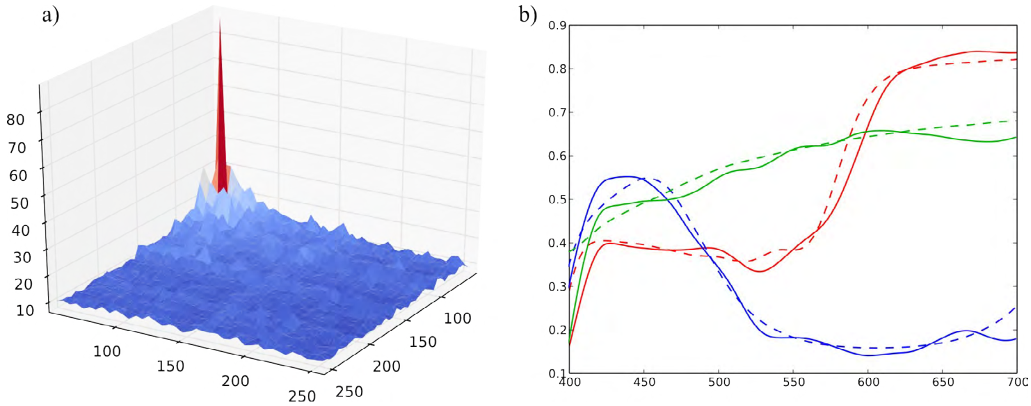

Figure 2: a) Slice of the spectral reflectance reconstruction error function on the R_lG_l plane, for the parameter B = 245; b) example spectrum reconstruction results for three samples.

The three dimensional grid of the projected color samples was chosen as the domain for evaluation of the error function.The sampling was made in the range between 50 and 255, with the step of 5 levels for each of the nominal CMY channels. Fig. 2a depicts the plot of the CM slice of the objective function for Y = 245. It clearly shows, that for intensities above a certain threshold, the error variations are very small. It means that the spectrum reconstruction performance does not depend much on the projected intensities, unless they are lower than a border value. The data evaluation shows, that the threshold equal to 150 is sufficient. Additionally it proves that the overall accuracy of the spectral reflectance reconstruction is determined by the shape of the light source SPD, rather than by proportions of its subranges.

Fig. 2b presents simulated reconstruction of spectral curves for three exemplary samples. Their reference characteristics, indicated by the dashed lines, come from real reflectances, measured by a spectrophotometer.

3. EXPERIMENTAL RESULTS

The reflectance spectrum reconstruction, based on the acquisition with structured light projection, was verified experimentally. The 3D scanner was set in the laboratory, where it was shielded from light sources other than the DLP projector. Three illumination patterns with cyan, magenta and yellow hues were used as lighting for in the multispectral acquisition.

The ColorChecker Passport target was captured as a point cloud. The color patches were extracted by a semiautomatic segmentation of the 3D data, so that an average value was found for each patch in every band. These data served as input for calculation of the Wiener inverse model of the spectrum reconstruction. The model was verified with measurement of the same color target and a set of painted samples, which did not took part in the model estimation. Additionally the setup was used to scan two paintings' reproductions, made in different techniques. The first one was the fragment of V. van Gogh impasto on canvas and the other was a limestone wall painting with an antique theme. The 100x100mm samples were digitized as point clouds with the resolution of 100 points per square millimeter. Fig. 3 shows point clouds with reconstructed color and spectral curves recovered in chosen places, along with their RMS and GFC error metrics (Imai at. al. 2002).

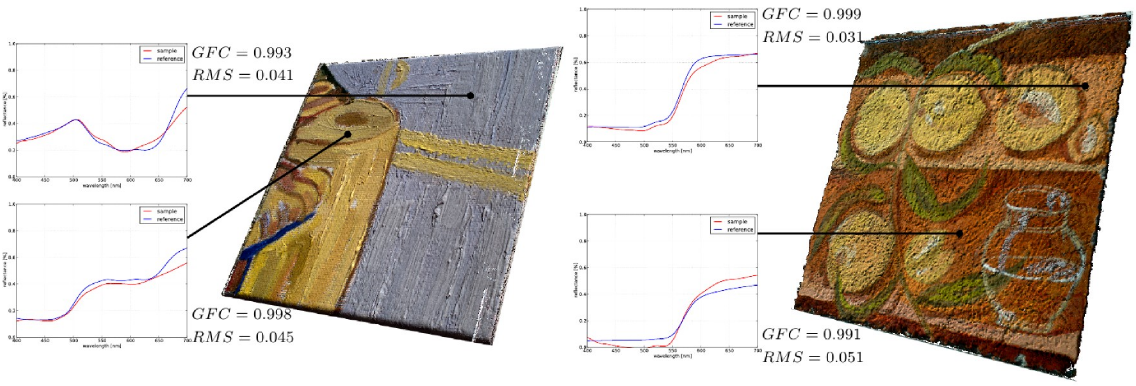

Figure 3: Measurement results of the painting samples.

4. CONCLUSIONS

The presented work shows a successful fusion of the shape measurement method with structured light projection, with the spectral reflectance estimation. It provides a starting point for further analysis of such integrated solutions, which open new possibilities in cultural heritage digitization.

The analysis leads to a conclusion that, having a flexibility of choice of the projected colors, they can be adjusted to achieve the same exposure in all acquired band images. This way the signal to noise ratio and quantization errors are similar and easier to compensate for. Moreover, the linear model of intensity registration provides data giving very accurate spectral reconstruction, which is generally not achievable in practice. This means, that the experimental factors such as noise, uneven illumination, ambient light and camera nonlinearity play important role in the reconstruction accuracy and elimination of them should provide better spectral reflectance reconstruction.

ACKNOWLEDGEMENTS

This work has been partially supported by the Ministry of Culture and National Heritage (Poland) by KULTURA+ framework (2011-2015) and Statutory Work of Warsaw University of Technology.

REFERENCES

Fischer, C. and I. Kakoulli. 2006. Multispectral and hyperspectral imaging technologies in conservation: current research and potential applications. *Reviews in conservation*, 7: 3-16.

Imai, F. H. and M. R. Rosen, and R. S. Berns. 2002. Comparative Study of Metrics for Spectral Match Quality. In *The First European Conference on Colour Graphics, Imaging and Vision*, 492-496.

Jiang, J. and J. Gu. 2012. Recovering spectral reflectance under commonly available lighting conditions. In *IEEE Computer Vision and Pattern Recognition Workshops (CVPRW)*, 1-8.

Kang, H. R., 2006. *Computational Color Technology.* Washington: SPIE Press.

Mansouri, A. and A. Lathuilière, F.S. Marzani, Y. Voisin, and P. Gouton. 2007. Toward a 3d multispectral scanner: an application to multimedia. *IEEE Multimedia* 14(1): 40-47.

Mączkowski, G. and R. Sitnik, and J. Krzesłowski. 2012. Data Acquisition Enhancement in Shape and Multispectral Color Measurements of 3D Objects, In *Image and Signal Processing*. 7340, 27-35.

Shrestha, R. and A. Mansouri, and J. Hardeberg. 2011. Multispectral imaging using a stereo camera: concept, design and assessment. *EURASIP Journal on Advances in Signal Processing.* 2011(57).

Simon-Chane, C. and R. Schütze, F. Boochs, and F. S. Marzani. 2013. Registration of 3D and multispectral data for the study of cultural heritage surfaces. *Sensors.* 13: 1004-1020.

Sitnik, R, 2002. *A fully automatic 3D shape measurement system with data export for engineering and multimedia systems*. PhD thesis, Warsaw University of Technology.

Tonsho, K. and Y. Akao, N. Tsumura, and Y. Miyake. 2001. Development of goniophotometric imaging system for recording reflectance spectra of 3D objects. In *Proc. SPIE 4663, Color Imaging: Device-Independent Color, Color Hardcopy, and Applications VII*, 370-378.

Address: Grzegorz MĄCZKOWSKI, Institute of Micromechanics and Photonics, Warsaw University of Technology, Św. Andrzeja Boboli 8, Warsaw, 02-525, POLAND
E-mail: g.maczkowski@mchtr.pw.edu.pl, lech@mchtr.pw.edu.pl r.sitnik@mchtr.pw.edu.pl

Multispectral Imaging System based on Tuneable LEDs

Muhammad SAFDAR,[1] Ming Ronnier LUO,[1,2] Yuzhao WANG,[1] Xiaoyu LIU[1,3]
[1] State Key Laboratory of Modern Optical Instrumentation, Zhejiang University, Hangzhou, China
[2] School of Design, University of Leeds, Leeds, UK
[3] College of Science, Harbin Engineering University, Harbin, China

ABSTRACT

A modified multiplexed illumination based multispectral imaging system was proposed using RGB camera and LED illumination, which used RGB camera and different combinations of RGB LEDs. The system was developed, optimised for its performance and compared with a commercial hyperspectral imaging system which uses line-scan and Push-Broom technology developed by Isuzu Optics. The Isuzu system was tested first by capturing different targets and its performance was found excellent. Three optimal combinations each of 3 LEDs (one from each of red, green and blue regions) were selected to illuminate the scene. Three exposures of RGB camera were used to estimate the 9-band spectral image of the scene using linear regression method. Some further improvements were made like optimization of camera spectral sensitivities, uniformity correction of exposures and adaptively assigning different weights to different LEDs and training samples. With these improvements the performance of the system was improved by about 50%. The sytem was tested by using four different target charts for training and testing. For different trainnig and testing sets, the performance of the system was lacking behind Isuzu system by 1 ΔE_{00} units which is obvious because of using low intensity LEDs. It can be concluded that the developed system is self-illuminated, energy efficient, easily realisable, cost effective and fast in acquisition.

1. INTRODUCTION

Multispectral imaging is preferred over conventional RGB imaging because of high color accuracy, non-metameric match and is not limited to visual range. Typically, multispectral imaging systems are developed using filter wheel, filter array, stereo camera or monochrome camera with multiplexed illumination which are expensive and time consuming methods. Much attention has been paid to the multiplexed LED illumination based systems during last decade because of their robustness, high switching capability and cost effectiveness (Shurestha 2013). Spectral imaging has wide spread applications including heritage and culture (Cotte 2003), biometrics (Rowe 2005), astronomy (Rosselet 1995), remote sensing (Swain 1978), medical imaging (Everdell 2009) and many others.

Many different methods of multispectral imaging have been proposed already and are available in literature. Multispectral imaging based on multiplexed LED is of prime interest in this paper (Tominaga 2012). In such a system, n different LEDs are illuminated in a sequence and the scene is captured under each light using a monochrome camera in result of which n band spectral image is obtained. Such a system has been used in several applications including film scanner (Shurestha 2012), biometrics (Rowe 2005) and medical imaging (Everdell 2009). Other types include filter wheel based, tuneable filter (Hardeberg 2002, Shurestha 2011) and filter array (Baone 2000, Miao 2006) based systems.

In State of the art multiplexed illumination based system, n band multispectral image is obtained by using n LEDs and n number of exposures of monochrome camera. While in modified multiplexed illumination based system, three LEDs, one from each of red, green and blue regions are illuminated at a time and RGB camera is used to capture the scene. So in this way, n band spectral image can be obtained by n/3 number of exposures (Shurestha 2013).

In the Current work, modified multiplexed illumination based system has been developed and some improvements have been made including uniformity correction, optimization of camera spectral sensitivity functions, and assigning optimal weights to different LEDs used as well as to training samples. The developed system was tested by using different training and testing color targets including four different charts named MCCC- Classic, MCCC-SG, DigiEye Digitizer and Oil Painting Pigments. Its performance was compared with a commercial hyper-spectral system (Hyper-spectral Microscope with EMCCD camera, VNIR-400~900nm) by Isuzu Optics. The commercial system uses line-scan and push-broom technology which is fast and robust comparing with typical filter based systems. This section is followed by method, results and discussion, and conclusions drawn in the end.

2. METHOD

In this paper, modified multiplexed illumination system was devleoped, improved and its performance was compared with a commercial hyper-spectral system. A commercialy available 16 channel LED illuminant, each channel of which is computer controlable, was used to illuminate the scene. Nine LEDs were selected out of sixteen, three from each of red, green and blue regions. The selected nine LEDs are narrow band, lying within and covering more less the whole visible range of 400-700nm (Figure 1). One combination of three LEDs, one from each region, was illuminated at a time and scene was captured using Canon 5D Mark II camera with RGB sensors. Three optimal combinations of LEDs were selected which give the minimum color difference. Four different color charts were used for training and testing (Figure 1). A computer system was used to synchronise illumination and capture. So the system is simple, self illuminated and computer controlled. The schematic daigram is shown below (Figure 2).

For each light the scene was captured once using Canon 5D Mark-II camera. These three exposures were used to estimate the 9-band spectral image of the scene using linear regression method. In this method, the reflectance values were back predicted using SPDs of the LEDs used, spectral sensitivities of the camera and reflectance values of the training set of samples measured using Data-Color SF600. Some further improvements were made like optimization of camera spectral sensitivities, uniformity correction of exposures and adaptively assigning different weights to different LEDs and training samples. With these improvements the performance of the system was improved by more than 50% of that of original for initial test done using MCCC-Classic. Main errors are caused by acquisition noise due to non-uniform and low intensity of the LED sources used. The performance of the developed system was compared with a commercially available hyper-spectral system. The commercial system was first tested by comparing its results with reflectance data measured using Data-Color SF600. The performance of the commercial system was found excellent. The Isuzu Optics used line-scan and push-broom technology to develop a hyper-spectral imaging system. The performance of both systems was measured using latest CIE color difference formula named CIEDE2000 (Luo 2001). Our developed system's performance was lacking behind Isuzu's system by about 1 ΔE_{00} units.

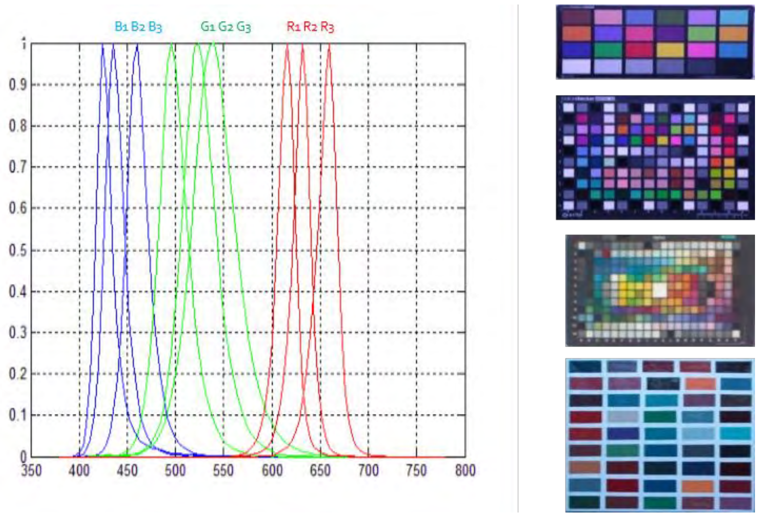

Figure 1: SPDs of selected 9 LEDs and four color charts used for training and testing.

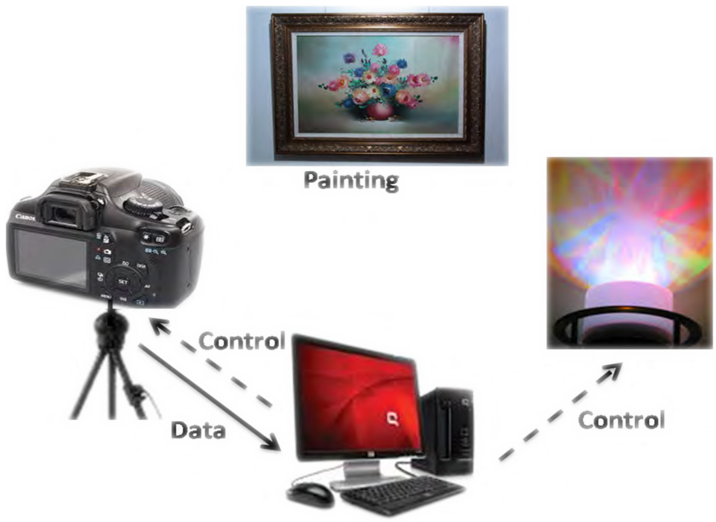

Figure 2: Schematic diagram of developed system.

3. RESULTS AND DISCUSSION

Both systems were tested by comparing results with measured reflectance data using Data-Color SF600. The results of Isuzu's system were found very close to the measured reflectance values and hence its perfromance was found excellent. The developed modified multiplexed illumination system was improved by introducing some modifications. The camera spectral sensitivities were optimized using an adaptive algorithm. The captured RGB images were stored in raw data form and then uniformity was corrected by using a unifrom white board. The uniformity corrected real matrices were then used to back predict reflectance data of each pixel. Different weights were adaptively assigned to SPDs of selected 9 LEDs. And in the same way different weigts were assigned to reflectance vectors of different training samples. The black level was also adjusted. In result of these improvements the performance of developed system was improved by about 50% compaing with original system. The performance of developed system was compared with Data-Color measurements and Isuzu's system as well. The performance of developed system was found lacking behind Isuzu's system by 1 CIEDE00 units. The results of developed system for four different training and testing targets are shown in Table 1. Oil paiting pigments chart was only used for self prediction because it does not include grey patches. First column respresents training sets while all other columns repesent testing results against four test targets. The results were presented in terms of color difference between measured and estimated reflectance calculated using CIEDE2000 formula. The developed system reduces acquisition time by 5 times because of fast switching capability of LEDs and computer control. The use of RGB camera is more convinient and its focus and resolution can be set by user. Moreover, such a system costs much less comparing with state of the art technology.

Table 1. Summary of the results of developed system for different trinig and testing sets.

Charts	MCCC-Classic	MCCC-SG	DigiEye-DigiTizer	Oil Paintig Pigments
MCCC-Classic	3	4.4	4.5	3.5
MCCC-SG	3.0	2.8	3	3.7
DigiEye-DigiTizer	2.9	3.2	2.5	3.8
Oil Paintig Pigments	X	X	X	3.9

As for different traning and testing samples the color defference is less than 3 on everage, so the improved multiplexed illumination spectral imaging system can give acceptable results for real time applications (Song 2000). Some paintings were also captured using develped system and images were found close to those captured using commercial system.

4. CONCLUSIONS

A modified multiplexed ilumination system was developed using tuneable LEDs and RGB camera. The developed system was then improved by optimising SSFs, applying uniformity correction, and adaptively asigning different weights to different SPDs of LEDs and different training samples. Dark levels were also adjusted adaptily. It was found that the performance of developed system improved after above mentioned modifications. The improved system is much faster and cost effective comparing with state of the art spectral imaging systems.

The performance of commercial system was also tested which was found excellent. The developed system was compared with the commercial one. The developed system was lacking a bit behind commercial system in terms of performance but was found more faster and cost effective. The developed system can be used for many applications including biometrics, medical imaging and especially for culture and heritage. It can be concluded that the developed system is self-illuminated, energy efficient, easily realisable, cost effective and fast in aquisition.

More work is being carried out to use high intensity and more uniform LED pannel and the expected results using the current method are less than 2 ΔE_{00}.

REFERENCES

Baone G. A., and Qi H. 2000. De-mosaicking Methods for Multispectral Cameras Using Mosaic Focal Plane Array Technology. The 8th International Symposium on Multispectral Color Science 6062 75-87.

Cotte P., Dupouy M. 2003. CRISATEL High Resolution Multispectral System. In PICS 161-165.

Everdell N. L., Styles I. B., Claridge E., Hebden J. C., and Calcagni A.S. 2009. Multispectral Imaging of the Ocular Fundas Using LED Illumination. Novel Optical Instrumentation for Biomedical Applications IV, SPIE Proceedings 3771.

Hardeberg J. Y., Schmitt F., and Brettel H. 2002. Multispectral colour image capture using a liquid crystal tuneable filter. Optical Engineering, 41(10) 2532-2548.

Lou M. R., Cui G., and Rigg B. 2001. The Development of CIE 2000 Color Difference Formula: CIEDE2000, Color Res. App., 26(5) 340-350.

Miao L., Qi H., Ramanath R., and Snyder W. 2006. Binary Tree Based Generic De-mosaicking algorithm for Multispectral Filter Array. IEEE Transactions on Image Processing 15(11) 3550-3558.

Rowe P. K., Nixon K. A., and Corcoran S. P. 2005. Multispectral Fingerprint Biometrics. Proc. of 6th Annual IEEE Information Assurance Workshop (IAW) 14-20.

Rosselet A. C., Graff W., Wild U. P., Keller C. U., and Gschwind R. 1995. Persistent Spectral Hole Burning Used for Spectrally High-Resolved Imaging of the Sun. Imaging Spectrometry, SPIE Proc. 2480.

Shurestha R., and Hardeberg J. Y. 2013. Multispectral Imaging Using LED Illumination and An RGB Camera. Proc. of 21st CIC, 8-13.

Shurestha R., Mansouri A., and Hardeberg J. Y. 2011. Multispectral Imaging Using a Stereo Camera. EURASIP Journal on Advances in Signal Processing 2011(1).

Shurestha R., Hardeberg J. Y., and Boust C. 2012. LED based Multispectral Film Sacanner for Accurate Color Imaging. The 8th International Conference on Signal Image Technology and Internet based Systems 811-817.

Song T., and Luo R. 2000. Testing Color Difference Formula on Complex Images Using a CRT Monitor. The 8th Color Imaging Conference (IS&T), 44-48.

Swain P. H., and Davis S. M. 1978. Remote Sensing: The Quantitative Approach. Mcgraw-Hill, New York., 1978.

Tominaga S., Horiuchi T. 2012. Spectral imaging by synchronizing capture and illumination. J. of Opt. Soc. Am. A, 29(9) 1764-1775.

Address: Prof. Ming Ronnier Luo, State Key Laboratory of modern optical instrumentation, Zhejiang University, Hangzhou, China

E-mails: msafdar87@zju.edu.cn, m.r.luo@leeds.ac.uk, wangyuzhao@zju.edu.cn, wangflxy@zju.edu.cn

Evaluation of Hyperspectral Imaging Systems for Cultural Heritage Applications Based on a Round Robin Test

Sony George, Irina Mihaela Ciortan, Jon Yngve Hardeberg
The Norwegian Colour and Visual Computing Laboratory
Gjøvik University College, Gjøvik, Norway

ABSTRACT

There has been an increasing interest in using spectral imaging for cultural heritage applications as it provides valuable scientific knowledge on the materials and techniques employed by the artist. In order to select the suitable device for various kinds of applications in the cultural heritage sector, it is necessary be able to evaluate the diverse set of available spectral imaging devices. The resulting spectral images are influenced by several device parameters (sensor characteristics, spectral sensitivity, spectral range, noise, dynamic range, optics, data formats) and imaging conditions (illuminant intensity and spectral power distribution, imaging geometry, illuminant non-uniformities etc.). This paper describes the details and preliminary results of a Round Robin Test (RRT) conducted to ensure the quality and comparability of measurements performed by different spectral imaging laboratories involved in cultural heritage imaging. The present RRT is considered as an external spectral image quality assurance tool in cultural heritage applications. Results from this RRT will be used to standardize spectral imaging procedures, and also to determine certain characteristics of reference materials which are useful for accurate documentation and analytical studies.

1. INTRODUCTION

The study of the paintings and other artworks that represent the cultural heritage is key to effective and adequate restoration and conservation procedures. Spectral imaging has been proved as a promising technology to perform scientific documentation and analysis of cultural heritage objects (Liang, 2012, Hardeberg et al. 2014). This non-invasive technique was found useful for achieving several objectives. Even though the general classification of spectral imaging is based on the number of bands – multispectral and hyperspectral systems, spectral imaging devices vary according to the technology used for capturing the data. This includes the sensor, electronics, optics and the imaging conditions also. Thus, the spectral characteristics of the same object acquired with different setups might vary.

The spectral imaging techniques have been initially developed in the remote sensing domain and later adopted in many other disciplines (Martinez et al. 2002). Many of the imaging systems used in the cultural heritage imaging are not designed to be applied in this domain, but they are adapted for this purpose. Due to this reason, the imaging systems has to be studied to understand the sensor characteristics, imaging geometry, reference objects which generate high quality data in cultural heritage sector. The EU funded COST action COSCH, Colour and Space in Cultural Heritage, is one of the initiatives that aim to investigate and enhance the use of spectral imaging for cultural heritage objects.

A Round Robin Test is a widely accepted tool to study the influence of various parameters, which may vary between individual laboratories and instruments. In this exercise, the same test objects was circulated among the participating laboratories and measured by different instruments to evaluate the quality of the data. This RRT has been conducted as a part of the European project COSCH and more than 16 laboratories have been participating in this programme. Each participating laboratory uses one or more imaging systems. Five test targets has been chosen for this RRT and each of these objects has different typologies which represent commonly used elements in cultural heritage imaging. The test targets includes a Spectralon wavelength calibration standard, X-Rite ColorChecker Classic, X-rite white reference, a painted panel reconstructed with medieval Tuscan technique, and an antique Russian icon on copper. The main discrepancy between the instruments might be caused by the different sub components, which has been used to build the acquisition setups, and the processing workflow. One of the main objectives of this RRT is to identify these elements and to recommend solutions to form an inter-instrument and inter-lab agreement.

Analysis of the hyperspectral data from two imaging systems to understand the quality in terms of image noise has already reported (Vitorino et al. 2015). This paper describes methodologies and preliminary results of the hyperspectral image data obtained by three of the participating laboratories.

2. METHOD AND MATERIALS

One of the most important factors that influences the result of any round-robin test practice is the choice of test targets. Utmost care has been taken to choose the targets, which replicate the common reference targets used while performing the spectral acquisition of cultural heritage objects. Details of the test targets are explained briefly in the following section.

2.1 Test Targets

Test target 1: Spectralon reference. The Spectralon® multi-component wavelength calibration standard is one of the most commonly used reference standards to keep track of the reflectance/absorbance of the measured object. Spectralon is impregnated with a combination of three rare earth oxides (holmium oxide, erbium oxide, dysprosium oxide), is a stable and chemically inert reflectance standard, commonly used for establishing the accuracy of the wavelength scale of reflectance spectrophotometers. Spectralon has a size of 90mm of diameter, and opaque, homogenous, smooth surface, and exhibits sharp absorptions at specific wavelengths span over UV-VIS-NIR region of the electromagnetic spectrum. This object was selected as one of the reference objects in this RRT in order to assess the wavelength accuracy and the spectral resolution of each spectral system.

Test target 2: X-rite ColorChecker Classic. The X-Rite® ColorChecker Classic target is a twenty-four patch color chart with standard colors which are the representation of true colors of natural matter (such as skin, foliage and sky), additive and subtractive primary colors, various steps of grey, and black and white. Each square patch has a size of 40mm and total size of 279.4mm x 215.9mm. The ColorChecker is a very commonly used item for conventional photography and also as a standard color reference to evaluate color reproduction processes, to guarantee that the information obtained is valuable and represents the true colors of the object that has to be studied and documented (Berns 2001).

Test target 3: X-rite White Reference. The ColorChecker® white balance target is a spectrally neutral reference standard to deliver accurate white reproduction. White balance reference is used to measure the light distribution in the objects location and it guarantees precise, uniform, neutral white under any lighting condition.

Figure 1. RRT test objects (a) Spectralon reference (b) ColorChecker Classic (c) White balance (d) Painted panel (e) Icon

Test target 4: Painted panel. In addition to the above listed reference targets, a painted panel is also included in the test objects. The panel was reconstructed by Elena Prandi and Marina Ginanni (Restoration Laboratories of the Soprintendenza SPSAE e per il Polo Museale della città di Firenze, Italy), in order to reproduce the medieval Tuscan technique as described by Cennino (1954). This panel was made in a wooden support and includes several layers of different pigments and underdrawings. The painted panel was included in the RRT items to evaluate the relevant spectral region for pigment analysis and to unveil underdrawings especially in the NIR region.

Test target 5: Icon. Test targets 1-4 were mainly proposed as reference objects for spectral imaging in cultural heritage. However, it is also desirable to study the current challenges in this field, which arises when dealing with objects of different properties like metallic or glossy surfaces. This will help to form best practices for imaging such items. A Russian icon, "Virgin of Kazan" dated 1899 owned by Lindsay MacDonald (University College London, UK) was chosen as a test target. The icon is in the form of a colored image printed on copper plate, with wooden support as the substrate. Due to the metallic plating, the illuminant generates specular reflections, which often reduces the quality of imaging. The aim of including this icon in this RRT is to understand the imaging instruments response to such challenging objects and investigate ways to address such issues.

2.2 Experimental Procedure

The same set of test objects was circulated among the participating laboratories. Each participant was provided with the general instructions of the test and performed the image acquisitions in the same manner they usually work with their instrument. Details of the spectral instrument and the image acquisition conditions have been collected with a Test report form. Basic processing steps were requested to be performed by every laboratory in order to get the object spectral reflectance data. Ground truth data for the test objects was measured using point spectrometers and used as reference for comparison for the data sets.

3. RESULTS AND DISCUSSION

In the present paper, we discuss the comparison between three sets of hyperspectral image data obtained from three laboratories. As shown in Table 1, the instrument specifications are different in several aspects and also the original purpose of not all these spectral systems are for cultural heritage imaging.

Spectral image quality highly depends on the end objective and the application domain. Defining attributes for every application is a challenging task (Shrestha et al. 2014). Most of the existing studies are in the remote sensing domain and are mostly related to the accuracy in classification. For cultural heritage applications, a standard has not been well established to evaluate the spectral imaging systems. In Table 2, a set of quality specifications is proposed. The values in the table are given for the three laboratories and hyperspectral imaging systems presented in the current study, but the attributes are meant to be a standard of quality that will be extended to all the imaging systems involved in the Round Robin Test.

Table 1. Details of the hyperspectral imaging systems.

Participant	No of bands	Wavelength (nm)	Imaging geometry	Spatial resolution	Bit depth	Original purpose of system
Lab 1	61	400-1000	0- 45	275 ppi	16 bit	Measurement and color control of spatially complex patterns
Lab 2	160	400-1000	0- 45	150 ppi	16 bit	Airborne applications
Lab 3	450	400-900	0- 45	300 ppi	12 bit	Art scanning

Table 2. Quality specifications of the 3 hyperspectral systems

Class of attributes	System / Attributes	Lab 1 **Pushbroom Hyperspectral Imaging System VIS-NIR**	Lab 2 **Hyperspectral Camera**	Lab 3 **Line Scanning Spectral System**
System Attributes	**Spatial sampling**	275 ppi	150 ppi	300 ppi
	Spectrum coverage	Visible + near infrared (400-1000nm)	Visible + near infrared (400-1000nm)	Visible + near infrared (400-960nm)
	Number of bands	61	160	450
	Band separation	~10 nm	~3.7nm	~1.25nm
	Number of bits	18	12	16
Set-up Information	**Position of the target**	Horizontal	Horizontal	Vertical
	Complexity	Medium	Medium	Medium
	Portability of the system	Low	Low	Low
	Cost	High	High	High
Post-processing	**File format**	.tif	Proprietary	.cub
	Compatibility with ENVI	No	Yes	Yes

It is noted that spectral data obtained from Lab 3, resulted in least spectral and colorimetric error compared with data from Lab 1 and Lab 2. This imaging system has better spectral and spatial resolution with 450 bands and 300 ppi. Since this system has originaly designed for art scanning applications, close range scanning might have resulted in better spectral data. Painted panel was made by mixing different materials and the spectral measurements was performed at visually similar spatial locations in the same bands. The imhomogeneity in painted material might have caused slightly higher values in RMSE compared to the ColorChecker. The overall trend of error metrics of spectral data from the 3 instruments is comparable.

In addition to the quality system specifications in Table 2 and the spectral and color accuracy metrics in Table 3 and Table 4, a set of image quality attributes has been defined to be taken into consideration as well in the final report of quality evaluation for the RRT Test objects, ColorChecker and Painted panel spectral images are compared spectrally and colorimetrically. In this analysis, measurements performed with a point spectrometer are considered as the ground truth. The metrics Root Mean Square Error and the CIELAB color difference are computed to quantify the spectral and the colorimetric quality respectively. The attributes refer to the quality of the image captured by the spectral systems, in terms of image sharpness, uniformity, noise and specularities that characterise the spectral digital captures of the cultural heritage objects studied in the RRT. The proposed attributes will be analysed in future work.

Table 3. RMSE and CIELAB color difference computed for the each of the 24 patches of the Color Checker, between the values measured with the three imaging systems and the ground truth data.

	Color Checker Patch	1	2	3	4	5	6	7	8	9	10	11	12	13
Lab 1	RMSE	0.11	0.12	0.02	0.03	0.09	0.10	0.12	0.09	0.09	0.05	0.11	0.11	0.04
	CIELAB diff	8.24	5.44	1.43	9.54	4.11	6.28	17.76	7.77	11.55	3.90	13.61	17.34	9.93
Lab 2	RMSE	0.05	0.03	0.05	0.02	0.01	0.05	0.07	0.03	0.04	0.04	0.02	0.09	0.03
	CIELAB diff	1.33	1.54	1.76	2.22	1.43	6.38	6.89	4.52	2.18	4.14	3.59	7.42	6.41
Lab 3	RMSE	0.01	0.01	0.01	0.01	0.01	0.01	0.01	0.01	0.01	0.01	0.01	0.01	0.01
	CIELAB diff	2.31	1.84	1.03	1.46	1.54	1.94	2.19	2.25	1.20	1.42	2.68	2.00	0.69
	Color Checker Patch	**14**	**15**	**16**	**17**	**18**	**19**	**20**	**21**	**22**	**23**	**24**	**Mean**	
Lab 1	RMSE	0.11	0.11	0.14	0.10	0.04	0.14	0.05	0.02	0.02	0.01	0.01	**0.08**	
	CIELAB diff	15.12	15.55	17.42	12.03	6.84	6.88	5.55	4.25	3.21	4.03	4.81	**8.86**	
Lab 2	RMSE	0.02	0.02	0.03	0.08	0.03	0.14	0.09	0.04	0.02	0.04	0.02	**0.04**	
	CIELAB diff	5.37	3.52	2.18	3.07	5.93	7.72	2.86	0.93	2.14	2.67	3.65	**3.74**	
Lab 3	RMSE	0.01	0.02	0.02	0.02	0.01	0.02	0.01	0.01	0.01	0.01	0.01	**0.01**	
	CIELAB diff	2.11	2.18	1.51	2.84	3.28	0.43	0.51	0.40	0.69	0.34	1.20	**1.58**	

Table 4. RMSE and CIELAB color difference computed for the each stripe of the Painted Panel, between the values measured with the three imaging systems and the ground truth data.

	Painted Panel	1	2	3	4	5	6	7	8	9	10	11	12	Mean
Lab 1	RMSE	0.04	0.03	0.12	0.14	0.12	0.11	0.03	0.02	0.06	0.05	0.08	0.02	**0.07**
	CIELAB diff	6.52	4.20	11.18	12.96	15.15	15.94	7.08	5.92	8.70	7.19	6.48	7.57	**9.08**
Lab 2	RMSE	0.04	0.01	0.09	0.04	0.07	0.12	0.06	0.04	0.02	0.02	0.21	0.04	**0.06**
	CIELAB diff	1.87	3.15	3.61	7.16	7.19	7.23	8.96	2.57	4.37	5.35	6.39	4.29	**5.18**
Lab 3	RMSE	0.01	0.01	0.01	0.01	0.02	0.01	0.00	0.01	0.01	0.01	0.02	0.01	**0.01**
	CIELAB diff	3.73	4.97	5.56	3.54	2.31	0.83	0.78	1.00	1.05	1.99	1.01	4.39	**2.60**

4. CONCLUSIONS

In this paper we have presented the preliminary analysis of hyperspectral data generated from a Round Robin Test. In addition to the technical comparison of spectral imaging systems, a quantitative evaluation of the image data has also been performed for three laboratories. In future work, this quality analysis will be extended to the full set of multispectral and hyperspectral devices involved in the RRT and more metrics will be added towards an in-depth evaluation.

ACKNOWLEDGEMENTS

The authors would like to thank all the participating laboratories in EU COST Action TD 1201 COSCH (Colour and Space in Cultural Heritage, http://www.cosch.info), particularly Work Group 1: Spectral object documentation. Part of this study was funded by an STSM action. The authors also acknowledge the Research Council of Norway for co-funding this research though project 221073 in the SHP programme: HyPerCept – Colour and Quality in Higher Dimensions.

REFERENCES

Berns, R.S. (2001) The Science of Digitizing Paintings for Color-Accurate Image Archives: A Review. *Journal of Imaging Science and Technology*, 45(4), 305-325

Cennino, C (1954). Il Libro dell'Arte (The Craftsman's Handbook), translated by D. V. Thompson. Dover, New York.

Hardeberg, J.Y., et al. (2015) Spectral Scream: Hyperspectral Image Acquisition and Analysis of a Masterpiece. To appear in Public paintings by Edvard Munch and some of his contemporaries. Changes and conservation challenges, Tine Frøysaker, Noëlle Streeton, Hatmut Kutzke, Biljana Topalova-Casadiego and Françoise Hanssen-Bauer, eds., Archetype Publications, London, UK

Liang, H. (2012) Advances in Multispectral and Hyperspectral Imaging for Archaeology and Art Conservation. *Applied Physics A: Materials Science & Processing*, 106(2), 309-323

Martinez, K. et al.: (2002) Ten Years of Art Imaging Research. *Proceedings of the IEEE*, 90(1), 28-41

McCamy, C.S. et al. (1976) A Color-Rendition Chart. *Journal of Applied Photographic Engineering*, 2(3), 95-99

Shrestha, R. et al. (2014) Quality evaluation of spectral imaging: Quality factors and metrics. *Journal of the International Colour Association*, 12:22–35.

Vitorino, T. et al., (2015) Accuracy in Colour Reproduction: Using a ColorChecker Chart to Assess the Usefulness and Comparability of Data Acquired with Two Hyper-Spectral Systems. *Computational Color Imaging, Lecture Notes in Computer Science 9016, 225-235*

Address: Dr. Sony George, The Norwegian Colour and Visual Computing Laboratory
Faculty of Computer Science and Media Technology, Gjøvik University College
P.O. Box 191, N-2821 Gjøvik, Norway, http://www.colourlab.no
E-mails: sony.george@hig.no, jon.hardeberg@hig.no, irina.ciortan@gmail.com

Spectral Gigapixel Imaging System for Omnidirectional Outdoor Scene Measurement

Motoki HORI, Naoto OSAWA, Keita HIRAI, Takahiko HORIUCHI, Shoji TOMINAGA
Graduate School of Advanced Integration Science, Chiba University

ABSTRACT

This paper presents a system for acquiring spectral gigapixel images of omnidirectional outdoor scenes. The system is constructed using two programmable high-speed RGB video cameras with telephoto lenses and a programmable rotating table. The captured image size is 2048 × 1088 pixels, and the camera can capture images at a rate of more than 100 frames per second. The telephoto lens covers a horizontal angle of 14.5° and a vertical angle of 10.8°. The rotating table can be automatically controlled by a computer. It can rotate 360° in the horizontal plane and 180° in the vertical plane. Two different types of color filters are mounted on the two RGB video cameras for multi-band image acquisition. By combining these color filters with the camera sensitivities, we can obtain six-channel spectral sensitivity functions. Then, spectral power distributions can be recovered from the captured six-band images by using the Wiener estimation algorithm. From the experimental results, the average RMSE in the proposed system is estimated to be 0.01427. For achieving gigapixel omnidirectional images, we capture the images for 60 horizontal and 21 vertical directions. Then we synthesize a gigapixel omnidirectional image by combining the above captured 1,260 images. This synthesized image covers a spherical field of 360° and comprises approximately 1.9 gigapixels (60000 × 32000 pixels). As a result, our spectral gigapixel image makes it possible to view the omnidirectional details, and also to reproduce accurate spectral power distributions in the scene.

1. INTRODUCTION

Omnidirectional imaging is a useful technology for landscape archiving applications such as Google Street View (Anguelov, 2010) and "Aftermath of the 2011 Tohoku earthquake and tsunami" (A project by The University of Tokyo and Tohoku University) (Sakurada, 2013). In addition, omnidirectional images are currently being applied to virtual experiences through head mounted display systems (Hale, 2014). Hence, it is clear that omnidirectional imaging has been widely used in our daily life.

A variety of omnidirectional imaging systems have also been developed. For example, a camera system with mirrors and panorama stitching algorithms using multiple images are well-known approaches (Szeliski, 2010). For covering 360° spherical field of view, recently a Ladybug camera system has been utilized (PointGrey Research, Ladybug5, 2014). This system has six cameras for synthesizing an omnidirectional image.

For high-quality omnidirectional scene archiving, it is also important to achieve accurate scene spectral information and high-resolution images. In other words, the technology of a spectral gigapixel imaging system for omnidirectional natural scenes is significant for the next-generation natural scene archiving. So far the imaging systems were developed separately through spectral imaging, gigapixel imaging, and omnidirectional imaging and had different applications. In addition, some integrated systems with above two functions were also proposed for specific purposes. For examples, a 360° omnidirectional gigapixel imaging system has been developed by using a telescopic camera and an automatically-controlled rotating table (Gigapixel Panorama Photo, 2013). In our previous work, we had developed a system for acquiring spectral images for time-lapse omnidirectional natural scenes (Hirai, 2014). However, there are no imaging systems for acquiring spectral, gigapixel and omnidirectional images concurrently.

In this paper, therefore, we present a system for acquiring spectral gigapixel images of omnidirectional outdoor scenes. In general, a gigapixel image is generated by combining huge amount of images that are captured using telephoto lenses. Then, we capture more than one thousand multi-band images for generating a spectral gigapixel image of an omnidirectional outdoor scene. For realizing this capture, we develop a system using two programmable high-speed RGB video cameras with telephoto lenses and a programmable rotating table.

2. PROPOSED SYSTEM AND IMAGE SYNTHESIS

2.1 Proposed Imaging System

Figure 1 shows the proposed imaging system for acquiring spectral gigapixel image of omnidirectional scenes. Our system consists of two programmable high-speed RGB video cameras with a telephoto lens, and programmable rotating table. Two different types of color filters are mounted on the two video cameras.

The video camera is a Baumer HXG20 with an image size of 2048 × 1088 pixels and a bit depth of 12 bits, which can capture images over 100 frames per second (fps). The cameras also have liner response characteristics. This specification of the camera is enough for reducing the acquisition time. The lens is Kowa telephoto lens, which covers a horizontal angle of 14.5°and a vertical angle of 10.8°. The rotating table is CLAUSS RODEON VR station HD, which can be automatically controlled by a computer and allow 360° movement in the horizontal plane and 180° in the vertical plane.

Two different types of color filters (KODAK No.34A, FUJIFILM SP-18) are mounted on the two color video cameras for six band image acquisition. Figure 2 shows the overall spectral sensitivity functions of the proposed imaging system. We reconstruct spectral power distributions (color signals) from the six-band images based on the Wiener estimation algorithm.

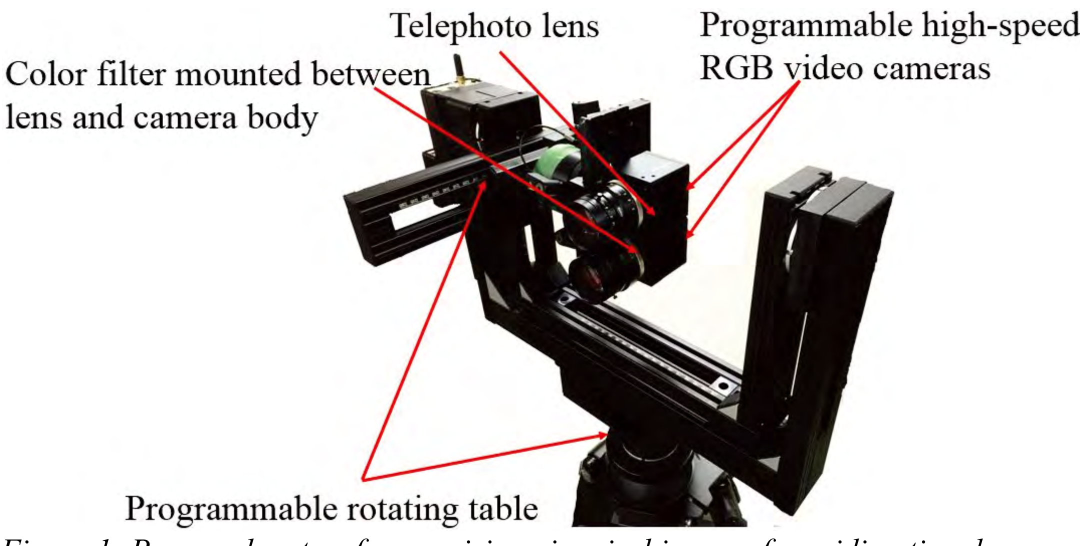

Figure 1: Proposed system for acquiring gigapixel image of omnidirectional scenes.

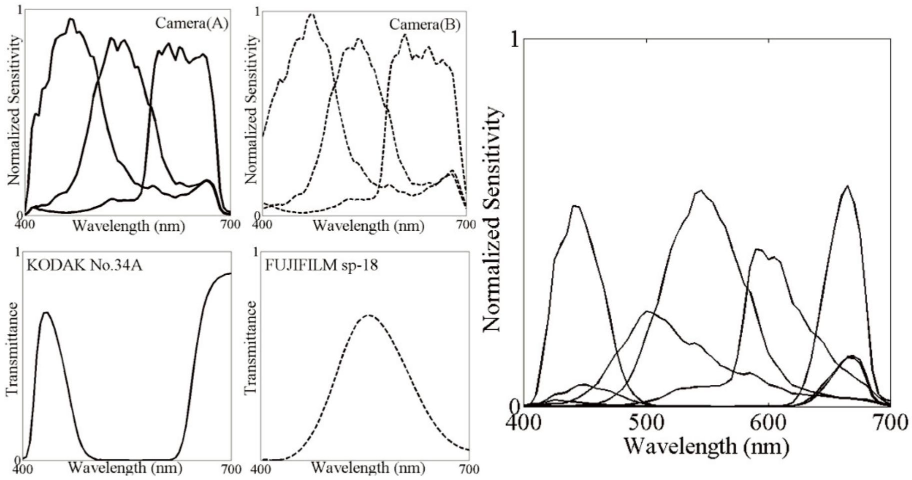

Figure 2: Spectral sensitivity functions spectral of the proposed six-band imaging system.

2.2 Image Synthesis

Figure 3 shows the flowchart for synthesizing a spectral gigapixel image of an omnidirectional scene. In our measurement system, we capture HDR images in 1260 directions (60 images in the horizontal plane and 21 images in the vertical plane). Each HDR image is generated by combining fifteen low dynamic range (LDR) images captured at 15 different exposure times.

Because the original images are captured using the stereo camera system, there is a disparity (displacement) between images captured using KODAK No.34A filter and Fujifilm SP-18 filter. Hence, we have to completely align the two images for the combined six-band images such that there is no registration error. We have implemented the Phase Only Correlation (POC) technique (Takita, 2003) for image registration.

Then, all captured images are transformed into the polar coordinate system (Szeliski, 1997) for representing the omnidirectional images. For synthesizing an omnidirectional image, we utilize a total of 1260 images. The use of the programmable rotating table allows us to control and record the horizontal and vertical directional angles of each captured image. In other words, the relative polar coordinates can be determined for the polar coordinate images. Then, we can simply synthesize an omnidirectional image from the 1260 polar coordinate images based on the recorded directional angles.

Finally, we recover the spectral images from the six-band images based on Wiener estimation technique (Hirai, 2012). The Wiener estimation is well known and widely utilized for recovering spectral information from noisy observations.

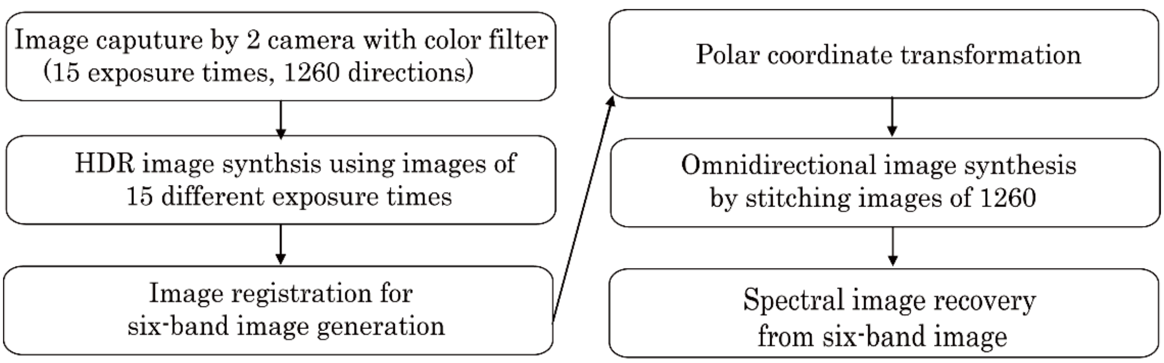

Figure 3: Flowchart for a spectral gigapixel image of an omnidirectional scene.

3. RESULTS AND DISCUSSION

Table 1 summarizes the performance of the proposed system. The six-band images are acquired using two color video cameras with two different types of color filters. In our image acquisition system, we require no filter exchange because we employ multiband imaging based on stereo one-shot technique. An omnidirectional image is synthesized from 1260 images. The pixel size is approximately 1.9 gigapixels. However, our system requires a higher acquisition time for capturing more than 1000 images.

Table 1. Summary of the configurations and performances of the proposed system.

Number of channels	Six-bands
Filter exchange	Not required
Multi-band technique	Stereo one-shot
Photographing direction	1260 directions: 60 horizontal and 21 vertical
Pixel size	Approx. 1.9 gigapixels (60000 × 32000)
Total acquisition time	Approx. 2 hour 17 min
Acquisition time for each directional image	Approx. 5 seconds (including both capturing and rotating processes)

For resolution comparison, we compare the proposed system with the conventional system (Hirai, 2014). Figure 4 shows the comparative rsults. The resolution of the conventional system is 7260 × 3630 pixels. The conventional system focuses on temporal resolution (acquisition time) rather than spatial resolutions, because the conventional system had been developed for acquiring time-lapse spectral images of omnidirectional natural scenes. As shown in Figure 4, we can see the details of distant objects.

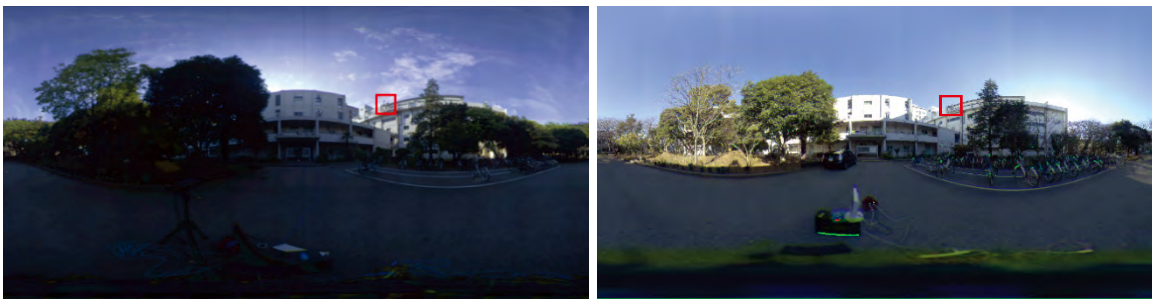

(a) Conventional system (7260×3630 pixels) *(b) Proposed system (60000 × 32000 pixels)*

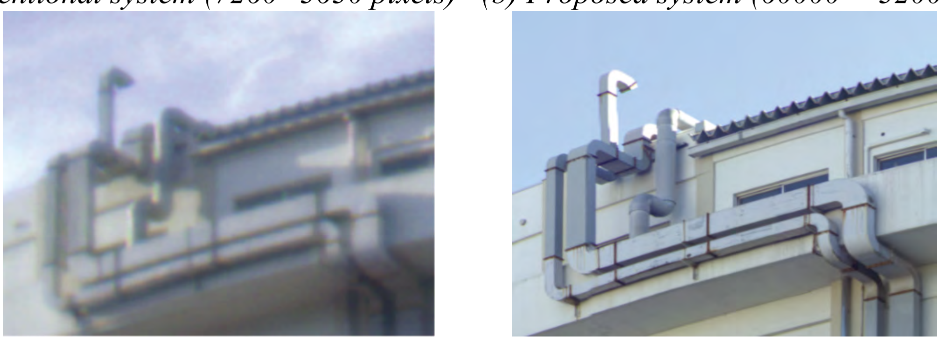

(c) Close-up of the red square in (a) *(d) Close-up of the red square in (b)*

Figure 4: Resolution comparison between the conventional and proposed system.

Next, for validating the accuracy of the recovered spectral power distributions, we compare the estimated results with the ground truth. In this experiment, we estimated spectra of X-rite ColorChecker under D65. The ground truth data was measured by a spectrophotometer. Figure 5 shows the estimation results of the spectral power distributions. The average normalized RMSE shown in Figure 5 is 0.0147, and the average ΔE is 1.315. The results show that the proposed system can estimate the spectral power distribution accurately. In addition, the proposed system has the ability to reproduce accurate color and spectra of omnidirectional scenes in high resolution.

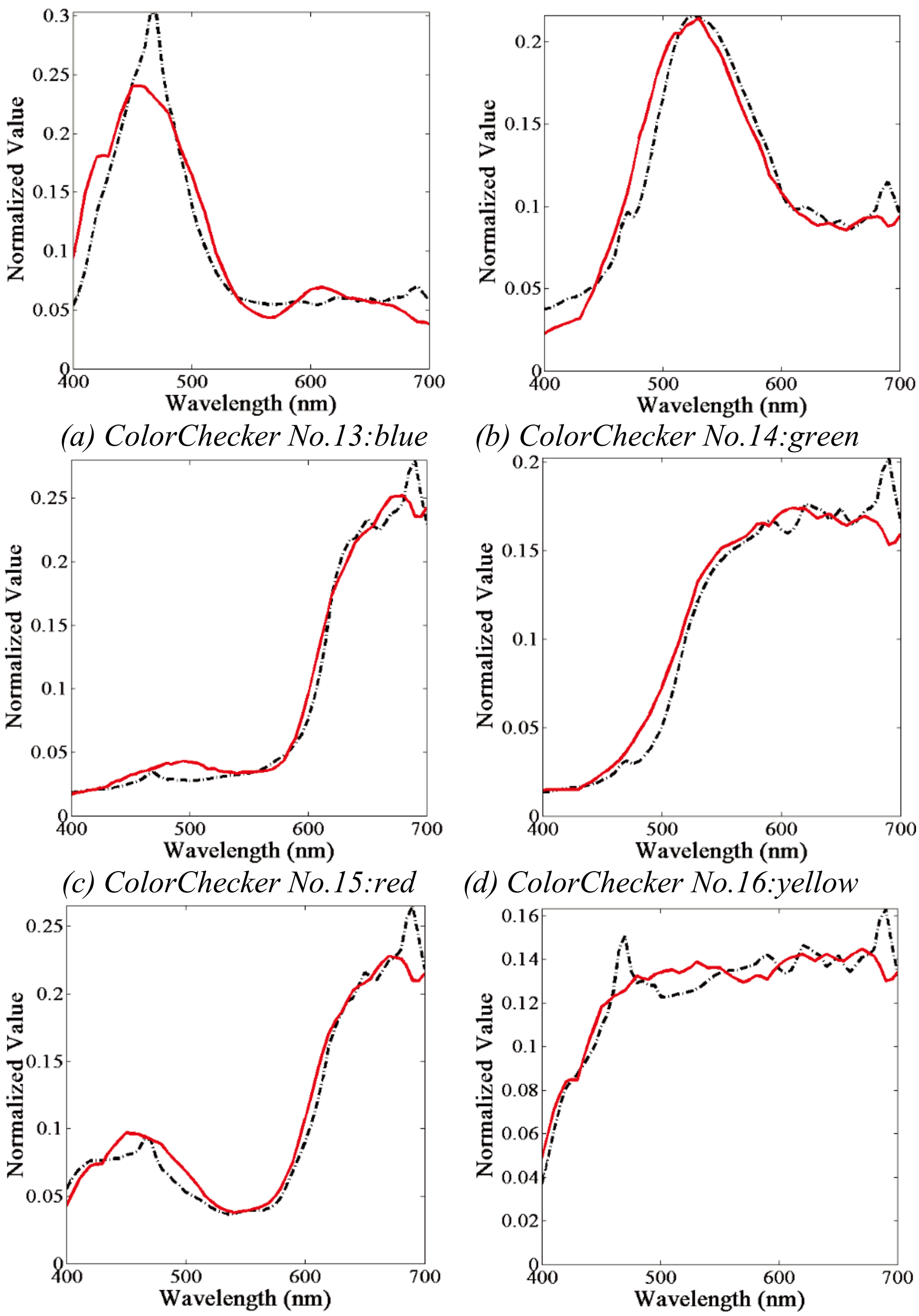

(a) ColorChecker No.13:blue *(b) ColorChecker No.14:green*

(c) ColorChecker No.15:red *(d) ColorChecker No.16:yellow*

(e) ColorChecker No.17:magenta *(f)ColorChecker No.19:white*

Figure 5: Estimation result of spectral power distributions of the selected six colors: blue, green, red, yellow, magenta, and white.(Red line : actual value , Black line : estimation)

4. CONCLUSIONS

This paper proposed a spectral gigapixel imaging system for omnidirectional outdoor scene measurement. The system was constructed using two programmable high-speed RGB video cameras with telephoto lenses and a programmable rotating table. Next, we generated gigapixel images from 1260 directional images. We also recovered spectral information from six-band images. As a result, an approximately 1.9 spectral gigapixel image of an omnidirectional scene was realized. We also showed the proposed system could accurately provide spectral power distributions of an omnidirectional scene (RMSE: 0.01427, ΔE: 1.315).

As future work, the acquisition time of the proposed system should be reduced. Another issue is the optimal color filter selection for acquiring accurate spectral information of an omnidirectional natural scene.

ACKNOWLEDGEMENTS

We would like to acknowledge the JSPS Grant-in-Aid for Young Scientists (B) No. 25730104 to partially support this work.

REFERENCES

Anguelov, D., C. Dulong, D. Filip, C. Frueh, S. Lafon, R. Lyon, A. Ogale, L. Vincent, and J. Weaver. 2010. Google Street View: Capturing the world at street level. *Computer*, 43(6):32-38.

Sakurada, K., T. Okatani, and K. Deguchi. 2013. Detecting Changes in 3D Structure of a Scene from Multi-view Images Captured by a Vehicle-mounted Camera. In *CVPR2013*, *Proceedings*, *26th IEEE CVPR*, 137-144.

Hale, S., and M. Stanney. 2015. *Handbook of Virtual Environments: Design, Implementation, and Applications, Second Edition*. Florida: CRC Press.

Szeliski, R. 2010. *Computer Vision: Algorithms and Applications. Texts in Computer Science*. Berlin: Springer Science & Business Media.

Point Grey Research. Ladybug5, http://wwx.ptgrey.com//Products/Ladybug5/. Accessed: February 27, 2015.

Gigapixel Panorama Photo, http://360gigapixels.com/petrin-prague-photo/. Accessed: February 27, 2015.

Hirai, K., N. Osawa, T. Horiuchi and S. Tominaga. 2014. An HDR Spectral Imaging System for Time-Varying Omnidirectional Scene. In *ICPR2014*, *Proceedings*, *22nd IEEE ICPR*, 2059-2064.

Takita, K., T. Aoki, Y. Sasaki, T. Higuchi and K. Kobayashi. 2003. High-accuracy Subpixel Image Registration based on Phase-only Correlation. *IEICE Trans. Fundamentals*, vol.E86-A, no.8, 1925-1934.

Szeliski, R., and H. Y. Shum. 1997. Creating Full View Panoramic Image Mosaics and Environment Maps. In *ACM SIGGRAPH 97*, 251-258.

Hirai, K., and S. Tominaga. 2012. A LUT-based Method for Recovering Color Signals from High Dynamic Range Images. *Proceedings*, *IS&T/SID's Twentieth CIC*. 88-93.

Address: Motoki Hori, Graduate School of Advanced Integration Science, Chiba University, Yayoi-cho 1-33, Inage-ku, Chiba, 263-8522, JAPAN
E-mails: aaca2805@chiba-u.jp, hirai@faculty.chiba-u.jp, horiuchi@faculty.chiba-u.jp

HANDHELD HYPERSPECTRAL IMAGING SYSTEM FOR THE DETECTION OF SKIN CANCER

Xana DELPUEYO,[1] Meritxell VILASECA,[1] Santiago ROYO,[1] Miguel ARES,[1] Ferran SANABRIA,[1] Jorge HERRERA,[1,2] Francisco J. BURGOS,[1] Jaume PUJOL,[1] Susana PUIG,[3] Giovanni PELLACANI,[4] Jorge VÁZQUEZ,[5] Giuseppe SOLOMITA,[6] Thierry BOSCH[7]

[1] Centre for Sensors, Instruments and Systems Development (CD6), Technical University of Catalonia (UPC), Terrassa, Spain.
[2] Instituto Tecnológico Metropolitano (ITM), Medellin, Colombia
[3] Hospital Clínic i Provincial de Barcelona, Barcelona, Spain
[4] Università di Modena e Reggio Emilia, Modena Italy
[5] Carril Instruments, S.L., Barcelona, Spain
[6] Mavig GmbH, Munich, Germany
[7] Institut National Polytechnique de Toulouse (INPT), France

ABSTRACT

Skin cancer detection is currently carried out using visual inspection through the dermoscope. Later, histological examination with a surgical extraction of the lesion is required for a complete and precise diagnosis. In this study, a new handled tool based on a hyperspectral system is proposed as a means of obtaining objective color and spectral information of the lesions to help in the diagnosis of skin cancer. The system includes light-emitting diodes (LEDs) as a light source as well as a digital camera. Preliminary images taken with the system and the corresponding results indicate the usefulness of the system. The prototype presented in this study will be integrated in the near future in a multiphotonic platform, including also 3D images, blood flow analysis and confocal microscopy, for in-vivo imaging of skin cancer lesions as a diagnosis service.

1. INTRODUCTION

Skin cancer represents one in three of all cancers worldwide and its incidence in Europe, USA and Australia is increasing rapidly. The melanoma, which only represents 4% of all skin cancers, is the most aggressive one causing the greatest number of deaths (Kuzmina et al., 2011). About 90% of skin cancers are caused by ultraviolet light from daylight or tanning booths. The World Health Organization estimates that 60,000 people die every year for sunlight excess: 48,000 from melanoma and 12,000 from another type of skin cancer. On the other hand, the survival rate in 5 years really increases if the pathology is detected and treated early.

Nowadays, visual inspection through the dermoscope is the technique most widely used by dermatologists for the detection of skin cancer. It consists of a handheld device with a magnifying lens and a white and uniform illumination field. The light is often polarized to remove specular reflection from the skin surface to obtain information of deeper layers. Dermoscopy allows the specialists identifying different structures, patterns and colors of the skin lesions suggesting if they are benign (seborrheic keratosis, haemangiomas, lipomas, warts) or malignant (melanoma, basal cell carcinoma). This is confirmed by a histological examination later on requiring a surgical extraction of the lesion, which is the gold standard for clinicians. By means of this procedure, a lot of false positives are still obtained and thus, the direct annual costs of diagnosis and treatment of skin cancer are high (Braun et al., 2005).

In order to improve the detection and diagnosis of skin cancer, in the last years color and spectral imaging technology have started to be used to enhance and analyze color and spectral properties of skin. They are caused by chromophores such as melanin, hemoglobin, water etc., which might differ among skin lesions of different etiologies.

In this context, some prototypes such as those developed by Spigulis et al. (Bekina et al., 2012), Kapsokalivas et al. (Kapsokalivas et al., 2013), and also some commercial devices such as the SIAscope V system (Emery et al., 2010), have already been proposed as a means of improving skin cancer diagnosis. However, most of them only use three spectral bands in the visible range (typically three colour RGB channels) and additionally another one located at the near infrared range.

For the reasons exposed above, in this study we propose a new handheld hyperspectral system with more spectral bands for the diagnosis of skin cancer, trying to improve the results obtained with the existing devices. In this work, we present the methodology carried out to setup and characterize the whole system, including the protocol followed in order to select the most suitable spectral bands to detect skin cancer lesions. Furthermore, the first results corresponding to real lesions analyzed at a clinical site are also presented. This work is within the framework of the European Project DIAGNOPTICS "Diagnosis of skin cancer using optics" (ICT PSP seventh call for proposals 2013), the aim of which is developing a multiphotonic platform including hyperspectral and 3D techniques, blood flow analysis and confocal microscopy for in-vivo imaging of skin cancer lesions as a diagnosis service (Ares et al., 2014). These technologies are envisaged to improve the detection ratio and the evaluation of the prognosis of skin cancer at earlier stages, compared with the conventional approach used nowadays.

2. METHOD

2.1 System design and components

The system developed has a cylindrical shape of about 10 cm in length, 7.5 cm of width and a weight of 0.5 kg. It includes a 12 bit-depth monochromatic camera and an objective lens, which allows recording skin lesions at 4 cm with a 15x20 mm field of view as their size is usually smaller.

A ring light source including light-emitting diodes (LEDs) with different spectral emissions within the visible and near infrared range (400 nm to 1000 nm) was designed to illuminate the sample. This illumination source was located onward of the objective lens to avoid the light of the LEDs reaching the sensor directly. The spectral bands of the system were chosen according to the spectral properties and absorption peaks of the skin chromophores and also taking into account market availability of LEDs. In order to obtain a uniform field of illumination on the sample and enough energy to acquire spectral images with low exposure times, 32 LEDs were finally included in the light source.

Moreover, two polarizers allow changing the degree of polarization of light and thus obtaining information from different skin depths. Specifically, the first polarizer is located in front of the LEDs and the second in front of the objective lens. Light polarization can be changed into 3 different positions: 0º - parallel polarizers, 45º and 90º - crossed polarizers.

The first prototype developed, which is a light, compact and ergonomic device to be used at a clinical site, is shown in Figure 1. The handheld hyperspectral head can be placed on a base between measurements, making all the procedure comfortable for the physician. Moreover, this base has also a storing function as the power supply and the electronic boards and other parts of the system are placed inside.

Figure 1: Different views of the handheld hyperspectral system.

Furthermore, the base also incorporates a calibrated sample resembling the light human skin that can be sheltered from external agents like dust by positioning it in the "in" and "out" positions (Figure 2). This sample is used in the preliminary calibration of the system that is done every day before starting measurements and that will be a key step when computing spectral results from the images acquired (see next section).

Figure 2: View of the base of the handheld hyperspectral system with the calibrated sample in the "out" and "in" positions, respectively.

2.2 Software development

A specific software was developed for controlling all components of the system (camera and LEDs), allowing for its proper operation. The software (Borland Builder C++) included autoexposure algorithms for adjusting the exposure time of each spectral band taking into account the LED emission level and also the typical reflectance and absorption properties of the skin. It also includes security controls avoiding LEDs to be switched on if the program is not running. A user interface was also developed for its use at a clinical site. A complete acquisition lasts 40 seconds approximately.

An additional software implemented in Matlab® was created to process all the images of the lesions. It included calibration algorithms as a means of computing reflectance values, chromaticity coordinates, colour differences etc., which might enhance subtle differences between benign and malignant lesions enabling a better diagnosis.

3. RESULTS AND DISCUSSION

Figure 3 shows spectral images obtained with the developed system corresponding to a common nevus lesion at different spectral bands between 400 nm and 1000 nm, and different degrees of polarization. As it can be seen, the degree of polarization allows removing the specular reflection of the skin surface (0º), obtaining information from deeper layers (90º), basically in the case of short (blue) wavelengths. This is important as for instance, melanomas can grow deeper than other lesions.

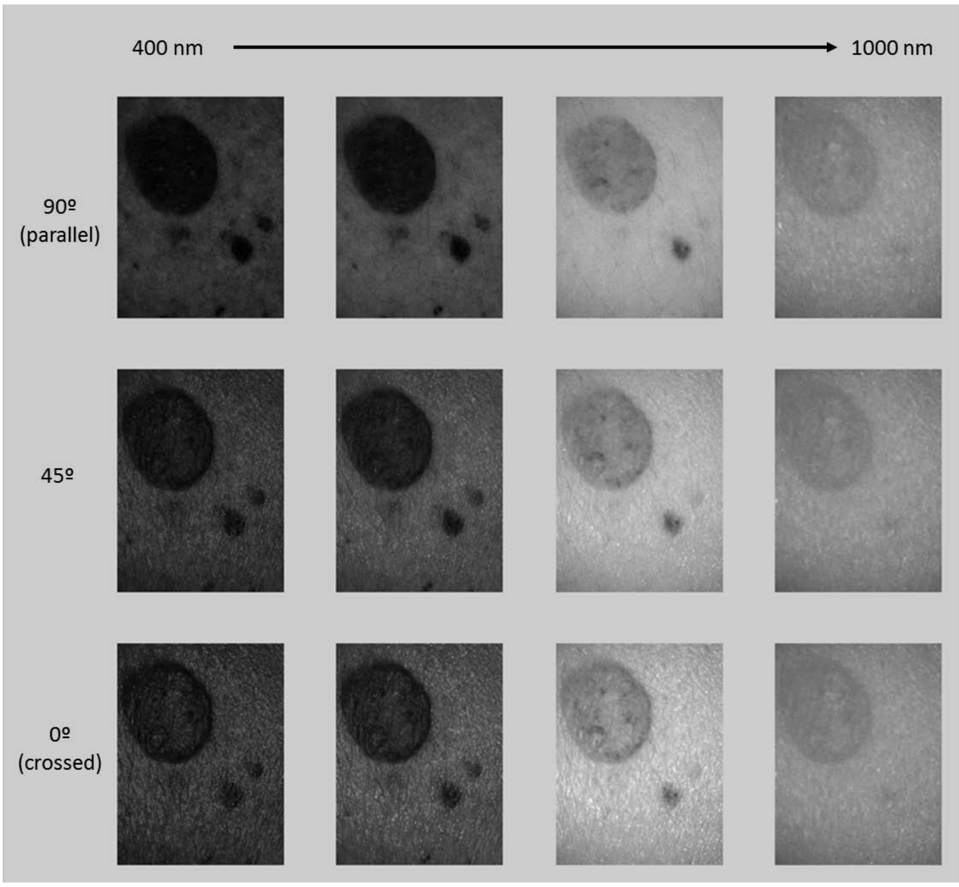

Figure 3: Images of a benign lesion (common nevus) obtained with the system using different spectral bands and three degrees of polarization (0º, 45º, 90º).

Figure 4 shows the spectral reflectance curves computed from two different areas of a skin sample: one corresponding to common skin and the other to a nevus. As it is shown the reflectance curves associated to each of them differ completely. As it was expected, nevus had lower reflectance values because its higher amount of melanin absorbs more light.

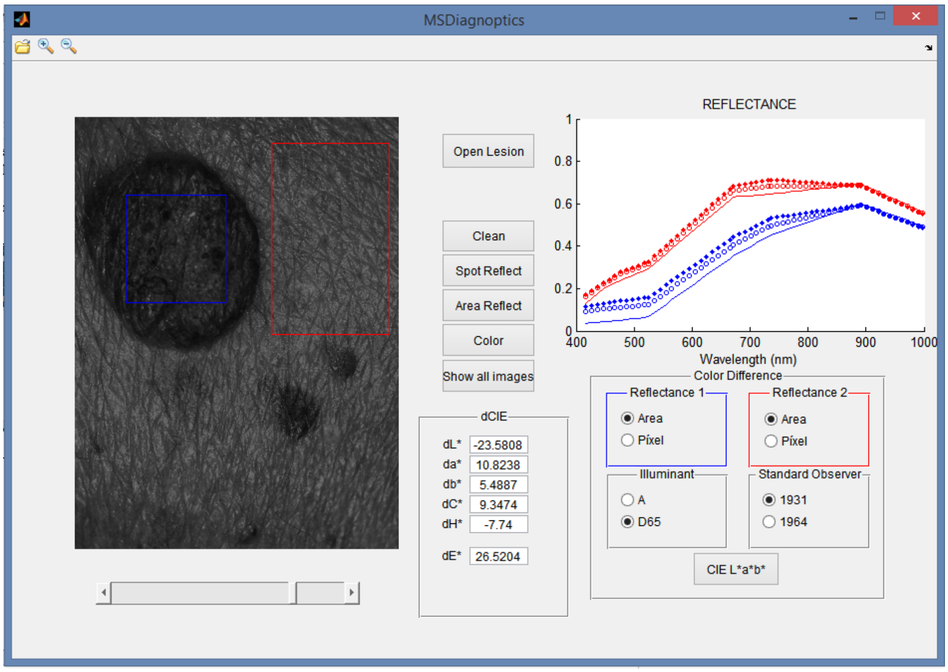

Figure 4: Spectral reflectance of common skin (red area) and common nevus (blue area)

4. CONCLUSIONS

In this study, a first prototype of a handheld hyperspectral system with several spectral bands in the visible and near infrared ranges of the electromagnetic spectrum for improving the diagnosis of skin cancer was presented. The developed system allows obtaining precise spectral information from the skin lesion analysed with a high spatial resolution in a fast and easy way. The use of LEDs as a light source enabled to build a system with reduced size and cost.

Current work is focused on the acquisition of images from a great variety of skin lesions in a clinical environment, including benign and malignant lesions (Hospital Clínic i Provincial de Barcelona, Spain), as well as the development of algorithms to obtain more reliable and objective diagnosis, helping dermatologists in their daily clinical practice. Skin lesions can be generally categorized according with their clinical presentation, taking into account different easily recognizable aspects, including from shape to colour. Therefore, it is expected that this last one will be a key in the diagnostic procedure as spectral reflectance profiles obtained with the new system will be related with the lesion etiology.

ACKNOWLEDGEMENTS

This research was supported by the European Commission of Research & Innovation under the grant DIAGNOPTICS "Diagnosis of skin cancer using optics" (ICT PSP seventh call for proposals 2013, 2014-2016).

REFERENCES

Ares, M., Royo, S., Vilaseca, M., Herrera, J.A., Delpueyo, X., Sanabria, F., 2014. Handheld 3D Scanning System for In-Vivo Imaging of Skin Cancer. In the 5th

International Conference on 3D Body Scanning Technologies, Proceedings, ed. by Hometrica Consulting. Switzerland: 231-236.

Bekina, A., Diebele, I., Rubins, U., Zaharans, J., Derjabo, A., Spigulis, J., 2012. *Multispectral assessment of skin malformations using a modified video-microscope,* Latvian Journal of Physics and Technical Sciences 49(5), 4-8.

Braun, R.P., Rabinovitz, H.S., Oliviero, M., Kopf, A.W., Saurat, J.H., 2005. *Dermoscopy of pigmented skin lesions,* Journal of the American Academy of Dermatology 77(2), 104-110.

Emery J.D., Hunter, J., Hall, P.N., Watson, A.J., Moncrieff, M., Walter, F.M., 2010. *Accuracy of SIAscopy for pigmented skin lesions encountered in primary care: development and validation of a new diagnostic algorithm,* BMC Dermatology, 10(9), 1:9.

Kapsokalyvas, D., Bruscino, N., Alfieri, D., de Giorgi, V., Cannarozzo, G., Cicchi, R., Massi, D., Pimpinelli, N., Pavone, F.S., 2013. *Spectral morphological analysis of skin lesions with a polarization multispectral dermoscope.* Optics express 21(4), 4826-40.

Kuzmina, I., Diebele, I., Jakovels, D., Spigulis, J., Valeine, L., Kapostinsh, J., Berzina, A., 2011. *Towards noncontact skin melanoma selection by multispectral imaging analyasis,* Biomedical Optics Express 16(6), 060502.

Address: MSc Xana Delpueyo,
Centre for Sensors, Instruments and Systems Development (CD6). Technical University of Catalonia (UPC), Rambla Sant Nebridi 10, Terrassa, 08222, SPAIN.
E-mails: xana.delpueyo@cd6.upc.edu, mvilasec@oo.upc.edu, santiago.royo@upc.edu

Empirical Disadvantages for Color-Deficient People

Joschua SIMON-LIEDTKE[1] and Ivar FARUP[1]
[1] The Norwegian Colour and Visual Computing Laboratory, Gjøvik University College

ABSTRACT

Trichromatic color vision in humans evolved most likely because it provides behavioral advantages in assisting attentional mechanisms, object recognition and, possibly, also detection of emotion states in other humans. Behavioral experiments, namely visual search and object recognition experiments, with normal-sighted observers have shown to support these hypotheses. We argue that the same types of experiments can be used to show that trichromacy does indeed give a behavioral, empirical measureable advantage before dichromacy or anomalous trichromacy by comparing behavioral responses of normal-sighted observers to color-deficient observers. More precisely, we suggest the use of visual search experiments to measure attentional responses, sample-to-match and object recognition tasks to measure objection recognition, and emotion detection to measure emotional responses. We furthermore implemented a visual search task to measure the performance of the attentional mechanism that showed that for the given experiment normal-sighted observers do indeed have an advantage over color-deficient observers.

1. INTRODUCTION

Trichromatic vision is based on the response of photosensitive receptors on the retina of the human eye, so-called *cones*, with sensibilities to light of different wavelengths. Color-deficient people typically have either reduced sensibility for one of the cones or lacking one of the cones altogether. Consequently, this will lead to a decreased ability of distinguishing certain colors. Color-deficient people truly encounter certain problems in daily life both in natural settings – for example when picking berries, determining whether a steak is raw or well-done etc–, and especially in social settings where color coding is heavily used in communication – for example when reading geographic and public transportation maps. More severely, they are excluded from certain professions that rely heavily on different colored signals, like pilots, train conductors etc. However, behavioral disadvantages of color-deficient people in natural and social settings is still only marginally researched. More specifically, two main questions remain: What is the behavioral advantage of trichromatic color vision in comparison to dichromatic color vision? And are there measurable behavioral differences between normal-sighted and color-deficient observers?

Studies suggest that color influences behavioral responses in the field of attention, object recognition, and interpretation of emotional states. Firstly, Treisman and Gelade (1980) proposed the feature-integration theory of attention stating that visual attention can be split up in a pre-attentive early state and a later stage. Color is used especially in the first stage to make elements “pop out” depending on their color contrast. Secondly, Bramão et al. (2012) suggested that colors helps to support object recognition at different states of visual processing. Thirdly, Changizi, Zhang, and Shimojo (2006) suggested that trichromatic color vision is used to better discriminate changes in skin spectra that arise to signal emotions, for example in socio-sexual contexts, and/or may indicate danger.

The previously mentioned research have in common that the hypotheses have been tested only on normal-sighted observers using both colored and black-and-white images showing that normal-sighted observers react faster and more accurate to colored than to black-and-white images. In this paper, we argue firstly that the same methodologies can be used to measure empirical differences between normal-sighted and color-deficient observers supporting the hypothesis that trichromatic color vision manifests an evolutionary advantage for attentional mechanism, object recognition and emotion detection over dichromatic or anomalous trichromatic vision. More precisely, we suggest the use of behavioral experiments involving visual search, object recognition, object identification, object class identification and emotion detection tasks for colored images to empirically measure disadvantages and advantages of color-deficient observers over normal-sighted observers. Secondly, we implemented a visual search experiment – the Visual Search Daltonization Evaluation Method (ViSDEM) – that is used to compare response times and accuracies for tasks involving the attentional mechanism of normal-sighted and color-deficient observers. We found out that color-deficient observers have indeed a slight behavioral disadvantage over normal-sighted observers.

2. BACKGROUND AND METHODOLOGY

Behavioral responses related to attention of trichromats, further called normal-sighted observers, and anomalous trichromats or dichromats, further called color-deficient observers, can be measured by visual search experiments as introduced by Treisman and Gelade (1980). In the basic implementations, the observer has to identify a target stimulus, like a symbol, object etc., among a number of distractors that differ in size, shape, color etc. In another experimentation design that we proposed (Simon-Liedtke, Farup and Laeng 2015), the observer is shown different natural images and a question/task related to the content of the image. The observer is then asked to answer as fast and as accurate as possible for each picture. For both experiments, response times (RTs) and accuracies (ACCs) of the answers are recorded, and analyzed by comparing RTs and ACCs of normal-sighted and color-deficient observers. We assume that according to our previously discussed hypothesis the normal-sighted observers will be able to respond faster and more accurately than the group of color-deficient observers.

Bramão et al. (2012) identified several object recognition experiments to access performance of color vision on object recognition. Images of different objects are shown to the observers, and the participant are asked to answer to certain questions. In the object verification task the observer has to state whether an object or a non-object is shown, in the category verification task the observer has to state whether the object is natural or artificial, and in the name verification task the observer has to state the correct name of the object. RTs of each observation were recorded and analyzed. We suggest implementing the same setup to compare performances of normal-sighted and color-deficient observers. Namely, we suggest the use of the object verification task, the category verification task, and the name verification tasks with colored objects, for which the RTs and ACCs are recorded. If our hypothesis about trichromatic vision is true, we assume that normal-sighted observers will be able to identify objects faster and more accurately than color-deficient observers.

The analysis of emotion detection through skin identification has to-date not yet been conducted. Thus, we propose an emotion detection experiment similar to the one that Adolphs *et al.* (2000) conducted based on the experiments to evaluate the universality of facial expressions proposed by Ekman (1999). Images of people imitating different facial expressions are shown to participants that are asked to name the emotional state that the expressions are meant to represent. Since the influence of emotion detection has to yet been analyzed to-date, the experimentation has to be conducted in two stages. In the first stage, normal-sighted and color-deficient observers are shown different images of facial expressions both colored and grayscale from males and females belonging to different emotion categories. In the second stage, only colored images are presented to both normal-sighted and color-deficient observers. For both stages we record the RTs and ACCs of the observations. If color vision in general and trichromatic color vision in particular facilitates emotion detection as expected, we expect, firstly, that observers in both groups will react faster and more accurate for the colored images than for the grayscale images, and, secondly, that for colored images normal-sighted observers will react faster and more accurate than color-deficient observers.

3. IMPLEMENTATION

To-date, we implemented a visual search experiment to analyze influence of color on attentional mechanism for normal-sighted and color-deficient observers: The method is originally designed to evaluate daltonization methods, and is called Visual Search Daltonization Evaluation Method (Simon-Liedtke, Farup and Laeng 2015). Fortunately, the results can also be interpreted in order to support for the previously discussed hypothesis that normal-sighted observers have a slight empirical measurable advantage to color-deficient observers. In our experiment, the observer looks at a range of images, for each of which we define certain tasks. The task consists of a statement, which the observer has to agree, respectively disagree to. The statement is connected to colors of objects, people etc. in the image like for example “The feather in the image has the same color hue as the background.” or “There is green powder in the image.” We conducted the experiment with 23 observers, of which 10 were normal-sighted and 13 deutan color-deficient, and we used 7 different sets of images. For more details on the implementation, please check our previous paper (Simon-Liedtke, Farup and Laeng 2015). We analyzed the confidence interval of the ACCs for both observer groups, and compared the medians of RTs for both groups according to a Mood’s median test.

4. RESULTS AND DISCUSSION

Figure 1 shows both RTs and ACCs of both normal-sighted and color-deficient observers. The median RT for the group of normal-sighted group is much lower than for the group of color-deficient observers. A Mood’s median test revealed a p-value of $4 \cdot 10^{-6}$ indicating that the medians of both populations are indeed significant different. The confidence interval (CI) of the ACCs for the group of normal-sighted observers is much higher than the CI of the ACCs for the group of color-deficient observers. Both observations agree with the assumptions we made prior to the experiment, namely that color-deficient people react less accurate and slower than normal-sighted observers. In other words, the results indicate that color-deficient people do indeed have behavioral disadvantages connected to their attentional system, and that these differences are indeed measureable with our proposed methodology based on visual search tasks.

5. CONCLUSIONS

We proposed a range of behavioral experiments through visual search, object identification and emotion detection tasks in order to test the hypothesis that trichromatic color vision provides evolutionary advantage for attention, object recognition and emotion detection. We suggest that color-deficient observers will respond slower, and less accurate to these tasks when compared to normal-sighted observers. Furthermore, we implemented a visual search experiment that shows that deutan color-deficient observers do indeed react slower and less accurate than color-deficient observers in a visual search experiment measuring attentional reactions.

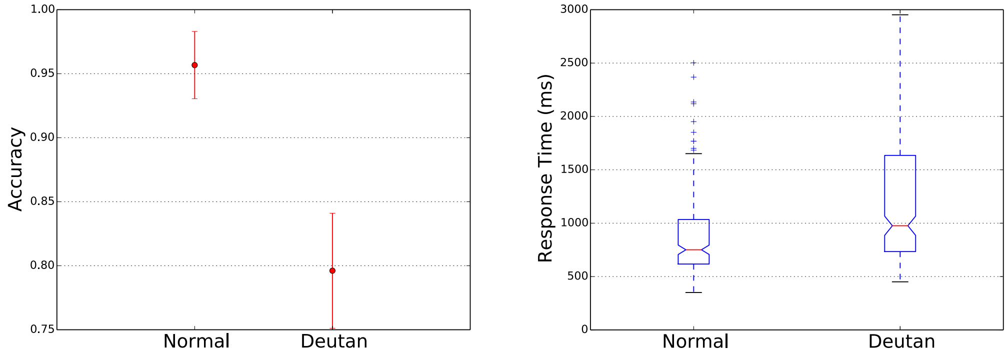

Figure 1: Accuracies (ACCs) and response times (RTs) of the visual search experiment for normal-sighted and deutan color-deficient observers indicating that color-deficient people do indeed react less fast and less accurate than normal-sighted observers. The median RTs of both groups are significant different according to the Mood median test.

ACKNOWLEDGEMENTS

We want to thank Prof. Bruno Laeng from the University of Oslo with his help in developping the behavioral experiments, and we also want to thank Kajsa Møllersen for her help in analyzing the data.

REFERENCES

Adolphs, Ralph, Hanna Damasio, Daniel Tranel, Greg Cooper, and Antonio R. Damasio. 2000. A role for somatosensory cortices in the visual recognition of emotion as revealed by three-dimensional lesion mapping. In *The Journal of Neuroscience*: 2683–2690.

Bramão, Inês, Luís Faísca, Karl Magnus Petersson, and Alexandra Reis. 2012. The Contribution of Color to Object Recognition. In *Advances in Object Recognition Systems*: 73–88.

Changizi, Mark A., Qiong Zhang, and Shinsuke Shimojo. 2006. Bare skin, blood and the evolution of primate colour vision. In *Biology letters*: 217–221.

Ekman, Paul. 1999. Facial expressions. In *Handbook of Cognition and Emotion*: 301–320.

Simon-Liedtke, Joschua T., Ivar Farup and Bruno Laeng. 2015. Evaluating color deficiency simulation and daltonization methods through visual search and sample-to-match: SaMSEM and ViSDEM. In *Proceedings of SPIE/IS&T Electronic Imaging 9395, Color Imaging XX: Displaying, Processing, Hardcopy, and Applications*. San Francisco, CA, USA.

Treisman, Anne M. and Garry Gelade. 1980. A feature-integration theory of attention. In *Cognitive Psychology*: 97–136.

Address: Joschua Thomas Simon-Liedtke, The Norwegian Colour and Visual Computing Laboratory, Gjøvik University College, Teknologivegen 22, 2815 Gjøvik, Norway
E-mails: joschua.simonliedtke@hig.no

Spectral reflectance recovery using natural neighbor interpolation with band-divided linear correction

Tzren-Ru Chou* and Tsung-Chieh Sun,
Dept. of Graphic Art and Communications,
National Taiwan Normal Univ., Taiwan, R.O.C

ABSTRACT

In this paper, we proposed an accurate recovery method of object spectral reflectance using the traditional natural neighbor interpolation, shortly named as NNI, with band-divided linear correction. Our method consists of two stages of recovery procedures. First, the NNI interpolation was used to construct the spectral reflectance from the real samples of color checkers. Secondly, the spectra resulting from NNI were further fine-tuned according to the difference between its sRGB color under illuminant of D_{65} and the original input one of ground true. Some experiments were performed to evaluate the performance of the proposed method. The 1269 checker spectra from Munsell book was used as the test samples under the training samples from Macbeth 24 color checkers. The largest color difference was 1.4869, and the average one was 0.0726. The experimental results showed that the proposed method was very accurate for the recovery of spectral reflectance.

1. INTRODUCTION

The purpose of this study is to obtain a precise estimation of the spectral reflectance. Essentially, such a recovery problem was usually to transform the RGB channel values into a spectrum to simulate the reflectance of an object. There were many previous works for the reconstruction of spectral reflectance, for instance, principle component analysis (PCA) (Fairman and Brill 2004), PCA modification (Lee et al. 2012), interpolation (Abed et al. 2009), such as hybrid methods (Kim et al. 2012), others like regression analysis (RA) (Harifi et al. 2008) (Amiri et al. 2014) or based on metamerism (Chou and Lin 2012).

PCA is a classical method for the reconstruction of spectral reflectances with good performance, but the value of estimation is out of the range from 0 to 1. This unnaturalness phenomenon may lead to an unexpected result during the reconstruction. On the other hand, the interpolation may establish more natural results (Amidror 2002), but could suffer from the extrapolation for the scatter data, such as the samples of color checkers. Further studies were needed to solve these shortcomings.

This paper proposed a new interpolation method with much more accuracy. The NNI was the basic reconstruction model. Eight additional pre-determined spectra were imposed for the corners of the sRGB color space to guarantee all the test samples in the gamut spanned by the known samples. And then, the traditional NNI were further fine-tuned according to the color difference under the illuminant of D_{65}. Three pre-specified wavelengths, denoted S, M, and L, were selected as the control points to adjust the spectral curve toward the correct direction.

The reminder of this paper is divided into three sections. Section 2 is our method in full details. Section 3 is our experiment results and discussion. Finally, the conclusions are drawn in Section 4.

2. METHOD

The method consists of two stages of the recovery procedures. First, the NNI interpolation was used to construct the spectral reflectance from the real samples of color checkers. Eight additional pre-determined spectra were imposed for the corners of the sRGB color space, named virtual extreme spectra, to guarantee all the test samples in the gamut spanned by the known samples (Figure 1).

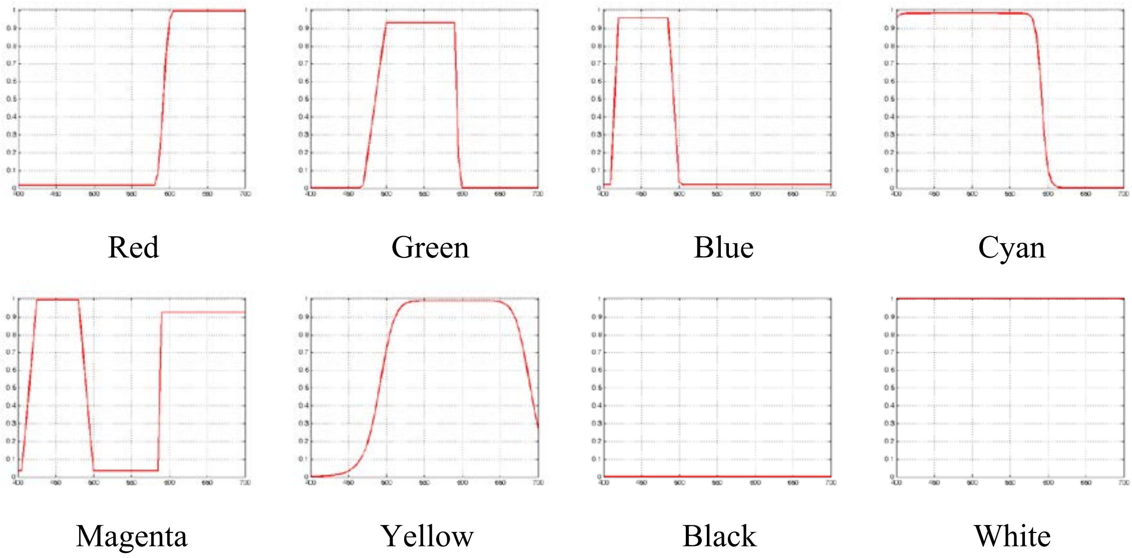

Figure 1: Eight additional pre-determined spectra

2.1 Method of natural neighbor interpolation

The natural neighbor interpolation developed by Robin Sibson is based on Voronoi tessellation of a discrete set of spatial points. In this method, the scattered points are used to form many tetrahedra in 3D space, and an interpolation model is performed within each tetrahedron (Amidror 2002). For example, we simulated a color x in the sRGB space to get the spectral reflectance. The x1, x2, and x3 in Figure 2 are the data of training samples with their RGB values are (255, 30, 30), (210, 150, 110), and (254, 200, 100), respectively. The color point x will be interpolated to the right place according to the RGB values as shown in Figure 2. The following diagram illustrates that the new Voronoi polygon is separated from the polygon formed by the neighbor color x1, x2, and x3. Then, the interpolating weight of x affected from each neighbor point can be determined according to the proportion of the partition volumes.

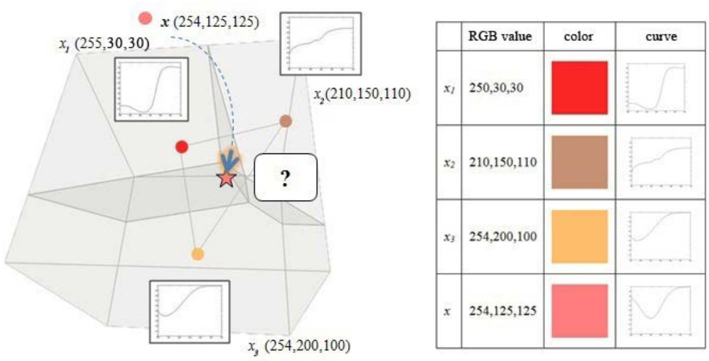

Figure 2: The interpolating model of NNI

2.2 Band-divided linear correction model

The spectra resulting from NNI were further fine-tuned according to the difference between its sRGB color under illuminant of D_{65} and the original input one of ground true. Three pre-specified wave lengths, denoted S, M, and L, were selected as the control points to correct this NNI spectrum approaching to a new one with less color difference. The x-axis values of three control points are 465nm, 550nm and 610nm, selected by the nearest dominant wavelength of blue, green and red in the sRGB gamut (Bergquist 2012). This correction was composed of 4 piecewise linear transformations related to 4 bands from 400nm to S, from S to M, from M to L, and from L to 700nm respectively as shown in Figure 3. We can get more accurate spectrum by solving the matrix as following equation (1). Equation (2) shows its expansion of the matrix form.

$$\begin{bmatrix} \Delta R \\ \Delta G \\ \Delta B \end{bmatrix} = \begin{bmatrix} c1 & c2 & c3 \\ c4 & c5 & c6 \\ c7 & c8 & c9 \end{bmatrix} * \begin{bmatrix} \Delta h_s \\ \Delta h_m \\ \Delta h_l \end{bmatrix} \qquad (1)$$

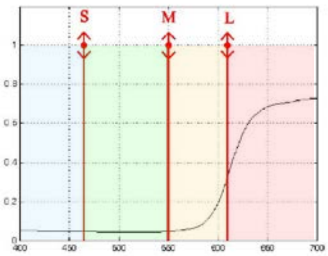

Figure 3: The L, M, and S control points

$$\begin{aligned} \Delta R &= c1 * \Delta h_s + c2 * \Delta h_m + c3 * \Delta h_l \\ \Delta G &= c4 * \Delta h_s + c5 * \Delta h_m + c6 * \Delta h_l \\ \Delta B &= c7 * \Delta h_s + c8 * \Delta h_m + c9 * \Delta h_l \end{aligned} \qquad (2)$$

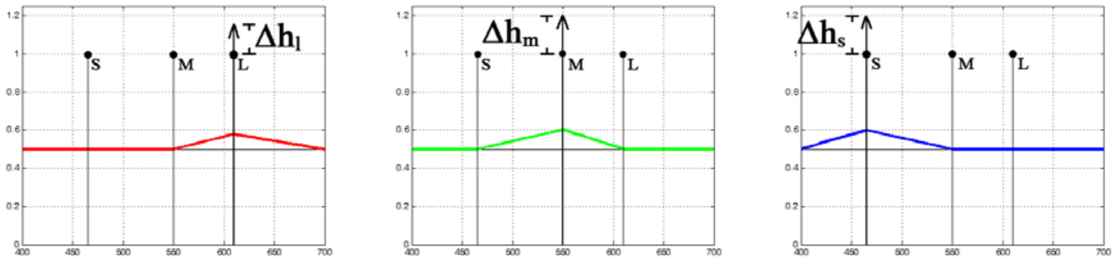

Figure 4 Changes of spectral curve after pulling the L, M and S control points

Figure 4 illustrates an example of the band-divided linear correction. Firstly, assuming the original spectrum is flat with its reflectance of 0.5, the control point L is pulled up of Δh_l. The Δh_l will lead to the linear transformation of the spectrum, denoted by the red line, during both bands from M to L, and from L to 700, with the change of ΔR about 0.0784.

The control points of M and S behave in the same manner, and are denoted by the green and blue lines in Figure 4, respectively.

The following presents the formulas for the correction of the spectra due to the changes of Δh_l, Δh_m, and Δh_s. The wavelength is represented by the discrete form of 61 values from 400nm to 700nm with the interval of 5nm. The linear correction is formed by 4 connected bands, from 400nm to S, from S to M, from M to L, and from L to 700nm.

1. If the x-axis value of point (x, p) is in the range between x-axis value of 400nm and S, the coordinate (x, p') on the spectral curve is calculated by equation (3) from the original one (x, p). $X_S - X_{400}$ means the separating distance between the control point S and (400nm, 1.0), that is, the point of the highest reflectance at 400nm.

$$\mathrm{p}' = p(1 + \Delta\mathrm{h}_s) * \frac{x}{X_S - X_{400}} \tag{3}$$

2. If the x-axis value of point (x, p) is in the range between x-axis value of S and M, the coordinate (x, p') on the spectral curve is calculated by equation (4) from the original one (x, p). $X_M - X_S$ means the separating distance between the control point S and M.

$$\mathrm{p}' = p(1 + \Delta\mathrm{h}_m) * \frac{x}{X_M - X_S} + p(1 + \Delta\mathrm{h}_s) * \frac{(X_M - X_S) - x}{X_M - X_S} \tag{4}$$

3. If the x-axis value of point (x, p) is in the range between x-axis value of M and L, the coordinate (x, p') on the spectral curve is calculated by equation (5) from the original one (x, p). $X_L - X_M$ means the separating distance between the control point M and L.

$$\mathrm{p}' = p(1 + \Delta\mathrm{h}_l) * \frac{x}{X_L - X_M} + p(1 + \Delta\mathrm{h}_m) * \frac{(X_L - X_M) - x}{X_L - X_M} \tag{5}$$

4. If the x-axis value of point (x, p) is in the range between x-axis value of L and 700nm, the coordinate (x, p') on the spectral curve is calculated by equation (6) from the original one (x, p). $X_{700} - X_L$ means the separating distance between the control point L and (700nm, 1.0), that is, the point of the highest reflectance at 700nm.

$$\mathrm{p}' = p(1 + \Delta\mathrm{h}_l) * \frac{(X_{700} - X_L) - x}{X_{700} - X_L} \tag{6}$$

2.3 Sample Preparation and Experimental Procedure

The simulating system was implemented in MATLAB® R2012 with Multi-Parametric Toolbox. The dataset consisting of 1269 spectra of Munsell book and 24 color samples of Macbeth color checkers with 8 sRGB extreme spectra were used in our experiments. All the reflectance data were fixed between 400 and 700nm of the interval of 5nm. The result of recovery spectra was evaluated by ΔE_{2000} color difference formula under illuminants D_{65} for CIE1931 standard observer. Figure 5 shows the experimental scheme.

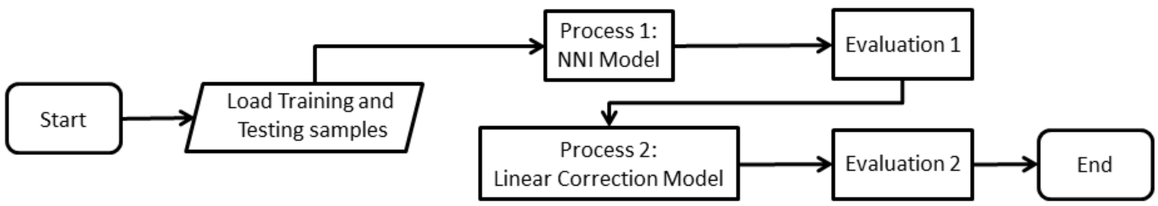

Figure 5: Flowchart of the experimental scheme

3. RESULTS AND DISCUSSION

Three experiments were performed to evaluate the performance of the new NNI with eight pre-defined spectra and the additional correction stage. At first, the 1269 checker spectra from Munsell book was used as the test samples under the training samples from Macbeth 24 color checkers. The largest color difference of ΔE_{2000} was 1.6366 based on the illuminant of D_{65}, and the average difference was 0.0915. And, the color differences were further improved, if the band-divided correction was adopted. Then, the largest ΔE_{2000} was 1.4869, and the average difference was 0.0726. In addition, the entire gamut of sRGB was also evaluated. The spectra recovered from the specified RGB channel values lead to the largest color difference was 1.6671 and the average one was 0.0315 under the illuminant of D_{65}, based on the training samples of Macbeth color checkers. The largest difference was 1.4915, and the average one was 0.0126, based on the training samples of Munsell book checkers. These experimental results showed that the proposed method was very accurate for the recovery of spectral reflectance.

4. CONCLUSIONS

In this paper, we proposed a new method to reconstruct the spectral reflectance of object. This new solution proposed not only gives more accurate results, but also avoids the extrapolation problem causing by the phenomena out of gamut. It is worth mentioning that our reconstructed reflectance ranges from 0 to 1, and it matches the phenomenon in the natural world. The method we proposed is successful to prevent the situation of improper data. Finally, the estimated spectral reflectance could be quite useful in various fields of color research, such as spectral camera designing, automatic white balancing, and digital lighting, etc.

REFERENCES

Amidror, I. 2002. Scattered data interpolation methods for electronic imaging systems: A survey. *Journal of Electronic Imaging, 11*(2): 157–176. doi: 10.1117/1.1455013

Abed, F.M., Amirshahi, S.H. and Abed, M.R. 2009. Reconstruction of reflectance data using an interpolation technique. *Journal of the Optical Society of America A, 26*(3): 613-624. doi: 10.1364/JOSAA.26.000613

Amiri, M.M. and Amirshahi, S.H. 2014. A hybrid of weighted regression and linear models for extraction of reflectance spectra from CIEXYZ tristimulus values. *Optical Review, 21*(6): 816-825.

Bergquist, J. 2012. Display with arbitrary primary spectra. *SID Symposium Digest of Technical Papers, 39*(1): 783-786. doi: 10.1889/1.3069786

Chou, T.R. and Lin, W.J. 2012. Optimal estimation of spectral reflectance based on metamerism. In *Proceeding of SPIE-IS&T Electronic Imaging 2012*, 8292, 829213-829213-10. doi: 10.1117/12.907606

Fairman, H.S. and Brill, M.H. 2004. The principal components of reflectances. *Color Research and Application, 29*(2): 104–110. doi: 10.1002/col.10230

Harifi, T., Amirshahi, S.H. and Agahian, F. 2008. Recovery of reflectance spectra from colorimetric data using principal component analysis embedded regression technique. *Optical Review, 15*(6): 302-308. doi: 10.1007/s10043-008-0049-1

Lee, M.H., Park, H., Ryu, I. and Park, J.I. 2012. Fast model-based multispectral imaging using nonnegative principal component analysis. *Optics Letters, 37*(11): 1937-1939.

Kim, B., Han, J. and Park, S. 2012. Spectral reflectivity recovery from the tristimulus values using a hybrid method. *Journal of the Optical Society of America A, 29*(12): 2612-2621. doi: 10.1364/JOSAA.29.002612

Munsell Color Science Laboratory. 2011. Useful Color Data. Available online, http://www.rit.edu/cos/colorscience/resources.php. Accessed: Oct 29, 2014.

University of Joensuu Color Group n.d. Spectral Database. Available online, https://www.uef.fi/fi/spectral/spectral-database. Accessed: Oct 29, 2014.

Address: Prof. Tzren-Ru Chou, Department of Graphic Art and Communications, National Taiwan Normal University, No.162, Sec. 1, Heping East Road., Taipei, Taiwan
E-mails: trchou@ntnu.edu.tw,

The research grant of the project is being sponsored by the Ministry of Science and Technology, R.O.C. (103-2221-E-003-012-)

Evaluation of gastrointestinal tissue oxygen saturation using LEDs and a photo detector

Yoshitaka MINAMI,[1] Takashi OHNISHI,[2] Koki KATO,[3]
Hiroyuki WASAKI,[3] Hiroshi KAWAHIRA,[2] Hideaki HANEISHI [2]
[1] Graduate School of Engineering, Chiba University
[2] Center for Frontier Medical Engineering, Chiba University
[3] Departure of Information and Computer Engineering,
Kisarazu National Collage of Technology

ABSTRACT

Accurate diagnosis of gastrointestinal viability in the reconstructive and resection surgery is strongly required to avoid anastomotic leak. Realization of quantification of gastrointestinal viability is really desirable. In this paper, we propose a method for estimating the tissue oxygen saturation (StO_2) of gastrointestinal organ using some LEDs in NIR region and a photo detector. We determine an organ absorbance model equation based on the Beer-Lambert law and estimate StO_2. However, the absorption coefficients of tissues in organs are unknown. First, we apply the nonnegative matrix factorization to the organ absorbance data obtained in advance to retrieve the absorption coefficients of each tissue. Furthermore, we define the band-based absorption coefficients that are suitable for emission characteristics of the LEDs to correct the error due to the LED bandwidth. Using the band-based absorbance coefficients, we re-defined the organ absorbance model equation. Then we estimate concentrations of organ tissues and calculate StO_2 by the ratio of oxygenated hemoglobin concentration and de-oxygenated hemoglobin concentration. Using transmittance spectra obtained in animal experiments, we simulated the performance of the proposed method and found that good estimation results will be obtained.

1. INTRODUCTION

Anastomotic leak leads to prolongation of hospitalization and increases postoperative morbidity, resulting in the increase of patient burden. Thus, correct determination of gastrointestinal viability at the time of anastomosis is very important. The determination is performed by visual inspection of surgeon now (Murai et al, 2013). However, the criterion of determination is neither quantified nor unified. Therefore, a quantitative method for viability determination of intraoperative organ is required (Urbanavicius et al, 2011).

As one of the quantification methods for organ viability determination, pulse oximeter is prevalent (La Hei et al, 2001). It can measure the oxygen saturation in artery blood. The measured value is sometimes expressed as SpO_2 because it utilizes pulsation. In contrast, it cannot measure that in veins and microcirculations that have no strong pulsation. Thus, the pulse oximeter is not suitable for evaluating viability of distal gastrointestinal organ.

In MCS2014, we presented a method for estimating the tissue oxygen saturation (StO_2) of gastrointestinal organ by near infrared (NIR) region spectroscopy. We performed animal experiments and obtained successful estimation results. However, a bulky setup for measurement is not suitable for clinical use.

In this paper, we investigated the feasibility of a more compact setup using several spectral bands of LEDs in NIR region and a photo detector. We first constructed a method, then predicted the performance of the proposed setup through computer simulation using transmittance spectra obtained in animal experiments.

2. METHOD

2.1 Outline

We build an organ absorbance model equation based on the Beer-Lambert law and estimate StO_2 by calculating the ratio of concentrations between oxygenated hemoglobin (HbO_2) and de-oxygenated hemoglobin (Hb). However, there are various light-absorbing materials other than blood in organs. Therefore, a model equation considering their influences is required. Thus, we model organ absorbance $A_{\text{spectral}}(\lambda)$ using absorption coefficients $\varepsilon(\lambda)$ and amounts C as

$$A_{\text{spectral}}(\lambda) = \varepsilon_{\text{HbO}_2}(\lambda)C_{\text{HbO}_2} + \varepsilon_{\text{Hb}}(\lambda)C_{\text{Hb}} + \varepsilon_{\text{other}}(\lambda)C_{\text{other}} \,. \tag{1}$$

Here, $\varepsilon_{\text{other}}(\lambda)C_{\text{other}}$ represents the influences of scattering and/or absorption by tissue other than blood. Spectral characteristics of the third term, $\varepsilon_{\text{other}}(\lambda)$, are unknown although oxygenated and de-oxygenated hemoglobin absorption coefficients, $\varepsilon_{\text{HbO2}}(\lambda)$ and $\varepsilon_{\text{Hb}}(\lambda)$, are already known.

Futhermore, as we assume to use several specral band of LEDs, we need to modify the wavelenth based model given by Eq. (1). In the proposed method, StO_2 is estimated as show in Fig. 1. In the preparation step, the absorption coefficients for LED wavelengh bands are estimated using the specral data. This is performed only once. In the intraoperative step, StO_2 is intraoperatively estimated using measured absorbance.

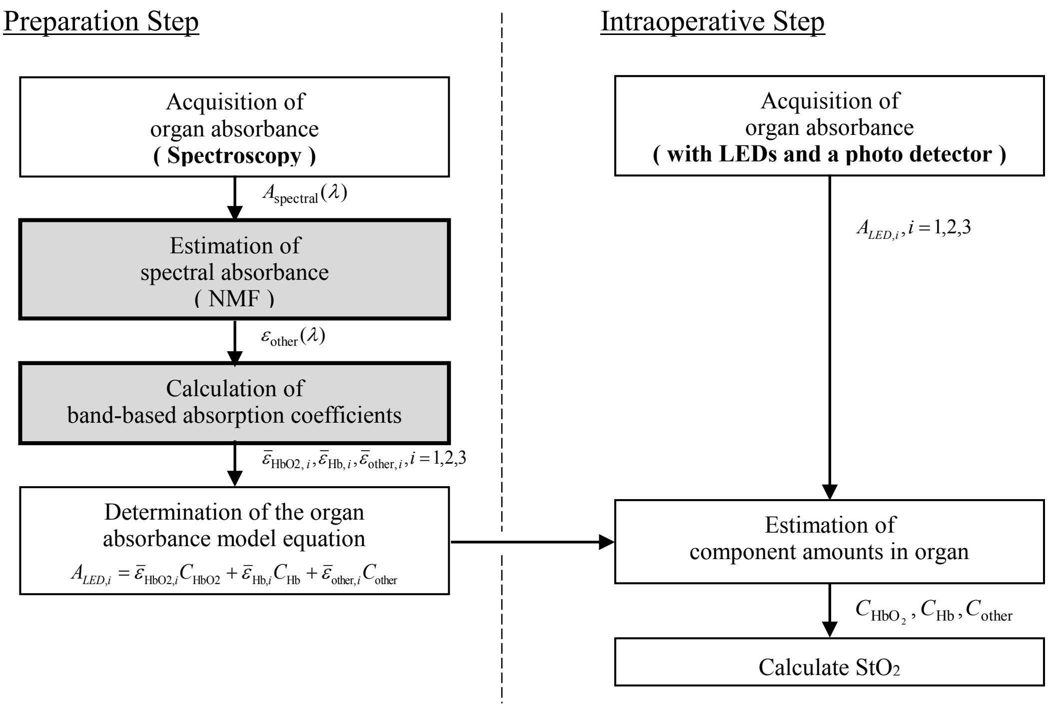

Figure 1: Flowchart of the proposed method.

2.2 Details of each step

As mentioned above, a simple system using LEDs can not use the wavelngth based model given by Eq. (1). In the preparation step, first of all, the spectral transmittance are measured. Then absorption coefficients $\varepsilon(\lambda)$ and amounts C are estimated. Then, using the amounts C, known spectral emittance of LED, spectral sensitivity of the sensor, the absorbtion coefficients for LEDs are calculated. In the intraoperative step, a simple matrix operation output the amounts C from the obained data. Detailed procesdure is given below.

(1) *Estimateion of spectral absorbance*

In the preparation step, we obtain the n transmittance spectra in advance and calculate absorbance by Eq. (2).

$$A^{(k)}(\lambda) = -\log\{T^{(k)}(\lambda)\},\ k = 1,...,n\ . \tag{2}$$

Here, $A^{(k)}(\lambda)$ and $T^{(k)}(\lambda)$ represent k-th absorbance and transmittance, respectively. Using these learning data, we estimate $\varepsilon_{\text{other}}(\lambda)$ by nonnegative matrix factorization (NMF) (Lee et al, 1999, 2001) that is a kind of blind source separation method.

NMF represents a given matrix by a weighted sum of two nonnegative matrices. We decompose the absorbance matrix **A** into two nonnegative matrices, **C** and **E**, as

$$\mathbf{A} = \mathbf{CE}\ . \tag{3}$$

Here **C** and **E** correspond to the amount of components for each subject and absorption coefficients of components in organs, respectively (Galeano et al, 2013) (Pauca et al, 2006). We call **C** and **E** as amount matrix and absorption coefficient matrix, respectively. Fig. 2 shows a schematic diagram of NMF. We use absorption coefficients of oxygenated and de-oxygenated hemoglobin as the known information. Separation number is three in this time. Thus we obtain the absorption coefficients and the amounts of each component from the learning organ absorbances.

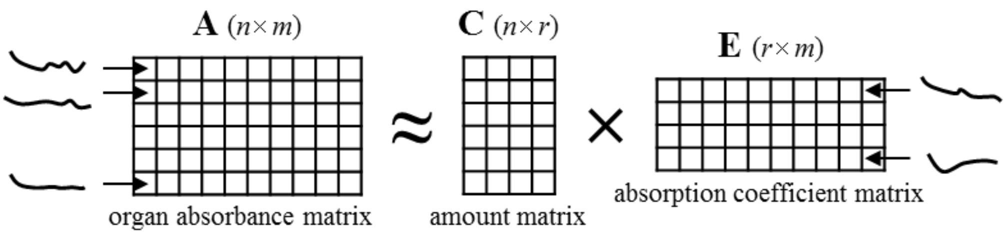

Figure 2: Schematic diagram of NMF.

(2) *Calculation of band-based absorption coefficients*

We assume a band-based model similar to Eq. (1) as

$$A_{\text{LED},i} = \bar{\varepsilon}_{\text{HbO}_2,i}C_{\text{HbO}_2} + \bar{\varepsilon}_{\text{Hb},i}C_{\text{Hb}} + \bar{\varepsilon}_{\text{other},i}C_{\text{other}},\quad i = 1,...,m\ . \tag{4}$$

Here, $A_{\text{LED},i}$ and $\bar{\varepsilon}_i$ represent the absorbance measured by i-th LED and a photo detector and the band-based absorption coefficients, respectively.

Absorbance of kth sample measured with i-th LED and the photo detector, $A^{(k)}_{LED,i}$ is represented as

$$A_{LED,i}^{(k)} = -\log \frac{\int_\lambda I_{LED,i}(\lambda) \times T^{(k)}(\lambda) \times S(\lambda) d\lambda}{\int_\lambda I_{LED,i}(\lambda) \times S(\lambda) d\lambda}, \ k = 1,\ldots,n, \ i = 1,\ldots,m . \quad (5)$$

Here, $I_{LED,i}(\lambda)$ and $S(\lambda)$ represent the spectral emission charactersitic of *i*-th LED and the spectral sensitivity of the sensor, respectively. These functions are assumed to be known. $T^{(k)}(\lambda)$ represents the transmittance spectra of *k*-th sample organ measured in the preoperative step. So $A_{LED,i}^{(k)}$ can be calculated.

Since we have $\{A_{LED,i}^{(k)}\}$ and the amounts $\{C_{HbO2}^{(k)}, C_{Hb}^{(k)}, C_{other}^{(k)}\}$ now, we represent Eq. (4) as a matrix form as

$$\mathbf{A}_{\mathrm{LED}} = \mathbf{C}\overline{\mathbf{E}} . \quad (6)$$

Here, $\overline{\mathbf{E}}$ represents the band-based absorption coefficient matrix.

Using simulated absorbance $\mathbf{A}_{\mathrm{LED}}$ and amounts of each component $\mathbf{C}$ calculated by NMF, we estimate $\overline{\mathbf{E}}$ as

$$\overline{\mathbf{E}} = \mathbf{C}^{+}\mathbf{A}_{\mathrm{LED}} . \quad (7)$$

Here, $\mathbf{C}^{+}$ represents a pseudo inverse matrix of $\mathbf{C}$.

The intraoperative step is conducted as follows. If the number of LED bands m=3, $\overline{\mathbf{E}}$ becomes a 3x3 matrix. So by multiplying the simple inverse matrix by the measured three values, the amounts of three components are obtained. If there are more than three LED bands, a least square method is applied to dermine C_{HbO2}, C_{Hb} and C_{other}. Then, we estimate the StO_2 by the ratio of obtained C_{HbO2} and C_{Hb}.

3. SIMULATION EXPERIMENTS & RESULTS

In this paper, we simulated the performance of the proposed method using transmittance spectra of swine small intestines. Using Eq. (5), we simulated absorbances obtained with three LEDs and a photo detector intraoperatively, and estimated StO_2 by applying proposed method. As a light emitting device, we assumed three LEDs made by Revox Inc. that have peak at 630, 690, 890 nm, and with a full width at half maximum (FWHM) of 20, 25, 45 nm, respectively. A photo detector made by Hamamatsu Photonics K. K. was assumed as a light receiving device.

3.1 Material

We measured small intestine absorbances of swine from 600 to 950 nm at 5 nm intervals. The measurement experiments were performed with prototype probe that consists of a compact spectrometer and a halogen light. Fig. 3 shows representative photos and some absorbances taken during the animal experiments.

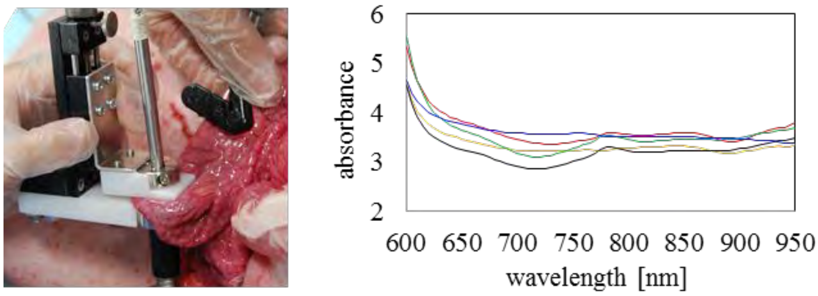

(a) (b)

Figure 3: (a) Represent photo of animal experiment.
(b) Some examples of obtained spectra data.

We have three kinds of measurement data. First one is for determination of the model equation. We have 32 spectra. Second one is for comparison with pulse oximeter. As a reference value, we measured oxygen saturation with a pulse oximeter. The measurement is performed in large vessel region of small intestine that had pulsation. We have 29 spectra and reference values. Last one is for evaluation of changes in the blood circulation state. We ligated the small intestine and created a poor blood circulation state. Thereafter we continued to obtain transmittance spectra of five intestines for three minutes at 20-second intervals after ligation.

3.2 Results

Fig. 4 shows StO_2 estimation results where (a) and (b) show comparison with reference value and StO_2 reduction for ligated intestines, respectively. In the comparison with pulse oximeter value, StO_2 was estimated with 2.4 % of average error and 8.4 % of maximum error, and we confirmed the linearity between estimated value and pulse oximeter value. Then, the capability of StO_2 estimation for various blood circulation state was confirmed. Furthermore, we confirmed the decrease of StO_2 with elapsed time after ligation for all time-dependent absorbance data of ligated intestines. From these experiments, the possibility of StO_2 monitoring in intraoperative organ was suggested by our proposed method using the simple setup.

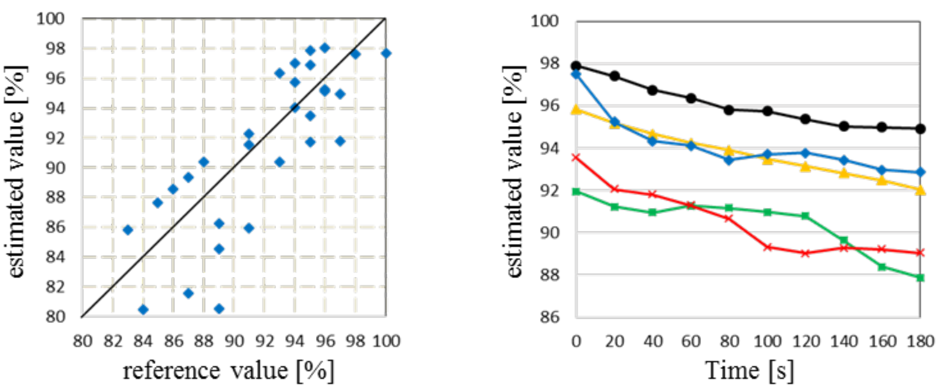

(a) (b)

Figure 4: (a) Comparison with pulse oximeter. (b) Estimation results to ligated intestines.

5. CONCLUSIONS

We proposed a StO_2 estimation method of intraoperative organ using a simple setup with some LEDs and a photo detector, and simulated the performance of the proposed method using spectra absorbance of swine small intestines. We confirmed the linearity between estimated value and reference value measured with a pulse oximeter, and achieved average error 2.7 %, maximum error 8.4 %. In the estimation experiment of ligated intestines, the reduction of StO_2 due to ligation was evaluated by our proposed method. Thereby, the possibility of StO_2 monitoring for intraoperative organs with a simple setup using three LEDs and a photo detector is suggested.

As a future work, we will prototype an actual equipment and evaluate our proposed method by applying to more swine small intestines in various blood circulation state.

ACKNOWLEDGEMENTS

This research was supported by KAKENHI, the Grant-in-Aid for Scientific Research B 25282151 and the Chiba University COE start-up program.

REFERENCES

Murai, K., H. Kawahira, and H. Haneishi. 2013. Improving color appearance of organ in surgery by optimally designed LED illuminant. *IFMBE Proc*. 39: 1010-1013.

Urbanavicius, L., P. Pattyn, D.V. Putte, and D. Venskutonis. 2011. How to assess intestinal viability during surgery: A review of techniques. *World J Gastrointest Surg.* 3(5): 59-69

La Hei, E.R. and A. Shun. 2001. Intra-operative plus oximetry can help determine intestinal viability. *Pediatric Surg. Int.* 17: 120-121

Lee, D.D., and H.S. Seung. 1999. Learning the parts of objects by nonnegative matrix factorization. *Nature* 401: 788–791

Lee, D.D., and H.S. Seung. 2001. Algorithms for non-negative matrix factorization. *Adv. Neural Process.*

Galeano, J., R. Jolivot, F. Marzani, and Y. Benezeth. 2013. Unmixing of human skin optical reflectance maps by Non-negative Matrix Factorization algorithm. *Biomedical Signal Processing and Control* 8: 169– 175

Pauca, V.P., J. Piper, and R.J. Plemmons, 2006. Nonnegative matrix factorization for spectral data analysis. Linear Algebra and Its Applications 416: 29–47

Address: Mr. Yoshitaka MINAMI, Graduate School of Engineering,
Chiba University, 1-33 Yayoi-cho, Inage-ku, Chiba, 263-8522 JAPAN
E-mails: y_minami@chiba-u.jp, t-ohnishi@chiba-u.jp, k.kato1060@gmail.com,
wasaki@j.kisarazu.ac.jp, {hk, haneishi}@faculty.chiba-u.jp

Proceedings

Poster Papers

COLOUR IMAGE, FASHION DESIGN AND IDENTITY

Dr. Larissa NOURY, Paris, France
«Couleur-Espace-Culture» / «Colour-Space-Culture»

The Colour, Art and Fashion design concerns the Harmonies of color associations of textile and other materials used for couturier’s aesthetic project. It is an illustration of collaboration of artists and couturiers on the harmonies of color associations in order to create a personal style and marque or brand identity. They were more closely tied at the turn of the 20th century than they are today. Artists did not see the difference between creating an original work of art, such as a painting, and designing a textile pattern that would be reproduced many times over. Each was a valid creative act in their eyes. There are a lot of vivid illustrations of the centuries-long love affair between fashion and art of color.

Fashion and identity

Beginning from the 19th century major changes both emerge in the role of fashion and in the place of art in society. Growing affluence and new social structures gradually turned both fashion design and art of color into ways of expressing personal taste and identity.

Our study raises a historic panorama of the colour in the fashion design during the XXth century, highlighting certain symbolic movements such as the Art nouveau, the Russian avant-garde, the modernism, pop art or the kinetic art. It lists the colour's harmonies for modern fashion design and describes the tools, ranges, palettes, techniques which allow personalizing a dress with fantasy and subtlety.

Art has often been a major source of inspiration for dress designers of XXth century: we remind some creations by Paul Poiret, Sonia Delaunay, Liza Schiaparelli, Coco Chanel, Yves Saint Laurent and Givenchy. In their practice art of color is in fashion image.

This connection between art and fashion is obvious from the end of XIXth century. Nowadays, the collaboration between artists and fashion designers continues. The personal artist’s inspiration of French colorist Larissa Noury comes from her own color harmonies of tactile painting, from within. Jean Marie Pujol, couturier who worked with Dior and Yves Saint Laurent at the time, designed several dresses to be painted by coloriste and designer Larissa Noury. Their unique collection of painted dresses means to perpetuate the art and fashion marriage in order to create an original color image.

Belle époque / Belle Epoch

The synthesis of practical considerations and of an aesthetic natural forms and lines is characterized by colour palettes of great richness. Modern times influences a great deal the development of fashion design and produced a profusion of the polychromy in it.

The large selection of paintings by Claude Monet and Pierre-August Renoir, Giovanni Boldini, Auguste Toulmouche, James Tissot, Jean Beraud and Alfred Stevens, – visual artists, who reflected the best on the fashion style of Belle Epoch, – is an example of what could be called fashion inspiration in fine arts. Artworks were created in realistic manner and do not have even a touch of stylization typical of modern art. Figures depicted in these paintings are precise and realistic. However, it would be fair to say that style itself is the subject matter instead of a particular model. Fashion is the main theme and inspiration for these paintings.

After a visit to the workshop in Vienna the avant-garde fashion designer Paul Poiret combined the idea of mixing art and fashion in his Parisian practice. He opened a Martine school (1911), a place which was also attractive for artists. He then employed Parisian artists such as Lepape, Ibibe, and Erte for fashion illustrations. He employed the artist Raoul Duffy to design fabric prints and to invent tissues. He went to art galleries and showed his artistic sensibilities by preferring Impressionist paintings at a time when they were new and unappreciated by the public. Poiret became very interested in modern art and said, "I have always liked painters. It seems to me that we are in the same trade and that they are my colleagues." The couturier considered himself firstly as an artist.

Russian constructivisme & suprematisme

The Russian avant-gard in Art and Design (1915-35) deserves to be mentioned. The word "revolution" has become a slogan for fashion design as well. The Russian constructivists defined the chromatic surfaces as fundamental coloured elements where the straight lines, the rectangular forms, the principal colors (yellow, red, blue, black and the white) are used to make a unified and inexistent on Nature composition.

Varvara Stepanova, Alexandre Rodchenko, Liubov Popova and others show their creativity through re-energizing new forms and meaning in art and dress design. The strong and independent colour, the uniformity of geometrical shapes and the lack of forces of gravity, - all those elements forms a kind of representation of an ideal cosmos. The key fragments of Russian revolutionary creativity still glow like radium, living on futuristic art and design into the imaginations of some most influential couturiers of the 20th and 21st century's. Christian Dior's Haute Couture was inspired by Malevich's painting in 2002.

Simultaneous Contrasts & Sonia Delaunay.

In the 1920s, abstract painting inspired a variety of fabric designs by successful designer and artist Sonia Delaunay. Married to Robert Delaunay and a close friend with artists like Mondrian, Arp, Vantongerloo and Kandinsky, she was a member of the contemporary artistic avant-garde in her own right. It was her own abstract paintings that she translated into rhythmic designs composed of squares, lines, circles, diagonals and colour planes. In all, Delaunay created over 2,000 of these fabric designs, around 200 of them produced especially for fashion house Metz & Co in Amsterdam.

Surrealism & Elsa Schiaparelli

Fashion designer Elsa Schiaparelli, Coco Chanel's main rival in the 1920s and '30s, produced clothing and hats heavily influenced by Surrealism. Her sweaters incorporating knitted ties or sailor collars were a sensation and she worked in close cooperation with artists like Salvador Dalí and Jean Cocteau. An example of her work with Dalí is her famous lobster dress and the original design of the very imaginative patterns such as the 'shoe hat' and surrealistic shoes and gloves. Dali said: **"Surrealism is destructive, but it destroys only what it considers to be shackles limiting our vision".**

Art deco & Coco Chanel

The designer's passionate interests inspired her fashions. Her apartment and her clothing followed her favorite color palette, shades of beige, black, and white, which composes a bases for style of art deco. Elements from art deco design, her art collection and even theatrical interests provided themes for her collections. The ornament of the dress, in both pattern and color palette, resembles the Asian lacquered screens which the designer loved and collected. The convergence of Art Deco line, the modernist impulse was married with pure form and Japanese’s potential.

Art of Neoplasticism

Piet Mondrian changed the face of modern art. His influence extends to painting, sculpture, graphic design, and fashion. In search of plastic harmony he introduced a universal language of shapes and primary colors that goes beyond the painting, Mondrian was the central figure and the most famous of the De Stijl movement. This style was baptized as neoplasticism and intended to achieve real objectivity by releasing the work of art from its dependence on the momentary individual perception and temperament of the artist. Yves Saint Laurent has created his famous dress with Mondrian’s colour composition.

Yves Saint Laurent, Diane Von Furstenberg, Nike, Moschino, Kara Ross, Christian Louboutin, Vans also used the codes of Neoplasticism. They proclaimed a new polychrome design "neo-plastician" who applies sharp and pure colors in their achievements. They intend to propose a theory of a relationship between design and painting, like "a place of modern painting in architecture". Théo van Doesburg defined the chromatic surfaces coloured as fundamental elements where the straight lines, the rectangular shapes, the principal colors (yellow, red, blue, black and the white) are used to make a unified composition.

In the 1950s, **Mrs Carven** produced a special designs dresses inspired by Optic illusion, and since then the emergence of Minimalist art has given rise to a widespread taste for sober, often asymmetrical designs. Not only paintings but also sculpture inspired couturiers for a news creation. **Mrs Grès** was known as a sculptor of fabric, since she used to create long, draped Grecian-style dresses with delicate pleats. Her favorite fabric was silk jersey and her signature was cutout gowns which would leave parts of the skin exposed. The perfect construction of her designs would always bring out a sophisticated feel of classical antiquity and ‘extreme purity’. Her clients included 20th century fashion icons such as the Duchess of Windsor, Jacqueline Kennedy and Grace Kelly. Madeleine **Vionnet** was known as the “architect among dressmakers”. Her vision was all about comfort and fluidity in movement. Her name is associated with the ‘bias cut’ which she introduced in order to help accentuate the natural curves of the female body. Inspired by ancient Greek art, the French designer remains known for her Grecian-style dresses and revolutionary clothes, worn by stars such as Marlene Dietrich and Greta Garbo.

Since the Second World War there has been frequent interaction between art, architectural design and fashion. Le Corbusier **was the designer of Minimalism.** He was one of the principal actors of the rationalist modern and purist movement with his slogan "Order. Reason. Purity. Truth. Structure. Bleaching”. But he was also one of the first architects that organized and classified the color in the scale of environmental polychromy. **Minimalist in fashion is** a case of André Courrèges who has opened his own couture house in 1961. He wanted to "modernize the women." From there, he created the futuristic collections, with clean and original shapes. He was then nicknamed "Le Corbusier of fashion."

Pop-art , op-art & hippie culture in fashion

The emerging hippie culture rejected the dictates of Paris haute couture, adopting instead an eclectic, highly individual look, mixing vintage and ethnic clothing with fashions inspired by contemporary psychedelic Pop art, nature, fantasy, and ethnographic art For instance Jean-Charles de Castelbajac was inspired by Andy Warhol and his **Pop-art** "Campbell's Soup" painting , he has always been inspired by contemporary art; he brings a joyful colour pallet from BD, cartoons, art graphics in his collection. **Op-art** produces at the spectator a physiological and psychological optical effect in environmental design and fashion.The artists as Victor Vazarely, Yvaral, Cruz Diaz and other representatives of "Optical Art" continue to influence modern fashion design and modern life today. Especially artists of "Op Art" inspired the fashion and interior design created by fashion designer Jean-Paul Gaultier.

The creativity work of Friedrich Hundertwasser remains before all that of a painter and a designer fighting against the austerity and the monotony of the industrial design. The unusual achievement of Hundertwasser with application of colour material and the use of irrational geometrical forms is a demonstration of kind of spatial contrasting harmony.

In 2007, Christian Dior designed a unique piece: hand painted and enhanced with spectacular embroidery Manteau Suzurka-San. Dior Haute Couture was inspired by The Great Wave of Kanagawa, emblematic work of Japanese artist Hokusai. Focusing on the relationship between art and creations of the house of Dior, we can say that the original works have been in one way or another influenced by different artists.
During his whole existence Yves Saint Laurent revolutionized fashion and gave the woman her freedom of movement that has inspired artists, poets and painters. "The profession needs an artist to exist," he said. He loved paintings, especially those of as Matisse, Mondrian, Braque, Picasso, and Van Gogh. Saint Laurent paid tribute in 1988 to Georges Braque, whose famous birds seem to fly stuck to the bride's dress. Then he designed a jacket inspired by "The Iris" of Van Gogh. It took 800 hours to sow the whole Van Gogh image. Flakes, tubes, seed beads, ribbons were all embroidered by hand to make the effects and lighting as it was on the canvas. Yves Saint Laurent, a veritable artist influenced in some way other couturiers.

Nowadays, fashion designs have increasingly been regarded as autonomous works of art. Some creations by designers like Jean-Paul Gauthier have been inspired by "futurism" and use the "tromp-l'oeil" effect. For instance stylish French can-can dress has been inspired by the "Moulin rouge" dancer. And we can see some kind of butterfly as a "camouflage" for his new fashion collection. The fashion house of "Martin Margiela" has been inspired by quotations from Frank Llloyd Wright, paintings of Gauguin and graphic codes of pop art that were transposed on dresses in an open way; yet fashion-art chemistry worked well together. Faces are covered with the now famous masks in combination with a kind of cap and remind us of motifs between science fiction and oriental legacy; sham tattoos on the tissue placed directly on the skin were hallucinating and sexy. Art of green fashion design show us the tendency to the ecological way of thinking. The very famous botanist Patrick Blanc, world known for his green wools & fashion designer Jean-Paul Gauthier have created a “green” wedding dress in 2002.

The latest movement is a combination of light & urban design as well as light and fashion design. Renowned for its distinctive colour palettes and creative designs **Franck Sorbier** used just two designs and stunning visual effects to narrate a medieval French fairytale on the runway in Paris. The Haute Couture Autumn/Winter 2012/2013 collection retold the 17th century story: Donkeyskin, a widowed king set on marrying his own daughter, who escapes his clutches by demanding a series of impossible gowns, the colour of the sky, moon or sun. “The collection is a bridge between the past, the present and what the future could be,” explained Franc, who had teamed up with software giant Intel for the high-tech side of the project.

All these examples show us that the variety of colour harmony in art and actual fashion design is a true colour 3D conception, with nuances and details, with specific colour codes and combinations, constantly changing in space and time. We can distinguish 4 colour associations or fundamental groups: “Colour”, “Value”, “Nuance” and “Mixed”; Inside of each group different components lose their own characteristics to the profit of a global perception. We can distinguish also 24 complementary intermediate colour groups (colour will be expressed on *NCS – Natural Colour System*).

These families of colours reflect their global impressions and comply with the laws of *“gestalt theory”*.

<u>Aleatory :</u> Values of hue, saturation and brightness are pulled at random in every action.

<u>Antagonistic achromatic:</u> Two opposite values of tints on the achromatic axes with various brightness levels.

<u>Antagonistic chromatic:</u> Two opposite values of tints on the chromatic circle with various brightness and saturation levels.

<u>Bichrome:</u> Two values of tints in right angle on the chromatic circle with various brightness and saturation.

<u>Camaïeu:</u> Colours of close tints on the chromatic circle with various brightness and saturation.

<u>Partial contrast:</u> Two tones with diverse brightness and saturation which binds a gradation between these two values.

<u>Degrading:</u> Continuous progression between two colours, both in tint and in saturation or in brightness.

<u>Progression moving:</u> Progression between two colours, in very distinctive ways as a step of colours in a staircase.

<u>Fusion:</u> Two colours merge gradually into a third whose colour is in the middle of the first two but the saturation is lower if the shades are remote.

<u>Equally chromatic:</u> Unity of tint, diverse saturation and brightness.

<u>Equally bright:</u> Unity of brightness, variations of tints and saturation.

<u>Equally saturated:</u> Unity of saturation, variations of tints and brightness.

Isolated: A colour in opposition of tint, saturation and brightness compare to a neutrality of the background.

Monochromatic: A colour with very close variations of saturation or brightness.

Multicolored: Multicolour is a complete harmony of all chromatic colours that are completed by the Neutral.

Neutral: A simple gradient from black to white. The harmony is very common in contemporary art, fashion design & architecture.

Nuanced: Low saturated group and close colours in brightness.

Progression in saturation: Unity of tint and brightness, progress in saturation.

Polychromatic: Composition of different chromatic colours.

Quadrichromatic : Four colours in right angles on the chromatic circle, degraded by saturation and by brightness.

Tone in the tone: The same colour tone which is corresponding to the different materials play some kind of contrast.

Trichromatic: Three colours in an equilateral triangle on the colour wheel, gradient in saturation and brightness.

United: The combination of very close colours in relief materials which give us a unique colour perceived from a long distance.

Translucent: Luminous effect of colour composition due to transparency of used materials.

Tactile colour & Haute Couture

My inspiration as a colorist and designer comes from my own painting, from within. Jean Marie Pujol, couturier who worked with Dior and Yves Saint Laurent at the time, designed several dresses to be painted using my technique to perpetuate the union of art and fashion. With this personal style we created a series of hand painted dresses presented during exhibitions and international events. An evolution of coloured strata in constant transformation, beauty of nature, the interaction of forms and images... It is towards this universe of harmony that I invite you. Everything lies in the pondering of both visual and tactile beauties which conceal thus a created space. A perception an eye discovers which is then transfigured and transformed by the feeling of touch.

« Beauty has as many meanings as man has moods.
Beauty is the symbol of symbols.
Beauty reveals everything, because it expresses nothing.

When it shows us itself, it shows us the whole fiery-colored world. »

Oscar Wilde, 1890

This type of art, beyond the visible, enriches us by its power and its self-fulfilment.

Address : Dr. Larissa NOURY, « Couleur-Espace-Culture »/ « Colour-Space-Culture »
14 rue de la Chapelle, 75018 Paris, France. E-mails: larinoury@gmail.com
www.larinoury.fr , www.CEC.larinoury.fr

Contemporary Art and the Unfoldings of Colour

Laura CARVALHO[1]
ProCor Brazilian Colour Association
School of Arts and Communication, University of São Paulo, Brazil

ABSTRACT

Contemporary art legitimates colour by leading it away from the traditional techniques of painting, and it transgresses platforms by thinking about new modalities of image: it puts the spectator and the space as central elements of the chromatic experience. Colour is the sensation given by the image – and the latter is no longer assimilated from traditional constituents (canvas, paint) – in installations and urban interventions. The passengers on streets and avenues are captured by the unexpected, and colour is inserted within the city's landscape as a sensorial input to be perceived. From the 60's onwards, the role of colour on the realms of contemporary visuality has been deeply rethought by art. Carlos Cruz-Diez (Venezuela), Hélio Oiticica (Brazil) and Daniel Buren (France) are leaders of this conceptual turning point: they established new chromatic formulations for installations and urban interventions; they made colour a way of awaking within the spectator the everyday sensitivity and the attention to the landscape.

1. INTRODUCTION

The 20th century was determinant for the colour judgement on the realms of art and culture. Modern art emancipates colour as a pictorial element, it deposes *mimesis* from its well-privileged field and it begins to consider the chromatic material within the domain of subjectivity. Contemporary art, on the other hand, evaluates the modern perspective, takes away from colour its character of personal expression in order to create new parameters – more objective and impersonal ones – on the way it turns into image.

It is not possible to accompany the fast transformation of the colour role in the art of the 20th century without taking into account Marcel Duchamp's legacy to the contemporary art (Temkin 2008). The French artist, through *readymade*, articulates his critique to the institutionalization of the work of art and the primacy of the object made by the artist: painting, its auratic dimension and its disarticulation with the social dynamics. Duchamp incorporates everyday objects – the common, the ordinary ones – in the field of artistic production in order to depose the handicraft character of art and its exclusive relation with the artistic genius.

[1] Laura Carvalho is Brazilian colour researcher and production designer for the cinema. Graduated on Audiovisual Arts by the University of São Paulo and Master of Arts in Theory and Aesthetics of Cinema by the same institution. Her academic research establishes a parallel between colour, cinema and visual arts, notably modern and contemporary art. Such academic research has brought results presented in conferences in Brazil and overseas, including countries as Spain (2012) and United Kingdom (2009, 2010). Presently works as production designer and scenographer for film, performance and theatre.

Duchamp was not notably a colour artist, but the debate he engendered resounds on the way colour was taken in within art from the decades of the 50's and 60's. The manufactured or industrial colour assumes certain distance from its handicraft process of production; the tube paints are replaced by those found at stores not dedicated to the artistic production, such as the masonry and automotive paints. At that moment, there was not a disarrangement between the artistic practice and the everyday life elements, and colour enters the world of art as a present element in the real world.

As for the installation and urban intervention - the focus of this text - the artists validated Duchamp's methodology on a two-folded way: not only did they question the museum as a space which endorses the value of art, but they also thought about the way of inserting art into the contemporary visual culture, through colour and urban landscape.

Hélio Oiticica, Carlos Cruz-Diez and Daniel Buren (having considered the different contexts they developed their work) stand out in their use of colour in the poetics of the expanded field (Krauss 1979), taking here the famous term coined by Rosalind Krauss. They do not move away from their personal preferences for determined shapes or shades – as, for instance, Buren's stripes, Cruz-Diez's geometry and Oiticica's primary colours -, however, they dimension their aesthetical choices according to their colours, materials and the design found in the field of industrial production.

That does not mean that those artists' visual scheme is a submission to the world of capitalist production; instead, through colour release in 3D space, Oiticica, Cruz-Diez and Buren adopted a critique to the institutional spaces of art and the way the everyday experience neglects our vision. For them, colour shows space in its social nature.

2. HÉLIO OITICICA

The Brazilian artist develops his journey along with his search for solving artistic problems through colour. Oiticica not only stands out in the Brazilian contemporary production, as well as he is one of the best developers of colour within a prism that takes into consideration the debates occurred around art and the insertion of his project into an underdeveloped context, such as the Brazilian one.

For him, colour needed to get out from the screen frame and reach space projection. This colour dodge aimed at dismantling the traditional art categories, as painting and sculpture. Throughout the years, this artist created a series of projects, identified by specific names: Núcleo (core), Penetrável (penetrable), Parangolé (colorful costumes made of fabric and plastic) and Bólide (fireballs). Let us focus on the Penetrable series, especially the *Magic Square* series.

From architectonic scale, *Magic Square#5* (1978, Figure 1) searches the spectator's involvement through colour. Nine brick 4,5 X 4,5m squares constitute ample coloured walls simulating labyrinths. Colour embodies the work structure; masonry paints cover the square faces, whose nuances may vary among white, magenta, blue, red, orange and yellow. Other elements from the industrial universe are used in the work, such as acrylic blue.

Oiticica, with this bold arrangement, assumes the hybrid qualities of the work, flirting with painting, sculpture and architecture. In Magic Square#5, the labyrinth structure enables the public to go through the colour fields, to walk on its walls, to learn on them, to observe the blue light that passes through the acrylic board, to pay attention to the landscape that involves the installation. The device he created reaffirms the project collective character. The word "square" takes at least two different meanings: the first, allusive to the architectonic dimension of the work (in relation to the fixed measured squares) and the other that relates to the public square space and its relation with the surroundings, making the installation prone to promote meetings among people and to promote the encounter between people and their surroundings.

Figure 1: Hélio Oiticica, Magic Square#5, 1978

The big dimensional work is clearly an exogenous element to the landscape it is inserted in (as it is the case of *Magic Square#5*, located at Tijuca Forest in Rio). Through colour, the walls stand out from their surroundings and activate the public's sensorial experience, carrying out a physical and social dimension of the work. It is physical because it demands the audience's bodily presence inside the installation, and it is social because the spectators walk around its labyrinths and they are invited to free themselves away from the dull and anti-creative everyday life (Pedrosa 2004), in order to acquire a new experience through art. The formal set projected by Oiticica opens up a magical dimension, as if the installation were from a fantastic nature inside a landscape that notably does not belong to it.

Hélio's project mixes intellectuality and intuition, this chromatic arrangement distances itself from a symbolic propensity of colour, denying possible associations between colour and its cultural meaning. The artist deeply debates the importance of colour on the social net where the installation in fixed in. The palette he searches is not the painter's one, not the architect's one, but it is a visual data which presents itself independently, lightly and loosely, and it is able to grab the spectator in a universe of sensations.

3. CARLOS CRUZ-DIEZ

In the Latin-American context and its situation in the international art, the Venezuelan Carlos Cruz-Diez has a relevant development of colour in the 3D field. He begins from a careful study of colours in the realm of science, graph art and painting, moved by the curiosity in associating scientific research and artistic production in the search for new industrial materials to be inserted in his works.

From easel painting to designer and illustrator, Cruz-Diez persisted on the way colour might be registered as an image. Thus, his extensive career deals with diverse materials (cardboard, wood, aluminium, plastic, LED light bulbs, etc.) adapted to specific aesthetic assumptions. For having this diversity of materials that enable a range of concepts, his art meets kinetic art, geometrical art, constructive art, expanded cinema and site specific.

Comparably to Oiticica and Buren, Cruz-Diez also presents himself opposed to the symbolic associations of colour, not conditioning it to a mythical character of interpretation. What he proposes is for colour to be emancipated from its cultural charge in order to be recreated according to the spectator's experience. Colour is a live and mutant organism, whose acknowledgement depends on people's interaction with his work, as if our vision were also something unstable to be transformed. His investigation of colour resulted in the study of added, subtracted or reflected colour and it took him to create some series of works: Adición Cromática (chromatic addition), Inducción Cromática (chromatic induction), Fisicromía (physichromia), Ambientación Cromática (chromatic environment) and Cromosaturación (chromosaturation).

Chromatic Addition is founded upon the concept of colour irradiation, when two colours get in touch and optically generate a third one. Some determining works of Chromatic Addition merge into Chromatic Environment: for instance, when the phenomenon of irradiated colour is present in urban shapes, in the zebra crossing (Figure 2) – a feature that used site specific experience in many different countries – or yet in panels or floorboards associated to the airport architecture (*Pisos y muros de Color Aditivo en el hall central del aeropuerto*, Caracas, 1974).

Figure 2: Carloz Cruz-Diez, Chromatic Addition – Liverpool One, 2014.

Chromatic Induction, on the other hand, is based on the phenomenon of post-image or retinal persistence. Linear structures capture the complementary colour and thus the presence of colour is given both physically (primary colour) and virtually (complementary). Once more, the zebra crossings, under the effect of Chromatic Induction, enter as an efficient visual resource in the integration of art and urban space.

At last, Chromosaturations promote a physical colour experience. They stimulate ways of thinking, seeing and acting. Cruz-Diez made this series throughout decades and kept modifying its shapes and support, either in transparent material constructions or using LED light bulbs. He made, for example, projects in the city of Paris, *Chromosaturation pour une allée publique* (1969), which enabled the collective experience of colour through an installation in the urban environment. A simple event such as this one invites the passer-by to turn into a prospective public, a spectator that is capable of exploring their perceptive domains about the installation space and about the urban space on which the work was constructed. As a whole, Cruz-Diez's efforts, throughout his vast production, is on a social dynamics of colour, by promoting an individual and collective experience that reconditions man's vision and makes him recognize the power of his look.

4. DANIEL BUREN

The French artist assumes *readymade* as a new repertoire of the contemporary visual culture. Buren does not nullify Duchamp's critical position; he just reconfigures art from his observation of the consumer society. The artist sets the repetition of shape (the famous white-and-colour stripes of 8,7cm, his identity mark) in different support, making the work merge into the landscape of the city and to its emphatic symbolic production of the mass culture.

Buren attributes the creation of this visual tool, the so-called stripes, to the observation of the fabric found at the Market in Saint-Pierre, Paris. These are meaningless signs, from an apparent neutrality and immutability. His colours also do not share a culturally given symbolism or a prescribed emotional charge. These are his projects named *Affiches Sauvages* (developed from 1968, Figure 3) and *Papiers Collés* (from 1969), bold proposals that carried out the discussion around image in the urban space, its banality in relation to the social life events.

Figure 3: Daniel Buren, Affiches Sauvages, 1968.

His method consists of gluing those works to walls as if they were mere posters, reproductive and ordinary ones, in which the artist's identity remains anonymous. The works merge in the visual assortment, characteristic of the contemporary society. The more palatable it could seem at first, the arrangement of colourful stripes created by Buren sieves aggressiveness, even present in the title of the series: "wild posters".

The urban intervention is a gesture of visually modifying a given reality, without asking for permission to any public or private institution in order to do so. Both series are nor exempt from ambiguity: along with their mimesis in a set of information, the works are intentionally glued and they make their presence in the own visuality of the contemporary culture on a non-institutional way. Actually, they are not marketing work because they had not been created by a marketing agency and they are not worthy the title of work of art (in the auratic and bourgeois sense of the term) because the artist remains anonymous and refuses the museum as a cultural privileged space of art.

Buren proposes a break in the everyday normality and demands from the spectator the attention to the uninteresting, the observation of the disintegration of the stripes as his authorial mark and of his artistic genius. He refuses painting as an aesthetic resource and little by little transforms his works in objects of the common world (which might be flags, towels, posters, etc.). Despite the apparent static shape of his works, they accompany an external spatial transformation; they are entangled in the architectonic, economic and political set of the city. The artist gives visibility to the urban architecture and he makes the museum invisible as an institution space of art (Rorimer 2002).

5. CONCLUSION

One of the most important premises of contemporary art in relation to colour was putting the artist as an observer of the social reach of the art from the dynamics it establishes with the urban space. In spite of having come from different contexts whose works get connected in debates of different theoretical perspectives, Oiticica, Cruz-Diez and Buren reintegrate colour into art: both architecture and colour as ways of the contemporary visual culture. The works invalidate the museums as official places of art and they take off their symbolic value associated to meanings of cultural nature. The movement from colour to space – both in installation and in the city – transforms the everyday experience into an aesthetic experience. For them, colour, art and life do not diverge, they merge in the attempt of re-establishing and updating the public's eye over the everyday events.

REFERENCES

Batchelor, D. 2008. *Colour - Documents of Contemporary Art*. Whitechapel Gallery/The MIT Press.

Buren, D. 2009 (1969-70). Beware!, *Art in Theory, 1900-2000*. Blackwell Publishing 861-867.

Cruz-Diez, C. 2009 (1989). *Reflections on Color*. Juan March Foundation/Cruz-Diez Foundation.

Jimenez, A. 2014. *Carlos Cruz-Diez Conversa com Ariel Jimenez*. Cosac Naify.

Krauss, R. 1979. *Sculpture in the Expanded Field*, October, spring 31-44.

Machado, T. 2011. *O Efeito Beaubourg na Perspectiva de Daniel Buren*, Angelus Novus (2) 142-161.

Oiticica, H. 1960-61. *Vários Escritos*. Itaú Cultural.

Pedrosa, M. 2004 (1961). Os projetos de Hélio Oiticica, *Acadêmicos e Modernos*. EDUSP 341-343.

Rorimer A. 2002. *Daniel Buren, From Painting to Architecture*, Parkett 66 61-68.

Salzstein, S. 1995. *Autonomia e Subjetividade na Obra de Hélio Oiticica*, Novos Estudos CEBRAP (41) 150-160.

Temkin, A. 2008. "Color shift", *Color chart: Reinventing Color, 1950 to Today*. The Museum of Modern Art 16-27.

Address: Laura CARVALHO, ProCor Brazilian Colour Association and University of São Paulo, Caio Prado Street, 207, São Paulo,01303-001,BRAZIL
E-mails: contato@lauracarvalhoarte.com, laura.carvalho.h@gmail.com
Website: lauracarvalhoarte.com

Comparison of Slovene color identities by researchers A. Trstenjak and M. Tusak with colors on Slovenian municipality flags

Vojko POGACAR,
Faculty of Mechanical Engineering, University of Maribor

Abstract

Combinations of specific forms and colors represent most effective method to distinguish between different identities. When forms (objects, items) are similar or even identical, then only colors remain most reliable discriminatory factor.

Medieval time in Europe were mainly dominated by the general illiteracy and forms of visual identities such as shields, coats of arms and flags, which were important to unambiguously distinguish the different actors - especially when they have emerged as opponents in fighting or games, or any expression of belonging, labeling property, possession, etc. In 11th century, when designing coats of arms and flags, a series of disciplines from heraldry, vexillology, sfragistics, insigniology, iconology emerged, which were applied among philosophical sciences at that time. However, today they are complementary Sciences of Art History.

The aim of this paper is to present colors, appearing on Slovenian municipality flags and to compare them with the findings on Slovenian color preferences by psychologist Anton Trstenjak 40 years ago and by psychologist Max Tusak around 20 years ago.

In last fifty years Slovenia gained a multitude of new flags appeared due to new municipalities on the basis of local features or attractions which were designed in accordance with modern trends in design. On the other hand, part of the municipal flags represent the heritage of the past, their historical traditions and well-known local attractions, etc. These "older" flags are generally based on heraldic and vexillological principles.

The three studies were done in different time frames, separated by decades. Psychologist Anton Trstenjak presented the color preferences of Slovenian population on a sample of 1,000 students in secondary schools. Psychologist Max Tusak, who worked with Anton Trstenjak, has carried out two decades later, a similar survey on a sample of students in four different types of secondary schools. In the third study, decades later, we made a research of the colors on Slovenian municipality flags, which represent color preferences of population in a given environment. Some structural analysis of color histograms was performed to find out representation of the colors in the flags. The results were given into the Periodic color model to comparatively analyse current state and illustrate the changes. In final study we found a lot of differences and changes over time in color preferences among decades, but we found also exception, mostly concerning similar preferences with color blue.

1. INTRODUCTION

Combinations of specific forms and colors represent most effective method to distinguish between different identities. When forms (objects, items) are similar or even identical, then only colors remain most reliable discriminatory factor.

Medieval time in Europe were mainly dominated by the general illiteracy and forms of visual identities such as shields, coats of arms and flags, which were important to unambiguously distinguish the different actors - especially when they have emerged as opponents in fighting or games, or any expression of belonging, labelling property, possession, etc. (Stanic, R. and Jakopic, T. 2005). In 11th century, when designing coats of arms and flags, a series of disciplines from heraldry, vexillology, sfragistics, insigniology, iconology emerged, which were among philosophical sciences applied at that time. However, today they are complementary Sciences of Art History.

In last fifty years, Slovenia gained a multitude of new flags appeared due to new municipalities on the bases of local features or attractions (Heimer Z. 2005), which were designed in accordance with modern trends in design. On the other hand, part of the municipal flags represent the heritage of the past, their historical traditions and well-known local attractions, etc. These “older” flags based on vexillology and heraldic principles, but the semantic undertones bearing important messages for the study of today’s Slovenian identity.

2. METHOD

The aim of this paper is to present colors, appearing on Slovenian municipality flags and to compare them with the findings on Slovenian color preferences by famous Slovenian psychologist Anton Trstenjak 40 years ago and by psychologist Maks Tusak around 20 years ago. Although the three color studies were done separated by decades in different timeframe, they show us that the most preferred common color through all times were blue. In a comparison of all three investigations, we would like to bring some conclusions in relationship to Slovenian identity background through aspects of color symbolism and psychological frames of color language.

2.1 Samples of Anton Trstenjak

Anton Trstenjak was PhD in philosophy and theology, beside that he was ordained a priest in 1931 in Maribor. He was one of the first Slovene, who made deeper researches in a field of color. All mentioned facts were in that times of deep socialism politically inappropriate and also life dangerous. Governmental behaviour was suspicious in most of scientific researches in which they haven’t have a proper control and knowledge what they mean and for what purpose they are done. They were too afraid of “bad western influences” which could spoil our society and out of such trivial reasons many of his colleges were imprisoned for many years. So, it is important to know in what kind of circumstances were done this first research of Slovenian color preferences. He made his research on a sample of 1.000 younger Slovenian students from secondary schools, among 15 to 22 years old, 500 male, 500 female, 500 citizens and 500 from province. The research was supported by adequate questionnaire, based on colors of clothing and fashion. To make the research frame more real and understandable, he posed a questions like: 1. Which color is generally referred favourite at all? 2. Which color is the most prefered in clothes? 3. Which color is the most unpleasant at all? 4. Are they in the choice of colors (clothes) follow fashion or their own, irrespective of fashion? 5. Have they prefer a single or multi-colored dress? 6. Are they prefer to dress abstract (geometric) or specific image-like, that they represent something? 7. Do they like the color changes, regardless of whether the new color is "his" or just fashionable?

This last question is particularly important because it is one of the main characteristics of each mode, precisely in the fact that rotational dictate of someone else always affect individual taste.

In general, the research examined the popularity and unpopularity of colors. In making this determination, an important difference arises whether it is a personal preference of color or for its applied use. For example, someone who likes red color will not buy a red coat, but something more socially acceptable. In clothing, therefore we get completely different results. Trstenjak draw attention to this duality that, personal color preferences differ from socially consensual. These colors are then located in the field among indifferent colors. Under such, just a little bit simplified interpretation, we can better understand the respond to colors, based on individual emotional level with a difference of social consensus and rational selected colors on the other side (Trstenjak A. 1996: 310-322).

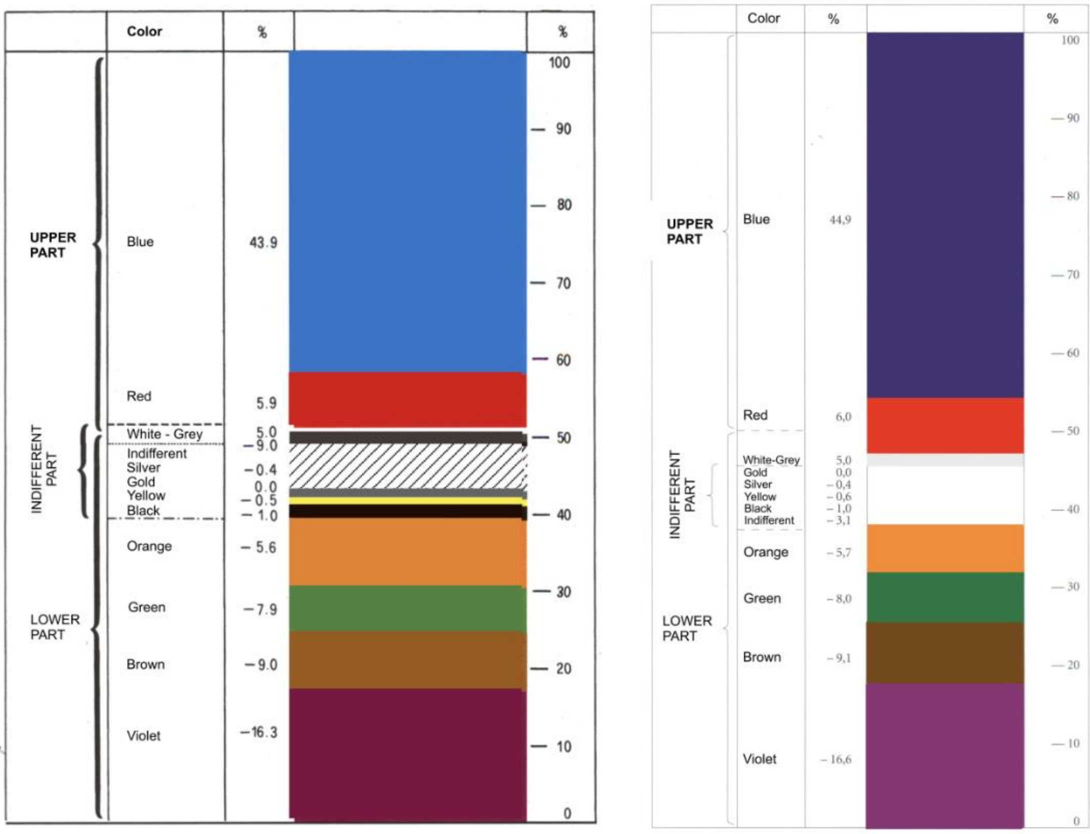

Figure 1: Color preferences of Slovenian student population by A. Trstenjak (left table) was done in 1975, first published in 1979 and second (right table) in 2001 by M. Tusak. The differences in printed colors are evident. It is also obvious that the colors were meant more in symbolic as in colorimetric sense (Trstenjak A. 1996: 312, Tusak, M., 2001: 87-118).

Trstenjak research was done around 1975 and presented in his book Psychology of colors, edited in 1979. As the research based on his questionnaire, we may suppose that each participant had slightly individual interpretation of exact colors tone, what means, that colors were understood wider, more loose and generally. Confirmation of this thesis can be found in the presentation of his results (Figure 1), when Trstenjak was still alive. The table in Figure 1 was first presented in his book as a blue color, closer to Cian - that time called Process blue. In second edition Cian turn to much deeper blue, closer to Blue out of RGB system. Also the other colors changed, but for further analyses it is not so important for us.

2.2 Samples of Maks Tusak

Psychologist Maks Tusak, who worked some time with Anton Trstenjak, also continued his research in the frame of improved Trstenjak's methodology. Two decades later in 1995 he carried out a similar survey on a sample of four different types of population on secondary and one elementary school in amount of more than 4000 participants. He also used the similar or even the same questionary method, and the results presented in Figure 2 also showed general similarities to Trstenjak's research. Tusak results of research are published in 2001 and presented on eight tables: 1st refer to male students and 2nd to female students of gymnasium, 3rd to male students 4th to male students of technical school, 5th to male students and 6th to female students of vocational schools and 7th and 8th to male end female of elementary school.

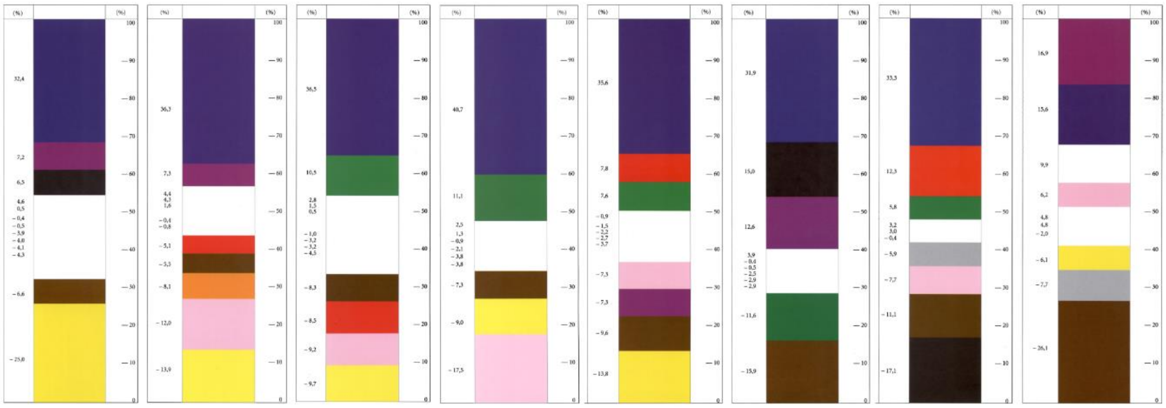

1 2 3 4 5 6 7 8

Figure 2: Color preferences of Slovenian elementary and secondary school's population by Maks Tusak performed in 1995 and published in 2001. (Tusak M. at all. 2001: 87-118.)

In all 8 tables in Figure 2 it comes out that the Blue is the most prefered, except at last one, where the Blue color is on second place, but general amount of Blue and Violet together figure as common positive opposition to unlike brown (Tusak M. at all. 2001: 87-118.).

2.3 Color samples of Municipality flags

A decade later in year 2005, we made a research of the colors on 193 Slovenian municipality flags, which represent color preferences of population in a given environment. It was published in (Pogacar V., at all. 2006: 6 f.). The research of Trstenjak and Tusak present as well positive as negative and indifferent color preferences, but our research was focused only on positive part. Technically based or research on structural and histogram analysis of colors on municipality flags. We presumed that the part of historic flags as leftovers of the heritage were already peoples identity out of habit. On the other hand, we have a multitude of newly created municipalities with flags, which are also selected consensually in accordance with the criteria of the wider local community and, in principle, reflect a consensual color identity. Perhaps the colors of the flags even more accurate represent personal color preferences, because they are not tied to any pragmatic use, but linked with symbolic and presentational level. Our result was also in accordance with previous researches of Trstenjak and Tusak: the average of Slovenians most prefered color is Blue, but an additional important conclusion comes out in this research, that the Green appeared as second most prefered color and it takes almost a half part of positive side. That way is clearly expressed tendency, which can be noticed as wide spreaded in nowadays Slovenia. These slightly trends were noticed in some parts of Tusak's research by pupils of technical and partly in vocational and elementary schools (Figure 3).

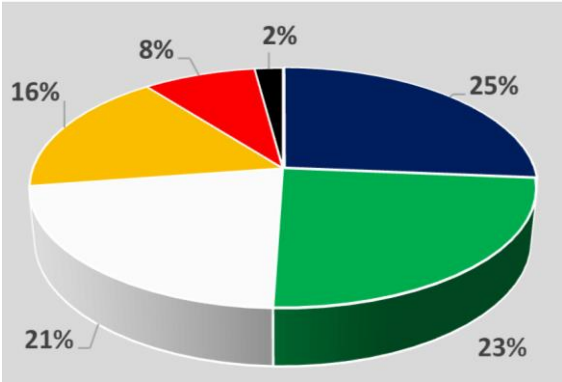

Figure 3: The everage of used colors on Slovenian municipality flags shows on the first place the same result as the previous researches of Trstenjak and Tusak, but in second place was ranked the green, which is no surprise since this is observed also in the nowadays Slovenian daily lives.

3. RESULTS AND DISCUSSION

In final study we found a lot of differences and changes over the time in color preferences among decades, but we found also exception, concerning to similar preferences in color Blue. But the most important changes in our opinion, appeared on the second place with Green and probably white. Green means the other half stated at the positive side of the color identity and its importance is increasing with the growth of Slovenian self-esteem. To interpret the pragmatic side of this thesis, we used our previous developed PCM (Periodic Color Model) (Pogacar V. 2005 and 2007), where we can analyse and compare symbolic meanings of prefered colors and future trends. All three research results given into PCM showed the general color tendencies (Figure 4).

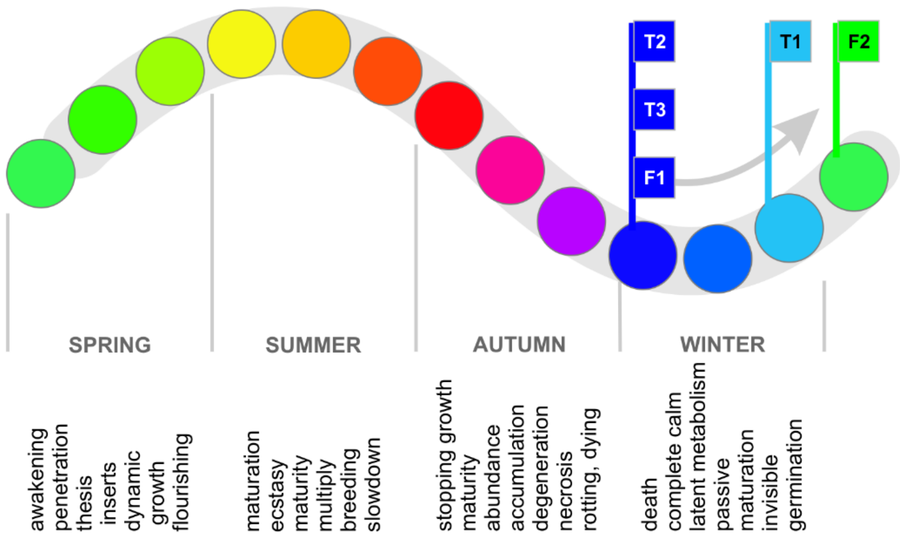

Figure 4: The interpretation in Periodic Color Model is shown general tendencies of the Research of Trstenjak (T1), (T2) and of Tusak (T3) and of Flags (F1). The Flag color

(F2) on the second place shows probably in which direction goes general color preferences in Slovenia nowadays.

4. CONCLUSIONS

And finally, all in research identified trends are already noticed in nowadays manifestations in sport disciplines and also on many other fields, mostly related to Slovenian state identity (Figure 5). But on the other hand, our State's flag doesn't reflect our research conclusions at all, because it was selected under the pressure of time in a year of liberation (1991), when Slovenia separated from former Yugoslavia. This flag is clearly reflecting a heritage and conception of previous times.

Figure 5: The pictures tell more than a thousand words: color identification through Slovene dresses on Olympic games in Sochi 2014 already confirmed predictions of our results in research.

REFERENCES

Heimer Z. 2005. *Slovenian municipal flags.* http://zeljko-heimer-fame.from.hr/hrvat/si-obc01.html

Pogacar V. 2005. Colors in relationship to time cycles. In AIC 2005: Proceedings, ed. by J.L. Nieves and J. Hernandez-Andres. Granada, Spain. 1449-1452.

Pogacar V. 2007. *The principles of Dynamic Color Model development.* Book of. In AIC 2007: Proceedings, Hangzhou, China, 14-17.

Pogacar V., A. Skrbinek, D. Zimsek. 2006. Colors of the national symbols. In 37th ISNT [and] 2nd ISNG [and] 7th IS of SCA. *Proceedings,* ed. by B. Simoncic et al. Ljubljana: Faculty of Natural Sciences and Engineering, 6 f.

Stanic, R. and Jakopic, T. 2005. *Osnove heraldike in istovetnostni simboli slovenskih občin*. Ljubljana: Lecnik.

Trstenjak A. 1978. *Človek in barve.* Ljubljana: Delavska univerza Univerzum.

Trstenjak A. 1996. *Psihologija barv.* Ljubljana: Institut Antona Trstenjaka.

Tusak M. 2001. Psihologija barve. In *Interdisciplinarnost barve vol. 1.* (Monograph DKS). ed. by S. Jeler and M. Kumar. Maribor: Društvo koloristov Slovenije, 87-118.

Address: Prof. Vojko POGACAR, Lab for Product Design, Faculty of Mechanical Engineering, University of Maribor, Smetanova 17, 2000 Maribor, SLOVENIA
E-mail: vojko.pogacar@um.si

A Comparison of Color Schemes and Images in the Package Design of Sweets in the US and Japan

Kyoko HIDAKA
Faculty of Art and Design, Tama Art University

ABSTRACT

This study compares the color schemes and design of packages of sweets in the US and Japan from the viewpoint of the cultural history of color. To visualize this comparison, color charts representing typical Japanese and American sweets packages are presented. The central aim of the comparison is to clarify cultural differences in color that characterize appetizing sweets, between the US and Japan. The research method was as follows: I purchased a total of 120 items, 20 items each of hard candy, chocolate, and chewing gum sold nationally, both in the US and Japan in 2013-14. Using ColorMunki Design of X-Rite, I measured the color scheme of these packages and listed the data in the form of color charts. These data are significant in revealing the fundamental cultural differences in the package design in these nations, a valuable insight for the field of international marketing and graphic/package design. Generally, there is a strong tendency for Japanese sweets packages to use a warm and light color scheme, whereas American ones apply a vivid multicolor scheme. Japanese sweets manufacturers produce various novelty items that promote seasonal and regional marketing, whereas American mass-produced sweets and its coloring are generally aimed at children and their dreams. Therefore, the color scheme of and the images on packages of US sweets resemble American comics.

1. INTRODUCTION

This paper compares the color schemes of the package design of sweets in the US and Japan from the the cultural history of color perspective. To visualize this comparison, color charts representing typical Japanese and American sweets packages are presented. The main objective of this paper is to clarify the cultural differences in color that characterize appetizing sweets between the US and Japan. Hues in the color scheme of these package designs are primarily examined.

Sugita reported that colors that infants see everyday largely influence the human color sense[1]. The development and innateness of color sense is still the subject under discussion. Even so, I hypothesized that the color scheme of the packaging of sweets can be a root cause of forming color culture since human beings habitually see packages of sweets from childhood. The result of this comparison can expose the cultural distinction in the color perspective and will be valuable in international marketing when exporting Japanese sweets. As precedence research, Birren published a series of books on color and consumer psychology[2]. Kawasome presented a paper examining the relation between food color and

---

[1] Sugita, Y. 2010.

[2] Birren, F. 1961.

human appetite. Iyenger, in her book, *Art of Choosing*, wrote on the issue of how people choose color.

2. METHOD

The research method was as follows. I purchased 120 items: 20 items each of hard candy, chocolate, and chewing gum sold nationally, both in the US and Japan in 2013-14. The names of stores were Wegmans, ACME, and Hudson News in New York and New Jersey; and 100 Lawson, Aeon, and Okashi-no-Machioka in Tokyo and Kanagawa. Both in the US and Japan, retail stores displayed an average of 18-30 competing products on the same shelves.

Using ColorMunki Design of X-Rite, I measured the color scheme of these packages and listed the data in the form of color charts. I selected 100 representative colors, including 5 colors each from 20 items. Then I sorted these 100 colors into Munsell's 10 hues: red, orange, yellow, yellow-green, green, blue-green, blue, blue-purple, purple, and red-purple, in addition to achromatic grayscale, including white, gray, and black. Figures 1-6 represent the hues of hard candy, chocolate, and chewing gums, which are frequently used.

For reference, I compare the typical colors of the sweets packages in the US and Japan in Munsell notations and RGB variables (Figure 7 and Tables 1-3).

Moroever, as an example of the cultural image influencing color, I mention one case of sweets package and American comics (Figures 8-9).

3. COLOR SCHEMES

3.1. Hard Candy

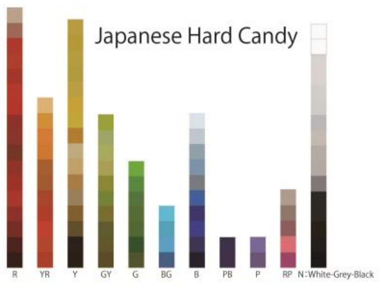

Figure 1: Japanese Hard Candy.

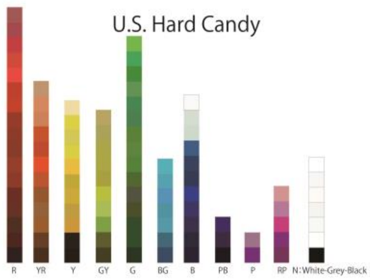

Figure 2: US Hard Candy.

Figure 1 shows that Japanese hard candy packages tend to use warm hues, such as red to yellow and light gray; however, they use less green to purple. The use of warm hues and grayish colors gives bright and soft impression overall. Furthermore, the Japanese data show middle ranges of value and chroma.

Figure 2 shows the similarity with the Japanese data, which also use warm hues. However, there are two differences: first, there is no use of gray, and second, there is frequent use of green. The tendency of not using gray in the US hard candy packages makes it look very colorful and vivid. The US hard candy uses low value (brightness) and high chroma (vividness).

3.2. Chocolate

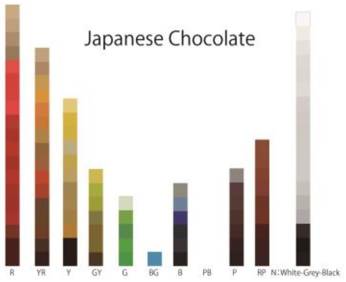

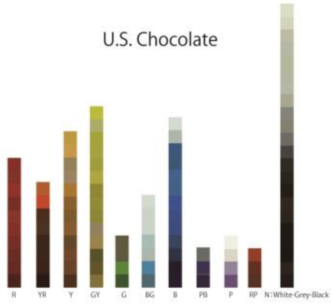

Figure 3: Japanese Chocolate. *Figure 4: US Chocolate.*

Figure 3 shows that the colors frequently used in Japanese chocolate packages are red, brown (orange and red-purple low in value and chroma), black, and light gray. Moreover, they use gold frequently for product logos. Red, brown, black, and gold are four hues that seem to be typical colors for Japanese chocolate. In Japan, black reminds bitterness and red reminds sweetness. Additionally, brown is in between red and black; to make brown hue, people mix these two colors. Typical products such as Glico’s Pocky and Lotte’s Ghana milk chocolate also use red packages. The bitterer taste and more cacao ingredients the products have, the darker are the hues of the package from brown to black.

In contrast, Figure 4 displays the frequent color scheme in the US. They use brown, dark gray, yellow-green, and blue. The Hershey chocolate currently uses brown in red-purple hue and silver gray. American traditional chocolate snacks, such as Milky Way and Reese, use orange and green, which are not found in the Japanese color scheme.

3.3. Chewing Gums

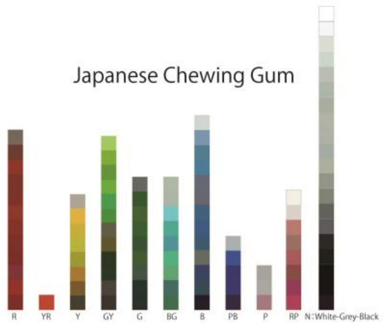

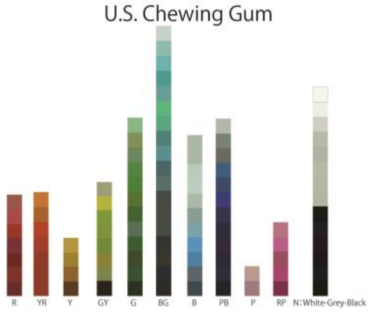

Figure 5:Japanese Chewing Gums. *Figure 6: US Chewing Gums.*

Both Japanese and US chewing gums frequently use yellow-green to blue-purple and silver (gray) for their packages. These hues represent cool, refreshing sensation of menthol flavor. On the contrary, they scarcely apply orange and brown for their overall background. Figure 5 shows that the most frequent hue in Japan is silver (gray). Japanese chewing gums use metallic colors and do not apply many hues to give an impression of a cool, sharp feeling. Black is also often used to express a sharp stimulus. Moreover, Japanese have an image of healthiness in green color. A unique Japanese chewing gum flavor is Japanese plum, and its red packaging reminds one of ripe plum.

American chewing gums use more blue-green than those of Japanese. In terms of value, Japanese chewing gums use high to medium range of colors, whereas the American package applies low range of colors. Furthermore, Figure 6 shows that the use of orange in the US is more frequent than in Japan.

4. BLUE COLORED SWEETS AND PACKAGE

Quoting the article from Birren, Kawasome reported that blue food reduces appetite[3]. It seems that previous research papers have spread such stereotype to the public, especially package designers and food manufacturers. Therefore, food packages in Japan frequently use warm colors, such as red, which is confirmed in this study. However, in the US, even though "blue" and "fluorescent color" in food rarely exists naturally, this survey found that these colors are widely used in both the packaging and food.

5. RESULTS AND DISCUSSION

5.1. The Typical Packaging Colors of the US and Japan

Figure 7: Typical Colors in Packages.

This section compares the typical colors from the result of this survey and examines the cultural distinction. Figure 7 illustrates a list of typical colors used in packages, sequenced from the first to fifth place. The left column is of the Japanese hard candy, chocolate, and chewing gum, and the right column is of the US. Comparing these three types of sweets, the divergence of hue is remarkable, particularly in chocolate.

In Japanese packages, the illustrative images of fruits, green tea, or milk are often used to inform and evoke these flavors. Accordingly, the colors of these items reflect the color of the packages. In Japan, the use of color in packages of long sellers, basic items versus seasonal, limited, or regional novelties are poles apart. The seasonal, limited ones use more drastic color schemes, whereas the long sellers do not often change the design and colors.

American package design generally applies colors in high chroma and low value. Unlike Japanese, American sweets tend to use illustrative images of contents rather than ingredients. Seasonal and limited novelties are also popular in the US, but it seems that these are rather event based, such as Halloween, Easter, and Christmas with its symbolic colors[4].

---

[3] Okuda, H., Tasaka, M., Yui, A., and Kawasome, S. 2002.

[4] Red & green for Christmas, yellow & pink for Easter, and orange & black for Halloween.

Table 1. Comparison of the Typical Colors of Hard Candy in Japan and the US.

Japan	Munsell (HVC)	RGB	USA	Munsell (HVC)	RGB
1	6.6R 4/11	179: 57: 44	1	7.6R 4/12	195: 67: 45
2	4.9Y 6/7	187: 158: 66	2	1.9G 4/6	72: 134: 82
3	3.5YR 5/9	213: 122: 57	3	9.2R 4/10	197: 83: 46
4	N 8.0	207: 205: 199	4	4Y 7/9	234: 187: 65
5	1GY 6/7	153: 161: 60	5	1.2B 6/5	88: 161: 176

Table 2. Comparison of the Typical Colors of Chocolate in Japan and the US.

Japan	Munsell (HVC)	RGB	USA	Munsell (HVC)	RGB
1	6.2R 4/11	180: 57: 50	1	N7.0	180: 181: 159
2	8.6YR 5/5	173: 130: 72	2	0.2GY 6/7	164: 163: 59
3	6.7R 1/3	72: 35: 29	3	1YR 1/1	49: 38: 32
4	N8.0	207: 199: 195	4	7.6PB 3/8	65: 81: 142
5	N1.0	32: 28: 24	5	7.3YR 4/5	137: 96: 47

Table 3. Comparison of the Typical Colors of Chewing Gum in Japan and the US.

Japan	Munsell (HVC)	RGB	USA	Munsell (HVC)	RGB
1	5.1GY 7/1	176: 181: 168	1	9.2G 4/3	82: 129: 117
2	1.7PB 3/4	66: 96: 124	2	8GY 3/4	69: 98: 50
3	9.2GY 5/8	78: 140: 59	3	1.3P 2/2	56: 54: 74
4	3.3R 3/7	128: 50: 40	4	7.9RP 5/9	188: 93: 136
5	9GY 3/4	61: 92: 49	5	1.2GY 7/1	183: 185: 169

5.2 American Comics and Sweets Package

The mass-produced snacks and sweets sold in American supermarkets and convenience stores are mostly for children, and its coloring is generally aimed at children and their dreams. Professor Story of University of Minnesota pointed out a tendency to use toys and cartoon characters for food advertisement to make children recognize brands[5]. In particular, M&M (Figure 8), Kellogg's cereal, and Oreo cookies use this marketing strategy[6].

[5] Story, M., and French, S. 2004.

[6] Ibid.

Figure 8: M&M Pretzel flavor in 2013.

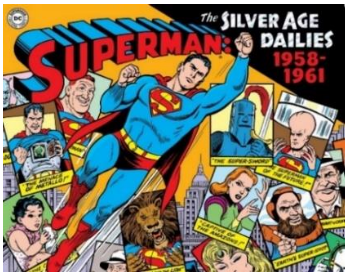

Figure 9: "Superman: Silver Age Dailies Vol. 1: 1959-1961" the Library of American Comics, 2013, Superman TM and © DC Comics, Inc.

Thus, it is predictable that the color scheme of these snacks and sweets packages resemble toys and cartoons. In Figure 9, Superman's color, which are blue, green, and red shows similarity to the one used in the US sweets. In Japan too, children purchase sweets because of bonus toys and the popular anime cartoon characters that are seen on the package. Yet, the colors of Japanese toys and cartoons may not be as vivid as those of the US.

6. CONCLUSIONS

The packages of long seller sweets can become the evidence of color sense in every country. In Japan, warm and light colors are used in the basic long sellers, and color scheme variations are seen in seasonal, regional, and limited items. In the US, marketing to children and color scheme of American comics deeply influence the design and colors of sweets packages. Humankind forms the color culture by looking at these items on a daily basis since childhood.

ACKNOWLEDGEMENTS

I would like to express my heartfelt thanks to Asahi Group Foundation for their support.

REFERENCES

Birren, F. 1961. *Color Psychology and Color Therapy*, University Books.

Iyengar, S. 2010. *The Art of Choosing*, Grand Central Publishing.

Okuda, H., Tasaka, M., Yui, A., and Kawasome, S. 2002. *Correlation between the Image of Food Colors and the Taste Sense: The Case of Japanese Twenties*, Journal of Cookery Science of Japan 35(1), 2-9.

Story, M. and French, S. 2004. *Food Advertising and Marketing Directed at Children and Adolescents in the US*, International Journal of Behavioral Nutrition and Physical Activity 1-3.

Sugita, Y. 2010. *Experience in Early Infancy for Color Perception*, Journal of the Color Science Association of Japan 34(2) 164-167.

Address: Dr. Kyoko HIDAKA, Department of Graphic Design, Faculty of Art and Design
Tama Art University, 2-1723 Yarimizu, Hachioji-shi, Tokyo, 192-0394, JAPAN
E-mail: kh2017@nyu.edu

Human monochromatic impressions on multichromatic / colorless phenomena and concepts

Ayana DEGUCHI[1], Akira ASANO[1], Chie MURAKI ASANO[2*], Katsunori OKAJIMA[3]
[1]Faculty of Informatics, Kansai University
[2]Faculty of Human Ecology, Yasuda Women's University
[3]Faculty of Environment and Information Sciences, Yokohama National University

ABSTRACT

This research experimentally investigates human association of colorless or abstract concepts and phenomena with a single color. This association is called *affinity* between concepts/phenomena and colors in this research. The respondents of the experiments were asked to express various colorless or abstract concepts and phenomena, presented by words, by a single color based on their impressions. The reason why the color was selected is also asked. According to the experimental results, it is found that there exists a color or a category of colors selected by most of respondents for each of several concepts and phenomena. The reasons answered for such concepts and phenomena indicate that the color is selected because most of the respondents agree with an association of the concept or phenomenon with a common concrete object, and the color derived from the object is selected. The model of color affinity is also applied for the selection of a single color for expressing a multichromatic phenomenon, and the existence of the affinity is observed through the experiments.

1. INTRODUCTION

Color is a human perception of a physical property of light. It indicates that a color perception is caused by actual stimuli of light with a distribution of spectra (Gonzalez and Woods, 2008). However, it is observed that humans often visualize even abstract or shapeless concepts and phenomena with some colors in mind, by an association of the concepts or phenomena with concrete objects containing some colors. For example, it is usual in Japan that the concept "spring season" is visualized with pink color, which is derived from cherry blossoms.

It is observed in the above example that a concept or a phenomenon can be associated with a color through the relationships between the concept/phenomenon and an intermediate object and between the intermediate object and the color. We call the relationship *affinity* between a color and a concept/phenomenon in this research, as shown in Fig. 1. High affinity indicates a tight relationship, that is, most of people select a common single color for a concept/phenomenon. In case of the above example, the affinity between the concept "spring" and the color "pink" is high if most people agree with associating spring with pink color. There have been a lot of research works on the association of color with concepts (Elliot and Maier, 2014), whereas our experiments investigate the association of concepts with colors.

The model of color affinity is also applicable not only to abstract concepts but also to multichromatic objects. We consider the situation that one is asked to express a multichromatic object, which is shown not by actual things or photos but by words. If one color is preferred

* Current affiliation: Faculty of Human Life and Environmental Sciences, Nagoya Women's University

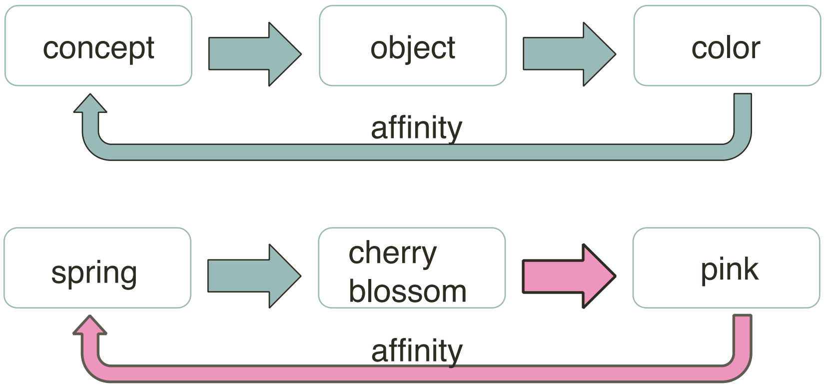

Fig. 1. The model of color affinity.

to express the color of multichromatic objects, the affinity between the color and the object in mind is high. For example, the rainbow has a continuous spectrum of colors. If a color is significantly preferred to express the rainbow when the respondents are asked to express the rainbow in mind by one color, the affinity between the color and the rainbow is high. It is expected that there are cultural characteristics.

We experimentally investigated the applicability of the model of color affinity for several abstract and colorless concepts/phenomena, and a multichromatic object. The respondents of the experiments were asked to express various colorless or abstract concepts, for example "summer," "Internet," etc., and a multichromatic phenomenon, "rainbow," presented by words, by a single color based on their impressions. The reason why the color was selected was also asked. We carried out the experiments for more than 100 respondents in Japan.

It is observed through our experiments that several concepts/phenomena have high affinity with specific colors, and some have high affinity to specific color categories. The intermediate objects are also observed in these cases. The result for the multichromatic phenomenon,"rainbow," indicates that all colors in the spectrum is not evenly selected and the affinity with a specific color is observed. It is shown by an additional experiment that the affinity is influenced by the background color and the arrangement of color stripes in the rainbow.

2. EXPERIMENTS

Our experiments are based on questionnaires for respondents. The respondents of the experiments are restricted to those who have mainly lived in Japan, in order to control the dependence on culture and circumstance. The following words, which were in Japanese in the experiments, were presented to each respondent. These words indicate colorless and/or abstract concepts and phenomena, and one multichromatic phenomenon, "rainbow."

Abstract concepts and phenomena
"spring", "summer", "Internet", "dream", "winter", "time",

Colorless phenomena
"water", "hot water", "air", "wind"

Multichromatic phenomena
"rainbow"

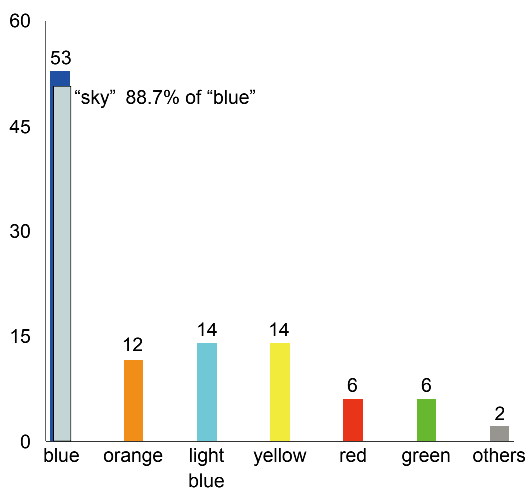

Fig. 2. Result for "summer."

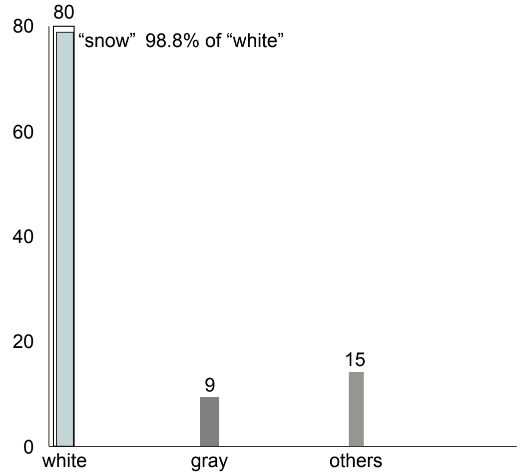

Fig. 3. Result for "winter."

The respondents were requested to answer a color in mind by a word for expressing each of the presented words. The answer was strictly restricted to a word expressing one single color. The respondents were also requested to answer the reason why the answered was selected for each of the concepts and phenomena. The number of the respondents is 107, and most of them are university students in Osaka, middle western city of Japan. Some of them are "friends" of Akira Asano, one of the authors, on Facebook, living in Japan.

3. RESULTS AND DISCUSSION

We show the results of the experiment for several concepts and phenomena where interesting characteristics on the affinity were observed.

3.1 "summer"

Figure 2 shows the number of respondents who answered each color to the concept "summer." The number on each bar indicates the number of respondent who answered each color. The result shows that 49.5% of the respondents answered "blue" to "summer." According to the reasons answered by the respondents, 88.7% of the respondents selecting "blue" associated "blue" with "sea" or "sky." It is observed that the affinity between "summer" and "blue" is high, and the intermediate object in the color affinity model is "sea" and "sky."

3.2 "winter"

Figure 3 shows the number of respondents who answered each color to the concept "winter." The result shows that 76.9% of the respondents answered "white" to "winter." According to the reasons answered by the respondents, 98.8% of the respondents selecting "white" associated "white" with "snow." It is observed that the affinity between "winter" and "white" is very high, and the intermediate object in the color affinity model is "snow."

The participants are mainly from around Osaka, middle western city of Japan. Since it snows only several days in one winter in this region, the winter scenery in this region is usually not white, but rather brown because of the defoliation of trees. The impression may be not from their actual experience but from their knowledge.

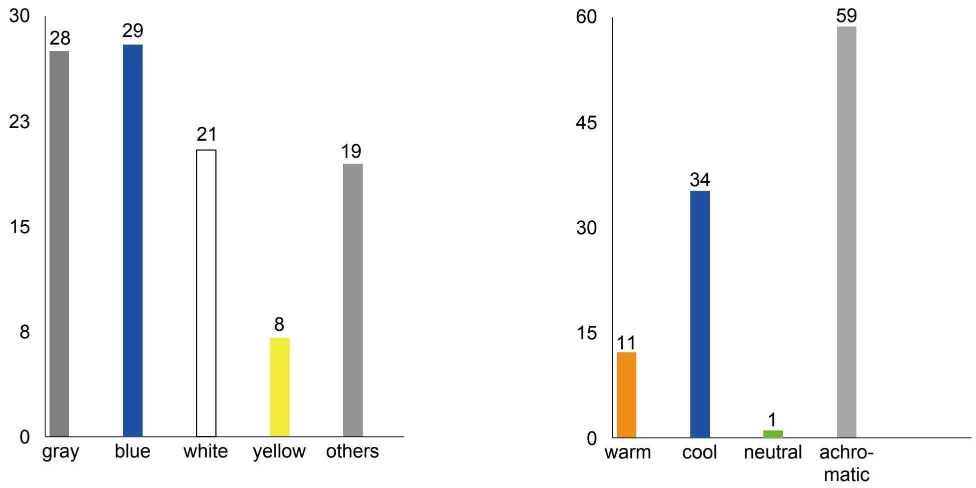

(a) *(b)*

Fig. 4. Results for "Internet." (a) preferred colors. (b) another categorization.

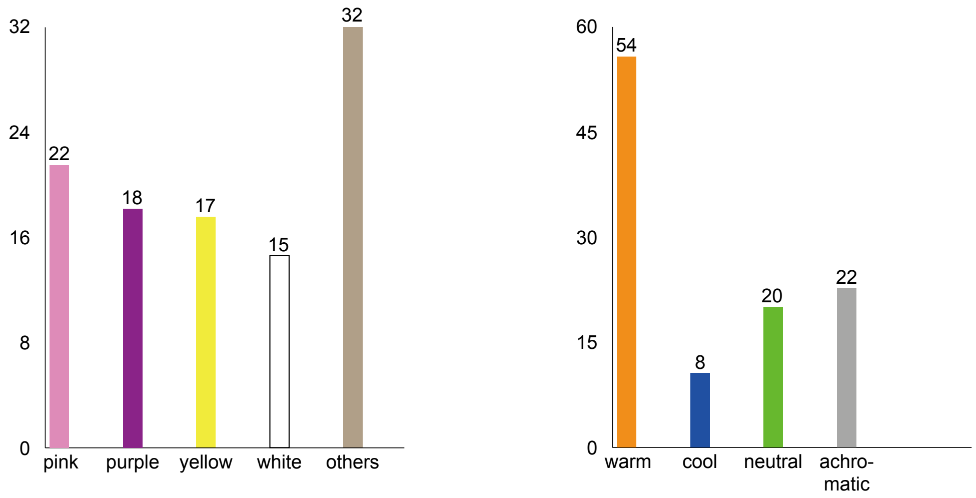

(a) *(b)*

Fig. 5. Results for "dream." (a) preferred colors. (b) another categorization.

3.3 "Internet"

Figure 4(a) shows the number of respondents who answered each color to the concept "Internet." It indicates that no specific color is closely related to this concept, and no affinity between "Internet" and any color is observed. Figure 4(b) shows the result by categorizing the answered colors into warm, cool, neutral, and achromatic colors. It shows that 56.2% of the respondents selected achromatic colors to express "Internet." The reasons answered by the respondents selecting achromatic colors were mainly negative impressions, for example "network crimes," "mixture of good and bad things," and "complex chaos." It suggests that a concept related to negative idea may be associated with achromatic colors.

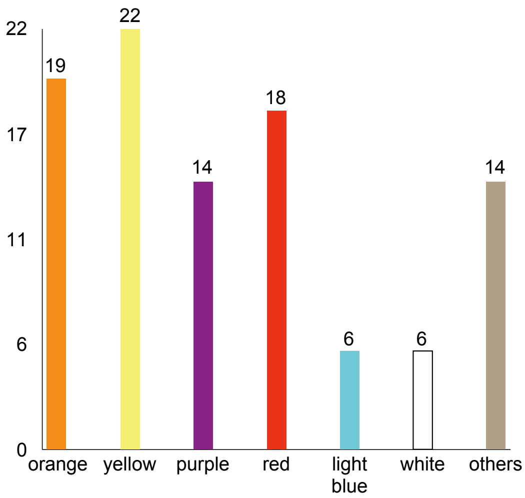

Fig. 6. Results for "rainbow."

3.4 "dream"

Figure 5(a) shows the number of respondents who answered each color to the concept "dream." It indicates that no specific color is closely related to this concept, and no affinity between "dream" and any color is observed. Figure 5(b) shows the result by the categorization similar to Fig. 4(b). It shows that 51.9% of the respondents selected warm colors to express "dream." The reasons answered by the respondents selecting warm colors were mainly positive impressions, for example "brightness" and "hope." It suggests that a concept related to positive idea may be associated with warm colors.

3.5 "rainbow"

Figure 6 shows the number of respondents who answered each color to the multichromatic phenomenon "rainbow." No affinity to any specific color is observed, but orange, yellow, purple, and red are preferred. The reasons answered by the respondents selecting warm colors were mainly "significant," "impressive," and "beautiful in the background blue sky." The reasons for "purple" were mainly "significant," "impressive," "purple is on the edge of the rainbow." Such answers as "The rainbow is watched in the cool sky" were found as the reason for cool colors.

It is interesting that none of the respondents answered "green," except one answer of "yellow-green," although green is physically obviously observed in the spectrum of the rainbow. We assumed a hypothesis that green is difficult to remember because the contrast between green and the background blue sky, and that between green and adjacent colors. A photo of the actual rainbow is shown in Fig. 7 for reference. We carried out two small experiments to confirm the hypothesis. We showed respondents 1) a color stripe similar to the rainbow with blue background on a display, and 2) the same color stripe with orange background, and asked which color was remembered best. The results was that warm colors were preferred in case 1), whereas in case 2) some respondents answered that blue and green were easy to memorize. We also showed a rearranged color stripe where green was between red and orange, and asked the same question. The result was that some respondents answered that blue and green were easy to memorize, also in this case. These results suggests that the results depend on contrasts among neighboring colors.

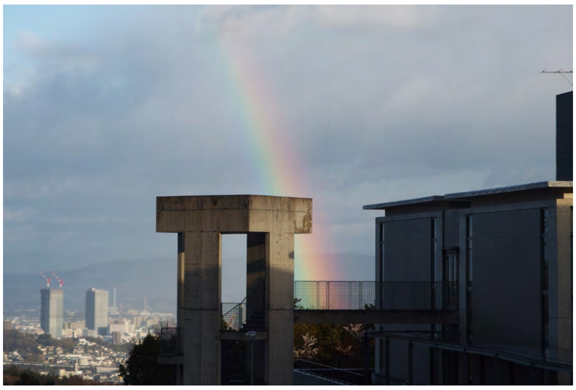

Fig. 7. Actual rainbow[1].

4. CONCLUSIONS

This research considers a model of color affinity, which means the association of an abstract or colorless concept/phenomenon with a color via an intermediate concrete object. We experimentally investigated the applicability of the model to several concepts and phenomena. We also investigated the applicability to a multichromatic object. We expect that further investigation of colors derived from concepts and phenomena may yield the inverse relationships, i. e. concepts or phenomena derived from colors.

The dependence of color affinity on each culture is an interesting problem. When we asked university students in Thailand to express the rainbow in one single color, 12 of 37 students selected green. The result was different from our experiments in Japan, and it is said that green is preferred in a lot of situations in Thailand.

REFERENCES

Gonzalez, C. and Woods, R. E. 2008. *Digital Image Processing, Third Edition, Chapter 6.,* Pearson Education.

Elliot, A. J. and Maier, M. A. 2014. *Color Psychology: Effects of Perceiving Color on Psychological Functioning in Humans,* Annual Review of Psychology, 65, 95-120.

Address: Prof. Akira Asano, Facutly of Informatics, Kansai University
Ryozenji-cho 2-1-1, Takatsuki, Osaka 569-1095, JAPAN
E-mail: a.asano@kansai-u.ac.jp

[1] Photographed by Akira Asano in Kansai University Takatsuki Campus, Osaka, Japan, on Apr. 4, 2014.

How to create a colour education that fosters price-winning design students

Ivar JUNG
Department of Design, Linnaeus University, Sweden

ABSTRACT

This paper has the objective to describe a price-winning approach to colour education. The colour education of today is an important building block for all future design. If we can provide our students with state of the art colour education we will get the best future design when it comes to the use of colours. That will include all kinds of design e.g. graphic design, architecture and product design.

In 2014 there was a national competition called *Prisad Färg* (Award-winning Colour) organized by Swedish Colour Centre Foundation that celebrated its 50 years anniversary. The competition was open to all students of design, architecture, fine art, graphic design and advertisement. Design students from the product design programme at the Linnaeus University won no less than two out of three awards.

The subject of colour is introduced very early in the programme. Students of product design have two weeks of colour theory and workshops in their first semester. In this basic theoretical course the students get to know different colour systems and the advantage of using systems to think, visualise and communicate colour. In the workshops they can train their eyes and skills in mixing and combining colours with different amount of complexity. The workshop ends with a task where students explore the colour language in different contexts and cultures. This lays a ground for four more weeks of colour projects with a exploratory approach. The students phrase their own colour questions and seek answers through research and visual colour representations. In the second year students progress to understanding different contexts of colour. The students continue with light theory and light projects for five more weeks and then proceed with light and colour in space contexts for another five weeks. The three-fold strategy: early introduction, emphasis on colour and continuous progression, has proved to be successful.

1. INTRODUCTION

Colour education is not a priority issue for the main part of Swedish design and architectural education. The competition, *Awarded-winning colour*, was in itself an attempt to emphasize the importance of colour education on a university level as a seed for advanced future colour design and colour research.

To express yourself you need a language. Colour is an important part of the language of visual communication. It is used more or less consciously in the fields of art, design, architecture and visual media. If we regard colour as a media for communication we need to provide our design students with the best tools for using that language. The more skilled the students are in the language of colour, the more they use it and also dare to make advanced colour design. An uncertain and unskilled designer tend to use only "safe" colours and colour combinations and can not use the variety of possibilities in the language of colour to create an excellent design.

2. SYSTEMATIC COLOUR EDUCATION

The aim of colour education at the product design BA programme at Linnaeus University, Sweden is to provide the students with skills to concisely use colour as a tool to make a more efficient design.

To discuss colours students normally use our everyday language and use traditional colour names. However, in order to engage in a professional discussion about colours the spoken language has to be complemented with an efficient and precise vocabulary. Therefore one of the first steps is to provide the students with a common language regarding colours. At Linnaeus University, we have found the NCS colour system (Hård et al 1996) a helpful tool for communication about colour and colour combinations. One of the great advantages with this system is that it allows students to visualise the relations between colours in a visual system consisting of the colour wheel and colour triangles. The same basic structure is also found in other colour systems as e.g. Munsell. NCS is also useful for the students to discover that the naming of colours regarding hue, and perceived amount of blackness, chromaticness and whiteness is a tool for making cognizant colour combinations.

The students learn that there is a variety of different colour systems used for different purposes and in alternative contexts. They learn about Munsell, Pantone, CIELab, CMYK, RGB and how they are related. The main language used in the learning program is the NCS system, mainly because it is clearly based on human perception, easy to understand for students and easily communicated. The design students appreciate the visual representation, which helps them to work with colours in a systematic way.

The foundation of understanding of colour systems makes it is easier for students to proceed to understand different theories regarding colour combinations. The students explore in theory and practice different principles of colour combinations such as complementary colours, likeness and contrasts regarding chromaticness, hue, blackness and whiteness. The students make colour combinations of increasing complexity in workshops and write down their analyses and reflections. At first they have to make their colour work physical with gouache and acrylic colours to give the students a sense of the colour pigments and materiality of colour. The next step is to explore the possibilities of working with colour in the digital world in different computer programmes.

3. COLOUR AND CULTURE

To explore the language of colour the students, on their second week of colour education, are given sixteen different words such as "warm", "cold", "young", "old" that they are asked to express with colour chords consisting of three chosen colours in a given form. This can be compared with a musical chord consisting of three notes. The colour chords are organized on the wall in groups where all chords made from one of the words are clustered together. In this way it is possible to see if there is a common colour language for those words (Figure1). The result is that certain words have a clear likeness when it comes to the chosen colours, while other words have a wider variety. This is a good opportunity for starting a discussion and exploring if there is such a thing as a common colour language and to what extent it is primarily cultural, contextual or individual. To explore these matters the students have to research the use of colours in different contexts, such as art, design, packaging, architecture and visual communication. They also look into the use of colours in different parts of the world, in different cultures and in different historical contexts. This gives a broad understanding of the use of colours and colour combinations in different cultural contexts.

Figure 2: Students analysing their colour chords from different words

The three-week-long theoretical and practical block evokes new questions for the students. These are channelled into an individual research question that the student will explore theoretically and practically for further three weeks. The result is presented to the group and also documented in an individual workbook where the teachers can follow the students individual work process, which includes reflections and further questions raised during the project.

4. LIGHT AND SPACE

In the second year the students are supposed to gain a deeper understanding of the perceived colour in relation to light and space. Students explore/observe their perception of colour in different environments and spaces and systematically write down and discuss their observations. The students learn how the perceived colour changes under the influence of different light and spatial conditions. The students build models where they make experiments with light and colours. They also make full-scale experiments with different light sources and different lighting design before they make their own design of a lamp and build it as a functioning prototype. This creates knowledge of the complexity of the relation between perceived colour and the contexts. The basic theory can be found in books but students also need to explore and see how colours in light and space are really perceived and experienced in the real context, to be able to have a full understanding of the impression of light and space on colours.

To ensure that the students will practice and use their colour skills throughout their entire study period they are asked to present and motivate the chosen colours in every project they do. That helps them always remember that the aspects of colour are as important as any other design aspect when it comes to the visual expression.

5. COLOUR RESEARCH

It is important to connect the colour education to current colour research. In the library the students can find literature with colour research to inspire them and inform them, but the students are also used as subjects in various colour studies, both in the lecturers' own projects and in studies carried out by researchers from other universities. In one of the design department's own research studies, 20 students compared perceived colours in glass with 1950 NCS opaque colour charts (Figure 2) and also with NCS colour charts on a computer screen (JUNG et al 2011). In another international linguistic study, 20 students participated and listed Swedish colour names to be compared to colour names in ten other languages. This student participation creates an interest and understanding of colour research. It also shows the dignity and variety of the field of colour. Participation points out the possibility for a future career in research, which may be about questions identified during their colour education that have not yet been answered.

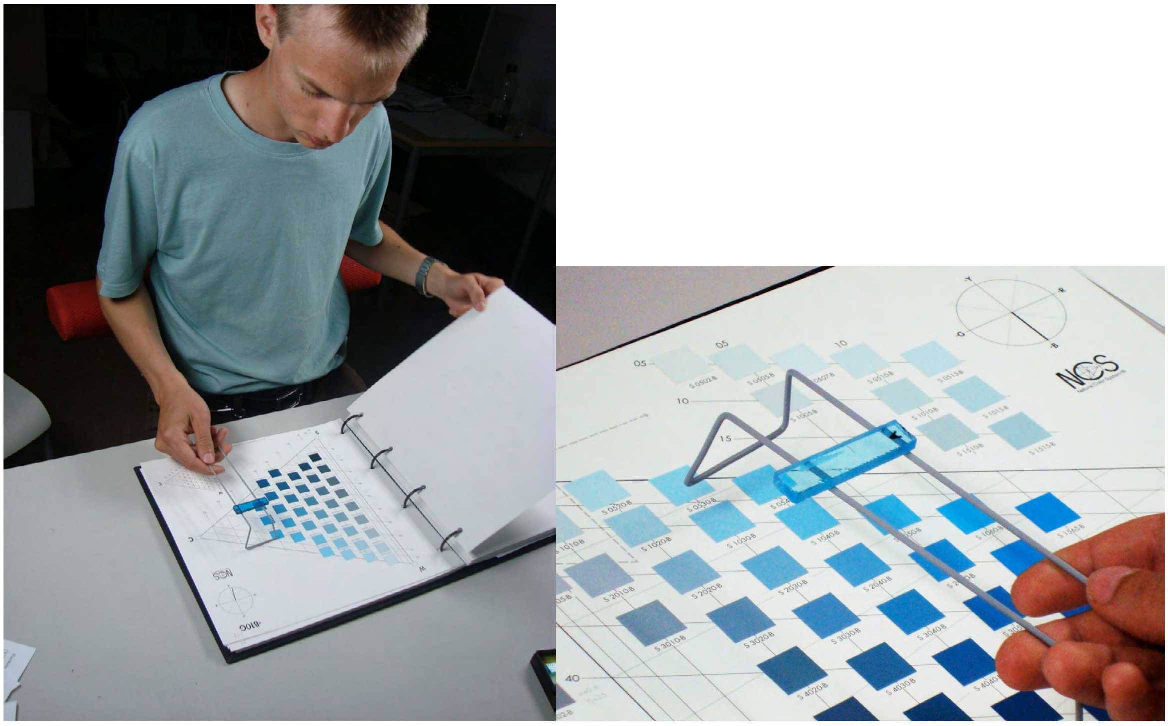

Figure 2: Student participating in research study, perceived colour in glass.

6. CONCLUSIONS

It is essential to introduce colour at an early stage of the BA programme. This means that the students are considering colour as a part of their design and a part of the visual expression. If not introduced early, colour will just be something added to the design at the end and not an integrated part of the design process. Students have different skills and levels of experiences when it comes to colour when they arrive on the programme. This emphasises the need for learning and practicing a colour system, which can be a language that helps the student to think about and communicate colour in a precise way. The introduction of colour systems in general and NCS in particular creates a possibility for students to visualise and understand the relations between colours in their future work. The conclusion is that it is the clear strategy for colour education that is repeatedly implemented throughout the entire programme that fosters award-winning students.

REFERENCES

Bimler, D. L., M. Uusküla 2014, *The map is the itinerary: Cognitive color space reconstructed from listing data for 11 European languages Perception* **43** ECVP Abstract Supplement, page 68.

Hård, A., L. Sivik and G. Tonnquist. 1996a. NCS, Natural Color System – from Concept to Research and Applications. Part I. *COLOR research and application* 21(3): 180-205.

Hård, A., L. Sivik and G. Tonnquist. 1996b. NCS, Natural Color System – from Concept to Research and Applications. Part II. *COLOR research and application* 21(3): 206-220.

Jung, I., P. Jokela, P. Brandt, and O. Victor. 2012. *What is the colour of a glass of wine? Color in food: Technological and Psychophysical Aspects*. Boca Raton: CRC Press. 35-41.

Jung, I., P. Jokela, P. Brandt, and O. Victor. 2011. *Percieved colour in transparent materials and objects*. In *AIC 2011 Interaction of Colour & Light in the Arts and Sciences, Midterm Meeting of the International Colour Association, Zurich, Switzerland, 7–10 June 2011: Conference Proceedings, CD,* edited by Verena M. Schindler and Stephan Cuber. Zurich: pro/colore, 2011.

Address: Senior lecturer Ivar JUNG, Department of Design,
Linnaeus University, S-391 82 Kalmar, SWEDEN
E-mail: ivar.jung@lnu.se

INFLUENCE OF ODORS FUNCTION AND COLORS SYMBOLISM IN ODOR-COLOR ASSOCIATIONS: COMPARATIVE STUDY BETWEEN RURAL AND URBAN REGIONS IN LEBANON

Léa NEHMÉ[1], Reine BARBAR[2], Yelena MARIC[3] and Muriel JACQUOT[4]

[1]LIBio (Laboratoire d'Ingénierie des Biomolécules), Université de Lorraine, 2 avenue de la Forêtde Haye, BP 172, 54505 Vandoeuvre-lès-Nancy, France.
[2]Departement of Food Science, Faculty of Agricultural and Food Sciences, Holy Spirit University of Kaslik, Lebanon, P.O.BOX 446, Jounieh, Lebanon
[3]myrissi, 24-30 rue Lionnois, BP 60120, 54003 Nancy Cedex
[4]Innovative Crossmodal Interactions Modeling (InnoCIM), ENSAIA, Université de Lorraine, 2 av. de la Forêt de Haye, 54500 Vandoeuvre-lès-Nancy, France

ABSTRACT

The purpose of this study was to assess the intra-cultural impact on the relationship between odor and color on one hand, and on the parameters of the smell on the other hand, within the same country, Lebanon, unlike the preliminary studies that evaluated the cultural effect between two different countries. To assesss this intra-cultural effect, sensory analyzes were performed on 200 subjects in two campus of the Holy Spirit University: two regions were considered, Zahleh campus representing the rural community, and Kaslik campus representing the urban community. The experiment was based on a set of 24 odors, some of them are internationally recognized, others nationally, and some of them are mainly recognized in the rural area. Statistical analyzes revealed anintra-cultural impact, given the existence of significant differences for some odors: shallots score the biggest difference, where it is more recognized in the urban area and more familiar, and they link it to brown color while at Zahleh it is linked to black color. Caramel, smoke, orange blossom, molasses and *Jellab* (the last two being purely national odors) also show significant differences in color choice between the two regions. Similarly, scores of familiarity, of intensity, pleasantness and edibility indicate some differences for few odors. These sensory analyzes have shown for the first time in Lebanon the impact of habits, environment and lifestyle on the relationship between odor and color, between rural and urban areas.

1. INTRODUCTION

According to UNICEF (2012) the definition of 'urban' varies from country to country, and, with periodic reclassification, can also vary within one country over time, making direct comparisons difficult. An urban area can be defined by one or more of the following: administrative criteria or political boundaries (e.g., area within the jurisdiction of a municipality or town committee), a threshold population size (where the minimum for an urban settlement is typically in the region of 2,000 people, although this varies globally between 200 and 50,000), population density, economic function (e.g., where a significant majority of the population is not primarily engaged in agriculture, or where there is surplus employment) or the presence of urban characteristics (e.g., paved streets, electric lighting, sewerage). The task of defining urban population has always been particularly challenging. The United Nations itself recognizes the difficulty of defining urban areas globally, stating that, "because of national differences in the characteristics that distinguish urban from rural areas, the distinction between urban and rural population is not amenable to a single definition that would be applicable to all countries” (UN, 1998). Rural areas are usually defined as “what is not urban” (UN, 1998 and 2004), and so inconsistencies in the definition of what is urban lead to inconsistencies in characterizing what is rural. In Lebanon , Kaslik area is considered as urban, due to the fact that the definition given by the UNICEF for urban cities is applicable on it. While Zahleh is considered as rural.

Crossmodal correspondence is one of the terms that have been used to describe the tendency that people have to associate certain features, or stimuli across the senses (Spence, 2011).

Throughout the years the relationship established between different senses attracted the attention of researchers, in particular the relationship between vision and hearing. While the intermodal correspondence between vision and olfaction has been less studied, it has been proven that this relation is consistent and durable. Various studies highlighted those facts: subjects noted the same results when the same sensory analysis were repeated after two years (Wada *et al.,*2012 ; Maric & Jacquot, 2013).

Previous studies showed that people tend to match basic tastes with a host of other non gustatory stimuli such as color (Spence *et al.,* 2010) or shapes (Spence and Deroy, 2014). On the other hand growing number of studies started to investigate cross-cultural differences in the way in which people match gustatory information with non gustatory ones. For instance, Levitan *et al.* (2014)investigated color-odor association between 6 different cultural groups. While Velasco *et al.* (2014) studied the color-flavor association between 3 different countries. Wan *et al.* (2014) showed cross-cultural differences in crossmodal correspondences between basic tastes and visual features between 4 countries.Maric *et al.*investigated in 2012 cross cultural differences between Lebanese and French populations.

These cross cultural studies have been carried out from two points of views: to understand cultural differences in food acceptance and preference (Yeh *et al.,* 1998) and to evaluate the effect of individual experience and knowledge of odors and colors, on odor and color perception, in order to understand how olfactory stimuli or visual stimuli influence psychology and behavior (Hudson & Distel, 2002). But while these studies evaluated the cross-cultural differences, rare are the studies focusing on the differences in one culture (one country).

The aim of the present study is to focus on the intra-cultural effect within the same country, Lebanon. The intra-cultural differences related to habits, environment and lifestyle between Zahleh (rural area) on one side and the urban area Kaslik on the other, were investigated in orderto analyze their impact on the odor-color association, on familiarity, pleasantness and edibility. The effect of the geographic area of residence can stimulate potential differences between the perception of the color-odor relationship among those residents in rural and urban areas in Lebanon.

2. METHOD

2.1 Sample Preparation

Participants:

Two hundred participants, aged between 18 and 60 years were recruited for these experiments, 100 from the rural area of Bekaa and 100 from the urban area of Kaslik in Lebanon.For the coastal region of Kaslik, subjects were either students or employees of the Holy Spirit University of Kaslik. In Zahleh participants were either students or residents of the region of Zahleh. Taking into consideration the differences between residents in both areas: Zahleh residents usually live, study and work in Zahleh so they are practically growing on the rural traditions of their area, where they are more engaged in agriculture and more familiar with the Lebanese "*mouneh*", which is a Lebanese word used to describe the fact of preserving food. *Mouneh* is prepared during the summer months in order to be consumed during the harsh days of winter. The main purpose is to transform foods that perish into foods with long shelf life, durable, lasting throughout a whole season. While Kaslik citizens are less familiar with these traditions.All subjects were naive about the stimuli. It was recommended not to wear perfume on the day of the experiment nor to eat or drink coffee 30 minutes before the session.The subjects were also tested for abnormalities of vision using the Ishihara test.

Olfactory Stimuli:

18 natural food and floral odors were chosen as olfactory stimuli. Our selection aimed firstly, to cover a wide variety of odors related to food and drinks, and secondly, to raise the intra-cultural differences of the same color-odor association for national aromas. To evaluate the level of the relationship between odors and colors, we chose two similar odors (peppermint*vs*. chlorophyll; lime *vs*. lemon).All odors were presented in a single aromatic intensity, except for the smell of plum (yellow fruit Mirabelle, specialty of the French Lorraine region), which was presented twice, with two different intensities. The samples were preparedby injecting 1 ml of each odor in a small piece of cotton placed in a little opaque glass vial. No visual factor was therefore present.

The samples were identified by three-digit codes and refrigerated between each two sessions. Samples were placed at room temperature 15 minutes before the analysis.The samples of international odors (rose, violet, orange blossom, lavender, cucumber, wild strawberry, lime, lemon, pineapple, smoked, shallot, caramel, chlorophyll, peppermint, mirabelle (high intensity), mirabelle (low intensity)) were purchased from the laboratories Mathé (Maxville, France), using the corresponding essential oils, while the two national odors (pomegranate molasses, *jellab*) were prepared in the Holy Spirit University of Kaslik campus. They were purchased directly from the products of the market (Kasatlé Chtoura brand).

Visual stimuli:

24 different color patches (4cm in diameter) were presented in a color chart. This color chart consisted of a white A3 size page containing twenty-one color patches arranged in circle from red to purple, and three achromatic colors (white, grey, black) presented separately in the lower left corner. Each color patch was identified by a code (one capital letter and one figure). Color charts were printed on coated paper. The print was calibrated to ensure consistent colors between participants. L*a*b coordinates were measured for each color chip by means of a Datacolor system (Pantone® ColorVision™ Spyder Master Suite Spectro), and converted in L*C*H* (Lightness, Chroma, Hue) coordinates, to get the exact position in the CIELAB color space (Figure 1).

Figure 1:the color chart used in sensory analysis

2.2 Experimental Procedure

Task location and procedure:

In each area, sessions were conducted in sensory testing facilities with separated booths. Each testing booth had white walls and standardized white light source. After completing the Ishihara Color Vision test, each subject was presented with the olfactory stimuli in a random order, and with the color chart. For each olfactory stimulus, participants were asked to open the glass bottle and smell its content orthonasally. Afterwards, participants were instructed to select among the 24 color patches one color that they felt closely matched the odor. After having made their choice, they rated the difficulty of odor-color association and the odor perceived intensity, familiarity, pleasantness, and edibility. Participants were not required to name the odors they smelled.

Data analysis:

All data were processed by SPSS 16.

3. RESULTS AND DISCUSSION

3.1 Relation between odor and color

Choice of color for each odor:

The results revealed that the participants of each area did not choose colors uniformly but rather tended to choose some colors over others when matching the odors. Indeed, all 18 olfactory stimuli led to significant preferences in the choice of color ($p < .05$ in all cases) in both areas.

Among the odors tested for the study, six indicated a significant difference in the choice of a color for a specific odor, between the two areas of Kaslik and Zahleh: caramel ($p=0.04<0.05$), shallot ($p=0.00<0.05$), orange blossom($p=0.00<0.05$),smoked ($p=0.01<0.05$), pomegranate molasses ($p=0.035<0.05$) and *jellab* ($p=0.036<0.05$).

For both Zahleh and Kaslik residentswe could note that the participants have registered in their majority the light brown color (or honey-color) as being the color of caramel but the difference lies in the choice of both purple and yellow color in Kaslik and brown color in Zahleh (Khi-Square=29.78, dl=21, $p= 0.04<0.05$)

Shallot registered a significant difference (Khi-Square= 39.36, dl=17, p=0.00<0.05) in the choice of associated colors between Zahleh and Kaslik. Zahleh residents tend to choose black and grey colors while Kaslik residents tend to choose the browncolor.

Orange blossom registered a significant difference (Khi-Square= 46.88, dl=23, p=0.00<0.05) in the choice of odors among both areas (Figure 2). So there is a relationship between the choice of color for orange blossom odor and the regions (urban *vs.* rural) where participants of the urban area of Kaslik have chosen in their majority the white color and more frequently the color pink, whereas in Zahleh the majority chose pink and gray colors.

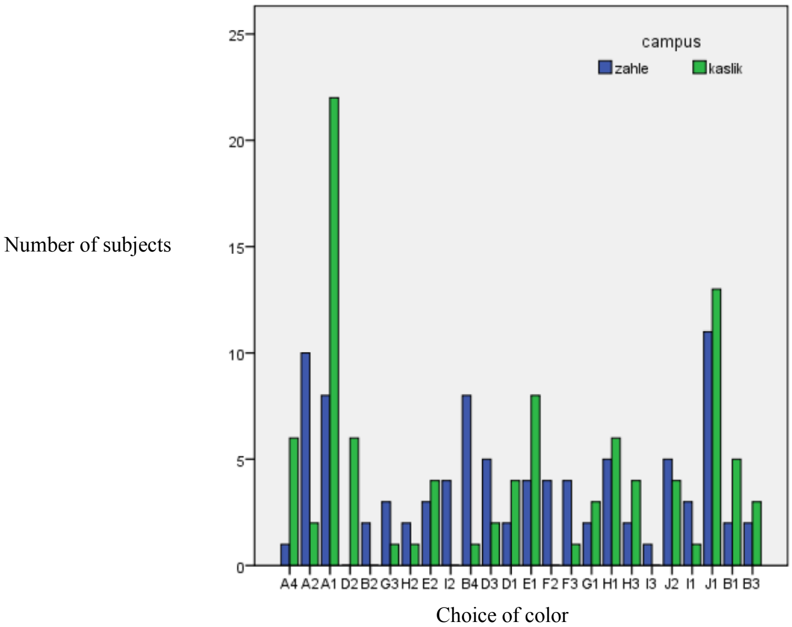

Figure 2:Graph representing the difference in the choice of color for the smell of orange blossom between Zahle and Kaslik

Smoke odor indicated a significant difference between the twolocations and the choice of color (Khi-Square= 34.11, dl=19, p=0.01<0.05). The most dominant color given by subjects of Kaslik is brown while in Zahleh the choice of color is more diversified tending to black and gray.

Pomegranate molasses recorded a significant difference (Khi-Square= 33.25, dl=22, p= 0.035<0.05). Zahleh subjects selected the color brown while Kaslik citizens selected in their majority the white color followed by the light pink.

Jellab displayed a significant difference (Khi-Square= 33.521, dl=23, p=0.036<0.05). The majority of participants in urban area of Kaslik selected the white color. While the participants of Zahleh selected pink, purple and red colors.

Difficulty of associating a color with an odor in the two areas:

Three odors registered difficulty of association with a color. They revealed a significant difference between the difficulty of association and the two areas: Pineapple; Peppermint; Chlorophyll.

Participants of Kaslik area found it more difficult (than Zahleh participants) to associate a color for these 3 odor samples: Pineapple (Khi-Square= 4.554, dl=1, p=0.033<0.05), peppermint (Khi-Square=3.910, dl=1, p=0.048<0.05) and chlorophyll (Khi-Square=3.910, dl=1, p=0.048<0.05).

3.2 Odor Parameters

Odor intensity :

The only significant difference was found for the odor of cucumber. Data analysis indicates that the mean intensity chosen by participants in Zahleh area is 5.60, superior to the mean in Kaslik which is 4.03. Moreover, the difference between the two regions is significant. So there is a relationship between the region and the average intensity detected for cucumber odor.

Odor familiarity:

Among the odors, data analysis detected significant differences in odor familiarity between Zahleh and Kaslik for 4 odor samples: Shallot, smoked, *jellab* and mirabelle (high intensity).

The mean value of familiarity parameter of shallot for Zahleh is 5.77 which is inferior to Kaslik (7.05). And there is a significant difference between the 2 areas (t-test= -2.163, dl=192, p=0.031<0.05) which indicates that Kaslik citizens tend to find shallot odor more familiar than Zahleh participants.

The mean value of familiarity score for smoked odor in Zahleh is 6.44 inferior than the mean in Kaslik (7.81). In addition, there is a significant difference between the two regions (t-test= -2.32, dl= 184, p=0.021<0.05). Therefore there is a relation between the area and the familiarity for the smoked odor. Kaslik participants found smoked odor familiar while in Zahleh the answers were heterogenic, some participants found it familiar while others did not.

Jellab odor shows a mean value of familiarity of 6.90 in Zahleh and of 5.62 in Kaslik with a significant difference (t-test= 2.338, dl= 188, p= 0.020<0.05). Residents in Zahleh found*jellab* odor more familiar than those living in Kaslik.

Mirabelle (high intensity) registered a mean familiarity score of 6.62 in Zahleh and of 7.68 in Kaslik. In addition significant difference was found between familiarity and area (t-test= -2.075, dl= 189, p= 0.039<0.05). Mirabelle (high intensity) was found to be more familiar in Kaslik.

Odor pleasantness :

Shallot registered the only significant difference among the 2 regions (t-test= -2.806, dl=186, p=0.038<0.05). Data analysis recorded a mean value for pleasantness for Zahleh residents (1.93) inferior to Kaslik (2.95). Kaslik citizens registered shallot odor as more pleasant.

Odor edibility:

Four odorsscored a significant difference between Zahleh and Kaslik concerning their edibility: shallot, rose, lime and mirabelle (low intensity).

The difference between the two variables, area and odor edibility for shallot was registered as significant (Khi-Square= 5.602, dl=1, p= 0.018<0.05). That indicates the presence of a relation between odor edibility and area of living. Kaslik residents still finds it more edible than Zahleh residents.

Rose odor samples registered a significant difference between the two variables area of living and odor edibility (Khi-Square=7.681, dl=1, p=0.0006<0.05). Both areas tend to describe it as edible. But Kaslik residents tend to find it more edible than Zahleh participants.

Significant difference was found in lime odor between the two variable odor edibility and area of living (Khi-Square=4.638, dl =1, p= 0.031<0.05). Both regions tend to consider lime odor as edible but Kaslik residents describe it as more edible than Zahleh residents.

The difference between odor edibility and region for mirabelle (low intensity) was found to be significant (Khi-Square=4.058, dl=1, p=0.034<0.05). Both regions tend to describe it as edible, but Kaslik residents tend to describe it as more edible.

3.3 General discussion

Among the 18 odor samples used in this study, shallot odor revealed the most striking difference between Kaslik and Zahleh. Residents of urban area (Kaslik) find shallot odor familiar, more pleasant, more edible and link it to brown color in comparison with Zahleh residents who linked it to black color. This could be due to the fact that shallot is usuallymore planted and consumed in urban areas, because it is sensitive to cold weather and need warm weather to grow. Therefore Kaslik residents find it more familiar and pleasantthan Zahleh residents which explain their choice of the black color.

In their study, Maric, Barbar and Jacquot (2012) found a significant difference between Lebanese and French participants in the attribution of a color to orange blossom odor.In Lebanon, orange blossom is associated to traditional Lebanese desserts and sugar pastries products, with color associations of white and pink.In France, this odor is more associated with hygiene products justifying the shades of bluechosen by the participants, typical color for non-food items. According to their study culture-dependent experiences affect our capacity to use, identify, like and consume odors. Thus odor-color associations can be similar or different among countries. When we recognize odors that seem familiar, semantic association is made upon the choice of colors. Even if subject is not able to identify exactly an odor, he might still beable to categorize it, for example, as a floral or fruity odor, edibleor non-edible odor.Both usage and association models affect odor-color associations revealing the complexity and multi-dimensional aspects of this linkage. In Lebanon orange blossom registered a significant difference between the residents of rural and urban areas, rural residents attributed first pink color followed by grey color, while urban residents attributed white color followed by pink color. Orange blossom is widely used in the Lebanese food, specifically pastries. The color of its extract is light pink color, which explain the use of the pink color in both areas. Orange blossom is used as well as a beverage mainly in urban areas, it is called by the Lebanese white coffee (café blanc) which can explain the choice of white color by Kaslik residents. The choice of grey color in Zahleh is due to its use in case of faintings to awaken people up. This relation with an unpleasant event justifies the choice of the grey achromatic color.

Smoked odor registered a significant difference as well in the choice of colors: Zahleh residents attributed to it the brown color for reminding them of the barbecue odor, while Kaslik residents associated it to black color for reminding them the pesticide odor and fuel combustion odor.

For the caramel smell almost the same odors were selected, but the difference lies in the fact that at Kaslik, 10 participants from 97 noted a clear purple color for caramel. Fact that has not been registered for Zahleh participants. Choosing clear purple color for caramel by Kaslik residents could be as a result of the use of the caramel flavor in sweets and candies, that are colourful and exist in urban areas supermarkets and rarely at the small stores of rural areas.

For national odors (*jellab* and pomegranate molasses) rural residents were able to detect easily these odors in comparison with urban residents. Due to the fact that these products are mainly produced in the Lebanese mountains, where the residents following the traditions prepare grapes, dates and pomegranate syrups to use them during winter and the cold season, when these fruits are rarely present. And they include them as well in food: *jellab* is usually drank during the fasting period and pomegranate molasses are used in Lebanese dishes like *fattouch*.

Concerning the rest of the odor samples, interesting remarks could be made. For chlorophyll odor, participants in urban area tend to link it with white color or light green for it reminds them of mint flavoured chewing-gum. While in Zahleh participants linked it to green color for it reminds them ofmint plants that areusually widely planted in the Lebanese mountains.

What seemed obvious was the difficulty that the subjects had in trying to connote a precise color to an odor,without guessing the origin of this aroma.Indeed, all subjects were trying to guess the smell, to imagine the object, then to link it to a specific colorwhich is consistent with the results of Morrot, Brochet & Dubourdieu study (2001).For odors they have not recognized, they scored directly "yes" to the question of the difficulty of association. For example, it was difficult to connote a color to the smell of peppermint and the smell of mint chlorophyll in both regions, but this was more acute for the region of Zahleh (rural), taking into consideration that both of these smells are extremely known in urban areas, because of their use in candies, food, gums and even fragrance and detergent. It wasn’t the case for the smell of ananas that registered a difficulty of association to a color in both regions but was more common in Kaslik.

The smell of wild strawberry reminded participants in both rural and urban areas, the smell of *shisha* or Lebanese *hookah*, which explain the choice of both purple and red colors given that tobacco used to prepare the shisha is red colored.

In addition participants detected unpleasant odors faster than pleasant ones. It has been noticed that participants disliking an odor detected it easily when these odors where in some cases undetectable by other participants.

On the other hand molasses, registered lower rate of pleasantness in Zahleh, while familiarity rate was higher than in Kaslik, and the color chosen by the majority is dark brown, more appropriate than the white color given by the subjects in Kaslik. A question arises here, why residents of the rural area would note a low rate of pleasantness for molasses while it is used in their daily culinary traditions dishes. Let us not forget, however, that the samples of the two national odors, *jellab* and molasses, have not been taken from essential oil extract, but they were prepared directly from the product of the market, which is why after having opened the sample several times, the smell had become so slight that some subjects had difficulties to detect it. Always talking about the intensity of the odor,we noticed a significant difference in the score of intensity for the smell of cucumber, it was noted more intense in Zahleh.

Concerning edibility rates, subjects that could not detect the odor noted it directly as non-edible. Rose and lime odors were considered more edible, more familiar and more pleasant in Kaslik. This indicates a linear relation between edibility and pleasantness. The more the odor is edible, the more it is considered as pleasant.

One of the hypotheses that could explain these observations is that the residents of the rural area recognize more easily the smell of flowers. Due to the fact that it reminds them of gardening and green space in their area, while subjects living in the urban area recognize the smell of flowers as an ingredient used in pastries, gum and food products in the market.

4. CONCLUSIONS

The purpose of the present study was to evaluate the intra-cultural effect on the relation between odor and color. Past studies highlighted cross cultural effects on odor-color associations, where according to Maric, Barbar and Jacquot (2012) the construction of odor- color correspondences proved to be culture-dependent: If participants of different countries, have the same usage purpose for a product they will associate it to similar colors. If not, significant differences will be revealed as it was the case for orange blossom.

The present study aims to emphasize the intra-cultural effect within the same country. The Lebanese residents tend to have different color-odor association between rural and urban area. Taking into consideration that Lebanon is a small country of 10452 km^2 the current study proved the effect of culture, not only internationally but also within the same country,in terms of environment, intra-cultural and culinary habits and ease of access to more local productions,on the relation between odor and color, and its effect on odor parameters.

REFERENCES

Hudson, R., and Distel, H. 2002. The individuality of odor perception. In Rouby, C., Schaal, D., Dubois, D., Gervais, R., and Holley, A. (Eds.), *Olfaction, taste and cognition, Cambridge*, London: Cambridge Press.

Levitan, C., Ren, J., Woods, A., Boesveldt, S., Chan, J., McKenzie, K., Dodson, M., Levin, J., Leong, C., and Van den Bosch, J. 2014. Cross-Cultural Color-Odor Associations. Available online at Plosone, http://journals.plos.org/plosone/article?id=10.1371/journal.pone.0101651.

Maric, Y., and Jacquot, M. 2013. Contribution to understanding odour-color associations. *Food Quality and Preference* 27: 191-195.

Maric, Y., Barbar, R., and Jacquot, M. 2012. As pink as an orange blossom odour: a French-Lebanese cross-cultural study. In *AIC Color 2012*, Proceedings, Interim Meeting of the International Colour Association.

Morrot, G., Brochet, F., Doubourdieu, D. 2001. The Color of Odors. *Brain and Language* 79: 309-320.

Spence, C. 2011. Crossmodal correspondences: A tutorial review.*Attention, Perception & Psychophysics* 73: 971-995.

Spence, C., and Deroy, O. 2014. Tasting shapes: A review of four hypothesis. *Theoria Historia Scientiarum* 10: 207-238.

Spence, C., Levitan, C.A., Shankar, M. U., and Zampini, M. 2010. Does Food Color Influence Taste and Flavor Perception in Humans? *Chemosensory Perception* 3: 68–84.

UNICEF. 2012. available at http://www.unicef.org/sowc2012/pdfs/SOWC-2012-DEFINITIONS.pdf

United Nations. 1998. *Principles and Recommendations for Population and Housing Censuses*. Revision 1. Series M, No. 67, Rev. 1 (United Nations publication, Sales No. E.98.XVII.8).

United Nations. 2004. World *Urbanization Prospects, the 2003 Revision*. United Nations Publication sales No. E.04.XIII.6

Velasco, C., Wan, X., Salgado-Montejo, A., Woods, A., Onate, G., Mu, B., and Spence, C. 2014. The context of color-flavor associations in crisps packaging: a cross cultural study comparing Chinese, Colombian, and British consumers. *Food Quality Preference* 38: 49-57.

Wada, Y., Inada, Y., Yang, J., Kunieda, S., Masuda, T., Kimura, A., Kanazawa, S. and Yamaguchi, M.K. 2012. Infant visual preference for fruit enhanced by congruent in-season odor. *Appetite*58: 1070-1075.

Wan, X., Velasco, C., Michel, M., Mu, B., Woods, A.T., and Spence, C. 2014. Does the shape of the glass influence the cross modal association between color and flavor ? A cross cultural comparison. *Flavor* 3: 3.

Yeh, L.L., Kim, K.O., Chompreeda, P., Rimkeeree, H., Yau, N.J.N., and Lundahl, D.S. 1998. Comparison in use of the 9-point hedonic scale between Americans, Chinese, Koreans, and Thai. *Food Quality and Preference* 9: 413-419.

Differences of generation dependences of preferences between colors and styles in women's fashion

Chie MURAKI ASANO[1*], Kanae TSUJIMOTO[1], Akira ASANO[2], Katsunori OKAJIMA[3]
[1]Faculty of Human Ecology, Yasuda Women's University
[2]Faculty of Informatics, Kansai University
[3]Faculty of Environment and Information Sciences, Yokohama National University

ABSTRACT

This research investigates generation dependence of preferences in fashion, and shows differences of dependences between colors and styles of dresses. It has been assumed that the tendency of age independence is found not only in the fashion-style but also in the color preference of fashion. In this paper, we investigated the preference of twenties students and their mothers, who are generally forties, in the fashion-style and color of fashion. As a result, a significant difference was confirmed in the fashion style between the student generation and the mother generation, especially in the taste of characteristic parts. However, the tendency of color preferences are found different from what have been assumed; Although it has been usually believed that elderly women prefer dark and dull colors, young students also preferred dark colors, while their mothers preferred dull colors to dark tone, according to our surveys for winter cloths. The mothers also preferred bright colors, especially in summer cloths, similarly to young students.

1. INTRODUCTION

It has been widely accepted that the preference of colors in fashion is different by the age group (Beke et al., 2008). However, it is said that the preference in fashion of forties' women has recently become less different from it of twenties. The fashion trends and their transitions were clear and charismatic leaders of fashions appeared successively in 1970s and 80s, when the forties' women were young. On the contrary, there are a lot of fashion trends simultaneously, and main stream of fashion trends in the whole society and their transitions are unclear in the 21st century. It may be the reason why the preferences have become less different between forties' and twenties' women.

It has been assumed the tendency of age independence is found not only in the fashion-style but also in the color preference of fashion. In this paper, we investigates the preference of twenties students and their mothers, who are generally forties, in the fashion-style and color of fashion. It examines precisely what kind of the preferences has really become less different. The research will be utilized for marketing in fashion industries.

As a result, a significant difference was confirmed in the fashion style between the student generation and the mother generation, especially in the taste of characteristic parts. However, it was shown that any significant difference was not confirmed in the color preferences, although some difference was observed. It has been usually said that elderly women prefer dark and dull colors, however, according to our surveys, young students also preferred

* Current affiliation: Faculty of Human Life and Environmental Sciences, Nagoya Women's University

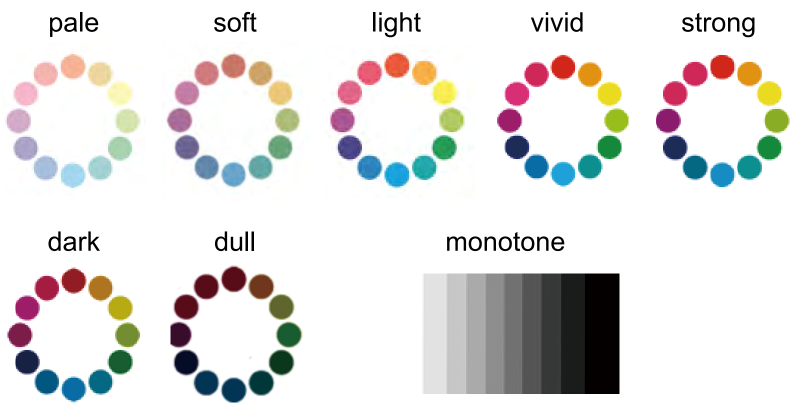

Fig. 1. Example of hue circle for each tone.

monochromes, especially in autumn-winter dresses. Mothers group also preferred bright colors, especially in spring-summer ones, similarly to the young students.

2. METHODS

The participants of our survey were 200 female university students and 60 of their mothers in Japan. We made a questionnaire on the preferences of colors and styles of dresses. The questionnaire sheet was written in Japanese.

Preferences of colors were surveyed not by selecting hues but by selecting from the following words indicating tones in the PCCS color system: pale, soft, light, vivid, strong, dark, and dull tones, and monotone. This is because it has been assumed that the generation dependence of color preferences is mainly on vividness or dullness and the target of our survey is confirming this assumption (Baucom and Grosch, 1996). Preferences of hues depend higher on each person than on generations. The example of the hue circle for each tone was presented on the questionnaire sheet, as shown in Fig. 1.

Preferences of styles were also surveyed on the details of the tops and the bottoms, e.g. shapes and lengths of skirts, sleeve lengths, etc. These style were explained by illustrations on the questionnaire sheet. Preferences on spring-summer and autumn-winter dresses were separately surveyed.

3. RESULTS AND DISCUSSION

We show the results of the surveys for preferences of styles and colors by young women and their mothers. For the sake of the limitation of paper length, some parts of styles showing significant generation differences are selected.

3.1 Materials

We surveyed preferences of materials, selected from cotton, hemp, wool, silk, cupra, rayon, tencel, nylon, polyester, and acrylic fibers, which are usually used for textiles. Each respondent selected one material from the list for each of summer and winter cloths. Figures 2(a) and (b) show the preferences in summer and winter cloths, respectively. Figure 2(a) indicates that hemp is preferred by young women to their mothers for summer cloths, while cotton is preferred by the mothers to the young women. It may be because hemp is difficult to handle

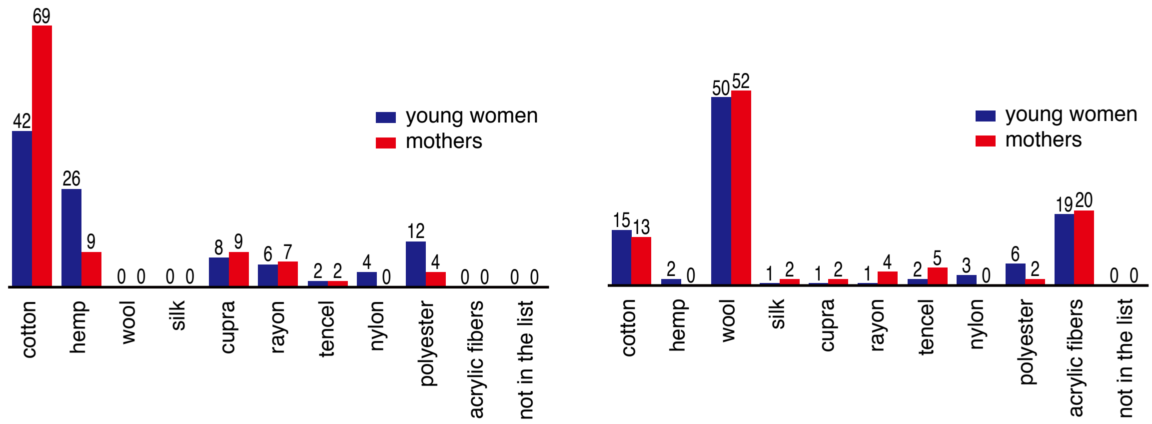

(*a*) *summer cloths.* (*b*) *winter cloths.*

Fig. 2. Preferences of materials (%).

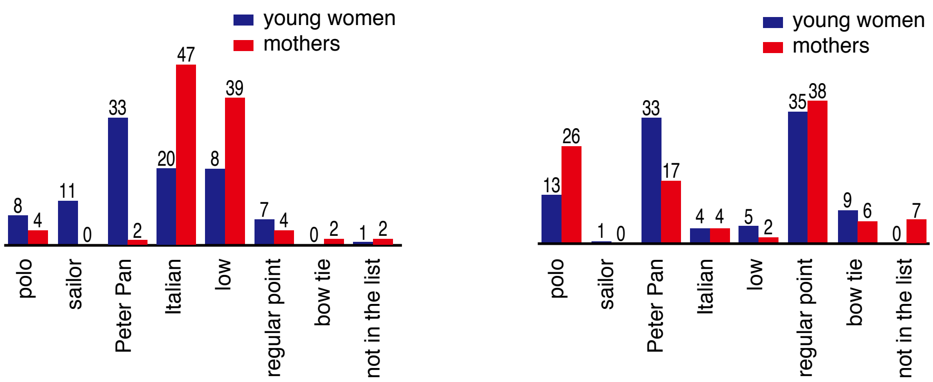

(*a*) *summer cloths.* (*b*) *winter cloths.*

Fig. 3. Preferences of collar shapes (%).

in home laundry and it has not been preferred by the mothers group, but its wrinkles caused by laundry process are rather preferred as a kind of fashion by young women. Figure 2(b) indicates that the preferences of winter cloths are similar for young women and their mothers.

3.2 Collar shapes

We surveyed preferences of collar shapes, selected from polo, sailor, Peter Pan, Italian, low, regular point, and bow tie collars. Figures 3(a) and (b) show the preferences in summer and winter cloths, respectively. Figure 3(a) indicates that the preferences of Peter Pan collar by young women and their mothers in summer cloths are significantly different. Since Peter Pan collar is a narrow-necked style, it may be considered uncomfortable by the mothers. Italian and low collars, which are preferred by the mothers, are low-necked styles. Figure 3(b) indicates that the difference of the preferences of Peter Pan collar is similar in winter cloths. The opposite difference appears in polo collar in winter cloths.

3.3 Colors

Figure 4(a) and (b) show the results of the survey of color preferences in summer and winter cloths. Color tones instead of color hues were surveyed, as explained in Section 2. Figure

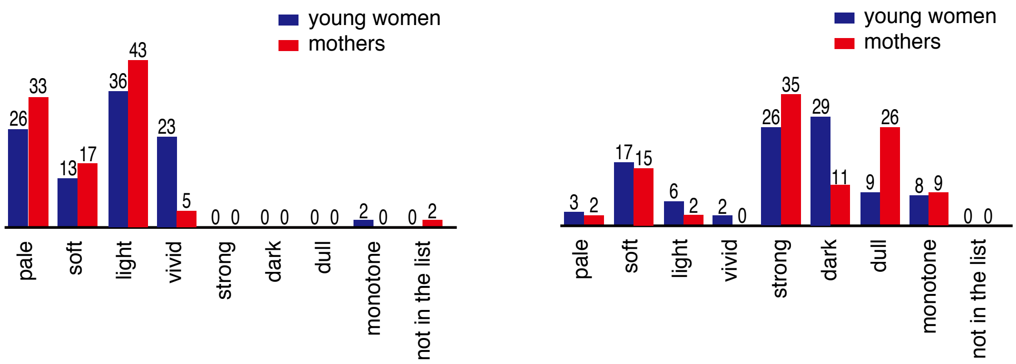

(*a*) *summer cloths.* (*b*) *winter cloths.*

Fig. 4. Preferences of colors (%).

4(a) shows that the majorities of the preferences both by young women and their mothers in summer cloths are almost similar, and the only difference is found in vivid color. Neither dark nor dull tone were selected by any of the young women or their mothers, although it has been usually believed that elderly women prefer dark and dull tone. Figure 4(b) shows that the only differences in winter cloths are found in dark and dull colors. Young women preferred dark colors, while their mothers preferred dull colors, according to our survey. This is also different from the above assumption for elderly women.

4. CONCLUSIONS

Although it has been assumed that the tendency of age independence is found not only in the fashion-style but also in the color preference of fashion, our research has shown that a significant difference is confirmed in the fashion style between the student generation and the mother generation, especially in the taste of characteristic parts. However, the tendency of color preferences are found different from what have been assumed; Although it has been usually believed that elderly women prefer dark and dull tone, young students also preferred dark tone, while their mothers preferred dull tone to dark tone, according to our surveys for winter cloths. The mothers also preferred bright tone, especially in summer cloths, similarly to the young women. The results, as well as further survey and investigations, will help business strategies of fashion industry.

REFERENCES

Beke, L., Kutas, G., Kwak, Y., Sung, G. Y., Park, D. S., and Bodrogi, P. 2008. *Color preference of aged observers compared to young observers,* Color Research and Application, 33(5), 381-394.

Baucom, A. H. and Grosch, R. J. 1996. *Hospitality Design for the Graying Generation: Meeting the Needs of a Growing Market,* John Wiley & Sons.

Address: Prof. Akira Asano, Facutly of Informatics, Kansai University
Ryozenji-cho 2-1-1, Takatsuki, Osaka 569-1095, JAPAN
E-mail: a.asano@kansai-u.ac.jp

Effect of Color Appeared in Signage to Identify Gender of Thai

Chanida SAKSIRIKOSIL[1]*, Kitirochna RATTANAKASAMSUK[2] and Ploy SRISURO[1]

[1]Department of Advertising and Public Relations Technology, Faculty of Mass Communication Technology, Rajamangala University of Technology Thanyaburi,Thailand.

[2] Color Research Center, Faculty of Mass Communication Technology, Rajamangala University of Technology Thanyaburi,Thailand.

ABSTRACT

This research aimed to study the effect of color appeared in signage to identify gender of Thai people. Colors used in this study were light blue and dark blue, identified as male; red and pink, as female and black as neutral color. Two symbols, as for male and female, were in aforementioned five colors. So the total was ten images. These symbol images were showed within 2 seconds. The subjects were 50 Rajamangala University of Technology Thunyaburi students. For the first evaluation, the subjects assessed the color of the symbols whether or not that color was identified as male or female. For the second evaluation, the subjects assessed the details of the symbols whether or not they were male or female. Then these two evaluations were compared. The results showed that the factor that most affecting gender identification was the details in the symbols. Color appeared in symbol is not relevant to gender identification in this experiment.

1. INTRODUCTION

Color is what we all see because it has physical properties. The color is what we see with our eyes. It also tells a story or information to human and creature. These data, such as food, are very important to our life. Creatures differentiate color of plants and animals so they can tell what can or cannot be eaten. Or they can tell the time from the color of the sky. Even the color can also be used to differentiate the human tribes, such as black is represent Africans, yellow for Mongoloid in Asia, and white for Caucasian in West and Scandinavian. (Pungrassamee and Ikeda 2008)

Colors are involved in our daily, considering the various appliances we use. Humans have known to use color since the old days, for example, the painted images on cave walls hundred years ago. Colors are around us as we are learning today. Colors are used to identify the ripe fruit that can be eaten or not. In addition, it also used to convey the meaning of writing, such as the color used in traffic signs on the road (Tangkijviwat 2014)

Red sign means danger. Yellow means caution. Green, often seen on the road, means harmless. Therefore, green has been used for many things, such as, in medical condition or to convey the emotion.

Colors are often used for designing advertising media in order to create the beauty and the eye-catching material, as well as it is used to convey the meaning of the typography in order to make the audience easily understand the message. (Itsadul 2007)

From the aforementioned reason, colors are very useful for daily life and also affect the interpretation. They can be conveyed without a written text and can easily be interpreted and understood. Therefore, this research was to study the influence of the color of the symbols that affect the classification of male and female of Thailand. Colors in Thailand have not been used as a standard to represent female and male. Unlike many other countries, such as Japan, colors are used to convey the meaning of female and male, such as red is used for lady's room and black or blue is used for men's room. In this study, the researcher chose dark blue and light blue as the color identified as male, red and pink as female and black as neutral.

2. METHOD

Female and male symbols were presented on a monitor placed inside an experimental room. Ten symbols were created by the combination of two gender (female and male) and five different colors (dark blue, light blue, black, red and pink) as shown in Table 1. These symbols were presented on a white background as shown in Figure 1. The room illuminance was kept constant throughout the experiment. The viewing distance is fixed at 30 cm. 50 undergraduate students of Faculty of Mass Communication Technology were participated in this experiment.

Table 1. Chromaticities of color symbols.

Colour name	Y	x	y
Red	35.6	.527	.339
Pink	34.7	.416	.217
Black	3.63	.286	.312
Drak blue	33.0	.154	.121
Light blue	42.5	.186	.187
White	200	.295	.326

The experiment started by asking the subject to enter in the experimental room and adapt to the room illumination for 2 minutes. A symbol image was presented to the subject one at a time. Each symbol was displayed for 2 seconds. Then, the symbol was disappeared and replaced by gray background in order to make the observer ready for the next assessment.

There were two tasks for each subject. For the first task, the subject was asked to identify if that symbol represent the female or male. In case of the second task, the observer was asked to identify if that color of the symbol represent the female or male.

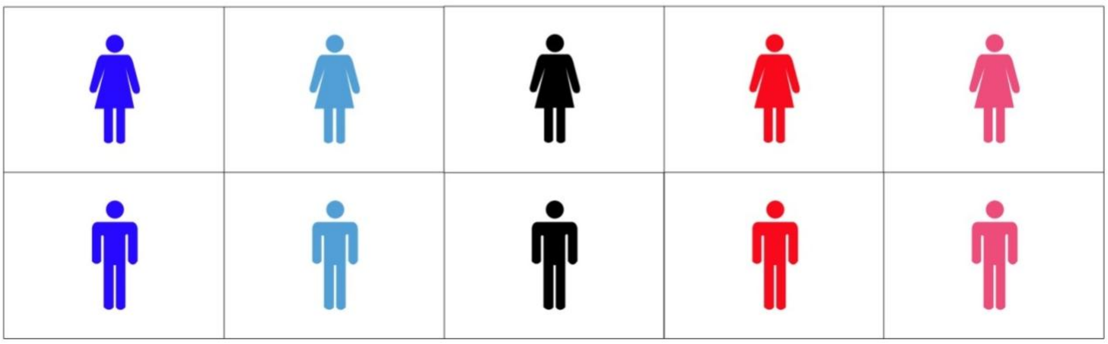

Figure 1: Color and symbol used in the study

3. RESULTS AND DISCUSSION

The result of the first task was shown in Figure 2. Almost all the Thai subject could correctly identify the gender of symbol even though that symbol was created in any colors. The results implied that color appeared in symbol has no effect on gender identification in this experiment.

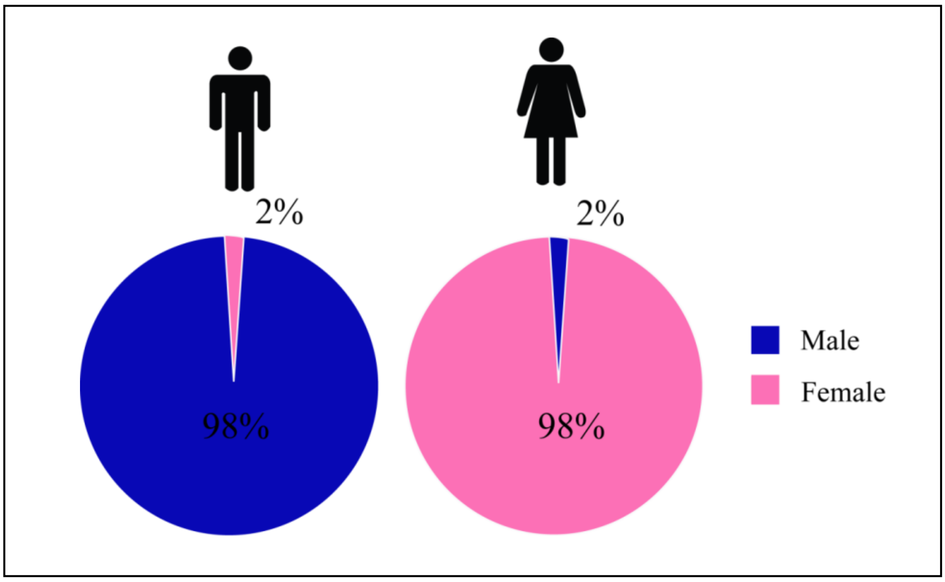

Figure 2: Gender identification by Symbol's details

The results from the second task were shown in Figure 3. We hypothesized that red and pink should associate with female identification, whereas blue and light blue should associate with male identification. Our results seemed to follow our hypothesis. 86% of Thai thought that pink was strongly represented the female and 60% of Thai associated red color with female. In case of male, dark blue and light blue associated with male by 74% and 54% respectively. However, color which strongly associated with male was neutral color like black.

If the saturation of color is considered, it seems that low saturation color such as light blue and pink obtained higher female identification than the vivid color. According to the hypothesis, red was represented female. However, 24% of the subject thought that it was represented male and 16% thought that it was represented both gender.

This concludes that, for Thai, even though there was some association between color and gender. But this association was not relevant to the gender identification in symbol. It was possibly due to no usage of color code to express gender in Thailand. Unlike some countries, for example, Japan, the male toilet symbol is generally blue or black and the female toilet is generally red. We expected that the obtained result would be different if the subjects were Japanese who are familiar to the color coding for gender identification in their daily life. Further experiment is required to confirm this expectation in the future.

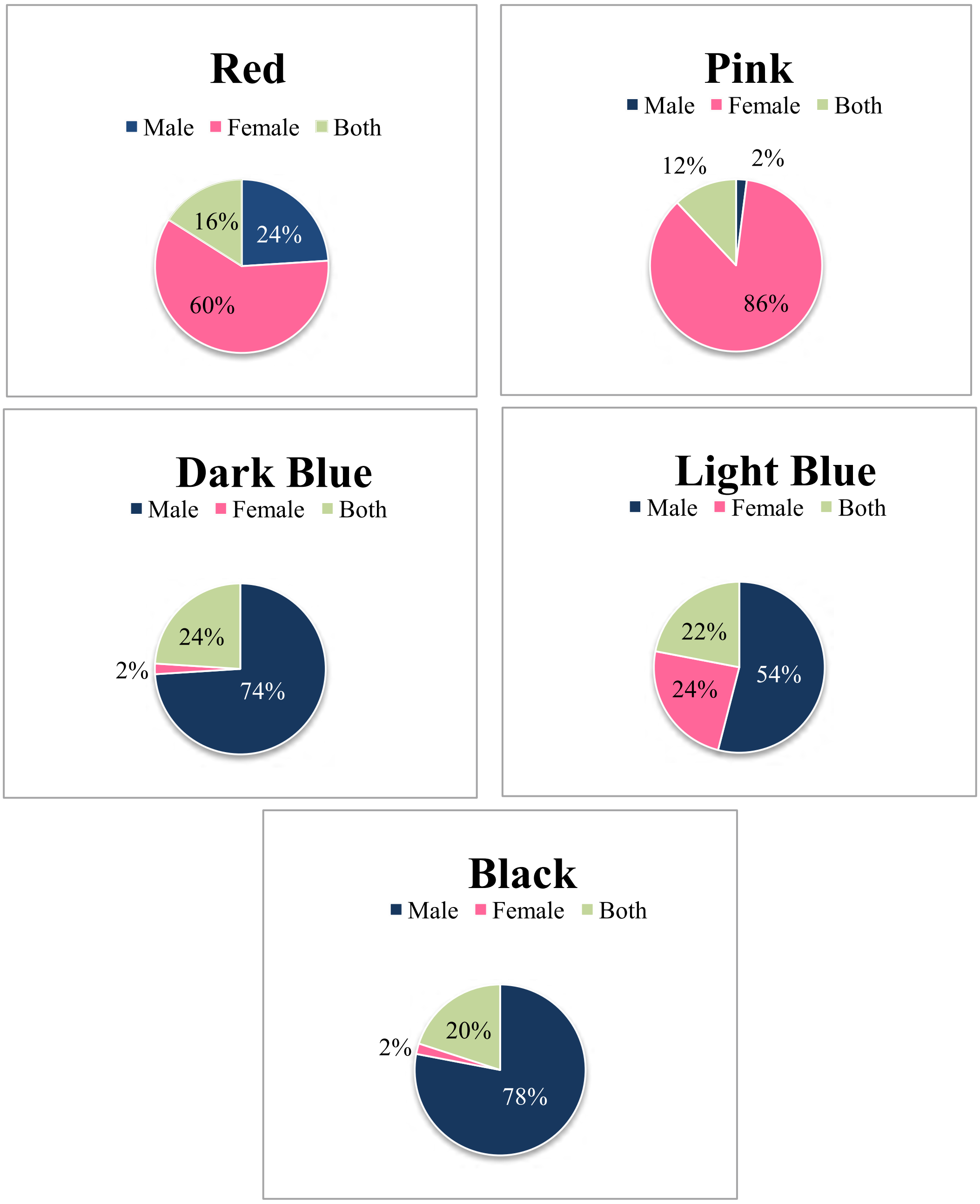

Figure 3: Gender identification by Symbol's color

4. CONCLUSIONS

The study found that the factor influencing gender identification in Thailand was the detail of the symbol but not the color of the symbol. From the first task, the subject correctly identified gender of the symbol. The subject also had the answers in the same direction whether the symbols were alternately colored. In the second task, the subject had different opinions when asked to identify the gender after seeing the color of the symbol. Almost the subjects agreed that pink was represented as female. Blue and black were represented as male. However, this association was not relevant to the gender identification in symbol.

ACKNOWLEDGEMENTS

We would like to thank the Faculty of Mass Communication Technology and the Department of Advertising and Public Relations Technology for the opportunity to conduct this research. As well as 50 subjects and other party who are not mentioned here who helped with this research.

REFERENCES

Ludwig, C. and others. 2010. *Adult age differences in the Color Stroop Test*, Archives of Geriatrics 51, 135-142.

Itsadul, P. 2007. *Vector Graphic in Printed Advertising,* Thammasart University, Bangkok.

Pungrassamee, P., and Ikeda, M. 2008. *Colr and Color Vision,* Chulalongkorn University Press, Bangkok.

Jewbang, T. 2007. *Learning Theory of Colour,* O.S .Printing House. Bangkok .

Tangkijviwat, U. 2014. *Color Science & Technology [PowerPoint Slides]*, Rajamangala University of Technology Thanyaburi.

Address: Chanida Saksirikosol, Department of Advertising and Public Relations,
Rajamangala University of Technology Thanyaburi,
39 Rangsit-Nakhonnayok Klonghok Thanyaburi Pathumthani, THAILAND
E-mails: dadahz69@gmail.com,chanida_69@hotmail.com,

Development of three primary-color transparent cubes for learning subtractive color mixing visually

Keiichi MIYAZAKI
Cubics Design

ABSTRACT

Since the principle of subtractive color mixing is more difficult to understand than additive color mixing, we have developed a teaching materials to learn the subtractive color mixing visually[1]. Teaching materials are three types of transparent cube with three colored surfaces, and one big color mixing transparent cube composed of eight stacked cubes. By making full use of the optical design, three types of cube is devised to be interesting in appearance and rainbow-colored beauty of color mixing. The process of making one big cube by stacking eight cubes, is devised to be able to enjoy the color mixing like solving the puzzle.

1. INTRODUCTION

It is said that young people have been lost interest in science, efforts to improve the learning motivation by fun experience, with facilities such as RiSuPia[2], have been made. If you try to learn the color science, usually, it is necessary to learn a variety of terminology and definitions related to visual characteristics as well as physical optics.

The purpose of this study is to provide teaching materials that can experience the fun and beauty of color for learning the subtractive color mixing used for printing or photo reproduction.

For example, building blocks of Cubicus[3](Figure 1(1)), because it has both beautiful appearance and puzzle features likes contemporary art, is very attractive as the teaching materials for visual learning. Therefore, by developing a new teaching materials for learning a subtractive color mixture incorporating the art puzzle elements, we want to make learn color mixing visually.

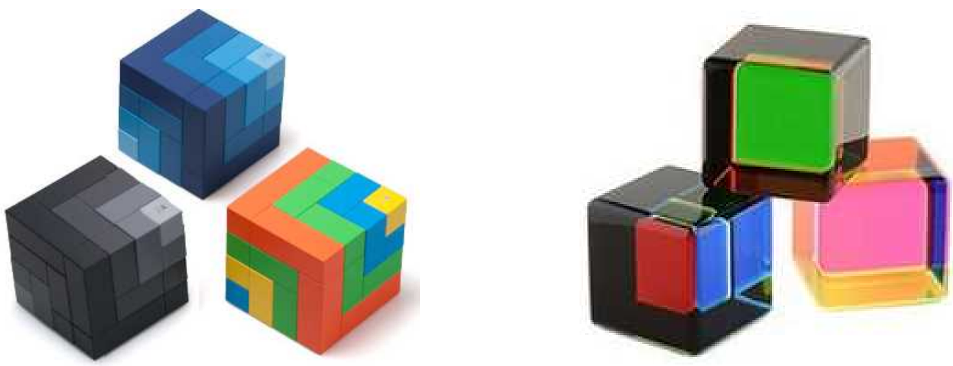

Figure 1: (1)Cubicus of Neaf *(2)Vasa Cubes of VASA*

2. METHOD

2.1 Color Mixing by Transparent Cube

Building blocks made of opaque plastic timber is not suitable for teaching materials of subtractive color mixing. However, if the transparent cube is used, such as Vasa Cubes[4] in Figure 1 (2), by making use of two parallel faces or two adjacent surfaces, it is possible to express the subtractive color mixing as shown in Fig. 2 (1). Each of the two color mixing, is referred to as the parallel surface color mixing(PCM) and the adjacent surface color mixing(ACM). When two transparent cubes are stacked as shown in Fig. 2 (2), it is also possible to represent the subtractive color mixing.

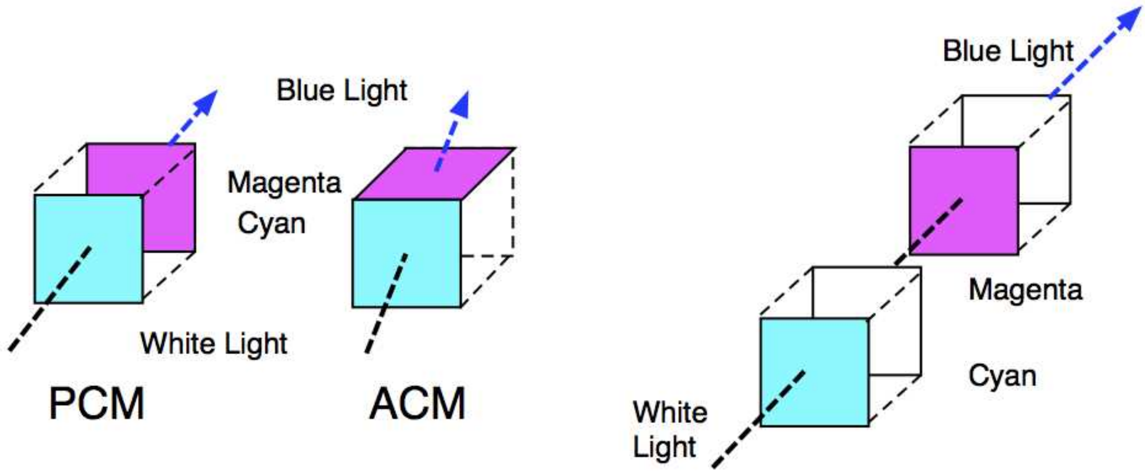

(1)Color mixing by one cube *(2) Color mixing by two cubes*

Figure 2: Subtractive color mixing by transparent cube

2.2 Tri-Mixing Color Cube

Since the cube has six faces, it is possible to represent the three sets of PCM information per cube as shown in Figure 3. Thereafter, a transparent cube with information of three sets of PCM is referred to as a tri-mixing color cube. It is possible to represent additional color mixing by the combination of some tri-mixing color cubes placing two or more cubes as shown in Figure 2 (2).

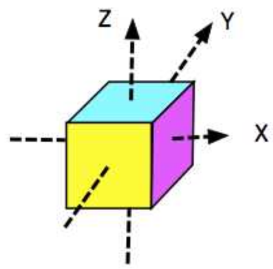

Figure 3:Tri-mixing color cube

3. Results and Discussion

3.1 Mixing Color of PCM-CUBE and ACM-CUBE

Using the six faces of the cube (from 1-6 dice surfaces), tri-mixing color cubes assigned the CMY to the arrangement of the PCM and ACM were shown in Figure 4. Comparing the number of colors that could be observed at the same time, PCM-CUBE(with three different mixing color pairs of PCM) had 6 colors, and ACM-CUBE(with three different mixing color pairs of ACM) had four colors. Considering the cause of the difference at looking of cubes, and decomposing the cube to check the placement of the CMY, gave a good opportunity to be interested in subtractive color mixing.

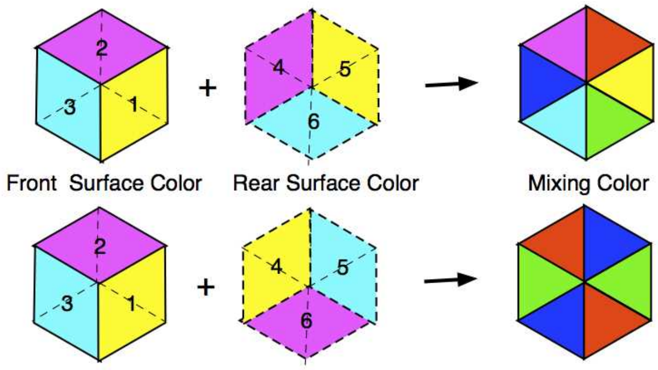

Figure 4:Surface color and mixining color of PCM(upper) and ACM(lower) CUBEs

3.2 Unexpected Color Mixing

In color mixing by stacking tri-mixing color cube, unexpected color mixing(UCM) occured in an oblique direction as in Figure 5, and UCM becomes the noise of stacking color mixing. Since the cause of the UCM was mainly ACM, in order to reduce ACM, a solid transparent cube was experimentally

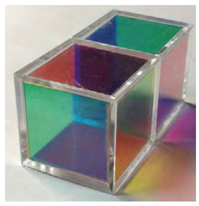

Figure 5 : An example of UCM

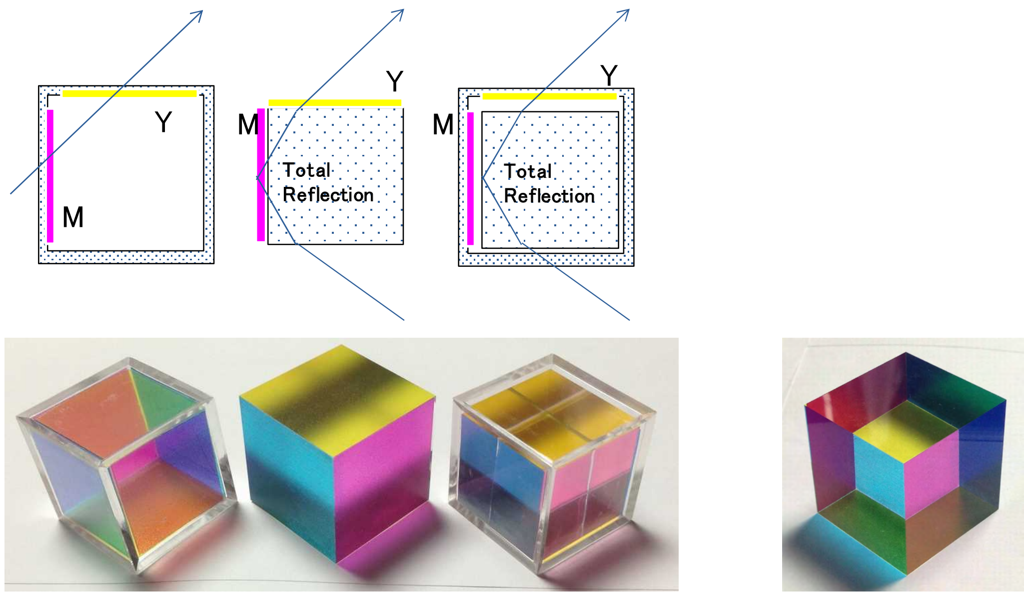

(1) Box(ACM) (2)Solid-FrontView (3)Box&Solid (2)Solid-RearView

Figure 6:Optics(upper figure) and appearance(lower figure) of cubes in Table 1

put inside the ACM-CUBE in Figure 6(1). And then, ACM of box and solid type in Figure 6(3) was nearly invisible by the total reflection of internal transparent solid cube.

3.3 Transparent Color of Tri-Mixing Color Cube

Transparent color with three types of tri-mixing color cube was summarized in Table 1. Row (3) in Table 1 had no ACM(no RGB) even viewed from any direction, and didn't occur UCM, then we called this type of tri-mixing color cube as tri-primary color cube. Row (2) in Table 1, as shown in Figure 5(2:Rear View), had a colorful and beautiful ACM.

Table 1.Transparent color of tri-mixing color cube[No. is same as Figure 6]

No.	Optical Structure	Surface Color						Parallel Viewing			Adjacent Viewing											
		Front			Rear						Front → Rear						Rear → Front					
	Dice※ Number	1	2	3	6	5	4	1→6 6→1	2→5 5→1	3→4 4→3	1→4	1→5	2→4	2→6	3→5	3→6	4→1	5→1	4→2	6→2	5→3	6→3
PCM	Box	Y	M	C	C	Y	M	G	R	B	R	YY	MM	B	G	CC	R	YY	MM	B	G	CC
(1)		Y	M	C	Y	M	C	YY	MM	CC	G	R	B	R	B	G	G	R	B	R	B	G
(2)	Solid	Y	M	C		–		Y	M	C	Y	Y	M	M	C	C	G	R	B	R	B	G
(3)	Box & Solid	Y	M	C		–		Y	M	C	Y	Y	M	M	C	C	C	M	C	Y	M	Y

※1→2 means viewing from 1 to 2 direction

3.4 Stacking Tri-Primary Color Cubes

An interesting example of stacking color mixing was stacking up the RGB tri-primary color cube from eight CMY tri-primary color cubes. When stacking eight CMY tri-primary color cubes, CMY tri-primary color cubes changed to one large RGB tri-primary color cube by subtractive color mixing, as shown in Figure 7(1). Furthermore, when replacing four CMY tri-primary color cubes to RGB tri-primary color cubes, as shown in Figure 7(2), color of whole cube changed to BLACK.

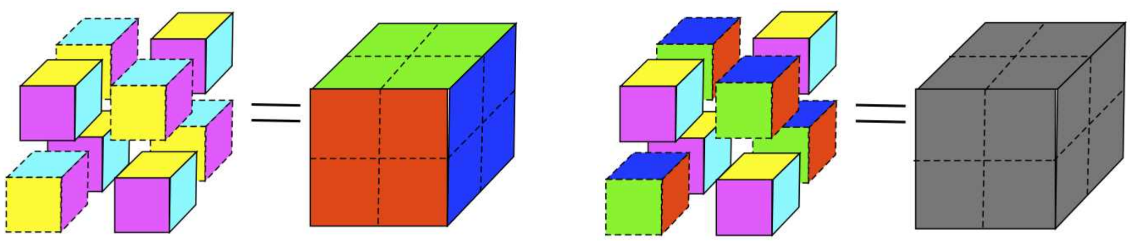

(1) 8 x CMY = RGB *(2) 4 x CMY + 4 x RGB = BLACK*

Figure 7: Arrangement of stacking eight cubes to one bigger cube

The image obtained by observing actual RGB cube stacked by eight CMY cubes from three directions was shown in Figure 8. It could be seen that the UCM does not occur.

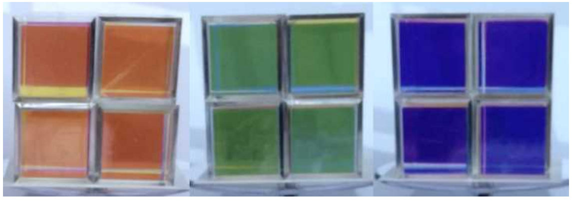

Figure 8: One big RGB cube without UCM resulting from the stacking method of Figure 7(1)

4. CONCLUSIONS

Tri-mixing color cubes which can be observed CMYRGB six colors simultaneously, and a method for building one RGB cube by stacking eight CMY tri-primary cubes have been developed. Next, we will promote use of tri-mixing and tri-primary color cubes at schools to teach the subtractive color mixing, and to verify the validity as a teaching material.

ACKNOWLEDGEMENTS

I wish to acknowledge valuable discussions and reading the manuscript with Dr. Noboru Ohta.

REFERENCES

[1] Keiichi Miyazaki, 2014, J. Color Sci. Assoc. Jpn., 38(6), in Japanese.
[2] RiSuPia, http://www.panasonic.com/global/corporate/center/tokyo/risupia.html
[3] Mikado Koyanagi, 2004, Edu-toy - NAEF and European Wooden Toys, in Japanese.
[4] Vasa Mihich, 2007, VASA

Address: Keiichi Miyazaki, Cubics Design
1-16-3 Sakae-cho, Odawara-shi, Kanagawa, 250-0011, JAPAN
E-mail: mgg02366@nifty.com

Multicolor LED Lighting Device with a Microprocessor for Demonstrating Effects of Lighting on Color Appearance

Takashi NAKAGAWA[1]
[1] Faculty of Information Engineering, Fukuoka Institute of Technology

ABSTRACT

The author has assembled multicolor LED lighting devices to demonstrate effects of lighting on color appearance. The most recent device, containing eight color LEDs and three white LEDs, is controlled by a microprocessor Arduino MEGA to realize flexible lighting conditions. In this paper, the author first describes the employed LEDs and discusses the importance of variety of LEDs that enables variety of light spectrum. He then describes and compares two versions of multicolor lighting devices he has assembled and shows that the equipment of a microprocessor greatly enhances the usability in the demonstration of color experiments.

1. INTRODUCTION

There are phenomena that can be demonstrated with lighting devices: metamerism, additive color mixture, color rendering, etc. Performance of LED lighting apparatus depends on the assortment of LED colors. However, wavelength ranges of available LEDs are restricted to those of mass production. Recently, power LEDs of various colors are available in chips. So, the author has fabricated multicolor lighting devices with chip LEDs.

2. LEDS

The lighting devices were made with Philips LUXEON Rebel chip LEDs: deep red (DR, λ_D = 655nm at 350mA), red (R, λ_D = 627nm), red orange (RO, λ_D = 617nm), amber (A, λ_D = 590nm), green (G, λ_D = 530nm), cyan (C, λ_D = 505nm), blue (B, λ_D = 470nm), royal blue (RB, λ_D = 448nm), cool white (CW, 6500K), neutral white (NW, 4100K), and warm white (WW, 3100K). Figure 1 shows the package outline. Light is emitted through the dome lens on the top surface. There are a thermal pad and two electrical contact pads on the bottom surface.

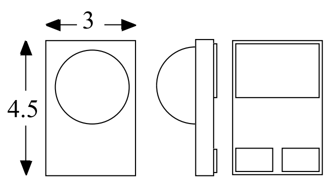

Figure 1. Package outline.

Figure 2 shows the relative spectrum power distributions of color LEDs and neutral white LED (cited from the supplier's data sheets). There is a vacant range of wavelength between blue and cyan as well as green and amber.

Figure 3 is the chromaticity diagram of LEDs. Trianguar marks in the outer area indicates color LEDs, and marks in the inner area indicates white LEDs.

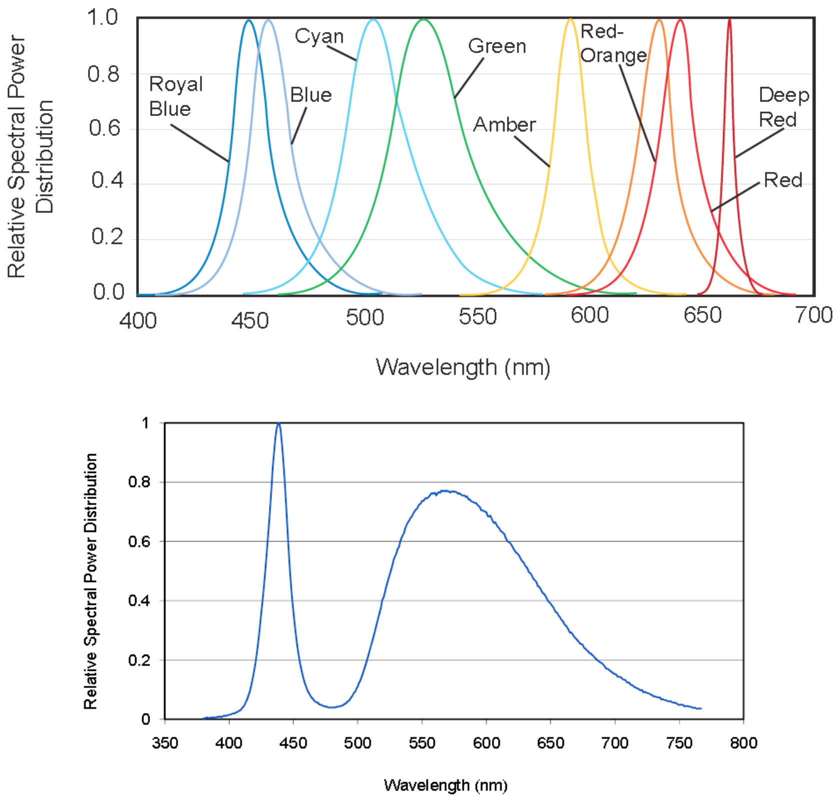

Figure 2. Relative spectrum power distributions of LEDs.

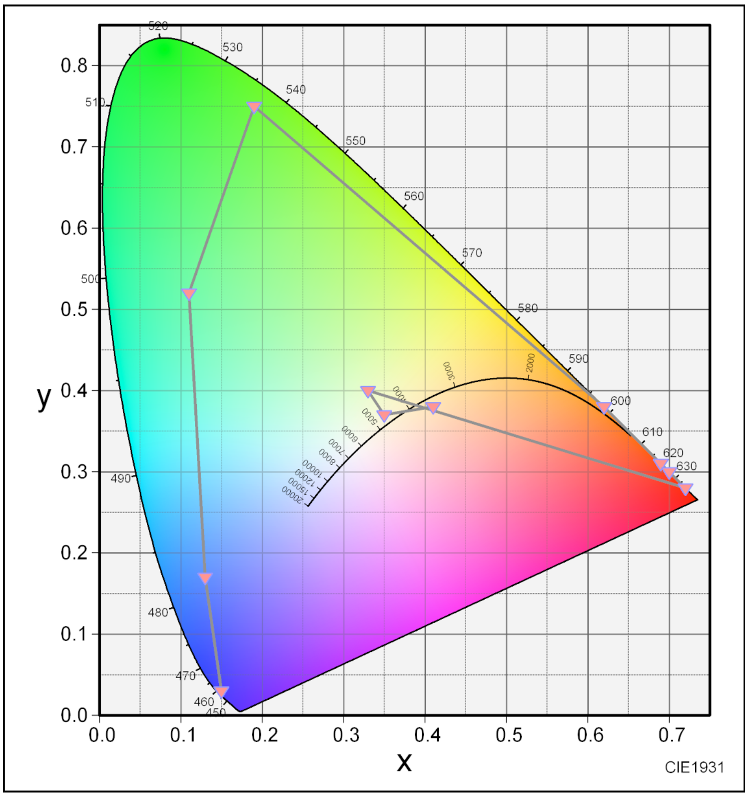

Figure 3. chromaticity diagram of LEDs.

It is well known that the chromaticity coordinate (x,y) of the color light L produced by summing three color lights L_1 (x_1,y_1), L_2 (x_2,y_2), L_3 (x_3,y_3) can be calculated as a weighted average of (x_1,y_1), (x_2,y_2), (x_3,y_3) where the weights are sums of color tristimulus values. In other words, it is possible to produce a color light L by summing three color lights L_1, L_2 and L_3, if the chromaticity coordinate (x,y) of L is inside of the triangle $L_1L_2L_3$ on the xy chromaticity diagram.

From Figure 3, it is obvious that there are many different combinations of three LEDs that can produce the same white color. For example, by using LEDs B, C and A, the color of neutral white LED can be obtained, whereas the same color can be also obtained by using RB, G and DR. To demonstrate this phenomenon, LED powers must be finely adjusted. This is possible by using Arduino MEGA.

Although the white color lights produced by the above three different ways (a) lighting NW, (b) lighting B, C and A, and (c) lighting RB, G and DR, have the same chromaticity coordinate (x,y), their spectrum power distributions are different. This difference causes the difference of body colors of two objects with different spectral reflections. Thus, our lighting device can be used to demonstrate metamerism and color rendering property of light.

Therefore, it is important that the lighting device has many LEDs of different colors.

3. THE LIGHTING DEVICES WITHOUT MICROPROCESSORS

Figure 4 shows the lighting devices without microprocessors. Each of them contained pairs of 8 color LEDs. Their fabrication was easy because wiring was simple: each color was simply switched ON or OFF. Yet they were useful for demonstrating metamerism.

Figure 4. An AC driven lighting device (left) and a portable one (right).

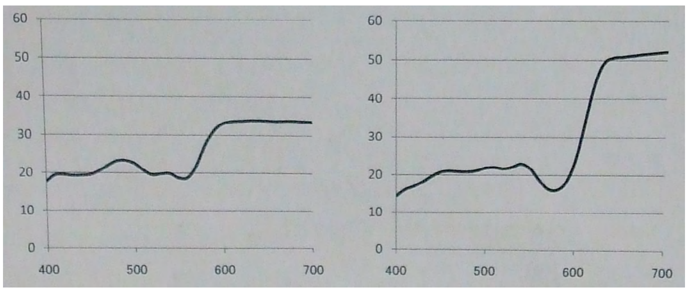

(a) under the daylight

(b) lighted with green and amber

Figure 5. Spectral reflectance of a metameric pair.

Figure 6. Color appearances.

Figure 5 shows the spectral reflectance of a metameric pair sheet provided by the manufacturer. Figure 6 shows their photographs under the daylight (a) and under the mixture of green and amber LED lights. We see in (b) that the left sheet appears brown while the right sheet appears green. This difference of color appearance can be explained using their spectral reflectance and the spectral power radiation of LEDs.

There is a problem in soldering chip LEDs. Chip LEDs are weak to the high temperature over 300°C. Therefore, the author used a temperature-controlled soldering iron for wiring and a temperature-controlled hot plate for the soldering of chip thermal pads to the radiation plate. Figure 7 shows the schematic diagram of the reflow technique where the chip has been previously attached to a supporting card paper and the radiation copper plate has been previously covered with solder.

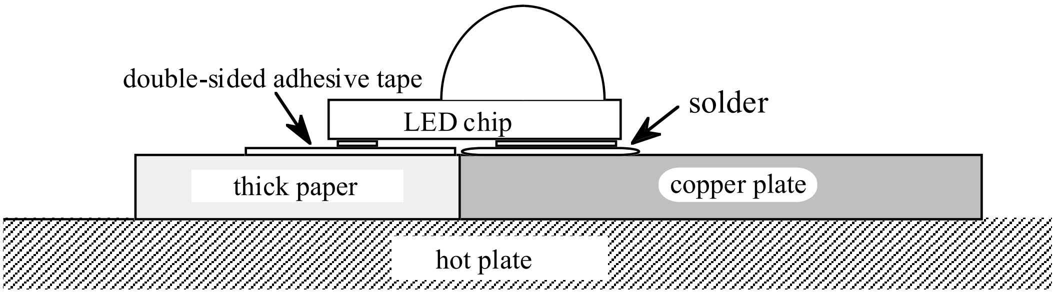

Figure 7. Soldering thermal pads of an LED chip on the radiation plate.

4. THE LIGHTING DEVICE WITH A MICROPROCESSOR

To freely control radiation levels of LEDs, the author employed an Arduino Mega 2560 microprocessor with 54 digital I/O pins of which 15 provides 8-bit PWM output. Figure 8 shows the outline of the electrical connection. PWM outputs to control LED lighting drive two subsystems: FETs that drive LEDs and the bar graph display units. A bar graph display unit is composed of a 10-segment LED bar graph display and its driver IC. These units are employed to display the radiation spectrum.

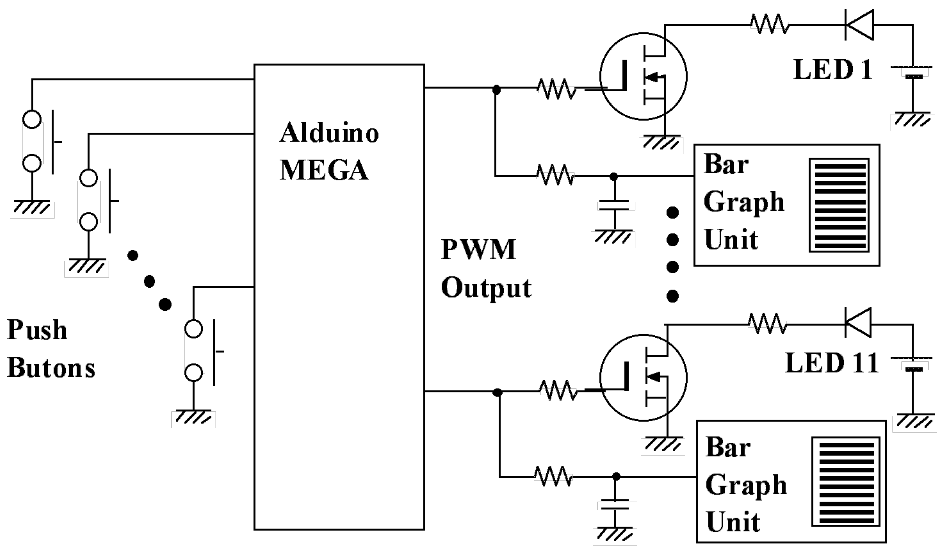

Figure 8. The outline of electrical connection.

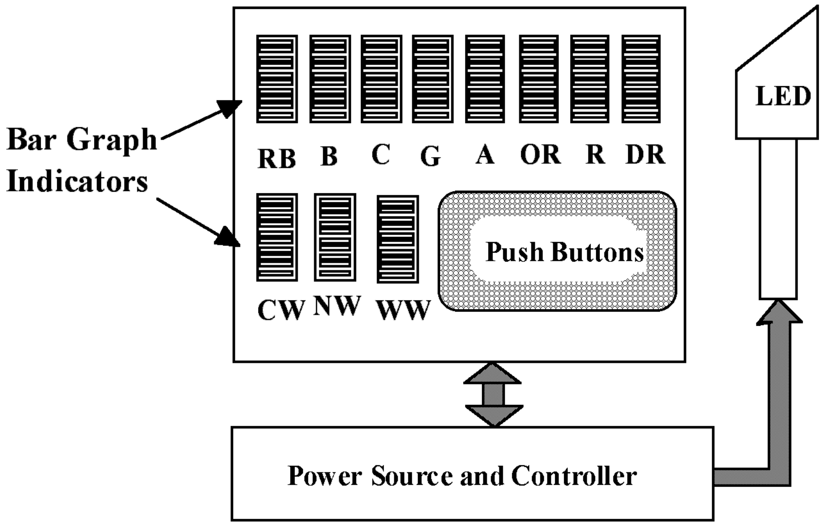

Figure 9. Rough composition of the lighting device.

Figure 9 shows the rough composition of the system. Power source and Arduino is contained inside a metal case, push buttons and bar graph indicators are on the surface of the case. The light radiation unit is connected to the power and controller unit case.

5. THE OPERATION OF THE LIGHTING DEVICE

With Arduino MEGA, various modes of operation can be realized. Some modes are as follows: (1) single LED lighting, (2) sequential lighting of single LEDs, (3) LED combination lighting, (4) sequential combination lighting, (5) On site adjustment of LED lighting, (6) Registration of the adjusted lighting and recalling.

With this flexibility, we can make various modes of demonstration. For example, we can show that the same color can be obtained with different combinations of primary colors, we can demonstrate metamerism and we can check color rendering.

5. CONCLUTION

By using multiple color LEDs, we can make lighting devices to demonstrate various color phenomena, and the ability of flexible demonstration is greatly enhanced by controlling with microprocessors.

REFERENCES

Takashi, Nakagawa: *Multicolor LED Lighting ApparatusFabricated to Demonstrate Metamerism*, Proceedings of ACA 2013, pp.118-120.

Address: Takashi NAKAGAWA, Kokubu 3-15-12, Dazaifu-shi, Fukuoka-ken, 818-0132, JAPAN
E-mails:nakagawa@fit.ac.jp, na32ka@yahoo.co.jp

The Effect of Environment Colour on Behavioural Inhibition.

Nicholas CICCONE, Stephen WESTLAND School of Design, University of Leeds, UK

ABSTRACT

The interplay between colour and behavioural inhibition (a trait of impulsivity) has yet to be researched despite the growing interest and activity in the field of impulsivity and behavioural inhibition (Webster and Jackson, 1997). The implications of gaining a better understanding of this area will help improve crime prevention strategies, the use of colour in marketing, the design of environments and product development. For example, in Japan and, recently, in the UK blue lights have been installed on railway platforms to discourage suicide attempts. However, the robustness of research into the veracity of claims about colour and impulsive behaviour remains to be tested.

This study addresses this by conducting a preliminary experiment in this area. Participant's behavioural inhibition was measured using reaction times gained from a computer based Go No-Go signal task within in a pop up colour studio. The luminance and chroma of the lighting environment was kept constant but the hue was manipulated between red, blue and green using a 24-bit LED stage lighting system; a white control lighting environment was also used. Results obtained through one way and mixed design ANOVA's found that: In the red light participants task reaction times were significantly faster than under white light. Highly impulsive participants showed significantly slower reaction times under all conditions except for green where a significant interaction was found. Additional work is underway to replicate the preliminary study using more advanced psychophysical techniques.

Keywords: *Colour, Impulsivity, Environment, Go no-go task, Crime prevention, Marketing.*

1. INTRODUCTION

For the purpose of this study impulsivity will be seen as reduced executive function and Inhibitory control (Logan, 1997). Behavioural Inhibition is the ability to suppress a pre-potent response (Nigg, 2000). Logan (1997) investigated if the inability to inhibit a pre-potent responses was a reflection of true impulsive behaviour through a stop signal task. It was found that go-signal responses were unaffected by impulsivity levels, but stop-signal tasks took longer with more impulsive subjects. Evidence indicates that in normal cohorts behavioural measures of inhibitory control are accurately related to represent levels of impulsivity (Enticott, 2006).

There are two main paradigms used when explaining the neurologically arousing effect of colour. The process is either; a learned or associated response (Grossman, 1999) or the result of the activation of an internally innate mechanism (Adams, 1973; Hupka, 1997).

An associative response to colour is caused by past experiences which effect an individual's physiological arousal, a process known as 'associative learning'. An unpleasant (fear) stimulus could be paired to a particular colour for example red with blood and pain. After several similar associations future exposures to that colour elicits the same neurological response to the paired stimulus but with only the colour being present (Bierley, 1985).

The general consensus on arousal caused by innate mechanisms is that the effect of the colour is dependent on where it falls within the colour spectrum (see figure 1). Longer light wavelength colours (yellow, orange and red) result in greater neuronal activation whereas shorter wavelengths (green and blue) have a sedative effect (Wright & Rainwater 1962).

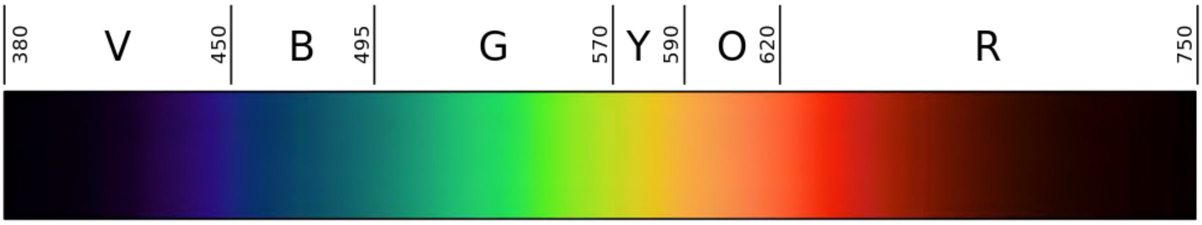

Figure 1: Colour spectrum with wavelengths (nm).

Neural activity has been associated with behavioural arousal and inhibitory control relating to individual differences in impulsivity. An fMRI study found a "positive correlation with activation (arousal) in the bilateral ventral amygdala, parahippocampal gyrus, dorsal anterior cingulate gyrus (BA 32), and bilateral caudate" to impulsivity. In addition to this there was a negative correlation when activation was seen in the dorsal amygdala and ventral prefrontal cortex (BA 47). This suggests that impulsivity is indeed influenced by the level of corticolimbic arousal (Brown, 2006).

Interestingly an effect has been found in relation to physiological arousal and impulse buying. A stimulating store environment was found to cause a momentary loss of self-control increasing instances of impulse purchases (Mattila and Wirtz 2008). These findings are consistent with psychology studies which highlight that over-stimulation or high arousal lessens a person's self-regulation (Baumeister *et al.*; 1998).

2. METHOD

A white pop-up studio was erected in a colour neutral room (white and black items only) with a marked x position for light positioning from behind the participant. A laptop equipped with Inquisit (by Millisecond Software version 4) and the Go/No Go experiment code installed on it with a touchpad was placed at a comfortable height for the participant to see the screen. A light emitting diode (LED) RGB capable light was used for colour accuracy and low temperature emission and placed in a position behind the participant facing towards the marked X. A Chroma meter displaying the International Commission on Illumination (CIE) was used to ensure similar luminosity levels within the popup studio in each condition while changes were made to the chroma (see figure 2).

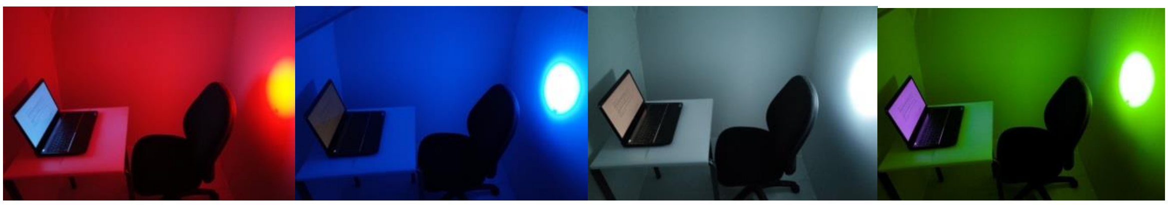

Figure 2: The four colour conditions.

2.1 Procedure

Participants entered the pop up studio and were instructed to sit at the desk and read the participant pack. This consisted of an information sheet about the general nature of the project, a consent form, the Ishihara colour deficiency test and the Barratt Questionnaire. An acclimatisation period of at least 10 minutes passed before the experiment began. The experiment file was then run on a laptop. Subjects were given adequate time to read the instructions and had an opportunity to ask any questions before the test was completed. The experimenter then turned on the LED light to the relevant colour setting for the participant and trial number. The main room light was then switched off and the participant was instructed to begin the task. After the first sets of trials were complete the experimenter changed the light to the second colour setting. The subject then completed the task for a second time. This process was then completed for each of the colour conditions. On completion of the last Go/No-Go task the main lights were turned on before the LED light was switched off. The participant were then given a full debrief of the purpose of the experiment thus concluding the test phase of the research.

2.2 PARTICIPANTS

This study used 27 participants (12 females and 15 males) with an average age of 20.9 years. Opportunity sampling was used to recruit individuals. Participants were screened to check: (i) They had had no previous experience in a similar study or any in-depth prior knowledge of colour research in the area being studied. (ii) That no one suffered from either claustrophobia or epilepsy. (iii) Normal colour perception through the use of the Ishihara test of colour perception deficiency (Ishihara 1917). (iv)That there was no high risk individual that may be suffering from impulsivity based pathologies using the Barratt Impulsivity Scale (Barratt 1959).

2.3 THE GO NO-GO TASK

The Go No-Go Task used in this study is a simplified version of the test used by Fillmore (2003). It measures impulse control by the level of ability shown by an individual to inhibit a behavioural response. The task consists of 200 trials, 50 in each condition (white, red, blue, green light) and took approximately 20 minutes to complete. The participant was shown a pre-target stimuli with a 60% chance of a go signal (black circle) and a 40% chance of a no go signal (black circle).

3. RESULTS AND DISCUSSION

3.1 PAIRED SAMPLE T-TEST

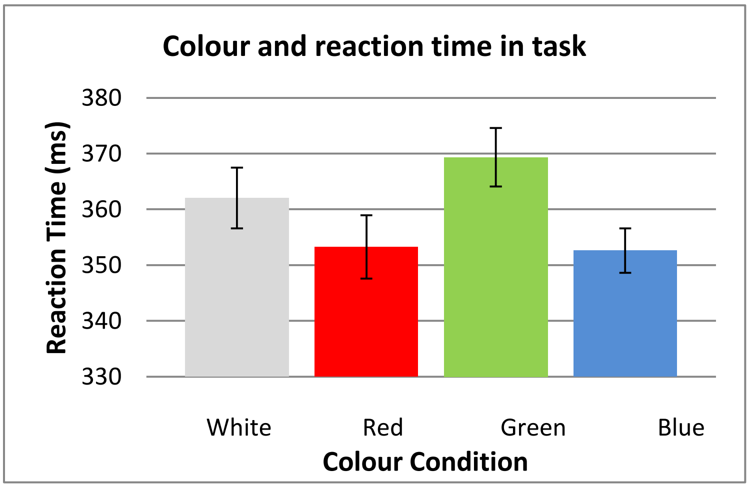

A paired sample T-Test found a significant effect of colour and Go No-Go task reaction times between white (M=362.03, SD=28.3) and red (M=353.3, SD=29.5); t(26)2.25, P=.033.

3.2 MIXED ANOVA

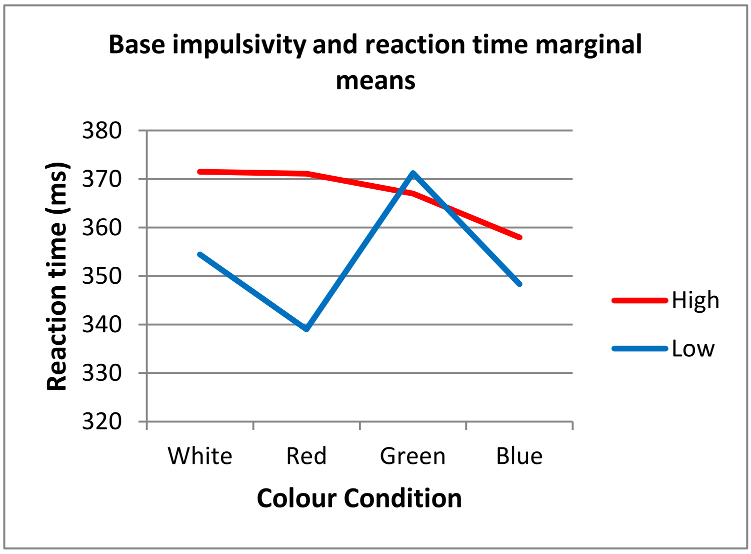

The sample was split into two groups; low and high base impulsivity determined from The Barrett Impulsivity Questionnaire (a score over 70 was considered high). A significant main effect of colour was found $F(2.23, 55.72) = 4.59$, $p = .012$ and a significant interaction between colour and impulsivity $F(2.23, 55.72) = 4.84$, $p = .009$. The Mauchley test for spherecity was significant p=.036 so a Greenhouse-Geisser correction was used.

4. Conclusions

Colour has previously been demonstrated to manipulate level of psychological arousal increases of which have been linked to greater impulsivity. Kosslyn (2003) found increases in physiological arousal and glandular responses when exposed to the colour red. The pituitary gland stimulates the adrenal medulla releasing epinephrine causing a higher psychological state with peaked behaviour and emotional responses (Fuller, 1982). Long wavelength colours have also been found to cause greater general neuronal activation compared to shorter wave length ones which have a sedative effect (Wright and Rainwater, 1962). Theories linking increased arousal to increased impulsivity include the one-dimensional concept (Eysenck, 1982; Doux, 1996) and the three-dimensional arousal model (Boucsein, 1992; 1997). If these theories are correct than red would be expected to cause increased impulsivity and thus a lower level of behavioural inhibition however this was not supported by the findings the T-Test showed significantly faster reaction times in the red light condition (M=353.3, SD=29.5); t(26)2.25, P=.033) compared to the control condition white (M=362.03, SD=28.3. This may suggest that the increased neuronal activation and arousal caused by red had a counteractive effect on the negative effect on the test caused by increased impulsivity. Faces of a competitor that are red are an indicator of testosterone levels related to anger and aggressiveness (Changizi, 2009). This combined with research associating colour within the context of evaluating threat (Elliot, 2009; 2007. Moller, 2009; Mathews, 1985) demonstrates the importance of red as a threat signal in humans. The human perceptual system assigns resources based on importance of the stimuli (Bishop, 2008) and this could be an explanation for these results however further research is needed to investigate the interaction between attention and impulsivity and effectiveness of behavioural inhibition.

Highly impulsive subjects had generally slower reaction times across the lighting conditions, compared to those of low base impulsivity. This was expected as in previous studies lower impulsivity has been associated with generally faster reaction times across colour conditions (Derefinko et al. 2008). Whereas highly impulsive participants have slower response times . A study of ADHD (a condition characterized by high impulsivity) found that typically participants had more errors and slower inhibition compared with controls (Roberts, Milich, 2011).

The faster reaction times in the red condition in those with low impulsivity can be explained through arousal theories (Kosslyn, 2003; Fuller, 1982, Wright and Rainwater 1962, Eysenck, 1982; Doux, 1996, Boucsein, 1992; 1997) and the selective processing of threat cues discussed previously (Elliot, 2009; 2007. Moller, 2009; Mathews, 1985). Red causes a higher level of alertness and therefore causes increases in attentional controls thus a faster response can be made without necessarily increasing impulsivity.

In contrast there was an interaction seen in reaction times and green light in those with low impulsivity. Under arousal theory states that impulsivity may be due to physiological under-arousal when in a state of rest than greater increases in arousal when stimulated (a rebound effect; Corr, 1995). This could support the interaction. The colour green is commonly associated with go & safe (McShane, 1999) It is possible that this memory schemata made through previous memory consolidation (Tse, 2007) negatively interacted with the stop signals. Rapid error-prone processing was used because of the cognitive matching between green and go when under green light (Dickman, 1990). More cognitive resources and time were therefore needed to correct this conflict.

The faster reaction times in the blue condition may be the result of reduced impulsivity through the relaxing effect of the colour. Anecdotally participants reported after the study that during the blue condition they felt calm. The sedative effect of blue has been previously reported by Wright and Rainwater (1962) notably this could have caused these faster reaction times through decreases in impulsivity levels however this still needs further investigation.

REFERENCES

Adams, F.M. and Osgood, C. E. (1973).”A Cross-Cultural Study of the Affective Meanings of Color”, Journal of Cross Cultural Phychology 4 (2).

Barratt, E. S. (1959). Anxiety and impulsiveness related to psychomotor efficiency. Perceptual and Motor Skills, 9(2), 191-198 doi: 10.2466/PMS.9.3.191-198

Baumeister, R., Bratslavsky, E., Muraven, M., & Tice, D. (1998). Ego depletion: Is the active self a limited resource. Journal of Personality & Social Psychology, 74(5), 1252–1265.

Bierley, C., McSweeney, F. K., & Vannieuwkerk, R. (1985). Classical conditioning of preferences for stimuli. *Journal of Consumer Research*, 316-323.

Bishop, S. J. (2008). Neural mechanisms underlying selective attention to threat. *Annals of the New York Academy of Sciences*, *1129*(1), 141-152.

Boucsein, Wolfram (1992), Electrodermal Activity. New York, London: Plenum Press.

Boucsein, Wolfram (1997), "Aktivierung," Handbuch Arbeitswissenschaft, eds. Luczak, Holger and Walter Volpert, Stuttgart: Schaeffer-Poeschel, 309-312.

Brown, S. M., Manuck, S. B., Flory, J. D., & Hariri, A. R. (2006). Neural basis of individual differences in impulsivity: contributions of corticolimbic circuits for behavioral arousal and control. Emotion, 6(2), 239.

Changizi, M. A. (2009). The vision revolution: How the latest research overturns everything we thought we knew about human vision. Dallas,TX: BenBella Books.

Corr, P. J., Pickering, A. D., & Gray, J. A. (1995). Sociability/impulsivity and caffeine-induced arousal: Critical flicker/fusion frequency and procedural learning. Personality and Individual Differences, 18(6), 713-730.

Derefinko KJ, Adams ZW, Milich R, Fillmore MT, Lorch EP, Lynam DR. (2008). Response style differences in the inattentive and combined subtypes of attention deficit/hyperactivity disorder. Journal of Abnormal and Child Psychology, 36, 745-758.

Dickman, S. J. (1990). Functional and dysfunctional impulsivity: personality and cognitive correlates. *Journal of personality and social psychology*, *58*(1), 95.

Doux Le, Joseph (1996), The Emotional Brain: The Mysterious Underpinnings of Emotional Life, New York: Simon & Schuster. PP.11-27

Elliot, A. J., Maier, M. A., Binser, M. J., Friedman, R., & Pekrun, R. (2009). The effect of red on avoidance behavior. Personality and Social Psychology Bulletin, 35, 365–375.

Elliot, A. J., Maier, M. A., Moller, A. C., Friedman, R., & Meinhardt, J. (2007). Color and psychological functioning: The effect of red on performance attainment. Journal of Experimental Psychology: General, 136, 154–168.

Enticott, Peter G.; Ogloff, James R.P.; Bradshaw, John L. (2006). "Associations between laboratory measures of executive inhibitory control and self-reported impulsivity". Personality and Individual Differences 41 (2): 285–94. doi:10.1016/j.paid.2006.01.011.

Eysenck, M. W. (1982). Attention and arousal: Cognition and performance. New York: Springer-Verlag.

Fillmore MT, Rush CR, Marczinski CA (2003).Effects of d-amphetamine on behavioral control in stimulant abusers: the role of prepotent response tendencies Drug and Alcohol Dependence, 71, 143-152.

Fuller, R. W. (1982). Pharmacology of brain epinephrine neurons. Annual review of pharmacology and toxicology, 22(1), 31-55.

Grossman, R.P. and Wisenblit, J. Z. (1999), "What we Know about Consumers Color Choices", Journal of Marketing Practice Applied Marketing Science, 5 (3) pp.77-89.

Hupka, R. B., Zaleski, Z., Otto, J., Tarabrina, N. V. (1997), "The Colors of Anger, Envy, Fear, Jealousy: A Cross Cultural Study", Journal of Cross-Cultural Psychology 28 (2), pp. 155-172.

Ishihara, S. (1917). Test for Coiour-Blindness. Tokyo: Hongo Harukicho.

Kosslyn, S. M. & Thompson, W. L. (2003), "When in Early Visual Cortex Activated During Visual-Mental Imagery Theory and Meta-Analysis", Psychological Bulletin 129 (5), pp. 722-747.

Logan, Gordon D.; Schachar, Russell J.; Tannock, Rosemary (1997). "Impulsivity and Inhibitory Control". Psychological Science 8 (1): 60–4. doi:10.1111/j.1467-9280.1997.tb00545.x. JSTOR 40062847.

Mathews, A., & MacLeod, C. (1985). Selective processing of threat cues in anxiety states. Behaviour research and therapy, 23(5), 563-569.

Mattila, A and Wirtz, J (2008), "The Role of Store Environmental Stimulation and Social Factors on Impulse Purchasing," Journal of Services Marketing, Vol. 23, No. 1, 562-567.

McShane, C. (1999). The origins and globalization of traffic control signals.Journal of Urban History, 25(3), 379-404.

Moller, A. C., Elliot, A. J., & Maier, M. A. (2009). Basic hue-meaning associations. Emotion, 9, 898–902.

Nigg, Joel T. (2000). "On inhibition/disinhibition in developmental psychopathology: Views from cognitive and personality psychology and a working inhibition taxonomy". Psychological Bulletin 126 (2): 220–46. doi:10.1037/0033-2909.126.2.220. PMID 10748641.

Roberts W, Fillmore MT, Milich R (2011). Separating automatic and intentional inhibitory mechanisms of attention in adults with Attention-Deficit/Hperactivity Disorder .Journal of Abnormal Psychology, 120, 223-233.

Tse, D., Langston, R. F., Kakeyama, M., Bethus, I., Spooner, P. A., Wood, E. R., ... & Morris, R. G. (2007). Schemas and memory consolidation. Science,316(5821), 76-82.

Webster, Christopher D., and Margaret A. Jackson, eds. *Impulsivity: Theory, assessment, and treatment*. Guilford Press, 1997.

Wright, B., & Rainwater, L. (1962). The meaning of color. Journal of General Psychology, 67, 89-99.

CONTACT

Nicholas Ciccone: ps10n2c@leeds.ac.uk

Stephen Westland: S.Westland@leeds.ac.uk

Influence of light incident angle and illuminance intensity on visual comfort and clarity

Yinqiu YUAN, Li-Ching CHUO, Hsin-Pou HUANG, and Ming-Shan JENG
Green Energy and Environment Research Laboratories, Industrial Technology Research Institute, Taiwan

ABSTRACT

This study focused on the influence of the combination of light source position and illuminance intensity on visual comfort for reading/writing. Two psychophysical experiments were conducted in a darkened room, 34 Taiwanese participated as the observers in both experiments. Each of them was asked to perform tasks of writing and reading in varied experimental lighting conditions. Evaluations of lighting quality were made by each observer. The results show that the position of the LED light had a strong impact on the observer response in terms of comfort. Although there was no significant difference in visual clarity between the three tested illuminance levels, 900lx was rated the most comfortable and was mostly preferred among the three illuminance levels.

1. INTRODUCTION

A wide variety of factors can affect visual comfort evaluation in an illuminated room, such as illuminance intensity, the correlated colour temperature (CCT), illumination uniformity, glare, colour rendering quality and so on. Enormous efforts have been made in investigating the influence of these factors on perceived visual comfort. For example, Lee (2011) found that the performance of visual accuracy in reading E-paper was best at ambient illumination of 1500lx. Xu and Zhu(1990) found that visual performance decreased as the illumination of display increased. Isono (2004) and his colleagues found that in terms of visual fatigue, there was no significant difference in reading electronic materials and conventional paper materials. Viewing difference and angle can also influence visual comfort. According to Shieh and Lee (2007), it was found that, in reading paper materials, the best viewing distance was at 360mm, which is less than the distance 500mm in reading E-paper. In terms of the effect of viewing angle, Shieh and Lee (2007) reported that the display screen tilted at 29.51 below horizontal eye level was evaluated the most comfortable for reading. Although the previous research findings provided evidence that light source was importance for visual satisfaction, there has been few study to investigate the influence of the combination of light source position and illuminance intensity.

To address the issue, the presented research conducted two psychophysical experiments to investigate the relationship between perceived visual comfort and positions of light source, as well as the effect of illuminance intensity.

2. METHOD

To address the issue, two psychophysical experiments were conducted in a darkened room, with a size of 42cm (height) by 222cm (width) by 230cm (depth). Thirty-four Taiwanese (including 17 males and 17 females) participated in both experiments. Half of the observers were over 175cm and the other half below 165cm. All of the observers have passed the Ishihara test for colour deficiency. A same wall-mounted LED lamp was used for providing experimental lights in both experiments.

2.1 Sample Preparation

To investigate the influence of light incident angle on visual comfort in Exp-1, a wall-mounted directional LED luminaire with fixed CCT of 4000K and illuminance of 500lx was used as experimental light. The position of the lamp can be varied horizontally by changing the angle of an adjustable folding arm that supported the lamp. This resulted in 7 angles of incident light on the writing panel: -24.45, -22.50, -14.40, 0, 14.40, 22.50 and 24.45 degrees, in which the negative angle values mean that the incident light came from the right side above the observer, and positive angle values mean the light came from the left side. Figure 1 shows the lighting conditions under each of the seven experimental incident angle of light.

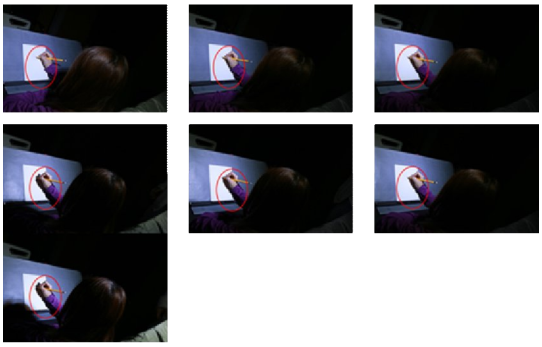

Figure 1: Lighting conditions caused by the 7 experimental incident angles of light.

The light intensity of 600lx, 900lx and 1200lx were selected as experimental illuminance levels (measured at the centre of reading panel) in Exp-2. The incidental light angle was fix at 24.50 during the experiment. The same group of observers took part in the experiment to evaluate visual comfort, preference and clarity for the tested light intensities.

2.2 Experimental Procedure

In Experiment 1, each observer performed a writing task on a matt ISO paper placed on a flat panel, with a tilt angle of 45 degrees, lit by a wall-mounted directional LED luminaire with fixed CCT of 4000K and illuminance of 500lx. This luminaire was positioned above the observer's head and adjustable to achieve varied incident angle of light. In the experiment, 7 angles of incident light on the writing panel were generated including -24.45, -22.50, -14.40, 0, 14.40, 22.50 and 24.45 degrees. During the experiment, the observer was allowed to adjust the viewing distance between his/her body and the writing panel as preferred. The observer was asked to perform a writing task on the panel under each experimental incident angle and give rating for each angle in terms of visual comfort.

In Experiment 2, the incidental light angle was fix at 24.50 which was found the most comfortable angle in Experiment 1. The illuminance intensity of the lamp can be adjusted by a DC power supply at 600lx, 900lx and 1200lx. The same group of observers performed a reading task on the same paper and the same panel as in Experiment 1. Each observer was asked to evaluate visual comfort, preference and clarity to each of experimental illuminance.

3. RESULTS AND DISCUSSION

The significance of influence by gender, observer's height, viewing distance and incident angel of light on visual comfort was analysed using ANOVA. Table 1 shows the results. It is clear that among the four factors, light incident angle had the most significant influence on visual comfort with p-value of 5.13E-12. In terms of significance of effect by gender, observer's height and viewing distance, the results of ANOVA indicate no significant effect was caused by neither of the three factors, with p values being far less than 0.05, Table 1 shows the detailed figures. This suggests that the position of light source can dramatically affect induced visual comfort. Figure 2 demonstrates the trend of the influence. Positive angles means the experimental light source was placed at the observer's left hand side, while negative angles were those of right hand oriented. The perceived visual comfort was found to increase as the angle of incidence becomes larger and larger, indicating a tendency that the observers (all right-handed) felt more comfortable when the lamp was situated on the left hand side than on the right hand side.

Figure2: *Effect of incident angle on visual comfort*

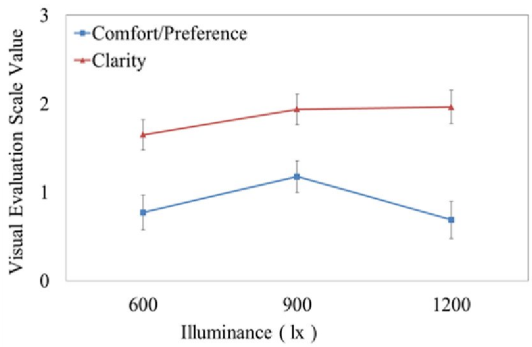

Figure 3: *Influence of illuminance intensity on visual comfort/preference and clarity*

In terms of the influence of illuminance intensity on visual comfort, preference and clarity, there was no significant difference between 600lx, 900lx and 1200lx. However, 900lx was rated the most comfortable and preferred intensity among the three tested illuminance levels. In addition, little gender difference and height difference was found in judging visual comfort, preference and clarity affected by illuminance intensity.

Table 1. ANOVA results for the significance of gender, observer's height, viewing distance and incident angel of lighting for the impacts on visual comfort

Dependent Variable : Visual comfort	Source	Gender	Height	Viewing distance	Incident angle
	Mean Square	1.143	1.829	0.008	16.104
	F	0.561	0.898	0.004	7.905
	p	0.457	0.347	0.996	5.13E-12

4. CONCLUSIONS

The experimental results show that the position of the LED light had a strong impact on the observer response in terms of comfort. The perceived visual comfort was found to increase as the angle of incidence becomes larger and larger, indicating a tendency that the observers (all right-handed) had higher visual satisfaction when the lamp was situated on the left hand side than on the right hand side. Although there was no significant difference in visual clarity between the three tested illuminance levels, 900lx was rated the most comfortable and preferred among the three illuminance levels. This indicates that uncomfortable illuminance does not necessarily cause a decline in visual clarity. The research result is useful for lighting design in indoor environments.

ACKNOWLEDGEMENTS

This work was supported in part by Bureau of Energy, Ministry of Economic Affairs, Taiwan R.O.C. for project “Research and Development of LED Lighting and Lighting System Efficiency Technology” (104-E0201).

REFERENCES

Isono, H., S. Takahashi. , Y. Takiguchi. and C. Yamada. 2004. Measurement of Visual Fatigue from Reading on Electronic Paper. In IDW 2004,Proceedings,ed. by Niigata. Niigata Convention Center, 1647-1648.

Lee, D. S., Y. H. Ko. , I. H. Shen. and C. Y. Shen. 2011. Effect of light source, ambient illumination, character size and interline spacing on visual performance and visual fatigue with electronic paper displays. Journal of Displays 32:1-7.

Shieh, K. K. and D. S. Lee. 2007. Preferred viewing distance and screen angle of electronic paper displays. Journal of Applied Ergonomics 38:601-608.

Xu, W.and Z. Zue. 1990. The effects of ambient illumination and target luminance on colour coding in a CRT display. Journal of Ergonomics 33:933-944.

Address: Dr. Yinqiu YUAN, Green Energy and Environment Research Laboratories, Industrial Technology Research Institute, No.195, Sec. 4, Zhongxing Rd., Zhudong Township, Hsinchu County 310, TAIWAN
E-mails: AlinaYuan@itri.org.tw, lichingchuo@itri.org.tw, itri451595@itri.org.tw, msjeng@itri.org.tw

Colour Terms in the Interior Design Process

Douha Y ATTIAH, Vien CHEUNG, Stephen WESTLAND and David BROMILOW
School of Design, University of Leeds

ABSTRACT

Colour is a very important topic that interior designers need to consider. Considerable research has been conducted in the area of colour application in interior design; in this study we are concerned with colour terms in interior design, mainly the terms designers use and know about. Fifteen interior designers with varied professional backgrounds, but based in the Middle East (Saudi Arabia, Dubai, Bahrain, Lebanon, Egypt, and Turkey), were interviewed. Previously we reported that fourteen out of fifteen designers stated that colour thinking and decision making take place at the early stages of their design processes; eight of them reported that colour takes place in the first step when meeting clients and starting the project (Attiah *et al*., 2014). This study documented 137 terms which the fifteen designers use whilst brainstorming and working on a design project; subsequent analysis of these terms could form a basis for understanding how interior designers communicate the abstract properties of colour as part of their design processes. In this paper we show how the 137 terms were categorised according to a framework of four categories of colour terms: emotional, descriptive, cultural and functional. In addition, seventeen words (scientists names and technical terms), which are widely used in colour science (such as: CIELAB, Saturation, Itten) were shown to the designers; their knowledge was shown to be incomplete.

1. INTRODUCTION

The field of interior design is an interdisciplinary practice that is concerned with the creation of interior environments to articulate identity and atmosphere through the manipulation of spatial volumes, placements of specific elements, and dealing with special surfaces (Coates *et al.*, 2009). Colour is an important element for both 2D and 3D surfaces of the interior, thus it plays a big role in the aesthetical success or failure of the interior. For this purpose, we are trying to look at the possibilities of enhancing better colour schemes for interiors through enhanced colour communication; hypothesising that some minor execution problems may be due to lack of technical knowledge and ineffective colour communication between designers themselves, designers and public (clients), designers and less-experienced designers, and contractors or working people.

2. METHOD

2.1 Case Studies

Prior to approaching designers we analysed (Figure 1) three different semi-public interiors in the UK and their colour schemes. The analysis considered colours in every aspect of each interior (colour in lights, materials, and surfaces, etc.) and how all these appear together in the final analysed space. We found that the terms we used in the study need to be categorised for a better discussion, thus we have assigned groups where we found the terms could fall onto four groups: *Cultural, Descriptive, Emotional,* and *Functional*. Table 1 shows the description of each group.

Figure 1: Three different semi-public interiors in the UK: restaurant (left), hotel lobby (middle) and bar (right).

Table 1: Four groups of colour terms category.

Groups	Descriptions	Examples
Cultural	When the colour is used in the interior to depict a certain era or when the colour is inspired or used to show a cultural background.	• renaissance • modern
Descriptive	When a scientific colour term or name is used to describe a colour.	• hue • shade
Emotional	When the colour is used in the design to convey or leave a certain impact on users' feelings.	• warm • cosy
Functional	When the colour is used in the space to create a specific effect such as to make the ceiling higher.	• deep • enlarging

2.2 Interviews

A semi-structured individual interview approach was conducted to try to find out what designers really think, and to prevent designers impacting on each other (as in a focus group). A total of 15 designers were recruited from different cultural backgrounds, age groups, working experiences, and places of work around the Middle East. The duration of each interview was 45-120 minutes for each participant. Data were both qualitative and quantitative and in this study the focus will be on two of the fourteen interview questions, which are described in Sections 2.2.1 and 2.2.2.

2.2.1 Collecting terms

Name terms you always use in your daily design life/career describing colour choices/decisions/schemes?

Designers freely expressed the terms that they usually use in their daily professional lives. A total of 137 words were collected (Attiah *et al.*, 2014). The analysis included counting the usage frequencies for frequently-used terms and categorising the terms according to the four groups in Table 1.

2.2.2 Testing knowledge

What do you know about each given term/name. Summarise what you know about each? If not familiar cross the word out.

Designers were given a sheet of seventeen colour terms (Table 2) and asked to write what they know about each. They were free to cross out what they believe they do not know. For each completed term the responses were categorised as being complete but with ambiguous description (CA), correct but incomplete (P), correct (C) or incorrect (X). Table 3 shows an example for one of the designer's responses.

Table 2: Seventeen colour terms.

Munsell	Colour intensity	Ostwald	Newton	Hue	Colour saturation
Chroma	Itten	Colour lightness	NCS	CIELAB	Colour value
Pantone	RAL system	Colour vividness	Colour temperature	Colour harmonies	

Table 3: An example of colour terms answer sheets.

Colour terms	Answers	Category
Munsell	---	Do not know
Colour intensity	The saturation level of the colour	CA
Ostwald	---	Do not know
Newton	---	Do not know
Hue	Black-white shade	X
Colour saturation	The intensity of the shade	CA
Chroma	---	Do not know
Itten	---	Do not know
Colour lightness	Lighter shade	X
NCS	---	Do not know
CIELAB	---	Do not know
Colour value	Within the same colour shades	P
Pantone	Graphic design; like RAL	P
RAL system	Used a lot with contractors	X
Colour vividness	Darker shade	X
Colour temperature	Cold vs warm colour	C
Colour harmonies	How colours work together	C

3. FINDINGS AND DISCUSSION

3.1 Collected terms

The 137 words were analysed for similarity and 76 unique terms were collected. Table 4 lists the 76 terms and their usage frequncies. Warm/cool was the most mentioned term with a frequency of 10.

Table 4: Collected terms and their usage frequencies (terms with a frequency greater than 4 are highlighted yellow; terms with a frequency greater than 2 are highlighted grey).

accent	2	contrast	3	harmony	3	renaissance	1
achromatic	2	country	1	Honest	1	saturation	1
active	1	cozy	2	hue	3	shade	5
analogous	2	dark	1	maroon	1	shocking	1
armani beige	1	daylight	1	metallic	2	sophisticated	1
artificial	1	earth tones	3	modern	1	split complementary	1
babies	1	elegant	1	monochrome	4	stressful	1
beiges	1	family of colours	1	moody	1	strong	2
bold	2	fashionable	2	mustard	1	tetrad	1
bright	2	feminine	1	natural	5	tint	4
Brown-scale	1	fire	1	neutral	7	tone	2
champagne	1	flashy	2	office/formal	1	tone down	1
childish	1	fresh	1	pale	1	transparent	1
chroma	1	funky	3	pastel	6	trendy	2
classic	1	gipsy	1	posh	1	triad	1
colour scheme	3	green design	1	powerful	1	ultra bright / neon	1
comfort	1	grey-scale	1	pewter	1	value	2
complementary	3	Happy	1	refer to samples	1	warm/cool	10
contemporary	1	harmonies	1	relaxing	1	youth	1

3.2 Categorised terms

Table 5: Categorised terms in the Descriptive, Emotional, Cultural and Functional groups and their usage frequencies (terms with a frequency greater than 4 are highlighted yellow; terms with a frequency greater than 2 are highlighted grey).

Descriptive		Descriptive		Emotional		Cultural		Functional	
accent	2	maroon	1	active	1	classic	1	comfort	1
achromatic	2	metallic	2	babies	1	contemporary	1	cozy	2
analogous	2	monochrome	4	bold	2	country	1	elegant	1
armani beige	1	mustard	1	childish	1	fashionable	2	feminine	1
artificial	1	natural	5	comfort	1	funky	3	fresh	1
beiges	1	neutral	7	cozy	2	gipsy	1	green design	1
bold	2	pale	1	elegant	1	modern	1	office/formal	1
bright	2	pastel	6	fresh	1	renaissance	1	sophisticated	1
brown-scale	1	pewter	1	funky	3	trendy	2		
champagne	1	refer to samples	1	happy	1	youth	1		
chroma	1	saturation	1	honest	1				
colour scheme	3	shade	5	moody	1				
complementary	3	strong	2	posh	1				
dark	1	tetrad	1	powerful	1				
earth tones	3	tint	4	relaxing	1				
family of colours	1	tone	2	shocking	1				
fire	1	tone down	1	sophisticated	1				
flashy	2	trasparent	1	stressful	1				
grey-scale	1	triad	1	strong	2				
harmonious	1	ultra bright / neon	1	warm/cool	1 0				
harmony	3	value	2						
hue	3	warm/cool	10						

54% of the filtered terms were categorised as *descriptive* according to Table 1. Table 5 summarises the categorised terms. All the fifteen designers included *descriptive* terms. *Functional* terms such as *green design* and *formal* were mentioned the least (10% of the terms were categorised as *functional*). 24% of the terms were categorised as *emotional* and 12% as *cultural*. 44 terms were descriptive, 20 were emotional, 10 were cultural, and 8 were functional. Some terms were put in more than a category, for example: *bold*, *warm/cool*, and *strong* can be both *descriptive* and *emotional*.

3.3 Technical colour terms

Table 6 shows the seventeen colour terms and a summary of the frequency responses in each of the categories: complete but with ambiguous description (CA), correct but incomplete (P), correct (C) and incorrect (X).

Table 6: Summary of responses from technical colour terms.

Colour terms	CA	P	C	X	Do not know
Munsell	0	2	3	0	10
Colour intensity	9	0	0	5	1
Ostwald	0	1	1	0	13
Newton	0	2	2	2	9
Hue	0	0	5	6	1
Colour saturation	6	0	0	6	0
Chroma	1	0	0	2	9
Itten	0	1	1	0	13
Colour lightness	1	4	1	9	0
NCS	0	0	0	0	15
CIELAB	0	0	0	1	14
Colour value	0	3	3	4	5
Pantone	0	1	5	3	6
RAL system	0	0	3	1	11
Colour vividness	1	1	1	5	7
Colour temperature	0	0	12	2	1
Colour harmonies	0	0	13	0	2

As shown in Table 6, the terms that received the most correct responses were colour temperature (12 out of 15) and colour harmonies (13 out of 15). Most other terms wee poorly understood. The least known terms were: NCS, CIELAB, Itten and Ostwald (15, 14, 13 and 13, respectively, out of 15 do not know). Ambiguity was shown mainly between colour saturation and intensity.

In terms of the four groups in Table 1, this study has shown that designers in the Middle East mostly use descriptive colour terms in their daily profession. However, their technical knowledge of colour terms and names, was found to be weak or incomplete in all but a few cases. This does not mean that the knowledge on all colour terms in this study is necessary for achieving well-chosen colour schemes. The findings therefore show a potential need for better technical colour knowledge in relation to design in the region.

4. CONCLUSIONS

Paterson (2003) suggested that any attempt to define or describe colour by means of words is doomed to failure; whereas we believe that an efficient verbal communication and knowledge on colour can result in better interior setups consequently. Although some of the colour terms in this study (such as Itten, Ostwald and Newton) may not have an impact on the colour choices in the design process, and indeed we previously found that most of these designers prefer to get inspired when thinking of the colours than sticking to a theory (Attiah *et al*, 2014), good technical knowledge on precise colour descriptions such as intensity, saturation and hue will enable effective colour communications. This study led us to rethink if designers' knowledge needs to be rethought of in the region, and if we can suggest a framework for designers for better colour and design discussions using the resulted categories (Table 2). A future study can include comparing Middle-East participants' results and Western designers' (for example, in the UK and USA).

ACKNOWLEDGEMENTS

We would like to thank the designers as the results of this study would not be possible without their dedicated time for the interviews.

REFERENCES

Attiah, D.Y., Cheung, V., Bromilow, D. and Westland, S. 2014. *Colour planning in the interior design process*, Proceedings of The Second Conference of Asia Color Association, 187-191, Taipei, Taiwan.

Coates, M., Brooker, G. and Stone, S. 2009. *The Visual Dictionary of Interior Architecture and Design*. AVA publishing.

Paterson, I. 2003. *A Dictionary of Colour*. Thorogood publishing Ltd.

Address: Douha Attiah, School of Design, University of Leeds, Leeds LS2 9JT, UK
E-mails: sd10dya@leeds.ac.uk, t.l.v.cheung@leeds.ac.uk, s.westland@leeds.ac.uk, d.bromilow@leeds.ac.uk

Effects of Classroom Wall Color on Students

Fazıla DUYAN, Rengin ÜNVER
Faculty of Architecture, Yıldız Technical University

ABSTRACT

It is a known fact that properties of physical environment act as stimulus and affects student's behavior and learning performance. The physical environment factors playing significant roles in achievement and reaching educational goals are size, heat, sound, light, color. In this paper, the results of an experimental research study which investigates preferences of 8-10 years-old subjects on their classroom's wall colors will be presented. Five colors (5R 7/8, 5Y 7/8, 5G 7/8, 5B 7/8, 5P 7/8) were selected by using Munsell Color System. The students have had lessons under different wall color in five weeks. The preferences of students were collected by surveys for each wall color.

1. INTRODUCTION

Effects of stimuli generated by physical properties such as volume, dimensions, temperature, sound, color and light on occupants emotions, behavior and performance is a well-known fact. In this respect, the effect of color, as one of the primary physical environmental elements of classrooms where the majority of learning takes place, on students is obvious. Therefore, a research project entitled "The Effect of Lighting and Color Schemes on Student's Performance in Classrooms of Primary School" had been initiated. This research has been supported by Yıldız Technical University Scientific Research Projects Coordination Department. Project Number: 2013-03-01-DOP01. The project consists of three basic stages.

- Determination of students' personal and classroom wall color preferences using color samples,
- Determination of students' preferences by painting classroom walls,
- Determination of the effect of classroom wall colors on student performance.

In this paper, studies to determine classroom wall color preferences of student groups between the ages of 8-10 by means of applying different colors on classroom walls, which is the second stage of the research project, will be explained. The findings made at this stage of the research will enable data gathering that would be instructive providing students with more pleasing educational environments, in terms of "surface color" which is one of the physical environmental elements.

2. METHOD

Procedures followed, on the second stage of "The Effect of Lighting and Color Schemes on Student's Performance in Classrooms of Primary School" research project, by painting classroom walls to determine 8-10 ages student preferences can be briefly listed as follows:

- Selection of the primary schools.
- Identification of classroom wall colors and application on the walls.
- Determination of classroom color preferences through surveys.
- Assessment of survey results.

The research has been conducted with different socio-cultural and economic backgrounds, in two elementary schools, one of which is a state school and the other is a private school at same location in Istanbul. 18 girls and 25 boys from the Private School, 21 girls and 13 boys from the State School, in total 77 students have been participated. All students were tested for color vision deficiencies prior to participation using Ishihara color vision test. In order to prevent the color of classroom equipment influencing the color of the walls, benches and panels were wrapped with dark medium gray (N 5/0) clothes and classroom cabinets covered with cartons of the same color. The lamps that were used in the present luminaries had been replaced with fluorescent lamps with higher color rendering index (Ra). Colors that were selected for the study had been applied on the walls for 5 consecutive weeks. The surveys were carried out on 10^{th} March-11^{st} April 2014. Students underwent their education in a different wall colors each week and preference surveys were conducted at the end of each week.

2.1. Identification of classroom wall colors

Results, obtained from the survey conducted to determine classroom color preferences at the first stage of the project, were used in the second stage. Value and chroma for selected colors remained constant and hue has changed according to Munsell Color System. Five wall colors that were going to be used in research on the second stage of the project are red (5R 7/8), yellow (5Y 7/8), green (5G 7/8), blue (5B 7/8) and purple (5P 7/8).

2.2. Application of Determined Colors and Preference Tests

Chosen five colors were applied to the classrooms during weekends and students were trained for the duration of the week. On the last day of the week (Friday) students were given a classroom wall color preference survey. In order to rate participant's preferences, a ten step Likert-type scale was used, ranging from 0 (disliked) to 9 (strongly liked). The sample pictures are shown in Figure 1 and 2.

Figure 1: Red, Yellow and Green Classroom

 

Figure 2: Blue and Purple Classroom

2.3. Assessment of Survey Results

Data collected from surveys to determine preferences of student groups 8 to 10 years of age on colors applied to classrooms are studied in five groups as given below:

- Girls (private and state)
- Boys (private and state)
- Private school (girl and boy)
- State school (girl and boy)
- All students (girl and boy; private and state school)

Scores are given in terms of ratings from 0 to 9 on Likert-type scale as the average responses of students and shown in Table 1:

Table 1. Preference Scores of Students

	GIRLS	BOYS	PRIVATE SCHOOL	STATE SCHOOL	TOTAL
RED 5R 7/8	6,62	5,61	4,74	7,74	6,06
YELLOW 5Y 7/8	6,10	6,82	6,44	6,47	6,45
GREEN 5G 7/8	7,00	7,34	6,42	8,12	7,17
BLUE 5B 7/8	7,54	8,53	8,12	7,91	8,03
PURPLE 5P 7/8	7,95	6,37	6,53	7,97	7,17

Girl preference results: In both schools girls have stated their classroom wall color, all five color pretty close to each other. The purple wall color was preferred the most and the yellow the least (Table 1 and Figure 3).

Boy preference results: Red turned out to be the least preferred color in both schools, whereas blue turned out to be the most preferred. Second to the most preferred color was green wall color. Red was the least favored wall color (Table 1 and Figure 3).

Private school (girl+boy) preference results: As seen in Table 1 and in Figure 4, private school students liked the color blue the most. Average rating given by students to color blue is 8,1. Blue wall color is followed by purple (5P 7/8), yellow (5Y 7/8) and green (5G 7/8.) Red wall was the least liked color among students with a rating of 4,47 points (Figure 4).

State school (girl+boy) preference results: Color preferences at the State school, green took the first place, followed by blue, purple and red with close scores (8,12 to 7,74 points). The least preferred color was yellow with 6,47 points (Table 1 and Figure 4).

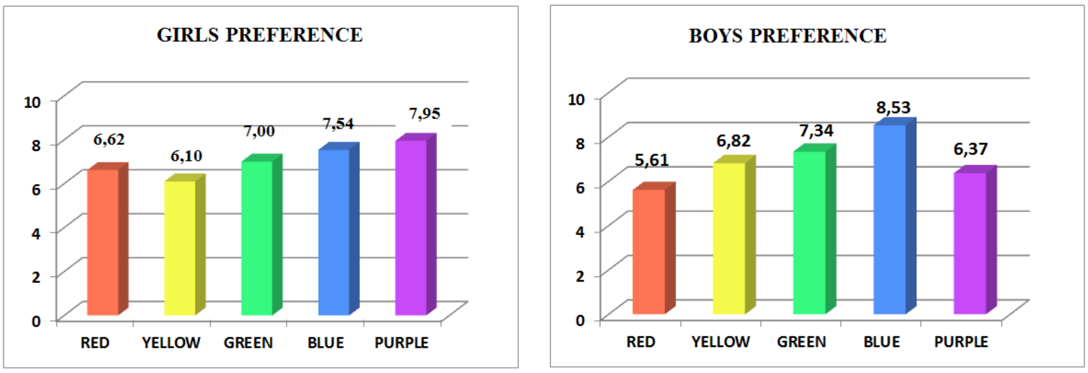

Figure 3: Female and Male Classroom Wall Preference Results

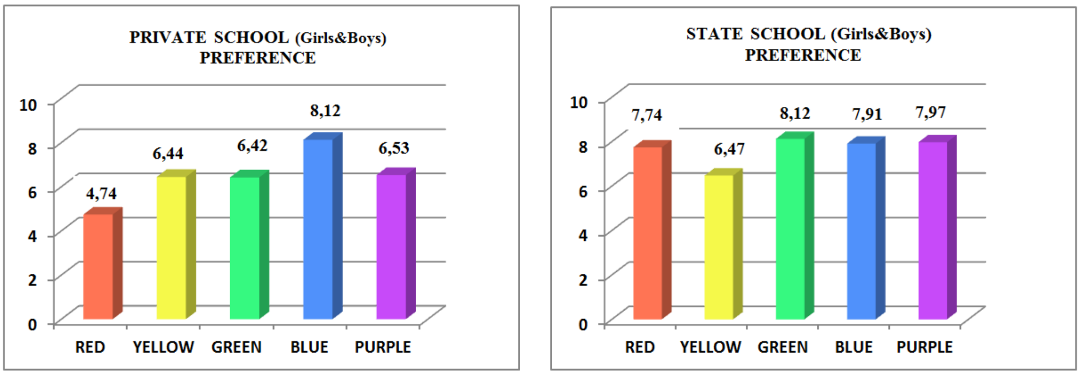

Figure 4 : Private and State School (Girl&Boy) Classroom Wall Preference Results

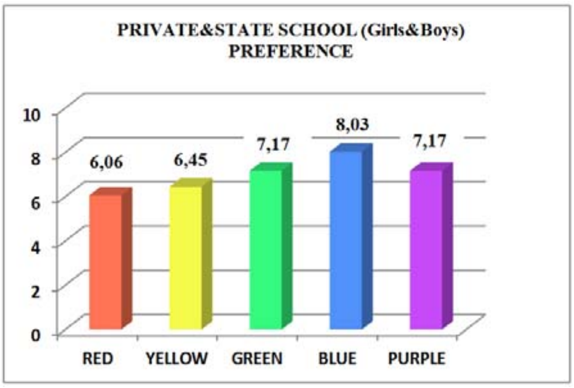

Figure: 5. Total Classroom Wall Preference Results

All students (boy&girl; private school & state school) preference results: The preference results for all the students participated are seen in Table 1 and Figure 5. According to these results blue with a score of 8,03 is the most preferred color. Blue is followed by purple and green with the same score of 7,17. The least preferred color is red with a score of 6,06.

3. CONCLUSION

In order to determine 8-10 years old students' classroom color preferences, five different colors were applied each week successively and a survey was conducted each week. Collected data was evaluated by gender (girls and boys), by school (private and state) and by sum of both gender and schools. Results could be summarized as follows:

- In both schools, purple was preferred the most and yellow the least by girl students. While blue is the most preferred and red is the least preferred color among boys. Girls rated blue with a high score that is close to purple's.
- On school basis, while private school students liked the blue most and red the least, state school students preferred green the most and yellow the least. State school students rated red higher in contrast to private school students.
- Blue is the most preferred color in both private and state schools and by both genders while red is the least preferred color.

In this research where student preferences are gathered, the highest inclination had been towards blue in every group. In this research conducted with 3rd grade elementary school students, it has been concluded that participants are most pleased studying in an environment painted blue (5B 7/8).

In order to enable the primary school students to receive education in a happier environment, the results from the first stage of the project and from the consequent similar studies should act as a guideline for the school headmasters and designers who have an important role in classroom color prefer all.

REFERENCES

Baytin, Ç., A. Kıran, M. Tunbiş 2005. Colour Preferences in Architectural Design Studious. *Architectural Science Review*, University of Sydney, 48(4) 317-328.

Schloss, K. B., E. D. Strauss, S. E. Palmer 2013. Object Color Preferences, *Color Research and Applications,* 38(6) 393-411.

Park, J. G. P. 2014. Correlations between Color Attributes and Children's Color Preferences, *Color Research and Applications*, 39 (5) 452-462.

Wang, H., R. R. Randall 2008 Computer Classroom Wall Colour Preference and They Relationship with Personality Type of College Students, *Colour, Design & Creativity*, 4 (2) 1-13.

Address: Prof. Dr. Rengin Ünver, M.Sc Fazıla Duyan,
Yıldız Technical University, Faculty of Architecture, Unit of Building Physics,
34349, Beşiktaş-Istanbul, TURKEY,
E-mails: faziladuyan@gmail.com, renginunver@gmail.com

A Study on the Evaluation Process of Facade Colour Parameters

Esra KÜÇÜKKILIÇ ÖZCAN, Rengin ÜNVER
Yıldız Technical University

ABSTRACT

Contemporarily, many material alternatives for facades has been emerged due to the improvements in the building and material technology along with the increased painting opportunities. Thus an excessive range of façade colours appear in cities causing inharmonious colour appearances and colour pollution in settlements. To avoid any inappropriate situations due to colour pollution in the design process, building façade colours should be determined considering factors such as architectural and environmental (natural and built) features as well as colour perception. Therefore, a systematic façade colour design approach for various scales including all the stages has been developed as a Research Project at Yıldız Technical University. This paper basically prepared with the aim of introducing the developed façade colour design approach which is constituted of several stages, mainly includes a detailed analysis of the first stage of the Research Project.

1. INTRODUCTION

Façade colour is one of the most important factors affecting the architecture of the building and the appearance, image / identity of the settlements. Therefore, any decision about the façade colour of a building changes the appearance and image of both the building and its environment. Contemporarily, many material alternatives for facades has been emerged due to the improvements in the building and material technology along with the increased painting opportunities. Furthermore, in the design process façade colour is being determined according to the likes, preferences and personal desires of architects, occupants, employers, etc. without caring the environmental parameters and colour perception factors in practice. Thus, an excessive range of façade colours appear in cities causing inharmonious colour appearances and colour pollution in settlements.

To avoid any inappropriate situations due to colour pollution in the design process, building façade colours should be determined considering factors such as architectural and environmental (natural and built) features as well as colour perception. But in practice, complex relationships of related factors constitute a major problem for the colour designers, architects, etc.

There are a range of important studies examining the façade colour design and the effects of related environmental and perceptional factors but the holistic approaches for the whole façade colour design process are very limited. Therefore, a systematic façade colour design approach for various scales including all the stages of urban master colour plan has been developed as a Research Project entitled “An Aproach to Façade Colour Design”. This research has been supported by Yıldız Technical University Scientific Research Projects Coordination Department. Project Number: 2013-03-01-DOP02. This paper basically prepared with the aim of introducing the developed façade colour design approach which is constituted of several stages, mainly includes a detailed analysis of the first stage of the Research Project.

2. APPROACH FOR FAÇADE COLOUR DESIGNING

While preparing urban colour plans, general criteria involving the whole settlement and appropriate colour designs need to be done. Colour planning criteria show similarities for all settlements. But every settlement has a unique architecture, natural and built environments, total area, population, building intensity and distribution, and these particularities show diversities from each other. Various particularities of the settlements create differences in generating urban colour plans. When considering these varieties, for considerably big, complex and constantly evolving cities like Istanbul, preparing master colour plans involving all the buildings in the city, requires very detailed and hard work.

In this research project, which began following these informations, it is needed to improve an Approach for Façade Colour Designing in preparing urban master colour plans. The project has been started with determining the main procedures for the urban colour planning process according to the Approach for Façade Color Designing. Therefore, Approach for Façade Color Designing is thought to consist of four basic phases. These phases are listed as:

a. Determining regions (district, quarter, neighborhood, square/street) and buildings of the settlement that have priority in making the colour design.

b. Making the environmental colour analysis of urban regions and buildings

c. Determining and evaluating the particularities affecting the colour perception of urban regions and buildings

d. Making colour proposals for urban regions and buildings

Since this paper is limited, only the first one of the above mentioned phases is explained in details.

3. DETERMINING REGIONS AND BUILDINGS THAT HAVE PRIORITY IN COLOUR DESIGNING

Although colour planning criteria are similar in new and current settlements, since the particularities of the current settlements are various and independent from each other, it is difficult to determine the colour planning criteria and this requires more detailed studies. Therefore, particularly in big settlements, beginning with the determination of regions and buildings having priority in colour designing and creating an evaluation system to fasten the process would be useful in colour planning preparations. But, determining this priority depends highly on many factors as socio-cultural structure, economic structure and aesthetic features. In this study, assuming that the main role in cityscape is obtained by buildings, the priority in colour designing is thought to be determined by "effects of urban regions and buildings on cityscape".

For this purpose, an evaluation system called "Degrees of Affecting the Cityscape" (DAC) has been created in order to determine the regions and buildings having priority in colour designing. This evaluation system helps measuring the building and the region it is part of. After setting the evaluation system in general, some criteria regarding the features of regions and buildings that affect the cityscape are determined. Subsequently, a questionnaire (public survey) has been realized in order to measure the influence degrees of the regions and buildings on the cityscape and prioritize these criteria.

3.1 The Evaluation System on Measuring Influence Degrees of Regions and Buildings on Cityscape

The flow diagram of the evaluation system for determining the degrees of affecting the cityscape is fundamentally set from urban scale to building scale (from macro scale to micro). However, after many examinations, it is found that the environmental factors in the phases from urban scale to neighbourhood scale are very different from the factors in the phases from neighbourhood scale to building scale. Therefore, the influence evaluation system (DAC) is limited within neighbourhood scale and building scale (from middle scale to micro) and presented in Figure 1.

After setting the evaluation system in general, some criteria regarding the features of regions and buildings that affect the cityscape are determined. Some literature examinations are made for the criteria in question, and after these examinations, criteria regarding effective regions and buildings in cityscape are determined and evaluated in details. In this context, the main criteria determined to establish the neighborhood, square/street, road, building ect. Having priority in colour designing process, are handled in two main groups as region scale and building scale (Table 1). Nine criteria for each group, thus totally 18 criteria, and subcriteria for each criterion, are generated.

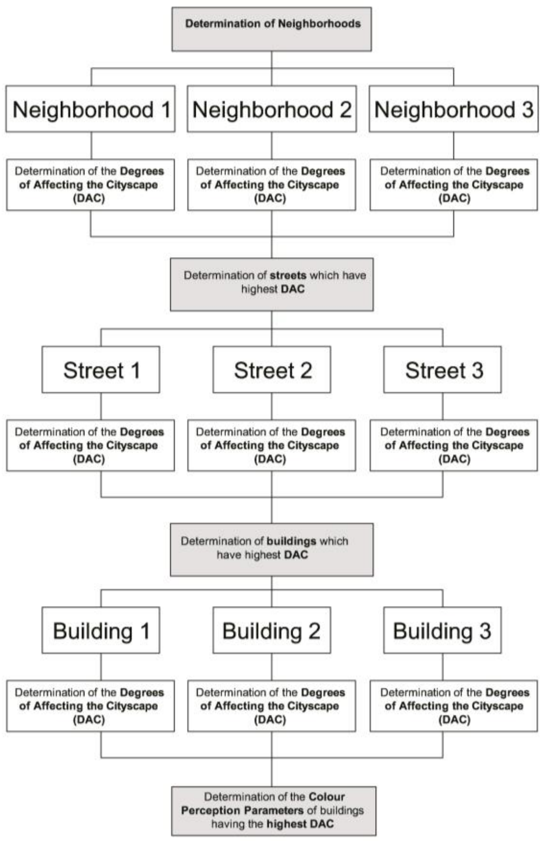

Figure 1: The phases of the fundamental method about determining the degrees of affecting on cityscape of urban regions and buildings

Table 1. Criteria regarding the groups : region scale and building scale

Basic Criteria for region Scale		Basic Criteria for Building Scale	
1	Architectural qualification	1	Architectural qualification
2	Building heights	2	Effect on environmental scape-Height
3	Effect on environmental scape	3	Effect on environmental scape-Width
4	Function	4	Function
5	Presentational effect	5	Presentational effect
6	Symbolic quality	6	Symbolic quality
7	Location in the city	7	Location
8	Topography	8	Façade material
9	Building intensity	9	Building colour

3.2 Survey Study

In order to determine the degrees of affection of regions and buildings on cityscape via the criteria decided to establish the prior regions and buildings in colour designing and presented in Table 1, a public survey has been realized.

There are totally 24 questions in this questionnaire. In the questionnaire, under every question regarding city region, building and environmental factors, there are various criteria and each participant has been asked to answer the question by rating every criterion based on Liekert Scale. In five degrees rating prepared according to Liekert Scale, expressions as “not effective at all, a little effective, effective, fairly effective, very effective” are used and each expression is related to a point, such as “not effective at all – 1 point; a little effective – 2 points; effective – 3 points; fairly effective – 4 points; very effective-5 points”.

The participants are mostly architects and city planners as well as other professions which are closely involved in the subject. Information about age, education status, profession and etc. are given in Table 2.

Table 2. The quantity and percentage (proportion) regarding personal information of the participants of the questionnaire

Personal Information		Quantity/Number
Sex	Female	61
	Male	39
Age	22-40	73
	40-55	17
	55-70	10
Education status	University degree	29
	Master	38
	PhD	33
Profession	Architect	67
	Civil Engineer	12
	City planner	10
	Other	11

Results obtained by the questionnaire are separately analysed and numerically evaluated for each question and criterion. Since the basic criteria are high in number, and thus not so easily evaluated directly, in evaluating the basic criteria the "method of factor analysis" through the SPSS 15.0 Computer Statistics Program has been used. The analysis for region and building scales are separately realized for each basic criterion. In order to determine the basic criteria on building scale, a four factor groups' analysis has been made with the evaluation of all the participants. In this four factors group analysis, in the 1st factor group there are respectively criteria of façade material and colour; in the 2nd factor group there are respectively quality, height, presentational effect; in the 3rd factor group there are respectively architectural qualification and location in the city; in the 4th factor group there are function and effect on environmental scape-width.

Following these results, in order to determine the regions and buildings that have priority in façade colour designing, basic criteria present in the 1st and 2nd factor groups of the region and building scales are decided to be taken into consideration. Speaking more clearly, basic criteria given in Table 3 are determined as the most effective features of regions and buildings that have affects on city/urban region scape and within the Evaluating System created for determining the regions and buildings that have priority in façade colour designing, subcriteria of these basic criteria are used to evaluate the degrees of affecting the cityscape.

Table 3. Basic Criteria to be Used for Determining the Influence Degrees of Regions and Buildings on Cityscape

Region Scale	**Building Scale**
Building heights	Façade material
Building intensity	Colour
Topography	Symbolic quality
Function	Effect on environmental scape-Height
Architectural qualification	Presentational effect

In order to determine the degrees of affection the cityscape by regions and buildings, the points given for subcriteria of the basic criteria in the questionnaire are summed, then divided by the number of the participants and thus the points according to Liekert Scale are obtained for each criterion. The features of urban regions and buildings shall be evaluate according to the points obtained and the priority in colour designing for these regions and buildings shall be done according this grading system.

4. CONCLUSION

A successful colour design can be obtained by examining appropriately each scale of the city, streets, squares, urban regions and the city itself, examining natural and built environments, many factors and data regarding visual perception and colour planning. In this context, colour master plans for every settlement should be prepared following the basic colour planning criteria.

Within the research project entitled "Approach for Façade Colour Designing", of which general features and its first phase are presented in this paper, in the preparation of colour master plans process, studies relevant apparoach for façade colour designing are still going on. Other data obtained in several phases of the approach, are going to be presented in subsequent publications.

REFERENCES

Küçükkılıç Özcan, E. and Ünver, R. 2014. *Yerleşimlerde Yapı Yüzü Renk Tasarımına Yönelik Bir Yaklaşım Önerisi*, Mimarlık Dergisi 379 60-65 (in Turkish).

Buether, A. 2014. *Colour Design Principles Planning Strategies Visual Communication*, An Edition Detail Book Institut für Internationale, ISBN 978-3-920034-96-6.

Ünver, R. and Dokuzer Öztürk, L. 2002, *Toplu Konutlarda Yapı Yüzü Renk Tasarımında Temel İlkeler ve Öneriler*, Yıldız Teknik Üniversitesi Araştırma Fonu Bitirme Raporu, Proje No: 99-03-01-02 (in Turkish).

Address: M.Sc Esra KÜÇÜKKILIÇ ÖZCAN, Prof. Dr. Rengin ÜNVER
Yıldız Technical University, Faculty of Architecture, Unit of Building Physics
34349, Beşiktaş, Istanbul, TURKEY
E-mails: esrakucukkilic@gmail.com, renginunver@gmail.com

Correlation between Personal and Classroom color Preferences of Children

Rengin ÜNVER, Fazıla DUYAN
Faculty of Architecture, Yıldız Technical University

ABSTRACT

The appearance and perception of colors make a strong impact on us in our daily lives. Our emotions, actions, perceptions, performances and health are influenced by colors of the environment. The color preferences of people differ based on the objects they use and spaces they live in. As people age, their tastes and choices evolve in years, which results in a change in their color preferences. In the related literature, there are various studies about color preferences but subjects of these studies are usually adults and children's color preferences studies are limited.

In this context, a research has been realized to investigate the correlation between the personal and classroom wall color preferences of children. 74 girls and 78 boys, in total 152 corresponding to the age group of 8-10 have participated in the survey. In the study, 10 hues having different values and chromas, in a total of 84 different colored samples were used and "personal color preferences" and "classroom wall color preferences" of children were determined through a survey. This paper aims to explain the method and findings of the research.

1. INTRODUCTION

Educational environments, especially classrooms where students spend a large part of the day have a significant impact on students' lives. As other physical components in an environment, it is a fact that colors of classroom affects students' performance and behaviors. However, classroom colors are determined by school managers or designers and students' preferences and opinions are not considered.

Therefore, in 2013, a research project entitled "The Effect of Lighting and Color Schemes on Student's Performance in Classrooms of Primary School" was started. This research has been supported by Yıldız Technical University Scientific Research Projects Coordination Department. Project Number: 2013-03-01-DOP01. The project was constructed in three parts; determination of personal and classroom wall color preferences of students using colored samples, determining personal and classroom wall color preferences of students using colored samples, determining students preference of the painted classroom walls in different colors and determining the effect of classroom wall colors on performance of students.

This paper presents the findings of the first step of this research project, which consists of the studies conducted for determining personal and classroom wall color preferences of students' in the age group of 8-10, using colored samples.

2. METHOD

The method of the first step of the research entitled "The Effect of Lighting and Color Schemes on Student's Performance in Classrooms of Primary School" can be summarized follows:

- Selection of the primary schools.
- Identification of the colors that are used in the personal and classroom color preferences.
- Determination of individual and classroom color preferences through surveys.
- Evaluation of survey results.

Two primary schools (private and state) in the same district of Istanbul were selected. The students in the private school have better social, cultural and economic conditions than the public school. 33 girls and 38 boys from the private school, 41 girls and 40 boys from state school, in total 152 students participated. Before the survey, the color vision deficiencies of the students were tested using an Ishihara Color Vision Test. The surveys were carried out in their classrooms on 1-13rd December 2013. Each student had spent approximately 20 minutes for the surveys. Average illuminance (daylight+artificial lighting) level on the working plane in the classrooms was 350-450 lux. The desks were covered with a matt grey cloth.

2.1. Identification of the Colors that are used in the Personal and Classroom Color Preferences.

84 colors selected for the determination of students color preferences in the survey was constructed taking into consideration findings from the first survey that was realized in 2012 with 119 (60 girls, 59 boys) students (Duyan and Unver, 2013). Principally, Hue, value and chroma dimensions of selected colors were determined by using Munsell Color System.

Tablo 1. Munsell Color System Notations for Colors.

HUE (Munsell)	VALUE/SATURATION			
	9/2			
5R (5R)	8/2			
RED	7/2	7/6	7/10	
	6/2	6/6	6/10	6/12
	9/2			
5YR (15)	8/2	8/6	8/8	
ORANGE	7/2	7/6	7/10	7/12
	6/2	6/6	6/10	
	9/2	9/6	9/10	8/12
5Y (25)	8/2	8/6	8/10	
GREEN	7/2	7/6	7/10	
	6/2	6/6		
	9/2	9/6	8,5/10	
5GY (35)	8/2	8/6	8/10	
GREEN-YELLOW	7/2	7/6		
	6/2	6/6		
	9/2			
5G (45)	8/2	8/6		
GREEN	7/2	7/6	7/10	
	6/2	6/6	6/10	

HUE (Munsell)	VALUE/SATURATION		
	9/2		
5BG (55)	8/2	8/4	
BLUE-GREEN	7/2	7/6	7/8
	6/2	6/6	6/8
	9/2		
5B (65)	8/2	8/4	
BLUE	7/2	7/6	7/8
	6/2	6/6	6/8
	9/2		
5PB (75)	8/2	8/6	
PURPLE-BLUE	7/2	7/6	
	6/2	6/6	6/10
	9/2		
5P (85)	8/2	8/4	
PURPLE	7/2	7/6	7/8
	6/2	6/6	6/8
	9/2		
5RP (95)	8/2	8/6	
RED-PURPLE	7/2		
	6/2		

In this context, in terms of hue, 10 hues (5R, 5YR, 5Y, 5GY, 5G, 5BG, 5B, 5PB,5P, 5RP) having different values and chroma, in a total of 84 colors were decided to use. Lower values were not selected in the previous survey (2012) by the students, therefore 6 and upper values were used in this survey. Chroma of colors were determined between 2 and 10 or 12 which are followed each other four step. For equal size in perceptual color differences, 1:4 was used as the ratio of units for value and saturation in the study according to the recommendations in the literature. Thus, values were selected as 6,7,8,9 and saturation determined as 2, 6, 10 or 12. The Munsell notations of the colors are given in Table 1.

Colored samples which were used in the study were generated using gouaches. Then the samples were measured by spectrophotometer. The colored samples were prepared in two different dimensions (Small: 3,5 x 3,5 cm; Big: 7x7 cm). The small size samples were pasted and grouped on grey cartons (N 5/0, size A4) for the same hue and 10 different hue pages were arranged. The big size colored samples were pasted on grey cartons (N 5/0, size B5) and 84 different samples were obtained. Some examples of the colored samples used in the surveys are given in Figure 1.

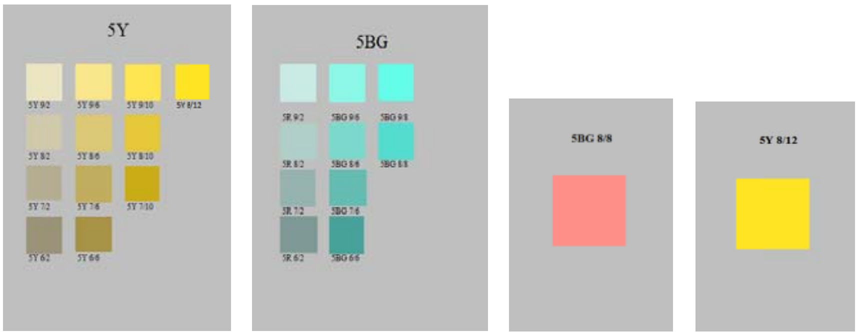

1a: Hue page samples *1b:Big sized samples*

Figure 1: Color Samples

2.2. Determination of Personal and Classroom Wall Color Preferences

Two-step process for determining the color preference was carried out. In the first step, 10 different Hue pages (size: A4) were shown to the subjects and asked to choose one color from each Hue pages and to note on the survey page. In the following step the chosen samples were presented as Big size (7x7 cm, B4) and the subjects were asked to select their most favorite color. This process was repeated both personal color and classroom wall color preferences (Figure 2).

Figure 2: Pictures from Survey

3. EVULATION of SURVEY RESULTS

The data obtained from surveys were examined in three parts; girls, boys and total (girl& boy).

3.1. Results of Personal Color Preferences

Girls Personal Color Preferences: The first preference of 74 girls in total on the personal color are 5P 7/8 purple (11%) and 5RP 8/9 red-purple (11%). Second most preferred colors are 5P 6/8 purple and 5R 7/8 red at the same rate (9%). Third preferred color is 5BG 7/8 blue-green. According to the results, girls tend to the red, purple as shown in Figure 3.

Boys Personal Color Preferences: Boys prefer strongly 5B 6/8 blue in 21%. Then they prefer 5BG 7/8 blue-green, 5PB 6/10 purple-blue and 5R 6/12 red at the same rate (8%). Based on the results, boys tend to the bluish colors.

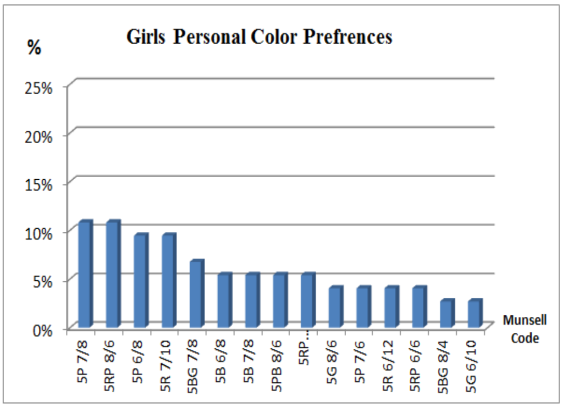

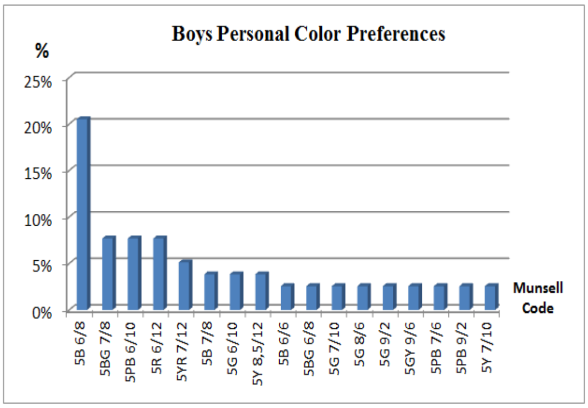

Figure 3: Girls and Boys Personal Color Preferences

Girl and Boy Students Personal Color Preferences: In total, both genders prefer mostly 5B 6/8 at 13% rate. The second most preferred color is 5BG 7/8 blue-green (7%) and the third one is 5R 6/12 red (6%). Girls prefer 5B 6/8 blue at a 5% rate. The blue color BG 6/8 was the first most preferred color because it was selected by a high rate of boys.

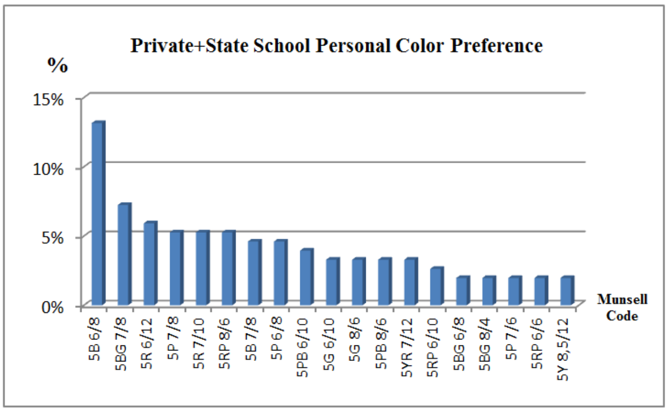

Figure 4: Personal Color Preferences (Private & State)

3.2. Results of Classroom Wall Color Preferences

Girls Classroom Wall Color Preferences: Classroom wall color preference of girls are in respectively 5 RP 6/10 red (8%), 5GY 8/10 green-yellow (5%), 5P 7/8 purple (5%) and 5RP 9/2 red-purple (5%).

Boys Classroom Wall Color Preferences: Most preferred color of boys for classroom wall color of boys is 5B 6/8 blue (12%). Second preferred colors are 5B 7/8 blue (6%) and 5YR 7/12 orange (6%).

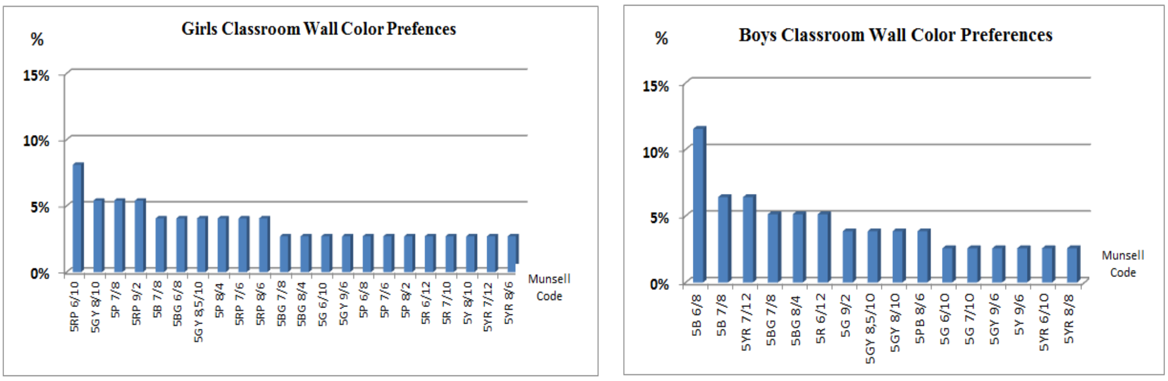

Figure 5: Girls and Boys Classroom Wall Color Preferences

Girls and Boys Students Classroom Wall Color Preferences: As shown in Figure 6, a total of 152 students' most preferred wall color is 5B 6/8 at the 6% rate. 5B 7/8 blue, 5GY 8/10 green-yellow, 5RP 6/10 red-purple and 5YR 7/12 orange follow to 5B 7/8 blue at the 5% rate.

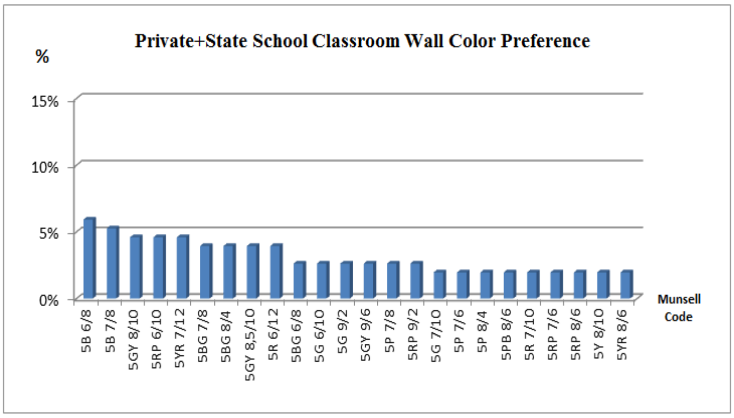

Figure 6: Girls and Boys Classroom Wall Color Preferences

4. CONCLUSION

The first, second and third preferences on the personal and classroom wall color results are given in Table 2 as girls, boys and total. According to the findings, girls prefer mostly red, purple hues on personal color preference. Whereas, boys prefer strongly blue. As personal color preference, both of the two genders preferences focus in blue

As classroom wall color preference, girls focus in order to red-purple, green-yellow, purple and red-purple. Boys significantly tend to 5B 6/8 blue as wall color preferences. Second preferred colors are 5B 7/8 blue and 5YR 7/12 orange sharing at the same rate. In total (girls and boys), the first preferred color is 5B 6/8 blue where the high rate of boys choosing this color is a determinant. The second, preferred color is shared between 5B 7/8, green-yellow, red-purple and orange.

Table 2: Distribution of the Preferences on the Individual and Classroom Colors.

Preference	PERSONAL									CLASSROOM WALL								
	GIRLS			BOYS			TOTAL			GIRLS			BOYS			TOTAL		
	Munsell Code	Color	%	Munsell Code	Color	%	Munsell Code	Color	%	Munsell Code	Color	%	Munsell Code	Color	%	Munsell Code	Color	%
1.	5P 7/8		11	5B 6/8		21	5B 6/8		13	5RP 6/10		8	5B 6/8		12	5B 6/8		6
	5RP 8/9		11															
2.	5P 6/8		9	5BG 7/8		8	5BG 7/8		7	5GY 8/10		5	5B 7/8		6	5B 7/8		5
	5R 7/10		9	5PB 6/10		8				5P 7/8		5	5YR 7/12		6	5GY 8/10		5
				5R 6/12		8				5RP 9/12		5				5RP 6/10		5
																5YR 7/12		5
3.	5BG 7/8		7				5R 6/12		6									

As a result of the findings, in both personal and classroom wall color preferences, girls liked to warm color like red, purple hues. The boys tended to blue (5B 6/8) in both personal and classroom wall color preferences. In total, the students preferred 5B 6/8 blue as a first color in both personal and classroom wall color preferences. Consequently, it can be said that there is a parallel correlation between personal color preference and classroom wall color preference of students.

REFERENCES

Baytin, Ç., A. Kıran, M. Tunbiş 2005. Colour Preferences in Architectural Design Studious. *Architectural Science Review*, University of Sydney, 48(4) 317-328.

Duyan F., R. UNVER 2013. A Study on Individual and Classroom Color Preferences of Children between the Ages of 8-10. *In AIC Color 2013, Proceeding*s, ed.

Schloss, K. B., E. D. Strauss, S. E. Palmer 2013. Object Color Preferences, *Color Research and Applications,* 38(6) 393-411.

Park, J. G. P. 2014. Correlations Between Color Attributes and Children's Color Preferences, *Color Research and Applications*, 39 (5) 452-462.

Wang, H., R. R. Randall 2008 Computer Classroom Wall Colour Preference and They Relationship with Personality Type of College Students, *Colour, Design & Creativity*, 4 (2) 1-13.

Address: Prof. Dr. Rengin Ünver, M.Sc Fazıla Duyan,
Yıldız Technical University, Faculty of Architecture, Unit of Building Physics,
34349, Beşiktaş-Istanbul, TURKEY,
E-mails: renginunver@gmail.com, faziladuyan@gmail.com

Research on the Coexistence of Color between Buildings and Exterior Advertising that Create a Cityscape ~ focusing on the Okamoto district of Kobe ~

Yoshihumi TAKAHASHI[1], Ikuko NARITA[2]
[1]Hosei University Graduate School of Regional Policy Design
[1]Couwa Sign Co. Ltd.
[2]Sense Up Planning. Ltd

ABSTRACT

In line with the Landscape Act of 2004, the Exterior Advertising Code was revised. At the same time, a new principle was put into place which includes not only improving aesthetic and scenic beauty but also the overall creation of a more favorable cityscape. There are a number of issues addressed by the Exterior Advertising Code, such as illegal signboards, restrictions on surface area, as well as delaying the rules to adjust to rapid growth in technology. Furthermore, in order to improve the cityscape, there is an increase in color restrictions being placed throughout the country. Indeed, many municipalities have implemented restrictions on color of high chroma for signboards. But could the solution be that simple? There should be a way to create an even better and more attractive cityscape by incorporating the colors of exterior advertising. Therefore, we reconsidered and studied the possibilities of a coexistence between the colors of buildings and exterior advertising. The survey was conducted by focusing on a mixed commercial and residential area in the Okamoto district of Kobe, Japan. We conducted a fact-finding survey on the colors of buildings and exterior advertising in the district, as well as a meeting with the Beautiful City Okamoto Council that drew up "The Exterior Advertising Rules and Guidelines." As a result, we found out that with respect to the regional style of the buildings throughout the entire district, some cityscapes are actually being harmonized with the colors of signboards.Therefore, it is conceivable that the colors of signboards do not prevent a landscape from forming scenic beauty, yet rather become an important factor for beautification. This form of cityscape was even supported by the the local residents themselves, who led the town planning over many years to formulate the guidelines for conforming the colors of exterior advertising.

1. INTRODUCTION

In line with the Landscape Act of 2004, the Exterior Advertising Code was revised. At the same time, a new principle was put into place which includes not only improving aesthetic and scenic beauty, but also the creation of a more favorable cityscape. According to Article 2 in the Exterior Advertising Code, the exterior advertising is "displayed outside in public permanently or a certain period of time and is presented on signboards, standing signboards, billboards, noticeboards, buildings and other structures and those similar thereto. "The Exterior Advertising Code itself does not contain detailed regulations. Thus, specific regulations are mostly determined by each municipality. This can be observed as a preceding example of decentralization. (Koide and Anpu 2007: 9-15). Once local authorities have become a part of landscape administrative bodies, they are then allowed to set up regulations on exterior advertising independently. This enables them to adapt suitable advertising in accordance with the local characteristics of their region. There is a lack of accumulated research on the standard measurements regarding the control of exterior advertising. Therefore, even the municipalities that have a positive attitude towards the utilization of exterior advertising for the improvement of the cityscape find themselves in a cycle of trial and error. On top of this, there are a number of conflicting issues regarding exterior advertising, such as illegal signboards, restrictions on surface area that do not take regional character into account, as well as delaying the adjustment of rules in accordance with rapid growth in technology. In regards to colors, there is an increasing number of color restrictions placed throughout Japan with the aim to create a more satisfactory cityscape. A number of areas have implemented restrictions on color of high chroma for signboards. But could the solution be that simple? There should be a way to create an even better and more attractive cityscape by incorporating the colors of exterior advertising. Therefore, we reconsidered this principle and studied the possibilities of a coexistence between the colors of buildings and exterior advertising. The investigation was conducted in the Okamoto district of Kobe, the area of the Beautiful City Okamoto Council that drew up "The Exterior Advertising Rules and Guidelines" and have been taking an active part in utilizing exterior advertising for beautification.

2. METHOD

The study method we performed involves a quantitative color analysis of the Okamoto district of Higashinada-ku, Kobe-shi. Based on the results from the survey, we examined how the coexistence of colors between buildings and exterior advertising influence the quality of cityscape color. We also studied the initiatives of the local residents who led town planning over many years in order to formulate the guidelines for conforming the colors of exterior advertising. Lastly, for the survey of the actual color condition, we employed a visual colorimeter supervised by Japan Color Research Institute. The survey was then conducted from 10:00 to 15:00 in August, 2014.

3. RESULTS

3-1 Community Development of the Beautiful City Okamoto Council

The Beautiful City Okamoto Council was formed on September, 1982. According to the community development agreement of Okamoto district, the area includes the entire area of 1-chome Okamoto, Higashinada-ku, Kobe-shi and a part of 5-chome Okamoto and 3-chome Kitamachi, Honzan. The Beautiful City Okamoto Council established rules such as, "Community Development," to form a community that allows citizens to play a part in making decisions about their own city. It has been over thirty years since the establishment of the council and the cityscape in Okamoto has shown a dramatic change.

In recent years, the soaring land prices have accelerated the increase in national chain stores, while the number of privately-owned local shops continues to decline. This is indeed the case in Okamoto city, whose cityscape of common signboards is being infiltrated by the growing number of stores that are putting up unnecessarily gaudy and thoughtless signboards with harmful colors. Due to these factors, in 2009 the authorities of Okamoto city began research for the formation of "The Exterior Advertising Rules and Guidelines for Okamoto." This set of rules was finally approved at the 32nd general meeting in 2014.The rules outline that signboards are an indispensable element of what construct the cityscape. This also explains that signboards that harm the beautiful landscape are unsuitable for the city and will be restricted under the rules.

Moreover, “The Exterior Advertising Rules and Guidelines for Okamoto” aims to increase suitable signboards for the overall image of Okamoto. Attractive signboards should enhance the city’s charm so that citizens will be even more proud of their city – in turn, this would eventually make the city more appealing for outside visitors as well.

There are three keywords that symbolize the universal elements and essential values of the city of Okamoto. These are the following: open sky, Mt. Rokko, and stories told by unique paved stones. Naturally, colors significantly influence these images. Considering these aspects, Okamoto city determined the suitable colors for exterior advertising as a way to maintain its fine cityscape. The city took on the positive challenge to place the colors of signboards in a way where they can coexist with the founding characteristics of the city.

Through the hearing surveys provided, various measures have been taken, such as the publishment of the quarterly magazine, “Beautiful Town Okamoto,” and a signboard contest that follows with the purpose of drawing up “The Exterior Advertising Rules and Guidelines.” These were all conducted to specifically visualize how the city should appear. The hearing surveys revealed that it takes steady efforts and enthusiasm to achieve successful community development.

3-2 The color investigation result of the Okamoto district

We performed the color investigation of the Okamoto district. We analyzed it with the quantitative investigation into outer wall (79 places) of the building and outdoor advertising goods (219 places) and grasped the characteristic of the color.

1) The color investigation result of buildings

We measured the color of the outer walls of 79 buildings. As a result, a building of the hue of YR and Y accounts for 60%. About the value, 8-9, 50% and less than 3 are 7%. About the chroma, 1-3, 63% and 4-6, 14% and 7-13, 0% and 14 are 1%. Achromatic color accounts for 22%, but black isn't and white is 13%. There are a lot of YR and Y of the high value and the low chroma overall. Light beige, white and gray of the high value are admitted the local color of this district.

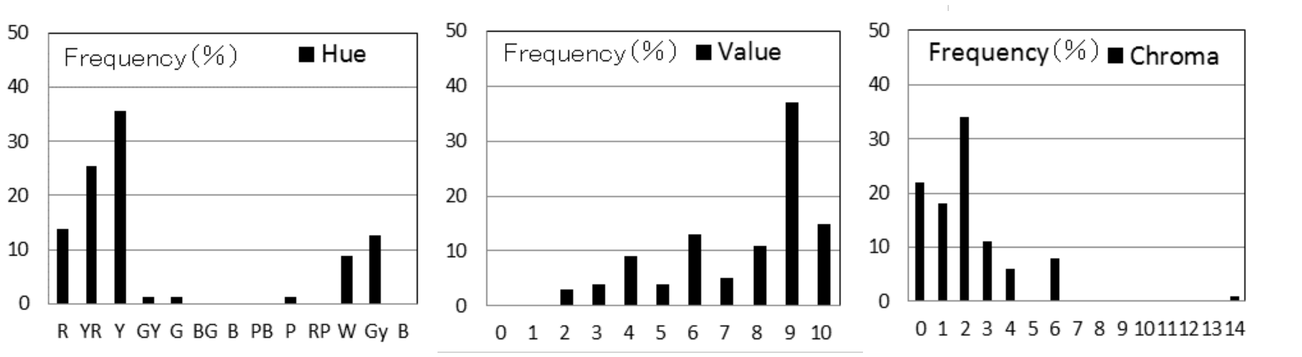

Figure 1: Color distribution map of buildings

2) The color investigation result of exterior advertising

We measured the color of exterior advertising goods of 219 places. As a result, it was white (29.2%) that there was the most. It accounts for 47.5% only by achromatic color. There are a lot of R (14.6%) and YR (8.7%) by chromatic color. Low and medium value is 43.9%. The medium and high chroma accounts for 35.1%. There are a lot of achromatic color, vivid red and orange for the feature of the overall color.

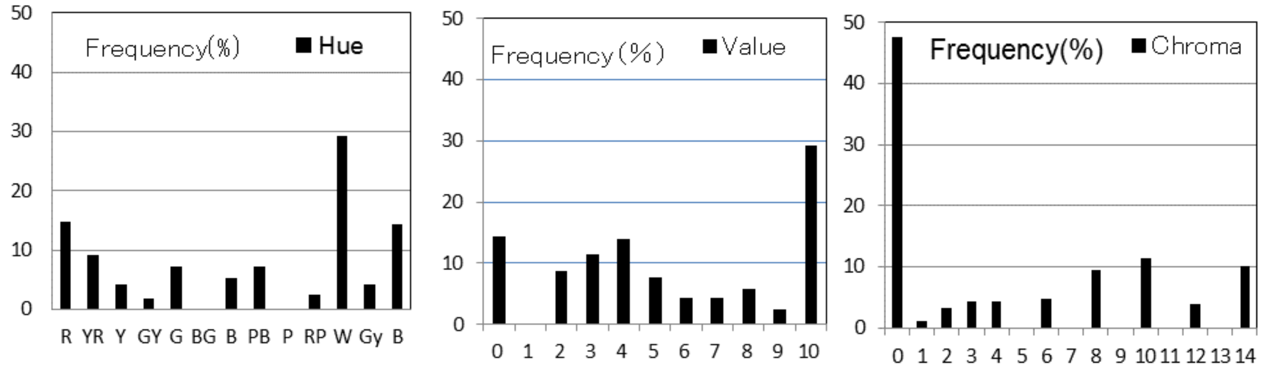

Figure2: Color distribution map of the exterior advertising goods

3) The features of the colors in Okamoto district

We found out that the local color of the building is admitted clearly. A commercial store and housing are intermingled in this Okamoto district. We can think a possibility that the color of the exterior advertising goods influences the quality of the color landscape in this whole district is high. A color of medium-high chroma is used for most of colors of the outdoor advertising goods backed by the white that is a local color.

Because the use area of those colors is small, the color of the outdoor advertising goods is accent color. In the Okamoto district we can recognize it to be a local color including the color of the outdoor advertising goods as well as buildings.

4. CONCLUSION

In the Okamoto district, the signboard colors harmonize with the building colors that were already established in the whole city over the years. That means exterior advertising colors have naturally and successfully created a part of the cityscape without becoming detrimental. We can conclude that this achievement was only made possible through the tremendous effort put forth by the local initiatives of The Beautiful City Okamototo Council, who have successfully made an ideal city come true.

REFERENCES

Koide K, and H, Anpu. 2007. *Munincipal Activities for Exterior Advertising and Hereafter*. Urban City + Design. 26 : 9-15.

Address: Yoshihumi TAKAHASHI,
Hosei University Graduate School of Regional Policy Design,
Couwa Sign Co. Ltd.,
2-19-11 Matsugaoka, Nakano-Ku,Tokyo, 165-0024, JAPAN,
E-mails: ytaka0502@gmail.com

Colour management in the colour design process

Per JUTTERSTROM
NCS Colour AB

ABSTRACT

Colour management in the colour design process in all manufacturing industries are changing due the development in technology and the change of needs from the end customers. With todays widely available colour measurement technology there are no secrets when it comes to the colour shades used by different industries as well as paint companies. Also with the higher demands from the end customers to expect the availability of any colour they want, the number of colours are escalating for different products in general, and for the coatings industry in particular, with number of colours exploding in the paint companies databases often with the consequences that colours are more or less visual identical but having different names.

By taking a more holistic approach to the management of colours in the colour design process and using a scientific system as a platform there are many benefits when it comes to make the colour design process more efficient and by doing that to save time and money in the management of colours. The starting point in that process is how to make a useful analysis of existing colours, both with digital applications as well as visual adjustments and comparisons with other colours on the market with the aim to develop a range that can deliver all the colours that is necessary for a market success.

This will also result in quality improvements and a more understandable offering of the colour range to the end customers.

This paper will present some case studies examining the importance of this holistic approach in the colour design process and how that result can be developed into more useful colour collections.

1. WHAT IS COLOUR?

According to my built in dictionary on this computer where this paper is written, colour is ”the property possessed by an object of producing different sensations on the eye as a result of the way it reflects or emits light”. We can all agree that colour is a visual sensation, that it makes us able to navigate in our daily life, orientate and make social statements by picking certain colours for our clothes, our homes, our cars or any other items.

2. NEED FOR COLOUR SYSTEM

Since colour is something that we as a human beings can see, a colour system should be based on visual perception. There are several systems for colours on the market, some of them based on colour research in different professional areas, not only in technical meanings, but also historical, social and psychological, physical etc., while others are basically collections based on purely commercial aspects or spun from technical processes such as tinting colours in different substrates.

Colour systems can be described by their purpose and can be divided into different levels of sophistication. The most basic of the colour systems are simply different collections of colours. The German RAL Classic is a clear example of such a ”system”, or to be more precise - a collection of colours. RAL is a collection of popular colours that are frequently used in the industrial area. Each colour has an unique four digit number to identify them (e.g. RAL 1003 etc.), however this number does not tell or give the user any added information about the actual colour, it is just an identification. Other collections such as British Standard could be added to this category.

The next level includes the system that has a production driven purpose. This could be tinting systems for tinting machines, or RGB for computers, Pantone for print etc., where colours also gives the information how it is mixed.

The most sophisticated level of colour systems are those based on colour perception and on scientific research. NCS (Natural Colour System) is one of those systems, the American Munsell is an other one and also, the no longer on the market, DIN (Deutsche Industrie Norm) system. Common for those systems are that they are all visually based, with a spectrum that covers the colour space and with some kind of logical steps where the relation of the colours can be described. This is also reflected in their way to notate the colours. There is actually a correlation between the name and the actual colour we can see.

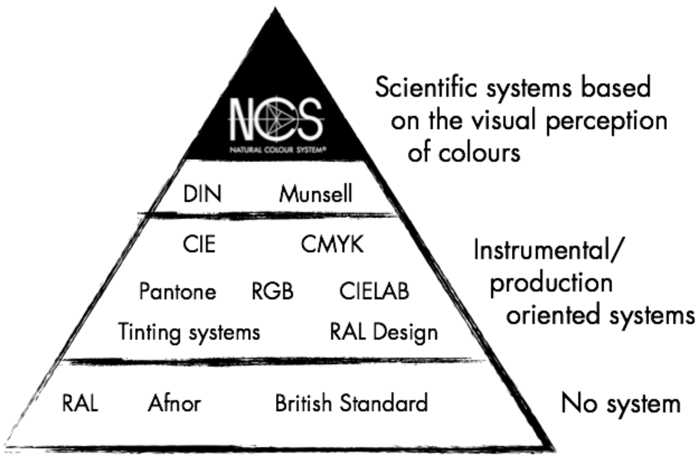

Figure 1. To illustrate the different levels for colour systems and collections on the market.

3. THE HOLISTIC APPROACH

With the globalized economy of today with the demand of quicker design processes and with outsourced production of the products to foreign countries the management of colours are more critical than ever.

Since there is no international standard for colours and manufacturing companies and industries are competing with the colour range on the market, the management of the colours are usually a big part of the design and production process. For manufacturing of products the colours are usually the most difficult part to manage when it comes to

accuracy and consistency. Often with the result that the “same” colour appears different due to different materials and application techniques.
For the paint industry this often results in overlapping colours, e.g. colours that are basically the same but with different names and notations, which also creates a situation where it is difficult to manage the issues of, colour accuracy and consistency in the production. It also makes it difficult to get a holistic view from marketing, sales and production point of view.

4. CASE STUDIES

By taking a holistic approach in the design process and using a visual based colour system, the management of colours can be done in a more simplified way, no matter if there are just a few colours for a range of products or a more extensive range for a paint industry.

4. 1. Product manufacturer

A manufacturer of household goods used to have 50 different colours for their range of products. The products were produced in different materials and applications such as powder coating, industrial coating, plastics, vinyl etc. with the result of difficulties to manage the wide range of colours and materials in terms of accuracy and consistency.

By comparing the used colours with the colours from competitors on the market and make an analysis and illustrate this in a visually based colour system, the company were able to reduce the number of colours from 50 down to only 6 but with a maintained strong offering to the market in terms of good and useful colours. It also made them able to differentiate from the competitors and make huge savings in the management process of their colour range.

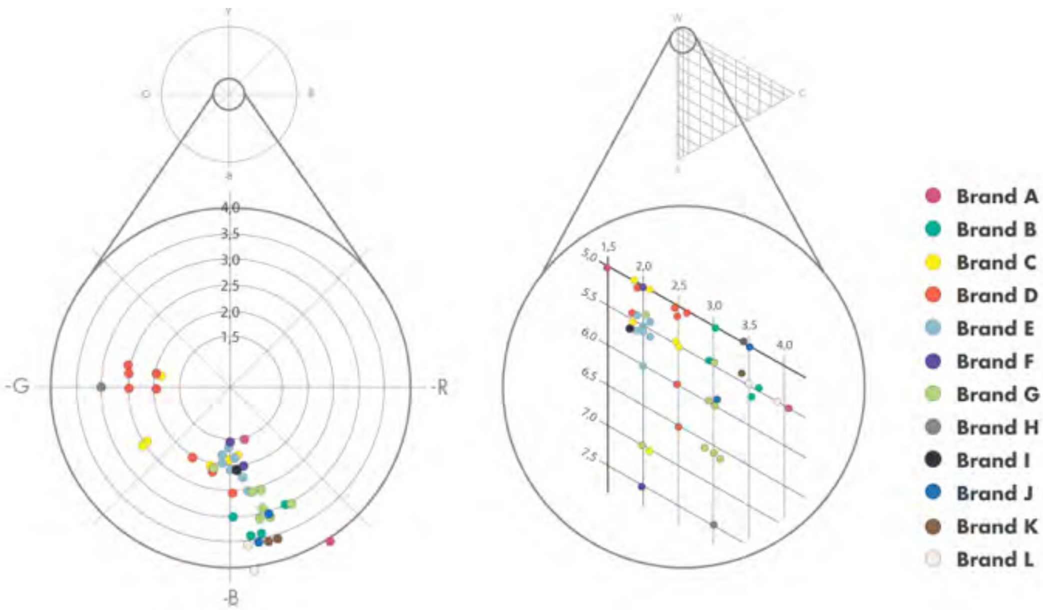

Figure 2. Comparisons for different producers of household goods and how the colours are located in the NCS colour system

4. 2. Paint producer

With the introduction of automatic tinting machines in the decorative coatings business, the options for the customer have dramatic increased in number of shades.

As a walk in customer in a paint shop, we expect the shop to be able to present and instant deliver a wide range of different shades. We also expect to be guided with colour sample material so we can see with our own eyes how the final colour will look like. Sometimes we also bring a piece of painted material that we would like to find the very same colour for, or a colour that goes well with it. Because of the possibilities in the modern tinting technology and the implementation of information technology, paint shops can carry thousands of formulas for different shades and quality of products. Not only for the brand that the shop sell, but also for other common colour collections on the market with competitors selections etc.

A mid sized decorative paint producer in the Middle East took the decision a few years ago to update their colour range and to get away from the clutter and overlapping colours in their tinting system. The primarily used fan deck was the Nova colour card with approx. 2000 colours with some additional influx from other fan decks such as British Standard, RAL, NCS, competitors etc. resulting in a database with more than 5000 formulations. The aim was be better represented in the colour space and cover more areas and give the end customer a better range of colours that is considered to be richer even though the number of colours are less.

By taking all the these different colours and using a visual based colour system as NCS, the ground work was to illustrate the range of the colours and identify areas where there were overlapping colours as well as areas with missing colours.

By mapping all the colours all those areas were easily identified and it made it possible to refine the colour range in a more efficient way.

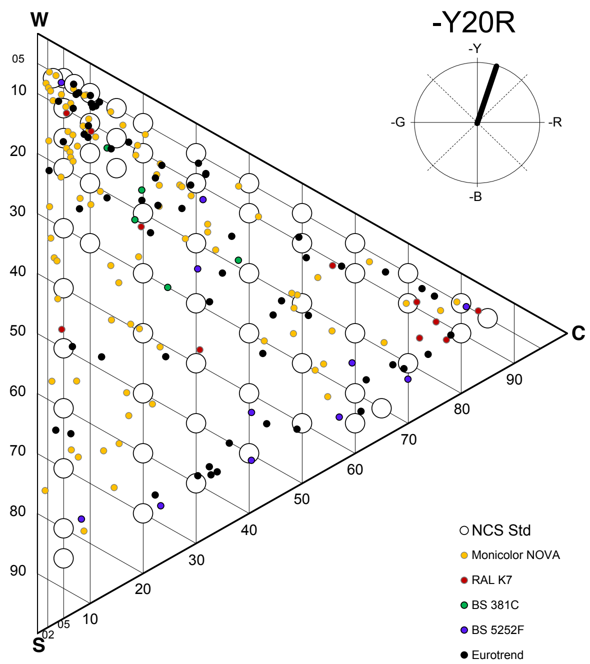

Figure 3: Different colour cards measured and notated into a visual colour system that gives the ability to see the correlation between the colours and how they actually are related.

By then identify the most important areas, a new range of colours could be developed that meet the demand from the market as well as create a more useful range.

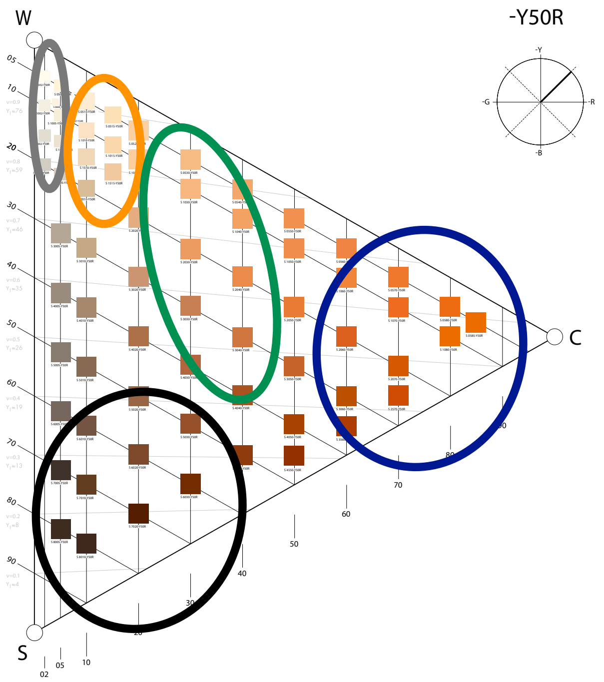

Figure 4: Areas that needed to be included in the new range.

This work ended up in a new collection with 915 colours, all carefully selected and with an even distribution in the colour space, eliminating overlaps and creating a more comprehensive range for the market.

By making this reduction, this paint producer was able to increase their efficiency and cut time and costs in the handling of different formulations.

5. CONCLUSIONS

Modern technology in the productions process gives infinity possibilities of different colour shades on manufactured products or in paint. However, from both a customer point of view and for the management of the production and handling for the producer, the huge number of colours will not really add any benefits in the end. Instead customers are more helped with less clutter and a more balanced colour range.

Customers want more options, but they also need guidance and a straight offer for their colours.

The challenges manufacturing industries as well as the coatings industry is to optimize their offering, by using advanced technical systems but also to benefit from colour systems based on visual perception – since colour is something we all can see.

REFERENCES

SIS (Swedish Standards Institution). 2004. *NCS Colour Atlas, Swedish Standard SS 019102*, Stockholm.

Hard A, Sivik L, Tonnquist G. 1996. NCS Natural Color System – from Concept to Research and Applications, Part I and II. *Color Reserach & Application*, Volume 21, Number 3, June 1996.

Bergström B. 2008. *Colour Choices – A practitioner´s guide to colour scheming and design*. Formas.

Hard A, Sivik L. 1977. Distinctness of Borderline Related to the Natural Color System. In *Proc of the 3rd AIC Congress, Color 77, Bristol*: Adam Hilger Ltd.

Hard A, Sivik L. 1978. Distinctness of Border as a Measure of Color Contrast - Effects of background color and border length. Report to BFR.

Hard A, Sivik L, 1983. Distinctness of border -A concept for a uniform color space. *Fackskrift nr F27*. Scand. Color Inst, Stockholm

Hard A, Sivik L, 1986. Distinctness of border: An alternative concept for a uniform color space. *Color Research and Application*, Vol.11, No.2.

Hard A, Sivik L, 1976. Distances between Colours - A Comparison of Different Structures, *Göteborg Psychological Reports*, Vol. 6, No. 7. (also in Edberg, G. (ed) Gruppen för Arkitekturpsykologi Symposium, nr 4, KTH, Stockholm, 1974.)

Hard A, Sivik L. 1977. Methodological Studies of Color Changes Due to Distance and lighting: Direct Assessment Using the Natural Color System. In *Proc of the 3rd AIC Congress, Color 77, Bristol*: Adam Hilger Ltd.

Address: Per Jutterstrom
NCS Colour AB, PO Box 49022, 100 28 Stockholm, Sweden
E-mail: per.jutterstrom@ncscolour.com

Exploring combinations of color patterns in Nature

Akemi YAMASHITA,[1] Naoko TAKEDA,[2]
[1] Okayama Prefectural University
[2] Tecnológico de Monterrey

ABSTRACT

In recent years the philosophy of Biomimicry is increasing, Nature is a result of many years of evolution, provides us an infinitely rich combination of wisdom and beauty. Observing, exploring and imitating Nature's best strategies we can obtain innovating ideas to solve any kind of needs and problems. That is why many researchers of any field of science and art base their studies on its creations.

We find the Lepidoptera (butterfly and moth) egg, caterpillar and its metamorphosis from pupa to adult, a source of inspiration with a great potential for achieving results to be applied in product and graphic design.

The focus of this research is the study of some species that have bright colors to flaunt in the context they are, in the other hand some that pass unnoticed by its neutral colors. Information as the color and graphic patterns of egg, larvae, pupa and butterflies and moths are collected from many source to obtain a comparative graphical table of pattern color combination. The objective is to design a palette of color patterns as a tool useful to do original creations for graphic and industrial design products, convenient for daily life and suitable to different environments as hazardous, quiet, modern, classical, cheerful, sporting to mention some. In this occasion we design some foldable umbrellas and their covers.

INTRODUCTION

Through the development of technology, in these days, the population living in artificial environment as cities is increasing, away from Nature. The coexistence with animals, plants, insects, is more and more difficult. It is reflected as a recent incident in Japan, covers for elementary school notebooks that had been featured with photographs of insects for long time, have been recalled because they are no longer familiar to children, even more they are considered as ugly beings.

One fundamental principle of nature is the optimization of resources, obtaining more with less. Specialists consider that Nature respond with functions according to the context that defines them, in the most economical manner. So, in nature there are no coincidences, every form, structure, movement, texture, odor, color, reaction has a reason.

Butterflies and moths are just an example of what marvelous the Nature is, of course the complete metamorphosis they undergo, but also the birth of larva from egg, their transformation to caterpillar and then to pupa.

Lepidoptera is one of the most widespread and widely recognizable insect orders in the world. In Japan exist around 5800 variations of butterfly and moth, around 3 hundred are butterflies and the remainder are moths. This project illustrates the scope of some of those lepidopteras color patterns, which provide a wide variety combination of designs and colors many of them difficult to imagine, that is why these invites us to deepen a research on them. The environment around lepidoptera is the reason of their motives, to camouflage or to draw attention to one objective: survive.

Within this body of information we can infer that the pattern and the color combination of each stage of lepidopteran species have a reason to be as the way as they are. Even there are still remaining many unknowns to discover, scientific around the world are discovering interesting features about their colorations useful to be apply on the development of design products.

2. METHOD

1. Selection of the Lepidoptera inhabiting in Japan.
   We select the most common Lepidoptera species to analyze, as Namiageha (Asian swallow tail) and others that have interesting patters and colors.
2. Observation and analysis of each step of transition
   We observe some species from egg until adult: colors, patterns, textures, movement, feeding, the transition when casting of the skin, pupa and silk.
   Common swallow tail butterfly, known as Namiageha in Japanese, lay a individual brilliant yellow and spherical egg on the host plant (citrus like mandarin and oranges or Japanese peppers plants), most of the cases on the underside of the leaf to protect them from the predators like bees. The egg become dark and transparent before larva get out, larva has as first food the egg's shell. The aspect of the larva is textured with thorns, black body with white spots. They transform to green caterpillar as mimicking the color of the host plant. The color of pupa could be green or brown. The wings of the butterfly are striped black and white with small orange and blue circles as accent colors.
3. Revise printed literature and web information
   The most of butterflies and moths after mating have a host plant where they lays eggs, the plant will be the food of larvae during caterpillar's instars until reach fully mature, and then develop into a pupa, chrysalis in the case of butterflies and cocoon for moths. Butterfly and moth are cover by scales throughout their bodies and wings, over millions of years of evolution, result a wide range of patterns and colorations from drab to brightly colored and complex-patterned.

Namiageha principally mimics in the following aspect:

- In the first stage of larvae is mimicking bird droppings, showing that are not taste good.
- Caterpillar turns green color as the host plant. The two eyes like spot are mimicking the face of a snake or a cat, which are enemy of the birds. Those eyes are oval conformed by 3 colors, black, red (warning color) and in the middle a white line like iris (exactly as the cat eyes).
- The larva chooses the place to become a pupa, the texture, odor, the diameter or the branch influence to become a green or brown chrysalis.
- In the adult stage, the shape of the back wings have an elongation as swallows have, near presents an orange dot, those characteristics are mimicking a face in backwards to deceive the enemy.

4. Conformation of color scheme. See 2.1
5. Development of patterns. See 2.2
6. Application in a product design See Result and Discussion.

2.1 Conformation of color scheme

Table 1 shows roughly the analysis of the colors and patterns of Lepidoptera.

	Scientific name	Japanese name	Larval food		egg		Larvae or Caterpillar		Pupa or Chrysalis		Adult	
					Pattern	color	Pattern	Color scheme	Pattern	Color scheme	Pattern	Color scheme
1	*Parantica sita*	Asagimadara	*Asclepiadaceae*									
2	*Papilio xuthus*	Namiageha	*Zanthoxylum piperitum*									
3	*Byasa alcinous*	Jacouageha	*Aristolochiaceae*									
4	*Lycaena phlaeas*	Benishijimi	*Polygonaceae*									
5	*Araschnia burejana*	Sakahachichou	*Boehmeria spicata*									
6	*Polygonia c-aureum*	Kitateha	*Humulus japonicus*									
7	*Argyreus hyperbius*	*Tsumagurohyoumon*	*Viola*									
8	*Cyrestis thyodamas*	Ishigakechou	*Ficus*									
10	*Zophoessa callipteris*	Himekimadarahikage	*Sasa nipponica*									
11	*Choaspes benjaminii*	Aobaseseri	*Meliosma rigida*									
12	*Monema flavescens*	Iraga	*Diospyros kaki Thunb.*									
13	*Parasa sinica*	Kuroshitaaoiraga	*Quercus acutissima*									
14	*Parasa lepida*	Hiroheriaoiraga	*Zelkova serrata*									
15	*Milionia zonea*	Kiobiedashaku	*Podocarpus macrophyllus*									
16	*Malacosoma neustrium*	Obikareha	*Prunus mume*									
17	*Saturnia japonica*	Kususan	*Castanea crenata*									
18	*Lymantria dispar*	Maimaiga	*Quercus acutissima*									
19	*Cucullia Maculosa*	Haiirosedakamokume	*Artemisia indica var.maximowiczii*									
20	*Hebomoia glaucippe*	Tsumabenichou	*Crateva religiosa*									
21	*Idea leuconoe*	Oogomadara	*Parsonsia laevigata*									
22	*Damaus genutia*	Sujigurokabamadara	*Cynanchum boudieri*									
23	*Arichanna gaschkevitchii*	Hyoumonedashaku	*Pieris japonica*									
24	*Macroglossum passalus*	Negurohoujakku	*Daphniphyllum teijsmannii*									
25	*Papilio protenor*	Kuroageha	*Zanthoxylum piperitum*									

Table 1. Colors and Patterns of some Lepidoptera

Table 2. shows in detail the study of color and pattern which were conducted for Namiageha from egg to adult stages and the host plant.

Larval food		egg	Larvae: shed their shell about four times as they grow		Larvae: 5th instar larvae	pupa: pupation	pupa: last instar	newly-emerged butterfly	newly-emerged butterfly	adult
	process of growth									
	Color Scheme									

Table2. Color and Pattern of Namiageha from egg to adult stage.

2.2 Development of patterns

In the section on Results and Discussion are described the results obtained of the development of some analyzed patterns.

3. RESULTS AND DISCUSSION

The developed patterns were applied on a common product as an umbrella (parasol), wich are used in the daily life.

This is the first step of the project, that is why Namiageha was chosen as main sample to develop new patterns. On the figure 1 are shown three variations of motives developed from the same Namiageha butterfly. Above in the figure are the inner of the hind wings, applied to the inside of the umbrella, below are the outside of the hind wings applied to the outside of the umbrella. Each pair represent one umbrella.

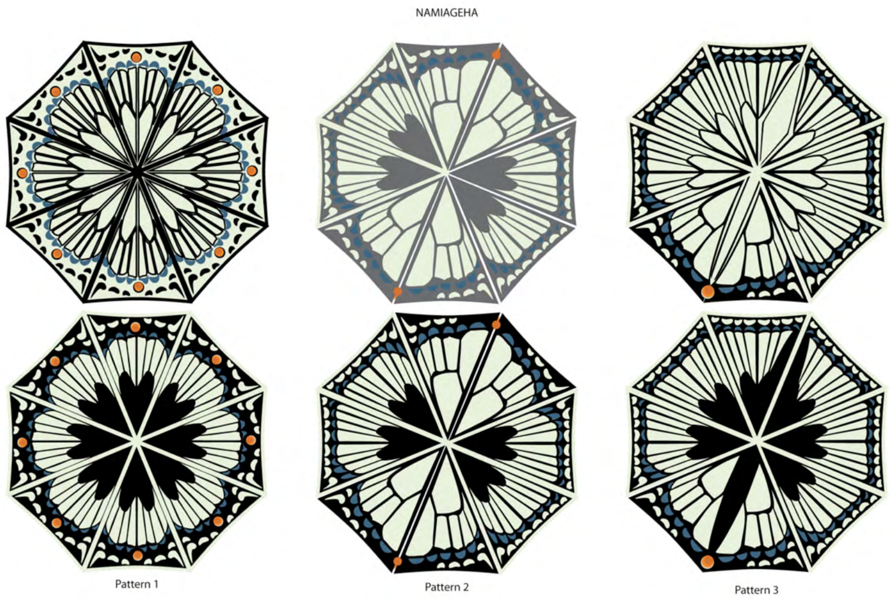

Figure 1: Patterns apply to canopy cloth of umbrella inspired by Namiageha's butterfly, both side of the hind wings.

As metaphor of the transition from larva to pupa, a reversible cover for the foldable umbrella was designed, one side refers to the green larva, and the reverse side to pupa in two colours as the Namiageha chrysalis could become. Fig. 2

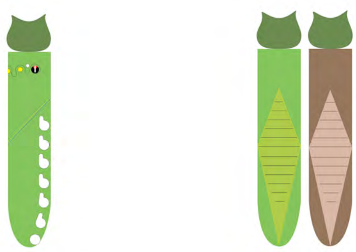

Figure 2: Patterns inspired by Namiageha's caterpillar and chrysalis

Others samples of lepidoptera attractive in their different stages were developed.The figure 3 shows Iraga (Monema flavescens) moth, Sujigurokabamadara (Danaus genutia) and Aobaseseri (Choaspes benjaminii) butterflies.

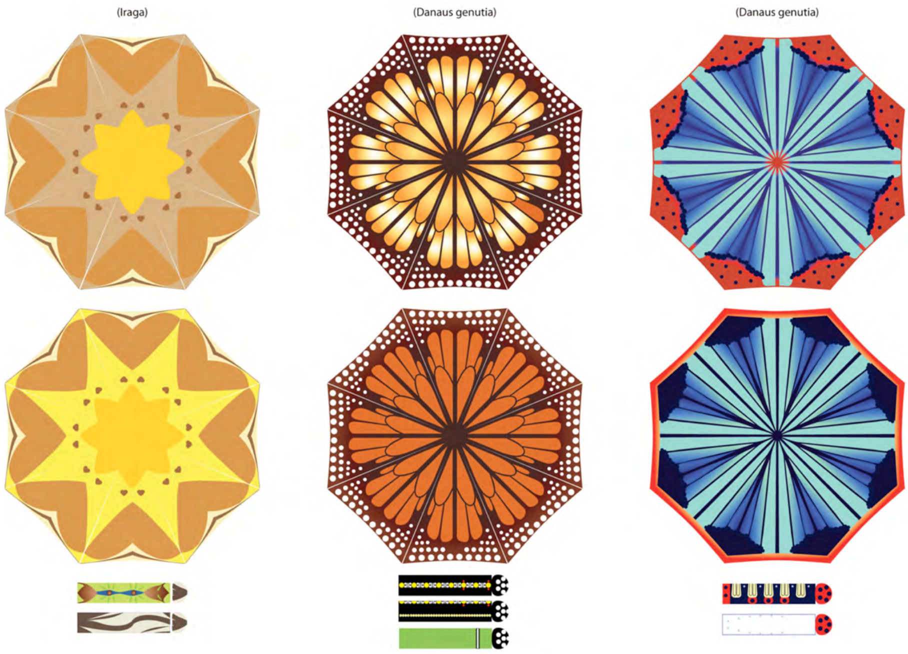

Figure 3: Patterns inspired by others butterfly and moth both side of the hind wing, caterpillar and pupa

Consider that it is the first step, the graphics resulting until now, have been applied to the design of umbrellas for women, this is the first stage of the project. The theme chosen for them, was striking, with the same principle further applications could be develop as an umbrella for emergency, umbrellas for children, signals. So well, camouflage in the context is also a intersanting issue to be developed.

The pattern could be applied also to products like parachute, glider, tarp, architecture, outdoor wear, traffic safety equipment and soon.

On the other hand, it is our intention continue developing the palette of colors and designs, considering more butterflies and strengthening aspects of camouflage and mimicry.

4. CONCLUSIONS

The wide variety of lepidoptera is an endless source of useful patterns for design development. Inspired by only one butterfly we can get several variations, if we take in account that there are more than 5,000 species only in Japan, we can infer that it is possible to get at least 5000 graphic patterns. We consider that the color scheme obtained is a potential tool, useful to develop different design depending the needs and the context in which the product will be used.

ACKNOWLEDGEMENTS

We would like to express our special gratitude to Prof. Sakai Wahei, emeritus professor of Kanazawa College of Art, who influence us to love Nature.

We would also like to thank Mr. S. Ueyama who allowed us to use his valuable photographs.

REFERENCES

1) Ruxton,G and Sherratt, T 2005. *Avoiding Attack: The Evolutionary Ecology of Crypsis*, Warning Signals And Mimicry

2) Harman, J 2013. *The Shark's Paintbrush Biomimicry and How Nature is Inspiring Innovation*, Japanese version.

3) Ruse, M 2003. *DARWIN and Design*, Harvard University Press.

4) Yasuda,M 2010. *The Handbook of Japanese Caterpillar* vol.1, bunichi Co.Ltd.

5) Yasuda,M 2010. *The Handbook of Japanese Caterpillar* vol.2, bunichi Co.Ltd.

6) Futahashi, R and Fujiwara, H. 2008. *Juvenile Hormone, Regulates Butterfly Larval Pattern Switches*, Science 22, Vol. 319 no. 5866 p.1061.

7) Fujiwara, H. 2007, *Nisete Damasu Gitai no Fushigi na Sekai*, DOJIN Sensho 2

8) Yamaguchi, J et al, 2013 *"Periodic Wn1 expression in response to ecdysteroid generates larval spot markings on caterpillar"*, Nature Communications Online Edition. Recuperated on 2015-02-22 http://www.nature.com/ncomms/journal/v4/n5/abs/ncomms2778.html

9) Ueyama, S. *"Osaka-shi to sono shuhen no Cho"* 27 September 2014 http://butterflyandsky.fan.coocan.jp/index.html

Address: Prof. Akemi Yamashita, Department of Visual Design, School of Design, Okayama Prefectural University, 1-1-1 Kuboki, Soja, 711-1197, JAPAN
Prof. Naoko Takeda, Department of Industrial Design, School of Art and Design, Tecnologico de Monterrey, Puebla, Mexico.
E-mails: yamashita@dgn.oka-pu.ac.jp, naoko@itesm.mx,

Visual Impressions Induced by Colours of Facial Skin and Lips

Mei-Ting LIU, Hsing-Ju HUNG, Wen-Ling DENG, Li-Chen OU
Graduate Institute of Colour and Illumination Technology, National Taiwan University of Science and Technology, Taiwan

ABSTRACT

Two psychophysical experiments were conducted to investigate visual impressions induced by colours of facial skin and lips. The first experiment focused on the effect of facial skin tone. The visual impressions were measured in terms of bipolar scales including active/passive, vibrant/dull, healthy/unhealthy, extraordinary/common, cute/not-cute, sexy/not-sexy, natural/unnatural, sensible/insensible, beautiful/ugly, young/old, delicate/strong, innocent/worldly and like/dislike. A total of 75 skin tones were tested using the face images, assessed by 35 observers with normal colour vision. The face images were presented on a 27-inch liquid crystal display (LCD) with a display luminance of 79 cd/m^2, situated in a darkened room. The experimental results show that the lightness of skin tone had little effect on all scales studied. There was a strong effect of hue on the impression of skin tone for all scales. The second experiment used face images with 3 skin tones and 45 lip colours, resulting in 135 combinations, as the stimuli, each assessed by 30 observers with normal colour vision. The experimental results show that observers' impression was significantly affected in terms of "beautiful/ugly", "extraordinary/common", "vibrant/dull" and "delicate/strong". The lightness, chroma, and hue of lip colours were all found to have significant effects on all scales. Male and female observers were found to agree with each other in terms of "harmonious/disharmonious" while they had different responses in "delicate/strong ".

1. INTRODUCTION

Facial expression is the most direct and honest reflection of a person's emotions. Interactions between two human beings often begin with the observations of each other's faces, which have this unparalleled ability to immediately convey the emotional states of the persons. To a certain degree, faces could even reveal what kind of person someone is. Using the information gathered through observing the faces, a person could make different choices in his or her approach to other human beings.

There have been studies into visual impressions of skin tones and make-ups. For instance, B. Fink et al. (2008) tracked the observers' eye gaze while they viewed images of varied skin colour distribution. It shows that skin colour distribution is highly correlated with age, health conditions, and attractiveness. Y. Yuan et al. found in 2011 that there are differences between male and female observers' responses in "attractiveness", "cooperativeness", and "masculinity" while using virtual face images for skin tones research. Zeng and Luo found in 2011 that the preferred skin tones for Oriental and African faces were more reddish than real skin tones. In addition, varied from the lightness of skin tone, the observers' preferences for chroma and hue of skin tone were different.

In recent decades, computer animation is developed rapidly. Virtual characters have been seen more and more in a wide range of applications in daily life. In order to enhance the realistic of virtual characters, it is important to use the suitable facial make-up to show the personality of the characters. According to the analysis of experimental results in present research, design guidelines can be provided to computer animation and other related industries.

The aims of present research include:

- To investigate the connection of virtual character's skin tone and observers' visual impressions.
- To investigate the connection of virtual character's make-up and observers' visual impressions.
- To realise the interaction of the colours on the face.
- To give different colour collocation for individual virtual character.

2. METHOD

The present research had two parts. The first part was aimed to investigate visual impressions induced by facial skin tone. The second part was to investigate visual impressions induced by facial colours including colours of facial skin and the lips. The visual impressions were measured in terms of bipolar scales including active/passive, vibrant/dull, healthy/unhealthy, extraordinary/common, cute/not cute, sexy/not sexy, natural/unnatural, sensible/insensible, beautiful/ugly, young/old, delicate/strong, innocent/worldly and like/dislike. These scales were selected on the basis of a questionnaire survey conducted before the main experiment. There were 35 observers (including 10 females) in the first experiment to conduct the questionnaire.

2.1 Experiment condition

The liquid crystal display (LCD) used in this research was EIZO ColorEdge CX270, which was calibrated to sRGB by X-rite i1 Pro. In order to present the right experimental colour, the display used the GOG model for colorimetric characterisation. Both of the experiments used the same LCD situated in a darkened room.

The reference white for the first experiment had a luminance of 78.76 cd/m^2, of which the chromaticity coordinates (x, y) was (0.3083, 0.3291). The reference white for the second experiment had a luminance of 81.92 cd/m^2, with chromaticity coordinates of (0.3092, 0.3277). The visual distance was about 1 metre for the first experiment and 0.5 metres for the second experiment.

2.2 Observers

Observers of both experiments were students of National Taiwan University of Science and Technology, aged from 22 to 29 years. There were 35 observers (including 19 females) participated in the first experiment. In the second experiment, among the 30 observers (including 14 females) were 19 observers taking part in both experiments. All of the observers passed the Ishihara test for colour deficiency.

2.3 First experiment

The experimental images were 5*5 in size, and were put together for every 25 images presented against a mid-grey background. Each image was framed with the reference white. Between any two slides, there was a full-screen slide with mid-grey background for at least 1 second to avoid the afterimage effect. The observers had no time limit to evaluate each test image using the 13 scales.

2.4 Second experiment

According to the results of the first experiment, the highest score of combination of chroma and hue in "natural/unnatural" was picked up, which had $C^*_{ab}=36$, $h_{ab}=45$ degrees. Colours with lightness values of 50, 60 and 70 corresponded to the light, medium, deep tones.

A total of 95 lip colours, which were acquired in terms of tristimulus values from our market research using a spectrophotometer Xrite-962. These were then converted into CIELAB values. Based on these 95 colours, a total of 135 colours were selected systematically from CIELAB space were selected for recolouring the lips in the experimental facial images.

Five semantic scales were used in the second experiment, of which two, "beautiful/ugly" and "extraordinary/common", were selected according to the Principal Component Analysis (PCA) results. The other three scales, "vibrant/dull", "delicate/strong" and "harmonious /disharmonious" were selected on the basis of the component loading results.

3. RESULTS

The results of the first experiment converted the data on the basis of the categorical judgment method to determine the scale values. Figure 1 shows the scale values of "natural/unnatural" plotted against hue angle.

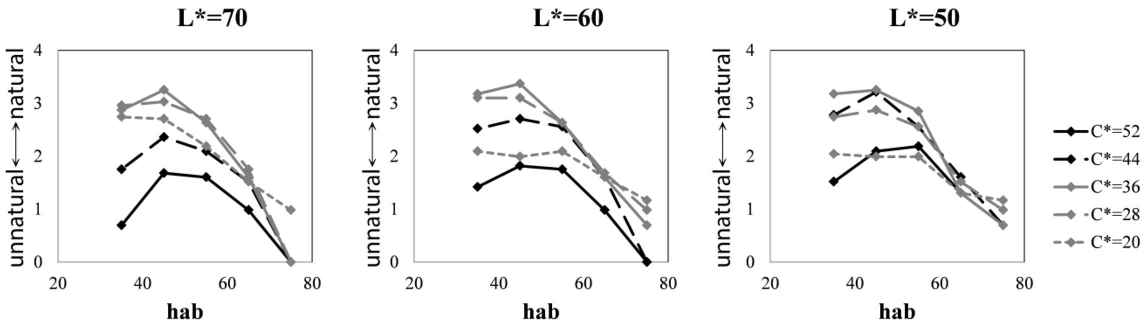

Figure 1: the scale values of "natural/unnatural" in the first experiment

All the other scales show trends similar to the graphs. ANOVA was conducted to see whether there was any influence of lightness on each scale. According to the results, the lightness of skin tone had little effect on all scales, and the hue of skin tone had significant effects on all scales except vibrant/dull and sexy/not sexy. No matter what the lightness of skin tone was, observers preferred the reddish skin tone for chroma values of 20, 28 and 36. Observers preferred orange skin tone for chroma values of 44 and 52.

The second experiment was to investigate the influence of lightness of skin tone in terms of the 5 semantic scales. No matter what the lightness of skin tone was, the higher the chroma of lip colour was, the higher the scale value was for all scales. In other words, if the chroma of lip colour that virtual character used was higher, there were more chances for observers to have the association with the 5 scales, "beautiful/ugly", "extraordinary/common", "vibrant/dull", "delicate/strong", and "harmonious /disharmonious".

Except "extraordinary/common", when the lightness values of skin tone were 50 and 60, the variability of chroma of lip colour had no significant effect on scale values. In addition, no matter which chroma of lip colour coordinate, the scale values were the lowest for lip colours with a lightness value of 70.

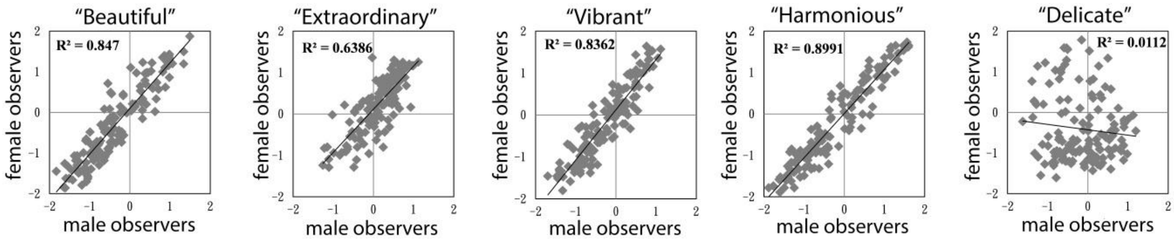

Figure 2: comparisons between male and female observers in the second experiment

According to figure 2, the comparisons of male and female observers, "delicate/strong" show a wide spread in the scatter graph. The result suggests that the image which felt delicate for male observers did not felt so for female observers. Figure 3 shows that female results show larger variability than male in rating different images. This suggests that male observers were not as sensitive as female observers in terms of visual impressions of skin tones and lip colours.

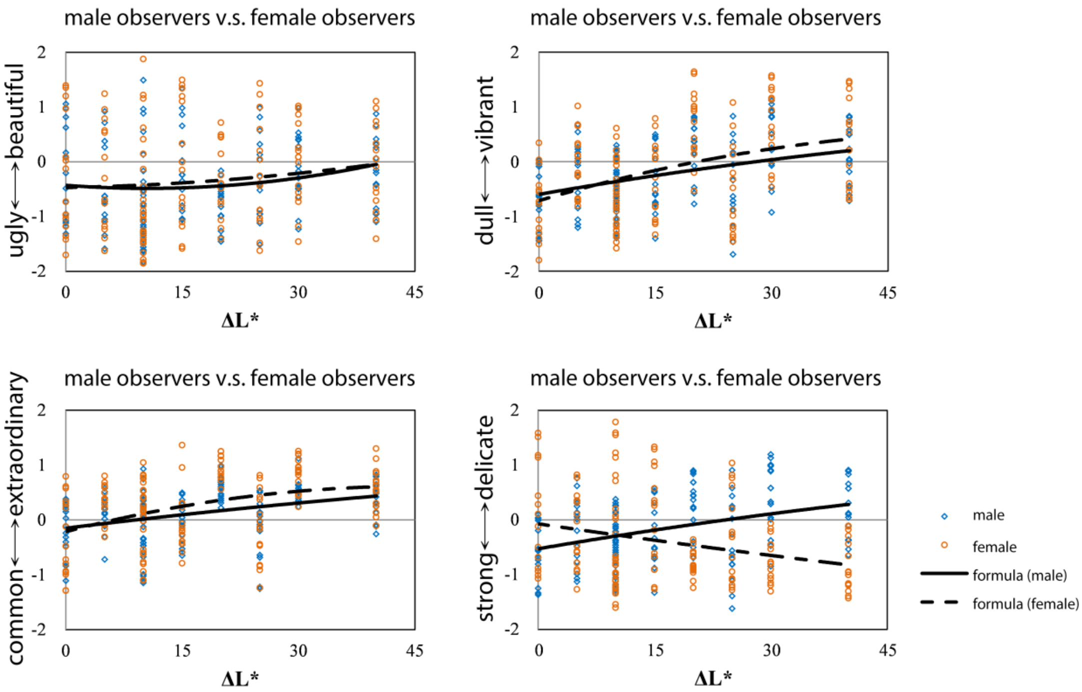

Figure 3: comparisons of "delicate/strong" between male and female observers

According to the comparison of the two experiments using ANOVA, there were strong difference in the values of "beautiful/ugly", "extraordinary/common", "vibrant/dull", and "delicate/strong" between whether a virtual character had make-up or not. Another result was that the lightness, chroma, and hue of lip colour had significant influence on all scales. In addition, there was significant interaction between the lightness and hue of lip colour in "extraordinary/common" and "vibrant/dull". There was also significant interaction between the chroma and hue of lip colour in “harmonious /disharmonious” and “vibrant/dull”.

For skin tones with a lightness value of 50, the lightness of lip colour would need to be higher for the facial image to feel more beautiful and more harmonious. For those with lightness of 60, the lip colours with lightness of 45 were found to be the most beautiful and most harmonious. For skin tones with lightness of 70, observers tended to associate the virtual character’s face with being ugly, dull, strong and disharmonious for lip colours with a lightness value of more than 70.

4. CONCLUSION

Ou and Luo (2006) have developed a two-colour harmony model based on contextless colour patches. This quantitative model was tested using the current experimental data, i.e. the CIELAB values of the skin and lip colours used in Experiment 2. As figure 4 shown, the test result shows a correlation coefficient of only 0.0045, indicating poor predictive performance of the colour harmony model for colour combinations of facial skin and the lips in a facial image.

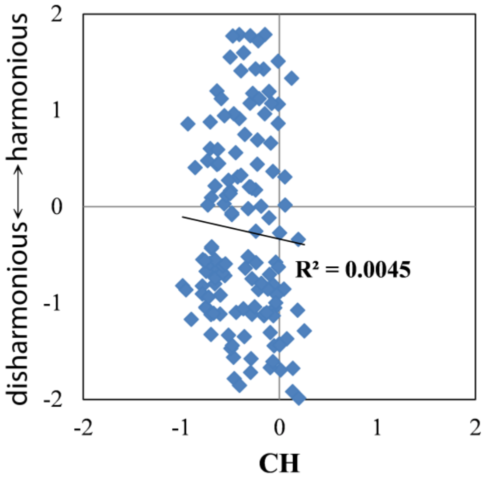

Figure 4: the colour harmony model by Ou & Luo v.s. the result of the present research

The virtual characters used in the computer simulation of the experiments were based on Southeast Asian females. It is thus recommended that, for a more comprehensive investigation of facial skin colours, virtual characters of various races and genders be used in future studies. Additionally, the races and cultural backgrounds of the observers should also be included as factors in order to compare any discrepancies between the visuals and different groups of observers. All of the observers in the experiments were between the ages of 22 to 29 years, making it difficult to eliminate the possibility that age might by one of the factors influencing the results of the study.

AKNOWLEDGEMENTS

This work was supported in part by the Ministry of Science and Technology, Taiwan (MOST 103-2221-E-011-138).

REFERENCES

Egges, A., S. Kshirsagar, N. M. Thalmann. 2003. A model for personality and emotion simulation. Knowledge-Based Intelligent Information and Engineering Systems. *Lecture Notes in Computer Science* (Vol. 2773) : 453-461.

Fink, B.,P.J. Matts, H. Klingenberg, S. Kuntze, B. Weege, K. Grammer. 2008. Visual attention to variation in female facial skin colour distribution. *Journal of Cosmetic Dermatology* (Vol. 7, No. 2) : 155-161.

Yuan, Y., L. C. Ou, M. R. Luo. 2011. Gender differences in social perception for skin tones. Proceedings of AIC Midterm Meeting, Interaction of Colour and Light in the Arts and Sciences.

Zeng, H., M. R. Luo. 2011. Colour and tolerance of preferred skin colours on digital photographic images. *Colour Research and Application* (Vol. 38, No. 1) : 30-45.

Ou, L. C., M. R. Luo. 2006. A colour harmony model for two-colour combinations. *Colour Research and Application* (Vol. 31, No. 3) : 191-204

Address: Graduate Institute of Color and Illumination Technology,
National Taiwan University of Science and Technology, Taiwan
E-mails: blueh919@gmail.com, b9934036.ntust@gmail.com,
fd70517@gmail.com, lichenou@mail.ntust.edu.tw

International Comparison of Uses of Color for Pictograms

Yuki AKIZUKI,[1] Michico IWATA,[2] Hirotaka SUZUKI[3]
[1] Faculty of Human Development, University of Toyama
[2] Faculty of Science and Engineering, Setsunan University
[3] Faculty of Engineering, Kobe University

ABSTRACT

Pictogram is a square including representative figure which indicates function or purpose of the facility. These pictograms are used in countries with different languages spoken, so although with different degrees of recognition, they are able to make people understand the space intuitively. Our study therefore conducts comparative survey on colors of pictograms in order to grasp the possibilities for pictograms to be attached to certain images pertaining colors, and to establish basic data for designing signs. We surveyed on colors of pictograms at international public facilities in 14 cities in 7 countries. The results of Toilet-Pictogram indicates tendency that European countries use achromatic colors without gender difference, and China uses multiple colors. All of pictograms of Unisex-Toilet use one same color, without differentiating genders. Gender image attached to particular color for pictogram is only seen in Japan, not elsewhere. In order to design signs in international perspectives, it is important to consider differences of culture, religion gender as well as color image.

1. INTRODUCTION

Japan enacted Basic Act for Promoting a Tourism-Oriented Country in 2007, which considers tourism one of the major growing industries in the 21st century, and tries to accept more foreign visitors. Recently, major stations and airports put signs in two languages (Japanese and English), and guideboards in tourist destination such as Kyoto are now also written in the two languages. But many cities still have Japanese only signs, which cause trouble for foreign visitors to use facilities or move around.

Pictogram is a square including representative figure which indicates function or purpose of the facility. ISO7001:2007, “50 passenger/pedestrian Symbol Signs” developed by American Institute of Graphic Arts, and JIS Z8210:2002 standardize various pictograms, and new pictograms are being proposed as needed. These pictograms are used in countries with different languages spoken, so although with different degrees of recognition, they are able to make people understand the space intuitively. They are useful in constructing urban building space becoming more and more international. JIS Z9103 is applied to pictograms for fire preventive equipment and evacuation signs, but other pictograms tend to have white background and black foreground internationally. On the other hand, in Japan, pictograms for toilets have distinct tendency of color (blue for men, red for women). There are various ways to use color for pictograms.

Our study therefore conducts comparative survey on color of pictograms in order to grasp the possibilities for pictograms to be attached to certain images pertaining color, and to establish basic data for designing signs.

2. METHOD

In 2008 and 2009, we surveyed on color of pictograms at international airport terminals, major railway stations, city halls, museum/historical buildings, major commercial centers, hotels, and parks in 14 cities in 7 countries. One spot of one facility is the subject, and if there is a pictogram, its background and foreground color are measured on the spot by visual photometry using a color chart (Figure 1) based on PCCS color coordinate system. Table 1 shows the correspondence with Mansell color system and PCCS color system.

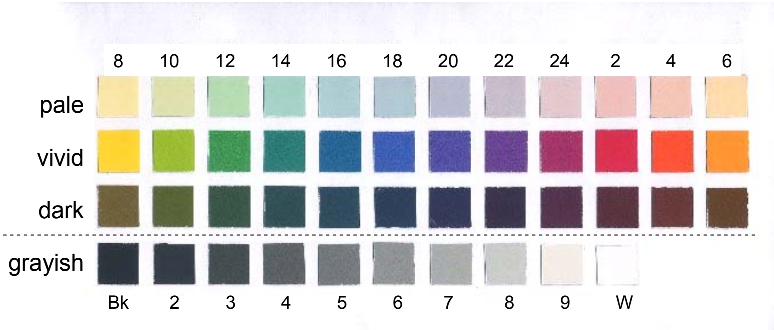

Figure 1. Color Chart based on PCCS color coordinate system.

Table 1. Correspondence table with Mansell color system.

	pale (p)	vivid (v)	dark (dk)
2	4R 8 / 3.5	4R 4.5 / 14	4R 2.5 / 6
4	10R 8 / 3.5	10R 5.5 / 14	10R 3 / 6
6	8YR 8.5 / 3.5	8YR 7 / 14	8YR 3.5 / 6
8	5Y 9 / 3	5Y 8 / 13	5Y 4 / 5.5
10	3GY 8.5 / 3	3GY 7 / 12	3GY 3.5 / 5
12	3G 8 / 3	3G 5.5 / 11	3G 3 / 4.5
14	5BG 8 / 3	5BG 4.5 / 10	5BG 2.5 / 4.5
16	5B 8 / 3	5B 4 / 10	5B 2.5 / 4.5
18	3PB 7.5 / 3	3PB 3.5 / 12	3PB 2 / 5
20	9PB 7.5 / 3	9PB 3.5 / 12	9PB 2 / 5
22	7P 7.5 / 3	7P 3.5 / 12	7P 2 / 5
24	6RP 8 / 3	6RP 4 / 13	6RP 2.5 / 5.5

grayish(g)	
Bk	N1.5
2	N2.0
3	N3.0
4	N4.0
5	N5.0
6	N6.0
7	N7.0
8	N8.0
9	N9.0
W	N9.5

3. RESULTS AND DISCUSSION

3.1 Color for Toilet-Pictogram

Table 2 shows the results of used color combinations for Toilet-Pictgram country by country. We collected 56 data at 25 male's toilets and 31 female's toilets. The results indicates a tendency that European countries use achromatic colors without gender difference, and China (Hong Kong, Macau and Taipei) uses multiple colors.

We also surveyed 33 unisex toilets in 5 countries. The results is shown in Table 2. 27 toilets use pictograms including both male and female symbols, and 6 toilets use only the letters "WC". All of them use one same color, without differentiating genders. In Japan, unisex toilets usually have pictogram with two different colors for each symbol. But these survey results show colors are not tied to symbol's meaning internationally.

17 toilets for disabled people were surveyed in 5 countries, and the results are shown in Table 2, too. In Japan, green color is often used for the pictgram of disabled-accessible

facilities. However there are no green pictgram for disabled-accessible toilet in any country, and there are some red pictgram for it in China.

Table 2. Color Combinations for Toilet-Pictgram.

(1) Toilet-Pictogram for Male

figure	ground	Germany	Switzerland	Austria	UK	Sweden	Finland	China
Red	Yellow							
	Gray							
	White							
Yellow	Yellow						1	
Blue	Gray							1
	White					3		2
Black	Yellow		1					
	Green						1	
	Gray	3				1		
	White	1		1			2	2
Gray	Gray							1
White	Red							2
	Yellow							
	Blue						1	
	Black				1			
	Gray	1						

(2) Toilet-Pictogram for Female

figure	ground	Germany	Switzerland	Austria	UK	Sweden	Finland	China
Red	Yellow							1
	Gray							1
	White							1
Yellow	Yellow						1	
Blue	Gray					3		1
	White							
Black	Yellow		1					
	Green						1	
	Gray	4				1		
	White	2		1			2	2
Gray	Gray							
White	Red							2
	Yellow							2
	Blue						3	
	Black				1			
	Gray	1						

chromatic pictogram   achromatic pictogram

(3) Toilet-Pictogram for Unisex

figure	ground	Germany	Switzerland	Sweden	Finland	China
Red	White					1
Yellow	Blue		1			
	Black					1
Green	White	1				
Blue	Green			1		
	Gray					1
	White					
Black	Yellow	3				
	Blue					1
	White	5		1	1	
Gray	Black			2		
White	Red					1
	Yellow					1
	Green				1	2
	Blue				3	2
	Black			1		1
	Gray	1				

(4) Toilet-Pictogram for disabled people

figure	ground	Germany	UK	Sweden	Finland	China
Red	White					1
Yellow	Blue					
	Black					
Green	White					
Blue	Green					
	Gray					1
	White			2		
Black	Yellow					
	Blue					
	White	4		1		
Gray	Black			1		
White	Red					1
	Yellow	2				
	Green					
	Blue				2	1
	Black		1			
	Gray					

chromatic pictogram   achromatic pictogram

3.2 Color for Emergency-Pictogram

Coloring of emergency evacuation sign is regulated by ISO and JIS. Among 74 pictograms of emergency in this survey, 88% pictograms have the color combination of white figure and green (3G5.5/11.0) background, whether it is at an exit or in a passage. In Japan, the color combination of the passage evacuation signs is reversed (with green figure and white background). Same arrangement is seen in 6 cases in only China (Taipei and Hong Kong).

Therefore it suggests that the color combination difference in passage evacuation signs is only seen in East Asia region including Japan. Also, 2 cases in China (Hong Kong and Macau) use non-safety color for emergency evaluation pictogram, 5B8.0/3.0 and 5Y4.0/5.5.

Among 34 pictograms of fire equipment, 90% pictograms use ISO regulated red (10R5.5/14.0) figure and white background. But 4 cases in China use other colors.

3.3 Most Frequently-Used Color for Pictogram

The frequently-used colors are examined with all 438 cases. The results shows in Figure 2. The most frequently-used color as figure is white (252 cases) and then black (103cases), these two explain 80% results. For background, the most frequently-used color is again white (100cases) but the second is 3G5.5/11.0 (70cases) followed by 3PB3.5/12.0 (61cases) and black (42cases). Considering that 3G5.5/11.0 is designated color for emergency evacuation signs, 3PB3.5/12.0 might be the most popular color for chromatic background. For the two color combination, the most frequent one is black figure and white background. The most chromatic combination is white figure and 3PB3.5/12.0 background, which is typically seen in airports and stations. Figure 3 shows some typical examples.

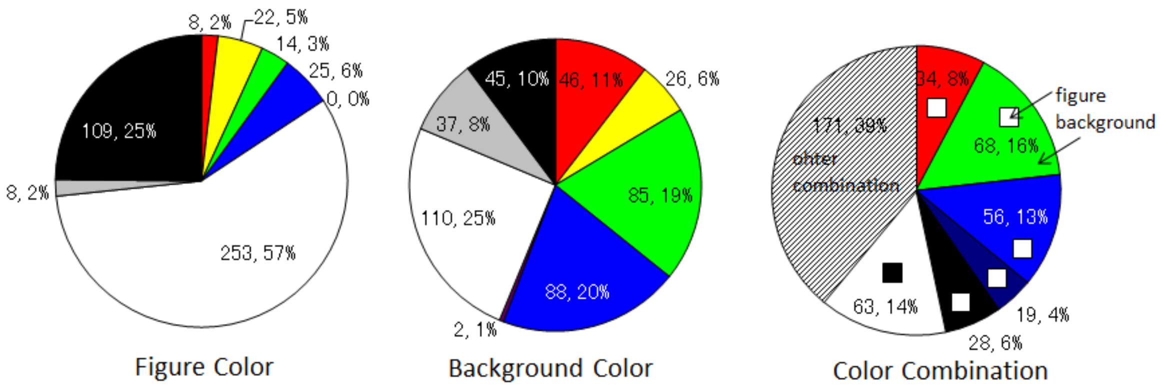

Figure 2. Frequently-Used Color for Pictograms.

Figure 3. Typical Example for Color Combination of Pictgram.

4. CONCLUSIONS

Gender image attached to particular color for pictogram is only seen in Japan, not elsewhere. In order to design signs in international perspectives, it is important to consider differences of culture, religion gender as well as color image. On the other hand, as our study shows there is some common tendency of color use.

It is useful to accumulate data further, to realize ideal sign designing to support space recognition.

And then, our survey finds some pictograms not honoring ISO color regulation. In order to ascertain that pictogram functions as common language, and to let them function for safety, further action will be called for to eliminate such cases.

ACKNOWLEDGEMENTS

This research was supported of Grant-in-Aid for Scientific Research of Japan Society for the Promotion of Science, No.20404020, Prof. Michico Iwata of the leader. We would like to thank Mr. Kazuya Osawa who helped our research analysis.

REFERENCES

ISO7001:2007. *Graphical symbols - Public information symbols*.
JIS Z8210: 2002. *Public Information Symbols*.
JIS Z9103: 2005. *Safety Colours – General specification*.

Address: Associate Prof. Yuki AKIZUKI, Faculty of Human Development,
University of Toyama,3190 Gofuku, Toyama, 930-8555, JAPAN
E-mails: akizuki@edu.u-toyama.ac.jp, michico@led.setsunan.ac.jp,
hirotakasuzuki@people.kobe-u.ac.jp

The Influence of Colour on the Perception of Cartographic Visualizations

Zbyněk ŠTĚRBA,[1] Jan D. BLÁHA[2]
[1] Department of Geography, Masaryk University in Brno, Czech Republic
[2] Department of Geography, J. E. Purkyně University in Ústí nad Labem, Czech Republic

ABSTRACT

The contribution provides an overview of the ways colour is used in cartographic visualizations and how it affects perception of these visualizations. Colour is generally considered as the most important graphic variable for expressing spatial information in cartographic visualizations. Through appropriate use of colours, the content of a map can be significantly accentuated, which enhances its legibility and comprehensibility profoundly. Appropriate use of colours is a very important factor in many cartographic applications, such as emergency management tools, in which cartographic visualization helps to transfer the required information effectively. A well-chosen colour scheme with appropriate contrasts is the best way to depict the overall character of an area or a phenomenon. The present paper describes the most significant approaches to colour use in cartography, which can be of immense help when communicating information to map users.

1. INTRODUCTION

When creating cartographic products, the form of depiction of the map's content is one of the primary outcomes of a cartographer's work. At the same time, the way various map symbols are depicted is a factor which is most likely to influence users' interpretations of the map. Different means of cartographic information transmission evolved gradually, but the greatest boom came with the development of thematic cartography, whose methods provided extra space for invention in the design of cartographic symbology.

The classic text in the field of cartographic symbology is Jacques Bertin's Semiology of Graphics (Sémiologie Graphique). The book, published in 1967, was the first to define basic cartographic means of expression, also referred to as graphic variables. Apart from the feature's position on the map, which represents the spatial location itself, external characteristics of a symbol can be described through various variables communicating different types of information. These variables, co-indicators of a symbol's content, include size, intensity, shape, orientation, structure and colour (among others).

Out of these, colour is generally considered as the most important graphic variable for expressing spatial information in cartographic visualizations. Colour can be used to display a relatively large amount of information in a single map without reducing the map's legibility and comprehensibility. Colour can also be easily combined with other variables, increasing their communication potential. Finally, in both thematic and topographic maps, colour is one of the principal enhancers of aesthetic quality, making the map much more visually attractive.

2. METHOD

Cartographic products are generally very powerful tools for communicating visual and spatial information. Through appropriate use of colours, the content of each map can be significantly accentuated, increasing the map's legibility and comprehensibility rapidly. Conversely, use of inappropriate colours and colour combinations can significantly undermine users' perception of the visualized information. Colour is used as a communication means in most elements and symbols within a map. Therefore, it both helps to communicate cartographic information and increases the legibility of the map and its aesthetic quality (Bláha, 2011). Hence, colours and colour contrasts influence the aesthetics of a map and the user's emotional response, as well as the map's usability.

Colour perception is definitely influenced by physiological, psychological, and other subjective factors. It is therefore always necessary to consider specific contexts in which the map will be used, such as light conditions (outdoor v. indoor use, etc.), type of cartographic product (analogue v. interactive map), map size (or display size of the display device), typical situations in which the map will be used, as well as potential cultural specifics (Bláha, 2013). Chesneau et al. (2005) argue that colours are able to elicit emotional responses that might significantly influence decision-making in map users. This effect is stronger in colour than in any other graphic variable. Drápela (1983) also views colour as a specific means of expression occupying a special position among cartographic variables and points out different aspects which should be considered when using colour effects in map design. Krygier & Wood (2005) describe several examples of inappropriate colour use in maps and emphasize the counterproductive impact of inappropriate colours on map legibility, which may manifest especially as erroneous or slow map interpretation. Inappropriate colour use also involves employment of inadequate colour ranges for displaying qualitative and quantitative data. On the other hand, use of appropriate colours and colour combinations can increase overall comprehensibility and legibility of the map substantially.

2.1 Colour contrast

An important thing to consider when designing map products is the contrast between different colours. This is because the effect of colours in maps – just like in any other graphic visualization – always depends on their combinations with other colours. Colour contrast can greatly enhance effective representation of the target information. A well-applied palette of contrasting colours is a perfect means of depicting the overall character of an area or a phenomenon, as the perceiver can immediately see the spatial distribution as well as the quantity and quality of different features on the map. Appropriately selected contrasts intensify the perception of the figure and the ground through dividing the map field into "layers" representing base and extension information (see Stachoň et al., 2013). As Krygier & Wood (2005) point out, contrast must be taken into consideration in any map design. It is therefore necessary to choose colours carefully to make them suitable for a particular background. Colours that are chosen arbitrarily and carelessly may produce uneven contrasts, which, in turn, may result in ambiguous perception of some of the features on the map, which become semantically indiscernible and unclassifiable.

In general, contrast refers to a situation when a clear difference can be observed between two juxtaposed objects or phenomena (Itten, 1987). Hence, contrast can result from differences in size, temperature or – in this case – colour. These observed differences are always relative because they arise through comparisons between two or more objects. Perception of colour and colour contrasts is a largely subjective process, which makes it hard to quantify or describe in detail. In the past (especially since the early 19th century), a relatively large number of authors commented on the issue of colour contrast (for overview, see Chesneau et al., 2005). However, it was not until Johannes Itten[1] that colour laws were finally formulated with sufficient objectivity, and principles of colour perception postulated which are often used in cartography to this day. Itten's principles systematically and explicitly define and describe seven basic types of contrasts observable in colour perception: contrast of hue, light-dark contrast, cold-warm contrast, complementary contrast, simultaneous contrast, contrast of saturation, and contrast of extension (for more detail and examples, see Bláha & Štěrba, 2014).

It has to be noted that, in reality (and all the more on the map), the above contrast types complement and mingle with each other and therefore cannot be treated as completely separate variables. For example, simultaneous contrast especially affects areas which also show the contrast of extension. Extension (relative area size), in turn, tends to influence colour saturation and colour lightness. On the other hand, the perception of colours as cool or warm, particularly with regard to their function as depth cues, is mostly independent of relative area size. All of this indicates that there might be certain hierarchy among different contrast types. Map design, just like visual arts, uses the law of cool and warm colours. When reading a map, similarly coloured (cool or warm) areas create an impression of similar depth, independent of area size. This effect is even more marked in cartography than in visual arts, where contrasts were originally studied. An impression of depth can also be achieved through the contrasts of saturation and light and dark, which is why figure elements on the map should always be depicted in deep and dark colours. When applied appropriately, the effects of individual contrasts will be multiplied.

Design of cartographic symbology should follow certain rules which are implicitly contained in the above principles. There are also other methods of increasing contrast that can be used to enhance the distinctness of particular features on the map. For example, Kennely & Steward (2010) design chloropleth maps with additional shading within the individual categorized polygons to create an illusion of a (pseudo)three-dimensional visualization. This effect enables further differentiation of individual elements within the same interval, adding new information represented – thanks to the impression of plasticity – by the polygon's "height". To a certain extent, this impression is also enhanced by appropriate choice of colour contrast – i.e. if features representing greater values are depicted in intensive and more saturated colours, there will be a stronger perception of ground features (polygons representing low values) and figure features (polygons representing high values). Obviously, a similar method could be used to visualize qualitative phenomena, namely to accentuate the contrast between warm and cool colours. Adequate choice of colour combinations and contrasts should, naturally, be also directed by the purpose for which the map is designed.

---

[1] Johannes Itten (1888 – 1967) was a Swiss designer, expressionist painter and theoretician closely associated with the arts and architecture group *Bauhaus*. He was especially interested in colour theory and studied the impact of colour on visual perception.

2.2 Effect of colour on the perception of a map

Colour perception, in general, is a very complex process. Apart from the properties discussed above, this is also caused by the fact that individual colours create different impressions in different people. Moreover, colour perception is strongly influenced by the context, i.e. colour properties of the surrounding objects as well as other external factors (Kryger & Wood, 2005).

MacEarchen (2004) notes that cartographers harnessed the knowledge of individual differences and variation in colour perception, and of the way people interpret cartographic information differently depending on the employed colour combinations, relatively early in the past. The best illustration is the cartographic visualization of elevation layers by means of hypsometric tints. This convention, established by Karl Peucker[2] in the late 19th century, is used in various analogous forms in atlas designs to this day (Thrower, 2008). The principle of this method consists in the fact that perception of distance (or depth) varies with changing colour tints or hues. This creates an impression of depth perspective and facilitates the process of information transmission. For example, hues of long wavelengths (orange and red) are perceived as closer on the map than hues of short wavelengths (blue and green). This phenomenon is often employed in spectral ranges (or, more often, their parts) used in cartographic visualizations. As specified by Imhof (2007), this stereoscopic effect does not result directly from physiological processes, but arises from a psychological illusion that is formed in people's minds. It is also advisable that similar colour ranges additionally involve the cold-warm contrast, which amplifies the overall impression of distance. Hence, colour ranges that include cool colours as well as warm colours (e.g. red – orange – light blue – dark blue) show particularly good properties in cartographic products.

Drápela (1983) describes the effect of colour, especially colour excitability, on the expression of positive and negative qualities of a phenomenon. "Calm" colours include shades and tints of yellow, blue and green. These colours create the most placid impression in people. "Excitable" colours, on the other hand, are represented by the other pole of the spectrum, namely by the red colour. The colour which is considered most excitable is non-spectral purple, which is physically composed of light with the shortest and longest wavelength (red and blue). This effect is probably caused by an increased struggle of the visual system to form a sharp image of purple-coloured objects on the retina. These properties are partly used – in analogy with traffic conventions – also in emergency maps to display potential hazards (see Konečný et al., 2011).

Cartographers who design maps are sometimes limited by various rules, standards and other conventions whose meaning is largely historical. Adherence to these rules is usually implicitly required by the user, and any deviations might lead to incorrect interpretations of the cartographic material. Such general conventions are summarized, for example, by Robinson et al. (1995), who find it natural that green colour represents areas covered by vegetation, brown colour indicates mountain ranges and yellow colour is used to depict areas with poor moisture supply (dry land, areas without vegetation cover, etc.). Besides mere conventionality, however, these expectations are fuelled by the connotations evoked by different colours, i.e. associations they tend to produce in most people (e.g. blue suggests moisture and cold, brown is associated with soil, etc.). Apparently, conventions

---

[2] Karl Peucker (1859 – 1940) was an Austrian theoretical cartographer.

such as these should be observed especially in maps designed for the general user. The more specialized a map is, the more its design should adhere to the rules and standards typical for that particular domain. As another example, Vasilev (2006) discusses how habitual practices of colour use in maps may vary due to regional or national differences. Apart from several, mostly topographical features (*blue* for bodies of water, *green* for forests and *brown* for mountains), individual colours may imply different meaning in different geographical areas. This could be caused not only by differences in culture and cultural traditions, which may produce different emotional impacts of a particular colour on the individuals, but also by differences in actual colour perception characteristic of the context or environment in which the cultural community lives. Finally, colours can also be perceived differently due to variations in individual dispositions.

3. CONCLUSIONS

In cartography, appropriate use of colours plays a crucial role in effective communication of the target information. A well-chosen colour scheme with suitable contrasts provides the best way of depicting the overall character of an area or a phenomenon. For these reasons, appropriate use of colours is especially important in domains such as emergency management where cartographic visualisations are extremely helpful in obtaining all of the needed information. Colour can be a very effective tool for displaying emergency situations. It can be used to depict possible hazards, ongoing events, or the current state of restoration processes in the afflicted areas. However, it must be noted that the domain of emergency management cartography tends to be particularly affected by conventions in colour use, which might be very limiting for cartographers designing these types of products.

In general, cartographic products for emergency management are employed by users who need to obtain the target information as quickly as possible, with a substantial level of accuracy. Decisions based on unclear cartographic visualisations could lead to misunderstandings that may finally turn into weighty losses. Through the employment of adequate colour contrasts, one can achieve optimum differentiation between the figure (most important) and the background (less relevant) information. This effect helps to significantly increase the efficiency and effectiveness of perception of the target information, which has a strong impact on the overall usability of a map.

ACKNOWLEDGEMENTS

This work was supported by the project „Employment of Best Young Scientists for International Cooperation Empowerment“ (CZ.1.07/2.3.00/30.0037) co-financed from European Social Fund and the state budget of the Czech Republic.

REFERENCES

Bláha, J. D. (2011). Aesthetic Aspects of Early Maps. In Ruas, A. (ed) *Advances in Cartography and GIScience. Vol. 1, Selection from ICC 2011 Paris*, 53–71.

Bláha, J. D. (2013). Cultural Aspects of Cartographic Creation: Use of Mental Maps in Cross-cultural Research. In *Proceeding of 26th ICC Dresden*, 1–15.

Bláha, J. D., Štěrba, Z. (2014). Colour Contrast in Cartographic Works Using the Principles of Johannes Itten. In *Cartographic Journal*: 51(3), 203-213.

Chesneau, E., Ruas, A., Bonin, O. (2005). Colour Contrasts Analysis for a better Legibility of Graphic Signs on Risk Maps. In *22nd International Cartographic Conference 9-16 July* [online], A Coruna, 2005, 10 s,

Drápela, M. V. (1983). *Vybrané kapitoly z kartografie*, 1. vyd., SPN Praha, Brno, 1983, 128 s.

Imhof, E. (2007). *Cartographic Relief Presentation*, 1. vyd., 2007, ESRI Press Redlands, 416 s., ISBN 978-1-58948-026-1.

Itten, J. (1987). *Kunst der Farbe: subjektives Erleben und objektives Erkennen als Wege zur Kunst*, Maier, Ravensburg.

Konečný, M. et al.(2011). Dynamická geovizualizace v krizovém managementu. Brno: Masarykova univerzita, 379 p. ISBN 978-80-210-5858-3.

Krygier, J., Wood. D. (2005). *Making Maps: a Visual Guide to Map Design for GIS*, 1. vyd., New York: Guilford Press, 2005, 303 s., ISBN 1593852002.

MacEachren, A. M. (2004). *How Maps Work: Representation, Visualisation and Design.* New York: The Guilford Press, 2004, 513 s., ISBN 0-89862-589-0.

Robinson, A. H., Morisson, J. L., Muehcke, P. C., Kimerling, A. J., Guptill, S. C. (1995). *Elements of Cartography*, 6. vyd., Wisley&Sons, 1995, 664 s., ISBN 0-471-55579-7.

Stachoň, Z., Šašinka, Č., Štěrba, Z., Zbořil, J., Březinová, Š. and Švancara, J. (2013). 'Influence of Graphic Design of Cartographic Symbols on Perception Structure', *Kartographische Nachrichten*, 63(4), pp. 9.

Thrower, N. J. W. (2008). *Maps & Civilization: Cartography in Culture and Society*, 3. vyd., The University of Chicago Press, 2008, 352 s., ISBN 978-0-226-79974-2.

Vasilev, S. (2006). Cartographical Symbolic. In *International Conference on Cartography and GIS* [online], Borovetz, 2006.Gage, J. 2008. *Signs of Disharmony: Newton's Opticks and the Artists*, Perspectives on Science 16(4) 360-377.

Address: Zbyněk Štěrba, Ph.D., Department of Geography, Faculty of Natural Sciences, Masaryk University, Kotlářská 2, Brno, 611 37,Czech Republic
E-mails: zbynek.ste@gmail.com, jdg@seznam.cz

Evaluation of colour appearances displaying on smartphones

X. Gao [1*], E. Khodamoradi [1], L. Guo [2], X. Yang [2], S. Tang [3], W. Guo [3], Y. Wang [3]

[1] Department of Computer Science, Middlesex University, London, NW4 4BT, UK
[2] Department of Information Science, Fuzhou University, Fuzhou, China
[3] Biomedical Engineering Center, Fudan University, Shanghai, China

*Corresponding Author: Prof. Xiaohong Gao, x.gao@mdx.ac.uk

ABSTRACT

Despite of the limited size and capacity of a mobile phone, the urge to apply it to meet quotidian needs has never been unencumbered due to its appealing appearance, versatility, and readiness, such as viewing/taking pictures and shopping online. While a smartphone can act as a mini-computer, it does not always offer the same functionality as a desktop computer does. For example, the RGB values on a smartphone normally cannot be modified nor can white balance be checked. As a result, performing online shopping using a mobile phone can be tricky, especially when buying colour sensitive items. Therefore, this research takes an initiative to investigate the variations of colours for a number of smartphones while making an effort to predict their colour appearance using CIECAM02, benefiting both phone users and makers. The paper studies models of Apple iPhone5, LG Nexus 4, Samsung, and Huawei, by capitalising on comparisons with a CRT colour monitor that has been calibrated under the illuminant of D65, to be in keeping with the usual way of viewing online colours. As expected, all the phones present more colourful images than a CRT does.

1. INTRODUCTION

A smartphone is a mobile phone with more advanced computing capability and connectivity than basic feature phones, offering functionalities of typically personal assistance, media player, digital camera, and a GPS navigation unit in addition to the basic calling/receiving facilities. At present, the global smartphone audience has reached 1 billion consumers [eMarkter] and expects to arrive at 1.75 billion by the end of 2014. As such, mobile sales are not only focusing heavily on smartphones, but also on the more affordable option of feature phones that do not have an operating system. As a result, mobile penetration has surpassed 100% in many regions of the world, including North America, Western Europe, Central and South America, Central and Eastern Europe, and the Middle East [WeAreSocial]. Among those smartphone users, about half of them go online by using the phone regularly. Table 1 lists the top 10 most popular smartphones on the market.

Table 1. Top 10 smartphone list as of May 2014 [Counter].

Rank	Brand	Model
1	Apple	iPhone 5s
2	Samsung	Galaxy S5
3	Samsung	Galaxy S4
4	Samsung	Note 3

5	Apple	iPhone 5c
6	Apple	iPhone 4S
7	Xiaomi	MI3
8	Samsung	Galaxy S4 mini
9	Xiaomi	Hongmi Redrice
10	Samsung	Galaxy Grand 2

One of the unexpected by-products of smartphones remains in the field of digital photography. It appears that more photos are taken by using Smartphones than normal cameras. For example, the Apple iPhone 5 is currently the most popular 'camera' on Flickr.com [Flickr]. As a direct result, large amount of money are being investigated by mobile developers to create photo apps in an attempt to satisfy the demands of 'serious' camera phone photographers.

While using smartphone to perform everyday activities, colour remains one of the key factors, in particular in online shopping. Similar to any other digital device, a phone represents a digital image in a RGB colour space. Therefore when an image is to be processed, it is usually firstly converted into the colour space of, say, hue, lightness and colourfulness. In this way, the dependency of RGB space on hardware devices can be circumvented, i.e., a colour in one device usually does not appear nor measure the same as the one in another device even with the same RGB values in both devices. This is because the range of R, G, or B values are manually set to be the same (such as [0, 255] for an 8-bit computer) for all devices regardless their physical measurements. On the other hand, hue, colourfulness and lightness, space agrees more with human vision theories. To further improve the fitness between users' perception and retrieved results, CIE has recommended a colour appearance model CIECAM02 to predict colours appear on any media under a number of viewing conditions [Moroney]. Stemmed from Hunt's early colour vision model [Luo (a) 1993, Luo (b) 1993] employing a simplified theory of colour vision for chromatic adaptation together with a uniformed colour space, CIECAM02 can predict the change of colour appearance as accurately as an average observer under a number of given viewing conditions. In particular, the way that the model describes a colour is reminiscent of subjective psychophysical terms, i.e., hue, colourfulness, chroma, brightness and lightness.

To begin with, CIECAM02 takes into account of measured physical parameters of viewing conditions, including tristimulus values (X, Y, and Z) of a stimulus, its background, its surround, the adapting stimulus, the luminance level, and other factors such as cognitive discounting of the illuminant. The output of the colour appearance model predicts mathematical correlates of perceptual attributes.

With regard to the representation of the colour appearance of an image, in this investigation, the perceptual colour attributes of lightness (J), colourfulness (M) and hue (H) are employed.

2. METHOD

Thirty test colours are randomly selected from the Munsell colour book while making an effort to cover as much CIE 1931 colour space as possible. Psychophysical experiments are then carried out on both 19" CRT colour monitor with its illuminant calibrated to D65 and mobile phones. As illustrated in Figure 1, each test colour is placed at a centre against a grey background (with 20% of luminance of reference white) and surrounded by the reference white, reference colourfulness and surrounding colours. The test field in the centre subtends a visual angle of 2^o at a viewing distance of ~60cm. Ten subjects with normal colour vision are selected to conduct the experiments using the technique of magnitude estimation which they have been trained in advance to apply skilfully. Specifically, for each test colour, each subject is asked to estimate its appearance in terms of lightness, colourfulness and hue contents verbally that are then recorded by an operator sitting nearby.

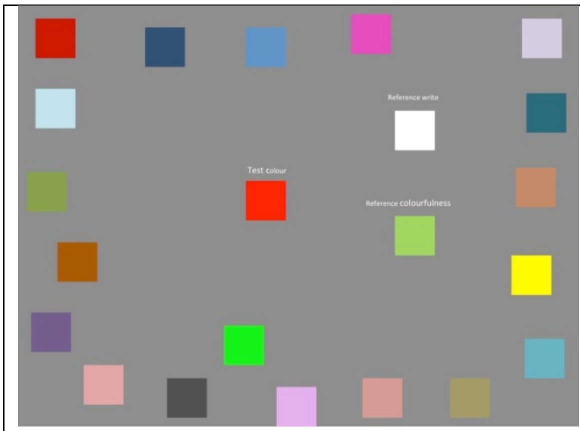

Figure 1. The paradigm of the experimental pattern.

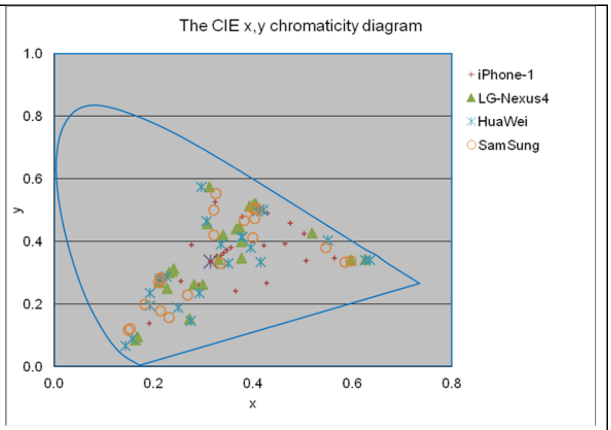

*Figure 2. The x, y data of the thirty sample colours plotted on the CIE xy Chromaticity diagram for the four phones to be studied in this research. The big * refers to the reference white.*

In addition, each colour on each phone has been measured using a colour meter CS-100A, simulating subjects' viewing position. Specifically, the reference white, reference colourfulness, and background are measured at least 3 times, e.g., at the beginning, the middle and the end of the colour sample sequence, to check the repeatability of the phone. In total, 6 phones, including three iPhone5, one Huawei, one SamSung, and one LG Nexus4, are measured and estimated. The same work is also performed on the CRT monitor, Philips Brilliance 201B. The measured data are presented in a CIE xy Chromaticity diagram as illustrated in Figure 2.

3. RESULTS AND DISCUSSION

3.1 iPhone

Three handsets of iPhone 5 are investigated in this paper. Figure 2 compares the subjects' estimation results between CRT and iPhone 5 where correlation coefficient (r) values are 0.76, 0.62 and 0.96 respectively for Lightness, colourfulness, and hue estimations.

For lightness, the estimation on mobile iphones tends to be 16% more than that on CRT mornitors, whereas 11% increase of colourfulness for mobile phones is evidenced. In Figure 4, a hue-colourfulness plot is presented, where small circles (o) represent the colours from CRT and big square (□) from iPhone5.

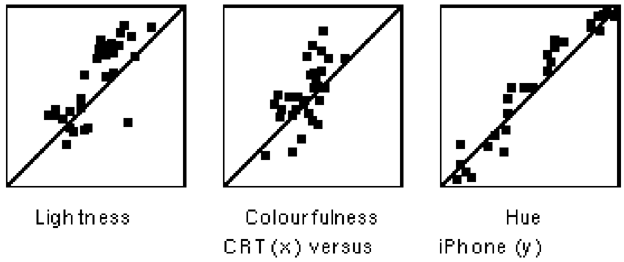

Figure 3. Comparison of subjective estimations of the thirty samples for CRT (x-axis) and iPhone 5 (y-axis).

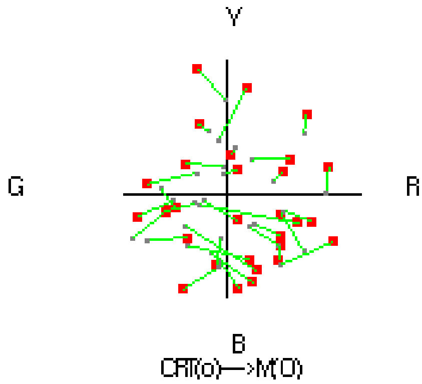

Figure 4. Subjects' estimation for the same group of colours on both CRT and Iphone5. Small circle(o) refers to the estimation for CRT whereas big solid square (▪) on Iphone.

3.2 Modelling of Iphone appearance using CIECAM02

Since the colour appearance model CIECAM02 is developed for the media of CRT, refection and transparency, it may not be well equipped to predict smartphones. After the setting of environmental parameters to 'dim' condition where F =0.9, c = 0.59, and Nc=0.90 to compensate lightness differences between CRT and iPhone, the comparison results are given in Figure 6 for the three phones, where colourfulness is adjusted according to Eq. (1).

$$Colourfulness\_smartphone = 1.8 * Colourfulness\_CIECAM02 \qquad (1)$$

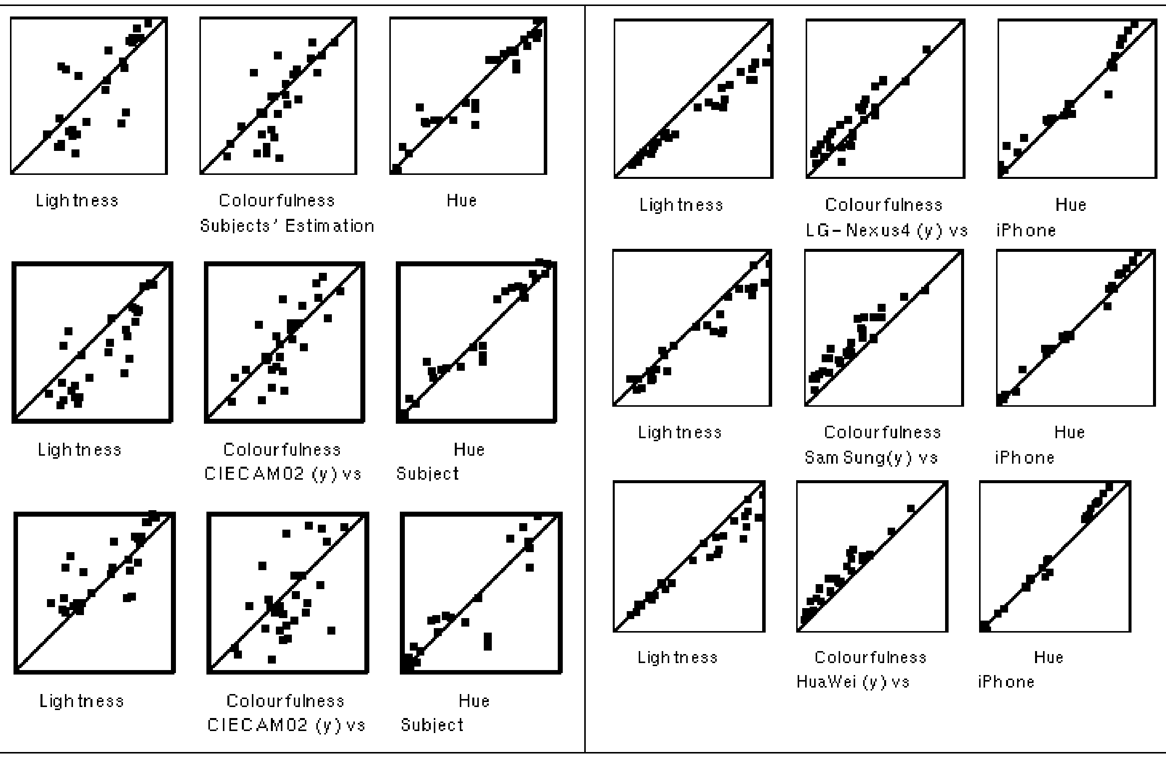

Figure 6. Comparison of CIECAM02 predictions with subjects estimations.

Figure 7. Comparison of iPhone (x-axis) with phones of LG-Nexus4 (top), Samsung (middle) and Huawei (bottom) by modified

It can be seen that after the correction using Eq. (1), the modified CIECAM02 can predict smartphones accurately.

3.3 Comparison with other smart phones

After the modelling of iphones using CIECAM02, a number of other smartphones are evaluated as well, including, a LG-Nexus4, SamSung, and HuaWei. Figure 7 presents the comparison results by the calculations using CIECAM02 for all the phones, whereas Figures 8 demonstrates a colour checker depicted on these phones.

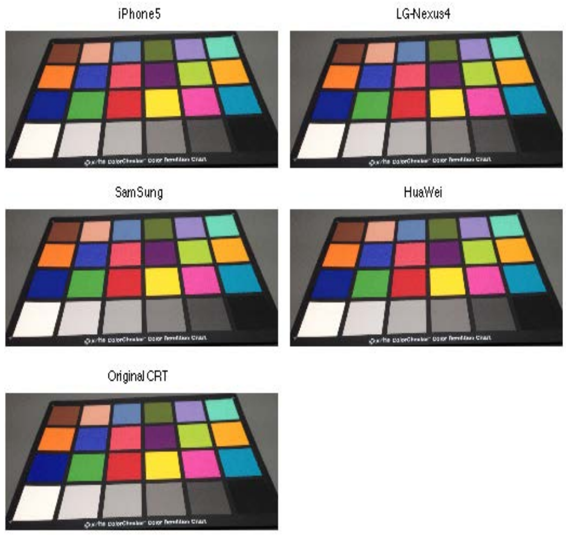

Figure 8. Colour checker depicted using four phones and CRT

When comparing with the other smartphones, in terms of hue, all three phones tends to be more reddish for purplish colours than those displayed on an iPhone, whereas the rest maintains near the same. With regard to lightness, for lighter colours, all three phones unanimously appear darker than on iPhones with LG-Nexus being the darkest with 25% darker, whereas 18% and 16% darker are evidenced for HuaWei and SamSung respectively. However, the opposite phenomenon occurs when it comes to the representation of colourfulness. All three phones of LG-Nexus4, SamSung, and HuaWei appear more colourful than those displayed on an iPhone. For example, the colours on a LG-Nexus4 phone appears systemically 10% more colourful than those depicted on an iPhone. In addition, for both HuaWei and SamSung phones, they appear again to be 17% and 22% more colourful, especially for colourful samples, the tendency presenting across all three phones. Since these findings are based on only one phone of each type, future study will focus on the investigation of large samples with more similar phones.

4. CONCLUSIONS

With 85% smartphone users perform their everyday tasks [Salesforce] using the device due to its ability and connectivity, smartphone continues to revolutionize how people perform their everyday activities. It is expected that this work will contribute to this revolutionary and complement users with some information when they perform online shopping buying colour incentive goods.

In summary, in terms of the measurement on each phone, encouragingly, the variations among the same kind of phones are insignificant with less than 3 ΔE CIELAB units. In addition, when comparing with subjects' hue estimations, all phones and the CRT monitor appear to have similar hue values, indicating that the hue values have been well reserved on those phones although some variations among phones are observe red. However, when it is viewed on a phone, a colour appears to show at variance with colourfulness by appearing much more colourful. Furthermore, the correlation coefficient (r) for CIELUV L* are 0.963, 0.959, 0.960, and 0.940 for iPhone, LG Nexus4, HuaWei and SamSung respectively, and are 0.890, 0.876, 0.761, and 0.764 respectively for CIELUV C* when comparing with the counterparts on the CRT monitor. Therefore, the iPhone tends to be the best with fewer scatterings. To predict a colour on a mobile phone using CIECAM02, the predictions rest on a number of environmental parameters settings, e.g., f = 0.9, c = 0.59, and nc = 0.90, which gives closer results with less scattering. Consequently, for an image with truthful colour to be displayed on a mobile phone, the forward and reverse model of CIECAM02 will have to be applied. Specifically, for iPhone5, nearly half of the colourfulness predicted by CIECAM02 need to be factored into. Further studies are in place to take more number of phones into consideration.

ACKNOWLEDGEMENTS

This research is in part funded by EU WIDTH project (2011-2014) under Marie Curie Scheme. Their financial supported is gratefully acknowledged.

REFERENCES

Counter Point Research, http://www.counterpointresearch.com/top10. Retrieved in February 2015.

eMarkter, http://www.emarketer.com/, retrieved in February, 2015.

Flickr: https://www.flickr.com/cameras. Retrieved in February, 2015.

Luo MR, Gao XW, Phodes PA, Xin HJ, Clark AA, Scrivener SAR, Quantifying colour appearance - Part IV., Transmissive media, *Color Research and Application*, vol. 18, 1993, pp. 191-206.

Luo MR, Gao XW, Phodes PA, Xin HJ, Clark AA, Scrivener SAR, Quantifying colour appearance - Part III., Supplementary LUTCHI colour appearance data, *Color Research and Application*, vol. 18, 1993, pp. 98-113.

Moroney N, Fairchild MD, Hunt RWG, Li C, Luo MR, Newman T, The CIECAM02 Color Appearance Model, *In IS@T/SID Tenth Color Imaging Conference*, 2002, pp. 23-27.

Salesforce: www.salesforce.com , retrieved in February 2015.

We are social, http://wearesocial.net/, retrieved in February, 2015.

Colour Management for High Dynamic Range Imaging

Keith D. M. FINDLATER
School of Design, University of Leeds

ABSTRACT

High dynamic range (HDR) composite images can be used to create photo-realistic and hyper-real images. Parameters including contrast ratios and tone mapping functions are used to control HDR image processing. However, the dynamic range of real world scenes is highly variable and digital cameras need to be characterised for different scenes. This research aims to investigate and compare colour management processes and image processing between standard and HDR image capture. It will also assess the advantages of HDR images by revealing perceived differences and to ascertain the boundaries where HDR imaging becomes a significantly advantageous process to use.

The proposed research method initially sets up an optimised camera characterisation using standard capture of a scene in controlled lighting conditions. The subject luminance range will then be extended beyond the dynamic range of the camera sensor through experimentation by controlling illumination and the subject using calibrated digital colour test charts. HDR capture techniques will then be employed to create composite images from multiple exposures and single images, from which colour reproduction can be assessed in comparison with the original scene. This process will be used for a range of types of scenes using natural and artificial light sources.

This research aims to extend existing methods of colour management to the HDR domain, to develop new methods if necessary, and to ascertain to whom colour management of HDR Images would be beneficial.

1. INTRODUCTION

An illuminated scene will have numerous defining characteristics that will affect the production of images captured by a camera. In photography, these are captured using a lens system and recorded onto either photo-sensitive silver halide film or electronic digital sensors. These camera systems have different design specifications for capturing varying types of scene, for example, by introducing interchangeable lenses and sensor formats to change the shape and angle of the photographed scene (Allen *et al.*, 2011).

The subject luminance ratio is the luminance range of a scene between the darkest shadow and the brightest highlight. A digital camera sensor or photographic film will be capable of recording a limited range of subject reflectances as a tonal range. The sensitivity is optimised for specific types of photography, varying from low level light to very bright scenes. The sensor is exposed to the scene for a period of time through a lens with a measured aperture. This exposure is set so that the sensor records the full tonal values of the subject. This process has been optimised by camera manufacturers so that a photographer can capture a desired image by arranging a scene along with camera settings and control of image or film processing to capture a desired image.

For a brightly illuminated scene, the range of reflectances of a subject can be too great for the tonal range of the captured image. This results in clipping, where tonal detail in the brightest highlights and darkest shadows are recorded as maximum and minimum image tones. The photographer has the option to accept this result, or attempt to reduce the subject luminance range by changing the lighting conditions, exposure control or image processing, to meet a desired outcome.

High Dynamic Range imaging is a field of research into ways of increasing the range of reflectances that a camera sensor can capture of a subject. The limiting factors include the dynamic range of the sensor and display or the reflectance range of the printed image. However, the commercial and consumer use of digital cameras is widespread using basic sRGB colour gamut for online, digital and printed platforms.

Colour management is the process of adjusting an image to account for differences between various image capture and display devices to ensure colour fidelity. For conventional imaging, methods for colour management have been extensively studied and various solutions are available (Westland *et al.*, 2012). However, much of HDR imaging has been to generate aesthetically pleasing images rather than to obtain colorimetrically accurate ones. This research aims to extend existing methods of colour management to the HDR domain, to develop new methods if necessary, and to ascertain to whom colour management of HDR Images would be beneficial.

2. PROPOSED WORKFLOW

The two components of this research involve investigating colour characterisation methods for cameras and then combining this with methods for generating HDR images. Once a workflow is established then more detailed research can begin into the nuances of comparative performance between single captured images with HDR images of different types of natural and artificial scene.

2.1 Sample Preparation

For standard camera characterisation, a digital reflective colour chart is normally used as a reference target to generate measured data for a scene under controlled uniform lighting conditions. The known CIE colour coordinates of the patches in the chart and their corresponding captured camera RGB values can be used to constrain a model that can predict CIE values given RGB values.

For HDR imaging, it is not clear that the colour patches in the standard colour charts have a high-enough dynamic range. A test scene needs to be created where the subject luminance range is extended beyond the dynamic range of the camera sensor by controlling illumination and the subject using calibrated digital colour test charts. One solution could be based on having two adjacent reflective colour test charts that fill the image capture area. Localised controlled lighting would be introduced so that, for example, one colour test chart is much brighter than its adjacent. Once optimized, this would be the starting point for creating a controlled test target for the characterisation of HDR images. Another possibility is to use self-luminous display targets.

The advantage of a controlled scene, such as the DigiEye System, is to be able to produce repeatable results for analysis. However, the ultimate aim would be to compare the capture of normal and HDR images under variable natural daylight and artificial light sources.

2.2 Camera Characterisation for a Display

The first stage is to establish a standard digital imaging workflow from a real scene to display output. This optimised workflow will be the camera characterisation for a display using standard capture of a scene in controlled lighting conditions.

This process uses principles of additive colour mixing using Grassman's Laws and the 1931 CIE system. The RGB values of the camera image are converted into XYZ values. These values are then converted and outputted to sRGB values or other colour space used by the display.

Once the camera is characterised for a display for a standard image, the same can be used for subsequent HDR captured images.

2.3 High Dynamic Range Image Capture

Many sensors in digital SLR cameras capture 12-bit RAW or 8-bit Jpeg files in a single image, corresponding to a dynamic range of exposure values of up to 9 stops between the brightest highlight and the darkest shadow. Firstly, the digital SLR camera will be characterised for display for a fixed colour target under uniform and constant illumination. This would be used for comparison with subsequent HDR images captured of a reference scene with a large subject luminance range.

High Dynamic Range images can be captured using different methods.

The Multiple Exposures Technique is where a sequence of images is captured with incremental changes in exposure time of a fixed scene from a fixed viewpoint (Nightingale, 2012). The number of images and the choice of exposure times are variable and this will be researched to produce a optimised HDR capture process. The resulting component images are merged into a single HDR image using a computational tone mapping process. The alternative method is to capture a single image using a sensor with an extended dynamic range capture capability.

The resulting HDR images will be assessed for colour fidelity by comparing the image colour data with the scene reference data, resulting in the characterisation of HDR images for display. Analysis of the differences between different Multiple Exposures Techniques and tone mapping processes will also be made. Differences between Standard Colour Capture and High Dynamic Range Imaging will be investigated for a variety of types of illuminated scene.

McCann & Rizzi found that glare occurs when a bright object in a scene reduces contrast everywhere within the field of view of the camera. The effect of glare increases with greater dynamic range, so this research would be looking to observe any limits to any corresponding increased colour fidelity (McCann & Rizzi, 2012).

Other limiting factors would include the performance of the imaging sensor, also optical limits in acquisition and visualisation. Other results would include comparison of colour fidelity on single and multiple exposure for scene capture.

A practical issue will be to override the automated proprietary functions in the chosen camera's firmware to provide experimental RAW data for analysis.

Initially for this research, the tone mapping functions will be used for creating photo-realistic HDR composite images only for comparison with standard digital characterisation for a display.

3. CONCLUSIONS

As mentioned earlier, the purpose of this paper is to outline the early stages of my PhD research into Colour Characterisation for High Dynamic Range Imaging. This paper will raise awareness and help refine my research plans by attending AIC Tokyo 2015.

The emphasis of my initial research will be to establish a workflow for the Colour Characterisation of HDR images. The differences and merits of HDR imaging techniques including Multiple Exposure techniques, sensors with extended dynamic range capture capability and tone mapping functions will be investigated.

Experimental data will also be collected to see whether observers notice a significant improvement between the resulting colours between captured standard and HDR images for different scenes. This will help see how successful the HDR imaging processes have been.

Other areas of investigative research will include comparisons of colour characterisation for different HDR tone mapping functions; the success of HDR characterisation for different types of scene using Natural and Artificial Light Sources.

Ultimately, my research aims to determine a number of questions. What are the best conditions for using HDR imaging for colour reproduction? What situations are best served by using colour reproduction for HDR imaging? What are the benefits and advantages of HDR imaging? Within what boundaries is HDR imaging a better process to use and for what applications? At what point will people significantly prefer viewing HDR images for different subject matter? What archival storage implications are there for HDR imaging?

ACKNOWLEDGEMENTS

I would like to thank my PhD supervisors Professor Stephen Westland and Dr Vien Cheung for their guidance and support with writing this paper.

REFERENCES AND BIBLIOGRAPHY

McCann, J.J., Rizzi, A. 2012. *The Art and Science of HDR Imaging (First Edition).* Wiley, Chichester.

Westland, S., Ripamonti, C., Cheung, V. 2012. *Computational Colour Science using MATLAB (Second Edition).* Wiley, Chichester.

Nightingale, D. 2012. *Practical HDR – A complete guide to creating High Dynamic Range images with your digital SLR (Second Edition).* ILEX, Lewis.

Allen, E., Triantaphillidou, S. et al. 2011. *The Manual of Photography (Tenth Edition).* Focal Press (Elsevier), Oxford.

Address: Keith D. M. FINDLATER, School of Design,
The University of Leeds, Leeds, West Yorkshire, LS2 9JT. ENGLAND U.K.
E-mails: sdkdmf@leeds.ac.uk, keith@keithfindlater.com

Development of a Wide-Gamut Digital Image Set

Stephen WESTLAND, Qianqian PAN, Yuan LI, Soojin LEE
School of Design, University of Leeds, UK

ABSTRACT

A great many imaging devices are consistent with the sRGB colour space. However, wide-gamut display devices exist that conform to colour spaces that have wider gamuts such as Adobe (1998) RGB. There is a shortage of standard image sets that contain colours that are outside of the sRGB gamut. Such images could be useful, for example, for testing various performance metrics in wide-gamut display systems. The purpose of this work is to develop a wide-gamut image set and make it widely available on the internet for the imaging community. Three digital SLR cameras were used to capture a large number of images that contained saturated colours. The colour space of the cameras was set to Adobe RGB and the file format was set to record raw. The images were converted to 48-bit TIFF images in the Adobe colour space and on average had about 18% of their pixels outside of the sRGB gamut. MATLAB was used to process the images and to ascertain the proportion of pixels that were outside of the sRGB gamut in each case. Images have been made available on a website – in both raw and tiff formats – and are categorised according to their colour and also according to the description of the objects for which the pixels are out of gamut. Example, object classifications include textiles, jewellery, arts, plants, foodstuffs and electronics. A total of 100 wide-gamut images were selected and have been made available to the community.

1. INTRODUCTION

Trichromacy is a crucial concept in colour imaging. The majority of digital cameras capture colour using three sensors, usually referred to as RGB, that capture different wavelength properties of the scene. Digital cameras often output images in a standard colour space known as sRGB (Süsstrunk *et al.*, 1999). The sRGB colour space has a gamut that is illustrated in Figure 1 by the black solid lines. The vast majority of image display devices also conform, at least approximately to the sRGB colour space so that they have a limited colour gamut. The vast majority of consumer images are defined in the sRGB colour space.

However, some capture and display devices are based on other colour spaces and one of the most common of these is the Adobe 1998 RGB space (Süsstrunk *et al.*, 1999). This colour space encompasses about 50% of the colours in CIELAB and improves on the gamut of sRGB in the green-cyan colours in particular. The Adobe RGB colour gamut is illustrated by the white lines in Figure 1. As can be seen the major difference between the two colour spaces is the chromaticities of the green primary which, for the Adobe space, is much more saturated. Images that contain colours that are outside of the sRGB colour space are referred to as wide-gamut images. There is some need to have standard wide-gamut images that can be widely available to the scientific community because these can be used to evaluate, for example, properties of so-called wide-gamut devices. With the widespread use of commercialised wide-gamut displays, the demand for wide-gamut content is increasing (Murakami *et al.*, 2013). The majority of LCD displays are based on the sRGB colour gamut whereas AMOLED displays support the Adobe RGB colour space;

based on an analysis of gamut volumes, AMOLED displays have been shown to be able to display 60-80% more discernible colours than the LCD displays (Li *et al.*, 2014). Wide-gamut images can also be useful for evaluating gamut-mapping algorithms (Langendijk *et al.*, 2009).

There have been several approaches to collect wide-gamut images. One approach is to use a spectral camera because this can capture a very wide colour gamut (Murakami *et al.*, 2013) or, alternatively, a multispectral camera (Murakami *et al.*, 2012). However, spectral cameras can be expensive, bulky and sometimes require extensive calibration and these constraints make them not so suitable for capturing images outdoors. A second approach has been to artificially expand the gamut of existing sRGB-specified images. However, in this paper we use consumer-grade digital SLR cameras that have the capacity to record images in Adobe RGB colour space. The aim of the work is to capture a large number of naturally occurring images that contain pixels that are outside of the sRGB colour gamut and to make these images widely available to the community for use.

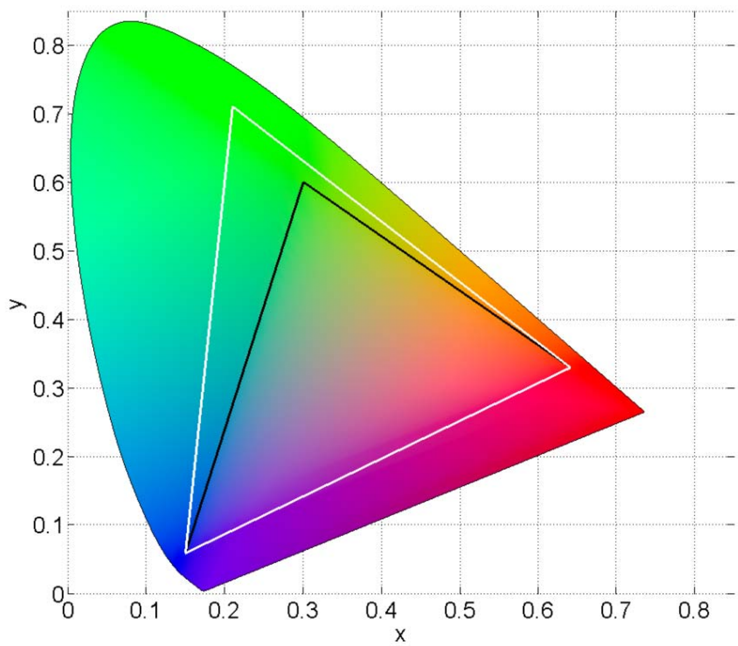

Figure 1: CIE 1931 chromaticity diagram showing the gamut of sRGB (black line) and Adobe 1998 RGB (white line).

2. METHOD

Three different digital SLR cameras were used to capture the images. Table 1 lists the cameras and their settings.

Images were captured as raw files and converted to 16-bit TIFF files with the Adobe sRGB colour space. Note that some images were captured in portrait mode and others were captured in landscape mode.

Table 1: Details of the camera files used in the work.

Device Name	Colour Space	File Type	Conversion File Type	Image Size
Nikon D90	Adobe RGB	RAW	16-bit TIFF	4288 × 2848
Nikon D7000	Adobe RGB	RAW	16-bit TIFF	4298 × 3264
Canon EOS 100D	Adobe RGB	RAW	16-bit TIFF	5184 × 3456

2.1 Image Processing and Selection Criteria

A large number of images were captured and these were processed and then selected to produce a set of 100 images with content outside of the sRGB gamut. A MATLAB program was therefore written to analyse each image. The first step was to convert the raw image to 16-bit Adobe RGB TIFF files. This was done using Corel PaintShop Pro (in the case of the Nikon images) and Canon Image Browser EX (for the Canon images). The second step was to convert from Adobe RGB to CIE XYZ, using the linear transform

$$\mathbf{T} = \mathbf{MC}$$

where **T** is a matrix of 3 × N XYZ values (where N is the number of pixels in the image), **C** is a matrix of 3 × N linear RGB values, and **M** is the 3 × 3 matrix thus:

$$\mathbf{M} = \begin{bmatrix} 0.57667 & 0.18556 & 0.18823 \\ 0.29734 & 0.62736 & 0.75290 \\ 0.27230 & 0.07069 & 0.99134 \end{bmatrix}$$

The linear RGB values were obtained from the camera RGB values according to the equation

$$C(i,j) = \left((D(i,j) + 0.055)/1.055\right)^{2.199}.$$

for channel i = 1 to 3 and pixel j = 1 to N and where $D(i, j)$ is the 16-bit RGB value normalized to the range 0-1 for channel i and pixel j. The third step was to convert from XYZ values to sRGB values. The normalized XYZ values **T** were converted to linear sRGB values using the matrix equation

$$\mathbf{S} = \mathbf{AT}$$

where **T** is a matrix of 3 × N normalised XYZ values, **S** is a matrix of 3 × N linear sRGB values, and **A** is the 3 × 3 matrix thus:

$$\mathbf{A} = \begin{bmatrix} 3.2406 & -1.5372 & -0.4986 \\ -0.9689 & 1.8758 & 0.0415 \\ 0.0557 & -0.2040 & 1.0570 \end{bmatrix}$$

The proportion of pixels that were outside of the sRGB gamut was calculated as being thr proportion of pixels for which either A(1, j), A(2, j) or A(3, j) was less than zero or greater than 1 at this stage. However, for display and subsequent storage as sRGB values the linear values A were processed thus

$$RGB(i,j) = 1.055S(i,j)^{1/2.4} - 0.055$$

if $S(i,j) > 0.0031308$ and otherwise

$$RGB(i,j) = 12.92S(i,j).$$

Figure 2 shows the flowchart of the colour-imaging workflow.

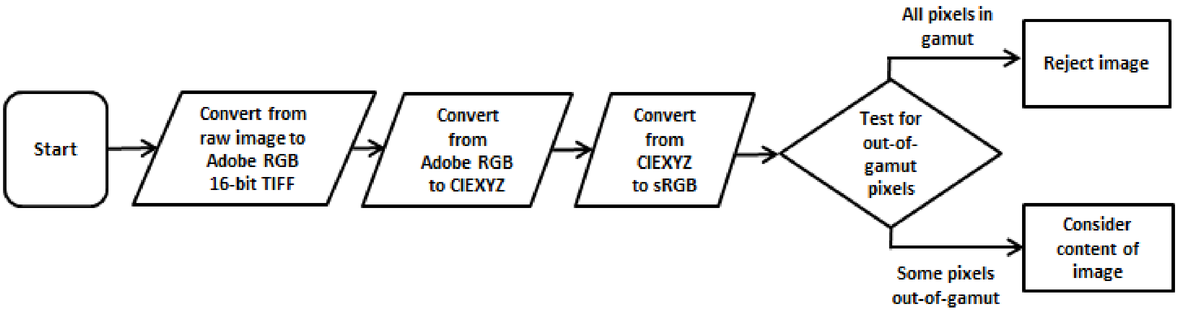

Figure 2: Flowchart illustrating workflow.

The approach of using an Adobe RGB camera system to obtain the images means that only colours that are blue, green, yellow and orange can be captured that are outside of the sRGB gamut. This is because the gamut boundaries of the two RGB systems in the red-magenta-blue region are the same (see Figure 1). A wide variety of content was aimed for including natural (precious stones, animals, plants, food) and manmade (light, textiles, plastics/paints, modern).

3. RESULTS AND DISCUSSION

Figure 3 illustrates some example output from the image processing described earlier. The left-hand upper pane shows the original image (as an sRGB representation) and the left-hand lower pane highlights the pixels that are out of the sRGB gamut (in this image pixels that are inside the gamut are darkened and the out-of-gamut pixels retain their original colour). The yellow colours of the flowers, for example, are out of gamut. The right-hand pane shows a CIE chromaticity diagram and the chromaticities of every pixel in the image. The sRGB and Adobe RGB gamuts are shown as white triangles. It is clear that some of the pixels in the yellow region are out of gamut. However, recall that gamuts are three dimensional and the out-of-gamut pixels have been identified as those that are outside of the three-dimensional sRGB gamut (as described in the Methods) and are highlighted in pink in the right-hand image. Note that in this example some pixels that are inside the sRGB triangle are actually out of gamut. In Figure 3, it can be seen that 43.8% of the pixels for this particular image were out of gamut. On average the images had about 18% of their pixels outside of the sRGB gamut with the minimum and maximum being 1% and 82% respectively.

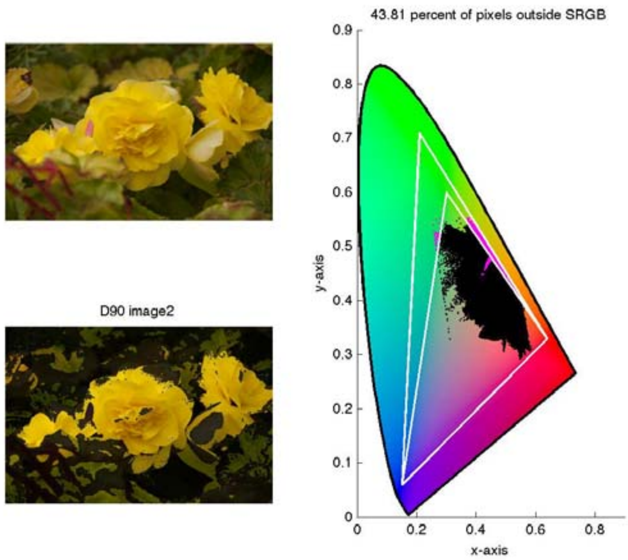

Figure 3: Flowchart illustrating the sample process.

As can be seen in Table 2, the number of images with out-of-gamut blue, green, yellow and orange components was 47, 43, 29 and 12 respectively; these numbers sum to more than 100 because some images contained two or more different colours that were outside of the gamut. Blue and green colours were most prevalent. In terms of categories, animal and jewelry were the most difficult to obtain.

Table 2. Summary of images included in the final database.

		blue	green	yellow	orange
natural	jewellry	2	0	0	0
	animal	0	0	1	0
	plants	0	5	4	2
	food	4	5	7	3
manmade	light	3	6	5	3
	textiles	6	1	3	1
	dyeing	17	11	4	3
	modern	15	15	5	0

The images are publically available at the following website which has been developed to support the images and their use within the scientific community - http://widegamutimages.wordpress.com/.

4. CONCLUSIONS

A total of 100 images have been captured with pixels that are outside of the sRGB gamut. On average the images had about 18% of their pixels outside of the sRGB gamut with the minimum and maximum being 1% and 82% respectively. The image contents represent a wide variety of subject matter including natural (precious stones, animals, plants, food) and manmade (light, textiles, plastics/paints, modern) objects. The images

The colour space of the cameras was set to Adobe RGB and the file format was set to record raw. The images were converted to 48-bit TIFF images in the Adobe colour space and on average had about 18% of their pixels outside of the sRGB gamut. MATLAB was used to process the images and to ascertain the proportion of pixels that were outside of the sRGB gamut in each case. Images have been made available on a website – in both raw and tiff formats – and are categorised according to their colour and also according to the description of the objects for which the pixels are out of gamut. Example, object classifications include textiles, jewellery, arts, plants, foodstuffs and electronics. The images have been made freely available to the scientific community for download.

REFERENCES

Süsstrunk, S., Buckley, R. and Swen, S. 1999. *Standard RGB Color Spaces*, Proceedings of the 7th IS&T Color Imaging Conference, 127-134.

Murakami, Y., Yamaguchi, M. and Ohyama, N. 2013. *Dictionary-Based Estimation of Spectra for Wide-Gamut Color Imaging*, Color Research and Application, **38** (2), 120-129.

Li, Y., Westland, S., Pan, Q. and Cheung, V. 2012. *Methods to assess the relative number of discernible colours for displays*, Proceedings of the 22nd IS&T Color Imaging Conference, 189-194.

Langendijk, E.H.A., Hotz, A.S. and Hinnen, K.J.G. 2009. *Wide Gamut Color Mapping and Image Enhancement using Image Segmentation*, Proceedings of the 17th IS&T Color Imaging Conference, 181-185.

Murakami, Y., Iwase, K., Yamaguchi, M. and Ohyama, N. 2008. *Evaluating Wide Gamut Color Capture of Multispectral Cameras*, Proceedings of the 16th IS&T Color Imaging Conference, 189-194.

.

Address: Prof. Stephen WESTLAND, School of Design,
University of Leeds, Woodhouse Lane, Leeds, LS2 9JT, UK
E-mails:s.westland@leeds.ac.uk,texqp@leeds.ac.uk

Construction of display profiles using simplicial maps and application to color reproduction of displays

Masashi YAMAMOTO,[1] Jinhui CHAO[1, 2]
[1] Graduate School of Science and Engineering, Chuo University
[2] Faculty of Science and Engineering, Chuo University

ABSTRACT

In this paper, we present an algorithm for color device calibration based on 3D-LUT using tetrahedral interpolation for displays. In particular, instead of test in which tetrahedron an input point lies, we proposed a fast algorithm to build a tetrahedron which contains an arbitrary input point for non-uniform grids. Performance of the proposed method is evaluated with color difference for single color inputs and natural images.

1. INTRODUCTION

To achieve a uniform color reproduction between different devices, a framework for color management and device calibration proposed by ICC using device profiles has been widely used e.g. Green (2010). Currently, most color devices are furnished with a profile by the device manufactures. Certain commercial software of profile making are also available.

However, variations exist between individual devices even by the same manufactures or due to device aging. The profile often describes device characteristics by a product of three 1D (usually monotonous) functions which is a rough approximation of a 3D nonlinear map. It might be useful for CRT but not enough for e.g. LCD displays with highly nonlinearity.

A solution is to use 3D look-up table (3D-LUT) in particular tetrahedronal interpolation. Lee(2005), Barsotti(2014), Kang(1996). However, besides a large number of measurements required, there seemed no efficient way to test which tetrahedron for a non-uniform grid an input point lies before to apply the inversion transformation. Existing approaches repeat try-and-error to test if the point is contained in a tetrahedron turned out to be inefficient.

In this paper, we present 3D-LUT calibration of displays using tetrahedronal interpolation in terms of simplicial maps. This formulation provides a conceptually clearer description of device calibration. The algorithm is different from existing approaches based on 3D-LUT using tetrahedral interpolation in the way to determine which tetrahedron an input point lies in. Instead of try to test if the point lies in a tetrahedron, we directly build a tetrahedron which contains the input point.

The following three implementations of the proposed method with different computational costs are investigated: 2D maps of the chromaticity plane, 3D maps of the color space which compensate chromaticity and brightness simultaneously, and (2+1)D maps which compensate chromaticity and brightness separately. The (2+1)D version shown to be a reasonable trade-off between performance and cost.

The proposed method and commercial profile makers are compared in terms of quantitative color difference between input and output colors. Besides, natural images are also used as input data for subjective comparison. Both experiments confirmed effectiveness of the proposed method.

2. PROPOSED METHOD

2.1 Simplicial linear maps and convex combination

A *m*-simplex is a *m*-D polytope which is the convex hull of its *m*+1 vertices $x_1, \ldots, x_{m+1}$:

$$S = \{x = a_1 x_1 + a_2 x_2 + \ldots + a_{m+1} x_{m+1},\ a_i \geq 0,\ \sum_{i=1}^{m+1} a_i = 1\}$$

E.g. a 2-simplex is a triangular, a 3-simplex is a tetrahedron. A set of points in R^n can be regarded as a collection of simplices or a simplicial complex.

Here $a = (a_1, a_2, \cdots, a_m)^T$ are called convex or barycentric coordinates of x with respect to $\{x_i\}$, which can be obtained as follows including the inverse of an $m \times m$ matrix X.

$$a = X^{-1}(x - x_{m+1}),\ X = (x_1 - x_{m+1}, \ldots, x_m - x_{m+1}) \quad (1)$$

E.g. m = 2 and m = 3, denote $x_i = (x_{i1}, \cdots, x_{im})^T$,

$$\begin{pmatrix} a_1 \\ a_2 \end{pmatrix} = \begin{pmatrix} x_{11} - x_{31} & x_{21} - x_{31} \\ x_{12} - x_{32} & x_{22} - x_{32} \end{pmatrix}^{-1} \begin{pmatrix} x_1 - x_{31} \\ x_2 - x_{32} \end{pmatrix} \quad (2)$$

$$\begin{pmatrix} a_1 \\ a_2 \\ a_3 \end{pmatrix} = \begin{pmatrix} x_{11} - x_{41} & x_{21} - x_{41} & x_{31} - x_{41} \\ x_{12} - x_{42} & x_{22} - x_{42} & x_{32} - x_{42} \\ x_{13} - x_{43} & x_{23} - x_{43} & x_{33} - x_{43} \end{pmatrix}^{-1} \begin{pmatrix} x_1 - x_{41} \\ x_2 - x_{42} \\ x_3 - x_{43} \end{pmatrix} \quad (3)$$

A point x lies insides the *m*-simplex if and only if all its barycentric coordinates $a_i \geq 0$.

A map $y = f(x)$ is a linear simplicial map if $f(x_i) = y_i, i = 1, \cdots, m+1$ and when $x = \sum_i a_i x_i,\ y = f(x) = \sum_i a_i y_i$. The linear simplicial maps then can be used to approximate C^0-class or continuous maps.

Characterization of a device is to produce a profile or a forward model as a map p from a device color space to the PCS or vice versa. Then calibration of the device is basically to apply the inverse map of p on the input color in PCS to compensate or correct the characteristics of the device in order to obtain a truthful color reproduction. E.g. for a display, the profile is measurements of the output RGB values for certain target colors in PCS. Such a forward map p is approximated by a linear simplicial map in 3D-LUT and the inverse map p^{-1} by tetrahedronal interpolation. Then an input x is first transformed to $z = p^{-1}(x)$ of which the output $p(z) = p \circ p^{-1}(x) = x$ reproduces the input faithfully.

The inverse f^{-1} of a linear simplicial f such that $x = f^{-1}(y)$ is also linear simplicial, which can be calculated as follows.

Given a point y, one needs first to find a simplex in which the point lies. Denote the vertices of the simplex as $y_1,\ldots,y_{m+1}, y_i = f(x_i)$. The second step is to calculate the barycentric coordinates b_i of y with respect to y_i such that $y=\sum_i b_i y_i$. The inverse map is then given by

$$x=f^{-1}(y):=\sum_i b_i x_i \tag{4}$$

Since $f(x)=\sum_i b_i f(x_i)=\sum_i b_i y_i = y$, the map (4) does give the inverse image of y.

2.2 Test if a point is inside a tetrahedron

In order to calculate the inverse map, a 3D-LUT requires to find the tetrahedron in which the input point x lies. This is however non-trivial for non-uniform grid which is the typical case for device calibration.

It is usually done by choosing a tetrahedron whose vertices are closted to x. Then calculate the convex coordinates a_i and check if the convex inclusion conditions $a_i \geq 0$ are satisfied. If not one needs to try another tetrahedron. In fact, since trials have to be repeated to avoid the cases shown in Figure 1(a), these calculations seemed to be the most time-consuming step in the 3D-LUT processing.

There are also other ways e.g. Amidror. I. (2002) to test if the straight line connecting x with a point lie in the tetrahedron intersects a face of the tetrahedron. x lies insides when there are no such a intersection for all 4 faces of the tetrahedron. However since the calculation to test the above intersection in a face or a triangular requires as the first step to calculate the convex coordinates of x with respect to the tetrahedron, this method seemed to be less efficient than direct application of the convex inclusion condition.

2.3 A new method to build a tetrahedron containing a point

Firstly, we reduce all 3D processings to 2D ones since calculations of barycentric coordinates and convex inclusion for triangulars are much easier than for tetrahedrones. Secondly, instead of repetition of test in which tetrahedron the input point lies, we directly produce a tetrahedron which contains the point without try-and-error.

To explain the idea, assume that an input point $x=(\alpha,\beta,\gamma)^T$ is given. Then one can draw a line λ through x in parallel to one coordinates axis e.g. X_1. Here we used X_1 as the L values in the CIELUV space. This line will intersect with two triangulars near to x. (We omit the lucky case when the line intersects a vertex or grid point of the triangulars.) In particular, the projections of the two triangulars onto the plane $[X_2, X_3]$ of the 2nd and the 3rd coordinates, which are two triangulars again will contain the projection (β,γ) of the input point x onto $[X_2, X_3]$. Search for these two triangulars is easy since it is virtually in the $[X_2, X_3]$ plane among the grid points whose the 2nd and the 3rd coordinates are close to (β,γ) We di this for the L levels below and about α.

Then we chose the desired tetrahedron with vertices of one of triangulars, e.g. $\langle x_1, x_2, x_3 \rangle$ and x_4 as the intersection point of the line λ with the other triangular. (See Figure 1(b)).

In fact, the barycentric coordinates of the intersection w between the line λ and the triangular $\{x_1, \ldots, x_3\}$ can be found the following 2D calculation.

Denote $x_i = (x_{i1}, x_{i2}, x_{i3})^T$

$$w = c_1 x_1 + c_2 x_2 + (1 - c_1 - c_2) x_3 \tag{5}$$

$$\begin{pmatrix} c_1 \\ c_2 \end{pmatrix} = \begin{pmatrix} x_{12} - x_{32} & x_{22} - x_{32} \\ x_{13} - x_{33} & x_{23} - x_{33} \end{pmatrix}^{-1} \begin{pmatrix} x_2 - x_{32} \\ x_3 - x_{33} \end{pmatrix} \tag{6}$$

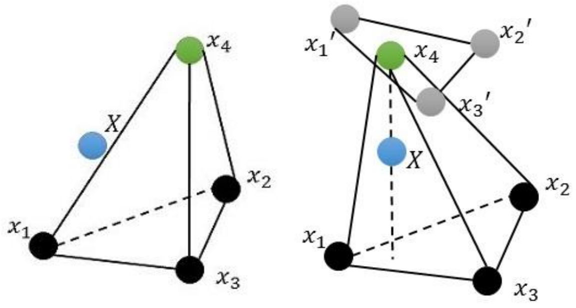

(a) x_4 is an invalid vertex *(b) x_4 as intersection of a line through X*

Figure 1: Build a tetrahedron containing a point X

Notice here that the inverse image of w under the profile map is the convex combination with the same barycentric coordinates of the inverse images of x_i.

2.4 Algorithm

The algorithm for display calibration with PCS as CIELUV space is described as follows:

Step 1: Build the profile or forward map by measurement on a display for target colors. The data are averaged among three measurements;

Step 2: For an input color $x = (\alpha, \beta, \gamma)^T$, for L levels below and above α, find the two triangular including (β, γ) in [$u^* v^*$] plane;

Step 3: Draw the line λ along L axis and find the fourth vertex x_4 by (6) therefore build the tetrahedron containing x;

Step 4: Calculate the convex coordinates of the input color x with respect to measured data by eq.(3);

Step 5: The inverse map (4) was applied to input color data as a preprocessing for color reproduction.

This algorithm is applied in three stages in the order of increasing complexity: firstly to $u^* v^*$ plane in CIELUV which we called 2D correction, secondly $u^* v^*$ and L axis separately which we called (2+1)D correction and finally the CIELUV space which we called the 3D correction.

2.5 Environment

Measurements and photos of the displays were all taken in a darkroom. CA-210 by KONICA MINOLTA was used as the colorimeter and each colorimetry value was obtained from average of three measurements. The target colors are consisted of 695 sample points on CIELUV space derived from 113 lattice points on the $u^* v^*$ chromaticity plane and 11 levels of brightness as L = 25, 30, …, 75. Furthermore, color difference between input color data and measured color data was evaluated by the distance ΔE in CIELUV space. E.g. for

$a = (L_a, u_a, v_a)$ and $b = (L_b, u_b, v_b)$, $\Delta E = \sqrt{(L_a - L_b)^2 + (u_a - u_b)^2 + (v_a - v_b)^2}$.

3. EXPERIMENTAL RESULT

Experiments on single color input and natural image are conducted for evaluation.

The table 1 shows the result applying the proposed method on 695 target colors. The color difference between input color and output color measured on display are shown for colors under calibration. The proposed method is compared with Spyder4Elite, a commercially available ICC profile maker. The proposed methods provided very closer reproduction of the input in 2D, (2+1)D and 3D cases. In Figure 2, we show the photos of two displays both showing the same color input twice on top and bottom. The top images are without calibration and the bottom were calibrated color. The improvement of agreement between the two displays can be easily observed.

Table 1: Comparison of color difference on displaying single color input

	Spyder4Elite	2D calibration	3D calibration	(2+1)D calibration
Average ΔE	16.415	7.255	1.712	3.361
Standard Deviation	7.806	1.039	1.245	1.938
Max ΔE	38.440	11.646	10.577	16.606
Min ΔE	1.070	4.147	0.200	0.284

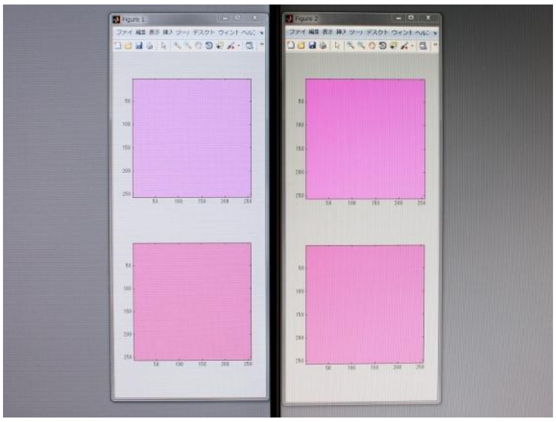

Figure 2: Comparison of the outputs of a single color input before and after calibration

Result of applying proposed method to natural images are shown in Figure 3.

Figure 3: Comparison of a natural image before and after calibration

ACKNOWLEDGEMENTS

The authors wish to thank Takehiro NAKATSUE, Hiroaki ETO of Sony Corporation for information on 3D-LUT and literatures Kang H.R. (1996), Aristova A. (2010).

REFERENCES

Green, P. 2010. *Color Management Understanding and Using ICC Profiles.* New Jersey: Wiley.

Kang, H.R. 1996. *Color Technology For Electronic Imaging Devices*. Washington: SPIE.

Aristova, A. 2010. Smoothness of color transformations. Available online, hdl.handle.net/11250/144133. Accessed: January 21, 2015.

Barsotti, J, T. Schulte. 2014. Display Profiling Solutions A Report On 3D LUT Creation. Available online, www.spectracal.com/Documents/White%20Papers/Display%20Profiling%20Solutions.pdf. Accessed: January 23, 2015.

Lee H.C. 2005. *Introduction to Color Imaging Science*. Cambridge: Cambridge University Press.

Amidror, I. 2002. Scattered data interpolation method for electronic imaging systems: a survey. *Journal of Electronic Imaging* 11(2): 157-176.

Yamamoto, M., J. Chao. 2014. Construction of display profiles using simplicial maps and application to color reproduction of displays. In *Proceedings of 29th SIP SYMPOSIUM*, IEICE Japan: Kyoto, 393-398.

Address: Prof. Jinhui CHAO, Faculty of Science and Engineering,
Chuo University, 1-13-27, Kasuga, Bunkyo-ku, Tokyo, 112-8551, JAPAN
E-mails: a10.7tb8@g.chuo-u.ac.jp, jchao@ise.chuo-u.ac.jp

"Psycolorsynthesis": An Introduction of 10-Color Communication Method

Chiori OHNAKA
Office Color Palette

ABSTRACT

"Psycolorsynthesis" is a newly developed concept derived from psychosynthesis. While harmonizing one's plural selves to attain integration of the personality is what Assagioli (1965) calls psychosynthesis, this paper shows that colors can play a critical role to attain this integration. 10-color communication method is introduced to demonstrate that colors enhance the awareness of self as well as others' understandings. And this awareness brings about personality integration. The method applies colors as an effective medium for people to express themselves regardless of their social status and contexts. The method calls for a workshop with a group of 8 to 12 people, and let each of them use a set of color cards (normally about 200 colors). It consists of two modules: communication with self by making a color identification data (ID) arranged from 10 selected favorite colors and communication with others by giving 2 colors to other participants as a gift.

Data collected from more than 300 workshop participants identify that approximately 80% of them show clear correlations between 10 self-selected favorite colors and colors received from others as a gift. In addition, workshop observation suggests that communication with a medium of colors clearly enhance relaxed interactions among participants and result in becoming aware of self and others. 10-color communication method demonstrates that the power of colors can overcome risks, worries, and fears that

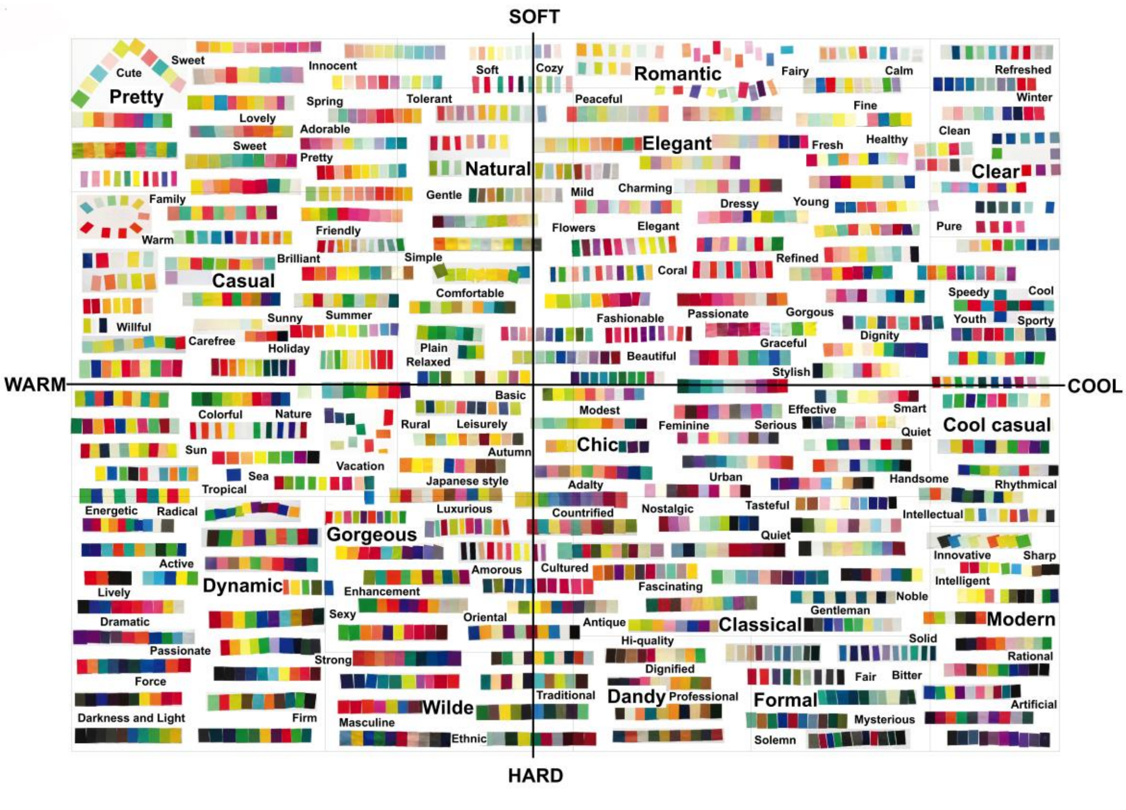

Figure1

people have deal with when they attempt to share their inner-colors. When colors applied to people as their representations, each color-ID (representing each person) is unique and distinctive, for which nobody can say better or worse compared with others' color-IDs (representing other persons). This communication method can effectively be applied to improve the practices of social activities such as recruiting and counseling.

1. INTRODUCTION

This paper introduces a new color communication method and shows, with the evidence of collected data, that the method can be an effective way for enhancing the awareness of self as well as others' understandings. In 10-color communication method that this paper introduces, colors are used as representations of one's multiple aspects of inner-selves (hereafter "inner-colors"). While mutual understanding is the essential goal of communication, few can actually understand self, let alone understand others. To begin with, one may not necessarily express one's feelings and thoughts freely due to socially expected norms and/or conflicting interests that one might have vis-à-vis others. This paper shows that colors enable people, regardless of their social status and contexts, to express themselves through inner-colors freely and to gain self-confidence The data collected from the communication workshops show that this straightforward method not only develops the awareness of self and others' understandings but also and more importantly provides participants with self-synthesizing and healing experiences. In this regard, this method can be named "psycolorsynthesis" after psychosynthesis (Assagioli, 1965).

The paper firstly explains the two modules of 10-color communication workshop and color-IDs, followed by the results of the workshop to show features of color-IDs and remarkable findings of color correlations. The paper then suggests how 10-color communication can potentially be effective when applied to social practices such as recruiting and counseling.

2. METHOD

The method calls for a workshop with a group of 8 to 12 people, and let each of them use a set of color cards[1]. It consists of two modules of communication as follows.

2.1 Module1: Communication with self

For the first module, each participant is asked to select 10 favorite colors, cut them squarely from the provided color card set, paste the selected 10 color pieces on a sheet straightly in his/her own favorite arrangement with glue. A frequently asked question is if selected color cards shall be arranged in order of his/her preference. And its answer is to arrange straightly as one feels the color-ID the most beautiful. This method specifically uses 10 colors for the following reason; while beautiful color combinations are two-color, three-color, four-color, five-color, and six-color combinations, a ten-color-ID can contain combinations such as 2-2-2-2-2, 3-3-4, 5-5, 6-4, 2-2-2-4, and so forth. Thus, not only mere color combinations but also groupings of the combinations show the feature of one's personalities and patterns.

---

[1] "Color Cards 199a " produced by Japan Color Enterprise Co., LTD contains 199 selected colors based on Practical Color Co-ordinate System(PCCS) and better serves for this workshop.

Once color-IDs are made, participants take a close look at each of their color-IDs that are sticked on a board, express in words whatever they intuitively sense and feel for each color-ID. Words can be nouns, adjectives, and short sentences. For example, "I feel bright like Sun shine." When participants express in words for each color-ID, each participant takes notes what others say about his/her own color-ID.

2.2 Module2: Communication with others

For the second module, each participant selects two colors that most fit the image of each of other participants, and then cut the two colors in square and give them to the participant as a gift. In this way, everybody receives two colors each from other participants. Each participant pastes all the received color squares on a sheet as he/she likes. Then, again, participants take a close look at each of the sheets sticked on a board, express in words for each of the sheets. When participants received colors and then received words for collected colors, participants realize how they are perceived by others. Finally, participants take out their own color-ID sheets and gifted color-square sheets from the board, and compare and analyze these two sets of colors.

3. RESULTS AND DISCUSSION

3.1 Color-IDs representing diverse inner-colors

In Module1, when participants expressed their feelings for each color-ID, they could talk freely as if they were playing a game. Participants shared many inspiring words to enjoy this process. On the other hand, when a participant took his/her turn to receive words from others, the participant realized that each word received from others was a representation of him/her-self. Through receiving many words, each participant becomes aware of one's inner-selves.

Color-IDs on Figure 1 are 188 (65 men and 123 women in the age range of between 20s and 50s) sample results collected from Module1 color communication workshops conducted for Japanese. Presented words for color-IDs mean that popular words that the owners of color-IDs received from other participants. This figure shows that they are all unique, different, and extremely diverse[2]. Yet, careful observation offers some tendencies.

Figure2

Color-IDs of women tend to be found in areas with presented words such as "Cute," "Pretty," and "Casual," while those of men are found in areas with "Dynamic," "Classical, "Cool. Having said that though, color-IDs for both women and men can be found any areas in the figure. Thus, one cannot identify men/women from color-IDs.

[2] Total possible combination is more than 10^{29}, while the total world population is about 10^{10}.

Color-IDs on Figure 2 are collected from 20 female university students. Looking at these color-IDs, people imagine words in mind. Women are likely to express their feelings in words. At beginning, theorists might feel not at ease finding words, yet colors gradually relax them to utter words as they feel. Some people are rather reserved to express their feelings. For this color communication workshop, however, it was observed that the bulk of participants were comfortable to express their feelings in words about presented color-IDs. As far as their topic was color-IDs, they seemed not to have any hesitation to share their feelings. Color-IDs are independent from their social positions and have an affinity for intuitive feelings. Participants apparently felt at home. They were talkative and open-minded as they enjoyed pleasant interactions. Many participants said that this communicative interactions to express and receive feelings each other were a healing experience.

Figure3

Color-IDs on Figure 3 are collected from 20 men. Which color-IDs are atttrative for you? What do you imagine persons making these color-IDs? Because color-IDs are simple and visual, anybody can participate in sharing feelings. Through color-IDs, people appreciate the diverisity of people's identities.

3.2 Comparing and analyzing results of Module1 and Module2

Figure 4 shows 15 color-IDs (from Module1) and corresponding 15 sets of colors that each participant received from others (from Module2). The 15 participants consist of 13 female university students, a lecturer, and a professor. The more colors one receives from others, the more one can understand one's inner-colors that are reflected on one's appearance. While vividness and brightness of one's inner-colors may change according to the time place, occasion and physical condition to some extent, their hue basically remains more or less the same. As one practices this workshop several times, one can realize one's inner-colors' patterns. One's preference, ways of thinking, and behavioral patterns are reflected in one's color arrangement. The comparison between one's own color-ID and colors received from others remarkably shows that many of them have resembling compositions to a great extent. This result suggests that one's inner-colors, which are practically invisible, are actually appearing outside oneself, and thus, others can sense one's inner-colors from one's appearance and express them in colors with a significant degree of accuracy.

Experiencing this remarkable result leads participants to astonishingly realize that their inner-colors are visualized by others. One can become aware of inner-colors of others, which people would not expect to be aware of. Inner-colors, which one thinks that one may hide as far as one does not express, can actually be aware of by others through one's appearance, atmosphere, behavior, voices, etc. When the impression of color-ID differs from that of colors one receives, the difference suggests that one have an unrecognized inner-colors that others can visualize. Does that mean that one does not realize one's own appealing selves? Or does one show a different image of selves to others? This, in any event, provides one with a valuable opportunity to become aware of selves through realizing how one is perceived by others.

Through this workshop, participants understand that color-IDs make their invisible subconscious mind visible. This experience makes each participant begin to become his/her own self-counselor. That one can visualize one's inner-colors through one's color-ID provides an opportunity for the one to critically reflect oneself for personal growth. Participants also become aware that people have intuitive abilities to read "invisible." This is not supernatural power. People have intuition to read others' inner-colors. Colors can convey one's inner-selves to others.

3.3 Practical applications

(1)*Recruiting*: 10-color communication method can benefit both recuiting companies and applicants because it removes unnecessary biases from recruiting processes. Computer based recruiting methods that analyze one's expected performance based on sexes, ages, academic background, working histories, obtained licenses, etc. tend to only appreciate talents appeared on selected aspects of abilities. Semantic differential (SD) method, which has widely been applied in a broad range of practices, tends to strengthen dichotomies such as good-bad, strong-weak, superior-inferior, and to develop unnecessary hierarchy due largely to its linear relationships. It would be fine to apply SD method for analyzing the tendency of personalities. However, applying SD method for recruitment may be problematic as people who happen to be allocated at the top of the unnecessary hierarchy are selected despite the fact that it does not necessarily make sense.

Figure 4

This may obvioulsy result in mismatched recruiting due to the lack of matching personalities to expected yet unwritten subtle tasks that a given job position requires. In contrast, complementary and neighboring color relationships of a color wheel, and the theory of color harmony never creates hierarchy. The concept of color harmony suggests creativity from mixing colors and mutual enhancement from complementary colors.

Analyzing his/her color-ID that is obtained through 10-color communication method, his/her personal features can much accurately be understood. The power of colors can eliminate unnecessary hierarchical biases. Thus, taking visualized inner-colors in account when matching a person to a specific job works for the benefit of both recruiting companies and applicants through sound selection processes.

(2)*Counseling*: 10-color communication method can effectively be applied to personal counseling. People naturally arrange colors in a way they feel beautiful. Through this arrangement, one is coordinating to harmonize plural selves inside. This coordination is what Assagioli (1965) calls psychosynthesis. The process of becoming aware of self through the color communication workshop resembles psychosynthesis that asserts "the direct experience of the self, of pure self-awareness …. is true." While Assagioli (2007) emphasizes the possibility of progressive integration of the personality, 10-color communication method contributes to the awareness of self as well as others, which, in turn, brings about the integration of the personality. In this regard, this 10-color communication method can be called "psycolorsynthesis."

4. CONCLUSIONS

The author conducted 10-color communication workshops for a total of more than 300 people. The paper has shown that this method contribute to become aware of self and others' understandings. Specific findings from the workshops and collected data are follows: (1) color-IDs can represent inner-selves of people, (2) results of color-IDs show that they are all unique, distinctive, and extremely diverse, (3) about 80% of sample data showed clear correlations between color-IDs and received colors, (4) one's inner-colors, which are invisible, is actually appearing outside oneself, and therefore, others can sense one's inner-colors from one's appearance and express in colors with a significant degree of accuracy, (5) 10-color communication method can enhance participants to actively engage in communicative interactions with other participants, (6) through communication with a medium of color-IDs, participants can overcome risks, fears, and worries that they face when they attempt to share their inner-selves, (7) the method provides an opportunity for participants to reflect their own inner-colors in a way they can use for their personal growth, (8) the method has significant potential to make recruiting and counseling more effective.

ACKNOWLEDGEMENTS

I thank all participants of the workshops. Without their participation, I could not have even thought of writing this paper. It is because astonishing and inspiring experiences that they enjoyed, I decided to share the power of colors through AIC2015 poster session.

REFERENCES

Assagioli, Robert. 1965. *Psychosynthesis.* Penguin books.
Assagioli, Robert. 1973. *The Act of Will.* Synthesis Center Press.

Address: Chiori Ohnaka, Office Color Palette
Ariake1-4-11-203, Koto-ku, Tokyo, 135-0063, JAPAN
E-mail: chiori@officecolorpalette.com

Perceptually inspired gamut mapping between any gamuts with any intersection

Javier VAZQUEZ-CORRAL, Marcelo BERTALMÍO
Information and Telecommunication Technologies Department, Universitat Pompeu Fabra, SPAIN

ABSTRACT

Gamut mapping transforms the color of an input image within the range of a target device. A huge amount of research has been devoted to two subproblems that arise from this general one: gamut reduction and gamut extension. Gamut reduction algorithms convert the input image to a new gamut that fits inside the one of the image , i.e. the gamuts' intersection is equal to the target gamut, while gamut extension algorithms convert the input image to a gamut that embodies the original image gamut, i.e. the gamuts' intersection is equal to the source gamut. In contrast to the two aforementioned cases, very little attention has been paid to the most general problem, where the intersection of source and target gamut is not equal to one of the two gamuts. In this paper we address this most general problem of gamut mapping between any two gamuts presenting any possible intersection. To deal with this problem we unify the gamut extension and gamut reduction algorithms presented in Zamir –et al- (Zamir 2014), which are based in the perceptually inspired variational framework of Bertalmío –et al- (Bertalmío 2007) that presents three competing terms; an attachment to the original data, a term for not-modifying the per-channel image mean (i.e. not modifying the white point), and a contrast enhancement term. In particular, in this paper we show how by defining a smooth transition on the contrast enhancement parameter over the chromaticity diagram we can simultaneously reduce the input gamut in some chromatic areas while increasing it in some other without introducing neither color artifacts nor halos.

1. INTRODUCTION

Gamut mapping is defined as the modification of the gamut of an input image to make it fit into a destination gamut. This problem is usually divided into two sub-problems that are treated separately: gamut reduction and gamut extension. The former is when the destination gamut is smaller than of the original image. This situation occurs both in the printing industry where images must be carefully mapped to those colors that are reproducible by the different inks and in the cinema industry where cinema footage needs to be passed through a gamut reduction method in order to be displayed on a television screen (Kennel 2007). Conversely, gamut extension is devoted to the case where the destination gamut is bigger. This is currently needed for state-of-the-art cinema projectors which are able to display a wider variety of color than those obtained by cameras.

There exist a huge number of gamut reduction algorithms and just a few gamut extension algorithms in the literature and we refer the reader to the book of Morovic (Morovic 2008) for a detailed explanation of them. Gamut reduction algorihms are usually divided into two classes: global (or non-local, non-adaptative) and local (or adaptative). Global methods involve point-to-point mapping of colors from source to target gamut. In contrast, local methods share two important properties of human perception: i), they better preserve the color gradient between two out-of-gamut colors instead of mapping them to the same in-gamut color and ii), two out-of-gamut colors with identical lightness and chromaticity map to two different in-gamut colors depending on their spatial context in the image. Recently, Zamir -et al- (Zamir 2014) presented a local method that is based on a perceptually based contrast reduction of the colors. This method was also modified to take into consideration the saliency of the original image (Vazquez-Corral 2014). Regarding gamut extension, the simplest method consists of simply taking any GRA and use the one-to-one mapping in the reverse direction to perform gamut extension, as Morovic comments in his book. Other methods that exist in the literature are (Kang 2003, Kim 2004, Laird 2009). Recently, Zamir -et al- showed how that by modifying the contrast parameter on their reduction method, a gamut expansion method was obtained (Zamir 2014, Zamir 2015).

In this work we do not focus on any of these two particular problems, but in the most general one: the case where the intersection between the two gamuts is not one of them (this intersection is the destination gamut in case of the reduction, and the image gamut in case of the extension). In particular, we explain how we can introduced some locality in the algorithms of Zamir -et al- in order to simultaneously perform reduction on those parts of the original image that exceed the destination gamut whilst performing extension on those parts of the image that are in the surface of the image gamut but far from the destination gamut. In particular, we will show the ability of this method to harmonize different images.

The paper is organized as follows. In the next section we explain the Zamir -et al- methodology. Later on, we explain how we introduce locality which allows us to extend or reduce each of the parts of the image. Results are presented in section 4. Finally in section 5 we sum up the conclusion of this work.

2. ZAMIR –ET AL- METHOD

Zamir –et al- (Zamir 2014) method is a modification of the perceptually-inspired image energy functional defined in Bertalmío -et al- (Bertalmio 2007). In particular, the image energy functional considered is Zamir –et al- is

$$E(I) = \frac{\alpha}{2}\sum_x (I(x)-\mu)^2 - \frac{\gamma}{2}\sum_x\sum_y w(x,y)|I(x)-I(y)| + \frac{\beta}{2}\sum_x (I(x)-I_0(x))^2 \tag{1}$$

where α and β are constant and positive weights, γ is a constant and real weight, I is a color channel (R, G or B), w(x,y) is a normalized Gaussian kernel of standard deviation σ, I_0 is the original image, μ is the mean average of the original image, and I(x) and I(y) are two intensity levels at pixel locations x and y respectively.

The resulting evolution equation for the previous functional can be expressed as

$$I^{k+1}(x) = \frac{I^k(x) + \Delta t\left(\alpha\mu + \beta I_0(x) + \frac{\gamma}{2}R_{I^k}(x)\right)}{1+\Delta t(\alpha+\beta)} \tag{2}$$

where the initial condition is $I^{k=0}(x) = I_0(x)$. The function $R_{I^k}(x)$ indicates the contrast function:

$$R_{I^k}(x) = \frac{\sum_{y\in\Im} w(x,y)s\left(I^k(x) - I^k(y)\right)}{\sum_{y\in\Im} w(x,y)} \tag{3}$$

where x is a fixed image pixel and y varies across the image domain. The slope function s() is a regularized approximation to the sign function, which appears as it is the derivative of the absolute value function in the second term of the functional; in (Bertalmio 2007) they choose for s() a polynomial of degree 7.

Zamir –et al- presented the importance of the weighting parameter of the contrast term (γ) for the gamut mapping problem. In particular, they showed that for γ smaller than 0, the gamut of the image was reduced, while for γ bigger than 0, the gamut of the image was extended. Moreover, they also showed that the smaller the value of γ, the smaller the gamut of the resulting image.

Zamir –et al- therefore chose a set of γ values smaller than 0 for creating a gamut reduction algorithm and a set of γ values bigger than 0 for creating a gamut extension algorithm. They, however, did not try study the case of selecting both negative and positive values of the γ parameter for the same image, in order to obtain a more general gamut mapping algorithm. This problem is the one we are tackling in this paper. In the next section we explain how given an input image and a target gamut (coming from a different image or from a display) a local γ value for each image pixel can be obtained, allowing the method to perform reduction in some parts of the image and extension in the others.

3. LOCAL CONTRAST COEFFICIENTS

To start with let us shed some light in the situation we will face. Let us call Y_1 the gamut of the image to modify and Y_2 the gamut we want to obtain. When plotting these gamuts in the chromaticity diagram three different regions will be presented. The first region will be the one where both gamuts intersect, and we denote it as Φ. The second region will present those colors in the input image that are not presented in the destination gamut. We call this region Ψ. Finally, the last region, that will call Ω, will be formed by the colors present in the destination gamut that are not present in the input image. Therefore, our goal is to reduce section Ψ while at the same time increasing section Φ to cover the section Ω. In other words, we want to reduce those colors presented only in the input image, while at the same time, expanding colors of the input image presented in the destination gamut to cover the full destination gamut. An illustration of the aforementioned procedure can be found in Figure 1.

Mathematically, we will proceed as follows to obtain the γ value corresponding to each chromatic color. First, we erode the region Φ to obtain the core region of the intersection between the two gamuts.

$$\Phi_{er} = \Phi \oplus D_\tau \tag{4}$$

where D_τ is a disk of radius τ.

Then, we define those points where we want to perform a bigger reduction, i.e., the points of section Ψ that are at a further distance of Φ, and we will give them a value that depends on the minima gamma we consider (γ_{min}). In particular, if we call Γ the map of the

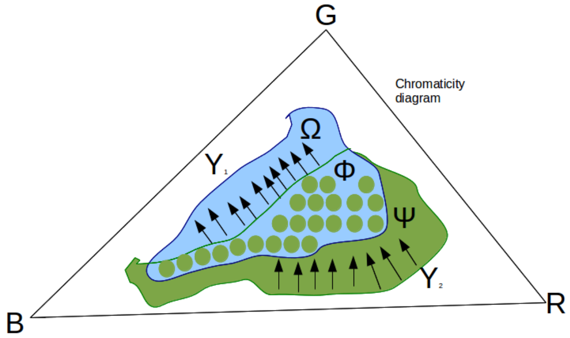

Figure 1: Explanation of the different regions found in our problem. See first paragraph of section 3 for details.

different gammas presented in the chromaticity diagram, and we call z any point presented in the chromaticity diagram, we obtain

$$\Gamma(z) = \left\{ \gamma_{min} \cdot \frac{d(z, \Phi_{er})}{\max_{\hat{z} \in \Psi}(d(\hat{z}, \Phi_{er}))} \right\} \; if \; z \in \Psi and \; \frac{d(z, \Phi_{er})}{\max_{\hat{z} \in \Psi}(d(\hat{z}, \Phi_{er}))} < \delta_1 \quad (5)$$

where all the values obtained will be negative.

Later, we look for the points in Φ that are in the border with respect to Ω. These points are the ones where we want to perform a bigger expansion to cover the region Ω. Their value will be based on the maxima gamma we consider (γ_{max}).

$$\Gamma(z) = \left\{ \gamma_{max} \cdot \left(1 - \frac{d(z, \Omega)}{\max_{\hat{z} \in \Phi}(d(\hat{z}, \Omega))} \right) \right\} \; if \; z \in \Phi \; and \; \frac{d(z, \Omega)}{min_{\hat{z} \in \Phi}(d(\hat{z}, \Omega))} < \delta_2 \quad (6)$$

where all the values obtained will be positive.

Finally, we look for the points we want to keep static when performing our method.

$$\Gamma(z) = 0 \; if \; z \in \Phi_{er} \quad (7)$$

Once all these different values have been defined in the matrix Γ, all the rest of the values are obtained by interpolation. Finally, for each pixel of the input image, its gamma value is obtained by searching its correspondence in Γ.

4. RESULTS

Figure 2 shows a result of our method. In the upper row of the figure we show the input image (left), the image from where we obtain the reference gamut (right) and the result of our method (center). In the bottom row we present: i) left: the gamut intersection between the images, where the red region represents Φ, the yellow region represents Ψ, and the blue region Ω represent, ii) center: the map of Γ, and iii) an image with the gammas used at each pixel. We would like to fix the reader attention both in the sky and in the sand, where our method is able to match the colors of the original image to those of the reference one. The parameters used in this image are δ_1=0.25, δ_2= 2, σ=3, γ_{max} =0.3, and γ_{min} =-0.75.

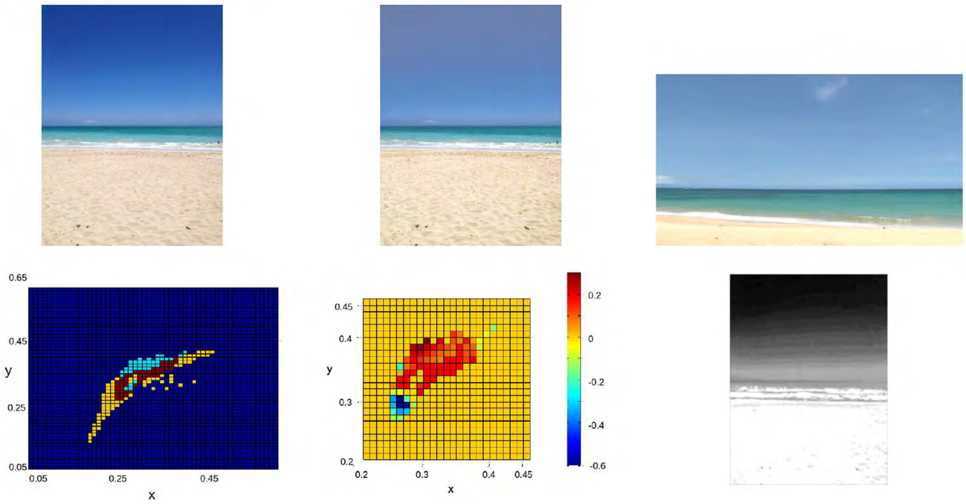

Figure 2: Results of our method. Upper row: Input image (left), Reference image (right) and our result (center). Bottom row: the gamut intersection between the images, where the red represents Φ, yellow represents Ψ, and blue represents Ω (left) , the map of Γ, (center) and the gammas at each pixel (right).

More results are presented in Figure 3, where we show the input image (left), the reference image from where the gamut is obtained (right), and our result (center). Again, we want to notice our ability to match the original image to look closer to the reference image. In thefirst case, we see how the white color has tent to the yellow of the reference image, while the blue has got the electric tone of the tub. In the second image, the orangish background has been moved towards the red of the reference image. Finally, in the last one, blue of the sky has been modified as there have been also modified other regions of the input image to look greener.

5. CONCLUSIONS

In this work we have presented a modification of Zamir –et al- algorithms in order to perform full gamut mapping, i.e., to being able to simultaneously reduce gamut of colors in some parts of the image while extending the colors in some other parts. The results presented are promising. Some future lines to improve our results may be the consideration of the full 3D gamut (a first attempt is presented in Figure 4) and the search of further applications such as semantic transfer.

ACKNOWLEDGEMETS

This work was supported by the European Research Council, Starting Grant ref.306337, by the Spanish Government, grant red.TIN2012-38112, and by the Icrea Academia Award.

REFERENCES

M. Bertalmío, V. Caselles, E. Provenzi, and A. Rizzi. 2007. *Perceptual color correction through variational techniques.* IEEE Transactions on Image Processing, 6(4):1058–1072.

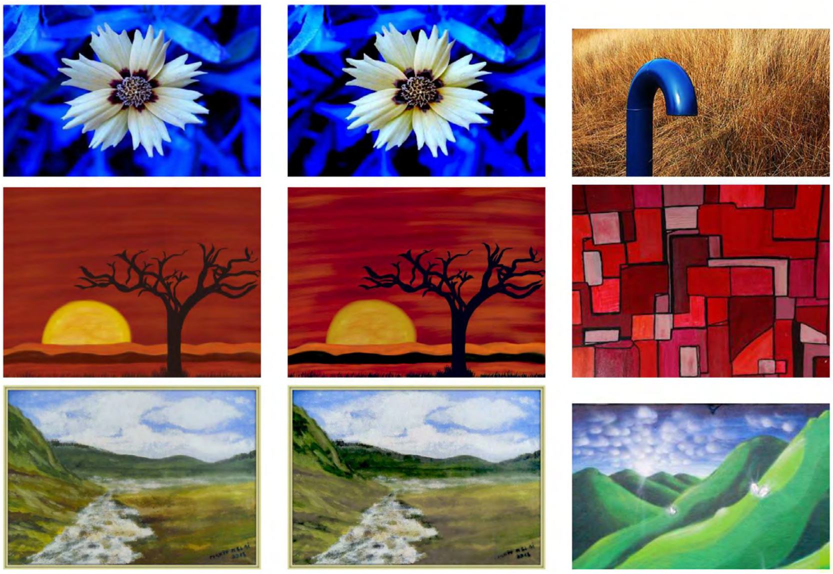

Figure 3: Results of our method. Left: original image. Right: reference image. Center: Our result

Figure 4: Example of the 3D case for our method. Left: original image. Right: reference image. Center: Our result

B. H. Kang, J. Morovic, M. R. Luo, and M. S. Cho. 2003. Gamut compression and extension algorithms based on observer experimental data. ETRI journal, 25(3):156–170.

G. Kennel. 2007. *Color and mastering for digital cinema: digital cinema industry handbook series*. Taylor & Francis US.

M. C. Kim, Y. C. Shin, Y. R. Song, S. J. Lee, and I. D. Kim. 2004. *Wide gamut multi-primary display for hdtv.* In Proc. of CGIV, pages 248–253.

J. Laird, R. Muijs, and J. Kuang. 2009. *Development and evaluation of gamut extension algorithms.* Color Research & Application, 34(6):443–451.

J. Morovic.2008. *Color gamut mapping,* Wiley.

J. Vazquez-Corral, S.Zamir, and M. Bertalmio. 2014. *Considering saliency in a perception inspired gamut reduction algorithm*. Is&T Color and Imaging Conference (CIC2014).

S. Zamir, J. Vazquez-Corral, and M. Bertalmio. 2014. *Gamut mapping in cinematography through perceptually-based contrast modification.* Selected Topics in Signal Processing, IEEE Journal of, 8(3):1–1

S. Zamir, J. Vazquez-Corral, and M. Bertalmio. 2015. *Gamut Extension for Cinema: psychophysical evaluation of the state of the art and a new algorithm*. IS&T/SPIE Electronic Imaging.

Address: Dr. Javier Vazquez-Corral, and Dr. Marcelo Bertalmío, Information and Telecommunication Technologies Department, Universitat Pompeu Fabra, Roc Boronat 138, 08018 Barcelona, Spain
E-mails: {javier.vazquez,marcelo.bertalmio}@upf.edu

Color Correction Operation for 3D Scanning Models

Kai-Lin Chan[1], Lin Lu[2], Tzung-Han Lin[1], Hung-Shing Chen[1, 2],
Chia-Pin Cueh[3], and Kang-Yu Liu[3]

[1] Graduate Institute of Color and Illumination Technology, National Taiwan University of Science and Technology

[2] Graduate Institute of Electro-optical Engineering, National Taiwan University of Science and Technology

[3] Printing Technology Research Institute, Taiwan

ABSTRACT

Color performance of 3D scanning model depends on color quality of the range images of a 3D object. In this study, color correction operation for 3D scanning models was established, which was composed of 2D color correction and 3D luminance correction Firstly, 2D color correction was executed, which contains lighting uniformity correction, gray balance correction and camera color correction. After 2D color correction, each range image is correction by 3D luminance correction considering its 3D depth information. A direct color measuring method using a 2D colorimeter is used to capture precise color information of the reference ColorChecker and the 3D object, which can apply to the proposed color correction operation.

1. INTRODUCTION

Nowadays, 3D scanner is capable of acquiring more realistic 3D objects. However, the color correction of 3D scanning models is still a challenging topic. The precise color reproduction of a 3D object highly depends on lighting conditions, material properties and geometrical shapes. To improve the color reproduction abilities of 3D object, we develop practice color correction operation for 3D scanning models by means of the using of 2D color correction and 3D luminance correction.

We initially fabricate a color 3D scanner based on a laser and a stereo camera, and we carry out the software for calculating 3D models. Likewise, this 3D scanner consists of a turntable with motor control unit, for rotating a 3D object to specific positions, and several LED white light bulbs. All the signal of construction is delivered by Arduino unit (Figure 1). During the 3D scanning process, eight range images of a 3D object are obtained and further integrated into one using digital 3D model [1].

Since color information of the scanning model is determined by the combination of all range images, the practice solution of the 2D color correction is useful for solving the color information. However, these color-calibrated 2D range images are still affected by 3D depth information of a 3D object. Therefore, another practice solution is to perform the 3D luminance correction. It is expected that the scanning model could make duplicate object achieve the same as the realistic object by means of the total color correction solution.

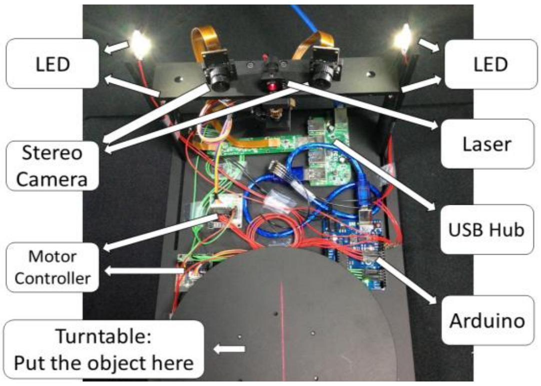

Figure 1: 3D scanner construction

2. METHOD

A 3D scanning system was developed in our laboratory. The 3D scanner is designed for scanning the object and taking the range images of the object by a set of stereo camera. Besides, the equipment and tools used in this study are arranged in Table 1.

Table 1: The equipment and tools in this study

No	Item	No	Item	No	Item
1	Topcon UA-1000A	2	X-rite ColorChecker Passport	3	3D printed Ball
					
4	X-rite SpectraLight III	5	X-rite White Balance Card		
					

In a 3D scanning process, we capture a color image, and then scan the object to obtain a series of full-color range images. To obtain a completed shape, the scanned object is rotated to eight specific positions by a turntable. Finally, all range images are merged into one solid model. However, in the merge process, the overlapped region may have duplicated vertexes and colors. To simplify the algorithm, we store the RGB color values for each vertex instead of for each polygon. To decide the reasonable color information of a vertex, we blend the colors which are from the projection positions of all visible images. In practice, the colors of all vertexes are set white after all scanned range images are merged. In this study, our developed color correction operation for 3D scanning models composes of 2D color correction and 3D luminance correction.

2.1 2D Color Correction

As mentioned above, the colors of the scanning models cover eight range images for a 3D object. Therefore, 2D color correction of scanning models depends on the calibrating colors of each range image. The standard ColorChecker was used, and its tristimulus values of 24 color patches emitted by D_{65} simulator in the light cabinet was measured by a 2D colorimeter (Topcon UA-1000A), which are regarded as the reference color values during 2D color correction process (Figure 3).

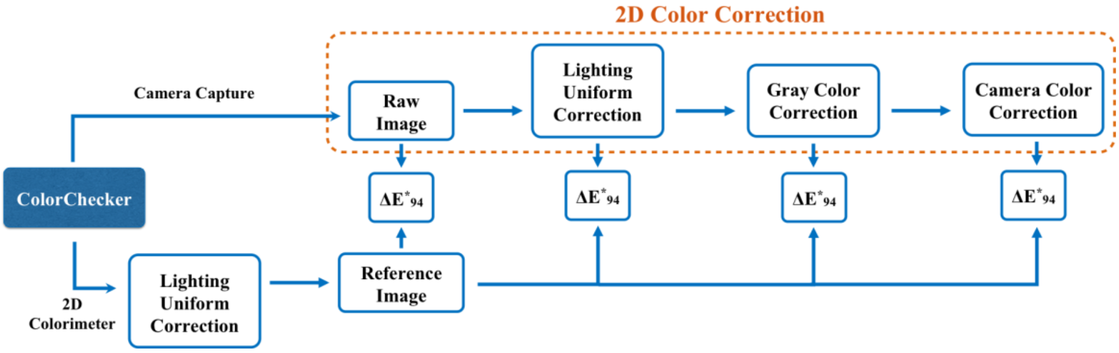

Figure 2: Schematic of 2D color correction

Lighting Uniformity Correction

Since the illuminant in light cabinet possibly irradiates on the white board non-uniformly in the beginning, the luminance distribution on ColorChecker would have the similar phenomenon. Due to the non-uniform luminance, the luminance and color information of a 3D object should not be reproduced accurately. To solve this problem, luminance uniformity should have a high priority at the first step for calibrating image. A uniform white board is placed at the same position of the object. When the background white was captured by a camera, its 8-bit RGB values can be converted to CIExyY. The Y distribution represents the lighting distribution of a range image. According to its original Y distribution, the inverse luminous mask (brightness compensating mask) can be designed to compensate the uniformity of a digitalized image. The original digital image was also converted to CIExyY. Its luminous distributions carry the entrywise product with the brightness compensating mask, then a digitalized image with lighting uniformity correction would be achieved.

Gray Balance Correction

The captured raw images look greener than normal one if the camera has no color calibration. To confirm this problem, the example of RGB tone curves was plotted using the six gray-scale patches on ColorChecker, as shown in Figure 3(a). At each luminance level, the green signal values are higher than red and blue signal values. Therefore, it is necessary to adjust RGB tone curves to the similar curve shape (Figure 3(b)).

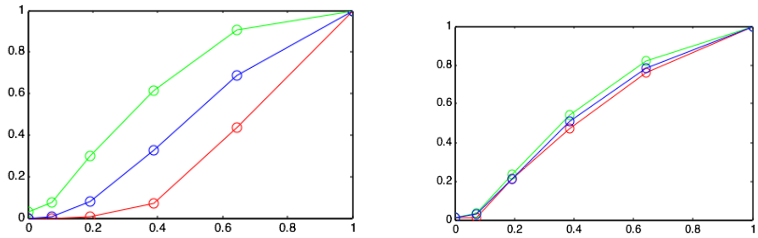

(a) Before correction (b) After correction

Figure 3: Gray-scale tone curves before and after gray balance correction

Camera Color Correction

After gray balance correction, the corrected image is only calibrated for gray-scale colors. The other colors on ColorChecker could be still error in comparison with the reference values. Therefore, we try to use polynomial regression to perform camera color correction. It is helpful for resolving an unknown matrix by two groups of known matrices by Eq. 1. If [A] and [B] are the known matrices, and [T] is the unknown matrix. Then [T] can be found by using Eq. 2. $[A]^T$ is transpose of [A], and $[A]^{-1}$ is the inverse of [A]. When the tristimulus values [X Y Z] of each range image's pixel with gray balance correction are set as the [A], and the target value is set as the [B]. Therefore, the computed [T] can make the tristimulus values of the input image be close to the target values.

$$[A] * [T] = [B] \quad (1)$$

$$[T] = ([A]^T * [A])^{-1} * [A]^T * [B] \quad (2)$$

Furthermore, [A] could be written by the forms of the 1st order regression in Eq. 3, or the 2nd order regression in Eq. 4 as follows.

$$[A]= [X, Y, Z, K] \text{ for 1st order regression} \quad (3)$$

$$[A]=[X^2, Y^2, Z^2, XY, YZ, XZ, X, Y, Z, K] \text{ for 2nd order regression} \quad (4)$$

Here, [B] is defined as [X Y Z], where XYZ are the vectors of the tristimulus values, which are translated from the 8-bit RGB values of an image according to sRGB standard, and K is the constant [2].

2.2 3D Luminance Correction

Before resolving the luminance problem caused by 3D depth of a real object, 2D color correction is necessary first. Then lightness difference (ΔL^*) is computed for checking the performances of the 3D luminance correction. Finally, all range images with 3D luminance correction are projected again to form the new 3D object using 3D scanning model (Figure 4). Firstly, the representative luminance values on the surface of a 3D object under the specific lighting condition were measured by a 2D colorimeter. The luminance values of 37 training points were chosen to obtain reference luminance values by using a 2D colorimeter capturing (Figure 5(a)). On the other hand, the luminance values at the same 37 positions on the captured range image after 2D color correction were computed (Figure 5(b)). Then the 2nd order regression similar to Eq. 1 was used to compute the correcting luminance values of the test image. Matrices [A] and [B] are described by Eq. 5, where Y means the luminance value.

$$[A] = [Y, Y^2]; \quad [B] = [Y] \tag{5}$$

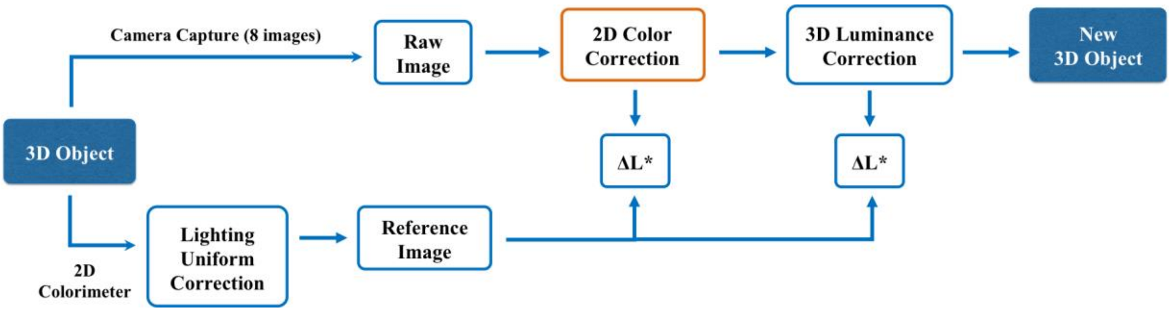

Figure 4: Schematic of 3D luminance correction

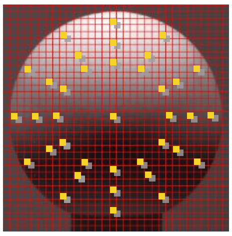

(a) Raw image

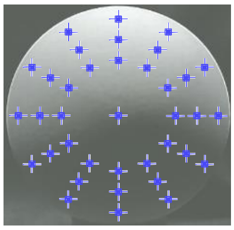

(b) Image after camera color correction

Figure 5: Training points for measuring luminance values

3. RESULTS AND DISCUSSION

The computed range images based on 2D color correction, which covered from raw image to camera color correction, are arranged in Table 2. Besides, the computed range images based on 3D luminance color correction are also arranged in Table 3.

Table 2: Images at 2D color correcting stages and color difference values

Stage	ColorChecker	3D Ball	ΔE^*_{94}
Raw Image	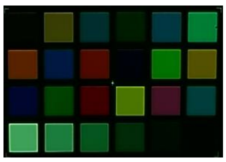		43
Luminance Uniformity Correction	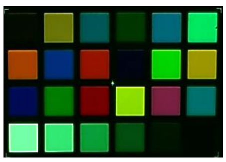		34
Gray Balance Correction	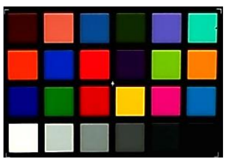		22

1st Order Regression			10
2nd Order Regression	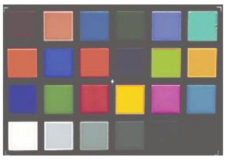		6

Table 3: Images of 3D luminance correction and the lightness difference (ΔL^*)

	Reference 2D Colorimeter	2D Color Correction	3D Luminance Correction
Image	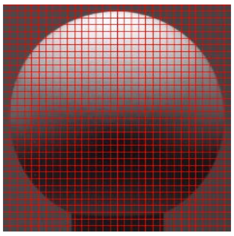	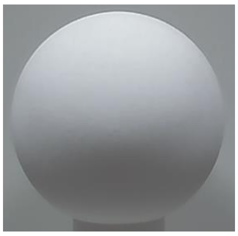	
ΔL^*	--	14	5

4. CONCLUSIONS

Color correction operations for 3D scanning system were developed, which made reproduced colors of a 3D object much better than non-calibrated colors. A direct color measuring method using a 2D colorimeter is used to capture precise color information of the standard ColorChecker and the 3D object, which can apply to the proposed color correction operation. The mean ΔE^*_{94} values were reduced from 43 to 6 after 2D color correction, and the mean ΔL^* values were reduced to 5 after 3D luminance correction. Future work is to correct not only 3D depth luminance but also the color shift problem of a real 3D object during 3D scanning process.

REFERENCES

[1] T. H. Lin, "Resolution adjustable 3D scanner based on stereo cameras," Asia Pacific Signal and Information Processing 2013, Kaohsiung, Taiwan, 2013.

[2] R.W.G Hunt and M. R. Pointer, Measuring Colour, 4th Edition, 2011

Postal address: Graduate Institute of Color and Illumination Technology,
No.43, Sec. 4, Keelung Rd., Da'an Dist., Taipei 106, Taiwan

E-mails: M10325002@mail.ntust.edu.tw, zmes159753@gmail.com, thl@mail.ntust.edu.tw, bridge@mail.ntust.edu.tw, james@ptri.org.tw, terryliu@ptri.org.tw

Correcting for induction phenomena on displays of different size

Marcelo BERTALMÍO
Universitat Pompeu Fabra, Spain

ABSTRACT

In this work we introduce a model for visual induction based on efficient coding and which elaborates on a previous approach. We show that this new model is able to qualitatively replicate psychophysical data on visual induction, and we propose a method by which an image can be pre-processed in a screen-size dependent way so that its perception, in terms of visual induction (i.e. ignoring the color capabilities of the displays), may remain constant across displays of different dimensions.

1. INTRODUCTION

In visual perception, induction designates the effect by which the lightness and chroma of an stimulus are affected by its surroundings. When the perception of an object shifts towards that of its surround the phenomenon is called assimilation; in the opposite case, when the perception of an object moves away from that of its neighborhood, we talk about contrast. Visual induction manifests itself both in achromatic and chromatic form, and the ocurrence of assimilation or contrast is determined by the spatial frequency of the stimulus (Helson 1963, Fach and Sharpe 1986), with assimilation being associated to large spatial frequencies and contrast to lower ones. There is evidence of neural activity at V1 that correlates with visual induction phenomena (Pereverzeva and Murray 2008).

A common observer looks at images on displays of vastly different sizes, from cinema screens to mobile phones, and in general the usual viewing distance is not proportional to screen dimensions. For instance, a comfortable distance to view a 50 inch TV screen may be 10 feet, or 120”, whereas for a mobile phone screen of 5 inches the usual viewing distance is around 15” (Heinonen 2013). This difference in the ratio of screen size over viewing distance implies a different angle of view for each screen, and therefore a change in the spatial frequency of the image content when viewed on different displays. As a consequence, the visual induction phenomena will also change from one screen to another: the same image may show significant assimilation effects when displayed on a screen, and less assimilation or even contrast when displayed on another.

In a recent work (Bertalmío 2014) we proposed a neural activity model which was able to predict lightness induction. It is in the form of the Wilson-Cowan equations (Wilson and Cowan 1972), that model the activity of neural populations along time and represent interactions with the use of a sigmoid function:

$$\frac{\partial a(x,t)}{\partial t} = -\alpha a(x,t) + \gamma \sum_{y} \omega(x,y) S(a(y,t))dy + \beta h(x,t) \qquad (1)$$

where **a** is the activity, x and y are cortical positions, t is time, w is a spatial summation kernel that decreases monotonically with distance, S is a sigmoid function in the range [0,1], **h** is an external input, and α, β,γ are constants. The work by Wilson and Cowan is very influential and has been used extensively for many different problems in computational neuroscience. Regarding vision in particular, Wilson and Cowan point out that their model reproduces several visual perception phenomena, including edge enhancement.

Bertalmío et al. (2007), in an image processing context, proposed the following evolution equation to perform local histogram equalization:

$$\frac{\partial a(x,t)}{\partial t} = -\alpha(a(x,t) - \frac{1}{2}) + \gamma \sum_y w(x,y)s(a(x,t) - a(y,t)) + \beta(h(x,t) - a(x,t)) \quad (2)$$

where **a** is an image channel (R,G or B), x and y are pixel coordinates, t is the evolution parameter, 1/2 is the target global mean average, w is a spatial summation kernel, s is a sigmoid function in the range [-1,1], **h** is the original image channel, and α,β,γ are constants. In this method, the input image **h** is processed by running the above evolution equation (with initial condition **a**=**h**) until steady state: the output image will be **a** at the last iteration step, when the evolution has stopped.

We can see then that this evolution equation has the form of the Wilson-Cowan equations, linking them to efficiency of representation, color constancy and the Retinex theory (Bertalmío et al. 2009, Bertalmío and Cowan 2009) and other visual perception phenomena. But as a limitation we must note that this method always increases contrast, so it's incapable of reproducing assimilation, as shown in Figure 1.

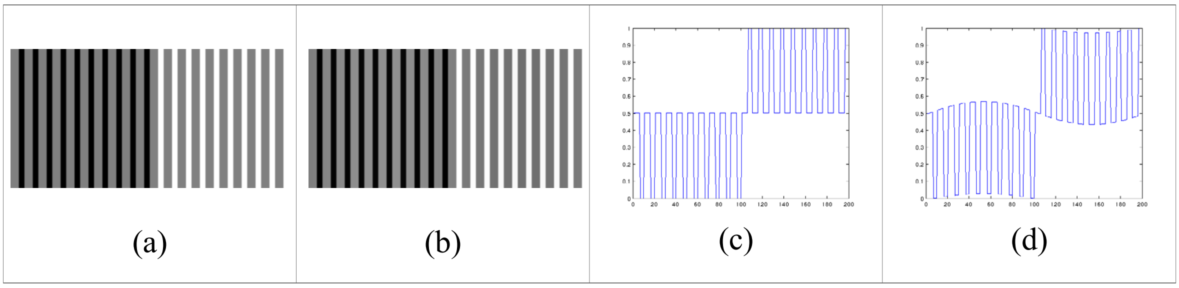

Figure 1: (a) Original image, example of lightness assimilation: the grey bars have all the same value but appear different over black and white backgrounds. (b) Result of applying the model of (Bertalmío et al. 2007) to image (a). (c) Profile of a line from image (a). (d) Profile of a line from image (b): notice how the model of (Bertalmío et al. 2007) actually emulates lightness contrast rather than assimilation. Figure taken from (Bertalmío 2014).

It was in order to overcome this issue that we recently proposed (Bertalmío 2014) the following modification:

$$\frac{\partial a(x,t)}{\partial t} = -\alpha(a(x,t) - \mu(x,t)) + \gamma(1 + (\sigma(x,t))^c) \sum_y w(x,y)s(a(x,t) - a(y,t)) + \beta(h(x,t) - a(x,t)) \quad (3)$$

where μ(x) is a Gaussian average, σ(x) is the local standard deviation and c is a global, fixed parameter. Results now show both assimilation and contrast, and the model is related to efficient coding by performing (local) histogram equalization, spectrum whitening and contrast enhancement. But the aforementioned changes to the 2007 model, specifically multiplying the contrast term by a weight depending on the local standard deviation, don't fit too well with the basic postulates of Wilson and Cowan's theory.

Our contribution in this work will then be to introduce a new model for visual induction that, while still based on efficient coding and the aforementioned approaches, is now able to comply better with the theory of Wilson and Cowan as well as to qualitatively replicate psychophysical data on assimilation and contrast results, both on achromatic and chromatic data. Finally, we will propose a method by which an image can be pre-processed in a screen-size dependent way so that its perception, in terms of visual induction (i.e. ignoring the color capabilities of the displays), may remain constant across displays of different dimensions.

2. METHOD

2.1 Proposed model

Going back to the generalized form of the Wilson-Cowan equations used in Bertalmío et al. (2007)

$$\frac{\partial a(x,t)}{\partial t} = -\alpha(a(x,t) - \frac{1}{2}) + \gamma \sum_y w(x,y)s(a(x,t) - a(y,t)) + \beta(h(x,t) - a(x,t)) \tag{4}$$

we replace the target global mean average 1/2 with μ(x), which is a local average:

$$\frac{\partial a(x,t)}{\partial t} = -\alpha(a(x,t) - \mu(x,t)) + \gamma \sum_y w(x,y)s(a(x,t) - a(y,t)) + \beta(h(x,t) - a(x,t)) \tag{5}$$

The value for μ(x,t) is computed by a convolution with a kernel K obtained as a weighted sum of two Gaussians, a wider one with less weight and a narrow one with larger weight, as shown in Figure 2.

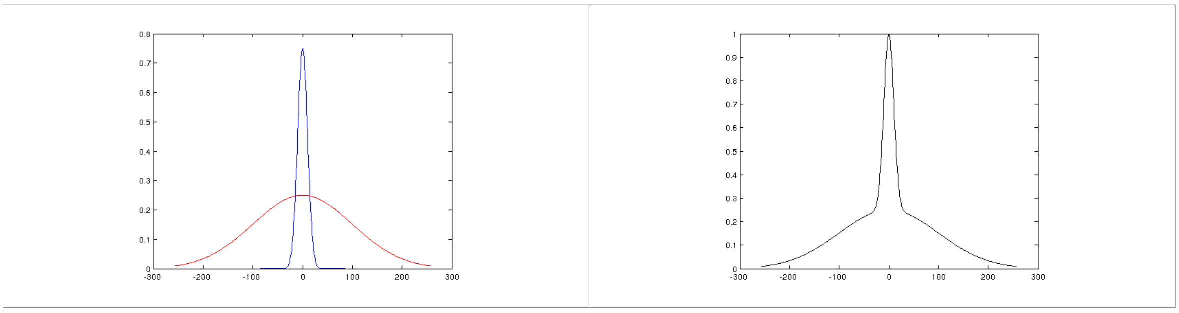

Figure 2: Left: scaled Gaussians. Right: resulting kernel K for computing the local mean.

The model given by Eq. (5) now complies with the basic postulates of Wilson-Cowan. Again, how we apply it in practice to an input image **h** is by running Eq. (5) to steady state, with **a**=**h** as initial condition, and the output will be the image **a** at the last iteration. The results thus obtained show both assimilation and contrast, as it can be seen in Figure 3 and Figure 4. We want to point out that all these achromatic and chromatic induction results have been obtained with the same set of parameter values and kernel sizes, i.e. the change from assimilation to contrast is only due to the spatial content of the images since the model is fixed.

2.2 Pre-correcting for changes in induction

With Eq. (5) we can qualitatively replicate the psychophysical results of the induction experiments of both (Helson 1963) for achromatic stimuli and (Fach and Sharpe 1986) for chromatic images. In both cases, observers were presented with stimuli consisting of gratings, identical bars over a uniform background, and reported the strongest assimilation effects for the largest spatial frequencies (thinnest bars); the strength of the effects would decrease with the increase in bar width, turning into contrast effects for wide bars. Using Eq. (5) we obtain the same type of results, as the green induction vs. bar-width plots in Figure 5 show.

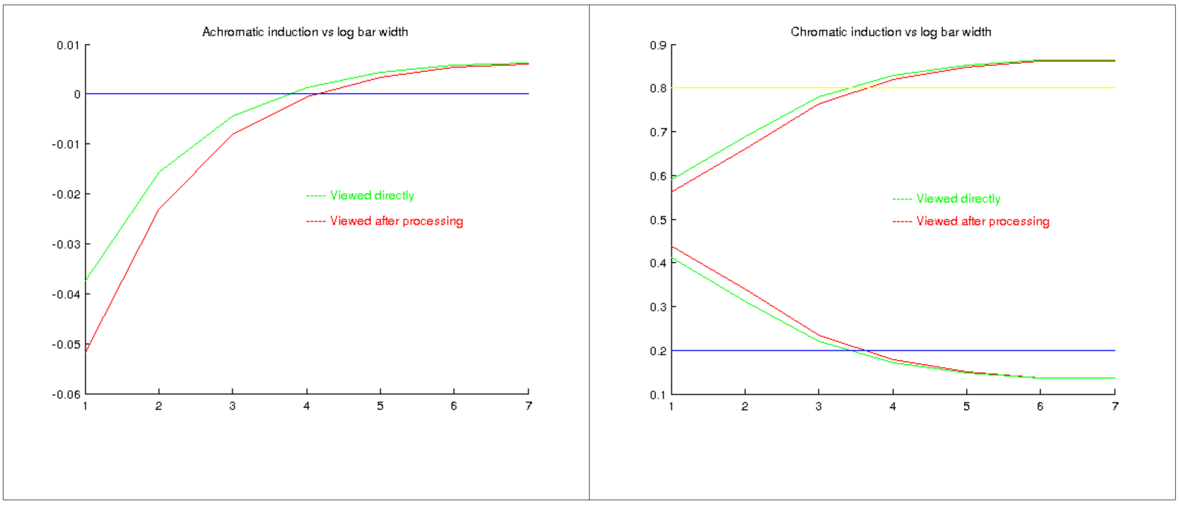

Figure 5: Predicting induction phenomena and correcting for changes in screen size. Left: achromatic grating, assimilation below blue line, contrast above blue line. Right: yellow-blue grating; top plots correspond to yellow, and yellow line separates assimilation from contrast effects; bottom plots correspond to blue, and blue line separates assimilation from contrast effects. Images in this figure approximate the plots of both (Helson 1963) for achromatic stimuli and (Fach and Sharpe 1986) for chromatic images, which were obtained through psychophysical tests.

Now for pre-correcting for changes in induction what we would need is the following. Given an image I, and with the correct choice of parameters, Eq. (5) will predict the induction effects that will be observed when looking at said image on a screen. If we now move away from the screen or, equivalently, look at the image on a screen of smaller size, the spatial frequencies of the image will increase and therefore Eq. (5) will predict a shift towards assimilation effects. Then what we would want to have is a pre-processing technique that applied to I produces an image I' whose induction vs. bar-width plot moves to the right. This would imply that the same induction effects would be seen by looking at I on the large screen as by looking at I' on the small screen. It turns out that what we need to do as pre-processing is simply to run the same Eq. (5) but with a different choice of parameters: giving more weight to (and reducing the standard deviation of) the Gaussian of kernel K which has smaller width, and reducing the value of the parameter β, which sets the strength of the contrast term. Example of plot shifts produced with this technique can be seen in red in Figure 5.

4. CONCLUSIONS

We have presented a method, related to neural models of vision and efficient coding in the visual system, that is able to qualitatively replicate psychophysical data on visual induction. We have also proposed a technique by which an image can be pre-processed in a screen-size dependent way so that its perception, in terms of visual induction, may remain constant across displays of different dimensions. These are very preliminary results, and currently we are working towards an accurate and automatic determination of all parameters involved, extensive testing on natural as well as artificial images and a full psychophysical evaluation.

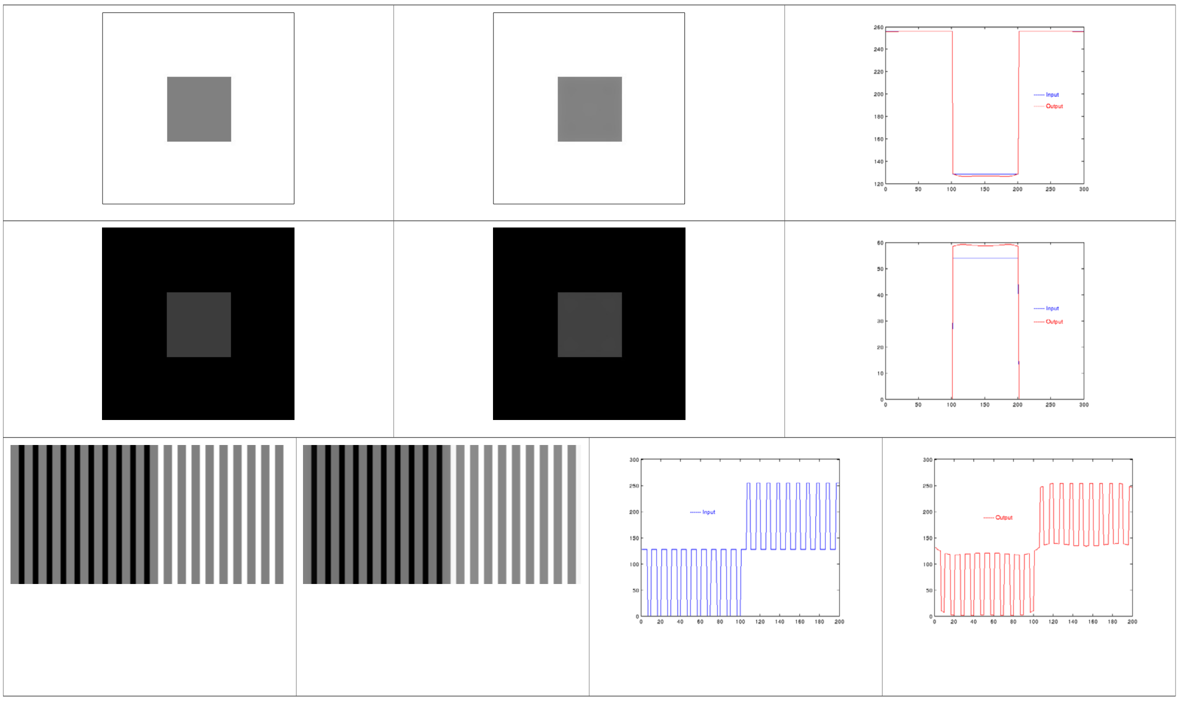

Figure 3: Achromatic induction examples. Top and middle rows: contrast. Bottom row: assimilation. In each row the first image is the input and the second image is the output result of applying our model.

Figure 4: Chromatic induction examples. Left: input. Right: output from our model. Original figure from (Stockman and Brainard 2009).

ACKNOWLEDGEMENTS

This work was supported by the European Research Council, Starting Grant ref. 306337, by Spanish grant ref. TIN2012-38112 and by ICREA Academia.

REFERENCES

Bertalmío, M., Caselles, V., Provenzi, E., & Rizzi, A. (2007). Perceptual color correction through variational techniques. *Image Processing, IEEE Transactions on, 16*(4), 1058-1072.

Bertalmío, M., Caselles, V., & Provenzi, E. (2009). Issues about retinex theory and contrast enhancement. *International Journal of Computer Vision, 83*(1), 101-119.

Bertalmío, M., & Cowan, J. D. (2009). Implementing the Retinex algorithm with Wilson–Cowan equations. *Journal of Physiology-Paris, 103*(1), 69-72.

Bertalmío, M. (2014). From image processing to computational neuroscience: a neural model based on histogram equalization. *Frontiers in computational neuroscience*, *8*.

Fach, C., & Sharpe, L. T. (1986). Assimilative hue shifts in color depend on bar width. *Perception & psychophysics*, *40*(6), 412-418.

Heinonen, C. (2013). http://referencehometheater.com/2013/commentary/image-distance-is-everything-4k-and-hidpi-displays/

Helson, H. (1963). Studies of anomalous contrast and assimilation. *JOSA*, *53*(1), 179-184.

Pereverzeva, M., & Murray, S. O. (2008). Neural activity in human V1 correlates with dynamic lightness induction. *Journal of Vision*, *8*(15), 8.

Stockman, A., & Brainard, D. H. (2009). Color vision mechanisms. The Optical Society of America Handbook of Optics, 3rd edition, Volume III: Vision and Vision Optics. New York: McGraw Hill.

Wilson, H. R., & Cowan, J. D. (1972). Excitatory and inhibitory interactions in localized populations of model neurons. *Biophysical journal*, *12*(1), 1-24.

Address: Prof. Marcelo BERTALMÍO, Department de Tecnologies de la Informació i les Comunicacions, Universitat Pompeu Fabra, Roc Boronat 138, 08018 Barcelona, SPAIN
marcelo.bertalmio@upf.edu

KANSEI evaluation of color images presented in different blue primary displays

Toshiya Hamano,[1] Takashi Fuseda,[1] Tomoronori Tashiro,[2] Tomoharu Ishikawa[1]
Hiroyuki Shinoda,[3] Kazuhiko Ohnuma,[4] Keisuke Araki,[2,5] Miyoshi Ayama[1]
[1] Graduate School of Engineering, Utsunomiya University
[2] Center for Optical Research & Education, Utsunomiya University
[3] College of Information Science and Engineering, Ritsumeikan University
[4] Graduate School of Engineering, Chiba University
[5] Canon Inc.

ABSTRACT

Recently, Rec.ITU-R BT.2020 has been published, and the new era for a super-wide color gamut has been started. It is generally accepted that the wider the color gamut, the better the color reproduction performance of the display. However, few have been reported on the comparison of color gamut from image preference or naturalness point of view. Among the three primaries, blue primary is considered to affect most on the color tone or color shade. Therefore, to investigate the best blue primary for color display from KANSEI-evaluation point of view, evaluation experiment was carried out using four different blue primaries of 430nm, 450nm, 470nm, and 480nm. Before the experiment, test image selection was carried out. Color distributions of more than 2620 images were analyzed based on our categorical color database, and 15 color images are selected as the test images from them. In the experiment, the test image was projected by the 2 projectors, one was for blue signal and the other one was for the red and green signals. Interference filters of λp = 430nm, 450nm, 470nm, and 480nm were inserted in front of the projection lens of the B projector to achieve different blue primaries. Images from the two projectors were carefully superimposed. Evaluation experiments were carried out with 2 luminance levels of 60 cd/m^2 for 430nm, 450nm, 470nm, and 480nm, and 170 cd/m^2 for 450nm, 470nm, and 480nm. The semantic differential method was used to quantify subjective evaluations of images using 14 adjective pairs. Results of the 4 blue primaries comparison, 430nm, 450nm, and 470nm blue primaries showed similar performance except for the skin color image. Results of the 3 blue primaries comparison, 470nm showed the best performance.

1. INTRODUCTION

Rec.ITU=R BT.2020 has been published in 2012. Its primary colors are 630nm, 532nm, and 467nm(ITU 2012). It is a new standard for broadcasting a super-high vision such as 4K or 8K in the future. In general, it has been considered that the wider color gamut is the better one. Performance of color gamut is usually assessed by how much of the spectrum reflectivity data of the real existence object can be reproduced (Masaoka et al. 2010). However, few have been reported on the comparison of color gamut from image preference or naturalness point of view. Evaluations using these words are called KANSEI-evaluation. "KANSEI" has the meaning called "mental sense of subjectivity" in Japanese. It is a higher order function of the human brain.

Among the tree primaries of R, G, and B, blue primary is considered to affect most on the color tone or color shade of image. Therefore, to investigate the best blue primary for color display from KANSEI-evaluation point of view, evaluation experiment was carried out using four different blue primaries of 430nm, 450nm, 470nm, and 480nm.

2. METHOD

2.1 Test images

Color distributions of more than 2620 images were analyzed based on our categorical color database (Ashiguchi 2009), and 15 color images are selected as the test images from them. Each pixel of image is labelled as a certain color category among 14 categories as shown in the right-hand side of Figure 1, using the color conversion from (RGB) to (L*a*b*) via (XYZ). In the categorical color database proposed by Ashiguchi et al., L*a*b* color space is gridded and each grid is labelled with one color among 14 categories. Using this categorical color database, all pixels of an image are divided into 14 color categories, and then the pixel ratio for each of color categories are calculated. In the next step, the image is denoted as one of the 15 groups shown in Table 1, according to the criterion shown in the right column of Table 1. Figure 1 shows the example of "blue image" , of which pixel ratios are indicated in the right-hand side.

Tabe 1 Criterion of the color group of image from pixel ratios of categorical colors

Group	Criterion	Group	Criterion
red	red > 40%	yellow-green	yellow + green > 60%
green	green > 40%	red-blue	blue + light blue + red > 60%
blue	blue + light blue > 40%	pink	pink > 40%
yellow	yellow> 40%	purple	purple > 40%
orange	orange > 40%	multi-colors	all color categories < 25%
red-green	red + green + orange > 60%	monochromatic	black + dark gray + gray + light gray
blue-green	blue + light blue + green > 60%		+ white > 80%
yellow-blue	blue + light blue + yellow > 60%	skin	Images of human face and skin

red	0%
blown	0%
pink	0%
orange	0%
yellow	0%
green	6%
blue	5%
light blue	74%
purple	0%
black	0%
dark gray	5%
gray	1%
light gray	0%
white	8%

Figure 1: The image and the analysis data of the image.

2.2 Experimental environment

Figure 2 shows the experimental apparatus of two projectors that project images.Test images were projected by the 2 projectors, one is for blue signal and the other one is for the red and green signals. Interference filters of λp = 430nm, 450nm, 470nm, and 480nm were inserted in front of the projection lens of the B projector to achieve different blue primaries. Projection from two projectors has been neatly matched. White balance of different blue primary conditions was set nearly the same chromaticity coordinates by inserting proper ND filters in front of the two projectors as well as adjusting the gain control. Figure 3 indicates color gamuts of different blue primaries in the CIE 1976 u'v' chromaticity diagram. Evaluation experiments were carried out with 2 levels of average luminance, 60 cd/m2 for 430nm, 450nm, 470nm, and 480nm, and 170 cd/m2 for 450nm, 470nm, and 480nm.

Average distance of vision is about 150cm. The size of the presented image is 42 × 58cm, visual angle is 16°×22°.

Figure 2: Two projectors that project images

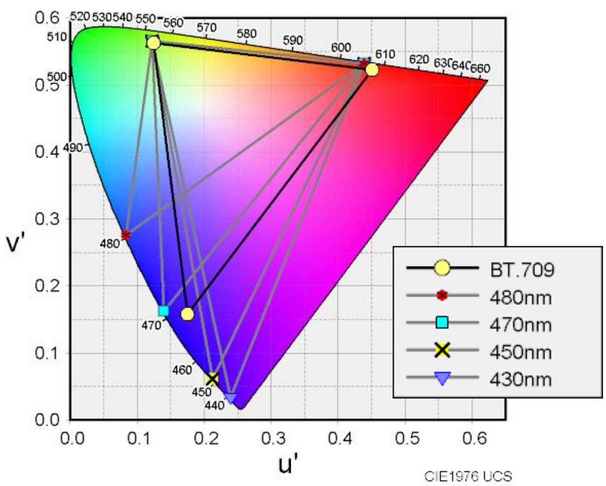

Figure 3: Color gamuts of different blue primaries. Solid line denotes bt.709.

2.3 Experimental Procedure

Tabel 2 shows 14 adjective pairs used in the experiment. “Unappetizing - Delicious” was used only in the images of foods and drinks. These word pairs were chosen from previous studies on the assessment of color image quality (Ayama et al. 2010, Kishimoto et al. 2011). The observer entered the experiment booth, and adapted to a dark environment for five minutes. Then test image was presented with one of the 4 or 3 blue primaries. Blue primary is changed every five pieces. The observer was instructed to evaluate each test image by indicating a score between two bipolar adjectives, on a seven-point scale from -3 to 3. There was no time limit for observer to see each image and make judgement. Fourteen observers participated in the 4 primaries experiments, while 17 observers in the 3 primaries experiments.

Table 2. Adjective pairs used in KANSEI evaluation

	negative	positive		negative	positive
1	Dark	Bright	8	Mundane	Impressive
2	Pale color	Deep color	9	Unnatural	Natural
3	Weak contrast	Strong contrast	10	Discomfort	Comfort
4	Dirty	Beautiful	11	Calm	Powerful
5	Blurry	Clear	12	Flat	Chiseled
6	Plain	Showy	13	Dismal	Cheerful
7	Dislike	Like	14*	Unappetizing	Delicious

*used only in the images of foods and drinks

3. RESULTS AND DISCUSSION

Figure 4 shows rating score of each evaluation word pair in the experiment using 4 and 3 different blue primaries, in the left-hand and right-hand side, respectively. Each point denotes the average of all observers’ scores. Results of the 4 blue primaries experiment, 430nm, 450nm, and 470nm blue primaries showed similar performance for each evaluation word. 480nm blue primary is a remarkably bad result. Results of the 3 blue primaries comparison, 470nm showed the great result than 450nm.

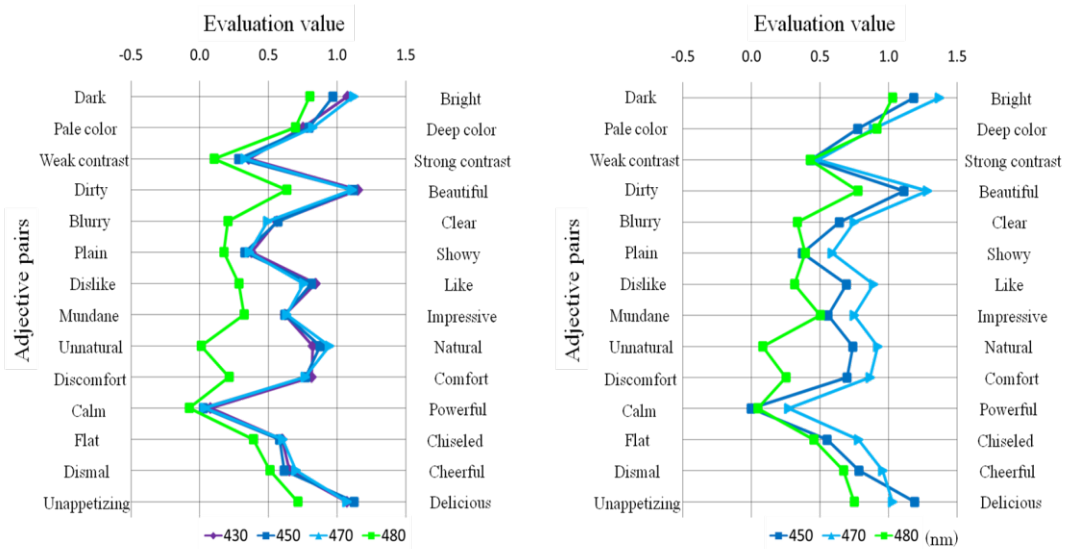

Figure 4: Left: Rating score of each evaluation word pair in the experiment using 4 different blue primaries. Right: The same figures using 3 different blue primaries.

In order to see the effect of different blue primaries more clearly, difference between the maximum and the minimum values of the evaluation word pairs were calculated for each of the test images. We found that effect of blue primary is relatively clearly indicated in the results of the following 5 adjective pairs of “Pale color vs Deep color”, “Dirty vs Beautiful”, “Dislike vs Like”, “Unnatural vs Natural”, and “Discomfort vs Comfort” in the results of the 4 blue primaries. “Dirty vs Beautiful” changes into “Dark vs Bright” in the results the 3 blue primaries. A average scores of these evaluation words were calculated.

Figure 5 shows average scores of the selected adjective pairs (1,2,7,9, and 10 in Table 2) for “purple”, “red-blue”, “blue”, “blue-green”, “yellow-blue”, and “skin” images in the 3 blue primary experiments. As shown in the figure, 470nm showed the best performance, while 480nm showed the worst. Generally, marked difference of evaluation was found in the bluish, greenish, and purple images, while no difference was observed in other color images such as red, yellow, and pink, etc.

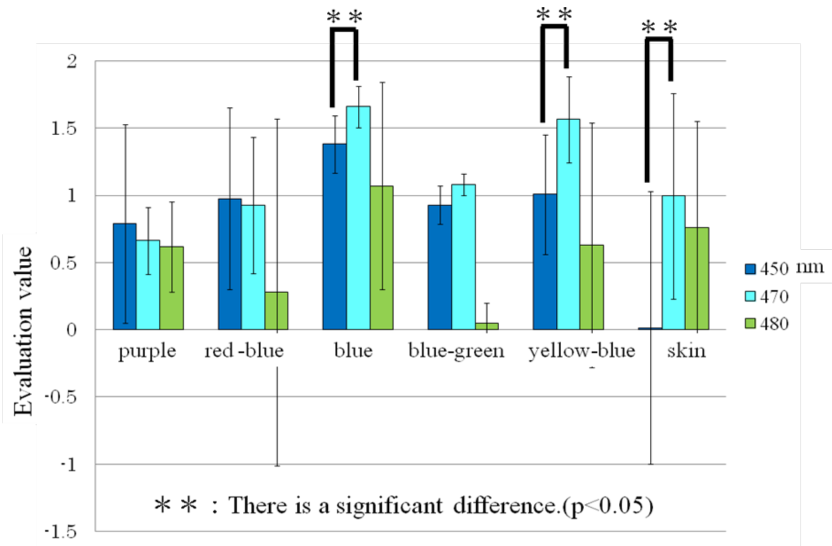

Figure 5: Average results of subjective evaluation of 6 color images in 5 adjective pairs (1,2,7,9,and 10 in Table 1) in the 3 blue primary experiment.

4. CONCLUSIONS

It was shown that 470nm blue primary showed the best performance for 15 test images in the KANSEI evaluation using 13 to 14 adjective pairs in the 3 blue primary experiment. It is suggested that the choice of the blue primary in the BT2020 is appropriate from the KANSEI-evaluation point of view.

A serious comment would be given to this study that the test images are chosen from the stock photos that are usually optimized in the color gamut of ITU-R BT.709-5 (ITU 2004) often called as sRGB. Among the blue primaries used in this study, 470nm is the closest to the blue primary of sRGB. If a picture is taken by a color camera with 430nm blue primary, the color signals are optimized, and displayed using the same blue primary, then the evaluation results of 430nm might be the best. Relation between the best color gamut from KANSEI-evaluation point of view and the selection of blue primary in the steps of taking a picture, optimization of color signal, and displaying the image, is the future issue. It is worth noting that for the “purple” image, 450nm showed the best performance in the 3 blue primary experiment as indicated in Figure 5, and 430nm blue primary showed the best score in the 4 blue primary experiment. This suggests that colors in the display stage is the most important for the image assessment from KANSEI-evaluation point of view.

ACKNOWLEDGEMENT

This research is partly supported by the Grant-in Aid from the Japan Society the Promotion of Science (No. 25390091) in 2013-2015, and the research grant from the Center for Optical Research and Education, Utsunomiya University.

REFERENCES

Ashiguchi, T., T. Yaguchi, K. Kijima, 2009. Application of categorical colors to area segmentation for road image, *Electronic Imaging 2008, Color Imaging XIV,Proceedings of SPIE*, 7241:.72410K-1-27410K-8,

Ayama, M., T. Shirakawa, T. Shimizu, H. Oguro, M. Sato, T. Eda, T. Ishikawa, and M. Kasuga. 2010. Kansei evaluation of color image - Influence of screen size, brightness and saturation contrast-, *Kansei Engineering*, 9 (2): 177-187

Kishimoto, Z., M. Kanazawa, Y. Murakami, M. Yamaguchi, H. Haneishi, N. Oyama. 2011. Analysis of psychological factors in high-fidelity color image reproduction system, *Image Electronics Journal*, 40 (6): 1017-1026

Masaoka, K., Y. Nishida, M. Sugawara, and E. Nakasu. 2010. Design of Primaries for a Wide-Gamut Television Colorimetry., *IEEE transactions on broadcasting*, 56 (4): 452-457.

ITU. 2004. Parameter values for the HDTV standards for production and international programme exchange. In Recommendation ITU-R BT.709-5

ITU. 2012. Parameter values Ultra-high definitiontelevision systems for production and international programme exchange. In Recommendation ITU-R BT.2020

Address: Toshiya Hamano, Graduate School of Engineering, Utsunomiya University,
7-1-2 Yoto, Utunomiya,Tochigi,321-8585, JAPAN
E-mails: mt146647@cc.utsunomiya-u.ac.jp

New Proposal for Advanced Measurement Technology for Image Clarity

Hideo Kita, [1] Shigeo Suga, [1] Jack A. Ladson[2]
[1]SUGA Test Instruments Co., Ltd.
[2]Color Science Consultancy

ABSTRACT

Evaluation of object surface structure traditionally involves the assessment of optical properties known as Gloss[1] and Haze[2]. More recently an advanced optical property of surfaces, known as Image Clarity, has gained major importance because Image Clarity provides an accurate assessment of the optical property of an object, while the traditional properties do not. The optical phenomenon of Image Clarity exists in both the reflection and transmission modalities for opaque and transparent products. We have evolved the design of instruments used to measure this phenomenon by using a narrow, diffraction limited optical beam and a CCD array as a detector. Results are obtained by analyzing the surface optical transfer function which uses Fast Fourier Transforms[3] for computational speed.

This optical surface evaluation technique affords several improvements over previous technologies[4]. This analytical technique allows assessment of the classical appearance properties and new appearance methods and metrics. Classically, the traditional appearance properties are gloss, haze, orange-peel and image clarity. Further, the measurement time of the new instrument is more rapid than bench top instruments allowing for near real-time measurement as well as continuous monitoring of moving plastic sheets or other processes in need of continuous examination. Both short and long wave surface phenomena are assessed with equal accuracy, and both precision and accuracy are improved by the new design. The rapidity of measurements affords a manufacturer the opportunity to assess the impact on surface quality of the product by controlling parameters in the manufacturing process.

Correlation is obtained with traditional assessments; such as gloss and haze. Additionally, the advanced technique correlates with visual product assessments. The fact that the new design is smaller and lighter than previous instruments provides the very important property of portability and usability to the instrument. The device is the latest in solid-state technology, ensuring reliability.

End users come from processes that require control of the quality of surface reflectance or transmittance and maintaining of product quality. These are industries and applications, such as; automotive enamels, coated surfaces, displays, films, glasses, material

1 ASTM D 523, Standard Test Method for Specular Gloss, ASTM International, West Conshohocken, PA

2 ASTM D 1003Standard Test Method for Haze and Luminous Transmittance of Transparent Plastics, ASTM International, West Conshohocken, PA

3 http://mathworld.wolfram.com/FastFourierTransform.html

4 ASTM D5767-95(2012) Standard Test Methods for Instrumental Measurement of Distinctness-of-Image Gloss of Coating Surfaces, ASTM International, West Conshohocken, PA

smoothness, paper processing, paper smoothness, painted panels, photographic hard reproduction media photographs, plated surfaces, plastics, polished surfaces, printed materials, surface texture and other industries where quality of surface structure or the quality aspects of components appearance is important.

1. INTRODUCTION

The method and apparatus for detecting certain surface phenomenon, such as, but not limited to, gloss, sheen, crazing, blistering, mud-cracking, cratering, haze, fog, orange-peel, distinctness of image[5] and texture of various frequencies is presented. The apparatus consists of a collimated beam illuminating the surface to be analyzed. A knife edge, commonly referred to as a slanted edge in image analysis, interrupts the reflected beam whose local intensities are captured by a Digital Still Camera containing a CCD/CMOS array. The images are scanned in the time domain and transformed to frequency domain using Fast Fourier Transforms (FFT). Certain frequency patterns prove to be associated quantitatively with certain of the mentioned appearance degradation phenomenon.

2. APPEARANCE MEASUREMENT

The appearance of an object is attributable to many factors. In this article, we concern ourselves with the appearance attributes that are associated with color appearance. The attributes of color are lightness, hue and chroma. The attributes of appearance are related to the optical surface structure. Gloss is classically used in many industries to evaluate surface appearance of an object. However, soon one discovers that gloss does not correlate with visual appearance and surfaces with the same gloss have totally different appearances. This issue was first addressed by Richard Hunter[6] in the 1980's. Hunter discovered that the appearance of an object is related to the spread of a light beam reflected from an object or transmitted through an object. Quantifying the spatial deviation of a light beam from a perfectly un-deviated beam at various spatial frequencies allows us to see deviations in surface structure that are consistent with appearance attributes; such as, gloss, DOI, orange peel and other optical imperfections caused by a less than perfect optical surface.

3. SAMPLE PREPARATION

The importance of proper sample preparation cannot be over stated. Sample conditioning is appropriate and necessary. We condition the sample before sample measurement. This typically involves the necessary time for allowing sufficient time for the sample(s) to stabilize in the measurement environment. The measurement environment is defined in ASTM[7], as; condition the test specimens at 23 ± 2°C [73.4 ± 3.6°F] and 50 ± 5 % relative humidity, Rh, for not less than 40 hours prior to test, in accordance with Procedure A of ASTM Standard Practice D618[8] . Samples are prepared in exactly the same manner each time they are collected before measurement.

---

5 ASTM D5767-95(2012) Standard Test Methods for Instrumental Measurement of Distinctness-of-Image Gloss of Coating Surfaces, ASTM International, West Conshohocken, PA

6 Hunter Lab, www.hunterlab.com, Model Dorigon II DOI/Haze Meter

7 ASTM International, West Conshohocken, PA

8 ASTM Standard Practice D 618.- Procedure A, ASTM International, West Conshohocken, PA

4. SELECTING SAMPLES

Select sample(s) that are representative of the entire batch should be selected for appearance measurement. Choose samples that are truly representative of the materials collected. For statistical analysis collect samples from various sources or differences in location at different times. These are the guidelines that we follow in our selection protocol.

1. The sample must also be representative of production and the attributes that are of interest. If samples are non-representative of the batch or are spoiled, damaged, or irregular, then the sample measurement may introduce a bias into the colour appearance measurement chain.
2. Choose a sample randomly.
3. Examine the sample to ensure that it is representative of production. This methodology will avoid biasing the results.
4. Follow the corporate SOP for handling instructions.
5. If sampling procedures are adequate, a different sample selected from the same batch should result in comparable measured values.

5. APPARATUS

An illustrative schematic diagram of the apparatus appears in Figure 1. A CCD camera is focused on the film surface to be analyzed. A knife edge interrupts the beam reflected from the surface under analysis from a collimated light source. The distance between the camera and the surface under analysis is slightly variable and under operator control because different optical surface phenomena will be found at different focal depths. The pixels of the image will be raster scanned across the image of the knife edge and Fast Fourier Transform (FFT) used to convert from time (spatial) domain to frequency domain. Certain patterns in the frequency domain act as fingerprints for certain characteristic surface degradation phenomena.

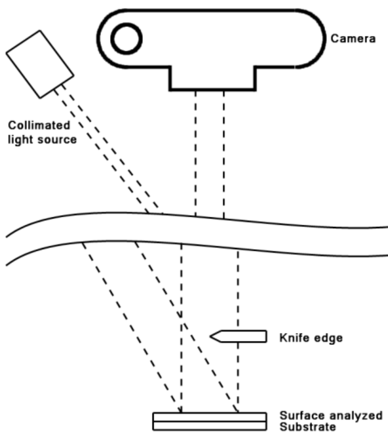

Figure 1: Schematic diagram of the apparatus

The variability in measurement angle relative to the sample and the light source allows measurements to be made in reflection and transmission and other intermediate angles. Other intermediate angles are useful for identifying different surface structures attributable to different optical effects.

This design implementation uses the slanted edge in accordance with ISO12233[9] . The slanted edge significantly reduces the aliasing that commonly occurs in high density linear array detectors. A linear dimensional array is used to compute the discrete derivative along the slanted edge. These data are combined to create a one-dimensional edge spread function. This over sampling produces an accurate assessment of the spatial frequency factor, SFR. Noise produces a bias in the SFR. However, when the data from the array are combined this significantly reduces the electronic and optical noise. We also use noise smoothing algorithms to reduce the influence of noise to an acceptable limit.

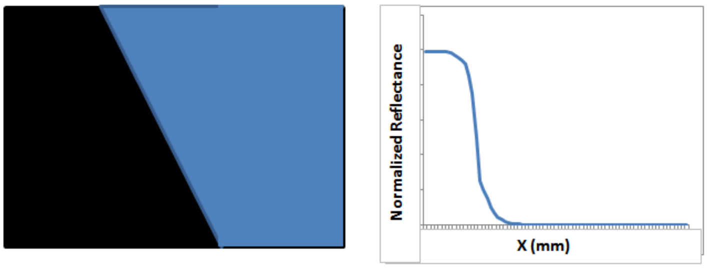

Figure 2: Slanted edge and data

In addition, certain characteristic patterns emerge from various depths within the fractured film itself. Therefore, it is necessary that the camera maintain a narrow focal plane and the focal plane is moved to various levels within the fractured film by mechanically changing the length of the specimen to camera axis by amounts proportional to a fraction of the film's thickness. This variance accommodates another feature of the method that the analysis may be accomplished without resort to variation of relative angles between camera, specimen, and the illumination.

6. METHOD

6.1 Standardization

Standardization of the photometric scale is accomplished by scanning a black polished glass representing zero (0) followed by scanning a white polished glass, representing full scale (100%).

6.2 Test Scan

Images are captured using physical and optical conditions identical with those of the standardization. Images are scanned along the entire x-axis if the image across the specimen perpendicular to the axis of the knife edge. In most cases, a single scan contains insufficient data to obtain repeatable results. In this case we form a histogram at each x-pixel location and combine data from the array. The histographic function is treated as the time domain function and submitted to FFT for analysis. The results in the frequency domain are then compared to scans of known specimens and experimental conditions. Here we show the acquired data and its corresponding modulation Transfer Function as a result of applying the image analysis transform.

9 International Organization for Standardization, ISO Central Secretariat, Chemin de Blandonnet 8, CP 401, 1214 Vernier, Geneva, Switzerland, http://www.iso.org/iso/home/store.htm

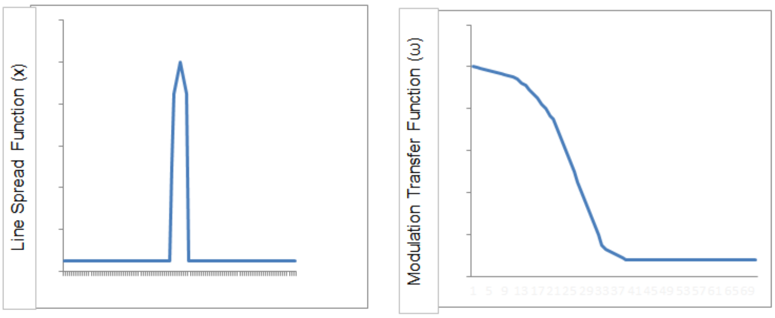

Figure 3: Line Spread Function and Moduration Transfer Function

7. RESULTS

By examining the data and applying algorithms we have minimized the sources or error which may introduce a bias into the modulation transfer function.

The image quality fundamental standards; such as, Orange Peel, Gloss, and other surface structural phenomenon, serve as crucial ground-truth information for evaluating Image Quality algorithms. Specifically, to quantify how well our Image Quality algorithm can predict the fundamental effect values from a particular analysis technique. We evaluate the algorithm's performance in terms of three performance criteria recommended by the Video Quality Experts Group (VQEG) [141][10]: (1) prediction accuracy, (2) prediction monotonicity, and (3) prediction consistency.

The prediction accuracy will be quantified and evaluated by measuring how well the algorithm's predictions correlate with known established standards values and by measuring the average error between the algorithm's predictions and those values. The Pearson correlation coefficient (PPMCC) and the root-mean-squared error (RMSE) are used to evaluate the performance.

8. CONCLUSIONS

Our experimental data show that this method of analysis provides increased analytical sensitivity, and discrimination and classification of various surface effects. These data in turn allow the user to perfect and control their manufacturing process where the appearance of high quality surfaces is important.

ACKNOWLEDGEMENTS

This development is a successful joint venture between the United States and Japan.

REFERENCES

PS Burns - IS&T PICS, 2002 Refined Slanted-edge Measurements for Digital Camera and Scanner Testing

Monie, S. A.; Stief, B. C.; Krupkin, N. V.Evaluation of Glossy Inkjet Papers Using Distinctness of Image (DOI) Measurement, NIP & Digital Fabrication Conference,

10 Arthur Webster, U.S. Dept. of Commerce, NTIA/ITS, Boulder, Colorado U.S.A.,Email: webster@its.bldrdoc.gov

2003 International Conference on Digital Printing Technologies. Pages 458-910., pp. 763-768(6)

Ming-Kai Tse*, David Forrest and Eugene Hong, An Improved Method for Distinctness of Image (DOI) Measurements,

Address: Hideo Kita, Calibration Dept, SUGA Test Instruments Co., Ltd.,
5-4-14, Shinjuku, Shinjuku-ku, Tokyo, 160-0022, JAPAN
E-mails: kita@sugatest.co.jp

Analysis of color appearance of metallic colors and pearlescent colors using multi-angle spectrophotometer

Yu-Wen Chiu[1], Hung-Shing Chen[2], Chia-Pin Cueh[3], Kang-Yu Liu[3]

[1] Graduate Institute of Color and Illumination Technology, National Taiwan University of Science and Technology, Taiwan
[2] Graduate Institute of Optical-Electronic Engineering, National Taiwan University of Science and Technology, Taiwan
[3] Printing Technology Research Institute, Taiwan

ABSTRACT

Many industrial products and packages use metallic or pearlescent inks to produce special effects. However, there is little specific comparison on special-effect inks and traditional inks to signal their feature difference. Using RAL color charts as examples, this paper provides three types of ink materials (solid, pearlescent and metallic colors) to discuss their appearances under varying illumination types and measurement geometries. The viewing angle-dependent color samples are measured using multi-angle spectrophotometer under different illuminating and measurement geometries. In addition, solid color samples with two levels of gloss coatings are also measured to analyze their color appearances.

1. INTRODUCTION

During the last few decades, there has been a rapid growth of special-effect performances due to the development of effect inks and post-processing technologies. The special effects generated by using metallic and pearlescent inks allow the creations of different fantastic optical effects. For examples, traditional inks only produce selective absorption and scattering, which show monotone color perception, and uniform appearance effect with independent observation angle, so called solid color. On the other hand, pearlescent inks can create special interference effect because they are composed of multi-layer structure, i.e., high refractive metal oxides coated low refractive mica flakes, leading to color change with different observation angles. Furthermore, metallic inks are usually generated by shinny and thin metal flakes, which tend to lie parallel to the surface and create highly specular reflection (Figure 1). Their appearances could vary with the illumination geometries and viewing conditions[1-3]. Because color appearances of ink materials with effect coating could vary with the viewing geometries and illumination geometries, the use of multi-angle spectrophotometer is necessary in the quantification of angle-dependent color appearances.

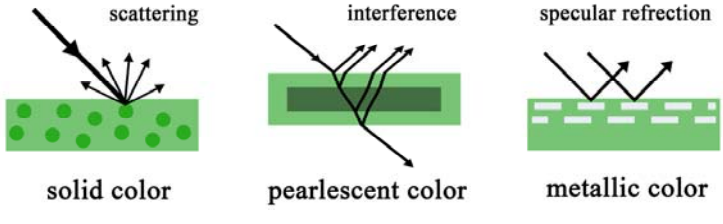

Figure 1: Optical effects of solid, pearlescent and metallic inks

In addition, it is well known that gloss coating has a notable effect on surface appearance. The spike of specular lobe reflection locates in the specular angle region, where the lightness and chroma extremely change. The shape of specular spike is lower and broader in matte materials than in glossy one. Matte surface appears higher lightness and lower chroma than the corresponding glossy surface[4]. Recent researches have explored the characteristics of special color appearance, and the surface appearance issues related to illumination and viewing conditions also pay more attentions[1-2]. Our objective in this study is to measure appearances of different ink materials and different gloss levels through multi-angle spectrophotometer.

2. METHOD

The method to carry out this study was using multi-angle spectrophotometer, BYK-mac instrument from BYK Gardner (Figure 2), which can objectively measure total appearance under different viewing angles and lighting conditions. The lighting conditions include directional illumination and diffused illumination. Under directional illumination, color appearance including CIELAB values is assessed at given 45° lighting angle and viewing under six aspecular angles -15°/ 15°/ 25°/ 45°/ 75°/ 110°. The aspecular angle is the viewing angle measured from the direct specular direction. Positive angle means in direction towards incident illumination, negative angle means away from incident illumination (Figure 3). Besides, sparkle grade is assessed under directional incidence angle 15°/ 45°/ 75° and observed from the normal direction. Under diffused illumination, graininess is evaluated from the normal direction[5] (Figure 4).

Figure 2: BYK-mac instrument

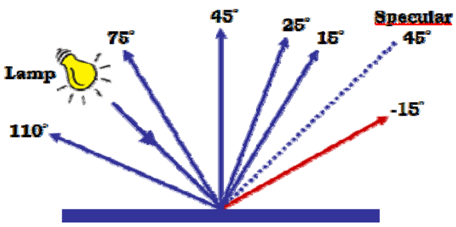

Figure 3: Color measurement geometry

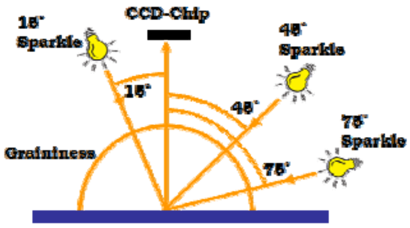

Figure 4: Effect measurement geometry

2.1 Experimental Design

In order to investigate the appearances of different ink materials and gloss levels in the particular illuminating conditions and viewing geometries, we measured a series of samples using a multi-angle spectrophotometer, BYK-mac. CIELAB values and the effect parameters including sparkle grade and graininess were analyzed. This study consisted of two experiments, Experiment 1 (Exp-1) of which was intended to elicit the appearance of three type of ink materials including solid, pearlescent and metallic effects varied with different lighting and measurement geometric conditions. Experiment 2 (Exp-2) focused on color changes of solid colors regarding two levels of gloss impressions, gloss and semi-matte (Figure 5).

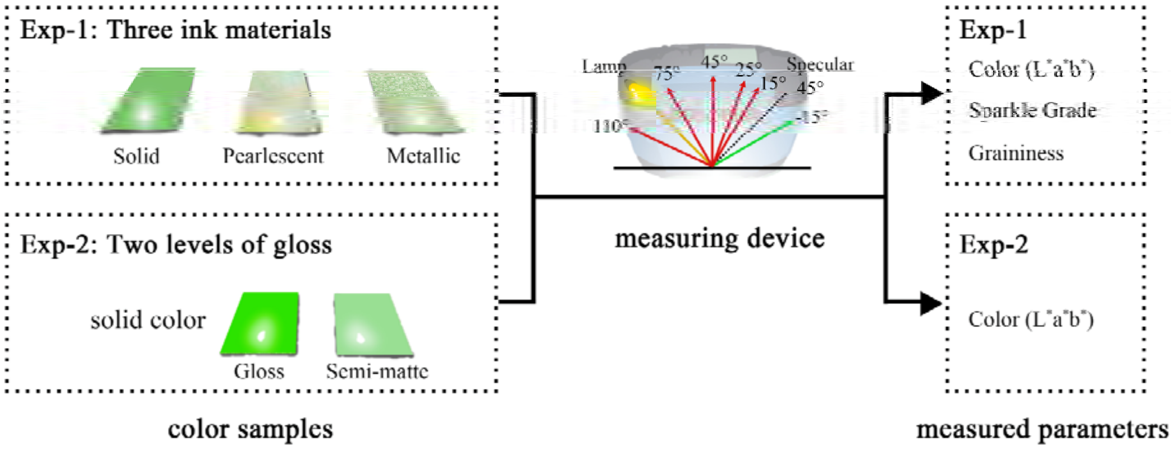

Figure 5: Experimental schematic

2.2 Sample Preparation

For Exp-1, total eight solid, eight pearlescent and eight metallic color samples were prepared. Colors of samples included red, orange, yellow, green, blue, violet, light grey and dark grey. For Exp-2, considering gloss as a specific appearance attribute, two levels of gloss in the solid color samples so called semi-matte and gloss samples were prepared. The solid color samples with gloss used in Exp-2 are the same as Exp-1. All color samples were chosen from the RAL color system. Solid and pearlescent colors were chosen from the RAL CLASSIC K5 collection, and metallic colors were chosen form RAL EFFECT E4 collection. The list of test samples is showed in Table 1.

Table 1: The list of color samples

Exp	Exp-1, Exp-2	Exp-2	Exp-1	Exp-1
Ink type	Solid color		Pearlescent color	Metallic color
Gloss level	gloss	semi-matte	gloss	gloss
Red	RAL 3020 Traffic red		RAL 3032 Pearl ruby red	RAL 450-M
Orange	RAL 2009 Traffic orange		RAL 2013 Pearl orange	RAL 410-M
Yellow	RAL 1023 Traffic yellow		RAL 1036 Pearl gold	RAL 270-M
Green	RAL 6024 Traffic green		RAL 6035 Pearl green	RAL 220-M
Blue	RAL 5017 Traffic blue		RAL 5025 Pearl gentian blue	RAL 640-M
Violet	RAL 4006 Traffic purple		RAL 4011 Pearl violet	RAL 570-M
Light grey	RAL 7042 Traffic grey A		RAL 9022 Pearl light grey	RAL 110-M
Dark grey	RAL 7043 Traffic grey B		RAL 9023 Pearl dark grey	RAL 840-M

3. RESULTS AND DISCUSSION

Experiment 1: Appearances of Ink Materials

The a^*b^* loci for eight color samples with three ink materials (solid, pearlescent and metallic colors) in a^*b^* color plane are illustrated in Figures 5(a) through 5(c). For solid colors, the measured color values of aspecular viewing angle -15° are close to the a^*b^* center. With the aspecular angle increases, a^* and b^* values increase. In case of pearlescent colors, chroma changes with measuring angle are significant and become greyish as measuring angle become larger. No significant trend was uncovered in metallic color samples.

The L^*C^* loci for eight color samples of three ink materials in L^*C^* color plane are illustrated in Figures 5(d) through 5(f). The measurement results showed that lightness (L^*) of all samples becomes larger with measuring angle accordingly up to specular direction. The lightness change is dramatic in pearlescent and metallic colors. In case of solid color samples, chroma changes with measuring angle are significant and become larger as measuring angle become larger. In contrast, chroma changes in pearlescent color samples with measuring angle are significant and become smaller as measuring angle become larger.

On the other hand, the measured effect parameters of sparkle grade and graininess are showed in Figure 6. The solid color samples have little sparkle effect because they are made by traditional solid inks. The pearlescent colors and metallic colors are made by metallic flakes which enable to generate grainy shining effects. In particular, the metallic samples appear with larger flake size, are more significant in the sparkle and graininess effects.

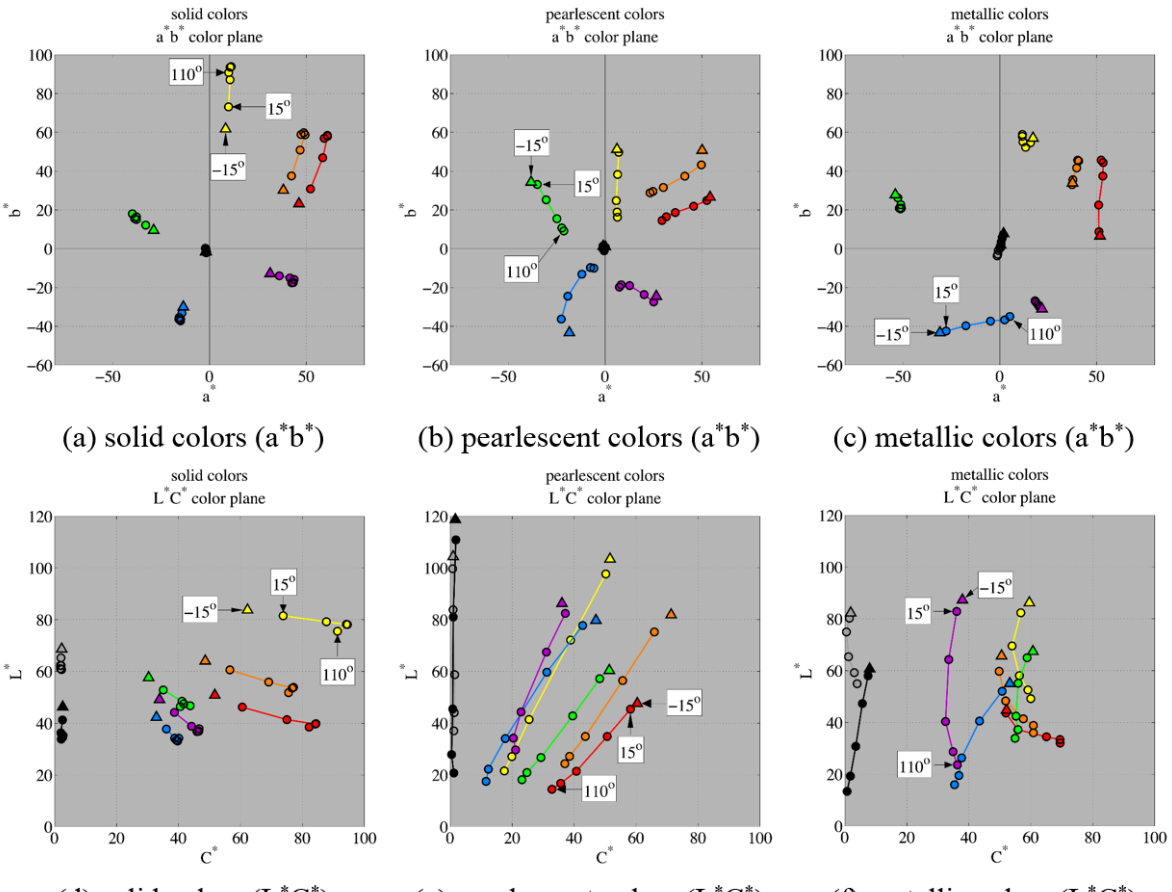

(a) solid colors (a^*b^*) (b) pearlescent colors (a^*b^*) (c) metallic colors (a^*b^*)

(d) solid colors (L^*C^*) (e) pearlescent colors (L^*C^*) (f) metallic colors (L^*C^*)

Figure 5: The LAB color values of three different ink colors (in a^*b^* / L^*C^* planes)

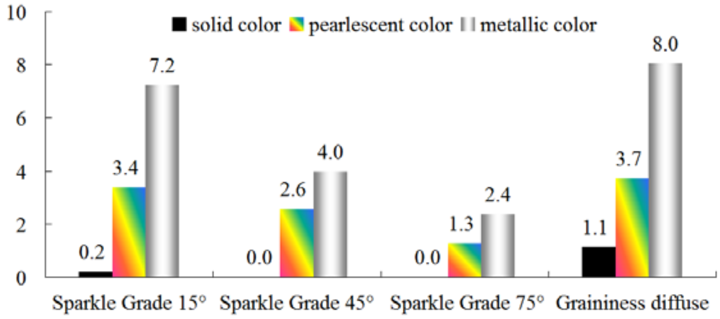

Figure 6: The effect parameters of three different ink colors

Experiment 2: Solid Color Appearances Regarding Gloss Levels

The a^*b^* loci of eight solid color samples with two levels of gloss (gloss and semi-matte) in a^*b^* plane are illustrated in Figure 7. For semi-matte colors, the measured color values of aspecular angle -15° and 15° are closer to the a^*b^* center than the glossy colors. Far from the specular region, the measured color values of gloss samples and semi-matte samples are rather identical. The L^*C^* loci of the solid color samples with two levels of gloss are illustrated in Figure 8. As expected, the main impact of gloss coating was the lightness value close to the aspecular angle of -15°, 15°. The lightness value of the semi-matte surface was higher than the gloss one, while the chroma value of the semi-matte surface was lower than the gloss one.

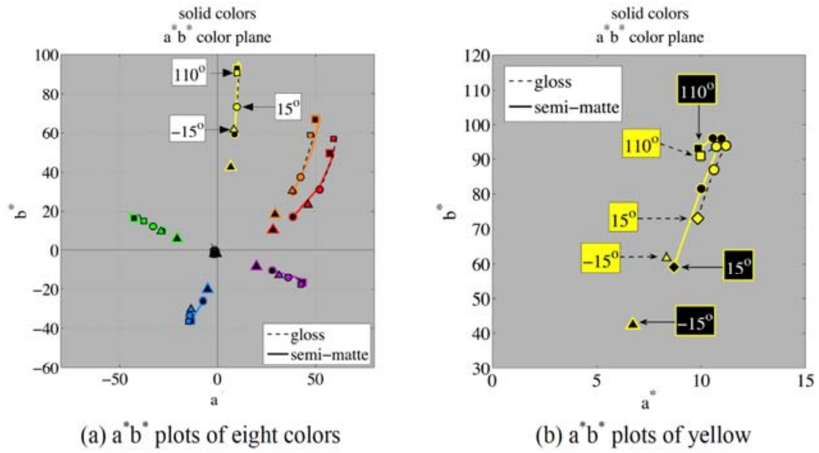

Figure 7: The a^*b^* plots of two surface processing

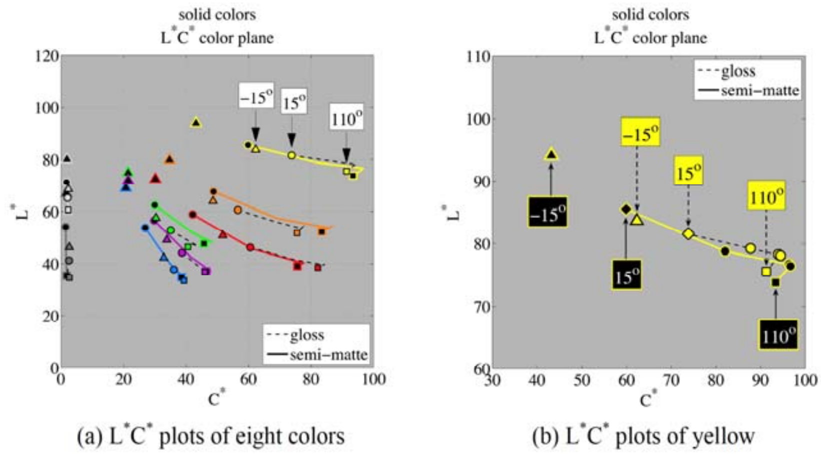

Figure 8: The L^*C^* plots of two surface processing

4. CONCLUSIONS

The viewing angle-dependent color samples with solid, pearlescent and metallic colors are measured using multi-angle spectrophotometer under different illuminating and measurement geometries. In addition, the solid color samples with 2 levels of gloss coatings are also measured to analyze their color appearances. The analysises in this paper are performed using a multi-angle spectrophotometer to obtain CIELAB color values and the effect parameters (sparkle grade and graininess). Experimental evaluation results show color appearances of three type ink materials (solid, pearlescent and metallic colors) are quite different. Besides, the main impact of gloss coating is the lightness value close to the aspecular angle of -15°, 15°. From the comparison of solid color samples between gloss type and semi-matte type, semi-matte surface appears higher lightness and lower chroma than glossy one. Our current implementation uses RAL color charts, but the development of special-effect inks technology is diversity. Our future work is to implement more ink materials to realize more multi-angle color performance of special-effect inks.

REFERENCES

1. Cramer, W.R., Gabel, P.W., 2001, *Measuring Special Effects*, Paint & Coating Industry, 9, p.36-46.
2. M. E. Nadal and T.A. Germer, 2002, *Colorimetric characterization of pearlescent coatings*, Proc. SPIE 4421, p.757–760.
3. McCamy CS., 1996, *Observation and measurement of the appearance of metallic materials. I. Macro appearance*, Color Res Appl, 21, p.292–304.
4. Mikula, Ceppan, et al., 2003, *Gloss and Goniocolorimetry of Printed Materials*, COLOR research and application, 28, p.335-342.
5. "BYK-Gardner Digital Catalog, 2013", from http://www.byk.com/en/support/instruments/download-catalog.html

Address: Prof. Hung-Shing Chen, Department of Optical-Electronic Engineering, National Taiwan University of Science and Technology, 43, Keelung Road, Section 4, Taipei, Taiwan

E-mails: M10325003@mail.ntust.edu.tw, bridge@mail.ntust.edu.tw, james@ptri.org.tw, terryliu@ptri.org.tw

HDR imaging – Automatic Exposure Time Estimation A novel approach

Miguel A. MARTÍNEZ,[1] Eva M. VALERO,[1] Javier HERNÁNDEZ-ANDRÉS,[1] Javier ROMERO,[1]
[1] Color Imaging Laboratory, University of Granada, Spain.

ABSTRACT

Digital imaging of common scenes can be a very challenging task if the scene radiances present a high dynamic range (HDR). HDR imaging techniques are applied to overcome this issue. The most popular technique is based in the combination of differently exposed low dynamic range (LDR) images. However there is a lack of a robust method for determining either the amount of LDR pictures needed, or their exposure time settings, without any prior knowledge of scene content. In a recent publication, we proposed a novel method for estimating the set of exposure times (bracketing set) needed to capture the full dynamic range of HDR scenes including daylight skies. Now we extend the applicability of this method to any imaging system or application (scientific, industrial or artistic). The proposed method is adaptive to scene content and to any camera response and camera configuration (raw, jpeg, etc). Our method works on-line, since the exposure times are estimated as the capturing process is ongoing. Therefore, it requires no a-priori information about scene content. The resulting bracketing sets are minimal for the scene being captured. The user can set a tolerance for the maximum percentage of pixel population that is underexposed or saturated. We can use this method separately for each color or spectral channel. This method can thus also be used for multispectral imaging systems.

1. INTRODUCTION

The use of HDR imaging techniques converts our digital camera in a tool for measuring the relative radiance outgoing from each point of the scene, and for each color channel. This final HDR image is called HDR radiance map. In order to generate it, we need to know the relationship between camera response values and relative irradiance impinging on the sensor (which is proportional to the radiance outgoing from the scene). This relationship is represented by the camera response function (CRF), which is easily calculated as proposed by Debevec and Malik (2008).

Merging different low dynamic range (LDR) images into a HDR radiance map using the CRF, is a very well known technique widely used in many imaging fields from photography to scientific or industrial applications. However, when the captures take place, there is no method that allows us to determine either how many LDR shots are going to be needed or what exposure times to be used, without having any prior knowledge of the radiance content of the scene being captured. Authors care the most about optimizing the signal to noise ratio (SNR) of the resulting HDR radiance map, rather than controlling the number of shots and the final total exposure time. For this purpose, they assume known information about scene content before starting the capturing process, like known illuminant or radiance levels, or they assume a camera with linear CRF (Granados et al. (2010), Hirakawa and Wolfe (2010), Gallo et al. (2012)). Their bracketing set selection is based in finding an intermediate exposure time, and increasing and decreasing it for the contiguous shots a fixed number of stops (Stunpfel et al. (2004), Bilcu et al. (2008)). Other authors capture a large number of exposures, and afterwards select which ones to use for an optimal SNR reconstruction (Hassinoff et al. (2010), Gallo et al. (2012)). Only Barakat et al. (2008), proposed a method for finding minimum bracketing sets for any given camera. They studied the radiance ranges covered by their camera using every exposure time setting available on it. Afterwards, they selected only those exposure times that covered the full dynamic range of the camera with some overlap, eliminating redundant shots that do not add any new radiance range to the final HDR image. To make this method adaptive to scene content, they included a stopping condition if they found no underexposed or saturated pixels respectively. This way they are limiting their capturing possibilities to usually 4 or 5 possible exposure times, and they do not control the SNR of the resulting HDR radiance map.

In this work we extend the applicability of the proposed method from natural scenes with daylight skies to any general or particular HDR imaging application. Numerical results of a different set of HDR radiance maps generated for daylight outdoors scenes, and a comparison with the method proposed by Barakat et al. (2008), are shown and explained in Martínez et al. (2015). Here we captured a set of 24 HDR scenes including both outdoors (with and without sky) and also indoors scenes, and also both in very bright and very dim lightning conditions.

We aimed for a method that can be used for any camera, whether it is linear or not. We wanted it to be adaptive to scene content and also to work on-line, as the capturing process is ongoing, without the need of being fed with any information about the scene. We also wanted the method to be tunable. The default configuration is to find a minimum bracketing set for the given camera and scene. However this would also mean reduced SNR compared to captures with larger number of shots and longer exposure times. Therefore, the user can tune the balance between shorter captures or higher SNR levels. We also included a parameter to bound the radiance range to be captured if we are not interested in recovering the full dynamic range, neglecting the extreme low or high radiances present in the scene (deep shadows or brilliant highlights).

We compared the SNR performance of our method, using 5 different tunning conditions (AEE-A to AEE-E), against the best SNR case that our camera can achieve. The latest case is called the ground truth (GT), and it is an HDR radiance map generated using every available exposure time that our camera offers (optimal SNR case).

2. METHOD

We present here the results obtained using a consumer camera model Canon EOS 7D working in sRGB jpeg mode (non linear). Nonetheless, the method was successfully tested as well in two linear scientific cameras (monochrome Retiga 1300 and RGB Retiga 1300C working in raw mode), yielding similar results as the ones presented here (Martínez et al. (2015)).

Our Canon camera was driven from a laptop computer via USB interface. The method proposed was implemented using Matlab and worked on-line. For the generation of GT images we just captured all 55 available exposure times in the camera.

Our method uses an initial shot as starting point. It can be any exposure time, as long as the resulting LDR image has some useful pixels (neither underexposed nor saturated). A good initial exposure time is the one implemented in the auto-exposure setting of most consumer cameras. If the camera used does not implement this function, then any intermediate exposure time would work good.

Once this image is captured, we calculate its cumulative histogram. This cue will give us information of the pixel populations which were correctly exposed in this first shot. The idea of using cumulative histograms to control sensor responses to pixel populations in the scene was taken from Grossberg and Nayar (2002), who originally used it to select pixel populations for CRF estimation.

We will consider at this point two sensor response levels: low (Lo) and high (Hi). Our algorithm will consider underexposed any sensor response that is below Lo level, and saturated whatever is above Hi level. This way, the user can tune the method. If Lo and Hi levels are set very close to the extreme sensor response values (say 0 and 255 for 8 bits data), the overlap between consecutive shots will be minimal, yielding thus a minimum bracketing set as output. If otherwise the Lo and Hi levels are selected far from these extremes, then the redundancy between consecutive shots will increase and the SNR of the resulting HDR radiance map will be higher at the cost of more shots and longer total exposure time.

So if thanks to the cumulative histogram of the image, we know the sensor responses at the Lo and Hi limits (DC_{Lo} and DC_{Hi}), and we also know the CRF, and the exposure time used (ΔT_0), we can determine the relative irradiance values (E_{Lo} and E_{Hi}) for the areas of the image which lie just in the limits of the correct exposure, as shown in equation 1:

$$E_{Lo}=\frac{CRF^{-1}(DC_{Lo})}{\Delta T_0} \quad E_{Hi}=\frac{CRF^{-1}(DC_{Hi})}{\Delta T_0} \qquad (1)$$

Now the aim is to find new exposure times, that shift the sensor responses corresponding to these irradiance values, to the opposite limit (Lo or Hi) that they were found in. For this purpose now we determine that the new longer and shorter exposure times (ΔT_{longer} and $\Delta T_{shorter}$), are calculated as shown in equation 2:

$$\Delta T_{longer}=\frac{CRF^{-1}(DC_{Hi})}{CRF^{-1}(DC_{Lo})}\cdot\Delta T_0 \quad \Delta T_{shorter}=\frac{CRF^{-1}(DC_{Lo})}{CRF^{-1}(DC_{Hi})}\cdot\Delta T_0 \qquad (2)$$

When the new exposure times are estimated, the algorithm will order to the camera, to acquire new pictures using them. For the new LDR images captured, the same procedure will be followed to find longer and/or shorter exposure times if needed. The stopping condition for this process would be to check in the cumulative histograms of the new LDR images captured, if the pixel population above Hi level or below Lo level is below some threshold percentage set by the user (zero for full range).

3. RESULTS AND DISCUSSION

We captured a set of 24 indoors and outdoors HDR scenes using our method. In every scene captured, the full dynamic range was recovered successfully, except for the case of direct sunlight, like figure 1. We see all its LDR exposures and the tone-mapped version of its HDR radiance map generated. We can also see the cumulative histograms of each LDR image. In figure 2, some other HDR tone-mapped radiance maps are shown, corresponding to outdoors and indoors scenes where the irradiance levels were lower than daylight skies'.

In order to study the SNR performance of the proposed method for different tuning conditions, we created a controlled illumination indoors scene to avoid illumination changes during the experiment. This is important because during the whole capturing process we need no changes in the radiance conditions coming from the scene to happen. This is a key factor to consider the irradiance on the sensor as a constant and not as a variable. With natural illumination this radiance stability is not controllable. We generated 6 sets of 10 HDR radiance maps. 5 of them were generated using our method with different tuning conditions (AEE from A to E). The other one was generated using all available exposure times in the camera (GT).

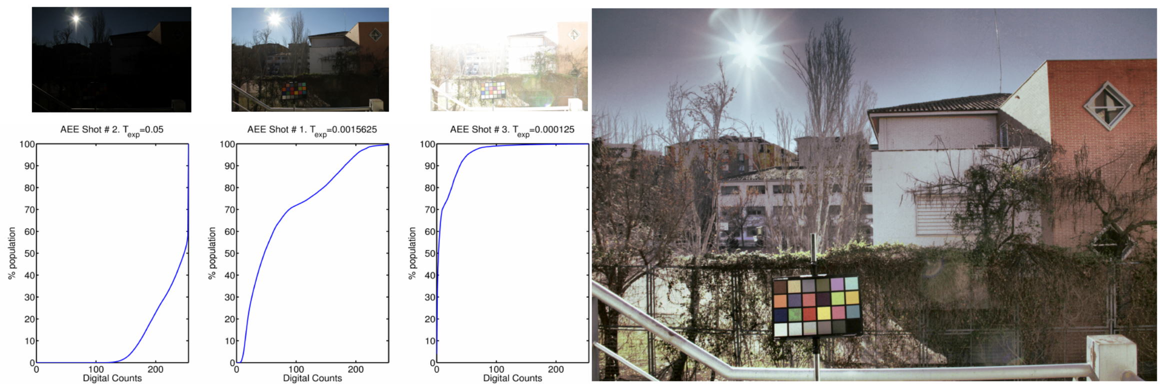

Figure 1: LDR images and histograms, and tone-mapped HDR radiance map.

Table 1. Numerical results of SNR study.

Condition	Lo level	Hi level	# of shots	ΣΔT (s)	SNR (dB)	std(SNR)
AEE A	3	252	3	8.313	23.82	2.42
AEE B	5	250	3	21.31	25.81	2.94
AEE C	10	245	3	30.2504	26.62	6.68
AEE D	30	225	4	30.252	28.14	3.45
AEE E	55	200	6	31.468	28.55	4.57
GT	X	X	55	151.4308	31.38	6.52

Numerical results are shown in table 1. We can see the total number of shots, total exposure time, average SNR and standard deviation of SNR and the Lo and Hi levels tuned.

As we can see, the minimum bracketing set achieved to recover the full dynamic range of the scene happened when setting the Lo and Hi levels close to the 8 bits sensor responses extremes. As we move these levels further from the extremes of the range, the number of shots and/or the total exposure time increase, and so does the average SNR. This is expected as for longer exposure times the signal is higher as well as because higher number of shots means to average more LDR images thus reducing the noise to a lower level.

In figure 3 we can see the HDR radiance map of the HDR indoors scene generated, as well as the SNR histograms of each of the tuning conditions tested.

Figure 2: Tone-mapped HDR radiance maps of outdoors and indoors scenes.

These results prove the ability of the proposed method to recover full range HDR radiance maps for any lightning condition, finding minimal bracketing sets, as well as the ability to control the balance between total exposure time (number of shots) and SNR. Therefore, for each application, the user can decide if faster acquisitions are more important or higher SNR are key factor, sacrificing capture speed.

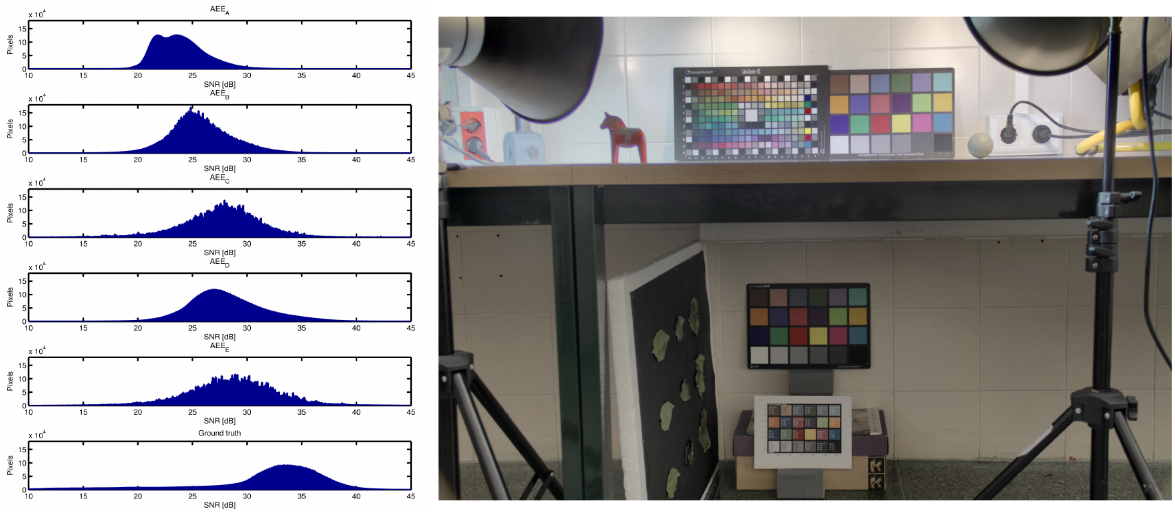

Figure 3: SNR histograms and tone-mapped HDR radiance map of indoors scene.

4. CONCLUSION

We have extended the applicability of a recently proposed method for estimating the bracketing set needed for a HDR radiance map capture via multiple LDR exposures. Our method adapts to any camera whatever camera response function has, as well as to any scene content. There is no need to know any information about scene content prior to the capture. Only a first exposure of the scene where some pixels are neither underexposed nor saturated is sufficient. We have captured several HDR scenes and in all of them the full dynamic range was covered except for direct sunlight.

We have also tested the ability of our method to be tuned in order to increase the SNR performance, at the cost of increasing also the total exposure time. We have seen how the more shots the method adds to the capture, the more similar the SNR performance is with the optimal one achievable by the camera.

The proposed method is therefore suitable for HDR imaging in any application, artistic, industrial or scientific, independently of the number of spectral channels or camera response function that the imaging system has.

ACKNOWLEDGEMENTS

This work was supported by the Ministry of Economy and Competitiveness of Spain, under research grant DPI2011-23202.

REFERENCES

Debevec, P. and Malik, J. 2008. Recovering high dynamic range radiance maps from photographs. In ACM SIGGRAPH 2008 proceedings 31.

Granados, M. Ajdin, B. Wand, M. and Theobalt, C. 2010. Optimal HDR reconstruction with linear digital cameras. In IEEE Conference on Computer Vision and pattern recognition 215-222.

Hirakawa, K. and Wolfe, P. J. 2010. Optimal exposure control for High Dynamic range imaging. In IEEE International Conference on Image Processing 3137-3140.

Gallo, O. Tico, M. Manduchi, R. Gelfand, N. and Pulli, K. 2012. Metering for exposure stacks. In Computer Graphics Forum 31, 479-488.

Stumpfel, J. Tchou, C. Jones, A. Hawkins, T. Wenger, A. and Debevec, P. 2004. Direct HDR capture of the sun and sky. In Proceedings of the 3rd International Conference on Computer Graphics, Virtual Reality, Visualization and Interaction in Africa 145-149.

Bilcu, R. C. Burian, A. Knuutila, A. and Vehvilainen, M. 2008. High Dynamic Range imaging on mobile devices. In the 15th IEEE International Conference on Electronics, Circuits and systems 1312-1315.

Hassinoff, S. W. Durand, F. and Freeman, W. T. 2010. Noise-optimal capture for high dynamic range photography. In IEEE Conference on Computer Vision and Pattern Recognition 553-560.

Barakat, N. Hone, A. N. and Darcie, T. E. 2008. Minimal-bracketing sets for high-dynamic-range image capture. In IEEE Transactions on Image Processing 1864-1875.

Martínez, M. A. Valero, E. M. Hernández-Andrés, J. 2015. Adaptive exposure estimation for high dynamic range imaging applied to natural scenes and daylight skies. Applied Optics Vol. 54, No. 4, B241-B250.

Grossberg, M. D. and Nayar, S. K. 2002. What can be known about the radiometric response from images?. In Computer Vision ECCV 189-205.

Address: MSc. Miguel Ángel Martínez, Color Imaging Laboratory, Department of Optics, Faculty of Sciences. University of Granada 18071, Granada, SPAIN.
E-mails: martinezm@ugr.es, valerob@ugr.es, javierha@ugr.es.

Real-time Green Visibility Ratio Measurement

Motonori DOI [1], Akira KIMACHI [2], Shogo NISHI [2]

[1] Department of Telecommunications and Computer Networks,
Osaka Electro-Communication University
[2] Department of Engineering Informatics, Osaka Electro-Communication University

ABSTRACT

The green visibility ratio is one of the important indices for urban environment assessment. The green visibility ratio is defined as the ratio of vegetation green in an image. The green area is usually detected manually. There is a product for automatic green visibility ratio measurement, which measure the green visibility ratio using color information only. Some artificial green objects often exist in the urban scene. Therefore, the discrimination of the vegetation green from other green objects is required for automatic green visibility ratio measurement. This paper presents a new method for the detection of vegetation green area based on the brightness changes in vegetation area. The experimental results showed the feasibility of the proposed method. We implemented a prototype system of the real-time green visibility ratio measurement by using the proposed method.

1. INTRODUCTION

There are some indices for urban environment assessment, such as the green plot ratio (Ong 2003) or the green visibility ratio (Ohki 2009). The green visibility ratio (GVR) is often used by Japanese local governments. The GVR is defined as the ratio of vegetation green in an image. The green area is usually detected manually. There is a product for automatic GVR measurement (Takizawa 2013), which measures the GVR using color information only. Some artificial green objects often exist in the urban scene. Therefore, the discrimination of the vegetation green from other green objects is required for automatic GVR measurement.

This paper presents a method for vegetation green area detection and a real-time GVR measurement system by using the proposed method. The vegetation green detection method is based on the analysis of color and image texture.

2. VEGETATION GREEN VS. NON-VEGETATION GREEN

Vegetation green and non-vegetation green have different characteristics in images. Natural vegetation green is defined as green colors observed in leaves of trees and grasses. Leaves are interlaced and have shades and shadows. Vegetation green areas exhibit large brightness changes caused by the shades of leaves, as shown in a sample scene in Figure 1, which contains bamboo leaves and a green chalkboard. These brightness changes in green areas allow humans to correctly identify vegetation areas.

In contrast, non-vegetation green areas arise from artificial green objects such as signboards, in an outdoor natural scene. These green areas usually exhibit uniform color or only small color variation. For example, the chalkboard in Figure 1 is recognized as a uniform surface with a certain color.

3. IMAGE PROCESSING FOR DETECTING BRIGHTNESS CHANGE

We define the vegetation green area as a green color area that undergoes frequent brightness changes. A simple, but effective, image processing technique for detecting brightness changes is edge detection because in image processing edges are defined as a local structure with large brightness changes and thus often related to object contours. The result of edge detection for the image in Figure 1 is shown in Figure 2, which represents the intensity of edges in grayness. The area of bamboo leaves produces many edges, whereas the chalkboard yields few edges associated with letters and attached sheets.

Edges are detected by differential operators in general. The most popular differential filter is the Sobel filter, which consists of two operators for detecting vertical and horizontal edges. Figure 3 shows these operators with the size of 3 pixels square. In the

Figure 1: A picture containing vegetation green (bamboo leaves) and non-vegetation green (a green chalkboard).

Figure 2: Edges extracted from Figure 1, with gray values denoting edge intensities.

1	0	-1
2	0	-2
1	0	-1

(*a*) *Vertical edge filter*

1	2	1
0	0	0
-1	-2	-1

(*b*) *Horizontal edge filter*

Figure 3: Sobel edge filters.

case of vertical edge detection, the differential in pixel values between the leftmost and the rightmost pixels in the 3x3 neighborhood of a target pixel is calculated. In general, the outputs of vertical and horizontal edge detection are combined.

4. AUTOMATIC DETECTION OF VEGETATION AREA

We propose a method for detecting vegetation areas by edge detection and subsequent image processing. The scheme of the method is shown in Figure 4.

First of all, the image of a scene is captured. Then, from the captured image, green color pixels are detected as those with a high G ratio and low R and B ratios to the sum of R, G and B values of the pixel. Meanwhile, edge pixels are detected with the Sobel filters for the G channel of the image, and assigned a flag “1”. The vegetation green pixels are then detected by AND operation between the green color pixel and the flag of edge pixels. Next, the vegetation green pixels are binarized. The vegetation area has some holes by non-uniformity of the texture. Therefore, recursive dilation and erosion operation is done for closing holes in the vegetation green area. Finally, the ratio of the number of pixels in the vegetation area to those of all pixels in the image is calculated.

5. EXPERIMENTS

We conducted experiments for evaluating the effectiveness of the proposed method. We took several pictures containing trees and artificial green objects in urban scenes as shown in Figure 5. The size of these images was 816 x 612 pixels. The vegetation areas were detected from these images.

Figure 6 shows the green color areas in Figure 5, that was determined by the ratios of R,G and B. When a pixel had the ratios of R and B larger than 0.4 and that of G smaller than 0.35, it was regarded as a non-green color pixel. Moreover, the green colors close to

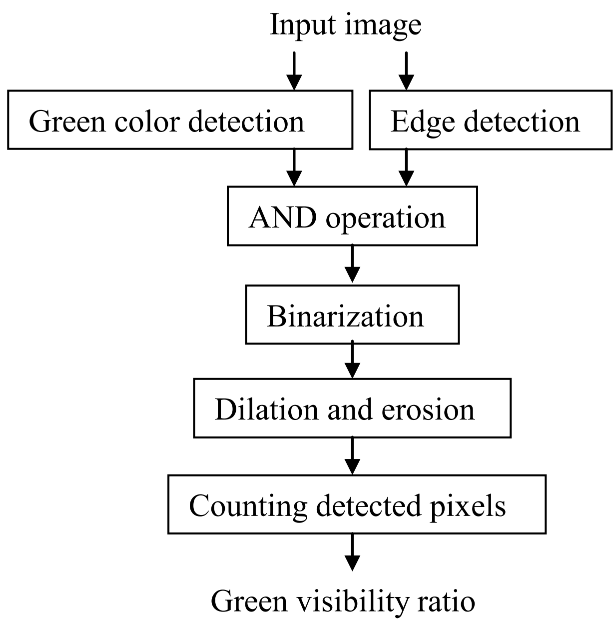

Figure 4: Scheme of vegetation green area detection.

white or black were also regarded as non-green. In Figure 6, non-green color pixels are painted in white. Detected green color areas in both images contain both vegetation green and artificial green. In this experiment, we used a simple color detection procedure. Even if we use more complicated color detection method, the detected vegetation green area will contain artificial green in some cases.

The results of the vegetation detection are shown in Figure 7, which depicts the vegetation areas as white. Successive operations of three dilations, six erosions and three dilations were applied for closing holes. These result images show that the proposed method detects correct vegetation areas of trees and leaves from the complicated scene.

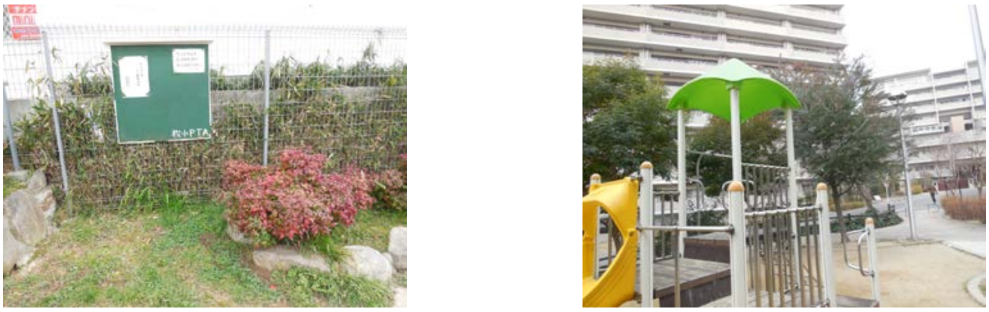

(*a*) (*b*)

Figure 5: Pictures for evaluation

(*a*) (*b*)

Figure 6: Green color areas detected from pictures in Figure 5.

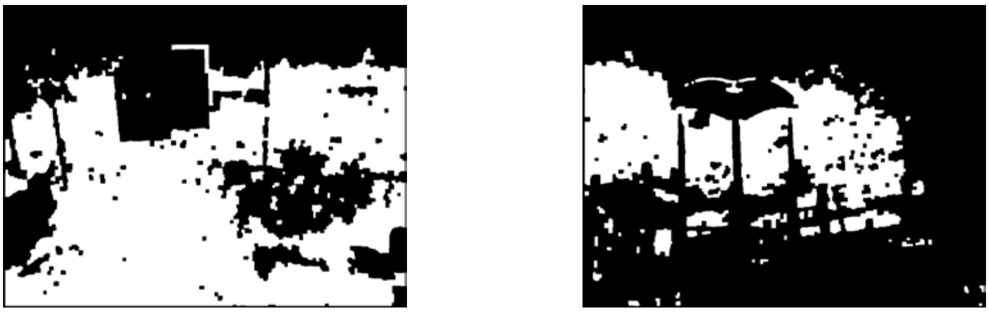

(*a*) (*b*)

Figure 7: Results of vegetation area detection for pictures in Figure 5.

Artificial green objects, which also appeared in the image, are nearly completely eliminated, though some part of object contours are wrongly detected. The GVRs were 41.3% for Figure 7 (a) and 24.0% for Figure 7 (b).

6. IMPREMENTATION

We implemented a prototype system for real-time GVR measurement by the proposed method. The system consists of a laptop computer (Mouse Computer W170HN, CPU: Intel Core i5-2450M 2.50GHz, Memory: 8GB) and a USB camera (Logicool HD Pro Webcam C920). The size of the input images was VGA (640 x 480 pixels). We developed the system by using Microsoft Visual Studio 2010 and the Open CV library, which is an open source library for computer vision programming.

Figure 8 shows a part of the PC monitor image during real-time processing. The left window shows the input image and the right shows the detected vegetation area and its GVR, 21.9% in this scene. The frame rate was about 5 fps.

7. CONCLUSIONS

This paper has proposed a method for vegetation green area detection from complicated scenes consisting of leaves and artificial green objects. The method detects green color areas with brightness fluctuation, which appear in leaf areas of images. The brightness fluctuation is detected as edges by the Sobel filters. We conducted experiments with images containing trees and artificial green objects. The experimental results show the correct detection of tree areas and thus demonstrate good feasibility of the proposed method. We implemented a prototype system for real-time GVR measurement by the proposed method. The system detected vegetation green areas and calculated GVR at a frame rate of 5 fps.

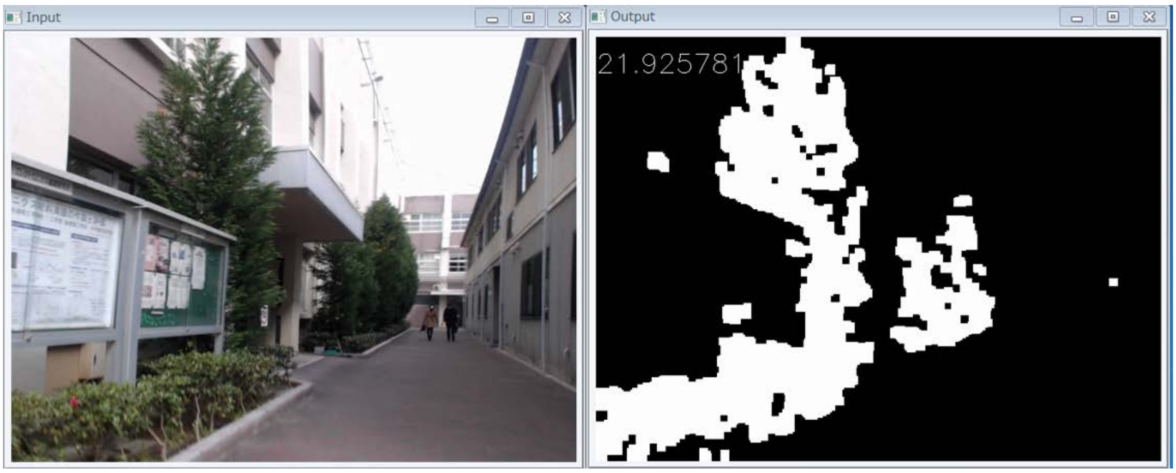

Figure 8: Screen shot of real-time processing.

REFERENCES

Ohki. T., et al., 2009. Proposal of the Green Landscape Evaluation Method That adopts Each View Angle Green Visibility Ratio, In *the 23rd Conference on Environmental Information Science*, 367-372. (in Japanese, with English abstract)

Ong. B. L., 2003. Green plot ratio: an ecological measure for architecture and urban planning, *Landscape and Urban Planning* 63: 197-211.

Takizawa. S., et al., 2013. Development of an instrument for the urban-green measure, In *the 44th Annual Meeting of Color Science Association of Japan*, 314-315. (in Japanese)

Address: Motonori Doi, Department of Tele-Communication and Computer Networks,
Osaka Electro-Communication University,
18-8 Hatsu-cho, Neyagawa, Osaka 572-8530, JAPAN
E-mails: doi@isc.osakac.ac.jp, kima@oecu.jp, s-nishi@isc.osakac.ac.jp

Evaluation of 20 p/d-safe colors used in image color reduction method for color deficient observers

Takashi SAKAMOTO
National Institute of Advanced Industrial Science and Technology (AIST)

ABSTRACT

This manuscript describes an evaluation of the safe colors used in the author's previous study on color vision deficiency. In my previous manuscript, a color reduction method especially designed for protan and deutan color vision deficiency (commonly known as red-green color blindness) was proposed. This method enables the replacement of protan- and deutan-confusion colors in target images with preliminarily selected protan- and deutan-safe (p/d-safe) colors. In this study, the chromaticity distribution of 20 p/d-safe colors is analyzed and evaluated using the CIELAB color space and a quasiuniform color space theoretically derived from the LMS (the response of the long, medium, and short cones of the human eye) color space. The results of the evaluation are described in this manuscript taking into consideration the uniformity of the chromaticity distribution of 20 p/d-safe colors, the color distance between each color, and the image processing utility of the color reduction implemented as a look-up table. The results of this study suggest that the chromaticity distribution of the 20 p/d-safe colors and the number of colors applied for the proposed color reduction method have to be optimized.

1. INTRODUCTION

A color vision deficiency such as protan and deutan defects occurs when the cells in the human retina fail to function normally or lack one or more types of cone cells. In many cases, the dysfunction is caused by specific genetic factors that affect a considerable number of people. In Japan, for example, approximately 5% of males and 0.2% of females suffer from either protan or deutan defects. Globally, more than 200 million people suffer from some form of congenital color vision deficiency. Such people have difficulty distinguishing particular sets of colors. For example, protan and deutan observers confuse red with green, deep-red with black, pink with sky blue, blue-green with gray, and pea-green with yellow. These particular sets of colors are called confusion colors.

A congenital color vision deficiency is caused genetically and is currently incurable by means of surgery and other medical procedures, visual training, or electrotherapy. The most reasonable and effective means to assist those suffering from a color vision deficiency is to improve their visual environment using imaging devices (e.g., TVs, projectors, electronic bulletin boards, PC monitors, and smartphones). An image color enhancement is the most effective method to replace sets of colors that cause color confusion in color deficient observers.

Sakamoto (2015) proposed an image enhancement method using image color reduction that enables protan and deutan observers to distinguish between confusion colors. The proposed method is based on a simple color mapping and does not require a complex computation. This method is significant for its simplicity and use of a unique color palette. The color palette comprises 20 protan- and deutan-safe (abbreviated to p/d-safe) colors and was originally proposed by Ito et al. (2013). Ito and his colleagues have not intended to apply their color palette to photographic and image processing. In contrast, Sakamoto (2015) proposed the idea that a color palette consisting of preliminarily selected p/d-safe colors is applicable to the color reduction processing of photographic images. Sakamoto (2015) found that a color reduction method using 20 or less p/d-safe colors is effective for replacing confusion colors and enhancing a target image for protan and deutan observers.

Sakamoto (2015) also described a few problems related to the color selection of the p/d-safe colors. Twenty or less colors may be unsuitable for high-definition color image processing because there are too few colors to replace, and the image degradation caused by the color reduction was noticeable in the color processing results. The most appropriate and effective solution for this may be to increase the number of colors used in a p/d-safe color palette. If so, the chromaticity distribution of the colors in the p/d-safe color palette must be analyzed and optimized to avoid color confusion.

This manuscript describes an evaluation of the 20 p/d-safe colors used in Sakamoto (2015) and shows the analysis results of the uniformity of the chromaticity distribution of 20 p/d-safe colors, the color distance between 20 p/d-safe colors, and the utility of the color reduction implemented as a look-up table.

2. METHOD

2.1 Twenty p/d-safe colors

Twenty p/d-safe colors for protans and deutans were proposed by Ito et al. (2013). These colors consist of nine vivid and strong colors, seven soft and pale colors (excluding two alternative low-saturation colors), and four achromatic colors. These colors are selected on the basis of visual tests for protan and deutan observers such that they are easily identified, classified, and distinguished from each other by protan and deutan observers. However, Ito et al. (2013) did not describe a chromaticity distribution of the 20 p/d-safe colors. Figure 1 shows these 20 colors, their index numbers, and the sRGB [IEC 61966-2-1:1999 standard RGB color space (1999)] tristimulus values for each color, as defined in Ito et al. (2013).

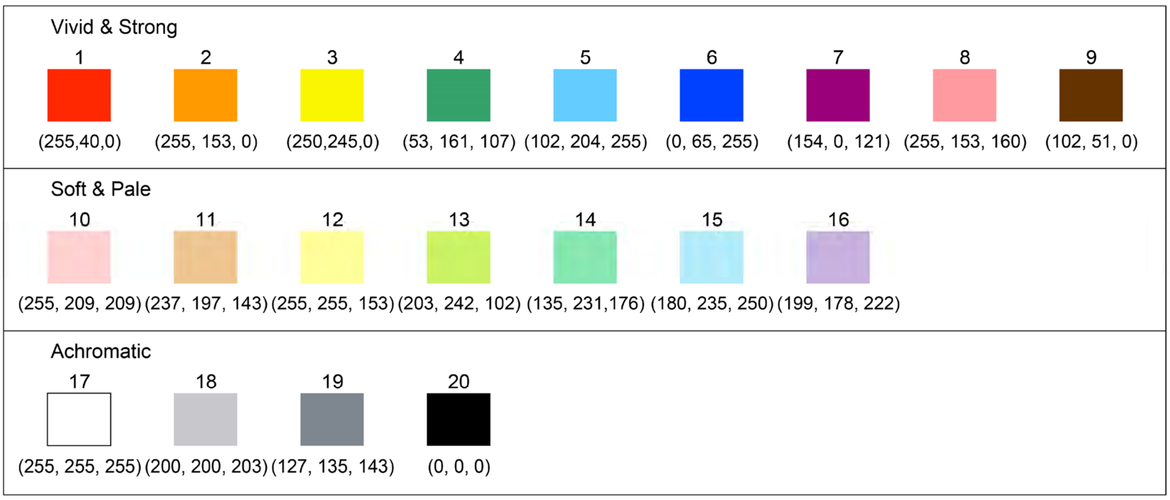

Figure 1: Twenty p/d-safe colors, their index numbers, and sRGB tristimulus values.

2.2 Simulation of protanopia and deuteranopia

Protanopic and deuteranopic color vision under the Joint ISO/CIE Standard Illuminant D65 (1999) condition is simulated according to the method proposed by Brettel et al. (1997). This study replaces the transformation matrix used in Brettel et al. (1997) with a Hunt–Pointer–Estevez matrix, as documented in Hunt (1995). This alternative matrix is used because the original matrix of Brettel et al. (1997) does not consider the illuminant D65 and sRGB color space.

Protanopic and deuteranopic simulated images are calculated as follows [with regard to the color spaces, sRGB, XYZ, and LMS are documented in Hunt (1995), Brettel et al. (1997), and IEC 61966-2-1 (1999)]: (1) the sRGB coordinates of the target image are converted into XYZ tristimulus values based on the reference document; (2) the XYZ tristimulus values are converted into LMS coordinates; (3) the LMS coordinates are modified according to the reduction in the cone types in the human retina, e.g., protanopia can be expressed by means of the M and S axes of the LMS coordinates; (4) the modified LMS coordinates are back-converted into XYZ tristimulus values; and (5) the sRGB coordinates of the simulation image are calculated from the XYZ tristimulus values.

2.3 CIELAB and $L^{\#}M^{\#}S^{\#}$ color spaces

The chromaticity distribution of the 20 p/d-safe colors and their protanopic and deuteranopic simulated colors are examined and analyzed using CIELAB, which is a perceptually uniform and standard color space [CIE 1976 color space, as documented in Hunt (1995)]. The lightness L* represents the darkest black at zero and the brightest white at 100. The a* and b* axes represent the degrees of chromaticness, and acromatic colors at a* = 0 and b* = 0.

The CIELAB color space represents a color difference by its Euclidean distance between colors. CIELAB can evaluate color differences perceived by observers with normal color vision but cannot deal with color differences perceived by observers with protan and deutan defects immediately. To deal with protanopic and deuteranopic color differences, the CIELAB values of protanopic and deuteranopic simulated colors must be known. Brettel et al. (1997) may be utilized for this purpose, but this procedure lacks precision because the simulation method is only an approximation of protanopic and deuteranopic views.

To avoid the approximation related to the protanopic and deuteranopic simulation, this study utilizes the LMS color space that can deal with and indicate protanopic and deuteranopic views of colors immediately in the form of tristimulus values. However, there remains another issue with the color differences in that the LMS color space is not perceptually uniform. In order to overcome this issue, this study proposes a new perceptually quasiuniform color space $L^{\#}M^{\#}S^{\#}$ and utilizes it for an analysis of the chromaticity distribution of the 20 p/d-safe colors. $L^{\#}$ is nonlinear transformation of the L axis of the LMS color space, and it is obtained by using the same nonlinear formula for the L* axis of the CIELAB color space. $M^{\#}$ and $S^{\#}$ are also obtained using a similar procedure for the M and S axes of the LMS color space.

3. RESULTS AND DISCUSSION

3.1 Chromaticity distribution analysis using CIELAB

Figure 2 shows the chromaticity distribution map of the 20 p/d-safe colors along the a* and b* axes. Black squares represent views of normal color vision, red circles represent simulated views of protanopic color vision, and blue triangles represent simulated views of deuteranopic color vision. The solid lines and filled dots represent the vivid and strong colors that are indicated as No. 1 to No. 9 in Figure 1. The dashed lines and open dots represent the soft and pale colors that are indicated as No. 10 to No. 16 in Figure 1. Achromatic colors (No. 17 to No. 20) are not indicated in Figure 2.

Figure 3 shows the chromaticity distribution map of the 20 p/d-safe colors along the L* and b* axes. Black squares, red circles, and blue triangles represent the same color vision categories as shown in Figure 2. Additionally, the green diamonds and solid lines represent the achromatic colors that are indicated in Figure 1 as No. 17 to No. 20. The other solid lines and filled dots represent vivid and strong colors, and the dashed lines and open dots represent soft and pale colors that are in the same color categories as in Figure 2.

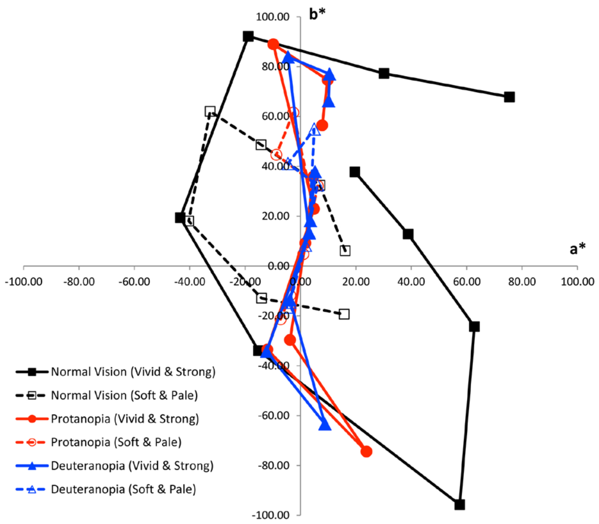

Figure 2: Chromaticity distribution map of the 20 p/d-safe colors along the a and b* axes.*

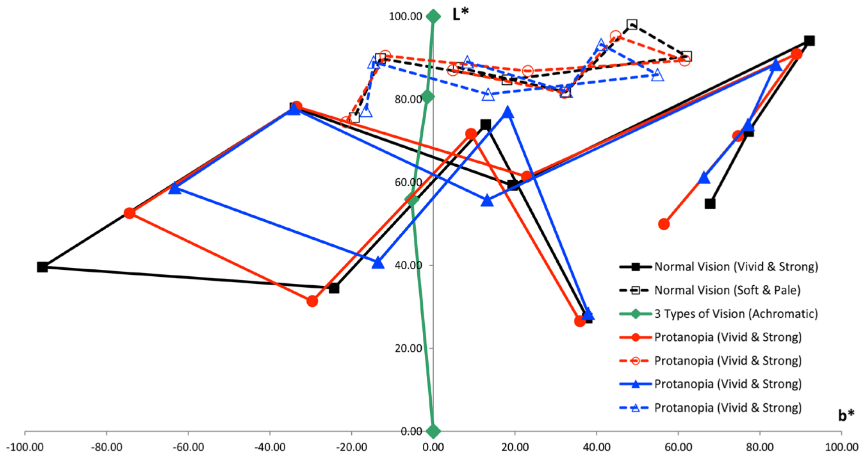

Figure 3: Chromaticity distribution map of the 20 p/d-safe colors along the L and b* axes.*

Figure 2 suggests that protanopic and deuteranopic observers can hardly perceive color differences along the a* axis. From Figure 3, we know that protanopic and deuteranopic observers can distinguish between 20 colors using the L* and b* axes. In addition, we know that vivid and strong colors have longer color distances between each other than soft and pale colors, which suggests that soft and pale colors are more difficult to distinguish amongst each other. Figure 2 also suggests that achromatic color No. 18 has lower color distances between it and soft and pale colors such as No. 10, No. 15, and No. 16, which suggests that pale gray (No. 18) may be confused with pale pink (No.10), pale blue (No. 15), and pale violet (No. 16).

3.2 Chromaticity distribution analysis using $L^{\#}M^{\#}S^{\#}$

Figure 4 shows the chromaticity distribution maps of the 20 p/d-safe colors; the left-side distribution map describes protanopic views of colors using the $M^{\#}$ and $S^{\#}$ axes, and the right-side distribution map describes deuteranopic views of colors using the $L^{\#}$ and $S^{\#}$ axes. Black squares represent the vivid and strong colors that are indicated as No. 1 to No. 9 in Figure 1. Green circles represent the soft and pale colors that are indicated as No. 10 to No. 16 in Figure 1. Achromatic colors (No. 17 to No. 20 in Figure 1) are represented by blue triangles, and the dashed lines represent the ideal achromatic line (equal-energy line). The red circles will be used in further discussion.

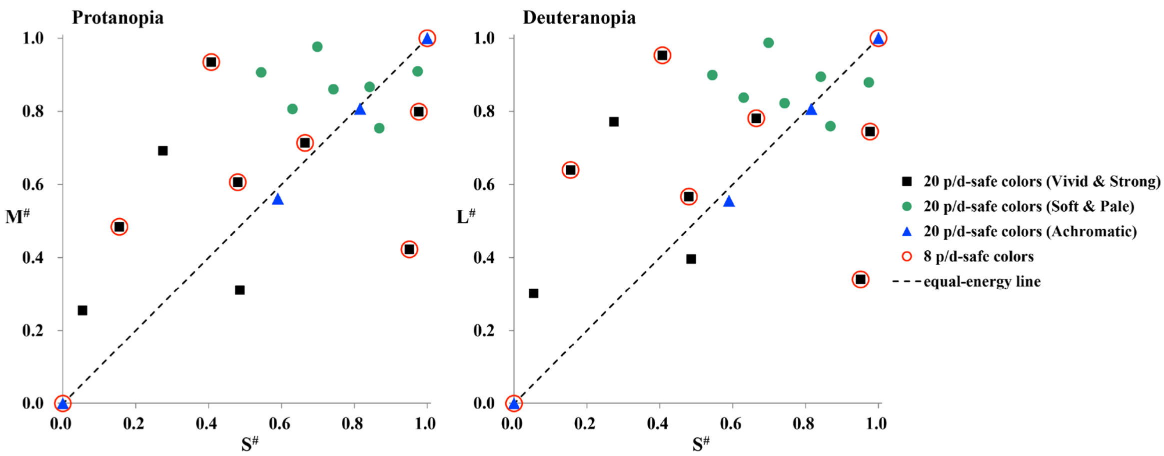

Figure 4: Chromaticity distribution map of the 20 p/d-safe colors using $L^{\#}$, $M^{\#}$, and $S^{\#}$.

Figure 4 suggests that vivid and strong colors have longer color distances between each other than soft and pale colors, which suggests that soft and pale colors are more difficult to distinguish amongst each other. Figure 4 also suggests that achromatic colors such as pale gray (No. 18) and gray (No. 19) have lower color distances between them and the other chromatic colors such as green (No. 4), pale pink (No. 10), pale green (No. 14), and pale violet (No. 16).

Figure 3 and Figure 4 also suggest that the 20 p/d-safe colors include few low-lightness colors, so the number of colors should be increased, and low-lightness colors such as deep blue and deep green should be utilized for the p/d-safe color palette. On the other hand, the number of soft and pale colors seems to be too high to distinguish between them. Soft and pale colors and gray may be redesigned to have uniform color differences between each color.

4. CONCLUSIONS

This study evaluated the chromaticity distribution of the 20 p/d-safe colors used in Sakamoto (2015). The evaluation revealed that the 20 p/d-safe colors had a lopsided distribution in the CIELAB and proposed $L^{\#}M^{\#}S^{\#}$ color spaces. The number of soft and pale colors may be too high to distinguish between them, and the number of low-lightness colors may be few, thereby allowing for an increase in the number of colors.

Eight p/d-safe colors, as indicated by the red circles in Figure 4, are easy to use in image color processing, and these eight colors have sufficient color differences between them. Therefore, these eight colors and the other color sets comprised of a few pale and dark colors, and gray colors may enable the construction of an appropriate p/d-safe color palette for the image color reduction method.

ACKNOWLEDGEMENTS

This work was partly supported by grants from KAKENHI (24650362).

REFERENCES

Brettel, H., F. Vienot, and J. Mollon. 1997. Computerized simulation of color appearance for dichromats. *Journal of the Optical Society of America A* 14 (10) 2647–2655.

Hunt, R. W. G. 1995. *The Reproduction of Colour*. Wiley.

International Electrotechnical Commission. 1999. *IEC 61966-2-1:1999 Multimedia systems and equipment - Colour measurement and management - Part 2-1: Colour management - Default RGB colour space - sRGB*, Geneva, Switzerland. International Electrotechnical Commission.

Ito, K., Japan Paint Manufacturers Association, DIC Corporation, Color Universal Design Organization, Maekawa, M. 2013. *Color Universal Design Color Set Guide Book 2013*. Taisei-sha (in Japanese).

Joint ISO/CIE Standard. 1999. ISO 10526:1999/CIE S005/E-1998. *CIE Standard Illuminants for Colorimetry*. International Organization for Standardization.

Sakamoto, T. 2015. Image color reduction method for color-defective observers using a color palette composed of 20 particular colors. *Proc. SPIE* 9395 (939514) 1–6.

Address: Dr. Takashi SAKAMOTO, Human Technology Research Institute,
National Institute of Advanced Industrial Science and Technology (AIST),
AIST Central 2, Umezono 1-1-1, Tsukuba, Ibaraki, 305-8568, JAPAN
E-mail: takashi-sakamoto@aist.go.jp

Silkscreen Printing on Cotton Fabrics with Soil Colorant

Somporn JENKUNAWAT[1], Pratoomtong TRIRAT[2] and Kulthanee SIRIRUK[3]
[1] Faculty of Agricultural Technology, RMUTT
[2] Faculty of Mass Communication Technology, RMUTT
[3] Phanomwan Technology College, Thailand

ABSTRACT

Recently, there is an increasing interest in natural or eco-colorants. Soils are natural colorants that have been used since ancient times before synthetic colorant quickly replace them. In this study 3 types of soil: black-, yellow- and red soils were used as sources of colorants of silkscreen ink for printing on cotton fabrics. Soil colorants were prepared by grinding soil into fine powder, then dissolved with water and left overnight for sedimentation. The supernatant liquid was discarded and the sediment was collected as soil colorant. Soil colorants were mixed with water based silkscreen medium for silkscreen inks. Physical properties of 3 types of silkscreen inks from soil colorants were measured. The result showed that density of silkscreen ink of black soil, red soil and yellow soil colorant were 1.02, 0.53 and 0.75 and the CIE (L*a*b*) values were L* = 47.79, a* = 7.57 b*= 19.54; L* = 72.18, a* = 17.88 b*= 27.55; L* = 72.26, a* = 15.18 b*= 38.91, respectively. Silkscreen inks from soil colorants were printed on cotton fabrics with the resolution of image printed at 30 LPI. The printed cotton fabrics were measured for halftone, dot gain, density, and wash-resistant. The results showed that silkscreen ink printed on cotton fabrics gave good quality line at 1-6 points for every soil colorant. The halftone was 10-50 per cent for red- and yellow soil while black soil halftone was 10-40 per cent. Densities of printed cotton fabrics before washing were 1.02, 0.53 and 0.75 for black-, red- and yellow soil, respectively. After washing printed cotton fabrics for three times the results showed that densities were changed to 0.99, 0.52 and 0.73, respectively. Dot gain of black soil at 10 - 20 per cent showed normal dot gain and gave a good printing quality but dot gain more than 60 per cent appeared solid ink density. While red- and yellow soil dot gain was 10-40 per cent showed normal dot gain and gave a good printing quality but dot gain more than 70 per cent showed solid ink density. In addition, quality of printed cotton fabrics not only depends on printing ink but also the worker has to have printing experience.

1. INTRODUCTION

Soil is the most important natural resources. The differences of soil when we looking is colors. In agriculture soil color means the fertile of the soil but for painter or artist soil colors were used as coloring agents. Soil series in Thailand was report including soil color (Boonsompopphan et al, 2008). The identification of soil series also showed the difference of soil color and properties. Blavet et al (2002) reported that the mean angular hue and mean redness rating of a soil are significantly linked to annual soil waterlogged rate. Hyun Jin Jeong studied her master degree on soil as fabric dyes. She collected 45 different soils across South Korea and United Kingdom and categorize them into seven different color families. Jeong apply soil-based paint directly to fabric (Earth dyeing, 2014). Trirat et al (2014) and Chotaku et al (2014) reported used soil dyes for colored handmade paper and printing ink, respectively. Nowadays, environmental have been more concerned especially toxic materials. Authors aim to reduce the use of harmful chemicals by replacing it with a friendly natural material that can be easily obtained such as the soil to replace chemical colorants.

2. METHOD

Three types of soil color were collected from the areas of Pathumthani province: red, yellow and black soil. Soil colorants were prepared by drying and grinding soil into fine powder. To make soil colorant, 100g of soil powder was added into 500 ml of clean water and mixed well by the blender. The mixture was filtered through muslin sheet to remove debris, and the mixture was left overnight for sedimentation. The supernatant liquid was discarded and the sediment is collected as soil colorant. Soil colorant was mixed with water based silkscreen medium for making silkscreen ink by adding 75 ml of soil colorant into 100 ml of water-based resin, and the mixture was mixed well by hand. Prepare screen frame by using T48 screen. Silkscreen inks from soil colorants were printed on cotton fabrics with the resolution of image printed at 30 LPI by using square-shaped rubber with the off contract of 3.0 mm. Printed cotton fabrics were measured for density, CIE-L*a*b* values, dot gain, the quality of silkscreen printing ink from soil colorants on cotton fabric. Printed cotton fabric was test for wash resistant by using washing machine with the ratio of detergent and water at 15g: 5L. The printed cotton fabric was washed for three times. Printed cotton fabric was washed for 5 minute and then rinsed with water for another 5 minutes, after that they were dried by sun light and density was measured after drying.

3. RESULTS AND DISCUSSION

The density and CIE L*a*b* of silkscreen ink were shown in tables 1. The result showed that density of silkscreen ink of black soil, red soil and yellow soil colorant were 1.02, 0.53 and 0.75 and the CIE (L*a*b*) values were L* = 47.79, a* = 7.57 b*= 19.54; L* = 72.18, a* = 17.88 b*= 27.55; L* = 72.26, a* = 15.18 b*= 38.91, respectively. The quality of silkscreen printing ink on cotton fabric showed that all types of colorants gave the line size from 1-6 point. The screen dot of water-based screen printing ink of red soil at 10 per cent was not appeared (Table 2). Similarly to yellow soil that could print only 7 percent while the black ink had 36.8 per cent. Water-based screen printing of black soil had dot gain from 10 per cent, but from 30 per cent it gave higher dot gain up to 80.8 per cent. When compared at 10 per cent, the black ink had more dot gain than red and yellow ink about 26 per cent. The results revealed that water-based screen printing ink able to print on figure with big screen dot or line printing. All type of soil colorants gave line printed of 1-6 point and area of halftone of black soil was 10-40 per cent while red and yellow soil had 10-50 per cent (Table 3).

*Table 1. The density and CIE L*a*b* of silkscreen printing ink on cotton fabric from 3 types of soil.*

Soil type	Density	CIE *L*a*b**		
		L*	a*	b*
Black	1.02	47.79	7.57	19.54
Red	0.53	72.18	17.88	27.55
Yellow	0.75	72.26	15.18	38.91

Table 2. The dot gain of silkscreen printing ink from 3 types of soil on cotton fabric.

Screen dot (per cent)	Black soil	Red soil	Yellow soil
10	36.8	0.0	7.0
20	64.1	21.0	32.1
30	80.8	40.1	51.0
40	85.9	66.9	58.2
50	90.0	73.3	82.1
60	93.8	83.4	84.8
70	93.8	92.0	90.5
80	93.9	94.1	97.1
90	98.3	99.4	99.0
100	100.0	100.0	100.0

Table 3. Line size and area of halftone of cotton fabric printed with silkscreen printing ink from 3 types of soil.

Soil type	Line size (Point)	Area halftone (per cent)
Black	1-6	10-40
Red	1-6	10-50
Yellow	1-6	10-50

Printed cotton fabrics were measured for density and then were washed for wash resistant. It was found that density was slightly decreased from before washed. Densities of printed cotton fabrics before washing were 1.02, 0.53 and 0.75 for black-, red- and yellow soil, respectively. After washing printed cotton fabrics for three times the results showed that densities were changed to 0.99, 0.52 and 0.73, respectively (Table 4).

Table 4. The density of silkscreen printing ink from 3 types of soil on cotton fabrics before and after washing.

Soil type	Before washing	First washing	Second washing	Third washing
Black	1.02	1.01	1.00	0.99
Red	0.53	0.53	0.52	0.52
Yellow	0.75	0.74	0.74	0.73

4. CONCLUSIONS

Different types of soil gave different color. Silkscreen printing ink from soil colorants gave a good printing quality on cotton fabric. The result revealed that water-based screen printing ink able to print on figure with big screen dot or line printing. The results showed that silkscreen ink printed on cotton fabrics gave good quality line at 1-6 points for every soil colorant. The halftone was 10-50 per cent for red- and yellow soil while black soil halftone was 10-40 per cent. Dot gain of black soil at 10 - 20 per cent showed normal dot gain and gave a good printing quality but dot gain more than 60 per cent appeared solid ink density. While red- and yellow soil dot gain was 10-40 percent showed normal dot gain and gave a good printing quality but dot gain more than 70 per cent showed solid ink density. Densities of printed cotton fabrics before washing were 1.02, 0.53 and 0.75 for black-, red- and yellow soil, respectively. After washing printed cotton fabrics for three times the results showed that densities were changed to 0.99, 0.52 and 0.73, respectively.

ACKNOWLEDGEMENTS

The authors would like to thanks students and officials of Faculty of Mass Communication Technology that took part in the experiment. We would also like to thank the Faculty of Agricultural Technology and Faculty of Mass Communication Technology, Rajamangala University of Technology Thanyaburi, Thailand for their support on our research and travel expense for the conference.

REFERENCES

Blavet, D., J.C. Leprun, E. Mathe and Pansu M. 2002. Soil colour variables as simple indicators of the duration of soil waterlogging in a West African catena. 17^{th} WCSS, 14-21 August 2002, Thailand. 1333-1-1333-11.

Boonsompophan, B., T. Vearasilp, T. Attanandana and R.S. Yost. 2008. Field identification of soil series-enabling Thai farmers share experience and knowledge. *Soil Science,* Vol.173, No.10:736-744.

Chotaku, S., P. Trirat , K. Siriruk. 2014. Water-Based Screen Printing Ink by Soil Dyes on Cotton Fabric for Community Products. AIC 2014: 312-314.

Jeong, Hyun Jin. 2014. *Earth dyeing*. Online:www.ecouterre.com/soil-as-fabric-dye-earth-dyeing-hits-pay-dirt/. Access: 25 May, 2014.

Trirat, P., S. Jenkunawat and V. Songcharoen. 2014. Dyeing paper by soil colorants for produce packaging paper. *Journal of the color science association of Japan,* Vol.38, No.3: 276-277.

Address: Somporn JENKUNAWAT, Faculty of Agricultural Technology,
Rajamangala University of Technology Thanyaburi, 39 Moo 1,
Rangsit-Nakornayok Road., Klong 6, Thanyaburi,
Pathumthani 12110, Thailand
E-mails: sompornjen@gmail.com

Estimation of the Environment Illumination Color Using Distribution of Pixels

Noriko YATA, Yuki ARAI, Yoshitsugu MANABE
Graduate school of advanced integration science, Chiba University

ABSTRACT

Techniques for estimating the illumination color of the imaging environment from an image are needed. This paper proposes a new technique to estimate the illumination color by examining pixel distributions in a characteristic space for each of the objective surfaces. A two-dimensional log-chromaticity differences space of the differences between logarithms of R and G, and B and G is used as a space of amount of characteristic. The proposal method to estimate the color of illuminations is a clustering of the characteristic values for each color temperature using support vector machine. In this study, the distributions of target pixels correspond to the surfaces of objects under different illumination conditions are plotted in the characteristic space. The training data are obtained from images of seven colors objects. In the results of the verification experiment for test data, the rate of correct estimation is 86.5 %. It can be expected to improve the illumination estimation accuracy through using combinations of different colors.

1. INTRODUCTION

We can perceive the colors of objects impervious to changing the illumination light in everyday life. On the other hand, colors of pixels in images depend on the surfaces conditions of the objects and the environment illuminations. It is difficult to determine which factor is cause of the changing color of pixels. The problem can be solved by performing the estimation of an illumination color and surface conditions of objects from a image. White patch retinex and gray world algorithm and others have been proposed as algorithms for representing the colors of objects without depending on the illumination light conditions. These algorithms are not performed an appropriate illumination estimation when white point is not present in the image or the scene has partial colors (Ebner 2007). The purpose of this study is to estimate the correlated color temperatures of the illumination light of the shooting environment from a single image that has partial color without white point.

2. METHOD OF CORRELATED COLOR ESTIMATION

The proposal method estimate the illumination color by clustering the pixel distribution in a feature space for each characteristic of the surfaces of objects. We focused on the log-chromaticity differences (LCD) that is proposed for shadow removal in images (Finlayson and Hordley 2001) as suitable features for the clustering. The method uses the LCD values in two-dimensional axes as the differences between the logarithm of R and G (log (R/G)), and B and G (log (B/G)) that represent colors of each pixel. The distribution of pixels color under various illuminations in LCD space is shown in Figure 1.

The method to estimate the correlated color temperatures of illuminations is a clustering of the LCD values for each color temperatures using support vector machine (SVM). The four values of log (R/G), log (B/G), angular coordinate in LCD space, and brightness obtained from target pixels are used to perform clustering for each image by SVM.

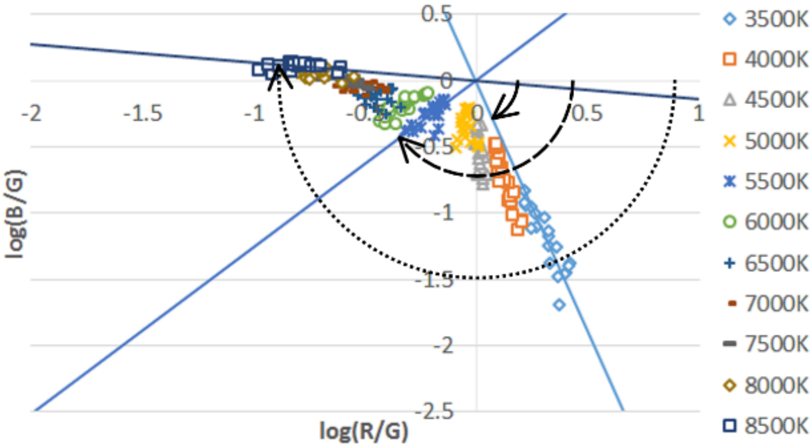

Figure 1: The distribution of pixels color and angular coordinate in LCD space.

3. EXPERIMENTATION AND RESULTS

3.1 Data preparation for Experiment

Illumination lights were configured to capture images for correlated color temperature estimation in the following way. The illumination lights was generated based on the spectral radiance of each color temperature using a spectral light source device. The actual spectral distributions and color temperatures of the illumination lights were measured using a spectral irradiance meter, and the measured values were defined as correct color temperatures of the illumination lights. In this study, the illumination light color temperatures of eleven types were set in 500 K increments of 3500 K to 8500 K for training data, and 24 types for test data. The correct classes and the color temperatures of the training data and the test data shown in Table 1.

The images of cylindrical papers with shading under controlled illuminations in dark room were used as test data for the experimentation. The colors of objects are seven types of white, gray, blue, green, orange, purple and yellow. The target pixels are taken from place of change to the shade from the bright part of the object, avoiding the specular reflection regions.

3.2 Verification Accuracy and Application to Color Correction

The results of estimation by proposed method are described follow. In the results of the verification experiment for the test data, the number of the estimated classes matched to the correct color temperatures has been 21 of 24 illumination conditions, and the rate of correct estimation has been 86.5 %. The proposed method has estimated the wrong class in three conditions of 3801 K, 7616 K, and 8136 K. Although our proposed method could not perform appropriate estimation for the three test data, all of these have been classified next to the correct class.

The color temperatures of the illumination lights were estimated using the images of new objects and the illuminations with different color temperatures with training data. The objects were cloth of four colors. Color corrections of the images were performed based on the estimated color temperatures, and the results were compared with white patch retinex (WPR) method. The examples of the color correction results are shown in Figure 2. Images shown in Figure 2 (a) and (d) are image before color correction, and the color temperatures of each image are 3285 K and 8597 K. Images shown in Figure 2 (b) and (e) are the results

Table 1. Correct classes and the color temperatures of the data.

Correct class	Color temperatures of training data (K)	Color temperatures of test data (K)
3500	3548	3289
4000	4055	3801
4500	4489	-
5000	4955	4939, 5009, 5093, 5161
5500	5552	5432, 5634
6000	6011	6106, 6207
6500	6512	6416, 6527, 6595, 6680
7000	6985	7091, 7096, 7098
7500	7496	7443, 7616
8000	7915	7885, 8114, 8136
8500	8485	8431, 8572

(a) Original image A (3285K) *(b) Proposed method for A* *(c) WPR for A*

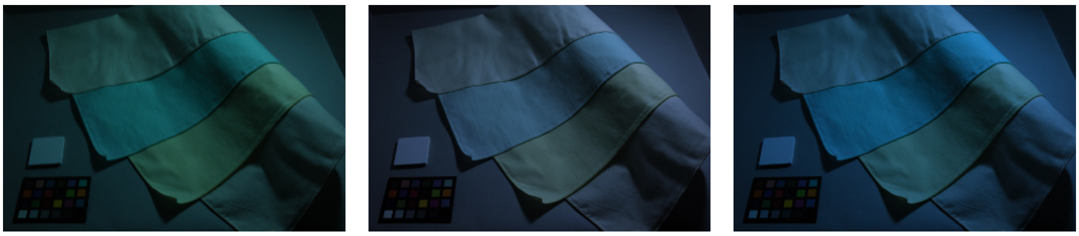

(d) Original image B (8597K) *(e) Proposed method for B* *(f) WPR for B*

Figure 2: The results of color corrections.

of our proposed method. Images shown in Figure 2 (c) and (f) are the results of WPR which use the information of white point. It can be seen that these images had been corrected from bluish or yellowish by both methods. The color differences ΔE^*_{ab} between the corrected images and the reference image were compared to quantitatively evaluate the color correction result by the proposed method and WPR. The reference was corrected image of the illuminated by 6382 K light. The differences were calculated on 24 colors of

Table 2. The mean color differences of ColorChecker.

Color temperatures of original images (K)	Proposal method	WPR
3285	12.24	15.02
4051	12.57	13.61
4492	13.13	13.01
5001	10.25	10.58
5608	7.14	6.62
6085	5.07	3.67
7102	3.69	3.84
7671	6.46	6.61
8156	7.10	8.07
8597	8.60	9.39

ColorChecker (x-rite). The mean color differences of ColorChecker shown in Table 2. The maximum value of the color difference of the proposed method has been smaller than that of WPR. The color differences of 5608K and 6085K however have been larger because the color temperatures of the estimated classes were incorrect in these conditions.

4. CONCLUSIONS

The new technique to estimate the illumination color was proposed in this paper. It was performed by examining the pixel distribution in a feature space for each characteristic of the surfaces of objects. The proposed method has shown better results than the WPR in verification of the accuracies of the estimated classes and the colors of corrected image.

It can be expected to improve the estimation accuracy using combinations of different colors objects to obtaining training data. Moreover, it is necessary a verification under illumination light such as fluorescent lamps and LED lights because neither of the training data and the test data was obtained from images taken in the same environment using the spectral light source device.

REFERENCES

Ebner, M. 2007. *Color Constancy*. New York: John Wiley and Sons.

Finlayson, G.D. and S.D. Hordley. 2001. Color Constancy at a Pixel. *Journal of Optical Society of America A* 18(2): 253-264.

Address: Noriko YATA, Graduate school of advanced integration science,
Chiba University, 1-33, Yayoi-cho, Inage-ku, Chiba-shi, Chiba 263-8522, JAPAN
E-mails: yata@chiba-u.jp, manabe@faculty.chiba-u.jp

A Spectral Reflectance Measurement System for Human Skin by Using Smartphone

Seungwan HONG, Norihiro TANAKA, Kosuke MOCHIZUKI
Faculty Business and Informatics, Nagano University

ABSTRACT

This paper describes a method for estimating the spectral reflectance of human skin based on multi-spectral imaging by using a smartphone. A spectral reflectance of human skin is very useful for a health care and beauty in cosmetic fields. By this system, anyone can measure spectral reflectance of human skin with smartphone and color chart. First, we develop a multi-spectral camera model of a smartphone for describing a light reflection process of a smartphone camera system. A camera of the smartphone has an automatic exposure and an automatic white balance function. The camera output (RGB) is modeled with spectral reflectance of human skin, spectral distribution of illumination, camera sensitivity and time parameter in the visible wavelength [400–700 nm].Second, we propose a simplified method for estimating spectral reflectance using a smartphone camera based on the multi-spectral camera model. We assumed that the spectral reflectance of a human skin surface can be described as linear combination of some basis functions. On the assumption that the system conversion matrix from the camera output to spectral reflection is estimated based on statistically analysis of tuple of spectral reflectance and camera outputs (RGB).Generally, smartphone camera has an automatic exposure and an automatic white balance function. The exposure and white balance is fixed correctly with a color chart. Third, we implement a position detection method for improving accuracy of human face and color chart position calibration. In the results, we can estimate spectral reflectance in arbitrary part of the human face. Finally, to confirm accuracy of the proposed method, we measured spectral reflectance of human face with a smartphone. The estimation results were compared with direct measurement of spectral reflectance with spectrophotometer. Consequently, it was possible to obtain the estimation results of spectral reflectance of human skin with high precision.

1. INTRODUCTION

Smartphone is useful as color device at any time. And also, because computer and digital color camera is implemented in the smartphone, the smartphone may be considered a color device for easily performing multi-spectral imaging. However it is difficult to estimate spectral information from the color image by the smartphone[1]. The camera of smartphone has an automatic exposure and automatic white balance function. These functions destabilize of estimating spectral information form the image.

In this study, we develop a method for estimating spectral reflectance of human skin from the smartphone. The human skin surface has inhomogeneous reflection properties and spectral reflectance. This paper will describe a method for estimating the spectral reflectance of human skin based on multi-spectral imaging by using smartphone. First, we develop an automatic detection system for color chart and human face in an image taken by smartphone. The system is developed based on machine leaning method[2]. The color information of color chart and geometry of face position in the image are used for calibrating camera characteristics and image recognition. Second, we proposed method for estimating spectral reflectance of human skin using smartphone. Finally, to confirm the feasibility of our method, we demonstrate the spectral estimation system for the smartphone.

2. DETECTION OF COLOR CHART AND HUMAN FACE

In this study, we need to know the position of the color chart and face in the measured image. Haar Feature-based Cascade Classifier method[2] is used as face detection and recognition system. And also, the method is used for the detection of color chart position. Haar Feature-based Cascade Classifier method is a sort of machine learning method. The machine learning can be carried out by using the learning data suitable for detection of color chart and human face. Firstly, to train Classifier, collect positive and negative samples from images that have notable features. Then, obtain several numbers of weak classifier by combining the features. Haar Feature-based Cascade Classifier method is not using a single strong classifier but using several weak classifiers in serial order for detecting an object. At first, low recognition rated classifier is applied on detecting a face. Then, gradually raise the rate of classifier to narrow the error range. This method can save time and memory for recognizing object during detection. In this project, 244 positive samples and 3000 negative samples are used for training color chart. As a result 7 weak classifiers are generated and the classifier detects color chart from an image by cascade method.

3. CAMERA MODEL OF THE SMARTPHONE

In order to estimate spectral reflectance using smartphone, the image data taken by smartphone is modeled based on multi-spectral reflectance[1][3]. Generally, the camera of the smartphone has an automatic exposure and an automatic white balance function. The camera output is modeled in visible wavelength[400-700nm] as

$$\begin{bmatrix} R \\ G \\ B \end{bmatrix} = \int_{400}^{700} E(\lambda)S(\lambda) \begin{bmatrix} r_{\mathrm{r}}(\lambda,t) \\ r_{\mathrm{g}}(\lambda,t) \\ r_{\mathrm{b}}(\lambda,t) \end{bmatrix} d\lambda \,. \tag{1}$$

$E(\lambda)$ is the spectral distributions of light sources. $S(\lambda)$ is the spectral reflectance of the objects. $r_{\mathrm{r}}(\lambda,t), r_{\mathrm{g}}(\lambda,t), r_{\mathrm{b}}(\lambda,t)$ are, respectively, the spectral sensitivity functions of sensor RGB. t is time parameter.

4. ESTIMATION METHOD OF THE SPECTRAL REFLECTANCE

In this study, we use two cameras[3]. The first one is the camera system which calibrated to remove influence of spectral sensitivity and illumination environment beforehand. The second one is uncalibleted camera of spectral sensitivity and illumination environment. As for the model, sensitivity properties change in time t. We measure a k-colored color chart in calibrated camera. The camera output of the calibrated camera assumes it matrix $\mathbf{\Lambda}_{\mathrm{C}}$ of 3×k. The camera output of the uncalibrated camera assumes it matrix $\mathbf{\Lambda}_{\mathrm{U}}(t)$ of 3×k including sensitivity change t by automatic exposure and white balance of the camera. We can describe the relations of the camera output of both in the next expression using color conversion matrix **T**.

$$\mathbf{\Lambda}_{\mathrm{C}} = \mathbf{T}(t)\mathbf{\Lambda}_{\mathrm{U}}(t) \tag{2}$$

We estimated $\mathbf{T}$ as $\mathbf{T}(t) = \mathbf{\Lambda}_{\mathrm{C}}\mathbf{\Lambda}^{+}{}_{\mathrm{U}}(t)$ using pseudo inverse matrix $\mathbf{\Lambda}_{\mathrm{C}}$ of matrix $\mathbf{\Lambda}_{\mathrm{C}}$. In this study, we get conversion matrix $\mathbf{T}(t)$ in time t by measuring a color chart becoming the standard at the time of photography at the same time. We can calculate heaviness coefficient matrix like the next expression when We express an image of uncalibrated camera of number of the pixels n then in matrix $\mathbf{C}_{\mathrm{U}}$ of $3 \times$n. If this $\mathbf{W}(t)$ can be calculate, the spectral reflectance can be estimate.

5. EXPERIMENTAL RESULTS

The proposed method was applied to estimate of spectral reflectance of human skin. We used a Motorola Atrix4G phone as the smartphone. Machine learning system is implemented with Open CV libraly. Figure 1 shows estimation results of the experiment. Figure 1(a) shows human face and color chart detection results. The red square is face detection result. The Green squire and red circles are color chart and color patach detection results. Figure 1(b) is estimation results of spectral reflectance. The blue line is the graph of estimation results and red squire in the red cirlce is estimation area of spectral reflectance.

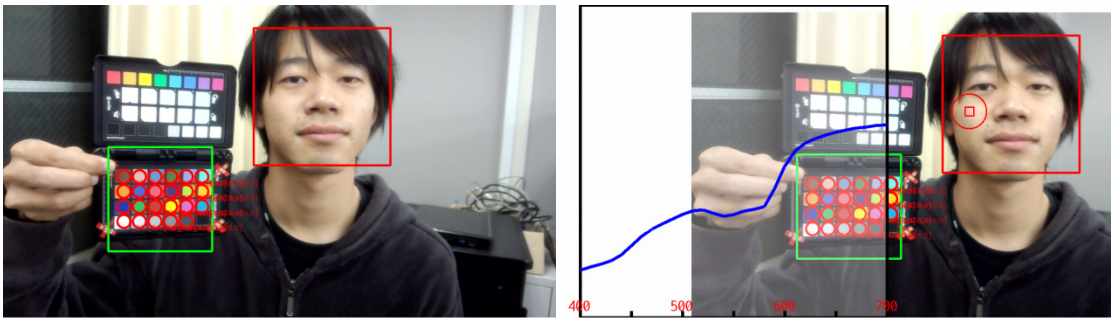

(a) face and color chart detection (b) estimation results of spectral reflectance

Figure 1. Estimation results

6. CONCLUSIONS

In this paper, we have developed a method for estimating spectral reflectance of human skin from the smartphone. The human skin surface has inhomogeneous reflection properties and spectral reflectance. This paper described a method for estimating the spectral reflectance of human skin based on multi-spectral imaging by using smartphone. First, we developed an automatic detection system for color chart and human face in an image taken by smartphone. The system is developed based on machine leaning method. The color information of color chart and geometry of face position in the image are used for calibrating camera characteristics and image recognition. Second, we proposed method for estimating spectral reflectance of human skin using smartphone. Finally, to confirm the feasibility of our method, we demonstrate the spectral estimation system for the smartphone.

ACKNOWLEDGEMENTS

This research was supported by KAKENHI (24500299).

REFERENCES

[1] S. TOYA, N. TANAKA and J. WOO: Estimation of Human Skin Properties using Smartphone, International Colour Association (AIC), 2012.
[2] P. VIOLA and M. JONES, Rapid object detection using a boosted cascade of simple features, Computer Vision and Pattern Recognition(CVPR), 2001.
[3] N. TANAKA, H. ARAI, J. WOO: Color Image Rendering of Human Skin Based on Multi-spectral Reflection Model, Vol. 36, suppl., pp.242-243, 2012.

Address: Faculty of Business and Informatics, Nagano University, 658-1 shimonogo, ueda-shi, Nagano 386-1298,Japan
E-mails:holyidea0824@yahoo.co.jp, n-tanaka@nagano.ac.jp, k-mochiduki@nagano.ac.jp

Colour Management for High Quality Reproduction on Uncoated Papers

Maja STRGAR KURECIC, Lidija MANDIC, Ante POLJICAK, Diana MILCIC
Faculty of Graphic Arts, University of Zagreb

ABSTRACT

The goal of this research was to establish the consistent and predictable workflow from the screen to the print on uncoated paper, taking into account specific constraints of the substrate and the reproduction process. The substrate is a major factor in determination of the attainable full-tone density and affects the reproducible color contrast, which both have a large impact on overall print quality. The specific restrictions on uncoated paper are determined by a rough surface on which there is always a large dot gain, reduced relative printing contrast compared to a print on coated paper, as well as the reduced gamut of colors that can be reproduced. By implementing color management ICC profiles characterized for specific uncoated printing substrate and by conducting proposed correction methods in the prepress, as well as optimizing the thickness of ink in printing, it is possible to achieve high quality color reproduction.

In the experimental part of this work special test target was designed and printed in offset on three different types of uncoated paper and one type coated paper. The test target was composed of ten types of color strips for instrumental measurements of dot gain, relative printing contrast, raster tonal value, full-tone density, etc. In addition, a photograph for visual assessment of prints was included. To be able to objectively compare the color differences of prints, spectrophotometric measurements of color strips were also made and analyzed.

1. INTRODUCTION

In recent years, the appeal of uncoated paper has undergone a dramatic image change in the eyes of designers and printers, contributing to the growing demand for uncoated stock. There is a wide range of high quality uncoated paper on the market today, available in many different textures, colours, weights and finishes. Because of their tactile properties and natural surface, uncoated paper creates a much stronger impression and lasting value compared to coated paper. On the other side, coated paper has an advantage in the standardised reproduction process and achieves higher quality printing results. The challenge is to ensure that uncoated print results are able to match the performance of colour prints on coated paper.

Each production step and each production device in the reproduction workflow can be a source of error. Figure 1. shows typical production steps of prepress to print where colour and tone value variations can occur.

The two main reasons of colour differences are the tone value increase (dot gain) and overprint changes (colour balance). On uncoated paper, the ink dots are absorbed slowly into paper surface and dots expands in size (dot gain). This makes the dots less sharp and colours slightly dull. Without proper corrections and compensations in the prepress the images printed on uncoated paper look darker, with colours not as clean, saturated and bright as they could be. Also, dark areas often lose details and have low contrast. Incorrectly done prepress can affect the stability in the press, prolonged ink drying times and problems like set-off and smearing, both in press and in binding.

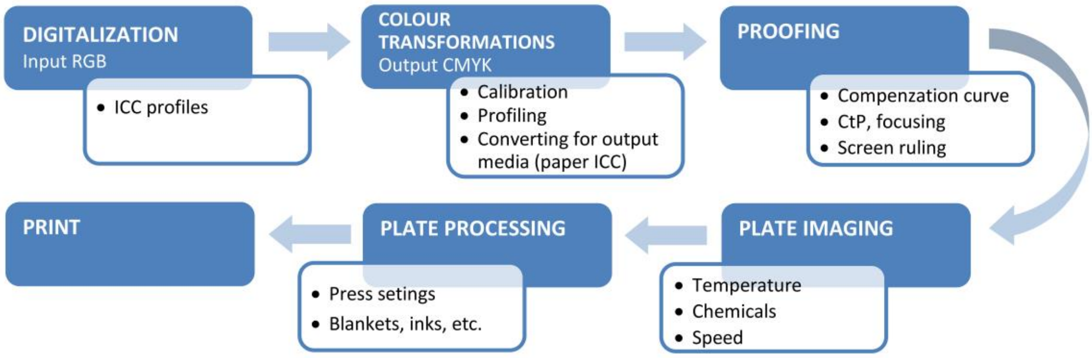

Figure 1: Production workflow

To keep the digital reproduction under control it is essential to regularly record and evaluate the colour and tone value variations. The most important things when printing on uncoated paper are: minimizing the dot gain and controlling the ink density. The tone value progression (RTV) should be checked in at least ten different halftone steps from 0% - 100% in every process colour. Also, 2- and 3-color overprint should be checked for controlling the grey balance. The transfer processes between different phases of prepress and printing is described by characteristic tone curve. It contains a great amount of information about the tone gradations from paper colour to solid tone. A distinction is made between characteristic tone curves for printing plates, proofs and printing.

Implementing Colour Management into the production workflow makes the exchange of colour data more consistent and predictable. The first step towards the standardisation of reproduction process is calibration of all equipment used in the graphic chain. That means taking it to a chosen operating state and ensuring that it remains in this state. Second step is characterization (profiling) which quantifies the colour space, colour gamut, or colour behaviour of the particular device under known conditions. When all devices are both calibrated and characterized it is possible to convert colours back and forth depending on the need and production workflow. This could be soft or hardcopy proofing.

2. METHOD

In the experimental part of this work a special test target was developed and printed in sheet fed offset machine on three different types of uncoated paper and one type coated paper.

2.1 Test Target Development

Special test target was developed for the process control and for evaluation of print quality on uncoated papers. Target consists of control elements for checking most important parameters by instrumental measurements and by visual control (Figure 1). The size of the target is adjustable to the standard formats of offset printing machines. All elements of the test target were designed in Adobe InDesign and Adobe Photoshop applications. File conversion was made with output Fogra Uncoated 29 profile.

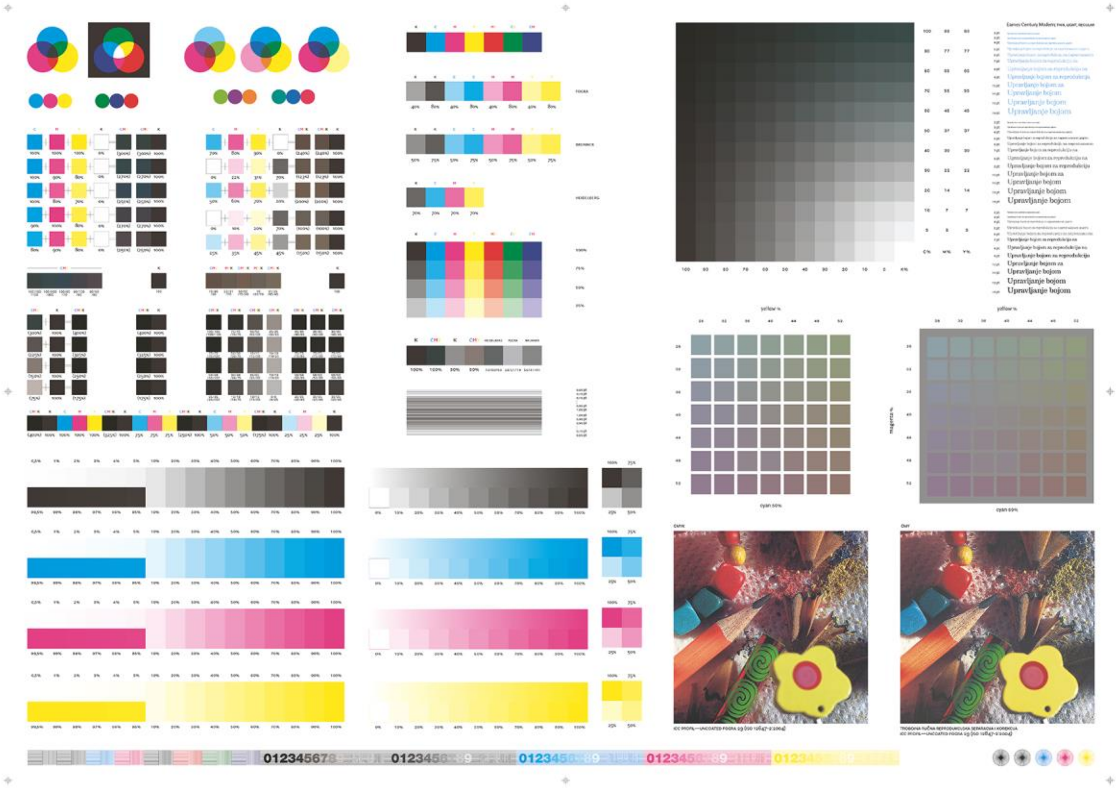

Figure 1: The test target

Each element of the test target was designed to higlight a particular aspect of the printing process. The main elements were: colour patches with primary colours in different combinations and with different RTV values, and with different UCR and GCR shares, patches with tone values from 0% - 100% in ten different halftone steps in every proces colour and the strip with continious tone, strip with minimal (0,5% - 5%) and maximal (99,5% - 95%) RTV, four color matrix for visual assessment of grey balance, photos reproduced with standard and custom profile, typographic elements from 2pt - 18pt, etc.

2.2 Preparing and Printing Test Target

The rasterization process was done with Harlequin Navigator RIP, Version 9. Offset plate (Thermostar P970) was exposed and processed with CTP system Luescher Xpose! 230 Thermal. Target was printed with Heidelberg Speedmaster 74-4-P3-H sheetfed offset machine. Offset ink used was Inkredible Resista (Michael Huber-Munchen). Coated paper used was Artic volume white (150 g/m^2). Three different uncoated papers used were: Munken Lynx (170 g/m^2), Munken Pure (170 g/m^2) and Maestro print (140 g/m^2).

2.3 Measurement Procedure

Spectral measurement of colour paches were conducted using Gretagmacbeth Eye-one Pro spectrophotometer in accordance with the ISO 13655 standard. The illumination corespond to D50, measurement geometry was 0/45, 2° observer. For process control during the print run black backing was used and dry ink was measured. For visual observation of prints Gretagmacbeth The Judge II light testing box was used under standard illuminant D50. The parameters observed were: coloure balance (colour tone), image gradation (lighter/darker), contrast range (high/low contrast) and register.

3. RESULTS AND DISCUSSION

Due to the large amount of results obtained, here will be presented only those that show the greatest differences in reproduction between different types of paper. Some of the results obtained by spectral measurement are shown in the Tab 1, Tab 2, and Fig 2.

Table 1. CIELAB colour values for solid tones of primary and secondary colours for offset printing on two paper types (one coated and three uncoated papers) compering to standard ISO 12647 values.

Paper type	ISO 12647 (PT 2)			Arctic Volume White 150 g/m^2			ISO 12647 (PT 4)			Maestro Print 140 g/m^2			Munken Lynx 170 g/m^2			Munken Pure 170 g/m^2		
	L*	a*	b*	L*	a*	b*	L*	a*	b*	L*	a*	b*	L*	a*	b*	L*	a*	b*
K	16	0	0	21	1	1	31	1	1	36	1	2	36	1	3	36	1	4
C	54	-36	-49	58	-34	-50	58	-25	-43	63	-24	-43	63	-25	-40	63	-27	-36
M	46	72	-5	50	75	-5	54	58	-2	56	58	-5	57	59	-2	57	57	0
Y	88	-6	90	89	-4	96	86	-4	75	89	-4	77	90	-4	79	90	-3	80
R	47	66	50	48	69	45	52	55	30	53	56	29	54	56	30	55	55	31
G	49	-66	33	51	-63	31	52	-46	16	56	-44	22	57	-43	23	57	-42	24
B	20	25	-48	27	22	-45	36	12	-32	40	11	-30	40	12	-27	40	9	-26
W_{paper}	92	0	-3	92	1	-4	92	0	-3	90	1	-6	91	1	-2	91	0	4

Table 2. Density values for quarter tones measured on prints (dry ink) printed on two paper types (one coated and three uncoated papers).

Paper type	Arctic Volume White 150 g/m^2				Maestro Print 140 g/m^2				Munken Lynx 170 g/m^2				Munken Pure 170 g/m^2			
RTV %	100	75	50	25	100	75	50	25	100	75	50	25	100	75	50	25
K	1,25	0,65	0,30	0,13	1,04	0,68	0,41	0,24	1,05	0,69	0,41	0,23	1,04	0,67	0,39	0,22
C	1,00	0,53	0,26	0,10	0,86	0,58	0,37	0,22	0,85	0,57	0,37	0,21	0,85	0,57	0,36	0,20
M	1,06	0,60	0,29	0,12	0,90	0,62	0,38	0,22	0,90	0,64	0,39	0,23	0,89	0,63	0,39	0,22
Y	0,88	0,48	0,23	0,08	0,83	0,53	0,31	0,18	0,83	0,54	0,34	0,20	0,85	0,56	0,36	0,23

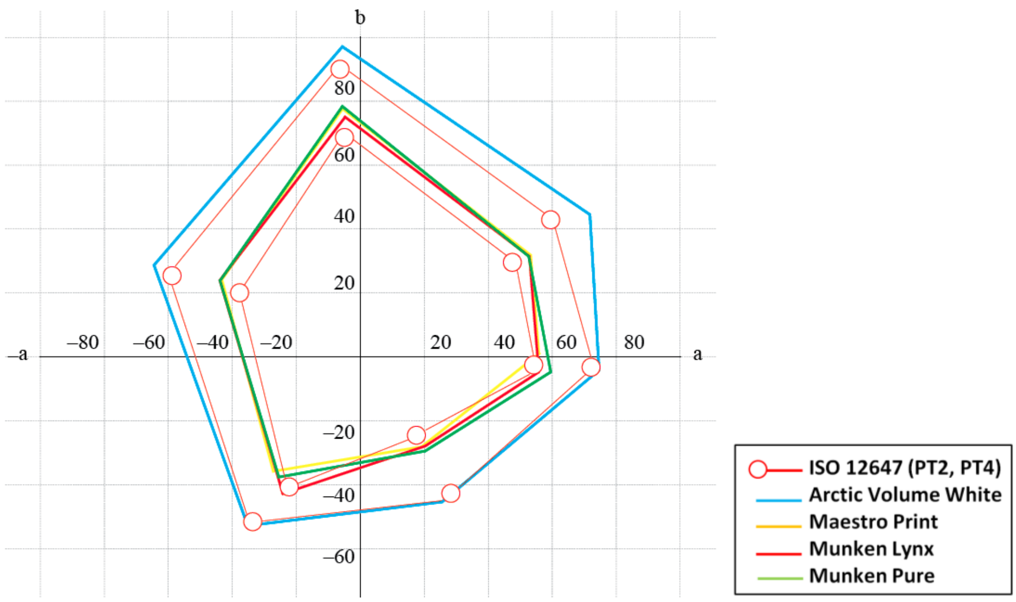

Figure 2: Comparison of colour gamut obtained on different types of paper plotted in CIELAB diagram.

Even though the numbers show that the print on uncoated papers does have a smaller densities and reduced colour gamut, our eyes can percieve the image to be similar to the orignal through good procesing. This research show that image adjustments made in prepress can improve percieved quality of prints on uncoated papers. Image adjustments should be conducted in the controled conditions on calibrated monitor by applying the simulation of paper colour and the output device profile. The paper type settings, together with an ICC profile, is fundamental to the whole process of prepress. It is recommended to adjust the density of an image by adjusting tone curves. By reducing the mid-tones and three-quarter tones by 12-15% the dot gain could be compensated. Also, important parts of an image should not involve tone values that lie outside the printable tone value range. Printable tone range for uncoated paper is from 4% for highlights dots to 85% for the darkest shadows. Total ink coverage (TIC) must be decreased to suit uncoated paper. It should not be over 280%. Too high TIC without proper curve compensation can result in ink set-off and drying problems. It is important to check that the ICC profile has the correct TIC value. By using the Under Colour Removal (UCR) or Gray Component Replacment (GCR) methods when defining the separations it is possible to reduce the TIC without detracting from the image's quality and achieving a more even degree of inking. Also, screen ruling should not be too high. Recommendation is to use 80-120 lpi for high bulk paper and 133-150 lpi for low bulk paper.

4. CONCLUSIONS

Offset printing is an unstable printing process and there is high potential for saving costs and time by standardisation. By folowing the propositions of the graphic industry printing standard ISO 12647 for adjustments acording to five predefined paper types and by using paper ICC profile depending on the output media, it is posible to secure and stabilise the reproduction process and printing quality. But, even though using the ICC profiles will help in many ways, it must be stated that every profile will have some level of generalization. In some cases, when high quality level is required, the specific (custom) profile, that will handle a specific offset press and a specific paper quality, should be used. It implies fine-tuning the system by customizing curves for particular paper/ink/print conditions.

The research show that well-planed and prepared separations are crucial for the quality of the print on uncoated paper. Adjustments made in the prepress, concerning the dot gain, contrast, saturation, colour balance and total ink coverage, sets the main quality level on the end results. The only thing that can be optimized during printing, if needed, is ink film thickness. Uncoated paper needs more ink to reach the same density as on a coated paper. A general recommendation for uncoated paper is to lower ink density to avoid over inking. But, if the prepress is done correctly and the total ink coverage is low (250-260%), the ink density can be kept relatively high without the risk of over inking. This will provide more colourful image.

ACKNOWLEDGEMENTS

This research was conducted under the scientific project (128-1281957-1958), supported by the Ministry of Science, Education and Sports of the Republic of Croatia.

REFERENCES

ISO 12647-1:2004 Graphic technology - *Process control for the production of half-tone colour separations, proof and production prints - Part 1: Parameters and measurement methods.*

ISO 12647-2:2004 Graphic technology - *Process control for the production of half-tone colour separations, proof and production prints - Part 2: Offset lithographic processes.*

ISO 13655:2009 Graphic technology - *Spectral measurement and colorimetric computation for graphic arts images.*

ISO 13656:2000 *Graphic technology - Application of reflection densitometry and colorimetry to process control or evaluation of prints and proofs*

Address: Assistant Prof. Maja STRGAR KURECIC, Department of Graphic Design and Image Reproduction, Faculty of Graphic Arts, University of Zagreb, Getaldiceva 2, 10000 Zagreb, CROATIA
E-mails: mstrgar@grf.hr, lmandic@grf.hr, ante.poljicak@grf.hr, diana.milcic@grf.hr

A Real-Time Multi-spectral CG Rendering Method for Building with Scene Illumination

ChihiroSAKURAI, NorihiroTANAKA, Kosuke MOCHIZUKI
Faculty Business and Informatics, Nagano University

ABSTRACT

This paper describes a real-time CG rendering method for building with scene illumination data. However, the multi-spectral scene rendering method with high accuracy scene illumination information needs a huge amount of calculation processing time. Therefore, we improve rendering performance of multi-spectral rendering system with omnidirectional illumination data. First, we develop a scene rendering system with multi-spectral reflection model include multi-spectral omnidirectional illumination data. The illumination data is measured with fish-eye lens and digital camera. The illumination data is generated as multi-spectral omini-directional image. Second, to reduce the time for rendering processing of scene illumination, we develop a real-time rendering method for implementing to Graphics Processing Unit (GPU). Moreover, we render a building with a rendering method based on Image Based Lighting (IBL). To improve rendering performance, we develop a multi-spectral irradiance map from the multi-spectral omni-directional image for GPU. Finally, to confirm validity of the proposed method, Nagano university campus is rendered by proposed method. And also, we compared CG reproduced image to the real scene.

1. INTRODUCTION

In the fields of digital archive of buildings, walk-through rendering method is required. To walk around various places with viewing landscape, we develop a rendering method for buildings with scene illumination. The scene illumination is very important for object color[1]. The rendering method need to render precise lighting, shading, gross and soft shadow et al. in the real scene illumination [2]. For the realistic rendering, the system needs to calculate illumination distribution characteristics in the scene and light reflection process on an object precisely[3][4]. Moreover, it is important that the CG rendering system can reproduce scene illumination precisely[5]. By the conventional RGB-based rendering technique, it is difficult to calculate scene illumination precisely. Because multi-spectral information is physical data peculiar to an object, the multi-spectral data is independent of color device such as a camera.

This paper describes a real-time CG rendering method for building with scene illumination data. However, the multi-spectral scene rendering method with high accuracy scene illumination information needs a huge amount of calculation processing time. Therefore, we improve rendering performance of multi-spectral rendering system with scene illumination data. We develop a scene rendering system with multi-spectral reflection model include multi-spectral scene illumination data. The illumination data is measured with digital camera.

Second, to reduce the time for rendering processing of scene illumination, we develop a real-time rendering method for implementing to Graphics Processing Unit (GPU). And also we develop a data compression algorithm for multi-spectral data for improving resolution and performance. Finally, to confirm validity of the proposed method, Nagano university campus is rendered by proposed method. And also, we demonstrated walk-through in the campus scene.

2. DIGITAL ARCHIVE METHOD

2.1 Measuring Structure

In this study, we need a real-time rendering speed for providing the presence that a user experiences. To render a high quality CG image of a structure while reducing the number of polygons, we develop rendering system for digital archivine of structures. To efficiently display 3D CG of structure with high accuracy using required minimum measured data by performing required minimum 3D vertex measurement. The dimension of the structure is measured by using laser distance meter. And also, the equipment such as furniture in the room is measured by using digital camera. The size of equipment is measured by using measure and image data. To make up for 3D vertex data shortage, the texture mapping is used for describing object surface material.Figure 1 shows measurement scene of interior dimensional size of the building and its equipment in the room. Figure 1(a) shows laser measurement of internal dimention of buildings. Figure 1(b) is measurement process of equipment in the room. The equipment is measured 3D verstex as 3D shape and its texutre image. It is synthesized for each measurement data to generate a composed CG data of the equipment.

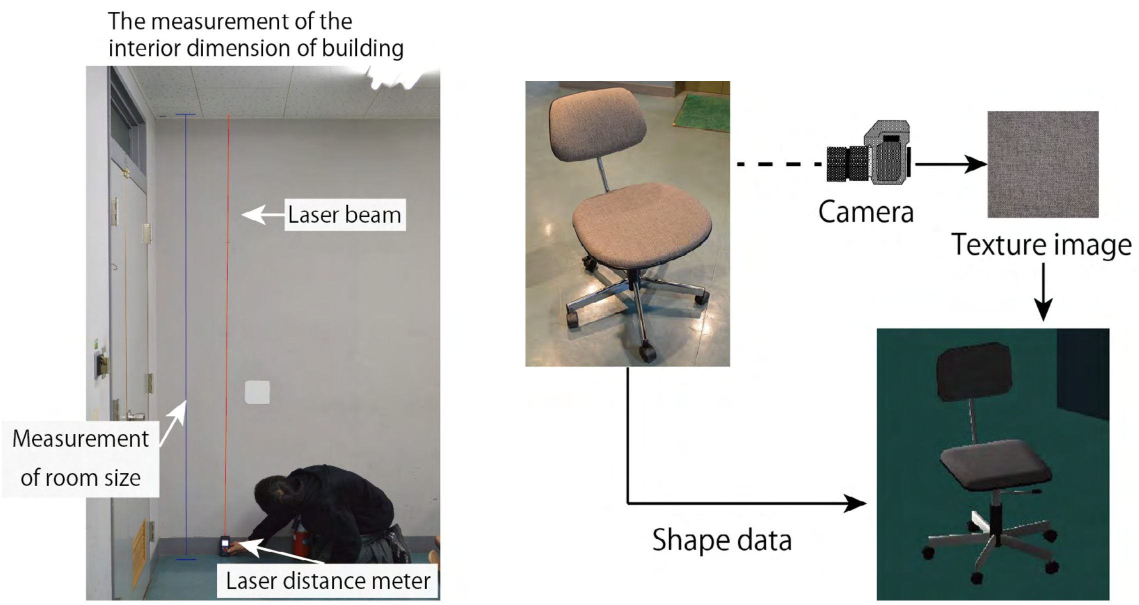

(a) Interior dimention of building (b) Equipment in the room

Figure 1. Measurement of the building and equipment

2.2 Multi-spectral model

Figure 2 shows scene illumination in a building. In this study, he scene illumination is described as spectral distribution of light source and object surface reflectance. We propose a method for estimating spectral distribution based on statistical method with color patches and a spectrophotometer. In this method, we assume that principal illumination in the scene consist of one type light source. We described the spectral information as 61 dimensional vector that is sampled at 5nm intervals in the visible light wavelength region (400-700nm). To estimate the spectral distribution of light source in the scene illumination, we developed multi-spectral camera model. In the model, the estimated spectral distribution **e** is described as

$$\bar{\mathbf{e}} = \boldsymbol{\rho}\mathbf{M} \tag{1}$$

where $\boldsymbol{\rho}$ is camera output. **M** is 3×3 translation matrix. $\boldsymbol{\Lambda}$ and $\mathbf{P}$ are 61×*m* matrix of m-tuple spectral distribution and 3×*m* matrix of *m*-tuple camera outputs, respectively. **t** is 61×3 matrix of camera sensitivity. The relation of these matrixes is described as $\mathbf{P} = \boldsymbol{\Lambda}\mathbf{t}$. We estimated **t** as $\mathbf{t} = \boldsymbol{\Lambda}^{+}\mathbf{P}$ using pseudo inverse matrix $\boldsymbol{\Lambda}^{+}$ of matrix $\boldsymbol{\Lambda}$. Then, 3×1 matrix **e** of the spectral distribution of light source can be estimated as $\mathbf{e}^{T} = \boldsymbol{\rho}^{T}\mathbf{t}^{-1}$ using inverse matrix $\mathbf{t}^{-1}$ of **t**. The translation matrix **M** is described as **t**.

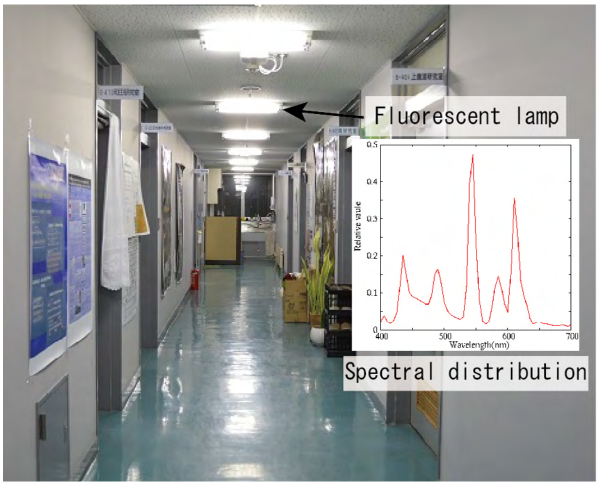

Figure 2. Multi-spectralscene illumination in the building

3. RENDERING METHOD

Figure 3 shows proposed multi-spectral rendering system. The multi-spectral real-time rendering system was developed for digital archive data for the building. In this system, the rendered CG image is based on multi-spectral image rendering. The CG images are precisely created under an ambient light environment in the scene. The system is developed as interactive walk-through system in the building. And also, the whole scene is modelled as multi-spectral scene light reflection model. In this study, the color signal of the visual system is calculated from the reflection model and illumination map. Therefore, the object color is calculated from the color signal and CIE color matching function $\bar{x}(\lambda), \bar{y}(\lambda), \bar{z}(\lambda)$ as a tristimulus value (CIE XYZ), which is computed as follows.

$$\begin{bmatrix} X \\ Y \\ Z \end{bmatrix} = \int_{400}^{700} S(\lambda)E(\lambda) \begin{bmatrix} \bar{x}(\lambda) \\ \bar{y}(\lambda) \\ \bar{z}(\lambda) \end{bmatrix} d\lambda \qquad (2)$$

The tristimulus value is independent of any display device. To render the RGB value precisely, we must calibrate the display device. The device RGB of the color display is obtained from the XYZ value via a transformation matrix and gamma correction, which collectively specify the intrinsic values of the display device. These values are estimated by measuring the corresponding relationship between the tristimulus and device RGB values, with a spectral radio photometer (TOPCON TECHNOHOUSE SR-3A-L1). The proposed method is implemented on a GPU, assuming a color monitor as the display device.

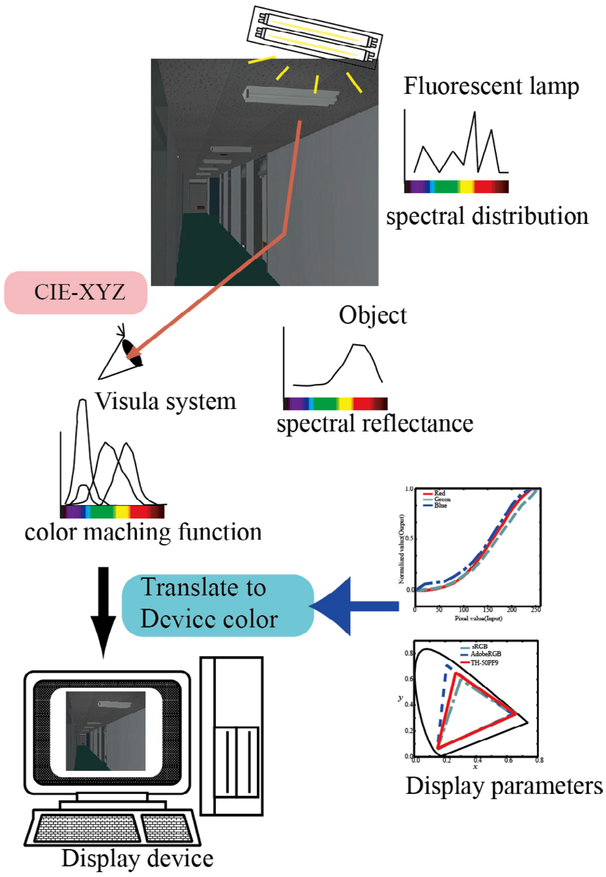

Figure 3. Multi-spectral rendering system with scene illumination data.

4. EXPERIMENTAL RESULTS

The proposed method was applied to digital archive of Nagano university campus. Once all vertex and texutre datas were estimated, we could reproduce the object in 3D CG of campus scene. Thus, we rendered the object shown in Figure 4. We have compared the reproduced CG with the picture of the real scene. Figure 5 shows rendering results at various location in Nagano University.

Figure 4.Renderingu results(comparison between Original Scene and Reproduced CG)

Figure 5. Rendering results at various location in f Nagano University.

4. CONCLUSIONS

This paper described a real-time CG rendering method for building with scene illumination data. We improved rendering performance of multi-spectral rendering system with scene illumination data. The multi-spectral scene rendering method with high accuracy scene illumination information needs a huge amount of calculation processing time. First, we proposed method reducing 3D shape data without lowering image quality. Second, to reduce the time for rendering processing of scene illumination, we develop a real-time rendering method for implementing to Graphics Processing Unit (GPU). Finally, to confirm validity of the proposed method, Nagano university campus is rendered by proposed method. And also, we compared CG reproduced image to the real scene.

ACKNOWLEDGEMENTS

This research was supported by KAKENHI (24500299).

REFERENCES

[1] C. C. Chiao, T. W. Cronin, and D. Osorio, "Color signals in natural scenes: Characteristics of reflectance spectra and effects of natural illuminants", J. Opt. Soc. Am. A 17, 218,2000.

[2] P. E. Debevec," Rendering Synthetic objects into real scenes:bridging traditional and image-based graphics with global illumination and high dynamic range photography", Proc. Of SIGGRAPH 98, pp.189-198,1998

[3] N. Tanaka, K. Mochizuki and J. Woo, "A Real-time Rendering Method of Art Objects Based on Multi-spectral Reflection Model", Proc. of IASDR, 4 pages,2009.

[4] N. Tanaka, K. Mochizuki: A digital archive method based on multispectral imaging with goniometric multiband camera,The Bulletin of Japanese Society for the Science of Design. 61(3) 35-44 2014.

[5] C. Iwasaki, N. Tanaka: A CG Reproduction Method of Human Skin under Omni-directional Illumination,Proceedings of International Association of Societies of Design Research (IASDR) 2013

Address: Prof. Norihiro TANAKA, Faculty of Business and Informatics,
Nagano University, 658-1 Shimonogo,Ueda, Nagano,386-1298 , JAPAN
E-mails: j13033cs@nagano.ac.jp,k-mochiduki@nagano.ac.jp, n-tanaka@nagano.ac.jp

Color mapping between a pair of similar facial images with and without applying cosmetics

Lin Lu, Hung-Shing Chen, Neng-Chung Hu

Graduate Institute of Electro-optical Engineering, National Taiwan University of Science and Technology, Taiwan

ABSTRACT

The aim of this study is to develop an automatic facial makeup technology, which can make a raw facial image reproduce the preferred cosmetic colors according to the chosen facial color template. The developed facial makeup method named Facial Color Morphing Algorithm (FCMA). Discriminative Response Map Fitting (DRMF) was also introduced to find the main facial organs (e.g. eyes, nose, mouth etc.) and the face outline. The facial image was divided by a series of triangles according to the facial feature points detected by DRMF. In addition, affine transformation and bilinear interpolation are applied to perform facial skin-color mapping between the test image and the morphing image. The simulated results indicate that our developed algorithm works well in representing preferred facial colors.

1. INTRODUCTION

An image-dependent color palette will be a better choice to achieve high image quality for displays (Chen et. al., 2014). However, it is difficult to analyze facial color differences between two similar facial images. In this study, image morphing technology (Howard Anton, 2005) is applied to map facial colors between the pair of faces which have a little different shapes. Besides, Discriminative Response Map Fitting (DRMF) (Asthana A. et al., 2013) is used to find the feature points of a human face. The aim of this study is to develop an automatic facial makeup technology, which can make a raw facial image reproduce the preferred cosmetic colors according to the chosen facial color template. The experimental schematic is shown in Figure 1.

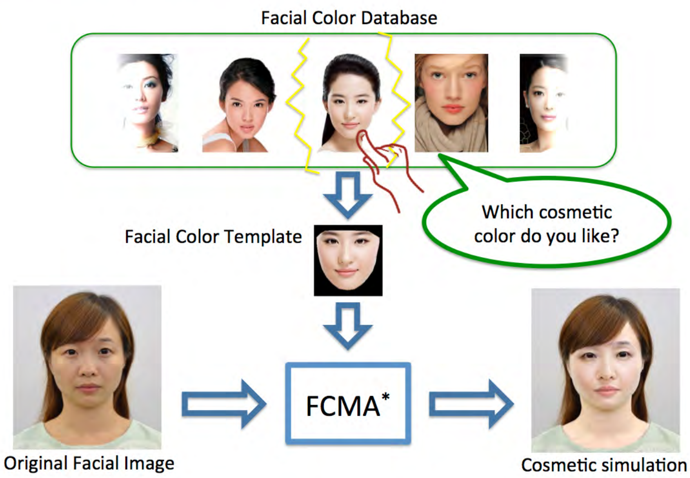

(FCMA: Facial Color Morphing Algorithm)

Figure 1: Experimental schematic

2. METHOD

Figure 2 demostrates the experimental flowchart in this study. The test image is defined as a raw image without cosmetics, and it is desired to make up her new face according to the chosen facial color templates. The simulated makeup results are mainly achieved by our developed algorithm, named Facial Color Morphing Algorithm (FCMA).

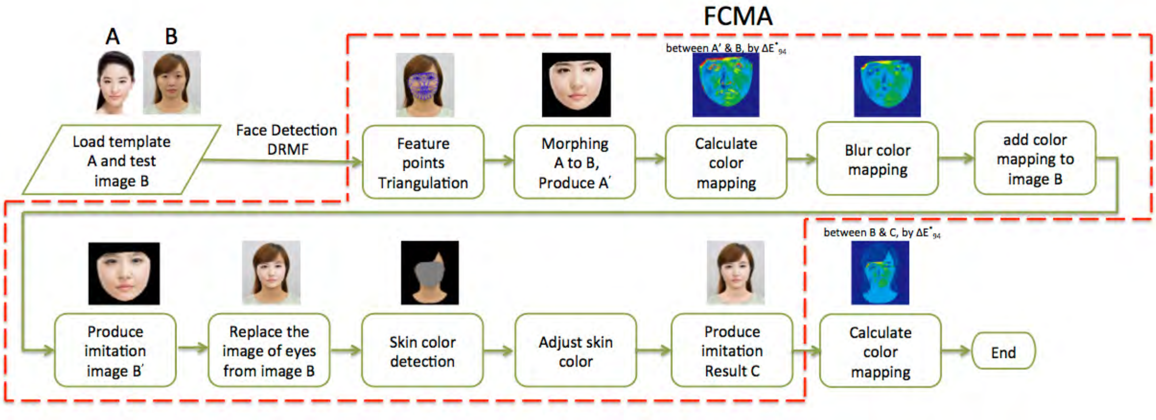

Figure 2: Experimental flowchart

2.1 Test Image and Facial Color Template

A test image, which is the raw face of a young woman without makeup (Figure 3(a)), is inputted into the FCMA. Also two template images with cosmetics of the young models are found from the website, which are seen as facial color templates (Figure 3(b)-3(c)). It is hoped to makeup the test image more pleasant to approach a similar skin color appearance to the chosen facial color template.

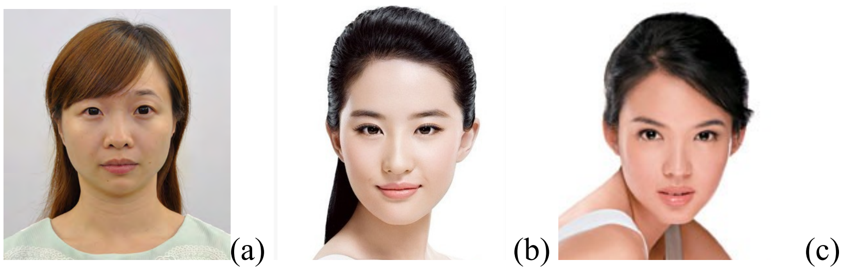

Figure3: Test image and template images; (a) test image,(b) and (c) facial color templates

2.2 Face Detection and Transformation

DRMF was applied to execute the facial feature point detection for the test image and the template image, respectively. As shown in the example of Figure 4(a), the red points represent the feature points of a facial image found by DRMF. It can be observed that most of the feature points almost cover the main facial organs (e.g., eyes, nose, mouth etc.) and the face outline.

When the feature points of the test image and the template image were found by DRMF, we let all feature points in an image produce feature line connections between a pair of the nearest points, and these feature lines do not cross each other. Finally, an image can be divided into a series of polygon grouped with many triangles (Figure 4 (b)) by face triangulation. Notice that numbers and orders of inner triangles between the test image and the template image should be equal.

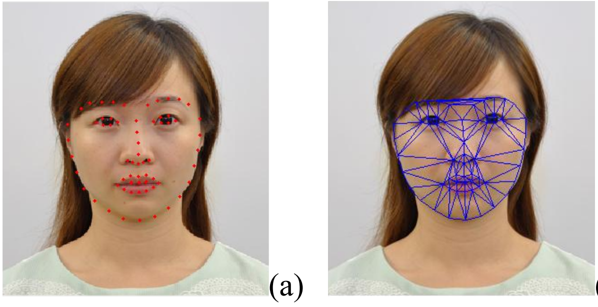

(a) (b)

Figure 4. Face detection; (a) feature points in test image (b) face triangulation

2.3 Image Morphing

Image morphing is performed in the template image mainly, which concept is based on affine transformation (Figure 5(a)). When a triangle T_1 in one image has three vertices V_1, V_2, V_3 and the point V is in T_1, then it can be expressed by Equation 1. Therefore, the coefficients (C_1, C_2, C_3) can be expressed by a triangle T_2 in the other image, which vertices W_1, W_2, W_3 can also satisfy Equation 2. So the point W inside the triangle T_2 can be determined by the coefficients(C_1, C_2, C_3). The point V and point W have a unique relation in affine transforming process.

$$\begin{cases} V = C_1V_1 + C_2V_2 + C_3V_3 \\ C_1 + C_2 + C_3 = 1 \\ C_1, C_2, C_3 > 0 \end{cases} \tag{1}$$

$$W = C_1W_1 + C_2W_2 + C_3W_3 \tag{2}$$

When all triangles in an image are computed by affine transformation, then image morphing is finished. The morphing example is shown in Figure 5 (b). The left part is the original image, and the right part is the morphing result. Note that they have the same facial shape of the test image, but different facial colors at this stage.

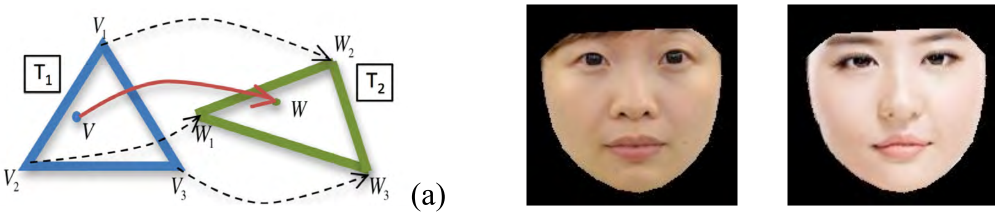

(a) (b)

Figure 5: (a) Triangulation and interpolation, (b) Images before and after affine transformation

During image morphing processing, the calculated (x, y) position at point W in Figure 5(a) calculated may not integer value. If the point W is selected as the position with the nearest calculated integer value, it could lead a morphing result unsmooth. Therefore, bilinear interpolation is suggested to solve this problem. As shown in Figure 6, bilinear interpolation based on four nearest points was used to perform interpolation points of all mapped RGB pixels (see Eq. 3). It is expected that the morphing image become smoother. In Equation 3, x_i and y_i mean the location of a pixel needed to interpolate. The combinations of x_1, x_2, y_1 and y_2 are the locations of four points which are nearest (x_i, y_i). $f(x, y)$ means the RGB values located on z axis corresponding to the position (x, y).

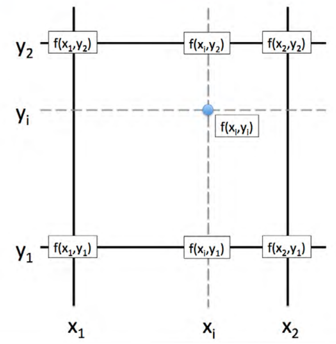

$$
\begin{cases}
f(x_i,y_1)=\dfrac{x_2-x_i}{x_2-x_1}\cdot f(x_1,y_1)+\dfrac{x_i-x_1}{x_2-x_1}\cdot f(x_2,y_1)\\
f(x_i,y_2)=\dfrac{x_2-x_i}{x_2-x_1}\cdot f(x_1,y_2)+\dfrac{x_i-x_1}{x_2-x_1}\cdot f(x_2,y_2)\\
f(x_i,y_y)=\dfrac{y_2-y_i}{y_2-y_1}\cdot f(x_i,y_1)+\dfrac{y_i-y_1}{y_2-y_1}\cdot f(x_i,y_2)
\end{cases}
\quad (3)
$$

Figure 6: Bilinear Interpolation

3. RESULTS AND DISCUSSION

As shown as the example in Figure 7, which are the results based on affine transformation and DRMF, but with two kind of interpolation methods. The left part is the nearest interpolation, and the right part is bilinear interpolation. We can observe that the edges of eyes and mouse are not smooth in the left images, but smoother edges appear in the right images. Therefore, the morphing images using bilinear interpolation are suggested in this study.

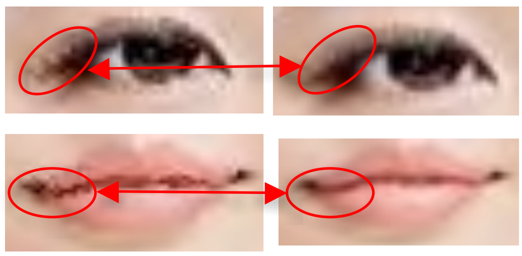

Figure 7 : Image interpotation comparisons; the nearest interpolation (left part) and bilinear interpotation (right part)

Image color differrences were calculated by ΔE^*_{94} color different formula between the test image and the morphing image. Referring to sRGB standard, the 8-bit RGB values of all image's pixels were transformed into XYZ tristimulus color space, then their XYZ value were transformed into $L^*a^*b^*$ color space. When a test image and a morphing image are compared (Figure 8), the color difference map indicates there is a large area with ΔE^*_{94} range of 0 to 5. However, there are several coutour areas with larger color different values (e.g., $\Delta E^*_{94} > 7$). Therefore, coutour smoothing is necessay to solve this problem.

(a) *(b)* *(c)*

Figure 8 : Facial color mapping results : (a) test image, (b) morphing image, (c) color differeence map

As shown in Figure 9, the sub-images (a), (c) and (e) are the results before smoothing in ΔL^*, Δa^* and Δb^* channel respectively, and (b), (d) and (f) are the results after smoothing in ΔL^*, Δa^* and Δb^* channel respectively. We can observer that ΔL^*, Δa^* and Δb^* channels before smoothing have a little strong contours. Therefore, the Gaussian blur filter is introduced into the initial morphing result to smooth large color differences in the coutour area. The ΔL^*, Δa^* and Δb^*channels after smoothing show much smoother results than the ones before smoothing. Then the smoothed ΔL^*, Δa^* and Δb^* channels are added to the original L^*, a^*, b^* channels again to restore a new facial image. Note that the eyes parts in a new face are still kept the same as the origial. Finally, Table 1 arranges the results that test facial image mapped by two facial template colors, which are (a) test image, (b) template color image, (c) color mapping result, (d) optimized mapping image and (e) color difference map.

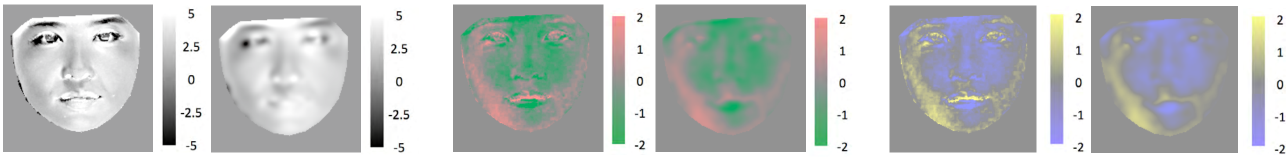

(a) (b) (c) (d) (e) (f)

Figure 9: ΔL^*, Δa^* and Δb^* channels; (a), (c) and (e) are before smoothing, (b), (d) and (f) are after smoothing

Table 1: Facial color mapping results

(a) Test image	(b) Templete color	(c) Color mapping result	(c) Optimized image	(d) Color difference map
				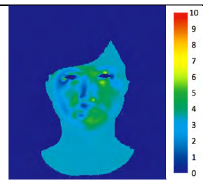
				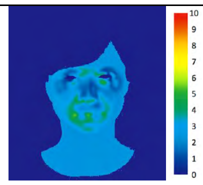

4. CONCLUSIONS

In this study, we developed an automatic facial makeup technology named Facial Color Morphing Algorithm (FCMA), which can make an original facial image without makeup reproduce the preferred cosmetic colors according to the facial color template database. Discriminative Response Map Fitting (DRMF) was also introduced to find the main facial organs (e.g. eyes, nose, mouth etc.) and the face outline information. In addition, affine transformation and bilinear interpolation was applied to perform facial skin-color mapping between the test image and the morphing image. The simulated results indicate that our developed algorithm works well in representing preferred facial images.

REFERENCES

Hung-Shing Chen, Shih-Han Chen, Yen-Hsiang Chao, Ronnier Luo and Pei-Li Sun, "*Applying Image-based Color Palette for Achieving High Image Quality for Displays*," Color Research and Application, Volume 39, Issue 2, pp. 154-168. 2014.

Howard Anton, 2005, *"Elementary Linear Algebra, 9th Edition "*, *Warps And Morphs,* New York : John Wiley & Sons.

Asthana A., S. Zafeiriou, S. Cheng and M. Pantic, CVPR 2013, *Robust Discriminative Response Map Fitting with Constrained Local Models*.

Address: Master. Lin LU, Graduate Institute of Electro-optical Engineering, National Taiwan University of Science and Technology, 43, Section 4, Keelung Road, Taipei, 10607, TAIWAN

E-mails: M10219005@mail.ntust.edu.tw, bridge@mail.ntust.edu.tw, nchu@mail.ntust.edu.tw

The consistent color appearance based on the display-referred

Yasunari KISHIMOTO,[1] Hitoshi OGATSU,[1] Hirokazu KONDO[2]
[1] Key Technology Laboratory, Fuji Xerox Co., Ltd.
[2] Imaging Technology Center, FUJIFILM Corporation

ABSTRACT

We report the results of testing of our hypothesis that using the largest gamut display as a reference and by producing colours to printers with different color gamuts, the use of a 'consistent color appearance' rendering including color and tone reproduction produces optimal results. The results obtained by two subjective assessments indicate that 'consistent color appearance' for various gamut sizes, from multi-color inkjet with a wide color gamut to newsprint with a narrow color gamut. 'Consistent color appearance' will provide an automatic process which enhances value of future digital printing.

1. INTRODUCTION

In recent years, printing for applications such as advertising and presentations are working to improve their quality and to reduce their color variation. This includes the use of color standards such as JapanColor, and the certification body. However, color differences between the target color gamut of the color standard and each output color gamut has been a problem as users can not fully utilize the color reproduction capability of wide color gamut printers and in addition them can not appliy to a narrow gamut printer. As shown in Fig. 1 and Fig. 2 (Case 2) the input images in the traditional offset print workflow (ISO 12647-2) are restricted to a standard color gamut such as JapanColor for color matching with the use of a print reference (ISO 22028-1). The characterized reference printing conditions (CRPCs, CGATS.21-2 2013) were specified as standard seven printing conditions from multi-ink wide color gamut printing to coldset inks for newspaper printing (narrow color gamut). These are intended as the basis for similar looking color for a variety of printing systems with print reference. They pay particular attention to gray balance and operational stability to produce similar results. Johan Lammens (2004) reported that the CMYK input images should apply color re-rendering following color rendering to the intended printing system for effective use across a variety of printing systems. In some cases it is important for a variety of printing systems to have a display reference and cross-media reproduction is often used as shown in Fig. 2 (Case 3). The International Color Consortium (ICC) has developed the concept of 'consistent color appearance' which should have a balance between color matching and consistent tone reproduction across multiple devices. Similar concepts are being studied in CIE Reportership R8-13 that it is include ITU-R BT. 2020 wide gamuts (Andreas Kraushaar 2013, Paul Sherfield 2013, CIE 156 2004). Furthermore, when preparing advertising for multiple media, the color gamut of different reproduction systems such as signage displays, inkjet or offset printing, the designer or prepress process involves making color adjustment of each color reproduction manually.

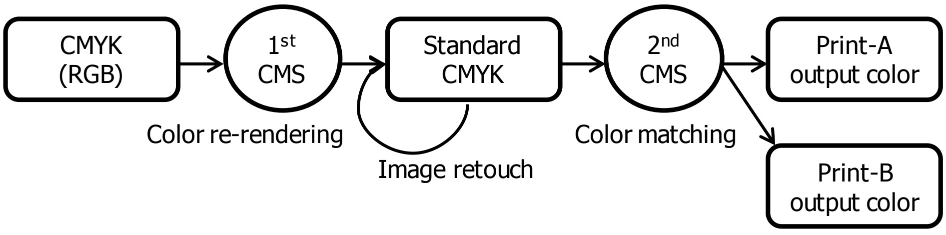

Figure 1: Examples of a standard traditional printing workflow based on CMYK print-referred.

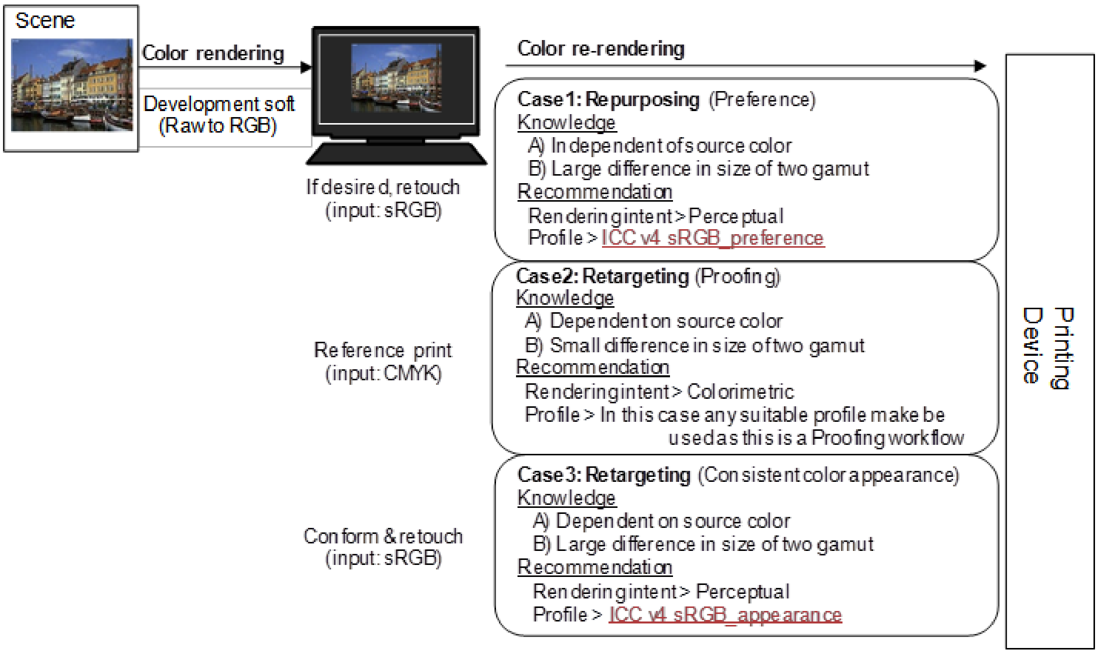

Figure 2: ICC color re-rendering as described in the ICC White Paper 42 update (2014).

This approach achieves a similar look between the display reference and the prints. Few reports are available on achieving a similar look between the display reference and prints from a variety of printing systems. This paper describes the results of an investigation of consistent color appearance. When color reproductions show highest similarity between the display reference and each print, and across the set of prints, when viewed under a common viewing condition they have by definition a 'consistent color appearance'. Similarity is judged by subjective assessment.

2. METHOD

We built the following hypothesis to test whether consistent color appearance is achieved based on a display reference. When display reference and outputs of respective printer have a similar looking image (color and tone) in a common viewing condition based on the common color reproduction aims (re-targeting of the display reference), outputs of all printer have a similar look. First, fundamental output colors corresponding to a limited number of common target colors (input color) are obtained by a full search of the colors on the reference images the can be producted by each printer. The number of colors is affected by the performance of experimental redering. Second, the new retargeting rendering is developed from fundamental output colors in each printing condition. Finally, we examined whether the same output was chosen as the preferred rendering by two subjective assessments.

2.1 Repeating subjective assessment and development of new retargeting rendering

The subjective assessment verified the closeness of appearance between the display reference image and all available print sample and judged its closeness of appearance. The reference images were selected as s set of images that covered the input color space. In addition, the assessment was limited to the relationship of a set of key image colors. New guidelines were made for fundamental output colors based on the result of the assessment. Common target colors were added as appropriate until the appearance of the two images looked similar. We repeated the process of making new print samples from fundamental output colors using the new guidelines and conducting this assessment until we judged the appearance of the image to be the nearest possible. This experiment was repeated even when multiple color gamuts of different printer and paper combinations.

As a result, we obtained a set of common target colors for multiple gamuts, and as shown in Fig. 3 and used these to develop a new retargeting rendering. The rendering is composed of two steps: (1) generate common appearance between the display reference and prints without considering gamut limitations (the common color reproduction), and (2) to control influence of the gamuts. In the common color reproduction, the relative Y matching (Rel.-Y) can maintain colors of highly sensitive color for skin tones, gray balance and so on with different output systems and paper types. Except for color close to the display white point, the effect of the Rel.-Y is superior to ICC absolute colorimetric reproduction and ICC relative colorimetric reproduction (ISO 15076-1 20124), because the luminance of display white point is close to the luminance of the paper white point in the viewing environment condition. This confirmed from not only our experimental data but also some market data. If the colors close to the white point in display system become out of gamut colors using Rel.-Y, they are adjusted in the consistent color rendering.

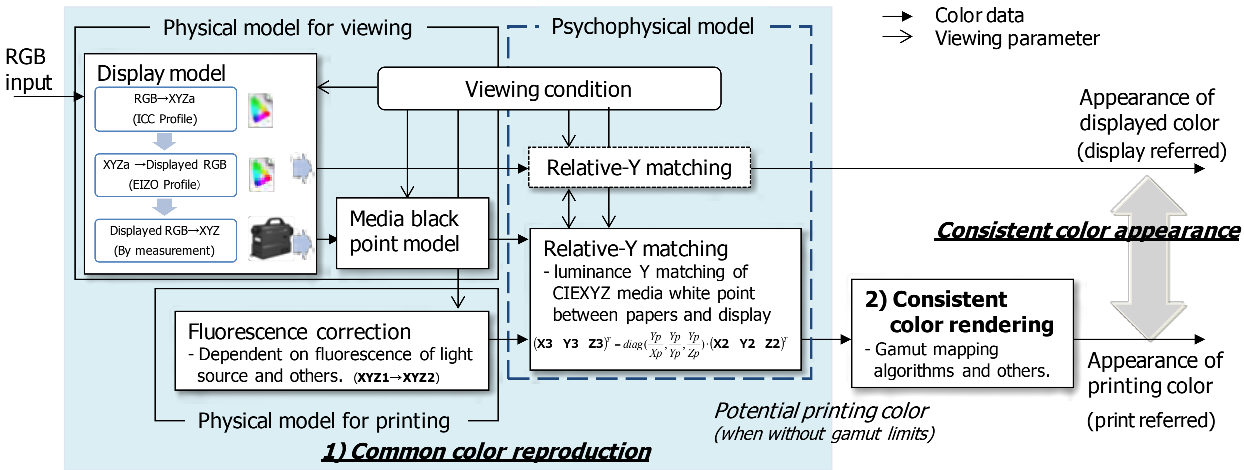

Figure 3: Schematic diagram showing a new retargeting rendering for 1) the common color reproduction without gamut limits, and 2) consistent color rendering. Using the relative-Y matching (Rel.-Y) equation, Xp, Yp, and Zp is the white point CIEXYZ; X2, Y2, and Z2 is the input CIEXYZ; X3, Y3, and Z3 is the Rel.-Y generated CIEXYZ.

2.2 Verification Experiment

The verification examined by using two subjective assessments (Table 1, 2). The first assessment was to rank the closeness of the appearance of the images on standard gamut in comparison with the display reference, and second assessment was to rank the closeness of the appearance of the images between images on standard gamut output and image on wide gamut output.

Table 1. Assessement conditons.

Test subject	20 persons.
Environment condition	ISO 3664 P2 conditon.
Display	EIZO CG221.
Test image	4 images (ISO 12640-4 SCID, high chroma image, portrait, and landscape).
Subjective assessment method	7 rank order scales (mentioned in Table 2).

Table 2. Print sample output conditions.

Color gamut	2 gamuts (Standard print, wide gamut by multiple-ink inkjet).
Paper	2 papers (plain paper, inkjet proofing paper).
Sample output	7 samples as combination of 3 methods (Commercial ICC profile builder, default condition of the each printing systems, and proposed rendering) and 2 printers (above-mentioned gamuts).

3. RESULTS AND DISCUSSION

As shown in Fig. 4, assessment of the average score of 4 images is divided into two groups. The group having a low degree of closeness of appearance with the reference image is a default condition used with factory setting on a commercial printing system. The group that has a high degree of closeness were made by a commercial ICC profile builder. It is suspected that in some cases closeness of appearance is achieved using the same algorithm for different printers. The proposed rendering showed the best result where the appearance of the image was judged to be the closest to display reference. Thus it is possible to achieve consistent color appearance by making the print output where the appearance of the image is close to the display reference.

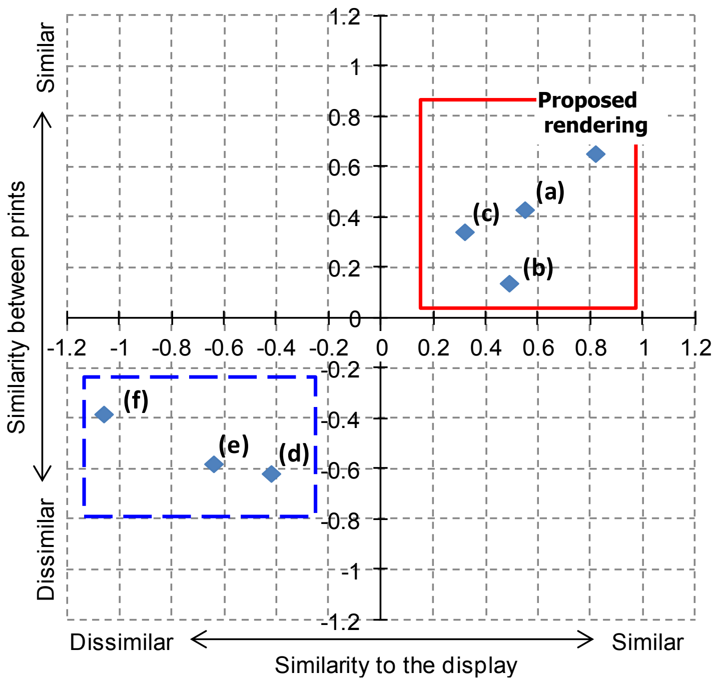

Figure 4: The results from the experiment. The (a), (b) and (c) is a condtion of a commercial ICC profile builder, the (d), (e) and (f) is a condition using a printer with color gamut corresponding to each print output.

4. CONCLUSIONS

In traditional printing workflow based on CMYK print reference there was a limitation that the full colour reproduction capability of a printing system cannot be used Furthermore, when producing advertising materials on multiple media designer or prepress process must control each color to look for similar colors and the display reference becomes important. Consistent color appearance aims to achieve similar output between the display reference and the prints on a variety of printing systems. We developed a new retargeting rendering by acquiring basic target color data using repeated subjective assessment. The rendering showed the result that the continuity (a color and tone) of the image was close visually between the display reference and the prints of two printing systems. Our results have demonstrated that the consisitent color appearance is feasible.

REFERENCES

ISO 3664:2009. *Graphic technology and photography -- Viewing conditions.*

ISO 12640-4:2011. *Graphic technology -- Prepress digital data exchange -- Part 4: Wide gamut display-referred standard colour image data [Adobe RGB (1998)/SCID].*

ISO 12647-2:2013. *Graphic technology -- Process control for the production of half-tone colour separations, proof and production prints -- Part 2: Offset lithographic processes.*

ISO 13655:2009. *Graphic technology -- Spectral measurement and colorimetric computation for graphic arts images.*

ISO 15076-1:2010. *Image technology colour management -- Architecture, profile format and data structure -- Part 1.*

ISO 22028-1:2004. *Photography and graphic technology -- Extended colour encodings for digital image storage, manipulation and interchange -- Part 1: Architecture and requirements*.

ANSI CGATS.21-2 2013. *CRPCs*, http://www.idealliance.org/downloads/iso-15339-reference-print-conditions-2011 .

CIE 156:2004. *Guidelines for the Evaluation of Gamut Mapping Algorithms.*

Lammens, J. Morovic, J.Nielsen, M. Zeng, H 2004. *Adaptive re-rendering of CMYK image data*, CGIV 2004 Final Program and Proceedings (5) 454-458.

International Color Consortium 2014. *Using the sRGB_ICC_v4_appareance.icc profile,* ICC White Paper 42 http://www.color.org/profiles/srgb_appearance.xalter and http://www.color.org/whitepapers.xalter

Andreas Kraushaar 2013. *Common Appearance - Introduction, Concept and Overview*, ICC Frankfurt Graphic Arts Color Experts' Day, http://www.color.org/events/frankfurt/Kraushaar_ICCFrankfurt2013_CommonAppearance.pdf .

Paul Sherfield 2013. *Common Color appearance*, ICC Frankfurt Graphic Arts Color Experts' Day, http://www.color.org/events/frankfurt/Sherfield_ICCFrankfurt2013_Common_Appearance.pdf .

Address: Yasunari KISHIMOTO, Key Technology Laboratory, Research & Technology Group, Fuji Xerox Co., Ltd., 430 Sakai, Nakai-machi, Ashigarakami-gun, Kanagawa, 259-0157, JAPAN

E-mails: Y.Kishimoto@fujixerox.co.jp, ogatsu.hitoshi@ fujixerox.co.jp, hirokazu.kondo@fujifilm.com

The study of museum lighting: the optimum lighting and colour environment - the proposal for the colour quality index -

Yuki NAKAJIMA, Takayoshi FUCHIDA,
Graduate School of Joshibi University of Art and Design

ABSTRACT

The purpose of this study is to develop the new calculation method to evaluate the colour rendering values taking illuminance into consideration based on the subjective experiments. We carried out the experiments to examine subjectively impression of the test colour samples (the two-colour samples, the multicolour sample and the picture samples) under various light sources and illuminance. The results showed that subjective colour feelings were influenced by illuminance as well as the spectral power distributions of light sources, and also subjective impression depended on the hue of colour samples, especially on whether the sample contained red. It was also found that subjective impression could be evaluated by "colour quality" such as subjective vividness and brightness by factor analysis. We defined "the colour quality index" called Gx and Rxi to evaluate the new colour rendering properties representing illuminance-effects and hue-effects. It was confirmed that the new index Gx and Rxi correlated practically subjective results.

1. INTRODUCTION

The lighting environment of a museum must be carefully controlled not to give any damage against deterioration of artworks. The CIE publication (157: 2004) recommends illuminance and a limiting exposure time to control of damage to artworks by optical radiation. In case of the exhibition of Japanese paintings for example, illuminance is regulated to constrain under 50 lx not to give colour fade damage as less as possible.

The present ISO/CIE standard recommends for museum lighting that General Colour Rendering Index *Ra* is better than 80. However, *Ra* does not include illuminance effects. The calculation method taking into consideration of illuminance does not exist at present. Low illuminance means the decrease of inherent colour appearance of artworks because artworks will lose brightness and colourfulness at low illuminance. As known as the Hunt-effects, chromatic objects look more vivid when illuminance increase, on the other hand they look darker and dull when illuminance decreases.

We clarified on the previous paper that *Ra* would not be sufficient when colour rendering properties were evaluated at low illuminance, and showed that the colour rendering properties at very low illuminance could be evaluated by Gamut Ratio (Nakajima et al. 2013, Nakajima et al. 2014). As for the relationship between colour rendering properties and chromatic samples whether the sample contained red, Rea (Rea et al. 2008) and Wei (Wei et al. 2014) showed the importance of red.

The purpose of this study is to clarify colour rendering properties at low illuminance and also to try to develop the new calculation method to evaluate the colour rendering values taking into consideration of illuminance based on the subjective evaluation experiments.

2. METHOD

The two types of experiments were performed by a haploscopic viewing method. The evaluation booth (Figure 1) separated at the center was used. The different light source was installed at the top of the each box. The wall of the booth was painted in matted gray (N6). The observer evaluated subjective colour feelings of the test colour samples of the test side compared with colour feelings of those of the reference side by Semantic Differential method. Figure 2 shows the eleven adjective pairs and the seven categorized scale. Ten females observers in the experiment 1 and 17 females observers in the experiment 2 were participated.

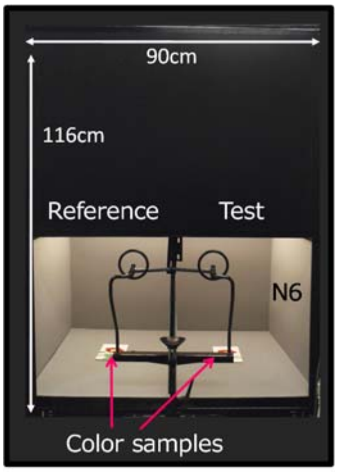

Figure 1: The evaluation booth.

No.	(—) ⟷ (+)	No.	(—) ⟷ (+)
1	dirty-beautiful	6	heavy-light
2	uncomfortable-comfortable	7	dark-bright
3	muddy-clear	8	cool-warm
4	sober-flashy	9	dislike-like
5	passive-active	10	dull-vivid

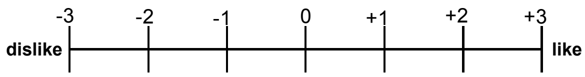

Figure 2: the adjective pairs and the seven categorized scale.

2.1 The reference and the test lighting

The reference light source was the fluorescent lamp specially designed for a museum lighting (FL-EDL: *Ra*96, 3060 K). The four types of test light sources were used in the two experiments, the two fluorescent lamps (FL-EDL: *Ra*96, 3060 K and FL-WW: *Ra*55, 3460 K), and the two LED lamps (LED-RGB: *Ra*21, 3050 K and LED-BY: *Ra*84, 3060 K). LED-RGB composed of the combination of red, green, blue LEDs had the special effect emphasizing saturation of colour. LED-BY composed of blue-LED and yellow phosphor had the effects rendering object colour dull. Table 1 shows the specifications of light sources, and Figure 3 shows the spectral power distributions of the test and the reference light sources. Illuminance of the test side was set at 700 lx and 10 lx respectively at the table top of the booth, and the illuminance of the reference side was fixed at 700 lx.

Table 1: The specifications of the light sources.

Light sources		CCT	*Ra*
Reference	FL-EDL	3060	96
Test	FL-EDL	3060	96
	LED-BY	3060	84
	FL-WW	3460	55
	LED-RGB	3050	21

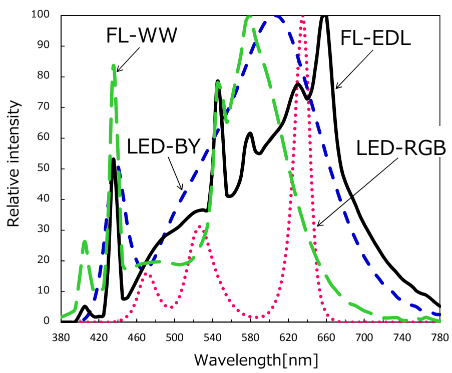

Figure 3: The spectral power distributions of the light sources.

2.2 Test colour samples

The seven kinds of the test colour samples (the two-colour pairs, the multicolour sample, the picture samples) were used in the experiment 1 (Figure 4). The test colour samples were categorised in two groups, red-include and red-exclude. The muti-colour sample was made up of the mineral pigments and the gold leaf for Japanease-style arts.

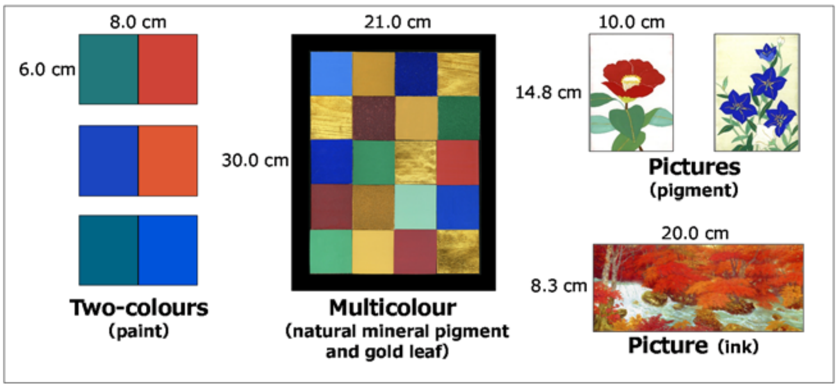

Figure 4: The test colour samples in the experiment 1.

The nine test colour samples were used in the experiment 2 (Figure 5). The original sample (Japanese painting by the artist Meiji HASHIMOTO) was selected by the reason that the sample did not include red at all. The each test sample had the small leaf images (green-yellow-yellow red-orange-red-red purple-blue purple-blue) sprinkled in the original image as addition. The hue angle of the leaf image, the spectral reflectance of the leaf image was shown, and the $a_M b_M$ coordinates (CIECAM02: Colour Appearance Model) was shown in Figure 5, Figure 6, and Figure 7.

Hue	Original	Green	Yellow	Yellow Red	Orange	Red	Red Purple	Blue Purple	Blue
Image	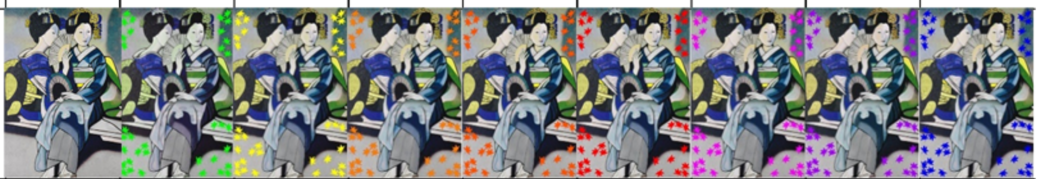								
Hue angle		133	95	39	28	20	355	347	265

Figure 5: The test colour samples in the experiment 2.

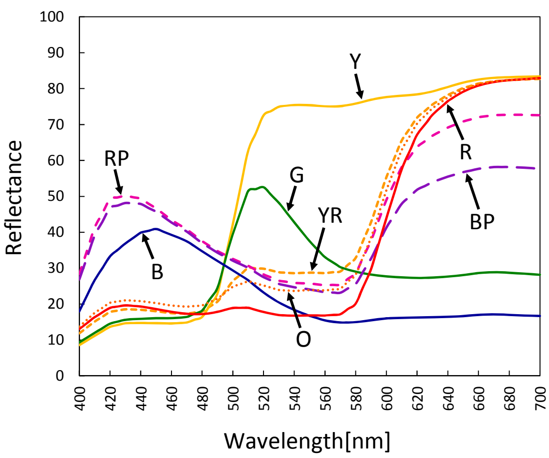

Figure 6: The spectral reflectance of the leaf images.

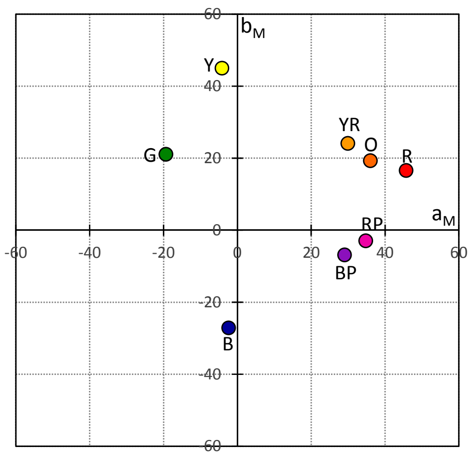

Figure 7: the $a_M b_M$ coordinates (CIECAM02) of the leaf images.

3. RESULTS AND DISCUSSION

3.1 Results of the experiment 1

Figure 8 shows the subjective evaluation profiles for the colour samples. As shown in Figure 8, the results of the subjective experiment were divided into two groups, the results of the red-include samples and those of the red-exclude samples. In the results of the red-include samples, it was clearly shown that the subjective impression under LED-RGB and those under the other test lamps were different. However in the results of the red-exclude samples, the subjective results were not different for the test lamps.

To examine which colour was most influenced when the observer evaluated the subjective evaluation of the test colour samples, the observer was asked two questions, one was which colour the most attention was when you judged the evaluation, and the other was which colour the most difference from the reference colour was. As shown in Figure 9 (a), the observer's judgement for the most attention colour was "red" regardless of illuminance and the light sources. On the other hand, the observer's evaluation for the most different colour from the reference colour varied by illuminance and the light sources shown in Figure 9 (b). The results suggested that "red" was the most important in colour rendering terms.

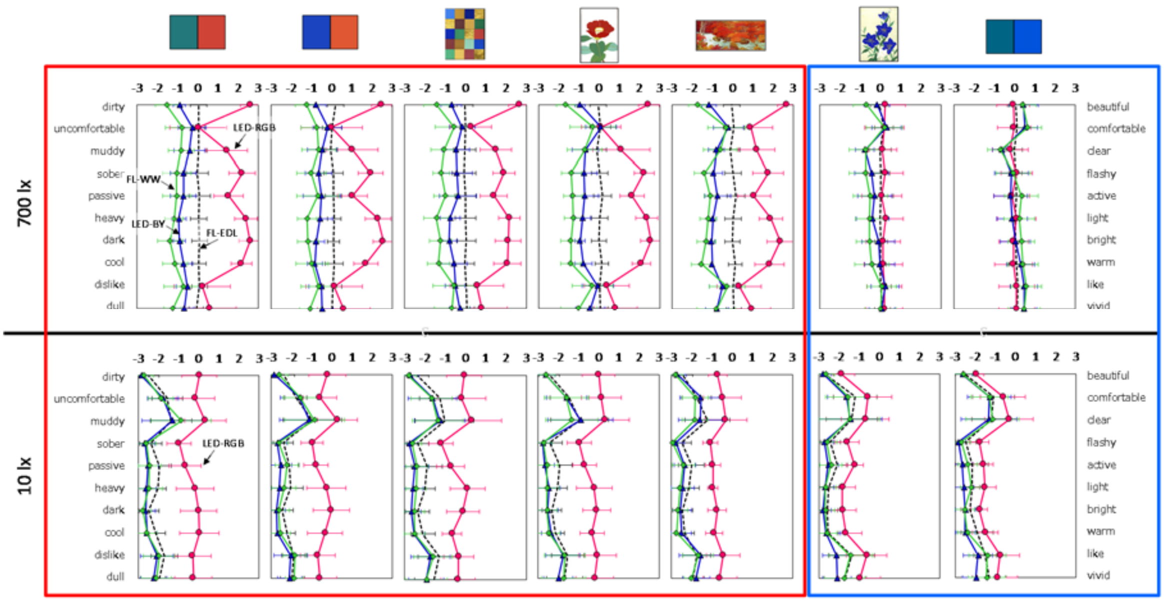

Figure 8: The subjective evaluation profiles of the colour samples.

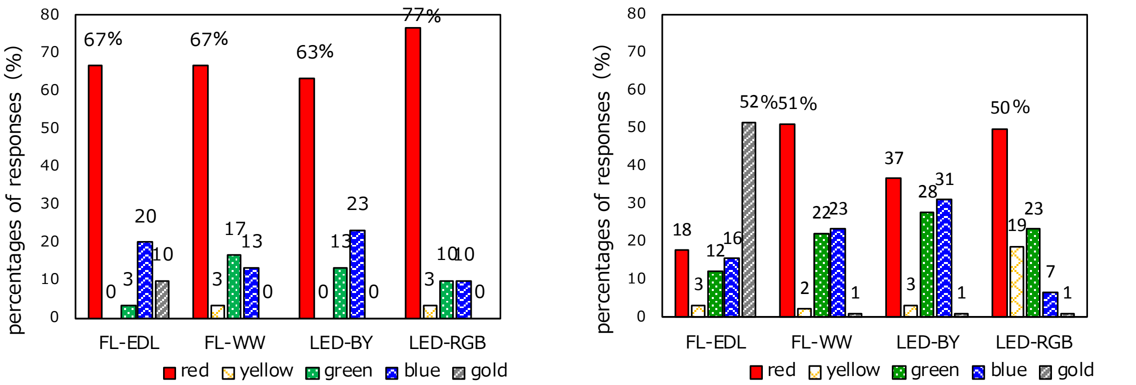

(a) *the most attention color* (b) *the most different colour from the reference*

Figure 9: Percentages of observer's responses to two questions at 700 lx.

3.2 Results of the experiment 2

The evaluation structure when impression of colour samples under various illuminations were sujectively observed was analysed by factor analysis. Factor analysis revealed the two main factors "color quality" and "preference". Figure 10 shows that the relationship between the subjective evaluation results for each factor and the hue angle of the leaf image by CIECAM02, and the relationship between ΔM and the hue angle. ΔM shows the difference between the colourfulness (M) under the test light source and that under the reference light sources. The results of “colour quality factor” were different from those of “preference factor” and it was clearly shown that the subjective impression of “colour quality facor” depended on the hue angle of the test colour, especially had the peak at about hue angle 20° (red) under LED-RGB and LED-BY. On the other hand, in the case of preference factor did not change for the hue angle as well as the test light sources. The results showed that the subjective feelings could be evaluated by “colour quality” of the colour samples such as vividness, brightness, flashyness, clearness and activeness.

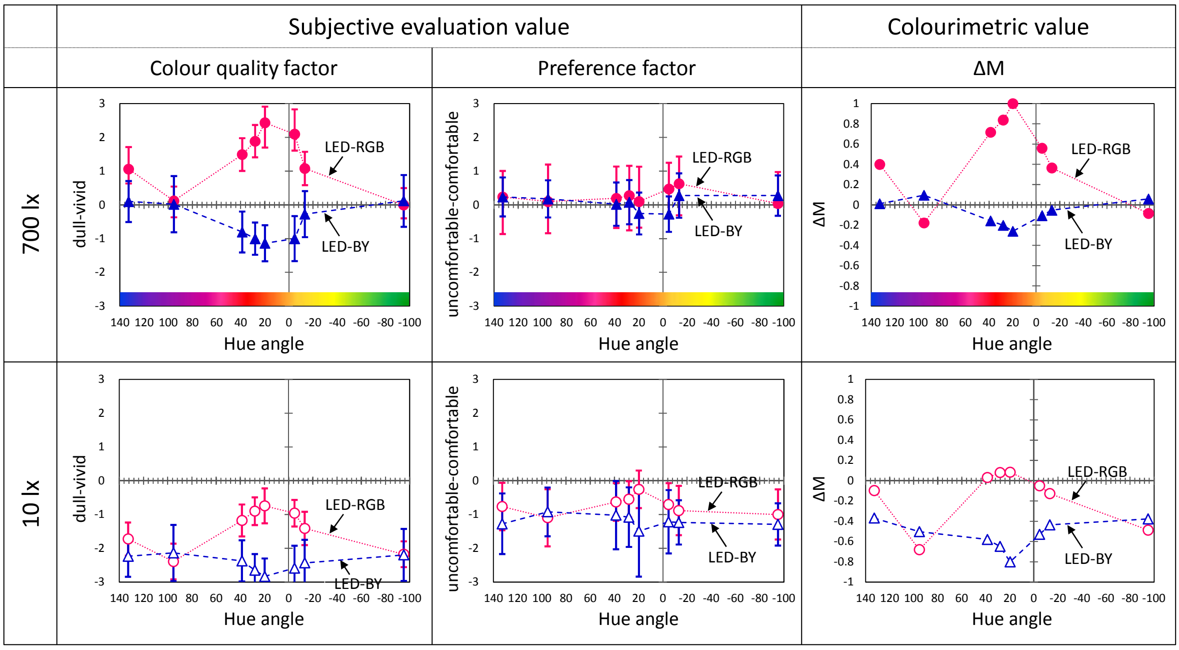

Figure 10: The relationship between the subjective evaluation results, ΔM and the hue angle.

As shown in Figure 10, the results of the subjective evaluation of “colour quality factor” were very similar with those of the colorimetric ΔM. It was clearly shown that “colour quality feeling” could be explained by the colorimetric ΔM.

Figure 11 shows that ΔM correlates closely with the subjective evaluation results of colour quality factor. The results suggested that the subjective evaluation results of colour quality factor could predict by ΔM based on colorimetric colourfulness.

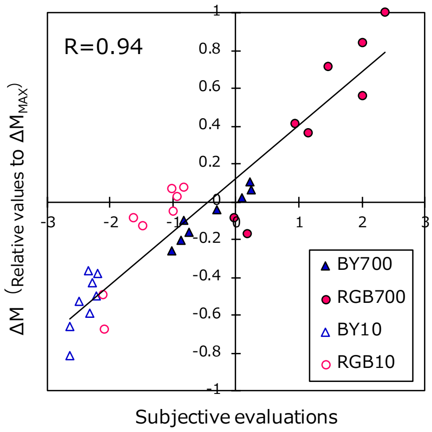

Figure 11: The relationship between ΔM and the subjective evaluation results.

3.3 Colour Quality Index (Gx and Rxi)

We defined "colour quality index" called Gx and Rxi to evaluate colour rendering properties taking into consideration of illuminance-effects as well as hue-effects based on the subjective evaluation results of the experiment 1 and the experiment 2.

3.3.1 The test colour samples and the reference light source

The saturated 20 colours made by Japan Colour Research Institute were used for the calculation of Rxi and Gx as the test color samples. Figure 12 and Figure 13 show the spectral reflectance and the $a_M b_M$ coordinates of CIECAM02 (FL-EDL, 700 lx).

The reference light source was FL-EDL specially designed for a museum lighting (3060 K, *Ra*96). The illuminance of the reference lighting was set at 700 lx for the calculation.

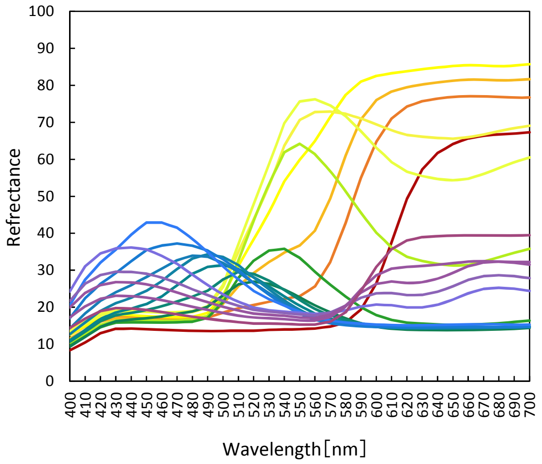

Figure 12: The spectral reflectance of the test colour samples.

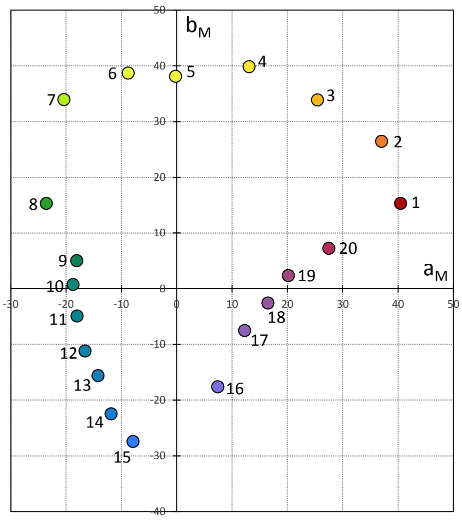

Figure 13: The $a_M b_M$ coordinates of the test colour samples.

3.3.2 Rxi

Gx is the colour quality index showing the subjective impression not for the individual test colour, but for the overall test colour samples. Gx is calculated by the ratio between the gamut of the test colour samples under the test light source and the that of the reference light source.

$$\mathrm{Rxi} = 100 + 100 \cdot \left(\frac{M_{iT(E)} - M_{iR(E)}}{M_{iR(E)}}\right) \quad (i=1\sim20) \qquad (1)$$

where $M_{iT(E)}$ is M of the test colour sample i under the test light source and any illuminance. $M_{iR(E)}$ is M of the test colour sample i under the FL-EDL and 700 lx.

Figure 14 shows the relationship between the color quality index (Rxi) and the subjective evaluation for colour quality by the experiment 2. These Rxi values were calculated by the test color samples chosen hue angle close to the hue angle of the test color samples (see Table 2). Rxi was correlated to the subjective results (R=0.94).

Table 2: The hue angle of the test color samples and the leaf images.

No of TCS	8	5	2	1	19	18	15
Hue angle	147	90	36	21	7	351	254

Leaf images	G	Y	YR	R	RP	BP	B
Hue angle	133	95	39	20	355	347	265

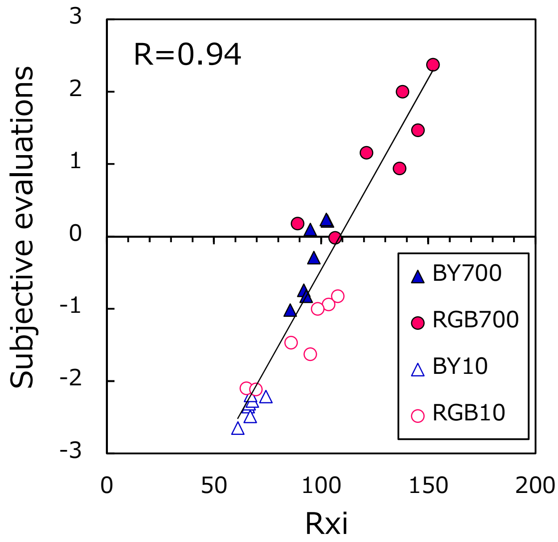

Figure 14: The relationship between Rxi and the subjective evaluation results.

3.3.3 Gx

Gx is the colour quality index showing the subjective impression not for the individual test colour, but for the overall test colour samples. Gx is calculated by the ratio between the gamut of the test colour samples under the test light source and the that of the reference light source by Equation 2.

$$Gx = 100 \cdot \left(\frac{G_{T(E)}}{G_{R(E)}}\right) \qquad (2)$$

$$a_{xi} = a_{Mi} \cdot W_{hi} \quad (i=1\sim20) \qquad (3)$$

$$b_{xi} = b_{Mi} \cdot W_{hi} \quad (i=1\sim20) \qquad (4)$$

$$W_{hi} = \frac{R_{xi}}{100} \quad (i=1\sim20) \qquad (5)$$

where $G_{T(E)}$ is th gamut area of the test colour samples under the test light source at the illuminance E lx. $G_{R(E)}$ is the gamut area of the test colour samples under FL-EDL at 700 lx. In addition, the $a_M b_M$ coordinates under the test light source were calculated with the weighting coefficient W_{hi} by Equation 3 to Equation 5. W_{hi} was defined at the test colour samples No.1~No.3 (reddish colours), No.9~No.11 (greenish colours)

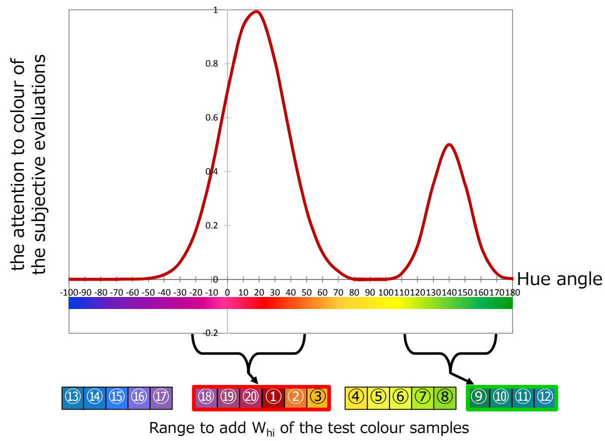

Figure 15: The relationship between the attention colours and the corresponding test colors.

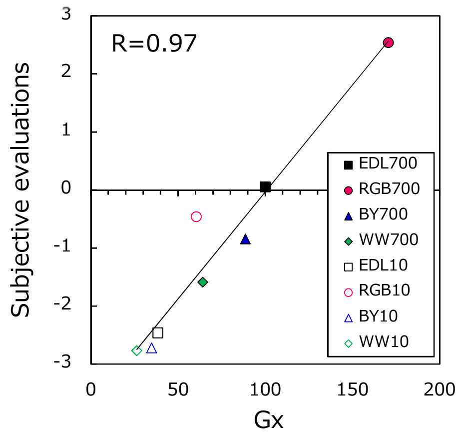

Figure 16: The relationship between Gx and the subjective evaluation results.

and No.18~No.20 (reddish colours) by the hue dependency of the subjective evaluation results as shown in Figure 15.

Figure 16 shows the relationship between Gx values and the subjective evaluation results by the experiment 1. As shown in Figure 16, Gx correlated very closely to the subjective evaluation results (R=0.97).

4. CONCLUSIONS

The colour quality indices Gx and Rxi supplementing *Ra* especially when evaluated at low illuminance were defined to represent the new colour rendering properties which could explain illuminace effects as well as hue dependency of the test colour sample. It was shown that Gx and Rxi correlated to the subjective evaluation of the test colour samples under various light sources. These new indices could be expected to use practically.

ACKNOWLEDGEMENTS

We would like to express our sincere appreciation and gratitude to Dr. Kenjiro Hashimoto for kind discussion, and to thank Japan Colour Research Institute and KONICA MINOLTA INC. for their supports. We also thank to the students of Graduate School of Joshibi University of Art and Design for their observer participation to our subjective experiment.

REFERENCES

Publ. CIE 157：2004. *Control of damage to museum objects by optical radiation*.

Hunt, R.W.G. 1952. *Light and dark adaptation and the perception of colour*, J. Opt. Soc. Am. 42(3) 190-199.

Nakajima, Y. and Fuchida, T. 2013. *Affective evaluation on color samples illuminated by LED illumination ~influence of illuminance level*, CIE2013 Paris Conference.

Nakajima, Y. and Fuchida, T. 2014. *Development of a new calculation method of color rendition taking illuminance into consideration*, CIE2014 Malaysia Conference.

Rea, M.S. and Freyssinier-Nova, J. P. 2008. *Color rendering：A tale of two metrics*, Color Res. Appl. 33(3) 192-202.

Wei, M., Houser, K.W., Allen, G.R. and Beers, W.W. 2014. *Color Preference under LEDs with Diminished Yellow Emission*, LEUKOS, 10(3) 119-131.

Address: Yuki Nakajima, Graduate School of Joshibi University of Art and Design,
1900 Asamizodai, Minami-ku, Sagamihara-shi, Kanagawa, 252-8538, JAPAN
E-mails: limesun.yn@gmail.com, fuchida11001@venus.joshibi.jp

Developing Test Targets for Color Management of Full Color Three-dimensional Printing

Yu-Ping SIE,[1] Pei-Li SUN,[1] Yun-Chien SU,[1] Chia-Pin CUEH,[2] Kang-Yu LIU[2]
[1] National Taiwan University of Science and Technology
[2] Printing Technology Research Institute, Taiwan

ABSTRACT

To evelate color fidelity of a 3D printer, several targets with different shapes and measurement methods were designed in this research, including Multi-direction Color Target which tests the color on different orientations, TC 2.83 C5 Target which can generate ICC profile rapidly with i1 Profiler, and 729-color Target which is material-saving and it use a DSLR to quickly calibrate its colors. The influence of different surface normals and post-processing methods also have been evaluated. Our experimental results show the color variations of different orientations are noticible and the color accuracy of top direction can be improved by applying 3D color LUTs with interpolation.

1. INTRODUCTION

The development of 3D printing technology has accelerated over the past few years (Stanic and Lozo, 2012). However, only few products can make full color models (Xiao, Zardawi, Noort and Yates, 2013). In traditional two-dimensional (2D) printing, color target is applied to estimate the color performance and make color management work. If we apply the same method to 3D printing, some problems will be encountered. For example, 3D printing can produce 3D objects with curved surfaces, which have various surface normals towards different directions (Jackson et. al, 2006). The same RGB input show different colors in different orientations. To optimize its color quality, it’s necessary to develop new methods to evaluate the color characteristics of a 3D printer. The efficiency of 3D printing color management must be considered because of high-cost in materials and low-speed in printing.

2. METHODS

In this research, several targets with different shapes and measurement methods were designed. Each target was developed based on different purposes including color evaluation of different surface directions, compatibility of commercial color measuring tools such as X-rite i1 Publish Pro 2, evaluating colors and generating ICC profile (ICC, 2012) with limited material and process time.

2.1 Target Design

Multi-direction Color Target is designed to estimate color performance of surfaces in 26 directions (Figure 1). The target is combined with 13 pieces in different surface directions, like a puzzle, and each piece has two sides with several color patches on it. The biggest piece, which is printed on top and bottom, has 225 color patches for general color management. The 225 colors consist of 6-level RGB and 9-level grayscale. The other pieces have 4 or 14 color patches and can represent the color differences in various surface normals. 4 pieces are consist of CMYK colors, and they are rotated for evaluating the color quality of 8 corner directions. 8 pieces of 14-color patches are consist of CMYKRGB primary colors and mid-tone CMYKRGB colors, and they are rotated for evaluating the color quality on 16 different directions, including front, back, right, left, and other 45 degrees oblique angle directions. The size of each color patch is 9×9 mm^2, and each pecies has 4.5 mm interval. The target can be measured by X-Rite i1 Publish after combined the 26 pieces in a correct order. In our model, the target is designed as a puzzle. Each piece has a unique shape to avoid mistakes in combining the pieces.

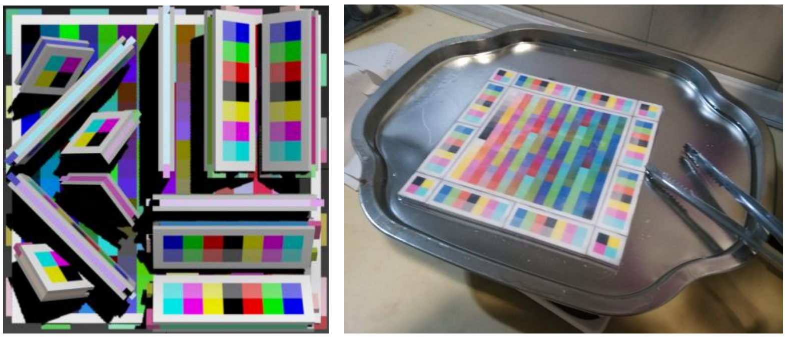

Figure 1: Multi-direction Color Target. The left figure shows the arrangement of each pieces in modeling software Autodesk 3DsMax. Each piece is arranged to face particular direction. The right figure shows a real target after the assembling.

TC 2.83 C5 Target was designed by X-rite. It is a RGB-based test chart, which arranged 283 color patches in C5 size and can be measured by X-Rite i1 Pro 2 spectrometer with a handheld scanning ruler and generates ICC profile rapidly and simply.

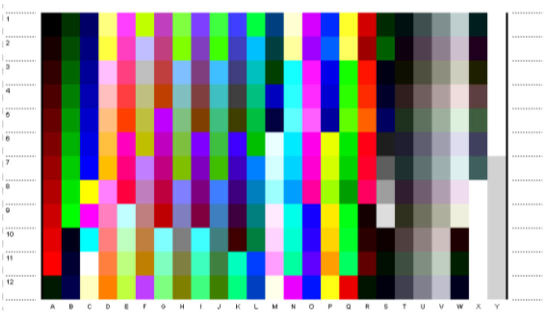

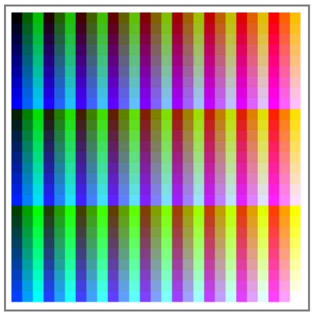

Figure 2(left): TC 2.83 C5 Target. Figure 3(right): 729-color Target. Both height and width of the target are 10 cm. The color patch set in RGB values from top-left to bottom-right is (0, 0, 0), (0, 0, 31), (0, 0, 63)…, (255, 255, 223) and (255,255,255), which is a set of 9-level RGB values. The size of each color patch is 0.35 × 0.35 cm.

729-color Target has 729 color patches in small area (10x10 cm). 729-color patches are consist of 9-level RGB colors, which is proper to RGB printer. It designed to be a material-saving target. However, because of the size of color patches, it cannot be measured directly by any spectrophotometer. Thus, it is necessary to design a process to measure the color patches by a calibrated DSLR camera. Taking a photo of the target and ColorChecker passport in a viewing booth simultaneously, the RGB values in particular light source can be read and applied to color management.

2.2 Modeling and Printing

The targets was modeled with Autodesk 3DsMax. The models are exported into VRML format and attached with PNG files for texture mapping, which are supported by 3D

Systems Projet 460 Plus Color 3D printer. The printer support RGB 3-channel color input and have CMY inkjet heads to print full-color 3D model. All of the glue-jet and the material of model which is gypsum-like powder are made by 3D Systems. The color inkjet heads are provided by HP.

2.3 Post-Processing

The models printed by Projet 460 Plus still need post-processing to enhance the purity of color and strength of material. To investiage the differences between various post-processing methods, some often-used coating material like Color-bond™, salted water, and paraffin wax were tested. These post-processing methods are detialed as follows:

The processing of Color-bond™ is to coat some "z-bond 90" on the model. The liquid infiltrates the model and coagulates. It is the most recommented method of post-processing because it can make the 3D model stronger and more colorful. To make sure that the color patches won't be influented by hand processing, we skipped scrubbing the targets by sandpaper which is a often-used process to make model surface flatter and more colorful.

Salted Water post-processing is also recommented. To make salted water, it is need to mix up epsom salt and water with 1:6 ratio. Spray salted water on the model and wait for it to be dried. The process called "Water Cure." The material become weak after sprayed salted water, so it is necessary to put the model carefully before it dried.

Paraffin Wax is also a material for post-processing, which is cheap and has good color performance. To melt the paraffin wax, it is needed to heat it until 60 to 70 degrees. Put the model into melted paraffin wax to infiltrate the model. Take the well-infiltrated model out and wait for cooled. The model will be a little swallowed after processed, but doesn't make influence on color measuring.

3. RESULTS AND DISCUSSION

To evulating the color performance of 3D printer, we made some process to measure the color patches for every targets we designed. For Multi-direction Color Target and TC 28.3 C5 Target, we used X-rite i1 to measure the color patches. The color differences between different surface normals were found to be visible by human eyes. We also tested 3 kinds of post-processing methods including Color-bond™, salted water and paraffin wax using the Multi-direction Color Target.

For the color patches on 729-color Target, we designed a process to obtain the CIELAB values of 729 color patches from measured spectra or XYZ stimulus data of ColorChecker and RGB image taken with camera in the light booth. For building an ICC profile for 3D printer with a fast and materal-saving method, we developed a program to make a 3D Look-Up-Tables (LUTs) for 729-color Target. To evaluate the LUTs, we read the B2A1 and A2B1 tables generated by i1 Profiler using TC 2.83 C5 Target. Both the TC 2.83 C5 Target and 729-color Target are Color-bond™ processed.

3.1 Color Difference across Different Orientations

For the Multi-direction Color Target, which combined 13 pieces, can be measured by X-rite i1. We also can connect X-rite i1iO and set patch numerial as 21 by 21 array to measure all of them automatically. After we measured the spectra for every color patches, we divided the color patches into 26 groups, which represent different surface direction. Calculating the XYZ values from spetral data with ASTM D50 Veneble sheet, the color patches on the target can be evaluated.

To analyze color difference on different surface normal, we regard the color patches on top (+z direction) surface as the standard color and compare the color differences of the other color patches with the same RGB inputs. Figure 4 shows the average color differences on each surface normal and average differences on L*, a* and b* in the Color-bond™ post-processed Multi-direction Color Target. Figure 5 compares color differences between CMYK colors. The mean and maximum color difference is up to 6.71 and 22 ΔE_{00} (CIE, 2012) respectively, which is noticible by human eyes. Color differences on different surface normal are mostly depended on the differences of lightness, and happened in black color which mixed by equal amount of cyan, magenta and yellow inks. The differences were caused by many different sources, such as moving direction of inkjet heads, asporbsion of the powder, dust, and force of gravity. Color image quality of 3D printing can be improved if we take the color variations across different orientations into account.

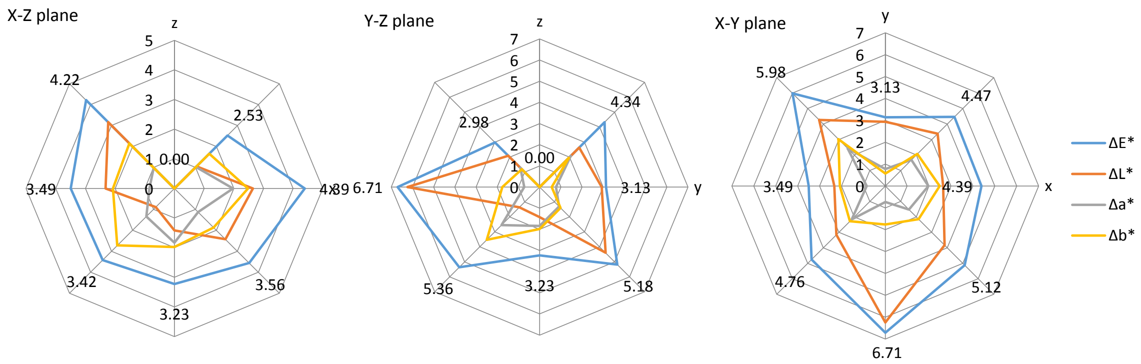

Figure 4: Average color differences on each surface normal and average differences on L, a* and b*.*

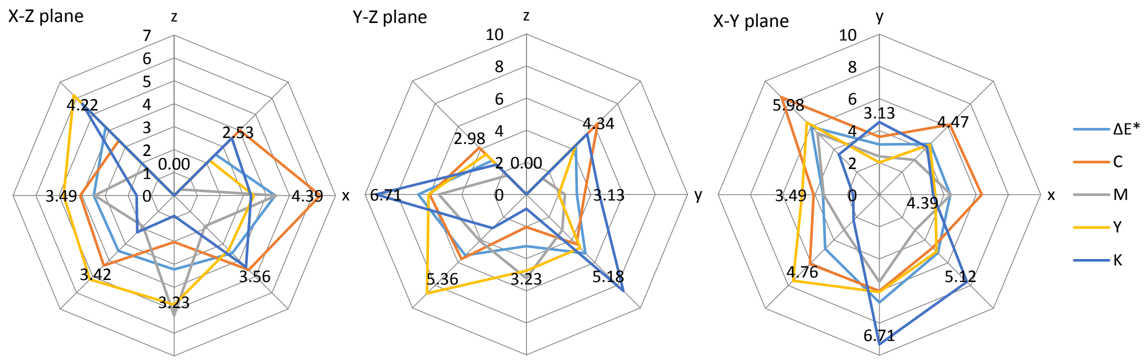

Figure 5: Average color differences on each surface normal and color differences on CMYK colors.

3.2 Color Difference on different post-processing method

Post-processing plays an important role on not only material strength but color performance. To compare the effects of post-processing, we printed 4 sheets of Multi-direction Color Target and applied non-post-processed, Color-bond™, salted water and paraffin wax respectively. Figure 6 shows the color differences between CMYKRGB colors in sRGB color space and printed target. Color performance on non-post-processed target is pale, while post-processed targets show better color density. Paraffin wax processed target has similar effect with Color-bond™. It means we also can get good color quality with the low-cost method.

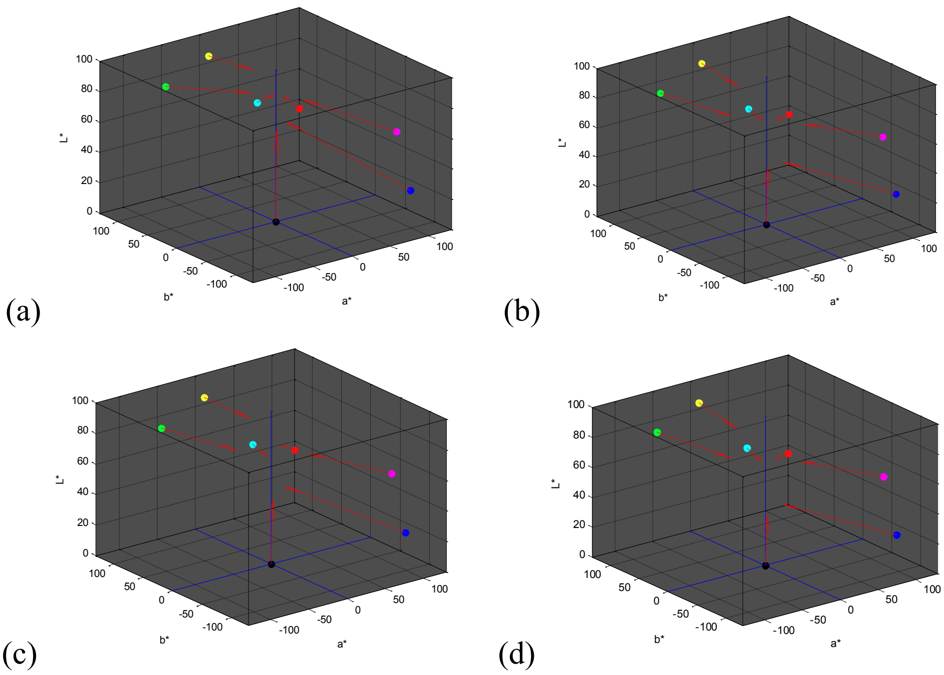

Figure 6: Color difference of CMYKRGB colors in (a) non-post-processed, (b) Color-bond™, (c) salted water and (d) paraffin wax.

3.3 Build look-up-tables with 729-color Target

The method to measure color patches from 729-color Target was different with the other targets. We put the target and a ColorChecker Passport into a light tooth (SpectraLight III) under D65 light source, and took a RGB photo with digital camera Canon EOS 5D Mark II (Figure 7a). The spectra or XYZ stimulus data of 24 colors on ColorChecker Passport were measured by Topcon SR-UL1R spectrometer.

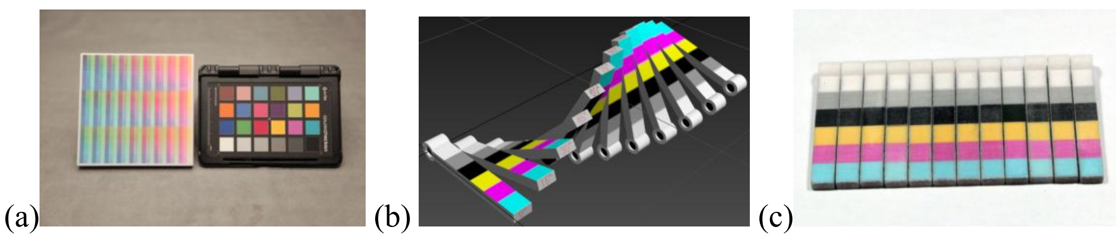

Figure 7: (a)729-color Target with ColorChecker Passport under SpectraLight III light booth.(b)3D model of Multi-angle Color Target. (c) Visual Comparison of target (c).

The purpose of measuring the color patches is to build an ICC Profile for 3D printer. Reading the RGB values of 729 colors from the target and 24 colors from the ColorChecker, the XYZ stimulus values of 729 color patches can be calculated by a polynomial regression with the measured spectra or XYZ stimulus data of 24 colors on

ColorChecker Passport and transform into CIELAB color space. We made a BtoA1 LUTs (Lab to RGB) in ICC profile from the LAB values of 729 color patches, and calculated the inverse LUTs as A2B1 (RGB to Lab) with tetrahedral interpolation. Applying the LUTs to colors in gamut of 3D printer, we can obtain similar output colors as the LUTs in ICC profile generated via TC 2.83 C5 Target. The mean and maximum color errors for the top surface were 2.8 and 9.5 ΔE_{00} in its in-gamut inverse transform. It is much better than no color management where the mean and maximum errors were 11.5 and 30.8 ΔE_{00} respectively.

We also developed some other test targets for evaluating image and object quality of a color 3D printer. Figure 7b is an example. The Multi-angle Color Target is printed in 12 different angles. Once we put all 12 pieces together, the user can visually compare the difference of CMYKGy primary colors in different printing angles (see Figure 7c).

4. CONCLUSIONS

In this work, we developed 3 types of test targets to evaluate color performance of a 3D printer. It was found that color performance changes along with different surface directions and post-processing methods. We also built ICC-based 3D LUTs in a material-saving way. Establishing different processes for 3D printing is important to make color management well and efficiently. In the future, we can keep on finding other factors which cause color differences in 3D printing, and make a complete color management system for 3D printers.

ACKNOWLEDGEMENTS

This study was partly supported by Ministry of Science and Technology of Taiwan (MOST 103-3111-Y-462-107).

REFERENCES

CIE Central Bureau, Vienna 2012. *Colorimetry – Part6: CIEDE2000 colour-difference formula,* CIE DS 014-6/E:2012

Jackson R. et al. 2006. *Methods and Systems for Producing a Desired Apparent Coloring Through Rapid Prototyping,* EU patent, EP#1558440-B1

ICC, *Specification ICC.1:2010. Image technology colour management — Architecture, profile format, and data structure,* International Color Consortium.

Stanic, M. and B. Lozo, *Color and Permance Issues in 3D Ink-jet Printing,* MIPRO2010

Xiao, K., Zardawi, F., Noort R. and Yates, J. M. 2013. *Development of Skin Colour Reproduction using 3D Colour Printing*, 12th International AIC Congress, 1805-1808.

Address: Yu-Ping SIE, Graduate Institute of Color and Illumination Technology,
National Taiwan University of Science and Technology,
43, Section 4, Keelung, Taipei, 10607, TAIWAN
E-mails: m10225006@mail.ntust.edu.tw

The Effect of Training Set on Camera Characterization

Semin OH,[1] Youngshin KWAK[1], Heebaek OH[2]
[1] Human and Systems Engineering Department, Ulsan National Institute of Science and Technology
[2] Aclover Co. Ltd

ABSTRACT

It is well known that the performance of the camera characterization model is strongly affected by the training set used to extract the model parameters. In this study, the effect of training color types (color paper vs. LCD monitor) on the camera characterization model performance is investigated. As training sets, 'Patch set' and 'Monitor set' were prepared. For 'Patch set', 114 color patches in Macbeth Colorchecker and Gretagmacbeth Colorchecker-SG chart were displayed in the viewing booth illuminated with D65 simulator and each color was measured with spectroradiometer and also with the camera. In the case of 'Monitor set', 150 colors were shown on the wide-gamut LCD monitor in a dark room covering around Adobe RGB color gamut. Similar to 'Patch set', each color was measured using a camera and the spectroradiometer at the same position. The performance test results showed that each model predicts the training data set well but the performance is significantly deteriorated when different type of data set was used. This result clearly indicates that the observer metamerism between CIE standard observer and camera sensors should be considered when three channel camera is used to measure color.

1. INTRODUCTION

These days there are many attempts to use a camera as a color measurement device, which requires camera characterization model. It is well known that the performance of the camera characterization model is strongly affected by the training set used to extract the model parameters. Training sets used in previous researches mostly consisted of paper-based colors (Kobus and Brian 2001; Vien et al 2004; Vien and Stephen 2005). However, if monitor colors are used as a training set, more various colors with high chroma can be generated to characterize a camera. In this study, the effect of a training set on the camera characterization model performance is investigated by using two different training sets, 'Patch set' and 'Monitor set'.

2. METHOD

For all measurement, Toshiba Teli CCD camera was used. Its resolution is 1280x960 and camera gamma was fixed to 1. For the comparison with camera measurement value, spectroradiometer CS-2000 was used. As a camera characterization model, simple 3x3 matrix was used since the camera RGB values showed the linear relationship with the luminance of the measured color.

As training sets, 'Patch set' and 'Monitor set' were prepared. For 'Patch set', 114 color patches in Macbeth Colorchecker and Gretagmacbeth Colorchecker-SG charts were shown in the viewing booth illuminated with D65 simulator and each color was measured with spectroradiometer and also with the camera. Below figure shows the measurement settings for 'Patch set' (Figure 1). The illuminance in the center of viewing booth was 1090 lux and luminance of reference white was 278.22 cd/m^2. The chromaticities of the color patches were mostly distributed within the range of sRGB gamut (Figure 3a).

Figure1: Measurement settings for 'Patch Set'.

In the case of 'Monitor set', 150 colors were shown on the wide-gamut LCD monitor in a dark room covering around Adobe RGB color gamut (Figure 3b). The luminance of the peak white was 262.74 cd/m^2. Similar to 'Patch set', each color was measured using a camera and the spectroradiometer at the same position. Figure 2 shows the measurement settings for 'Monitor set'.

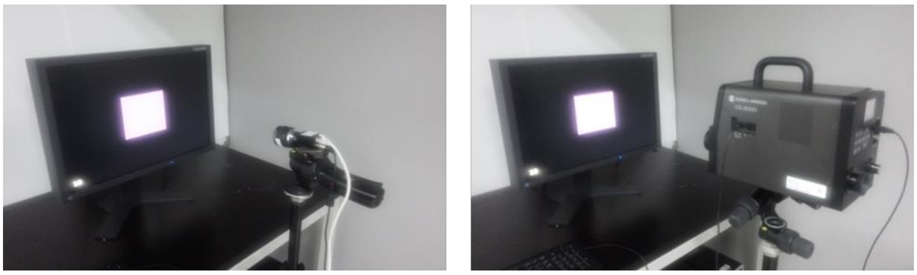

Figure2: Measurement settings for 'Monitor Set'.

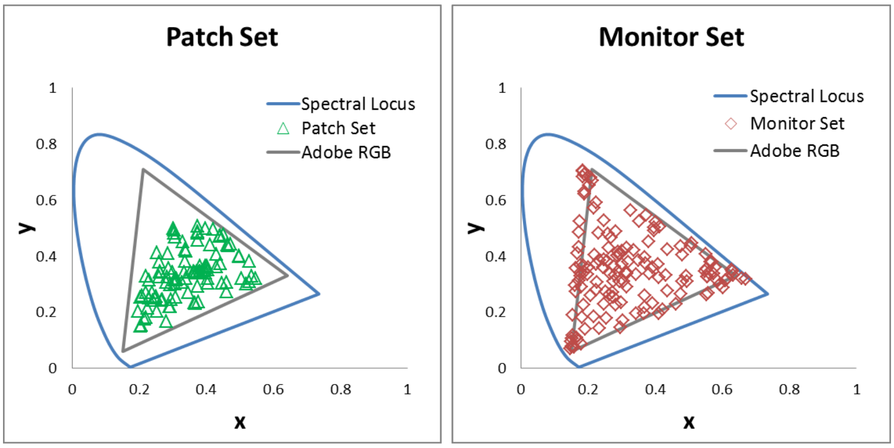

(a) (b)

Figure 3: Chromaticity coordinates of '(a) Patch Set' and '(b) Monitor Set'

3. RESULTS AND DISCUSSION

To optimize the model parameters, 'Patch Set' and 'Monitor set' were used seperately by minimizing the CIELAB ΔE^*_{ab} values between the measured and the predicted CIELAB values. For CIELAB calculation, the white color in the viewing booth was used as the reference white since that color showed the highest luminance. Then, the performances of two camera characterization models obtained using two different data set were evaluate using the same data sets.

Table 1. the Performance Test Result.

ΔE^*_{ab}	Patch Model	Monitor Model
Patch Set	1.38 ± 1.22	11.48 ± 11.08
Monitor Set	13.58 ± 12.14	4.05 ± 2.24

As shown in Table 1, each model predicts the training data set fairly well but the performance is significantly deteriorated when different data set was used. This result implies that the type of color stimuli – color paper or monitor color – affects the camera characterization model's significantly.

To evaluate the effect of type of the color stimuli more directly, trisimulus values of MCC chart colors except neutral colors were reproduced on the monitor and then measured using both the camera and the spectroradiometer. Figure 4 compares the spectrums of 'Patch Set (MCC)' and 'Monitor Set (MCC)'. The CIELAB color difference between the patch and the monitor was around 1.5 ΔE^*_{ab}. Therefore the main difference between two data sets was the spectral characteristics not the tristumulus values XYZ.

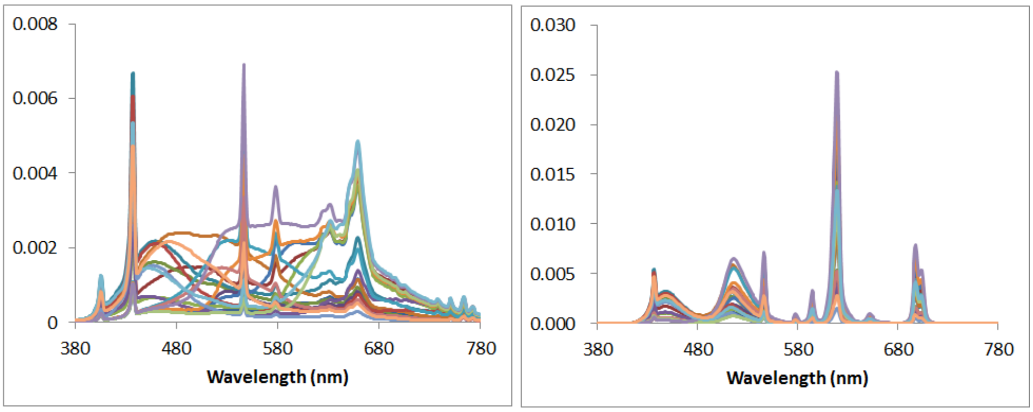

Figure 4: Spectrum of 'Patch Set (MCC)' and 'Monitor Set (MCC)'

To visualize how the CIE standard observer and the camera tested in this study see the test colors differently, chromaticity coordinates, xy and rg, were calcuated using CIE XYZ and camera RGB values. As shown in Figure 5, RGB values are very different between two data sets while XYZ values are similar to each other. It clearly indicates that the observer metamerism should be seriously considered when three channel camera is used to measure color.

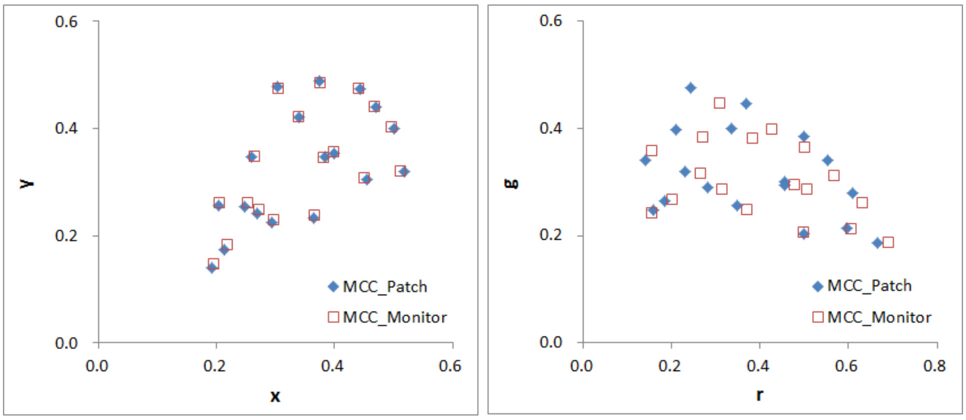

Figure 5: CIE xy and Camera rg chromaticity coordinates of 'Patch Set (MCC)' and 'Monitor Set (MCC)'

4. CONCLUSIONS

The effect of training color types (color paper vs. LCD monitor) on the camera characterization model performance is investigated. As training sets, 'Patch set' consisting of 114 color papers and 'Monitor set' consisting of 150 colors generated using LCD monitor were prepared. Then each color was measured using a camera and the spectroradiometer at the same position to develop the camera characterization models.

The performance test results showed that each model predicts the training data set fairly well but the performance is significantly deteriorated when different data set was used. This result indicates that the observer metamerism between CIE standard observer and three channel camera sensors is quite serious. Therefore, different camera characterization model should be used depnding on the spectral characteristics of data sets.

REFERENCES

Kobus Barnard and Brian Funt 2001. *Camera Characterization for Color Research*, Color research and application 27(3) 152-163.

Vien Cheung, Stephen Westland and Mitch Thomson 2004. *Accurate Estimation of the Nonlinearity of Input/Output Response for Color Cameras*, Color research and application 29(6) 406-412.

Vien Cheung and Stephen Westland 2005. *Characterization of trichromatic color cameras by using a new multispectral imaging technique*, Journal of Optical Society of America A 22(7) 1231-1240.

Address: Prof. Youngshin Kwak, Human and Systems Engineering Department
UNIST, Banyeonri, Eonyangeub, Uljugun, Ulsan, SOUTH KOREA
E-mails: smoh@unist.ac.kr,yskwak@unist.ac.kr, ohb@aclover.co.kr

Reproducing the Old Masters: A study in replicating dark colours with inkjet printing

Melissa OLEN,[1] Joseph PADFIELD[2]
[1] Centre for Fine Print Research, University of the West of England
[2] Scientific Department, The National Gallery, London

ABSTRACT

This paper presents work carried out to extend the available range of printable dark colours by incorporating the use of alternative direct channel and multiple pass printing techniques not usually employed within current inkjet printing workflows. These methods aim to improve the colour match between the colours measured within printed reproductions and those measured within paintings in the collection of the National Gallery, London. For this study, a number of colour measurements were taken from the dark paint passages of one particular National Gallery painting, *The Supper at Emmaus*, by Michelangelo Merisi da Caravaggio. Reproductions of the painted colours were printed using the alternative printing techniques, along with traditional inkjet print reproduction workflows. The colour of various printed reproductions were then measured and compared with the original measurements taken from the painting. The results of this comparison show that the proposed alternative direct channel and multiple pass printing techniques are capable of producing a range of dark colours which more closely matched the original paint passages.

1. INTRODUCTION

One of the major difficulties in producing inkjet reproductions of Old Master paintings is the accurate replication of the colours found within dark paint passages. Reproducing these very dark colours is normally achieved by mixing the available coloured inks with high proportions of black. However, this high concentration of black ink tends to dominate the printed passages, leading to a smaller perceivable gamut of printed dark colour and the original subtle variations seen in the painted colours being perceptively lost. Reproducing the colour of dark paint passages in old master paintings, using inkjet printing, can be very difficult. Limited sets of inks and media obviously restrict the print process in its ability to replicate the vast number of colours and surface qualities observed in paintings.

In order to investigate the practical application of direct channel and multiple pass printing methods described in previous research undertaken by the authors (Olen, Padfield, & Parraman 2014), this paper examines how well a selection of colours measured from a suitable target painting in the National Gallery, London, can be reproduced. Containing a range of dark paint passages, *The Supper at Emmaus*, by Michelangelo Merisi da Caravaggio, was chosen as a target painting for this research. While difficult to accurately print, the colours in the dark paint passages of this target painting can be easily distinguished under normal viewing conditions. This paper presents measurements and evaluation of the alternative printing methods based upon six of the measured paint passages. This research aims to investigate the potential benefits of incorporating these alternative printing techniques into future reproduction workflows, expanding the available gamut of darker colours and improving the overall colour accuracy of inkjet printing in fine art reproduction.

2. METHOD

For this evaluation measurements were gathered from both the target painting, *The Supper at Emmaus*, and from a series of colour patches printed using a Canon iPF8400 multichannel inkjet printer.

To ensure the safety of the target painting and to avoid disrupting public access the colour measurements needed to be carried out before the National Gallery opened, utilising a Konica Minolta CS1000a Spectroradiometer, which allowed for measurements to be taken without touching the surface of the painting.

Alternatively, measurements of prepared colour charts, produced with the Canon inkjet printer, could be taken outside of the public galleries using a handheld X-Rite i1Pro spectrophotometer, allowing for faster measurement of many more patches. Testing and analysis was undertaken to ensure consistent and comparable results were achieved with both devices.

2.1 Measurement of Target Painting

For each measurement, the spectroradiometer was placed on a tripod directly in front of the painting, roughly perpendicular to the surface and a portable D50 light bank was placed to the side at an approximate forty-five degree angle. For each sampled area a white control measurement was taken of a white calibration tile before and after the actual colour measurement. This allowed the measured spectral reflectance of the colour to be divided by the averaged whites in order to obtain an illuminant independent measurement. The six colours sampled from the Caravaggio target painting include the red in Christ's drapery, the green of his disciple's shirt, the blue in the pitcher on the table, and a sample of the black, yellow, and red in the table cloth. The location of each measurement is depicted by a white dot in Figure 1.

Figure 1: Location identification of each colour measurement taken of Michelangelo Merisi da Caravaggio's 'The Supper at Emmaus.'

2.2 Experimental Procedure for Matching Inkjet Colour

To evaluate the capabilities of the Canon inkjet printer using direct channel and multiple pass printing capabilities the authors first designed a custom colour chart composed of a range of near neutral dark colours. The Canon printer was selected for the study, controlled with the Caldera VisualRIP+, with which the cyan, magenta, yellow, red, green, blue, and black ink channels can be controlled independently. Whilst the printer can use all seven channels to generate a single colour, to keep the number of reference samples manageable for this study the chart was limited to include up to three colours, plus black. For each four colour combination, variations were included where each colourant, or a set of two colourants, decreased in coverage in ten percent intervals. While the chart did not sample the entirety of the shadow region of the printer's gamut, it provided close approximations from which further refinement could be applied. In total the chart consisted of 2,290 colour patches, each with a unique colourant combination. This chart was printed in multiple passes through the printer, where one colour was printed onto the paper with each pass. In this instance, the sequence in which the colours were printed was kept consistent for all patches.

The spectral reflectance curves of all of the 2,290 reference patches were compared with the spectral reflectance curves measured for the six paint passages. Using the adjusted spectral reflectance of the painting measurements as reference, the root-mean-square (RMS) error for each of the patches was calculated, as this method has been shown to be an accurate measurement of spectral differences (Viggiano 2004). This allowed for the identification of the closest approximation that best replicated the spectral distribution of the reference colour. Table 1 depicts the colourants, and their percentage of coverage, present in the patches with the smallest deviation from each of the sampled painting colours. Several of the colourant combinations follow the common approach of subgrouping colourants using only analogous colours (Sharma 2003: 370), such as the red drapery of Sample 1, which contains magenta, red, and black. However, in the case of sample 3, the blue pitcher, the calculations identified the colour patch containing both cyan and red as having the best approximation. While this reflectance was later found to have a spectral redundancy to a combination of unequal percentages of CMYK, it was also noted that redundancies do not occur for all non-analogous subgroupings. Therefore the data set continues to employ triadic and analogous-complimentary subgroupings where the selected colourants span across the gamut.

Table 1.Percentage of ink colourant combinations for approximate colour matches.

Sample	Cyan	Magenta	Yellow	Red	Green	Blue	Black
1 : Red Drapery		70		100			100
2 : Green Shirt			80		80		100
3 : Blue Pitcher	70		100	70			100
4 : Black in Cloth				50	50		100
5 : Yellow in Cloth			60	60			100
6 : Red in Cloth		40		100			100

For comparative analysis a smaller chart was also prepared containing the six reference measurements from the painting converted to L*a*b* colour values. This chart was printed four times following suggested, as well as common, colour management workflows using custom ICC profiles. Two were printed using the control of Adobe Photoshop and the Canon printer driver, and two were processed through the Caldera VisualRIP+ using its CMYKRGB mode. For each of these two workflows, one set of prints was produced using the absolute colorimetric rendering, as recommended by Frey and Farnand (Frey & Farnand 2011) for cultural heritage reproduction, and the second set was printed using perceptual rendering, which is typically found useful for images requiring a remapping of the dynamic range to maintain detail information (BS ISO 15076-1:2010).

3. RESULTS AND DISCUSSION

The spectral reflectances of the collected painting references, direct channel / multiple pass print, and colour managed samples can be seen in Figure 2. For all six of the samples the method of direct channel / multiple pass printing produces a better match to the reference than the colour managed print samples. While this is partially to be expected due to the potential limitations of a colorimetric workflow compared to a spectral one (Morovič et al. 2012), it can be further attributed to the direct channel / multiple pass method's ability to produce colour that is unattainable through the current implementation of either of these workflows. With the ability to apply colours in layers, the direct channel / multiple pass method generates a higher density in the final colour output, which can be seen here as the method's spectral reflectances fall below the other inkjet printed samples. Furthermore, the ability to utilise non-customary combinations of colourants allows for increased control over the hue for each of the dark samples, creating a closer approximation to the reference measurement from the painting.

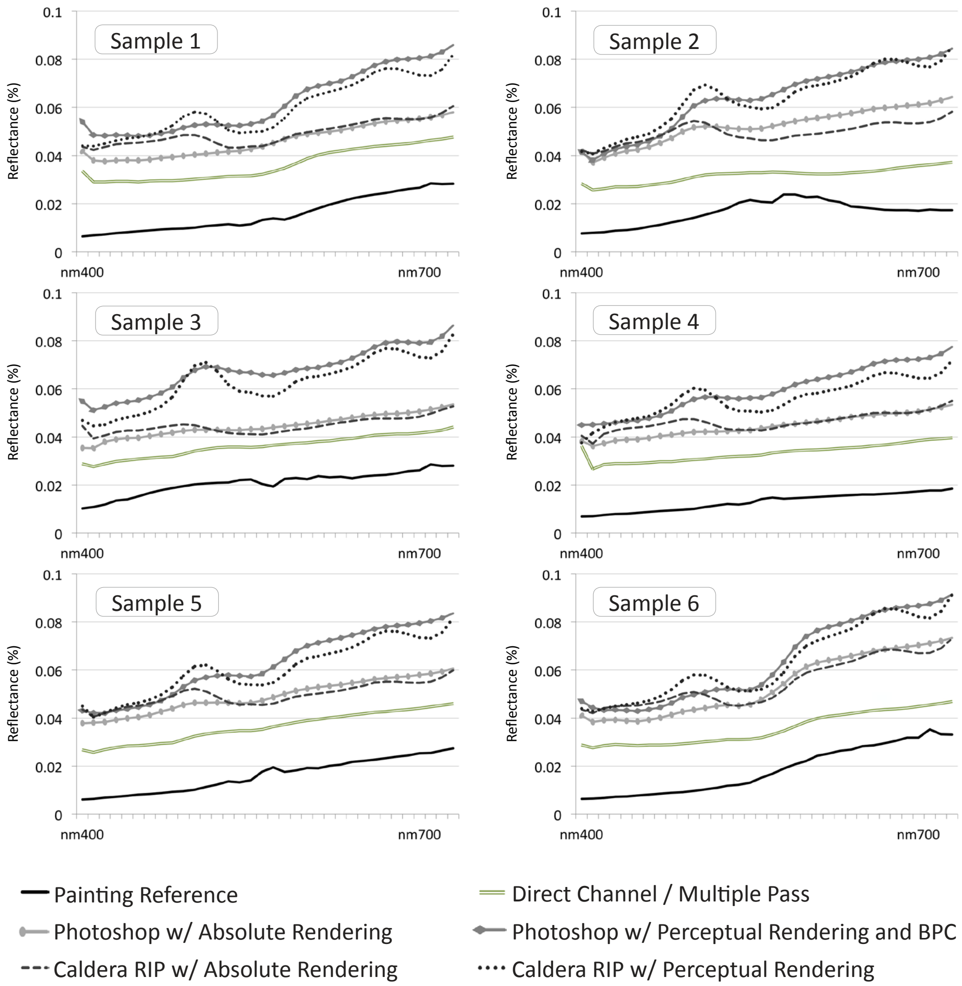

Figure 2: Spectral reflectances of direct channel / multiple pass print and colour managed samples shown against the reflectances of the painting for all six sampled colours.

Calculation of the root-mean-square error between the reference measurement of the painting and the printed samples shows that the direct channel / multiple pass printing method outperforms the colorimetric workflows more significantly in some cases compared to others, as can be seen in Figure 3. In the instances of Samples 1 and 3, the difference between the direct channel / multiple pass print and the colour processed through Adobe Photoshop and the Canon printer driver with absolute colorimetric rendering are relatively small, especially when considering the RMS error present in the direct channel / multiple pass method. However, when considering the overall improvement in colour reproduction, the benefits of this printing method can be seen.

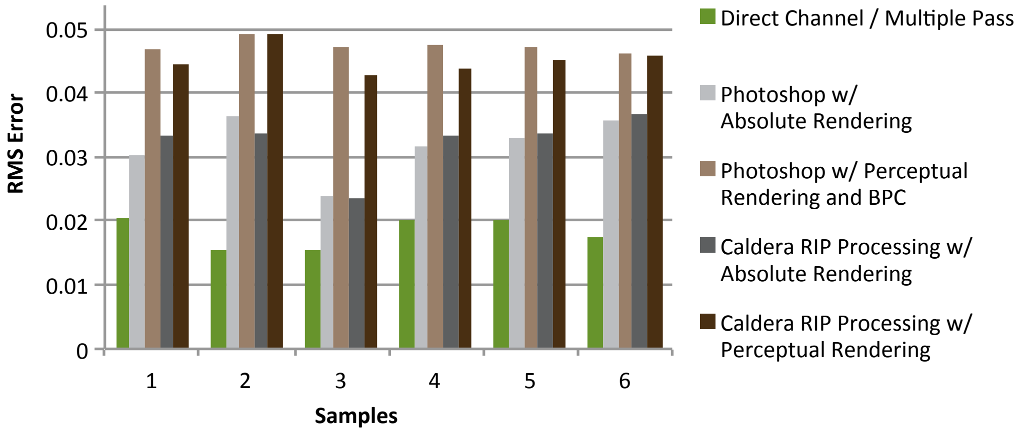

Figure 3: Chart of root mean square errors against painting reference measurements.

4. CONCLUSIONS

In this paper a working method has been shown for evaluating the capabilities of direct channel and multiple pass printing to better reproduce colours in the dark passages of Old Master paintings, using Caravaggio's *The Supper at Emmaus* as an example. It has also been shown the direct channel / multiple pass print method obtains increased colour accuracy compared to common colorimetric workflows, and achieves greater density and spectral distribution.

While the results of this study are promising, further research and refinement of this process is required. The data set in the test colour chart is limited and would benefit from a secondary search of more closely related colour patches. Also, the greatest discrepancy between the adjusted spectral reflectance from the painting and the colour reproduction is in the darkness of the colour. Limitations of the substrate used in the study could have attributed to the inability to achieve the same dark values as the original painting. Further investigation into alternative media and/or varnish coatings will be beneficial.

ACKNOWLEDGEMENTS

This work was supported by the Marie Curie Initial Training Networks (ITN) CP7.0 N-290154 funding. The authors would like to express thanks to Carinna Parraman who has been invaluable in helping develop this research. They also would like to thank Caldera for providing licensing of their software to conduct these tests.

REFERENCES

Olen, M., Padfield, J., and Parraman, C. 2014. *Reproducing the old masters: applying colour mixing and painting methodologies to inkjet printing*, Proc. SPIE 9015 Color Imaging XIX. doi:10.1117/12.2040647.

Viggiano, JA. 2004. *Metrics for Evaluating Spectral Matches: A Quantitative Comparison*, Proc. Conference on Colour Graphics, Imaging and Vision. pp. 286-291.

Sharma G. 2003. *Digital Color Imaging Handbook*. CRC Press.

Frey, F. and Farnand, S. 2011. *Benchmarking Art Image Interchange Cycles: Final Report 2011,* Rochester Institute of Technology.

BS ISO 15076-1:2010: *Image technology colour management. Architecture, profile format and data structure*. Based on ICC.1:2010 2010, British Standards Institute.

Morovič, P., Morovič, J., Arnabat, J., García-Reyero, J.M. 2012. *Revisiting Spectral Printing: A Data Driven Approach*, Proc. 20th Color and Imaging Conference. pp. 335-340

Address: Melissa Olen, Centre for Fine Print Research, School of Art and Design,
University of the West of England, Bower Ashton Campus,
Kennel Lodge Rd, Bristol, BS3 2JT, UK
E-mail: melissa.olen@uwe.ac.uk

A New Metric for Evaluating the Closeness of Two Colors

Yasuki YAMAUCHI, Yusuke IIDA, Yuki KAWASHIMA, Takehiro NAGAI
Graduate School of Science and Engineering, Yamagata University

ABSTRACT

Color difference metrics such as CIEDE2000 and CIE76 are suggested to use when the color differences are relatively small. We would also need a new metric which can well express large color differences. Evaluating the difference of two colors would be equivalent to evaluate how close those two colors are. Instead of directly comparing the color difference/closeness, it would be also possible to compare colors with some intervening color. In this study, we try to propose a new metric based on the hypothesis mentioned above. We assume that each color has several "corresponding colors", which give the impression or the appearance of that color to be identical or at least similar. If those colors form a trend-line, it would be way to make a new metric by describing how far a given color would be from this trend-line. We call a series of the color on the same trend-line "consistent color". In Experiment 1, we tried to find consistent colors for 12 reference colors. In order to find a trend line of consistent color for each reference color, a subject changed the test color on the surface of a given gamut until the test color appeared the most similar, or closest to the reference color. By fitting the closest colors of different gamut, we could obtain the trend line for consistent color appearance. Then, we tried magnitude estimation experiment to evaluate how close the displayed colors were to a given test color. Although there seems to be many issues to be solved, from our preliminary experiment, we would say that it is possible to judge how consistent a presented color is to the reference color, which may lead to define a new metric.

1. INTRODUCTION

In order to estimate the difference of colors, metrics describing color difference such as CIEDE2000 and CIE76 are widely used. They are suggested to use when the color differences are relatively small. When it comes to evaluate two colors whose color difference, such as lightness and saturation, are large, we would need a new metric which can well express their differences. Evaluating the difference of two colors would be equivalent to evaluate how close those two colors are. Instead of directly comparing the color difference/closeness, it would be also possible to compare colors with some intervening color.

In this study, our final goal is to propose a new metric based on the hypothesis mentioned above. We assume that each color has several "corresponding colors", which give the impression or the appearance of that color to be identical or at least similar. If those colors form a trend-line, a new metric to be proposed should describe how far a given color would be from this trend-line. We call a series of the color on the same trend line "consistent color". This concept is close to that proposed in ICC as the term "common color appearance". A new Reportership TC8-13 has been just started its activity in CIE, aiming to validate this concept.

As the first step, we need to find consistent colors. As Experiment 1, we tried to find consistent colors for several reference colors. In order to find a trend line of consistent color for each reference color, we need several different color gamut whose surface will cover differently. We used several CRPCs (Characterized Reference Printing Condition) proposed by CGATS. A subject could change the test color on the surface of a given CRPC until the test color appeared the most similar, or closest to the reference color. By fitting the consistent colors of different CRPCs, we could obtain the trend line for consistent color appearance.

Secondly, we tried to verify our concept with magnitude estimation experiments as a preliminary experiment to evaluate how close the displayed colors are to a given test color.

2. METHOD

2.1 Apparatus

The experiments were conducted in a booth whose walls were covered with black velvet. A schematic view of the apparatus is shown in Figure 1. A fluorescent light (Toshiba, N-EDL, CCT 5000K) lit the inside the booth in order to prevent subjects from dark adaptation. The illuminance of the booth was approximately 100 lx. An LCD monitor (NEC MultiSync LCD-PA241W, 24.1 inch), controlled with Psychtoolbox, was placed in front of the subject in order to present stimuli. The gamut of this monitor covered almost the entire Adobe RGB space. The distance between a monitor and a subject was approximately 80 cm. Subjects could move their head freely. The adjustment of the test color was conducted with a trackball and a keyboard.

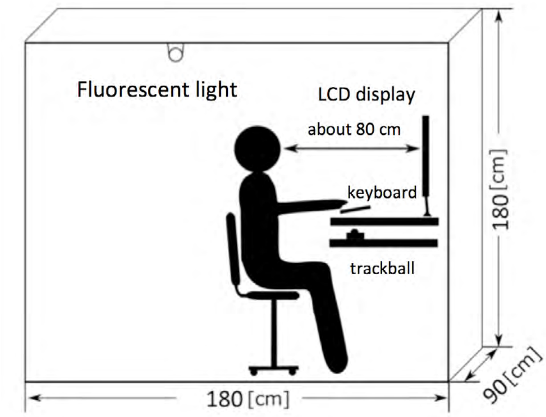

Figure 1: Experimental setup

2.2 Stimuli

In Experiment 1, 36 reference colors were used in total in the experiment, 3 different luminance levels for 12 different hues. The hues were chosen as those of CUSPs of three primaries (RGB) and their mixtures (CMY), and also those of the midpoints between 2 contiguous colors of RGBCMY. They are shown in Figure 2, which is represented on CIECAM02 a*-b* plane.

As for the luminances of the stimuli, the luminances of RGBCMY and their midpoints were used, which will be referred to as “middle range”. Two other conditions were used in the experiment:

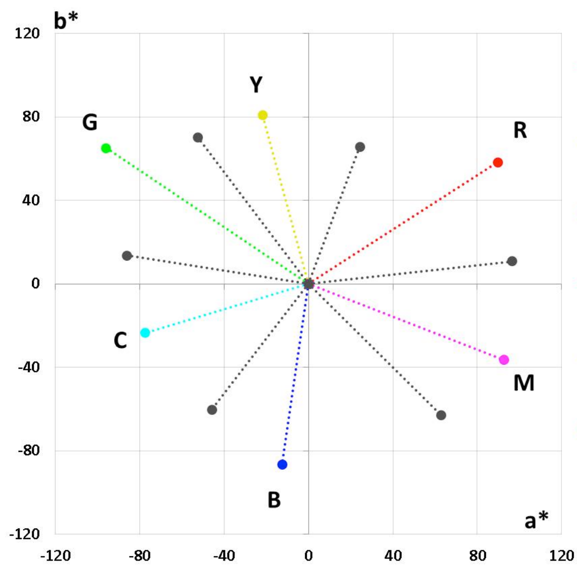

Figure 2: 12 different hues used in the experiment

1) “high-range”, whose luminances were the midpoints between each of 12 reference colors and that of white, and 2) “low-range”, whose luminances were the midpoints between each of the reference colors and that of black.

We adopted three different CRPCs: CRPC7, CRPC5 and CRPC3. Adobe RGB space was used to display the reference colors. Their size projected on a*-b* plane are shown in Figure 3.

The test stimulus was the color on the surface of one of the CRPC, which are controlled by the manipulation of the trackball and the keyboard.

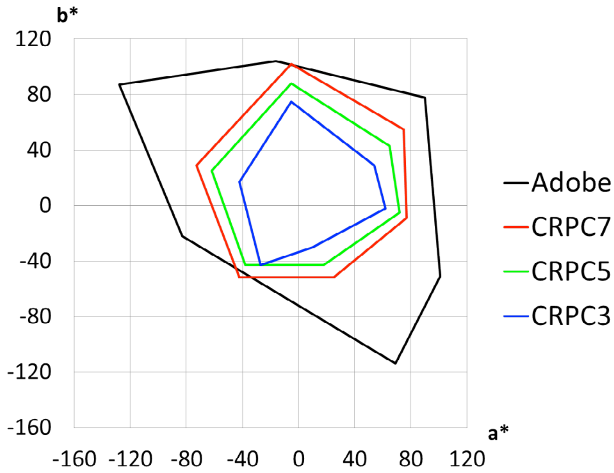

Figure 3: Color gamuts used in the experiment

All the squares extended 2 deg, with a separation of 1 deg. The background was fixed to gray.

The reference colors which were shown during the setting increased as the difference of the color gamuts became larger (multiple reference method). In this method, the corresponding color of CRPC 7 was first searched. Then, the corresponding color of CRPC 5 was explored. Here both the reference color and the corresponding CRPC7 color were displayed in a row. Schematic diagram of the stimulus presented to the subjects is shown in Figure 4.

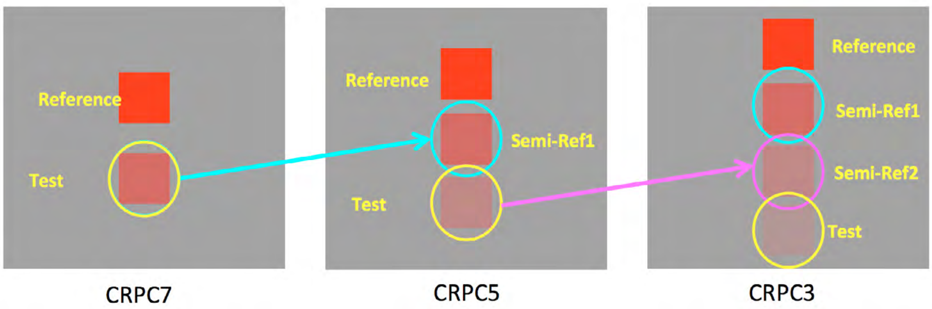

Figure 4: Multiple reference method used in the expeirment

In the next step (Preliminary Experiment 2), we showed one of the series of the reference colors: reference color and three colors of different CRPCs, in a row. The test color, which were apart from the trend line were shown below the row. We used three different colors of the same saturation (C*) for each side of the trend-line. The subject answered the score how different the test color is from the trend line, e.g. the subject rated “0” when the test color was on the trend-line.

2.3 Procedure and subjects

After adapting for 3 minutes under the fluorescent light in the booth, the experiment was started.

In each trial, a test stimulus and the reference color (or the reference colors in some conditions of 3)) was displayed on a monitor. The hue and their luminance range used in that trial was randomly selected. By controlling a trackball, the subject could change the color to move along the surface of a given color gamut. Each trial started when the subject hit any button on the keyboard. The stimulus was presented continuously. There was no restriction in time for observing stimuli.

As mentioned above, in the preliminary Experiment2, a trial was consisted of rating a test color displayed on the screen. The stimulus was continuously presented to the subject until the rating was completed.

10 color normal male subjects participated in the experiment. All the subjects were naïve for the purpose of the research.

3. RESULTS AND DISCUSSION

The results of the experiment are shown in Figure 5. Left and right panel refers to the luminance condition of "middle range" and "low range", respectively. They are shown in a*-b* color plane. The results are the mean values obtained from all the subjects. Solid circles are the reference colors (Adobe RGB). Solid squares, diamonds, and triangles indicate the results obtained from CRPC7, CRPC5 and CRPC3, respectively. Error bars show the standard deviation among the subjects.

Dashed lines shows the equal hue angle trends relative to the reference colors. If the consistent colors show the same trends to the equal hue, they should line up on the same line.

As clearly shown in the figures, the consistent colors of several colors have more or less the same hue angle, i.e. they line up on the same line. The colors of the 1st quadrant of the middle range and the yellow of all the ranges are the distinct results among them.

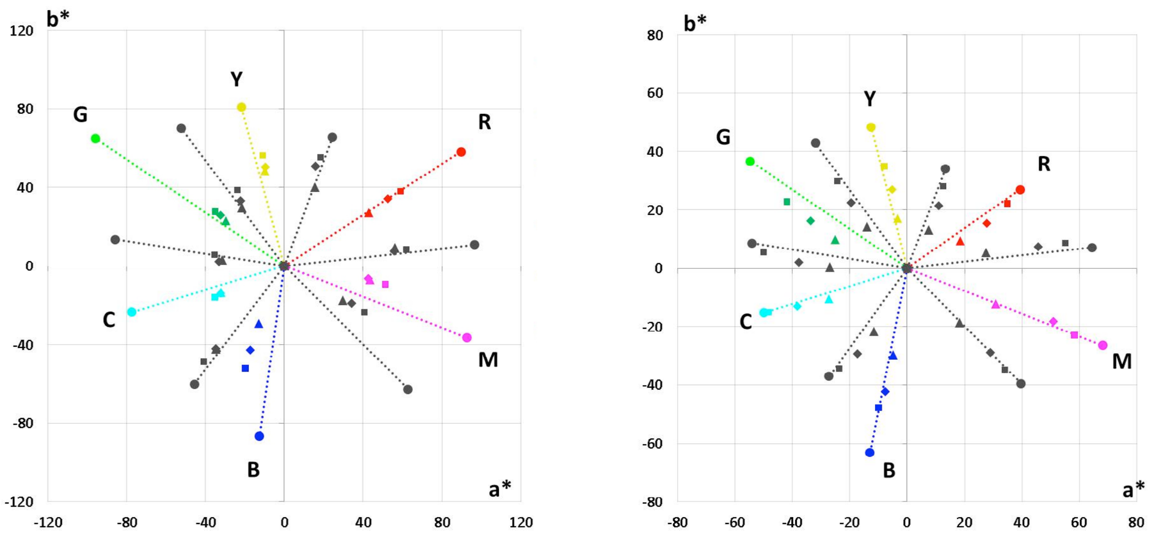

Figure 5: Consistent color trends of 12 colors (Left: "Middle range", Right: "Low range")

As for the consistent color of the blue, the colors of intermediate saturations were apart from the hue angle of the reference color. The tendency was similar to that reported by

Hung(1995), which was investigating the constant hue loci of several colors. It means that our subjects conducted an experiment with the judgment of the hue for the primary criteria.

The results of the preliminary experiments showed that in some hues, the subjects rated higher rates to the test colors which are further from the trend line. However, the results were dependent on the subjects and colors. Some subjects, however, did not show such a clear trends.

4. CONCLUSIONS

In our research, we tried to propose a new metric which can well describe the difference of two colors with the concept of the consistent color. So far, we haven't come to the stage for proposing a new metric, but we could obtain the trend-lines of the color which give the similar or the "close" appearance to the reference color. This might be a way of verifying the concept of the consistent colors. Moreover, the trend-lines showed a similar behavior as the constant hue loci. This finding indicate that when the judgment of the closeness of the color should be done, hue is the primary factor in its process.

Although we haven't obtained a clear result, we could show a possibility to evaluate the difference of the color apart from the consistent color loci quantitatively. In order to verify the concept, we need to explore our experimental conditions more in detail. We are expecting our findings will lead to propose a new metric that can be used to express the difference of the colors.

REFERENCES

CIE 2001, CIE Publication No. 142-2001, Central Bureau of the CIE

CGATS, https://www.npes.org/programs/standardsworkroom/cgatstechnicalstandards.aspx

Zhu, S.Y, Luo, M.R. and Cui, G.H. 2002, *New experimental data for investigating uniform color spaces*, Proc. SPIE 4421, 9th Congress of the International Colour Association, 626

Hung, P. and Berns. R.S 1995, *Determination of constant Hue Loci for a CRT gamut and their predictions using color appearance spaces*, Color Research & Application 20 (5) 285-295.

Address: Prof. Yasuki YAMAUCHI, Department of Informatics, Graduate School of Science and Engineering, Yamagata University, 4-3-16 Jonan, Yonezawa, Yamagata, 992-8510, JAPAN
E-mails: yamauchi@yz.yamagata-u.ac.jp, tkk25057 @st.yamagata-u.ac.jp, kawashima.yu@yz.yamagata-u.ac.jp,tnagai@yz.yamagata-u.ac.jp

Image and Color Space Clustering for Image Search

Akinobu HATADA,[1]
[1] Graduate School of Human Sciences, Kanagawa University, Japan.

ABSTRACT

Image search is one of application like Google internet search. But normally internet search engine use text context, not image. Google provides image search system, today. It seems recognize image as what it is and generate text key word as search key. Final search result is web page list, and image list of same theme. For example, Eiffel tower image is given as search source, it report Eiffel tower web page and list of Eiffel tower picture. It seems searching picture that contains same subject in source image.

Image search by image is yet another thema. (Abhinav Shrivastava, etal, 2011) is a quite similar research as previous case. Abhinav approach is by way of massive caliculation. (Hatada, 2014) report more simple approach by way of pre-caliculated index data, that based on color region on image.

Search speed is a big value for search engine. Nobody never look up Google if it spend one hour for every searching request. Image searching. It means caliculation in searching phase should light. In other hand, making index data for each searching target is easy to allowing spend time.

In this study report indexed data by color information and image clustering approach as image search application.

1. INTRODUCTION

Image search like Web page search is one of interest application. Today, what we call web search is "full text search" in strictly. It search web page by text key word, and search result is sorted by certain order, which called ranking (Brin and Page, 1998). Today, Google provides image search service (Google Search by Image). User is able to having an experiment of search by image at Google site, today. It seems searching picture that picture including same major content of source picture. For example, searching by picture of Eiffel tower; try to show web page of Eiffel tower or picture which include Eiffel tower.

Either case of text, image or voice, search engine is includes data analysing unit, characteristic data storage, data matching unit and ranking unit. Data analysing method is most important unit, because it determines search engine's character or capability. For example, data analysing method is definitively different between text data case and image data case.

One of popular image characteristic data is vector data. Vector data is line of subject edge in image. Usually many numbers of vector data is generated by single image. This style of search engine would suitable to subject recognition. In above case, pick up a word "Eiffel tower" from Eiffel tower's picture is required subject recognition. Once text word is provided, search system can find web page by its key word. If text word is not appeared by image, search engine could search by vector data itself. Vector data is comparable and matching process is able to developing.

(Abhinav etal, 2011) is also uses this kind of data. As their presentation, it seems pretty good result. But it requires massive calculation in searching process.

(a) Daytime Picture

(b) Night Picture

Figure 1: Tow Pictures Takes Same Place and Different Time.

Figure 1 shows two pictures. These picture takes same place and simular angle, but different times. These picture includes same contents like buildings. According my observation, many people don't think these are simular picture, as far as these are including same content. This fact means that content in picture is not key point of evaluating landscape. If two picture have same vector dates, it is not galantee they are simular. By this observation, our research effort developed by color information.

2. METHOD

In previous study, filling region is employee as characteristic data. In this study, clustering data is improved as characteristic data. All of images are normalized to 1024 x 768 size and rotation.

2.1 Characteristic Data

Characteristic data from image is using filling region information. Filling region is an area that determined by flood filling algorithm (Figure 2). In previous experiment, image colors are reduced 64 from 16 million of it. Filling region is simple and provided useful information as characteristic data. It is not include position data. It means image rotation is not matter about in phase of image search, but it claimed that important data is missing.

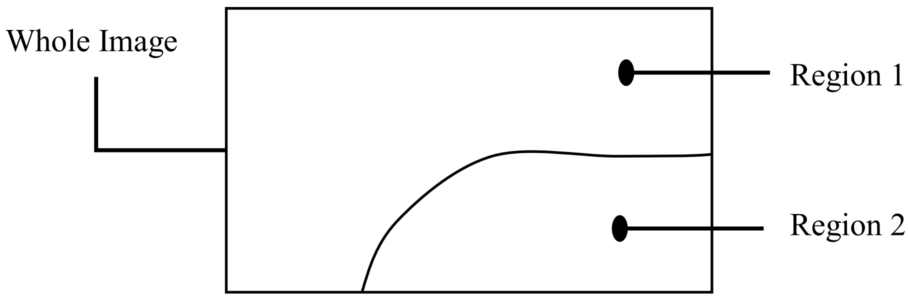

Figure 2: Filling Region.

Cluster a kind of concept that representing some vector space. It includes clustering point in analysing data space(Figure 3).

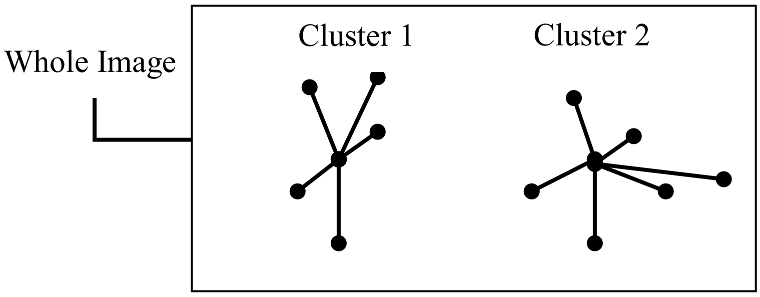

Figure 3: Cluster.

2.2 Clustering Approach

Around clustering study, K-means algorithm and its application is one of major topics, that reported by (Steinhaus, H., 1957) or (MacQueen, J. B., 1967) etc. There are also a lot of study is easy to found in imaging processing research area. A point of those studies is, how makes clusters well. In original K-means algorithm should provide number of initial cluster, and it takes large effect to clustering result. (YAMAMOTO and MURAKAMI, 2003) tried to calculate number of cluster according image data. This study also uses color data. Actually, it uses color distance as cluster combining threshold. But their experiment includes several ad-hoc methods to integrate clusters, i.e. omitting small clusters. It also not disclosing how many cycle is required until K-means loop.

Avoiding problem of loop cycle evaluation, and ad-hoc small cluster omitting issue, this study improve yet another approach. In point of view of vision psychology, human eye is sensitive to lightness rather than colour hue. Actual example is shown in Figure 4. It shows edge of colour image (a) and grey scaled edge (b).

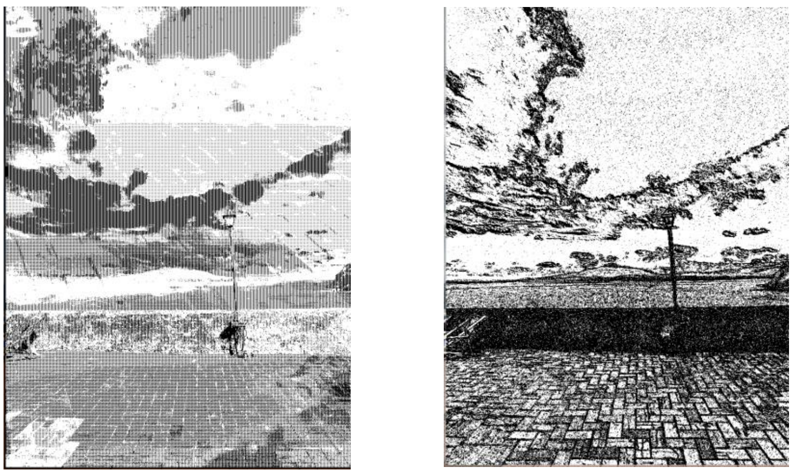

(a) by colour image (b) by grey scaled image

Figure 4: Edge Example.

Edge data from colour image is noisy than grey scaled data. Then this study employee grey scaled data as bases of image clustering. Grey scale is 8 steps and it is decided adapted to image data. In additionally, reduce less than 1% area cluster is processed.

In result of it, 322 sample landscape data converted about 20 clustered data (Figure 5).

"GrayScale",	"x",	"y",	"Count"
177,	57,	117,	12716
250,	152,	260,	55718
255,	486,	97,	98754
250,	301,	277,	20636
129,	40,	293,	9749
177,	96,	594,	20664
0,	971,	496,	10386

Figure 5: Generated Cluster Data (Sample).

2.3 Scoring

Matching score is calculated according (exp.1). Comparing source cluster and destination image's clusters and pick up most neighbor cluster and takes a differential.

$$De = k \sum_{Color} \frac{1}{(R1 - R2)^2 + 1} \qquad \text{(exp.1)}$$

De: Differential value of two images
k: adjustment value.
R1 and R2 is number of region in two images.

3. RESULTS AND DISCUSSION

Sample result is shown at Figure 6. Search trial shows some interesting result.For example, a case of Figure 6 hit similar composition of image. In previous study, search result did not care about this kind of effect.

Source image Result Image(s)

Figure 6: Sample Search Result.

4. CONCLUSIONS

This trial shows some interesting result, but it is not enough. In this study, clustering seems to good idea of including location data to charateristic data. But grey scale information may not enough as search key. Color data should concern about cluster property in future study.

REFERENCES

Abhinav Shrivastava, Tomasz Malisiewicz, Abhinav Gupta, Alexei A. Efros, 2011, *Data-driven Visual Similarity for Cross-domain Image Matching*, ACM Transactions on Graphics (TOG) - Proceedings of ACM SIGGRAPH Asia 2011 ,Volume 30 Issue 6, December 2011, Article No. 154

Akinobu Hatada, 2014, *Image comparing by color information*, ACA2014 Proceedings, 140-143

Brin, S.; Page, L., 1998, *The anatomy of a large-scale hypertextual Web search engine*. Computer Networks and ISDN Systems 30: 107–117.

Steinhaus, H., 1957,. *Sur la division des corps matériels en parties*. Bull. Acad. Polon. Sci. (in French) 4 (12): 801–804

MacQueen, J. B., 1967, *Some Methods for classification and Analysis of Multivariate Observations*, 1. Proceedings of 5th Berkeley Symposium on Mathematical Statistics and Probability. University of California Press. pp. 281–297

Kyuuich YAMAMOTO and Shinichi MURAKAMI, *A Study on Image Segmentation by K-Means Algorithm*, Report of Information Processing Society of Japan [Audio-Visual combined information processing] 2003(125), 173-178, 2003-12-18, Information Processing Society of Japan

Address: Akinobu Hatada, Graduate School of Human Sciences, Kanagawa University
3-27-1 Rokkakubashi Kanagawa-ku Yokohama, 221-8686, JAPAN
E-mails: r201270904ui@kanagawa-u.ac.jp

Restoration of color appearance by combining local adaptations for HDR images

Yuto KUBO,[1] Takao JINNO,[1] Shigeru KURIYAMA[1]
[1] Toyohashi University of Technology

ABSTRACT

Image colors are often degraded due to saturation or fade-out for the scenes illuminated by colored lightings. This research improves such degradation for high dynamic range (HDR) images that can fully capture the brightness and chroma at high bit-depth. The dynamic range should be compressed to fit that of ordinary color monitors, and color appearance model (CAM) is widely used for authentically reproducing colors in compressions. This model can take the feature of human visual system that can adaptively perceive colors according to the brightness within a local area. This adaptation model, however, is inapplicable to an image including both brightly- and dimly-lit areas. We propose a method of combining such local adaptations for different brightness on a single image. Our method enables unified color restoration for HDR images while retaining the global consistency of brightness variations, and its effectiveness is experimentally demonstrated for the indoor scene illuminated by a color LED.

1. INTRODUCTION

With popularization of color LED lightings, accurately restoring the chromaticness of captured images become important for demonstrating their effectiveness, which may be utilized for lighting design, advertisement, etc. Most of ordinary digital cameras, however, lack the capability in color restoration, owing to the insufficient dynamic ranges of their image sensors.

HDR images can fully capture the scene radiance at high bit-depth, and displaying them on ordinary monitors of lower bit-depth requires compressing their dynamic range. The range compression based on iCAM06 (Kuang 2007) can reproduce the color appearance. Since the scenes including glaring colored light source have very wide dynamic range, iCAM06 cannot sufficiently restore the colorfulness owing to its limited compression rate.

Our previous study (Kubo 2014) divides an input HDR image into the areas of lights and surroundings, for separately compressing their dynamic ranges. It can reproduce the color appearance for each image region whose dynamic range is lower enough for accurate restoration. This approach, however, often causes a contrast inversion along the boundary of areas to which different adaptation parameters are set. This paper therefore proposes the dynamic range compression by introducing a local adaptation of white point with a bilateral filter. This can reproduce the local color appearance of an HDR image on an ordinary low dynamic range (LDR) image, without causing any contrast inversion.

2. DYNAMIC RANGE COMPRESSION

Methods of dynamic range compression are roughly categorized as the following types:

(a) Non-linear function whose global parameter is changed for a whole image, which can retain brightness gradients without causing any contrast inversion

(b) Non-linear function whose parameters are changed for each pixel, which can preserve the details of the scene

(c) Non-linear function based on the color appearance model (Kuang 2007) (Reinhard 2010)

where the last category is most suitable for our target, especially, those based on the iCAM06 model.

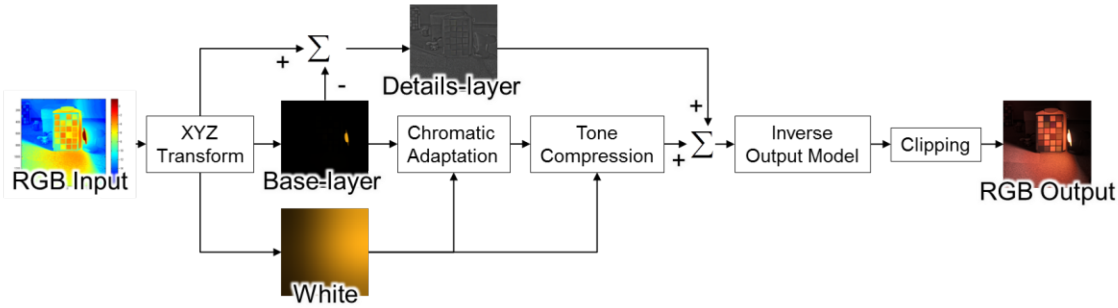

Figure 1: Flowchart of iCAM06.

2.1 iCAM06

Human visual system consists of many non-linear response functions and adaptations for maximizing sensing performance against real world of very wide dynamic range, and many range compression algorithm for HDR image is developed by imitating this functionalities.

The iCAM06 was developed for HDR image rendering by extending iCAM framework (Johnson 2003) that can reproduce the color appearance based on CIECAM02 (Moroney 2002). The CIECAM02 predicts the color appearance attributes from the tristimulus values; this process, however, cannot be suited to compress the dynamic range of the HDR image into LDR one. The iCAM06 introduces an empirical range clipping mechanism by rounding off the values outside the 1th and 99th percentile. Although this clipping is suitable for most of the HDR scenes, color degradation is inevitable for the scenes including very wide dynamic range, e.g. the scene including both dim regions and colored lights, as shown in Figure 2.

Figure 1 shows the flowchart of the iCAM06. The iCAM06 separates the HDR image into the details-layer and the base-layer, and compresses only a wide dynamic range of the base-layer based on the Retinex theory (Rahman 1997) by applying a tone compression. The tone compression consists of cone and rod response functions, which have local adjustments according to an adaptation luminance map. This map is estimated by filtering the input HDR luminance using a Gaussian kernel whose standard deviation is 5 (Kuang 2004).

(a) HDR luminance map (b) iCAM06 (clipped) (c) iCAM06 (normalized)

Figure 2: Range compression for a colored light.

2.2 Effect of iCAM06

Figure 2 shows (a) brightness distribution, (b) the clipped effect of iCAM06, and (c) the normalized effect without clipping, for HDR scene including a colored lighting. Figure 2(b) shows that the colorfulness of the lighting is faded out due to the effect of clipping, whereas it is retained in Figure 2(c). This demonstrates the insufficiency of the range compression rate of iCAM06 for very wide dynamic range scenes.

Figure 3 shows a converted image with iCAM06 and its adaptation luminance, which reveals that the emitted light strongly affects the adaptation white for a whole image. This suggests that restoring the colors of lighting and surrounding areas requires stronger compression of the dynamic range in a separate manner, by using more local adaptation.

3. METHODOLOGY

Our target is to reproduce the color appearance when converting HDR images into LDR ones, which can be attained by more locally changing the adaptation luminance in the iCAM06.

Narrowing the field of view (i.e. decreacing the standard deviation of Gaussian filter) is effective for reducing the chromatic degradation of the lighting area; it, however, causes a halo effect on the boundary against the surrounding and brightens the black colored objects of low reflectance in unnatural ways. For improving these defects, the edge-preserving smoothing operation with a bilateral filter is applied to calculate the local adaptation. This filter is comnputed at the input luminance I of each pixel p as

$$\mathrm{BF}\left[I_p\right] = \frac{1}{W_p} \sum_{q \in S} G_{\sigma_s}(\|p-q\|) G_{\sigma_r}\left(\left|I_p - I_q\right|\right) I_q, \tag{8}$$

$$\mathrm{G}_\sigma(\mathrm{x}) = \frac{1}{2\pi\sigma^2} \exp\left(-\frac{x^2}{2\sigma^2}\right), \tag{9}$$

where $\|p-q\|$ denotes the Euclidean distance of pixel coordinates, $\left|I_p - I_q\right|$ denotes the luminance difference, and $\mathrm{W_p}$ is the normalization term. Both $\mathrm{G}_{\sigma_\mathrm{s}}$ and $\mathrm{G}_{\sigma_\mathrm{r}}$ denote the normal distribution function whose standard deviations representing a view field size σ_s and masking effect σ_r are adaptively controlled for avoiding halo effect. We found that a bilateral filter can yield the local adaptation more effectively than that is yielded with a Gaussian filter.

4. EVALUATION

4.1 Experimental setup

We investigated the effects of the dynamic range compression of iCAM06, whose tone compression (Section 2.1) uses our adaptation luminance, for the scenes illuminated by a red LED bulb (CIE xy chromaticity: $\mathrm{x} = 0.62$, $\mathrm{y} = 0.33$) against various values of σ_s and σ_r.

As a quantitative evaluation, we calculated the differences between reference chromaticity $(\mathrm{u}_\mathrm{r}', \mathrm{v}_\mathrm{r}')$ and mean chromaticity $(\mathrm{u}', \mathrm{v}')$ for each pixel of the output image, where the references are obtained by measuring with a color illuminometer at the following locations:

(A) a white patch of the front chart as shown in Figure 4A.
(B) a white patch of the rear chart as shown in Figure 4B.
(C) the area of the red colored bulb.

The resolution and the range ($\max(\mathrm{I}) - \min(\mathrm{I})$) of the input image were 2736×1824 and 6.47, and σ_s and σ_r were determined as $\sigma_s = \min(height, width)/s$ and $\sigma_r = (\max(I) - \min(I))/r$, respectively.

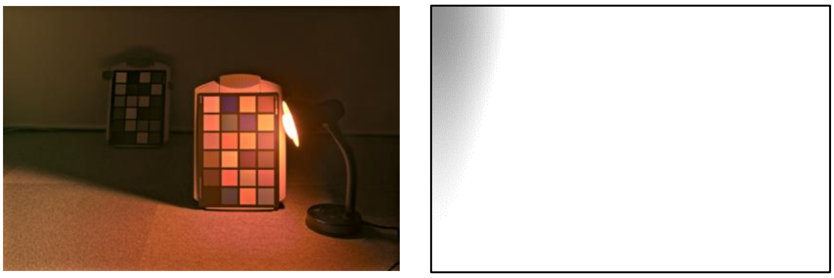

Figure 3: Resulting image with iCAM06 (left) and its clipped adaptation luminance (right).

Figure 4: Experimental environment.

4.2 Observation

Figure 5(a) shows the converted images with our method and Figure 5(b) shows the corresponding adaptation luminances. The results with small σ_s can preserve the color of the red colored bulb but causes the halo effects at the front chart and the bulb and reducing the global contrast. Our method can, however, reduce the halo effects by setting smaller σ_r as shown in the upper row of Figure 5(a). Unfortunately, our mtehod also unnaturally brightens the black colored objects as shown in Figure 5. This negative effect is caused by neglecting the reflectance components for bilateral filtering. We solved this problem by extending the bilateral filter to a cross bilateral filter with a Lighting or Shading map, which is obtained by intrinsic image estimation algorithms.

Figure 6 shows the chromatic differences of our method against the iCAM06, sampled at three areas whose brightness are middle (A), low (B) and high (C). The difference is lower in images restored with our method than those obtained with the iCAM06, where our local adaptation effect is relatively noticeable at the areas (B) and (C). The color reproducibility of the iCAM06 is promoted at the area (A) because the middle brightness area is not affected by clipping or weak range compression.

Consequently, we have found that our method can restore local color appearance more accurately by setting σ_s and σ_r by smaller values. These settings, however, decrease a global contrast of the output image, because of the trade-off between the color reproducibility and the global contrast. This paper does not evaluate the chromatic differences for the lower reflectance areas, where (A) and (B) are the higher reflectance areas and (C) is the light bulb area. We should measure the reference chromaticity with a spectral radiance meter at the various reflectance areas for more accurately evaluating the chromatic differences.

5. CONCLUSION

This article has proposed a color restoration scheme for the scenes of very wide dynamic range caused by colored lightings. Our method calculates the local adaptation white more effectively with the bilateral filter, and adaptively utilizes iCAM06 to reproduce the color appearance of HDR images.

We should improve the remapping mechanism for lower reflectance areas by introducing more accurate quantitative evaluation for color reproducibility of various reflectance areas.

It is also challenging task to restore colors for the scenes illuminated by many lightings of different colors. Our future work also includes psychological experiments in actual lighting environments or with various color monitors.

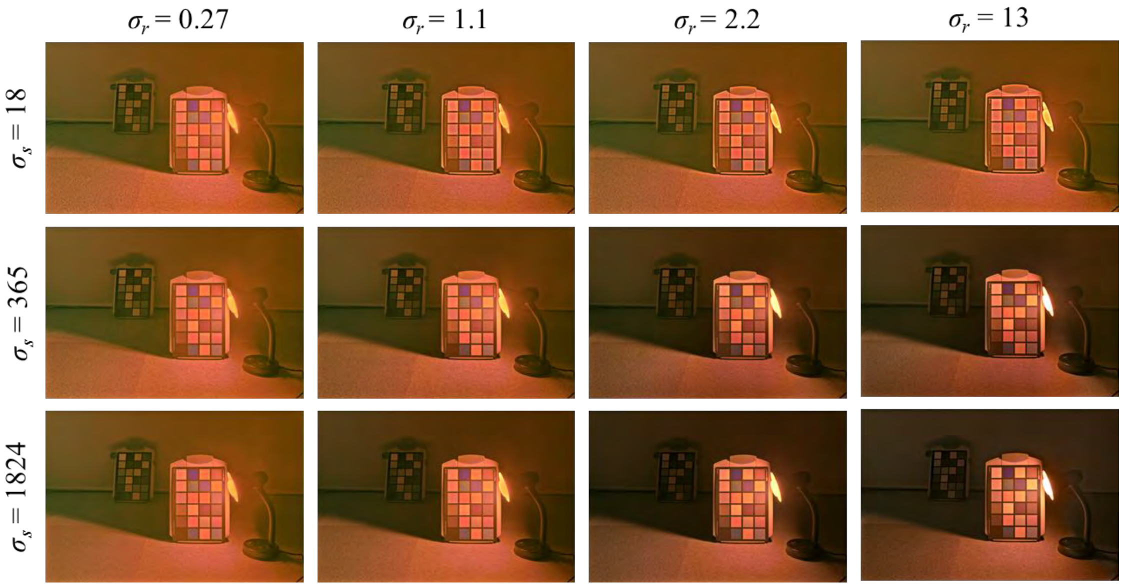

(a) Converted images for various parameters

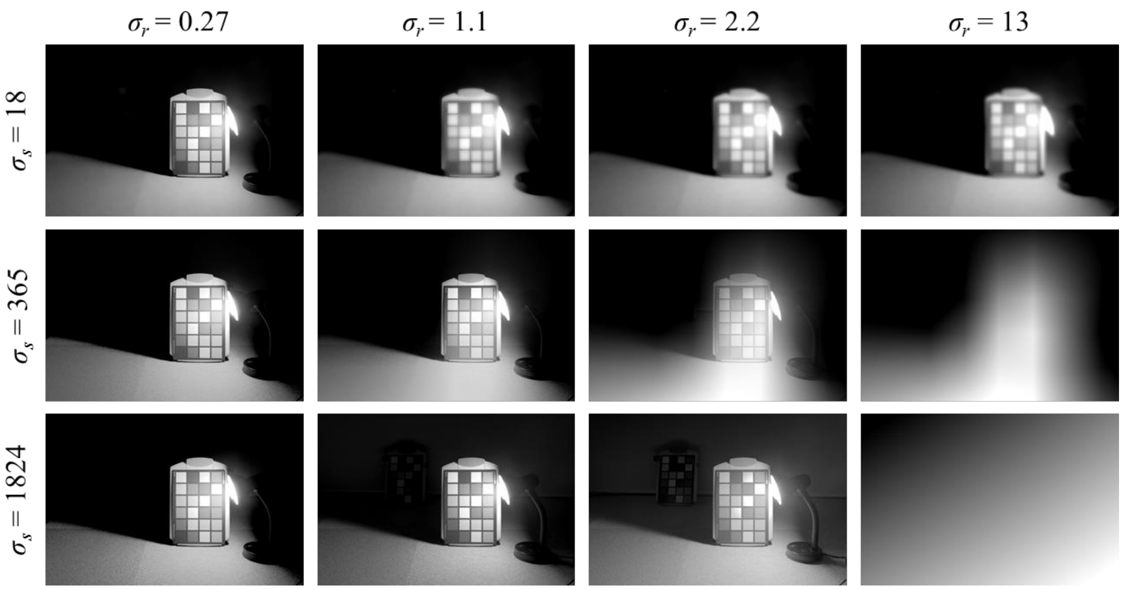

(b) Adaptation luminance (clipped)

Figure 5: Output images and adaptation luminacnes.

REFERENCES

J. Kuang, G.M. Johnson and M.D. Fairchild 2007. iCAM06: *A refined image appearance model for HDR image rendering*, Journal of Visual Communication 185, pp406–414.

E. Reinhard, G. Ward, S. Pattanaik, P. Debevec, W. Heidrich and K. Myszkowski 2010. *High Dynamic Range Imaging Acquisition, Display, and Image-Based Lighting*, Morgan Kaufmann, pp91–118.

N. Moroney, M.D. Fairchild, R.W.G. Hunt, C. Li, M.R. Luo and T. Newman 2002. *The CIECAM02 Color Appearance Model*, IS& T/SID 10th Color Imaging Conference pp23–27.
Z. Rahman, D.J. Jobson and G.A. Woodell 1997. *Multi-Scale Retinex for Color Image Enhancement*, Proc. International Conference on Image Processing 3 pp1003–1006.
J. Kuang, H. Yamaguchi, G.M. Johnson and M.D. Fairchild 2004. *Testing HDR image rendering algorithms*, Color Imaging Conference pp315–320.
Y. Kubo, T. Jinno and S. Kuriyama 2014. *Color Restoration of Color Lighting Effects*, 47th Annual Conference of IEIJ, 8-20.

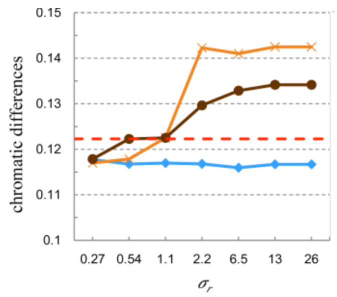

(A) white patch of the front chart

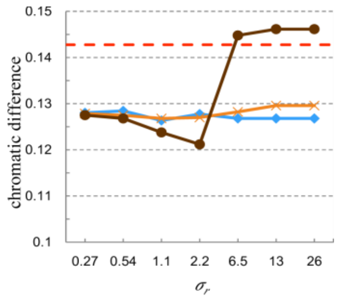

(B) white patch of the rear chart

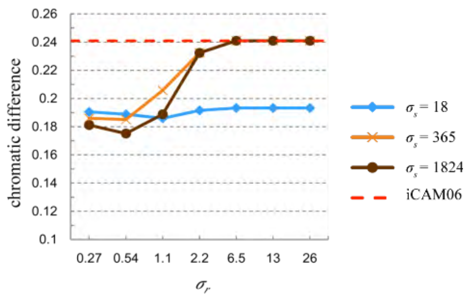

(C) light bulb

(upper row) chromatic differences when setting the various σ_r against the fixed σ_s

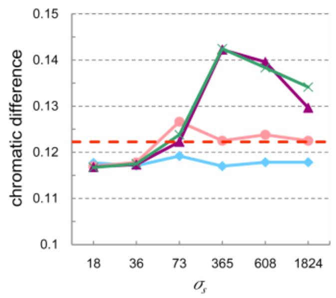

(A) white patch of the front chart

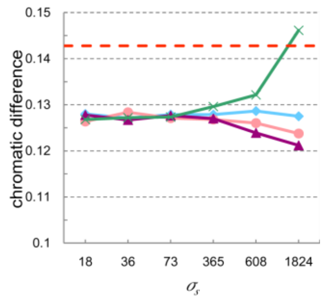

(B) white patch of the rear chart

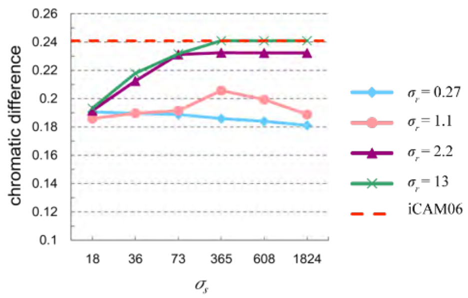

(C) light bulb

(lower row) chromatic differences when setting the various σ_s against the fixed σ_r

Figure 6: Chromatic difference against measurement.

Address: Assistant Prof. Takao JINNO, Department of Computer Science and Engineering, Toyohashi University of Technology, 1-1 Hibarigaoka Tenpaku-cho, Toyohashi, Aichi 441-8580, JAPAN.
E-mails: kubo@val.cs.tut.ac.jp, jinno@cs.tut.ac.jp, sk@tut.ac.jp

Image Quality index for perceiving three-dimensional effect in mobile displays

Chun-Kai CHANG, Hirohisa YAGUCHI, Yoko MIZOKAMI
Graduate School of Advanced Integration Science, Chiba University

ABSTRACT

This article mainly describe two color indices, one is image quality index for color (IQI_{color}) for evaluating image qualities of color and sharpness. Another is image quality index for 3D perception (IQI_{3D}) for evaluating depth perception. The result shows IQI_{color} represents perceived that image color qualities sufficiently and IQI_{3D} provides an easy way to discriminate the depth effects between heterogeneous displays.

1. INTRODUCTION

Recent years, with the rapid development of technology in mobile displays, from traditional cell phones to brand-new smart phones, wider-gamut, higher resolution and higher contrast mobile displays have appeared on the market. In such cases, we could perceive that they have three-dimensional effects but in different levels. In order to understand the differences in perceiving these effects between mobile displays, and precisely estimate in which condition mobile displays perform it well, we consider two indices. One was for evaluation of image quality index of color and sharpness, the image quality index for color IQI_{color}, another was for evaluation of depth perception, the image quality index for depth perception IQI_{3D}.

2. METHOD

First, we prepared nine mobile displays, including one AMOLED tablet, one LCD tablet, four AMOLED phones and three LCD phones. Table 1 illustrates each basic specification.

The IQI_{color} and IQI_{3D} are both specified with chromatic contrast and luminance contrast that are the common factors in the color clarity of display. The procedures of obtaining colorimetric specifications are shown below.

Step 1. Basic color patches, R, G, B, C, M, Y, W and Bk were presented on each display by using 4% pattern which length and width were one fifth of display size, and measured with a Konia Minolta CS-2000 spectroradiometer.

Step 2. The luminance and the tristimulus values X, Y, and Z of color patches are measured with a Konica Minolta CS-2000A spectroradiometer in dark room at 1 lux.

Step 3. XYZ were transferred to the lightness J, the colorfulness M, and the hue h of the CIECAM02, then transferred to a' and b' of the CIECAM02-UCS.

Step 4. The color volumes and luminance contrast of the display were calculated.

Table 2 illustrates the x,y chromaticity coordinates and the maximum and minimum luminance in R, G, B and W color patches.

Part 1: Image quality index for color (IQI_{color})

In chromatic contrast, we defined a relative color volume in the CIECAM02-USC color space (Luo et al., 2006) using the volume color gamut efficiency (Inui, 2000) which can be described as volume of display color gamut divided by volume within optimal color. As the volume within optimal color is 2,334,000 in CIELAB unit (Inui, 2000), the relative color volume in CIECAM02-USC ($RCV_{\text{CAM02-USC}}$) unit can be simply described as follow,

$$RCV_{\text{CAM02-USC}} = (\text{Volume of display color gamut}) / 2{,}000{,}000 \quad (1)$$

In luminance contrast, we used luminance ratio as a luminance contrast index instead of usual Michelson contrast. Although the luminance of black in AMOLED displays is approaching to 0, we defined our contrast ratio index (*CRI*) as 8 log unit for some facilitating calculation reasons as follows,

$$CRI = \log (L_{\max} / L_{\min}) / 8 \quad (2)$$

The image quality for color and luminance contrast could be represented as a function of color volume and contrast ratio as following equation.

$$IQI_{\text{color}} = (RCV_{\text{CAM02-USC}} * CRI)^{1/2} \quad (3)$$

Table 1. Each basic specification of mobile display

	Display size (inch)	Diagonal size (inch)	Number of pixels	Resolution (ppi)
AMOLED phone 1	4.91 x 2.8	5.7	1920 x 1080	386
AMOLED phone 2	4.32 x 2.45	5.0	1920 x 1080	441
AMOLED phone 3	4.40 x 2.49	5.1	1920 x 1080	432
AMOLED phone 4	4.17 x 2.37	4.8	1280 x 720	306
LCD phone 1	4.13 x 2.34	4.8	1280 x 720	308
LCD phone 2	5.07 x 2.84	5.9	1920 x 1080	373
LCD phone 3	4.29 x 2.45	5.0	1920 x 1080	443
AMOLED tablet	8.85 x 5.49	10.5	2560 x 1600	288
LCD tablet	7.6 x 5.77	9.7	2048 x 1536	264

Table 2. Chromaticity coordinates of mobile displays

Display primaries	(*x,y*) Chromaticity coordinates				Luminance (cd/m^2)	
	R	G	B	W	White $L_{\max}$	Black $L_{\min}$
AMOLED phone 1	(0.655, 0.336)	(0.223, 0.722)	(0.144, 0.043)	(0.299, 0.328)	395.37	7×10^{-5}
AMOLED phone 2	(0.665, 0.334)	(0.223, 0.724)	(0.142, 0.045)	(0.301, 0.331)	316.37	6×10^{-5}
AMOLED phone 3	(0.662, 0.337)	(0.227, 0.711)	(0.141, 0.046)	(0.302 0.320)	440.58	3×10^{-5}
AMOLED phone 4	(0.668, 0.331)	(0.213, 0.724)	(0.140, 0.051)	(0.303, 0.325)	254.16	8×10^{-4}
LCD phone 1	(0.635, 0.331)	(0.302, 0.557)	(0.149, 0.061)	(0.293, 0.293)	465.03	5×10^{-1}
LCD phone 2	(0.637, 0.335)	(0.303, 0.610)	(0.155, 0.066)	(0.311, 0.344)	438.61	5×10^{-1}
LCD phone 3	(0.648, 0.342)	(0.265, 0.645)	(0.153, 0.037)	(0.300, 0.327)	401.25	1×10^{-1}
AMOLED tablet	(0.660, 0.339)	(0.237, 0.709)	(0.141, 0.048)	(0.303, 0.319)	350.71	6×10^{-5}
LCD tablet	(0.641, 0.338)	(0.305, 0.609)	(0.154, 0.048)	(0.306, 0.322)	389.56	3×10^{-1}

A visual experiment of image quality

In this experiment, excepting 2 tablet displays for size reasons, we prepared 7 mobile displays, and carried out a visual evaluation of image quality by a paired comparison method using three natural images called “Wineglass”, “Wool” and “Harbor” from SHIPP (Standard High Precision Picture) data shown in Figure 1 (a)-(c). Each image was selected for a particular purpose as follows,

Wineglass: tone reproduction of light and neutral color.

Wool:color reproduction of high chroma image.

Harbor: evaluation of image processing for fine detail of geometrical structure.

(a) Wineglass (b) Wool (c) Harbor (d) Venice

(e) Wine & Table (f) Houses (g) Trees (h) Swan

Figure 1. Test images

Visual image quality performance is provided by Z-scores from the experiment. The Z-scores represent the image quality as a distance from mean in terms of standard deviation. Table 3 shows the final result of calculation in image quality indices and Z-scores from a visual experiment for image quality. Figure 2 shows the Z-score of each device in three images, and the error bars indicate standard deviation. When using mobile displays, our impression of image would also be affected by the modulation transfer function (MTF) of display indirectly, we consider another formula to explain this result instead of Equation (2) as describe below,

$$IQI_{\text{total}} = (RCV_{\text{CAM02-USC}} * CRI * RI)^{1/3} \quad (4)$$

Where the resolution index RI is given by the following Equation. The number of 582 ppi corresponds to the limit of retinal resolution for visual acuity 2.0 at the viewing distance of 30 cm, are regarded as normalization base. Table 3 shows pixel per inch (ppi) and resolution index (RI) for mobile displays.

$$RI = ppi / 582 \quad (5)$$

Although Equation (4) shows a good relationship between the three parameters, we tried to develop a total image quality index with weighting coefficients as following equation. From least square method, the weighting coefficients w_{CV} , w_{CR} and w_{R} as 0.2, 0.4 and 0.4 respectively, perform the highest correlation between IQI_{total} and Z-score as shown in Figure 3.

$$IQI_{\text{total}} = w_{\text{CV}}\, RCV_{\text{CAM02-USC}} + w_{\text{CR}} CRI + w_{\text{R}} RI \quad (6)$$

Part 2: Image quality index for 3D perception (IQI_{3D})

In this part, 3D depth effect will be verified by two psychophysical experiments, a paired comparison method and an observers' subjective evaluation. Comparing to IQI_{color}, we added two tablet displays and reduced one LCD phone from the experiment. Test images called "Venice", "Wine & Table", "Houses", "Trees" and one short movie "Swan" are also shown in Figure 1 (d)-(h). Total 15 observers with normal visual acuity participated in this experiment.

(a) The method of successive categories

In this session, the observers were asked to evaluate the depth perception of displays directly in 5 stages, by using the method of successive categories in binocular and monocular visions in a dark room. The successive categories are shown in Figure 4.

(b) The method of paired comparison

We carried out a paired comparison method to evaluate depth perception for 6 mobile displays, totally 15 combinations. Observers answered which mobile phone presented stronger 3D effect in each image and movie.

Table 3. Image quality indices and visual evaluation result

Device	RCVCAM02-USC	CRI	RI	IQI_{total}	Z-score
AMOLED phone 1	0.811	0.837	0.664	0.763	2.698
AMOLED phone 2	0.811	0.840	0.757	0.801	1.680
AMOLED phone 3	0.857	0.886	0.742	0.823	2.491
AMOLED phone 4	0.760	0.686	0.526	0.637	-1.730
LCD phone 1	0.513	0.363	0.526	0.458	-2.284
LCD phone 2	0.503	0.364	0.642	0.503	-1.227
LCD phone 3	0.703	0.372	0.761	0.594	-1.626

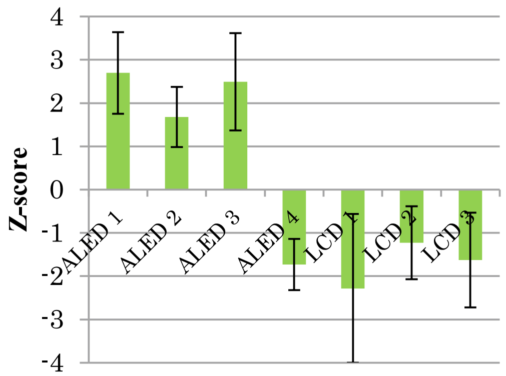

Figure 2. Visual image quality results of paired comparison method of IQI_{color}

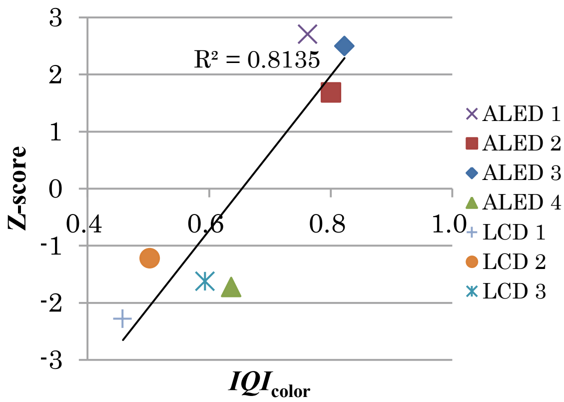

Figure 3. The relationship between IQI_{total} & Z-score

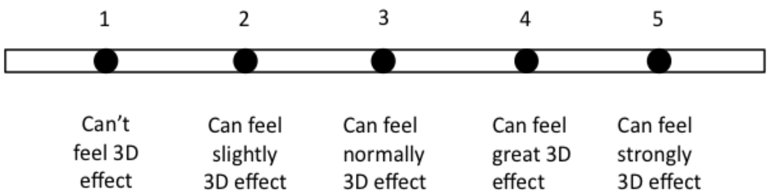

Figure 4. Category of 3D perception

As Part 1, after completing above experiments, an image quality index for depth perception will be established. It would be considered that the feeling of depth could be affected by color volume, luminance contrast, resolution and display size. We have already defined the color volume and the contrast ratio as Equations (1) and (2), but we use pixel per degree (ppd) instead of pixel per inch in resolution index as follows,

$$RI_{\mathrm{retina}} = ppd \,/\, 100 \quad (7)$$

The number of 100 comes from rough number of cones in a visual angle of one degree in a foveal retina. Display size are also be defined as a field size in retina as follows,

$$RDS_{\mathrm{retina}} = [(\text{Display size in degree}) / 1440]^{1/2} \quad (8)$$

The number of 1440 comes from a full visual field with binocular vision, 48º by 30º. Both of the display resolution in retina, RI_{retina} and the display size in visual angle, RDS_{retina} depend on the viewing distance. As the same way, we derive $IQI_{3\mathrm{D}}$ as Equation (6).The weighting coefficients w_{CV} , w_{CR}, w_{R} and w_{DS} are 0.3, 0.3, 0.2 and 0.2, having a high correlation with Z-score. Table 4 shows the $\mathrm{IQI}_{3\mathrm{D}}$ result of each mobile display.

$$IQI_{3\mathrm{D}} = w_{\mathrm{CV}}\ RCV_{\mathrm{CAM02\text{-}USC}} + w_{\mathrm{CR}}CRI + w_{\mathrm{RS}}\ RI_{\mathrm{retina}} + w_{\mathrm{DS}}\ RDS_{\mathrm{retina}} \tag{9}$$

Table 4. $IQI_{3\mathrm{D}}$ evaluation results

Device	$\mathrm{RCV}_{\mathrm{CAM02\text{-}USC}}$	CRI	RI_{retina}	RDS_{retina}	IQI_{3D}
AMOLED phone 1	0.811	0.837	0.837	0.470	0.752
AMOLED phone 2	0.811	0.840	0.926	0.413	0.763
AMOLED phone 3	0.857	0.886	0.909	0.420	0.789
AMOLED phone 4	0.760	0.686	0.639	0.399	0.642
LCD phone 1	0.513	0.363	0.645	0.395	0.471
LCD phone 2	0.503	0.364	0.792	0.481	0.515
AMOLED tablet	0.834	0.840	0.623	0.864	0.800
LCD tablet	0.562	0.382	0.574	0.825	0.563

3. RESULTS AND DISCUSSION

Figure 5 and Figure 6 shows the results of psychophysical experiments in $IQI_{3\mathrm{D}}$. In Figure 6, we normalized the successive categories from 0 to 1. We can see the all AMOLED displays have a high preference than LED displays. Finally, we conducted a one-way ANOVA in each result of the experiments, showing some of differences reach their significant levels as shown in green shaded cells in Table 5 and Table 6. The results indicated the threshold is 0.09 when observers can discriminate 3D depth effect easily. As the same way in Table 6, the base rate of subjective evaluation can be earned from the difference ratio in $IQI_{3\mathrm{D}}$ and subjective evaluation is 0.9158, thus we can know roughly how much the subjective 3D depth feeling will be according to $IQI_{3\mathrm{D}}$ value.

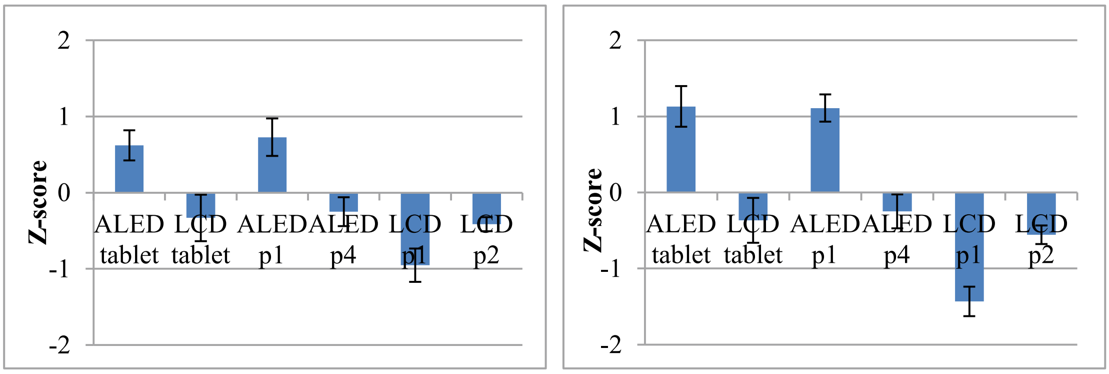

Figure 5. Visual image quality obtained by paired comparison method,
Left side: result of binocular, Right side: result of monocular

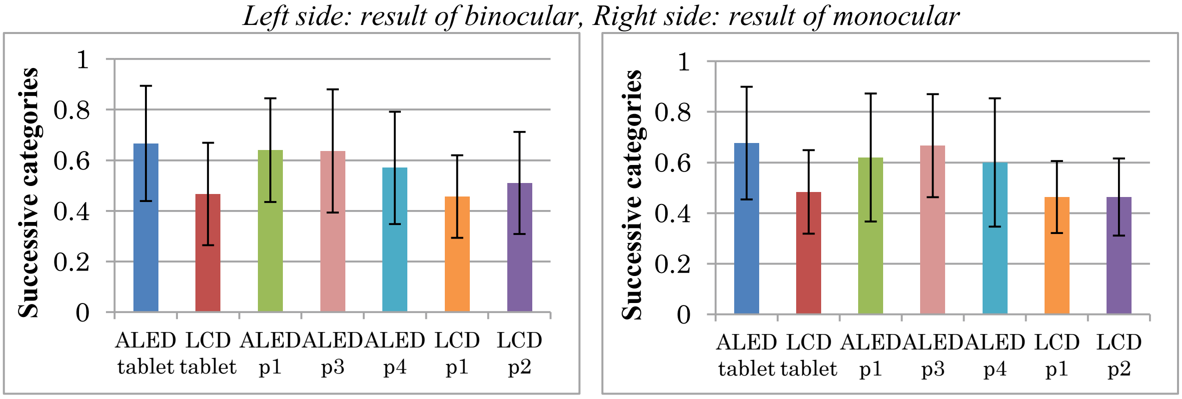

Figure 6. Visual image quality obtained by successive categories experiment
Left side: result of binocular, Right side: result of monocular

Table 5. The differences of IQI_{3D} in paired comparison

	ALED p1	ALED p4	LCD p1	LCD p3	ALED tablet	LCD tablet
ALED p1	0	-0.110	-0.280	-0.227	0.275	-0.189
ALED p4	0.110	0	-0.170	-0.117	0.158	-0.078
LCD p1	0.280	0.170	0	0.053	0.328	0.091
LCD p3	0.227	0.117	-0.053	0	0.275	0.038
ALED tablet	-0.048	-0.158	-0.328	-0.275	0	-0.237
LCD tablet	0.189	0.078	-0.091	-0.038	0.237	0

Table 6. The differences of IQI_{3D} in subjective evaluation

	ALED p1	ALED p3	ALED p4	LCD p1	LCD p3	ALED tablet	LCD tablet
ALED p1	0	0.037	-0.110	-0.280	-0.227	0.048	-0.189
ALED p3	-0.037	0	-0.147	-0.317	-0.264	0.011	-0.226
ALED p4	0.110	0.147	0	-0.170	-0.117	0.158	-0.078
LCD p1	0.280	0.317	0.170	0	0.053	0.328	0.091
LCD p3	0.227	0.264	0.117	-0.053	0	0.275	0.038
ALED tablet	-0.048	-0.011	-0.158	-0.328	-0.275	0	-0.237
LCD tablet	0.189	0.226	0.078	-0.091	-0.038	0.237	0

4. CONCLUSIONS

We developed image quality index for color (IQI_{color}) for evaluating the image qualities of color and sharpness, and image quality index for 3D perception (IQI_{3D}) for evaluating depth perception. In IQI_{color}, we found that as bigger values displays had, the better image qualities were perceived. In IQI_{3D}, there are the same tendencies with IQI_{color} in perceiving 3D depth effect. The results also suggest that the IQI_{3D} difference of 0.1 could cause an easily perceptible difference of depth between different displays.

REFERENCES

Mark D. Fairchild, 2013. *Color Appearance Models, 3rd Ed.* Wiley-IS&T, Chichester, UK

Masao Inui, 2000. The Quantification of Color Gamut Efficiency, *J. Soc. Photogr. Sci. Technol. Japan,* 63, 277-281.

M. Ronnier Luo, Guihua Cui, and Changjun Li, 2006.Uniform Colour Spaces Based on CIECAM02, *Color research and application* 31(4): 320-330.

Society for Information Display (SID) 2012.Information Display Measurements Standard ver.1.03, 82-84

Address: C.-K. CHANG, Graduate School of Advanced Integration Science,
Chiba University, 1-33 Yayoicho, Inage-Ku, Chiba, 263-8522, Japan
E-mail:hibadina0520@yahoo.com.tw
yaguchi@faculty.chiba-u.jp, mizokami@faculty.chiba-u.jp

Imageries of Edible Souvenirs Evoked by Colours and Visual Textures of Packages

Shuo-Ting WEI
Department of Visual Communication Design, TransWorld University, Taiwan

ABSTRACT

The current study aims to investigate the relationship between imagery and appearance of packing papers for edible souvenirs in terms of colours and visual textures. To achieve this, an experiment of categorical judgments was carried out. 25 observers provided integers from 1 to 7 to show their opinions for 100 stimuli with 12 different textures. The 20 bipolar scales of imagery were assessed for each stimulus. The results showed that only the imagery of roughness was significantly influenced by texture. For the effect of colour on imagery, we found that packing papers with light colours are more likely to be considered soft and relax. Red and orange were considered warm and friendly colours, whereas cyan and blue were associated with cool and unfriendly. The 20 imageries for the appearance of packing papers can be explained using 4 principal imageries. They explained 80.41% of total variations.

1. INTRODUCTION

In the recent few years, Taiwan's travel industry has witnessed a surge in tourist numbers and the spending by tourists in souvenirs has increased accordingly. This has led to a larger yet more competitive market of tourism souvenirs, i.e., commemorative merchandise associated with a location to provide tourists a memento of their visit and to encourage an opportunity for a return visit. Thus, seeking approaches to highlight features and to create a unique identity (e.g., product feature, brand images…etc) for tourism souvenirs has received a great deal of attention from package designers. Among many aspects, colors and visual textures of packaging materials are two essentials of design that conveys product features and brand images. In this study, we aim to examine the relationship between imagery and appearance of packing papers for edible souvenirs in terms of colours and visual textures.

Many of the relevant studies regarding the imagery of colour, or colour emotion, tended to agree that imagery of heat, i.e. warm and cool, is highly associated with hue. The imageries of hardness (i.e. hard and soft) and weight (i.e. heavy and light) are associated with lightness. Activity and clearness, on the other hand, tend to be associated with chroma (Kobayashi, 1981; Sato et al., 2000; Ou et al., 2004; Lee & Lee, 2005; Gao et al., 2007). In the recent years, the relationship between colour and imagery was proved to be impacted by visual textures. Lucassen et al. (2011) investigated the influence of texture on the imagery of colours. They concluded that texture cannot be ignored in colour emotion studies as they found that the imagery of hardness is fully determined by texture, and in decreasing extent for masculine–feminine, heavy–light, and warm–cool. Simmons & Russell (2008) also found that the imagery of pleasantness was impacted by texture. People tended to feel unpleasant for colour samples with textures. The extent of unpleasantness was determined by types of textures.

2. METHOD

Visual assessments using the categorical judgment method (Torgerson, 1958) were conducted to obtain psychological responses with regard to imageries of packing papers. The experimental settings and procedures are described below.

2.1 Stimuli Preparation

A hundred of packing papers were selected in this study as the materials for stimuli preparation. As shown in Figure 1, the papers include 12 different textures. Each texture has multiple colours from 1 to 21. These papers are frequently used in graphic design and package design. Figure 2 shows the CIELAB values of the 100 papers, which gives a good coverage in a^*-b^* plane. The reason why colours of lightness below 20 were missing is because surfaces of the papers are matt, which naturally produces diffuse reflection of light. The packing papers were presented in a form of 20*12*4 cm^3 boxes in the experiment as visual stimuli, as shown in Figure 3. This was to simulate the papers being seen in the context of souvenirs.

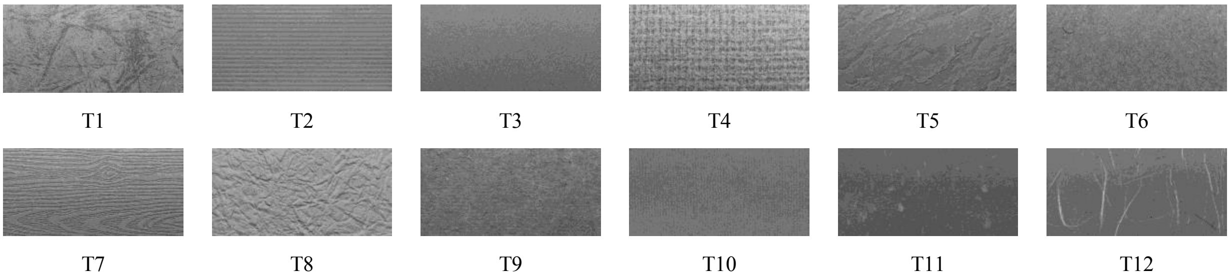

Figure 1 The 12 textures of packing papers examined in this study.

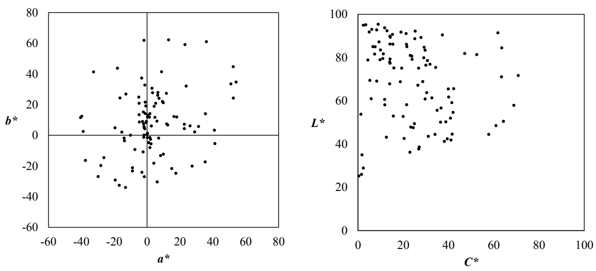

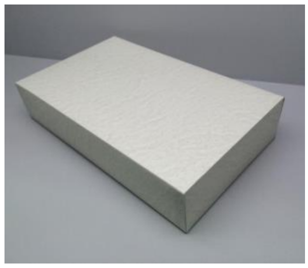

Figure 2 The colours of packing papers in CIELAB (a) a-b* plane and (b) L*-C* plane.*

Figure 3 An example of the visual stimuli

2.2 Scales of Imagery

Twenty bipolar scales of imagery were used in this study to measure observers' opinions about appearance of packing papers in terms of colour and texture. These scales includes heavy – light, complex – simple, natural – artificial, rough – smooth, local – international, active – passive, dislike – like, old – new, romantic – realistic, casual – formal, realistic – exaggerated, fresh – overdue, hard – soft, relax – serious, cheap – expensive, warm – cool, friendly – unfriendly, delicious – insipid, plain – gorgeous and loose – tight. These scales are relevant to package design (e.g. romantic – realistic), colour appearance (e.g. warm–cool), texture appearance (e.g. rough – smooth) or food souvenir (e.g. delicious – insipid). They were chosen by five package designers using KJ method, i.e. affinity diagram.

Integer eget neque ac ex lobortis consequat. Morbi non eros arcu. Donec convallis sem et augue cursus, vel rutrum orci sollicitudin. Quisque vel nulla felis. Sed scelerisque mollis consectetur. Integer lacinia nec ex nec consectetur. Phasellus finibus sollicitudin volutpat. Nunc eget nibh lacus. Vivamus commodo convallis turpis, et dignissim ex suscipit id. Phasellus lorem massa, auctor nec porttitor a, dignissim id tellus. Nam laoreet ut ante vitae pulvinar. Proin est ipsum, iaculis sit amet ipsum nec, mattis hendrerit nisi. Quisque nec orci sed metus interdum molestie sit amet vitae arcu. In hac habitasse platea dictumst. Sed volutpat lectus at lorem vehicula blandit. Donec fermentum ligula sit amet augue finibus ornare congue a purus.

2.3 Observers

Twenty five observers participated in this study, including 13 females and 12 males. All of them were undergraduate students at the TransWorld University, Taiwan. All of them major in graphic design. The ages of these observers ranged from 20 to 22 with an average of 21. All observers passed the Ishihara test to ensure normal colour vision.

2.4 Experimental Procedures

The experiment was carried out in a dark room. The visual stimuli were presented in a viewing cabinet and illuminated using D65. The observers were seated approximately 30cm from the near edge of the viewing cabinet. During the experiment, the observers provided integers from 1 to 7 to show their opinions for the 100 stimuli. The 20 bipolar scales of imagery were assessed for each stimulus. The whole experiment was divided into 4 sessions of equal numbers of assessments. The observers completed the 4 sessions within two weeks.

3. RESULTS

3.1 Consistency of Responses

The consistency of observers' responses was firstly investigated by examining intra- and inter-observer agreements using the measure of *root mean square* (RMS). For intra-observer agreement, the results revealed that most of the RMSs between repeated assessments were around 1 unit with the mean RMS of 1.07 units for female observers and 1.08 units for male observers. This indicates high intra-observer agreement, as the differences between repeated assessments for both male and female were around 1 category of the 7-category measurement scale.

In the case of inter-observer agreement, the mean values of RMS were 1.37 for female and 1.33 for male observers. This indicates that the differences between individual observers' responses and the responses of the majority were less than 1.5 categories of the 7-category measurement scale, suggesting reliable inter-observer agreement.

3.2 Gender Differences

Gender differences were investigated using the measure of *root mean square* (RMS, see equation 1), too. It was found that the RMS value is 0.92, which is slightly smaller than 1 unit of the 7-category measurement scale. This suggests small differences of experimental results between female and male observers. Hence, the imageries of the visual stimuli were determined by mean scores of the 25 observers' raw data.

3.3 The Influence of Textures

The results of the stimuli with beige and cyan colours were selected to analyse the influence of textures. We found that only the imagery of rough – smooth was significantly influenced by texture. Figure 4(a) illustrates the results of rough – smooth against 9 different textures with error bars of 95% confidence interval. Dots and crosses denote beige and cyan samples, respectively. The figure shows that the texture of flax (T4) and texture of kneaded paper (T8) were considered rough textures ($p<.05$). Although in average the texture of wood (T7) was considered rough, the results did not significantly lower than the score 4.

Hard – soft, the scale that was concluded by Lucassen et al. (2011) to be fully determined by texture, did not show the same result in the current study. As shown in Figure 4(b), most of the 9 textures were considered soft for both beige and cyan colours. In addition, beige colour looked much softer than cyan colour ($p<.05$) for the stimuli with the textures of T2, suggesting that colour influences the imagery of hard – soft.

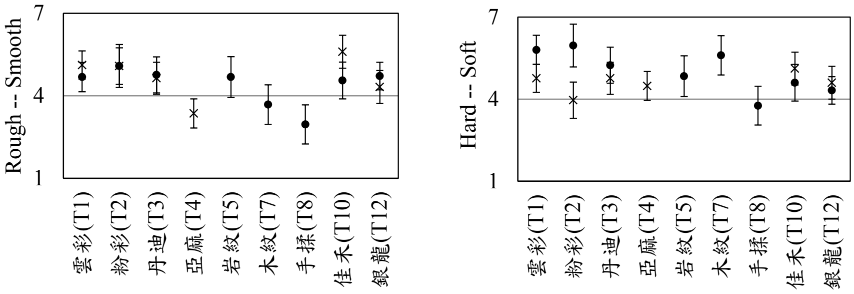

(a) *(b)*

Figure 4 (a) Roughness and (b) hardness scores of the 9 textures with beige (dots) and cyan (crosses) colours.

3.4 The Influence of Colours

The influence of colours was examined in terms of lightness, hue and chroma. We found that some scales of imagery were affected by lightness and chroma. However, Chroma of packing papers neither correlated well with the scales of imagery nor showed any clear nonlinear trend.

The scales of heavy – light, hard –soft and relax – serious were highly correlated with lightness. The correlation coefficients R equals .88, .74 and -.80, respectively. This suggests that packing papers with light colours are more likely to be considered soft and relax no matter what kind of texture is used. Figure 5 shows the scatter plots of hue against the scales of warm – cool and friendly – unfriendly. It was found that both scales of imagery were associated hue with clear nonlinear trends. Red and orange were considered warm and friendly colours, whereas cyan and blue were associated with cool and unfriendly.

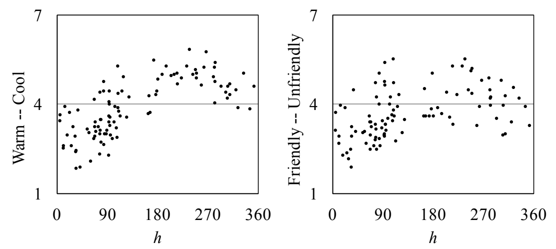

Figure 5 the scatter plots of hue angle against warm – cool and friendly – unfriendly.

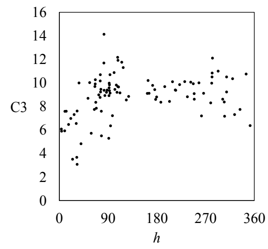

Figure 6 the scatter plot of hue angle against the component C3.

3.5 Principal Imageries

Principal Component Analysis (PCA) was carried out to investigate whether there is any underlying principal component that can be used to explain the experimental results of the 20 scales of imagery. As a result, 4 principal components were found and they explained 80.41% of total variations. The components and the included scales of imagery are given in Table 1. Component C1 was highly correlated with lightness of packing papers (R = -.84). C2 and C3 were moderately with yellowness-blueness (i.e. b^*) and Chroma, respectively (R = -0.51 and -0.63). The scatter plot of C3 against hue also revealed a clear nonlinear trend as shown in Figure 6. No clear trend was found between the component C4 and colour attributes.

Table 1 The 4 principal components and their relevant imageries.

Components	C1	C2	C3	C4
Scales of imagery	complex – simple rough – smooth dislike – like old – new local - international heavy - light casual - formal	cheap - expensive loose - tight natural - artificial hard - soft plain - gorgeous relax - serious	realistic - exaggerated romantic - realistic active - passive	warm - cool friendly - unfriendly delicious - insipid fresh - overdue

4. CONCLUSIONS

This study aims to investigate the imagery of packing papers for edible souvenirs. More specifically, we examine the relationship between imagery and appearance of packing papers in terms of colours and visual textures. To achieve this, visual assessments using the categorical judgment method were conducted to quantify psychological responses with regard to imageries of packing papers. A hundred packing papers with the 12 different textures were visually assessed by the 25 observers using the 20 bipolar scales of imagery. The results revealed that only the imagery of rough – smooth was significantly influenced by texture. For the effect of colour on imagery, we found that heavy – light, hard –soft and relax – serious were highly correlated with lightnes, suggesting that packing papers with light colours are more likely to be considered soft and relax. The scales of warm – cool and friendly – unfriendly were associated with hue angle. Red and orange were considered warm and friendly colours, whereas cyan and blue were associated with cool and unfriendly. Chroma of packing papers neither correlated well with the scales of imagery nor showed any clear nonlinear trend. The results of PCA suggest that imagery of packing papers for edible souvenirs can be adequately explained using 4 principle imageries.

ACKNOWLEDGEMENTS

This research is partially supported by TransWorld University and sponsored by Ministry of Science and Technology, Taiwan, R.O.C. under Grant no. MOST 103-2221-E-265-002-

REFERENCES

Gao, X., Xin, J., Sato, T., Hansuebsai, A., Scalzo, M., Kajiwara K., Guan, S., Valldeperas, J., Lis. M., and Billger, M. 2007. Analysis of Cross-cultural Color Emotion, *Color Research and Application* 32: 223-229.

Ishihara, S. 2003. *Ishihara's tests for colour deficiency. 38 Plates Edition*. Tokyo: Kanehara Trading.

Kobayashi, S. 1981. The Aim and Method of Color Image Scale. *Color Research and Application* 6: 93-107.

Lee, Y. and Lee, J. 2005. The Development of an Emotion Model Based on Colour Combinations. *International Journal of Computer Studies* 30: 122-136.

Lucassen, M.P., Gevers, T., Gijsenij, A. 2011. Texture Affects Color Emotion, *Color Research and Application* 36: 426-436.

Ou, L., Luo, M. R., Woodcock, A. and Wright, A. 2004. A study of Colour Emotion and Colour Preference Part I: Colour Emotions for Single Colours, *Color Research and Application* 29**:** 232-240.

Sato, T., Kajiwara, K., Hoshino, H. and Nakamura, T. 2000. Quantitative Evaluation and Categorizing of Human Emotion Induced by Color, *Advances in Color Science and Technology* 3: 53-59.

Simmons, D. and Russell, C. 2008. Visual Texture Affects the Perceived Unpleasantness of Colours. *Perception* 37, ECVP Abstract Supplement, 146-146.

Torgerson, W.S. 1958. *Theory and methods of scaling*. New York: John Wiley & Sons.

Address: Dr. Shuo-Ting Wei, Department of Visual Communication Design,
TransWorld University, No.1221, Zhennan Rd., Douliu City, Yunlin County 640, Taiwan
E-mail: tim.stw@gmail.com

A Study of the preference and orientation of "the sense-oriented"

Takashi INABA
Nippon Color & Design Research Institute Inc.

ABSTRACT

To decide the color of the product, it is desirable to reflect the preference of the users. When only one or two color use is permitted for a new product, it is important to choose novel and distinguishable colors. In order to achieve this, we offer a method to identify individuals with strong interest in colors, design, art and trends as “sense-oriented”, and refer to them as an index upon determining the colors of products.

The “sense-oriented” females, obtained through a survey of 1,440 subjects, wish others to consider them as fashionable figures, and prefer the elegant and classy image. Moreover, they hold a preference for high-quality materials, brilliant colors such as red and gold, and cold colors with hues of B and BG. They are also enthusiastic consumers and set a high value on texture.

1. INTRODUCTION

Upon deciding the color of a product, it is important to reflect the users’ color needs. When it is possible to have color variations for a single product, the colors can be set for each user group with different needs. If that is not the case, it is a common solution to choose a popular color among the general population which consequently results in a situation where many products have the same color, which leads to the lack of distinction and novelty.

The introduction of the method to identify individuals who actively adopt new colors and using their preferred colors on new products will bring novel colors to the market, which could potentially lead other users to follow and consume those colors. The process is to first select people with strong interest in colors and design, then within that group determine individuals who are interested in the field of that product, who will then serve as the index for the target as color leaders.

In this research, as the primary step, people with strong interest in colors, design and trends were selected, then were compared to those who lack interest in the subject area for color and image preference.

2. METHOD

The survey was conducted online on 1,440 male and female subjects, ages ranging from 18 to 69 years old. The questionnaire consisted of two parts: Part 1 Questionnaires to research the awareness of colors, design, art and trends, and Part 2 Questionnaires to research color preference by presenting visuals.

20 questionnaires, such as "Have you confidence in your sense of color ? ", "Do you often go to the event or exhibitions of art and design ?" and "Do you buy cheaper thing even

though that is not your favorite color and design ? ", were set to select out individuals with strong interest in colors, design and trends. The subjects answered the questionnaires on a 5 point scale.

In the questionnaire to research the preference by presenting visuals, 48 colors selected from Hue & Tone system were used in order avoid bias (Figure 1).

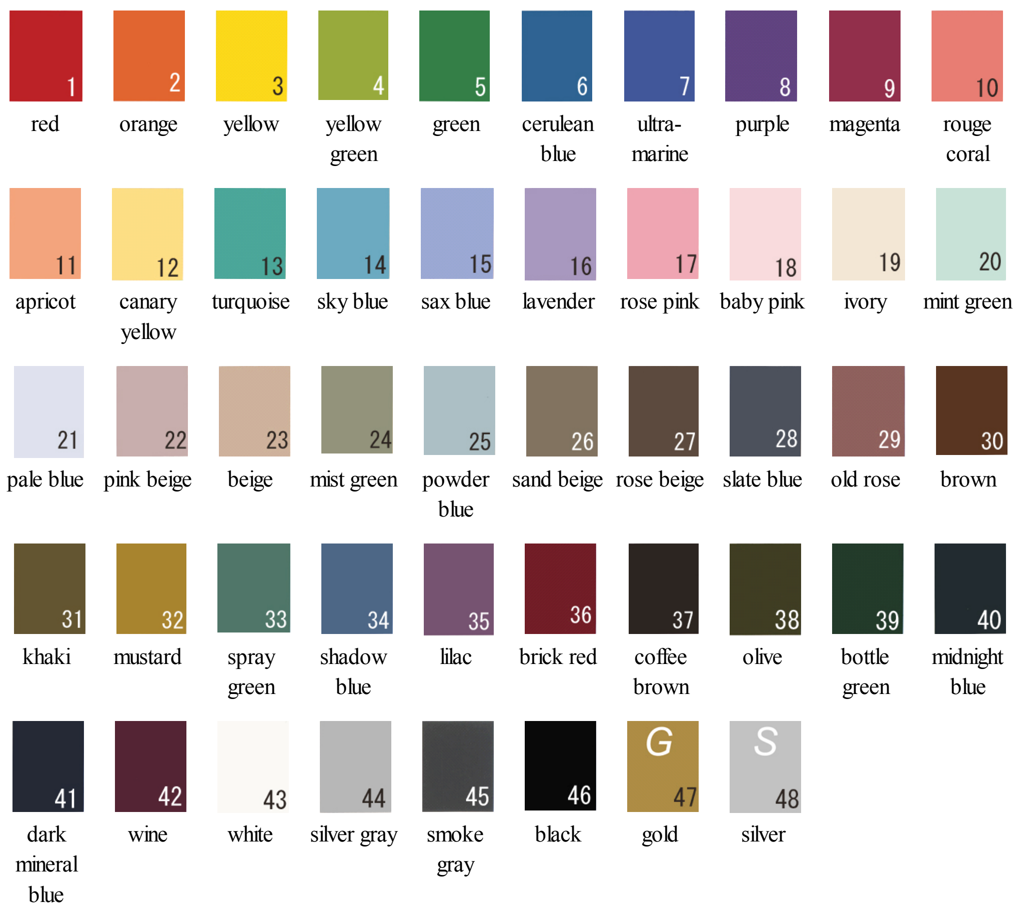

Figure 1: Color Samples.

3. RESULTS AND DISCUSSION

Factor analysis was performed on the data from the questionnaires on colors, design, art and trends (maximum likelihood method, Promax factor rotation with Kaiser's normalization). Pattern matrix is shown in the Table 1.

Factor 1 indicates the acquisition of information, such as familiarity with events regarding design and art, and the knowledge of trend colors and designs. Factor 2 indicates the actual actions taken, such as adopting colors and designs into their daily lives or how much they put emphasis on colors and designs upon purchasing items.

Cluster analysis was then conducted. As a result, 1,440 subjects were divided into four clusters. Regarding the component ratio, Cluster 1 is the smallest at 15.6% whereas Cluster 2 is the largest at 35.0% as shown in Table 2. Figure 2 presents the cluster center of each cluster.

Table 1. Pattern matrix(Factor analysis).

	FACTOR 1	FACTOR 2
Do you know "Milano Salone","Tokyo Designer's Week" ?	0.977	-0.250
Do you often go to the event or exhibitions of art and design ?	0.910	-0.140
Are you engaged in color and design on business (or study) ?	0.873	-0.173
Do you have a favorite designer of product or fashion ?	0.863	-0.024
Are you well informed of art and design ?	0.845	-0.028
Do you often watch TV programs, Web sites, magazines on art and design ?	0.828	0.012
Do you know the latest trendy colors ?	0.780	0.043
Do you like finding the information of trends about color and design in magazines or on the Internet ?	0.582	0.230
Do your family or friends ask you for advice how to use colors ?	0.548	0.322
Do you often go to fashionable shops and town ?	0.508	0.325
Do you pay attention to a new package of beverage, confectionery and foods ?	0.417	0.317
Do you buy cheaper thing even though that is not your favorite color and design ?	-0.474	0.830
Do you think color and design enrich people's life ?	-0.090	0.786
Do you know the color that suits yourself ?	-0.003	0.719
Are the colors and design of your clothes and room coordinated by your own taste ?	0.077	0.701
Do you like making the coordination of fashion or interior ?	0.181	0.695
Do you want to buy a product that nobody has the similar design ?	0.030	0.658
Do you often buy a product because you are attracted by its color and design ?	-0.036	0.643
Do you check the color of your clothes and accessories so that it won't be the same with others around you ?	0.173	0.612
Are you praised for the color coordination of your clothes and accessories ?	0.229	0.611
Do you like going window-shopping or looking display of products ?	0.256	0.562
Have you confidence in your sense of color ?	0.265	0.543
Do you try to use the colors that match to the season ?	0.264	0.540
Can you explain the good points of the product design that you chose ?	0.444	0.453
Do you want to use trendy colors into your daily life ?	0.336	0.401

Cluster 1 holds a positive position for both Factor 1 “information” and Factor 2 “actions”, which indicates that Cluster 1 considers their sense, interests in colors, design and trends, to be essential. They were categorized as “sense-oriented”. Cluster 2 regards sense as an important factor, though not as much as Cluster 1, therefore were categorized as “semi sense-oriented”. Cluster 3 and Cluster 4 were identified as “average” and “low-interest”, respectively. Regarding the component ratio of sex, Cluster 1 had the highest female ratio, whilst Cluster 4 had the highest male ratio.

Table 2. Component ratio.

		%
Cluster1	"sense-oriented "(sensibility as important)	15.6%
Cluster2	"semi sense-oriented" (sensibility a little)	35.0%
Cluster3	"average"	26.9%
Cluster4	"low-interest"	22.5%
		N=1440

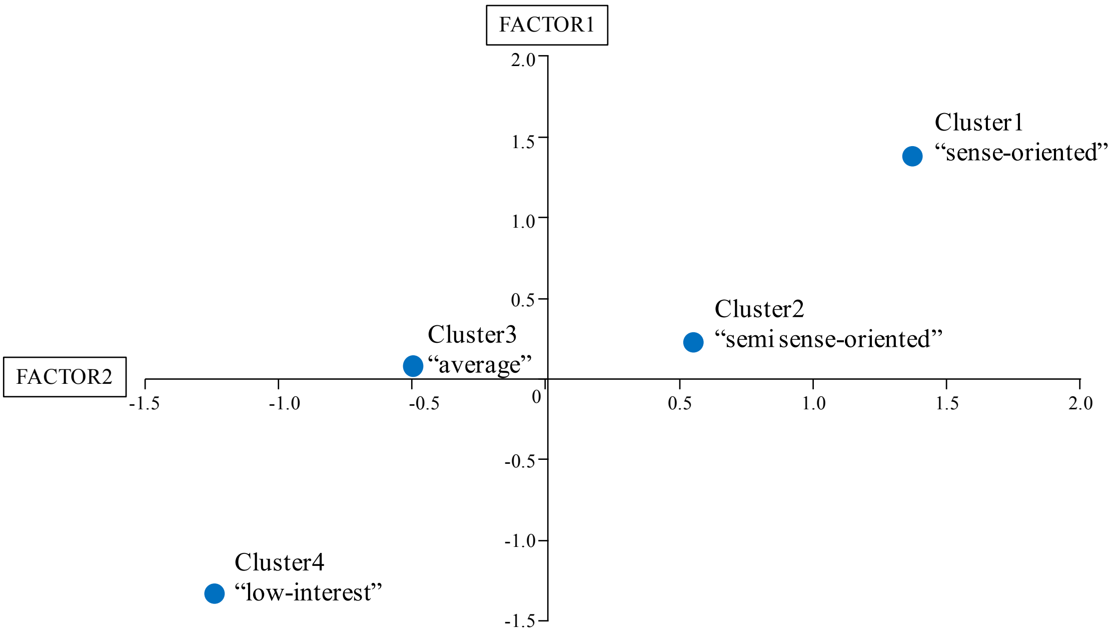

Figure 2: Cluster score matrix.

A comparison was then performed between Cluster 1 "sense-oriented" and the other clusters for color and image preferences. Since color preference differs by gender, the analysis was separately performed on males and females. The following is the result of the female subjects.
Figure 3 presents the result of individuals from the "sense-oriented" cluster and individuals from other remaining clusters choosing a single favorable color. Additionally, a Chi-squared test was performed to investigate the presence of a significant difference between the two groups. As a result, there was a significant difference in turquoise, red and gold ($P<0.01$), and lavender, white, ultra marine, mint green and dark mineral blue ($P<0.05$).

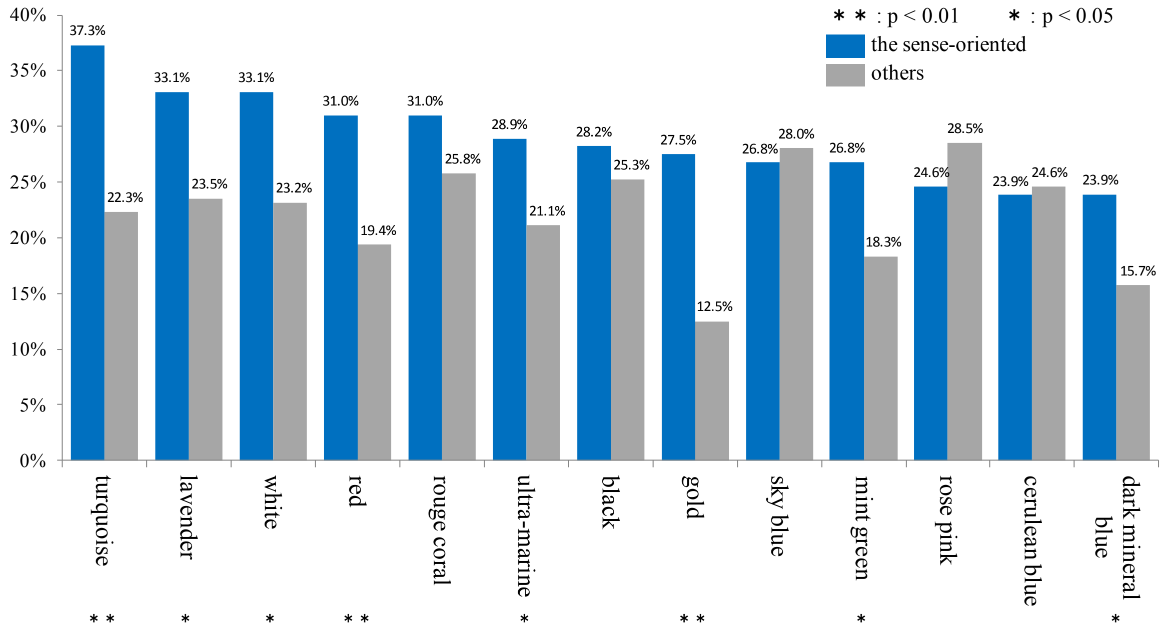

Figure 3: Color Preferences.

Moreover, in the material category, cashmere and silk were P<0.01, and porcelain and linen were P<0.05 (Figure 4).

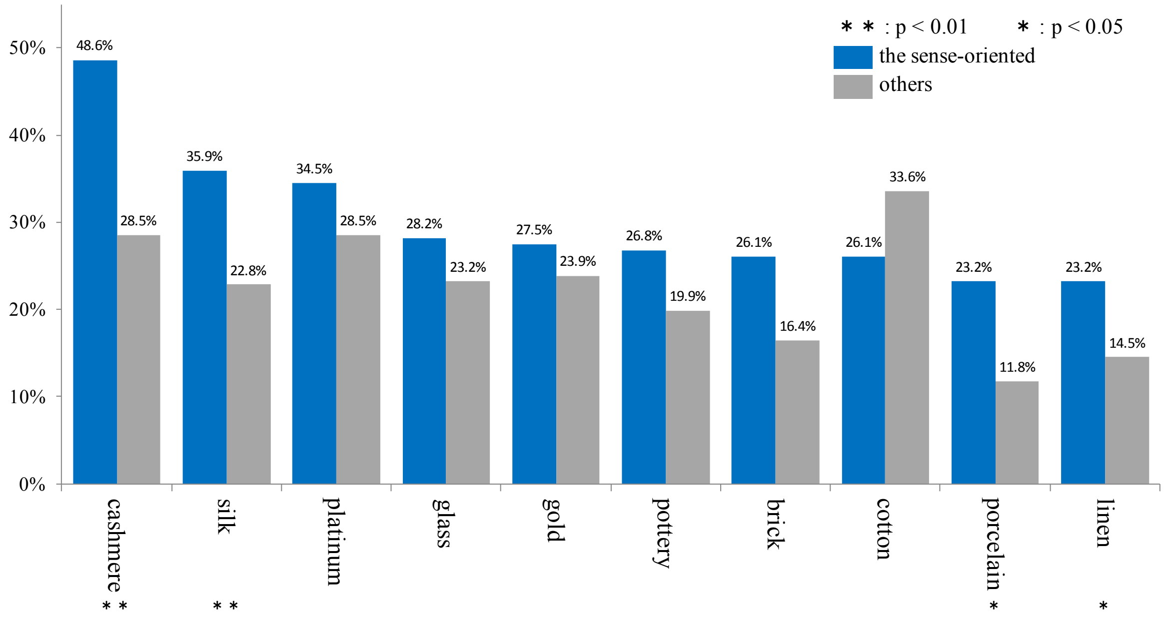

Figure 4: Material Preferences.

When the subjects were asked to choose a favorite image word, elegant (P<0.01), and refined, polished and feminine (P<0.05) presented a significant difference (Figure 5).

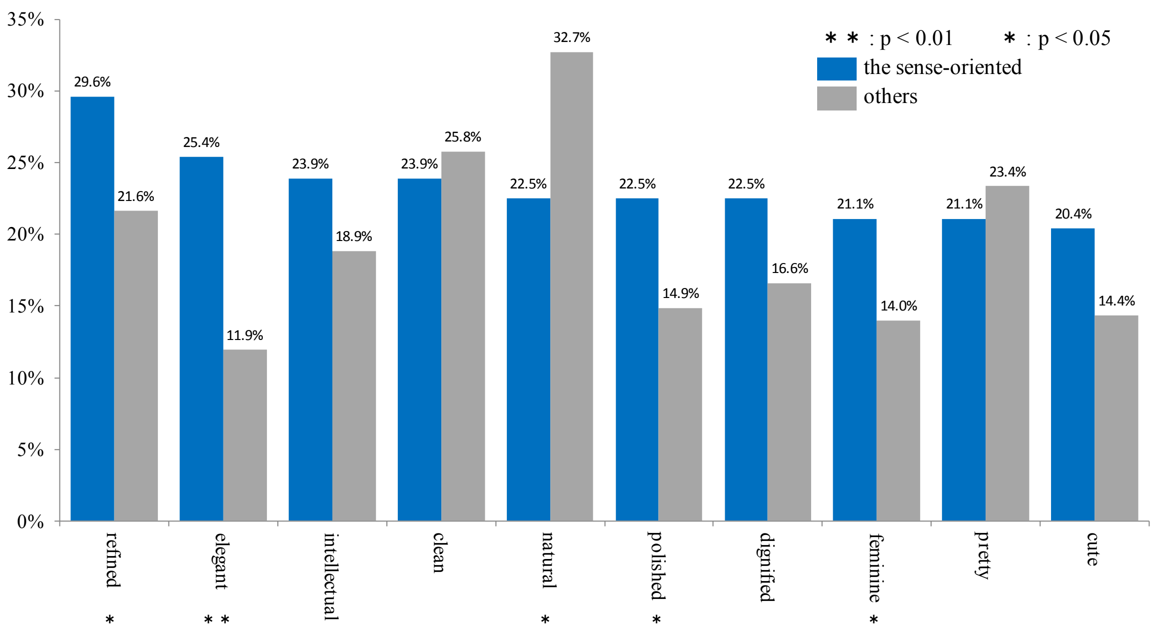

Figure 5: Favorite Image Word.

In the questionnaire on how they wish to be viewed by others, fashionable, person with good taste and intelligent (P<0.01), and polished (P<0.05) presented a significant difference.

In the questionnaire regarding their perspective on purchasing, there was a significant difference ($P<0.01$) between "sense-oriented" and others in the following:

I love shopping (sense-oriented 36.6%, others 23.9%)
I buy items I like even if it is slightly out of my range (35.9%, 18.9%)
I put a high value on the sense of touch and the texture upon purchasing (35.2%, 17.0%)
The country of origin of the product is significant to me (33.1%, 15.2%)
I will put emphasis on the design if the price is the same (30.3%, 15.9%)
I am confident in my judgment to choose a good product (27.5%, 10.9%)
I have my own preference for specific brands and companies (23.2%, 8.1%)

The above results indicate that the "sense-oriented" females desire to be viewed as fashionable and favor elegant and polished images. Regarding their perspective on purchasing, they are proactive buyers with specific preference for the countries of origin of the product and the brands. Moreover, their value on not only the appearance of the product but also the texture of it became apparent as they favored high quality materials such as cashmere and silk.
They favor vibrant, brilliant colors such as red and gold, along with colors in several tones which give out a cool impression such as turquoise, ultra marine, mint green and dark mineral blue.

4. CONCLUSIONS

By presuming that it is crucial to reflect user preference upon deciding the best color for a product, the method to select individuals with strong interest in colors, design and trends among product users, and using their preference as an index to select colors and designs for products was presented.

A survey was conducted on 1,440 subjects, with questionnaires to evaluate the subjects' value on their sense, and questionnaires to study their favorite colors and materials, which was then used to select a "sense-oriented" group. The results indicated that the "sense-oriented" females value their sense, quality and elegance, and have high buying intention. Furthermore, when compared to females in the non-"sense-oriented" groups, they favor brilliant warm colors with high saturation, and cold colors in various tones which convey a cool impression.

In this manner, the efficacy has been partially verified regarding the method to refer to "sense-oriented" females as an index to select product colors in the process of product development.

Address: Takashi INABA, Nippon Color & Design Research Institute Inc.,
3-5-2 Hongo Bunkyo-ku, Tokyo, 113-0033, JAPAN
E-mails: inaba@ncd-ri.co.jp

Color Preference Measured by Paper-Format Implicit Association Test

Shinji NAKAMURA,[1] Aya NODERA[2]
[1] Faculty of Child Development, Nihon Fukushi University
[2] Faculty of Human Culture and Sciences, Fukuyama University

ABSTRACT

In a history of research concerning color preference, preference judgment has been measured via explicit behaviors, such as verbal report or so on. In many recent psychological studies, however, it has been indicated that expressed attitude measured with explicit methods often differs from underlying implicit attitude. In the present studies, we tried to analyze an implicit attitude toward color, using implicit association test (IAT). Paper-and-pencil style IAT (paper-IAT) makes us enable to execute psychological experiments simultaneously in a massy group to collect preference data from considerable number of participants. In a paper-IAT, the participants were asked to manually tick a list of discrimination targets (printed on paper). We can assess relative implicit color preferences by calculating differences of number of the items that the participants could make judgments. 234 undergraduate participants took part in paper-IAT experiments to measure relative preference between red and green, blue and yellow, and also black and white. Target colors were presented by either color names or object names which can easily make the participants recall specific colors. Two separated IAT experiments were repeated with an interval of five weeks. Results of psychological experiments indicated that correlations between implicit color preference measured by IAT and explicit color preference measured by visual analogue scale (VAS) were significant in chromatic color evaluations (red-green and yellow-blue), but not in the case of achromatic color (white-black). It was also shown that correlations between two repeated IATs were significant. These results suggested that paper-IAT holds a considerable reliability in measuring relative implicit color preference, and we can utilize it for measurements of color preference in a group experiment.

1. INTRODUCTION

Color preference has been one of the biggest concerns in the color sciences for long years. The color preference has been measured by various methods in accordance with the researcher's interest. In most cases, the methods in measuring color preference would be based on the participants' explicit behavior, such as verbal report or so on. Typically, an investigator may simply ask the participants to select their most preferred or hated color from a set of candidate colors. In many recent psychological studies, however, it has been indicated that explicitly expressed attitude often differs from underlying implicit attitude. Thus, in the present investigation, we tried to analyze implicit attitude toward color, using implicit association test (IAT; Greenwald et al, 1998). IAT is recognized as one of the most conventional methods in measuring implicit attitude in psychological studies. In IAT, participants discriminate target words into two criteria. In the condition where two psychological concepts which are mutually associated with each other are paired in discriminatory criteria, the participant's reaction is facilitated (reaction time is reduced), and vice versa in the condition where the psychological concepts without implicit association are paired. IAT utilizes differences of reaction time in categorical judgment in order to measure participants' implicit attitude without their conscious and arbitrary indication.

In our previous reports, we tried to measure implicit associations between specific color combinations (red-green and white-black) and psychological concepts of pleasantness /unpleasantness, and found that significant positive correlations between IAT scores and explicitly measured color preference (by visual analogue scale [VAS]) in the case of chromatic color (red-green), but not in the achromatic case (white-black) (Nakamura & Nodera, 2014). The previous experiments employed four different styles of target color presentation, namely color name, color patch, object name and object picture. Correlations of IAT scores across the different targets were considerably high, indicating that IAT can be reliable and quite stable in measuring participant's implicit color preference.

The previous investigation successfully demonstrated that IAT can be utilized as one of the possible implicit measurements concerning the participant's color preference. On the other hand, conventional IAT measurement requires considerable test durations in isolated individual experiments. It makes researchers difficult to collect data from mass participants and grab general tendencies concerning color preference in specific groups. In the present studies, we tried to measure the participants' implicit color preference using paper-and-pencil style IAT (paper-IAT; Lemm et al, 2008). It makes us enable to execute psychological experiments simultaneously in a massy group to collect preference data from considerable number of participants. In a paper-IAT, the participants were asked to manually tick a list of discrimination targets (printed on paper), instead of a computer-based key pressing in the case of conventional IAT.

2. METHOD

Before participating IAT sessions, the participants' explicit color preferences were measured with visual analogue scale (VAS). In VAS session, the participants answered degree of preference/hate towards six colors (white, black, red, green, blue and yellow), by drawing slash ("/") on line whose ends were correspond to "completely dislike (0)" and "completely like (100)." In IAT session, they were participated in IAT trials measuring implicit associations between pleasantness/unpleasantness and targeted colors. Target color combinations were red-green, blue-yellow or white-black. IAT sheets were supplied to the participants. Each sheet was composed by 20 rows and three columns of target words, belonging to either the following four categories; target color1, target color2, pleasant and unpleasant (see figure 1). The target color was presented as 1) color name or 2) object name. In both cases, the target color was presented in Japanese with Chinese character. Table 1 indicates the objects employed in the object name conditions to represent the target colors. Pleasant and unpleasant words were also presented as nouns which represent the target concepts (e.g., happiness, peace or fortune for pleasant, and misery, pollution or evil for unpleasant words, in Japanese with Chinese character).

The participant's task was to discriminate and categorize the word, and tick a check mark at corresponding box (either left or right) located both sides of each target word. They executed two discrete discriminations simultaneously; colors and pleasant/unpleasant. Time limitation for discrimination in each sheet was 20 seconds. In a case of red-green evaluation, for example, two IAT sheets were employed. The participants were requested to

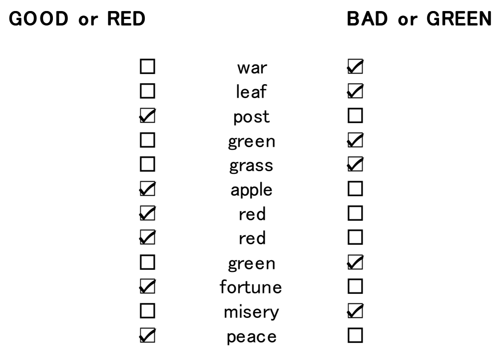

Figure 1 Sample of Paper-IAT sheet employed in the experiment. The participants were required to check the left box for “red” or “good” target and the right box for the “green” or “bad” target. In a real sheet, there were 20 rows and 3 columns of target words, and the color name and the object name were tested in a different trial.

Table 1 Objects employed in object-name IAT trials

color	object			
red	tomato	apple	post	strawberry
green	melon	leaves	grass	(green)pepper
blue	earth	space	sea	sapphire
yellow	banana	lemon	dandelion	sunflower
white	rice	snow	tofu	rabbit
black	ink	tire	coal	(black)seaweed

check “red” and pleasant words (and “green” and unpleasant words) at the check box located in same side in one of the sheets, and “green” and pleasant (“red” and unpleasant) were paired in the other one. The participants who exhibited greater implicit associations of psychological concept of pleasantness with the red, rather than with the green, can make more discrimination in the red-pleasant sheet than the green-pleasant sheet, and vice versa for the participants who implicitly preferred the color green. Thus, we can assess relative implicit preference between red and green, by differentiating numbers of checked items between two sheets.

Both VAS and IAT sessions were repeated with interval of 5 weeks (Test1 and Test2) in order to examine reliability of paper-IAT as an implicit measurement for color preference. The participants were undergraduate students. 275 students were participated in Test1 and 282 students were participated in Test2. 234 students who took part in both tests were set to be subjects to the following analyses (76 male and 158 female, ages ranged from 18 to 23). In this study, VAS and IAT scores were calculated for explicit and implicit indices which would represent relative color preference between red and green, blue and yellow or white and black. VAS scores were accomplished by difference between two raw VAS values divided by sum of them. IAT scores were also defined by difference of numbers of checked items between two target colors, divided by sum of them; e.g., in a case of red-green evaluation, scores were indicated by (red-green)/(red+green). With the standardization by sum of raw values, we can archive relative measurements avoiding the effects of general variations of the raw values. Both for VAS and IAT scores, positive values were assigned to relative preference to red, blue or white. Thus, score 0 means that there was no difference of preference, greater positive score means that the participant’s greater preference in red, blue or white, and vice versa for negative value. We obtained three VAS scores (three color combinations; red-green, blue-yellow and black-white) and six IAT scores (three colors and two color presentations [color name and object name]) from each participant in each test.

3. RESULTS AND DISCUSSION

Table 2 indicates Peason's coefficiates of correlation between Test1 and Test2 for both VAS and IAT scores. VAS scores demonstrated quite high correlations ranging from 0.69 to 0.75 for each color combination. For IAT scores, correlations were relatively low as compared with VAS, but still significant and considerable with regard to the numerous participants took part in this investigation (ranging from 0.36 to 0.46). Thus, IAT scores obtained in this experiment can be a reliable measrement for implicit color preference, exhibiting a certain range of robustness against repeating tests with interval of five weeks.

Table 2 Coefficients of correlations between Test1 and Test2

	red-green	blue-yellow	white-black
VAS	0.69	0.75	0.73
color-name IAT	0.36	0.40	0.39
object-name IAT	0.45	0.42	0.46

Table 3 Coefficients of correlations between VAS and IAT scores

Test1	red-green	blue-yellow	white-black
VAS-ColorName	0.37	0.32	0.15
VAS-ObjectName	0.32	0.37	0.11
ColorName-ObjectName	0.28	0.31	0.30

Test2	red-green	blue-yellow	white-black
VAS-ColorName	0.36	0.28	0.06
VAS-ObjectName	0.29	0.32	-0.03
ColorName-ObjectName	0.32	0.34	0.29

Table 3 indicates correlations between VAS and IAT (both for color and object names) in Test1 and Test2. In red-green and blue-yellow evaluations, VAS and IAT were mildly correlated (from 0.28 to 0.37). Implicit color preference mesured by paper-IAT and explicit preference measured by VAS were consistent with each oterh in the case of evaulation for chromatic color combination, suggesting shared underlying foundations for both types of preferences. On the other hand, in white-black evaluation, correlations bween VAS and IAT were not significant and quite low (from 0.03 to 0.15). This might be due to the fact that IAT scores were slightly biased toward white preference, whereas there were no such biases in VAS scores. This means that the participants who explicitly reported black preference exhibited black avoidance in implicit measurements, and sugests that there would be some discontinuities between explicit and implicit measurements of achromatic color preference. Table 3 also indicates correlation btween color-name IAT and object-name IAT. Coefficients supposed to be in medium range (from 0.28 to 0.34) evinced that the discrimination targets presented by either the color name or the object name successfully elicited identical psychological concept concerning color to the participants.

Above mentioned results in this research were generally consistent with our previous investigation employing conventional computer-based IAT. Thus, we can conclude that paper-IAT can be used as cost effective alternative with less equipment requirments and applicable for mass group experiments in measuring implicit color preference.

4. CONCLUSIONS

The current investigations tried to apply paper format IAT (paper-IAT) as implicit measurement of color preference. Psychological experiments indicated that paper-IAT exhibited a considerable reliability and mild but significant correlations against conventional and explicit measurments of color preference (VAS) in the case of chromatic color evaluations. Thus, we can utilize it for measurements of implicit color preference in a group experiment.

REFERENCES

Greenwald, A. G., McGhee, D.E., and Shwarz, J.L.K. 1998. Measuring individual differences in implicit cognition: The implicit association test. *Journal of Personality and Social Psychology,* 74(6): 1464-1480.

Lemm, K. M., Lane, K. A., Sattler, D. N., Khan, S. R., and Nosek, B. A. 2008. Assessing Implicit Cognitions with a Paper-Format Implicit Association Test. In M. A. Morrison & T. G. Morrison (Eds.), *The psychology of modern prejudice* (pp. 123-146). Hauppauge, NY: Nova Science Publishers.

Nakamura, S., and Nodera, A., 2014. Implicit association test can be applied for measuring color preference. *The 2nd Conference of Asia Color Association, Conference Proceedings* p.77-81.

Address: Shinji Nakamura, Faculty of Child Development,
Nihon Fukushi University, Okuda, Mihama-cho, Aichi, 470-3295
JAPAN
E-mails: shinji@n-fukushi.ac.jp, nodera@fuhc.fukuyama-u.ac.jp

SSVEP response study for low semantic images

Syntyche Gbèhounou,[1] Enrico Calore,[2] François Lecellier,[1] Alessandro Rizzi,[2] Christine Fernandez-Maloigne[1]

[1] Department SIC of XLIM Laboratory, UMR CNRS 7252; Poitiers, France
[2] Dipartimento di Informatica, Università degli Studi di Milano, Milan, Italy

ABSTRACT

In this paper, we have studied the relation between Steady-State Visual-Evoked Potentials (SSVEP) responses, the emotion valence and some low level images features. In the literature numerous papers refer to this kind of study made on IAPS (Lang, Bradley, & Cuthbert, 2008). This database is dedicated to emotion study and it contains many images carrying a strong semantic. From the experiences on this dataset, the amplitude, latency and topography of the SSVEP response have been proven to be correlated to the arousal and valence of the shown pictures. Our aim is to test if this conclusion can be extended for low semantic images: could SSVEP response also be used to study the affective content of natural images that were not specially created to elicit emotional responses?

We chose 12 images from our new database SENSE (Studies of Emotion on Natural image databaSE) developed for this kind of task. From the obtained results we can confirm that for the considered natural images, there is a clear and strong correlation between the pictures and the SSVEP response elicited in the observers.

1. INTRODUCTION

An Evoked Potential (EP), in the context of EEG signals, is an electrical potential elicited by the presentation of a stimulus that can be recorded from the nervous system. In particular, in the case of non-invasive EEG recordings, it can be acquired from an electrode positioned on the surface of the scalp. Visually Evoked Potentials (VEP) are EP aroused by a visual stimulation and Steady-state VEP (SSVEP) are a particular case of VEP. The stimulus is presented multiple times at a frequency at least higher than 3.5Hz, but more commonly higher than 6Hz. Then, a periodic response called SSVEP can be observed in the recorded scalp EEG signal, in particular in the occipital brain region, where the visual cortex resides. The SSVEP response have been studied deeply in the field of vision research starting from the seventies (Regan, 2009) and it is still considered in the fields of cognitive neuroscience and clinical neuroscience. Moreover in the last years it has been adopted widely for the implementation of Brain-Computer Interfaces (BCI) (François-Benoît Vialatte, 2010) and various researches are being conducted to provide applications for new Human-Computer Interactions (HCI) systems.

In the literature, multiple evidences exist suggesting the SSVEP response not being only a mechanical reaction of the brain to a flickering stimulus, it is known to be modulated by the user's attention and affective state (Yee Joon Kim, 2006) (Paolo Toffanin, 2009). In particular, in these works, flickering pictures from the International Affective Picture System (IAPS) (P.J. Lang, 2008) have been shown to a group of users during the acquisition of their EEG. These studies conclude that the amplitude, latency and topography of the SSVEP response are correlated to the arousal and valence of the shown pictures.

The aim of our research is to test if the SSVEP response could be used to study the affective content also of natural images that were not specifically created to elicit emotional responses. In fact, the majority of the studies is done on IAPS which is a semantic image set.

The rest of the paper is organized as follows: we describe in Section 2 the considered database and evaluation protocol. We present in Section 3 the results of our different analysis and we conclude and provide some future works in Section 4.

2. EXPERIMENTAL METHOD

2.1 Description of the database

Our studies were made on a natural and low semantic image database called SENSE (Studies of Emotion on Natural image databaSE) (Syntyche Gbèhounou, 2013). In this paper, "low-semantic" means that the images do not induce a strong emotional response. This dataset is composed of 350 images such as animals, food and drink, landscapes, historic and touristic monuments as shown in Figure 1.

Figure 1: Some images from the database SENSE we used.

The images of SENSE are assessed according to the nature and power of their emotional. For the nature, that corresponds in part to the valence, observers had choice between "Negative", "Neutral" and "Positive" and the power varies from "Low" to "High". The nature rating corresponds to the emotion valence information.

For our evaluations we only recorded the SSVEP response of 12 colored images from SENSE. They were chosen according to the percentage of observers that defined the final nature of the emotion in order to consider conclusive images.

2.2 The test description

During the tests, we recorded the EEG of the 4 participants looking at the 12 colored images. The participants to our tests were volunteer and did not receive a financial reward.

The images are evaluated during three trials and presented in a pseudo-random order. For each trial, an image was displayed for 8s and flickering at 10Hz. After displaying the image to assess, a black image is displayed for 5s.

The EEG was recorded from 4 electrodes positioned on the occipital area on Pz, POz, PO3 and PO4 location according to the 10-20 system as shown in Figure 2.

We studied different correlation between the SSVEP responses recorded across different trials and observers to be sure that there is a significant modulation of the response due to the pictures content.

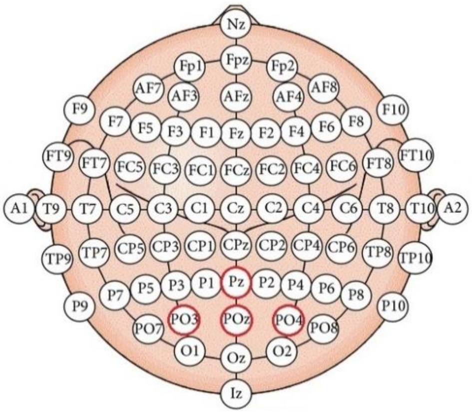

Figure 2: 10-20 system with the four location we considered.

3. RESULT ANALYSIS AND DISCUSSION

In particular we looked for a correlation between the intensity of the SSVEP response of 4 subjects computed with a relatively novel state-of-the-art technique (O. Friman, 2007) (Zhu, 2011).

To study the potential correlation we used the Pearson's correlation computed by PSPPIRE software[1].

At first, we evaluated the correlation between the computed SSVEP responses and the pictures across different trials and observers to be sure that there is a significant modulation of the response due to the pictures content. We had two configurations:

1. We computed the SSVEP response for the whole displaying duration (8s) using the "Minimum Energy" algorithm (O. Friman, 2007);
2. We computed with the same algorithm the SSVEP response for each second of viewing and then averaged it.

The results are presented in the Table 1 for the first configuration and in Table 2 for the second one. The SSVEP response used is the mean value for the duration considered.

Table 1. Correlation between the trials the complete duration of SSVEP response recording: the duration time is equals to 8s

		Trial 1	Trial 2	Trial 3
Trial 1	Pearson' Coef	1	**0.56**	**0.49**
	Significance	-	**0**	**0**
Trial 2	Pearson' Coef	0.56	1	**0.40**
	Significance	0	-	**0**
Trial 3	Pearson' Coef	0.49	0.40	1
	Significance	0	0	-

Regarding the results in the tables 1 and 2 (the Person's coefficients and the significance values ≤0.05) we reject the null hypothesis of correlation between the three trials for both configurations. Moreover, for the second one a stronger correlation has been found

[1] https://www.gnu.org/software/pspp/tour.html

between trials. This confirms, at first, that the SSVEP responses we have computed are consistent and correlated to the pictures.

Table 2. Correlation study in the second configuration: the duration time is equals to 1s

		Trial 1	Trial 2	Trial 3
Trial 1	Pearson' Coef	1	**0.62**	**0.61**
	Significance	-	**0**	**0**
Trial 2	Pearson' Coef	0.62	1	**0.68**
	Significance	0	-	**0**
Trial 3	Pearson' Coef	0.61	0.68	1
	Significance	0	0	-

To complete this study, we compute the average luminance, the energy of Gabor features and the emotion valence for each image. Then we analysed the possible correlation between them and the SSVEP response for the images selected. The idea is to try to study the potential link between the SSVEP response and these low level features in order to better understand and analyze the emotional impact of images.

The energy of Gabor features is based on Gabor filters (S.E. Grigorescu, 2002) which are directly related to Gabor wavelets. The two-dimensional Gabor filter is defined by the function $g_{\lambda,\Theta,\varphi}(x,y)$ as the multiplication of a cosine/sine (even/odd) wave with a Gaussian window, as follows:

$$g_{\lambda,\Theta,\varphi}(x,y) = \cos(2\pi\frac{x'}{\lambda} + \varphi)\exp(\frac{-x'^2+\gamma^2 y'^2}{2\sigma^2}), \quad (1)$$

with $x' = x\cos\Theta + y\sin\Theta$ and $y' = y\cos\Theta - x\sin\Theta$.

For Gabor features, we considered 12 different angles $\Theta\,\epsilon\,[0,\pi[$ every $\frac{\pi}{12}$ and 2 phases $\varphi\,\epsilon\,\{0,-\frac{\pi}{2}\}$, leading to 24 filters. We chose an isotropic Gaussian ($\lambda = 1$) with standard deviation $\sigma = 0.56\lambda$. This choice is justified by the properties of the visual cortex that can be model with Gabor filter as said Grigorescu and al. (S.E. Grigorescu, 2002).

The energy of Gabor features is the combination of the results of the 12 filtering for each phase.

The luminance and the energy of Gabor features given in the tables 1 and 2 are the average for the values computed for each pixel. Considering the obtained results, we cannot conclude to a correlation between the SSVEP responses recorded and the low level features chosen. The result for the second trial and the average value of SSVEP response through the whole test is not relevant. This probably comes from the selected images which, on the contrary of IAPS ones does not provoke a strong emotion. We also think that more observers must be suitable and the correlation with other features could be tried as well, since the most important features may not have been in the tested set. Moreover, using more EEG electrodes and more complex signal processing techniques, to take into account the SSVEP response propagation from the occipital to the parietal and frontal areas of the cerebral cortex, as proposed in (Gary Garcia-Molina, 2013), more information about the valence and/or arousal of the emotion involved in the SSVEP response elicitation could be deduced. It is in fact demonstrated that the modulation of the SSVEP response, due to the user's affect state, changes across different scalp locations in correlation with the arousal and valence of the emotion (Kemp A. H., 2002).

Table 3. Correlation study between the emotion valence, the luminance, Gabor energy and the SSVEP responses of the images used for our tests: Duration time t=1s. The average SSVEP response presented in this table corresponds to the mean response compute through the tree trials.

		Valence	**Luminance**	**Gabor energy**
Trial 1	Pearson' Coef	-0.15	0.14	0.13
	Significance	0.30	0.33	0.39
Trial 2	Pearson' Coef	-0.17	0.12	0.08
	Significance	0.25	0.43	0.61
Trial 3	Pearson' Coef	-0.03	0.04	0.09
	Significance	0.82	0.80	0.53
Average	Pearson' Coef	-0.13	0.12	0.11
	Significance	0.34	0.43	0.44

Table 4. Correlation study between the emotion valence, the luminance, Gabor energy and the SSVEP responses of the images used for our tests: Duration time t=8s. The average SSVEP response presented in this table corresponds to the mean response compute through the tree trials.

		Valence	**Luminance**	**Gabor energy**
Trial 1	Pearson' Coef	-0.16	-0.24	0
	Significance	0.27	0.10	1
Trial 2	Pearson' Coef	0.07	**-0.33**	0.13
	Significance	0.65	**0.02**	0.36
Trial 3	Pearson' Coef	0.01	-0.07	-0.10
	Significance	0.95	0.63	0.51
Average	Pearson' Coef	0.23	-0.27	0.02
	Significance	0.11	0.06	0.87

3. CONCLUSIONS

From this study we can confirm that for the used natural images there is a clear and strong correlation between the pictures and the SSVEP response elicited in the observers.

On the other side, we cannot at this stage identify which are the main image features modulating the SSVEP response; a clear statistical significance could be reached performing the experiment on a higher number of subjects and/or using a higher number of images.

Due to the kind of our database, it could be interesting also to plan new evaluations with the aid of an "eyetracker" to study during the observation duration the change in the SSVEP response according to the gaze region.

REFERENCES

François-Benoît Vialatte, M. M. (2010). Steady-state visually evoked potentials : focus on essential paradigms and future perspectives. *Progress in neurobiology, 90*(4), 418-438.

Gary Garcia-Molina, T. T. (2013). Emotional brain–computer interfaces. *International Journal of Autonomous and Adaptive Communications Systems, 6*(1), 9-25.

Hovagim Bakardjian, T. T. (2011). Emotional faces boost up steady-state visual. *NeuroReport, 22*(3), 121–125.

Kemp A. H., G. M. (2002). Steady-State Visually Evoked Potential Topography during Processing. *NeuroImage, 17*(4), 1684-1692.

O. Friman, I. V. (2007). Multiple Channel Detection of Steady-State Visual Evoked Potentials for Brain-Computer Interfaces. *IEEE Transactions on Biomedical Engineering, 54*(4), 742-750.

P.J. Lang, M. B. (2008). *International affective picture system (IAPS): Affective ratings of pictures and instruction manual. Technical Report A-8.* University of Florida.

Paolo Toffanin, R. d. (2009). Using frequency tagging to quantify attentional deployment in a visual divided attention task. *International Journal of Psychophysiology, 72*(3), 289-298.

Regan, D. (2009). Some early uses of evoked brain responses in investigations of human visual function. *Vision Research, 49*(9), 882–897.

S.E. Grigorescu, N. P. (2002). Comparison of texture features based on gabor filters. *IEEE Transactions on Image Processing, 11*(10), 1160 – 1167,.

Syntyche Gbèhounou, F. L.-M. (2013). Can Salient Interest Regions Resume Emotional Impact of an Image? *Lecture Notes in Computer Science , 12*(4), pp. 515-522.

Wang Shangfei, W. G. (2013). Analysis of Affective Effects on Steady-State Visual Evoked Potential Responses. *Advances in Intelligent Systems and Computing, 194*, 757-766.

Yee Joon Kim, M. G. (2006). Attention induces synchronization-based response gain in steady-state visual evoked potentials. *Nature neuroscience, 10*(1), 117-125.

Zhu, G. G.-M. (2011). Optimal spatial filtering for the steady state visual evoked potential :BCI application. *5th International IEEE/EMBS Conference on Neural Engineering*, (pp. 156-160).

MY OWN COLOURS

KRISTIINA NYRHINEN

“The nature has always been the most important source for the art in Finland.”

Is this the truth or is it a cliché or a mantra that we Finns keep on repeating, while we have the opportunity to tell someone about our art.

The truth is that we as a country have a large surface, but we are small in population. The countryside surrounds every city, even the capital is close to the nature. It takes less than an hour to be on the fields and forests alone or enjoy solitude on the small island nearby.

In my generation almost everyone has roots in the countryside, grandparents and relatives still live there. Also many families living in the city have a little summer cottage somewhere in the woods, isolated by the lake.

I lived my childhood in the countryside by a large lake. The changes of the four seasons were easy to observe there. The first signs of the spring were seen in the lighter colours and brightening light. Suddenly the ice disappeared and the lake was blue and glittering again. Also in the autumn when the funny scratchy noise was heard from the lake as a fanfare before the first cold night and a very thin ice was formed on the lake. The winter had come.

Now I live and work in a city close to the capital but still in the forest. I can’t feel the changes of the seasons so easily and clearly as before. I’ve grown to know the seasons inside me and I can see its influence in my artwork. I don’t know the trees and vegetable world very good but I enjoy the atmosphere and the colouring of the forest and meadows.

My early work, the huge, transparent textiles, in the public buildings was highly influenced by the big lake near my home and water in general. I’ve used water like materials and shades to reflect the rich palette of the water.

In my childhood I’ve looked my mother planting and watering plants in the garden. From her garden she harvested vegetables for the table and flowers for the eyes.. And now in three years time I have a small patch of land of my own where I care for my peonies and lilies. Now my textile works have changed a lot. I’ve studied flower petals, how they grow and fade away. And I’ve noticed that the form becomes more exciting and the colours become darker. I reflect the garden of my mothers in my art, the hues of blue, red and yellow. I work with the metaphor of ageing and fading-out.

I have focused in three main ideas in my poster: the nature, water and ageing and fading-out.

My earliest memories from my childhood are the short moments in the nature; I’m walking on a small path feeling the sun on my face and wind blowing and carrying the small grains of sand to my cheeks. I remember the colour and the shape of the sunspot on the wooden floor of my home when I’m sitting there with my colouring box. In wintertime when the lake was covered with ice and snow I used to ski there and wonder about the ultramarine shadows of the bushes. The lake was a great source of imagination. It had a huge amount of shades all around the year, ranging from clear blue to depressing grey to almost violent black, and all hues had a strong influence to the people who lived nearby.

All the other memories of my childhood consist memories of colours and sense of the materials. Through my eyes and the sense of touch the observation has been carved to my memory. Now, thinking back to my textile works I've realised my aim was to reach for the "golden" days of the free and happy childhood. I'm trying to build the solid scenery of my lost childhood what my adultery has separated for good.

In my textile work colour and material are equals. In my art the colour and the material unite essentially. When I begin to create and sketch something new, colour and material come hand in hand. I choose the material that brings out the best intensity in colours and brings the best result in realising the idea. The works for the public buildings have the special demands, concerning mostly materials and techniques the sustainability in general. I never compromise concerns the colours, I worked as long it took to find the best among the colour samples.

Transparency has always been characteristic in my work, either they are huge in close relationship with the architecture or tiny mini textiles. The lightness and many layers in textiles with different shades and different impressions seen from different angles always gives me great pleasure and satisfaction that only textile art can give.

I have to agree on the hypothesis that nature plays a great role in importance for the Finnish artist. My main goal is not to imitate the nature, but use it as a source and a key to my memory to catch the significant moments and emotional incidents in my life.

Water

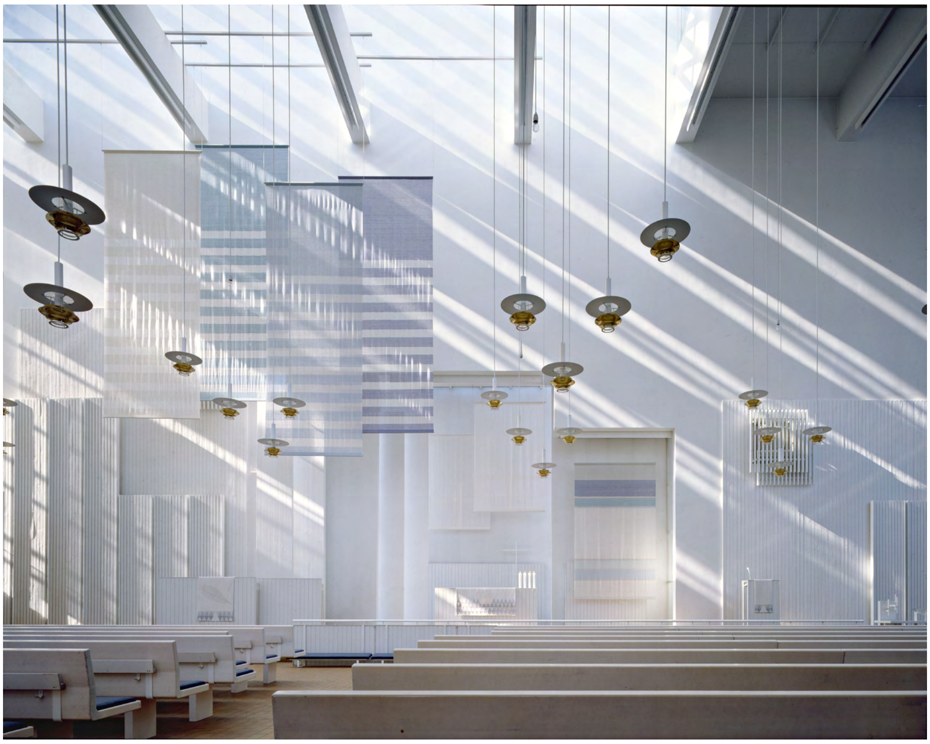

Myyrmäki Church, Textile Art Work by Kristiina Nyrhinen.
Architect Juha Leiviskä 1984

Nature

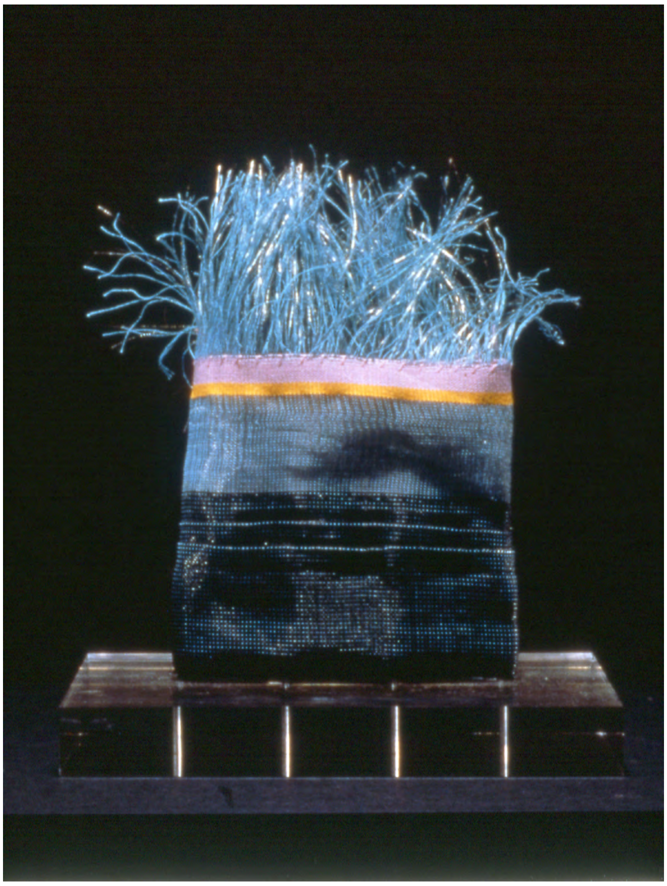

“The Wind in The Willows”

Contact:

Textile Artist

Kristiina Nyrhinen

Kristiina.nyrhinen@gmail.com

Suvikuja 3 A 10,

02120 Espoo

FINLAND

Hue and Tone Effects on Color Attractiveness in Mono-Color Design

Uravis TANGKIJVIWAT, Warawan MEKSUWAN,
Color Research Center, Rajamangala University of Technology Thanyaburi

ABSTRACT

In the marketing world, color of a product play an important role to catch a customer's attention. Althought a colorful object is more powerful to be attractive, a mono-color design is considered as competitor due to eco-anxiety. This research, hence, examined the influence of hue and tone on color attractiveness. Thirty-three color chips were chosen from the Munsell notation varying in hues and chromas. The results showed a vivid color was more attractive. In addition, warm colors were greater to draw attention than cool colors. Color appearance mode also affected to color attractiveness. Colors appearing in light source color mode and unnatural ojbect color mode were attracted. Furthurmore, we found that perceived color attributes related to color attractiveness.

1. INTRODUCTION

One cannot deny the fact that nowadays there are serious competitions in the market. Marketing practitioners know that a product's color may play an important role in a consumer's purchase decision (Grossman, 1999). About 62-90 percent of the assessment is based on color alone. So, prudent use of colors can contribute not only to differentiating products from competitors, but also to influencing moods and feelings –positively or negatively- and therefore, to attitude towards certain products (Singh, 2006). For building up a market share, designers must be created products which are interesting and attract the customer's attention.

One of the important roles for catching a customer's attention is to color attractiveness of product package. It indicates a characteristic that which product can be distinguished most clearly among various products. It said to be that a colorful package attracts a subject's attention and to arouse the desire to consume in marketing (Shun, 2001). Regarding the environmental conservation matter, ecological design, eco-design, seeks to conform to the environment and substantially reduce material consumption. Monochromatic design in printing has been noted as alternative technique as eco-design. Amount of ink on substrates for this design is less than that for color printing in the printing process. Moreover, this design reduces the printing troubles and cost of a product. Although monochromatic design seems to conform to eco-design, the color attractiveness is required for a product design. It would like to know how to catch customer's eyes with the monochromatic design. Several factors are said to be responsible for color attraction for instance differences in age, gender, culture and so on (Radeloff, 1990; Zellner, 2010). The major aim of this study, hence, is to investigate the effect of monochromatic color on attractiveness.

2. METHOD

2.1 Experimental Setting

As shown in Figure 1, the apparatus was composed of two rooms separated by a wall with a 1^{o} square aperture (T). The subject's room was covered inside with white wallpaper of about N9 and illuminated by daylight type fluorescent lamps (FL_S). The intensity of the lamps was adjusted by a light controller. The room illumination was measured by an illuminometer (I_S) placed on a shelf below the aperture at distance of 44 cm. Many objects such as artificial flowers, dolls, books, and dolls were put into this room. Color chips to serve as the test stimuli were attached to a rotating wheel placed in the test chart's room. They were also illuminated by adjustable daylight type fluorescent lamps (FL_T).

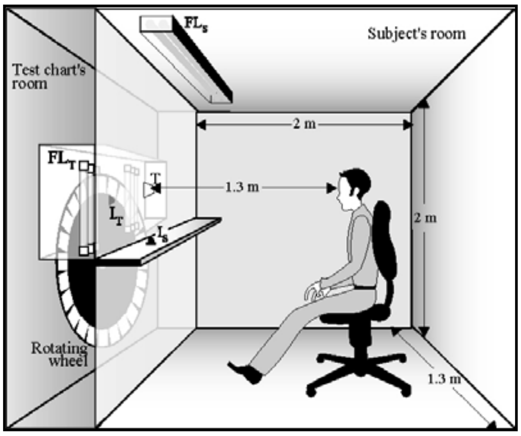

Figure 1: Schematic diagram of the apparatus

2.2 Color Stimuli and Conditions

Thirty-three color chips selected from the Munsell Color notation were used as the test stimuli. The color chips included one achromatic color (N5) and eight hues (5R, 5YR, 5Y, 5GY, 5G, 10BG, 10B, and 5P) varied in different chromas (2, 5, and 8). The Munsell value of all color chips was 5. The experimental conditions were composed of the combination of subject's room illuminance levels (50 and 500 lx) and test chart's room illuminance levels (500 and 700 lx).

2.3 Subjects

Five subjects ranging from 22 to 27 years in age took part in this experiment. All subjects had normal or corrected-to-normal visual acuity. They were screened for color deficiencies using the Ishihara plate.

2.2 Experimental Procedure

The subject sat in subject's room and looked at the test stimuli through the aperture from a distance of 130 cm. There were three tasks for each subject. In the first task, the subject was asked to assess the degree of color attractiveness for each color by using the scale which was divided into 6 levels, as -3 (do not attract) to +3 (extremely attract). The word "attractiveness" here means salient or conspicuous, which is to get attention of viewers. In the second task, the subject judged the color appearance mode of each color chip as object color mode (OB-mode), unnatural object color mode (UN-mode), and light source color mode (LS-mode). And the last one, the subject was asked to assess the amount of chromaticness, whiteness, and blackness for each color chip base on the NCS. These three components have 100% in total. Within each session, 16 or 17 color chips were randomly presented under four conditions to make 96 or 102 judgments. Each subject has done three sessions per condition. No time limits were set for making the judgments. Subjects were tested individually.

3. RESULTS AND DISCUSSION

For each color chip, the attractiveness scores for the five subjects were averaged. As shown in Figure 2, the mean score for each color chip is plotted against different Munsell chromas. Results showed that the higher the chroma of the color chip, the higher the attractiveness score, regardless of hues. For instance, the mean score of chroma 2, 5, 8 and maximum under $I_S50:I_T500$ condition are -0.1, 1.1, 2.0, and 2.7, respectively. Therefore, it was found that the vivid color attracts subject's attention. The same tendency occurred in all conditions. Our result agreen well with previous researches. Tanaka *et al.* (2000) proposed that chroma is linearly correlated to attractiveness. In our results, moreover, warm colors such as 5R, 5YR, 5Y and 5P were greater to draw attention than cool colors. Many previous researches reported that warm colors are considered arousing (Bellizzi and Hite, 1992; Cahoon, 1969) and active (Madden *et al.*, 2000; Richards and David, 2005), and lead to higher levels of anxiety (Jacobs and Suess, 1975). Tanaka *et al.* (2000) suggested that the closer the hue of a color to red was, the more salient the color would be.

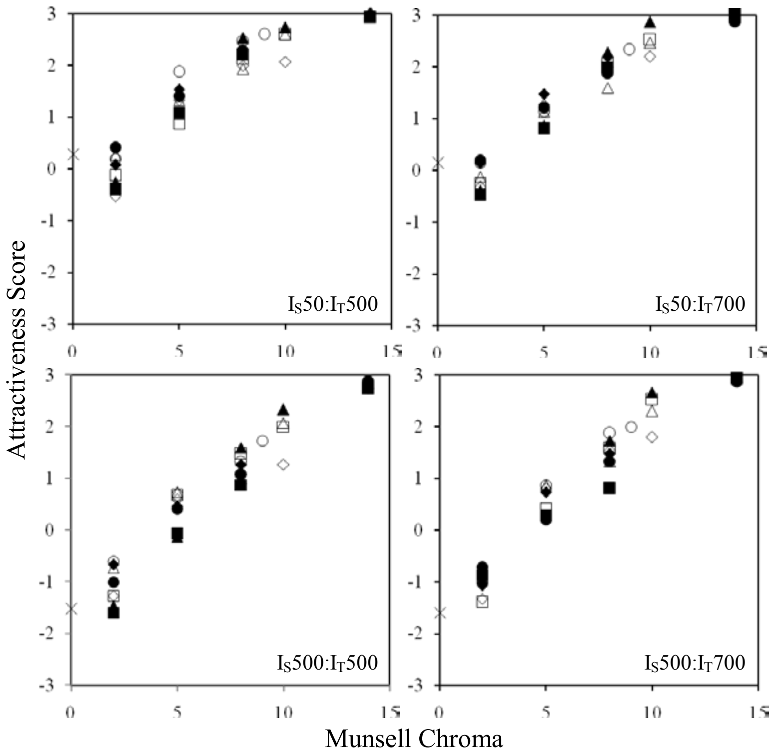

Figure 2: The attractiveness score from average result across all subjects by plotting against Munsell chroma for different Munsell hues; 5R(◆), 5YR(●), 5Y(■), 5GY(▲), 5G(◇), 10BG(○), 10B(□), 5P(△), N5(×).

Because a perception of color varies in a different illuminations, an effect of color apperance mode on attractiveness was considered. The color apperance mode judgment accummulated from all subjects were expressed in term of the color apperance mode index (i_{CAM}) by following equation:

$$\text{Color appearance mode index } (i_{CAM}) = \frac{-1(N_{OB}) + 0(N_{UN}) + 1(N_{LS})}{N_{OB} + N_{UN} + N_{LS}} \quad ,(1)$$

where N_{OB}, N_{UN}, and N_{LS} are the numbers of response in OB mode, UN mode, and LS mode. If $i_{CAM} > 0.5$, the color chip is classified in LS mode; if $i_{CAM} < -0.5$, UN mode; and if $-0.5 < i_{CAM} < 0.5$, OB mode.

Table 1. Mean and Standard Deviation of the attractiveness score across eight hues.

	$I_S50{:}I_T500$		$I_S50{:}I_T700$		$I_S500{:}I_T500$		$I_S500{:}I_T700$	
Chroma	Mean	SD	Mean	SD	Mean	SD	Mean	SD
2	-0.1	0.26	-0.1	0.34	-1.1	0.38	-1.0	0.25
5	1.1	0.24	1.3	0.31	0.4	0.34	0.6	0.29
8	2.0	0.21	2.2	0.21	1.2	0.25	1.5	0.32
Maximun	2.7	0.31	2.7	0.30	2.2	0.56	2.5	0.43

Note. For each chroma, n = 120

In Figure 3, the mean attractiveness score for the color chips that appeared in the LS and UN modes were higher than those in OB mode. This showed that color that appeared in LS and UN modes paid attention to viewers. In a light source color and unnatural object color modes, subjects perceived color too bright than adjacent surrounding. The bright color with dimmed background is an outstanding color. This result agrees with previous results. Tanaka *et al.* (2000) reported that background has an influence over color attractiveness. However, Mackiewicz (2007) noticed that a color of background had a little effect on viewers' ratings of the attractiveness of color combinations.

Next, possible correlations between color attractiveness and perceived color attributes were determined. The elementary color naming method was used to assess the perceived color attributes of the color chips in three color appearance modes. The amounts of the perceived color attributes were expressed as average values across all subjects for each color chip under each condition. In Figure 4, the attractiveness scores were plotted against perceived chromaticness, whiteness, and blackness. As shown in Figure 4 (a) and (b), it was found that the perceived blackness significantly related to the attractiveness score as negative correlation in OB mode (-0.854) and perceived whiteness in UN mode and LS mode (-0.879 and -0.889) as shown in Table 2. On the other hand, the attractiveness score increased with increasing perceived chromaticness as shown in Figure 4. There was a significant correlation between the perceived chromaticness and the attractiveness score in all color appearance modes. This result corresponded with the results of Munsell chroma. This showed that both physical chromaticness and perceived chromaticness have an influence over color attractiveness. Our result indicates that the color attractiveness may be described as the perceived color attributes.

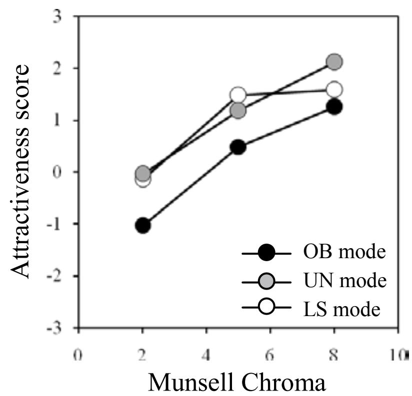

Figure 3: Mean color attractiveness plotted against Munsell chroma for different color appearance modes.

Table 2. Pearson correlation coefficients between attractiveness score and perceived color attributes.

	OB mode	UN mode	LS mode
Perceived chromaticness	0.924	0.960	0.948
Perceived whiteness	-0.785	-0.879	-0.889
Perceived blackness	-0.854	0.490	-0.698

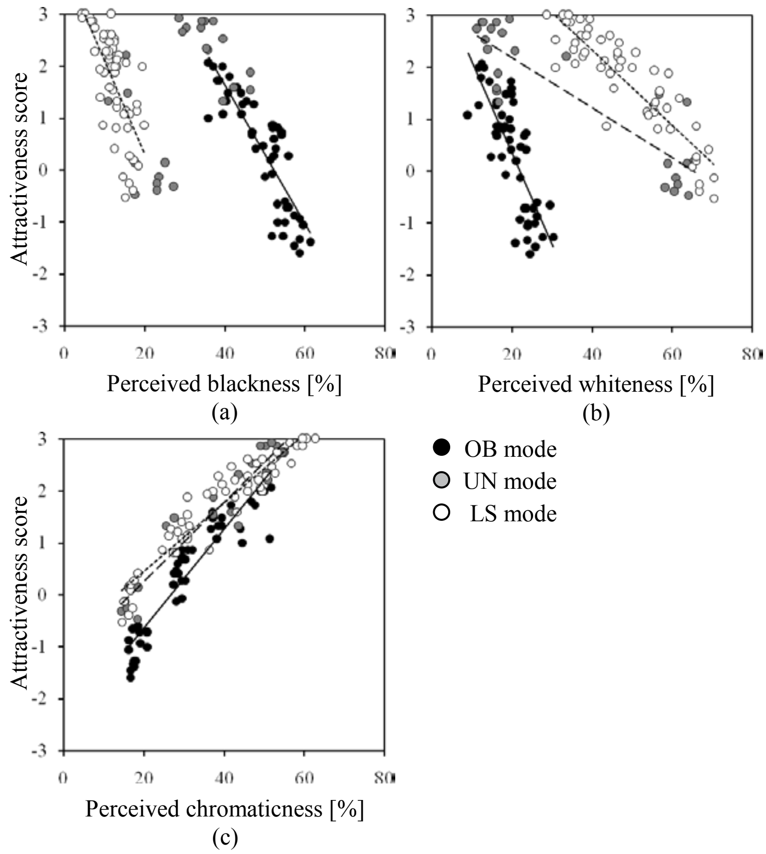

Figure 4: Scatter plot of attractiveness score and perceived color attributes: (a) perceived blackness, (b) perceived whiteness, and (c) perceived chromaticness.

4. CONCLUSIONS

In this study, thirty-three color chips varying in hues and tone were assessed under four conditions covered three color appearance modes. Findings showed that color with high chroma yielded higher attractiveness scores and warm color is to get attention of viewers. In a comparison among three color appearance modes, the color attractiveness in the unnatural object color mode and in light source color mode were significantly higher than those in the object color mode. Furthermore, the color attractiveness was significantly related to the perceived color attributes. They play a role as underlying mechanism on the determination of color attractiveness. Thus, it may be possible to use these components as a scale for predicting color attractiveness on the different color appearance modes. Our empirical finding delivers the idea to choose a proper hue and tone to get more attractiveness in mono-color design. However, this study is limited in color stimulus and a small number of subjects. In further research other factors are required for instance color combinations, tone combinations, a great number of subjects, circumstances, and so on.

REFERENCES

Bellizzi, J.A., and Hite, R.E. 1992. *Environmental color, consumer feelings, and purchase likelihood.* Journal of Psychology and Marketing 9(5) 347-363.

Cahoon, R.L. 1969. *Physiological arousal and time estimation.* Journal of Perceptual and Motor Skills 28(1) 259-268.

Grossman, R.P. and Wisenblit, J.Z. 1999. *What we know about customers' color choiese,* Journal of Marketing Practice: Applied Marketing Science 5(3) 78-88.

Jacobs, K.W., and Suess, J.F. 1975. *Effects of four psychological primary colors on anxiety state.* Journal of Perceptual and Motor Skills 41(1) 207-210.

Madden, T.J., Hewett, K., and Roth, M.S. 2000. *Managing images in different cultures: A cross-national study of color meanings and preferences.* Journal of International Marketing 8(4) 90-107.

Mackiewicz, J. 2007. *Perceptions of clarity and attractiveness in power point graph slides.* Journal of Technical Communication 54(2) 145-156.

Radeloff, D.J. 1999. *Role of color in perception of attractiveness.* Journal of Perceptual and Motor Skills 71(1) 151-160.

Richards, A., and David, C. 2005. *Decorative color as a rhetorical enhancement on the World Wide Web.* Journal of Technical Communication Quarterly 14(1) 31-48.

Shun, L.Y. 2001. *The effects of store environment on shopping behaviors: Acritical review.* Journal of Advances in Consumer Research 28(1) 190-197.

Singh, S. 2006. *Impact of color on marketing*, Journal of Management Decision 44(6) 786-789.

Tanaka, S., Iwadate, Y. And Inokuchi, S. 2000. *An attractiveness evaluation model based on the physical features of image regions,* In Pattern Recognition, *Proceedings,* ed. by A. Sanfeliu. Barcelona, 793-796.

Zellner, D.A., Lankford, M., Ambrose, L. and Locher, P. 2010. *Art on the plate: Effect of balance and color on attractiveness of, willingness to try and linking for food.* Journal of Food Quality and Preference 21(5) 575-578.

Address: Uravis TANGKIJVIWAT, Color Research Center,
Rajamangala University of Technology Thanyaburi,
39 Rangsit-Nakornayok Rd., Klong Hok, Thanyaburi, Pathumthani 12110 THAILAND
E-mails: uravis_t@yahoo.com

A study on silver metallic color preference
-A comparison of responses between Japanese and Thai people-

Mikiko KAWASUMI[1], Kamron YOUGSUE[2], Chanprapha PHUANGSUWAN[2], Kanrawee TAWONPAN[2], and Ken NISHINA[3]
[1] Faculty of Science and Technology, Meijo University, Japan
[2]Faculty of Mass Communication Technology, Rajamangala University of Technology Thanyaburi, Thailand
[3]Department of Techno-Business Administration, Nagoya Institute of Technology, Japan

ABSTRACT

This paper describes the outcome of the research on the comparative studies in Asian countries on silver metallic color preference of industrial products. We are doing research on the relationship between the customers' impression and the color of a products' surface. In this revised survey, we increased the number of the respondents in a wide range of age, and then compared the results between Japanese and Thai people. We could confirm the previous results in detail and some interesting topics were newly found.

1. INTRODUCTION

Japanese industries export various products such as cameras, games, laptops, etc., and those products are very popular in overseas markets. We've researched the designing conditions for more attractive surfaces of the industrial products in cooperation with a material manufacture. It is significant for us to understand the customers' visual preference for each product in each nation. The appearance of a product is one of the important factors for the customers' visual impressions. What kind of impression do you desire for metallic products? And what kind of silver metallic color do you prefer for each product? The desired impression and color preference of the customers may be different by age, gender and nationality. Manufacturers hope to develop the attractive metallic silver with a tint according to the customers' preference. In this survey, we've prepared every question of our questionnaire in Thai language in order to increase Thai respondents who live in local region including local elderly people. I'll show you the comparative results between Japanese and Thai people.

2. METHOD

A questionnaire was used for our investigation and written in Japanese, Thai, and English. Figure 1 shows a part of our questionnaire on the Web. Computer graphics were used to represent the metallic surface products such as a fridge and a DVD player. Those have slightly different silver colors: reddish, yellowish, bluish, and so on, and each of color was controlled in ten hues of the Munsell color system: **P**, **RP**, **R**, **YR**, **Y**, **GY**, **G**, **BG**, **B**, and **PB** (Figure 2). We set five target feelings: "clean / pure", "relaxing / comforting", "stylish / chic", "high-quality", and "favorite" as shown in Table 1, which were chosen as the most important feelings for the metallic product by Japanese customers in our previous investigation. We translated these English adjectives to Thai language carefully. The respondents answered with the color that they felt was the most "clean / pure", for example, for seven target products: a fridge, a television, a DVD player, a laptop computer, a digital camera, a smartphone, and a music player (Figure 3). Also, we asked other many questions such as the preference of gold / silver, the most important desired feelings, etc.

Figure 1: A part of questionnaire.

Table 1: Five target feelings.

in Japanese	in English	in Thai
清潔感のある	Clean / pure	สะอาด/บริสุทธิ์
スタイリッシュな	Stylish / chic	มีรสนิยม/แฟชั่น
上質な	High-quality	คุณภาพสูงสุด
落ち着いた	Relaxing / comforting	ผ่อนคลาย/สะดวกสบาย
好きな	Favorite	ชอบ

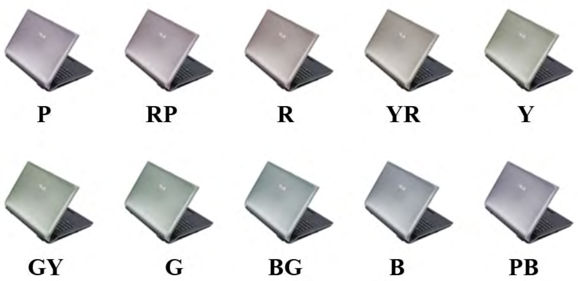

Figure 2: Ten colored products.

Figure 3: Seven target products.

Table 2: Number of respondents.

Nation	Male	Female	Total
Japan	213	207	421
Thailand	136	185	321
Total	349	392	742

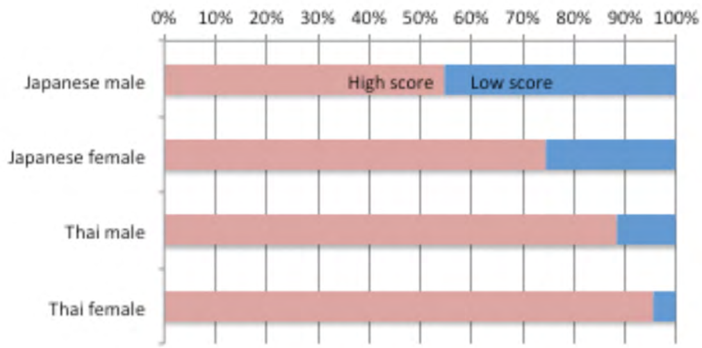

Figure 5: Percentage of persons with high color consciousness.

Rajamangala University of Technology Thanyaburi

Department of Social Welfare Development Center for Older Persons

Figure 4: Scenes of answering questionnaire.

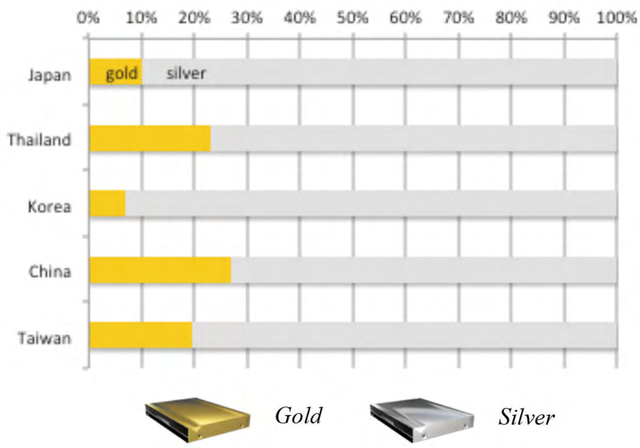

Figure 6: Which do you prefer, gold or silver?

We requested that the screen size of a computer should be not less than twelve inches, because it may be hard to distinguish the differences among ten hues on a small display. The required time was about twenty minutes on average for the people under forties. It took a lot of time over forty minutes for elderly people, because we instructed every question in their mother tongue in the next seat and wrote down each answer on the paper sheet, as shown in right side of Figure 4. We formed small groups, and several participants (3 – 6 persons) could answer at the same time. Finally, more than seven hundred persons from Japan and Thailand have cooperated with us in total (Table 2). Japanese people participated in Japanese questionnaire, and Thai people joined in Thai or English.

3. RESULTS AND DISCUSSION

Firstly, we newly found from other additional questions that Thai people's color consciousness is very high in comparison with Japanese, as shown in Figure 5. In Figure 6, you can see that most people prefer silver metallic color for the industrial products, though Thai people prefer gold more than Japanese. The necessity of more investigation about silver metallic color could be confirmed.

Figure 7 shows our main results, the comparative results for five feelings between Japanese and Thai people. The horizontal axis shows ten hues of the Munsell color system, and the vertical the percentage of choice for the hue. Different line types indicate seven target products. As the result, it became clear that both nationalities preferred the bluish silver color as the feeling of "clean / pure" in every product. Especially, Munsell **B** had the largest followers in both nations, and **BG** was also higher in Japan. Many Thai people selected **BG** in every product for "relaxing / comforting", in contrast, many Japanese selected **YR** and **B**. Also, Japanese and Thai people were similar in the tendency for "high-quality" and different for "stylish / chic".

Table 3 shows the correlation between "favorite" and other four feelings. We could confirm that "favorite" has strong correlations with "clean / pure" and "high-quality" in every product in Thailand. On the other hand, in Japan, you can see that it has a little bit strong correlation with "clean / pure" and "stylish" only in family-use products such as a fridge, a TV, and a DVD player.

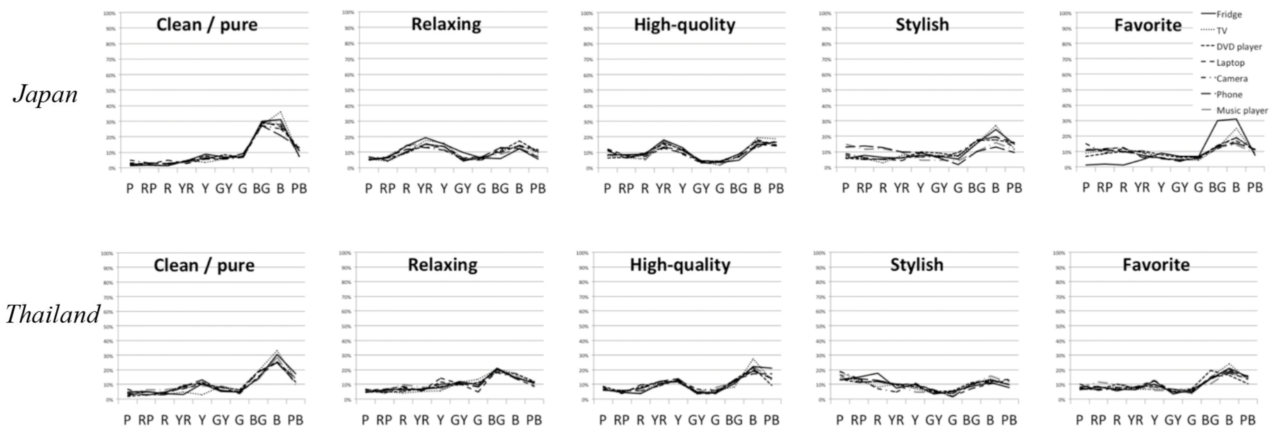

Figure 7: Comparative results between Japan and Thailand

Table 3: Correlation coefficient between "favorite" and other four adjectives.

Japan

	Clear / pure	Relaxing	High-quality	Stylish / chic
Fridge	0.51	0.02	0.06	0.51
TV	0.61	0.15	0.31	0.69
DVD player	0.65	0.57	0.57	0.59
PC	0.37	0.16	0.41	0.41
Camera	0.25	0.21	0.31	0.36
Smart phone	0.29	0.05	0.16	0.57
Music player	0.18	0.02	0.05	0.20

Thailand

	Clear / pure	Relaxing	High-quality	Stylish / chic
Fridge	0.92	0.28	0.84	0.01
TV	0.85	0.32	0.67	0.19
DVD player	0.75	0.62	0.56	0.19
PC	0.75	0.33	0.90	0.14
Camera	0.88	0.46	0.81	0.12
Smart phone	0.75	0.35	0.77	0.26
Music player	0.59	0.15	0.56	0.50

Table 4: Top ten of desired feeling for the metallic products

Japan

1	上質な (High-quality)
2	シンプルな (Simple)
3	清潔な (Clean)
4	スタイリッシュな (Stylish)
5	スマートな (Smart)
6	上品な (Elegant)
7	高級な (Luxurious)
8	美しい (Beautiful)
9	落ち着いた (Comforting)
10	カッコイイ (Cool)

Thailand

1	Fine-quality
2	Clean
3	Comforting
4	Modern
5	High-quality
6	Stylish
7	Smart
8	Luxurious
9	Creative
10	Classic

In addition, we asked about the important desired feelings for the metallic products by using adjectives at the ending of our questionnaire. Table 4 shows the top ten of adjectives that the respondents chose. Many Thai and other ASEAN people chose "modern" as the important desired feeling. But it is not included in the top twenty in Japan. We need to additionally examine the silver color preference that Thai people feel is the most "modern".

Moreover, we examined how much the response was affected by his/her "birthday color" in Thailand, because Thai people have his/her own special color depending on birthday that based on an ancient Buddhist wisdom. However those were not found to have a correlation.

4. CONCLUSIONS

We've examined the relationship between the customers' desired feelings and the surface colors of metallic products by an online survey, and our questionnaire was written in mother tongue for Japanese and Thai people. As the results, we could compare the characteristic of preference between two nations and some interesting topics were found. For instance, they have difference tendencies in "relaxing / comforting" and "stylish / chic".

The results from this survey are very useful for a manufacturer to fit the design concept in each nation. It is necessary for us to continuously analyze the data from cultural and social points of view and link to predict the customers' preference in future.

ACKNOWLEDGEMENTS

We appreciate the help received from Department of Social Welfare Development Center for Older Persons, Bureau of Social Welfare Services, Department of Social Development and Welfare, Ministry of Social Development and Human Security in Thailand, Rajamangala University of Technology Thanyaburi (RMUTT) in Thailand, Nagakute Silver Human Resources Center in Aichi in Japan, Meijo University, Nagoya Institute of Technology, and other many persons.

We wish to acknowledge valuable discussions with the members of Color Research Center in RMUTT in Thailand.

REFERENCES

Saito, M., 1994. *A cross-cultural study on color preference in three Asian cities: Comparison between Tokyo, Taipei and Tianjin.* Japanese psychological Research 36(4): 219-232.

Xin, J.H., Cheng, K.M., Taylor, G., Sato, T., Hansuebsai, A., 2004a. *Cross-Regional Comparison of Colour Emotions Part I, Part II: Quantitative Analysis.* Color Research and Application 29(6): 451-457, 458-466.

Kawasumi, M., 2013. *A Comparative Study in Asian Countries on Color Preference for Factory Products*. In 1st Conference of Asian Color Association, Proceedings, ed. by Payackso V., Thanyaburi: Rajamangala University of Technology Tanyaburi, 26-27.

Kawasumi, M., 2014. *Comparative studies in Asian countries on color preference of industrial products*. In 2nd conference of Asian Color Association, Proceedings, ed. by Tien-Rein LEE. Taipei: Chinese Culture University, 268-271.

Address: Mikiko Kawasumi,
Faculty of Science and Technology, Meijo University
1-501 Shiogamaguchi, Tempaku-ku, Nagoya 468-8502 JAPAN
E-mails: future@meijo-u.ac.jp, ykamron@gmail.com, karamennn@gmail.com,
ktawonpan@gmail.com, nishina@nitech.ac.jp

COLORS' RELATIONS TO OTHER THINGS IN MY WORKS

Helena LUPARI
Textile artist
Board member of Finnish Color association
Senior lecturer emerita (School of Arts, Design, and Architecture, Aalto University Department of Textile Arts)

I see my works in textile art as traveling through colors, shapes and materials. First I thought that technique was most important (I discovered how I can weave twelve layers´ fabrics).

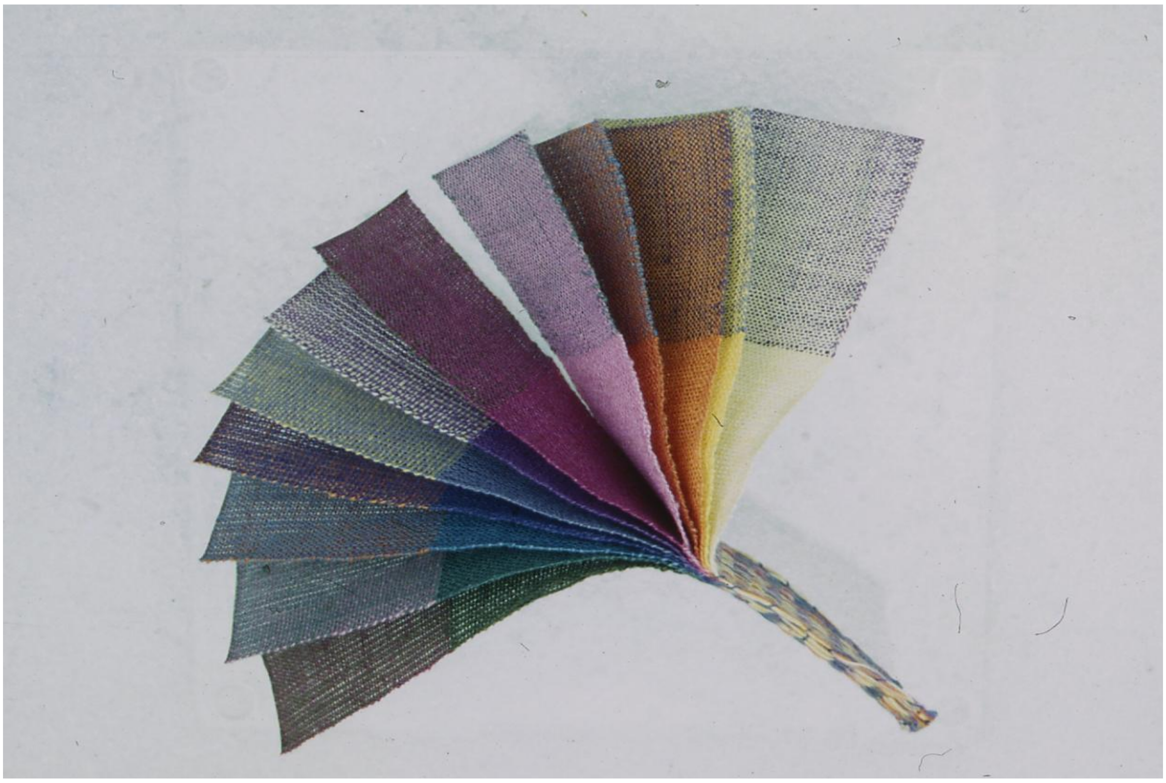

Now I'm more interested in how to get the color, the sculptural shape, the material and the light work well together, to give an emotional experience.

Making textile art is an endless way of questions:

How much I can think of myself, my ideas, my wishes, other people and all the demands of the commercial point of view. As for colors, everyone has his or her own color taste. Should I and can I give new experiences of it and what is the ultimate meaning of my work.

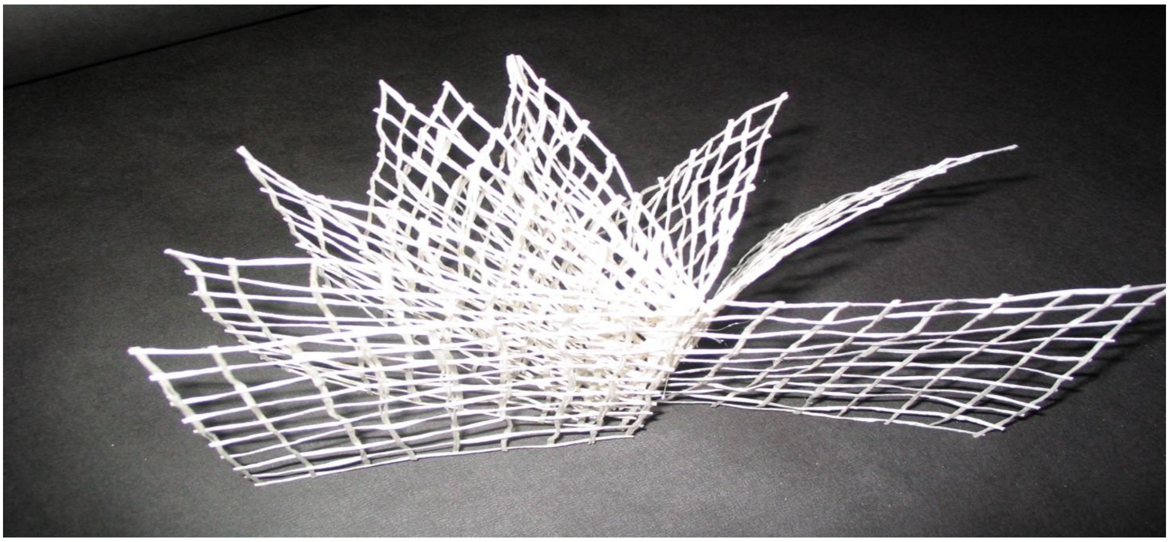

The art piece must be so strong that it takes its space where ever it will have its role in the future and the co-operation with the environment. How important is the color right now? Does it shout or whisper? Both shouting and whispering could be strong items. And the emotional point of view! Is it white clean and pure or black, dark or silent? For me the color is the first thing I see in an art piece. It opens the work.

It calls or draws you away.

I'm fascinated in architectural bridges. They lead you somewhere and at the same time they combine you with someone. They inspire me and when the structure is strong the color must support it like material does too. I found the Japanese flat silk yarn so sensitive and strong at the same time. I dyed it and it took the color precisely the way I wanted.

In textile Art there are so many ways to use color as a tool.

The color combinations are most demanding, can you make the colors alive and interesting new versions.

The right color gives more to the material but you can also kill the feeling.

The best thing in colors is that it is like poetry, you just have to let your imagination be free.

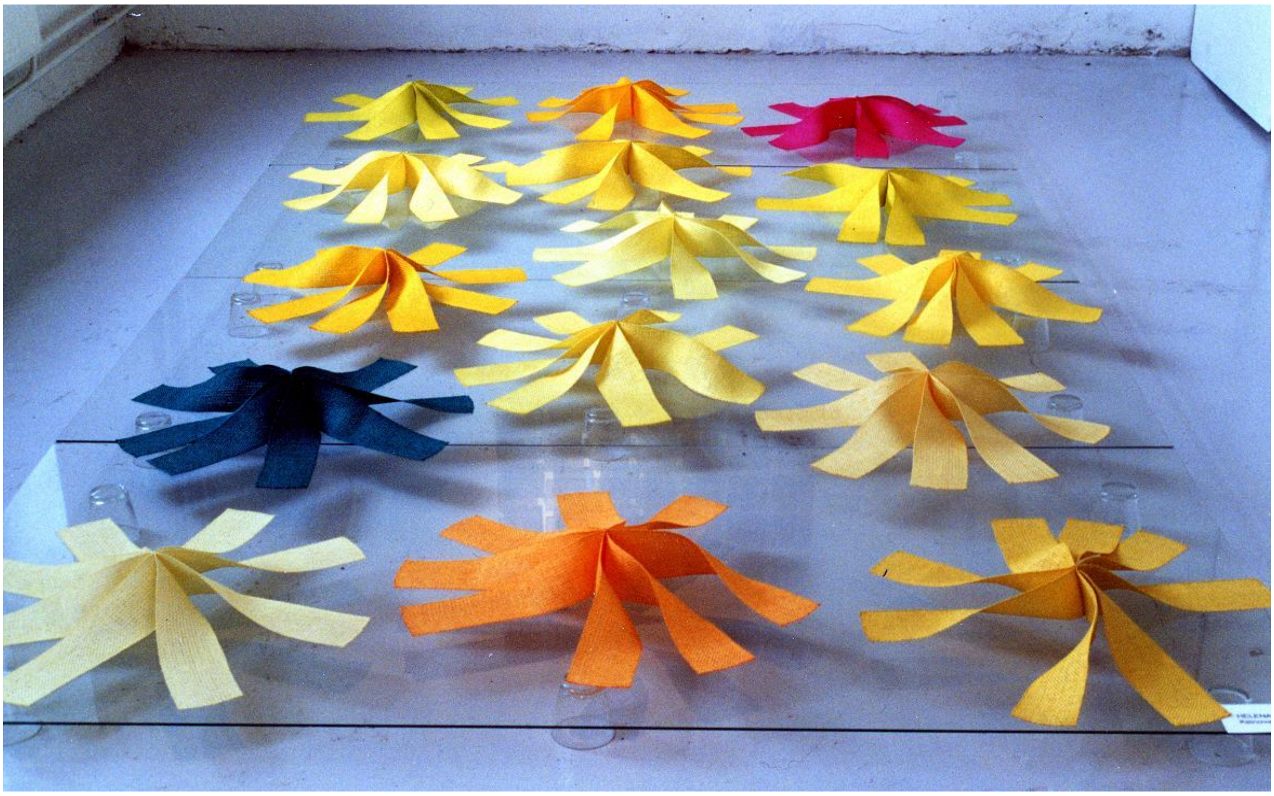

Address: Senior lecturer emerita Helena LUPARI,
Jokitie 12 C, 00780, Helsinki, FINLAND
E-mail: helena.lupari@kolumbus.fi

Color Preference of Preschoolers: Compared to Adults' Surmise

Wei-Chun HUNG, Pei-Li SUN, Li-Chen OU
Graduate Institute of Color and Illumination Technology, National Taiwan University of Science and Technology

ABSTRACT

The aim of this study is to investigate the color preferences of young children aged 4~5 and to compare with the viewpoint of adults in color preferences of the children. Based on the truth that preschoolers receive minor influence from environment comparing with adults, it's interesting to know as if adults' opinions agree with the young children'. The effects of gender and the association of objects also were analyzed. In this study, 15 color samples were chosen to produce color patches, mini T-shirts and candy-shaped packaging as test samples. The experimental results show there are gender differences in the preschoolers' color preferences. Age and the association of objects also influence the color preferences. Adults chose stereotype colors – pink for girls and blue for boys – especially in guessing the preschoolers' favorite color patches. However, the preschoolers prefer wide range of colors including neutral colors.

1. INTRODUCTION

Previous studies show that color preference of human varies across different culture (Choungourian, 1968), gender (Hurlbert and Ling, 2007), age (Taylor, Schloss, Palmer, and Franklin, 2013), race and educational background (Schloss, Strauss and Palmer, 2013). Personal experience and personality also would affect the choice of preferred colors (Palmer, and Schloss, 2010). In addition, the preference could be object dependent (Schloss, Strauss and Palmer, 2013). For example, an individual would prefer black shoes but dislike a black wash machine.

"Girls wear pink and boys wear blue" is one of gender stereotypes nowadays. However, before the 1920s, parents dressed infants and toddlers, girls and boys alike, in white dresses, suggesting that color and dresses were not used to distinguish between girls and boys (Chiu et al., 2006). Gender identity imposed by the parents might play an important role on the pink frilly dresses of girls (Ruble, Lurye, Zosuls, 2007). It is interesting to know the color preference of patches and dresses across different genders and different ages. The results will be useful for designing learning materials for children.

2. METHOD

A series of psychovisual experiments were conducted to investigate the preferred colors of preschoolers. Young adults also participated to the experiments for comparing the results. Three types of objects including color patch, T-shirt and candy-shaped packaging were used for preferred color selection. The independent variables of the experiments were Gender, Object Type, and Age Group.

2.1 Test Samples

In the experiments, every participant must select one of 15 colors to be his/her favorite color for each test session. The 15 colors include pure red (R), orange (O), yellow (Y), green (G), blue (B), purple (P), black (K), gray (Gy), white (W), plus six additional colors selected from Angela Wright's Personality Type 1 Morning Light Color (Wright, 1998) which is common used to produce children's products. It contains pink (LR), light orange (LO), light yellow (LY), light green (LG), light blue (LB) and light purple (LP). These six colors are relatively brighter and less saturate. 45(=15*3 repeated) color patches were printed out on uncoated papers using an inkjet printer and then folded them manually as the color patches, the mini T-shirts and the candy-shaped packaging respectively as shown as Figure 1.

Figure 1: Test samples: (a) color patches, (b) mini T-shirts, and (c) candy packaging

2.2 Experimental Setup

The experiments were conducted under a dark room. The participants were asked to fully adapt to the dark surround in front of a LED light booth with about 835 lux illuminance for two minutes. After the adaptation, the participants were asked to choose their preferred color of a set of samples inside the light booth. The participants divided into two age groups. The preschoolers include 19 children (10 male and 9 female) aged 4 to 5 from a kindergarten in Taipei. And the adults include 15 postgraduate students (9 males, 6 females) aged 23 to 25 from our university. All of them passed Ishihara color vision test. Each of them has to answer a questionnaire. The preschoolers have three sessions for choosing favorite color patch, mini T-shirt and candy packaging sequentially. However, the adults have four sessions including two sessions to choose their own favorite color patch and mini T-shirt, and two sessions to guess the favorite colors of boys and girls. Figure 2 show the sequence of answering the questionnaire of each test session for either the preschoolers or the adults.

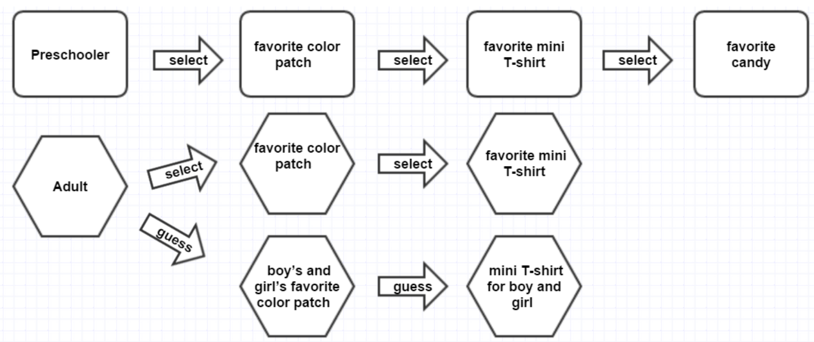

Figure 2: The sequence of answering the questionnaire for different test session.

3. RESULTS AND DISCUSSION

3.1 Gender Differences of Preschoolers

We would like to know whether the preschoolers have gender differences in color preferences. The preferred colors of the preschoolers for color patches listed in descending order are: pink, light green, light blue, light yellow, gray, white, light purple, red, purple, and blue (see Figure 3). Pink (34%) and light green (30%) are the most favorite colors for the girls and the boys respectively. Furthermore, the boys selected light blue (20%) as the second favorite color whereas the girls selected light yellow (22%) as the second. In comparison with the two genders, none of the boys like pink as their favorite color whereas girls are not interesting in green, but girls rank light blue (11%) as their third favorite color. Boys are interested in red more than girls and girls prefer light yellow more than boys. Light blue, gray, and white are favorite colors for both boys and girls. In general, the preschoolers prefer bright colors with low chroma. In summary, there are significant gender differences in preschoolers' color preferences based on Chi-square test on 4 color groups (pink, light blue, neutral colors and all the others).

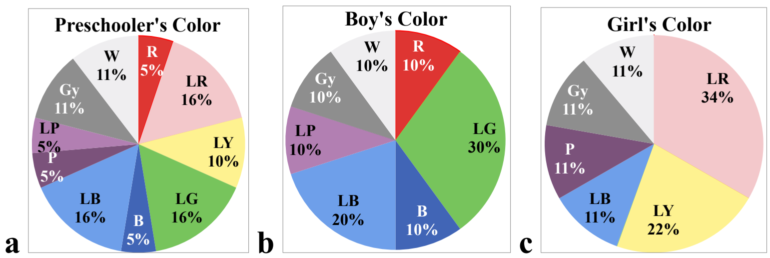

Figure 3: Color (patch) preference: (a) preschoolers, (b) boys, and (c) girls.

3.2 Preschoolers vs. Adults

We also would like to know whether age influenced the choice of favorite colors. The preferred colors of the adults listed in descending order are: light blue, pink, light green, red, orange, light orange, yellow, light yellow, green (see Figure 4). Pink (33%) and light blue (45%) are the most favorite colors for the females and the males respectively. It confirmes the stereotype colors for the two genders. Furthermore light blue are favorite for both males and females. In compared with the preschoolers (referring to Figure 3), adults also preferred light color. However, the latters are not interested in neutral colors. Adult has the same tendency as the preschoolers that males do not like pink whereas females are not interesting in green. In the top three chosen colors (light blue, light green and pink), adults and preschools are the same. Moreover, adults like orange and preschoolers like purple and neutral colors. Regardless of age, females like pink (adult and preschooler both are 34%) and warm color, males like cool color more. Surprisingly, some preschoolers are interest in neutral color, and none of them like orange color. Light blue was preferred by all genders and age groups. In short, there are some age differences in color preferences.

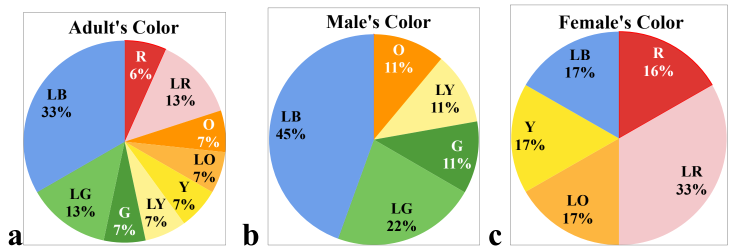

Figure 4: Color (patch) preference: (a) adults, (b) males, and (c) females.

The results of Chi-square test show insignificant differences between the proportional distributions of boy and girl subjects in color preference of warm and cool colors. Conversely, there is significant difference between the proportional distributions of male and female ($\chi 2$ =5.402, d.f. =1, p=.041). (see Figure 5)

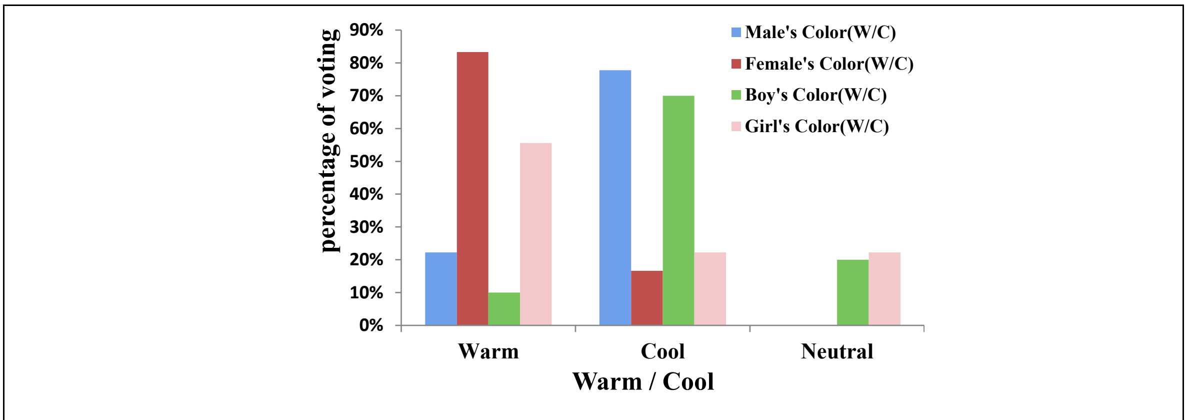

Figure 5:Color preferences (Warm/Cool) of males and females, boys and girls in percentage of each group.

3.3 The Impact of Object Type

We are interested to know if object type influencing the color preference significantly. Color preferences of different group of participants on T-shirts and candies are shown in Figure 6. As we can see, the boys prefer a T-shirt in black (30%) but the girls more like a T-shirt in white (23%). It seems that children like neutral colors when buying a T-shirt. Their secondary choice was light blue. The red, pink and orange are top three preferred colors of the candy packaging among the preschoolers. Boys like orange (20%) and girls like red (45%)and pink (44%) in choosing a candy. The result implies color and taste has some connection. A red or pink candy might taste sweeter in participants' memory. It should be a psychological effect. The results of Chi-square test show that the color preference of patch (p=0.001) and candy packaging (p=0.002) of the preschoolers have significant gender difference but T-shirt doesn't (p=0.09) at 95% confidence level. In terms of the effect of object types in the preschooler group, only T-shirt versus candy packaging for girls (p=0.003) have significant different color preferences. Moreover, in the adults group, color patch and T-shirt of both males and females show significant preferance differences. The males prefer a light blue T-shirt (45%) whereas the females like a red T-shirt (33%).

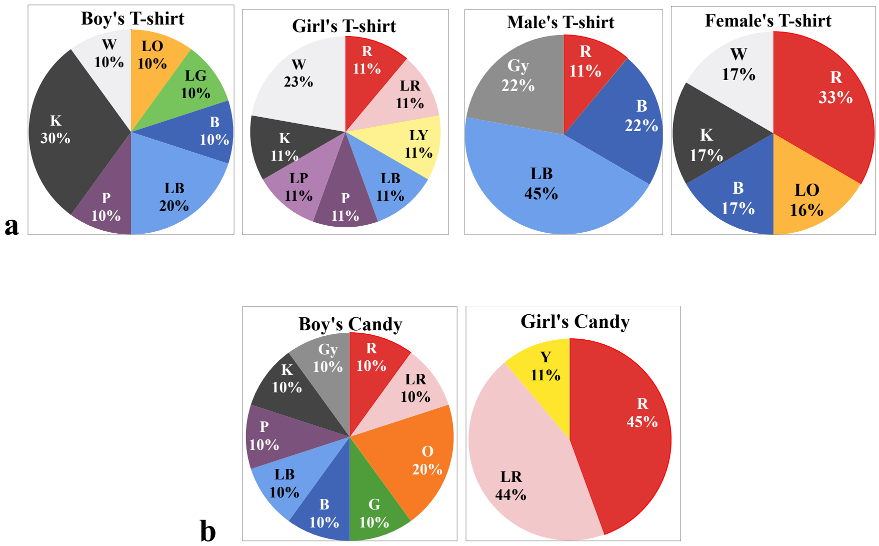

Figure 6: Color preference between objects. (a) T-shirts and (b) candies.

3.4 Adults' Surmise

We are also interested to know how accurate is the adults' surmise on preschoolers' color preferences on different type of objects. A comparison between Figure 3 and 7a confirms that adults picked stereotype colors for the preschoolers especially in guessing the preschoolers' favorite color patches. 73.3% adults surmised that the girls like Pink and 47% adults surmised that the boys like Blue (or light blue). The results are a little bit different from the preschoolers' shown in Figure 3. In reality, preschoolers chose more color categories such as gray and white. On the other hand, adults' surmise on the preschoolers' preferred T-shirt colors are quite inaccurate. The adults think the girls like light pink but in reality, the girls like a wide range of colors including white, black and purple (Figure 6a). The adults also think boys like light colors especially in light yellow and green. However, the boys prefer black instead of the light yellow.

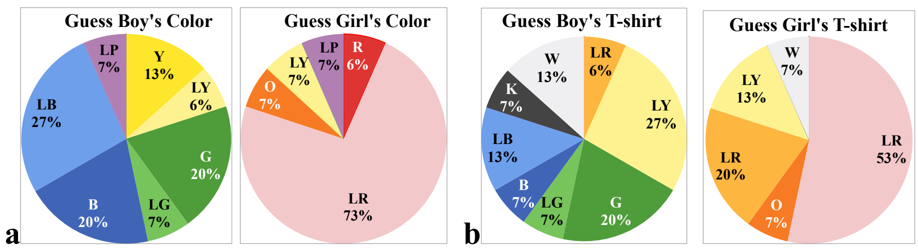

Figure 7: Adults' surmise on: (a) favorite color patch, and (b) favorite T-shirt color of the preschoolers.

4. CONCLUSIONS

This study aims to explore the color preferences of preschoolers and to compare with the viewpoint of adults in color preferences of the children, and the effects of gender, age and the association of objects also were investigated. The results show there are gender differences in the preschoolers' color preferences. Age and the association of objects also influence the color preferences to some degree. Adults chose stereotype colors – pink for girls and blue for boys – especially in guessing the preschoolers' favorite color patches. However, the preschoolers prefer wide range of colors including neutral colors. We hope the results can break the gender stereotypes, prompt product designers to rethink the color usage for children and let children select more neutral and variety of colors for their everyday life.

ACKNOWLEDGEMENTS

We sincerely thank Cheng-Hsun Chung, Wei-Wen Yuan, Yu-Wen Chiu, Yu-Cin Cai, Li-Ci Su, and Fan-Ling Hsiao for their assistance of this research.

REFERENCES

Chiu, S.W., Gervan, S., Fairbrother, C., Johnson, L.L, Owen-Anderson, A.F.H., Bradley, S.J, Zucker, K.J. 2006. *Sex-dimorphic color preference in children with gender identity disorder: A comparison in clinical and community controls*. Sex Roles, 55, 385-395.

Choungourian, A. 1968. *Color preferences and cultural variation.* Perceptual and Motor Skills, 26(3), 1203-1206.

Hurlbert, A. C., and Ling, Y. 2007. *Biological components of sex differences in color preference*. Current Biology, 17(16), R623 – R625.

Karp, E. M., and Karp, H. B. 1988. *Color Associations of Male and Female Fourth-Grade School Children*, The Journal of Psychology, 122 (4), 383-388.

Palmer, S. E. and Schloss, K. B. 2010. *An ecological valence theory of human color Preference*, Proceedings of the National Academy of Sciences USA 107(19), 8877 – 8882.

Ruble D.N., Lurye L.E., Zosuls K.M. 2015. *Pink frilly dresses (PFD) and early gender identit*y. Princeton Report on Knowledge, http://www.princeton.edu/prok/issues/2-2/pink_frilly.xml.

Schloss K.B., Strauss E.D., Palmer S.E.2013. *Object Color Preferences*. Color Research & Application 38(6), 393-411.

Taylor, C., Schloss, K., Palmer, S.E., and Franklin, A. 2013.*Color preferences in infants and adults are different*, Psychonomic Bulletin & Review 20(5), 916-922.

Wright, A. 1998. *The Beginner's Guide to Colour Psychology*, Colour Affects Ltd.

Ruble, D.N., Lurye, L.E., Zosuls, K.M. 2015. *Pink frilly dresses (PFD) and early gender identit*y. Princeton Report on Knowledge, http://www.princeton.edu/prok/issues/2-2/pink_frilly.xml.

Wright, A. 1998. *The Beginner's Guide to Colour Psychology*, Colour Affects Ltd.

Address: Wei-Chun HUNG, National Taiwan University of Science and Technology, No.43, Sec. 4, Keelung Rd., Da'an Dist., Taipei 10607,Taiwan
E-mails:m10325009@mail.ntust.edu.tw

Influence of the typical color in object memory task

Mikuko SASAKI, Yasuhiro KAWABATA
Department of Psychology, Graduate School of Letters, Hokkaido University

ABSTRACT

This paper presents the results of a study on changes in color memory. We presented colors from two adjacent color categories to participants, and found that color memory may change in the direction towards the typical color of each object when two object images of the same color are presented. On the other hand, no significant differences between the color conditions were found for objects that do not have a typical color. These results suggest that knowledge about an object's color may affect the recognition and categorization of the color.

1. INTRODUCTION

When people see the color of an object, they recognize it using their accumulated knowledge. Many studies have discussed the role of color in object memory (Tanaka, Weiskopf & Williams, 2001; Nagai & Yokosawa 2006). The color of an object is categorized immediately, and stored with its shape and texture in the memory trace. If the hue of an object is typically within a particular range, these information is stored with other knowledge of the object. As the color yellow comes to mind when one hears the word "lemon," colors that are strongly associated with objects are referred to as typical colors. Delk and Fillenbaum suggested that the knowledge of an object's typical color could indeed affect an object's color perception (Delk and Fillenbaum, 1965). Moreover, several studies have reported that when objects are presented in their typical colors, recall performance is higher than when objects are presented in non-typical colors (Ratner & McCarthy, 1990). In general, it is thought that objects presented in their typical color are stored in greater detail than are objects without a typical color. However, the accuracy of color memory based on typical color might be rather low. In addition, Mitterer and Ruiter (2008) reported that observers use knowledge of an object's color to recalibrate their color categories. But the role of typical color in color categorization is not enough discussed. Thus, the present study examines whether the degree of association object and its color influences categorization.

2. METHOD

In this experiment, we used as stimuli colors that are difficult to clearly categorize as (e.g., intermediate colors of red and orange). Images of two objects that have a typical color and an image of an object without a typical color were presented in the same color. We compared the amount and direction of change in memory for each condition. We additionally examined whether color categories determined by using color chips are the same as when determined using object images. From these results, we consider the effect of typical color on categorization of color memory.

2.1 Participants

A total 68 students (67 Japanese, 1 Chinese, 28 male, 40 female, average age = 20.3 ± 1.3) participated in this experiment.

2.2 Stimulus

In the memory task, 18 photo images of familiar objects were prepared as stimuli. These images were classified into an A, B, or C condition depending on the color property of the objects (Figure 1). Conditions A and B consisted of objects that have a typical color. The typical colors of the objects in conditions A and B were adjacent, such as red and orange. If the image in condition A was a tomato, for example, condition B was a persimmon. There were 6 pairs of stimuli in conditions A and B. The objects classified into condition C did not have a typical color. In addition, the three object conditions were presented with two color conditions of consisting of colors intermediate from the typical and non-typical colors of objects A and B. The objects and their typical colors are listed in Table 1. Participants performed two of these six conditions. In addition, 7 color selection charts were created for each condition (Figure 2). In each chart, the correct color and six other neighboring colors were indicated: three neighboring colors clockwise from the correct on the Mansell hue ring were selected, and three colors counterclockwise from correct color on the Mansell Hue ring were selected. The color difference ΔE (the L*a*b* color space) between each chart was about 13.6 on average. In the color categorization task, 48 colors, including the same color used in the memory tasks and those on the color charts, were selected as stimuli for assessing color categorization.

Table 1. Stimulus objects of the 3 object conditions.

	Red-Orange	Orange-Yellow	Yellow-Light green	Green-Blue green	Blue-Violet	Purple-Red purple
Object A	tomato	orange	banana	cucumber	grape	eggplant
Object B	persimmon	lemon	peas	ramune bottle	blueberry	red radish
Object C	tea pot	cap	flash light	polo shirt	camera	ribbon

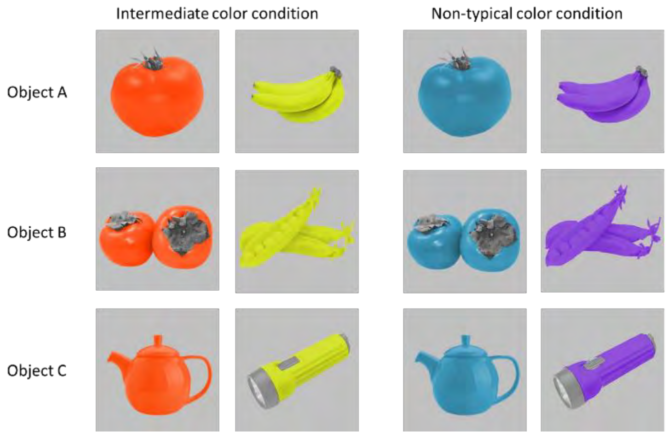

Figure 1. Example of stimulus images.

Firure 2. Example of a screen in color recognition task.

2.3 Experimental Procedure

After instruction, participants began the memory task. All images were displayed on 24.1-inches LCD screen. The observation distance to the screen was 80 cm, and the view angle was 5-7 degrees. In this task, color images appeared for 2 sec each at the center of the screen, and the participants observed the image. A total of 12 color images were presented. Next, participants completes a 5-10 min interference task in which they subtracted two-digit numbers or practiced typewriting. After this interference task, all participants began the object recognition task. In the recognition task, participants were asked to select the object they observed during the memory task from the object list and mark it with a check. There were 24 object names, including the correct answer, on the list. Following this, the participants were asked to choose the color of the objects observed during the memory task. At first, grayscale images were displayed for 2 sec. Next, seven images of the same shape but painted in different colors were presented. These seven images appeared in random positions. The participants were instructed to indicate which object were same color as that presented during the memory task by clicking on the image with an optical mouse. When they clicked the mouse, the next trial began. There were a total of 12 trials. Then, participants were instructed to classify 48 color chips of the color category. The 48 color chips (3 cm × 3 cm) were singly presented at random, and participants were to indicate whether the presented color applied to any color category on the screen (see Figure 3). Nine color names and frames were presented on the screen, and participants were to move the color chips using the mouse. The color categories that were prepared in advance were red, orange, yellow, yellow-green, green, light blue, blue, purple, and brown. Participants were allowed to create a new category if they did not think any of the displayed categories were accurate. The experiment concluded following the color category task.

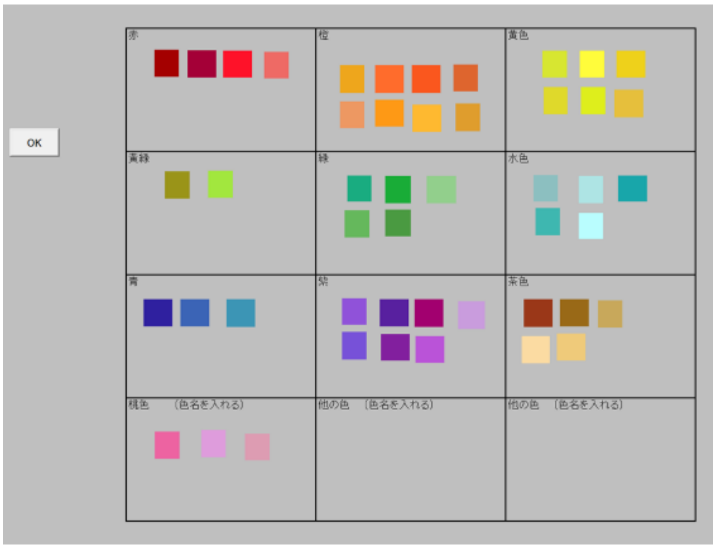

Figure 3. A screen example after color categorization task.

3. RESULTS AND DISCUSSION

To compare recognition of object names across the conditions, we calculated the number of correct objects participants selected from the list. The average of correct rates for each condition were compared in a 3 (object: object A, B, C) × 2 (color: intermediate vs non-typical) ANOVA. There was a significant effect of object [$F(2, 130) = 3.26$, $p < .05$]. Object A (93.6%) was associated with a significantly higher percentage of correct answers than was object C (85.8%). If an object was presented in a color close to the typical color of object A, recognition of the object name was better than objects without a typical color. Thus, when an object is associated with color, its color information facilitates recognition of the object.

Next, we investigated recognition of the object color rather than the object name. From the results of the recognition task, it was examined whether the selected color changed in either direction and how far it shifted from the stimulus color. The differences between the 12 selected colors and 12 stimulus colors were calculated using the L*a*b* color space. Change in direction was calculated as + changes clockwise on Mansell hue circle, and - changes in the counter-clockwise direction. The amount of change in each trial was analyzed AVOVA. There was a significant effect of color [F (1, 130) = 6.7, p < .05] (Figure. 4). Analysis results of the average change in direction did not indicate any significant effects of color and object, but did show a significant interaction [F (2, 130) = 7.16, p < .01]. Examination of the simple main effects revealed that in the close color to the typical color of objects A and B, the changes in direction were significantly different between objects A and B (p < .001), and objects A and C (p < .001). In addition, in the intermediate color condition of objects A and B, there was a clear change in direction relative to the non-typical color condition. The left side of Figure 4 indicates that in the object B condition, the direction changed to clockwise, and in the object A condition, it changed to counterclockwise. In addition, we calculated the number of different category cases between the stimulus color and the selected color in the color categorization task. Results of the $\chi 2$ test showed a significant difference between objects that have typical color and objects that do not have a typical color (p < .05). This suggests that when the participants viewed an object with a color close to the typical color, they selected a color belonging to a different category of the color they saw in the memory task. Thus, information regarding the typical color of an object influenced color category boundaries.

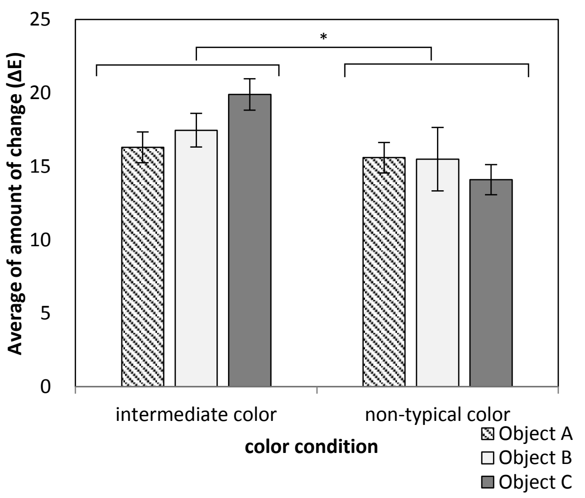

Figure 4. difference between stimuli color and selected color.

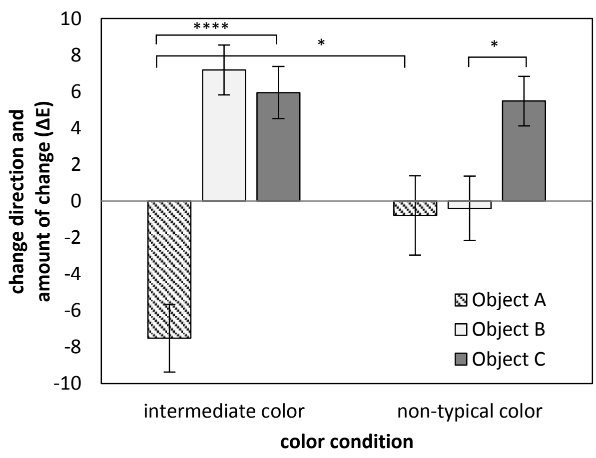

Figure 5 change direction and amount of change.

4. CONCLUSIONS

From these experiments, it has become clear that human color memory shifts to its own typical color of the object when 2 objects of a different typical color are painted with an intermediate color. Moreover, the present results suggest that in the case of objects that do not have a typical color, color condition does not impact memory. It is suggested that the strength of an association between an object and its color involves the accuracy of color memory. Further, it is possible that information regarding the representative color does not necessarily promote accuracy of detailed color memory. In the object condition that have a typical color, the participants often selected a color that belong a different category from a stimulus color's one. Colors close to an object's typical color promote readjustment of color category boundaries when recognizing the object.

REFERENCES

Delk, J.L., & S. Fillenbaum. 1965. Differences in perceived color as a function of characteristic color. *American Journal of Psychology* 78: 290–293.

Mitterer, H., J.P. Ruiter. 2008. Recalibrating Color Categories Using World Knowledge. *Psychological Science* 19(7): 629-634.

Nagai, J., K. Yokosawa. 2006. Color diagnosticity or category: Which determines the role of color in visual object recognition?. *The Japanese Journal of Cognitive Psychology* 3(2): 181-192.

Ratner, C., & J. McCarthy. 1990. Ecologically relevant stimuli and color memory. *Journal of General Psychology* 117: 369-377.

Tanaka, J., D. Weiskopf, & P. Williams. 2001. The role of color in high-level vision. *Trends in Cognitive Sciences* 5: 211–215.

Address: Mikuko SASAKI & Yasuhiro KAWABATA,
Department of Psychology, Graduate School of Letters, Hokkaido University,
Kita 10 Nishi 7, Kita-ku, Sapporo, 060-0810, JAPAN
E-mails: sasaki-m@let.hokudai.ac.jp, kawabata@let.hokudai.ac.jp

Neural basis of color harmony and disharmony based on two-color combination

Takashi IKEDA,[1] Naoyuki OSAKA[2]
[1] Graduate School of Engineering, Osaka University
[2] Graduate School of Letters, Kyoto University

ABSTRACT

Prior to functional imaging study, individual color harmony scores were determined by rating experiment. Each participant rated 351 two-color combinations stimuli presented against a gray background on a 9-point scale. Based on the results, we made individual data sets for each participant to optimise the subjective experience of color harmony and disharmony; then we selected 30 stimuli in each class according to highest, middle, and lowest scores. We conducted functional magnetic resonance imaging to determine the brain regions activated by harmonious and disharmonious color combinations in comparison to neutral combination. Each participant was instructed to rate a stimulus on a 3-point scale. During the presentation of Harmony stimuli, we found that the left medial orbitofrontal cortex was activated, while, bilateral amygdala and right inferior frontal gyrus were activated under the presentation of Disharmony stimuli. To quantify the relationship of two colors, we introduced five indexes based on CIELAB color space, i.e. difference in lightness (ΔL^*), mean lightness ($meanL^*$), difference in chroma (ΔC^*), mean chroma ($meanC^*$), and difference in hue (ΔH^*). This experiment revealed that there were no significant differences between Neutral and Harmony stimulus combinations, however, Disharmony stimulus had significant differences in ΔL^*, $meanL^*$, $meanC^*$ and ΔH^* in comparison to Harmony or Neutral. We found that color disharmony depended on perceptual properties of the actual stimulus. Taken together, our findings suggest that color disharmony depends on its stimulus properties and unconscious neural processes mediated by the amygdala, whereas color harmony is harder to discriminate based on color characteristics and is supported by processing aesthetic value within the medial orbitofrontal cortex.

1. INTRODUCTION

To make our daily lives more comfortable, we tend to gravitate toward harmonious color combinations. This can be seen in the clothing combinations we select, and so on. Research on color harmony theory has a long history. Theory of Colours, a book published by Goethe in 1810, established a wheel describing principal components of colors, which are consisted of three primary (yellow, red, and blue) and three secondary colors (orange, green, and violet); it was thought that harmonious relationships existed between colors that were opposite (complementary) each other on this wheel (Von Goethe 1970). Additionally, Munsell (1907) developed a color order system that was based on three perceptual properties: hue, value (lightness), and chroma. More recent study has focused on how to generate harmonious color combinations based on hue, chroma, and lightness using CIELAB to quantitatively assess differences in uniform color space (Ou and Luo 2006).

Previous studies revealed that color harmony could be predicted by these three properties. However, the neural mechanisms which underlie the aesthetic and emotional aspects of color, specifically harmony or disharmony, are still poorly understood. It is known that color information is first processed on the retina followed by higher visual cortices (McKeefry and Zeki 1997). Since, color harmony has been reported to exert a pleasing effect (Judd and Wyszecki 1963), brain regions activated by harmonious or disharmonious color combination should be able to process both perceptual and affective, in particular aesthetic aspects of color. Moreover, disharmonious color combinations might elicit an opposite, negative emotion.

Previous studies have indicated that color harmony can be influenced by many factors such as shape, size, the number of colors, and the relative positions of colors in a combination (Hård and Sivik 2001, Burchett 2002). Therefore, in the current study, we first examined the association between perceptual properties and color-harmony score with 351 color combinations presented against a gray background. The use of different pairs of color combinations allowed us to assess the relationship between two colors and the three perceptual properties: lightness, chroma, and hue. We then conducted functional magnetic resonance imaging (fMRI) to examine the brain regions which were activated during the presentation of harmonious and disharmonious combinations compared with the neutral stimuli. This method appears to be the simplest way to examine the neural correlates of aesthetic preference of color.

2. METHOD

2.1 Participants

Eighteen participants (6 females and 12 males, aged 19–30) attended the fMRI study All participants had normal or corrected-to-normal vision, and none had a history of neurological or psychiatric disorders. Moreover, none of the participants had any special experience with art or color design. We used Ishihara plates for the color vision test under a fluorescent light simulating D65 illuminant. Written informed consent was obtained from all participants, the experiments were conducted in accordance with the ethical guidelines of the Declaration of Helsinki, and all methodology was approved by the Committee of Medical Ethics, Graduate School of Medicine, Kyoto University.

2.2 Experimental Procedure

In the fMRI experiment, participants viewed stimuli on a screen projected (U2-X2000, PLUS Corporation, Japan) through a mirror attached to the head coil. Earplugs were used to reduce the noise from the MRI scanner. We calibrated the projector using a luminance colorimeter (CS-100A, Konica Minolta, Japan). We made a color palette that contained 27 colors (six hues across four tones and three achromatic colors, see Figure 1). These colors were chosen from the Practical Color Co-ordinate System (PCCS: developed by Japan Color Research Institute), which has been determined to be suitable for making harmonious color combinations.

From the results of the preliminary experiment, we made individual data sets for each participant to optimise the subjective experience of color harmony and disharmony; we selected 30 stimuli in each condition according to highest, middle, and lowest given scores individually.

The fMRI experiment was conducted in a 3-T MRI scanner (Trio, Siemens, Germany). A forehead strap and form pads were used to reduce head motion. Functional images were taken with a gradient echo echo-planar pulse sequence (TR = 2500 ms, TE = 30 ms; flip angle = 90°, voxel size = 3 mm × 3 mm × 3 mm; 36 axial slices). To minimise signal loss in the orbitofrontal cortex caused by local susceptibility gradients, we used a tilted acquisition sequence at 30° to the AC-PC line (Deichmann et al. 2003). Following the acquisition of functional images, anatomical T1-weighted images (MPRAGE sequence, voxel size = 0.94 mm × 0.94 mm × 1 mm, 208 slices) were collected.

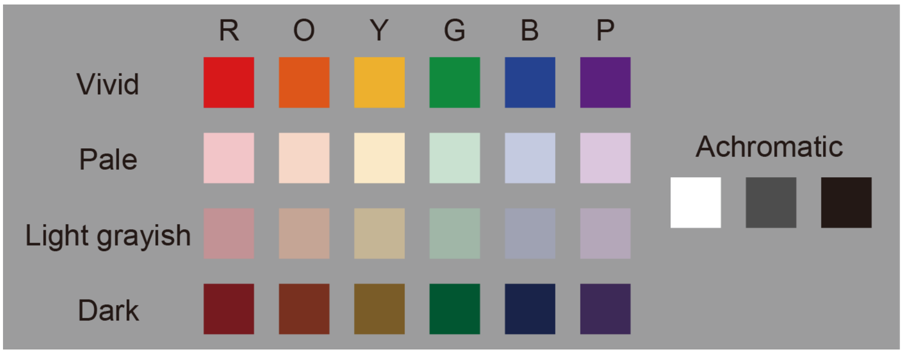

Figure 1: Color pallet used in this experiment.

Following the presentation of a black fixation cross (for 1000 ms), participants were instructed to rate a stimulus on a 3-point scale (1 = disharmony, 3 = harmony) within 2500 ms by pressing three buttons on the response box in their right hand. After the rating, we set a pseudo-randomised inter-trial interval (2000, 2500, or 3000 ms) before starting the next trial. Participants rated for 180 trials (30 stimuli × 3 data sets × 2 repetitions) and 60 catch trials in which they had to press any button as soon as the black fixation point turned white. All trials were presented in a pseudo-randomised order.

2.3 Image Processing and Analysis

Image processing and analysis were performed using SPM8 (Wellcome Department of Cognitive Neurology, London, UK) running on MATLAB (MathWorks Inc., Sherborn, MA, USA). First, we conducted slice acquisition timing correction to functional images. These images were realigned to the mean image for correction of head movement. T1-weighted anatomical images were then normalised to the MNI space, and its parameter was applied to normalise the realigned functional images. Images were then smoothed with an isotropic Gaussian kernel of 6-mm full width-half maximum, and low-frequency noise was removed using a high-pass filter (time constant 128 s).

Individual analysis was performed with a fixed effect model. Statistical parametric maps were calculated to identify voxels with event-related BOLD signal changes using the general linear model (GLM). Trials were classified into three conditions (Harmony, Neutral, and Disharmony) by the responses of each participant during functional scanning. Each event defined as the onset of a stimulus presentation was convolved with a canonical hemodynamic response function (HRF) to provide regressors for the GLM. Head movement parameters calculated in the realignment step and onsets of the catch trials convolved with HRF were included in this model as regressors of no interest. Lastly, contrast images for 'Harmony vs. Neutral' and 'Disharmony vs. Neutral' were run through a second-level *t*-test to make statistical maps at the group level. The statistical threshold was set at $p < 0.001$ (uncorrected).

3. RESULTS AND DISCUSSION

Table 1 shows activated regions during presentation of Harmony and Disharmony stimuli when compared to Neutral stimuli as baseline. During the presentation of Harmony stimuli, we found that the left medial orbitofrontal cortex (mOFC) was activated, while, bilateral amygdala and right inferior frontal gyrus were activated under the presentation of Disharmony stimuli (Figure 2). These results are reported as MNI coordinates.

Table 1. Activated areas in each contrast.

Contrast	Anatomical label	BA	Coordinates *x*	*y*	*z*	*Z*	*k*
Harmony > Neutral	Medial Orbitofrontal Cortex	10/11	-4	56	-2	3.53	9
Disharmony > Neutral	Cerebelum		22	-44	-36	5.53	57
	Inferior Frontal Cortex	45/47	50	32	-2	4.26	33
	Hippocampus		-20	-38	10	4.15	27
	Amygdala		-10	-4	-14	4.07	24
	Precentral Gyrus	6	56	-4	36	3.91	57
	Amygdala		20	-8	-20	3.78	14
	Anterior Cingurate Cortex	32	-6	48	14	3.71	24
	Middle Temporal Cortex	39	46	-56	20	3.70	21
	Cerebelum		-14	-50	-32	3.68	33
	Superior Temporal Cortex	39	46	-32	20	3.57	41
	Celeberum		14	-38	-32	3.56	14
	Middle Temporal Cortex	38	-60	-8	-20	3.53	15
	Inferior Frontal Cortex	45	42	22	12	3.45	14

(BA : Brodmann Area)

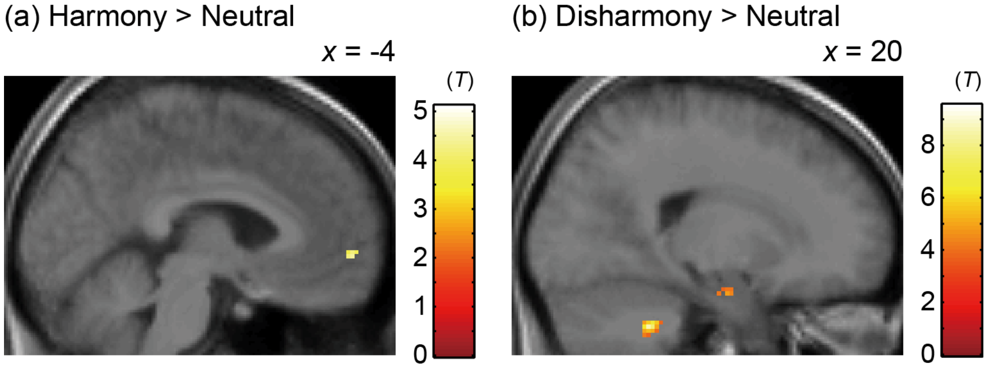

Figure 2: Statistical parametric maps rendered on a slice of T1-weighted image.

The fact that harmonious stimuli combinations activated the mOFC was consistent with previous studies showing that this region was activated when individuals felt an aesthetically pleasing experience in the musical context (Blood et al. 1999) and the visuo-spatial context (Kawabata and Zeki 2004, Vartanian and Goel 2004, Ishizu and Zeki 2011). Therefore, activation of the mOFC is not restricted to experiences of color harmony, but is involved in various aesthetic experiences regardless of modality.

We also found that disharmonious stimuli combinations activated bilateral amygdala and several cortical regions including the right IFC, anterior cingulate cortex, and middle/superior temporal cortex. It is well established that the amygdala plays an important role in evaluating the biological significance of affective visual stimuli. This subcortical region has been shown to activate when emotionally negative stimuli are presented, and furthermore, the activation of the amygdala might involve unconscious processing of affective visual stimuli (Pessoa and Adolphs 2010).

To quantify perceptual properties of two colors, we introduced five indexes made from CIELAB color space, i.e. difference in lightness (ΔL^*), mean lightness (*meanL**), difference in chroma (ΔC^*), mean chroma (*meanC**), and difference in hue (ΔH^*) (Note: we avoided using mean hue since we determined it to be an unsuitable index; for example, the mean hue of red and green is yellow). From the results of one-way ANOVAs, we determined that main effects of *meanL** [$F(2,34) = 24.44$, $p < 0.001$], ΔL^* [$F(2,34) = 14.08$, $p < 0.001$], *meanC** [$F(2,34) = 13.02$, $p < 0.001$], and ΔH^* [$F(2,34) = 23.04$, $p < 0.001$] were significant; however, the main effect of ΔC^* [$F(2,34) = 1.10$, $p = 0.344$] was not significant. Additionally, multiple comparisons using Shaffer's modified Bonferroni procedure revealed that there were significant differences between Disharmony and Neutral, and between Disharmony and Harmony ($p < 0.05$; Figure 3). However, there were no significant difference between Neutral vs. Harmony ($p > 0.05$) in any indexes. Perceptual characteristics of disharmonious stimuli were different from those of neutral and harmonious stimuli. This results suggest that disharmonious combination can be determined by perceptual characteristics, including darkness, saturation, and complementary color combination.

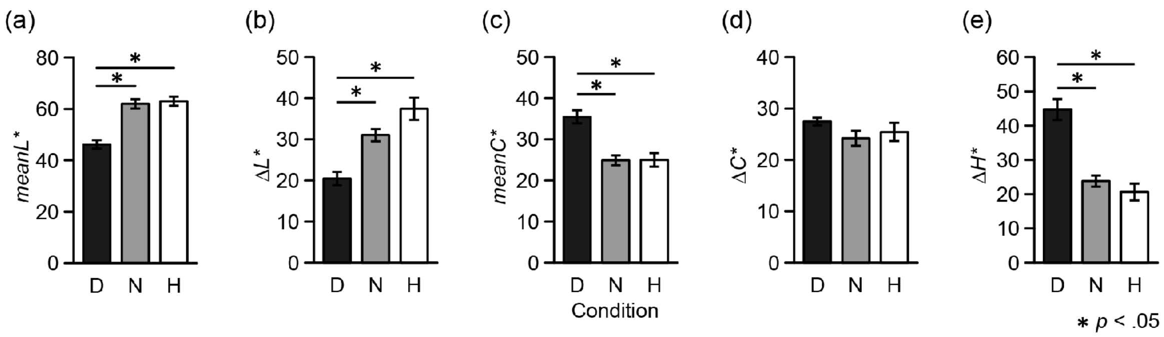

Figure 3: Five indexes of color combination stimuli across the three conditions.

Previous studies have treated the scoring of color harmony as a bipolar single scale; however, the results of our fMRI experiments suggest that color harmony contains two processes. First, color disharmony depends on the stimulus itself and the unconscious neural process that is mediated by the amygdala. In contrast, color harmony is hard to determine based on color characteristics alone, and this is supported by processing aesthetic value within the mOFC.

4. CONCLUSIONS

Harmonious color combination was represented in mOFC. However, amygdala was activated by a disharmonius color combination, which was easily determined by perceptual characteristics in the CIELAB color space. A bipolar single scale on color harmony might consist of independent neural mechanisms.

ACKNOWLEDGEMENTS

This work was supported by JSPS KAKENHI Grant Numbers 23700314, 22220003.

REFERENCES

Blood, A. J., R. J. Zatorre, P. Bermudez and A. C. Evans (1999). Emotional responses to pleasant and unpleasant music correlate with activity in paralimbic brain regions. *Nature Neuroscience* 2 (4): 382-387.

Burchett, K. E. (2002). Color harmony. *Color Research and Application* 27 (1): 28-31.

Deichmann, R., J. A. Gottfried, C. Hutton and R. Turner (2003). Optimized EPI for fMRI studies of the orbitofrontal cortex. *Neuroimage* 19 (2 Pt 1): 430-441.

Hård, A. and L. Sivik (2001). A theory of colors in combination - A descriptive model related to the NCS color-order system. *Color Research and Application* 26 (1): 4-28.

Ishizu, T. and S. Zeki (2011). Toward a brain-based theory of beauty. *PloS One* 6 (7): e21852.

Judd, D. B. and G. Wyszecki (1963). *Color in business, science, and industry*. New York, Wiley.

Kawabata, H. and S. Zeki (2004). Neural correlates of beauty. *Journal of Neurophysiology* 91 (4): 1699-1705.

McKeefry, D. J. and S. Zeki (1997). The position and topography of the human colour centre as revealed by functional magnetic resonance imaging. *Brain* 120: 2229-2242.

Munsell, A. H. (1907). *A color notation*. Boston, MA, Geo. H. Ellis Co.

Ou, L. C. and M. R. Luo (2006). A colour harmony model for two-colour combinations. *Color Research and Application* 31 (3): 191-204.

Pessoa, L. and R. Adolphs (2010). Emotion processing and the amygdala: from a 'low road' to 'many roads' of evaluating biological significance. *Nature Reviews: Neuroscience* 11 (11): 773-783.

Vartanian, O. and V. Goel (2004). Neuroanatomical correlates of aesthetic preference for paintings. *Neuroreport* 15 (5): 893-897.

Von Goethe, J. W. (1970). *Theory of colours*. Cambridge, MA, MIT Press.

Address: Takashi IKEDA, Ph.D., Graduate School of Engineering,
Osaka University, 2-1 Yamadaoka, Suita, Osaka, 565-0871, JAPAN
E-mails: tikeda@ams.eng.osaka-u.ac.jp, nosaka@bun.kyoto-u.ac.jp

Psychological hue circle of blind people and development of a tactile color tag for clothes

Saori OKUDERA, Ken SAGAWA, Yuko NAKAJIMA, Natsumi OHBA,
Shoko ASHIZAWA
Department of Clothing, Faculty of Human Science and Design,
Japan Women's University

ABSTRACT

Totally blind people have a strong interest in color though they are not able to see it. Women, in particular, like to know the color of their clothes and enjoy color coordination of their wear. In order to meet this need, psychological mechanism of color identification of blind people was investigated and a method to convey color information was developed by means of the tactile sense.

In the study of investigating color identification of the blind who has no experience of seeing color in his/her life, psychological distances (or distinctness) among a total of 10 fundamental colors (red, orange, yellow, … etc.) were measured in a 5 point scale from "very far" (point 5) to "very close" (point 1). From these perceptual distances and using the MDS (multi-dimensional scaling) method, a possible placing of those 10 colors was derived. The result obtained when averaged over 16 subjects was that the 10 fundamental colors showed a clear hue circle with exactly the same order of colors as those obtained for the sighted people.

On the basis of this experimental result, a tactile tag designed with a hue circle was developed in which ten small tactile dots were lined up on a circle each representing fundamental color with one bigger dot or hole to show the color for identification. Tactile experiments were done also to confirm the appropriate size of the color circle and a tactile dot size. And finally, a color tag was developed from a few materials (acrylic button, embroidery, and artificial leather) and was attached to a T-shirt for the field test which showed successful color identification by blind people.

1. INTRODUCTION

Color is one of the important information in our daily life not only for functional means such as traffic signals for safety but also for some emotional purpose like ladies' fashion. Unfortunately totally blind people are not able to use and enjoy those color information. This study was triggered by a request from a blind lady that she would like to know by herself the color of clothes she is wearing.

In order to develop a method to meet her request, a few questions were raised: (1) what is the effective way to let her know the color; voice or Braille or some other means, (2) how the blind person, the congenitally blind person in particular, understands the color, (3) what is the feasible way to apply the method to clothes.

The 2nd question is most interesting in color science, and some studies were already done (Shepard and Cooper, 1992; Shinn and Ohmi, 2012). Those studies provided us some important insight about the color recognition of the blind people. However, it was difficult to draw any definite conclusion and this lead us to the need for carrying out a new experiment which give us a directly useful result for developing a method for conveying color information to blind people.

In addition to this scientific interest, we were clearly aware that this type of study should extend to the level practically useful. This means the development of a color tag that can be attached to clothes. Tactile marking was one possible way to develop and the suitable design for this was investigated.

2. HUE CIRCLE OF BLIND PEOPLE

In order to investigate the identification and psychological representation of color in totally blind people, particualry in those who have never seen the color from the birth (congenitally blind), an experiment was carried out in which the psychological distances or distinctness of any two colors were scaled in 5 points scale, and by applying the multi-dimensional scaling (MDS) to those scaled distance data, the scheme of color of blind people was investigated.

2.1 Experiment

A total of 10 fundamental colors addressed in Munsell hue circle, such as red(R), orange(YR), yellow(Y), green-yellow(GY), green(G), blue-green(BG), blue(B), pueple-blue(PB), purple(P), and red-purple(RP), were selected as test colors and any two-colors combination was made by those fundamental colors and presented verbally to the subject who was totally blind. The subjet was asked how those two colors were considered different or close to each other.

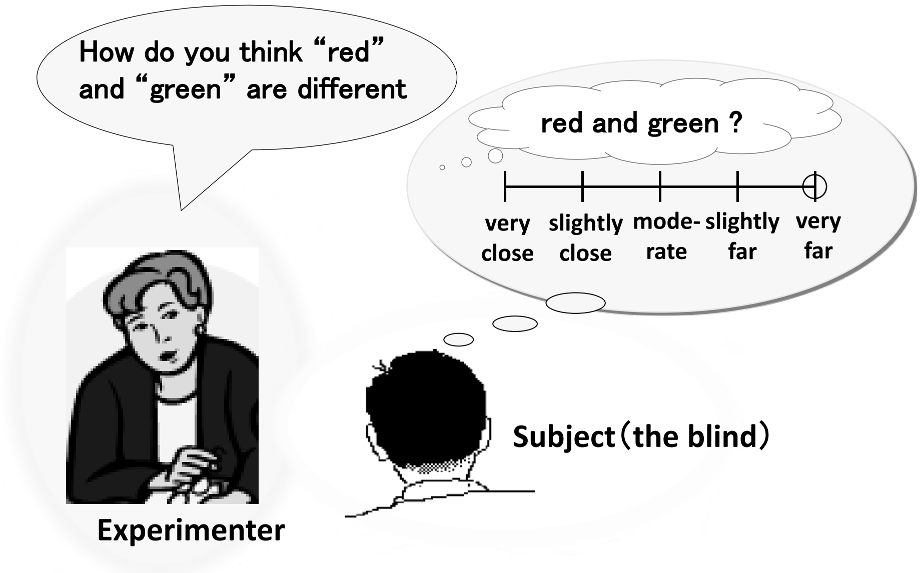

Figure 1: Experimental procedure to evaluate the psychological difference of two colors

Figure 1 illustrates this procdure. The experimenter picked up any of two colors among 10 fundamental colors and asked the blind subject the difference of those two colors. The subject estimated the difference from his/her own understanding of those colors and responded the difference in 5 points scale from very close (point 1) to very far (point 5). For example, as shown in Figure 1, if he/she regarded red and green are very different he/she gave the answer of “point 5, very far”. This procedure was repeated for one subject until a total of 45 pairs of colors were presented.

A total of 16 subjects, all totally blind, participated in the experiment. Ten subjects are congenitally or almost congentially blind, and the remaining 6 subjects lost their sight at ages between 5 to 18 years old and have clear experience of seeing color. Male and female were just evenly balanced.

2.2 Results and discussion

The data were originally obtained in a form of 10 x10 matrix for all the combination of 10 colors and a half of the matirx was entered by data avoiding the same entry in the matrix. These data, individual or averaged over 16 subjects, were analyzed by the MDS method to seek for the best possible placement of those 10 colors to satisfy the numerical relationships reported by subjects among the colors. The MDS analysis was done for each individual data as well as for the averaged one.

Figure 2 shows the result obtained for the averaged distance data for the 10 test colors. Two dimentional space is mathematically sufficient to discribe the relationships of the colors and in this space the ten test colors were reasonbly placed as shown in Figure 2. It is clear that the 10 colors form a beautiful circle with the color order exactly same as normal color vision. It is noted that the hue circle obtained by MDS only expresses the relationships among colors and, therefore, the direction of the color order, such as clockwise or unticlockwise, does not matter.

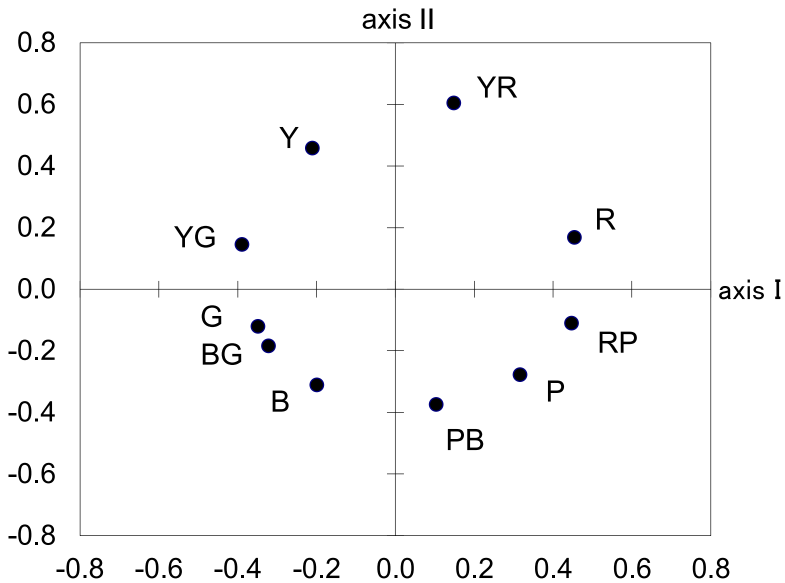

Figure 2: Placing of 10 test colors in a two dimensional space obtained from psychological distances of the colors and analyzing with the MDS method

Although the averaged data shows a clear circle as shown in Figure 2, it is not all the 16 subjects who exhbits such a clear hue circle. As shown in Figure 3(b) as an example, some subject did not show the hue circle, while some other subject exhbited a clear hue circle more or less as shown in Figure 3(a) as an example. Three subjects failed to show the hue circle, while the remaining 13 subjetcs showed it. It was found that those subjects who did not show a clear hue circle were all male and they had not been interested in color at all in his/her daily life and they ware mostly the blackish colors selected by their families. This means that the blind people take and understand the color information from their daily conversation which contains much of color terms, and if they have no interest in getting such color informaiton the concept of hue cirlce does not seem to be establsihed.

Previsous studies on the color representation of the blind (Shepard et al, Shin et al) mostly indicated that the hue circle was not established or understandable by the blind. On the contrary the present study, being based on relatively larger number of subjects, showed that the hue circle or at least the relationship of colors of hue cirlce was understandable by blind people except for some cases.

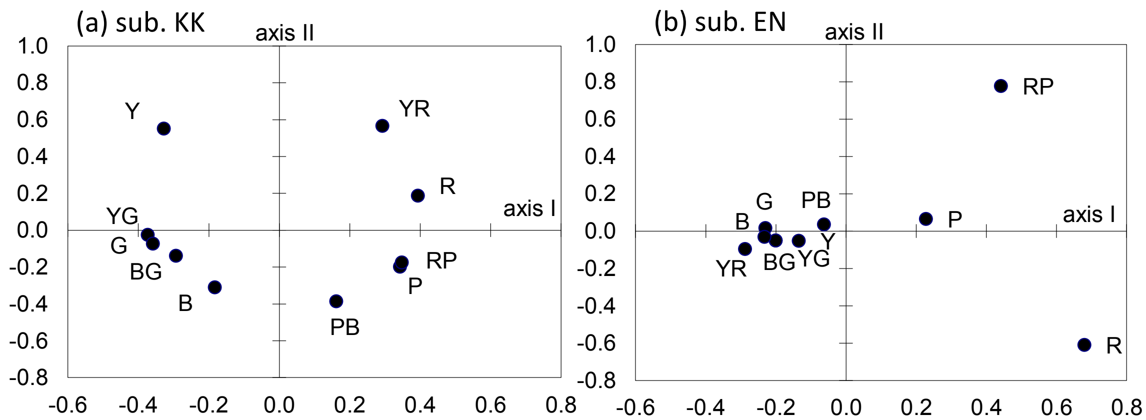

Figure 3: Two typical example of color placing obtained by MDS for the blind subjects showing (a) a clear hue circle, and (b) no hue circle

3. DESIGN AND DEVELOPMENT OF COLOR TAG FOR COLOTHES

Being based on the experimental results described above, a tactile tag for clothes was designed so as to inform color information to the blind. As shown in Figure 4, the tactile tag consists of a total of 10 small tactile dots which forms a circle and each dot represents a fundamental color of a hue circle. With red at the top and placing orange, yellow, green-yellow, etc in clockwise until it comes to the red-purple, and by enlarging or making a hole for one of the ten dots (in case of green, see Figure 4) it is possible to tell a blind person the color of clothes which the tag indicates through touching the dot or the hole. At the center of the circle three achromatic colors, white, gray, and black, are placed, and if the color is pale or desaturated, an inner circle is used.

Tactile experiment was also done to confirm the appropriate size of the circle and the dot.

Finally, we made a set of test tags from a few different materials (acrylic button, embroidery, and artificial leather) and attached them to T-shirts of different colors. Figure 5 shows some examples of the tag of each material and T-shirts the tags attached. Ten blind people participated in the color identification experiment of T-shirts color with the tactile tags. They showed almost perfect performance in identifying colors of the T-shirts (93 %

correct). The feeling of touch on the tag was also evaluated by psychological experiement and the result was also satisfactory. Among those test tags, the acrylic button was found to be the best for identifying color, and the artificial leather for tactile feeling.

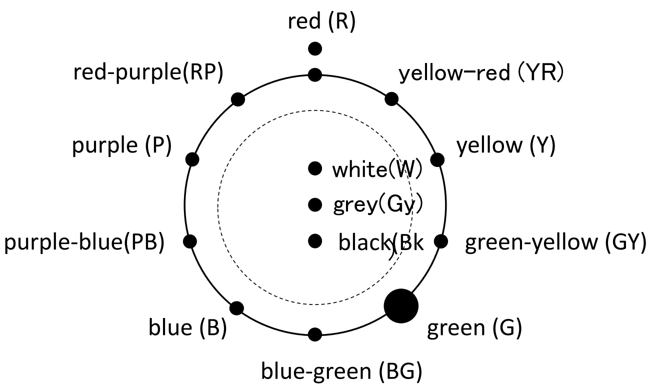

Figure 4: A color tag designed for representing color for the blind by tactile dots

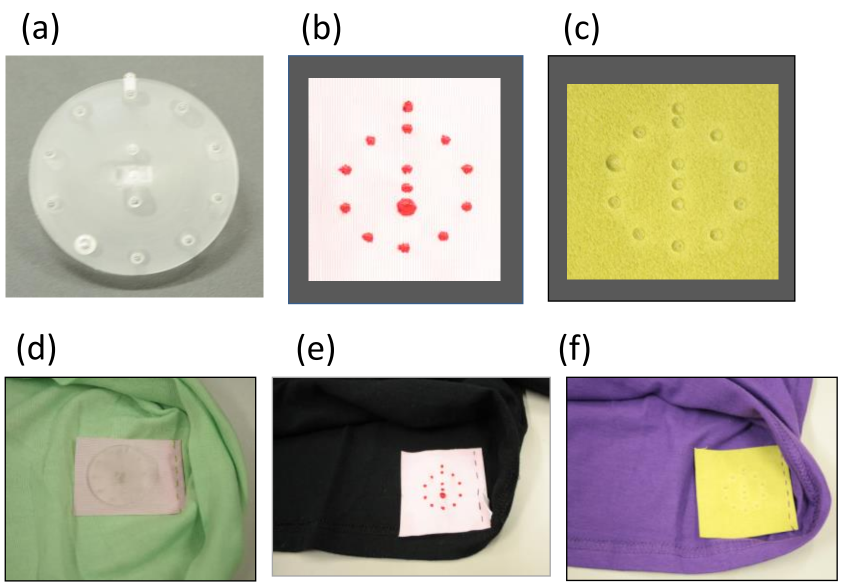

Figure 5: A color tag actually developed and attached to T-shirts. (a) and (d) are acrylic button, (b) and (e) are embroidery, and (c) and (f) are artificial leather.

4. CONCLUSION

Through psychological scaling experiment on color distinctness of blind people and analysing those data by multi-dimentioanl scaling (MDS), the relationships among fundamental colors were found to be nearly same for blind people as those for people with normal color vision. This means that hue circle was quite reasonable to tell the color to the blind people. A tactile color tag which has a hue circle made by ten tactile dots representing fundamental colors with three dots at the center representing achromatic white, grey, and black colors, was developed for informing blind people the color of their clothes. The successful test results of color identification by the tag confirmed that the idea of tactile color tag with the hue circle was very useful.

ACKNOWLEDGEMENTS

This research was suported by a grant from Ministry of Education, Culture, Sports, Science, and Technology in Japan. Support is also from Japan Braille Library in carrying out the experiments.

REFERENCES

Shepard, R.N. and Cooper, L.A. 1992. Representation of colors in the blind, color-blind, and normally sighted, Psychological Science, 3(2), 97-103.

Shin E. and Ohmi G. 2011. Color Vocabularies and Their Cognitive Contents in the Congenitally Blind, 35(3), 203-211.

Address: Dr. Ken SAGAWA, Department of Clothing, Human Science and Design,
Faculty of Human Science and Design, 2-8-1, Mejirodai, Tokyo 112-8681, JAPAN
E-mails: sagawa@fc.jwu.ac.jp

Examination of Method for Decreasing Unpleasantness Caused by Strong Brightness of Smart-phone Displays in Dark Adaptation

Itsuki MIYAMAE,[1] Hyojin JUNG,[2] Saori KITAGUCHI,[1] Tetsuya SATO[1]
[1] Department of Design Engineering and Management, Kyoto Institute of Technology
[2] Venture Laboratory, Kyoto Institute of Technology

ABSTRACT

The aim of this research is to suggest a method for decreasing the unpleasantness by the strong brightness on a display which the user of a smart-phone has under dark adaptation. In this research, a questionnaire survey was conducted about the unpleasantness which subjects feel to the dazzle of a smart-phone display to 21 smart-phone users. Then, a visual experiment using iPod touch (same form to iPhone) manufactured by Apple Inc. was conducted that 30 subjects evaluated the impression and the unpleasantness caused by the brightness of the smart-phone display with different brightness and background colours. The replies obtained in the questionnaire survey and the experimental results were analyzed. It authorized whether a significant difference would be between each evaluation result, and investigated correlation with luminance level and illuminance. Through the analysis of the experimental results, the followings were found out;

The 3 kinds of impressions to the brightness in each conditions, which are 'dazzle', 'fatigue' and 'irritation', have high correlation to luminance level and illuminance.

The favourite luminance level to use a smart-phone display was found out. In addition, at the time of dark adaptation, it was found out that brightness lower than the brightness given by the self-adjustment function of a smart-phone display reduces the unpleasantness. Moreover, the unpleasantness can be reduced by changing a background colour to black, even if the brightness was given by the self-adjustment function.

1. INTRODUCTION

Nowadays, smart-phones and tablet PCs are used very much in our daily life, and the opportunity to work by seeing their displays has been increased. Many of such display media have a self-luminous display. The display media is used under various lighting conditions. Therefore, in order to adjust users' visual sensitivity under the various lighting conditions, the regulation function of the display can adjust luminance according to the luminance of surrounding environment, and users can see images and characters on brightness by the display automatic self-adjusted luminance. However, it is not clear whether the brightness self-adjusted is suitable for smart-phone users or not.

The aim of this study is to suggest a method for decreasing users' visual stress such as unpleasantness. The unpleasantness which the user of a smart-phone has under dark adaptation is given by the strong brightness on a smart-phone display. In order to know about the details of the impressions relating to visual stress such as unpleasantness and dazzle when smart-phone users use their smart-phones, a questionnaire was conducted to university students. A visual experiment for evaluating 6 impressions of 'dazzle', 'readability', 'unnaturalness', 'fatigue', 'irritation' and 'unpleasantness', which were chosen using the results of the questionnaire, was also conducted. In addition, the subjects were asked to choose the most favourite luminance level samples used in the visual experiment.

2. METHOD

A questionnaire survey was conducted to 21 smart-phone users, and a visual evaluation experiment was also conducted. Then, a visual experiment was conducted that 30 subjects evaluated the impression and the unpleasantness caused by the brightness of the smart-phone display with different brightness and background colours. The results obtained were statistically analyzed using correlation analysis and analysis of variance.

2.1 Questionnaire Survey

In order to know about problem such as dazzle and displeasure when smart-phone users use their smart-phones, a questionnaire was conducted to 21 university students. The questions were use situation, problem under use, and next action when users have the problem. As one the results obtained in the questionnaire, visual problems under use are shown as below:

Replies for a question about visual problems under use (n=21)

13 replies: I feel dazzling for my smart-phone display lightness when dark such as midnight

6 replies: I can’t read the screen of my smart-phone in the outdoors.

2 replies: My eyes get tired when I use my smart-phone for a long time.

2.2 Sample Preparation for Visual Experiment

An iPod touch manufactured by Apple Inc., which has the same form and similar function to iPhone, was used in this visual experiment. The details of the iPod touch is as followings; white colour, IPS retina screen, 1136x640(px), 800:1 contrast ratio, and 500cd/m^2 maximum luminance.

The display sample on the iPod touch was an e-mail which were written in Japanese. Black and white characters were used for the white and black background colours, respectively. The background colours are white and black. All of the content was the same e-mail. The display samples on white and black background were shown in Figure 1.

Figure 1: Samples used in this visual experiment: White and black background.

We used 6 luminance level samples (w0, w25, w50, w75, w100) in this research, which have different luminance on white/black background. The luminance levels of white background samples are w0, w25, w50, w75, w100, and the luminance levels of black background sample is b35. The luminance level of b35 is the luminance level given by self-adjustment function in the dark experimental room used in this study.

In addition, w50 and b50 luminance level samples were used at the first of the visual evaluation. b50 was used only for practice of subjects. The relationship between luminance levels of iPod touch and illuminance values onto subjects is shown in Table 1. The illuminance values were measured 5 times for each sample by an illuminance meter T-10 manufactured by Minolta Inc., and the measured values were averaged excluding unexpected values.

Table 1. Lighting levels of iPod touch of illuminance values onto subjects.

Luminance level	w0	w25	w50	w75	w100	b35	b50
Illuminance (lx)	0.19	2.17	5.53	10.64	23.79	0.38	0.68

2.3 Subject and Evaluation Item

The subjects are university students who are 18 to 24 years old. The number of the subjects was 30 (15 male and 15 female). The evaluation items are ‘dazzle’, ‘readability’, ‘unnaturalness’, ‘fatigue’, ‘irritation’, and ‘unpleasantness’ which were selected using the results of the questionnaire. The visual experiment was conducted using Semantic Differential Method (5 points evaluation, 1 to 5 score). The subjects were asked to evaluate 7 samples including 2 practice samples with the 5 levels. After the visual experiment, they were also asked to select the most suitable display sample.

2.4 Experimental Procedure

The subjects separately carried out the visual experiment at different date and time. The subjects entered into a dark experimental room, and they took 5 minutes for getting the dark adaptation with a iPod touch in their hands. After getting the dark adaptation in a dark room, the visual evaluation was started. The subjects were asked to evaluate each sample in 30 seconds, to reduce the influence of light adaptation. The subjects took a rest for 2 minutes after the evaluation of one sample. The samples were w0, w25, w50, w75, w100, b35 and b50 which had been prepared in advance. At the first, the subjects were asked to evaluate w50 and b50 as practice. After the practice, the evaluation for each 6 samples (w0, w25, w50, w75, w100 and b35) were randomly given and evaluated for ‘dazzle’, ‘readability’, ‘unnaturalness’, ‘fatigue’, ‘irritation’, and ‘unpleasantness’ impressions. After the evaluation for all samples, the subjects were asked to choose the most favorite sample used in dark condition.

3. RESULTS AND DISCUSSION

The visual results for 6 kinds of impressions, which are ‘dazzle’, ‘readability’, ‘unnaturalness’, ‘fatigue’, ‘irritation’, and ‘unpleasantness’, were totaled and calculated their average values respectively. Then, the correlation of each impression to luminance level and illuminance were analyzed. The values of luminance levels were directly used the level numbers of iPod touch. Table 2 shows the correlation coefficients of the 6 impressions to luminance level and illuminance.

Table 2. Correlation of the 6 impressions to luminance level and illuminance.

	Dazzle	Readability	Unnaturalness	Fatigue	Irritation	Unpleasantness
Luminance level	0.77	0.07	0.18	0.67	0.67	0.39
Illuminance	0.69	0.14	0.23	0.62	0.62	0.41

The 6 impressions have some correlation among themselves. Table 3 shows the correlation coefficients between 'unpleasantness' and other 5 impressions. This may mean that 'unpleasantness' is synthetically evaluated using other impressions.

Table 3. Correlation between 'unpleasantness' and other 5 impressions.

	Dazzle	Readability	Unnaturalness	Fatigue	Irritation
Correlation coefficient	0.54	0.48	0.66	0.68	0.70

The 6 impressions discussed in this study are relating to visual stress. Total of subjects' evaluation values for each sample through SD method was used as total visual stress index. Table 4 shows the total visual stress index. The lowest visual stress was w0, and the second lowest one was b35. The highest visual stress sample was w100.

Table 4. Total visual stress index of the 6 impressions.

Luminance level	w0	w25	w50	w75	w100	b35
Visual stress index	410	453	598	620	725	431

Table 5 shows favourite luminance level chosen by subjects. 15 subjects, a half of the subjects, chose w25. 10 subjects chose b35, and 4 subjects chose w0. W75 and w100 were not chosen.

Table 5. Favorite luminance level chosen by subjects: Frequency and percentages (n=30).

Luminance level	w0	w25	w50	w75	w100	b35
frequency	4	15	1	0	0	10
%	13.3	50.0	3.3	0.0	0.0	33.3

Comparing with the results of visual stress analysis, we found favourite samples used in dark condition are about the same to the low visual stress samples. However, the most favourite sample w25 was the third lowest visual stress sample, not the lowest visual stress sample. This means that the lowest luminance level is not the most favourite level and users choose the most favourite level with using some other factors.

4. CONCLUSIONS

It authorized whether a significant difference would be between each evaluation result, and investigated correlation with luminance. Through the analysis of the experimental results, the followings were found out;

1. The 3 kinds of impressions to the brightness in each conditions, which are 'dazzle', 'fatigue' and 'irritation', have correlation to luminance level and illuminance. The correlations between visual evaluation and illuminance levels are 0.77, 0.67 and 0.67, respectively, and those between visual evaluation and luminance level are 0.69, 0.62 and 0.62, respectively. The 'unpleasantness' evaluation result has correlation 0.39 and 0.41 to luminance level and illuminance.
2. The favourite luminance level to use a smart-phone display was found out. In addition, at the time of dark adaptation, it was found out that brightness lower than the brightness

given by the self-adjustment function of a smart-phone display reduces the unpleasantness. Moreover, the unpleasantness can be reduced by changing a background colour to black, even if the brightness was given by the self-adjustment function.

3. The lowest luminance level is not the most favourite level. Users may choose the most favourite level using some other factors. Too low luminance level may be not so good for users' favour. The details and the factors should be investigated more.

The summary of this study suggests us the following ways to reduce the problems such as unpleasantness under dark lighting condition; One is to use w25 that having low luminance white background however not so dark. Another is to change from white background colour to black background and use white characters.

REFERENCES

Horiba, Y. and M. Kamijo 2011. *Comparative Study on Readability for Electronic Display Media Luminance and Impression Evaluation*, Journal of the Japan Society of Kansei Engineering, 10(4) 445-456.

Aoki, K. and Y. Umemura 1986. *Research on the Relationship between Work Time and the Screen Luminance of Visual Display Terminal*, Journal of the Japan Ergonomics Society 22 (Suppl) 116-117.

Address: Prof. Tetsuya SATO, Department of Design Engineering and Management,
Faculty of Science and Technology, Kyoto Institute of Technology,
Matsugasaki, Sakyo-ku, Kyoto, 606-8585, JAPAN
E-mail: tsato@kit.ac.jp

A Spectral-based Color Vision Deficiency Model Compatible with Dichromat and Anomalous Trichromat

Hiroaki KOTERA, KOTERA Imaging Laboratory

ABSTRACT

This paper proposes a spectral-based color vision deficiency model with compatibility both for dichromats and anomalous trichromats. The spectral projection model based on Matrix-***R*** extracts the lost spectrum as a difference in the *fundamentals* between the normal and the color deficient. The lost spectrum is re-used for image daltonization by an optimal spectral shift algorithm to maximize the spectral visibility or minimize the visual gap from the normal. The model dramatically improved the scene visibility. The proposed model is designed based on the ***original key ideas*** of

1) Extraction of *fundamental* $\boldsymbol{C^*}_{LMS}$ (spectrum visible to the normal) from sRGB camera images by a pseudo-inverse projection without spectral image.

2) Foundation of projection matrix-$\boldsymbol{R}_{DEF}$ onto dichromatic and anomalous trichromatic spectral spaces by combining the cone spectral tables of DeMarco & Pokorny & Smith.

3) Extraction of *fundamental* $\boldsymbol{C^*}_{DEF}$ (spectrum visible to the dichromat or anomalous trichromat) by operating the matrix-$\boldsymbol{R}_{DEF}$ on the *fundamental* $\boldsymbol{C^*}_{LMS}$.

4) Introduction of complete OCS (Opponent-Color Space) to keep the perfect achromatic grayness in the opponent-color stage.

5) Estimation of lost spectra $\boldsymbol{\Delta C^*}_{DEF}$ as the difference between visible spectra $\boldsymbol{C^*}_{LMS}$ to the normal and $\boldsymbol{C^*}_{DEF}$ to the dichromat or anomalous trichromat.

6) Scene visibility correction (daltonization) by reviving the lost spectrum $\boldsymbol{\Delta C^*}_{DEF}$ with the optimal spectral shift into the visible waveband.

1. INTRODUCTION

Typical Color Vision Deficiency (CVD) is classified to dichromacy and anomalous trichromacy. Dichromacy is caused by the absence of one of the L, M, or S photopigments. While, anomalous trichromacy is explained by a spectral shift in the cones caused by arrangement of exon DNA in X-chromosome. The first CVD simulator is modeled to find the corresponding color pairs between the normals and the dichromats (Brettel et al, 1997). The troublesome corresponding pair procedure is simplified by a systematic color transform model (Capilla et al, 2004) and advanced to 2-step model including opponent-color stage (Pardo and Sharma, 2011). The color-blind simulators based on Brettel are widely accepted, but any of them didn't step into the spectral analysis. The author proposed a spectral-based dichromatic vision model (Kotera, 2011, 2012) based on Matrix-***R*** theory. The model clarified for the first time what spectra are visible or invisible to the dichromats and which parts are lost from the fundamentals in normal vision. The lost spectra analysis first interpreted the reason behind the *red-green opponent-color* blindness. The anomalous trichromatic vision is modeled by a simple spectral shift (Yang, 2008) or (Machado et al, 2009) but without dealing spectral losses. This paper proposes a versatile model compatible with both of dichromacy and anomalous trichromacy. The paper demonstrates the spectral daltonization algorithm for correcting the color blindness, which is designed to maximize the visibility for the confusing colors and minimize the visual spectral gap from the normals based on the mathematical evaluation criterion.

2. SPECTRAL PROJECTION ONTO COLOR DEFICIENT SPACE

2.1 Visible, Invisible and Lost Spectra based on Extended Matrix-*R* Theory

Based on *Matrix-**R*** theory (Cohen, 2001), *a* spectral input ***C*** is decomposed into the *fundamental* C^*_{LMS} and the *metameric black* ***B*** through the projection matrix R_{LMS} as

$$C = C^*_{LMS} + B,\ C^*_{LMS} = R_{LMS}C,\ \ B = (I - R_{LMS})C$$

$$R_{LMS} = A_{LMS}(A^t_{LMS}A_{LMS})^{-1}A^t_{LMS}\ for\ \ A_{LMS} = \left[l(\lambda)\ m(\lambda)\ s(\lambda)\right] : cone\ sensitivity$$

The fundamental C^*_{LMS} denotes the visible spectra to normal vision, while ***B*** is by-passed and lost as an invisible spectrum with zero tristimulus value. While, the spectra visible to the color deficient are much more lost through the matrix R_{DEF} corresponding to each type of color deficient (Figure 1: sample for Protanopia).

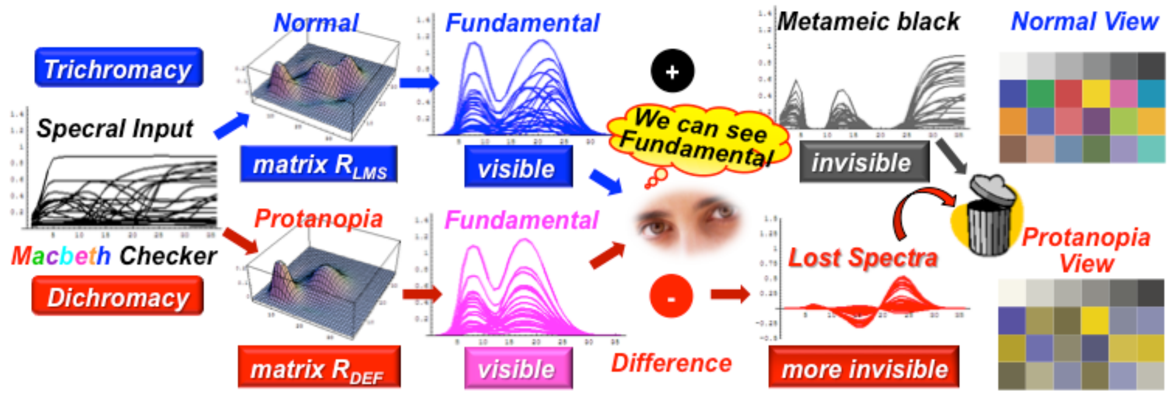

Figure 1: What color spectra are visible and lost to the color deficient?

2.2 Foundation of Projection Matrices onto Color Deficient Spectral Space

In this paper, typical four types of color deficiencies are simulated with *LMS* cone spectral sensitivities for normal and anormalous trichromat (DeMarco & Pokorny & Smith, 1992). The projection matrix R_{DEF} for each color deficient is created from a set of dichromatic and anomalous trichromatic cone responses (Figure 2).

$$R_{DEF} = A_{DEF}(A^t_{DEF}A_{DEF})^{-1}A^t_{DEF}\ := R_P\ or\ R_D\ or\ \ R_{aP}\ or\ R_{aD}$$

$$A_{DEF}\ := A_P\ or\ A_D\ or\ \ A_{aP}\ or\ A_{aD}$$

$$A_P = \left[m(\lambda)\ s(\lambda)\right]\ for\ protanopia,\ \ A_D = \left[l(\lambda)\ s(\lambda)\right]\ for\ deuteranopia$$

$$A_{aP} = \left[l_a(\lambda)\ m(\lambda)\ s(\lambda)\right]\ for\ protanomaly,\ \ A_{aD} = \left[l(\lambda)\ m_a\ s(\lambda)\right]\ for\ deuteranomaly$$

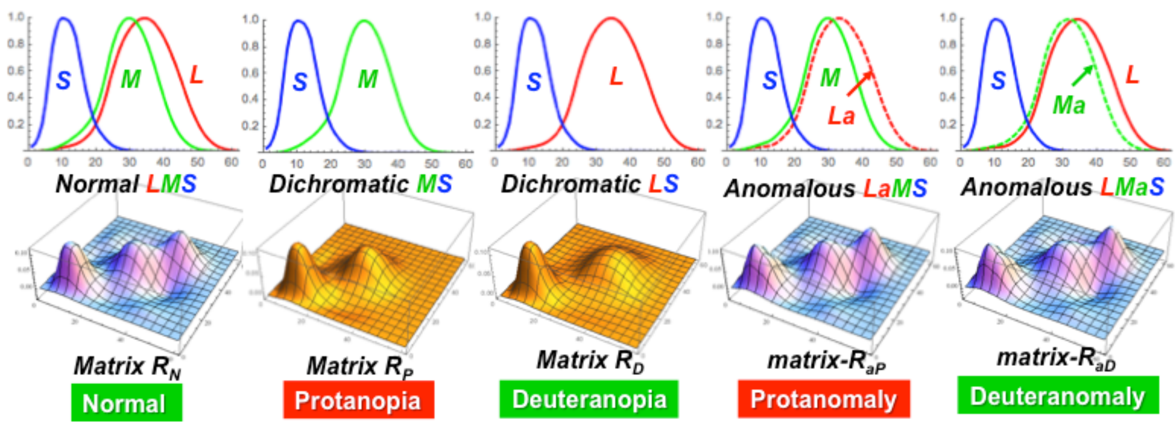

*Figure 2: Matrix-**R**$_{DEF}$ projection operators onto spectral CVD space.*

3. SIMULATION MODEL & RESULTS

3.1 Versatile Simulation Model for Dichromatic and Anomalous Trichromatic Vision

The proposed model simulates the color deficient appearance including the spectral-based daltonization and gray balance process in OCS. The model works compatible with both dichromat and anomalous trichromat by just selecting the projection matrix $\boldsymbol{R_{DEF}}$. First, the *fundamental* $\boldsymbol{C}^*_{LMS}$, visible spectrum to normal is captured with a sRGB camera and secondly projected to the *fundamental* $\boldsymbol{C}^*_{DEF}$ visible to the deficient. Thirdly, the lost spectrum $\Delta\boldsymbol{C}^*$ is calculated by taking the difference in $\boldsymbol{C}^*_{LMS}$ and $\boldsymbol{C}^*_{DEF}$. Next, the lost spectra $\Delta\boldsymbol{C}^*$ is re-used to daltonize the confusing color visibility by the optimal spectral shift algorithm. Finally, the corrected *fundamental* spectra are displayed on sRGB monitor throiugh the inverse transforms of (spectral to *LMS*), (*LMS* to *OCS*) and (*OCS* to *sRGB*). In the opponent-color process, the achromatic grayness is kept in the complete orthonormal *YCrCb OCS* (Kotera, 2014) (Figure 3).

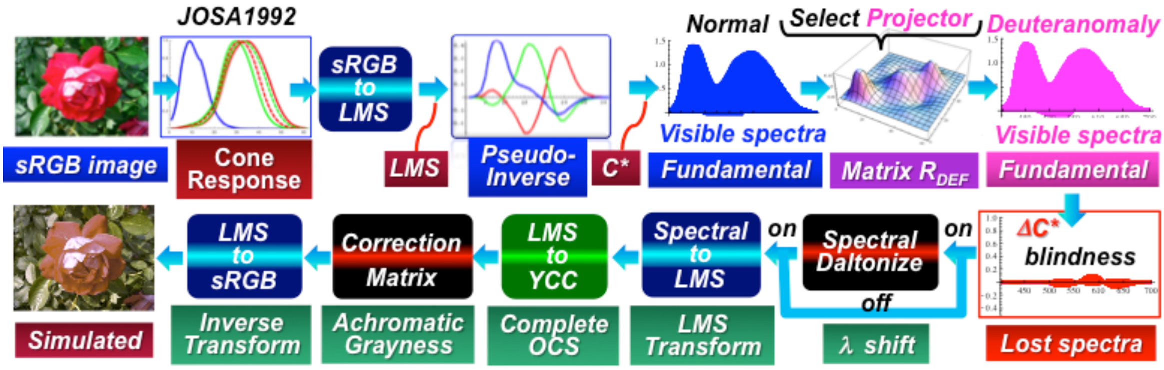

Figure 3: Spectral CVD model compatible with dichromacy and anomalous trichromacy.

3.2 Getting *Fundamental* for Scene from sRGB Camera Image

Since the *fundamental* $\boldsymbol{C}^*_{LMS}$ (spectrum visible to normal) carries the tristimulus value $\boldsymbol{T}_{LMS}$ as same as the input spectrum $\boldsymbol{C}$, it's exactly recovered by the pseudo-inverse transform (Kotera, 1996) from $\boldsymbol{T}_{LMS}$. Hence, the actual scene spectrum visible to normal vision is obtained from sRGB image without using expensive spectral camera as follows.

$$\begin{aligned}\boldsymbol{C}^*_{LMS} &= \boldsymbol{P}_{INV}\boldsymbol{T}_{LMS} \ \text{, where } \boldsymbol{P}_{INV} = \boldsymbol{A}_{LMS}(\boldsymbol{A}^t_{LMS}\,\boldsymbol{A}_{LMS})^{-1} \\ &= \boldsymbol{P}_{INV}\left(\boldsymbol{M}_{XYZ\to LMS}\right)\left(\boldsymbol{M}_{sRGB\to XYZ}\right)\boldsymbol{sRGB}_{IMG} \ ;\ \boldsymbol{M}_{P\to Q} = P \text{ to } Q \text{ transform matrix}\end{aligned}$$

3.3 Lost and Visible Spectra to Color Deficient

The fundamental $\boldsymbol{C}^*_{DEF}$ (spectrum visible to the color deficient) is obtained by operating the matrix $\boldsymbol{R}_{DEF}$ on the trichromatic fundamental $\boldsymbol{C}^*_{LMS}$ and the lost spectra $\Delta\boldsymbol{C}^*_{DEF}$ from the normal vision is given by taking the difference in $\boldsymbol{C}^*_{LMS}$ and $\boldsymbol{C}^*_{DEF}$ as

$$\boldsymbol{C}^*_{DEF} = \boldsymbol{R}_{DEF}\boldsymbol{C} = \boldsymbol{R}_{DEF}\boldsymbol{C}^*_{LMS},\ \ \Delta\boldsymbol{C}^*_{DEF} = \boldsymbol{C}^*_{LMS} - \boldsymbol{C}^*_{DEF} = \left(\boldsymbol{R}_{LMS} - \boldsymbol{R}_{DEF}\right)\boldsymbol{C}^*_{LMS}$$

3.4 Reviving Lost Spectra for Daltonizing Color Deficient Visibility

Though the lost spectrum $\Delta\boldsymbol{C}^*_{DEF}$ is invisible if left as it is, we can revive it for daltonizing the confusing color visibility by shifting its distribution into the visible wavelength region.

ΔC^*_{DEF} is shifted by λ_{SHT} in a manner of rotate-left and added to the *fundamental* C^*_{LMS}. The daltonized *fundamental* ${}_{DAL}C^*_{LMS}$ is given by

$$ {}_{DAL}C^*_{LMS}(\lambda) = C^*_{LMS}(\lambda) + \Delta C^*_{DEF}(\lambda - \lambda_{SHT}) $$

The optimal shift wavelength λ_{OPT} is determined to maximize the function $\Psi_{OPT}(\lambda_{SHT})$.

The total evaluation function $\Psi_{OPT}(\lambda_{SHT})$ is defined by combining the spectral fitness $\Psi_{FIT}(\lambda_{SHT})$ and the spectral difference $\Psi_{DIF}(\lambda_{SHT})$ to and from the normal vision as

$$ \begin{aligned} &\lambda_{OPT} = \lambda_{SHT} \; for \; \Psi_{OPT}(\lambda_{OPT}) = \max_{\lambda_{SHT}=0}^{\lambda_{max}-\lambda_{min}} \{\Psi_{OPT}(\lambda_{SHT})\} \\ &\Psi_{OPT}(\lambda_{SHT}) = w\Psi_{FIT}(\lambda_{SHT}) + (1-w)\{1 - \Psi_{DIF}(\lambda_{SHT})\} \end{aligned} . $$

$\Psi_{FIT}(\lambda_{SHT})$ and $\Psi_{DIF}(\lambda_{SHT})$ are estimated by summing up the power spectra (squared norm) for all the pixels g_j (j=1~J) in sRGB image as follows (Kotera, 2012).

$$ \Psi_{FIT}(\lambda_{SHT}) = \sum_{j=1}^{J} \left\| \{\Delta C^*_{DEF}(\lambda - \lambda_{SHT}), g_j\} \right\|^2 $$

$$ \Psi_{DIF}(\lambda_{SHT}) = \sum_{j=1}^{J} \left\| \{\Delta C^*_{DIF}(\lambda - \lambda_{SHT}), g_j\} \right\|^2 \; for \; \Delta C^*_{DIF}(\lambda) = (R_{LMS} - R_{DEF})\, {}_{DAL}C^*_{LMS}(\lambda) $$

The weighting factor w is adjusted to maximize the visibility for the confusing colors (w=1) or minimize the visual spectral gap (w=0) from the normals after the daltonized image is viewed by the color deficient. Very fortunately, in many cases for dichromats, the function $\Psi_{FIT}(\lambda_{SHT})$ takes its maximum value at $\lambda_{SHT} = \lambda_{OPT}$ and simultaneously, the function $\Psi_{DIF}(\lambda_{SHT})$ goes down to a quasi-minimum point around at the same wavelength. The proposed algorithm dramatically improved the image visibility and naturalness after daltonization with default weight w=0.5 much better than that by popular simulator Vischeck (Brettel model). (Figure 4: sample "wild strawberries" for Deuteranopia).

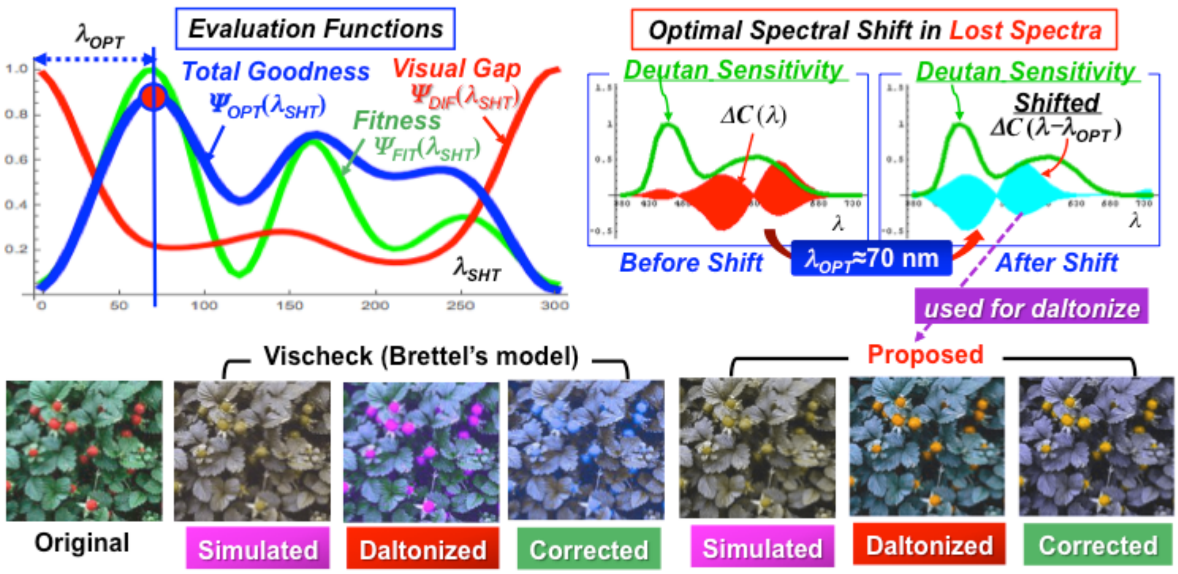

Figure 4: Daltonization for correcting CVD visibility by reusing lost spectra

3.5 Keeping Achromatic Greyness in Opponent-Color Process

Following the cone response **stage-1**, the *LMS* stimulus is encoded to a luminance-chrominance YC_RC_B signals in the next opponent-color **stage-2**. Since the opponent-color system is thought to work for the color deficient as well as the normal, the YC_RC_B signals should keep the achromatic grayness. Because a simple anomalous trichromatic simulation model (S. Yang, 19xx) only with **stage-1** caused coloring problem for the neutral gray input, the correction process to guarantee the achromatic grayness is introduced to the pathway in **stage-2** (Machado et al, 2009).

In this paper, an achromatic greyness process different from Machado's is introduced. Assuming *EE* (Equal-*Energy*) white spectrum input $\boldsymbol{W}_{EE}(\lambda)$ to the normal vision, the visible spectrum ${}_{EE}\boldsymbol{C}^*_{LMS}$, its *LMS* cone response $\boldsymbol{T}_{LMS}$, and the corresponding *opponent-color* signals YC_RC_B should satisfy the achromatic grayness of (Y=1, $C_R = C_B$ =0) as

$$\left[Y\ C_R\ C_B\right]^t_{EE} = M_{LMS\to YCC} \cdot {}_{EE}\boldsymbol{T}_{LMS} = \left[1\ 0\ 0\right]^t : \textit{achromatic grayness}$$

$${}_{EE}\boldsymbol{T}_{LMS} = \left[L\ M\ S\right]^t_{EE} = \boldsymbol{A}_{LMS} \cdot {}_{EE}\boldsymbol{C}^*_{LMS}(\lambda) : \textit{LMS tristimulus value for EE white}$$

$${}_{EE}\boldsymbol{C}^*_{LMS}(\lambda) = \boldsymbol{R}_{LMS}\boldsymbol{C}^*_{EE}(\lambda) = \boldsymbol{R}_{LMS}\boldsymbol{W}_{EE}(\lambda)\ \textit{for}\ \boldsymbol{W}_{EE}(\lambda) = \left[1\ 1\ 1\ \cdots\cdots\ 1\right]^t$$

The linear transform matrix $\boldsymbol{M}_{LMS\to YCC}$ to meet this condition is obtained by coupling $\boldsymbol{M}_{LMS->XYZ}$ (CIECAMO2) with $\boldsymbol{M}_{XYZ\to YCC}$ (Complete OCS, Kotera, 2014) as

$$M_{LMS\to YCC} = \left(M_{XYZ\to YCC}\right)_{Kotera}\left(M_{LMS\to XYZ}\right)_{CIECAMO2} = \begin{bmatrix} 0.4889 & 0.1336 & 0.3775 \\ 1.0038 & -0.7900 & -0.2138 \\ 0.0344 & -0.4718 & 0.4374 \end{bmatrix}$$

Indeed, YC_RC_B values to *EE* white for normal is verified to keep the perfect grayness as

$$\left[Y\ C_R\ C_B\right]^t_{EE} = M_{LMS/YCC} \cdot \boldsymbol{A}_{LMS}\boldsymbol{W}_{EE}(\lambda) = \left[1.00\ \ -8.3\times10^{-17}\ \ -1.1\times10^{-16}\right]^t \cong \left[1\ \ 0\ \ 0\right]^t$$

Since the spectrum ${}_{EE}\boldsymbol{C}^*_{DEF}$ visible to color deficient for *EE* white is lost by $\Delta\boldsymbol{C}^*_{DEF}$ against normal vision, its *LMS* or YC_RC_B responses deviate from $[1\ 1\ 1]^t$ or $[1\ 0\ 0]^t$ as given by

$${}_{DEF}\left[Y\ C_R\ C_B\right]^t_{EE} = M_{LMS\to YCC} \cdot {}_{EE}\boldsymbol{T}_{DEF}$$

$${}_{EE}\boldsymbol{T}_{DEF} = \left[L\ M\ S\right]^t_{EE} = \boldsymbol{A}_{DEF} \cdot {}_{EE}\boldsymbol{C}^*_{DEF}(\lambda)\ {}_{EE}\ \textit{for}\ \boldsymbol{C}^*_{DEF}(\lambda) = \boldsymbol{R}_{DEF}\boldsymbol{R}_{LMS}\boldsymbol{W}_{EE}(\lambda)$$

Actually, the deviations from YC_RC_B =[1 0 0] are estimated for each type of deficient as

$[Y\ C_R\ C_B]_{EE}$=[0.912 -0.180 -0.006] (protanopia)
$[Y\ C_R\ C_B]_{EE}$=[1.005 -0.032 -0.019] (deuteranopia)
$[Y\ C_R\ C_B]_{EE}$=[1.005 0.012 0.001] (protanomaly)
$[Y\ C_R\ C_B]_{EE}$=[1.002 -0.013 -0.008] (deuteranomaly)

Hence, the inverse correction matrices to guarantee the achromatic grayness are inserted in the route between (*LMS* to YC_RC_B) and (YC_RC_B to *sRGB*) transforms in Figure 3.

3.6 Simulation Results in Comparison with Other Models

The simulation results for the dichromat and anomalous trichromat are compared with typical color blindness simulators with some daltonization effects (Figure 5). Though the simulated CVD appearances look to be much the same across the models, the proposed daltonization function worked better clearly than others for rescuing the dichromatic blindness, but not so distinct for the anomalous trichromats, due to the smaller lost spectra.

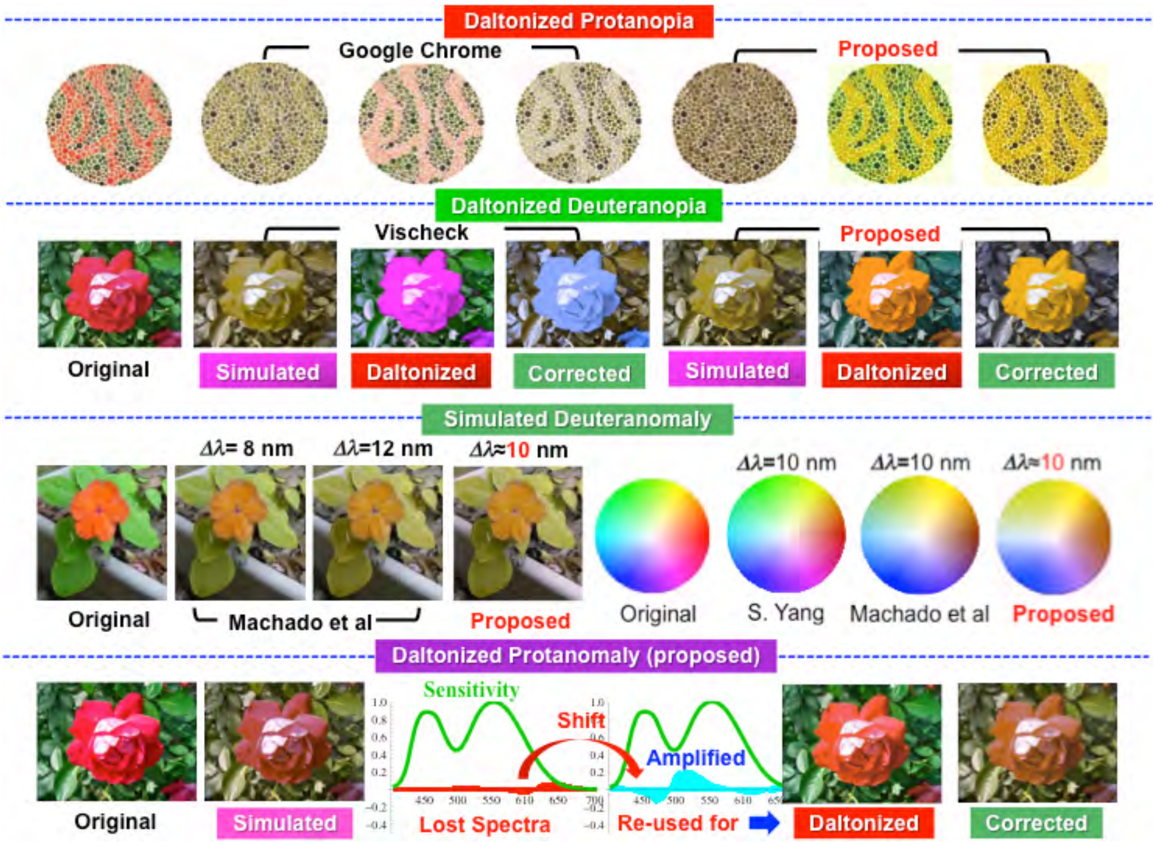

Figure 5: Comparisons in CVD simulation and daltonization effects

4. CONCLUSIONS

A Spectral-based CVD model developed from dichromacy into anomalous trichromacy. The proposed algorithm, quite different from 2D-3D corresponding pair process based on Brettel's, can estimate the visible, invisible, and lost spectra from a usual sRGB image. The model demonstrated how the lost spectrum is revived and used for daltonizing the scene visibility much better than other methods. Though its effects are remarkable for the dichromats, but still insufficient for anomalous trichromats and needs more future works.

REFERENCES

Brettel, H. et al 1997. *Computerized simulation ...dichromats*, JOSA, A, 14, 10, 2641-2655
Capilla, P. et al 2004. *Corresponding-pair procedure: a new ......*, JOSA. A, 21,2, 176-186
Pardo and Sharma 2011. *Dichromatic …… in a two stage model*, IEEE IVMSP WS, 12-17
Kotera, H. 2011. *A Study on Spectral Response for Dichromatic Vision*, CIC19, 8-13
Kotera, H. 2012. *Optimal Daltonization by Spectral Shift for Dichroma ...*, CIC20, 302-307
Yang, J. 2008. *Qualification anomalous …* , EURASIP, J. Image & Video Processing, 1-12
Machado, G. M. et al 2009. *A Physiologically…*, IEEE Trans., Vis & CG, 15, 6, 1291-1298
Cohen, J. B. 2001. *Visual Color and Color Mixture*, Illinois Press
DeMaro, Pokorny, and Smith 1992. *Full-spectrum cone sensitivity …*, JOSA, 9, 1465-1476
Kotera, H. 1996. *Recovery of Fundamental Spectrum from Color Signals*, CIC4, 141-146
Kotera, H. 2014. *A Complete Opponent-Color Space with Golden Vectors*, CIC22, 65-70

Address: Dr. Hiroaki KOTERA, KOTERA Imaging Laboratory,
3-20-20, Oyumino-Cyuoh, Midori-ku, Chiba 266-0032, JAPAN
E-mails: hiroimage@asahi.email.ne.jp

Colour Information in Design

Seahwa WON, Stephen WESTLAND, Kishore BUDHA, Bruce CARNIE
School of Design, University of Leeds

ABSTRACT

This study is concerned with identifying which types of colour information are useful in design. An analysis of the literature (299 journal papers and 10 textbooks) identified thirteen types of colour information. The importance of these thirteen types was explored through an online survey (N=62) with participants (identified through LinkedIn with a strong interest in packaging and branding) and face-to-face interviews (N=10) with senior designers and brand managers. The results from the online survey and the interviews were broadly consistent (r^2=0.66) and identified *harmony, perception, meaning, psychology,* and *printing* as being particularly important.

1. INTRODUCTION

Gradually the world would become more colourful (Leeuwen, 2011). In a demonstration of this statement, we can find the proliferation of colour in product categories that were previously largely black or white – e.g., kettles, toasters. In the retail industry, colour in packaging is a key differentiator as most warehouse supermarkets more or less offer the same shopping experience through their formats of stocking and display. Colour conveys products' messages, and influences consumers' attention and their purchase decision-making. Yet despite the importance of colour in design, it has tended to be regarded as secondary. Throughout the design process, a considerable range and volume of information is generated, used, referred to, and consulted with (Baya *et al*., 1992). Useful information in design can assist to save duplication of effort and time and to simulate creative energies (Wodehouse and Ion, 2010). According to the Cambridge Dictionary of Sociology (Turner, 2006), information is defined as uncertainty reduction, patterned abstraction, and knowledge. In the Oxford Dictionary of Environment and Conservation (Park and Allaby, 2013), information is interpreted data which is useful for making decisions or arriving at new facts. In the Oxford Dictionary of Psychology (Colman, 2009), information is knowledge acquired by learning. Synthesising these conceptions of information, this study defines colour information as interpretations, abstractions and knowledge about colour data in various fields, which include natural sciences, technology, art, psychology, cultural studies, history, and design. Colour is a meta-discipline that crosses various academic boundaries such as science, design, art, history and education. Due to the multi-disciplinary nature of colour, it is not clear whether colour information is effectively utilised in the design process. Furthermore, although developing technology makes it easy to access to variety formats of colour information via publications, websites, or mobile Apps, there are many unreliable sources especially on the internet. Colour information is a relatively new area that has not yet been addressed in detail by design research practically or theoretically. In this sense, it is noticeable that there is currently a lack of study on colour as information in design. This study will provide valuable insights for designers and brand managers informing which colour information are useful for their design process.

2. METHOD

Multiple methods such as analysing literature, online survey and face-to-face interviews with designers and brand managers were carried out to explore which colour information is useful in design. Firstly, 299 journal papers were searched by the keyword 'colour' in Colour Research and Application (CRA) which is a primary journal for colour field for 2011-2013 and ten academic books on colour which could be generally found in library were investigated using title analysis. The title of a document gives a compact summary (Senda and Sinohara, 2002), and the title analysis provides insight into topics of relative current interest (Ruben, 1992). The title terms presented in the 299 journals and the ten books were counted using online word frequency. In the CRA journal, titles predominantly focus on 'harmony', 'measurement', 'printing', 'perception, 'preference' and 'light'. In the ten colour references, titles and contents frequently concern; *design, harmony, theory, printing, art, history, perception, psychology, trend, naming, symbolism, culture* and *preference*. Analysing these terms, thirteen types of colour terms were identified (Table 1). The thirteen types of colour terms are not intended to be definitive or exhaustive. For example, there is no obvious rationale to restrict this survey to hard-copy books or journals and exclude internet sources. Nevertheless, these terms for colour information provide a holistic overview of current topics and relative interest in the colour academic field. Using these thirteen types of colour information, an online questionnaire and face-to-face interviews were conducted to identify useful colour information in the design process. For the online survey, LinkedIn was used as the main online platform to recruit relevant designers and brand managers to participate in the survey. Sixty-two responses were collected for the online questionnaire. For the interviews, ten senior designers and brand managers were interviewed.

In the online survey participants were asked to rate (using a slider bar) on a scale of 0-100 how important each of the thirteen types of colour information were to them in their design work (where 0 = no importance at all and 100 = vital). In the interviews participants were asked whether they considered each type of information to be important (so their responses were binary).

3. RESULTS AND DISCUSSION

Table 1. The thirteen types of colour information used in this study

Colour in art and design: famous artists' or designers' colours.
Colour harmony: colour combinations which arouse a pleasing effect.
Colour history: how a particular colour was developed.
Colour and light: principles of light such as wavelengths and frequencies.
Colour meaning: what is meant by a colour in different cultures or product categories
Colour measurement: measuring properties of colour or using colour measurement devices.
Colour notation: colour numbers or names to describe or communicate colour.
Colour perception: which colours attract consumers' attention.
Colour preference: individual's favourite colour.

Colour printing: the quality of colour printing.	
Colour psychology: behaviour and mental experience on colour.	
Colour theory: supposition or a system of ideas intended to explain colour.	
Colour trend: colours which are on-trend or popular.	

Figure 1 represents the results of the online survey. The figure shows the mean score for importance for each information type. The error bars show ± 1 standard error of the mean. Without performing formal statistical analysis (which will be presented in a future paper) it is clear that the standard deviations of the mean are small compared to the differences in mean scores in many cases. *Printing* gave the strongest response. *History* gave the weakest response. *Printing, harmony, meaning, psychology* and *perception* are all important. *Notation, theory, preference* and *trend* are of lesser importance. The others seem not important at all.

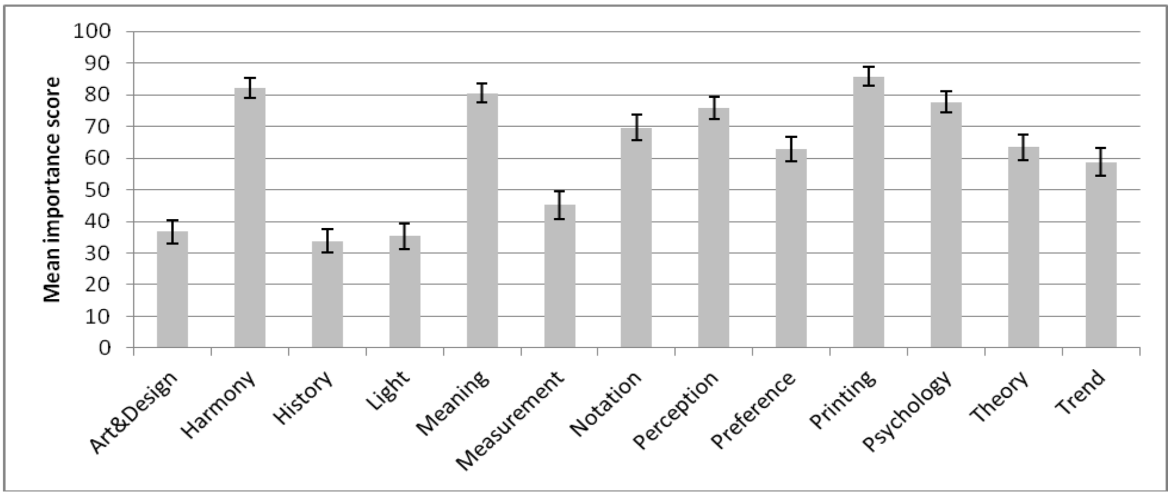

Figure 1: The result of online survey.

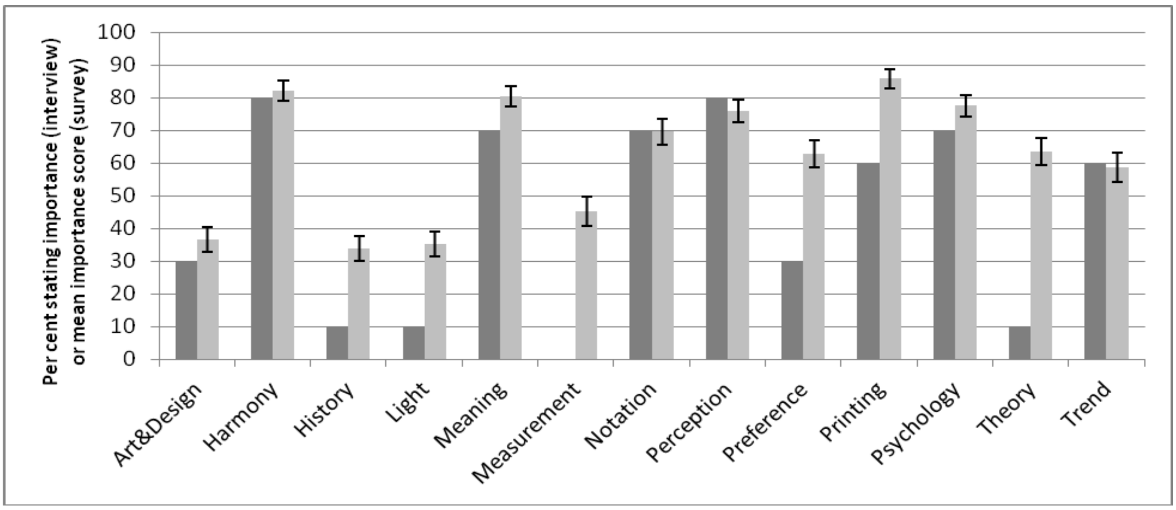

Figure 2: The result of face to face interview (dark grey) and the result of online survey (light grey).

Statistical analysis of the interview responses is more difficult partly because the sample size was low (N=10) and partly because the responses were binary rather than interval data. Nevertheless, if the per cent of participants who state that a colour information type is important is calculated (Figure 2) then it can be seen that *harmony, perception, meaning, notation* and *psychology* gave the strongest response.

If the per cent importance (from the interviews) is compared with the mean importance scores (from the surveys) then there is strong agreement (see Figure 2) between the two studies ($r^2 = 0.66$). Taken together, if the average of the per cent importance and the mean importance scores is calculated then the following types are deemed to be important *harmony, perception, meaning, psychology,* and *printing* because the mean is greater than 70%.

4. CONCLUSIONS

This work sought to identify the types of useful colour information in the design process. A review of the literature identified thirteen terms for further study. Results from an online survey (N=62) and interviews (N=10) showed strong agreement with *harmony, perception, meaning, psychology,* and *printing* identified as areas of importance in the design process.

REFERENCES

Baya, V., J. Gevins, C. Baudin, A. Mabogunje, G. Toye and L. Leifer. 1992. An Experimental Study of Design Information Reuse, In *Proceedings of the 4th International Conference on Design Theory and Methodology, ASME*. Scottsdale, Arizona, 141-147.

Leeuwen, T. V. 2011. *The language of colour: an introduction,* London: Routledge.

Turner, B. S. 2006. *The Cambridge Dictionary of Sociology,* Cambridge: Cambridge University Press.

Park, C. and M. Allaby. 2013. *A Dictionary of Environment and Conservation*, Oxford: Oxford University Press.

Colman, A. M. 2009. *A Dictionary of Psychology,* Oxford: Oxford University Press.

Senda, Y. and Y. Sinohara. 2002. Analysis of Titles and Readers: For Title Generation Centered on the Readers, In *Proceedings of COLING 2002.* Taipei, 421–424.

Ruben, B. D. 1992. The communication-information relationship in system-theoretic perspective, *Journal of the American Society for Information Science* 43(1): 15-27.

Wodehouse, A. J. and W. J. Ion 2010. Information Use in Conceptual Design: Existing Taxonomies and New Approaches, *International Journal of Design* 4(3): 53-65.

Address: Seahwa Won, School of Design,
University of Leeds, Leeds, LS2 9JT, UK
E-mails: sdsw@leeds.ac.uk

Relationship between Perceived Whiteness and Color Vision Characteristics

Ichiro KATAYAMA,[1] Koichi IGA,[2] Shoko ISAWA,[3] Tsuneo SUZUKI[4]
[1] Faculty of Biology-Oriented Science and Technology, Kinki University
[2] Color Universal Design Organization
[3] Faculty of Contemporary Human Life Science, Tokyo Kasei Gakuin University
[4] Faculty of Law, Keio University

ABSTRACT

We used a liquid crystal color display to present various near-white stimuli, equivalent to a Munsell Value of 9.5 and a Munsell Chroma of 0.25, and had observers with normal color vision (N-type) and observers with color vision deficiencies (P-type, Pa-type, D-type, Da-type) evaluate respective relative whiteness. Compared to N-type observers, observers with color vision deficiencies, regardless of their color vision type, showed a tendency to evaluate perceived whiteness as being lower for the stimuli ranging from reddish hue to yellowish hue, including the long-wavelength component. Differences in evaluation results among observers with color vision deficiencies were smaller than those of N-type observers.

1. INTRODUCTION

Fluorescent whitening agents and bluish dyes are added to white clothing and printer paper to evaluate the increased perceived whiteness of these objects. This is done to take advantage of the color components that contribute to the perception of brightness (Katayama and Fairchild 2010). Until now, research on the effects of color on perceived whiteness has been conducted on observers with normal color vision (Ganz 1979). However, comparisons with color deficient observers (Gegenfurtner and Sharpe 1999), who account for a certain portion of the population, have not to be made. This study investigates the relationship between the color vision characteristics of observers and perceived whiteness, with regard to near-white stimuli of a variety of hues.

2. EXPERIMENTAL APPARATUS AND METHOD

We used a liquid crystal color display (Eizo CG223W), on which a white point was adjusted to match the chromaticity of the standard illuminant D65. Twelve types of near-white stimuli were then presented to the observers. We adjusted the hues of the stimuli to be exactly 10PB, 3PB, 5B, 7BG, 9G, 3G, 3GY, 5Y, 4YR, 4R, 7P and N in Munsell notation; the lightness was adjusted to 9.5 in Munsell notation; and the Munsell Chroma was set to 0.25 with the exception of the achromatic stimulus N, using a color luminance meter (Minolta CS-100). Figure 1 shows the chromaticity distribution of the stimuli. The rectangle mark in the figure indicates the chromaticity point of D65 and the two oblique lines indicate the boundaries of the tint index, $T_w = 2$ and $T_w = -4$, for the CIE whiteness formula. The viewing angles of the square-shaped stimulus were approximately 4 degrees and the stimulus pair was displayed on an N7 equivalent achromatic background for the side-by-side comparison.

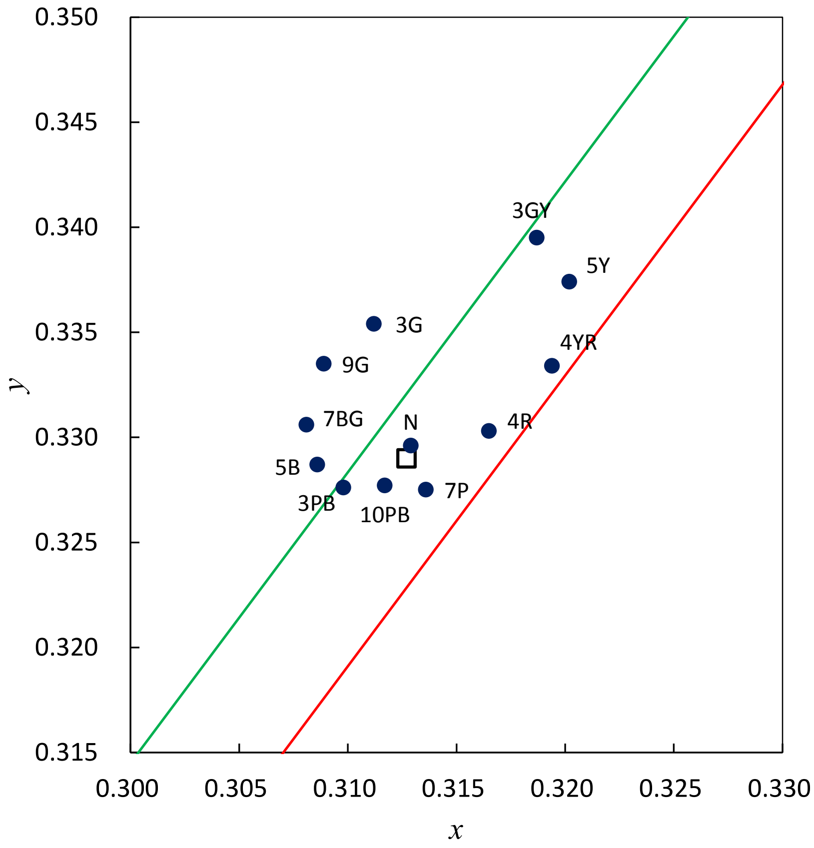

Figure 1: Chromatisity distribution of the stimuli.

After the observers adapted to the N7 background displayed on the liquid crystal color display for one minute, they were asked to select the stimulus which they thought to be whiter from the pair of near-white stimuli. The stimulus pairs were presented in random order, and the observers evaluated each of them twice.

3. OBSERVERS

The observers consisted of 15 persons with normal color vision (N-type), seven persons with Dichromatic Protanopia (P-type), four persons with Anomalous Trichromatic Protanomaly (Pa-type), seven persons with dichromatic Deuteranopia (D-type), and three persons with Anomalous Trichromatic Deuteranomaly (Da-type). The color vision characteristics of the observers were confirmed using the Ishihara Color Test and the Panel D-15 Test. The average age of the observers were as follows: N-type; 27.0, P-type; 55.1, Pa-type; 56.0, D-type; 50.4 and Da-type; 66.3. All of the N-type observers were female and all of the observers with color vision deficiencies were male.

4. RESULTS AND DISCUSSION

By testing the consistency of the results of the paired comparisons made by each observer, it was confirmed that the results were statistically significant. The differences in the results between the P-type and the Pa-type observers, and the differences in the results between the D-type and the Da-type observers were small. Therefore, we analyzed them as P_Pa-type

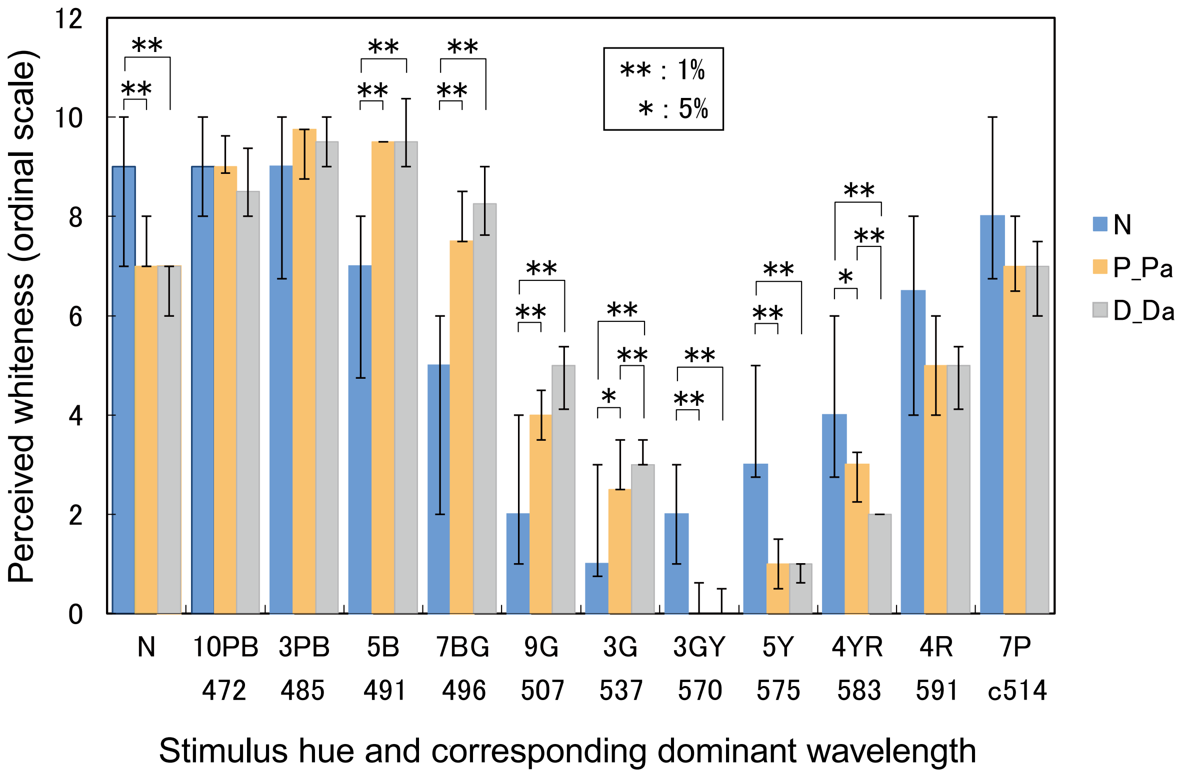

Figure 2: Median of the perceived whiteness for each stimulus from the evaluation results of each observer group (N-type, P_Pa-type, D_Da-type).

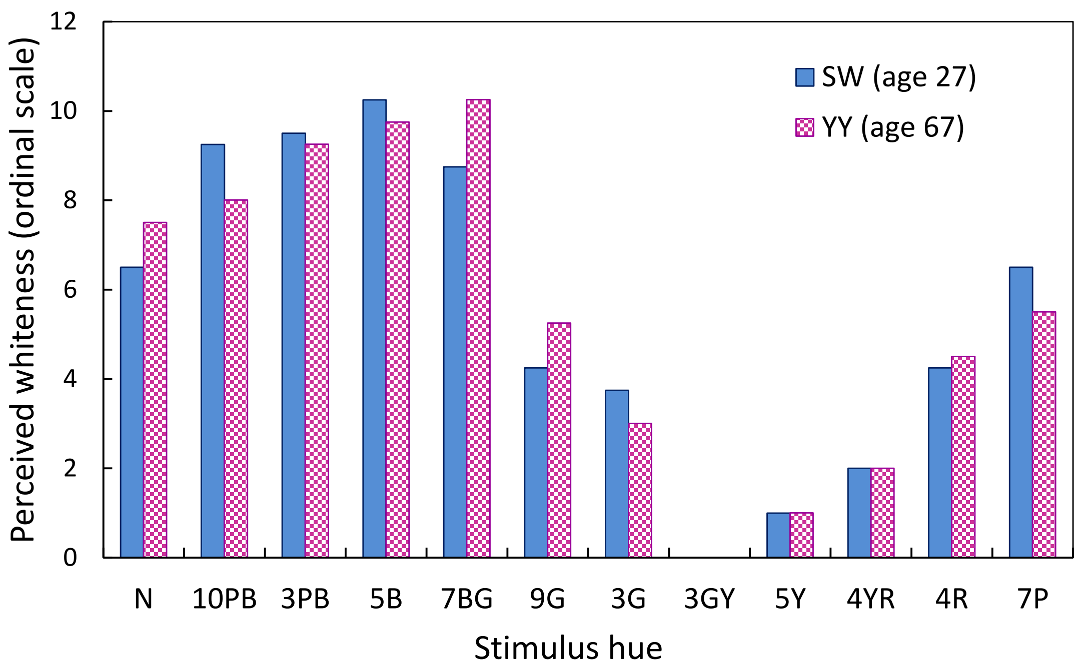

Figure 3: Comparison between the youngest and the oldest D-type observer.

and D_Da-type, respectively. We obtained the median of the perceived whiteness for each stimulus from the evaluation results of each observer group (N-type, P_Pa-type, D_Da-type). The results are shown in Figure 2. The abscissa represents the Munsell Hue and dominant wavelength of each stimulus, and the ordinate represents the relative rank value for perceived whiteness. In this figure, a higher ordinate value denotes a higher perceived whiteness. The error bars represent the median plus or minus the 25th percentile. Multiple comparison results among the three observer groups are also denoted.

The overall evaluation results show that there was a tendency for perceived whiteness to be evaluated as low for stimuli ranging from green hue to yellow-green hue regardless of color vision characteristics. However, some differences were observed among the three observer groups. The average age of the observers with color-vision deficiencies was higher than that of the N-type observers. Thus, we investigated the effect on whiteness evaluation with age. Among the D-type observers, the evaluation results of the youngest observer (SW: 27 years of age) and those of the oldest observer (YY: 67 years of age) are shown in Figure 3, respectively. The abscissa in the figure represents the Munsell Hue of the stimulus, and the ordinate represents the rank value for the perceived whiteness. As Figure 3 shows, large differences in evaluation results between the observers were not observed. Similarly, in the other observers with color vision deficiencies, no differences in evaluation tendencies were observed. Thus, our study focused only on color vision characteristics.

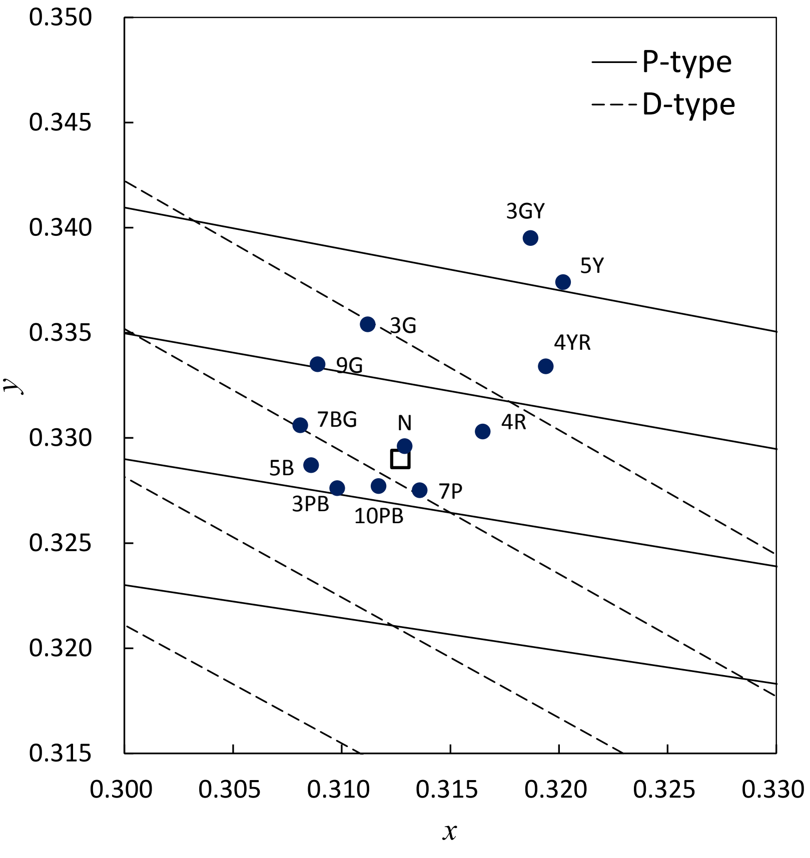

Figure 4: Relationship between the chromaticity of the stimuli and the color confusion loci.

The evaluation results for P_Pa-type and D_Da-type observers were similar, and significant differences were observed only for 3G and 4YR stimuli. However, significant differences were observed in the results between N-type and color deficient observers regarding eight stimuli. Overall, the P_Pa-type and the D_Da-type observers had a tendency to evaluate perceived whiteness as being lower for the stimuli, ranging from reddish hue to yellowish hue, including the long-wavelength component, compared to the N-type observers. This is thought to be caused by the P_Pa-type and the D_Da-type observers having lower sensitivity in long-wavelength for brightness perception compared to the N-type observers.

Next, Figure 4 shows the relationship between the chromaticity of the stimuli and the color confusion loci. The solid lines in the figure represent the P-type color confusion loci and the broken lines represent the D-type color confusion loci. In conjunction with the results shown in Figure 2, the P_Pa-type and the D_Da-type observers evaluated perceived whiteness at almost the same level as the greenish and reddish stimuli along the color confusion loci. Also, the length of the error bars shown in Figure 2 indicates that inter-observer variability in color deficient observers was smaller than that for N-type observers. This might be due to N-type observers having individual internal criteria when evaluating reddish-white or greenish-white as being whiter.

5. CONCLUSIONS

The results of examining the relationship between the perceived whiteness and color vision characteristics showed the following conclusions:

(1) Regardless of color vision characteristics, perceived whiteness was evaluated as being low for near-white stimuli with hues ranging from green to yellow-green.

(2) The difference in results between P-type and Pa-type observers, and the difference in results between D-type and Da-type observers was small.

(3) The results for P_Pa-type and D_Da-type observers were similar, and significant differences were observed only for 3G and 4YR stimuli.

(4) Compared to N-type observers, P_Pa-type and D_Da-type observers had a tendency to evaluate perceived whiteness as being lower for reddish stimuli and to evaluate perceived whiteness as being higher for greenish stimuli.

(5) The inter-observer variability for color deficient observers in the evaluation was smaller than that for N-type observers.

REFERENCES

Ganz, E. 1979. *Whiteness perception: individual difference and common trends*, Applied Optics 18(17) 2963-2970.

Gegenfurtner, K.R. and L.T. Sharpe 1999. *Color vision: from gene to perception*. Cambridge: Cambridge University Press.

Katayama, I. and M.D. Fairchild 2010. *Quantitative Evaluation of Perceived Whiteness Based on a Color Vision Model*, Journal of Color Research and Application 35(6) 410-418.

Address: Ichiro KATAYAMA, Department of Biomechanical and Human Factors Engineering, Faculty of Biology-Oriented Science and Technology, Kinki University, 930 Nishimitani, Kinokawa, Wakayama, 649-6493, JAPAN
E-mails: katayama@waka.kindai.ac.jp, iga@cudo.jp, isawa@san.kasei-gakuin.ac.jp, suzukitn@hc.cc.keio.ac.jp

An Experiment of Color Rendering with 3D Objects

Laura BLASO,[1] Cristian BONANOMI,[2] Simonetta FUMAGALLI,[1] Ornella LI ROSI[1]
Alessandro RIZZI,[2]
[1] Italian National Agency for New Technologies, Energy and Sustainable Economic Development ENEA, UTTEI-SISP
[2] Department of Computer Science, Università degli Studi di Milano

ABSTRACT

The Color Rendering Index was developed by CIE in order to measure how accurate a light source is at reproducing the color appearance of the lighted scene. This index has been used for many years by research and industry but unfortunately it tends to fail the scoring of the new LED-based lighting systems, as demonstrated by many experiments.

Many attempts to develop a more reliable index have been done, but a definitive method has not been found yet. In developing alternative color rendering indices, the aim is to achieve an index able to help in choosing a light source, maximizing the perceived quality of its color appearance reproduction. An index with a very high or a very low score is easy to interpret, but the goal is to attain a color-rendering index able to scale changes in color shift proportional to our vision between the two extremes.

One aspect not enough investigated in literature, is the influence of the characteristics of the observed scene in the color appearance preservation under varying illuminants. The presented work aims at investigating appearance variation of real non-flat objects under varying light sources, according to human color sensation. During the experiment participants had to compare a set of 3D color samples observed under a reference light source and under a test light source. Participants' answers were recorded through a questionnaire. Finally, results are compared with a set of alternative color rendering indices.

1. INTRODUCTION

The Color-Rendering Index (CRI) is the actual standard to specify the visual rendering properties of a light source (CIE, 1995). With the advent of new types of lighting devices, the CRI has shown its limits, that is the ability of having measurements in accordance with the human visual system perception (Joist-boissard, Fontoynont and Blanc-gonnet, 2009; Brueckner, Bodrogi and Khanh, 2009; Sandor and Shanda, 2005). The standard method for calculating the Color-Rendering Index does not succeed in predicting the visual response under narrow band light sources, such as three-band fluorescent lamps or white LEDs (Narendran and Deng, 2002; Bodrogi et al., 2004). These types of light sources show a rather low Color-Rendering Index, but a pleasant visual appeal and a good preservation of color. Many attempts to standardize a new method for the calculation of the color rendering have been made, but no one seems to be definitive.

In general, color rendering indices are computed in relation to a reference light source, therefore a maximum score is expected when considering light sources very close to the reference one. Difficulties arise in having a color rendering index able to scale changes in color shift proportional to human vision. Aim of the test here presented is to assess how our visual system judges the color rendering of various light sources, in order to have a baseline to compare with available color rendering indices.

2. METHOD

The main goal of this research is to collect data about the color appearance variation according to the used light source, in order to analyze the relation between a set of color rendering indices and the evaluation given by users.

2.1 The Task

The experiment, involving 48 students of a high-school (21 females and 27 males), aged between 14 and 18 years, aimed to compare 3D color samples (orange, green, white, blue, yellow, and red bricks, part of the toy showed in Figure 1) observed under a reference light source and under a test light source (Table 2). Building a 3D scene introduces shadows and inter-reflections, created by complex geometries, in order to reproduce what happens in everyday scenes.

Observers were requested to evaluate the differences between each pair of brick color. A two-stage approach was proposed: at first, a qualitative assessment to make a rough categorization, evaluating if bricks are identical, similar, or different; in the second stage, participants had to assign a number between 0 and 100, according to the category previously chosen.

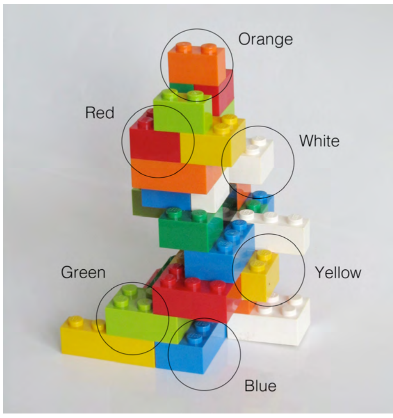

Figure 1: 3D building used in the experiment.

2.2 Experiment Setup

Four wood boxes have been constructed with size: 1 m × 1 m × 0.8 m. The inside of each box was covered with white paper. The upper part of the box was screened with a panel, to avoid direct light reaching the observers' eyes. Four identical plastic brick constructions have been placed inside the four boxes. Two light sources are housed in each box, and only one at a time was turned on. The experiments have been conducted in a dark room without time limits. Observers accomplished the experiment after a light adaptation period. The whole test has been carefully explained in advance and continuously supervised by one of the authors, to solve any possible doubt of the observers.

2.3 Light Source

Six light sources have been tested: three fluorescent, one halogen, and two LED lamps. Another halogen light source was used as reference, having the color-rendering index equal to 100. In Table 1, some of the features of the light sources used in the experiment are described.

Table 1. Light sources used in the experiments.

Light source	L.S. #1	L.S. #2	L.S. #3	L.S. #4	L.S. #5	L.S. #6	Ref. L.S.
Power (W)	20	11	11	8	3	30	42
Flux (lm)	1250	650	600	345	270	806	630
Lux (lx)	913	546	457	338	171	470	390
CCT	2969	7566	4393	3441	3178	3239	3050
Type	Fluo.	Fluo.	Fluo.	LED	LED	Halo. IRC	Halo.

Note that the second light source (L.S. #2) has a CCT of 7566 K, very different from the others. The choice of utilizing this lamp lied in the will to test it as an extreme condition. Time has been given to the observers to adapt to the average luminance level, similar in all the boxes.

2.4 Results

In Table 2, a set of calculated color-rendering indices is shown: Standard CIE CRI, CRI R96a (CIE, 1999), CQS (Davis and Ohno, 2006), CRI2012 (Smet et al., 2013), CRI-00 (Geisler-Moroder and Dur, 2009), CRI-CAM02 UCS (Li et al., 2012), GAI (Freyssinier-Nova and Rea, 2010), RCRI (Bodrogi and Brueckner, 2009), as well as the indices estimated by the users. Although the GAI and CQS are not fidelity indices, it was decided to test them too, for comparison purposes. Data are plotted for each light source in Figure 2, where the column filled in black represents the participants' answers.

In the following some comments about the effect of the different light sources are given.

L.S. #1 (Fluorescent): the observers give a score of 86. The standard CRI, the CAM02UCS and CQS give a score around 80 to the light, in line with the result of the observers.

L.S. #2 (fluorescent): R96a (with a score of 79) is the method that better estimates observers' evaluations (78).

L.S. #3 (Fluorescent): even if in all the cases the algorithms underestimate the observers' result (82), each method produces a good approximation of the result, with scores in a range between 74 (RCRI) and 80 (CRI00, CAM02UCS, CQS).

L.S. #4 (LED): all the methods give a good approximation to the observers' evaluation (80), with the exception of GAI which underestimates the result.

L.S. #5 (LED): the various methods give very different scores. CQS (71) and CRI2012 (69) get closer to the result of the observers (70).

Table 2. Color rendering indices calculated for each light source for the methods described and users evaluation.

Light source	L.S. #1	L.S. #2	L.S. #3	L.S. #4	L.S. #5	L.S. #6
Std. CRI	80	83	78	83	63	98
CRI 00	76	86	80	84	63	98
GAI	45	98	79	61	40	57
R96a	58	79	78	84	62	75
CAM02UCS	79	85	80	84	67	97
CQS	80	85	80	82	71	96
RCRI	71	89	74	89	62	100
Ra2012	68	69	76	85	69	99
User 3D	86	78	82	80	70	91

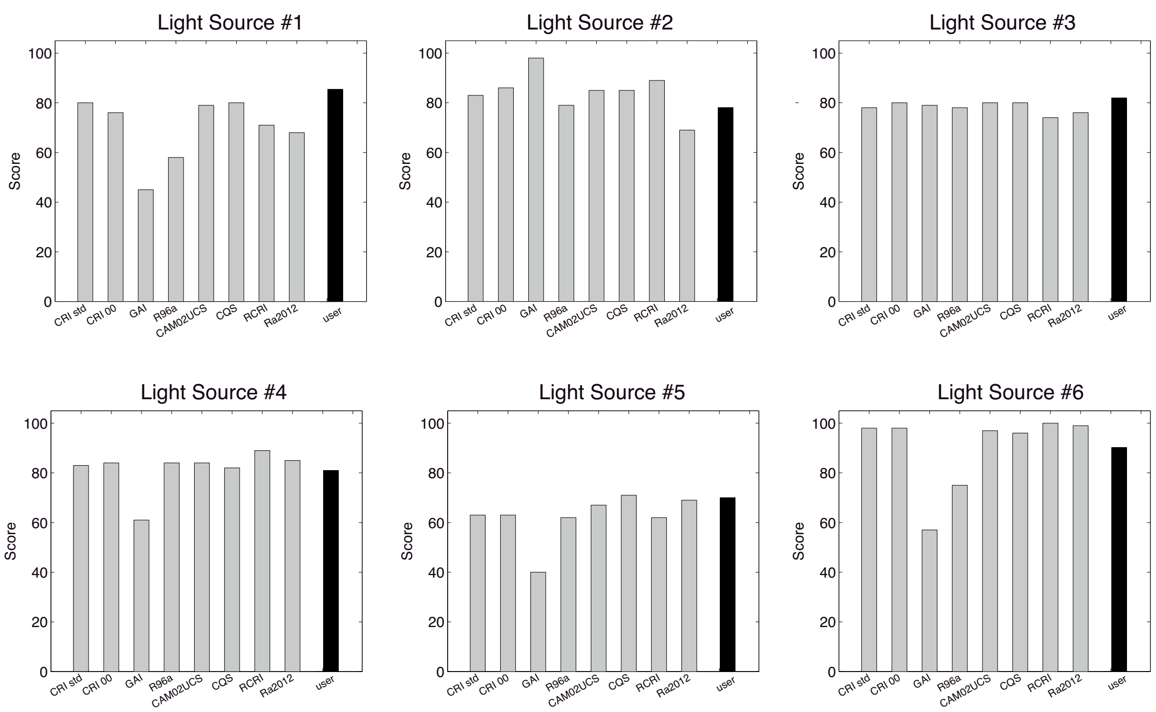

Figure 2: Comparison between the calculated and perceived color rendering indices for each light source. The bars represent: the standard CIE CRI Ra, CRI 00, GAI, R96a, CAM02UCS, CQS, RCRI, CRI2012, and the index evaluated by the users (black bar).

L.S. #6 (Halogen). All the methods except GAI (57) and R96a (75) overestimate the observation result (91). This is due to the fact that the halogen light source has a spectrum that can be approximated with a black body radiation. Therefore, the reference light source calculated by the various methods is almost identical to the light source to test, resulting in a high CRI.

The Pearson correlation coefficients have been calculated: the method that better represents the sensation of the observers, for this experiment setup, is the Standard CRI (0.875), followed by CAM02UCS (0.821), CQS (0.819), CRI 00 (0.779), CRI2012 (0.630), RCRI (0.629), R96a (0.115), and GAI (0.02).

For more details about the experiments and the results, refer to the work of Fumagalli, Bonanomi and Rizzi (2015).

4. CONCLUSIONS

A test involving users have been designed, in order to attain a data to better understand the mechanism of color rendering assessment. During the experiment participants had to compare a set of 3D color samples observed under a reference light source and under a test light source. Users' result were then compared to a set of CRIs available in literature.

Assessing color rendering among various light sources is a complex task. This process involves many aspects that can lead to different results: the colors under test, the user's experience, the context in which colors are analyzed, and many other factors. Calculating the correlation indices between user observations and a set of CRIs shows that the standard CRI is the method that best performs in this case.

REFERENCES

Bodrogi, P., P. Csuti, F. Szabo,and J. Schanda. 2004. Why Does the Colour Rendering Index Fail for White Rgb Led Light Sources? In *CIE Expert Symposium on LED Light Sources*, Tokyo, 1–4.

Bodrogi, P., and S. Brueckner. 2009. Re-defining the Colour Rendering Index. In *CIE Proceedings*, Budapest,

Brueckner, S.,P. Bodrogi, and T.Q. Khanh. 2009. Colour Rendering of New White Led Light Sources Visual Tests. In *Proceedings of 11 Lux Europa*, Istanbul, 397–404.

CIE, 1995. Method of Measuring and Specifying Colour Rendering Properties of Light Sources. CIE Technical Report 13.3.

CIE, 1999. Colour Rendering. TC 1–33 Closing Remarks. CIE Pubbl. No. 135/2.

Davis, W., and Y. Ohno. 2006. Development of a Color Quality Scale. In *Proceedings in Sixth International Lighting Research Symposium on Light and Color*, Orlando, FL.

Freyssinier-Nova, J.P., and M.S. Rea. 2010. A Two-metric Proposal to Specify the Color-rendering Properties of Light Sources for Retail Lighting. Tenth International Conference of Solid- State Lighting, In *Proceedings of SPIE*, San Diego, CA.

Fumagalli S., C. Bonanomi, and A Rizzi. 2015. Experimental assessment of color-rendering indices and color appearance under varying setups. *Journal of Modern Optics* 62: 56-66.

Geisler-Moroder, D., and A. Dur. 2009. Color-rendering indices in global illumination methods. *Journal of Electron. Imaging* 18: 043015-1–043015-12.

Jost-boissard, S., M. Fontoynont,and J. Blanc-gonnet. 2009. Colour Rendering of Led Sources: Visual Experiment on Difference, Fidelity and Preference. In *CIE Light and*

Lighting Conference with Special Emphasis on LEDs and Solid State Lighting, Budapest.

Li, C., M.R. Luo, C. Li, and G. Cui. 2012. The CRI-CAM02UCS colour rendering index. *Color Research Application* 37: 160–167.

Narendran, N., and L. Deng. 2002. Color Rendering Properties of Led Light Sources. In *Proceedings of SPIE*, Seattle, WA, 61–67.

Sandor, N., and J. Schanda. 2005. Visual Colour-Rendering experiments. In *10th Congress of the International Colour Association*, Granada, 511–514.

Smet, K.A.G., J. Schanda, 2013. L. Whitehead, and R.M. Luo. CRI2012: A Proposal for Updating the CIE Colour Rendering Index. *Lighting Research and Technology* 45: 689-709.

Address: Doct. Laura BLASO, Department of Applied Optics, School of Engineering, Italian National Agency for New Technologies, Energy and Sustainable Economic Development ENEA, UTTEI-SISP, Via Enrico Fermi 2749, 21020 Ispra, VA, ITALY
E-mails: laura.blaso@enea.it, cristian.bonanomi@unimi.it, simonetta.fumagalli@enea.it ornella.lirosi@enea.it, alessandro.rizzi@unimi.it

Adapting and adapted colors under colored illumination

Mitsuo IKEDA[1], Chanprapha PHUANGSUWAN[1], and Kanwara CHUNVIJITRA[2]
[1]Color Research Center, Rajamangala Univ. of Tech. Thanyaburi, Thailand
[2]Faculty of Mass Communi. Tech., Rajamangala Univ. of Tech. Thanyaburi, Thailand

ABSTRACT

The state of chromatic adaptation was investigated by measuring the adapted color for the adapting color by the environment-stimulus independent illumination technique. Seven colors were employed for a subject room and the subject judged the color appearance of an achromatic test patch placed in a test room through a window between the two rooms. The angle from the adapting color to the adapted color was obtained. The angles were read out from other works available in journals and they were all plotted on one graph. The angle did not follow the opponent relation. That is, the unique red adapting color did not cause the adapted color to be the unique green. There were only two adapting colors that gave the opponent colors in the adapted color. The effect of saturation of the adapting color on the adapted color was investigated and no significant effect was found.

1. INTRODUCTION

The state of chromatic adaptation could be known by the apparent color of an achromatic patch placed at the center of a uniform colored background, the phenomenon being known as the simultaneous color contrast. If the background is red the apparent color or adapted color is green, for example. The adapted green is very pale, however, to be used to investigate the chromatic adaptation in detail. Vivid adapted color can be obtained by the two rooms technique or the environment-stimulus independent illumination technique developed by Ikeda and his colleagues[1)]. Even if the psychophysical color expressed by x and y chromaticity coordinates are made equal for a wide area of the retina in both techniques, the uniform colored background and the two rooms, the color appearance of the test patch obtained is almost achromatic by the former, while it is very vivid by the latter[2)]. In the present experiment the two rooms technique was employed and the color appearance of an achromatic test patch was measured by the elementary color naming method for seven different colors of illumination for a subject room. To show the relationship between the color appearance of illumination of the subject room and the color appearance of a test patch the angle from the former to the latter was calculated on the polar diagram used in the opponent colors system. An additional experiment was carried out, where the saturation of the illumination of the subject room was changed and the color appearance of the test patch was measured.

2. APPARATUS

Figure 1 shows the apparatus composing of two rooms, a subject room and a test room separated by a wall on which a large window W of the size 40 cm wide and 30 cm high was opened so that the subject could see an achromatic test patch T made of a white board without any scratches and placed against the back of the test room. It was illuminated by two fluorescent lamps Lt of the daylight type.

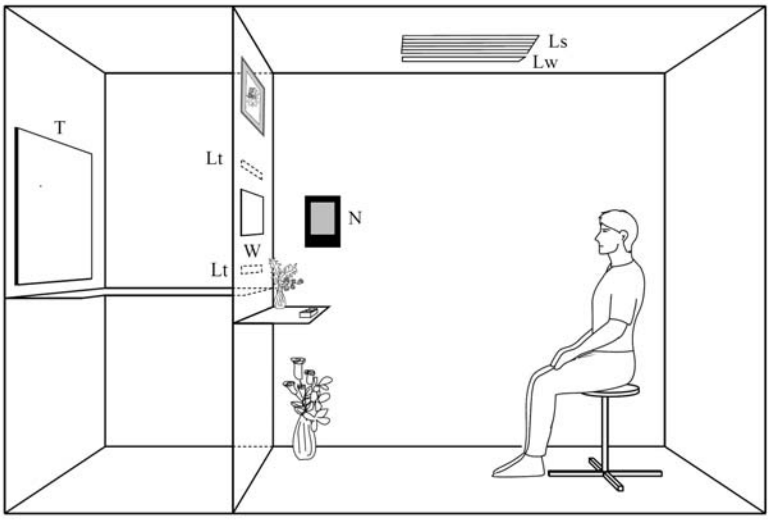

Fig. 1 Apparatus composing of a subject room (right) and a test room (left).

The distance from the subject to the window W was 180 cm and the visual angle of W became 13° × 10°. The subject room was decorated with various objects to simulate a normal room. The five ceiling fluorescent lamps in the subject room Ls were covered by a colored film to give a colored illumination to the subject room. One of the lamps was adjustable in its intensity. To change the saturation of the color another fluorescent lamp Lw was attached to the ceiling.

Seven different colored films were employed for the subject room and their chromaticity coordinates u'v' are shown by open circles in Fig. 2 denoted as CRC3. The illuminance measured on the front shelf in the subject room was kept at 50 lx for all the colors. The subject's task was to judge the color appearance of the window W by the elementary color naming method. The measurement was repeated for five times at different sessions. The horizontal illuminance near to T on the shelf of the test room was kept at 9 lx. In the additional experiment on saturation five colors of illumination of different saturation were employed for red and green illumination as shown in Fig. 3, by open circles for red and open squares for green. The illuminance was not particularly controlled and it varied for different saturation.

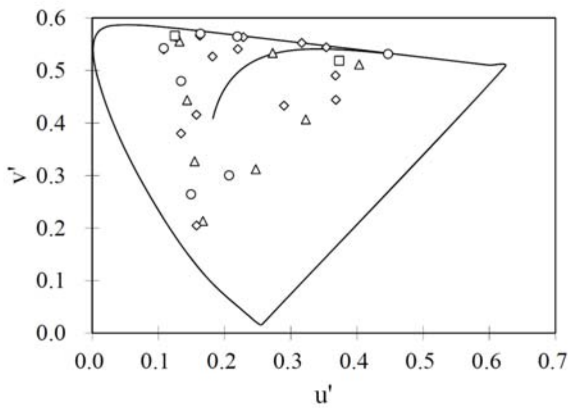

Fig. 2 Colors employed for the subject room illumination. △, Rits[3]; ◊, CRC1[4]; □, CRC2[2]; ○, CRC3, present work.

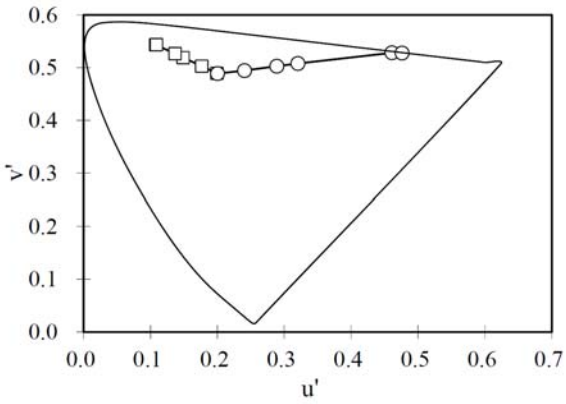

Fig. 3 Colors employed for the subject room illumination in the saturation experiment. ○, red; □, green.

An achromatic patch N of N6 in Fig. 1 was used for the measurement of the color appearance of the subject room. At the measurement the window W was made small, 2 x 2 cm^2, through which a subject looked at N and judged color with the elementary color naming method. The horizontal plane illuminance in front of the white board was kept at 130 lx. The measurement was repeated for five times.

Five subjects participated in the main experiment and two of them in the additional experiment, all normal in color vision as tested by the 100 hue test.

3. RESULTS AND DISCUSSION

For any color of illumination the entire field of the window appeared uniformly colored. Subjects perceived as if a colored paper was pasted on the window, which implied that the subjects perceived the window as an object placed in the subject room. Results of subjects CP and KC from the main experiment are shown in Fig. 4 by a polar diagram for the case of reddish blue illumination. R, Y, G, and B indicate the unique hues of red, yellow, green, and blue and the hue appearance obtained by the elementary color naming is shown by the angle from the unique red. The amount of chromaticness is shown by the radiant distance from the center becoming 100 % at the outmost circle. Open circles show the color appearance of the subject room judged from the test room through a small window, which we called the adapting color. Open squares show the color appearance of the test patch of white board judged from the subject room on the large window, which we called the adapted color. Small symbols indicate five repetitive judgments and large symbols connected by lines through the origin indicate their average. We see that the variance within a subject is not large but the variance among subjects is large.

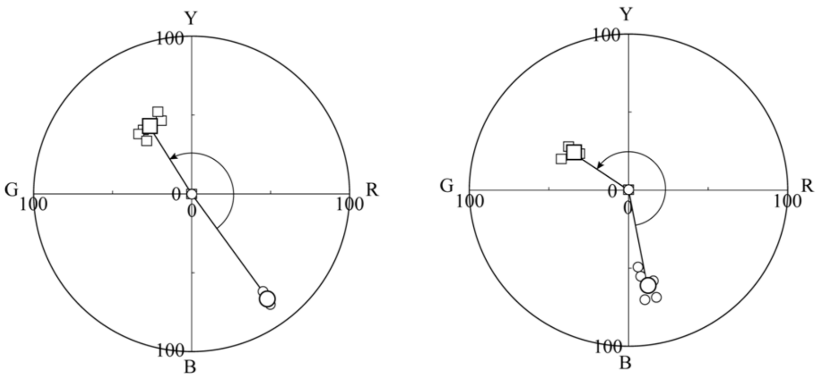

Fig. 4 Adapting and adapted colors for a reddish blue illumination color. ○, adapting color; □, adapted color. Subjects CP (left) and KC (right).

We are interested in the relationship between the adapting color and the adapted color and we obtained the angle from the former to the latter, $\Delta\theta$ measured in anticlockwise as shown in the diagram of the subject CP and KC. It was 176° in CP and 225° in KC. We took the average of $\Delta\theta$ for all five subjects for all the seven colors of illuminations and plotted them for the adapting angle. The results are shown by open circles in Fig. 5. The abscissa gives the adapting angle in degree and the ordinate the angle difference $\Delta\theta$. A horizontal dotted line indicates $\Delta\theta = 180°$.

In the past there are other similar data available, though for different purposes in some cases[2-4)]. We read out $\Delta\theta$ from their papers which are listed in Table 1 together with number of subjects, the window size, number of colors investigated, and the color appearance mode. The present work is specified as CRC3. The illumination colors

Table 1 Works used to obtain $\Delta\theta$ plotted in Fig. 5.

Authors	Sub	Test size	Colors	Mode
Rits	5	6cm circluar	8	Object
CRC1	5	4x4 cm^2	14	Object
CRC2	4	4x4 cm^2	2	Object
CRC3	5	40x30 cm^2	7	Object

triangles for Rits[3)], open diamond for CRC1[4)], open squares for CRC2[2)], and open circles for the present work, CRC3, in Fig. 2.

All the angles $\Delta\theta$ read out from these works are plotted together for the adapting color by different symbols in Fig. 5. For the data of CRC1, CRC2, and CRC3 the standard deviations of subjects are shown by short vertical bars. It is clear from these data that $\Delta\theta$ is not necessarily 180° for the adapting color. In fact the exact opponency between the adapting color and the adapted color takes place at only two adapting colors, yellowish green and reddish blue. The data can be approximated by a sine curve as shown by a thick line.

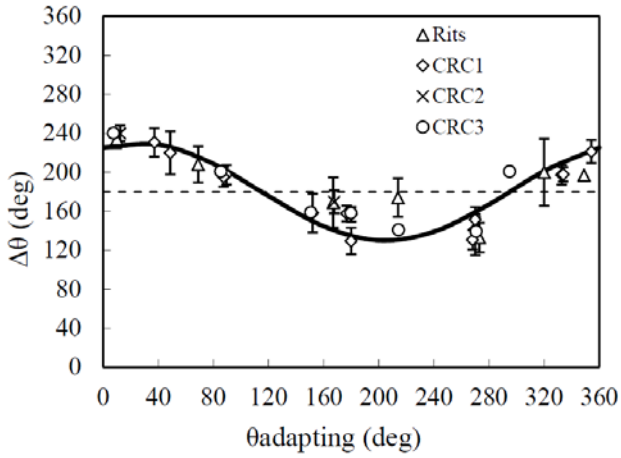

Fig. 5 The angle from the adapting color to the adapted color plotted for the adapting color. Data from four researches are plotted together.

The data in Fig. 5 were obtained by various authors and the experimental condition was inevitably different among them as to the illuminance and the saturation. To see the effect

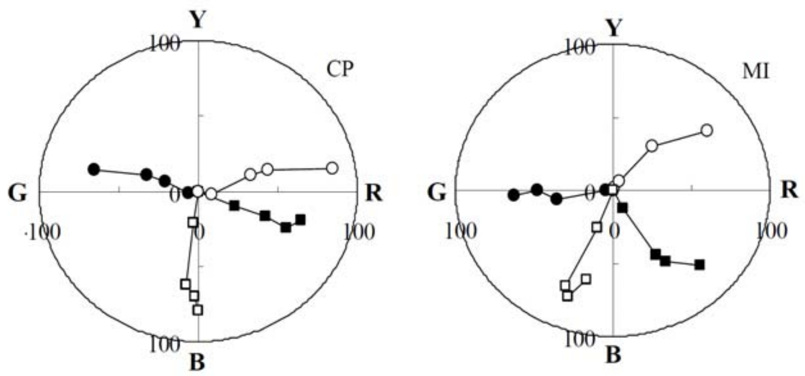

Fig. 6 Adapting and adapted colors for a red (open symbols) and green (filled) illumination. Circles, adapting color; Squares, adapted color. Subjects CP and MI.

of the saturation of the illumination in the subject room the additional experiment was done where the saturation was changed in the red and green colors that were employed for the main experiment as shown in Fig. 3. The results of the color appearance of the test patch are shown for the two subjects CP and MI in Fig. 6. Circles show the color appearance of the illumination and squares that of the test patch. There is observed change in the color appearance of the test patch for different saturation of the illumination but small.

The effect of the luminance of the test patch was investigated by Ikeda et al.[3]. Again there was observed the effect but small.

To conclude the adapting and adapted colors are roughly opposite in the opponent colors diagram but not exact. When the angle from the former to the latter is plotted the curve obeys sinusoidal shape.

REFERENCES

1) Ikeda, M. and S. Fukumura, 1995. Formation of a recognized visual space of illumination with increasing initial visual information. Jr. Illum. Engng. Inst. Jpn. 79: 392-399. [in Japanese].

2) Ikeda, M., W. Naksuwan, and C. Phuangsuwan, 2014. Chromatic adaptation is not for object but for illumination. Jr. Col. Sci. Assoc. Jpn 38: 174-175.

3) Ikeda, M., Y. Mizokami, S. Nakane, and H. Shinoda, 2002. Color appearance of a patch explained by RVSI for the conditions of various colors of room illumination and of various luminance levels of the patch, Opt. Rev. 9: 132-139.

4) Spirat, P., C. Phuangsuwan, and M. Ikeda, 2014. Chromatic adaptation to illumination investigated with two rooms technique, Jr. Col. Sci. Assoc. Jpn 38: 176-177.

Address: Prof. Mitsuo IKEDA, Color Research Center, Rajamanjala University of Technology Thanyaburi, 39 Moo 1 Klonghok Klongloung, Patumthani, 12110, THAILAND
E-mails: kaymitsuo@gmail.com

Color constancy depends on initial visual information

Chanprapha PHUANGSUWAN,[1] Mitsuo IKEDA,[1] Kanwara CHUVIJITRA,[2]
[1] Color Research Center, Rajamangala University of Technology Thanyaburi, Thailand
[2] Faculty of Mass Comm. Tech., Rajamangala University of Technology Thanyaburi

ABSTRACT

The concept of the recognized visual space of illumination RVSI asserts that the color appearance of objects is determiend by the adapted brain to the color of illumination of the space where the objects are placed and then the color constancy holds. Without any object in a space there should be no recognition of the space and no color constancy. The object necessary for the recognition of a space is called the initial visual information IVI. In this paper number of flowers was increased to increase the IVI complexity and the color appearance of a white board placed in the space was measured to see the effect of IVI for the color constancy. Only a small piece of a flower already gave a space recognition and the color constancy to some extent. With increase of complexity of IVI the white board became more white and many flowers surrounded by side walls gave almost perfect color constancy. As an additional experiment still smaller IVIs were investigated and it was found that even a pair of white petals already helped the brain to construct a space perception.

1. INTRODUCTION

The color constancy is a well known property of the visual system and many scientists studied on this phenomenon from two different approaches. One is to emphasize the cone adaptation at the retina and the other is to emphasize the brain adaptation. The former is expressed as the bottom up thinking and the latter the top down thinking. Ikeda's RVSI concept is one of the top down thinking and the present paper was carried out along the theory[1)]. The RVSI theory says that when a person enters a room he/she recognizes the space, understands the illumination filling the space, and adapts to the illumination[2)]. He sees objects in the space with the adapted brain and sees a white object as almost white whatever the illumination color may be, the phenomenon being called the color constancy. It was clearly shown by Pungrassamee et al.[3)] and Ikeda et al.[4)] that the color appearance of an achromatic patch returned achromatic when a subject could recognize the existence of the space where the patch was placed to confirm the RVSI concept. A question how much information or initial visual information IVI of the space is needed to recognize the existence of the space is an interesting question and Phuangsuwan et al.[5)] showed only a small information could construct the space recognition for the color constancy to take place. Their finding showed that the first smallest IVI that they employed was already enough to produce the color constancy. In the present paper several IVI, which were considered very small IVI, were employed to know IVI necessary to construct a space recognition and thus to produce the color constancy.

2. APPARATUS AND EXPERIMENT

The two rooms technique or the environment-stimulus independent illumination technique was employed to carry out the experiment. It was composed of two rooms as shown in Fig. 1, a subject room where a subject stayed and a test room where a test patch was placed. There was opened a large window W of the size 40 cm wide and 30 cm high on the separating wall through which a subject observed a test patch for judging the color of the patch by the elementary color naming method. The entire apparatus was of the size, 300 cm deep, 120 cm wide, and 200 cm high. The subject room was decorated by objects to simulate a normal room. At the viewing distance of 180 cm the window W was the size 13° x 10° arc of visual angle. At the back wall of the test room a white board WB of about L* = 94 was vertically placed, which served as a test patch. It is large enough to fill out the window W when a subject observed it.

The inside of the subject room was pasted by a white wall paper of about L* = 86. The room was illuminated by five fluorescent lamps of the daylight type Ls. The intensity of one of them was adjustable by a light controller. The lamps were covered by a color film to give a colored illumination for the subject room. Four color films, red, yellow, green, and blue were prepared and the illuminance was adjusted to 50 lx when measured on the front shelf. Figure 2 shows their chromaticity points by open circles. Diamond and square symbols indicate the white board WB and D65. The test room was illuminated by the same fluorescent lamps Lt as the subject room at one of four horizontal plane illuminances, 0.5, 1, 3 and 9 lx when measured just in front of WB and on a shelf at the height 85 cm from the floor.

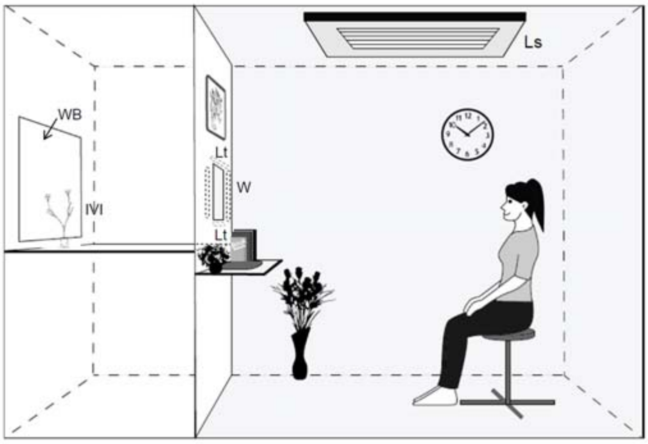

Fig. 1 A scheme of apparatus.

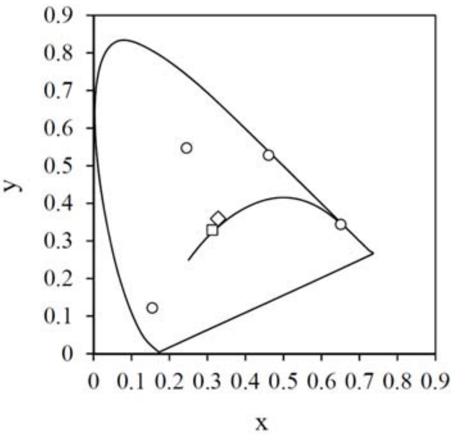

Fig. 2 Colors of illumination.

We first prepared seven initial visual information IVI, I_1 through I_7, as shown in Fig. 3. They were made of artificial flowers, white carnation, green leaves, red rose, and green fern. They were inserted into a white vase with blue line decoration.

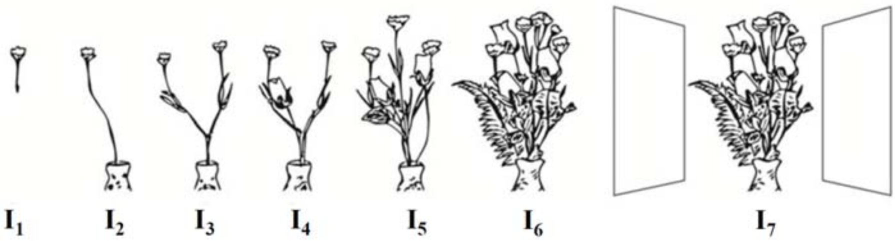

Fig. 3 Initial visual information.

The IVI I_7 was the same flower as I_6 but with walls at both sides to help subjects to perceive a more complete space[6, 7]. The wall was a cardboard of pale yellow with some texture of very low contrast. The lightness was L* = 82. Beside these seven IVI we showed subjects no object at all, which was denoted as I_0. IVI I_1 could not be put in a vase and was hung by a thin string from the ceiling. Each IVI was placed near WB as shown in Fig. 1 and the flower(s) sometime touched WB. Subject could not see the bottom portion of the vase as indicated in Fig. 3.

The subject's task was to judge the color of the white board WB nearby the flowers but avoiding their shadow by using the elementary color naming method. Five repetitions were conducted for the measurement for each condition; IVI, illuminance level, and illumination color. Five subjects, MI, MK, CP, KC, and PL with normal color vision participated in the experiment.

3. RESULTS AND DISCUSSION

Without any object but the white board only in the test room, namely with the condition of I_0, subjects saw only uniform color over the window W and pasted on W. In other words the subjects recognized the color belonging to the subject room. With I_1 the subjects could notice the white board in the test room implying the perception of the space.

In Fig. 4 the amount of chromaticness perceived on WB is shown on the ordinate for IVI number on the abscissa. The data points from I_7 are plotted at 9. Those were obtained for 1 lx illuminance of the test room and for the red adapting color. Squares were from the subject MI and circles from KC. Short vertical bars show the standard deviation of five repetitions. In these cases the SD of MI is larger for almost every IVI than KC but in some other conditions (not shown) MI showed smaller SD than KC. Difference between the two subjects is not small but in both subjects showed a similar tendency of decrease of chromaticness for larger IVI. With I_0 subjects saw adapted color on the window W as if there was pasted a paper of that color. With I_1 or with one piece of carnation flower they suddenly recognized the existence of the space of the test room and could perceive the surface of white board, which eventually decreased the amount of chromaticness as seen in Fig. 4. The chromaticness of the white board continuously decreased and the whiteness increased for larger IVI. With I_7 the white board appeared almost white to imply the color constancy.

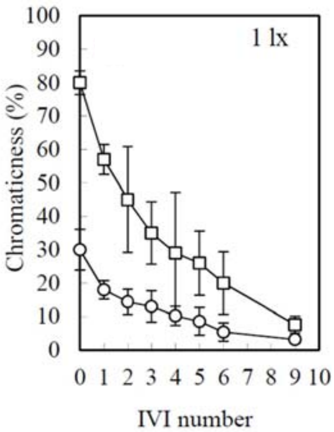

Fig. 4. Chromaticness plotted for IVI for red illumination. Squares, subject MI, and circles, KC.

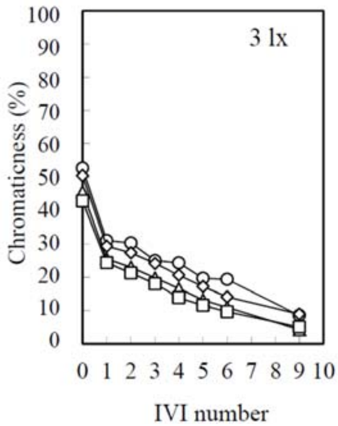

Fig. 5. Chromaticness plotted for IVI for red (circles), yellow (triangles), green (diamonds), and blue (squares).

Figure 5 shows the averaged amounts of chromaticness of five subjects for four illumination colors for different IVI, circles for red, triangles for yellow, diamonds for green, and squares for blue in the case of 3 lx test room illumination. Four curves showed very similar tendency. The drop of chromaticness at I_1 from I_0 was quite large. Amount of chromaticness of about 50% dropped down to about 30% with only one flower of carnation.

The average of four curves of Fig. 5 was taken and they are shown by circles in Fig. 6. In the figure the numbers of I_1 through I_6 were all increased by 6 so that the number of I_1 became I_7 (revised), for example. The number of original I_7 was also revised to become 14.3. The revision of the IVI number was conducted to approximate all the data points on a regression line as shown by a solid line, which can be written as Chr = - 2.9 × IVI + 47.9. In this way of plotting we can see that there remains a wide gap between I_0 and I_1 or I_7 (revised). It is amazing that even one piece of carnation flower already worked as initial visual information to construct an RVSI for the test room to some extent. With I_7 or $I_{14.3}$ (revised) the chromaticness went down to about 10% to show almost complete color constancy. The side walls were very effective for the recognition of a space and eventually for the color constancy.

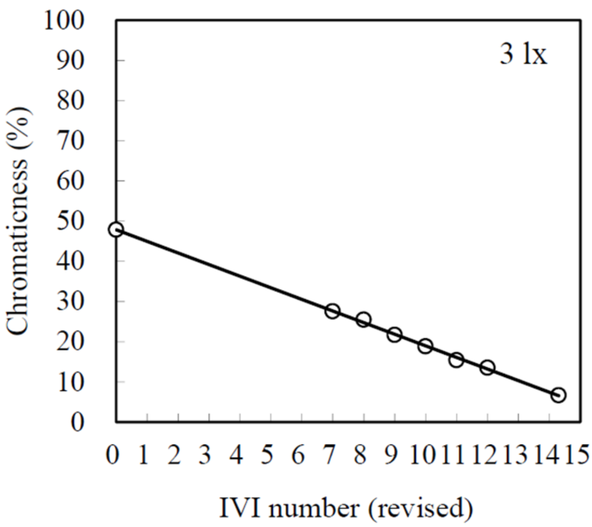

Fig. 6. Chromaticness plotted for the revised number of IVI.

An additional experiment was conducted to fill data points between I_0 and I_1 in Fig. 6 by further reducing the amount of IVI. The new IVIs are a pair of white petals, a green leave, and a white bud of carnation flower with a short green stalk as denoted I_A, I_B, and I_C, respectively, and shown in Fig. 7. Those were directly pasted on white boards WB. In the experiment the previous I_1, I_3, and I_5 were mixed proving 6 IVIs altogether. Four colors of illumination were employed at 50 lx same as the main experiment and only 3 lx of illumination in the test room was investigated. Five subjects, MI, TT, CP, KC, and KT participated in the experiment, three of whom, MI, CP, and KC participating in the previous experiment also.

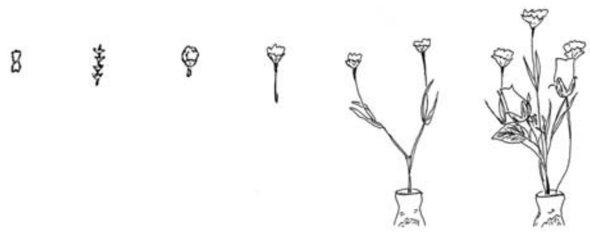

I_A I_B I_C I_1 I_3 I_5

Fig. 7. Initial visual information in additional experiment.

IVI was randomly presented for one illumination color and the judgment was repeated 5 times for each IVI, and also for each illumination color.

Amount of chromaticness is shown in Fig. 8 for all the five subjects in the case of yellow illumination. The abscissa gives the IVI and the ordinate the chromaticness in percentage. With I_0 the chromaticness was very high and it gradually decreased for increasing IVI. There is a large individual variance but the property of a gradual decrease was held in common. The average of five subjects was taken for four colors of illumination, respectively, and is shown in Fig. 9 by different symbols. The property of gradual decrease of chromaticness for increase of IVI is seen commonly among the colors

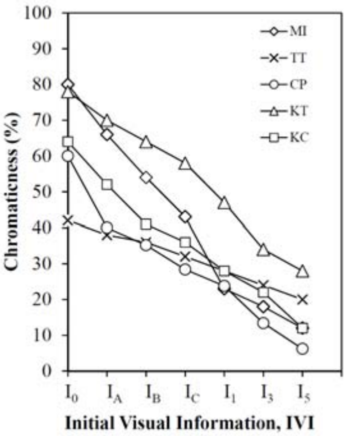

Fig. 8. Chromaticness plotted for IVI from 5 subjects.

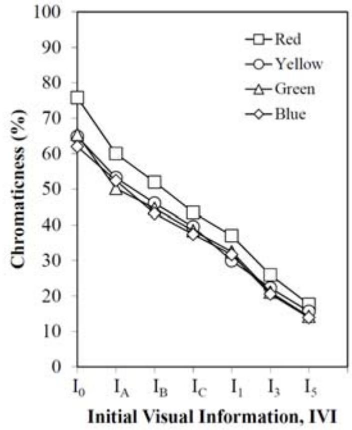

Fig. 9. Chromaticness plotted for IVI for illumination colors.

though the vertical positions of curves differ slightly. However, the vertical position should vary depending on the saturation of the illumination color and the relatively close vertical position of four curves is a coincidence by chance.

To fill the gap between I_0 and I_1 in Fig. 6 the results of three subjects who participated both in the main experiment and the additional experiment were averaged for all the colors in both cases. The results are shown in Fig.10 by open circles for the main experiment and filled circles for the additional experiment. They come very close with each other constructing one straight line of Chr = - 4.2 × IVI + 61.3 when the IVI number was slightly revised, I_A to 2, I_B to 4, and I_C to 5.5. The dashed line was obtained by this formulae.

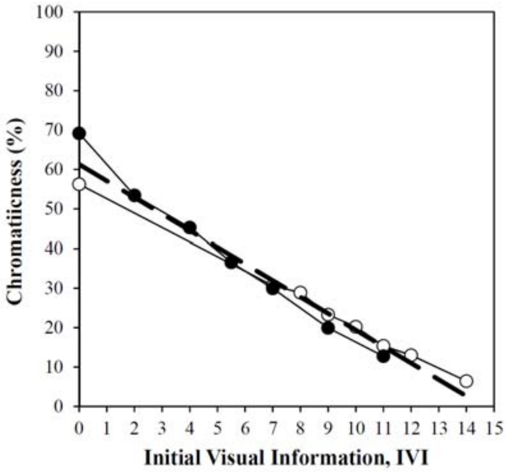

Fig. 10. Chromaticness for revised IVI. The average of three subjects.
○*, the main experiment;* ●*, the additional experiment*; — — —, regression line.

To conclude only a pair of white petals already worked as meaningful initial visual information to construct a space perception and the color constancy.

REFERENCES

1) Ikeda, M. and S. Fukumura, 1995. Formation of a recognized visual space of illumination with increasing initial visual information. Jr. Illum. Engng. Inst. Jpn. 79: 392-399. [in Japanese].

2) Ikeda, M., 2004. Color appearance explained, predicted and confirmed by the concept of recognized visual space of illumination. Opt. Rev. 11: 217-225.

3) Pungrassamee, P., M. Ikeda, P. Katemake, and A. Hansuwebsai, 2005. Color appearance
Determined by recognition of space. Opt. Rev. 12: 211-218.

4) Ikeda, M., P. Pungrassaamee, P. Katemake, and A. Hansuwebsai, 2006. The brain adaptation to the color of illumination and not the retinal adaptation to the color of objects that determines the color appearance of an object in the space. Opt. Rev. 113: 388-395.

5) Phuangsuwan, C. and M. Ikeda, 2014. Effect of initial visual information on construction of a space perception and on the color constancy. Proc. ACA2013Thanyaburi: 36-39.

6) Yamauchi, R., M. Ikeda, and H. Shinoda, 2003. Walls surrounding a space work more efficiently construct a recognized visual space of illumination than do scattered objects. Opt. Rev. 10: 166-173.

7) Cunthasaksiri, P., H. Shinoda, and M. Ikeda. 2004. Recognized visual space of illumination: A new account of center-surround simultaneous color contrast. Col. Res. Appl. 29: 255-260.

Address: Dr. Chanprapha PHUANGSUWAN, Color Research Center,
Rajamangala University of Technology Thanyaburi, 39 Moo 1 Klonghok Thanyaburi,
Patumthani, 12110, Thailand
E-mails: karamennn@gmail.com

Neighboring Color Effect on the Perception of Textile Colors

Youngjoo CHAE, John H. XIN, Tao HUA
Institute of Textiles and Clothing, The Hong Kong Polytechnic University, Hong Kong

ABSTRACT

In this study, the effect of the spatial and colorimetric attributes of neighboring color on color perception in textiles was investigated. Totally 240 woven color combinations were constructed in which each of three test colors, that is, cyan, magenta, and yellow, is placed with 20 different neighboring colors in varying proportions in stripe paradigms. The test colors were then visually assessed by 12 normal color-vision observers using a magnitude estimation method estimating the lightness, colorfulness, and hue values through the comparison with reference samples consisting solely of each test color. According to the obtained visual estimates, each test color has the different color attribute most affected by neighboring colors: lightness for magenta, colorfulness for yellow, and hue for cyan. In terms of overall color, cyan was perceived most differently from its actual, i.e. physically measured, color under the influence of neighboring colors. It was also revealed that these neighboring color effects generally become more apparent and varied with an increment in the size of the neighboring colors.

1. INTRODUCTION

Color is an attribute of visual sensation perceived in the context of various internal and external factors such as its size, shape, surface property, surround/background, and illumination geometry. This study focuses on the effect of surround, i.e. neighboring color, on color perception. The neighboring color effect can be described as *simultaneous contrast* in which a stimulus changes in color appearance depending on the particular relationship with its neighboring color. The simultaneous contrast has been importantly applied in the fine art and design practice, and textile design is one of the areas where this phenomenon is most frequently used in many different forms to create new color appearances.

Previous studies (Jameson & Hurvich 1961; Luo et al. 1995; Ware & Cowan 1982) in general investigated the simultaneous contrast effect in a center-surround paradigm with a single fixed proportion of the two color fields. Stripes, another most often used pattern in textile applications, also have this effect although the extent would be less large as one color in the pattern is not completely surrounded by another. Also in the previous studies, four psychological primaries, red, yellow, green, and blue, were usually used as test colors induced, and only a limited number of inducing colors were included.

The work described here investigated the effect of a large range of neighboring colors in different sizes and arrangements on the perception of cyan, magenta, and yellow in striped woven textiles. The principal aims of the work were to 1) analyze the varying extents of the neighboring color effect depending on the test color, 2) discover the color attribute most affected for each test color, and 3) investigate the effect of the spatial attributes of the neighboring colors.

2. METHOD

2.1 Sample Preparation

In total, 243 woven fabric samples were constructed in 1/4 sateen weaves using a LX3202 Staubli jacquard machine. Among them, three are reference samples consisting of a single test color, that is, one of cyan, magenta, and yellow, and 240 are test samples that are test/neighboring (induced/inducing) color combinations in striped paradigms (Table 1). In the samples, white yarns (L^*=92.97; a^*=-0.46; b^*=1.58) were consistently used for warp, and cyan (L^*=50.48; a^*=-19.76; b^*=-38.14), magenta (L^*=51.20; a^*=62.45; b^*=0.86), and yellow (L^*=84.87; a^*=-0.60; b^*=88.37) yarns were used for weft in varying proportions to produce 21 woven colors varying in lightness, colorfulness, and hue (in case of test colors, each single color was used for warp and weft). All the yarns were made of polyester, and the yarn diameter and fabric density were 0.125mm and 47×40/cm, respectively.

Table 1. Sample designs.

	Reference sample	Test sample (T* + N**)			
	100%T	20%T+80%N	40%T+60%N	60%T+40%N	80%T+20%N
Design	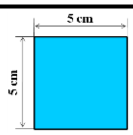	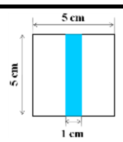	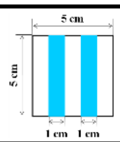	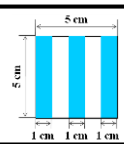	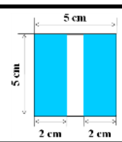
Number	1	20	20	20	20
Design	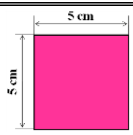	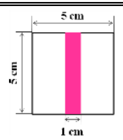	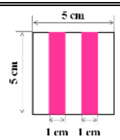	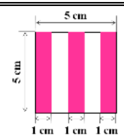	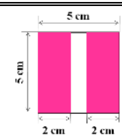
Number	1	20	20	20	20
Design	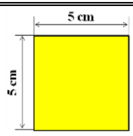	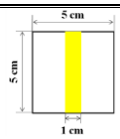	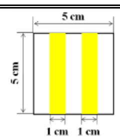	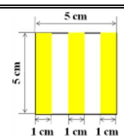	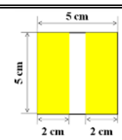
Number	1	20	20	20	20
Total	1×3=3	80×3=240			


***T: Test color**


****N: Neighboring color**

2.2 Visual Assessment

Twelve normal color-vision observers conducted visual assessment using a magnitude estimation method for test samples, i.e. test/neighboring color combinations, in the Verivide CAC 120 light cabinet set to the CIE standard illuminant D65 (illumination/viewing angles: 45/0). The test samples were given one by one in a random order with a relevant reference sample, i.e. a single test color, and its physically measured color attributes. Based on the given data, observers were asked to estimate the lightness L*, colorfulness C*, and hue h˚ values of each test color in the test samples through the comparison with the reference sample.

3. RESULTS AND DISCUSSION

Totally 2,880 estimations were made for 240 test samples, that is, three test colors placed with 20 different neighboring colors in four different proportions. The mean estimates were distributed in CIELAB color space as shown in Figure 1 in which crosses represent physically measured test colors (cyan: L*=54.36, C*=40.11, h˚=238.53; magenta: L*=56.95, C*=57.20, h˚=357.04; yellow: L*=84.52, C*=72.33, h˚=95.18), and diamonds are the visually assessed test colors. In each test color set, there was a discrepancy not only between the measured and the perceived colors, but also between the perceived colors depending on their proportions in the test samples. Also, a different distribution range was observed for each test color. These findings indicate that the extent of the neighboring color effect differs according to test colors and their proportions.

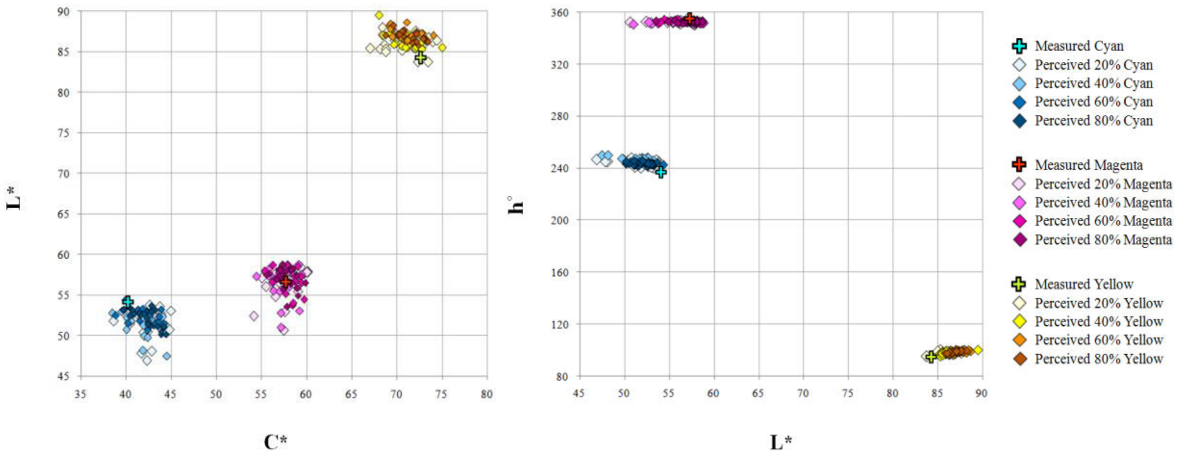

(a) *(b)*

*Figure 1: Distribution of physically measured and visually assessed test colors on (a) CIE L*C* plane and (b) CIE L*h˚ plane.*

The mean color ranges of perceived cyan, magenta, and yellow were calculated and compared in terms of lightness, colorfulness, and hue as shown in Figure 2. In general, cyan has the widest range of estimated h˚ values, magenta has the widest range of estimated L* values, and yellow has the widest range of estimated C* values. This indicates each of these color attributes for each test color is most affected by neighboring colors (in terms of the variation between estimates). According to the proportions of test colors, there was a general tendency that the color ranges of the perceived test colors become wider when their proportions become lower. It implies when a color is placed with or surrounded by another color in a dominant size rather than a small size, the effect of the neighboring color becomes more apparent and varied.

As the discrepancy between the measured and the perceived test colors, cyan was found to be perceived most differently from its actual color, especially in terms of hue (Δh˚=5.9), under the influence of neighboring colors having the average $\Delta E_{CMC(2:1)}$ value of approximately 4. In the perception of lightness and colorfulness, cyan and magenta, regardless of their proportion, were generally perceived as darker and more saturated than the actual colors, while yellow was perceived as lighter and less saturated with neighboring colors.

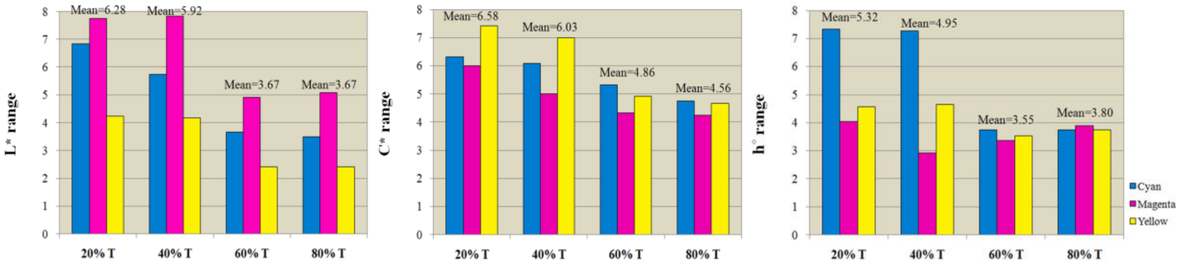

(a) *(b)* *(c)*

Figure 2: Comparison of the ranges of perceived (a) L, (b) C*, and (c) h° values according to test colors and their proportions.*

4. CONCLUSIONS

Three woven test colors, that is, cyan, magenta, and yellow, placed with 20 different neighboring colors in varying proportions were visually assessed to investigate the effect of neighboring color on color perception in textiles. The obtained visual estimates revealed the most affected color attribute of each test color, i.e. hue of cyan, lightness of magenta, and colorfulness of yellow. In terms of overall color, cyan was perceived most differently from its actual color under the influence of neighboring colors. In addition, these neighboring color effects were found to become more apparent and varied in general with an increment in the size of the neighboring colors.

Further work will be done to discover the significant attributes of neighboring colors affecting each of the perceived lightness, colorfulness, and hue of test colors through statistical analyses. These significant neighboring color effects will be modeled.

ACKNOWLEDGEMENTS

This research was supported by the Research Grants Council (RGC) under the Hong Kong PhD Fellowship Scheme.

REFERENCES

Jameson, D. and Hurvich, L.M. 1961. *Opponent Chromatic Induction: Experimental Evaluation and Theoretical Account*, Journal of the Optical Society of America 51(1) 46-53.

Luo, M.R., Gao, X.W., and Scrivener, S.A.R. 1995. *Quantifying Colour Appearance. Part V. Simultaneous Contrast*, Color Research and Application 20(1) 18-28.

Ware, C. and Cowan, W.B. 1982. *Changes in Perceived Color due to Chromatic Interactions*, Vision Research 22(11) 1353-1362.

Address: Prof. John H. XIN, Institute of Textiles and Clothing, The Hong Kong Polytechnic University, Hung Hom, Kowloon, HONG KONG
E-mails: fchae@hanmail.net, john.xin@polyu.edu.hk, tao.hua@polyu.edu.hk

The impact of light at the perception of colours in architecture

State of the art study and suggestions for further research

Shabnam ARBAB, Barbara Szybinska MATUSIAK
Faculty of Architecture and Fine, Norwegian University of Science and Technology (NTNU)

ABSTRACT

This paper presents results of the state of the art study carried out at Light & Colour Group at NTNU in 2014. The aim was to present an overview of contemporary research dealing with the impact of natural light, sometimes modified by different glazing types, at the perception of colours in architecture. This was considered as an essential exercise for identifying areas that are missing from the research map of this topic. Based on this study, suggestions for future research were formulated.

About 100 papers were found in: Science Direct, Scopus, Sage and Wiley online libraries using the following keywords: Light, Coloured light, Colour, Vision, Colour shift, Colour temperature, Visual perception, Window Glazing, Transmittance, Spectral composition, Visual comfort and Smart window.

The most interesting founding is that a considerably large number of papers, especially from the last 10 years, present studies of a new generation of dynamically responsive glazing called "smart windows". Smart window notion comprise different glazing technologies that can be reversibly switched from a closed to a transparent state resulting in thermal and optical properties that can be dynamically controlled (Lee et al. 2004). Most of the reported studies examined the effect of switchable glazing on visual and thermal comfort, but very little has been found regarding the effect of different types of smart windows on the perception of surface colours and consequently on colour shift.

1. INTRODUCTION

All of us live within three-dimensional reality that is changing continuously. Our perceptive and cognitive systems have been formed within this context. Colour and light together construct our mental image of space. The experiences of colour and light are interdependent and cannot be analysed separately (Arnkil et al. 2012).

Obviously, one of the lively elements of the built environment is light. It offers a vital connection between the individual, the building and the nearby outdoor environment. Light in a building can be perceived from various viewpoints such as: its necessity for working and living, whether natural or artificial, its source (if artificial), and finally its adverse feature, i.e. expense. Daylight has been the main source of light during centuries and is still appreciated as the most favourable for human health and well-being, therefor is should be considered as a main source of light, while electrical light as a supplement enabling illumination when and where it is impossible to illuminate by natural light.

We know that colour is not the property of objects, spaces or surfaces; it is the sensation caused by certain qualities of light that the eye recognizes and the brain interprets.

Therefore, light and colour are inseparable, and, in the design of the human habitat, equal attention must be devoted to their psychological, physiological, visual, aesthetic, and technical aspects.

The colour of surrounding influences experience of light and the need for lighting. The qualities of light (intensity, directionality, distribution, etc.) are essential for our perception of colour. Colour and light in constructed spaces influence our experiences and feelings, our comfort and our physiological well-being. A thorough investigation of the simultaneous and interrelated human perception of light and colour in architectural space was carried out by the Scandinavian research group SYN-TES (Fridell Anter and Klaren 2010) and a systematic literature review was carried out by Karin Fridell Anter (2013).

The current development in the glass and glazing technologies results with new products, e.g. windows, glass-façades or glass roof elements e.g. with high-tech coatings on the glass. Increasingly often they have chromatic features that influence the spectral power distribution of the light passing through them. We may compare many modern glazing products to a colour filters situated in the building envelope openings. Such filters may change the perception of colours in interiors and the perception of outdoor colours while observed through a "filter-glazing". A colour shift of surface colours may occur. Also one of the crucial aesthetic issues in architecture, namely the visual appearance of building facades, depends considerably on the optical qualities of the glazing.

The impact of different spectral compositions of light on colour perception could be one of the interesting research topics. To find more about the actual state of the art in research, a comprehensive literature study was carried out in the Light & Colour Group, at the Norwegian University of Science and Technology, NTNU, in Trondheim, Norway.

2. METHOD

The literature review helps to ensure that the design of a new research project is original, but at the same time it often gives inspiration for new and creative ideas. Additionally, the review of different studies enables comparing and combining of results and that have a value that no single study can have. Another special reason to do literature review is that it let researchers to address broad questions (Prinstein 2012).

The present study involves different methods, from clearing the area of interest, searching in database to finding and studying relevant articles. In this study the narrative review approach was used. This is a more traditional approach that provides qualitative descriptions of the results of many previous studies.

The search was carried out online on literature available at Norwegian University of Science and Technology (NTNU). Considering English language publications starting from the year 1938 was the only limitation for the review.

Selected keywords (Table 1) were combined in the chosen databases. Each combination of words also resulted in a link called related articles in the databases. Combination of two or three keywords in addition to a single word helped to narrow the search result and to find the articles that were really relevant. We ended up skimming a long list of abstracts to identify the related articles. We used Science Direct, Scopus, Sage and Wiley online libraries and because of using the same keywords, there were some overlapping's in the results. Actually it was advantageous; we could be sure that those articles have good quality. The variety of articles about the colour and light was high but most of them were related to thermal and emotional effects of light or colour. Screening was done by reading the abstracts and choosing the most relevant for the following two topics: light and colour interaction and perception of colour under different lighting sources.

Table 1. Keywords used in database search.

Keywords		
Light	Coloured light	Transmittance
Colour	Colour shift	Spectral composition
Vision	Colour temperature	
Window	Visual perception	
Glazing	Visual comfort	
Smart window	Visual environment	
Electrochromic Glazing		

Additionally, some webpages were visited to find out the state of the art regarding technical development in industry.

4. CONCLUSIONS

The scope of this article limits us to present only the most interesting findings. We have found that the need of knowledge about spatial (as opposite to flat) visual perception was often neglected in colour research. By reviewing the existing we found that the perception of colour illuminated by light having different spectral composition and passing through different glazing types is one of the research gaps in this regards.

As expected, numerous papers deal with light and colour at the general level. The most interesting finding is that a considerably large number of papers, especially from the last 10 years, present studies of a new generation of dynamically responsive glazing called "smart windows". Smart window notion comprise different glazing technologies that can be reversibly switched from a closed to a transparent state resulting in thermal and optical properties that can be dynamically controlled (Lee et al. 2004). One example of smart window technology is the electro-chromic (EC) glazing which is controlled by a small applied voltage. In the closed state the EC glazing has a very strong chromatic feature, e.g. a dark blue colour. Most of the reported studies examined the effect of switchable glazing on visual and thermal comfort, but very little has been found regarding the effect of different types of smart windows on the colour shift, and consequently on the perception of visual environment.

According to the literature review, glazing type is not necessarily considered as an issue effecting visual perception. There is a general lack of understanding regarding the performance and effect of smart windows, as a new generation of dynamic responsive glazing in real-world environments, on colour perception.

According to Kumar (2005), formulating a research question is considered as "the first and most important step in the research process". The state of the art study aided us to formulation of the two main research questions for the future research:

1. *How is the perception of colour influenced by light?*

2. *What will be the consequences of using smart window technology for visual environment?*

The secondary questions will be:

What are differences between standard glazing and different glazing types form smart window technologies?

What is the impact of light passing through a smart window at the total indoor visual environment?

How does the colour of the façade made of smart windows looks from different distances?

To what extent are different colours of light accepted in interiors?

This research project (PhD) started with the exploration of the impact of color temperature of light at the perception of surface colors. The experiment expolring this issue (question 1) was done in September 2014 in connection with the "Colour in the City" exhibition in September 2014 in Trondheim and is described in the paper (Arbab and Matusiak 2015).

Further, the consequences of using smart window technology for the visual environment in interiors will be examined (question 2). All behavioral data analysis requires a combination of empiricism and interpretation, and it can be argued that both quantitative and qualitative approaches, components, data, and/or strategies for analysis are necessary to adequately understand human behavior, whether individual, group, or societal (Bazeley 2012).

In order to carry out comprehensive analysis about the impact of light on color perception there is a need to merge qualitative and qualitative approaches; the strengths of both could provide the best understanding while it can give meaning to numbers by narrative, pictures and words (Johnson and Onwuegbuzie 2004). Nagy Hesse-Biber (2010) asserts that triangulation adopts a positivistic perspective by default. This method is employed when a researcher seeks to validate quantitative statistical findings with qualitative data results. Yet the assumption underlying triangulation is the positivistic view that there is an objective reality in which a given truth can be validated.

The theoretical and empirical studies draw our attention to a number of objectives for future study regarding various aspects of visual adaptation and the difficulties of measuring and describing human experiences of light and color in the diverse and complex situations of real life.

The main methodology will be experimental research to evaluate the different aspects of visual perception in three different experimental phases that are parts of a long-term study on the relation between light characteristics and color perception

According to the Joroff and Morse Model, range of research in this project would be somehow social science research.

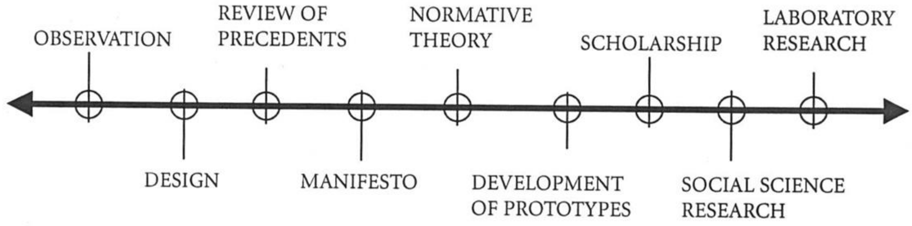

Figure 1. Michael Joroff and Stanley Morse's conceptual framework for architectural research (Joroff and Morse 1983).

At the last, statistical analyses would be needed to compare qualitative and quantitative measures. The intention is to further understand the interaction between light and color as perceived by humans.

ACKNOWLEDGEMENTS

The authors would like to express appreciation to Professor Tore Haugen for the useful comments, remarks and engagement and to NTNU for sponsoring this work.

REFERENCES (MOST IMPORTANT ONES ONLY)

Albers, J. 2006. *Interaction of Color: Revised and expanded edition*, Yale University Press.

Arbab, S., Matusiak, B. S. Perception of colours illuminated by coloured light. In AIC 2015, *Proceedings of Colour and image*. Tokyo.

Arnkil, H., Fridell Anter, K., Klarén, U. and Matusiak, B. PERCIFAL: Visual analysis of space, light and colour. In AIC 2011, Interaction of Colour & Light in the Arts and Sciences, Midterm Meeting of the International Colour Association, Zurich, Switzerland, 7–10 June 2011: Conference Proceedings, CD, 2011. pro/colore, 2011, 229-232.

Arnkil , H., Fridell Anter, K. & Klarén, U. 2012. *Colour and Light, Concepts and confusions*.

Azens, A. and Granqvist, C. 2003. Electrochromic smart windows: energy efficiency and device aspects. *Journal of Solid State Electrochemistry,* 7**,** 64-68.

Bazeley, P. 2012. Integrative analysis strategies for mixed data sources. *American Behavioral Scientist,* 56**,** 814-828.

Beaufort, C. From motion to emotion: The color-light event and the experience of the interval. In AIC 2011. Switzerland.

De Mattiello, M. L. Colour and light in architecture. In AIC 2004 Color and Paints, Interim Meeting of the International Color Association, Proceedings, 2005. Jose Luis Caivano, 190.

Fridell Anter, K. 2000. *What colour is the red house? Perceived colour of painted facades.* Stockholm: Royal Institute of Technology (KTH).

Fridell Anter, K. And Klarén, U. 2010. SYN-TES: Human Colour And Light Synthesis Towards A Coherent Field Of Knowledge. In *CIE 2010, Proseedings of "Lighting Quality and Energy Efficiency"*.

Fridell Anter, K. 2013. Spatial interaction between light and colour, an overview over current international research. *Nordic light and colour.* Trondheim: NTNU, the faculty architecture and fine art

Gerard, R. M. 1958. *Differential effects of colored lights on psychophysiological functions.* University of California, Los Angeles.
Green-Armytage, P. 2006. The value of knowledge for colour design. *Color Research & Application,* 31**,** 253-269.
Hesse-Biber, S. N. 2010. *Mixed methods research: Merging theory with practice*, Guilford Press.
Häggström, C. & Fridell Anter, K. 2012. Interior colour design effects on preferred level of light. In *AIC 2012*.
Johnson, R. B. and Onwuegbuzie, A. J. 2004. Mixed methods research: A research paradigm whose time has come. *Educational researcher,* 33**,** 14-26.
JorofF, M. L. and Morse, S. J. 1983. *A proposed framework for the emerging field of architectural research*, Laboratory of Architecture and Planning, Massachusetts Institute of Technology.
Klarén, U., Arnkil, H. and Fridell Anter, K. 2012. Levels of experiencing colour and light. *Nordic light and colour***,** 39.
Kumar, R. 2005. *Research methodology: a step-by-step guide for beginners,* London, SAGE.
Lancaster, M. 1996. *Colourscape*, Academy Editions.
Lee, E., Yazdanian, M. and Selkowitz, S. 2004. The energy-savings potential of electrochromic windows in the US commercial buildings sector.
Mahnke, F. H. 2012. *Color in Architecture — More Than Just Decoration* [Online]. Available: http://archinect.com/features/article/53292622/color-in-architecture-more-than-just-decoration.
Matusiak, B. 2004. The impact of lighting/daylighting and reflectances on the size impression of the room. Full-scale studies. *Architectural Science Review,* 47**,** 115-119.
Naseri, G. H. and Tamizi, M. 2011. Assessing the Function of Light and Color in Architectural View. *World academy of science, engineering and technology.*
Noė, A. 2005. *Action in perception*, MIT Press.
Prinstein, M. J. 2012. *The portable mentor: Expert guide to a successful career in psychology*, Springer.
Valberg, A. 2007. *Light vision color,* John Wiley & Sons.
Valdez, P. & Mehrabian, A. 1994. Effects of color on emotions. *Journal of Experimental Psychology: General,* 123**,** 394.
Veitch, J. A. 2005. Light, lighting, and health: Issues for consideration. *Leukos,* 2**,** 85-96.
Vogels, I., De Vries, M. and Van erp, T. Effect of Coloured Light on Atmosphere Perception. AIC 2008, 2011 Stockholm, Sweden.
Wijk, H. 2001. Colour perception in old age. *Colour Discrimination, Colour Naming, Colour Preferences and Colour/Shape Recognition. G öteborgs Universitet, Gothenburg University, Gothenburg*.
Zinzi, M. 2006. Office worker preferences of electrochromic windows: a pilot study. *Building and Environment,* 41**,** 1262-1273.

Address: Shabnam Arbab, Dept. of Arch. Design, Form and Colour Studies, Norwegian University of Science and Technology (NTNU), Alfred Getz vei 3, 7491 Trondheim, Norway
E-mails: Shabnam.arbab@ntnu.no, barbara.matusiak@ntnu.no

Evaluation of Cloth Roughness and Smoothness by Visual and Tactile Perceptions: Investigation of Cloth Photography Method for Online Shopping

Tomoharu ISHIKAWA,[1] Yuya AKAGAWA,[1] Kazuma SHINODA,[1] Shigeru INUI,[2]
Kazuya SASAKI,[1] Keiko MIYATAKE,[3] Miyoshi AYAMA[1]
[1] Utsunomiya University
[2] Shinshu University
[3] Kyoritsu Women's University

ABSTRACT

The purposes of this study were to clarify differences that arise in the assessment of cloth texture, particularly cloth roughness or smoothness, using visual and tactile evaluations, and to investigate a method for producing cloth photographs for online shopping websites that observers could use to assess the degree of roughness or smoothness of the cloth. Two evaluation experiments were conducted. The first experiment was a visual evaluation (VE), in which the surface textures of actual pieces of cloth were evaluated solely by visual examination. The other was a visual and tactile evaluation (VTE), in which cloth textures were evaluated using both visual and tactile examination. The characteristics of cloth roughness and smoothness were examined in each experiment. The results showed that the roughness of many types of cloth was overestimated when VTE was conducted and that smoothness was underestimated when VE was conducted. The second experiment was conducted to evaluate cloth surface textures using digital photographs of pieces of cloth taken at different distances between the cloth and the camera. Object distances that produced the same or similar evaluation results were examined and clarified using VE of the photographs. We thus confirmed that the method used in this study can be used to take photographs that users of online shopping websites can use to determine the degree of roughness or smoothness of cloths.

1. INTRODUCTION

In recent years, online shopping for clothes has grown in popularity.[1] However, because most retailers offer only visual information such as pictures of clothes, there may be discrepancies between an item's visual image and its actual appearance and physical comfort. To address this problem, visual and tactile measures that can be used to assess differences between images of clothes in pictures and the look and feel of the actual items are required. In a previous study (Ishikawa et al. 2013), we conducted two fabric identification experiments to assess an observer's accuracy in identifying both an actual piece of cloth and a photograph of the same cloth, based on his/her visual and/or tactile responses. These experiments involved the participants' performing the following: 1) blind touch identification of an actual piece of test cloth after they observed a photograph of the

[1] http://www.soumu.go.jp/johotsusintokei/whitepaper/ja/h23/index.html

same cloth and 2) visual identification of an actual piece of cloth while they reviewed a photograph of the same cloth. The results indicated that even if an actual piece of cloth and a high-quality photograph are presented to observers, some types of cloth are identified at a low level of accuracy. Therefore, there are considerable differences between perceiving the actual characteristics of a piece of cloth and evaluating a photograph of the cloth. Although the latter evaluation method is mostly established in the field of psychophysiology, the photography method is largely based on the photographer's abilities. If the photography conditions corresponding to the evaluation results for the cloth texture are clarified, many types of cloth could be identified at high levels of accuracy. Many previous studies clarified that the terms roughness and smoothness are important words in evaluating cloth texture (Brockman 1966, Kawabata 1980, Sakita 2006, Ishikawa et al. 2014a). Therefore, a method to photograph a piece of cloth that can make it easy to evaluate cloth texture in terms of roughness or smoothness was investigated in this study to improve the accuracy of the online shopping experience. In Experiment 1, two evaluations were conducted. One was a visual evaluation (VE), in which the surface textures of actual pieces of cloth were evaluated solely by visual examination. The other was a visual and tactile evaluation (VTE), in which cloth textures were evaluated using both visual and tactile examinations. The characteristics by which roughness and smoothness were evaluated were examined in each experiment. The results showed that roughness was overestimated for many types of cloth when VTE was conducted and that smoothness was underestimated when VE was conducted. In Experiment 2, the surface textures of pieces of cloth were evaluated using digital photographs shot at different distances between the cloth and the camera. Object distances that produced the same or similar evaluation results were examined and clarified using VE of the photographs. We thus confirmed that the method examined in this study can be used to take photographs from which users of online shopping websites can determine the degree of roughness or smoothness of fabrics.

2. EXPERIMENT

2.1 Experiment 1: VE and VTE using actual cloths

2.1.1 Experimental conditions

Eight types of test fabrics were prepared for use in VE and VTE testing. The fabrics used were ones which, in a preliminary experiment, designers were able to differentiate from each other based on touch. The base colors of the fabrics were white and beige, and the materials used included polyester and triacetate. Figures 1(a-f) are photographs of the fabric samples. The fabric stimuli presented in the VE and VTE testing were produced by affixing the test fabrics shown in Figure 1 to 400 mm x 275 mm boards. In the VE testing, roughness and smoothness were evaluated using visual perception alone, whereas in the VTE testing, roughness and smoothness were evaluated using both visual and tactile perception. In both sets of tests, participants sat in chairs and observed the fabric stimuli on a table at a distance of 40 cm from their eyes. The horizontal illuminance of the fabric stimuli was 499 lx. Roughness and smoothness were rated separately on 7-point unipolar rating scales (0 = not like that; 2 = a little like that; 4 = like that; 6 = very much like that). The participants were ten engineering students in their twenties.

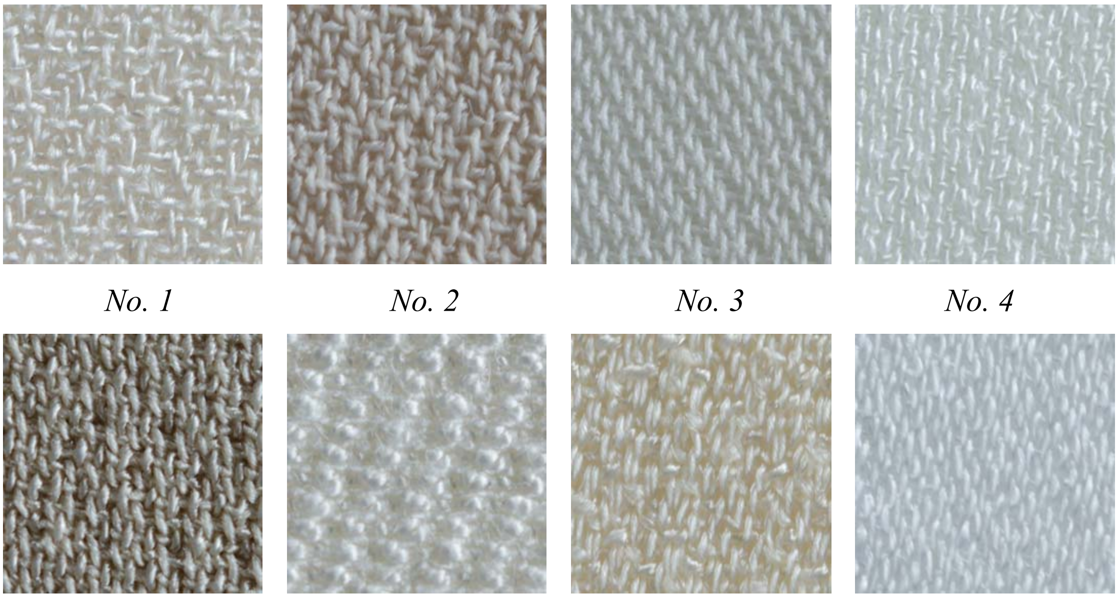

No. 1 No. 2 No. 3 No. 4

No. 5 No. 6 No. 7 No. 8

Figure 1: Test cloths.

2.1.2 Results and Discussion of Experiment 1

Figures 2(a-b) show the results of the smoothness and roughness ratings. The mean VE and VTE ratings are indicated for each fabric. As Figure 2(a) shows, for six of the eight fabric types, the VTE rating for smoothness was lower than the VE rating. In contrast, Figure 2(b) shows that for the same six fabrics, the VTE was higher than the VE rating. These results indicate that touching a fabric led to rating it as rougher (less smooth). The results also suggest that because judgments based on visual perception of fabric texture tend to lead to rating it as smooth, it is necessary to include indicators that emphasize the roughness of a fabric.

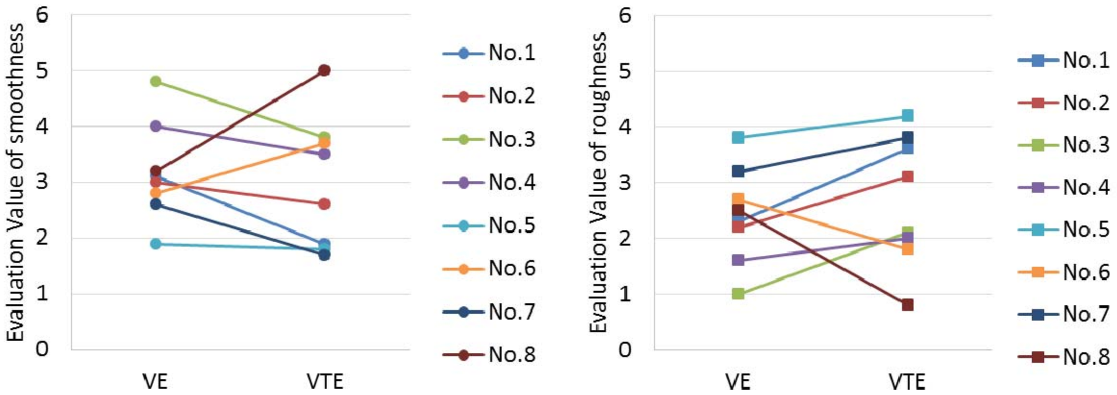

(a) Results for smoothness *(b) Results for roughness*

Figure 2: Results of VE and VTE

2.2 Experiment 2: VE using photographs of cloths

2.2.1 Experimental conditions

The fabrics were photographed to produce images for use in the experiment. When photographing fabrics, methods that involve adjusting the magnification of the lens can be considered, but because of the possibility of color aberration and other unwanted effects, a different photographic method was selected, in which the camera lens and other settings are held constant while the distance from the camera to the object is varied. The fabric stimuli used in Experiment 1 were fixed in place, and 13 different photographs of each fabric were taken using a Nikon D7000 camera and an AF-S Micro NIKKOR 60-mm F2.8G ED macro lens, with the photographic distance varied from 0.185m to 1.4 m. At the time of shooting, the camera was set to an ISO sensitivity of 100, an aperture of f/6.3, and a shutter speed of 1/30 s. An Apple Cinema Display A1081 (1680 × 1050 resolution) was used in the ratings experiment, and the images were clipped to 1680 × 1050 px and displayed across a full screen.

2.2.2 Results and Discussion of Experiment 2

Figures 3(a-b) display the results of the fabric smoothness and roughness ratings at various photographic distances. The figures show a trend of smoothness ratings tending to increase and roughness ratings tending to decrease as the photographic distance increases. In addition, over the range of photographic distances, there is little fluctuation in the relative smoothness and roughness rankings of the fabrics, indicating that fabric smoothness and roughness ratings change almost uniformly in response to changes in photographic distance, regardless of fabric type.

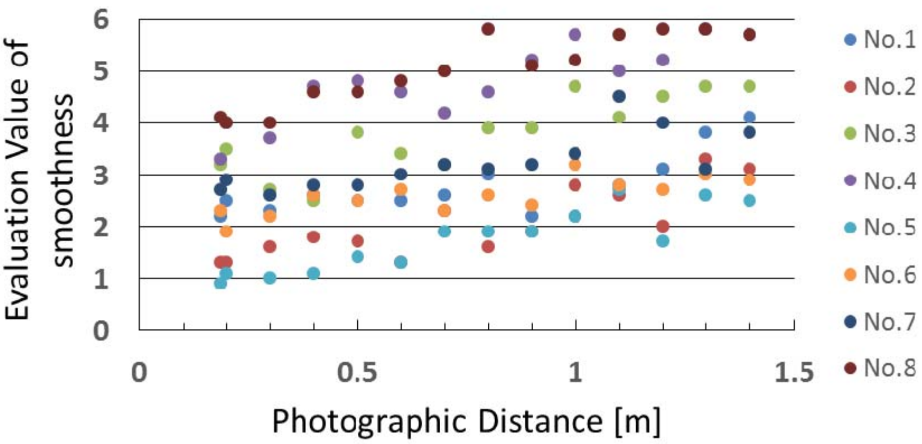

(a) Result of smoothness

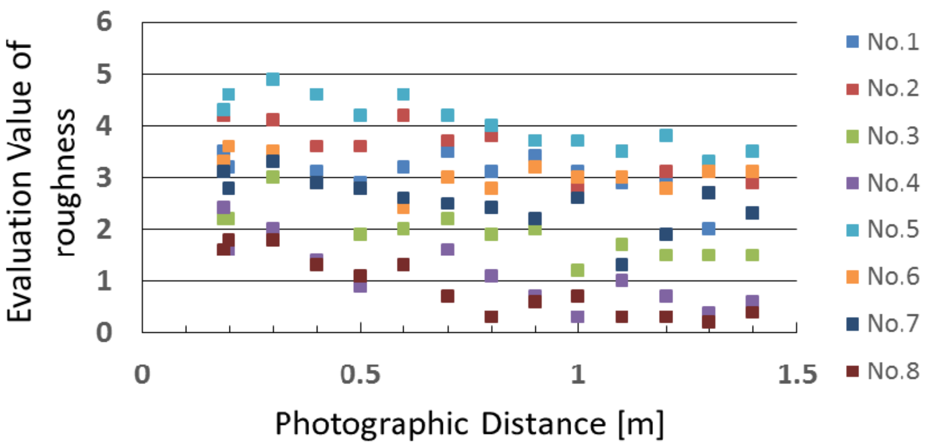

(b) Result of roughness

Figure 3: Result of photography's VE against change in photographic distance

3. ANALYSIS AND DISCUSSION

Through analysis of correlations and mean errors, we examined which of the conditions in Experiment 2 yielded results that were most consistent with the results of the VE and VTE ratings of smoothness and roughness of fabric stimuli in Experiment 1. The results indicated that for VE ratings, a photographic distance of 0.5 m represented the condition for which the results of Experiments 1 and 2 were most consistent, with a correlation of approximately 0.7 and a mean error value of approximately 0.1. On the other hand, for VTE ratings, the photographic distance range of 0.5 to 0.7 m represented conditions for which the results were most consistent, with correlations centered at approximately 0.7 and mean error values centered at approximately 0.1. These findings suggest that for the photographic environment used in this study, photographs taken at a distance in the range of 0.5 to 0.7 m from the object best capture the smoothness and roughness of actual pieces of fabric when they are seen and touched. In the future, it may be necessary to confirm this with replication studies that simulate actual online shopping.

4. CONCLUSIONS

To investigate the methods used to photograph fabrics for online shopping, the differences in the ratings of the roughness and smoothness of the textures of various fabrics were examined, and the differences in rating results obtained for fabrics evaluated by visual examination alone versus fabrics evaluated by both visual and tactile examination were investigated. Fabrics examined by the former method (visual evaluation alone) tended to be perceived as smoother than fabrics examined with the latter method (visual and tactile evaluation). Roughness and smoothness ratings were then obtained for fabrics using photos taken from various distances. By investigating which photographic conditions were consistent with the actual roughness and smoothness ratings, we determined the most suitable distances at which photographs should be taken to assist online shopping website users in accurately assessing fabric texture. In the future, in addition to conducting studies to verify these results, we plan to analyze the relationships between the special features of fabric photographs (such as spatial frequency, contrast, and average brightness) and roughness and smoothness, and thereby identify the key image features in the evaluation of roughness and smoothness In addition, we plan to investigate other related issues, such as the influence that differences in experience with and knowledge of clothing can have on such evaluations (Ishikawa et al. 2014b).

ACKNOWLEDGEMENTS

This research was supported by JSPS KAKENHI Grant Numbers 24220012 and 25330316.

REFERENCES

Brockman, H. L. 1966. *The theory of fashion design*, John Wiley & Sons: 301-324.

Sakita, K. 2006. *Fashion Branding: New Luxury Branding & MOT*, Takarazuka University of Art and Design Press (in Japanese).

Kawabata, S. 1980. *The Standardization and Analysis of Hand Evaluation: Second Edition*, The Hand Evaluation and Standardization Committee, The Textile Machinery Society of Japan: 100.

Ishikawa, T., R. Tsuji, K. Sato, K. Sasaki, H. Shimizu, and M. Ayama. 2013. *Basic Study on Recognition Mechanism for Cloth Textures in Online Shopping - Involvement of Visual and Tactile Perception* -, 5th International Congress of the International Association of Societies of Design Research 2013.

Ishikawa, T., S. Nakamori, K. Sasaki, K. Miyatake, and M. Ayama. 2014a. *Investigation of Appearance and Tactile Sensation Scales for Evaluating Clothes in Online Shopping*, International Conference on Kansei Engineering and Emotion Research.

Ishikawa, T., K. Sasaki, H. Shimizu, and M. Ayama. 2014b. *Online Shopping and Individual Consumer Adaptation: The Relationship Between Fabric-Identification Ability and Prior Knowledge, Industrial Application of Affective Engineering*, Springer International Publishing Switzerland: 209-218.

Address: Associate Prof. Tomoharu ISHIKAWA, Graduate School of Engineering,
Utsunomiya University, 7-1-2 Yoto, Tochigi, 321-8585, JAPAN
E-mails: ishikawa@is.utsunomiya-u.ac.jp

STUDY OF COLOR PREFERENCES OF GAC FRUIT BLENDED WITH MIXED MUSHROOM JUICE

Wattana WIRIVUTTHIKORN, Somporn JENKUNAWATT
Faculty of Agricultural Technology, Rajamangala University of Technology Thanyaburi (RMUTT)
2 Soi Phaholyothin 87 Soi 2 Phaholyothin Road Thanyaburi PathumThani 12130 Thailand.

ABSTRACT

The effect of different ratios of mushroom and gac fruit juice on sensory and color properties of mixed mushroom (Shitake, Golden and Angel) and gac fruit juice were studied. Mixed mushroom and gac fruit juice prepared to do a variety test by using bael as sweetener, namely sensory evaluation and color measurement. Firstly, preparation of mixed mushroom juice and gac fruit juice were sliced into small pieces and washed with clean water. Blending of aliquots were performed continuously until homogeneous by using an electric blender. After that, juices were heated at temperature 80°c. Physical properties (color measurement) was measured by Hunter and Sensory evaluation was done by using 9-hedonic scaling test. The results showed that the values of L*, a* and b* depending on different ratio of mixed mushroom and gac fruit juices. The using of higher gac fruit juice gave much lightness, but less of gac fruit revealed higher intensity of a* and b*. Sensory evaluation showed that the the highest average of the mean of attributes color and overall acceptability were treatment 5 with an average 6.93 and 7.73, respectively. There were significant differences ($P \leq 0.05$) for attributes color and overall acceptability. Treatment 5 revealed that gave the best overall acceptability and color. From the information above can be used in developing color of products in form of health drinks, covers the essential nutrients needed in the future to meet the demands of consumers, which has increased steadily and expanded, in the large level in beverage industry.

1. INTRODUCTION

The aspect and color of the food surface is the first quality parameter evaluated by consumers and is critical in the acceptance of the product. The color of this surface is the first sensation that the consumer perceives and uses as a tool to accept or reject food. The determination of color can be carried out by visual (human) inspection or by using a color measuring instrument. In order to carry out a more objective color analysis, color standards are often used as reference material. Unfortunately, their use implies a slower inspection and requires more specialized training of the observers. For this reason it is recommendable to determine color through the use of color measuring instrumentation. At present, color spaces and numerical values are used to create, represent and visualize colors in two and three dimensional space (Trusell Saber and Vrhel, 2005). Gac fruit has high levels of carotenoids, especially β-carotene and lycopene, are found in gac fruit aril, the brightly colouredflesh covering the seeds. (Aoki.et al. (2002) The advantages of mixed mushroom extracts (Shitake, Golden and Angel) are studied as possible treatments for diseases, such as cardiovascular disorders. Some mushroom materials, including polysaccharides, glycoproteins and proteoglycans are under basic research for their potential to modulate immune system responses and inhibit tumor growth. (Gao et al., 2005)

The aim of this study was to evaluate effect of different ratios of mixed mushroom and gac fruit on color measurement in gac fruit blended with mixed mushroom juice and sensory evaluation.

2. METHOD

2.1 Mixed Mushroom Juice and Gac Fruit Juice Preparation

Fresh mushrooms (Shitake, Golden and Angel) and gac fruit are the main ingredients (see Table1.) in the production of mushroom juice and gac fruit juice were sliced into small pieces and washed with clean water. Blending of aliquots were performed continuously until homogeneous by using an electric blender. After that, juices were heated at temperature 80°c for 15 minutes and cooling at room temperature (Batu, 1990; Wirivutthikorn and Jenkunawatt, 2014)

Table 1. Mushroom Juice and Gac Fruit Juice Production.

Ingredients	Treatment				
	1	2	3	4	5
Mixed mushroom juice (ml)	65	55	50	50	55
Gac fruit juice (ml)	20	20	25	35	25
Sugar (g)	15	25	25	15	20
Dried bael (g)	15	15	15	15	15

2.2 Sensory Evaluation

The sensory evaluation was carried out 30 panelists consisting of panelists in Rajamangala University of Technology Thanyaburi, Thailand. Sensory evaluation was done by 9-hedonic evaluation. Panelists are asked to determine the level of preferences on each treatment using hedonic scale of 9 points (1: dislike extremely, 2: dislike very much, 3: dislike moderately, 4: dislike slightly, 5: neither like nor dislike, 6: like slightly, 7: like moderately, 8: like very much, 9: like extremely) based on attributes of color and overall acceptability. (Wirivutthikorn and Jenkunawatt, 2014)

Color Measurement

The sample of mixed mushroom juice and gac fruit juice from each treatment were prepared for color measurement using a Spectro Dens A407077 Premium (D-61462, Germany). Color was recorded and shown using brightness (L*), redness (a*) and yellowness (b*)

3. RESULTS AND DISCUSSION

1. Color of Juice

Table 2. Value of L,a*,b* .*

Value	Treatment				
	1	2	3	4	5
L*	35.3	33.2	35.9	40.4	31.1
a*	-0.1	3.6	3.4	-1.7	1.7
b*	12.6	18.0	2.9	4.0	22.5

From the above results, The values of L*, a* and b* and physical appearance depending on different ratio of mixed mushroom and gac fruit juices. The using of higher gac fruit juice gave much lightness, but less of gac fruit revealed higher intensity of a* and b* (Wirivutthikorn and Jenkunawatt, 2014)

2. Sensory Evaluation

In sensory evaluation, the highest average of the mean of attributes color and overall acceptability were treatment 5 with an average 6.93 and 7.73, respectively. There were significant differences ($P \leq 0.05$) for attributes color and overall acceptability of juice in each treatments. Treatment 5 indicated that the highest scores both of color and overall acceptability (Wirivutthikorn and Jenkunawatt, 2014)

4. CONCLUSIONS

The uses of different ratios of raw material preparation has effects on quality of mixed mushroom and gac fruit juice. Treatment 5 revealed that gave the best overall acceptability and color.

ACKNOWLEDGEMENTS

The authors would like to thanks students and officials of Faculty Agricultural Technology Rajamangala University of Technology Thanyaburi (RMUTT) Thailand that helped part in the research. We would also like to thank the Faculty of Agricultural Technology for their support facilities and budgets on our research and travel expense for this conference.

REFERENCES

Aoki, H., Kieu, N. T. M., Kuze, N., Tomisaka, K. and Chuyen, N. V. 2002. Carotenoid pigments in gac fruit.). *Journal of Biotechnology* 66(11): 2479-2484.

Batu, A. 1990. *A study on production of a white hard grape pekmez byadding different additives.*. MSc. Thesis. Food Engineering Department, Engineering Faculty, Ege University. Bornova, Izmir.

Gao, Y. et al. 2005. Effects of water-soluble Ganoderma lucidum polysaccharides on the immune functions of patients with advanced lung cancer. *J. Med Food* 8(2):159-68.

Trusell, H. J., Saber, E. and Vrhel, M. 2005. Color image processing. *IEEE Signal Processing Magazine* 22(1): 14–22.

Wirivutthikorn, W. and Jenkunawatt, S. 2014. *Preference Colors of Gac Fruit Blended with Pineapple Juice.* Tien-Rein LEE (Editor –in-Chief). The 2 nd Conference of Asia Color Association URBAN COLOR FOR LIFE 4-7 September 2014, Taipei, Taiwan. 304-307.

Address: Wattana Wirivutthikorn Faculty of Agricultural Technology, Rajamangala University of Technology Thanyaburi (RMUTT) 2 Soi Phaholyothin 87 Soi 2 Phaholyothin Road Thanyaburi PathumThani 12130 Thailand.

E-mail: wattana_w@mail.rmutt.ac.th,sompornjen@gmail.com

Luminance Contrast of Thai Letters Influencing Elderly Vision

Kitirochna RATTANAKASAMSUK
Color Research Center, Faculty of Mass Communication Technology,
Rajamangala University of Technology Thanyaburi

ABSTRACT

We investigated the effect of luminance contrast between text and background on legibility of Thai letters. Three groups of subjects; young (18-23 yrs.), elderly (58-66 yrs.), and simulated elderly (young wored cataract experiencing goggle) participated in this research. The stimulus configuration was a row of ten random Thai letters presented on an LED display. The letter's size was 0.35 degree at 246 cm viewing distance. The luminance contrast between text and background was composed of five levels of positive polarity and five levels of negative polarity. The subjects viewed the stimuli in a room which illuminated at 0 and 300 lux. The first task of each subject was to report those 10 random letters. Reading performance was calculated in term of percentage of correct answer. For the second task, the subjects was asked to rate the reading easiness of those letters. The results showed that the elderly required higher contrast letter than the young. For positive polarity, reading performance and easiness score of the real elderly were slightly lower than those of the other two groups. For negative polarity, result of the real elderly under 0 and 300 lux was slightly different. However, at low luminance contrast, reading performance and easiness score of the young under 300 lux was suddenly declined and significantly different from reading performance under 0 lux. For all groups of subject, minimum required contrast for easy reading is higher than minimum required contrast for correct reading. Even though all groups of subject could read the lower contrast letter but they felt that the lower contrast is not easy to read.

1. INTRODUCTION

Number of elderly population in Thailand has been growing. In 2025, the percentage of elderly people will be more than 15% and will become more than 25% in 2050 (Institute for Population and Social Research 2006; United Nations 2002). Therefore, we cannot discard this severe situation and have to prepare for the aging society. It is important to study the elderly vision in order to prepare the elder-friendly environment so that the elderly can maintain their quality of life and also their performance to live by themselves. One important aspect for the elderly is their loss of vision due to the cataract. Their crystalline lens become hazy which caused more scattered light in their eye. Therefore, they cannot see some small details clearly such as small Thai letters. In this research we then investigated the effect of luminance contrast between text and background on legibility of Thai letters. We selected an LED display as a source to present the letters becuse nowaday LED display is generally used to present information. However, its characteristic was not the same as the reflected paper because the LED display is a self emitting source. We thought that the LED display generally emit stronger light intensity than the reflected light from paper. We varied the luminance contrast between text and background and examined the reading performance and easiness of young and elderly people.

2. METHOD

2.1 Apparatus

The apparatus was composed of two rooms (a test room and a subject room) separated by a wall. The dimension of this apparatus was shown in Figure 1. Inside the test room, an LED display (Toshiba LED40PU200T) was placed and connected to a PC via HDMI cable. This LED display was used for presenting stimuli. The test room was covered by a black curtain to minimize external light. In the subject room, the internal wall was covered by a white wall paper. The room was also decorated by some stuff such as artificial flower, a doll, and books on a shelf in order to simulate the daily life used rooms. There was a set of four fluorescence lamps attached to the room's ceiling. The intensity of this set of four fluorescence lamps was adjustable to obtain the required illluminance level. The illuminance in this room was measured by a chroma meter (Konica Minolta CL-200A) placed on the shelf closed to the front wall. On the front wall which connected to the test room, a 5 cm × 30 cm aperture was cut at the subject eye's level. The subject looked through this aperture to see the stimuli which were presented on the LED display. The distance between the front wall and the subject's eye was fixed at 2 m.

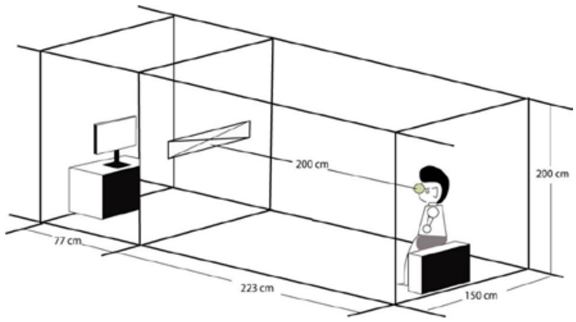

Figure 1: Schematic diagrams of the apparatus.(Rattanakasamsuk 2013)

2.2 Subjects

Three groups of subjects participated in this experiment. The first group was 30 undergraduated student (age between 18-23 years old.). We named this group as "*young*". The second group was five elderly people (age between 58-66 years old). This group was named as "*elderly*". For the third group, 30 young subjects were asked to wear cataract experiencing goggle during experiment. This cataract experiencing goggle was developed by Obama et al. (Obama et al. 2004). It was made from 58% transmittance filter, 14% of haze values filter and yellow filter in order to simulate the elderly vision. These 30 subjects was called "the simulated elderly". All subjects had normal or corrected to normal visual acuity.

2.3 Stimuli and Experimental Conditions

The stimulus configuration was a row of ten random Thai letters presented on an LED display. The letter's size and viewing distance were kept constant at 0.35 degree and 246 cm, respectively. The luminance of *"black"* and *"white"* background was constant at 0.01 and 147 cd/m^2, respectively. Two polarities of luminance contrast between letter and background was applied to the stimuli as shown in Figure 2. The first one was positive polarity (dark letter on *white* background). Five levels of luminance contrast for the positive polarity were set at -1.30, -0.95, -0.54, -0.37, 0.65, and 4.17. The second one was negative polarity (light letter on *black* background). Five levels of luminance contrast for the negative polarity were set at 0.30, 1.23, 2.48, 3.18, 3.60, and 4.17. Note that all luminance contrast was presented in term of log Weber contrast. The illuminance of the subject room was set at 0 lux for simulating night-time condition and set at 300 lux for simulating the indoor viewing condition.

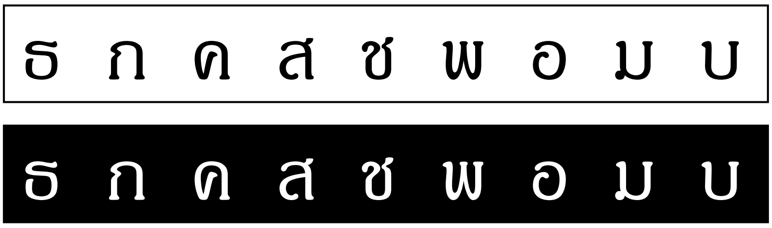

Figure 2: Example of stimuli. (Top) positive polarity and (Bottom) negative polarity.

2.4 Experimental Procedure

There were two tasks for each subject. The first task was reading performance task. The subject was asked to report each random letter. The reading performance was calculated by percentage of correct answer. The second task was reading easiness task. When the subject saw the stimuli, they were asked to rate the easiness of reading with five levels of score from 0 to 4. While 0 means *"unable to read/very difficult to read"*, 4 means *"very easy to read"*. These two tasks were done in separated sessions. Therefore, in each session, the experimenter selected one of the experimental conditions from the combination of two illuminance levels (0 or 300 lux), two contrast polarities (positive or negative polarity) and two tasks (reading performance or reading easiness). The subject was asked to sit in the experimental room and look around inside the room for two minutes. After two-minute adaptation, a line of ten random Thai letters was presented. The subject was asked to complete either reading performance task or reading easiness task. After finishing each trial, the new 10 random letter with different luminance contrast was presented. The subjects repeated the tasks until all five luminance contrast were presented.

3. RESULTS AND DISCUSSION

Positive Polarity (Dark Letter on White Background)

Figure 3 showed result of positive polarity. The two top panels showed results of reading performance task, and the two bottom panels showed result of reading easiness task. The left and right panels showed result obtained under subject room's illuminance at 0 and 300 lux. Circle, square, and triangle represented average result obtained from young, simulated elderly, and elderly respectively. The dashed lines were the regression line which obtained by fitting the data with logistic functions as shown in Equation 1.

$$y = \frac{1}{1+e^{(-ax-i)}} \qquad (1)$$

For reading performance task, we calculated the minimum required contrast for good reading performance at 75% correct answer. The results were shown in Figure 4 (Left). It clearly showed that the result of the young was not the same as the elderly and the simulated elderly. The reading performance of the young was better than that of the other two groups. The young could also read lower contrast letter under both 0 and 300 lux conditions. However, there was difference between the real elderly and the simulated elderly. The Reading performance of the simulated elderly seems not to be strongly influenced by environment light. On the other hand, reading performance of the elderly was significantly affected by environment. In case of 0 lux condition where all environments was dark but the adjacent background only looked bright, the reading performance was significantly lower than that in the 300 lux.

For reading easiness task, we calculated the minimum required contrast for easy reading at easiness score 3. The results were shown in Figure 4 (Right). The results showed that even all subjects could see the low contrast letter but they felt that the letter was uneasy or uncomfortable to read. They required contrast between letters and background at least -0.528, 0.095 and 0.253 for the young, the simulated elderly and the elderly, respectively.

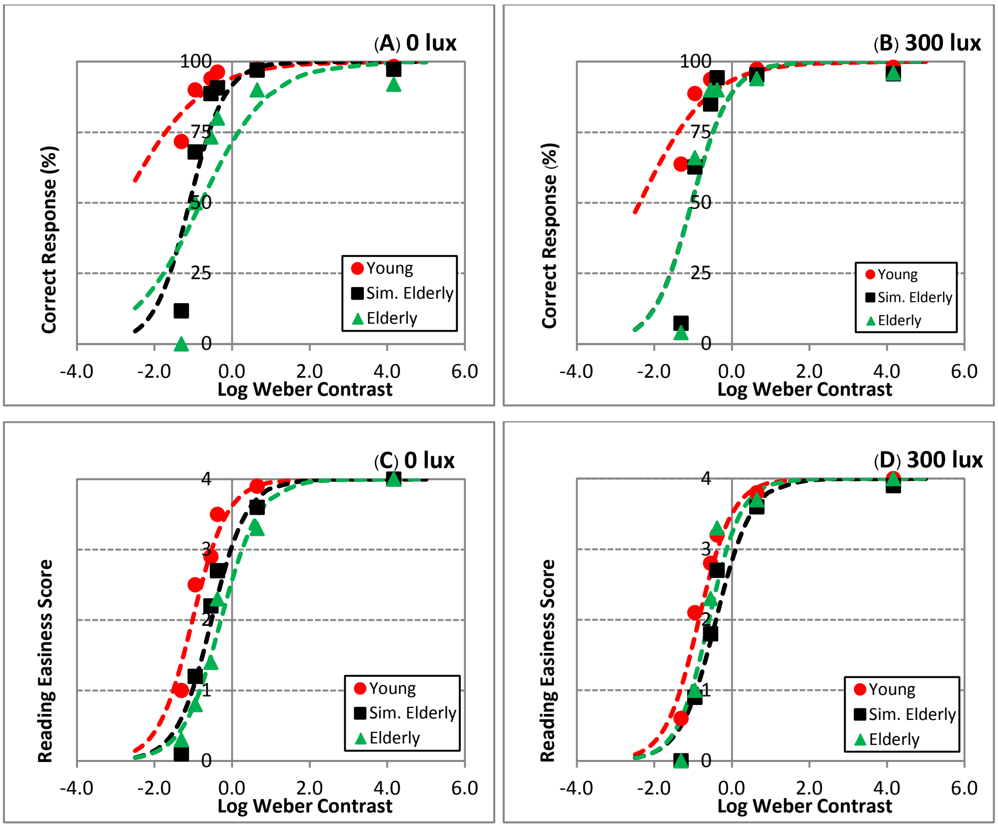

Figure 3: Result of positive polarity. (Top) reading performance task (Bottom) reading easiness task.

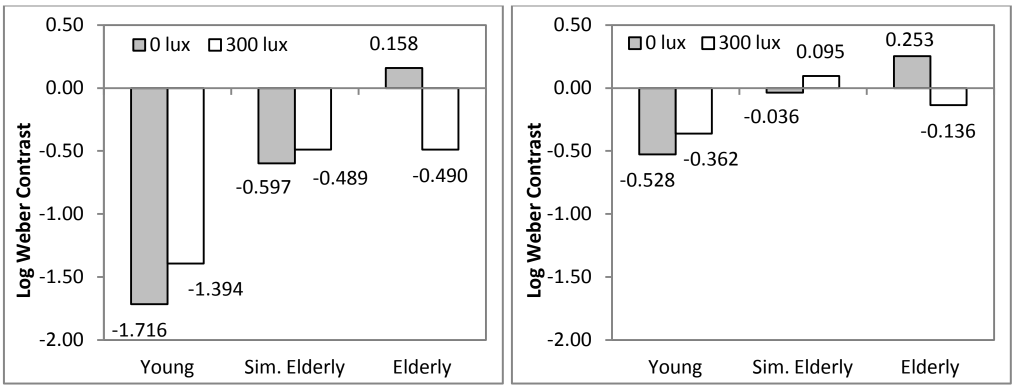

Figure 4: Minimum required contrast for positive polarity from (Left) reading performance task and (Right) reading easiness task.

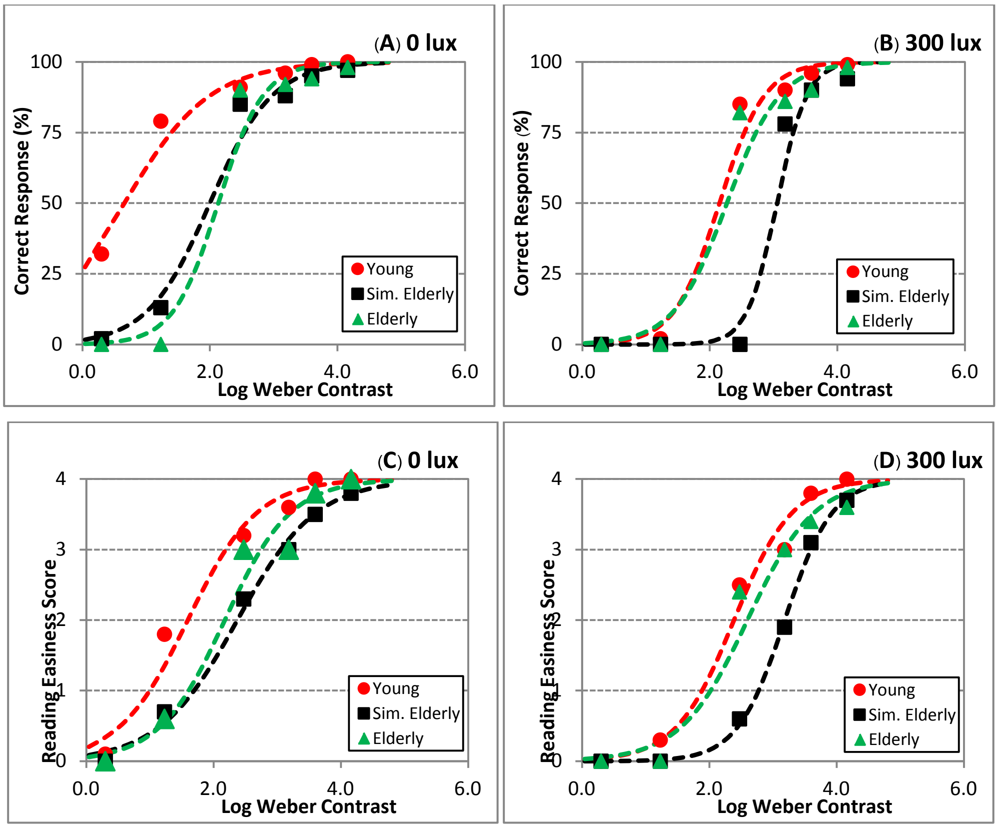

Figure 5: Result of negative polarity. (Top) reading performance task (Bottom) reading easiness task.

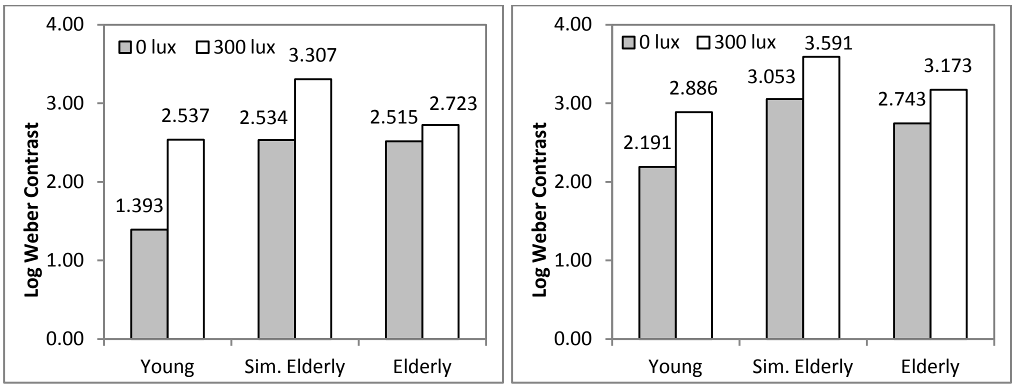

Figure 6: Minimum required contrast for negative polarity from (Left) reading performance task and (Right) reading easiness task.

Negative Polarity (Bright Letter on Black Background)

The results of negative polarity were shown in Figure 5 and 6. At any contrast level, the reading performance of the young was still better and the easiness score was still higher than the simulated elderly. These lowering reading performance and easiness score of the simulated elderly were mainly due to the cataract experiencing goggle. The goggle caused scattered light which disturbed the sharpness of letter and possibly covered some minor detail of the letter so that the subject could not clearly and comfortably see the letter. However, we found that the room illuminance showed slightly effect on reading performance of the elderly. The minimum required contrast for the elderly under both case were nearly identical. But the room illuminance strongly affected the reading performance of the young and the simulated elderly. The reading performance of both groups was suddenly declined when the room illuminance increased. We asked the subject to describe their perception. Both young and simulated elderly reported that when the room was bright (300 lux condition), they felt like a lot of reflected light come through their eyes. This situation caused them to unable to see the bright letter on the black background clearly. But when we asked the elderly, they reported that no noticeable difference on their perception between 0 and 300 lux condition. This report was unexpected because we all know that the scattered light in the eye of the elderly and the scattered light from cataract experiencing goggle should be higher when the environment was bright. Therefore the elderly should be more under influence of room illuminance than the young. But our results contradict to this fact.

4. CONCLUSIONS

Our results showed that the elderly required higher contrast letter than the young. For all groups of subject, minimum required contrast for easy reading is higher than minimum required contrast for correct reading. Even though all groups of subject could read the low contrast letter but they felt that the low contrast is uneasy to read.

ACKNOWLEDGEMENTS

We thank Prof. Mitsuo Ikeda, Assoc. Prof. Tomoko Obama for their support and valuable comments to this experiment.

REFERENCES

Institute for Population and Social Research, Mahidol University 2006, *Population Projections for Thailand, 2005-2025.*

United Nations, Department of Economic and Social Affair Division 2002, *World Population Ageing 1950-2050,* Population Division, New York.

Obama, T., Uozato, H., Terauchi, H., and Matsuoka, M. A. 2004. *Qualitative Determination of Senile Cataract Experience Filters*, Journal of Color Science Association of Japan, 28, 245–252 (in Japanese).

Rattanakasamsuk, K. 2013. *Elderly Vision on Legibility of Thai Letters Presented on LED Panel, Proceeding of ACA2013Thanyaburi,* Pathum Thani, pp70-73.

Address: Kitirochna RATTANAKASAMSUK,
Color Research Center,Faculty of Mass Communication Technology,
Rajamangala University of Technology Thanyaburi,
39 Muh 1 Rangsit-Nakon Nayok Rd., Klong 6,Thanyaburi,
Pathum Thanim, 12110, THAILAND
E-mails: kitirochna@gmail.com

Color rendering analysis based on color pair evaluation under different LED lighting conditions

Qing WANG,[1] Haisong XU,[1,*] Jianqi CAI,[2] Wei YE [3]
[1] State Key Laboratory of Modern Optical Instrumentation, Department of Optical Engineering, Zhejiang University
[2] Visual Health and Safety Institute, China National Institute of Standardization
[3] State Key Laboratory of Industrial Control Technology, Zhejiang University

ABSTRACT

Most color rendering measures are concentrated on the precise rendering of a single color under the test illuminant comparing with the standard illuminant, and few studies estimate an illuminant by the rule of the color difference between color pairs. Hereby, this study focuses on the color discrimination of two colors under individual illuminants. Based on the psychophysical method of gray scale, a visual experiment was carried out to test the effects of LED lightings on the color difference of color pairs with Munsell color samples. A panel of 10 observers participated in the color discrimination evaluations under 12 lighting conditions, including 2 levels of illuminance and 6 correlated color temperatures (CCTs) ranged from 2000K to 10000K in a LED light booth. The experimental results indicate that the illuminant has obvious impacts on the visual color differences, but the effects are different for the color pairs with differences of hue, lightness or chroma.

1. INTRODUCTION

Solid-state lighting technology based on light emitting diodes (LEDs) is now emerging as a cost-competitive and energy efficient alternative to conventional lightings. The narrowband LED light sources make them different from other light sources and so are important for the evaluation of color rendering. One of the key characteristics of light sources for interior lighting is their color rendering property. If the color rendering is poor, the light source would not be useful for interior lighting. The CIE color rendering index (CIE-R_a) is the most widely used measure for quantifying the color rendering performance of light sources. However, many papers have been published that the CIE-R_a is not appropriate for evaluating the color rendering property of LED lighting (Ohno, 2005). Hence, some other matrics, such as CRI-2012 (Smet, 2013) and Color Quality Scale (CQS-Q_a/-Q_p) (Davis, 2010), have been developed to focus on color fidelity or preference. In addition, the color discrimination index (CDI) (Thornton, 1972) suggested by Thornton evaluates color appearance under the illumination provided by the conventional light sources, which is used to predicte how well the lighting can discriminate color differences in hue.

2. METHOD

2.1 Sample Preparation

Almost all procedures for color rendering evaluation are based on the calculation of the color rendering of either a set of selected multiple color samples or of a gamut of colors. This is correct when the spectrum of the light source is more or less continuous. However, the uneven spectra of LED light sources make it difficult to account for the color differences that occur with many different color samples. Hereby, this study focuses on the color discrimination of two colors under individual illuminants. In this study, the 6 test CCTs of 2000 K, 2700 K, 3450 K, 5000 K, 6500 K and 10000K as well as 2 illuminance levels of 500 lx, and 1000 lx were adopted, which were combined as 12 predefined lighting conditions in total. All experimental setups were achieved by a light booth of Just Normlicht consisting of six kinds of narrowband LEDs with wavelength peaks across the visible spectrum, with its inner wall being painted as the neutral color of Munsell N6. The measured relative spectral power distributions (SPDs) of the 12 test lighting conditions actually used in the assessments, via the tele-spectroradiometer of Konica Minolta CS-2000, are shown in Figure 1. A panel of 10 subjects with normal color vision participated in the visual experiments, all of whom were graduate students in Zhejiang University.

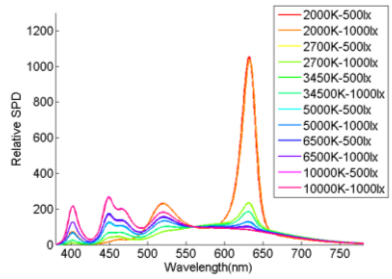

Figure 1: The relative spectral power distributions of 12 test lighting conditions.

A total of 16 groups of color samples were selected from Munsell color order system, as listed in Table 1, including all the 5 primary hue and 5 middle hue. Each color sample group comprised a reference color sample and several test color samples, and the color differences between the reference color and the test colors were one of the three cases, i.e. hue differences or chroma differences or lightness differences. Therefore, there were 73 pairs of color differences in total, involving 16 pairs of hue differences, 26 pairs of lightness differences, and 31 pairs of chroma differences.

Table 1. The 16 groups of color samples selected from Munsell color order system.

Reference	Test color samples					
5Y6/4	7.5Y6/4	5Y5/4	5Y7/4	5Y6/6	5Y6/2	
5GY6/8	2.5GY6/8	5GY6/10	5GY6/6	5GY7/8	5GY5/8	
2.5G6/6	5G6/6	2.5G6/8	2.5G6/4	2.5G7/6	2.5G5/6	
10BG6/4	10BG6/2	2.5BG6/4	7.5BG6/4	10BG7/4	10BG6/6	10BG5/4
10P6/8	10P7/8	10P6/10	2.5RP6/8	10P6/6	7.5P6/8	10P5/8
5Y8/10	5Y8/8	5Y8.5/10	5Y7/10	5Y8/12		
5YR8/4	7.5YR8/4	2.5YR8/4	5YR8/2	5YR8/6	5YR7/4	
7.5P4/10	7.5P3/10	7.5P5/10	7.5P4/12	10P4/10	7.5P4/8	5P4/10
10PB4/10	10PB3/10	10PB4/12	10PB5/10	10PB4/8		
7.5B5/10	7.5B4/10	5B5/10	7.5B6/10	10B5/10	7.5B5/8	
7.5GY7/10	7.5GY6/10	7.5GY8/10	7.5GY7/8	5GY7/10		
2.5GY8/10	2.5GY7/10	2.5GY8/12	2.5GY8/8			
10YR7/12	10YR7/14	10YR7/10	10YR6/12	10YR8/12		
10R6/12	2.5YR6/12	10R5/12	10R6/10	10R6/14		
5R4/14	5R4/12	5R5/14	7.5R4/14			
7.5RP4/12	7.5RP5/12	7.5RP4/10	5RP4/12	10RP4/12		

2.2 Experimental Procedure

The experiment was carried out in a dark room with a psychophysical method of gray scale, and all the subjective estimations must rate the color differences of the Munsell sample pairs by referring the gray scale. Note that there are 9 levels of gray scales at the interval of 0.5, with the lowest gray scale of 1 representing the largest color difference and the greatest scale of 5 labelling the least color difference. The viewing angles for each color pair was 2° with the illumination and viewing geometry of 45/0. The whole experiment was divided into 12 sessions according to the 12 test lightings assigned randomly to the subjects, and in each session all the 73 color pairs must be rated by the individual subjects. A brief description about the experiment was presented to the subjects before each session, which began with a 3-min dark adaptation. Next, at the beginning of each test lighting condition, 1-min light adaptation was carried out (Ohta, 2006), and then the subjects were asked to estimate the color differences. Totally 8760 assessments were collected from this study [10 subjects × 73 pairs × 6 CCTs × 2 illuminances].

3. RESULTS AND DISCUSSION

3.1 Chromaticity differences of 73 color pairs under 6 CCT LED lightings

As some typical examples, Figure 2 depicts the chromaticity coordinates of the reference colors and their corresponding test colors for 4 groups of color samples in CIE1976UCS under the 6 CCTs of LED lightings, respectively. The 6 dots in each subfigure represent the chromaticity coordinates of the reference color for the corresponding color group under the 6 CCT lightings, respectively, and the crosses label the chromaticity coordinates of the test colors and the lines illustrate the differences of chromaticity coordinates between the reference and the test colors.

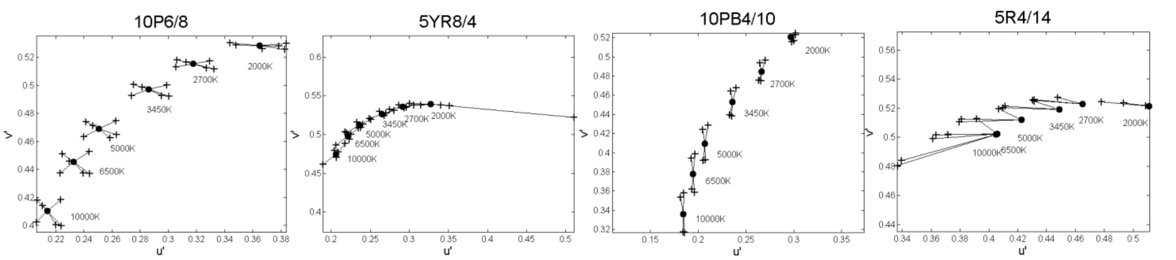

Figure 2: The chromaticity coordinates differences of 4 groups of color samples as typical examples under 6 CCTs of LED lightings, respectively, in CIE1976UCS diagram.

As shown in Figure 2, the chromaticity differences between the reference color 5YR8/4 and the test color 5YR8/2 under the CCT 2000 K is extremely large with comparison to those under the other 5 CCT lightings, implying that 2000 K is the most appropriate condition for discriminating this color pair among the 6 tested CCT LED lightings. While the chromaticity differences of the reference color 10PB4/10 with its test colors are very small under 2000 K, which indicates that the purple-blue is very difficult to be distinguished under such a low CCT of lighting. Moreover, the reference color 5R4/14 and its test colors show the largest chromaticity differences under 10000 K, which means so high a CCT as 10000 K is a rather helpful LED lighting condition for distinguishing the highly chromatic red colors. These results indicate that a lighting condition would induce great color differences for some specific colors but little color differences for other colors.

Therefore, a hypothesis could be proposed that a lighting endowed with high color discrimination property would show large mean color difference for the test color pairs.

3.2 Correlation of visual color difference with color rendering indices

In the gray scale comparison experiment, the subjective assessment for pairs of color differences was refereed by the grade values (G) of 9 levels gray scale, which must be converted into the visual color differences (ΔV). To do this, the transfer equations were fit between the ΔE^{*}_{ab} values of the 9 gray scales and the corresponding grades (G). With the quadratic equations, the ratings of 73 Munsell test color pairs can be converted to their visual color differences (ΔV), which could be regarded as the indicators to analyze the color discrimination property of the light source. Table 2 lists the Pearson correlation coefficients between the visual color differences (ΔV) and several related color rendering indices for the sample pairs, respectively, with hue difference, chroma difference, lightness difference, as well as all the test sample pairs. Among all cases, hue differences have relatively high correlations with all color rendering indices except for CRI-2012 (with s-curve function and simulated samples in its calculation, rather different from others), which means that hue difference is the most obvious component of the total color difference and so contributes evidently to the color rendering metrics of the lightings. On the other hand, CDI shows the strongest correlation with the hue difference due to its focusing on the color discrimation property of light sources by computing the gamut area of object colors in uniform chromaticity diagram. However, the correlations of ΔV with the related color rendering indices for the color sample pairs of chroma difference, lightness difference and overall color difference are poor, indicating no significant relevancy between them.

Table 2. The Pearson correlation coefficients betwen the visual color difference (ΔV) and the related color rendering indices.

ΔV	CIE-R_a	CQS-Q_a	CQS-Q_p	CRI-2012	CDI
Hue difference	0.64	0.51	0.58	-0.12	0.90
Chroma difference	0.03	0.02	0.33	-0.05	0.55
Lightness difference	-0.24	-0.10	0.15	0.20	-0.31
Overall color difference	0.26	0.24	0.45	0.01	0.48

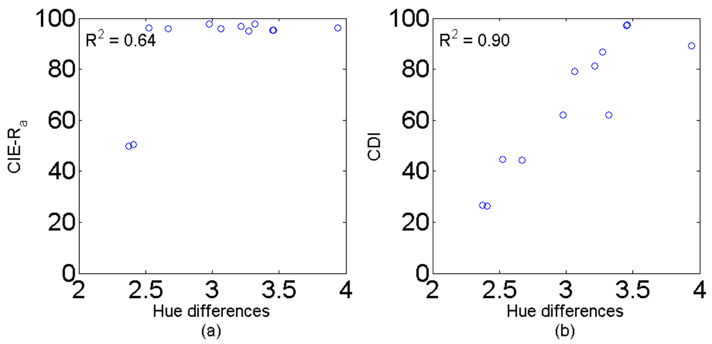

Figure 3: The relationships of hue differences with CIE-R_a (a) and CDI (b).

As mentioned above, the sample pairs with hue differences appear high correlations with the color rendering indices, among which CDI achieves the greatest Pearson correlation coefficient. Figure 3 illustrates the relationships between hue differences and CDI values, along with CIE-R_a, the present standard, as a comparison. The very likely reason may be that the indices except for CDI mainly focus on the fidelity or preference rather than the color discrimination property of the tested light sources. Thereby, a further study will be carried out in the future to investigate the essential relationships between the color discrimination ability and color rendering property of the LED lighting.

4. CONCLUSIONS

In this study, a psychophysical experiment was implemented to discuss the color discrimination property of LED light sources via the gray scale method using color sample pairs with various color differences under 12 lighting conditions. It is indicated that the LED lightings have obvious impacts on the visual color differences, while the effects are dependent upon the type of color differences, i.e. hue difference, chroma difference or lightness difference. In detail, hue difference shows strong correlation with CDI among all the situations. Hence, it needs further investigation to explore a way of assessing the color rendering property of an LED light source based on its color discrimination characteristics.

ACKNOWLEDGEMENTS

This work was funded by the National Science and Technology Support Program of China [Grant No. 2012BAK28B01-7].

REFERENCES

Davis, W. and Ohno, Y. 2010. Color quality scale, Optical Engineering 49 (3) 033602-033602.

Ohno, Y. 2005. Spectral design considerations for white LED color rendering, Optical Engineering 44 (11) 111302-111302.

Ohta, N. and Robertson, A. 2006. Colorimetry: fundamentals and applications. John Wiley & Sons.

Smet, K. A. G. *et al. CRI2012: A Proposal for Updating the CIE Color Rendering Index*, Lighting Research and Technology 45 689-709.

Thornton, W. A. 1972. Color-discrimination index, JOSA 62 (2) 191-194.

Address: Prof. Haisong XU, State Key Laboratory of Modern Optical Instrumentation, Department of Optical Engineering, Zhejiang University, Hangzhou 310027, China
E-mails: chsxu@zju.edu.cn

The Relationship between Whiteness Perception of Watercolor Illusions and Color Vision Characteristics

Shoko ISAWA,[1] Koichi IGA,[2] Ichiro KATAYAMA,[3] Tsuneo SUZUKI,[4]
[1] Faculty of Contemporary Human Life Science, Tokyo Kasei Gakuin University
[2] Color Universal Design Organization
[3] Faculty of Biology-Oriented Science and Technology, Kinki University
[4] Faculty of Law, Keio University

ABSTRACT

The relationship between how the white color regions of graphics are perceived and the color vision characteristics for the subjects with normal color vision and defective color vision was studies by using the conventional watercolor illusion graphics and newly-developed watercolor illusion graphics. The results revealed that the whiteness perception and the evaluation tendencies of the color in the white region were nearly identical regardless of color vision characteristics in both graphics.

1. INTRODUCTION

When a double-lined outline of a graphic is drawn in two chromatic colors, the color of the inner outline looks like bleeding in the enclosed regions. This phenomenon is known as the watercolor illusion (Pinna et al. 2001). Until today, we have shown that the perceived whiteness of the regions enclosed with the double-lined outlines varies with the combination of outline colors and that the combination of a blue inner line and a yellow outer line, a red inner line and a green outer line, or a blue inner line and a green outer line can increase the whiteness perception (Isawa and Suzuki 2011, 2012). In addition, we invented a new watercolor illusion graphic with horizontal stripes drawn in two chromatic colors and evaluated the perceived whiteness of the white region to confirm the same result as in the case of conventional watercolor illusion graphics (Isawa et al. 2009, Isawa and Suzuki 2014). However, it is unknown that whether or not the change in the whiteness perception attributed to the optic illusion occurs among the subjects with defective color vision because the series of research targeted the subjects with normal color vision. Thus, this study investigated the relationship between the whiteness perception of the watercolor illusion and the color vision characteristics of subjects.

2. EXPERIMENTAL OVERVIEW

The subjects consisted of 12 participants with normal color vision (N-type), 11 participants with protanopia or protanomaly (P-type), and 11 participants with deuteranopia or deuteranomaly (D-type).

The conventional watercolor illusion graphics and the new watercolor illusion graphics consisting of horizontal stripes in two chromatic colors were used as stimuli to be evaluated. In the new graphic, the outer colors of the double-lined outlines in the conventional graphic are placed on both sides of the white color region, and the horizontal stripes of the inner colors of the double-lined outlines are overlapped on them. In the following descriptions, the conventional watercolor illusion graphic is hereinafter referred to as WC, and the newly-developed watercolor illusion graphic as HS for simplicity. The stimuli placing the WC and the HS on the left and the right were presented to the subjects and the subjects were asked to compare the whiteness of each white color region. Three combinations of graphics were presented and were shown in Figure 1. The stimuli were printed on the photo papers.

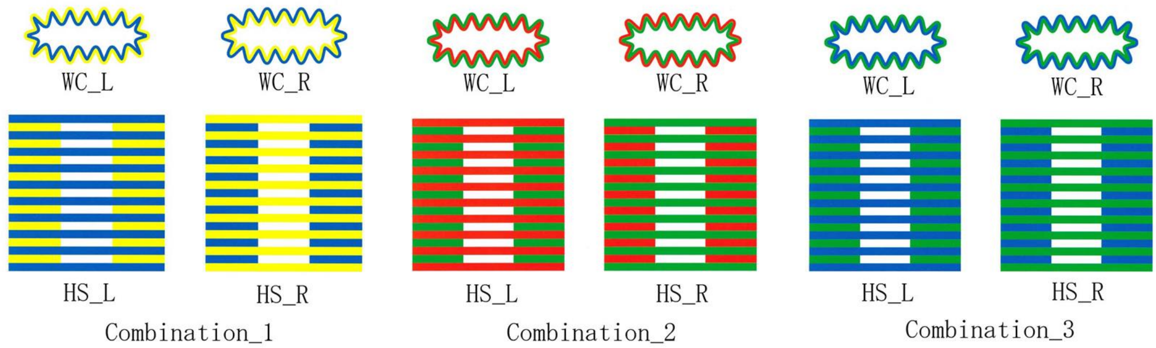

Figure 1: Stimulus combinations used in the experiment.

3. RESULTS AND DISCUSSION

All the subjects answered that the whiteness in the white region seemed different between the right and the left graphics on both the WC and the HS, except for the Combination 2 (combination of red and green). For the Combination 2, extremely few subjects with defective color vision answered that the whiteness in the white region in both left and right graphics seemed the same. Table 1 shows the number of the subjects who answered that the white region in the left and right graphics seemed the same. The denominator of each cell indicates the number of subjects.

Table 1: Number of the subjects who did not distinguish the whiteness difference between the left and the right graphics.

	Combination_1 Blue-Yellow		Combination_2 Red-Green		Combination_3 Blue-Green	
	WC	HS	WC	HS	WC	HS
N-type	0/12	0/12	0/12	0/12	0/12	0/12
P-type	0/11	0/11	1/11	1/11	0/11	0/11
D-type	0/11	0/11	2/11	0/11	0/11	0/11

For the Combination 1, regardless of color vision characteristics, 28 subjects out of all the 34 subjects answered that the white regions in the WC_L and the HS_L are “whiter”, “more clearly white” and “more vividly white” when comparing to the ones in the WC_R and the HS_R. For the Combination 2, more than half of the P-type subjects answered that the white regions in the WC_L and the HS_L are “more clearly white”, “more vividly white” and “more freshly white” when comparing to the ones in the WC_R and the HS_R. However, more than half of the D-type subjects answered that the white regions in the WC_R and the HS_R are “more brightly white”, “more beautifully white” and “whiter” when comparing to the ones in the WC_L and the HS_L. Two-thirds of the N-type subjects answered that the white region in the WC_L is “whiter” for the WC graphics; however, a little less than half of the N-type subjects answered that the white region in the HS_L is “whiter” for the HS graphics. Thus, a difference was found between the WC and the HS graphics. For the Combination 3, regardless of color vision characteristics, majority of the subjects answered that the white regions in both the WC_L and the HS_L are “whiter” when comparing to the ones in the WC_R and the HS_R. Most of the N-type subjects described the white regions of the WC_R and the HS_R as “yellowish white”, while only a few of the P-type and the D-type subjects described them as “yellowish white”. Table 2 shows the main results on how the subjects described the appearance of the white region of each graphic.

Table 2: Summary of the answers obtained from the subjects.

	Blue-Yellow			
	WC(Watercolor illusion)		HS(Horizontal Stripe pattern)	
	In comparison with Right, Left looks	In comparison with Left, Right looks	In comparison with Right, Left looks	In comparison with Left, Right looks
	whiter	dull yellow	clear bright white	dull white
N-type	clear white	yellowish	whiter	yellow white
	strong white	dull	clear white	yellowish
	strong white	yellowish	clear vivid white	dull yellow
P-type	clear white	dull and yellowish white	clear white	yellowish
	whiter	yellowish white	bright strong white	yellowish white
	whiter	a little yellowish	whiter	yellowish
D-type	clear and bluish white	yellowish white	strong white	yellowish white
	bluish white	dull and grayish	bluish white	natural white

	Red-Green			
	WC		HS	
	In comparison with Right, Left looks	In comparison with Left, Right looks	In comparison with Right, Left looks	In comparison with Left, Right looks
	pinkish white	a little coolish white	clear white	a little greenish white
N-type	pale pink	greenish white	pinkish white	whiter
	whiter	greenish	pale pink	greenish
	clear white	a little white	clear white	a little dull
P-type	whiter	less vivid white	white	a little dark and yellowish
	a little pink	simple white	a little pink	a little greenish
	a little reddish	whiter	reddish	whiter
D-type	yellowish	light white	a little pink	clear white
	dull white	a little greenish	pinkish	light and white

	Blue-Green			
	WC		HS	
	In comparison with Right, Left looks	In comparison with Left, Right looks	In comparison with Right, Left looks	In comparison with Left, Right looks
	bluish white	yellowish	clear white	yellowish
N-type	clear white	dull white	whiter	dull white
	whiter	greenish	bluish	yellowish white
	whiter	a little yellowish	clear and vivid white	a little yellowish
P-type	clear white	greenish	whiter	greenish
	bluish and vivid	dull white	strong white	dull white
	whiter	greenish white	whiter	dull white
D-type	bluish white	natural white	vivid white	yellowish white
	light white	yellowish	bluish white	greenish white

Reading through the answer results of the subjects, there is no effect of color vision characteristics on the whiteness perception due to the watercolor illusion in blue/yellow and blue/green combinations, while the whiteness perception varied depending on the color vision characteristics in red/green combination. In addition, for the combination of red and green, N-type subjects' whiteness perception due to the watercolor illusion was found to differ between the WC and the HS graphics.

4. CONCLUSIONS

The effect of chromatic color combinations on the whiteness perception in the watercolor illusion graphic was studied on the subjects with normal color vision and the subjects with defective color vision by using two types of watercolor illusion graphics. The results are summarized below.

(1) It was found that the change of whiteness perception attributed to the watercolor illusion was nearly in common regardless of the color vision characteristics.
(2) When combining red and green, it was found the whiteness perception in the white region was slightly different depending on the color vision characteristics.
(3) Excluding the combination of red and green, no difference in the whiteness perception in the white region was found between the conventional watercolor illusion graphics and the newly-developed watercolor illusion graphics.

REFERENCES

Isawa, S., T. Suzuki and A. Komachiya. 2009. *Effect of adjacent chromatic colors on whiteness perception.* Journal of the Color Science Association of Japan 33 Supplement: 90-91.

Isawa, S. and T. Suzuki. 2011. *The improvement of perceivable whiteness by the watercolor illusion.* Journal of the Color Science Association of Japan 35 Supplement: 114-115.

Isawa, S. and T. Suzuki. 2012. *The quantification of whiteness change by the watercolor illusion.* Journal of the Color Science Association of Japan 36 Supplement: 154-155.

Isawa, S. and T. Suzuki. 2014. *Comparison of Adjacent Chromatic Colors and Watercolor Illusions in Whiteness Perception –The New Type of Watercolor Illusion-.* Journal of the Color Science Association of Japan 38(3): 240-241.

Pinna, B., G. Brelstaff and L. Spillmann. 2001. *Surface color from boundaries: a new 'watercolor' illusion.* Vision Research 41(20): 2669-2676.

Address: Shoko ISAWA, Department of Modern Home Economics, Faculty of Contemporary Human Life Science, Tokyo Kasei Gakuin University,22 Sanban-cho, Chiyoda-ku, Tokyo, 102-8341, JAPAN
E-mails: isawa@san.kasei-gakuin.ac.jp, iga@cudo.jp, katayama@waka.kindai.ac.jp, suzukitn@hc.cc.keio.ac.jp

INFLUENCE OF DAYLIGHT ILLUMINATION IN THE VISUAL SALIENCY MAP OF COLOR SCENES.

Juan OJEDA, Juan Luis NIEVES and Javier ROMERO
Department of Optics, Faculty of Sciences, University of Granada

ABSTRACT

Visual saliency maps code topographically local conspicuity over the entire scene. They are based on image properties such as color, luminance or orientation. And because object colors depend on both the spectral reflectance of the surfaces and the spectral power distribution (SPD) of the light impinging on them it is plausible to check also the influence of that SPD on the saliency maps of color images. Preliminary results suggest some differences among the saliency maps under different daylight correlated color temperatures (CCTs), being minimum and maximum along the Orientation and BY channels, respectively.

1. INTRODUCTION.

The color signal of objects depend on the spectral reflectance of their surfaces and the SPD of the light impinging on them. The aim of this study is to determine the influence of daylight in the saliency maps of color images.

Studies in humans have shown that color can influence visual attention but only few studies concentrate on this issue. Amano and Foster (2014) found local color properties yield a better explanation of fixation position than other local achromatic properties. Hamel et al. (2014) improve the predictive power of Marat saliency model for video (2009) by incorporating color information to it. The analysis of neurophysiologically relevant color features by Frey et al. (2008) shows that the influence of color on overt attention depends on the type of image.

The saliency map is a biologically plausible model for bottom-up overt attention proposed by Koch and Ullman in 1985. In the review of the model by Itty et al. (1998), the visual saliency maps are topographical codifications of fixation position in visual search over the entire scene based on different image features such as luminance, orientation or color.

2. METHOD AND RESULTS.

In this work we have used a set of 1100 RGB 400x400 pixels images sorted in different semantic categories: Forests, Fields, Shores, Mountains, Beaches, Rivers (these six belong to Natural images) and Highways, Cities, Buildings, Interiors and Streets (that belong to Non-natural or artificial images). Every category has two subcategories: with or without objects pictures. The pictures are from the authors and from the SUN Database (Xiao et al. 2010).

2.1 Images simulation under different SPD of daylight.

Every RGB image was normalized to the range [0..1] and simulated under five different SPD of daylight characterized by their respective CCTs: 2735K, 4505K, 6479K, 10181K and 25889K between 400-700 nm. The simulation was made using Judd color matching functions (Judd 1951) and the Bradford chromatic adaptation matrix (Süsstrunk et al. 2001)

The real daylight SPDs were measured in Granada, Spain, from sunrise to sunset under different atmospheric conditions and covering a vast range of CCTs from 4800 up to 30,000 K (Hernández-Andrés et al. 2001). The simulated daylight SPDs were obtained with SBDART, a software tool to compute plane-parallel radiative transfer energy in clear and cloudy conditions within the Earth's atmosphere and at the surface (Ricchiazzi et al 1998) to cover CCTs below 4800 K.

Figure 1 shows an example (Forest picture with objects) of simulated images under the working SPDs of this work. We can see how the appearance of the image depends on CCT, the image looks more bluish when CCT is high and reddish when CCT is small. But is there any influence and/or change in the saliency maps for different CCTs?

Original Picture	2735K	4500K
		
6479K	10181K	25889K
		

Figure 1. Original and simulated pictures under five illuminants of CCTs 2735K, 45005K, 6479K, 10181K and 25889K.

2.2 Saliency maps of color images under different daylight.

In the Itti-Koch algorithm (Itti et al. 1998) every picture is separated by linear filtering in three features: Intensity (Luminance), Color (which is classified in two opposite chromatic sub channels RG and BY) and Orientation (which is divided in four sub channels for different angles). The features maps are computed by a set of center-surround differences between a center fine scale and a surround coarser scale defined as the interpolation to the finer scale and a point-by-point subtraction.

A map normalization operator $\mathcal{N}(.)$ is applied to the features maps to globally promote them with a small number of strong peaks of activity (conspicuous locations) and suppress them with numerous comparable peak responses. These normalized features maps are reduced to central scale and added point-by-point yielding three conspicuity maps: Intensity, Color and Orientation. The saliency map is the average of the three conspicuity maps normalized by $\mathcal{N}(.)$ operator.

The Itti algorithm implemented by Harel (2013), which is a simplified version of Itti-Koch algorithm, was applied to the simulated images using a 0.5 threshold value. The conspicuity maps for each channel (including RG and BY chromatic sub channels) and the picture saliency map were found.

In Figure 2 we can see an example of conspicuity and saliency maps for a Forest picture with objects. The rows correspond to Luminance and Orientation channels, Chromatic RG and BY sub channels conspicuity maps and the global saliency map of the picture, columns show the CCTs of the different illuminant used in the study. Figure 2 suggest some changes in the color saliency maps (across their RG and BY sub channels) depending on the CCT.

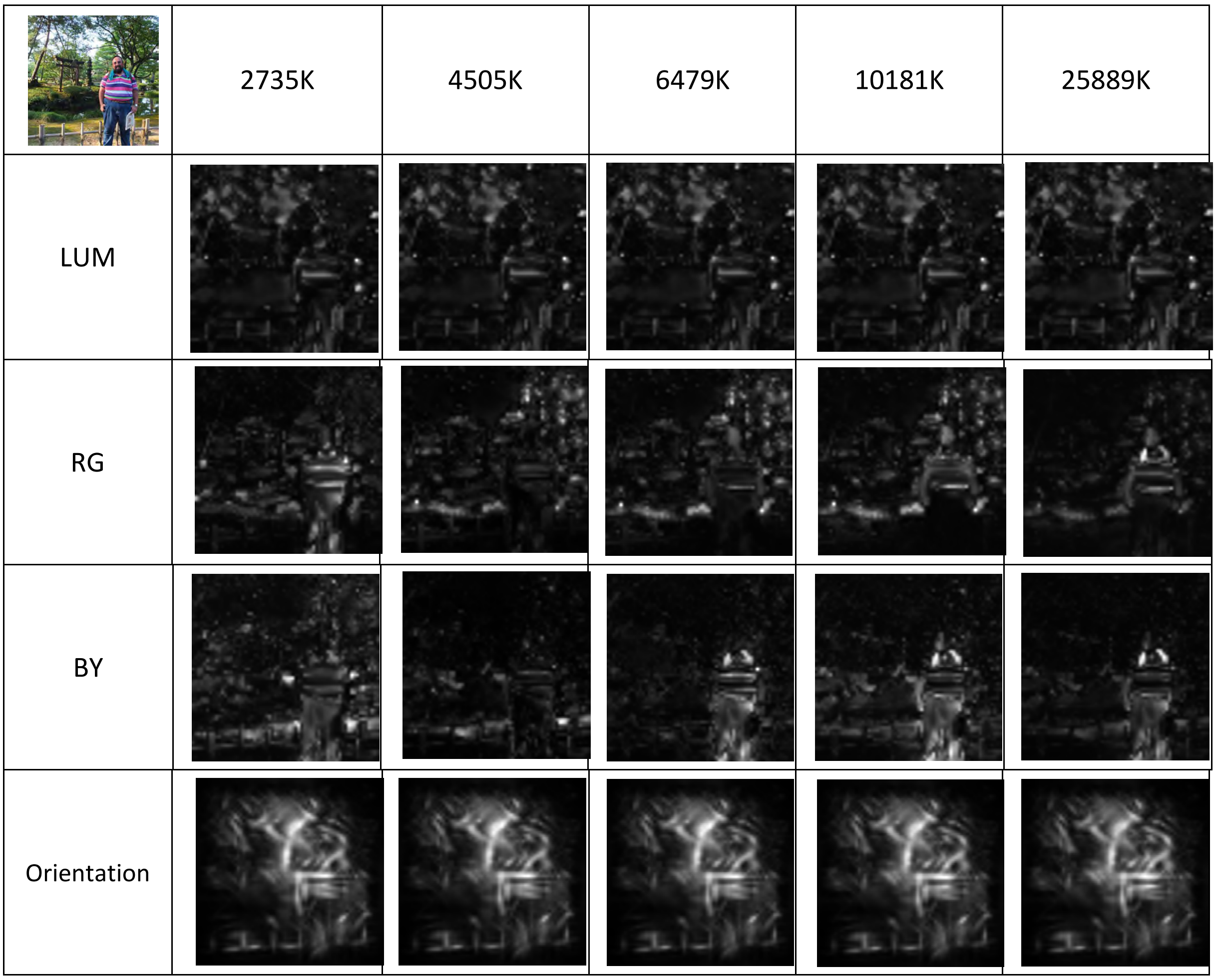

GLOBAL	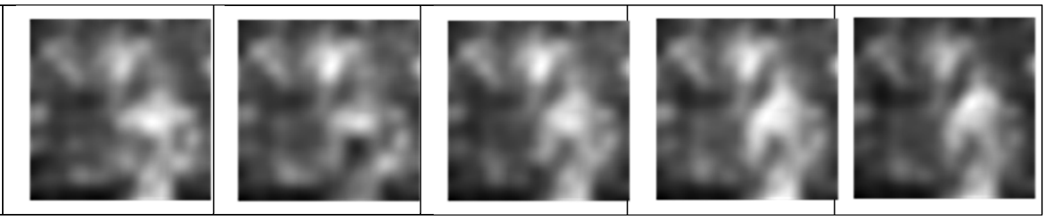

Figure 2. Example of the Luminance (LUM), Chromatic RG and BY sub channels and Orientation conspicuity maps and the saliency map (GLOBAL) of an image under five illuminants of CCTs 2735K, 45005K, 6479K, 10181K and 25889K.

To test if those changes were or not relevant the percentage of number of pixels with saliency above the threshold was calculated as a measure of the saliency for every channel of the pictures. Figure 3 shows the average percentage of pixels above 0.5 for natural and artificial images for Lum and Orientation channels, RG and BY chromaticity sub channels under the different illuminants.

a

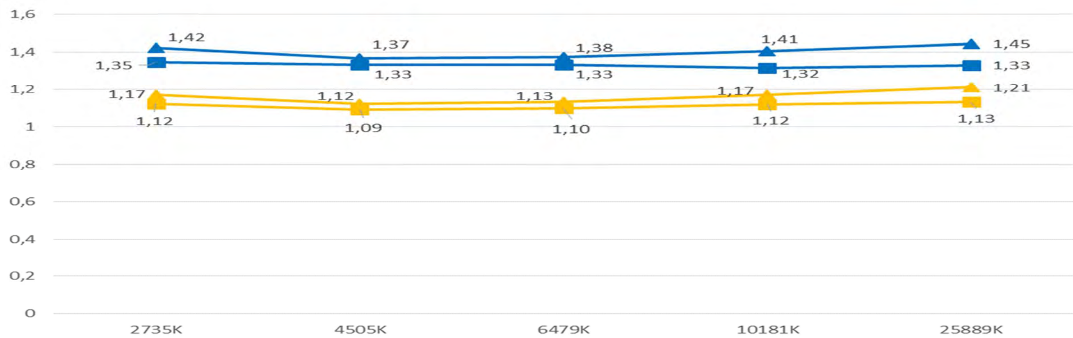

b

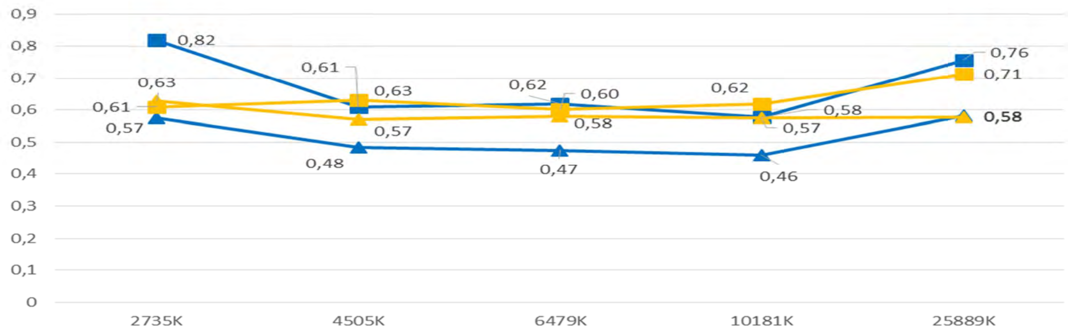

c

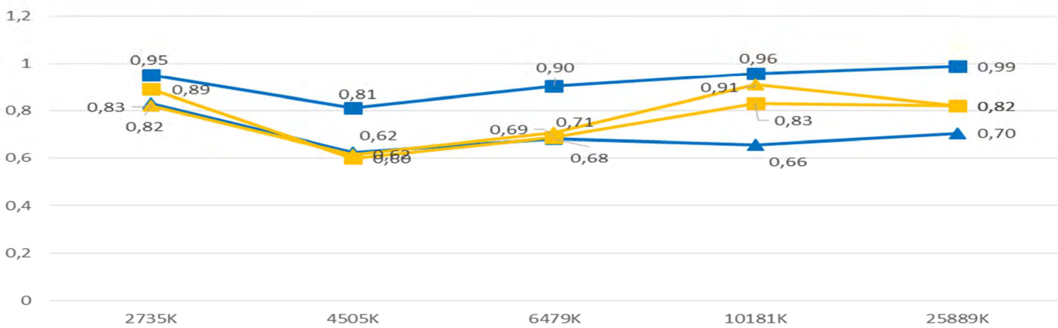

d

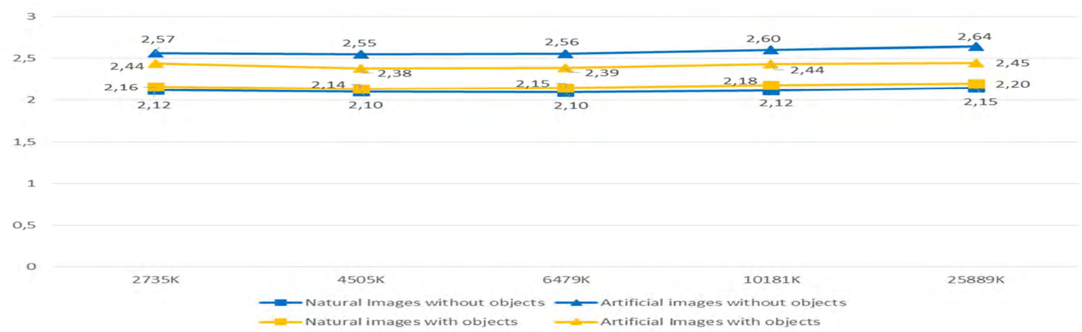

Figure 3. Graphs of the average percentage of pixels with saliency above 0.5 as a function of CCT: Luminance (a), RG (b) and BY (c) Chromaticity sub channels and Orientation (d).

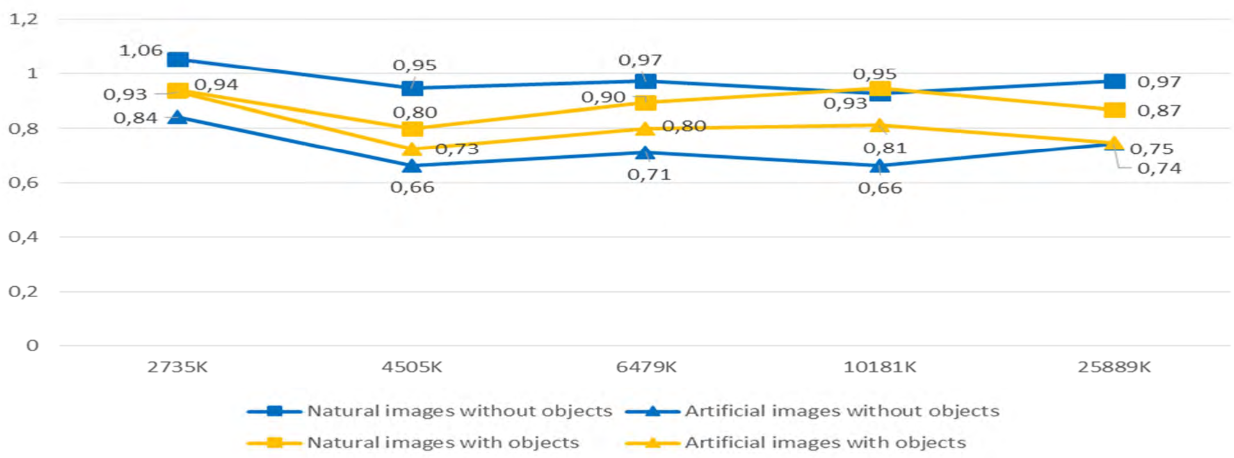

Figure 4. Graph of the average percentage of pixels with saliency above 0.5 as a function of CCT in the Color channel.

3. CONCLUSSIONS

In the range of working daylights used (CCT from 2,735 K to 25,889 K) Figure 3 results suggest differences among the saliency maps. These differences are minima in the Orientation channel and significant for the two chromatic RG and BY (maxima) sub channels.

Nevertheless those differences are small if we consider just one Color channel instead of two separately RG and BY sub channels in the Itti-Koch algorithm (Figure 4). It is a matter of further analysis to study if the use of combined or separately chromatic channels can influence invariant features (including conspicuity maps) linked to the pictures.

ACKNOWLEDGMENTS

This work was funded by the Spanish Ministry of Economy and Competitiveness through the research project DPI2011-23202.

REFERENCES

Amano K. and D.H. Foster 2014. Influence of local scene color on fixation position in visual search. *J. Opt. Soc. Am. A.* 31: 254 – 262.

Frey H-P., C. Honey and P. König 2008. What's color got to do with it? The influence of color on visual attention in different categories. *Journal of Vision* 8(14):6 : 1–17.

Hamel S., N. Guyader, D. Pellerin, and D. Houzet 2014 Contribution Of Color Information In Visual Saliency Model For Videos. *In 6th International Conference on Image and Signal Processing 2014 (ICISP 2014), Jun 2014, Cherbourg, France.*

Harel J 2013. A Saliency Implementation in MATLAB. Available online http://www.klab.caltech.edu/~harel/share/gbvs.php

Hernández-Andrés J., J. Romero, J.L. Nieves and R.L.Jr. Lee 2001. Color and spectral analysis of daylight in southern Europe. *J. Opt. Soc. Am. A.* 18: 1325-1335.

Itti L., C. Koch and E. Niebur 1998. A model of saliency-based visual attention for rapid scene analysis. *IEEE Transactions on Pattern Analysis and Machine Intelligence,* 20: 1254–1259.

Judd, D. B. 1951. Report of U.S. Secretariat Committee on Colorimetry and Artificial Daylight. *In Proceedings of the Twelfth Session of the CIE, Stockholm* (vol. 1, pp. 11). Paris: Bureau Central de la CIE .

Koch C. and S. Ullman 1985. Shifts in selective visual attention: Towards the underlying neural circuitry. *Human Neurobiology*, 4: 219–227.

Marat, S., T. Ho Phuoc, L. Granjon, N. Guyader, D. Pellerin and A. Guérin-Dugué 2009. Modelling spatio-temporal saliency to predict gaze direction for short videos. *International Journal of Computer Vision* 82(3) 231–243

Ricchiazzi P., S. Yang, C. Gautier and D. Sowle 1998. SBDART: a research and teaching software tool for plane-parallel radiative transfer in the earth's atmosphere. *Bull. Am. Meteorol. Soc.*: 2101–2114.

Süsstrunk, S., J. Holm and G.D. Finlayson 2001. Chromatic Adaptation Performance of Different RGB Sensors. *Proc. IS&T/SPIE Electronic Imaging 2001: Color Imaging*, Vol. 4300: 172-183.

Xiao J., J. Hays, K. Ehinger, A. Oliva and A. Torralba 2010. SUN Database: Large-scale Scene Recognition from Abbey to Zoo. *IEEE Conference on Computer Vision and Pattern Recognition.*

Address: Juan Luis Nieves, Dept. of Optics, Faculty of Sciences,
University of Granada, Campus Fuentenueva, 18151-Granada, SPAIN
E-mails: jojojog@hotmail.com, jnieves@ugr.es, jromero@ugr.es

Comparison between Multispectral Imaging Colors of Single Yarns and Spectrophotometric Colors of Corresponding Yarn Swatches

Lin LUO,[1] Hui-Liang SHEN,[2] Si-Jie SHAO,[1] John H. XIN[1]
[1] Institute of Textiles & Clothing, The Hong Kong Polytechnic University
[2] Department of Information Science and Electronic Engineering, Zhejiang University

ABSTRACT

While colors of single yarns and yarn swatches can be separately acquired by multispectral imaging systems and spectrophotometers, color comparison between single yarn and yarn swatch has not yet been well investigated. This paper compares multispectral imaging colors of single yarns and spectrophotometric colors of corresponding yarn swatches, using 100 pairs of single yarn and yarn swatch samples. Colors of the yarn swatch and single yarn samples were measured by a spectrophotometer Datacolor 650 and a multispectral imaging system, namely Imaging Colour Measurement (ICM), respectively. Lightness (L*) and hue (a* and b*) distributions, as well as color difference between single yarn and yarn swatche were analyzed in detail. Experimental results show that lightness (L*) and hue (a* and b*) values of single yarns acquired by multispectral imaging system are approximately 0.91, 0.88, and 0.91 times those of yarn swathes measured by spectrophotometer. The average color difference between single yarns and yarn swatches is 2.79 CMC(2:1) units.

1. INTRODUCTION

In textile and garment industries, spectrophotometers are widespread instruments that measure colors of fabrics. However, spectrophotometers cannot acquire spectral reflectance of single yarns but yarn swatches, which are individual yarns winded on a background card. A spectrophotometer can only measure the average color of a sample area presented in the aperture (Luo 2014). A single yarn is too small to cover the entire aperture of a spectrophotometer. In contrast, multispectral imaging (MSI) systems (Luo 2013, Shen 2007a, Shen 2007b) can provide not only the spectral information but also the spatial information of a sample. The spatial information facilitates direct color measurement of single yarns from multispectral images.

While colors of single yarns and yarn swatches can be separately acquired by multispectral imaging systems and spectrophotometers, color comparison between single yarn and yarn swatch has not yet been well investigated. This paper compares colors of single yarns and yarn swatches measured by multispectral imaging system and spectrophotometer using 100 pairs of single yarn and yarn swatch samples.

2. METHOD

2.1 Sample Preparation

100 pairs of single yarn and yarn swatch samples were prepared to carry out the experiment. These samples were collected from a garment manufacturing company in Hong Kong. The

material of these samples was cotton and yarn count was 80 Ne. As shown in Figure 1, single yarns (Figure 1a) were carefully winded on a white background card to constitute yarn swatches (Figure 1b).

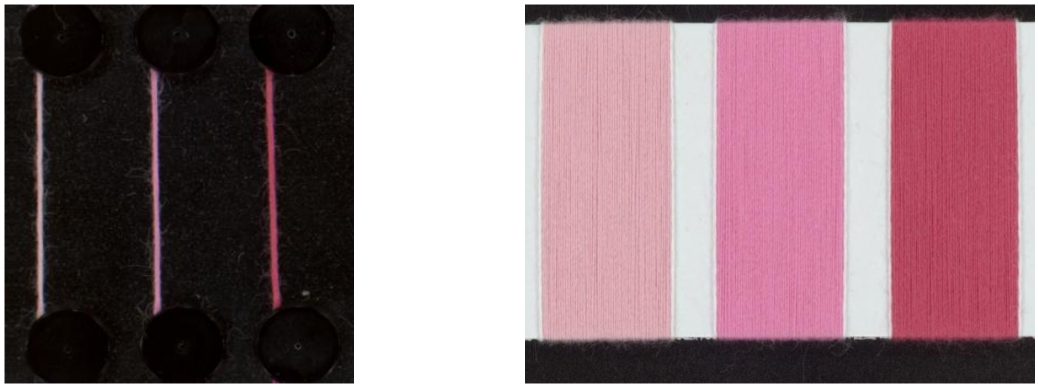

(a) (b)

Figure 1: Example of single yarns and corresponding yarn swatches. (a) single yarns; (b) corresponding yarn swatches.

2.2 Spectrophotometric Measurements

A Datacolor 650 spectrophotometer was employed to acquire reflectance of the yarn swatches. All the measurements were conducted under the 1964 CIE standard observer. The specular component excluded (SCE) and UV excluded modes were applied. Figure 2a shows reflectance of the 100 yarn swatches measured by the Datacolor 650.

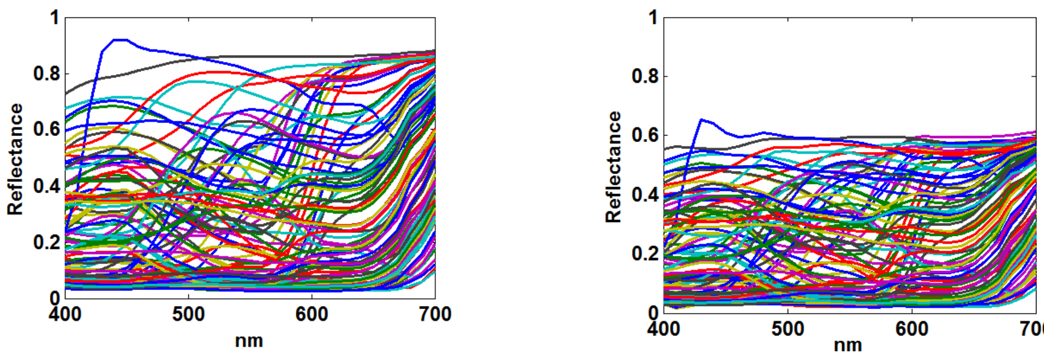

(a) (b)

Figure 2: Reflectance of yarn swatch and single yarn samples measured by Datacolor 650 and ICM. (a) reflectance of yarn swatches; (c) reflectance of single yarns.

2.3 Multispectral Imaging Measurements

The reflectance of single yarns was acquired by a multispectral imaging system, namely ICM (Luo 2014). The ICM system was calibrated by reflectance of Macbeth ColorChecker Digital acquired by the Datacolor 650 spectrophotometer. The calibration result was 0.232 CMC(2:1) units. The reflectance of a single yarn measured by ICM was specified as the average reflectance of all the pixels on it:

$$R(\lambda) = \frac{\sum R(\lambda, x, y)}{N} \quad (1)$$

where $R(\lambda, x, y)$, $R(\lambda)$ and N denote the measured spectral reflectance at pixel (x, y), the specified reflectance, and the number of pixels in the chosen area, respectively. Figure 2b shows the spectral reflectance of the 100 single yarn samples measured by ICM.

3. RESULTS AND DISCUSSION

3.1 Lightness Distribution

The first experiment analyzed lightness distribution (L*) of the single yarn and yarn swatch samples under CIE Standard Illuminants D65, F2, and A, as shown in Figure 3a-c. The black lines denote lightness values of single yarns acquired by the ICM are the same to those of corresponding yarn swatches measured by Datacolor 650. When a dot approaches to the black line, lightness of a single yarn is closer to that of corresponding yarn swatch. A dot above the black line represents lightness of a single yarn is larger than that of the corresponding yarn swatch, *vice versa*. The correlation (R) values between lightness values of the 100 pairs of single yarns and yarn swatches under D65, F2, and A are 0.997, which implies that dependence between lightness values of single yarns and yarn swatches are high. The least squares fitting method (Banerjee 2014) was applied to find the linear relationship between lightness of single yarns and yarn swatches, which are shown as red lines in Figure 3a-c. The coefficient of determination (R^2) is 0.994. Note that slopes of the regressed lines are 0.910, 0.910, and 0.900 for D65, F2, and A, which means that if yarn swatches with lightness as measured by Datacolor 650 is 1.0, lightness values of single yarns acquired by ICM are 0.910, 0.910, and 0.900 for D65, F2, and A. Therefore, it can be concluded that lightness of a single yarn measured by ICM is smaller than that of corresponding yarn swatch measured by Datacolor 650.

3.2 Hue Distribution

The second experiment analyzed hue distribution (a* and b*) of the yarn swatch and single yarn samples measured by Datacolor 650 and ICM, as shown in Figure 3d-i. The meaning of black and red lines is the same as in Figure 3a-c. The coefficients of R and R^2 are (0.991, 0.991, 0.992) and (0.981, 0.982, 0.984) for a* values of yarn swatches and single yarns under D65, F2, and A. For b* values, R and R^2 are (0.996, 0.996, 0.996) and (0.992, 0.992, 0.991). Note that slopes of the regressed lines are (0.88, 0.88, 0.88) and (0.91, 0.91, 0.90) for a* and b* distributions of yarn swatches and single yarns under the three CIE Illuminants. It can be concluded that a* and b* values of a single yarn measured by ICM is smaller than those of corresponding yarn swatch measured by Datacolor 650.

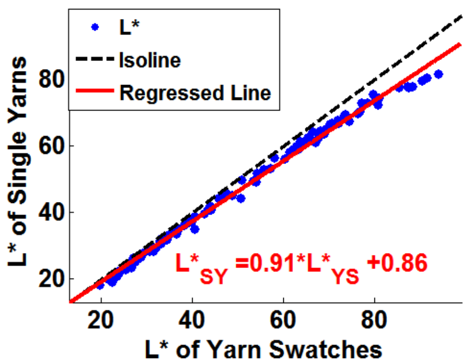

(a)

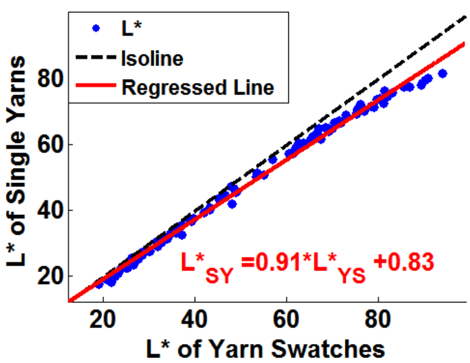

(b)

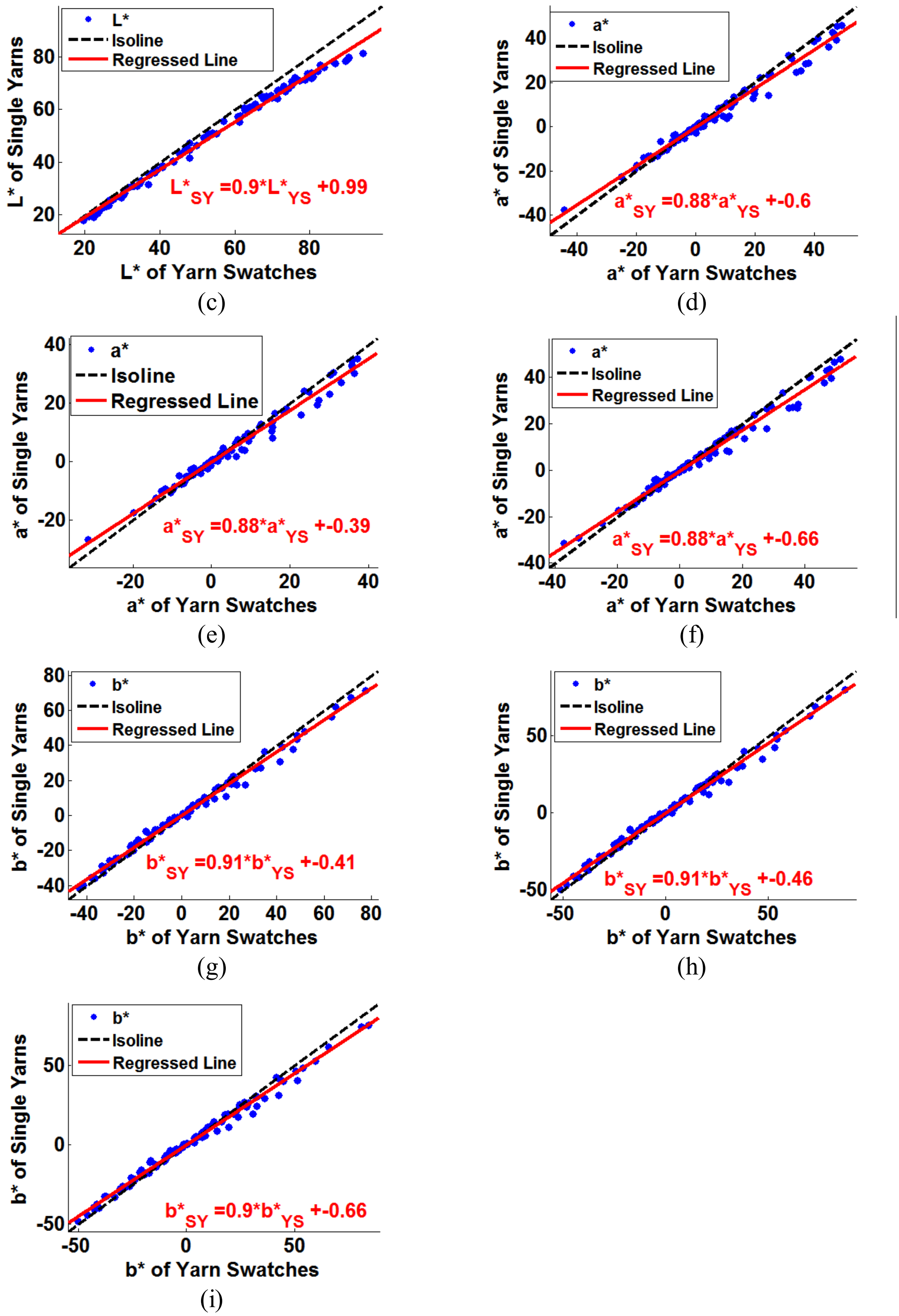

Figure 3: Lightness and hue distributions of single yarn(SY) and yarn swatch(YS) samples under D65, F2, and illuminant A. (a-c), lightness distributions under D65, F2, and A; (d-f), a distributions under D65, F2, and A; (g-i), b* distributions under D65, F2, and A.*

The coefficients of R, R^2, and slope between the 100 pairs of single yarns and yarn swatches under D65, F2, and A are summarized in Table 1. It can be concluded from Figure 3 and Table 1 that lightness (L*) and hue (a* and b*) values of single yarns measured by ICM are approximately 0.91, 0.88, and 0.91 times those of yarn swathes measured by Datacolor 650.

Table 1. Summary of the relationship between colors of yarn swatches and single yarns measured by Datacolor 650 and ICM.

	L*			a*			b*		
	D65	F2	A	D65	F2	A	D65	F2	A
R	0.997	0.997	0.997	0.991	0.991	0.992	0.996	0.996	0.996
R^2	0.994	0.994	0.994	0.981	0.982	0.984	0.992	0.992	0.991
Slope	0.910	0.910	0.900	0.880	0.880	0.880	0.910	0.910	0.900

3.3 Color Difference

The final experiment analyzed color difference between the 100 pairs of single yarns and yarn swatches under 9 CIE Standard Illuminants (A, C, D50, D55, D65, D75, F2, F7, and F11). The CMC(2:1) formula was applied to calculating the color difference (ΔE). Table 2 illustrates the statistics of color difference between the 100 pairs of single yarns and yarn swatch samples. The average color difference is 2.79 CMC(2:1) units with the standard deviation 1.55 CMC(2:1) units. The large color difference implies that color of a yarn swatch acquired by a spectrophotometer is different from that of corresponding single yarn measured by a multispectral imaging system. It can be concluded from Figure 3, Table 1, and Table 2 that the large color difference between single yarns and yarn swatches stems from that CIELAB values of single yarns measured by a multispectral imaging system are smaller than those of corresponding yarn swatches acquired by a spectrophotometer.

Table 2.Color difference between the 100 pairs of single yarns and yarn swatches under 9 CIE Standard Illuminants.

Statistics	A	C	D50	D55	D65	D75	F2	F7	F11	Average
Mean	2.83	2.80	2.82	2.82	2.81	2.81	2.67	2.77	2.80	2.79
Median	2.34	2.34	2.34	2.35	2.34	2.36	2.23	2.36	2.28	2.33
Std.	1.60	1.55	1.59	1.58	1.57	1.56	1.42	1.52	1.55	1.55
Max.	7.34	7.08	7.26	7.22	7.14	7.07	6.89	6.82	7.02	7.09
90th	5.45	5.07	5.21	5.16	5.09	5.06	4.73	4.97	5.09	5.09

4. CONCLUSIONS

Colors of single yarns and corresponding yarn swatches acquired by a multispectral imaging system and a spectrophotometer are compared in this paper, using 100 pairs of single yarns and yarn swatch samples. The colors of these samples were measured by a spectrophotometer Datacolor 650 and a multispectral imaging system, namely Imaging Colour Measurement (ICM). Lightness distribution (L*), hue distribution (a* and b*), and color difference between single yarn and yarn swatch samples were analyzed in detail. Experimental results show that lightness (L*) and hue (a* and b*) values of single yarns measured by ICM are approximately 0.91, 0.88, and 0.91 times those of yarn swathes measured by Datacolor 650. The average color difference between single yarns and yarn swatches is 2.79 CMC(2:1) units.

While these results demonstrate that colors of single yarns acquired by a multispectral imaging system are different from those of yarn swatches measured by a spectrophotometer, there is still much work to be done. First, the fundamental principle of color difference between single yarns and yarn swatches needs to be explored. Second, quantitative relationship between colors of single yarns and corresponding yarn swatches needs to be established. Together, these efforts should facilitate development of color measurement from fabric to single yarn in textile.

ACKNOWLEDGEMENTS

This work was supported by the Innovation and Technology Commission of the Hong Kong SAR Government and the Hong Kong Polytechnic University under the HKRITA project (ITP/001/10TP and ITP/048/13TP), and by the National Natural Science Foundation of China (under grant 61371160).

REFERENCES

Banerjee S., and A. Roy. 2014. *Linear algebra and matrix analysis for statistics*. Boca Raton: CRC Press.

Luo, L., S. J. Shao, H. L. Shen, and J. H. Xin. 2013. An unsupervised method to detect dominant colour regions in yarn dyed fabric images. *Coloration Technology* 129: 389-397.

Luo, L., K. M. Tsang, H. L. Shen, S. J. Shao, and J. H. Xin. 2014. An investigation of how the texture surface of a fabric influences its instrumental color. *Color Research and Application* doi: 10.1002/col.21923.

Shen, H. L., P. Q. Cai, S. J. Shao, and J. H. Xin. 2007a. Reflectance reconstruction for multispectral imaging by adaptive Wiener estimation. *Optical Express* 15: 15545-15554.

Shen, H. L., and J. H. Xin. 2007b. Improved reflectance reconstruction for multispectral imaging by combining different techniques. *Optical Express* 15: 5531-5536.

Address: Lin LUO, Room QT803, Chow Yei Ching Building, ITC, The Hong Kong Polytechnic University, Hung Hom, Hong Kong, China
E-mails: stluolin@gmail.com, shenhl@zju.edu.cn,
tcsjshao@polyu.edu.hk, tcxinjh@polyu.edu.hk

New color rendering index based on color discriminability and its application to evaluate comfortability of illuminants

Yasuhisa Nakano, Toshiki Nagasaki, Ryu Toyota, Jiro Kohda, Takuo Yano
Department of Frontier Sciences, Hiroshima City University

ABSTRACT

We proposed a new way of evaluating color rendering property of illuminants based on color discriminability. From the experimental data collected from extended Munsell 100 hue test, in that number of hue is increased to 180, we found that maximum error of color discrimination task under various illuminants are correlated to a minimum color difference among 8 TCSs (Test Color Samples used for the CIE CRI evaluation) when they are plotted on the CIELUV uniform color space under each illuminant. We called this index CDC (Color Discriminability Criterion) as color discriminability is improved as CDC increases. There was a tendency that illuminants having lager CDC seem more comfortable because color chips appear more colorful under such illuminants, but some of illuminants having large CDC seem uncomfortable because red colors appear too prominent. Spectra of such illuminants are unbalanced as some spectrum region is too low and another region is too high. To evaluate the balance of a spectral irradiance distribution, we introduced another index, that is the minimum lightness (L*) value among 8 TCSs under the test illuminant. The index is called CL (Critical Lightness) because lack of energy in certain spectrum region can be improved by making CL larger. We found that one feels more comfortable under such illuminants that have lager CDC and lager CL.

1. INTRODUCTION

Color rendering is one of the important properties of illuminants. CIE CRI (Color Rendering Index) is widely used to evaluate this property. Recently, white LED light sources begin to spread as new illuminant, but the CIE CRI sometimes fails to describe its visual impression (Bodrogi et al. 2004). So, the higher CIE CRI is not necessarily means better visual impression of the illuminant. One of the problems of the CIE CRI is that it is a relative evaluation of a test illuminant compare to the standard illuminant that has the same correlated color temperature as the test illuminant. One can say if visual impression of the test illuminant is close to the standard illuminant, but cannot say if it is good or bad.

To overcome this disadvantage of the CIE CRI, we first tried to evaluate color rendering property of illuminants based on performance on color discrimination task. We conducted the experiment similar to Munsell 100 hue test, and performed color discrimination task under illuminants having various spectra. Assumption here is that errors of color order will be smaller under such illuminants having better color rendering property. By analyzing data from this experiment we found a new index correlated to the performance of color discrimination task. We called this index CDC (Color Discriminability Criterion).

Then, we investigated if this index could be used as an index for visual comfortability of illuminants. We conducted the second experiment to evaluate visual impression of illuminants using semantic differential method. In this paper, we describe above two experiments in detail and discuss about how we can construct a new method of evaluating color rendering property for wide variety of illuminants based on visual comfortability.

2. METHOD

2.1 Experiment 1: Munsell 180 Hue Test

To increase the number of color chips of Munsell 100 Hue Test (Macbeth Farnsworth-Munsell 100 Hue Test) from 85 to 180, we first measured spectral reflectances of the 85 real color chips using the spectrophotometer (GretagMacbeth Spectrolino). Then, the principal components of the 85 spectral refrectances were calculated to interpolate spectral reflectance of a color having an arbitray chromaticity coordinates. CIELAB uniform color space was used to interpolate 85 color chips, and 180 chromaticity coordinates were selected along interpolated locus in every 2^{O} hue angle, then spectral refrectance functions were synthesized using the 4 principal components obtained above. Munsell color test was performed on the calibrated CRT display (Mitsubishi RDF19S) by simulating tristimulus values of the color chips under given spectral irradiance of the test illuminants.

Tests were conducted under fifteen illuminants having different CDC values as shown in Table 1. Spctral irradiance distribution functions were synthesized mathematically using 7 Gaussian functions peaked at 430, 470, 510, 550, 590, 630, 670 nm. Band width of each Gaussian function was 30 nm. The illuminants in gray cells in Table 1 were standard illuminants for each CCT (Correlated Color Temperature). Two subjects participated in this experiment.

Table 1. CDC values of the test illuminants used in Experiment 1.

CCT	4200K					5000K					7500K				
CDC	14.8	19.1	27.2	31.5	25.3	13.9	19.3	30.4	36.0	26.1	11.2	18.3	33.0	39.8	24.5

2.2 Experiment 2: Absolute Evaluation of Visual Impression of Illuminants

Images taken by the multi-spectral camera were displaied on the calibrated CRT display (Sony GDM-2000TC) to simulate tristimulus values of every pixel in the image under given spectral irruminance of the test illuminants (Nakano et al. 2005). Subjects observed displaied image in the dark room and asked to grade visual impression using fifteen adjective pairs.

Test images were rendered using 30 illuminants synthesized in the same way as previous experiment. CDC values of each illuminants were shown in Table 2. Gray cells are for standard illuminants. Four subjects participated in this experiment.

Table 2. CDC values of the test illuminants used in Experiment 2.

CCT	CDC									
4200K	14.8	16.0	17.0	17.8	19.1	19.2	25.8	27.8	28.8	25.3
5000K	16.8	17.1	18.2	18.7	23.4	23.7	30.4	31.1	33.0	26.1
7500K	13.1	15.0	15.8	19.1	26.7	34.5	36.1	38.5	39.8	24.5

3. RESULTS AND DISCUSSION

Figure 1 shows three examples of the results in Experiment 1. Top panels show spectral irradiance distribution functions of the test illuminants. Middle panels show chromaticity coordimantes of 8 TCSs for CIE CRI under each test illuminant plotted in CIELUV uniform color space. CDC is defined as smallest color difference among 8 TCSs as shown in each panel. Bottom panels show error score plots for Munsell 180 Hue Test. Results of two subjects were averaged because tendency was the same between them. Dotted lines show original score data and thick solid lines show moving average among 9 neighboring data to smooth original data.

Clear tendency was observed that maximum error score increases as CDC value decreases. Correlation coefficient between CDC and maximum error score was -0.82. This means that we can evaluate color rendering property of test illuminants in terms of color discriminability performance using CDC.

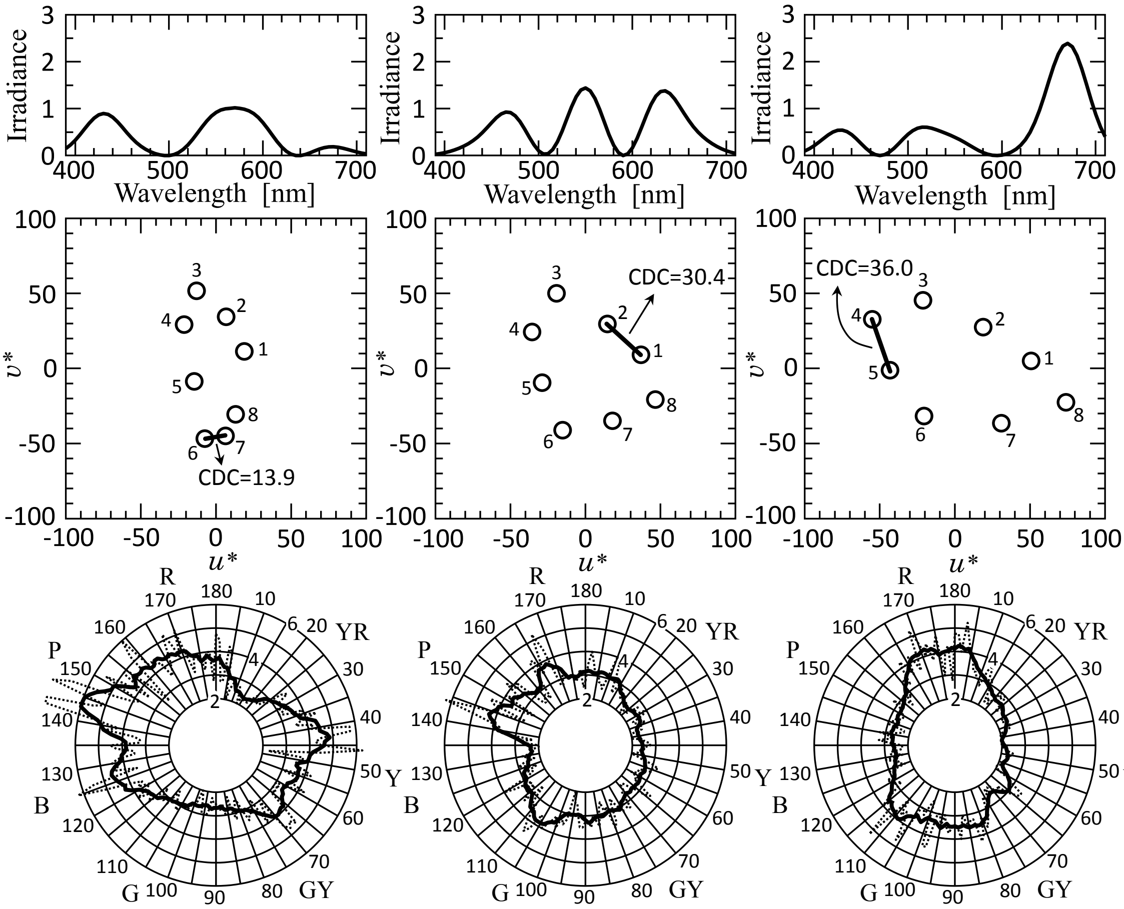

Figure 1: Examples of the results in Experiment 1 selected from 5000K illuminants.

While doing this experiment, we noticed that color chips became more colorful as CDC values increases, and felt comfortable for such illuminants that have lager CDC values. As the results of the next experiment show, however, correlation between CDC and comfortability is not necessarily high. Right hand illuminant in Figure 1, for example, has largest CDC value among 5000K illuminants, and color discrimination performance is good, but it is not necessarily comfortable because red colors are too prominent.

Figure 2 shows the results of Experiment 2. Left panel shows first two principal component vectors derived from score matrix of 15 adjective pairs (rows) for 30 illuminants (column). Scores were averaged for 4 subjects because the tendency was the same among them. Third vector and beyond were neglected because contribution rates were small. First vector is likely to relate to "colorfulness" impression of illuminant, because components of adjectives related to colorfulness show higher values compare to other components. Second vector is likely to relate to "fidelity/comfortability" impression of illuminants. Right panel shows score plot of 30 illuminants, in that, abscissa indicates score of "colorfulness" impression, and ordinate indicates that of "fidelity/comfortability" impression. Size of each symbol was set according to the score of "comfortable-unpleasant" adjective pair. Larger the size, the illuminant was evaluated as more comfortable. From these results, we can say that visual impression of color rendering arose by any illuminant can be evaluated using two factors, "colofulness" and "fidelity/comfortability", and comfortability become higher when both factors show higher score.

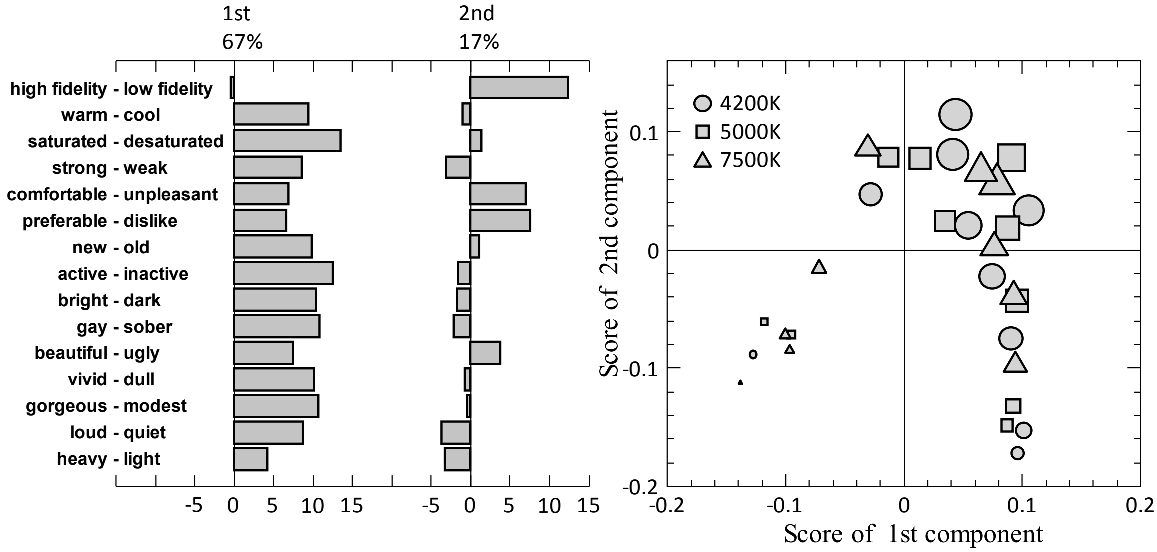

Figure 2: Principal component vectors derived from score matrix of 15 adjective pairs for 30 illuminants (left panel), and score plot for30 illuminants (right panel).

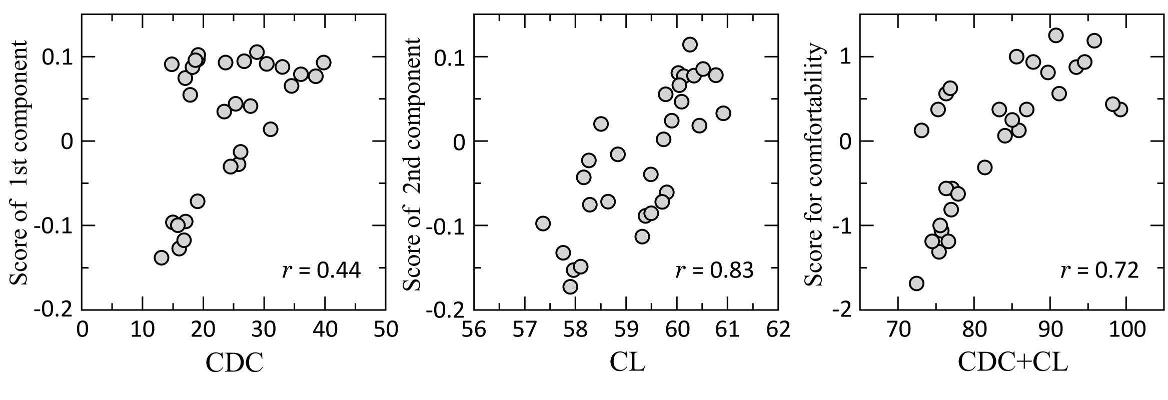

Figure 3: Correlations between scores and CDC, CL or CDC+CL.

It is convenient if we can evaluate these two scores just by using spectral irradiance distribution function of illuminant in practical situations. It is easy to imagine that CDC might be related to the score of first component, but we need another index to evaluate the score of second component. We introduced a new index, that is the minimum lightness (L*) value among 8 TCSs under the test illuminant. We called this index as CL (Critical Lightness), and the purpose of the index is to evaluate the balance of the spectral irradiance distribution of the illuminant. If energy in middle wavelength region is lacking in spectral irradiance distribution, for example, lightness of greenish test color sample will be lower. By increasing CL, such energy lack problem can be prevented, hence the balance of the spectral irradiance distribution is preserved.

Figure 3 shows correlations between CDC and score of first component (left panel), between CL and score of second component (middle panel), and between CDC+CL and score of "comfortable-unpleasant" adjective pair (right panel). Though, some of correlation coefficients are not so high, we can see that CDC is related to "colorfulness" impression, and that CL is related to "fidelity/comfortability" impression. If that is the case, we can expect that the illuminant having larger CDC and larger CL values will be more comfortable. This is confirmed by plotting the correlation between CDC+CL and "comfortability" score as shown in right panel in Figure 3.

4. CONCLUSIONS

CDC (Color Discriminability Criterion), that is defined as smallest color difference among 8 TCSs used for CIE CRI, can be used to evaluate color rendering property of illuminant in terms of color discriminability performance. By adding another index CL, that is defined as minimum lightness (L*) value among 8 TCSs, we can also evaluate visual impression of color rendering in terms of "comfortability". These indices will be useful when designing and evaluating spectral power distribution of new light sources such as LED and EL.

REFERENCES

Bodrogi, P., Csuti, P., Szabó, F., Schanda, J. 2004. *Why does the CIE colour rendering index fail for white RGB LED light sources?*, Proceedings of the CIE Symposioum 2004 on LED Light Sources, Tokyo, Japan, 24-27.

Nakano, Y., Tahara, H., Suehara, K., Kohda, J., Yano, T. 2005. *Application of multispectral cameras to color rendering simulator*, Proceedings of the 10th Congress of the International Colour Association – AIC Colour 05, Granada, Spain, 1625-1628.

Address: Dr. Yasuhisa Nakano, Department of Frontier Sciences, Graduate School of Information Sciences, Hiroshima City University, 3-4-1 Ozukahigashi, Asaminami-ku, Hiroshima, 731-3194 , JAPAN
E-mail: ynakano@hiroshima-cu.ac.jp

Color monitoring method under high temperature during oven cooking

Yuji NAKAMORI,[1] Hiroyuki IYOTA,[1] Hideki SAKAI,[2]
Taiki MATSUMOTO[1] and Shuhei NOMURA[1]
[1] Graduate School of Engineering, Osaka City University
[2] Graduate School of Human Life Science, Osaka City University

ABSTRACT

The oven is one of the most popular appliances used for food processing tasks such as heating and baking, both in industry and domestic households. In general, the temperature of the oven chamber is monitored and regulated automatically during the baking process, and automated baking is performed using programmatic control. In this case, the only parameters used are those of time and temperature, without reference to color information. In contrast, when food is cooked manually (i.e. using a frying pan), we intuitively monitor the appearance of food visually, judging whether it is ready or not by its color, without measuring the time and temperature. This is because appearance monitoring in real-time, that is, in-situ color measurement, allows an optimization of the appearance of food, and provides a result that can be aesthetically appealing. Appearance is in fact one of the most important factors for food consumers. For these reasons, we have developed color-monitoring equipment, together with a method for baking in the oven. In our previous study, we reported on an in-situ color monitoring method that comprised a halogen light, an optical fiber and a spectrometer, used as a light source and a measuring instrument, respectively. Sliced white bread was used as the sample material. In this study, we investigated this real-time monitoring method using a charge-coupled device (CCD) camera for color detection. We constructed a small oven for our experiments using a conventional home oven as a basis, and examined the monitoring method at a temperature of approximately 200°C. The cooking and previously reported prediction expressions were also used. As we were considering practical usage in the home, infrared heaters installed in a commercially available oven (100V-600W-2200K) were used as the light source. The experimental results demonstrate their applicability for this purpose. Suitable methods for automatically determining the optimal conditions of the monitoring system, allowing for the preferences of users, are also proposed.

1. INTRODUCTION

The oven is one of the most popular items of cooking equipment in the home. Normally, oven users are able to control two crucial parameters of the heating environment, temperature and time. The latter is mostly determined by visual observation during heating. However, as it is not possible to observe the oven constantly during the heating process, it is difficult to know when the contents are ready, even if the oven temperature is regulated automatically and a timer has been installed. Therefore oven-cooked food is sometimes overcooked and so unsuitable for consumption. In addition, accidents may occur due to the abnormal expansion of food on a tray in the oven. For these reasons, color-monitoring equipment, has been developed, together with a method for oven cooking (Iyota *et al*. 2013, Matsumoto *et al*. 2014). It was also necessary to develop a food monitoring method that could remain inside the oven at high temperatures. Here a charge-coupled device

(CCD) camera was used to replace the role of visual monitoring, in order to improve the automatic control function. In this paper, we investigated a color monitoring method to be used during cooking at high temperatures, using a CCD camera and comparing the measured lightness, L*, using a spectrometer. An electric near-infrared radiant heater was used as the light source, and placed on the upper side of a commercially available oven suitable for home use.

2. METHOD

2.1 Experimental Apparatus

The experimental apparatus employed in this study is given in Figure 1. A conventional oven, suitable for use in the home, has been modified for use in these experiments. The fan and the convection heater (3) (with a power of 1360 W) were placed at the innermost side of the oven chamber, as shown in Figure 1. The oven chamber temperature was regulated automatically by a temperature controller. In addition, there was an electric radiant heater (2) (with a power of 600 W) placed at the top of the chamber, in order to bake food by a process of radiative heat transfer. The voltage supplied to this heater was controlled using a variable transformer. The color temperature of the heater at a power of 100 V was 2200 K, in the visible to near-infrared wavelength range. This heater was also used as a light source in the study. The CCD camera (4) (Imaging Source, DFK41AU02, 1/2 inch, 1280 × 960 pixels) and lens (5) were used to observe the food from the viewing hole composed of heat-resistance glass provided on the upper surface of the oven. At a lens focal distance of 8 mm, images of the bottom side of the chamber in a circle of approximately 100 mm diameter, were recorded using a personal computer, connected via USB. For comparison, spectroscopic measurements obtained using a spectrometer connected to the oven through an optical fiber were taken simultaneously.

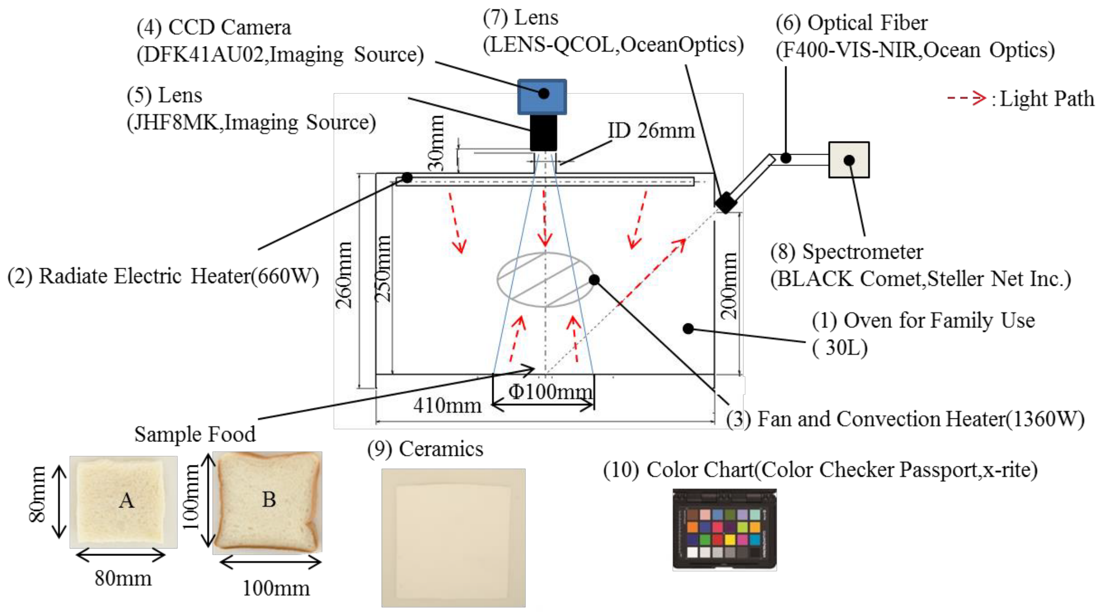

Figure 1. Experimental apparatus for the real-time color monitoring method (1-8) and the materials used for color and grayscale correction (9-10).

Two sizes of sliced white bread, with a thickness of 17 mm, were used as the food samples. The dimensions of sample A were 80 mm × 80 mm, with the surrounding crust removed, while the dimensions of sample B were 100 mm × 100 mm, including a brown crust. The oven temperature was maintained at 200 ± 5 ℃. We measured the voltage and the current of the radiation heater during heating, and confirmed that the electric resistant of the radiant heater, the heater temperature and the power remained constant (the change in the current value was less than 0.04 A).

After preheating the oven, the image of a white porous ceramics plate (9) was recorded for white balance correction. The plate was composed of a silicate compound (Miyagawa Kasei Industry Co.), with a reflectance of 0.88 in the 380-780 nm wavelength range. In terms of the total color (R, G, and B) light-receiving gain of the CCD sensor, the R and B gains were adjusted separately to equal 80% of the upper limit for each color. Values of the total color = 460, red = 18, and blue = 69 were used, together with a shutter speed of 1 / 2000 s. Next, the image of a 24-color chart (10) (Color Checker Passport, X-rite Co.) was recorded for the grayscale correction. Finally, after quickly placing the food sample (slice of bread) in the oven and closing the oven door, a continuous measurement of the sample color change was obtained. Images from the CCD camera and spectral data from the attached spectrometer were recorded by the personal computer approximately every 60 seconds, using the time stamp information.

2.2 Image analysis

The food images obtained were reduced from their original size of 1280 × 960 pixels to 800 × 600 pixel images. These images were then processed as follows:

(1) White balance correction:

Every pixel of the images was corrected using the white balance image data (taken from the white porous ceramic plate). The spatial distributions of the illumination, the color temperature, and the peripheral light of the lens were collected by performing this white balance correction.

(2) Grayscale correction:

An achromatic set of six colors in the color chart at position (10) in Fig. 1 was used for the grayscale correction. First, we determined the regression equation for converting the lightness of the corresponding portion in the color chart image, after applying a white balance correction to the standard values in the color chart. After determining the lightness of an image sample using the white balance correction, the image lightness was used to correct the values in this equation. The spectral data obtained using the spectrometer was also simultaneously used to determine the lightness, and the results compared with the values measured using the CCD camera.

3. RESULTS AND DISCUSSION

3.1 Determining measurement accuracy

Table 1 shows the variation with color of the standard lightness value, L^*_{std}, on the color chart, the value $L^*_{(1)}$ after the white balance correction, the value $L^*_{(1)(2)}$ after the additional grayscale correction, and the absolute value $|L^*_{std}-L^*_{(1)(2)}|$ of the error between L^*_{std} and $L^*_{(1)(2)}$."

The maximum error obtained was 5.71 (No.15, red). Lightness was obtained from the RGB values with the greatest proportion arising from the G component. The standard G value for No.15 red is the second smallest among the 24 colors of the color chart. Therefore, the error in the measurement becomes large compared to that of the other colors. It is considered to exhibit the maximum measured error. The average error was found to be 2.32. This value was obtained for a CCD camera, giving the L^* measurement accuracy for current color measurement.

Table 1. The difference between the lightness of 24 colors. Measured L values are given for comparison with standard color chart values.*

No.	ColorChecker color name	L^*_{std}	$L^*_{(1)}$	$L^*_{(1)(2)}$	$\lvert \Delta L^* \rvert$
1	dark skin	38.02	11.61	36.37	1.65
2	light skin	65.67	38.42	65.62	0.05
3	blue sky	50.63	20.89	47.57	3.06
4	foliage	43.00	13.79	39.10	3.90
5	blue flower	55.68	27.15	54.48	1.20
6	bluish green	71.00	44.67	71.08	0.08
7	orange	61.13	38.05	65.28	4.15
8	purplish blue	41.12	15.28	40.94	0.18
9	moderate red	51.33	27.36	54.70	3.37
10	purple	31.10	8.57	32.46	1.36
11	yellow green	71.90	46.99	72.97	1.08
12	orange yellow	71.04	49.15	74.67	3.63
13	blue	30.35	8.42	32.26	1.90
14	green	55.03	25.73	52.95	2.08
15	red	41.34	20.44	47.05	5.71
16	yellow	80.70	61.15	82.99	2.29
17	magenta	51.14	28.97	56.39	5.25
18	cyan	51.15	22.84	49.78	1.37
19	white	95.82	87.61	94.61	1.20
20	neutral 8	80.60	61.37	83.12	2.52
21	neutral 6.5	65.87	39.40	66.51	0.65
22	neutral 5	51.19	21.24	47.97	3.22
23	neutral 3.5	36.15	9.66	33.88	2.27
24	black	21.70	3.14	25.16	3.46

3.2 Lightness change in baking food

The change in lightness given by baking two samples of different sizes, samples A and B, is shown in Figure 2. A difference in the color changes exhibited by samples A and B was observed. This result shows the importance of real-time color measurement for automatic oven operation.

The difference between color change, L^*_{fs}, in the baking process that was obtained using the optical fiber and spectrometer, and the color change resulting from the baking, $L^*_{(1)(2)}$, obtained using the CCD camera, were in agreement within ± 5. These results indicate that it is possible to monitor the lightness change of food during baking using a CCD camera with an electric radiative heater as the low color temperature light source.

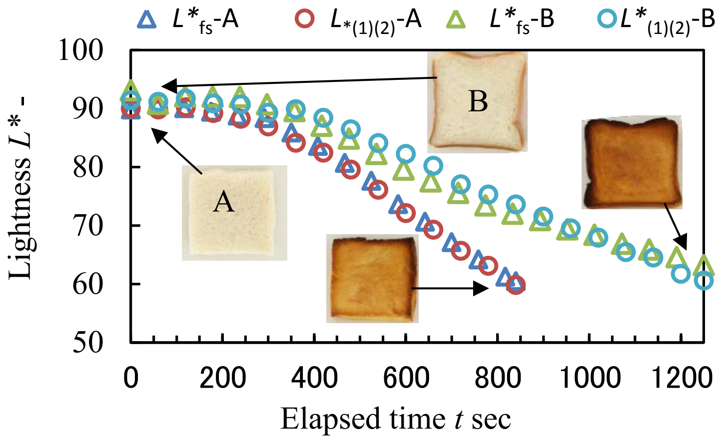

Figure 2. Lightness, L, obtained during the baking process using a CCD camera and a spectrometer vs. elapsed time.*

4. CONCLUSIONS

In this study, we monitored only the L* changes for images of food samples that changed from white to brown, captured using a CCD camera. We are examining the use of other types of food samples, in order to develop a user-friendly and safe automatic oven control.

REFERENCES

Iyota, H. *et al*. 2013. *Color measurement methods for optimization of oven operation (baking of sliced bread with superheated steam and hot air)*, Food Science and Technology Research, 19(6), 939-947.

Matsumoto, T. *et al*. 2014. *Development of food appearance monitoring system for oven cooking*, Proc. ACA 2014, 200-203.

Address: Yuji NAKAMORI, Department of Mechanical Engineering, Faculty of Engineering, Osaka City University, 3-3-138, Sugimoto, Sumiyoshi-ku, Osaka, 558-8585, JAPAN
E-mails: nakamori_yuji@yahoo.co.jp, iyota@mech.eng.osaka-cu.ac.jp, hsakai@life.osaka-cu.ac.jp, yanasegawaxpjp@gmail.com shuhei072522@gmail.com

Woodblock printing as a means for 2.5D and 3D surface evaluation

Teun BAAR,[1] Melissa OLEN,[2] Carinna PARRAMAN,[2] Maria ORTIZ SEGOVIA[1]
[1] OCE – Canon Group
[2] University of the West of England

ABSTRACT

Inspired by the traditional Chiaroscuro woodblock printing techniques of the 16th century, we have explored the use of producing relief print impressions as a means to evaluate the surface rendered with 2.5D and 3D printing technologies. By transferring the surface characteristics of 3D or 2.5D down to 2D, we benefit from the availability of classic quality measurements.

As a benchmark of our idea, we employed different methods to control the modulation of a surface by either carving (laser cutting, CNC engraving) from an existing material (acrylic, wood, model board) or building relief using additive fabrication (Makerbot, Océ 2.5D printer prototype). For print analysis we created a set of two targets to test spatial resolution and edge detail. Following traditional printmaking processes the plates were inked, and subjected to a high level of downward pressure in a press to create impressions (i.e. the surface is embossed by the physical force). All of the plates were inked and printed in the same way. Instead of evaluating the quality of the relief plates created with each of the processes directly, we perform the evaluation on the impressions made with the plates. Each of the testing plates was adapted from optical frequency test patterns in order to access spatial resolution and edge detail in print. The Modulation Transfer Function (MTF), describing the print accuracy for different frequencies in horizontal, vertical and diagonal directions, was obtained for each of the methods based on the impressions.

In this paper, we discuss the results of our relief surface evaluation method with several technologies and the possible extension of our solution for the evaluation of more complex features.

1. INTRODUCTION

Although there exists an increasing interest in printing techniques possessing the ability to control the surface topology of the printout, there is limited focus on the evaluation of quality in the resulting prints. Due to limitations and instabilities of the printing process, the print will probably be distorted in shape and surface texture. Polzin et al. (2013: 37-43) designed a test target for 3D printing systems to evaluate such limitations, as the resolution and characteristics such as object strength and surface roughness. These results can be used to assess the accuracy and limits of a 3D printer and the feasibility of reproducing different shapes. Lui et al. (2014: 90180) proposed several measurements of 3D printed test charts for the evaluation of 3D printing systems, which also required measurements of the print surface topology. Although topography and micro-imaging methods can be used to measure surfaces, perceptual quality evaluation from surfaces rendered by additive printing methods is still a challenge, as discussed in a previous work by Baar et al. (2013: 1-6). In this paper, we propose to evaluate the print systems based on impressions produced with corresponding relief prints, as a means to evaluate the surface rendered with 2.5D and 3D printing technologies, thereby reducing from 3D or 2.5D down to two dimensions.

Traditionally, relief prints are created through the combination of a raised printing surface and the surface qualities of the printing woodblock (end-grain hardwood, chipboard, linoleum, acrylic), which is then inked and printed under great downward pressure. The woodblock surface is manipulated by engraving, cutting and abrasion (traditional tools include sharp V shape or U shaped chisels). In order to obtain a high quality printed image, the inked plate needs to produce well defined lines and solid areas with uniform colour.

Similar to traditional relief printing, we created plates by wood carving methods, using a laser cutter and a CNC engraving machine. Additionally, we introduced the use of two additional printing systems to generate printing plates. In the following section the target images used for assessment are described, as well as a description of each of the processes. Following this, we describe the results of our print quality assessment for each of the processes, based on the obtained relief prints.

2. TEST TARGETS FOR RELIEF PLATES

Each of the techniques used to modulate the surface texture carries advantages and disadvantages, both in terms of costs and creation time, and also in their ability to create small details and large smooth surfaces accurately. We used two resolution targets to assess the performance of the surface modulation processes.

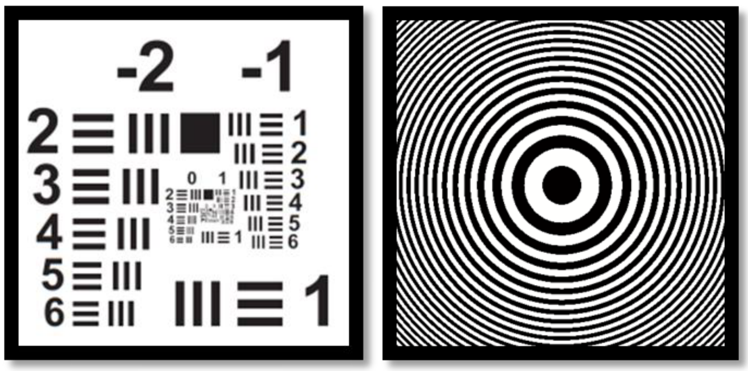

Figure 1: Test targets to assess resolution limitations of each of the relief plates. Black corresponds to high relief and white to a lower (carved out) surface.

The first sample is the USAF resolution test chart (1951), shown on the left of Figure 1, where a set (*element*) of three horizontal and vertical lines is depicted for different dimensions. Six elements together form a *group,* identified by the larger number on top. In accordance with the standard, this target is printed such that the first element of *group* -2 is 10mm long. By determining the element that corresponds to the smallest set of lines that are still distinguishable, the corresponding maximum representable resolution is calculated by:

$$Resolution = 25.4 \cdot 2^{group+\frac{element-1}{6}} \quad cycles/inch \qquad (1)$$

For the second target we used a Zone plate ring pattern with a spatial frequency that increases from 5 up to 50 cycles per inch at the border, as shown on the right of Figure 1. A Modulation Transfer Function (MTF) could then be obtained from the printed target, describing the reproduction accuracy of the print for different frequencies in horizontal, vertical and diagonal direction, as described by Park, Schowengerdt and Kaczynski (1984: 2572-2582).

3. EVALUATION OF RELIEF PLATES AND IMPRESSIONS

We used five different processes for the creation of our test target printing plates. Relief was built up using additive (printing) fabrication, with both a commercially available Makerbot 3D printing system (using PLA filament to build 3D objects) and an Océ 2.5D digital printer prototype (where several layers of ink are superimposed to modulate the surface texture). Other relief plates were obtained by carving from an existing material, including wood and acrylic. Here, the non-printing areas were cut from these materials using a laser or CNC engraving machine.

3.1 Comparing Relief Plates

The two relief plates have been created using each of the technologies previously described. For each process, the target was input as a raster greyscale image (e.g. Tiff or Jpg file format), with the proper resolution used for each individual process. Each plate was made to have identical dimensions, including a depth in between 1.5 and 2mm (maximum distance between low and high parts of the plate). The time needed to create the plates varied from 20 minutes for the laser cutter to 46 hours using the CNC engraving. By observation of the relief plate, the maximum plate resolution was determined using the USAF resolution target and finding the smallest (textured) line pairs that could still be distinguished, from which a resolution limitation could be calculated following equation 1.

Table 1. Comparing relief prints from different processes.

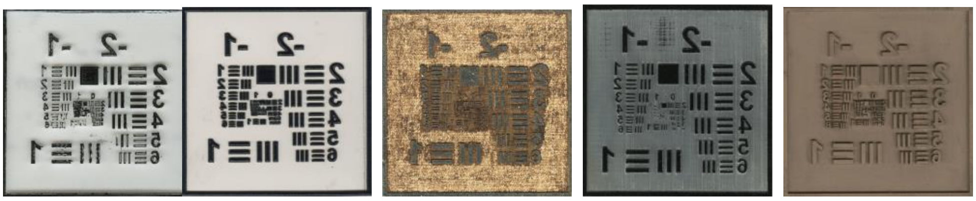

relief plate process:	MakerBot 3D	Océ 2.5D	Laser cut wood	Laser cut acrylic	CNC engraving
input resolution:	253dpi	450dpi	300dpi	300dpi	600dpi
depth:	2mm	2mm	1.5mm	1.5	2mm
creation time:	2 hours	3 hours	20 minutes	20 minutes	46 hours
max. plate resolution:	g: -1 e: 4 18 cy/inch	g: 1 e: 2 57 cy/inch	g: 1 e: 1 51 cy/inch	g: 0 e: 4 36 cy/inch	g: 0 e: 5 40 cy/inch

The 3D printer showed the poorest reproduction ability, as it was unable to exceed a resolution of 18 cycles per inch. Artefacts for resolutions higher than 10 cycles per inch were observed with the frequency test, mainly caused by the filament traces left on unintended areas. The laser cutter failed to fully remove all the wooden and acrylic material, which led to some variation in the depth of the low parts of the printing plate. Furthermore, due to laser temperature, the material curves and edges are oddly sharp because of the material melting on the edges of the relief, forming unexpected textures. It should be noted that the wooden relief plates (made using the laser cutter and CNC engraving) require additional surface treatment. The resin ‘shellac’ was used to prepare the surface in these two cases. In comparison, the Océ 2.5D plate presented the highest achievable relief frequency and it did not require any additional cleaning or treatment following its production method. However, the OCE 2.5 plate exhibits one of the highest production times. It should be noted that the technique of using a printing system to build the relief showed the artefact of soft edges, less sharp than the plates created with the carving methods.

3.2 Comparing the Impressions of Relief Plates

Following a traditional printmaking process, the plates were inked and printed on an Albion press. Instead of evaluating the quality of the surface rendered by each of the methods directly, we performed the evaluation on the impressions made with the plates, accessing various aspects, such as density of ink, uniformity of the surfaces, sharpness of the edges and spatial resolution at different angles. Similarly to Table 1, Table 2 shows the maximum achievable resolutions based on the relief prints created with each of the processes. Compared to the resolution of the printing plates, the resolutions of the relief prints were found to be lower. Out of the tested processes, the highest achievable frequency was found for the plates made with the Océ 2.5D printer and CNC engraving machine.

Table 2. Comparing impression of USAF test target for different relief print processes

relief plate process:	MakerBot 3D	Océ 2.5D	Laser cut wood	Laser cut acrylic	CNC engraving
maximum resolution:	g: -1 e: 4 18 cy/inch	g: 0 e: 4 35 cy/inch	g: 0 e: 2 29 cy/inch	g: 0 e: 1 25 cy/inch	g: 0 e: 2 29 cy/inch

As previously introduced, the Zone plate was used as second target to analyse the print accuracy for different frequencies. For evaluation of print quality, the final prints from each of the relief plates were scanned, as shown in Figure 2. The first row of Figure 2 shows the input, a horizontal section of the Zone Plate from the centre to the right border, where the frequency increases from 5 to 50 cycles per inch. The next row is the result after printing, using the plate created with the MakerBot 3D printer, where resolutions over 25 cycles per inch could not be achieved. The following couple of rows show the resulting relief print for each of the other processes. For each relief printed image a section in horizontal direction is shown on top of a (rotated) section in the vertical direction. The horizontal direction is here referred to as the direction in which the print-head/laser/cutting tool moves.

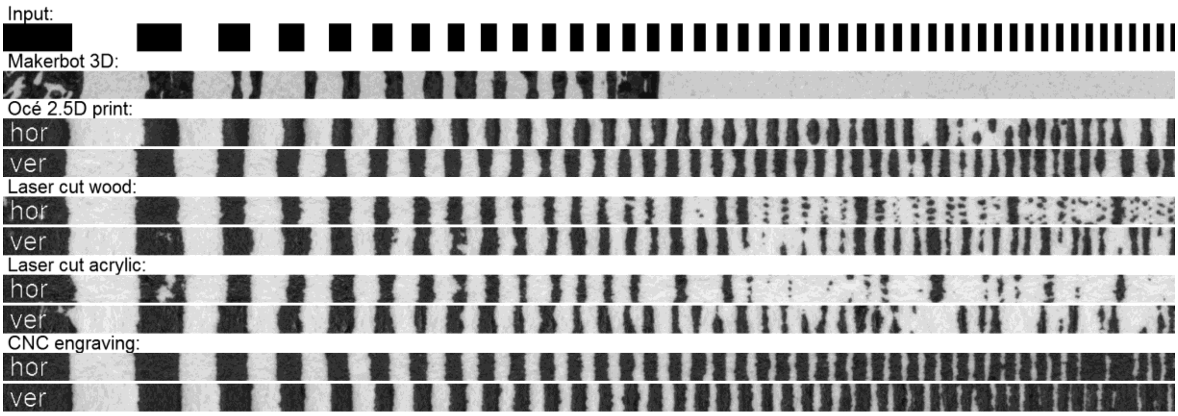

Figure 2: Scan of impression of Zone Plate for each of the processes. Only a selection is shown from the centre of the Zone Plate to the border, increasing from 5 up to 50 cycles per inch, both in the horizontal and vertical direction.

Although conclusions on the accuracy of printing different resolutions could subjectively be drawn from Figure 2, an objective measure is obtained by determining a Modulation Transfer Function for each of the printed outputs. The MTF is defined as the ratio of the modulation of the input signal and the output signal,

$$MTF = \frac{Modulation(output)}{Modulation(input)}. \tag{2}$$

Similar resolution targets are mainly used to assess the frequency response of optical measurement instruments where problems like aliasing do not occur and therefore the modulation can be simply determined based on minimum and maximum response values per frequency. In the case of the impressions shown in Figure 2, this would lead to an incorrect assessment of the performance, because the higher frequencies are not obtained but minimum and maximum values are still present in the calculation. We therefore determine the modulation via the Fourier domain:

$$Modulation(f) = \frac{F(f)}{F(0)} \tag{3}$$

Using equations 2 and 3 the MTF's are determined for each of the processes and shown in Figure 3, indicating how well several frequencies are reproduced. An important observation is the dependency on the direction of the output, as presented in the left graph of Figure 3. Here it can be seen that in the vertical direction (orthogonal to the direction of the laser and print head movement) a higher resolution can be obtained.

The MTF of the Océ 2.5D and CNC engraving process presented the highest achievable resolution, while the laser cut with the acrylic material shows the worst performance. These results are in agreement with the observations made earlier and indicated in Table 2. Based on the USAF test target, critical frequencies appear to occur at the 80% point of the MTF. An interesting observation was made from Figure 2 and 3 where the frequency response of the Océ 2.5D relief plate shows a peak at 45 cycles per inch, exactly around one tenth of the printer resolution. Although the impression of the CNC relief plate on the print (Figure 2) is nicely inked on the high frequencies, the inked lines are a bit thicker compared to the white spaces in between, which results in a low frequency response as shown in the MTF plot of Figure 3.

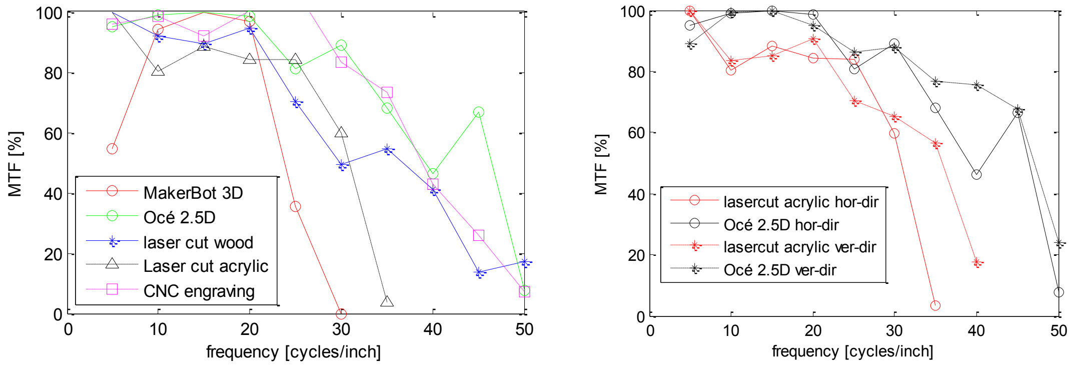

Figure 3: Modulation Transfer Functions based on the relief prints, comparing the different processes (left) and showing the direction dependency (right).

5. CONCLUSIONS

We have shown how several techniques can be used to create printing plates for the relief printing process. Imitating the Chiaroscuro woodcuts prints, we used two methods of carving printing plates out of wood and acrylic, along with two 3D printers, where plates were created by superimposing several layers of ink to modulate the surface texture.

Impressions of the relief plates were obtained through a relief printing process, from which limitations of reproducible frequencies were determined. In our investigation we found that spatial frequencies above 45 cycles per inch were poorly reproduced. The Océ 2.5D printing technique achieved the highest accuracy, preforming slightly better than the CNC engraving machine and laser cutting process. On the other hand we observed the effect of rounded edges in relief plates that were printed, while carving methods appeared sharper.

Current experiments have focussed on surface structures generated from raster images as input. Future work will be undertaken to investigate the performance differences using a vector format, which should result in more clearly defined cut lines. This would be more directly related to the creation of hand-carved woodblocks which could be included as a ground-truth comparison.

ACKNOWLEDGEMENTS

This work was supported by the Marie Curie Initial Training Networks (ITN) CP7.0 N-290154 funding.

REFERENCES

Baar, T., H. Brettel, and M.V. Ortiz-Segovia (2013). A survey of 3D image quality metrics for relief print evaluation. In *Proc. Colour and Visual Computing Symposium*: 1-6.

Liu, X., L. Chen, M.V. Ortiz-Segovia, J. Ferwerda, and J. Allebach (2014). Characterization of relief printing. In *Proc. SPIE 9018, Measuring, Modeling, and Reproducing Material Appearance*: 90180.

Park, S., R. Schowengerdt and M. Kaczynski 1984. Modulation-transfer-function analysis for sampled image systems. *Journal of Applied Optics* 23: 2572-2582.

Polzin, C., S. Spath and H. Seitz 2013. Characterization and evaluation of a pmma-based 3d printing process. *Rapid Prototyping Journal* 19(1): 37-43.

E-mails: Teun.Baar@oce.com, Melissa.Olen@uwe.ac.uk

The Relationships between Colors of Neck, Cheek, and Shaded Face Line Affects Beauty of Made-up Face

Youhei Ishiguro, Mamiko Nakato, Erika Tokuyama, Nao Matsushita, Minori Yamahara
Momotani Juntenkan., LTD

ABSTRACT

The color choice of make-up foundation is one of the most important step to make a beautiful finish of made-up face, and a difficult problem for many users. For these users, there are many advices in markets. Such as "You should look for a nearest matching color to the color of your face line". However, there have been several questions. 1) Where is the best region of a face (or neck) for the color matching? 2) Is color matching to a certain region the best way to make a beautiful finish? In this study, visual evaluation tasks were conducted using images of Japanese female faces applied make-up foundations having various colors. As results, the index value indicated the relationship between colors of several regions had a strong negative correlation with scores of beauty evaluated by these tasks. In detail, these results suggested that participants used the coincidence of 2 color directions from the color of shaded face line to the color of cheek or neck in L*a*b* color space, to evaluate the positive feeling about the color choice of make-up foundation.

1. INTRODUCTION

Make-up foundation is one of the basic make-up items. This item is usually applied to a whole face, and this finish is shown as a skin tone. Therefore, if the color of this item was far from the natural skin color, the finish is certainly not beautiful. This fact means that the best color of this item to make a beautiful finish is different for each users, because natural skin colors of each user are different. For this reason, the color choice of make-up foundation has been difficult problem for many users. For these users, there are many advices in markets. Such as "You should look for a nearest matching color to the color of your face line". And there are several systems that could give these advices automatically using image analysis (e.g. Jain, et al, 2008: 331). However, several different regions have been recommended as the region for color matching in these advices, and it has not been clarified where the best region is. Furthermore, it has not been verified whether the color matching to a certain region is the best way to make a beautiful finish. There is a contradictory common opinion that many Japanese females want to make them face brightened. Considering each positions of these regions, cheek is usually applied region, and neck is usually non-applied region. Thus, we could observe the relationship between colors of applied region and non-applied region in neck and cheek. And then, it is predicted that the positive feeling about that color choice could be evaluated by using this color difference. However, the boundary is usually not clear, and there is the region of shaded face line. It is generally known that an existence of boundary regions or shades interfere to percept of a color difference between both sides. Furthermore, the color factor effected by shading of human skin is not only brightness but hue and saturation, because of the complex reflection structure of human skin. In other words, human skin has character about the shading color direction that is from the color of shaded region to the color of brightened region in L*a*b* color space. Therefore, we guessed that the main factor of the positive feeling about that color choice is not the color difference between cheek (applied region) and neck (non-applied region), but the coincidence of 2 color directions from the color of shaded face line to the color of cheek, or neck.

2. METHOD

The index value was developed as evaluating the positive feeling about the color choice of a make-up foundation. It was calculated from images of faces applied a make-up foundation using image analysis, and based on our hypothesis about the main factor of that positive feeling. And then, 2 visual evaluation tasks were conducted to verify this index value.

2.1 Index value

Calculating method of the index value is shown as follows. Firstly, each regions were defined. Figure 1(a) shows the line from neck to cheek was set up arbitrary in the image of face. And the darkest pixel in the line was defined as the region of shaded face line. Then, L*a*b* values of these 3 regions were gotten from each pixel value of the smoothed image. Figure 1(b) shows the 3D angle of 2 color directions from the color of shaded face line to the color of cheek or neck. The index value was defined the logarithm of this 3D angle. This value became lower when these directions were coincided, and became higher when these directions were divorced.

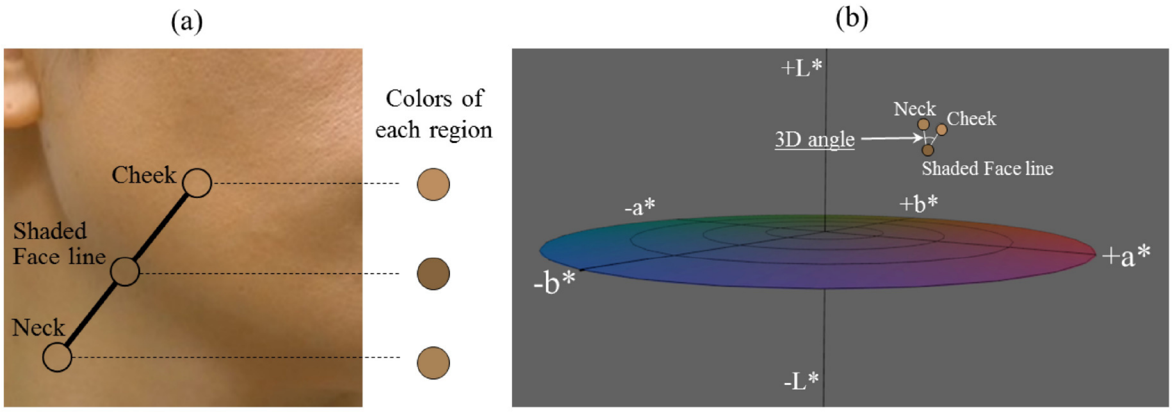

*Figure 1: (a) shows each regions in the image of face. (b) shows the 3D angle of 2 color directions in L*a*b* color space.*

2.2 Visual Evaluation Tasks

The first task were used 40 images of 4 Japanese female faces applied 10 make-up foundations having various colors. Figure 2(a) shows some images of them. 34 participants observed these images and replied scores (1: beautiful, -1: not beautiful, 0: not either) about these color choices. In the second task, simulated images were used. For the simulation, 12 original images of the first task were selected as the group having a mid-range index value. And then, 108 simulated images were made from these original images to 9 conditions (2 parameters, 3 steps) as shown in Figure 2(b). The parameter of horizontal axis was the color of neck, and to change the angle of the color direction from the color of shaded face line to the color of neck. Therefore, this parameter changed that coincidence of color directions, without to change the color of face and the color difference between neck and shaded face line. The comparison parameter of vertical axis was the the color of face, and to change the color difference from the color of shaded face line to the color of whole face. Therefore, this parameter changed the brightness of face without to change the color of neck and the coincidence of these color directions. Participants of the second task were 6, and other regulations of the second task were followed the first task.

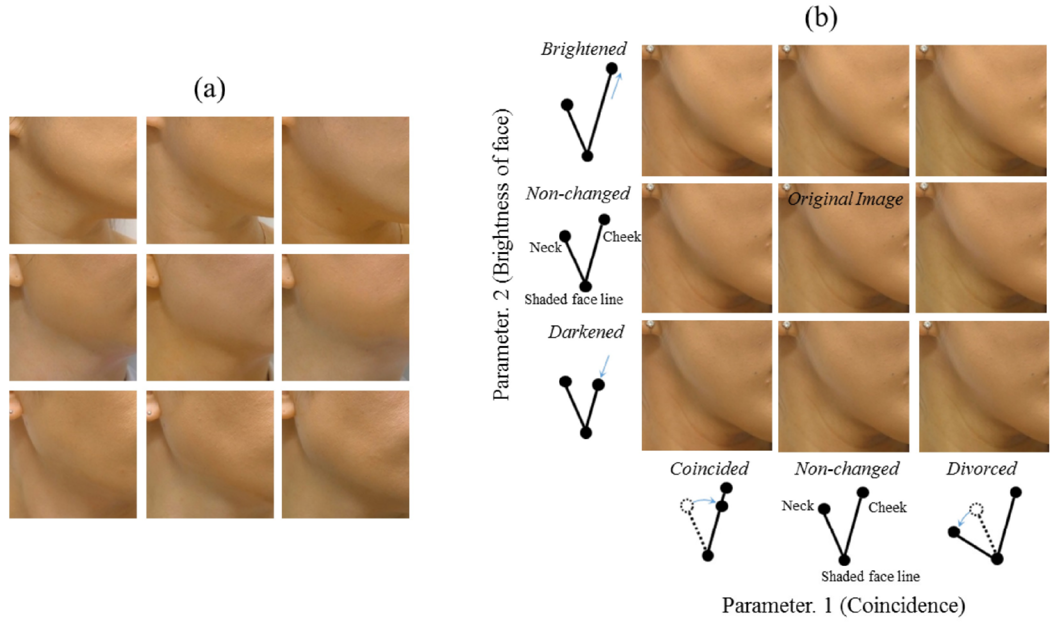

Figure 2: (a) shows faces applied make-up foundations having various colors for the first task. (b) shows faces simulated to control an index value or a brightness of face for the second task.

3. RESULTS AND DISCUSSION

As shown in Figure 3(a), the index value had a strong negative correlation with scores of the first task. This correlation coefficient was 0.73. The other hand, the correlation coefficient of the logarithm of ΔE (the color difference between colors of neck and cheek) versus these scores was 0.57 and significantly lower ($p<.05$). This reason was that shading degrees of neck and cheek were partialy different in these images, and this difference caused large ΔE. Our proposed index value was based on the consideration about this difference of shading degrees. Because this difference is usually shown in natural scenes.

Figure 3(b) shows results of the second task. Values of the vertical axis in this figure are differences of the average scores of each row groups as shown in Figure 2(b) against the score of original image. Therefore, these values indicate the effect of these 2 parameters which are the coincidence of color directions and the brightness of face. These p values were caluculated by using *Student's T-test* versus the average score of non-changed images of each parameter. One of the knowledge verified from these results is that the positive feeling of that color choices does not depend on the single color of any certain region, but depend on relationships between colors of several regions. Because these parameters were not related one either color of neck or face, and if it depended on a color of any single region without any relationships, either one of these parameters could not effect these scores. As the effect of brightness of face, the effect of darkned was significantly shown, but the effect of brightened was not significantly shown. For this reason, it is considered that the effect of brightness of face is little when the brightness is over a certain level. On the other hand, The effect of coinsidence of color directions was shown more significantly about either coinsided or divorced. For these reasons, it was verified that the coincidence of that color directions was important for the positive feeling of that.

Considering L*a*b* values of each regions in natural schenes, the color of shaded face line has usually lower value of L* and higher values of a* and b* than the color of non-shaded face line. This phenomenon affects the relationship between colors of these regions strongly. For this reason, we concluded that the color value of shaded face line in natural scenes is more importart than the color value of non-shaded face line, such as the value measured by a color difference meter or any other tools having the function of avoiding the influence of shades.

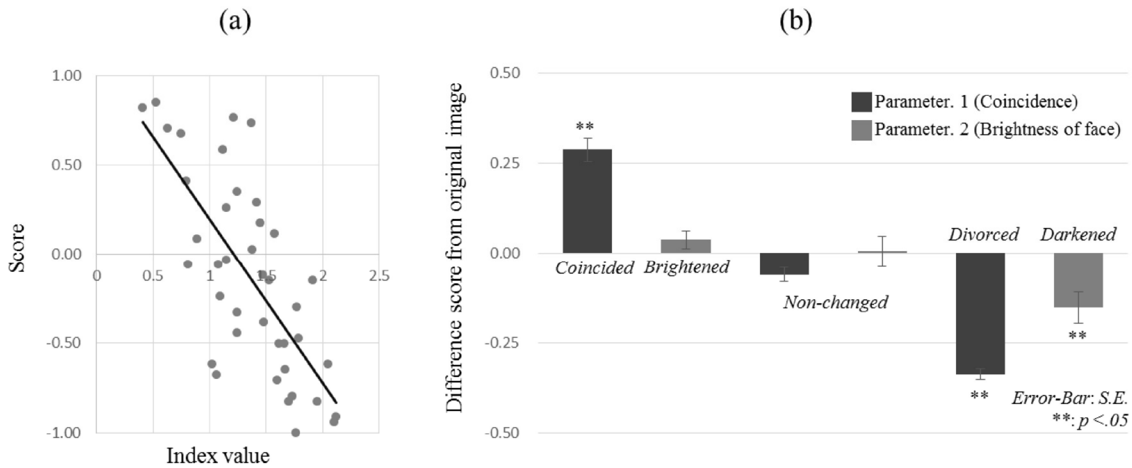

Figure 3: (a) shows results of the first task. (b) shows results of the second task.

4. CONCLUSIONS

It was suggested that the main factor of positive feeling about the color choice of make-up foundation is the coincidence of 2 color directions from the color of shaded face line to the color of cheek or neck in L*a*b* color space.

REFERENCES

Jain, J, et al. 2008. *Color Match: an imaging based mobile cosmetics advisory service,* Proceedings of the 10th international conference on Human computer interaction with mobile devices and services. 331-334.

Address: Youhei Ishiguro, R&D Department, MOMOTANI JUNENKAN LTD,
4-30, 2-Chome, Ichioka, Minato-ku Osaka, 552-0012, JAPAN
E-mails: y-ishiguro@e-cosmetics.co.jp

Experimental Method Suggested for Optical Observation of Anisotropic Scattering

Akio KAWAGUCHI,[1] Hirofumi NINOMIYA[2]
[1] Research Reactor Institute, Kyoto University
[2] Ninomiya Jewellery Co.Ltd.

ABSTRACT

Experimantal methods are suggested for observation of scattering considered with spatially anisotropic distribution. Applying “transferring surface” which has controled curvature and orientation can achieve easy and rapid observation of emmision or radiation from a sample set at an unique point; emmision (such as emitted or scattered light from the irradiated sample) with spatial anisotropy is projected or reflected on “transferring surface” and transfered intensity is detected as two-dimensional images veiwed with observing instruments. In this report, we adopted parabollic curved surface as “transferring surface”. Such indirect observation can provide experimental merits as rapid and wide-range measurements with high resolution, and (observed) transferred intensity can be also revised through estimation of reflecting property on “transferring surface”; in the case of passively irradiated materials, it means effective experiments for bidirectional reflectance distribution function (BRDF). The method can be appliable for vairous scattering: both spontaneous light source and irradiated materials, discrete scattering and gradated (or diffused) one, observation of spatial distribution and color dispersion, and more. Measurements using straight light beams as incidence and “transfering surface” suggested analysis of distribution of light scattered by jewels (diamonds) and sheeny cloths (silk textiles).

1. INTRODUCTION

There are some genres for viewing estimation of commercial products where objective standards hardly exist or convictive explanations are not enough scientifically discussed. Estimation for jewels represented by diamonds is such typical operation which may be often regarded dubiously because the products are occasionally expensive; amateurs or customers have to trust judgments given by professionals or sellers.

On the other hand, as estimation for jewels, chemical analysis for the samples or measurement for their geometrical shapes may be objective.(Schumann, 1977: 68) However, conclusion indicated by such procedures are independent from optical process or viewing impression. Or, some instruments appeal results given by optical measurements but scientific explanations as physics are not sufficiently indicated.

Even for either spontaneous light source or materials irradiated by external light, visual effects and functionality are determined by spatial distribution of light from the objects. Viewing illuminated materials that do not emit light spontaneously, perception for the viewed objects depends on spatial distribution of scattered light: distribution for intensity, wavelength dispersion, solid angle width, orientation of scattered light direction, etc.

However, it is sure that all scattered light should be originated with external light incidence though their directions are unknown and do not have to be known, generally. In this sense, *"isotropic"* lighting or illumination, which is regarded as general and natural environments recommended for visual estimation, can be approximated by summation of *straight* incident beams with many enough direction.

Authors have been investigating objective and convictive estimation for viewing diamonds and jewels, which are recommended to be judged with isotropic lighting environment such as orthodoxy "through a north window, on a fine day". As mentioned above, however, such isotropic lighting can be approximated by straight light beam(s) and, then, optical property can be discussed as physical light scattering. Furthermore, suggested methods are generally applicable for estimation of other materials showing anisotropic light scattering.

2. METHOD

2.1 Samples

As a jewel sample, a diamond cut as "round brilliant cut" design was prepared: weight c.a. 0.2 ct., cut grade "very good (VG)", girdle diameter c.a. 3mm.(Figure 1) As sheeny textiles, three kinds of silk textile (Japanese "Nishijin-Ori") sheets were investigated. (A: white, B:pink , C: light blue, in Figure 1)

Figure 1: Jewel and Textile samples.

2.2 Optical Instruments and Layout: Mechanics and Fundamentality

As light source, laser beam (red) and LED (white) were used. Since each beam was collimated as straight incidence of 8 mm in diameter, which is larger enough than the jewel sample, they covered whole volume of the jewel sample. Beams were alternately introduced to the sample on the same path using a half mirror and the incident beam can move in angle range of Θ = 0-90 deg. and Φ = 0-270 deg. (Figure 2)

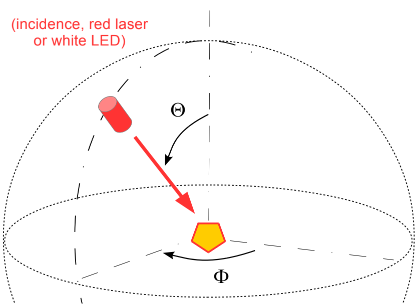

Figure 2: Orientation of light source; meridian coordination, Θ, and horizontal one, Φ.

Then, the sample position was a centre of light source running on a circle track with a rotating table; it was always irradiated by the incidence for all range of (Θ, Φ). Additionally, the position is also designed as a focus of following “parabolic surface”.

The beams emmited from the sample were observed through “transfering surface”, which can be available as plane surfaces or curved ones generally. Presently, we adopted parabollic curved surface which was coated by white powder (MgO) and was a circle of A = 200 mm in diameter with a slit of 10 mm width to introduce incident beams; emmission from the sample was observed as images projected on “transfering surface” as a curved screen. (Figure 3a)

When the sample position coincides with the focus of the parabollic curve (“origin” in Figure 3b), beams emitted from the focus point (“red lines” in Figure 3b) are transferred to parallel beams (“orange lines” in Figure 3b); emitted direction, (θ, ϕ) is transferred to observing coordination, (r, ϕ): $r = r(\theta) = A(1\text{-}\cos\theta)/\sin\theta$ or $\cos\theta = (A^2\text{-}r^2)/(A^2+r^2)$. And, intensity scattered form the sample, I(θ, ϕ), is also transferred to $I_{obs}(\theta, \phi) \approx I(\theta, \phi)\rho_s(\theta/2)/D^2$, $D = A/(1+\cos\theta)$, ρ_s: reflectivity on transfering surface. Scattered beams projected on parabolic “transfering surface” were observed from a CCD camera at a point along the axis of the parabolic surface with sufficiently far distance, c.a.900 mm. (camera: Lumenera Lc370c, 3M-pixel; lens: Kowa LM25JC5M, f = 50mm) Actual surface (white area in Figure 3a) was manufactured applying part of parabollic curve, y > 0, and screen diameter, A, corresponds to x = -2 ~ +2, in Figure 3b.

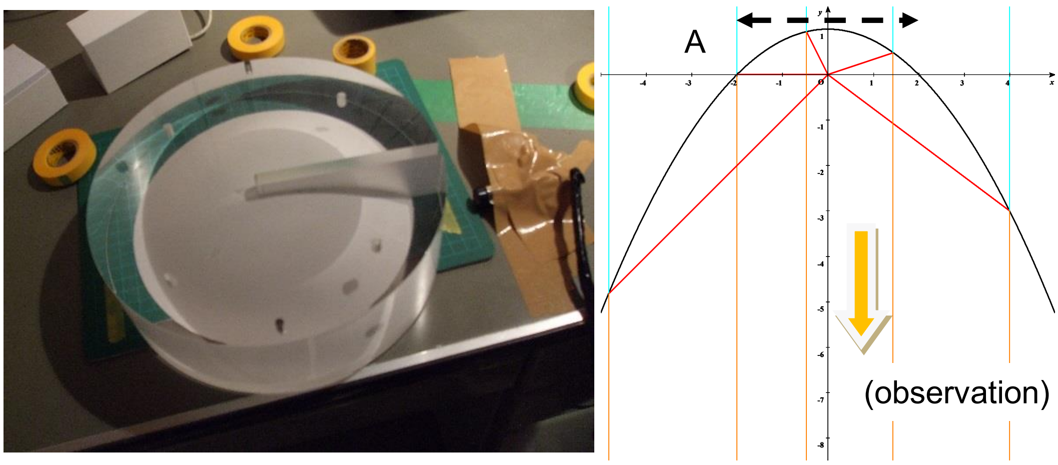

Figure 3: (a, left) Parabolic surface (behind acrylic pillar) and (b, right) its fundamentality.

2.3 Analysis for Scattered Beams from Jewel.

As light source, red laser beam was used for investigation of the jewel sample. The sample was set at the sample position with tweezers owing three wires, and its “table facet” which was the top and largest plane of the design was (almost) oriented to Θ=0 direction. Scattered beams emitted from the sample projected as “light spots” on the parabolic screen, and the view observed from the CCD camera was saved as image datum in a PC. Moving orientation of the light source (Θ, Φ) as 82 positions and controlling sensitivity of the camera (low and high), taken 82 shots were converted to “two-value (zero-one)” images to estimate statistical distribution of size of “light spots”.

For statistical analysis from the images, image analysing software, “WinROOF (Mitani

Corporation)", was applied. Distribution of size of "light spots" was summed for all (82) directions and was averaged for per one shot.

2.4 Observation for Silky Textiles.

For observation of silk textiles, white LED was used as light source moving in range of Θ = 0-75 deg. and Φ = 0-90 deg. Each textile samples was set at the sample position with a double-coated tape on the top of a flat-head pillar; normal plane of the textiles was oriented to Θ=0 direction. Quantitative analysis for the textile samples was not considered in present work because of inaccuracy of reflectivity on the "transfering surface".

3. RESULTS AND DISCUSSION

3.1 Emitted Beams from Diamond: Scattering by "Round Brilliant Cut" Design.

For a "round brilliant cut" diamond, which has 58 facets generally, one incident beam was scattered as number of $10^3 \sim 10^5$ (or much more, actually) emitted beams projected as "light spots". And such corelation of orientation between the *straight* incidence and each spot should be correctly indicating corelation between illuminating light (unknown and just before going into the jewels) and observation of the jewels as brilliancy or glare. If so, estimation for distribution of solid angle width of emitted beams (or size of "light spot") is fully meaningful since it is discussion of probability that each emitted beam can detected by an observer's eye.

Then, considering statistical tendency of distribution of size of "light spot", histogram plot is indicated; $\ln\{N(\Omega)+1\}$ vs. Ω, where Ω is a solid angle value (steradian) for each spot, $N(\Omega)$ is number of data contained in interval sections and "+1" term is introduced to avoid errors in logarithm function. As a typical result, statistical distribution of solid angle distribution of emitted beams is indicated in Figure 4.

Both plots for high sensitivity of camera and low one show existence of <u>region applicable with "linear approximation" in low Ω range</u> (emphasized with red dotted ovals in Figure 4); it means that, in low Ω range (as tendency of small or tiny "light spots"), statistical distribution of $N(\Omega)$ follows an exponential rule, $N(\Omega) \sim \exp\{-\lambda\Omega\}$ ($\lambda > 0$).

On the other hand, even if number of tiny "light spots" is much large, bigger sized "light spots" which volume is relatively small may be more effective or more impressive

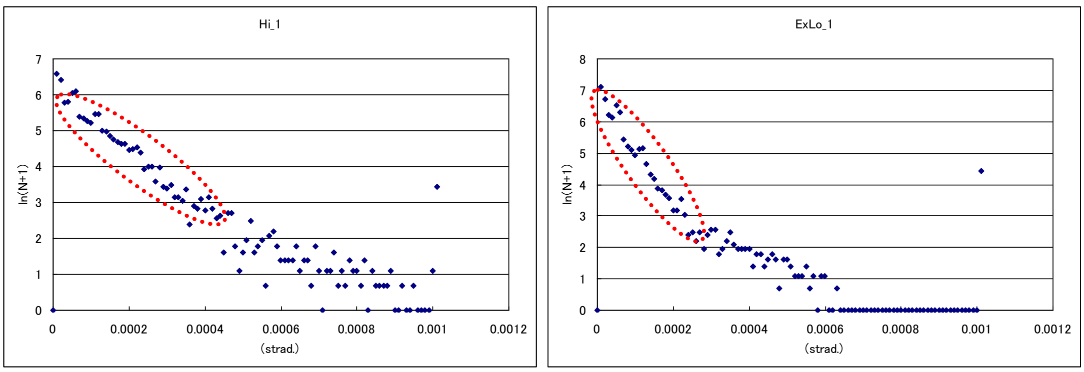

Figure 4: Histogram plots, $\ln\{N(\Omega)+1\}$ vs. Ω, and "linear region" in low Ω range; interval step is 1×10^{-5} strad., alternating camera sensitivity high (left) and low (right).

when customers actually look the jewels. Above “exponential distribution in low Ω range” is expected to clarify scientific objectivity for effective impression of jewels.

Furthermore, though directions of the emitted beams are innumerable, the suggested method can provide data for spatial bias about their orientation and wave distribution. Such factors are expected to be efficiency on observers’ impression.

Unfortunately, though above statistical distribution of size or solid angle can provide scientific grounds for facts of brilliancy of jewels, we have not yet arrived at relationship between the experimental data and professional jewelers’ judgment. Considering intensity distribution of the “light spots”, correspondence between statistical distribution of Ω and estimation judged by jewelers have to be discussed and concluded in near future.

3.2 Anisotropic Diffuse Scattering by Silk Textiles.

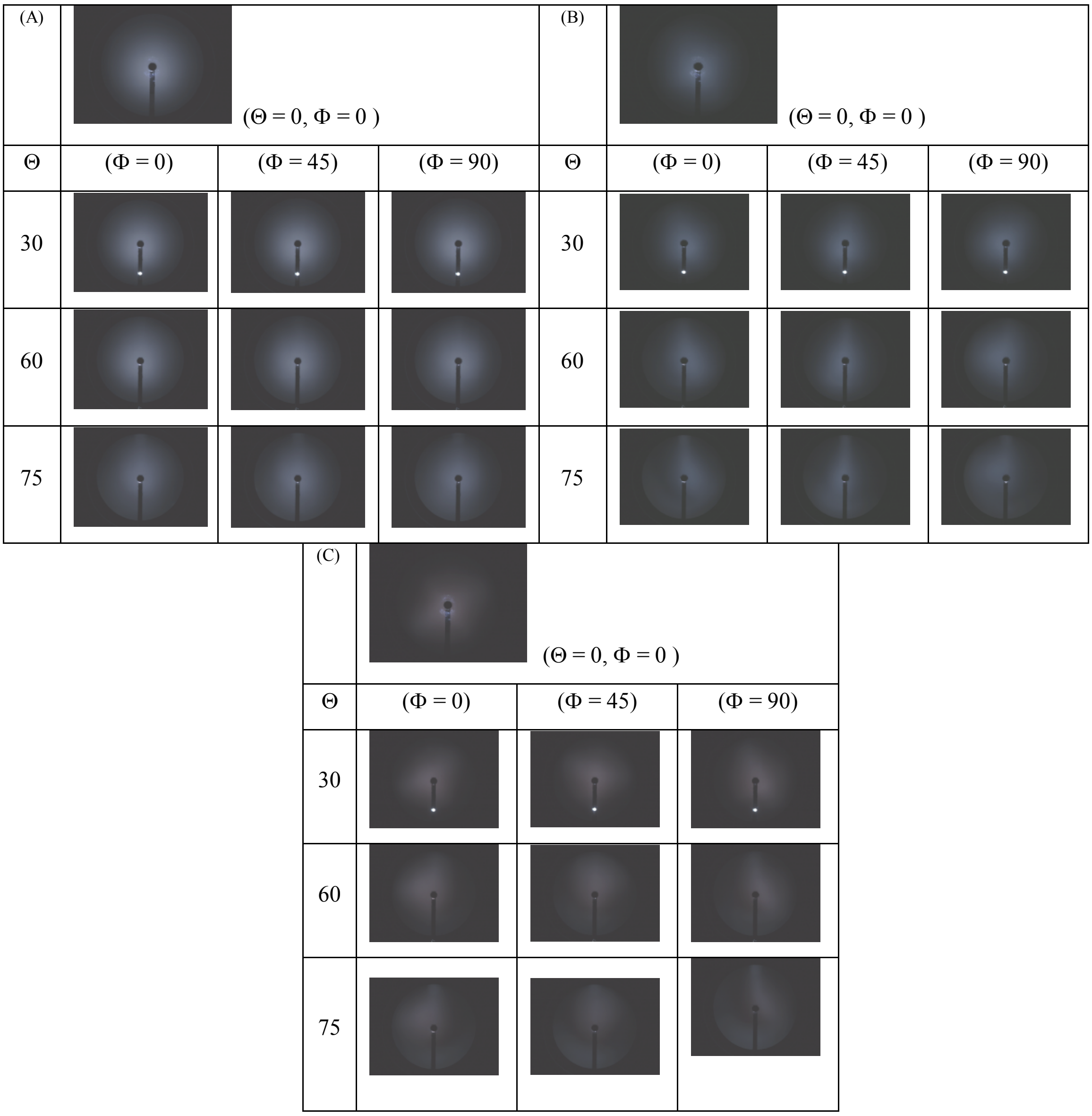

Figure 5: Scattered light distribution observed as 2-dim images for three silk textiles irradiated with white LED incidence; “black band” viewed on center is a slit for incidence.

Applying the method and instruments for observation of scattering as "light spots" from jewel samples, we can observe anisotropic light scattering from glossy materials such as silk textiles. However, since reflectivity function, $\rho_s(\phi)$ (ϕ: reflective angle at each point on the "tranfering surface"), has not tuned correctly and quantitatively, the present image data are estimated or discussed qualitatively.

Observation results for three silky textiles (A/B/C) irradiated with a white LED beam alternating incident orientation: Θ = 0, 30, 60, 75 deg. and Φ = 0, 45, 90 deg. Obviously, both dependency on colours of each sample and anisotropy of intensity, $I_{obs}(\Theta, \Phi; \theta, \phi)$ which is function for orientation of the light source (Θ, Φ) and direction of scattered light (θ, ϕ) or ($r(\theta)$, ϕ), were recognized in the images. (Figure 5) It is noticeable that anisotropy in intensity of scattered light was frequently observed in area missing "incidence plane", which corresponds with plane parallel to "black band (slit)" in Figure 5; these figures are two dimensional detection of bidirectional reflectance distribution function (BRDF) for the silk textiles.

In measuring orientation of scattered or emitted intensity, usual orthodox experiments use a point-detector (a single camera) on a goniometer which catches intensity for some direction. Such direct detection is the most accurate procedure to estimate intensity or dispersion. However, it also has demerits: antinomy, "scanning range" or "resolution" vs. "measuring time", or insufficiency in observation for irregular bias or distribution under gradation. Indirect method of observation with "transferring surface" can introduce consistence between measuring time and resolution requiring standardization of 2-dim image and reflectivity of "transferring surface".

4. CONCLUSIONS

Indirect observation of light scattered from objects applying "transferring surface" has potential advantages to estimate irregularity or anisotropy in light scattering. When jewel samples such as cut diamonds are irradiated with a single straight incidence, scattered beams are emitted as "light spots" for innumerable direction. Since correlation between insidence and emitted beams is approximation of recognization, statistical and orientaional analysis are expected to provide objectivity for human's judgments. Presently, "exponential distribution", $N(\Omega) \sim \exp\{-\lambda\Omega\}$ ($\lambda > 0$), is found for distribution of low range of solid angle (Ω) as statistical tendency. And, under standardization of 2-dim image and reflectivity of "transferring surface" and experimental devices, acquiring two dimensional distribution, (θ, ϕ) or ($r(\theta)$, ϕ), for scattered light as image data can provide more effective observation for objective estimation of glossy samples. .

REFERENCES

Schumann, W., 1977. *GEMSTONES of the World*: London: N.A.G. Press.

Address: Dr. Akio KAWAGUCHI, Research Reactor Institute, Kyoto University,
2-1010 Noda, Kumatori T., Osaka, 590-0494, JAPAN
E-mails: akawagch@rri.kyoto-u.ac.jp

Color measurement of meat in cooking under LED lightings with different spectral distributions

Akari KAGIMOTO[1], Risa SHIOMI[2], Shino OKUDA[2], Mami MASUDA[3],
Katsunori OKAJIMA[4], Hideki SAKAI[5] and Hiroyuki IYOTA[6]
[1]Graduate School of Human Life and Science, Doshisha Women's College
[2] Faculty of Human Life and Science, Doshisha Women's College of Liberal Arts
[3] Graduate School of Environment and Information Sciences,
Yokohama National University
[4] Faculty of Environment and Information Sciences, Yokohama National University
[5] Graduate School of Human Life Science, Osaka City University
[6] Graduate School of Engineering, Osaka City University

ABSTRACT

We measured the colors of meat during cooking under the standard illuminant D65 and several LED lighting conditions which differ in the spectral power distribution. First, we prepared three kinds of minced meat, beef, chicken and pork, which were shaped into 2 cm cubes. Each cubes of the minced meats was baked with an oven at the temperature of 200 degrees Celsius. We made a spherical dome for measuring average chromaticity values of an object in the condition of no shadow. The dome equipped fluorescent lamps of the standard illuminant D65 and two kinds of LED lamps: RGB LED lamps and white LED lamps. We measured the average chromaticity of the top surface of minced meat cubes at a raw stage and 22 cooking stages using a two-dimensional luminance colorimeter under eight lighting conditions in the spherical dome. According to the results, the chromaticity values gradually decreased with the increases cooking time under all lighting conditions. It was also shown that the color appearance while the beef has been cooked depends on the lighting conditions.

1. INTRODUCTION

Color appearance is a powerful indicator of food quality (Hutchings 2010). When we cook meat, it is needed to be adequately heated to prevent food-poisoning among other aspects of safety and good hygiene. Therefore, the color appearance of cooked meat is important in order to confirm how it has been cooked. Color appearance depends on the lighting condition such as the illuminance and the spectral power distribution. It has been reported that the color appearance of food is different under the following three kinds of light sources: LED light, Halogen incandescent and compact fluorescent lamp (Ixtaina et al. 2010). In addition, the colors of meat during storage under fluorescent lamps with different spectral power distributions (Saenz et al. 2005) and the color appearance of food in cooking process under D65 fluorescent lamp were measured (Sakai and Iyota 2013). This study aims to clarify quantitatively the color changes of meat during cooking under LED lighting conditions. We conducted measurements of the color of meat during cooking under several LED lightings with different spectral power distribution.

2. METHOD

2.1 Measured objects

We prepared three kinds of minced meat: beef, chicken and pork. We shaped these minced meats into a cube, 2 cm on a side. Each cube of the minced meat was baked with an electric oven [NE-M156-W, Panasonic] at the temperature of 200 degrees Celsius. We set 22 stages of the cooking time; in 30 seconds intervals till 5 minutes, 1 minute intervals from 5 till 10 minutes, 2 minutes intervals from 10 till 20 minutes and 5 minutes intervals from 20 till 30 minutes.

2.2 Apparatus

We made a spherical dome for measuring the chromaticity values of an object with no shadow. Figure 1 shows the apparatus for color measurement of the minced meat. The inner wall of the dome was painted white, L^*=93.59, a^*=-0.38 and b^*=2.40, measured with a spectrophotometer [CM-700d, KONICA-MINOLTA] in the setting of a D65 light source. The dome is equipped with two RGB LED lamps [iColor Cove MX Powercore, Philips Color Kinetics] and two white LED lamps [iW CoveMX Powercore, Philips Color Kinetics] with three kinds of LED chips with different correlated color temperature. It also had two fluorescent lamps of a standard illuminant D65 [FL20S D-EDL-D65, TOSHIBA]. These lamps were placed below the stage. The cubes of minced meat were put on the stage in the middle of the spherical dome. The top surface of the minced meat cube was measured by using a two-dimensional luminance colorimeter [UA-1000A, TOPCON Co. Ltd.] from the above.

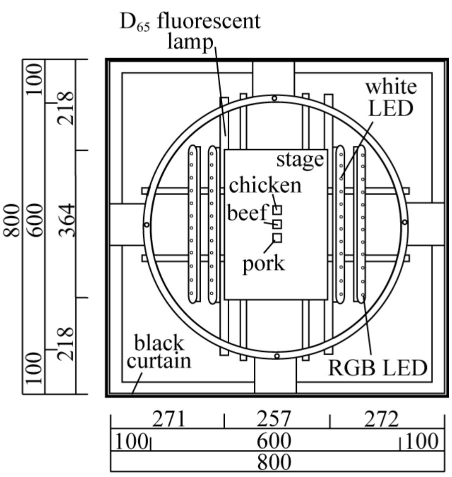

a) Plan

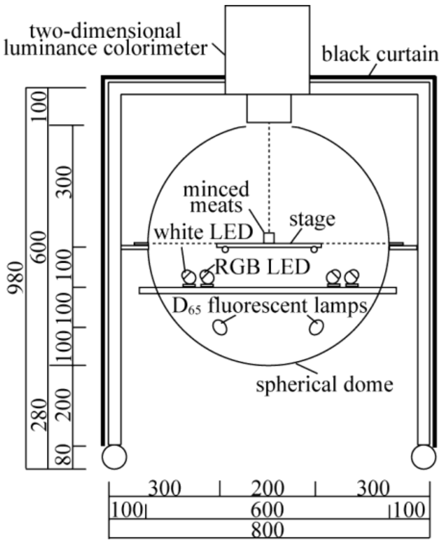

b) Section

Figure 1: Apparatus for color measurement

2.3 Lighting conditions

We set eight kinds of lighting conditions: seven kinds of LED lighting conditions and the standard illuminant D65. Table 1 shows the lighting conditions. Figure 2 illustrates spectral power distributions of the eight lighting conditions.

Table 1. Lighting conditions

Lighting conditions	CCT (K)	Ra	u'	v'	duv
LED-1	2894	82	0.255	0.523	0.00
LED-2	4134	59	0.229	0.486	-0.01
LED-3	4137	91	0.221	0.502	0.00
LED-4	4164	82	0.221	0.502	0.00
LED-5	6272	74	0.196	0.474	0.01
LED-6	6286	94	0.201	0.468	0.00
LED-7	6296	83	0.201	0.468	0.00
D65	5760	99	0.200	0.480	0.01

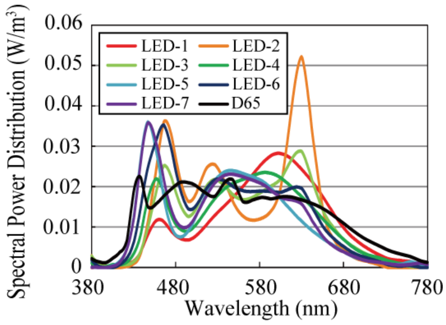

Figure 2: The SPDs of the eight lighting conditions.

3. RESULTS AND DISCUSSION

Figure 3 shows the mean values of chromaticity (L^*,u^* and v^*) of the top surface of minced beef at 23 cooking stages under each lighting condition. It was shown that the L^*, u^* and v^* values gradually decreased with increasing cooking time under all lighting conditions. The color appearance of the minced beef was different by the lighting condition as shown in Figure 4. The beef looked reddish under the lighting condition of LED-1 though the beef had been sufficiently cooked. On the other hand, under the lighting condition of LED-5, the beef looked dusty-red at each cooking stage. Therefore, the color appearance of the beef during cooking depends on the lighting condition.

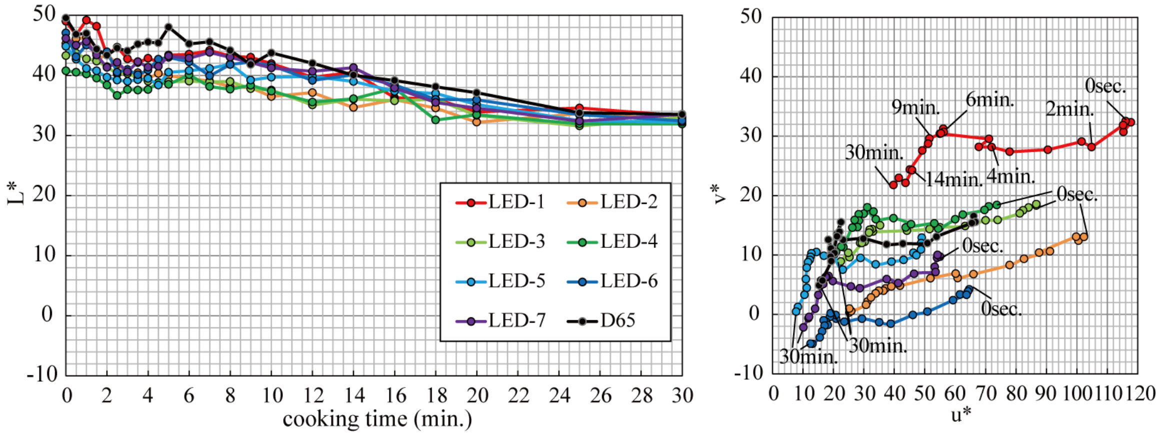

Figure 3 : The values of the average chromaticity of minced beef

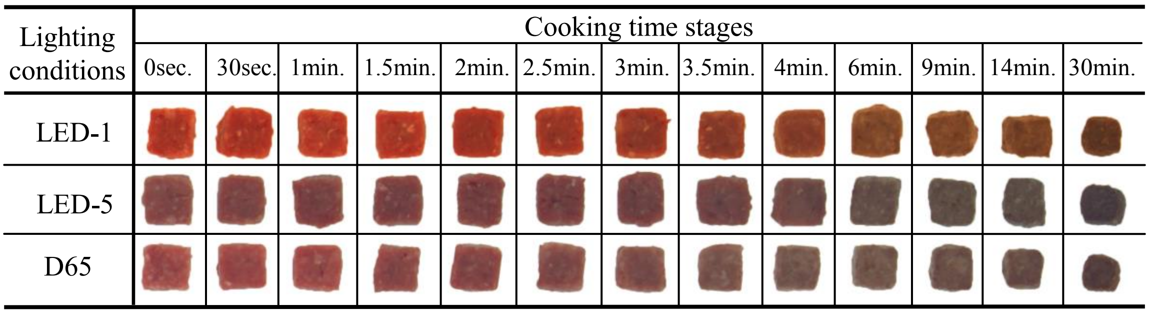

Figure 4 : The digital image of minced beef under the conditions of LED-1, LED-5 and D65

Table 2 shows the color differences (ΔE^*_{uv}) of the measured chromaticity under all lighting conditions. The color differences were obtained in the calculation as below (Equation 1).

$$\Delta E^*_{uv} = |L^*u^*v^*_{\text{LED-}i} - L^*u^*v^*_{D65}| \qquad \text{Equation 1}$$

$L^*u^*v^*_{\text{LED-}i}$: chromaticity value under i-th LED lighting condition

$L^*u^*v^*_{D65}$: chromaticity value under the standard illuminant D65

It was shown that the color difference values greatly differed among the LED lighting conditions. In particular, the color difference was large at the raw stage (0 second).

Table 2. The color difference (ΔE^*_{uv}) of the measured chromaticity under LED lighting conditions and those under D65 lighting condition

Lighting conditions	LED-1	LED-2	LED-3	LED-4	LED-5	LED-6	LED-7
0 second	54.06	34.95	21.58	11.78	18.04	12.65	14.32
8 minutes	39.26	20.65	15.16	11.57	9.15	13.97	9.17
14 minutes	37.15	15.44	11.04	9.39	8.15	11.20	5.60
20 minutes	27.85	11.53	7.05	5.44	10.68	13.46	12.49
30 minutes	28.32	10.03	9.65	5.93	10.22	11.39	7.55

4. CONCLUSIONS

We measured the color change of minced meat during cooking under various LED lighting conditions and compared their color appearance with those under the standard D65 lighting. It was clarified that the chromaticity values gradually decreased with increasing cooking time under all lighting conditions and that the color appearance of beef during cooking depends on lighting conditions.

ACKNOWLEDGEMENTS

This research was supported by JSPS KAKENHI Grant Number 25282006.

REFERENCES

Huchings, J. 2010. *Food, expectations, colour and appearance*, AIC 2010 Proc. 17-22.

Ixtaina, P., Presso, M. and Bredice, F. *Colour appearance in LED lighting*, AIC 2010 Proc. 302-305.

Saenz, C., Hernandez, B., Beriain, M. J. *Meat Color in Retail Displays with Fluorescent Illumination*, Color Research & Application 30(4) 304-311.

Sakai, H. and Iyota, H. *Sensory Evaluation of Preference of Baked Food Color,* AIC 2013 Proc. 57-60.

Address: Akari Kagimoto, Life style design studies,
Graduate School of Human Life and Science,
Doshisha Women's College, 602, genbu-cho, Kamigyo-ku, Kyoto, 602-0893, JAPAN
E-mails: inkdg001@dwc.doshisha.ac.jp, shd071@dwc.doshisha.ac.jp,
sokuda@dwc.doshisha.ac.jp, masuda-mami-mz @ynu.jp, okajima@ynu.ac.jp,
hsakai@life.osaka-cu.ac.jp, iyota@mech.eng.osaka-cu.ac.jp

Color temperature and Illuminance of Main Streets with Day and Night Illumination in the Center of Osaka, Japan

Haruyo OHNO
Faculty of Media and Arts,Otemae University

ABSTRACT

There are many topics on the beauty of the scenery concerning color planning. The author considers it is very important to designate lighting planning[1)] for urban color planning. This paper includes a survey concerning lighting atmospheres of the urban districts and questionnaire survey in Osaka City. As a result of the survey, the mean value of illuminance was considerably similar between each street at night-time but not at daytime, on the other hand, that of chromaticities did not show significant difference between night-time and daytime. The questionnaire survey indicated the street lighting was effective in making people feel bright and safe.

1. INTRODUCTION

Nowadays with an aim of creating comfortable, delightful and interesting urban environment, various factors in the actual environment[2),3)] are used to promote attractive plans. In color planning, not only the surface color but also lighting planning are very important. The author obtained data from two main sources: 1) measurement data on daylight and night illumination, and 2) questionnaire survey obtained from young people in Osaka. Firstly two areas were selected as survey sites, one northern and the other southern areas in the center of Osaka City. Five streets were picked up in each area. In every measuring point, the horizontal and vertical Illuminance, as well as the horizontal and vertical color temperature were measured both in daylight and night illumination for three days. Questionnaire survey was carried out to find any difference in psychological perceptions relating to lighting on these streets.

2. METHOD

The author investigated the illumination of Osaka city by using measurement data and the visual perception of those illuminations. This research includes data collected from two main sources: 1) measurement data in daylight and night illumination, and 2) questionnaire survey obtained from young people.

2.1 Measurement Data

10 survey locations were selected for this study as shown in Table 1. These streets were located in the center of Osaka city, Umeda, a northern area, and Namba, a southern area. Five streets, grouped into three district features, the shopping arcade, the downtown and the main street, were picked up from each area. For each street, we monitored 16 measurement points with 20 meter interval covering 300 meter length, total 160 measuring points. Data was recorded 6 times during the collection period between July to

November 2009, at daytime and at night-time for three days. We measured the values of horizontal and the vertical illuminance and the horizontal and vertical chrommaticities of daylight and night illumination. Data were recorded in daytime (10:00 to 16:00) and at night-time (18:00 to 22:00). Thus each points had total of 24 measurement values. MINOLTA-CL-200 was used to identify the illuminance and the relative color temperature. At the same time the author also evaluated the visual perceptions of the lighting circumstances at these monitoring points. There were 11 items that the author considered; brightness, confusion, beauty, warmth, exoticism, nature, calm, plane, ordinary, harmony

Place	Shopping Acade		Downtown	Avenue	
Umeda	Higashi Dori	Ohatsutennjin Dori	Cyayamachi	North Nishiumeda	South Nishiumeda
Namba	Shinsaibashi	Sennichimae	Doutonbori	North Midou	South Midou

and pleasant for psychological evaluations.

Table 1 Survey Locations

2.2 Questionnaire Survey

Questionnaire survey was carried out to find any difference in psychological perceptions relating to lighting on these streets in Osaka city November 2009 by e-mail. 100 subjects were asked to give their visual perception of the street lightings. They were all students in their twenties and had visited those streets both at daytime and night-time.

3. Results and Discussion

3. 1 **Shopping Arcade**

These streets have an arcade, shops facing each other and the road 7m in width.

1) Illuminance

The horizontal illuminance data of daytime at Higashidori is shown in Fig.1. The mean value of the horizontal illuminance at each point ranges from 800lx to 3,700lx. The higher illuminance 20,000lx is observed at the 160m point on the street as there is an intersection on that point. The vertical illuminance of this street ranges from 300lx to 2,000lx as shown in Fig. 3. To compare with measurement data of other street, the mean value of three days are used to evaluate the illumination of each street. At night, the horizontal illuminance ranges from 250lx to 900lx and the verticl illuminance from 40lx to160lx,

2) Relative Color Temperature

Figure 2 and 3 shows the results of the relative color temperature versus the horizontal illuminance and the vertical illuminance, respectively. The relative color temperature ranges from 4,700K to 5,800K for the horizontal illuminance and from 4,600K to 5,300K for the vertical illuminance. In the daytime, the color of the light source is blue or whitish blue. These illuminance data shows some difference, but little difference for the visual perception according to the paper described by the authors, within the measured environment..At night, the relative color temperature ranges from 4,400K to 4,900K for the horizontal illuminance and from 3,600K to 4,800K for the vertical illuminance. The colors of the light source is reddish .

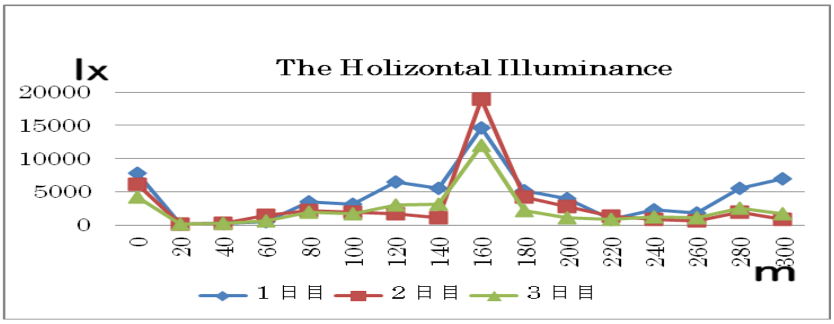

Fig.1 The horizontal illuminance from daylight at Higashidori shopping arcade

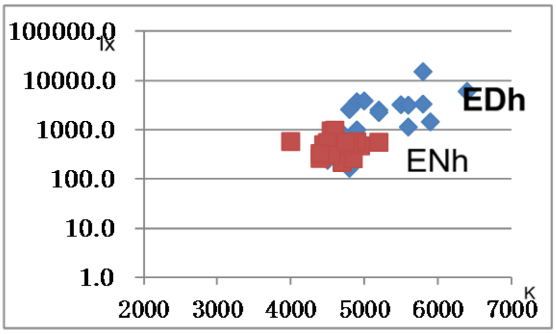

Fig.2 The relationship between horizontal Illuminance and relative color temperature at day and night (Higashidori)

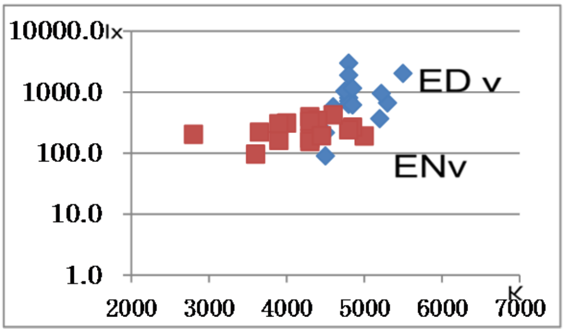

Fig3 The relationship between vertical illuminance and relative color temperature at day and night(Higashidori)

3.2the downtown

These streets have roads 7m wide in north area and 14m wide in south area, respectively and open to sky. Shops are facing each other and are around 15m in height.

1) Illuminance

In daytime at Cyayamachi Street, the horizontal illuminance ranges from 13,400lx to 22,000lx and the vertical illuminance from 3,800lx to 7,300lx. At night, the horizontal illuminance ranges from 20lx to 80lx and vertical illuminance from 10lx to 50lx. These values are quite low as compared with those of shopping arcade.

2) Relative Color Temperature

The relative color temperature ranges from 5,900K to 6,100K for the horizontal illuminance and from 5,700K to 6,000K for the vertical illuminance in the daytime. The color of these light sources is whitish blue. At night, the relative color temperature ranges from 2,500K to 3,300K for the horizontal illuminance and from 2,600K to 3,200K for the vertical illuminance. The colors of the light sources are reddish and orange. In daytime, these data are similar to those observed in shopping arcades, but different at night-time.

3.3 Main Street

The roads of these streets are 15m wide in north area and 45m wide in south area, and open to sky. The buildings are around 30m in height and most of shops are located on the first or second floor.

1) **Illuminance**

In daytime at North Street of Nishiumeda, the horizontal illuminance ranges from 100lx to 5,700lx and the vertical illuminance from 500lx to 2200lx. At night, the horizontal illuminance ranges from 8ix to 44lx and the vertical illuminance from 5lx to 25lx, These night data at night are quite low as compare with those of shopping arcade at night.

2) Relative Color Temperature

The relative color temperature ranges from 5,800K to 6,300K for the horizontal illuminance and from 5,500K to 5,800K for the vertical illuminance during the daytime and the colors of these light sources is whitish blue. At night, the relative color temperature ranges from 2,400K to 3,900K for the horizontal illuminance and from 2,600K to 3,200K for the vertical illuminance. The colors of the light sources are reddish and orange. These data are similar to those of downtowns at daytime and night- time.

3.4 Questionnaire Survey

Questionnaire surveys were carried out to find any difference from visual perceptions relating to lighting on these streets, the author got the street lighting was effective in making people feel bright and safe, but not clear to find delightful and interesting lightings.

4. CONCLUSIONS

The illuminance of daylight at the shopping arcade area is about 1/2 as compared with two other area, but it is more than 5 times higher than those of two other areas at night. The color of the light source from daylight at the shopping arcade is whitish and that of other areas is whitish blue, .and from nightlight the former is reddish, the latter are reddish and orange, Although the data obtained in this research may not be enough to indicate clear conclusion, however the author can recommended how to improve illumination on the street and how to change them to achieve a better visual impact and perception.

ACKNOWLEDGEMENTS

The author expresses her gratitude to the sutudents of Otemae University for their cooperation in this research, as well as Miss Mayumi Kaneko and Miss Azusa Matsumoto, then a graduation these research workers respectively .

REFERENCES

1)K.Itoh, H.Ohno: Practical Integrated Lighting Design with Daylight-Cumulative occurrence Rate of the Horizontal Illuminance from an Unobstructed Hemisphere of Sky, Transactions of A.I.J. No.215,junuary 1974

2)H.Ohno,N.Koizumi: Mood perception of Interior Colors in a Gym, AIC Color 01, The 9 th Congress of the International Color Association, Proceedings of SPIE Vol.4421(2002.8), pp404-408

3)M.Kono, N.Hara, H.Ohno:Effect of colored light and illuminance levels on subjective Contrast between chromatic Patches and achromatic backgrounds, J.Illum. Engng. Inst.Jpn.Vol.94,No11,2010 pp735-742

Address: Haruyo OHNO, Otemae University, 2-2-2 Inano,Itami,Hyogo,664-0861, JAPAN E-mail: ohnoh@otemae.ac.jp

Changes of Color Names and Coloring Materials in Japan

Norifumi KUNIMOTO
Tokyo Polytechnic University, Faculty of Arts

ABSTRACT

It is necessary to organize the historical changes in the Japanese colors. The color of Japan had several changes historically, and at least three changes exist. The first change is introduction of the color notion in 6^{th} century. Around the 6th century, by trade with the China (such as the Tang dynasty) and the countries of Korean Peninsula, "Saishiki(coloring)", the manufacture of pigments, the notion of color like "Goshiki(5 colors)" were conveyed to Japan. After that, various color names appeared in Japan. The second change took place in Heian period. After 10^{th} century, enhancement of the Japanese culture led to the development of literature, dresses and their ornaments at salon culture in the Court. In this time, new color "Kasane" was created in dresses. It describes the colors which layered or put in order and likened the color to the plants or the natural phenomenon. From this time, some colors even if they were made of another color materials had been called as the same color names.The third change is change to the new coloring materials. In Europe, synthetic dyes was developed in the 19th century, and the "painting" changed. In Japan, at the Meiji Restoration, "Westernization" was called for. Then the inflow of techniques and materials of oil painting and watercolor painting took place. Simultaneously, the color theories developed in Europe were also brought to Japan. The color mixing and the three primary colors were studied immediately in Japan. After passing through such changes, some "new" colors were come to be called by color names of "old" materials. Since the situation of such multistory changes are not researched, this research organize the historical change of "the color of Japan", and it clarifies the multi-layered color names of Japan.

1. INTRODUCTION

It is difficult to define "The color of Japan", because has a various color names and color materials. Therefore, it is necessary to organize the historical changes in the Japanese colors. If you look at the historical change of color names, materials and theories, you would recognize three major changes. In order to organize complex color names and materials about "The color of Japan", I would like to arrange the historical changes of colors in Japan.

2. THE FIRST CHANGE

The first change is introduction of the color notion in 6th century. Before that, a few natural dyes and mineral pigments were already used in Japan. Because of the lack of the historical materials, the actual circumstance of formation and classification about color names are not clear. There were also few coloring materials used as pigments. Around the 6th century, by trade with the China (such as the Tang dynasty) and the countries of Korean Peninsula, "Saishiki(coloring)", the manufacture of pigments, the notion of color like

“Goshiki(5 colors)” were conveyed to Japan. After that, various color names appeared in Japan. "Goshiki" is five colors about "red", "blue", "black", "white", "yellow". Goshiki is a concept that was associated with the five elements (Wu Xing), and is also a systematic color classification (Figure 1). Wood represents green which include blue. Fire represents red. Earth represents yellow. Metal represents white. And Water represents black. In China, the five colors is important as a formal color. Before the five colors introduced into Japan, red color of Aka-Tsuchi(赤土 minerals of red clay), and blue green color of Yama-Ai(山藍 plants of Mercurialis leiocarpa) were familiar colors in Japan. The first Japanese colors were considered to be those colors.

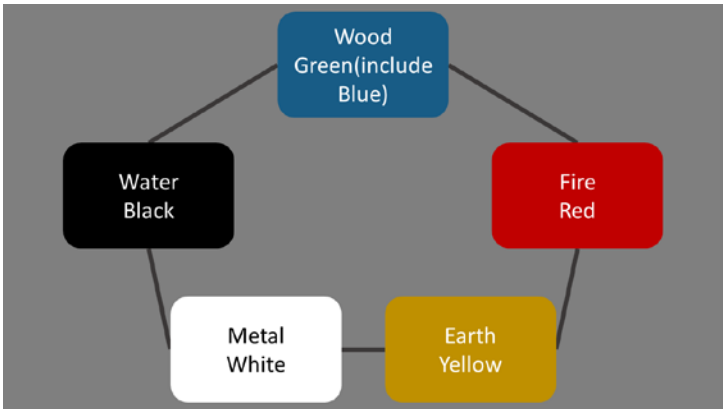

Figure 1: Gogyo and Goshiki(5 Elements and 5 Colors).

Berlin and Kay pointed out establishment order of color terms. It is white and black is first established, and then the red, yellow, and green is followed[1]. Satake Akihiro consider the "Aka(red)", "Kuro(black)", "Shiro(white)", "Ao(Blue)" has been established from the representation on the initial literature of Japan. He thought that Aka comes from Akarui(bright), Kuro comes from Kurai(dark) , white comes from is Shiroi(clearly), Ao comes from Aoi(vague) (Figure 2). However after introducing of the five colors to Japan, due to strong influence by the culture of Chinese characters, the Japanese idea of the color comes the five colors as it base.

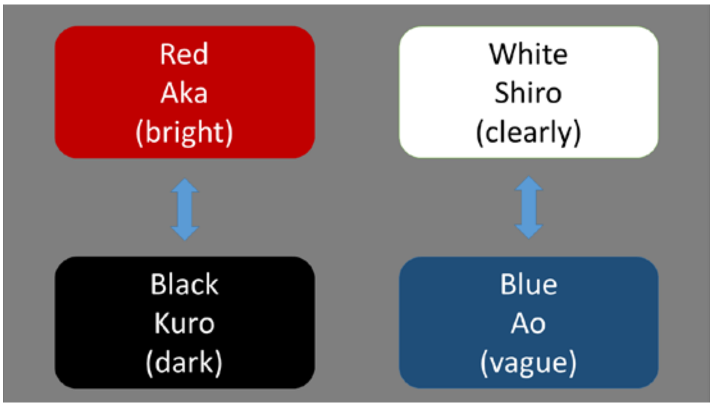

Figure 2: Appearance of Japanese Color Names.

---

[1] Brent Berlin, Paul Kay 1969(1999).*Basic Color Terms: Their Universality and Evolution.*University of Chicago press 1999 14-25.

3. THE SECOND CHANGE

The second change took place in Heian period. The abolition of official envoys to Tang dynasty, and the imitation of the Chinese Tang culture were over at the end of 9th century.The pigments of pictures and sculptures like "Syusa(朱砂)", "Konjyo(金青)" and etc were scribed in manuscripts "Shosoin-Monjyo" of the 8th century. At that era, various pigments were obviously classified and were used.Color name of material derived have been written many in "Shoku-Nihongi" and "Shosoin-Monjyo" of the 8th century.By construction of Todai-ji Temple has been made as a national business, Buddhist art was developed. And production of paintings and sculptures has been actively produced. The many kinds of coloring materials inscribed on the historical materials indicates that the understanding and arrangement of the color materials and color names were made. However at 894 AD, Japanese missions to Tang dynasty were abolished, and the era of imitation of the China's Tang culture was finished. After 10th century, enhancement of the Japanese culture led to the development of literature, dresses and their ornaments at salon culture in the Court. In this time, new color "Kasane" was created in dresses (Figure 3). It describes the colors which layered or put in order and likened the color to the plants or the natural phenomenon(Figure 4). While new many colors appeared as Kasane, the discovery and development of new color materials weren't made. However, increasing of rich color expression in conjunction with development of the literature had represented the extension and understanding of Japanese color cultural development.

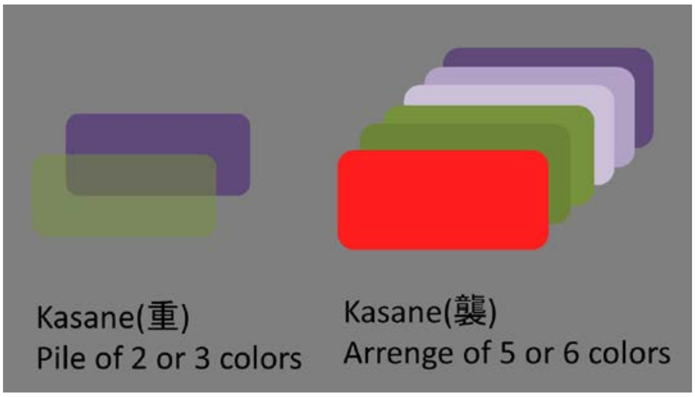

Figure 3: Images of Kasane colors.

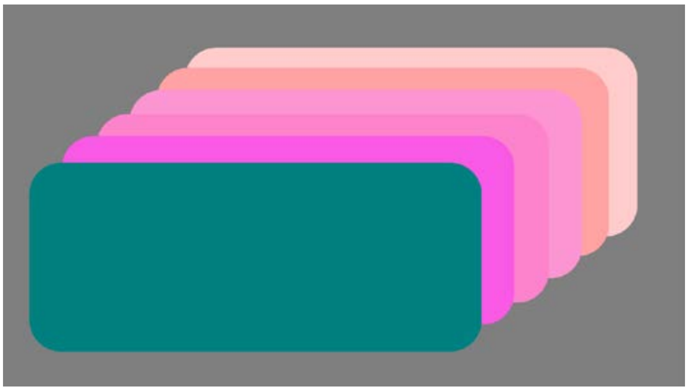

Figure 4:Mood of Kobai（紅梅 Japanese apricot, Prunus mume）color, from “Masasuke Syozoku-syo” Historical Material of Heian period.

Before introducing of 5 colors to Japan, the color name had been represented by the materials. However, the skill and knowledge of the dye plant cultivation which continued from Asuka and Nara period had begun to be lost gradually. From around this time, some colors even if they were made of another color materials had been called as the same old color names. Because of that, the Japanese color names have such overlapping complexity. And, the establishment of this multi-layered color names was not limited to the Heian period, and was occured gradually.

4. THE THIRD CHANGE

The third change is change to the new coloring materials. In Europe, synthetic dyes were developed in the 19th century, and the "painting" had changed. In Japan, through the Meiji Restoration, "Westernization" was called for. In either politics, economy, industry or culture, Japanese people were willing to learn the knowledge and technology of the West. This circumstance was same in the arts. Then the inflow of techniques and materials of oil painting and watercolor painting took place. Furthermore it brought about change of the coloring materials of Japanese fine arts and traditional handicrafts. In the Meiji era, imported European coloring materials had to be called in more than one color name which called the color names from European pronunciation and Japanese color names. In addition, assigned Japanese color names to imported materials were meant sometimes another color material. Simultaneously, the color theories developed in Europe were also brought to Japan. The color mixing and the three primary colors were introduced and studied as soon also in Japan. Theories of George Field (1777–1854), David Brewster (1781–1868), Hermann von Helmholtz (1821–1894), James Clerk Maxwell (1831–1879) et al were introduced. As the expansion of color science in Japan, there was "Shikisai-Gaku (Color Science)" by Michiya Yano to introduce a lot of knowledge about color science of Europe, and there was remarkable teaching at the field of art education by Shirahama Akira. In addition, "Shikisai Shin-Ron" of Beisaku Taguchi was the first Japanese color theory. "Beni(紅 red of safflower)","Yellow (Yellow)","Ai (藍 Blue of Indigo)" had written as the three primary colors in that book. It was remarkable that "Beni(red)" and "Ai(blue) had been written as color classification.

Figure 5: Beisaku Taguchi,"Shikisai-Shinron"

5. CONCLUSIONS

Thus, after three major changes of colors, Japanese color has been established. Currently, some "new" colors may be referred as the color name of "old" materials. For example, the color with a name such as "Roku-Syo(緑青 Malachite)" and "Gun-Jyo(群青 Azurite)" originally refers to the color material by the natural pigment from around the 8th century. "Dosabi(Patina or Verdigris)" and one of "Shin-Iwa-Enogu(新岩絵具. Colored glass powder which are made from spraying the synthetic dyes) " are called as "Roku-Syo" today.

In the history of Japanese color culture, there have not been studied about major changes as described above. In this paper, I summarized the major changes of Japanese color. Because of such changes of color, there appeared the multi-layered color names. In addition, it was also pointed out emerging about the color of the same color names while different color materials. Then, I pointed out reason for further complicatedness of Japanese color that caused by flowing of European culture to Modern Japan. In order to explore the peculiarities of color materials and color names in Japan, I would challenge deeper investigation and research about the color names and color materials of a turning point of changes of colors in the future.

REFERENCES

Brent Berlin, Paul Kay 1969(1999).*Basic Color Terms: Their Universality and Evolution.*University of Chicago press 1999.

Akihiro Satake.1955.*Kodai Nihongo ni okerru Shikimei no Seikaku*. Kokugokokubun 250 (24-6) 340-346

Norifumi Kunimoto.2013. *Manufacture and selling of paints in Japanese modern era.*Journal of the Color Science Association of Japan 37(3)284-285

Address: Norifumi KUNIMOTO, Faculty of Arts, Tokyo Polytechnic University, Irifune 3-1-6-304 Chuo-Ku Tokyo, 104-0042, JAPAN
E-mails: n-kunimoto@br4.fiberbit.net

"DIFFERENCES IN THE DRAWINGS AND THE COLOR OF THE VIOLENCE IN CHILDREN FROM THREE DIFFERENT CULTURES."

Dra.Georgina Ortiz Hernandez
Universidad Nacional Autónoma de México, AMEXINC
Dra. Mabel López
Universidad de Buenos Aires, GAC

ABSTRACT

The violence is a social phenomenon, that, although it has been present in all the history of the human beings is not inherent to all the individuals, and it is known that the social environment contributes to its development.

The fear produced by the violence is intensified in the child population and that is why we considered important to know what the children think about the violence, how they perceive it and, if it is possible, how they feel it. We seek these answers through two media that are familiar and not dangerous for them: color and drawing. Both are privileged elements for the research of violence through a visual image, the color, informs about the emotional states through the analysis of the meanings and formation of chromatic patterns found in the drawings (Ortiz, 2011). That is why we can say that humans live in a symbolic world of color.

The research presented here in is oriented toward the investigation and the study of the way in which the children draw and color violent scenes, since their drawings will let us know their personal experiences.

Our objectives were:

-To know the influence of the native and urban cultures in the representation and use of colors of violence.

- To know the colors and the meanings that children from ten to twelve years use in their graphic representations of violence and not violence.

We used a qualitative method using rhetorical and semiotic analysis of the images for their interpretation**.**

Key words: Color; drawing; children; culture.

INTRODUCTION

Mexico is one of the countries where the violence has exceeded the criminal limits and it has become a part of the daily environment, in which the children are innocent participants since they live the violence, directly or indirectly in their familiar, academic, and social environments through the media and electronic games.

That is why, to study how children perceive their socio-cultural environment, we use drawings and its components. One of these components is color; through it, we can get information about the assessment of intelligence, mood, psycho-physical development, nature of conflicts and development potential (García González, 2000).

However, although there are common elements in their drawings, regardless their ethnicities, we can say that culture gives different nuances to the drawings according to their natural and social environment (Kellogg Rhoda, 2007). Regarding color, we must remember that it is a communicating element that must be decoded by following the rules of the culture in which it develops, as it is based on meanings of signs and symbols (Ortiz 2010).

Moreover, color is related to emotions (Ortiz, 2011), and they reinforce another kind of expressions like drawing, i.e. they make rhetoric from the graphic expression (López, 2014).

OBJECTIVE

To know, through pictorial manifestations and the use of color, how the culture of their place of origin and development influence the children in their perception of violence.

METHOD

Two traditional methods were used for the analysis of the graphic expressions: the quantitative and qualitative, because there are no general or specific parameters for their study.

The drawings obtained in three different samples will be presented: Nayarit (Lindavista), Guerrero (Chilpancingo de los Bravos, Apaxtla, San Marcos) and Mexico City, the latter in order to point to local differences.

Population and sample

The sample application in Nayarit and Guerrero was discretionary; while in Mexico City sample it was probabilistic. These three samples were different according to the possibilities of the interviewers; the smallest one was from the state of Guerrero, where only 15 children were interviewed. The other two samples were randomly matched with this number, so a total of 45 drawings will be analyzed.

RESULTS

General data

The population was composed by 45 respondents of elementary school students from 5^{th} and 6^{th} grade. Their age range from 10 to 12 years old with a mean value of 11.00 and a standard deviation of 0.7385; 20 (44.4%) were girls and 25 (55.6%) were boys.

Violence

To find out if the respondents were subjected to violence, they answer several questions ranging from family violence to violence perceived in videogames. The results were the following:

- The boys suffer more violent acts (56%) compared to the girls (40%).

- The girls of Guerrero suffer less violence (29%) compared to boys (50%); this situation was opposite in the sample from Mexico City.
- Most of the violence was physical and it was received from a family member, especially in the case of girls (50%). In contrast, the sources of the violence for boys were their friends and schoolfellows (20%), one or both parents (20%) and another family member (20%).
- The places where the violence took place vary according to their gender; for girls it was their own homes and for males the school and the streets.

In the school environment we observed that:

- In almost all the cases, the violence came from the students (42.9% for girls and 50% for boys).
- The sample from Mexico City had the highest percentage of affirmative answers, both in girls (58.3%) and boys (63.6%).

It was also inquired whether the children had suffered any violent situation in the street:

- 80% of the girls and 60% of the boys gave a positive answer.
- The main act of violence suffered by them was physical aggressions.
- 58.8% of the girls had suffered physical aggressions compared to 40% of the boys.

The results of the analysis by entities were:

- Nayarit:
    - 42.9% of the girls suffer physical aggressions.
    - 60% of the boys did not specify what kind of abuse they suffer.
- Guerrero
    - The boys did not explain the situation.
    - The girls preferred not to answer.
- Mexico City
    - The most recurrent act of violence for both, girls (66.7%) and boys (80%), was physical aggressions.

Drawings

By analyzing the drawings of the three different populations, similarities and differences were found.

- The number of characters in the drawings range from 1 to 26
- The statistical mode was 2
- The mean value was 3.68 human figures per drawing.

Some of the similarities found were:

- Most human figures depicted were figurative with different complementary elements such as clothes, decorations and, in some of them, movement.
- Regarding size, in most of them, the aggressors were bigger than the victims.
- The aggressors depicted were mainly men, so it is not surprising that the aggressions were committed mainly against women or children.

The most relevant differences found were:

Nayarit

- For the children in this sample, the violence is an attack on the property of others and, especially, against nature. The main causes are the roads; in them, they draw cars without windows, cars running over pedestrians, or cars transporting people with guns. In one of the drawings, one truck carrying bread is assaulted; this drawing can be an indicator whether of much poverty and hunger or of a very high criminal activity.
- Most of the aggressors cannot be identified because they faces are hidden by masks or bandanas; some of them have empty faces or just have eyes, but their gender can be recognized through other features of the body. Most of them are men.
- In the drawings in which the aggressors have faces, they show happiness or anger when they committed an act of violence. Some of the victims are smiling when they suffer the act of violence.
- The range of weapons used in the acts of violence is not as wide. They used mainly guns, rocks, and knives, drugs and physical strength.
- The acts of violence include blood and dead people.

Guerrero

- The violence against nature did not appear. The aggressions were between two persons, mainly carrying weapons.
- The acts of violence were located in different scenarios such as the house, the school or any place that promotes social relations.
- In this sample, a plurality of identifiable forms of violence (physical, verbal, psychological, gender) was found, mainly because the children drew different scenarios in one sheet.
- The representation of violence lies mainly in men and their faces did not show expressions.
- The blood is present as a characteristic element of physical violence.
- The faces of the victims did not show happiness unlike the sample from Nayarit.

Mexico City

- In this sample, the natural landscapes have completely disappeared and although there are scenes in the streets, most of the aggressions were located in the school environment.

- Fantastic aggressors such as monsters appear, so we can infer that the factor of the media influence is present. We can see this specially in one drawing where the aggressor can also be considered as a victim.
- Regarding the weapons, the guns are preferred as in the other samples.

Colors

As in the analysis of the drawings, similarities and differences between the uses of colors were found.

Some the similarities found in the three samples are:

- Most of the analyzed drawings do not have a background color so, the color of the paper (white) is the predominant one and it is where the drawing is created.
- Regarding the use of color:
  - most of the girls used soft colors while boys used strong shades;
  - the boys used fewer colors than girls;
  - Most participants did not illuminate the faces, so they were white, with the exception of the sample from Mexico City.

The results of the analysis by entities were:

Nayarit

- The most common colors were green, blue and brown. They are used mainly in natural landscapes such as mountains, rivers, trees and flowers.
- Most of the animals in the representations of violence lacked color.
- The colors used in the aggressors clothes, and in some cases in the victims, are darker (regularly black and brown).
- Most of the cars were blue; in contrast with the blue of the sky, they were drawn with darker tones. It is important to mention that they belong to the aggressors.
- The houses depicted showed a wider variety of colors compared to the other two samples, but the preferred color was blue, followed by black, white and yellow.
- Regarding the color of the aggressors, girls perceived it as black and brown.
- The color black was mainly used to hide the identity of the aggressor.
- Unlike girls, boys did not relate directly the color black with the aggressor but with the victim (usually in their pants) and they illuminate the aggressors with the colors red and dark blue.
- The color red represented blood.
- The victims appeared naked to their aggressors.
- The weapons were mainly guns and the most frequent colors in them were white and black.
- All the knives were totally white.
- We also found the use of rocks as weapons, they were mostly brown. We can infer that if they do not have access to "advanced" weapons, they can use things in their immediate context to exert power over others. In one drawing we can see a somber scene abut funerals and cemeteries, where the dark colors are related to emotions of sadness but we can also see a social coexistence of people unlike the scenes of violence that are much more individualized.

Guerrero

It is important to note that this is the poorest group and that when they received the box of colors and they were informed that it was a gift for them, they were so happy that they kept it as something very precious without using it.

- The number of colors used in this sample was lower compared to the other two samples. We found a trend to draw only with the pencil without worrying about the use of color. This trend was observed more in boys than in girls. For this reason, the discussion of the use of color in this group is limited.
- The girls used a greater number of different objects for the characters and a greater number of colors. The trend is similar to the one from Nayarit; they used the colors brown, green and blue that are a true reflection of the things they saw daily in the natural world.
- We observed more frequently the figure of the sun (in the sample from Nayarit we only found one); it generally was yellow or red.
- The dark colors, like the black and brown, are representative of the aggressors for the boys, and for the girls it was the color green; the same color that represented mountains and trees before now represents violence.
- Regarding the victims, we found that both genders draw them with the colors white and red in their clothes.
- The clothes of the feminine characters usually corresponds with the feminine stereotype, thus the color pink was used in them.
- The color red, used for the presence of blood, was found in the aggressors and not in the injured or dead people.
- The tendency to draw colorless faces is still present, but we can observe colors such as pink or yellow in the faces, especially in the victims.
- In the case of the viewers of violence (new characters drawn), we found that they try to pass unnoticed because they are drawn only with a pencil stroke; in just one drawing the viewer has colors but, in this case, there is a house interposed between him and the act of violence.
- The most present weapons were, again, guns; they were drawn only with the pencil, so its color was grey; they were followed by white ties or belts for both genders.

Mexico City

- In this sample, the natural landscapes have completely disappeared.
- The factor of the media influence is present, especially in one drawing where the aggressor, which can also be seen as a victim, is a multicolor Godzilla type character; so, in this visual context we found a tendency to caricaturize the violence. The only color used that was used also in the other samples is the green and, again, it is used in the landscapes.
- The color blue is used more often in the sky than in the water, indiscriminately for both genders.
- The color of the aggressor (or the violence) is the white, this finding contradicts many of the researches which determine that the colors black and red represent this phenomenon; it is true that the color red is still one of the mostly found in all the samples in this research, but the color black is more related to the victims (except in girls where it is related to the aggressors) and the color white (in boys) is most related to the clothes of the aggressors.
- The color of the faces in this sample is more varied, the flesh color is more used and also the brown to represent brown skins, that in most drawings are from the aggressors, especially for the girls in both, Mexico City and Guerrero samples.

- Regarding the weapons, the guns, the preferred weapons along all the research, are represented more frequently with the colors white and black.

Comparatives

The results of the comparison of the three samples are the following:
BACKGROUND:

- The color of the space or the place represented mostly lacked color. In the few cases where the background has color we observe that the most used colors were brown and transparent and in second place green.
- Regarding the use of color by entity, the following chart indicates that the urban sample use the greater number of colors.

Color of the space									
	NAYARIT		**GUERRERO**		**MEXICO CITY**				
Garden					*transparent*	*orange/*	*blue*	*transparent/*	*green*
Street			*transparent*		*transparent/*	*blue*			
Countryside	*transparent*	*green*	*transparent*	*green*	*green/*	*blue*			
House	*transparent*								
Driveway	*transparent*								
Town	*transparent*	*green*							
No determined	*transparent*		*transparent*		*transparent*				

Characters:

- We found a maximum of 10 characters.
- By analyzing the color of the characters in the drawings of violence we found that:
    - Most of the girls did not illuminate the faces
    - The second more used color were flesh color.
- In the Nayarit sample we found that the aggressor used Balaclava helmets, so their faces were black.
- The faces of most of the characters that were not covered were colorless.

Color of the face			
Nayarit	*transparent*		
	flesh		
	black		
	brown		
Guerrero	*transparent*		
	yellow		
	blue		
Mexico City	*flesh*		
	pink		

	orange
	transparent
Total	*transparent*
	flesh
	pink
	brown

- Regarding the color of the accessories, we found that the most used was the black; again, it was the urban sample the one that used more colors.

Colors in accessories										
	NAYARIT					**GUERRERO**	**MEXICO CITY**			
Buttons							*red*	*green*		
Horns							*red*	*green*		
Hat/cap							*black*			
Hair accessories							*pink*	*orange*	*purple*	*black*
Belt	*green*	*black*	*yellow*	*blue*	*brown*	*transparent*				
Balaclava helmets	*green*	*black*				*black*				
Bracelets			*yellow*							

Weapons

The results regarding weapons were the following:

Colors in weapons											
	NAYARIT				**GUERRERO**			**MEXICO CITY**			
Guns	*grey/ pencil*	*transparent*	*purple*	*black*				*black*	*transparent*	*blood*	*transparent*
Machine guns	*transparent*							*black*			
Panque								*brown*			
Ball								*green*	*transparent /*		*black*
Rifle with bayonet					*grey/ pencil*			*transparent*			
Hands/ fists	*transparent*		*grey/ pencil*		*brown*		*grey/ pencil*	*pink*	*orange*		
Knives	*transparent*		*grey/ pencil*		*transparent*						
Brick/ rocks	*brown*		*transparent*		*transparent*	*brown*	*grey/ pencil*				
Chainsaw	*transparent*		*grey/ pencil*								

Belt		*black*		
Stick		*transparent*		
Other		*transparent*		

The number of houses in the drawings was also recorded. The results were the following:

- We obtain a statistic mode of 1 and a mean value of 2.8 houses. Most of them were not lit. In most of the cases we found the use of the colors brown, brown and black, and blue.
- In Mexico City sample we found one case of a house painted with color blue.
- In Nayarit and Guerrero samples there was a trend of not using colors in most of the cases.

Colors in houses		
Nayarit	*Transparent*	
	brown/	*Black*
	blue/	*Purple*
	red/	*Orange*
	Green	
	Blue	
	Brown	
Mexico City	*Blue*	
Guerrero	*Transparent*	
	Brown	
	red/	*Yellow*

Curiously we only found land transports in the sample from Nayarit, because for them, the driveways and vehicles are signs of violence.

Colors in transports					
	NAYARIT				**MEXICO CITY**
Airplane					*Transparent*
Car	*pink*	*purple*	*black*	*orange*	
Van	*blue*				
Truck	*Transparent*				

Regarding another elements present in the drawings where color was used, we found the following:

- In most cases, they were colorless; however, we found the use of the colors brown and green followed by the filling with the pencil and the black.
- In Nayarit, the most used color in these objects was blue, followed by brown and green, related to nature.
- In Guerrero it was more common to let them colorless, but in second place was the use of the black, followed by red.
- In the sample from Mexico City, there was only one case of using of the color red.

Colors in another elements						
	NAYARIT					
Flowers	green	red	orange	transparent		
Lake	blue	pencil				
River	blue	brown	transparent	green	green/ white	/red
Rock	brown	pencil	green	blue		
Smoke	pencil	brown	transparent	blue	black	orange
Bag/briefcase with money	green					
Road/ driveway	blue	brown	transparent			
Cigar	pencil	brown	transparent	black	blue	orange
Balaclava helmet/mask	black					
Bushes	green	orange	transparent			
Flag	green	blue	green/ white	red		
Mountains	blue	transparent	pencil	green	orange	
Fence/wall	brown	pencil				
Grass	green	blue	red	brown	Green/ white/	red
Tomb	blue	brown	transparent			
Casket/coffin	blue	brown	transparent			

Colors in another elements				
	GUERRERO			
Flowers	Red	transparent	brown	
River	Red	transparent		
Smoke	Black	transparent		
Bag/briefcase with money	Black	transparent	pencil	yellow
Road/driveway	transparent			
Cigar	Black	transparent		
Balaclava helmet/mask	Black	pencil	yellow	transparent
Mountains	Brown	red	transparent	
Grass	Green			
Deer	Red	transparent		
Ball	transparent			
Rocks	Brown	black	red	transparent
Jewels/valuables	Black	yellow	pencil	transparent
Public lighting	Black	yellow	pencil	transparent

Colors in another elements	
	MEXICO CITY
Balloon	Red

CONCLUSIONS

When we analyzed the drawings we found that the respondents were in the first phase of the **intellectual realism** (Loquat, 1978) in which they draw the things they see and they try to copy the models represented as well as elements that are visible. Although in this phase, they also use items that should not be visible, this situation, in turn, causes the suppression of visual elements that are not important for them, so they recurred to the use of transparency, although, few cases were found in this report.

Other characteristics of this phase that we found in the analyzed drawings were the lack of perspective; this allowed them to put the maximum possible number of elements in certain form, so the quadrupeds, birds and fish are always in side face while the human figures are always frontwards.

Regarding our objective, we found that the differences are greater than the similarities. This confirms the hypothesis that the natural environment has an influence in the use of the perception of violence through drawings and colors in the drawings of violence.

Such differences were, among others, that in the sample from Nayarit, we can see a widespread concern for the natural environment manifested in the excessive presence of driveways. In this research, the brown or grey driveways were interpreted as violence to the natural environment, disappearance of nature for purposes of modernization / urbanization.

This situation was different in the sample from Guerrero, a place that, in the last few years, has been characterized by high levels of violence. This maybe the reason why the children visualize violence in their social environment and some of them included in different planes different scenes, that although they are related with the general subject their characters, scenarios and objects are not related with each other.

It is important to highlight that although the box of colors was a gift for all the participating children, the group from Guerrero chose to keep them instead of use them and that when they received it, they showed an expression of joy and surprise as if they had never had a gift like this.

BIBLIOGRAPHY

Fernández S., F. (2007) Dibujo de la figura humana: Análisis del funcionamiento diferencial de los criterios en la Revista Interamericana de Psicología /interamerican Journal of Pschology 2007 vol 41 num. 2 pp 215-220

Rhoda Kellogg Child Art Collection. Washington, DC., Microcard Editions, Inc., 1967. Digital Reedition: Birute Gujer, Dieter Maurer, Claudia Riboni, Karin Wälchli. www.early-pictures.ch/kellogg/, 2007. (Technique and Design: Christian d'Heureuse, Jürgen Ragaller)

Luquet (1978) El dibujo infantil. Barcelona, médica-técnica. Madrid

Ortiz,G. (2011) El significado de los colores. Editorial Trillas. México

Ortiz G. (2014) Usos, Aplicaciones del Color. Editorial Trillas, México

Puleo, R. E. (2007) Análisis comparativo de dibujos infantiles en niños(as) de la ciudad de Mérida (1-6 años de edad) tesis de licenciatura Universidad de los Andes Venezuela

Scott , L:H: (1985) Measuring inteligence whith the Goodenough Harris Drawing Test. Psychological Buletin 89,1, 483.505 citado por Fernández

COLOR AND IMAGE OF THE CITY IN ENVIRONMENTAL DESIGN OF KAZIMIR MALEVICH

Yulia GRIBER,
Smolensk State University

ABSTRACT

The article is devoted to the description and the systematization of Malevich's strategies for color design in urban space. The article demonstrates the ideas of Malevich on how color functions as an important symbol in environmental design and how a new color 'edition' helps to change the impressions about the existing social structure of urban society, and also serves as a means of promotion of some quarters, districts and even whole towns. The text contains the description of the main results of Malevich's experimental research into the role of color in the built environment. These studies include the principles of color organization of the scenic architecture, Suprematism facade coloration, and architectural painting of Malevich, implemented in 1919 in Vitebsk. The principles of form and space organization in Malevich's projects are analyzed. The color structure, color constellations, and how they contribute to the creation of image and spatial illusion in the city are characterized. An important aim of the article is the examination of the impact of unique methods and ideas of Malevich on contemporary and subsequent architectural color usage. In particular, it reveals the link between the work of Malevich and Russian avantgarde projects, especially to abstract axonometric compositions of geometric solids such as the Prouns of El Lissitzky. It also shows the ways in which the ideas on environmental color design of Malevich continue to exist in the modern popular culture of the city.

1. INTRODUCTION

Kazimir Malevich is well known as a prominent painter. However, he also had a lot of interesting ideas about color environmental design, and his town-planning painting had a significant impact on the color development of cities.

2. METHOD

As the basic research method was used a complex (integrated) approach based on the appropriate methodological arsenal. An important means of this study was a comparative analysis and its methodology as well. A case study using such field methods of qualitative research as project analysis and historical documentation of color, content analysis, comparison of individual cases and a systematic qualitative data analysis was conducted by the description of the Malevich's scenic architecture, his Architectons and Planits, projects of spatial Suprematism, facade coloration, and architectural painting, implemented in 1919 in Vitebsk.

3. RESULTS AND DISCUSSION

The starting point of the research was the thesis that we have been using color to create idiosyncrasies in urban space as long as we have been living in cities. Color in a city is accessible to individual citizens or "actors" who desire a means of "self-expression" and "impression management" (Goffman 1959) they wish to make upon others. However, together with these individual actors in the color space of the city we find collective actors as well, and the influence of these actors on color characteristics of the city is much more essential. Having a great amount of resources, the collective actors "modify the city" by use of color. Collective actors can create color illusions implying that urban spaces have particular qualities that are not present in reality.

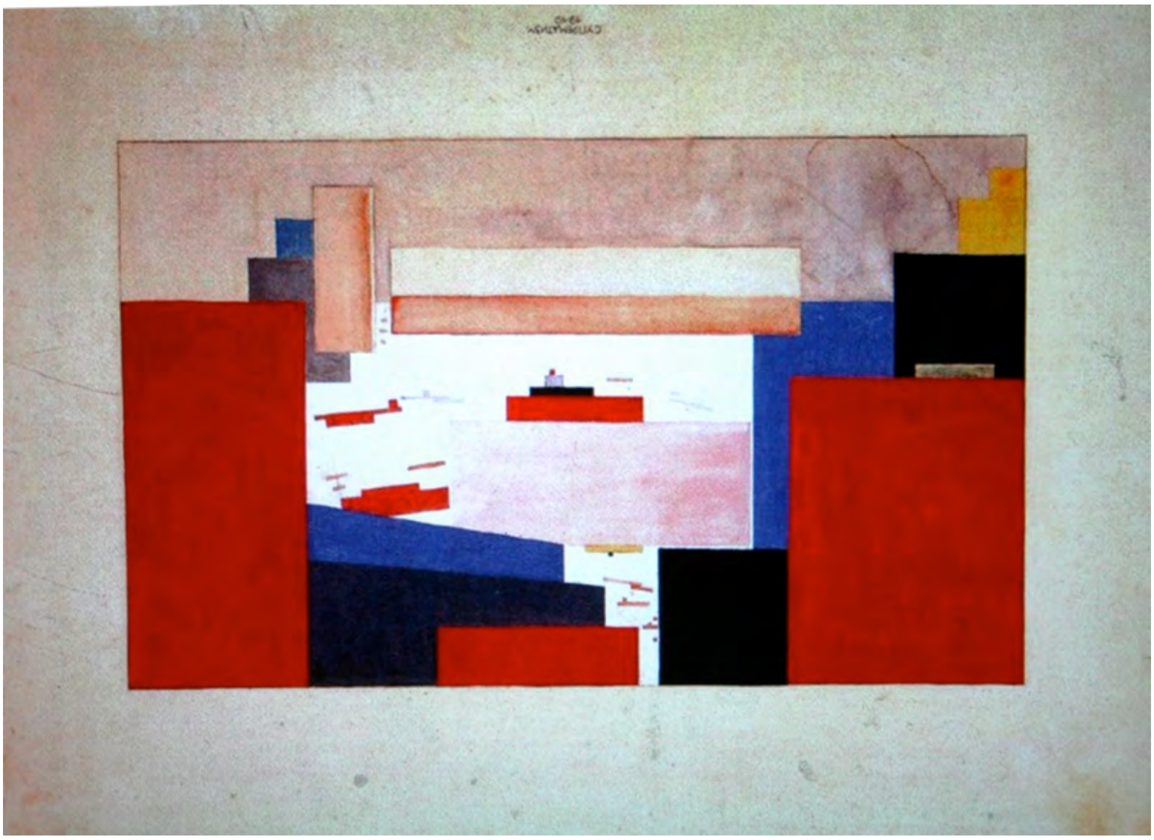

Figure 1: Kazimir Malevich. Study for a curtain (1919).
Source: cultobzor.ru

3.1 Philosophy of Malevich

The political power of color in the color design of urban space was extensively used in socialist societies. Architects were working at the creation of a visual environment that corresponded to the socialistic structure. A rather exact and idealized image was produced, which transformed the architecture itself.

Malevich obviously realized that socialism changed not only the political system but also the ideology of people. It created new conditions for the development of color planning and urban color design, forced new ways for the production and distribution of color images in urban culture. His idea was that architects could not get rid of the existing architecture; however, they were able to use that accumulated architectural material as a basis for expressing new ideas and creating a new image of the city by means of color.

Malevich considered color as an important symbol in environmental design. His idea was, that a new color “edition” can help to change the impressions about the existing social structure of urban society, and also can serve as a means of promotion of some quarters, districts and even whole towns.

3.2 Malevich’s projects

The main results of Malevich’s experimental research into the role of color in the built environment include the principles of color organization of the scenic architecture, the Architectons and Planits, the spatial Suprematism, facade coloration, and architectural painting of Malevich, implemented in 1919 in Vitebsk.

The scenic architecture of Malevich was his first experience of color design in three-dimensional space. As a stage designer of the Futurist opera “Victory over the Sun” premiered in 1913 in Saint-Petersburg he intended to underline parallels between literary text written in zaum[1] language by Alexei Kruchenykh, musical score written by Mikhail Matyushin, and the art of painting and the color (Figure 1).

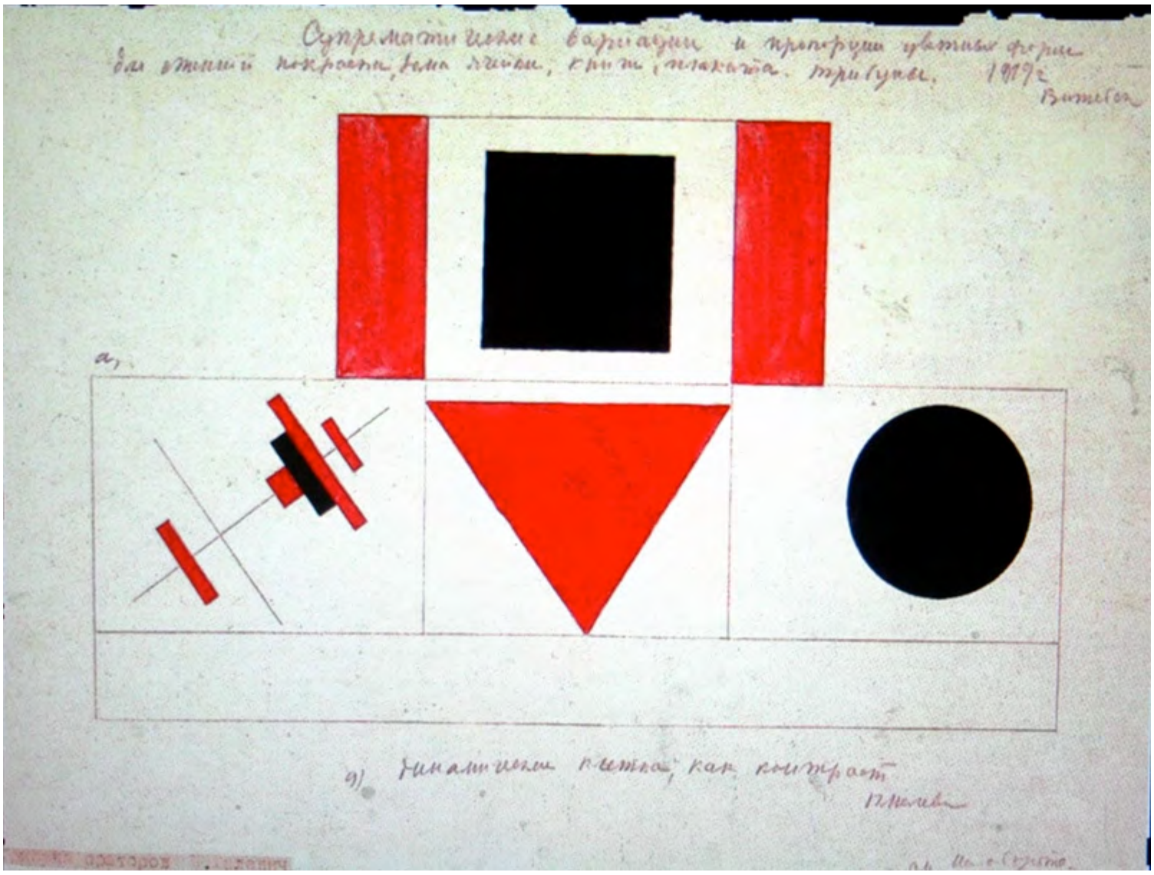

Figure 2: Kazimir Malevich. Design for the speaker's rostrum (1919).
Source: Arskaya et al. 2000

In 1919, during Malevich’s tenure (1919–1922) in the Soviet town of Vitebsk, Malevich’s spatial Suprematism confronted the real built environment. The Vitebsk experiment involved many different objects of urban space: Malevich and his disciples

[1] Zaum (Russian: за́умь) are the linguistic experiments in sound symbolism and language creation of Russian-empire Futurist poets such as Velimir Khlebnikov and Aleksei Kruchenykh.

created drawings for murals on buildings and interiors, signboards for the stores and shops, propaganda panels that decorated the sides of streetcars, speaker's rostrums (Figure 2), and even the decorations on the ration cards used during the period of War Communism, crockery, textiles.

The prominent filmmaker Sergey Eisenstein depicted his reception of the transformation of "sooty and cheerless" provincial city, typically "built of red brick" into a Suprematic one:

> But this city is especially strange. Here the red brick streets are covered with white paint, and green circles are scattered around this white background. There are orange squares. Blue rectangles. This is Vitebsk in 1920. Its brick walls have met the brush of Kazimir Malevich. And from these walls you can hear: 'The streets are our palette!' (Eisenstein 1963: 279).

3.3 The principles of form and space organization

The essential characteristic of space representation in the town-planning painting of Malevich was the "two-dimensionality" of the basic forms he used in the urban space decoration (Figure 3). All the compositions comprises the same repeated elements – squares, circles, crosses, triangles of various sizes and colors, vivid against the typical of Malevich's Suprematism white ground. The white canva was for him a field of pure light, a means emboding infinite space with no gravity inside. Spread over the façade both horizontally and vertically, the dynamically distributed colored forms of various sizes were included in a series of smaller and more complex compositions. Dynamic positioning of shapes testified to Malevich's desire to restructure the rigid solidity of the original building while creating a feeling of "non-objectiv" environment.

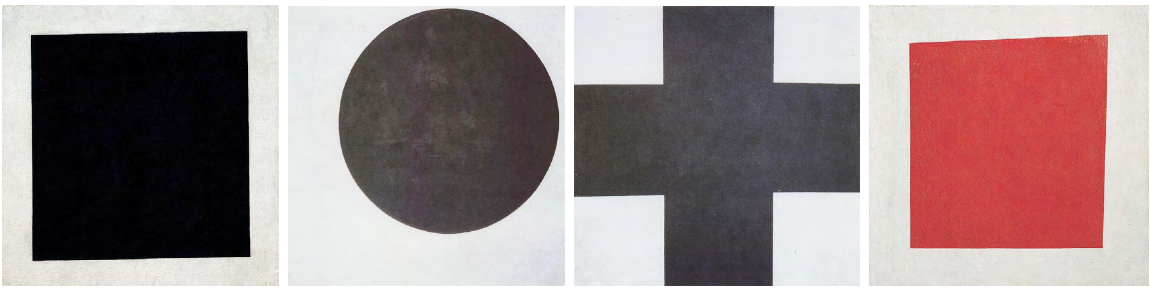

Figure 3: The basic Suprematism forms. The Black square (1923).The Black circle (1923). The Black cross (1923).The Red square (1915).
Source: Arskaya et al. 2000

3.4 The color structure

In urban space Malevich knowingly used a simplified coloration. The color system of the town-planning painting of the artist had a definite brief structure. Two main colors, the black and the white, were used in it. These two colors had quite clear and well-defined semantics. Malevich considered the black as "the most concentrated materiality" and "the sign of economy". The white was identified as "nonfigurative art", "renovation", "purity", "order", "high geometry of consciousness" (Malevich 2001: 80). All other colors did not have any expressed independent fixed symbolism in the art concept of Malevich. They were identified and semantically belonged to the third class. Only symbolism of the red was mentioned in some of his works as a "signal of revolution" (Malevich 2001: 80).

Thus, Malevich created the color dictionary of his town-planning painting, abandoning the symbolic meanings of a number of colors and shades, eliminating their cultural meanings. Similar "color blindness" was typical of the early stages of the color language evolution, the basic principles of which were affirmed in the works of Berlin and Kay (1969). In particular, just the same tendency was evident in the language of the African tribe Ndembu. Recurring one of the early stages of the color terms development, the color dictionary of the town-planning painting of Malevich was based on the three-termed classification. Such a parallel is not unique in the history of art and indicates that different types of color simplifications continue to exist in the artistic consciousness, repeating certain stages in the evolution of color language.

3.5 The impact of Malevich's ideas on architectural color usage

The unique methods of Malevich (the two-dimensionality of basic forms, color-structuring of space, etc.) and his architectural ideas on spatial Suprematism have the great impact on contemporary and subsequent architectural color usage. In particular, there is an evident link between the work of Malevich and Russian avant-garde projects, especially to spatial Suprematism and abstract axonometric compositions of geometric solids such as the Prouns of El Lissitzky (Figure 4). The ideas on environmental color design of Malevich continue to exist in the modern popular culture of the city, where they work rather as metaphors (Figure 5).

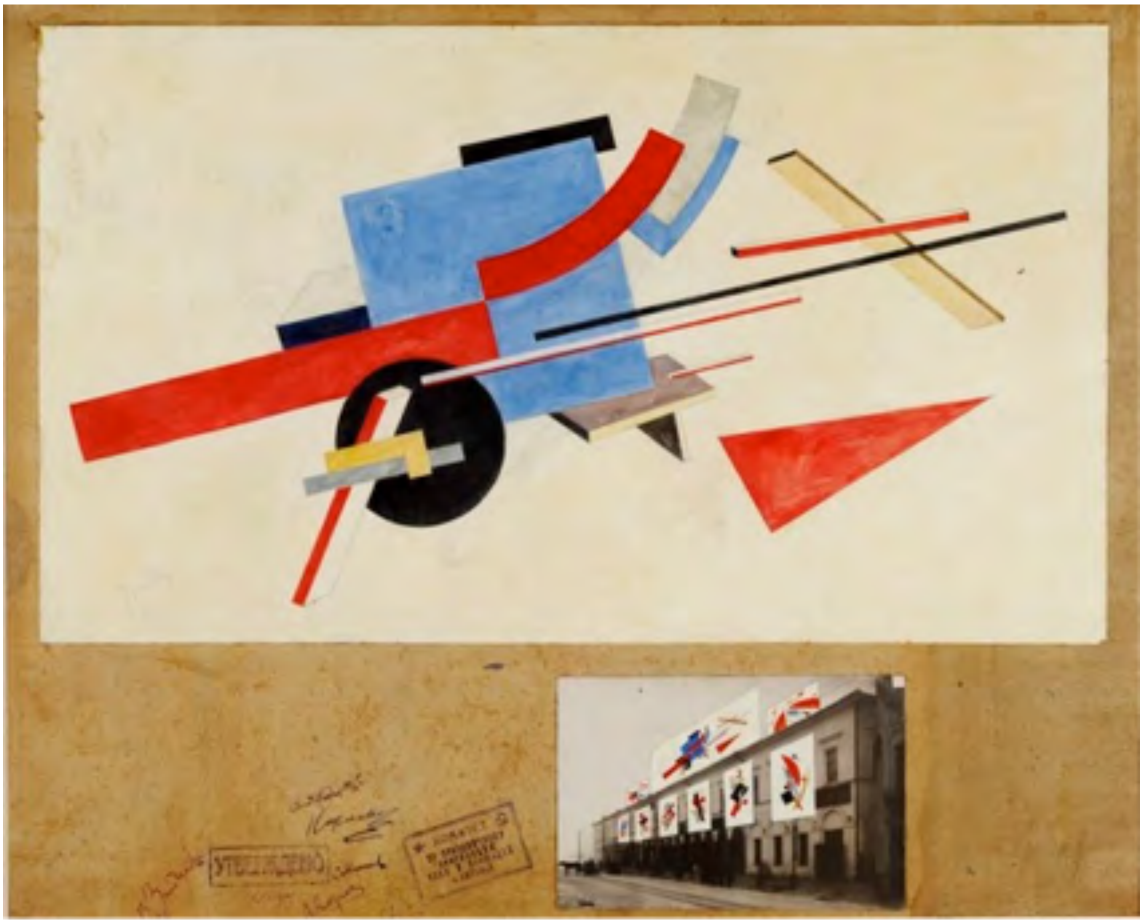

Figure 4: El Lissitzky. Study for a builging exterior in Vitebsk (1919). Source: designblog.rietveldacademie.nl

4. CONCLUSIONS

Malevich’s ideas on urban color design have the great theoretical importance to the development of conceptual and methodological approaches toward the study of color phenomena in environmental design. The systematization of Malevich’s strategies of color planning has not only theoretical but practical significance as well. This is a new chapter in color education, and will be used in the restoration and reclamation of monuments as well as in new construction and city image developement.

Figure 5: The residential area “Malevich” (Yekaterinburg, Russia)
Source: us-invest.ru

ACKNOWLEDGEMENTS

I wish to acknowledge the help during the planning and development of this research work provided by the Malevich Society.

REFERENCES

Arskaya, I. et al. *Kazimir Malevich in the State Russian Museum.* 2000. Saint-Petersburg: Palace Editions.

Berlin, B., and P. Kay. 1969. *Basic color terms: their universality and evolution*. Berkeley: University of California Press.

Eisenstein, S. 1963. Zametki o V.V. Mayakovskom [Notices about V.V. Mayakovskiy]. In *V.V. Mayakovskiy v vospominaniyakh sovremennikov*. Moscow: Izdatel'stvo khudozhestvennoy literatury.

Goffman, E. 1959. *The presentation of self in everyday life.* New York: Doubleday Anchor.

Malevich, K. 2001. *Chernyy kvadrat [The black square].* Saint-Petersburg: Azbuka.

Address: Prof. Dr. Yulia GRIBER, Department of Sociology,
Smolensk State University, 4 Prshevalskiy Street, Smolensk, 214000, RUSSIA
E-mails: y.griber@gmail.com, julia_griber@mail.ru

Comparative Study about Preference Tendency to Spatial Color Based on Color Recognitions and Emotions among Nations: Focused on Korean and Malaysia

Ji-Young OH[1], Heykyung PARK[1], Mai NEO[2], Jian-Yuan SOH[1], Min-Jae LEE[1],
[1] U-design Department, Design Institute, Inje University
[2] Faculty of Creative Multimedia, Multimedia University

ABSTRACT

Korea is changing rapidly from a single-raced nation into a multi-national due in part to the increasing number of Chinese and Southeast Asian immigrants. This gives rise to a multitude of social problems, one of them being the difficulties faced by children of the second generation multi-cultural families who enroll to elementary schools in Korea. This should be solved urgently as it is predicted to be an unavoidable problem in future. Only by understanding and accepting mutual cultural differences will the solution to these multi-cultural societal problems be remedied. This study aims to investigate the differences in preference tendencies among nations with respect to their recognition of colors and emotions within spatial color environments. The study's sample consisted of Korean and Malaysian design students, whose colour preferences and vocabulary appraisals of the environmental colors in Korean school health rooms were solicited. The collected data was analyzed to ensure the reliability and the results show strong support for comparison studies on colour preferences among nations.

1. INTRODUCTION

In South Korea today, foreign workers from China and Southeast Asia have been growing in numbers due to the economic shortcomings of their home countries. This increasing number of foreignen workers in South Korea is causing the number of multicultural families to increase, and consequently, results in cultural and social conflicts and problems. Due to this globalization, these second generation immigrants enroll into Korea elementary schools. As such, these younger generation begin to experience maladjustment and difficulties. Therefore there is an urgent need to solve the problem as soon as possible. Since 2003, the Ministry of Education of South Korea organized the "Health Room Modernization" program as a means to solve this problem. The result of this initiative is the design and development of elementary school health rooms. These elementary school health room should include health guidance, prevention education and counseling.

As the multi-cultural society continues to grow, there is a need to educate the younger generation to recognize and understand the color changes of the environments. This can be done through understanding the differences between cultural sensibilities, which, in turn, would help alleviate these cultural conflicts and problems. Limberg (2000) has claimed that color could influence the feelings and emotions of a human with a very strong impact, Schmitt(1995) concurs and states that color has a significant influence on people's feelings and emotions. Every color has different meaning depending on the person's culture, so it is important to understand the difference between perception and color preferences of each culture. Therefore, this study aims to identify the characteristics differences between two countries, Korea and Malaysia, and investigate their sensitivity in color perceptions and color preferences.

2. METHOD

2.1 Composition of health room color

The "Korean Government's Health Room Modernization Service" was conducted in 10 Elementary School health rooms (A-J) in Busan, South Korea. Our research team went to all 10 locations, using a spectroscopic to collect the color data, took some photographs and collected information about each school. Looking at the configuration of colors of each, only one main color was been applied to the floors YR(90%); for walls, there were two similar main colors with similar hues YR(43.6%), Y(41%); and for furnitures, a variety of colors was applied Y(32.5%), GY(32.5%), YR(20%), G(5%), B(5%). This was seen through all 10 schools observed. Table 1 shows the distribution of spatial colors in each of the health rooms.

Table 1. Distribution of health room's spatial color

School	A	B	C	D	E
Space Image					
색상 분포도	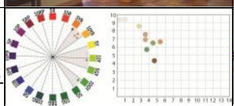	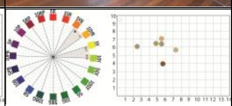	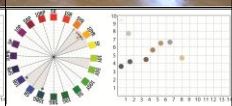	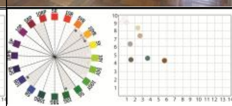	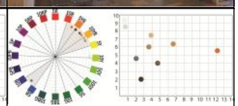
School	F	G	H	I	J
Space Image		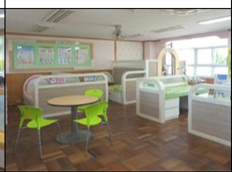			
색상 분포도	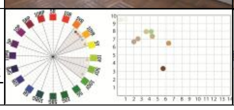	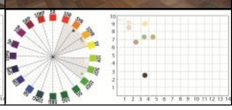	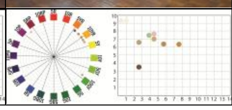	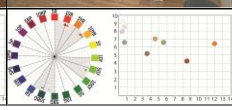	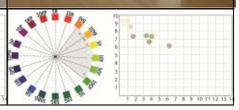

Each health room used most of the nine colors, and YR, where the Y color was seen to be used as the main color. School B had less colors configurations, and thus presented the simplest color scheme. School I's health room had a total of 6 colors, and was the school with the most color scheme. Color YR was seen to be the color most often applied, approximately 3-4times. School A applied the most YR as its main color, whereas color Y was applied most frequently in school B. School C's Value and Chroma levels were both heavy and appeared to be have the least decent color scheme, where as School J had high Value but low Chroma levels, and appeared to have the color characteristics of softness. Schools E and I appeared to have the most contrasting colors, where its colours had high saturation levels, which resulted in strong color contrast characteristics in its the applied colors.

2.2 Survey

To investigate the differences between Korean and Malaysian preferences and emotional state towards these health room environments' colors, a survey was conducted on a sample of 160 students. These students were made up of Koreans (males = 26, females = 54) and Malaysians (males = 29, females = 51). They were asked to choose a color to symbolize their country, follow by their most preferred and least preferred color palette color among the 10 School health rooms. Following that, they were then give the emotional evaluation form, which would solicit their preferences with respect to the health rooms' color environment.

3. RESULTS AND DISCUSSION

3.1 Koreans and Malaysians Perception of National Color

In order to examine the cognitive aspects of color of each country (South Korea and Malaysia), students were asked to choose a color that they felt symbolized each country. As shown in Table 2, Korean subjects reported Red (55%) and White (31.3%) colors to symbolize their nation, due on part to the effect of both the uniform color of the Korean football team (Red Devil) as well as the notion of White representing the Korean traditional spirit. On the other hand, In contrast, Malaysian subjects reported White (37.5%), Red(26.3%), Blue(25%) to symbolize South Korea, mainly because of South Korea's national flag and their perception of South Korea as a clean and high-tech industry.

Table 2. Korean and Malaysian's perception of symbolic color for the two countries

	Korea's symbolizing color										Malaysia's symbolizing color									
Color	Red	Orange	yellow	Green	Blue	Purple	Brown	Black	White	Etc.	Red	Orange	yellow	Green	Blue	Purple	Brown	Black	White	Etc.
Korean (%)	55	2.5	1.3	0	10	0	0	0	31.3	0	10	27.5	16.3	31.3	3.8	1.3	8.8	0	1.3	0
Malay (%)	26.3	0	1.3	2.5	25	5	0	1.3	37.5	1.3	35	3.8	21.3	8.8	31.3	0	0	0	0	0

The Korean subject provided a variety of colors to symbolize the country Malaysia, with Green (31.3%), Orange (27.5%) being the colours with the highest percentages of students. The answer Green was chosen because of the green plants and fruits representive of the tropical climate of Malaysia, and the color Orange were chosen as of the color of Malaysians.

According to a study by Abdulrahman (2015), in Malaysia the color Green referred as the color that symbolizes danger and disease. The 31.3% of Koreans who answered that the color that symbolized Malaysia was Green will indicate shortage of recognition and may cause disrespect to the Malaysian culture, even if a small number of Malaysian answered Green, they appeared to be foreigners residing in Malaysia.

3.2 Environment Color Palette of Preferences and Sensibility Evaluation

Korean and Malaysian students were also asked to pick their three most preferred color palettes and their three least preferred color palettes, which were followed with an emotional assessment survey to elicit the reasons for their choices.

Table 3. Health room's color spatial palette

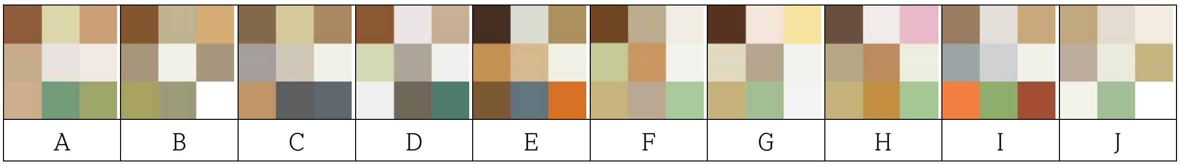

As can be seen in Table 3, the top three colors that Koreans preferred was A, B, and C. These three color palettes have similar low brightness (range: 6.3 - 6.8), and showed that they preferred calm and soft colors. As for the emotional assessment results, Koreans preferred Calm feeling (32.5%), Soft feeling (22.5%), however Clear feeling (12.5%), Breezy feeling (12.5%), and Natural feeling (12.5).

On the other hand, Malaysians was found to favour Natural color feel with high brightness color in palette A, H, J. As for the emotional assessment results, Malaysian students preferred palettes that were similar to the Korean students with highest ratio of Calm feeling (28.8%), follow by Happy feeling (20%), Soft feeling (17.5), Natural feeling (16.3). From Korean student's answers, Happy feeling was the lowest, but interestingly, was one of the highest chosen by Malaysian students. This result showed that Malaysians valued happiness more over Koreans. This is shown in Table 4 below.

Table 4.Emotional Assessment for preferred color palette

Vocabulary	Soft feeling	Clear feeling	Happy feeling	Breezy feeling	Calm feeling	Natural feeling	Others
Korean (%)	22.5	12.5	3.8	12.5	32.5	12.5	3.8
Malay (%)	17.5	7.5	20	7.5	28.8	16.3	2.5

As shown in Table 5, Korean students' least preferred color palette appeared to be E, H, I. Koreans did not prefer a color palette that had high saturation levels, because they felt that the color did not seem to be balanced. As for the emotional assessment results, Koreans did not prefer Muddy feeling (33.8%), Artificial feeling (28.8%). In contrast, Malaysians preferred color palette H, although the Koreans does not. This clearly shows that there is a difference in the color preferences between Malaysians and Koreans.

Malaysians' least preferred color was found in C, D, and E. Generally, Malaysians disliked muddy and dull feelings as shown in the result. Koreans preferred color palette C, although Malaysiana did not appear to like it. This proven even though the same color palette is chosen, people from different cultures can still have completely different emotion feelings towards it.

Table 5. Emotional Assessment for least preferred color palette

Vocabulary	Hard feeling	Muddy feeling	Sad feeling	Dull feeling	Active feeling	Artificial feeling	Others
Korean (%)	5	33.8	8.8	13.8	0	28.8	10
Malay (%)	11.3	21.3	3.8	37.5	13.8	8.8	3.8

3.3 Comparing the Emotional Evaluation on Color Palette and the Scale of Spatial Color Image

In addition, analysis and comparison between the evaluation assessment of color palette preferences and the actual spatial color image scale were conducted. As Table 6 shows, Korean students chose images A, B, C as their most preferred spatial color, because they preferred the Calm feeling, Soft feeling, Clear feeling, Breezy feeling, Natural feeling. This showed that Koreans equally prefer Naturally, Graceful, Decorous colors and partially towards the Elegant color. This result shows that the collected data of evaluation assessment of color palette preferences matches with the actual spatial color image scale.

Table 6 Spatial color image scale

School	A	B	C	D	E
Image Scale	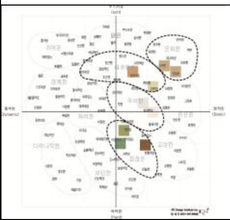	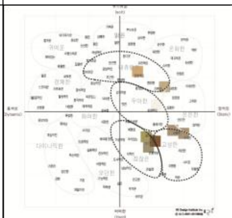	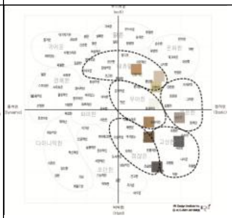	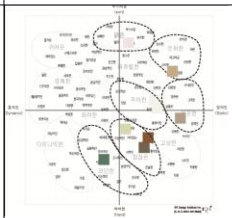	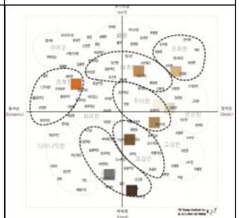
Voca.	Mildly, Naturally, Graceful, Decorous	Naturally, Graceful, Decorous, Elegant	Naturally, Graceful, Ambient, Decorous, Elegant	Clearly, Mildly, Ambient, Graceful, Decorous, Modernistic	Mildly, Graceful, Decorous, Modernistic, Breezy
School	F	G	H	I	J
Image Scale	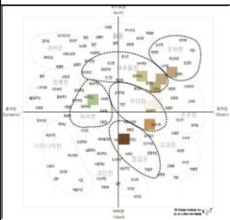	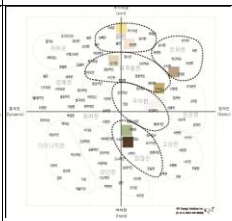	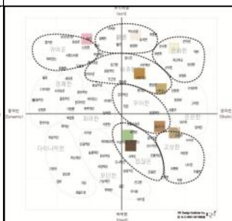	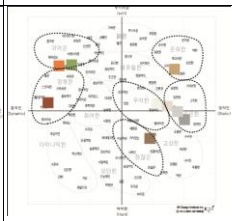	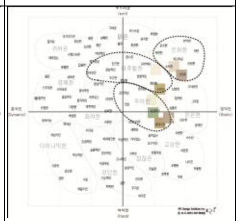
Voca	Mildly, Naturally, Graceful, Decorous, Glamorous	Clearly, Mildly, Naturally, Graceful, Decorous,	Lovely, Clearly, Mildly, Naturally, Graceful, Decorous, Elegant	Lovely, Breezy, Mildly, Ambient, Graceful, Decorous,	Mildly, Naturally, Graceful,

Malaysian students chose images A, H, J as their most prefer spatial color, because they preferred the Calm feeling, Soft feeling, Clear feeling, Breezy feeling, Natural feeling. Malaysians appear to prefer Naturally, Graceful, Decorous colors follow by Lovely and Mildly colors. By analysing the preferred color palette, the results showed that Malaysians preferred the Happy feeling, follow by Lovely feeling and Mildly feeling. This result shows that the collected data of evaluation assessment of color palette preferences matches the actual spatial color image scale.

4. CONCLUSIONS

There are several conclusions that can be drawn from this study's results. Firstly, when Korean and Malaysian subjects did the same survey of choosing the symbolic color for each country, their results showed that the colors in their national flags are higher in ratio. However, Malaysians reported that the color Green symbolized disease, whereas the sKorean thought Green symbolized Malaysia because of the the country's tropical climate, plants, and fruits. This results showed that people from different culture background have different points of view on the same color.

Secondly, Korean and Malaysian subjects were asked to choose their most preferred and least preferred spatial color images and evaluate their emotional sensitivities towards the 10 color palettes. Results show that Koreans preferred color palettes that have calm and gentle emotions feelings, whereas Malaysians favored color palettes that had happy and natural emotion feelings. In adition, Koreans did not prefer color palettes that were artificial and harmonious, and Malaysias dis not like the color palette that had dull and muddy feelings.

Thirdly and finally, comparing and analysing the emotional evaluation on color palettes and the scale of spatial color images, the results show to matche very well. This shows that the collected data were reliable, in future research will further this study by doing more comparison with other countries.

ACKNOWLEDGEMENTS

This work was supported by the National Research Foundation of Korea Grant funded by the Korean Government (NRF-2014S1A5B8044097).

REFERENCES

Bernd H. Schmitt 1995. Language and visual imagery: Issues of Corporate Identity in East Asia. *Columbia J. world bus*. 30: 28-36.

Abdulrahman S. AL-Rasheed. 2015. An experimental study of gender and cultural differences in hue preference. *Frontiers in Psychology* 6: 1-5.

Kim, Y.S., Park M.S., and Kim Y.M. 2011. A Comparative analysis of perception of color between Korean and Chinese: focusing on young men and women. *Journal of Korea Society of Color Studies* 25(3): 77-86

Je, N., and Choi G. 2011. Comparative Study of University Student' Favorite Colors between Korea and Canada -centering on general and special favorite colors-. *Journal of Korea Society of Color Studies* 25(4): 35-48.

Address: Prof. Heykyung PARK, Department of U-design, Design Institute,
Inje University, 197 Inje-ro, Gimhae, KOREA
E-mails: dehkpark@inje.ac.kr, drmaineo@gmail.com, ojy1245@gmail.com,
matthias2001my@hotmail.com, mjleeworld@nate.com,

The analysis of door color on the Traditional Palace of the Kingdom of Joseon

Lu Chen,[1] Jin sook, Lee,[2]
[1] The Doctorial course, Dept of Architecture Engineering,
Chungnam National University ,Korea
[2] Professor, Dept of Architecture Engineering ,
Chungnam National University, Korea

ABSTRACT

This study is a part of the architectural element color analysis on the Traditional Palace(Gyeongbokguang,_Changdeokgung and Changgyeonggung) which belongs to Kingdom of Joseon. This study is based on main architectural element door analysis on the Traditional Palace of the Kingdom of Joseon. In this paper, we adopt Munsell Color System and NCS Color System to study color usage on the door of the Traditional Palace. The objective is find out the color distribution range and the character on the doors and analyze the results based on cultural tradition of Korea. This study includes by three steps. First was mainly of the study which is subjects information searching.The second step used the Munsell Color System and NCS Color System to analyze the study subjects to get the color distribution range and the character of distribution range. The third step was the analysis of the door color from step two and got the results like followings. Firstly, the range of door color distribution concentrated from 5R to 5YR by the Munsell Color System. And color adopted is low and middle value and chroma. Secondly, the color of door distributed in the range of 5 and 6. The character of the color in this area is dark, while the dark tones and dark tones correspond to nearly colorless. Lastly, it found out the relationship between color and culture. The major color of Korea architecture are used by asymmetrical balance with natural, and harmonious color.The color of the palace also has same character, the color impression is not serious and dignified sense. The impression is relaxed and stable integration of the nature feeling. Future research will analyze other architectrual element color on the Traditional Place of the Kingdom of Joseon.

1. INTRODUCTION

With the development of history, most of Asian like the lifestyle and culture of western Traditions lifestyle and cultural are gradually neglected. The culture of nations which once owned themselves also has been gradually forgotten. However, with the development of economy, the international status of Korea has been improved. People of the country pay attention to their own nation culture and lifestyle. People start to search for the source of nation culture.

This study is a part of the architectural element color analysis on the Traditional Palace(Gyeongbokguang, Changdeokgung and Changgyeonggung) of the Kingdom of Joseon. In this paper, we adopt Munsell Color System and NCS Color System to study color usage on the door of the Traditional Palace of the Kingdom of Joseon.The purpose of this study is find out the color distribution range and the character on the doors and analysis the results based on cultural tradition of Korea. This study was the base of the architectural element color analysis on the Traditional Palace between China and Korea. I did this study just for two reasons. The first reason was the past research had compared a long time. And the other reason was compared with other method such as photo analysis method in past resarch, this one raises precision and error was kept below 0.1. So I decided to do this study for researching color distribution range and the character on the Traditional Palace again.

2. METHOD

2.1 Sample Preparation

In this paper,three Traditional Palace were selected and founded in the Joseon Dynasty which is Gyeongbokguang,Changdeokguang and Changgyeongguang.The 3 research subjects were located in Seoul. This study aims are the color of the main building doors. (Figure 1).

Figure 1: Gyeongbokguang, Changdeokguang, Changgyeonggung

2.2 Experimental Procedure

To measure the color of doors,the current study used CM-2600d,_NCS COLOR SCAN 2.0 to measure physiological signals.CM-2600d used Munsell Color System to measurement the color of doors. NCS COLOR SCAN 2.0 used NCS Color System to measurement the color of doors. Before measuring the color of doors, I used my hand to wipe the surface of the door. After the measurement of color was done throgh the machine on the surface of the door. To minimize the mistake with the surface, extraneous substances were wiped off the surface of the door.

The measurement method used as follows. The subject was seated comfortably in the outside and the day had no strongly sunlight. I used my hand to wipe the surface of door.Next,two color measurement machines were taken for 10 seconds in the surface of the door. In order to reduce the error of result of measurement.I measured different positions just like red square region in the surface of door. And the other way to reduce the error of result of measurement, I used color measurement machines to measure the color of door for many times. At last, I took the average of the result of color measurement and recorded in the paper(Figure 2).

Figure 2: Measurement color used two color measurement machines.

3. RESULTS AND DISCUSSION

This study used the Munsell Color System and NCS Color System to analyze the study subjects to get the color distribution range and the character of distribution range. Munsell Color System, this system consists of three independent dimensions which can be respresented cylindrically in three dimensions as an irregular color solid: hue, measured by degrees around horizontal circles; chroma, measured radially outward from the neutral vertical axis; and value, measured vertically from 0 (black) to 10 (white). Munsell Color System determined the spacing of colors along these dimensions by taking measurements of human visual responses. NCS Color System is based on the color opponency description of color vision. The system is usually used for matching colors rather than mixing colors.

The result of color measurement can be classified into the two following groups. In the first group,CM-2600d used Munsell Color System to measurement the color of doors. The result of color measurement was shown as in Figure3 and Figure4.In the second group, NCS COLOR SCAN 2.0 used NCS Color System to measurement the color of doors. The result of color measurement was shown as in Figure 5.

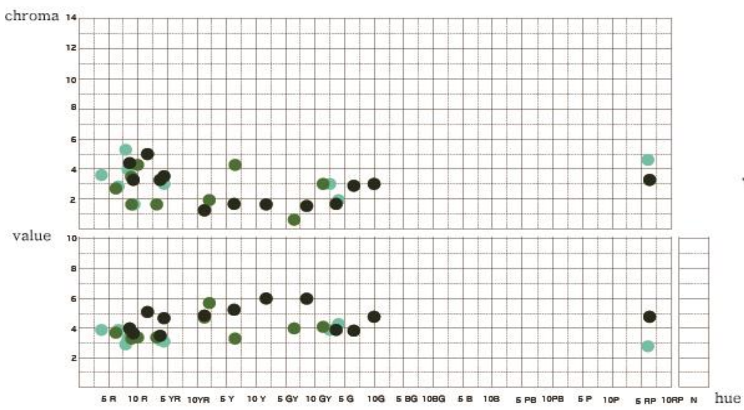

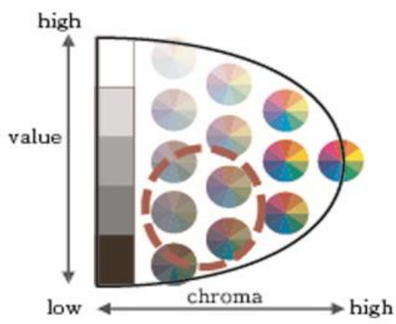

Figure 3: Measurement color by CM-2600d and Analysis by Munsell Color System

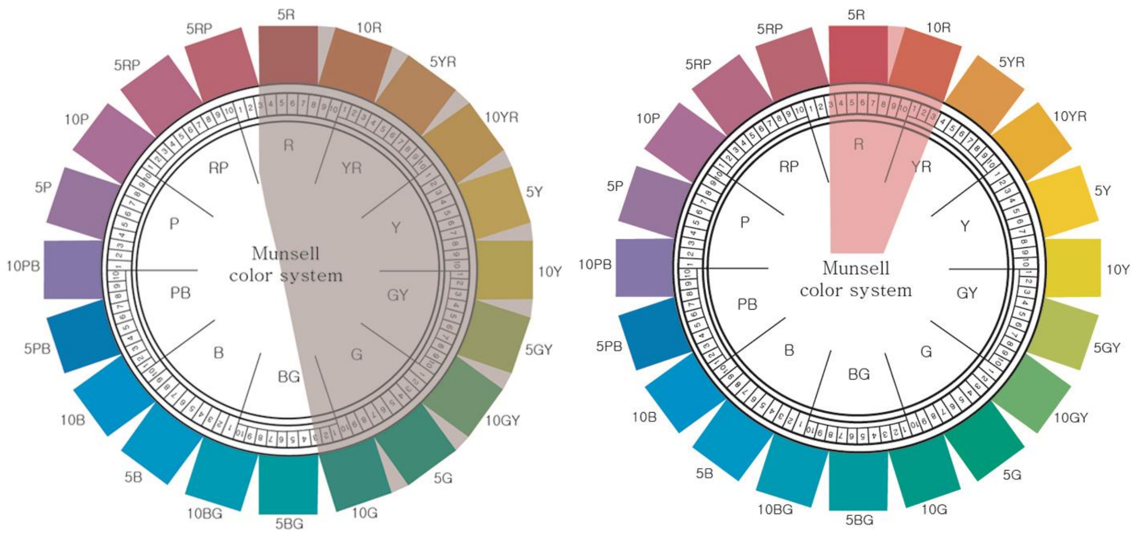

Figure 4: Measurement color by CM-2600d and Analysis by Munsell Color System

The result of the first group is anyalyzed by Munsell Color System.The range of door color distribution is from 1-5 in the direction of chroma.And the range of door color distribution concentrated from 2-5 in the direction of chroma.The range of door color distribution is from 3-6 in the direction of value. And the range of door color distribution is from 3-5 in the direction of value. And color adopted by door is low and middle value and chroma.The range of door color distribution is from 5R to 10G in the black shadow region.The range of door color distribution concentrated from 5R to 5YR in the red shaow region by Munsell Color System.

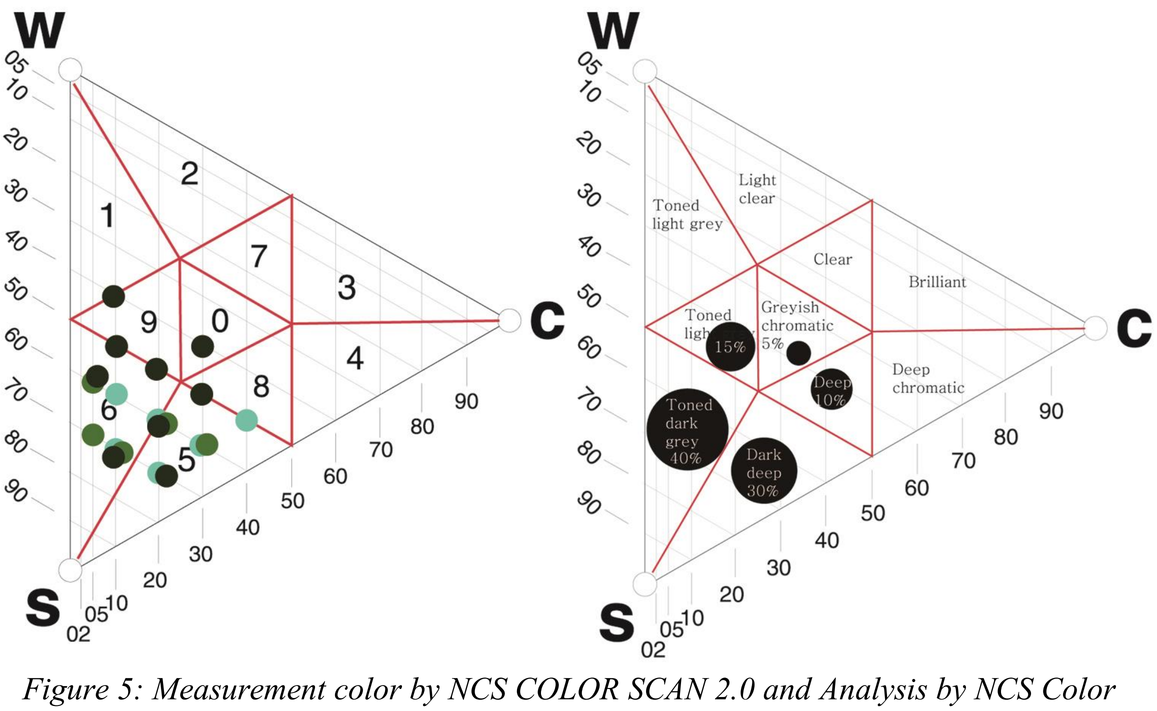

Figure 5: Measurement color by NCS COLOR SCAN 2.0 and Analysis by NCS Color System

The result of the second group is anyalyzed by NCS Color System.The color of door distributed in the range of 5, 6, 8 and 9. The color of door distributed concentrated 5 and 6. The character of the color in this idea is Toned dark grey and Dark deep tones correspond to nearly colorless.

4. CONCLUSIONS

The purpose of the current study was to analyze the door color on the Traditional Palace of the Kingdom of Joseon.Based on the result, the color adopdted by door is low and middle value and chroma by the Munsell Color System. And the color adopted by door is Toned dark grey and dark deep tones correspond to nearly colorless by the NCS Color System.

Following the result, the traditional palace color of the Kingdom is associated with traditional Korean culture. Korean traditional culture thinks that the relationship for person and nature should be a harmonious unity. Under the influence of this idea, people prefer to use the natural unity of color and materials. Even though Korea also has a hirerarchy society but not too fierce so that during the brightness design shows available, the colors are most unsophisticated which are put more attention in the spiritual feelings.The major color of Korea architecture are used by asymmetrical balance with natural, and harmonious color.The color of the palace also has same character, the color impression is not serious and dignified sense. The impression is relaxed and stable integration of the nature feeling. As such, future research will analyze other architectural element color on the Traditional Palace of the Kingdom of Joseon. And it will analyze architectural element color on the Traditional Palace of China. It will find out the same and different character between China and Korea.

REFERENCES

Kim Yeon-Jung, Lee Yeon-sook, 1999. *Furniture of Eastern-Korea and Japan to the center*, monthly Interior Design Korea.

Kim Kook-sum.2004. *Comparative Analysis on Design Characteristics of Traditional Residence in Korea, China ,Japan*, Korea.

Ru Jinghua, Peng hualiang. 1998. *Palace Architecture*, SpringerWienNewYork(2)150-161

Joo Namchul.1999. *The design elements of the Korean architecture*. Ilgisa.

Seo, Soo-Yeon.2012. *A Study on comparative analysis of characteristic for color design in Kora Japanese residential space*, Korea

Address: Prof. Jin sook Lee, Department of Architectural Engineering, School of Engineering,
University of ChungNam National University, 99 Daehak-ro,Yuseong-gu, Daejon, 305-764, KOREA
E-mails: chenluzhuxi@naver.com, js_lee@cnu.ac.kr

Comparison among three methods for Thai colour naming.

Pichayada KATEMAKE,[1] Dimitris MYLONAS,[2] Lindsay MACDONALD,[3] Amra PRASITHRATHSINT[4]
[1] Faculty of Science, Chulalongkorn University
[2] School of Electronic Engineering and Computer Science, Queen Marry University
[3] Civil, Environmental & Geomatic Engineering, University College London
[4] Faculty of Arts, Chulalongkorn University

ABSTRACT

We conducted experiments in colour naming and colour categorisation in Thai to facilitate colour communication within and across cultures. In this study, we compare the frequency and location of Thai basic colours terms (n=11+1) in three experimental methodologies - two conducted in controlled viewing conditions (classical and category) and one over the Internet. Although the frequencies of colour names across the methods were different, they produced ranks within each method that were only slightly different compared with the ranks obtained in the other 2 methods. In terms of hue and lightness the agreement was relatively good for most colour terms but we found large differences in chroma.

1. INTRODUCTION

There are five published studies about Thai colour naming. Three of them are made by linguists and were published in Thai language.

The first study was focused on colour names and on colour perception in Utaradit, north of Thailand (Witchurote, 1986). One hundred and twenty observers participated but only 33 colour names were verbally stated. More than 90 percent of observers could name white, red, yellow and green. Seventy percent could name black, pink, sky blue, and orange. The number of known colour names was significantly different among gender, age and profession. The colour names that could be identified with highest precision were white, black and yellow.

The second research was the comparative study of Zhuang on Thai colour terminologies (Prasithrathsint, 1988). Four observers, with ages between 30 and 40 years, living in 4 geographic regions: central (Bangkok), north (Chiang-mai), north east (Nakhon-ratchsima) and south (Nokorn-sri-thammarat), were interviewed and were randomly showed 217 printed colour samples one by one. The process was repeated twice. The colour samples were printed by Graf-G process inks from Dainippon Ink and Chemicals. Basic colour terms were defined on the criteria of Berlin and Kay, distinguishing the following 3 cases: 1. Identical 12 basic colour terms were identified using: a). observers from Bangkok; b). observers from Chiang-Mai; 2. Eleven basic colour terms were identified using observers from Nakhon-ratchsima; 3. Ten basic colour terms were identified using observers from Nokorn-sri-thammarat.

The 12 basic colour terms identified in the first case, are: white /*khaw*/, black /*dam*/, red /*dang*/, yellow /*leaung*/, green /*khiaw*/, sky blue /*fa*/, blue /*nam-ngen*/, brown /*nam-tan*/, grey /*thaw*/, purple /*muang*/, pink /*chom-pu*/ and orange /*som*/. In the second case, all former colour terms were identified but blue and sky blue were identified with the same colour term. In the last case, grey and brown were identified with the same colour term while pink could not be associated to any colour term, the rest of colour terms being as in case 1. Despite the subjectiveness of the observation procedure, useful data was collected and, based on it, further studies were developed.

In 2003, there was a third research, a comparative study of colour terms made for the Sukhotai period (13-15 A.D.) and for the present time (Engchuan, 2003). Thai colour names that were found in recorded documents originating in Sukhotai period were corroborated with colour samples and natural colour objects. The colour name identification process was carried out with 10 female and 10 male observers, having the age between 30 and 45 years. This study showed that there were 5 basic colour terms in Sukhotai period: white /*khaw*/, black /*dam*/, red /*dang*/, yellow /*leaung*/, green /*khiaw*/, and 12 in present time: white /*khaw*/, black /*dam*/, red /*dang*/, yellow /*leaung*/, green /*khiaw*/, sky blue /*fa*/, blue /*nam-ngen*/, brown /*nam-tan*/, grey /*thaw*/, purple /*muang*/, pink /*chom-pu*/ and orange /*som*/.

In addition to the 3 studies conducted by linguists, there were 2 more studies performed by colour scientists on traditional Thai colour names. The first study resulted in the subjective identification of 50 colour names and was published in a Thai local journal in 1988 (Siripant, 1988). The second study is based on an objective identification method first published in 2011 (Katemake et al., 2013), which was subsequently improved, resulting the first Traditional Thai Colour Name Dictionary that presents 147 traditional Thai colour names analysed, identified, quantitatively described, explained, transliterated and translated (Katemake and Preda, 2014). Most of the traditional Thai colour names take the names of specific objects from nature and environment to be part of their name in combination with basic colour terms.

In December 2013, we started collecting unconstrained colour names with their colour coordinates from hundreds of Thai speakers in an online colour naming experiment (Mylonas & MacDonald, 2010) with an aim to facilitate colour communication across cultures over the Internet. In this study, we attempt to validate our findings by comparing the frequency and the location of colour centroids in CIELAB, against two experimental methodologies conducted in controlled viewing conditions.

2. METHOD

Three experiments of colour namings: classical (CS), category (CT) and online (OL) were carried out. The method of online experiment is already publised (Mylonas & MacDonald 2010, Mylonas & MacDonald 2015), therefore we will only describe the principle.

2.1 Stimuli Preparation

One thousend three hundred matt Munsell sheets were used in both CS and CT experiments. Samples of 5 x 5 cm were cut from each Munsell sheet, were pasted on white cardboard and were framed with neutral grey for the classical experiment. For the CT experiment, cut samples of 2 x 2 cm size were pasted on white paper with magnetic sheet and marked with Munsell notation and barcode on the opposite side. In OL experiment, 600 Munsell codes were selected from the Munsell Renotation Dataset with an addition of neutral samples and were converted to sRGB colour coordinates in order to display the colours on a monitor against a neutral mid-grey backgroud. The chosen size for each displayed colour was 147 pixels width and 94 pixels height, which for a pixel density of 3.3 pixels per mm would be 4.5 x 3.0 cm, subtending an angle of 3.4 degrees at 50 cm viewing distance (Mylonas & MacDonald, 2015).

2.2 Subjects

In the CS experiment, 10 paid subjects participated (5 males and 5 females) with an averaged age of 26.9 years (σ=6.9). The subjects were undergraduates, graduates and lecturers, all having normal colour vision and half of them having basic knowledge of colour science. In the CT experiment, 8 paid subjects were involved (5 males and 3 females), undergraduates, graduates and lecturers, with an average age of 25.6 years (σ=7.7). In the OL experiment, 266 subjects participated but only the responses from 214 subjects (156 males and 58 females) could be used for analysis. Their education level ranged from primary school to Ph.D and their averaged age was 29 years (σ=9.8).

2.3 Apparatus and procedure

In the CS experiment, Munsell samples were placed in a viewing booth of 116x56x83 (WxLxD) with neutral grey interior walls. D65 fluorescent lamps, with the colour rendering index (CRI) of 98 and total illuminance of 1200 lux, were installed on the booth's ceiling. The viewing distance was 60 cm. This resulted in an approximately subtended angle of 4.8 degrees for the sample size of 5 x 5 cm. In the CT experiment, 1300 Munsell samples with magnetic base were randomly positioned on a 100x200x92 (WxLxH) cm iron-table with neutral grey background. The D65 fluorescent lamps, having the same CRI and illuminance as in the CS experiment, were installed on a white ceiling placed 90 cm far from the table surface. The ceiling was sustained by a framework outranging the experimental area in order to have no walls within the subjects' viewing range. The viewing distance depended on the height of subjects. For an average height of 160 cm, the viewing distance was approximately 74-78 cm. The subjects' variable sized top part of the body was another factor affecting the viewing distance. This gave an approximately subtended angle of 1.5 degrees for the sample size of 2 x 2 cm.

For the CS experiment, 2 samples were cut from each Munsell sheet, resulting 2600 samples. One set of 1300 samples, one sample for each Munsell colour, was randomly separated in 6 boxes. From the second set of 1300 Munsell samples, 200 samples were randomly selected and placed into a 7th box. The samples from the 6 boxes were shown to the subjects one at a time in random order in the viewing booth. The subjects were asked to say "open" when opening the grey cover for viewing each sample and they were asked to name each colour, as fast as possible, using basic colour terms or non-basic colour terms, without using foreign words. The time needed for each subject to name each colour was recorded as response time for the considered subject/colour pair. The 7th box with 200 samples was used for checking the consistency of the obtained data. The total observations were 15,000. In the CT experiment, 1300 Munsell samples were placed simultaneously on the iron-table. The samples were shown randomly to subjects who were asked to select and group colours according to each subject's opinion on colour similarities and based on each subject's choice for naming the colour-group. The colour names were written down for each resulted group and the colour samples from each group were placed separately into small boxes. The subjects were allowed to build colour-name groups simultaneously and/or sequentially. The total observations were 10,400. We measured each Munsell sample under the experiment lighting condition with Konica Minolta CS-1000 in the same angle and distance that subjects were seated.

The OL experiment (www.colournaming.com/th) consisted of six procedural stages: i) adjusting the display condition ii) giving display information iii) testing colour vision iv) naming colours of 20 randomly selected colours, v) giving cultural information and vi) summary of the results (Mylonas & MacDonald, 2010).

3. RESULTS AND DISCUSSION

In the laboratory experiments, the subjects were asked to name the colours in Thai language without using foreign descriptive terms or Thai words of foreign influence. More colour terms were obtained in the CS experiment, when one sample at a time was shown to the subjects, than in the CT experiment, when various samples were shown simultanously. The average ratio was 6 to 1. We analysed the data in terms of colourname frequencies and colour centroids. The colour names were divided into 3 groups: G1) basic colour names according to Berlin and Kay (Berlin and Kay 1969) definition plus *fa* (sky blue) G2) monolexemic terms and G3) colour names that include G1+identifier, G2+identifier, 2 colour-word and 2 colour-word + identifiers. The reason why we added *fa* (sky blue) to the basic colour names is that *fa* (sky blue) has been used to represent blue before the word *nam-ngen* (blue) was known. With CS and CT method, G1 were 23.03% and 61.90%, G2 were 1.34% and 2.88% and G3 were 75.25% and 35.22% respectively.

The frequencies of colournames grouped in G1 are shown in Figure 1. The colourname with the highest frequency obtained in the CS method was *thaw* (grey): 20.32%, because the matt Munsell samples within the first step of chroma, which is much higher than other steps, were mostly named *thaw* (grey) by subjects. However, when subjects were shown these samples along with other samples, the resulted frequency dropped to 9.38%. The colour names that had the top six highest frequencies were: 1) for CS: *thaw* (grey), *khiew* (green), *muang* (purple), *nam-tan* (brown), *chom-pu* (pink) and *fa* (sky blue); 2) for CT: *khiew* (green), *muang* (purple), *chom-pu* (pink), *fa* (sky blue), *nam-tan* (brown) and *thaw* (grey); 3) for OL: *muang* (purple), *chom-pu* (pink), *fa* (sky blue), *khiew* (green), *nam-ngen* (blue) and *nam-tan* (brown). This shows that *fa* (sky blue) is more frequent than *nam-ngen* (blue), which indicates that *fa* (sky blue) might be more appropriate to be considered in the Berlin and Kay 11 basic colour terms than *nam-ngen* (blue).

Colour centroids of G1 colourname-group (n=11+1) determined in all three experiments, are shown in Figure 2. The CIEDE2000 colour differences in CIELAB between CS and CT were relatively small (mean DE_{00}=3.26) because the same type and number of colour samples and the same type of illumination were used in both methods. The differences between CS and OL (mean DE_{00}=12.5) and between CT and OL (mean DE_{00}=12.5) were mainly observed in chroma. The largest hue difference was observed in *nam-ngen* (blue). The lightness difference was small across the samples, *dam* (black) being an exception. The colour centroids obtained for *thaw* (gray) in the 3 methods were close to each other.

The advantage of the CS over the CT method is that a greater number of non-basic, non-monolexemic colour names could be recorded. This method is similar to OL in terms of presenting samples sequentially to the subjects. The disadvantage of CS compared to CT relies in the time consuming procedures of colour naming and analysis.

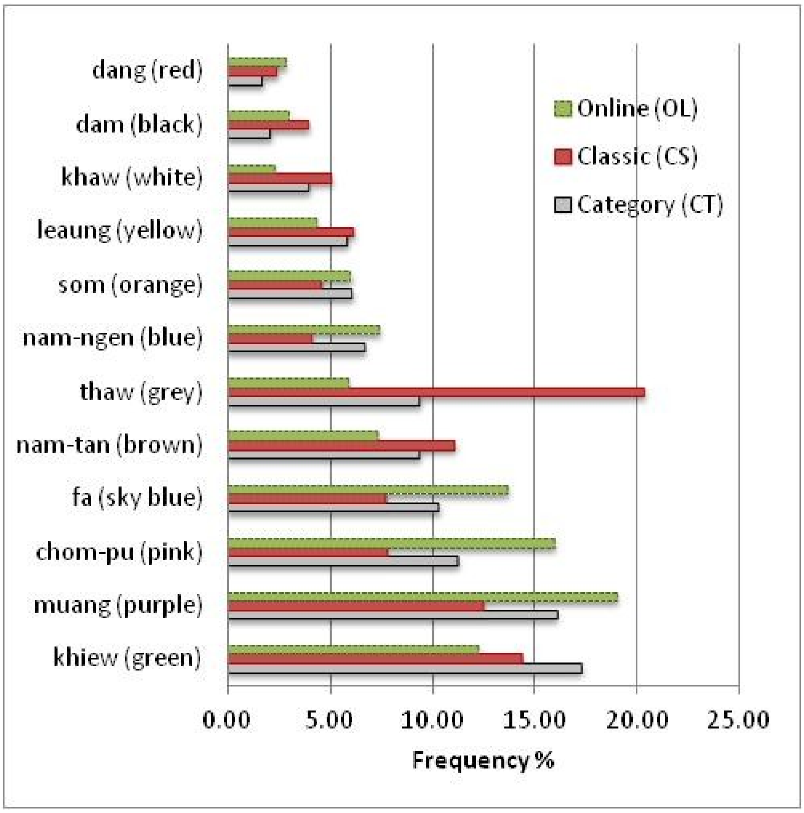

Figure 1: Frequencies of basic colour terms plus fa (sky blue).

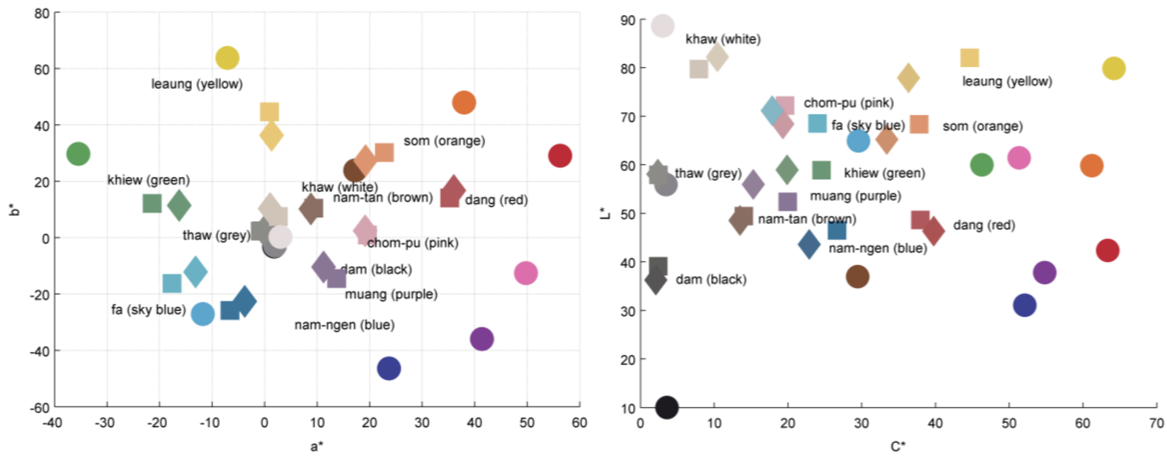

Figure 2. Colour centroids of basic colour terms plus fa (sky blue) obtained by CS (square), CT (diamond) and OL (circle) methods, D65/10º, left plot is CIE a b* showing hue and chroma differences and right plot is CIE L* C* showing lightness and chroma differences.*

4. CONCLUSIONS.

In this study, we presented a comparison of the frequency and location of basic colour terms in Thai among three experimental procedures. The small differences observed between the two laboratory procedures (CS vs. CT) might be due to the same type of colour samples and illumination used in both methods and the effect of size and surrounding. The relatively larger differences between online and laboratory (CS vs. OL and CT vs. OL) observed mainly in chroma might be the result of different sampling and different display medium and the constrain of subjects in the laboratory setting to use foreign influenced words. Our initial results are encouraging, but further work is still needed to develop a comprehensive colour naming model to facilitate colour communication across cultures including the analysis of basic and non-basic colour names and their response times.

ACKNOWLEDGEMENTS

We thank all participants in 3 experiments and Dr. Eng. Razvan I. Preda for scientific proof reading of manuscript.

REFERENCES

Berlin, B., and P. Kay. 1969. *Basic color terms: Their universality and evolution*. Berkeley, CA: Cambridge University Press.

Engchuan, S. 2003. Color terms and the concept of color of the Thais in Sukhotai period and at the present time In AIC Color 2003, Bangkok: Chulalongkorn University.

Katemake, P., R.I. Preda, and D. Hoontrakul. 2013. *Identification of traditional Thai colours used for mural paintings and Khon masks*. Color Research and Application; 38(3): 229-234.

Katemake, P. and R.I. Preda. 2014. *Complete study of traditional Thai colors used in mural paintings: traditional Thai color name dictionary*. Color Research and Application 39(6): 616-629.

Mylonas, D. and L.W. MacDonald. 2010. Online colour naming experiment using Munsell colour samples In *Proceedings of 4th IS&T/SID on Colour in Graphics, Imaging, and Vision.* Joensuu, Finland, 27-32.

Mylonas, D. and L.W. MacDonald. 2015. *Augmenting basic colour terms in English.* Color Research and Application (27 JAN 2015 DOI: 10.1002/col.21944)

Prasithrathsint, A. 1988. A comparative study of Zhaung and Thai kinship systems In *the 4th International Conference on Thai Studies*. Yunnan, China: Kunming.

Premsrirat, S. 1991. The Khmu color system and its elaborations In *24th International Conference on Sino-Tibetan languages and Linguistics*, Bangkok and Chiangmai.

Witchurote, P. 1986. *Color terms and color perception of speakers of the Thai dialect of Uttaradit at Tambon Na-in, Amphoe Pichai, Uttaradit Province*. M.A.Thesis, Chulalongkorn University.

Siripant, S. 1988. *Methods of notation of Thai mural painting colours by CIE and Munsell systems*. J Sci Soc Thailand 14 121–136.

Address: P.KATEMAKE, Faculty of Science, Chulalongkorn University, Phayatai Rd., Patumwan, Bangkok, THAILAND
D. MYLONAS, School of Electronic Engineering and Computer Science, Queen Marry University, Mile End Rd, London E1 4NS, UK
E-mails:pichayada.k@chula.ac.th, d.mylonas@qmul.ac.uk

A Study on Elements Perceived as Traditional among Fabrics and Colors for Hanbok

JiHyun Sung[1], YungKyung Park[2]
[1] The master's course, Dept. of Color Design, Ewha Womans Univ
[2] Professor, Dept. of Color Design, Ewha Womans Univ

ABSTRACT

Recently, traditional Korean clothes Hanbok, being perceived as inconvenient and out of style, are evaded from young people and daily life. Thus, this study felt the need to develop colors and materials of Hanbok and sought to investigate which kinds of fabric and color the young generation might feel as traditional or modern. On the premise that the extent of people's perception as traditional might differ by color or fabric, the study arranged 100 color sample chips composed of various fabrics such as cotton, satin, chiffon, organdie and fabric for Hanbok, and conducted questionnaire survey among 15 women in their 20s and 30s. As a result, the study found that regardless of fabric types, colors with high lightness were dominantly perceived as modern, while those with low lightness as modern. And as the significant difference the study also found that while fabrics perceived as traditional had no big difference, chiffon and organdie-transparent and thin fabrics-were not perceived as modern. Based on these findings, this study expects that if fabric for Hanbok were used excepting fabrics such as chiffon and organdie, also along with colors with high lightness, it will contribute to modernization and popularization of Hanbok.

1. INTRODUCTION

As Korean people's overall lifestyle has been westernized since the modernization in the mid 19th Century, traditional Korean clothes Hanbok, being perceived as inconvenient and out of style, just maintains its status as a high-class formal dress to be worn in the events such as first birthday party and 70th birthday party. As for reasons for that phenomenon, Soo Ae Kweon, Jong Myoung Choi, Eun Kyung Lee (1998) attributed to 'inconvenience in activity', 'cumbersomeness' and 'difficulty of handling', while Kyung-Hee Hong(2007) attributed to 'inconvenience', don't like the image', and 'don't like to attract the attention of others' for the reason why traditional Hanbok is averted in daily life. This tells people's perception has not changed in the course of over 10 years time, highlighting the urgency of Hanbok's modernization .

Under the circumstances. this study, in an attempt to develop various colors and materials for Hanbok, sought to investigate which kinds of material and color the young generation might feel as traditional or modern, including modern material as well as material for Hanbok. If materials and colors of Hanbok were to be used in a modern style based on the findings of this study, the study expects, it will contribute to modernization and popularization of Hanbok.

2. METHOD

Prior to experimental design, the study established two hypotheses to identify how color is to be perceived as traditional depending on fabric - the purpose of this study. One is that same color may generate different feelings of being traditional depending on fabrics. Another is that same fabric may generate different feelings of being traditional depending on colors.

2.1 Collection of survey data

Building on these hypothesis, the study conducted a questionnaire survey by comparing fabrics actually used in Hanbok with those generally used in modern clothes. As the first step, the study collected recently-used samples of fabrics for Hanbok and then collected fabrics such as cotton, satin, chiffon and organdie largely used for modern clothing. It selected 100 samples in total by matching fabrics identical or similar with fabric for Hanbok.

2.1.1 Types and features of fabric

Looking at features by the fabric type used in this experiment, fabric for Hanbok has fine and precise structure as well as diverse textures and designs, whereas cotton has a bit rough surface due to relatively thick threads and its structure of plain weave. Satin, closely woven by thin threads, has soft surface and lustre. Unlike the above fabrics, chiffon and organdie have such a loosely woven structure as to be visible the other side, while they are distinct in that chiffon is soft and organdie is quite stiff.

2.2 Composition of questionnaire and analysis methods

100 random sample chips produced by the above method were distributed to the subjects of the survey. The questionnaire comprized three choices; they were supposed to choose 'traditional' and 'modern' if they found each sample to be so and 'neutral' if they found the sample didn't belong to any specific category. And the subjects were asked to check if each sample were perceived 'traditional' or not.

The survey was conducted among female graduate students in their 20s and 30s who were sensitive to colors, and based on the analysis of frequency of answered outcomes, the study analyzed the distribution of CIELAB values of the samples.

3. RESULTS AND DISCUSSION

The result of classifying totally 69 samples with distinct differences - those with the most votes and getting seven or more votes beyond the majority at the same time - showed that 31 samples were perceived as traditional, 17 were as modern, and 21 as neutral. However in an effort to investigate definite colors perceived either traditional or modern, the study excluded the samples that were answered as 'neutral' or didn't have clear distinction with one vote difference or the tie.

3.1 Analysis by the color

Looking at the distribution of CIELAB color coordinate of the samples consistently perceived as traditional or modern regardless of fabric types out of the samples with same color but different fabric, the samples perceived as modern were evenly distributed for their chroma but were mainly situated at high lightness, while the samples perceived as traditional were centered on low chroma and low lightness. And the colors perceived as traditional were mainly revealed as R group, RP group, B group. On the other hand, the colors perceived as modern were evenly distributed among R group, Y group, G group except B group <Figure 1>. <Table 1> shows the colors perceived as either traditional or modern regardless of fabric types.

Table 1. Color with consistent images

Traditional	Modern

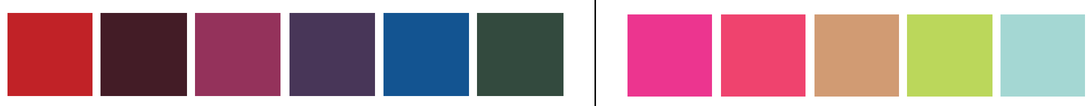

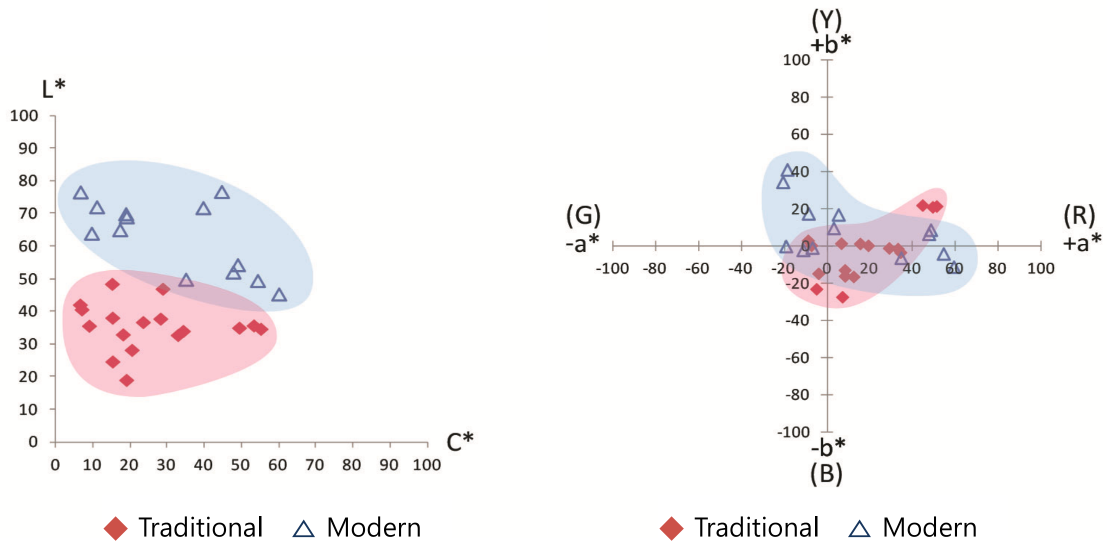

Figure 1. Color distribution with consistent images

3.2 Analysis by the fabric

Looking at fabric types selected by each image, all fabrics such as fabric for Hanbok, cotton, satin, chiffon and organdie were perceived as traditional, whereas only fabric for Hanbok except chiffon/organdie, cotton, satin were perceived as modern.

And looking at the rate selected as traditional or modern in proportion with the sample number of each fabric type as per <Table 2>, organdie, chiffon, fabric for Hanbok and cotton were more selected as traditional, while satin had the same perceived rate between being traditional and modern.

Based on these findings, the study was able to identify that fabrics with traditional image had no big difference, while thin and transparent fabrics such as organdie, chiffon were not perceived as modern.

Table 2. Selection rate of the image by the fabric

Fabric type	No. of samples	Traditional		Modern	
		n	%	n	%
Hanbok	24	8	33.3	5	20.8
Satin	24	8	33.3	8	33.3
Chiffon	16	3	18.8	0	00.0
Organdie	8	6	75.0	0	00.0
Cotton	28	6	21.4	4	14.3
Totall	100	31	31.0	17	17.0

n : No. of selected samples by the fabric

3. CONCLUSIONS

As a matter of fact, Hanbok does not get good response from contemporary young generation despite a diverse range of the industry's efforts to modernize and popularize it. And in an attempt to find ways to overcome this circumstance by modernizing materials and colors of Hanbok, this study used 100 color chips composed of fabric for Hanbok and modern fabric and conducted the survey on whether how people might perceive either traditional or modern depending on fabrics and colors.

Based on 31 and 17 samples perceived as traditional and modern respectively, the study conducted analysis of sets composed of identical or similar colors regardless of fabric types and as a result found that the scope of colors perceived as Hanbok were situated at high lightness and that of colors perceived as traditional were centered on low chroma and low lightness. On the other hand, the colors perceived as modern were evenly distributed among R group, Y group, G group except B group. Looking at the analysis by the fabric, fabrics with traditional image had no big difference, while thin and transparent fabrics such as organdie, chiffon were not perceived as modern.

Based on these findings, the study revealed that important factors influencing people to perceive either traditional or modern included R group colors with low lightness and low chroma - colors absolutely felt as traditional regardless of fabric types - and colors with high lightness -colors felt as modern - as well as thin and transparent fabrics such as organdie and chiffon.

If, building on these, the Hanbok industry were to produce Hanbok using colors with high lightness - perceived as modern - or using mainly fabrics other than organdie and chiffon, and ultimately combining colors perceived as modern with fabrics other than organdie and chiffon, it is expected to contribute to modernization and popularization of Hanbok.

REFERENCES

Soo Ae Kweon, Jong Myoung Choi, and Eun Kyung Lee. 1998. *A Study on the Actual State of Wearing Korean Traditional Clothes and Purchasing Factor*, Journal of Korean Living Science Association 7(1) 129-138

Kyung-Hee Hong. 2007. *남녀대학생의 전통한복에 대한 태도, 평가 및 인식에 관한 연구,* Proceedings of the Korean Society of Clothing and Textiles Conference 2007(1), 132-132

Address: Prof. YungKyung Park, 1302, International Education Building, Ewhayeodae-gil, Seodaemun-gu, Seoul, 120-750, KOREA
E-mails: gray-hole@hanmail.net, yungkyung.park@ewha.ac.kr

THE POSITIVE IMPACT OF IMAGE BY COLOUR FOR VULNERABLE PEOPLE

MariaElena Chagoya

Image by Colour coach, Tasmania, Australia

ABSTRACT

The participants of "the Positive Impact of Image by Colour for Vulnerable People "project learned to re-discover their positive self-image, build their self-esteem and feel more confident to achieve their life goals all through simply enhancing their physical appearance and the colour of their clothing.

They have benefited from this advice by feeling more confident, finding work and having hope after major life changes.

The first part of the project was presented in the AIC 2014, in Oaxaca, Mexico, it was well received .
I would be honoured to present the results of this continuing project in Tokyo 2015.

1. INTRODUCTION

The proposal of this presentation at 2015 AIC Midterm Meeting in Tokyo is about how Image by Colour has helped vulnerable people.
I am currently volunteering my services in Australia to help people who are vulnerable, disdvantaged or feeling isolated from society. For example:
Victims of discrimination and racism , as victims of domestic violence ,victims of bulling , People with disabilities , women with emotional or physical hurts, whose self-worth was very low, refuges and migrants need to start a new life in Australia.

People with mental ill-health and mental disorders are particularly vulnerable to infringement of their civil and human rights and to discrimination [1].

Racism can isolate and exclude people preventing them from having equal opportunities to integrate to the society, The impact and negative effects increase distrust, fear and resentment , depression stress and anxiety. [2]

In Australian studies, self-reported racism has been associated with substance use, emotional and behavioural difficulties, and suicide risk for young Aboriginal people [3]

A 2009 joint report by the Women's Centre for Health Matters (WCHM), the Domestic Violence Crisis Service (DVCS) and Women with Disabilities ACT (WWDACT), *Women With Disabilities Accessing Crisis Services* found women with disabilities are more likely to experience abuse or violence than women without disabilities .[4]

The Image by Colour service supports respect of their diversity by creating a genuine, unique and harmonious image. This influences, from the first contact, the impression others have of them, trought to show the correct colour in their garments

2. METHOD

Coaching by customized instructional, training and guidance intervention designed to improve the performance and capacity of the participants, team. The Image by Colour, coaching is characterized by intense, sustained non-judgmental and assistance, support by giving feedback to set goals, identify obstacles, and develop plans trought their image and colours and strategies to achieve goals.

Image by colur coaching was integrated by one- to one colour analysys, support their individual needs in his vulnerable status and their guardrobe and also by "peer coaching" , that help to encourage with a very positive feedback of the participants to each other.

Imageby colour Coaching was provided to each particpant:

Hel ping Relationship and tools characterized by the provision of assistance, tesmtimonlila, personal colours and set of garments to start to use their right colours.

Particpipants receibed caring by created environments characterized by qualities such as helpfulness, concern, empathy, kindness, consideration, good will, responsiveness, and ways to love theirself.

2.1 Sample Preparation

The participants achieved to identify by couching one –to-one the difference between warm and cool colours . Identified their natural colours and subtones can use to achieve the feeling of the confidence to look younger , more vibrant and energetic. Their skin colour are smooth and their texture looks radiance, with healthy gleam in their eyes.

The participants identified wrong colours that affect their appearance: look older, exhausted, ill or dull.

The participants identified how enhance use their own friendly colours based on their skin, hair, eyes, persona and culture.

The participants identified their season and how combine their seasonal colours and enhance by their personality how combine, contrast and coordinate colours for their own benefit for different occasions through clothing, accessories and right hair colour.

The participants with severe level of disability received also one- to-one coaching, with less possibilities to identify why their range the colours was causing the positive impact of the colour , however the mood and attitude was recognized for them and cares. Trough their careers, who received all the information we continue the experimental procedure with this vulnerable sector.

2.2 Experimental Procedure

The participants in a team with peer gain a personal perception that why psychologists have determined that the colour is the first concept about a person's appearance. Its impact is immediate and long-lasting.

The participants recognize how the right and incorrect colours used in a period of 6 months was affecting their mood, apparent age, their attitude on life and the overall impression can make on others. They was using the "wrong colour" for some hours 2 days a week to measure trhe impact with others and in their own perception of them.

By groups the participants ask each other: What kind of first impression do you make?A first impression is the most important impression you'll ever make--and you get only one chance to make it .[5]

Left side wrong colours - Right side right colours

3. RESULTS AND DISCUSSION

Table 1. Positive Impact of Image by Colour		
	Increase selfesteem	Increase confidance in participants
• Economical disvantage	• 12	• 12
• Disability	• 6	• 6
• Feelings of Devaluation	• 25	• 25

Table 1. Positive Impact of Image by Colour

In the process ot the project the Positive Impact of Image by Colour for Vulnerable People the participants also experimented by wearing cloth new and brand name with status of expensive cloth but not in their range of positive colours, as consequence they have the opportunity to compare how they feel how the people treat them. The general impression is with that kind of cloth means wrong colours in expensive garners only cause the effect to focus the attention in the cloth, not in the person.

The discussion was centred about new cloth and good quality or famous brand names are better elements to create a positive image don't matter what is the colour.

Their validate that by wearing old, but in good condition garments in the right colours the participants by the coach of Image by Colour obtain the skill to coordinate an effective, smart and functional wardrobe that will help create a positive image of them with less effort and money.

The key of the reflection for the vulnerable sector is that a lot of them are accepting use garments are reusable, recycle or old by receiving as present, donation or by buying in : opportunity or second hand stores.

The result to wear in the last period of the project their correct sub tone and degradation of colours in the range of "best" colours enhance their harmony was a very satisfaction result for all of them and relatives to see then with a very happy and confident face.

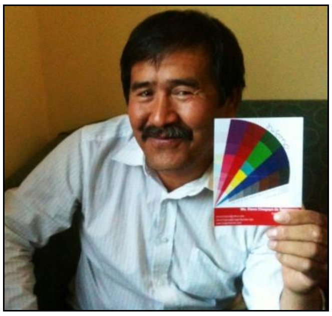  

4. CONCLUSIONS

All vulnerable sector, women and men, not just statues, famous or rich people can develop their self identify while gaining respect for their diversity through an enhanced genuine and harmonious self image.

To find, use and coordinate a range of positive and friendly colours is the key to portray you and create a positive image of yourself.

Be mindful that the holistic synergy in the vulnerable sectors need the support of the social workers, doctors or therapists and the valuable psychological support are parallel a this service. However dear lovers of the colour :

The benefit to support vulnerable people , who start to be selective , admire and value their image which already started to love in the mirror, the feeling of confidence to enhance to use their skills, talents . Enhance their proud of their unique diversity , background and personality is the best humble but impressive , important and impact job that the colour for Vulnerable people is causing..

ACKNOWLEDGEMENTS

Multicultural Council of Tasmania, the Migrant Resource Centre, City Mission, Advocate of Disability, Autism Association, Yemaya Family Violence centre, City Park Radio, Tafe Tasmania

REFERENCES

1 National Mental Health Policy 2008.

2 Pachter L, Garcia Coll C., *Racism and child health:* a review of the literature and future directions. *J Dev Behav Pediatr* 2009; 30: 255-263.

3 Zubrick SR, Silburn SR, Lawrence DM, et al. *Western Australian Aboriginal child health survey: the social and emotional wellbeing of Aboriginal children and young people.* Perth: Telethon Institute for Child Health Research, 2005.

4 Women's Centre for Health Matters, Domestic Violence Crisis Service, and Women with Disabilities ACT, *Women With Disabilities Accessing Crisis Service*s, 2009.

5Demarais A. , Ph.D., and Valerie White V., Ph.D.,2005 *First Impressions: What You Don't Know about How Others See You.* Random House Inc

Address: Maria Elena Chagoya
Country : Mexico
Make up Artist & Image by Colour Coach
Country of residence:
6 Atlas st. Launceston, Tasmania , Australia 7250
Email : elenachagoya@yahoo.com Mobile: 0435 152612
www.imageporcolour.com.au

Faith in the power of color: Spiritual revival from the East Japan Earthquake disaster

Yumi AWANO
Tokyo Zokei University

ABSTRACT

The Pacific Ocean coastal area of Tohoku, Japan suffered extensive damage due to a massive earthquake and tidal wave, which occurred on March 11, 2011. The entire infrastructure and memories of towns disappeared in a short moment. 15,891 people died, 2584 people were missing, and 6,152 people injured. Though the landscape changed beyond recognition, people seemed to experience a revival to the living world through the use of color. I discovered this when my eyes beheld the color in the landscape. This contrast between a relative figure and the background, can be considered as *hare* and *ke*, using Japanese concepts. Color is the accent spread on a level landscape as *hare*, meaning uncommoness. It works as a spice. For example, there was the cheerful color of *senbazuru* (one thousand paper cranes), *dashi* (a kind of float with a variety of decorations in festival parades), *tairyohbata* (good catch flag), and the flowers blooming on rubble of the collapsed schoolhouse painted by high school students and their teacher. These colors can be considered a sign of courage, or maybe as an anchor, or perhaps as many good wishes.

Color is a flower. Furthermore, while there is life, there is color. The faith of the entire culture and daily customs are formed as a result of personal modest daily beliefs. In this article, I wish to make certain that color accompanies the people of Tohoku to recover from this calamity. I will use these ideas as a clue to explore a relation between the Japanese spirit and treatment of color.

1. INTRODUCTION

Tohoku, Japan has a severe climate but has been blessed with the rich harvest from the sea, woods and fields. Many customs, traditions, and festivals bringing people into contact with nature have been handed down through the generations. The scenery of the coastal area was changed completely by the serious tsunami damage of the East Japan Earthquake on March 11, 2011. Several tidal waves caused by the intense earthquake destroyed almost everything, while reaching inland to the forest floor, carrying almost everything along in the undertow. The amount of wreckage was almost insurmountable. If I look at this from another perspective, the wreckage at least left some fragments of life before the tsunami. This situation caused most people inner conflict. It was a time of countless funerals. Sky, soil, and plants - this landscape without any artifact from the modern era closely resembled an ancient era (Figure 1,2). In those days, human beings constructed their life by using only basic tools and materials. People's minds as well as the material civilization were injured now.

When I visited there with a great deal of anxiety, I was convinced that color could bring out people's vitality to get them through their unprecedented loss. For example, I could see the cheerful color of *senbazuru* (one thousand paper cranes), *dashi* (a kind of float with a variety decorations in festival parades), *tairyobata* (good catch flag), and the flowers blooming on rubble of the collapsed schoolhouse, painted by high school students and their teacher. The brilliance of tint produced an attractive contrast in the landscape that had lost its focal point.

Figure 1:Migratory birds return as usual to the salt water paddy field in winter. (Rikuzentakata,December 23,2012)

Figure 2:"The miracle pine tree" also gave courage an anchor, and wishes to many survivors.(August 17,2012)

2. LANDSCAPE OF COLOR AS *HARE*

In this section, I will introduce the three phases after this calamity to consider the power of color as well as a healing: that of natural sight, traditional rite, and activity of people.

2.1 Flowers

Snow fell after the disaster in March; weeds covered up a scar in the ground in summer. Below, in figure 3 and 4 the scene looks like a calm grassland. But a vacant house in the midst of the grassland can be seen. A curtain fluttered from a broken window. The residential area from the past was quietly spread under the sky. Though the rubble was almost all disposed of, fragments of someone's life were still scattered throughout the bushes. Between the sky and the aimless ground, my eyes were attracted to yellow and red flowers. Then, I noticed that there were floral tributes placed here and there. I respectfully restrained from taking pictures since the flowers represented a private requiem. It was the season of *Obon* (a memorial service event for dead persons and ancestor spirits).

Figure 3,4; At Ishinomaki, Miyagi(August 8,2012)

2.2 *Senbazuru* (One thousand paper cranes)

There were dead cedar woods here and there at the foot of the mountains. Sea water reached the woods and left damage to the tree roots. After passing several such mountains, a colored banner on a protection wall suddenly appeared (Figure 5,6). The plates of *Tatsuganesan* were on a slope of lost woods. Other plates stating, "Thank you very much to everyone in the world" were on the protection wall, too. Banners of vivid colors were a length of *senbazuru,* one thousand folded paper cranes. *Senbazuru,* which is many folded paper cranes linked together, is the offering or charm which is an enduring symbol of wishes for a recovery from illness and also for longevity. These colored *senbazuru* banners, appealed with gratitude citing, "We make an effort to be fine."

Figure 5

Figure 6

Figure 5,6; on the way to Minami Sanriku cho from Kesen cho (August 8,2012)

The Japanese Kanji character for *Engi* (Luck) is found here. Sometimes, a small shrine is built at the entrance to a particular place, like a village, or the entrance to a mountain. Often, *Engi* marks the spot where a miracle took place. Every so often, it is used to repel vice or bad things. Engi can also be used as a memorial. This place became a new small shrine (Figure 7,8). One thousand folded paper cranes and floral tributes have been offered. The prayer says "Rest in Peace."

Figure 7

Figure 8

Figure 7,8; At the Disaster Prevention Office in Minami Sanriku cho (August 8,2012)

2.3 *Tairyohbata* (good catch flag)

A revival market *Isatomae Fukko* market was established at the foot of a mountain in Minami Sanriku cho(Figure 9). The Kanji of *Fukko* (revive) is the same sound as *Fuku*

Figure 9: Isatomae Fukko market in Minami Sanriku cho (August 8,2012)

(lucky) + *ko* (happy), so people like to use the latter kanji. Many cheerful good catch flags were waving with several other flags. The good catch flag is a lucky charm that wishes safety for a ship and offers a prayer for a big catch of fish. It is very familiar to the people of this region. The color red is believed to hold power like a talisman, and also represents rejoicing in Japan. There is also a practical use for red color in flags since it is easy to spot on a ship while sailors are at sea.

2.4 *Dashi* (a kind of float with a variety decorations in festival parades)

Figure10: Dashi, at Rikuzentakata (August 8,2012)

There is “Fighting Spirit Star Festival" which originated around 900 years ago in Kesencho, Rikuzentakata. At the neighboring town of *Takata*, "The Moving Star Festival" is also held every year nowadays. This festival takes place at the beginning of the *Obon*. Both festivals feature gorgeously decorated floats. People were able to hold the customary festival even though they were lacking many materials used prepare for the festival. Even though the festival decorations were only intended to be used once, they were assembled with the utmost care. This attention to detail might relate to*date. Date* is closely related to some important concepts in Japan, for example *kabuku, furiu* (or f*uryu*),and *basara*.. The spirit entailed in heavily decorating something is related to the *furiu* concept. Some of the dances and floats are named using *furiu*. Originally *furiu* was considered as something excessive. Recordings of this in the literature increased around the late Heian era to Kamakura era. The Kanji characters for *furiu* mean amorous in ancient Chinese language. Such meaning is included in the interpretation about *iro* in Japanese. *Iro* means mainly color, or amorous. Considering the common concept as explained earlier, it is possible to recognize excessive decorations and dramatic color as a natural progression. The remaining float became a spatial landmark in the grassland (Figure.10), although it is hard to remember its origins.

2.5 Persimmon

Persimmon is one of the predominant colors of autumn. The persimmon that has finished ripening on a branch is called *undakko* in the dialect of this district. The pronunciation of it is similar to the sound of the word meaning, "hold the luck" in Japanese, though the origin of this dialect has another meaning. Therefore, this brilliant color seems like an edible hope. People and birds share these gifts. Before it becomes *undakko*, people pick some of them to make dried persimmons. After peeling the skin, if they are kept hanging outside, sugar from the fruit seeps out. Fresh persimmons worn smooth through exposure to natural air glitter as they reflect the gentle sunshine in late autumn. (figure.11,12,13,14)..

Figure 11,12: "Undakko" in nature,
Figure13,14: dried persimmon in field, at Rikuzentakata (December 23,2013)

2.6 Flowers blooming on the rubble

This disaster brought a many emotional difficulties for the people of the area. Everyone suffered extreme stress during the earthquake, and in the aftermath as they adjusted to a long period of being refugees. In such a situation, a teacher of fine arts from Hohara High School in Fukushima reached a sense of peace by drawing a picture. Then she started the project "Blooming flowers on the rubble" with her students. Though some of her students were not familiar with painting, everybody could make a flower bloom through their drawings (Figure15,16). The rubble used in this project is fragments of a collapsed schoolhouse. The teacher and her students gathered the pieces to be used for the paintings. Those "Flowers blooming on the rubble" will be placed beside the rebuilt schoolhouse in the near future. Sometimes they encouraged the refugees who lived in temporary housing by this project. Through this activity, they could exchange a smile with people here. The students of the project "Blooming flower on the rubble" graduated last March.

How much did the color comfort the silent rubble? Color becomes a flower here.

Figure 15,16; project "Blooming flower on the rubble" by students in Hobara High School and their teacher Atsumi Bansho, at the exhibition in Ginza, (February 23,2013)

3. FAITH IN THE POWER OF COLOR

On the way to Tokyo, I felt out of place, looking at the solid buildings and crowded houses since my eyes had experienced the ruin, the prefabricated temporary buildings or the containers in the disaster area. At this cityscape, the power of color seemed less important. What is existence of color? The evidence of contrast between an accent color and the natural color from the ancient era or the gray of an artifact can be related to vitality. There is a relationship between *hare* and *ke*. The landscape which pauses is daily life as *ke a*nd the tint of accent is *hare* as extraordinariness. When considering Japanese concepts, we can believe that color is related to the performing arts and entertainment. Try to take care with all things, realizing at the same time that there will always be change. It can be thought of as a kind of Japanese elegance. Variations in the festival is proof of *hare*. *Hare* appears with an upsurge, then disappears to become *ke*.

4. CONCLUSION

As stated above, the power of color is rooted in personal small daily beliefs. Faith in culture and customs is formed after understanding personal modest daily beliefs. Vitality is required to see color. Sensitivity to color is not only for discovery but is also a kind of proof of being alive.

ACKNOWLEDGEMENTS

I wish to express my gratitude to Dr. Masaru Kumagai, Dr .Makoto Manabe, Dr, Naoto Tomioka, Dr. Lois Lydens, EGTaku, Atsumi Bansho, and friends in Iwate, Miyagi, Fukushima and Tokyo.

REFERENCES

Yoshihiko Amino, 1993, *A Viewpoint of Japanology -Society and State of islands*,Tokyo:Shogakukan
Katachi no Bunka Kai,2012, *Encyclopedia about form of Japan*, Tokyo:Kosakusya

Address: Prof. Yumi AWANO, Media Design Major,Tokyo Zokei University
1556 Utsunuki-cho, Hachioji, Tokyo, 192-0992, JAPAN
E-mail: awano@zokei.ac.jp

Types of Smart Cities | Cities Built from the scratch and Old Cities transformed into Smart Cities: What kind of colours can we use?

Ana C. OLIVEIRA,[1]
[1] Lisbon Architecture Faculty – Lisbon, Portugal

ABSTRACT

Cities are the habitat of the knowledge based economy. Cities produce and attract human capital and are today giant interface of communication, Cities possess the critical mass for the production and diffusion of knowledge, innovation and integration of human networks, which enable sustainable growth. At the same time cities are the true heart of innovation. The aim of this paper is to create architectonic interventions on this new cities for the creation of spaces that all human beings felt comfortable as they are inside old cities and with modern and sustainable fields. This kind of new cities concept has to have more than only architecture Buildings and beautiful construction. They have to produce concepts of community for habitants and not only a networking but technologies. So this is the “bad” part inside this type of new U-biquous cities. All the Data from this cities has to be incorporate inside an Open Community Data, where the citizens participate actively on the decisions, and an empowering citizens in the construction of a participatory e-society. A city is not only a walkable place according to Jeff Speck: ” …the author of "Walkable City: How Downtown Can Save America, One Step At A Time," a walk has to be useful, safe, comfortable, and interesting if you're going to get people out of their cars and into the sidewalks.”. A city, and the Architecture that we have inside the city has to produce feelings and sensations to the population. A city is not an object as a simple “fridge”. So, the focus is on the public spaces and on common areas inside the Buildings, how they connect with each other’s is an objective and the Colors that we use, we see and we find are points that we can´t forget. The aim of this research is to determine some Architectural concepts that can help not only for cities, but especially for planners and architects, their role, their tools and theirs strategies. The paper argues that the strategic plan applied on this New Smart Cities it is helpful for the future sustainability of the maintenance of the space. Architecture systems could produce outcomes on the techno-economic scenario analysis and on the socio-economic impacts.

1. INTRODUCTION

“Smart Cities” are part of our modern society and are strong models on our generation, but as everything, we have the positive face and the negative face, it always depend of how spaces are used. These spaces are a reflection of the enormous technological advances provided by years and years of studies promoted by the human being, that in certain actions that go beyond the physical barrier allowing the people to live in a space at the beginning of virtually, without borders. Like many inventions changed the history, the Smart Cities are revealed as a tendency for new generations marking determining and creating a new type of culture. At the end, what are real Smart Cities? What are Smart Cities?[1]“…Across the world, the stride of migration from rural to urban areas is increasing. By 2050, about 70 per cent of the population will be living in cities, and India is no exception. It will need about 500 new cities to accommodate the influx…" according to this statement Human beings are trying to react to the law of supply and demand, and trying to find a way to be able to solve a future problem. Cities are modern creations[1]"…It is a city where information technology is the principal infrastructure and the basis for providing essential services to residents…" The origins can be at some especial lines[1]"…The concept of smart cities originated at the time when the entire world was facing one of the worst economic crises. In 2008, IBM began work on 'smarter cities' concept as part of its Smarter Planet initiative. By the beginning of 2009, the concept had captivated the imagination of various nations across the globe…" On article of 11 November 2014, on the SustainableCitiesCollective, Nina Bianchi e Kat Hartman, describe Smart Cities as[2] "…a skeptical image of a "remote-control city…". The definition says[3]"…A city can be defined as 'smart' when investments in human and social capital and traditional (transport) and modern (ICT) communication infrastructure fuel sustainable economic development and a high quality of life, with a wise management of natural resources, through participatory action and engagement…". But Smart City means efficiency, but efficiency is where the human being is also involved in its development. Smart Cities are characterized as[3]"…Smart cities as «innovation ecosystems» could offer ample opportunities for sustainable, user-driven «intelligent services»…". If these spaces are well architectural designed, they can become multicultural areas and spaces of knowledge and development where the human being wants to live and feel with quality of life. However, the economic pressures have led some errors in planning and management. A city cannot provide this feeling[4]"…No other city in South Korea, has attracted more attention than Songdo, the skyscraper-intensive, apparently eco-friendly 'smart city' built along reclaimed waterfront land in Incheon, home of the country's largest international airport called Songdo International City, so called because of the 'ubiquitous' data-gathering technology. In recent centuries, and from 70's by Michael Graves and his concept of Re-design cities, or even the city model of Corbusier and several authors as Paolo Portoghesi were big influences on urban design. Colin Rowe also have been present as another influential but more focused on the American's city design. Léon Krier, Rodrigo Perez, Peter Eisenman, Daniel Libeskind and recently Norman Foster, are major influencers in these new concepts of Smart Cities. Maria Teresa Bilotta expose on her article on 22 December 2014 that Songdo is the first Smart City in the world [5]. It is a sustainable city, Green and full of technology and innovation. A city that contains a Central Park as referrer point, a semi imitation of Central Park in New York. A city that has 10 years of development. However, according Antony M Townsend, in his Smart Cities book [6] "…Songdo was originally conceived as «a weapon for fighting trade wars» the idea was «to entice multinationals to set up Asian operations at Songdo»… with lower taxes and less regulation…". Really Songdo since its inception that introduced the concept of a Free Economic Zone, an area with different regulation of the rest of the country, but it's not working like that and it has a lot of problems.

2. METHOD

This idea is based on logic with the concept and the implementation of Green Architecture and elements that create the Green Color on a city - the logic of Sustainable Urban and Energy. This initial question arises a sub - question to identify response that is characterized by knowing which color it has to be more present on the sustainable design method to be used. On 17 December 2014, The Guardian, by Steven Poole[7] said, "…The truth about smart cities: ‘In the end, they will destroy democracy…” and further underlines also “…The smart city is, to many urban thinkers, just a buzzphrase that has outlived its usefulness: ‘the wrong idea pitched in the wrong way to the wrong people’. So why did that happen – and what’s coming in its place?...” This research improve these cities to be projected and built today, improving its existence, its sustainability and improve the type of intervention in a new systems on the existing cities. There are situations that are not identifiable, as described Alain de Botton[8]”… Beautiful houses not only fail as guarantee of happiness, as can also be accused of failing to improve the character of those who live there …”, may not only be the image of buildings could describe the development of a city. Nerveless, Alain de Botton[8]identify a reality “…We have to ask what should be exactly the look of beautiful building …”. Zygmunt Bauman, on his book Trust and Fear at the Cities says[9]“…submit ourselves to the limits of our faculties: we know very well that we will never come to dominate completely the nature and our body also will never be immortal or also immune to the relentless course of time. Thus, we do not have, because another remedy that is not content with what exists. This is a finding that has no reason to discourage us or break the will to live, but rather should serve us encouragement and infuse us energy. While we can not completely extirpate the pain, we can, in some cases, eliminate it in part and in others relieve it. The question is to know about it persist, again and again, without faint…”.

2.1 Sample Preparation

A list of questions and analysis at experts ideas connected with the Smart Cities State of Art create this new type evaluation to apply in existing cities and in Future Cities.

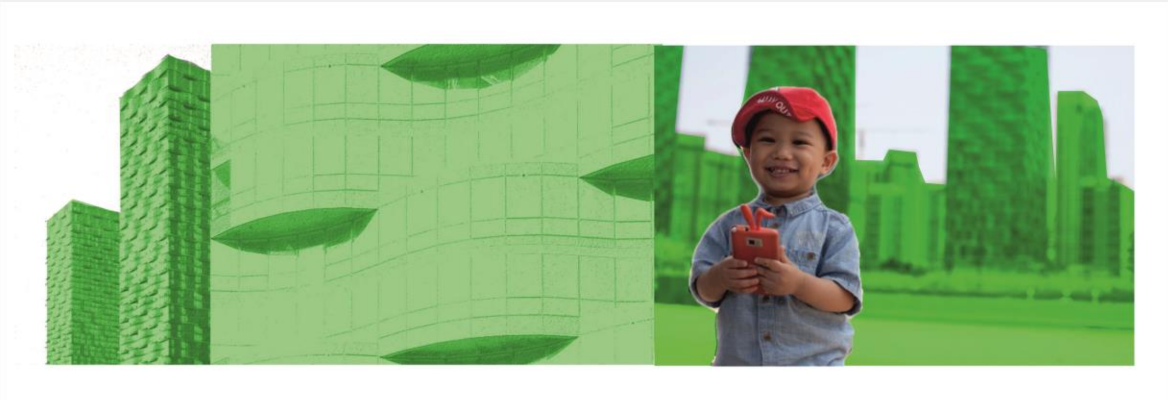

Figure 1: Songdo building Sharp I - by Ana Oliveira – transformed image

2.2 Experimental Procedure

This idea was based on interviews on experts, where were identified Colors on Smart Cities and the influences of colors on Smart Cities, searching for the best color to apply on the buildings and state of art of the predominant colors. Experts: CIKUTOVIC, Marco - AES Gener, Engineering Manager – Chile; DIAS, Solemain - Chadwick International School - Admitions Director, Brazil, DUMELIE, Geoff - Chadwick International School - Village School Counselor – Canada; HAN, Jisop - Opus Design and KPF - Director design – South Korea; JACKSON, Emma - Metroland Media Group - Canada-; KIM, May - Collins International - Real State advisor – Korea; MORE, David G. - Gale International - Project Manager – England; Polycarp, Clifford - Green Climate Found - Director Manager

– India, helped to create this analysis. Different colours were identified. And Green was the selected color. Green is a Sustainable color in all opinions.

Create an orientation basis on the demonstration of how architecture on city's can be changed according to the real importance and action in which the Green Architecture can produce big results in our days.

Figure 2: Flowchart illustrating the sample process.

With a Data Base and the Smart City concept, create a first a conclusion and a possible application on a Case Study.

3. RESULTS AND DISCUSSION

All Populations need to be informed and guided to preduce results from the initial planning of interventions inside Smart Cities. The solutions pass as well with improvement on the comunication with Universal Language because cities are not static are organic. People aspect cities with Quality and not ghost towns [10].

All this concepts with Green Architecture can be applied on Old Cities without the needing of a total demolishement. For choosing a color it's important knowing how people live and how people relate to city's too much important. Jan Gehl [10] explain [11] "... Cities are the places where people meet to exchange ideas, trade, or simply relax and enjoy Themselves ... The compact city - with development grouped around public transport, walking, and cycling - is the only environmentally sustainable form of city... the city must Increase the quantity and quality of well-planned beautiful spaces que are human in scale, sustainable, healthy, safe, and lively ... Cities ... They provide the structure que Enables cities to come to life, and to Encourage and accommodate diverse Activities, from the quiet and contemplative to the noisy and busy. The human city ... Creates pleasure for visitors and passers-by, as well as for those who live, work, and play there every day ... The Jan says: "We shape cities, And They shape us" ... "

The Green color is Balance and create positive feelings. Green color is Harmony and refreshment. Green color is Universal Love and equilibrium. It could have some negative feelings as stagnation and blandness as well. The Green color is on the center of the spectrum, a very important concept that people doesn't realize. A place with plenty of green transmit the water presence and a nature feeling. History and old elements are very important for the lives of human beings and Green produce that.

Symbols in a city are an automatic human reaction. Jan Gehl [10] also notes the following [11] "... walking, stopping, resting, staying and conversing. Unpredictability and unplanned, spontaneous actions are very much part of what makes moving and staying in city space such a special attraction."

Country	City	Color	RGB	
USA	San Francisco	Auburn	#841B2D	
Mozambique	Maputo	Camouflage Green	#78866B	

Thailand	Bangkok	Chamoisee	#A0785A	
Cuba	Havana	Cerulean Blue	#2A52BE	
Argentina	Buenos Aires	Columbia Blue	#C4D8E2	
Peru	Lima	Chocolate (Web)	#D2691E	
Germany	Berlin	Ash Grey	#B2BEB5	
Italy	Sicilia	Citrine	#E4D00A	
South Korea	Seoul	Dark Gray (X11)	#A9A9A9	
Austria	Vienna	Deep Violet	#330066	
China	Macau	Buff	#F0DC82	
United Kingdom	London	French Bistre	#856D4D	
Scotland	Edinburgh	Fern Green	#4F7942	
India	New Delhi	English Red	#AB4B52	
USA	New York City	Electric Yellow	#FFFF33	
Portugal	Lisbon	Cosmic Latte	#FFF8E7	
China	Beijing	Ebony	#555D50	
Italy	Rome	Camel	#C19A6B	
Japan	Tokyo	Amethyst	#9966CC	
France	Paris	Champagne	#F7E7CE	
Morocco	Marrakech	Café Au Lait	#A67B5B	
South Korea	Songdo	Cadet Grey	#91A3B0	

Table 1. Summary of the results from the experiment.

The Green color[14]represent fresh air. The color of the interior and exterior spaces are human influencers as is proved. Peter Zumthor [12] also transmits in his book Atmospheres [13] "... I enter the building see the room and - in the fraction of a second - have this feeling about it. We have perceive atmosphere through our emotional sensibility - a form of perception that works incredibly and Which We humans evidently need to help us survive ... I have no idea why that is so, but it's like that with architecture too ... ". Population, cities, governments, companies will benefit with this new concept. More oxygen, more quality with a Green color.

4. CONCLUSIONS

All of the Smart Cities are not follow the original concepts of Sustainable spaces, its important to change that. For trasforme and create a sustainable city, the amount the is needed is very big, so the direct focus on the population has to be very strong and productive. All Smart Cities have to improve to maintain the population, becouse only with this focus, the space is prepare to make and produce results to create mechanism to apply on new technologies or ether to transform the Spaces in Sustainable and autonoms areas. The Green color, in this case, can be applied in Songdo and in other Smart Cities in Asia because of the polution, but in the future, other colors can be supporting this idea. For now the Green is the solution.

ACKNOWLEDGEMENTS

The last ten years of my life were dedicated for Academic valorization, with a concluded master at the end of 2008, with my MBA in the middle of 2013 and now on the last months of the PhD between Lisbon, Milan, New York and South Korea. I want to express to all the people who helped me on this journey, and who have been in my best and worst moments, my deepest gratitude. To my advisor, Professor Arch. *Carlos Alho* from Lisbon Architecture University (FAUTL) for their valuable support. To my mother, for all the dedication and to my father for always being present and ready to help with pragmatism. To my love, for making me see the world in such a different and courageously, and his unconditional support. In general also thank all the friends who motivated me repeatedly with positive words of encouragement.

REFERENCES

A. Puri, 15-Aug-2014. What are smart cities? The Hindu, [1]

Smart City Development and Definition | Sustainable Cities Collective. [Online]. Available: http://sustainablecitiescollective.com/big-city/1011486/what-makes-city-smartanyway?utm_source=hootsuite&utm_medium=twitter&utm_campaign=hootsuite_tweets. [Accessed: 18-Nov-2014]. [2]

Wikipedia, the free encyclopedia, 12-Oct-2014*, Smart city*. [3]

C. M. in Songdo, Welcome to Paju Book City, the Guardian. [Online]. Available:http://www.theguardian.com/cities/2014/jul/16/welcome-to-paju-book-city-the-south-korean-town-inspired-by-hay-on-wye. [Accessed: 08-Jan-2015]. [4]

M. T. B. in Songdo, Songdo, South Korea: the world's first smart city - in pictures, the Guardian.http://www.theguardian.com/cities/2014/dec/22/songdo-south-korea-world-first-smart-city-in-pictures. [Accessed: 06-Jan-2015]. [5]

Anthony Townsend*, My Work*. [6]

S. Poole, The truth about smart cities: 'In the end, they will destroy democracy, the Guardian. http://www.theguardian.com/cities/2014/dec/17/truth-smart-city-destroy-democracy-urban-thinkers-buzzphrase. [Accessed: 06-Jan-2015]. [7]

A. de Botton, *A Arquitectura da Felicidade*, 1 vols. D.Quixote, 2009. [8]

Z. Bauman, Confiança e Medo na Cidade, Relógio D'Água Editores - tradução Miguel Serras Pereira., 1 vols. Antropos, 2005. [9]

Wikipedia, 01-Jan-2015, *Jan Gehl*, [10]

J. Gehl, 1st ed., vol. 1, 1 vols. Washington, Covelo, London: Island Press, 2010, Cities for People. [11]

Wikipedia, 09-Jan-2015, *Peter Zumthor*.[12]

P. Zumthor, *Atmospheres*. [13]

Wikipedia, List of colors: A–F http://en.wikipedia.org/wiki/List_of_colors:_A%E2%80%93F

Colour Affects, http://www.colour-affects.co.uk/psychological-properties-of-colours[14]

Address: Prof. Carlos Alho, Department of Architecture and Urbanism,
Lisbon Architecture University, Rua Sá Nogueira, Pólo Universitário, Alto da Ajuda,
1349-055, PORTUGAL
E-mails: anaoliveira@lineontime.com

The Use of English Colour Terms in Big Data

Dimitris MYLONAS,[1,3] Matthew PURVER,[1]
Mehrnoosh SADRZADEH,[1] Lindsay MACDONALD,[2] Lewis GRIFFIN,[3]
[1] School of Electronic Engineering and Computer Science, Queen Mary Univ. of London
[2] Dept. of Civil, Environmental & Geomatic Engineering, University College London
[3] Dept. of Computer Science, University College London

ABSTRACT

This study explores the use of English colour names in large datasets from informal Twitter messages and the well-structured corpus of Google Books. Because colour names in text have no directly associated chromatic stimuli, the corresponding colour categories of colour words was assessed from responses in an online colour naming experiment. A comparison of the frequency in the three datasets revealed that the mapping of colour names to perceptually uniform colour spaces does not reflect natural language colour distributions.

1. INTRODUCTION

Colour plays a central role in visual perception and can be a powerful tool to differentiate emotions, ideas and identities. We are able to see millions of different colours but we tend to organise them into a smaller set of colour categories and give them names such as yellow, peach or sky blue. There is a growing interest in the language of colour, and over recent years colour naming models have been used for gamut mapping (Motomura, 1997), image processing (Moroney *et al.,* 2008) and colour selection (Heer & Stone, 2012).

In this paper we explore natural language processing and data visualisation methods for understanding the use of colour names by analysing a large pool data from Twitter and Google Books. Because colours in language have no direct reference to chromatic stimuli, we accessed the associated colour categories of each colour name from the responses of hundreds of participants in an online colour naming experiment (Mylonas & MacDonald, 2010).

Twitter is an open micro-blogging platform that allows millions of users around the world to broadcast and receive in real time short messages, known as *tweets*, of up to 140 characters long. Twitter's conversations are public by default and organised by community-driven practices. This provides researchers with the opportunity to analyse multilingual everyday conversations outside of formal institutional environments.

In 2001, Google created a large corpus of n-grams based on ~4% of all books ever published. N-grams refer to the sequence of n words found in all digitized books. The first edition of the corpus consisted of over 500 billion words published between 1500 and 2000 in English, French, Spanish, German, Chinese, Russian and Hebrew (Michel *et al.* 2011). A new edition of the corpus provides syntactically annotated n-grams and their counts with part-of-speech (POS) tags from over 6% of all books ever published in 8 languages (Lin *et al.* 2012). POS taggers classify words as nouns, verbs and adjectives, etc. and provide an instructive form of word-category disambiguation in a given context.

An online colour naming experiment (Available at: http://colournaming.com) was designed to collect broad sets of multilingual colour names with their corresponding colour ranges in sRGB and Munsell specifications. Over the past seven years (2008-2015) the server has gathered responses from thousands of participants in fourteen languages: English, Greek, Spanish, German, Catalan, Italian, simplified and traditional Chinese, French, Korean, Danish, Lithuanian, Thai and Portuguese. The server also gathered the response time for each colour name and associated metadata regarding the cultural background, colour deficiency, hardware/software components and viewing conditions of the participants (Mylonas & MacDonald, 2010).

The Munsell system is the most widely used apparatus in colour naming research, despite its limitations, as it provides a pragmatic colour space to map colour names to perceptual colour coordinates. The system divides the colour space evenly into five primary hues (yellow, red, blue, purple and green) and five intermediate hues. Purple was included as a primary because there are about twice as many perceptible hue steps between blue and red as between red and yellow, or yellow and green, or green and blue (although in nature we might find relatively fewer purple colours). A renotation was carried out (Newhall *et al.,* 1943) with the objective to represent perceptually uniform hue, saturation and lightness spacing based on the principle of the Just Noticeable Difference (JND). The Munsell colours do not represent typical naturally occurring colours as their pigment spectra are smoothed in comparison to naturally occurring spectra and while it covers all the most important regions of colour space, some areas are not well represented (Buchsbaum & Bloch, 2002).

Considering that colour coding may reflect the colours available in our environment, previous studies have focused on uniform colour spaces and image statistics of natural scenes (McDermott & Webster, 2012). In the present study we asked instead whether colour language is efficiently represented in perceptual colour spaces and examined whether the statistics of colour in written language follow the distribution of colour names mapped to an approximately uniform colour space in an online colour naming experiment.

2. METHOD

We analysed 10,000 responses in the online colour naming experiment from 500 UK-resident English speakers, of which 90.3% reported normal colour vision. Colour name responses most often were of a single word (monolexemic) but could consist of an unlimited number of words. We identified the most frequent 50 monolexemic colour terms responded 20 times or more in responses from non-deficient observers over the age of 16. To access the associated colour categories of each colour name we retrieved all colour samples given the same name.

To explore the usage of colour names in informal, online conversations, we took the 50 most frequent monolexemic colour terms from experiment responses, and measured their probability in 1,036,103 random tweets from the Twitter API. We filtered Twitter's public stream with the geo-location coordinates of [-5.4,50.1,1.7,55.8] that correspond to a rectangle with edges approximately at the edges of Britain. We excluded tweets in other languages than English {'lang':'en'}. Each tweet was tokenised into unigrams using the Natural Language Toolkit (Bird *et al.*, 2009) and typographical conventions were removed resulting in 129,355,280 tokens.

Messages in Twitter are limited to max 140 characters and often consist of non-standard English that makes the task of word-category disambiguation challenging. For example, it is difficult to determine whether the word *orange* is being used metonymically as an adjective to describe the colour of an object, like an orange table, or is being used literally to describe a type of citrus fruit. To investigate the use of colour names in context and disambiguate their syntactic role, we also counted the probability of the 50 most frequent monolexemic colour terms from experiment responses in the syntactically annotated Google Books corpus of all digitised English books between 1500-2000. The frequency of occurrence of each unigram was counted by dividing the number of instances of each unigram in the given years by the total number of tokens (n=468,491,999,592) in the corpus for the same years (Lin *et al.,* 2012).

2.1 Sample Preparation

The 600 total test samples in the colour naming experiment were specified in the sRGB colour space and selected from the Munsell Renotation Data (Newhall *et al.,* 1943). The original dataset consisted of 2729 colour samples specified in CIE *xyY* colour space and viewed against a neutral grey background under illuminant C. Since achromatic colours were not included, nine neutral samples, one for each Munsell Value and a White and a Black sample at the extremes of the sRGB cube were added. Colour samples lying outside the sRGB gamut were discarded. Given the cylindrical coordinate system, the sub-sampling of the remaining in-gamut colour samples followed a similar approach to the advice of Billmeyer to Sturges & Whitfield (1995), namely to equalize the perceptual distances between samples (Mylonas & MacDonald, 2010).

2.2 Experimental Procedure

The procedure in the online colour naming experiment consists of six steps (Figure 1). First, we ask the observers to adjust his or her display to sRGB settings, and the brightness in order to make visible all twenty-one steps of a grey scale ramp. In the second step the participant answers questions relating to the lighting conditions, the environment and properties of the display. Then, in the third step, the participant is screened for possible colour deficiencies with a simple web-based Dynamic Colour Vision Test developed at the City University London (Barbur 2004). The fourth and main part is the *unconstrained colour-naming task*: any colour descriptor, either a single word, or a compound, or terms(s) with modifiers can be entered to describe each of twenty samples presented in sequence and randomly selected from the 600 in total samples. Along with the colour name typed on a keyboard, the response times (RTs) of onset of typing are recorded, defined as the interval between presentation of the colour stimulus and the first keystroke. In the fifth step we collect information about the participant's residency, nationality, language proficiency, educational level, age, gender and colour experience. In the last step we provide the participant with a summary of the responses.

Figure 1: Flowchart of the experimental procedure (Available at: http://colornaming.com)

3. RESULTS AND DISCUSSION

The probability of the most frequent monolexemic colour terms from experiment responses in Twitter messages is shown in Figure 2. For clarity, we have chosen a cut-off of 30 most frequent terms in Twitter given that non-expert observers are able to identify 30 colour names in their native language without training (Derefeldt & Swartling, 1995). *Black* and *white* were the most frequent colour terms followed by *red*, *cream* and *blue*. *Yellow* was found in the 9th position while *indigo* and *teal* were ranked at the bottom of the list. The absence of context in this approach produced an issue of word-category disambiguation. For example, we were not able to disambiguate whether *cream*, *orange* and *salmon* were used as nouns or as adjectives. In Twitter messages this is a particularly challenging problem as the character limit and conventions of text communication forces users to compress more information into fewer characters without conventional use of grammar and syntax. For well-structured corpora such as books and articles, POS taggers achieve higher accuracy.

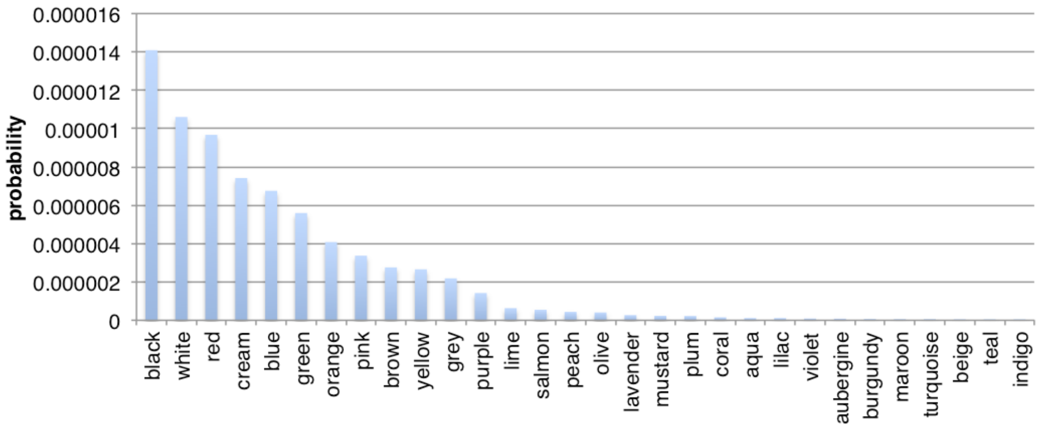

Figure 2. Top 30 most frequent colour terms in ~1 million Twitter conversations

Figure 3 shows the probability of the 30 most frequent English colour terms used as adjectives in the syntactically annotated Google Ngrams Corpus from the 50 most frequent monolexemic colour terms from experiment responses. *White, brown* and *red* were the most frequent colour terms followed by *blue*, *black, green* and *yellow*. The least frequent terms were *khaki*, *turquoise* and *maroon*.

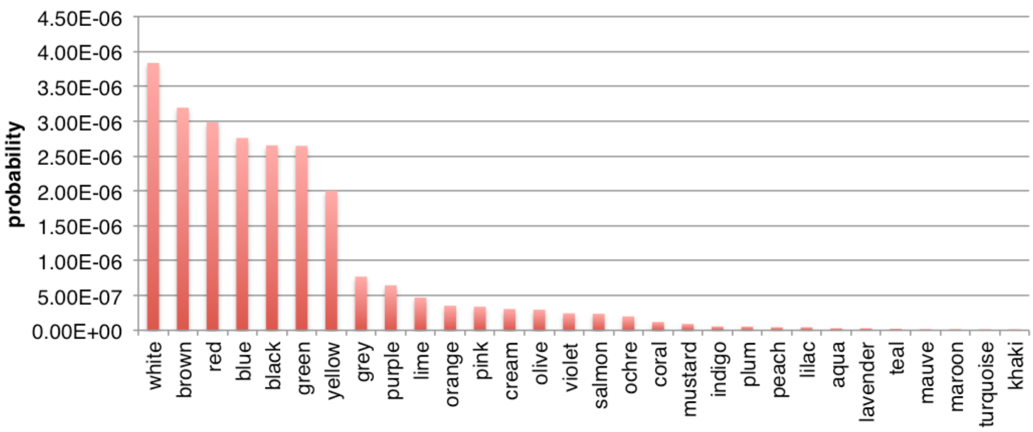

Figure 3. Top 30 most frequent English colour terms used as adjectives in Google books Ngrams between 1500-2000.

We retrieved the 30 most frequent colour terms with the highest average rank across Twitter and Google Books (*white, black, red, blue, brown, green, cream, yellow, orange, grey, pink, purple, lime, olive, salmon, mustard, peach, coral, violet, plum, lavender, lilac, aqua, indigo, maroon, teal, turquoise, burgundy, aubergine and beige*) and obtained all colour samples given the same name by hundreds of participants in the online colour naming experiment.

Figure 4 shows these colour categories by the size and their associated colour names. *Purple* was the largest colour category in the experiment followed by *blue* and *pink*. *Lilac* and *turquoise* were found in the 6th and 7th positions respectively. The colour categories with the smallest size were *coral, cream* and *lime*.

Comparing the distributions of colour names in the three datasets shows that while *white* was the most frequent colour term in Google Books and second in Twitter, in the online experiment it was found in the 26th position. *Purple* on the other hand was the largest category in the online experiment while in Twitter was the 12th and in Google Books the 9th most popular colour term. *Red* was found in the 3rd position in both Twitter and Google Books but in the experimental dataset was found in the 12th position.

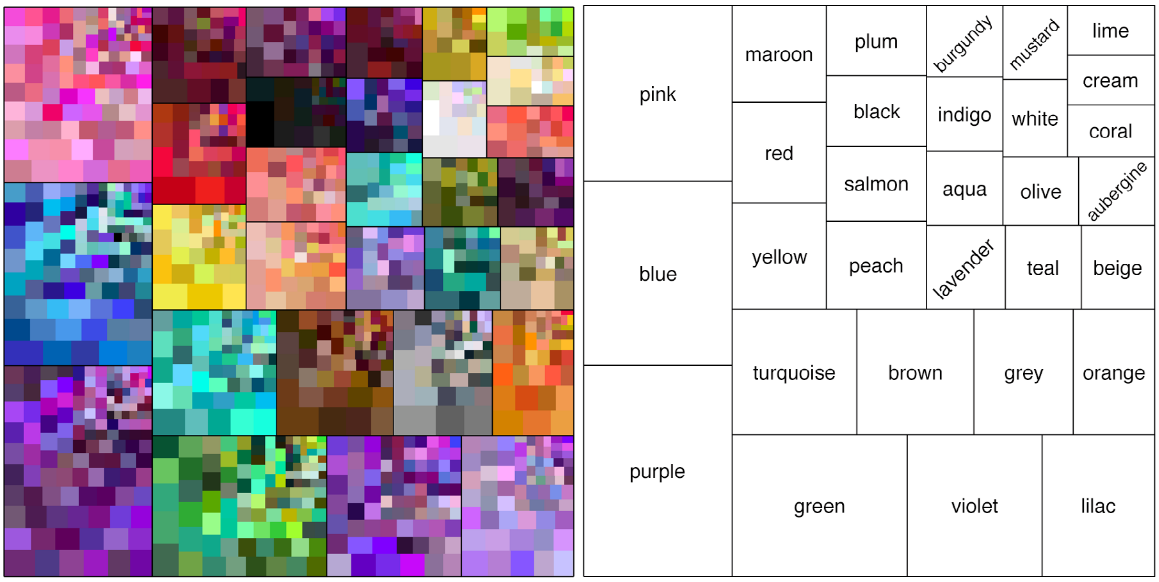

Figure 4. Treemap associated with the size of colour categories in the online colour naming experiment: (left) colour samples of each colour name; (right) colour name.

4. CONCLUSIONS

In this study we have presented the use of colour names in Twitter messages and Google Books and we visualised their associated colour categories using responses from an online colour naming experiment. The comparison of the colour distributions in the three datasets revealed that the mapping of colour names to perceptually uniform colour coordinates does not reflect natural language colour distributions. Future plans include the examination of the geometry of lexical colour spaces.

ACKNOWLEDGEMENTS

We thank all the volunteers who have contributed in this study as participants in the online experiment. This work was supported in part by the QMUL Media and Arts Technology programme, EPSRC Doctoral Training Centre and by the UCL Computer Science, EPSRC Doctoral Training Grant.

REFERENCES

Buchsbaum, G. and O. Bloch 2002. Color categories revealed by non-negative matrix factorization of Munsell color spectra. *Vision Research*, 42(5), 559-563.

Barbur J.L., A.J. Harlow, G.T. Plant 1994. Insights into the different exploits of colour in the visual Cortex. *Proc Royal Society London B Biology Sci*. 258: 327-334.

Bird, S., E. Klein & E. Loper 2009. *Natural Language Processing with Python*. Beijing; Cambridge Mass.: O'Reilly Media.

Derefeldt, G., & T. Swartling 1995. Colour concept retrieval by free colour naming. Identification of up to 30 colours without training. *Displays*, 16(2), 69–77.

Heer, J. and M. Stone 2012. Color naming models for color selection, image editing and palette design. *In Proc. CHI 2012*, Austin, TX, USA, ACM Press: 1007-1016

Lin, Y., J.-B. Michel, E.L. Aiden, J. Orwant, W. Brockman and S. Petrov 2012. Syntactic Annotations for the Google Books Ngram Corpus. *In Proc. ACL 2012 System Demonstrations*. Stroudsburg: Assoc. Comp. Linguistics.

Michel, J.-B., Y.K. Shen, A.P. Aiden, A. Veres,… E.L.Aiden 2011. Quantitative Analysis of Culture Using Millions of Digitized Books. *Science*, 331 (6014), 176-182.

McDermott, K. C., & M.A. Webster 2012. Uniform color spaces and natural image statistics. *Journal of the Optical Society of America A*, 29(2), A182–A187.

Moroney, N., P. Obrador and G. Beretta 2008. Lexical Image Processing. *In Proc. 16th Color Imaging Conf.*, Portland: IS&T, pp. 268-273

Motomura, H. 1997. Categorical Color Mapping for Gamut Mapping. *In Proc. 5th Color Imaging Conf.,* Scottsdale: IS&T/SID, pp. 50-55.

Mylonas, D. and L. MacDonald 2010. Online Colour Naming Experiment Using Munsell Samples. *In Proc 5th European Conf. on Colour in Graphics, Imaging and Vision (CGIV)*, Joensuu: IS&T, pp. 27-32

Newhall, S.M., D. Nickerson and D.B. Judd 1943. Final Report of the O.S.A. Subcommittee on the Spacing of the Munsell Colors. *Journal of the Optical Society of America A*, 33(7), 385-411.

Sturges, J. and A. Whitfield 1995. Locating basic colours in the Munsell Space. *Color Research and Application*, 20(6): 364-376.

Address: Dimitris MYLONAS, Department of Computer Science,
University College London, Gower Street, London, WC1E 6BT, UK
E-mails: d.mylonas@ucl.ac.uk, m.purver@qmul.ac.uk, mehrnoosh.sadrzadeh@qmul.ac.uk,
lindsay.macdonald@ucl.ac.uk, l.griffin@cs.ucl.ac.uk

A Proposal of a Colour Universal Design Game for Learning Dichromats' Confusion Colours

Shigehito KATSURA,[1] Shoji SUNAGA[2]
[1] Graduate School of Advanced Integration Science, Chiba University
[2] Faculty of Design, Kyushu University

ABSTRACT

The products based on the idea of colour universal design have spread by development of check tools for colour universal design in Japan. One of the next issues is how to educate colour universal design to a designer. We developed a game for learning the confusion-colour combinations of dichromats. In this paper, we introduce a development process of the game and some comments to the game from game players.

1. INTRODUCTION

It is well known that there is diversity in colour vision. Congenital colour-vision deficiency is one kind of colour vision types. Colour vision defectives cannot discriminate any colour combinations that are called confusion colours (Wyszecki and Stiles 1982). Therefore, colour vision defectives cannot receive information defined by the confusion colours in visual media or on visual displays. A colour universal design has been proposed against such a dichromats' disadvantage. A basic idea of colour universal design is to avoid using such dichromats' confusion-colour combinations. Some colour-universal-design aiding tools, for example Variantor (Miyazawa, Onouchi, Oda, Shinomori, and Nakauchi 2006) and Vischeck (Dougherty and Wade 2002), have been developed recently. However, the role of these tools is to check whether confusion colours are being used by simulating the dichromats' colour appearance, but is not to improve the designers' knowledge of dichromats' confusion colours. The knowledge of dichromats' confusion colours would allow designers to choose colours based on the colour universal design.

The purpose of this paper was to propose a colour-universal-design aiding tool to improve the designers' knowledge of dichromats' confusion colours. We developed a game which players can learn the confusion colours in order to improve the knowledge of dichromats' confusion colours.

2. DEVELOPMENT OF A GAME

2.1 The Conception of the Game

The conception of this game is that the player's knowledge of dichromats' confusion colours is empirically improved by playing the game. There are two approaches to accomplish the education of colour universal design for designers. One is the approach of making a designer learn the colour combinations that dichromats can discriminate. Using the colour combination learned, the colour design would be a universal design. For example, the colour pallet for universal design recommended by Japan Paint Manufactures Association (Ito 2011) is based on this idea. The other approach is for a designer to learn the typical confusion-colour combinations of dichromats. Namely, he/she learns colour combinations that should not be used for colour universal design. Currently, it is not clear which approach is better.

We adopted the latter approach, because we have thought that the latter approach would yield a designer the question whether the confusion-colour combinations are being used in visual displays whenever he/she looks at them.

2.2 The Features of the Game

It is the most important point of the game that a player plays the game frequently. Therefore, we gave the following features to the game.

1) The rule of the game is very simple.
2) One game finishes within 3 minutes at longest.
3) The game has contingency so that the player would not get bored it.
4) The game can run on a smartphone or a tablet terminal so that the player can play it anytime anywhere.

We chose an iOS programming with Xcode on MacOS X as a platform of the game development and developed the game guessing the confusion-colour combinations.

2.3 Calculation of Confusion-Colours Combinations

The confusion-colour combinations were calculated in the LMS colour space defined by the cone fundamentals proposed by Smith and Pokorny (1975). Eight colours were randomly chosen in the parallelepiped defined by the gamut of a colour display. The RGB primaries and the gamma characteristic of the sRGB standard were applied to those of the colour display, respectively. A confusion colour paired to each of the eight colours was randomly determined by shifting to the direction paralleled to the missing fundamental axis in the parallelepiped. An example in the case of the "Protan" is shown in Figure 1.

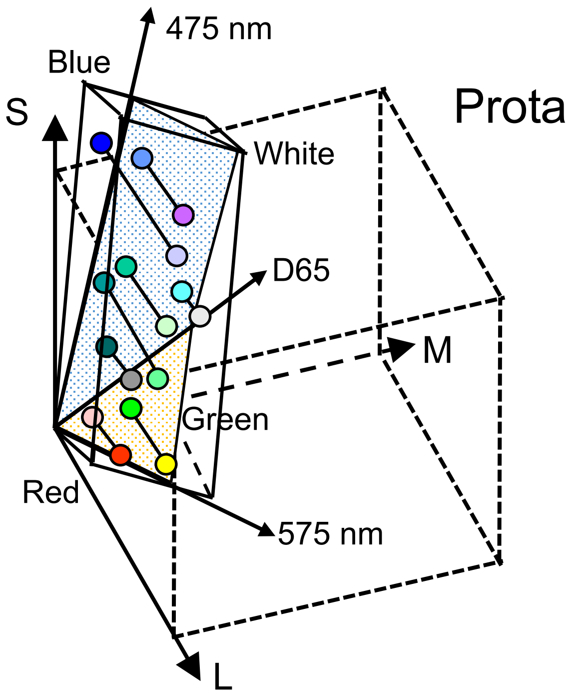

Figure 1: Method of determining the paired confusion colours.

3. HOW TO ENJOY THE GAME

The game screen is shown in Figure 2. The screen consisted of a Segmented Control and sixteen colour patches. Sixteen colour patches constitute eight pairs of the confusion colours as mentioned in Section 2.3. How to play the game and the rule of the game are as follows.

1) A player selects one type of dichromacy to learn from the Segmented Control: “Protan”, “Deutan”, and “Tritan”.
2) Eight confusion-colour pairs of the selected dichromacy are computed. Sixteen colour patches consisting of eight pairs are randomly assigned to a four-by-four arrangement and are displayed.
3) The player chooses two colour patches that are guessed to be a confusion-colour pair by tapping.
4) If the chosen two colour patches are a confusion-colour pair, the player will get 1 point and can move to a next choice. Otherwise, the game will be over.

We expect that the game player’s knowledge of dichromats' confusion colours would be empirically improved by repetition of the game play.

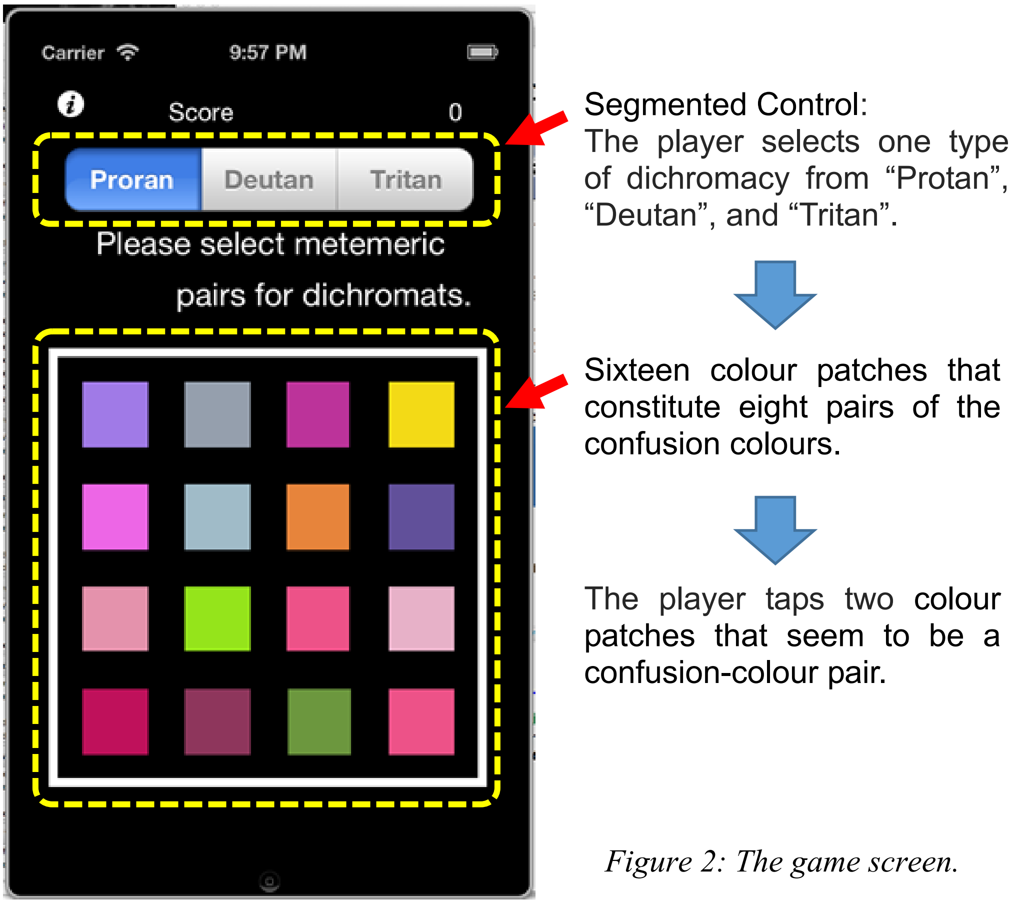

Figure 2: The game screen.

4. COMMENTS TO THE GAME

We got some comments from the game players who were students at school of design, Kyushu University. They were interested in the game guessing the confusion-colour pairs. Almost the comments were that it was difficult to choose the confusion-colour pairs without any knowledge of dichromats' confusion colours. Therefore, other supplementary materials may be required for the player in order to provide a basic knowledge of dichromats' confusion colours. Further, even if they have some knowledge of those, it was hard for them to complete the game when similar confusion-colours pairs were displayed. It may be necessary to add a constraint on the random colour-choice algorithm in order to avoid displaying similar confusion-colours pairs.

5. CONCLUSIONS

We developed a game for designers to improve the knowledge of dichromats' confusion colours. In this paper, we have described the development process of the game and players' comments to the game. However, we have not examined validity of the game in learning the confusion-colour combinations yet. We will examine whether the game player's knowledge of dichromats' confusion colours will be empirically improved by playing the game in the future study.

ACKNOWLEDGEMENTS

This study was supported by Grants-in-Aid for Scientific Research, Japan Society for the Promotion of Science; contract grant numbers 26282005 (B) and 25242004 (A).

REFERENCES

Dougherty, B. and A. Wade 2002. Vischeck, http://www.vischeck.com/.

Ito, K. 2011, *The Color Palette for Universal Design*, Irodori 29 : 12-13 (in Japanese).

Miyazawa, K., T. Onouchi, H. Oda, K. Shinomori, and S. Nakauchi 2006. *Functional Spectral Filter Optically Simulating Color Discrimination Property of Dichromats*, Perception 35(Supplement) : 197-198.

Simith, V.C. and J. Pokorny 1975. *Spectral Sensitivity of the Foveal Cone Pigments between 400 and 500 nm*, Vision Research 15(2) : 161-171.

Wyszecki, G. and W.S. Stiles 1967. *Color Science: Concepts and Methods, Quantitative Data and Formulae*, New York: John Wiley and Sons.

Address: Shigehito KATSURA, Graduate School of Advanced Integration Science,
Chiba University, 1-33 Yayoi-cho, Inage-ku, Chiba, 263-8522, JAPAN
E-mails: shige_k@graduate.chiba-u.jp
Shoji SUNAGA, Faculty of Design,
Kyushu University, 4-9-1 Shiobaru, Minami-ku, Fukuoka, 815-8540, JAPAN
E-mails: sunaga@design.kyushu-u.ac.jp

Colour Management: Managing the Intuitive Issue, the Gamut Issue and the Engagement Issue.

Phil HENRY,[1] Stephen WESTLAND,[1]
[1] School of Design, University of Leeds

ABSTRACT

This research directly challenges the established and continued practice to implement colour-picker arrangements that are underpinned by colour science principles. Computer Aided Design software has evolved to empathetically resolve familiar real-world design challenges, whilst colour selection interfaces are predominantly governed by unfamiliar technical colour-spaces and additive colour behaviour (the intuitive issue). Importantly, the work confronts the current norm where colour-picker arrangements offer a user little insight into the potential colour difference between the various hardware components until hard copy proofs are produced (the *gamut* issue). Perhaps, more problematical still is the less obvious issue relating to an interface design strategy that allows users to *easily* select colour from the full monitor gamut (the *engagement* issue). The consequence of presenting exaggerated, yet easily accessed colour choice, in a technologically enhanced workflow can seemingly lead users to confidently select colours with little reflection on their tacit colour knowledge. This workflow can effectively negate inherent colour aptitudes which in the case of designers is likely based on paint and more naturally aligned to printer capabilities.

1. INTRODUCTION

The important concept that underpins this investigation is the hypothesis that creative digital colour users will benefit from a colour–picker interface that is designed to be consistent with their intuitive colour knowledge i.e. subtractive colour (Henry *et al.*, 2013; Henry, *2013*). This notion is seen to have particular significance for problematic digital colour tasks where the creative objective is to achieve an acceptable colour-match between the monitor display and colour printer. Such colour-sensitive objectives are often a creative requirement in the colour critical industries of fashion, textiles and graphic design. Hard copy proofs (colour-printouts) are regularly used as an integral part of the design development process, being central to effective in-house discussion, customer approval or in some cases as contractually binding manufacturing standards. Equally important is the understanding that this work doses not seek to invalidate technical colour management protocols but rather shares the views of other researchers in the observation that design communities working in colour critical environments often struggle to effectively apply ridged colour management workflows in a fluid and ever evolving design context (O'Neill *et al.*, 2008; Hirschler, 2010). A note worthy observation supported anecdotally in both industry and education contexts is the relationship between increased expectations in colour fidelity in direct relation to any increased investment in technical colour engagement. Subsequently, any disappointing results often lead to mistrust in the quality/capabilities of hardware, software or even user proficiency.

2. SUMMARY OF EXPERIMENTAL WORK

2.1 The Intuitive Issue

In the initial work the ability of users to predict colour mixtures in additive and subtractive systems was tested (the intuitive issue); it was shown that users can better predict the results from subtractive systems and it was assumed that experience with physical colorant system (e.g. paints) during childhood may be where the knowledge required is gained. This finding led to the hypothesis that a colour-picker tool based on subtractive colour mixing might be better, or more *intuitive,* than one based on RGB additive colour mixing. A series of experiments were conduced by which the accuracy of a colour match (where a participant tries to match or select a colour to match a given target) was assessed for a tool based on subtractive CMY primaries and compared with one based on additive RGB primaries. The subtractive CMY tool did, in fact, give better performance. However, most contemporary software presents a colour-selection environment rather than a colour-mixing environment; that is a colour map, for example, rather than RGB sliders. Therefore the new subtractive CMY tool was also tested against more contemporary solutions, (*Figure 1*.), and, in some circumstances, was shown to still give a better performance. The new subtractive tool works well when it has been explained to users (in terms of paint-mixing) whereas a similar explanation for the additive tool is unsuccessful.

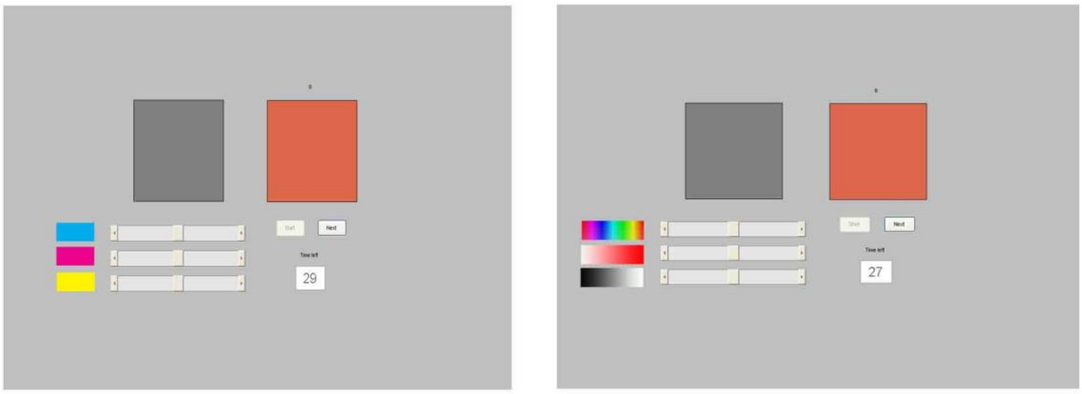

Figure 1: Examples of experimental colour-picker tools, a CMY slider bar (left) consistent with the experimental paradigm and an HCL arrangement (right) modelled on standard configurations.

2.2 The Gamut Issue

Further work explored more challenging cross-media colour matching scenarios questioning why users tend to select very bright and saturated colours on screen (i.e. *the gamut issue)*. Several conclusions were arrived at: (1) firstly, users are drawn to saturated colour and if presented with these will tend to select them (without even thinking about the consequences); (2) secondly, users tend to remember colours as being brighter and more saturated than they were (*Figure 2*.); (3) thirdly, the way in which the interface is designed encourages functional-fixedness (Dunker, 1945) and does nothing to challenge the user to think about the differences in gamuts, for example, between display and print.

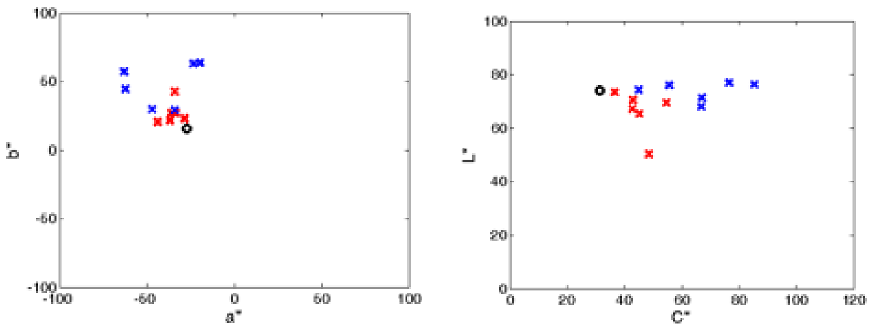

Figure 2: CIELAB coordinates (a and b*) (L* and C*) of one of the six targets (black circle) and the matches made by the observers on-screen (blue X) and in print (red X)*

2.3 The Engagement Issue

Previous studies of user colour-interface experience focuses their assessments on ease-of-use; how easily the participants could excel in basic colour-matching tasks when using different colour-picker arrangements. However, more current HCI (Human Computer Interaction) thinking has identified reservations with regards to interface strategies centred on ease-of-use preferring interfaces that exhibit aspects of possibilities-in-action. An underpinning and distinguishing quality of our colour-picker tool is the opportunity for a user to engage-in-use and connect with their existing colour knowledge, as well as gain an improved understanding regarding the nature of the digital colour challenges they are dealing with and use their skills and knowledge to make well-informed decisions. This new strategy is counter to existing colour selection strategies that seemingly encourage poor colour choice by presenting colour options that are not compatible with printing and only provide users with a relatively passive role in accepting colour outcomes governed by often concealed colour management infrastructures (i.e. the engagement issue).

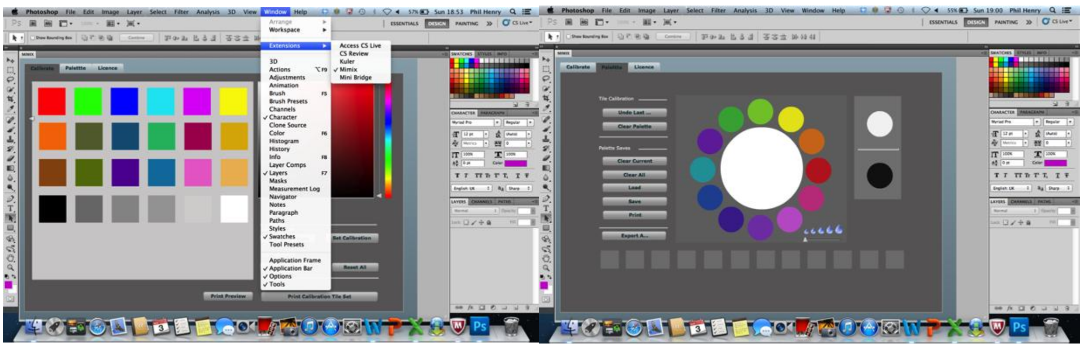

Figure 3: Illustrates views of the initial characterisation/colour matching exercise which introduces user to the gamut issue and the colour mixing interface which mimics subtractive/paint mixing

4. DISCUSSION

The results of this work challenge the established colour science convention suggesting that colour management methods are the most viable answer to tackling colour fidelity issues prevalent in many design industries, notably Textiles, Fashion and Graphics. Unquestionably, existing colour management does offer effective solutions providing the technical structures are correctly implemented and the practical constraints understood. However, a key criticism highlighted on all existing workflows is a procedure that allows users to make contextually poor colour decisions based on the colour information and options presented by the majority of colour-picker arrangements. Why, in the first instance, mislead the design expert with exaggerated colour options, then expect that any required compromises in creativity will be adequately resolved by colour science proficiency?

CONCLUSIONS

The final outcome of this research project is fully functional colour-creation software ColourMimix; it is developed as colouring tool for designers providing the means to create original palettes reproducible within the colour-space of a selected printer, ink set and substrate combination. This is achieved without the need for expensive and complicated colour management hardware or software; as an alternative the designer is in control from the outset using their colour judgment to set up the colour-picker tool to display only printable colour selections on the monitor screen. The software incorporates a unique intuitive interface and provides an alternative user-centred approach to managing digital colour. More detailed information regarding the software can be found at www.ColourMimix.co.uk and https://creative.adobe.com/addons.

REFERENCES

Duncker, K., 1945. *On Problem-Solving, Chapter in Dashiell J., F., ed., Psychological Monographs 58, No. 5.*

Henry P., Westland S. & Cheung V., 2013. *Colour selection strategies in colour design, Proceedings of the 12th Congress of the International Color Association, 1157-1160, Gateshead, UK.*

Henry P., 2013. *The design of a new colour-picker tool, Proceedings of the NIP, 98-101 Seattle, USA.*

Hirschler, R., 2010. *Electronic Communication in the Textile and Apparel Industry, REDIGE - V1 N1*

O'Neill,J., *Martin, D., Colombino, T., Roulland, F. and Willamowski, J., 2008. Colour Management is a Socio-technical Problem. Proceedings of CSCW 08.*

Address: Dr Phil HENRY, , School of Design, University of Leeds, Centre For Colour Design Technology, Leeds, LS2 9JT, ENGLAND

E-mails: p.m.henry@leeds.ac.uk, s.w.westland@leeds.ac.uk,

Suggestion for Teaching Natural Colors through Investigation and Analysis of Current Color Education for Children in Korea

Shin SANGEUN, Choi SUERAN, Kim SAETBUL, Kim YOOSUN[1]
[1]Sahmyook Environmnental GreenDesign Research Institute

ABSTRACT

Modern people experience color in various ways and thus should have sufficient color education. Especially, color education is important for children, who are more affected by colors than adults. However, it is difficult to teach art since color education for children in Korea is taught by non-experts and consists of artificial colors, according to the results of a survey interviewing teachers of the Nuri Curriculum for children aged 3-5 years. Moreover, there is a lack of appropriate color education for children, and color is recognized as an important art activity. In this study, we suggest that Forest Experience Education as a method of color education for children based on the literature and interviews using qualitative analysis. Current color education for children in Korea utilizes parts of the Forest Experience Education curriculum but does not focus on natural colors or color use, even though there is a sense of seasons and many experiences of natural objects. Hence, we have developed guidelines on color activities for children involving color theory, sense, system, etc., implementation of basic color theory by early childhood teachers, and suggestions for natural color education based on standard colors (KS). Therefore, color education for children in Korea can upgrade the understanding of natural colors, and activities are expected to continue interest in color education.

1. INTRODUCTION

1.1 Background of Study and Purpose

Color education for modern people is being gradually recognized as useful. Professional color education is effective in utilizing colors and should be started during infancy. It is possible to know the mentioned contents which study the relationship between the child's intelligence and the ability of the color use, stated Lowen feld who is the art educationalist, the children have be highly intelligent and result various of color application as the tendency of the reference on the art is high, they live in the good educational environment for art, and the more children learn the art education. In other words, aesthetic sensibility of children is affected by their preceding education. Thus, art educators, historians, and psychologists should concentrate on art activities during childhood. For example, Paul Klee who is an artist in Germany had experience with the visual arts from childhood, and his artistic instincts consolidate music and the visual arts. There are positive effects of color education for children after becoming an adult. However, current color education for children (Nuri Curriculum) is not motivating and tends to concentrate on step-by-step skills.

1.2 Theoretical Study

The various activity progresses along the vitalization of the recent forest experience education, it tends to start in infancy. This is able to know directly or indirectly to search the advance of program on the various forest experience education, the foundation of Forest kindergarten, and the management.

Practically, early childhood education focuses on the seasons and experience of natural objects. First, for seasons as it is connected with the activity of the subject if we see the activity of the related nature included the instruction of Nuri Curriculum for teacher. The comment concentrated on the subject of "animals, plants, and natures" it tends to be concentrated on the contents around the subject, especially the contents of the season.

When using natural objects, it process variously as the very effective activity in the environment of city which is not enough to meet the nature, as the activity helping the weakness processing rapidly due to the future of the change of environment and the feature of location. Recent color education for children is based on Forest Experience Education, which is recognized as artistic education for children. In Forest Experience Education, all of nature becomes a playground, while using the forest for the education space regardless of the season and weather, the purpose is that learning the harmonious relationship between human and nature from childhood according to the reason of the well-rounded development and there is to develop the body and mental for children harmoniously. There are official organizations for Forest kindergartens in Germany and Denmark but in a state of developing the plan of the program and the invention of the forest kindergarten in Korea. For this reason, color education for children should be based on the seasons, the activity of subjects, and forest experience education, it is the lack of connection and not concentrates on the nature color and the color activity.

Humans attain the superiority over reaction of Type by a twenty two-month-old baby but do superiority over reaction of color from a four-year-old, transition period around a five-year-old is confused the reaction of type and color, and reaction of type attain supervisory over the reaction of type around a nine years old. Children respond more sensitively to color than shape. Thus, we studied children receiving Nuri curriculum (ages 3-5 years) who attended a daycare center and kindergarten from 2013 (Ministry of Education) to examine the current conditions of color education for children in Korea.

2. METHOD

2.1 Research Object

Humans attain the superiority over reaction of Type by a twenty two-month-old baby but do superiority over reaction of color from a four-year-old, transition period around a five-year-old is confused the reaction of type and color, and reaction of type attain supervisory over the reaction of type around a nine years old. Children respond more sensitively to color than shape. Thus, we studied children receiving Nuri curriculum (ages 3-5 years) who attended a daycare center and kindergarten from 2013 (Ministry of Education) to examine the current conditions of color education for children in Korea.

2.2 Research Method

2.2.1 Quantitative study

The method of study is as blow. To survey the present condition of color education for children related to Nuri curriculum, we studied and classified three articles on the present conditions of color education, present conditions of color activity, and satisfaction of color activities through a survey and interview of 50 professional early childhood teachers in Seoul and Gyoung-gi.

2.2.2 Qualitative study

Based on the results of the qualitative study, we interviewed early childhood teachers and investigated related books and theses.

3. RESULTS AND DISCUSSION

3.1 Results of quantitative Study

Figure 1 shows the answers to the survey question 'How important is it to use a teaching aid related to art activities for children?' Twenty-nine answered that it is important to apply art activities for children. Four people answered ‘yes’, 12 people said ‘somewhat’, and seven people answered ‘no’. Regarding the question ‘Have you ever experienced difficulties in making teaching aids or lack understanding of color?’, 40% answered that they lacked information as the majority and lack knowledge of existing color activities and teaching aids, and lack knowledge of the question ‘If you have difficulties in making teaching aids or lack understanding of color, what is the reason?’ Importance of color is recognized by professional early childhood teachers to teach the children, the suitable color education for children and the contents of activities among the art activities for the children are lack.

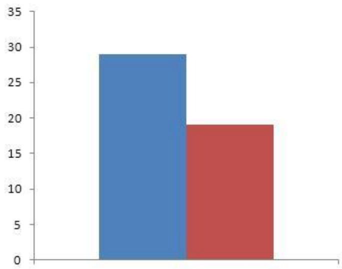

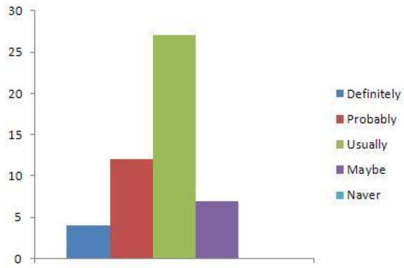

Figure 1:Art activities from children&Importance of color.

Figure 2. Difficult experience of the art activity/teaching aids according to the lack of understanding

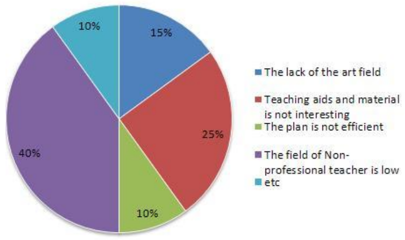

Figure 3:The cause of difficult experience of the art activity/teaching aids according to the lack of understanding

We investigated color education for professional early childhood teachers as well as books and teaching aids for art activities for children regarding the question question 'If you have difficulties in making teaching aids or lack understanding of color, what is the reason?' to search "the lack of information on the related field" and "the lack of the existing activities for color and the variety of teaching aid" to take first ranking and second, respectively. In the survey, an overwhelmingly majority of 43 people among 50 answered 'no'. Most color education is experienced at university, and total time to compete the course takes an average of 4 hours.

Finally, "non-artificial color" is 29% by the high rate and follows the aesthetic shape, inexpensive price, etc. regarding the art text book and teaching aid to improve. Art activities for children and education are important themselves based on an in-depth interview with early childhood teachers except the survey, there was the situation not to recommend high-quality color activity for children due to the understanding on the color field and the lack of information or the suitability of activity and teaching aid for many discretion and autonomy

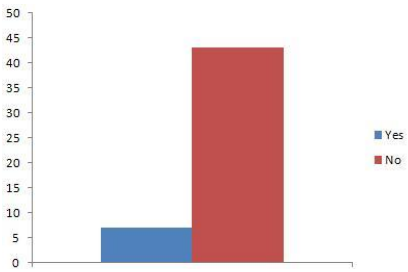

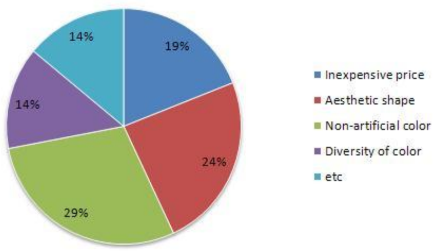

Figure 4:The experience related on the color education figure

Figure 5:The improvement of producing teaching aids of art activity from children

3.2 Qualitative and quantitative studies

First, it need to give the basic education for color theory the early childhood teacher who markedly lack of curriculum related on the color as the result of the Figure 2 of a quantitative study and as the Figure 4 having much difficult in doing art activity or the production of teaching aid according to the lack of color understanding. These lead to a sense of seasons, experience of natural objects, color, art activities in the Nuri curriculum, and education of natural colors in Figure 5.

According to contents of the Figure 1, we adjusted standard colors (Korean Industrial Standard, KS) in Korea to the color education and activities practically not to build the system and concept of color even though the importance for the color education is growing more, to mix the system and concept of color in the above Nuri curriculum in the activity of experience of around the fun and interests .

Next, this is present the various color activities and the teaching method. we try to suggest the activities aimed for natural color in the field of art experience of the observation, expression, feelings and the utilization of teaching aid, for example, in art activities for children to develop the activities for the color researching to be able to searching for in the natural objective using standard color(KS), to make the natural colored palette for children to be able to express and feel the natural color extracted natural objective to apply the concept of color management, through activity of the observation on the change of color of the natural object such as tree, flower, etc. to add the concept of the brightness and chroma to apply the color perception.

4. CONCLUSIONS

Color education for children in Korea lacks focus on natural colors and utilization but the various actives progresses recently according to the vitalization of for natural ecology. Thus, we suggest that color education for children should focus on natural colors based on qualitative and quantitative studies. First, basic education of color theory should be administered by early childhood teachers using Nuri curriculum. There are not many chances to learn about color even though early childhood teachers learn a wide range of art and music. Difficulties in early childhood education are lack of teaching-learning materials for adapting the Nuri curriculum *(2013: Park, Noh cited re-quotation)*. Color education in adapting to children is unfamiliar. Above all, art activities for children are influenced greatly by the ability of early childhood teachers.

Second, we developed color activities based on standard color (KS) excluding artificial colors the artificial color is from the understanding on need to give various chance to meet the natural color as the contents pointed out by the early childhood teacher to improve the color cognition and visuals

of children live the city life mostly.

Third, we provided guidelines for various color activities. Art activities should be performed twice per week in practice unlike the child participated in the activity to interestingly because the teacher have to depend on the certain guide line or plan when teaching. But the detailed suggestion does not present the various color activities to help this. This study is expected to lead to the color education from children in Korea to upgrade understanding on the natural color, the activities, and the consistent interest and study as presenting the direction of the color education from children and the natural color education.

ACKNOWLEDGEMENTS

Thank you for the family to support at all times and Environmental Green Design Research Institute both in joy and in sorrow

REFERENCES.

Kim, Kim & Shin, 2011. *A Study on Kindergarten Color Environmental Design for Creative Education Environment - Focused on Case Study of Kindergarten-Color Design-*, Seoul National University of Science and Technology, Science Museum Exhibition Design, Korea Science Arts Forum , Vol.9

Shin. 2014. *An Experimental Study on Cognitive Processes Stroop Effects and Children's Pattern*, Multimedia Association, Arts and Media, Vol.13, No 2.

Jang. 2012. *A Study of Forest Kindergarten as European Ecological alternative Education and Plan to Develop Domestic Forest Kindergarten*, research in Eco-centered Early Childhood Education Vol.11. No.3

Yoo, Kim, Yoo, 2014. *Effect on Multi-Intelligence of Young Children based on Nature-Friendly Educational Activities Program for children aged 5,* the Early Childhood Education Research Vol.19, No. 4

Seo, Park, Kim, 2009. *The Effects of Art Activity Using a Nature Object on Children's Art Ability and Eco-Friendly Attitude*, Korea Infant Care Education Vol. 58

Lee. 2005. *An Analysis of the color program of the children in the USA and in the UK* ,
Ewha Womans' University, The Education of Graduate School, master's thesis

Choi, Yeon. 2013. *Picture book analysis for the adoption of the field of "art activity" to the Nuri curriculum*, children's literature education study Vol. 14, No. 4

the Forest Experience Education for Little Children during tewelve month centered Natural observation, Korea: ShinJung

Gwon, Mun, Gwon, Sung, Shin. 2012. *child development*, Korea : ChanJiSa

The Ministry of Education.2014. http://www.childschool.moe.go.kr. Accessed: August 30, 2014

Address: Researcher Shin Sangeun , Sahmyook Environmental GreenDesign Research Institute, Hwarang-ro(street) 248, 504 room, 2 science hall of Sahmyook University, Seoul, 139-742, KOREA
E-mails: greencolor@syu.ac.kr, kyscolor@syu.ac.kr, greendesign@syu.ac.kr

Color Mixture Learning using Personal Computer for Basic Design

Tomoko MITSUTAKE, [1] Katsuyuki AIHARA, [2] Yosuke YOSHIZAWA, [3]
[1] Nippon Designers School / Design Consultant
[2] Tokyo Zokei University / Designer
[3] Chiba University, Organization for promotion of Academic Affairs

ABSTRACT

Media expressions by graphic designers have been digitalized from the 21st century. This paper is about a trial of basic education for designer in the digital environment.

There are two significances to introduce PC into basic education for designer. One is that physical color simulation can be done easily. The result of the Additive and the Subtractive color mixture can be expressed easily. We needed a lot of training to mix color well without PC. The second is that accurate drawing can be done easily and accurately to manage element of color and figure by the numerical value with graphics software. The basic operational directions of a graphic (translation, zooming, rotation and reflection) are also easy. More complex repeating work can also be performed quickly. These are very great advantages for design learner.

This design exercise is based on "color mixture". At first, each method of training is indicated. And after, student's impressions are also indicated. Significance of these trainings is shown from student's impressions.

1. INTRODUCTION

Basic design in the digital environment (the color and morphology manipulation) is a theme for this research. We focus on "the color mixture". Because of the color mixture by the three primary colors are used much for reproduction with the color for industrial design. We paid attention to symmetry of a graphic by morphology manipulation. Because of the most of graphics software are designed based on morphology.

The industrial color reproduction and understanding of graphics software are very important in present design. The significance in which combines these modern industrial technology with basic education for designer is important. The color design which made "color mixture" is a theme for the design exercises indicated as below. At first, the training of Additive, Subtractive and Juxtaposed color mixture were indicated. And next, student's impressions were also indicated.

2. METHOD

Attribute of the person for learning: Begineer of the graphic design. Student of the night graphic design department in Nippon Designers School. Number of students: 6 male and 17 female students, average age: 21 years old. Class name: Basic Design & Art 1（refer to 2-1 “Subtractive color mixture” and 2-2 “Additive color mixture”）, Visual design（refer to 2-3 “Juxtaposed color mixture”）

2.1 Subtractive color mixture

2-1-1 Training of CMY color mixture with a colored pencil and the painting on paper (for water-color painting use). Exercises for various CMY color mixture by painting applied "4-level gradation" in each CMY color.(Figure 1)

2-1-2 An exercise of the CMY color mixture with "the transparency film". Layers with the films can make CMY color mixture.(Figure 2, Figure 3, Figure 4)

Figure 1

Figure 2

Figure 3

Figure 4

2-1-3 Training of the CMY color mixture simulation of the exercise of 1-1 with the PC software. Each CMY color is divided in "4-level gradation" into "every layer" and simulate a subtraction color mixture.

In this study, we use Adobe Illustrator. Training method is as follows. (Figure 5)

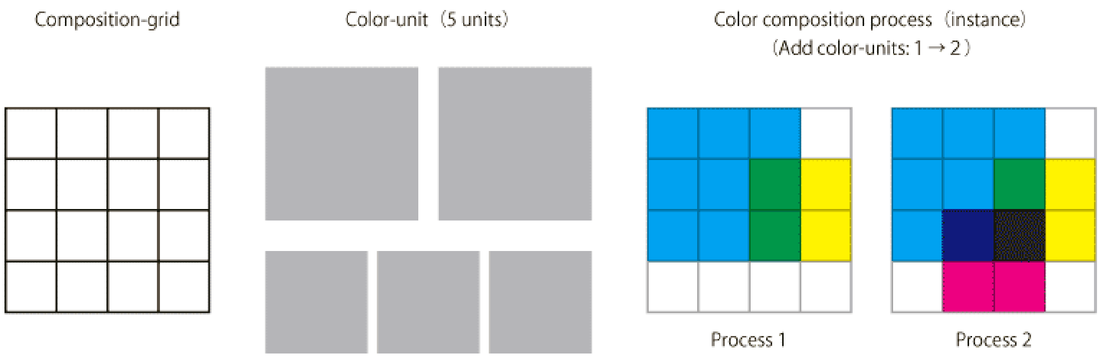

Figure 5: Practice process for CMY color mixture simulation.

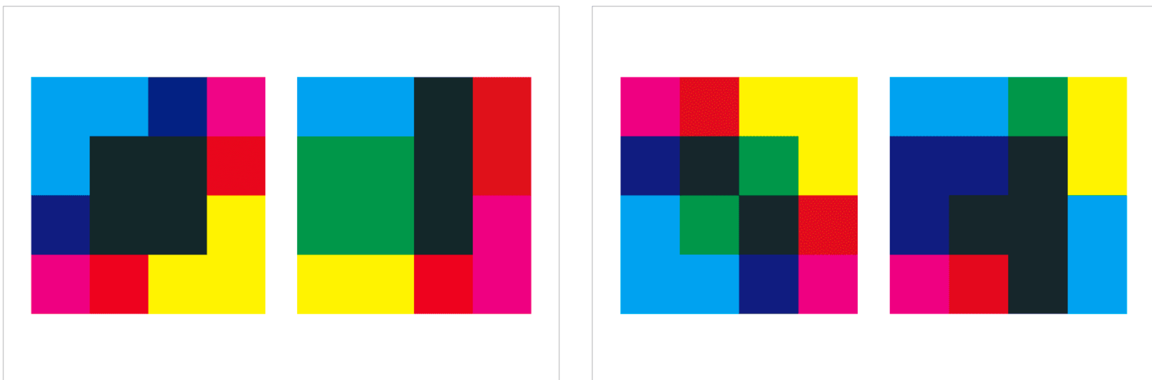

Figure 6: Student work examples.

2.2 Additive color mixture

2-2-1 Exercise for the Additive color mixture with the lights transmitted the each RGB color cellophane. （Figure 7）

Figure 7: Simulate the mixing result in the RGB color of flashlight.

2-2-2 Exercise for RGB color mixture simulation with PC software ("5-level gradation" and WEB safe colors in each RGB).

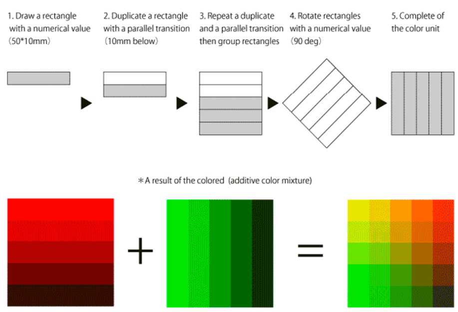

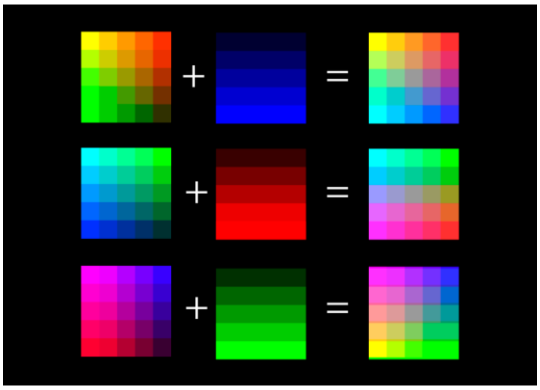

Figure 8: Working process for RGB color mixture. *Figure 9: RGB color mixing simulation.*

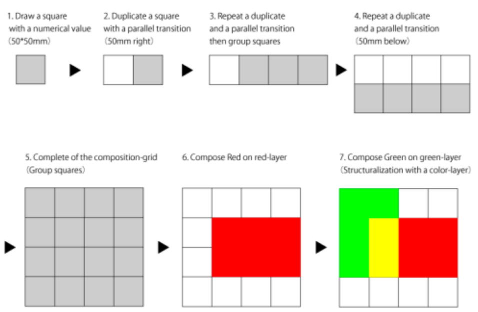

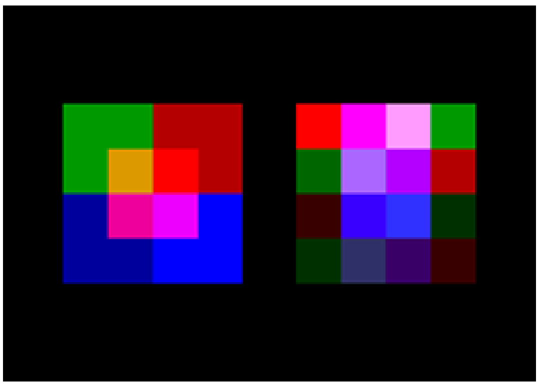

Figure 10: Practice process for RGB color mixture. *Figure 11: Student work examples*

2.3 Juxtaposed color mixture

As an example of the juxtaposed color mixture, to design the color pattern of the plain weave with the PC. Based on an example of the checked pattern using CMY, to create the pattern by student's color choice. Condition: To choose three colors of the option and design by Juxtaposed color mixture.

A work procedure: Each color plane assumes it a square of 3mm (step 1). To place the first color, the second color into checks form (step 2). To copy, rotate 90 degree and put on it (step 3). The third color locates it as a lower color of the ground. This is defined as “basic unit” of the Juxtaposed color mixture (step 4). To copy the basic unit, and a design of the checked pattern is completed in A4 size [length:298mm, height:210mm](step 5). To print the pattern to a piece of A4 size cloth. A book jacket is made to the size of the book by folding. A production process and the students’ work are as follows.

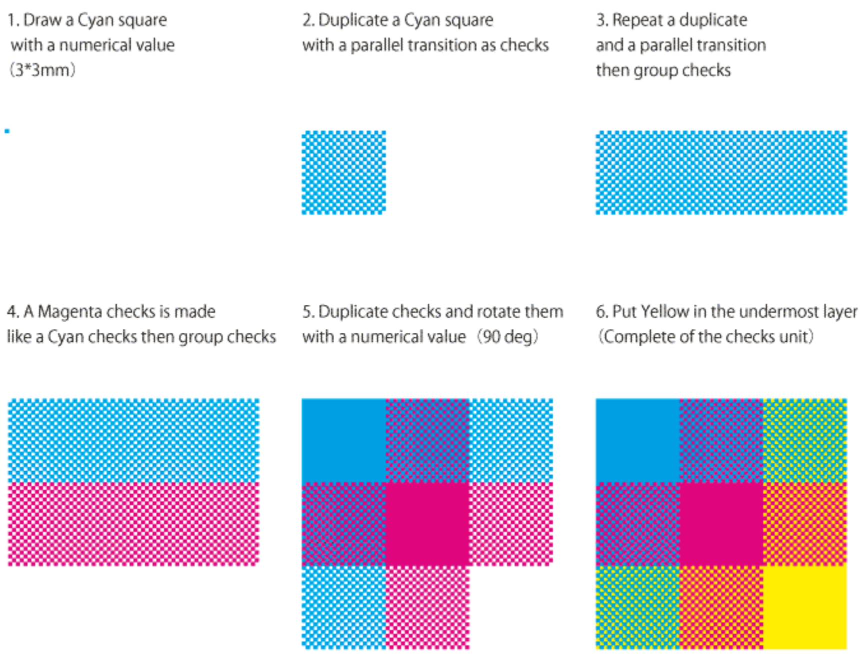

Figure 12: Working process for Juxtaposed color mixture

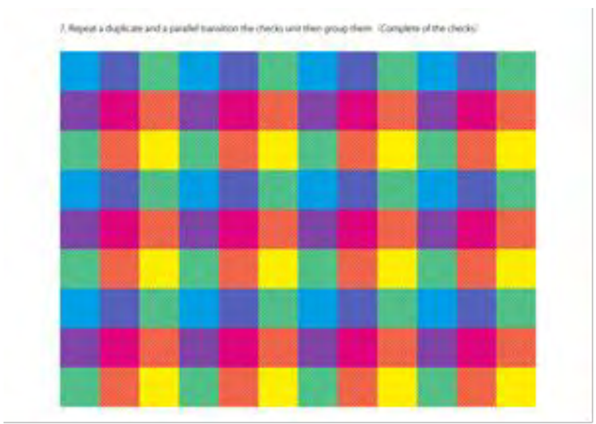

Figure 13: Replicate the basic unit of checked pattern to A4 size

Figure 14: Student work examples

3. RESULTS AND DISCUSSION

A production process and the work of the student are as follows.
"A function called color multiplication was convenient and understood well and it was interesting."
"I felt that it was easy to make a translucent design and the design with the united feeling."
"I had color constitution like today's class (in this training), and even other classes only changed a position to be piled up a little and an impression changed completely and was interesting".
"I was able to imagine only that I mixed paint when I heard the word color mixture, but I came to be able to imagine the color mixture to use "transparence origami" and the layer by this class"
"It was different from the image only to make colors juxtaposition when I only put one's color that I imaged when I mixed it. Therefore, it was necessary to simulate it many times and was serious. But I think it a very good study."
From these comment after the trainings, significance of the training is suggested.
The color is a very important topic in education for designer. When a learner handles the color, they face two problems. One is a color material and the color mixture. The color material with physical properties such as paint, it is difficult to predict the color mixing result, a number of empirical knowledge. In now, we also design using the color display and also need knowledge of RGB color. Another is the color scheme. Various color theories have been proposed, but in the actual design, it is difficult to well adapt their theory.

By introducing the PC for color education, these problems are easily solved. Additive and Subtractive color mixture are both physical phenomena. The PC software, a simulation of physical phenomena is easy. In particular color learning Additive color mixture was difficult with conventional color education. Also, in Juxtaposed color mixture, a huge number of fine color surface are needed. To create manually these color plane is difficult, but PC can create easily with graphics software.
Learning of color scheme is often used a color space that is abstracted such color wheel. This method is obtained by utilizing the geometric relationship of the color space. Color is treated as abstracted code (such as color number) in the space. This method is suitable to understand the color scheme theory, prior to the "toning" has been coloring material (such as colored paper) is required.
Learning the color, "toning" is also an important issue. For toning, it is necessary to understand the color caused by the three primary colors and color mixing principle, and also mixed toning to determine the interrelationship of color. Therefore, understanding of

color mixing is the basis of the color scheme learning. This is an extremely benefit for beginners.

4. CONCLUSIONS

Among the practical challenges, "Juxtaposed color mixture" is very significant of practice (design of book jacket). In this exercise, relation between the principle of color mixing (juxtaposed color mixture) and the design work (checked pattern) including the design process is very easy to understand for the learner. Among the design education, education related to basic design & art such as colors is difficult to resolve with only abstracted theory. Also when theorizing, it is also important to consider whether to theorize at any stage. For example, in this study, we showed the theory (explicit knowledge) back to a more primitive stage called "color mixture" rather than " harmony theory" for the color scheme.

In the future, same as Additive and Subtractive color mixture, we would like to advance the research including its design process such as directly linked the modeling representation and formal knowledge and also help the first scholars for training challenges.

REFERENCES

Mitsutake, T., Aihara, K., YOSHIZAWA, Y., 2013. *A study of the color composition training by RGB Additive Color Mixture.* Journal of the Color Science Association of Japan 37(3), 342-343.

Mitsutake, T., Aihara, K., YOSHIZAWA, Y., 2014. *A study of the color composition training by RGB Additive Color Mixture. No.2,* Journal of the Color Science Association of Japan 38(3), 216-217.

Mitsutake, T., Aihara, K., YOSHIZAWA, Y., 2014. *A proposal of the color composition training by Adobe Illustrator.* Journal of the Japan Society of Basic Design and Art P.10.

Mitsutake, T., Aihara, K., YOSHIZAWA, Y., 2014. *A study of the color composition training by CMY Subtractive color mixing,* Journal of the Color Science Association of Japan 38(6), 480-481.

Address: Tomoko MITSUTAKE, Nippon Designers School, 4-16 Sakuragaoka-cho, Shibuya-ku, Tokyo, 150-0031, JAPAN
E-mails: tomokomit@mac.com, aihara@zokei.ac.jp, yosuke_yoshizawa@chiba-u.jp

The art of colour harmony: the enigmatic concept of complementary colours

HARALD ARNKIL
Aalto University School of Arts, Design and Architecture

ABSTRACT

This paper explores the theory and practice of colour harmony based on the equilibrium of complementary colours. For centuries artists relied for their colour choices on studio experience and artistic knowledge handed down from master to apprentice while "scientific" colour theory remained mostly the preoccupation of scholars and philosophers. Many of the latter kind of theory were based on a comparison of visual harmony with theories of musical harmony, astronomy and mathematics (Kemp 1990; Gage 1993, 1999). This paper presents some reflections on those theories and argues that they have led the research of the aesthetics of colour astray for centuries.

1. INTRODUCTION

Complementary colour is a concept that is often referred to in textbooks on colour and in discussions on colour harmony. Complementariness in colours is sometimes described as oppositeness, although strictly speaking complementariness and oppositeness are two different concepts. Since ancient times artists and designers have either intuitively or consciously exploited the phenomenon of oppositeness in colours to achieve highly different visual effects. Some have aimed at maximum visual tension, others at harmony through equilibrium. Colour educators have tended to seek universal laws and principles or empirical evidence that would explain "scientifically" the phenomena and effects of colour experience. The principle of harmony through balance of opposites or of complementaries is an integral part of numerous colour harmony theories (Munsell 1905; Ostwald 1917; Itten 1961). What is meant by opposites or complementaries varies from one theory to the other and thus necessarily affects the interpretation of harmony in those theories.

The concept of harmony – and hence of colour harmony – is historically entwined in mathematics and theory of music and is not free of these associations even today (Arnkil 2013). The notion prevails that colours are separate entities belonging to an *a priori* system, and that they have fixed physical identities and locations in a system rather like the 12 tones of the diatonic scale in Western musical harmony. But what could harmony through equilibrium mean? Colour has no measurable weight, area or mass, which is perhaps why in art colour harmony has been understood as balance of metaphorical visual forces. (Kandinsky, Klee, Munsell). A scientific view of equilibrium presupposes a precise identification and quantification of energy, power, mass, etc. In the case of colour these forces have sometimes been identified as complementary wavelength distributions or opponent neurobiological processes. (Pridmore 2009). The latter type of investigation can contribute to the development of more sophisticated mathematical models of human colour vision, but is unlikely to deepen our understanding of the aesthetic function of colours in art and design. As artists through the centuries have shown, it is possible to identify balancing, opposite or antagonistic relationships in certain types of colour combination without attempting to pin down a precise calculable definition of those relationships. Such relationships need not lead to a "harmonious" visual outcome, but offer instead multiple expressive possibilities. The outcome depends always on several visual factors and variables of colour that cannot be left of the equation.

2. A SCIENTIFIC FOUNDATION FOR THE ART OF COLOUR?

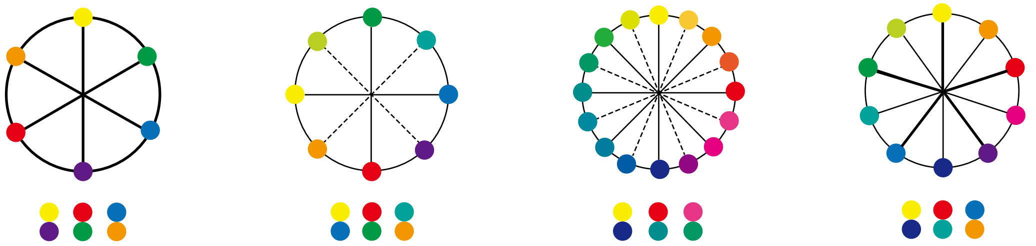

Figure 1. Schematic illustration of some colour wheels and their complementary hues. From left to right: Delacroix/Chevreul/Blanc; Hering; Ostwald; Munsell.

Almost every colour primer that says something about complementary colours makes reference to a colour wheel, stating that colours found diametrically opposite on the wheel are complementary to each other. (Itten 1973: 34, 78; Hope & Walch 1990: 89; Holtzschue 2002: 52–53; Hornung 2005: 15; Stone 2006: 236). Some textbooks insist that these relationships are extremely precise, because of their scientific foundation (Itten 1973: 34). Others, while forwarding a colour wheel -based harmony theory, admit that this principle is made rather uncertain by the fact that the colour relationship depends entirely on how the wheel is constructed. (Feisner 2006: 50). The origin of the various colour wheels, their differences, and their potential problems for predicting colour harmony are thoroughly discussed in Westland et al 2007. The wheel or circle as a symmetrical symbol of perfection suggests in itself completeness and harmony. This symbolism was idealized by the early Romantic painter Philipp Otto Runge in his spherical representation of the harmony of colours. 150 years later Johannes Itten modelled his own colour sphere and colour star on Runge's sphere and made them an iconic image of colour harmony in his book *Kunst der Farbe/The Art of Colour* (Itten 1973), The book was originally published in 1961, but is still immensely influential in colour pedagogy.

The two most famous colour systems that have made claims about both scientific colour ordering and colour harmony are the now forgotten Ostwald system and the still thriving Munsell system. Wilhelm Ostwald based his uniform hue difference scale on complementary wavelength pairs (Pridmore: 234), thus placing the concept of complementaries at the centre of his theory of colour harmony. Although Munsell also put great emphasis on "balance" in visual aesthetics, he abandoned in his hue circle his initial "compensatory" colour pairs in favour of perceptual uniformity. (Kuehni & Schwarz 2008: 115). The fitting together in one and the same colour space of perceptual uniformity of colour difference and symmetrically opposed complementary hues remains and unresolved challenge for colour science.

2.1. Opponent colours and opponent processes

In 1872 the German psychologist Ewald Hering (1834–1918) presented his theory of colour opponency which stated that a colour cannot appear both red and green at the same time and that there can be neither bluish yellows nor yellowish blues. It was first thought that Hering's opponent colour theory was irreconcilable with the Young–Helmholtz theory of trichromacy, but gradually it was realized (and proven also empirically) that they describe two different levels of the colour vision process. (Kuehni & Schwarz 2008: 100). Could Hering's opponent colours be called complementary and if so, does their complementariness have a neurological basis? Hering hypothesized that the neural opponency of red with green and yellow with blue was based on antagonistic physiological processes (Valberg 2005: 279). At first there seemed to be no evidence to support this hypothesis but the discovery of opponent-process colour-coded cells in the 1950s and 60s, first in the retinas of fish, then in primates and later in the human visual cortex seemed to finally prove the neurobiological basis of complementariness in these colours. It is worth remembering, though, that an important role of that process is not to only to provide us with good discrimination of reds from greens and blues from yellows, but to pack the signals from the three cone receptor channels into a more economical form through a process of signal subtraction. Hence we are much more attuned to colour *differences per se* than to *absolute* colours in any sense of the word.

Building on Helmhotz's and Hering's legacy, the CIE has produced ever more precise colour difference models. Do these improved scientific models contain the answer to complementary colours and colour harmony? Professor Anders Hård showed in 1985 in his article *Är komplementärfärger mer olika än andra färgpar?* (Are complementary colours more dissimilar than other colour pairs?) how ambiguous the concept of complementarity is even within a scientific frame of reference. He also concludes that artists "grasped the new scientific theories of subtractive complementaries, complementary stimuli and simultaneous and successive contrasts, as acceptable explanations, proof or definitions of phenomena *that they had since long ago known and worked with*." (Hård 1985, my italics). In a more recent article by Anders Hård and Lars Sivik the authors say:

> In color literature and encyclopedias, the concept "complementary colors" is defined in several different ways … As far as we understand, it is not possible to decide whether simultaneously perceived Color Elements are complementary according to any of these definitions unless one has acquired, through specific experimental learning, the knowledge of the particular definition in question. (Hård & Sivik 2001).

Hård and Sivik also point out that in their experiment carried out with 35 architecture students of architecture, showed no evidence that complementary colour combinations are experienced as more harmonious than other combinations: "The colors that were hue (Φ), chromaticness (c), and redness (r) identical, on the other hand, were judged as more harmonious than all the others, while the constellation where all the colors were completely different was judged as least harmonious." Neither were the complementary colour pairs perceived as more different than other combinations. The experience of difference depended rather on NCS lightness difference. (Hård & Sivik 2001: 26). The findings of Li-Chen Ou and Ronnier Luo corroborate these findings: in their 2003 study, equal hue and moderate lightness difference were among the most important contributing factors in harmony and there were no results for complementary colours. (Ou & Luo 2003).

2.2. Other dimensions of complementary colours

Complementariness is closely related to simultaneous contrast otherwise known as colour induction. (Pridmore 2009). Colour induction is in some degree present in nearly all colour juxtapositions, but it is most dramatic in colour combinations where a colour field of high chromaticness induces an opposite hue in an adjacent, more neutral colour field. This perceptually induced opposite hue is said to be the complementary of its adjacent hue stimulus. Another related phenomenon is that of *vibrating boundaries*, sometimes also called "simultaneous contrast" or "simultaneity" in art parlance. There are several explanations for this phenomenon (see e.g. Livingstone 2002), but it is most often attributed to complementary colours enhancing each other when juxtaposed in the form of hard-edged areas. So-called 'simultaneity' in the form of juxtaposed areas of saturated complementary-type colours in highly rhythmic designs were typical of the works the Robert and Sonia Delaunay. It is debatable whether they can be called 'harmonious' or that either artist even aimed at harmony. The effect is rather of vibrancy and a sense of rhythmic movement. Indeed, the proclaimed aim of Robert Delaunay was the creation of movement and a novel evocation of time and space through colour. (Gage 2006: 36–37) In the Pop- and Op-Art of the 1960s complementary-type contrasts in equiluminant combinations often created a restless, vibrating or kinetic effect whose very aim was the opposite of harmony. Such effects were widely used in advertising and especially in the graphic images of the 1960s pop culture and psychedelia.

Although complementary and antagonistic colours do not automatically create harmony in a colour composition, they may occupy an otherwise special place among colour combinations. Michel Eugène Chevreul (1786–1889) stated that colours appeared to their best advantage when juxtaposed as pairs of complementaries. In Chevreul's colour circle, the three primary colours red, yellow and blue are placed at angles 60° in relation to each other, yielding the complementary pairs: red/green, yellow/violet, blue/orange, etc. Summarizing his findings on various types of colour juxtapositions, he concludes: "*This* [juxtaposition of complementaries] *is the only association where the colours mutually improve, strengthen and purify each other without going out of their respective scales."*(Chevreul 1987: 134). But he goes on to say: "This case is so advantageous to the associated colours, that the association is also satisfactory when the colours are not absolutely complementary. So it is also when they are tarnished with grey." (Ibid.).

3. DISCUSSION

Chromatic contrast not only provides us information about lighting, space and material qualities, but also affords us pure enjoyment and aesthetic pleasure, but sometimes also displeasure. Artists or designers can learn to control these factors only by experience, by tirelessly testing various options and by training their sensitivity to the multiple layers of visual experience at play in any art or design task. Josef Albers has demonstrated how creating with colours has very little to do with rigid rules and much with alertness, flexibility and tactical skill, with "thinking in situations". (Albers 2013: 42, 68). He referred to theories of complementary colours, but never asserted that they were a guarantee of harmony. In fact, harmony was for Albers no more desirable than disharmony. Just as music consists of consonances and dissonances, so must visual art. (Albers 2013: 39–43). In contrast to his former teacher and colleague Johannes Itten, Albers had a deep distrust of formal rules of colour harmony – mainly because of they did not address the relational and situational nature of colour design. (See Albers 2013: 42). There have been attempts even in Albers's time to quantify variables such as surface area, complexity and colour intervals in mathematical representations of colour harmony (Moon & Spencer 1944). However, most of the models are able to include a very limited number of hues or other variables in the algorithm. Even the most sophisticated computational colour harmony models to date leave out crucial factors affecting the experience of harmony. These include the spatial array, cultural context, figuration, symbolism, texture, materiality and evocation of light and atmosphere. Computational rules of colour harmony so far appear to be self-predicting. There is no guarantee of their success outside their own form of presentation and mode of appearance, as even the creators of such models admit. (See: Ou & Luo 2003, Conclusions). A continuation of computational harmony studies with more naturalistic stimuli could be extremely challenging, but perhaps worth trying.

4. CONCLUSIONS

The concept of complementariness in colours has no single established definition. The "harmony" or "disharmony" of colours, whether based on complementariness or other relationships, is not scientifically quantifiable, but a qualitative aspect that requires artistic knowledge, sensibility and attention to several simultaneous layers of experience. The experience of visual balance is not dependent on any precise and quantifiable chromatic relation. The experience of visual harmony depends on multiple factors that can only be addressed through the sensibility, skill and experience of the designer or artist. Rules of harmony that are based on fixed, abstract formulae do not sufficiently take into account the multiple variables involved in real-life applications of colour and do not sufficiently address the needs of contemporary art and design. Complementary, opposite or antagonistic colours can, when used with skill, afford visual balance to the chromatic composition of images, objects or spaces, but they can also result in visual tension, restlessness, even discomfort. The latter effects can be and often are the very goal in today's designs or artworks. Present-day colour harmony research has received little or no attention from artists, designers and architects. The reason may be that "harmony" is too limited a concept for the needs of visual communication, expression and good design in contemporary life. Many of the confusions and misunderstandings concerning the role of colour in art, design and architecture arise from a lack of clearly articulated artistic knowledge about colour. It has sometimes resulted in artists taking recourse to science that they do not understand and scientists applying to art methods and rules which are blind to the multifaceted nature of art. The discussion between science and art in colour research can be useful only when the strengths and limitations of each approach are clearly identified.

References

Arnkil, H. 2013. Colour Harmony: from Dualism to Living Perception. Proceedings of the AIC 2013: 12th International AIC Congress, Newcastle, UK. Lindsay MacDonald, Stephen Westland, Sophie Wuerger (eds.). The Colour Group (Great Britain).

Albers, Josef 2013. *Interaction of Color*. 50th Anniversary Edition. Yale University Press.

Chevreul. M. E. 1987. *The Principles of Harmony and Contrast of Colors and their Application to the Arts*. Schiffer Publishing Ltd.

Feisner, E.A. 2006. *Color: How to Use Color in Art and Design*. Laurence King Publishing Ltd.

Gage, J. 1999. *Colour and Meaning: Art, Science and Symbolism*. Thames and Hudson.

Gage, J. 2006. *Colour in Art*. Thames and Hudson.

Holtzschue, L. 2002. *Understanding Color: an Introduction for Designers*. John Wiley & Sons.

Hope, A. and Walch, M. 1990. *The Colour Compendium*. Van Nostrand Reinhold.

Hornung 2005. *Colour: a workshop for artists and designers*. Laurence King Publishing Ltd.

Hård, A. 1985. *Är komplementärfärger mer olika än andra färgpar?* Färgrapport F31. Chalmers Tekniska Högskola/Skandinaviska färginstitutet AB.

Hård, A. and Sivik, L. 2001. *A Theory of Colors in Combination—A Descriptive Model Related to the NCS Color-Order System*. Color Research and Application Volume 26, Number 1.

IItten, J. 1973. T*he Art of Color: The Subjective Experience and Objective Rationale of Color*. Van Nostrand Reihold.

Kemp, M. 1990. *The Science of Art – Optical themes in western art from Brunelleschi to Seurat*. Yale University Press.

Livingstone, M. 2002. *Vision and Art: the biology of seeing*. Harry N. Abrams, Inc.

Kuehni, R.G. and Schwarz, A. 2008. *Color Ordered: A Survey of Color Order Systems from Antiquity to the Present*. Oxford University Press.

Moon, P. and D.E. Spencer (1944) *Aesthetic Measure Applied to Color* Harmony. Journal of the Optical Society of America, Vol. 34, Issue 4, pp. 234-242.

Ou L; Luo M.R. 2003 *A Study of Colour Harmony for Two-Colour Combinations*. Proceedings: 6th Asian Design International Conference, Tsukuba 6th Asian Design International Conference, Tsukuba.

Pridmore, R.W. 2009. *Complementary Colors: The Structure of Wavelength Discrimination, Uniform Hue, Spectral Sensitivity, Saturation, Chromatic Adaptation, and Chromatic Induction*. Color Research and Application, Volume 34, Number 3, June 2009. Wiley Periodicals Inc.

Stone, T.L. 2006. *Color Design Workbook - A Real-World Guide to Using Color in Graphic Design*. Rockport Publishers.

The Concise Oxford Dictionary of Current English. Seventh Edition 1982. Oxford University Press.

Valberg, A. 2005. *Light Vision Color*. John Wiley & Sons Ltd

Address: Harald Arnkil, Aalto University School of Arts, Design and Architecture
Centre for General Studies, Department of Art
PO Box 31000, FI-00076 AALTO, Finland
E-Mail: harald.arnkil@aalto.fi

A Study on Influence of the Culture and Art Experience of Senior Citizens from Relationships between Culture and Art Education Space and Color Emotion Assessment

Hyeyun SON,[1] Yunsun PARK,[2] Jinsook LEE[3]
[1] Dept. of Design & Crafts, Hongik University
[2] Dept. of College of Design & Art, Hongik University
[3] Dept. of Architectural Engineering, Chungnam National University

ABSTRACT

Accordingly in this research, properties of evaluation vocabularies according to colors used in each Korean cultural art education indoor space is evaluated. Through analyzed resources, influence on senior citizen's color sensibility evaluation by the relationship between cultural art education space and color sensibility evaluation is analyzed. In order to achieve the goal of this research, SPSS statistic program 21 is used to conduct reliability analysis and T-test analysis. As a result of the research, among the three elements, ceiling, wall and floor in educational space, wall is the most influential when applied with color. Second, in oriental calligraphy room which has clear use and purpose, and used for visual art education space, color sensibility is clearly demonstrated per use of different colors. Third, there were difference in the sensibility each individual feels from the color of the wall between a group of individuals who has experienced cultural art and the group of individuals who has not experienced cultural art. There was significant difference in grey, pink, wine and yellow-green. The conclusion of this research is believed to be used as an important data to plan indoor education space color palette for senior cultural art education spaces.

1. INTRODUCTION

As the number of facilities allowing senior citizens to explore cultural art is increasing in Korea, geographical distance to/from cultural art center, transportation method is getting easier and the opportunities of experimenting various cultural art is growing. The difference in details and degree of emotional sensibility each individual feels from the colors in interior spaces are expected between individuals who have experienced cultural art and who have not. In the coming future and forward, Korean government is anticipated to generously support and invest in improving life quality by adopting cultural art experiences as universal opportunities. Consequently, as a first step in this research, emotional sensibility of senior citizens, the true users of cultural art education spaces are studied as a part of indoor color palette plan. As a second step, the purpose of this research in distinguishing the differences in emotional sensibilities between individuals who have experienced cultural art and who have not to identify the properties and use them resources for designing cultural art spaces since emotional sensibility of users who have experienced cultural art can be referenced in making color palette plans for indoor spaces distinctively designed for educational purposes.

2. METHOD

2.1 Experiment Outline

This research includes preliminary survey and main study. Physically and mentally healthy 57 senior citizens (31 females and 26 males) at ages between 55 and 63 without conditions of color blindness participated in this experiment. Preliminary survey was used to identify biological information along with physical and psychological conditions. The main study is conducted as color sensibility category in cultural art education space using general statistics and Likert's 9-point scale. Especially, the application of color in indoor space is limited to walls by referencing advanced researches. According to the preliminary survey conducted in this research, 94.09% of senior citizens responded that walls have the biggest affect to interior space images and sensibilities.

Figure 1: Basic 15 Colors for Color Sensibility Evaluation.

Accordingly, prior to conducting this survey, sufficient explanations on color stimulant in indoor spaces are provided. Survey participants were asked to evaluate emotional sensibilities they feel by looking at images of indoor spaces that best demonstrate the basic 15 colors (red, yellow-red, yellow, green-yellow, green, blue-green, blue, bluish violet, purple, reddish purple, pink, brown, white, grey and black) on 9-point scale.

2.2 Evaluation Subjects and Vocabulary Selection

Oriental calligraphy room that is designated as a social educational space located as a part of senior citizen welfare center which conduct cultural art educations such as photography, oriental calligraphy, oriental painting, art and architecture is selected as an evaluation subject. The basic colors are selected based on KS color system and the colors are applied to walls which has the most visual influence within indoor spaces. Vocabularies used in the evaluation are derived from the 2014 research of Lee, Jin-sook. As shown in (Table 1), total of sixteen pair of evaluation vocabularies are selected and SD (Semantic Differential Method) is used to conduct the sensibility evaluation.

Table 1. Color Sensibility Evaluation Vocabulary

No.	Vocabulary	No.	Vocabulary
1	Happy – Not Happy	**9**	Enjoyable – Irritating
2	Hopeful - Hopeless	**10**	Interesting - Boring
3	Stable - Stimulating	**11**	Calm – Excited
4	Comfortable - Tense	**12**	Active - Static
5	Pleasant - Unpleasant	**13**	Bright - Dark
6	Warm - Cold	**14**	Light - Heavy
7	Clear - Dozy	**15**	Confident - Fearful
8	Influential – Influenced	**16**	Strong - Weak

2.3 Evaluation Method

In this research, in order to evaluate the reliability of each evaluation vocabulary, reliability analysis (Cronhach-ɑ) is conducted using SPSS statistics program 21. Moreover, in order to evaluate fundamental properties of evaluation vocabularies based on colors, descriptive analysis is conducted. Lastly, T-test is conducted to analyze the effect of education space color on participant's sensibility between those who have experienced cultural art and those who have not.

3. RESEARCH RESULT

3.1 Reliability Analysis

Reliability analysis is a value that allows to verify how accurate and consistently the evaluation vocabularies are measured by survey participants. In other word, it is the probability of resulting in the same measurement regarding the same concept repeatedly.
Generally in the social science area, the standard that interprets Cronbach ɑ value sees that the value above 0.6 is credible. The total Cronbach a value is demonstrated as 0.940 therefore no specific vocabulary is removed. All 16-pairs of vocabularies are used as evaluation vocabularies.

3.2 Descriptive

In order to identify the property of evaluation vocabularies as results of cultural art education indoor space colors, the average value of evaluation vocabularies evaluated by the senior citizens is used to conduct descriptive statistics. Analysis result according to applied color is as shown in the following.
For color red, [stimulating], [Tense], [Exciting] and [Strong] were the most frequent sensibility vocabularies. [Bright] was the most frequent sensibility vocabulary for yellow-red. For yellow, [Happy], [Hopeful], [Pleasant], [Warm], [Clear], [Enjoyable], [Active] and [Confident] were the most frequent sensibility vocabularies. Especially in yellow, [Interesting], [Bright] and [Light] were the highest sensibility vocabularies. Yellow-green had [Pleasant], [Enjoyable] and [bright] as the most frequent sensibility vocabularies. Green had relatively frequent sensibility vocabularies in [Pleasant], [Clear] and [Strong]. Turquoise blue had relatively frequent sensibility vocabularies in [Stable], [Clear] and [Strong]. Blue had relatively frequent sensibility vocabularies in [Heavy] and [Calm]. [Cold] was the most frequent sensibility vocabulary for blue. [Cold], [Dark] and [Heavy] were the most frequent sensibility vocabularies for bluish violet. Purple had low distribution in overall, but among them, [Clear] and [Strong] were the most frequent sensibility vocabularies. Reddish purple had relatively high frequency in [Exciting], [Heavy] and [Strong] sensibility vocabularies. [Happy], [Active] and [Light] were the most frequent sensibility vocabularies for pink. [Heavy] was the most frequent sensibility vocabulary for brown. For white, [Pleasant] and [Calm] were the relatively frequent vocabularies and [Bright] and [Light] were the most frequent sensibility vocabularies for white. For grey, [Calm] and [Heavy] were relatively frequent. [Not Happy], [Hopeless], [Unpleasant], [Cold], [Irritating], [Boring], [Dark], [Heavy] and [Fearful] were the most frequent sensibility vocabularies for black.

3.3 Sensibility vocabulary evaluation analysis in cultural art education space

T-test analysis is conducted to evaluate the influence on education participants' sensibility by different colors applied to education spaces by conducting sensibility vocabulary evaluation analysis. T-test is an analysis method that compares the average between two groups. In this research, through an independent sample t-test analysis, the sensibility evaluation result gained from two groups, one who has experienced cultural art and another who has not experience cultural art is analyzed as t-value and significance probability value. Moreover, among total analysis result, only values that demonstrated significant differences are used. Oriental calligraphy room that has clear educational purpose within the space is used as an object space and the category of art education conducted in the objective space is applied as shown in (Table 2). Through questions that allow multiple confirmations, the participants are identified as individuals who have experienced cultural art and who have not.

Table 2: Cultural Art Category used in Calligraphy Room

Cultural Art Category	.Oriental calligraphy room
Applied Education Area	Photography, Architecture, Art
Number of Individuals who have experience cultural art	31

It is a result of comparison between two groups: one who has experience photography, architecture and art and another group who has not. In the calligraphy room, varying from whether individuals who have experienced the cultural art or not, yellow-green(6) had t-value of 2.769, pink(15) had t-value of -3.032, grey(3) had t-value of -3.030, grey(4) had t-value of -3.448, and grey(5) had t-value of -2.948. There was less than 0.01 of difference in significance level. Moreover, Reddish purple(5) had t-value of 2.546, pink(5) had t-value of -2.311, pink(14) had t-value of -2.361, grey(1) had t-value of -2.127, grey(8) had t-value of -2.330, grey(11) had t-value of -2.139, grey(12) had t-value of -2.198, grey(13) had t-value of -2.127, and grey(14) had t-value of -2.031. There was less than 0.05 of difference in significance level. In total of 14 categories of yellow-green, purple, pink and grey, statistically difference was demonstrated between the two groups.

4. RESULTS AND DISCUSSION

Based on the advanced technology statistical analysis result, color sensibility vocabulary properties are demonstrated in sensibility evaluation. Vocabularies show vocabularies that have the average value of 6-7 for each color and is in descending order. For colors that do not have numbers higher than 6 demonstrate vocabularies that fall in to the high values. Furthermore, they are vocabularies that are evaluated in educational spaces that have sensibility properties each color has.

Based on the result of independent sample T-test analysis conducted to analyze sensibility between the group who has cultural art experience and another group who does not have the experience, there were total of 14 differences in sensibility vocabulary in yellow-green, reddish purple, pink and grey. Especially, there was major difference in sensibility vocabulary for grey.

For the group who has no cultural art experience, yellow-green was described as [Cold] when the group who has cultural art experience described the color as [Warm]. More individuals in the group who has no cultural art experience felt [Pleasant] for color reddish purple. Moreover, for pink, the group who has no cultural art experience felt [Pleasant], [Light] and [Confident]. Lastly, for grey, the group who has no cultural art experience felt

[Happy], [Comfortable], [Pleasant] and [Influential] whereas the group who has the experience felt [Not Happy], [Tense], [Unpleasant] and [Influenced]. Many individuals in the group who has no experience felt [Stable] and [Calm]. Additionally, whereas the group who has no cultural experience showed medium value in sensibility evaluation of [Active-Static], [bright-Dark] and [Light-Heavy], the group who has the experience felt [Static], [Dark] and [Heavy]. Lastly, in yellow-red, green and purple, there was no difference in all evaluation vocabulary categories.

5. CONCLUSIONS

In this research, sensibility vocabulary evaluation is conducted among senior citizens based on different colors applied to cultural art education space. The evaluation is used to analyze the influence of cultural art education space on senior citizens' sensibility. Research result can be summarized as following:

First, according to the preliminary survey and main study result, in indoor spaces, wall color is the most influential part of the space that allows one to recognize the space and delivers sensibility.

Secondly, yellow and black are colors that deliver most sensibilities described in color sensibility vocabularies. Whereas individuals feel positive emotions towards the color yellow, individuals feel negative emotions towards black. Each color sensibility vocabulary is determined as indoor space color properties.

Third, according to the T-test analysis result, the sensibility derived from color is different in individuals who have experienced cultural art and individuals who have not. Hence, at this point, where the number of cultural art educational spaces for senior citizens and related programs are gradually increasing, sensibility of the users should be incorporated in designing cultural art education spaces.

The result of this research proposes conclusions that can improve the cultural art education quality and help design indoor spaces. This is expected to lead to bring positive influence to senior citizens who utilize cultural art education spaces and improve the leisure life satisfactory level. Additionally, government and municipal groups should establish various and appropriate spatial color plan, improve cultural art educational space facilities and allow planning color palette plans according to spatial properties.

Thus far, research results that demonstrates sensibilities that senior citizens feel according to different indoor spaces and educational space properties have been gathered. In the future, emotional sensibility will be evaluated through color experiences in various cultural art education spaces. Research result as such is expected to prove importance of color as environmental factor in senior citizens facility evaluation category. Furthermore, as a follow-up research, systematic color model development and utilization measure researches will be needed for senior citizen's cultural art educational space.

.

REFERENCES

Jinsook Lee, 2014. *An Analysis Sensitivity Adjectives Evaluation to apply Color to the Indoor Living Space*. Journal of Korea Society of Color Studies 28(2) 74-76.

Valdez Patricia & Mehrabian Albert, 1994. *Effects of Color on Emotions*. Journal of Personality and Social Psychology 123(4) 394-409.

Address: Ph.D. Candidate, Hyeyun SON, Dept. Hongik University of Design & Crafts,
Department of Applied Optics, 94, Wausan-ro, Mapo-gu, Seoul, Korea, 121-791
E-mails: sonhyeyun@hanmail.net, yspark@wow.hongik.ac.kr,
js_lee@cnu.ac.kr

Impressions of buildings derived from the combined effects of exterior colour, material, and window shape

Kazumi NAKAYAMA[1], Masato SATO[2]
[1] None
[2] Division of Environmental Science, Kyoto Prefectural University

ABSTRACT

External appearance is determining factor in the overall impression of a building, and is greatly affected by the building's architectural surfaces. This study focuses on colour, material, and window shape as elements that affect the visual impression of a building's appearance to ultimately understand the extent to which they impact impressions of a building's appearance. A series of experiments was conducted to determine impressions derived from surface designs of an office building using the semantic differential method. The parameters were exterior colour, materials used, and window shape. In all, 29 colours were selected from the Munsell Coulor System, and three types of materials were selected from commonly used exterior materials in Japanese office buildings. Two types of window shapes were selected from commonly used exterior designs of office buildings. In order to display these elements to the study participants, 174 perspectives of buildings were created as stimuli, using a computer graphics program. Evaluations were sought from 38 observers using 30 semantic differential rating scales. Image profiles were then drawn using the average of each stimulus from the results of the experiments. Three factors—'evaluation', 'potency', and 'warmth'—were extracted and can be characterized by the above parameters. An impression evaluation was determined by the effect of the combination of these elements; however, according to the factor scores, the impact from impressions of colour, material, and window shape was not a constant trend. The results of this study show that colour is the most affective element with respect to impressions regarding architectural appearance; however, because material and window shape also have an impact, it is important to ensure that designs are created through a combination of these elements.

1. INTRODUCTION

The impression of an architectural object's appearance is affected by the components of the surface (i.e. colour, material, window shape). Several previous studies have been conducted on exterior colour and its effect on the overall impression of a building. The impression of exterior colour and impression of colour itself are evaluated by the same factors—the evaluation factor, activity factor, and warmth factor.

Regarding colour, the evaluation factor is related to chroma, activity factor is related to value, and warmth factor is related to hue. In recent years, there has been an increase in the type of exterior materials available for use, such as glossy materials or a different colour for the joints between tiles, which influence appearance. In addition, window shape also affects the impression. In this study, colour, material, and window shape were selected as elements that affect the visual impression of a building's appearance. The strength of impact that these elements have on impression, and the mutual relationships among them, has not been made clear in previous studies; thus, this study seeks to illustrate the extent to which these elements impact the impressions of a building's appearance.

2. EXPERIMENTAL METHOD

A series of experiments was conducted to determine impressions derived from surface designs of an office building using the semantic differential method. The parameters were exterior colour, materials used, and window shape. Twenty-nine colours were selected from the Munsell Color System (see Table 1), and three types of materials and two types of window shapes were selected from commonly used exterior materials used in newer Japanese office buildings.

Table 1. Assigned colours.

Hue	Value／Chroma				Hue	Value／Chroma			Hue	Value	
5R	8/4	6/10	5/6		5BG	8/3	7/8		N	9	7
5YR	8/6	7/12	6/4	3/2	5B	8/4	6/8	4/8			
5Y	9/3	8/14	7/4	6/10	5PB	8/3	6/8				
5GY	9/4	7/6	5/2		5P	8/4	6/8				
5G	8/4	5/10			5RP	7/2	7/8				

The three types of materials were mortar, porcelain tile, and metal panel. Window shape included a single window and a ream window. In order to display these elements to the study participants, 174 perspectives of buildings were created as stimuli, using a computer graphics program. The shape of the example building was a simple form, with window shapes set and exterior materials rendered in the surface colour white (N9.5). Figure 1 shows the images of the rendered building in two dimensions. Using these two-dimensional images, colour simulations were carried out to change only wall colour. The stimuli were presented to participants on a 21-inch CRT display at random. Evaluations were sought from 38 observers using 30 semantic differential seven-point rating scales.

	Material -1	**Material- 2**	**Material- 3**
	Mortar	Porcelain tile	Metal panel
Window-1 Single window			
Window-2 Ream window			

Figure 1. CG images.

3. RESULTS AND DISCUSSION

3.1 Semantic Differential Rating

Image profiles were drawn using the average of each stimulus from the results of the experiments. Figure 2 shows the image profiles of the 5Y pattern (mortar and single window) which is used with a large number of colours in architectural walls. The impressions were different according to the degree of value or chroma under the same hue. For example, 5Y9/3 is a commonly used colour on building exteriors in Japan, and the impressions were ‘natural’ and ‘friendly’. In addition, the impressions of 5Y7/4 were ‘natural’ and ‘sober’, and the impressions of 5Y6/10 were ‘rural’ and ‘unfashionable’. 5Y8/14 is a vivid yellow, and its impressions were ‘tired’ and ‘ignoble’. In the case of the same hue, as value increased, the impressions were either ‘brighter’ or ‘paler’, and as chroma increased, the impressions changed to be more ‘dynamic’ and ‘heroic’. Figure 3 shows the effect of the window shape or materials used in the case of the image profile for 5Y9/3. In this figure, the case of mortar and single window indicates 0, and difference value of the other cases is shown. In Figure 2, the degree of change of the impressions is not large compared to Figure 3. In adjective pairs such as ‘elegant-inelegant’, depending on the window shape or the materials, evaluation toggled between positive and negative. On the other hand, adjective pairs such as ‘originative’, ‘satisfactory’ showed almost no change. That is, in regard to some adjective pairs, impressions were often affected by window shapes or the materials. Focusing on the materials, impressions of mortar were ‘bright’ and ‘casual’, impressions of metal panels were ‘refreshing’ and ‘urban’, and impressions of tile were ‘friendly’ and ‘tasteful’. When comparing the ream window and single window, impressions of ream window tended to be ‘cold’ and ‘casual’.

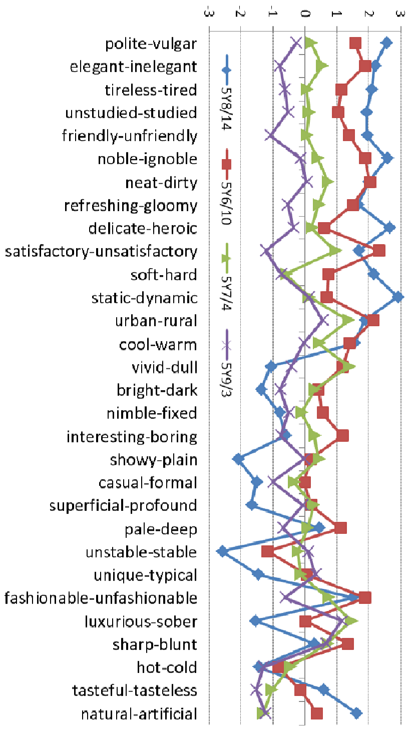

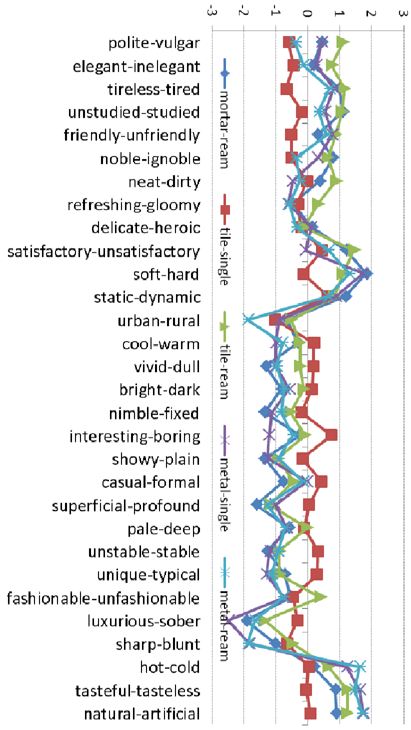

Figure 2. Image Profiles. (5Y, Mortar, Single) Figure 3. Image Profiles. (5Y9/3)

3.2 Evaluation of Tolerance

Using factor analysis, the semantic differential rating data were separately analysed, with the factor loading of each scale shown in Table 2. Three factors—‘evaluation’, ‘potency’, and ‘warmth’—were extracted from the results of this factor analysis. In the first factor (evaluation), the highest scores were obtained in the cases of achromatic and low chroma colours, while factor scores were low in the high chroma colours. Comparing among the different hues, the factor score was lowest in 5P. The materials and window shapes were not as clearly affected by the factor scores. The second factor (potency) was influenced by value, observed as high-value stimuli that were evaluated higher than others. Comparing hue factor scores reveals a higher tendency in 5P and 5GY. The score was highest in the cases of the metal panels. The third factor (warmth) illustrated whether the coolness or warmth of hue was reflected in the evaluation. In this third factor, the effects of the material and window shape were not clearly observed.

Table 2. The factor loading of each scale.

Adjectives	Factor 1	Factor 2	Factor 3	Adjectives	Factor 1	Factor 2	Factor 3	Adjectives	Factor 1	Factor 2	Factor 3
polite-vulgar	0.968	-0.146	-0.022	vivid-dull	0.026	0.946	-0.007	hot-cold	-0.121	0.085	0.940
elegant-inelegant	0.939	0.187	0.003	bright-dark	0.188	0.938	0.092	tasteful-tasteless	0.200	0.128	0.896
tireless-tired	0.922	-0.249	0.155	nimble-fixed	0.170	0.936	-0.064	natural-artificial	0.397	-0.341	0.787
unstudied-studied	0.911	-0.323	0.105	interesting-boring	0.128	0.932	0.027				
friendly-unfriendly	0.903	0.108	0.364	showy-plain	-0.359	0.902	-0.045				
noble-ignoble	0.891	-0.321	-0.066	casual-formal	-0.240	0.888	0.207				
neat-dirty	0.837	-0.134	-0.358	superficial-profound	-0.103	0.873	-0.297				
refreshing-gloomy	0.837	0.488	-0.083	pale-deep	0.524	0.781	-0.110				
delicate-heroic	0.832	0.301	-0.212	unstable-stable	-0.636	0.721	-0.109				
satisfactory-unsatisfactory	0.736	0.299	0.313	unique-typical	-0.555	0.710	-0.199				
soft-hard	0.669	-0.595	0.339	fashionable-unfashionable	0.668	0.704	-0.080				
static-dynamic	0.655	-0.552	-0.395	luxurious-sober	-0.530	0.645	-0.025				
urban-rural	0.627	0.355	-0.596	sharp-blunt	0.439	0.644	-0.561				
cool-warm	0.594	0.517	-0.531					Accumulated contribution(%)	39.196	75.229	89.208

Factor scores' mean score for each stimulus was calculated for confirmation. Figure 4 shows four examples of the factor scores in the case of the single window.

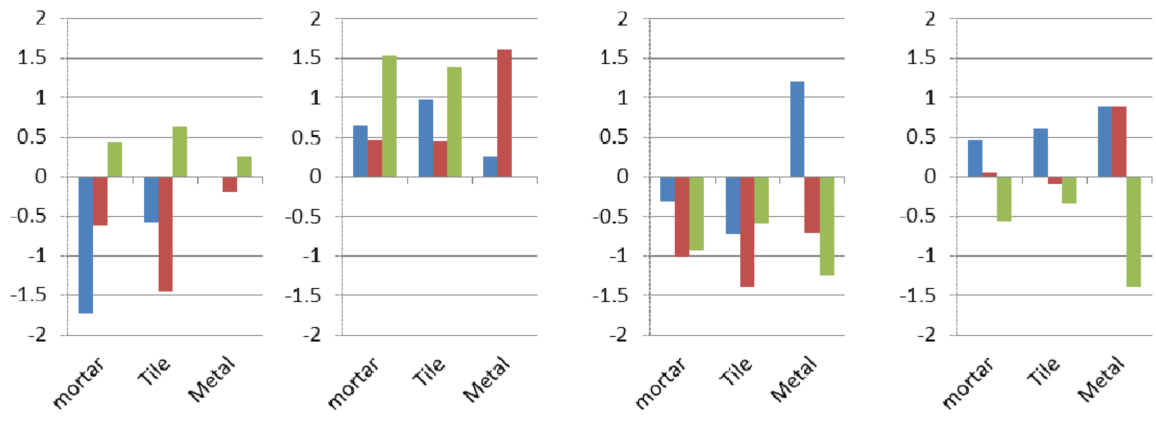

a) 5Y6/10 *b)5Y9/3* *c)5B4/8* *d)5PB8/3*

Figure 4. Factor Score. (single window)

Focusing on the first factor, factor scores of metal panels were higher by one point or more than the other walls in the case of cool colours. Focusing on the second factor, factor scores of metal panels were higher compared to other materials of the same colour. Focusing on the third factor, factor scores of metal panels were lower with almost colour. Features of the material due to their inherent differences are reflected in the trend of impressions between mortar and tile, but metal panel showed a different tendency.

Impressions of the first factor were affected by the window shape in 5Y9/3; however, the impact of the materials was observed more strongly than window shapes in 5B8/4 (see Figure 5).

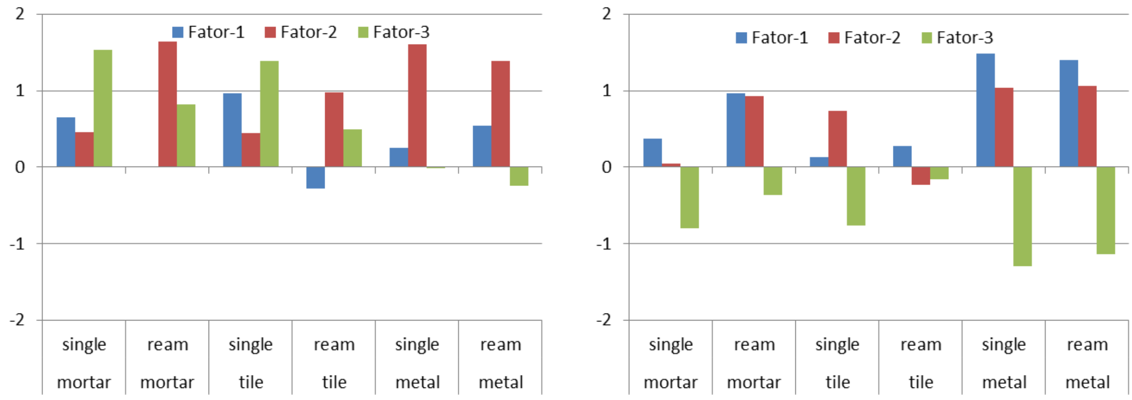

a) 5Y9/3 *b) 5B8/4*

Figure 5. Factor score. (combination comparison between materials and window shape)

In the second factor, the factor scores of the ream window were equal or higher than the factor scores of the single window; however, factor scores of the ream window were low in the case of 5B8/4 (tile). In the third factor, the single window had higher factor scores than the ream window in any material in 5Y9/3; however, the scores were reversed in 5B8/4. Effects of the impression due to the difference of window shape were different based on the combination of materials and colours.

4. CONCLUSIONS

As a result of the factor analysis, three factors were extracted that describe the impressions and mutual relationships among colours, wall materials, and window shapes. Colour was shown to be the most affective element with respect to impressions regarding architectural appearance; however, material and window shape also have an impact. Effects of the impressions were different based on the combination of colours, window shapes, and materials; therefore, it is important to ensure that designs are created through a combination of these three elements.

REFERENCES

K. Nakayama, and M. Sato, 2006. Effect to Impressions of a Building Derived from Exterior Color, Material and Windows. In *Summaries of Technical Papers of Annual Meeting, D1, AIJ,* 361-364.

Address: Prof. Masato Sato, Division of Environmental Sciences,
Kyoto Prefectural University, 1-5 Hangi-cho, Shimogamo,
Sakyo-ku, Kyoto 606 -8522, Japan
E-mail: ma_sato@kpu.ac.jp

Analysis of Current Colors of Native Plants Growing Naturally in Korea

Yoosun KIM, Sueran CHOI, Saetbyul KIM, Sangeun SHIN
Sahmyook University Environmental Green design Research Institute

ABSTRACT

Although there are numerous magazines and specialty publications covering a range of plants from foliage plants to wild flowers, plant colors are often misunderstood. Although color atlases for the design field have been developed, they are limited in their applicability to plants. The RHS color chart published by the Royal Horticulture Society is used as the standard for classifying flower colors by adjusting chroma and brightness based on principle hue. Although the RHS color chart is used in Korea for classification of plant colors, its specificity for British flowers limits its applicability to Korean wild plants. As it is not generalized in the ordinary domain other than by plant majors, it is hard to share information in other fields except for the relevant field. In addition, there are limits in terms of peripheral temperature, humidity, light conditions, and subjective perception of color. This research tried to develop an objective and rational standard color atlas for native plants growing naturally in Korea.

From February 2013 to January 2014, wild plants were photographed using Colorchecker Passport (Standard Colorchip), and colors were extracted using the Lightroom program. In analyzing native plants by season, a total of 187 color values were extracted, and Yellow Green showed the highest extraction yield with 37.9% of 116 colors extracted in the spring, followed by Yellow with 29.3% extracted in the spring. Of the 63 colors extracted in the summer, Yellow Green showed the highest extraction yield at 36.5%, whereas Yellow showed 31.7% and Orange and Reddish Purple both showed 9.5%. Of the eight colors extracted in the fall, Yellow Green and Yellow showed extration yields of 37.5%, whereas Purple and Reddish Purple both showed 12.5%. In the winter, native plants hibernated and were not extracted. Based on this research, the availability of natural colors will increase. Studies on color atlases on plants in Korea should be conducted.

1. INTRODUCTION

1.1 Purpose and Implication of the Research

Native Korean plants are all plants that exist and grow naturally in mountains and fields of Korea. A large variety of plants are categorized as native Korean plants, including endemic plant species that only exist in Korea (An 2008). In 1952, Nakai reported that there are 2,898 species of native Korean plants and over 4,000 more species of native Korean plants have been discovered since then, including 407 Korean special species (Lee 2001, Yoon 2002). Korea is a peninsula in the northern hemisphere temperature region (adjusted to the south of China and surrounded by the ocean on the east, west, and south), which means there is a comparatively wider variety of native plants compared to other countries (Koo 1999). In this era of globalization, development of native plants, which have climate and cultural specificity, is essential (Oh 2002). Consequently, there are many recent studies on native plants. As well as their physiology and growth/development, including thier habitat environments (Lee 1990), category and ecology (Jeong 1991), cultivation (Ha 1998), and breeding(Yoo 1984). Yet, there is still a lack of research on the color of native plants, such as stainability of natural plant extracts (Park 2004) and applicability of fruit colors from native plants (Kim 2011). There are also many different variables affecting colors, including surrounding temperature, humidity, lighting, and subjective factors in perceiving colors (Han 2006). Especially, plant colors are of a much wider variety than fragmentary manmade colors, which means they can be more emotionally expressive. However, due to limitations in collecting objective data and application methods thereof, the full range of plant colors is not being fully used (Kim 2012). Color atlases, which are objective analysis tools, are being continuously developed, For example, there are also numerous accurate published color atlases such as Seoul Color and Guides to Public Design Color Standards. However, such color atlases are insufficient when applied to colors of plants. The RHS (Royal Horticulture Society) color chart, which is a color standard in the field of horticulture, is currently used for categorizing colors of plants in Korea. Yet, there is a limitation in matching colors of native Korean plants with the color chart defined in England with their own flower colors (Kim 2014). Furthermore, such color charts are not widely used in various fields other by plant majors, which means there is a difficulty in sharing information amog fields other than plant-relatedones. Thus, this study was designed to prepare fundamental data for designing an objective and reasonable standard color chart for Korean native plants.

2. METHODS

2.1 Research Target and Range

To analyze colors of native Korean plants, a total number of 140 plants were selected through relevant research references (Yoon 2002), advice from three professional florists, and local investigations as follows: 86 species that bloom in spring, 48 that bloom in summer, and six that bloom in autumn.

2.2 Experimental Procedure

2.2.1 Investigation Method for Colors of Native Plants

From February of 2014 to January of 2014, pictures of target native plants were taken using a DMC-LX5 Panasonic camera. The pictures were taken under the same lighting conditions (clear daytime at same time range) using a Colorchecker Passport (Standard Colorship)(Figure 1) of X-Rite, which provides standards for processing using color modification programs (Figure 2). In order to accurately modify the white balance, the pictures were saved as RAW files (Baek 2012).

Figure 1: The Colorchecker Passport(Standard Colorchip) used in the study

Figure 2: Taking pictures of the targets(native plants) using Colorchecker Passport

2.2.2 Native Plants Color Analysis

Prior to the color analysis, a monitor-modification process was performed using the Eye-One Xtreme iO bundle of X-rite in order to increase accuracy of the color reproduction process. Adobe Photoshop Lightroom 5.6 program was used to reproduce the original colors of the targets, with sRGB designated as the standard RGB color range (Baek 2012) and the image files saved by exporting the pictures. Using the Adobe Photoshop CS5 program, color coefficients of each image were investigated (Figure 3), and the color chips were produced to reproduce the colors as images (Figure 4). Since plants have various patterns and colors, different colors could be extracted from a single species (Kim 2014). Both background and pattern colors were extracted from patterned plants, and only the background color was extracted from solid-colored plants. For a collection of objective data, the above process was repeated three times.

Figure 3: Investigation of color coefficients(RGB) using Adobe Photoshop CS5 Program

Scientific name	R	G	B	Color image
Paeonia lactiflora Pall.	208	2	133	

Figure 4:Creation of color image using the color coeffiecients(RGB)

2.2.3 Color system of Korea Industrial Standard (KS)

The KS is managed by the Korea Technology Standards Association, and the color standards are matched with the KS according to the Industrial Standardization Act (Moon 2011). The KS color system consists of 10 basic colors: red (R), yellow red (YR), yellow (Y), green yellow (GY), green (G), blue green (BG), blue (B), purple blue (PB), purple (P), and red purple(RP) (Park 2007)(Figure 5).

Figure 5: Basic colors of KS color system

3. RESULTS AND DISCUSSION

3.1.1 Analysis of Native Plant Colors (Spring)

Of the 85 spring native plants, a total of 116 color coefficients, including pattern colors, were extracted. Specifically, GY group colors showed the highest extraction yield of 37.9%, followed by Y group colors (29.3%), P group colors (13.8%), and RP group colors (10.3%). The R (5.2%) and YR (3.4%) group colors were extracted in small proportions (Table 1).

Table 1. Analysis of Native Plant Colors (Spring)

No	L*	a*	b*	R	G	B	H	V	C	C	M	Y	K	Color
1	16.05	25.19	11.14	89	35	42	8.83R	1.55	5.44	19	41	38	45	
2	19.22	32.83	18.04	106	31	39	9.12R	1.87	7.57	19	49	46	38	
3	25.50	20.93	8.76	107	60	65	5.98R	2.49	4.42	19	38	36	38	
4	42.35	22.36	11.41	152	96	99	5.27R	4.11	5.02	20	41	40	20	
5	55.16	53.58	5.56	221	191	201	1.87R	7.68	2.66	13	25	21	0	

3.1.2 Analysis of Native Plant Colors (Summer)

Of the 45 summer native plants, a total of 63 color coefficients, including pattern colors, were extracted. Specifically, GY group colors showed the highest extraction yield of 36.5%, followed by Y group colors (31.7%), RP group colors (9.5%), and O group colors (9.5%) (Table 2).

Table 2. Analysis of Native Plant Colors (Summer)

No	L*	a*	b*	R	G	B	H	V	C	C	M	Y	K	Color
1	27.16	22.36	12.60	114	62	63	7.60R	2.65	4.90	19	40	39	35	
2	48.72	13.60	6.22	154	117	122	4.52R	4.72	3.16	20	34	32	19	
3	72.32	20.70	14.47	230	168	167	6.94R	7.07	5.51	9	34	34	0	
4	36.63	41.54	19.74	162	63	74	4.93YR	3.56	9.42	20	58	54	146	
5	50.18	51.52	62.68	218	82	2	0.19YR	4.86	14.88	14	67	99	0	

3.1.3 Analysis of Native Plant Colosr (Autumn)

Of the seven autumn native plants, a total of eight color coefficients were extracted. Specifically, Y and GY group colors showed the highest extraction yield of 37.5%, followed by RP group colors (12.5%) and P group colors (12.5%) (Table 3).

Table 3. Analysis of Native Plant Colors (Autumn)

No	L*	a*	b*	R	G	B	H	V	C	C	M	Y	K	Color
1	55.73	-0.79	50.87	154	145	57	9.73Y	5.41	6.95	20	23	58	19	
2	81.41	-6.47	84.08	223	210	1	9.82Y	8.01	11.52	12	17	99	0	
3	92.05	-6.47	73.37	255	237	0	9.14Y	9.10	12.65	0	7	100	0	
4	74.96	-0.04	33.45	199	192	139	0.55GY	7.34	0.55	20	22	43	1	
5	96.74	-6.36	7.71	246	247	242	7.5GY	9.57	7.50	3	3	5	0	

3.1.4 Analysis of Native Plant Colors (Winter)

In winter, all native plants hibernate, so no colors were extracted.

3.1.5 Integrated Native Plant Color Analysis

As a result of the analysis of colors of Korean native plants, GY and Y group colors showed the highest extraction yields from plants in all three seasons. Although in small proportions, RP group colors were also found from plants in all three seasons (Table 4).

Table 4. Intergrated Native Plant color analysis

Color name		R	YR	Y	GY	G	BG	B	PB	P	RP	Total(%)
Season	Spring	5.2	3.4	29.3	37.9	0.0	0.0	0.0	0.0	13.8	10.3	100.0
	Summer	4.8	9.5	31.7	36.5	0.0	0.0	0.0	0.0	7.9	9.5	100.0
	Autumn	0.0	0.0	37.5	37.5	0.0	0.0	0.0	0.0	0.0	12.5	100.0

4. CONCLUSIONS

Colors of Korean native plants were analysed, and no colors were extracted from plants in winter, when all native plants hibernate. In the three other seasons, GY and Y group colors were found in large proportions from native plants. Although in small proportions, RP group colors were found as well.

Currently there is no color chart for colors of Korean native plants, so this study is expected to increase the applicability of plant colors and can be used as fundamental data for investigating Korean native plants in the future. Moreover, there is a necessity for continuous production of relevant research from various approaches.

REFERENCES

An Y.H. 2008. *(The)native plants of Korea,* Paju: Gimmyoung.

Baek J. S. 2012. Digital photography workflow with Lightroom 4. Seoul: Easyspub.

Ha S. K., J. K. Jeon, and S. T. Choi. 1988. Studies on Flower Bud Differentiation and Forcing of Pulsatilla koreana. *Kor. J. Hort. Sci. Technol* 29(1): 46-52.

Han S. W., N. Y. Lee, and J. S. Lee. 2006. Application to RGB Image Data for Analysis of Leaf Color in Succulent Plants. *Kor. Soc. For People, Plants and Environment* 9(4): 88-94.

Jeong J. H., and K. S. Kim. 1991. Morphological Characteristics of Korean Native Lilies. Kor. J. Hort. Sci. Technol 32(3): 411-418.

Kim M. Y. 2011. A Study on the Native Fruiting Plants for Ornamental Applications. *In a master ´s thesis.* The Graduate school of Chung-ang University.

Kim Y. S. 2012. Utilization of Floricultural Design Based on Colors from Plants. *The Korean Society of Floral Art & Design* 27: 113-125.

Kim Y. S., S. R. Choi, and B. Jeon. 2014. Suggestion of Color Atlas based on Analysis of Ornamental Foliage Plant Colors Distributed in Korea. *Journal of Korean Society of Color Studies* 28(1): 156-165.

Koo M. Y., J. M. Joe, and Y. W. Kim. 1999. Study on the Roadside Beautification Native Plant Material Developed in Korea. In *Journal of Biseul.* Dae gu: Keimyung University, 10: 233-266.

Lee J. S., P. S. Yoon, and S. J. Jeong. 2001. The Present Condition and Direction of Study about Korean Native Plants -The Study for the period between 1960 and 1996-. *The Korean Society of Floral Art & Design* 5(0): 43-54.

Lee M. J., and Sang C. K. 1990. Growth Conditions of Hepatica asiatica Nakai in the Habitats for the Cultivation as a Floricultural Crop. *Kor. J. Hort. Sci. Technol* 31(1): 81-89

Moon E. B. 2011. *Textbook of Color Design*. Gyeonggi: Ahn Graphics.

Oh H. W. 2002. (A) Study on the Utilization of Korean Native Plants for Interior Landscape. *In a master's thesis.* Seoul: Seoul Women's University.

Park Y. J., J. H. Jeong, S. J. Kim, and B. K. Heo. 2004. Dyeability of 46 Kinds of Native Herbaceous Plant Extracts onto Skeletonizing Leaves for Flower Design. *J. Kor. Flower Res. Soc.* 12(4): 317-322.

Park Y. S. 2007. *(A) dictionary of color.* Seoul: Yelim.

Yoo M. S., and J. H. Yoo. 1984. Studies on Propagation of Bittersweet (Celastrus orbiculatus). Kor. J. Hort. Sci. Technol. 667-674.

Yoon P. S. 2002. *(New)Native Botany,* Seoul: Daesun.

Address: Researcher. Saetbyul KIM, Sahmyook University Environmental Green design Institute, Hwarangro-815 Nowon-gu, Seoul, 139-800, KOREA
E-mails: kyscolor@syu.ac.kr,hellosran@naver.com,, 01034210528@hanmail.net, greencolor@syu.ac.kr

Effects of Accent Colour on the Apparent Distance to a Wall and the Apparent Volume of an Interior Space: The Validation Experiment in an Actual Space

Wataru KAMIJO, Keishi YOSHIDA, Masato SATO,
Division of Environmental Sciences, Kyoto Prefectural University

ABSTRACT

This study was conducted to evaluate the effects of an accent colour on a wall, based on the apparent distance to the wall and the apparent volume of the interior space. Psychological experiments were conducted in an actual experimental space. Based on the presence of the accent colour on the wall, the apparent distance to the wall and apparent volume of the interior space may vary. They depend on the size of the accent colour area, as well as its hue. If the wall contains a greater amount of the accent colour, the wall will seem to advance and the interior space will appear cramped. Conversely, if the wall contains a lesser amount of the accent colour, the degree of the effect will be smaller.

1. INTRODUCTION

Colours produce many psychological effects, such as contrast, assimilation, advancing, receding, and area effects, among others. The authors studied the advancing and receding effects of the colours on the apparent distance to a front wall located in an interior space painted in a single colour. Notably, houses contain many accessories, such as curtains, blinds, paintings, etc. These components are perceived as accent colours in an interior space. Thus, the study also sought to evaluate the effects of the accent colours on a wall, considering the apparent distance to the wall and the apparent volume of the interior space by using scale models. However, as these effects need to be confirmed in an actual space, this study evaluated the effects of an accent colour on a wall in an actual experimental space. Consideration was given to the apparent distance to the wall and the apparent volume of the interior space. It was found that accent colours on a wall have effects on the apparent distance to a wall and the apparent volume of an actual interior space.

2. EXPERIMENTAL METHOD

Psychological experiments were conducted in an actual experimental space (see Figure 1). Two distinct spaces of the same size (i.e., the standard space and the comparison space) were set side by side. They were separated by an N8 curtain. The walls of the spaces were painted with N8. Fluorescent lamps of high colour-rendering type were installed. The average interior illuminance level was approximately 500 lx. An extremely thin square panel painted in a single colour was hung in the center of the wall of the comparison space. There were three experimental conditions based on the panel size: (1) a large panel (hereafter referred to as EC50) occupying 50% of the wall; (2) a mid-sized panel (hereafter referred to as EC10) occupying 10% of the wall; (3) a small panel (hereafter referred to as EC2) occupying 2% of the wall (see Figure 2). A total of seven panel colours were selected. Table 1 shows the assigned panel colours. A total of 22 experimental patterns were created. They included combinations of seven colours, and were constructed with panels of three different sizes as well as without a panel. The subjects consisted of twelve females and two males with age ranging between 20 and 24. The subjects had no colour-vision deficiencies. The experimental panels were randomly presented to each subject. The fourteen subjects were asked to evaluate the apparent distance of the front wall of the comparison space based on their comparisons of both spaces. The comparisons were rated by using a seven-point rating scale. The magnitude estimation method was adopted to evaluate the apparent volume of the comparison space. The subjects were also asked to compare the ratio of the apparent volume of the comparison space with that of the standard space, whose value was set to 100.

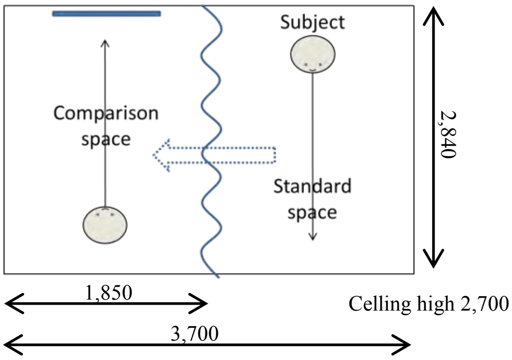

Figure 1: The plan of the experimental spaces.

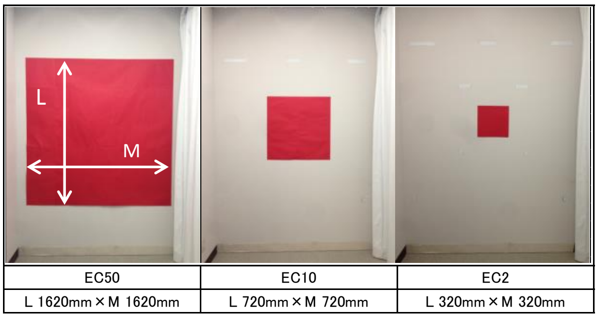

Figure 2: The panel sizes.

Table 1. The assigned panel colour.

NO.	Colour term (Designation of the study)	Hue	Value	Chroma
1	RED (R)	5R	4	12
2	YELLOW (Y)	5Y	8	10
3	GREEN (G)	7.5G	5	8
4	BLUE (B)	10B	5	8
5	PURPLE (P)	5P	4	6
6	BLACK (Bk)	N	2	–
7	WHITE (W)	N	9.5	–

3. RESULTS AND DISCUSSION

3.1 Apparent distance to the frontal wall

Figure 3 shows the apparent distance to the wall for each colour in each panel size. For EC50, the wall seemed to advance for all the colours except W. The degree of advancement was greater for the warm colours, as well as for Bk and P. For EC10, the wall seemed to advance for all the colours. The degree of advancement was greater for the warm colours. For EC2, the wall seemed to advance for all the colours except B and G. As in the previous cases, the degree of advancement was greater for the warm colours. The values increased proportionally to the area of the panel.

To clarify the relationship between the apparent wall distance and the experimental factors, an analysis of variance was conducted using the General Linear Model procedure. The experimental factors chosen were the hue and area of the panel. The effects of all the factors were statistically significant (Level of significance: 0.05). Figure 4 shows the profile plots of each significant experimental factor. With respects to the hue of the panel, the front wall appeared to advance significantly for all the colours except B. The degree of advancement was greater for the warm colours. With respects to the area of the panel, the front wall appeared to advance for all the sizes, with a decreasing degree of advancement following the order EC50, EC10, EC2.

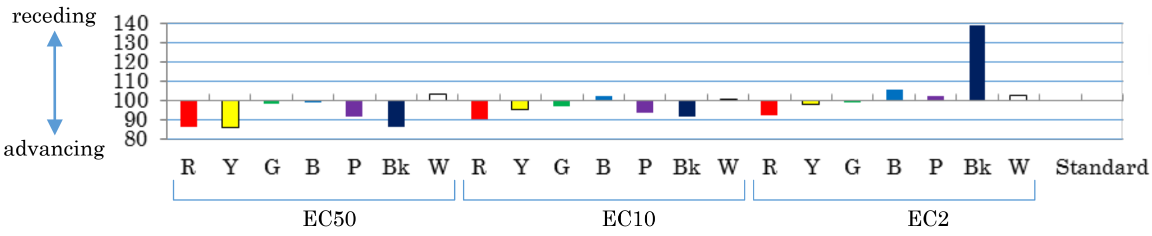

Figure 3: Apparent distance to the wall for each colour in each size.

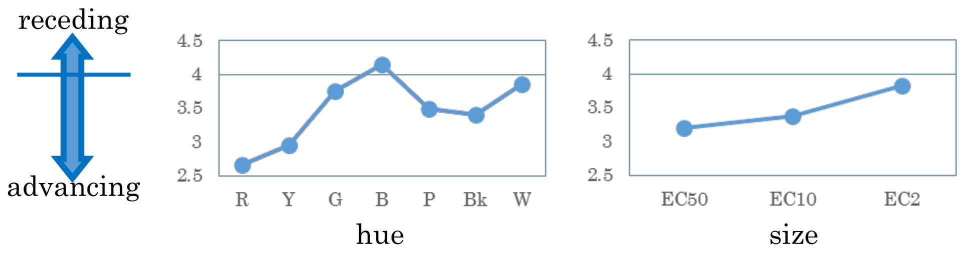

Figure 4: The profile plots of each significant experimental factor.

3.2 Apparent volume of the interior space

Figure 5 shows the average apparent volume of the interior space for each colour in each panel size. For EC50, the interior space appeared smaller for all the colours except W. The degree of shrinkage was greater for the warm colours, as well as for Bk and P. The values of EC10 showed a similar tendency to those of EC50. However, the degree of shrinkage for EC10 was smaller than that observed for EC50. For EC2, the interior space appeared smaller for the warm colours, while it appeared larger when blue and black were used.

In addition, an analysis of variance was conducted. The effects of all the factors were statistically significant (Level of significance: 0.05). Figure 6 shows the profile plots of each significant experimental factor. With respects to the hue of the panel, the value of the interior space appeared significantly cramped for all the colours except B and W. The degree of restriction was greater for the warm colours. With respects to the area of the panel, the value of the interior space appeared cramped in EC50 and EC10. For EC2, the volume appeared equivalent to the standard space.

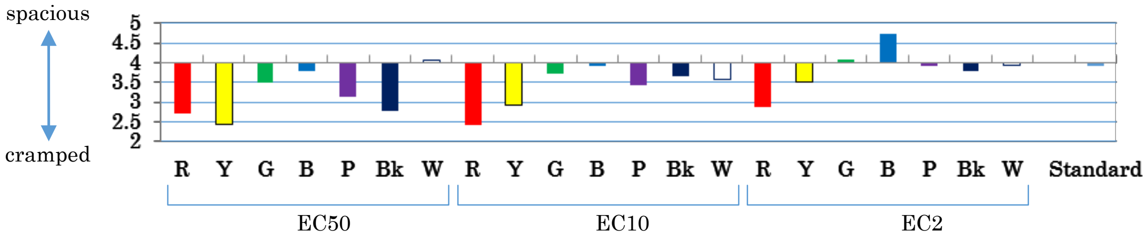

Figure 5: Apparent distance to the wall for each colour in each size.

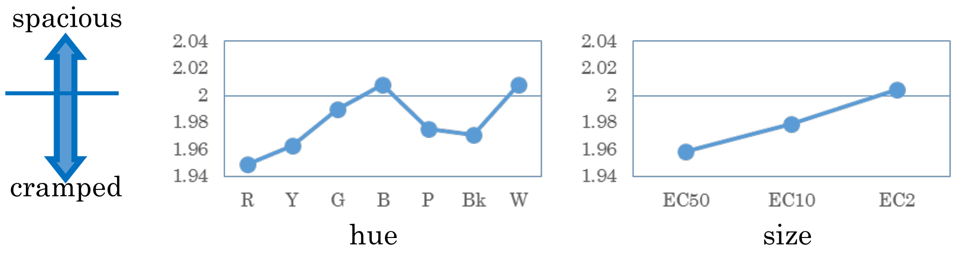

Figure 6: The profile plots of each significant experimental factor.

3.3 Relationship between the apparent distance and the apparent volume

The correlation coefficient between the apparent distance and apparent volume was quite high: 0.837.

4. CONCLUSIONS

The following conclusions were obtained by conducting experiments in the actual space. In relation to the presence of an accent colour on the wall, the apparent distance to the wall and the apparent volume of the space can vary. The apparent distance to the wall and the apparent volume of the space depend on the area of the accent colour, as well as its hue. If the wall contains a greater amount of an accent colour, the wall seems to advance and the interior space appears cramped. However, if a cold colour is contained, the wall seems to recede and the interior space appears more spacious. The degree of the advancement was greater for warm colours, in line with the perceptual effect reported in previous research. It was found that the presence of an accent colour on a wall influences the apparent distance to a wall and the apparent volume of an actual interior space.

REFERENCES

Sato, M., 2012. *Advancing and receding effects of colours on apparent distance to a wall of an interior space*, J. Environ. Eng., AIJ 77(677) 559-565.

Sato, M. and Goto, M., 2013. *Effects of accent colour on apparent distance to a front wall and apparent volume of an interior space*, 12th AIC congress proceeding volume 2, New castle, 555-558.

Address: Prof. Masato Sato, Division of Environmental Sciences,
Kyoto Prefectural University, 1-5 Hangi-cho, Shimogamo,
Sakyou-ku, Kyoto 606-8522, JAPAN
E-mails: ma_sato@kpu.ac.jp

Metamer Mismatching as a Measure of the Color Rendering of Lights

Hamidreza Mirzaei and Brian Funt
School of Computing Science, Simon Fraser University

ABSTRACT

We propose a new method for evaluating the colour rendering properties of lights. The new method uses the degree of metamer mismatching for the CIE XYZ corresponding to flat grey (constant reflectance of 0.5) quantified in terms of the metamer mismatch volume index proposed by Logvinenko et al. (Logvinenko 2014). A major advantage of this method is that unlike many previous color rendering indices it does not depend on the properties of a chosen set of representative test objects.

1. INTRODUCTION

Evaluating the colour rendering properties of lights is an important issue in the lighting industry. It is well known that the colours of objects viewed under lights of identical correlated colour temperature may look very different under the different lights. Several color rendering indices have been used in the past. Perhaps the most widely used is the CIE colour rendering index CIE Ra (CIE 1995), which is based on computing the average color difference induced by the illuminant for a fixed set of reflectances. The CIE Ra is a color fidelity measure. There have also been preference-based measures such as Judd's flattery index (Judd 1967) and Thornton's colour preference index (Thornton, 1972), in which the focus is more on the subjective preferability of lights. More recently Smet et al. (Smet 2010, Smet 2015) have suggested a memory-color-similarity measures, Sa and Rm (a non-linear scaling of Sa), based on how a light affects the colors of a sample set of familiar objects (green apple, banana, orange, lavender, Smurf, strawberry yoghurt, sliced cucumber, cauliflower, Caucasian skin, sphere painted Munsell N4 grey) in comparison to the average subject's memory of the colors of those objects as determined by psychophysical experiments.

The CIE Ra is defined in terms of a reference illuminant and the test light being evaluated. For test lights of CCT less than 5000K the reference illuminant is chosen to be the ideal blackbody radiator of the same CCT. For test lights with CCT of 5000K or greater, the reference light is chosen to be the standard CIE daylight D-series illuminant of the same CCT. There are 8 test color samples (Munsell papers) whose color differences, after an adjustment for chromatic adaptation, under the test and reference lights are evaluated.

The CIE Ra has been widely criticized, especially for the evaluation of LED lights. One of the key problems with it is that it is based on measuring the colour differences that arise across a small sample of 8 (sometimes generalized to 14) coloured papers. Not only may such a sample not represent what the colour differences for all other possible surface reflectances may be, it also gives manufacturers the opportunity to tune the spectra of their lights to perform well on the standard sample.

Variants of metamer mismatching have been previously used as a measure of the color rendering of daylight simulators. In particular, the CIE Metamerism index is a measure based on calculating the average color difference between each of a set of reflectance pairs that are initially metameric matches under the reference light but not necessarily metameric matches under the target light. However, this method is limited to the specific reflectances used. Whitehead et al. (Whitehead 2012) extend this general idea by using a large number of randomly generated metameric spectra and then assessing the fraction of them that noticeably change colour when the illuminant changes. In contrast, the method proposed here is based on measuring the size of the metamer mismatch volume, which is the volume of colour signals (i.e., XYZs) induced under the second light by the set of all theoretically possible reflectances that make a metameric match under the first light.

1. METAMER MISMATCH INDEX

The background for the proposed measure of colour rendering is the concept of metamer mismatching. Consider a colour signal XYZ (in CIE standard coordinates) observed under a first light. Metamer mismatching refers to the fact that the possible XYZ that might be observed under a second light is only constrained to lie within a convex volume of possible XYZ values. The size of the volume depends on the XYZ and the lights involved; however, the volume for the XYZ of flat grey is the largest. The metamer mismatch volume represents the range of possible XYZ that can arise under the second light and so provides a measure of how varied the XYZ under the second light can be—the less the variation, the better the color rendering.

The boundary of the metamer mismatch volume can be calculated using the code of Logvinenko et al. (Logvinenko 2014), which finds the maximum amount of metamer mismatching that can occur for any given XYZ and pair of lights. Figure 1 shows an example of the metamer mismatch volume for the XYZ of flat grey for a change in illuminant from an ideal 2900K blackbody radiator to a 2900K LED. Even though the two illuminants are of the same CCT the metamer mismatch volume is quite large: it fills a sizable fraction of the entire object-color solid. The object-colour solid is the set of all possible XYZ that can arise for all possible reflectance functions $\rho(\lambda)$ (i.e., $0 \leq \rho(\lambda) \leq 1, 380 \leq \lambda \leq 780$nm). The metamer mismatch volume depicted is the set of all possible XYZ that could arise under the second illuminant for any reflectance that is metameric to flat grey under the first illuminant.

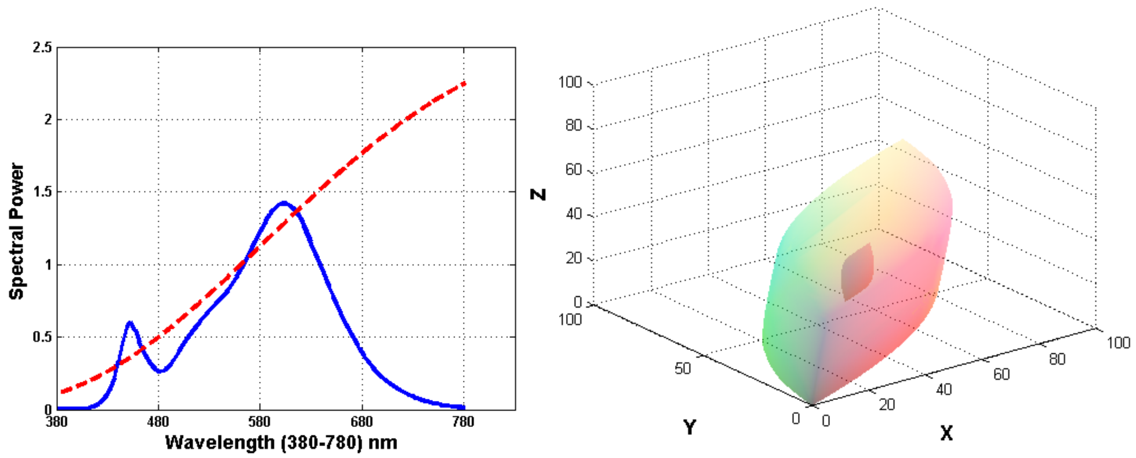

Figure 1: Left: Spectra of a 2900K LED (blue) and that of an ideal 2900K blackbody radiator (dashed red). Right: Metamer mismatch volume (for the XYZ of flat grey lit by a 2900K blackbody) shown inside the object-colour solid of the 2900K LED for the case when the illuminant is changed from the blackbody to the LED. Coordinates are the CIE 1931 XYZ space.

Since both the object color solid and the metamer mismatch volume change with the second illuminant, we consider size of the metamer mismatch volume relative to the size of the object color solid it generates. In particular, both scale with the intensity of the second illuminant. Hence, the metamer mismatch volume index (MMVI) (see Logvinenko et al., 2014 Eq. 15 for a formal definition) for a given XYZ and a pair of illuminants is defined as the ratio:

$$MMVI = \frac{\text{volume of the metamer mismatch volume for the given illuminant pair}}{\text{volume of the object color solid under the second illuminant}} \quad (1)$$

Note that this ratio is also independent of any linear transformation of the color coordinate space and so will be the same for any LMS space obtained as a linear transform of CIE XYZ as for CIE XYZ itself.

In terms of colour rendering, the larger the MMVI, the poorer the colour rendering of the second light relative to the first light is likely to be. Since the MMVI is volume based, we find it more intuitive to consider MMVI^(1/3). The Metamer Mismatching Colour Rendering Index (MMCRI) is then defined as:

$$MMCRI = (1 - \sqrt[3]{MMVI}) \times 100 \quad (2)$$

where the MMVI is for that of the XYZ of flat grey under the first illuminant. The scaling by 100 is simply to make its range match that of the CIE CRI Ra.

4. COMPARISON TO OTHER COLOR RENDERING INDICES

The MMCRI can be computed for any pair of illuminants as a measure of the color rendering properties of the second light relative to the first. However, the CIE CRI Ra for a light L is defined relative to an 'ideal' illuminant (blackbody or D-series) of the same CCT as L. For comparison with Ra we use the same choice of 'ideal' illuminant as the first illuminant when computing the MMCRI of L.

We have computed the MMCRI and CIE Ra for several light spectra across a range of CCTs and technologies and compared them. In particular, we measured the spectra of several commercially available LED lights and also used the spectra of the CIE standard illuminants. When plotted as in Figure 2 we see a good correlation between the two indices—an indication that the MMCRI behaves reasonably—but with notable differences for some illuminants. It is exactly such differences that the proposed new method is intended to reveal. In particular, we note that F11 and F12 have a high CIE Ra but a low MMCRI. Since F11 and F12 are both dominated by three narrowband peaks, it seems unlikely that their color rendering properties are very good, and this is confirmed by the MMCRI.

As second test, we make use of the set of lights Smet et al. included in their paired comparison experiment (Smet 2010). Smet's set contains: a halogen lamp (H), a fluorescent lamp approximating CIE F4 (F4), a Neodymium incandescent lamp (Nd), a Philips Fortimo LED module with a green filter (FG), an RGB LED lamp (RGB) and a LED cluster (LC) optimized to obtain a high Sa, all of which are plotted in Figure 3. The various color rendering measures are compared in Table 1.

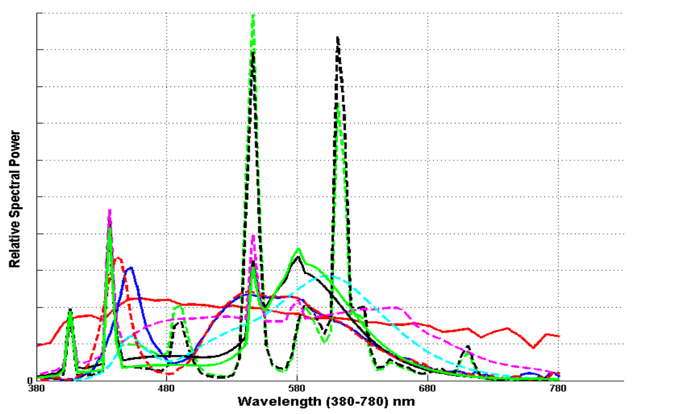

(2a)

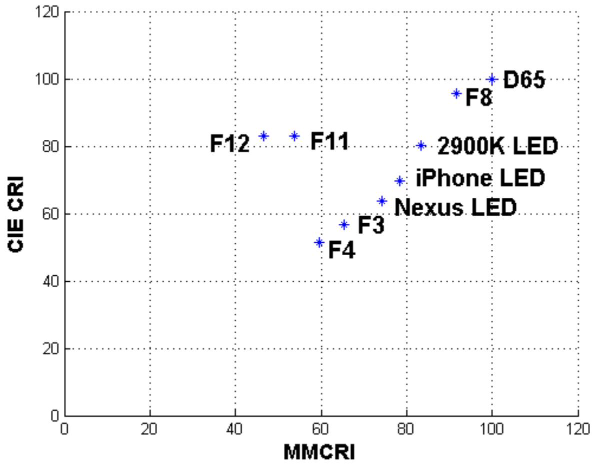

(2b)

Figure 2: (2a) The illuminant spectra used for testing: D65 (red), F3 (black), F4 (dashed green), F8 (dashed magenta), F11 (dashed green), F12 (dashed black), 2900K LED (dashed cyan), Nexus LED (dashed red) and iPhone LED (blue). (2b) CIE CRI versus MMCRI.

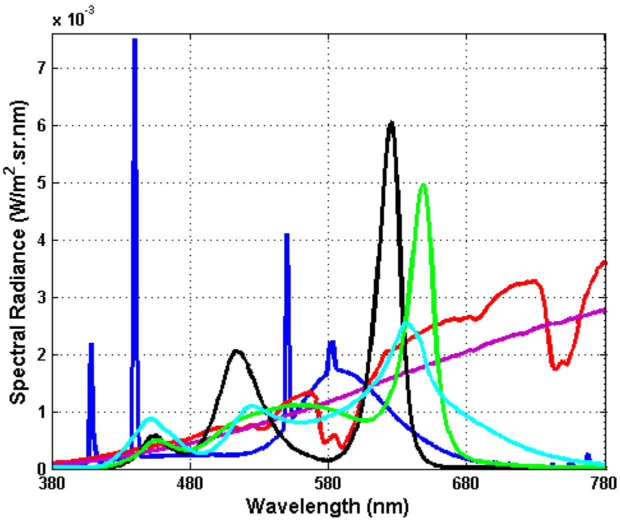

Figure 3: The spectral power distributions of the six light sources (provided by Smet) and used for the comparison of the color rendering measures listed in Table 1. The lights (see text) are F4 (blue curve), FG (green), Nd (red), LC (cyan), H (purple) and RGB (black).

Table 1. Comparison of Color Rendering Measures. Measures include: Sa, memory color similarity (Smet 2010), Ra (CIE CRI), NIST CQSa Color Quality Scale (Davis 2010), and MMCRI (proposed metamer mismatch index). The data reported in the table for Sa, CIE CRI Ra and NIST CQSa are quoted from Table 2 of Smet et al. (Smet 2010, page 26235). The MMCRI results were computed based on the MMVs for a change from the blackbody radiator having the CCT of the given illuminant to the given illuminant. The lights were approximately equal illuminance ranging from 239 to 251 lux, and CCT ranging from 2640 to 2878. The spectra of the lights are plotted in Figure 3.

Light source	Sa		CIE Ra		NIST CQSa		MMCRI	
	Sa	Rank	Ra	Rank	CQSa	Rank	MMCRI (Grey)	Rank
F4	0.6672	5	52.8	5	53.9	5	55.53	5
FG	0.7787	3	80.6	3	87.2	3	83.99	3
Nd	0.7841	2	73.7	4	87.0	4	89.46	2
LC	0.7899	1	81.0	2	89.0	2	74.95	4
H	0.7662	4	99.6	1	97.2	1	99.64	1
RGB	0.6548	6	31.9	6	50.5	6	49.30	6

The results in Table 1 show a general agreement in ranking across all the methods in that the same lights are given ranks 3 (FG), 5 (F4), and 6 (RGB). Ra and CQSa rankings for all six lights are identical. MMCRI agrees with Ra and CQSa on 4 of the rankings, but swaps the rankings of Nd and LC, ranking Nd 2nd, in agreement with Sa and the reported popularity of Neodymium lights in terms of their sales. Since LC is an LED cluster designed to optimize Sa, it is not surprising that it is ranked first by Sa. Similarly, since H is a halogen light closely approximating a blackbody radiator, it is also not surprising that MMCRI, Ra and CQSa all rank it first since they assume that a blackbody is the ideal light source in terms of color rendering. This is an assumption that Smet et al. (Smet 2012) challenge, but as yet no general alternative has been proposed.

It should be noted that the Sa rankings in Table 1 do agree with the 'preference' and 'fidelity' rankings reported in Table 3 of Smet et al. (Smet 2010, p. 26237). However, one problem Table 1 reveals about the Sa measure is that it ranks many of the lights almost identically. In particular, FG, Nd, LC and H all have Sa values of 0.778 ±0.012. Effectively, Sa divides the lights into just two groups: (FG, Nd, LC, H) and (F4, RGB). In comparison, with MMCRI there are clear differences in the scores such that there are four distinct groups: (F4, RGB), (LC), (FG, Nd) and (H).

4. CONCLUSION

A new measure of the color rendering properties of lights is proposed based on the general concept of metamer mismatching. The amount of metamer mismatching—effectively the range of theoretically possible color signals arising under a second light—is taken as an indicator of the difference in the color rendering properties of the second light relative to the first. The greater the degree of metamer mismatching, the poorer the color rendering is considered to be. Previous color rendering indices have been based on a fixed selection of object reflectances. Although there have been attempts to optimize the set of test reflectances (Smet 2013) a finite set will always remain the source of some bias. In comparison, the proposed method, through the calculation of the metamer mismatch volume, takes into account all theoretically possible reflectances

ACKNOWLEDGEMENTS

Funding was provided by the National Research and Engineering Research Council of Canada. The authors wish to thank Kevin Smet for providing his spectral data.

REFERENCES

CIE 1995. *Method of measuring and specifying colour rendering properties of light sources.* CIE Publication, No. 13.3.

Davis, W., and Y, Ohno. 2010. Color quality scale. *Opt. Eng*. **49**(3), 033602.

Judd. D., 1967. *A flattery index for artificial illuminants.* Illum. Eng. 62, 593–598.

Logvinenko A., B. Funt and C. Godau. 2014. Metamer mismatching. *IEEE Trans on Image Processing*, 23, 34-43.

Smet, K., W. Ryckaert, M. Pointer, G. Deconinck, and P. Hanselaer. 2010. Memory colours and colour quality evaluation of conventional and solid-state lamps. *Optics Express,* 18(25), 26229-26244.

Smet, K., and L. Whitehead. 2011 Meta-Standards for Color Rendering Metrics and Implications for Sample Spectral Sets. In *Proc. CIC'19 19th Color Imaging Conference*, 76-81.

Smet, K., W. Ryckaert, M. Pointer, G. Deconinck, and P. Hanselaer. 2012. A memory colour quality metric for white light sources. *Energy and Buildings*, 49, 216-225.

Smet K., J. Schanda, L. Whitehead, and R. Luo. 2013. CRI2012: A proposal for updating the CIE colour rendering index. *Lighting Research and Technology*. 45(6), 689-709.

Smet, K., and P. Hanselaer. 2015. Memory and preferred colours and the colour rendition evaluation of white light sources. *Lighting Research and Technology*.

Thornton. W. A. 1972. A validation of the color preference index. *Illum. Eng*. 62, 191–194.

Whitehead L., and M. Mossman. 2012. A Monte Carlo method for assessing color rendering quality with possible application to color rendering standards. *Color Research & Application.* 37(1), 13-22.

Address: Professor Brian Funt, School of Computing Science, Simon Fraser University, 8888 University Drive, Burnaby, British Columbia, Canada V5A 1S6.
E-mails: hmirzaei@sfu.ca, funt@sfu.ca.

Visual Impression of a Real Room Affected by Lighting Conditions and by Colour and Texture of the Walls

Jau-Yi WU, Henry PAN, Li-Chen OU
Graduate Institute of Color and Illumination Technology,
National Taiwan University of Science and Technology, Taiwan

ABSTRACT

Colour scheme plays an important role in the process of interior design. Different combinations of wall colours, textures and lighting conditions can bring out differences in terms of semantic feelings and aesthetic judgements. That makes an important issue to find out appropriate combinations of colours and light sources for an interior environment. To address the issues, interior colour design was taken as an example in our psychophysical study of wall colour and lighting conditions.

The aim of this study is to investigate visual impression of a real-room space, a "shooting studio" with a size of 3m (width) x 3m (depth) x 2.5m (height). The backgrounds for the three "walls" were made of coloured cloth sets that can be changed easily by a rail system. The lighting conditions were varied by adopting different light sources. Six wall colours were used in the study: grey, white, black, light brown, light blue and light green. Six lighting conditions were adopted, generated by two correlated colour temperatures (CCT), 6500K and 2700K, and three lighting directions, including (a) light travelling up and sideway, (b) a non-directional floor lamp and (c) light travelling down). This resulted in 6 (background colours) x 6 (lighting conditions) = 36 experimental conditions. In addition to these 36 experimental conditions based on cloth background, 12 extra experimental conditions based on paper background were also used to investigate whether the results were influenced by the background texture (i.e. cloth vs. paper). The 12 paper-background experimental conditions were selected randomly from the 36 cloth-background experimental conditions in terms of wall colours and light sources.

Ten semantic scales, including like/dislike, comfortable/uncomfortable, warm/cool, spacious/small, bright/dark, clean/dirty, relaxing/tense, elegant/inelegant, classical/modern and harmonious/disharmonious, were used to measure the emotional effects of combinations of the wall colours and the lighting conditions. Twenty-two observers with normal colour vision, including 11 males and 11 females, participated in the study. During the experiment, each observer was asked to sit in the room and to rate for each experimental condition using the 10 semantic scales.

As a result, the 10 scales were classified using principal component analysis into two underlying factors, "brightness" and "warmth". The "brightness" factor was found to correlate closely with bright/dark, clean/dirty and spacious/small. The "warmth" factor was highly correlated with the remaining scales. Note that "like/dislike" was correlated more closely with the "warmth" factor (R=0.75) than with the "brightness" factor (R=0.45), implying that warmth was more important than brightness to increase the preference. High

correlation was found between the cloth-background and the paper-background experimental conditions in terms of all semantic scales, with the highest correlation coefficient 0.92 for classical/modern, followed by 0.90 for spacious/small, and the lowest correlation being 0.66 for both like/dislike and comfortable/uncomfortable. This suggests that the texture of walls had a stronger impact on preference and comfort than on the other scales.

1. INTRODUCTION

Other than colour harmonization, conditions such as adjacent colouring area proportions, and lighting are issues of consideration in the process of allocating colours in the real time environment. Therefore, this research is using real-room environment as the condition, for considering colour harmony appearance and reality application adding different lighting condition. Expecting this research could get the colour harmony theory closer to the practical application. Academia and industries has always been interested in the topic: Impression of the interior environment. Instead of setting a real-room as the experiment condition, There are lots of existing research using computer-simulated interior graphics as the stimulus. Now a days, colour harmony research apply modern colour science technology, some of the colour harmony quantitative model were using in the interior graphics and put forward a satisfied predictive. However, could the model apply to a real interior environment is still unclear.

2. METHOD

Different lighting condition and wall colour were used to find out the colour harmony model[1] in the real-room. For the goal to investigate whether the results were influenced by the background texture (i.e. cloth vs. paper), 12 extra experimental conditions based on paper background randomly picked from the 36 conditions using cloth background. Analysing the data that collected from both experiment using cloth and paper background to find out whether they show the similar correlation with colour harmony model.

2.1 Sample Preparation

Observers: a total of twenty-two observers with normal colour vision, including 11 males and 11 females, participated in the study.

Stimuli: a “shooting studio” with a size of 3m (width) x 3m (depth) x 2.5m (height). The backgrounds for the three “walls” were made of coloured cloth sets that can be changed easily by a rail system. The lighting conditions were varied by adopting different light sources. Six wall colours were used in the study: grey, white, black, light brown, light blue and light green. Six lighting conditions were adopted, generated by two correlated colour temperatures (CCT), 6500K and 2700K, and three lighting directions, including (a) light travelling up and sideway, (b) a non-directional floor lamp and (c) light travelling down). This resulted in 6 (background colours) x 6 (lighting conditions) = 36 experimental conditions. 12 of the 36 conditions were randomly picked to replace the cloth-background to the similar colour paper-background, as illustrated in *Figure 1*. This experiment was using Super Seamless paper-background to find an similar colour that matched the cloth-background as the wall colour condition. The same six wall colours were used in paper background: grey, white, black, light brown, light blue and light green. CIELAB values of cloth-background are shown in *Table 1* and paper-background are shown in *Table 2*.

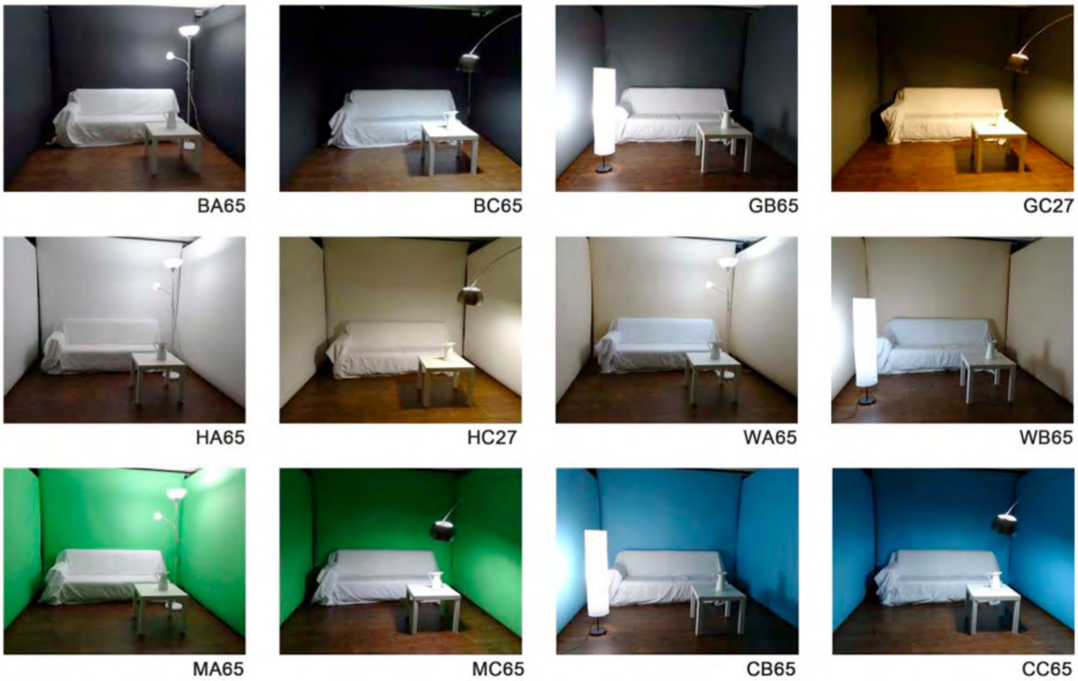

Figure 1: The 12 paper-background experimental condition

Table 1: CIELAB reference value of Cloth-background.(X-rite 962)

	L*	a*	b*	C^*_{ab}	h_{ab}
Black	16.8	0.1	-1.5	1.5	273.9
Grey	40.5	1.8	-11.2	11.4	279.2
White	93.8	2.0	-8.2	8.5	283.9
Light Yellow	88.4	2.1	14.4	14.5	81.6
Light Blue	54.7	-7.5	-2.8	8.0	200.5
Light Green	65.7	-14.7	43.0	45.5	108.9

Table 2: CIELAB reference value of Paper-background(X-rite 962)

	L*	a*	b*	C^*_{ab}	h_{ab}
Black	25.05	-0.26	-0.69	0.73	249.58
Grey	42.99	-1.54	-0.06	1.54	182.35
White	95.18	1.35	-3.5	3.75	291.05
Light Yellow	85.89	5.25	14.34	15.27	69.89
Light Blue	69.61	-18.18	-16.6	24.62	222.39
Light Green	71.95	-27.5	31.54	41.85	131.08

Scales: A survey were emitted, asked 19 observers (8 males and 11 females) to list 15 adjective in the impression of a "living room" before the experiment. Pick out the 8 most repeated adjective and add "like/dislike" "harmonious/disharmonious" to find out the colour preference and colour harmony in the real-room environment. Result as Figure 1. Ten semantic scales, including like/dislike, comfortable/uncomfortable, warm/cool, spacious/small, bright/dark, clean/dirty, relaxing/tense, elegant/inelegant, classical/modern and harmonious/disharmonious, were used to measure the emotional effects of combinations of the wall colours and the lighting conditions.

2.2 Experimental Procedure

Every observer will sit in the room and adapted for 30 seconds. Then start to value the real-room experimental condition in 10 semantic scales. Each of the semantic scales were forced choice in 6 categories. As a case of "spacious/small", the categories were"very spacious", "spacious", "slightly spacious", "slightly small", "small" and "very small". Every observer has to do the complete experiment twice to make sure the repetitive of experiment. The 12 stimuli were randomly picked in the experiment.

3. RESULTS

The aim of the study was to investigate visual impression of a real-room induced by lighting conditions and the wall colour. To see there was any difference between cloth and paper background in the observer responses, the experimental data were divided in to two groups of back ground texture. The correlation coefficients of the 10 scales between 12 cloth and paper background experimental conditions are shown in *Table 3*.

Table 3. Correlation coefficients of the 10 scales between 12 cloth and paper background

like/dislike	bright/dark	warm/cool	spacious/small	comfortable/ uncomfortable
0.656	0.807	0.773	0.904	0.664
clean/dirty	relaxing/tense	elegant/ inelegant	classical/ modern	harmonious/ disharmonious
0.855	0.718	0.721	0.922	0.722

As the result in *Table 3*, most of the observer's data were highly correlated. "Classical/modern" is the highest; "spacious/small" "clean/dirty" and "bright/dark" comes second; "like/dislike" is the last. As we could know, the difference between background texture didn't had significant influence in the scale of "classical/modern" "spacious/small" "clean/dirty" and "bright/dark". Therefore, difference between background texture did influence the result of "like/dislike". For reference in *Table 4*, most of the adjectives were scored slightly higher in paper background than cloth background. Texture of the background could possibly in a similar change tendency of observer's data, a degree of score difference may be observed.

Table 4. The average score of the raw data (paper and cloth background in 10 scales)

	Cloth background	Paper background
Like	3.40	3.94
Comfortable	3.40	4.02
Warm	2.84	3.45
Spacious	3.47	3.70
Bright	3.80	3.68
Clean	4.04	4.17
Relaxing	3.28	3.89
Elegant	3.50	3.90
Classical	2.65	3.37
Harmonious	3.58	4.04
average	3.40	3.82

4. CONCLUSION

This study aimed to investigate the influences of background texture on the visual impression of a real-room environment. The results show that (1) observers had higher preference in paper background which seems to be like the real wall texture. (2) Although general scores of paper background were higher than cloth in 10 scales, the experimental data show high correlation coefficients for the 10 scales between cloth and paper background. This could explain that observers will have a similar scoring trend in the same lighting condition and different background texture.

ACKNOWLEDGEMENTS

This work was supported in part by the Ministry of Science and Technology, Taiwan (MOST 103-2420-H-011-002-MY2)..

REFERENCES

Ou, L., Luo, M. R., Woodcock, A. and Wright, A. 2004. A study of colour emotion and colour preference, Part I: Colour emotions for single colours. *Color Research and Application* 29, 232-240.

Ou, L. and Luo, M. R. (2006) *A colour harmony model for two-colour combinations*, Color Research and Application, vol. 31, pp 191-204.

Torgerson, W. S. (1958) *Theory and Methods of Scaling,* John Wiley & Sons, New York.

Address:43, Section 4, Keelung Road, Taipei, Taiwan
E-mails:m10125003@mail.ntust.edu.tw, m10225011@mail.ntust.edu.tw,
lichenou@mail.ntust.edu.tw

Suggesting appropriate color range for indoor space based on EEG measurement

Hanna KIM[1], Heewon LEE[2], Mijin LEE[3], Jinsook LEE[2]

[1]Noroo Paint & Coatings Co., Ltd, NPCI, Korea
[2]Dept. of Architectural Engineering, Chungnam National University, Korea
[3]Samsung C&T Corporation, Design ENG Team, Korea

ABSTRACT

In Color influences the human body in physiological and psychological manner, and interest in research on revealing such influence through brain wave measurement is increasing. The current study observed human physiological reaction in different indoors color environment, through an analysis of brain wave in the range of 8 to 13Hz, commonly known as the alpha wave. The frequency of RSA (8-11Hz/4-50Hz), or “slow” alpha wave, and RFA (11-13Hz/4-50Hz), or “fast” alpha wave, were studied. Centering on the changes to the brain wave after the color stimulus, the current study analyzed what influence 9 different colors had on the human body. Four groups came out in the result: 1) Red, Green-Yellow, Blue-Green, Yellow-Red incurred decreased RSA and increased RFA; 2) Yellow increased RSA and decreased RFA; 3) Blue and Purple increased both RSA and RFA. 4) Green and White decreased both RSA and RFA. The results of the current study is useful in that they can be used as a practical data for classifying colors appropriate for various purposes in residential spaces.In residential spaces, these colors are more appropriate for living rooms, in which rest combined with basic activities takes place, rather than bedrooms, in which rest leading to sleep takes place.

1. Introduction

1.1 Background

Colors have their unique wavelengths and are physical elements that greatly influence the physiological and psychological health of humans. The techniques related to color therapy and color correction that use color characteristics are applied in various industries, but there exists no quantified data or systematically conducted research. Therapy that treats diseases using the full color spectrum is referred to as chromotherapy. It has seen increased use in the field of medicine, with several studies touting the effectiveness of this method. [1] Moreover, while there are a number of fragmentary hypotheses on the influence that indoor colors have on the human body, it is time to have research that objectifies conclusions with systematic experimental evaluation.

Therefore, the study created a mockup environment designed to quantify the human body response to the unique wavelengths of colors and performed experimental evaluation of human body response through measurement of brain waves.

1.2 Previous Research

The leading method that has been used in the earlier studies to investigate the physiological responses in the human body consists in analyzing the changes in brain wave caused by color stimulation. Studies examining brain wave responses to colors suggest that colors can actually exercise influence on brain activity. Several clinical studies have been conducted to examine whether color therapy might help relieve symptoms related to diseases such as epilepsy and Parkinson's. [2][3] Earlier studies on colors and brain wave responses have shown that certain neural patterns can deliver physiological and psychological relaxation and excitement. While there exist differences in methods used in several previous studies, the physiological and psychological responses are summarized as follows. Pressey examined the physiological and psychological changes generated by the colors red, blue, and white. The color red was shown to stimulate sensory nerves. In other words, red activates blood circulation by stimulating all five senses: olfaction, vision, audition, gustatory, and tactile. Pressey found that the presence of red increased blood pressure, heart rate, and breathing caused increased perspiration in the skin, muscle contraction, and frequent eye blinking. Blue works to decrease blood pressure, heart rate, skin responses, and eye blinking. Finally, he found that white was related to psychological tension and stress. While white facilitated increases in blood pressure and heart rate, it did not cause the same magnitude of changes as did the color red. Studying children's responses to color design, Hong (1994) found that children who spent six months in a room painted blue showed much less nervousness or hostile speech compared to those who did not do so. Park and others (1999) conducted an experiment where a colored structure was composed of red, blue, and white walls, and participants had their blood pressure and heartbeat checked during a 20-minute interval. The authors found significantly higher heart rate from red to white, white to no color, and no color to blue. In addition, higher blood pressure was observed from red to white, white to blue, and blue to no color. Lower blood pressure was observed from no color to red, red to blue, and blue to white. These results suggest that blood pressure and heart rate decrease in line with "colder" colors and increase along with "warmer" colors.

1.2 Study Aims

As confirmed in previous literatures, alpha wave occurs in a state of comfort, such as when the body is relaxed; the more relaxed the body is, the greater the amplitude. A characteristic of this wave is that it appears continuously and regularly, with the most presence in parietal and occipital regions of the brain, and seen the least in the frontal region. Especially stable alpha wave is observed when the body is in a relaxed state with eyes closed, while the wave is deterred when the body is emotionally excited or when it is staring into an object with eyes open. What changes may occur to the alpha brain wave, then, when subjects are exposed to various indoors color environments? The goal of this study is to classify frequencies comprising alpha wave, 8 to 13 Hz, into segments, to analyze physiological reaction of the human body to various indoors color environments. The results will serve to provide a practical data on what effects indoors color environment has on the human body.

2. Methodology

The experimental set up included a windowless room that was 1,500 mm × 1,500 mm × 2,400 mm for the ceiling, wall, and floor lengths, respectively. Light was installed at 600 mm × 600 mm on the center of the ceiling while a dimming system was installed to ensure a light intensity of 100 lx for the different colors using the standard D65 illuminant. Stimulation was applied with three basic colors for respective wavelengths, a high-level chroma was selected, and paint was applied using nine colors. To prevent noise while measuring brain waves, acoustic noise and outside light were removed, and the room was kept at a temperature of 20 to 21 degrees Celsius with 50 to 55% humidity.

Color	Munsell	NCS	Experimental environment
	5R 4/14	S 2070-R	
	2.5YR 6/14	S 0580-Y50R	
	5Y 8.5/12	S 0570-Y10R	
	2.5GY 8.5/10	S 0570-G70Y	
	7.5G 5/8	S 2565-G	
	7.5BG 5/8	S 2555-B30G	
	10B 5/10	S 2060-B	
	7.5P 3/10	S 4050-R50B	
	N9.5	S 0500-N	

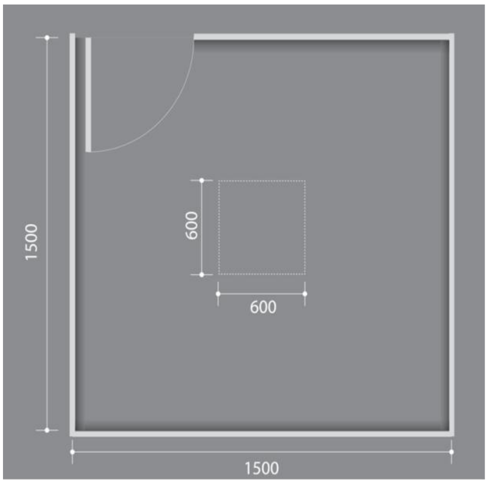

Fig.1. Experimental Environment

2.1 EEG Measurement and Analysis

To assess brain wave patterns, the current study used PC-connected equipment, QEEG-8 (LXE3208, Laxtha Inc., South Korea), to measure physiological signals. The measurement of brain waves was done through monopolar derivation across eight sites on the surface of the subject’s head. In accordance with the International 10/20 system, electrodes were placed on left and right sides of the prefrontal (Fp1, Fp2), frontal (Fp3, Fp4), parietal (P3, P4), and occipital lobes (O1, O2). The reference electrode was placed behind the right earlobe, and the ground electrode was placed behind the left earlobe. Gold-coated tray-shaped disk electrodes were used. To minimize friction with the skin, extraneous substances were wiped off the surface of the subject’s head. Electrodes were smeared with adhesive electrode gel (Elefix z-401ce, Nihon Kohden) to provide a better signal.

The measurement method used was as follows. The subject was seated comfortably in a chair within the white room. After attaching the electrodes, the subject was allowed to relax and adjust to the space for five minutes. Next, EEG measurements were taken for 60 seconds in the green, blue, and red rooms (room order was counterbalanced across subjects). In order to account for any potential afterimage from experiencing one color to the next, the subject took a one-minute break in the white room before moving to another room. Since protracted brain wave measurements tend to be distracting, the 60-second time limit was used to ensure quality data collection. In addition, subjects were instructed do mental counting in order to stay alert and avoid any other cognitive distraction. Following EEG measurement in each room, to prevent any additional afterimage effects from colors, a white stimulus was presented in between the evaluation objects and to provide subjects with a one-minute break. Measurements were repeated three times to ensure stable data collection.

Raw data were collected with Telescan (CD-TS-2.2, Laxtha Inc., South Korea), a real-time data and time series analysis program. Data for the 4–50-Hz band were obtained through frequency filtering, which was subjected to another conversion in order to perform an analysis as to the relative and absolute power for different channels. In addition, to ensure stable data collection during this analysis, the first second at the beginning and end of each recording session was removed, leaving 58 seconds available for further analysis. For all data analysis, the raw data CDF file was converted to a .txt file, and then to a Microsoft Excel file, to quantify and average EEG data signals for all 30 subjects. SPSS 20.0 statistical software was used for the converted data while differences in the three Power Spectrum values within the β-wave area was accomplished using the Friedman Test.

2.2 Subject Composition

A total of 57 subjects, including 16 teenagers, 26 individuals in their 20s or 30s, and 15 individuals in their 60s, were recruited for the current study. Since EEG signals vary largely across individuals, subjects with high or low EEG signals (i.e., outliers) were removed from the analyses. Therefore, a total of 21 subjects remained in the final sample: 7 teenagers, 7 individuals in their 20s or 30s, and 7 in their 50s or 60s.

3. Result

RSA (8-11Hz/4-50Hz), also known as “slow” alpha wave, occurs when the body feels comfort while it is slightly sleepy. RFA (11-14Hz/4-50Hz), “fast” alpha wave, occurs when the body feels comfort while it is concentrating. The current study aspires to measure what effects 9 different colors have on the human body, based on the characteristics of such ranges of the alpha brain wave. The result of brain wave measurement in 9 different color stimulus environments can be classified into the three following groups. In the first group, 8-11Hz range decreases after color stimulus as shown in fig. 3, but the 11-13Hz range increases. Red, Green-Yellow, Blue-Green, and Yellow-Red are the colors that cause such physiological change. In residential spaces, These colors are more appropriate for living rooms, in which rest combined with basic activities takes place, rather than bedrooms, in which rest leading to sleep takes place.

Contrary to the results in the first group, in the second group 8-11Hz range occurs more frequently after color stimulus, as shown in fig. 4, while 11-13Hz is displayed less frequently after the stimulus. Yellow is the color that causes such physiological change. The color is deemed more appropriate for bedrooms in which rest leading to sleep takes place, rather than for living room where basic activity takes place alongside relaxation.

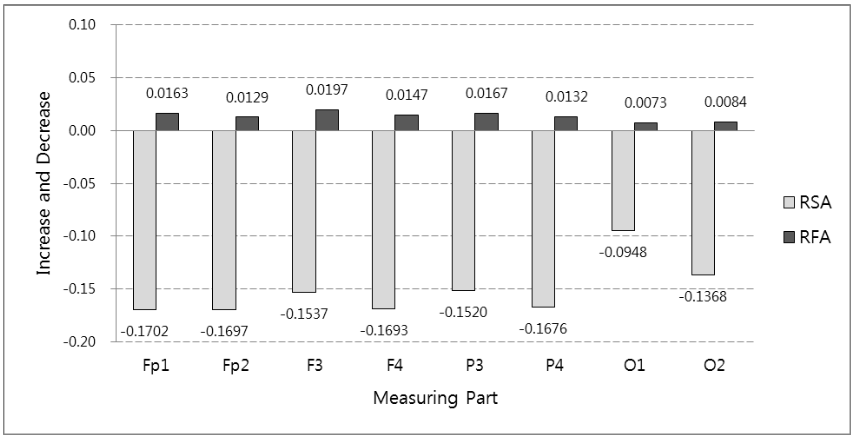

Fig. 3. Increase and decrease each ranges of the alpha brain wave in Red space

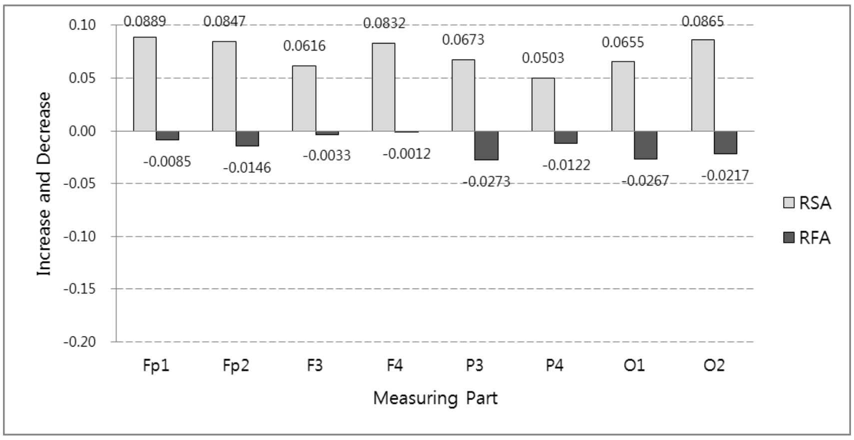

Fig. 4. Increase and decrease each ranges of the alpha brain wave in Yellow space

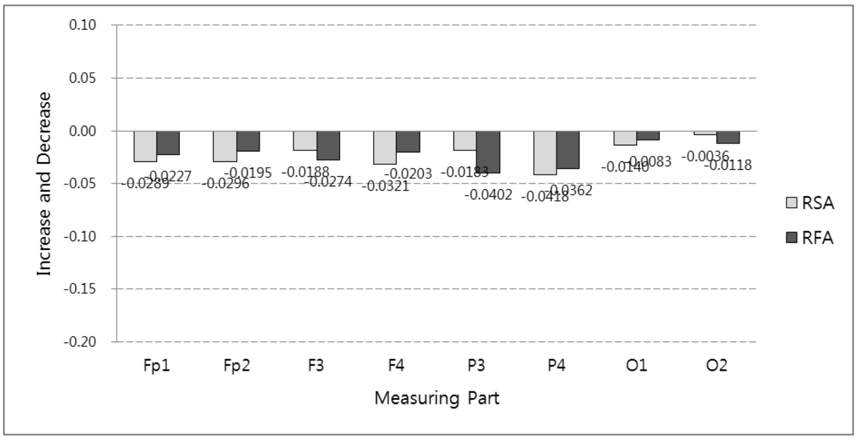

Fig. 5. Increase and decrease each ranges of the alpha brain wave in Green space

The third group displayed increased 8-11Hz wave and 11-13Hz wave after color stimulus except prefrontal lobe. Blue and Purple cause such physiological change. The fourth group displayed decreased 8-11Hz wave and 11-13Hz wave after color stimulus, as shown in fig. 5. Green and White cause such physiological change. These colors are less appropriate for living rooms and bedrooms where relaxation takes place; study rooms or workrooms, in which residents focus on certain activities, would benefit more from using these colors.

4. Conclusion

The purpose of the current study was to analyze human physiological reaction in various indoors color environments, by segmentalizing the range of alpha brain wave (8-13Hz), that increase when the body feels comfort. Based on the result, the study classified colors that are appropriate for different spaces in a residential space, which makes the results of this study a practical data on the effects of indoors color environment on the human body.

The 9 colors used in the current study, however, are colors with high levels of chroma to give a clear stimulus for the purpose of analyzing the effects of color. This makes it difficult to implement the results of this study on an actual residential space. As such, future research will have to delve into the issue raised by brightness and chroma, with a basis on the findings of this study on color.

Acknowledgements

This research was supported by the National Research Foundation of Korea on the auspices of the 2014 governmental finances (the Ministry of Science, ICT, and Future)(No. 2008-0061908)

References

Rosenthal, N. E., & Wehr, T. A.(1987), Seasonal affective disorders. Psychiatric Annals. 17(10) 670-674.

Haug et al., 1995; Katsuura, Shimomura & Iwanaga, 2009; Starchenko, & Boitsova, 2010

Mesri, & Dellepiane, 1991; Haug et al., 1995; Sholomovet al., 2009

Jin, B.H. 2011. Electroencephalogram. Korea Medical Book Press, Seoul

Vernon, D., T. Egner, N. Cooper, T. Compton, C. Neilands, A. Sheri, and J. Gruzelier. 2003. The effect of training distinct neurofeedback protocols on aspectsof cognitive performance. International Journal of Psychophysiology 47:75-85

Vernon, D., A. Frick, and J. Gruzelier. 2004. Neurofeedback as a treatment of ADHD: A methodological review with implications for future research. Journal of Neurotherapy 8(2):53-82

Park Ji-hyeon et al. (1999), “A Study on the Influences that Colors Have on Physiological and Coordination Movement,” Collected Academic Papers 22 from Department of Physical Therapy, College of Health Science in affiliation with Korea University.

Faber Birren, Principles of Color: A Review of Past Traditions and Modern Theories of Color Harmony, translated by Kim Jin-hwan (1995), Sigongsa, p.74.

Address: Ph.D Hanna Kim, 127 Eulji-ro, Jung-gu, Seoul
Noroo Paint & Coatings Co., Ltd, NPCI, Korea
E-mails: hnkim@noroo.com, bluesky4r@paran.com,
mj0919.lee@samsung.com, js_lee@cnu.ac.kr

Development of the Interior Color Coordination Recommendation System of Living Space for University Student Living Alone Using Genetic Algorithm

Tatsunori MATSUI[1]. Keiichi MURAMATSU[2], Kazuaki KOJIMA[3], Mai KAWASHIMA[1], Miho SAITO[1]
[1] Faculty of Human Sciences, Waseda University
[2] Graduate School of Science and Engineering, Saitama University
[3] Learning Technology Laboratory, Teikyo University

ABSTRACT

In this research, we constructed by genetic algorithm an interior color design system for college students who are living alone. As the first step, we investigated what color configurations college students living alone usually used for interior furnishings, as well as the affective impressions elicited by those color configurations. Next, we studied the colors associated with the adjectives which express spatial conceptions. On the basis of the results, five candidate fitness functions were determined. Then we ran the systems each adopting one of the candidate fitness functions, and evaluated their performance against actual human preference. It turned out that the system with the the fitness function wherein the three evaluation functions shared the same weight approximated the psychological data most precisely, which inferred that the ability to pinpoint the colors associated with the adjectives expressing spatial conceptions might play a vital role in generating the color configurations required by users.

1. BACKGROUND

Nowadays a lot of college students are interested in the interior furnishings of their rooms, but, especially to those living alone, practical difficulties such as economic pressure and the need of a good feeling usually add up to a significant barrier. Considering that in the recent years the shops selling cheap colored furniture are increasing in number, we get an idea that it is possible to improve interior furnishings by just changing their color configuration. Hence, in this research, we construct a system which can propose appropriate color schemes for interior furnishings through genetic algorithm (GA).

2. STUDY OF ROOMS OF COLLEGE STUDENTS LIVING ALONE

2.1 Objective

In order to select the sorts of furniture employed in the interior color design system, in this study we screened the interior furnishings in the rooms of college students living alone.

2.2 Subjects.

20 college students (10 males & 10 females, ages: 20.70 ± 1.34) who are living alone in the Kanto region participated in this study.

2.3 Method

From the photos of the subjects' rooms, we recorded the colors, the number of items, and the positions of each sort of furniture. Then, via subjective color measurement, we divided the sorts of furniture into two categories: The sorts of furniture belonging to the first category possessed great color variation while those belonging to the second group had small color variation.

2.4 Results

The category characterized with great color variation included shelf, bedstead, coverlet, bedsheet, curtain, table, rag, chair, desk, television table and pillow. The category characterized with small color variation included television, bed, wall and ceiling. The colors of the furniture in the latter category were fixed in the interior color design system constructed in this research.

3. STUDY OF RELATIONSHPS BETWEEN INTERIOR COLOR CONFIGUATION AND AFFECTIVE IMPRESSION

3.1 Objective

This study is intended to clarify the factorial structure of the affective impression elicited by color configuration of interior furnishings in the rooms of college students living alone through a psychological experiment using Semantic Differential method. The interpretation of the factors extracted in this experiment is carried out in the form of propositions.

3.2 Pilot Study

Objective: This pilot study aims to determine the range of color selection for each sort of furniture depicted in the experimental stimuli. Each experimental stimulus is a picture representing a certain color configuration of interior furnishings.

Method: We measured the colors of the sorts of furniture engaged in this research using the color system NOCS developed by Nakagawa Color Lab.

Results: With regard to the sorts of furniture with a high degree of color variation, the shelves had four colors, bedsteads four colors, coverlets 14 colors, bedsheet 13 colors, curtains 22 colors, tables three colors, rags 12 colors, chairs eight colors, desks three colors, television tables two colors and pillows 13 colors. The fixed colors of television, bed, wall and ceiling were also specified. The details of the color variation are shown in Table 1.

Table 1: Colors used in Experimental Stimuli (Munsell values)

interior	H	V	C
coverlets	10R	8	2
	5B	8	1.5
	5B	6.5	6
	5GY	7	10
	5P	3	7
	5PB	1.5	4
	5R	4	14.5
	5RP	6.5	7.5
	5Y	9	9.5
	5Y	6.5	3
	5YR	6	11
	5YR	4	2.5
	N	1	
	N	9	
pillows	10Y	7.5	11
	10YR	7.5	2.5
	10YR	5.5	1
	10YR	4.5	2.5
	5GY	7	10
	5PB	1.5	4
	5R	4	14.5
	5RP	6.5	7.5
	5Y	9	9.5
	5YR	7.5	10
	5YR	4	7.5
	N	1	
	N	9	
tables	N	1	
	N	9	
	10YR	8	3
desks	N	1	
	N	9	
	10YR	8	3

interior	H	V	C
bedsheet	10R	7.5	6.5
	10Y	7.5	11
	10YR	5.5	1
	10YR	4.5	2.5
	5B	9	1.5
	5GY	8	6.5
	5GY	8	8
	5PB	1.5	4
	5R	8.5	1.5
	5R	4	14.5
	5Y	9	9.5
	N	1	
	N	9	
bedsteads	10YR	8	3
	N	1	
	N	6	
	N	9	
rags	10GY	2	4.5
	10R	7	9.5
	5GY	8.5	1.5
	5GY	5	5.5
	5PB	1.5	4
	5R	4	14.5
	5RP	8.5	2.5
	5RP	3.5	6
	5Y	9	9.5
	5YR	2.5	2.5
	N	1	
	N	9	
shelves	10YR	2.5	2.5
	10YR	8	3
	5YR	6.5	5
	N	1	

interior	H	V	C
curtains	5R	4	13
	10R	7.5	6.5
	10R	7	9.5
	10YR	4.5	2.5
	5B	8	1.5
	5G	2.5	3
	5G	8	1
	5GY	8	6.5
	5P	1.5	4.5
	5P	5.5	2.5
	5R	7	7.5
	5R	4.5	1.5
	5RP	6.5	7.5
	5RP	3.5	15
	5RP	2.5	8
	5Y	8.5	7
	5YR	2.5	2.5
	5YR	2.5	4.5
	5YR	7.5	2
	5YR	6	11
	N	1	
	N	9	
chairs	10YR	7	6.5
	5PB	3	14.5
	5PB	5.5	9.5
	5R	4	14.5
	5RP	6	9.5
	N	1	
	N	3	
	N	9	
television tables	10YR	8	3
	N	9	

Totally 102 college students (54 males & 48 females, ages: 21.45 ± 1.25) took part in this experiment. The subjects were divided into three groups:

Group A: 19 males & 15 females (ages: 21.03 ± 1.23); Group B: 18 males & 16 females (ages: 21.03 ± 1.23); Group C: 17 males & 17 females (ages: 21.03 ± 1.24).

3.4 Evaluating Method

60 adjectives gathered from previous researches, e.g. “light”, “clean” and “calm”, all of which express spatial conceptions, were used in this experiment. Every adjective is a two-point (“match” or “does not match”) rating scale.

3.5 Experimental Procedure

30 pictures (shown in Figure 1), used as the experimental stimuli, were generated by Interior Designer Pro 2 on the basis of the results of the aforementioned pilot study. The color configuration in every stimulus picture was randomly determined. The stimuli were displayed to the subjects by iPad (Retina Display MD370J/A). Every subject group was assigned a different set of ten stimuli. The order of stimulus displaying was counter-balanced.

Figure 1: Experimental Stimuli

3.6 Results and Discussion

In the process of factor analysis, maximum likelihood estimation was used to extract the factors, and the Promax method was employed to rotate the factors. The rotated factor loadings matrix is calclated which shows that 13 factors, i.e. “Pop”, “Cool”, “Elegant”, “Natural”, “Formal”, “Eccentric”, “Light”, “Classical”, “Tropical”, “Dandy”, “Profound”, “Quiet” and “European”, have been extracted in this experiment. When interpreting a factor, we distinguished the stimuli whose factor scores are greater than zero on the factor from the stimuli whose factor scores are less than zero on the factor, and then examined the two groups respectively. Take the factor “Pop” as an example. The stimuli in the high-factor-score group used more colors with high or intermediate saturation than those in the low-factor-score group. In the high-factor-score group, coverlets in highly saturated red and those in highly saturated yellow were used more frequently than in the low-factor-score group. On the other hand, in the low-factor-score group, blue coverlets and achromatic coverlets were employed more frequently than in the high-factor-score group. In the light of it, the characteristics of the high-factor-score group on this factor could be expressed in the following four propositions: 1) The group uses many highly saturated colors; 2) The group uses many intermediately saturated colors; 3) Many of the coverlets in this group are highly saturated red; and 4) Many of the coverlets in this group are highly saturated yellow. As to the low-factor-score group on this factor, its characteristics could be expressed in the following three propositions: 1) Many of the coverlets in this group are blue; 2) Many of the coverlets in this group are achromatic; and 3) The group uses very few highly saturated colors. In the same manner, we made clear, in the form of proposition, the characteristics of the other factors by scrutinizing their associated high-factor-score group and low-factor-score group. As a result, totally 46 propositions were formulated.

4. STUDY OF COLOR SELECTION RANGE OF INTERIOR FURNISHINGS

4.1 Objective

This study is targeted to preclude the interior color design system from outputting color configurations of interior furnishings which seldom appear in the real life.

4.2 Method

Based on the results of the pilot study described in Subsection 3.2, focusing on the colors employed in the experimental stimuli, we specified subjectively the range of color selection for each sort of furniture.

4.3 Results

We assigned a wide color selection range to every sort of furniture with a high degree of color variation shown in the results of the pilot study. On the other hand, we assigned a narrow color selection range to every sort of furniture with a low degree of color variation shown in the results of the pilot study.

5. SETTING AND RUNNING OF GENETIC ALGORITHM PROGRAM

5.1 Outline

The users were required to select five or more adjectives which appropriately described the ideal interior design for their rooms from the adjective list introduced in Subsection 3.4. The users were also asked to report their genders and whether they had any experience of living alone. This personal information served as one part of the input information to the GA system. The outputs of the GA system were the $L^*a^*b^*$ values of the color configurations of interior furnishings which were expected to match the adjectives selected by the users.

5.2 Parameter Setting

Encoding: The chromosome structure encoded 33 variables, that is, the $L^*a^*b^*$ values of the colors of the 11 sorts of furniture employed in the system.

Crossover & Mutation: The crossover operator and the mutation operator were applied respectively to the two furniture categories introduced in Section 2, namely the category characterized with great color variation and the one characterized with small color variation. And, the $L^*a^*b^*$ values of each sort of furniture were treated as one set.

5.3 Fitness Function

Based on the results of the study introduced in Section 3 and the study on color-adjective association, we determined the fitness function $F(x)$ as a liner sum of 3 sub functions (details shown on the poster).

6. EXPERIMENT FOR TESTING SYSTEM PERFORMANCE

6.1 Objective

This experiment aims to clarify the effectiveness, the users's satisfaction and the deficiencies of this interior color design system via real-world testing.

6.2 Subjects

8 college students (2 males with experience of living alone, 2 males without experience of living alone, 2 females with experience of living alone and 2 females without experience of living alone; ages: 22±0.58) living in the Kanto region participated in this experiment.

6.3 Experimental Procedure

The achromatic version of the stimulus picture No.8 used in the study introduced in Section 3 (shown as Figure 2) was displayed to the subjects for the reason that this picture contained the most achromatic colors among the stimuli used in that study.

The subjects were required to imagine themselves as college students living alone and select from the adjective list described in Subsection 3.4 five or more adejctives which best depicted their ideal images of the color configuration of the interior furnishings in the room.

The personal information of the subjects and the adjectives selected by them were input into five variants of the system each defined by a set of α, β and γ values, i.e. the weights of the three evaluation functions in the fitness function. The $L^*a^*b^*$ values encoded by the first chromosome in the last generation of the evolution process of each system variant were employed to colorize the stimulus picture used in this experiment, producing a chromatic picture as the output of the system variant. Prior to the colorization, the $L^*a^*b^*$ values of the resulted five pictures were transformed into RGB values.

The α, β and γ values characteristic of each system variant are shown as follows:

(1) α=5, β=3, γ=2. (This set of values was set as default in that it best fitted the empirical rules.)
(2) α=1, β=0, γ=0. (This set of values allowed only the first evaluation function to take effect.)
(3) α=0, β=1, γ=0. (This set of values allowed only the second evaluation function to take effect.)
(4) α=0, β=0, γ=1. (This set of values allowed only the third evaluation function to take effect.)
(5) α=1, β=1, γ=1. (This set of values allocated equal influence to the three evaluation functions.)

Then, the five pictures were displayed to the subjects one after another, and the subjects were asked to evaluate on a 5-point rating scale to what extent the pictures matched their ideal images. The subjects were also required to write down the reasons for their ratings in the form of free answer. During the data analysis, the ratings of every stimulus were averaged across the subjects, and the average ratings of the stimuli were compared with one another. Prior to the averaging, the five degrees on the rating scale were transformed to the quantitative values "100", "50", "0", "-50", "-100" from the end "match well" to the other end "match badly".

6.4 Results

Output Example: Take as an example the outputs of the five system variants to the input information of Subject A. As the adjectives best depicting his ideal image, this subject selected "calm", "good-looking" , "stylish", "heart-warming", "gentle", "kind", "natural", "simple", "monotone", "unified", "light", "clean", "warm", "trig", "refined", "modern", "chic" and "formal". The pictures generated based on the output information of the five system variants corresponding to these adjectives are shown as Figure 2.

Overall Tendency: With regard to the first evaluation function, the fitness of a large number of stimuli remained almost the same over time, converging eventually to a relatively low value. A possible explanation for this phenomenon is that this evaluation function best fitted the empirical rules, thus being heavily constrained.

Next, we compared the average ratings of the five pictures. The picture with the highest average rating was the one output by the fifth system variant. In the fitness function of the system variant, the three evaluation functions shared the same weight.

In addition, many subjects wrote in their free-answer questionares that "although the picture matches my ideal image, I don't like the colors of the interior furnishings in the picture" or "the colors of the interior furnishings in the picture aren't my favorate ones, so I don't think the picture matches my ideal image". In view of it, it is resonable to believe that the color preference of an individual can influence his/her evaluation of the color configuration of interior furnishings. Especially, when the subjects disliked the colors of the sorts of furniture of a large size, such as coverlet, they tended to give negative responses. Besides, a proportion of the subjects had color-adjective association different from the general condition. As a result, to these subjects, using colors as the general condition suggested often brought about negative responses.

No.1, Syatem 1 No.2, System 2 No.3, System 3 No.4, System 4 No.5, System 5

Figure 2: Output Picture No.1 - No.5 for Subject A

7. CONCLUSIONS

In this research, we contructed an interior color design system that could visualize users' ideal images of color configuration of indoor furnishings. The only information users are required to input into the system is a set of adjectives depicting their ideal images of indoor color configuration. The results of the real-world system test demonstrated that the fitness function in which the three evaluation functions shared the same weight best matched users' ideal images. It infers that the more precisely the system simulates users's general impression to the adjectives expressing spatial conceptions, the better the outputs of the system approxiamte users' ideal images. In addition, based on the results of the study on the relationships between interior color configuration and the elicited affective impressions as well as the results of the real-world system test, we can say that color preference has a great impact on the evaluation of color configuration of interior furnishings. It suggests the possibility of improving the simulating accurary of the system by integrating the information about users' color preference into the input information to the system..

ACKNOWLEDGEMENTS

This work was supported by Grant-in-Aid for Scientific Research (B) (2011-2013, Leader: Miho SAITO) from Japan Society for the Promotion of Science (JSPS). Also, authors sincerely thank Mr. Fang Siyuan for his valuable comennts to this research.

REFERENCES

Sawashima, T. 2012. *University Student's Attitude to Housing Field of Home Economics Education and Interior Coordination*, Journal of Faculty of Culture and Education of Saga University 17(1) 89-97.

Matsui, T., et al. 2012. *Supporting System for Color Coordination of Bridal Space Using Genetic Algorithm*, Journal of the Color Science Association of Japan 32(Supplement) 52-53.

Kobayashi, S. 2001. *Kara Imeji Sukeru Kaiteban (version 2)* Kodansha Ltd.

Koga, K. 2005. *Karafuru Haishoku Resson + Mihonjo* Gijutsu-Hyohron Co., Ltd.

Shikisai no Arekore (Color, abc-xyz): http://www.geocities.jp/s_inoue777view/index.html

Address: Prof. Tatsunori Matsui, Faculty of Human Sciences, Waseda University,
2-579-15 Mikajima Tokorozawa, Saitama, 359-1192, JAPAN
E-mails: matsui-t@waseda.jp

Chromatic integration of the architectural surfaces with environment: analysis and classification of case studies

Alessandro PREMIER,[1] Katia GASPARINI[2]
[1] University of Udine, Italy
[2] Iuav University of Venice, Italy

ABSTRACT

The introduction and application of new products in the building market, joined to the continuous elaboration and re-interpretation of already known materials, in particular of those dedicated to the facades, produces new effects on the perception of the chromatic truth of the places where these are employed. Among these products and materials there are someone, employed in multiple shapes, finishes and textures, those use has been consolidated in the realization of facade claddings (concrete, metals, glass, plastics, composites, smart etc.). Their use in the context in which these facades are located produces particular chromatic effects, different from those of the tradition, or similar to it: chromatic agreements, contrasts (see Itten), dematerialization of the building envelope etc. Is it possible to lead a chromatic analysis of meaningful cases having the target to supply useful instruments to the design phase?

This study has the proposal to complete a chromatic surveying of famous buildings by the means of common graphical instruments such as the pixel filter: a tool useful to identify the dominant tones that can be obtained from a photographic relief. Captured colors can be inserted in a diagram to classify their combinations: one dominant, two colors, three colors, four colors, contrast of light and dark, contrast of warm and cool colors, etc..These kind of studies would have to lead us to the definition of a table of chromatic harmonies and contrasts. The study means to consider all the elements of the context: sky, green, water, buildings etc, so as to be able to contemplate also the chromatic variants due to the change of the luminous or atmospheric conditions. Knowing that "varying the field of vision whichever chromatic manifestation can be obtained, just because seeing it is not never an objective fact, but it is participation, subjective interpretation" (Tornquist 1999).

1. INTRODUCTION[1]

This research, which began in 2003/2004 with a dissertation on the color of metal claddings, followed several developments in the following years, first within the research unit Colour and Light in Architecture at Iuav University of Venice and currently under the research center Eterotopie - Color, Light and Communication in Architecture. The research aims to identify and classify the color design strategies adopted by many designers to achieve specific color effects: integration with the landscape, contrast, highlight of certain parts of the building and so on. Relapse is the last possible embodiment of a system of guidelines for the design already integrated, as regards the sun screens, in the book "Superfici Dinamiche" (Franco Angeli, 2012), as regards the metals in "Facciate metalliche" (Utet , 2012) and for media buildings in “Schermi Urbani” (2012).

2. METHOD[1]

The research analyzed architectural envelopes made with different materials and technologies, from traditional up to innovative materials: plaster, wood, ceramics, concrete, GRC, metal, glass, plastics, textiles, composites, smart. For each category of façade material we analyzed a representative sample of case study, than we used multiple images, then transformed with a computer tool to get the main colors of the composition: the pixel filter. The pixel filter allows, blurring the original image, to detect the dominant colors of the analyzed photo (we always tried to use images of the building with a good portion of the context). The result can be approximated to one, two, three or four main colors that could constitute chromatic agreements or contrasts obtainable from color theory and its recent developments.

> The chromatic fact is the pigment, i.e. the coloring material that can be determined and analyzed from a physico-chemical point of view, which assumes its content and meaning through human perception through the retina and the brain. The eye and the mind can achieve an exact perception only for comparison or contrast. [...] The color evaluation, in contrast to the physico-chemical facty of color, constitutes the psycho-physical fact of color that I define the chromatic effect. Physical reality and color effects are identified only in harmonic chords. In all other cases, the reality of the color is changed simultaneously, producing a new, different effect (Itten 1961: 17).

In addition to issues related to the change in the size of the visual field, we took note of the limits imposed by the studies that have made an important contribution on the three-dimensional use of the color material.

> Even photography is the two-dimensional representation - that we read as truth - a three-dimensional reality. A higher order can not be explained by a lower one, therefore it is not possible to realistically represent a work created in three dimensions through the use of two dimensions (Tornquist 1999: 108).

The goal of the research was to understand how most important contemporary designers use color to achieve desired color effects of integration or contrast with the surrounding environment.

> If in the field of materials we assumes, for example, a base material subjected to a process of transformation, we get something that is different from the material we used and which is the product. Similarly, when you design, you introduce into the design process (similar to a machine) the basic materials, consisting of all the information needed to design [...] and you transform them into the particular product represented by all the documents of the design (Ciribini 1984: 12).

The process we performe in the color composition seems to look very similar.

2.1 Case studies[1]

Among the case studies, for the plaster surfaces, there is the Housing and Office Complex Zeleni Gaj, šiška, in Ljubljana, 1999-2001, by Bevk Perovic 'Architects. The surfaces of the facades are colored in gray, while the top floor set back from the facade is white. The neutral color of the facades highlights the lodges and the wooden frames. The pixel filter highlights the gray tones that tend to mix the building with the environment of other residential projects.

Among the buildings with wooden envelope we analyzed the Damiani Holz & Ko Building in Bressanone, 2012, by Modus Architects. The envelope made entirely of laminated spruce wood contrasts with the blue sky and the green mountains (contrast of complementary colors), while the base in grey concrete blends with the color of the horizontal surfaces.

Among the buildings with ceramic cladding there is the Central St. Giles in London, 2010, by Renzo Piano. The large facades of ceramic material are characterized by the colors orange, green, yellow and red. The pixel filter reduces the composition in two main colors: red and green, two complementary colors. The context instead merges into a uniform gray given by the buildings of the surrounding city.

Another case study for ceramic materials is the Music Hall and House in Alguena, Spain, 2011, by COR Asociados. The cladding of the music hall is completely covered with pearlescent ceramic with a mirror finish. This finish reflects the colors that surround the building blending with the environment. In fact, with the pixel filter the building seems to disappear, leaving only the colors of the blue sky and of the earth.

Among concrete envelopes we analyzed the Asylum Les Cabanyes in Barcelona, 2008-2010, by Arqtel architecture. The building is entirely made in grey concrete, while the parts set back from the front edge are brightly colored. Window holes and lodges have surfaces colored in red, orange, yellow and green. With the pixel filter gray surfaces seem to disappear highlighting the blue sky and the colors red and green in the portico. The contrast of complementary colors is just in front of the building.

Among GRC claddings there is Soccer City Stadium in Soweto in South Africa, by Boogertman + Partners and Populous. The large envelope is clad in panels of GRC colored by earthy colors. The shape looks like a traditional African pot: the Calabash. The pixel filter shows that the building merges with the color of the earth in contrast with the blue sky in a game of primary colors contrast (red and blue).

Among the metal claddings we analyzed the Parking Structure Art Façade in Indianapolis (USA), 2014, by Urbana. The large flat facade of the parking is characterized by metal strips colored in blue and yellow. The strips, similar to many post-it, are bent and positioned so that the building, from one side, appears completely blue and from the other side completely yellow. The building was designed to be seen in motion so that the façade, while being static, seems dynamic, due to a change in color between yellow and blue. The pixel filter highlights how this contrast of primary colors is only in front of the building.

A similar game was played by Architecture Studio in the glass envelope of Advancia School of Business, in Paris, 2010. The facades are characterized by blades of frosted glass in red and yellow color. In some places the alternation of the two colors produces an effect of interpenetration. The color contrast is only in the façades of the building.

Among the buildings with plastic claddings we analyzed the Civic Center Roberto Gritti in Ranica (BG) Italy, 2009, by DAP Studio. The polycarbonate shell is colored only on the inner face so as to present a lighter color in the outside. The colors are cold: purple, blue and green and are immersed in the surrounding natural background. With the pixel filter the building seems to dematerialize.

Among the buildings with textile surfaces there is the Basketball Arena in London, 2012, by Wilkinson Eyre Architects. The envelope is made with a membrane made of polyester fiber coated with PVC. The membrane is stretched over a curved tubular structure in aluminum so as to assume a wavy and jagged shape. On the completely white facades there is a contrast of light and dark color (by shadows) that highlights the shapes drawn by the designers.

Among claddings made with composite materials there is the Seeko'o Hotel in Bordeaux, 2007, by Atelier King Kong. The building envelope, made of Corian ©, is completely white. The building is so completely divorced from the context: almost an alien in shape and color.

Among the envelopes with smart materials there is La Defense Offices in Almere (NL), 2004, by UNStudio. The insulating glass facades are integrated with dichroic film produced by 3M that changes color according to the angle of incidence of sunlight. The facades then veer from green to red and vice versa, creating a contrast of simultaneity.

> The contrast of simultaneity is the phenomenon by which our eye, subjected to a given color, requires at the same time – simultaneously - the complementary color, and not receiving it, it creates it by itself (Itten, 1961: 52).

2.2 The special case of media and smart façades[2]

The research also included the architectural media and smart façades.

The case study analysis has shown a different color performance of these façades, probably due to the used technology.
For the media façades category were analyzed architectures whose envelope was bright and made with digital technologies. In particular, we have analyzed the façades designed by the Berlin group realities:united. They use the BIX system inside architectural envelope (for example: KunstMuseum Graz and Spot Facade in Berlin). Than we analyzed the façades made with LED technology, with LED packets or with the mediamesh system.

For the smart façades type, were analyzed façades system with glass panels, with a smart film interposed. In this case were chosen façades with variable color smart materials as the chromogenic material (thermochromic, photochromic, electrochromic, Lcd) and dichroic film.
One of the case studies is the project: La Defense Offices in Almere, described earlier. The characteristic of media façades analyzed is the division of the façade cladding in many lighting components. These components are visible within easy reach in front of the building. When the façade is seen from far away or when the façade is off the surface is uniform.

When the media envelope is switched on, each component becomes a pixel, a pixel in urban dimension that interacts with the environment.

The façade made with the BIX system are different from those covered in LEDs, because the size of the light components is different. The components of the BIX system are bright fluorescent lamps, they are at least 30 cm and transmit white light. Therefore, the media façade works only in two colors: black or white, corresponding to the controls on / off of the lamp. The pixels are big and the façade transmit 20 frames / sec maximum. They are defined *low resolution façades*. The LEDs, however, are very small components and they are placed very close together, they are colored and they transmit images with many frames / sec. They realize colorful and high resolution façades.

Feature of the smart facades is color uniformity. The materials for smart façades are active or inactive, to shield the facades. So, they may be of a single color (blue or gray) when they are active. When the film is inactive we perceive a glass envelope that reflects the surrounding environment.

It is different for dichroic films (pleochromic materials), whose change in color varies according to the solar incidence.

3. RESULTS AND DISCUSSION[1]

Analyzing the data that emerge from the study above we can infer some design strategies that seem to be used by the designers to achieve certain color effects:

- Merger with natural elements of the environment (ground, sky, vegetation).

- Dematerialization of the building (gray, mirrored surfaces).

- Contrast of primary colors (red-blue). For example, between the building and the sky.

- Contrast of complementary colors (i.e. red Vs green). For example, between building and vegetation.

- Combinations of colors only in the facade (multicolored facades).

- Highlighting specific architectural elements (projecting parts, backward elements, etc.).

- Contrast of light and dark to highlight some forms.

- Color totally divorced from the context: to create a "stranger".

3.1 The “non-color” of media and smart façades[2]

From the analysis, that has been synthesized here, we can see the special case of media and smart facades and their relationship with the visibility and color perception. It is difficult to lay down a rule of color design for these façades and find a measure of their interaction with the environment.

The reasons are to be found in the components and materials used. So, summarizing:

- In the low resolution media facades (eg system BIX) the chromatic interaction with the environment is influenced by the color of the cladding components, of their texture, the type of material (eg. blue plastic, white aluminum panel, frosted glass, etc.). Also, you can find a relationship between color, environment and facade materials only when the media system is off.

- The high-resolution media facades (by LEDs) are already a pixel system, like the analysis system used for this research. Elaborating further the image, the mix of thousands of colored pixels gives as results a "non-color". Usually it is black, gray or brown.
- In smart façades, when the system is off, the color effect is given from the reflection on the glass facades, which are therefore neutral (non color). When the system is "on" the result is a "non-color", the cladding is gray, rarely it is blue.

- The facades using pleochromic smart materials (dichroic film), however, may result in a contrast of simultaneity, according to the incidence of sunlight.

4. CONCLUSIONS

As it is widely known to those involved in the environmental chromatic design, color is an essential aspect in the design process and today it can not be overshadowed. For too long the schools of architecture in Italy have put aside this issue despite knowing that we live in an environment full of colors, perhaps today more than yesterday. The contemporary colors are closely related to the materials and technologies that produce them and they can not be used without a proper knowledge of these technologies. Despite the desire of some academy to keep in the corner these studies, now it seems increasingly essential to place them in evidence and to intensify the research efforts in this direction.

ACKNOWLEDGEMENTS

Eterotopie – Colour, Light and Communication in Architecture – Research Centre: www.eterotopielab.org

REFERENCES

Ciribini, G. 1984. *Tecnologia e progetto. Argomenti di cultura tecnologica della progettazione*, Turin: Celid.

Gasparini, K. 2012. *Schermi Urbani. Tecnologia e innovazione: nuovi sistemi per le facciate mediatiche*. Milan: Wolters Kluwer Italia.

Itten, J. 1961. *Kunst der Farbe*, Ravensburg: Otto Maier Verlag.

Premier, A. editor, 2014. *Innovazione sostenibile per l'architettura: materiali, tecnologie e progetti*. Rimini: Maggioli.

Tornquist, J. 1999. *Colore e luce. Teoria e pratica*. Milan: Istituto del Colore.

Address: Arch. Alessandro PREMIER, Eterotopie Research Centre,
130 Via San Pelaio, Treviso (TV), 31100, ITALY
E-mails: alessandro.premier@iuav.it, katia.gasparini@iuav.it

Color appearance of red printing ink for color vision deficiency

Terumi KATO[1], Yoko MIZOKAMI[1], Masami SHISHIKURA[2], Shinichiro TANIGUCHI[2], Tomomi TAKESHITA[3], Fumiko GOTO[3] , Hirohisa YAGUCHI[1]
[1] Graduate School of Advanced Integration Science, Chiba University
[2] DIC Corporation
[3] DIC Color Design, Inc.

ABSTRACT

In package printing industry, spot color ink generated by mixing base inks has been used more often than cmyk process ink. In particular, red color ink is required not only for designability but also for using to refer notes on many packages. Therefore, it is important to investigate conspicuous red color inks for various illuminant conditions and color vision deficiency. We made red spot color inks which consisted of several base inks, and printed on coated papers using those spot color inks. Observers with normal color vision and color vision deficiency evaluated the redness of the printing samples and their discriminability results from a black background under two illuminance levels (500 lx and 1 lx). The results of evaluation for redness show that the samples whose hue are from 2.5R to 7.5R and high chroma obtain the high score at 500 lx in general. At 1 lx, samples with yellowish red hue and high chroma obtain the high score of redness for observers with color vision deficiency, especially for protan. The results of discriminability from black is more correlated with the lightness of samples at 1 lx than at 500 lx. The samples with high chroma are highly discriminable for both normal and deutan observers. The scores of protan observers for yellowish red hue and high chroma are high at 1 lx as same as the results of redness. Better discriminability for those samples would be due to the higher middle-wavelength (yellowish color) components in the spectral reflectance of those samples.

1. INTRODUCTION

A model color palette for color universal design was provided to be using for cmyk process print, paint, and display (ref.1). In various package prints (e.g. foods, sanitary product), special color such as a corporate color or a product brand color is used. To reproduce the special color, spot color ink which is generated by mixing base inks has been used more often than the process ink. The combination of the base inks is not necessarily unique, and it is common to exist several combinations to reproduce the same color. Package makers have traditionally selected one from among plural combinations with consideration of physical factor (e.g. light resitance). For package design, however, it is important to convey the product image and to inform notes of product to consumers. Red color inks in particular are often used to printing notes of package products. Accordingly, not only criterion with physical factor, but also a psycophysical factor,“Color appearance” is necessary to select the combination. Package products are seen by a lot of consumers with different types of color vision, and under various illuminant conditions. Therefore, it is important to investigate conspicuous spot color inks, especially red color inks for various illuminant conditions and color vision deficiency. In some cases, packages are seen in outdoor in the evening under low illuminance level as well as indoor. It was reported that not only chroma and lightness but hue of red color chips changed with illuminance (Shin *et al*., 2004). (3) Also, the categorical color perception of color vision deficiency was reported (Kagawa *et al*., 2013). They showed that the color categories of ordinary deuteranomals were almost the same as those of normal trichromats, whereas those of extreme deuteranomals were different under 500 lx.

In this study, we investigate how the color appearance of red spot color inks is influenced by illuminant conditions and color vision deficiency.

2. METHOD

We made red spot color inks which consisted of several base inks, and printed on coated papers. Observers with normal color vision and color vision deficiency evaluated the redness of the printing samples and their discriminability from a black background under various illuminant conditions.

2.1 Sample Preparation

Observers made evaluatations in the booth that inside walls were coverd with gray paper. The test color samples presenetd on desktop of the booth illuminated by high color-rendering fluorescent lamps with correlated color temperature about 5000 K. We tested two illuminance levels, 500 lx and 1 lx

The test samples were 37 color prints with target colors that approximated Munsell values and chromas in hues from 10RP to 10R (Table 1). The spot color inks of samples were mixed with base color inks for offset printing (NCP F-GLOSS, DIC Graphics). The mixing formula to reproduce the target colors was estimated by a computer color matching system. We checked whether each target color was inside of printing ink gamut. Colors out of gamut were replaced to printable colors by gamut mapping. We printed on coated papers using those spot color inks with ink proof machine (R.I Tester). We used art coated papers (Mitsubishi Tokubishi Art N), and cut the printed papers to small 75 mm x 45 mm samples. These printed papers were measured by a spectrophotometer (SpectroEye, X Rite).

2.2 Experimental Procedure

We conducted four conditions in this experiment, evaluation for redness and discriminability from a black background under high illuminance level condition (500 lx) and under low illuminance level condition (1 lx). Observers adapted to an illuminant level for 3 min under 500 lx and 20 min under 1 lx. After the adaptation, observers put each test sample on the desktop and evaluated all 37 test samples individually. The evaluation of all samples was replicated three times for each condition. For the evaluation of redness, the observers viewed each sample on a white backgound and scored using five scale. The white backgroud was a white paper without fluorescent whitening agents. The observer scored five and one point(s) to the most and the least reddish sample, respectively. For the evaluation of discriminability from black, the observers viewed each sample on black backgound and scored in the same way as redness. Score five means that an observer percived the sample as the most discriminative, and one means as the least discriminative.

Four protan, four deutan, and five normal trichromat observers participated in the experiment.

Table 1: Target colors of Samples

No.	Target Color	No.	Target Color	No.	Target Color
1	10RP V4.5/C18	12	3.75R V5/C18	26	8.75R V4/C9
2	1.25R V4/C9	13	5R V4/C9	27	8.75R V5/C9
3	1.25R V4/C13	14	5R V4/C13	28	8.75R V5/C13
4	1.25R V5/C9	15	5R V5/C9	29	8.75R V6/C9
5	1.25R V5/C13	16	5R V5/C13	30	8.75R V6/C13
6	1.25R V5/C18	17	5R V5/C18	31	8.75R V5.5/C18
7	2.5R V4/C9	18	6.25R V5/C18	32	10R V4/C9
8	2.5R V4/C13	19	7.5R V4/C9	33	10R V5/C9
9	2.5R V5/C9	20	7.5R V4/C13	34	10R V5/C13
10	2.5R V5/C13	21	7.5R V5/C9	35	10R V6/C9
11	2.5R V5/C18	22	7.5R V5/C13	36	10R V6/C13
		23	7.5R V6/C9	37	10R V6/C18
		24	7.5R V6/C13		
		25	7.5R V5/C18		

3. RESULTS AND DISCUSSION

We present the averaged results from each type of color vision for the evaluation of redness and discriminability on the black background under two illuminance levels.

3.1 Sample Color (Lightness, Chroma, and Hue)

The correlation coefficients of redness and discriminability from a black background with lightness (L^*), chroma (C^*), hue (H^*) were calculated, respectively. The redness evaluation from deutans had some correlation with chroma at 500 lx. At 1 lx, redness evaluations from both protans and deutans had correlation with chroma, and lightness had some correlation with the results of protans and deutans. The results of discriminability from a black background correlated with lightness at both illuminance levels. The correlation of the discriminability with chroma at 500 lx was stronger than at 1 lx. For protans, the results of discriminability correlated with hue at 500 lx.

In results of redness evaluation at 500 lx, the samples from 2.5R to 7.5R and high chroma obtained the high scores. The samples with low lightness obtained higher score for protans than deutans and normal trichromats. At 1 lx, the sample colors with middle or high lightness and high chroma obtained high score rather than the others. Samples with yellowish red hue and high chroma obtained the high score of redness, especially for protans.

Figure 1 shows the hue samples of high chroma which obtained the high score of the discriminability from the black background for deutans and normal trichromats at 500 lx and 1 lx. For protans, the yellowish red hue and high chroma colors obtained high score in the same way as redness. The scores at 1 lx increased with increasing lightness as same as 500 lx. The above inclination to increase was conspicuous than 500 lx; e.g. In case of 7.5R and Chroma 9, No.19 (Value = 4), No.21 (Value = 5), No.6 (Value = 6). The influence of hue at 1 lx upon the discriminability was less than those at 500 lx.

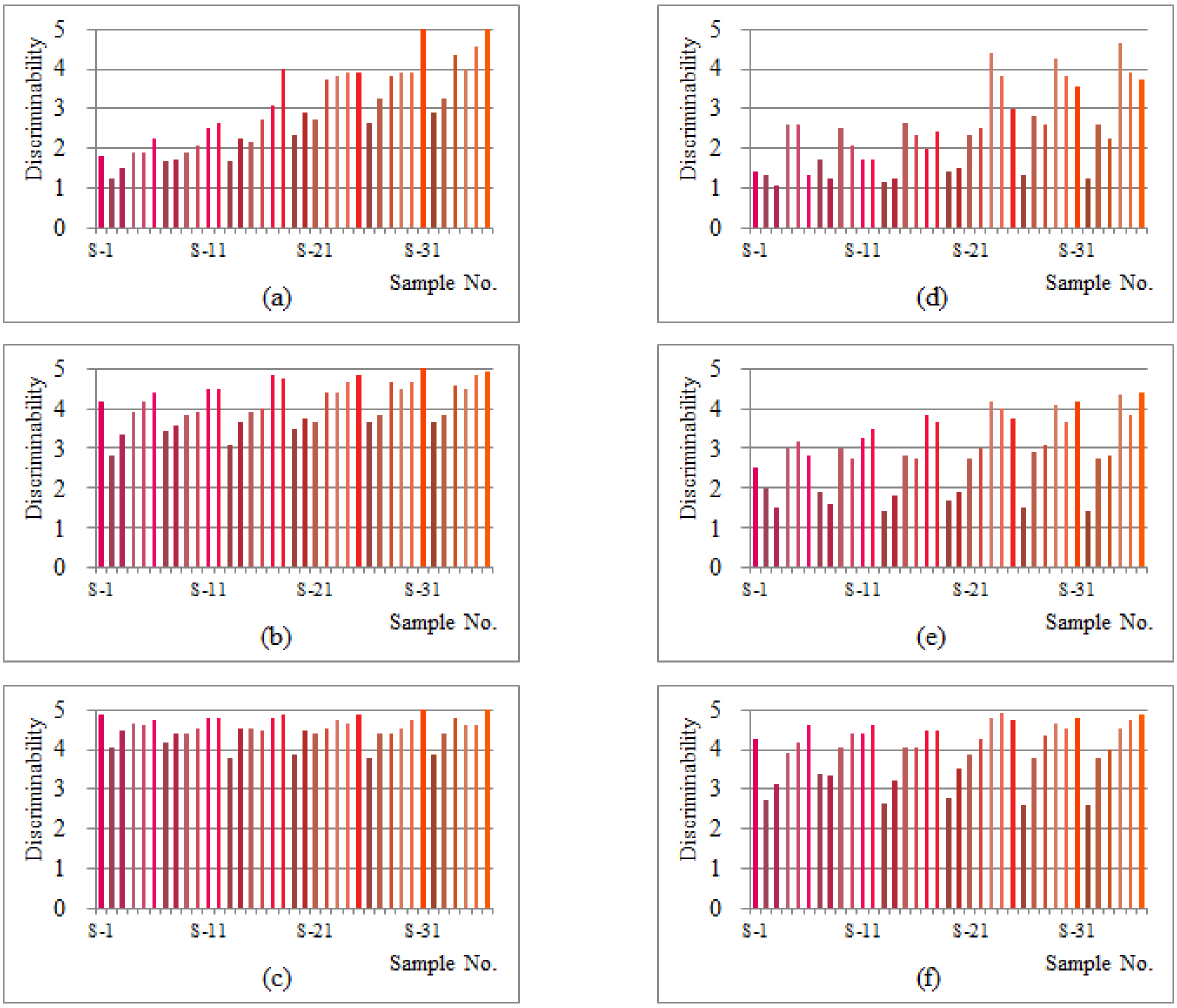

Figure 1: The discriminability from a black background; Left side is for 500 lx, (a) protans, (b) deutans, (c) normal trichromats, Right side is for 1 lx, (d) protans, (e) deutans, (f) normal trichromats,

3.2 Illuminance level

In the preceding, we presented results that evaluation for redness and discriminability from the black background were changed by illuminance level. We investigated the affection of illuminance with samples of high chroma whose hue were from 2.5R to 10R. The shifts of redness and discriminability scores by illuminance level were plotted in Figure 2. The discriminability results of samples from 2.5R to 5R decreased with the shift of illuminance level from 500 lx to 1 lx, whereas, scores of yellowish-red hue colors (8.75R and 10R) shifted less than the other colors.

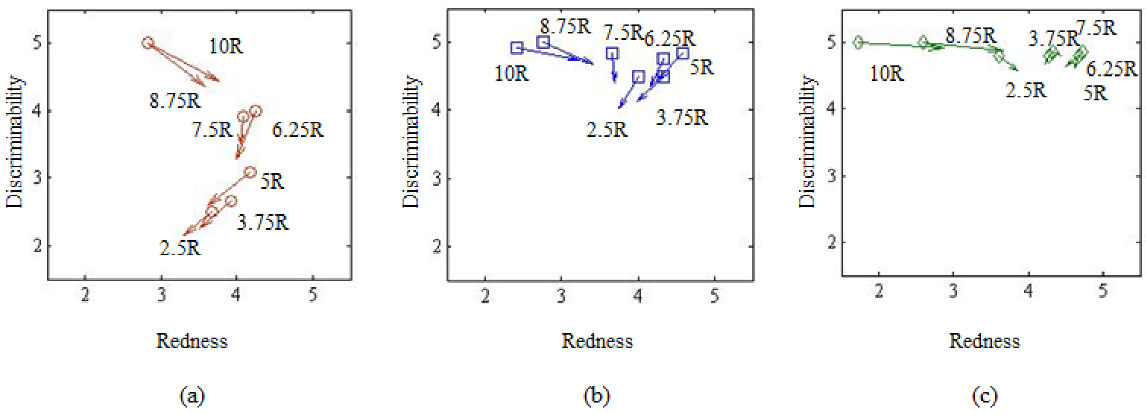

Figure 2: The shifts of redness and discriminability scores by illuminance level (from 500 lx to 1 lx) (a) protan, (b) deutan, and (c)normal trichromats

3.3 Spectral reflectance of sample

As the above result, the discriminability results at 1 lx were worse than at 500 lx for most of samples. However, we also obtained the opposite results, especially in protans, to above in several samples as shown in Figure 1; e.g. discriminability results of No.23 (7.5R6/9), No.29 (8.75R6/9) and No.35 (10R6/9) at 1 lx were higher or the same as those at 500 lx. Therefore, we extracted seven colors each that discriminability results improved or reduced. Those spectral reflectances are shown in Figure 3. The presence of middle-wavelength (yellowish color) components was found in samples with improved discriminability. We consider that the Purkinje shift influenced above tendencies.

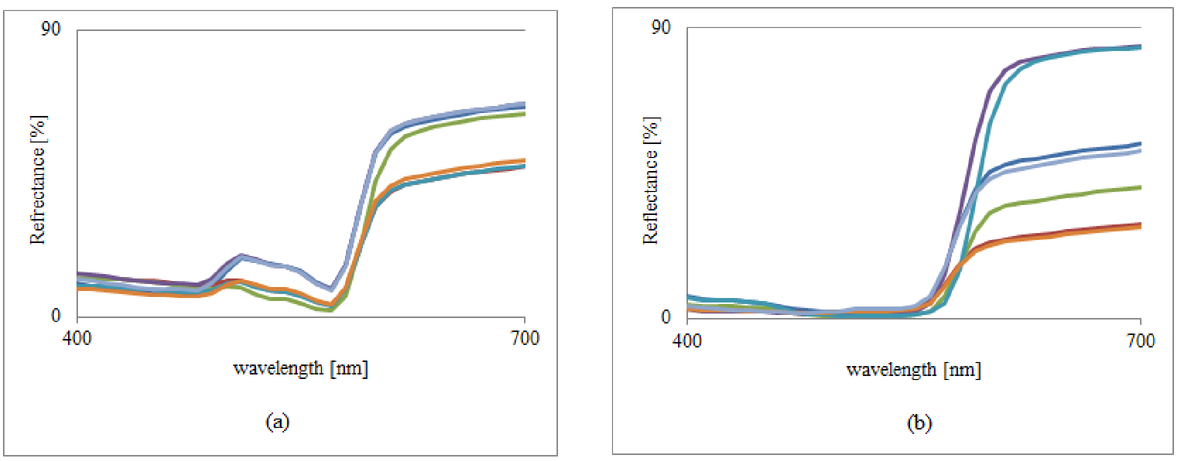

Figure 3: The spectral reflectances of seven colors, (a) improved discriminability, and (b) reduced discriminability.

4. CONCLUSIONS

We investigated the color appearance of red spot color inks by the evaluation of redness and discriminability from a black background in order to find conspicuous package print color inks for various illuminant conditions and different types of color vision deficiency. The redness was tend to vary with observers, though our experimental results showed the samples of around 2.5R to 7.5R and high chroma generally obtained high score at 500 lx. High chroma samples highly scored on the discriminability at 500 lx for deutan and normal trichromats. Above all others, yellowish-red hue samples obtained noticeable discriminability score for protan at 1 lx. Those samples were improved discriminability according to decrement in illuminance level, and the presence of middle-wavelength (yellowish color) components in spectral reflectance. Better discriminability at 1 lx for those samples would be due to the higher middle-wavelength components implying the influence of the Purkinje shift.

Our results suggest that we are able to predict an appropriate red spot color ink for various illuminants, color vision deficiencies, and application usages. In addition, we would investigate more detail of influence by spectral reflectance of inks as a future issue.

ACKNOWLEDGEMENTS

We would like to thank Consortium for a model color palette for color universal design; Dr. Kei Ito, The University of Tokyo, Japan Paint Manufacturers Association and Color Universal Design Organization.

REFERENCES

http://jfly.iam.u-tokyo.ac.jp/colorset/

J. C. Shin , H. Yaguchi and S. Shioiri 2004. *Change of Color Appearance in Photopic, Mesopic and Scotopic Vision*, Opt. Rev. 11-4, 265-271.

Y. Kagawa, H. Yaguchi and Y. Mizokami 2013. *The role of color clues in categorical color perception of deuteranomalous trichromats*, Journal of the Color Science Association of Japan 37-2, pp.103-112. (in Japanese).

Address: Masami SHISHIKURA, Central Research Laboratories, DIC Corporation, 631, Sakado, Sakura, Chiba, 285-8668, JAPAN
E-mails: katot@chiba-u.jp, mizokami@faculty.chiba-u.jp, masami-shishikura@ma.dic.co.jp, shinichiro-taniguchi@mc.dic.co.jp, tomomi-takeshita@dic-color.com, fumiko-gotou@dic-color.com, yaguchi@faculty.chiba-u.jp

A Study on the utilization of Korean Saekdong Color In the Textile arts

Kum-Hee Ryu
Professor, Dept. of Textile Stylist, Gangdong University

ABSTRACT

For the arrangement, structure, and ratio of Saekdong, they are typical stripe patterns symbolizing the philosophy and outlook on the universe of Korean people rather than a simple sense of beauty; such can be called Korea's traditional color senses and the harmony of color arrangement featuring moderated modern beauty. Korean people expressed strong aesthetic consciousness of the intention of good omen through Saekdong, the peculiar color sensitivity made by patching cloth of various colors and maintaining it as the traditional color pattern unique to Korean people. The colors most used for Saekdong were the 4 colors of Obang colors excluding black, wherein a mix of various colors were combined with blue, red, yellow, and white to ensure soft color transfers. In particular, the unique sense of rhythm created from the repetitive arrangement of a specified unit amid the asymmetrical natural sense of balance of the left and right of the original colors and the mixed colors is the excellent plastic art element of Korean Saekdong. Therefore, this study was carried out based on the writer's report on studying textile art works of diverse genres to revitalize Saekdong, which shares Korea's identity as well as the aesthetic consciousness of world generality.

INTRODUCTION

Saekdong is is a typical color arrangement that symbolizes today's Korea. The unique color composition and plastic characteristics are products of representative aesthetic awareness wherein the cultural senses inherent to Korean people are condensed and have been closely used during the daily life of Korean people. In particular, the writer has completed modern textile arts expression by reflecting the color sensitivity of Saekdong on various experimental plastic art works such as <The Cord of Life - motif with black(even though excluding black, Saekdong) and white color > done by the writer in the past.

<Work1: Saekdong Image Design – Scarf 05A>

The morphological elements of works are as follows: First, as the relief plastic element of patch work, the work expresses relief form through the plastic art combination and coloring of diversified materials - not the existing needlework technique - based on the plastic section division and patching technique of Korea's wrapping cloth. The writer sought

<Work1: Saekdong Image Design – Scarf 05B>

diverse colors of the Saekdong colors reinterpreted on the delicate textile materials and the contemporary plastic expressions in the geometric configuration resulting from the material patching. Second, as a pictorial Saekdong object element, the Saekdong object was assigned as the first accent color of the color planning of the works to express the coexistent energy of life, attempting to reflect the sensitivity of the Saekdong colors on the plastic work as much as possible by extracting strong metaphorical color language from the Saekdong pattern and to compose a with the principal and auxiliary colors and No. 2 and No. 3 accent colors. Third, the existing shape of the large plastic works of Obang colors worked for a long period of time as a linear element combining the Saekdong colors with motif as depicted in the form of line, the symbolic expression element forming the motif. The Saekdong colors were introduced to the monotone motif containing much energy, as a contemporary textile design.

METHOD

The following is < Color Planning Table for Textile Arts > and explains in detail how the Author use 'Korean Color Palett' for real works to express modern colors of Saekdong. Especially in the color planning for modeling works, They are expressed the energy of life on the works by using the colors of Saekdong cloth to give accents to an entire picture. Besides, proposes composition table of the color arrangement with dominant and secondary colors and work index colors. In detail, the color planning can be divided into 6 types, which are expressed in diagram and particularly summarized by work.

[Type I] The vivid colors extracted from Saekdong colors are arranged as secondary color on the geometric solid and added the 2nd and 3rd contracting accent colors to Saekdong to give the color sensation of Saekdong to the modern modeling work as much as I can.

[Type II] The first, second and third assistant color to the accept colors, which are clear and vivid due to their high chroma used in Saekdong object, through watery color contrast of low brightness and calm color tone or the expressions of scattered color drawing of modern Saekdong colors

[Type III] To create a unique composition with Saekdong colors which are accent colors, It use greyish pastel images in which all of dominant and secondary colors are toned down to express the hidden white image of Korean people.

[Type IV] Unlike other works for which the colors of Saekdong cloth are used as accent color for, Saekdong pattern of multiple colors is arranged on the wide cloth of the first and second accessary color. As dominant color, black and white, which is the colors of motif for mono-tone are mixed to maximize the visibility of the motif.

[Type V] The colors of Saekdong fill the entire picture of the work. Being arranged along with accent colors and secondary colors, the numerous paths and traces of Saekdong colors are expressed for piling image in the space

[Type VI] Red and blue, which are two of five cardinal colors are used as dominant and secondary color, respectively, for contrast effect. This contrast elevates the expansibility of image. In addition, the motif pattern in black and white is arranged on the front, composing the picture as secondary color along with white color line that is dominant color. All these are an attempt for multilateral color planning.

RESULTS AND DISCUSSION

The color planning of modeling works by [Type I~ **IV**] is as follows.

Color Planning – type I

C O L O R	Work 1
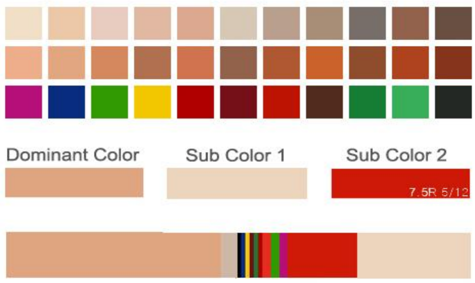	

Color Planning - type II

C O L O R	Work 2
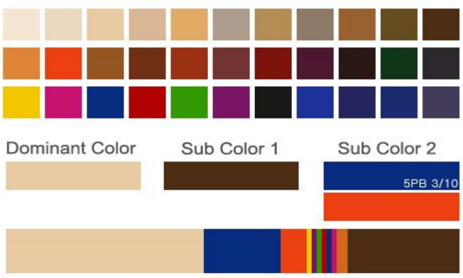	

Color Planning - type III

C O L O R	Work 3
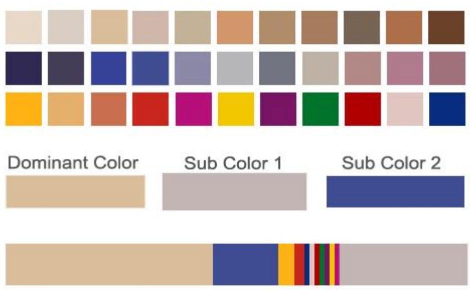	

Color Planning - type IV

COLOR	Work 4
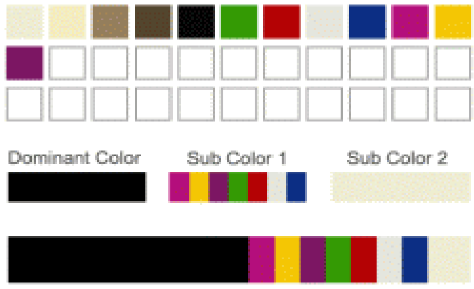	

CONCLUSIONS

One important precautionary point that should not be overlooked in relation to diversified modern textile art works under this study is that it has attempted at the modern plastic expression of the Saekdong colors with the premise that the image of the results should carry unique global competitiveness having specific nationality. To date, there have been many plastic works and prior studies and analysis carried out on colors regarding plastic works and Korean-style image expression. Through the diverse and aggressive plastic experiments carried out on colors unique to Korean people, gone will be the times when such colors might be ignored owing to traditionality.

They also provide an opportunity to use such colors positively as the global color sensitivity contents based on the plastic superiority of the Saekdong colors of Korea. We hope that various color tests and experiments are carried out continuously in the future to modernize the Saekdong patterns.

REFERENCES

Kum-Hee Ryu, *A Study on the Contemporary Plastic Art Expression of Korean Saekdong Color (Ph.D. Dissertation 2012), Seoul(Korea)*

National Museum of Contemporary Art: *Korea Traditional Sstandard Color name and Color, Seoul(Korea):Daehwa Publishing Ltd.*

National Museum, Beauty of Korea*: Color, Costume, Jewelry, Bo, Seou(Korea)l: Dongcheon cultural history Publishing Co.*

Korea Society of Color Studies Corp., *Color Design*, *Seoul(Korea): Jigu Publishing Co.*

Gisuk Keum*, Korean Costume art, Seoul: yeolhwadang*

Yongsook Kim, Economics*, Color View Point of the Korean people, Korea Culture and Arts Foundation.*

Fred W. Billmeyer, Jr. Max Saltzman, *Principles of Color Technology*, John Wiley & Sons Inc.

Jerstorp / Köhlmark, *The Textile Design Book*, Lark Books, A&C Black,

Jean Philippe Lenclos, *Couleurs de Monde*, Moniteur.

John Gage, *Color and Culture*, University of California Press.Marion Boulton Stroud, *Innovation in Pattern & Print at The Fabric Workshop, NewYork: W. W. Norton.*

Mark D. Fairchild, *Clolor Appearance Models,* 2/e, NewYork: John Wiley & Sons Ltd..
Roys.Berns*, Principles of Color Technology, Sigmapress*

Address: Prof. Kum-Hee Ryu, Department of Textile Stylist, Gangdong University, Janghowon P.O.Box 1, Echeon-City, Gyeonggi-Do, 467-900, KOREA
E-mails: fausta@gangdong.ac.kr

Color adjustment for an appealing facial photography

Kyeong ah Jeong,[1] Hyeon-Jeong Suk,[1]
[1] Department of Industrial Design, KAIST

ABSTRACT

This study investigated the relationship between the color adjustments and preference judgment of facial. Four facial photographs were given and subjects were asked to choose more attractive and likeable photography between a pair of facial photographs displayed in two identical smartphones. All stimuli were adjusted with 5 color adjustments comprised of Lightness, Contrast, Saturation, and a* and b* values in CIELAB color space. Through an orthogonal design, a total of 28 combinations were planned including 3 holdouts. Based on the judgments for the paired comparisons, Conjoint analysis was performed and the impact of each attribute and the levels of within each attribute were identified. Contrast had the biggest impact followed by Lightness, Saturation, and hue values, a* or b*. This tendency was found across all four photographs. The results provide guide to improve the quality of facial photograph, and limitations are discussed.

1. INTRODUCTION

Called as 'Selfie' in the social network services (SNS), a facial photography is one of the popular behaviors of SNS users. Due to a growing concern about more attractive and professional Selfies, most of the SNS are offering image filters. The profile images on Social Network have a characteristic that can be exposed toward unspecified individuals(Zhao, Grasmuck, and Martin 2008), and they are regarded as one of the most powerful ways to express ones' desired impressions on the network(Ellison, Heino, and Gibbs 2006). Studies on self-presentation analysis revealed that people tend to upload their online profile images not actual versions but edited versions which are reflected their own ideal images(Ellison, Heino, and Gibbs 2006). Under this circumstance, the photo editing applications try to meet social network users' demands to change their profile photos. Consequently, the photo editing applications contain filter bundles which modify the image characteristics and thereby improve impressions of photos. In this regard, we tries to find an underlying relationship between the color adjustments that affects judgment of facial photography.

2. METHOD

2.1 Material and color adjustment

We purchased four portrait photos from iStock®, and the four consisted of two males and two females (Figure 1). When selecting the four photography, we intended to avoid the external effect such as background color, clothes(Elliot and Niesta 2008), and the initial facial expressions. Accordingly, we chose neutral facial expression and then removed the background and modified the clothe either in black or white. For the graphical editing, we used the Photoshop CS6.

Figure 1: Original photos of 4 stimuli (from left, male A, male B, female A, female B)

As the color attributes for the adjustment, we manipulated the following five aspects: 1) The Lightness: direct adjustment of L*; 2) Contrast: a sigmoid adjustment to L*); 3) Saturation: multiplicative adjustment to C^*_{ab} at a constant h_{ab}; 4) and 5) a* and b* values: adjustment at a* and b* coordinates in the CIELAB system. What particular in our study was that we articulated the a* and b* indenpendently, whereas most of the related studies grouped a* and b* into several nominal categories. Then we varied the levels of each attribute somewhat differently as presented in Table 1. While altering the levels of color attributes, we basically pursue maintaining aesthetically acceptable quality, and thus we referred to a previous study in that the acceptable range of deviation of color attributes were proposed (Fernandez, Fairchild, and Braun 2005). Subsequently, with regard to the Lightness, Contrast and Saturation, we applied 5 levels, whereas we did 3 levels for both a* and b*. We created the adjusted images in MatLab® 2014b.

Table 1. Summary of the levels of adjustment value on five color attributes.

Color Attributes	Levels				
	(a)	(b)	(c)	(d)	(e)
Lightness	-10	-5	Original	5	10
Contrast	0.03	0.04	Original	0.05	0.06
Saturation	0.8	0.9	Original	1.1	1.2
a* value	-2.5	Original	2.5		
b* value	-2.5	Original	2.5		

In order to reduce the number of combination from the entire factorial designs (1,125 = 5x5x5x3x3) while minimizing the loss of information, we created only 25 combinations by through an Orthogonal Design. After having added another 3 combinations as the holdouts, we prepared a total number of 28 combinations for the subjective assessment. Considering the Selfie context, we displayed the photos on a smartphone whose screen size is 2.4 inches in width and 4.2 inches in height.

2.2 Method

A total of 30 college students composed of 16 males and 14 females participated in experiment. The avrage age of the subjects was 21.57 years with a standard deviation of 3.37 years.

The experiments consisted of two parts. In the first part, we asked the subjects to evaluate each of the four original photography using a set of criteria. The criteria included the following five aspects proposed by Willis and Todorov (2006): Attractiveness, Likeable, Competence, Trustworthiness and Aggressiveness. We intended to identify the baseline of each photography, and subjects made judgments of each photography using 7-point Likert scale (1 = strongly disagree, 5 = strongly agree). In the latter part, we adopted a pair comparison method, and thus provided each subject with a pair of photography displayed in two identical smarphones. Since we prepared 28 combinations, a total of 378 paired comparisons (28*27/2 = 378) were acquired. We requested subjects to choose a more attractive photography than the other within 2 seconds, and all could easily make the decision.

The experiment room was lit with 6500K and illuminance was 650 lx. Under this illumination, the luminosity reflected from a white area in the content image was measured as 203 cd/m^2.

2.3 Results and analyses

Based on the assessments in the first part, we compared the mean differences among the 4 photographs with regard to the 5 criteria, and found that there were differences of initial impressions among the four. Repeated measure One-way ANOVA yielded the statistical difference an alpha level of 0.01. For example, in terms of degree of 'Attractiveness', Female A got the highest score(5.23) followed by Male B, Female B, and Male A. Therefore, we should take the individual difference into consideration during the analysis of the data.

Table 2. Mean and standard deviation of the 4 photographs when original. (N = 30)

Attributes	Male A	Male B	Female A	Female B
Attractiveness	4.20 (0.85)	4.93 (1.05)	5.23 (1.10)	4.33 (0.96)
Likeable	4.43 (0.90)	3.97 (1.10)	4.70 (0.99)	5.00 (0.95)
Competence	4.57 (0.97)	5.33 (1.06)	5.27 (0.98)	4.03 (0.81)
Trustworthiness	4.40 (1.00)	4.17 (1.44)	3.87 (1.04)	5.00 (0.87)
Aggressiveness	4.20 (0.81)	5.10 (1.03)	5.73 (0.91)	3.70 (1.06)

Then we accumulated the judgments of paired comparisions, and transformed the data into the rank orders. Based on the 60 cases (30 subjects x 2 sets of photographs) of ranked data, we performed a Conjoint analysis in SPSS® 21 to identify the relevance of each attribute(i.e. relative importance) as well as each level within each attribute(i.e. utility). The following Figure 2 presents the averaged importance values of 60 cases. Among the five color attributes, Contrast had the greatest impact while b* did the smallest one. A

Repeated measure One-way ANOVA confirmed that the averaged values of relative importance were statistically significant [$F(4,236) = 117.42$, $p = 0.00$]. Moreover, a strong positive correlation was found between the ranks of 25 combinations and those of 3 holdouts (kendall's tau = 0.87, $p = 0.00$), supporting a high level of reliability.

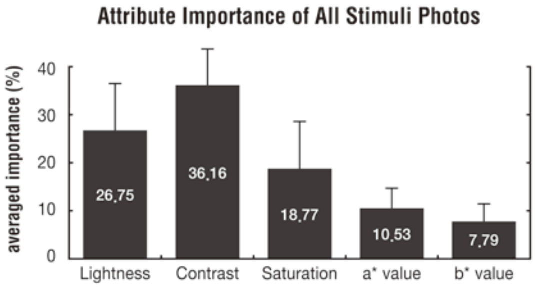

Figure 2: Relative importance of the five attributes.

Futhermore, the utility scores of each of the 5 attributes were revealed (Figure 3), and we formed the best combination as follows: 3.78 + 4.52 + 1.97 + 1.20 + 0.40 = 11.87 (maximum of sum of utility).

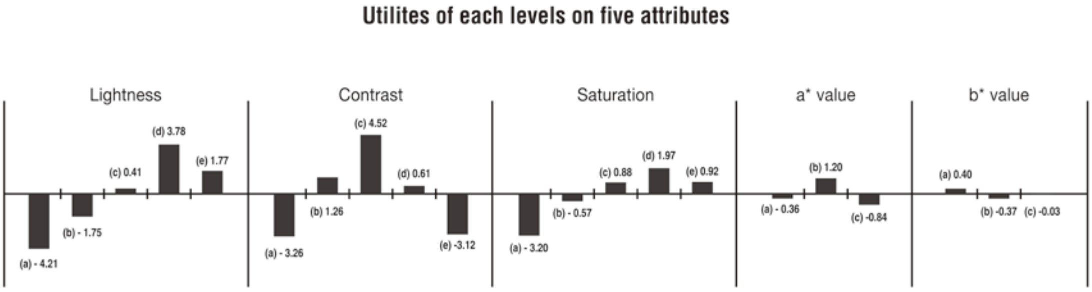

Figure 3: Utility of each level on five attributes

Also we observed quite similar tendency between males and females indicating that the color adjustment can be applied to both genders. In both gender groups, Contrast had the strongest impact followed by Lightness, Saturation, a*, and then b*. The only slight

Figure 4: (Above) Original photos (Below) Adjusted to be the most appealing

difference was found in the utility scores of b*. More bluish female photographs(negative b*) were preferred while more yellowish male photogrpahs(positive b*) were preferred.

In addition, we concerned about the individual difference among the four photographs with regard to the initial impressions. However, the Conjoint analysis yielded similar tendency across the four different faces. This implies that the color adjustment to make a facial photographs to be more attractive can be universally applied to different faces (Figure 4).

4. CONCLUSIONS

This study revealed the relative importance of color attributes for the impressions of facial photography. The empirical study showed that Contrast was the most effective on both female and male photos whereas b* value change was the least. In particular, the most attractive/likeable combination of color attributes on photos was proposed in the following procedure; 5 amount increase of Lightness value, 1.1 multiple amount of Saturation value, original Contrast value, original a* value and 2.5 amount negative shift of b* value. When the utility scores within each attribute were compared, it was found that original contrast was the most preferred. However, further investigation should be carried out with non-professional photographs whose aesthetic quality is not professionally controlled. Nevertheless, a consistent tendency was found across all four photographs, which implies that there is a ground truth with regard to the preference for facial photographs. In a future study, the empirical study should expand to include different initial quality of the photographs and different ethnic groups not only as stimuli but also for the judgment.

REFERENCES

Elliot, Andrew J, and Daniela Niesta. 2008. Romantic red: red enhances men's attraction to women. *Journal of personality and social psychology* 95 (5):1150.

Ellison, Nicole, Rebecca Heino, and Jennifer Gibbs. 2006. Managing impressions online: Self‐presentation processes in the online dating environment. *Journal of Computer‐Mediated Communication* 11 (2):415-441.

Fernandez, Scot R, Mark D Fairchild, and Karen Braun. 2005. Analysis of Observer and Cultural Variability while Generating. *Journal of Imaging Science and Technology* 49 (1):96-104.

Willis, Janine, and Alexander Todorov. 2006. First impressions making up your mind after a 100-ms exposure to a face. *Psychological science* 17 (7):592-598.

Zhao, Shanyang, Sherri Grasmuck, and Jason Martin. 2008. Identity construction on Facebook: Digital empowerment in anchored relationships. *Computers in human behavior* 24 (5):1816-1836.

Address: Prof. Hyeon-Jeong Suk, Department of Industrial Design,
Korean Advanced Institution of Science and Technology, 291 Daehak-ro, Yuseong-gu,
Daejeon, 205-338, KOREA
E-mails: kyeongah17@kaist.ac.kr, h.j.suk@kaist.ac.kr

Understanding popular relationships among colors through the network analysis for crowd sourced color data

EunJin KIM,[1] Hyeon-Jeong Suk[1]
[1] Department of Industrial Design, KAIST

ABSTRACT

This study makes a unique attempt to adopt Social Network Analysis(SNA) in order to exploit the potential of the crowd sourced large-scale color data. We anticipate understanding the trend of color combinations and the way of generating harmonious color schemes. Basic concepts in SNA are introduced along with the method of constructing a color network from the existing color database called Adobe Kuler®. In relation to the characteristics of SNA, the implication of adopting SNA is discussed while demonstrating its benefits through findings from the network analysis of a color database. Various ways of visualization of the color data are suggested to illustrate the difference among them. In addition, quantitative metrics are calculated which identify the relative importance of individual colors and the entire structure of a network. The result reveals key players of a color network and subgroups of colors which are harmonized well to each other.

1. INTRODUCTION

Utilizing a harmonious color scheme is often essential to make an aesthetically pleasing art work and design. In order to support a proper color choice, there have been studies that are focused on developing algorithms or tools to generate a set of color (Shen et al. 2000, Wijffelaars et al. 2008, Hu et al. 2014). However, constructing a satisfied color scheme is still challenging due to the limited practicality and weak theoretical background of existing models. In this regard, this research aims to investigate patterns of color combinations through exploring the latent relationships among colors in color schemes. A network analysis was adopted to examine the relationship of colors that are generated by crowd, and to identify key players of the color combinations and the subgroups that consist of closely related colors.

2. APPLICATION OF SNA FOR A LARGE-SCALE COLOR DATA

Social Network Analysis (SNA) has been successfully utilized in various fields to understand the structure of a community, a society and even a biological system (Ennett and Bauman 1993, Böde et al. 2007, Blanchet and James 2012). Compared to traditional research methods, SNA focuses on the relationships and emerging structures formed by relationships (Scott 2012). Due to this characteristics, SNA has been supported the identification of new paradigms and latent patterns beneath the structure. Nowadays, a growing number of researches adopt SNA to investigate the structure, determinants, and impacts of relationships between actors. To our best knowledge, however, it has been yet applied to the large-scaled color data, especially a database of color schemes built by crowd. A color scheme can be easily interpreted as relational data among colors that belongs to a same scheme. In addition, Adobe Kuler®, one of the largest color scheme database, provides not only the color schemes but also the ratings for each scheme that are given by numerous users. It is expected that existing color schemes and their ratings can provide relevant guidelines to identify a harmonious combinations of colors that is applicable to a new art work. Thus we made an attempt to explore the color schemes of Adobe Kuler using SNA.

Table 1. Summary of the charcateristics of SNA and its implications on a color network .

Characteristicss of Social Network Analysis	Related SNA metrics	Implications of applying SNA to a color network	Related examples from SNS studies
Quick and easy visualization of big database	-	An easy and intuitive understanding of popular colors (See 4.1)	-
Identifting the relative importance of a social actor depending on the network position	Closeness centrality	Identifying universal colors which are easy to match with diverse colors (See 4.2)	A user who can reach to all other users with fewer steps using a friendship network
Identifying the subgroups of a network according to the relational data.	Modularity	Identifying a group of colors that are often used together in order to construct a color scheme (See 4.3)	A group of users that have intimate and dense friendships with each other

Application of network analysis to a crowd sourced database has several advantages. First of all, SNA enables a quick and easy visualization of large scaled data. Due to the visual properties of color data, an immediate visualization of data facilitates initial analysis and interpretation of the entire dataset. Secondly, network analysis focuses on the relational data, and this focal point is much more appropriate to investigate the compatibility of a color rather than its popularity that can be easily captured and compared by conventional methods. SNA provides quantitative metrics such as closeness centrality that measures the relative importance of a node in the aspect of connectivity a node has. This can be employed to identify universal colors that have been belonged to many color schemes with diverse combinations. SNA also supports a clustering of nodes using a modularity algorithm that identifies subgroups of intimate colors based on the relational data.

In conclusion, SNA allows rich and informative analysis to investigate latent but practical knowledge that traditional methods are hard to discover. Table 1 summarizes the characteristics of SNA and its implication on the study of color database with the comparison of examples from Social Network Service(SNS) studies (Perry-Smith 2006, Newman 2006) .

3. CONSTRUCTING A COLOR NETWORK

3.1 Data collection and processing

In order to construct a color network, we utilized 44,986 color themes of Adobe Kuler(Adobe Color CC) which were collected and distributed by O'Donovan et al (2011). We filtered out 7,118 popular color themes whose scores are higher than 4.0 out of 5.0. Then we transformed each color theme into nodes and links data. A node indicates a single color, and a link is a connection between a pair of colors which are included in the same color scheme. Since every color scheme consists of five colors, we were able to extract five nodes and ten links (10= (5 x 4)/2) from each color scheme.

In addition, the RGB scores as it was initially crawled were mapped into the CIE1976L*a*b space. The L, a, b scores were rounded off to every 5(for example a color with L:71, a:14, b:13 was transformed to L:70, a:15, b:15). Consequently the color quantization aggregated multiple colors into one, and helped to construct a concise and denser network.

3.2 Visualization in Gephi®

Utilizing the quantized Lab values of Adobe Kuler data, a color network with 4,922 nodes and 26,401 edges was generated. An opensource software Gephi was utilized in order to visualize the network and anlyze it. Figure 1 shows a visualized color network which is composed of colors that are used more than 50 times.

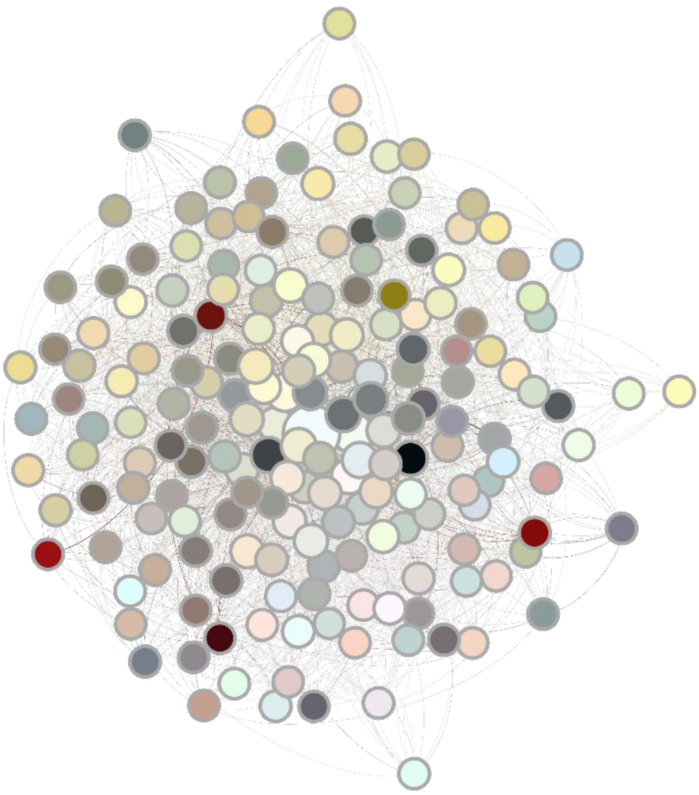

Figure 1: A color network of colors which are utilized more than 50 times

4. FINDINGS FROM THE NETWORK ANALYSIS

4.1 Identifying key players through a visualized network

As previously mentioned, SNA has notable characteristics and advantages that are different from other research methods. First, it provides an effective way of visualization which enables an intuitive understanding of the entire data. Figure 2 shows three networks which utilized the same data but devised different filtering criteria to emphasize the key players of a color network. The left network provides a look of network that are composed of colors utilized more than 20 times (degrees). It covers 37.85 % of the entire links, and shows the general tendency of the color utilized by crowd. The middle one shows popular colors that are utilized more than 70 times. As shown in the graph, most of reddish colors appeared in the low range of L, whereas bluish colors more frequently had higher L values. The right figure was generated by applying the criterion of degrees more than 200. In this case, only a few colors are visualized, and it is really easy to identify the extremely popular colors that are frequently utilized throughout the database. To summarize, SNA provides an easy and effective way of representing the data while investigating the relationships with diverse perspectives. It also provides an intuitive view to compare more than two different color networks. Especially when it combines with time-dependent data, it is expected that the trend change of popular colors can be traced and compared easily using the color network.

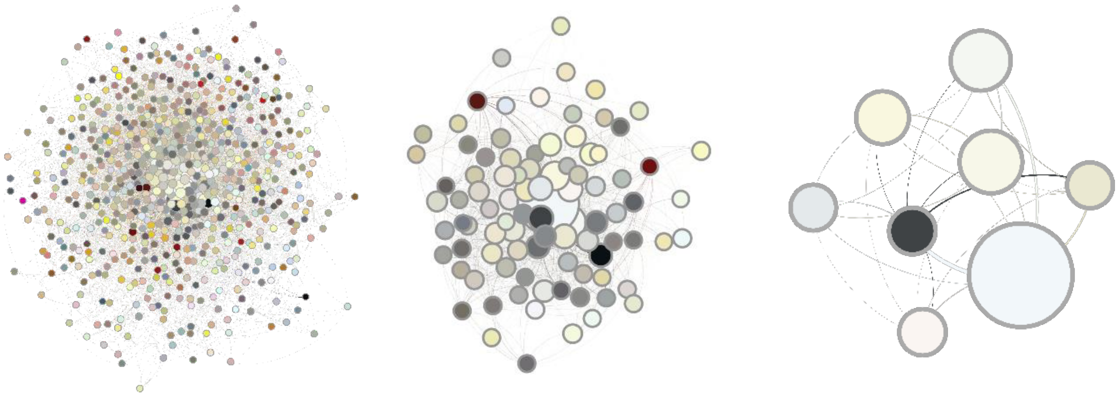

Figure 2: Networks with different filtering criteria - nodes of 20, 70, 200 degrees respectively

4.2 Identifying universal colors using a closeness centrality measure

A color scheme is often constructed with more than 2~3 colors. Hence, it is important to identify colors that can be universally matched with other colors instead of capturing single color with a extreme popularity. In this regard, a color which has a closer relationship with other colors is more meaningful than a color which has been frequently used as a member of a color scheme. The measure of closeness centrality relates to the concept of universal match, and it calculates the average distance from each node to every other nodes in the network. For instance, the value 2 of closeness centrality indicates that the node can reach to other nodes within two degrees in average. The higher closeness centrality implies that a color can be connected to other colors with a shoter distance, and it increases the possiblity that a color belongs to various color schemes. Therefore, a color with a higher closeness centrality can be regarded as a universal one which is compatable to any combinations.

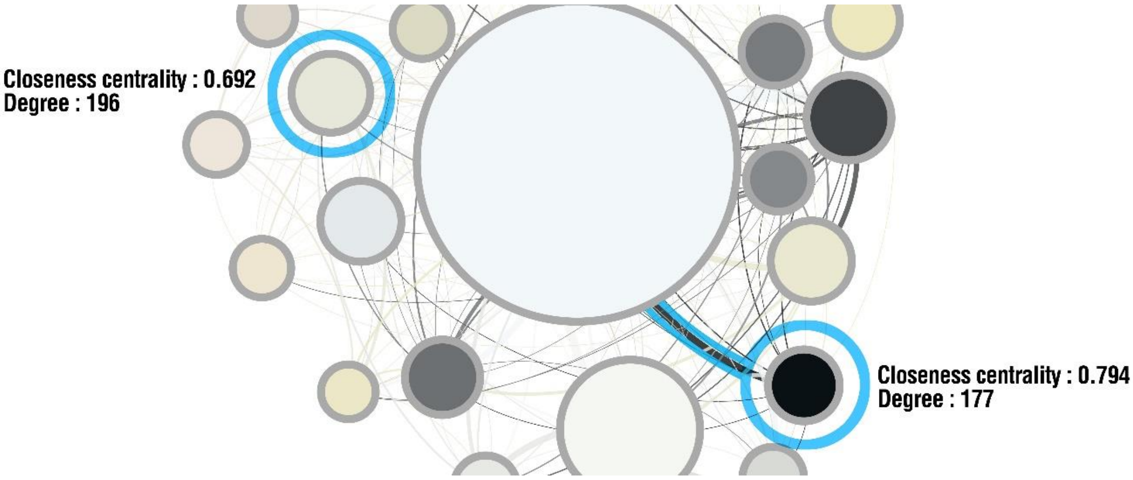

Figure 3: A partial network to compare two colors with different closeness centralities

In a network, colors which show higher closeness centralities often overlap with the popular colors which are utilized more frequently than others, but not always the same. Figure 3 shows two colors in a network with a closer look; the highlighted color on the right side of the network represents a color with a higher closeness centrality (0.794) whereas the left one represents a popular color utilized more frequently but less central (0.692). As shown in the graph, the color with higher centrality has strong relationships with other colors that are popular as their size represent. However the left one with a lower centrality value has relatively less links with other popular colors. The strong connectivity with other popular colors increase the possibility that the right color reach to other colors to construct various combinations. In general, colors with remarkable centralities have extreme L values and lower chromaticities throughout the entire graph.

4.3 Identifying groups of harmonious colors using a Modularity measure

The modularity algorithm looks for nodes that are more densely connected together than to the rest of the network (Newman 2006). The nodes that belong to the same modularity group has a strong relationship with each other because they have been frequently utilized in the same color scheme together. Therefore the modular membership of a color can be employed to construct a color scheme which has been proved as harmonious combination by numerous users. As shown in the Figure 4, color schemes that consist of colors from the same modular groups are relatively more harmonious than schemes composed of colors with different modular memberships.

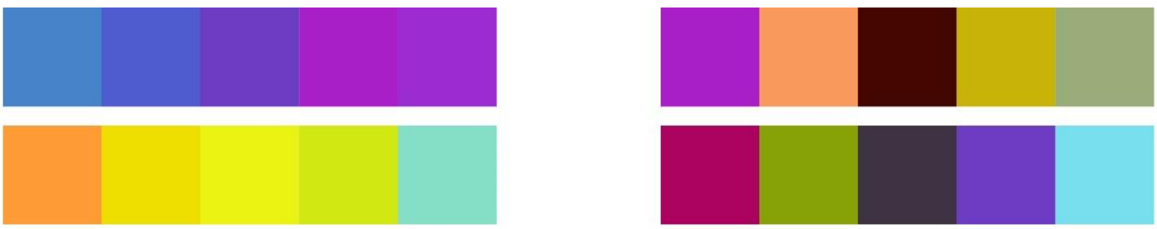

(a) Colors from the same Modularity group

(b) Colors from the different Modularity group

Figure 4: Color schemes that are generated using the Modularity of colors

5. CONCLUSION

In this study, Social Network Analysis has been adopted in order to explore the crowd-generated color big data. We have discussed the method to construct a network using the exsiting color database, and have introduced relevant metrics and methods that are applicable to the color data. The constructed network was analyzed and interpreted by visualizing it with different filtering criteria, and by calculating network measurements such as closeness centrality and modularity. The measurement of closeness centrality reveals that colors with extreme L values and low chromaticities are more compatable with other colors. We also generated color schemes by employing the modularity memberships of colors, and the colors from the same modular groups produeced more harmonious color schemes. In conclusion, the network analysis provides a noble way of investigating color data in the perspective of relatinships among colors, and suggests findings that conventional methods are hard to reveal. However this study is intended as a priliminary research to introduce the implication and benefits of applying a network analysis. For further studies, it is required to develop relative analysis methods and verify its significance in order to enhance reliability and practicality of network analysis in color studies.

REFERENCES

Böde, Csaba, István A Kovács, Máté S Szalay, Robin Palotai, Tamás Korcsmáros, and Péter Csermely. 2007. Network analysis of protein dynamics. *Febs Letters* 581 (15):2776-2782.

Blanchet, Karl, and Philip James. 2012. The role of social networks in the governance of health systems: the case of eye care systems in Ghana. *Health policy and planning*:czs031.

Ennett, Susan T, and Karl E Bauman. 1993. Peer group structure and adolescent cigarette smoking: A social network analysis. *Journal of Health and Social Behavior*:226-236.

Hu, Guosheng, Zhigeng Pan, Mingmin Zhang, De Chen, Wenzhen Yang, and Jian Chen. 2014. An interactive method for generating harmonious color schemes. *Color Research & Application* 39 (1):70-78.

Newman, Mark EJ. 2006. Modularity and community structure in networks. *Proceedings of the National Academy of Sciences* 103 (23):8577-8582.

O'Donovan, Peter, Aseem Agarwala, and Aaron Hertzmann. 2011. Color compatibility from large datasets. In *ACM SIGGRAPH 2011, Proceedings*, Canada, 1-12.

Perry-Smith, Jill E. 2006. Social yet creative: The role of social relationships in facilitating individual creativity. *Academy of Management Journal* 49 (1):85-101.

Scott, John. 2012. *Social network analysis*. 3rd ed: SAGE Publications Ltd.

Shen, Yu–Chuan, Wu–Hsiung Yuan, Wen–Hsing Hsu, and Yung–Sheng Chen. 2000. Color selection in the consideration of color harmony for interior design. *Color Research & Application* 25 (1):20-31.

Wijffelaars, Martijn, Roel Vliegen, Jarke J Van Wijk, and Erik ‐ Jan Van Der Linden. 2008. Generating color palettes using intuitive parameters. In *Computer Graphics Forum, Proceedings*, 743-750.

Address: Prof. Hyeon-Jeong Suk, Department of Industrial Design, KAIST
Bldg. N25, 291 Daehak-ro, Yuseong-gu, Daejeon, 305-701, KOREA
E-mails: kejkim8@kaist.ac.kr, h.j.suk@kaist.ac.kr

Eliciting the Color Bizarreness Effect Using Photographs

Aiko MORITA, Saki FUNAKOSHI[1]
Graduate School of Education, Hiroshima University

ABSTRACT

Color typicality has seemed to affect on performance of a picture memory task. When an object is typically colored, the color is remembered more accurately than when it is atypically colored. In contrast, incongruent stimuli have been found to increase attention, resulting in higher performance on memory tasks compared with congruent stimuli, the so-called "bizarreness effect". The previous study by these authors investigated the color bizarreness effect in line drawings. The current study manipulated the object color of photographs, rather than that of line drawings. We expected that the strangeness of the bizarrely colored stimuli is larger in photographs than that in line drawings. The objects pictured were exactly the same as those in the previous study, which found a color bizarreness effect with line drawings. The participants in this study comprised 30 university students. In an initial learning session, 28 photographs of objects were presented one at a time. They were colored in typical colors (e.g., yellow banana, purple eggplant) or bizarre colors (e.g., blue banana, orange eggplant). The recall performance results did not show a bizarreness effect or a typicality effect. Why the bizarrely colored photographs did not produce color bizarreness effect is discussed. Previously, the authors examined the color bizarreness effect using line-drawings. The procedure was exactly the same as this current experiment except that the stimuli were line-drawings, not photographs. That experiment did produce bizarreness effect. An ad-hoc analysis found that the strangeness of the filler stimuli, that is, typically-colored stimuli, affected the bizarreness effect; because the typically-colored photo stimuli seemed to be a little unnatural, bizarreness effect decreases. This mechanism for the color bizarreness effect can be applied to create striking text or advertisements.

1. INTRODUCTION

The so-called bizarreness effect is the theory that people have better memory for bizarre items as compared to common items, a finding referred to as the bizarreness effect (Geraci, McDaniel, Miller, & Hughes, 2013). Many of the studies on this theory have used bizarre images or sentences as stimuli. However, some studies triggered this effect using pictures (e.g., Gounden & Nicolas, 2012), advertisements (e.g., Subbotsky & Matthews, 2011), or personal information (e.g., Brandt, Gardiner, & Macrae, 2006).

The mechanism of the bizarreness effect has yet to be clarified, but one of its underlying factors is that bizarre stimuli attract attention. Another factor is that bizarre or unexpected items activate particular encoding processes. When the event is more elaboratively processed, bizarre items are encoded with a richer set of cues that are especially useful in retrieval (McDaniel, DeLosh, May, & Brady, 1995).

The present study investigated the mechanism producing the color bizarreness effect. While color typicality evidently affects performance of picture-memory tasks, some studies have reported that when a line drawing is typically colored, it is more accurately remembered than when it is bizarrely colored (e.g., Morita, 2013; Ratner & McCarthy, 1990). In such cases, it is possible that the color bizarreness effect scarcely occurs. In contrast, we found a color bizarreness effect with line drawings as participants recalled more bizarrely colored line drawings than commonly colored ones (Morita & Funakoshi, in press).

Our present study used exactly the same objects as in the previous study (Morita & Funakoshi, in press), but showed them in photographs rather than line drawings. We mentioned above that some studies found a color typicality effect for pictures; however, few have examined the color bizarreness effect. Thus, we arranged conditions to induce the bizarreness effect. We examined whether we could find the color bizarreness effect when using photographs.

2. METHOD

2.1 Participants

The participants in this study were 30 university students, and the experiment consisted of small groups of one to five participants.

2.2 Stimuli

We selected 28 objects based on the our previous studies that used line drawings (Morita & Funakoshi, in press). We then chose photographs of the objects from a database of psychological photographs and websites.

Of the 28 objects, 12 were assigned to target stimuli, which were were colored with either a common or bizarre color. Another 12 objects were assigned to filler stimuli. The bizarreness effect can be expected to be larger when there are more common items employed. For example, Hirshman, Whelley, & Palij (1989) found that the effect occurred when there were four bizarre sentences and 12 common sentences, but not when there were 12 bizarre sentences and four common sentences. To prevent primacy and the recency effect, the remaining four objects were assigned to dummy stimuli, which were presented as the first and last items on the list. Target items were counterbalanced across participants. A participant was presented six bizarrely colored targets, six commonly colored targets, 12 commonly colored fillers, and the dummy stimuli.

To compare the effect, the bizarre color and the common color of these stimuli were the same as in Morita & Funakoshi (in press) using line drawings. Adobe Photoshop was used to color the photograph stimuli (Figure 1).

Figure 1: Examples of commonly colored and bizarrely colored stimuli.

2.3 Experimental Procedure

The experiment consisted of a learning session and a free recall test session. In the initial learning session, 28 photographs of objects were presented one at a time by PowerPoint. One trial consisted of a gaze point (1 sec), photograph of the object (2 sec), and the object name attached to the photograph (1 sec). Participants judged whether it was easy to identify the object, and rated on a three-point scale. After viewing the 28 stimuli, participants were made to perform to a distraction task; spending 2 minutes answering a questionnaire. In the last test session, participants were asked to recall the names of the objects presented in the learning session.

3. RESULTS AND DISCUSSION

Figure 2 shows the mean proportions of recall of the common and bizarre targets. The mean recall rate of filler stimuli was 56.7%. A *t*-test found no significant difference between the recall performance under two conditions; the bizarreness effect did not occur.

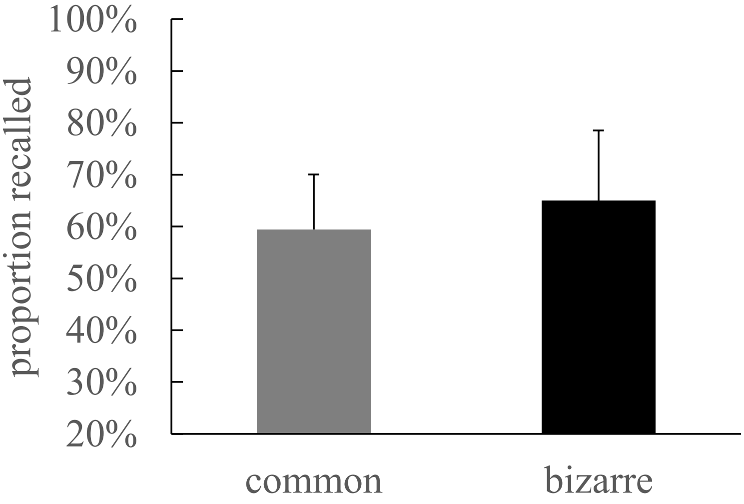

Figure 2: Mean proportion of recall of commonly colored and bizarrely colored stimuli.

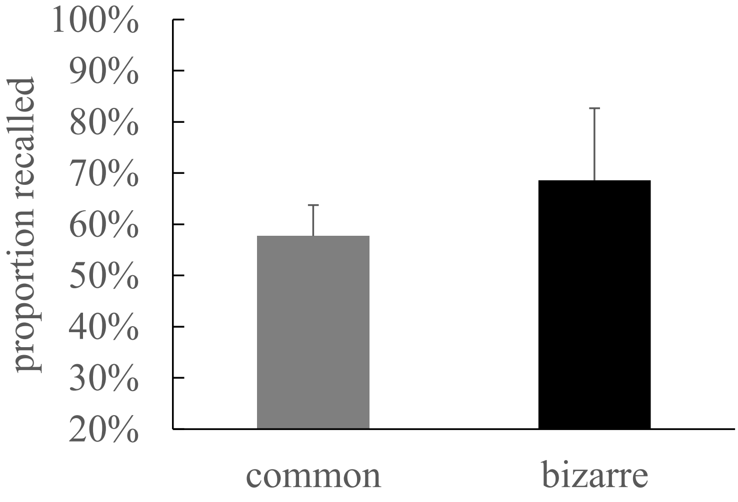

Figure 3: Mean proportion of recall of commonly colored and bizarrely colored stimuli excluding five participants.

However, five participants had a recall rate of below 50% for all stimuli. It is possible these five did not perform the task sincerely. Thus, we analyzed the recall rate for the target stimuli again, excluding these five participants' data (Figure 3). A *t*-test found that bizarrely color targets were recalled marginally better than commonly colored ones.

The study's objective was to investigate whether the color bizarreness effect could occur under conditions arranged to induce the bizarreness effect. The current study used photographs, expecting that the strangeness of the bizarrely colored stimuli would be greater this way as opposed to using line drawings.

The results showed no significant difference between common and bizarre colors. When excluding five participants from apparently underperforming participants, the bizarreness effect was found to occur at a marginal level. Though this experiment was conducted under conditions for inducing the bizarreness effect, the effect seldom surfaced.

In comparing our present and past studies, we note the procedure was exactly the same except the previous stimuli were line drawings rather than photographs. Ad-hoc analysis found that somewhat strange attributes of the filler (typically colored) stimuli affected the bizarreness effect. This was because the typically colored photo stimuli seemed slightly unnatural, and thus the bizarreness effect decreased.

This experiment added insight about the mechanism of the bizarreness effect. We suggest that the process differs between the differently colored objects. Rappaport, Humphreys, & Riddoch (2013) reported that a search for a common color-form conjunction was uniquely efficient. That study suggested that learned bindings can be computed with minimal attentional limitations. In contrast, the search for bizarrely colored objects was slow, consistent with serial attention being required to distinguish targets and nontargets. Here we suggest that bizarrely colored stimuli need additional processing with attention. This additional processing is found to produce the bizarreness effect and, thus, observance of the color bizarreness effect should come as no surporse. In contrast, memory performance is enhanced to the extent that the context forms and integrated unit with the target. A common object will yield superior memory performance because a more elaborate trace is laid down and because in such cases the structure of semantic memory can be used more effectively to facilitate retrieval (Claik & Tulving, 1975). This rich elaboration is indicated to produce a typicality effect.

4. CONCLUSIONS

In this experiment, neither of these two effect occurred clearly. We could not conclude that bizarrely colored objects are easier to remember. It seems to be difficult to produce the bizarreness effect using color manipulation. This may be dependent upon the color-shape conjunction or strangeness of the color.

REFERECCES

Craik, F. I. M. and Tulving, E. 1975. Depth of processing and retention of words in episodic memory, *Journal of Experimental Psychology: General* 104: 268-294.

Brandt, K. R., Gardiner, J. M. and Macrae, C. N. 2006. The distinctiveness effect in forenames: The role of subjective experiences and recognition memory, *British Journal of Psychology* 97: 269-280.

Geraci, L., McDaniel, M. A., Miller, T. M. and Hughes, M. L. 2013. The bizarreness effect: evidence for the critical influence of retrieval processes, *Memory and Cognition* 41: 1228-1237.

Gounden, Y. and Nicolas, S. 2012. The impact of processing time on the bizarreness and orthographic distinctiveness effects, *Scandinavian Journal of Psychology* 53: 287-294.

Hirshman, E.H., Whelley, M.M. and Palij, M. 1989. An investigation of paradoxical memory effects, *Journal of Memory and Language* 28: 594-609.

McDaniel, M. A., Einstein, G. O., DeLosh, E. L., May, C. P. and Brady, P. 1995. The bizarreness effect: It's not surprising, it's complex, *Journal of Experimental Psychology: Learning, Memory, and Cognition* 21: 422-435.

Morita, A. and Funakoshi, S. in press The effect of color bizarreness on picture memory, *The 14th European Congress of Psychology*.

Subbotsky, E. and Matthews, J. 2011. Magical thinking and memory: distinctiveness effect for TV commercials with magical content, *Psychological Reports* 109: 369-379.

Rappaport, S. J., Humphreys, G. W. and Riddoch, M. J. 2013. The attraction of yellow corn: reduced attentional constraints on coding learned conjunctive relations, *Journal of Experimental psychology: Human Perception and Performance* 39: 1016-1031.

Ratner, C. and McCarthy, J. 1990. Ecologically relevant stimuli and color memory, *Journal of General Psychology* 117: 369-377.

Address: Dr. Aiko MORITA, Department of Psychology, Graduate School of Education, Hiroshima University, 1-1-1, Kagamiyama, Higashi-Hiroshima City, 739-8524 JAPAN
E-mails: amorita@hiroshima-u.ac.jp

Texture in Color Emotions

Ivana TOMIC,[1] M. Mar LAZARO,[2] Ana CARRASCO-SANZ,[2] Ana BENJUMEA,[2]
Li-Chen OU,[3] Jose A. GARCIA,[2] Igor KARLOVIC,[1] Rafael HUERTAS[2]
[1] Faculty of Technical Sciences, Graphic Engineering and Design, Novi Sad (Serbia)
[2] Department of Optics, Faculty of Science, University of Granada (Spain)
[3] Applied Science and Technology, National University of Science and Technology (Taiwan)

ABSTRACT

Regarding the visual sensation much effort is put into investigating so-called color emotions, building the models by selecting emotion scales and through them assessing human reaction to selected colors. Most of the previous studies had recorded color emotions in subjects viewing uniform color patches. However, when dealing with the real world objects, perception of the color is usually connected with the perception of objects surface properties i.e. texture. In this work we had done a pilot study to assess and possibly describe the effect of texture on color emotions and also to select a set of attributes which can be appropriate for describing the reaction to the texture.

1. INTRODUCTION

There are an extensive number of studies that tried to capture and model the effect of color on human emotions (Gao and Xin, 2006; Ou et al., 2004; Ou et al, 2012, etc.). In these studies solid colors are used as stimuli, while the emotion scales are based on pairs of words, usually adjectives, with the opposite meaning (for example: heavy-light, modern-classical, clean-dirty, masculine-feminine, etc.). As seen from these examples, adjectives used to describe emotions are rather opinions and descriptions of specific reaction to a certain color and the effect it produces. Even though these descriptors do not capture the essence of emotions, they do provide very important information about human reaction to a certain color. Hence, for the purpose of our study we will adopt the term color emotions for describing the reaction to the colored sample, in general.

It is stated that color can be perceived differently, and consequently evoke different emotions, if it is combined with the texture (Zhang and Wandell, 1996). Lucassen et al. (2011) show that "texture fully determins the response on the hard-soft scale and plays an important role in decreasing weight for the masculine-feminine, heavy-light and warm-cool scales." This study was done with synthesized images, where all the samples were visible during the decision process.

The aim of this study was to provide us with some basic information for better understanding of the effect that texture has on human reaction to color. In this part of a study we decided to use a limited number of natural textures. We started testing whether the adjectives used in the color emotion studies are actually appropriate when dealing with textures, so we conducted a survey on 94 respondents of different nationalities. The method and some preliminary results are presented in the next sections.

2. METHOD

2.1 Selection of the Color Centers and Texture Samples

For the purpose of our study thirty chromatic and three achromatic color centers were chosen. Samples had L^* values of 20, 50 and 80. In case of the chromatic samples, h_{ab} was 18°, 90°, 162°, 234° and 306°, while C^*_{ab} was chosen to be the maximum and half the maximum value in sRGB color space. For the hue centers, the above-defined angles represent better the unique hues (Kuehni, 1979).

Next step was defining the textured samples. The goal was to define a set with a reasonably low number of them with enough of the variance regarding texture strength. Samples were chosen from the KTH-TIPS and KTH-TIPS2 database (Mallikarjuna et al, 2006; Fritz et al, 2004) by taking into account the results presented in Gebejes et al (2012; 2013), where GLCM method (Haralick et al., 1973) was used for the characterization of the samples. Since the Homogeneity parameter was shown to have the best correlation with visual perception (Gebejes et al, 2012) five textured color images were selected according to their Homogeneity values (0.571, 0.696, 0.787, 0.869 and 0.949), as seen in Fig. 1. Please, note that for the solid colors Homogeneity takes value of 1. Among some different possibilities, visual appearance of the textures was taken into account in the final decision. Thus, a total of 198 samples (combining 33 color centers with five textures, plus the solid colors) were generated.

Figure 1. Textured color images ordered by decreasing Homogeneity.

2.2 Color to Texture Fusion

Color to texture fusion was performed in CIE LCH color space. It is assumed that resulting hue does not depend on the hue of the source image, while lightness and chroma are computed from both the source image and the target color as in (Milic et al., 2010). Thus, hue channel corresponds to the selected target hue, while lightness and saturation channels were normalized with the respect to the mean values of the source image as:

$$P_t^i = P_t + \left(P^i - P_{mean}\right) \qquad (1)$$

where P_t^i is the target lightness/chroma of a pixel i, P_t is the lightness/chroma of the target color, P^i is the source lightness/chroma of a pixel i and P_{mean} is the mean value of the lightness/chroma of the source image. Fig. 2 shows the results of color to texture fusion for the 5 considered textured images in the case of medium-lightness, saturated blue center (L^*=50, C^*_{ab}=39, h_{ab}=234°).

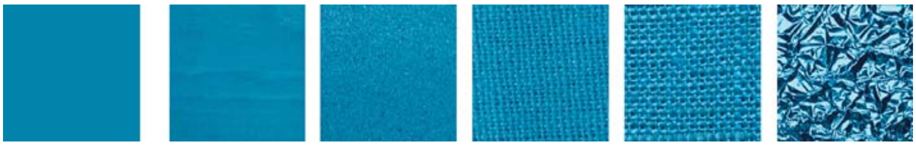

Figure 2. One of the blue target colors and resulting images of the color to texture fusion for all the textures considered in Fig. 1.

2.3 Scales for Texture Emotion

We conducted a survey with the goal to define the most appropriate scales for assessing emotions related to textured samples. The basic idea was to obtain responses from people belonging to different nationhood, and that words pairs used were the most "universal" as possible – meaning not culturally dependent. Our examinees were asked to imagine some texture(s) and to describe, with ten adjectives, their emotions and sensations toward it. In total, we obtained the responses from 94 people. Most of the examinees were from Spain and Serbia (34 of the both nationhood). The rest of the group contained Hungarians, Norwegians, Americans, German, Italian, Romanians, Portuguese, Dutch, Irish, Russian, Bulgarian, Indian, French and Israeli. Questions were posed in English and, due to the large number of examinees from Spain and Serbia, also in Spanish and Serbian. Adjectives obtained in Spanish and Serbian were translated into English and were assessed by language professors.

2.4 Task of the Observers

In this part of the work 26 observers participated 16 females and 10 males, with ages ranging from 21 to 58 and with normal color vision (tested with the Ishihara Color Vision Test).

The 198 samples were presented in dark viewing condition on a LCD monitor (HP 2510i of 25" of the size and operated with a resolution of 1920x1080 pixels). Monitor was calibrated with Eye-One Display colorimeter by taking into account the chromacity coordinates of the sRGB color space. Accuracy of color patches displayed on the screen was measured by the Photo Research SpectraScan PR-704 spectroradiometer. The luminance of the referent white of the screen was 105 cd/m^2. Samples were observed against a neutral background as shown in Fig. 3. The size of the color patches displayed on the LCD screen was 115x115 mm, while the distance of observation was around 50 cm; no chinrest had been used. Thus, the CIE 1964 Supplementary Standard Observer has been assumed according to the samples size and observers' position.

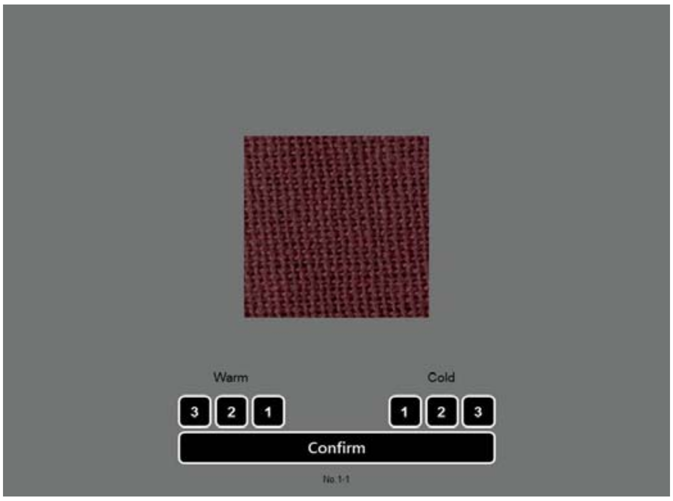

Figure 3. Screenshot of the observers' task

Previous to each session, the observers were adapted to the background conditions for two minutes and adaptation between samples displaying was of 1 second. For each displayed sample, the observers were asked to select one of the words of the pairs and give a score between 1 and 3. Taking warm-cold as an example, numbers 1 to 3 represent the intensity of the reaction, either warm or cold, where 1 means 'slightly' and 3 means 'very'. Value zero was not allowed. For each displayed sample, the answer for two of the words pairs was asked consecutively. The experiment was divided into 3 sessions; one for the words pairs soft-hard and warm-cold, another for smooth-rough and heavy-light, and other for natural-unnatural and like-dislike. Each session lasts for around 30 minutes. Observers performed the sessions in random order and different days.

3. RESULTS AND DISCUSSION

In assessing the results of the survey it was noticed that most of the responses were actually descriptions of texture surface roughness. Overall, we obtained 430 different adjectives where only small amount of them can be regarded as emotional reactions. The words with the highest frequency of the appearance were: soft (12.3%), rough (10.2%), cold (5.8%), warm (5.8%), smooth (4.7%), even (4.7%), hard (3.3%), and pleasant (2.8). It can be seen that among the most frequently used adjectives there are words with somehow opposite meaning (*soft-rough, cold-warm*). This is similar, but not completely in accordance, with the pairs used in color emotion studies (Ou et al., 2004): *warm–cool, hard–soft*.

Following scales were chosen among those with the highest frequency: *soft-hard, warm-cold,* and *smooth-rough.* Besides these, we included two pairs that are frequently used in the color emotion studies and were also found among the responses of our examinees: *heavy-light* and *natural-unnatural*. Additional scale describing preferences is also used in the form *like-dislike*. Thus, in total we chose six pairs of words: soft-hard, warm-cold, smooth-rough, heavy-light, natural-unnatural and like-dislike. Chosen scales can be divided into 3 groups according to the primary potency factors (Ou et al, 2004); *Like-dislike* and *natural-unnatural* can be categorized as evaluative factor, *soft-hard, smooth-rough* and *heavy-light* as potency, while *warm-cold* as activity factors.

The inter-observer variability was computed with a modified version of RMS:

$$RMS = \sqrt{\frac{\sum_i \left(x_i - \bar{x}_i\right)^2}{N}} \qquad (2)$$

where x_i represents an observer's color emotion response to the stimulus i; x_i represents the mean value for all observers within the group for stimulus i; N is the total number of stimuli. Finally, we average over the 26 observers. The lower the RMS value, the more the observers' responses agree with each other within the group and thus, the more accurate the responses.

Table 1 summarizes the test results, which are similar, though slightly lower than in previous works of color emotions (Ou et al., 2012). Considering all the samples, the warm/cold responses were the most accurate within the group, while the like/dislike and natural/unnatural, the evaluative factors, the least. This is also in agreement with the previous works (Ou et al., 2012). The stronger textures (less homogeneous) produce higher variability for all the scales except soft/hard. It seems that texture in some way helps observers to decide about soft/hard but scatter the responses for the rest of scales.

Torgerson's law of categorical judgment was used to convert the raw data (with scales ranging from -3 to 3) into z-score related scale values. Table 2 shows the Pearson correlation coefficient between the emotion scales.

Table 1. Inter-observer variability RMS values for the six color emotion scales.

Homogeneity	Soft/ Hard	Warm/ Cold	Smooth/ Rough	Heavy/ Light	Natural/ Unnatural	Like/ Dislike	Mean
0.57	1.06	1.22	1.25	1.83	1.25	1.72	1.39
0.70	1.61	1.59	1.80	1.66	1.76	1.65	1.68
0.79	1.47	1.57	1.68	1.50	1.79	1.66	1.61
0.87	1.03	1.39	1.05	1.27	1.64	1.68	1.34
0.95	1.48	1.37	1.56	1.36	1.59	1.59	1.49
1 (solid)	1.84	1.40	1.53	1.52	1.62	1.49	1.57
All	1.51	1.45	1.60	1.58	1.65	1.66	1.58

Table 2. Pearson coefficient for the emotion scales.

	Soft/ Hard	Warm/ Cold	Smoot/ Rough	Heavy/ Light	Natural/ Unnatural	Like/ Dislike
Soft/Hard	1	0.5783	0.6131	-0.7232	0.2898	0.3969
Warm/Cold	0.5783	1	0.2278	-0.4175	0.2901	0.4467
Smooth/Rough	0.6131	0.2278	1	-0.2996	0.1381	0.1235
Heavy/Light	-0.7232	-0.4175	-0.2996	1	-0.0055	-0.1739
Natural/Unnatural	0.2898	0.2901	0.1381	-0.0055	1	0.6597
Like/Dislike	0.3969	0.4467	0.1235	-0.1739	0.6597	1

From Table 2 it can be deduced that the chosen emotion scales are quite independent. The higher correlation (-0.7232) appears between two potency factors heavy/light and soft/hard, in a negative way. The more heavy a stimulus appears the harder it is perceived, which seems logical. The next higher correlation (0.6597) is between the two evaluative factors, like/dislike and natural/unnatural, in a positive way. Then, the more natural stimulus appears the more it was favored, as could be expected. The fewer correlated scales are natural/unnatural and heavy/light, with a coefficient of -0.0055.

4. CONCLUSIONS

A textured images set to perform an experiment about texture emotions, had been generated according to perception dissimilarity: 198 samples, mixing 6 different textures (one of them is the case of solid color) with 33 color centers. Furthermore, specific emotion scales for the study of texture emotions had been developed. Preliminary results, with 26 observers, indicate a good inter-observer variability, in agreement with previous works, and a good selection of the chosen emotion scales, which are independent.

ACKNOWLEDGEMENTS

This work was supported by the research project FIS2013- 45952-P ("Ministerio de Economia y Competitividad," Spain) with European Union FEDER (European Regional Development Funds) support and the Serbian Ministry of Science and Technological Development, Grant No.:35027.

REFERENCES

Fritz, M., E. Hayman, B. Caputo and J. O. Eklundh. 2004. *THE KTH-TIPS database*. Available online, http://www.nada.kth.se/cvap/databases/kth-tips/ Accessed: September 10, 2014.

Gao, X.-P. and J.H. Xin. 2006. *Investigation of human's emotional responses on colors*. Color Research & Application 31 (5): 411–417.

Gebejes, A., I. Tomić, R. Huertas, and M. Stepanić. 2012. A preliminary perceptual scale for texture feature parameters. In *Proceedings of GRID12*. Novi Sad: Faculty of Technical Sciences, 195-201.

Gebejes, A., R. Huertas, I. Tomić, and M. Stepanić. 2013. Selection of optimal features for texture characterization and perception. In *Proceedings of CVCS 2013*. Gjøvik: The Norwegian Color and Visual Computing Laboratory, 1-5.

Haralick, R. M., K. Shanmungam, and I. Dinstein. 1973. *Textural Features of Image Classification*. IEEE Transactions on Systems, Man and Cybernetics 3(6): 610-621.

Kuehni, R.G. and R. T. Marcus. 1979. *An Experiment in Visual Scaling of Small Color*. Color Research & Application 4 (2):83–91.

Lucassen, M.P., T. Gevers, and A. Gijsenij. 2011. *Texture affects color emotion*. Color Research & Application 36 (6): 426–436.

Mallikarjuna P., A. T. Targhi, M. Fritz, E. Hayman, B. Caputo, and J. O. Eklundh. 2006. *THE KTH-TIPS2 database*. Available online, http://www.nada.kth.se/cvap/databases/kth-tips/. Accessed: September 10, 2014.

Milic, N., R. Slavuj, and B. Milosavljevic. 2010. The color mapping method based on the LCH color space for simulating textile printed texture images. In *Proceedings of GRID10*. Novi Sad: Faculty of Technical Sciences, 167-172.

Ou, L.C., M.R. Luo, A.Woodcock, and A. Wright. 2004. *A study of color emotion and color preference. Part I: Color emotions for single colors*. Color Research & Application 29 (3): 232–240.

Ou, L.C., M.R. Luo, P.L. Sun, N.C. Hu, H.S. Chen, S.S. Guan, A. Woodcock, J.L. Caivano, R. Huertas, A. Treméau, M. Billger, H. Izadan, K. Richter. 2012. *A cross-cultural comparison of colour emotion for two-colour combinations*. Color Research & Application 37 (1), 23–43.

Zhang, X. and B. A. Wandell. 1996. A spatial extension of CIELAB for digital color image reproduction. In *Proceedings of the Society of Information Display Symposium*. San Jose, USA. 731-734.

Address: Prof. Rafael HUERTAS, Department of Optics, Faculty of Science, University of Granada, c/ Cuesta del Hospicio s/n, Granada, 18071, SPAIN
E-mails: tomic@uns.ac.rs, mlazaro@ugr.es, acarrasco@ugr.es, ana.beca.88@gmail.com, lichenou@mail.ntust.edu.tw, jgarcia@ugr.es, karlovic@uns.ac.rs, rhuertas@ugr.es

Individual's Color Preference and Personality of Feeling Active and Passive Good Emotion, Pleasantness and Comfortableness

Shin'ya TAKAHASHI[1], and Takashi HANARI[2]
[1] School of Humanities, Tokaigakuen University
[2] School of Culture-Information Studies, Sugiyama Jogakuen University

ABSTRACT

We investigated relationship between individual's color preference and his/her personality of feeling pleasantness and comfortableness, that is, active and passive kinds of good emotion. A hundred university students answered the degree of liking of twelve basic colors; red, orange, yellow, yellow-green, green, blue, purple, pink, brown, white, black, and gray. In addition, they were asked to read six short sentences, three of which depicted pleasant affairs (P sentences) and the remaining three depicted comfortable affairs (C sentences), and to answer how strong he/she will feel good emotion presented as ten emotional words. Based on an exploratory analysis of the data, we selected two emotional words ('glad' and 'excited') as indicators of pleasantness, and two words ('relieved' and 'relaxed') as indicators of comfortableness. Correlation analysis and multiple regression analysis between the degree of liking each color and the degree of feeling these indicator words showed that the individual who is sensitive to pleasantness on P sentences tends to like black and purple, and the individual who is sensitive to comfortableness on C sentences tends to like orange, green, and yellow-green. These colors were suggested to have some association with our active and passive aspects of good feeling.

1. INTRODUCTION

Color preference is one of the most intriguing topics in the field of color psychology. The underlying idea of the color preference research as a subject of psychology would be that a certain color makes a certain person feel good for a certain reason. Thus, researchers try to clarify 'what color' is preferred by the individual having 'what personality and/or attribute' for 'what reason.' Indeed, anyone has some color(s) associated with good feeling.

Kuno, Ohno, and Nakahata (1987) proposed, in the field of thermal sensation, that our good feeling could be distinguished into two types, active one and passive one. The active good feeling is called pleasantness, which is characterized by activeness, change, and surprise. For example, when we move from the extremely hot open air to an air-conditioned room, we would feel excitingly good, that is pleasantness. On the other hand, the passive good feeling is called comfortableness, which is characterized by passiveness, stability, and ordinariness. For example, when we stay in a room neither hot nor cold (in other words, not being conscious of the room temperature), we would feel calmly good, that is comfortableness. Though the original idea by Kuno et al. (1987) stems from the thermal comfort research, Takahashi (2003) discussed that the distinction between pleasantness and comfortableness could be applied to visual comfort, and even to more general concept of human's good emotion and sense of well-being.

In the present study, we take the first step to investigate possible relationship between individual's color preference and his/her personality of feeling pleasantness and comfortableness. It was aimed at contributing to our better understanding of the color preference in the light of an untouched factor of its psychological process.

2. METHOD

2.1 Participants

A hundred university students, forty-five males and fifty-five females, participated in our research. Their mean age was 18.5 years old (SD = .56).

2.2 Procedure

All data were collected through questionnaire. The questionnaire was composed of two parts. The first part included twelve visual analog scales on which participant answered his/her degree of liking of twelve basic colors; red (5R 4.5/14), orange (10R 6/11), yellow (5Y 8.5/12), yellow-green (5YG 6.5/9), green (5G 4.5/10), blue (2.5PB 4/11), purple (10P 4/11), pink (5RP 6.5/9), brown (7.5R 4/6), white (N9.5), black (N1.5), and gray (N5.5). These colors were presented as printed color chips (6 mm × 16 mm). Participants drew a slash, according to the degree of liking each color, on the line with the left-end indicating 'don't like at all (0% liking)' and the right-end indicating 'like the most (100% liking)' (Figure 1).

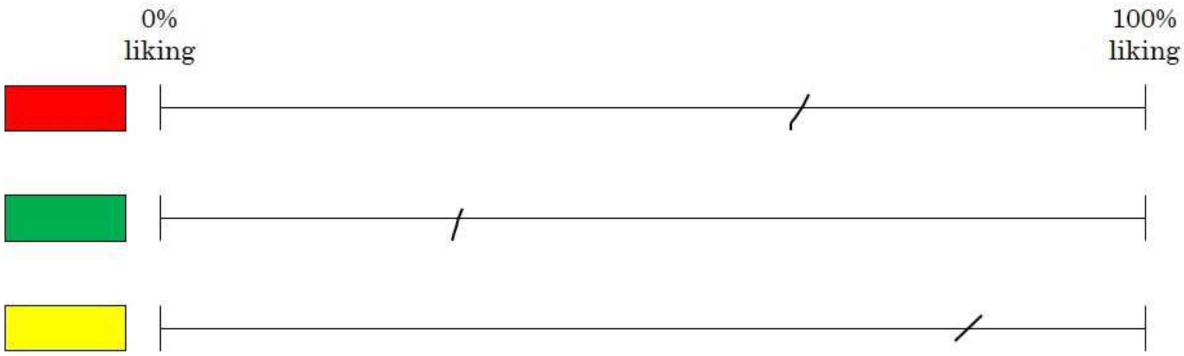

Figure 1: Samples of the visual analog scales.

The second part showed participants six short sentences, each of which depicted good affair. Three of them depicted pleasant situation (P sentences), and the remaining three depicted comfortable situation (C sentences) (Table 1). For each sentence, participants were asked to imagine how strong he/she will feel emotions presented as ten emotional words, and answer the degree on 11-point scales (0: 'don't feel at all' – 10: 'feel the most'). Five of ten words intended to measure the pleasant feeling; 'glad,' 'wakening,' 'pleasing,' 'delightful,' and 'excited.' Another five intended to measure the comfortable feeling; 'relieved,' 'heart-warming,' 'calm,' 'comfortable,' and 'relaxed.

2.3 Data processing

As for results of the visual analog scales, position of the slash was measured and converted

Table 1. Brief sentences depicting imaginary good affairs. Please note actually richer Japanese expression was given so as to emphasize pleasant or comfortable situation.

P sentences	P1: Cool the flushing body by the blast of cold air. P2: Win a prize of 5,000 yen in the lottery. P3: Notice cherry blossoms in full bloom.
C sentences	C1: No problem was pointed in a health examination. C2: Stay relaxed in a moderately air-conditioned room. C3: Take a walk through the trees on the plateau.

into the preference score ranging from 0 (the left-end) to 100 (the right-end). Ratings for each emotional word were averaged for three P sentences (P1, P2, P3) and for three C sentences (C1, C2, C3) in each participant.

3. RESULTS AND DISCUSSION

3.1 Preference scores

Mean preference scores for each color, separately for male and female participants, are shown in Table 2, which are ordered by the grand mean (for all participants). Compared to our previous data (Takahashi and Hanari, 2008), a drop of black's score, which was formerly 73.4 and ranked first, is remarkable. Otherwise almost the same sketch was replicated. As for the sex difference, pink and yellow were liked more by females than by males, which was the case in the previous data.

Table 2. Mean preference scores in all, male, and female participants. ** $p < .01$

	White	Blue	Red	Black	Yellow	Orange	Y-G	Green	Pink	Purple	Gray	Brown
All	79.9	72.3	69.2	66.2	65.1	64.6	60.3	58.8	58.2	54.5	52.7	44.7
Males	76.6	71.8	67.4	62.7	56.8	66.1	60.7	61.0	49.6	57.1	57.1	44.6
Females	82.6	72.6	70.7	69.1	** 71.8	63.4	60.0	57.1	** 65.2	52.3	49.2	44.8

3.2 Color preference and feeling pleasantness and comfortableness

Using data of all participants, mean ratings for each emotional word were compared between P sentences and C sentences. As the results, ratings for 'glad' and 'excited' were found to be higher for P sentences than for C sentences ('glad': P 8.04, C 6.02, 'excited': P 6.50, C 4.45). Thus these words were chosen to be pleasantness indicators, and the mean of these ratings for three P sentences was calculated in each participant to show his/her pleasantness sensitivity (P score). Contrarily, ratings for 'relieved' and 'relaxed' were found to be higher for C sentences than for P sentences ('relieved': P 4.91, C 7.07, 'relaxed': P 5.17, C 6.98). Thus these words were chosen to be confortableness indicators, and the mean of these ratings for three C sentences was calculated in each participant to show his/her comfortableness sensitivity (C score).

Next, correlations between each participant's P score and C score and his/her preference

Table 3. Correlations between P and C scores and color preference scores. ** $p < .01$, * $p < .05$

	White	Blue	Red	Black	Yellow	Orange	Y-G	Green	Pink	Purple	Gray	Brown
P score	.034	.113	.071	.416**	.062	.119	.068	.132	.063	.282**	.191	.052
C score	.211*	.197*	.214*	.151	.252*	.376**	.311**	.364**	.113	.146	.107	.116

scores for each color were obtained. As shown in Table 3, P score was positively correlated with black and purple, whereas C score was positively correlated with orange, green, and yellow-green. These results were also supported by the multiple regression analysis with P score and C score as explanatory valiables and the preference score for each color as a target valiable. It was shown that black and purple preferences were significantly regressed by P score; standardized partial regression coefficient (β) was .442 ($p < .001$) and .275 ($p < .05$), respectively. And, orange, green, and yellow-green preferences were significantly regressed by C score; $\beta = .419$ ($p < .001$), .395 ($p < .001$), and .365 ($p < .001$), respectively.

4. CONCLUSIONS

The present study investigated relationship between the color preference and personality of feeling good emotions, and found that pleasantness-sensitive individual tends to like black and purple, while comfortableness-sensitive individual tends to like orange, green, and yellow-green. Considering that preference for any colors did not correlated with both P score and C score, pleasantness and comfortableness would be clearly distinguished from each other in terms of the color preference, each having unique psychological mechanism related with the preference for certain colors. Roughly speaking, orange, green, and yellow-green would be categorized as 'nature colors,' having peaceful impression that might be loved by comfortableness-sensitive people. Contrastingly, purple would have somewhat artificial and surprising impression that might have affinity with pleasantness-seeking. Relationship between black and pleasantness seems not to be easily explained. In the next step, individual's reason for liking those key colors should be examined to understand psychological process of the color preference more deeply.

REFERENCES

Kuno, S., H. Ohno, and N. Nakahata. 1987. A two-dimensional model expressing thermal sensation in transitional conditions, *ASHRAE Transactions* 93(2): 396-406.

Takahashi, S. 2003. A pilot study of visual environmental psychology (2): Some issues concerning visual pleasantness, *The Journal of the Faculty of Letters, Nagoya University, Philosophy* 147: 61-75. [In Japanese]

Takahashi, S. and T. Hanari. 2008. Cognitive factors in color preference (2): Generalization of previous findings by using modified procedures, *Journal of the Color Science Association of Japan* 32(4): 282-289. [In Japanese]

Address: Prof. Shin'ya TAKAHASHI, Department of Psychology, School of Humanities, Tokaigakuen University, 2-901 Nakahira, Tempaku, Nagoya, 468-8514, JAPAN
E-mails: takahashi-s@tokaigakuen-u.ac.jp, hanari@sugiyama-u.ac.jp

Colour Emotions for Antioxidant-Enriched Virgin Olive Oils

Luis GOMEZ-ROBLEDO[1], Piedad LIMON[2], Ruperto BERMEJO[2], Manuel MELGOSA
[1] Department of Optics, University of Granada (Spain)
[2] Department of Physical and Analytical Chemistry, High Politechnical School of Linares, Jaén University (Spain)

ABSTRACT

This work looks for relationships between 9 specific colour emotions applied to a set of extra virgin olive oils which have been coloured by using a lutein and ß-carotene enriched extract from microalgae. 6 extra virgin olive oils have been coloured with 2 different concentrations of this colorant obtaining a total of 18 different samples. 20 non-expert Spanish observers were asked to describe the colour appearance of the samples using 9 different pairs of adjectives (Aromatic-Odourless, Bitter-Sweet, Fresh-Rancid, Healthy-Unhealthy, Like-Dislike, Natural-Artificial, Spicy-Non spicy, Tasty-Insipid and Textured-Smooth). Results of spectroradiometric measurements performed under the same conditions than visual observations showed that increasing concentrations of the colorant changed the colour of the sample towards a reddish hue. The microalgae antioxidant-enriched colorant changed the colour of the olive oils mainly in hue, in such a way that, on the average, more than 70% of the total CIELAB colour-difference between pure and lutein and ß-carotene enriched virgin olive oils was a hue difference. Torgerson's law of categorical judgment was applied to the results in our colour-emotion experiment showing that there is a high correlation between some pairs of emotions whose meanings are more related to colour preference (Fresh-Rancid, Healthy-Unhealthy, Like-Dislike, Natural-Artificial and Tasty-Insipid). Bitter-Sweet, Spicy-Non spicy, and Textured-Smootj are not correlated with any other emotion. Finally, combining results from colour measurements and colour-preferences we found that if the samples are too reddish their appearance tends to generate a dislike emotion. Therefore, virgin olive oils with high CIELAB hue-angles (greenish hues) seem to be the most appropriate ones to be enriched by these extracts from microalgae.

1. INTRODUCTION

The amounts of carotenoids that are found in human tissues are almost exclusively from dietary origin, mainly from fruits and vegetables, or from supplements. It has been reported that the uptake of ß -carotene reduces the risk of age-related macular degeneration (Teikari, J.M.: 1998). In addition, it has been shown that olive oil with extract from microalgae known as *Scenedesmus almeriensis* brought changes in olive oils, quality, composition, colour and stability giving. Therefore, olive oil with an addition of microalgae extract could be a good convoy to improve and enhance the intake of carotenoids in a daily basis (Limon, P: 2015). Although this change in colour may not change its taste or smell, the subjective perception of these factors can change (Zellner, DA: 2003) and colour emotion techniques help to quantify the expectation of a product when it is perceived by human eye (Wei, S: 2014).

This work has two main objectives. Firstly, we want to analyse how does the colour of virgin olive oil changes when we add lutein and ß-carotene enriched extract from the Scenedesmus almeriensis microalga. Secondly, we want to check how does the human perceived this change in colour by using colour semantic methods (Ou, L: 2004).

2. METHOD

Six samples of different extra-virgin olive oils have been selected, five of them obtained in the same harvest season: Fuenroble, Santuario Mágina, Oro de Bailén, Castillo de Canena and Melgarejo 1; and another one from the previous harvest season Melgarejo 2. For each one of these samples we have prepaired three different samples by adding different concentration of extract of microalgae: 0.00 mg/ml (A), 0.10 mg/ml (B) and 0.21 mg/ml. A total of 18 samples have been used, 6 oils × 3 concentrations. Each one of the samples was poured into bottles with dimensions of 1.5 cm X 1.5cm X 6.0 cm and a capacity of about 20 ml. These bottles have rectangular prism shape and their flat faces allow having an homogenous colour of the oils, this fact makes easier their colour measurement and their colour perception. All the samples were kept in a controlled environment during all the experiment.

Colour measurement of the samples has been made placing the samples in a Verivide Portable cabinet (Verivide, Leicester, United Kingdom) using a D65 light source simulator, the walls of the cabinets were covered by white non fluorescent paper in order to avoid shades in the samples and have a lighter background behind the samples. The colour was measured using a Konica Minolta CS2000A spectroradiometer (Konika Minolta, Nieuwegein, Netherlands) in the same position that the observers performing the visual experiment (figure 1). Tristimulus values were computed assuming CIE64 standard observer. Three replicas of the measurements were made.

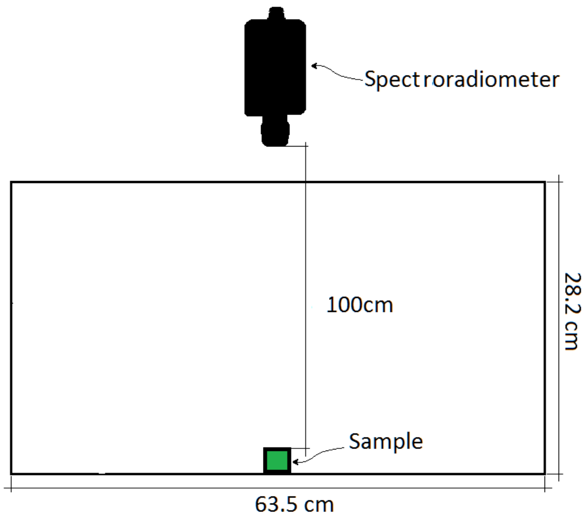

Figure 1: Geometry of the colour measurement of the samples

20 Spanish observers were asked to describe each one of the samples following 9 pairs of opposite descriptors: Aromatic-Odourless, Bitter-Sweet, Fresh-Rancid, Healthy-Unhealthy, Like-Dislike, Natural-Artificial, Spicy-Non spicy, Tasty-Insipid and Textured-Smooth. These 9 descriptors were obtained from 15 interviews to olive oil tasters, trying to describe olive oil appearance in an appropriate way.

For each pair they had to choose one of the descriptors and after that they had to decide if that descriptor describe the oil as “a little”, “moderately” or “very”. For example, an oil can be described as: *moderately aromatic, a little bitter, very rancid, moderately unhealthy, very dislike, very artificial, a little tasty and very textured*. Each one of the samples was shown to each observer 3 times, in the same conditions as it was measured by the spectroradiometer, following a random order. A total of 1080 judgements were made (20observers ×18 samples×3 replicas).

Torgerson’s law of Cathegorical Judgement was applied to the mean of the answers of the observers. This law allow us to create psycophysical scales where each *z* score means the intensity in which a stimulus is percieved inside that emotional scale.

3. RESULTS AND DISCUSSION

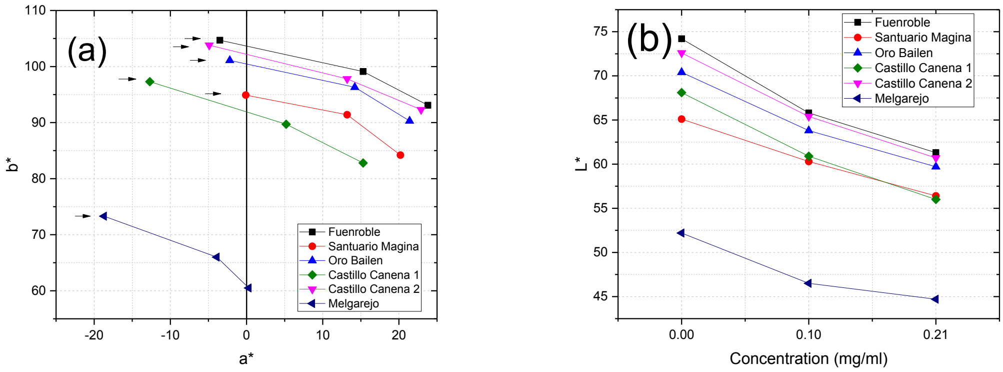

*Figure 2: Colour coordinates of the samples changing the concentration of microalgae extract. (a) Plane a*b* (black arrow indicates direction of color change when extract concentration is increased). (b) Lightness dependence with concentration.*

Figure 2 shows results corresponding to colour measurements. In figure 2 we can see that adding lutein and ß-carotene produced a decrease of lightness L^* and b^* coordinates and an increase of a^* coordinate. In Table 1 we have summarized colour change of the oils from pure extra-virgin olive oil to oils with the 2 concentrations of microalgae extract. Second and third columns in Table 1 indicate a high colour change, clearly perceptible by human observers with normal coclor vision. Last column indicates that the colour change is mainly due to a hue change. Combining data from Figure 2 and Table 1 we can conclude that enriching the oils with lutein and ß-carotene extract makes the oils become more reddish and darker. All the oils except Melgarejo (the greenest oil) undergo a color change from yellow to yellowish-orange hues.

Table 1: Mean colour change from pure extra-virgin olive oils in CIELAB and CIEDE2000 units. Three last columns show percentage of change in Lightness, Chroma and Hue in CIELAB units.

Change	ΔE_{00}	ΔE_{ab}	$\%\Delta L^*$	$\%\Delta C^*_{ab}$	$\%\Delta H^*_{ab}$
From 0.00 mg/ml to 0.10 mg/ml	10.5	18.8	12.4	10.7	76.9
From 0.00 mg/ml to 0.21 mg/ml	16.4	29.2	13.2	15.3	71.6

Results from visual experiment are summarized in Table 2. In this table we have correlation coefficents between *z* scores of different emotions. We can see that there are a high correlation between Fresh-Rancid, Healthy-Unhealthy, Like-Dislike, Natural-Artificial and Tasty-Insipid. That means that when an oil is perceived as Fresh it is perceived also as Healthy, Natural and it likes. This result agrees with the meaning of these descriptors, all of them are related with preferences and can be interpreted as like-dislike. The remaining emotions are descriptors that are related with taste and smell but for observers who are not olive oils experts they do not give a value of preference to the oil.

Table 2: Correlation coefficient (r^2) of z scores obtained from colour emotion experiment. Yellow cells show correlation coefficients greater than 0.8.

	Aromatic Odourless	**Bitter Sweet**	**Fresh Rancid**	**Healthy Unhealthy**	**Like Dislike**	**Natural Artificial**	**Spicy Non spicy**	**Tasty Insipid**
Bitter Sweet	0.02							
Fresh Rancid	0.68	0.06						
Healthy Unhealthy	0.73	0.05	0.98					
Like Dislike	0.71	0.04	0.96	0.98				
Natural Artificial	0.73	0.03	0.98	0.99	0.98			
Spicy Non Spicy	0.00	0.66	0.19	0.19	0.16	0.16		
Tasty Insipid	0.87	0.00	0.83	0.87	0.86	0.86	0.05	
Textured Smooth	0.05	0.43	0.43	0.40	0.39	0.39	0.78	0.19

Emotional responses corresponding to the pair of emotions Like-Dislike are plotted in Figure 3, in left axis we can check the z-score and in right axis we can see the linguistical meaning of the z-scores . The oils are percieved as less liked when the concentration of microalgae additive increases for most of the samples, and this trend is very similar for the emotions well correlated with Like-Dislike. If we add an additive that makes the oil more reddish, the olive oil is percieved as less natural and it does not like. There is only one exception, the oil Melgarejo follows an opposite trend to the other samples: when the concentration of lutein and ß-carotene increases, the emotion “like” increases. The explanation to this behaviour can be explained with colour measurements (figure 2). This sample is the only one in which its colour goes from a greenish colour to a yellower and the rest of the samples go towards a reddish colour.

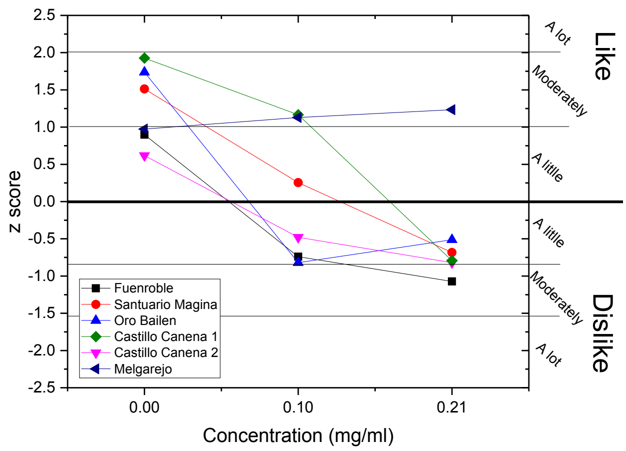

Figure 3: Emotional responses for each sample in scale Like-Dislike. Right axis and horizontal lines shows the linguistic term associated to each z score.

4. CONCLUSIONS

Colour measurements show that adding lutein and ß-carotene enriched extract from microalga Scenedesmus almeriensis to extra virgin olive oils produces a change in colour of the oils. That makes them decrease slightly in their chroma and lightness, and produces a high decrease from greenish or yellow to reddish. The obtained colour differences are far from a just-noticeable colour difference, the change in colour being clearly perceptible by human eye.

From the studied descriptors by a colour-emotion experiment some of them are highly correlated. The meaning of these emotions can be related to the terms Like-Dislike. From the 6 studied oils there is only one that is liked more when we add extract from microalgae, because it changes from green to yellow.

ACKNOWLEDGEMENTS

Research Project FIS2013-40661-P, Ministry of Economy and Competeteviness (Spain), with European Regional Development Fund (ERDF).

REFERENCES

Limón, P., Malheiro R., Casal S., Acién-Fernández, F.G., Fernández-Sevilla, J.M., Rodrigues, N., Cruz, R. Bermejo R., and J.A. Pereira. 2015. Improvement of stability and carotenoids fraction of virgin olive oils by addition of microalgae scenedesmus almeriensis extracts. *Food Chemistry* 175 (0) (5/15): 203-11.

Ou, L.C., Luo M.R., Woodcock A., and A. Wright. 2004. A study of colour emotion and colour preference. part I: Colour emotions for single colours. *Color Research & Application* 29 (3): 232-40.

Teikari, J. M., Rautalahti, M., Haukka, J., Jarvinen, P., Hartman, A. M., Virtamo, J., Albanes, D., and O. Heinonen. 1998. Incidence of cataract operations in finnish male smokers unaffected by alpha tocopherol or beta carotene supplements. *Journal of Epidemiology and Community Health* 52 (7) (Jul): 468-72.

Wei, S.T., Ou, L. C., Luo, M. R., and J. B. Hutchings. 2014. Package design: Colour harmony and consumer expectations. *International Journal of Design* 8 (1): 109-26.

Zellner, D. A., and P. Durlach. 2003. Effect of color on expected and experienced refreshment, intensity, and liking of beverages. *American Journal of Psychology* 116 (4): 633-47.

Address: Luis Gómez-Robledo, Department Optics, Faculty of Sciences,
University of Granada, Severo Ochoa s/n, 18170 Granada, SPAIN
E-mails: luisgrobledo@ugr.es, pidilv@gmail.com, rbermejo@ujaen.es, mmelgosa@ugr.es

A Study on Difference in Color Sensibility Judgment between Professionals & Non-Professionals

Younjin Lee
Senior researcher, Ewha Color Design Research Institute

ABSTRACT

This study conducted a subjective evaluation experiment on 35 kinds of single colors on 43 sensibility adjective scales to compare the contribution of hue and tone to color sensibility judgment in both professionals and non-professionals. As a result, it showed that professionals had higher acuity for color sensibility than non-professionals and it was not hue but tone that made greater contribution to color sensibility judgment. Besides, it was identified that professionals held dominance over non-professionals in such a tendency, corresponding to findings of precedent studies suggestive of stronger contribution of tone than hue.

1. INTRODUCTION

There are 3 basic attributes of color as criteria for feeling and judging color sensibility, in other words, hue, value and chroma. It may be expressed as a three-dimensional color system of hue × value × chroma, particularly as the Hue & Tone system that is defined as a 2-dimensional hue × tone through combining value and chroma as the tone. As such, separating value and chroma from hue results from the fact that value or chroma is more effective and easier to feel and express a variety of color sensibilities than hue.

There are many comparative analytic studies on the color image and sensibility that separated hue from tone. Reports mention cases of inducing color image or sensibility both by hue and by tone but many raise an opinion that tone makes a dominant contribution over hue (Suk & Irtel 2010, Lee, Sa & Chung 2012). On the other hand, according to the research by Suzuki & Nakatani (1990) suggesting that there is a difference in response to hue and tone among certain groups, practitioners in art and design fields showed a difference in the structural factor for color sensibility since they were good at rousing various kinds of sensibilities by colors compared with general people, reacting to tone more strongly rather than hue.

Considering such points above, setting people as two groups, professionals and non-professionals based on the number of experiences in art, color and design fields, this study aimed at examining about what contribution hue and tone make to color sensibility through the inter-group comparison in terms of their difference and commonness.

2. METHOD

2.1 Evaluation scales

As for the evaluation scales, this study organized 43 monopolar scales as 7-step each using sensibility adjectives systemically selected from the previous study (Lee, Lee & Kim 2012). Table. 1 shows 43 sensibility words extracted from the cluster analysis in the precedent study.

2.2 Subjects

48 subjects participated in the evaluative experiment, composed of 30 female non-professionals (10 persons in their 20s, 30s, 40s respectively) and 18 professionals (9 in their 20s, 6 in their 30s, 3 in their 40s). As for the criterion dividing subjects into both groups, persons who are engaged in color & design business or studies as a major were classified into a professional group and non-majors into a non-professional group. The entire 48 subjects had a normal color perception ability.

Table 1: 43 sensibility words extracted from cluster analysis.

Words extracted from cluster analysis			
mild	exotic	natural	masculine
cool	strong	stylish	luxurious
soft	unique	elegant	charming
pure	sturdy	delicate	eco-friendly
cute	cheery	dynamic	traditional
neat	lovely	hopeful	interesting
deep	casual	classic	high-tech
retro	mature	cheerful	mysterious
light	simple	romantic	sophisticated
clean	sensual	modern	unconventional
bright	modest	emotional	

2.3 Sensibility Evaluation on Single Color

Evaluation scales were created from adjectives (Korean) in Table 1, and subjective assessment experiments were performed using single colors systematically selected from color space. Color stimuli were selected so that a minimum number of stimuli could effectively represent a color space. 35 colors were systematically selected from the PCCS Color System: 6 primary hues and 5 tones for each hue group, and 5 additional achromatic colors. The stimuli were distributed within appropriate range in CIELAB Color Space. Each color stimulus was presented on a medium gray background (L^* = 50) on a LCD monitor. Table 2 shows hue & tone classification for the 35 colors, and CIELAB values obtained from measurement by Minolta CS-1000 Spectroradiometer.

35 colors were randomly presented, and each color was assessed against 43 adjective scales utilizing 7-step evaluation scale. 7-step evaluation scale works as follows: when evaluating against "cold" scale, "7" is checked if coldness was strongly sensed, "1" if no coldness was felt, or "4" for moderate coldness. The viewing distance was 50cm from the monitor, and 10º in visual angle. Each color stimulus was placed at the center of the monitor, and evaluation scales were located beneath. One experiment session took 1 hour 20 minutes including a 5 minute break.

Table 2: Specifications of the 35 color samples.

Sample	Tone	Hue	L^*	a^*	b^*	C^*	h
1	Pale	Red	85.3	5.7	2.7	6.3	26
2		Orange	90.1	3.3	12.6	13.0	75
3		Yellow	90.2	-2.1	16.5	16.6	97
4		Green	85.4	-12.7	6.8	14.4	152
5		Blue	80.5	-1.6	-5.7	5.9	254
6		Purple	80.5	4.2	-3.1	5.2	323
7	Lignt$^+$	Red	77.0	34.7	10.2	36.2	16
8		Orange	85.7	13.9	38.1	40.6	70
9		Yellow	91.6	-1.4	48.7	48.7	92
10		Green	80.0	-22.9	8.6	24.4	159
11		Blue	69.4	1.8	-29.7	29.7	274
12		Purple	71.6	23.4	-16.7	28.8	324
13	Vivid	Red	45.6	60.4	24.4	65.2	22
14		Orange	70.6	42.0	63.7	76.3	57
15		Yellow	83.4	11.0	78.3	79.1	82
16		Green	56.4	-56.7	24.9	61.9	156
17		Blue	45.4	0.5	-44.7	44.7	271
18		Purple	35.4	41.6	-30.7	51.7	324
19	Dark	Red	25.1	28.1	8.1	29.2	16
20		Orange	35.4	14.0	33.3	36.1	67
21		Yellow	40.7	0.7	37.8	37.8	89
22		Green	30.5	-22.1	9.3	24.0	157
23		Blue	20.3	-0.7	-22.2	22.2	268
24		Purple	20.2	19.0	-14.7	24.1	322
25	Grayish	Red	40.7	9.8	3.8	10.5	21
26		Orange	45.8	5.0	11.3	12.4	66
27		Yellow	45.9	-0.7	14.1	14.1	93
28		Green	40.8	-9.9	4.6	11.0	155
29		Blue	35.6	-1.1	-8.7	8.8	263
30		Purple	35.5	8.3	-6.6	10.6	322
31	Achromatic	White	95.1	-0.2	0.3	0.4	124
32		Light Gray	75.7	1.0	-0.6	1.2	329
33		Mid Gray	56.1	-0.1	0.2	0.2	117
34		Dark Gray	35.6	-0.1	0.1	0.1	135
35		Black	15.3	-0.1	0.3	0.3	252

3. RESULTS AND DISCUSSION

3.1 Difference in Emotional Words Used by Among Professionals & Non-Professionals

For professional and non-professional groups, the mean, SD, maximum and minimum values of estimations on 35 colors were calculated for the entire subjects (see Table 3). Differentials of SD, maximum and minimum values show that both groups discerned a color stimulus to some extent. Also, it may be said that professional group has a higher acuity compared with non-professionals since there was remarkably greater standard deviation in professional group.

Table 3: Mean, SD, MAX & MIN for Professionals & Non-Professionals.

	Non-Pro	Pro
Mean	3.70	3.75
SD	0.82	1.20
MAX	5.31	5.98
MIN	2.30	1.91

3.2 Difference Among Professionals & Non-Professionals According to Hue & Tone

This study compared non-professionals with professionals by setting hue and tone as factors for judging color sensibility. In other words, for both groups, it examined whether they are influenced by hue or tone, otherwise by both, what interaction hue and tone have in judging changes of 43 kinds of sensibilities to 35 color stimuli. ANOVA was conducted on 6 (hue) × 5 (tone) × 2 (group) using the mean of color stimulus estimation corresponding to each red, orange, yellow, green, blue, purple hue (6 levels, referred to as a "color factor" hereafter) and that of color stimulus estimation corresponding to each pale, light$^+$, vivid, dark, grayish tone (5 levels, referred to as a "tone factor" hereafter).

Firstly, it showed that hue had no contribution to judging sensibility ($F(5)$= 2.160, *n.s.*). There was no difference in such a tendency between groups (hue×group $F(5)$= 0.673, *n.s.*). On the other hand, this study identified contribution by tone ($F(4)$= 32.794, p < .001). Furthermore, groups differed from each other in such a tendency (tone×group $F(4)$= 3.742, p < .01). Also, it revealed that there existed interaction between hue and tone (hue×tone $F(20)$= 5.485, p < .001), showing no difference between groups (hue×tone×group $F(20)$= 1.053, *n.s.*).

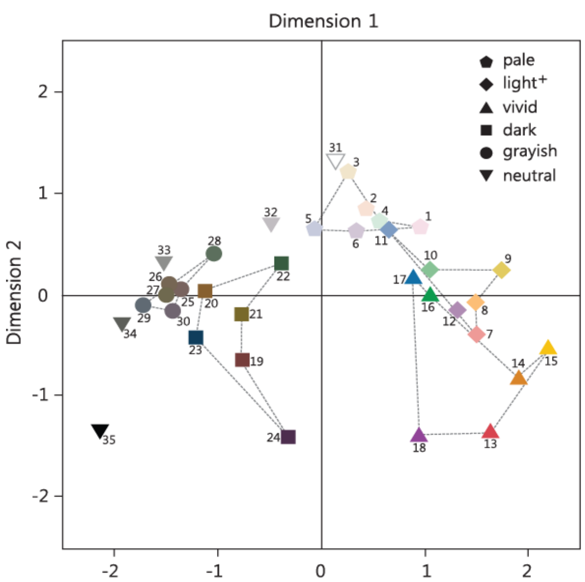

Fig. 1a: MDS plots for non-professionals.

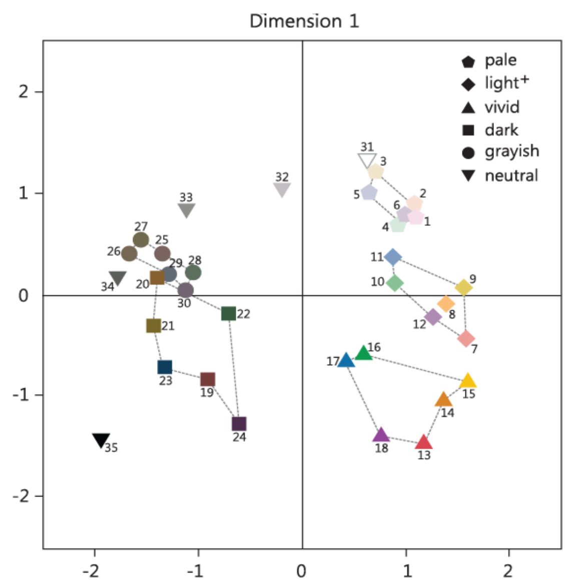

Fig. 1b: MDS plots for professionals.

3.3 Relationship between Color Sensibility Judgment & Tone

Analysis using MDS was conducted to identify what dimension color sensibility judgment has and examine whether professional and non-professional groups have a differed structural dimension based on hue and tone. As shown from a 2-dimensioanl MDS plot in <Fig. 1a>, <Fig. 1b>, research findings showed that there was difference in the distribution of 35 color stimuli between professional and non-professional groups. In <Fig. 1a>, <Fig. 1b>, since similar tones hold together closely in both groups, it showed that objects formed a group by tone rather than by hue and may be interpreted that professional group is more distinct in its degree than non-professionals.

MDS results showed that both professional and non-professional groups formed a dimension of color sensibility judgment based on the tone. Besides, professional group revealed a dimensional structure based on the tone more clearly. Such a result supports ANOVA of the paragraph above that there was difference between both groups by tone factors and suggests that professional group has an advantage in classifying color stimuli by tone through schematization.

4. CONCLUSIONS

In this study, we compared the contribution of hue and tone dimension to color sensibility judgment through subjective evaluation experiment using 43 sensibility adjective scales and 35 single colors, assessing both color professionals and non-professionals. The results were as follows.

Firstly, the color professional group displayed higher acuity for color sensibility judgment than the nonprofessional group, which is attributable to its higher discrimination capability for color stimulus differences and shift in sensibility. Secondly, hue and tone was defined as factors serving as judgment criteria for color sensibility, and their contribution was examined using repeated measures ANOVA. The results revealed that tone was more influential than hue in determining color sensibility, and the amount of its contribution differed between the subject groups. Thirdly, we applied a multidimensional scaling method (MDS) to analyze the structural dimension of color sensibility on hue and tone in both subject groups. The two-dimensional MDS plots in the color professional group revealed the tone dimension much more clearly than the hue dimension, implying a stronger contribution of tone to color sensibility judgment.

REFERENCES

Suk, H.J. and Irtel, H. 2010. *Emotional response to color across media*, Color Research & Application 35(1) 64-77.

Lee, M.S., Sa, J.K. and Chung, K.H 2012. *A comparative analysis of the characteristics and images of costume colors in the traditional plays of Korea, China, and Japan*, Color Research & Application 37(4) 302-312.

Suzuki, N. and Nakatani, M. 1990. *Color-affection, inspired in the hyper-sensitive by a color of the upper part of clothing*, Journal of the Color Science Association of Japan 14(3) 45-57.

Lee, N.K., Lee, Y.J. and Kim, S.J. 2012. *Sensibility factors of single color for product design*, In : Proceedings of 14th Congress of the International Colour Association(AIC).

Address: Dr. Younjin LEE, Ewha Color Design Research Institute,
Ewha Womans University, 52, Ewhayeodae-gil, Seodaemun-gu, Seoul, 120-750, KOREA
E-mails: hacomama@ewha.ac.kr

Age Effects on Garments Color Harmony

Min HUANG,[1] Zeyang LI,[1] Guihua CUI,[2*] Haoxue LIU,[1] M. Ronnier LUO[3]
[1]School of Printing and Packing Engineering, Beijing Institute of Graphic Communication
[2]Physics & Electronic Information Engineering, Wenzhou University
[3]School of Design, University of Leeds

ABSTRACT

In order to investigate the age effects on garments color harmony in two-color combinations, 300 color pairs were generated from 24 colors that uniformly selected from CIELAB color space. 59 observers with normal color vision aging from 20 to 79 were divided into two groups according to their ages: junior (20-45 years), and senior (46-79 years). They were encouraged to assess the garments color harmony of the above-mentioned color pairs presented as jackets and trousers on a vicenarian and a quinquagenarian model. The experiments were carried out on a well-characterized LCD monitor with a method of categorical judgment. The color harmony assessments for different age groups on the garments were analyzed.

1. INTRODUCTION

Color conveys different information in our daily life. Two or more color combinations can invoke different color emotion, preference and harmony (*Ou et al. 2012*). The results have revealed that the abstract colors (i.e. colors without any context or specific object assigned) and the specific colors invoke different results. The influence of the application scenarios on the color harmony is an area worth studying, there are some experiments were conducted for juice packages (*Wei et al. 2013*), fashion design (*Luo et al. 2011)* and interior images (*Ou et al. 2011)*. The culture, gender, age (*Ou et al. 2012)* and character of a person also have influences on her/his color preferences, which may be partly related to specific ageing color-vision changes.

In this study, 300 color pairs were generated from 24 colors uniformly selected in CIELAB color space. 59 observers with normal color vision aging from 20 to 79 were organized to assess the garments color harmony of the above color pairs presented on vicenarian and quinquagenarian models. The experimental results were used to analyze the relationships between the mean harmonious/ disharmonious response for different age groups.

2. METHOD

24 colors were chosen to be exhibited on a vicenarian and a quinquagenarian model. It is worth mentioning that some of these colors could not be reproduced on real garments due to the limitation of textile dyestuffs and color gamut actually available. However, they remained in the study considering for the theoretical research. Figure 1 shows the distribution of 24 color centers in the CIELAB $a^*_{10}b^*_{10}$ and $L^*_{10}C^*_{10,\mathrm{ab}}$ planes. It can be seen that these color centers had a good coverage in CIELAB space.

300 color pairs were generated from two-color combinations of the 24 colors as shown in Figure 1. For example, the 1st color was set as the jackets and the 1st, 2nd, 3rd…24th color were arranged as the trousers, respectively, and so on. Considering in daily life, the color combinations for female garments are much more concern than that for the male's and with regards of the experimental workload, only two female models, a vicenarian and a quinquagenarian, were selected as the tested models (see Figure 2). The color stimuli were shown on the screen as garments in irregular patterns and different sizes. The ratios of jackets' to trousers' areas measured in terms of pixels were 69% and 216% for the vicenarian and quinquagenarian model, respectively.

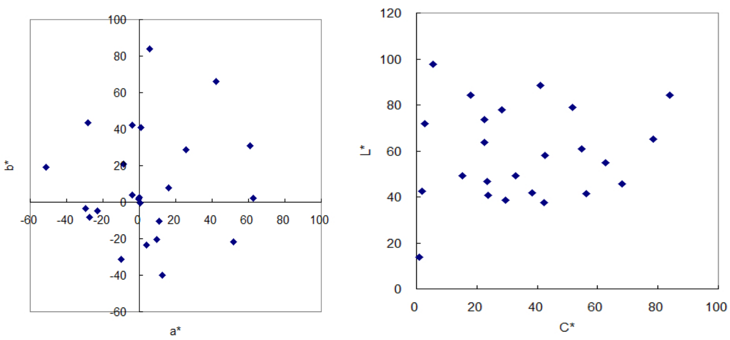

(a) (b)

Figure.1: Distribution of colors selected for the current experiment of garments color harmony in the CIELAB (a) $a^*_{10}b^*_{10}$ and (b) $L^*_{10}C^*_{10,ab}$.

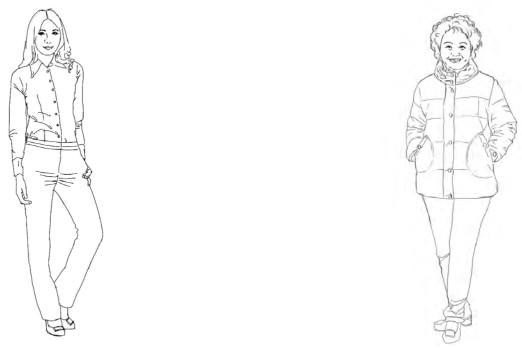

(a) (b)

Figure. 2. Models for the (a) vicenarian and (b) quinquagenarian used in the experiment.

The psychological method used in the experiments by Ou (*Ou et al. 2012*) and Szabó (*Szabó et al. 2010*) has been adopted in the current study as shown in Fig. 3. The background of the monitor and images were set to a gray with L^*, a^*, b^* of 80.78, 1.22, -1.29. In the experiment, each assessment includes 630 judgments for the two models (30 reduplicative for each model) and was divided into six sessions, each including 105 images displayed on the screen of an EIZO CG19 monitor. The approximate duration of each session is about 30 minutes, no time limit for each session. The images presented to the observers were in a random order. 59 Chinese observers (26 female and 33 male) with normal color vision were organized to assess color harmony of the garments. They were divided into two age groups: junior group (31 persons with an average age of 31.0 from 20 to 45) and senior group (28 persons with an average age of 59.7 from 46 to 79), 15 observers replicated the assessments of the 630 images 2-4 times for evaluation of the intra-observer variability. Finally, there are 42 and 40 sets of assessments were gathered for the junior and senior group, respectively. The total number of visual assessments is 630× 82=51660. The intra-observer and inter-observer variability were determined by averaging the root mean square error (*RMSE*) (*Ou et al. 2012*) between each individual data and the overall mean. As a result, the average intra-observer variability was 0.89 and the average inter-observer variability was 2.06.

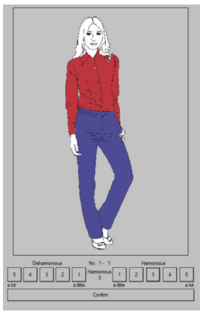

Figure. 3. The experimental layout of the color harmony evaluation

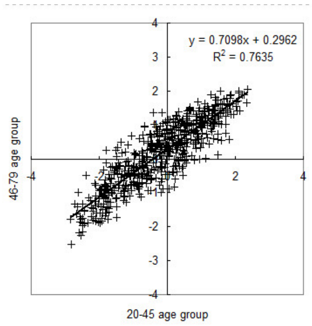

Figure. 4. Observers' responses to garments color harmony of 2 age groups

3. RESULTS AND DISCUSSION

Comparisons were made between observers' responses of different ages for 600 garments color harmony presented on the vicenarian and quinquagenarian models using scatter diagram; the mean scale values for the junior were plotted against that for the senior group (see Figure. 4). Positive and negative numbers mean "harmonious" or "disharmonious", respectively. This indicated that as one ages, although the observers' aesthetical standards for judging garments color harmony have been varied and show some different trends, the junior observers are more "extremes" than the senior observers in their harmonious.

The harmony scores for the 600 garments by the 2 age groups were ranked, the most harmonious and disharmonious garments were shown in Figure.5. For the 2 age groups, the most harmonious garments almost appeared at the vicenarian model and the most disharmonious garments appeared at the quinquagenarian model. Figure.5a and 5b indicated that the less colorful and the cool (green, blue and purple) colors for the jackets, the colors similar to neutral colors for the trousers were easy to arouse harmonious sense. Figure.5c and 5d indicated that the garments with the higher chroma were easy to arouse disharmonious sense, which is not accord with Luo *et al*'s fashion design experimental results (*Luo et al. 2011)* while have some trends with their uniform color patch results *(Ou et al. 2011).*

4. CONCLUSIONS

For the same two-color combinations on the garments, all the observers had higher scores to the 300 garments for the vicenarian model than those for the quinquagenarian model. The senior group was more tolerant than the junior group, especially for the harmony assessments of the quinquagenarian model. The model/style and age both have significant influence on the aesthetical standard of garments color harmony.

(a) the most harmonious judged by the junior group

(b) the most harmonious judged by the senior group

(c) the most disharmonious judged by the junior group

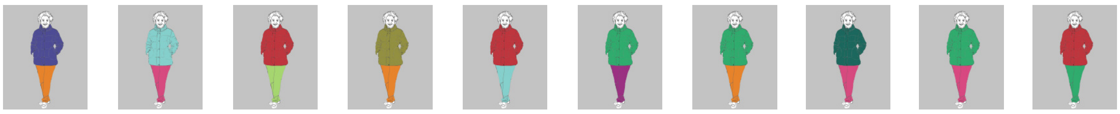

(d) the most disharmonious judged by the senior group

Figure. 5. The most harmonious and disharmonious garments for the 2 age groups

ACKNOWLEDGEMENTS

This research was supported by National Natural Science Foundation of China (grant 61308081), the Top Young Talents (CIT&TCD201404127) and Young Talents of Beijing Municipal Commission of Education (YETP1465)

REFERENCES

Luo M. R., and L. Ou, 2011. Colour harmony for fashion design. In Proceedings of AIC midterm meeting: Interaction of Colour & Light in the Arts and sciences, pp540-543.

Ou L., P. Chong, M. R. Luo, C. Minchew, 2011. Additivity of Colour Harmony. *Color Research & Application* 36:355-372.

Ou L., M. R. Luo, P. Sun, etc, 2012. Age Effects on Colour Emotion, Preference, and Harmony. *Color Research & Application* 37:92-105.

Szabó F., P. Bodrogi, J. Schanda, 2010. Experimental Modeling of Colour Harmony. *Color Research & Application* 35:34-49.

Wei S., L. Ou, M. R. Luo, J. Hutchings, 2013. Psychophysical models of consumer expectations and colour harmony in the context of juice packaging. *Color Research & Application* DOI: 10.1002/col.21867

Address: Prof. Guihua Cui, School of Physics & Electronic Information Engineering, Wenzhou University, Wenzhou, Zhejiang, 325035, China

E-mails: guihua.cui@gmail.com, huangmin@bigc.edu.cn, 347034425@qq.com, liuhaoxue@bigc.edu.cn, m.r.luo@leeds.ac.uk

Effects of Color and Aroma of Roasted Tea on the Predicted Taste and Palatability

Atsushi HARUTA,[1] Kosuke Asano, [1] Akihisa TAKEMURA,[1]
Shino OKUDA,[2] and Katsunori OKAJIMA [3]
[1] Faculty of Science and Engineering, Setsunan University
[2] Faculty of Human Life and Science, Doshisha Women's College of Liberal Arts
[3] Faculty of Environment and Information Sciences, Yokohama National University

ABSTRACT

We can predict the taste of tea by the appearance and the flavor without drinking. Thus it is useful to reveal the multimodal effect of color and aroma on the predicted taste and palatability of tea quantitatively. In the present study, we focused on the roasted tea, because it is one of the most popular tea in Japan and has typical roasted flavor. Visual stimuli and olfactory stimuli: four roasted tea samples those were brewed two hours from 2, 6, 18 and 36 grams of tea leaves (a tea bag) and one liter of water, were evaluated by twenty participants in their twenties. The experiment consisted of three sessions. First, participants observed a visual stimulus without any olfactory stimulus (visual evaluation). Next, they smelled one olfactory stimulus without any visual stimulus (olfactory evaluation). Finally, they observed one of the visual stimuli while smelling one of the olfactory stimuli (visual-olfactory evaluation). Evaluated items were "intensity of color and aroma", "predicted sweetness, bitterness, umami taste, deep flavor, roasted flavor", and "predicted palatability". It was revealed that not only color but also aroma of roasted tea effected on the predicted taste and palatability. Moreover, we tested whether the visual-olfactory evaluation (Z) can be explained the sum of the visual evaluation (X) and the olfactory evaluation (Y) with weighting factors as the formula "$Z = aX + bY$". The results show that weighting factors of "predicted palatability" are (a, b) = (0.36, 0.41). Finally, we compared weighting factors of roasted tea and those of green tea which were calculated in our previous study, and found that olfactory weighting factor of "predicted palatability" in the case of roasted tea is slightly larger than that in the case of green tea ((a, b) = (0.51,0.49)).

1. INTRODUCTION

Before drinking tea, the appearance and the flavor must be very important cues. Therefore, it is quite meaningful to reveal the relation between the appearance and the flavor in predicting the taste and palatability of tea before drinking tea. A previous study (Okuda et al., 2013) reported the effect of visual and olfactory "predicted palatability" on multi-sensory evaluation in the case of green tea. Under the condition without the trial to drink, there are few previous researches about the psychological evaluation of drinks. Okuda revealed the effect of visual and olfactory "predicted palatability" on multi-sensory evaluation are nearly equal in the case of evaluation of green tea (Okuda 2013). Roasted tea is also one of the most popular tea in Japan, with characteristic flavor in the roasted process. Thus it is expected the tendency of evaluation in roasted tea is different from the case of green tea. In this study, it was revealed the effect of mono-sensory (visual and olfactory) "predicted tastes and palatability" on multi-sensory evaluation.

2. METHOD

2.1 Visual and Olfactory Stimuli

Visual stimuli and olfactory stimuli were four roasted tea samples those were brewed two hours from two, six, eighteen and thirty six grams of tea leaves (packs of tea bag) and one liter of water. As visual stimulus, each two hundred milliliters tea was poured into a glass, which was six centimeters in diameter, eleven centimeters tall. As olfactory stimulus, each ten milliliters tea was packed in a fifteen milliliters brown bottle (Figure 1).

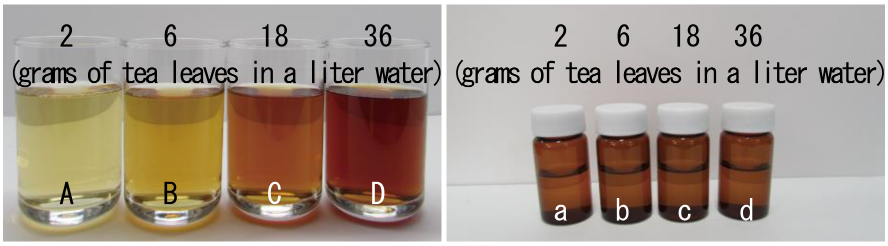

Figure 1: Visual stimuli and olfactory stimuli (roasted tea).

2.2 Procedure

The above stimuli were evaluated by twenty participants (eight women and twelve men) in their twenties. The experiment consisted of three sessions. First, participants observed a visual stimulus without showing any olfactory stimulus (visual evaluation). Next, they smelled one olfactory stimulus without showing any visual stimulus (olfactory evaluation). Finally, they observed one of the visual stimuli while smelling one of the olfactory stimuli (visual-olfactory evaluation). Presentations of stimuli were conducted in the experimental booths (Figure 2). Each booth had a desk and a fluorescent lamp of the standard illuminant D65 on the ceiling. The inside walls and the desk were white (N9). The illuminance of the center of the desk was three hundred lx.

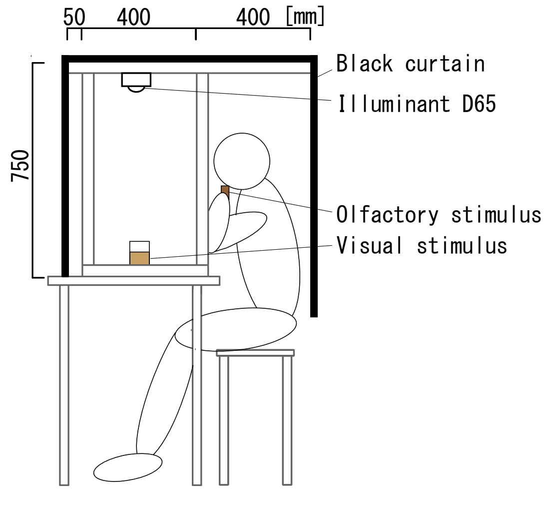

Figure 2:Experimental booth (cross-section view).

Participants evaluated about "intensity of color and aroma" and "predicted tastes (sweetness, bitterness, umami taste, deep flavor, roasted flavor)" on numerical scales of zero to ten, and "predicted palatability" on a categorical scale from ‘very palatable’ to ‘very unpalatable’. Participants were received proper rewards.

3. RESULTS AND DISCUSSION

Figure 3 shows the mean evaluations about "Predicted tastes (sweetness, bitterness, umami-flavor, roasted-flavor and deep-flavor)" and "Intensity of color" in the visual-olfactory experiment. As the color of tea was deep, all evaluations were high except for "sweetness". It may be difficult to evaluate "Sweetness" of tea by only the color. As the aroma of tea was strong, all evaluations were also high, however, the differences between ‘c’ and ’d’were small. In the stimuli combination those were well-matched visually and olfactory, the visual-olfactory evaluations were close to the visual evaluations, as compared among the visual-olfactory evaluations and the visual evaluation.

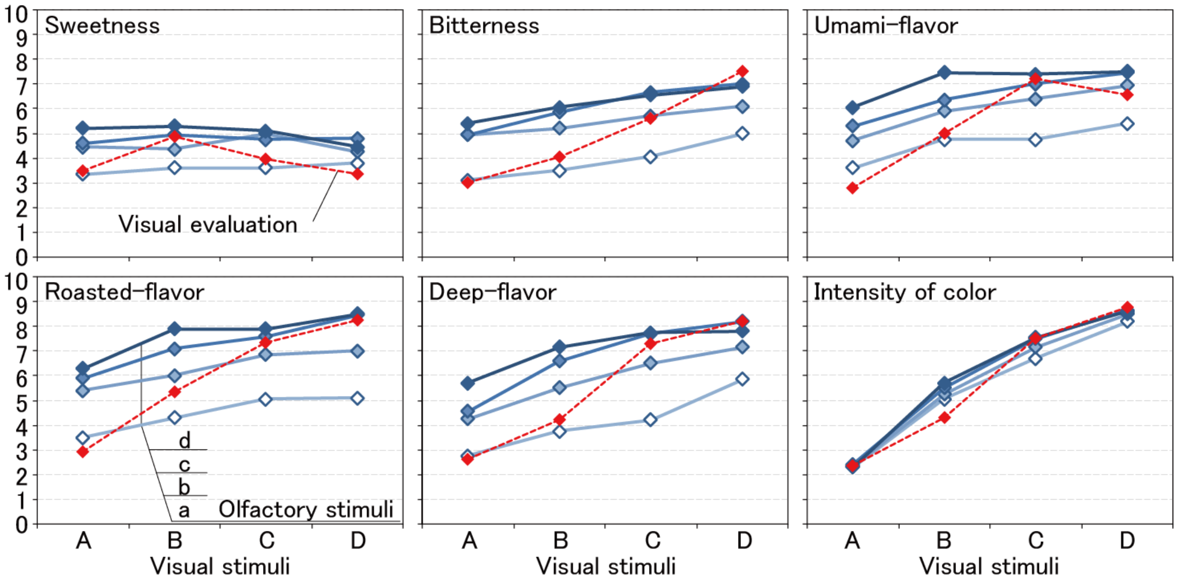

Figure 1. Comparison ’Predicted tastes’ and ‘Intensity of color’ between in the visual-olfactory evaluation and visual experiment.

Figure 4 shows the mean evaluations about "Predicted palatabiluty" in the visual-olfactory experiment. The highest palatability was obtained at ‘C’ stimuli, instead of ‘D’ in the visual stimuli. In the olfactory stimuli, stronger aroma was palatable. As compared among the visual-olfactory evaluations and the visual evaluation, those were close evaluations in the stimuli ‘A’ and ‘D’. However, in the stimulus ‘C’, the visual evaluation was higher than all visual-olfactory evaluations.

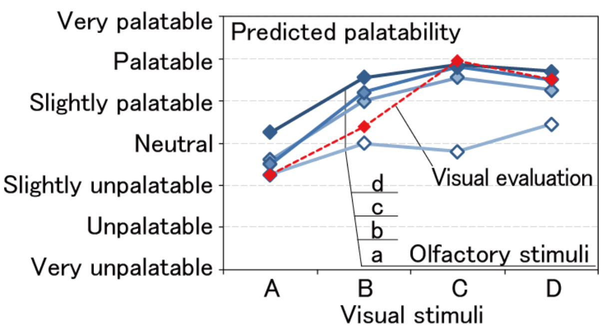

Figure 2. Comparison ’Predicted palatability’ between in the visual-olfactory evaluation and visual experiment.

It was proposed that mono-sensory evaluations, those were the visual evaluation and the olfactory evaluation, decided to the multi-sensory evaluation as below (equation (1)).

$Z = \alpha X + \beta Y$ *equation. (1)*

X : evaluation values in the visual experiment

Y : evaluation values in the olfactory experiment

Z : evaluation values in the visual-olfactory experiment

α : contribution ratios of vision

β : contribution ratios of olfaction

Evaluation values (X , Y and Z) were assigned in the equation (1), and contribution ratios α and β were calculated by the least square method (Table 1).

Table 1. Contribution ratios of vision and olfaction in the case of roasted tea.

Evaluation item	α	β	r	α : β
Sweetness	0.15	0.56	0.84	1 : 3.73
Bitterness	0.31	0.57	0.97	1 : 1.84
Umami-flavor	0.38	0.61	0.96	1 : 1.61
Roasted-flavor	0.34	0.71	0.98	1 : 2.09
Deep-flavor	0.44	0.55	0.97	1 : 1.25
Predicted palatability	0.36	0.41	0.90	1 : 1.14

In all evaluation items, high correlation coefficients (‘ r ’) between evaluated ‘ Z ’, and calculated ‘ Z ’ by deciding ‘ α ’ and ‘ β ’ were obtained. It was cleared ‘ β ’ was larger than ‘ α ’ in all evaluation items. This indicates that the olfactory evaluation of roasted tea might have larger effect on the multi-sensory evaluation than the visual evaluation.

Contribution ratios in green tea stimuli (Okuda et al.,2013) were shown in Table 2. Comparing between Table 1 and Table 2, the magnitude relation between ‘ α ’ and ‘ β ’ was almost close except for in "predicted palatability". The contribution ratio might be different between the species of tea leaves, or the matured stages.

*Table 2. Contribution ratios of vision and olfaction in the case of green tea (*Okuda 2013*).*

Evaluation item	α	β	r	α : β
Sweetness	0.26	0.74	0.53	1 : 2.91
Bitterness	0.24	0.78	0.98	1 : 3.31
Roasted-flavor	0.25	0.75	0.96	1 : 2.98
Deep-flavor	0.39	0.62	0.98	1 : 1.59
Predicted palatability	0.51	0.49	0.91	1 : 0.96

4. CONCLUSIONS

We revealed contribution ratios of vision and olfaction cues to multi-sensory "predicted tastes" and "palatability" evaluations. Moreover, we compared contribution ratios in roasted tea and green tea stimuli, and found that they are almost similar except for "predicted palatability".

REFERENCE

S. Okuda, A. Takemura and K. Okajima 2013. *Effect of color and odor of green tea on expected taste*, Japanese Journal of Sensory Evaluation 17(1) 62. (In Japanese)

Address: Assistant Prof. Akihisa TAKEMURA,
Department of Living and Environmental Design,
Faculty of Science and Engineering, Setsunan University,
17-8 Ikedanaka-machi, Neyagawa City, Osaka, 572-8508, JAPAN
E-mails: a-takemu@led.setsunan.ac.jp, sokuda@dwc.doshisha.ac.jp, okajima@ynu.ac.jp

A study of relationship between physical value and psychological value in PCCS

Tadayuki WAKATA & Miho SAITO
Faculty of Human Sciences, Waseda University

ABSTRACT

The purpose of this study is to examine the effect of psychological Lightness and Saturation on color image by analyzing its tone. This study adopted two methods. First, we investigated the dimensions of the color image; second, we measured the psychological Lightness and Saturation of color. Further, we examined the relation between the dimensions of color image and psychological Lightness and Saturation using a Structural Equation Modelling(SEM). As a result, the correlation relationship was observed between factor scores and physical values. Furthermore, psychological Lightness and Saturation were integrated, their relationship with the dimensions of color image. SEM was performed to investigate these results, and consequently, the relational model of physical value and psychological value was constructed.

1. INTRODUCTION

In colorimetry, color is classified on the basis of three attributes: hue, value, and chroma. These are physically independent, and many color order systems have adopted them; for example, the Munsell system. However, these attributes are not psychologically independent. For instance, in the Helmholtz-Kohlrausch effect, it was observed that lightness perception is affected by chroma. Therefore, it indicates a psychological interaction between value and chroma. Practical Color Co-ordinate System (PCCS) is a color order system developed in Japan, and it comprises three attributes: Hue, Lightness (value), and Saturation (chroma). Moreover, PCCS is characterized by the tone, which is a combination of Lightness and Saturation. Many studies have included three or four dimensions of color image. Our previous study by factor analysis identified two dimensions of color: activity and potency. These factors corresponded with the physical value of color, i.e., potency of Lightness and activity of Saturation in PCCS.

The purpose of this study is to examine the effect of psychological Lightness and Saturation on color image by analyzing its tone.

2. METHOD

This study adopted two methods. First, we investigated the dimensions of the color image; second, we measured the psychological Lightness and Saturation of color.

2.1 Stimuli

The stimuli used were 12 tones (vivid, bright, strong, deep, light, soft, dull, dark, pale, light grayish, grayish, and dark grayish), five hues (2R, 8Y, 12G, 18B, 22P), and five achromatic colors. These were classified into four types. 1) Tone stimuli, with each tone consisting of five hues arranged in a circle, in which the color chip was 3 × 3 cm and the mount was 12 × 12 cm(Fig1); 2) hue stimuli, with each hue consisting of 12 tones arranged in a row, in which the color chip was 3 ×1.5cm and the mount was 5 × 21 cm(Fig2); 3) Gray scale, with five achromatic color steps arranged in a row, in which the color chip was 3 ×1.5cm and the mount was 5 × 10.5 cm(Fig3) ; and 4) single color stimuli in which the color chip was 3 ×3 cm and the mount was 10 × 10 cm(Fig4), with each color being pasted on a neutral gray mount.

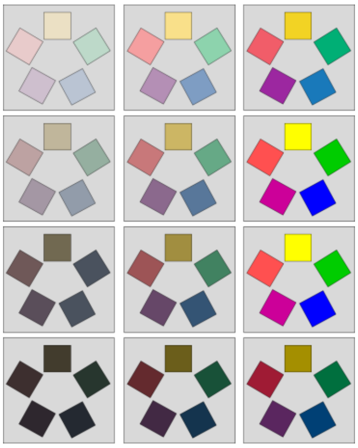

Fig1. Tone stimuli
(There are 12 in total)

Fig2. Hue stimuli
(There are 5 in total)

Fig3. Gray scale

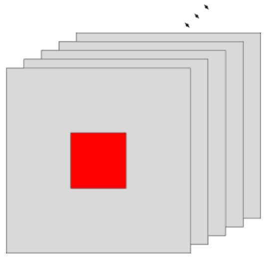

Fig4. single color Stimuli
(there are 65 in total)

2.2 Questionnaire

Two questionnaire type scales were used. First, the semantic differential method (SD method) was used to investigate color image dimensions. Then, the visual analog scale (VAS) was used to measure psychological color lightness and saturation. The SD method had 15 adjective-pair words(beautiful-ugly, clear-muddy, bright-dark, dull-sharp, cheerful-gloomy, loud-quiet, dynamic-static, strained-loosen, light-heavy, gaudy-subdued, soft-hard, blurred-distinctly, warm-cool, preferable-hateful, plain-rich), and had a seven-point scale. The VAS had two adjective pair words(bright-dark and vivid-dull). The questionnaire was presented on an iPad.

2.2 Experimental Procedure

There were 30 participants (8 male and 22 female, average age 21.6 ± 2.0 years) in this experiment. The experiment was conducted in a university classroom under fluorescent light. The participants were divided into four groups, and each group was presented with a different stimuli order and a different adjective pair word order. The subjects were required to look at each color and answer the questionnaire.

3. RESULTS AND DISCUSSION

3.1 Factor analysis

A factor analysis was used to evaluate the results of the SD method. The result of the factor analysis (Maximum likelihood method, *Promax* rotation) revealed four factors (Table1). The factor loadings differ from Osgood's factors(Osgood et.al.: 1964) and

Oyama's factors(Oyama et.al.: 1965). The first factor was Activity. Evaluation and Potency were intermingled in the second factor. The third factor and fourth factors were symbolized imageries, such as shade, and they were based on a combination of stimuli. Furthermore, this tendency was observed in Wakata and Saito (2012). Table2 shows a correlation relationship between factors scores; for example, the correlation between factor 1 and factor 2 (r = .684). The factor analysis showed that the dimensions of color images are not independent.

3.2 Correlation

The correlation coefficients between the VAS value (Lightness and Saturation) and factor scores were calculated (Table3). As a result, a correlation relationship was observed between the Lightness and Saturation(r= .723); it suggested that psychological Lightness and Saturation depend on each other. This result was consistent with the Helmholtz-Kohlrausch effect. Relationships were observed between the VAS values and the factor scores; for example, the relationship between the Saturation (VAS) and factor 1 (r = .896), and the Lightness (VAS) and factor 2 (r = .896). Factor1 is Activity and Factor2 is Potency and Evaluation. The correlation coefficients suggested that the dimensions of color images correspond to psychological values.

3.1 Structural Equation Modelling

The result of the factor analysis and correlation coefficients showed a relationship between the physical value and psychological value in terms of the dimensions of color images. Next, the model of this relationship was built using Structural Equation Modelling (SEM). The model consisted of mainly two parts: first, a factor analysis model of the color images obtained through the SD method (it was based on the resulting *3.1factor analysis* of factor 1 and factor 2). Second, a factor analysis model of psychological Lightness and Saturation was obtained by the VAS. Furthermore, the VAS factor affected the factors of the color image. The result was shown by a path diagram(Fig5). The coefficients were used in standardized values. The following fit parameters were used: Comparative Fit Index (CFI), Goodness of Fit Index (GFI), and Root Mean Square Error of Approximation (RMSEA). As a result, CFI and GFI were high, but RSMEA was observed to be p = 0.099. This

Table1. Factor lodgings (Factor Analysis)

			Fac1	Fac2	Fac3	Fac4
dynamic	-	static	1. 002	-. 247	. 082	-. 066
loud	-	quiet	. 980	-. 310	. 130	-. 040
warm	-	cool	. 649	. 131	-. 378	-. 270
gaudy	-	subdued	. 613	. 346	. 056	-. 078
cheerful	-	gloomy	. 528	. 359	-. 051	. 035
preferable	-	hateful	-. 272	1. 028	. 011	-. 192
beautiful	-	ugly	-. 163	1. 007	. 017	-. 071
clear	-	muddy	. 001	. 622	. 182	. 271
bright	-	dark	. 405	. 477	-. 164	. 078
soft	-	hard	. 115	. 097	-. 672	. 176
strained	-	loosen	. 072	. 042	. 616	-. 050
blurred	-	distinctly	. 315	. 254	. 572	-. 098
dull	-	sharp	. 353	. 169	. 415	. 202
plain	-	rich	-. 247	-. 133	-. 148	. 789
light	-	heavy	. 229	. 156	-. 344	. 451

Maximum likelihood method, *Promax* rotation

Table2. Correlation matrix (between factors)

	Fac1	Fac2	Fac3	Fac4
Fac1	1. 000	. 684	. 082	. 400
Fac2	. 684	1. 000	-. 060	. 573
Fac3	. 082	-. 060	1. 000	-. 273
Fac4	. 400	. 573	-. 273	1. 000

Table3. Correlation matrix (between VAS values and factors scores)

	(VAS) Saturation	(VAS) Lightness	Fac1	Fac2	Fac3	Fac4
Saturation (VAS)	1. 000	. 723	. 896	. 852	. 324	. 424
Lightness (VAS)	. 723	1. 000	. 825	. 896	-. 292	. 773
Fac1	. 896	. 825	1. 000	. 876	. 023	. 557
Fac2	. 852	. 896	. 876	1. 000	-. 157	. 795
Fac3	. 324	-. 292	. 023	-. 157	1. 000	-. 612
Fac4	. 424	. 773	. 557	. 795	-. 612	1. 000

model was adopted from the aforementioned parameters. The factor of psychological value showed that the factor influence of Saturation (.973) was greater than that of Lightness (.631). The emergence of this factor depended on Saturation. Therefore, We consider that Japanese「明るい:akarui」is included in「あざやか:azayaka」. Furthermore, the factors of the color image showed a correlation relationship (r =.729). PCCS defines Saturation as a psychological value; Lightness was also similarly defined. This is considered to be related to the structure of this model.

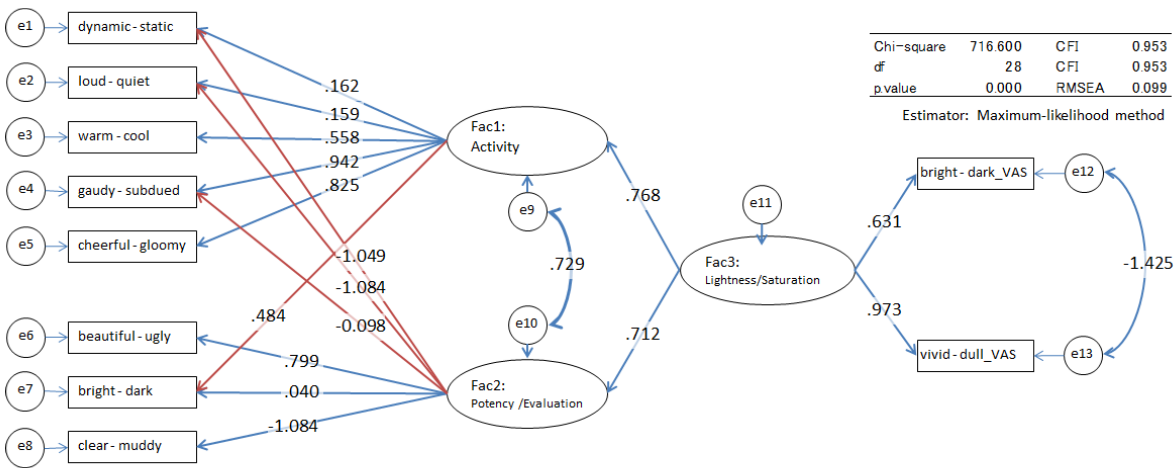

Fig5. Path diagram (SEM)

4. CONCLUSIONS

This study showed that psychological Lightness and Saturation were not independent and suggested the existence of a high level concept common to both variables. Through the use of this concept, a definition for the correspondence between the physical value and psychological value has been achieved.

REFERENCES

Osgood. C. E., Suci. G. J. and Tannenbaum. P. H. 1964. *The measurement of meaning*, University of Illinois Press.

Oyama. T., Soma. I., Tomiie. T. and Chijiiwa. H. 1965, *A factor analytical study on affective responses to colors*, ACTA CHROMATICA 1(4) 164-173.

Wakata. T., Saito. M., 2012. *The impression of tones and hue in gradation of Practical Color Co-Ordinate System (PCCS)*, International Color Association 2012 Taipei, Taiwan, 322-325.

Address: Tadayuki WAKATA, Saito Lab, Faculty of Human Sciences, University of Waseda,2-579-15, Mikashima,Tokorozawa, Saitama ,359-1192, JAPAN
E-mails:t.wakata@ruri.waseda.jp, miho@waseda.jp

Psychological effects of meal tray color on the visual palatability of meals among individuals with low vision – the effect of brightly toned colors

Keiko TOMITA[1], Maya INAMURA[1], Kimiko OHTANI[2]
[1] Faculty of Agriculture, Kinki University
[2] Graduate School of Life and Environmental Science, Kyoto Prefectural University

ABSTRACT

The psychological effects of six meal tray colors (b2, b4, b8, b12, b16, b24 on the Practical Color Coordinate System) on the visual palatability of meals for individuals with low vision were investigated. Images for each tray color were described according to the semantic differential method using 36 antonymic adjective pairs. Participants were divided into either a low-vision group in which subjects wore low-vision simulation glasses or a healthy group with good vision. Using factor analyses, two components, "activity" and "relaxation", were extracted from 36 antonymic adjective pairs. Tray color b8 was positive for both components in terms of visual perception among both low vision and healthy subjects. In addition, b8 showed higher visibility than the other colors. Tray color b8 was the most useful color for visual perception, universal color design, and comfort of the six brightly colored trays.

1. INTRODUCTION

According to the World Health Organization, 347 million people worldwide have diabetes. In such individuals, a lack of control of dietary intake can lead to serious complications, such as diabetic retinopathy, which leads not only to low vision, but also blindness. Although cooking and eating to maintain dietary control under low vision is difficult (Hiroshi T., 2002), most color schemes (Shoko A., 1994, Yuji M. 2009) which represent an important factor in appetite, for tableware made for individuals with low vision only come in combinations of black and white. This study examined the psychological effects of meal tray color on the visual palatability of meals for individuals with low vision.

2. METHOD

Pictures of meals on trays taken with a single-lens reflex camera (Nikon D3000), which was adjusted to white balance selected under the daylight and fluorescent light setting (6500K), were used as samples. The color of the trays was changed using a liquid-crystal display (LCD) while the color of the meals was not adjusted. An image survey of meals on the color-adjusted trays was performed under low vision as described below.

2.1 Sample preparation methods

Pictures of 218 meals which were served for approximately 2.5 months in a nursing home in Japan were taken under D65 using a standard light source device (Macbeth Judge II: Sakata Engineering Co., Ltd.). Meals on trays that created a good color scheme together (not including the dishes on the trays) were selected using the semantic differential (SD) method with the 218 meals divided into seven grades. Sample photos of these meals were then selected.

2.2 Color conversion methods

Pictures of the Practical Color Coordinate System (PCCS) color chart *(Table 1)* were taken under D65 with a standard light source device (Sakata Engineering Macbeth Judge II) using a digital single-lens reflex camera (Nikon D3000). RAW corrections were made using the X-rite Color Checker Classic (Sakata Engineering). The colors of the trays with the meals found to be the most appealing according to the SD method were converted to six bright tones (b2, b4, b8, b12, b16, b24 on the PCCS) using Photoshop (Adobe Systems) on a LCD screen. The legitimacy of color conversion was confirmed using a brightness meter (Konica Minolta CS-2000).

Table 1. Munsel and RGB values of the six tray colors

PCCS color name	Munsel value	RGB value		
		R	G	B
b2	4R 6/12.0	241	93	105
b4	10R 6.5/1.5	247	119	77
b8	5Y 8.5/11.0	242	211	36
b12	3G 6.5/9.0	0	178	117
b16	5B 5.5/8.5	0	143	179
b24	6RP 5.5/10.5	204	92	135

2.3 Image research methods

The subjects were university students (mean age, 21.7±0.76 years; 309 females, 118 males) who sat in front of a LCD screen onto which pictures of the meals and six tray colors were projected. After viewing the pictures of the meals and trays, the subjects answered a questionnaire. All experiments were performed in a room with a fixed fluorescent lamp on the ceiling. The subjects were divided into two groups: a low-vision group in which subjects wore low-vision simulation glasses; and a healthy group without simulation glasses and good vision. The results of the two groups were compared. In this study, two research methods were used. One was the paired comparison method which consisted of looking at two LCD screens at once, while the other method consisted of looking only at one LCD screen. The number of subjects for each method is shown in *Table 2*.The scale of the tray pictures was 60%. Illuminance on each table was 505±11.4 lx, room temperature was 25±1.3℃, and humidity was 57±14.7%. The questionnaire comprised the following three sections: attributes; physical and/or mental condition; and image of tray. Images for each tray color were described according to the SD method, using 36 antonymic adjective pairs. All subjects took part in the experiment at least 1 h after eating.

Table 2. Number of participants by research method and group

	Low-vision group (N/tray color)	**Healthy group** (N/tray color)	**Total** (N/tray color)
Single LCD	31	30	31
Paired comparison method	31	30	31
Total	62	60	122

Table 3. Two components ("activity" and "relaxation") were extracted from the 36 antonym-adjective pairs by factor analysis

Antonymic adjective pairs			**Components**	
			Activity	**Relaxation**
Cheerful	-	Gloomy	0.903	-0.120
Exhilarated	-	Melancholy	0.885	-0.098
Pleased	-	Lonesome	0.872	-0.094
Warm	-	Cool	0.872	0.063
Intimately	-	Lonely	0.872	0.034
Lively	-	Unlively	0.854	-0.205
Conversational	-	Silent	0.841	0.078
Happy	-	Unhappy	0.827	0.190
Energetic	-	Weary	0.825	-0.247
Appetizing	-	Unappetizing	0.804	0.300
Delicious	-	Undelicious	0.777	0.321
Cordial	-	Uncordial	0.776	0.273
Open	-	Closed	0.763	0.052
Fleshly	-	Unfleshly	0.727	0.218
Feminine	-	Musculine	0.631	-0.204
Stable	-	Unstable	0.050	0.812
Calm	-	Excessive	-0.279	0.786
Restful	-	Unrestful	-0.278	0.785
Heartwarming	-	Vigorous	-0.319	0.752
Relaxant	-	Tense	0.157	0.742
Ordinary	-	Original	-0.066	0.724
Natural	-	Artificial	0.162	0.701
Healing	-	Unhealing	0.223	0.701
Simple	-	Decorative	-0.188	0.664
Eigenvalue			10.422	5.520
Cumulative contribution ratio(%)			43.43	66.43
Cronbach's coefficient alpha			0.964	0.899

3. RESULTS AND DISCUSSION

3.1 Single LCD

Using factor analyses, two components, "activity" and "relaxation", were extracted as shown in *Table 3*. Tray color b8 was positive for both components in terms of visual perception for both low vision and healthy subjects *(Figure 1)*. In addition, b8 was evaluated to have higher visibility than the other colors tested.

3.2 Paired comparison method

Tray color b8 was the most clearly visible among both low vision and healthy subjects. B8 among healthy group was evaluated to have a comfortable and restful feeling without garish image, although a bright tone had high value and chroma.

4. CONCLUSIONS

Among the six brightly toned trays, tray color b8 was shown as the most useful color in terms of visual perception, universal color design and comfort.

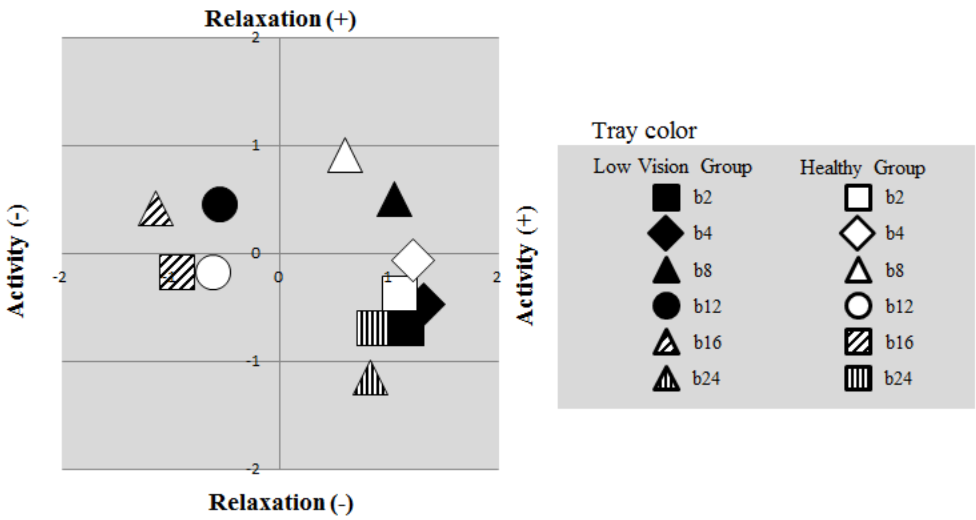

Figure 1. Scores of each tray color for the components "activity" and "relaxation"

ACKNOWLEDGEMENTS

This study was partly supported in part by a Grant-in-Aid from JSPS KAKENHI (Grant Number 21500760).

REFERENCES

Hiroshi, T. 2002. *Low Vision Care – In order to improve the QOL for the visually impaired - Second edition*, Tokyo: IGAKU-SHOIN Ltd.

Shoko A. and Mitsuo I. 1994. *Size effect in color conspicuity*, Color Science Association of Japan, 18(3), 200-204

Yuji M., Toshiaki H., Mitsutoshi K. and Kazuhiko N. 2009. *A study on the eye movement of low vision persons – Case study in an eye clinic -*, J. Archit. Plann., AIJ, Vol. 74(641), 1531-1538.

Address: Prof. Keiko TOMITA, Department of Applied Optics, School of Engineering, Kindai University, 3327-204 Naka-machi, Nara City, Nara, 631-8505, JAPAN
E-mails: keitomi@nara.kindai.ac.jp, i-maya@nara.kindai.ac.jp, ohtani@kpu.ac.jp

A Comparison Between the Impact of Short and Long Wavelengths of Light on Sleepiness and Mood

Mengxi YUN[1], Sayaka ARITAKE[2], Sunao UCHIDA[2], Miho SAITO[3]
[1]Graduate School of Human Sciences, Waseda University
[2]Faculty of Sport Sciences, Waseda University
[3]Faculty of Human Sciences, Waseda University

ABSTRACT

It is widely acknowledged that light of a certain wavelength induces alertness, disturbing the duration of sleep. More precisely, among the wavelengths, short wavelength light (blue light) exerts a greater stimulus on circadian rhythm, compared with long wavelength light (red light). Previous studies have demonstrated that blue light exposure impacts on nocturnal alertness, suggesting the impact of chromatic light on the quality of sleep. On the other hand, some investigations have suggested sleeping in blue room is better for sleep rather than red room. Therefore, based on the contradiction, the present study was designed to figure out the psychological impact of short and long wavelengths light (blue and red light) on sleepiness and mood.

1. INTRODUCTION

Since sound sleep is indispensable for health of body and mind, the increasing number of people who are suffering from sleep problems is a concern, raising questions about how to promote high-quality sleep. One of the factors thought to be associated with high-quality sleep is the bedroom circumstance. Among them, the light illumination of the bedroom is one of the most important factors. Light of a certain wavelength is also known to modify human circadian rhythm. The timing, light intensity and light wavelength, are three important factors for circadian entrainment, which is associated with the sleep and alertness rhythm (Dumont et al., 2007). Many studies have reported that exposure to short wavelength light (blue light) prior to sleep stimulates the circadian rhythm most, impacting on alertness and reducing the quality of sleep (Cajochen et al., 2005). Moreover, blue light exposure at night has also been shown to be a factor contributing to mood disorder (Bedrosian et al., 2013; Dumont et al., 2007).

On the other hand, an investigation examining bedroom color conducted by a hotel company (Travelodge, 2013), concluded that sleeping in a blue bedroom is far more conducive to a good night's sleep than sleeping in a red bedroom. Further, several studies have reported that red is the color which stimulates the sympathetic nervous system (SNS) most, whereas blue activates the parasympathetic nervous system (PNS), producing a calming effect (Jacobs & Hustmyer, 1974; Sakuragi & Sugiyama, 2011). These studies together appear to contradict the findings noted before, although the former studies investigated the light color itself, while the latter investigated the reflection of the color of the walls.

In the present study, we examine the effects of bedroom lighting on night sleep. The present study compares the impact of short and long wavelength lights on both sleepiness and mood, using both questionnaires and a behavioral task to elicit effects.

2. METHOD

2.1 Participants

Ten healthy subjects (5 males and 5 females) aged 23 to 35 years who reported not taking medication and having no visual defects or psychological disorders, participated in the experiment after giving oral consent. The experiment consisted of having subjects exposed to light of both short (blue) and long (red) wavelengths. The experiment was conducted over a two-day period, with one condition being presented on each day. The order of the experimental conditions was determined randomly. The subjects were asked to ensure that they had sufficient sleep on the days prior to the experiment. They were also requested to refrain from vigorous exercise, and from consuming alcohol or caffeine on both days of the experiment.

2.2 Measures

Visual Analogue Scale. The Visual Analogue Scale is an effective way of measuring subjective momentary feelings, such as pain, and sleepiness. (Wewers & Lowe, 1990; Sakuragi & Sugiyama, 2011). The present study used the VAS to evaluate subjects' physical sleepiness and mental state.

Psychomotor Vigilance Tests. Psychomotor Vigilance Tests (PVT) use reaction times to particular tasks to objectively determine sleepiness (PVT; PC-PVT v1.1.0 developed by Biotechnology HPC Software Applications Institute) (Khitrov, et al., 2014). A PVT was administered for 10 minutes after exposure to each of the experimental light conditions in order to measure sleepiness at the behavioral level.

Profile of Mood States. The Profile of Mood States (POMS)-Brief Form Japanese Version was used to assess subjective mood. POMS categorizes mood into six subscales: Tension-anxiety, Depression- dejection, Anger-hostility, Vigor, Fatigue and Confusion. POMS also enables the measurement of changes of mood which occur over a short period of time (Yokoyama, 2006). The present study used POMS to evaluate the change of mood over a period of 30 minutes.

2.3 Apparatus and Procedure

Before being exposed to each experimental light condition, each subject was asked to complete both VAS and POMS questionnaires in order to establish the baseline of sleepiness, mental state and mood. After the completion of the questionnaires, each subject was escorted to a soundproof chamber (length 266cm×width 170cm×height 201cm). In the chamber, the apparatus for presenting the chromatic light was located at the center of the ceiling, directly above the subject's head. Each subject was requested to keep his or her eyes open for the entire duration of light exposure, ensuring the delivery of the chromatic light. Figure 1 shows the image of the experimental environment in which both red light and blue light was presented. Two chromatic light conditions were presented using a blue LED peaking at 462 nm, and a red LED peaking at 630 nm (Figure 2). Each subject received light exposure for 30 minutes. The illuminance of several points in the experimental soundproof chamber was measured; red light: 21.81lx, blue light: 3.22lx at subject eyes' level. After exposure to each lighting condition, respectively, subjects undertook a 10-minute PVT test in the chamber and finally, repeated, in post-test fashion, completing the same VAS and POMS questionnaire used in the pre-test. Figure 3 illustrates the experimental procedure and the data collection activity periods.

Figure 1: Simulated experimental environment of the clamber with red light illumination (left) and with blue light illumination (right).

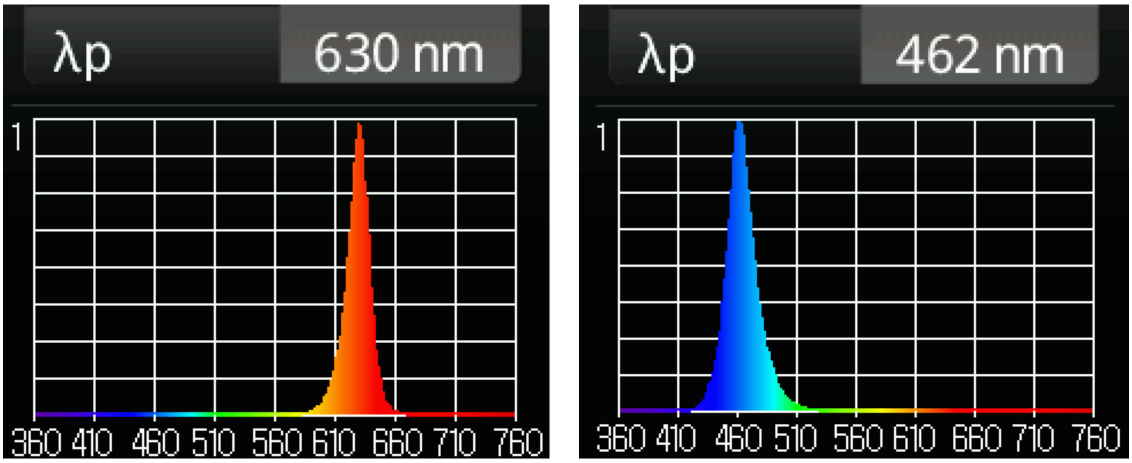

Figure 2: Spectral distribution of red LED light (left) and blue LED light (right).

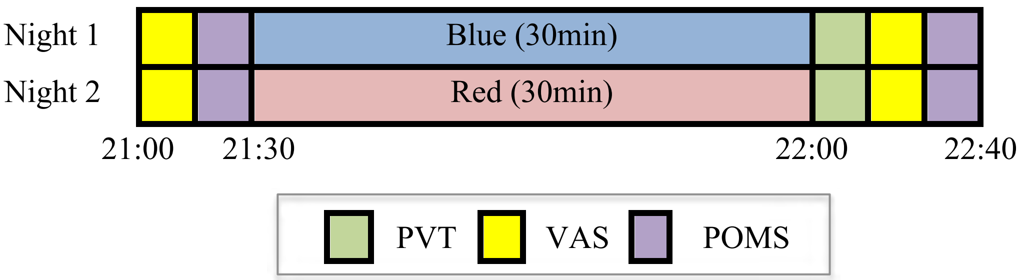

Figure 3: Experimental procedure and data collection times for each subject.

3. RESULTS AND DISCUSSION

3.1 VAS Results

In terms of reported sleepiness, a paired t test revealed significantly increased sleepiness only under the blue condition ($t(9)=-3.485$, $p<0.01$). Both blue and red conditions indicated significant variation in mental state instability (red: $t(9)=2.423$, $p<0.05$; blue: $t(9)=3.692$, $p<0.01$). However, when changes under the red condition were compared with changes under the blue condition, no significant difference was found.

3.2 POMS Results

To establish the comparative impact of light of both long and short wavelengths on mood, a paired t test was used for each subscale. In the Vigor subscale, under both the red condition and under the blue condition, vigor was significantly reduced (red: $t(9)=3.613$, $p<0.01$; blue: $t(9)=3.647$, $p<0.01$). Further, for the Confusion subscale, the reported degree of confusion showed a significant increase only under the blue light condition ($t(9)=-2.717$, $p<0.05$). However, as with VAS, the POMS results showed no significant difference between the red or blue light experimental condition.

3.3 PVT Results

The results of a paired t test showed no significant difference between the red and blue light conditions on sleepiness, as determined by behavioral tasks.

3.4 Discussion

After exposure to blue light for 30 minutes, sleepiness increased significantly (VAS results), whereas red light failed to induce any significant changes in sleepiness. This result is consistent with the statement that the secret to a good night's sleep is to sleep in a blue bedroom rather than red bedroom, as reported by a hotel company (Travelodge, 2013). Meanwhile, the significant increase of sleepiness under blue light condition indicates a discrepancy between the actual outcome and the conclusion of previous studies, that short-wavelength light stimulates the suprachiasmatic nucleus (SCN) most, leading to circadian rhythm disorder and sleep problems. This inconsistency raises the possibility of the existence of other light-sensitive pathways regulating sleep besides the retinohypothalamic tract (RHT).

With respect to mood, both red and blue light exposure contributed to mood instability. However, only under the blue light condition, subjects seemed to become more confused. This result is consistent with the conclusion that blue light leads to mood disorder. Since mood change before sleep also influence the quality of sleep, it is necessary to integrate and compare the reported sleepiness with the impact of mood when evaluating the real quality of real sleep.

Given that the questionnaires and behavioral method have limitations for determining the quality of sleep directly and subjectively, taking into consideration the possibility of other light-sensitive pathways regulating sleep proved by the present study, further study is needed to analyze electrophysiological measures in order to more accurately clarify the impact of different wavelengths of light on sleep.

4. CONCLUSIONS

Exposure to light of a short wavelength (blue light) for 30 minutes elevates nocturnal sleepiness. Mood instability possibly caused by both the short and long wavelengths of light (blue and red light), especially higher confusion led by blue light could influence quality of sleep. These results require further experimental investigation using polysomnographic examinations after exposure to the light conditions used in this study.

REFERENCES

Bedrosian, T. A., Vaughn, C. A., Galan, A., Daye, G., Weil, Z. M., Nelson, R.J. 2013. Nocturnal light exposure impairs affective responses in a wavelength-dependent manner. *The Journal of Neuroscience*, 33(32): 13081-13087.

Cajochen, C., Munch, M., Kobialka, S., Krauchi, K., Steiner, R., Oelhafen, P., Wirz-Justice, A. 2005. High sensitivity of human melatonin, alertness, thermoregulation, and heart rate to short wavelength light. *The Journal of Clinical Endocrinology & Metabolism,* 90(3): 1311-1316.

Dumont, M., & Beaulieu, C. 2007. Light exposure in the natural environment: Relevance to mood and sleep disorders. *Sleep Medicine,* 8 (2007): 557-565.

Jacobs, K. W., & Hustmyer, F. E. 1974 Effects of four psychological primary colors on GSR, heart rate and respiration rate. *Perceptual and Motor Skills* 38: 763-766.

Khitrov, Y. M., Laxminarayan, S., Thorsley, D., Ramakrishnan, S., Rajaraman, S., Wesensten, J. N., Reifman, J. 2014. PC-PVT: A platform for psychomotor vigilance task testing, analysis, and prediction. *Behavior Research Methods*, 46: 140-147.

Sakuragi, S., & Sugiyama, Y. 2011. Effect of partition board color on mood and autonomic nervous function. *Perceptual and Motor Skills,* 113, 3: 941-956.

Travelodge. 2013. *The secret to a good night's slumber is to sleep in a blue bedroom.* Market Wired. Available online, http://www.marketwired.com/press-release/the-secret-to-a-good-nights-slumber-is-to-sleep-in-a-blue-bedroom-1791681.htm

Wewers, M. E., & Lowe, N. K. 1990. A critical review of visual analogue scales in the measurement of clinical phenomena. *Research in Nursing and Health*, 13: 227-236.

Yokoyama, W. 2006. *The guidance and case explanation of POMS brief form.* Tokyo: Kanekoshobo.

Address: Mengxi YUN, Department of Human Informatics and Cognitive Sciences, Graduate of Human Sciences

Prof. Miho SAITO, Department of Human Informatics and Cognitive Sciences, Faculty of Human Sciences

Waseda University, Mikajima 2-579-15, Tokorozawa, Saitama, 359-1192, JAPAN

E-mails: mugi@ruri.waseda.jp

miho@waseda.jp

Experimental Study of Common Factors between Impressions of Wall-Paper Colors and Sounds in Living Environments

Miho SAITO,[1] Yuriko OISHI,[1] Taiichiro ISHIDA,[2]
[1] Faculty of Human Sciences, Waseda University
[2] Graduate School of Engineering, Kyoto University

ABSTRACT

In order to investigate and extract common factors between the impressions elicited by the change of wall-paper colors and those elicited by the change of sounds in living environments, 30 undergraduate and graduate students were asked to evaluate a model of living rooms with 9 different wall-papers colors by the SD method. Secondly, they were required to evaluate each of four pieces of computer-generated music by the SD method. They were then evaluated by the same SD method regarding their impression of a model of a living room while listening to one of four pieces of music. The data obtained in the three experiments were analyzed by Factor analysis. From among the results of three experiments, two factors, 'pleasant' and 'mild', were extracted. Their possible role in the formation of impressions how colors and sounds relate to the concept of a comfortable living room are discussed.

1. INTRODUCTION

In daily life, psychological impressions are formed through multiple sensory modalities rather than a single sensory modality. The experience of such cross-modal perception is quite natural and common because two or more different sensory modalities usually interact in the brain. This explains why people sometimes associate a paticular color with a certain genre or piece of music. People also often express their memories associated with various colors. Consequently, understanding the relationships between the impressions derived from multiple sensory modalities and the impressions of visual information, especially colors, helps clarify the structure of the impressions derived from multiple sensory modalities. In other words, color may play an important role as a node of cross-modal perception. For instance, Ward et al. (2006) reported that sound-color synesthetes, as a group, tend to see lighter colors for higher sounds. Saito et al. (2013) investigated the harmonious relationship between color and music. They found that changes in the key of music corresponds to changes in the lightness of *PCCS* tone. On the other hand, results indicating that changes in tempo correspond to changes in lightness and saturation in *PCCS* tones from lower levels to higher levels suggest that tempo has a multi-dimensional relationship with lightness and saturation. From a cross-modal point of view, it was also suggested that the components of music can be classified by means of the components of color. To further clarify the relationship between music and color on the assessment of a living room being comfortable or not, the present study investigates the triangulation of these factors in a living environment. In the present study, we investigate factors common to the impressions elicited by the change of wall-paper colors and the impressions elicited by the change of sounds in living environments, using the model of a living room.

2. METHOD

2.1 Participants and Apparatus

The number of subjects who participated in the experiments was 30 undergraduate and graduate students (12 males, and 18 females, ages: mean=21.8 years, SD=1.34). The experimental stimuli were as follows: 1) A model of a living room (Width 500mm x Depth 400mm x Height 300mm) with all of its white miniature interior materials (three sofas, a table, and a curtain) illuminated by *Panasonic* natural white. (See Fig.1) Wall-papers were 9 different colors of the *PCCS* (Practical Color Co-ordinate System), namely: pale tones and grayish tones x 2R, 8Y, 12G, 18B and white. (See Fig. 2 and Fig.3); 2) Sound stimuli: 4 pieces of music composed using our own computer-software in two different octaves of C major, namely C3 major (low) and the second higher octave (high), at two different tempos (BPM=120 and 210). The scores of the four pieces of computer-generated music can be seen in Appendices.

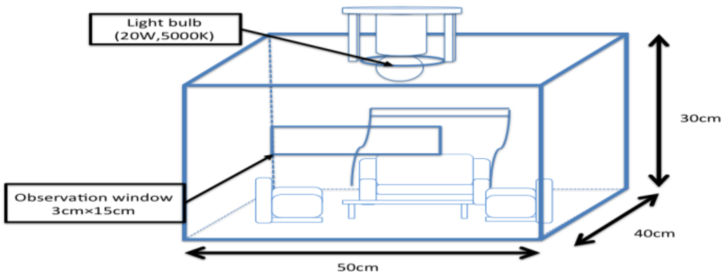

Figure 1: Model of the living room

2.2 Procedure

The participants were asked to look into the model of the living room through an observation window and rate each stimuli on a seven-point scale following the semantic differential (SD) method. In our experiment, 17 adjective-pairs (pleasant-unpleasant, like-dislike, harmonious-unharmonious, ordered-disordered, familiar-unfamiliar, sophisticated-unsophisticated, clear-unclear, soft-hard, cheap-luxurious, nondistinctive-distinctive, cheerful-gloomy, quiet-noisy, bright-dark, gaudy-subdued, warm-cool, calm-restless, feminine-manly) were used. The evaluation was also followed by free comments relating to the first impression, the positive or negative feelings, and the extent of comfortableness, together with some verbal questions, such as feeling free or not, and favorite and disliked colors.

The study comprised three experiments: First, the participants were asked to give their psychological evaluations of each living-room model by the SD method, and provide free comments. Second, they were asked to evaluate each of the four pieces of computer-generated music by the SD method. Finally, they were asked to evaluate, by the same SD method, each model of a living room while listening to one of the four pieces of music.

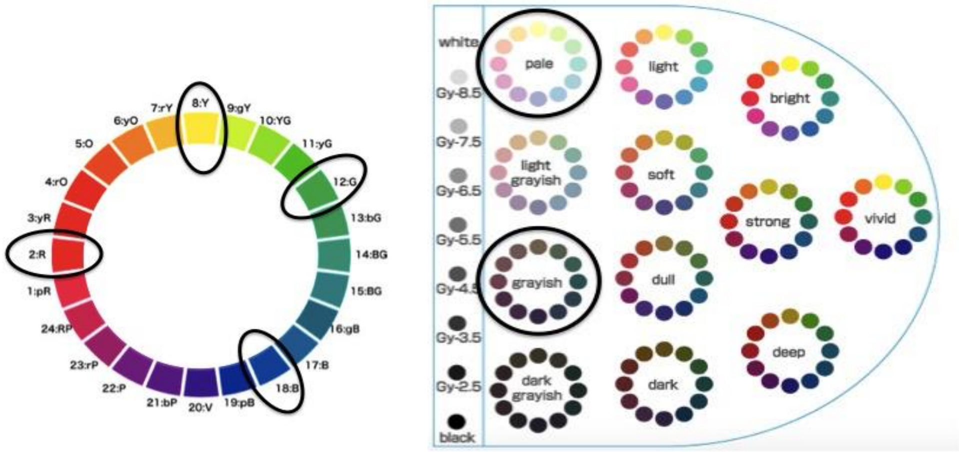

Figure 2: Hues and tones of PCCS used in the experiments

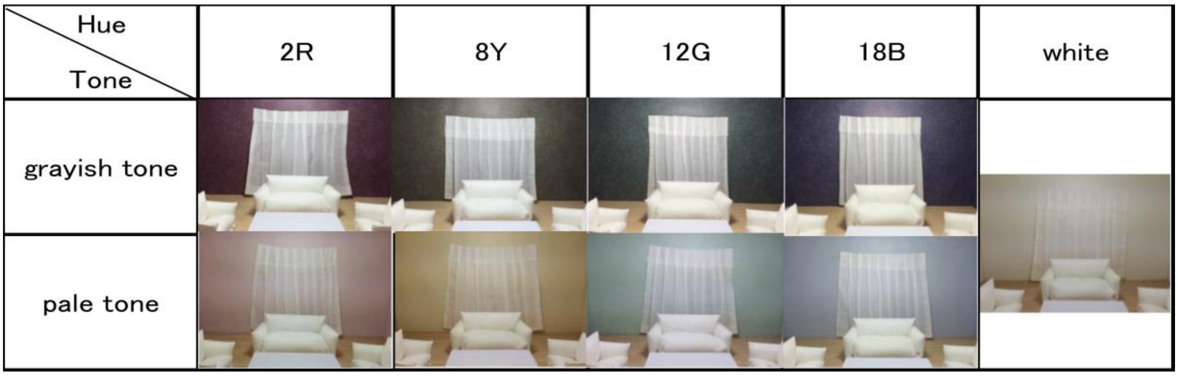

Figure 3: Hue and tone of the wall-paper in the models

3. RESULTS AND DISCUSSION

3.1 Factor Analysis

The data obtained in the three experiments were analyzed independently by Factor analysis (Maximum likelihood method, *Promax* rotation) with two similar factors emerging. Using factor analysis (Major factor method, *Varimax* rotation), a data analysis of all three experiments was repeated, as a result of which two factors, ‘pleasant’ and ‘mild’, were identified. Table 1 indicates factor loadings of the analysis of all of the data from three experiments. As the first factor included the scales of pleasant-unpleasant, like-dislike, harmonious-unharmonious, ordered-disordered, familiar-unfamiliar, sophisticated-unsophisticated, clear-unclear, and soft-hard, it was designated the 'pleasant' factor. The second factor, which consisted of the scales of cheerful-gloomy, quiet-noisy, bright-dark, gaudy-subdued, warm-cool, calm-restless, and feminine-manly, was designated the 'mild' factor. Hence, it is possible that these two factors, 'pleasant' and 'mild', are common to the formation of impressions about a living room being comfortable or not.

Table 1: Matrix of factor loadings

Ajective pairs	Factor	
	PLEASANT	MILD
pleasant-unpleasant	.889	.105
like-dislike	.843	.139
harmonious-unharmonious	.804	.101
ordered-disordered	.735	-.028
familiar-unfamiliar	.725	.283
sophisticated-unsophisticated	.592	-.045
clear-unclear	.563	.242
soft-hard	.457	.440
cheerful-gloomy	.313	.765
quiet-loud	.196	-.731
bright-dark	.470	.725
gaudy-simple	-.108	.664
warm-cool	.340	.609
calm-restless	.522	-.539
feminine-masculine	.155	.509
Contribution ratio	32.5	22.5
Cumulative contribution ratio	32.5	55.0

3.2 Scatter Plot

Fig. 4 below shows a scatter plot of the factor scores of all three experiments. The combination of wall-papers pale in tone appears in the first and fourth quadrants, indicating that no matter what the tempo was, the pleasant and harmonious impression was influenced by the tone of the wall-paper colors, that is, a pale tone was preferred to a grayish tone. As for the impression of cheerfulness and mildness, the tempo of the music seemed to play an important role because while the stimulus combined with a high tempo were mainly scattered in the first and second quadrants, those associated with a low tempo were located in the third and fourth quadrants

3.2 Multiple Regression Analysis

Multiple regression analysis was performed to ascertain the effect of music and wall-paper colors on the impression of the living room. The highest multiple coefficient of determination was 0.311 for 'feminine – manly', indicating that no effective equation of regression was obtained as a whole. However, the partial regression coefficient of the impression only for wall-paper color was higher than that for music. It is suggested that the impression of wall-paper color may be the dominant factor in regard to the conception of a comfortable living room.

4. CONCLUSION

An applied study was carried out to elucidate common factors between the impressions elicited by the change of wall-paper colors and those elicited by the change of sounds in a living environment. Three experiments were conducted and Factor analysis was applied to the participants' evaluations of wall-paper colors of living rooms, relating to sounds, as presented by music of low and high key, and slow and fast tempo. Two main factors, 'pleasant' and 'mild' were extracted from all the experimental data indicating that these two factors feature significantly in the conception of a harmonious living room. Moreover, the results of multiple regression analysis suggest that the impressions of wall-paper colors are related to pleasant and harmonious feelings about a living room. Further studies are required to apply the result of this study to actual living environments.

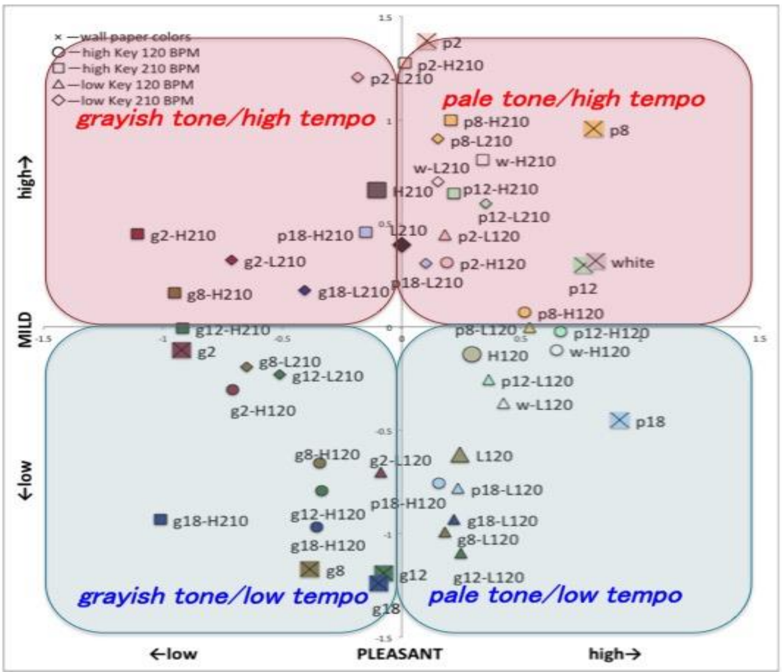

Figure 4: Scatter plot

ACKNOWLEDGEMENT

This work was supported by Grant-in-Aid for Scientific Research (B) (2011-2013) from Japan Society for the Promotion of Science (JSPS).

REFERENCES

Saito, M., T. Wakata, and R. Senga 2013. *Harmonious relationship between color and music focusing on psychological evaluation of key and tempo*, Proceedings of International Color Association 2013 Newcastle, UK. 1793-1796.

Ward, J., B. Huckstep, and E. Tsakanikos 2006. *Sound-colour synaesthesia: to what extent does it use cross-modal mechanisms common to us all?*. Cortex 42(2) 264-280.

APPENDICES

Appendix 1. The score of the computer-generated music: Higher octave

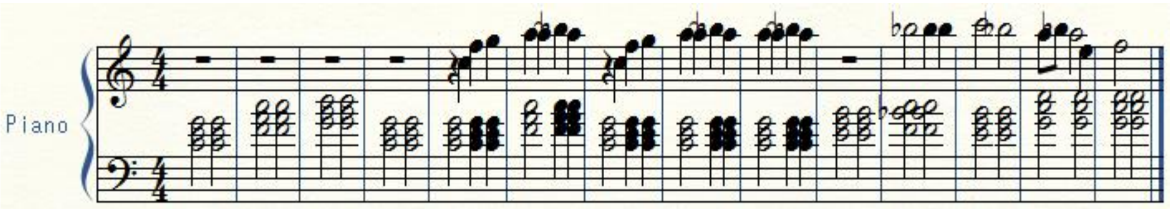

Appendix 2. The score of the computer-generated music: Lower octave
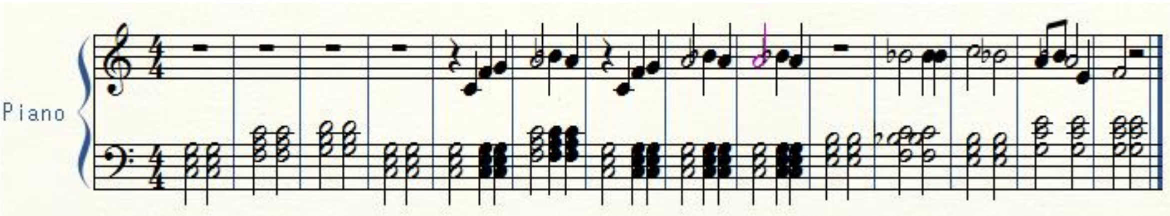
Address: Prof. Dr. Miho SAITO, Faculty of Human Sciences,
Waseda University, 2-579-15, Mikajima, Tokorozawa, 359-1192, Japan,
E-mails: miho@waseda.jp, yuriko-oishi@moegi.waseda.jp, ishida@archi.kyoto-u.ac.jp

The Investigation of Factors Influencing the Impression of Color Harmony

Yuh-Chang WEI[1], Wen-Guey KUO[2]
[1]Department of Information Communications, Chinese Culture University, Taipei, Taiwan
[2]Department of Textile Engineering, Chinese Culture University, Taipei, Taiwan

ABSTRACT

Color harmony has been systematically investigated since 1956 at Budapest using specific pattern samples. To quantify the impression of color harmony, Szabó et al. (2010) developed a CH formula for two and three-color combinations and a harmony rendering index (HRI) quantifying the change of the value of CHF for certain test color sample combinations under the test light source. Ou et al. (2011) developed an additive CF formula for two and three-color combinations and first by using complex images in predicting multicolor harmony. Kuo et al. (2011) developed a pilot CH formula by using textile pattern samples of color images of fashion apparel for two and three-color combinations, and using a psychophysical method of magnitude estimation instead of previous psychological method of category judgment. In Kuo and Wei (2013) CHF performance test study, the results show that test models still cannot have good agreement with model prediction and visual test results of color harmony via textile pattern samples of color images of fashion apparel. The findings indicate that factors influence the accuracy of color-harmony predicting models need to be further investigated.

1. INTRODUCTION

Color harmony is a complex issue and contains a wide variety of factors. Since last centuries, color order systems were developed by Munsell, Ostwald and Itten, and nowadays by Nemcsics to establish harmonic sets of colors. Further studies of color harmony focused on an interrelationship of colors. Judd and Wyszecki defined harmony as "when two or more colors seen in neighboring areas produce a pleasing effect, they are said to produce a color harmony". There are a number of principles of harmony, such as 'powerful', 'soft', 'splendid', 'completeness, according to Goethe, 'order' according to Ostwald, 'similarity' and 'contrast' according to Nemcsics and Chevreul, and 'Balance' according to Munsell. Color difference-related color harmony as proposed by Moon and Spencer. Other color systems, such as 'aesthetic uniformity' by Coloroid system, 'similarity' and 'color perception' by Natural Color System. Although those principles shared in common regarding color harmony, such as hue, chroma and lightness, but the consistency and predictability of color harmony varied from above mentioned factors.

The recent development in color harmony research adopted CIE colorimetry and psychophysical scaling methods for measuring and modeling color harmony in terms of visual response based on comparisons of a variety of pairs of color consisted of equal hue, or equal chroma, or unequal lightness. Most previous studies on color harmony were typically concerned with whether the color harmony scale can be expressed with a small number of categories, or factors, by using the psychological method of category judgment (Torgerson,1958) or the psychophysical method of magnitude estimation (Kuo, 2007) instead. To modelling color harmony has being studied since 1956 at the Budapest Technical University by Nemcsics (2007). There are advanced color harmony models concerning additive factors that affected predictability, such as light source quality, color emotion, cultural difference, preference, and live-dependency multi-color image test samples, subsequently proposed by Szabó et al. (2010), Ou et al. (2011), and Kuo et al. (2011). However, there still exists a difference among those models in which various types of test color samples and visual experiments were conducted, according to the experimental results analyzed by Kuo et al. (2013).

2. EXPERIMENTAL MODELING OF COLOUR HARMONY

2.1 Two-color Harmony Experiment

In the common two-color harmony experiment, color stimuli consisted of two squared color patches presented side by side, with a gray background (see Fig. 1). These stimuli are generated from selected colors, combining all colors from this set of selected colors. This set also contains monochromatic two-color combinations with the same hue. The test sample colors are selected systematically from the CIE color space containing achromatic and chromatic colors. The experiment is repeated to examine repeatability of observer responses. The same experiment is also used to investigate dichromatic two-color combinations, which consists of two samples of different hue.

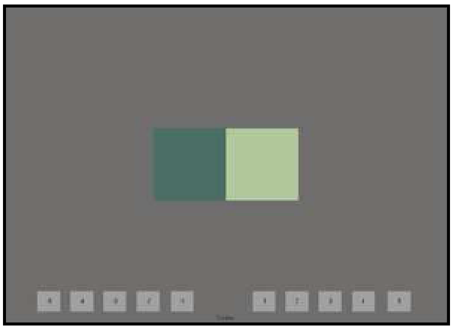

Fig. 1: Example of two-color combination (Szabó et al., 2010)

2.2 Three-color Harmony Experiment

In the common three-color harmony experiment, color stimuli consisted of three squared color patches presented in a triangle position or in a wheel, having a vertex in the middle, with a gray background (see Fig. 2a & b). The three-color harmony experiment arrangement is similar to two-color harmony experiment. The test sample colors are selected systematically from the CIE color space containing achromatic and chromatic colors. Monochromatic three-color combinations are composed form these set of samples, selecting three of them with the same hue. The experiment is repeated to examine repeatability of observer responses. The same experiment is also used to investigate trichromatic three-color combinations, which consists of three samples of different hue.

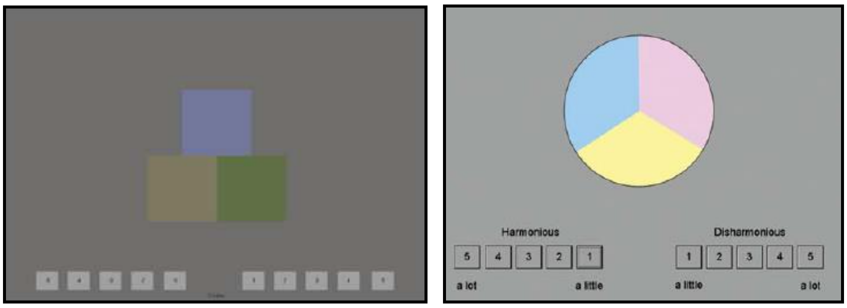

a b

Fig. 2: Example (a) of three-color combination by Szabó et al. (2010); Example (b) of three-color combination by Ou et al. (2011)

2.3 Two and Three-color Harmony Experiment for Complex Color Images

To use complex images of interior decoration (Ou et al., 2011) or fashion apparel (Kuo et al., 2011) as the stimuli (see Fig. 3a & b), there are the latest researches, not only to test two and three-color harmony models, but also to be considered more relevant than a combination of color patches to the art and design practice. Meanwhile, in Ou's study, effect of image configuration and cultural difference are first examined. The results indicate that additive approach, considered as a trichromatic model, is proved effective. The experiment environment including grey background, viewing conditions and data collection methods were the same as those used two and three-color harmony experiments.

a b

Fig. 3: Example (a) of image of interior decoration by Ou et al. (2011); Example (b) of images of fashion apparel by Kuo et al. (2011)

3. COMPARISONS OF THE PERFORMANCE OF COLOR HARMONY MODELS

3.1 Stability of Visual Assessment

In Kuo et al. (2013) study, a series of color-harmony assessing experiments are carried out respectively by fifteen observers using the magnitude estimation method. The coefficient of variation (CV%), proposed by Coates et al. (1981), is used to indicate the observer variation. The equation is as follow:

$$CV(\%) = 100[\Sigma(x_i - y_i)^2 / n]^{1/2} / \tilde{y},$$

where n is the number of samples in x_i and y_i sets of data, and $\tilde{y}$ is the mean value of the y_i set data. The larger the value of CV is, the worse the agreement between the two sets of data compared. For a perfect agreement, the value of CV should be zero. The results show that a general stability can be found for the visual results, i.e. the total mean value of 78 in CV unit. And, the result of assessing stability for the observers in this study is less or equal to that for those experiments of color appearance or color difference assessment (Kuo and Luo, 1996).

3.2 The Performance Factor (PF)

The performance factor (PF) developed by Luo and Rigg (1987) is used to indicate the agreement between two sets of data and defined as the following equation:

$$PF = 100\,(\gamma + V_{AB} + CV/100 - r),$$

Where CV and γ were proposed by Coates et al. (1981), V_{AB} derived by Schultze and Gall (1971), and r is the correlation coefficient between the two sets of data compared. For a perfect agreement between two sets of data, the PF value should be zero. All estimations of the performance of the color difference formula on predicting visual color differences in the following data analysis are, in terms of PF/4 unit, being able to indicate the percentage error between two sets of data. Meanwhile, the higher the value of PF/4 obtained, the worse the agreement between data sets.

Table 1. Estimation on the performances of the color-harmony models derived by Ou et al. and Szabó et al., and Kuo et al., in predicting visual color-harmony data, H_{v2} and H_{v3} standing for the visual assessing values of the samples with two and three color-combinations respectively, by means of the performance factor (PF/4)

Models / Values of PF/4 / Items	Ou's	Szabó's	Kuo's
H_{v2}	191	137	197
H_{v3}	156	115	191
Mean	174	126	194

3.3 Comparisons of the Performance of Three Color-Harmony Models

The performances of color-harmony models, such as model Szabó et al. (2010), model Ou et al. (2011) and pilot model Kuo et al. (2011), in predicting visual color harmony were examined using the experimental visual-harmony data obtained from this study using 162 color images of fashion apparel containing 141 and 21 test samples with two-color and three-color combinations respectively by means of the performance factor (PF/4). The results showed that the model Szabó has the best performance in predicting the visual color harmony among tested models, having the mean values of 126 in the unit of PF/4 as shown on Table 1. However, above test models still cannot have good agreement between model prediction and visual results of color harmony.

4. Discussions and Suggestions

4.1 Agreement of Factors Attribute to Color Harmony

According to previous studies, by Szabó et al. (2010) and Ou et al. (2011), on two and three-color harmony, the test results agree that the factors influence color harmony, that is, ‘equal hue’, ‘equal chroma’, ‘unequal lightness’, ‘high lightness’, and ‘hue preference’. But, it is also found that test results do not show agreement with two conventional principles of color harmony, which are ‘complementary hue’ and ‘equal lightness’ (Szabó et al., 2010; Ou et al., 2011). Obviously, there are other factors that attribute to color harmony need to be taken in account and require further investigation in future research.

4.2 Future Directions for Further Investigation

In Kuo and Wei (2013) study of the performance among three color harmony models using the complex images test samples, surprisingly, the test results show that additive CH model, proposed by Ou et al. (2011), does not have the best performance in predicting visual color harmony, which is different from the test results as reported in Ou’s study. But, indeed, the additive approach opens up a research direction in predicting multicolor harmony whether is more relevant to the art and design practice. There are other factors, such as ‘cultural difference’, ‘light source color quality’, 'color harmony index (HRI)’, proposed by Szabó; ‘context’, ‘image configuration’, ‘color size’, proposed by Ou, and ‘live-dependency complex image’ test samples, proposed by Ou and Kuo. In addition to improve the consistency and predictability of color harmony, there are ongoing researches on Color Rendering Index (CRI) and better uniform color space (CIELAB or CIECAM02) to achieve accordance.

REFERENCES

Coates, E., Fong, K.Y. and Rigg, B., 1981, ’*Uniform Lightness Scales,*’ J.S.D.C. 97 179-183.

Kuo, W.G. and Kuo Y.C., 2000, *The Investigation on the Relationship between DRP Color Image Scale and CIEL*a*b* Color Space*, Proceedings of the Conference on the Color Application and Color Science in 2000 137~144.

Kuo, W.G., 2007, *The Feasibility of Establishing New Color Image Scales Using the Magnitude Estimation Method*, Color Research and Application 32 (6) 463~468.

Kuo, W.G., Lee, C.K., Wei, Y.C. and Huang, Y.Y., 2011, *Effect of different sample patterns on color harmony*, Proceedings of 12th International Conference on Color Design, Application and Science in 2011 187~194.

Kuo, W.G., Wei, Y.C., Lin, S.M, Lee, C.K. and Hong, C.C. 2013, *Investigation on Various Color-Harmony Models in Predicting Color Harmony for Color-Apparel Images*, Proceedings of 12th International AIC Color Congress in 2013 103

Luo, M.R. and Rigg, B., 1987, *BFD (l:c) color-difference Formula Part I- Development of the Formula*, J. Soc. Dyers Colour. 103 86-94.

Luo, M.R., Lo, M.C. and Kuo, W.G., 1996, *The LLAB(l:c) Color model*, Color Res. Appl. 21 412-429.

Nemcsics, A., 2007, *Experimental determination of laws of color harmony. Part 1: harmony content of different scales with similar hue*, Color Research and Application 32 (6) 477~488.

Ou, L.C., Chong, P. and Luo, M.R., 2011, *Additivity of color harmony*, Color Research and Application 36 (5) 355~372.

Schultze, W. and Gall, L., 1971, *Application of Color Difference Formulae to Highly Saturated Colors Differing Only in Lightness and Saturation*, J. Color Appear. 1(1) 17-24.

Szabó, F., Bodrogi, P. and Schanda, J., 2010, *Experimental modeling of color harmony*, Color Research and Application 35 (1) 34~49.

Torgerson, W.S., 1958, *Theory and Methods of Scaling,* John Wiley & Sons, New York, USA 205~246.

Address: Dr. Wen-Guey Kuo, Department of Textile Engineering
Dr. Yuh-Chang Wei, Department of Information Communications
Chinese Culture University, No. 55 Hua Kang Road, Yang Ming Shan, Taipei 11104, Taiwan
E-mails: kuow@staff.pccu.edu.tw, ycwei@faculty.pccu.edu.tw

The hidden image – a strategy to put an unwanted phenomenon in its true light

Salome EGGER,
Nottingham Trent University, UK

ABSTRACT

In the everyday we are surrounded by images and the plethora of visual material is overwhelming us. We do not anymore look properly at images and we assume that what we see is correct. We do not doubt our sight and do not expect that the same image could appear with different colours. This proposal depicts the journey of the exploration of the physical colour phenomenon called metamerism, where a colour pair looks even in a given light situation, but may appear different in a changed light source. In the field of colour most practitioners aim to avoid metameric colour pairs, as it is seen as a problem so far. By contrast, the fascination of the subtle colour change and the interest to work with this 'error', uncovering the potentiality of something that has not previously been appreciated, is a main driver of this research. This research investigates the creation and steering of metameric pairs of colours and their impact upon viewers. Yarns, as the basic material of the fabrics, have intentionally been dyed to be metameric. Knit has been chosen as the medium to create therewith images. The fabrics, thereby created, change colour depending on the switched on 'white' light source and they are revealing hitherto unnoticed visual contrasts. The aim is to give visibility and to lead to a new consideration of this 'trivial' phenomenon. Light breathes life into the colours of the fabrics and the images unveil the phenomenon offering to the audience this wonderful magic of the relativity of colour perception. The interaction of light and colour creates different views of one image and through these artworks metamerism becomes experiencable and the vitality of colours becomes reality.

1. INTRODUCTION

The impetus for this research project resulted from my daily routine as a designer. The zippers I had carefully selected for a knitted cardigan didn't match, and I discovered that this was due to an optical phenomenon called metamerism. It turned out that the colour of a material may appear different under different light sources: when the spectral composition of light changes it can result in differences of the spectral diffuse reflectance of the material surface, causing the initially uniform colour of the material to appear different (Hunt 2011). As in the above example, metameric colours can be a professional irritation and to date, colour metamerism is generally discussed as a problem. This research, by contrast, seeks to explore the poetic and aesthetic experience of this 'unwanted' physical colour phenomenon in order to reconsider its affect, and put in its true light. Through a series of art installations and performances, the project is intended to create and sustain the sense of wonder when metamerism is experienced, allowing an audience to encounter it consciously, and from a new conceptual angle. It is a transdisciplinary exploration of the perception of colours, lighting and environment bringing together the fields of art, science and technology, using the craft of dyeing and knitting. Ideas have been tested in several performances and installations; this paper will outline progress so far, and concentrate upon part of this research journey, the installation "Trilogy of light", a performative installation with three wall-mounted knitted 'canvases', showing three times the same image of a lamp, but with interchanged colours. The work is illuminated by at least two different light sources, switched on and off alternately, and changing at set intervals, thus enabling the images depicted to reveal unexpected subtle colour changes.

2. METHODS, MATERIAL & MEDIUM

This research is situated within art & science (Wilson 2010), therefore the methodology cross-fertilises approaches from various disciplines: it mobilises the science of textile chemistry and physics, knowledge from the humanities, the craft and aesthetic theory of design and visual art, and it uses a mix of qualitative, quantitative and explorative methods. In the twenty-first century, artists, scientists and technologists are collaborating and cooperating with each other on increasingly hybrid inquiries. As well as enabling the specific intentions of this project, the mixed methods enhance links between disciplines, and seek to develop new ways of working and thinking, such that alternative perspectives offer a fruitful way for generating new knowledge.

2.1 Preparation of material: Yarn dyeing

The first part of the research was quantitative, and mainly dedicated to the development of adequate conditions for the dye explorations; it was necessary to generate proper research results to enable preparation of the metameric material. The goal was to find colours, which can be dyed in the manner, that they would look visually the same in daylight D65 but would look different under A and TL84[1]. Knowing that mixed colours tend to be the most metameric, recipes in the range of greyish, brownish and greenish colours have been calculated by the Datacolor System. The research aimed for colour recipes, which would allow three variations responding in a different way to the fixed three light sources. The first colour should stay stable in all the three lights, the second should change visibly in the fluorescent light (TL84) and the third should change in Tungsten (A). The first dyestuff combinations, which showed visually attractive changes, were an olive green and the decision has been taken to proceed with this, and to determine the best way to create and manipulate the effect on the basis of one colour.

2.2 Knit as material and medium

Knit has been chosen as the material to combine the purposefully metameric dyed yarns. I am a trained textile artisan and a knitwear designer, with knit as my core competence: the use of textile techniques as a medium for these artworks is a logical consequence. Jessica Hemmings' makes clear that knit contributes

> "… to a vast array of disciplines, including contemporary and traditional crafts, modern literature, fine art, feminism, activism and history" (Hemmings 2010).

---

[1] D65 and A are Standard Illuminates, defined by the International Commission of Illumination, (CIE), D65 is a definition of day light with a temperature of about 6504 Kelvin. A corresponds to incandescent light with a temperature of about 2856 Kelvin. TL84 instead is a definition of a fluorescent lamp with a temperature of about 4000 Kelvin. (Hunt 2011).

Like Hemmings, this project seeks to acknowledge and expand the contribution knitting can make to different disciplines[2].

With the first dyed yarn, different fabrics were produced using stripes, jacquard and more complex structures; these were then observed under defined light sources and the effects evaluated according to the subjective aesthetic visual judgement of an artist. These initial explorations were the crucial basis for developing subsequent concepts for installations and performances.

2.3 Light, Performances & Installations

It had been the intention to construct a light cabinet to test the work, but during the research the colour change triggered by common light sources shifted this: it was decided to work with everyday light sources underlining the prosaicness of the phenomenon. Several bulbs were purchased from an ordinary shop, inserted in various lamps and observed against three coloured fabrics. Fluorescent energy saver bulbs produced visually attractive colour changes, as did the incandescent bulbs (halogen and the old banned bulb).

As the research aims to make visible the phenomenon, and to change the usually negative perception, it became clear that installation and performance could be an effective method for exploration and testing. Each installation and performance requires a certain light setting dependent on the concept of each work. As it is rarely possible in gallery installation settings to show artworks in daylight, the unicolour variation gets lost; by contrast performances give an opportunity to lead the audience from rooms with daylight to those with different artificial illumination. In practice it has been difficult to control the setting of the light sources and the installation was not yet always ideal. Further research is needed to explore a broader range of illumination options and settings.

3. EXPERIMENTS, RESULTS AND REFLECTION

3.1 Installations and Performances

"green-green-green"

For the performance "green-green-green" a dress was developed, which acts as a 'canvas' during performances and gives the performer the chance to move around in a building with the audience taking advantage of the available light sources. It became clear that it was important to start the performances in daylight, as viewers experience a greater sense of wonder when something apparently unicolour becomes colourful. What was especially interesting in terms of changing perceptions, was that one observer saw a unicolour dress in the beginning in the daylight situation, but after the performance she could not revert to seeing a single colour now she knew that different colours were present. The live experience of engaging with performances reliant upon specific light generates powerful sensory affect through which a poetic physical experience can unfold (Figure 1).

---

[2] As well Turney (Turney 2009) stresses the important cultural contribution of knitting.

Figure 1 Image of the Performance: "green-green-green", 2014, Nottingham UK

"green-green-green_1_03:11"

Subsequent developments involved images of the performer knitted with a Jacquard technique. By reducing the colour range of the images with the software Photoshop to just three colours, images were produced with the three metameric green dyed variations of yarn. "green-green-green_1_03:11" (Figure 2) was tested in the 'Knitting Nottingham' exhibition, Bonington Gallery, Nottingham UK where it was framed as a performative installation: as Erika Fischer-Lichte argues, the key aspects of performativity are unpredictability and a transformative power (Fischer-Lichte 2012). The installation is time-based and the image performs a colour change, which is not predictable. This subtle and aesthetic wonder can change the perception of the phenomenon. Leavy (Leavy 2009: 255) formulates it like this:

> "The arts can grab hold of people's attention in powerful ways, making lasting impressions. Art is immediate. …; a piece of visual art can stop people in their tracks and jar them into seeing something differently; …".

In this exhibition, the Tungsten spotlight was working appropriately, but the fluorescent light was put just underneath the artwork and unfortunately was not strong enough to experience the second colour variation accurately.

Figure 2: "green-green-green_1_03:11", 2014, Bonington Gallery, Nottingham UK

"Trilogy of light"

In order to consider the specific types of light to be used within the research, it was necessary to explore a range of light sources, and as a by-product an archive of images of lamps and light was created (Figure 3). At a certain point, this material became interesting in itself, and this subject matter formed the source in turn for the image in three knitted squares forming "Trilogy of Light" (Figure 4).

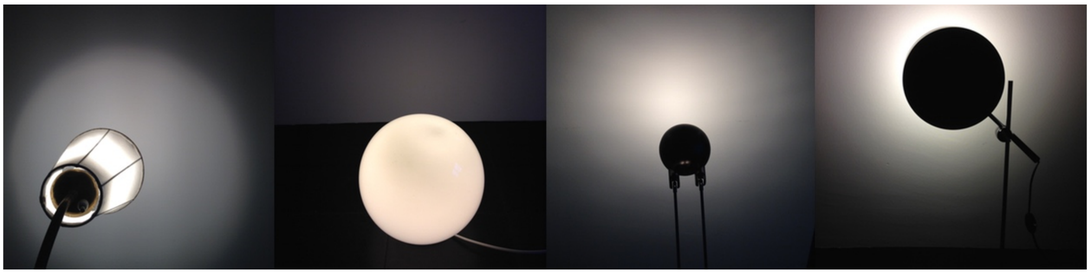

Figure 3: Various photos of lamps and light

Figure 5: "Trilogy of light" in Tungsten

Each knitted square has an image of the same lamp, made using differently dyed yarns to create three different metameric options. In daylight the human eye is not capable of perceiving the differences of colour and the image is hidden: the colour variations only occur when artificial lights are used. In this installation, the same cone of light is shown three times, but each 'canvas' reacts differently to the same light situation. It is a double game: the light itself is a form on the image, made visible by the form of the lampshade. Böhme (Böhme 1995) asserted, that we could see light only, if it appears as a medium. In fact the canvas acts as a medium; the lamp is the carrier of the light source and the light source of the standard lamp in front of the installation is the trigger. Through this combination the phenomenon comes alive. The knitted trilogy, provoked by various light sources, plays with perception and offers a visual and aesthetic experience. In this research the image is a medium to enable insight. A new point of view of this 'unwanted' physical colour phenomenon is generated. The conscious witnessing of the phenomenon enables a new experience. For Böhme (Böhme 1994) all light artists are tutors because their works are exercises of perception: as they offer the possibility to sense, observe and to feel the impact of light, to understand something of the context of light, room and perception, which is often forgotten and unobtrusive in the daily life. I see the performances and installations in this sense.

4. CONCLUSIONS

The artwork "Trilogy of light" as part of this research leads to a new consideration of the unwanted metameric phenomenon and therefore it is offering new insight. New knowledge is created through practice-based research; creating artworks, which are able to be experienced and which can be showed in different contexts to diverse audiences. The research has been tested with audiences through a series of performances and installations across the last year. It has been interesting to have responses from fellow researchers, artists, children and so on: all encountered the wonder of the subtle colour change and proved to be astonished by this banal phenomenon. Those working in colour education have already asked for demonstration material, so an educational output is possible.

This performative artwork is an embodied experience; research through practice and exploring through observing. The artworks open the phenomena to further questions. After performances or discussions about the research, it was confirmed that everybody knows the phenomenon, but nobody really knows it. The performances piqued the curiosity of audiences and changed their understanding as the hidden image shows its true colours, when it is provoked by various light situations: new insight is created and leads to a conscious appropriation of the physical colour phenomenon. The research is still on going and there is further development of installations and performance needed with the goal to communicate with images and words and to debate and test the research in the public domain. This work is a contribution in the field of colour and light and aims to reach a broad audience to spread the new observation of this phenomenon and to explore subtle instances of 'wonder' provoked by encounters with metameric phenomena. Working to consider how the poetics of this experience generate new aesthetic and artistic knowledge, it will take up John Dewey's contention that in the use of the senses a possibility of insight is embodied.

ACKNOWLEDGEMENTS

A special thanks to Joanne Lee, Nottingham Trent University, UK, for her professional guidance and valuable support.

REFERENCES

Böhme, G. 2013. *Atmosphäre: Essays zur neuen Ästhetik*. Berlin: Suhrkamp.

Böhme, H. 1994. *Das Licht als Medium der Kunst*. Berlin: Humboldt-Universität zu Berlin, Heft 66

Dewey, J. 2005. *Art As Experience.* New York: Perigee Books.

Fischer-Lichte, E. 2012. Performativität: eine Einführung. transcript.

Hemmings J. 2010. *In the Loop: Knitting Now*. London: black dog publishing. Available online, http://jessicahemmings.com/index.php/books/in-the-loop/. Accessed: February 26, 2015

Hunt, R.W.G. R. Pointer and M. Pointer, 2011. *Measuring Colour*. Wiley.

Leavy, P. 2009. *Method meets art: arts-based research practice*. New York: Guilford Press.

Turney, J. 2009 *The Culture of Knitting*. New York: Berg Publishers

Wilson, S. 2010. *Art + science now: how scientific research and technological innovation are becoming key to 21st-century aesthetics.* London: Thames & Hudson.

Address: Salome EGGER, School of Art and Design, Nottingham Trent University,
Zeigerweg 8, 3014 Bern, SWITZERLAND
E-mails: salome.egger2010@my.ntu.ac.uk

Does colour really affect pulse rate and blood pressure?

Soojin LEE, Stephen WESTLAND
School of Design, University of Leeds, UK

ABSTRACT

It is commonly believed that colour affects our heart rates and our blood pressure. However, evidence for this is limited. In this study, 42 participants took part in an experiment to explore the effect of the colour of an environment. Physiological measurements were taken of blood pressure and pulse rate after exposure to coloured-light environments for about 20 minutes. It was found that pulse rate was raised under red light compared with blue and green light. It was also found that blood pressure was raised under red light. However, no statistically significant effects were observed.

1. INTRODUCTION

There are two possibilities why a certain colour could induce a particular reaction (Kaiser, 1984). Firstly, it could be explained as physiological autonomic reactions to colour. Secondly, the responses could be evoked (possibly, for example, as colour associations) from observers' perception of the world. It is still debated *whether the reaction comes from nervous autonomic systems or a cognition process of past culturally based experiences with colour, or the two mechanisms simultaneously* (Kaiser, 1984).

For autonomic nervous systems typically, the following techniques have been employed: electroencephalogram (EEG), galvanic skin response (GSR), skin conductance response (SCR), palmar conductance, respiration movement, blood pressure, and heart rate. Although a significant effect of colour on these autonomic systems (except heart rate) was found by Gerard (1958), a later study found that only for GSR was there a significant physiological effect of colour (Jacobs and Hustmyer, 1974). A review of the literature in 1984 revealed very little evidence that colour can affect heart rate or blood pressure (Kaiser, 1984). More recently, Spath (2011) did find a decrease in blood pressure and heart rate when participants relaxed in a pink room; however, the experiment was not controlled and it is possible that participants may have shown a similar reduction if they had relaxed in a white room, for example. The question of whether colour (and coloured light in particular) can induce physiological changes is therefore still open and this study addresses it.

2. METHOD

The study was conducted in a lighting laboratory at University of Leeds (UK). The room was equipped with controllable LED lighting. A personal colour environment was constructed using a pop-up photographic studio (see Figure 1) which was illuminated externally with lighting of one of four colours (white, red, green and blue). The light inside the environment was diffuse (apart from a patch that was behind where the participants sat) and was adjusted so that a measurement of the interior of the environment had a luminance of 4.21-4.27 cd/m². Note that this level was determined primarily by the blue-light condition which has low luminance even at the brightest setting. Since it was important that each light was set to the same luminance the luminance of the blue light was a controlling factor.

A total of 42 participants took part in the study; 22 females and 20 males aged 21-35 years. No major medical or visual disabilities were detected. All subjects were run separately. The subjects were divided (randomly but balanced with approximately equal gender and nationality in each group) into three groups according to the three different coloured lights (red, green, and blue). Therefore, there were 14 participants for each colour condition.

Figure 1: The personal-colour environment in the four different conditions. Note that the computer was only present during pre-experimental measurements and was not in the environment during the actual experiments.

Each participant was first exposed to the white-light condition (control) and asked to complete an action-behaviour tendency (ACS-90) questionnaire (Kuhl, 1994) during which they became adapted to the light. The questionnaire results are not being considered in this paper. After completing the ACS-90 questionnaire each participant's blood pressure and pulse were measured. The colour of the light was changed (to either red, green or blue, depending which group they were in) and in order that the participants spent the same amount of time under each light, they were asked to complete a short logic test. On average participants spent about 20 minutes under each lighting condition and blood pressure and pulse rate were measured at the end of this period.

Different participants were exposed to red, blue and green light and therefore a direct comparison between the heart rates, for example, under the different lights cannot be carried out. Instead, in this work we consider the change in heart rate (and blood pressure) for each participant when they first adapted to white light and then adapted to a coloured light.

3. RESULTS AND DISCUSSION

Table 1 shows the pulse rate results and shows that, on average, there was an increase in pulse rate under the red light (compared with the white light) and a decrease under the green and blue lights. However, none of the differences were statistically significant ($p > 0.05$).

Table 2 shows the blood pressure results and shows that, on average, there was an increase in blood pressure (both systolic and diastolic) under the red light. However, none of the differences were statistically significant ($p > 0.1$).

PR		
red	green	blue
0	-9	0
2	-7	0
-5	-5	-3
-5	1	5
1	-6	-7
-4	-6	4
-1	-16	-4
7	0	-5
6	5	-3
7	8	2
-1	2	-4
7	2	8
-8	6	1
-1	1	0
0.3571	-1.7143	-0.4286

Table 1: The difference between the pulse rate measured under the test light and the control light is calculated for each participant. The mean differences for each of the three test lights are shown in the bottom row.

BP (Systolic)			BP (Diastolic)		
red	green	blue	red	green	blue
-6	10	1	-1	1	-5
-7	3	0	1	2	-4
7	-10	1	1	-5	-2
-7	0	4	-8	8	4
-5	-5	3	-6	-9	-1
-4	-1	2	-1	-2	-1
8	-12	-3	-1	-5	1
5	0	-5	2	0	-1
3	-16	-1	10	-1	0
-4	-4	9	6	12	8
11	-5	-5	8	3	-3
5	8	3	11	2	-26
2	-5	0	-5	0	2
23	10	-7	17	12	-10
2.2143	-1.9286	0.1429	2.4286	1.2857	-2.7143

Table 2: The difference between the blood pressure measured under the test light and the control light is calculated for each participant. The mean differences for each of the three test lights are shown in the bottom row. Data are shown for systolic and diastolic conditions.

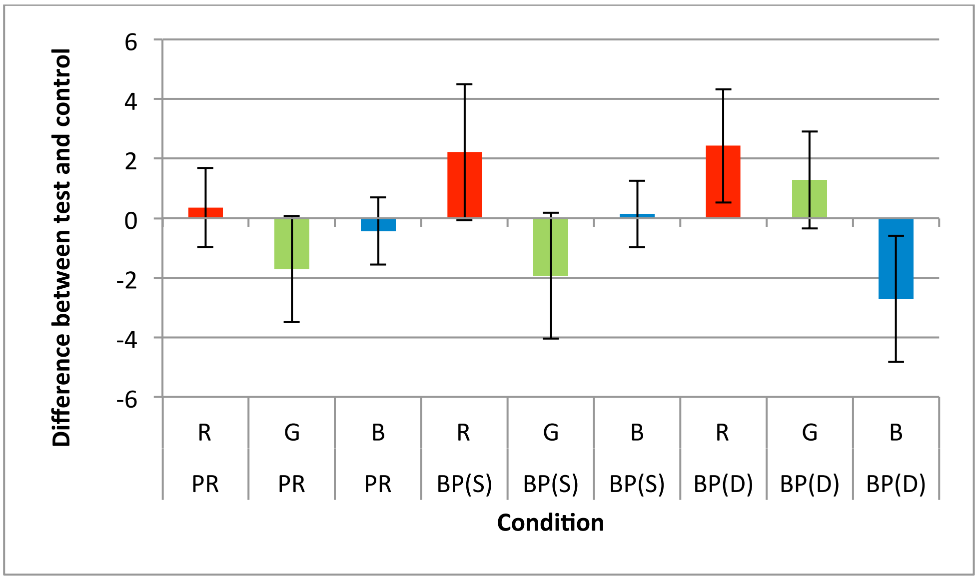

Figure 2: Summary of the physiological measurements. The mean differences in pulse rate PR, systolic blood pressure BP (S) and diastolic blood pressure BP (D) between the test and control light conditions are shown.

4. CONCLUSIONS

In this study, 42 participants took part in an experiment to explore the effect on their physiological response. Measurements were taken of blood pressure and pulse rate. When compared with the control condition (white light), the pulse rate increased under the red-light condition and decreased under the blue- and green-light conditions. The effects were not statistically significant, however; this is consistent with Jacobs and Hustmyer (1974) who found no effect of colour on heart rate.

When compared with the control condition, blood pressure (systolic and diastolic) increased under the red-light condition. However, there was no statistically significant effect of the test colour on blood-pressure change. This is consistent with Kaiser (1984) who noted that he had "unpublished data which show no differences in systolic blood pressure as a function of observers looking at grey, red, blue, green, or pink".

Despite anecdotal evidence that colour affects blood pressure and heart rate, in this study we find no statistically significant effect despite using colour environments that were very intense and likely to be far more colourful than the environment in most practical applications. However, it cannot be ruled out that in this study there were simply too few participants to find a significant effect since although there were 42 participants there were only 14 for each colour condition. The observation that red did increase blood pressure and pulse rate (although not significantly) is intriguing however and further work is probably needed with much greater numbers of participants to be able to make a robust and general conclusion. All that can be said is that, in this study, no effects were found. It seems likely, that even if a further study with more participants finds a significant effect then the effect may not be very meaningful since the magnitudes of the differences (even under the relatively extreme conditions used in this study) were quite small.

REFERENCES

Gerard, R. M. 1958. *Differential effects of colored lights*. Unpublished Ph.D. dissertation, University of California at Los Angeles.

Jacobs, K. W. and Hustmyer, F. E. 1974. Effects of four psychological primary colors on GSR, heart rate and respiration rate. *Perceptual and Motor Skills*. **38**(3), pp.763-766.

Kaiser, P. K. 1984. Physiological response to color: a critical review. *Colour Research and Application*. **9**(1), pp.29-36.

Kuhl, J. 1994. A theory of action and state orientations. In: Kuhl, J and Beckmann, J. ed. *Volition and personality: action versus state orientation*. Seattle: Hogrefe & Huber Publishers, pp.9-46.

Späth, D. 2011. The psychological and physiological effect of 'cool down pink' on human behavior. In: Schindler, V. M. and Cuber, S. ed. *AIC 2011, Interaction of Colour & Light in the Arts and Sciences, Midterm Meeting of International Color Association, Zurich, Switzerland, 7/10 June 2011, Zurich*. Zurich: pro/colore, pp.751-754.

Address: Prof. Stephen WESTLAND, School of Design,
University of Leeds, Woodhouse Lane, Leeds, LS2 9JT, UK
E-mails: s.westland@leeds.ac.uk, ml12s8l@leeds.ac.uk

Effects of Font Size on Visual Comfort for Reading on a Tablet Computer

Hsin-Pou HUANG, Yi-Ho BAI, Li-Chen OU
Graduate Institute of Applied Science and Technology, National Taiwan University of Science and Technology, Taiwan

ABSTRACT

To investigate the effect of display size on visual comfort for e-reading, two psychophysical experiments were conducted. During Experiment 1(iPad 2-size) and Experiment 2(iPod touch 4-size), 20 older and 20 young observers were presented with 190 pairs of document layouts. Each observer was asked to pick one of the two layouts, of which the observer felt more comfortable to read the text. The font size of Experiment 1 was bigger than the font size of Experiment 2. The scale values for the observer response were determined using the paired comparison method. The results of Experiment 1 and Experiment 2 show that older observers tended to prefer strong text-background lightness difference in a document layout, while young observers tended to prefer moderate lightness difference. The scale values from iPad 2-size to iPod touch 4-size for older and young observers shown that the difference of visual comfort between black background and others background is increased. However, the difference of visual comfort between white background and others background only increased for young observer. This phenomenon for young observers was different from the scale values for older observers.

1. INTRODUCTION

There have been extensive studies into the impacts of text-background contrast on visual comfort using desktop computer displays (Scharff 2002; Buchner 2007). Little was known, however, as to whether the findings also apply to e-reading devices, such as iPads or Kindle. There are more and more people using tablet computer displays for e-reading, it is important to know how users use these devices effectively and avoid any visual discomfort. The previous study(Darroch et al. 2005) shown that designers of interfaces for handheld computers provide fonts in the range of 8-12 point to maximize readability for the widest range of users. The equipment was HP iPAQ hx4700 which has a 65,000 colour TFT screen with a resolution of 640x480 pixels was used to present the text. The resolution of HP iPAQ hx4700 is smaller than the resolution of tablet computer such as iPad 2 or iPod touch 4. Our study aims to investigate the effect of display size(font size) for older and young observers reading on a tablet computer.

2. METHOD

To investigate the effect of display size on visual comfort for e-reading, two psychophysical experiments were conducted. During Experiment 1 and 2, each observer was asked to pick one of the two layouts, of which the observer felt more comfortable to read the text. The only difference of these two experiments is the font size of article shown on the iPad 2. Based on the 5 achromatic colours, 20 text-background combinations were generated, considering both positive and negative polarity conditions. Table 1 shows colorimetric measurement data for the 5 colours including luminance and the CIE values. The pair of document layout was composed by 2 text-background combinations from 20 text-background combinations. This resulted in 190 paired comparisons. Each document layout was presented on the same text, the only difference being the lightness values of the text and of the background for the two document layouts.

Table 1.CIE colorimetric data for colour samples used in Experiment 1 and Experiment 2

Colour	Luminance	(L*)	(x, y)
1. black	0.52 cd/m^2	1.19	(0.2638, 0.2552)
2. dark grey	12.59 cd/m^2	20.71	(0.3010, 0.3126)
3. medium grey	84.25 cd/m^2	53.17	(0.3004, 0.3114)
4. light grey	202.73 cd/m^2	76.69	(0.3010, 0.3125)
5. white	397.34 cd/m^2	100	(0.3005, 0.3115)

Twenty older(aged 60 years) and twenty young(aged 20-30 years) observers were presented with 190 pairs of document layouts on an iPad 2(as shown in Figures 1 (a)) during Experiment 1. Twenty older(aged 60 years) and twenty young(aged 20-30 years) observers were presented with 190 pairs of document layouts in a simulated iPod touch 4 size also shown on the iPad 2(as shown in Figures 1 (b)) during Experiment 2. The font size of Experiment 1 was bigger than the font size of Experiment 2. The display was situated in a darkened room, with the only light source coming from the iPad 2. The display peak white had a luminance value of 397.34 cd/m2, with CIE chromaticity (x, y) = (0.3005, 0.3115). The viewing distance was around 300mm between the observer and the iPad 2, which was placed with a tilt angle of 15 degrees against a desk.

(a)

(b)

Figure 1: Examples of screen layouts for (a) Experiment 1 and (b) Experiment 2

3. RESULTS AND DISCUSSION

The scale values of visual comfort were determined using the paired comparison method (Thurstone 1927). The scale values obtained from Experiment 1 for older observers were plotted against the lightness difference value, as illustrated in Figure 3 (a). Obviously the CIE lightness difference between text and background affect the observer response. It is clear from the graph that the higher the lightness difference between text and background, the higher the visual comfort for older observers. Note this tendency does not seem to be affected by the background luminance. On the other hand, Figures 3 (b) shows that in general, for the lightness difference over 80 for young observers, the visual comfort value remains unchanged or even starts to decline. This tendency for young observers is different from that for older observers as described above.

Figure 4 (a) shows the results of Experiment 2 for older observers. As illustrated in the graph, the higher lightness difference between text and background, the higher visual comfort for older observers. Such a trend does not seem to be affected by the font size of the article shown on the iPad2. This suggests that the older observers tended to prefer higher lightness difference between text and background in a document layout. For young observers, on the other hand, Figure 4 (b) shows that in general, the larger lightness difference between text and background, the higher visual comfort value, while for the lightness difference over 80 or so, the visual comfort value remains unchanged or even starts to decline.

The scale values from iPad 2-size(Experiment 1) to iPod touch 4-size(Experiment 2) for older and young observers shown that the difference of visual comfort between black background and others background is increased. However, the difference of visual comfort between white background and others background only increased for young observer.

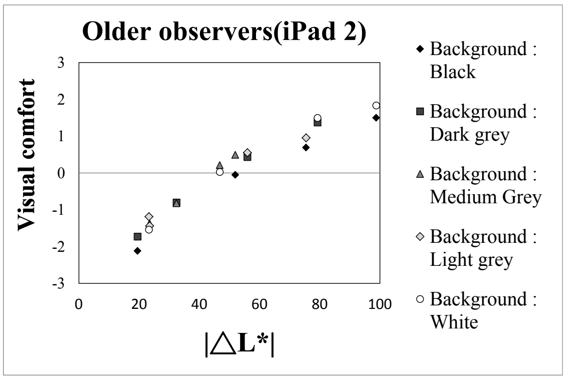

(a)

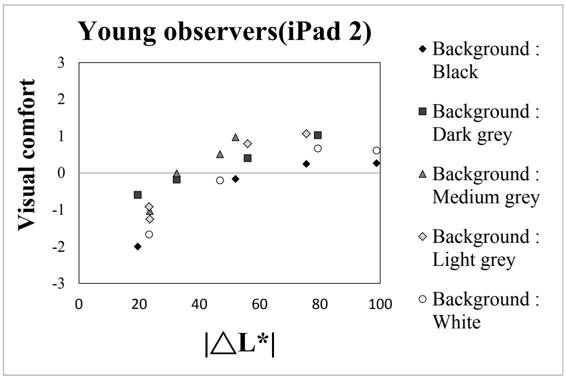

(b)

Figure 3: Visual comfort plotted against CIE lightness difference (△L) between text and background as results of Experiment 1 for (a) Older observers and (b) Young observers*

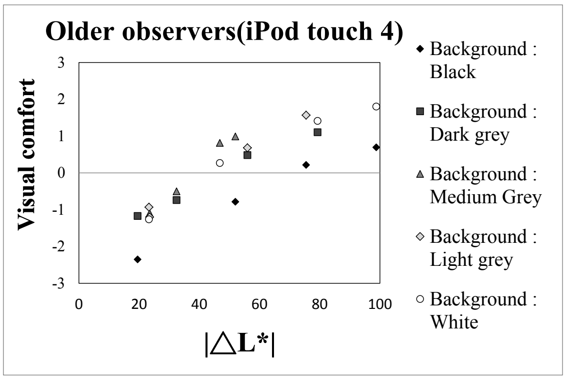

(a)

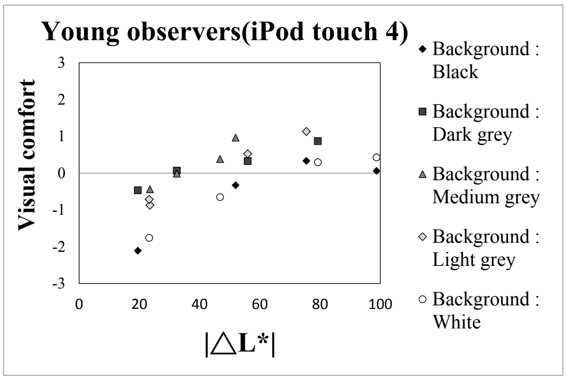

(b)

Figure 4: Visual comfort plotted against CIE lightness difference (△L) between text and background as results of Experiment 2 for (a) Older observers and (b) Young observers*

4. CONCLUSIONS

Two psychophysical experiments were conducted to investigate the visual comfort for different font size, including young and older observers. According to the experimental results, older observers tended to prefer large lightness difference (Experiment 1 and 2) between text and background shown on the iPad 2. For young observers, on the other hand, a document layout with a medium lightness difference (Experiment 1 and 2) between text and background tended to be most comfortable to read. This suggests that the font size has little influence on the tendency of visual comfort for older and young observers. Note that the visual comfort of black background is the lowest scale values for older observers. In contrast, the visual comfort of black and white background is the lowest scale values only for young observers. This phenomenon for young observers is different from the scale values for older observers.

AKNOWLEDGEMENTS

This work was supported in part by the Ministry of Science and Technology, Taiwan (MOST 103-2221-E-011-138).

REFERENCES

Scharff, L.F.V. and A.J. Ahumada Jr. 2002 *Predicting the readability of transparent text*, Journal of Vision, vol. 2, pp 653-666.

Buchner, A. and N. Baumgartner. 2007 *Text-background polarity affects performance irrespective of ambient illumination and colour contrast*, Ergonomics, vol. 50, pp 1036-1063.

Darroch, I., J. Goodman, S. Brewster, and P. Gray. 2005 *The effect of age and font size on reading text on handheld computer*, International Federation for Information Processing, LNCS 3585, pp253-266.

Thurstone, L. L. 1927 *A law of comparative judgment*, Psychological Review, vol. 34, pp 273-286.

Address:Hsin-Pou Huang, Graduate Institute of Applied Science and Technology, National Taiwan University of Science and Technology, Keelung Road., Da'an Dist, sec. 4,No. 43, Taiwan
E-mails: j133212001@gmail.com, D1002203@mail.ntust.edu.tw, lichenou@mail.ntust.edu.tw

Influence of spectral component of white light on the discomfort glare

—Contribution of image and non-image forming pathways—

Toshihiro TOYOTA, Taka-aki SUZUKI
Industrial Research Institute of Shizuoka Prefecture

ABSTRACT

Discomfort glare is a remarkable issue on novel light sources such as solid state illuminating light sources (LEDs and OLEDs). In this research, we focused on the fact that solid state light sources differ greatly in spectral characteristics from conventional light sources. In our previous studies, we conducted subjective evaluation experiments using metameric lights with different spectral characteristics and the same photometric value to find out whether there are differences in discomfort glare. The results showed that although each luminance of test light was the same, discomfort glare has a clear dependency to spectral distribution of the test lights. In particular, excitation quantity around specific wavelengths had been correlated with discomfort glare evaluation. Therefore, we investigated the contribution of ipRGCs as non-image forming pathways and rods as image-forming pathways to the discomfort glare. We then found a correlation between the quantity of them and the psychophysical evaluation of discomfort glare.

1. INTRODUCTION

Recently, discomfort glare is a crucial issue regarding novel light sources such as LEDs or LEDs. There are many optical characteristics between traditional light sources and novel light sources. In particular, spectral distributions of those light sources are quite unique.

Our previous studies showed a clear dependency between spectral characteristics and discomfort glare perception (Toyota et al. 2014). In those studies, a series of spectral distribution of test light that had the same chromaticity as daylight [T = 6500 K, xy chromaticity (x, y) = (0.3127, 0.3290)] and the same luminance for all of those as metameric white lights was designed by combining several monochromatic lights with 20 nm spectral bandwidth. We employed several limitations to simplify the spectral designing process because it is well known that there are innumerable spectral distributions that correspond to the same chromaticity (Schmitt 1976). The central wavelength of each monochromatic light was preliminarily fixed (as shown in Table 1) and the combining ratio of each monochromatic light was optimized. Each test light was represented by a digitally-controlled spectrally programmable light engine (OneLight Spectra, OneLight Corp.). A series of subjective discomfort glare ratings by nine levels conforming to a conventional manner was conducted. Results showed that discomfort glare perceptions varied even if test light of the chromaticity and luminance had the same photometric value (as shown in Figure 1). Discomfort glare perception seems to be particularly related to the spectral intensity around the wavelength of 500 nm of white lights.

The aim of this study is to discuss whether the mechanism of the discomfort glare perception could be influenced by the spectral characteristics of light sources. We focused on the relationship between results of the discomfort glare ratings and several cellular responses. In particular, we are interested in how image or non-image forming pathways contribute to the discomfort glare perception.

Table 1. Spectral conditions of metameric white lights as test lights.

Condition	Central wavelength [nm]			Photometric value		
	λ_1	λ_2	λ_3	Lv [cd/m^2]	x	y
T1			507	18356.74	0.3117	0.3265
T2	450	610	533	18137.53	0.3132	0.3292
T3			555	18467.40	0.3125	3.3280
D1	450	568		18618.26	0.3156	0.3326
D2	491	610		18444.05	0.3156	0.3326
Broad				18275.97	0.3010	0.3297

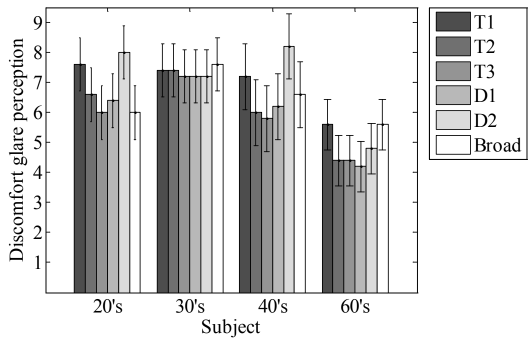

Figure 1: Discomfort glare ratings for metameric white light.

2. METHOD

We investigated the relationship between spectral characteristics and the discomfort glare perception mechanism focusing on the following perspectives.

(1) Luminance deviation caused by artifacts of reproducing the test light.

(2) Image forming pathways: rod photoreceptors.

(3) Non-image forming pathways: intrinsically photosensitive melanopsin retinal ganglion cells (ipRGCs).

2.1 Contribution of the luminance deviation

In the spectral distrubution designing process, chromaticity and luminance for all of the metameric white lights were fixed at the same value. Furthermore, fine tuning of each spectral distribution of the test light was performed to correct the representation error of the light engine. However, someone might claim that such variation of discomfort glare perception could be caused by residual errors of luminance correction. Therefore, we validated the relationship between discomfort glare ratings and luminance for each test light as combination of the quantity of L-cones and M-cones stimulation.

2.2 Contribution of image forming pathways

As another possibility of the deviations of discomfort glare perception, they might be influenced by scotopic vision or mesopic vision, because a series of experiments was performed in a darkroom in previous studies. We also tested contributions by the quantity of rods stimulation using scotopic luminous efficiency function (Judd 1951) to the discomfort glare ratings.

2.3 Contribution of non-image forming pathways

It is well known that ipRGCs are responsible for the mechanisms of circadian rhythms and the pupil responses (Tsujimura 2010). Moreover, recent studies have also shown melanopsion contributes to light perception mechanisms (Brown et al. 2012). Therefore, we also focused on the contribution of ipRGCs as non-image forming pathways to the discomfort glare perception.

To calculate the quantity of ipRGCs stimulation, an action spectrum combining spectral sensitivity of S-cones and rods (Brainard et al. 2001, Thapan et al. 2001, Rea et al. 2002) was employed as showin in Equation 1.

$$C(\lambda) = S(\lambda) + 0.67V'(\lambda) \qquad (1)$$

Figure 2 shows a series of spectral distributions of metameric white light that was used in experiments, a composite action spectrum as sensitivity of ipRGCs and spectral sensitivity of rods as a solid line, a dotted line and a dashed line, respectively.

3. RESULTS

Results of the discomfort glare rating were normalized to control the individual difference because the discomfort glare rating scale refers to individual judgement. All of the rating score was converted to follow normal distribution $N(0, 1)$ in each subject.

3.1 Calculation results for quantity of stimulation

Figure 3 shows the relationship among each quantity of stimulation. Luminance as L-cones+M-cones and ipRGCs or rods were independent. However, the quantity of ipRGCs and rods were highly correrated (r = 0.9995).

3.2 Relationship between each pathway and the results of discomfort glare rating

Figure 4 shows the relationship between each pathway and result of discomfort glare rating.

The luminance deviation for a series of test lights was irrelevant to the results of the discomfort glare ratings as shown in Figure 4 (a). In contrast, the quantity of rod stimulation and ipRGC stimulation are positively correlated with the discomfort glare perception ratings (r = 0.6648 and r = 0.6650, respectively) as shown in Figure 4 (c).

The results showed that a mechanism of the discomfort glare perception may be taking into the spectral contexts of the light sources.

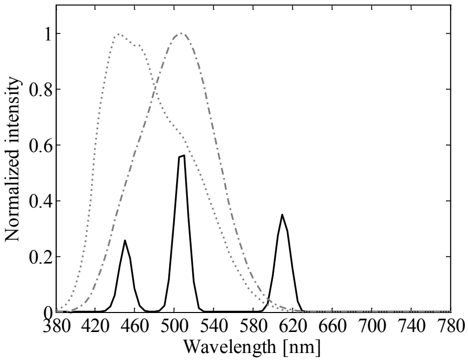

(a) T1

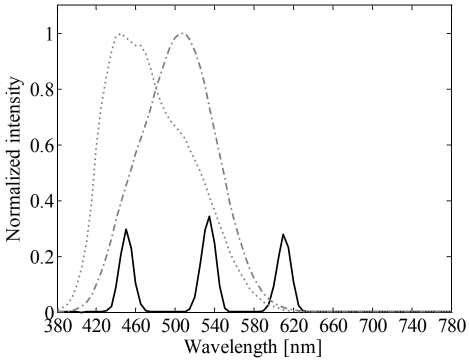

(b) T2

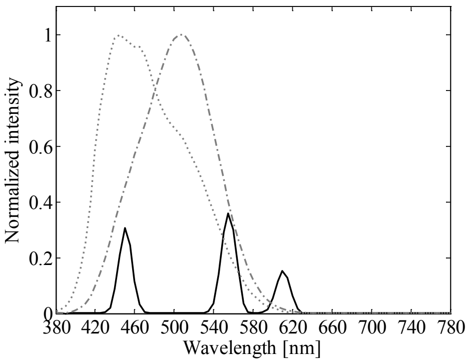

(c) T3

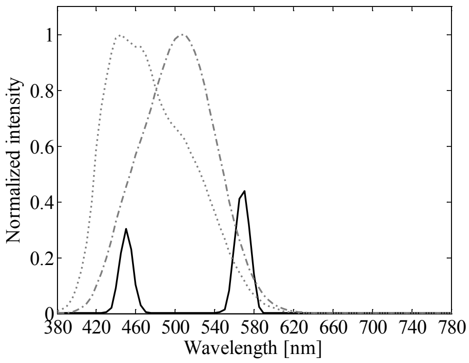

(d) D1

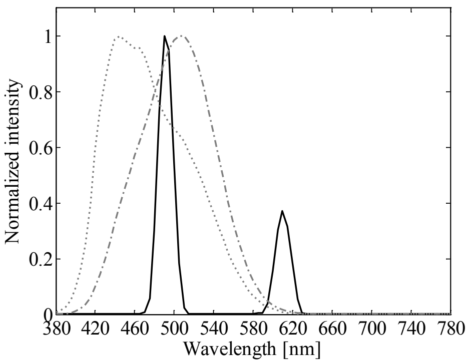

(e) D2

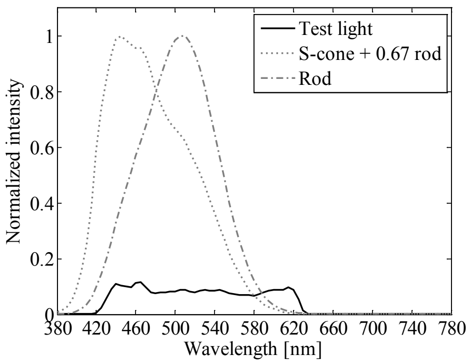

(f) Broad

Figure 2. Spectral distributions of test lights.

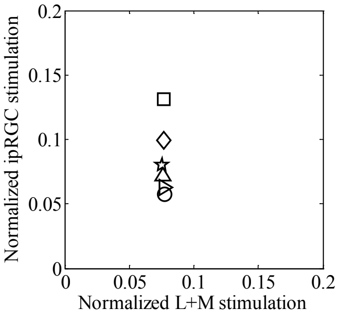

(a) L+M vs. ipRGCs

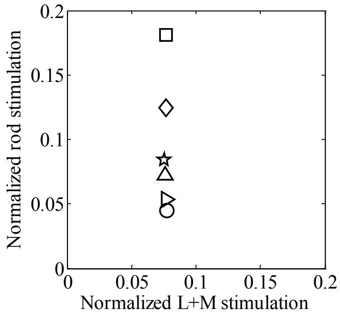

(b) L+M vs. Rods

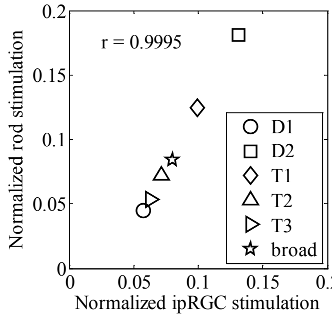

(c) ipRGCs vs. Rods

Figure 3. Quantity of stimulation

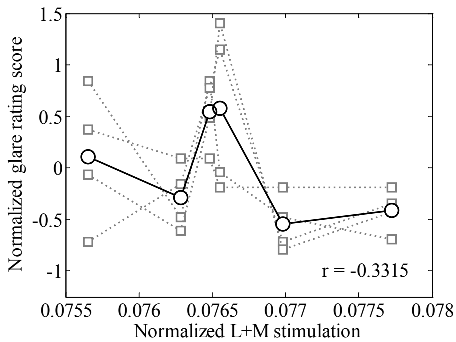

(a) L+M vs. Glare

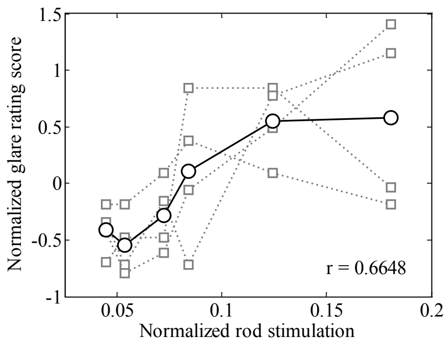

(b) Rods vs. Glare

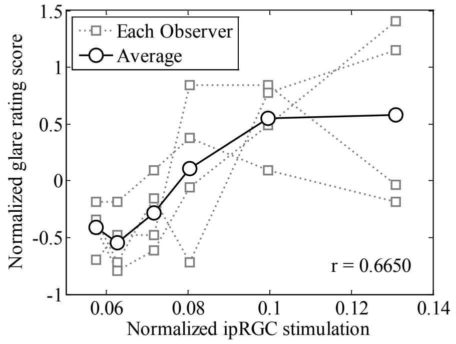

(c) ipRGCs vs. Glare

Figure 4. Comparison with glare evaluation and quantity of stimulation

4. CONCLUSION

In this study, we investigated the relationship between the results of the discomfort glare ratings and the quantity of cellular responses of visual or non-visual image forming pathways. Results suggest that the mechanism of the discomfort glare perception is influenced by both an image forming pathway that involves a scotopic vision and a non-image forming pathway.

Going forward, we will consider conducting simultaneous measurements of discomfort glare ratings and pupil diameters to explore the contribution of non-image forming pathways to the discomfort glare perception.

REFERENCES

Toyota, T., T. Suzuki, W. Shichi, T. Funai, and T. Mano. 2014. Effect of Spectral Characteristics of Metameric Illuminant on Glare Perception. In *Proceedings of the 14th International Symposium on the Science and Technology of Lighting*, ed. by R. Devonshire and G. Zissis. Sheffield, South Yorkshire, UK: FAST-LS Ltd, 513–516.

Schmitt, F.J.M. 1976. A method for the treatment of metamerism in colorimetry. *Journal of the Optical Society of America* 66: 601–608.

Judd, D.B. 1951. Report of U.S. secretariat committee on colorimetry and artificial daylight. In *Proceedings of the twelfth session of the CIE*, Paris: Central bureau of the CIE, 11.

Tsujimura S., K. Ukai, D. Ohama, A. Nuruki, and K. Yunokuchi. 2010. Contribution of human melanopsin retinal ganglion cells to steady-state pupil responses. *Proceedings of the Royal Society London. Series B: Biological Sciences* 277: 2485–2492.

Brown T.M., S. Tsujimura, A.E. Allen, J. Wynne, R. Bedford, G. Vickery, A. Vugler, and R.J. Lucas. 2012. Melanopsion-based brightness discrimination in mice and humans. *Current Biology* 22: 1134–1141.

Brainard G.C., J.P. Hanifin, J. M. Greeson., B. Byrne, G. Glickman, E. Gerner, and M. D. Rollag. 2001. Action spectrum for melatonin regulation in humans: evidence for a novel circadian photoreceptor. *Journal of Neuroscience* 21: 6405–6412.

Thapan K, J. Arendt and D.J, Skene. 2001. An action spectrum for melatonin suppression: evidence for a novel non-rod, non-cone photoreceptor system in humans. *Journal of Physiology* 535: 261–267.

Rea, M.S., J.D. Bullough, and M.G. Figueiro. 2002. Phototransduction for human melatonin suppression. *Journal of Pineal Research* 32: 209–213.

Address: Dr. Toshihiro TOYOTA, Machinery Division, Industrial Research Institute of Shizuoka Prefecture, 2078 Makigaya, Aoi-ku, Shizuoka-shi, Shizuoka 421-1298, JAPAN
E-mail: toshihiro_toyota@iri.pref.shizuoka.jp

Low-chroma colors suppress luminance-driven brain activation measured by fMRI

Ippei NEGISHI[1] , Keizo SHINOMORI[1]
[1] School of Information, Kochi University of Technology

ABSTRACT

The interaction between color and luminance information has been suggested by psychophysical research in human visual perception. To reveal the mechanism of the interaction, we measured brain activation while observing visual stimuli consisted of luminance and color information and varied the intensity of color information.

In the experiment, subject observed 10 color patches and achromatic background pattern. There were 4 conditions in saturation (value 0, 2, 4 and 6 in Munsell color system) of the patches in 4 levels. We measured brain activity while subject observed the stimuli. The brain activity was analysed in several visual fields.

The results showed that brain activations were the highest in the condition of chroma 0, and those of chroma 6, 4, and 2 conditions were following. It seemed that the brain activation for achromatic background pattern was suppressed by color patches and that is confirmed by additional control experiment. The amount of the suppression was more large in low chroma level condition.

1. INTRODUCTION

The interaction between color and luminance information has been suggested in human visual perception. Some reports suggested that luminance information is suppressed by the presence of color information psychophysically (Switkes et al. 1988, Kingdom 2003, Kingdom et al. 2010), though the mechanism of the suppression is not fully revealed.

To reveal the mechanism of the suppression, we measured activities of visual fields by fMRI, while seeing achromatic pattern and color patches. We manipulated saturation of the color patches as an index of color information intensity. It is also unclear in which level in visual cortex the suppression occurs. So we identified V1, V2, V3, V3A/B, hV4 and LO1 of each subject and analyzed the brain activity of those visual fields.

2. METHOD

13 subjects participated in the experiment (12 male and 1 female, mean age = 22.7 years old). All subject had normal color vision (tested by Ishihara Color Vision Test, SPP Color Vision Test and Panel D-15 Color Vision Test), and normal or corrected to normal visual acuity.

2.1 Apparatus

We used 3T MRI scanner (Verio, Siemense) for collecting fMRI images. Subject observed visual stimuli on the screen through the mirror (Figure 1). The viewing distance was 69 cm and the viewing angle was 31.5 degree × 25.2 degree, and the resolution of visual stimuli was 1280 pixel × 1024 pixel. The projector was controlled by CRS ViSaGe and calibrated by CS-200 color meter.

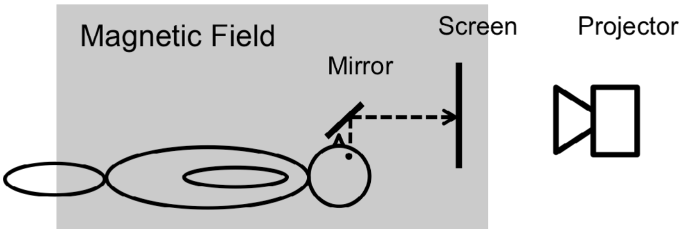

Figure 1: Experimental apparatus

2.2 Visual Stimuli

We presented 10 patches on the background pattern consisted of more than 700 achromatic oval patches (Figure 2). The patches were placed in the circle and the diameter of each circle was 3.0 degree. The patches were filled by 10 hues (5R, 5YR, 5Y, 5GY, 5G, 5BG, 5B, 5PB, 5P and 5RP on Munsell color system), and the position of each hue was randomized for each trial. The chroma of patches was set at one of 4 levels (6, 4, 2 and 0 in Munsell chroma). The Munsell value of the patches was constant (Value = 5) in all conditions (Figure 3). White fixation point was presented in the center of the stimuli.

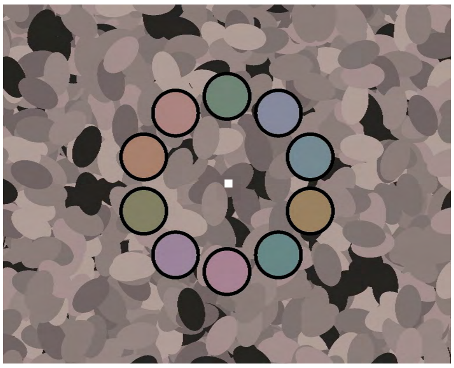

Figure 2: Overview of visual stimuli

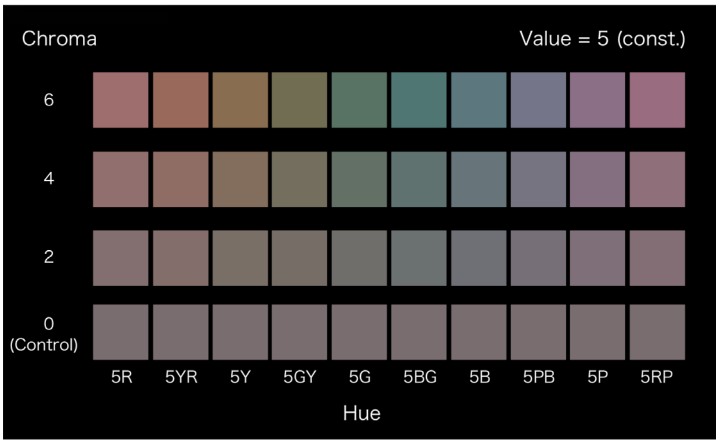

Figure 3: Hues of patches in each chroma level condition

2.2 Experimental Procedure

Each subject conducted 18 blocks of experiment. 1 block contained 12 trials (3 trials for each chroma level condition and presentation order was randomized in each block). Each trial contained stimulation phase and rest phase. The stimulation phase lasted 15 second and the visual stimuli and its scrambled pattern were presented alternatively at 1Hz. During the stimulation phase, subject watched the fixation point at the center of visual stimuli. The rest phase also lasted 15 second. In the rest phase, nothing were projected on the screen except that simple white figure is presented in first 5 second. Subject perform easy cognition task in first 5 second and rested in last 10 second. Brain activity was measured every 2.5 second during the block. (Figure 4)

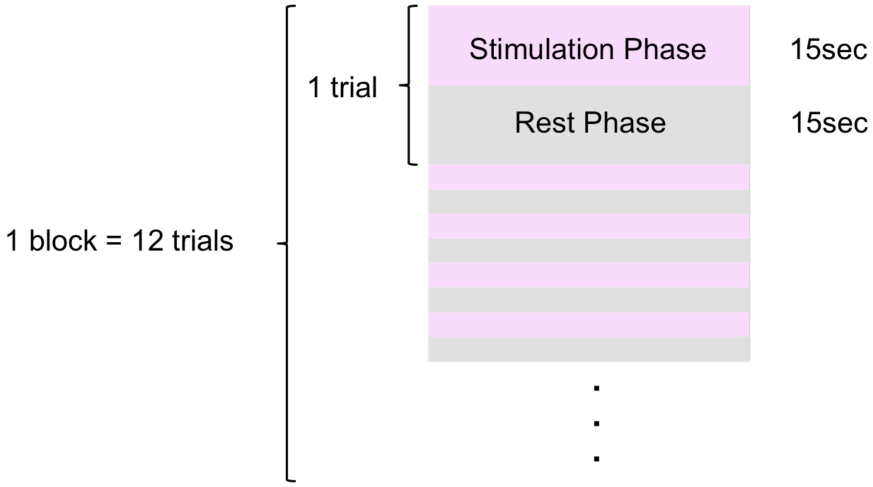

Figure 4: Experimental time course

3. RESULTS AND DISCUSSION

V1 and other visual fields were identified by travelling wave method (Wandell et al. 2007). Figure 5A shows the time course of normalized BOLD responses in V1 for each chroma level condition. Anterior half of the time course corresponds to the stimulation phase and posterior half of the time course corresponds to the rest phase. The responses of chromatic (chroma 2, 4 and 6) conditions were smaller than achromatic (chroma 0) condition. One way ANOVA indicated that there is significance main effect of chroma level condition. Post-hoc comparisons indicate significant difference between chroma 0 and 2 conditions.

To confirm that the results is not reflect brain activity driven by color information directly, we conducted control experiment in which the background pattern of visual stimuli was removed. Figure 5B shows the result of control experiment. There are no significant main effect of chroma level condition and differences in any combinations of the chroma level condition. These results suggest the presence of suppression on luminance information by color information in main experiment. In V2, V3, V3A/B, hV4 and LO1, the time courses of BOLD responses were similar to those of V1. It seems that the suppression occurs in early visual cortex, and the effect spreads to higher visual cortex.

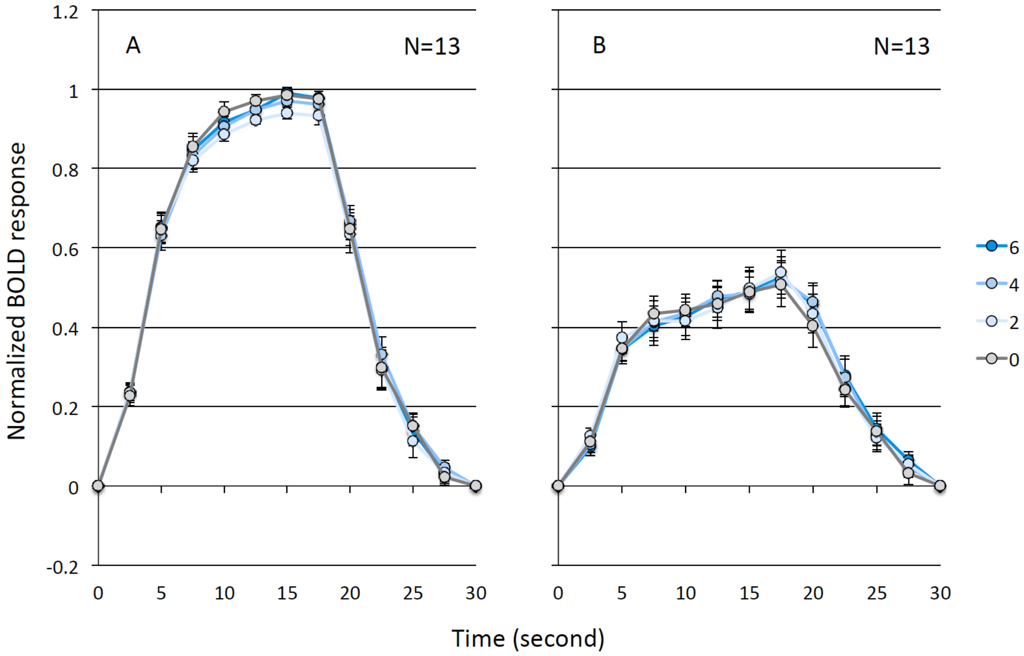

Figure 5: Normalized BOLD responses in V1

4. CONCLUSIONS

Brain activation by luminance information was suppressed when color information was attouched. The amount of suppression was larger when the color information was weak. The suppression was observed in V1, V2, V3, V3A/B, hV4 and LO1.

ACKNOWLEDGEMENTS

This research was supported by JSPS KAKENHI Grant Number 24300085 to IN and KS.

REFERENCES

Kingdom, F.A.A. 2003. *Color brings relief to human vision*, Nature Neuroscience 6 (6) 641-644.

Kingdom, F.A.A., J. Bell, E. Gheorghiu and G. Malkoc 2010. *Chromatic variations suppress suprathreshold brightness variations*, Journal of Vision 10(10) 1-13.

Switkes, E., A. Bradley and K. K. De Valois 1988. *Contrast dependence and mechanisms of masking interactions among chromatic and luminance gratings*, Journal of the Optical Society of America A 5(7) 1149-1162.

Wandell, B., S. Dumoulin and A. Brewer 2007. *Visual Field Maps in Human Cortex*, Neuron 56 366-383.

Address: Ippei NEGISHI, School of Information, Kochi University of Technology
185 Tosayamaca-cyo-Miyanokuchi, Kami city, Kochi, 782-8502, JAPAN
E-mails: negishi.ippei@kochi-tech.ac.jp, shinomori.keizo@kochi-tech.ac.jp

A new evaluation method using the 100-hue test and age trends in color distinction ability

Masayuki HARADA [1]
[1] Graduate School of Design and Architecture, Nagoya City University

ABSTRACT

It has often been noted that sight becomes yellowish with aging because of the lenses of the eyes taking on a yellow hue. As a result, the ability to distinguish color is diminished; however, the degree of decline in color distinction ability varies among individuals. Therefore, it is important to be able to determine how advanced the degree of decline is. However, there are no convenient methods for individuals to identify their status quickly.

This study proposes a new way of achieving this objective using the 100-hue test, which requires calculating the error scores of four trays and estimating color distinction ability by the size of the error score values. However, it cannot explain the extent to which color difference can be distinguished. This new index digitizes color distinction ability using probability and statistics theory and can estimate distinction ability as the color difference.

1. INTRODUCTION

It has often been noted that sight becomes yellowish with aging because of lenses of the eyes taking on a yellow hue. As a result, the ability to distinguish color is diminished. This can cause missteps and visual recognition failures, leading to accidents, collisions, or falls; the degree of the decline in color distinction ability, however, varies among individuals.

Yellow vison with aging was first regarded as a problem of vital function with the investigation by Boettner and Wolter (1962) on the optical transmittance of sample eyeballs. In Japan, Yoshida and Hashimoto (1990) aimed to clarify this problem. From measurements of the colors of the pictures taken with lenses or filters with the same wavelength transmittance characteristics as yellow vision, they estimated the sight of old people. However, their approach did not consider color adaptation as a physiological mechanism and the overestimation of effects of yellow vision. It is therefore desirable to estimate yellow vision as a psychophysical value by an experiment using old subjects.

The 100-hue test is a standard evaluation method of color distinction ability of a subject and has been studied by various researchers. Verriest (1963) conducted experiments under conditions of standard light C of illuminance level 100 lx with 480 subjects aged 10–64 years using the Farnsworth–Munsell 100-hue test and found that the error scores of senior subjects becomes high in the blue–green and red areas. In Japan, Yano et al. (1993) studied the influence of illuminance level and light color temperature on color distinction ability using the same 100-hue test as that used in this study. They made it clear that the distinction ability of senior subjects was inferior in every hue, especially the purple–red area, compared with young subjects and that the influence of light color temperature was small with a high illuminance level; however, the error scores of old subjects increased with a low illuminance of 100 lx, and the error scores of both young and old subjects increased with a low illuminance of 10 lx.

However, the error score is an ordinal scale comparing the relative magnitude relationship only. It does not provide enough information about the scale of difference of color caps distinguished by the subject. A new evaluation method is needed to measure this. In this paper, we propose a new evaluation method using the 100-hue test and report an example analysis using the new evaluation method.

2. PROPOSAL OF THE NEW INDEX OF THE COLOR DISTINCTION ABILITY USING THE 100-HUE TEST

2.1 100-hue test

The 100-hue test (Farnsworth, 1943) was developed by Dean Farnsworth in the 1940s to evaluate the color distinction ability. Figure 1 is a 100-hue test (ND-100) devised by Japan Color Enterprise Co., Ltd. This 100-hue test consists of 100 color caps that have the same value and chrome. The 100 color caps were lined up at equal intervals along the length of the test equipment, displaying 100 color difference units (NBS units) on the CIE 1964 (U*V*W*) color space. The 100 color caps were divided into four trays, each with 25 caps. The other two next-color caps were fixed at either end of each tray. Subjects were asked to replace the 25 removable caps as the hue gradually changed.

Figure 1: 100-hue test

2.2 Error score

The error score is the traditional evaluation index usually used in the 100-hue test. This score was calculated from the test order of the color caps lined by a subject by the procedure indicated in Table 1, and it indicated the degree of error. A high error score implied low color distinction ability. Table 2 shows a calculation example. However, the error score cannot provide information as to the degree of difference between color caps distinguished by the subject.

Table 1 : Calculation procedure of the error score

Step 1) Write the number of the color cap placed by a subject in space of "Test order" on table 2.
Step 2) Calculate the difference between the next 2 numbers of "Test order," and write the difference in a blank space between "・" and "・" on the "Difference" line.
Step 3) Add the next 2 numbers of "Difference," and write the calculation result in a blank space under "・" of the "Add" line.
Step 4) Subtract 2 from numerical values on the "Add" line and write the result on the "Error score" line.
Step 5) Add 25 error scores and it will be the sub-total error score. In total, 4 sub-total error scores and "total error score" will be obtained.

Table 2 : A calculation example of the error score

Position	100 1 2 3 4 5 6 7 8 9 10 11 12 13 14 · ·
Test order	(0) 1 2 3 5 4 6 9 8 7 10 11 12 13 14 · ·
Difference	1 · 1 · 1 · 1 · 2 · 1 · 2 · 3 · 1 · 1 · 3 · 1 · 1 ·
Add	2 2 3 3 3 5 4 2 4 4 2 2 2 2 ·
Error score	0 0 1 1 1 3 2 0 2 2 0 0 0 0 ·

2.3 Development of a new color distinction index

It seemed appropriate to consider all color caps instead of the next color cap only for an accurate estimation of color distinction ability. Even when a subject has a confusion between color caps, the possibility exists that the subject has lined up the color caps in the right order by chance. Therefore, it is necessary to include a concept of the expectation value in a new evaluation index in order to take accidents into account.

The concept and procedure of this new index was as follows. Before deriving the value "n(i)," the confusion amount "C(i)" was defined. The C(i) calculation procedure was as follows. The difference between any two color cap numbers was defined as the distance between the two. The author assumed that the color cap was placed in the wrong position when the color cap that should be placed on the left side of color cap No.i was placed on its right side, or vice versa, and the confusion amount C(i) was defined by the equation

$$C(i) = \Sigma\, \gamma\, d_{ij} \qquad \cdots\cdots \text{equation (1)}$$

where "i" is the number of the target color cap, "d_{ij}" is the distance between color cap Nos.i and j, "γ" is a variable with a value of either "0" or "1" : when color cap No.j was placed in the wrong order in relation to color cap No.i, "γ" becomes "1", and when placed in the right order, "γ" becomes "0." Equation (1) provides the total distance between color cap No.i and all color caps placed in wrong orders. Table 3 is a calculation example where the confusion amount C(7) of No.7 become 7.

Each color cap usually has two color caps of the same distance. As the color caps were divided into 4 trays, however, the color cap No.27, for example, has only one cap with a distance of more than 2 (the color cap with a distance of 2 is only No.29). Therefore, when the color cap was lined up by mistake in such a case, a weighting factor (=2) was adopted. Calculation example 2 is indicated in Table 3.

Next, "n(i)" can be inferred from the confusion amount C(i). The "n(i)" value indicated the distance between the two confused color caps. Before n(i) was defined, the following two assumptions were made :

Assumption 1 : When confusion does not occur, all color caps are lined up in the correct order.

Assumption 2 : When confusion occurs, the color cap is lined up in the correct order with a probability of 1/2 and is lined up in the wrong order with a probability of 1/2.

When taking into account these assumptions, in a case where confusion does not occur at all, the expected value of C(i) is "0." When confusion occurs with the color caps with a distance of 1, two color caps with a distance of 1 will be lined up in the wrong order with a probability of 1/2 each. Therefore, when confusing color cap No.i with a color cap with a distance of 1, the expected value of the confusion amount C(i) will be 1 [= 1(distance) × 1/2 (probability) × 2 (caps)]. When confusion has occurred with a color cap with a distance of 2, two color caps with a distance of 1 and two color caps with a distance of 2 will be lined up in the wrong order with a probability of 1/2 each. Therefore, C(i) will be 3 [= 1 (distance) × 1/2 (probability) × 2 (caps) + 2 (distance) × 1/2 (probability) × 2 (caps)].

Equally, when confusion occurs with color caps with a distance of N, the expected value of the confusion amount C(i) will be expressed as

$$C(i) = \Sigma\,(i \times 1/2 \times 2) = N\,(N + 1)/2 \quad \cdots\cdots \text{equation (2)}$$

Equation (2) can be solved from N. It is possible to define the n(i) value using the confusion amount C(i) derived from an experimental result [see equation (3)].

$$N = n(i) = [-1 + \sqrt{(1 + 8 \times C)}]/2 \quad \cdots\cdots \text{equation (3)}$$

Table 3 : Calculation examples of n(i)

<u>**Calculation example 1**</u>: The confusion amount C(i) and n(i) value of color cap No.7

Order	100	1	2	3	4	5	6	7	8	9	10	11	12	13	14 ･････
Test order	(0)	1	2	3	5	4	10	9	8	7	6	11	12	13	14 ･････

When looking at color cap No.7,
the color caps placed on the right side by mistake are … No.6
the color caps placed on the left side by mistake are … No.8, No.9, No.10
Therefore, $C(7)= \Sigma\,(\gamma \times d_{7j})= 1 + 1 + 2 + 3 = 7$.
And $n(7) = \{ -1 + \sqrt{[1 + 8C(7)]}\}/2= [-1 + \sqrt{(1 + 8 \times 7)}]/2 = 3.275$.
In conclusion, it is presumed that the subject confused the color cap No.7 with the color cap of distance 3.275.

<u>**Calculation example 2 (weighting)**</u>: The confusion amount C(i) and n(i) of color cap No.27

Order	25	26	27	28	29	30	31	32	33	34	35	36	37 ･････
Test order	25	26	30	28	27	29	31	32	33	34	35	36	37 ･････

When looking at color cap No.27,
the color caps placed on the right side by mistake are … none
the color caps placed on the left side by mistake are … No.28, No.30
The color cap No.25 is fixed. The color cap of distance 3 from No.27 is only No.30.
Therefore, the weighting factor (=2) is adopted on No.30.
There, $C(27) = \Sigma\,(\gamma \times d_{27j}) = 1 + 3 \times 2 = 7$.
And, $n(27)= \{-1+ \sqrt{[1 + 8 \times C(27)]}\}/2 = [-1+ \sqrt{(1 + 8 \times 7)}]/2 = 3.275$
In conclusion, it is presumed that the subject confused the color cap No.27 with the color cap of distance 3.275.

3. ANALYSIS OF AGE TRENDS IN COLOR DISTINCTION ABILITY USING THE NEW INDEX

3.1 The experimental outline

An experiment was conducted in the room with only artificial lighting from three wavelength fluorescent lamps. The average illuminance on a desk surface was 411 lx.

There were 34 subjects (nine people in their 50s, seven in their 60s, and seven in their 70s as the old groups, and 11 in their 20s as the young group). The subjects were checked using the Ishihara color blindness test plate, and the color vision of all subjects was normal. The subjects familiarized themselves with the 100-hue test before the experiment.

3.2 Relationship between age and color distinction ability

The average n(i) value for each subject for each tray was calculated. The results are indicated in Figure 2. As an overall tendency, old subjects had high n(i) values. In particular, the n(i) values of subjects in their 60s and 70s were high in the second tray consisting of the color caps in the green–blue area and in the fourth tray consisting of the purple–red area. And the individual variation was seemed to be large. Some subjects in their 50s, 60s, and 70s had the same n(i) values as the subjects in their 20s.

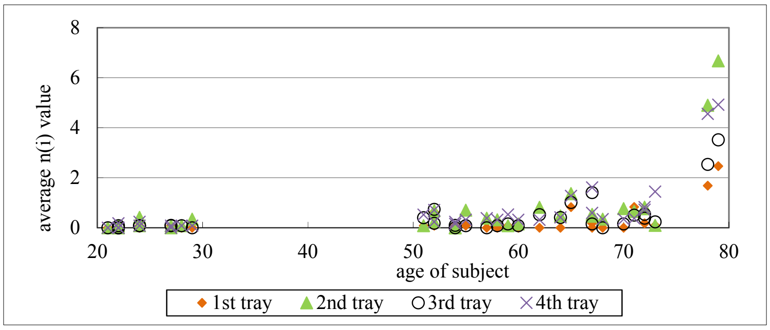

Figure 2: Average n(i) of each subject for each tray

Next, the average n(i) for each color cap for each age group was calculated. The calculation result is indicated in Figure 3. From No.10 to No.35 and from No.70 to No.80, the n(i) value was low for every age group, and the differences between the n(i) values among age groups were small. On the other hand, the differences between the n(i) values among age groups were large from No.35 to No.60 and from No.85 to No.5. The older group tends to have higher n(i) values.

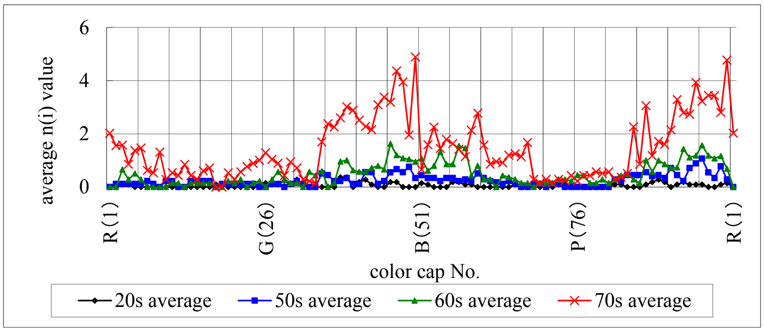

Figure 3: Average n(i) of each color cap for each age group

One hundred color caps were divided into 10 hues of the Munsell color system to make the result indicated in Figure 3 easier to understand. Figure 4 shows the n(i) value of each hue for each age group. As seen in Figure 4, the subjects in their 20s can distinguish all color caps almost perfectly. The older subject group had higher n(i) values on almost all of the hues than the young group. Particularly, the distinction ability falls suddenly for those in their 60s and 70s. This tendency was conspicuous in the hues of G, BG, B, and RP. On the other hand, the decline in the distinction ability in the hues of YR, Y, GY, and PB was inconspicuous. Although no subjects in their 30s and 40s participated in this experiment, it can be surmised that color distinction ability does not fall gradually with age but rather that the decline in color distinction ability appears as a sudden change after the 50s.

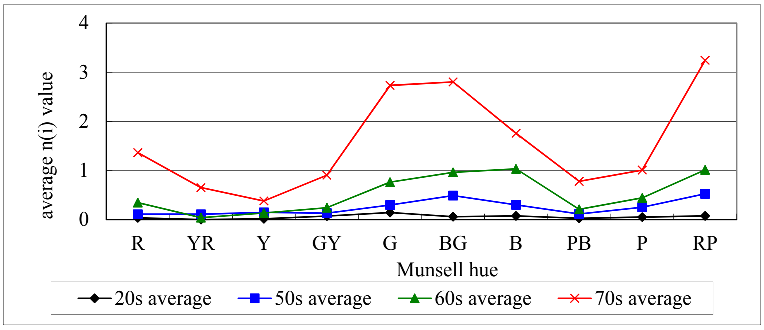

Figure 4: Average n(i) of each hue for each age group

4. CONCLUSIONS

Yellowing vison with aging is widely known, but there were no ways to assess color distinction ability correctly and easily. The error score of the 100-hue test is used as one measure of judgment, but it cannot explain the extent to which color difference can be distinguished. The new index proposed in this paper is different from the error score in two ways. First, a relationship between the target color cap and all other color caps is taken into consideration in the new index. Second, the new index is based on a concept of probability and statistics. This new index, the n(i) value, displays distinction ability as the difference between the color caps, but if the color difference between the color caps is known, the distinction ability can be estimated as the color difference.

The results of the test of 34 subjects in their 20s–70s was analyzed using this new evaluation index. The results indicated that color distinction ability in the G–BG–B area and the RP–P area falls conspicuously in subjects in their 50s and over. Individual variation was found to be large, with some subjects in their 50s to 70s having the same distinction ability as those in their 20s.

ACKNOWLEDGEMENTS

The author would like to thank everyone who cooperated with the experiment. This work was supported by JSPS Grants-in-Aid for Young Scientists (B) Number 13750577. In addition, Katsutoshi Murawaka (at the time, a graduate student of Nagoya University) cooperated substantially in implementing the study. The author would like to thank Enago for the English language review. A part of the contents of this paper was reported in reference (Harada et al., 2002).

REFERENCES

Boettner, E.A., and J.R. Wolter. 1962. Transmission of the ocular media. *Investigative Ophthalmology* 1 (6): 776-783.

Farnsworth, D. 1943. The Farnsworth-Munsell 100-Hue and Dichotomous Tests for Color Vision. *Journal of the Optical Society of America* 33: 568–574.

Harada, M., K. Murawaka and S. Kuno. 2002. Studies on the Age-related Yellow vision and Color Discrimination Properties: Part.1. *Proceedings of Kinki Chapter Architectural Research Meeting* 42: 253-256 (in Japanese).

Verriest, G. 1963. Further Studies on Acquired Deficiency of Color Discrimination. *Journal of the Optical Society of America* 53 (1): 185-195.

Yano, T., Y. Shimomura, K. Hashimoto and S. Kanaya. 1993. The effect of illuminance level, the correlated color temperature of the light source, and the observer's age on color discrimination properties. *Journal of the Color Science Association of Japan* 17 (2): 107-118 (in Japanese).

Yoshida, A, and T. Hashimoto. 1990. Disappeared Signs Analyzed By Spectral Transmissivity: Study of Yellow Vision Field by Age (1). *Summaries of technical papers of Annual Meeting Architectural Institute of Japan E*: 669-670 (in Japanese).

Address: Assistant Prof., Masayuki HARADA, Nagoya City University, 2-1-10 Kita-chikusa, Chikusa-ku, Nagoya, 464-0083, JAPAN
E-mail: harada@sda.nagoya-cu.ac.jp

Study on image statistics when color attracts human attention

Yasuhiro HATORI,[1,2] Ichiro KURIKI,[1] Kazumichi MATSUMIYA,[1] Satoshi SHIOIRI[1,2]
[1] Research Institute of Electrical Communication, Tohoku University
[2] CREST, Japan Science and Technology Agency

ABSTRACT

Computational models of human visual attention predict candidate locations in a visual scene to which human may pay attention by using bottom-up visual features such as orientation, color, and luminance (Itti et al., 1998). These features are assumed to contribute equally to constitute a single saliency or conspicuity map. A previous study applied a machine learning technique to seek the optimal weights for the features, and showed that the weight for orientation is larger than those for other features (Zhao and Koch, 2011). Although the result suggests the dominance of orientation for the deployment of attention based on low-level features, it has not been clarified whether relative efficiency among low-level features is always constant in individual images. First, we computed orientation-based and color-based saliency maps of around 500 natural images, and evaluated prediction accuracy by means of the area under the curve (AUC). The results showed that orientation-based saliency outperforms color-based saliency, on average, which is consistent with the result of the previous study. The images were sorted based on the difference of AUC scores between color and orientation so that we classify the images into two categories: color-dominant and orientation-dominant images. For around 25% of the images, color information was more effective than orientation information to predict gaze locations. We also obtained image statistics of the images in CIE $L^*a^*b^*$ color space to characterise what properties of the images yeilded the better performance in color-based saliency. We found that skewness and kurtosis of a^* were significantly larger in color-dominant images than those in orientation-dominant images. These results suggest that the simple image statistics could determine low-level visual features that attract attention in humans.

1. INTRODUCTION

Brain selects and processes important or meaningful information and ignores others. Such a selection mechanism is called visual attention, which allows us to process parts of external world relevant to ourselves among enormous information. However, fundamental mechanism of visual attention is less understood. Several psychophysical studies argued relationships between attended locations and gaze positions (e.g., overt attention; Posner 1980), and therefore, most computational studies tried to predict human gaze locations. One of the most successful concepts to predict gaze shifts is the saliency map which visualizes attractiveness of each spatial position in a given image (Koch and Ullman, 1985; Itti et al., 1998). In this saliency map approach, it is assumed that the different low-level features attract human attention independently. Low-level visual features such as orientation, color, and intensity (luminance) are extracted topographically, and they are combined into a saliency (conspicuity) map.

Most of the models hypothesize that individual features contribute equally to constitute a saliency map (e.g., Itti et al., 1998). A previous study has made an attempt to seek the optimal weights for the low-level visual features to predict gaze positions among natural images, and showed that the contribution of orientation tended to be larger than other low-level features (Zhao and Koch, 2011). Although the result suggests that orientation information is useful to predict gaze shifts, it has not been investigated whether relative efficiency among low-level features should always be constant for individual images.

First, we investigated performance of orientation and color information to predict gaze shifts in individual natural images. We obtained saliency maps from single features, and found the dominance of orientation-based saliency map in the prediction of gaze locations compared to that of color-based saliency map on average, reproducing the finding of the previous study (Zhao and Koch, 2011). We compared prediction accuracy of gaze shifts between orientation-based and color-based saliency maps of individual images, and found that color-based saliency predicted gaze shifts more accurately for approximately 25% of natural images. This result suggests that efficient visual features for predicting gaze shifts could be different among images.

We examined characteristics of the images that yielded the dominance of color information. It is reported that brain takes advantages from the statistical structures of natural images by means of efficient processing (Hoyer and Hyvärinen, 2000; Olshausen and Field, 1997), so that image statistics are candidates for explaining the better performance of color-based saliency. In the present study, we utilized four statistics (mean, variance, skewness and kurtosis) of the images in CIE $L^*a^*b^*$ color space. We found that skewness and kurtosis of a^* are significantly larger when color capture gaze shifts, suggesting that simple image statistics could be the descriptor of low-level features which capture human's attention.

2. METHOD

2.1 The model

Implementations of saliency map have been published elsewhere (e.g., Itti et al., 1998; Hiratani et al., 2013; Judd et al., 2009; Zhao and Koch, 2011). The essence of computation is given below. Low-level visual features (orientation, color, and intensity) that are represented in early visual cortices are extracted topographically from an input image, yielding feature maps.

The attractiveness of a visual feature is not determined by itself, rather depends on context. For instance, one feature (e.g., a red bar) surrounded by similar features (e.g., magenta bars) is less attractive compared to the case that the feature surrounded by dissimilar features (e.g., green bars). In the model, this mechanism is realized by a map-normalization operator which reduces attractiveness of a feature that has multiple peaks of values (Itti et al., 1998).

Range of values in each feature maps is different so that the maps are normalized. Feature maps are summed linearly to obtain final output (saliency map) that represents attractiveness of each spatial position. In the present study, we obtained saliency map from single features (orientation or color) in order to investigate predictability of each visual features.

2.2 Natural images and eye-tracking data

Natural images and eye-traking data when perticipants looked the images were taken from MIT dataset (http://people.csail.mit.edu/tjudd/WherePeopleLook/index.html). We choosed natural images whose size is 1024×768 pixels (n = 463). The choosen natural images included various objects (e.g., animals, foods, buildings, and vehicles), and various scenes (e.g., outdoor/indoor and urban/nonurban scenes). 15 subjects perticipated in experiments for eye-tracking. More details of the experiment are described in other pubulished article (Judd et al., 2009).

2.3 Evaluation of the model

Prediction accuracy of a saliency map is evaluated by Receiver Operating Characteristics (ROC) in terms of Area under the ROC Curve (AUC). AUC is popularly used to evaluate the performance of a saliency map (Judd et al., 2009; Zhao and Koch, 2011). Obtained saliency map was binarized at p % threshold of the map. Then, we obtained the rate of human fixations within the map. A hit rate curve is plotted as the function of threshold by changing threshold p. The area under the hit rate curve indicates the prediction accuracy of the model.

3. RESULTS AND DISCUSSION

The purpose of this study is to investigate whether efficiency of individual features to predict gaze locations is kept constant on individual images, and to identify chracteristics of natural images that lead the better performance of color information. We obtained saliency map from either orientation or color, and showed that orientation-based saliency outperforms color-based saliency on average (AUC scores are 0.69±0.12 for orientation, 0.60±0.15 for color; mean ± SD. This is consistent with the result of the previous study (Zhao and Koch, 2011). We analysed performance of each feature by taking the difference of AUC scores between color-based and orientation-based saliency map of individual images. Natural images were classified as color-dominant and orientation-dominant images. The number of color-dominant images was 120 out of 463. Figure1 shows the examples of color-dominant and orientation-based dominant image. The color-dominant images tended to contain one or two large objects of which color and luminance are different from a background, and the orientation-dominant images tended to have monochromatic objects as salient image features.

We examined the characteristics of images that lead the better performance of color-based saliency map. It has been reported that brain takes advantages from statistical structures of natural images (Hoyer and Hyvärinen, 2000; Olshausen and Field, 1997), so that we obtained four image statistics (mean, variance, skewness, and kurtosis) of the images in CIE $L^*a^*b^*$ color space. Figure2 shows skewness and kurtosis of the top 15 color-dominant and the top 15 orientation-dominant images. There are significant difference of skewness and kurtosis of a^* between color-dominant and orientation-dominant images (skewness of a^* is 1.43±3.94 for color dominant images and 0.13±1.12 for orientation dominant images, t-test, $p < 0.05$; kurtosis of a^* is 13.32±89.65 for color dominant images and 6.78±35.06 for orientation dominant images, t-test, $p < 0.05$; mean ± SD). The finding agrees with the concept of saliency. For instance, one colored object becomes highly salient when surrounded by achromatic objects (in this case, skewness and kurtosis of *a** or *b** are expected to become larger). In contrast, human seeks other cues such as orientation if color does not provide useful information (e.g., a uniform colored image yields low skewness). The result demonstrated that the image statistics determine low-level visual features which capture human attention.

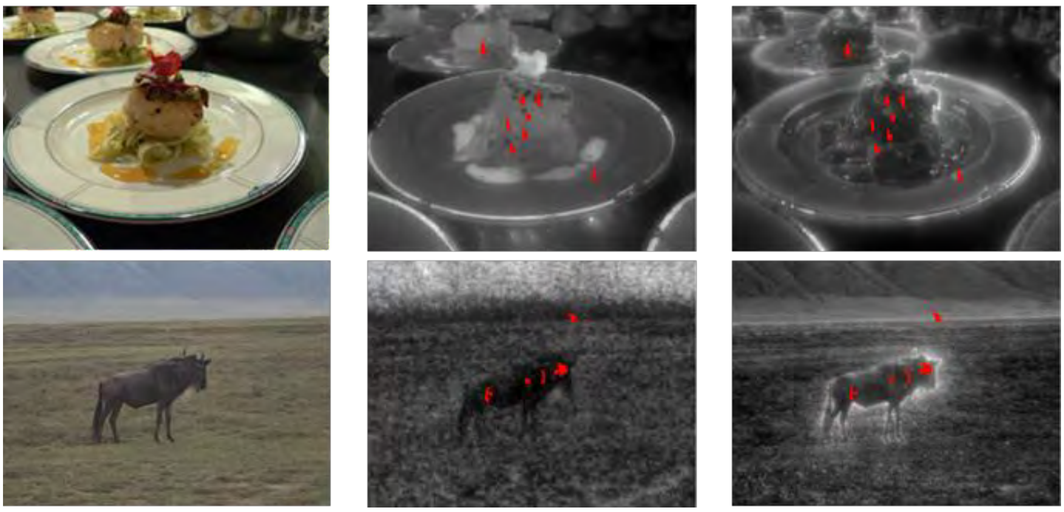

Figure 1: Example outputs of the model. The image which is accurately predicted by color-based (top row) and orientation-based saliency maps (bottom row). Input images (left column). Color-based saliency map (center column) and orientation-based saliency map (right column). Intensity of the maps represents estimated attractiveness at each spatial position. Gaze shifts in one subject are superimposed to the saliency maps. Red symbols represent fixation points.

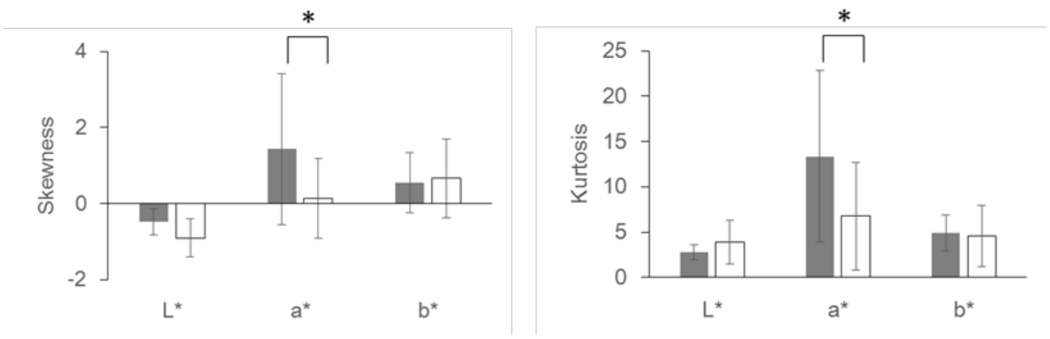

*Figure 2: Skewness (left) and Kurtosis (right) of natural images in CIE L*a*b* coordinates. Gray and white bars indicate averaged statistics of 15 color-dominant and orientation-dominant images, respectively. Error bars indicate standard deviations.*

4. CONCLUSIONS

This article demonstrated that effectiveness of the low-level visual features that capture attention is different among natural images. Although the number of analysed images is limited, color-dominant images had larger skewness and kurtosis in *a** than those of orientation-dominant images. The result provides the idea that the simple image statistics could determine low-level visual features that attract attention in humans.

ACKNOWLEDGEMENTS

We would like to thank Dr. Tilke Judd for providing the natural images and the collected eye-traking data.

REFERENCES

Hiratani, A., Nakashima, R., Matsumiya K., Kuriki, I., and Shioiri, S. 2013. Considerations of self-motion in motion saliency, *Proceedings of the International Joint Workshop on Advanced Sensing/ Visual Attention and Interaction -Toward Creation of Human-Harmonized Information Technology-* 783-787.

Hoyer, P. O., and Hyvärinen A. 2000. Independent component analysis applied to feature extraction from colour and stereo images, *Network* 11, 191-210.

Itti, L., Koch, C., and Niebur, E. 1998. A Model of Saliency-Based Visual Attention for Rapid Scene Analysis, *IEEE Transactions on Pattern Analysis and Machine Intelligence* 20(11) 1254-1259.

Judd, T., Ehinger, K., Durand, F., and Torralba, A. 2009. *Learning to Predict Where Humans Look,* IEEE International Conference on Computer Vision 2106-2113.

Koch, C., and Ullman, S. 1985. Shifts in selective visual attention: towards the underlying neural circuitry. *Human Neurobiology* 4 219-227.

Olshausen, BA., and Field, DJ. 1996. Emergence of Simple-cell Receptive Field Properties by Learning a Sparse Code for Natural Images, *Nature*, 381(6583), 607-609.

Posner, M.I., 1980. Orienting of attention, *The Quarterly Journal of Experimental Psychology* 32(1), 3-25.

Zhao, Q., and Koch, C. 2011. Learning a Saliency Map using Fixated Locations in Natural Scenes, *Journal of Vision* 11(3):9 1-15.

Address: Research Institute of Electrical Communication, Tohoku University,
2-1-1 Katahira, Aoba-ku, Sendai, Miyagi, 980-8577, JAPAN
E-mail: hatori@riec.tohoku.ac.jp

Prior knowledge modulates peripheral color appearance

Bilge SAYIM,[1] Erik MYIN,[2] Tilde VAN UYTVEN,[3]
[1] Laboratory of Experimental Psychology, University of Leuven (KU Leuven)
[2] CST, Literature and Philosophy, Philosophy, University of Antwerp
[3] Royal Academy of Fine Arts Antwerp

ABSTRACT

Color perception deteriorates with increasing eccentricity in the visual field. Here, we investigated peripheral color perception using a painting method, asking how prior knowledge affects color appearance. A professional artist was presented with complex, cluttered images in the visual periphery. The task was to paint as accurately as possible how each image appeared. Eye tracking assured that the image was only viewed in the periphery. The resulting paintings were strongly compromised. After finishing a painting, the target image was freely viewed to acquire knowledge about it. Next, the same image was presented at the same peripheral location and painted again. There were two conditions for the second painting. In the first condition, the image was again masked when not fixating the fixation dot (as during the first presentation). In the second condition, the image was not masked, allowing saccades to the image. In both conditions, the paintings resulting from the first presentation showed clear differences compared to the second presentation. Salient color regions in the images that were not painted during the first presentation, were painted during the second presentation. Color changes were less pronounced in the first than in the second condition. Importantly, several image features were remembered but not painted during the second presentation, showing - in addition to subjective reports – the perceptual nature of the effect. Our results indicate that prior knowledge of peripheral targets strongly shapes perception.

1. INTRODUCTION

Color sensitivity deteriorates with increasing eccentricity (Moreland, 1972). The extent of this deterioration is still unclear. For example, it has been proposed that color vision is absent at eccentricities larger than 40 degrees of visual angle (Moreland & Cruz, 1959). However, it has also been shown that, depending on the stimulus properties, color can still be discerned at larger eccentricities, even up to 90 degrees (Noorlander, Koenderink, den Ouden, & Edens, 1983). Peripheral vision is not only characterized by diminished color sensitivity. One of the major limiting factors of peripheral vision is crowding - the deleterious influence of neighboring items on the perceptibility of a target (e.g., Levi, 2008). For example, an isolated letter that is easily recognized in the periphery is indiscernible when other letters are presented in close proximity. Crowding depends on several factors, e.g., eccentricity (Bouma, 1970), target-flanker similarity (Kooi et al., 1994), grouping (Sayim, Westheimer, & Herzog, 2010), and prior knowledge (Zhang et al., 2009). The influence of crowding on color perception is rarely investigated. However, it has recently been shown that the perception of hue and saturation deteriorates when the target is crowded (van den Berg, Roerdink, & Cornelissen, 2007). Using visual noise

(Greenwood, Bex, & Dakin, 2010), and letters and letter-like symbols (Sayim & Wagemans, 2013), it has been shown that crowding does not only impede performance but also changes appearance.

Here, we used a painting method to investigate appearance changes in complex, cluttered images, asking first, how color appearance is influenced by crowding, and second, whether knowledge about target images modulates appearance. This explorative painting method in conjunction with complex images allowed us to explore these questions simultaneously, using the entire image as a target. We found strong modulation of color appearance, and a clear influence of knowledge on target perception.

2. METHOD

We investigated peripheral color appearance with a painting method. A professional artist (the last author of this manuscript, TvU) was presented with complex, cluttered images in the right visual field. The task was to capture as accurate as possible how the image appeared.

2.1 Apparatus

Stimuli were presented on a Sony Trinitron GDM-F520 CRT monitor driven by a standard accelerated graphics card. The screen resolution was set to 1152 by 864 pixels; the refresh rate was 120 Hz. A chin and head rest was used to restrict head movements. The screen was viewed from a distance of 58 cm. Eye positions were monitored by an SR Research EyeLink 1000 running at a sampling rate of 1000 Hz. An elevated, inclined drawing board was placed in front of the head and chin rest to allow for painting without leaving the head rest. Colored crayons were used to paint. MATLAB (Mathworks, Natick Massachusetts, USA) in combination with the Psychophysics toolbox (Brainard, 1997) was used for stimulus presentation.

2.2 Stimuli

Stimuli consisted of two complex, cluttered images (Figure 1). Images were 15.0 degrees wide, 10.2 degrees high, and were presented on the horizontal midline of the screen, centered at 12 degrees eccentricity in the right visual field. The first image consisted of various shapes, such as ellipses, rectangles, and lines (the “Miro”-Image, Figure 1A, left). The second image consisted of an arrangement of rectangles with different sizes and colors (the “Mondrian”-Image, Figure 1B, left). Both images varied strongly in color and luminance. Images were presented on a gray background (50.5 cd/m^2). A fixation dot was presented at the center of the screen. To prevent central viewing of the stimulus, the target images were masked by a pattern mask of the same size as the target whenever the participant did not fixate the center of the screen (except during the second “Mondrian” painting; see Procedure).

2.3 Procedure

Each target image was painted twice. The participating artist (TvU) fixated on the fixation dot in the center of the screen. For the first painting of each image, the target image was only presented when fixating the fixation dot, otherwise it was masked. The task was to reproduce the appearance of the stimulus in as much detail as possible. After completion of the painting, the image was shown foveally for visual inspection. Next, the target image was again presented in the periphery and painted once more. In the “Miro”-condition, the target image was again only shown when fixating the fixation dot, and masked otherwise. In the “Mondrian”-condition, the target image was not masked. There was no time restriction for (peripheral) viewing of the target image, and finishing a painting, allowing the participant to focus attention on all areas of the presented target. The painting of one image took about 40 minutes.

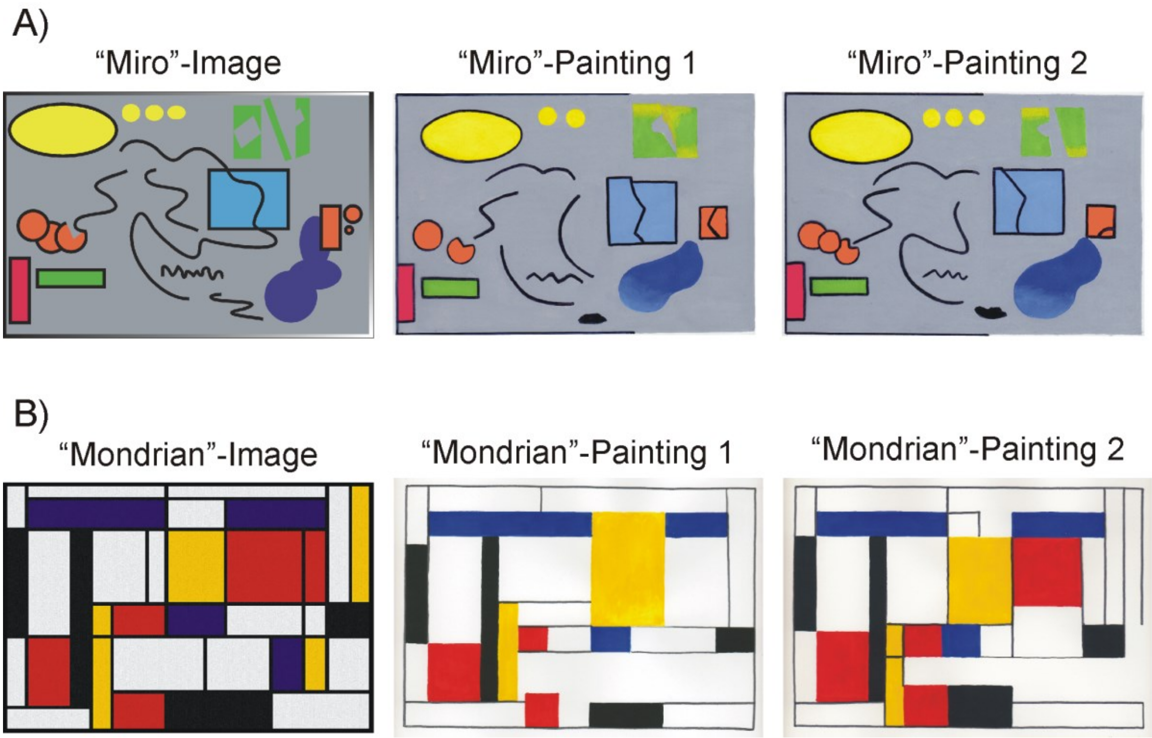

Figure 1: Original images and painting results. Target images (left column) were presented at 12 degrees in the right visual field. (A) In the “Miro”-condition, the target image was masked during the first (“Miro”-Painting 1) and second (“Miro”-Painting 2) presentation when the fixation dot was not fixated. B) In the “Mondrian”-condition, the target image was masked during the first presentation when the fixation dot was not fixated (“Mondrian”-Painting 1); during the second presentation, it was not masked (“Mondrian”-Painting 2).

3. RESULTS AND DISCUSSION

The results show a strong decrease in accuracy with increasing eccentricity (Figure 1). Sections of the target images closer to the fovea were reproduced more accurately, i.e., more similar to the target image, than sections farther in the periphery (note that due to the imprecision of the painting method, only large, categorical differences are of interest here). In the first painting of the “Miro”-Image (Figure 1A, center, “Miro”-Painting 1), several shapes and parts of shapes are depicted distorted or left out entirely. For example, instead of an orange rectangle and two orange discs (right outer edge of the painting), a single square structure was painted. However, clear differences between the target image and the painting occurred also closer to the fovea. Instead of depicting three circular/ oval items in the upper left quadrant, only two items were painted. Similarly, close to the left edge (below the horizontal midline) an empty/ gray gap was introduced between the two painted orange discs. Noticeable deviations of color appearance occurred in sections far in the periphery. In particular, uniformly colored items were depicted to contain additional hues (the green pattern in the upper right quadrant was depicted in green and yellow), or varied in regard to saturation (the bluish structure in the lower right quadrant). After free visual inspection, i.e., acquisition of detailed knowledge of the target image, the image was again presented in the visual periphery when fixating the center of the screen, and painted a second time (Figure 1A, right, "Miro"-Painting 2). The second painting was clearly different compared to the first painting. In particular, the previously missing circular/oval items were depicted in the second painting. Reports by TvU pointed at strong changes of perception compared to the first painting, e.g., "I now see clearly that there are three yellow discs". Subjective reports also indicated a general reduction of vagueness of color appearance ("the green is clearer now").

The first painting of the "Mondrian"-Image shows similar effects as the first "Miro"-Painting. Several (missing or added) white gaps, and missing regions with different hues show that peripheral color perception was compromised, again increasing with eccentricity. The two red rectangles and the yellow rectangle in the upper right quadrant, as well as the blue and yellow rectangles in the lower right quadrant are entirely missing. Subjective reports indicated that the large yellow rectangle sometimes appeared in parts orange – similar color mixtures and perceptual switching between different color categories at the same location were reported with other paintings (results not shown here). The second painting of the "Mondrian"-Image showed clear differences compared to the first. A large difference occurred in the upper right quadrant where a red square/rectangle present in the image was painted instead of a white region depicted in the first painting. Also, the number of deviating white gaps was reduced in the second painting.

Our results reveal a strong loss of accurate perception of detail which increased with eccentricity, reflecting the combined effect of crowding and reduced sensitivity in the peripheral visual field. In particular, the loss of large regions with strong color contrast are noticeable, raising questions regarding their visibility, for example, in standard detection experiments (note that crowding usually does not influence detection). Differences between the first and second paintings indicate appearance changes by knowledge, both when knowledge was only acquired between trials ("Miro"-condition), as well as between trials and during the second trial ("Mondrian"-condition). The large difference between the first and second trial in the "Mondrian"-condition (the red rectangle in the upper right quadrant), suggests that intermittent acquisition of knowledge strongly changed appearance. Importantly, several details of the images were remembered during the second paintings but not perceived and therefore not painted, indicating that perceptual changes, and not abstract memory, underlie these results. For example, the blue and the two yellow rectangles in the right half of the "Mondrian"-Image were remembered but not depicted (Figure 1B, right). The still clearly visible decrease of accuracy with eccentricity supports this interpretation, as do subjective reports regarding the perceptual nature of the appearance changes. Note that to paint the image, all regions of the image were (covertly) attended several times allowing maximum reduction of uncertainty about appearance. Similar, even though less pronounced, differences between the first and second painting in the “Miro”-condition show that the effect is not due to the continuous presentation of the image in the Mondrian-condition.

4. CONCLUSIONS

Our results show that peripheral vision can be strongly modulated by knowledge. In particular, images that were unknown to the participant and only viewed peripherally (first painting) resulted in different perceptions when additional knowledge was acquired about the images (second painting). The large color effects in the unknown images cannot be explained by diminished color perception in the periphery as images were sufficiently close to the fovea where color vision is good. Abstract memory does not explain the appearance differences between the first and second paintings because several details were remembered but not perceived. Rather, we suggest that our results are due to vague percepts caused by crowding which are strongly susceptible to prior knowledge (see also, Sayim & Wagemans, 2013). Future experiments will show in how far the presentation of highly complex images modulates effects of crowding. We propose that the painting method is useful to explore the perception of complex stimuli, in particular to capture perceptually vague phenomena, as painting is more precise and efficient than, e.g., verbal descriptions when stimuli are complex. Finally, we suggest that artists who depict peripherally viewed scenes (e.g., Pepperell, 2012) for scientific or artistic purposes may benefit from the use of unknown images and gaze contingent presentation.

ACKNOWLEDGEMENTS

This work was supported by an FWO Pegasus Marie Curie fellowships awarded to BS, and a BOF grant by the Royal Academy of Fine Arts awarded to BS, EM, and TvU. Additional funding by the Methusalem program of the Flemish Government (METH/08/02) awarded to Johan Wagemans. Our thanks to Vebjørn Ekroll for helpful comments.

REFERENCES

Bouma, H. 1970. *Interaction effects in parafoveal letter recognition*. Nature, 226(5241): 177-178.

Brainard, D. H. 1997. *The Psychophysics Toolbox*. Spatial Vision, 10(4), 433–436.

Greenwood, J.A., Bex, P.J., & Dakin, S.C. 2010. *Crowding changes appearance.* Current Biology, 20(6), 496-501.

Kooi, F. L., Toet, A., Tripathy, S. P., & Levi, D. M. 1994. *The effect of similarity and duration on spatial inter-action in peripheral vision.* Spatial Vision, 8, 255–279.

Levi, D. M. 2008. *Crowding – an essential bottleneck for object recognition: a mini-review.* Vision Research, 48(5): 635-54.

Moreland, J. D. 1972. *Peripheral color vision.* In Handbook of sensory physiology, vol. VII/4 (eds Jameson, J. and Hurvich L. M.), pp. 517–536. Berlin, Germany: Springer.

Moreland, J. D., & Cruz, A 1959. *Colour perception with the peripheral retina*. Optica Acta, 59, 117–151.

Noorlander, C., Koenderink, J. J., den Ouden, R. J., & Edens, B. W. 1983. *Sensitivity to spatiotemporal colour contrast in the peripheral visual field.* Vision Research, 23, 1–11.

Pepperell, R. 2012. *The perception of art and the science of perception*. In B. E. Rogowitz, N. P. Thrasyvoulos, & H. de Ridder (Eds.), Vision and Electronic Imaging XVII .

Sayim, B. & Wagemans, J. 2013. *Drawings of the visual periphery reveal appearance changes in crowding.* Perception, 42 (ECVP Supplement), 229. (Abstract)

Sayim, B., Westheimer, G., & Herzog, M. H. 2010. *Gestalt Factors Modulate Basic Spatial Vision.* Psychological Science, 21(5), 641-644.

van den Berg, R., Roerdink, J. B. T. M., and Cornelissen, F. W. 2007. *On the generality of crowding: Visual crowding in size, saturation, and hue compared to orientation.* Journal of Vision, 7(2):14, 1–11.

Zhang, J. Y., Zhang, T., Xue, F., Liu, L., & Yu, C. (2009). *Legibility of Chinese characters in peripheral vision and the top-down influences on crowding.* Vision Research, 49, 44–53.

Address: Dr. Bilge SAYIM, Laboratory of Experimental Psycholgy, University of Leuven (KU Leuven), Tiensestraat 102 - box 3711, Leuven B-3000, Belgium. E-mail: bilge.sayim@ppw.kuleuven.be

Decision of Validness in Custom Color Name of JIS Z 8102

Yosuke YOSHIZAWA[1]
[1] Organization for Promotion of Academic Affairs, Chiba University

ABSTRACT

This paper is about a trial to decide valid color names from 122 foreign custom color names in JIS Z 8102 (Japan Industrial Standard). In Japan, "Systematic" and "Custom color name" are often used. Especially, custom color name have a lot of origin – ex. plant, material ,region name etc. But it was not revealed whether each custom color name is valid or not. To decide valid color names, 56 subjects had Color Matching Task and color cluster was constructed from the result of color choice task in each name. Based on the cluster and Berlin & Kay's 11 basic colors, 26 colors were decided as validness.

1. INTRODUCTION

Generally, color names tend to be used for daily communication in color. Especially in Japan, "Systematic" and "Custom color name" are used based on JIS Z 8102 (Japan Industrial Standard). Custom color names have origin in plant, material, food and so on. But it was not revealed whether each custom color name is used accurately or not.

To clarify this question, 3 indices "Color distance between a given standard color of JIS Z 8102 and subject's choice for it in CIE L*a*b*", "Familiarity of color name" and "Imaginableness of color name" were acquired from color choice experiment and questionnaires to subjects (2009, Yoshizawa et al). These indices lead new 2 parameters "Degree of recognition" and "Distance in color space" in each color name for decision of how much recognition in each custom color name.

In another aspect, distinguishes between in custom color names included basic color – ex. Chinese red, Chartreuse Green, cobalt blue and so on - were clarified, and valid color names were decided in each group with included basic color based on Berlin & Kay's 11 color words (2009, Yoshizawa et al).

Against this aspect, the aim of this research is to reveal validness of Custom Color Name in 122 foreign custom color name of JIS Z 8102（except of color names "Gold" and "Silver"）.

First, cluster analysis makes some color name clusters from data of color choice experiment in each 122 name. Finally, representational color is decided based on Berlin & Kay's 11 basic color names and color difference between a given standard color of JIS Z 8102 and subject's choice for it in CIE L*a*b*" in each cluster and validness of each custom color can appear.

2. METHOD

2.1 Color Matching Task

Each subject was given the task of matching color names with the respective colors. Figure 2 shows a related tool. Subjects read a custom color name written on a card and chose a color from 468 color chips. In case they could not match a color with its name, they had to choose a color chip. Custom Color Chart and PCCS 201-L (both are Color Chart: Japan Color Enterprise Co. Ltd.) were used as color chips. 468 colors were attached on the board. White fluorescent lights (FLR 40-S-W/M-x36, by Panasonic, Japan) were used as the source of light and were adjusted at 500lx on the color chips.

2.2 Subjects

56 Japanese college students participated in this test (30 men and 26 women in the age range of 19–28 years). Of all the subjects, 72.2% belonged to the design section; however, they had little opportunity to study color names in detail.

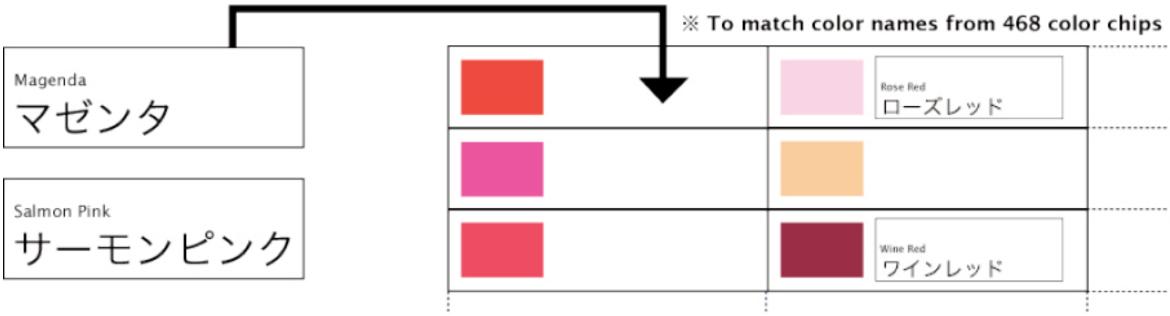

Figure 1: Image of color matching task.

3. RESULT & DISCUSSION

3.1 Cluster Analysis

In each color chart, parameters L*,a* and b* of CIE L*a*b* acqired with i1 (color measurement instrument by x-rite Co. Ltd.). Average of L*, a* and b* in each color were used for constructing cluster with Ward method（Figure 2 & 3 : Average value of Color distance [ΔE] between a given standard color of JIS Z 8102 and subject's choice for it in CIE L*a*b*" in each color name are shown in Figure 2 & 3）

3.2 Cluster Analysis

To decide valid color names from the cluster, three regulation were considered : a) To follow Berlin & Kay's 11 basic color (pink marker in Fig 2 & 3), b) To follow color name qualified ΔE: Color distance based on ASTM Method E93-53 (as possble as), and c) To decide the lowest color name as a represental color in each cluster except a) & b).

Based on these regulation, 26 valid color were decided (Cluster Decision Line [red line] in Figure 2 & 3)

Color Name	Munsell	ΔE(*)
Rose Pink	10RP 7/8	23.7
Pink	2.5R 7/7	23.0
Magenta	5RP 5/14	31.0
Carmine	4R 4/14	39.0
Salmon Pink	8R 7.5/7.5	22.4
Wine Red	10RP 3/9	13.0
Old Rose	1R 6/6.5	32.4
Cochineal Red	10RP 4/12	19.9
Coral Red	2.5R 7/11	32.2
Scarlet	7R 5/14	25.7
Poppy Red	4R 5/14	12.7
Ruby Red	10RP 4/14	13.6
Rose Red	7.5RP 5/12	21.6
Rose	1R 5/14	17.3
Strawberry	1R 4/14	16.8
Cherry Pink	6RP 5.5/11.5	21.6
Signal Red	4R 4.5/14	8.7
Red	5R 5/14	11.9
Tomato Red	5R 5/14	10.4
Chinese Red	10R 6/15	33.6
Burgundy	10RP 2/2.5	48.3
Burnt Sienna	10R 4.5/7.5	46.3
Burnt Umber	10YR 3/3	36.0
Umber	8YR 5.5/6.5	40.3
Raw Umber	2.5Y 4/6	40.9
Orchid	7.5P 7/6	52.0
Bronze	8.5YR 4/5	26.1
Terracotta	7.5R 4.5/8	41.5
Tan	6YR 5/6	34.4
Pansy	1P 2.5/10	69.7
Raw Sienna	4YR 5/9	53.1
Buff	8YR 6.5/5	38.4
Sepia	10YR 2.5/2	31.6
Leghorn	2.5Y 8/4	40.7
Lilac	6P 7/6	50.4
Rose Gray	2.5R 5.5/1	23.7
Bordeaux	2.5R 2.5/3	38.8
Vermilion	6R 5.5/14	59.2
Chocolate	10R 2.5/2.5	12.9
Cocoa Brown	2YR 3.5/4	12.5
Brown	5YR 3.5/4	15.7
Baby Pink	4R 8.5/4	20.7
Shell Pink	10R 8.5/3.5	26.3
Peach	3YR 8/3.5	26.1
Nail Pink	10R 8/4	27.9
Cork	7YR 5.5/4	19.1
Blond(e)	2Y 7.5/7	30.4
Ecru Beige	7.5YR 8.5/4	26.3
Beige	10YR 7/2.5	20.0
Cream Yellow	5Y 8.5/3.5	15.8
Maroon	5R 2.5/6	57.6
Heliotrope	2P 5/10.5	55.9
Ash Gray	N 6	13.6
Gray	N 5	9.4
Slate Gray	2.5PB 3.5/0.5	21.4
Steel Gray	5P 4.5/1	13.5
Jaune Brilliant	5Y 8.5/14	105.2
Mauve	5P 4.5/9	44.7
Charcoal Gray	5PP 3/1	19.2
Hyacinth	5.5PB 5.5/6	39.2
Wistaria	10PB 5/12	48.8
Lamp Black	N 1	7.8
Black	N 1.5	2.4

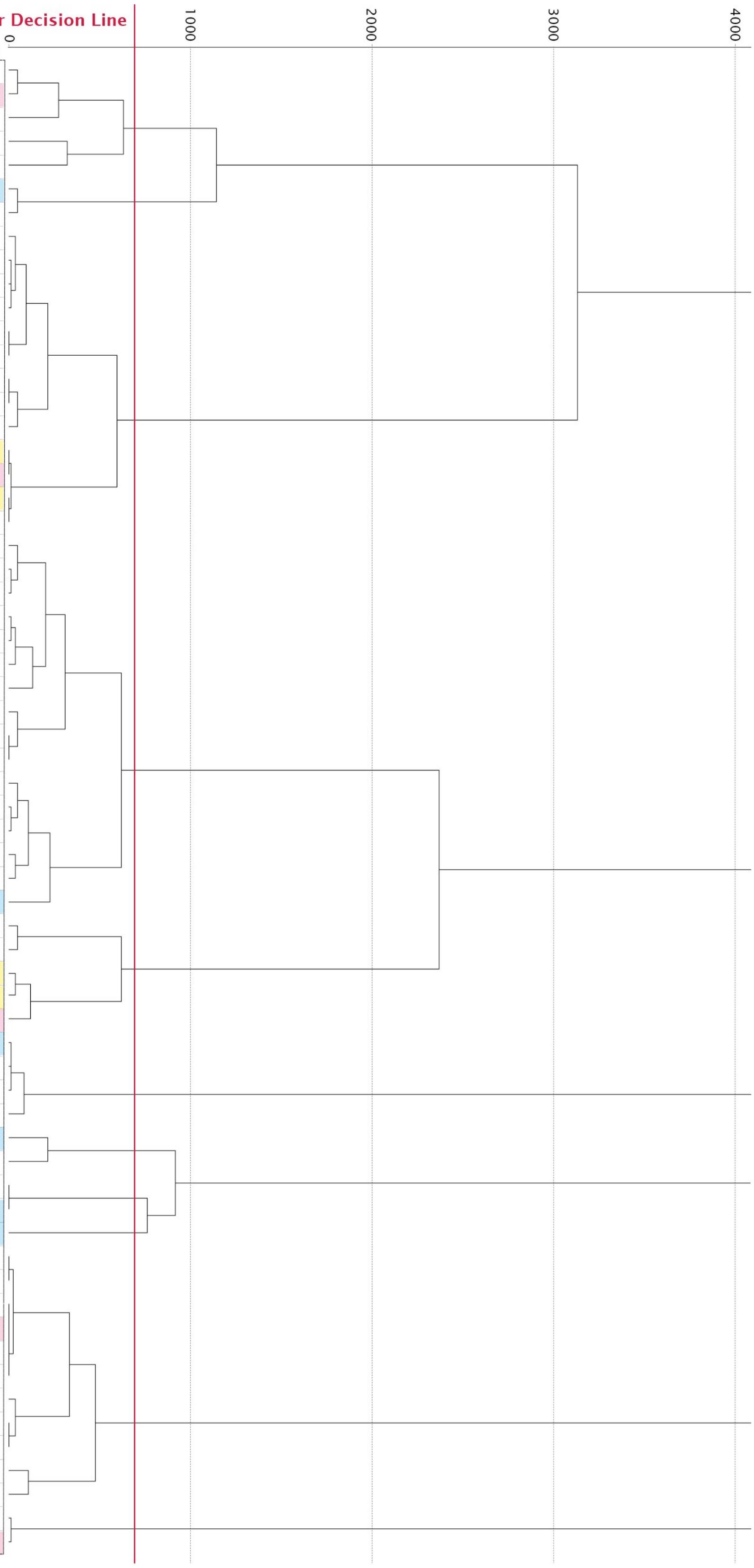

: Berlin & Kay's 11 basic color names

: ΔE of Color Name ≦ Berlin & Kay's basic color name in same cluster

: Color Name of the most lowest ΔE except &

*ΔE : Average Color Distance acqired from color choice task

Figure 2: Color Name Cluster from color matching task (#1)

Color Name	Munsell	ΔE(*)
Violet	2.5P 4/11	23.7
Purple	7.5P 5/12	19.5
Lavender	5P 6/3	33.7
Baby Blue	10B 7.5/3	20.4
Sky Gray	7.5B 7.5/0.5	18.0
Ivory	2.5Y 8.5/1.5	29.5
Silver Gray	N 6.5	10.2
Pearl Gray	N 7	12.7
White	N 9.5	0.7
Snow White	N 9.5	2.5
Carott Orange	10R 5/11	21.4
Orange	5YR 6.5/13	16.8
Mandarin Orange	7YR 7/11.5	22.5
Aprocpt	6YR 7/6	40.6
Golden Yellow	7.5YR 7/10	33.2
Naples Yellow	2.5Y 8/7.5	30.3
Yellow	5Y 8.5/14	6.6
Lemon Yellow	8Y 8/12	15.8
Marigold	8YR 7.5/13	21.6
Yellow Ocher	10YR 6/7.5	32.7
Chrome Yellow	3Y 8/12	33.0
Canary	7Y 8.5/10	33.0
Khaki	1Y 5/5.5	27.3
Olivedrob	7.5Y 4/2	29.9
Olive	7.5Y 3.5/4	26.0
Olive Green	2.5GY 3.5/3	31.4
Chartreuse Green	4GY 8/10	64.9
Malachite Green	4G 4.5/9	30.5
Peacock Green	7.5BG 4.5/9	32.3
Mint Green	2.5G 7.5/8	21.3
Green	2.5G 5.5/10	17.5
Emerald Green	4G 6/8	21.6
Leaf Green	5GY 6/7	32.6
Grass Green	5GY 5/5	34.2
Apple Green	10GY 8.5	30.1
Sea Green	6GY 7/8	62.3
Cobalt Green	4G 7/9	38.6
Ivy Green	7.5GY 4/5	36.3
Bottle Green	5G 2.5/3	31.4
Billiard Green	10G 2.5/5	26.4
Forest Green	7.5G 4.5/5	17.5
Viridian	8G 4/6	27.6
Nile Blue	10BG 5.5/5	33.4
Prussian Blue	5PB 3/4	28.5
Horizon Blue	7.5B 7/4	35.8
Saxe Blue	1PB 5/4.5	24.9
Marine Blue	5B 3/7	27.0
Cerulean Blue	9B 4.5/9	19.4
Cobalt Blue	3PB 4/10	19.7
Ultramarine Blue	7.5PB 3.5/11	28.4
Oriental Blue	7.5PB 3/10	29.6
Blue	2.5PB 4.5/10	13.0
Peacock Blue	10BG 4/8.5	29.9
Turquoise Blue	5B 6/8	23.8
Sky Blue	9B 7.5/5.5	24.2
Cyan	7.5B 6/10	31.7
Iron Blue	5PB 3/4	20.4
Midnight Blue	5PB 1.5/2	24.4
Navy Blue	6PB 2.5/4	20.3

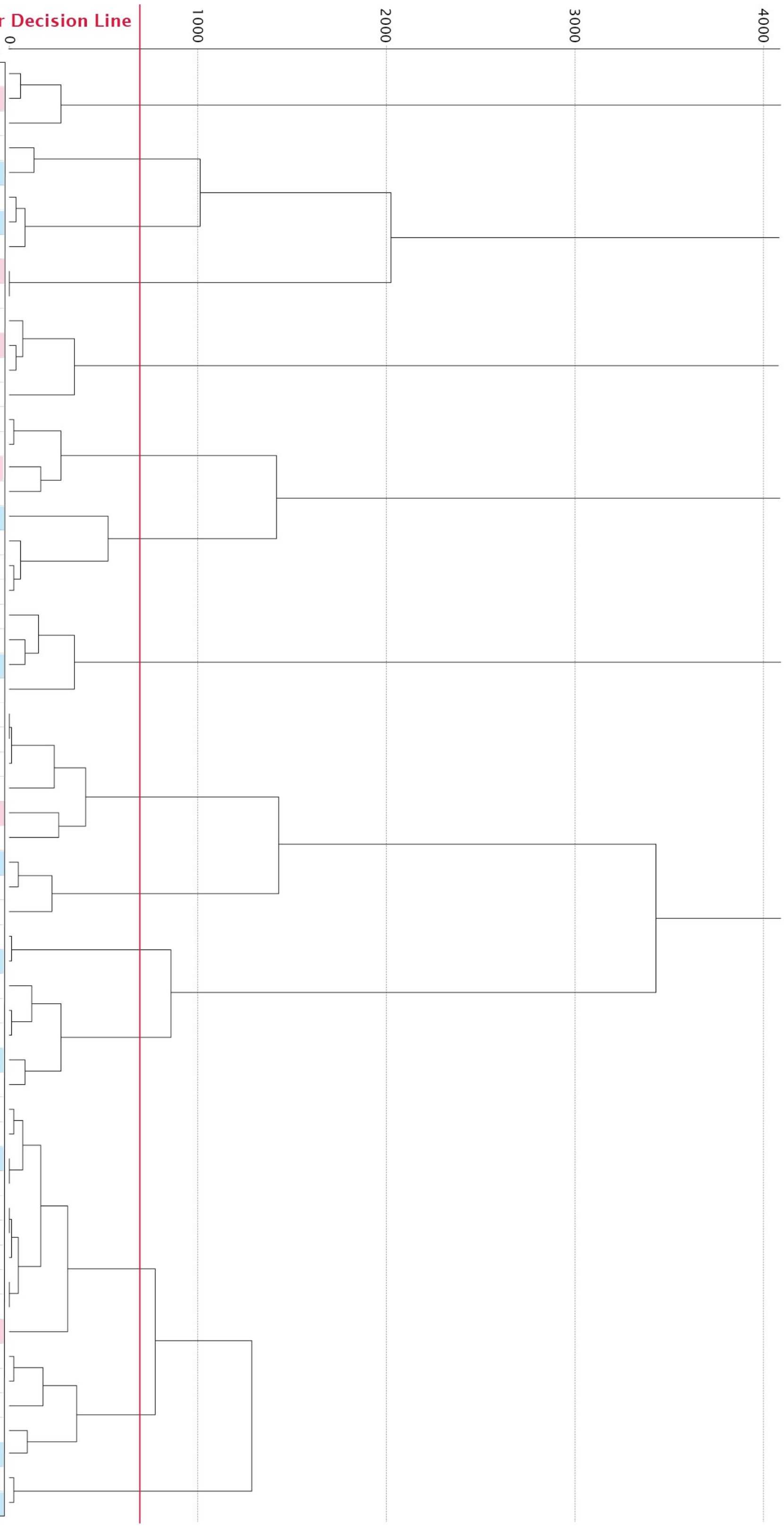

: Berlin & Kay's 11 basic color names
: ΔE of Color Name ≦ Berlin & Kay's basic color name in same cluster
: Color Name of the most lowest ΔE except &

*ΔE : Average Color Distance acqired from color choice task

Figure 3: Color Name Cluster from color matching task (#2)

4. CONCLUSIONS

In this paper, to decide vail custom color name in the JIS, the cluster was formed by indices - L*, a*and b* from color choice task in each 122 foreign custom color name.

Berlin & Kay's 11 color names and ΔE: Color distance were applied for the decision. In the future, it will be necessary to clarify the significance with ANOVA in each cluster.

In another case, even if a color name's ΔE: Color distance is low, it is difficult to decide to recognize and use accurately.

Based on them, clarification in use of custom color names will focus on increasing custom color names used correctly and usably.

REFERENCES

Berlin, B & Kay, P 1969, *Basic Color Terms : Their Universality and Evolution*, Univ. of California. Press.

Yoshizawa, Y. et.al 2009, *Recognition of Custom Color Name #1 : Relationship between Distance in Color Space, Familiarity of Color Names and Imaginableness of Color Names. And Trial of Determination in Recognition*, CSAJ 33(2) 96-107

Yoshizawa, Y. et.al 2009, *Research on the Recognition of Custom Color Names : #2 Distinguishment and Basic Color Tendency of Custom Color Names in Color Choice Task*, CSAJ 33(3) 218-229

Yoshizawa, Y. et.al 2009, *Recognition of Non-Japanese Custom Color Names: Relation among Distance in Color Space, Familiarity of Color Names, and Imaginableness of Color Names*, IASDR 2009 Proceeding CD-ROM.

ASTM 1953, Method E 93-53

Address: Yosuke YOSHIZAWA, Organization for Promotion of Academic Affairs,
Chiba University, 1-33 Yayoi-cho, Chiba, 263-8522, JAPAN
E-mails: yosuke_yoshizawa@chiba-u.jp
URL: http://evolutional-blue.com

Evaluation of color appearance under LED and OLED lighting based on the data obtained by a new color category rating method

Taiichiro Ishida,[1] Yasuki Yamauchi,[2] Takehiro Nagai,[2] Hiroyuki Kurimoto,[2] Yuhei Shoji,[2] Tatsuya Tajima[1]
[1] Graduate School of Engineering, Kyoto University
[2] Graduate School of Science and Engineering, Yamagata University

ABSTRACT

We conducted the experiments to evaluate the appearance of colors under white LED, OLED and fluorescent lamps using color chips systematically selected from the Munsell color space. We introduced a new color category rating method that was extension of the method reported by Uchikawa et al. (1994) to obtain more detailed description of color appearance. The results of the experiment 1 showed that the color category rating under each of three illuminants were similar in general, however, there were noticeable differences in some color regions. We carried out the additional experiment (Exp.2) in which color appearance was evaluated by the conventional elemental color naming method. The analysis of the results showed that multiple regression models based on the color category rating well explained the elemental naming responses, indicating the possibility that color category rating data can be transformed into the elemental color description.

1. INTRODUCTION

Technologies of solid-state lighting, such as light-emitting diode (LED) and organic electroluminescent lighting (OLED), are progressing rapidly in recent years. LED lighting is now widely used in our living environments. However there are still arguments about color appearance under these lighting environments. In this study we examined color appearances under a white LED, OLED and FL (fluorescent lamp) using a new method to describe the appearance of colors.

2. EXPERIMENT 1:

The experiment 1 was conducted to evaluate the appearance of colors under a white LED, OLED and FL using color chips systematically selected from the Munsell color space (shoji et al., 2013). We introduced a new color category rating method that was extension of the method proposed by Uchikawa et al. (1994) in a way to obtain more detailed description of color appearance.

2.1 methods

Subjects answered color appearance of a chip by selecting up to three colors out of 11 basic color terms; red(R), orange(Or), yellow(Y), green(G), blue(B), purple(P), pink(Pk), brown(Bn), black(Bk), gray(N) and white(W). Also tye assined a weighting score to each of the selected colors to make a total of 10. After adapting to a given illuminant (FL, LED or OLED) for 5 minutes, a subject responded with the color category rating method for each of 146 color chips presented on the gray background. The size of color chips from the subject was about 2 deg. The illuminance was set 500 lx at the location of the color chip. Each of the subjects repeated twice for each light source condition. 10 subjects (University students) participated in the experiments. The specifications of the light sources are given in Table 1. Figure 1 shows the relative spectral power distribution of the FL, LED and OLED used in the experiment.

Table 1: Specification of the light sources

	FL	LED	OLED
product	FL20SS-ENW/18HF	LEL-AW6N/2	P03B0909-NA12A
x	0.343	0.349	0.351
y	0.356	0.358	0.369
Tc	5200 K	5000 K	4900 K
Ra	84	81	81

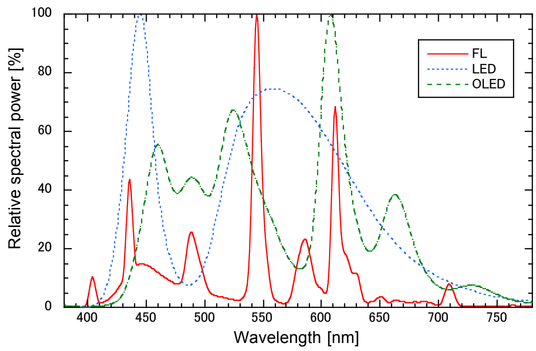

Figure 1: Relative spectral power distribution of the light sources

2.2 Results

Figure 2 shows the results of the experiment 1 (V=5, C=6) under light sources FL, LED and OLED. The color category ratings were averaged over the subjects. While the color

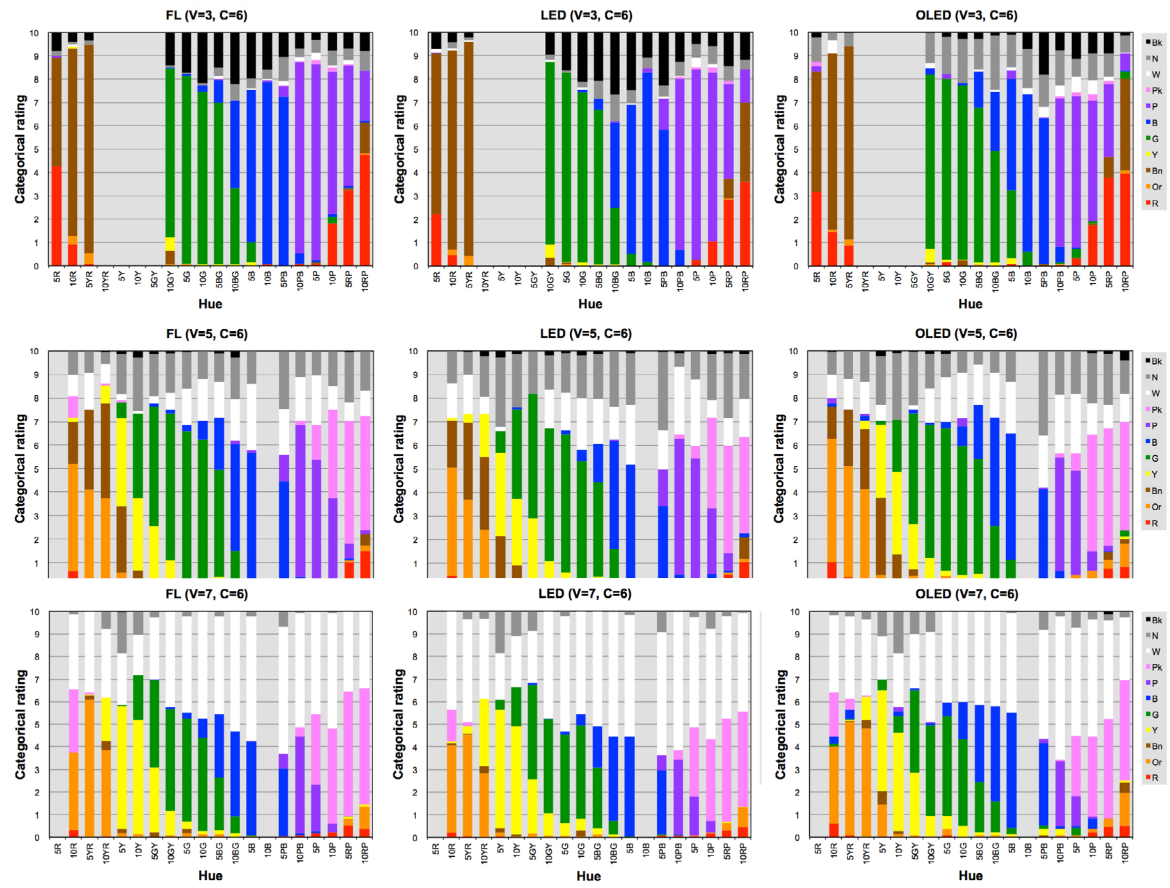

Figure 2: The results of color categorical rating for the color chips (V=3, 5,7, C=6).

category ratings under each of three illuminants look similar in general, noticeable differences in categorical rating were found in some parts of the colors. For example, the color chips between 10R to 10YR were given higher "orange" rating under the OLED than other light sources.

3. EXPERIMENT 2:

To know quantitative changes of the color appearances, we considered possibility to transform color category rating data to elemental color rating data. Then we carried out the additional experiment (Exp.2) in which color appearance was measured by the ordinary elemental color naming method.

3.1 Methods

In the experiment 2, the subjects described color appearance by giving achromatic rates (black/white), followed by chromatic rates (red/green, yellow/blue) to bring the total to 10. The number of the Munsell color chips tested in the experiment 2 was reduced to 76 from 146 in the experiment 1. Other procedures and conditions were the same as in the experiment 1.

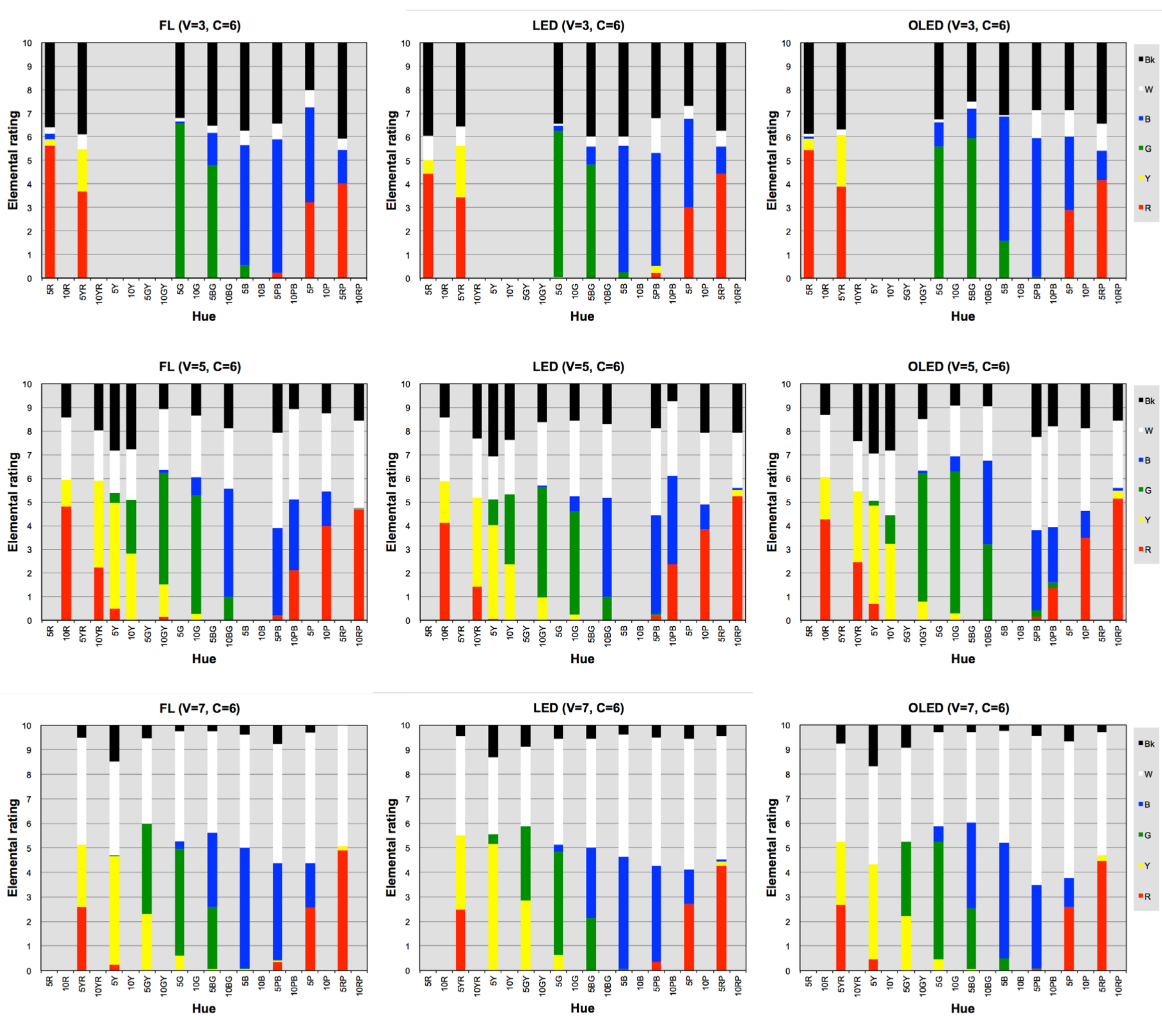

Figure 3: The results of elemental color naming for the color chips (V=3, 5, 7, C=6).

3.2 Results

Figure 3 presents the results of the experiment 2 (V=5, C=6) under the light sources FL, LED and OLED. The elemental color naming scores were averaged over the subjects. The results of the experiment 2 show typical changes of color appearance along the hue circle. Although the color appearance show a similar change in three light source conditions, there are also some differences such as higher redness and greenness of V=5 under OLED and lower chromaticness under LED.

DISCUSSION

Each color category must be described as combination of elementary colors. For example, "purple" may be described as combination of "red", "blue" with some weighting factors. Then we considered that it might be possible to transform color category rating data to elemental color naming description. Relationship between the color category rating (Exp.1) and elementary naming (Exp.2) was analyzed with the multiple regression analysis; explanatory variables were 11 category ratings and objective variables were 6 elementary naming responses. The results of the regression were summarized in Table 2. Figure 4 shows correlation of elemental color ratings predicted by the multiple regression model and those evaluated by the subjects in the experiment 2. It is clearly shown that regression models based on the color category rating data well explain the elementary naming responses, indicating the color category rating can be transformed into the elementary color description.

Table 2: Regression coefficients to predict elemental colors from color category ratings

Elemental color	Color category (explanatory variables) R	Or	Y	G	B	P	Pk	Bn	W	N	Bk	cor-ration R
Red	0.924	0.528	-0.037	-0.006	-0.007	0.334	0.732	0.292	0.016	-0.007	-0.033	0.984
Green	0.010	-0.013	0.007	0.847	0.004	-0.007	-0.017	0.019	0.022	0.022	-0.145	0.981
Yellow	-0.022	0.407	0.872	-0.012	-0.009	-0.001	-0.003	0.188	0.007	0.016	-0.034	0.982
Blue	-0.027	-0.013	-0.030	0.030	0.920	0.468	0.009	0.012	0.022	0.006	-0.060	0.982
White	0.033	0.047	0.139	0.045	0.015	0.055	0.226	0.070	0.939	0.512	-0.134	0.979
Black	0.083	0.044	0.050	0.099	0.083	0.150	0.053	0.421	-0.008	0.449	1.395	0.971

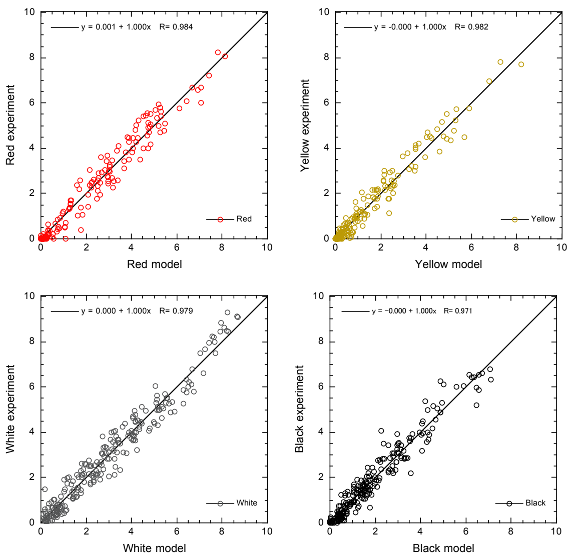

Figure 4: Correlation of elemental color ratings predicted by the model and those evaluated by the subjects in the experiment 2.

Comparison of the predicted elemental naming data derived from the regression model with the experimental data is shown in Figure 5 for the color chips (V=3, 5, 7, C=6) under the FL condition. As shown in the figure, the model based on the color category rating data well predicts changes of color appearance.

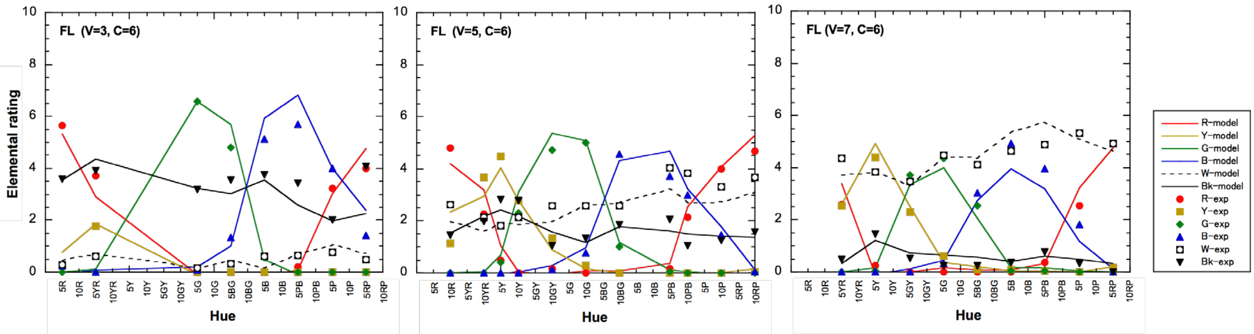

Figure 5: Comparison of the elemental rating predicted by the regression model (lines) with the experimental data (symbols) plotted for the color chips (V=3, 5,7, C=6) under the FL condition.

This study was primarily motived by to examine color appearance under LED and OLED lightings. To see the changes in color appearance, predicted elemental color naming values assigned to the color chips used in the experiment 1 were derived from the regression model based on the color category rating data. Arrows in figure 6 indicate the predicted changes of color appearance from FL to LED or OLED conditions plotted on red-green and yellow-blue axes.

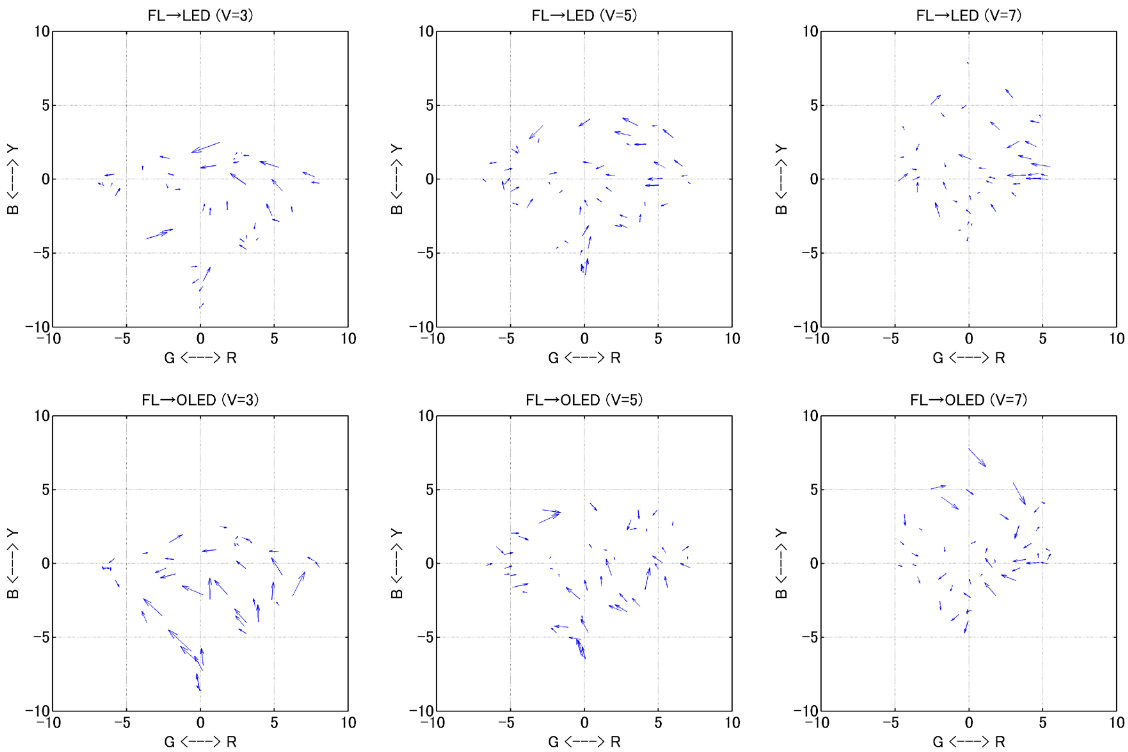

Figure 6: Predicted changes of color appearance from FL to LED or OLED lighting plotted on red-green and yellow-blue axes.

General changes of arrows in figure 6 indicate that the color chips under the LED used in the experiment may appear slightly desaturated compared with the FL. We can also see some enhancement of color appearance toward "orange" under the OLED.

Further discussion is needed to connect our data to evaluation of color appearance under solid-state light sources in a more general way. In addition, it is worth to examine usefulness of the color category rating method.

REFERENCES

Shoji, Y., T. Tajima, T. Nagai, T. Ishida and Y. Yamauchi. 2013. Measurement of color appearance with color category rating method under organic light emitting diode. Proceedings of the 1st Asia Color Association Conference, ACA2013: 207-210.

Uchikawa, K., I. Kuriki and H. Shinoda. 1994. Expression of color appearance in aperture and surface color modes. Journal of the Illuminating Engineering Institute of Japan, 78: 83-93 (*in Japanese*)

Address: Taiichiro ISHIDA
Department of Architecture and Architectural Engineering
Graduate School of Engineering, Kyoto University
Kyotodaigaku-Katsura, Nishikyo-ku, Kyoto 615-8540, JAPAN
e-mails: ishida@archi.kyoto-u.ac.jp
yamauchi@yz.yamagata-u.ac.jp
tnagai@yz.yamagata-u.ac.jp

Influence of position of colored panels to entire pattern's visibility.

Ryota Nakaya,[1] Ippei Negishi,[1] Keizo Shinomori,[1]
[1]School of Information, Kochi University of Technology

ABSTRACT

Visibility is related to the decision of area to pay attention in field of view, and must be considered in interface or advertisement. However, it has not been revealed how the visibility is determined in daily and complex scene, which contains various factors. In this study, we focused the color and its position from various factors, and measured the visibility of each color panel in a different arrangement by the paired comparison test. We evaluated the effect of arrangement of color stimuli for visibility by the selection rate of each figure pattern. Analysis of variance on the selection rate of each figure pattern by the pair comparison method revealed that one figure pattern category defined by certain features of the arrangement showed significantly lower selection rate than other categories. Additionally to such pattern categories, there were additional common features in patterns that showed exceptionally higher or lower selection rates, over all arrangement patterns. These results suggest that the arrangement of color patch affects the visibility of entire figure.

1. INTRODUCTION

In daily life, visibility of objects is heavily involved in decision of area to pay attention in field of view. The visibility is a kind of degree to attract the attention of the people with the target, and must be considered in the interface or advertisements from its feature. Such the feature in natural scenes has commonly been called as "attractiveness" especially in attention research. In this study, however, we call this kind of feature as "visibility", mostly because we would employ the paired comparison method in which a simple detection of the object in short time can be considered as a dominant key factor. Contrary, if the method of the measurement would be replaced to trace of eye movement or target detection method, the data would be more influenced by attention capture referred as the attractiveness.

Such the visibility should strongly be influenced by color, meaning that influenced by lightness and saturation. The correlation between color and visibility has been demonstrated (Shinomori et.al. 2013; Suzuki et al. 2013; Toyota et al. 2014) that the visibility by the paired comparison method can reasonably be predicted by the features of the colors. However, shape and size of a target and positional relationship of the colored parts also can affect the visibility, meaning that the degree of visibility also involves multiple factors. Unlike the experiment environment for limiting factors, multiple factors should alter the visibility in daily environments. Therefore, it is difficult to determine the degree of visibility, which is strongly concerning to concept of conspicuity in many cases, only by the effect of color, separately. In this sense, integrated previous research, such as to clarify this complex mechanism, does not exist. However, it is still too difficult to determine the mechanism of visibility using the stimulus involving many factors, limited number of factors should be selected for measurements of the visibility. Therefore, in this study, we focused the color and its position and measured the visibility with different arrangements of color panels in equal lumiannce by the paired comparison test. From the results, we considered the effect of arrangement of partly colored stimuli for visibility from the selection rate.

2. METHOD

Measurement in this experiment was carried out using the equipment installed in a dark room (Figure 1). We used a LCD display for stimulus presentation and a general numeric keypad for response. Observers were nine students (5 male and 4 female) in the mean age of 21.0 year old. They were naïve observers and authors were not included. Observers were screened by color vision tests of Ishihara-plate (38 plates edition), Standard Pseudo-isochromatic Plates (SPP) and D-15 and were confirmed to have normal color vision.

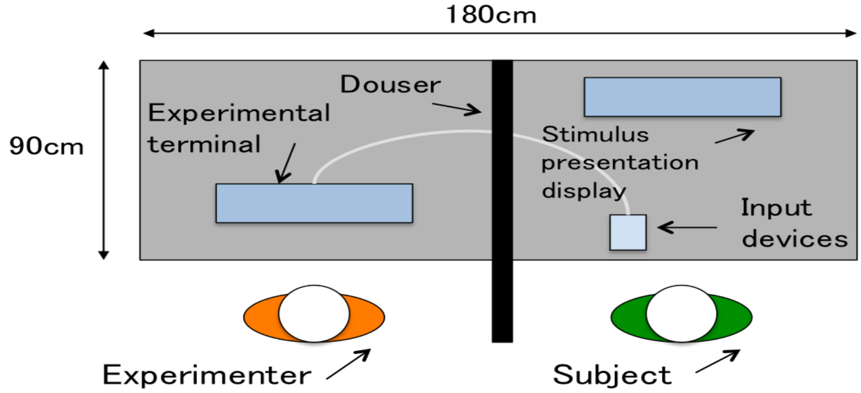

Figure 1: Apparatus

2.1 Stimulus

In this experiment, we use a set of figure patterns as the stimulus, those were consisted of 7 gray panels and two colored panels arranged to make a square shape of 3 × 3 panels. The size of the gray and colored panels were 1.8 cmx1.8 cm (1.5 ° x 1.5 ° in visual angle), making the entire figure of 4.4 ° x 4.4 °. The color for the colored panel was red, which had shown to have the highest visibility in previous studies (Shinomori et.al. 2013; Suzuki et al. 2013; Toyota et al. 2014). Panel's colors, red and gray were equated in luminance (24.68 and 24.64 cd/m^2, respectively) and their CIE 1931 xy chromaticity coordinates were (0.495, 0.323) and (0.289, 0.294), respectively, measured by a luminance and color meter (CS-200, Konica Minolta Co. Ltd.).

The set of stimulus figure pattern was composed of 36 kinds of patterns depending on the position of red (colored) panels. The patterns were classified to four categories for analysis by characteristics of the arrangement of the colored panels as shown in Figure 2; Category 1 was the classification having a rectangular arrangement of colored panels contacting with one side, meaning the adjacency in a vertical or horizontal direction. Category 2 was the classification with an arrangement characteristic of the color panels in contact with one vertex, meaning the adjacency in the oblique direction. Category 3 was the classification with a configurationally features in the column direction or the same row direction, but without adjacency. Category 4 was the classification without the configurationally feature nor the adjacency, meaning that colored panels were not in the same row or column. Show below an example of each category.

Figure 2: Examples of stimulus figure patterns belonging to four categories.

2.2 Experiment Technique

Before the experiment, the observer adapted to a dark background of the monitor screen for five minutes. In the experiment, two stimulus figure patterns were pseudo-randomly selected from 36 patterns and presented to the observer as shown in Figure 3. The observer made a response of choosing stimulus figure pattern in higher visibility from two as one trial. Trials were continued until all the combinations would be completed in the pair comparison in one session, although we did not make the comparison between the same pattern. The pair of patterns were pseudo-randomly changed after observer's response, thus, the order of pattern presentation were also change in every time of the experiment. Additionally, we tried to avoid a possible influence on determination by the presentation of preceding patterns and by retinal adaptation, which could be different between gray and colored panels. Location of the stimulus patterns presented on the screen was changed slightly between trials (shifted in any (random) direction with a random amount of distance up to 3.3 °). The paired comparison for all combinations were performed in one session and one observer performed 3 sessions. The observers took at least 5 minutes break between sessions and any time when the observer required.

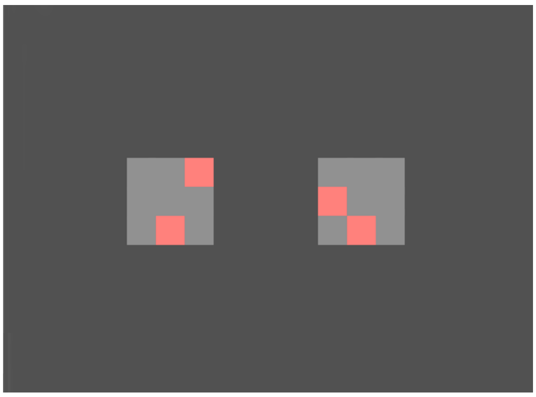

Figure 3: Example of presentation stimulus

3. RESULTS AND DISCUSSION

In this experiment, we defined a selectivity (0 to 1) as the probability of selecting one stimulus figure pattern against all other patterns (thus, not including against the same pattern) in the pair comparison method, as a reference for determining the degree of visibility. Based on the mean selectivity of all observers, ranking of the visibility in the entire patterns was determined and presented in Figure 4. The average of the selectivity for all patterns belonging to one category were also calculated and presented in Figure 5.

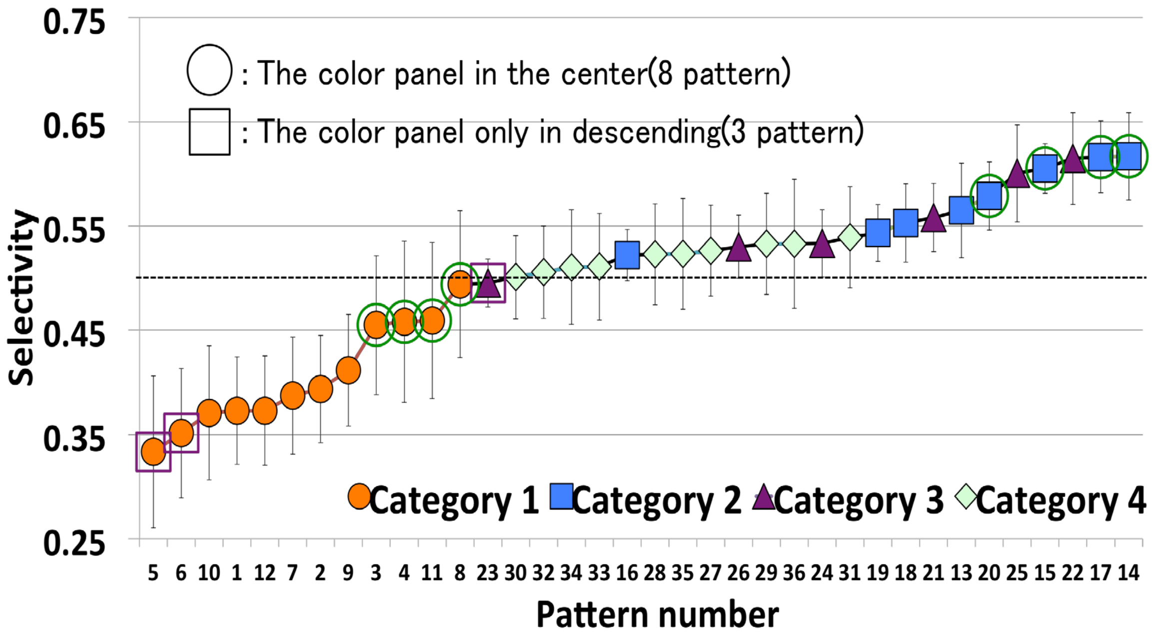

Figure 4: Ranking of the selectivity for each pattern.

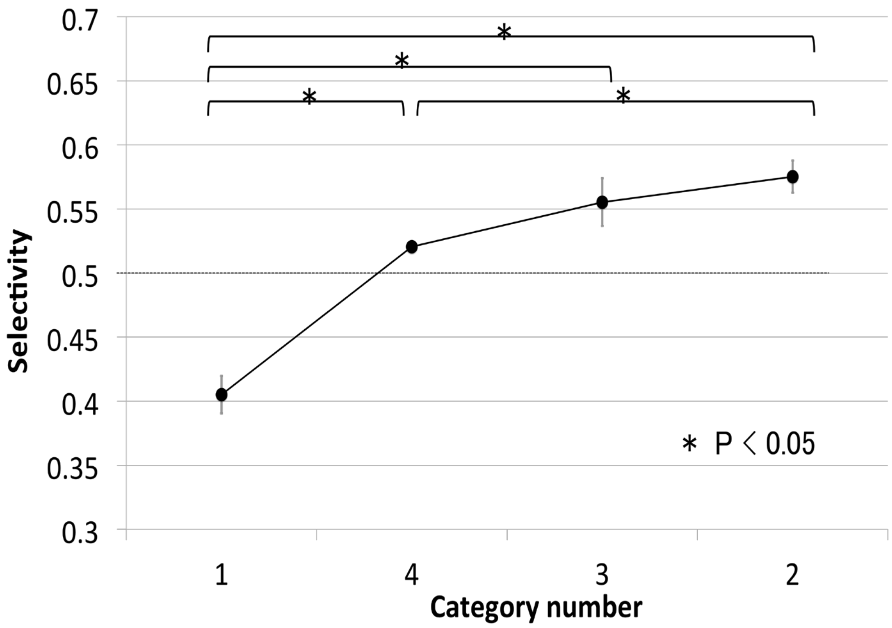

Figure 5: Ranking of the averaged selectivity for each category

The selectivity between categories, category 2 showed the highest selectivity as shown in Figure 5. Category 1 had the lowest selectivity, showing large difference in selectivity for other categories. Result of analysis of variance for selectivity between categories, category 1 showed a significantly lower selectivity ($p < 0.05$) compared to other categories, category 4 showed a significantly lower selectivity ($p < 0.05$) compared to category 2. The overall pattern selectivity in Figure 4 indicated that the patterns belonging to the same category, other than the category 3, were close in the ranking. This tendency caused the significant ranking order between categories as shown in Figure 5. Category 3 had divergence in the ranking order, although it tended to have higher rankings. However, in category 3, the ranking of pattern 23 exceptionally located in a lower order of the selectivity compared to other patterns in the same category. That is the pattern classified as colored panels are only in the most descending (bottom) column, explained more details in the later paragraph.

The main difference in the selectivity between category 1 and other categories was a way of the contact between colored panels. From this feature, patterns belonging to the category 1 were recognized as one colored rectangular in the pattern. On the other hand, other categories were recognized as the pattern having two colored panels independently. Therefore, a plurality of colored stimuli can be considered to give a stronger influence on the visibility of the subject than the single colored stimulus.

The main difference between categories 4 and 2 was an existence of the contact point and category 4 did not have the contact point between colored panels. Therefore, it is conceivable that the contact point has some influence on the visibility of the pattern. Combined with the analysis for category 1, for higher visibility, it is necessary to be recognized as separated colored stimuli while having the contact point.

We would like to mention about two special features of the pattern found in different categories; the first one is the arrangement in which one colored panel was placed in the center at the entire stimulus figure pattern. Such patterns, denoted by circles in Figure 4, commonly had the highest selectivity in the belonging category. It suggests that the color stimulus at the central portion is positively affecting the visibility. However, this feature did not go over the category border in the selectivity ranking, suggesting that this special feature can infuence to the visibility in the lower level compared to influences of contact points and arrangement that we used for classifying categories.

The other special feature of the pattern was for exceptionally lower selectivity compared to others in the same category. That is the pattern classified as colored panels are only in the most descending (bottom) column as mentioned above. Other two patterns with this special feature were both located in the rank of the lowest selectivity. The colored stimulus lopsided in the bottom column can be considered to have negative impact on visibility compared to other features. However, again, this feature did not go over the category border in the selectivity ranking, suggesting the same consideration to the pattern with the center stimulus.

We, however, did not know whether the same results would be obtained under the different conditions such as increasing the number of panels. If the number of panels will be increased, however, it may not be possible to perform the experiment practically because of the experimental time should become enormous in the paired comparison method. Thus, in the future, it is necessary to verify the effectiveness of these arrangement and positional features using a new method.

4. CONCLUSIONS

In this study, we found that the arrangement relationship between the two colored panels used for the classification of categories in this study is one of the stronger factors that influence the visibility of the overall stimulus figure. Additionally, we found several positional features, which affect the visibility of the stimulus in terms of the position relationship of the colored panel, such as the central positions and the bottom positions. The visibility of the color stimulus can be changed by such positional features, however, they are weaker and simly adding the effect to the arrangement features from the lower (weaker) level.

ACKNOWLEDGEMENTS

This research was supported by JSPS KAKENHI Grant Number 24300085 to IN and KS.

REFERENCES

Shinomori, K., T. Suzuki, N. Murai, Y. Ozaki and S. Nakauchi 2013. *Function-oriented color selection technique using subjective estimation (paired comparison of images) and psychophysical evaluation (reaction time measurement)*, Proceedings of AIC Colour 2013, 3, 1165-1168.

Suzuki, T., K. Shinomori, N. Murai, Y. Ozaki and S. Nakauchi 2013. *Evaluation of visibility of color under a range of spectral illumination using physically based spectral rendering images: Comparison of reaction times for colored handrail in the bathroom*, Proceedings of AIC Colour 2013,1, 135-138.

Toyota, T., K. Shinomori, T. Suzuki and S. Nakauchi 2014. *Practical color visibility evaluated by response time of search and selection rate in paired comparison*, i-Perception, 5(4), 273.

Address: Ryota Nakaya, Shinomori Lab, School of Information, Kochi University of Technology,
185 Tosayamada- Miyanokuchi, kami-city, Kochi 782-8502, JAPAN
E-mails: 150334p@ugs.kochi-tech.ac.jp

A color coordination support system based on impression from color and readability of text

Yoshihiko AZUMA, Kazuhiro YAMAMOTO, Miyuki KOBAYASHI, Eri KOMIYAMA
Faculty of Engineering, Tokyo Polytechnic University

ABSTRACT

Readability of color scheme is one of important factor at general text design including graphic design, or web design. Each color and color schemes owe unique psychological effects. In general text design, color choice should consider these unique psychological effects. However, this considerable color choice must need high degree of skills. In present study, authors constructed a semi-automatic color coordination support system based on psychological color theory. The color coordination support system was able to nominate font colors that specified by background color. Nominees were based on psychological color theory and readability. Readability of color schemes were measured and formulated from subjective evaluation experiments for various combinations of font and background colors.

1. INTRODUCTION

General text design including graphic design, or web design must maintain readability. Text readability is constructed from color scheme of font and background. Designers are always considering balance of interested graphical design and readability. Thus, general text design needs knowledge and skills of color including psychological effects. Knowledge and skills of color is not easy to acquire. It suggest, knowledge and skills of color is hard to suit for general text design with readability maintained. In present study, authors were tried to developing a color coordinate system for readability secured. This system is able to nominate font colors considering with psychological effects for background color of user selected. Color coordinate system nominees were evaluated readability and psychological effect factors.

2. SYSTEM CONSTRUCTION

Color coordinate system was postulated that does not depend on knowledge and skills of color. Unique and key factor of functions are,

1) selectable background color for high degree of freedom in design.

2) color schemes of system nominees were ranked order of readability.

Those two functions are implemented for considering with balance of interested graphical design and readability.

2.1 Impression from color

Images of something else were impressed from colors. It is look like some color perception generated some psychological description. Impression from color is an important factor in graphic design. Color coordinate system nominated colors from keywords. Keywords and impression are shown in Table.1. Twenty-seven words were selected with reference of preceding study[1]. Relations of keywords and colors were defined on the basis of PCCS

(Practical Color Co-ordinate System[2] by Japan Color Research Institute) as shown in Figure 1.In Table.1, digits of “1” mean that PCCS colors give impressions in corresponding columns, and digits of “0” mean that they give no impressions. The reasons why PCCS was adopted are,

1) Results by preceding studies are available that investigated the relation between color and impression from color based on PCCS.
2) PCCS is able to handle colors by their only two attributes, hue and tone.
3) The number of PCCS colors are limited to about two hundreds, so easy to process by program.

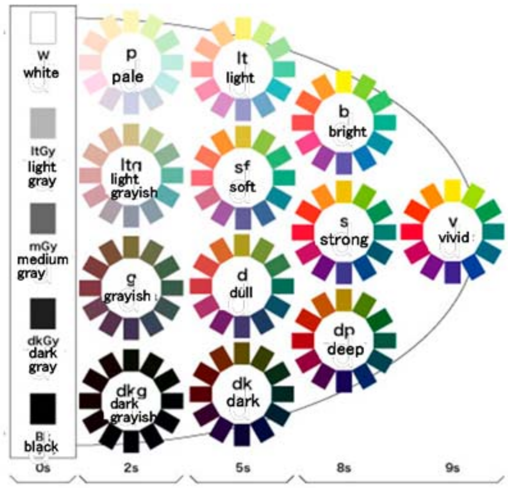

Figure 1: PCCS tone chart[2].

In present study, 201 colors (including 192 chromatic cards in twelve tone and 9 achromatic cards.) were used from PCCS harmonic cards. CIE XYZ values of 201 colors were measured by spectrophotometer (Spectrolino). D65 illuminant was used in colorimetric calculation. The XYZ values were converted to RGB values to display colors on LCD monitor with sRGB color gamut.

Table 1. Rlation between PCCS color and impression.

color notation \ impression	warm	cool	light	heavy	loud	quiet	bright	dark	dynamic	static	weak	happy	sad	merry	mirthless	sweet	spicy	·sour	bitter	masculine	feminine	healthy	unhealthy	classic	romantic	sporty	·ethnic.
v1	1	0	0	0	1	0	0	0	0	0	0	0	0	0	0	0	0	0	0	0	1	0	0	0	0	0	0
v2	1	0	0	0	1	0	0	0	1	0	0	0	0	0	0	0	0	0	0	0	1	0	0	0	0	0	0
v3	1	0	0	0	1	0	0	0	1	0	0	0	0	1	0	0	0	0	0	0	0	0	0	0	0	0	0
v4	1	0	0	0	1	0	0	0	0	0	0	0	0	1	0	0	0	0	0	0	0	1	0	0	0	0	1
v5	1	0	0	0	1	0	0	0	1	0	0	0	0	1	0	0	0	0	0	0	0	0	0	0	0	0	0
v6	1	0	0	0	1	0	0	0	0	0	0	0	0	1	0	0	0	0	0	0	0	0	0	0	0	0	0
v7	1	0	0	0	1	0	1	0	0	0	0	0	0	0	0	0	0	0	0	0	0	0	0	0	0	0	0
v8	1	0	0	0	1	0	1	0	1	0	0	0	0	1	0	0	0	1	0	0	0	0	0	0	0	0	0
v9	0	0	0	0	0	0	0	0	0	0	0	0	0	0	0	0	0	1	0	0	0	0	0	0	0	0	0
v10	0	0	0	0	0	0	0	0	0	0	0	0	0	0	0	0	0	1	0	0	0	0	0	0	0	0	0
v11	0	0	0	0	0	0	0	0	0	0	0	0	0	0	0	0	0	0	0	0	0	0	0	0	0	0	0
v12	0	0	0	0	0	0	0	0	0	0	0	0	0	0	0	0	0	0	0	0	0	0	0	0	0	1	0

2.2 Readability of color scheme

Readability of font color for background color was obtained from subjective evaluation experiments for multiple combinations of font and background colors, that was conducted in our previous study. Readability was formulated from the results, as given in the following equation.

$$y = 0.0927\ |L_1^* - L_2^*| + 0.00635\ |C_1^* - C_2^*| + 0.843\ , \qquad (1)$$

where, y reperesents readability, and L_1^* and C_1^* are metric lightness and chroma in CIELAB color space for background color, respectively. Similarly L_2^* and C_2^* are metric lightness and chroma for font color, respectively.

3. PTOCESS FLOW

Control software of color cooordinate system was built with C++ programing language for Wndows PC. Process flow chart of software is shown in Figure 2. Operation and display screen of the system is shown in Figure 3.

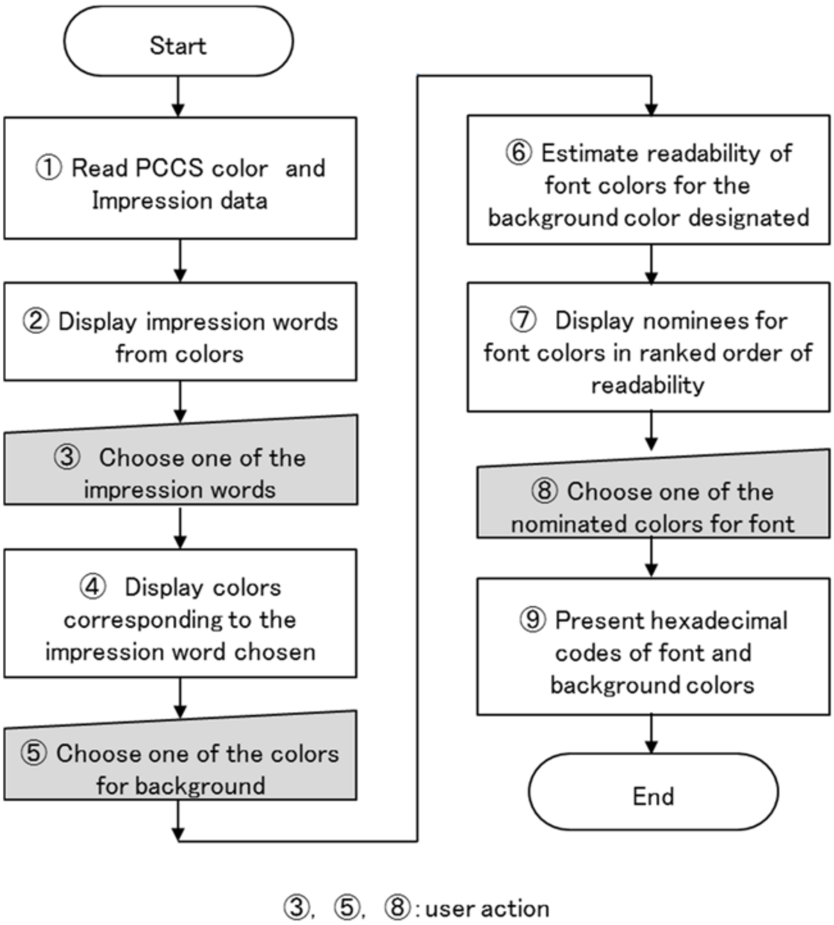

Figure 2: Process flow chart.

Impression words are displayed in window ①, and the corresponding colors for background are displayed in window ② when a user chooses one of the impression words and clicks on the execution button. Then, font colors on background color designated are ranked in order of readability and presented in window ③ when a user chooses one of the colors for bckground. The readability of font color for bckground color is calculated with Equation 1.When clicking one of the color schemes in window ③, RGB values of font and background colors are displayed in window ④.

Figure 3: Operation and display screen.

4. RESULTS AND DISCUSSION

Table 2 shows examples of color scheme results obtained using the color coordinate system. It was confirmed that a fairly reasonable result was obtained for given impression words. Figure 4 shows examples of nominated font colors in ranked order of readability for background color having impression of cool. The order of readability seems to be almost valid. High ranked font colors were white or yellow with high lightness, while low ranked font colors have various hues. In present study, impression from font color is not taken account. If text area is large, impression from font color should be considered.

Actually this system was applied for graphic design of can package and confirmed to be effective in creating images as intended[3].

Table 2. Examples of color scheme results

Impression	Font color	background color	Color sch eme result
happy	55, 55, 55	254,125,116	I Love Color!
sad	238,235,237	79,98,104	I Love Color!
dynamic	233,229,224	252,45,62	I Love Color!
static	76,58,58	122,184,169	I Love Color!

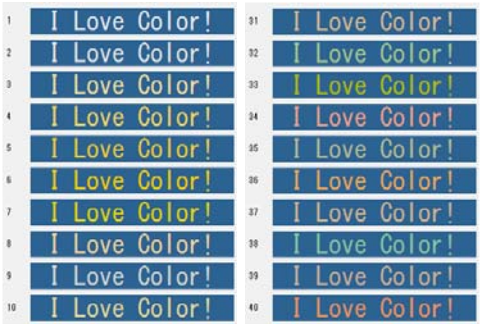

Figure 4: Nominated font colors in ranked order of readability for cool background color.

5. SUMMARY

A semi-automatic color coordination support system was constructed and evaluated. This system was able to nominate font colors in ranked order of readability for background color designated by impression from color. The system is expected to be an effective tool for color scheme for users not having enough knowledge and skills of color.

REFERENCES

1) Kawasaki, H. 2002. *Introduction to color coordination for color coordinator.* Tokyo:Japan Color Research Institute.
2) Japan Color Research Institute. 2007. PCCS. Available online, www.sikiken.co.jp/pccs. Accessed: February 21, 2015.
3) Azuma, Y., Yamamoto, K. 2013. A color recommendation system based on psychological images of colors and readability of texts. In *the Japanese Society of Printing Science and Technology 130th Conference*, *Proceedings*, Kyoto: Kyoto TERRSA, 65-68.

Address: Yoshihiko AZUMA, Department of Media and Image, Faculty of Engineering, Tokyo Polytechnic University, 1583 Iiyama, Atsugi-shi, Kanagawa 243-0297, JAPAN
E-mails: azuma@mega.t-kougei.ac.jp

Study on Visual Recognition of Specula Reflection about Silk and Cotton Textile

Eun Jung LEE,[1] Masayuki OSUMI,[2]
[1] Dept. of Fashion Design, Sejong University
[2] Office Color Science Co., Ltd.

ABSTRACT

In this study, optical property of textile was measured, and applied for human visual assessment by computer graphics to clarify the mechanism about visual recognition of silk and cotton textile. The measuring textile samples were 19 white or non-dyed textiles including silk, cotton, polyester materials, and these were plain and twill weavings. Sample was stretched on 20cm diameter cylinder surface with tensile force to sense reflectance profile with various illuminant and detect optical dimension, and measured by gonio-photometric spectral imaging system. After measuring, spectral image at 550nm wavelength of each samples was respectively analyzed and calculated to get skewness and deviation profiles of optical dimension. To analyze visual recoginition, the human visualizing assessment test was applied as magnitude estimation method combined by polar coordinates to apply two different parametric objects, angle was meaning of material type that is silk or cotton feel, and distance from origin was meaning of textile feel. The display device presented monochrome visual stimulus with this coordinates. The images of this experiment were created from metric profile and combined with typical short fiber texture like a cotton broad cloth and typical long fiber texture like a silk taffeta cloth, and variables were intensity of specula profile and texture images. As the result of this study, the boundary area of textile feel, and also silk/cotton material feel were calculated. The silk feel was approximately related with intensity of specula profile, and textile feel was approximately related with intensity of texture.

1. INTRODUCTION

The various texture and design of fabric are created by combined fiber material, spinning, weaving and finishing effects. Especially, silk and cotton fabrics are the most popular and typical cloths in human life, and also there were a lot of them represented by drawing or painting on the arts. Basically, visual recognition of silk and cotton textile is the very interesting subject.

2. METHOD

2.1 Textile measuring by Spectral Imaging (Metric Data Acquisition)

For instrumentation, liquid crystal tunable filter (Perkin Elmer, LCTF) is used as the spectrum method. And Pertie Cooling, monochromatic-CCD camera equipped with anti-blooming and white LED were used in the process. As LCTF is 10nm in half-band width, and the CCD camera with 772 X 580 pixel and closing-up distance shot in the 40 cm distance far from the apex of the sample cylinder. In this case, the resolution is 180 dpi. LED lamps were aligned through a like shape with vertical 15° through 45° angle to the sample planes from 30 cm distance. These measured samples were all attached to the planes of a cylinder with 20cm in diameter. From the lamp with the vertical 15° angle to the sample plane, it was able to get the optical geometric conditional information as a specular angle to the X axis of the result image ranges from -60° to 90°, or the one with 45° ranges from -30° to 120°. Figure 1 shows which instrument and optical geometric condition was used and based.

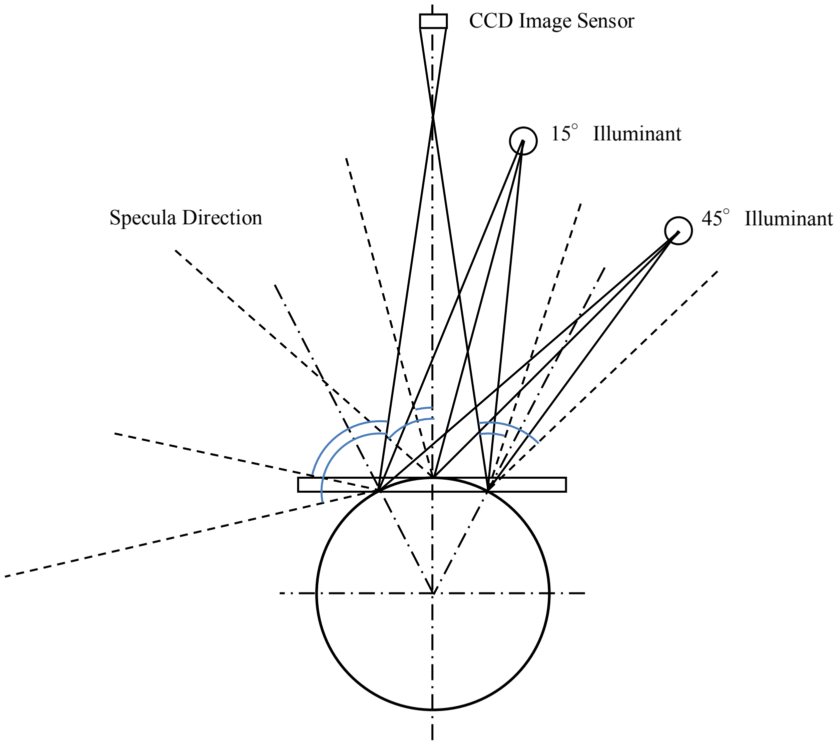

Figure 1: Optical geometry of spectral imaging system.

Measured samples were 19, including cotton, silk, synthetic fiber textile, and mat surface paper. Among these, the most representative profiles were 4; cotton broad, silk taffeta, polyester taffeta and mat surface paper. These were interpreted while using mathematical method to figure out reflectance profile to optical geometric conditions using images with 550nm. These image and L* profile of each measuring are shown in Fig.2.

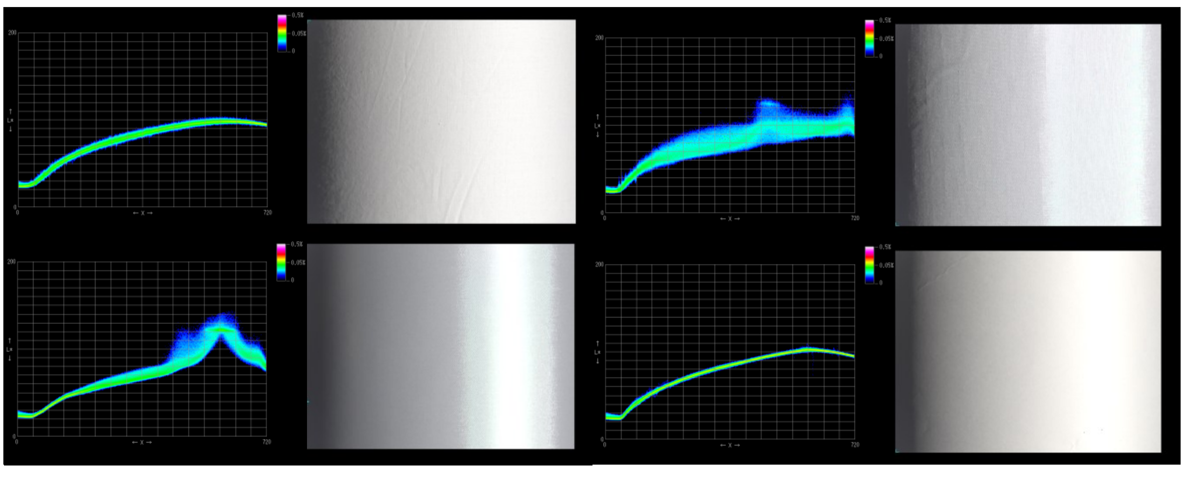

Figure 2: Measuring result of 4 chosen textile and paper.

2.2 Human visualize assessment (Visual Data Acquisition)

With basics of profile from measurement data, presentation stimulation recording based on magnitude estimate was carried out to measure perception levels. Experimental stimulations used gloss constituents from each basic reflectance profile of cotton, silk, synthetic fabric. And finally, texture such as short and long fiber, their carried combination as stimulating parameter and 32 images are created with skewness range between -0.6 to 0.8 and kurtosis range between 1.8 to 2.5 of luminance distribution. The texture intensity calculated by Laplancian filter, and created image has 1.4 to 24. The list of the used parameters in every experiment was shown in Table 1.

Table 1. The list of parameter.

Sample	Skewness	Kurtosis	Texture Intensity	Sample	Skewness	Kurtosis	Texture intensity
1	-0.46	1.86	1.41	17	0.80	2.48	6.85
2	-0.59	1.99	16.93	18	0.79	2.48	10.06
3	0.79	2.48	13.30	19	0.79	2.48	13.30
4	-0.41	1.86	15.43	20	0.79	2.47	16.55
5	-0.59	1.99	11.44	21	0.17	2.01	4.07
6	-0.59	1.99	13.78	22	0.17	2.01	7.17
7	0.79	2.48	11.44	23	0.17	2.01	10.37
8	0.79	2.47	17.49	24	0.17	2.01	13.61
9	-0.41	1.86	13.22	25	0.17	2.01	16.86
10	-0.60	1.99	4.55	26	0.11	1.79	2.29
11	-0.48	1.93	8.77	27	0.11	1.79	4.73
12	-0.59	1.99	16.89	28	0.11	1.79	7.82
13	-0.59	1.99	20.32	29	0.11	1.80	11.01
14	-0.58	2.00	24.02	30	0.11	1.80	14.23
15	0.80	2.49	1.48	31	0.11	1.80	17.47
16	0.80	2.49	3.74	32	-0.17	1.79	2.28

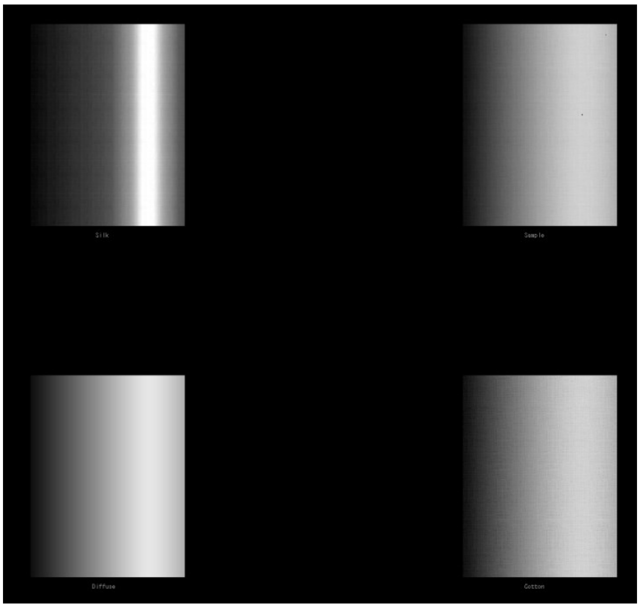

Figure 3: Test sample image for human visualize assessment.

As the parameters, from the gloss parts, cotton, silk, synthetic fabric, diffusing cotton and each respective reflectance profile, and also short and long fabric type textures were prepared to be paired variably for making different stimulations. For these stimulations, the image from the diffusing cotton profile with the 0 intensity of texture was placed on the origin point in XY coordinates, on (X,Y) = (1.0, 0.0) for the image of short fabric type texture from cotton profile, on (X,Y) = (0.0, 1.0) for the image of long fabric type texture form silk profile, on X axis for cotton likeness, on Y axis of the 2 dimensional coordinates for silk likeness, and finally on (X,Y) = (1.0, 1.0) for each given stimulation. For answer process, XY coordinates were shown and mouse clicking over the 2 dimensional coordinates was conducted. In this manner, fabric likeness coincides with the distance from the origin point, cotton likeness with X axis, silk recognition intensity with Y axis, and all of these were alternatively displayed. Also, while answering, there were 4 sorts of answers as following; 1 is cotton recognizing, another is 2 for silk recognizing, 3 for recognizing non-cotton or silk, and the last is 4 for not recognizing any fabric. The subjects in the experiment were 20 with normal eye vision, consisting of male 0 and female 0. 4K display (Samsung, the U32D970Q, 31.5 inch, 16:93820X2190 pixel, 208dpi, 350Cd/m2) was used for indicating display(See Fig 3.).

3. RESULTS AND DISCUSSION

Figure 4 shows the visual assessment test results and the plot results from the whole answers' values. And x and y are the values of answers on 20 points surely gotten from experiments. Also, 20 people were asked to report whether they can recognize or not. From the silk and cotton, there are 2 divisions in area. In the center was either recognizing as other fabric or not recognizing as any fabric. So were cotton and silk in the center and also admitted in the strong gloss area. For the suggested stimulation area, it goes almost up to not-recognition which will be the properly suggested range.

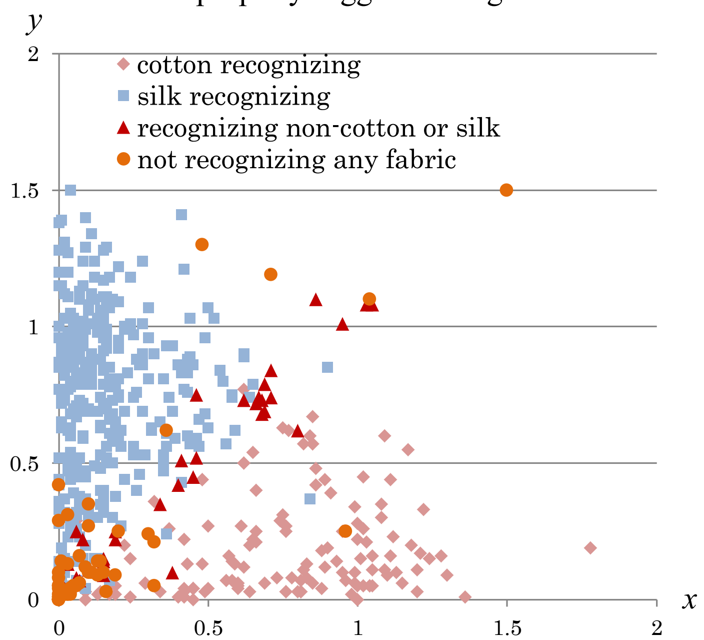

Figure 4: The human visualize assessment test result.

Figure 5 shows what the results of instrumentation would be like if only stimulation revised by one gloss profile is suggested. Above all, the level of recognition was low, and more or less than 48 percent or almost up to half answered that they couldn't recognize any fabric in this stimulation group. This is because the No. 1 matt with gloss profile and the No. 32 with combined by 4 profiles were recognized bad, and these 2 were followed by

72.5% of answers that reported that they were not recognized as any fabrics. However, in the perfect diffusing profile of the No.10, 35% recognized it as cotton, 85% as fabric including cotton and etc. Also, in the high kurtosis profile of the No.15, 35% reported that it was silk, and 65% said it was a fabric, which produced pretty high scores. Either the No.10 or 15 originally starts from fabric gloss profile, and highly likely to be recognized as fabric even though not undergoing texture test. Besides, cotton is reported from perfect diffusing and silk is recognized from high kurtosis. Although the nuance between profiles for matt and perfect diffusing exists, there is a pretty conspicuous difference in recognition as fabric. Figure 6 illustrates which results should possibly come out when the perfect diffusion profile is added and revised by texture parameter. As the texture increased, levels of recognition as textile fabric went up, too, and even a slightest addition of texture was made, levels of recognition as textile fabric rapidly increased. The No.11 stimulation where the perfect diffusion profile is added by a newly produced short type texture was perfectly reported as cotton by every subject. Meanwhile, in case that long type texture was added, levels of recognition as fabric was 100% as same as the one discussed from the No.11. But, for its proportional results, a half of the subjects said that it was cotton, and the other said it was silk. This didn't resort to the trend from gloss profile, but predominantly on types of texture in which cotton equals to short type fabric and silk equals to long type fabric. The short type texture increased, so proportionally did levels of recognition as cotton.

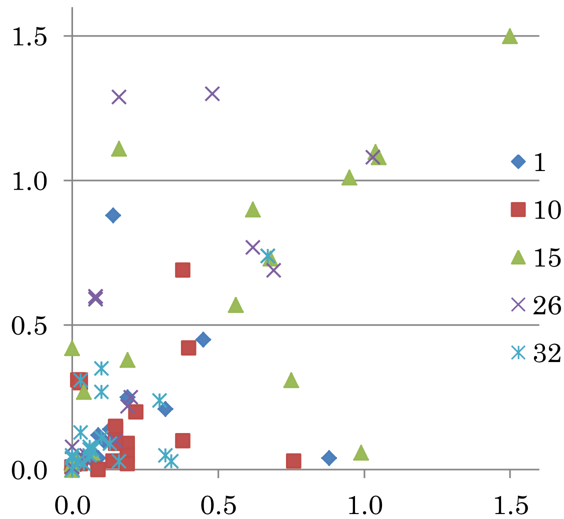

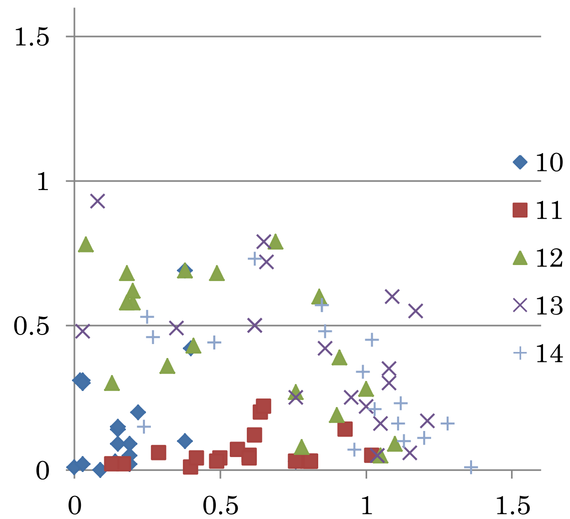

Figure 5, 6: The human visualize assessment test result.

For the next, Figure 7 shows what comes when short type is combined to high kurtosis profile. When the high kurtosis profile was given, the level of recognition as silk was high. Also, herein was reported back as textile fabric by 91% of the subjects placed in this stimulation group, and as silk by 83% in the same group. In addition, even though being the short type, levels of recognition as fabric increased as texture intensity went up. In this case, because gloss far exceeded other parameters in effects, it forcefully affected whether it could be recognized as silk or cotton even though texture was also involved in increases for recognition as fabric. The perfect 100% rate of answers was from the recognition as silk from the No.18 to No.20. Also, Figure 8 indicates the results combined by the compound of high kurtosis profile and the perfect diffusion profile and the short type texture as the one Figure 0 shows. As including the No.15, the 89% rate of answers was from the recognition as textile fabric, and from this, the 78% recognized it as silk. In this step, recognition barely changed, and also the gloss profile was dominant, so the level of recognition as silk was high without depending on texture intensity or its type. There is one interesting fact that when intensity for short type texture fabric increased, it was highly proportionally recognized as silk, so about 100% perfect rate reported it was silk where there was somewhat appropriate texture in these 3 suggested stimulation groups.

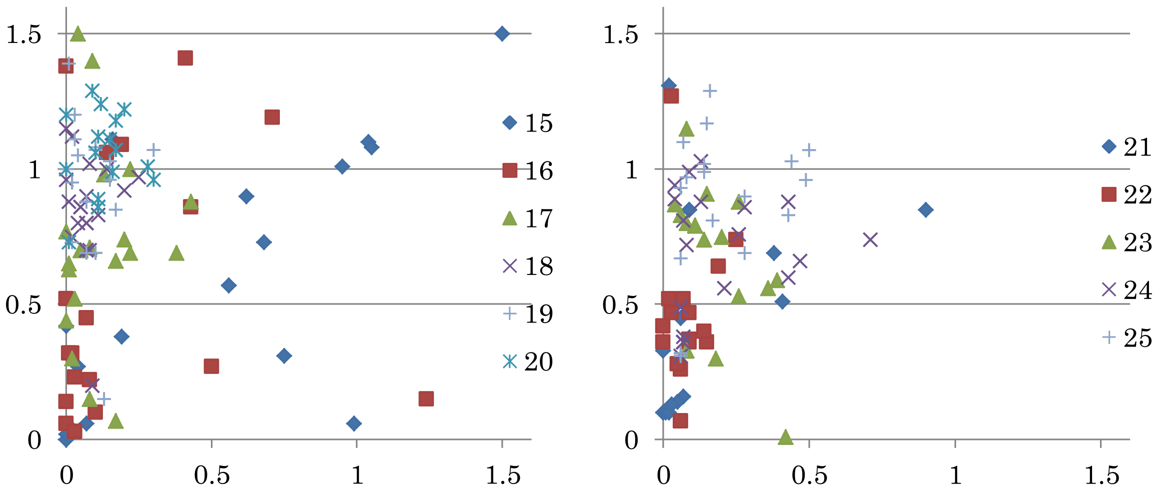

Figure 7, 8: The human visualize assessment test result.

4. CONCLUSIONS

The high gloss textile material has various luminance distribution profiles, so it is recognized as silk without depending on its shape. On the other hands, the low gloss textile material is highly affected by luminance distribution profile in its recognition, and also by the smallest difference of shape without texture. The level of recognition as fabric rapidly increases revised by the texture input. In the diffuse reflection, the types of texture have an impact on recognition of basic fabric material.

REFERENCES

Motoyoshi, I. 2007. *Image statistics and the perception of surface*, Nature vol.447:206-209.

Kuo, CFJ. 2008. *Automatic Recognition of Fabric Nature by Using the Approach of Texture Analysis*, Textile Research Journal vol.76(5):375-382.

Motoyoshi, I. 2012. *Variability in constancy of the perceived surface reflectance across different illumination statistics*, Vision Research 53:30-39.

Adelson, E.H. 2008. *Image statistics and surface perception*, SPIE-IS&T Electronic Imaging vol.6806:680602.

Sakurai, K. 2013. *Exploring texture element of realistic cloth,* IPSJ SIG Technical Report vol.2013-CG-151 No.2:624

Ishikawa, T. 2011. *Fundamental Study on Texture Recognition of Cloth Image and Material*, Journal of Japan Kansei Engineering vol.10 No.4:497-504

Address: Prof. Eun Jung LEE, Department of Fashion Design, Sejong University,
209 Neungdong-ro, Gwangjin-gu, Seoul, KOREA
E-mails: lej624@gmail.com, masayuki-osumi@nifty.com

An Experiment on Color Differences Using Automotive Gonioapparent Samples

Manuel MELGOSA,[1] Luis GÓMEZ-ROBLEDO,[1] Esther PERALES,[2] Elisabet CHORRO,[2]
Francisco Miguel MARTÍNEZ-VERDÚ,[2] Thomas DAUSER[3]
[1] Department of Optics, University of Granada, 18071 Granada, Spain
[2] Color and Vision Group, Department of Optics, Pharmacology and Anatomy, University of Alicante, 03690 Sant Vicent del Raspeig, Alicante, Spain
[3] AUDI AG, I/PG-C41, 85045 Ingolstadt, Germany

ABSTRACT

A panel of 9-11 observers with normal color vision has assessed a set of 61 color pairs in a multiangle color cabinet using a gray scale method. The main goal was to test the potential relationship between perceived lightness differences and lightness flop. The samples in our color pairs were nearly achromatic (C^*_{ab}<10) and with gradual changes of lightness flop in the range 0.5-4.0 CIELAB lightness units per degree. The average color difference in the color pairs was 3.0 CIELAB units. The percentage of lightness difference in the total color difference was above 85% in all color pairs, with an average value of 93.7%. Observers' variability in our experiment was low, with an average standard deviation of visual differences of 0.6 CIELAB units, or an intra- and inter-observer variability of 15.4 and 17.5 *STRESS* units, respectively. The CIEDE2000 color-difference formula provided the best predictions of our visual results with a *STRESS* value of 27.4. However, the predictions made by CIEDE2000 and a set of 11 different advanced color-difference formulas were not statistically significant different, with their *STRESS* values changing in a short range from 27.4 to 33.0 units. Our results show no clear relationship between perceived lightness differences and lightness flop, perhaps because the perceived lightness gradients in the samples in our experiment were small. None of the weighting functions for lightness proposed by recent color-difference formulas (e.g. CMC, CIEDE2000, CAM02-SCD, OSA-GP-Euclidean, AUDI2000, etc.) was particularly useful to predict the results of our visual experiment. However, power functions seem an appropriate option to improve the predictions of current visual results. Specifically, an exponent 0.55 in the CIEDE2000 and AUDI2000 formulas provided *STRESS* values of 18.5 and 18.3 units, respectively, which are considerably lower than the original ones and close to inter-observer variability.

1. INTRODUCTION

Automotive industry needs successful color-difference formulas to establish reliable tolerances in color quality-control. This goal must be achieved for all modern materials employed in this industry, which includes materials exhibiting both homogeneous (solid) and goniochromatic (effect) colors. Goniochromatism can be defined as the property related to the change in any of all attributes of color of a specimen on change in angular illuminating-viewing conditions, without any change in light source or observer. In industrial applications the difference in appearance of a material viewed over two different aspecular angles (i.e. two viewing angles measured from the specular direction) is usually designated as "flop" (ASTM, 1995). Currently, AUDI2000 (Dauser, 2012) is the only color-difference formula considering sample pairs with flop effects in the computation of color differences.

In two previous papers (Melgosa et al., 2014a and 2014b) we analyzed the performance of different advanced color-difference formulas using automotive sample pairs, with particular attention to the performance of the term of lightness flop in the AUDI2000 color-difference formula. In the first paper (Melgosa et al., 2014a), we reported results of an experiment where the sample pairs had a small size of 3.5x3.7 cm and almost random amounts of lightness flop. In the second paper (Melgosa et al., 2014b) we employed samples with a bigger size of 10x10 cm and systematic increasing amounts of lightness flop, but the color differences in a considerable number of these color pairs were not lightness differences. This made difficult to achieve clear conclusions on the relationship between lightness differences and lightness flop, as proposed in the AUDI2000 color-difference formula. The current paper reports a new experiment where, in addition to sample pairs with the highest available size and a systematic increase of lightness flop, the color differences in all color pairs were predominantly lightness differences. Specifically, in all color pairs in the current experiment the percentage of lightness difference (ΔL^*) in the total color difference (ΔE^*_{ab}) was higher than 85%, and the uncertainty in observers' visual assessments was considerably low. In this way, we expect to achieve new conclusions on the relationship between perceived lightness differences and amount of lightness flop, which may be particularly useful to test/improve the AUDI2000 color-difference formula.

2. METHODS

From a set of 476 samples produced by AkzoNobel for the automotive industry, we have selected 61 nearly achromatic color pairs with increasing amounts of lightness flop. Figure 1 shows the average color coordinates and lightness flops of the two samples in each color pair, as measured using a BYK-mac multi-angle spectrophotometer (aperture 23 mm; illuminant D65; CIE 1964 standard colorimetric observer). Our samples had C^*_{ab}<10 and a wide lightness range (Fig. 1, left). For our color pairs, the average values of lightness and the angular lightness flop had a good positive correlation (Fig. 1, right), in such a way that, for example, it was not possible to find color pairs with low lightness and high angular lightness flop. We have defined the angular lightness flop for each color sample as $|L^*_{\gamma i+1}-L^*_{\gamma i}|/(\gamma_{i+1} - \gamma_i)$, where the angles were γ_i=15° and γ_{i+1} =25°, or γ_i=25° and γ_{i+1}=45°, according to the viewing conditions. The two samples in each color pair had very similar angular lightness flop, the angular lightness flop of each color pair being defined as the average. We can note that the angular lightness flop in our color pairs was above 0.5 (i.e. we have not highly homogeneous or solid colors) and covered a relatively wide range (Fig. 1, right). With respect to the color differences in our color pairs, they had average and standard deviations values of 3.0 and 1.9 CIELAB units, respectively. It is important to emphasize that the highly predominant contribution in such color differences was a lightness difference, in such a way that the percentage of lightness difference, measured as $100(\Delta L^*/\ \Delta E^*_{ab})^2$, had an average value of 93.7%, with no color pair with percentage lower than 85%.

Each one of the 61 selected color pairs was visually assessed using a byko-spectra effect light booth (BYK Additives and Instruments) placed in a dark room. Specifically, 31/30 color pairs were assessed at the University of Alicante/Granada (Spain) by 9/11 observers with normal color vision, the viewing angles being γ_i=15° for 30 color pairs, and γ_{i+1} =25° for the remaining 31 color pairs. After an adaptation time of around 3 min, the color pairs were presented in random order to each observer, whose task was to judge the magnitude of perceived color differences using the Gray Scale for Change in Colour of the Society of

Dyers and Colourists. This Gray Scale (9 color pairs with color differences in the range 0-15 CIELAB units, approximately) was just placed above the color pairs. The visual sessions never lasted more than 20 min to avoid observers' fatigue. Each observer performed 3 non-sequential assessments of each color pair, in such a way that a total of 1827 visual assessments were recorded in our experiment. The raw gray scale results reported by the observers were transformed into true visual differences (ΔV) in CIELAB units using a fourth degree polynomial function (Guan et al., 1999). We removed as outliers all visual answers below Q1-1.5*(Q3-Q1) or above Q3+1.5(Q3-Q1), where Q1 and Q3 are the first and third quartiles in the population of all visual answers, respectively.

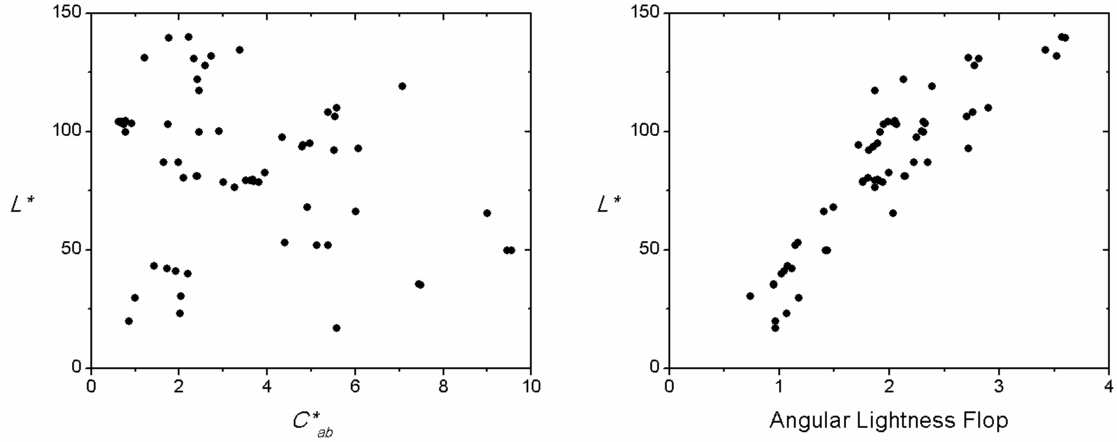

Figure 1: Average CIELAB color coordinates of the two samples in the 61 color pairs (left); average values of lightness against average angular lightness flop (see definition in main text) for the 61 color pairs (right).

We have tested the predictions of the visual results in our experiment by a set of 12 modern color-difference formulas. Detailed information on such color-differences formulas can be found in the original papers or in recent reviews (Melgosa et al., 2013; Melgosa et al., 2014a). The *STRESS* index (García et al., 2007) has been used to measure the merit of each tested color-difference formula, as well as the intra- and inter-observer variability in our experiment (Melgosa et al., 2011). Low *STRESS* values (always in the range 0-100) indicate better performance of a color-difference formula or low observer variability. A color-difference can be considered successful when it achieves a *STRESS* value lower than the ones corresponding to the intra- and interobserver variability.

3. RESULTS AND DISCUSSION

After removing outlier answers, the average standard deviation of the visual differences measured in our experiment was 0.6 CIELAB units. This means that observers' accuracy in our visual experiment was considerably high, in agreement with our values for intra- and inter-observer variability, which were 15.4 and 17.5 *STRESS* units, respectively. Results in Table 1 indicate that predictions of our visual experiment by 12 color-difference formulas were enough similar, as indicated by a short range of *STRESS* values between 27.4 and 33.0 units. Parametric factors in all tested color-difference formulas were assumed as $k_L=k_C=k_H=1.0$. The CIEDE2000 formula, which is the currently CIE/ISO recommended color-difference formula, provided the best predictions of our visual results with a *STRESS* value of 27.4, but it must be indicated that the predictions made by CIEDE2000 and the remaining 11 color-difference formulas were not statistically significant different. It is also important to note that the *STRESS* values for all tested color-difference formulas were at least 10 units higher than the intra- and inter-observer variability in our experiment, which means that the predictions made by all these color-difference formulas were unsatisfactory.

Table 1. STRESS values for 12 tested color-difference formulas (k_L=k_C=k_H=1.0).

CIELAB	CIELUV	CMC	BFD	CIE94	CIEDE2000	DIN99d	AUDI2000	CAM02-SCD	CAM02-UCS	OSA-GP-Euc.	OSA-GP
30.9	31.0	33.0	32.5	31.0	27.4	28.9	32.7	29.3	28.7	31.1	30.0

We have plotted the ratio *ΔL*/ΔV* against the angular lightness flop for our 61 color pairs (Fig. 2, left), in order to ascertain potential relationships between lightness tolerances and lightness flop. Note that the ratio *ΔL*/ΔV* is equal to the lightness tolerance (or the weighting function for lightness usually designated as S_L) when the CIELAB chroma and hue differences are null. This last approach is enough acceptable in our current situation of color pairs with highly predominant lightness differences. From the results shown in Fig. 2 left, it cannot be concluded that lightness tolerances increase with angular lightness flop, as proposed by the AUDI2000 color-difference formula. Therefore, optimizing the coefficients in the weighting function for lightness in the AUDI2000 formula with respect to our current visual results seems meaningless. However, there seems to be an enough clear non-linear relationship between our visual results and the predictions made by the AUDI2000 color-difference formula (see Fig. 2, right). Similar relationships can be also found for the other color-difference formulas considered here, suggesting that a simple power function may improve the performance of most color-difference formulas (Huang, 2015).

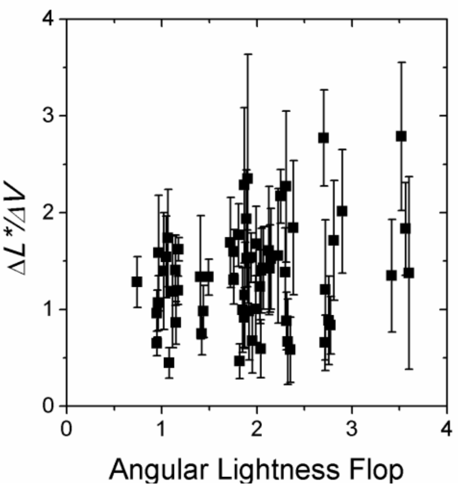

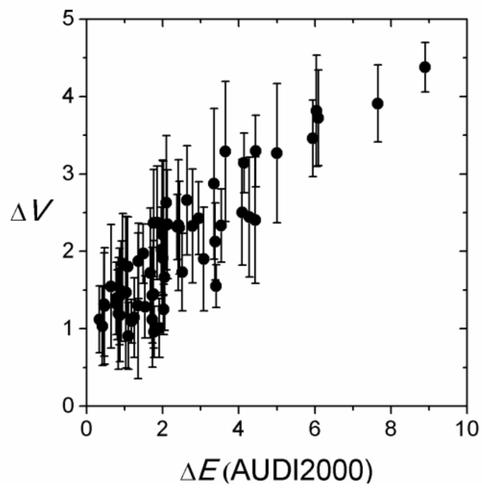

Figure 2: Relationship between approximated lightness tolerances and angular lightness flop (left); visual differences against predictions made by the AUDI2000 formula (right). Error bars indicate the uncertainty associated to the variability in observers' assessments.

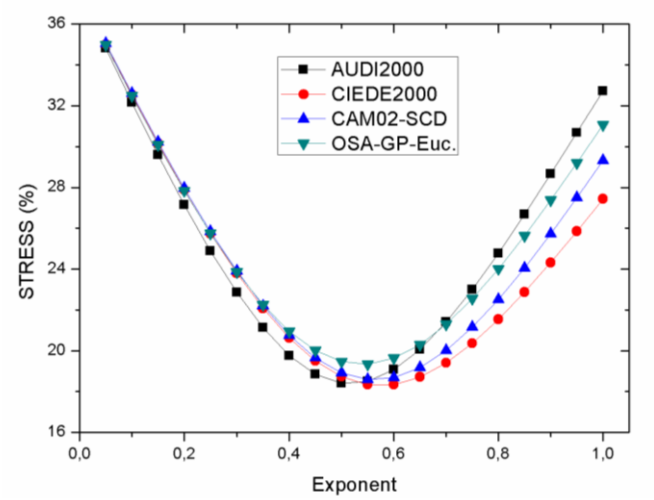

Figure 3: STRESS values for power functions with different exponents in four color-difference formulas, with respect to the visual results found in our experiment.

It can be noted (see Fig. 2, right) that ΔV values are overestimated for very small color differences (perhaps as a consequence of false alarm rates and the fourth degree polynomial function employed to convert from raw to true visual differences), and underestimated for very large color differences. These two deviations may be accounted in color-difference formulas by using simple power functions with appropriate exponents α; that is, simple transforms like $\Delta E' = \Delta E^{\alpha}$. Power functions led to a considerable improvement in the predictions of the visual results found in our experiment by different color-difference formulas, as shown for four specific color-difference formulas in Fig. 3. Note that exponents around 0.5-0.6 considerably decreased the *STRESS* values reported by the original color-difference formulas in about 8-10 *STRESS* units, and the new *STRESS* values are very close to the inter-observer variability in our experiment (17.5 *STRESS* units). Specifically, the use of an exponent 0.55 in the CIEDE2000 or the AUDI2000 color-difference formulas provided values of 18.5 and 18.3 *STRESS* units, respectively.

4. CONCLUSIONS

We have developed a visual experiment where 61 color pairs with mainly lightness differences and different amount of angular lightness flop were visualy asssessed with low uncertainty by a panel of 9/11 observers with normal color vision. From the results in this experiment it cannot be concluded that lightness tolerances increase with angular lightness flop, as proposed by the AUDI2000 color-difference formula, perhaps because the perceived lightness gradients in the samples in our experiment were small. Predictions of our visual results by a set of 12 modern color-difference formulas were not significantly different and unsatisfactory. However, such predictions may considerably improve using power functions with exponent around 0.5.

ACKNOWLEDGEMENTS

This research was supported by the Ministry of Economy and Competitiveness of Spain, research projects FIS2013-40661-P and DPI2011-30090-C02, with European Regional Development Fund (ERDF). Authors are grateful to all volunteer observers participating in the visual experiment. AkzoNobel Automotive & Aerospace Coatings (Sassenheim, the Netherlands) produced the samples used in this experiment. The loan of a byko-spectra effect light booth used in the part of the experiment carried out at the University of Granada is acknowledged to BYK Additives and Instruments (Geretsried, Germany).

REFERENCES

American Society for Testing and Materials. 1995. *Standard terminology of appearance.* ASTM E284 95a.

Dauser, T. 2012. Color Management at AUDI. Available online, http://www.detroitcc.org/files/Color%20Management%20at%20AUDI%20(DCC%20March%202012).pdf . Accessed: February 27, 2015.

García, P.A., R. Huertas, M. Melgosa, and G. Cui. 2007. Measurement of the relationship between perceived and computed color differences. *J. Opt. Soc. Am. A* 24:1823-1829.

Guan S., and M.R. Luo. 1999. Investigation of parametric effects using small colour differences. *Color Res. Appl.* 24: 331-343.

Huang, M., G. Cui, M. Melgosa, M. Sánchez-Marañón, C. Li, M.R. Luo, and H. Liu. 2015. Power functions improving the perfformance of color-difference formulas. *Opt. Express* 23: 597-610.

Melgosa, M., P.A. García, L. Gómez-Robledo, R. Shamey, D. Hinks, G. Cui, and M.R. Luo. 2011. Notes on the application of the standardized residual sum of square index for the assessment of intra- and inter-observer variability in color-difference experiments. *J. Opt. Soc. Am. A* 28:949-953.

Melgosa, M., A. Trémeau, and G. Cui. 2013. Colour difference evaluation. *Advanced Color Image Processing and Analysis*, Chapter 3, pp. 59-81. Editor: C. Fernandez-Maloigne (Springer).

Melgosa, M., J. Martínez-García, L. Gómez-Robledo, E. Perales, F.M. Martínez-Verdú, and T. Dauser. 2014a. Measuring color differences in automotive samples with lightness flop: A test of the AUDI2000 color-difference formula. *Opt. Express* 22: 3458-3467.

Melgosa, M, L. Gómez-Robledo, G. Cui, C. Li, E. Perales, F.M. Martínez-Verdú, and T. Dauser. 2014b. Measuring color differences in gonioapparent materials used in the automotive industry. In *23rd Congress of the International Commission for Optics (ICO23),* colour_84-123. Conference Abstracts (ISBN: 978-84-697-1027-2), p. 26. Paper accepted for publication in a forthcoming issue of *Journal of Physics*.

Address: Prof. Manuel MELGOSA, Department of Optics, Faculty of Sciences,
University of Granada, 18071 Granada, SPAIN
E-mails: mmelgosa@ugr.es, luisgrobledo@ugr.es, esther.perales@ua.es,
elisabet.chorro@ua.es, verdu@ua.es, thomas.dauser@audi.de

Legibility of printed Thai letters comparison on young and elderly

Boonchai WALEETORNCHEEPSAWAT[1]

[1]Faculty of Science and Technology, Sukhothai Thammathirat Open University

ABSTRACT

Elderlies' vision deteriorates by cataract when they are aged. Printed labels represent visual environment and have been found to be expressed by so small letters, which are too difficult for elderlies to read. Design of labels and sign consist of fonts and colors. Thai letters are unique in shape and composition, and can have effect on legibility. The proper color-pairs used for combination of fonts and backgrounds are also needed to guarantee highly legible for efficient vision. This research aimed to compare the legibility of printed Thai letters for young and elderlies in terms of different background contrasts under normal daily situation and illumination. Elderlies aged 60-80 years old and young subjects aged 20-40 years old participated in this experiment. Subjects experimented with adjustment method to find out the legibility of letter charts capable for correct reading. Three achromatic charts of black letters on White, N5, and N4 backgrounds were used for monochrome chart. The charts in different backgrounds each contain 24 lines of Thai letters varying in sizes that are logarithmically even distributed. The viewing distance of 1.2 meter with natural lighting situation in the day time was used for this experimental illuminance. The result showed that for the similar illuminance, legibility of the young not much affected by the darkening of background compare to the substantial legibility decrease of the elderlies when background darkening. The darker background or the lower contrast charts caused higher decrease in legibility for elderlies than the young.

1. INTRODUCTION

Thailand is emerging the elderly society soon as the elderly population in Thailand is increasing substantially. The ageing physical change affect the quality of life, especiallly the visual performance. When people get older they get cataract and their visual performance deteriorates. It is an urgent matter to investigate the performance of elderly vision and to provide proper infrastructure and environment to assure them the quality of life. In this study we pay attention to letter size and background contrast of product labels as the elderly people get information from labels for their daily living. Legibility by elderly people has been investigated by some researchers, Elliott et al. for English, and Ayama et al. for Japanese. They all showed deterioration of the visual acuity by elderly people. But in our knowledge, none investigated for Thai letters and no proposal was made for the Thai letter size recommended for labels to suit elderly people. Thai letters are different from English or Japanese letters.

Legibility at the high contrast stimuli is better than the legibility of lower contrast. Different color pairs of letters and backgrounds also give different legibility which affect the visual performance of elderly and young people differently. We want to know the degree of legibility difference between the elderlies and youngs under normal daily lighting situation in order to set the guideline for graphical labels designing that create by young designers' vision to suit the proper vision of elderlies.

2. METHOD

The adjustment experimental method was used for this study. Subjects were divided into two groups: ten young and eleven elderlies. The elderlies live with their family and performed experiment in their home or in the temple community area during the social gathering event, which was the relaxing atmosphere. Young subjects are recruited from home and office.

2.1 Apparatus

The apparatus for this field experiment composed of test chart and mask, light meter, and measuring tape. The Thai letters test chart was designed to test the legibility especially for Thai subjects. The chart contains 24 lines of Thai letters varying in sizes that are logarithmically even distributed from line to line. There are 3 charts of different backgrounds in White, N5 and N4 to represent different contrast background as shown in Figure 1.

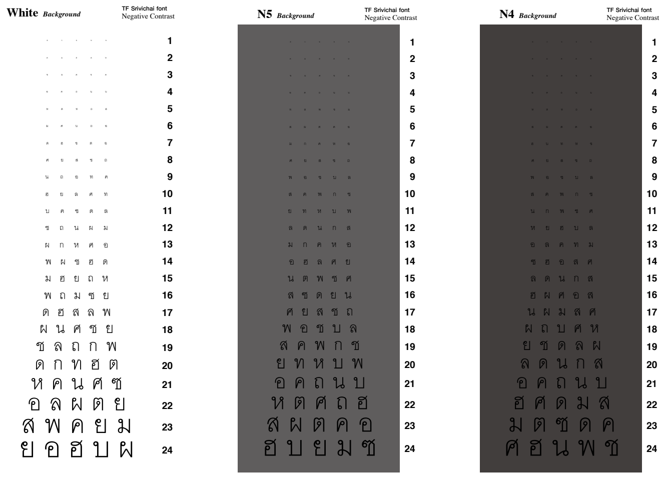

Figure 1. Thai letters test chart in White, N5 and N4 backgrounds.

2.2 Procedure

The subject recruitment was done by two steps. First, check the age to fit in the required range of 20-40 years for young, and 60-80 for elderly. Second, to interview and exclude of any eye decease or abnormal eye condition such as severe cataract. The recruited subjects sat in 1.2 meters distance and illuminance measured. The experiment started with the white background color chart. Mask with window that open to see only one line at a time was used to hide the rest of different letter sizes. The test chart of white background was shown to subject with a mask that open only one line of letters at a time. Subject was asked to tell the overall sharpness of letters shown, and to fine tune to the line that was legible with confident. The larger size letter is shown if subject cannot read correctly, and the smallest line number that fulfill the confident correct reading was recorded. Subjects tell the line number of each chart that can see clearly, and the line number is recorded. The same procedure was done to test chart of N5 and N4 background respectively. Each subject experimented for one time.

3. RESULTS AND DISCUSSION

The legibility data recorded by line number from the experiment was calculated into letter height. The results of legibility are shown by letter height of elderly and young form the three backgrounds test chart and shown in Table 1.

The averaged age for elderly and young are 68.4 and 31.0 years old respectively. There are 11 elderly subjects and 10 young subjects participated in the experiment. The result from all subjects in each groups are averaged in letter height that legible at the distance of 1.2 meter. The illuminance at the experimental area were averaged 913 lx for elderlies and 900 lx for young.

Table 1. Legibility of elderly and young in daily situation on 3 backgrounds

						Letter height (mm)		
	Age (avg)	Subjects	Sex	Lx (avg)	Dist(m)	Nw	N5	N4
Elderly	68.4	11	2M/9F	913	1.2	4.6	6.5	8.7
Young	31.0	10	4M/6F	900	1.2	1.7	2.0	2.2
Gap of difference						2.9	4.5	6.5

The experimental result showed the legibility in term of the letter height that fully legible to the subjects. Legibility of elderlies worse than the legibility of young in all levels of background contrasts. The gap of difference become higher with the darker background from 2.9 mm on white background to 4.5 mm on N5 background and 6.5 mm on N4 background. Figure 2. shows the letter height of elderlies and young in different background contrast charts. The black circle showed legibility of the elderlies, and open circle showed legibility of the young. Lower letter height represents better legibility. This imply that elderlies suffer in higher degree than young people if the contrast of stimuli is decrease.

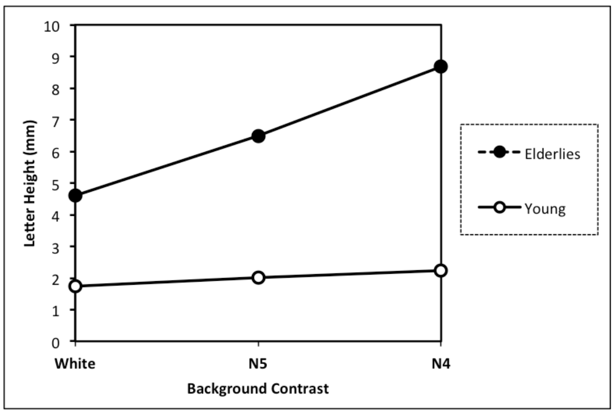

Figure 2. Letter height difference between elderlies and young for test chart in White, N5 and N4 backgrounds.

4. CONCLUSIONS

Legibility of elderlies worse than the legibility of young in all levels of background contrasts. The deterioration increase for the lower contrast of stimuli. This imply that elderlies suffer in higher degree than young people if the contrast of stimuli is decrease. For the designing of graphical labels, legibility of elderlies must be concern. Under the same illuminance and distance conditions, young designers can put the degree of letter height difference or legibility difference shown in this experiment into account for the assignment of letter height suitable for elderlies in their design.

ACKNOWLEDGEMENTS

I would thank all my subjects especially the elderlies in the provincial area for their kind cooperation in this experiment. I gratefully acknowledge Associate Professor Pontawee Pungrassamee, Dr. Tomoko Obama and Professor Mitsuo Ikeda for their kind support of my research training. I also thank Sukhothai Thammathirat Open University for allowing me to attend AIC2015 conference.

REFERENCES

Ayama, M., Ujike, H., Iwai, W., Funakawa, M., and Okajima, K. 2007. Effects of contrast and character size upon legibility of Japanese text stimuli presented on visual display terminal. *Optical Review 14,* 48-56.

Elloit, D. B., and Situ, P. 1998. Visual acuity versus letter contrast sensitivity in early cataract. *Vision Research, 38,* 2047-2052.

Ikeda, M., and Obama, T. 2008. Desaturation of color by environment light in cataract eyes. *Color Research and Application, 33,* 142-147

Owsley, C., Sekuler, R., and Siemen, D. 1983. Contrast sensitivity throughout adulthood. *Vision Research, 23,* 689-699

Address: Assistant Professor Dr. Boonchai WALEETORNCHEEPSAWAT
Faculty of Science and Technology, Sukhothai Thammathirat Open University, Thailand
E-mails: Boonchai.wal@stou.ac.th, bwddstou@gmail.com

On the perceived brightness of whites

Dragan SEKULOVSKI,[1] Kees TEUNISSEN,[1] Mart PEETERS,[2]
YueJun SUN,[2] Remy BROERSMA[2]
[1] Philips Research Europe
[2] Philips Lighting

ABSTRACT

One of the most fascinating observations in the perception of whiteness is the fact that objects with a slight bluish tint appear whiter than objects with a neutral reflection, which resulted in a widespread use of fluorescent agents in white surfaces. The increased whiteness additionally induces a feeling of increased brightness of the white surfaces. This result, however, is shown to hold for two objects under the same light source. In this work, we explore the relation between the perceived whiteness and perceived brightness of the same surfaces lit by different light sources. Using simultaneous viewing and an interleaved, forced choice staircase procedure, a scene lit by two light sources, producing a chromaticity difference of 0.007 $\Delta u'v'$, was matched on perceived brightness. The matching was done for three illuminance levels: 150, 300, and 500 lux. The results of 18 participants show a surprisingly large effect of the relatively low chromaticity change on perceived brightness. The illuminance level at which the whiter scene looked equally bright with the reference was found to be on average 20% lower. The effect was influenced by the light level and was smaller (12% at 150 lux) at lower light levels. No effect of age, gender, or lighting expertise was found. However, a small group of participants had markedly different answers and showed no effect of perceived whiteness on their judgment of brightness.

1. INTRODUCTION

Whiteness perception of objects is an important part of the visual experience and has been a topic of considerable interest in the color world. As early as 1979 an overview paper by Ganz (1979) cited more than 300 papers on the topic and Wyszecki and Stiles (2000) give 20 different formulas for measuring perceived whiteness of objects. One of the most fascinating results in the perception of whites is that a perfect white diffuser (with 100% reflectance in the visible wavelength range) can be perceived as less white than an object with a lower reflectance, if the lower reflectance object has a slight bluish tint. If, however, the reflectance of the tinted object is lowered in a way that keeps the amount of tint the same, at some point the perfect white diffuser is perceived as whiter again. Thus, for the perception of whiteness, there is a trade-off between the lightness of an object and the amount of bluish tint that produce the same increase in perceived whiteness. This trade-off ratio can be estimated from whiteness formulas that take both lightness and chromaticity into account, like the CIE Whiteness equation (CIE 2004). Furthermore, participants in whiteness experiments often note that surfaces that appear whiter also appear lighter or brighter.

The increase of the perception of whiteness by shifting the chromaticity towards blue has been used in the paper and textile industry, where the natural tint of the raw material is yellowish. From using blue dyes, as early as 1929 (Krais, 1929) the industry has shifted to using fluorescent whitening agents (FWAs). FWAs transfer part of the ultraviolet and violet part of the electromagnetic spectrum (λ < 430 nm) to the blue-cyan part of the spectrum of visible light (for which the human eye is more sensitive), thus shifting the chromaticity of the surface towards blue and increasing perceived whiteness.

Most of the classical work on whiteness has been on the perception of whiteness of objects and the illumination has always been treated as a given. The newly rekindled interest in whiteness, however, has been driven by the influence of the illumination on the appearance of white surfaces. In particular, the influence of LED lighting on the appearance of white surfaces containing fluorescent whitening agents was brought to attention by among others Zwinkels and Noel (2011). As most LED light sources do not emit ultraviolet and violet light, the FWAs in the white objects are not activated which results in poorer whiteness rendering compared to daylight and other electric light sources.

The difference in whiteness rendering of different electric light sources also brings differences in the perceived brightness of whitened surfaces. This brings the interesting question of the influence of whiteness rendering of an electric light source on the perceived brightness of the environment that the source illuminates. In this work, we present an experiment designed to explore the effect that the increased perception of whiteness, due to activation of FWAs, has on the perception of brightness of a simple scene containing white surfaces.

2. EXPERIMENTAL METHOD

To find the effect of increased whiteness on the perception of brightness, we designed a brightness matching experiment using LED light sources with and without FWA activation. The illuminance in the center of a simple scene was used as a correlate of brightness and the brightness matching was done using simultaneous viewing. The light source with no FWA activation, called the reference light source, was presented at three preset light levels and the intensity of the light source with FWA activation, called the test source, was tuned using a staircase procedure until an equal perceived brightness was achieved. Additionally, to check the measurement error of the method, the same procedure was used to match the brightness of two reference sources.

2.1 Experimental setup

The experiment was conducted using two identical viewing boxes with the experimental light sources mounted in the center of each box. Both the vertical and the horizontal planes of the boxes were covered with standard office paper from the same batch and having the same FWA properties. All the outside edges of the box were covered with black cardboard perpendicular to the edge. This included the edge between the boxes and ensured a separation of at least 10 degrees of visual angle between the two sides of the stimulus.

Each box had two different LED light sources. The first, reference, light source was a standard warm white spot light module with chromaticity on the black body locus of u'v' = (0.252, 0.521) and did not activate FWAs. The second, test light source, was a spot light module with added violet radiation to activate FWAs. Both modules were positioned at a close distance to each other at the center of each box and were used without a reflector. The difference in the chromaticity of the light reflected from the paper under the light sources was 0.007 Δu'v'. The light sources were driven using a 16 bit DMX driver connected to a computer. The setup was calibrated and checked for thermal effects. Within the ranges of light levels used in the experiment, the thermal effects were negligible. Based on the calibration measurements, a transfer function was fitted modeling the illuminance at the target position for a given DMX control value for each module/driver combination.

2.2 Stimuli and procedure

From the viewing distance of 1 meter from the viewing boxes, the participants simultaneously observed both stimuli. Each box had a size of 60 degrees visual angle with a 10 degree visual angle black separator between the boxes.

The brightness matching was done at three reference illuminance levels of 150, 300 and 500 lux. For each reference light level, a range of light levels for the test light source were defined and a staircase procedure was used to traverse over the levels. Two staircases per reference light level were used: one with the reference on the right side; and one with the reference on the left side. Additionally, two staircases were added with both sides showing the reference source and changing one of the sides to produce a brightness match. All staircases started from a random light level of the test source ranging from 50% to 150% of the reference light level. All staircases were presented randomly interleaved to account for possible reference bias of the participants. At each staircase step, the participants had to indicate which box was perceived as having a higher brightness using the left and the right arrow keys on a keyboard. The procedure was explained to the participants before the beginning of the experiment. The term brightness was not explained such that all participants had their own interpretation of the term.

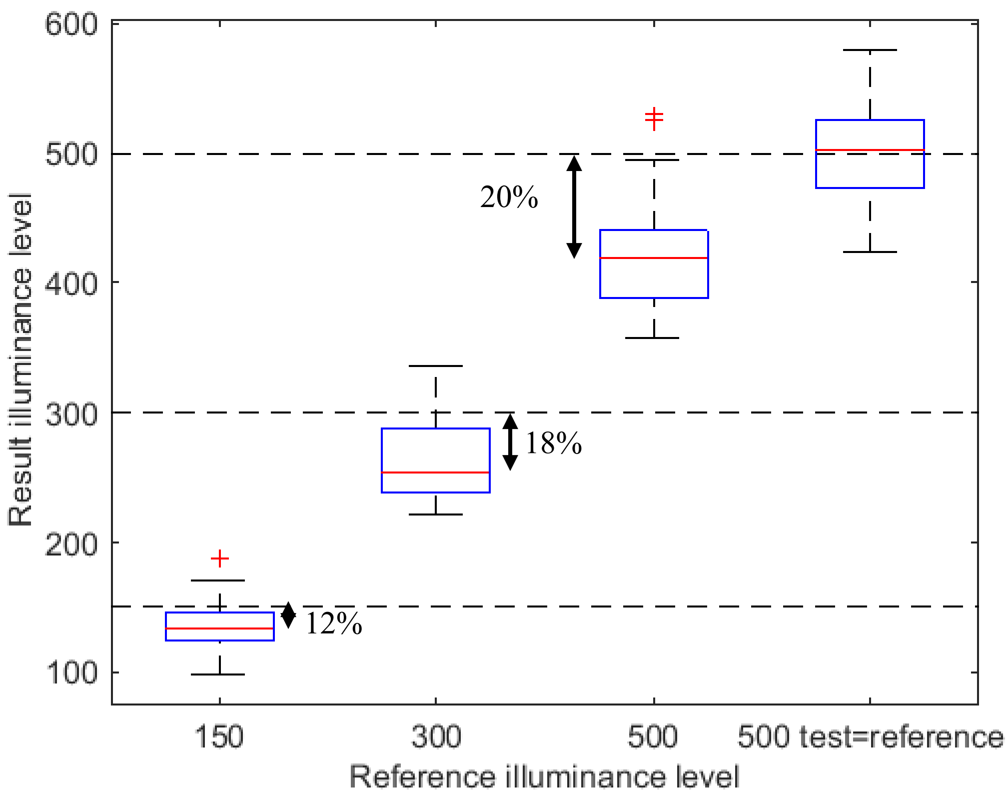

Figure 1: A boxplot of the resulting matched illuminance levels for the three reference illuminance levels (150, 300, and 500 lux) in the experiment.

2.3 Participants

18 participants with ages from 22 to 58 took part in the experiment. Five participants were female and twelve of the participants were lighting professionals. All participants were members of the staff or interns of Philips Research in Eindhoven, the Netherlands.

3. RESULTS AND DISCUSSION

The results of the experiment are expressed as the illuminance level produced by the the test source at the center of the scene for a given illuminance level of the reference source. Figure 1 gives an overview of the obtained results. The difference in illuminance between the reference source and the median illuminance of the test source for which an equal brightness was obtained was 12%, 18% and 20% for reference illuminance levels of 150, 300, and 500 lux, respectively (see Figure 1).

The clear effect of the chromaticity change on perceived brightness, as visible in figure 1, is also supported by statistical testing. All single sample t-tests for the cases with different chromaticies showed a significant difference from the mean illuminance of the reference source ($p < 0.001$ in all cases). For the additional staircases with the same test and reference light source, a single sample t-test did not show a significant effect ($p = 0.798$). The measurement error also depended on the light level and ranged from 19 lux for the lowest light level to 41 lux at the highest light level. There was also no difference between the measurement error in the regular cases and the additional case where the reference light source was used both as a reference and as a test source.

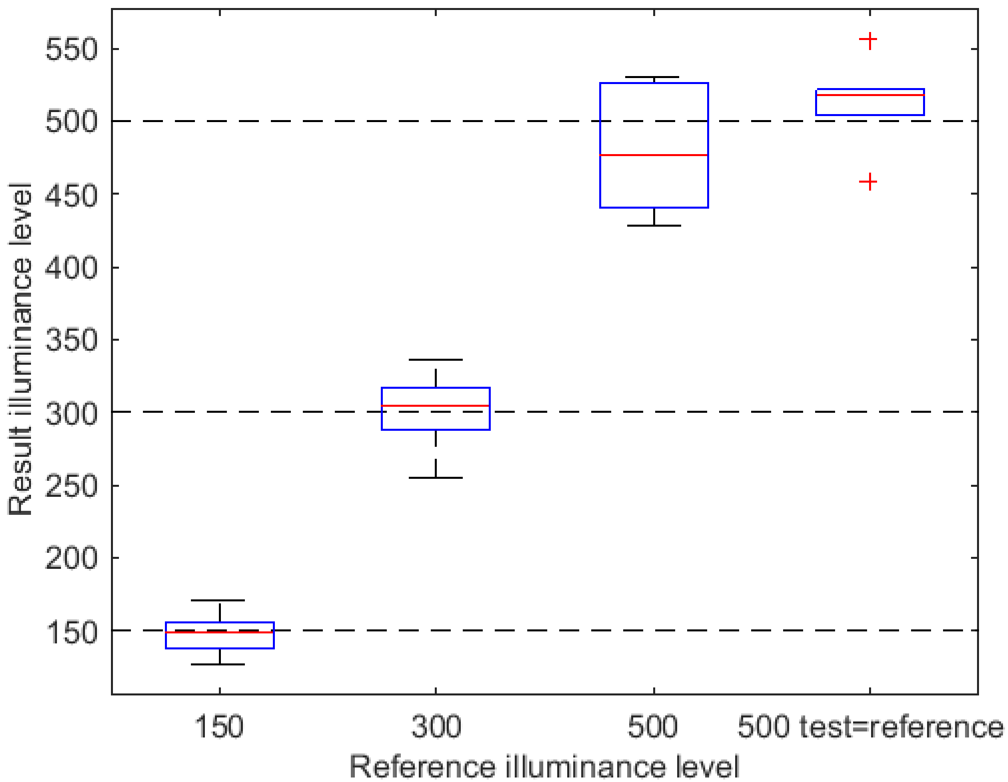

Figure 2: A boxplot of the resulting matched illuminance level for the illuminance levels in the experiment for the group of 3 participants not showing a significant effect.

No significant effects of age, gender, or lighting expertise were found using an ANOVA procedure. A hierarchical cluster analysis procedure identified a small group of three participants with markedly different answers than the rest of the participants. The results of the participants in this group were significantly higher than the other participants and showed no significant difference from the illuminance of the reference source for all light levels. Figure 2 depicts the result of this group of participants. It is interesting to estimate the size of this group in the general population as the size estimated from this experiment can be biased due to the selection of the participants in the experiment.

The results show that for an average observer, the activation of FWAs not only increases the perception of whiteness of surfaces, but also the overall brightness of the surrounding that contains white surfaces. Consequently, an equivalent brightness impression can be obtained by using up to 20% less intensity. This result can be particularly important in applications where both the perceived brightness and the natural whiteness rendering of surfaces is important, as for example is the case in fashion retail. In this case, only using the illuminance in the space could be a poor indicator of the suitability of a light source. For more accurately predicting the object as well as space appearance, whiteness rendering and in particular the activation of FWAs have to be taken into account.

4. CONCLUSIONS

We present results of an experiment that was designed to explore the change in brightness appearance caused by change of illumination that results in a change in whiteness perception. A LED light source that activates fluorescent whitening agents was shown to match the brightness of a LED light source that does not activate FWAs with up to 20% less intensity. No effect of age, gender, or lighting expertise was found. However, three participants had markedly different answers and showed no effect of perceived whiteness on their brightness judgment. The presented results show the need of taking the whiteness rendering of electric light sources into account when comparing the perceived brightness they produce.

REFERENCES

Wyszecki, G., and W. S. Stiles. 2000. *Color science, concepts and methods, quantitative data and formulas,* 2nd edition. New York: John Wiley and Sons.

Ganz, E. 1979. Whiteness formulas: a selection. *Applied Optics* 18 (7): 1073-1078

CIE 2004. *Colorimetry*, 3rd edition. CIE Technical report 15.3:2004

Zwinkels, J. C. and M. Noel, CIE whiteness assessment of papers: impact of LED illumination. In *27th Session of the CIE*, *Proceedings*. Sun City, South Africa.

Krais, P. 1929. On a new black and a new white. *Melliand Textileber* 10: 468

Address: Dragan SEKULOVSKI, Philips Research Europe,
High Tech Campus 36, Eindhoven, 5656 AE, NETHERLANDS
E-mails: dragan.sekulovski@philips.com,kees.teunissen@philips.com,
mart.peeters@philips.com, youjun.sun@philips.com, remy.broersma@philips.com

Smart lighting providing different optimal visiual illumination for different objects

Neng-chung HU,[1] Horng-Ching Hsiao,[2] Li-Chi Su[1]
[1] Dept. of electronic engineering, National Taiwan University of Science and Technology, Taiwan
[2] Dept. of electrical engineering, National Taiwan University of Science and Technology, Taiwan

ABSTRACT

Unlike commonly mentioned smart lighting with the purpose of energy saving, the optimal visual smart lighting can provide different CCT conditions of lights for different scenes to achieve the best visual preference which is given as $\text{Preference} = W_1 \cdot \text{Lightness} + W_2 \cdot \text{Saturation}$.

1. INTRODUCTION

When mentioned “Smart lighting”, it always denotes the lighting provides different energy saving functions depending on different purposes. In this energy saving smart lighting, it contains a white light illumination and a sensor system to sensing the environment to give more light or less light for energy saving. However , in this article, we mean the smart lighting that will provide illuminations of different color temperatures, and the detemination of which illumination is suitable for a given scene depending on the preference of the scene shined by different color temperatures of lights.

2. METHOD

This smart lighting contains two major parts, namely the color sensing unit and dynamic LED lighting unit. The dynamic LED lighting unit is composed of 4-channel LEDs that can provide the light conditions of CCTs 2700K、3000K、3500K、4000K、4500K、5000K、5700K、6500K、9000K and 12000K. The corresponding color rendering indexes of these lighting conditions are greater than 85. The color sensing unit has RGB sensors to collect the raw data of the responded values of the R-, G-, B- sensors of the scene illuminated by different CCT of lights, followed by a process of converting these R-, G-, B-values to the tristimulus values, X, Y, and Z of the scene by a correcting matrix obtained from a training set of 35 pictures, the correcting matrix is as follow:

$$
B = \begin{bmatrix} 4358.3024 & 1609.936151 & 2725.901567 \\ 1508.600055 & 6270.02137 & 1625.804137 \\ -1489.288606 & -7835.489888 & 21395.36667 \end{bmatrix}
$$

$$
\begin{bmatrix} \hat{X} \\ \hat{Y} \\ \hat{Z} \end{bmatrix} = B \begin{bmatrix} R \\ G \\ B \end{bmatrix}
$$

, where $\hat{X}, \hat{Y}, \hat{Z}$ are the calculated tristimulus values of the scene obtained from the sensor. These values are to approximate the true tristimulus values of the scene. Then the calculated tristimulus values are transfered to saturation, lightness, and Chroma, thru a simplified formula which can be executed by 8051 microprocessor. Lightness L^* is given as $L^* = W_L \cdot \hat{Y} + W_o$,where W_L and W_o are weighting factors and different CCT has different weighting factors. Saturation is given as $S = a_2 D_i^2 + a_1 D_i + a_0$, where $D_i = |\hat{x}_i - \hat{x}_n| + |\hat{y}_i - \hat{y}_n|$. Thus, the values of the preference of the scene lighted by the ten light conditions are obtained according to saturation, lightness, and Chroma as $\text{Preference} = W_1 \cdot \text{Lightness} + W_2 \cdot \text{Saturation}$. The light with the largest preference value is the best one. The block diagram the smart lighting is show in Fig.1 .

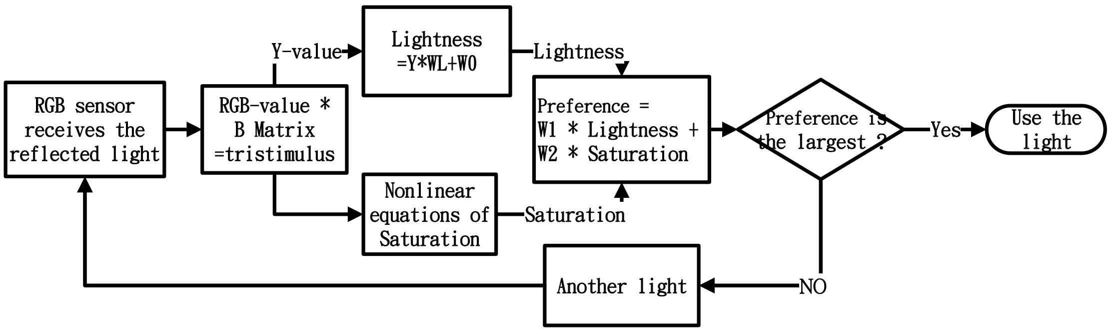

Fig.1 The block diagram of the smart lighting.

An experiment is conducted by 15 subjects to evaluate the preference score ranged from 1 to 6 of a picture illuminated by different lighting condition. This subjective evaluation result is the same as the result obtained from the proposed LED smart lighting.

3. RESULTS AND DISCUSSION

Light	L	S	By Preference	By subjective method
3000K	16.3465	0.164717	56.4527	0
4000K	17.2814	0.119807	59.3057	23.07692308
5000K	18.0860	0.132568	**62.1165**	**46.15384615**
6500K	17.4197	0.13599	59.8857	19.23076923
7000K	17.2438	0.244627	60.0416	7.692307692
8000K	17.68257	0.121796	60.6769	3.846153846
9000K	17.62066	0.117943	60.4408	0

Light	L	S	By Preference	By subjective method
3000K	16.4280	0.34982	58.0085	0
4000K	18.4476	0.19025	63.7388	11.538462
5000K	18.8790	0.16308	65.0108	26.923077
6500K	19.6493	0.23361	**68.1053**	**30.769231**
7000K	18.4708	0.21149	63.9643	23.076923
8000K	19.15526	0.10344	65.5333	0
9000K	19.14104	0.10209	65.4758	7.6923077

Light	L	S	By Preference	By subjective method
3000K	18.12557	0.08966	61.9537	11.538462
4000K	19.80246	0.24447	**68.6985**	**34.615385**
5000K	19.63744	0.13432	67.3784	19.230769
6500K	19.4456	0.12581	66.6705	11.538462
7000K	19.15356	0.14842	65.8386	7.6923077
8000K	19.64262	0.13077	67.3714	11.538462
9000K	17.62066	0.117943	60.4408	0

Light	L	S	By Preference	By subjective method
3000K	16.42798	0.3539	58.0367	11.538462
4000K	18.93377	0.21413	**65.5493**	**26.923077**
5000K	18.73747	0.06517	63.8549	11.538462
6500K	18.60633	0.05612	63.3485	23.076923
7000K	18.18996	0.20488	62.9684	19.230769
8000K	18.79869	0.0556	63.9959	3.8461538
3000K	16.42798	0.3539	58.0367	11.538462

Light	L	S	By Preference	By subjective method
3000K	16.58972	0.32635	58.3934	0
4000K	18.51785	0.24989	64.3892	11.538462
5000K	19.63744	0.30126	**68.5329**	**30.769231**
6500K	18.96093	0.10146	64.8620	23.076923
7000K	18.60951	0.16739	64.1288	19.230769
8000K	19.22571	0.1468	66.0715	0
9000K	19.2102	0.1516	66.0522	15.384615

Five test pictures are for testing to see whether the selected optimal CCT is the same as the method selected by 26 subjects. As we can see the CCT selected by calculative preference according to L^* and S is exactly the same as selected by subjective method.

4. CONCLUSIONS

An LED smart lighting with 10 different CCT conditions and a color sensing system is proposed. For different scenes, the smart lighting determine the optimal lighting CCT condition based on the best preference value of the given scene shined by the ten lighting CCT conditions. Thus, for a giving scene, the smart lighting selects a lighting condition with the best preference for the scene.

ACKNOWLEDGEMENTS

This work was supported by Ministry of science and Technology of ROC, under NSC-102-2221-E-011-101.

REFERENCES

Martirano, Luigi. "A smart lighting control to save energy." Intelligent Data Acquisition and Advanced Computing Systems (IDAACS), 2011 IEEE 6th International Conference on. Vol. 1. IEEE, 2011.

Bhardwaj, Sachin, T. Ozcelebi, and Johan Lukkien. "Smart lighting using LED luminaries." Pervasive Computing and Communications Workshops (PERCOM Workshops), 2010 8th IEEE International Conference on. IEEE, 2010.

Patricia Valdez, Albert Mehrabian, " Effects of Color on Emotions", journal of experimental psychology general, Vol.123, No.4, pp.394-409(1994)

Address: Neng-chung Hu, Dept. of Electronic Engineering,
National Taiwan University of Science and Technology,
43, Sec. 4, Keelung Road, Taipei, Taiwan
E-mails: nchu@mail.ntust.edu.tw

Prediction of acceptable lightness difference in painting on automobile surface with different materials based on multi-angle measurement

Kohei Wakai / Cre-Inno.inc k-wakai@shikisa.com

ABSTRACT

It is difficult to judge whether variation in color occurring at a coat formation process is within an acceptable range. Even if we examine parts visually and their color appears fine, it would appear different when they are assembled into a car. Moreover, we often judge their color using color measurement apparatus, the measurement cannot necessarily reflect the color acceptance correctly. Since the measured color is only reference information, we always have to look at and check a car actually assembled. This is inefficient and cause many restrictions when we supply those parts from distant factories. It will be a great help to engineers in those factories if we can predict whether the color of parts is correct only by a measured color difference.

Paints for cars appear to be different color when a viewing angle changes. One of reasons why an inaccurate judgment for the color of paints is because the difference is judged only by a color measured with a fixed angle. Therefore, it would be effective to use a multi-angle measurement. I analyzed the color measurement data of vehicles made at a factory, and examined the relation between lightness L* and acceptable delta L* of the painted surface of metal-body and plastics-parts .

The range of acceptable delta L* changes with painted colors. Some paints shows larger acceptable delta L* range than others. When L* is high, the number of colors with large acceptance range of delta L* increases in general, but there are some exceptions. Lightness observed at five angles differ. They become higher if the measuring angle is close to a specular reflection angle, and vice versa. Not only L* of the brightest and the darkest angle differs, but the upward approximate curves of L* in a middle angle range differ.

The boundary of acceptance and unacceptance was compared to the combination of these features.

As a result, it is suggested that three features can explain the acceptance range of delta L* of five angles, and each angle's coefficient is calculated based on angle difference from specular reflection angle.

1) For a color with a big difference of L* between the brightest and the darkest angle, the acceptance range of delta L* becomes larger.

2) If L* from a middle angle goes up rapidly, the acceptance range of delta L* becomes larger.

3) If the L* of surface is higher in each angle, the acceptance range of delta L* becomes larger.

Color measurement apparatus usually obtain color difference based on data at a particular angle in spite of angle dependency in color. Misunderstanding would be caused if a color difference is calculated by CIELAB solely based on those data .Difference of delta L* near actual appearance may be predicted by correcting calculation using this method.

1. INTRODUCTION

An automobile usually uses both metal and plastic as the exterior material. For example, a bumper is made of plastic, while a rear fender is made of the same material as a body structural part; and thus these will be painted in separate processes.

Once completed, a car should appear to be a single color product, and so we strive to have the colors on two different materials look the same now and in the future.

It is said to be ideal to use a color measurement apparatus to quantitatively evaluate color variations that can be generated during the manufacturing process, so that the variation can eventually be brought below an acceptable level and made less noticeable. This method, however, fails to coincide with the result of visual inspection, and needs to be improved.

In the current study, I formulated an equation to estimate the acceptable range in the lightness of any painted color, based on a comparison between visual inspection and a measured color value. The equation includes inclinations between acceptance angles and looseness as the parameters. Some other consideration other than the lightness correction might be needed for a perfect formulation, though, hopefully the method I propose here will help control any color variation which might be generated during the manufacturing process.

2. MULTI-ANGLE COLOR MEASUREMENT

Many paints used for automobiles change lightness or color if looked at from different angles. To prevent such variation, the painted surfaces are often examined using color measurement performed at multiple acceptance angles and entrance angles. At most automobile manufaturing companies, a portable type spectroscopic multi-angle color measurement apparatus with 45-degree incidence and five acceptance angles, X-Rite MA68 (Figs. 1 & 2), is used.

【Fig. 1 X-RiteMA68】

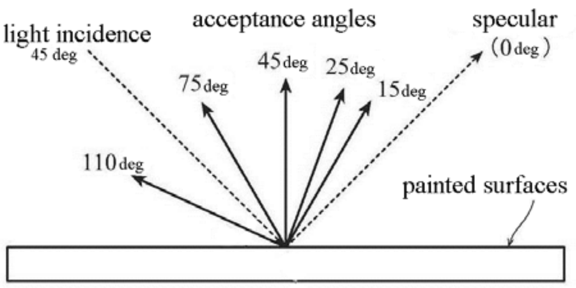

【Fig. 2 Optical System of Color Measurement Apparatus】

Measurement using this apparatus provides higher reflection intensity at an acceptance angle of 15 or 25 degrees, which is closer to the specular direction, rather than at the angle of 45 degrees, which is perpendicular to the painted surface; and lower reflection intensity at an acceptance angle of 75 or 110 degrees which is farther away from the specular direction.

The reflection intensity experimentally obtained for each wavelength is converted using tristimulus values Y to a certain value, which is then converted in terms of L* to get the relation of the lightness to the angles as shown in Fig. 3.

The case of a silver metallic color shows a highly-curved line over all the angles between 15 and 110 degrees. The case of white pearl shows a line where the lightness increases beyond 45 degrees, and solid colors show a flat line.

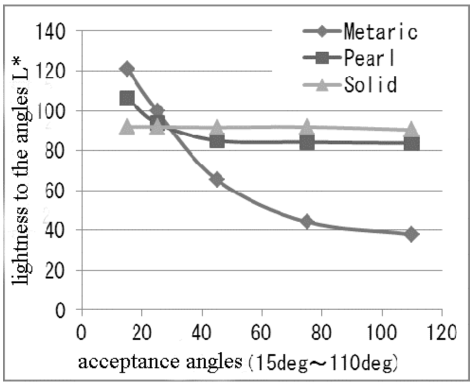

【Fig. 3 Silver Metallic, White Pearl, and Solid】

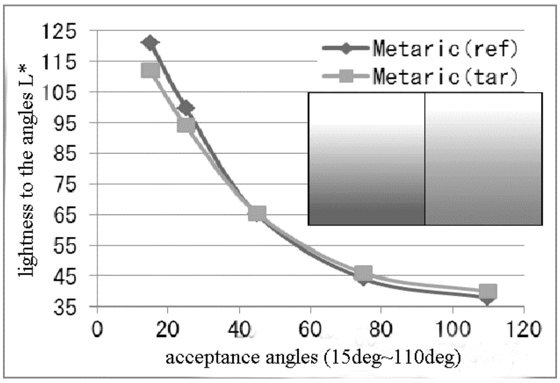

【Fig.4 Example of Change in Silver-Metallic Process】

3. CHANGE DURING PAINTING PROCESS

Paint of the same color might end up on painted surfaces as different colors due to many factors in a painting process.

The most significant change appears in lightness, which is hardly ever uniform over all the acceptance angles. The color measurement shows, for example, that L* at 45 degrees changes only by 0.3, while L* at 15 degrees changes more than 3.0. If we used an apparatus which could measure only at 45 degrees in order to establish a threshold, we couldn’t make a right judgment, because intrinsically a color space coordinate is defined so that a delta L* shall not exceed 0.3. Fig. 4 shows color differences in silver metallic colored paint when the painting conditions are changed. Target samples "tar" decreases at 15 and 25 degrees than "ref", but increases at 75 and 110 degrees adversely.The difference in lightness that is typical of metallic colored paints can be said to have become smaller.

4. DIFFERENCE BETWEEN DIFFERENCE IN LIGHTNESS (⊿L*) AND ACCEPTABLE RANGE

Color measurement can detect differences, yet even a difference of 3.0 in the delta L* in automotive paints doesn't usually come across as a big difference upon visual inspection, which is sometimes seen as a failing. However, by classifying the visual inspections and results of color measurement according to the kind of paint, I found that although there was a relationship between the delta L* value at which visual inspection resulted in a No Good judgment and the lightness of the paint, the type of paint involved had an even bigger impact.

Fig. 5 has a vertical axis with the delta L* value for multiple automotive parts that passed visual inspection and, of the various acceptance angles at which paint lightness was measured (for example, L* = 65 at 45 degrees, L* = 99 at 25 degrees, and L* = 120 at 15 degrees), charts the results for 15 degrees only.

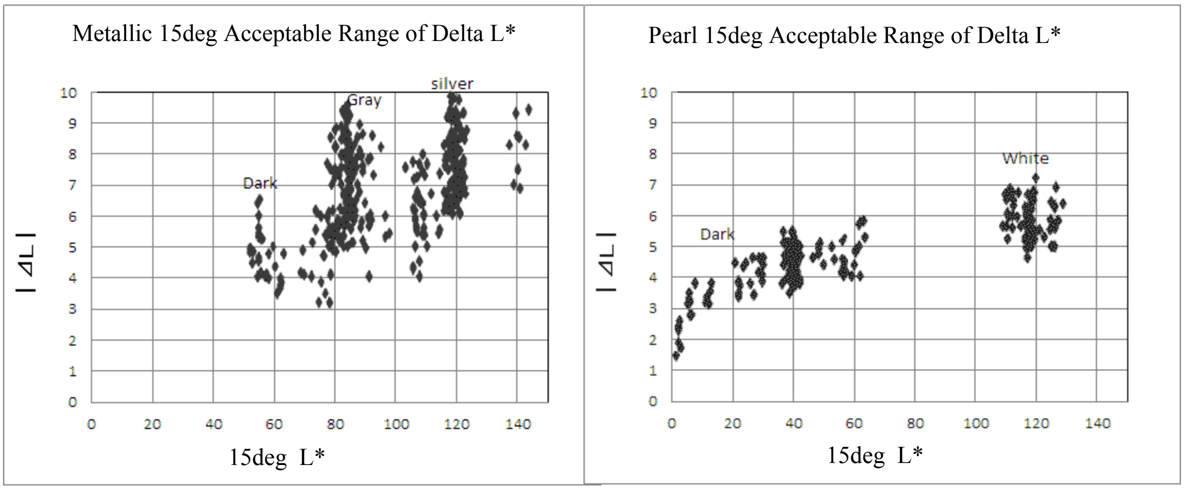

【Fig. 5 Acceptable Range of Delta L* vs. Paint Color Lightness L*. Left: Metallic, Right: Pearl】

Even if there is difference in color measurements, visual inspection may show no difference, allowing the painting to pass the inspection.

The difference is less noticeable for the metallic painting than for the pearl painting.

5. CHANGE OF LIGHTNESS OF PAINT COLOR (15 TO 110 DEGREES) AND ACCEPTABLE RANGE OF DELTA L*

I looked into the possibility of explanatory factors other than the relation among paint color type, L*(Paint Color lightness), and acceptable range of delta L*. The extent of the change of lightness depends on the paint color. A comparison of the acceptable range of delta L* with L*d, which is the difference between the lightness at 15 and 110 degrees and is substituted into the horizontal axis (Fig. 6), showed that the larger the L*d, the larger the visually acceptable range of delta L*.

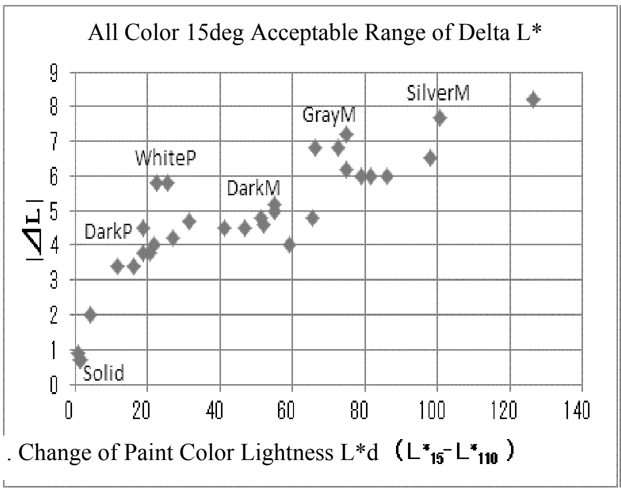

【Fig. 6 Acceptable Range of Delta L* vs. Change of Paint Color Lightness L*d】

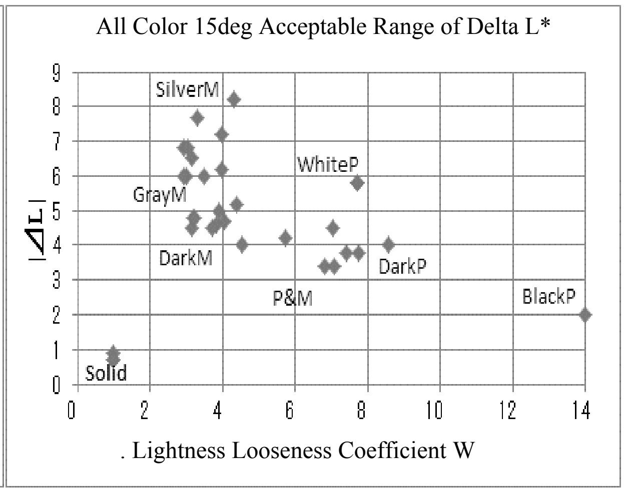

【Fig. 7 Acceptable Range of Delta L* vs. Lightness Looseness Coefficient W】

6. LOOSENESS COEFFICIENT FOR LIGHTNESS CHANGE CURVE AND ACCEPTABLE RANGE OF DELTA L*

The five acceptance angles can provide information not only on the maximum and minimum lightness but also on changes partway.

Since the curved line is similar to a catenary, I formulated Equation (1) with an angle as a variable; using Ld, which is the change of paint color lightness ($L^*_{15} - L^*_{110}$) as discussed in the previous section, as a gradient; and L^*_{110} as an intercept. The looseness coefficient W was then obtained from the values L^*_{25}, L^*_{45}, and L^*_{75}.

$$L^*_r = Ld * \gamma_{(r)} + L^*_{110} \cdots (1)$$

$$\text{where } \gamma_{(r)} = |\cosh(W \cdot D_r) - \cosh(W \cdot D_0)| / \gamma_0$$

$$\gamma_0 = |\cosh(W \cdot D_1) - \cosh(W \cdot D_0)|$$

$$D_r = (r-110)/(110-15)$$

$$D_1 = D_{15} = -1,\ D_0 = D_{110} = 0$$

The results show that W≈1 for the solid color, W≈4 for the silver metallic color, and W≈8 for the pearl white color, which shows a sharp upward curve. The visual acceptable range of delta L* shows that the relations seem to be inversely proportional, except in the case of the solid color.

7. ESTIMATING ACCEPTABLE RANGE OF DELTA L* USING THE RELATION BETWEEN DIFFERENCE OF LIGHTNESS AND CURVE SHAPE

A multiple regression analysis was conducted. Only L*d, L*r, and W were significant as shown in Fig. 8. Saturation was insignificant.

The size of the significant L*d, L*r, and W may help accurately predict the relation

	$L^*_{15} - L^*_{110}$ L*d	each deg L* L* i	Looseness Coefficient W	chroma C'max	chroma C'
15deg R^2=0.9697	** P:0.0000	* P:0.0255	** P:0.000	P:0.1685	P:0.1689
25deg R^2=0.9580	** P:0.0000	P:0.4671	** P:0.0023	P:0.1704	P:0.1765
45deg R^2=0.9705	** P:0.0000	** P:0.0100	** P:0.0083	P:0.2381	P:0.2234
75deg R^2=0.9565	** P:0.0000	** P:0.0020	** P:0.0011	P:0.0745	P:0.0640
110deg R^2=0.9601	** P:0.0000	** P:0.0000	** P:0.0002	P:0.4482	P:0.2069

【Fig. 8: Multiple regression analysis of acceptable range of lightness/saturation of paint viewed from five angles.】

between the difference perceived in visual inspection and the delta L* obtained from measurement.

If each coefficient for the acceptance angle r is expressed as S_{dr}, S_{Lr}, and S_{wr},

$$|\Delta L^*|_{r=} S_{dr} * L^*d + S_{Lr} * L^*r + S_{wr} * W \cdots (2)$$

Equation (2) indicates an estimated value.

The coefficients for r=15, r=25, r=45, r=75, and r=110 obtained by multiple regression analysis are expressed in Equations (3) to (7), which all consist of positive values.

$|\Delta L^*|\ 15 = +0.0481\ L^*d + 0.0140\ L^*15 + 0.3309W \cdots (3)$
$|\Delta L^*|\ 25 = +0.0443\ L^*d + 0.0081\ L^*25 + 0.1336W \cdots (4)$
$|\Delta L^*|\ 45 = +0.0277\ L^*d + 0.0097\ L^*45 + 0.0526W \cdots (5)$
$|\Delta L^*|\ 75 = +0.0183\ L^*d + 0.0105\ L^*75 + 0.0547W \cdots (6)$
$|\Delta L^*|\ 110 = +0.0128\ L^*d + 0.0115\ L^*110 + 0.0666W \cdots (7)$

To express the relation between an arbitrary aspecular angle (r degrees) and S_{dr}, S_{Lr} , and S_{wr}, an equation using the exponent function is formulated.

The relation between Ld and r is approximated by a sigmoid function to get Equation (8).

S_{dr} =0.03234/(1+EXP(6.6637*(RAD(r) −0.661)))+0.017875···(8)

The relation between S_{Lr} and r shows an almost straight line.

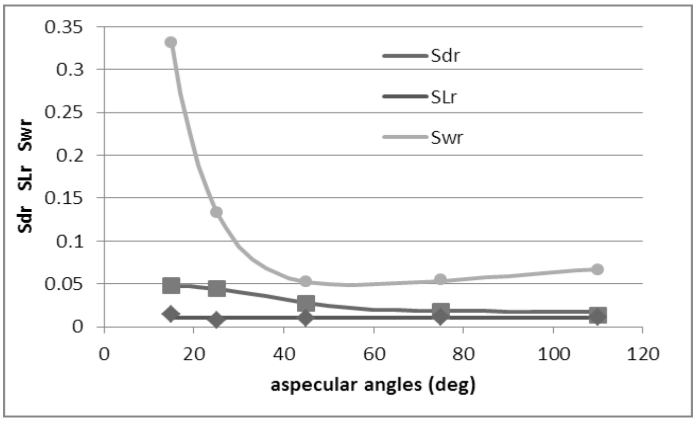

【Fig.9: Relation between Each Coefficient and Aspecular Angles】

S_{Lr} = 0.01···(9)

The relation with W is expressed using the combination of an exponent and a primary expression.

Swr = 1.558*EXP(−6.27*RAD(r))+0.023*RAD(r)+0.023···(10)

The results of Equations (8) to (10) are plotted in Fig. 9.

8. CONCLUSIONS

The closer the aspecular angle is to specular (0), the brighter the reflected light is for visual inspection and the more difficult the recognition of difference of lightness is. One of the objectives of the current study is to propose how to interpret the difference of lightness obtained by multi-angle color measurement.

Here, I showed that aspecular angles allow the calculation of lightness, change of the lightness, and weighted amount of the speed of the change for the measured aspecular angles. This method will help estimate the acceptable range of lightness with significantly better accuracy.

REFERENCES

1) Kohei Wakai 2014. *Study of the permissible width of Lightness in multi-angle color measurement and visual evaluation*, Journal of the Color Science Association of Japan,Vol38,No.6 448-449.

2) Nissan Motor Co., Ltd　JP 5640812 B2 2014.12.17

Visual Perception and Criteria for Good Lighting

Johanna ENGER,[1] Anahita DAVOODI,[1]
[1] Jönköping School of Engineering

ABSTRACT

The study is conducted as a subproject in a PhD-project titled Criteria for Good Lighting. The overall aim of the study is to, based on visual qualities - rather than physical measurements - research the possibility of creating lighting environments that inspires comfort and meets function while providing energy efficiency. The study's specific objective is to identify and formulate criteria for a good light environment based on visual qualities, and to create a light simulator based on these criteria.
This paper describes the implemented pilot study and the basis for the full-scale study in the next phase. The method has been designed from the perspective of light and colour as two factors that collectively create visual impressions and experience of the room.

The background is that lighting design today follow lighting standards and norms that often are based on photometry. Photometry describes the eye's sensitivity to light in different frequencies of light radiation and how well it is possible to discern details in different amounts of light radiation. As a tool for lighting design the photometry and thus current standards are partially inadequate because it is mainly based on the detail vision's need of high light levels, but it is through the peripheral vision we understand the space, and it occurs primarily when the eye registers differences between contrasts in brightness and colour. A new definition of lighting criteria needs to be based on an understanding of how the visual perception functions; how to meet both the detail vision's need of higher light levels and the peripheral vision's need of a legible spatiality.
The study is conducted in two phases. The first phase is a pilot study where small groups of people is interviewed in their work environments in order to find out how they experience their work place and to what extent the lighting affects the experience. A literature overview was carried out on relevant research in the field of light, colour and visual perception. In the second phase, a full-scale studies are conducted in an office environment where the subjects are interviewed in different room-settings.

1. INTRODUCTION

The objective is to better understand human visual perception in order to create more efficient lighting design adapted to human needs. The aim is to find quality measures that relate to human perception and experience and develop criteria for good lighting based on the human visual perception.

1.1 Levels of perception

We receive and process the impressions of the outside world through all the senses, on several levels - simultaneously. Biologically and physiologically, all humans are quite similar, but we are also social and cultural beings and also with individual preferences, needs and experiences. An environment that is created based on human needs should include all these aspects. (Fig. 1)

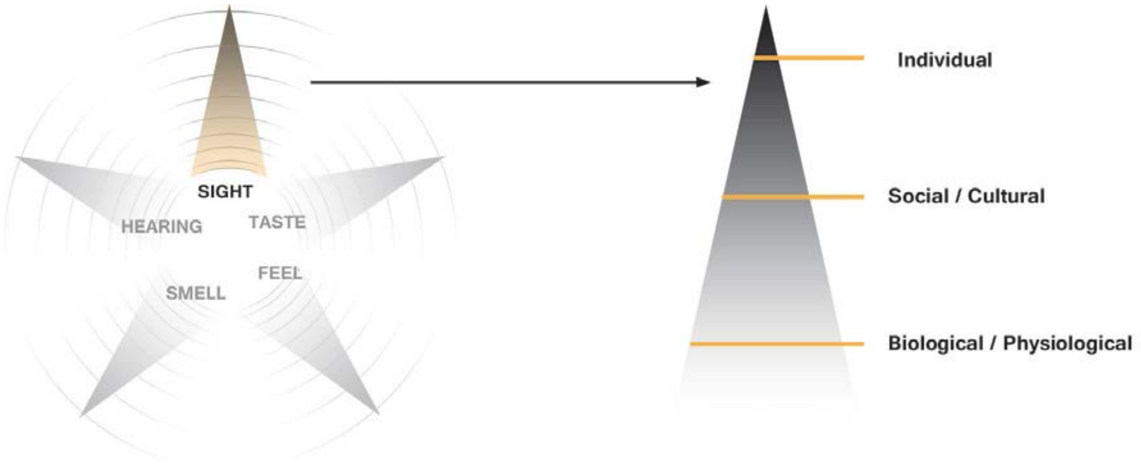

Figure 1: Levels of Perception (J. Enger)

The perception of light and colour is a complex process that is not yet completely understood, and it can not be explained solely by the eye's sensitivity to different levels of light radiation. Light radiation emitted from light sources and from reflecting surfaces with different colours and textures hits the retina and is converted to visual impulses of light and creates perception of space. Visual perception combines the impression of direct light and reflected light, which together create the overall appearance of the room and the light and colour experience. Light radiation is a physical concept and can be measured in absolute terms, whereas the experience of light is a relative experience created by the visual perception. Simultaneous contrast is a well known example of how the perception of brightness is created in the visual sense when a colour gives the impression to vary in brightness relative to the surrounding colour tone. (Fig. 2)

Our perception of light and colour also has an emotional aspect. While the perception of light is a prerequisite for us to orient in a space, the character of light also create an atmosphere of the room that affects us both as cultural and social beings belonging to a particular group, and also as individuals. This aspect may be as important as the physiological for the experience of an environment. If the experience of light is considered to be a sensuous process that takes place on several levels, a holistic perspective is needed in order to define criteria for a good light environment.

Figure 2: Simultaneous contrast. The grass has a solid grey tone but seems to shift in hue depending on the gradient in the background.

2. METHOD

2.1 Pilot study

In a preliminary study six people of mixed gender aged 30 to 60 years were interviewed, about their experience of the environment and lighting conditions of their workstations. Several typical offices were represented in the pilot study, such as private offices and office landscapes. At each occurrence the illuminance was also measured both at the workplace and in the center of the room. The aim of the study was to obtain a basis for the planning of the full-scale test rooms of the project's second phase.

The interviews began with a survey in which the subjects were asked to answer open questions about how they perceive their work environment in general and the lighting situation in particular. This was supplemented with a form in which they were to answer questions about the character of light in the room. The questionnaire was based on the method of analysis PERCIFAL (Klarén 2011). The respondents were asked to answer questions about, for example, perceived light level and perceived light colour, shadows and light distribution. A more detailed analysis of the same type with a detailed description of the room was then carried out by the interviewer in order to obtain comparative material.

2.2 Scenarios

The aim of the full-scale study is to examine the overall experience of light, colour and space based on the three levels of perception. The objective is to identify a number of different variables that together affect the light and spatial experience, to categorize them and to explore how these relate to the photometric values.

In the study, emotional values are of equal relevance as the perceptual impression. The study is conducted in office rooms of standard type and designed to create a distinct atmosphere with the Nordic light as a theme.

2.3 Nordic Light

The Nordic light is used as motif for the design because it offers great dynamics and varying light situations between seasons and different times of day that can be transferd to scenarios. The scenarios also relate to several examples of typical interior lighting that appeals to different groups of people.

In the essay *Nordic Daylight* Professor Barbara Matusiak investigates the character of the Nordic light in order to find out whether and how it differs from the light in other geographical locations (Matusiak B., Fridell Anter K. 2013). The study describes the artists' rendering of the Nordic light as well as estimations of the sun's angle over the year and climate data for the northern hemisphere. The conclusion is that it is possible to identify certain characteristics of the light at northern latitudes. A large part of the year, the sun appears from a low angle which creates distinct shadows in landscapes and textures and gives a warm light colour when the light is refracted in the atmosphere. The blue hour is a concept that is associated with northern countries and it also has its physical explanation. As the sun goes down under the horizon it continues to light up the sky that reflects a bluish light to the earth. Another feature that characterizes the light in the Nordic countries are long periods of overcast sky that gives a diffused and contrast-free, neutral light.

In test rooms the different light characters are portrayed in four different scenarios: 1. Sunset: vertical light with warm light colour that gives long shadows, and materials with a muted colour palette of warm tones. 2. Blue Hour: indirect bluish light, low light level. Low placed light sources with warm light. 3. Overcast: diffuse neutral and contrast-free light. Colours are painted in shades of gray with dark gray and black accents. 4. Midsummer: High level of light from a light source with high placement. Relatively warm light colour and distinct shadows. Materials in vivid mostly bright colours. (Fig. 3)

Figure 3: Nordic Light Scenarios (J. Enger)

2.4 Visual concepts

Several researchers and other individuals with knowledge of light have identified the need to formulate concepts that describe the visual impression of light in an environment. Yet there is still no widely accepted or complete system of concepts for light experience.

Christopher Cuttle has studied the relationship between light and visual perception and presents two groups of concepts that can be used as a tool in the design process. An important observation is the distinction between the light's spatial distribution described with flow and sharpness, and the light's ability to render object: shading, highlight and shadow. (Cuttle C. 2013)

The Nordic research project SYN-TES developed a method to analyse and describe light and spatial experience called PERCIFAL (Perceptual Spatial Analysis of Colour and Light). The method is not to evaluate the quality of light, but to analyse the character of light without evaluating the results. The visual concepts used in the method are: light level, light distribution, shadows, light patches, specular reflections, glare, colour of light and surface colour. (Klarén U. 2011).

2.5 Sensory science and Kansei Engineering

Other disciplines have created methods to not only analyze the character of a sensory experience, but also quantify and assess the outcome. The two examples described here has been developed to provide a basis for product development and ultimately marketing. The purpose of this study is not specifically focused on marketing strategies, but the analyses used in Sensory Science and Kansei Engineering are very suitable and possible to adapt in this context.

Sensory Science is described as "the science of what we can experience with our senses" and includes methods to express, evaluate and categorize the sensory experience (Gustafsson IB. Et. al. 2014). The discipline has a strong connection to gastronomy and the

food industry and can be described as the link between a product's chemical, physical and technical characteristics in relation to the affective and perceptual experience of it.
A product can be evaluated, for instance by having a test panel that compare various makes of food products. The participants evaluate the character of the respective products based on, for example, concepts such as richness, sweetness, acidity, etc., and also rank them according to preference. The result can be compiled into charts that provide information about which products panel prefer. It is also possible to draw conclusions about the qualities many people are attracted to or dislike.

The market's rapid feedback on different products and brands appeal has driven the development of knowledge on consumer behavior and product identity. A product's functional properties and technical performance is not sufficient to ensure success in the market, as consumers often choose product based on emotional values.

Kansei Engineering, also known as affective engineering was originally developed in Japan and it is a method used to evaluate products affective values. The dissertation *Engineering Emotional Values in Product Design* the author makes the definition: ”The main task is to translate feelings, perceptions, individual experiences and understandings into ‘hard’ measurements and mathematical models which in turn have to be falsifiable using both qualitative and quantitative methods.” (Schütte S. 2005)

The methodology makes it possible to identify cognitive, emotional and perceptual impressions of a sensual stimuli by studying both behaviours, physical reactions and verbal expressions. The result is valuable information that can be combined with a technical specification to optimize the design of a product to meet both the spoken and unspoken needs a specific target group.

2.6 Experimental Procedure
The full-scale study is carried out in small offices with identical layout and furniture of standard type. The lighting design and the colour scheme is based on the four scenarios described above, but the furniture and other inventory are neutral. Careful measurements of photometric values is made in every room.
The group of respondents consists of 30 individuals of mixed ages and gender about half of which have professional knowledge of light and the rest are laymen. The subjects respond to a questionnaire with the same design as that used the pilot study for evaluating the room's light character with given concepts. The following stage is based on the analysis methods developed in Sensory Science and Kansei Engineering but adapted to the context. An interview is carried out where the subjects are stimulated to describe the experience of the room's atmosphere and light character in their own words and concepts.

3. RESULTS AND DISCUSSION

The outcome of the pilot study made it clear that awareness of light and the need a good light environment varied between different people, and also personal preference in terms of light character in the work environment. Some people clearly expressed that they wanted an even light and high light level in the room, while others preferred a subdued light from many low-set light sources. Some of the interviewees were able to clearly define their needs, while others argued that light does not have much effect on the working environment. The results of the analysis form also showed that the interviewees and the interviewer usually had the same experience of the room's light level but that the measured illuminance not always corresponded with that.

Throughout all the interviews it became clear that the interviewees are not always separated the experience of light character from a functional or technical aspects of lighting. When asked about the overall experience of the environment, several persons used the concept of light in a broader sense. One room was for instance experienced such as light and airy. A plausible interpretation is that it does not refer to illuminance but rather to a sense of space that can be created by combining bright colours and sparse furniture.

The Full-scale study is not completed but the result is expected to provide is an extended knowledge about the experience of light and colour in relation to spatial context. More specifically, the results will give indications of the relationships between emotional experience, perceived light level and photometric values. The material from the interviews can provide a basis for an expanded system of concepts of light, colour and spatiality that can be used as a basis to formulate criteria for good light environments.

ACKNOWLEDGEMENTS

The author gratefully acknowledge the support of supervisors Professor Thorbjörn Laike and Lecturer Cecilia Häggström.

REFERENCES

Cuttle C. 2013. Introduction to a novel perception-based approach to lighting design. *Proceedings PLDC 4th Global Lighting Design Convention 2013*. VIA-Verlag Germany. 152-154

Gustafsson. I-B et. al. 2014. *Sensorik och marknadsföring*. Studentlitteratur AB, Lund. Denmark 2014

Klarén. U. 2011. *PERCIFAL- Perceptual spatial analysis of colour and light*. SYN-TES Report 2E. The Perception Studio / Konstfack–Univ. College of Arts, Crafts and Design.

Matusiak B. and Fridell Anter K. 2013. Nordic daylight*, Nordic Light and Colour*, NTNU. 25-38

Schütte S. 2005. *Engineering Emotional Values in Product Design – Kansei Engineering in Development. Dissertation 951*. Linköpings Universitet, Institute of Technology. Linköping 2005.

Address: Ms Johanna ENGER, School of Engineering, Jönköping University,
P.O.Box 1026. SE-551 11 Jönköping, Sweden
E-mails:johanna.enger@jth.hj.se

Space brightness affected by a scenic view through a window

Shogo YAMADA,[1] Ryosuke TANAKA,[1] Hiroyuki SHINODA,[2] Yasuhiro SEYA[2]
[1] Graduate School of Information Science and Engineering, Ritsumeikan University
[2] Department of Computer and Human Intelligence, College of Information Science and Engineering, Ritsumeikan University

ABSTRACT

There has been an increasing demand in the use of daylight through windows for maintaining bright visual environments while saving lighting energy. Recent studies have reported that although the horizontal illuminance is increased by daylight, space brightness is not as efficiently increased as expected by the illuminance. The purpose of the present study was to investigate the effects of daylight from a window on space brightness perception when various colors and objects outside a window, i.e., a scenic view, was visible. In an experiment, we used two scale models simulating an office: one was a room with a window (test room) and the other was one without it (reference room). Two types of scenic view, i.e., natural or urban landscape photographs behind the window, were used with or without a human-shaped board covered with full-length photograph of adult male. Daylight was simulated by fluorescent lamps and its intensity was manipulated by changing the number of the lamps. A room illuminance from ceiling lights without daylight (base illuminance) was also manipulated. Participants viewed the two models repeatedly and estimated brightness for the test room relative to that for the reference room. The results revealed that although the space brightness increased with increasing daylight intensity, the efficiency was much lower than that expected by the horizontal illuminance. The comparisons between the present results and the findings of a previous study revealed that brightness enhancement by daylight was lower with a scenic view than without it. Although a pattern of results was quite similar whether the human-shaped board was present or absent, the variance of brightness reported by participants was smaller in the human-shape board present condition than in the human-shape board absent condition.

1. INTRODUCTION

Although the diversification of lighting methods enables us to create various visual environments, recent studies have reported many situations in which horizontal illuminance (generally used as a brightness index) does not correspond to human perception. For example, a room with low horizontal illuminance is sometimes perceived as brighter than that with high horizontal illuminance. Many studies have examined human space brightness and proposed some indices corresponding to human perception (Yamaguchi & Shinoda 2007; Yamaguchi, Shinoda, & Ikeda 2002). In most of those studies, however, daylight from windows has not been taken into account. Considering that in real life situations, we are exposed to visual environments with windows, daylight should affect space brightness.

Several studies have investigated this topic by measuring magnitude estimation (ME) of perceptual brightness for a scale model of room with or without daylight from a window, and reported that the brightness become lower for a room with daylight than without it (e.g., Yamaguchi & Shinoda 2014). To our knowledge, most of those studies used frosted glass as a window and thus the scenic views from a window were invisible. Therefore, research on this topic using a window with a scenic view was scarce. In this study, we extended the previous findings by investigating the effects of daylight and various landscapes (that was viewed through a window) with or without the human-shaped board on space brightness by using ME method.

2. METHOD

In the experiment, we used two 1/8 scale models (Figure 1). Each model simulated an office with approximately 62 square meters. The size of each model is 800 mm (width) × 1,200 mm (depth) × 340 mm (height). The interior was all achromatic. The two models were located side by side: one was a room with a window (test room) and the other was one without a window (reference room). We simulated daylight from a window by using 8 fluorescent lamps attached outside the test room. The daylight intensity was munipulated by the number of lamps: 8, 4, 2, 1, or 0 (no-daylight). Behind the window, we attached one of four landscape photos (urban-distant view, natural-distant view, urban-near view, and natural-near view) with or without the human-shaped board covered with full-length photograph of adult male. The horizontal illuminance (base illuminance) of the test room without daylight was either 100, 300, or 1000 lx. The reference room was identical to the test room except that the room was illuminated only by artificial lighting from the ceiling witout simulated daylight (no window).

At the beginning of each trial, participants sequentially viewed the rooms. The task of participants was to estimate the brightness of the test room relative to that of the reference room. Participants were told that the brightness of reference room set to a value of 100. In addition to the experimental condition, we also conducted a control condition in which brightness of the test room was measured without daylight. The task was identical to that in the experimental conditions. There were 4 trials for each condition of daylight and base illuminance intensities, landscape, and human-shape board. The order of conditions was randomized across participants. Before the experiment, participants practiced several trials until they were familiarized with the task. Participants were five individuals. Two of those had experience of brightness evaluation experiment (Tanaka, Shinoda, & Seya, 2014).

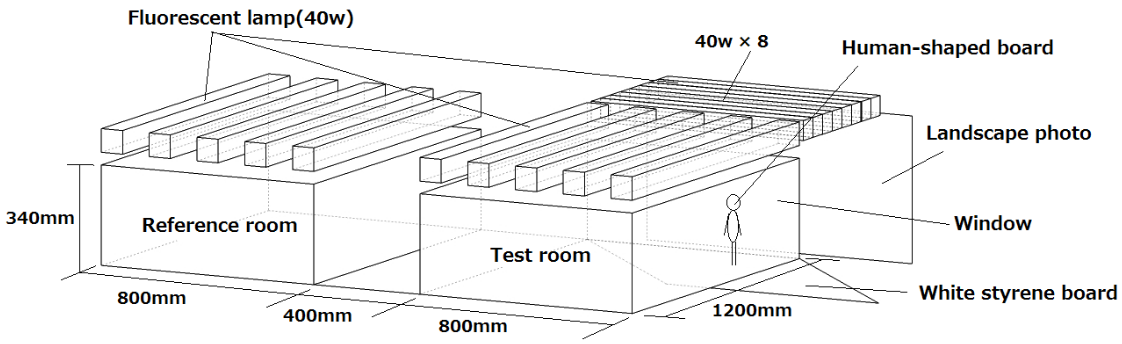

Figure 1: Experimental apparatuses.

3. RESULTS AND DISCUSSION

Figure 2 shows the mean ME values as a function of averaged horizontal illuminance separately for each daylight intensity and type of scenic view in the absence (left panels) or the presence (right panels) of human-shaped board. Upper, middle, and lower panels indicate the 100-lx, 300-lx, and 1000-lx base illuminance conditions, respectively. Square markers indicate ME values in the urban-distant view (solid line) and urban-near view (broken line) conditions. Circle markers indicate those in the natural-distant view (solid line) and natural–near view (broken line) conditions. Cross markers indicate ME values in the control condition (i.e., base line).

As seen in the figure, in the 100-lx and 300-lx base illuminance conditions, the ME values increased with increasing the horizontal illuminance, but they were lower in the daylight conditions (i.e., square and circle lines) than in the control condition (i.e., cross base line), irrespective of the scene view and human-shape board conditions. This indicates that although the participants perceived higher brightness with increasing daylight intensity, the efficiency of brightness enhancement was lower than that expected from the horizontal illuminance. On other hand, in the 1000-lx base illuminance condition, the rate of brightness enhancement was almost the same as that in the control condition, suggesting that, beyond a certain intensity of base illuminance, the efficiency of brightness enhancement would not be affected by daylight effects observed in low base illuminance conditions. These results are consistent with the findings of previous studies using a frosted glass as a window (Yamaguchi & Shinoda 2014).

The comparisons between the human-shape board absent (Figures 2a, c, e) and present conditions (Figures 2b, d, f) revealed that, overall, brightness was lower in the presence of the human-shape board than in the absence of it. The reason for the differences in the ME values with or without the human-shaped board is not clear. One possibility is that the board may have served as a cue indicating a room space and, as a result, participants may have been able to clearly separate spaces beyond and in front of a window. Consequently, participants may have been capable of estimating space brightness independently of the brightness outside a window.

Two participants had participated in our previous experiments in which the effects of daylight were investigated without a scenic view in the absence of the human-shape board. To further examine the effects of scenic view on space brightness, we compared the present results with the findings of previous study. Figure 3 shows the mean ME values as a function of averaged horizontal illuminance separately for each daylight intensity with (the present study) or without a scenic view (the previous study) in one participant. Upper-left, upper-right, and lower panels indicate the 100-lx, 300-lx, and 1000-lx base illuminance conditions, respectively. Square, circle, and cross markers indicate the results of the present study (Figure 2). Triangle markers indicate ME values without senic view (the frost glass was used as a window). The comparisons between the results with or without a scenic view revealed that, overall, brightness was lower with a scenic view than without it. The difference between the results of the two studies could be due to the participants' recognition of window. In the previous study, participants may have recognized a window of frosted grass as a light source, resulting in enhancement of space brightness. On the other hand, in the present study, the participants could separate spaces beyond and in front of a window. We consider that this participant more easily estimated space brightness.

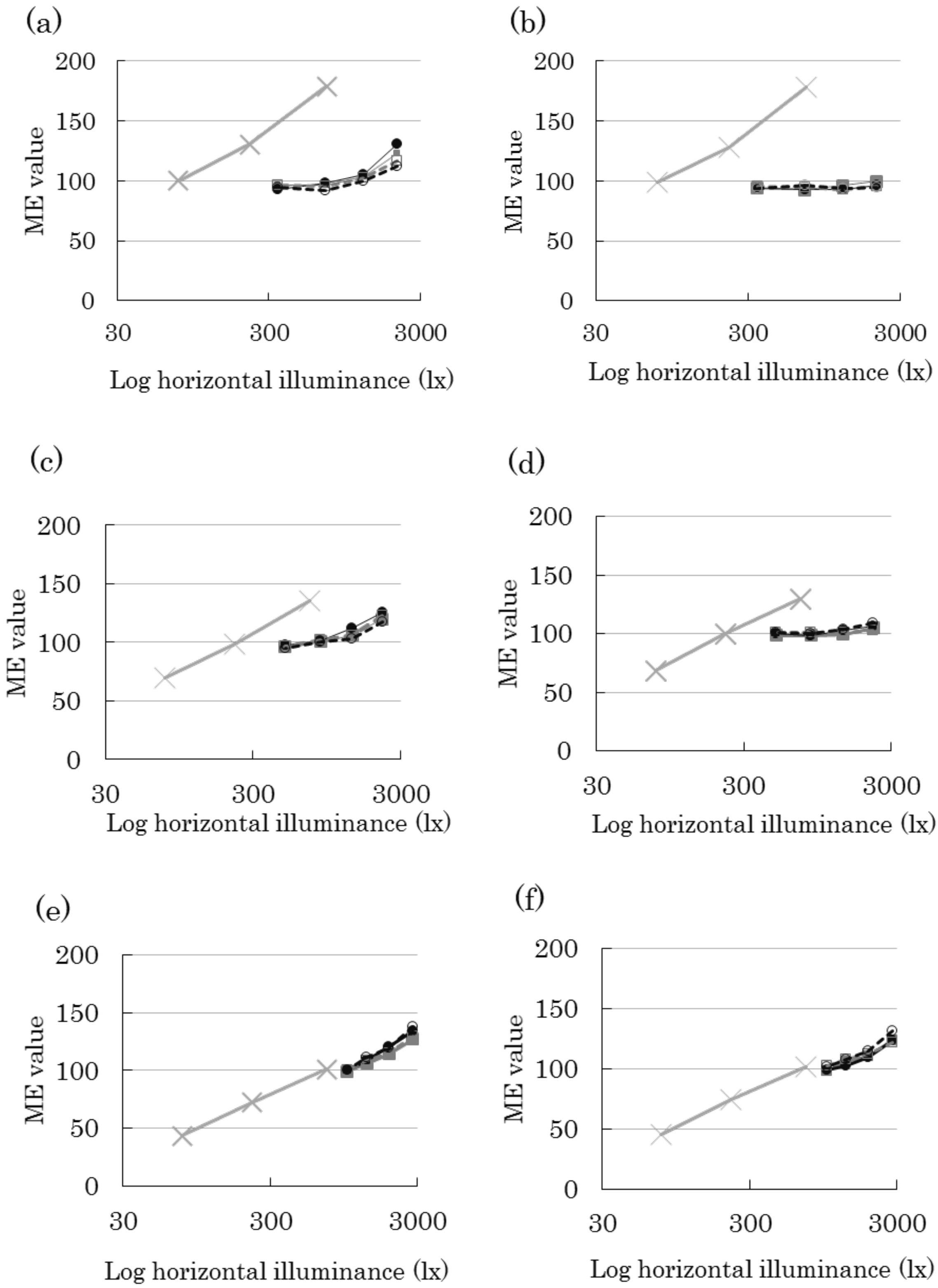

Figure.2: Mean ME values as a function of horizontal illuminance.

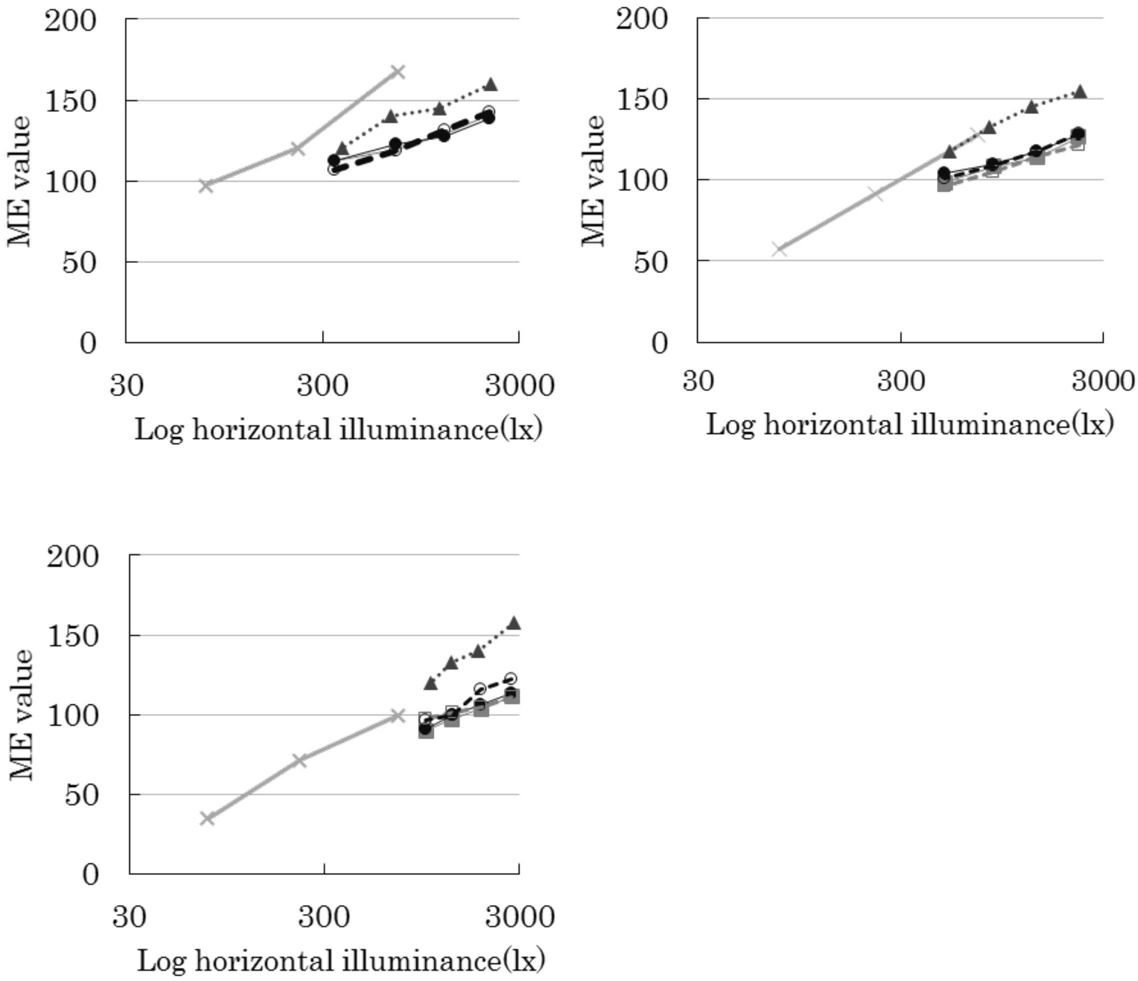

Figure.3: Mean ME values as a function of horizontal illuminance in one participant.

4. CONCLUSIONS

In this study, the effects on space brightness were investigated for various types of scenic view. Results showed increases in brightness with increasing horizontal illuminance by daylight, but the rate of brightness enhancement with a scenic view was lower than the rate of brightness enhancement without it. No difference between scenic views was found. Moreover, in the presence of the human-shaped board near the window, the brightness became lower than the case of space without the human shaped-board. Especially, for lower base illuminance, the tendency was more remarkable.

REFERENCES

Tanaka, R., Shinoda, H., and Seya, Y. 2014, *Brightness perception in daylight office with scene*, Perception 43 (Supplement) 163.

Yamaguchi, H., Maruyama, T., and Shinoda, H. 2014. *Space Brightness Evaluation for Day-Lit Offices*, Journal of Illuminating Engineering Institute of Japan 98 (11) 593-599 (in Japanese).

Yamaguchi, H., and Shinoda, H. 2007. *Space Brightness Evaluated Using Border Luminance of Color Appearance Mode*, Journal of Illuminating Engineering Institute of Japan 91 (5) 266-271 (in Japanese).
Yamaguchi, H., Shinoda, H., and Ikeda, M. 2002. *Brightness in Natural Environments Evaluated Using the Brightness Size of Recognized Visual Space of Illumination*, Journal of Illuminating Engineering Institute of Japan 86 (11) 830-836 (in Japanese).

Address: Shogo Yamada, Graduate School of Information Science and Engineering,
Ritsumeikan University, 1-1-1 Noji-higashi, Kusatsu, Shiga, 525-8577, JAPAN
E-mails: is0144ps@ed.ritsumei.ac.jp, is0024@ed.ritsumei.ac.jp,
hshinoda@is.ritsumei.ac.jp, yseya@fc.ritsumei.ac.jp

Influence of Surface Properties on Material Appearance

Ming-Kang LAN[1], Tien-Rein LEE[1], Vincent C. SUN[2]
[1] Department of Information Communication, Chinese Culture University, Taiwan
[2]Department of Mass Communication, Chinese Culture University, Taiwan

ABSTRACT

Color Research has developed prosperously in these years, particularly on "color appearance", which had made a significant breakthrough. Among them, textures, which is intimately related to color appearance, has got few attention. Features of textures possess enormous influences on surface color perception. Interactions between colors and surface materials have big stake on the accuracy of color display. Recently, the uprising of "material perception" researches have gradually filled up the insufficiency.

This research aims to explore the influences of material properties on the appearance of colors. By adopting the Cesia's theoretical mode (Caivano, 1996), based on three elements of material properties: Permeability, Lightness, and Diffusivity, with the utilization of a rotary color mixer device, in adjustment with properties combined of various ratios of mirror surface, matted surface, and transparent surface, we investigate each element's influences on objects' surfaces' color appearance and inspect influences of various texture on subject's psychological feelings. The aim is to know how those influences perform? What are the influences formed on people's mentality?

The purpose of the present research is to perform a quantitative survey on perceptions about material surface features in systematic ways, and to deliver results of practical data for subsequent researches on Cesia theory. The findings can provide advises on experimental operation, and broaden knowledge about influences of surface features on color appearance.

Key Words: Color Appearance, texture, Cesia, Permeability, Lightness, Diffusivity, material surface

1. INTRODUCTION

Color Research has developed prosperously in these years, particularly on "Color Appearance", which had made a significant breakthrough. In order to make out effectively, several business corporations have adopted colors as tool for marketing. However, most domestic research focuses on colors' influences on human mentality, and few has focused on texture's influences.

Texture, which is intimately connected to color appearance, has got rare attention. Features of texture possess enormous influences on color. Interactions between colors and surface material have big stake on the accuracy of color display. If we figure out patters of connection between texture and color, it's not only beneficial to our future generations in texture research; also, it can be practically applied to business commodity.

Regardless of the color, different textures have different effects on human mentality when people are looking at certain objects. Smooth and reflective objects like mirror, glass, etc. make people feel tough, heavy, and cold; whereas objects with rough surface like wooden furniture and fabric give people feelings of softness, lightness and warmth, and other uncountable emotions. Feelings aroused by objects are also experiences accumulated within human's mind.

Studies demonstrate that, surface material of products directly affects sales consequences, which indicates besides color, texture is another important factor affecting user's psychology. Texture itself is a huge research issue, and it will be bigger and intriguing when adding into color factor. There are thousand kinds of combinations as objects are composed of different colors and textures, but no previous research had figured out the variation or tendencies of this phenomenon. In this research, we intend to figure out patterns of connection by probing into mutual influences between colors and textures and contribute to advanced studies.

2. MEASUREMENTS ON SURFACE FEATURES

Former chairman of International Color Association (AIC) and Dr. Caivano in 1991 quoted "cesia" in his thesis available in the journal *Color Research and Application*, which refers to the system describing the optical property of texture, and the system was initiated by Jannello in the 1960s.

With Dr. Caivano's effort, cesia has been used as the system to describe Visual Textures, especially features concerning gloss and brightness. From physical measurements perspective, cesia can be presented with light's permeability and diffusivity, plus luminosity factor, forms a three-dimensional cesia space composed of permeability, diffusivity, and absorption. Just like Color Order Systems such as NCS and Munsell, cesia is an Order System describing surface characteristics.

Dr. Caivano's "cesia" is basically a way of describing visual sensation. Under different illumination and observing conditions, different cesia PDA indexes will turn out, and representing different visual sensation toward surface characteristics. Under standard measuring conditions, cesia data can be used as surface sensation index, besides trichromatic theory.

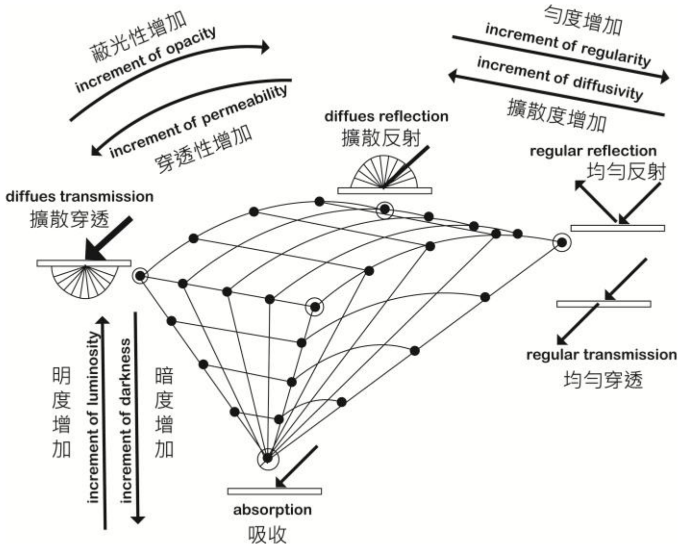

Figure 1: The solid of Cesia with the five primary sensations and the three kinds of variation.（Caivano, 1994）

3. EXPERIMENTAL METHODS

After entering experimental circumstances, experiment subjects will read the instruction first, and listen to the introduction of cesia system.

Experiment starts. The experiment includes five steps in response to five different combinations. These combinations are composed of different ratios of diffuse reflection, regular reflection, diffuse transmission, and regular transmission. In each step, a rotary table one the right side will be placed 100% texture, and another one on the left will be texture of different ratios in the random order (87.5%, 75%, 50%, 25%, 12.5%......).

In the first step, as the machine runs, we will begin to ask questions to our experiment subjects. Suppose texture on the right side is 100%, what is the ratio of texture on the left side? For instance, when it is 100% regular reflection on the right side, how many percent of regular reflection is on the left side? After they finish the questionnaire, we will change textures into different ratios without informing our experimental subjects, and ask them to make judges again. In all the five steps, ratios of experimental textures are random and nonrepetitive in every single step. Experiment ends as we finish all five steps.

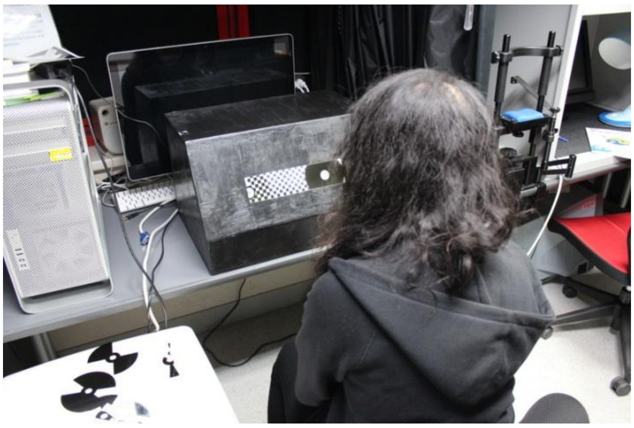

Figure 2: Experimental environment

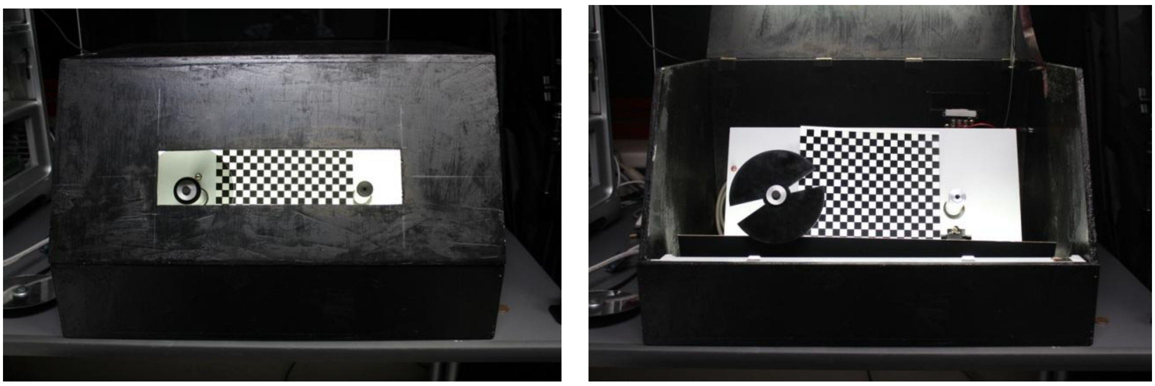

Figure 3: color mixer in special box

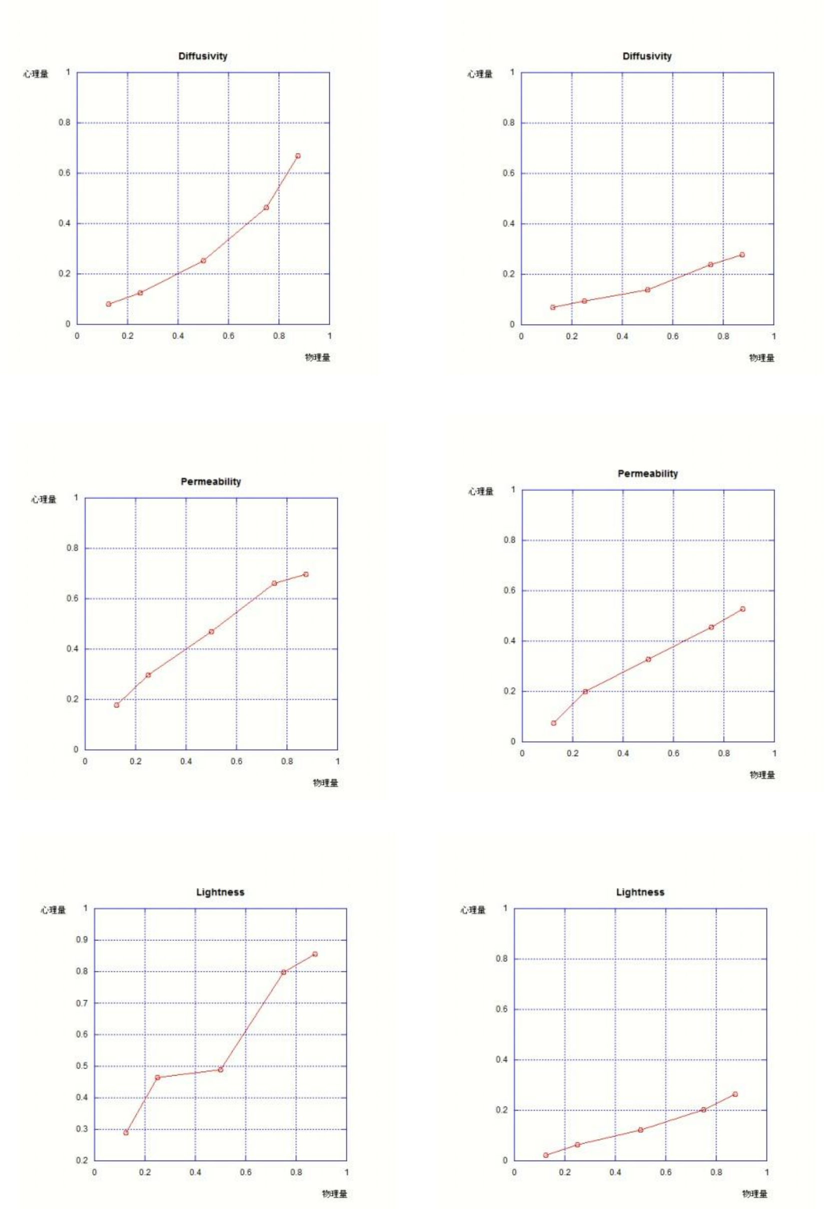

Figure 4 : The results of Permeability, Diffusivity and Lightness

REFERENCES

1. Caivano, J. L. (1991). "Cesia: A System of Visual Signs Complementing Color." Color Research and Application **Volume 16, Number 4**: P258-268.
2. Caivano, J. L. (1994). "Appearance (cesia): Construction of scales by means of spinning disks." Color Research and Application **19 (5)**: P351-362.
3. Jannello, C. (1963). "Texture as a visual phenomenon." Architectural Design **33**(8): 394-396.

Address: Department of Information Communication,
Chinese Culture University, No. 55, Hwa-Kang Rd., Taipei 11114, Taiwan
E-mails: lanmk76105@gmail.com, trlee@faculty.pccu.edu.tw,
csun@faculty.pccu.edu.tw

Visual evaluation of a wooden-finish room and the colorimetry of wood

Shigeko KITAMURA[1], Jun TSUCHIYA[2] and Shoji SUNAGA[3]
[1] School of Human Environmental Sciences, Mukogawa Women's University
[2] Center for Landscape Research, Kyushu Sangyo University
[3] Faculty of Design, Kyushu University

ABSTRACT

The use of wood as a building material or interior finish is known to induce a favorable psychological and physiological effect. There are many desirable aspects of wood, including the visual naturalness of wood grains, tactile warmth, tactile smoothness, natural smell, and others[1)2)3)4)]. Furthermore, the color and gloss of wood produced by aging are often desirable traits. Therefore, wood has long been used as internal and external building material in many circumstances. Although these effects are acquired by natural wood, the use of interior finishing paper with a printed image of wood grain[5)6)7)] has also increased. In this case, can we expect the same effect as seen for natural wood?

In this study, we begin by reporting the results of an experiment on the subjective visual evaluation of a wooden-finish room. Next, we provide an analysis of the spatial frequency of wood grain based on two-dimensional colorimetry. Furthermore, we consider the relationship between the evaluation of the wooden finish and the characteristics of the wood surface.

1. INTRODUCTION

It is generally considered that the visual impression of a wooden finish in a room depends on the surface color, difference of grain blend, and mutual influence of the proportion of wood-finish area and surface color[8)9)].

The purpose of this study was to clarify the factors influencing variation in the visual evaluation of wood color and area of wood finish in a room.

2. METHOD

2.1 Sample Preparation

Eleven types of wooden wallpaper samples[10)11)] with different colors were selected as the interior finish of a room (Table 1).

A 1/20-scale model that was finished with a reduced photocopy of wooden wallpaper was made for subjective evaluation. The scale model consisted of a living room, dining room, and kitchen. The area of wood finish in the rooms was changed in three conditions (Figure 1). The area of wood finish in the room was calculated from an indoor photograph taken from the subject's viewpoint. The subjective evaluation was accomplished under all 33 conditions corresponding to combinations of the 11 colors and 3 area proportions of the wooden finish.

Table 1: Wood Samples.

No	Tree species		Munsell color	L*	a*	b*
A	chestnut		2.5Y9/1	74.1	4.5	17.7
B	maple		10YR8.5/3	75.3	8.0	24.5
C	birch		5YR7/4	65.9	14.7	23.6
D	oak		7.5YR7/4	63.0	8.1	23.6
E	European walnut		7.5YR5/6	46.4	14.3	23.2
F	walnut		7.5YR5/3	64.8	7.9	22.2
G	teak		7.5YR4/4	42.5	12.5	19.9
H	European cherry		2.5YR5/6	59.1	10.8	21.1
I	mahogany		5YR3/3	32.7	7.2	7.8
J	black walnut		5YR4/2	28.0	2.1	1.5
K	plum		7.5YR2/4	47.3	28.1	31.9

41% *52%* *56%*

Figure 1: Examples of the scale model with different proportions of the wooden finish area

2.2 Experimental Procedure

The horizontal illumination on the desk of the scale model ranged from 800 to 900 lx. Forty-five students of Mukogawa Women's University participated in the experiment. The 45 observers used binoculars to provide subjective impressions of the scale model room through an observation window (65 × 250 mm). They based their evaluations according to a 7-step semantic differential scale using 9 pairs of adjectives, as listed in Table 2. The experiments were carried out from December 12th to 17th of 2013.

Table 2: Evaluation adjectives.

light	-	somber
spacious	-	cramped
bright	-	dark
classy	-	cheap
healing	-	not healing
warm	-	cool
natural	-	artificial
likable	-	dislikable
harmonious	-	disharmonious

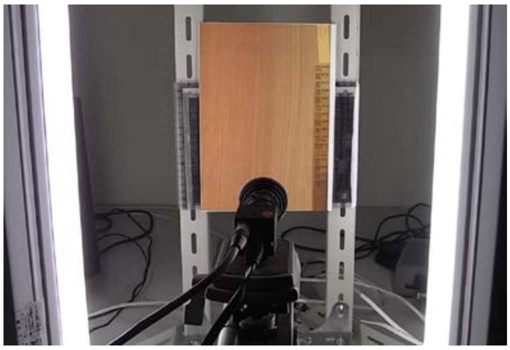

Figure 2 : Measurement equipment.

2.3 Colorimetry

The surface colors (CIE-XYZ) of the wallpaper samples were measured in a orthogonal direction by a luminance and chromaticity uniformity analyzer (UA-10, Topcon; Figure 2). The two-dimensional colorimetric distribution of the wood surface was determined with reference to previous studies[12)13)]. Specimens were illuminated by two fluorescent lamps with the same spectral distribution and the same light diffusion as the subjective evaluation experiment. Measurement specimens were eleven types of wooden wallpaper samples same as the subjective evaluation experiment. Wood grain on the specimens was the original size, not minified. Measurement area was 1280×960 pixels (200×150mm), and 256 × 256 pixels (40 × 40mm) of it was analyzed. This size was same as visual angle of the front wall observed by subjects in the subjective evaluation experiment.

3. RESULTS AND DISCUSSION

3.1 Factor analysis of the subjective evaluation

Factor analysis was performed to investigate the most relevant factors contributing to variation in the visual evaluations of a scale model room with a wood finish based on the adjectives provided (Table 2). As shown in Table 3, 2 main factors were extracted, Lightness and Harmony, which showed a cumulative contribution rate of 84.83%. There was barely any difference in the individual contributions of Lightness and Harmony, indicating that these 2 factors show equivalent efficacy on the subjective visual evaluation of a wooden-finish room.

Table 3. Factor structure.

		factor loadings		commonality
		1 Lightness	2 Harmony	
1	light	0.9932	0.0748	0.9921
	spacious	0.9874	0.0765	0.9808
	bright	0.9827	0.0834	0.9727
	classy	-0.9292	0.0437	0.8654
2	healing	0.1527	0.9650	0.9545
	warm	-0.0076	0.9232	0.8524
	natural	-0.1203	0.9225	0.8654
	likable	0.2289	0.8530	0.7800
	harmonious	-0.0020	0.6091	0.3710
eigenvalue		3.8809	3.7534	
contribution rate		43.12%	41.70%	
accumulated contribution rate		43.12%	84.83%	

3.2 Results of colorimetry and image analysis with the Fast Fourier Transform method

The CIE-XYZ value was obtained by two-dimensional colorimetry. The Y value is considered to correspond to the interval or contrasting density of the wood grain. Therefore, the Y value on each pixel of the input image was analyzed by the Fourier transform algorithm. The middle rows of Figure 3 show the images of specimens applied to Fourier transform analysis.

In addition, the spatial frequency from the center of the image outward was analyzed. The Hamming window function was applied as an approximation of spatial frequency. The bottom rows of Figure 3 show the relationships between spatial frequency and the modulation transfer function for each wood color. According to this relationship, the spatial frequency ratio was calculated to describe the characteristics of the wood grain, and was considered as an index of wood grain.

Figure 3 : Fourier transform and spatial frequency characteristics

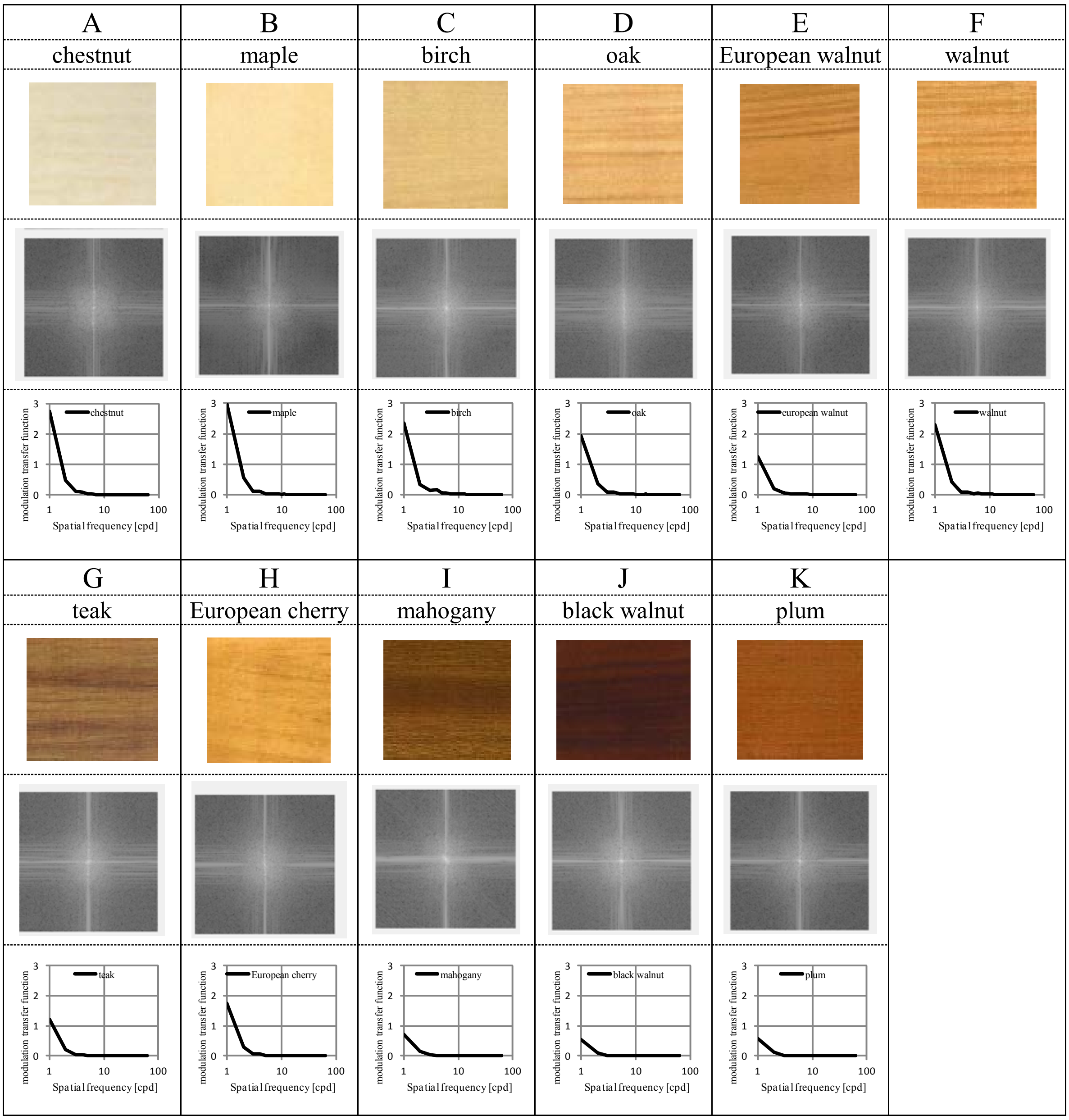

3.3 Relationship between subjective evaluation and colorimetry

The relationship between the two-dimensional colorimetric distribution of the wood surface and the factors of subjective evaluation was examined through multi-regression analysis, and the results are shown in Table 5. Lightness was influenced by the L* value and the proportion of wooden finish area in the room. Harmony was influenced by the proportion of wooden finish area, wood color (a* and b*), and wood grain.

Table 4 : Result of multi-regression analysis

	multiple correlation coefficient	partial correlation coefficient				
		L*	a*	b*	Spatial frequency ratio	area
F1 Lightness	0.9150	0.7398**	0.1767	-0.3648	0.1436	-0.6963**
F2 Harmony	0.7553	-0.2755	-0.5012**	0.5694**	0.3171	0.5435**

**: p<0.001

4. CONCLUSIONS

To clarify the influences of wood color and wood grain on the subjective evaluation of a wooden-finish room, we conducted a study to associate the results of a subjective experiment to those of image analysis based on two-dimensional colorimetry of wood.

These results lead to the conclusion that subjective evaluation of a room with a wooden finish consists of 2 factors: Lightness and Harmony. The lightness value of wood color and the proportion of wood area in the room influence the Lightness factor. Wood color and wood grain influence the Harmony factor. In addition, our results show that two-dimensional colorimetry and spatial frequency analysis with a Hamming window function seems to be an appropriate method for analyzing the characteristics of wood color.

ACKNOWLEDGEMENTS

We would like to express special thanks to Yuka Ono and Kaori Hamao, students at Mukogawa Women's University during the study period, for carrying out the experiments on subjective evaluation.

REFERENCES

1) Nakamura, M. 2012, *Appearance of wood and wooden interior,* Journal of Wood Science, 58(1)1-10.

2) Ito, J., Nakamura, M. and Masuda, M. 2006, *The influence of colors on the Psychological image of the wooden interior: Application of the image analysis in consideration of the accent color,* Journal of the Society of Materials Science, 55(4)373−377.

3) Broman, N. O. 2001, *Aesthetic properties in knotty wood surfaces and their connection with people's preferences*, Journal of Wood Science, 47, 192-198.

4) Tsuchiya, J., Kimura, A. and Iijima, Y. 2010, *Study on the evaluation for the texture of wood products: Part1.The different perception of visual and tactile texture on wood surfaces*, Summaries of Technical Papers of Annual Meeting, Architectural Institute of Japan, A(1)343-3444)
5) Sagawa, K., 2000, *Visual Comfort Evaluated by Number of Categorical Colors in Colored Image*, Color research and application, 25(3)193-199.
6) Akiyama, R., Aoyama H., and Oya T. 2014, *Study on Digital Style Design -Method to Generate Wood Grain Pattern Representing Required Impression-,* 80(5) 484-490.
7) Tashiro, T., and Nakamura, M. 2013, *Characterization of Colors Distributed on Lumber Surface by Imaging Spectroscopy*, Journal of the Society of Materials Science, 62(4)248-253.
8) Kitamura, S. 2006, *Two dimensional effect of texture for interior finishing materials*, Summaries of Technical Papers of Annual Meeting, Architectural Institute of Japan, D(1)349-352.
9) Nagayasu, T., Masuda, M., and Nakamura, M. 1998*, Effect of Wood Ratio and Area in Interior Space on the Psychological Images : In the Case of Experiment Using a Loft in a Log-house,* Forest research, 70, 19-27.
10) Nick Gibbs 2005, The Wood Handbook, Sanchoh Shuppan Inc.
11) Dai Nippon Printing Co. Ltd 2012.WS collection, Dai Nippon Printing Co. Ltd
12) Sunaga, S. and Yamashita Yukio 2003, *Causes of Color Conspicuousness in Scene Color Image*, Journal of the Color Science Association of Japan, 27(4) 285-297.
13) Sunaga, S. and Yamashita, Y. 2007, *Global color impressions of multicolored textured pattern with equal unique hue elements*, Color Research and Application, 32, 267−277.

Address: Associate Prof. Shigeko KITAMURA,
Department of Human Environmental Sciences, School of Human Environmental Sciences,
Mukogawa Women's University, 6-46 Ikebiraki, Nishinomiya, Hyogo,663-8558, JAPAN
E-mails: kitamura@mukogawa-u.ac.jp, a.jun@ip.kyusan-u.ac.jp,
sunaga@design.kyushu-u.ac.jp

Total Appearance of Metallic Coatings using a Stereo Capture System

Min-Ho JUNG, Vien CHEUNG, Peter A. RHODES
School of Design, University of Leeds

ABSTRACT

This paper describes a study which aims to define the total appearance of metallic coatings and then objectively characterise it. Total appearance here refers to the combination of three properties of perceptual attributes of the surface: glint, coarseness and brightness. This study took into account one specific viewing angles only when irradiated by an intense directed light source. 54 metallic panels were visually scaled and a computational model capable for predicting three perceptual attributes was developed.

1. INTRODUCTION

Over recent decades, textured coating provided by metallic surfaces has been an important factor in attracting customers of the automobile industry. This has meant that quantifying the appearance of coating products is essential for product development and quality control. The appearance of these coated products strongly depends on the viewing geometry, giving rise to a variety of properties of perceptual attributes such as texture, colour and gloss. Due to the visually-complex nature of such coatings, there remains an unsatisfied demand to develop techniques to measure the total appearance of metallic coatings. This study focused on characterising not only one dominant attribute, glint, but also minor attributes, coarseness and brightness, with an intense directed light source. The measurement of the total appearance of metallic coating was conducted from an investigation of the relationships between the three perceptual appearance attributes judged by observers and the physical parameters extracted by a stereo capture system.

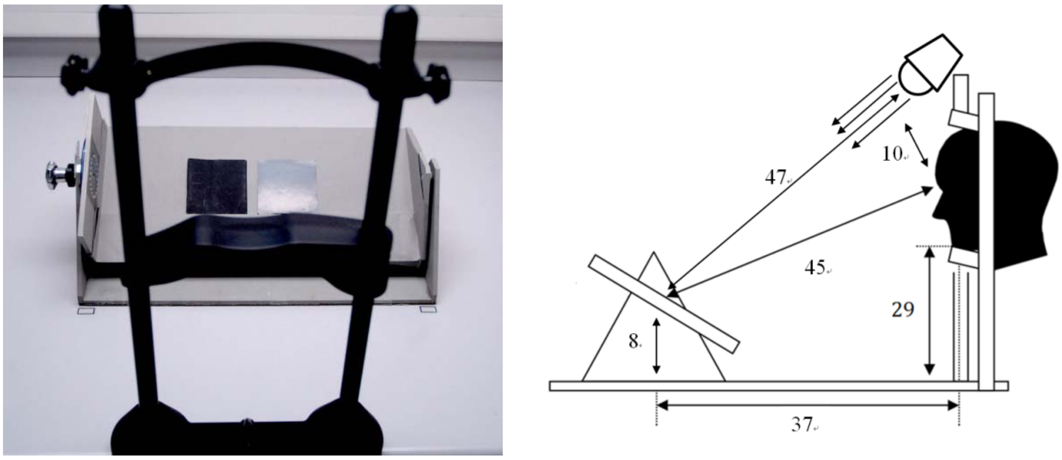

Figure 1: Experimental setup for total appearance – real setup (left) and schematic diagram of viewing condition (right).

2. PSYCHOPYSICAL EXPERIMENT

Visual assessments were carried out to quantify three properties of perceptual attributes of metalic-coagting panels: glint, coarseness and brightness. Ten observers with normal (or corrected to normal) visual acuity and colour vision participated in the assessments. They judged three perceptual attributes of 54 metallic panels under directional illumination by comparison with a reference sample. The session was carried out twice, each on a different day, in order to test repeatability. Each session lasted around 35 minutes, but was limited to 45 minutes so as to avoid visual fatigue. Figure 1 shows a LED spot light was used as the light source and it was located closely above the observer's head to minimise the angle between light source and observer.

3. DIGITAL IMAGING ANALYSIS

A computational model was developed to relate the results from the visual assessments to data obtained from the stereo capture system. This is a new alternative technique aimed at solving one of the most challenging problems in computer vision: stereo matching (Zhou and Boulanger, 2011). In the system, two images are captured by a same camera under two different lighting conditions to mimic stereoscopic vision. This not only addresses the problem of stereo matching (i.e. to find the corresponding pixels between two images) but also enhances the effect of perceptual attributes, especially glint. After capturing two images, digital imaging processing was implemented to extract relative features of perceptual attributes of metallic texture under directional light source.

3.1 Stereo Capture System

The stereo capture system consists of a digital camera and two LED spot lights shown in Figure 2. The system was designed to mimic human stereo vision. In the system, one digital camera was used as an image detector in contrast to a striking way with general type of stereo capture system with two or more lenses with a separate image sensor. Nevertheless, the system can reproduce the effective images of stereo perception without the big problems in stereo matching. This advantage of this system comes from illumination set up. Two LED spot lights are located at different lateral positions and Each LED source plays a role as each eye of human vision. Two scenes illuminated by two different lights are different due to illumination angle. The angle between a digital camera and light source was fixed as that of viewing geometry in visual assessment. In practice, two slightly different images for one sample were captured under two different lighting conditions: each image with single light on.

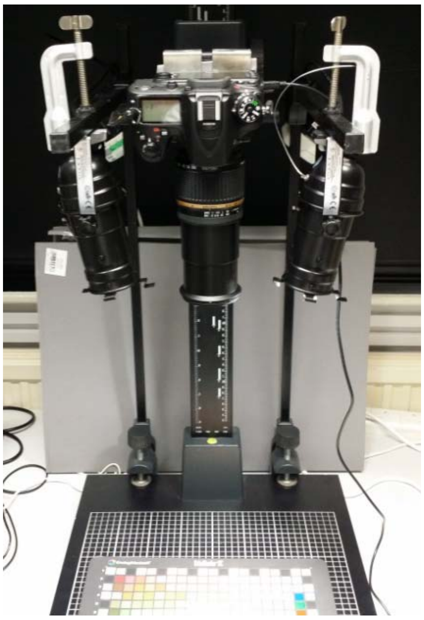

Figure 2: Stereo capture system.

3.2. Digital Image Processing

A camera characterisation method was applied to transform device-dependent RGB values to device-independent CIE XYZ tristimulus values. Luminance Y value of the images was used for the feature extraction. Illumination uniformity method was performed to minimise the effect of non-uniformity of the illumination intensity caused by the nature and geometry of spot light source used. The top-hat transform of an image was then employed to remove minor scratch of metallic-coating surface while leaving others undisturbed (Gonzalez *et al.*, 2004). Feature extraction starts on the assumption that the intensity distribution of the solid coating panels may be normal and symmetric histogram. This indicates that metallic-coating panels with the aluminium flakes have excessive part of histogram due to bright regions. According to assumption of normal distribution of the solid coating panels without aluminium flakes, Gaussian function was fitted to simulate the histogram and differential portion between both histograms was found. A global thresholding technique was applied to separate bright parts of metallic-coating panels. Two images obtained by these steps were combined into one image which is the largest elements of two images. Consequently, the image is the result which is similar to scene of stereo vision for digital image analysis.

4. RESULTS AND CONCLUSIONS

Figure 3 shows a comparison of two images; image (a) reconstructed by stereo image technic and image (b) captured by general image system with single camera. Two images represent not only the same metallic-coating panel but also exactly same area of the sample. Nevertheless, two images show different scene each other. Image (a) is similar to perception of human being with two eyes and gives more visual information than image (b). Intensity histogram of stereo image (a) testifies their difference in detail.

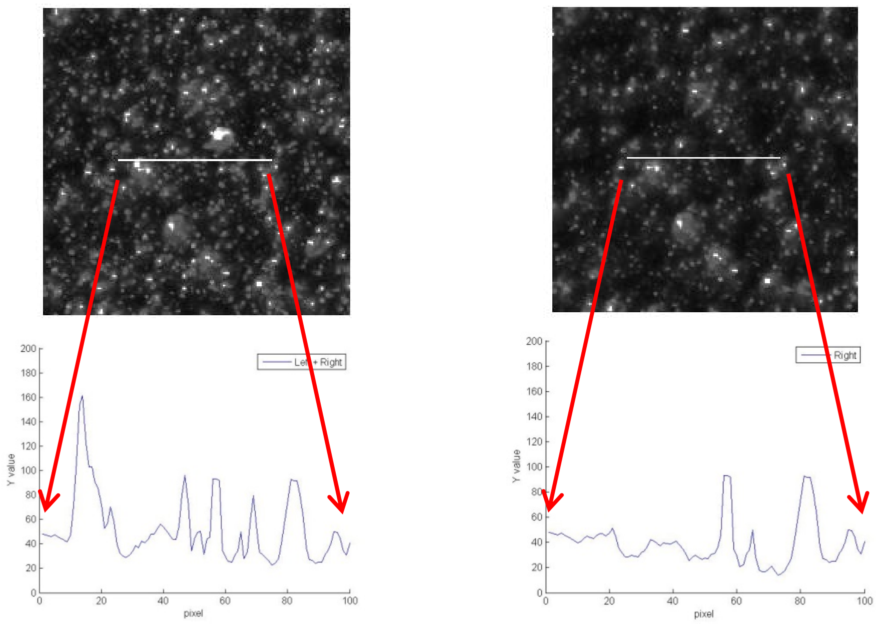

(a) (b)

Figure 3: The intensity comparison of two images captured from general acquisition and stereo capture system.

Observer variability of the three perceptual attributes: glint, coarseness and brightness was quantified using observer accuracy and repeatability. The statistical methods used in data analysis were the coefficient of determination, R^2, and coefficient of variation, *CV*. Table 1 shows that the observer accuracy and repeatability. Repeatability of coarseness was similar to that of glint but another was lower to that. The results of brightness do not provide signified statistics due to very low R^2 values obtained. It can be concluded that only glint of appearance attributes of metallic-coating panels is a meaningful property under specific viewing angles only when irradiated by an intense directed light source.

Table 1: A summary of observer accuracy and repeatability measures for all the samples.

		Accuracy			Repeatability		
	Logarithmic Scale	Glint	Coarseness	Brightness	Glint	Coarseness	Brightness
R^2	Mean	0.90	0.71	0.09	0.90	0.75	0.52
	Median	0.91	0.71	0.08	0.90	0.75	0.52
CV	Mean	13.67	12.15	4.26	10.42	11.76	4.64
	Median	12.49	10.33	3.50	10.89	10.09	3.49
	Raw Scale	Glint	Coarseness	Brightness	Glint	Coarseness	Brightness
R^2	Mean	0.85	0.74	0.58	0.82	0.75	0.52
	Median	0.87	0.76	0.59	0.85	0.77	0.47
CV	Mean	30.09	29.75	19.72	-	-	-
	Median	24.94	26.19	14.04	-	-	-

Using digital image processing, a dominant property of the total appearance of metallic coatings, glint, was extracted and compared with perceptual grade of observers in terms of twelve features: number of pixels, sum of those pixel values, number of particles, sum of mean value of each particle, pixel percentage against background, area percentage and six properties which are divided by the threshold *t* value (Kitaguchi, 2008). As shown in Figure 4 (h), sum of those pixel values divided by threshold value represent the highest correlation between both.

There are several statistic features with high correlation with perceptual glint along with representative property (h). To develop the model predictions, non-linearity step was applied and the performance of model was evaluated. Finally, power form using the property (h) gave the best performance.

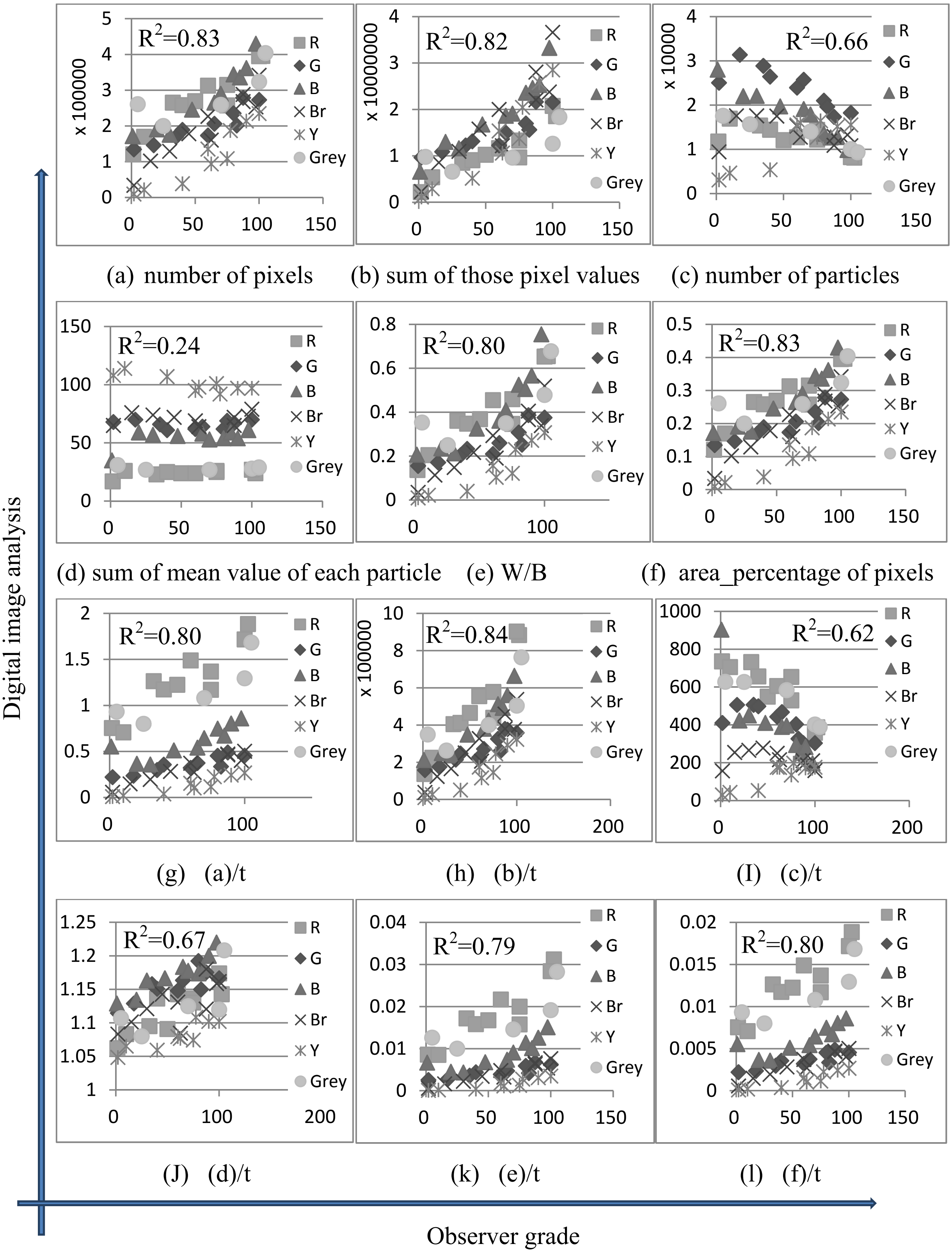

Figure 4: Observer grade VS digital image analysis

REFERENCES

Zhou, X. and Boulanger, P. 2011. Illumination Invariant Stereo Matching Based on Normalized Mutual Information and Census Methods. *Proceedings of Computer Graphics International Conference*.

Gonzalez, R.C., Woods, R.E., and Eddings, S.L. 2004. *Digital image processing using MATLAB*. New Jersey: Pearson Education, Inc.

Kitaguchi, S. 2008. Modelling Texture Appearance of Gonioapparent Objects. *PhD Thesis,* University of Leeds, UK.

Address: Min-Ho Jung, School of Design, University of Leeds, Leeds LS2 9JT, UK
E-mails: ccd6mhj@leeds.ac.uk, t.l.v.cheung@lees.ac.uk, p.a.rhodes@leeds.ac.uk

Statistical Image Analysis for Evaluating Face Shine: Cosmetic Research

Takanori IGARASHI,[1] Takahiro NAOKI,[2] Masataka SEO,[2] Yen-Wei CHEN[2]
[1] Skincare Products Research Laboratory, Kao Corporation
[2] School of Information and Engineering, Ritsumeikan University

ABSTRACT

Cosmetics, particularly base-makeup items such as foundation, are expected to provide beautiful shine with faces. In the process of cosmetics development, therefore, it is critical to understand features of face shine. In this study, we evaluate the feature using a novel statistical facial image analysis that characterizes the spatial distribution of brightness (texture) appearing on facial images. Since statistical methods require large amounts of facial images for learning data, we employed a facial image database designed for cosmetic purpose (the database is composed of facail images of Japanese females with and wtihout foundation). Then, to evaluate the features of face shine from the standpoint of facial "texture", we normalized each facial shape in the database to a mean shape by using a warping technique. These "shape-normalized facial images" are used as learning data for statistical texture analysis. We used principal component analysis to calculate eigenvectors of the facial texture. Each eigenvector represents a specific feature of the texture. Therefore, the facial image with different texture can be reconstructed by the combination of these eigenvectors. In this method, we first reconstructed facial images that had different acumulated cover ratio (ACR). Information regarding the differences between the reconstructed facial images was then used to extract textures that determined the features of face shine. By using this method, textural features of facial images with different types of face shine were evaluated. The results showed that texture that appeared in ACR of 82% ~ 97 % especially related to the deterioration of face shine. Since local unevenness of the facial skin such as pores are expressed in ACR 82% ~ 97 %, this result suggests that the local unevenness deteriorates face shine.

1. INTRODUCTION

As an important function of cosmetic foundation, which is a typical base-makeup, achieving a desirable cosmetic finish (face impression with makeup applied) has long been noted[1)]. In this regard, the importance of controlling the appearance of the face and its skin has been gathering interest in recent years[1)]. Among the efforts being made, study on face shine is particularly important. For example, as reported in a previous study[2)], the impression of a face can be flexibly controlled by varying the angular pattern of reflection from the skin, which suggests that feature of face shine is one of the key factors for controlling facial appearance. As is well known, the cosmetic finish is altered through skin sebum secretions, which cause an undesirable type of face shine (oily shine)[3)-5)]. In other research, the relationship between skin shine and skin age perceptions were investigated[6), 7)], and the result provides insights in designing cosmetics. As these previous cases show, study concerning face shine has been one of the most critical topics in cosmetic research.

In order to control feature of face shine with cosmetics, textural factors of face that generate the differences of the feature need to be assessed. In this study, a quantitative evaluation method for textural features concerning face shine is first proposed. Here, principal component analysis (PCA), which is useful for the analysis of facial images, was employed. Then, by using the method, the texture control points for achieving the desirable shine is identified.

2. EXTRACTION METHOD OF TEXTURE FROM FACIAL IMAGES

A novel method for the extraction of facial texture was developed by applying the Eigenface method[8)], statistical image analysis based on PCA.

2.1 Facial Image Database for Learning

PCA requires large amounts of facial images for learning data. We, therefore, employed a facial image database designed for cosmetic research named "Multi-angle View Illumination Cosmetic Facial Image Database: MaVIC [2)]. Facial images in MaVIC were captured Multi-angle Image Capturing System[2)] (Figure 1), which allows us to capture facial images from 20 directions under various illumination conditions. MaVIC is composed of facial images of 420 Japanese females. MaVIC possesses 100 pairs of facial images with and without foundation. In this study, frontal facial images illuminated from the frontal direction were chosen from MaVIC.

Figure 1: Multi-angle Image Capturing System.

Cosmetic foundation achieves desired appearances by controlling texture such as skin imperfections (*e.g.* pores and freckles) and face shine. Therefore, in the evaluation of facial appearance for the purpose of foundation development, analysis focused solely on facial texture (NOT facial shape) is crucial. For this reason, as the facial image database (DB) for statistical learning, we prepared a "shape-normalized facial image DB" in which facial shapes (contours, positions of noses and eyes, etc.) of the images chosen from MaVIC were entirely unified by a warping technique[9)] (Figure 2).

2.2 Eigenface Method

Employing the learning data of the aforesaid shape-normalized facial image DB, we computed eigenspace using the Eigenface method[8)]. In this method, facial image **x** is described using basis functions (eigenvectors) $\mathbf{v}_i$ and their coefficients y_i:

$$\mathbf{x} = \mathbf{m} + y_1\mathbf{v}_1 + y_2\mathbf{v}_2 + \ldots + y_{n-1}\mathbf{v}_{n-1} + y_n\mathbf{v}_n \qquad (1)$$

Here **m** represents the mean vector of all facial images, and n is the total number of eigenvectors (n = 307). The reconstruction of facial images based on Equation (1) showed that facial texture was restored as the accumulated cover ratio (ACR) increased (Figure 3).

2.3 Identification of ACR bands related to face shine

A method for extracting the feature of face shine from the reconstructed facial images with different ACR levels was developed. As is evident in the comparison between reconstructed facial images with different feature of face shine shown in Figure 3 (a) to (c), the differences did not clearly emerge for the “low-order” reconstructed images with low ACR (for example, ACR = 50% in Figure 3). The differences, however, are clearly recognized for the “high-order” reconstructed images with high ACR. Thus, textural factors that determine the feature of face shine can be emerged at specific high-order ACR bands. Consequently, we attempted to identify the ACR bands according to the following 6 steps:

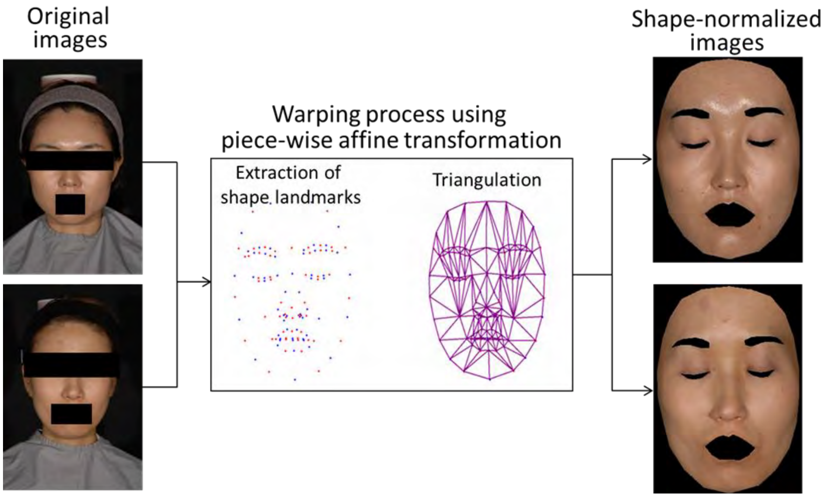

Figure 2: Shape-normalization via the warping technique.

1. Subjective evaluation was carried out to score the level of face shine for 19 facial images;
2. For the 19 facial images, reconstructed facial images were synthesized by varying ACR according to Equation (1) (ACR varying increment was 3%: Figure 4(a));
3. Residual images between adjacent reconstructed facial images were computed (Figure 4(b));
4. Variance of the computed residual images were calculated (Figure 4(c));
5. The obtained variances for various ACR bands were accumulated.
6. The cumulative values obtained in step 5 were compared with subjective scores obtained in step 1, and then ACR bands that have high correlation to the subjective scores were identified.

In this study, the computational process represented in the above steps (Figure 4) is named “Eigen subspace selection method”.

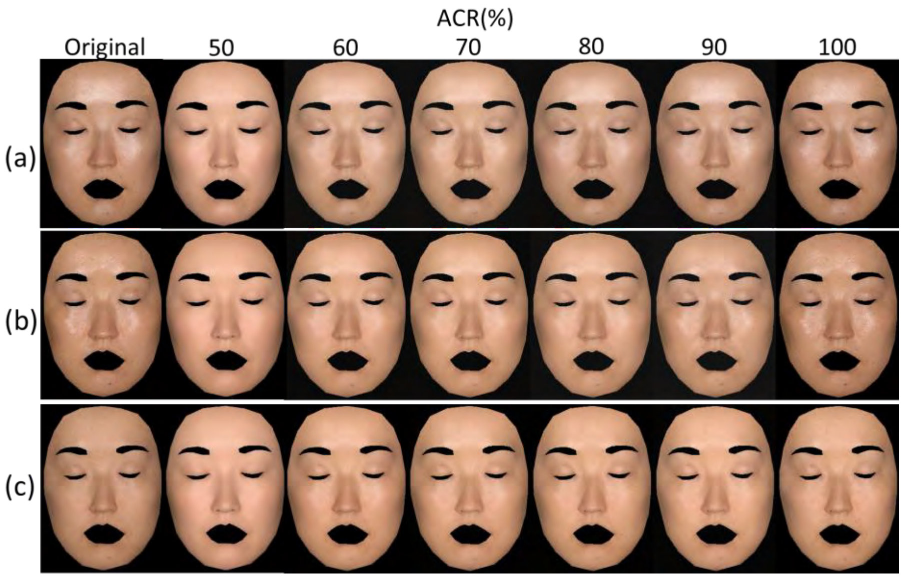

Figure 3: Reconstructed images of faces with different types of facial shine.

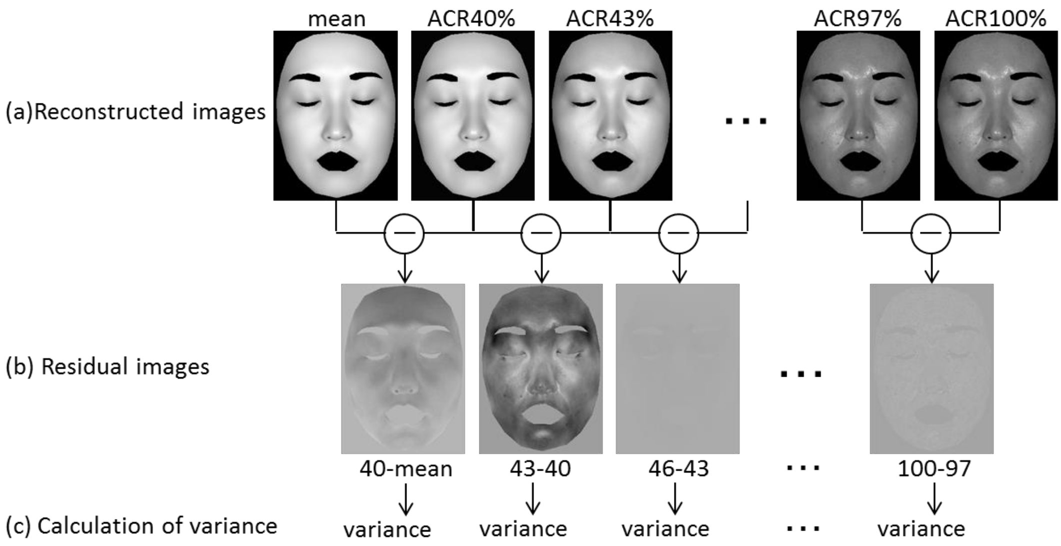

Figure 4: Computational process for the quantification of facial texture ("Eigen Subspace Selection Method").

3. RESULTS AND DISCUSSION

The subjective scores for the level of face shine are, as shown in Figure 5, highly correlated to the cumulative values of the variance for the ACR bands ranging from 64% to 97%. In particular, the correlation reaches the maximum at the ACR band from 82% to 97%. Therefore, face shine can be efficiently quantified by cumulative variance value at the band of ACR 82% ~ 97%. Figure 6 shows the example of facial images reconstructed using the eigenvectors of the ACR 82% ~97%. Interestingly, textures derived from face shine as well as fine (local) skin unevenness such as pores are clearly extracted in the reconstructed facial image.

Next, we evaluated the relationship between the cumulative values of variance at the ACR band from 82% to 97% and the desirability of face shine scored via subjective evaluation (the number of test images is 19). Consequently, as shown in Figure 7, the following results were obtained:

1. Facial images with undesirable shine have large cumulative variance at the ACR band;
2. Facial images with excessively matte impression have small cumulative variance at the ACR band;
3. Facial images with desirable impression like "perceived translucency" have an intermediate cumulative variance at the ACR band.

With respect to 1, facial images with both face shine and local skin unevenness such as conspicuous pores have a large cumulative ACR variance from 82% to 97%. This suggested that local skin unevenness is one of the main factors that deteriorate face shine. With respect to 2, the cumulative ACR variance from 82% to 97% becomes small when both face shine and local skin unevenness are excessively absent. In this case, the faces look unnatural, and consequently give negative impression even though skin unevenness is restricted. Finally, with respect to 3, the result shows that a moderate level of shine with suppressing local skin unevenness provides a favorable impression of facial appearance. These discussions provide us with important insights for the design of foundation: in order

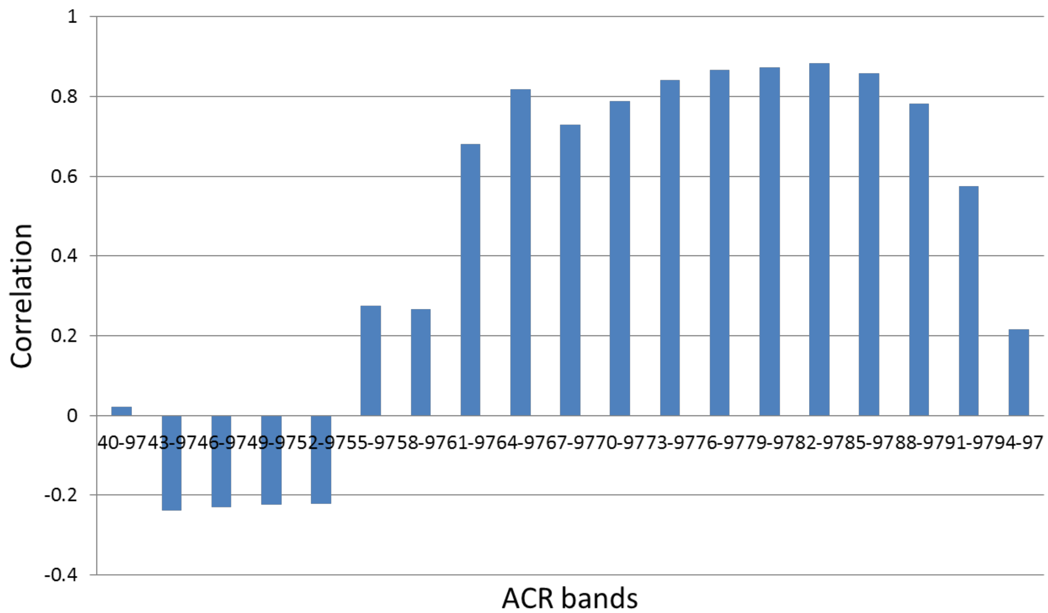

Figure 5: Correlation between the cumulative values of variance at various ACR bands and scores of the subjective evaluation for the level of face shine.

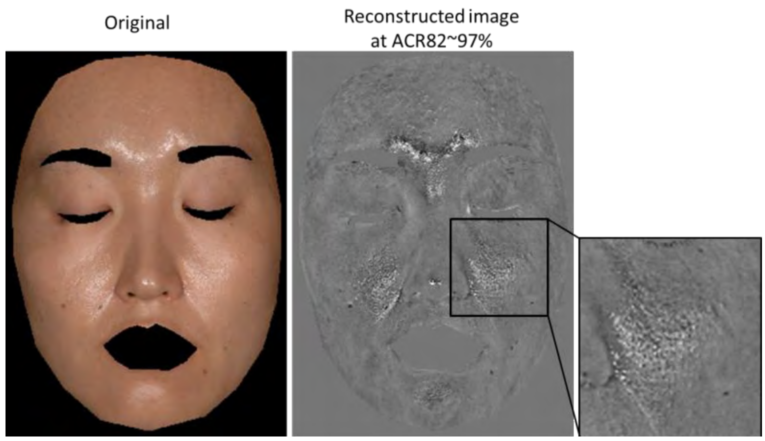

Figure 6: A typical facial image with shine (Original) and its reconstructed image at ACR 82~97%. In this ACR band, local skin unevenness such as pores is clearly extracted in the area of face shine.

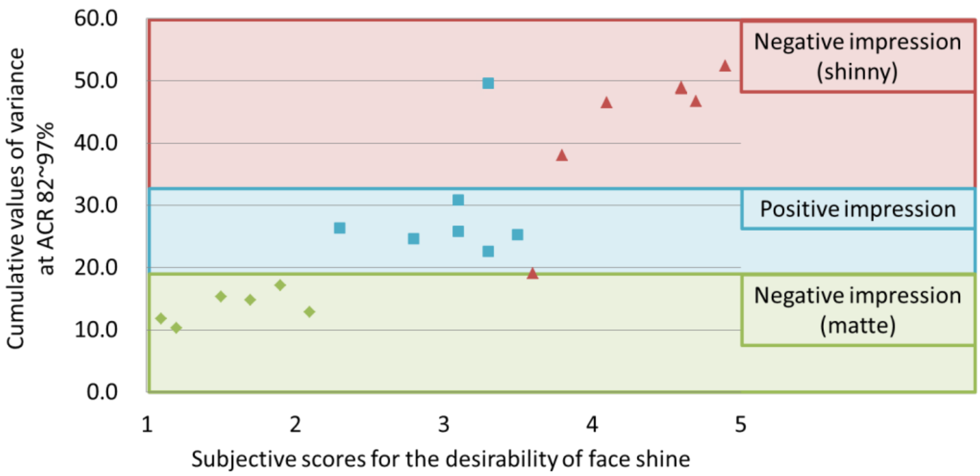

Figure 7: Relationship between subjective scores for the desirability of face shine and computational values via the proposed method ("Eigen subspace selection method").

to develop foundation that achieves desirable facial appearances, it is critical to effectively restrict local unevenness of facial skin with providing moderate shine.

4. CONCLUSIONS

We evaluate features of face shine based on the new-developed technique, “Eigen subspace selection method”. In this method, facial images that have different ACR are first reconstructed using PCA. Then, the variance of residual images from the reconstructed facial images is used to quantify textures that determine feature of face shine. The results show that texture extracted at ACR band from 82% to 97 % relates to the feature of face shine. At the band, local skin unevenness such as pores is mainly expressed. Therefore, the result suggests that restriction of the unevenness with providing moderate face shine is important for the development of foundation that achieves favorable facial appearances.

REFERENCES

1. Igarashi, T., Nishino, K., and Nayar, S.K. 2007. *The Appearance of Human Skin: A Survey*, Foundations and Vision in Computer Graphics and Vision 3 (1) 1-95.
2. Igarashi, T., Fukui, T., Qiao, X., Nakao, K., Kashimoto, A., Fukuda, K., and Chen, Y.W. 2008. *Face Designing: Technology to Control Facial Appearance Based on Multi-angle Image Analysis and Electromagnetic Simulation*, Proceedings of the 25th IFSCC Congress, Barcelona, Spain, 145-150.
3. Fujii, M., Misaki, Y., Sakaki, I. 2009. *Application of Image Processing Technique for Facial Gloss Evaluation*, Journal of the SCCJ, 43(2) 72-78. (in Japanese)
4. Ohtsuki, R., Hikima, R., Sakamaki, S., Tominaga, S. 2013. *Evaluation Method of Oily-shine Using Facial Image with Cosmetics Foundation*, Journal of the Color Science Association of Japan, 37(2) 113-123. (in Japanese)
5. Naoki, T., Seo, M., Igarashi, T., Chen, Y.W. 2013. *Optimal Color Space for Quantitative Analysis of Shinny Skin*, Proceedings of the 6th International Conference on Biomedical Engineering and Informatics (BMEI), 836-840.
6. Arce-Lopera, C., Igarashi, T., Nakao, K., Okajima, K. 2012. *Effects of Diffuse And Specular Refletions on the Perceived Age of Facial Skin*, Optical Review, 19(1) 167-173.
7. Arce-Lopera, C., Igarashi, T., Nakao, K., Okajima, K. 2013. *Image Statistics on the Age Perception of Human Skin*, Skin Research And Technology, 19(3) 273-278.
8. Turk, M., Pentland, A. 1991. *Eigenfaces for Recognition*, Journal of Cognitive Neuroscience, 3(1) 71-86.
9. Terada, T., Fukui, T., Igarashi, T., Nakao, K., Kashimoto, K., Chen, Y.W. 2009. *Automatic Facial Image Manipulation System And Facial Texture Analysis*, Proceedings of Fifth International Conference on Natural Computation 8-12.

Address: Takanori IGARASHI, Skincare Products Research Laboratory,
Kao Corporation, 2-1-3Bunka,Sumida-ku, Tokyo, 131-8501, JAPAN
E-mails: igarashi.takanori@kao.co.jp, is0027ff@ed.ritsumei.ac.jp,
s.dream.7342@gmail.com, chen@is.ritsumei.ac.jp

High Dynamic, Spectral and Polarized Natural Light Environment Acquisition

Philippe Porral[1], Patrick Callet[1,2], Philippe Fuchs[1]

[1]Robotics Lab, MINES ParisTech,France

[2]Applied Mathematics and Systems Laboratory, CentraleSupélec, France

ABSTRACT

In the field of the image synthesis, the simulation of material's appearance requires a rigorous resolution of the light transport equation. This implies taking into account all the elements that may have an influence on the spectral radiance, and that are perceived by the human eye. Obviously, the reflectance properties of the materials have a major impact in the calculations, but other significant properties of light such as spectral distribution and polarization must also be taken into account, in order to expect correct results. Unfortunately real maps of the polarized or spectral environment corresponding to a real sky do not exist.

Therefore, it seemed necessary to focus our work on capturing such data, in order to have a system that qualifies all the properties of the light and capable of powering simulations in a renderer. As a consequence, in this work, we develop and we characterize a device designed to capture the entire light environment, by taking into account both the dynamic range of the spectral distribution and the polarization states, in a measurement time of less than two minutes. We propose a data format inspired by polarimetric imaging and fitted for a spectral rendering engine, which exploits the "Stokes-Mueller formalism."

Keywords: global illumination, spectral rendering, polarization, HDRI, Stokes vectors, Mueller matrix

1. INTRODUCTION

The fundamental rendering equation (1) proposed in 1986, [Kajiya, 1986] formulates the mechanism of light/matter interactions.

$$L_o(x,\vec{\omega},\lambda) = \int_{\Omega} L_i(x,\vec{\omega}',\lambda) f(x,\vec{\omega},\vec{\omega}',\lambda)(\vec{\omega}'.\vec{n})d\omega' \tag{1}$$

Wherein:

- L is the light information.
- f is the Bidirectional Scattering Distribution Function (BSDF), characterizing the goniometric behavior of matter with a light hit.
- the additional factor is the indicator's angle on the impacted shape.

Obviously, this equation confirms the essential role of light. To expect a correct resolution, it is essential to take into account the totality of the physical nature of light, ie:

- *Intensity, wavelength, phase, polarization.*

Further author information: (Send correspondence to Philippe Porral.)
E-mail: philippe.porral@mines-paristech.fr, Telephone: +33 (0)1 40 51 94 37
E-mail: {philippe.fuchs, patrick.callet, thomas.muller}@mines-paristech.fr

Unfortunately, with a very few exceptions, in the current synthesis imaging softwares, the spectral composition and especially the light polarization is neglected. Sometimes this is justified by some simplifications, or by the unavailability of the necessary informations for rendering methods. This leads to inaccuracies, or worse, to significant errors as shown in figure (1) or just impossible image calculations.

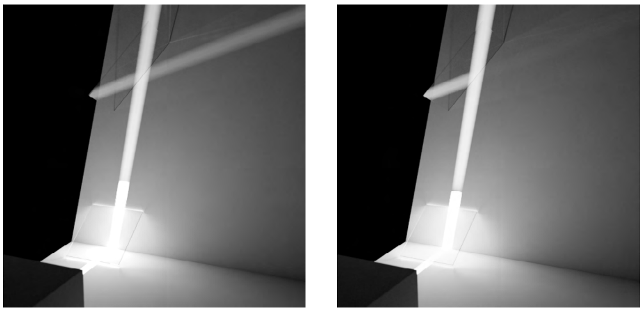

(a) *No polarization* (b) *With polarization*

Figure 1: *Brewster experience simulation. At an incidence equal to the Brewster angle θ, the TM wave (p polarization) is totally transmitted and the reflected beam disappears.*

In order to answer this need, we propose the development and characterization of a device for the acquisition of the natural light environments, taking into account the range of light intensity, the spectral distribution and the polarization. The obtained informations will be processed and stored in a specific format to make them usable in a spectral renderer adapted accordingly based on the ”Stokes-Mueller formalism”.

2. LIGHT ENVIRONMENT MODELS

2.1 Light Environment Models Classification

Since the first observation instruments seeking to discover the organization of the sky and understand the optical phenomena that take place there, several descriptions and models have been proposed and nowadays many scientific fields are involved in this knowledge. In figure (2) we propose a classification of models and tools currently available. We excluded works on specific visual phenomena as clouds, rainbows, halos … and focused on the only influence of the couple sun/sky on objects for an observer at a place and at a specific time.

We will see that although used in the synthesis imaging tools, with a few exceptions, they are either oversized or suffer from limitations.

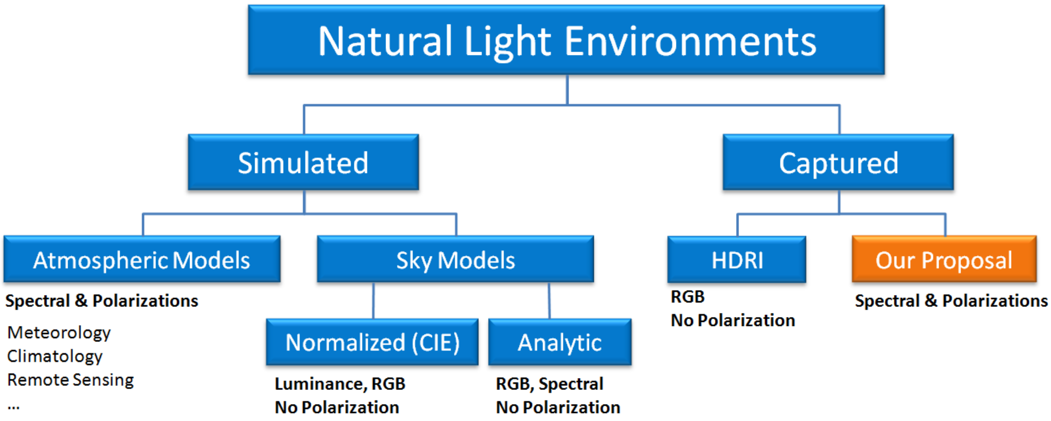

Figure 2: *Proposed classification of existing works on Light Environments*

2.2 Fundamentals

- Rayleigh scattering
  At the end of the 19th century, [Rayleigh, 1899] developed a theory of atmospheric scattering caused by the molecules of air. The results of his work formulate and specify the influence of this diffusion to the blue dominant color in the sky and the light polarization levels, follows a λ^{-4} rule.
- Mie scattering
  It is caused by particles whose size is in the same order of magnitude as the light wavelength [Horvath, 2009], such as water droplets, volcanic ash, mist . . . It does not vary significantly with the wavelength and is anisotropic. When there are relatively much larger particles in the atmosphere, the sky whitens, this phenomenon being especially common in the clouds or fog, which we perceive as white or gray.

2.3 Simulated Models

2.3.1 Atmospheric Models

In scientific fields such as: meteorology, climatology, astronomy, remote sensing . . . a lot of relevant models are available. They are based on different mathematical techniques for solving the radiative transfer equation and usually specialized in the study of very specific problems. In fact, they are inadequate or completely oversized for our proposal. Limited to operational solutions in the frequency band of the visible spectrum and taking into account the polarization, without being exhaustive, we can cite the software suite: libRadtran [Mayer and Kylling, 2005], MODTRAN-P [Pust and Shaw, 2011]. All these tools are used to model a majority of atmospheric conditions with high precision: direct solar spectral irradiance, diffusion, atmospheric transmission, and polarization states with input data such as: location, date and time, weather conditions, observation positions, temperature. All these tools have been widely validated by many experiments and observations in particular with the data tables proposed by Coulson [Coulson, 1988] as a reference. All these models produce synthetic skies that correspond to theoretical or ideal conditions.

2.3.2 Participating Media and Sky Models

In 1976, [McCartney, 1976] provides extensive data on diffusion phenomena in different weather conditions, characterized by the turbidity (T) parameter. In 1982, [Blinn, 1982] developed methods for simulating light scattering in volumes. This approach, based on results obtained in other scientific fields allows the computer graphics to benefit of these other sciences. Blinn was the first to apply the radiative transfer theory in application to the synthesis image generation in a participating environment. Many methods are available using analytical skies: [Nishita and Nakamae, 1986], [Tadamura et al., 1993], [Nishita et al., 1993]. More specifically, in the field of computer graphics, in 1999, [Preetham et al., 1999] proposed a model based on turbidity and designed for realistic rendering, that calculates the sky appearance under different conditions taking into account atmospheric perspective. In 2012, [Hosek and Wilkie, 2012] introduced a new and more accurate model improving the Preetham model. In almost all of the existing analytics sky models usable in synthesis imaging, polarization is neglected, with the exception of [Wilkie et al., 2004], to our knowledge.

2.3.3 CIE Models

The CIE models are particularly important as a reference and are very generic, therefore, they do not represent the reality for a given time and place as some simulation scenarios require.

CIE Standard: *Overcast Sky and Clear Sky* [Illumination, 1996] shows two extremes sky conditions, but of course in most cases, the reality is somewhere in between. In 1997, a new luminance distribution model has been proposed by CIE, which ranks all the skies in fifteen categories. In 2001, [Igawa and Nakamura, 2001] proposed to standardize all sky conditions by providing their own luminance distributions. A numerical equation then is introduced with the absolute values of the luminance and distribution of all types of sky, the clear skies and overcast, can be estimated. This sky proposed as an advanced normalized sky is called: *All Sky Model*. By in against all these models, the polarization is completely ignored.

2.4 Captured Models (HDRI)

The principle of high dynamic range imagery (HDRI) exists independently of computer graphics. The use of HDRI in renderer has been proposed [Debevec, 1998] and many publications are available on this subject. The HDR technique captures all the light information of a scene and reproduce all the details contained in both dark areas and bright ones whose dynamics exceeds that of the digital camera sensor.

2.4.1 Acquisitions

The traditional technique of capturing high dynamic images [Stumpfel et al., 2004] is the combination of several acquisition exposure time of the same scene with a Digital Still Camera (DSC), by setting a film sensibility, and a fixed aperture. We adopt this technique for the device that we propose, in addition it is important to note here that the HDRI cannot be viewed as such and are inseparable from the ”Tone Mapper” operators.

2.4.2 Limitations

Although often used in computer graphics, HDR images are insufficient, they are coded in a trichromatic system and provide no information about the polarization.

3. CAPTURE SYSTEM

The polarization of the light of sky itself has been the subject of many theoretical and experimental studies, literature is important: [van de Hulst, 1948], [Chandrasekar, 1950], [Coulson, 1988], [North and Duggin, 1997], [Voss and Liu, 1997]. Several solutions ensuring the capture of a sky with some or all the required features are available. All the existing devices are used in measurement of the sky polarization, or location-based applications. None thought of as capturing light environment system for synthesis of imaging applications. In 1997, [Voss and Liu, 1997] shown a system based on a Charge Coupled Device (CCD) to measure the distribution of the polarized radiance of the light of the sky. In 2006, [Pust and Shaw, 2006] proposed a comprehensive system based on ”Liquid Crystal Variable Retarders” (LCVR). In 2014 [Zhang et al][Zhang et al., 2014] proposed a similar system also based on LCVR, focusing mainly on settings and calibrations LCVR.

3.1 Adopted solution

After an accurate analysis of the information available in the literature, we discarded the solutions using LCVR, for reasons of electronic complexity. So we focused on a device similar to the one proposed in 2010 [Miyazaki et al., 2010], by supplementing it with measurements by spectral bands rather than only trichromatic. We focused on an optical system assembly with motorized filter wheels and slave as shown in figure (3).

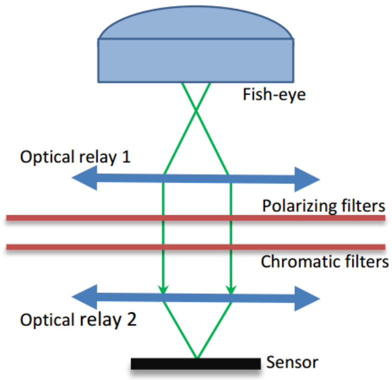

Figure 3: General principle of the proposed capture device

3.2 Hardware

The fish-eye is an objective of the brand ”SUNEX” with a NIKON mount type (F), focal length: 5.6 mm, fixed aperture: F / 5.6, field of view: $185°$, image circle: 14.5 mm. The optical relays have been specially designed with a particular care for ensuring an optimal collimation of the rays before the passage of the filters, as well as their focus on the sensor plane. Filters are carried by two servo motor and wheels, the first wheel comprises seven combinations of polarizing filters and an empty space. The distribution is as follows:

- $0°$ Polarizer: one polarizer at $0°$ orientation
- $45°$ Polarizer: one polarizer at $45°$ orientation
- $90°$ Polarizer: one polarizer at $90°$ orientation
- $0°$ Polarizer $45°$ WP: one polarizer at $0°$ orientation + one wave-plate at $45°$ orientation
- $0°$ Polarizer $135°$ WP: one polarizer at $0°$ orientation + one wave-plate at $135°$ orientation
- $90°$ Polarizer $45°$ WP: one polarizer at $90°$ orientation + one wave-plate at $45°$ orientation
- $90°$ Polarizer $135°$ WP: one polarizer at $90°$ orientation + one wave-plate at $135°$ orientation

The second wheel comprises 16 color filters from 400 to 800 nm with a pitch of 25 nm. The sensor is a CCD (KAI-08670) of the brand ”ON Semiconductor,” a resolution of 3600 (H) x 2400 (V) pixels (APS-H optical format). Connections to an external computer are made via an USB interface, both for the camera control and for the filter wheels, a specific program was carried out accordingly. The GPS coordinates, and the date/hour of use are recorded. An accelerometer measures the potential vertical faults. All these informations are automatically saved in a file for future use.

3.3 Calibrations

The following characteristics are taken into consideration, which describe the influence of the acquisition device on the incident light, by both the optics, the various filters and the sensor.

- The Mueller matrix of the fish-eye in function of the light incidence angle from the optical axis.
- The fish-eye angular distortion, ie the angular distance relative to the zenith angle of incidence, in theory they are equal.
- The sensor radiometric response.
- Light intensity evolution of the sensor as a function of incidence angle.
- Polarizing filters transmission according to the wavelength.
- The response curves of the color filters.

To determine the changes undergone by the incident light through the system, we must determine its Mueller matrix: $M(\theta)$ as a function of incidence angle θ. In the general case, this amounts to determine 16 values: $M_{1,1}(\theta)$, $M_{1,2}(\theta)$, $M_{1,3}(\theta)$ ... In our case, it is not necessary to determine all of the elements. The sensor is only sensitive to the incident light intensity, only the first line ($M_{1,1}(\theta)$, $M_{1,2}(\theta)$, $M_{1,3}(\theta)$, $M_{1,4}(\theta)$) must be determined. Generally the sky light is not circularly polarized [Coulson, 1988], so we do not need to acquire $M_{1,4}(\theta)$, anyway we will do it, at least to check.

4. SPREAD OF LIGHT BEAMS IN A RENDERING ENGINE

Simulation polarization effects in image synthesis has until recently been generally overlooked. One of the main reasons why the polarization has been neglected is the general feeling that the polarization effects have minimal contribution to the appearance of a scene. However, many real-world scenes present significant polarization effects; such as the brightness of the glazing, large water surfaces, discoloration metallic objects and thoughts. All things being equal, the rendering engine will be adapted accordingly:

- Ray Tracing conventional
  - Scalar intensity
  - Scalar reflection and transmission
- Ray Tracing polarized
  - Stokes vectors (4D)
  - Mueller matrices (4x4)

This requires a specific treatment rendering engine level, considering a vector mathematical formulation and not scalar. Very few articles are available.[Wolff and Kurlander, 1990], [Freniere et al., 1999], [Wilkie and Weidlich, 2010]

5. CONCLUSION

To provide an answer to the problem of inconsistency in terms of the nature of the data in traditional synthesis imaging tools, it is essential to have all the information in the same formulation. The light is obviously the key point. We propose a capture system for the light measurement designed for computer graphics to adapt and complement current methods of resolutions of the rendering equation. We hypothesize that the knowledge of this data, operating in a rendering engine, will:

- Improve trick play of colors and aspects.
- Simulate specific effects (absorption, dispersions, diffractions, interference...).
- Anticipate the phenomena of metamerism.
- Improve the match between real environments and simulations in augmented reality applications.

REFERENCES

[Blinn, 1982] Blinn, J. F. (1982). Light reflection functions for simulation of clouds and dusty surfaces. *SIGGRAPH Comput. Graph.*, 16(3):21–29.

[Chandrasekar, 1950] Chandrasekar, S. (1950). *Radiative Transfer*. Oxford Univ. Press.

[Coulson, 1988] Coulson, K. (1988). *Polarization and intensity of light in the atmosphere*. Studies in geophysical optics and remote sensing. A. Deepak Pub.

[Debevec, 1998] Debevec, P. (1998). Rendering synthetic objects into real scenes: Bridging traditional and image-based graphics with global illumination and high dynamic range photography. In *Proceedings of the 25th Annual Conference on Computer Graphics and Interactive Techniques*, SIGGRAPH '98, pages 189–198, New York, NY, USA. ACM.

[Freniere et al., 1999] Freniere, E. R., Gregory, G. G., and Hassler, R. A. (1999). Polarization models for monte carlo ray tracing.

[Horvath, 2009] Horvath, H. (2009). Gustav mie and the scattering and absorption of light by particles: Historic developments and basics. *Journal of Quantitative Spectroscopy and Radiative Transfer*, 110(11):787 – 799. Light Scattering: Mie and More Commemorating 100 years of Mie's 1908 publication.

[Hosek and Wilkie, 2012] Hosek, L. and Wilkie, A. (2012). An analytic model for full spectral sky-dome radiance. *ACM Trans. Graph.*, 31(4):95:1–95:9.

[Igawa and Nakamura, 2001] Igawa, N. and Nakamura, H. (2001). All sky model as a standard sky for the simulation of daylit environment. *Building and Environment*, 36(6):763 – 770. Building and Environmental Performance Simulation:Current State and Future Issues.

[Illumination, 1996] Illumination, I. (1996). *Spatial Distribution of Daylight - CIE Standards Overcast Sky and Clear Sky*. International Commission on Illumination.

[Kajiya, 1986] Kajiya, J. T. (1986). The rendering equation. In *Computer Graphics*, pages 143–150.

[Mayer and Kylling, 2005] Mayer, B. and Kylling, A. (2005). Technical note: The libradtran software package for radiative transfer calculations - description and examples of use. *Atmospheric Chemistry and Physics*, 5(7):1855–1877.

[McCartney, 1976] McCartney, E. J. (1976). *Optics of the atmosphere : scattering by molecules and particles / Earl J. McCartney*. Wiley New York.

[Miyazaki et al., 2010] Miyazaki, D., Ammar, M., Kawakami, R., and Ikeuchi, K. (2010). Estimating sunlight polarization using a fish-eye lens. *Information and Media Technologies*, 5(1):164–176.

[Nishita and Nakamae, 1986] Nishita, T. and Nakamae, E. (1986). Continuous tone representation of three-dimensional objects illuminated by sky light. In *Proceedings of the 13th Annual Conference on Computer Graphics and Interactive Techniques*, SIGGRAPH '86, pages 125–132, New York, NY, USA. ACM.

[Nishita et al., 1993] Nishita, T., Sirai, T., Tadamura, K., and Nakamae, E. (1993). Display of the earth taking into account atmospheric scattering. In *Proceedings of the 20th Annual Conference on Computer Graphics and Interactive Techniques*, SIGGRAPH '93, pages 175–182, New York, NY, USA. ACM.

[North and Duggin, 1997] North, J. A. and Duggin, M. J. (1997). Stokes vector imaging of the polarized sky-dome. *Appl. Opt.*, 36(3):723–730.

[Preetham et al., 1999] Preetham, A. J., Shirley, P., and Smits, B. (1999). A practical analytic model for daylight. In *Proceedings of the 26th Annual Conference on Computer Graphics and Interactive Techniques*, SIGGRAPH '99, pages 91–100, New York, NY, USA. ACM Press/Addison-Wesley Publishing Co.

[Pust and Shaw, 2006] Pust, N. J. and Shaw, J. A. (2006). Dual-field imaging polarimeter using liquid crystal variable retarders. *Appl. Opt.*, 45(22):5470–5478.

[Pust and Shaw, 2011] Pust, N. J. and Shaw, J. A. (2011). Comparison of skylight polarization measurements and modtran-p calculations. *Journal of Applied Remote Sensing*, 5(1):053529–053529–16.

[Rayleigh, 1899] Rayleigh, L. (1899). Xxxiv. on the transmission of light through an atmosphere containing small particles in suspension, and on the origin of the blue of the sky. *Philosophical Magazine Series 5*, 47(287):375–384.

[Stumpfel et al., 2004] Stumpfel, J., Jones, A., Wenger, A., Tchou, C., Hawkins, T., and Debevec, P. (2004). Direct hdr capture of the sun and sky. In *IN AFRIGRAPH*, pages 145–149.

[Tadamura et al., 1993] Tadamura, K., Nakamae, E., Kaneda, K., Baba, M., Yamashita, H., and Nishita, T. (1993). Modeling of skylight and rendering of outdoor scenes. *Computer Graphics Forum*, 12(3):189–200.

[van de Hulst, 1948] van de Hulst, H. (1948). Scattering in a planetary atmosphere. 107:220.

[Voss and Liu, 1997] Voss, K. J. and Liu, Y. (1997). Polarized radiance distribution measurements of skylight. i. system description and characterization. *Appl. Opt.*, 36(24):6083–6094.

[Wilkie et al., 2004] Wilkie, A., Ulbricht, C., Tobler, R. F., Zotti, G., and Purgathofer, W. (2004). An analytical model for skylight polarisation. In *Proceedings of the Fifteenth Eurographics Conference on Rendering Techniques*, EGSR'04, pages 387–397, Aire-la-Ville, Switzerland, Switzerland. Eurographics Association.

[Wilkie and Weidlich, 2010] Wilkie, A. and Weidlich, A. (2010). A standardised polarisation visualisation for images. In *Proceedings of the 26th Spring Conference on Computer Graphics*, SCCG '10, pages 43–50, New York, NY, USA. ACM.

[Wolff and Kurlander, 1990] Wolff, L. B. and Kurlander, D. J. (1990). Ray tracing with polarization parameters. *IEEE Comput. Graph. Appl.*, 10(6):44–55.

[Zhang et al., 2014] Zhang, Y., Zhao, H., Song, P., Shi, S., Xu, W., and Liang, X. (2014). Ground-based full-sky imaging polarimeter based on liquid crystal variable retarders. *Opt. Express*, 22(7):8749–8764.

Development of skin reflectance prediction model using skin data

Kaida XIAO[1,2], Megmeng WANG[3], Tushar CHAUHAN[2], Jingjing YIN [2], Changjun LI[1] , Ronnier LUO[3] and Sophie WUERGER[2]
[1] School of Electronics and Information Engineering, University of Science and Technology Liaoning, China
[2] Department of Psychological Sciences, IPHS, University of Liverpool, UK
[3] School of Design, University of Leeds, UK

ABSTRACT

A skin spectra prediction model was developed to transform camera RGB of skin image to skin spectral reflectance. Skin colour measurement and skin image capture were conducted for 61 Caucasians and 71 Chinese. Rather than using a standard colour chart, skin colour of subset of subjects were used to fit the model. Using the remaining subjects skin colour data, the proposed model were evaluated using CIELAB colour difference between device measured skin spectra and model predicted spectra under three typical illuminations (D65, CWF and A). Results showed that using small numbers of subject skin data, a satifistory colour reprpodcution can be achieved when a linear transform from camera RGB to CIE XYZ tristimulus values was applied.

1. INTRODUCTION

Interest in the spectral reflectance of human skin has been greatly stimulated by the increased need for accurate human skin colour for various industrial and medical applications, including skin colour reproduction for graphic arts, skin pigmentation prediction for cosmetic industry, skin colour measurement for the diagnosis of cutaneous disease and skin colour matching for body and maxillofacial soft tissue prostheses. While CIE Colorimetry is useful for defining skin colour under a particular illumination condition, skin spectral reflectance data contain all the necessary information to predict, model and simulate skin appearance under any illumination condition. Furthermore, skin spectra can also be linked to skin chromophores and therefore provide an opportunity to extract important health-related information using only optical, non-invasive skin measurements.

It has previously been shown that three basis functions obtained by Principal Component Analysis (PCA) are sufficient to accurately describe the spectral reflectance of human skin, thereby allowing the formulation of an algorithm for the estimation of the spectral reflectance of each pixel of an RGB image [1]. However, since human skin is a non-flat multi-layer material with non-uniform colour properties, we found large predictive errors on using a conventional method (i.e. a standard colour chart) for camera colour profiling. This could be caused by material differences between the skin colour chart and the human skin, and lack of uniformity (in both, the colour chart and the subjects' faces).

The aim of this study is to develop a new skin reflectance re-construction model to predict skin reflectance from facial images. Facial images from 132 subjects (71 Chinese and 61 Caucasians) were captured using a Nikon camera system under controlled viewing conditions. The reflectance of their skin from four facial areas was also measured using a Konica Minolta CM 700d spectrophotometer. Rather than using a standard colour chart, a reflectance re-construction model was developed using the skin colours of a subset of the subjects, and evaluated using the remaining subjects. The effect of the selection of training colours was investigated.

2. METHOD

2.1 Skin colour database

A skin colour database was collected at the University of Liverppol in collaboration with the University of Leeds. A Konica Minolta CM-700d spectrophotometer using the CM-SA skin analysis software was used to obtain skin colour measurements and spectral reflectance data in the range 400nm to 700 nm, sampled at intervals of 10nm. During the measurements, a viewing geometry of d/8 (diffuse illumination, 8-degree viewing) was used, with the specular component included and the aperture size set to 3mm. For each subject, skin colour measurements were obtained from four body areas - forehead, cheek, cheekbone and neck. Information on age, gender and ethnicity was also collected.

Subsequently, each subject sat in a Verivide facial image viewing cabinet with a diffused D65 lighting, and their facial image was captured by a Nikon D7000 DSLR camera. Verivide Digieye software was used to manually control camera setting, such as exposure, focus, ISO. Each facial image was saved as a camera RGB image.

To date, skin colours of 132 subjects (61 Caucasians and 71 Chinese) have been obtained. Figure 1 illstrutrates the chromaticities and lightness of skin colours in both the Chinese (solid diamonds) and the Caucausian samples (open squares) in CIELAB colour space [2]. Figure 1(a) shows the measured colours in the CIELAB a*-b* chromaticity diagram, whereas Fig 1(b) shows the same data in a chroma (saturation) - lightness diagram.

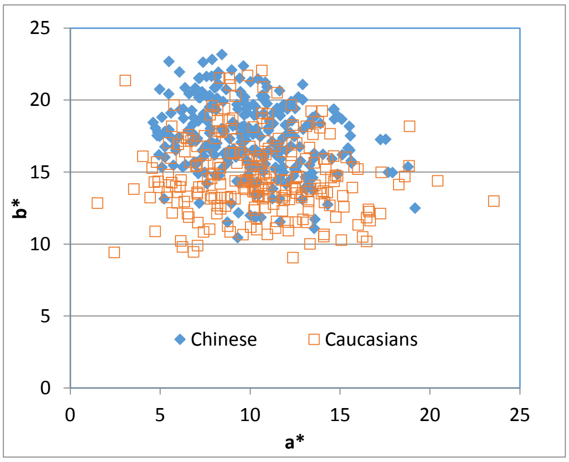

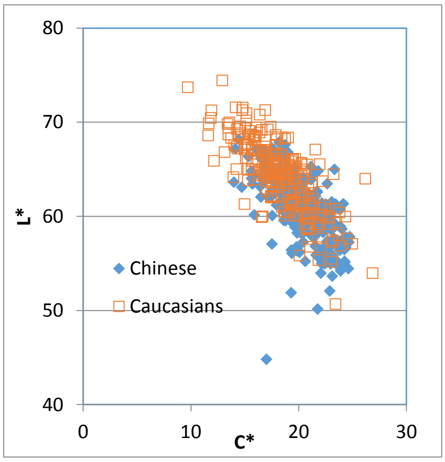

(a) (b)

Figure 1: Colour specifications of the new skin colour database.

2.2 Skin reflectance prediction model

Skin spectral reflectances were predicted from the camera RGB values by a two-step model. In the first step, camera colour characterisation was performed to transform RGB to to CIE XYZ tristimulus values using equation 1. Here, ζ (equation 2) denotes the relative colour density calculated from the CIE XYZ coordinates, ρ_k denotes a vector composed of power-products of device-dependent RGB coordinates up to the k^{th} degree, and M denotes the required transform [3]. Three forms of ρ_k as shown in equations 3, 4 and 5 were considered. These correspond to linear, 2^{nd} and 3^{rd} order regression models respectively. The performance of these regresssion models was compared.

$$\zeta = \rho_k \bullet M \tag{1}$$

$$\zeta = \begin{bmatrix} \log\frac{X}{X_w} & \log\frac{Y}{Yw} & \log\frac{Z}{Zw} \end{bmatrix} \tag{2}$$

$$\rho_1 = [R \quad G \quad B \quad 1] \tag{3}$$

$$\rho_2 = [R \quad G \quad B \quad R^2 \quad G^2 \quad B^2 \quad RG \quad GB \quad BR \quad 1] \tag{4}$$

$$\begin{aligned} &\rho_{31} = [R\ G\ B\ R^2\ G^2\ B^2\ RG\ RB\ GB\ RGB] \\ &\rho_{32} = [R^2G\ R^2B\ G^2R\ G^2B\ B^2R\ B^2G\ R^3\ G^3\ B^3\ 1] \\ &\rho_3 = [\rho_{31}\ \rho_{32}] \end{aligned} \tag{5}$$

In the second step, reflectance spectra were reconstructed, i.e. the spectra were derived from the CIE XYZ tristimulus values. Principle component analysis was performed using our new spectral skin database [4]. Using the basis functions (B) and the ASTM coefficient matrix (M_{ASTM}), spectral reflectance of skin colour can be predicted from the CIE XYZ tristimulus values using equations 6 and 7. M_{ASTM} combines spectral power distribution of the illuminant and the CIE 1931 colour matching function.

$$\beta = (M_{ASTM}B)^{-1}\begin{pmatrix} X \\ Y \\ Z \end{pmatrix} \tag{6}$$

$$r \approx \beta_1 b^{(1)} + \beta_2 b^{(2)} + \beta_3 b^{(3)} = B\beta \tag{7}$$

2.3 Selection of skin colour database

Three skin colour databases (Chinese, Caucasian and combined) were used. For each individual database, a subset of skin colours was used as the training set to develop the model, and the remaining spectra were used as the testing set to evaluate model performance. For the camera characterisation model, there is always a tradeoff between selection of training colours and the accuracy of the model performance. In general, a larger number of training colours provides a better model; but in most applications, a small number of training colours is desireable. To investigate the effect of the number of training colours, sub-sets ranging from 1% to 50% of the total number of samples were used for training. Training colours were chosen randomly from a uniform distribution and 400 iterations were performed.

2.4 Evaluation of the skin spectral prediction model

To evaluate performance of the skin reflectance re-construction, test skin colours were used to predict the skin spectral reflectances for each model. Colour differences for each pair of skin spectral (measured vs. prediced skin spectra) were calculated for three typical Illuminants (D65, A and CWF) using the CIELAB colour difference formular. A median mean was calcuated to represent model performance for all testing colours.

3. RESULTS AND DISCUSSION

For each level of training percentage (i.e. the proportion of skin spectra used as the training set), the goodness of the skin prediction model was evaluated using the remaining set of spectra as a test set. Figure 2 shows the mean colour difference (CIELAB) as a function of the training percentage, for the three different model assumptions: the linear transform (blue solid line), 2nd order polynomial regression (red dashed lines) and 3rd order polynomial regression (green dotted line). Results for the chinese, caucasians and cobmined database are shown in figures a,b and c respectively.

Our main result is that all three models converge to about $3\Delta E^*_{ab}$ preditive error, indicating that, in princple, an acceptable colour reproduction can be achieved [5]. The linear model converges much faster (at about 5%) than the 2nd order and 3rd order models (at about 10% and 20% respectively). The performence is very consistent across different ethnicities ; fastest convergence occurs for the combined skin data set which makes use of both the chinese and the caucasian skin spectra.

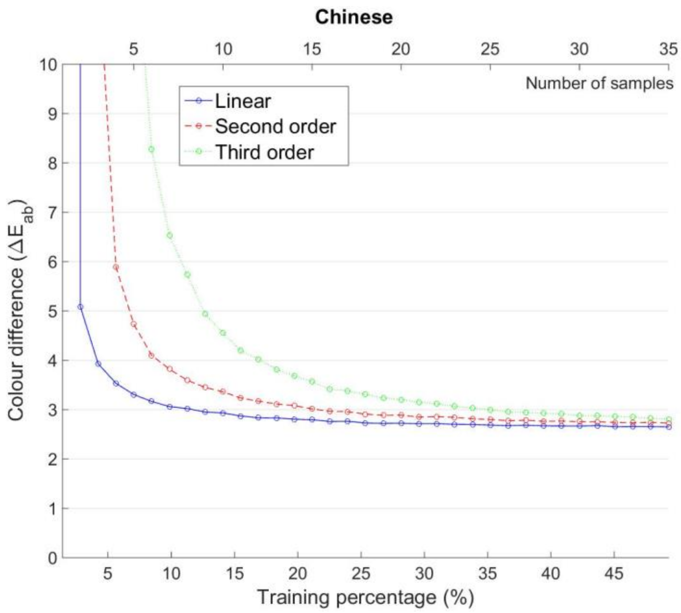

(a)

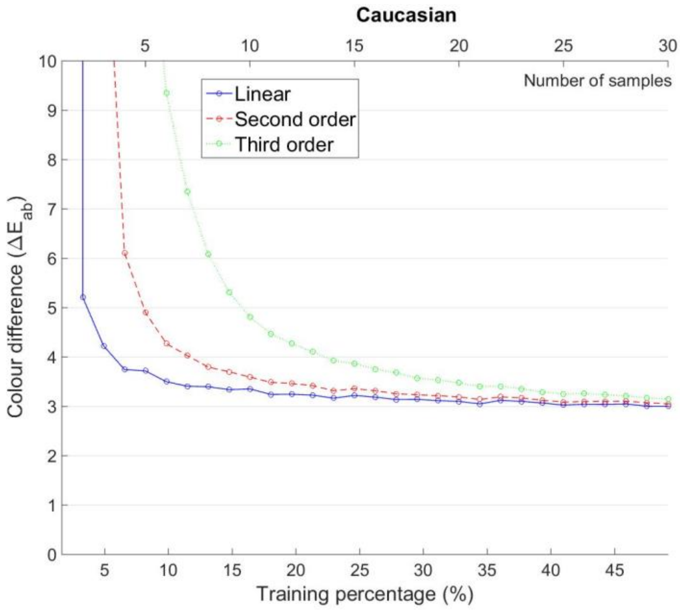

(b)

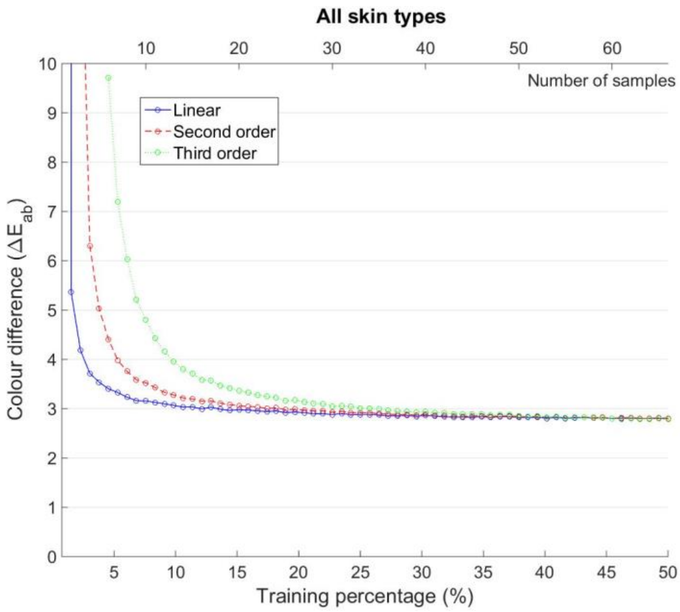

(c)

Figure 2 : Model performence for different training set percentages .

4. CONCLUSIONS

Using a large set of spectral skin data, a skin spectral prediction model was developed and evaluated using different proportions of training and test data. The best performance is achieved by assuming a linear transform from device-dependent camera RGB to device-independent CIE XYZ tristimulus values. Convergence is slighltly faster when skin spectra from both chinese and caucasian ethnic groups together with the linear transform are used.

ACKNOWLEDGEMENTS

This project was partially supported by the EPSRC grant EP/K040057/1, National Natural Science Foundation of China Grant 61178053 and Verivide Limited, UK.

REFERENCES

[1] F. H. Imai, N. Tsumura, H. Haneishi and Y. Miyake 1996, *Principal Component Analysis of Skin Color and Its Application to Colorimetric Color Reproduction on CRT Display and Hardcopy*, J. of Imag. Sci. and Tech., 40, 422-430.

[2] CIE Technical Report, Colorimetry, 3rd ed. Publication 15. Vienna: CIE Central Bureau; 2004.

[3] G. Hong, M.R. Luo, and P.A. Rhodes 2001, *A study of digital camera colorimetric characterization based on polynomial modelling*, Color Research and Application, 26, 1, 76-84.

[4] K Xiao, Z Qin, T Chauhan, C Li, S Wuerger 2014, Principal component analysis for skin reflectance reconstruction, Proceeding of IS&T 22nd Color & Imaging Conference, Boston, USA.

[5] RD Paravina, G Majkic, Del Mar Perez M, S Kiat-amnuay 2009. *Color Difference Thresholds of Maxillo Skin Replications*. Journal of Prosthodontics, 18: 618–625.

Address: Dr.Kaida XIAO, Department of Psychological Science, University of Liverpool,Eleanor Rathbone Building, Bedford Street South, Liverpool, L69 7ZA, UK

E-mails: k.xiao@liverpool.ac.uk, cjliustl@sina.com,s.m.wuerger@liverpool.ac.uk

Comparing CSI and PCA in Amalgamation with JPEG for Spectral Image Compression

Muhammad SAFDAR,[1] Ming Ronnier LUO,[1,2] Xiaoyu LIU[1,3]
[1] State Key Laboratory of Modern Optical Instrumentation, Zhejiang University, Hangzhou, China
[2] School of Design, University of Leeds, Leeds, UK
[3] College of Science, Harbin Engineering University, Harbin, China

ABSTRACT

Continuing our previous research on color image compression, we move towards spectral image compression. This enormous amount of data needs more space to store and more time to transmit. To manage this sheer amount of data, researchers have investigated different techniques so that image quality can be conserved and compressibility can be improved. The principle component analysis (PCA) can be employed to reduce the dimensions of spectral images to achieve high compressibility and performance. Due to processing complexity of PCA, a simple interpolation technique called cubic spline interpolation (CSI) was considered to reduce the dimensionality of spectral domain of spectral images. The CSI and PCA were employed one by one in the spectral domain and were amalgamated with the JPEG, which was employed in spatial domain. Three measures including compression rate (CR), processing time (Tp) and color difference CIEDE2000 were used for performance analysis. Test results showed that for a fixed value of compression rate, CSI based algorithm performed poor in terms of ΔE_{00}, in comparison with PCA, but is still reliable because of small color difference. On the other hand it has lower complexity and is computationally much better as compared to PCA based algorithm, especially for spectral images with large size images.

1. INTRODUCTION

In last two decades, demand of high speed data transfer and high level of data compression have increased and it has been a hot topic of research in the area of signal processing and communications. As images are always a reasonable part of data that is being transmitted or stored, image compression techniques play an important role to compress such data. The visual information is compressed by human visual system and still it provides high quality of image and true color information. This information motivated researchers to compress visual data or images in a way that the compressed information should be reliable and color information should not change. Almost the same rate of compression was achieved in early 90's for the color images.

Concerning multi-spectral or hyper-spectral imaging which have a number of spectral bands, their accessibility is hindered by the communication bandwidth and image size. These limitations may be alleviated by efficient image compression. J. Delcourt et al., proposed an adaptive multi-resolution based multispectral imaging technique substituted with JPEG algorithm (Delcourt 2010). Markas and Reif proposed two coder schemes, one to remove spectral redundancy and another wavelet based coder to remove special redundancy, in the multispectral images (Markas 1993). N. Salamati et al., proposed a coder that puts a threshold on DCT components due to high correlation between visible color RGB and near-infrared components of four channel multispectral images. They also compared their results with JPEG and PCA based compression techniques and found almost the same compression rate (Salamati 2012). Canta and Poggi, proposed address predictive vector quantization based technique for multispectral images (Canta 1997). In this work both spatial and spectral dependencies were exploited. L. Chang used Eigen-based segmentation for multispectral image compression (Chang 2004). M. Cagnazzo, et al., proposed classified transform coding based spectral image compression technique in order to lower the computational complexity (Cagnazzo 2006). Q. Du and J. E. Fowler, amalgamated PCA with JPEG for hyper-spectral image compression (Du 2007).

The joint photographic experts group (JPEG) proposed an algorithm called JPEG which is the most commonly used image compression standard. By selecting a tradeoff between image quality and rate of compression, it can achieve a degree of compression that is desired depending on the application (Skodras 2001). The cubic spline interpolation (CSI) is a best polynomial based interpolation technique that is smooth on the edges due to its strict constraint of continuity at second derivative. It is a computationally simple and robust technique. It can be combined with JPEG for image compression.

In the current work, we continued our previous research on color image compression (Safdar 2014), we have incorporated cubic spline interpolation (CSI) into the JPEG algorithm to compress multispectral images. The CSI was used to compress spectral domain while JPEG was employed to reduce spatial dimensionality. The results of both methods were compared and analyzed on the bases of computational complexity and quality of the image reduced due to compression.

2. METHOD

The principle component analysis (PCA) has widely been used for spectral reduction and spectral de-correlation in multivariate data analysis (Du 2007). PCA practically provides optimal and excellent de-correlation in statistical sense. At the time of training of all PCs, PCA is commonly known as the KarhunenLo`eve transform (KLT), in which case a hyper-spectral image with N spectral bands produces an N×N unitary KLT transform matrix. Because of being data dependent matrix, it must be communicated to the decoder in any KLT-based compression system. Alternatively, corresponding to the P largest eigenvectors, by training in the KLT transform matrix PCA can effectuate dimensionality reduction. The data volume passed to the encoder then has $P < N$, rather than N, spectral components, and the resulting N×P PCA matrix is communicated to the decoder.

The JPEG 1992 standard was used in the current work. The PCA transform matrix and data mean vector were generated in MATLAB; the Kakadu encoder performs the spectral transform (implicitly reducing the spectral dimensionality if $P<N$) and then embeds the mean vector as well as the inverse transform matrix into the JPEG2000 bit-stream. The encoder automatically allocates rate simultaneously across the P PCs to be coded; i.e., post-compression rate-distortion (PCRD) optimization is applied simultaneously to all code blocks in all PCs to optimally truncate the embedded bit stream for each code block. In the reconstruction process, the Kakadu decoder automatically extracts the transform matrix and mean vector and then applies them appropriately after the bit stream has been decoded (Du 2007).

Due to processing complexity of PCA, a simple algorithm is needed to reduce dimensionality of spectral data. The cubic spline interpolation (CSI) was considered here to reduce the dimensionality of spectral domain of multispectral images (MSIs). The CSI was employed in the spectral domain along with the JPEG that was employed in spatial domain. Down sampling stage before the baseline JPEG was skipped to avoid the loss of sheer information in both the algorithms. The performance results of both algorithms were then compared in terms of compressibility, processing complexity and reliability.

3. RESULTS AND DISCUSSION

Four spectral images were selected to test both compression algorithms. Selected four images that include human skin color, natural objects, dark colors and most widely used test color checker chart, are shown below (Figure 1). The images were named as Caucasian male, red rose, tomatoes and Macbeth color checker lab, respectively. Three measures including compression rate (CR), processing time (T_p) and CIEDE2000 were used for performance analysis. The CIEDE2000 is CIE color difference formula which is best correlated with the human visual perception (Luo 2001).

Figure 1: Selected test images

The images were calculated using MATLAB. The compression rate was fixed at 8 and performance of both algorithms was tested in terms of quality of visual performance and computational complexity. The average results of image calculations have been shown (see Table 1). The results in (Table 1) show that ΔE_{00} for PCA based algorithm is much lower as compared to CSI based algorithm. And both algorithms have different performance for different images of same size that is the effect of spatial non-uniformity on the compressibility. The Fig. 2 shows the logarithmic values of processing time of two algorithms at different image sizes. It can be seen from Fig. 2 that increasing the image size processing time of PCA based algorithm increases rapidly, while CSI based algorithm does not add that much computational complexity with the increase of image size.

Being color scientists, we believe that color difference less than 1.0 ΔE_{00} units is tolerable. Test results showed that for a fixed value of compression rate, CSI based algorithm performed poor in terms of ΔE_{00}, in comparison with PCA, but is still reliable because of small color difference with the original image data. On the other hand it has lower complexity and is computationally much better as compared to PCA based algorithm, especially for spectral images with large number of pixels that may take several minutes to process even on a powerful computer. With the increase of image size, complexity of PCA increases rapidly and hence takes more time to process.

Table 1. Summary of the results from spectral compression

Algo. Name	caucassian	Red Rose	Tomotoes	Macbeth
CSI and JPEG	0.5	0.8	0.7	0.6
PCA and JPEG	0.2	0.3	0.2	0.2

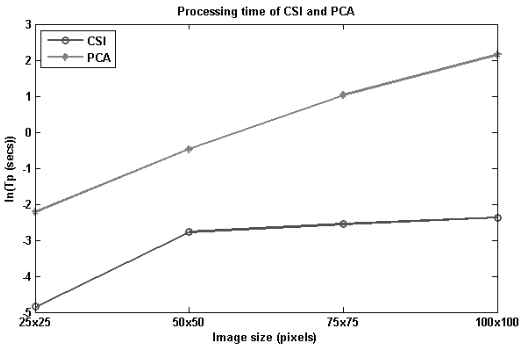

Figure 2: Processing time plotted against image size.

4. CONCLUSIONS

Two different techniques cubic spline interpolation (CSI) and principle component analysis (PCA) were employed one by one in the spectral domain and were amalgamated with the JPEG, which was employed in spatial domain. The performance results of both algorithms were then compared in terms of compressibility and processing complexity. Test results showed that for a fixed value of compression rate, CSI based algorithm performed poor in terms of ΔE_{00}, in comparison with PCA, but is still reliable because of small color difference with the original image data. On the other hand it has lower complexity and is computationally much better as compared to PCA based algorithm, especially for spectral images with large size. With the increase of image size, complexity of PCA increases rapidly and hence needs more time and memory to process.

REFERENCES

Delcourt J. et al. 2010. An Adaptive Multi-resolution Based Multispectral Image Compression Method. Image and Signal Processing. Springer Berlin Heidelberg, 54-62.

Markas T., and Reif J. 1993. Multispectral Image Compression Algorithms. Data Compression Conference 1993. DCC'93. IEEE, 391-400.

Salamati N., Sadeghipoor Z., and Susstrunk S. 2012. Compression of Multispectral Images: Color (RGB) Plus Near-infrared (NIR). Multimedia Signal Processing (MMSP), 2012 IEEE 14th International Workshop on. IEEE, 65-70.
Canta R. G., and Poggi G. 1997. Compression of multispectral images by address-predictive vector quantization. Signal Processing: Image Communication 11.2, 147-159.
Chang L. 2004. Multispectral Image Compression Using Eigenregion-based Segmentation, Pattern Recognition. 37(6) 1233-1243.
Cagnazzo M., et al. 2006. Low-complexity compression of multispectral images based on classified transform coding. Signal Processing: Image Communication 21(10) 850-861.
Du Q., and Fowler J. E. 2007. Hyperspectral Image Compression Using JPEG2000 and Principal Component Analysis, Geoscience and Remote Sensing Letters, IEEE 4(2) 201-205.
Skodras A., Christopoulos C., and Ebrahimi T. 2001. The JPEG 2000 Still Image Compression Standard. Signal Processing Magazine, IEEE 18(5) 36-58.
Safdar M., Luo M. R., and Liu X. Y. 2014. Using Different Color Model to Test JPEG and Modified JPEG. The 22nd Color Imaging Conference, Boston 189-193.
http://www.imageval.com/scene-database/
Luo M. R., Cui G. and Rigg 2001. The Development of CIE 2000 Color Difference Formula: CIEDE2000, Color Res. App., 26(5), 340-350.

Address: Prof. Ming Ronnier Luo, State Key Laboratory of modern optical instrumentation, Zhejiang University, Hangzhou, China
E-mails: msafdar87@zju.edu.cn, m.r.luo@leeds.ac.uk, wangflxy@zju.edu.cn

A system for analyzing color information with the multi-spectral image and its application

Junyan LUO[1], Yoko MIZOKAMI[1], Hirohisa YAGUCHI[1], Yohei TAKARA[2], Fuminori ANDO[2], Takahiro FUJIMORI[2], Naoki NORO[2]
[1] Graduate School of Advanced Integration Science, Chiba University
[2] EBA JAPAN CO., LTD

ABSTRACT

It has become easier to take a multi-spectral image of ordinary scene by newly developed multi-spectral cameras. We have constructed a system which can analyze chromaticity data from spectral data taken by a hyperspectral camera. We verified the accuracy of the data which taken by the hyperspectral camera. Although the accuracy would need to be improved, we were able to obtain chromaticity data useful for color analyses. We compared those color information and spectral distribution to analyze and simulate the color appearance of color deficiency for traffic signals with new LED and old type lamps. Using new XYZ tristimulus values derived from the cone fundamentals of CIE170-2 of red, green and yellow traffic lamps were calculated from the multi-spectral images. We also simulated the different degrees of color deficiency by shifting L or M cone spectral sensitivity. The simulated chromaticity coordinates of dichromat and anomalous trichromat are different from normal color vision for both old and new traffic signal in the case of red and blue signals. It was shown that our system can contribute to study and analyze various environments including color universal design using multi-spectral images and their data.

1. INTRODUCTION

With the development of multi-spectral cameras, it has become easier to take a multi-spectral image. This means that the information from a multi-spectral camera would be a strong tool to obtain and analyze the color information of various scenes. However, it is complicated to extract color information from raw spectral distribution data in a multi-spectral image since a precise color calibration and the calculations of colorimetric values such as chromaticity coordinates are required.

Recently, a portable hyperspectral camera has been developed, and it has become easier to take multi-spectral image data in various outside environments. With multi-spectral image data, we can do lots of things such as analyzing color statistics of natural scene, applying for color appearance models. In this paper, we will introduce a method how to transform a multi-spectral image to the CIE tristimulus values X, Y and Z. Meanwhile, it also can be simulated the color appearance of anomalous trichromat. As we all know, the CIE tristimulus values also can be convert to the CIE (x, y) chromaticity coordinates. With the CIE (x, y) chromaticity diagram, we can analyze the color between normal color vision and anomalous trichromat. This simulation model will be helpful for color universal design.

2. METHOD

We have constructed a system which can analyze color data from spectral data taken by a newly developed hyperspectral camera (NH-7, EBA Japan). The multi-spectral image data contains 1280 by 1024 pixels. Each pixel have the data of a spectral power distribution from 350 nm to 1100 nm. We used the range of visible spctrum between 380 nm and 780 nm.

First, uniformity and the shape of spectral distributions in an image due to the sensitivity of each sensor in the camera were calibrated based on a uniform reference xenon light through an integrating sphere. Then the CIE XYZ were calculated using the obtained precise spectral distributions and the color matching functions. It is also possible to transfer to the other chromaticity values such as the CIELAB and LMS cone stimulus values. With this system, we can analyze color statistics (e.g. average color and color distribution) of an image.

2.1 Model with CIE 1931 color matching function and further

The CIE1931 XYZ was calculated using the obtained precise spectral distributions and the CIE 1931 color-matching functions by following equations.

$$X = \int_{380}^{780} I(\lambda)\,\bar{x}(\lambda)\mathrm{d}\lambda \quad (1)$$

$$Y = \int_{380}^{780} I(\lambda)\,\bar{y}(\lambda)\mathrm{d}\lambda \quad (2)$$

$$Z = \int_{380}^{780} I(\lambda)\,\bar{z}(\lambda)\mathrm{d}\lambda \quad (3)$$

Where $I(\lambda)$ is a spectral power distribution obtatined from calibrated data, and $\bar{x}(\lambda), \bar{y}(\lambda), \bar{z}(\lambda)$ are the CIE1931 color matching functions. With the above Eqs. (1), (2) and (3) , the spectral power distribution can be transform to the CIE tristimulus values X, Y and Z.

$$x = \frac{X}{X+Y+Z} \quad (4)$$

$$y = \frac{Y}{X+Y+Z} \quad (5)$$

With Eqs.(4) and (5), the CIE tristimulus values can be turn to the CIE1931 xy chromaticity coordinates. This method use the color matching function to convert the spectral power distribution to xy chromaticity.

We verified the accuracy of this method using a hyperspectral camera (NH-7). We took the spectral data of a color checker in a booth illuminated by fluorescent lamps simulating D65. Then we calculated the CIE1931 (x, y) chromaticity data of some color in the color checker with the spectral data. Meanwhile, we also meansured the CIE1931 (x, y) chromaticity data of same color as above in the color checker with a spectroradiometer (PR-680, Photo Research).

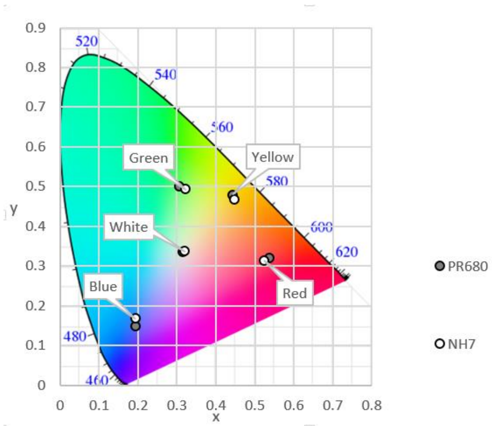

Figure 1: CIE1931 xy chromaticity diagram of 5 colors in color checker

Figure 1 shows the data of 5 colors which contains white, blue, green, yellow and red. Comparing the 2 sets of (x, y) chromaticity data, white shows good consistency. Other colors show small differencies. The data which taken by the multi-spectral camera (NH7) would be sufficient for general use, but we may need to improve the accuracy of the system further.

The advantage of our system is that we can obtain the chromaticity values of varoius color spaces, even which cannot calculate without spectral distribution of stimuli or can not convert each other based on their chromaticity values, by replacing the part of the color matching function. For example, the new color maching function to be proposed by CIE (http://www.cvrl.org/) which transformed from the CIE (2006) LMS functions (CIE 170-1:2006) requires a spectral distribution of stimuli for its calculation. We use this color maching function for the calculation of the simulation model of anomalous trichromat in the next section.

2.2 Simulation Model of color appearance for anomalous trichromat

As an example of application, we compared those color information and spectral distribution to analyze and simulate the color appearance of normal color vision, dichromat and anomalous trichromat. In the this method, we use the spectral image data and the second stage of color vision model data to simulate the color appearance of the anomalous trichromat. To develop our simulation, we make three assumptions (Yaguchi, 2013). First, we assume that anomalous trichromats posses green-shifted or red-shifted photopigments instead of one of the normal L or M-photopigments. The degree of anomalousness is presented by amount of shift. Secondly, luminance and the red/green, yellow/blue opponent color channels are defined by the linear combination of L, M, and S cone stimulus values based on the CIE cone fundamentals (CIE, 2006). Final assumption is that the equal energy white look white for all observers including anomalous trichromats.

As a result, the spectral sensitivity functions of the luminance channel, the red/green- and the yellow/blue-opponent color channels are derived with Eqs. (6), (7) and (8), where L_{EEW} and M_{EEW} are stimulus values of the equal energy white for normal trichromats, and L'_{EEW} and M'_{EEW} are those for anomalous trichromats.

$$\overline{y'}(\lambda) = 0.6899\left(\frac{L_{EEW}}{L'_{EEW}}\right)\overline{l'}(\lambda) + 0.3483\left(\frac{M_{EEW}}{M'_{EEW}}\right)\overline{m'}(\lambda) \quad (6)$$

$$\overline{r/g'}(\lambda) = 0.8344\left(\frac{L_{EEW}}{L'_{EEW}}\right)\overline{l'}(\lambda) - 1.0260\left(\frac{M_{EEW}}{M'_{EEW}}\right)\overline{m'}(\lambda) \quad (7)$$

$$\overline{y/b'}(\lambda) = 0.8344\left(\frac{L_{EEW}}{L'_{EEW}}\right)\overline{l'}(\lambda) - 1.0260\left(\frac{M_{EEW}}{M'_{EEW}}\right)\overline{m'}(\lambda) - \overline{s'}(\lambda) \quad (8)$$

Where $\overline{l'}(\lambda)$, $\overline{m'}(\lambda)$ and $\overline{s'}(\lambda)$ are the spectral sensitivity functions of L-, M-, and S-cone, respectively for the anomalous trichromat. The luminance, Y' and the stimulus values of red/green- and the yellow/blue-opponent colour channels, $C'_{r/g}$ and $C'_{y/b}$ for the anomalous trichromats are calculated with Eqs. (9), (10) and (11).

$$Y' = \int P(\lambda)\overline{y'}(\lambda)d\lambda \quad (9)$$

$$C'_{r/g} = \int P(\lambda)\overline{r/g'}(\lambda)d\lambda \quad (10)$$

$$C'_{y/b} = \int P(\lambda)\overline{y/b'}(\lambda)d\lambda \quad (11)$$

In the above equations, $P(\lambda)$ is the spectral radiance of the stimulus.

In order to simulate the appearance of the image for anomalous trichromats for color normal observers, the luminance and the stimulus values of the opponent color channels should be converted to the XYZ tristimulus values for normal observers. Using new XYZ tristimulus values derived from the cone fundamentals of CIE170-212, notified with X_F, Y_F, Z_F called the fundamental tristimus values are transformed from the luminance and the stimulus values of the opponent-color channels with Eqs. (12), (13) and (14).

$$X_F = Y' + 1.6541C'_{r/g} - 0.3675C'_{y/b} \tag{12}$$

$$Y_F = Y' \tag{13}$$

$$Z_F = Y' - 1.9349C'_{y/b} \tag{14}$$

Finally, we can use Eqs.(4), (5), transfer equation from X_F, Y_F, Z_F to (x_F, y_F) chromaticity.

3. MEASUREMENT

First, we used the hyperspectral camera (NH-7) to take multi-spectral image data of LED signal lamps and old type signal lamps placed in a street nearby the campus of Chiba University. After calibration we obtained their spectral power distributions. Using simulation model of color appearance for anomalous trichromatic as we mentioned in the method part, we can convert the data from spectral power distribution to the (x_F, y_F) chromaticity coordinates.

4. RESULTS AND DISCUSSION

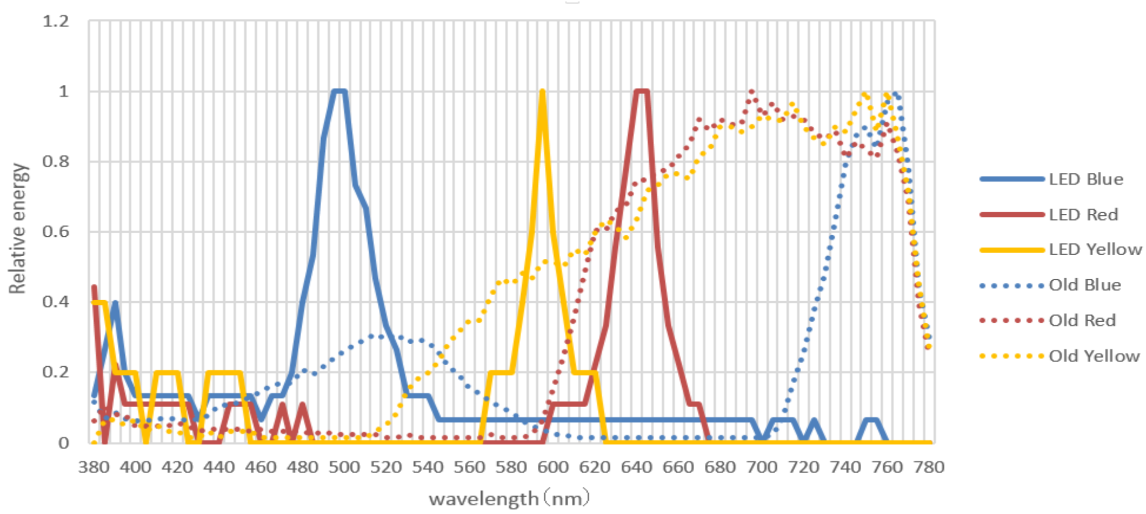

Figure 2: relative energy of LED/old signal lamp

Figure 2 show the reslut of the relative energy of LED/old signal lamp.

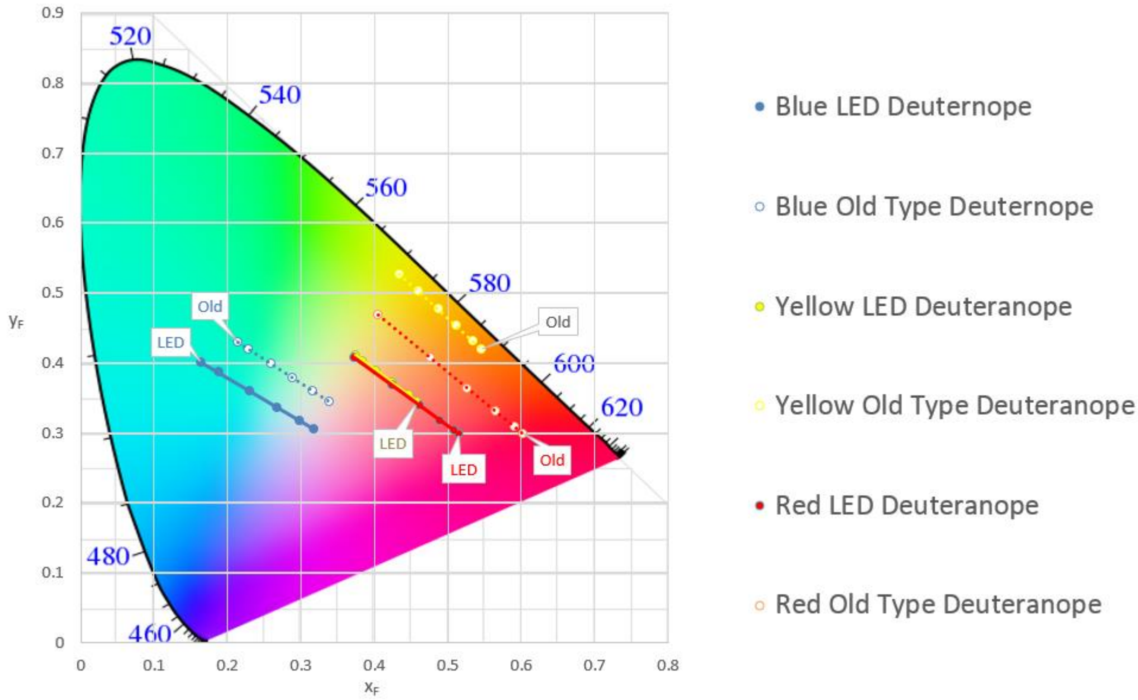

Figure 3: color simulation of Deuternope

Figure 3 shows the simulated color appearnce of deuteranope on the (x_F, y_F) chromaticity diagram. In this diagram, the point with a label is the start point which indicates the (x_F, y_F) chromaticity coordinates of normal color vision. End point is the chromaticity coordinates of the simulated color appeance of deuteranope. Points between start point and end point present deuteranope (M-100/300/500/700). "M-100/300/500/700" means that the strength of deficiency where the peak sensitivity of M-cone shits 100/300/500/700 cm^{-1} in wavenumber towards red. The locus of the red signal of LED lamp and the yellow signal of LED lamp overlap each other. It implys that deuteranope could confuse red and yellow signal of LED lamp.

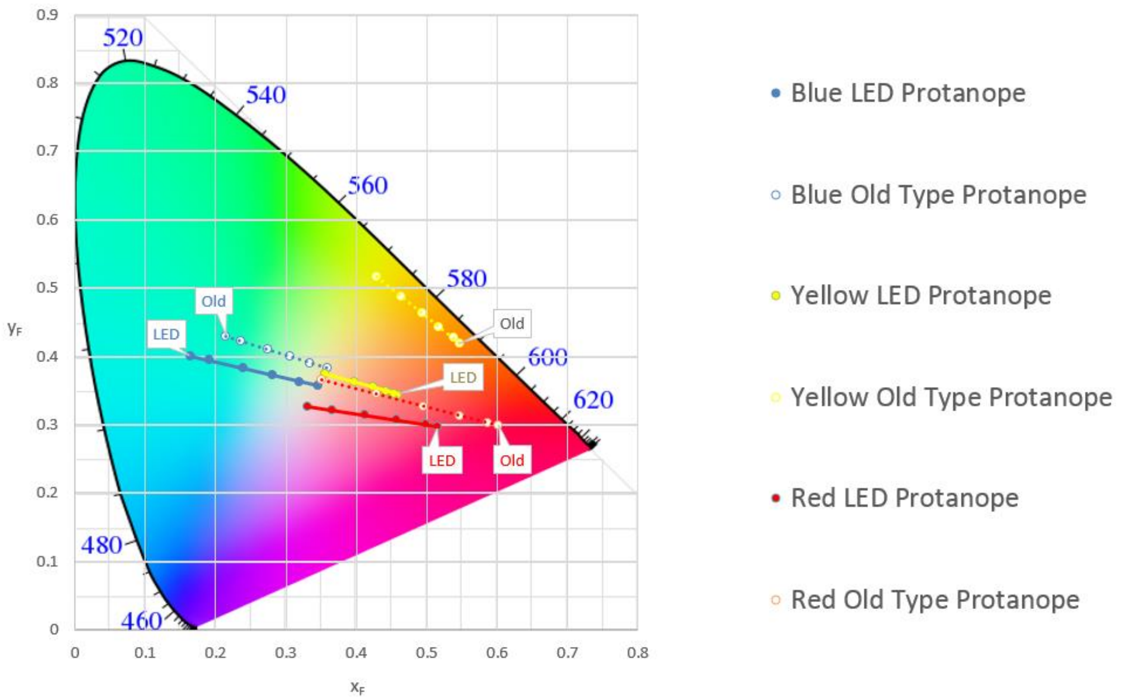

Figure 4: color simulation of Deuternope

Figure 4 shows a (x_F, y_F) chromaticity diagram of the simulated color appearance of protanope. In this diagram, the point with a label is the start point which means the (x_F, y_F) chromaticity of normal color vision. End point the simulated color appeance of protanope. Points between start point and end point present protanope (L-100/ L-300/ L-500/ L-700). "L-100/300/500/700" means the strength of deficiency where the peak sensitivity of L-cone shits 100/300/500/700 cm^{-1} in wavenumber towards green. The simulated color appeance of protanope for all signals, except for that of the old type/LED yellow signal, close each other. It implys that protanope could see the blue, red signal of LED signal lamp as similar color, and the blue and red of old signal lamp as similar color.

4. CONCLUSIONS

We constructed a system which can analyze color data from spectral data taken by a multi-spectral camera. First, uniformity of intensities and the shape of spectral distributions in an image were calibrated based on a uniform reference light. Then the CIE1931 XYZ was calculated using the obtained precise spectral distributions and the color-matching function. Although the accuracy would need to be improved, we were able to obtain chromaticity data useful for color analyses. We compared those color information and spectral distribution to analyze and simulate the color appearance of normal color vision, dichromat and anomalous trichromat based on a simulation model of color appearance for anomalous trichromat. With this model and the multi-spectral image data, we simulated the color appeance of LED and old signal lamp for the deuteranope and protanope. Our simulation suggests that anomalous trichromat could confuse some colors of traffic signal lamps. Since the multi-spectral data contains wavelength information, we can simulate other color appearance of various scenes and images not only for the abnormal color vision but also for a color vision with any individual color matching function.

REFERENCES

H. Yaguchi, J. Luo, and Y. Mizokami, Computerized simulation of color appearance for anomalous trichromats using the multispectral image, The 22nd Symposium of the International Colour Vision Society (2013 July, Winchester)

CIE 170-1:2006 Fundamental Chromaticity Diagram with Physiological Axes - Part 1

CIE 170-2: Fundamental Chromaticity Diagram with Physiological Axes - Part 2 (to be published, http://cvrl.ioo.ucl.ac.uk)

Address: Juanyn Luo, Graduate School of Advanced Integration Science, Chiba University, 1-33, Yayoi-cho, Inage-ku, Chiba-shi, Chiba, 263-8522 JAPAN
E-mails: aeta4997@chiba-u.jp, mizokami@faculty.chiba-u.jp, yaguchi@faculty.chiba-u.jp, takara@ebajapan.jp, ando@ebajapan.jp, ujimori@ebajapan.jp, noro@ebajapan.jp

Proceedings

MCS Poster Papers

Quality comparison of multispectral imaging systems based on real experimental data

Raju SHRESTHA, Jon Y. HARDEBERG
The Norwegian Colour and Visual Computing Laboratory, Gjøvik University College

ABSTRACT

In this paper, we evaluate and compare the quality of three fast and practical multispectral imaging systems we proposed along with a conventional filter wheel based system. The four systems being compared are a single shot 6-band stereo camera based system, two (a 6-band and a 9-band) RGB camera and LED illumination based systems, and a 6-band filter wheel based system, for which we used a commercial SpectroCam UV-VIS system from PixelTeQ. The systems are evaluated and compared based on spectral as well as colorimetric accuracies produced by the prototype systems. Mean metric values are most commonly used to compare different multispectral imaging systems. In this paper, we propose a cumulative distribution function based measure for a more effective and consistent comparison of the systems. We believe that the quality comparison framework and the methodology provided in this paper would be useful in identifying a most appropriate technique or system for a given application.

1. INTRODUCTION

Multispectral imaging (MSI) acquires images of a scene in a limited number of narrow or somewhat wider spectral bands. The spectral reflectances of the scene are then obtained from the sensor responses using a spectral estimation method. MSI provides a simpler, faster, and cheaper solution to spectral imaging compared to hyperspectral imaging. Many different types of multispectral imaging techniques and systems have been proposed in the literature. In a conventional filter-based multispectral imaging system, either a set of traditional optical filters in a filter wheel (Martinez 1991), or a tunable filter (Hardeberg et al. 2002, Nascimento et al. 2002) in front of a monochrome camera is employed, and images of a scene are acquired with each of these filters in a sequence. Use of RGB cameras increases the acquisition speed by a factor of three (Valero et al. 2007, Yamaguchi et al. 2008). Filter array based multispectral imaging (FAMSI) (Brauers and Aach 2006, Miao and Qi 2006, Lapray et al. 2014), which is based on the extension of filter array from 3-bands in the Bayer pattern to *n* bands provides a single-shot solution, however, at the cost of spatial details because of a demosaicing step it requires for bands separation. Another promising technique of multispectral imaging is based on multiplexed LED illumination (LEDMSI) (Park et al. 2007, Parmar et al. 2012, Shrestha et al. 2012).

Even though many different multispectral imaging systems have been proposed in the literature before, the existing state of the art multispectral imaging systems were still mostly slow, complex, and expensive. Because of this their acceptance and use has been limited. We proposed several fast, practical, and inexpensive solutions such as a single-shot 6-band stereo camera based (StereoMSI) system (Shrestha et al. 2011), a single-shot filter array based (FAMSI) system (Shrestha and Hardeberg 2013), and fast LED illumination based (LEDMSI) systems using RGB cameras (RGB-LEDMSI) (Shrestha and Hardeberg 2013).

In order to identify a suitable system to be used for a given application, it is important to evaluate and compare the performance and quality of different systems. In Shrestha and Hardeberg (2014), we evaluated and compared the three major different types of fast and practical multispectral imaging techniques: StereoMSI, FAMSI, and LEDMSI systems, along with a conventional filter wheel (FWMSI) and a liquid crystal tunable filter (LCTFMSI) based systems as well as a trichromatic color camera, both qualitatively and quantitatively, using simulated systems. Quantitative evaluation was done based on spectral and colorimetric accuracies from spectral reflectance images estimated from the multi-band images acquired with the systems. In this paper, we validate the evaluation and comparison of different MSI systems through real-world experimentation using prototype systems. The systems are evaluated and compared both spectrally and colorimetrically using the root mean square (RMS) and CIE ΔE^*_{ab} metrics respectively. For a more effective and consistent comparison of the systems, we propose a new cumulative distribution function (CDF) based measure.

In Section 2, we describe the four multispectral imaging systems used in the experiments. Section 3 presents the new 95%CDF measure. We then present experimental results in Section 4 and discuss the results in Section 5. We finally conclude the paper in Section 6.

2. MULTISPECTRAL IMAGING SYSTEMS USED

We built the three prototype systems: a StereoMSI, a 6-band RGB-LEDMSI, and a 9-band RGB-LEDMSI. For a FWMSI system, we used a commercial system. The four systems and their setups are briefly described here.

- **6-band StereoMSI system**: This is a single-shot MSI system built with a Fujifilm FinePix REAL 3D W1 stereo camera, and a pair of optimal filters placed in front of the two lenses of the camera. The two filters used are XF2021 and XF2030, selected from a set of 265 filters from Omega Optical Inc. The system acquires a 6-band image of a scene in a single-shot. More details of the system can found in Shrestha et al. (2011).
- **6-band RGB-LEDMSI system**: This system is built with a Nikon D600 RGB camera, and six LEDs from JUST Normlicht (2014)'s LED ColorControl light booth. This is considered as a constrained LEDMSI case where the number of LEDs is limited to six. A 6-band image is acquired in two exposures (or shots) under two different LED combinations. Each LED combination consists of three different LEDs whose peak wavelengths lie in the three different regions (red, green, and blue) of the camera sensitivities. For the details on the spectral sensitivities of the Nikon D600 camera, the six LEDs and their spectral power distributions (SPDs) we refer to the paper Shrestha and Hardeberg (2014). Optimal LED combinations for each exposure is selected using the LED selection method we proposed in Shrestha and Hardeberg (2013). The method picked 1-3-5 and 2-4-6 as the two optimal LED combinations for the two exposures.
- **9-band RGB-LEDMSI system**: This system is also built with the same Nikon D600 camera as in the 6-band system, but using nine optimal LEDs selected from the 22 LEDs available in an iQ-LED module from Image Engineering (2014). A 9-band image is acquired in three exposures under three different LED combinations. In this case, the LED selection method picked 1-6-11, 2-8-14, and 4-7-10 as the three optimal LED

combinations for the three exposures. SPDs of the LEDs can be found in Shrestha and Hardeberg (2014).

- **6-band FWMSI system**: A commercial SpectroCam UV-VIS system from PixelTeQ (2014), with six filters in its filter wheel is used for this. The six filters used are the band pass filters with *peakwavelength*(nm)_FWHM (Full Width Half Maximum) of 425_100, 475_100, 505_50, 550_100, 615_100 and 650_100. For an improved signal-to-noise ratio (SNR), we used appropriate integration times with different filters that result in higher camera signals but without any saturated pixel. We set the exposure times to 15, 10, 30, 15, 15, and 20 milliseconds for the six filters respectively. The gain value was set to one. For the spectral sensitivity of the SpectroCam UV-VIS camera and the spectral transmittances of the six filters used, we again refer to the paper Shrestha and Hardeberg (2014).

3. CDF BASED MEASURE FOR MSI SYSTEMS COMPARISON

There are many different types of quality metrics proposed to evaluate the performance and quality of a multispectral imaging system. The root mean square (RMS) error and CIE ΔE^*_{ab} are widely used spectral and colorimetric metrics respectively. Mean of these metric values are usually used to compare two MSI systems. In this paper, we propose a cumulative distribution function (CDF) based measure as an alternative, for a more effective and consistent comparison results.

CDF describes the probability that a real-valued random variable x with a given probability distribution will be found to have a value less than or equal to a (Everitt 2006), and it is expressed as $\mathrm{CDF}(x,a) = \mathrm{P}(x \le a)$, where $\mathrm{P}(x \le a)$ denotes the probability of x to be less than or equal to a. In our context, we can assume any estimation error such as RMS and ΔE^*_{ab} in each pixel of a scene as a random variable. CDF can be plotted with an evaluation metric value along the *x*-axis and the CDF (or percentage count) along the *y*-axis as illustrated in Figure 1.

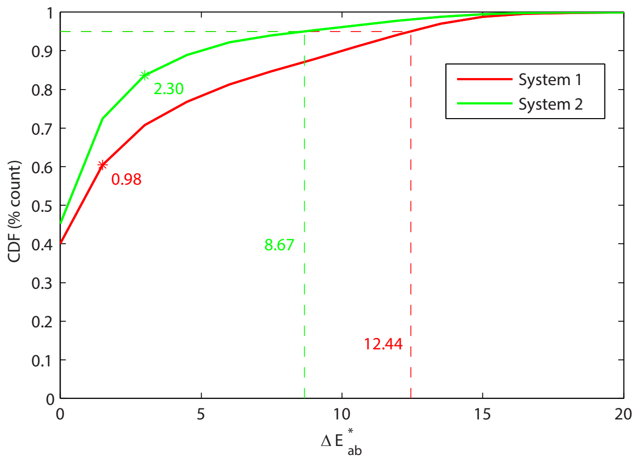

Figure 1: 95%CDF vs. mean metric values

In the illustration, two systems have mean ΔE^*_{ab} values of 0.978 and 2.295, indicating that System 1 is better than System 2. However, if we look at the CDF curves, we see that 95% of pixels produce ΔE^*_{ab} of 12.44 or less with the System 1, while the same number of pixels produces ΔE^*_{ab} of 8.67 or less with the System 2. In this aspect, the latter is much better than the former. Since CDF measure is more practical than the mean values, we propose this as a new measure for the comparison of any two MSI systems. By setting a CDF percentage count required to τ%, we can determine the corresponding metric value from the CDF, which we call it as τ%CDF. Since 95% is considered as a reasonably good value in statistics, we use 95%CDF in our experiments.

4. EXPERIMENTAL RESULTS

Multi-band images of a Macbeth ColorChecker DC (MCCDC) and a classic (MCC) are acquired with all the four systems. Spectral reflectances of the 24 MCC patches are estimated from the multi-band images, using Wiener spectral estimation method (Haneishi et al. 2000). For this, sixty-two patches from the MCCDC, selected based on the significant target selection method proposed by Hardeberg et al. (1998) are used for calibrating the system. Based on the estimated spectral reflectances from the four systems, they are evaluated and compared using both the mean and 95%CDF values corresponding to the spectral (RMS) and colorimetric (ΔE^*_{ab}) metrics.

Statistics of spectral and colorimetric estimation errors is given in Table 1. Figure 2 shows standard error plots with the bounds of the 95% confidence intervals, which shows statistical significance of the RMS and ΔE^*_{ab} estimations. Histograms and CDF plots for the RMS and ΔE^*_{ab} errors are given in Figure 3. From the table and the CDF plots, we see that the 6-band RGB-LEDMSI performs the best both spectrally and colorimetrically, with 95%CDF for RMS and ΔE^*_{ab} values of 0.03 and 1.95 respectively. The 9-band RGB-LEDMSI comes next, then the 6-band FWMSI system, and lastly the StereoMSI system. The error plots show the similar performance trends both in terms of the spectral and colorimetric estimations.

Table 1. Statistics of the spectral and color estimation errors produced by the four MSI systems.

MSI System	RMS				ΔE^*_{ab}			
	Max.	Mean	Std.	95% CDF	Max.	Mean	Std.	95% CDF
6-band FWMSI	0.067	0.030	0.017	0.059	6.100	3.041	1.280	5.400
6-band StereoMSI	0.112	0.036	0.028	0.080	9.609	3.769	2.796	7.900
6-band RGB-LEDMSI (JUST LED)	0.037	0.018	0.007	0.029	3.021	1.130	0.691	1.950
9-band RGB-LEDMSI (iQ-LED)	0.064	0.024	0.011	0.035	5.607	2.344	1.108	3.900

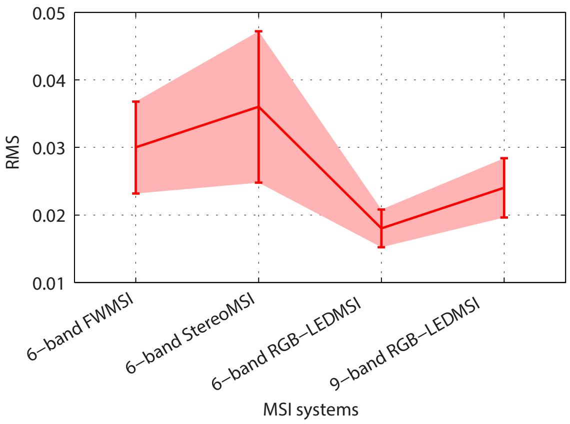

(a) RMS

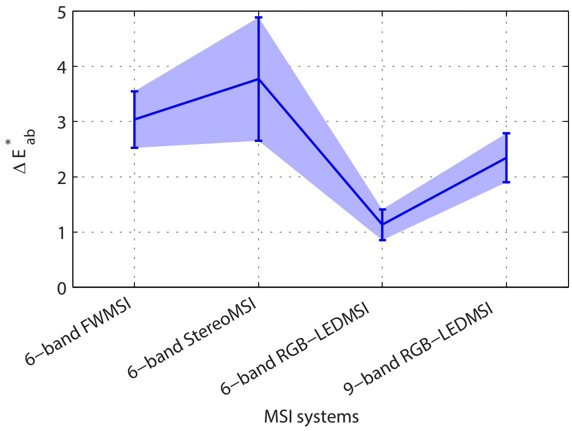

(b) ΔE^*_{ab}

Figure 2: Standard error plots for the four prototype MSI systems.

5. DISCUSSION

Standard error plots showed that the performance of the single-shot 6-band StereoMSI system is comparable to the traditional 6-band FWMSI system, indicating its feasibility. It is to be noted here that the stereo camera used had a minimum control on the internal processing in the imaging workflow, such as white balancing, demosaicing, etc. We can anticipate significantly improved results from a fully controllable camera.

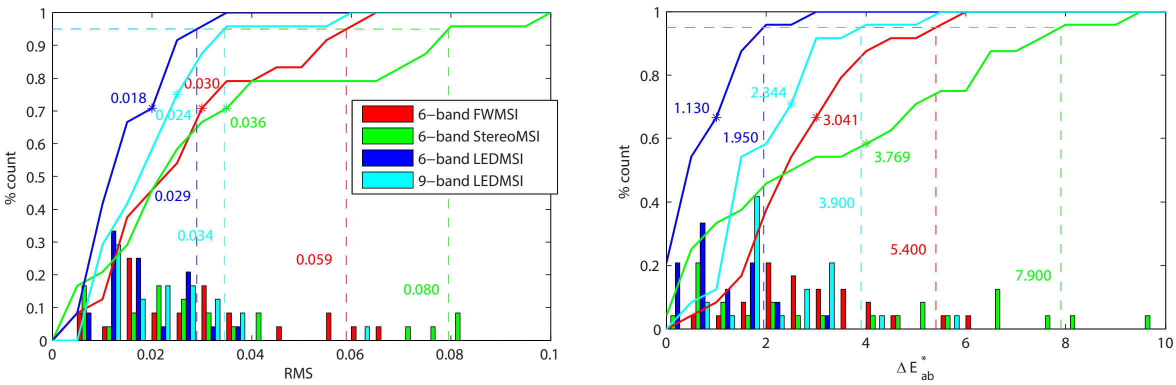

(a) *RMS* (b) ΔE^*_{ab}

Figure 3: Histograms and CDFs produced by the four MSI systems for the MCC target. Mean values are shown and marked with ''. 95%CDF lines (vertical dotted) and values are also shown.*

The 6-band RGB-LEDMSI has shown to perform better than the other three systems both spectrally and colorimetrically. The decreased performance of the 9-band RGB-LEDMSI system indicates that just increasing the number of LEDs (or bands) does not always lead to an improved performance. This is in line with the conclusion of our paper Shrestha and Hardeberg (2014), where we studied various factors influencing the performance of a LEDMSI system. Influence of noise increases with the increase in the number of bands. Moreover, increase in the number of bands does not always lead to capturing of significantly new information; and in such case, we cannot anticipate a better performance. This depends on the choice of LEDs. If we had a freedom of choosing from a large number of LEDs, and in the ideal case, with equal intensities uniformly spreading along the spectrum, we can anticipate some improvement in the results. Looking at the effective channel sensitivities of the two LEDMSI systems, we find much overlaps in the channels in the 9-band RGB-LEDMSI systems; while in the case of the 6-band RGB-LEDMSI system, the channels were reasonably well separated. Because of this, even though having three more bands, the 9-band system may not capture much new information, but suffers from more noise influence. Moreover, the illumination levels of the JUST LEDs were quite high, while that of the iQ-LED modules were weak and we had to increase integration times by increasing the camera shutter speed. This seemed to introduce more noise in the camera responses, and this might have had an effect on the performance of the system. By addressing these issues, performance of the 9-band RGB-LEDMSI system could probably be improved.

6. CONCLUSION

The proposed 95%CDF measure has shown to be an effective and consistent alternative to the most commonly used mean metric values for comparing any two multispectral imaging systems. The experimental results from the quality evaluation and comparison of the four MSI systems showed that the 6-band RGB-LEDMSI system performed the best producing the lowest 95%CDF values for both the RMS and ΔE^*_{ab}. StereoMSI provides a single-shot solution with the quality comparable to a classic 6-band FWMSI system. Increasing the number of bands does not always produce better results, but requires dealing with the other influencing factors such as noise, parameter selection etc. appropriately.

REFERENCES

Brauers, J. and T. Aach 2006. A Color Filter Array Based Multispectral Camera. In *The 12th Workshop on Farbbildverarbeitung*.

Everitt, B. S. 2006. *The Cambridge Dictionary of Statistics*, Cambridge University Press.

Haneishi, H., T. Hasegawa, A. Hosoi, Y. Yokoyama, N. Tsumura and Y. Miyake 2000. "System Design for Accurately Estimating the Spectral Reflectance of Art Paintings." *Applied Optics* **39(35)**: 6621-6632.

Hardeberg, J. Y., H. Brettel and F. Schmitt 1998. Spectral Characterisation of Electronic Cameras. In *Electronic Imaging: Processing, Printing, and Publishing in Color* **3409:** 100-109.

Hardeberg, J. Y., F. Schmitt and H. Brettel 2002. "Multispectral Color Image Capture Using a Liquid Crystal Tunable Filter." *Optical Engineering* **41**(10): 2532-2548.

Image Engineering. 2014. "iQ-LED Technology." Accessed: February, 2015, Available online, http://image-engineering-shop.de/shop/article_iQ-LED/IQ-LED.html.

JUST Normlicht. 2014. "Just LED ColorControl." Accessed: February, 2015, Available online, http://www.justnormlicht.com/just-led-technology.html.

Lapray, P. J., X. Wang, T. Jean-Baptiste and P. Gouton 2014. "Multispectral Filter Arrays: Recent Advances and Practical Implementation." *Sensors* **14**(11): 21626-21659.

Martinez, K. 1991. "High Resolution Digital Imaging of Paintings. The Vasari Project." *Microcomputers for Information Management* **8**(4): 277–283.

Miao, L. and H. Qi 2006. "The Design and Evaluation of a Generic Method for Generating Mosaicked Multispectral Filter Arrays." *IEEE TIP* **15**(9): 2780-2791.

Nascimento, S. M. C., F. P. Ferreira and D. H. Foster 2002. "Statistics of Spatial Cone-Excitation Ratios in Natural Scenes." *Journal of Optical Society of America A* **19**(8): 1484-1490.

Park, J. I., M. H. Lee, M. D. Grossberg and S. K. Nayar 2007. Multispectral Imaging Using Multiplexed Illumination. In *IEEE International Conference on Computer Vision* 1-8.

Parmar, M., S. Lansel and J. Farrell 2012. An LED-based Lighting System for Acquiring Multispectral Scenes. In *Digital Photography VIII* **82990:** 82990P.

PixelTeQ. 2014. "PixelTeQ SpectroCam." Accessed: February, 2015, Available online, http://www.pixelteq.com/product/spectrocam-uv/.

Shrestha, R. and J. Y. Hardeberg 2013. CFA Based Simultaneous Multispectral Imaging and Illuminant Estimation. *Computational Color Imaging*, Springer. **7786:** 158-170.

Shrestha, R. and J. Y. Hardeberg 2013. Multispectral Imaging Using LED Illumination and an RGB Camera. In *The 21st Color and Imaging Conference (CIC)*, IS&T. 8-13.

Shrestha, R. and J. Y. Hardeberg 2014. Evaluation and Comparison of Multispectral Imaging Systems. In *The 22nd Color and Imaging Conference (CIC)*, IS&T. 107-112.

Shrestha, R. and J. Y. Hardeberg 2014. How are LED Illumination based Multispectral Imaging Systems Influenced by Different Factors? *Image & Signal Processing*, Springer. **8509:**61-71.

Shrestha, R., J. Y. Hardeberg and C. Boust 2012. LED Based Multispectral Film Scanner for Accurate Color Imaging. In *The 8th International Conference on Signal Image Technology and Internet Based Systems (SITIS)*, IEEE Proceedings. 811-817.

Shrestha, R., A. Mansouri and J. Y. Hardeberg 2011. "Multispectral Imaging Using a Stereo Camera: Concept, Design and Assessment." *EURASIP Journal on Advances in Signal Processing* **2011**(1): 57-57.

Valero, E. M., J. L. Nieves, S. M. C. Nascimento, K. Amano and D. H. Foster 2007. "Recovering Spectral Data from Natural Scenes with an RGB Digital Camera." *Color Research & Application* **32**(5): 352-360.

Yamaguchi, M., H. Haneishi and N. Ohyama 2008. "Beyond Red-Green-Blue (RGB): Spectrum-based Color Imaging Technology." *Journal of Imaging Science and Technology* **52(1)**: 1-15.

Address: Gjøvik University College, P.O.Box 191, N- 2802 Gjøvik, Norway
E-mails: raju.shrestha@hig.no, jon.hardeberg@hig.no

LED-based gonio-hyperspectral system for the analysis of automotive paintings

Francisco J. BURGOS,[1] Meritxell VILASECA,[1] Esther PERALES,[2] Elísabet CHORRO,[2] Francisco M. MARTÍNEZ-VERDÚ,[2] José FERNÁNDEZ-DORADO,[1] José L. ALVAREZ-MUÑOZ,[3] Jaume PUJOL[1]
[1] Centre for Sensors, Instruments and Systems Development, Technical University of Catalonia
[2] Department of Optics, Pharmacology and Anatomy, University of Alicante
[3] Department of Optics and Optometry, Technical University of Catalonia

ABSTRACT

The potential of goniochromatic pigments is being widely exploited in several industries. One clear example is the automotive sector. In order to evaluate specific colorimetric features of these pigments, commercial gonio-spectrometers have been recently developed such as the BYK-mac®, the X-Rite MA98® and the Datacolor FX10®. With the same purpose, gonio-spectral imaging systems can be very useful as they provide spectral information with high spatial resolution from a large area overcoming some of the limitations of the commercial systems currently used. A novel gonio-hyperspectral imaging system based on light-emitting diodes (LEDs) is presented in this work. The proposed device is composed by two motorized rotation stages, two digital cameras and a LED-based light source that includes a linear actuator. The imaging set includes a visible CCD camera with enhanced sensitivity in the ultraviolet region of the spectrum and an InGaAs camera covering the near-infrared range. The light source consists of 29 different kinds of LEDs from 365nm to 1300nm. White LEDs were also incorporated to analyse texture descriptors used in the automotive sector. The geometries shared by the BYK-mac® and the X-Rite MA98® were evaluated (45ºx:-60º, 45ºx:-30º, 45ºx:-20º, 45ºx:0º, 45ºx:30º and 45ºx:65º) to compare their results with those obtained with the proposed system in terms of CIE L*a*b* coordinates. As a first approach, three samples of real automotive paintings were analised: one solid, one metallic and one pearlescent. The results of this study show the usefulness of the developed system in the assessment of colorimetric features of coatings containing goniochromatic pigments with a high spatial resolution.

1. INTRODUCTION

In the last decades, the automotive sector is widely using goniochromatic or effect pigments for any kind of car painting. The result is that, nowadays, 80% of the automotive finishes are effect coatings. These kind of pigments are divided in two categories: metallic pigments, which mainly show variations in lightness; and pearlescent pigments, which exhibit hue and chroma shifts as a function of the illumination and/or observation angle (Maile 2005; Pfaff 2008).

Commercial gonio-spectrophotometers have been recently launched to cover the need of characterising these particular coatings such as the BYK-mac®, the X-Rite MA98® and the Datacolor FX10®. Even though these devices offer very accurate colorimetric information, they only evaluate integrated information from a relatively small area over the sample. This fact can be considered a limitation, especially when dealing with materials that change their appearance all over the sample depending on how they are illuminated and observed. To overcome this, we propose a LED-based gonio-hyperspectral imaging system that guarantees the colorimetric evaluation of the appearance and the spatial distribution of it along an extended area pixel by pixel. As a first step, the goal of this work is to demonstrate that the developed system allows obtaining similar colorimetric results to those provided by commercial gonio-spectrometers when analysing a central area of the acquired image.

2. METHOD

2.1 Setup

The proposed LED-based gonio-hyperspectral imaging system consists of two motorized rotation stages, two digital cameras and a light source based on LEDs (Figure 1). One of the rotation stages (8MR151-30; STANDA, Lithuania) controls the angle of illumination by rotating the sample with respect to the light source while the other stage (8MR191-30-28; STANDA, Lithuania) controls the observation angle by moving the arm that supports the cameras. The system includes two monochromatic cameras, one visible CCD camera (CM-140GE-UV; JAI, Japan) with enhanced sensitivity in the ultraviolet range of the spectrum (200nm – 1000nm) and an InGaAs camera (C10633-13; HAMAMATSU, Japan) that covers the near-infrared range (900nm – 1700nm). The resolution of the visible camera is 1392x1040 pixels while that of the near-infrared camera is of 320x256 pixels. The illumination set includes 29 different groups of LEDs, a linear actuator (ZLW-0630-02-B-60-L-1000; IGUS, Germany) that holds the LED board and allows changing from one spectral channel to the next one and a collimating lens. The light source is constituted by 28 different spectral channels with peak wavelengths from 365nm to 1300nm (370, 395, 410, 448, 470, 490, 505, 530, 568, 590, 617, 627, 655, 670, 690, 700, 720, 735, 750, 770, 810, 850, 870, 940, 970, 1020, 1050 and 1300 nm). Moreover, the light source also incorporates white LEDs which are intended for the evaluation of texture descriptors such as sparkle, graininess and mottling. They are also used in the automotive industry to describe appearance of coatings besides colorimetric features.

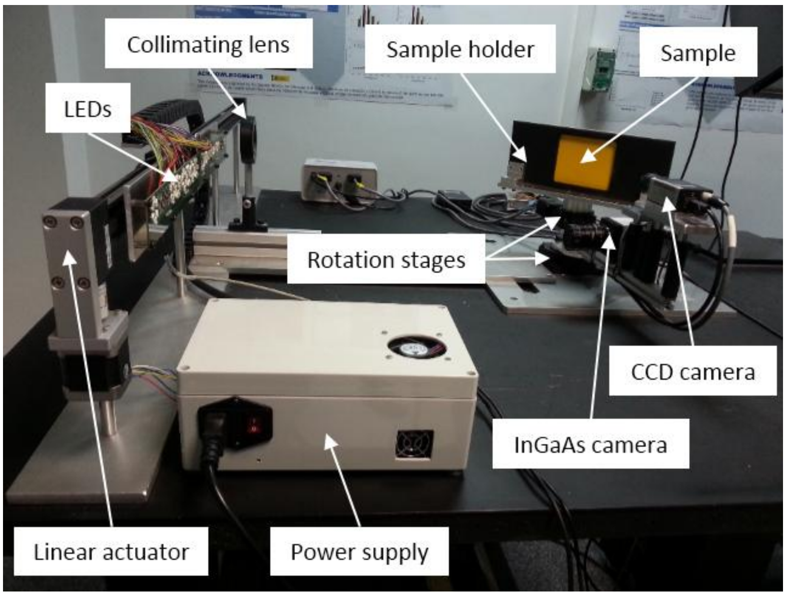

Figure 1: Setup.

2.2 Experimental Procedure

Three different samples were analyzed: one solid, one metallic and one pearlescent plates. Each one was measured at six different geometries: 45ºx:-60º, 45ºx:-30º, 45ºx:-20º, 45ºx:0º, 45ºx:30º and 45ºx:65º (Figure 2). The illumination direction was fixed at 45º from the normal direction of the sample while the observation arm was situated at six different positions with respect to the normal (-60º, -30º, -20º, 0º, 30º, 65º). These geometries were chosen because they are the angular positions that the BYK-mac® and the X-Rite MA98® share, thus allowing for a more accurate comparison of the results.

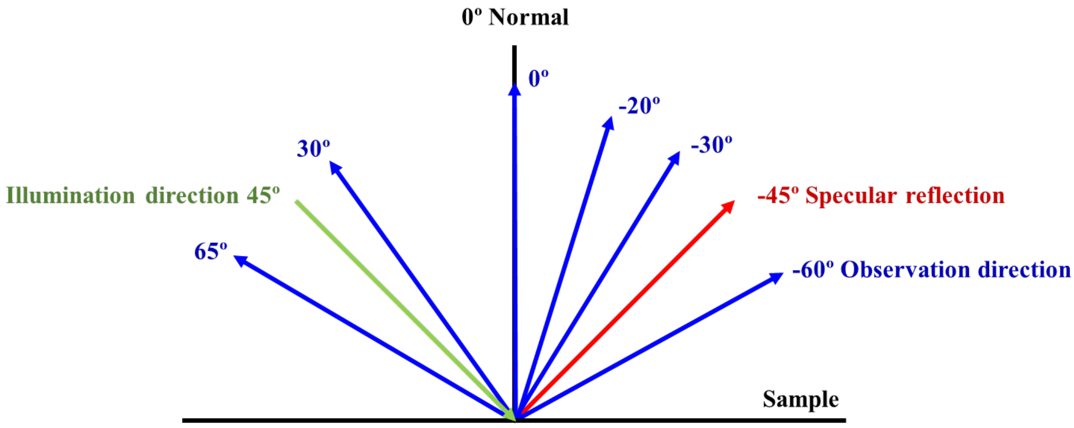

Figure 2: Measurement geometries (45ºx:-60º, 45ºx:-30º, 45ºx:-20º, 45ºx:0º, 45ºx:30º and 45ºx:65º).

2.3 Image and Colour Analysis

At each geometry and for each spectral channel, 10 images were captured and lately averaged to reduce noise. In addition, the following formula was applied to obtain the reflectance of each pixel of the image at a certain wavelength:

$$r(i,j) = c \cdot \frac{DL_I(i.j) - DL_{DC}(i.j)}{DL_W(i.j) - DL_{DC}(i.j)}, \qquad (1)$$

where $r(i,j)$ is the reflectance corresponding to a pixel, $DL_I(i,j)$, $DL_W(i,j)$ and $DL_{DC}(i,j)$ are the digital levels of the raw image, the reference white and the dark current, respectively, and c is the reflectance value of the calibrated reference white (BN-R98-SQ10C; GIGAHERTZ OPTIK, Germany).

Secondly, the tristimulus values XYZ CIE-1964 were computed based on the reflectance spectra from 400nm to 700nm (Nassau 1997). Posteriorly, the CIE L*a*b* coordinates were calculated for the illuminant D65 (Nassau 1997) and compared with those provided by the commercial gonio-spectrometers BYK-mac® and X-Rite MA98® in terms of colour differences (ΔE, CIELAB1976).

3. RESULTS AND DISCUSSION

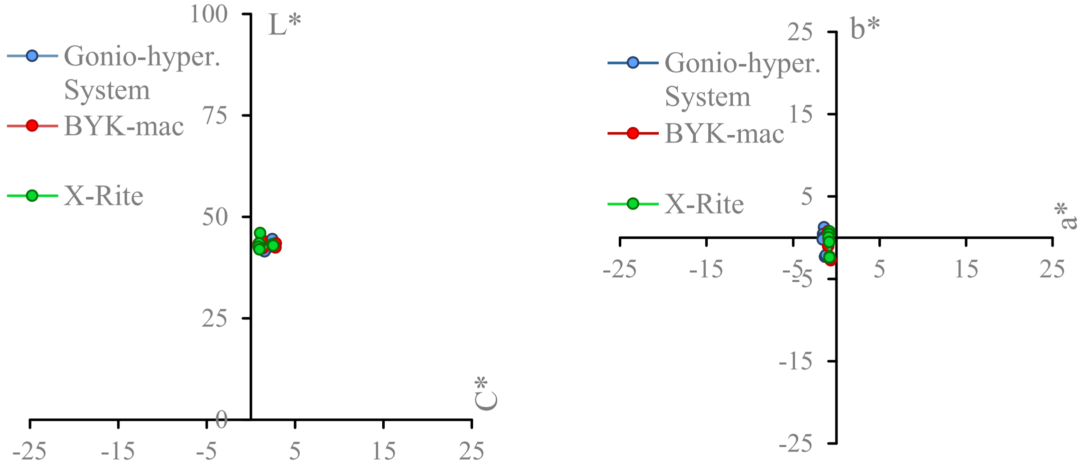

(a)

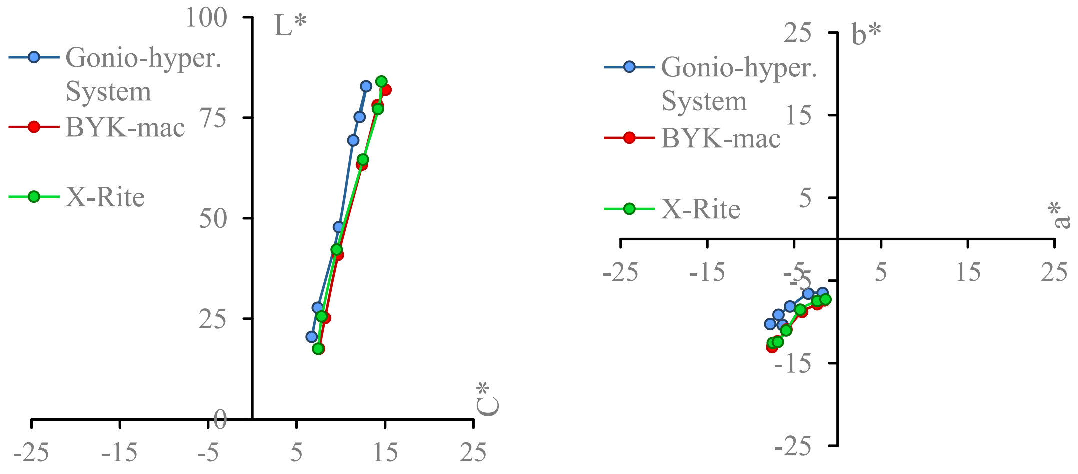

(b)

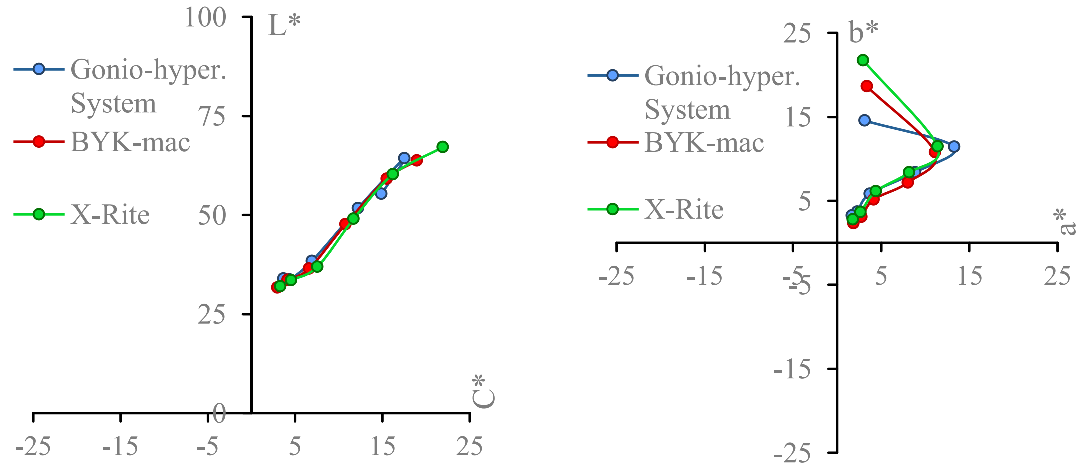

(c)

Figure 3: CIELAB diagrams of the solid (a), metallic (b) and pearlescent sample (c) for the three devices tested.

Figure 3 shows the colorimetric behavior of three samples (solid, metallic and pearlescent) measured with the BYK-mac®, the X-Rite MA98® and the proposed system. As expected, the solid sample (Figure 3 (a)) exhibited very small variations in L^*, a^*, b^* and C^* ($C^* = \sqrt{(a^*)^2 + (b^*)^2}$) since solid pigments have similar appearance at any direction. Nevertheless, metallic (Figure 3(b)) and pearlescent (Figure 3(c)) samples did behave different as a function of the observation angle. On one hand, the metallic sample experienced the largest changes in L^* parameter, while for C^*, a^* and b^* the variation was very small. The pearlescent sample was characterised by greater shifts in C^*, a^* and b^* parameters rather than in L^*. The three samples showed similar colorimetric performance for the three devices tested.

Table 1 contains the color differences between the CIE L*a*b* parameters obtained with the system and those measured with the BYK-mac® and the X-Rite MA98® gonio-spectrophotometers. The lowest color differences were found for the solid sample with differences of less than four units and rather constant along the different geometries. In the case of the metallic and pearlescent samples, the colour difference values varied depending on the measurement geometry. The highest values were found in those positions closer to the specular reflection (45ºx:-60º, 45ºx:-30º and 45ºx:-20º), reaching values up to 13 ΔE units. In spite of this, at the geometries further to the specular reflection (45ºx:0º, 45ºx:30º and 45ºx:65º) colour differences notably decreased becoming in some cases very small.

Table 1. CIELAB color differences (ΔE, CIE1976) when comparing the gonio-hyperspectral imaging system and the commercial devices for the solid (S), metallic (M) and pearlescent (P) samples.

Sample	ΔE	45ºx:-60º	45ºx:-30º	45ºx:-20º	45ºx:0º	45ºx:30º	45ºx:65º
S	BYK-mac	2.36	0.98	1.28	1.28	0.89	2.14
	X-Rite	3.85	0.98	1.18	0.92	0.58	1.64
M	BYK-mac	7.45	5.18	6.41	7.07	2.97	3.09
	X-Rite	9.24	6.08	5.24	5.65	2.54	3.09
P	BYK-mac	9.34	5.61	4.32	2.11	0.79	2.44
	X-Rite	13.82	4.44	2.78	1.66	0.40	2.00

4. CONCLUSIONS

A LED-based gonio-hyperspectral imaging system for the analysis of automotive paintings has been presented. This system showed a good colorimetric performance similar to that of the BYK-mac® and the X-Rite MA98® commercial gonio-spectrophotometers, in particular for solid pigments. Future work will be focused on diminishing the differences that the system exhibited in comparison with the commercial devices when dealing with goniochromatic pigments. However, preliminary results are already promising. In addition, texture descriptors will be also developed.

ACKNOWLEDGEMENTS

This research was supported by the Spanish Ministry of Science and Innovation under the grant DPI2011-30090-C02 and the European Union. Francisco J. Burgos would like to thank the Government of Catalonia for his Ph.D. grant. We would also like to thank the European Colour and Space in Cultural Heritage (COSCH) COST Action TD1210 for the financial support towards research visits and meetings.

REFERENCES

Maile, F. J., G. Pfaff, and P. Reynders. 2005. Effect Pigments—Past, Present and Future. *Progress in Organic Coatings* 54 (3): 150–163.

Nassau, K. 1997. *Color for Science, Art and Technology*. Amsterdam: Elsevier Science.

Pfaff, G. 2008. *Special Effect Pigments*. Norwich: William Andrew Publishers.

Address: Francisco J. BURGOS, Centre for Sensors, Instruments and Systems Development, Technical University of Catalonia, 10 Rambla Sant Nebridi, Terrassa, 08222, SPAIN

E-mails: francisco.javier.burgos@cd6.upc.edu, mvilasec@oo.upc.edu, esther.perales@ua.es, elisabet.chorro@ua.es, verdu@ua.es, mpepe3@gmail.com, alvarez@oo.upc.edu, pujol@oo.upc.edu

Multispectral image estimation from RGB image based on digital watermarking

Kazuma SHINODA,[1] Aya WATANABE,[2] Madoka HASEGAWA,[1] Shigeo KATO[1]
[1] Graduate School of Engineering, Utsunomiya University
[2] Faculty of Engineering, Utsunomiya University

ABSTRACT

In this paper, we propose a method of embedding the spectral information in an RGB image by the digital watermarking. The proposed method divides the multispectral image into two components before embedding: RGB image and residual. The RGB image is extracted from the multispectral image by using the XYZ color matching functions and a color conversion matrix. The original multispectral image is estimated from the RGB image by Wiener estimation, and the difference between the original and the estimated multispectral image is referred to as the residual. In our method, the estimated spectral residual data are compressed by JPEG2000 and embedded in the lower bit planes of the RGB image. The experimental results show that the proposed method leads to more than 10 dB gain relative to conventional methods in the peak signal-to-noise ratio comparison of recovered multispectral image while there are almost no significant perceptual differences in the watermarked RGB image. The experimental results show that the proposed method can improve the quality of the recovered multispectral image at the expense of a slight degradation in RGB image quality.

1. INTRODUCTION

Multispectral images (MSIs) have been studied for many fields such as remote sensing and medical applications. MSIs have been used for not only analysis applications, but also the color reproduction of RGB images under a different illumination (Yamaguchi et al. 2008). Converting MSI into RGB image is needed to display MSIs, therefore RGB format is essential for the field of computer graphics. Additionally, most of widely used formats in computer graphics are based on RGB. However, converting MSI to RGB image cuts spectral information except for visible components. In the color reproduction of RGB images, estimating of object spectrum is required and has been studied in some literature (Haneishi et al. 2000, Stigell et al. 2007, and Murakami et al. 2013). Converting MSI into RGB image will be required in some systems because the low-dimensional image such as RGB images can be utilized easily in the current imaging system, but it is difficult to recover the original spectra once it is converted.

The conventional spectral reconstruction methods can be separated into two types: estimate/reconstruct spectrum with additional data (Keusen 1996, Yu et al 2006, Shinoda et al. 2011, and Murakami et al. 2013), or without additional data (Haneishi et al. 2000 and Stigell et al. 2007). A high-dimensional signal can be estimated from a low-dimensional one more accurately if additional data is available, but the whole data structure becomes less compatibility with conventional sRGB systems. An efficient spectral estimation method while maintaining the conventional data structure such as a sRGB image has not yet been proposed.

We propose a new spectral estimation method using a digital watermarking by embedding additional spectral information into an RGB image. The RGB image is calculated from an original MSI, and then the original MSI is estimated from only the RGB image in the embedding side. The residual of the estimation is compressed and embedded into the lower bit planes of the RGB image. This watermarked image can be used as an RGB image without any knowledge about spectrum. If reconstruction of the spectrum is required in an application, the compressed residual data is extracted from the lower bit planes of the RGB image, and then the estimated MSI from RGB image can be corrected by the extracted residual data.

This paper is organized as follows. Our compression method is presented in Section 2. The results are given in Section 3. In Section 4, we conclude this paper.

2. RGB DIGITAL WATERMARKING FOR MSI ESTIMATION

The embedding and reconstructing flow of the proposed method is shown in Figures 1 and 2. In the embedding side, an original MSI is converted to an RGB image, then the lower bit planes of the RGB image are used for digital watermarking. At first, the RGB image is calculated from the original MSI by using the CIE XYZ color matching functions under the standard illuminant D65, and sRGB color space. Let $\boldsymbol{f}$ be a spectrum (MSI is regarded as a spectral reflectance in this paper), and $\boldsymbol{g}$ be RGB values. $\boldsymbol{g}$ is calculated as

$$\boldsymbol{g} = \boldsymbol{CTEf} = \boldsymbol{Hf}, \tag{1}$$

where $\boldsymbol{C}$ is the XYZ-to-RGB color transform matrix of sRGB, $\boldsymbol{T}$ is the CIE XYZ color matching functions, and $\boldsymbol{E}$ is the standard illuminant. The spatial position (x, y) is ignored in this paper because each pixel is processed independently. The lower n-bit planes of the obtained RGB image are then filled with zero at this stage for digital watermarking, and the truncated RGB image is defined as $\boldsymbol{g}'$. An MSI is estimated from the obtained RGB by using Wiener estimation. The Wiener estimation from $\boldsymbol{g}'$ to $\boldsymbol{f}'$ is defined as

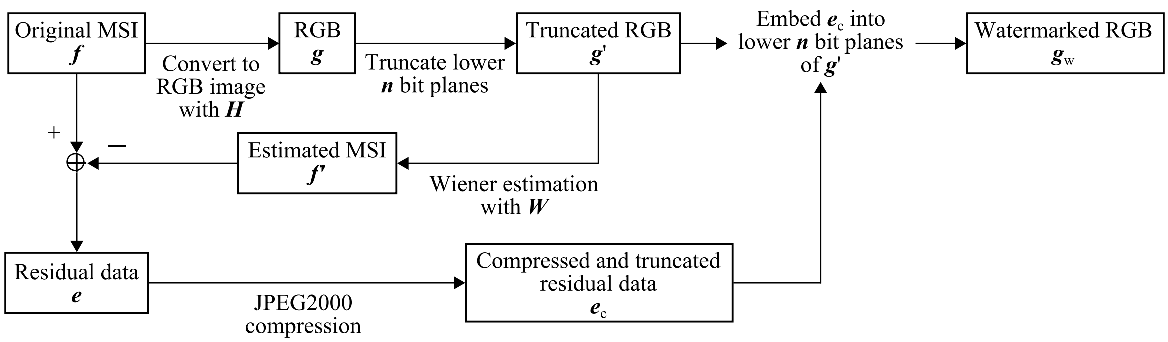

Figure 1: Proposed embedding process.

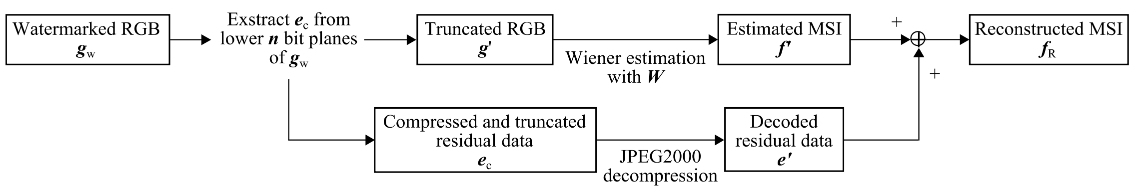

Figure 2: Proposed reconstructing process.

$$f' = Wg' \tag{2}$$

$$W = R_f H^T (H R_f H^T)^{-1}, \tag{3}$$

where W is a Wiener estimation matrix, and R_f is the autocorrelation matrix of f.

A residual spectral data can be obtained as

$$e = f - f'. \tag{4}$$

The obtained residual data is compressed by JPEG2000 with multi-component transform (JPEG2000-MCT) lossy mode with Karhunen-Loeve transform (KLT), and the truncated lossy code-stream is defined as e'. Here, if M is the total number of pixels of the RGB image, the compressed residual data is truncated into $M \times n$ bits before embedding. The compressed residual data is embedded into the lower n-bit planes of g'.

The reconstructing process is an inverse process of the embedding side as shown in Figure 2. The compressed residual data is extracted from the watermarked RGB image and is decoded by JPEG2000-MCT. The lower n-bit planes of the RGB image are filled with zero, then an MSI is estimated from the RGB image. This estimation process is completely the same as Eqs. (2) and (3). The reconstructed MSI can be obtained by adding the decoded residual data to the estimated MSI from RGB image.

The quality of the watermarked RGB image is slightly degraded because it has random bits in the lower n-bit planes, but the degradation can be suppressed as n is decreased. On the other hand, if n is increased, the reconstructed MSI quality is improved whereas the RGB image quality is decreased. The relation between the quality of RGB and MSI is thought to be trade-off. However, this is not always a completely trade-off because the estimated MSI quality from the RGB image is improved as n is decreased. The results and trade-off are discussed in Section 3.

3. RESULTS AND DISCUSSION

In this section, we show the peak signal-to-noise ratio (PSNR) of both watermarked RGB images and reconstructed MSIs. Figure 3 shows test images that consist of 512×512 pixels, 8 bits / pixel with 16 bands. The images were captured with a camera (Fukuda, 2002) equipped with 16-band filters. The residual data is encoded by using Jasper (Adams, 2015) with 9/7 real wavelet transform. The embedded information includes not only the compressed residual data but also the coefficients of the Wiener estimation matrix.

(a)

(b)

Figure 3: Test images with 512×512 pixels, 12 bits / pixel, and 16 bands. (a) Dishes (b) Toys.

Table 1. Comparison of reconstructed MSI and watermarked RGB PSNRs in dB..

Embedded planes	*Dishes*		*Toys*	
n	MSI	RGB	MSI	RGB
0	33.65	Inf.	27.73	Inf.
1	44.76	51.14	47.50	51.14
2	45.52	44.13	47.72	44.03
3	45.39	37.89	46.93	37.74
4	45.63	31.85	46.42	31.63
5	46.71	25.83	47.55	25.66
6	47.62	19.37	49.14	19.56
7	48.58	14.23	49.87	14.33

Table 1 shows the PSNR of watermarked RGB images and reconstructed MSIs depending on n. We also show the PSNR of the reconstructed MSI at $n = 0$, which corresponds to using only Wiener estimation. In $n = 1$, the PSNR of MSI shows over 40 dB while maintaining over 50 dB in RGB image. The proposed method shows the greatly higher PSNR of MSI than Wiener estimation while maintaining no perceived difference in RGB images.

It is thought that the relation of the image quality between reconstructed MSI and watermarked RGB is a trade-off, but note that there is an exception. Although the PSNR of MSI is larger when n is larger, we can see the degradation of the reconstructed PSNR at $n = 3$, 4 and 5 in *Toys* image. In this case, $n = 3$ to 5 is not a reasonable choice to obtain the balanced MSI and RGB images, therefore one of the trade-off point considering both MSI and RGB images is $n = 2$ in *Toys* image. This breakpoint depends on a test image, but the proposed method can decide an appropriate n at the embedding side because we can calculate the MSI and RGB PSNRs in the embedding side.

4. CONCLUSIONS

We proposed a new spectral estimation method using a watermarked RGB image. The proposed method embeds the estimation residual information of MSI into the lower bit planes of RGB image. The quality relation between MSI and RGB images is trade-off depending on the amount of the embedding residual data, but the perceived difference of the watermarked RGB image is not significant while maintaining higher MSI quality than Wiener estimation. Additionally, the proposed method can adjust the quality of MSI and RGB by changing the embedding amount. The future work is to give a compression tolerance to the watermarked RGB.

ACKNOWLEDGEMENTS

This work was supported by JSPS KAKENHI Grant Number 25870676. We would like to thank Masahiro Yamaguchi at the Tokyo Institute of Technology for providing the test images used in our experiments.

REFERENCES

M. Yamaguchi, H. Haneishi, and N. Ohyama. 2008. Beyond red-green-blue(RGB): spectrum-based color imaging technology. *Journal of Imaging Science and Technology*. 52 (1): 10201-1--10201-15.

H. Haneishi, T. Hasegawa, A. Hosoi, Y. Yokoyama, N. Tsumura, and Y. Miyake. 2000. System design for accurately estimating the spectral reflectance of art paintings. *Appl. Opt*. 39 (35): 6621-6632.

P. Stigell, K. Miyata, and M. Hauta-Kasari. 2007. Wiener estimation method in estimating of spectral reflectance from RGB images. *Pattern Recognition and Image Analysis*. 17 (2): 233-242.

Y. Murakami, M. Yamaguchi, and N. Ohyama. 2013. Dictionary-based estimation of spectra for wide-gamut color imaging. *Color Research and Application*. 38 (2): 120-129.

T. Keusen. 1996. Multispectral color system with an encoding format compatible with the conventional tristimulus model. *Journal of Imaging Science and Technology*. 40 (6): 510-515.

S. Yu, Y. Murakami, T. Obi, M. Yamaguchi, and N. Ohyama. 2006. Multispectral image compression for improvement of colorimetric and spectral reproducibility by nonlinear spectral transform. *Optical Review*. 13 (5): 346-356.

K. Shinoda, Y. Murakami, M. Yamaguchi, and N.Ohyama. 2011. Lossless and lossy coding for multispectral image based on sRGB standard and residual components. *J. Electron. Imaging*. 20 (2): 023003-1--023003-12.

H. Fukuda, T. Uchiyama, H. Haneishi, M. Yamaguchi, and N. Ohyama. 2002. Development of 16-band multispectral image archiving system. *Proc. of SPIE*. 5667: 136-145.

M. D. Adams. Jasper software version 1.900.1. Accessed February 3, 2015. Available at http://www.ece.uvic.ca/~frodo/jasper/.

Address: Dr. Kazuma SHINODA, Graduate School of Engineering,
Utsunomiya University, 7-1-2 Yoto, Utsunomiya, Tochigi, 321-8585, JAPAN
E-mails: shinoda@is.utsunomiya-u.ac.jp

Image Correction for a Multispectral Imaging System Using Interference Filters and Its Application

Shogo NISHI,[1] Shoji TOMINAGA[2]
[1] Dept. of Engineering Informatics, Osaka Electro-Communication University
[2] Graduate School of Advanced Integration Science, Chiba University

ABSTRACT

The present paper proposes a calibration method of a multispectral camera system using interference filters. A spectral image processing is effective to acquire an inherent information of an object in a general way. However, filter registration error often occurs when the interference filter is used. Therefore, a calibration method is presented for correcting observed images. The method is based on the phase analysis of images in Fourier domain. We use the phase correlation method for cariblating the registration error. Moreover, we describe a method for digital archiving of art paintings based the present imaging system.

1. INTRODUCTION

A multispectral imaging system can improve color accuracy in the captured images, compared with a general RGB camera system. Also the system makes it possible to estimate important surface properties such as spectral reflectance at each pixel point of an object surface. Therefore, a variety of multispectral camera/imaging systems have been proposed for the purpose of estimating spectral information such as spectral radiance in a scene and surface-spectral reflectance of an object. Some typical systems are constructed by using one or two additional color filters to a trichromatic digital camera (F.H. Imai, et al. 1999), combining a monochrome camera and color filters with different spectral bands (S. Tominaga, et al. 2007), using narrow band interference filters (S. Nishi, et al. 2011), or using a liquid-crystal tunable (LCT) filter. However, these imaging systems have several problems such as the stability of filtration, the accuracy of spectral estimation, and the time consumption for filter change. Therefore, these systems have advantages and disadvantages.

The present multispectral camera system is decomposed into two parts of a filtration system of an automatic filter changer and eight interference filters and a monochrome CCD camera system. This imaging system has an advantage of narrow band filtering, therefore it is excellent in the stability and the accuracy of spectral estimation. However, filter registration errors often occurr because it is difficult to optically align the filters with different indices of diffraction. These registration errors are called a longitudinal aberration and transverse aberration. Some calibration techniques for registration error have been proposed so far (J. Brauers, et al. 2008) (A. Mansouri, et al. 2005). In this research, we examine the calibration method that targets the transverse aberration. In addition, there is another factor to make calibration processing difficult. An image acquired by a multiband imaging system are different from the one acquired by a RGB camera. Namely, the pixel value is obviously different in each band images even if it takes a picture of the same scene. Therefore, it is difficult to correct a registration error between images using a general correlation technique.

In this paper we proposed a calibration method for the registration error caused by the interference filters. This method is easily applied to the digital archiving. In the following, we first describe an imaging system. Second a calibration method is presented for correcting observed images with the filter registration error. Third, we describe a method for digital archiving of art paintings based the present imaging system. Multispectral images of an oil painting are acquired using the imaging system, and the properties of the painting surfaces are estimated from the observed images. Moreover realistic images of the painting are rendered under arbitrary conditions of viewing and illumination. Finally, the feasibility of the proposed system is shown in experiments using real painting objects.

2. SPECTRAL IMAGING SYSTEM

Figure 1 shows the present imaging system. Our multiband camera system is composed of a monochrome CCD camera (Toshiba Teli CS3920), a C mount lens, an automatic filter changer, and eight interference filters whose central wavelengths are 420, 450, 490, 530, 570, 610, 650, and 670 nm. The full width at half maximum of filtration is about 10 nm. Figure 2 shows the composite spectral sensitivity functions for eight sensors. The CCD outputs are band-pass signals in the visible wavelength range, and they are finally integrated. The interference filter utilizes the interference effect of light occurred by a dielectric material and a metal thin film. It has the property that the spectral transmission characteristics depend on the index of refraction and the incidence angle. Moreover, note that the inner metal thin films are not always parallel to the incidence plane and the output plane. It can be considered that the registration error occurs in the acquired images for these reasons. Therefore, calibration is necessary to correct the registration error.

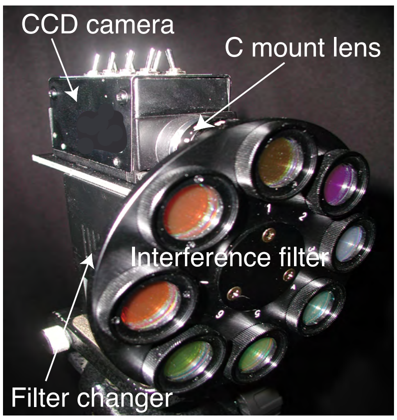

Figure 1: Imaging system.

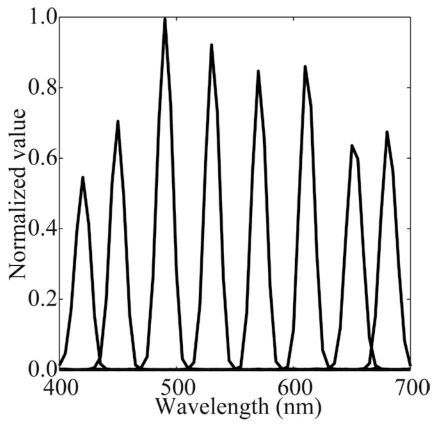

Figure 2: Spectral sensitivities of the imaging system.

3. CALIBRATION METHOD

The registration error is found when the spectral images captured with different wavelengths are aligned and superimposed. For instance, suppose that we take a picture of an object in a scene. The object images projected onto a focal plane are slightly shifted by passing through the filters. The alignment and focusing do only once with an arbitrary filter channel for the convenience of the experiment, and the adjustments are not done at all afterwards. Therefore, one of eight images is selected as a reference image and the remaining seven images are corrected as target images.

It is well known that an image acquired by a multiband imaging system is different from the one acquired by a RGB camera. That is to say, the pixel value is obviously different in each band images even if it takes a picture of the same scene. Therefore, it is difficult to correct a registration error between images using a general correlation technique. Therefore, we propose novel correlation method using phase images of each multiband image. A phase image is an image that normalizes an amplitude spectrum of an image by one. A phase correlation method (C. D. Kuglin, et al. 1975) is a technique for calculating the correlation by using the phase image. As previously mentioned, the amplitude spectrum of a spectral image is different in each acquisition band. Therefore, the proposal method can expect to correct without influence of the different amplitude spectrum in each image.

Here, let both $f(n_1, n_2)$ and $g(n_1, n_2)$ be $N_1 \times N_2$ images. Let $F(k_1, k_2)$ and $G(k_1, k_2)$ be the 2D discrete Fourier transforms of the image $f(n_1, n_2)$ and $g(n_1, n_2)$ respectively. Therefore, $F(k_1, k_2)$ and $G(k_1, k_2)$ are defined as

$$F\left(k_1,k_2\right) = \sum_{n_1,n_2} f\left(n_1,n_2\right) W_{N_1}^{k_1 n_1} W_{N_2}^{k_2 n_2} = A_F\left(k_1,k_2\right) \exp\left[j\theta_F\left(k_1,k_2\right)\right], \tag{1}$$

$$G\left(k_1,k_2\right) = \sum_{n_1,n_2} g\left(n_1,n_2\right) W_{N_1}^{k_1 n_1} W_{N_2}^{k_2 n_2} = A_G\left(k_1,k_2\right) \exp\left[j\theta_G\left(k_1,k_2\right)\right], \tag{2}$$

where k_1 and k_2 are the discrete Fourier index, and $W_{N1} = \exp[-j(2\pi / N_1)]$, $W_{N2} = \exp[-j(2\pi / N_2)]$. $A_F(k_1, k_2)$ and $A_G(k_1, k_2)$ are amplitude components, and $\theta_F(k_1, k_2)$ and $\theta_G(k_1, k_2)$ are phase components. The phase image of image $f(n_1, n_2)$ is defined as

$$f_p\left(n_1,n_2\right) = FT^{-1}\left[\frac{F\left(k_1,k_2\right)}{\left|F\left(k_1,k_2\right)\right|}\right], \tag{3}$$

where $f_p(n_1, n_2)$ is the phase image, and FT^{-1} is the 2D inverse discrete Fourier transforms. The cross spectrum $C(k_1, k_2)$ between $F(k_1, k_2)$ and $G(k_1, k_2)$ is defined as

$$C\left(k_1,k_2\right) = F\left(k_1,k_2\right)\overline{G\left(k_1,k_2\right)} = A_F\left(k_1,k_2\right) A_G\left(k_1,k_2\right) \exp\left[j\theta\left(k_1,k_2\right)\right], \tag{4}$$

where $\overline{G(k_1,k_2)}$ represents the complex conjugate of $G(k_1, k_2)$, and $\theta(k_1, k_2) = \theta_F(k_1, k_2) - \theta_G(k_1, k_2)$, it represents the phase difference spectrum. Therefore, the cross correlation using the phase image is defined as

$$C\left(k_1,k_2\right) = \frac{F\left(k_1,k_2\right)\overline{G\left(k_1,k_2\right)}}{\left|F\left(k_1,k_2\right)\right|\left|\overline{G\left(k_1,k_2\right)}\right|} = \exp\left[j\theta\left(k_1,k_2\right)\right]. \tag{5}$$

The amplitude of correlation peak shows the similarity of two spectral images, and the axis of correlation peak shows the relative registration error of two spectral images.

In order to improve the correlation accuracy in this paper, first, the captured image is divided into small regions. Then, the reference image and the target image are performed displacement detection by phase correlation method, and then, the registration error of these images are calibrated. In some band images, a region where image data is blank occurs at this time. Therefore, the image that contains a blank area is extracted from the acquired spectral images, and then, these images are calibrated again by the proposed method. Finally, the blank area is complemented by the above process. In this paper, we divide into the regions with a fixed size. However, it is also possible to vary the region adaptively depending on the degree of texture density of the acquired spectral images.

4. DIGITAL ARCHIVING OF ART PAINTINGS

We apply the proposed method to digital archiving of art paintings based the present imaging system. In this paper, it is intended for digital archive of oil paintings. We have to estimate the surface properties of oil paintings. Specifically, it is necessary to estimate the spectral reflectance of the painting surfaces, the surface shape and the light reflection model parameters (S. Tominaga, et al. 2008).

Surface reflection of oil paintings include specular reflection or gloss. Therefore the camera output for the painting surface is composed of the diffused reflection and the specular reflection. As the reflection properties, the surface-normal vector and the surface-spectral reflectance are estimated from the diffuse reflection component. The reflection model parameters are estimated from the specular component.

The surface-normal vector at each pixel point is computed by using a photometric stereo method. For estimating the surface-spectral reflectance the camera output is described as a model.

$$\rho_k = \sum_i S(\lambda_i) E(\lambda_i) R_k(\lambda_i) + n_k, \ (k = 1, 2, 3, \ldots, 8), \tag{6}$$

where $S(\lambda_i)$ is the spectral reflectance, $E(\lambda_i)$ is the spectral distribution of illumination, $R_k(\lambda_i)$ is the spectral sensitivities of the k-th sensor, and n_k is the noise. Let $\boldsymbol{\rho}$ be an eight-dimensional column vector representing all spectral camera outputs, and $\mathbf{s}$ be a n-dimensional vector representing the spectral reflectance $S(\lambda_i)$. Moreover, let $\mathbf{H}$ ($\equiv[h_{kj}]$) be a $8 \times n$ matrix with the element $h_{kj} = E(\lambda_i)R_k(\lambda_i)$. Then the above imaging relationships are summarized in the matrix form $\boldsymbol{\rho} = \mathbf{Hs} + \mathbf{n}$. When the signal component $\mathbf{s}$ and the noise component $\mathbf{n}$ are uncorrelated, a solution method minimizing the estimation error on $\mathbf{s}$ is given as the Wiener estimator

$$\hat{\mathbf{s}} = \mathbf{R}_{ss}\mathbf{H}^{\mathrm{t}}\left[\mathbf{H}\mathbf{R}_{ss}\mathbf{H}^{\mathrm{t}} + \sigma^2\mathbf{I}\right]^{-1}\rho, \tag{7}$$

where $\mathbf{R}_{ss}$ is an $n \times n$ matrix representing a correlation among surface spectral reflectances. We assume white noise with a correlation matrix $\sigma^2\mathbf{I}$.

A reflection model is needed for rendering realistic images of oil paintings. In our previous study (S. Nishi, et al. 2007), we found that surface reflection of most oil paintings can be described by the Cook-Torrance model. The model parameters of this mathematical model are estimated from the specular reflection component of the observed images.

Image rendering is then performed based on all estimates on the surface reflection, which are the surface-normal vectors, the surface-spectral reflectances, and the reflection model parameters.

5. EXPERIMENTAL RESULTS

First, we experimented to verify the validity of the proposal calibration method. Figure 3 shows the calibration result. In figure 3(a), we can see the registration error occurred in the

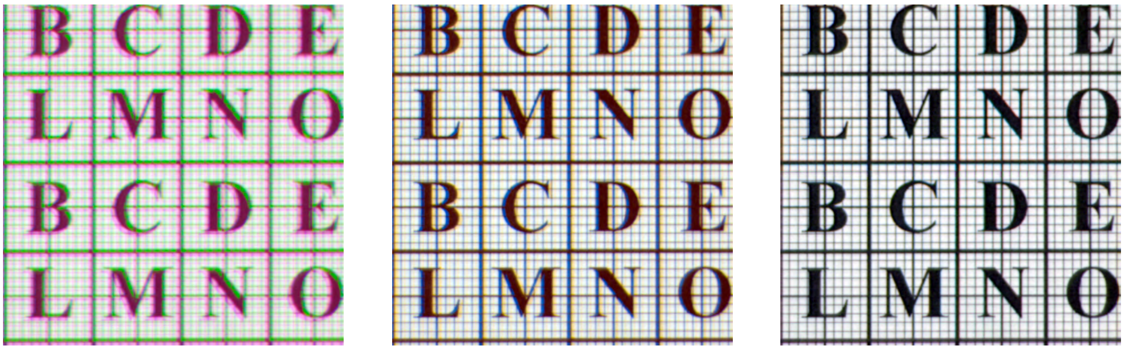

(a) (b) (c)

Figure 3: Calibration results.
(a)Before calibraion, (b)Calibration without division, (c)Calibraion with divison.

synthesized eight band images. This phenomenon is called chromatic aberration, which is one of the factors that the reproduced image is degraded. Figure 3(b) is the calibration result by the phase correlation method without division. The registration error is improved as compared with the results in Fig 3 (a). However, pale yellow or blue has appeared, it can be seen that the calibration is incomplete. Figure 3(c) shows the calibration result by proposed method. Color in Figure 3(b) disappears, the original achromatic appearance is reproduced. Therefore, the proposed method has been verified to be useful as a calibration method. Next, we acquired the multispectral images of an oil painting by the present imaging system and performed the proposed calibration method. By the method described in chapter 4, image rendering was carried out using the estimated surface properties of oil painting. Figure 4 shows the result of image rendering of part of oil paintings.

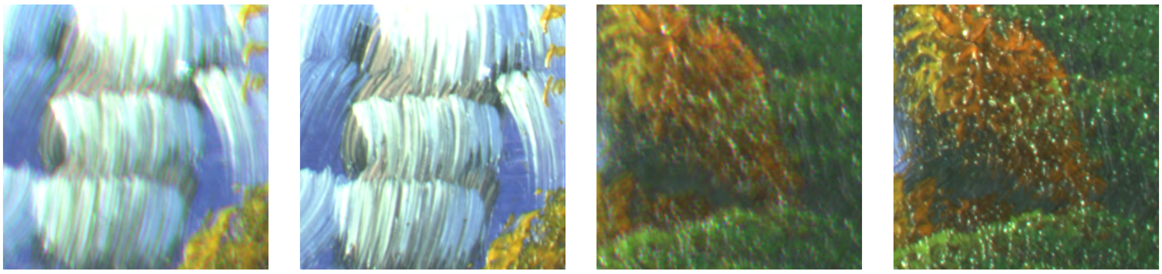

(a)Before calibration *(b)After calibration* *(c)Before calibration* *(d)After calibration*

Figure 4: Calibration result of part of oil paintings.

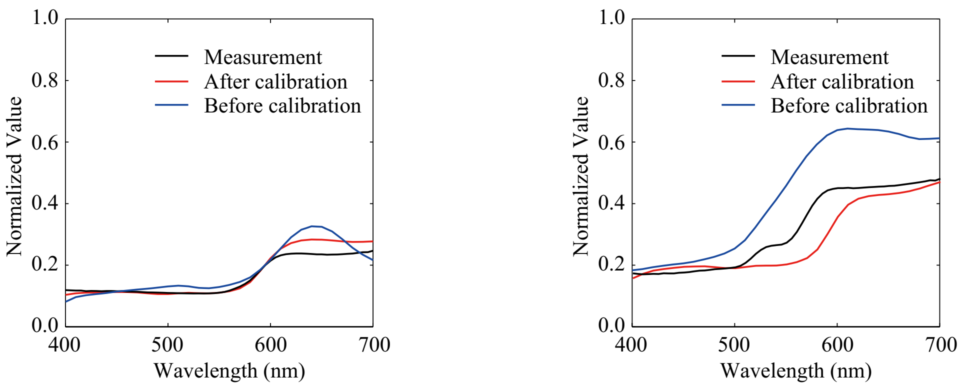

Figure 5: Estimation results for surface spectral reflectances of oil paintings.

Our proposed method is clearly beneficial by comparing with before calibration and after calibration. Figure 5 shows the estimation results for the surface spectral reflectance of part of oil painting. It can be confirmed that the estimation accuracy of surface spectral reflectance is excellent in comparison with the before calibration result.

6. CONCLUSION

This paper has proposed a method for the calibration of the registration error caused by the interference filters. The calibration method was based on the correlation technique using the phase images of acquired spectral image. In order to improve the correlation accuracy, the captured image was divided into small regions. Then, the reference image and the target image were performed displacement detection by phase correlation method, and then, the registration error of these images were calibrated. Therefore the calibration processing was able to perform with high accuracy. Furthermore, the calibration processing was capable of calculating fast for the correlation calculation in the frequency domain. Moreover, we applied this multiband camera system for the digital archive of art paintings. We have described a method for digital archiving of art paintings based the present imaging system. The availability of the proposed calibration method was shown by the experimental results.

REFERENCES

F.H. Imai, et al., 1999. Spectral estimation using trichromatic digital camera. In *Proc. of International Symp. Multispectral Imaging and Color Reproduction for Digital Archives*, 42–49.

S. Tominaga, et al., 2007. Omnidirectional scene illuminant estimation using a multispectral imaging system. In *Proc. of SPIE, Color Imaging XII*, 5667, 128–135.

S. Nishi, et al., 2011. Calibration of a Multispectral Camera System Using Interference Filters. In *Proc. of SPIE,* 8011, 80119E-1–7.

J. Brauers, et.al., 2008. Multispectral filter wheel cameras: Geometric distortion model and compensation algorithms, *IEEE Trans. on Image Processing*, 17 (12): 2368–2380.

A Mansouri, et al., 2005. Optical calibration of a multispectral imaging system based on interference filters. *Optical Engineering* 44 (2): 027004-1–12.

C. D. Kuglin, et al., 1975. The phase correlation image alignment method. In *Proc. IEEE Int. Conf. Cybernetics and Society*, 163–165.

S. Tominaga, et al., 2008. Spectral Image Acquisition, Analysis, and Rendering for Art Paintings. *Journal of Electronic Imaging* 17(4): 043022-1–13.

S. Nishi, et al., 2007. Measurement and Analysis of Reflection Properties of Art Paints. In *Proc. of AIC2007*, 170–173.

Address: Shogo NISHI, Department of Engineering Informatics,
Osaka Electro-Communication University,
18-8 Hatsu-cho, Neyagawa, Osaka, 572-8530, JAPAN
E-mails: s-nishi@isc.osakac.ac.jp, shoji@faculty.chiba-u.jp

Development of Multi-bands 3D Projector

Ryotaro MIWA, Yoshitsugu MANABE, Noriko YATA
Chiba University

ABSTRACT

Recently, devices that can display a three dimensional image is becoming inexpensive. We can enjoy a three dimensional image at home. On the other hand, a reproduction of more accurate color information and high-definition images are required in various fields. However, an accurate color reproduction is difficult because of the insufficient color gamut by RGB primary colors. There are some studies concerning to multi-primary color display devices, but the researching cost takes an expensive. Therefore, if it is possible to construct a simple system using a general 3D projectors and optical filters, it is considered that the 3D image with expanded the color gamut can be displayed. This paper proposes a method for expanding the color gamut of a 3D image by projection of the multi-primary color more than RGB 3 bands using two 3D projectors with different spectral characteristics. First, the optimal spectral transmission characteristics of notch filters is determined by a filter simulation based on the RGB characteristics of the projector. Second, the filters with the determined spectral transmission characteristics is produced, and the spectral characteristics of the projectors are changed by attaching the filter in front of the two projectors's lens. Furthermore, the experimental results are shown that the proposed system can expand the color gamut.

1. INTRODUCTION

Stereoscopic image technology is improved every day. Many people has experienced actual 3D image. On the other hand, a demand for color reproduction of images is increasing by the development of image and video communication system. It is possible to display a color image in some naturally by using the display device such as a projector. However, representation of all color range that can be human perception is difficult. Therefore, the spectral image is attracting attention in order to reproduce high-definition image recording spectral information. It is considered that the spectral information can reproduce a more accurate image by input to the display device. Furthermore, it is important to consider the color gamut problems of the display device for projecting onto a screen.

This paper focuses on approaches of using two projectors that are most attention in the color gamut extension. There are various existing studies with respect to the color gamut expansion using two projectors. The general projector can project RGB 3-bands color, so 6 bands color projection is made possible by two projectors with different optical filters. The color gamut of the image projected from the projector is known to expand by appropriately increasing the number of bands.

2. METHOD

This paper proposes a method of expanding the color gamut of a 3D image by projection of the multi-primary colors more than the RGB three bands. The proposed method is applied a color gamut expansion technique in the video presentation device using the two 3D projectors with different spectral characteristics. The optimal spectral characteristic of filters is simulated based on the spectral characteristic of 3D projector in order to realize the multi-primary color projection. Projecting images are generated from the spectral images.

2.1 Multi-band projector system

This section shows the outline of the color gamut expansion method of 3D image by multi-band projection. Figure 1 shows the proposed multiband 3D projection system. In particular, each projector is equipped with a filter that has different spectral transmission characteristics in front of the projector. The projected images from each projector are overlaied on the screen. RGB spectral characteristics changes to 6 bands information by using the filters. The desired color is reproduced by 6 bands information. Moreover the proposed system can display 3D images according to project synchronized right or left 6 band images in turn.

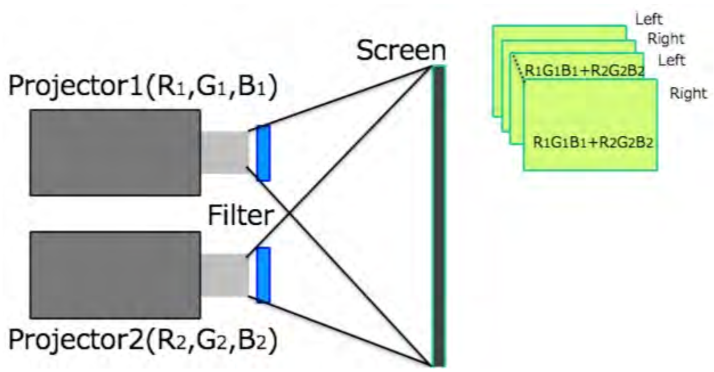

Figure 1: Proposed multiband 3D Projection System.

2.2 Filter simulation

First, the RGB spectral characteristics of 3D projector used in this study is measured. Measurement is performed in a dark room by using only the projected light from the projector. In the measurement, R (255,0,0), G (0,255,0), and B (0,0,255) are respectively projected on the screen. Each RGB spectral distribution are obtained using a spectral radiometer.

The optimal spectral transmission characteristics of each filter is simulated based on RGB spectral distribution of the projector, and the use of notch filter is supposed in this study. The filter characteristic is determined so that the color gamut becomes maximum when it is plotted on xy chromaticity diagram. The simulation performs between 380~780nm, and all wavelength is used in the range. The decision flow of the optimal spectral characteristics of filters is shown in Figure 2.

Filter simulation is calculated while changing the wavelength range which the transmittance becomes 0% in the each filter. Figure 3 shows the decided spectral characteristics of each filter and the spectral characteristics of the projector changed by the each filter. Red, green, and blue lines indicate the changed RGB spectral characteristics of the projector respectevely.

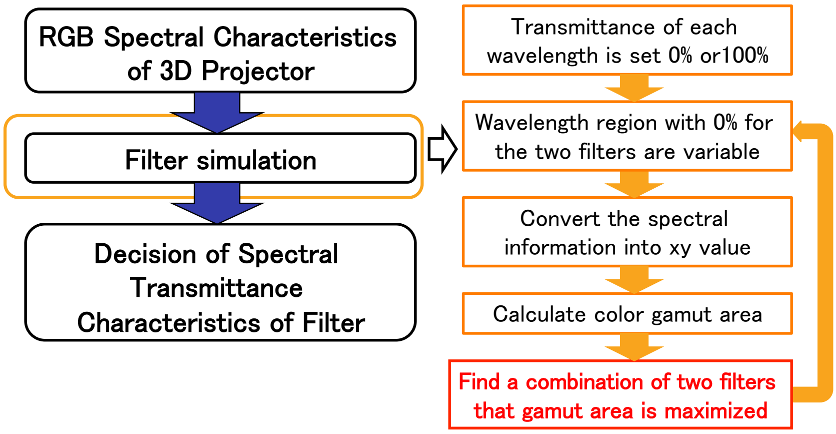

Figure 2: Flow of filter simulation.

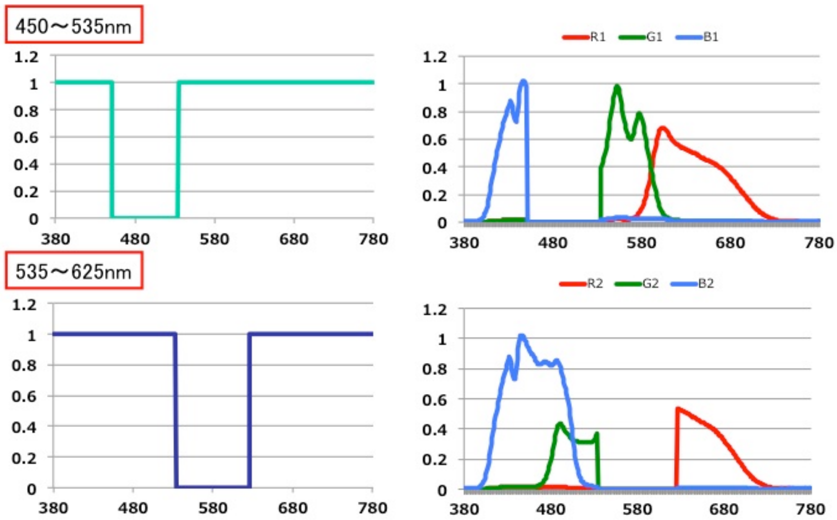

Figure 3: Simulation results.

3. EXPERIMENT AND DISCUSSION

This section shows the experimental results. The experimental system uses two VIEWSONIC PJD6253 as 3D projector. The resolution of projector is 1024 × 760 pixels. In addition, the spectral radiometer that measure spectral distribution is TOPCON SR3. Figure 4 shows the used projector and Figure 5 shows the produced filter experimentally based on the simulation result.

Figure 4: 3D projector.

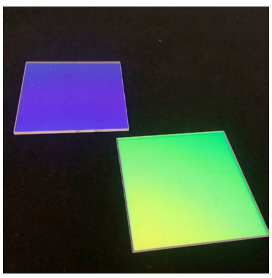

Figure 5: Produced Filter.

Figure 6 shows the spectral characteristics of two produced filters based on the decided spectral characteristics of filters by the simulation. It is possible to present the 6 bands information according to change RGB spectral characteristics by putting these filters in front of the projector's lens.

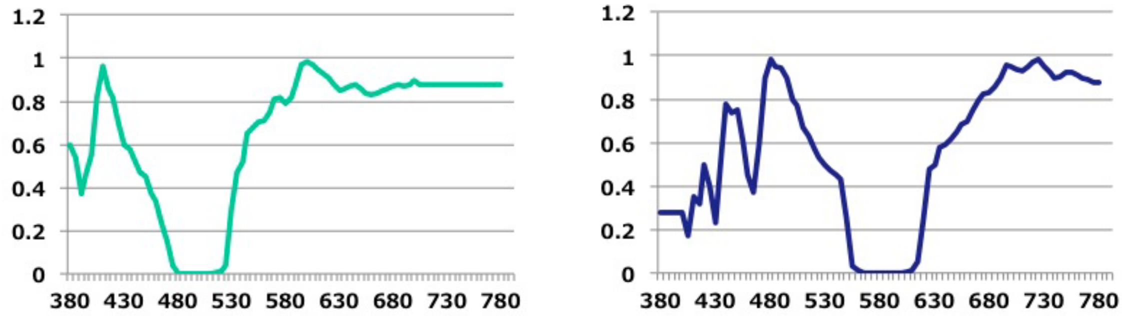

(a) Characteristics of the filter 1. *(b) Characteristics of the filter 2.*

Figure 6: Characteristics of the produced filters.

Table 1 and table 2 show xy values of the used projector's RGB and the proposed 6 bands projector with the produced filters based on simulation respectively. Figure 7 shows the color gamut of the used projector and the extended color gamut of the proposed system with the use of the produced filters. In figure 7, black line triangle indicates the color gamut of the projector's RGB, and red line hexagon indicates the color gamut of the prposed 6 bands projector. These measurement results show the proposed method can expand color gamut with the use of two 3D projectors and notch filter with different spectral transmission characteristics. The color gamut is covered extensively for red, green and blue regions. However, the extension of green region is not enough, because it is considered two filter of spectral characteristics affect the green area.

Using the prototype system an image is projected on a screen. This study uses a spectral image as a input image, not a normal RGB color image. Figure 8 shows the scene that project an image using the projectors put the produced filters. Lower projector is put filter 1 that cut the short wavelength, and upper projector is put filter 2 that cut middle wavelength. The projected image on the screen is shown in figure 9. This image shows that the target color image is reproduced by superimposing the two projected images.

Table 1. xy values of projector's RGB.

	x	y
R	0.625	0.344
G	0.345	0.565
B	0.147	0.085

Table 2. xy value of RGB with filter.

	x	y
R1	0.651	0.346
G1	0.423	0.569
B1	0.169	0.036
R2	0.697	0.288
G2	0.129	0.571
B2	0.131	0.091

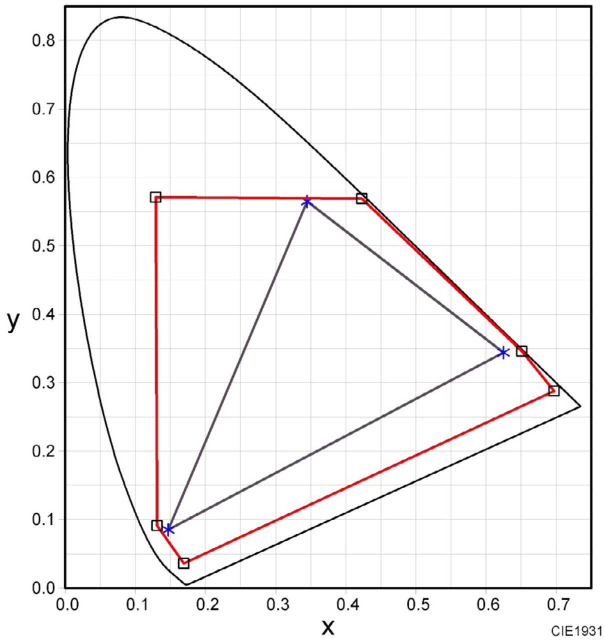

Figure 7: Extension of Color gamut using filters.

Figure 8: Two projectors put each filter.

Figure 9: Superimposed image.

4. CONCLUSIONS

This paper proposed a new method of expanding the color gamut of a 3D display system by the multiband projection using two 3D projectorsa and optical filters. The characteristics of the filter attached to the projector were simulated in order to realize multi-band projection. The optimal filter was decided based on the result of filter simulation, and the extent of color gamut was confirmed by plotting on the xy chromaticity diagram. Also, images created by processing spectral images were input to the projectors put each filter, and projected on the screen. The experimental results showed that the projected images had extend color gamut.

REFERENCES

Ajito, T. Obi, T. Yamaguchi, M and Ohyama, N. 1999. *Six-primary color projection display for expanded color gamut reproduction.* In proc. International Symposium on Multispectral Imaging and Color Reproduction for Digital Archives, pages 135-138.

Miyake, Y. and Yokoyama, Y 1998. *Obtaining and Reproduction of Accurate Color Images Based on Human Perception*, Proc. SPIE Color Imaging, 3300, 190-197.

Yamaguchi, M. 1999. *Multi primary Color Displays*, Color Forum Japan 99, 73-79

Address: Prof. Yoshitsugu MANABE, Graduate School of Advanced Integration Science, Chiba University, 1-33 Yayoi-cho, Inage-ku, Chiba, 263-8522, JAPAN
E-mails: manabe@faculty.chiba-u.jp, yata@chiba-u.jp

Perceived Quality of Printed Images on Fluorescing Substrates under Various Illuminations

Steven LE MOAN, Ludovic GUSTAFSSON COPPEL
Gjøvik University College, Norway

ABSTRACT

We design a quality assessment workflow to measure the perceived quality of prints across illuminants, while accounting for the fluorescence of the substrate as well as the ink UV absorption. Given an input multispectral image, we simulate the output of a CMYKRGB printer by means of a spectral gamut mapping and an extended cellular Yule-Nielsen modified Spectral Neugebaeur model allows us to account for both paper fluorescence and ink UV absorption. We demonstrate the relevance of considering these effects as they lead to substantial changes in the perceived image difference across illuminants. These findings are of particular interest for soft- and hard-proofing applications in spectral printing workflows.

1. INTRODUCTION

In printing, colorimetric workflows ensure that the print looks as good as possible under one specific illuminant (typically daylight), but without accounting for the fact that colours, and therefore colour differences, may change drastically from one illuminant to another (Le Moan, 2014). This effect is referred to as metamerism: two objects may seem to have the same colour under one light, but not under another. There are several applications that require having some control over the quality of a print under various viewing conditions, and for which colorimetric workflows are therefore not appropriate. Furniture catalogues or paint swatch books are among these applications as it is important that customers have a good idea of the colour of a piece of furniture or a particular pigment under the light of their living room for example. Only in a spectral workflow is one able to have such control, by using the pixels' spectral reflectance factor, rather than e.g. RGB or CIELAB values. Controlling quality in such workflows is however challenging due to the potentially large number of viewing conditions that need to be considered (e.g. all kinds of domestic lights) and because distances between pixels (such as the Euclidean distance) carry very little meaning in terms of perception, when computed in the "reflectance domain" (as opposed to the "colour domain").

There is a variety of so-called image-difference metrics in the literature, that aim at predicting the perceived difference between an original image and its reproduction (e.g. a simulated print), using features such as structure, contrast, detail visibility, etc… However, most of these metrics work with three-dimensional colour spaces optimised for one illuminant only. Recently, Le Moan and Urban (2014) proposed a scheme to extend one of these metrics, called CID, for spectral workflows by using a set of representative illuminants and combining the CID scores between the renderings obtained for each of them. The resulting multi-illuminant metric is referred to as Spectral Image Difference (SID) and it has been reported to significantly outperform traditional spectral difference metrics such as the root-mean square error (RMSE) when compared to subjective data. Although SID can be applied to control quality within a spectral printing workflow, it fails to consider paper fluorescence and its impact on the perceived quality of the print. It is well known however that fluorescing whitening agents (FWA) are used to make papers appear whiter (Coppel, 2012). These dyes absorb UV radiation and re-emit light in the blue region of the electromagnetic spectrum. In this study, we design a quality assessment workflow to investigate the influence of paper fluorescence on perceived image quality. Given an input multispectral image, we simulate the output of a CMYKRGB printer by means of a spectral gamut mapping (Urban, 2011) and an extended cellular Yule-Nielsen modified Spectral Neugebaeur model allows us to account for both paper fluorescence and ink UV absorption. We demonstrate the relevance of considering these effects as they lead to substantial changes in the perceived image difference across illuminants. These findings are of particular interest for soft- and hard-proofing applications in spectral printing workflows.

2. QUALITY ASSESSMENT WORKFLOW

2.1 Spectral separation and gamut mapping

Urban and Berns (2011) introduced a spectral gamut mapping strategy, based on a sequence of colorimetric mappings within paramer-mismatch gamuts. For example, given two illuminants γ_1 and γ_2 and given that γ_1 should be prioritized over γ_2, the spectral mapping aims at minimizing the colour difference under γ_2 while keeping the difference under γ_1 unnoticeable (i.e. lower than JND – Just Noticeable Difference). We used this approach and considered a cellular Neugebauer spectral model calibrated for an HP-Z3200 printer in the 7-channel CMYKRGB mode with an almost non-fluorescing EFI offset proof 9200 semimatt 200 g/m^2 paper. Note that, as in Urban and Berns' study, only 4-ink combinations including K were considered (e.g. CMYK, CKRG or MYKB), since it was observed that 5-, 6- or 7-ink combinations do not contribute much to the spectral variability of the printouts and are therefore of limited interest in the present study (in other words, most of the spectral gamut can be described with 4-ink combinations only).

2.2 Fluorescing substrate

When fluorescence is present, the reflectance factor is no longer independent of the illumination and must be estimated for each illuminant. For a halftone print on a fluorescing substrate, the incident light is first partly absorbed by the ink dots before it changes wavelength due to the fluorescence process, and is finally partly absorbed at that longer wavelength by the ink dots. Assuming opacity in the excitation wavelength band and introducing an equivalent scalar transmittance t_j' of the Neugebaur Primaries (NP) in the excitation band, Hersch (2014) proposed an extension of the spectral Yule-Nielsen modified Neugebauer model (Wyble, 2000) expressing the total reflectance factor R^{tot} from measurement of the substrate and NPs in one illumination without excitation radiation and in one illumination with excitation radiation:

$$R^{\mathrm{tot}}(\lambda) = \left[R_{\mathrm{p}}^{\mathrm{tot}}(\lambda) - R_{\mathrm{p}}^{*}(\lambda)\right]\left[\sum_{j=1}^{N} a_j t_j'\right]\left[\sum_{j=1}^{N} a_j t_{\mathrm{j}}(\lambda)^{\frac{1}{n}}\right]^{n} + R^{*}(\lambda)\,, \tag{1}$$

where $R_{\mathrm{p}}^{\mathrm{tot}}$ is the reflectance factor of the substrate in an illumination including the excitation wavelengths, R_{p}^{*} is the reflectance factor of the substrate in an illumination without fluorescence excitation, $t_{\mathrm{j}}(\lambda)$ is the transmittance of NP j at emission wavelength λ, R^{*} is the reflectance factor of the printed substrate without fluorescence excitation, and $N = 2^4$ (four inks) is the number of NPs. The Yule-Nielsen model is applied with factor n to account for the lateral light propagation within the substrate (optical dot gain).

Equation (1) states that the reflectance factor of a halftone is the sum of the reflectance of the halftone without excitation radiation (R^*) and of the paper substrate's fluorescent component attenuated by the weighted t'_j in the excitation band and the weighted t_j in the emission band of the FWA. The apparent transmittances in the excitation band t'_j are obtained by spectrally fitting Eq. (1) with *N*=1 to the measured reflectance of fulltone individual NP ($a_j = 1$) with (R_j^{tot}) and without (R_j^*) fluorescence excitation. Two i1 spectrophotometers (X-rite Inc.), with and without UV cut-off filter were used to determine t'_j and $t_\mathrm{j} = \left(R_j^*/R_\mathrm{s}^*\right)^{1/2}$ of the inks when printed on a fluorescing substrate whose fluorescent component was measured in the same way. We propose here to determine the paper's fluorescent component in different illuminations from the Donaldson matrix $D(\lambda_1, \lambda_2)$, which gives the bispectral reflectance from all excitation wavelengths λ_1 to all emission wavelength λ_2. From this matrix we computed the fluorescent component of the reflectance factor of the paper according to (Zwinkels, 1999),

$$R_\mathrm{p}^{\mathrm{tot}}(\lambda_2|E) - R_\mathrm{p}^*(\lambda_2) = \frac{1}{E(\lambda_2)} \sum_{\lambda_1<\lambda_2} D(\lambda_1, \lambda_2) E(\lambda_1), \quad (2)$$

where *E* is the spectral power distribution (SPD) of the illuminant. Note that, in practice, FWA tend to decrease $R_\mathrm{p}^*(\lambda_2)$ in the 400-420nm band (Coppel, 2011) but this effect is neglected in this study. It is also worth noting that the fluorescent component depends on this SPD in the emission band of the FWA. This means that two illuminants that have the same SPD in the excitation band do not necesseraly lead to the same fluorescent component (Coppel, 2013). The Donaldson matrix of a typical paper sample with 18 kg/T FWA measured with a bi-spectrophotometer (Coppel, 2011) was used here.

Once the ink surface coverages are determined by the spectral separation and gamut mapping for the non-fluorescence case, Eq. (1) is used to simulate the printed spectral images with fluorescence under illuminants CIED65 and CIEA. Figure 1 shows the relectance factor of the unprinted and fulltone patches in the different illuminants.

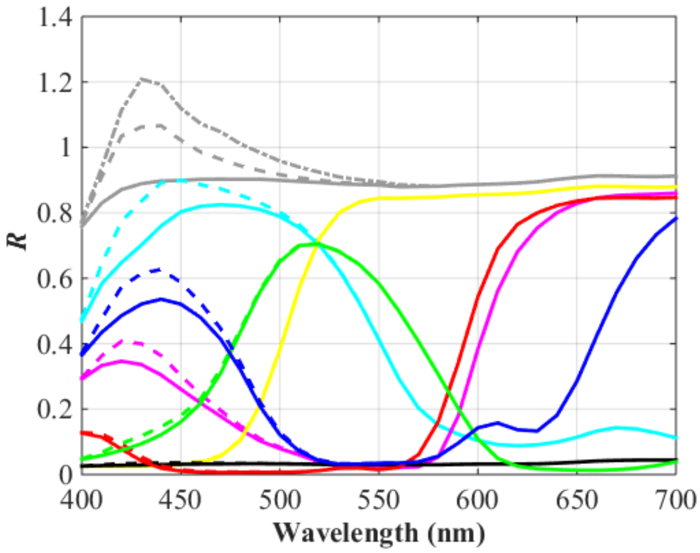

Figure 1. Measured reflectance factors R of the process inks and paper without fluorescence (solid) and simulated R with fluorescence in illuminant CIEA (dash) and CIED65 (dash-dot, only bare paper). The inks are represented by their respective colours. Note that light tones and ink combinations with only cyan, blue and magenta are the most subject to colour shifts due to fluorescence.

3. SPECTRAL IMAGE DIFFERENCE

In order to evaluate the perceived quality of the simulated prints, we used the Spectral Image Difference metric (Le Moan, 2014), with only the two illuminants under consideration. This metric evaluates the perceived image difference under each illuminant and computes the weighted mean value as the final score. Note that it uses a chromatic adaptation transform in order to account for the ability of our visual system to adjust to various viewing conditions. The resulting score was shown to correlate with human judgement to a great extent. For this particular study, we used the most recent implementation of the CID metric - on which SID is based - referred to as MSiCID (*Multi-Scale improved* CID) (Le Moan, 2015). Incidentally, we renamed the SID metric as iSID (*improved* SID). We define it as follows:

$$\mathrm{iSID}(\mathbf{I}_1;\mathbf{I}_2) = \alpha \mathrm{MSiCID}\left(\mathbf{i}_{1,D65};\mathbf{i}_{2,D65}\right) + \beta \mathrm{MSiCID}\left(\mathbf{i}_{1,A};\mathbf{i}_{2,A}\right), \tag{3}$$

where $\mathbf{I}_1$ and $\mathbf{I}_2$ are two spectral images, $\mathbf{i}_{x,\gamma}$ is the rendering of $\mathbf{I}_x$ for illuminant γ and α and β are weighting coefficients. We considered that CIED65 should be prioritized over CIEA as daylight is still the most used reference illuminant in many printing applications. Consequently, we used the following coefficients: $\alpha = 0.75$ and $\beta = 0.25$.

3. RESULTS

We used the 16 natural scenes from the two Foster hyperspectral image databases (Nascimento, 2002). They depict natural scenes (vegetation, urban areas…) and contain between 30 and 32 spectral channels, sampling the visible range of wavelength from 400 to 720nm. However, in order to fit the characteristics of our printer model (see Section 2.2), all images were modified to be in the range 400-700nm. For images whose spectral ranges starts at 410nm, the band at 400nm was assumed to be equal to the one at 410nm.

Table 1 gives the mean, standard deviation and maximum iSID scores obtained when comparing the simulated prints with and without fluorescence. Note that iSID scores range from 0 (no difference) to 1 (largest measurable difference). Figure 2 shows an example of images rendered for CIED65, with and without considering the fluorescence phenomenon. Figure 3 shows the DE2000 pixel-wise colour-difference maps for CIED65 and CIEA for one of the 16 spectral images considered in this study, for illustrative purposes. What we believe is particularly noteworthy here is that not considering fluorescence will likely result in a perceivable difference in the final print, up to 0.122 iSID units on the data tested, which is considerably high.

Table 1. Obtained iSID scores on each scene of the Foster database, between simulated prints with and without fluorescence and ink UV absorption (respectively $\mathbf{I}_{\mathrm{fluo}}$ *and* $\mathbf{I}_{\mathrm{no\_fluo}}$*).*

	$\mathrm{iSID}\left(\mathbf{I}_{\mathrm{fluo}};\mathbf{I}_{\mathrm{no\_fluo}}\right)$
Average	**0.057**
Standard deviation	**0.034**
Maximum	**0.122**

Figure 2. Simulated prints, without (left) and with (right) considering fluorescence and ink UV absorption, for CIED65. Note how these phenomena change particularly the colour of the flower petals, which consist mainly of magenta ink.

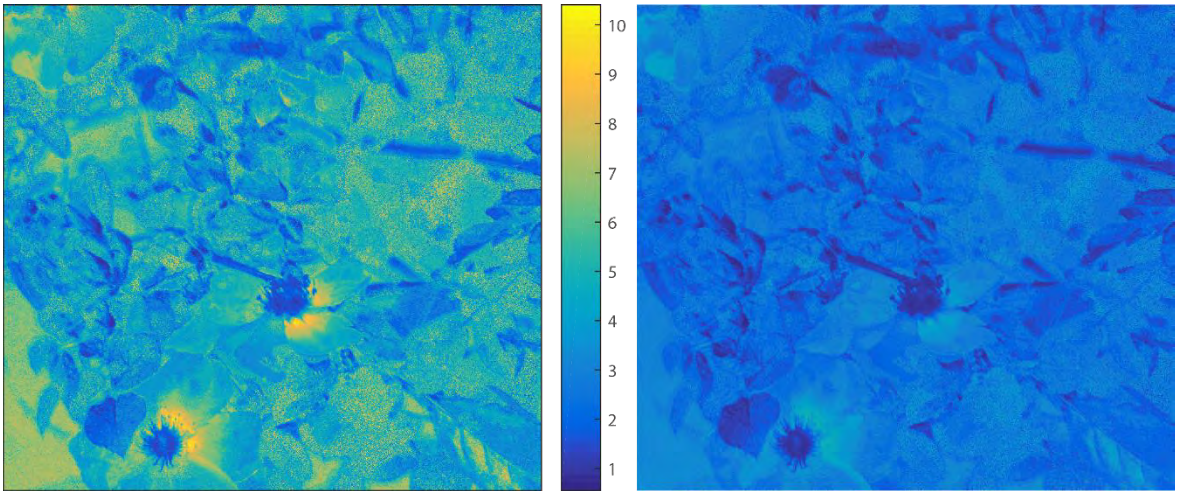

Figure 3. DE2000 colour-difference maps for CIED65 (left) and CIEA (right). Note that daylight, which contains more energy in the UV wavelengths and therefore engenders more fluorescence, yields colorimetric errors larger than 10 DE2000 for this particular image

4. CONCLUSIONS

We designed a quality assessment workflow to measure the perceived quality of prints across illuminants, while accounting for the fluorescence of the substrate as well as the ink UV absorption. Given an input multispectral image, we simulated the output of a CMYKRGB printer by means of a spectral gamut mapping and an extended cellular Yule-Nielsen modified Spectral Neugebaeur model allowed us to account for both paper fluorescence and ink UV absorption. We demonstrated the relevance of considering these effects as they lead to substantial changes in the perceived image difference across illuminants.

ACKNOWLEDGEMENTS

This work was supported by the Marie Curie Initial Training Networks (ITN) CP7.0 N-290154 funding.

REFERENCES

Coppel, L.G, Anderson A, Edström P. and Kinnunen J. 2011. *Limitations in the Efficiency of Fluorescent Whitening Agents in Uncoated Paper*. Nordic Pulp Paper Research Journal, 26(3), 319–328.

Coppel, L.G., 2012. *Whiteness and Fluorescence in Layered Paper and Board*. Doctoral Thesis No. 138, Mid Sweden University.

Coppel, L.G., Andersson M., Norberg O. and Lindberg S. 2013. *Impact of Illumination Spectral Power Distribution on Radiance Factor of Fluorescing Materials*, IEEE Proc. Colour and Visual Computing Symposium (CVCS).

Hersch, R.D. 2014. *Spectral Neugebauer-based Color Halftone Prediction Model Accounting for Paper Fluorescence*, Applied Optics 53(24), 5380–90.

Le Moan, S. and Urban, P., 2014. *Image-Difference Prediction: From Color to Spectral*, IEEE Transactions on Image Processing 23(5) 2058-2068.

Le Moan, S. and Urban, P. 2015. *Evaluating the Multi-scale iCID Metric*, IS&T/SPIE Image Quality and System Performance XII, 9396, 38.

Nascimento, S.M.C., Ferreira, F.P., and Foster, D.H. 2002. *Statistics of Spatial Cone-excitation Ratios in Natural Scenes*, Journal of the Optical Society of America A, 19(8), 1484–1490.

Urban, P. and Berns, R.S. 2011. *Paramer Mismatch-based Spectral Gamut Mapping*, IEEE Transactions on Image Processing 20(6), 1599-1610.

Wyble, D.R. and Berns, R.S. 2000. *A Critical Review of Spectral Models Applied to Binary Color Printing*, Color Research and Application, 25(1), 4-19.

Zwinkels, J.C. and Gauthier, F. 1999. *Instrumentation, standards, and procedures used at the National Research Council of Canada for high-accuracy fluorescence measurements*, Anal. Chim. Acta, 380, 193–209.

Address: The Norwegian Colour and Visual Computing Laboratory,
Gjøvik University College, Teknologivegen 22, 2815 Gjøvik, NORWAY
E-mails: steven.lemoan@gmail.com, ludovic.coppel@hig.no

To Predict Reality in Virtual Environments: Exploring the reliability of colour and light appearance in 3D-models

Beata STAHRE WÄSTBERG[1], Jacqueline FORZELIUS[1] and Monica BILLGER[2]
[1] Department of Applied Information Technology, University of Gothenburg
[2] Department of Architecture, Chalmers University of Technology

ABSTRACT

To predict how the not yet built environment is going to appear regarding light and colour is a crucial problem for architects and designers. 3D-visualization is an established design tool and used for representations of project proposals, often with the aim to make good-looking images that sell the design. In order for software such as 3Ds Max to become usable planning tools of light and colour in buildings, the visualization must be trusted to show the correct appearance in accordance with the physical preconditions of reality. This paper discusses the problems of translating reality to its digital counterpart. In previous studies from 2004-2006, a reference room was compared to different simulations. The result showed significant differences in colour and light appearance between the reference room and the virtual rooms. Since then, the technology within colour rendering has moved forward. New comparisons with the reference room were performed in 3Ds Max Design 2015, in order to explore the trustworthiness of colour and light representations today. The rendering techniques Mental ray and Vray were evaluated. Preliminary results show strong improvements regarding colour variations and shadows. However, there are still incorrectly reproduced contrast effects and interreflections between angled surfaces.

1. INTRODUCTION

This paper discusses the problems of translating reality to its digital counterpart. 3D-visualization is an established design tool for architects and designers. In many cases, the aim with the visualizations is to make good-looking images to sell the design. In order for software, such as 3Ds Max, to become usable planning tools of light and colour in buildings, the visualization must be trusted to show the correct appearance in accordance with the physical preconditions of reality. The complex interaction between light and objects makes the problem of lighting scenes central within computer graphics. There are few studies on colour appearance within real compared to virtual environments (Stahre and Billger, 2006, Billger et al, 2004). A method for comparing real environments with digital images was introduced by Meyer et al (1986). This method was built upon measurements of radiant energy flux densities in a simplified physical environment; *i.e.* the Cornell Box, compared to a simulation where radiosity was used. In order for the comparison to be as accurate as possible, both the image and the box were viewed simultaneously through a camera. Another study where simulations were compared to a real scene was carried out by McNamara et al (2005). The study aimed to determine how much computation is enough in order to create a trustworthy image, based on the human visual system rather than on physical correctness. For this the ray tracing based software Radiance was used. Objects were viewed in a real scene, *i.e.* a lighting booth, and compared to rendered images. Scenes were viewed monocularly in order to eliminate depth cues. Mania et al (2003) aimed for photo-realistic simulations and made great efforts to control colour and lights. In their study, the focus lay on mnemonic recall of individual objects in a room. Colour appearance was not visually assessed or discussed, though the study involved the translation of colours from reality to Virtual Reality (VR) in different viewing conditions. In order to achieve a more 'naturalistic' awareness state, the realism in the simulations was sometimes forgone. In recent years, interesting software development has been undertaken in photorealistic rendering (Pharr and Humphreys, 2010; Billeter, 2012; Maxwell Renderer, 2015).

In a previous study (Billger et al, 2004; Stahre et al, 2005; Stahre and Billger, 2006), interactive spatial 3D-models were compared to a full scale reference room. Important in this study was that the rooms were studied interactively from *within*. Various problems were discovered in 3Ds Max related to the rendering of light and colour in the models. Compared to reality, the virtual rooms showed incorrect reflections between surfaces; too simple chromatic information on light sources; too achromatic shadows; too few contrast effects; and too few colour variations. Since then, the technology within colour rendering and computer graphics has moved forward. In this study, we want to investigate if the stated problems are solved with today's software technology, focusing on 3Ds Max and its built-in renderer Mental Ray; as well as the external renderer VRay. The aim with this study is to identify problems and test solutions for simulating trustworthy visual appearance, focusing on colour and light, in digital modeling. The results persented here are based only on rendered views of the room.

2. METHOD

In the earlier studies carried out 2004-2006, a 25 m^2 multi-coloured reference room was compared with corresponding digital models (Fig 1A, B). The models were made in Lightscape and in 3Ds Max[1]. The 3Ds Max-model was exported to VR in order for the rooms to be interactively evaluated from within. 56 observers evaluated the different rooms using various evaluation techniques. Initially, studies were conducted in the reference room, and in Lightscape/3Ds Max. To compare the model and the reference room, the results of the visual assessments (verbal description, magnitude estimation and colour matching with the colour reference box) were analyzed. These results lead to adjustments of the digital models. In order to compare colours with their digital counterparts, a process was developed to translate real colours to digital values. Since the translation was complex, it was important to find an acceptable level of correctness. A basic prerequisite for correct colour appearance in the digital models was that the computer was calibrated. Most important however was that the *relationship* between differently coloured surfaces was as correct as possible compared to reality. If so, small displacements between colours on different displays were acceptable; as well as small translocations of the colour scale, since they were results from the adaptation to the surrounding light, and the light from the computer. For documentation and reference, physical measurements of the spectral composition were conducted for the room surfaces both in the reference room and in the models. Three different illuminations were used: incandescent light; fluorescent 827 (2700K); and fluorescent 830 (3000K). In order to get the simulation of the 6 fluorescent luminaries (2 ceiling armatures and 4 wall washers) as correct as possible, the manufacturer Fagerhult's own photometric light was used as IES-files, enabling a

[1] Halfway through the project, Lightscape was incorporated into 3Ds max, and ceased to exist as a free-standing product. The light calculation functions of Lightscape were incorporated into 3Ds max, which led to the use of this program for the continued studies.

simulation of the lighting originally used in the reference room. For the renderings, the default Scanline renderer in 3Ds Max was used, since this was at the time for the studies the only renderer in 3Ds max supporting photometric light using radiosity.

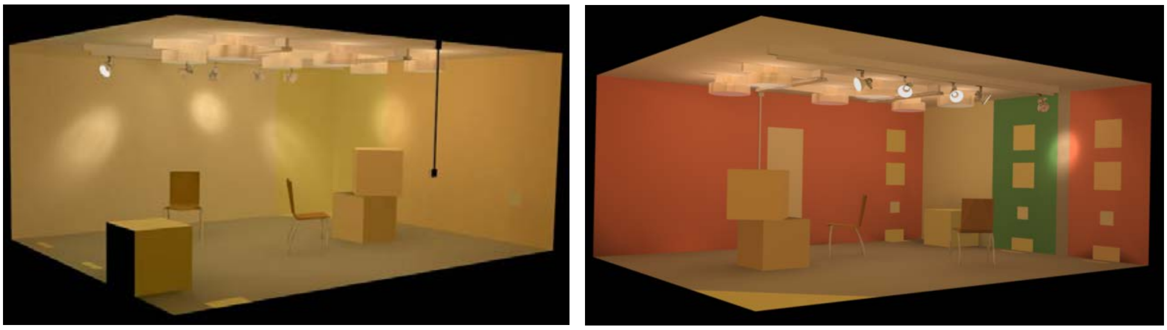

Figure 1A,B: The reference room, designed to show clear examples of how simultaneous contrast phenomena and reflections cause different appearances.

In our comparative study from 2014-2015, tests were performed in 3Ds Max Design 2015 in order to explore the trustworthiness of colour and light representations, with the aim to find out if our stated problems had been solved. For this, the same 3Ds Max-models were used as in previous studies, and evaluated against the same reference room. Focus lay on the flourescent illumination 830 (3000K). The light sources were not manipulated, and no additional illumination were allowed. The models were rendered with the built-in renderer Mental Ray, since it now supports photometric light, and the now existing external renderer VRay (Visual Dynamics, 2015). The default settings of 3Ds Max were used, following the recommended settings in the tutorials. A difference to earlier recommendations, used in the previous studies, meant that all colours in the model were based on bitmap-textures, and that Gamma 2.2. was applied by default in 3Ds Max (Aversis 3D-Tutorials, 2014). The evaluation in this study consisted of visual assessments made by the research team.

3. RESULTS AND DISCUSSION

3.1. Colour and light appearance in the reference room 2004-2006

The reference room was designed to show significant effects of illumination, reflections and contrasts. Our previous studies showed that in this room differently painted surfaces perpendicular to or opposite each other became more similar by reflections, causing large colour variations on equally painted surfaces. Each uniformly painted area showed different colour variations, and contrast effects were evident between differently painted surfaces on the same level (Figure 2A). A brightness phenomenon appeared, *i.e.* the light square on the yellow wall in the darkest corner was perceived as whitest and lightest of all surfaces, although five other areas in the room were painted in the same nuance (Figure 2B). Visual assessments showed that even small differences in colour appearance could be important for the experience. The colours also showed very different appearance in the different light situations. The white fluorescent illumination (3000K) was by most observers found to be cold or neutral, and experienced as having practically no colour, though some observers found it to be slightly yellowish. The more yellow 2700K fluorescent light was by the observers perceived as slightly warmer, and having a greenish tint.

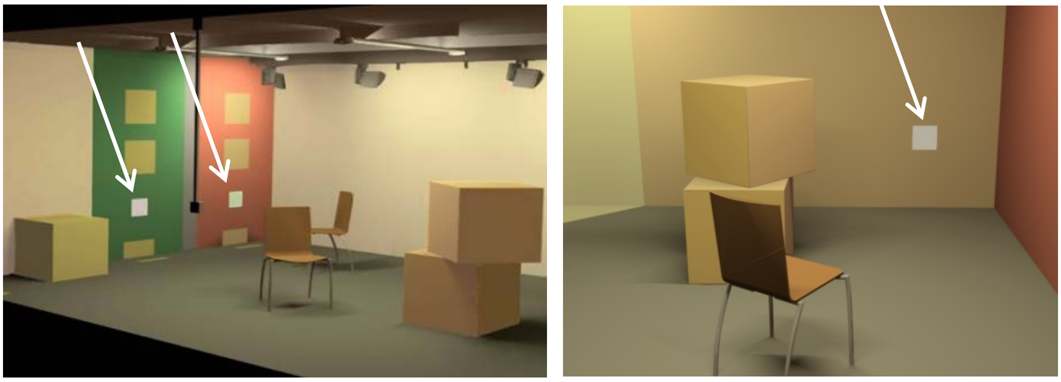

Figure 2 A: A contrast phenomenon made the greenish light square on the green background appear pinkish and the reddish light square on the red background appear greenish. B: A brightness phenomenon made the small square appear whitest and lightest. (Manipulations made to demonstrate the appearance in the reference room.)

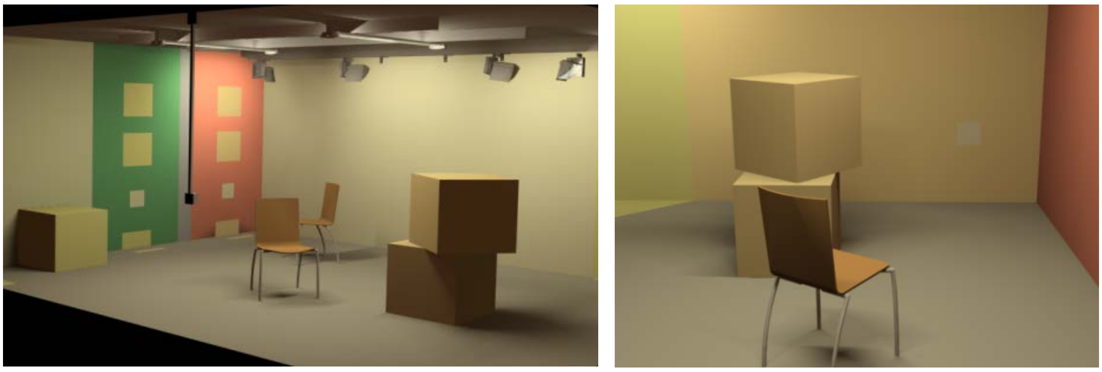

Figure 3A,B: The same views rendered with the Scanline renderer in 2004-2006.

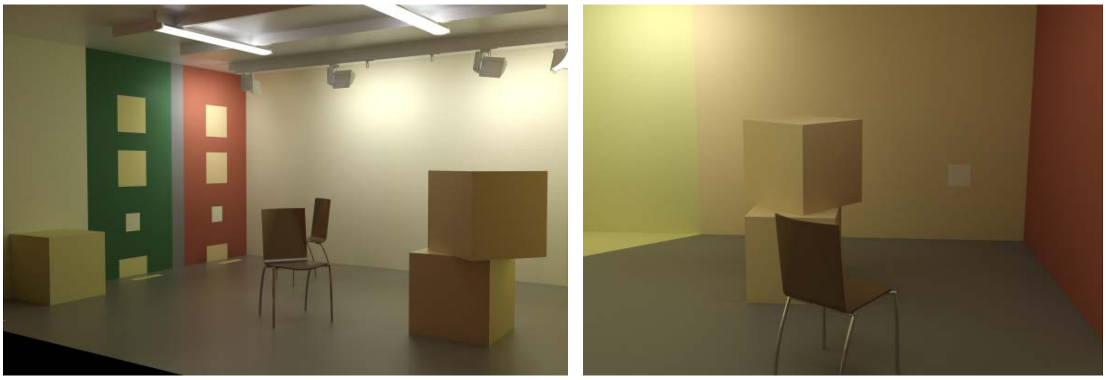

Figure 4A,B: The same views rendered with the Mental Ray renderer in 2014-2015.

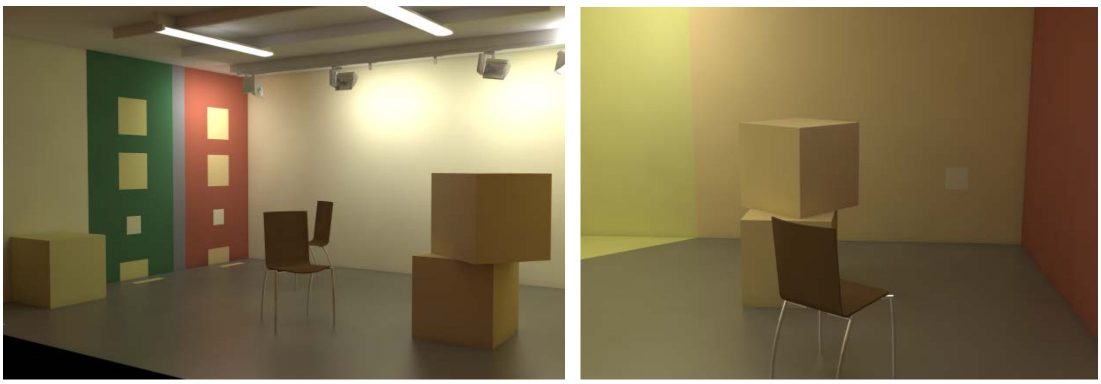

Figure 5A,B: The same views rendered with the VRay renderer in 2014-2015.

3.2. Colour and light appearance in 3Ds Max 2004-2006

In the virtual room, five significant differences in appearance compared to the reference room were pointed out, including: 1) Too few colour variations: The large colour variations on equally painted surfaces that appeared in the reference room did not show. Furthermore, the areas with the whitest nuances came out too greyish. 2) Too few contrast effects. Neither the contrast effects between differently painted surfaces on the same level (Figure 3A), nor the brightness phenomenon regarding the light square on the yellow wall (Figure 3B) appeared. 3) Incorrect reflections between surfaces perpendicular to, or opposite, each other. 4) Too simple chromatic information on light sources: The fluorescent lights 3000K and 2700K appeared identical, while they in reality caused distinctly different colour appearance. 5) Too achromatic shadows.

Moreover, problems with the parameter settings for the radiosity calculations were discovered. The recommended settings for physically correct results regarding colour bleed in 3Ds Max resulted in fewer colour variations compared to reality. Furthermore, the recommendation for colour bleed from the manufacturer of the light fixtures turned out to be too low.

3.3. Colour and light appearance in 3Ds Max 2014-2015

In both Mental Ray and Vray, preliminary results show general improvements on colour and light appearance. Concerning the stated problems from the earlier studies, the following observations were made. 1) The colour variations have visibly improved. 2) The contrast effects are still too few. No difference has been observed from previous studies. Neither the contrast effects between differently painted surfaces on the same level (Figures 4A,5A), nor the brightness phenomenon regarding the light square on the yellow wall (Figures 4B,5B) appeared to a satisfactory extent. 3) There are still incorrect reflections between surfaces: Reflections are not having enough impact on angled surfaces compared to opposite ones. For example, the short light wall appears greenish in all simulations; however in reality it is strongly affected by the red wall and appeared light beige without any green tint. 4) There is still too simple chromatic information on light sources: The lights 3000K and 2700K appeared almost the same. 5) The shadows appear close to reality, *i.e.* they are no longer achromatic. A specific difference between Mental Ray and Vray was that the light from the wallwasher spotlights created burned out areas in VRay (Figure 5A).

4. CONCLUSION

In our studies from 2004-2006, various problems related to the translation and comparison of light and colour appearance in real world settings to 3D-models were revealed. Even when the real world appearance was studied in detail, it turned out to still be difficult to simulate a trustworthy appearance in the models. In our new comparative study, results show strong improvements in 3Ds Max regarding colour variations, shadows and reflections. However, there are still incorrectly reproduced contrast effects and interreflections between angled surfaces. A conclusion drawn is that in 3Ds Max, even when the real appearance is known, the handling of various complex parameters makes the creation of an accurate colour and light appearance extremely problematic, even for expert users. Though some issues regarding the appearance by now are solved, others remain. The technology has reached the point were we by manipulations can render an almost perfect copy of a real scenario. However, it is still a problem to recreate correctness in the representation of colour and light when the real world appearance is *not* known. In order to be able to predict a future built scenario in 3Ds Max, one must have an extensive experience of both the real world appearance and various parameter settings in the software. Knowing the colour appearance of the real objects (rooms, buildings, etc) has proved to be essential in order to correctly recreate a trustworthy colour and light representation in 3Ds Max. Psychological phenomena and the way the human visual system works need to be included in the research as a complement to today's mathematical modeling of physical conditions.

ACKNOWLEDGEMENT

We thank Visual Arena Lindholmen for support and use of facilities.

REFERENCES

Aversis 3D-Tutorials, 2014, Available online, www.aversis.be/tutorials/vray/vray-20-gamma-linear-workflow_01.htm, Accessed: December 15, 2014

Billeter, M, Sintorn, E and Assarsson, U, (2012) Real-Time Multiple Scattering using Light Propagation Volumes In: Proceedings 13D '12 Proceedings of the ACM SIGGRAPH Symposium on Interactive 3D Graphics and Games, pp 119-126

Billger, M., Heldal, I., Stahre B. and Renström K., (2004): Perception of Colour and Space in Virtual Reality: A Comparison between a Real Room and Virtual Reality Models. In: Proceedings for IS&T SPIE 16th annual meeting on Colour Imaging, pp. 90–98.

Mania, K., Troscianko, T., Hawkes, R. and Chalmers, A. (2003). Fidelity metrics for virtual environment simulations based on spatial memory awareness states. *Presence: Teleoperators and Virtual Environments* 12(3): 296-310.

Maxwell Render, 2015, Available online, www.maxwellrender.com/

McNamara, A. M. (2005). Exploring perceptual equivalence between real and simulated imagery. In: Proceedings of the 2nd symposium on Applied Perception in Graphics and Visualization. A Coroña, Spain. pp 123 - 128.

Meyer, G. W., Rushmeyer, H. E., Cohen, M.F., Greenberg, D.P. and Torrance, K.E. (1986). An Experimental Evaluation of Computer Graphics Imagery. *ACM Transactions on Graphics* (TOG) 5(1): 30-50.

Pharr, M. and Humphreys, G., (2010) *Physically Based Rendering: From Theory to Implementation, Second ed*., Elsevier Inc. Morgan Kaufmann; 2 edition

Stahre B., Billger, M. and Fridell Anter, K., (2009). To Colour the Virtual World - Difficulties in Visualizing Spatial Colour Appearance in Virtual Environments, *International Journal of Architectural Computing* (IJAC), 02(07), 289-308

Stahre, B. and Billger, M., (2006): Physical Measurements vs Visual Perception: Comparing Colour Appearance in Reality to Virtual Reality. In: Proceedings for CGIV 2006, Leeds, United Kingdom, June 19–22, 2006, pp 146-151.

Stahre, B., Gatta, C., Billger, M. and Rizzi, A., (2005): Towards perceptual colour for virtual environments. In: Proceedings for 10th Congress of the International Colour Association AIC Colour 05, Granada, May 8–13, 2005, pp 219-222.

Visual Dynamics, 2015, Available online, www.vray.com/, Accessed: February 19, 2015

Address: Dr. Beata STAHRE WÄSTBERG, Department of Applied Information Technology, University of Gothenburg, Forskningsgången 6, 417 56 Göteborg, SWEDEN
beata.wastberg@ait.gu.se, jackie.forzelius@gmail.com, monica.billger@chalmers.se

Altering Perceived Depth of Objects with Colored Lighting

Ruth Genevieve ONG, Nan-Ching TAI
National Taipei University of Technology

ABSTRACT

Color stereopsis is a phenomenon in which colored objects on the same plane are perceived to be on different planes or depth, and prior studies about this indicate that long–wavelength colors were often perceived to be nearer, although there are occasions wherein a reverse or even no effect was perceived. However, very little research on how lighting can affect color stereopsis exist, especially in relation to color contrast between target objects and its surround or context. This study sought to test whether lighting can alter an object's perceived depth resulting from color contrast (thereby creating a color reversal), and whether the red target object will be perceived to be nearer under different colored lighting conditions. Seven lighting conditions were used to illuminate a scaled model of a gallery, and radiance maps were created to serve as visual stimuli for the psychophysical experiment. Results show that colored lighting can affect color–depth perception due to the resulting change in color contrast between the target objects and its context, and that under different colored lighting conditions, color reversal would occur due to the color contrast.

1. INTRODUCTION

Color stereopsis, or chromostereopsis, is a phenomenon in which colored objects located on the same plane are perceived to be on different planes, therefore creating a difference in depth or spatial layout. Many studies on the topic have expressed that a long–wavelength stimulus was more often perceived to be closer than short–wavelength stimulus even when both are equidistant from the observer (Luckiesh 1918; Payne 1964; Sundet 1978). When the reverse effect was perceived, that is, the short–wavelength stimulus was perceived as nearer than long–wavelength stimulus, a color reversal is said to have occurred.

Several studies on the possible causes of this color reversal and color stereopsis in general have been conducted (Vos 1960; Winn et al 1995), but most attribute the color stereopsis effect to "optical" causes. Thompson et al (1993) drifted from this convention when they proposed that color stereopsis could be due to a combination of luminance–based and color–based depth effects, thereby suggesting a perceptual basis for the effect. This perceptual basis for the color stereopsis effect seems promising, but only a few studies cover color–based depth effects, as most focus on the influence of luminance. Dengler and Nitschke (1993) claim that the color reversal effect can be due to border contrast between the colored stimulus or target and its immediate surround rather than just the "optical" causes, while Rempel et al (2011) cited Treisman's observations that color and contrast both influence perceived depth.

However, these studies (even for studies on luminance–based effects) usually discount the illuminant in their experiments, claiming that lighting had a negligible effect on the scene. But an illuminant is known to influence color appearances, especially if the lighting is spectrally different from daylight or a cool-white illuminant. Prior studies on target–surround contrast used achromatic surround in their experiments, but should the color of the light change, the surround or context may change along with it, as will the contrast between the target and surround. This study then seeks to discover how colored lighting would affect the color stereopsis effect (wherein red was perceived nearer than blue) by manipulating the color of the illuminant, and whether color reversal would occur under different colored lighting conditions.

2. METHOD

To investigate the effect of colored lighting on color–depth perception, a psychophysical experiment was conducted to test whether the red stimuli will still be perceived to be nearer than the blue stimuli under colored lighting. Two hypotheses were developed for this study: first, that the red object was perceived to be closer even under different colored lighting conditions (at least 50% of the observed responses); and second, that the proportions of observed responses across different lighting conditions are the same.

2.1 Experiment Setup

A 1:5 scaled model of an 18 meters × 6 meters gallery was designed to be the three-dimensional environment for the study. The scaled model was composed of three bays, with its interior surfaces (walls, floor, and ceiling) lined with plain grayish brown cardboard sheets. Two of the bays had a skylight to illuminate the gallery. One of the skylights had a colored filter while the other did not. Colored cellophane sheets were used as a "filter," to represent colored lighting.

The two cubes assigned to be the target objects were of equal dimensions (40cm × 40cm × 40cm), and were hung with a nylon string in order to appear as if they were floating in Bay C. Both cubes were spray painted with two colors, red and blue. The surfaces of the two cubes facing the observer were aligned with each other, and this same plane/surface was aligned to one edge of the skylight opening. The observer's standpoint (or in this case, the camera), was set about 12 meters away from the target objects. The blue cube was placed on the right side, while the red cube is on the left side. Figure 1 shows a cut-away view of the scene, indicating the location of the target objects, observer, and the skylights.

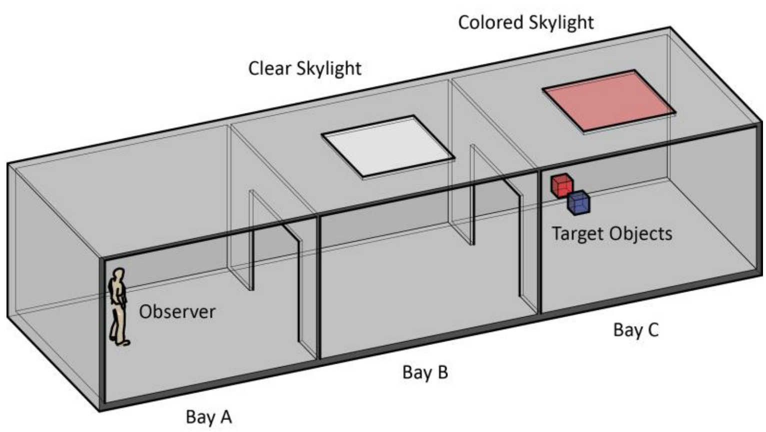

Figure 1: Cut-away view of experiment setup.

Six colored lighting were tested in this study: two variations each for the blue, red, and yellow lighting. The variations of the colored lighting were created through the layering of the cellophane sheets. The first, and lighter variation, used one layer of cellophane sheet, and the second, darker variation used four layers. The colored cellophane sheets covered the skylight opening in Bay C. A seventh test condition (neutral or uncolored) was included to serve as the control or baseline image. In this condition, there were no colored cellophane sheets over the skylight opening in Bay C. Using a room's fluorescent lamp as the light source for the scaled model, the light entering Bay C became colored due to the cellophane sheets.

2.2 Visual Stimuli

Instead of using physical objects as stimuli, which is a commonly employed color stereopsis experiments, we opted to create the visual stimuli through high-dynamic range (HDR) photography. Through radiance maps (the most common way of generating HDR content), issues about color constancy during changes in colored lighting can be minimized. A radiance map is produced by combining several low-dynamic range images to create a single HDR image.

Low-dynamic range images of the scene were captured using a tripod-mounted Canon 5D Mark III, with a 50mm prime lens attached to it. The camera was manually set to focus on the target objects. For each lighting condition, ten images of the scene were captured; each image was set to have one of the following shutter speeds: 1/15, 1/8 , 1/4, 1/2, 1, 2, 4, 8, 15, and 30 seconds. The captured images were then combined using Photosphere (Ward 2010) to create the radiance maps.

Since the typical display device cannot natively display HDR images, the radiance maps had to be tone mapped to properly display them on a typical display device. The Photoreceptor tone mapping operator was selected for this study as an example of one of the many tone mapping operators available (Reinhard and Devlin 2005). Figure 2 shows a compilation of the tone mapped HDR images of the seven colored lighting conditions.

Figure 2: Tone mapped HDR images of the scenes with colored lighting (L–R: Neutral, Blue 1, Blue 4, Red 1, Red 4, Yellow 1, Yellow 4).

2.3 Experimental Procedure

The tone mapped images were used as visual stimuli for a psychophysical experiment wherein observers were presented with one image of the colored lighting condition at a time, and they were asked to choose which of the target objects in the scene did they perceive to be nearer.

Ten trichromat observers (one of which is one of the authors) with normal or corrected-to-normal vision participated in the psychophysical experiment. The experiment was held in a completely dark environment. There was no lighting in the room except from the backlit laptop monitors (one used for presenting the visual stimuli, and another—which faced away from the observer—for recording the observers' responses). The visual stimuli were shown to observers using a 13" Intel Core i5–4258U 2.40Ghz MacBook Pro with Retina display, Intel Iris 1024 MB graphics, 2560 × 1600 resolution, and 60Hz refresh rate. The color settings of the monitor remained at default (Apple RGB color profile), and display brightness was at 75%.

Using the method of constant stimuli, each of the seven lighting conditions was shown ten times (for a total of 70 trials per observer) to the observers in block randomization. A black image was shown for about two seconds between each lighting condition to prevent the subject from total adaptation to the scene. Observers were tasked to verbally respond (forced choice) which of the two target objects in the scene appeared to be nearer based on the target objects' color. The responses of the observers were then recorded in a spreadsheet on a second laptop (display brightness was at the lowest level to decrease the amount of light in the room).

3. RESULTS AND DISCUSSIONS

By visually comparing the tone mapped images, the hue of the target objects did not seem to change, although the value and saturation appear to have been affected. The blue target object in the Blue 1 and Blue 4 lighting conditions look lighter than the blue target in the Neutral condition, while the blue target object in other lighting conditions seems to be more saturated than in the Neutral condition. The red target object in the Red 1 and Red 4 conditions appear to be less saturated than in the Neutral condition, but in other scenes the red target's saturation did not appear to change.

As for the context color (the wall behind the target objects), its color appearance changed accordingly with the colored lighting used in the scene. When the colored lighting was blue, the original context color became blue; the same goes for the red and yellow colored lighting. The grayish cardboard surfaces are no longer achromatic, even though the target objects retained their hue. The values of the surround also differed between the variations, with the dark variation of lighting creating a darker surround than the lighter variation. This change in the hue and value of the surround then changed the color contrast between the target and the surround, creating target–surround contrasts that may be higher or lower depending on the colored lighting.

Responses for the psychophysical experiment were tallied as red being nearer or blue being nearer. Figure 3 shows a graph of the medians of responses and the inter-quartile range for all seven lighting conditions. The dotted horizontal line signifies the median value of 5, the point wherein the red and blue stimuli are perceived to be equidistant from the observer. Median values above 5 indicate that red was perceived nearer than blue, and median values below 5 indicate that blue was perceived nearer than red. From the seven lighting conditions, only the Neutral, Blue 1, and Blue 4 lighting conditions have median values above 5. With red and yellow lighting, the blue target was perceived to be nearer, signaling the occurrence of color reversal.

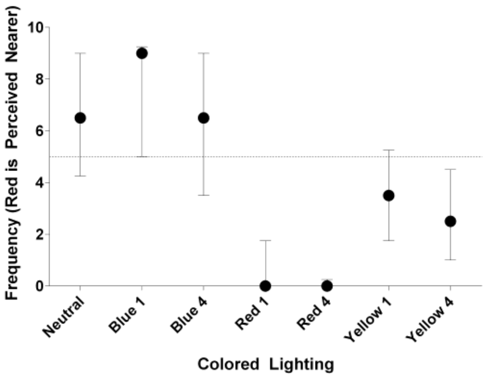

Figure 3: Median values and interquartile range in which the red stimuli was perceived nearer than the blue stimuli.

Considering that the responses for some of the lighting conditions were not normally distributed, a nonparametric analysis was selected to compare the proportions between various lighting conditions. The Friedman test was used to determine the differences in perceived depth of objects under colored lighting. Using SPSS, pairwise comparisons were then performed with a Bonferroni correction for multiple comparisons. Statistical significance was accepted at $p < 0.05$ level.

With $n = 10$ and $df = 6$, the perceived depths of the target objects were statistically significantly different under colored lighting, $\chi^2(6) = 28.326$, $p < 0.0005$. Post hoc analysis revealed statistically significant differences in perceived depth in the following pairs: Neutral lighting ($Mdn = 6.50$) and Red 1 lighting ($Mdn = 0.00$)($p = 0.033$); Red 1 lighting and Blue 1 lighting ($Mdn = 9.0$)($p = 0.011$); Red 1 lighting and Blue 4 lighting ($Mdn = 6.50$)($p = 0.013$); and, finally, Red 4 lighting ($Mdn = 0.00$) and Blue 1 lighting ($p = 0.023$); Red 4 lighting and Blue 4 lighting ($p = 0.028$). Other pairwise comparisons were not statistically significant.

The responses for when the red target object was perceived nearer under neutral or uncolored lighting were above the median value of 5. The responses for Blue 4 lighting were somewhat similar to that. The intriguing points were the results for the rest of colored lighting conditions. Our expectations for red being perceived to be nearer was at least and a little over 50%, but the responses for the other colored lighting conditions show a considerably different results, especially for the Blue 1, Red 1, and Red 4 colored lighting. For Blue 1 lighting, most observers (about 90%) perceived red to be nearer, while with Red 1 and Red 4 lighting, almost none of the observers perceived red to be nearer. Under yellow colored lighting, however, the responses were closer to the 50% proportion than the three previously mentioned colored lighting, but the responses were below the 50%, which means the observers perceived blue to be nearer instead of red.

While visual inspection of the pictorial images and statistical results have produced interesting results on the effect of colored light on depth perception, the full extent on the effect of colored lighting has yet to be explored. This study does support the perceptual basis of color stereopsis proposed by Thompson et al (1993), who believed that color could influence the perceived depth of objects.

The color stereopsis effect was also observed in this study, but only under colored lighting conditions that altered the color contrast of the target and surround. As the current study has tested only three chromatic illuminants, the point or threshold at which a positive color stereopsis effect (red in front of blue) shifts to a negative color stereopsis (color reversal) cannot be determined at this point. This study can only, at best, claim that color reversal is possible under colored lighting.

4. CONCLUSIONS

Visual inspection of the images and the results from the experiment show that colored lighting can indeed alter the color contrast between the target and its surround, thereby also altering the perceived depth of objects in a three-dimensional space. Under neutral (or uncolored) and blue lighting, red was perceived to be nearer than blue, but under red and yellow lighting, a color reversal occurs, wherein blue was perceived nearer than red.

ACKNOWLEDGEMENTS

We would like to thank all the persons who agreed to participate in our psychophysical experiment. The authors would also like to thank the Ministry of Science and Technology of Taiwan for the financial support they provided for this study (Grant NO: MOST 103-2221-E-027-055-).

REFERENCES

Dengler, M., and W. Nitschke. 1993. Color stereopsis: a model for depth reversals based on border contrast. *Perception and Psychophysics* 53(2): 150-56.

Reinhard, E., and K. Devlin. 2005. Dynamic range reduction inspired by photoreceptor physiology. *IEEE Transactions on Visualization and Computer Graphics* 11(1): 13–24.

Luckiesh, M. 1918. On 'retiring' and 'advancing' colors. *The American Journal of Psychology* 29 (2): 182–86.

Payne, M. C. 1964. Color as an independent variable in perceptual research. *Psychological Bulletin* 61(3): 199-208.

Rempel, A. G., W. Heidrich, and R. Mantiuk. 2011. The role of contrast in the perceived depth of monocular imagery. In *ACM SIGGRAPH Symposium on Applied Perception in Graphics and Visualization*, *Proceedings*. Toulouse, France: ACM, 115–115.

Sundet, J. M. 1978. Effects of colour on perceived depth: review of experiments and evaluation of theories. *Scandinavian Journal of Psychology* 19(1): 133-43.

Thompson, P., K. May, and R. Stone. 1993. Chromostereopsis: a multicomponent depth effect? *Displays* 14(4): 227–34.

Vos, J. J. 1960. Some new aspects of color stereoscopy. *Journal of the Optical Society of America* 50(8): 785–90.

Ward, G. (2010). *Photosphere* (version 1.8.6U). Mac. Anyhere Software.

Winn, B., A. Bradley, N. C. Strang, P. V. Mcgraw, and L. N. Thibos. 1995. Reversals of the colour-depth illusion explained by ocular chromatic aberration. *Vision Research* 35 (19): 2675–84.

Address: Ruth Genevieve ONG, College of Design,
National Taipei University of Technology, No. 1 Sec. 3 Zhongxiao East Road,
Taipei City, 106, TAIWAN
E-mail: ruth.genevieve@gmail.com

A Model for Estimation of Overprinted Colors on *Nishiki-e* Printings

Sayoko TAYA[1], Takuzi SUZUKI[2], Noriko YATA[1], Yoshitsugu MANABE[1]
1 Chiba University
2 National Museum of Japanese History

ABSTRACT

Nishiki-e, a type of *Ukiyo-e*, is Japanese historical multicolored woodblock printing. Some of *Nishiki-e* printing were lost over the years even though printing woodblocks were remained. For digital reproduction of lost Nishiki-e printings from remained woodblocks, accurate estimation of printed color is essential requirement. In this paper, a model for estimation of overprinted color using spectral reflectance and the order of every colorant is proposed and verified. The proposed model is based on Kubelka-Munk theory and Minato's method. Estimation of overprinted orange and green was tried. Reflectance of orange was estimated well compared with measured one. However, green was not estimated successfully. Improvement of the model in order to be applied to various overprinted color is our future work.

1. INTRODUCTION

Ukiyo-e is very famous Japanese historical visual art. Especially, multicolored woodblock printings in *Ukiyo-e* are called *Nishiki-e*. A *Nishiki-e* printing is produced by a set of printing blocks. National Museum of Japanese History, Chiba, JAPAN has thousands of *Nishiki-e* printings and hundreds of printing blocks. Some sets of printing blocks don't have printed *Nishiki-e* because they were lost over the years. It is beneficial that lost *Nishiki-e* printings can be reproduced from remained printing blocks from a viewpoint of restoration of cultural assets. However, any colorants should not be put on remained printing blocks immediately because these have great historical value and should not be damaged. Establishment of digital *Nishiki-e* reproduction technology is one of constructive approaches to satisfy both conservation and utilization of *Nishiki-e* materials.

Digital reproduction of *Nishiki-e* printings requires shape information and color information. In our previous work, painting region as shape information is available by measuring printing block of National Museum of Japanese History non-destructively (Taya 2015). This paper focuses on color information. Accurate color information is essential in order to reproduce *Nishiki-e* more realistically. *Nishiki-e* has two way of representing color. One way is to put only single colorant on paper, and the other is to put more than two colorants on paper one by one. Overprinted area and kinds of colorants used in the area can be discriminated from remained printing blocks. However, the order of overprinting of colorants is hard to know with non-destructive inspection.

In this paper, a model for estimating a spectral reflectance of an overprinted area using spectral reflectance and the order of every colorant is proposed and verified. Reflectance data obtained by measuring single colorant part of *Nishiki-e* printings are applied to the proposed model, and the estimated reflectance data are compared with measured reflectance data in the overprinted area to confirm the validity of the model. The order of overprinting also can be estimated from the result of estimation of reflectance.

2. PROPOSED MODEL

The proposed model is based on Kubelka-Munk theory (Kubelka 1948). We assume that overprinted area has a kind of layered structure of colorants.

In the case of two layered structure, inter-reflectance is occurred between the layers like the optics model shown as Figure 1. Then, reflectance of the whole layer is represented by Equation (1).

$$\begin{aligned} R_{1,2} &= R_1 + T_1^2 R_2 (1 + R_1 R_2 + R_1^2 R_2^2 + \ldots) \\ &= R_1 + \frac{T_1^2 R_2}{1 - R_1 R_2} \qquad (1) \end{aligned}$$

Overprinted color part has three layers of upper-colorant, lower-colorant and paper shown as Figure 2. However, lower-colorant may be absorbed by paper. Therefore, shown as Figure 2, the proposed model is constructed with two layers of the layer of upper-colorant and the layer consists of lower-colorant and paper.

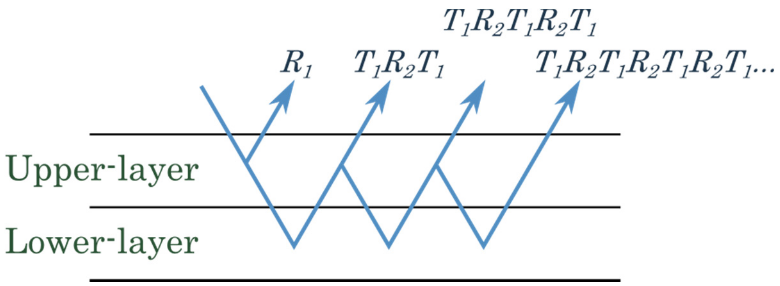

Figure 1: Optics model of two layers

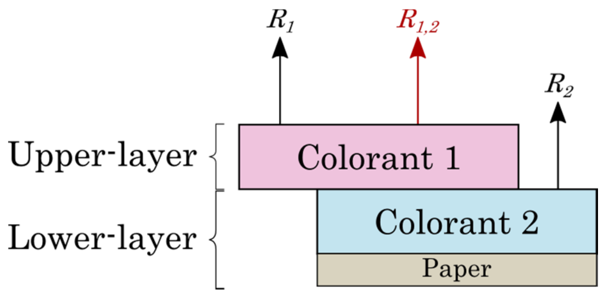

Figure 2: Layered structure of overprinted colorants

To calculate reflectance of the whole layer $R_{1,2}$, reflectance of upper-layer R_1, transmittance of upper-layer T_1 and reflectance of lower-layer R_2 are required. R_2 is measurable value from *Nishiki-e* printings, but R_1 and T_1 are immeasurable directly. They are calculated by Equations (2) and (3).

$$R_1 = \frac{1}{a + b\coth(bSD)} \qquad (2)$$

$$T_1 = \frac{b}{a\sinh(bSD) + b\cosh(bSD)} \qquad (3)$$

$$a = \frac{1}{2}\left(\frac{1}{R_\infty} + R_\infty\right), b = \frac{1}{2}\left(\frac{1}{R_\infty} - R_\infty\right)$$

In these equations, S means scattering coefficient, D means thickness and R_∞ means unique reflectance at upper-layer. Unique reflectance of layer indicates the reflectance in case that the layer has enough thickness to conceal the ground. That is, unique reflectance of layer is not influenced by the reflectance of ground at all.

Unfortunately, the unique reflectance of colorant used in *Nishiki-e* is immeasurable. There are two reasons. One is because there is not a part of colorant whose layer has enough thickness to conceal the ground. The other is because it is difficult today to generate the colorant used in those days when *Nishiki-e* printings are produced. Then, it is assumed that the method by Minato (Minato 1969) is available for colorants of *Nishiki-e*. The method estimates the unique reflectance of translucent layer from the difference of the reflectance of the layer on black ground and that on white ground. Equation (4) shows the estimation equation of the method.

$$R_\infty = \frac{-B + \sqrt{B^2 - 4A^2}}{2A} \qquad (4)$$
$$A = R_w B - R_b W$$
$$B = (W - B)(1 + R_w R_b) - (R_w - R_b)(1 + WB)$$

In this equation, R_w means reflectance of layer on white ground, R_b means reflectance of layer on black ground, W means reflectance of white ground and B means reflectance of black ground. Scattering coefficient S required in Equations (2) and (3) is calculated by Equation (5).

$$S = \frac{1}{bD}\coth^{-1}\left(\frac{1 - aR_b}{bR_b}\right) \qquad (5)$$

3. RESULTS AND DISCUSSION

Figure 3(a) shows the three measured points of red, yellow, and orange. Orange is overprinted by red and yellow. In Figure 3(b), the two estimated results that order is different are shown. A correlation coefficient between estimation 1 (red over yellow) and measured reflectance of overprinted colorants is 0.99, and that between estimation 2 (yellow over red) and measured one is 0.97.

Figure 3(c) shows the three measured points of blue, yellow, and green. Green is overprinted by blue and yellow. In Figure 3(d), the two estimated results that order is different are shown. A correlation coefficient between estimation 1 (blue over yellow) and measured reflectance of overprinted colorants is 0.78, and that between estimation 2 (yellow over blue) and measured one is 0.39.

In each overprinted colorants, the spectral reflectance is estimated differently by the order in which colorants overlap. Estimate results considering the order are deduced by the proposed model. About overprinted orange, estimation 1 is close to measured reflectance and the correlation coefficient of it is higher than that of estimation 2. Figure 4 is a photomicrograph of overprinted yellow. It is observed that red colorant is putted on printed yellow. The estimation is successful about the orange. However, about overprinted green, neither result is close to measured reflectance. The correlation coefficient is also the same.

4. CONCLUSIONS

A color model for estimation of overprinted color from each colorant information and its order using Kubelka-Munk theory was proposed. The estimated results were obtained from the model using the spectral reflectance of single colorants measured in *Nishiki-e* printings. The model well explains the difference of estimated spectral reflectance of overprinted colorants by the order. Estimated results of overprinted orange and green were also shown as an application of the proposed model. Reflectance of orange was estimated well compared with measured one. However, green was not estimated successfully.

In future work, improvement of the model will be required in order to be applied to various overprinted color.

ACKNOWLEDGEMENTS

Prof. Dr. Jun'ichi Ōkubo of National Museum of Japanese History supports our research as an expert researcher of *Nishiki-e*. Assist. Prof. Yoshiko Shimadzu of National Museum of Japanese History gave knowledge about several kinds of colorants.

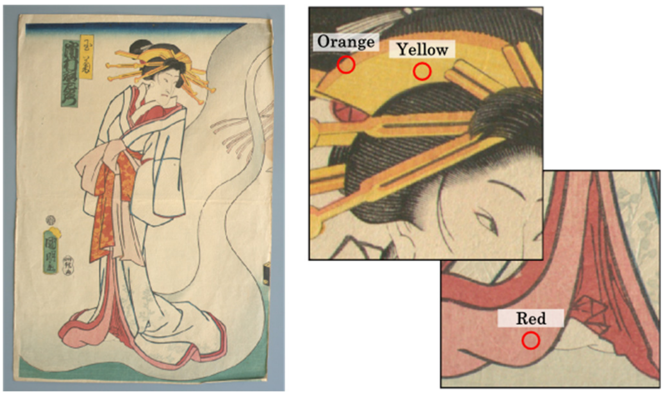

(a) Example 1: Red, Yellow, and Orange

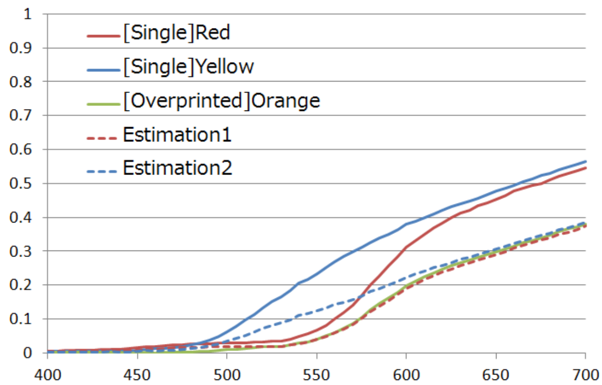

(b) Estimated reflectance of example 1

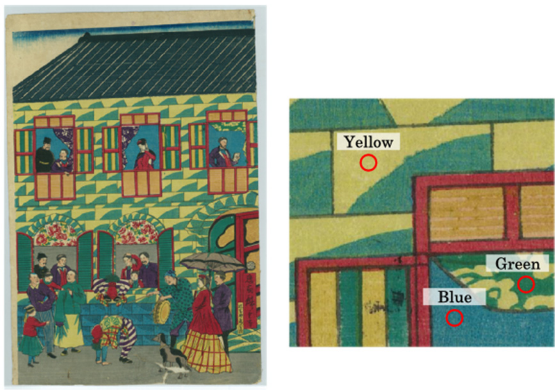

(c) Example 2: Blue, Yellow, and Green

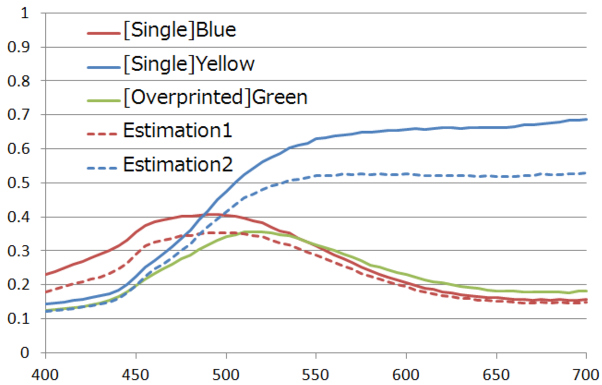

(d) Estimated reflectance of example 2

Figure 3: Examples of Nishiki-e Printings and these estimated results

Figure 4: photomicrographs of overprinted orange and background yellow

REFERENCES

KUBELKA, Paul. 1948. "New Contributions to the Optics of Intensely Light-Scattering Materials. Part I". In *Journal of the Optical Society of America*, 38(5): 448-457.

MINATO, Sachie. 1969. "Reference Color *ni yoru* Kubelka-Munk *ni-teisū riron no sanran keisū* (Scattering Coefficient of Two-Constant Kubelka-Munk Theory by Reference Color, In Japanese)". In *Journal of Faculty of Engineering, Chiba University*, 19(36): 203-208.

TAYA, Sayoko, Takuzi Suzuki, Noriko Yata, Yoshitsugu Manabe. 2015. "Extracting Convex Region of Printing Blocks for Digital Reproduction of *Nishiki-e*". In *The 2015 Joint Conference of the International Workshop on Advanced Image Technology (IWAIT) and the International Forum on Medical Imaging in Asia (IFMIA) Proceedings,* Tainan, Taiwan, January 2015: Poster Session 4, 520.

Address: Assoc. Prof. Takuzi SUZUKI, Research Department, National Museum of Japanese History, 117 Jōnai-chō, Sakura-shi, Chiba, 285-8502 JAPAN
E-mails: taya@chiba-u.jp, suzuki@rekihaku.ac.jp,yata@chiba-u.jp, manabe@faculty.chiba-u.jp

Ethical Considerations on Gene Therapy for Color-Deficient People

Joschua SIMON-LIEDTKE[1]
[1] The Norwegian Colour and Visual Computing Laboratory, Gjøvik University College, Norway

ABSTRACT

In 2009, a procedure for creating trichromacy in dichromatic monkeys has been proposed by Mancuso *et al*. The treatment could be used to "cure" color deficiency in human observers in the future, but to-date the method has not been adjusted and tested on humans yet. I believe that from an ethical view point the proposed method should be adjusted for humans and allowed for clinical trials, as long as the risks and harms are minimized, the treatment and its long-term benefits and risks have successfully been studied on animal trials, and as long as possible human trials follow certain international standards like for example the informed consent etc. Since color deficiency does not qualify as "real" disability, however, only somatic gene therapy as opposed to germ line therapy should be allowed, and private actors and the patients themselves should carry the main costs of development and application. From a social view point, other image improvement methods, like for example daltonization, should be prioritized for public funding in order to increase usability in general resulting in better navigation and communication for not only color-deficient people but other groups of people who have issues distinguishing color due to age, etc. as well.

1. INTRODUCTION AND BACKGROUND

The majority of people can differentiate between millions of different colors. Most scientists agree on that the perception of color leads to behavioral advantages connected to the attentional system, object recognition, and possibly detection of emotional states, as I discussed in a previous paper (Simon-Liedtke, Farup and Laeng 2015). Also, color has been used more and more in our modern world for communication in arts, navigation, traffic, and education. Color-deficient people are people that have difficulties distinguishing certain colors, however, most color-deficient people are not in fact color-*blind*. De Valois and De Valois (1993) explain that information from our eyes is processed in three distinctive pathways representing color attributes of intensity, red–green opponency and blue–yellow opponency. Most color-deficient people only have a reduced or missing perception along the red–green axis, but perceive fairly good color perception along the blue–yellow axis. In natural settings, color-deficient people might face discomfort (f.ex. collecting berries in the forest) but they are not in immediate threat of danger. It is especially in social contexts that color-deficient people are confronted with problems (Flatla and Gutwin 2012). Luckily, there are computational solutions in image processing to simulate color-deficient vision or daltonization methods that improve images for color-deficient people, as listed in a previous paper (Simon-Liedtke, Farup and Laeng 2015).

Mancuso *et al.* (2009) have proposed a procedure – aka the Mancuso-Neitz method – based on somatic gene therapy for creating trichromacy in dichromatic squirrel monkeys by injecting the missing cone pigment in the retina of dichromatic males. The procedure is implemented as somatic gene therapy, i.e. the genes are affected only in the treated cells directly (Anderson 1985), in opposite to germ line therapy, where the specific gene is modified in the genome as a whole (ebid.). Although this procedure might also be used to "cure" color deficiency in human observers, the method has not been adapted for humans to-date, and thus is not permitted for clinical trials on humans yet. Prior to approving clinical trials, there are certain international standards for these kind of clinical trials, like the Declaration of Helsinki (WMA 2013) that lists certain guidelines to ensure ethical conduct for test on humans like the right of informed consent, right to withdraw, privacy etc. On a national level, institutions and branches of government like the US Department of Health and Human Services (HHS) (1997) provide detailed guidelines about what can and cannot be done, and how it should be done, like for example that all trials have to be supervised. Therefore HHS introduces Institutional Review Boards (IRB) for monitoring trials. Furthermore, Anderson (1985) argues that the aspect of delivery, expression, and safety[1] has to be successfully fulfilled in animal studies as requirement before proceeding to clinical trials on humans. One main factor in the ethical debate about gene therapy for - people is whether this type of gene therapy would be defined either as somatic gene therapy to correct a genetic defect or as enhancement genetic engineering. In other words, whether color deficiency is defined as disability or as non-harmful anomaly. In this paper, I present arguments for and against allowing gene therapy for human observers, before I conclude with the proposition that gene therapy for color deficiency should indeed be allowed for humans under certain restrictions.

2. DISCUSSION

The ethical problem of gene therapy for color-deficient people gravitates around the two questions of if gene therapy for color deficiency should be allowed at all, and if yes, if the introduced Mancuso-Neitz therapy should be allowed for clinical trials on humans. The evaluation depends strongly on whether or not the nature of color deficiency is defined as natural variation, i.e. anomaly, or as mild disability. I argue for somatic cell gene therapy on a case-by-case analysis because it might facilitate color-deficient people to fulfill their life goals, and clinical trials have to follow certain international standards.

2.1 Is gene therapy for color deficiency ethical justifiable in general?

I argue that color-deficient people would benefit from gene therapy on a personal level but that most color-deficient people could function perfectly in society without it as well. On the one hand, banning gene therapy for color deficiency would lead to minor personal distress and discomfort for color-deficient people when navigating in social contexts, and it would manifest the exclusion of color-deficient people from certain professions like becoming a pilot, train conductor etc. Although, color-deficient people have indeed slight empirical measurable disadvantages to normal-sighted observers, I do not believe that color deficiency justifies as mild disability. Firstly, it does not lead to immediate danger or harm of the color-deficient person's life. In opposite to other disabilities, where people would suffer a notable decrease in quality of life, and exclusion from central aspects of daily life, color-deficient people manage most important tasks without difficulties since they learned to compensate for their deficiency when growing up. Exclusion occurs only in

---

[1] In other words, only the targeted cells should be affected, the exogeneous gene does lead to the creation of the additional pigment, and it does not harm the cell or the whole animal.

some peripheral aspects like mentioned professions, and society as a whole can usually compensate very well for a color-deficient person who is excluded from those professions. The benefit for color-deficient level on a personal level, on the other hand, can be huge, ranking from facilitating navigation in traffic to fulfilling lifetime professions. Inclusion and self-realization of all their citizens is an important goal in many Western democracies including Norway, the USA etc. Last but not least, the Mancuso-Neitz method could lead to development of tetracromacy in trichromatic people (Jordan 2010).

In conclusion, the resulting benefit for society as a whole from curing color deficiency is not very high, and, in my opinion, would not justify heavily public funding of development of such a therapy. Moreover, I want to underline that most problems for color-deficient people occur in a society that only focus on the needs of normal-sighted, i.e. trichromatic, people. Most problems can easily be solved by implementing guidelines known from universal design and usability, i.e. making all media that use color as communication more accessible for the color-deficient and other “visually disadvantaged” interest groups, like for example the elderly, as well. For this purpose, image processing provides the possibility of daltonization, i.e. the automatic image enhancement for the color-deficient, and other image enhancement methods. Also, I argue that it is unjustified to realize the treatment as a germ line therapy, meaning to change the genetic code in the genome such as to extinguish color deficiency altogether, since the effects of changing the gene pool are firstly hard to comprehend and do not justify the means, similar to the arguments about germ line therapy by Anderson (1985) in general. However, I do believe that gene therapy for color deficiency should be allowed as somatic gene therapy, if funded privately, since the presented therapy could help many color-deficient people to increase their personal quality of life, enable democratic inclusion and help them to fulfill lifetime professions.

2.2 Is the Mancuso-Neitz color deficiency gene therapy ready for clinical trials?

General ethical aspects circulate around the question of risks and harms for the health of people and animals involved in the process of developing the final treatment, and patients of the final treatment. In order to allow the presented Mancuso-Neitz method for clinical trials, we have to guarantee the integrity of health, human rights and the dignity of people and animals involved. Harms and unnecessary danger have to be averted. The current method to-date has only been tested on squirrel monkeys, on which it does not seem to have any negative effects, but the authors have not sufficiently listed long-term consequences of the treatment for the animals. If the presented results from Mancuso *et al.* (2009) are true, the results suggest sufficient integrity according to Anderson’s (1985) three requirements from animal studies. Namely, only cones have been affected, the modulated genes did create the additional and intended pigment, and no other cells were harmed. However, further studies have to be conducted on animals as well to document and investigate long-term effects. If these studies, too, test satisfactorily, the method could be allowed for human clinical trials given they comply with international standards defined by for example the HHS (1997) or the Declaration of Helsinki (WMA 2013). I argue that a new chapter for clinical trials on humans could be opened given that the long-term effect of the treatment have been studied on animals, an exact overview over benefits and risks of the treatment has been documented, and as long as the trials follow international standards like the right to informed consent, and the trials are planned and monitored according to national and international standards guaranteeing the reduction of risks for the patients. Moreover, as discussed before, I believe that the financial costs of the development should not be handled by the general public but by private actors.

3. CONCLUSIONS

In conclusion, I argue for the case of gene therapy for color-deficient on an individual level if international standards are fulfilled for the treatment, the risk is reduced to a minimum for the patient, and private actors handle the costs. Public funding should better be spent on other solutions that may help both color-deficient people and other groups with color vision that differ from the majority like for example the elderly. More precisely, the focus should be put on usability and daltonization. Concerning the Mancuso-Neitz gene therapy, I argue that clinical trials should be allowed if patients of this clinical trials are treated according to guidelines of international standards like informed consent, information about the risks etc., and the research is financed by private actors or the patient him/herself.

REFERENCES

Anderson, W. F. 1985. Human gene therapy: scientific and ethical considerations. *Journal of Medicine and Philosophy* 10: 275–292.

De Valois, Russell L., and Karen K. De Valois. 1993. A Multi-Stage Color Model. *Vision research* 33: 1053–1065.

Flatla, David, and Carl Gutwin. 2012. “So That's What You See!” Building Understanding with Personalized Simulations of Colour Vision Deficiency. In *ASSETS '12: The proceedings of the 14th international ACM SIGACCESS conference on Computers and accessibility*. Boulder, Colorado, USA: 167–174.

Jordan, Gabriele, Samir S. Deeb, Jenny M. Bosten, and J.D. Mollon. 2010. The dimensionality of color vision in carriers of anomalous trichromacy. *Journal of Vision* 10: 1–19.

Mancuso, K., William W. Hauswirth, Qiuhong Li, Thomas B. Connor, James A. Kuchenbecker, Matthew C. Mauck, Jay Neitz, and Maureen Neitz. 2009. Gene therapy for red–green colour blindness. *Nature* 461: 784–787.

US Department of Health and Human Services (HHS). 1997. Guidance for industry, E6 Good Clinical Practice: Consolidated Guidance. Washington, DC, USA: US Department of Health and Human Services. Also available online: http://clinicalcenter.nih.gov/ccc/clinicalresearch/guidance.pdf. (Last checked on 01/20/2015.)

Simon-Liedtke, Joschua T., Ivar Farup and Bruno Laeng. 2015. Evaluating color deficiency simulation and daltonization methods through visual search and sample-to-match: SaMSEM and ViSDEM. In *Proceedings of SPIE/IS&T Electronic Imaging 9395, Color Imaging XX: Displaying, Processing, Hardcopy, and Applications*. San Francisco, CA, USA.

World Medial Association (WMA). 2013, 1st edition in 1964. WMA Declaration of Helsinki - Ethical Principles for Medical Research Involving Human Subjects. Ferney-Voltaire, France: World Medial Association. Also available online: http://www.wma.net/en/30publications/10policies/b3/. (Last checked on 01/20/2015.)

Address: Joschua Simon-Liedtke, The Norwegian Colour and Visual Computing Laboratory, Gjøvik University College, Teknologivegen 22, 2815 Gjøvik, Norway

E-mails: joschua.simonliedtke@hig.no

Robust Cross-Domain Reflectance Estimation

Christoph GODAU
Institute of Printing Science and Technology, TU Darmstadt, Germany

ABSTRACT

A common step in multi-spectral imaging is the estimation of spectral reflectances from camera responses. Most practical spectral reconstruction methods rely on examples to learn a transformation from camera responses to reflectances. The main problem then lies in the selection of the training samples. It is often impractical to produce the required number of samples for a given algorithm and application. Instead, samples from a different "domain" are used: a standard color chart or printed samples. We compare the performance of linear and non-linear estimation algorithms, paying particular attention to the effect of using training and test samples from different domains, in our case different printers and papers.

1. INTRODUCTION

Color measurement using camera systems requires a transformation from the camera space to standardized color spaces. A common step in multi-spectral imaging is therefore the estimation of spectral reflectances from camera responses, which then allow for the calculation of most common colorimetric properties. Most practical spectral reconstruction methods rely on examples to learn a transformation from camera responses to reflectances.

The main problem then lies in the selection of training samples. It is often impractical to produce the required number of samples for a given algorithm and application. Instead, samples from a different "domain" are used: a standard color chart, printed or painted samples, depending on the application. The word "domain" refers to any systematic differences influencing the measurement results. Different paper types, printing inks, measurement conditions or gloss levels could all be seen as separate domains.

This is problematic because spectral estimation is an underdetermined problem, where the number of camera channels is typically much lower than the number of spectral bands to be estimated. One way to improve results is to incorporate prior knowledge about the reflectance domain, either directly through regularization (Heikkinen et al. 2007) and sparse representations (Zickler et al. 2006; Zhang et al. 2012; Lansel, Parmar, and Wandell 2009), or indirectly through an adaptive learning algorithm that is capable of capturing structural properties of the training data (Bengio, Courville, and Vincent 2012; a. Mansouri, Marzani, and Gouton 2005).

In this work we use the example of print inspection: we want to estimate the reflectance spectra of colors produced by a particular printer, but for training only standard color charts or samples printed on a different printer and paper are available.

2. METHOD

2.1 Spectral Reconstruction

The estimation of spectra from camera responses can be achieved by inverting the image formation process or by learning a transformation from examples.

Examples of direct spectral reconstruction (inversion of the image formation process) are the spatial Wiener filter (Shimano 2006) and an extension that includes a deblurring component (Christoph Godau and Urban 2013). We do not consider spatial information in this work, although it is possible to extend most approaches this way. The main advantage of spatial approaches are increased robustness to noise and preservation of structure in the image (Urban, Rosen, and Berns 2009), both of which are not relevant in our study since we perform measurements on relatively large and homogeneous regions.

A large number of indirect (learning-based) methods have been proposed for spectral estimation. In principle, any multi-dimensional regression method may be used. The simplest approaches estimate a linear transformation from camera responses to spectral reflectance, for example using the Moore-Penrose pseudoinverse or an iteratively reweighted robust least squares method (Dumouchel and O'Brien 1992).

More complex approaches add regularization and non-linear components to the estimation process (Heikkinen et al. 2007). We include the log-kernel estimation method in our comparison (Eckhard et al. 2014), which performs well for spectral estimation on printed samples with a camera system very similar to the one used in our experiments.

Another common approach is the use of a more compact representation for reflectance spectra. Each spectrum can then be described with a small number of coefficients or parameters, which may reduce the effect of noise and potentially makes it easier to invert the previously underdetermined system. There are many ways to obtain such representations, both linear (A. Mansouri et al. 2008; Kohonen, Parkkinen, and Jääskeläinen 2006) piece-wise linear (Lansel 2011) and non-linear (Tenenbaum, de Silva, and Langford 2000). We performed tests using these methods, but found that the reduced representations are most useful for estimation from very low dimensional systems (such as RGB).

2.2 Experimental Set-up

We use data from the following domains (different printers and papers) for our experiments:

- **Inkjet HP (IJ_HP):** Chart printed on an HP Z3100 7-ink system (CMYKRGB) on high-gloss photo paper.
- **Inkjet Epson (IJ_EP):** Chart printed on an Epson R2880 9-ink system (CMYK+light/vivid variants) on semi- to high-gloss paper.
- **Offset A (OFS_A):** Chart printed by a commercial CMYK offset printing service in high quality on semi-gloss paper.
- **Offset B (OFS_B):** Chart printed by a commercial CMYK offset printing service in normal quality on thinner semi-gloss paper.

On each system we printed the same color chart containing more than 2000 randomly colored patches. We then measured each patch using a spectrophotometer[1] and obtained camera response data using a 12-channel multi-spectral system[2], taking the average of the central region from each patch to reduce effects of noise, and normalizing responses to the [0,1] range. From each chart we then selected 1000 patches, maximizing the spectral

[1] XRite i1iSis, http://www.xrite.com/i1isis-with-obc

[2] Chromasens TruePIXA Multi-spectral line scan camera, http://www.chromasens.de/en/multi-spectral-camera-truepixa

difference between selected colors. The spectra and camera response data is available in the supplementary materials[3].

In our experiments we use the following learning-based methods for reflectance estimation:

- **Linear: Least Squares (LSQ):** Direct linear least-squares using the Moore-Penrose Pseudo-Inverse.
- **Linear: Robust Least Squares (RLSQ):** An iteratively reweighted least squares method, giving less weight to outliers[4].
- **Non-Linear: Neural Network (NN)**: A neural network with one hidden layer of size 12 trained using backpropagation[5].
- **Non-Linear: Log-Kernel (LKL):** The logarithmic kernel method which has previously been shown to perform well using a set-up similar to ours (C Godau et al. 2013), using the suggested parameters from (Eckhard et al. 2014) [6]

Note that the main goal is not the direct comparison of the reconstruction results, but rather of the methods ability to generalize across domains. Given sufficient knowledge about an application, the results reported here could likely benefit from adjusting relevant parameters or choosing an alternative representation. In particular we compare the generalization properties of linear vs. non-linear methods.

We then used each of the 4 sets to train the algorithms and evaluated the reconstruction quality using the CIEDE2000 color difference formula (Sharma, Wu, and Dalal 2005). Due to space restrictions we only present the mean error for each result, for more details please refer to the supplementary material. To avoid using the exact same data for training and testing, we used 10-fold cross-validation when test and training set were identical (diagonals in the result matrices in Table 1).

3. RESULTS AND DISCUSSION

The error matrices for the algorithms using all 12 camera channels are shown in Table 1, where columns indicate the training set and rows the test set. All methods performed well when test and training data where from the same domain (diagonals of each matrix), with the best result for each combination of training/test domain indicated in bold. Using the median instead of the mean resulted in overall smaller numbers, but the overall trends remained the same.

The biggest errors occur for the Inkjet HP chart; in particular the non-linear methods (neural net and log-kernel) performed much worse than the linear methods in estimating the HP Inkjet's spectra. This is probably due to the glossy paper, additional inks (RGB) and larger gamut of the printer. The differences in spectral properties can lead to arbitrarily

---

[3] http://www.idd.tu-darmstadt.de/re_search/colorg/color_publications/index.en.jsp

[4] Implemented using MATLAB and Statistics Toolbox Release 2014b, The MathWorks, Inc., Natick, Massachusetts, United States.

[5] Implemented using MATLAB and Neural Network Toolbox Release 2014b, The MathWorks, Inc., Natick, Massachusetts, United States.

[6] Implemented using the original code available online at http://www.ugr.es/~colorimg/suppl_docs/log_kernel.html

large errors depending on the properties of the non-linear terms, while linear methods typically perform consistently even for extrapolation. This problem actually becomes worse with a higher dimensionality.

Table 1: Error matrices for spectral reconstruction using 12 camera channels. Columns indicate the training domain, rows the test domain. Numbers show the average CIEDE2000 color differences to the spectrophotometer measurements, the best result for each training/test combination is highlighted in bold. When training and test sets are identical, we use 10-fold cross-validation.

LSQ	IJ_HP	IJ_EP	OFS_A	OFS_B
IJ_HP	**1.25**	**1.79**	2.11	**2.07**
IJ_EP	**0.89**	**0.37**	0.82	1.05
OFS_A	**0.81**	**0.58**	0.42	0.86
OFS_B	**0.98**	**0.78**	**0.78**	0.32

RLSQ	IJ_HP	IJ_EP	OFS_A	OFS_B
IJ_HP	1.98	1.82	**1.94**	2.54
IJ_EP	1.48	**0.37**	**0.62**	**1.02**
OFS_A	1.37	0.71	**0.41**	**0.81**
OFS_B	1.52	0.94	0.79	**0.31**

NN	IJ_HP	IJ_EP	OFS_A	OFS_B
IJ_HP	1.82	2.19	8.78	7.38
IJ_EP	2.30	0.29	1.33	1.33
OFS_A	2.20	0.74	0.48	1.35
OFS_B	2.00	0.97	0.78	0.36

LKL	IJ_HP	IJ_EP	OFS_A	OFS_B
IJ_HP	1.50	2.56	2.97	2.89
IJ_EP	23.70	**0.22**	1.11	1.24
OFS_A	21.33	1.05	0.43	0.88
OFS_B	20.32	0.99	0.99	**0.31**

Table 2: Error matrices for spectral reconstruction using 3 channels (RGB).

LSQ	IJ_HP	IJ_EP	OFS_A	OFS_B
IJ_HP	4.91	5.33	5.43	**4.71**
IJ_EP	**2.73**	2.07	2.50	2.33
OFS_A	**2.22**	1.93	1.78	1.81
OFS_B	**2.55**	2.39	2.29	1.69

RLSQ	IJ_HP	IJ_EP	OFS_A	OFS_B
IJ_HP	5.27	4.97	5.86	4.91
IJ_EP	4.24	1.49	2.62	2.25
OFS_A	3.74	1.94	1.86	1.79
OFS_B	3.16	1.99	2.41	1.71

NN	IJ_HP	IJ_EP	OFS_A	OFS_B
IJ_HP	2.65	**4.24**	5.53	5.42
IJ_EP	12.02	0.59	2.08	2.04
OFS_A	10.78	**1.56**	**0.68**	1.46
OFS_B	12.88	1.35	1.33	**0.46**

LKL	IJ_HP	IJ_EP	OFS_A	OFS_B
IJ_HP	**1.95**	4.52	**5.10**	5.60
IJ_EP	8.24	**0.45**	**2.00**	**1.78**
OFS_A	7.57	**1.56**	0.70	**1.44**
OFS_B	6.98	**1.34**	**1.25**	0.48

Overall, the linear estimators performed best on 12-channel data across domains. The log-kernel method performs well when training and test data are from the same distribution but performance deteriorates significantly when the data sets are different. The neural network performs does not perform particularly well in any combination, but the maximum errors are significantly lower than for the log-kernel.

In most camera systems the number of available channels is however much smaller. We therefore also tested the performance for a lower number of channels by only using 3 of the 12 available channels of our system (RGB). Surprisingly, the non-linear methods performed *better* in a number of configurations with only 3 channels than with 12. Table 2 shows the results for this scenario. While large differences between test and training sets are still a problem, both the neural net and the log-kernel significantly outperform the linear approaches, except for the problematic Inkjet HP data set. Another interesting result is that the "robust" least squares method appears to be more sensitive to domain changes than regular least squares, probably because it fits the training set more closely by giving less weight to outliers.

4. CONCLUSIONS

The non-linear methods (neural net and log-kernel) appear to be more sensitive to differences between test and training data, particularly when the dimensionality of the camera space increases (this might be an example of the *curse of dimensionality)*. For low-dimensional spaces, the advantage of a non-linear estimation is significant, but overfitting remains a problem when training and test domain differ significantly.

When the dimensionality of the camera system is sufficiently high (>6 channels in our case), a linear least squares solution provides the best results in terms of overall colorimetric error, especially across domains. Non-linear approaches provide significant benefits only when the training and test domains are similar *and* the number of camera channels is small.

It is obvious that all of these results heavily depend on the selected domains. The spectra of printed samples presumably have a low effective dimensionality (roughly proportional to the number of inks), other samples such as natural reflectances would most likely lead to different results.

REFERENCES

Bengio, Yoshua, Aaron Courville, and Pascal Vincent. 2012. "Representation Learning: A Review and New Perspectives." *CoRR* abs/1206.5 (1993): 1–30.

Dumouchel, William, and Fanny O'Brien. 1992. "Integrating a Robust Option into a Multiple Regression Computing Environment" (January 3): 41–48.

Eckhard, Timo, Eva M Valero, Javier Hernández-Andrés, and Ville Heikkinen. 2014. "Evaluating Logarithmic Kernel for Spectral Reflectance Estimation-Effects on Model Parametrization, Training Set Size, and Number of Sensor Spectral Channels." *Journal of the Optical Society of America. A, Optics, Image Science, and Vision* 31 (3) (March 1): 541–9.

Godau, C, M Klammer, T Eckhard, M Schnitzlein, D Nowack, B Frei, and P Urban. 2013. "Evaluation of a Multi-Spectral Camera System for Inline Color Measurement." *Annual Meeting of the German Colour Group*.

Godau, Christoph, and Philipp Urban. 2013. "Spatio-Spectral Image Restoration." In *Color and Imaging Conference*, 27–32. Society for Imaging Science and Technology.

Heikkinen, Ville, Tuija Jetsu, Jussi Parkkinen, Markku Hauta-Kasari, Timo Jaaskelainen, and Seong Deok Lee. 2007. "Regularized Learning Framework in the Estimation of Reflectance Spectra from Camera Responses." *Journal of the Optical Society of America. A, Optics, Image Science, and Vision* 24 (9): 2673–2683.

Kohonen, Oili, Jussi Parkkinen, and Timo Jääskeläinen. 2006. "Databases for Spectral Color Science." *Color Research & Application* 31 (5) (October): 381–390.

Lansel, Steven Paul. 2011. "Local Linear Learned Method for Image and Reflectance Estimation." PhD Thesis, Stanford University.

Lansel, Steven Paul, M. Parmar, and B. a. Wandell. 2009. "Dictionaries for Sparse Representation and Recovery of Reflectances." *Computational Imaging VII* 7246: 72460D–72460D–11.

Mansouri, a., F. S. Marzani, and P. Gouton. 2005. "Neural Networks in Two Cascade Algorithms for Spectral Reflectance Reconstruction." *Proceedings - International Conference on Image Processing, ICIP* 2: 718–721. doi:10.1109/ICIP.2005.1530156.

Mansouri, Alamin, Tadeusz Sliwa, Jon Y Hardeberg, and Yvon Voisin. 2008. "Representation and Estimation of Spectral Reflectances Using Projection on PCA and Wavelet Bases." *Color Research & Application* 33 (6): 485–493.

Sharma, Gaurav, Wencheng Wu, and Edul N. Dalal. 2005. "The CIEDE2000 Color-Difference Formula: Implementation Notes, Supplementary Test Data, and Mathematical Observations." *Color Research & Application* 30 (1) (February): 21–30.

Shimano, Noriyuki. 2006. "Recovery of Spectral Reflectances of Objects Being Imaged without Prior Knowledge." *IEEE Transactions on Image Processing* 15 (7) (July): 1848–56..

Tenenbaum, J B, V de Silva, and J C Langford. 2000. "A Global Geometric Framework for Nonlinear Dimensionality Reduction." *Science (New York, N.Y.)* 290 (5500) (December 22): 2319–23..

Urban, Philipp, Mitchell R Rosen, and Roy S Berns. 2009. "Spectral Image Reconstruction Using an Edge Preserving Spatio-Spectral Wiener Estimation." *Journal of the Optical Society of America A* 26 (8): 1865–1875.

Zhang, Wei-Feng, Peng Yang, Dao-Qing Dai, and Arye Nehorai. 2012. "Reflectance Estimation Using Local Regression Methods." In *Advances in Neural Networks--ISNN 2012*, 116–122. Springer.

Zickler, Todd, Ravi Ramamoorthi, Sebastian Enrique, and Peter N Belhumeur. 2006. "Reflectance Sharing: Predicting Appearance from a Sparse Set of Images of a Known Shape." *IEEE Transactions on Pattern Analysis and Machine Intelligence* 28 (8) (August): 1287–302..

Address:

Christoph Godau, Institute of Printing Science and Technology, TU Darmstadt,
Magdalenenstr. 2, 64289 Darmstadt, GERMANY
E-mail: godau@idd-tu-darmstadt.de

Colorama: Extra Color Sensation for the Color-Deficient with Gene Therapy and Modal Augmentation

Joschua SIMON-LIEDTKE[1]
[1] The Norwegian Colour and Visual Computing Laboratory, Gjøvik University College, Norway

ABSTRACT

Color-deficient people may be confronted with disadvantages and discomfort when navigating through a society that relies heavily on color as medium of communication in their daily lives. Daltonization as automated methods to improve color images for color-deficient people has traditionally been proposed by the field of image processing. Also, Sensory Substitution Devices from vision-to-touch or vision-to-hearing have been developed for the blind, and could be adapted to the needs of the color-deficient as well. And last but not least, a gene therapy for creating trichromacy in dichromatic monkeys has been proposed that might be applicable for humans as well in the future. All three approaches can be used to facilitate the life of color-deficient people with different up- and downsides to each method. Firstly, gene therapy holds the promise of a complete cure and regain of the lost color perception, while being highly intrusive and holding still unknown costs, risks and long-term effects on the patients' health. Secondly, SSDs provide an approximate substitution of the lost color sense, at the same time as it is somewhat intrusive and cannot copy all aspects related to the attributes of colors to a full degree. Thirdly, daltonization is probably most effective and can even help other groups of people that have problems distinguishing colors like the elderly, but it cannot fully emulate lost color perception. I argue that, while all three methods can promise interesting results, daltonization should be the method in focus of public attention when evaluating all alternatives in the light of usability and accessibility.

1. INTRODUCTION

Color deficiency exists in about 8% of the male population. Color-deficient people have problems distinguishing certain colors, or do not perceive certain colors at all. Most color-deficient people have problems with colors along the red–green axis. The problems of color-deficient people are closely related to reduced usability and accessibility in daily life situations. Discomfort and problems for color-deficient people in daily life are closely connected to social settings where our society heavily relies on color-coding as can be seen on how color is used in geographic maps, advertising, communication etc. We might use so-called daltonization methods, Sensory Substitution Devices (SSDs) – most commonly realized as vision-to-touch or vision-to-hearing – or even gene therapy. To evaluate each method, it makes sense to use categories such as efficiency, costs, feasibility etc. with special focus on the improvement in the light of accessibility and usability for a lesser or greater extend of people. In this paper, I am going to present the different methods, discuss their advantages and disadvantages in order to answer the question, how each of the presented approaches might help to increase accessibility and improve usability of electronic media for color-deficient people.

2. BACKGROUND

Daltonization methods are automated methods from the field of image processing to increase image quality for color-deficient people, some of which are mentioned in a previous paper (Simon-Liedtke, Farup and Laeng 2015). Daltonization methods help to regain lost information and to facilitate differentiation of colors that are otherwise hard to distinguish for color-deficient people by increasing global and/or local color contrast. Daltonization methods can be implemented on practically any computing device and various applications like for example on computers, smart phones, printers etc., for web browsers, camera interfaces, etc., as color profiles, filters, lookup-tables etc.

Sensory Substitution Systems (SSDs) have been developed mainly for the blind to translate visual information into other senses, like for example into touch and/or hearing by "systematically converting properties of vision […] into auditory properties […] or tactile properties […] by means of a man-made device" (Ward and Wright 2014). Ward and Wright (ibid.) mention several implementations related to the two main categories of Haptic SSDs, i.e. SSDs that translate to the sense of touch, and Auditory SSDs, i.e. SSDs that are translate to the sense of hearing. Haptic SSDs are for example the TVSS and the TDU that project tactile information to the back or the tongue of the user respectively (ibid.). In terms of Auditory SSDs, devices like "seeColOr" that encodes color as orchestral instruments, "The Vibe" or "The vOICe" that convert a two-dimensional gray-scale image into a two-dimensional sound image have been mentioned by Ward and Wright (ibid.). Also, the "eyeborg" project by Harbisson and Montandon (2013) deserves to be mentioned, in which a chip that is permanently attached to the back of the head of achromats maps light frequencies to sound frequencies, making color "hearable"

Mancuso et al. (2009) proposed a somatic gene therapy to create trichromacy in dichromatic squirrel monkeys. The treatment consists of a viral injection caring an L-opsin gene into the retina of male squirrel monkeys: A specie, of which females are usually trichromats whereas and of which males are dichromats. After the treatment, male squirrel monkeys displayed a clear trichromatic behavior. To-date, however, there are no published studies about the applicability for humans and/or long-term effects on the health of the squirrel monkeys.

Universal Design is defined by The Center for Universal Design (CUD) (2008) through a quote of Ron Mace as "the design of products and environments to be usable by all people, to the greatest extend possible, without the need for adaptation or specialized design". In universal design, we take into consideration the fact that people or groups of people have different needs and possibilities, which we do have to take into account when designing an (interactive) media outlet. CUD (1998) lists therefore seven principles facilitating the implementation of a successful universal design, including equitable use, flexibility, simplicity, perceptibility, error tolerance, low physical effort, and size and space. An important aspect of universal design is the question of usability, i.e. "the extent to which a product can be used by specified users to achieve specified goals with effectiveness, efficiency and satisfaction in a specified context of use" (ISO 1998). A usability evaluation should measure to which extent a color-deficient user is able to extract-correct visual information from a photography or an information graphic like maps, public transportation schedule etc. Next to the principles of universal design and usability, I include the following aspects of the discussed methods: Firstly, if there is any notable improvement for the color-deficient users, secondly, the aspect of practicality and feasibility, and, thirdly, the aspect of intuition and training.

3. DISCUSSION

Daltonization methods do not help color-deficient people to actually perceive more colors, but they help to change colors in a way that colors that are otherwise easily confused become more distinct from each other. These methods reach their limit in cases where a lot of colors are present in an image and the possibilities of rearranging color contrasts get exhausted. By contrast, most daltonization methods are efficient in terms of costs and computation. They are also easily implementable on most electronic output devices like computers, smart phones etc. for both screens and prints – after prior pre-processing. They can be realized as filters, apps, lookup-tables etc. making it easy to use for every color-deficient person that owns a smart phone, tablet or computer. Moreover, daltonization follows the usability guidelines of equitable use, flexibility, perceptibility, low physical effort, and size and space. I believe that the easy availability of daltonization methods, especially in combination with color deficiency simulation methods as listed in a previous article (Simon-Liedtke, Farup and Laeng 2015) also helps to increase awareness for color deficiency in normal-sighted people, since normal-sighted people as well can try out daltonization without huge costs or effort.

On the one hand, SSDs require a certain adaptation period before enabling simple and intuitive use, even though most participants reported to have adapted very well after the initial training phase (Ward and Wright 2014). Some implementations do not provide lesser physical effort with respect to the CUD guidelines, especially in the case that tactile information is obtained through fingers. However, other devices have been proposed that are attached to the body directly without further interaction (ibid.). Also, the physical nature of visual, haptic and acoustic stimuli may lead to obstacles. Consider for example the range of the senses: Things can be seen from very far away, whereas sound has undeniable range limitations, and touch can basically only be perceived from very nearby. This would make it difficult to translate certain visual information into other senses. Furthermore, SSDs might interfere with other stimuli. If sound is for example being used to transport color, there will be problems in conversations with others. Last but not least, SSDs are somewhat intrusive because it means that the color-deficient person has to carry around additional devices, like for example the “eyeborg” prosthetic, that might even be somewhat expensive. On the other hand, SSDs can make colors truly sensible: Harbisson, for example, reported that he actually started to hear colors (Harbisson and Montandon 2013). Ward and Wright (2014) point out that SSDs might lead to artificially acquired synesthesia, i.e. that participants start to both hear and see colors, respectively both feel and see. The argument of device costs can be limited to the degree that most modern smart phones are already capable of giving haptic or auditory feedback, a fact that might reduce costs and intrusiveness of SSDs. And last but not least, SSDs can be combined with virtually any form of sensor that measures any kind of electromagnetic radiation or fields, thus it might enable people to perceive UV- and/or NIR-radiation, electronic and/or magnetic fields etc.

Admittedly, gene therapy is a somewhat young field of research to-date, such that the full extend of the treatment, long-term risks and harms, costs etc. are not fully comprehensible. There are certain shortcomings in the documentation of aspects related to safety in the gene therapy study by Mancuso *et al.* (2009). And since no adaptation has been made for humans, there is no prediction about costs and harms for humans; let alone if the procedure is even applicable for humans. Moreover, the procedure is highly intrusive since it alters the genetic code of the participant. On the other hand, though, it is the solution that truly “cures” color deficiency leading to the only real sensation of the color dimensionality that is lost for color-deficient people. Moreover, it could be used to create tetrachromacy, i.e. the ability to perceive more colors than normal-sighted people can (Jordan *et al.* 2010)

4. CONCLUSION

Daltonization provides effective and easily implementable help of improving media outlets but it cannot create additional visual perception. SSDs show deficits concerning simplicity, physical effort, nature and range of the stimuli, integrability, compatibility and costs but provide huge advantages of SSDs related to equitable use, flexibility, perceptible information, error tolerance, size and space, and creation of a truly new sense. Thirdly, gene therapy raises question concerning safety and feasibility at the possibility of truly curing color deficiency. I, as a computer scientist, believe that daltonization to-date surely provides the best solution in daily life in the light of universal design, at the same time as the possibilities of SSDs and gene therapy should be further investigated.

REFERENCES

The Center for Universal Design (CUD). 1997. The Principles of Universal Design. Raleigh, NC, USA: The Center for Universal Design at NCSU. Also available online: http://www.ncsu.edu/ncsu/design/cud/about_ud/udprinciplestext.htm. (Last checked on 12/02/2014.)

The Center for Universal Design (CUD). 2008. About Universal Design. Raleigh, NC, USA: The Center for Universal Design at NCSU. Also available online: http://www.ncsu.edu/ncsu/design/cud/about_ud/about_ud.htm. (Last checked on 12/02/2014.)

Harbisson, Neil, and Adam Montandon. 2013. Cyborg Foundation. Barcelona, Spain: Cyborg Foundation. Also available online: http://cyborgproject.com/pdf/Neil-Harbisson-A-cyborg-artist.pdf. (Last checked on 10/13/2014.)

The International Organization for Standardization (ISO). 1998. ISO 9241-11 – Ergonomic requirements for office work with visual display terminals (VDTs). Geneva, Switzerland: The International Organization for Standardization.

Jordan, Gabriele, Samir S. Deeb, Jenny M. Bosten, and J.D. Mollon. 2010. The dimensionality of color vision in carriers of anomalous trichromacy. *Journal of Vision* 10: 1–19.

Mancuso, K., William W. Hauswirth, Qiuhong Li, Thomas B. Connor, James A. Kuchenbecker, Matthew C. Mauck, Jay Neitz, and Maureen Neitz. 2009. Gene therapy for red–green colour blindness. *Nature* 461: 784–787.

Simon-Liedtke, Joschua T., Ivar Farup and Bruno Laeng. 2015. Evaluating color deficiency simulation and daltonization methods through visual search and sample-to-match: SaMSEM and ViSDEM. In *Proceedings of SPIE/IS&T Electronic Imaging 9395, Color Imaging XX: Displaying, Processing, Hardcopy, and Applications*. San Francisco, CA, USA.

Ward, J. and T. Wright. 2014. Sensory substitution as an artificially acquired synaesthesia. *Neuroscience & Biobehavioral Reviews* 41: 26–35.

Address: Joschua Thomas Simon-Liedtke, The Norwegian Colour and Visual Computing Laboratory, Gjøvik University College, Teknologivegen 22, 2815 Gjøvik, Norway
E-mails: joschua.simonliedtke@hig.no

Benchmarking a Grating-Based Spectral Imaging System

M. James SHYU,[1] Ting-Yun LIN,[2]
[1] Department of Information Communications, Chinese Culture University, Taiwan
[2] Dynalab Inc.

ABSTRACT

Spectral imaging system handles image signals in spectral form. Different approach can be used to generate spectral image. Early spectral camera system uses tunable liquid crystal tunable filter for capturing narrow band signals. Newer multi-filter camera system uses optimized filters with monochromatic camera to captures spectral data and then to numerically process the data into finer spectral resolution. Another example is two-filter RGB camera system that captures image with RGB CCD sensor array through specifically optimized filter pair. Numerical process is followed to reconstruct the full spectral range. Active illumination is also a new approach proposed for faster acquisition of image in spectral form. A gating-based spectral imaging system is used by the authors as well. Each method deploys different hardware device resulting in difference color reproduction perfromance. In this study the colorimetric performance for spectral imaging system is under investigation. Two different calibration procedures were performed in the grating-based spectral imaging system. The 24-color ColorChecker were used as the baseline test target to generate color difference values as the performance metrics. Results indicate that this grating-based spectral imaging system is capable to yield similar colorimetric performance than the other spectral imaging system. With tighter calibration procedure, it has the potential to generate even better colorimetric performance than the other spectral imaging system. Nevertheless, all the spectral imaging systems studied here perform better than conventional RGB camera in color reproduction accuracy.

1. INTRODUCTION

Spectral imaging system is gaining more attention not only from the technical development point of view but also for the actual application of high accuracy color reproduction. There are various approaches to configure the imaging system to acquire imaging data in spectral form. One common way is to use optimized filters to capture integrated signals and reconstruct the spectral data by known vector characteristics (Berns et al., 2005a; Imai and Berns, 2009). Another newer way utilizes active illumination, like LED or DLP projector, to generate spectrally selected signals to reconstruct the full spectral data (Tominaga and Horiuchi, 2012). The other way uses grating-type device to capture the spectral signals directly. Each approach may deploy different hardware device or different computation method, therefore results in different operation procedures and colorimetric performance. There are different operational merits, like faster to capture or easier to process for different approaches among these spectral systems. However, it is the colorimetric performance that is focused in this study.

Some of the colorimetric performance analyses of high-end RGB digital camera in museum community can be found in prior benchmarking studies (Berns et al, 2005b; Frey and Farnand, 2011). Berns' more recent study summarized the colorimetric benchmarking of museum imaging system: average color accuracy in 2005 for four museums was 12.4 $\triangle E^*_{ab}$; average performance improved to 8.9 $\triangle E^*_{ab}$ among 22 participating museums in the range between 4.25 to 17.15 in 2010 (Berns, 2012). For more recent camera back systems incorporating color management default camera profiles, the average $\triangle E^*_{ab}$ for ColorChecker are ranged from 6.6 to 9.8 (Berns, 2012). These results are based on high-end RGB (tri-chromatic) cameras.

For spectral imaging system, the RIT Dual-RGB approach included a filter slider that can sequentially place two custom color filters to capture image. When optimized to minimize average $\triangle E^*_{ab}$ for the ColoeChecker, the colorimetric accuracy was reported for average $\triangle E^*_{ab}$ at 1.1 and 0.7 in $\triangle E^*_{00}$. Other custom-made test targets were also verified (Berns, 2012). On the other hand, an active spectral illumination approach is proposed at Chiba University. A special light source which is capable of emitting arbitrary spectrum in high speed was used with three algorithms (Tominaga and Horiuchi, 2012; Fong et al., 2008). The best colorimetric accuracy for mini ColorChecker was reported for average $\triangle E^*_{ab}$ at 1.88 with maximum $\triangle E^*_{ab}$ at 3.90 when narrowband algorithm was used. These prior results provide good references in benchmarking the colorimetric performance of spectral imaging systems.

In addition a grating type device, spectrograph, is capable to disperse incoming light into spectrum. With 2-D monochrome CCDs and X-Y scan-bed, a spectral scanning system can be established. It is the objective of this study to perform the colorimetric benchmark for this spectral scanning system that is used by the authors. The results are provided for general reference as one example of spectral imaging systems.

2. METHOD

A gating-based device (spectrograph by Specim) is deployed in this research to establish a spectral imaging system for digital archive of small museum objects. A special Xeon light is used as the illumination. Two optical fibers guide the illumination to both sides of the lens to form a 45/0 geometry. The image is captured in line-by-line manner. The incoming light of every pixel on the line is dispersed by the spectrograph into a series of spectrum perpendicular to the line direction to be projected on a monochromatic 2-D CCD sensor array. The two-dimensional signals on the CCD sensor array comprise the spectral signals on every pixel of the scan line.

The light source, lens, spectrograph device and monochrome CCD camera are mounted on an X-Y scan bed as shown in Figure 1. Each scan line includes 1600 pixels and each pixel consists of 800 samplings from different wavelengths in the visible bandwidth, which are consequently interpolated into samplings from 390 nm to 730 nm in 10 nm increments. Each wavelength reading is recorded in 12-bit encoding by the monochrome CCD camera. This configuration can avoid the potential registration problem from multiple exposures. After calibrating to a known reference standard and post-processing, spectral reflectance factor for every pixel can be generated. Colorimetric accuracy can be estimated by computing the color difference between the measured spectral reflectance factors of the original test color patches and the spectral reflectance factors of the reproduced values. Both $\triangle E^*_{ab}$ and $\triangle E^*_{00}$ are generated in D65 for comparison with prior studies. Average and maximum color difference are reported.

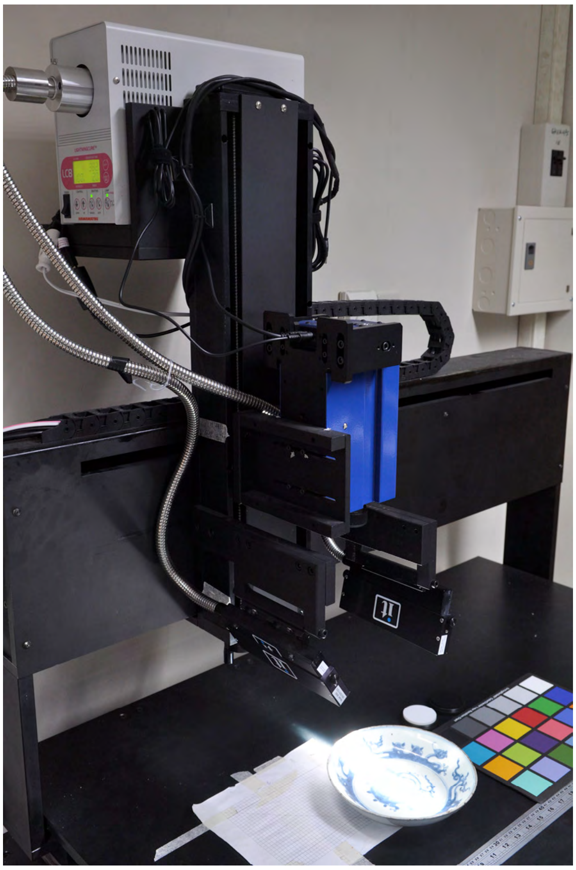

Figure 1: Spectral imaging system used in this study.

2.1 Sample Preparation

An X-rite mini ColorChecker (Passport) wae used as the testing target. The spectral reflectance factors of the 24 color patches were measured using a GretagMacbeth SpectroEye spectrophotometer. A pair of Labsphere reference target (2% and 99%) were used as calibration references as shown in Figure 2 altogether. A MATLAB program is developed to perform the calibration and to process all the spectral data.

Figure 2: Test targets and reference targets used in this study.

2.2 Experimental Procedure

This spectrograph with CCD camera generates 12-bit raw signals. After calibrating the raw signals with reference standards, spectral reflectance factor can be computed. In this study two rounds of calibration procedures are reported. The first one only uses two independent reference targets (2% and 99% Labsphere patches) in the calibration procedure. The 24 color patches in the ColorChecker Passport are used as independent test samples to verify the calibration results. After analyzing the first results, the second calibration procedure is proposed. Since the ColorChecker includes six levels of neutral color and its size is not to large, it is then feasible to just take the six neutral colors as the calibratoion references and to use the rest eighteen colors as independent test targets. It is assumed that more neutral targets can improve the reproduction accuracy within the calibration (linearization) process. This is the idea behind the second procedure.

3. RESULTS AND DISCUSSION

Two sets of color difference values are computed. The first procedure just uses a black and a white independent references to perform the calibration. The second procedure uses 6 neutral colors as reference to perform the calibration. Table 1 summarized the testing resutls in $\triangle E^*_{ab}$ units. Procedure one uses two independent reference targets, therefore the 24 color differences in the average of 2.11 $\triangle E^*_{ab}$ can be considered as the colormetric performance under this circustance, while the maximum difference is 4.40 $\triangle E^*_{ab}$. Procedure two takes the 6 neutral color patches in the ColorChekcer as the calibration (linearization) references, therefore taking the rest 18 colors to compute the average color difference reveals more independent information. It can be seen that procedure two yields better results than procedure one for the averaged 18 colors, which implies a larger range of linearization in this configuration can improve the performance. The averaged 6 colors is from the 6 neutral color patches in the ColorChecker, which is provided for cross-check.

Table 1. Summary of the results from the two procedures in $\triangle E^*_{ab}$. (noted for the small difference)*

Procedure/ $\triangle E^*_{ab}$	24 Colors (ave)	18 Colors (ave)	6 Colors (ave)	24 Colors (max)	18 Colors (max)	6 colors (max)
Black and White	2.11	2.45	1.10	4.40	4.40	2.42
Six neutral levels	0.827*	0.829*	0.821	1.81	1.81	1.10

Table 2. Summary of the results from the two procedures in $\triangle E^*_{00}$.

Procedure/ $\triangle E^*_{00}$	24 Colors (ave)	18 Colors (ave)	6 Colors (ave)	24 Colors (max)	18 Colors (max)	6 colors (max)
Black and White	1.19	1.28	0.91	1.72	1.69	1.72
Six neutral levels	0.52	0.42	0.821	1.40	0.65	1.40

The same data are computed in $\triangle E^*_{00}$ and is summaried in Table 2. As shown in Table 2, the trend is similar that procedure two yields better performance than procedure one. However, there is one exception that when finding the maximum difference, it always falls in the neutral color group in $\triangle E^*_{00}$ units for both procedures. When computed in $\triangle E^*_{ab}$ units, the maximum difference is always found not in the neutral color group. The different weightings in the two color difference formulas may cause the shift. This variation might deserve some attention in the museum community while selecting color different formula as performance metrics. Further studies might be needed though.

Another possible future work is to use just the darkest and lightest neutral color patches in the ColorChecker to perform the calibration for comparison. The other possible work is to use six independent color patches, like the Labsphere targets, as reference standards from dark to white for comparison. It is preferred though to use the ColorChecker's nutral colors for the calibration since this mini ColorChecker is so small that can be included in the scan easily. These can be good topics for future studies. Nevertheless, all these results are good benchmark values for this grating-type spectral imaing system.

4. CONCLUSIONS

There are various approaches to establish spectral imaging system. This study used grating-type spectrograph device to build a spectral scanning system. With a basic calibration procedure (reference to a black and a white patch), this system can reach an average color differnce for ColorChecker at 2.11 $\triangle E^*_{ab}$ or 1.19 $\triangle E^*_{00}$ with maximun difference at 4.40 $\triangle E^*_{ab}$ or 1.72 $\triangle E^*_{00}$. If tighter calibration (linerization) is used with the 6 neutral color patches in the ColorChecker, this system can reach an average color differnce for 18 chromatic colors in the ColorChecker at 0.83 $\triangle E^*_{ab}$ or 0.42 $\triangle E^*_{00}$ with maximun difference at 1.81 $\triangle E^*_{ab}$ or 0.65 $\triangle E^*_{00}$. These provide a benchmark reference for this grating-type spectral system. It is within a similar range for the colorimetirc performance of the other spectral imaging systems.

ACKNOWLEDGEMENTS

The authors would like to express their appreciation for the supports from the Color Culture and Informatic lab at Chinese Culture University in Taipei, Taiwan.

REFERENCES

Berns, R. S., L. A. Taplin, M. Nezamabadi, and M. Mohammadi. 2005a. Spectral imaging using a commercial color-filter array digital camera. *Proc. 14th Triennial Meeting The Hague, ICOM Committee for Conservation*, 743-750.

Berns, R. S., F. S. Frey, M. R. Rosen, E. P. Smoyer, and L. A. Taplin. 2005b. Direct digital capture of cultural heritage - Benchmarking American museum practices and defining future needs report. Rochester Institute of Technology, http://www.art-si.org/PDFs/Metric/Benchmark_Report_April.pdf. Accessed: Feb. 26, 2015.

Berns, R. S. 2012. Analysis of color management default camera profiles for museum imaging applications. *IS&T Archiving Conference*, Copenhagen.

Fong, A., B. Bronson, and E. Wachman. 2008. Advanced photonic tools for hyperspectral imaging in the life sciences, *SPIE Newsroom*.

Frey, F. and S. Farnand. 2011. Benchmarking art image interchange cycles: final report 2011. Rochester Institute of Technology, http://artimaging.rit.edu/wordpress/wpcontent/uploads/2011/07/MellonFinalReport_FreyFarnand.pdf. Accessed: Feb. 26, 2015.

Imai, F. H. and R. S. Berns. 2009. U. S. Patent 7,554,586, System and method for scene image acquisition and spectral estimation using a wide-band multi-channel image capture, June 30, 2009. Assignee: Rochester Institute of Technology (Rochester, NY).

Tominaga, S. and T. Horiuchi. 2012. Spectral imaging by synchronizing capture and illumination, *JOSA A*, Vol. 29, Issue 9, pp. 1764-1775.

Address: M. James Shyu, Department of Information Communications,
Chinese Culture University, 55 Hwa Kang Road, Taipei 11114, Taiwan
E-mail: mjshyu@faculty.pccu.edu.tw

Experimental Evaluation of Chromostereopsis with Varying Spectral Power Distribution of Same Color

Masaru TSUCHIDA, Minoru MORI, Kunio KASHINO, Junji YAMATO
NTT Communication Science Laboratories, NTT Corporation

ABSTRACT

On the assumption that chromostereopsis is caused by chromatic aberration of the eyes, not only color but also the spectral power distribution (SPD) of observed light should affect the phenomenon. To confirm this, we displayed two color patches with different SPDs but the same chromaticity values on an LCD and compared their depth impressions. The SPD of the LCD's backlight can be changed by selecting band-pass filters attached in front of the light source. One color patch had an SPD consisting of a single peak at one wavelength, the other had one consisting of two peaks at different wavelengths. Evaluation results show that the former seems to be placed in front of the latter.

1. INTRODUCTION

Choromostereopsis has been well known for over a hundred years as a visual illusion in which color affects depth perception [Hartridge 1918; Howeard 1995]. For example a red patch next to a blue patch on a black background is often perceived as being in front of the blue one (Fig. 1). The wavelength of red light is longer than that of blue light. Therefore chromostereopsis is thought to be caused by a chromatic aberration of the eyes. There are two models for explaining chromostereosis; longitude chromatic aberration and transverse chromatic aberration. However, with the former, the effect of monocular stereoscopy is weak. In addition, it is difficult to explain by longitude chromatic aberration why a minority of observers perceive blue in front of red. For these reasons, transverse chromatic aberration is thought to be the major factor in chromostereopsis [Vos 1960; Kishto 1960; Sundet 1976; Faubert 1994] (Fig. 2). Recently, several models explaining chromostereopsis [Sundet 1972; Ye et al. 1991; Kitaoka 2006] and

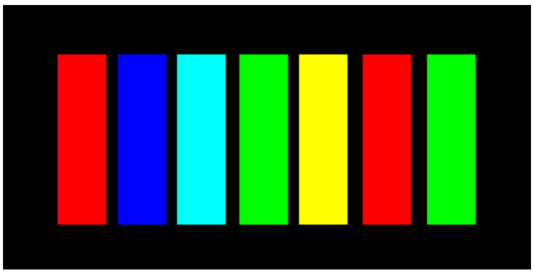

Figure 1: Color chart for confirming effect of chromostereopsis. Each colored rectangle is the same size.

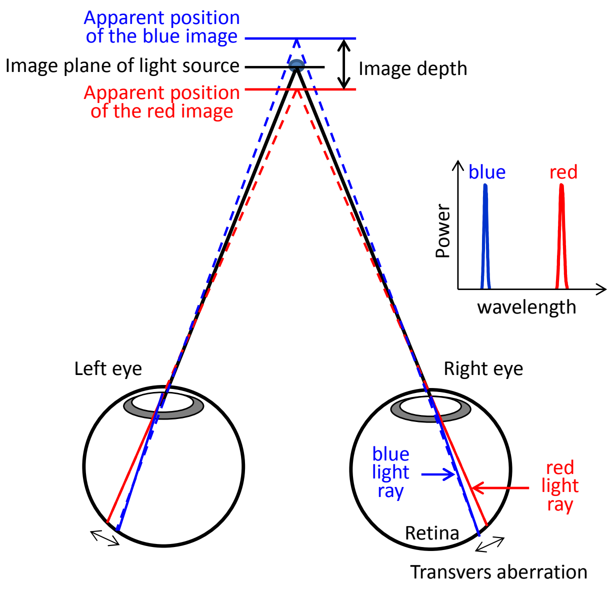

Figure 2: Transverse chromatic aberration model. Incident light ray (e.g. red and blue) is divided into two by refraction and transvers aberration occurs. This causes different apparent position of each color image.

methods for enhancing the stereoscopic effect [Steenblik 1987; Bailey et al. 1998; Ucke et al. 1998; Schemali et al. 2014] have been proposed.

Most previous research has only dealt with monochromatic light, i.e. light whose spectral power distribution (SPD) consists of a peak with a small full width at half maximum (FWHM) at the center wavelength. Some researchers have evaluated the relationship between depth perception and the FWHM and have confirmed that the effect of chromostereopsis among different colors is reduced when the FWHM is increased, especially when SPDs of each color overlap [Tsuchida et al. 2014]. However, there are cases where the chromaticity value of a color is the same but its SPD is different. Discussions concerning colors whose SPD is broad or consists of several peaks at different wavelengths with small FWHM are necessary. According to the transverse chromatic aberration model, a color with an SPD consisting of several peaks at each center wavelength causes blur on the retina. This should make the depth perception of the color patch weaker than that of a color patch with an SPD consisting of a single peak with a small FWHM at the center wavelength when their chromaticity values are the same.

To verifying this hypothesis, we compared depth perception of two color patches with different SPDs but the same chromaticity values. One color patch whose SPD consisted of a single peak at a wavelength was used as the target and its center wavelength was fixed. The other whose SPD consisted of two isolated peaks at different wavelengths was used as the reference, and the combinations of center wavelengths were changed. Target and reference color patches were displayed side by side on a liquid crystal display (LCD).

2. EXPERIMENTS

2.1 System Configuration

Our experimental system consists of an LC panel with a red-green-blue filter array, two xenon lamp systems, a metal halide lamp and band-pass filters (Fig. 3). The xenon lamp systems and the metal halide lamp are used to backlight the LCD. A band-pass filter is attached in front of the lens of the light-guide optical fiber of the metal halide lamp. Light from the metal halide lamp is used as a target color. Each lamp system consists of a xenon lamp, an ND filter, and a filter turret on which eight filters can be attached. Brightness and the filter turret can be controlled by software on a computer Light from the two xenon lamp systems is combined by light-guide optical fibers. The combination of band-pass filters and brightness of light are adjusted to match the chromaticity value to a target color. The SPD of the reference color has two peaks at different wavelengths. Target and reference color patches were displayed side by side on the LCD. The distance between each color patch was 0.5 cm. Images of color patches were 10 cm in height and 2.5 cm in width.

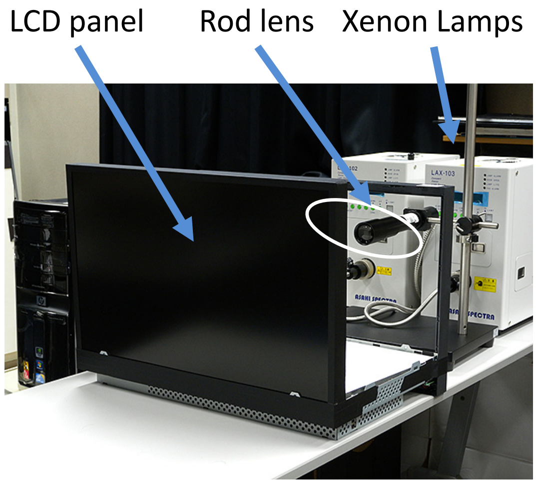

Figure 3: LCD system used in experiments. Interference filters are attached inside lamp housings.

The distance between the LCD and observers was approximately 50 cm. The experiments were conducted in a dark room.

The spectral locus on the chromaticity diagram between 520 and 630 nm is linear (see Fig. 4), and a target color can be synthesized by combining two lights whose center wavelengths are different. Then, these wavelengths were used for the experiments. Light that had passed through a band-pass filter whose center wavelength and FWHM were 570 and 30 nm, respectively, was chosen as a target color. To obtain enough brightness as target color, we chose a filter with relatively large FWHM. As a reference color, four combinations of light that had passed through the band-pass filter were chosen and their center wavelength were 520 and 610 nm, 530 and 630 nm, 540 and 610 nm, and 550 and 600 nm (note that the FWHM of the 630 nm filter was 30 nm; that of the other filter was 10 nm). There were few overlaps between SPDs of the target color and the third and fourth combinations (540 and 610 nm, and 550 and 600 nm).

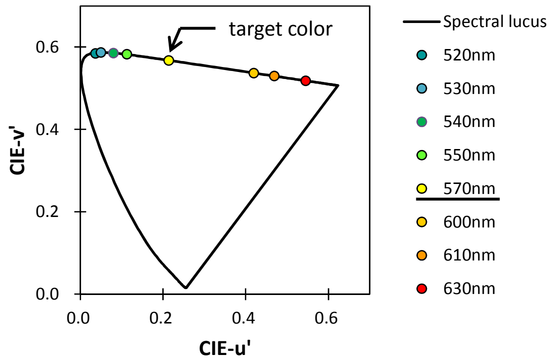

Figure 4: Chromaticity values of each color.

2.2 Results and Discussion

First, the brightness of each light from the lamps was adjusted to obtain the same chromaticity value between the target- and the reference color patches. Table 1 shows chromaticity values of each color patch, and their SPDs are shown in Fig. 5(a). Figure 5(b) is a chromaticity diagram plotting chromaticity values of each color patch. These results show that the same color with different SPDs were obtained. Note that we made one of the tristimulus values (CIE-Y) of each color the same to avoid the effect of difference in brightness.

Next, we compared the apparent depths of the target and reference color patch. The combination of lights, whose

Table 1: Measured chromaticity values of target and reference color patches.

	CIE-xyz			CIE-u'v'	
	x	y	z	u'	v'
570nm (target color)	0.475	0.523	0.002	0.228	0.565
520nm and 610nm	0.464	0.509	0.028	0.227	0.560
530nm and 630nm	0.471	0.517	0.011	0.228	0.563
540nm and 610nm	0.472	0.519	0.009	0.228	0.564
550nm and 600nm	0.469	0.528	0.003	0.224	0.565

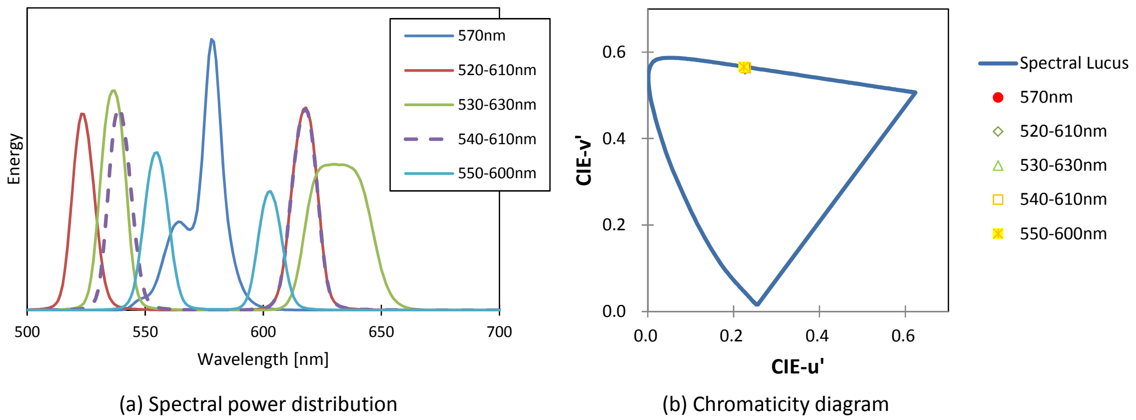

Figure 5: (a) Spectral power distribution and (b) chromaticity value of each combination.

Table 2: Standard deviations of each SPD of color patch.

	570nm (target color)	520nm and 610nm	530nm and 630nm	540nm and 610nm	550nm and 600nm
Standard deviation	8.08	46.71	45.67	39.07	23.90

center wavelengths were 520 and 610 nm, was used as the first reference color patch. In this case, the target color patch was perceived as located in front of the reference patch. The same result was also observed when center wavelengths of the reference color patch were 530 and 610 nm. However, the difference in the apparent depth between the target and reference color patches was reduced for the third and fourth reference color patches (540 and 610 nm, and 550 and 600 nm). Particulaly, the target and reference color patches seemed to be located at the same depth for the fourth reference color patch. These results infer that the apparent depths of target and reference color patches whose chromaticity values are same depends on variance of the SPD of each color patch. Table 2 shows standard deviations of each SPD.

It can be said that the experiment described above is equal to that using an eight primary color display. The displayed color could be presented using either one primary or two primaries. When the chromaticity values of displayed color patches are the same, the SPD of the color presented by one primary is narrower than that of the one presented by two primaries. The number of primaries for presenting color, distance between center wavelengths of two primaries, and the FWHM of each primary's SPD affect its apparent depth.

4. CONCLUSIONS

We experimentally showed that the spectral power distribution (SPD) of a displayed color affects depth perception. The SPD consisting of a single peak with a small full width at half maximum at a center wavelength was narrower than that consisting of two isolated peaks at each center wavelength. Even when chromaticity values of two displayed color patches were the same, the color patch with the narrower SPD seemed to be in front of the other patch. In cases where the SPD of each color overlapped, the effect caused by chromostereopsis was reduced or disappeard. We used eight monochtome colors between 520 and 630 nm in the experiments. We will conduct experiments using other colors in near future.

REFERENCES

Bailey, M, and Clark, D. 1998: Using ChromaDepth to obtain Inexpensive Single-image Stereovision for Scientific Visualization. *Journal of Graphics Tools archive, Vol.3, Issue 3, 1-9.*

Guerlac, H. 1967: *Newton's Optical Aether: His Draft of a Proposed Addition to His Opticks*, Notes and Records of the Royal Society of London 22(1) 45-57.

Hartridge, H. 1918: Chromatic aberration and the resolving of the eye. *Journal of Physiology, vol.52, 175-246.*

Howard, I. P., and Rogers, B. J. 1995: *Binocular vision and stereopsis*. New York and Oxford: Oxford University Press

Kishto, B. N. 1965: The colour stereoscopic effect. *Vision Research, vol.5, 313-329.*

Kitaoka, A., Kuriki, I., and Ashida, H. 2006: The Center-of-gravity Model of Chromostereopsis. *Ritsumeikan Journal of Human Sciences, vol.11, 59-64*. (http://www.psy.ritsumei.ac.jp/~akitaoka/chromostereopsis.pdf)

Schemali, L., and Eisemann, E. 2014: ChromoStereoscopic Rendering for Trichromatic Displays. *In proceedings of the Workshop on Non-Photorealistic Animation and Rendering. 57-62.*
Steenblik, R.A. 1989: Chromostereoscopic Microscopy. *In Proceedings of SPIE Vol.1083, 60-64.*
Sundet, J. M. 1972: The effect of pupil size variations on the colour stereoscopic phenomenon. *Vision Research, vol.12, 1027-1032.*
Sundet, J. M. 1976: Two Theories of Colour Stereoscopy, *Vision Research, vol.16, 469-472.*
Tsuchida, M., Kashino., K., and Yamato., J. 2014: Experimental Evaluation of Chromostereopsis with Varying Center Wavelength and FWHM of Spectral Power Distribution. *Springer LNCS 8509, 133-141.*
Ucke, D. 1998: 3-D Vision with Chromadepth^{TM} Glasses. *In proceedings of the international ICPE/GIREP. 23-28.*
Vos, J. J. 1960: Some new aspect of color stereoscopy. *Journal of Optical Society of America., vol.50, 785-790.*
Ye, M., Bradley, A., Thibos, L.N., and Zhang, X. 1991: Interocular differences in transverse chromatic aberration determine chromostereopsis for small pupils. *Vision Research, vol.31, 1787-1796.*

Address: Masaru TSUCHIDA, NTT Communication Science Laboratories,
3-1 Morinosato-Wakamiya, Atsugi-shi, Kanagawa, 243-0198, JAPAN
E-mails: tsuchida.masaru@lab.ntt.co.jp

HAZE AND CONVERGENCE MODELS: EXPERIMENTAL COMPARISON

Jessica El Khoury, Jean-Baptiste Thomas, Alamin Mansouri
LE2I, University of Burgundy, France
Email: jessica.el-khoury@u-bourgogne.fr

ABSTRACT

Bad environmental conditions like bad weather, such as fog and haze, and smoke-filled monitored closed areas, cause a degradation and a loss in contrast and color information in images. Unlike outdoor scenes imaged in a foggy day, an indoor artificial hazy scene can be acquired in controlled conditions, while the clear image is always available when the smoke is dispersed. This can help to investigate models of haze and evaluate dehazing algorithms. Thus, an artificial indoor scene was set up in a closed area with a mean to control the amount of haze within this scene. While a convergence model simulates correctly a small amount of haze, it fails to reproduce the same perceived hazy colors of the real image when haze density is high. This difference becomes obvious when the same dehazing method is applied to both images. Unlike simulated images, colors in real hazy images are resulted from environmental illuminants interference.

1. INTRODUCTION

Outdoor images are usually prone to degradation caused by atmospheric scattering particles. Indoor images captured and handled by monitoring sensors could be as well subject to color and contrast fadeout caused by occasional smoke emission, causing security failure. Many dehazing methods have been proposed to minimize this degradation and to recover original scene contrast [7, 12]. Although several articles have reported the shortage of color fidelity in recovered scenes [4, 9], none of the existing methods has deeply addressed this problem from a color point of view. In order to address this issue, we initiated to depict color shift between original clear image and the dehazed one of a simulated scene based on convergence model [3]. Recently, an artificial indoor hazy scene was installed to see how a real hazy scene could be faithfully represented by simulation.

The principal aim of this paper is to identify the limits that prevent a simulated hazy image formed by the convergence model to represent the same veiled object placed at a constant distance while changing fog density. Convergence model does not include the distance between the object and the camera and the effect of the fog that lies through the line of sight.

The rest of this paper is organized as follows. After briefly introducing dehazing and color convergence models and outlining the previous work in section 2, we describe in section 3 the experimental procedure of hazy images establishment. Experimental results and discussion are given in section 4, and conclusions and future works in section 5.

2. BACKGROUND AND PREVIOUS WORK

2.1 Haze and convergence models

According to D'Zmura *et al.* [1], translation and convergence in CIE xy lead to the perception of transparency. Color constancy revealed in presence of fog can be modelled by convergence model while taking into consideration shift in color and contrast. This was confirmed by asymmetric matching experiments.

Koschmieder [8] established a linear relationship between the luminance reflected by the object and the luminance reaching the observer. This linear relationship is based on the distance between the observer and the object. As Koschmieder stated, the problem of restoring true intensities and color, presents an underlying ambiguity that cannot be analytically solved unless scene depth data is available. The scene depth is equivalent to transmission.

Haze (1) and color transparency (2) are equivalently modelled:

$$I(x) = J(x)t(x) + A_\infty\big(1 - t(x)\big) \quad (1) \qquad b = (1-\alpha)a + \alpha f \quad (2)$$

$I(x)$ is the perceived intensity of the hazed image, $J(x)$ is the scene radiance of the original free-haze image and $t(x)$ is the direct transmission, which represents the non scattered light emanating from the object and is attenuated by the scattering along the line of sight ($t(x) = e^{-\beta d}$, β is the scattering coefficient and d is the scene depth). The airlight corresponds to an object at an infinite distance and it is called atmospheric light A_∞. The airlight $A(1 - t(x))$ is the light coming from an illuminant (*i.e.* sun) and scattered by the atmospheric particles towards the camera. In the transparency model, a represents the tristimulus values of a surface; a convergence application leads to new tristimulus values b. f is the target of convergence. α represents the amount of fog covering the surface. Light that reaches the eye from the surface is the sum of the original light emanating from the surface and the light that depends on the chromatic properties of the fog.

2.2 Previous work

Dehazing aims at the inversion of haze model, the automatic evaluation of parameters influences color recovering. In order to qualify this, we initiated previous work by studying how dehazing methods fail to recover accurately original colors of simulated hazy scene. In the previous work [3], we proposed a simulation of haze based on the convergence model. Color shift evaluation was done using this model. Unlike haze model, the transmission of the surface depends only on the amount of covering fog, which is a transparent filter, and it does not depend on the distance between the surface and the camera. We assumed that the effect of this distance is equivalent to α: when alpha increases, this gives the same impression as the distance increases through the haze. According to the convergence model, the simulation consists on embedding haze in CIE XYZ image of GretagMacbeth ColorChecker. We applied the same model to RGB image in order to perform a cross validation with two different spaces basis [3]. The dehazing method Dark Channel Prior (DCP) [6] was applied to recover original image. Thus, we realized by converting color to IPT color space [2] and CIE LUV, that this method boosts the color saturation without altering hue of highly chromatic colors.

3. EXPERIMENTAL SETUP

In order to provide stable basic conditions that simplify the evaluation of dehazing processes, we proceeded by creating controlled indoor hazy scene. This scene was set up in a closed room with a large window that allows a homogenous sunlight to get in, in order to avoid directionality of artificial light. At the back of the calibrated scene, the farthest point to the camera Nikon D7100 (6.9 m), where the covering airlight is considered to have the maximal value, we placed a GretagMacbeth ColorChecker, and we changed consecutively the amount of emitted haze. The smoke machine FOGBURST 1500 was used for haze emission, and the different levels of haze by evacuating progressively the emitted haze. We used also the Konica Minolta CS-2000 spectroradiometer for transmittance measurements of the haze.

The spectra of Figure 2 depict the transmittance of the white patch of each haze level. When the haze veil dominates the image, we can easily notice that transmittance curves represent the light scattered by haze particles adding to it the daylight reflected by the patch. The manner how the transmission intensity evolves through haze levels, we can notice that the luminance of haze density is exponentially evolving. From level 6 the transmittance intensity becomes to reach back and to be closer again to the transmittance spectrum of the clear image. This leads to deduce that the airlight causes the atmosphere to behave like a secondary light source of a different type than the outdoor global illumination.

According to the definition of convergence model parameters, b is the image that is covered by a given level of haze. a is the clear image, which is considered to be the one captured without embedding haze. f represents the tristimulus value of the captured target when it is covered by an opaque haze veil. Finally, α is calculated by inverting the convergence model and choosing the value corresponding to the black patch. We assume that the darkest patch does not reflect the daylight, and that the airlight over this patch is only due to the haze veil. The camera noise is removed by subtracting the tristimulus values of the black patch in clear image from the values of the same patch covered by different haze levels. Equiluminous veil embedded in simulated images where α is constant, is unnatural, and it cannot be represented by such physical veil.

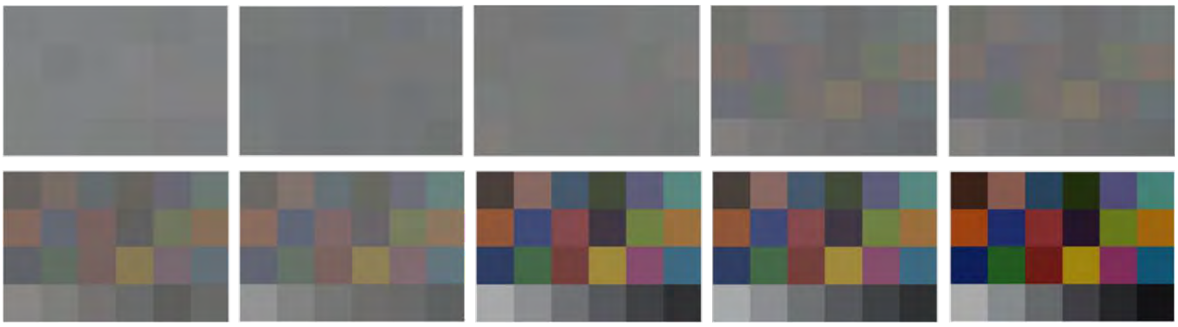

Figure 1 – Our database. The images of the GretagMacbeth ColorChecker taken under different haze levels. From left to right: Level 1; Level 2; Level 3; Level 4; Level 5; Level 6; Level 7; Level 8; Level 9; Clear image.

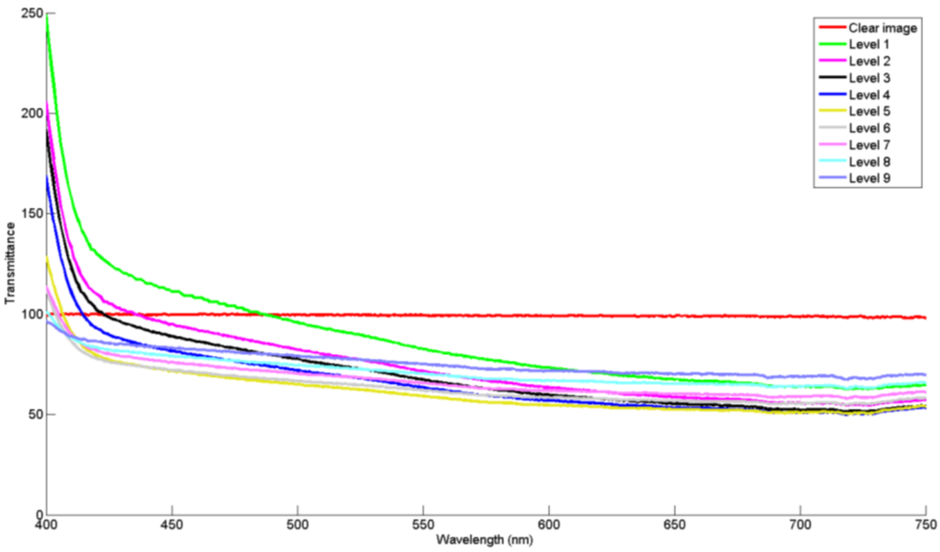

Figure 2 – Transmission curves of the white patch at different haze density levels. We notice that the short wavelength overcome the calibration. According to Rayleigh scattering [11], the strong wavelength dependence of the scattering ($\sim\lambda^{-4}$) means that shorter (blue) wavelengths are scattered more strongly than longer (red) wavelengths.

4. DISCUSSION

Haze that lies between the camera and the ColorChecker target modifies the light that emanates from it and reaches the camera. The light reflected from the target is added to the light scattered by the intervening particles. When the haze density greatly increases and the scattered light overcomes the light reflected by the target, the perceived colors components, hue and saturation, shift from their original values. This is clearly shown in Figure 3, where the simulation succeeds to represent the real scene of level 9 (with a little saturation difference related to the clear black patch) and fails for level 5. Referring to Figure 4, the distributions of points representing the red patch from level 5 to level 2 change between (a) and (b), while other points keep the same relative place between the end points (red and white) with a little shift in saturation (as shown in Figure 3 for Scene Level 9 and Simulated Level 9).

As it is defined above, the direct transmission is the light that reaches the camera without being scattered. Thus, the hue of this light is assumed to be independent of the reflected surface depth. The hue of airlight depends on the particle size distribution and tends to be gray or light blue in the case of haze and fog [11]. According to Figure 4, when the haze veil becomes great, the points placed on the chromaticity diagram of the patches, deviate from the line linking the haze veil color (white point) to the original unveiled color (red point), and they are biased toward blue/green area. Some points are also located outside the area between the red and white points. The deviation rate depends on the patch color, the airlight and the sunlight interference. When the amount of deviation in simulated scenes is smaller, all points representing a given patch at different haze levels remain between the red and white point.

When DCP is applied to Scene Level 5 (Figure 3), it accentuates the veiled colors by enhancing saturation. The recovered colors are totally different from those recovered from the Simulated Level 5, where the target and the veil are colorimetrically independent.

Figure 3 – The first line represents two different levels of scene images and the corresponding simulated images. The second line represents the recovered images by DCP of the first line images. From left to right (first line): Scene Level 9 – Simulated Level 9 – Scene Level 5 – Simulated Level 5. DCP fails to recover accurately the same colors for both images of Level 5 where haze density is high. Unlike the simulated scene, irradiance undergo illuminants interference and scattering effects.

This work confirms the previous conclusions considering that DCP saturates recovered colors. And the way it estimates the airlight and the transmission does not enables it to take into consideration the interference of different illuminants. As the retrieval of these parameters is limited to the pixels' intensities estimation, its mission remains limited to saturation enhancement, and original hues are not accurately recovered (Figure 3). On the other side, when the density of haze is small and the original hue is not altered, a simple adjustment based on convergence model could reinstate original saturation.

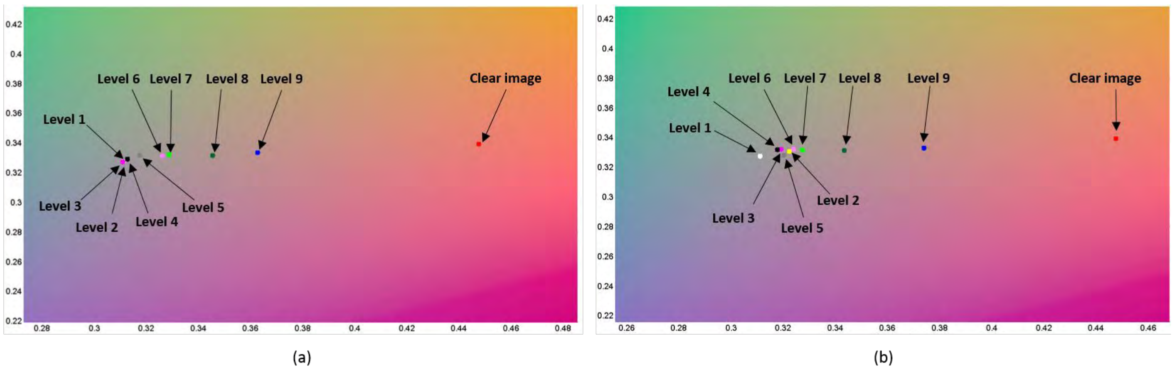

Figure 4 – The chromaticities of different haze levels placed on the chromaticity diagram of the red patch. (a) Real Scene, (b) Simulated Scene. Red: clear image – white: Level 1 – yellow: Level 2 – magenta: Level 3 – black: Level 4 - gray: Level 5 – pink: Level 6 – green: Level 7 – dark green: Level 8 – blue: Level 9. The distributions of points representing the red path from level 5 to level 2 are different between (a) an (b), while other points keep the same relative place between the end points (red and white) with a little shift in saturation.

5. CONCLUSIONS AND FUTURE WORKS

In this article we study the similarities between a simulated hazy image created by a convergence model and a real hazy scene. Physical luminous interaction modifies the perceived scene, while colors in the simulated image maintain their hue information and only their saturation component shifts between the original color (saturated), and the haze color (unsaturated). Convergence model fails to stand for hazy image when the density of haze becomes considerably high. Dehazing methods like DCP, aim just to remove the covered veil and to recover the color as it is not completely hidden, without taking into consideration the interaction of different phenomenon. Thus, a pre-processing aiming to adjust hue color, and a post-processing based on convergence model for saturation adjustments.

Future works shall focus on the validation of the color correction on dehazed images. We intend also to investigate the possibility to extend color-based image dehazing methods to multispectral-based image. Calibrated hazy images database should evidently considered as a benchmarking tool of colorimetric issues that are related to dehazing methods.

ACKNOWLEDGEMENTS

The authors thanks the Open Food System project for funding. Open Food System is a research project supported by Vitagora, Cap Digital, Imaginove, Aquimer, Microtechnique and Agrimip, funded by the French State and the Franche-Comté Region as part of The Investments for the Future Programme managed by Bpifrance, www.openfoodsystem.fr.

REFERENCES

[1] D'Zmura M., P. Colantoni, K. Knoblauch, and B. Laget. 1997. Color transparency. Perception (26): 471-492.

[2] Ebner F., and M. D. Fairchild. 1998. Development and testing of a color space (IPT) with improved hue uniformity. In Color and Imaging Conference, 8-13.

[3] El Khoury J., J.B. Thomas, and A. Mansouri. 2014. Does dehazing model preserve color information?. In 10th International Conference on Signal-Image Technology and Internet-Based Systems, 606-613.
[4] Guo F., J. Tang, and Z. Cai. 2014. Image Dehazing Based on Haziness Analysis. *International Journal of Automation and Computing 11(1)*, 78-86.
[5] Hagedorn J., and M. D'Zmura. 2000. Color Appearance of Surfaces Viewed Through Fog. *Perception* (29), 1169-1184.
[6] He K., J. Sun, and X. Tang. 2009. Single image haze removal using dark channel prior. In IEEE Conference on Computer Vision and Pattern Recognition, 1956-1963.
[7] Kaur H., and R. Mahajan. 2014. A review on various visibility restoration techniques. *International Journal of Advanced Research in Computer and Communication Engineering,* Volume 3, Issue 5.
[8] Koschmieder H. 1925.Theorie der horizontalen Sichtweite: Kontrast und Sichtweite. Keim & Nemnich.
[9] Kponou E., Z. Wang, and L. Li. 2013. A comprehensive study on fast image dehazing techniques. *International Journal of Computer Science and Mobile Computing,* Volume 2, Issue 9, 146-152.
[10] McCamy C. S., H. Marcus, and J. G. Davidson. 1976. A Color-Rendition Chart. *Journal of Applied Photographic Engineering* (2), 95-99.
[11] Nayar S., and S. Narasimhan. 1999. Vision in bad weather. In IEEE International Conference on Computer Vision (ICCV), 820-827.
[12] Sharma R., and V. Chopra. 2014. A review on different image dehazing methods. *International Journal of Computer Engineering and Applications,* Volume 6, Issue 3.

Hyperspectral Reflectance Reconstruction Using a Filter-based Multispectral Camera

Wei-Chun HUNG [1], Pei-Li SUN [1], Raymond JIANG [2]
[1] Graduate Institute of Color and Illumination Tech., Nat. Taiwan Univ. of Sci. & Tech.
[2] Graduate Institute of Applied Sci. & Tech., Nat. Taiwan Univ. of Sci. & Tech.

ABSTRACT

In this study, a filter-based multispectral camera is used to extent its data from 16 band to 61 bands within visual spectra. The camera provides uncorrected achromatic image for each filter-band. We corrected its lighting uniformity, estimated multispectral tone responses using a polynomial regression by not only achromatic samples but also color samples from a ColorChecker chart, interpolate its spectral data to 5nm interval using cubic interpolation. The maximum color errors greatly reduced from 21.97 to 5.2 ΔE. PCA based method also were tested. The maximum color error was further decreased to 1.9 ΔE.

On the other hand, the spectral filters of the camera are switchable. However, if we switch the filters, the spectral images captured from different filter sets cannot align each other accurately. A deblurring process and a Scale Invariant Feature Transform (SIFT) therefore are applied to align the sub-frame of a spectral image spatially.

1. INTRODUCTION

In multispectral imaging field, three types of spectral cameras are commonly used: (1) a line-scanning hyper-spectral camera (Grahn and Geladi, 2007), (2) a filter-based multispectral camera (Hill, 1998) and (3) a trichomatic camera with known principal components of the spectral reflectances (Imai and Berns, 1999). Each of them has its own pros and cons. The line-scanning hyperspectral camera is time-consuming in its spectral image acquisition, whereas the filter-based multispectral camera cannot provide accurate hyperspectral data with its limited bands. The trichomatic camera cannot predict the spectral data in high precision when the principal components of surface reflectances are unknown.

In digital archiving, hyperspectral data is useful for image restoration. In this study, a filter-based 8 band multispectral camera was used to extent its data from 8 band to 61 bands within visual spectra. The spectral filters of the camera are switchable. The spectral accuracy can be enhanced by using two sets of narrowband filters (16 wavebands) for image acquisition. The camera provides uncorrected achromatic image for each filter-band. Therefore, we have to write software to improve the accuracy of spectral estimation. On the other hand, the filter-based camera enables of capturing each frame up to 20 fps. However, the fast moving of the color wheel results in minor motion blur. In addition, if we change the spectral filter set manually, the spectral images captured from different filter sets cannot align each other accurately. The resulted spectral images will suffer from blurring or ghosting. Spectral correction and image alignment therefore are the two challenged issues for the post processing of spectral images.

2. APPARATUS

The spectral camera used in this study was Pixelteq SpectroCam VIS-NIR. It contains a filter wheel holding 8 easily changeable filter segments, digital progressive scan CCD scientific imager and operating in Visible / Near Infrared (VIS/NIR) range. In this study, two use two sets of spectral filters, one set starts from 400nm to 680nm in 40 nm interval. The other set starts from 420nm to 700nm in 40 nm. The bandwidth of each spectral filter is about 20nm. Figure 1 shows the spectral transmittances of the 16 VIS filters measured by a spectrophotometer. The image format of the spectral image is 16bit PNG file in 1280×1024 resolution. All measurement were done under a X-rite SectralLight III light booth. This spectral camera can use Fast Mode or Index Mode. The latter allows the user to set exposure time and gain for each channel. To achieve the best image quality, we set the exposure time and the gain value solely for each channel. The criteria of the adjustment is to set exposure time first to meet 80% gray level for No. 19 white patch on a X-rite ColorChecker chart. If the exposure time is up to its limit, adjust gain value to fullfil the criteria.

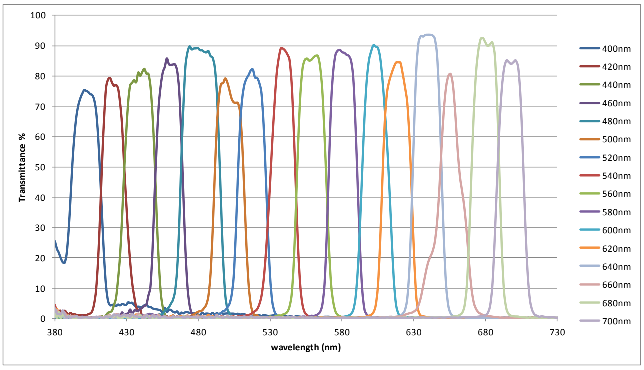

Figure 1: Spectral transmittances of 16 VIS filters.

3. SPECTRAL CORRECTION

X-rite ColorChecker was used to optimize the accuracy of reflectance reconstruction. The spectral reflectances of 24 patches on ColorChecker were measured by DataColor SF600 in its specularly excluding mode. Four commonly used light sources, A, D65 (filtered halogen), TL84 and CWF, were tested. And we found D65 shows best results on reflectance reconstruction as it provides smooth power spectra and more energy at short wavelength. The following test therefore all carried out under D65 light source. The spectral accuracy is judged by calcuating RMSE (root-mean-squared error) and color color differences (ΔE_{76}) under the four illumants. The measured and approximate spectral reflactances were compared in 400nm to 700nm range with 5nm intervals. The following steps were taken to optimize the accuracy.

2.1 Tone Correction

If we reconstruct the spectral reflectances of ColorChecker directly using the 16 band spectral images with nearest point interpolation, the mean and maximum color differences across the four light sources are 9.49 and 21.97 ΔE respectively. If only normalizes the data based on the reflectance of white patch, the maximum error can be reduced to 19.30 ΔE. The errors can be greatly reduced by black and white equalization shown as Figure 2, where the mean and maximum errors are 3.02 and 8.01ΔE respectively. The maximum errors can be further reduced to 7.42 by tone correction using first-order linear regression based on the grayscale No.19 to No.24 for each channel individually.

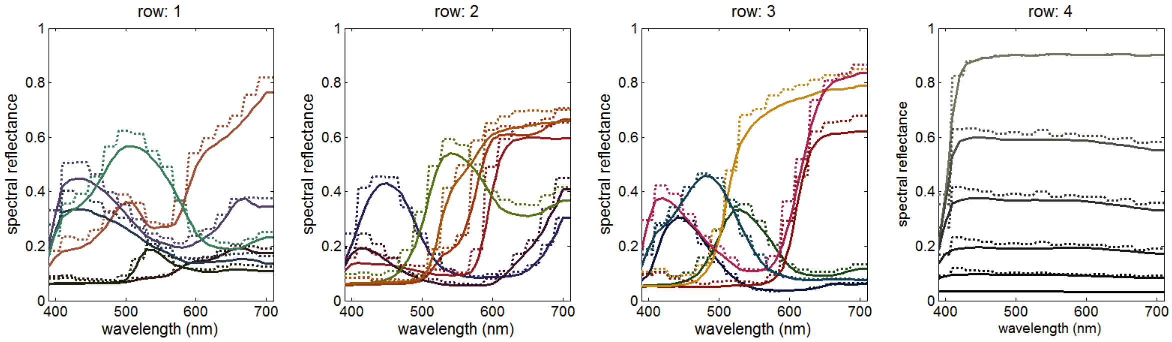

Figure 2: Spectral reconstruction of ColorChecker using black and white patches for tone correction. Solid lines: measurement. Dotted lines: approximation.

Table 1. Summary of the results from the experiment.

				mean					maximum				
band	tone	interpolate	uniform	A	D65	TL84	CWF	RMSE $*10^{-5}$	A	D65	TL84	CWF	RMSE $*10^{-5}$
16	no	nearest	no	9.15	9.50	9.67	9.63	72.59	18.05	20.75	21.78	21.97	183.49
	white	nearest	no	9.43	9.64	9.82	9.81	42.00	16.06	18.29	19.31	19.30	64.12
	black & white	nearest	no	2.74	3.00	3.15	3.19	13.03	6.76	7.82	7.96	8.01	30.07
	grayscale (1st)	nearest	no	2.59	2.72	3.18	3.01	8.78	5.77	6.29	7.42	6.74	19.54
	grayscale (1st)	linear	no	2.27	2.42	2.65	2.50	4.26	6.01	6.46	6.86	7.32	11.79
	grayscale (1st)	cubic	no	2.29	2.47	2.87	2.65	4.20	6.01	6.53	7.26	7.33	11.70
	grayscale (1st)	cubic	yes	1.60	1.89	1.89	1.85	1.75	4.69	6.42	6.08	6.28	5.21
	color (1st)	cubic	yes	1.44	1.62	1.48	1.54	**1.18**	3.91	5.16	5.10	4.94	**3.14**
	color (2nd)	cubic	yes	1.80	1.78	2.03	1.98	4.79	5.47	6.43	7.08	6.96	16.76
	PCA (n=3)	-	yes	6.16	7.98	7.71	6.28	11.64	15.00	17.81	20.17	15.41	26.52
	PCA (n=6)	-	yes	1.44	1.31	2.15	1.44	1.95	5.34	5.08	8.79	4.10	6.45
	PCA (n=9)	-	yes	0.20	0.22	0.65	0.30	**0.27**	0.86	0.97	1.95	0.90	**1.00**
8	color (1st)	cubic	yes	1.80	1.78	2.03	1.98	4.93	5.47	6.43	7.08	6.96	16.78

2.2 Spectral Interpolation and Uniformity Correction

Compared the color differences of three spectral interpolation methods – nearest, linear and cubic interpolations, the results have not significant differences. However, if we look at the RMSEs, both linear and cubic interpolations can reduce the maximum values to nearly a half. ColorChecker is a big color target. It won't recevie equal illuminance across each patches. An spectral image of X-rite WhiteBlacing chart therefore was taken in the same environment for equalizing the spatial uniformity of spectral data. After the uniformity correction, the maximum RMSE redcue from 11.70^{e}-5 to 5.21^{e}-5 where the mean and maximum color differences are 1.81 and 6.42 ΔE respectively. The best results we can achieve using a 16 band spectral image was applying first order regression not only from the grayscale but also from all 24 color patches in the spectral tone correction. The mean and maximum color differences are 1.52 and 5.16 ΔE respectively, and the approximate spectra are shown in Figure 3. However, if 2-nd order polynomial regression is applied, the maximum error increased. The reason could be that the characteristic curve of the CCD is almost linear to luminance, a non-linear tone correction is not necessary and the regression might overestimate the tone characteristics. If only 8 spectral filters are used, the mean and maximum color differences using the 1st order color regression are 1.90 and 7.08 ΔE respectively.

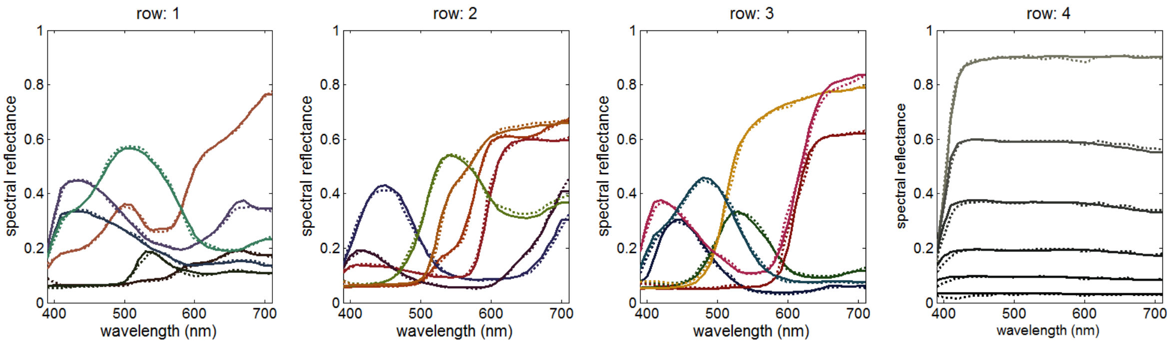

Figure 3: Spectral reconstruction of ColorChecker using color regression and uniformity correction. Solid lines: measurement. Dotted lines: approximation.

2.3 PCA-based Approach

Imai and Berns (1999) proposed a spectral estimation method for a trichomatic camera with known principal components of the spectral reflectances. A specrtral camera can be regarded as a multi-channel color camera and the results of spectral estimation should be more accuracte. We tested the method using 16, 8 and 4 narrowband filters and the results show that both 8 and 16 filters can reconstruct the spectral reflectances accurately when more than 6 basis functions are used. However, it the filters don't cover the whole spectral range or the number of basis functions is not enough, the results won't be acceptable. As the PCA-based approach only work when the PCA spectra of the target objects are known, it isn't recommended for normal spectral inspection.

3. DEBLURRING AND SUB-FRAME ALIGNMENT

As mentioned previously, the vibration of the color wheel might cause image blur and the manual swtiching of different filter set and slight moving of the target object might also result in blurring and even ghosting. To improve the spectral image qaulity, A deburring process should be applied to each spectral frame and an image alignment process must be done to generate a ghost-free and clear spectral image. In terms of deblurring, there are many methods such as Wiener filter (Gonzalez and Woods, 2007) can be used.

In terms of sub-frame alignment, a Scale Invariant Feature Transform (SIFT) (Lowe, 2004) therefore is applied to align the spectral images spatially. If we the two spectral band to match the SIFT key-points, only few of them can be found as Figure 4a. It is not s sufficient for geometry transform of the two images. However, if we choose adjacent wavebands for matching, many SIFT key-points can be found. Once we found enough correspondent key-points, after removing unusual moving vectors, a 3 by 3 transform matrix can be derived to project one sub-frame to the other. To optimize the image quality, the sub-frame near 550 nm should not be changed spatially.

(a) 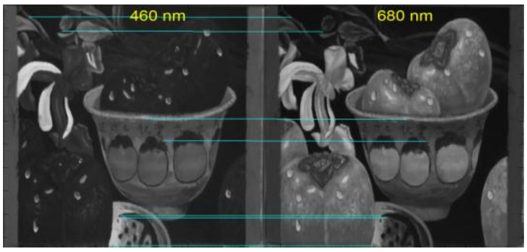

(b) 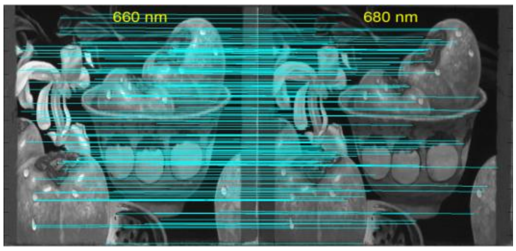

Figure 4: The results of SIFT key-points correspondence – (a) inconsecutive wavebands and (b) successive wavebands.

(a) 
(b) 

Figure 5: The results of deblurring and sub-frame alignment – (a) uncorrected and (b) uncorrected.

4. CONCLUSIONS

In this study, a filter-based multispectral camera is used to extent its data from 16 band to 61 bands within visual spectra. The camera provides uncorrected achromatic image for each filter-band. We corrected its lighting uniformity, estimated multispectral tone responses using a polynomial regression by not only achromatic samples but also color samples from a ColorChecker chart, interpolate its spectral data to 5nm interval using cubic interpolation. The maximum color errors greatly reduced from 21.97 to 5.2 ΔE. PCA based method also were tested. The maximum color error was further decreased to 1.9 ΔE.

On the other hand, the spectral filters of the camera are switchable. However, if we switch the filters, the spectral images captured from different filter sets cannot align each other accurately. A deblurring process and a Scale Invariant Feature Transform (SIFT) therefore are applied to align the sub-frame of a spectral image spatially.

REFERENCES

Gonzalez R. C. and Woods R. E., 2007. *Digital Image Processing* (3rd Edition), Prentice Hall.

Grahn H. and Geladi, P. 2007. *Techniques and Applications of Hyperspectral Image Analysis*. John Wiley & Sons.

Hill, B. 1998. Multispectral Color Technology: *A Way towards High Definition Color Image Scanning and Encoding*, Electronic Imaging 1998: 2-13.

Imai, F. H. and Berns, R. S., 1999. *Spectral estimation using trichromatic digital cameras*, in Proc. of the International Symposium on Multispectral Imaging and Color Reproduction for Digital Archives, Chiba University, Chiba, Japan, 1999, 42-49.

Lowe, D. G., 2004. *Distinctive image features from scale-invariant key points*, International Journal of Computer Vision 60(2): 91-110.

Address: Pei-Li SUN, Graduate Institute of Color and Illumination Technology,
National Taiwan University of Science and Technology,
43, Section 4, Keelung, Taipei, 10607, TAIWAN
E-mails: plsun@mail.ntust.edu.tw

Author Index

A

AIHARA, Katsuyuki *PS2-15*
AKAGAWA, Yuya *PS1-74*
AKIZUKI, Yuki *PS1-22*
ALVAREZ-MUÑOZ, José L. *PS2-71*
ANDO, Fuminori *PS2-69*
ANGELO, Kine *OS6-3*
ARAI, Yuki *PS1-39*
ARAKI, Keisuke *PS1-32*
ARBAB, Shabnam *OS2-1, PS1-73*
ARES, Miguel *MCS2-1*
ARITAKE, Sayaka *PS2-39*
ARNKIL, Harald *OS5-3, PS2-16*
ARRARTE-GRAU, Malvina *OS2-6*
ASANO, Akira *PS1-5, PS1-8*
ASANO, Kosuke *PS2-36*
ASHIZAWA, Shoko *PS1-64*
ATTIAH, Douha Y *PS1-14*
AWANO, Yumi *PS2-9*
AYAMA, Miyoshi *PS1-32, PS1-74*
AZUMA, Yoshihiko *PS2-53*

B

BAAR, Teun *PS1-83*
BAE, Hyunjoo *OS7-4*
BAI, Yi-Ho *PS2-44*
BARBAR, Reine *PS1-7*
BEIGPOUR, Shida *OS4-5*
BENJUMEA, Ana *PS2-31*
BERMEJO, Ruperto *PS2-33*
BERTALMÍO, Marcelo *PS1-29, PS1-31*
BILLGER, Monica *PS2-76*
BLÁHA, Jan D. *PS1-23*
BLASO, Laura *PS1-69*
BONANOMI, Cristian *OS5-2, PS1-69*
BOOKER, Alex *OS6-3*
BOSCH, Thierry *MCS2-1*
BROERSMA, Remy *PS2-57*
BROMILOW, David *PS1-14*
BUDHA, Kishore *PS1-67*
BURGOS, Francisco J. *MCS2-1, PS2-71*

C

CAI, Jianqi *PS1-77*
CALLET, Patrick *PS2-66*
CALORE, Enrico *PS1-56*
CARNIE, Bruce *PS1-67*
CARRASCO-SANZ, Ana *PS2-31*
CARVALHO, Laura *PS1-2*
CHAE, Youngjoo *PS1-72*
CHAGOYA, MariaElena *PS2-8*
CHANG, Chia-Chi *OS2-5*
CHANG, Chun-Kai *PS1-52*
CHAN, Kai-Lin *PS1-30*
CHAO, Jinhui *PS1-27*
CHAO, Wei-Hsuan *OS10-1*
CHAUHAN, Tushar *PS2-67*
CHEN, Hung-Shing *OS8-3, PS1-30, PS1-34, PS1-43*
CHEN, I-Ping *OS4-6*
CHEN, Lu *PS2-5*
CHEN, Yen-Wei *PS2-65*
CHEUNG, Vien *PS1-14, PS2-64*
CHIOU, Wei-Jei *OS4-6*
CHIU, Yu-Wen *PS1-34*
CHOI, Sueran *PS2-14, PS2-19*
CHORRO, Elísabet *PS2-55, PS2-71*
CHOU, Tzren-Ru *MCS2-3*
CHUNVIJITRA, Kanwara *PS1-70*
CHUO, Li-Ching *PS1-13*
CHUVIJITRA, Kanwara *PS1-71*
CICCONE, Nicholas *PS1-12*
CIORTAN, Irina Mihaela *MCS1-3*
CORDERO, Elisa *OS5-5*
CUEH, Chia-Pin *PS1-30, PS1-34, PS1-46*
CUI, Guihua *PS2-35*

D

DAUSER, Thomas *PS2-55*
DAVOODI, Anahita *PS2-60*
DEGUCHI, Ayana *PS1-5*
DELPUEYO, Xana *MCS2-1*
DENG, Wen-Ling *PS1-21*
DOI, Motonori *PS1-36*
DUYAN, Fazıla *PS1-15, PS1-17*

E

EGGER, Salome *PS2-42*
El KHOURY, Jessica *PS2-84*
ENGER, Johanna *PS2-60*

F

FANG, Jingyu *OS3-3*
FARUP, Ivar *OS3-2, MCS2-2*
FERNÁNDEZ-DORADO, José *PS2-71*
FERNANDEZ-MALOIGNE, Christine *PS1-56*
FINDLATER, Keith D. M. *PS1-25*
FINLAYSON, Graham *OS1-2, OS1-3*
FORZELIUS, Jacqueline *PS2-76*
FRIDELL ANTER, Karin *OS5-3, OS5-4*
FUCHIDA, Takayoshi *PS1-45*
FUCHS, Philippe *PS2-66*
FUJIMORI, Takahiro *PS2-69*
FUMAGALLI, Simonetta *PS1-69*
FUNAKOSHI, Saki *PS2-30*
FUNT, Brian *OS1-1, OS1-4, PS2-21*
FUSEDA, Takashi *PS1-32*

G

GAO, X. *PS1-24*
GARCIA, Jose A. *PS2-31*
GASPARINI, Katia *PS2-25*
GBÈHOUNOU, Syntyche *PS1-56*
GEORGE, Sony *MCS1-3*
GODAU, Christoph *PS2-80*
GÓMEZ-ROBLEDO, Luis *PS2-33, PS2-55*
GOTO, Fumiko *OS8-4, PS2-26*
GREEN, Phil *OS3-2*
GRIBER, Yulia *PS2-3*
GRIFFIN, Lewis *PS2-11*
GU, Haiting *OS7-2*
GUO, L. *PS1-24*
GUO, W. *PS1-24*
GUSTAFSSON COPPEL, Ludovic *PS2-75*

H

HAMANO, Toshiya *PS1-32*
HANARI, Takashi *PS2-32*
HANEISHI, Hideaki *MCS2-4*
HARADA, Masayuki *PS2-47*
HARDEBERG, Jon Y. *PS2-70*
HARDEBERG, Jon Yngve *Invited Talk (MCS) pp.27, MCS1-3*
HARDING, Mikaela *OS1-6*
HARUTA, Atsushi *PS2-36*
HASEGAWA, Madoka *PS2-72*
HASHIDA, Mio *OS8-1*
HASHIMOTO, Mitsumasa *OS8-4*
HATADA, Akinobu *PS1-50*
HATORI, Yasuhiro *PS2-48*
HENRY, Phil *PS2-13*
HERNÁNDEZ-ANDRÉS, Javier *PS1-35*
HERNANDEZ, Georgina Ortiz *PS2-2*
HERRERA, Jorge *MCS2-1*
HIDAKA, Kyoko *PS1-4*
HIRAI, Keita *MCS1-4*
HIRAO, Tetsuji *OS9-4*
HONG, Seungwan *PS1-40*
HORI, Motoki *MCS1-4*
HORIUCHI, Takahiko *OS9-1, MCS1-4*
HO, Ting-Tsung *OS2-5*
HSIAO, Horng-Ching *PS2-58*
HUANG, Hsin-Pou *PS1-13, PS2-44*
HUANG, Min *PS2-35*
HUANG, Wenjie *OS3-6*
HUA, Tao *PS1-72*
HUERTAS, Rafael *PS2-31*
HULL, Ben *OS1-4*
HU, Neng-Chung *PS1-43, PS2-58*
HUNG, Hsing-Ju *PS1-21*
HUNG, Ji-Yuan *OS10-1*
HUNG, Wei-Chun *PS1-61, PS2-85*
HUOLMAN, Ilona *OS5-1*

I

ICHIHARA, Yasuyo G. *OS8-5*
IGA, Koichi *OS8-4, PS1-68, PS1-78*
IGARASHI, Takanori *PS2-65*
IIDA, Yusuke *PS1-49*
IKEDA, Mitsuo *PS1-70, PS1-71*
IKEDA, Takashi *PS1-63*
INABA, Takashi *PS1-54*
INAMURA, Maya *PS2-38*
INUI, Shigeru *PS1-74*
ISAWA, Shoko *PS1-68, PS1-78*
ISHIDA, Taiichiro *PS2-40, PS2-51*
ISHIGURO, Youhei *PS1-84*
ISHIKAWA, Tomoharu *PS1-32, PS1-74*
ITO, Kei *OS8-4*
IWATA, Michico *PS1-22*
IYOTA, Hiroyuki *PS1-82, PS1-86*

J

JACQUOT, Muriel *PS1-7*
JENG, Ming-Shan *PS1-13*

JENKUNAWAT, Somporn *PS1-38*
JENKUNAWATT, Somporn *PS1-75*
JEONG, Chanung *OS7-3*
JEONG, Kyeongah *PS2-28*
JIANG, Raymond *PS2-85*
JIAN, Jia-Wun *OS8-3*
JINNO, Takao *PS1-51*
JUNG, Hyojin *PS1-65*
JUNG, Ivar *PS1-6*
JUNG, Min-Ho *PS2-64*
JUTTERSTROM, Per *PS1-19*

K

KAGIMOTO, Akari *PS1-86*
KAMIJO, Wataru *PS2-20*
KARLOVIC, Igor *PS2-31*
KASHINO, Kunio *PS2-83*
KATAYAMA, Ichiro *PS1-68, PS1-78*
KATEMAKE, Pichayada *PS2-6*
KATO, Koki *MCS2-4*
KATO, Shigeo *PS2-72*
KATO, Terumi *PS2-26*
KATSURA, Shigehito *PS2-12*
KAWABATA, Yasuhiro *PS1-62*
KAWAGUCHI, Akio *PS1-85*
KAWAHIRA, Hiroshi *MCS2-4*
KAWASHIMA, Mai *PS2-24*
KAWASHIMA, Yuki *PS1-49*
KAWASUMI, Mikiko *OS10-2, PS1-59*
KHODAMORADI, E. *PS1-24*
KIKUCHI, Kumiko *OS9-4*
KIMACHI, Akira *PS1-36*
KIM, EunJin *PS2-29*
KIM, Haechan *OS7-4*
KIM, Hanna *OS4-2, PS2-23*
KIM. Saetbul *PS2-14*
KIM, Saetbyul *PS2-19*
KIM, Yoosun *PS2-14, PS2-19*
KISHIMOTO, Yasunari *PS1-44*
KITAGUCHI, Saori *PS1-65*
KITA, Hideo *OS1-5, PS1-33*
KITAMURA, Shigeko *PS2-63*
KITANO, Toru *OS7-5*
KLARÉN, Ulf *OS5-3, OS5-4*
KOBAYASHI, Miyuki *PS2-53*
KOBAYASHI, Teruo *OS8-4*
KOHDA, Jiro *PS1-81*
KOJIMA, Kazuaki *PS2-24*
KOMATSU, Hidehiko *Invited Talk pp.33*
KOMIYAMA, Eri *PS2-53*
KONDO, Hirokazu *PS1-44*
KOTERA, Hiroaki *PS1-66*
KRYSANOVA, Sasha *OS6-4*
KUBO, Yuto *PS1-51*
KÜÇÜKKILIÇ ÖZCAN, Esra *PS1-16*
KUNIMOTO, Norifumi *PS2-1*
KUO, Wen-Guey *PS2-41*
KURIKI, Ichiro *PS2-48*
KURIMOTO, Hiroyuki *PS2-51*
KURIYAMA, Shigeru *PS1-51*
KWAK, Youngshin *PS1-47*

L

LADSON, Jack A. *PS1-33*
LAN, Chung-Chien *OS10-1*
LAN, Ming-Kang *PS2-62*
LAZARO, M. Mar *PS2-31*
LECELLIER, François *PS1-56*
LECH, Krzysztof *MCS1-1*
LEE, Eun Jung *PS2-54*
LEE, Heewon *OS4-2, PS2-23*
LEE, Jin sook *PS2-5*
LEE, Jinsook *OS4-2, OS7-3, PS2-17, PS2-23*
LEE, Mijin *PS2-23*
LEE, Min-Jae *PS2-4*
LEE, Soojin *PS1-26, PS2-43*
LEE, Tien-Rein *OS2-3, PS2-62*
LEE, Younjin *PS2-34*
LE MOAN, Steven *PS2-75*
LIANG, Ya-Chen *OS4-4*
LI, Changjun *OS3-1, PS2-67*
LIMON, Piedad *PS2-33*
LIN, Ting-Yun *PS2-82*
LIN, Tzung-Han *PS1-30*
LI ROSI, Ornella *PS1-69*
LI, Tianyi *OS3-1*
LIU, Haiyan *OS7-2*
LIU, HaiYan *OS3-5*
LIU, Haoxue *PS2-35*
LIU, Kang-Yu *PS1-30, PS1-34, PS1-46*
LIU, Mei-Ting *PS1-21*
LIU, Xiaoyu *OS7-2, MCS1-2, PS2-68*
LIU, XiaoYu *OS3-5, OS7-1*
LI, Yuan *PS1-26*

LI, Zeyang *PS2-35*
LÓPEZ, Mabel *PS2-2*
LU, Lin *PS1-30, PS1-43*
LUO, Junyan *PS2-69*
LUO, Lin *PS1-80*
LUO, Ming Ronnier *OS3-5, OS3-6, OS7-1, OS7-2, MCS1-2, PS2-68*
LUO, M Ronnier *OS3-1*
LUO, M. Ronnier *PS2-35*
LUO, Ronnier *OS8-3, PS2-67*
LUPARI, Helena *PS1-60*

M

MACDONALD, Lindsay *PS2-6, PS2-11*
MACDONALD, Lindsay W. *OS9-2*
MĄCZKOWSKI, Grzegorz *MCS1-1*
MAEKAWA, Mitsuyoshi *OS8-4*
MANABE, Yoshitsugu *PS1-39, PS2-74, PS2-78*
MANDIC, Lidija *PS1-41*
MANSOURI, Alamin *PS2-84*
MARIC, Yelena *PS1-7*
MARTÍNEZ, Eréndira *OS5-5*
MARTÍNEZ, Miguel A. *PS1-35*
MARTÍNEZ-VERDÚ, Francisco M. *PS2-71*
MARTÍNEZ-VERDÚ, Francisco Miguel *PS2-55*
MA, ShiNing *OS7-1*
MASUDA, Mami *PS1-86*
MASUDA, Yuji *OS9-4*
MATSUI, Tatsunori *PS2-24*
MATSUMIYA, Kazumichi *PS2-48*
MATSUMOTO, Taiki *PS1-82*
MATSUSHITA, Nao *PS1-84*
MATUSIAK, Barbara Szybinska *OS2-1, PS1-73*
MEKSUWAN, Warawan *PS1-58*
MELGOSA, Manuel *OS3-1, PS2-33, PS2-55*
MICHINAKA, Yusuke *OS10-3*
MILCIC, Diana *PS1-41*
MINAMI, Yoshitaka *MCS2-4*
MIRZAEI, Hamidreza *PS2-21*
MITSUBOSHI, Muneo *OS10-4*
MITSUTAKE, Tomoko *PS2-15*
MIWA, Ryotaro *PS2-74*
MIYAMAE, Itsuki *PS1-65*
MIYATAKE, Keiko *PS1-74*
MIYAZAKI, Keiichi *PS1-10*
MIYAZAWA, Kanae *OS8-2*
MIZOKAMI, Yoko *OS9-4, PS1-52, PS2-26, PS2-69*
MOCHIZUKI, Kosuke *PS1-40, PS1-42*
MOHAMMADZADEH DARRODI, Maryam *OS1-3*
MORI, Minoru *PS2-83*
MORITA, Aiko *PS2-30*
MUGHAL, Muhammad Farhan *OS3-6*
MURAKI ASANO, Chie *PS1-5, PS1-8*
MURAMATSU, Keiichi *PS2-24*
MYIN, Erik *PS2-49*
MYLONAS, Dimitris *PS2-6, PS2-11*

N

NAGAI, Takehiro *PS1-49, PS2-51*
NAGASAKI, Toshiki *PS1-81*
NAKAGAWA, Takashi *PS1-11*
NAKAJIMA, Yuki *PS1-45*
NAKAJIMA, Yuko *PS1-64*
NAKAMORI, Yuji *PS1-82*
NAKAMURA, Shinji *PS1-55*
NAKANO, Yasuhisa *PS1-81*
NAKATO, Mamiko *PS1-84*
NAKAUCHI, Shigeki *OS8-2*
NAKAYAMA, Kazumi *PS2-18*
NAKAYA, Ryota *PS2-52*
NAOKI, Takahiro *PS2-65*
NARITA, Ikuko *PS1-18*
NEGISHI, Ippei *OS8-1, PS2-46, PS2-52*
NEHME, Léa *PS1-7*
NEO, Mai *PS2-4*
NIEVES, Juan Luis *PS1-79*
NINOMIYA, Hirofumi *PS1-85*
NISHIGAKI, Masafumi *OS8-4*
NISHINA, Ken *PS1-59*
NISHI, Shogo *PS1-36, PS2-73*
NODERA, Aya *PS1-55*
NOGUCHI, Yuria *OS10-4*
NOMURA, Shuhei *PS1-82*
NORO, Naoki *PS2-69*
NOURY, Larissa *PS1-1*
NUDURUMATI, Srikrishna *OS3-2*
NYRHINEN, Kristiina *PS1-57*

O

O'DOWD, Paul *OS1-6*
OGATSU, Hitoshi *PS1-44*

OHBA, Natsumi *PS1-64*
OH, Heebaek *PS1-47*
OH, Ji-Young *PS2-4*
OHNAKA, Chiori *PS1-28*
OHNISHI, Takashi *MCS2-4*
OHNO, Haruyo *PS1-87*
OHNUMA, Kazuhiko *PS1-32*
OH, Semin *PS1-47*
OHTANI, Kimiko *PS2-38*
OISHI, Yuriko *PS2-40*
OJEDA, Juan *PS1-79*
OKAGAWA, Koki *OS8-4*
OKAJIMA, Katsunori *OS4-1, PS1-5, PS1-8, PS1-86, PS2-36*
OKUDA, Shino *PS1-86, PS2-36*
OKUDERA, Saori *PS1-64*
OLEN, Melissa *PS1-48, PS1-83*
OLIVEIRA, Ana C. *PS2-10*
ONG, Ruth Genevieve *PS2-77*
ORTIZ SEGOVIA, Maria *PS1-83*
OSAKA, Naoyuki *PS1-63*
OSAWA, Naoto *MCS1-4*
OSHIMA, Kosuke *OS7-5*
OSUMI, Masayuki *OS3-4, PS2-54*
OU, Li-Chen *OS2-5, OS4-4, OS10-1, PS1-21, PS1-61, PS2-22, PS2-31, PS2-44*

P

PADFIELD, Joseph *PS1-48*
PAN, Henry *PS2-22*
PAN, Qianqian *PS1-26*
PARK, Heykyung *PS2-4*
PARK, Jiyoung *OS7-3*
PARK, YungKyung *PS2-7*
PARK, Yunsun *PS2-17*
PARRAMAN, Carinna *OS1-6, PS1-83*
PEDERSEN, Marius *OS4-5*
PEETERS, Mart *PS2-57*
PELLACANI, Giovanni *MCS2-1*
PERALES, Esther *PS2-55, PS2-71*
PHUANGSUWAN, Chanprapha *OS10-2, PS1-59, PS1-70, PS1-71*
POGACAR, Vojko *PS1-3*
POINTER, Michael *OS3-1*
POLJICAK, Ante *PS1-41*
PORRAL, Philippe *PS2-66*
PRASITHRATHSINT, Amra *PS2-6*
PREMIER, Alessandro *PS2-25*
PUIG, Susana *MCS2-1*
PUJOL, Jaume *MCS2-1, PS2-71*
PURVER, Matthew *PS2-11*

Q

R

RATTANAKASAMSUK, Kitirochna *PS1-9, PS1-76*
REISINGER, Markus *OS9-3*
RHODES, Peter A. *PS2-64*
RIZZI, Alessandro *OS5-2, PS1-56, PS1-69*
ROMERO, Javier *PS1-35, PS1-79*
ROSSI, Maurizio *OS5-2*
ROYO, Santiago *MCS2-1*
RYU, Jiseon *OS4-2*
RYU, Kum-Hee *PS2-27*

S

SADRZADEH, Mehrnoosh *PS2-11*
SAFDAR, Muhammad *OS3-6, MCS1-2, PS2-68*
SAGAWA, Ken *PS1-64*
SAITO, Miho *PS2-24, PS2-37, PS2-39, PS2-40*
SAKAI, Hideki *OS4-3, PS1-82, PS1-86*
SAKAMOTO, Takashi *PS1-37*
SAKSIRIKOSIL, Chanida *PS1-9*
SAKURAI, Chihiro *PS1-42*
SAKURAI, Masato *OS10-3*
SANABRIA, Ferran *MCS2-1*
SASAKI, Kazuya *PS1-74*
SASAKI, Mikuko *PS1-62*
SATO, Kiyoshi *OS9-4*
SATO, Masato *OS2-2, PS2-18, PS2-20*
SATO, Tetsuya *PS1-65*
SAYIM, Bilge *PS2-49*
SCHINDLER, Verena M. *OS6-1*
SEJIMA, Kazuyo *Keynote Lecture pp.26*
SEKULOVSKI, Dragan *PS2-57*
SEO, Eunji *OS7-3*
SEO, Masataka *PS2-65*
SEYA, Yasuhiro *PS2-61*
SHAO, Si-Jie *PS1-80*
SHEN, Hui-Liang *PS1-80*
SHINODA, Hiroyuki *PS1-32, PS2-61*
SHINODA, Kazuma *PS1-74, PS2-72*

SHINOMORI, Keizo *OS8-1, OS8-2, PS2-46, PS2-52*
SHIN, Sangeun *PS2-14, PS2-19*
SHIOIRI, Satoshi *PS2-48*
SHIOMI, Risa *PS1-86*
SHISHIKURA, Masami *PS2-26*
SHOJI, Yuhei *PS2-51*
SHRADER, Stephen *OS6-5*
SHRESTHA, Raju *PS2-70*
SHYU, M. James *PS2-82*
SIE, Yu-Ping *PS1-46*
SIMON-LIEDTKE, Joschua *MCS2-2, PS2-79, PS2-81*
SINISCALCO, Andrea *OS5-2*
SIRIRUK, Kulthanee *PS1-38*
SITNIK, Robert *MCS1-1*
SOH, Jian-Yuan *PS2-4*
SOLOMITA, Giuseppe *MCS2-1*
SON, Hyeyun *PS2-17*
SRISURO, Ploy *PS1-9*
STAHRE WÄSTBERG, Beata *PS2-76*
ŠTĚRBA, Zbyněk *PS1-23*
STRGAR KURECIC, Maja *PS1-41*
SUGA, Shigeo *OS1-5, PS1-33*
SUK, Hyeon-Jeong *OS7-4, PS2-28, PS2-29*
SU, Li-Chi *PS2-58*
SUNAGA, Shoji *PS2-12, PS2-63*
SUNG, JiHyun *PS2-7*
SUN, Pei-Li *OS4-4, PS1-46, PS1-61, PS2-85*
SUN, Tsung-Chieh *MCS2-3*
SUN, Vincent C. *PS2-62*
SUN, YueJun *PS2-57*
SU, Yun-Chien *PS1-46*
SUZUKI, Hirotaka *PS1-22*
SUZUKI, Taka-aki *PS2-45*
SUZUKI, Takuzi *PS2-78*
SUZUKI, Tsuneo *PS1-68, PS1-78*

T

TAI, Nan-Ching *PS2-77*
TAJIMA, Tatsuya *PS2-51*
TAKAHASHI, Shin'ya *PS2-32*
TAKAHASHI, Yoshihumi *PS1-18*
TAKARA, Yohei *PS2-69*
TAKEDA, Naoko *PS1-20*
TAKEMURA, Akihisa *PS2-36*
TAKESHITA, Tomomi *OS8-4, PS2-26*
TANAKA, Midori *OS9-1*
TANAKA, Norihiro *PS1-40, PS1-42*
TANAKA, Ryosuke *PS2-61*
TANAKA, Yosuke *OS8-4*
TANGKIJVIWAT, Uravis *PS1-58*
TANG, S. *PS1-24*
TANIGUCHI, Shinichiro *PS2-26*
TASHIRO, Tomoronori *PS1-32*
TAWONPAN, Kanrawee *OS10-2, PS1-59*
TAYA, Sayoko *PS2-78*
TEUNISSEN, Kees *PS2-57*
THOMAS, Jean-Baptiste *PS2-84*
TOKUYAMA, Erika *PS1-84*
TOMIC, Ivana *PS2-31*
TOMINAGA, Shoji *MCS1-4, PS2-73*
TOMITA, Keiko *PS2-38*
TOYOTA, Ryu *PS1-81*
TOYOTA, Toshihiro *PS2-45*
TRIRAT, Pratoomtong *PS1-38*
TSUCHIDA, Masaru *PS2-83*
TSUCHIYA, Jun *PS2-63*
TSUJIMOTO, Kanae *PS1-8*
TSUJIMURA, Sei-ichi *OS4-1*

U

UCHIDA, Sunao *PS2-39*
ÜNVER, Rengin *PS1-15, PS1-16, PS1-17*

V

VALERO, Eva M. *PS1-35*
VAN UYTVEN, Tilde *PS2-49*
VAZQUEZ-CORRAL, Javier *PS1-29*
VÁZQUEZ, Jorge *MCS2-1*
VIÉNOT, Françoise *Judd Award Lecture pp.39*
VILASECA, Meritxell *MCS2-1, PS2-71*

W

WAKAI, Kohei *PS2-59*
WAKATA, Tadayuki *PS2-37*
WALEETORNCHEEPSAWAT, Boonchai *PS2-56*
WANG, Binyu *OS7-2*
WANG, BinYu *OS3-5, OS7-1*
WANG, Megmeng *PS2-67*
WANG, Qing *PS1-77*
WANG, Y. *PS1-24*
WANG, Yuzhao *MCS1-2*
WANG, YuZhao *OS3-5*

WANG, Zhifeng *OS3-1*
WASAKI, Hiroyuki *MCS2-4*
WATANABE, Aya *PS2-72*
WATANABE, Shunsuke *OS8-4*
WEI, Shuo-Ting *PS1-53*
WEI, Yuh-Chang *PS2-41*
WESTLAND, Stephen *PS1-12, PS1-14, PS1-26, PS1-67, PS2-13, PS2-43*
WIRIVUTTHIKORN, Wattana *PS1-75*
WON, Seahwa *PS1-67*
WUERGER, Sophie *PS2-67*
WU, Jau-Yi *PS2-22*

X

XIAO, Kaida *PS2-67*
XIN, John H. *PS1-72, PS1-80*
XU, Haisong *OS3-3, PS1-77*
XU, Jie *OS6-2*
XU, Liwen *OS1-1*

Y

YAGUCHI, Hirohisa *OS9-4, PS1-52, PS2-26, PS2-69*
YAMADA, Shogo *PS2-61*
YAMADA, Tetsuji *OS7-5*
YAMADA, Yuko *OS6-5*
YAMAHARA, Minori *PS1-84*
YAMAMOTO, Kazuhiro *PS2-53*
YAMAMOTO, Masashi *PS1-27*
YAMAMOTO, Sari *OS2-4*
YAMASHITA, Akemi *PS1-20*
YAMATO, Junji *PS2-83*
YAMAUCHI, Yasuki *PS1-49, PS2-51*
YANG, X. *PS1-24*
YANG, Yang *OS7-1*
YANO, Takuo *PS1-81*
YATA, Noriko *PS1-39, PS2-74, PS2-78*
YE, Ming *OS3-6*
YE, Wei *OS3-3, PS1-77*
YIN, Jingjing *PS2-67*
YONGSUE, Kamron *OS10-2, PS1-59*
YOSHIDA, Keishi *OS2-2, PS2-20*
YOSHIKAWA, Takahiro *OS10-3*
YOSHIMURA, Kohji *OS6-5*
YOSHIZAWA, Yosuke *PS2-15, PS2-50*
YUAN, Yinqiu *PS1-13*
YUN, Mengxi *PS2-39*

Z

ZAKIZADEH, Roshanak *OS1-2*
ZHU, Yuteng *OS3-6*

AIC 2015 Sponsors

Premium sponsor

BYK-Gardner GmbH

BYK-Gardner

BYK-Gardner is part of the BYK Additives and Instruments Division of Altana AG, a worldwide leader in the additives, special coatings and adhesives, effect pigments, sealants and testing instruments.

Innovation and Customer Focus - hand in hand

BYK-Gardner provides QC system solutions to those industries where color, appearance and physical properties add important value to their products. Innovative developments are the essential prerequisites to meet current and future needs of our customers. New technologies such as LED light sources or camera detection are the key to ensure not only accurate and reliable results in the most efficient way, but also a continuous improvement in correlation to the visual perception.

New products and application oriented solutions are the result of customer focus and partnership with our customers on a global basis. Therefore, BYK-Gardner is represented with subsidiaries and distributors in over 100 countries and regions.

Quality is our business

Our instruments are manufactured and controlled according to international standards ISO 9001, ISO/IEC 17025, ISO 50001, ISO 14001 guidelines and procedures.

Brand new manufacturing facilities, state-of-the-art production and advanced calibration equipment – all this makes BYK-Gardner products rank among the best in the market.

BYK-Gardner sets standards in color and appearance control.

Konica Minolta Inc.

Sensing Business Unit of Konica Minolta Inc. provides light and color measuring instruments based on the company's core optical technology to every corner of the world. As a pioneer in this filed, we developed the first light meter used on board a spacecraft in 1968 (Apollo 8) and the world's first portable spectrophotometer in 1982. Our products have recently become a staple in research and manufacturing environments, helping our partners to be innovative and successful in making breakthroughs with the least waste of time and effort by improving and assuring the quality of their products. This commitment to creating value for customers is the shared passion and the core principle behind the Konica Minolta brand. Color management is essential in almost all areas of manufacturing, including automotive, paint, plastic, chemicals, textiles, construction materials, medicine, cosmetics, and food. Our color control techniques are instrumental in measuring subtle color differences that human eyes cannot distinguish accurately. Konica Minolta's spectrophotometers and colorimeters are therefore widely utilized at quality control and R&D. We promise to do our best to contribute to the success of our customers by providing not only the state-of-the-art products, but the high level of customer-centric technical support and services worldwide.

Gold sponsor

EBA Japan Co.,Ltd.

EBA Japan CO.,LTD. treats spectral imaging technologies.
Our technologies clear and propose the path for your innovative future.
They can get spectroscopic information not for one pixel but for all pixels quickly.
Using the spectroscopic information map, you can convert colors to every color space coordinates and evaluate them in 3 dimensions (horizontal, vertical, spectral).
The spectral color imaging system is helpful in “Various display evaluations”, “Color rendering evaluation”, “Color evaluation of cultural assets” or “Evaluation of light source”.
We hope that “EBA Japan Imaging” will help you with your research and offer the hints for your future prosperities.

FUJIFILM Holdings Corporation

Fujifilm Group is transcending its conventional business fields of “Imaging and Information” to transform into a company that contributes to the development of culture, science, technology and industry, as well as improving health and environmental protection across society. To help enhance the quality of life toward realizing a society in which people enjoy spiritual and material wealth, we will strive to realize our corporate philosophy through the three business fields of Imaging Solutions, Information Solutions and Document Solutions.

Suga Test Instruments Co.,Ltd.

SUGA Test Instruments Co., Ltd. is a manufacturing company specialized in optical property measuring instruments.
Since 1959, SUGA Test Instruments, has developed Colour Meters and thereafter other unique color property, and accumulated rich experiences supporting gl-obal partners in improving and assuring the quality of partners' products.
SUGA Test Instruments, manufacturers, sells and provides services globally, portable and desk top, world-class colour meters, spectrometers, and unique & bench top gloss meters, haze meters and image clarity meters.
These colour appearance analyzers allow one to access and control the colour appearance properties of products and materials.
SUGA-only is a brand that you can rely and depend upon to solve all your colour appearance needs.

Silver sponsor

DIC Corporation / DIC Graphics Corporation

DIC is a fine chemicals company with a top share in printing inks, organic pigments and PPS compounds in the global market.
DIC provides a broad range of products that respond to the needs of society and its customers, and works to bring people "Color & Comfort by Chemistry."

Japan Paint Manufacturers Association

The Japan Paint Manufacturers Association (JPMA) was established in April 1948 as a voluntary organization of paint manufacturers industry. JPMA consists of about 258 members: Regular Members who are leading paint manufacturers in Japan, plus Supporting Members who are engaged in paint-related industries.

Murakami Color Research Laboratory

NIPPON DENSHOKU INDUSTRIES CO.,LTD.

NIPPON DENSHOKU INDUSTRIES CO.,LTD., is specialist for color measuring instruments.
It's been half a century since we have started to support the color management and will broaden our view and contribute to color business society.

OPTIS Japan

Since 1989, OPTIS has led the way in light simulation software. Our unique physics based simulation tools deliver the most accurate representation of optical and lighting systems and are fully integrated into the world leading CAD platforms. OPTIS solutions can also help you understand how color and spectrum work in your products and systems.

Spectral Application Research Lab. Inc.

Spectral Application Research Laboratory Inc. (SARLI) supplies a Spectral Imaging System (all own designs) which is able to examine the mixed state of natural and artificial materials more deeply. Our system consists of camera and drive device on sample side, and also a dedicated software application is built-in.

Systems Engineering Inc.

Topcon Technohouse Corporation

Topcon Technohouse Corporation provides various types of light and color measuring instruments and contributes to the development of many industries.
Our Luminance colorimeter BM series, Spectroradiometer SR-3/UL series, and Illuminance meter IM series have been used as standard in various industry fields such as Flat panel display, Illumination, and Automotive.

Basic sponsor

Canon Inc.

Canon specializes in an extensive range of imaging products such as digital cameras, printers, office multifunction devices, and others for consumers, businesses, and professionals. With years of expertise in image-processing technologies, Canon creates high-quality, unified color look possible even for input and output devices with differing color reproduction ranges.

Integra Inc.

Primary businesses of Integra Inc. are development, marketing and sale of computer software products and related services for engineering.
Main products of the company are software packages, Hybrid Light Simulation Software, lumicept for optical and illumination simulation where accuracy and speed to simulate propagation of light has the essential importance.

KLV. CO., Ltd

KLV is known as one of the top makers of light sources, optical parts, and optical products. We have contributed to the development of optical technology in many field including medical, biological, agricultural, environmental, and food sciences for the past 30 years in Japan.

SERIC Ltd.

We are a manufacturer of artificial solar light, branded SOLAX for color evaluation. We have many sales result to deliver our products for our customers, who are car manufacturers, paint companies, digital camera makers, cosmetic companies, and so. We recommend our product for color management as the professional sunlight maker.

Coffee Break sponsor

OFFICE COLOR SCIENCE Co., Ltd

Office Color Science Co., Ltd is specialized in computer system relating to color science. We have mainly developed Computer Color Matching (CCM) system and Color Quality Control system for Metallic and Pearlescent color. We pursue the possibility of color application and create value through our technology to enrich color design of industrial products.

色 と 像

AIC 2015 TOKYO